Essentials of Diagnostic Pathology
*Series Editor:* Farid Moinfar

Peter Spieler
Matthias Rössle

# Nongynecologic Cytopathology

## A Practical Guide

Springer

# Essentials of Diagnostic Pathology

Series Editor: Farid Moinfar, Graz, Austria

For further volumes:
http://www.springer.com/series/8171

Peter Spieler • Matthias Rössle

# Nongynecologic Cytopathology

## A Practical Guide

Springer

**Dr. Peter Spieler**
Kantonsspital St. Gallen
Institut für Pathologie
Rorschacherstraße 95
9007 St. Gallen – Switzerland
Email: pe.spieler@bluewin.ch

**Dr. Matthias Rössle**
UniversitätsSpital Zürich
Institut für Klinische Pathologie
Schmelzbergstraße 12
8091 Zürich – Switzerland
Email: matthias.roessle@usz.ch

ISSN 2194-6256 eISSN 2194-6264
ISBN 978-3-642-24718-7 ISBN 978-3-642-24719-4 (eBook)
DOI 10.1007/978-3-642-24719-4
Springer Heidelberg Dordrecht London New York

Library of Congress Control Number: 2012941429



*Cover design:* eStudio Calamar, Figueres/Berlin

Printed on acid-free paper

Springer is part of Springer Science+Business Media (www.springer.com)

# Foreword

Pathologists play a key role in the realization of personalized patient care. Their efforts have been central in providing appropriate diagnostic, prognostic, and predictive information. As an integral part of surgical pathology, the discipline of cytopathology also plays an important role in health care.

This volume, the first in the series *Essentials of Diagnostic Pathology*, has been written by two highly respected cytopathologists, Drs. Peter Spieler and Matthias Rössle, who have a great deal of experience in the field of clinical cytology. The book deals extensively with exfoliative and aspiration cytology of all major nongynecologic body sites. It offers a systematic and organized approach to the diagnostic criteria, main differential diagnoses, and major pitfalls in nongynecologic cytopathology. It also considers the application of possible ancillary studies in order to reach the correct diagnosis. Gynecologic cytopathology is not included in this work, but will be covered separately in a forthcoming book of the series entitled *Diagnostic Gynecologic Pathology*.

This practical guide will serve as a substantial reference monograph by virtue of the inclusion of more than a thousand high-quality illustrations of a wide variety of benign and malignant lesions. It is highly recommend to pathology residents, cytopathology fellows, cytotechnologists, and academic/community cytopathologists, for whom it will represent a valuable addition to the library and an excellent day-to-day reference manual.

Drs. Spieler and Rössle are to be congratulated for providing this beautiful work on nongynecologic cytopathology.

**Farid Moinfar, MD**
Series Editor: Essentials of Diagnostic Pathology
Professor of Pathology
Institute of Pathology
Medical University of Graz

# Dedication

This book is dedicated with great appreciation to my wife, Cathy Spieler-Menzi, in gratitude for her thoughtfulness and abundance of patience during the long four-year period of writing the manuscript and preparation for publication.

Matthias Rössle expresses his special thanks to his wife and best friend, Daniela Lang Rössle.

**Peter Spieler, MD**

# Preface

*He will manage to cure best who has foreseen what is to happen from the present state of matters.*

*Hippocrates*

We have faced two key challenges in creating this book: to maintain the high standard offered by previously published books and atlases on cytopathology, and to provide a reference of a different type that will be suitable for advanced practitioners of diagnostic cytology.

The incentive to write the book originated from a friend and colleague, Dr. Farid Moinfar, Professor of Pathology at University Hospital Graz, Austria. We are grateful to Dr. Moinfar for reviewing the chapter on fine-needle aspiration of the breast.

His enthusiastic encouragement inspired us to put to paper our knowledge in cytologic diagnostics. In the case of Peter Spieler this is based on 30 years of diagnostic experience in cytopathology and static digital DNA image cytometry, while Matthias Roessle has expertise in the practical application of immunocytochemistry and molecular methods in routine cytologic diagnostics.

This book provides comprehensive, extensively illustrated descriptions of the pathology of the full range of disorders of almost all the organ systems, an exception being the female genital tract. As analyses of cytomorphologic findings at various body sites sometimes prove extremely challenging, we offer a systematic approach based on cytologic criteria and present differential diagnostic algorithms that we hope will assist cytopathologists and cytotechnologists when analyzing problematic cases.

The management of disease is a multidisciplinary endeavor and often includes a cytologic analysis. Throughout this book we emphasize that a cytomorphologic diagnosis, either in itself or in conjunction with ancillary test results, constitutes a decisive factor when determining the course of further investigations and/or treatment.

**Peter Spieler, MD**
**Matthias Rössle, MD**

# Acknowledgments

The authors wish to thank a great many staff members in the Cytology and Histology Departments of the Institutes of Pathology, Kantonsspital St. Gallen, Kantonsspital Lucerne, and University Hospital Zurich, all located in Switzerland, for their loyal scientific, technical, and logistic support.

The authors also wish to express their sincere appreciation and gratitude to PD Sergio B. Cogliatti, MD, for his invaluable contribution to the lymph node chapter. As an expert in lymphoma pathology, he critically reviewed the entire chapter and incorporated valuable suggestions and improvements regarding diagnostics and adjuvant analyses at the cytology level. Despite his high work commitment in a busy, service-oriented institute, Dr. Cogliatti always found time for stimulating discussions, and rigorously scrutinized the technical explanatory notes. We also gratefully acknowledge the contribution of Dr. Walter Hoebling, PMPH, Director of the Institute of Pathology at Klinikum Wels-Grieskirchen, Wels, Austria, in providing a selection of illustrations for the section "Malignant Lesions of Soft Tissue and Bone."

Special thanks are due to Josefine Stani, CFIAC, and Joshua Korn, Vienna, Austria, for correction and review of the English text.

Finally, we wish to express our appreciation to our publisher, Springer-Verlag, and particularly to Gabriela Schroeder, Editorial Director; Ellen Blasig, Desk Editor; Sandra Lesny, Associate Editor; Claus-Dieter Bachem, Project Coordinator; Linda Northrup, Text Editor; and Alwin Metter, Production for their excellent professional work and cooperation.

# Contents

## 6 Central Nervous System



## 7 Eye



## 8 Oral Cavity and Oropharynx



## 9 Liver



## 10 Pancreas, Extrahepatic Bile Ducts, Ampullary Region



## 11 Gastrointestinal Tract

## 12 Kidney, Adrenal Glands, Retroperitoneum



## 13 Urinary Tract



## 14 Male Genital Organs



## 15 Lymph Nodes



## 16 Skin Lesions and Unusual Subcutaneous Lesions



## 17 Soft Tissue and Bone

# 18 Synopsis and Algorithms

# 1 Breast



Spieler/Rössle, *Nongynecologic Cytopathology. A Practical Guide. Essentials of Diagnostic Pathology*,
DOI 10.1007/978-3-642-24719-4_1, 

## Synopsis and Algorithms

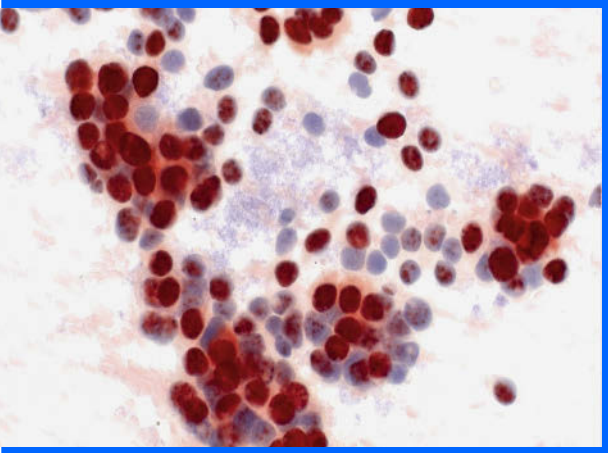

# Section 1.1
# Breast: Fine-Needle Aspiration Biopsy



## 1.1.1 Introduction

- Percutaneous fine-needle aspiration biopsy (FNAB) of the mammary glands has been widely used as a diagnostic tool from the middle to the end of the twentieth century [19, 33, 56]. However, for many years, the use of core-needle biopsy (CB) has increased. FNAB has been shown to be a simple, rapid, cost effective, and mainly complication-free technique that can replace a large number of surgical biopsies when performed by a well-trained physician. However, many clinicians and pathologists are unfamiliar with this interventional technique and especially its appropriate implementation [91].
- The best results with FNAB are obtained when every step of the procedure is performed by a skilled cytopathologist [38], that is:
  - Assessment of the relevant clinical history and the appearance of the target lesion on the image.
  - The choice of the interventional procedure (with or without image control).
  - Selection of the specimen-processing method (conventional smears vs. a liquid-based method vs. the cell-block technique).
  - Microscopic evaluation.
  - Application of ancillary diagnostic methods.
  - To make a final cytologic diagnosis.
- Inexperienced operators and inadequately trained physicians reduce the efficiency and diagnostic sensitivity of the method; FNABs often yield inadequate diagnostically inconclusive and potentially misleading material [33, 43, 78].
- It is a fact that the acceptance of FNAB has been delayed in many centers. Training of private physicians and physicians at primary care hospitals has been shown to be highly effective for the quality of aspirated material [16, 65, 97,104].
- The successful implementation of FNAB depends on the cytopathologists' skill and results; but multidisciplinary approach, and local situations in pathology and clinical institutions are highly important as well. Furthermore, close collaboration between the cytopathologists, radiologists, and surgeons in a specialized breast unit provides the most efficient interventional method and maximizes the quality of diagnostic results [63, 67, 69, 97,100].
- The assistance of a cytotechnologist (biomedical analyst), skilled in specimen preparation to make a preliminary judgment on the adequacy of the aspirated sample, is highly recommended for image-guided FNABs outside the cytology department.
- Physical examination, mammography, and FNAB known as the triple technique is still used in breast clinics as a routine practice with excellent results. If there is any doubt after triple assessment, needle-core biopsy or surgical excision must be performed. Furthermore, all cases with suspicious or equivocal FNAB results should be followed by a subsequent core biopsy before planning surgery.
- Judging from our experience and reports in the literature, FNAB has significant limitations in the diagnosis of carcinoma in-situ, lobular carcinoma, tubular carcinoma, and small nonpalpable tumors (< 1 cm) [50, 83].

- In spite of a tremendous increase in the application of core-needle biopsies, reports in the literature and guidelines indicate that FNAB is still a useful method in the diagnosis of a variety of breast disorders [12, 18, 29].

**Caution**

FNAB is not effective in the evaluation of microcalcifications

## 1.1.2 Aspiration Technique

- In cases with superficial nodules, the target lesion must be immobilized with one hand. Therefore, it is highly recommended to use a single hand-grip syringe holder (equipped with a syringe with an eccentric tip and the appropriate needle), in order to apply suction as soon as the needle is inserted into the target. The use of a vacuum system directly connected with the needle is also recommended.
- FNAB utilizes 21- to 27-gauge needles. Using larger needles in many cases yields blood-rich aspirates with only a few target cells, insufficient for a diagnosis. It is better to use a larger needle (21-gauge) to empty a cyst with thick content. In contrast, smaller needles (25- to 27-gauge) perform better in densely fibrotic lesions, highly vascular lesions, and tiny firm superficial lesions.
- It is important to perform excessive aspiration with multiple needle passes and suctions in a fan-like modality in order to collect an adequate sample. We agree with Wu and Burstein, who emphasize "Sampling in FNA is not as much a function of suction as of cutting" [107].
- Several papers describe the technique of needle sampling without suction [1, 110]. A more recent paper by Ibrahim and coauthors on FNABs without aspiration on breast lesions indicate a high inadequacy rate of 58.7% and a very low sensitivity of 34.5% [45]. We conclude that FNAB without suction cannot perform successfully on breast lesions because many solid tumors harbor densely fibrotic tissue that prevents harvesting sufficient diagnostic material.
- There are several excellent papers providing greater detail regarding the FNA biopsy technique [98, 107].

## 1.1.3 Indications for FNAB and Imprint Cytology

- All palpable masses are suitable for FNAB and there is virtually no contraindication for FNAB on lumps in the breast. The intervention should be performed with a certain respect and less vigorously than usual on patients with bleeding diathesis or anticoagulant use. FNAB has been shown to be very useful as an initial investigation on tumorous disorders in the male breast [40].
- There is a wide spectrum of lesions in the breast and in the surgical scar area after a mastectomy and lumpectomy, especially during and after radiotherapy. The majority of these lesions are benign. FNAB helps to achieve a quick diagnosis and prevents further surgery [55, 66].
- In a few cases the "scouting needle" FNAB technique may be applied when the patient refuses a more invasive procedure and in cases with a diffuse disorder of the breast with unremarkable imaging tests [23]. Vigorous aspiration with multiple passes in a suspected area, or four-quadrant aspiration in cases with diffuse breast enlargement is recommended. Negative cytologic findings require further investigations.
- The image-guided FNAB technique can be utilized in deep seated nonpalpable tumors which are recognized by ultrasound or magnet resonance imaging (see Sect. 1.1.5, p. 6).
- For multidisciplinary assessment in one-stop clinics, on-site cytopathologists can provide immediate diagnostic results on FNABs that enable clinicians to counsel patients and plan the appropriate treatment [67]. Several recent studies show that core imprint cytology is a reliable predictor of the core biopsy histology and, therefore, could be a useful supplement for rapid assessment in breast clinics [31, 48, 84].

Based on personal experience from the interdisciplinary cooperation with the specialists of the breast unit at our hospital, the indications for FNAB listed in Table 1.1.1. are the most significant.

## 1.1.4 Laboratory Techniques

### 1.1.4.1 Conventional Smears

Both wet-fixed and air-dried smears provide a reliable cytodiagnostic performance. Many cytopathologists prefer wet-fixed specimens followed by Papanicolaou staining because nuclear details are well preserved and match nuclear and cytoplasmic structures observed in paraffin sections.

For wet fixation, direct smears must be fixed immediately within 1–3 s after spreading the material. Slides can be dropped into a pot with an alcohol-based fixative or a spray fixative can be used.

### 1.1.4.2 Liquid-Based Cytology

(cytospin®, ThinPrep®, SurePath®, etc.)

- FNAB material is rinsed in a vial containing a cell medium. Thin-layer preparations can be performed as instructed by the manufacturer. The thin-layer method is best used by clinicians performing FNABs if the operators are not familiar with proper preparation and fixation technique [98].

**Table 1.1.1** FNAB indications for the breast, both with and without ultrasound guidance

| | |
|---|---|
| 1. | Minimally invasive diagnostic procedure on large palpable tumors with outpatients |
| 2. | Small palpable or ultrasound-relevant lesions > 3 mm, in particular those related to the skin or adjacent to the chest wall and prostheses, respectively |
| 3. | All lesions considered benign due to clinical and imaging findings |
| 4. | Cystic lesions |
| 5. | Complex mastopathic lesions calling for repeated monitoring over long periods |
| 6. | FNAB on multifocal and multicentric lesions during the same session for tumor staging |
| 7. | Structural changes in the mammary gland during pregnancy and in the lactation period |
| 8. | Tumors in the male breast |
| 9. | Recurrent lesions in the follow-up of known breast cancer, especially after radiation therapy and in surgical scars |
| 10. | Tumors in the breast with a well-known history of malignancies from organs other than the breast |
| 11. | Palpable and nonpalpable axillary nodular lesions |
| 12. | Patients with bleeding diathesis or those on anticoagulant medication |
| 13. | Rapid on-site / one-stop diagnostics in specialist breast units combined with ultrafast staining of the cytologic sample |

In many circumstances, the liquid-based method is superior to conventional smears because it provides a clear background, monolayer cell preparation, and good cell preservation.

- With this procedure, an optimal preparation can be achieved for special investigations, in particular for immunocytochemistry, fluorescence in situ hybridization, or static DNA cytometry. In addition, the rinse from the needle and syringe may be used for immunolabeled flow cytometry [52, 60].
- Regardless of the operator, hemolyzing fixatives (Cytolyt® and others) have been shown to be indispensable as an initial transport medium for blood-rich aspirates (particularly from thyroid and abdominal lesions). Combined with a thin-layer preparation, hemolyzing fixatives are a very useful modality for blood-rich FNABs. It lyses blood cells, yielding well-preserved cellular material and clear background.
- An accurate diagnosis in fine-needle aspiration is highly dependent on well-known cytoarchitectural and cellular patterns and the relation of cellular and background material to each other. Morphologic features may be altered using liquid-based methods. The procedure may raise diagnostic problems, especially in the differential diagnosis between benign florid ductal proliferation, atypical ductal proliferation, and malignant low-grade lesions [80] (Figs. 1.1 and 1.2).
- All recent reports in the literature indicate that liquid-based cytology is an accurate and feasible method for the investigation of breast lesions as well as in comparison with the conventional smear [8, 49, 52, 102]. However, liquid-based preparations require special experience concerning cell interpretation.

### 1.1.4.3 Cell-Block Technique

Application of cell-block production depends on the type and the amount of cytologic material available. The preparation of cell blocks is useful in situations where tissue fragments or clots are present in the original cytologic specimen, especially in the liquid-based setting.

### 1.1.4.4 Rapid-Staining and "Quick-Read" [58, 98]

- FNAB is a simple method, sampling and processing of cellular material takes little time. Therefore an immediate nearpatient diagnosis using a rapid cytodiagnostic approach is a useful procedure:
  - To ensure adequacy of the aspirate.
  - To identify cases which qualify for a second intervention in order to obtain more material for ancillary studies [98].
  - For critically ill patients demanding rapid therapeutic intervention.
- A modified Wright-Giemsa stain (Diff-Quik) can easily be used on air-dried preparations. On wet-fixed smears, an ultrafast Pap-staining technique can be applied [108].
- A very simple nuclear staining procedure is applied at our institution, mainly on outpatients. The fast stain provides information on the cell content of the aspirate and a reliable diagnosis within 3 min in a high percentage of cases:
  - Immersion of the slide in alcohol medium or fixation with a fixative spray;
  - Nuclear hematoxylin staining for 10 s;
  - Watering;
  - Slide mounted with water.

1

## 1.1.5 FNAB Supported by Imaging Methods

### 1.1.5.1 Ultrasound-Guided FNAB

[11, 15, 17, 32, 37, 41, 51, 62, 75, 81, 95, 103, 106]

- Ultrasound-guided FNAB (US-FNAB) is useful in the management of small and nonpalpable breast masses and lymph nodes, respectively, especially where the lesions are deep-seated, adjacent to the chest wall and implants or between the ribs. It is a valuable method, complementary to the ultrasound-guided large-core biopsy that reduces unnecessary surgical procedures (Fig. 1.3).
- It has been shown that high-frequency breast ultrasound (13 MHz) has a higher ultrasound diagnostic accuracy compared to ultrasound investigations with 7.5-MHz transducers [93].
- On the real-time ultrasound image, the aspirator has to make sure that the needle has penetrated the lesion.
- However, cytology frequently does not correlate with clinical and imaging findings in lesions smaller than 1 cm. In cases with equivocal FNAB results, the patients should undergo a histologic procedure. The negative and equivocal results are often due to technical limitations or biological properties of the target lesions:
  - Image-guided targeting of small lesions is often difficult.
  - Small benign and malignant disorders exhibit stronger fibrosis and sclerosis than voluminous tumors, providing a sparse FNAB sample.
  - Small breast cancers are likely to be well differentiated with equivocal cytological changes of malignancy.
  - US-FNAB on lesions, solely visible as calcifications (> 3mm) and suggestive of an in-situ lesion, is adequate in selected cases or in institutions where this procedure is an integrated component of outpatient management. Nevertheless, it is widely accepted that invasion in malignant breast lesions cannot be assessed by aspiration cytology [13, 70, 88, 89].
  - In our experience, US-FNAB, compared to freehand aspiration, yields better results also on large superficial palpable lesions where the needle is easily placed in the sonographically most suspicious area.

US-FNAB has turned out to be an extremely reliable diagnostic tool in our institution, particularly for small solid lesions. The results during a 1-year period are presented in Table 1.1.2.

### 1.1.5.2 Stereotactic FNAB

Management of nonpalpable and well-defined lesions on mammography is also possible with FNAB by the stereotactic approach [3, 5, 20, 22, 103]. However, today stereotactic needle biopsy using wide-core needles for histologic samples is largely preferred. The stereotactic core-needle biopsy yields more accurate results when compared with stereotactic FNAB [59].

### 1.1.5.3 FNAB Supported by PET-CT Imaging

Computed tomography (CT) combined with positron emission tomography (PET) resolves the problem of exact localization of a vague lesion with enhanced metabolic activity, which has a direct impact on the FNAB results. Many of the lesions can be detected by ultrasound and clarified using US-FNAB after being visualized by contrast-enhanced computer tomography imaging. The procedure is particularly valuable in the management of axillary lymph nodes, level II and III

**Table 1.1.2** Total US-FNAB on 218 female breasts during a 1-year period (2005)

164 US-FNAB with complete follow-up (core biopsy, excision, lumpectomy, autopsy, re-FNAB and clinics)
Follow up: minimum 12 to a maximum 24 months

| | B2 | B3 | B4 | B5 | Clinical follow-up |
|---|---|---|---|---|---|
| C2 | 9 | 1 | | 1 | 107 |
| C3 | 8 | | | | 2 |
| C4 | 1 | | 1 | 2 | |
| C5 | | | | 29 | 3 |

Specificity, 99.2%; complete sensitivity (including C3 + C4): 97.2%

The B/C scheme is elucidated in Sect. 1.1.6, p. 7.

Patient age: 15–89 years; mean, 50 years

Size of the lesions: 3–45 mm; mean, 16 mm

- Cytologic carcinoma diagnoses on 218 FNABs: **32 ( 15% )**;
- FNABs without histologic control (unequivocal triple assessment; see Sect. 1.1.1, p. 3): **51%**;
- FNABs not adequate (poor or missing diagnostic cell material): **7 (3.2%)**; histology: one carcinoma, one papilloma, five benign lesions.

[97]. PET-CT has also been reported to be a valuable method for identifying occult breast cancer [99].

#### 1.1.5.4 MR-Guided Breast Biopsy

Magnetic resonance (MR) imaging-guided stereotactic biopsy has been documented as a feasible procedure for routine clinical use [92]. It appears that using this method cytologic samples are less adequate for diagnosis when compared with histologic biopsies [79].

### 1.1.6 Reporting Categories and Cytologic Grading

- The *UK NHSBSP Guidelines for Non-operative Diagnostic Procedure and Reporting in Breast Cancer Screening, 2001* [74, 83] is an often recommended and used classification to assign the FNAB results. It contains the following five cytology categories (in agreement with the histologic scheme):
  - C1 inadequate
  - C2 benign
  - C3 atypia, probably benign
  - C4 suspicious, probably malignant
  - C5 malignant

  The classification turned out to be helpful in combination with a rapid on-site patient FNAB diagnostic service and for studies on large-scale FNAB material.
- In addition to cytometric methods (see Sect. 1.1.8.4, p. 8), grading systems using cellular and nuclear morphologic properties can be applied to cytologic samples. These results, as documented in the literature, show a close correlation with the histologic grade and indicate reliable information for an overall prognosis. These findings are important because prognostic information from the preoperatively performed fine-needle aspiration is increasingly required. [25, 44, 47, 85, 86, 111].

### 1.1.7 FNAB vs. Core-Needle Biopsy

Core-needle biopsy (CNB) is superior to FNAB in terms of sensitivity and specificity, and for a correct histological typing of breast lesions. Indeed, CNB exhibits a lower suspicious rate of breast lesions. The combination of FNAB and CNB increases sensitivity and decreases inadequate rates. The FNAB results are most accurate when experienced cytopathologists are available for the biopsy procedure and interpretation (the sensitivity of FNAB ranges from 90 to 97% in large series) [6, 9, 10, 26, 34, 57, 61, 63, 77, 105]. If performance requirements cannot be met, FNAB will be an inadequate method leading to an excess of false-negative results and be useless for clinical application in modern breast units.

A comprehensive review of the literature and analyses are discussed by P.D. Britton in *The Breast 1999*. He emphasizes that the results gained from research projects and many various centers are diverse [15].

### 1.1.8 Ancillary Studies

Ancillary studies can be conducted on direct FNAB smears, liquid-based preparations (cytocentrifuge, ThinPrep, etc.), and sections of cell-block material with reliable results.

Special studies on FNAB material are particularly useful in cases of small tumors, patients undergoing presurgical (neoadjuvant) therapy, tumor follow-up with relapses in the breast, and breast cancer metastases in distant organs [36, 64, 60, 68, 94].

A review of the literature on application of immunohistochemistry can be seen in a recent paper by I.T. Yeh and C. Mies [109].

#### 1.1.8.1 Analysis of Hormone Receptors

(Figs. 1.4 and 1.5)

Hormone receptor (estrogen receptor, ER; progesterone receptor, PR) status is important for the therapeutic choice (antihormonal treatment) and prognosis of breast cancer.

Several studies have revealed that immunocytochemical assay of hormone receptors can be applied in routinely fixed cytological preparations. Results show high accuracy and good concordance compared with the corresponding test on histologic sections [60, 68, 73, 96].

#### 1.1.8.2 Other Immunocytochemical Stains

Immunocytochemical (IC) assays, other than hormone receptor analysis and assessment of Her2/neu oncoprotein overexpression, are rarely used on cytologic material.

- Lobular breast cancer cells are mostly negative for E-cadherin and positive for high-molecular-weight cytokeratin marker 34BetaE12, while ductal cancer cells show an opposite staining pattern.
- While positive immunoreactions for low- and high-molecular-weight cytokeratins are characteristic of benign ductal epithelial proliferation (UDH), the vast majority of lesions with ductal intraepithelial neoplasia (atypical intraductal hyperplasia/ductal carcinoma in situ) are negative for high-molecular-weight cytokeratins (such as CK5/6, CK14, or CK34beta14). One should also note that CK34BetaE12 is characteristically positive in the vast majority of lobular intraepithelial neoplasia and less commonly positive in invasive lobular carcinoma [72].

1

In general, immunoprofiles that distinguish between benign, atypical, and malignant ductal lesions are beyond the cytodiagnostic challenge.

- Immunocytochemical analysis is essential in metastatic breast cancer [24, 42]. Secondary cancer, which mimics a primary breast neoplasia, must definitely be assessed because evaluation of the anatomic site of origin needs an appropriate panel of immunostains. Breast cancer cells are often positive for ER, PR, CK7, GCDFP15 and mammaglobin unless the tumor is poorly differentiated or the cells are poorly preserved.

#### 1.1.8.3 Her2/neu Status (Fig. 1.6)

- Many studies have shown that Her2/neu overexpression is a prognostic and predictive factor in breast cancer patients. Overexpression of the Her2/neu oncoprotein can be reliably detected in routine cytologic preparations [71].
- While IC detects the gene product, fluorescence in situ hybridization (FISH) detects gene amplification. Judging from data in literature, it seems that it is better to assess gene amplification of Her2/neu (as detected by FISH) than oncoprotein overexpression (as assessed by IC) [7, 90].
- The FISH technique is highly applicable in FNAB material because the nuclei are intact and no dissociation procedure is necessary [14, 36, 39, 76]. It is important to select widely spaced and isolated cells that are not covered by erythrocytes. Her2-status can also be evaluated on archived cytologic slides [39].

#### 1.1.8.4 DNA Ploidy, Grading

Numerous investigations over the last three decades have shown DNA ploidy to be a useful prognostic indicator, independent of clinical factors, with a good correlation between grading and ploidy of breast carcinoma [4, 21, 30]. Similar results are reported in the assessment of DNA ploidy and S-phase fraction with flow cytometry [82]. Computerized image analysis determines DNA content using the Feulgen stain on air-dried, wet-fixed, or archived FNAB samples.

In recent papers, a new classification of DNA content has been described. This method appears to be more relevant in predicting the aggressive potential of breast carcinomas than the previous one, which classified breast carcinomas into diploid, polyploid, tetraploid, and aneuploid groups. In addition, the new method classifies these cancers into stable and unstable subtypes [53, 54].

**Caution**

- Ancillary studies can be performed on cytologic preparations produced by various techniques. Technical details and individual processing have to be developed for each type of investigation depending on the specific equipment in each individual institution.
- Drying out the smears can prevent proper immunolabeling, which may provide false-negative results.

### 1.1.9 The Problem of Suboptimal FNAB Specimens

#### 1.1.9.1 Inadequate fixation

Fixation by immersion or a spray fixative for Pap-staining must be applied within 1–3 s; otherwise important diagnostic details will be effaced due to air drying (Figs. 1.7 and 1.8).

The most important cytomorphologic features for assessment of malignancy in ductal and lobular cells are nuclear shape and chromatin structure. However, inadequately fixed cell material from malignant lesions that occurs in regular clusters and exhibits pale nuclei with smooth margins intermingled with small dark bipolar nuclei could be interpreted as benign. On the other hand, less well-preserved cellular material from malignant lesions usually exhibits irregular dense clusters with overt cellular depolarization. Nuclei are eccentrically positioned and irregularly shaped. Isolated cells and cells in tiny aggregations make up a denser cytoplasm and a more granular chromatin pattern.

#### 1.1.9.2 Sanguineous Aspirates

Excessive blood in a cytologic preparation may completely mask the epithelial cell component hampering the diagnostic evaluation. The immediate transfer of the syringe content of blood-rich aspirates into hemolyzing fixatives helps to solve this problem. The subsequent processing of the material using a liquid-based method offers an accurate diagnostic tool (see also Sect. 1.1.4.2, p. 5).

#### 1.1.9.3 Marked Fibrosis

FNAB on fibrotic lesions yields aspirates with sparse cellularity. The only cellular material presented on smears may be small fragments of fibrotic soft tissue even by vigorous cutting motions during the aspiration procedure. A diagnostic core needle biopsy or excisional procedure is considered more appropriate than a repeated FNAB in lesions with marked fibrosis.

## 1.1.10 FNAB of Axillary Nodes

- Clinically suspicious nodes in the axilla are a common indication for FNAB. The sensitivity of physical examination of the axilla is low: 33–68% [27].
- Preoperative ultrasonography combined with US-FNAB of the axilla without palpable lymph nodes in breast cancer patients reduces the number of sentinel lymph node excisions and generates a significant cost savings [2, 35]. A sentinel lymph node biopsy together with a subsequent lymph node dissection is much more labor-intensive than a preoperatively positive FNAB result. Only the sonographically most suspicious nodes should be aspirated in order to reduce the number of FNABs on normal nodes to a minimum [27, 46, 87].
- Cells from small macrometastasis (metastasis larger than 2 mm) and micrometastasis (metastasis ≤ 2 mm) appear only occasionally in US-FNAB, and they are often lost on the imprints from the cut surface of sentinel nodes.
- It is important to be aware of the diversity of benign and malignant entities encountered in FNABs from axillary masses and nodules:
  - Breast cancer metastasis;
  - Primary breast cancer developed from ectopic mammary tissue;
  - Metastasis of tumors from sites other than the breast;
  - Fibrocystic changes or hyperplasia in ectopic breast tissue (Fig. 1.9);
  - Malignant lymphoma;
  - Lipoma;
  - Epidermal cyst;
  - Tumor-forming inflammation [28, 101]

**Caution**

Cells from small macrometastasis and micrometastasis in lymph nodes with a benign overall echographic node pattern appear only occasionally in US-FNAB material (false-negative results).

## 1.1.11 Further Reading


1. Akhtar M, Ali MA, Huq M, Faulkner C. Fine needle biopsy: comparison of cellular yield with and without aspiration . Diagn Cytopathol 1989;5:162-165.
2. Alkuwari E, Auger M. Accuracy of fine-needle aspiration cytology of axillary lymph nodes in breast cancer patients. A study of 115 cases with cytologic-histologic correlation. Cancer(Cancer Cytopathology) 2008;114:89-93.
3. Apesteguia L, Pina L, Inchusta M, et al. Nonpalpable, well defined, probably benign breast nodule: management by fine-needle aspiration biopsy and long-interval follow-up mammography. Eur Radiol 1997;7:1235-1239.
4. Auer GU, Caspersson TO, Wallgren AS, et al. DNA content and survival in mammary carcinoma. Anal Quant Cytol 1980;2:161-165.
5. Azavedo E, Svane G, Auer G. Stereotactic fine-needle biopsy in 2594 mammographically detected non-palpable lesions. The Lancet 1989;May 13:1033-1036.
6. Ballo MS, Sneige N. Can Core Needle biopsy replace fine-needle aspiration cytology in the diagnosis of palpable breast carcinoma. Cancer 1996;78:773-777.
7. Beatty BG, Bryant R, Wang W, et al. Her2/neu detection in fine needle aspirates of breast cancer with fluorescence in situ hybridization and immunocytochemical analysis. Am J Clin Pathol 2004;122:246-255.
8. Bedard YC, Pollett AF. Breast fine-needle aspiration. A comparison of ThinPrep and conventional smears. Am J Clin Pathol 1999;111:523-527.
9. Berg W. When is core breast biopsy or fine needle aspiration not enough? Radiology 1996;198:313-315.
10. Berner A, Davidson B, Sigstad E, Risberg B. Fine-needle aspiration cytology vs. core biopsy in the dignosis of breast lesions. Diagn Cytopath 2003;29:344-348.
11. Boerner S, Fornage BD, Singletary E, Sneige N. Ultrasound-guided fine-needle aspiration (FNA) of non-palpable breast lesions: a review of 1885 FNA cases using the National Cancer Institute-supported recommendations on the uniform approach to breast FNA. Cancer 1999;87:19-24.
12. Bofin AM, Lydersen S, Isaksen C, Hagmar BM. Interpretation of fine needle aspiration cytology of the breast: a comparison of cytological, frozen section, and final histological diagnoses. Cytopathol 2004;15:297-304.
13. Bondeson L, Lindholm K. prediction of invasiveness by aspiration cytology applied to nonpalpable breast carcinoma andtested in 300 cases. Diagn Cytopathol 1997;17:315-320.
14. Bozzetti C, Nizzoli R, Guazzi A, et al. Her2/neu amplification detected by fluorescence in situ hybridization in fine needle aspirates from primary breast cancer. Ann Oncol 2002;13:1398-1403.
15. Britton PD. Fine needle aspiration or core biopsy. The Breast 19998:1-4.
16. Brown LA, Coghill SB. Fine needle aspiration cytology of the breast: factors affecting sensitivity. Cytopathology 1991;2:67-74.
17. Buchbinder SS, Gurell DS, Tarlow MM, et al. Role of US-guided fine-needle aspiration with on-site cytopathologic evaluation in management of non-palpable breast lesions. Acad Radiol 2001;8:322-7.
18. Bulgaresi P, Cariaggi P, Ciatto S, Houssami N. Positive predictive value of breast fine needle aspiration cytology (FNAC) in combination with clinical and imaging findings: a series of 2334 subjects with abnormal cytology. Breast Cancer Res Treat 2006;97:319-321.
19. Ciatto S, Bonardi R, Cariaggi MP. Performance of fine-needle aspiration cytology of the breast-multicenter study of 23063 aspirates in ten Italian laboratories Tumori 1995 ;81:13-17.
20. Ciatto S, Rosselli del Turco M, Ambrogetti D, et al. Solid nonpalpable breast lesions. Success and failure of guided fine-needle aspiration cytology in a consecutive series of 2444 cases. Acta Radiol 1997;38:815-820.
21. Cornelisse CJ, van de Velde CJ, Caspers RJ, et al. DNA ploidy and survival in breast cancer patients. Cytometry 1987;8:225-234.
22. Coté J-F, Klijanienko J, Meunier M, et al. Stereotactic fine-needle aspiration cytology of nonpalpable breast lesions. Cancer(Cancer Cytopathol) 1998;84:77-83.
23. Daum GS, Kline TS, Artymyshyn RL, Neal HS. Aspiration biopsy cytology of occult breast lesions by use of the “Scouting Needle”. Cancer 1991;67:2150-2152.
24. David O, Gattuso P, Razan W, et al. Unusual cases of metastases to the breast. A report of 17 cases diagnosed by fine needle aspiration. Acta Cytol 2002;46:377-385.
25. Denley H, Pinder SE, Elston CW, Lee AHS, Ellis IO. Preoperative assessment of prognostic factors in breast cancer. J Clin Pathol 2001;54:20-24.

26. Dennison G, Anand R, Makar SH, Pain JA. A prospective study of the use of fine-needle aspiration cytology and core biopsy in the diagnosis of breast cancer. Breast J 2003;9:491-493.
27. Deurloo EE, Tani PJ, Gilhuijs KGA, et al. Reduction of the number of sentinel lymph node procedures by preoperative ultrasonography of the axilla in breast cancer. Eur J Cancer 2003;39:1068-1073.
28. Dey P, Karmakar T. Fine needle aspiration cytology of accessory axillary breasts and their lesions. Acta Cytol 1994;38:915-916.
29. E.C. Working Group on Breast Screening Pathology. Quality assurance guidelines for pathology, fourth edition. 6a: Cytological and histological non-operative procedures, ed. C.A.Wells, European communities 2006; pp:221-256.
30. Fallenius AG, Auer GU, Carstensen JM. Prognostic significance of DNA measurements in 409 consecutive breast cancer patients. Cancer 1988;62:331-341.
31. Farshid G, Pieterse S. Core imprint cytology of Screen-detected breast lesions is predictive of the histologic result. Cancer(Cancer Cytopathol) 2006;108:150-156.
32. Fornage BD, Sneige N, Singletary SE. Masses in breasts with implants: Diagnosis with US-guided fine-needle aspiration biopsy. Radiology 1994;191:339-342.
33. Gantenbein H, Spieler P. Fine needle aspiration biopsy of the breast. Schweiz Med Wschr 1986;116:1513-1518.
34. Garg S, Mohan H,Bal A, et al. A comparative analysis of core needle biopsy and fine-needle aspiration cytology in the evaluation of palpable and mammographically detected suspicious breast lesions. Diagn Cytopathol 2007;35:681-689.
35. Genta F, Zanon E, Camanni M, et al. Cost/accuracy ratio analysis in breast cancer patients undergoing ultrasound-guided fine-needle aspiration cytology, sentinel node biopsy and frozen section of node. World J Surg 2007;31:1155-1163.
36. Gong Y, Booser DJ, Sneige N. Comparison of Her2-status determined by fluorescence in situ hybridization in primary and metastatic breast carcinoma. Cancer 2005;103:1763-1769.
37. Gordon PB. Image-directed fine needle aspiration biopsy in nonpalpable breast lesions. Clin Lab Med 2005;25:655-678.
38. Grohs HK. The interventional cytopathologist. A new Clinician/Pathologist Hybrid. Am J Clin Pathol 1988;90:351-354.
39. Gu M, Ghafari S, Zhao M. Fluorescence in situ hybridization for Her2/neu amplification of breast carcinoma in archival fine needle aspiration biopsy specimens. Acta Cytol 2005;49:471-476.
40. Gupta RK, Naran S, Dowle CS, Simpson JS. The diagnostic impact of needle aspiration cytology of the breast on clinical decision making with an emphasis on the aspiration cytodiagnosis of male breast masses. Diagn Cytopathol 1991;7:637-639.
41. Haller U, Marincek B, Garzoli E, et al. Mammadiagnostik. Möglichkeiten und Indikationen konventioneller und neuer Technologien bei der Abklärung von Brusterkrankungen. Schweiz Aerztezeitung 1998;79:1198-1205.
42. Hejmadi RK, Day LJ, Young JA. Extramammary metastatic neoplasms in the breast: a cytomorphological study of 11 cases. Cytopathology 2003;14:191-194.
43. Howell LP, Gandour –Edwards R, Folkins K, et al. Adequacy evaluation of fine-needle aspiration biopsy in the breast Health Clinic setting. Cancer(Cancer Cytopathol) 2004;102:295-301.
44. Hunt CM, Ellis IO, Elston CW, et al. Cytological grading of breast carcinoma – a feasible proposition? Cytopathology 1990;1:287-295.
45. Ibrahim AE, Bateman AC, Theaker JM, et al. The role and histological classification of needle core biopsy in comparison with fine needle aspiration cytology in the preoperative assessment of impalpable breast lesions. J Clin Pathol 2001;54:121-125.
46. Jain A, Haisfield-Wolfe ME, Lange J, et al. The role of ultrasound-guided fine-needle aspiration of axillary nodes in the staging of breast cancer. Ann Surg Oncol 2008;15:462-471.
47. Jayaram G, Elsayed EM. Cytologic evaluation of prognostic markers in breast carcinoma. Acta Cytol 2005;49:605-610.
48. Jones L, Lott MF, Calder CJ, Kutt E. Imprint cytology from ultrasound-guided core biopsies: accurate and immediate diagnosis in a one-stop breast clinic. Clin Radiol 2004;59:903-908.
49. Joseph L, Edwards JM, Nicholson CM, et al. An audit of the accuracy of fine-needle aspiration using a liquid-based cytology system in the setting of a rapid access breast clinic. Cytopathology 2002;13:343-349.
50. Kerin MJ, McAnena OJ, Waldron RP, et al. Diagnostic pitfalls of fine needle aspiration cytology for breast disease. Irish Med J 1993;86:100-101.
51. Klijanienko J, Cote J-F, Thibault F, et al. Ultrasound-guided fine-needle aspiration cytology of nonpalpable breast lesions. Cancer(Cancer Cytopathol ) 1998;84:36-41.
52. Kontzoglou K, Moulakakis KG, Konofaos P, et al. The role of liquid based cytology in the investigation of breast lesions using fine-needle aspiration: a cytohistopathological evaluation. J Surg Oncol 2005;89:75-78.
53. Kronenwett U, Huwendiek S, Östring C, et al. Improved grading of breast adenocarcinomas based on genomic instability. Cancer Research 2004;64:904-909.
54. Kronenwett U, Ploner A, Zetterberg A, et al. Genomic instability and prognosis in breast carcinomas. Cancer Epidemiol Biomarkers Prev 2006;15:1630-1635.
55. Ku NNK, Mela NJ, Fiorica JV, et al. Role of fine needle aspiration cytology after lumpectomy. Acta Cytol 1994;38:927-932.
56. Lamb J, Anderson TJ. Influence of cancer histology on the success of fine needle aspiration of the breast. J Clin Pathol 1989;42:733-735.
57. Layfield LJ. Fine needle aspiration of the breast: review of the technique and a comparison with excisional biopsy. Current Diagn Pathol 1995;2:138-145.
58. Layfield LJ, Bentz JS, Gopez EV. Immediate On-site interpretation of fine-needle aspiration smears. A cost and compensation analysis. Cancer(Cytopathol) 2001;93:319-322.
59. Leifland K, Lagerstedt U, Svane G. Comparison of stereotactic fine needle aspiration cytology and core needle biopsy in 522 non-palpable breast lesions. Acta Radiol 2003;44:387-391.
60. Leung SW, Bedard YC. Estrogen and progesterone receptor contents. I. ThinPrep-processed fine-needle aspirates of breast. Am J Clin Pathol 1999;112:50-56.
61. Levine T. Breast Cytology – is there still a role? Cytopathology 2004;15:293-296.
62. Liao J, Davey DD, Warren G, et al. Ultrasound-guided fine-needle aspiration biopsy remains a valid approach in the evaluation of nonpalpable breast lesions. Diagn Cytopathol 2004;30:325-331.
63. Litherland J. The role of needle biopsy in the diagnosis of breast lesions. Breast 2001;10:383-387.
64. Ljung B-M, Chew K, Deng G, et al. Fine needle aspiration technique as for the characterization of breast cancers. Cancer 1994;74:1000-1005..
65. Ljung B-M, Drejet A, Chiampi N, et al. Diagnostic accuracy of fine-needle aspiration biopsy is determined by physician training in sampling technique. Cancer(Cancer Cytopathol) 2001;93:263-268.
66. Malberger E, Edoute Y, Toledano O, Sapir D. Fine-needle aspiration and cytologic findings of surgical scar lesions in women with breast cancer. Cancer 1992;69:148-152.
67. Manfrin E, Mariotto R, Remo A, et al. Is there still a role for fine-needle aspiration cytology in breast cancer screening? Cancer (Cancer Cytopathol) 2008;114:74-82.
68. Masood S, Frykberg ER, Garey L, et al. Application of estrogen receptor immunocytochemical assay to aspirates from mammographically guided fine needle biopsy of nonpalpable breast lesions. Southern Med J 1991;84:857-861.
69. Mayall F, Denford A, Chang B, Darlington A. Improved FNA cytology results with a near patient diagnosis service for non-breast lesions. J ClinPathol 1998;51:541-544.

70. McKee GT, Tambouret RH, Finkelstein D. Fine needle aspiration cytology of the breast: Invasive vs. in situ carcinoma. Diagn Cytopathol 2001;25:73-77.
71. Mitteldorf CA, Leite KR, Meirelles MI, Camara-Lopes LH. Overexpression of Her2/neu oncoprotein in cytologic specimens. Acta Cytol 2004;48:199-206.
72. Moinfar F. Essentials of diagnostic breast pathology. A practical approach. Springer-Verlag Berlin Heidelberg 2007.
73. Moriki T, Takahashi T, Ueta S, et al. Hormone receptor status and Her2/neu overexpression determined by automated immunostainer on routinely fixed cytologic specimens from breast carcinoma: correlation with histologic sections determinations and diagnostic pitfalls. Diagn Cytopathol 2004;30:251-256.
74. NHSBSP. Non-operative diagnosis subgroup of the national coordinating group for breast screening pathology. In: Guidelines for non-operative diagnostic procedure and reporting in breast cancer screening. publ No 50, NHS Cancer screening programmes, Sheffield, 2001; pp:1-56.
75. Okamoto H, Ogawara T, Inoue S, et al. Clinical management of nonpalpable or small breast masses by fine-needle aspiration biopsy (FNAB) under ultrasound guidance. J Surg Oncol 1998;67:246-250.
76. Oliveira AM, French CA. Applications of fluorescence in situ hybridization in cytopathology. Acta Cytol 2005;49:587-594.
77. Oyama T, Koibuchi Y, McKee G. Core needle biopsy(CNB) as a diagnostic method for breast lesions: Comparison with fine needle aspiration cytology. Breast Cancer 2004;11:339-342.
78. Padel AF, Coghill SB, Powis SJA. Evidence that the sensitivity is increased and the inadequacy rate decreased when pathologists take aspirates for cytodiagnosis. Cytopathol 1993;4:161-165.
79. Panizza P, De Cobelli F, De Gaspari A, et al. MR-guided stereotactic breast biopsy: technical aspects and preliminary results. Radiol Med 2003;106:232-244.
80. Perez-Reyes N, Mulford DK, Rutkowski MA, et al. Breast fine-needle aspiration. A comparison of Thin-layer and conventional preparation. Am J Clin Pathol 1994;102:349-353.
81. Pijnappel RM, van den Donk M, Holland R, et al. Diagnostic accuracy for different strategies of image-guided breast intervention in cases of nonpalpable breast lesions. Brit J Cancer 2004;90:595-600.
82. Pinto AE, Mendonca E, Andre S, et al. Independent prognostic value of hormone receptor expression and S-phase fraction in advanced breast cancer. Analyt Quant Cytol Histol 2002;24:345-354.
83. Quinn CM. The pathology of breast screening. Current Diagn Pathol 2001;7:81-90.
84. Qureshi NA, Beresford A, Sami S, et al. Imprint cytology of needle core-biopsy specimens of breast lesions: Is it a useful adjunct to rapid assessment breast clinics. The Breast 2007;16:81-85. 85.
85. Robinson IA, McKee G. Cytological grading of breast carcinoma. Acta cytol 1995;39:1257.
86. Robinson IA, McKee G, Nicholson A, et al. Prognostic value of cytological grading of fine-needle aspirates from breast carcinomas. Lancet 1994;343:947-949.
87. Sapino A, Cassoni P, Zanon E, et al. Ultrasonographically-guided fine-needle aspiration of axillary lymph nodes: role in breast cancer management. Brit J Cancer 2003;88:702-706.
88. Sauer T, Garred O, Lomo J, Naess O. Assessing invasion criteria in fine needle aspirates from breast carcinoma diagnosed as DCIS or invasive carcinoma:can we identify an invasive component in addition to DCIS? Acta cytol 2006;50:263-270.
89. Sauer T, Lomo J, Garred O, Naess O. Cytologic features of ductal carcinoma in situ in fine-needle aspiration of the breast mirror the histopathologic growth pattern heterogeneity and grading. Cancer 2005;105:21-27.
90. Sauer T, Wiedswang G, Boudjema G, et al. Assessment of Her2/neu overexpression and/or gene amplification in breast carcinomas: should in situ hybridization be the method of choice? APMIS 2003;111:444-450.
91. Saxe A, Phillips E, Orfanou P, Husain M. Role of sample adequacy in fine needle aspiration biopsy of palpable breast lesions. Am J Surg 2001;182:369-371.
92. Schnall MD, Orel SG, Connick TJ. MR guided biopsy of the breast. Magn Reson Imaging Clin N Am 1994;2:585-589.
93. Schulz-Wendtland R, Bock K, Aichinger U, et al. Ultrasound examination of the breast with 7,5, MHz and 13 MHz-transducers: Scope for improving diagnostic accuracy in complementary breast diagnostics? Ultraschall in Med 2005;26:209-215.
94. Shin SJ, Chen B, Hyjek E, Vazquez M. Immunocytochemistry and fluorescence in situ hybridization in Her-2/neu status in cell block preparations. Acta Cytol 2007;51:552-557.
95. Shulman SG, March DE. Ultrasound-guided breast interventions: Accuracy of biopsy techniques and applications in patient management. Semin ultrasound CT MRI 2006;27:298-307.
96. Skoog L, Humla S, Isaksson S, et al. Immunocytochemical analysis of receptors for estrogen and progesterone in fine needle aspirates from human breast carcinomas. Diagn Cytopathol 1990;6:95-98.
97. Spieler P, Ammann M, Schoenegg R. Fine needle aspiration cytology. Aspects of a minimally invasive diagnostic procedure. Pathologe 2007;28:325-333.
98. Suen KC, et al. The Papanicolaou Society of Cytopathology Task Force on standards of practice. Guidelines of the Papanicolaou Society of Cytopathology for fine-needle aspiration procedure and reporting. Modern Pathol 1997;10:739-747.
99. Takabatake D, Taira N, Aogi K, et al. Two cases of occult breast cancer in which PET-CT was helpful in identifying primary tumors. Breast Cancer 2008;15:181-184.
100. Tubiana M, Holland R, Kopans DB, et al. Commission of the European communities “Europe against cancer” programme. Management of non-palpable and small lesions found in mass breast screening. Eur J Cancer 1994;30A:538-547.
101. Velanovich V. Fine needle aspiration cytology in the diagnosis and management of ectopic breast tissue. The Amer Surg 1995;61:277-278.
102. Veneti S, Daskalopoulou D, Zervoudis S, et al. Liquid-based cytology in breast fine needle aspiration. Comparison with the conventional smear. Acta cytol 2003;47:188-192.
103. Vielh P, Klijanienko J. Stereotactic and ultrasound guided fine-needle cytology in nonpalpable breast lesions. Arch Anat Cytol Pathol 1998;46:237-240.
104. Wells CA, Perera R, White FE, Domizio P. Fine needle aspiration cytology in the UK breast screening programme:a national audit of results. The Breast 1999;8:261-266.
105. Westenend PJ, Sever AR, Beekman-de volder HJC, Liem SJ. A comparison of aspiration cytology and core needle biopsy in the evaluation of breast lesions. Cancer (Cancer Cytopathol) 2001;93:146-150.
106. Wilson R, Otto R, Hackeloer J. Guidelines for ultrasound guided breast biopsy. Ultraschall in der Medizin 2005;26:240-243.
107. Wu M, Burstein DE. Fine Needle Aspiration. Cancer Invest 2004;22:620-628.
108. Yang GCH, Alvarez II. Ultrafast Papanicolaou stain. Acta cytol 1995;39:55-60.
109. Yeh IT, Mies C. Application of immunohistochemistry to breast lesions. Arch Path Lab Med 2008;132:349-358.
110. Zajdela A, Zillhardt P, Voillemot N. Cytologic diagnosis by fine-needle sampling without aspiration. Cancer 1987;59:1201-1205.
111. Zoppi JA, Pellicer EM, Sundblad AS. Cytohistologic correlation of nuclear grade in breast carcinoma. Acta Cytol 1997;41:701-704.

1

**Figs. 1.1 and 1.2 Comparison between conventional smear and liquid-based (ThinPrep) preparation.**
A split FNAB sample composed of atypical ductal proliferation (Pap stain) was processed.
*Tentative cytologic diagnosis:* suggestive of low-grade DIN (DCIS).
*Histology of the lesion* revealed intermediate DIN (DIN2, DCIS G2).

**Fig. 1.1** The direct smear shows a cohesive papilliform cluster of slightly atypical ductal epithelial cells (high magnification) showing:
– A homogeneous cell pattern.
– Loss of cellular polarization.
– Single-file cell arrangement (arrows).
– Nuclear membrane irregularities.
– Loosely structured chromatin.
– Indistinct nucleoli.

**Fig. 1.2** A papilliform, somewhat flat and focally discohesive sheet is seen in ThinPrep preparation (same magnification as in Fig. 1.1).
In contrast to conventional specimens:
– The pseudo-heterogeneity of the cell population using liquid-based processing is caused by shrinkage of individual epithelial cells.
– The abnormal cellular arrangement is less characteristic.
– The nuclear indentations and nucleoli are more pronounced.
– The chromatin pattern appears coarser.

**Fig. 1.3 US-guided FNAB of small lesions: an example.**
A well-circumscribed nonpalpable breast cancer metastasis (7.3 mm) (arrow) between two ribs (arrowheads) was detected sonographically and diagnosed with ultrasound-guided FNAB.

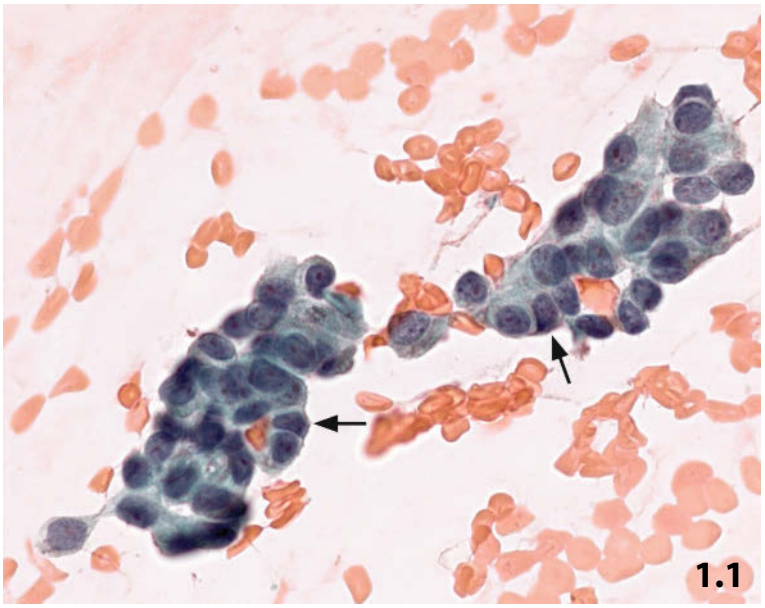
1.1

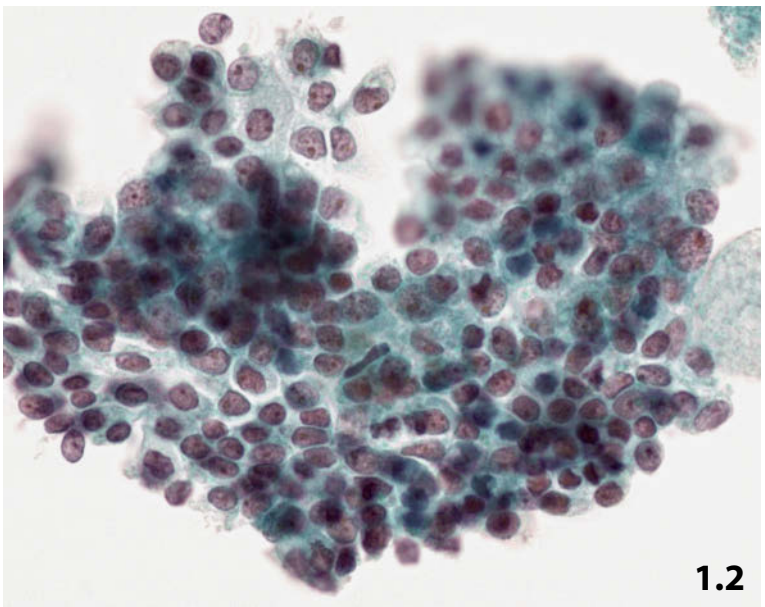
1.2

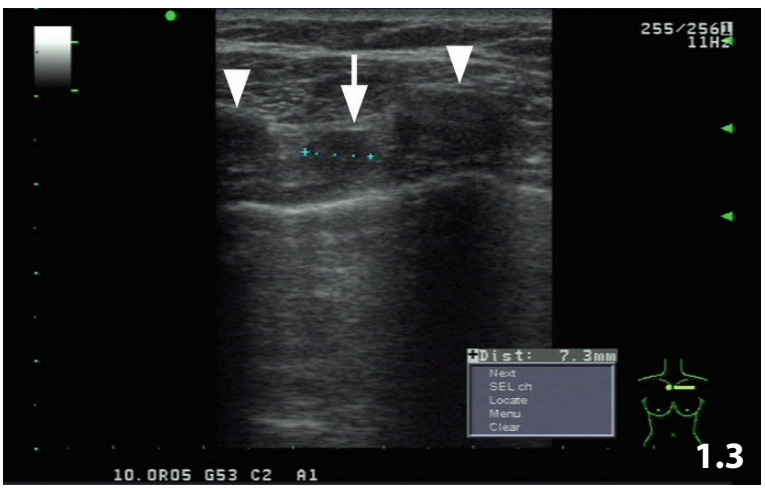
255/256
11Hz
Dist: 7.3mm
Next
SEL ch
Locate
Menu
Clear
10.0R05 G53 C2 A1
1.3

1

**Figs. 1.4 and 1.5 Hormone receptor analysis.**
Two cases of invasive ductal carcinoma of the common type (not otherwise specified, NOS).

**Fig. 1.4** (case #1) Strong positive immunoreactivity for estrogen receptors (Pap-prestained conventional smear).

**Fig. 1.5** (case #2) A case of infiltrating breast carcinoma showing a heterogeneous positive nuclear immunoreactivity for progesterone receptors (Pap-prestained ThinPrep specimen).

**Fig. 1.6 Fluorescence in situ hybridization (FISH) using smears from fine-needle aspirates.**
FISH study on a Pap-prestained liquid-based preparation (ThinPrep) of a primary breast cancer using a green probe against CEP17 and an orange probe against HER2/neu genes: more than two green signals (effective ratio in this case, 3.10) suggest polysomia, while evidence of gene amplification appears as multiple orange signals (HER2/CEP17 ratio in this case, 3.90) and as clusters of orange dots.

**Figs. 1.7 and 1.8 Inadequate fixation of conventional smears.**
Two examples of poorly preserved FNAB material from benign and malignant breast lesions (direct smears, Pap stain).

**Fig. 1.7** (case #1) A case of ductal proliferation without atypia shows epithelial clusters that are difficult to differentiate from low-grade malignancy. Note the irregular cell arrangement, the small cell rows, and the smudge chromatin pattern of the nuclei (high magnification) (arrows).

**Fig. 1.8** (case #2) A case with a ductal carcinoma of the common type. A malignant lesion may be suspected based on the compact three-dimensional and sharply outlined epithelial clusters, dispersed single cells, and mucoid cytoplasmic inclusions (high magnification). Smudge chromatin pattern due to delayed fixation prevents a definite diagnosis.

Erroneous interpretation (false-positive as well as false-negative diagnosis) may easily occur in poorly preserved cytological specimens. In such cases, an indeterminate cytologic report should be provided accompanied by a recommendation for repeated FNAB or histologic diagnosis.

**Fig. 1.9 Axillary nodes: FNAB as a perfect diagnostic tool.**
A 29-year-old pregnant woman (24 weeks of gestation) presented with a mass in the left axilla (1 cm in diameter). Direct smear shows multiple small clusters of activated ductal epithelial cells (low magnification, Pap stain). Cytological findings are compatible with hormonally stimulated ectopic mammary tissue. Note the enlarged rounded nuclei, large centrally placed nucleoli, loose granular chromatin, and granular cytoplasm.

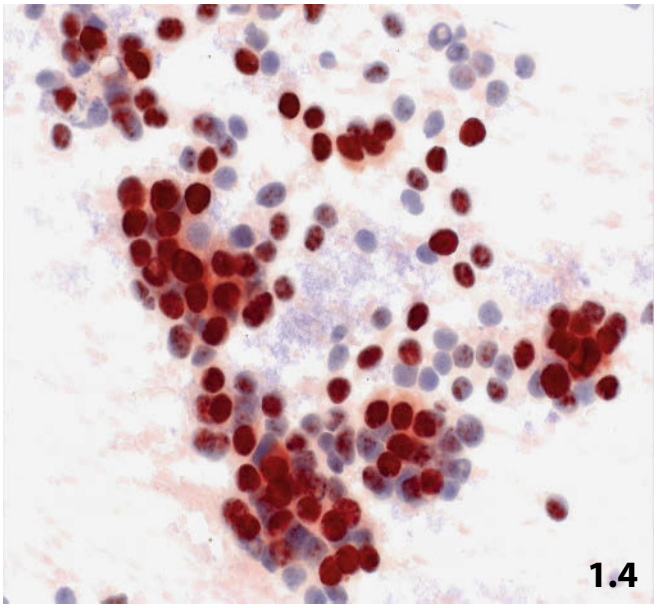
1.4

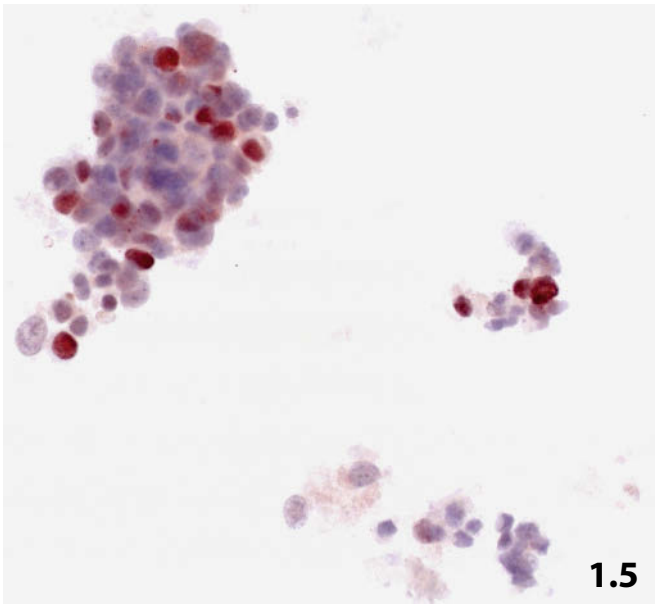
1.5

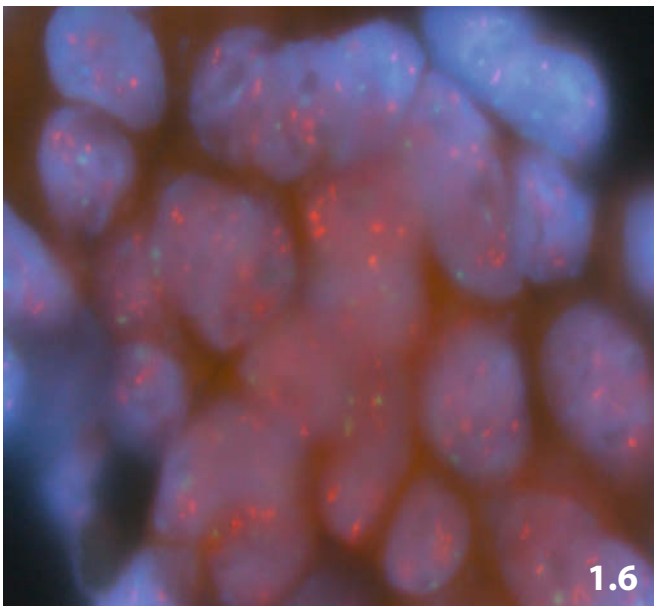
1.6

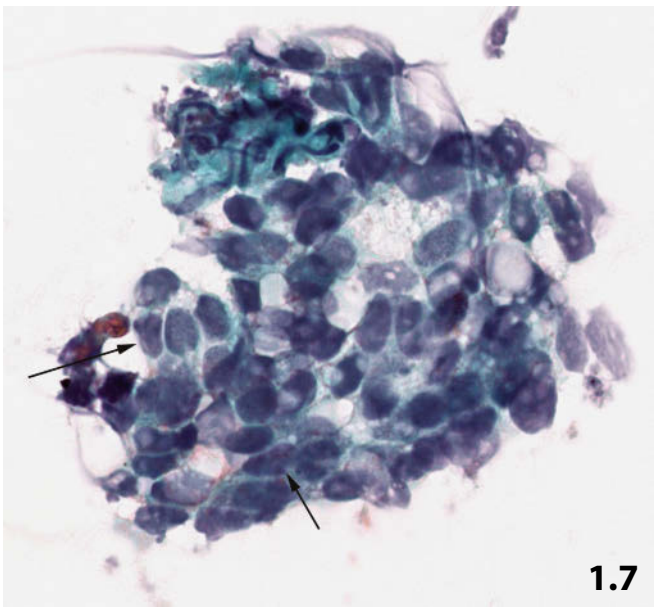
1.7

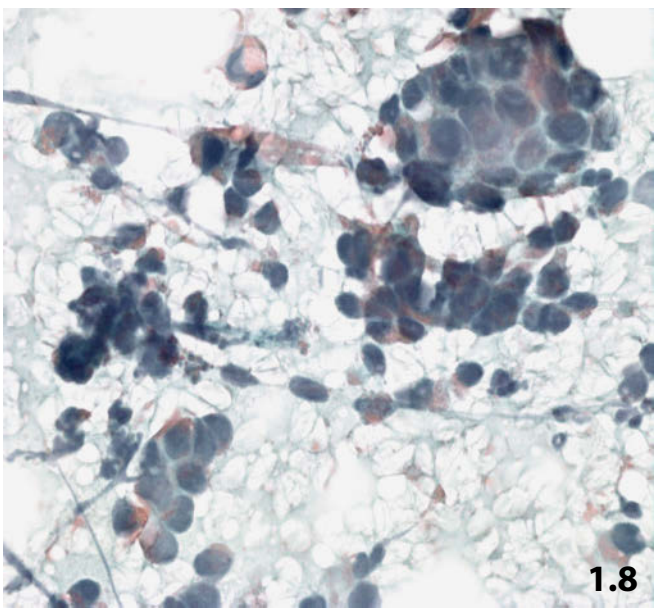
1.8

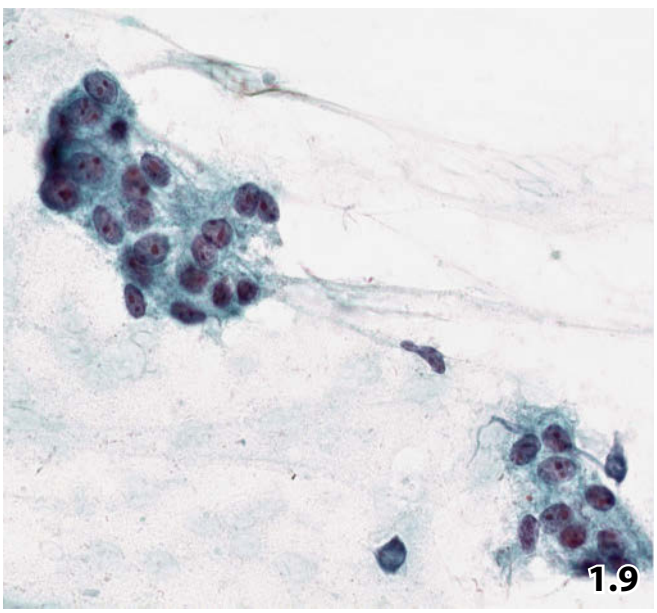
1.9

# Section 1.2
# Breast: Fine-Needle Aspiration Biopsy

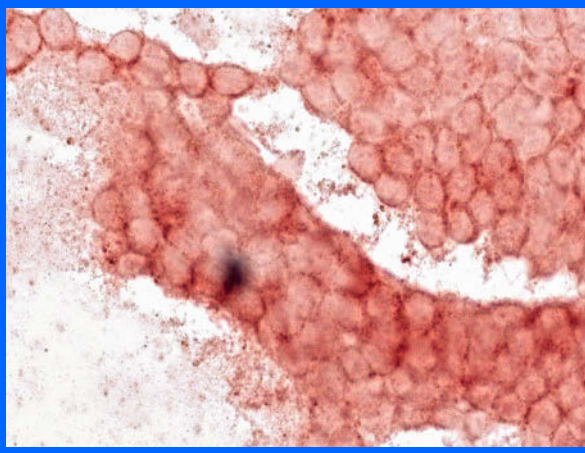

## Normal Findings
## Benign Disorders
## Benign Tumors
## Proliferative Breast Disease with Atypia

### 1.2.1 Histology and Cytology of Normal Breast Parenchyma

#### 1.2.1.1 Histology

The mammary gland is composed of 15–25 lobes. Each lobe or segment is drained by a collecting duct.

- The collecting duct connects the nipple to the lactiferous sinus. The terminal portions of the collecting ducts abutting on the nipple are lined by squamous epithelium.
- Segmental and subsegmental lactiferous ducts connect the lactiferous sinus to the terminal ductal lobular units
- Lobules comprise terminal ducts and secretory acini and are also called terminal ductules. Terminal ducts flow either extralobular or intralobular. Lobular parenchyma is surrounded by specialized stroma: collagen fibers, reticulin, and a large number of capillaries.

The duct system is lined by two cell layers (except for the distal ends of collecting ducts):

- Luminal epithelial cells are small and cuboidal, of intermediate size, or columnar shaped depending on the functional status of the gland.
- Myoepithelial cells are basally arrayed and surrounded by basement membrane material. The cells are usually small with elongated darkly stained, dense nuclei and tiny cytoplasm.
- The myoepithelial cells become larger and rounder with a clear cytoplasm due to glycogen accumulation in the luteal phase of the cycle.

#### 1.2.1.2 Cytology

- *Ductal epithelial cells* appear as regular flat sheets with honeycomb features. The cells are cuboidal to columnar in shape and focal overlapping is common. The nuclei are regular with a smooth contour and loose, evenly distributed chromatin. Small distinct nucleoli may occasionally be observed and are centrally located (Fig. 1.10).
- *Myoepithelial cells* appear as small, elongated, dark nuclei with an indistinct cytoplasm. They are loosely attached to the periphery of the cell clusters and only a few cells are dispersed in the background of the smear. Enlarged myoepithelial cells in the luteal phase of the cycle may be barely distinguished from epithelial cells or even histiocytes.
- *Fragments of the normal lobular unit* exhibit typical acini embedded in a loose stroma and a tubular terminal duct fragment of variable length is usually appended. The luminal epithelial cells are cuboidal to cylindrical, arranged in a single layer, and surrounded by myoepithelial cells. Luteal-phase myoepithelial cells can be recognized in this setting. Basal lamina encircles the terminal ductules and acinic structures as a distinct thin or gross membranous formation (Fig. 1.11).

**Caution**

One has to be aware of the varying size and shape as well as the nuclear and cytoplasmic features of epithelial and myoepithelial cells regulated by the menstrual cycle and the functional state of the gland.

## 1.2.2 Cystic Lesions and Duct Ectasia

**Etiology, Microscopic Features, and General Comments**

- Cyst formation is a dilatation of intralobular glands due to an accumulation of secretion. The epithelial lining often exhibits apocrine metaplasia.
- A small cyst cannot be distinguished from duct ectasia by cytology; however, small drops of fluid may be consistent with duct ectasia in cases without a palpable node.
- Duct ectasia implies a dilatation of the duct without obvious cyst formation and is clearly visualized by ultrasound imaging.
- Microscopic hallmarks (Figs. 1.12 and 1.13):
  - Foam cells in variable numbers, frequently degenerating.
  - Background debris.
  - Monolayer sheets of apocrine cells or bland duct cells, respectively.
- The aspirated cyst fluid may be clear, opaque, or turbid; its color varies from light yellow to dark brown-green. Many cyst fluids show poor cellularity.
- Increased numbers of neutrophils in a cystic lesion is due to reactive inflammation and should not be considered as secondary to an infection.
- Malignant cells in fluid from a benign-looking cyst occur extremely rarely. It is likely to be caused by a carcinoma involving the cystic wall.
- Ciatto and coworkers reported the results from a very large series of mammary cyst fluids [11].

**Apocrine Cells / Apocrine Metaplasia** [49] (Fig. 1.14)

Apocrine metaplasia occur in a large variety of benign cystic and solid tumorous lesions. Apocrine metaplasia usually indicates that there is no malignancy.

- Apocrine cells are characteristically arranged in flat sheets with their typically abundant granular cytoplasm and large round nuclei exhibiting a dark stain and one centrally located prominent nucleolus.

**Caution**

- Apocrine cells from the neighboring benign tissue may be intermingled with carcinoma cells.
- Malignant cells from a monomorphic apocrine carcinoma may look like benign apocrine metaplastic cells (see also: Sect. 1.3.8.1, p. 61).

**Problems and Differential Diagnostic Considerations**

- Blood-stained cystic fluid should raise strong suspicion of an intracystic neoplasia (mostly low-grade papillary tumors), especially in cases with degenerating erythrocytes and hemosiderophages. In many cases, the cytologic material is not diagnostic and an excisional biopsy is necessary.
- A few small papilliform clusters with activated epithelial cells may originate from needle passes through adjacent proliferative breast tissue .
- The strong enlargement of cells from the cyst-epithelial layer is due to a regenerative and reparative process. Cytoplasmic and nuclear polymorphism, hyperchromatic nuclei, and enlarged pleomorphic nucleoli may lead to a false-positive diagnosis of malignancy. The benign epithelial cells with reactive changes, however, display a low N/C ratio and nuclei with finely and regularly distributed chromatin or even patternless (Figs. 1.15 and 1.16).
- Cyst fluids infrequently contain strongly activated atypical foamy cells with mitotic activity (Fig. 1.17). Large-cell secretory carcinoma, Langerhans cell proliferation, and granular cell tumors can be excluded by immunocytochemical stainings: histiocytes are positive for CD68, carcinoma cells for pancytokeratins, Langerhans cells for CD1a, and granular cell tumor cells exhibit strong positivity for S-100 protein.
- It is mandatory to exclude a residual mass by palpation and sonography after removal of the cyst content. Residual lesions are mostly located in or adjacent to the wall of a cyst. In cases with residual findings, a second FNAB should be performed.

**Caution**

- The cystic fluid may contain huge amounts of neutrophilic granulocytes, which is particularly a sign of a reactive inflammatory process and not a sign of infection.
- Large atypical epithelial cells originating from the cyst wall due to a regenerative and reparative process should not lead to a false diagnosis of carcinoma

## 1.2.3 Mastitis and Abscess

### 1.2.3.1 Problem of Reactive Epithelial Atypia

Inflammatory disorders and infections in the breast cause tissue destruction followed by epithelial regeneration and repair. The inflammatory atypia should not be falsely diagnosed as carcinoma.

Cytomorphologic features consistent with reactive atypia are (Fig. 1.18):

- Loose and/or compact cell sheets focally infiltrated with neutrophilic granulocytes.
- Enlarged cells, N/C ratio within normal limits.
- Three-dimensional ballooned appearance of the nuclei with a finely spotted benign chromatin pattern and smooth borders.
- Enlarged round, centrally located nucleolus.
- Focal streaming pattern.

#### 1.2.3.2 Subareolar Abscess [61]

**Pathogenesis**

Several theories have been proposed concerning the development of the subareolar abscess. The most likely explanation is that the filling-up of the lactiferous duct lumen with keratinized debris is followed by rupture and an inflammatory reaction in the surrounding area as well as a foreign body reaction [59].

**Microscopic Features and Differential Diagnosis**

(Fig. 1.19)

- The lesion is located within the subareolar region immediately beneath the nipple. The anatomic site distinguishes a subareolar abscess from a ruptured epidermal inclusion cyst.
  - The microscopic hallmarks are: plenty of squamous cells, mostly anucleated, and a mixed inflammatory cell pattern along with a foreign body reaction.
- Squamous cells also occur in aspirates from malignant breast lesions, a majority of the cases represent metaplastic carcinomas. A careful assessment of the cytologic properties is important to achieve a correct diagnosis. Malignant squamous cells in metaplastic carcinomas are more pleomorphic, show mitotic activity, and tumor cell cannibalism. Conspicuous malignant squamous cells with a polymorphic cytoplasmic and nuclear shape may occasionally be found in subareolar inflammatory lesions [47].

### 1.2.4 Fat Necrosis and Suture Granuloma

#### 1.2.4.1 Fat Necrosis (Fig. 1.20)

Fat necrosis may follow a trauma, surgery, or irradiation. Breast carcinoma may cause focal marginal necrosis of the fatty tissue. The sonographic properties of a fat necrosis frequently match those of a breast carcinoma. A bioptic evaluation is necessary in the majority of cases.

- The microscopic hallmark is a mixture between well-preserved and degenerated fat cells, lipophages, and amorphous debris. Multinucleated macrophages and a few activated fibroblasts are added to a mixed inflammatory cell type.
- The diagnostic result is not reliable in cases of hypocellular aspirates.

#### 1.2.4.2 Suture Granuloma (Fig. 1.21)

A suture granuloma is located in or adjacent to a scar. A breast nodule caused by a foreign body type granulomatous reaction to surgical material could mimic a local recurrence of carcinoma.

- Suture material ingested in multinucleated macrophages shows up as tightly packed bars with strong birefringence under polarized light, but it can also be readily recognized in light microscopy.
- The hallmark is the excessive foreign body reaction (a cell pattern with many multinucleated macrophages).

### 1.2.5 Granulomatous Mastitis and Epithelioid Granulomatosis

**Microscopic Features and Differential Diagnosis**

- *Idiopathic granulomatous mastitis* is a rare, benign, chronic inflammatory condition with unknown etiology. However, secondary granulomatous mastitis may occur after acute inflammation, hematoma, acute fat necrosis, and surgery. Granulomatous lesions sometimes mimic breast cancer, clinically and radiographically [30].
  - The smears are abundant in cellular material: a mixed inflammatory cell pattern with predominant plasma cells and lymphocytes; striking small and large fragments of granulomatous tissue rich in activated fibroblasts; focal fibrosis and sclerosis of the matrix;
    a rather poor admixture of epithelial cell groups with inflammatory atypia can be observed (see Sect. 1.2.3.1, p. 17) (Figs. 1.18 and 1.22).
- *Sarcoidosis* of the breast is extremely rare. The differential diagnosis includes epithelioid type granulomatosis, secondary to infection of various organisms (fungi, leprosy, and brucellosis).
  - Activated histiocytes with epithelioid features and occasional Langhans-type giant cells are characteristic. Necrosis is not evident.
- *Tuberculosis* is a rare type of extrapulmonary mycobacterial infection, but in endemic areas tuberculosis should always be considered first and foremost in the differential diagnostic workup of granulomatous mastitis [41].
  - Hallmark: A necrotic caseous background with degenerating neutrophilic granulocytes and frequent calcifying deposits (Fig. 1.23).

**Caution**

Strongly activated, polymorphic fibroblasts accompanying inflammatory disorders of different origins may look like undifferentiated carcinoma cells. Immunocytochemical stains are helpful in ambiguous cases – pancytokeratins demonstrate a reliable positivity for carcinoma cells.

### 1.2.6 Pseudolymphoma of the Breast Nipple or Areola [8, 12]

**General Comments**

- Synonyms: Cutaneous lymphoid hyperplasia and lymphocytoma cutis.

- The lesion is an example of cutaneous B-cell pseudolymphoma that can generally be induced by arthropod bites, vaccination, drugs, and other antigenic stimuli. Lymphoproliferative lesions of the breast nipple and/or areola are in a substantial number of cases caused by antigenic stimulation by *Borrelia burgdorferi* following a tick bite.
- Pseudolymphoma, in most cases, appears as a nipple/areolar induration comprising eczema-like changes of the cutis. The lesion is clinically often suspected to be Paget disease, supported by occasionally enlarged axillary lymph nodes.

**Microscopic Features and Differential Diagnosis**

(Fig. 1.24)

- FNAB smears are cellular and dominated by an immature lymphocytic population with large numbers of immature blastic cells. Small lymphocytes, plasmacytoid cells, and histiocytes are observed as well.

The polymorphic cell population may easily be misdiagnosed as malignant lymphoma. Polymorphic blastic cells may look like malignant cells from a large-cell carcinoma.

**Additional Analyses**

- Immunocytochemistry: Carcinoma has to be excluded by negative immunostaining for cytokeratins. B/T cell enumeration on cytologic preparations may suggest B-cell non-Hodgkin lymphoma due to a preponderance of B lymphocytes.
- Molecular genetics: A polymerase chain reaction (PCR) of the IgH gene rearrangement will show a polyclonal result in most cases.
- PCR and/or serology may detect *Borrelia burgdorferi*.

**Caution**

- An immature lymphoproliferative lesion in the nipple area brings up the possibility of a *Borrelia burgdorferi* etiology following a tick bite. Molecular and serologic tests for *Borrelia burgdorferi* are compulsory in this typical clinical/morphologic setting.
- Beware of a false-positive carcinoma or lymphoma diagnosis based on cytologic features alone.
- Monoclonal rearrangement of the IgH gene and of T-cell receptor gamma gene using PCR has been described in single cases of mammary pseudolymphoma [8].

## 1.2.7 Plasma Cell Mastitis [67]

**Definition**

Plasma cell mastitis is a rare form of inflammatory, noninfectious mastitis. It is not observed during the postpartum and breastfeeding period in comparison to other inflammatory breast disorders. The autoimmune origin of this lesion has been discussed.

**Microscopic Features and Differential Diagnosis**

- Hallmarks: Abundant mature plasma cells and transformed lymphocytes.

A well-differentiated plasmacytoma must be excluded especially in cases with an equivocal clinical background. In situ hybridization or PCR gene amplification of kappa and lambda light chains are reliable methods to establish the clonality of a plasmacytoid population.

## 1.2.8 Noncellular Elements

### 1.2.8.1 Liesegang Rings [1, 20, 53] (Fig. 1.25)

- Liesegang rings are ring-shaped concretions with a concentrically laminated morphology. They can be occasionally found in degenerate chronic cystic lesions and inflammatory disorders. They can also be identified in FNAB aspirates from many organs, particularly benign cysts of the breast, complex renal cysts, and perirenal inflammatory disorders.
- The exact mechanism of formation and the composition of these structures is unclear.
- Liesegang rings are best observed using routine stains on air-dried or wet-fixed cytologic preparations.
- Liesegang rings may be confused with parasites, algae, calcifications, and psammoma bodies.

### 1.2.8.2 Collagenous Spherulosis [18]

Collagenous spherulosis of the breast (CSph) is a rare finding in FNABs, associated with benign breast lesions. The extracellular spheres consist of basement membrane material.

**Microscopic Features and Differential Diagnosis**

- The cellular aspirates comprise closely packed cohesive cell groups that surround the translucent acellular spherules. Nuclei exhibit benign features, smooth borders, and fine granular evenly distributed chromatin.
- Single, naked, bipolar nuclei occur in the background of the smears.

It is very important to differentiate CSph from its malignant look-alikes, which are described in detail in histologic and cytologic literature; the cribriform architecture may mimic atypical ductal hyperplasia, in situ and invasive cribriform ductal carcinoma, and above all adenoid cystic carcinoma. However, epithelial cells in CSph are bland or show reactive changes [52, 54, 70].

### 1.2.8.3 Mucocele-Like Lesions [9, 73]

- Mucocele-like lesions (MLLs) are cysts containing mucus that have ruptured into the surrounding tissue. Mucoid masses may appear diffuse or globular.

- Simple MLLs and MLLs in combination with benign ductal hyperplasia should not cause diagnostic problems: smears show scant cellularity, monolayer epithelial sheets, and no nuclear atypia.
- In cases of MLLs in combination with florid or atypical ductal proliferation, the cytologic features may overlap with a mucinous carcinoma [9]: cell-rich smears, dense three-dimensional clusters, significant nuclear atypia, and globular and diffuse mucus.
- A combination of FNAB cytology and image findings should provide a correct diagnosis. MLL presents sonographically as a cystic lesion and mucinous carcinoma as a distinct nodule in ultrasound and mammography.

#### 1.2.8.4 Silicone Granulomas [14]

Silicone may produce granulomas either at the site of injection or due to a migration of silicone-gel through the wall of an otherwise intact implant.

- The characteristics of silicon granulomas are numerous vacuolated histiocytes along with multinucleated giant cells and a minimal amount of inflammatory cells. Air-dried aspirates may reveal an amorphous thick glassy substance presumed to be silicone; however, if silicone were present it would most likely be lost by fixation.

Silicone granuloma may also appear in ipsilateral axillary lymph nodes in females with a breast prosthesis (Fig. 1.26).

#### 1.2.8.5 Amyloid Tumor [34, 59] (Fig. 4.62)

Amyloid deposits in the breast are extremely rare. Recognition of this protein is simple with experience of amyloid accumulation in other organs.

- Cytologic findings include homogeneous and cylindric material. The strands are refractile and brightly eosinophilic in Papanicolaou-stained smears.

Amyloid protein shows positive with Congo red and exhibits birefringence in a bottle-green manner.

### 1.2.9 Hormonal Stimulation During Pregnancy and Lactation (Figs. 1.9, 1.27, 1.28)

**General Comments and Differential Diagnosis**

Most nodular lesions in the breast during pregnancy and lactation are fibroadenomas, and secondary to hormonal stimulation of an otherwise homogeneous breast tissue area. Hormonally highly activated cell populations share morphologic properties with secretory carcinoma. A fatal misdiagnosis may occur if appropriate clinical information is not communicated. However, a carcinoma in a pregnant woman must always be excluded, because these cancers are highly aggressive with a poor survival rate.

**Microscopic Features**

Hallmarks

- Large cells often naked and stripped of cytoplasm.
- Ballooned round nuclei with finely granular, evenly distributed chromatin, and a centrally positioned prominent nucleolus.
- Abundant vacuolated and granular cytoplasm.
- Dirty secretory background.
- Epithelial cells are usually dispersed and show gross enlargement and a very low N/C ratio. Many naked nuclei are observed, occasionally degenerating.
- The dirty background of secretory material is due to disrupted cytoplasm.

#### 1.2.9.1. Lactating Adenoma (Fig. 1.29)

In addition to the characteristic cytologic features of hormonally stimulated breast tissue, lactating adenomas may be suspected if the preparations exhibit extreme high cellularity and numerous densely packed acinic clusters with myoepithelial cells at the periphery. Lactating adenomas and fibroadenomas may be difficult to classify in cytologic preparations of pregnant women; the characteristic tumor cytoarchitecture often becomes vague.

**Caution**

Strong hormonal cell activation often causes cellular changes similar to features of secretory carcinoma.

### 1.2.10 Fibrocystic Breast Changes

**General Comments**

Fibrocystic change is a histologic alteration including dilatation of intralobular glands, fibrotic changes of the connective tissue, which may be associated with mild epithelial hyperplasia, apocrine metaplasia, and focal adenosis.

Complex mastopathic lesions (combined fibrosis, cystic changes, and epithelial proliferation) frequently reveal differing benign diagnoses in cell and tissue samples obtained at the same time.

**Microscopic Features** (Fig. 1.30)

- Low cellularity, occasionally with fragments of adipose and fibrotic tissue.
- Regular benign cell sheets and acinic clusters admixed with myoepithelial cells.
- Most commonly, small sheets of apocrine cells.
- Isolated bipolar nuclei (believed to be derived from myoepithelial cells) and foam cells.

## 1.2.11 Proliferative Breast Disease with and without Atypia

### 1.2.11.1 Proliferative Breast Disease without Atypia

#### 1.2.11.1.1. Benign Ductal Hyperplasia

[17, 19] (Figs. 1.31–1.36)

**Microscopic Features and Differential Diagnosis**

Hallmarks

- High cellularity of the preparations with dense three-dimensional cell clusters, frequently papilliform. The cohesive clusters are regular with groups of elongated cells in a shoal of fish arrangement (streaming pattern) or a swirling pattern. No distinct loss of nuclear polarity.
- Moderate variability of nuclear size. Nuclei are round to oval with smooth borders, regular chromatin pattern, and variable small nucleoli.
- Focally enlarged epithelial cells showing indistinct nuclear indentations, bland chromatin pattern, and dark staining. Prominent regular nucleoli.
- Bipolar nuclei and myoepithelial cells between and overlaying clustered epithelial cells, and in the background of the smears.

- It is important for cytologists to avoid overdiagnosis in smears exhibiting marked benign ductal proliferation. Marked heterogeneity of the epithelial cell population over the whole smear is pathognomonic in benign hyperplasia. In most cases with cell-rich and well-processed aspirates, the morphologic features are adequate to distinguish between benign florid proliferation and true atypical lesions progressing to cancer [44]. However, histologic investigations with a core or excisional biopsy are recommended in equivocal cases.
- Fibroadenomas or papillomas may be suspected in cases with large arborizing cell clusters.

#### 1.2.11.1.2 Nipple Duct Adenoma [40, 65] (Fig. 1.37)

Synonyms: Nipple adenoma, florid papillomatosis of the nipple, subareolar duct papillomatosis.

**General Comments and Microscopic Features**

- Nipple duct adenoma is a benign tumorous proliferation of tubules in the subareolar area.
- The overall cytologic pattern is identical to florid benign ductal proliferation, as described above, but this particular lesion can be mistaken for carcinoma due to the following features:
  - Florid proliferation and papillary excrescents of the tubulus-lining epithelial cells may be striking.
  - Increased mitotic activity.
  - Cellular enlargement and higher N/C ratio. Pleomorphic nuclei and distinct nucleoli.
- Necrotic changes and surface erosion of the nipple area can be observed. Necrotic cell change is uncommon in benign proliferative breast disease but may occur in nipple duct adenomas.

**Caution**

Florid epithelial proliferation in combination with necrosis and striking clinical and image findings should not lead to a misdiagnosis of cancer.

#### 1.2.11.1.3 Juvenile Papillomatosis [55, 56, 60]

- Juvenile-type papillomatosis is a localized breast lesion that resembles fibroadenoma (Fig. 1.54). The disorder usually occurs in younger females.
- It is important to suspect the diagnosis on FNAB because there is a correlation between juvenile papillomatosis and breast cancer. The lesion may be an indicator for breast cancer mainly in females with recurrent lesions and a positive family history.
  - Cytologic smears appear with hypercellularity, corresponding to the histologic pattern: proliferative epithelial clusters, acini, apocrine cells, and a cystic background are observed; the latter may be predominant. Florid epithelial proliferation is common.

### 1.2.11.2 Proliferative Breast Disease: Ductal Hyperplasia with Atypia

[5, 19, 50] (Figs. 1.38–1.41, 1.43)

**Microscopic Features**

Cytologic features that help to determine atypical ductal proliferations with suspicion of progression to cancer:

- Dense and loose cell clusters.
- More irregular nuclear spacing.
- Loss of the nuclear polarity characterized by varying alignment of the nuclear longer axis.
- Cell dissociation.
- Anisonucleosis, irregularity of nuclear membranes.
- Coarsely granular and clumping chromatin and nuclei with variable hyperchromasia;
- Macronucleoli.
- Absence of myoepithelial cells related to atypical cell clusters.

Degree of three-dimensionality of cell clusters and nuclear overlapping is not a sign of malignancy.

**Differential Diagnosis**

Atypical ductal proliferation belongs to the category of low-grade ductal intraepithelial neoplasia. Overlapping morphologic and genetic features between atypical ductal hyperplastic lesions and low-grade in situ carcinoma make the reliable separation of these lesions difficult, if not impossible, on cytologic specimens.

Diagnostic difficulties may arise with low-grade malignant neoplasms (DCIS [2, 64], papillary carcinoma, tubular

carcinoma (Fig. 1.42)), and benign lesions with a florid proliferation of the epithelial component, for example fibroadenoma and papilloma.

**Caution**

- Shoal of fish arrangement (streaming pattern) of groups of elongated epithelial cells within large clusters is a distinct sign of benign proliferation (Figs. 1.31C, 1.34, 1.36).
- Strong nuclear overlapping and areas with enlarged, activated cell groups are not a sign of atypia in the sense of increased malignant potential.
- Cytologic features that help to determine atypical ductal proliferation suspicious of malignancy are:
  - Depolarization of nuclei characterized by varying alignment of the nuclear longer axis.
  - More irregular nuclear spacing combined with atypical cell features.
  - Cell dissociation, anisonucleosis, nuclear irregularity, coarsely granular and clumping chromatin, variable hyperchromasia, and a lack of bipolar nuclei.

The hallmarks of benign florid ductal hyperplasia and ductal proliferation with atypia are contrasted in Table 1.2.1.

**Additional Analyses**

Immunocytochemistry

Epithelial cells of benign proliferative lesions without atypia are positive for CK5/6, the cells of ductal intraepithelial neoplasia are, in the vast majority of cases, negative for CK5/6. It is emphasized that interpretation of a CK5/6-immunostaining pattern on cytologic material can be delicate: benign and atypical cells and clusters are randomly mixed and a correlation between morphologic and immunostaining results is equivocal, smears may be of low cellularity and negative immunostaining is not always conclusive; negativity due to technical problems is always possible. Lack of histoarchitecture prevents a comparison of staining results on various epithelial proliferation patterns.

DNA ploidy

Few papers refer to the successful application of DNA image cytometry to differentiate low-risk from high-risk breast borderline lesions [21].

### 1.2.11.3 Proliferative Breast Disease: Tubular Adenoma / Adenosis / Sclerosing Adenosis

#### 1.2.11.3.1 Tubular Adenoma / Adenosis (Fig. 1.44)

**General Comments and Microscopic Features**

- Adenosis and tubular adenoma are due to hyperplasia of lobuli; the latter may present itself as distinct breast mass.
- Different types of adenosis with a variety of epithelial cell types exist: columnar, apocrine, secretory, and myoepithelial differentiation.
- A specific diagnosis of adenoma / adenosis may not be possible cytologically but the cells clearly exhibit benign features:
  - Cellular smears exhibit benign proliferative breast disease (see Sect. 1.2.11.1, p. 21).
  - Characteristic tubular formations of various sizes.
  - Numerous isolated naked nuclei.
  - Scarce stromal component.

#### 1.2.11.3.2 Sclerosing Adenosis (Fig. 1.45)

**Microscopic Features and Differential Diagnosis**

In contrast to predominantly parenchymatous adenosis, sclerosing adenosis may raise diagnostic problems in cytologic aspirates.

- Due to the strong sclerotic stromal changes, aspirates exhibit low cellularity with many single cells in small clusters or in rows, as characteristically observed in frank carcinoma. Malignancy is suspected in cases where cells show eccentrically located irregular nuclei and densely structured irregular cytoplasm.

**Table 1.2.1** Cytomorphology of benign ductal proliferation vs. ductal proliferation with atypia (with an increased malignant potential)

| Features | Benign ductal hyperplasia | Ductal hyperplasia with atypia (in most cases mixed with benign hyperplasia) |
|---|---|---|
| **Cell clusters** | | |
| Three-dimensional and papilliform | Yes | Yes |
| Streaming cell pattern | Yes | No |
| Loss of polarization | No | Yes |
| Cell dissociation | No | Yes |
| **Nuclei** | | |
| Regular and smooth borders | Yes | No |
| Irregular and polymorphic | No | Yes |
| Hyperchromasia | No | Yes |
| Nucleoli | Small and indistinct | Large |
| N/C ratio | Low | High |
| Myoepithelial / bipolar cells | Yes - in clusters and background | No - in atypical clusters |

Other sclerotic disorders of the breast (radial scar, complex sclerosing lesion) may cause identical cell patterns of equivocal malignancy.

## 1.2.12 Gynecomastia [24, 28] (Figs. 1.46 and 1.47)

### Definition, Etiology, Clinical Appearance

- Gynecomastia denotes enlargement of the male breast due to hyperplasia of connective tissue and mammary ducts. There is rarely a formation of true lobules. The lesion is not uncommon and is a prior indication for FNAB.
- It is known as idiopathic and has a transient occurrence during normal adolescence, but it is also caused by endogenic and exogenic hormonal effects and drug administration (digitalis, reserpine, and others).
- Clinically, gynecomastia appears beneath the nipple as a firm, rubbery, mobile, and ill-defined lump.

### Microscopic Features and Differential Diagnosis

The overall cell pattern is comparable with that of florid ductal hyperplasia and fibroadenoma:

- Few large, dense, three-dimensional branching cell clusters.
- Variability of nuclear size. Nuclei are round to oval with smooth borders, regular chromatin texture, and nucleoli.
- Cellular stroma is often edematous or myxoid.
- Apocrine metaplasia and myoepithelial cells are focally present.

*Proliferative lesions in the florid phase* may exhibit an extremely polymorphic pattern. The microscopic features are similar to juvenile fibroadenoma of the female breast:

- Cells and nuclei with strong variation in size.
- Nuclei may show indentations and prominent nucleoli but increased N/C ratio and dark nuclear staining is infrequent.
- Occasional mitotic figures.
- The overall cell pattern is unlike carcinoma due to the marked cellular and cytoarchitectural polymorphism and the absence of unambiguous features of malignancy.

Papilloma, fibroadenoma, phylloides tumors, or stromal tissue lesions may originate in the male breast as well. They are morphologically indistinguishable from their female counterparts and are difficult to separate from gynecomastia in FNAB samples.

## 1.2.13 Hamartoma [23, 25, 26, 68] (Fig. 1.48)

### Definition and General Comments

- Hamartoma is composed of an abnormal mixture of hyperplastic tissue components that are normally present at that site. It is a local malformation, well circumscribed, and histologically well demarcated with a capsule-like condensation of fibrous tissue.
- The myoid hamartoma is a rare lesion dominated by smooth muscle tissue and has an uncertain origin (blood vessels, myoepithelium).
- It is not a precancerous lesion, but hamartoma may harbor a small cancer, especially in situ carcinoma [68].

### Microscopic Features

Hallmarks

- Highly cellular smears with an epithelial and stromal component. Cells occur singly and in clusters, and are enclosed in large tissue fragments.
- *Epithelial component:* lobular and ductal cells. Intact, acini-forming lobular units, embedded in fibrous stroma, are pathognomonic in cytologic preparations. Bland duct epithelium and clusters of proliferating ductal epithelial cells. Myoepithelial cells and bipolar nuclei can be observed.
- *Mesenchymal component:* large fragments of fibrous and adipose tissue focally with epithelial clusters attached or encased.
- The myoid hamartoma is a rare lesion dominated by smooth muscle tissue, it has an uncertain origin (blood vessels, myoepithelium).

Varying amounts of apocrine cells, smooth muscle tissue, angiomatous stroma, stromal giant cells, and foamy cells from cystic ducts are most often present. Focal calcification can be identified.

### Differential Diagnosis

Hamartoma matches the cytologic features of other benign breast lesions but the overall cell pattern clearly suggests this particular entity in adequate cellular aspirations.

Hyperplastic acini may be misinterpreted as adenosis and proliferating lobular units as fibroadenoma. The lesion is unlikely to be falsely interpreted as malignant.

## 1.2.14 Papilloma [10, 15, 27, 38, 45, 62].

### 1.2.14.1 Intracystic Papilloma (Figs. 1.49 and 1.50)

### General Comments

- Blood-stained aspirated fluid from a breast cyst should raise the possibility of an intracystic neoplasia, mostly low-grade papillary tumor. This is especially true in cases with degenerating erythrocytes and hemosiderophages in light microscopy.
- Distinguishing a benign papilloma from a low-grade papillary carcinoma is difficult in most cases. In addition, cytologically unequivocal benign-looking papillary tumors with a myoepithelial component may show a localized stromal invasion on surgical excision. Therefore,

each unambiguous papillary tumor and each suspected papillary neoplasm detected in cystic fluids must undergo an excisional biopsy [27].

- A few small papilliform clusters in nonbloody cystic fluid may originate from proliferating cyst epithelium or from needle passes through cyst-adjacent proliferative breast disease.

**Microscopic Features**

- Hallmarks: Papillary, arborizing clusters with fibrovascular cores are a definite sign of a papillary neoplasm.
- Bipolar myoepithelial cells beneath the epithelial cell layer (one or two layers) provide evidence of a benign tumor.
- The following cellular content in hypocellular cystic fluid supports a diagnosis of papilloma:
  - Small papilliform and stellate clusters with palisading cylindric cells.
  - 3–10 palisading columnar cells in a compact row.
  - Single cells with elongated and cylindric cytoplasm.
  - Bipolar nuclei at the periphery of the clusters or in the background.
- Palisade arranged cells are cuboid or columnar with bland nuclei.
- Apocrine metaplasia commonly occurs.
- Focal squamous metaplasia is the exception, intercellular bridges may be evident [16].

**Differential Diagnosis**

- Lack of myoepithelial cells raises high suspicions of papillary carcinoma: Epithelial cells are slightly enlarged, the nuclei are irregular with focal stratification. Subtle hyperchromasia and enlarged nucleoli are present. Fibrovascular cores tend to be filiform.
- Branching clusters of fibroadenoma with a marked palisade arrangement of cylindric epithelial cells and a large amount of cystic background material (due to preexisting dilatated tubular structures) may lead to a false interpretation of papilloma.

**Caution**

- Blood-stained cystic fluid with hemosiderophages has to raise a strong suspicion of an intracystic neoplasia.
- Distinction of papilloma from low-grade papillary carcinoma is difficult. An absence of myoepithelial cells is highly suspicious of papillary carcinoma. However, one should always bear in mind that the presence of myoepithelial cells in a papillary tumor does not exclude the possibility of an intraductal (intracystic) papillary carcinoma with microinvasion.
- Every tumor of a suspected or definite papillary nature should undergo surgical excision for histologic assessment.
- Small papilliform clusters in an otherwise bland cystic fluid may originate from needle passes through cyst-adjacent proliferative breast disease.
- Distinguishing papilloma from fibroadenoma can be difficult.

### 1.2.14.2 Intraductal Papilloma (Fig. 1.51)

- Microscopic features and differential diagnostic considerations are identical, as described for intracystic papilloma.
- However, intraductal papilloma – particularly in tumors located at the periphery of the mammary gland – are smaller in size yielding less cellular aspirates. Large papillary fronds with a fibrovascular core are uncommon.
- Papillary tumors that occur in terminal ducts are frequently multiple. Peripheral papillomas show more frequently cellular atypia or malignant degeneration compared to their centrally located counterparts [29, 48]. In this setting, histologic evaluation of surgical biopsy specimens is required.
- Centrally located papillomas are benign and malignancy is extremely rare.

## 1.2.15 Fibroadenoma and Phylloides Tumor

### 1.2.15.1 Fibroadenoma [31, 36] (Figs. 1.52 and 1.53)

Fibroadenoma (FA) is the most frequent benign breast tumor and occurs commonly in younger females. In contrast to fibrocystic changes, the lesion is in most cases freely movable, firm, and sharply outlined.

**Microscopic Features**

FNAB produces a characteristic smear including the following hallmarks:

- Marked cellularity.
- Finger-like fronds (antler-horn like clusters).
- Large numbers of isolated stripped epithelial cells and bipolar nuclei.
- Myxoid degeneration of stromal fragments.
- Additionally, large cohesive sheets occur with the monomorphic cells regularly arranged in a distinct honeycomb pattern admixed with myoepithelial cells. The nuclei are round and smoothly bordered, the chromatin is regular and finely dispersed. A nucleolus is frequently distinct, regular, and centrally placed.
- Apocrine cells and foam cells are observed in most cases in association with cystic duct changes.

- Multinucleated giant histiocytes are frequently observed.

Naked bipolar nuclei are believed to be derived from myoepithelial or stromal cells.

**Differential Diagnosis**

- Cellular aspirates of fibrocystic disease and proliferative breast disease may match several features with fibroadenoma.
- Juvenile fibroadenoma and fibroadenoma in pregnancy and the lactation period could easily be misinterpreted as carcinoma: abundant cellularity, nuclear polymorphism with huge nucleoli, loss of polarity, and discohesive clusters with large numbers of isolated cells are alarming cell features; Though the chromatin is fine and evenly distributed and the myoepithelial cells are overt (Fig. 1.54).
- FAs with a large number of isolated cells, cylindric or elongated cytoplasmic bodies, and virtual lack of pathognomonic cell clusters may raise the possibility of papilloma.
- Pleomorphic adenoma shares cytomorphologic similarities with FA and phylloides tumors. Pleomorphic adenoma is a rare benign heterogeneous tumor that originates in large ducts.
- Chondromyxoid matrix can be misinterpreted as mucus or colloid [32].

**Additional Comments**

- The epithelial fraction of the phylloides tumor is virtually identical to the epithelial pattern of fibroadenoma.
- A limited number of fibroadenoma coexisting with carcinoma are reported in the literature. Carcinoma is confined to or adjacent to the fibroadenoma. At our institution, we have observed the latter form of tumor combination in one patient. Most carcinomas were found to be lobular carcinoma in situ (lobular intraepithelial neoplasia) and less frequently ductal carcinoma in situ [43, 74].

**Caution**

- Juvenile fibroadenoma and fibroadenoma in pregnancy and lactation exhibit a marked polymorphic cellular pattern. Correct interpretation of the different cell types and the pathognomonic cytoarchitecture of clusters prevents a misdiagnosis of malignancy (Fig. 1.54).
- Coexisting intralesional or adjacent fibroadenoma and carcinoma are rare. The detection on cytologic samples is challenging as lobular carcinoma in situ is reported to be the predominant tumor type. In only one case from our archive have we noted single small atypical cells suspicious of lobular neoplasia.

#### 1.2.15.2 Phylloides Tumor [42] (Figs. 1.55, 1.56, 1.57)

Phylloides tumor is a biphasic fibroepithelial tumor characterized by a bland epithelial and a hypercellular mesenchymal component.

**General Comments and Microscopic Features**

- The epithelial component exhibits identical cytologic features and raises the same diagnostic problems as discussed in Sect. 1.2.15.1, p. 24.
- In contrast to fibroadenoma, the stromal component is clearly more cellular. Spindle-shaped fibroblastic cells harbor nuclei that may be bland, polymorphic, or sarcomatous in appearance.
- The cytodiagnosis of the malignant phylloides tumor is based on unequivocal sarcomatous features (Fig. 1.57).

Unless an excessive aspiration with multiple needle passes is performed, the stromal component will not be collected at all. Therefore, a final cytologic diagnosis is not possible in many cases.

The classification of phylloides tumors into a low-grade or malignant category is in most cases left to the histopathologist on large surgical excisional biopsies. Several reports have discussed the diagnostic features and options for classification of phylloides tumors in fine-needle samples [7, 57, 58, 71].

### 1.2.16 Adenomyoepithelioma

(Figs. 1.58, 1.59A, 1.60, 1.61)

Adenomyoepithelioma of the breast is a rare biphasic type neoplasm. It is characterized by the presence of both epithelial and myoepithelial cells [75].

**Microscopic Features**

- The slides are hypercellular and may contain uncommonly large cell clusters.
- Myoepithelial cells are admixed with proliferative ductal cells and acinic formations. The cohesive epithelial clusters are regular, encasing cohesive groups of elongated and spindle-shaped myoepithelial cells in a streaming pattern. The biphasic pattern may at once be detected with the light microscope's low magnification. Myoepithelial cells may also be present as single elongated cells and naked bipolar nuclei.
- Nuclei are bland, the N/C ratio is regular, and the chromatin texture is fine.
- Proliferative cell activity exhibits features as described in Sect. 1.2.11.1. "Proliferative Breast Disease without Atypia," p. 21, and should not be misinterpreted as carcinoma.

1

**Additional Comments**

- The cytologic features of adenomyoepithelioma are described in several reports in the literature. The authors emphasize the varying cytology that makes the diagnosis challenging. However, the combination of benign epithelial cells and clusters of spindle cells should lead the cytopathologist to a correct diagnosis. Immunocytochemical stainings (see below) clearly distinguish epithelial from myoepithelial cells.
- The tumor has the potential for local recurrence.
- A focal carcinomatous transformation or malignant change of one or both cell types may occur [46, 66] (Fig. 1.59B). Malignant adenomyoepitheliomas commonly show necrosis and increased mitotic activity.

**Differential Diagnosis** [69]

- Adenomyoepithelial lesions match cytologic features with those of fibroepithelial lesions (fibroadenoma, phyllodes tumor, hamartoma) and with pseudoangiomatous stromal hyperplasia.
- Adenomyoepithelioma may exhibit a practically pure bland spindle cell pattern which can also be encountered by fibromatosis and fibrous skin tumors.
- The predominance of highly atypical spindle cells combined with an irregular epithelial component may raise suspicion of a metaplastic carcinoma.
- Virtually all pure pleomorphic spindle cell tumors should lead to a differential diagnosis including metaplastic mammary carcinoma and primary or secondary sarcomas.

**Immunocytochemistry**

Epithelial cells reveal positivity for cytokeratins, whereas spindle-shaped cells are strongly positive for myoepithelial markers such as S-100 and smooth muscle actin (Figs. 1.60 and 1.61). Furthermore, SM-myosin heavy-chain, calponin, maspin, CD10, p63 are recommended for the detection of myoepithelial cells in adenomyoepithelioma.

## 1.2.17 Lipoma / Angiolipoma / Hibernoma

[42] (Figs. 1.62, 17.1, 17.3)

- The presence of fat tissue is common in FNAB. It represents a sampling of adipose tissue surrounding the target lesion.
- *Lipoma* (Fig. 17.1) can be diagnosed if a circumscribed mass is aspirated and the smears exclusively contain groups of enlarged, uniform, and ballooned adipocytes. The nuclei are small with bland chromatin. Occasionally, spindle cells and collagen fibers are admixed with the adipocytes.
- *Angiolipoma* can be cytologically well recognized. The basic pattern is the same as that of lipoma, but a branching vascular network can be observed spreading out among the smaller groups of adipocytes (Fig. 1.62).
- *Lipoma-like liposarcoma* may exhibit similar cytologic features as those of lipoma including myxoid matrix. It is practically impossible to distinguish between lipoma and lipoma-like liposarcoma based on cytology alone.
- *Hibernoma*. Brown fat is designated as hibernoma (Fig. 17.3) composed of adipocytes containing numerous small fat droplets. They give a reddish-brown staining to the cells and the tissue. The densely packed droplets mimic cytoplasmic granulation, which could lead to the misinterpretation of a granular cell tumor or an apocrine lesion in some cases.

## 1.2.18 Granular Cell Tumor (Figs. 1.63 and 1.64)

A granular cell tumor is a mesenchymal tumor suggested to be of neurogenic origin. The benign granular cell tumor has a distinctive cytomorphologic appearance that allows a diagnosis on cytologic samples [3, 22].

**Microscopic Features**

- Hallmarks:
  - Highly cellular FNAB specimens.
  - Uniformly large cells with a poorly defined and abundant, finely granular cytoplasm.
  - Cells are fragile, leading to a background of granular material.
- Cells are single or grouped in dense or loose clusters.
- The nuclei are small and may be eccentrically positioned with a bland granular chromatin.
- Nucleoli are inconspicuous.
- Mild nuclear polymorphism with distinct nucleoli may occur (Fig. 1.64).

**Immunocytochemistry and Cytochemistry**

(Figs. 1.63B and 1.63C)

- Positive immunostaining for S-100 protein, neuron-specific enolase, and vimentin.
- Tumor cells also stain for the macrophage epitope CD68.
- Positivity for alpha1-antichymotrypsin and myoglobin has been reported [33].
- Cytoplasmic granules of the tumor cells are PAS-positive and diastase-resistant.

**Additional Comments and Differential Diagnosis**

- These tumors are usually benign. Recognition on FNAB is important since granular cell tumors of the breast often mimic carcinoma clinically, and radiologically.
- Occasional cells with nuclear pleomorphism and prominent nucleoli should not be interpreted as signs of malignancy; they can be present in benign granular cell tumors. Nuclear pleomorphism together with hyperchromasia, coarse chromatin, and enlarged nucleoli throughout the whole cytologic sample are described as key features of malignancy [72]. Some authors emphasize that mitotic

figures and necrosis should be identified before a diagnosis of malignancy is rendered [35].

- Cytopathologists, who are not familiar with the cellular pattern of granular cell tumors, may easily be misled. The differential diagnosis of benign and malignant lesions include:
  - Abundant foam cells from a cystic fluid.
  - Apocrine and clear cell lesions, particularly apocrine breast carcinoma or metastasis of renal cell adenocarcinoma.
  - Malignant melanoma.
  - Histiocytoid (mostly invasive lobular carcinoma with histiocytoid features) carcinoma and lipid-rich carcinoma.

## 1.2.19 Rare Benign Breast Lesions

A number of rare tumors in the breast arising within the gland, from the skin and its adnexa, or in the surrounding connective tissue are reported in the literature. Large lesions can masquerade as malignant tumors on clinical and imaging results. A few of these lesions could cause difficulties in histologic and cytologic breast cancer diagnoses. The most challenging lesions in cytologic samples are discussed together with the corresponding benign lesions in this chapter and with malignant look-alikes in Sect. 1.3. "Breast: Malignant Lesions," p. 56. In rare instances, these lesions are observed in the male breast as well.

The disorders are mainly documented in the histological literature, selected entities are listed below. Recent publications with information on the cytodiagnostic features are cited:

- *Epithelial lesions:* Pilomatrixoma [4, 63] (Figs. 16.5–16.7) (see also Sect. 1.3.1.2 "Monomorphic Small-Cell Ductal Carcinoma: Differential Diagnosis," p. 57), Syringomatous adenoma [13].
- *Cystic lesions:* Epidermal inclusion cyst.
- *Mesenchymal lesions:* Fibromatosis, nodular fasciitis [37], fibrohistiocytoma, myxoma, leiomyoma, hemangiopericytoma, chondrolipoma, neurilemmoma [6] (see Sect. 17.1, "Soft Tissue and Bone: Benign Lesions," p. 1055).
- *Tietze's syndrome* [39, 51] (Fig. 1.65) is a painful nonsuppurative parasternal swelling of the costochondral junction due to microfractures of the upper ribs. The nodule is often suspected to be a tumorous lesion belonging to parasternal mammary tissue. The FNAB sample is hypocellular made up of small soft tissue fragments and activated fibroblasts. Cytologic findings together with characteristic clinical signs are diagnostic.

## 1.2.20 Further Reading


1. Aalaei S, Zarif A, Gattuso P, Siziopikou K. Liesegang rings. Breast J 2005;2005:522.
2. Abendroth CS, Wang HH, Ducatman BS. Comparative features of carcinoma in situ and atypical ductal hyperplasia of the breast on fine-needle aspiration biopsy specimens. Am J Clin Pathol 1991;96:654-659.
3. Adeniran A, Al-Ahmadie H, Mahoney MC, Robinson-Smith TM. Granular cell tumor of the breast: a series of 17 cases and review of the literature. Breast J 2004;10:528-531.
4. Ali MZ, Ali FZ. Pilomatrixoma breast mimicking carcinoma. Coll Physicians Surg Pak 2005;15:248-249.
5. al-Kaisi. The spectrum of the "gray zone" in breast cytology. A review of 186 cases of atypical and suspicious cytology. Acta Cytol 1994;38:898-908.
6. Bernardello F, Caneva A, Bresaola E, et al. Breast solitary schwannoma: fine-needle aspiration biopsy and immunocytochemical analysis. Diagn Cytopathol 1994;10:221-223.
7. Bhattarai S, Kapila K, Verma K. Phylloides tumor of the breast. A cytohistologic study of 80 cases. Acta cytol 2000;44:790-796.
8. Boudova L, Kazakov DV, Sima R, et al. Cutaneous lymphoid hyperplasia and other lymphoid infiltrates of the breast nipple: a retrospective clinicopathologic study of fifty-six patients. Am J Dermatopathol 2005;27:375-386.
9. Cheng L, Lee WY, Chang TW. Benign mucocele-like lesion of the breast: how to differentiate from mucinous carcinoma before surgery. Cytopathol 2004;15:104-108.
10. Choi YD, Gong GY, Kim MJ, et al. Clinical and cytologic features of papillary neoplasms of the breast. Acta Cytol 2006;50:35-40.
11. Ciatto S,Cariaggi P, Bulgaresi P. The value of routine cytologic examination of breast fluids. Acta Cytol 1987;31:301-304.
12. Colli C, Leinweber B, Müllegger R, et al. Borrelia burgdorferi-associated lymphocytoma cutis: clinicopathologic, immunophenotypic, and molecular study of 106 cases. J Cutan Pathol 2004;31:232-240.
13. Dahlstrom JE, Tait N, Cranney BG, Jain S. Fine needle aspiration cytology and core biopsy histo-logy in infiltrating syringomatous adenoma of the breast. A case report. Acta Cytol 1999;43:303-307.
14. Dodd LG, Sneige N,Reece GP, Fornage B. Fine-needle aspiration cytology of Silicone granulomas in the augmented breast. Diagn Cytopathol 1993;9:498-502.
15. Field A, Mak A. A prospective study of the diagnostic accuracy of cytological criteria in the FNAB diagnosis of breast papillomas. Diagn Cytopathol 2007;35:465-475.
16. Flint A, Oberman HA. Infarction and squamous metaplasia of intraductal papilloma. Human Pathol 1984;15:764-767.
17. Frost AR, Aksu A, Kurstin R, Sidawy MK. Can nonproliferative breast disease and proliferative breast disease without atypia be distinguished by fine-needle aspiration cytology? Cancer Cytopathol 1997
18. Gangane N, Joshi D, Anshu, Shivkumar VB. Cytological diagnosis of collagenous spherulosis of breast associated with fibroadenoma: report of a case with review of literature. Diagn Cytopathol 2007;35:366-369.
19. Gangopadhyay M, Nijhawan R, Joshi K, Gupta S. Cytology of "significant" breast ductal proliferations. Acta cytol 1997;41:1112-1120.
20. Gavin K, Banville N, Gibbons D, Quinn CM. Liesegang rings in inflammatory breast lesions. J Clin Pathol 2005;58:1343-1344.
21. Gherardi G, Marveggio C. Cytologic score and DNA-image analysis in the classification of borderline breast lesions: a prospective study on 47 fine-needle aspirates. Diagn Cytopathol 1999;20:212-218.
22. Gibbons D, Leitch M, Coscia J, et al. Fine needle aspiration cytology and histologic findings of granular cell tumor of the breast: review of 19 cases with clinical/radiologic correlation. Breast J 2000;6:27-30.

23. Gomez-Aracil V, Mayayo E, Azua J, et al. Fine needle aspiration cytology of mammary hamartoma: a review of nine cases with histologic correlation. Cytopathol 2003;14:195-200.
24. Gupta RK, Naran S, Simpson J. The role of fine needle aspiration cytology (FNAC) in the diagnosis of breast masses in males. Eur J Surg Oncol 1988;14:317-320.
25. Herbert M, Mendlovic S, Liokumovich P, et al. Can hamartoma of the breast be distinguished from fibroadenoma using fine-needle aspiration cytology? Diagn Cytopathol 2006;34:326-329.
26. Herbert M, Schvimer M, Zehavi S, et al. Breast hamartoma: fine-needle aspiration cytologic finding. Cancer 2003;99:255-258.
27. Jayaram G, Elsayed EM, Yaccob RB. Papillary breast lesions diagnosed on cytology. Profile of 65 cases. Acta Cytol 2007;51:3-8.
28. Kapila K, Verma K. Cytomorphological spectrum in gynecomastia: a study of 389 cases. Cytopathology 2002;13:300-308.
29. Katzer B, Pinterowitsch J, Bässler R Immunohistochemical studies of the differential diagnosis of papillary tumors of the breast Pathologe 1990;11:201-207.
30. Khamapirad T, Hennan K, Leonard M Jr, et al. Granulomatous lobular mastitis: two case reports with focus on radiologic and histopathologic features. Ann Diagn Pathol 2007;11:109-112.
31. Kollur SM, El Hag IA. FNA of breast fibroadenoma: observer variability and review of cytomorphology with cytohistological correlation. Cytopathology 2006;17:239-244.
32. Kumar PV, Sobhani SA, Monabati A, et al. Cytologic findings of a pleomorphic adenoma of the breast: a case report. Acta Cytol 2004;48:849-852.
33. Lee S, Morimoto K, Kaseno S, et al. Granular cell tumor of the male breast: report of a case. Surg Today 2000;30:658-662.
34. Lew W, Seymour AE. Primary amyloid tumor of the breast. Case report and literature review. Acta Cytol 1985;29:7-11.
35. Liu K, Madden JF, Olatidoye BA, Dodd LG. Features of benign granular cell tumor on fine needle aspiration. Acta Cytol 1999;43:552-557.
36. Lopez-Ferrer P, Jimenez-Heffernan JA, Vicandi B, et al. Fine needle aspiration cytology of breast fibroadenoma. A cytohistologic correlation study of 405 cases. Acta Cytol 1999;43:579-586.
37. Maly B, Maly A. Nodular fasciitis of the breast: report of a case initially diagnosed by fine needle aspiration cytology. Acta Cytol 2001;45:794-796.
38. Masood S, Loya A, Khalbuss W. Is core needle biopsy superior to fine-needle aspiration biopsy in the diagnosis of papillary breast lesions? Diagn Cytopathol 2003;28:329-334.
39. Mathew AS, El-Haddad G, Lilien DL, Takalkar AM. Costosternal chondrodynia simulating recurrent breast cancer unveiled by FDG PET. Clin Nucl Med 2008;33:330-332.
40. Mazzara PF, Flint A, Naylor B. Adenoma of the nipple. Cytopathologic features. Acta Cytol 1989;33:188-190.
41. Mirsaeidi SM, Masjedi MR, Mansouri SD, Velayati AA. Tuberculosis of the breast: report of 4 clinical cases and literature review. East Mediterr Health J 2007;13:670-676.
42. Moinfar F. Essentials of diagnostic breast pathology. A practical approach. Springer-Verlag Berlin Heidelberg 2007.
43. Morelli A, Diaz L, Vighi S, et al. Carcinoma and fibroadenoma of the breast. Medicina(B Aires) 1989;49:583-588.
44. MulfordDK, Dawson AE. Atypia in fine needle aspiration cytology of nonpalpable and palpable mammographically detected breast lesions. Acta Cytol 1994;38:9-17.
45. Nayar R, De Frias DV, Bourtsos EP, et al. Cytologic differential diagnosis of papillary pattern in breast aspirates: correlation with histology. Ann Diagn Pathol 2001;5:34-42.
46. Ng WK. Adenomyoepithelioma of the breast. A review of three cases with reappraisal of the fine needle aspiration biopsy findings. Acta Cytol 2002;46:317-324.
47. Ng WK, Kong Jh. Significance of squamous cells in fine needle aspiration cytology of the breast. A review of cases in a seven-year period. Acta Cytol 2003;47:27-35.
48. Ohuchi N, Abe R,Kasai M. Possible cancerous change of intraductal papillomas of the breast. A 3-D reconstruction study of 25 cases. Cancer 1984;54:605-611.
49. O'Malley FP, Bane A. An update on apocrine lesions of the breast. Histopathology 2008;52:3-10.
50. Ozkara SK, Ustün MO, Paksoy N. The gray zone in breast fine needle aspiration cytology. How to report on it? Acta Cytol 2002 ;46 :513-518.
51. Pappalardo A, Buccheri C, Salli L, Nalbone L. Reflexions on the Tietze syndrome. Clinical contribution. Clin Ter 1995;146:675-682.
52. Rabban JT, Swain RS, Zaloudek CJ, et al. Immunophenotypic overlap between adenoid cystic carcinoma and collagenous spherulosis of the breast: potential diagnostic pitfalls using myoepithelial markers. Mod Pathol 2006;19:1351-1357.
53. Raso DS, Greene WB, Finley JL, Silverman JF. Morphology and pathogenesis of Liesegang rings in cyst aspirates: report of two cases with ancillary studies. Diagn Cytopathol 1998;19:116-119.
54. Resetkova E, Albarracin C, Sneige N. Collagenous spherulosis of breast: study of 59 cases and review of the literature. Am J Surg Pathol 2006;30:20-27.
55. Rosen PP, Kimmel M. Juvenile papillomatosis of the breast. A follow up of 41 patients having biopsies before 1979. Am J Clin Pathol 1990;93:599-603.
56. Rosen PP, Cantrell B, Mullen DL, DePalo A. Juvenile papillomatosis (Swiss cheese disease) of the breast. Am J Surg Pathol 1980;4:3-12.
57. Scolyer RA, McKenzie PR, Achmed D, Lee CS. Can phyllodes tumours of the breast be distinguished from fibroadenomas using fine needle aspiration cytology? Pathology 2001;33:437-443.
58. Shabb NS. Phyllodes tumor. Fine needle aspiration cytology of eight cases. Acta Cytol 1997;41:321-326.
59. Silverman JF. chap.27 breast, in: comprehensive cytopathology, ed.M.Bibbo. W.B.Saunders Company, 1991;p:726.
60. Silverman JF. in: Comprehensive Cytopathology, ed. M. Bibbo. W.B.Saunders Company,1991 .
61. Silverman JF, Lannin DR, Unverferth M, et al. Fine needle aspiration cytology of subareolar abscess of the breast: spectrum of cytomorphologic findings and potential diagnostic pitfalls. Acta Cytol 1986;30:413-419.
62. Simsir A, Waisman J, Thorner K, Cangiarella J. Mammary lesions diagnosed as "papillary" by aspiration biopsy: 70 cases with follow-up. Cancer 2003;99:156-165.
63. Sivakumar S. Pilomatrixoma as a diagnostic pitfall in fine needle aspiration cytology: a case report. Acta Cytol 2007;51:583-585.
64. Sneige N, Gregg A, Staerkel A. Fine-needle aspiration cytology of ductal hyperplasia with and without atypia and ductal carcinoma in situ. Hum Pathol 1994;25:485-492.
65. Stormby N, Bondeson L. Adenoma of the nipple. An unusual diagnosis in aspiration cytology. Acta Cytol 1984;28:729-732.
66. Tavassoli FA. Myoepithelial lesions of the breast. Myoepitheliosis, adenomyoepithelioma, and myoepithelial carcinoma. Am J Surg Pathol 1991;15:554-568.
67. Tournant B. Lymphocytic plasma cell mastitis Arch Anat Cytol Pathol 1995;43:88-92.
68. Tse GM, Law BK, Ma TK, et al. Hamartoma of the breast: a clinicopathological review. J Clin Pathol 2002;55:951-954.
69. Tse GM, Tan PH, Lui PC, Putti TC. Spindle cell lesions of the breast – the pathologic differential diagnosis. Breast Cancer Res Treat 2008;109:199-207.
70. Tyler X, Coghill SB. Fine needle aspiration cytology of collagenous spherulosis of the breast. Cytopathology 1991;2:159-162.
71. Vladescu T, Klijanienko J, Caillaud JM, Lagacé R, Vielh P. Fine-needle sampling in malignant phyllodes tumors: clinicopathologic study of 22 cases seen at the institute Curie. Diagn Cytopathol 2004;31:71-76.

72. Wieczorek TJ, Krane JF, Domanski HA, et al. Cytologic findings in granular cell tumors, with emphasis on the diagnosis of malignant granular cell tumor by fine-needle aspiration biopsy. Cancer 2001;93:398-408.
73. Wong NL, Wan SK. Comparative cytology of mucocele-like lesion and mucinous carcinoma of the breast in fine needle aspiration. Acta Cytol 2000;44:765-770.
74. Yoshida Y, Takaoka M, Fukumoto M. Carcinoma arising in fibroadenoma: a case report and review of the world literature. J Surg Oncol 198529:132-140.
75. Yvengar P, Ali SZ, Brogi E. Fine-needle aspiration cytology of mammary adenomyoepithelioma: a study of 12 patients. Cancer 2006;108:250-256.

**Fig. 1.10 Benign ductal epithelium.**
High magnification showing a large flat sheet of uniform, cuboidal benign duct cells exhibiting evenly distributed granular and reticular chromatin, several chromocenters, small round nucleoli, and a moderate but distinct cytoplasmic rim. Small dark bipolar nuclei of myoepithelial cells are seen in varying microscopic foci (arrows) (FNAB, direct smear, Pap stain).

**Fig. 1.11 Normal lobular unit.**
A terminal duct-lobular unit with a loose stromal component. Small segments of terminal ducts (arrow) ending in acinic structures encircled by a thin basal lamina (arrowheads) (FNAB, direct smear, Pap stain, lower magnification).

**Fig. 1.12 Duct ectasia.**
Aspirate with morphologic features commonly observed in duct ectasia. Numerous large drops of proteinaceous secretion (stained eosinophilic or cyanophilic) and only a few small benign sheets of inactive ductal epithelial cells are present (FNAB, direct sediment smear, Pap stain, low magnification).

**Fig. 1.13 Typical cystic sediment devoid of epithelial elements.**
Ultrasound-guided FNAB of a cystic lesion (2 cm in diameter). High magnification shows a typical cystic sediment with mainly degenerating histiocytes/foam cells, cellular debris, small drops of secretion, and a few red blood cells (direct sediment smear, Pap stain).

**Fig. 1.14 Apocrine metaplasia.**
Flat sheets of apocrine metaplastic cells in a direct sediment smear of an aspirated cystic fluid. Note the cobblestone arrangement of the cells, the presence of distinct eosinophilic cytoplasmic granules, large centrally placed nucleoli, and the loose chromatin structure including chromocenters (Pap stain, high magnification).

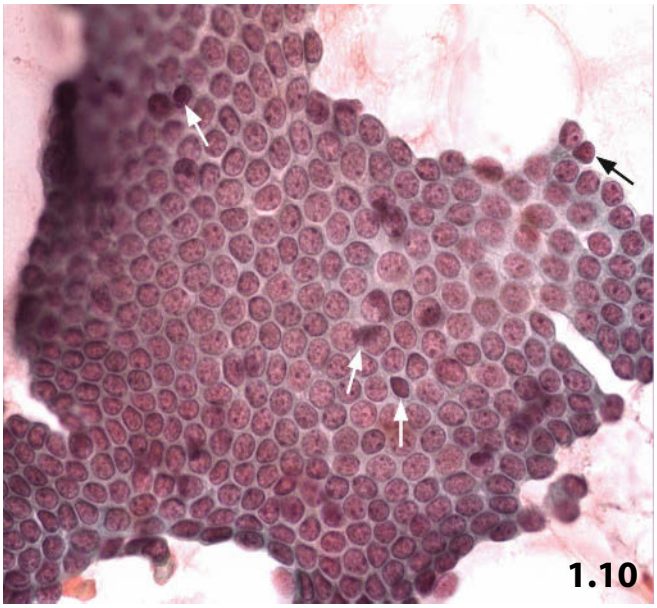
1.10

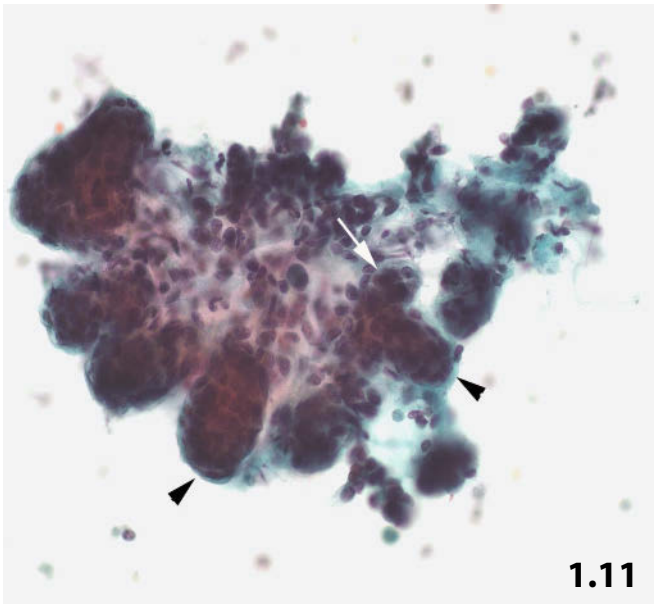
1.11

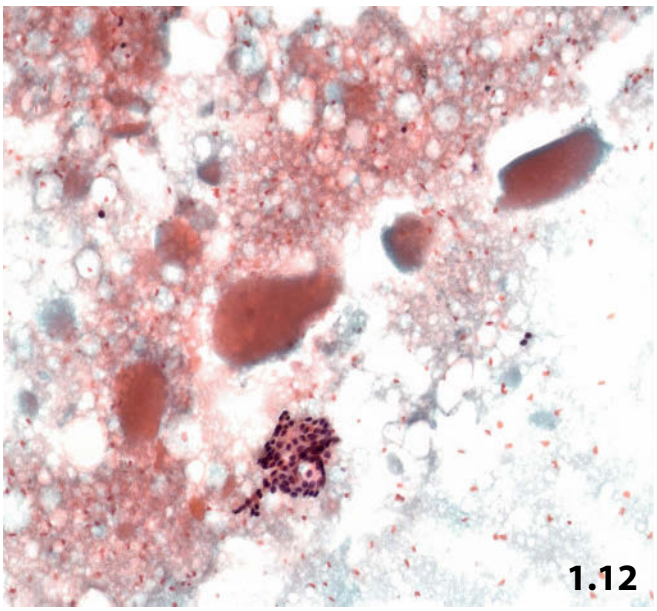
1.12

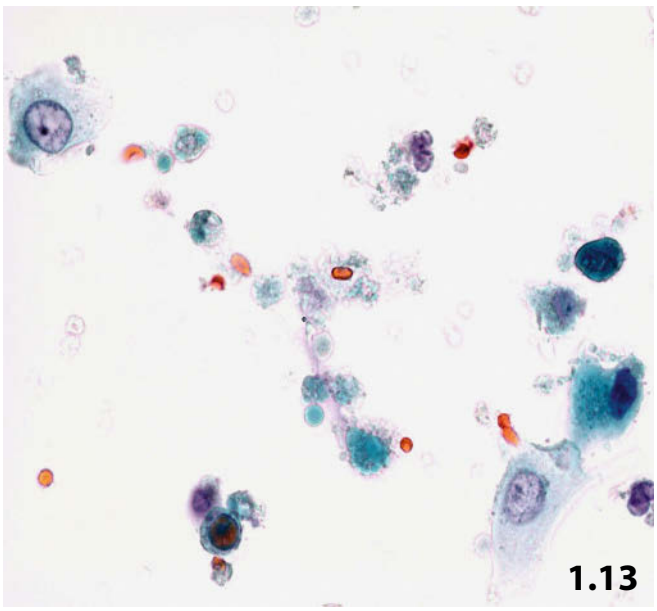
1.13

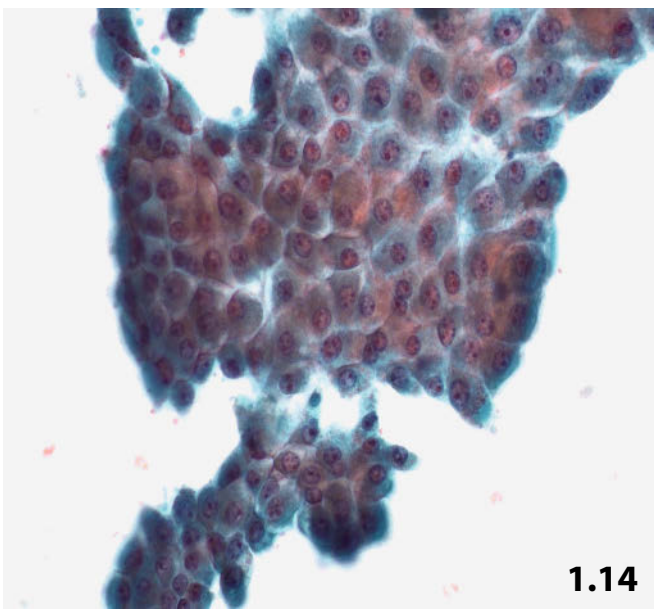
1.14

1

**Figs. 1.15 and 1.16 Regenerative changes of cyst lining epithelium.**
FNABs of mammary cysts from two patients. Direct sediment smears were Pap-stained

**Fig. 1.15** Fluid sediment includes sheets and clusters from the cyst-epithelial layer showing strong regenerative/reparative changes. Note the neutrophilic granulocytes admixed with epithelial cells (high magnification).

**Fig. 1.16A, B** Another example at lower magnification demonstrating the diagnostic problem of reactive cyst-lining cells. **A** Reactive epithelial cells exhibiting pronounced cytoplasmic elongation and a streaming pattern. The regular N/C ratio and chromatin structure favor a benign-regenerative process. **B** Immunocytochemistry for pancytokeratin (Lu-5) shows a strong positive reaction proving the epithelial origin of the elongated cells (Pap-prestained smear).

Variation in cellular size and shape, nuclear polymorphism, dark nuclear staining, and multi-nucleation may mislead to a diagnosis of malignancy. Prominent nucleoli are normally observed in activated epithelial cells.

**Fig. 1.17 Activated histiocytes/foamy cells versus malignant neoplasm.**
A 34-year-old woman presented with a symptomatic cyst in the left breast. FNAB yields cystic fluid showing a characteristic background, signs of acute inflammation, and strongly activated foamy cells (cellular enlargement, large nucleoli) with increased mitotic activity (upper right). The homogeneity of the histiocytic cell population, low N/C ratio, and bland chromatin exclude a malignant process (direct sediment smears, Pap stain, high magnification).

**Fig. 1.18 Inflammatory atypia of ductal epithelium.**
FNAB of a firm uneven infiltrate in the breast (measuring 4 cm) in a 48-year-old woman. Direct smears contain compact clusters of ductal cells with reactive atypias (the inflammatory component is not shown). Note the cellular enlargement and occasional pronounced nucleoli. The benign chromatin pattern and a focal streaming pattern (arrows) should be considered characteristic of a benign ductal proliferative disorder (direct smear, Pap stain, high magnification).
*Cytologic diagnosis:* granulomatous mastitis (diagnosis was confirmed by histology).

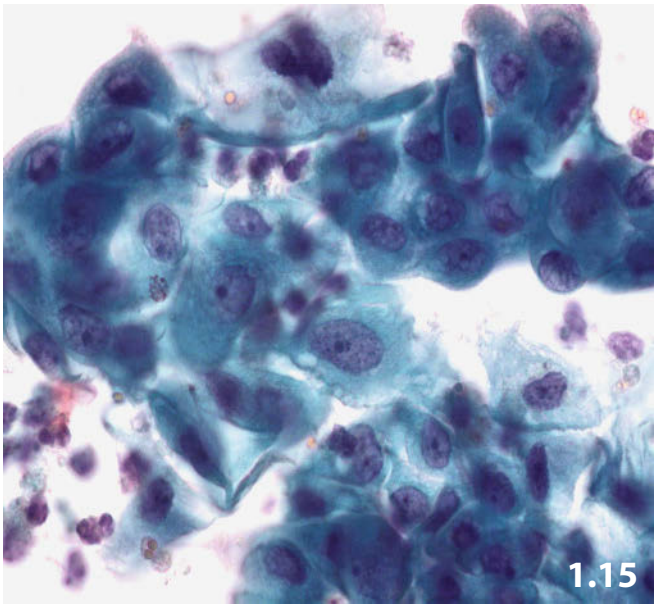
1.15

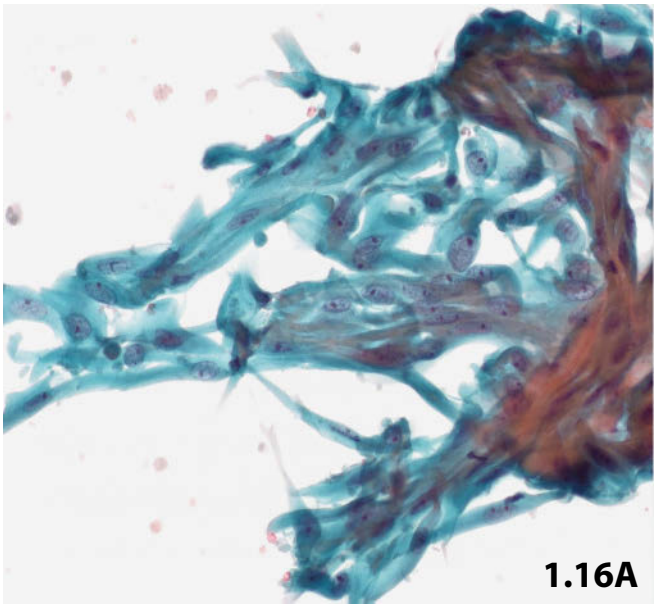
1.16A

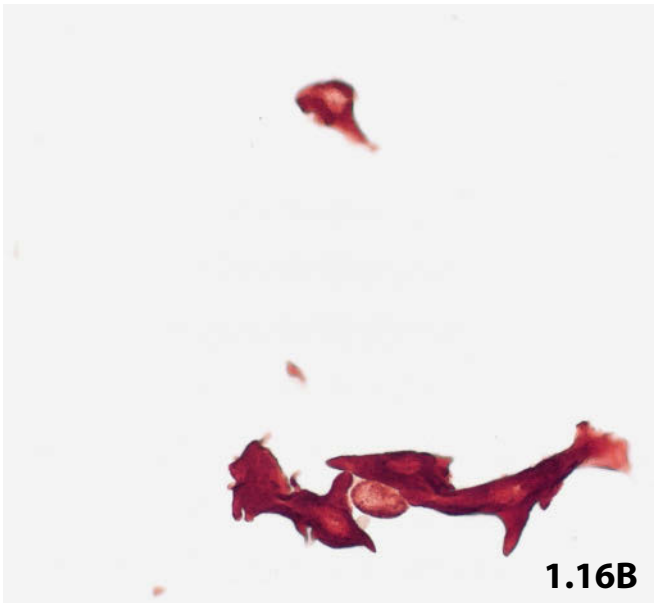
1.16B

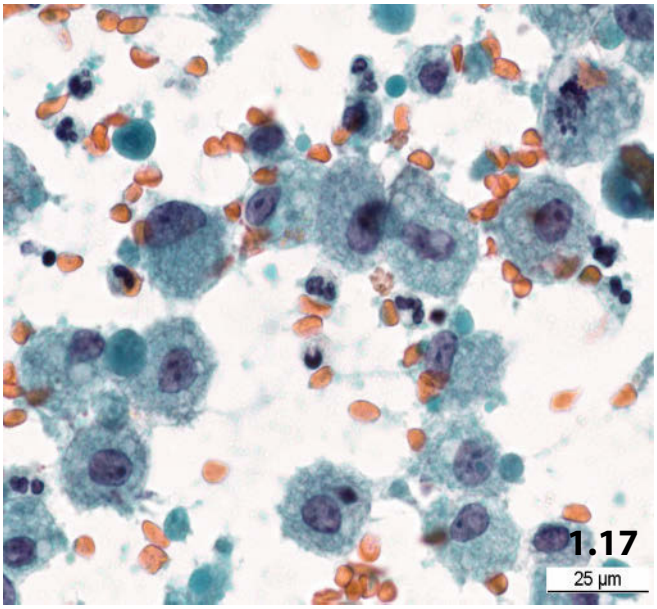

1.17

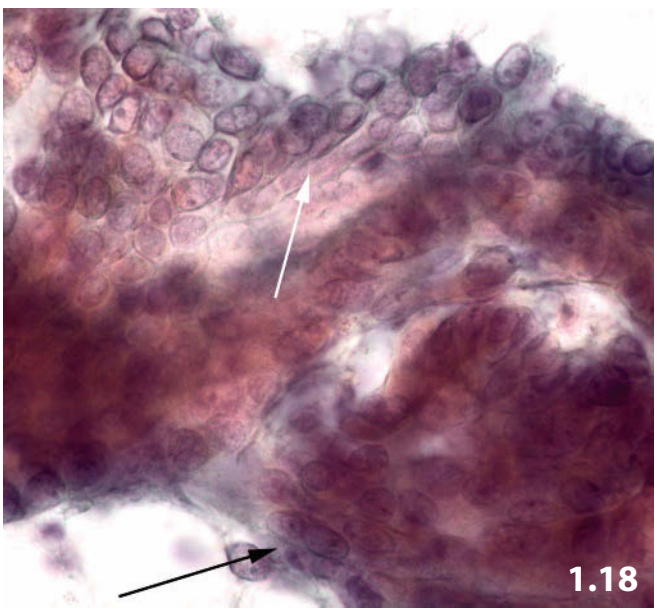
1.18

**Fig. 1.19 Subareolar abscess.**
FNAB of subareolar abscess shows a mixed inflammatory infiltrate mainly composed of histiocytes, foreign body giant cells (arrows), and proliferating fibroblasts. Nucleated and anucleated bland squamous cells are a key feature of this lesion. The single squamous cell (arrowhead) showing a small dark nucleus, and polymorphic eosinophilic cytoplasm should not be misinterpreted as malignant squamous cell (direct smear, Pap stain, low magnification).

**Fig. 1.20 Fat necrosis.**
A lump in the left breast of a 50-year-old woman after two surgical interventions 2 years before. FNAB shows material from necrotic fat tissue: amorphous material and shadowy lipocytes (asterisks) are embedded in sanguineous background. Granulomatous tissue fragments (arrows) are indicative of a later stage of lipomatous degeneration (direct smear, Pap stain, low magnification).

**Fig. 1.21 Suture granuloma.**
Suture granuloma provides refractile bars (birefringent upon polarization), both ingested in multinucleated macrophages and enclosed between proliferating fibroblasts (FNAB, direct smear, Pap stain, high magnification).

**Fig. 1.22 Granulomatous mastitis.**
FNAB of a retromammilar nodule in a 26-year-old woman. Low magnification shows a huge fragment of granulation tissue composed of mixed inflammatory cells, activated fibroblasts, multinucleated histiocytes, and fibrosis/sclerosis. In other areas of the smear (not shown, see also Fig. 1.18), cohesive epithelial clusters with reactive atypical changes were also observed. (direct smear, Pap stain).
*Cytologic diagnosis:* granulomatous mastitis, probably subareolar abscess in a late stage.

**Fig. 1.23 Tuberculosis.**
An 89-year-old woman with no specific clinical history presented with a large mass (8 cm) in her left breast. FNAB disclosed granular debris, calcifying deposits (center and left), and a few degenerating cells. A conclusive cytologic diagnosis could not be established. A Ziehl-Neelsen staining was not performed. (Pap stain)
*Subsequent tissue examination* revealed tuberculoma.

**Fig. 1.24 Pseudolymphoma.**
Example of a pseudolymphoma of the breast. The cell population is mainly composed of immature lymphocytes (note the large nucleoli and the irregular nuclear outline). Both immunoblasts and centroblasts (arrows) and numerous disseminated histiocytes (arrowheads) are readily identified (FNAB, direct smear, Pap stain, high magnification).

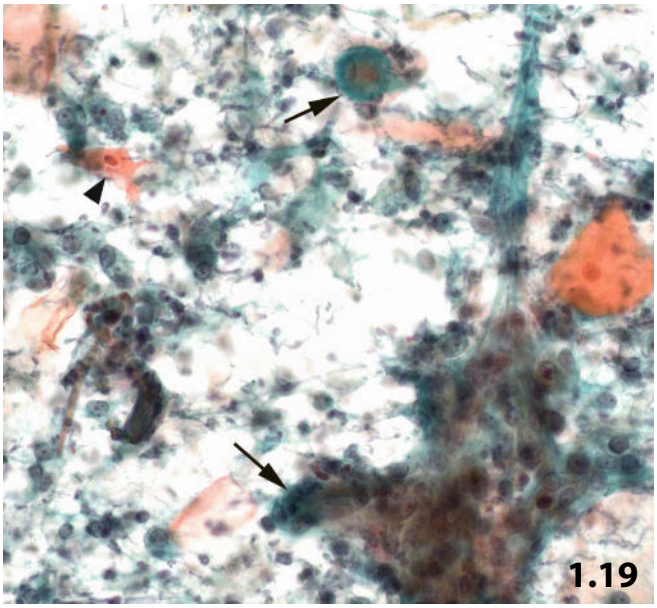
1.19

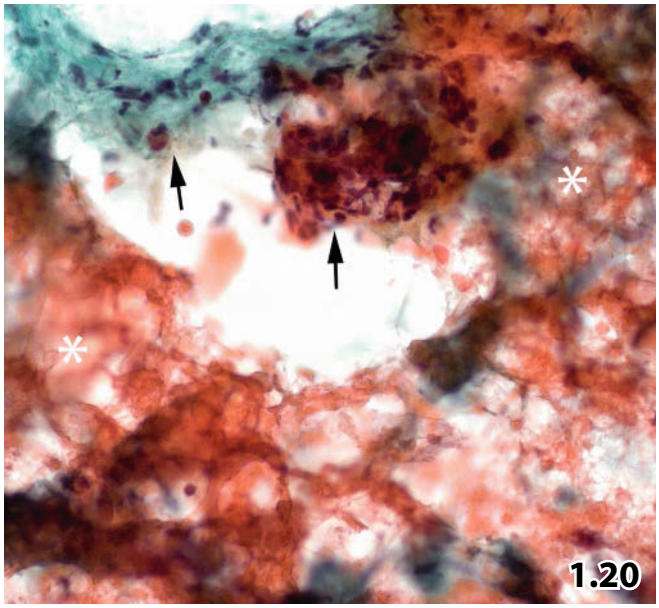
1.20

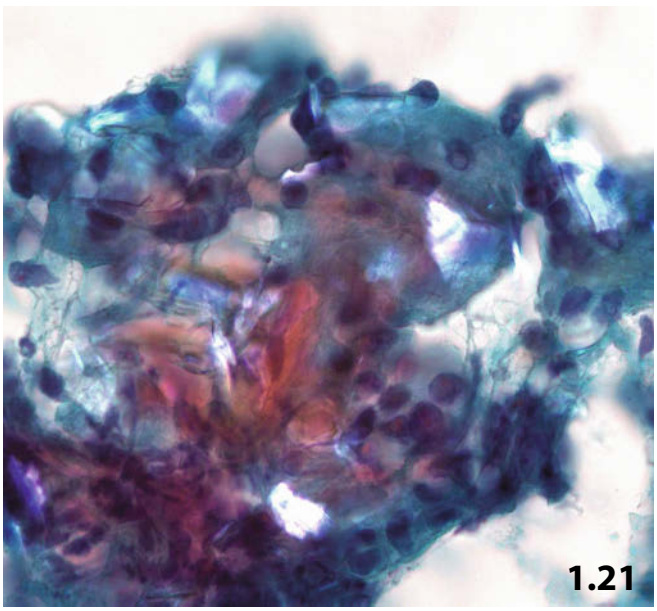
1.21

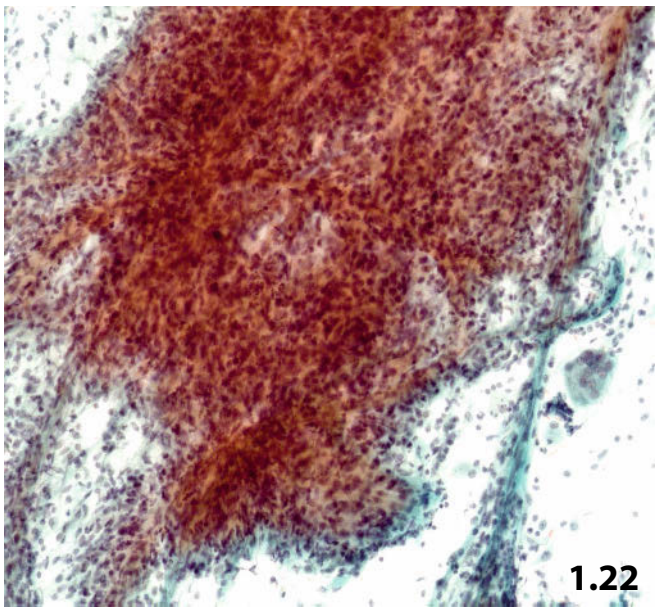
1.22

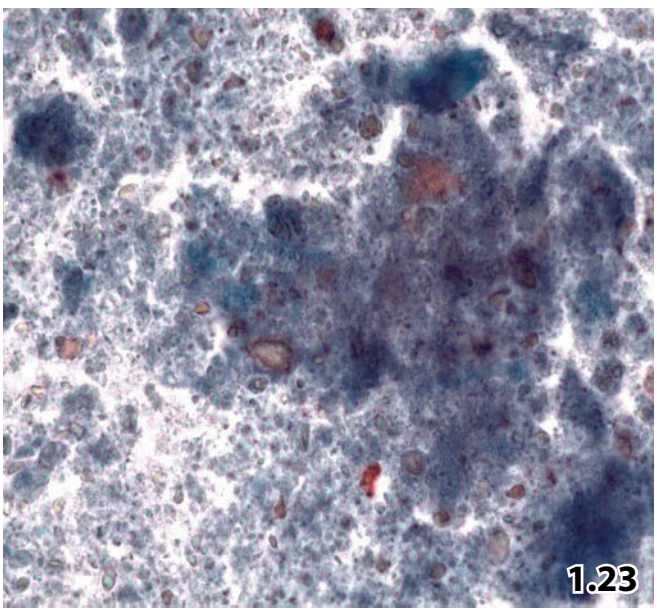
1.23

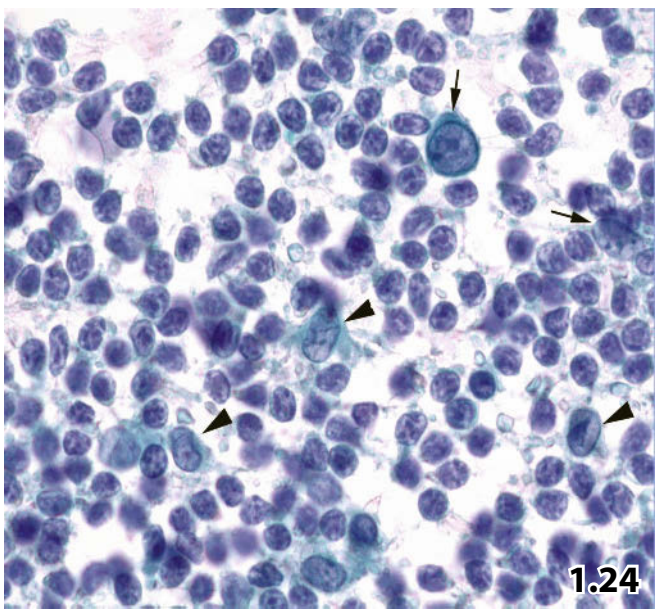
1.24

**Fig. 1.25 Liesegang rings.**
A 43-year-old woman presented with a palpable lesion in the periphery of her left breast. The result of radiologic imaging was suggestive of malignancy. FNAB yielded a few drops of fluid. Microscopic evaluation of the direct smear shows cystic background (one foam cell is shown) and numerous ring-shaped, concentrically laminated concretions: so-called Liesegang rings (Pap stain, high magnification).

**Fig. 1.26 Silicone granuloma.**
A 60-year-old woman presented with a palpable supraclavicular nodule and enlarged mediastinal lymph nodes by imaging. Thirteen years before, the patient had undergone left-side subcutaneous mastectomy for multicentric DCIS and subsequent implantation of a silicone prosthesis. FNAB of the palpable lymph node shows silicone granulomas: aggregation of activated mono- and multinuclear macrophages with evidence of small and large optically empty bubbles (extra- and intracytoplasmic). Note an asteroid body (arrow) in the center of the cell aggregate (direct smear, Pap stain, high magnification).

**Figs. 1.27–1.29 Hormonal stimulation of mammary epithelial cells.**
FNAB of nodular breast lesions in three pregnant women. Conventional smears Pap-stained For another example, see Fig. 1.9.

**Fig. 1.27** A 29-year-old woman (in week 18 of gestation) presented with a firm nodule. Clinical and ultrasound investigations suggested a fibroadenoma. Low magnification shows high cellularity, proteinaceous material, and edematous soft tissue in the background (lower left). The cellular appearance is characteristic of hormonal stimulation including enlarged epithelial cells, irregular and discohesive cell clusters, numerous naked and fragile nuclei, prominent nucleoli, finely dispersed chromatin, and abundant fading cytoplasm.

**Fig. 1.28** Details of hormonally stimulated epithelial cells are shown in liquid-based preparation (ThinPrep). Note the very prominent nucleoli and the characteristic background of the smear.

**Fig. 1.29** A female patient in week 33 of gestation. FNAB of a solitary nodule in the left breast revealed large acini with smooth rounded borders and abundant vacuolated cytoplasm. Numerous myoepithelial cells appear at the periphery of the acini and between the epithelial cells (low magnification).
*Tentative cytologic diagnosis:* suggestive of a lactating adenoma (the diagnosis was verified by histology).

In most cases, cytology cannot reliably distinguish between a hormonally stimulated nodular area of the breast tissue and hormonally stimulated benign neoplasms (adenoma, fibroadenoma, phyllodes tumor).

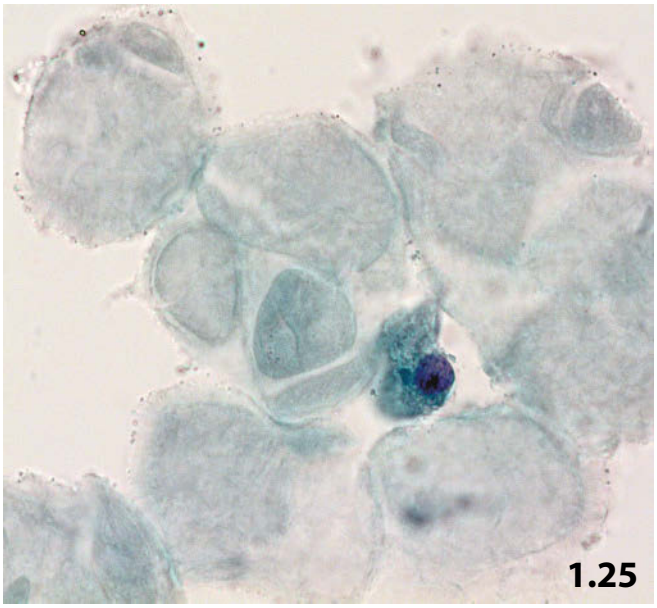
1.25

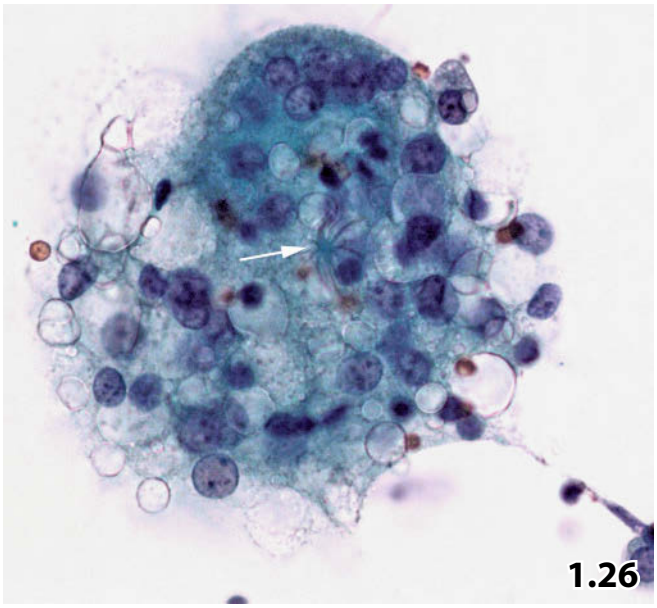
1.26

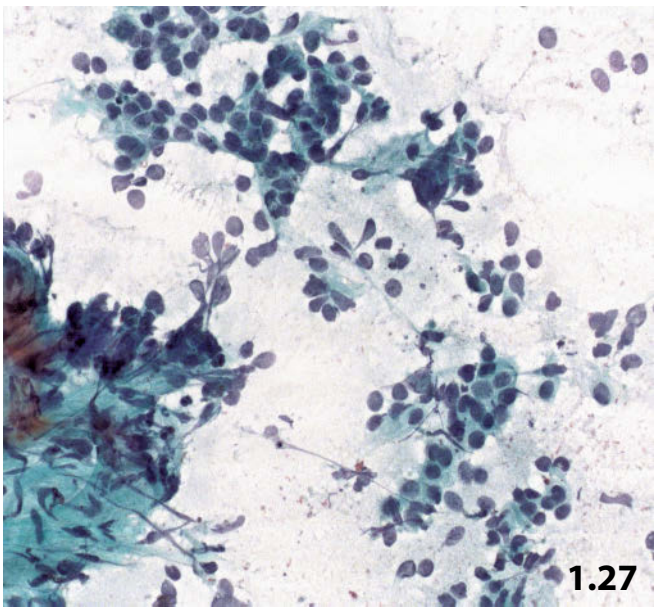
1.27

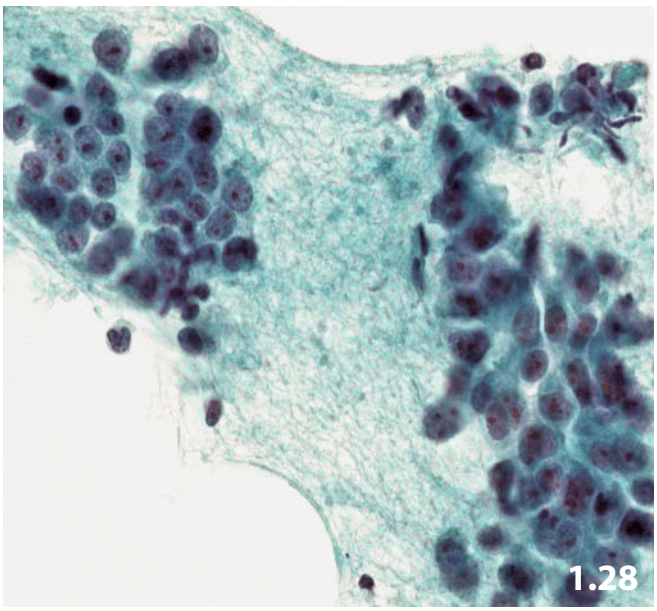
1.28

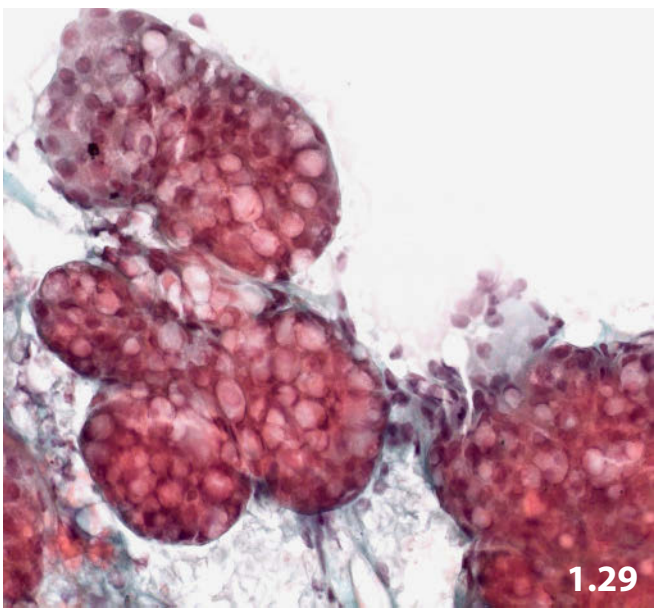
1.29

**Fig. 1.30 Fibrocystic changes.**
A cytologic example of fibrocystic changes of the breast (FNAB). Low magnification shows a hypocellular material from conventional smear composed of fragments of lipomatous (top) and fibrotic (bottom) tissue, and a few epithelial cells (arrows). Degenerating foam cells and a dirty background suggest cystic change (Pap stain).

**Figs. 1.31–1.33 Usual ductal hyperplasia (intraductal hyperplasia without atypia).**
Breast aspirations from three different patients exhibiting classic features of benign ductal hyperplasia in conventional smear and liquid-based specimen (Pap stain).

Fig. 1.31A–C (case #1) Usual ductal hyperplasia, cytologic appearance in different magnification scales. **A** At low magnification the lesion exhibits small and large compact epithelial cell clusters that are frequently papilliform. Stromal fragments may adhere to epithelial clusters (arrow). A few single columnar epithelial cells (arrowheads) and foam cells are present, the latter suggesting ectasia of the altered ducts (direct smear) **B** At higher magnification, nuclear polarization and the pathognomonic streaming pattern (arrows) are evident. The cell population is heterogeneous and the nuclei are bland. Focal palisading of elongated ductal cells (arrowheads) may cause diagnostic confusion with a true papillary lesion (direct smear). **C** High magnification exhibits the dual cell population of epithelial and myoepithelial cells (upper right) and transformation to apocrine metaplasia (left), which are indicative of benign epithelial proliferation. Note the streaming pattern of epithelial cells in each cluster (direct smear).

**Fig. 1.32** (case #2) A case with histologically confirmed usual ductal hyperplasia. Calcified particles and foreign body type multinucleated histiocytes can be present in cytologic specimens. Epithelial cells and clusters exhibit no atypia(not shown) (direct smear).

**Fig. 1.33** (case #3) Aspirate from a usual ductal hyperplasia processed using the liquid-based technique (ThinPrep). Note that the characteristic cytoarchitecture of the epithelial clusters (streaming or swirling pattern) is mainly lost. Cellular shrinkage produces both a certain nuclear polymorphism and small, dark nuclei. Therefore, it is often difficult to assess the characteristic heterogeneity of the hyperplastic cell population.

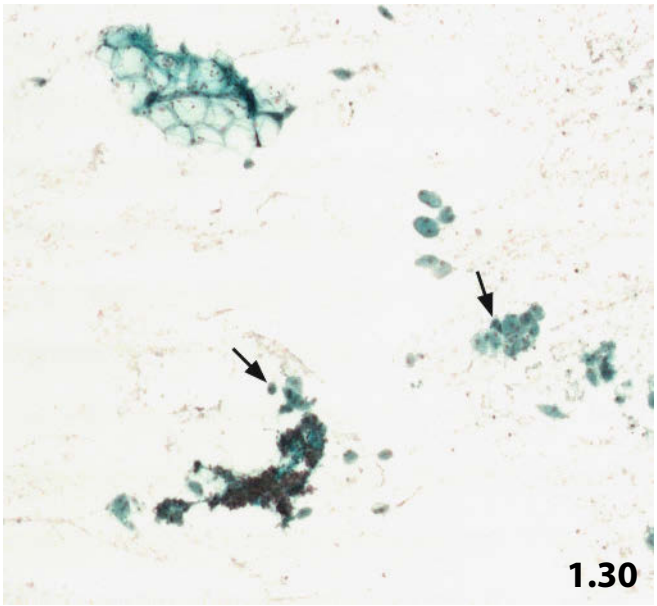
1.30

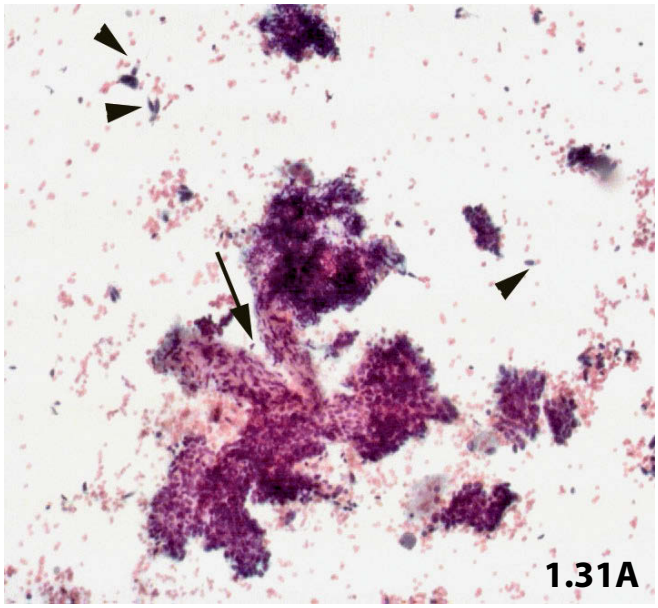
1.31A

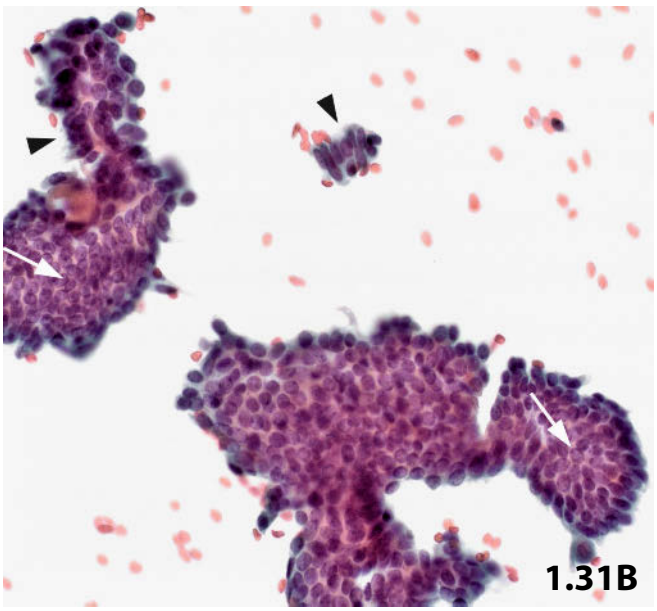
1.31B

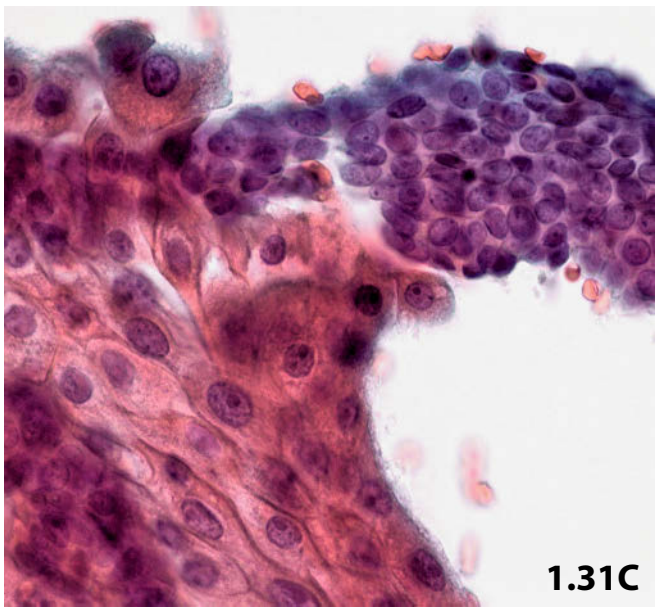
1.31C

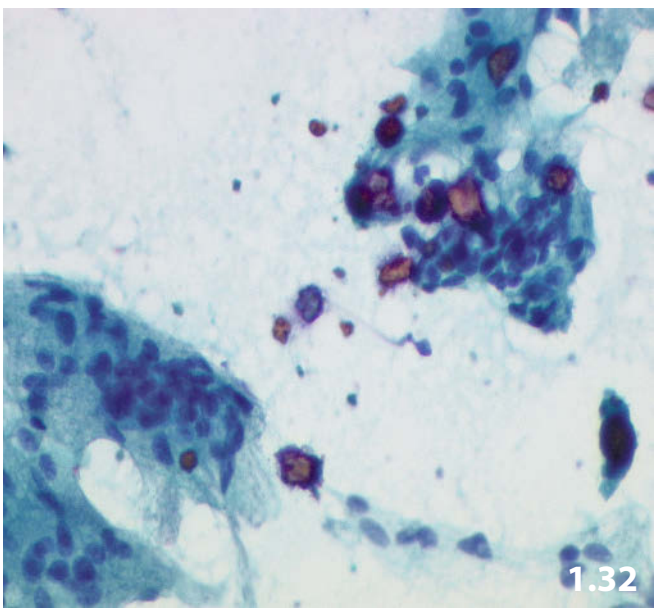
1.32

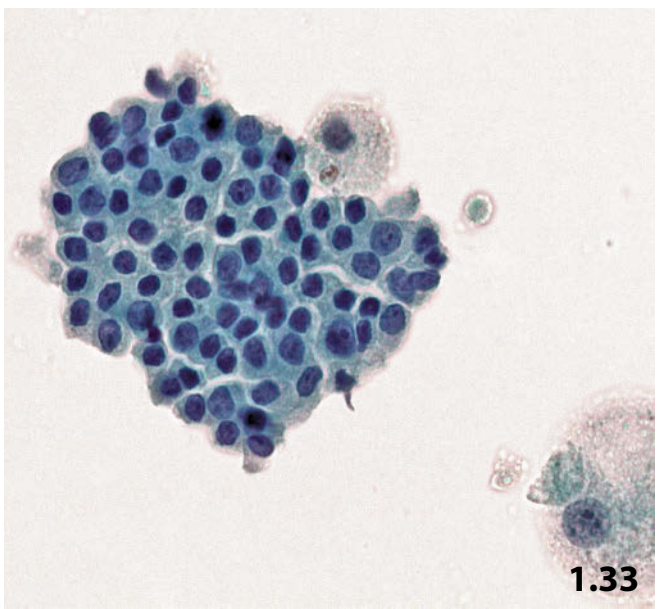
1.33

**Figs. 1.34–1.36 Benign florid ductal hyperplasia: diagnostic challenge.**
Florid ductal hyperplasia may mimic an atypical or even a malignant lesion in cytologic specimens. Three examples are presented (FNABs, direct smears, Pap stain).

**Fig. 1.34** (case #1) A compact three-dimensional epithelial cluster indicating florid ductal hyperplasia. Overall cytomorphology should be interpreted as benign despite nuclear enlargement and prominent nucleoli. Bland chromatin distribution, smooth nuclear outlines, dual cell pattern (myoepithelial cells are frequently in a deeper focal plane), a streaming pattern, and cluster cohesiveness are features consistent with ductal hyperplasia (high magnification).

**Fig. 1.35** (case #2) High magnification of a single epithelial cluster. Bland chromatin pattern and dual cell components of epithelial and myoepithelial cells (arrows) indicate a benign breast lesion. However, it is difficult to make a conclusive cytologic diagnosis due to the disintegration of the cell cluster, the single-file cell arrangement (left), the nuclear depolarization, and the nuclear irregularities.

**Fig. 1.36** (case #3) Low magnification from a third case shows a heterogeneous cell population, which makes it easy to diagnose a benign proliferative lesion: a cluster of a florid ductal hyperplasia (right) and a classic cluster composed of proliferating ductal cells (left). In addition, numerous stripped epithelial cells in the background of the smear suggest a benign lesion.

**Fig. 1.37A, B Nipple duct adenoma.**
A subareolar nodular lesion (1 cm in diameter) in a 14-year-old teenager was examined using FNAB. Aspirates were processed using conventional smears (Pap stain).
*Cytologic diagnosis:* nipple duct adenoma (verified by histologic examination). Age of the patient, location of the tumorous process, and predominantly bland nuclear features are consistent with the benign nature of the lesion.
**A** Extremely cellular smear (low magnification) showing large and compact, three-dimensional papillary clusters of duct epithelial cells. Numerous isolated cells showing elongated cytoplasm, and stripped nuclei are also present. **B** High magnification shows key features of this benign proliferative lesion such as tubular structures (right), compact ball-like clusters (arrow), high N/C ratio, occasional nuclear pleomorphism, and cellular debris. Nuclear pleomorphism and cellular debris can mislead to a false diagnosis of malignancy.

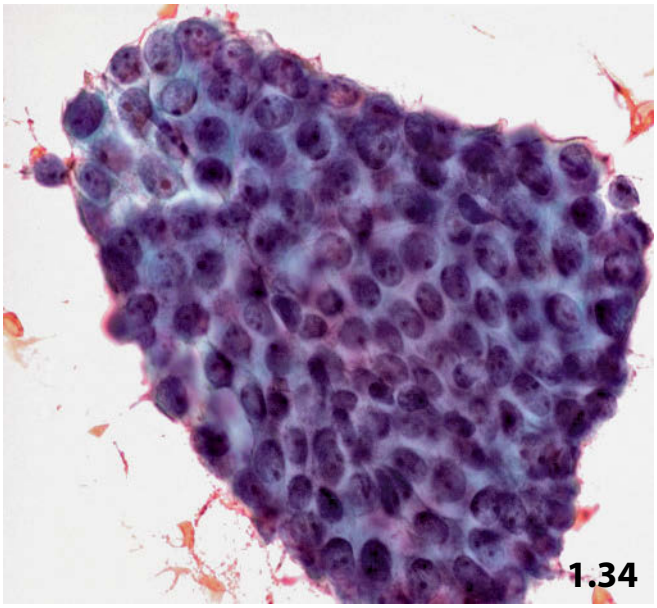

1.34

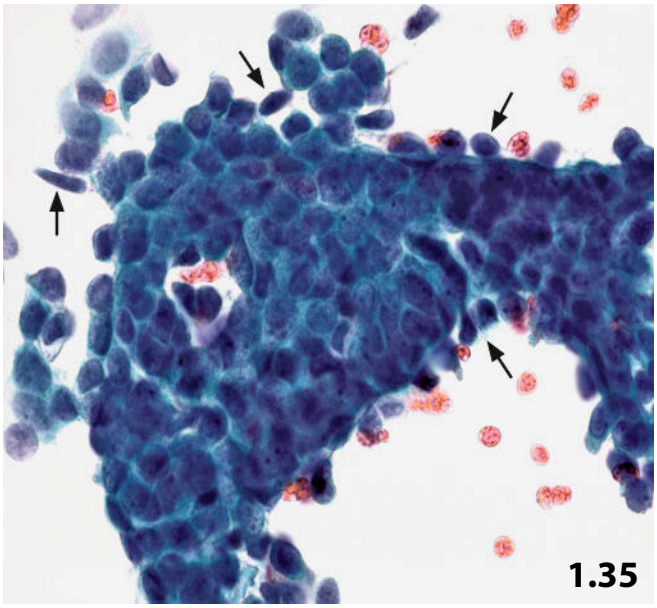

1.35

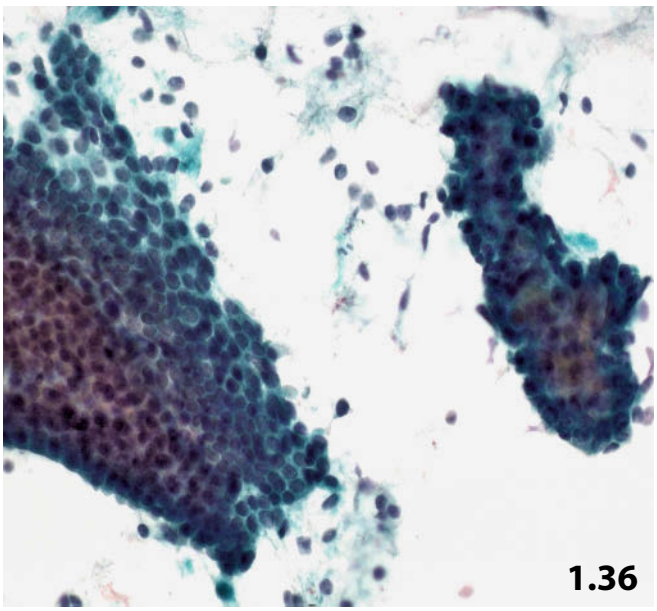

1.36

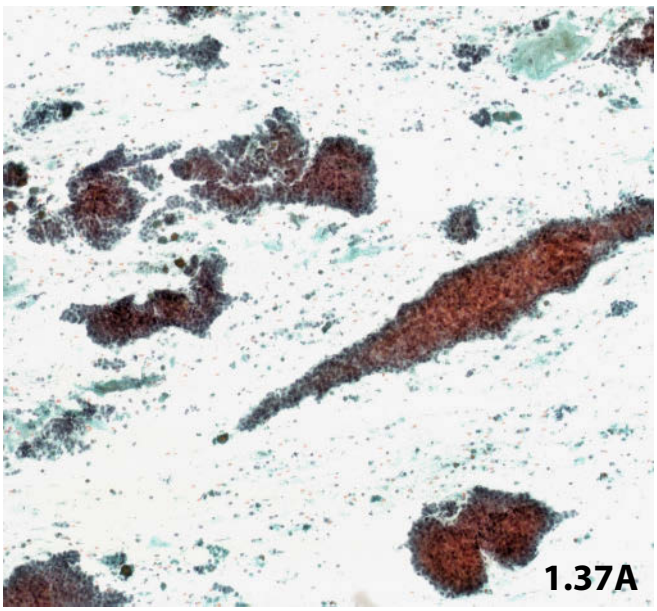

1.37A

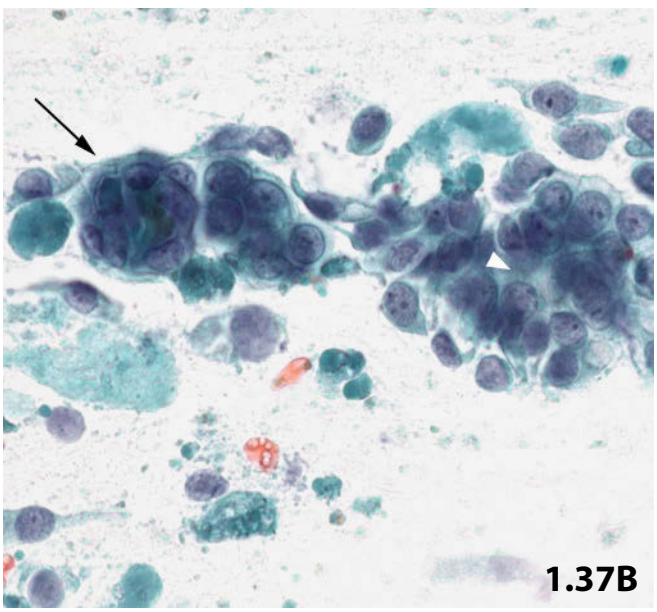

1.37B

**Figs. 1.38–1.43 Proliferative ductal breast lesions with atypia.**
Several examples highlight the cytologic characteristics of atypical ductal epithelial proliferation and emphasize difficulties distinguishing between atypical and malignant proliferation by cytology. Mammary FNABs of six patients are presented. Direct smears were stained according to the Papanicolaou technique.

**Fig. 1.38** (case #1) High magnification exhibits:
- A cell cluster aspirated from benign hyperplastic duct epithelium (lower right);
- Two compact irregular clusters composed of enlarged epithelial cells showing loss of polarization and pronounced nuclear irregularity

*Tentative cytologic diagnosis:* atypical proliferative breast disease. Intraepithelial neoplasia (DCIS) or invasive carcinoma cannot be excluded.
*Tissue diagnosis* (excisional biopsy): atypical ductal hyperplasia.

**Fig. 1.39** (case #2) Distinct papilliform epithelial cell clusters (marginal palisading of columnar cells), occasional sharply outlined margins, pronounced nuclear irregularities (best seen upper left) indicate an atypical proliferation (high magnification).
*Cytologic diagnosis:* proliferative papillary breast lesion with atypia, malignant lesion cannot be excluded.
*Tissue diagnosis* (excisional biopsy): atypical ductal hyperplasia.

**Fig. 1.40** (case #3) A microscopic field at lower magnification shows four benign cells with apocrine transformation and a benign proliferative epithelial cluster (upper right). Epithelial cells grouped in a third sheet (arrow) fulfil most features indicating malignancy. Loss of cellular polarity, nuclear irregularities, lucid nuclei, and dense eccentric cytoplasm are worrisome features.
*Cytologic diagnosis:* fibrocystic and proliferative breast disease with atypia, several atypical sheets suggest a neoplastic proliferation (DCIS?).
Tissue diagnosis (excisional biopsy): florid and atypical ductal hyperplasia associated with pronounced sclerosing adenosis.

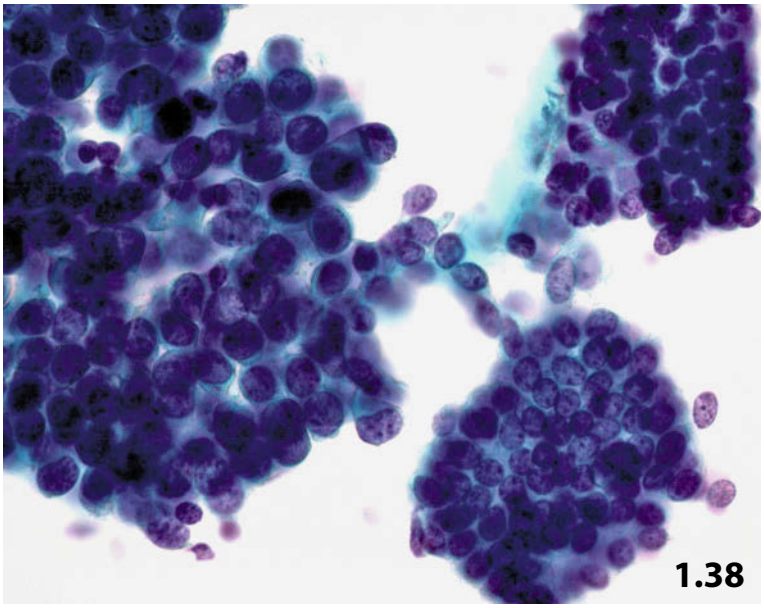

1.38

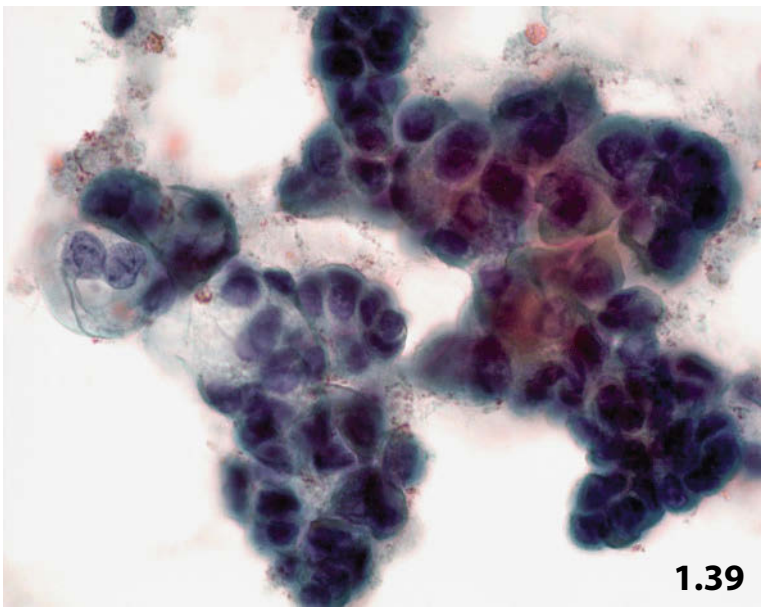

1.39

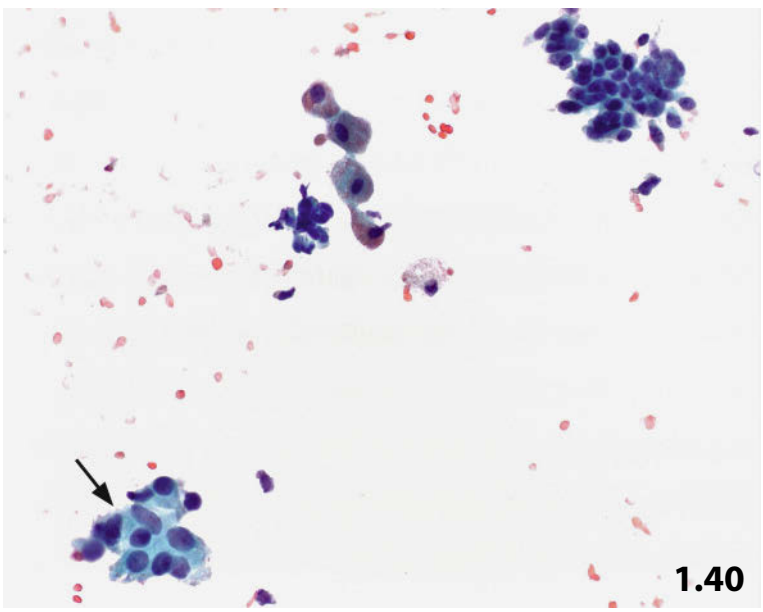

1.40

**Fig. 1.41A, B** (case #4) Atypical epithelial proliferation versus ductal carcinoma in situ.
Ultrasound-guided FNAB of a nodular breast lesion (10 mm in diameter) in a 36-year-old woman.
*Cytologic diagnosis:* atypical epithelial proliferation, most likely well-differentiated breast carcinoma.
*Tissue diagnosis:* low-grade DCIS.
**A** Cytologic appearance at low magnification may mislead to a false-negative diagnosis of usual ductal hyperplasia. However, several cytologic features are suspicious for malignancy, including distinct homogeneous cell population: absence of bipolar nuclei, sporadic sharply delineated clusters (arrows), rows with single-file cellular arrangement (lower left), and plasmacytoid appearance of single cells. **B** Cellular and structural details as stated above are shown at high magnification.

**Fig. 1.42** (case #5) Atypical proliferation versus tubular carcinoma.
FNAB of a palpable tumor (15 mm in diameter) in the breast of a 42-year-old woman. Clinical and image findings suggest a benign proliferative lesion. Low magnification shows cytologic features akin to those of the prior case (Fig. 1.41A). Additional features of atypia are the dense chromatin texture and the dissolved nuclear membranes. The sheet-like aggregation of the atypical cells presents diagnostic dilemmas.
*Tentative cytologic diagnosis:* proliferative epithelial lesion with atypia (ADH? Low-grade DCIS?).
*Tissue diagnosis* (excisional biopsy): tubular carcinoma.

**Fig. 1.43** (case #6) Atypical proliferation: postradiation changes.
A 76-year-old woman with a history of tumorectomy for invasive breast carcinoma followed by irradiation 1 year before. A palpable lesion beneath the scar was highly suggestive of tumor relapse. FNAB shows pronounced cellular atypia consistent with postradiation changes of ductal cells (high magnification). One must pay attention to the normal N/C ratio, benign nuclear features (delicate margins, pronounced membrane, bland chromatin structure), large nucleoli, and degenerated nuclei presenting vacuoles (arrows). As mentioned above, in conventional smears the elongated cytoplasm and the streaming cell pattern are key features of benign epithelial proliferative disorders.

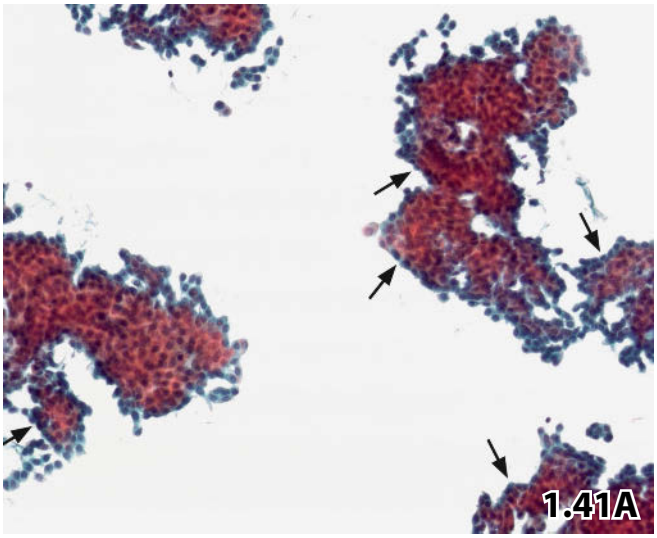
1.41A

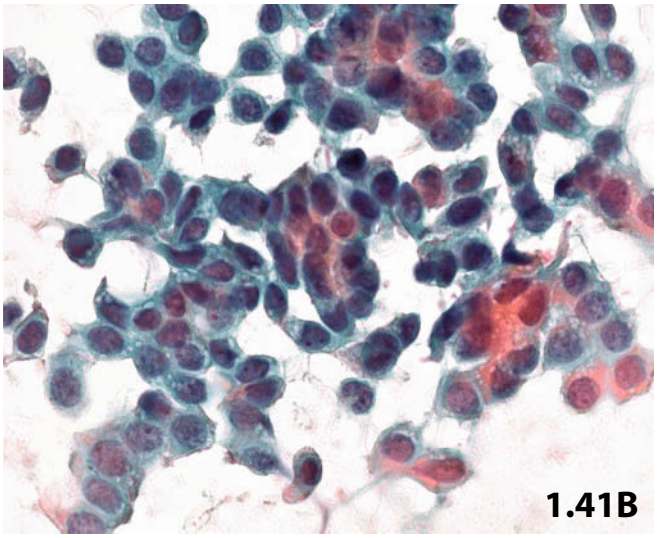
1.41B

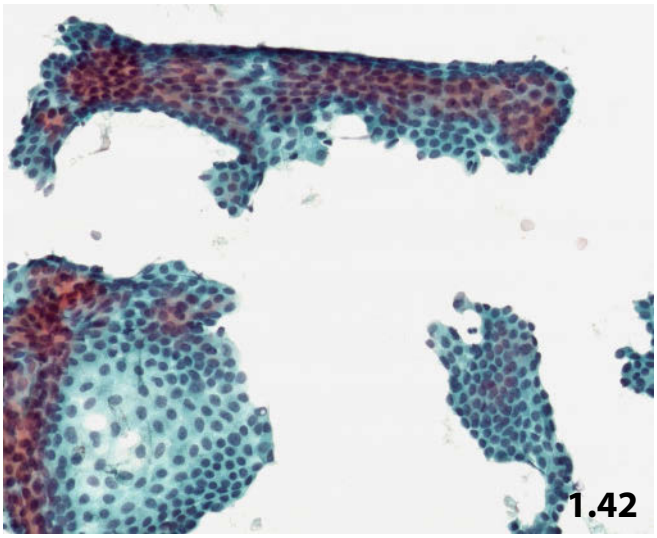
1.42

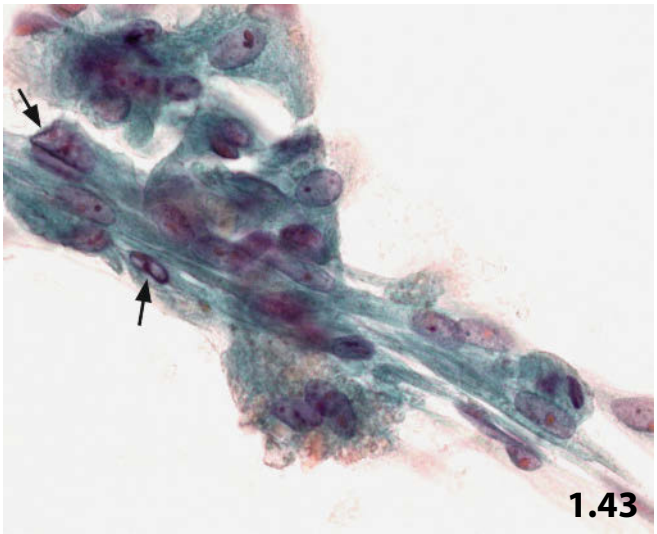
1.43

**Fig. 1.44 Tubular adenoma.**
Tubular adenoma yields highly cellular aspirates. Hyperplastic ductal cells, frequently arranged in tubular formations (upper left), and numerous isolated naked nuclei are characteristic features of this lesion. A few bipolar nuclei (myoepithelial cells) are also present (arrows). Usually, it is not possible to accurately distinguish between adenoma, adenosis, and ductal hyperplasia based on the cytologic features alone. (direct smear, Pap stain, lower magnification).

**Fig. 1.45A, B Sclerosing adenosis.**
Cytologically, it is difficult to distinguish between sclerosing adenosis and other benign proliferative disorders and low-grade malignant lesions. FNAB of a breast nodule (20 mm in diameter) in a 35-year-old woman. Direct smears were Pap-stained. The clinical and sonographic tentative diagnosis was fibroadenoma.
*Tentative cytologic diagnosis:* Severe proliferation of duct epithelial cells, possibly activated fibroadenoma. Well-differentiated carcinoma cannot be excluded, a histologic verification is highly recommended!
*Histologic diagnosis:* Florid sclerosing adenosis**.**
**A** Cytologic aspirate of sclerosing adenosis is usually characterized by low cellularity and small irregular clusters (low magnification). **B** At high magnification, cohesive epithelial clusters exhibit architectural and cellular features comparable to proliferative breast lesions with atypia, as described earlier. In such cases, a neoplastic process should always be considered.

**Figs. 1.46 and 1.47 Gynecomastia.**
Two examples of gynecomastia. Direct smears of the aspirated material were stained according to the May-Gruenwald-Giemsa and Papanicolaou methods.

**Fig. 1.46** (case #1) The overall cytologic appearance is comparable to florid ductal hyperplasia of the female breast (as described earlier). Note streaming and swirling pattern that is typical of benign ductal proliferations. In general, activated benign ductal cells are densely packed; however, dissociation and naked nuclei may focally occur (MGG stain, lower magnification).

**Fig. 1.47** (case #2) Similar cytologic appearance of another case of gynecomastia at high magnification (Pap stain).

**Fig. 1.48 Hamartoma.**
FNAB of a hamartoma in a 51-year-old woman. Low magnification shows fragments of epithelial and mesenchymal breast tissue (Pap stain). Ducts and lobuli (lower right) frequently exhibit proliferative cell activity. Mesenchymal tissue may come along with fibrosis and sclerosis; true sclerosing adenosis may occur. The overall cell pattern may closely mimic fibroadenoma in cases with a high proportion of clusters originating from proliferating ducts (arrows).

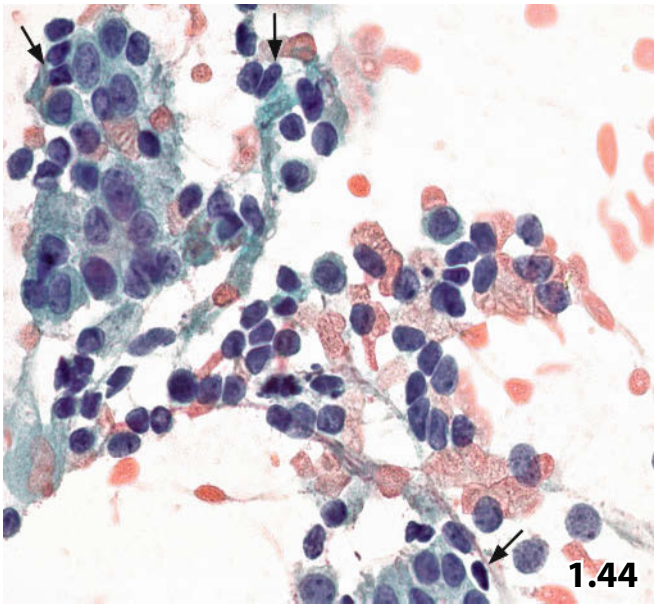
1.44

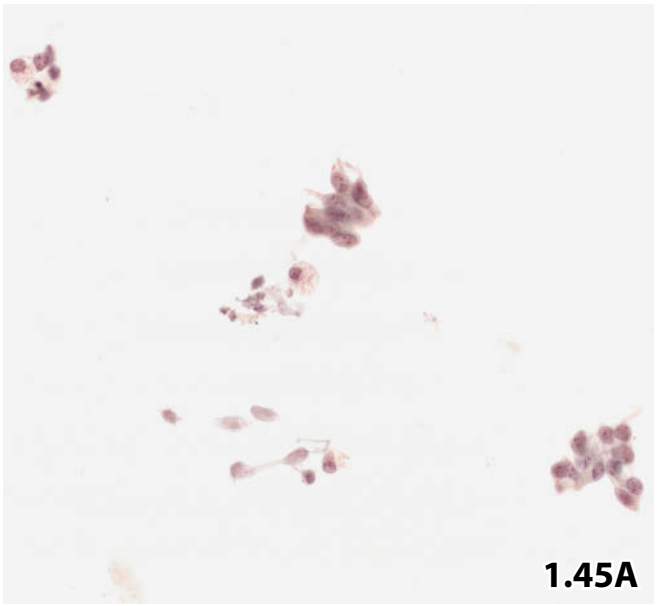
1.45A

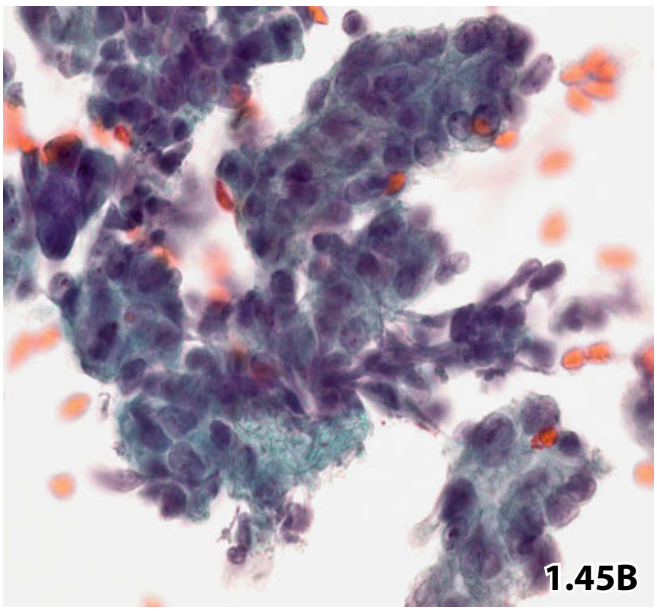
1.45B

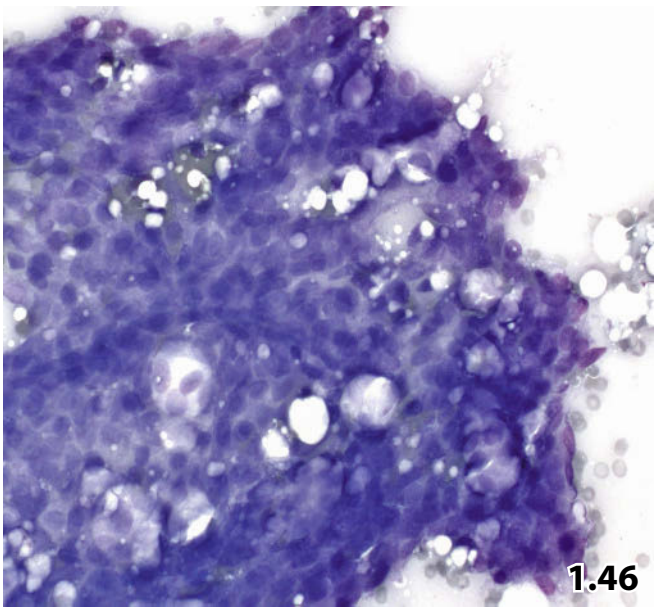
1.46

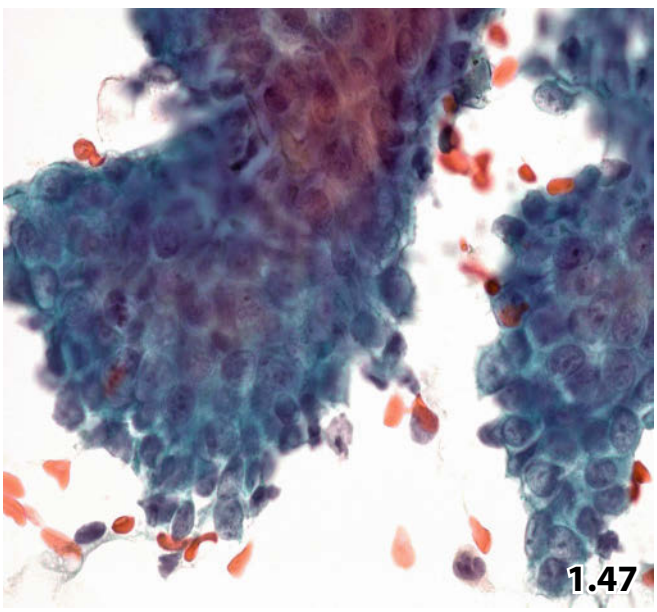
1.47

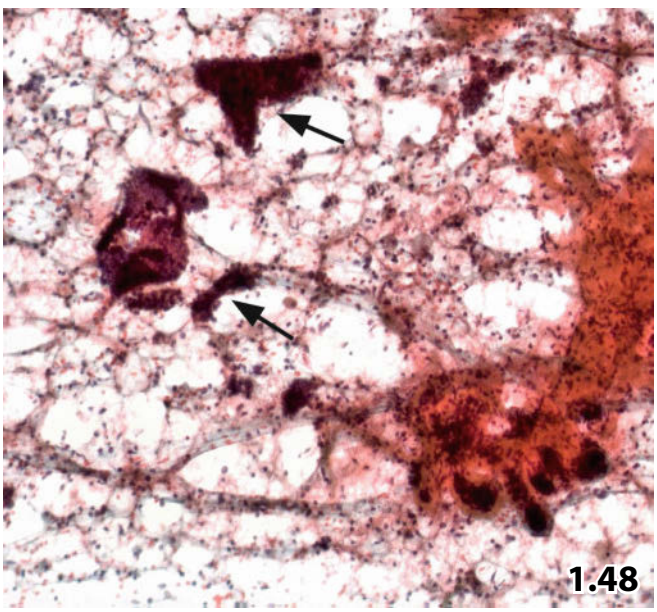
1.48

1

**Figs. 1.49 and 1.50 Intracystic papilloma.**
Two examples of intracystic papilloma exhibiting different cytology. Direct smears of the cystic fluid sediments were Pap-stained.

**Fig. 1.49** (case #1) FNAB of a mammary cyst containing a papilloma: a three-dimensional papillary cluster with a fibrovascular core (not completely in focus); the latter is ramifying into two almost bare branches (asterisk). Nuclei show benign morphologic features (low magnification).
*Cytologic diagnosis:* intracystic papillary tumor.
*Discussion:* the pronounced cell dissociation, high N/C ratio, and absence of myoepithelial cells are suggestive of low-grade papillary carcinoma and should call for excision or close follow-up.
*Tissue diagnosis* following surgical excision in the area of the earlier FNAB shows fibrocystic changes (the time interval between cytological and histological findings was 2 years!)
*Comment:* the divergence between cytologic and histologic diagnosis could not be elucidated.

**Fig. 1.50** (case #2) A second example of an intracystic papilloma. Cytologic preparations failed to show true papillary formations.
*Cytologic and histologic diagnosis:* Intracystic papilloma**. A** While true papillary clusters are absent, an accurate cytologic diagnosis can be made based upon papilliform and pseudopapillary clusters (devoid of fibrovascular cores) (low magnification). **B**: High magnification demonstrates palisading bland columnar cells.

**Fig. 1.51 Intraductal papilloma.**
Example of a centrally located intraductal papilloma in a 42-year-old man's left mammary gland. The lesion was accompanied by sanguineous nipple secretion. Mammography, galactography, and cytology of nipple discharge were highly suspicious of intraductal papilloma. Cytologic direct smears from the aspirated material (image-guided FNAB) contained large tissue fragments of a benign papillary neoplasm characterized by papillary tufts with broad fibrovascular cores (arrow) (low magnification, Pap stain). No histologic results were available.

**Figs. 1.52–1.54 Fibroadenoma.**
Fibroadenomas of the common and florid type are demonstrated using FNABs from three different patients (direct smears, Pap stain)

**Fig. 1.52** (case #1) Low magnification shows the characteristic cellular components: marked cellularity, large monolayered sheets, and cohesive epithelial clusters with branching antler-horn- or fingerlike pattern (arrows), numerous naked nuclei of epithelial and myoepithelial origin in the background, and myxoid degenerated stromal fragments (arrowheads).

The epithelial component of fibroadenoma may mimic florid ductal hyperplasia or papilloma. The myxoid stromal fragments constitute the most important clue in the assessment of a correct cytologic diagnosis.

**Fig. 1.53** (case #2) Papilliform, alternately monolayered (vague honeycomb pattern) and three-dimensional formations, interspersed with numerous bipolar myoepithelial nuclei, characterize fibroadenoma as well (higher magnification).

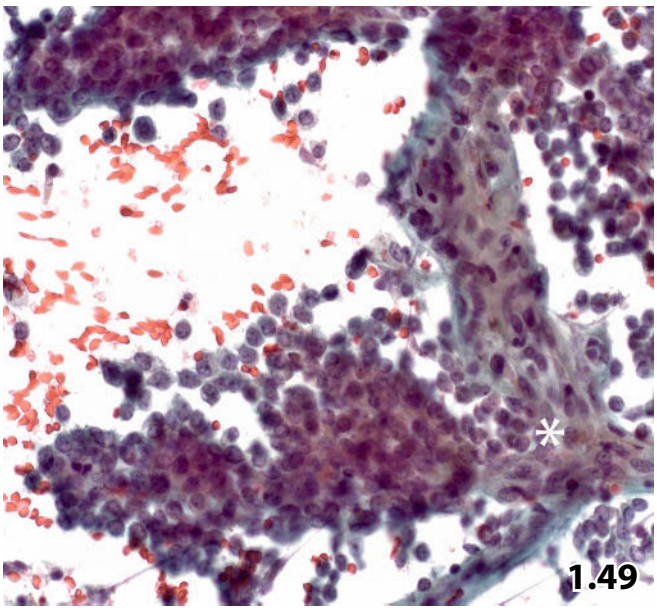
1.49

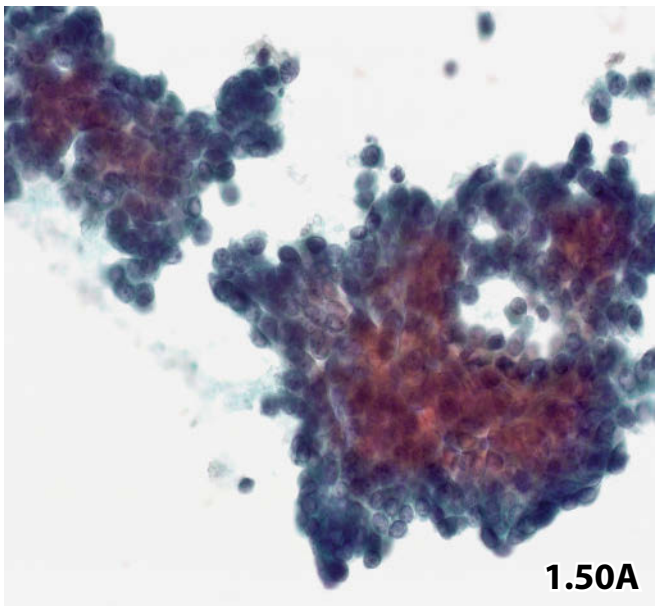
1.50A

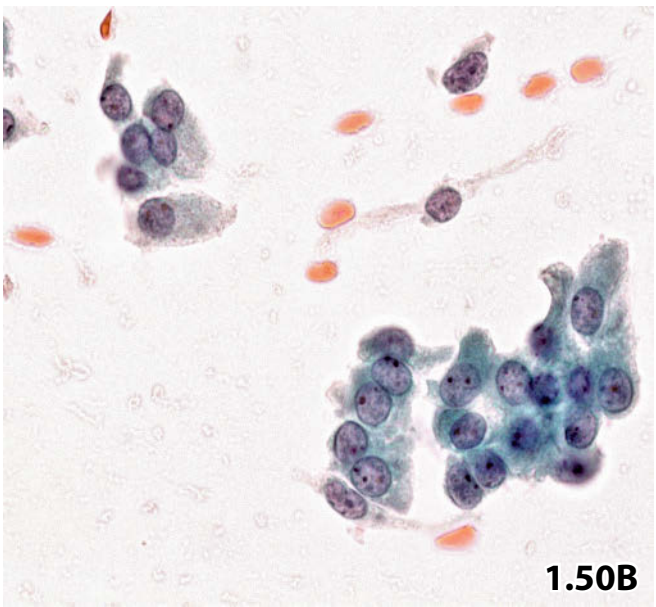
1.50B

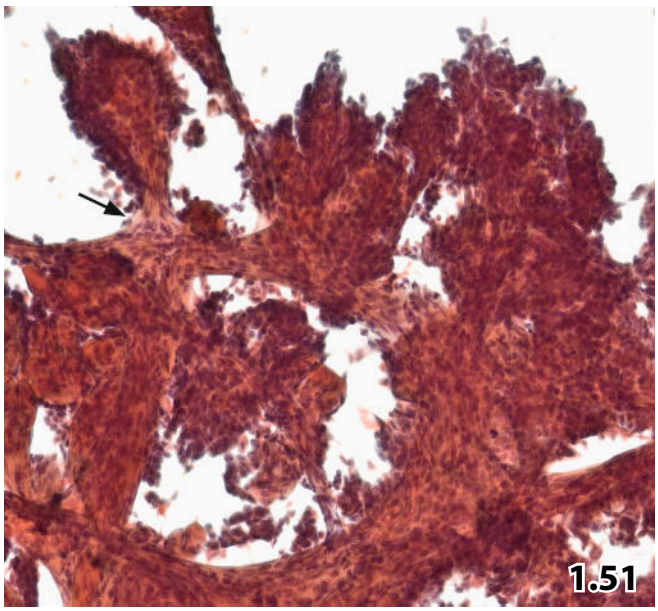
1.51

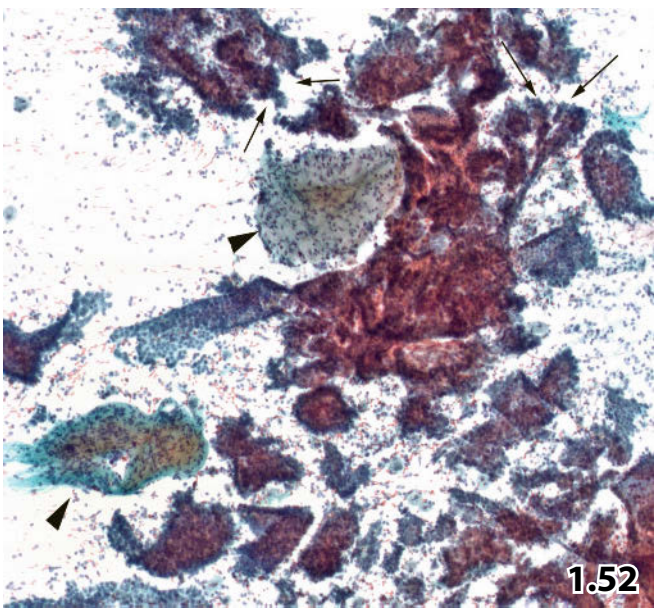
1.52

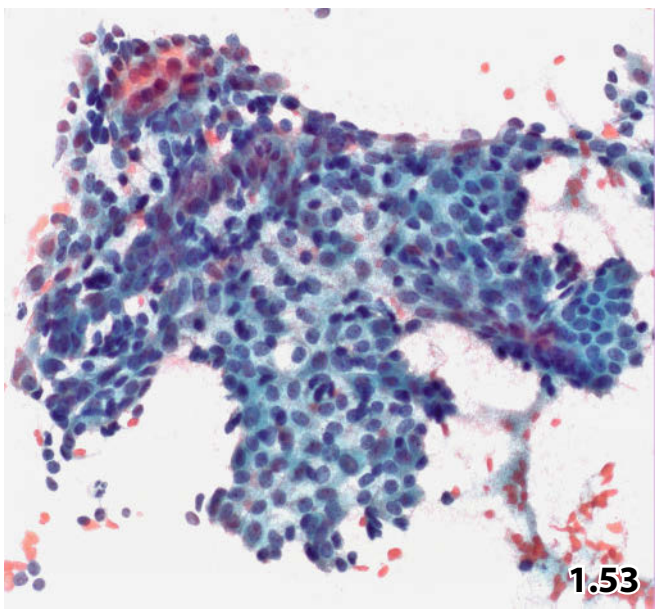
1.53

**Fig. 1.54** (case #3) Juvenile fibroadenoma.
Detail of an epithelial cluster from a fibroadenoma of florid type in a 37-year-old woman, also referred to as juvenile-type fibroadenoma. Cellular enlargement, loss of polarization, focal ball-like nuclear crowding (left margin), and mitotic activity may lead to a false-positive diagnosis of malignancy. The bland nuclear and cytoplasmic features and numerous naked nuclei in the background should exclude malignancy, however. Based on the cytologic features, distinguishing between florid fibroadenoma and juvenile papillomatosis is almost impossible.
*Cytologic diagnosis:* juvenile-type fibroadenoma (no histologic results available).

**Figs. 1.55–1.57 Phylloides tumor.**
Variants of phylloides tumors are presented. Cellular material sampled by FNAB was conventionally processed. Smears were Pap-stained.

**Fig. 1.55A, B** (case #1) A 48-year-old woman presented with a large tumor (9 cm in diameter) in her left breast.
*Cytologic diagnosis:* low-grade (benign) phylloides tumor.
*Tissue diagnosis* (tumor excision): low-grade (benign) phylloides tumor.
**A** Low magnification shows a biphasic appearance: proliferating epithelial clusters (left) and cellular stroma (right). The stromal component of the phylloides tumor is much more cellular than the fibroadenoma component. **B** The hypercellular mesenchymal area of the tumor represents activated spindle-shaped fibroblasts with bland chromatin texture, pronounced nucleoli, and abundant cytoplasm (high magnification).

**Fig. 1.56** (case #2) Example of a low-grade (benign) phylloides tumor that is predominantly composed of a proliferative epithelial component (lower magnification).
*Cytology:* fibroadenoma was favored by the presence of scant myxoid stroma (not shown) and foam cells (arrows). The hypercellular stromal component assessing the diagnosis of phylloides tumor has merely been detected in tissue sections.

**Fig. 1.57** (case #3) An 82-year-old woman presented with a firm and circumscribed nodule (15×20 mm) in her right breast. High magnification shows hypercellular stroma with significant nuclear atypia including variation in nuclear size and shape, hyperchromasia, coarse clumping chromatin, and multiple pleomorphic nucleoli. Cytology is suspicious for a malignant biphasic tumor.
*Tentative cytologic diagnosis:* cytologic sample with features intermediate between a benign and malignant phylloides tumor. A malignant mesenchymal neoplasia of a different histogenetic origin cannot be excluded.
*Tissue diagnosis:* high-grade (malignant) phylloides tumor.

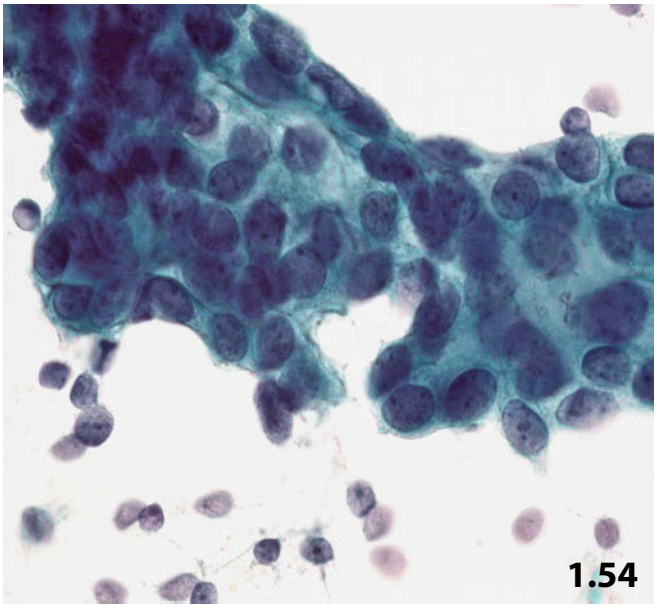
1.54

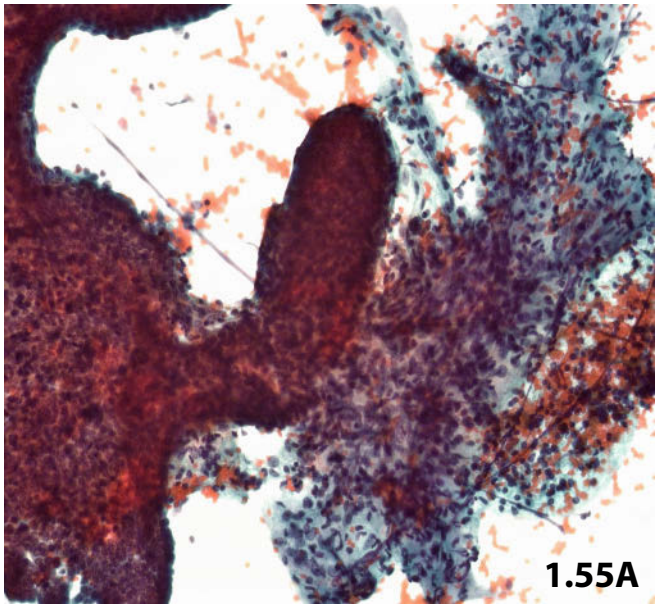
1.55A

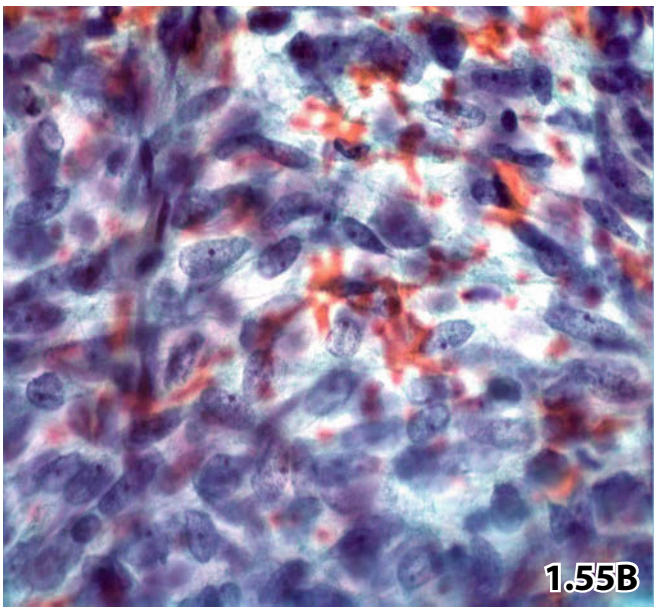
1.55B

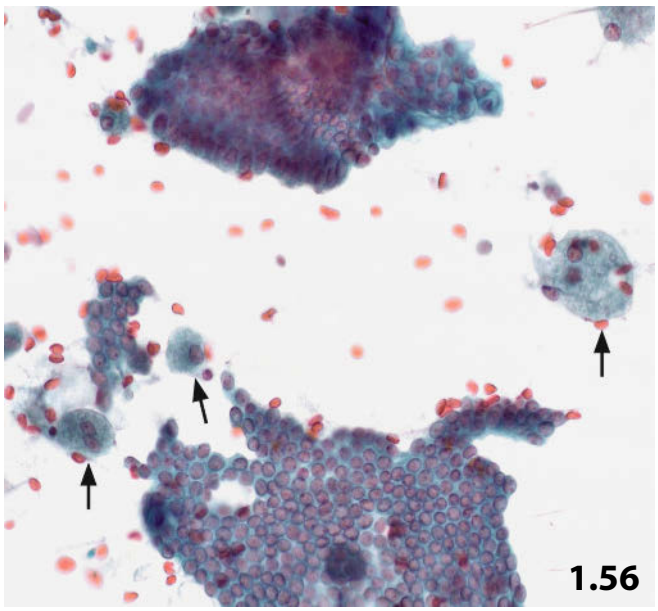
1.56

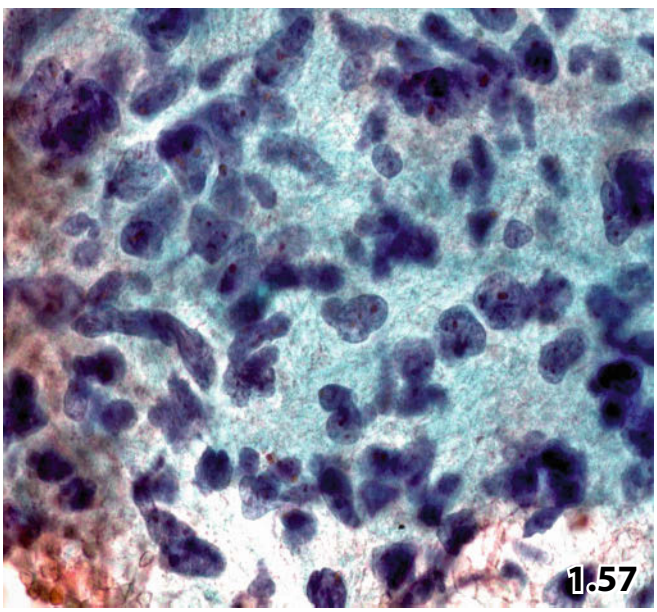
1.57

1

**Figs. 1.58–1.61 Benign and malignant adenomyoepithelial neoplasm.**
We focus on cytologic characteristics and immunocytochemical key features of a benign and a malignant myoepithelial neoplasm. The FNA direct smears were Pap-stained.

**Fig. 1.58** Voluminous cell clusters are usually aspirated from adenomyoepitheliomas. The tumor fragment presented here in low magnification exhibits the characteristic biphasic pattern: bundles of elongated myoepithelial cells (exhibiting a streaming pattern; arrows) are surrounded by compact epithelial clusters. The nuclei of both cell types are monomorphic and bland.
*Cytologic and histologic diagnoses:* benign adenomyoepithelioma.

**Fig. 1.59A, B** A 65-year-old woman with a breast lesion. Sonography suggested a breast carcinoma.
*Tentative cytologic diagnosis:* Adenomyoepitheliomatous tumor of uncertain malignancy status. Surgical excision and histologic examination are crucial.
*Comment:* this is a case of a myoepithelial tumor where cytology cannot reliably distinguish between adenomyoepithelioma with proliferative activity and adenomyoepithelial carcinoma.
*Tissue diagnosis:* invasive, poorly differentiated adenomyoepithelial carcinoma**.**
**A** Lower magnification shows the classic heterogeneous pattern of a myoepithelial tumor. Nuclei are bland except for the upper marginal area of the tissue fragment (direct smear).
**B** High magnification drawing attention to dissociated cells exhibiting enlargement, irregular nuclear outlines, and high N/C ratio. A few isolated epithelial cells and cell clusters show unequivocal malignant features.

**Fig. 1.60** Smooth muscle actin: conventional smear. The immunoreactivity for smooth muscle actin clearly separates the positive myoepithelial strands from the negative epithelial areas in a large tumor fragment of an adenomyoepithelioma. Note the nonspecific faint light-pink staining reaction in the cytoplasm of epithelial cells (upper left) (Pap-prestained direct smear, low magnification)

**Fig. 1.61** Smooth muscle actin: liquid-based preparation. The same immunoreactive pattern can be achieved on tumor cells in liquid-based preparations (Pap-prestained ThinPrep specimen, high magnification).

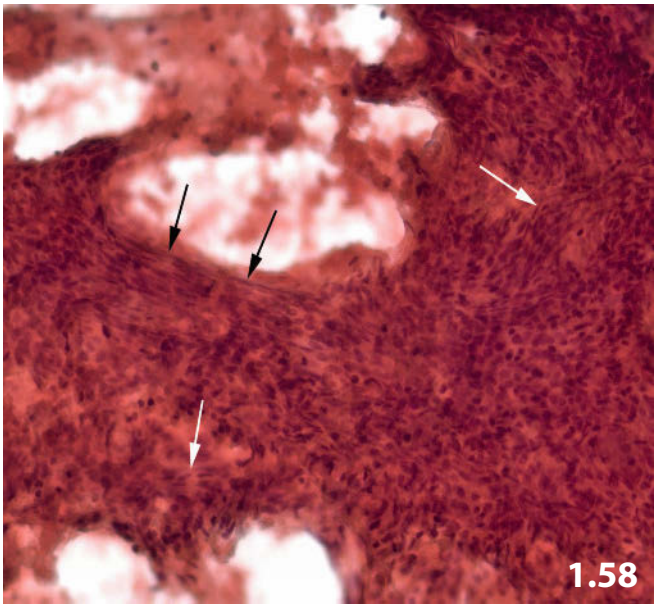
1.58

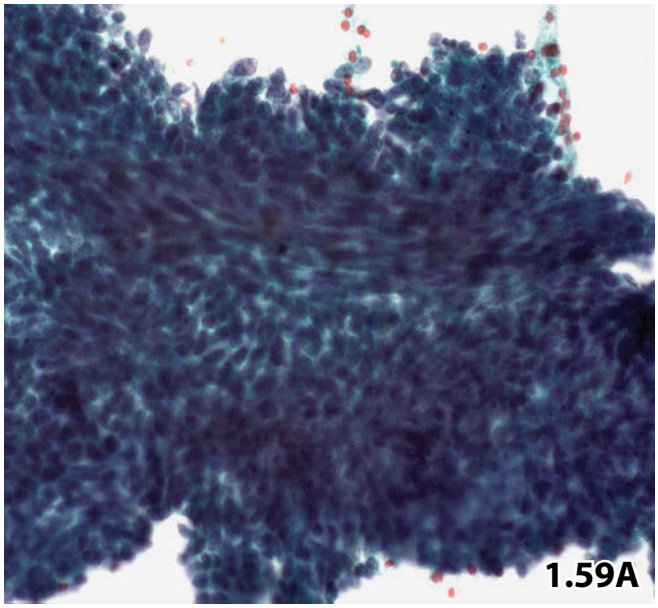
1.59A

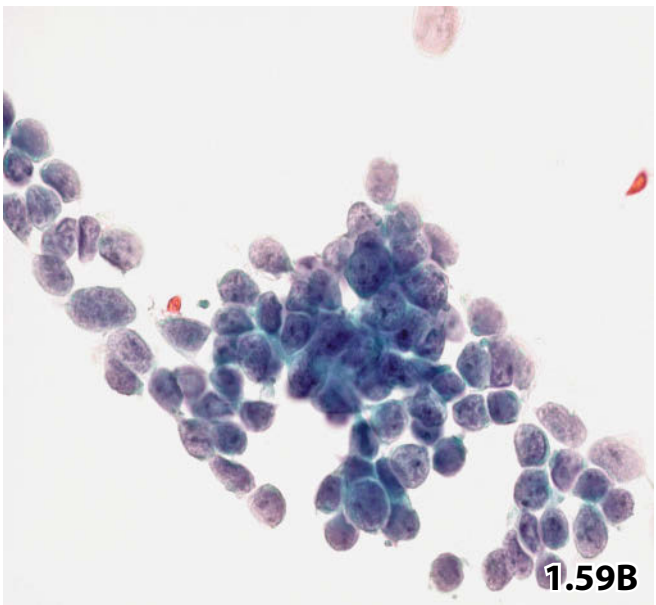
1.59B

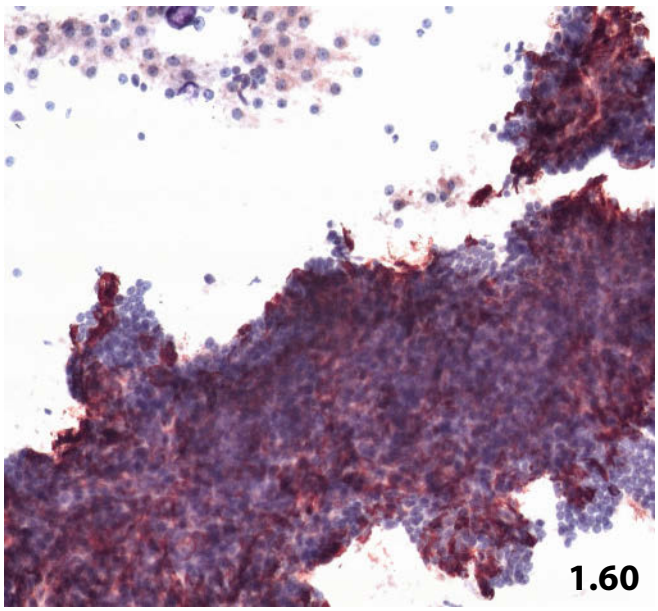
1.60

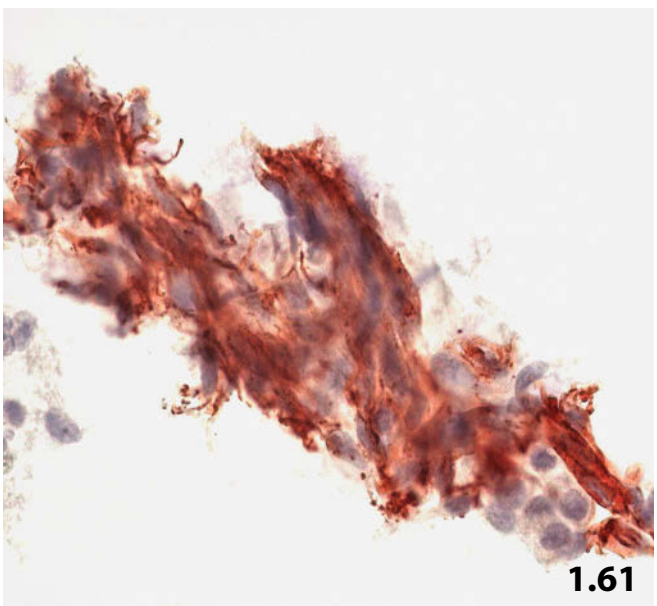
1.61

**Fig. 1.62 Angiolipoma.**
Example of an angiolipoma: branching capillary-sized vessels surrounding groups of lipocytes and single lipoid cells (FNAB, direct smear,, Pap stain, low magnification).

**Figs. 1.63 and 1.64 Granular cell tumor.**
Two examples of granular cell tumors displaying typical cytologic features and immunocytochemical/cytochemical properties. FNAB of nodular breast lesions was initially performed. Direct smears were Pap-stained.

**Fig. 1.63A–C** (case #1) A 37-year-old woman presented with a small (about 10 mm in diameter), firm, distinctly outlined nodule in her left breast. **A** With cytology, the lesion presenting loosely arranged cell clusters and isolated cells. The tumor cells exhibit abundant, ill-defined, uniform round to polygonal granular and somewhat fragile cytoplasm. Round to oval nuclei having indistinct nucleoli and evenly distributed granular chromatin. **B** An antibody for S100 protein decorates the tumor cells in the perinuclear area ( Pap-prestained smear). **C** Special stain for PAS displays a diffuse cytoplasmic reaction (Pap-prestained smear).

**Fig. 1.64** (case #2) Low magnification of another granular cell tumor focuses on the pronounced cytoplasmic fragility of the tumor cells and their tendency to degenerate. Note single cells with enlarged, hyperchromatic, and polymorphic nuclei (upper right) (low magnification).

**Fig. 1.65 Tietze syndrome.**
A 59-year-old woman presented with a painful small palpable nodule located close to the sternum. Physical investigation and radiography suspected a tumorous lesion in the upper inner quadrant of the right breast. Sonography provided no additional information.
The FNAB sample is hypocellular, disclosing a few small-sized fibrolipomatous fragments and activated fibroblasts (arrow).
Cytomorphologic features together with clinical and reevaluated sonographic findings provide a conclusive diagnosis of Tietze syndrome (no further work-up) (direct smear, Pap stain, higher magnification).

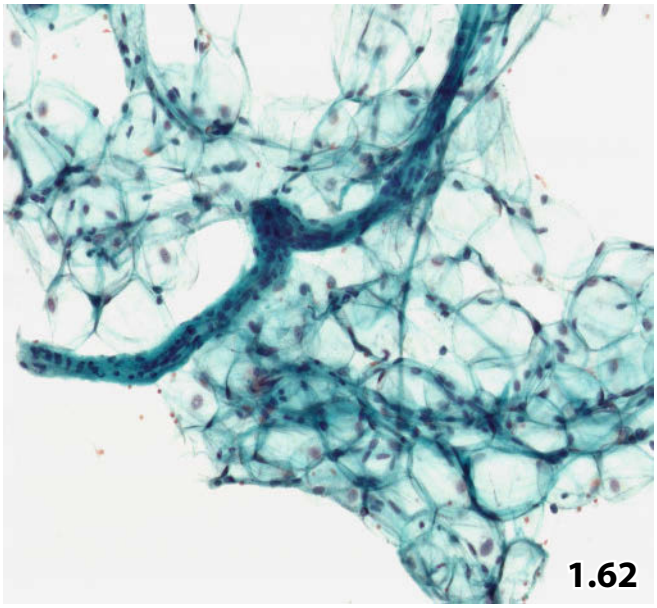
1.62

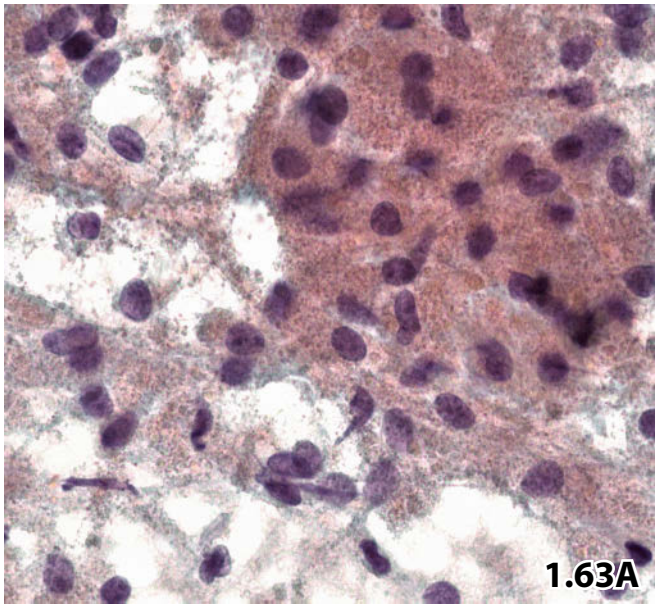
1.63A

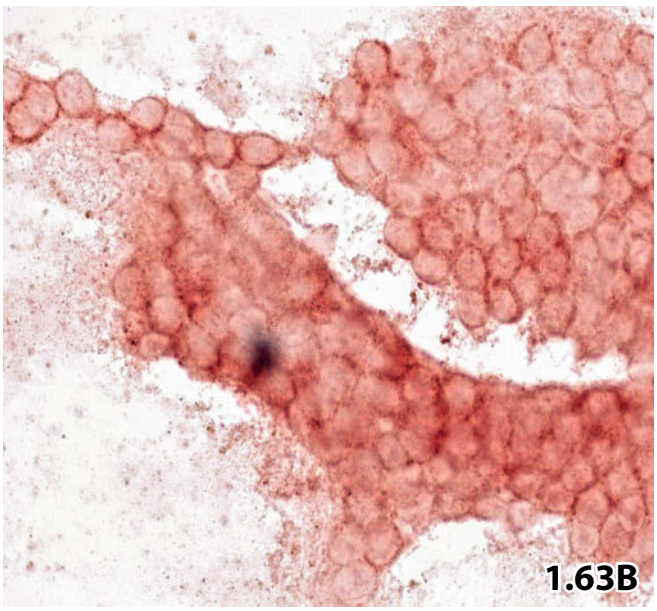
1.63B

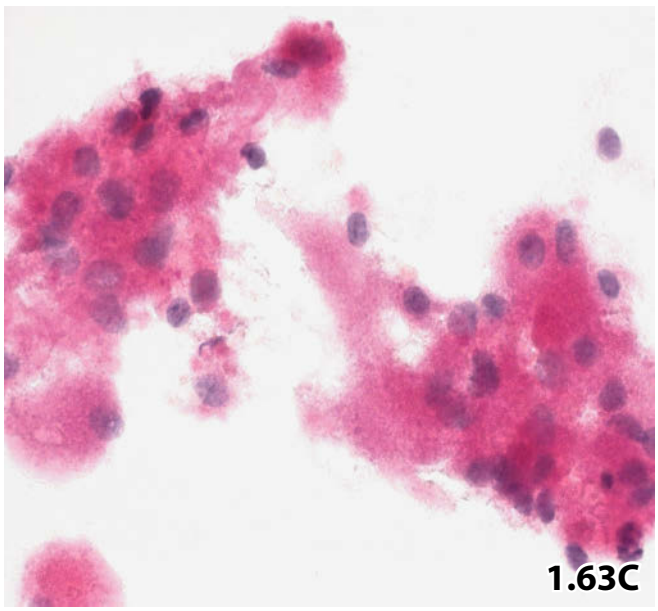
1.63C

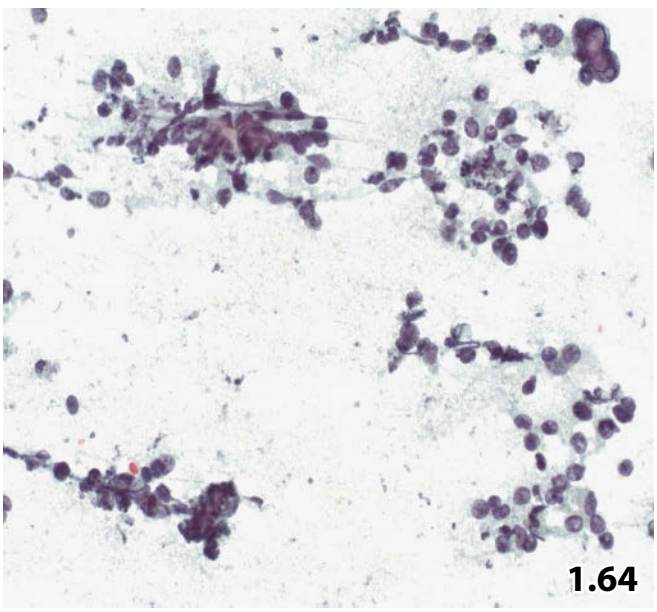
1.64

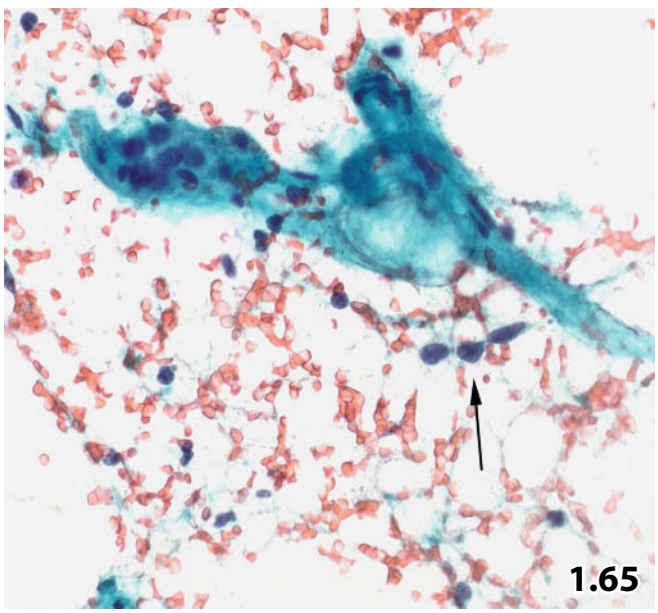
1.65

# Section 1.3
# Breast: Fine-Needle Aspiration Biopsy

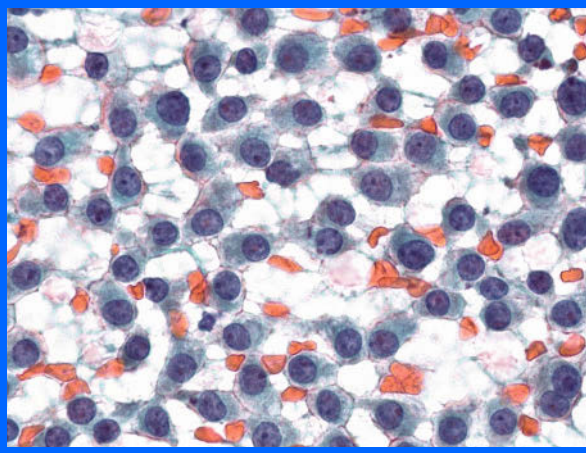

## Intraepithelial Neoplasia
## Malignant Lesions

### 1.3.1 Infiltrating Ductal Carcinoma

#### 1.3.1.1 Infiltrating Ductal Carcinoma of the Common Type (Figs. 1.66–1.71)

**Microscopic Features**

The samples are usually of a high cellularity and exhibit an overall monomorphic cell pattern. The tumor cells are of intermediate size and show unequivocal features of malignancy but usually indistinct nucleoli. Relative to our cytodiagnostic procedure, we refer to this tumor type as the common type of breast carcinoma; it is encountered in about 80% of all FNAB samples.

- *Tumor cells* present:
  - As cohesive groups, gland-like arrangements and three-dimensional dense clusters that are, at least partially, sharply demarcated.
  - Nuclear overlapping and loss of polarity are striking. Shoe-/boot-formed and V-shaped clusters are conspicuous.
  - A single-file cellular arrangement is frequent as individual epithelial cells in varying numbers. Clustered and single cells with eccentrically placed nuclei and triangular cytoplasm resulting in a plasmacytoid appearance are common.
- *Nuclei* exhibit:
  - A size of three to four erythrocytes.
  - Round to oval shapes with smooth and wrinkled membranes. In many cases, large numbers of malignant nuclei show molding and cleaving.
  - Either hyperchromasia or dyschromasia (lightly pink or blue); in any case, they differ from the staining of benign nuclei in the same smear.
  - Often distinct nuclear clearing, possibly nuclear grooves and inclusions.
  - Increased N/C ratio.
- *Chromatin texture* is variable:
  - Most frequently, dense and finely granular. Uneven distribution with a shift to one side of the nucleus is highly characteristic of malignancy (Fig. 1.82B).
  - Coarsely granular.
  - Dense and almost patternless, sometimes dusty or glassy.
- *Nucleoli* are absent in a large number of nuclei. If present, nucleoli are small and inconspicuous.
- *Cytoplasm:*
  - Densely structured, cyanophilic with Pap stain.
  - Triangular and eccentric, leading to a plasmacytoid appearance of the single cells.
  - Target-like inclusions with a centrally located core of mucus are pathognomonic.
- *Myoepithelial cells* are absent in both clusters as well as in the background material, except in cases where carcinoma is accompanied by a benign mammary epithelial tissue.
- *Necrosis* is infrequent in cytologic samples of this tumor type.

**Table 1.3.1** Breast cancer common type: classification of cytomorphologic features into two categories: definitive and indicative of malignancy

| Features | Definitive of malignancy | Indicative of malignancy |
|---|---|---|
| *Chromatin pattern* | Dense and finely granular or inconspicuous – homogeneous | Shifted to one side of the nucleus |
| *Nucleus*<br>– Margin | Multiple wrinkling saw-blade-like or molding/cleaving | |
| – Staining | | Hyperchromasia or dyschromasia (light pink-blue) or nuclear clearing |
| *Individual cells*<br>– Shape | Dense triangular cytoplasm frayed or plasmacytoid, and nuclear changes as described | |
| – Size | | Enlarged compared to benign cells |
| *Cell clusters* | Nuclear overlapping and loss of polarity<br><br>Shoe-/boot-shaped and/ or V-shaped and/or small rows (single-file-like) | |
| *Cytoplasm* | | Target-like inclusions<br>Core of mucus |
| *Myoepithelial cells* | | Absent |

The cytomorphologic key features are classified into two categories, shown in Table 1.3.1.

To us, this setting proved to be a rational basis for diagnosing breast carcinoma on FNAB samples provided that at least three proving features from three different categories and one indicative feature are present. False-positive diagnoses are practically eliminated, and the sensitivity for detecting a carcinoma has not lowered. Other categorical approaches in reporting results of breast FNAB have been published earlier [45, 65, 68, 104].

### Differential Diagnosis

- As stated in Sect. 1.2.11.3.2, p. 22, sclerosing adenosis may pose problems in excluding an invasive carcinoma. Aspirates of sclerosing adenosis may exhibit many isolated cells as well as cells in small clusters or in rows similar to frank carcinoma due to the substantial sclerotic stromal changes (Fig. 1.45A).
- A florid benign epithelial proliferation may partly match the cytologic criteria of carcinoma cells.
- Epithelial and soft tissue cell changes due to irradiation often strongly mimic carcinoma cells, especially in combination with a paucity of cells and fragments of connective tissue (Fig. 1.43). In such cases, a bioptic or excisional investigation is indispensable. Immunocytochemical tests for pancytokeratin can distinguish activated fibroblasts from epithelial cells, but not benign from malignant cells.

**Caution**

- Benign sclerosing breast conditions and actinic changes on epithelial and soft tissue cells can strongly mimic breast carcinoma.
- Cytologic smears only presenting individual carcinoma cells may occur (Fig. 1.70). A malignant lymphoma has to be excluded, particularly in cases where a large breast nodule is detected in an elderly woman (see Sect. 1.3.15, p. 65).
- A US-guided FNAB for carcinoma smaller than 15 mm may yield scarce material, causing difficulties in assessing a definite diagnosis:
  - Targeting of small lesions is difficult in certain cases.
  - Small malignant disorders can exhibit a stronger fibrosis and sclerosis than voluminous tumors, and less pronounced nuclear atypias.
  - Small carcinomas are commonly of the monomorphic cell type (see Sect. 1.3.1.2, below)

## 1.3.1.2 Infiltrating Ductal Carcinoma of the Monomorphic Small-Cell Type (Figs. 1.72–1.75)

### Microscopic Features

Carcinoma of the monomorphic cell type comprise up to 10% of all aspirates in institutions that perform large numbers of US-guided FNABs on small, nonpalpable breast lesions:

- Carcinoma cells are small, exhibiting an overall monomorphic pattern.
- The nuclear size does not exceed the diameter of two to three erythrocytes.
- The architectural and cellular criteria are identical, as listed above, but less distinct.
- A diagnosis of malignancy is based upon single cells and clusters with pathognomonic changes in cell-rich smears.

**Differential Diagnosis**

Possible pitfalls include a few benign, and malignant lesions:

- Benign proliferative breast lesions composed of mainly small cells must be differentiated from carcinoma of the small-cell type.
- Pilomatrixomas (synonym: Malherbe calcifying epithelioma) are benign tumors of the hair follicle that form firm nodules in the subcutaneous tissue. They may easily be misdiagnosed as a small-cell carcinoma of the mammary gland, especially in cases of voluminous intramammary lesions mainly composed of proliferating basaloid cells in the low presence or complete absence of the typical shadow (ghost) cells (derived from mature squamous cells) (Fig. 16.7). Due to microcalcification, the lesion may also be suspected of being cancerous on mammography [77]. Pilomatrixoma that develops from the skin of the breast is extremely rare [5]. The diagnostic problems for cytologists are well known from pilomatrixoma that originate from anatomic sites other than the breast [92].
- Small and monomorphic cell-type mammary cancers that have hyperchromatic nuclei and a tendency to appear in a chain formation should include the possibility of a metastatic small-cell carcinoma, most probably of pulmonary origin (Fig. 1.75A). Clinical evaluation and immunocytochemical tests (IC) should lead to a final diagnosis: IC pattern of small-cell lung carcinoma includes nuclear positivity for TTF-1 and cytoplasmic positivity for neuroendocrine markers (e.g., CD56, synaptophysin, and chromogranin A), and a negative immunoreactivity for hormone receptors (ER, PR).

**Caution**

- Lobular carcinoma and low-grade ductal intraepithelial neoplasia appear in many cases as monomorphic cell type (Figs . 1.77, 1.78, 1.79, 1.80) .
- Small breast carcinomas (< 15 mm) exhibit essentially a monomorphic cell pattern.
- An FNAB of small tumors may yield hypocellular samples that prevent a definite diagnosis of malignancy.

#### 1.3.1.3 Infiltrating Ductal Carcinoma of the Large-Cell Type (Fig. 1.76)

**Microscopic Features**

This tumor type is readily recognized as malignant in most cases.

- Highly cellular specimen.
- Loose aggregates of large polymorphic, highly atypical cells. Numerous isolated cells.
- Irregular nuclei, indentations and folding, coarse chromatin, hyperchromasia, mitotic activity.
- Large nucleoli, often multiple.
- Increased N/C ratio. The cytoplasm is bizarrely shaped and fragile.
- A necrotic background is common.

**Differential Diagnosis**

Tumorous or nontumorous florid benign and atypical epithelial proliferation, proliferative nipple duct adenoma with necrosis, marked lactational changes of the benign mammary epithelium, and actinic changes of epithelial and soft tissue cells should not lead to a false-positive diagnosis. Benign nuclear features, benign cyto-architecture of cell aggregations, and the presence of myoepithelial cells are characteristic features that exclude malignancy (see Sect. 1.2.11, p 21, and Table 1.2.1.).

### 1.3.2 Infiltrating Lobular Carcinoma

(Figs. 1.77 and 1.78)

#### 1.3.2.1 Classic Lobular Carcinoma

**General Comments and Microscopic Features**

- The cytologic assessment of lobular carcinoma fails in many cases due to a strong fibrosis, which yields inadequate aspirates comprised of disassociated small tumor cells with subtle pleomorphism [78].
- Furthermore, the cytologic differential diagnosis of ductal versus lobular invasive carcinoma is difficult. There are frequently overlapping cytologic features with lobular and ductal carcinoma and borderline lesions. However, some of the features are more characteristic of one entity than the other. Features that may be helpful in this respect have been compiled and discussed in several reports in the literature [18, 24, 33, 35, 57, 75].
- The cellular and architectural characteristics of the classic variant of lobular carcinoma most frequently mentioned and generally in agreement with our own diagnostic policy are:
  - A rather low cellularity.
  - The cell picture consisting of predominantly dissociated small to medium-sized tumor cells, distinct single-file-like formations, and a lack of large tumor cell clusters.
  - Eccentric nuclei, mucus containing cytoplasm (signet ring cells may be overt) and frequent targetoid inclu-

sions with a mucoid central core. Many cells show scant cytoplasm.
- Vesicular nuclei frequently with molding and cleaving (cleaving is in many cases difficult to identify).
- Chromatin is finely dispersed and nuclear clearing is pronounced.
- Tiny nucleoli, if any.

**Caution**

Intracytoplasmic targetoid-type lumina are not a specific criterion for lobular carcinoma. They may infrequently be observed in ductal carcinoma and exceptionally in proliferative breast disease [15].

**Additional Comments and Immunocytochemistry**

- Differentiation between lobular and ductal invasive carcinoma in mammary FNAB is of minor importance in routine cytology practice. However, the recognition of the lobular tumor entity may become important in cases of cytologic tumor samples that are distant from the breast, such as axillary lymph nodes with negative or equivocal mammary imaging results.
- Immunocytochemical positivity for CK7 and CK34betaE7 and negativity for E-cadherin indicate lobular carcinoma. Technical problems leading to negative immunoreactivity for E-cadherin have to be excluded.

### 1.3.2.2 Variants of Invasive Lobular Carcinoma

[6, 16]

- Pleomorphic lobular carcinoma share a variety of cytologic features with the classic types, such as cytoplasmic inclusions with mucus and cell clustering (single-file-pattern), but there is greater cellularity, a larger cell size, and nuclear pleomorphism. A misdiagnosis of duct carcinoma is possible. This tumor type is more aggressive than the common-type lobular carcinoma.
- Invasive lobular carcinoma with a solid, alveolar, and mixed type exhibit the same cellular characteristics as the classic tumor type. These subtypes cannot be classified properly based on cytology.

## 1.3.3 Intraepithelial Neoplasia (Carcinoma in Situ)

### 1.3.3.1 Ductal Intraepithelial Neoplasia

- Cytopathologists increasingly encounter cytologic samples from ductal carcinoma in situ / ductal intraepithelial neoplasia (DCIS/DIN) when nonpalpable small lesions have been aspirated by image guidance. A high percentage of detected cancers in mammography screening programs are DCIS [82]. In our institution, our experience has shown that DCIS may sporadically appear as a large and palpable nodule or may even expand throughout the whole gland in rare cases.
- In several studies [11, 54, 81, 83, 97], it has been demonstrated that in situ disease may exhibit characteristic cytologic features, and invasive cancer may be reliably diagnosed and differentiated from DCIS. However, the authors also emphasize that an invasive component in a DCIS cannot be excluded from cytologic criteria alone.

**Microscopic Features**

- Cytologic samples aspirated from DCIS show a high cellularity and a homogeneous cell population without myoepithelial cells.

*Low-grade DCIS:* (Figs. 1.79 and 1.80):
- A monotonous population of monomorphic small to medium-sized cells arranged mainly in clusters and combined with a high cohesiveness is highly suspicious for DCIS. There is an absence of tubular aggregates.
- An obvious loss of nuclear polarity of the atypical cells.
- Nuclear atypias are the same as those listed in Table 1.3.1, p. 57, but are less pronounced.

*High-grade DCIS* (Fig. 1.81):
- Pleomorphic malignant cells as described for infiltrating ductal carcinoma of the large-cell type (see Sect. 1.3.1.3, p. 58). The background of the smear is often dirty with necrosis (comedo necrosis) and associated with apoptotic and degenerated tumor cells.

**Caution**

- Atypical epithelial cells admixed to fragments of connective tissue (fatty or fibrous) are not a reliable indicator for tumor invasion [52].
- A distinction between DCIS and invasive carcinoma is not reliably based on cytologic features. However, low-grade DCIS in particular may exhibit a characteristic cytologic pattern that allows a tentative diagnosis.

### 1.3.3.2 Lobular Intraepithelial Neoplasia

Lobular carcinoma in situ / lobular intraepithelial neoplasia (LCIS/LIN) is rarely encountered in a preoperative FNAB of the breast because the entity does not present as a palpable nodule or as a distinct lesion in mammography and sonography studies. Ustün and coauthors documented the cytomorphologic features of lobular in situ carcinoma in the literature and postulated that there are "no reliable criteria that help to differentiate pleomorphic and dissociated lobular carcinoma in situ from invasive lobular carcinoma" [101].

### 1.3.4 Tubular Carcinoma (Figs. 1.42 and 1.82)

Tubular carcinoma is a well-differentiated carcinoma with an excellent overall prognosis.

However, the bland appearance of cells and sheets leads to limitations in the cytodiagnosis with regard to malignancy and specific tumor typing. An evaluation of large tumor series suggests that tubular carcinoma may be recognized or at least be suspected if distinct cytologic criteria are considered [26].

#### Microscopic Features and Differential Diagnosis

- Nuclear atypia are similar to those seen in lobular carcinoma: a slight variation in size with nuclear membrane irregularities. Chromatin is thinly dispersed and staining is bright. No hyperchromasia and generally small nucleoli.
- Solitary cytoplasmic vacuoles are occasionally seen.
- Cohesive flat sheets without myoepithelial cells are predominant. Additional three-dimensional tubular structures are recorded in many cases. Cell dissociation is uncommon.

Many types of hyperplastic breast disorders such as microglandular adenosis or microglandular-like breast lesions can lead to a misdiagnosis [20] (Fig. 1.42).

Some malignancies may also be considered in the differential diagnosis of tubular carcinoma: adenoid cystic carcinoma, low-grade papillary neoplasia, and invasive monomorphic ductal carcinoma [26].

**Caution**

- As tubular carcinoma tends to be relatively small, a myoepithelial component originating from the surrounding benign mammary gland tissue is common.
- Components of ductal intraepithelial neoplasia (DIN, DCIS) occuring adjacent to tubular carcinoma can likewise be encountered in cytologic aspirates.
- However, in some instances tubular carcinoma itself seems to contribute to the presence of myoepithelial cells [10].

### 1.3.5 Papillary Carcinoma

Papillary breast carcinoma can be observed as intracystic or ductal invasive papillary carcinoma and carcinoma in situ as well. This tumor accounts for less than 1% of all breast malignancies but is seen in a higher percentage in the male breast [9].

1. Distinguishing a benign papilloma from a low-grade papillary carcinoma is difficult in most cases. In addition, cytologically unequivocal benign-looking papillary tumors may already exhibit a focal invasion on surgical excision. Therefore, each unambiguous papillary tumor and each suspected papillary carcinoma must undergo an excisional biopsy. For further comments and a microscopic description, see Sect. 1.2.14, p. 23 (see also references indicated in Sect. 1.2.14, p. 23) (Figs. 1.49 and 1.83).
2. Less well-differentiated papillary carcinoma are identified by distinct architectural features and cellular atypia (Fig. 1.84).

#### Microscopic Features

- Cytologic samples are highly cellular.
- Three-dimensional papilliform clusters and true complex papillary fragments with fibrovascular cores are diagnostic.
- An atypical cell population that comprises columnar cells, either single or in palisade arrangement should also be diagnostic of papillary carcinoma (or at least raise suspicions).
- Cells of less well-differentiated papillary carcinoma are larger than those of low-grade papillary tumors and have an increased N/C ratio.
- Nuclear indentations, coarse chromatin, hyperchromasia, and conspicuous nucleoli are helpful in assessing frank malignancy.
- A presence of myoepithelial cells can be disregarded together with the overall cytopathologic setting.
- A necrotic background and hemosiderophages may be present above all in intracystic proliferating neoplasms.

**Caution**

- Micropapillary carcinoma of the breast is an unusual variant of invasive ductal carcinoma exhibiting cytologically with a pseudopapillary cell arrangement.
- In addition, a small number of mucinous carcinomas may reveal the cytologic equivalent of a histologic micropapillary pattern. The cytologic features should be recognized, this tumor variant is known to have an aggressive clinical behavior [32, 48, 72].

### 1.3.6 Mucinous (Colloid) Carcinoma (Figs. 1.85 and 1.86)

#### General Comments

- Mucinous carcinoma constitutes of 1–6% of all breast carcinomas. In histology, a pure variant of mucinous carcinoma is distinguished from a mixed variant; separation of the two tumor types is important because of the favorable prognosis of the pure variant [95]. Carcinoma is considered colloid type if at least 50% of the lesion is composed of extracellular mucus [87].
- It is not possible to differentiate cytologically between pure and mixed variants of mucinous carcinoma as needle sampling cannot represent the whole volume of the lesion. Therefore, it may be appropriate to render cytologic diagnosis as breast carcinoma with partial mucinous differentiation.

**Microscopic Features**

- Three-dimensional sharply outlined cell balls, flat sheets, and single cells floating in a thick mucinous material, often concentrically condensed (corresponding to the pure variant of mucinous carcinoma). Additional findings with ductal carcinoma-type cells not floating in mucus correspond to the mixed variant. Mucus stains pink, pale blue, or cyanophilic with the Papanicolaou staining procedure.
- Occasional signet-ring cells.
- Nuclei demonstrate a slight degree of atypia. They are bright and vesicular, lack hyperchromasia, and occasionally have a grooved membrane.
- Rare nucleoli.
- Most of the scattered tumor cells exhibit the same malignant features that have been described for ductal carcinoma.

**Differential Diagnosis**

- Mucocele-like lesions (MLL) are cysts containing mucus and may rupture into the surrounding tissue: cytologic samples show scant cellularity and monolayered sheets with an absence of nuclear atypia. In cases with additional florid or atypical ductal proliferation, the cytologic features may particularly overlap with mucinous carcinoma [14]. An excisional biopsy is advised in all equivocal cases [102, 105]. For further comments, see Sect. 1.2.8.3, p. 19.
- A marked myxoid stromal change in fibroadenoma could be misinterpreted as mucus. However, in most cases the epithelial key features of fibroadenoma (cell groups with finger-like branching and naked nuclei) are evident.
- Mucinous eccrine carcinoma is a rare malignant tumor of the skin with slightly atypical cells suspended in mucin. They occur in the axillary skin or present themselves as a metastasis in an axillary lymph node, which may lead to suspicions of a metastatic mucinous mammary carcinoma [96].

## 1.3.7 Medullary Carcinoma ( Figs. 1.87 and 1.88)

**General Comments**

Medullary carcinoma accounts for around 5% of all breast carcinomas. The patients have a high survival rate compared to patients with an ordinary invasive ductal breast cancer, despite its malignant appearance and poor biological markers: cytometric analyses yield marked aneuploidy and a high S-phase fraction, and most medullary carcinomas are negative for ER and PR [95]. The most conspicuous feature of this type of breast cancer is the pronounced lymphoplasmacytic infiltrate in the supporting and surrounding stroma.

**Microscopic Features**

- Highly cellular smears.
- The unequivocal malignant cells are arranged in clusters but mainly in syncytial sheets. Large numbers of individual scattered tumor cells and stripped nuclei.
- The nuclei are enlarged with variations in size and shape, a coarse chromatin pattern, and prominent polymorphous nucleoli. The cytoplasm varies in size and is most often vacuolated and fading away at the periphery.
- Numerous lymphocytes, plasma cells and occasional neutrophilic granulocytes are present in the background, intimately admixed with carcinoma cells.

**Differential Diagnosis**

The differential diagnosis includes several different tumor entities. It is important to take into consideration that lymphocytes and plasma cells can be seen in various breast lesions. Lymphocytosis may be part of a high-grade ductal carcinoma or may originate from an intramammary lymph node, from a metastasis in an intramammary lymph node, or from a malignant lymphoma [40, 74]. Further rare potential cytodiagnostic pitfalls have been reported in the literature [85].

**Immunocytochemistry** (Fig. 1.88)

- Negativity for ER and PR is reported in different series.
- In a recent publication, Milde and coauthors showed that a reliable classification of medullary carcinoma cannot be attained from using a large panel of immunocytochemical markers [58].
- Positive immunoreactivity for pancytokeratins and negativity for CD45 (LCA) of large malignant cells exclude large-cell non-Hodgkin lymphoma (NHL).
- The mixed lymphoid population is in most cases readily recognized as reactive and benign. In equivocal cases, an adequate immunopanel for lymphoid cells and polymerase chain reactions using nuclear DNA obtained from cytologic samples can differentiate between a benign and malignant lymphoproliferative process.

## 1.3.8 Breast Carcinoma Comprising Voluminous Granular or Clear and Vacuolated Cytoplasm

Such tumors are rarely encountered in cytologic practice. The cellular features alone may not be distinctive enough for an accurate diagnosis in individual cases. The most interesting tumor types concerning FNAB cytology are briefly described, including differential diagnostic considerations:

### 1.3.8.1 Apocrine Carcinoma (Fig. 1.89)

Apocrine carcinoma should be diagnosed when the tumor cells are clearly recognizable as apocrine-type epithelium with an abundant eosinophilic granular cytoplasm. A large cytoplasm with dense eosinophilic staining may also be diagnostic for this tumor type. A wide range of incidence and

prognosis is reported in the histologic literature due to a lack of clearly reproducible features for apocrine carcinoma diagnosis [95]. An update of apocrine mammary lesions has recently been published [64].

**Microscopic Features**

Hallmarks:

- Abundant cytoplasm with sharply defined margins.
- Variable eosinophilic granulation, frequently coarse granules - PAS positive.
- Large, round, and vesicular eccentrically located nuclei.
- Nuclei may be rounded or multilobated and contain (multiple) prominent nucleoli.
- Dense eosinophil staining, foamy, or vacuolated cytoplasm is possible.
- Cyst formation is usual.

**Immunocytochemistry**

Most apocrine tumor cells do not express estrogen or progesterone receptors, but many of them show positivity for androgen receptors [51, 95].

**Differential Diagnosis**

- Apocrine neoplasms exhibiting numerous cells with a prominent foamy and vacuolated cytoplasm can be confused with lipid-rich carcinoma (staining positive for neutral lipids).
- Carcinoma with squamous differentiation may mimic apocrine carcinoma.
- Granular cell tumor (glycogen content and immunocytochemical reactivity for S-100) is another lesion with prominent cytoplasmic granularity that may be confused with apocrine carcinoma (see Sect. 1.2.18, p. 26) (Fig. 1.63).
- Apocrine carcinoma of the axilla originating in the local apocrine glands can lead to a false diagnosis of an axillary metastasis of apocrine breast carcinoma.

**Caution**

- Both apocrine carcinoma and secretory carcinoma (see Sect. 1.3.8.2, see below) may masquerade as benign hormonally stimulated cell populations during pregnancy and lactation and vice versa.
- Distinguishing between cells from a monomorphic apocrine carcinoma and those from a benign apocrine metaplastic lesion may be difficult.

### 1.3.8.2 Secretory Carcinoma [29, 49, 86]

This tumor occurs more frequently during the first three decades of life and therefore it has also been designated as juvenile carcinoma. However, secretory carcinomas are also diagnosed in prepubescents and elderly women. Secretory carcinoma can be reliably diagnosed on FNAB samples if the characteristic cellular features with an abundance of secretory material are present.

**Microscopic Features and Cytochemistry**

Cytologic hallmarks:

- Several authors describe grape-like clusters with mucous globular structures and single globuli. These globular structures consist of vacuolated cells containing large cytoplasmic inclusions of a secretory product.
- The grape-like clusters correspond to microcystic and microfollicular patterns in histology.
- Only sparse extracellular mucus in an otherwise clean background.
- Absence of significant cellular atypia.

Cytochemistry renders a diffuse positivity for mucin with Alcian-blue stain and periodic acid Schiff (PAS) diastase resistance.

### 1.3.8.3 Lipid-Rich Carcinoma [2, 31, 41] (Fig. 1.90)

A lipid accumulation in the cytoplasm of common breast carcinomas is well known. Lipid has been shown to be a secretory product; it does not reflect a cytoplasmic accumulation of lipoid masses due to cellular degeneration [95]. Therefore, a breast neoplasia should only be designated as a lipid-rich carcinoma when virtually all tumor cells harbor abundant lipid causing a unique cytoplasmic vacuolization.

**Microscopic Features and Cytochemistry**

Cytologic hallmarks:

- Large cells with abundant rounded cytoplasm due to abundant fat storage. Lipid droplets should be considered if the cytoplasm exhibits a mix of multiple small and large well-defined vacuoles.
- Cells often occur singly and occasionally clustered.
- The eccentrically located nuclei have clumped or finely granular chromatin and prominent nucleoli.

A diagnostic key feature for lipid-rich carcinoma is evidence of Oil-red-O positively stained lipid droplets in almost all of the cells. The cytochemical reaction to establish the presence of lipid must be performed on air-dried slides. Pap-stained slides, previously fixed in 95% ethanol, lose the reactivity for neutral fat.

**Differential Diagnosis**

The pathognomonic cytologic features should distinguish this tumor type from other breast carcinoma entities. However, a distinct cytoplasmic granularity in a large number of lipid-rich carcinoma cells could give rise to a misinterpretation of apocrine carcinoma (Fig. 1.91).

### 1.3.8.4 Clear Cell (Glycogen-Rich) Carcinoma

[3, 17, 80]

#### Microscopic Features and Cytochemistry

The varying cytomorphologic appearances of glycogen-rich clear cell carcinoma (GRCC) often prevent an accurate diagnosis. A demonstration of glycogen is essential for definitive GRCC diagnosis.

Cytologic hallmarks:

- A mixed cell pattern comprising clusters, loose groups, and single cells.
- Large cells with abundant optically clear cytoplasm, which contains abundant glycogen.
- The nuclei exhibit hyperchromasia, varied irregularity of shape and may be eccentrically located. The nuclear pleomorphism matches that of common breast carcinomas (see Table 1.3.1, p. 57).
- Cytoplasm is finely granular and contains no lipids or mucins. Eosinophilic granularity may be occasionally observed.

For a definitive GRCC diagnosis, most tumor cells must show abundant cytoplasmic PAS-positive granular material, which is sensitive to diastase digestion. A PAS–diastase reaction can be performed on standard Pap-stained preparations.

#### Differential Diagnosis

- Glycogen-rich carcinoma share many cytologic features with those of other breast tumors; the greatest overlap is with the lipid-rich carcinoma (see Sect. 1.3.8.3, p 62).
- Other lesions that can be confused with GRCC are: high-grade ductal breast carcinoma (large-cell type), secretory carcinoma, clear cell neuroendocrine tumors, apocrine tumors, metastatic renal cell carcinoma, and other rare benign and malignant entities that have a large and clear cytoplasm [3].
- Glycogen-rich carcinoma may be combined with other types of breast carcinoma.

## 1.3.9 Adenoid Cystic Carcinoma

[21, 25, 79, 94] (Fig. 1.92)

Adenoid cystic carcinoma (ACC) is a rare variant of breast carcinomas and is known to have a favorable prognosis. Cytologic features of the cribriform type are similar to its counterpart in the salivary glands.

#### Microscopic Features

Cytologic hallmarks:

- Presence of two cell types - epithelial and myoepithelial, the latter are prominent.
- Samples are cell rich.
- Three-dimensional, well-outlined, thick and nest-like clusters composed of small basaloid myoepithelial cells and scattered foci of larger eosinophilic cells. The cells are arranged around cores of homogeneous acellular material.
- Cells are generally small and uniform, exhibiting minor nuclear atypia and scant cytoplasm.
- Numerous bipolar naked cells may occur singly in the background.
- Basement-membrane-like cylinders and spherical structures are common as background material. The acellular material is translucent with Pap-stain and metachromatic with MGG or Diff-Quik stain.

#### Immunocytochemistry

- Adenoid cystic carcinoma show variable positive immunoreactivity according to the heterogeneous cellularity. The immunoreactions on the myoepithelial cells are positive for smooth muscle actin, S-100 protein, calponin, and p63. Pancytokeratins (e.g., MNF-116) along with low- and high-molecular-weight CKs reveal a positive reaction in larger epithelial cells.
- Quinodoz and coauthors refer to the diagnostic utility of immunocytochemical studies using the collagen alpha (IV) chain antibody on cytologic material with suspected adenoid cystic carcinoma of the breast [73].

#### Differential Diagnosis

- Distinction of benign collagenous spherulosis from ACC is very difficult in cytologic preparations with a low cellularity and spheres associated with small benign epithelial cells.
- Spherulosis could possibly be confused with adenoid cystic carcinoma.
- Breast carcinomas of the ductal type with secretory material within their dilated glands, and cribriform carcinoma may mimic adenoid cystic carcinoma.

## 1.3.10 Metaplastic Carcinoma

[47] (Figs. 1.93 and 1.94)

#### Definition and General Comments

- Metaplastic carcinoma is an unusual tumor (<1% of all breast malignancies). Metaplastic carcinoma is a heterogeneous group of breast carcinomas and includes areas of squamous, spindle, chondroid, and osseous metaplasia.
- Carcinoma with predominant pseudosarcomatous metaplasia are difficult to separate from true sarcoma by cytology. They are highly malignant with poor survival.

#### Microscopic Features

- In most cases, the cytologic samples exhibit highly atypical and large tumor cells.
- A mixture of frank carcinoma cells and cells with a mesenchymal-like appearance should give rise to an accurate cytologic diagnosis.

- Carcinoma cells are morphologically similar to those in invasive ductal carcinoma and in breast carcinoma of the large-cell type.
- Spindle tumor cells may be relatively bland or may exhibit sarcomatoid features. The latter are large and extremely pleomorphic, with bizarre nuclei and a vacuolated cytoplasm. They may show phagocytotic activity as well.
- Atypical histiocyte-like multinucleated cells and fibroblast-like cells are frequent; intracytoplasmic vacuoles and debris are common.
- Chondroid and chondrosarcomatous differentiation may also be discerned in cytologic material; chondroid cells with variable atypia are observed against a background of a myxoid/chondroid substance [37].
- Osseous substance is unlikely to be sampled using FNAB.
- Squamous metaplasia may show up as malignant squamous cells with a deep eosinophilic cytoplasm.

**Differential Diagnosis** [89]

The differential diagnosis of metaplastic carcinoma should include:

- Tumors of mesenchymal origin: Pseudosarcomatous fasciitis, fibromatosis, primary and metastatic sarcoma of the breast.
- Tumors of epithelial origin: Pleomorphic large-cell mammary carcinoma, very poorly differentiated metastatic carcinoma (adenomatous or squamoid), and phylloides tumor comprising epithelial atypia.

**Caution**

Distinguishing between metaplastic carcinoma with a marked pseudosarcomatous proportion and primary or metastatic sarcoma of the breast is not possible using cytomorphological features alone.

**Immunocytochemistry**

In cases of malignant mesenchymal-looking tumors of the breast, metaplastic carcinoma has to be considered and should lead to immunocytochemical examinations for cytokeratin (pancytokeratin, CK5/6, etc.) (Fig. 1.94). A myoepithelial differentiation can be supported by immunocytochemistry for basal-cell-type CKs and with myoepithelial markers (SMA, S-100, p63, and others) [60].

## 1.3.11 Squamous Cell Carcinoma [27, 28]

The cytology is characterized by numerous malignant squamous cells with the classic morphology identical to its counterparts in many different organs:

- Densely keratinizing cytoplasm.
- Hyperchromatic dense nuclei and coarse or patternless chromatin, highly irregular nuclear membrane.
- Large polymorph nucleoli.
- Background necrosis.

The identification of this tumor type in a breast FNAB must always be followed by a search for other sources of a primary tumor. A diagnosis of primary squamous cell carcinoma of the breast should be accepted if no other primary tumor localization has been found.

## 1.3.12 Carcinoma with Osteoclastic Giant Cells [13, 36, 103] (Fig. 1.95)

Invasive ductal carcinoma with osteoclast-like giant cells is an extremely rare variant of breast carcinoma. Most reports emphasize that the tumor is clearly recognizable as malignant in cytologic samples.

**Microscopic Features and Immunocytochemistry**

- Smears show a biphasic component of malignant epithelial cells and giant cells.
- The *epithelial component* is characterized by irregular clusters and cell dissociation.Nuclear pleomorphism generally is slight to moderate (see Table 1.3.1, p. 57).
- The *giant cells* are scattered between carcinoma cells exhibiting osteoclastic features: huge cells with abundant cytoplasm. The nuclei are crowded to one margin of the cytoplasm harboring one conspicuous nucleolus.

CD68 positivity, and negativity for cytokeratins and EMA, confirm a histiocytic origin of the giant cells.

## 1.3.13 Carcinoma with Neuroendocrine Differentiation [50, 60]

**General Comments**

Breast carcinoma with neuroendocrine differentiation is defined either by a focally typical growth pattern indicating carcinoid tumor or by immunocytochemical positivity of some of the tumor cells with neuroendocrine markers (e.g., chromogranin A, synaptophysin, and neuron specific enolases (NSE)). The biological behavior of these tumors seems to be akin to morphologically similar carcinoma without neuroendocrine differentiation.

**Microscopic Features**

The characteristic growth pattern of the common type neuroendocrine tumor may be recognized both in histologic tissue sections and in cytologic smears:

- Monomorphic small to medium-sized cells in a rosette-like and alveolar arrangement and isolated cells in the background. A few strongly enlarged cells with homogeneous nuclei and deep blue in color may be observed.
- The regular nuclei exhibit indistinct wrinkled margins and thinly dispersed chromatin.
- Cytoplasm may be indistinct, dense, or plasmacytoid. Fine eosinophilic granularity is frequently observed.

**Differential Diagnosis**

- Cases with a preponderance of uniform small spindle cells should be suggestive of a pure endocrine tumor. Neuroendocrine tumors can metastasize into the mammary gland. It is not possible to distinguish primary from secondary endocrine cancer on cytologic findings alone. The patient's history and clinical information are essential for the final assessment.
- A small-cell pattern (oat cell type) should bring into consideration a primary small-cell neuroendocrine breast cancer, a metastasis from lung cancer, or Merkel cell carcinoma [55].

**Immunocytochemistry**

- All NETs are positive for at least one neuroendocrine marker such as CD 56 (NCAM), chromogranin A, synaptophysin, or NSE.
- TTF-1 nuclear positivity is an indicator of a pulmonary origin of a NET. Most NETs of other origins, including the intestinal tract, are reported to show a negative expression; nevertheless, small-cell carcinoma from other sites may occasionally show a nuclear positive staining.
- It is important to always apply a panel of antibodies in order to help ascertain the primary site of neuroendocrine tumors [43, 53].

## 1.3.14 Infiltrating Breast Carcinoma: Further Rare Special Types

### 1.3.14.1 Inflammatory Carcinoma

(Fig. 1.96 and 1.97)

Inflammatory carcinoma is defined as a presence of carcinoma cells in the dermal lymphatic vessels followed by lymphedema and associated with pathognomonic clinical features. The most impressive clinical signs include erythema, edema, peau d'orange, and diffuse infiltration of the breast. FNAB is only indicated in selected cases, since a target lesion is not clearly discernible, neither clinically nor by imaging. It occurs haphazardly that FNAB hits isolated carcinomatous lymphatic vessels. Cytologic findings are those of less well differentiated invasive ductal carcinoma.

### 1.3.14.2 Paget Disease (Fig. 1.98)

Paget disease appears as an eczema-like change of the nipple area and is occasionally combined with incipient ulceration. The lesion is morphologically determined by large carcinoma cells enclosed in deep layers of the epidermis and, in the majority of cases, is associated with underlying ductal intraepithelial neoplasia (high grade). Paget disease is occasionally accompanied by a centrally located breast nodule indicative for association with invasive ductal type carcinoma.

FNAB is highly recommended to clarify the nature of a nodular lesion. Scraping of eczematous areas of the nipple would be ineffective in many cases due to the basal location of the tumor cells.

**Microscopic Features and Differential Diagnosis**

- Scraped cell material exhibit blood, squamous cells, possibly detritus, and (if the lesion is deeply ulcerated) sparsely isolated large pleomorphic cells.
- Nuclei are round with pronounced irregularities, coarse chromatin, hyperchromasia, and irregular prominent nucleoli.
- The cytoplasm is distinct, clear or densely structured.

- Malignant melanoma has to be excluded in context with the clinical features. Melanoma cells typically are cytokeratin negative and positive for melanoma markers: Melan A, HMB-45, and S-100.
- Scraping that surprisingly yields cell-rich smears with malignant cells lacking large cytoplasm should raise suspicions of squamous carcinoma in situ (Bowen disease).

**Caution**

Intradermal tumor cells are encased in the basal epidermal layers, hence scraping of eczematous areas of the nipple will yield no carcinoma cells in most cases unless the lesion is ulcerated.

### 1.3.14.3 Other Sporadic Carcinomas

Acinic cell carcinoma [66], adenosquamous carcinoma, mucoepidermoid carcinoma [22, 70], breast carcinoma with choriocarcinomatous features [4], and other types are not further discussed. The lesions are expected to reveal similar cytoarchitectural features as those of their counterparts at other sites of the body.

## 1.3.15 Malignant Lymphoma and Myeloid Lesions

**General Comments**

- Malignant lymphoma in the breast may be a form of primary extranodal lymphoma or part of a systemic disease. The majority of primary breast lymphoma are of the intermediate or the high-grade type, and most of the disseminated lymphoma with breast involvement are of the low-grade type [19].
- Malignant lymphomas are observed within a wide age range of patients and exhibit clinically as a well-delineated mass. In particular, voluminous breast nodules in elderly female patients raise suspicions of malignant lymphoma.

- The reader is referred to Sect. 15.3."Lymph Nodes, Malignant Lesions," p. 950, for detailed information on hematopoietic and lymphoid lesions.

### 1.3.15.1 High-Grade Non-Hodgkin Lymphoma: Homogeneous Cell Pattern (Figs. 1.99–1.102)

The most frequent primary lymphoid tumor type in the breast is high-grade NHL. Diffuse large B-cell lymphoma account for the most frequent subtype in this tumor group followed by rare entities such as anaplastic large-cell lymphoma, Burkitt lymphoma, poorly differentiated plasmacytoma, T-cell lymphoma, and others [62, 67, 71, 91, 98].

#### Microscopic Features

- Tumor cells are single but may also be grouped loosely or in dense clusters, mimicking epithelial neoplasia (Figs. 1.99 and 1.100A).
- The cytologic samples are highly cellular with a wide morphologic spectrum of large pleomorphic cells, and a variable admixture of small and medium sized atypical lymphoid cells.
- The nuclei are irregular with indentations, coarse chromatin, hyperchromasia, and single or multiple pleomorphic nucleoli. Clear and multilobated nuclei should raise the possibility of T-cell NHL.
- Variable cytoplasm in size and density.

#### Additional Analyses and Differential Diagnosis

- FNAB specimens containing blastic-cell-type NHLs are easily classified as malignant. Yet, due to a low incidence of this tumor type, they may be misdiagnosed as poorly differentiated mammary carcinoma or as medullary carcinoma by cytologic evaluation alone. To avoid unnecessary surgical procedures, it is highly recommended to confirm an equivocal cytologic judgment by application of a basic immunopanel:
  - Carcinoma stain positive for pancytokeratins (e.g., MNF-116);
  - NHL stains positive for CD45 with few exceptions (Fig. 1.100B).
- Histology remains the major diagnostic tool for exact lymphoma typing. Still, it may be desirable to achieve a more precise cytology-based subclassification of lymphoma in patients in whom management without additional invasiveness is more suitable. The information can be achieved by an adjuvant set of immunocytochemical markers (IC) and by molecular genetic analyses on cellular material from FNAB, provided that a substantial number of slides are available.

  Selected lymphoma types along with their diagnostic characteristics are briefly mentioned below:
  - Diffuse large B-cell lymphoma (Fig. 1.100): Varied positive staining for pan-B-cell markers (CD20, CD79a), BCL-6 nuclear positivity in a high proportion of cases, MIB-1 (usually high proliferative index), CD30-positive in anaplastic variants. Translocation t(14;18) in a minority of cases.
  - Anaplastic large-cell lymphoma: CD30 usually positive, variable staining for CD45, T-cell markers, EMA and ALK. Translocation t(2;5) in a majority of cases [62].
  - Burkitt lymphoma (Fig. 1.101): Positivity for CD20, CD10, BCL-6, and MIB-1 (proliferative index nearly 100%). Negativity for CD5 and BCL-2. Characteristic cytoplasmic vacuolization and large numbers of starry-sky cells.
  - Plasma cell neoplasm (Fig. 1.102): CD38 and CD138 positive. CD45 and CD20 mostly negative!
  - Multilobated T-cell lymphoma: Multilobated T-NHL exhibit a pale cytoplasm and large nuclei of irregular configuration due to multilobation and hypersegmentation. Hyperchromasia and chromatin structure tends to be indistinct, and large nucleoli are frequent. T-cell NHL are identified by strong positive reactions of the tumor cells for CD45 (LCA) and variable positive immunostaining with T-cell antibodies (CD3, CD4, CD5, CD7, CD8). Sometimes CD30 positivity. The rare variant of multilobated B-NHL (IC: B-cell markers positive) and Hodgkin disease with Hodgkin/Reed-Sternberg cells (IC: CD15, CD30, PAX5 positive) should be excluded [71].
- Primary and metastatic neoplasms in the breast, which may be mistaken for large-cell lymphoma are amelanotic melanoma and sarcoma. Melanomas are suspected in most cases by the cytomorphologic characteristics and definitely determined by positive immunostaining for melanocytic markers. Sarcoma demonstrate negative immunoreaction for CD45 and immunopositivity for mesenchymal markers.

**Caution**

- FNABs with large numbers of pleomorphic malignant cells, whether isolated or clustered, call for basic immunostains to distinguish lymphoma from carcinoma.
- NHL of the large blastic-cell type may exhibit cellular groupings and clustering mimicking carcinoma.
- Plasmablastic lymphoma reveal negative immunostaining for CD45 and frequently for CD20.

### 1.3.15.2 Non-Hodgkin Lymphoma of the Mixed Cell Type and Hodgkin Lymphoma [91, 98].

#### General Comments

- *NHL* of low or intermediate grade is very difficult to distinguish from inflammatory conditions. Pseudolymphoma particularly induces pleomorphic lymphocytic patterns

composed of mature and immature T and B lymphocytes with plasmacytoid features (see also Sect. 1.2.6, p. 18) (Fig. 1.24).

- A similar pattern of activated lymphoid cells is observed as concomitant population in *classical Hodgkin lymphoma*. Absence of the pathognomonic multinucleated Reed-Sternberg cells and mononuclear Hodgkin cells in aspirates will make a definitive diagnosis difficult.

**Microscopic Features**

Cellular hallmarks of mixed-cell-type NHL are comparable to lymphocytes in benign reactive lymphoid disorders:

- Small lymphoid cells exhibit slightly enlarged irregular and angulated nuclei.
- The nuclei of small reactive and neoplastic lymphoid cells stain somewhat darker than bland lymphocytes.
- The chromatin pattern is dense and granular.
- A large number of nuclei contain distinct irregular nucleoli.

**Additional Analyses**

- Demonstrating the neoplastic nature (monoclonality) of lymphocytes requires immunocytochemical T/B enumeration or flow cytometric analysis (FCM). However, it is unlikely to separate inflammatory conditions from malignant lymphoma in many lymphoid breast disorders, due to a pronounced proliferation of B lymphocytes in benign lesions.
- Polymerase chain amplification (PCR) is a reliable method to assess clonality in lymphoid proliferations where immunocytochemical analyses are not diagnostic. Bear in mind that monoclonal rearrangement of the IgH gene and T-cell receptor gamma gene using PCR has been described in single cases of pseudolymphoma [12].
- A subclassification of lymphoma on FNAB samples may be desirable in rare cases due to clinical requirements. Fluorescence in situ hybridization (FISH) is an excellent method to recognize chromosomal translocations, among others, of the following lymphoma subtypes: lymphoma of follicle center cell origin: t(14;18) and mantle cell lymphoma: t(11;14).
- Hodgkin-typical malignant cells, if present, are immunocytochemically positive for CD15, CD30, and PAX5 and negative for CD45.

**Caution**

- Mammary infiltration of Hodgkin lymphoma may present itself as a mixed reactive lymphoid cell population lacking the typically malignant Reed-Sternberg and Hodgkin cells.
- Lymphoid populations of benign breast pseudolymphoma may occasionally exhibit monoclonal gene amplification by PCR.

### 1.3.15.3 Myelogenic Sarcoma

[7, 59, 63, 69, 90] (Figs. 15.103 and 15.104)

Foci of so-called myelogenic sarcoma or granulocytic sarcoma (chloroma) may develop in the breast as a solid tumor mass. These rare lesions may accompany or even precede myelomonocytic leukemias; the patient's history and a general clinical examination support a proper diagnosis.

Myeloid cells show distinct immunopositive staining for myeloperoxidase.

**Microscopic Features and Differential Diagnosis**

- *Immature and blastic myelogenic sarcoma, monocytic leukemia:*
  - Tumor cells are large and reveal mostly lobated or histiocytoid clear nuclei. The cytoplasm is vacuolated or granular.

  It is difficult to distinguish such a tumor from large-cell malignant lymphoma, undifferentiated carcinoma, and malignant melanoma.
- *Mature variant:*
  - The mixed pattern comprising myeloid precursors, immature granulocytes, and megakaryocytic elements should be differentiated from extramedullary hemopoiesis (Fig. 15.102).

More information is provided in Sects. 15.3.22, p. 975, and 15.3.23, p. 975.

## 1.3.16 Malignant Mesenchymal Lesions

[1, 60, 89]

- Nonepithelial tumors are rarely observed in FNAB breast samples. The cytologic aspirate will yield sparse cell material inadequate for diagnostic purposes in many cases. If possible, cell blocks should be made from a part of the material.
- An epithelioid transformation of miscellaneous soft tissue sarcoma could lead to a misinterpretation of invasive ductal breast carcinoma.
- A list of selected tumor entities as presented below, may be helpful for cytodiagnostic considerations. Very unusual sarcomas and those with no specific differentiation are not mentioned.

### 1.3.16.1 Malignant Fibrous Histiocytoma / Undifferentiated Pleomorphic Sarcoma

[89] (Fig. 1.103)

Many variants of this histogenetically ill-defined tumor type exist including pleomorphic, giant cell, myxoid, and inflammatory types. Metaplastic carcinoma has to be excluded.

Cellular elements may show a positive immunoreaction for various mesenchymal markers. A few cells may also express cytokeratin [60].

**Caution**

Be cautious of a tumor diagnosis in postirradiation patients!

### 1.3.16.2 Liposarcoma

Lipoblasts are the key feature! The pleomorphic and myxoid variant of liposarcoma should not cause any diagnostic problems with benign lipomatous tumors. In contrast, well-differentiated liposarcoma (lipoma-like liposarcoma) is mainly composed of lipocytes without nuclear atypia causing diagnostic uncertainties. Pleomorphic lipoma may lead to a false-positive tumor diagnosis [46]. Liposarcoma may be a component of malignant biphasic neoplasms.

### 1.3.16.3 Leiomyosarcoma [34]

Moderate to severe atypia and increased mitotic activity are key diagnostic features of a malignant leiomyomatous tumor. Leiomyosarcoma has to be distinguished from metaplastic carcinoma and malignant phyllodes tumors.

Tumor cells are immunocytochemically positive for myogenic markers such as smooth muscle actin and desmin, and negative for cytokeratins.

### 1.3.16.4 Malignant Myoepithelioma [84, 99].

This tumor exhibits a similar cell pattern as sometimes observed in leiomyosarcoma.

Tumor cells show immunopositivity for smooth muscle actin and desmin. A positive immunoreaction is also shown for keratin (MNF-116), S100-protein, and vimentin.

### 1.3.16.5 Angiosarcoma [39, 44] (Fig. 1.104)

Low-grade angiosarcoma displays minimal cellular atypia; distinction from hemangioma is not possible.

Identification of intracytoplasmic hemosiderin deposits is not a reliable feature for angiomatous tumors. It may be impossible to distinguish angiosarcoma from cell change after radiotherapy.

Neoplastic endothelial cells are immunopositive for CD31, CD34, and factor VIII and negative for cytokeratins.

### 1.3.16.6 Malignant Schwannoma [56, 93] (Fig. 1.105)

Schwannoma, particularly those with epithelioid cell features (loosely clustered large cells with abundant polygonal cytoplasm and possibly with a granular appearance) are difficult to distinguish from other types of malignant tumors, especially pleomorphic carcinoma, amelanotic melanoma, and stromal sarcoma.

A correct classification could be possible on FNAB samples if enough material is available to allow the use of an appropriate immunocytochemical panel comprising neuron-specific enolase, glial fibrillary acidic protein, cytokeratin, S-100 protein, and melanoma-associated antigens.

### 1.3.16.7 Osteogenic Sarcoma [100]

The following cytologic features may suggest osteosarcoma: smears with pleomorphic cells, spindly shaped to oval; background with scarce or abundant amorphous material, suggestive of osteoid; osteoclast-like giant cells and stromal fragments; in some cases cartilage may also be present. Primary metaplastic carcinoma of the breast often harbors foci of osteogenic and chondromatous tissue.

More information on malignant soft-tissue tumors (selected entities) is provided in Sect. 17.2, "Soft Tissue and Bone: Malignant Lesions," p 1092.

## 1.3.17 Metastatic Cancers (Figs. 1.106–1.110)

**General Comments**

- Neoplasms metastatic to the breast are not frequent; the rate is clinically observed in up to 2% of breast neoplasms [88]. An FNAB diagnosis of metastatic breast disease is essential in order to avoid unnecessary breast surgery and to start an immediate search for the primary lesion, clinically and using imaging techniques.
- Ancillary studies, and in particular immunocytochemistry, are mandatory in equivocal cases in order to assess a definitive diagnosis.
- The most common metastatic cancers in the female breast are: melanoma, lung cancer, ovarian carcinoma, and soft-tissue sarcoma followed by gastrointestinal and genitourinary tumors [30]. Malignant lymphoma should not be considered as true metastasis: these tumors are either primary (primary extranodal lymphoma) or part of a systemic disease.
- Carcinoma in the prostate is the most common metastatic disease in the male breast.
- Further comments on differential diagnoses between primary and secondary breast malignoma can also be found in the preceding sections of this chapter.
- Contralateral primary breast cancer should be interpreted as a second primary tumor rather than a metastatic disorder.

**Immunocytochemistry** [38]

*Primary breast carcinoma* exhibits a relatively selective immunopanel:

– CK7 **+**.
– Estrogen and progesterone receptors **+** (Figs. 1.4 and 1.5).
– Mammaglobin **+** (this marker is not very sensitive).
– GCDFP (gross cystic disease fluid protein) **+**. It is a poorly sensitive but highly specific marker if carcinoma of the salivary gland, skin adnexa, and prostate are excluded [42].
– CK20 negativity.

*Metastatic tumors*: In order to distinguish metastatic lesions from primary breast cancers, the most important immunoreactions and immunopanels are as follows:
– Melanoma is recognized by the specific melanoma markers Melan A, HMB-45, and S-100.
– Ovarian cancer shares many positive immunoreactions with breast cancer (e.g., steroid receptors, CK7). Positivity for CK20 may suggest mucinous ovarian adenocarcinoma. CA125 is not a reliable marker; however, a negative reaction suggests breast carcinoma.
– Pulmonary carcinoma. TTF-1 positivity excludes breast primary (Fig. 1.107B). Steroid receptors may also be sporadically expressed in lung cancer cells.
– Colon cancer exhibits strong positivity for CK20 and often nuclear positivity for CDX-2.
– Adenocarcinoma of prostate should be diagnosed without problems by application of specific antibodies against PSA and prostatic acid phosphatase (PAP).
– Malignant lymphoma cells are positive for CD45 (LCA) and negative for cytokeratins. (special lymphoma types, see Sect. 1.3.15, p. 65).

## 1.3.18 Male Breast: Malignant Neoplasms

- Male breast carcinoma accounts for 1% of all mammary cancers.
- Male breast carcinoma may be related to gynecomastia in rare cases.
- Mammary cancers in men generally present themselves a decade later than in women, with a median age of 63 years, and a lower incidence of bilaterality in comparison to the incidence in females [23].
- The large varieties of female breast carcinoma may also be seen in the male breast. Male breast carcinomas are morphologically indistinguishable from their female counterparts (Fig. 1.72). Papillary carcinoma appears more frequently in men than in women. A series of papillary neoplasms along with their cytologic features has recently been presented by Reid-Nicholson and coauthors [76]. Malignant soft-tissue tumors have rarely been observed [8, 61].
- Metastatic prostatic carcinoma in the breast exhibit unequivocal (organ-typical) cytologic criteria of malignancy in most cases: large uniform tumor cells including distinct vacuolated and granular cytoplasm, round nuclei with densely packed granular chromatin, and a large eosinophilic nucleolus.

  The positive immunocytochemical reaction for PSA and PAP is diagnostic for a metastasis of prostate cancer.

## 1.3.19 Further Reading


1. Adem C, Reynolds C, Ingle JN, Nascimento AG. Primary breast sarcoma: clinicopathologic series from the Mayo clinic and review of literature. Brit J of Cancer 2004;91:237-241.
2. Aida Y, Takeuchi E, Shinagawa T, et al. Fine needle aspiration cytology of lipid-secreting carcinoma of the breast. A case report. Acta Cytol 1993;37:547-551.
3. Akbulut M, Zekioglu O, Kapkac M, et al. Fine needle aspiration cytology of glycogen-rich clear cell carcinoma of the breast. Review of 37 cases with histologic correlation. Acta Cytol 2008;52:65-71.
4. Akbulut M, Zekioglu O, Ozdemir N, Kapkac M, et al. Fine needle aspiration cytology of mammary carcinoma with choriocarcinomatous features. Report of 2 cases. Acta Cytol 2008;52:99-104.
5. Ali MZ, Ali FZ. Pilomatrixoma breast mimicking carcinoma. Coll Physicians Surg Pak 2005;15:248-249.
6. Auger M, Hüttner I. Fine needle aspiration cytology of pleomorphic lobular carcinoma of the breast. Comparison with the classic type. Cancer 1997;81:29-32.
7. Barker TH. Granulocytic sarcoma of the breast diagnosed by fine needle aspiration (FNA) cytology. Cytopathology 1998;9:135-137.
8. Bhagat P, Kline TS. The male breast and malignant neoplasms. Diagnosis by aspiration biopsy cytology. Cancer 1990;65:2338-2341.
9. Bhatia A, Dey P, Saikia UN, Kumar Y. Fine needle aspiration cytology of papillary carcinoma of breast. Cytopathology 2007;18:321-324.
10. Bondeson L, Lindholm K. Aspiration cytology of tubular breast carcinoma. Acta Cytol 1990;34:15-20.
11. Bondeson L, Lindholm K. prediction of invasiveness by aspiration cytology applied to nonpalpable breast carcinoma and tested in 300 cases. Diagn Cytopathol 1997;17:315-320.
12. Boudova L, Kazakov DV, Sima R, et al. Cutaneous lymphoid hyperplasia and other lymphoid infiltrates of the breast nipple: a retrospective clinicopathologic study of fifty-six patients. Am J Dermatopathol 2005;27:375-386.
13. Cai G, Simsir A, Cangiarella J. Invasive mammary carcinoma with osteoclast-like giant cells diagnosed by fine needle aspiration biopsy: review of the cytologic literature and distinction from other mammary lesions containing giant cells. Diagn Cytopathol 2004;30:396-400.
14. Cheng L, Lee WY, Chang TW. Benign mucocele-like lesion of the breast: how to differentiate from mucinous carcinoma before surgery. Cytopathol 2004;15:104-108.
15. Crasta JA, Makhija P, Kumar KR, Sheriff S. Cytological features of lobular carcinoma of breast: how important are the intracytoplasmic lumina? Indian J Pathol Microbiol 2005;48:170-172.
16. Dabbs DJ,Grenko RT, Silverman JF. Fine needle aspiration cytology of pleomorphic lobular carcinoma of the breast. Duct carcinoma as a diagnostic pitfall. Acta Cytol 1994;38:923-926.
17. Das AK, Verma K, Aron M. Fine needle aspiration cytology of glycogen-rich carcinoma of breast: report of a case and review of the literature. Diagn Cytopathol 2005;33:263-267.
18. de las Morenas A, Crespo P, Moroz K, Donnelly MM. Cytologic diagnosis of ductal versus lobular carcinoma of the breast. Acta Cytol 1995;39:865-869.
19. Domchek SM, Hecht JL, Fleming MD, et al. Lymphomas of the breast: Primary and secondary involvement. Cancer 2002;94:6-13.
20. Evans AT, Hussein KAH. A microglandular adenosis-like lesion simulating tubular adenocarcinoma of the breast. A case report with cytological and histological appearances. Cytopathology 1990;1:311-316.

21. Galed-Placed I, Garcia-Ureta E. Fine needle aspiration biopsy diagnosis of adenoid cystic carcinoma of the breast. A case report. Acta Cytol 1992;36:364-366.
22. Gomez-Aracil V, Mayayo Artal E, Azua-Romeo J, et al. Fine needle aspiration cytology of high grade mucoepidermoid carcinoma of the breast: a case report. Acta Cytol 2006;50:344-348.
23. Goss PE, Reid C, Pintilie M, et al. Male breast carcinoma. A review of 229 patients who presented to the Princess Margaret Hospital during 40 years: 1955-1996. Cancer 1999;85:629-639.
24. Greeley CF, Frost AR. Cytologic features of ductal and lobular carcinoma in fine needle aspirates of the breast. Acta Cytol 1997;41:333-340.
25. Gupta RK. Fine needle aspiration cytodiagnosis of primary and metastatic squamous cell carcinoma of the breast. Acta Cytol 1997;41:692-696.
26. Gupta RK, Dowle CS. Cytodiagnosis of pure primary squamous cell carcinoma of the breast by fine needle aspiration cytology. Diagn Cytopathol 1997;17:197-199.
27. Gupta RK, Dowle C. Fine needle aspiration cytodiagnosis of adenoid cystic carcinoma of the breast. Diagn Cytopathol 1996;14:328-330.
28. Gupta RK, Dowle CS. Fine needle aspiration cytology of tubular carcinoma of the breast. Acta Cytol 1997;41:1139-1143.
29. Gupta RK, Kenwright D, Naran S, et al. Fine needle aspiration cytodiagnosis of secretory carcinoma of the breast. Cytopathology 2000;11:496-502.
30. Hajdu SI, Urban JA. Cancers metastatic to the breast. Cancer 1972;29:1691-1696.
31. Insabato L, Russo R, Cascone AM, Angrisani P. Fine needle aspiration cytology of lipid-secreting breast carcinoma. A case report. Acta Cytol 1993;37:752-755.
32. Jaffer S, Reid-Nicholson M, Bleiweiss IJ. Infiltrating micropapillary carcinoma of the breast. Cytologic findings. Acta Cytol 2002;46:1081-1087.
33. Jayaram G, Jayalakshmi P, Yip CH. Leiomyosarcoma of the breast. Acta cytol 2005;49:656-660.
34. Jayaram G, Swain M, Chew MT, Yip CH. Cytologic appearances in invasive lobular carcinoma of the breast. A study of 21 cases. Acta Cytol 2000;44:169-174.
35. Joshi A, Kumar N, Verma K. Diagnostic challenge of lobular carcinoma on aspiration cytology. Diagn Cytopathol 1998;18:179-183.
36. Kajo K, Machalekova K, Kviatkovska Z. Mammary carcinoma with osteoclastic-like giant cells - report of two cases. Cesk Patol 2006;42:71-75
37. Kato T, Tohnosu N, Suwa T, et al. Metaplastic breast carcinoma with chondrosarcomatous differentiation: fine needle aspiration cytology findings. A case report. Diagn Cytopathol 2006;34:772-775.
38. Kaufmann O, Deidesheimer T, Muehlenberg M, et al. Immunohistochemical differentiation of metastatic breast carcinomas from adenocarcinomas of other common primary sites. Histopathology 1996;29:23-240.
39. Kiyozuka Y, Koyama H, Nakata M, et al. Diagnostic cytopathology in type II angiosarcoma of the breast: a case report. Acta Cytol 2005;49:560-566.
40. Kleer CG, Michael CW. Fine needle aspiration of breast carcinomas with prominent lymphocytic infiltrate. Diagn Cytopathol 2000;23:39-42.
41. Lapey JD. Lipid-rich mammary carcinoma – diagnosis by cytology. case report. Acta Cytol 1977;21:120-122.
42. Lerwill MF. Current practical applications of diagnostic immunohistochemistry in breast pathology. Am J Surg Pathol 2004;28:1076-1091.
43. Lin X, Saad RS, Luckasevic TM, Silverman Jf, Liu Y. Diagnostic value of CDX-2 and TTF-1 expressions in separating metastatic neuroendocrine neoplasms of unknown origin. Appl Immunohistochem Mol Morphol 2007;15:407-414.
44. Liu K, Layfield LJ. Cytomorphologic features of angiosarcoma on fine needle aspiration biopsy. Acta Cytol 1999;43:407-415.
45. Logrone R, Kurtycz JE, Inhorn SL. Criteria for reporting fine needle aspiration on palpable and nonpalpable masses of the breast. Acta cytol 1997;41:623-627.
46. Lopez-Rios F, Alberti N, Perez-Barrios A, et al. Aspiration biopsy of pleomorphic lipoma of the breast. A case report. Acta Cytol 2000;44:255-258.
47. Lui PC, Tse GM, Tan PH, et al. Fine needle aspiration cytology of metaplastic carcinoma of the breast. Clin Pathol 2007;60:529-533.
48. Madur B, Shet T, Chinoy R. Cytologic findings in infiltrating micropapillary carcinoma and mucinous carcinomas with micropapillary pattern. Acta Cytol 2007;51:25-32.
49. Mardi K, Sharma J. A rare case of secretory breast carcinoma in an elderly woman: correlation of aspiration cytology and histology. Indian J Pathol Microbiol 2007;50:865-867.
50. Mardi K, Sharma J. Fine needle aspiration cytology of breast carcinoma with neuroendocrine features – a case report with histopathological and immunohistochemical correlation. Indian J Pathol Microbiol 2007;50:65-68.
51. Matsuo K, Fukutomi T, Hasegawa T, et al. Histological and immunohistological analysis of apocrine breast carcinoma. Breast Cancer 2002;9:43-49.
52. Maygarden SJ, Brock MS, Novotny DB. Are epithelial cells in fat or connective tissue a reliable indicator of tumor invasion in fine needle aspiration of the breast? Diagn Cytopathol 1997;16:137-142.
53. McCluggage WG, Sargent A, Bailey A, Wilson GE. Large cell neuroendocrine carcinoma of the uterine cervix exhibiting TTF-1 immunoreactivity. Histopathology 2007;51:405-407.
54. McKee GT, Tambouret RH, Finkelstein D. Fine needle aspiration cytology of the breast: Invasive vs. in situ carcinoma. Diagn Cytopathol 2001;25:73-77.
55. Mecca P, Busam K. Primary male neuroendocrine adenocarcinoma involving the nipple simulating Merkel cell carcinoma – a diagnostic pitfall. J Cutan Pathol 2008;35:207-211.
56. Medina-Franco H, Gamboa-Dominguez A, de la Medina AR. Malignant peripheral nerve sheath tumor of the breast. Breast J 2003;9:332.
57. Menet E, Becette V, Briffod M. Cytologic diagnosis of lobular carcinoma of the breast: Experience with 555 patients in the Rene Huguenin Cancer Center. Cancer 2008;114:111-117.
58. Milde S, Gaedcke J, v Wasielewski R, et al. Diagnosis and immunohistochemistry of medullary breast cancer. Patholoqe 2006;27:358-362.
59. Miura H, Konaka C, Kawate N, et al. Fine needle aspiration cytology of metastatic breast tumor originating from leukemia. Diagn Cytopathol 1992;8:605-608.
60. Moinfar F. Essentials of diagnostic breast pathology. A practical approach. Springer-Verlag Berlin Heidelberg 2007.
61. Mondal A, Mukherjee PK. Diagnosis of malignant neoplasms of male breast by fine needle aspiration cytology. Indian J Pathol Microbiol 1994;37:263-268.
62. Ng WK, Ip P, Choy C, Collins RJ. Cytologic and immunocytochemical findings of anaplastic large cell lymphoma: analysis of ten fine-needle aspiration specimens over a 9-year period. Cancer 2003;99:33-43.
63. Ngu IW, Sinclair EC, Greenaway S, Greenberg ML. Unusual presentation of granulocytic sarcoma in the breast: a case report and review of the literature. Diagn Cytopathol 2001;24:53-57.
64. O'Malley FP, Bane A. An update on apocrine lesions of the breast. Histopathology 2008;52:3-10.
65. Page DL, Johnson JE, Dupont WD. Probalistic approach to the reporting of fine needle aspiration cytology of the breast. Cancer(Cancer Cytopathol) 1997;81:6-9.
66. Peintinger F, Leibl S, Reitsamer R, Moinfar F. Primary acinic cell carcinoma of the breast: a case report with long-term follow-up and review of literature. Histopathology 2004;45:645-648.

67. Pereira EM, Maeda SA, Reis-Filho JS. Sarcomatoid variant of anaplastic large cell lymphoma mimicking a primary breast cancer: a challenging diagnosis. Arch Path Lab Med 2002;126:723-726.
68. Peterse JL, Koolman-Schellekens Mieke A, van de Peppel-va de Ham T, et al. Atypia in fine needle aspiration cytology of the breast: A histologic follow-up study in 301 cases. Seminars in Diagnostic Pathology 1989;6:126-134.
69. Pettinato G, De Chiara A, Insabato L, De Renzo A. Fine needle aspiration biopsy of a granulocytic sarcoma (chloroma) of the breast. Acta Cytol 1988;32:67-71.
70. Pettinato G, Insabato L, De Chiara A, et al. High-grade mucoepidermoid carcinoma of the breast. Fine needle aspiration cytology and clinicopathologic study of a case. Acta Cytol 1989;33:195-200.
71. Pettinato G, Manivel JC, Petrella G, De Chiara A. Primary multilobated T-cell lymphoma of the breast diagnosed by fine-needle aspiration cytology and immunocytochemistry. Acta Cytol 1991;35:294-299.
72. Pettinato G, Pambuccian SE, Di Prisco B, Manivel JC. Fine needle aspiration cytology of invasive micropapillary (pseudopapillary) carcinoma of the breast. Report of 11 cases with clinicopathologic findings. Acta Cytol 2002;46:1088-1094.
73. Quinodoz IS, Berger SD, Schafer P, Remadi S. Adenoid cystic carcinoma of the breast: utility of immunocytochemical study with collagen IV on fine-needle aspiration. Diagn Cytopathol 1997;16:442-445.
74. Racz MM, Pommier RF, Troxell ML. Fine needle aspiration cytology of medullary breast carcinoma: report of two cases and review of the literature with emphasis on differential diagnosis. Diagn Cytopathol 2007;35:313-318.
75. Rajesh L, Dey P, Joshi K. Fine needle aspiration cytology of lobular breast carcinoma. Comparison with other breast lesions. Acta Cytol 2003;47:177-182.
76. Reid-Nicholson MD, Tong G, Cangiarella JF, Moreira AL Cytomorphologic features of papillary lesions of the male breast: a Study of 11 cases. Cancer 2006;108:222-230.
77. Rousselot C, Tourasse C, Samimi M, et al. Breast pilomatrixoma manifested as microcalcifications on mammography: report of two cases. J Radiol 2007;88:978-980.
78. Sadler GP, McGee S, Dallimore NS, et al. Role of fine-needle aspiration cytology and needle-core biopsy in the diagnosis of lobular carcinoma of the breast. Brit J of Surgery 1994;81:1315-1317.
79. Saqi A, Mercado CL, Hamele-Bena D. Adenoid cystic carcinoma of the breast diagnosed by fine needle aspiration. Diagn Cytopathol 2004;30:271-274.
80. Satoh F, Umemura S, Itoh H, et al. Fine needle aspiration cytology of glycogen-rich clear cell carcinoma of the breast. A case report. Acta Cytol 1998;42:413-418.
81. Sauer T. Cytologic findings in malignant myoepithelioma: a case report and review of the literature. Cytojournal 2007;4:3.
82. Sauer T, Garred O, Lomo J, Naess O. Assessing invasion criteria in fine needle aspirates from breast carcinoma diagnosed as DCIS or invasive carcinoma: can we identify an invasive component in addition to DCIS? Acta cytol 2006;50:263-270.
83. Sauer T, Lomo J, Garred O, Naess O. Cytologic features of ductal carcinoma in situ in fine-needle aspiration of the breast mirror the histopathologic growth pattern heterogeneity and grading. Cancer 2005;105:21-27.
84. Sauer T, Young K, Thoresen SO. Fine needle aspiration cytology in the work-up of mammographic and ultrasonographic findings in breast cancer screening: an attempt at differentiating in situ and invasive carcinoma. Cytopathology 2002;13:101-110.
85. Sharma P, Jain S, Nigam S, et al. Malignant fibrous histiocytoma of the chest wall masquerading as medullary breast carcinoma: a case report. Acta Cytol 2006;50:577-580.
86. Shinagawa T, Tadokoro M, Kitamura H, et al. Secretory carcinoma of the breast. Correlation of aspiration cytology and histology. Acta Cytol 1994;38:909-914.
87. Silverberg SG, Kay S, Chitale AR, et al. Colloid carcinoma of the breast. Am J Clin Pathol 1971;55:355-363.
88. Silverman JF, Feldman PS, Covell JL, Frable WJ. Fine needle aspiration cytology of neoplasms metastatic to the breast. Acta Cytol 1987;31:291-300.
89. Silverman JF, Geisinger KR, Frable WJ. Fine needle aspiration cytology of mesenchymal tumors of the breast. Diagn Cytopathol 1988;4:50-58.
90. Silverman JF, Geisinger KR, Park HK, et al. Fine needle aspiration cytology of granulocytic sarcoma and myeloid metaplasia. Diagn Cytopathol 1990;6:106-111.
91. Singh NG, Kapila K, Dawar R, Verma K. Fine needle aspiration cytology diagnosis of lymphoproliferative disease of the breast. Acta Cytol 2003;47:739-743.
92. Sivakumar S. Pilomatrixoma as a diagnostic pitfall in fine needle aspiration cytology: a case report. Acta Cytol 2007;51:583-585.
93. Staklenac B,Pauzar B, Pajtler M, et al. An unusual tumor of the breast: cytological findings in a malignant schwannoma, epithelioid variant. Cytopathology 2004;15:160-162.
94. Stanley MW, Tani EM, Rutquist LE, Skoog L. Adenoid cystic carcinoma of the breast: diagnosis by fine needle aspiration. Diagn Cytopathol 1993;9:184-187.
95. Tavassoli FA. Pathology of the Breast, 2th edition, Appleton &Lange,Stamford Connecticut. 1999.
96. Terada T, Sato Y, Furukawa K, Sugiura M. Primary cutaneous mucinous carcinoma initially diagnosed as metastatic adenocarcinoma. Tohoku J Exp Med 2004;203:345-348.
97. Theocharous C, Greenberg ML. Cytologic features of ductal carcinoma in situ. Diagn Cytopathol 1996;15:367-373.
98. Topalovski M, Crisan D, Mattson JC. Lymphoma of the breast. A clinicopathologic study of primary and secondary cases. Arch Pathol Lab Med 1999;123:1208-1218.
99. Tosoni I, Zoebeli L, Spieler P, et al. Myoepithelial tumors of the breast. Schweiz Med Wochenschr 1997;127:1767.
100. Trihia H, Valavanis C, Markidou S, et al. Primary osteogenic sarcoma of the breast: cytomorphologic study of 3 cases with histologic correlation. Acta cytol 2007;51:443-450.
101. Ustün M, Berner A, Davidson B, Risberg B. Fine needle aspiration cytology of lobular carcinoma in situ. Diagn Cytopathol 2002;27:22-26.
102. Ventura K, Cangiarella J, Lee I, et al. Aspiration biopsy of mammary lesions with abundant extracellular mucinous material. Review of 43 cases with surgical follow-up. Am J Clin Pathol 2003;120:194-202.
103. Vicandi B, Jimenez-Heffernan JA, Lopez-Ferrer P, et al. Fine needle aspiration cytology of mammary carcinoma with osteoclast-like giant cells. Cytopathology 2004;15:321-325.
104. Wang HH, Ducatman BS. Fine needle aspiration of the breast. A probabilistic approach to diagnosis of carcinoma. Acta Cytol 1998;42:285-289.
105. Wong NL, Wan SK. Comparative cytology of mucocele-like lesion and mucinous carcinoma of the breast in fine needle aspiration. Acta Cytol 2000;44:765-770.

1

**Figs. 1.66–1.71 Infiltrating ductal breast carcinoma of the common type.**
Characteristic cytoarchitecture and cytomorphology of breast carcinoma is demonstrated using different preparation and staining techniques on fine needle aspirates.

**Fig. 1.66A–C** (case #1) Malignant cell clusters: Varying cytoarchitecture using different methodologies. **A** Conventional smearing and Pap staining convincingly shows:
– peculiar shape and partially well-defined delineation of a malignant three-dimensional cell cluster (arrows).
– single-file cellular arrangement (arrowhead) (high magnification).
**B** Air-dried smear and Diff-Quik method gives a better impression of nuclear polymorphism and cytoplasmic features (high magnification). **C** Liquid-based preparation (ThinPrep) usually provides altered cytoarchitecture and cellular shrinkage, causing diagnostic problems or leading to a false-negative diagnosis (lower magnification).

**Fig. 1.67A, B** (case #2) Cellular details of carcinoma cells are presented at high magnification in direct smear and liquid-based preparations. Both specimens are Pap-stained. **A** A conventional smear exhibits the classical cytoarchitectural, nuclear and cytoplasmic features of breast carcinoma (see Table 1.3.1, p. 57). **B** In the ThinPrep specimen, nuclear irregularities such as cleaving, molding, and grooves appear less distinct (due to nuclear shrinking), and nucleoli appear enlarged.

**Fig. 1.68** (case #3) Another fine-needle aspirate of a breast carcinoma has been processed using the the ThinPrep technique. The picture shows well-preserved structural details of loosely aggregated and dispersed carcinoma cells (high magnification)

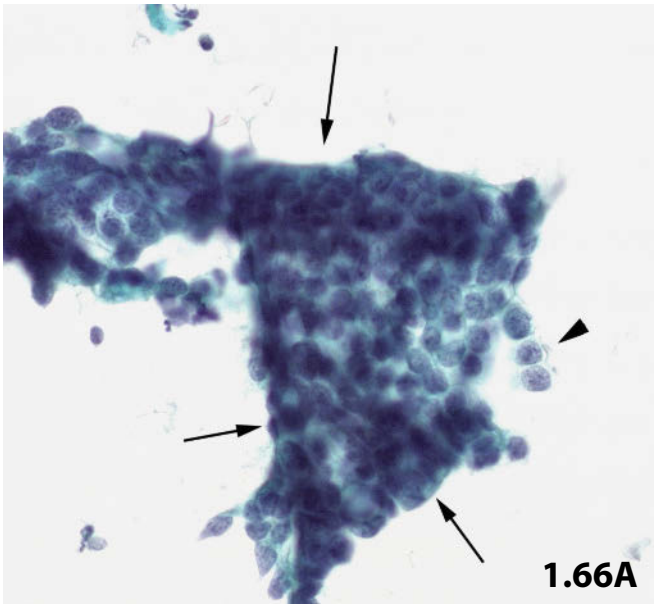
1.66A

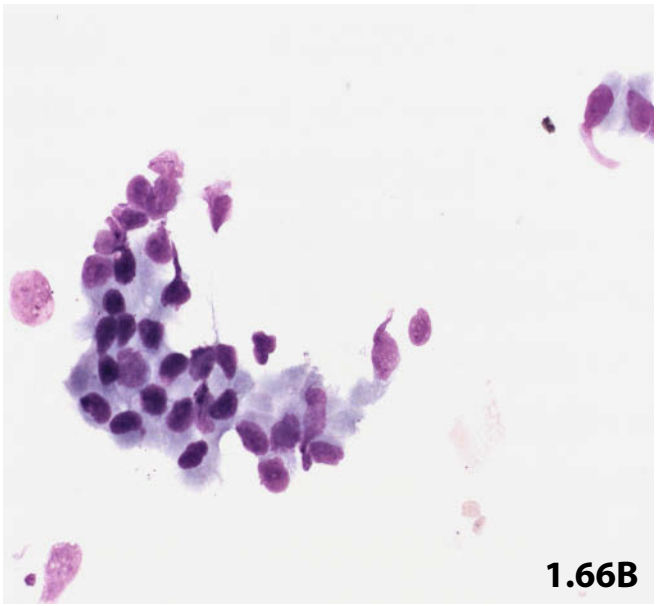
1.66B

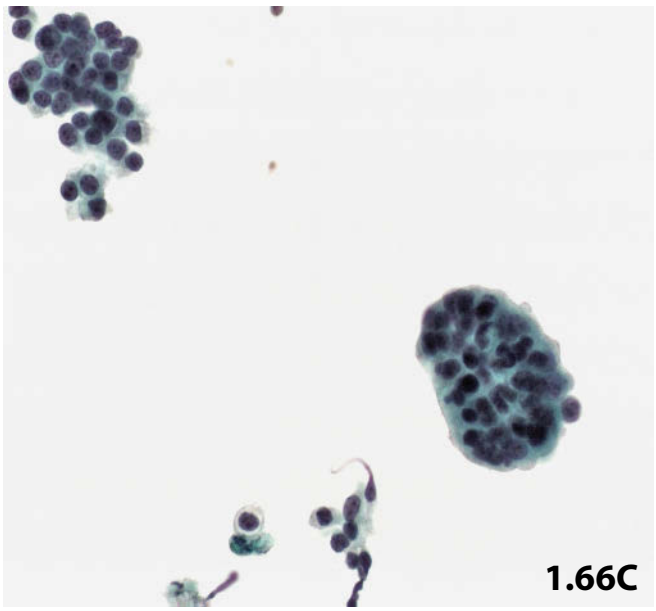
1.66C

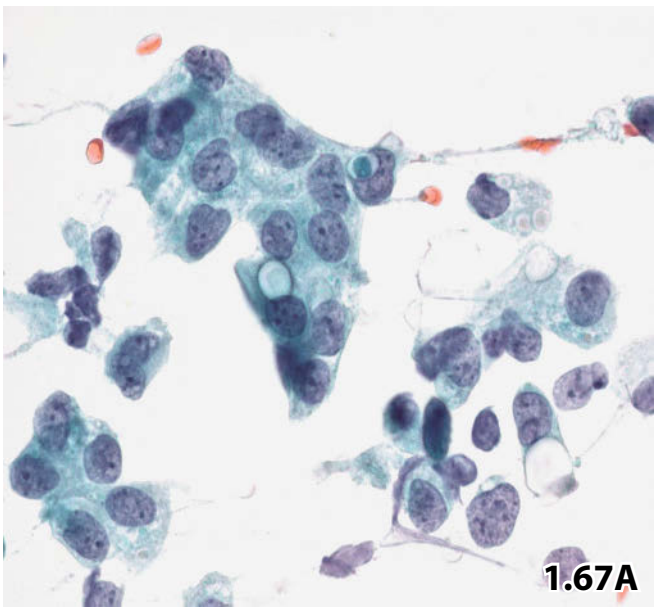
1.67A

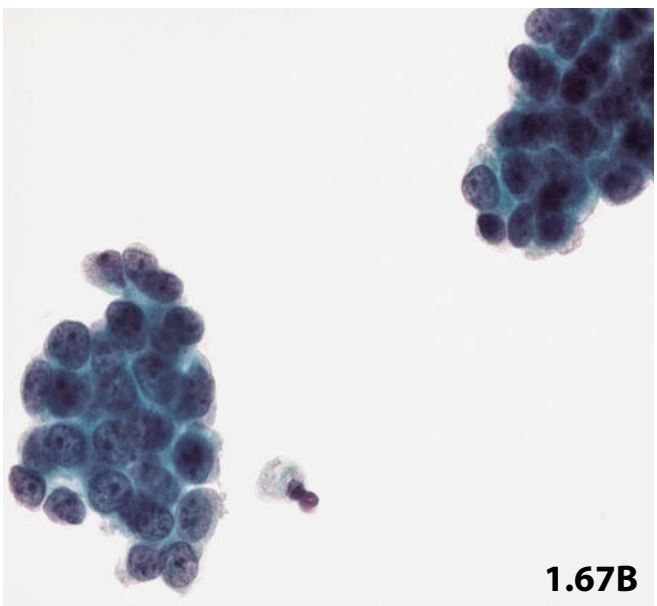
1.67B

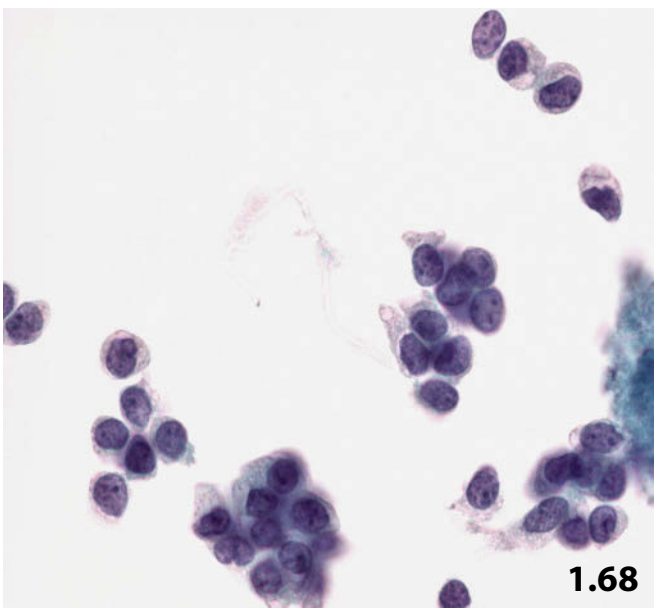
1.68

**Fig. 1.69** (case #4) The three most characteristic variants of malignant cell clusters occurring in conventional smears from breast carcinoma are presented (low magnification, Pap stain):
- Shoe-shaped structure (lower left);
- Gland-like cell arrangements (center);
- Single-file rows (upper right).

**Fig. 1.70** (case #5) FNAB of a breast carcinoma. Conventional smear (Pap stain) solely composed of isolated carcinoma cells showing distinct plasmacytoid features. Note both eccentric rounded nuclei and triangular cytoplasmic shape (high magnification).

**Fig. 1.71** (case #6) Detail of an aspirate specimen (Pap stain) shows nuclear clearing (arrows) of the tumor cells and fragile cytoplasm. Chromatin clearing is a typical nuclear feature of breast carcinoma.

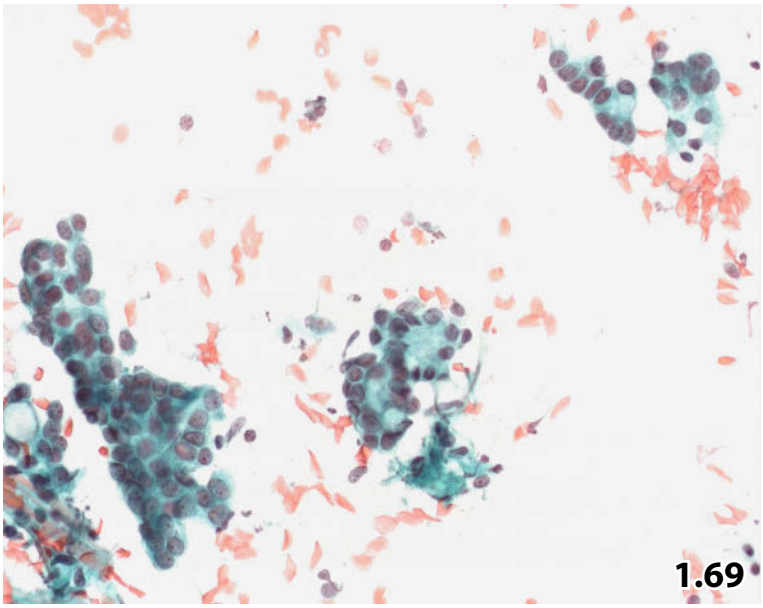
1.69

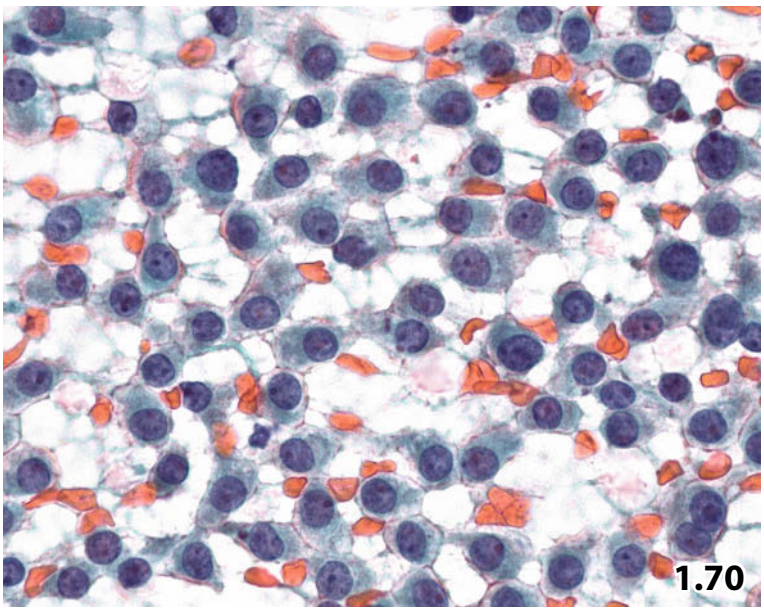
1.70

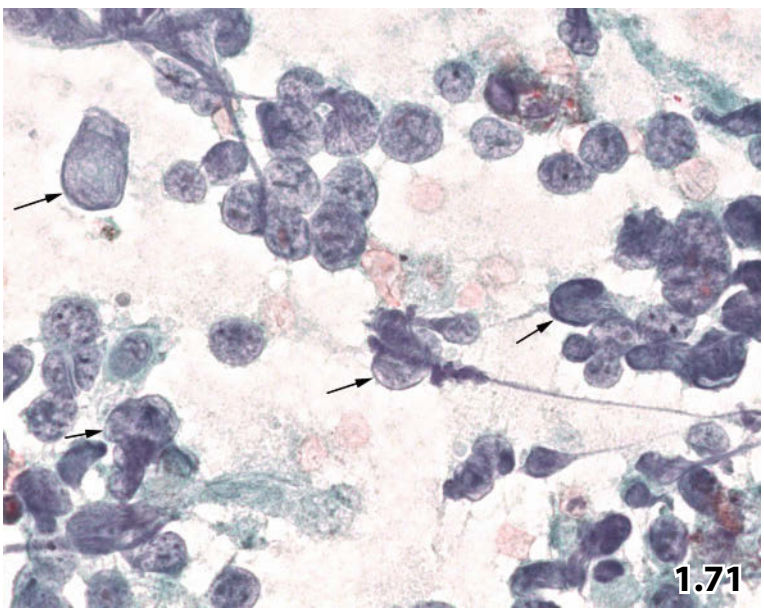
1.71

**Figs. 1.72–1.75 Infiltrating ductal breast carcinoma of the monomorphic small-cell type.**
Morphologic key features are shown in FNABs of primary breast lesions and of a metastatic cancer.

**Fig. 1.72** (case #1) FNAB of a tumor mass in a 61-year-old man's breast. Lower magnification demonstrates clusters of a small-cell breast carcinoma composed of a monotonous small-tumor-cell population. Both clusters and single cells exhibit the characteristic features of malignant transformation. Note the presence of microcalcification on the right (conventional smear, Pap stain).

**Fig. 1.73** (case #2) A female breast carcinoma composed of extremely small tumor cells. The low magnification shows monomorphic neoplastic cells lacking conclusive malignant features at first glance. However, the homogeneity of the cell population, cellular arrangement in rows, eccentric nuclei and nuclear clearing indicate malignancy (conventional specimen, Pap stain, lower magnification).

**Fig. 1.74** (case #3) A second example of breast carcinoma composed of small tumor cells. Detail shows several morphologic properties indicating malignancy such as cellular arrangement in rows, focally sharply outlined cell clusters, loss of nuclear polarization, nuclear clearing, eccentric nuclei, occasional low N/C ratio, and psammoma body (top) (direct smear, Pap stain).

In cases of small (monomorphic) cell breast carcinoma, diagnosis of malignancy is based upon cytologic smears rich in tumor cells in combination with careful cytologic evaluation regarding definitive signs of malignancy.

**Fig. 1.75A, B** (case #4) FNAB of an enlarged axillary lymph node in a female patient suffering from a breast carcinoma of the small-cell type. **A** The small uniform tumor cells may mimic both lymphocytes and cells from other (metastatic) small-cell neoplasms (lower magnification):
- Note indicators for small-cell carcinoma: compact cell ball (bottom right), rows of small cells (arrows), and immunoreactivity for MNF-116 (see Fig. 1.75B).
- Note specific indicators for breast carcinoma: dense finely granular chromatin, nuclear clearing, and cytoplasmic vacuoles (arrowhead).

**B** Immunoreactivity for pancytokeratin MNF-116 (Pap-prestained ThinPrep specimen) excludes lymphoid cells.

**Fig. 1.76 Breast carcinoma of the large-cell type.**
A ThinPrep specimen contains a cell population of large carcinoma cells. Nuclei exhibit macronucleoli and coarse clumping chromatin, unlike breast carcinomas consisting of common or small tumor cells (FNAB, Pap stain, high magnification).

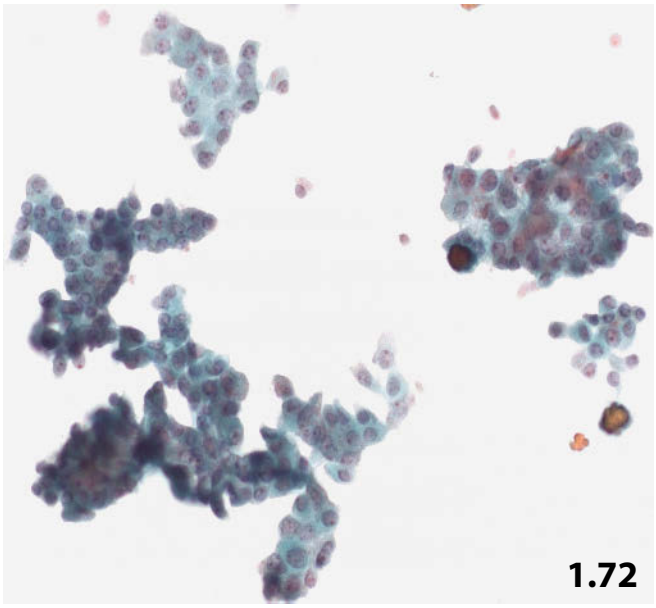
1.72

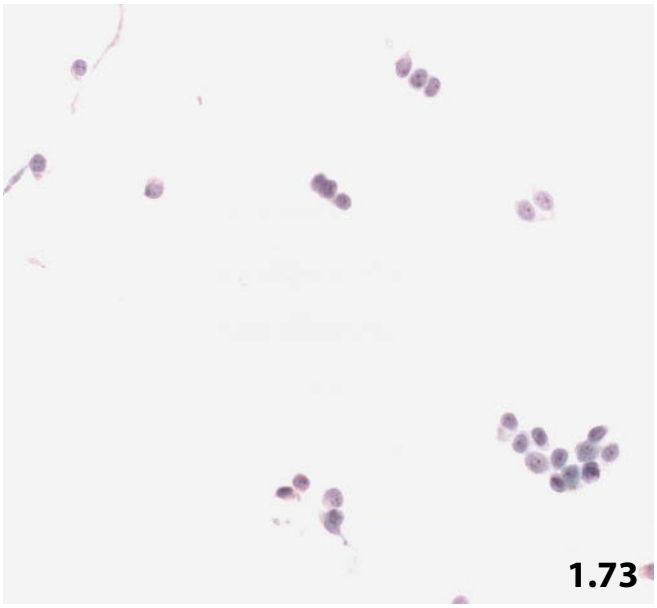
1.73

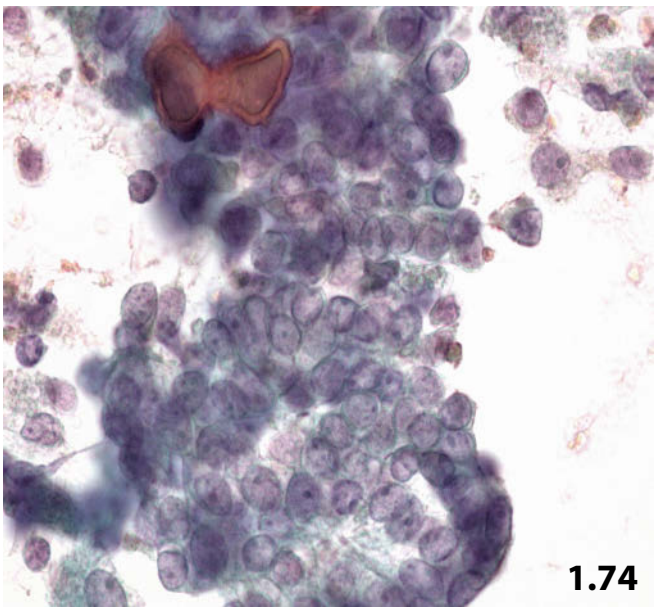
1.74

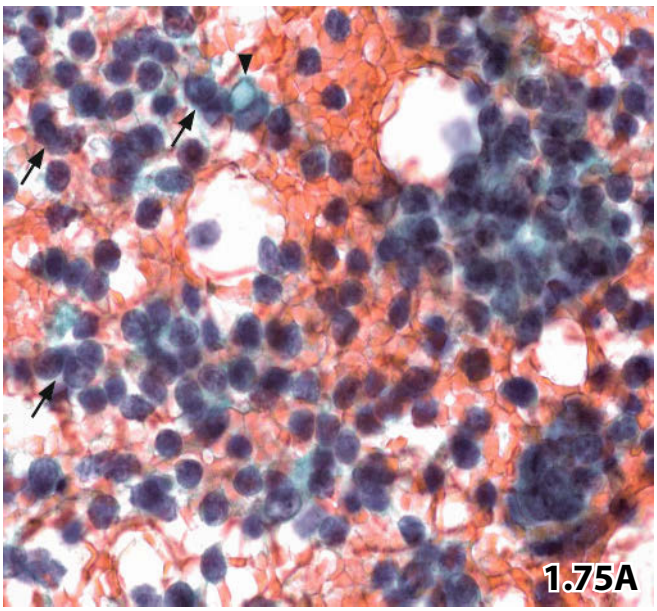
1.75A

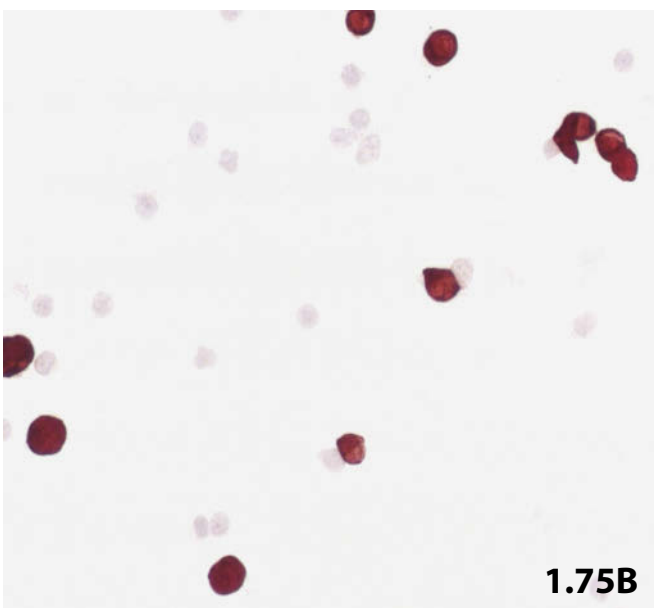
1.75B

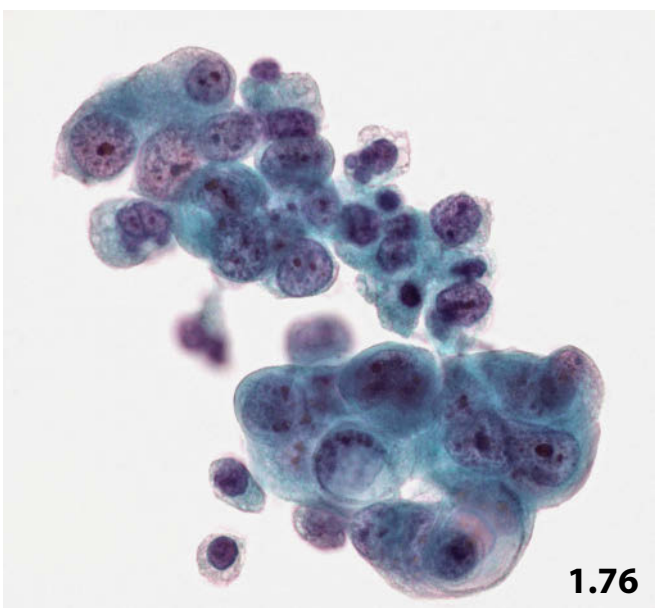
1.76

1

**Figs. 1.77 and 1.78 Infiltrating lobular carcinoma.**
Cytologic key features of invasive lobular carcinomas of the breast are highlighted in aspirates from two patients. Direct smears were Pap-stained.

**Fig. 1.77** (case #1) Numerous isolated tumor cells: the cell population is devoid of a myoepithelial component. The overall cell pattern is monotonous in appearance. Note finely dispersed chromatin, nuclear clearing, distinct nuclear irregularities, indistinct nucleoli, intracytoplasmic vacuoles, and plasmacytoid features (low magnification).

**Fig. 1.78** (case #2) Both loosely cohesive and compact clusters exhibiting characteristic features including sharp demarcation and single-file cell arrangement. Many of the cells show intracytoplasmic vacuoles occasionally containing pink-stained mucus (low magnification). Examples of target-like cytoplasmic inclusions (targetoid cells) are shown in Fig. 1.67A.

**Figs. 1.79 and 1.80 Low-grade ductal intraepithelial neoplasia (low-grade DCIS/DIN).**

**Fig. 1.79** Low grade ductal intraepithelial neoplasia is characterized by a monotonous cell population. Cells are usually arranged in large cohesive clusters, but very low magnification exhibits loss of nuclear polarity and isolated cells with eccentrically positioned nuclei (arrows) (FNAB, direct smear, Pap stain).

**Fig. 1.80** Higher magnification shows a very uniform epithelial cell population. The absence of myoepithelial cells, loss of polarization, nuclear overlapping, and dissociating cells with eccentric nuclei are suggestive of a low-grade neoplasia (low-grade DCIS or low-grade invasive carcinoma) (FNAB, direct smear, Pap stain).

One needs to keep in mind that the monotony or homogeneity of an epithelial cell population (lack of a myoepithelial cell component) comprising subtle nuclear atypia is suspicious of malignancy. One has to examine the smear preparation(s) carefully in order to establish the malignancy-characteristic nuclear outline (wrinkling, molding, and partial loss of the membrane).

As a rule, cytology cannot distinguish between DIN and invasive carcinoma. In individual cases, however, specific morphologic features may differentiate DIN from invasive neoplasia.

**Fig. 1.81 High-grade ductal intraepithelial neoplasia (high-grade DCIS/ DIN)**
Example of a high-grade ductal intraepithelial neoplasia. In general, features of clusters and single cells are the same as described for infiltrating ductal carcinoma. The background with apoptotic bodies, necrosis, and inflammation (upper right) is consistent with comedo-type DCIS (or invasive necrotic carcinoma). (FNAB, direct smear, Pap stain).

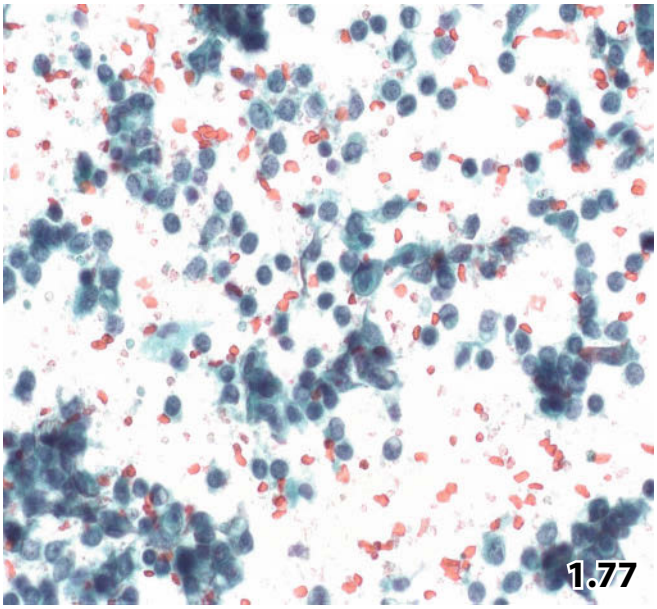
1.77

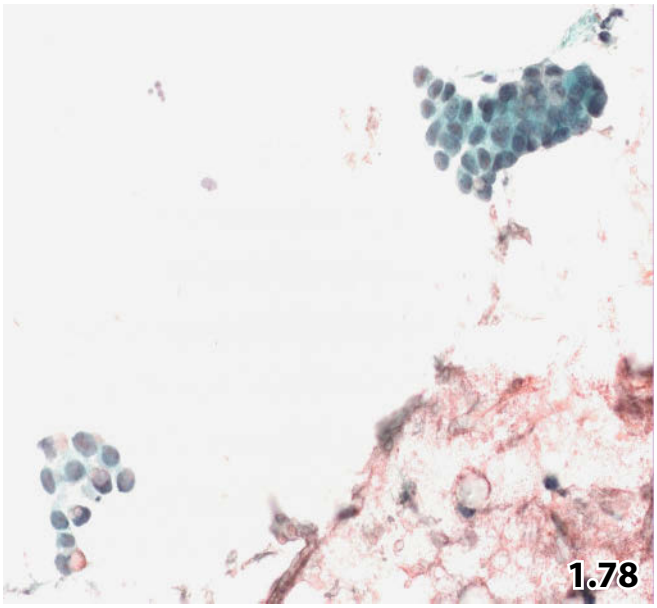
1.78

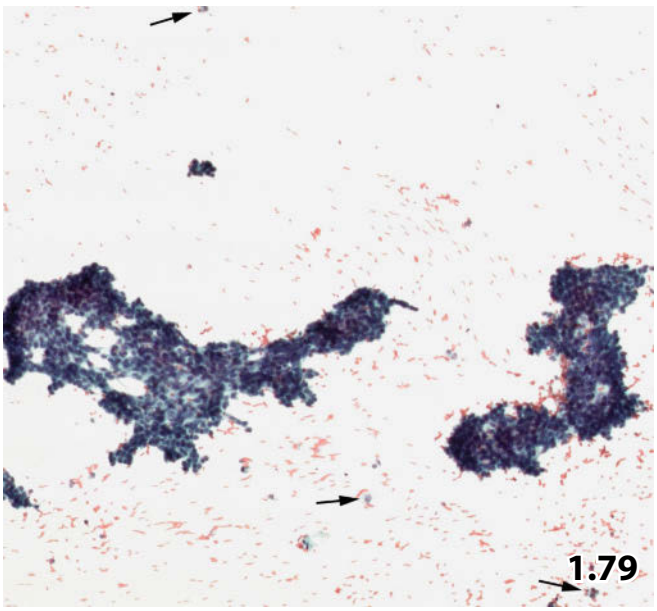
1.79

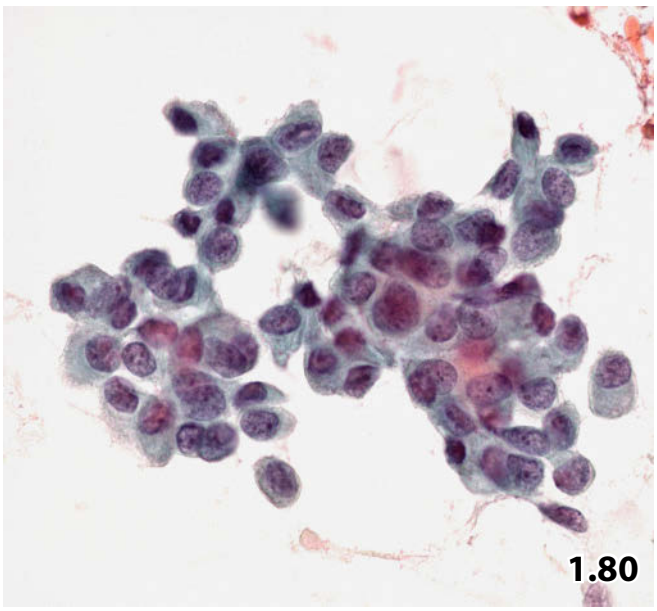
1.80

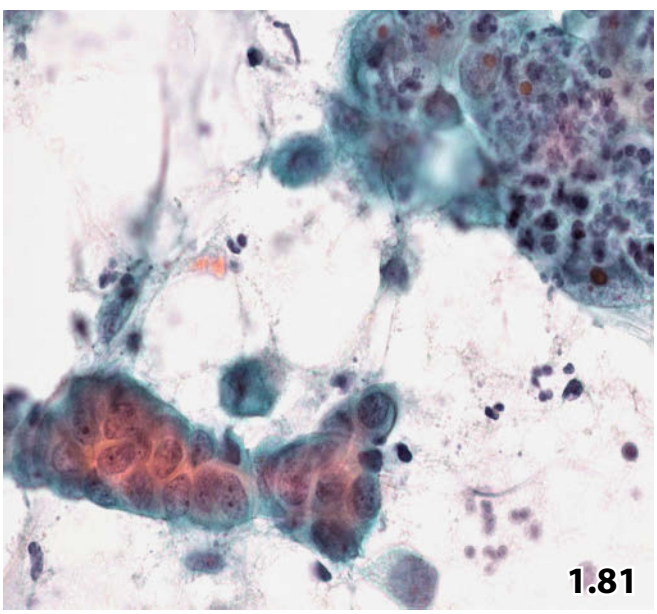
1.81

**Fig. 1.82A, B Tubular carcinoma.**
A 49-year-old woman presented with a palpable lesion in her left breast. FNAB was performed, direct smears were Pap-stained.
*Cytologic diagnosis:* low-grade (monomorphous type) breast carcinoma, most likely tubular variant.
*Histology:* tubular carcinoma was verified by subsequent histologic examination of the excised tumor mass**.**
**A** Numerous three-dimensional clusters containing tubules are encountered at low magnification. The population of small tumor cells appear monomorphic and monophasic, suggesting malignancy; the isolated cells show eccentric nuclei. **B** High magnification shows signs of nuclear malignancy including mild irregularity in size and shape, finely granular chromatin, and distinct nuclear clearing (yet only scarce irregularities of the nuclear outline!). Note the impressive presentation of the nuclei in a three-dimensional ballooned fashion, and the shift of chromatin to one side of the nucleus. Myoepithelial cells are absent.

**Fig. 1.83 Well-differentiated papillary carcinoma.**
A 46-year-old woman presented with a small lesion (< 1cm in diameter) in the recessus axillaris of her left breast. FNAB was performed. Direct smears were Pap-stained . The low magnification shows a branching papillary cluster composed of uniform cuboidal to columnar cells with evidently bland nuclei. A marginal palisading of columnar cells is seen (arrowheads). A fibrovascular core is present but not always in focus (arrows). It is difficult to determine whether the small dark nuclei belong to apoptotic epithelial cells or are of myoepithelial origin. (For comparison see also Figs. 1.49, 1.50, 1.51: benign intracystic/intraductal papillomas).
*Tentative cytologic diagnosis:* the cytologic differential diagnosis includes papilloma and well-differentiated intraductal papillary carcinoma. A conclusive cytologic diagnosis is not possible.
*Tissue diagnosis* (excisional biopsy): low-grade intraductal papillary carcinoma.

**Fig. 1.84A, B High-grade papillary carcinoma.**
A 44-year-old woman presented a sanguineous nipple discharge of short duration. A deep-seated lesion was detected by sonography and examined by ultrasound-guided FNAB. Direct smears were Pap-stained.
*Cytologic diagnosis:* poorly differentiated papillary carcinoma (verified by excisional biopsy).
**A** Low magnification showing a classical papillary cluster composed of a fibrovascular core and palisading columnar cells. The papillary fragment and the smaller papilliform clusters (absent fibrovascular core, lower left) exhibit irregular arrangement of the epithelial cells, nuclear overlapping, nuclear polymorphism, and a high N/C ratio. **B** High magnification displays highly atypical/ malignant epithelial cells.

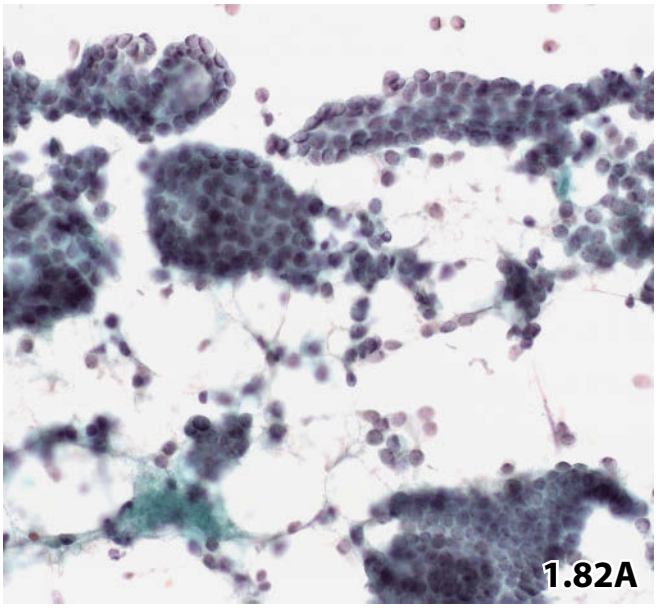
1.82A

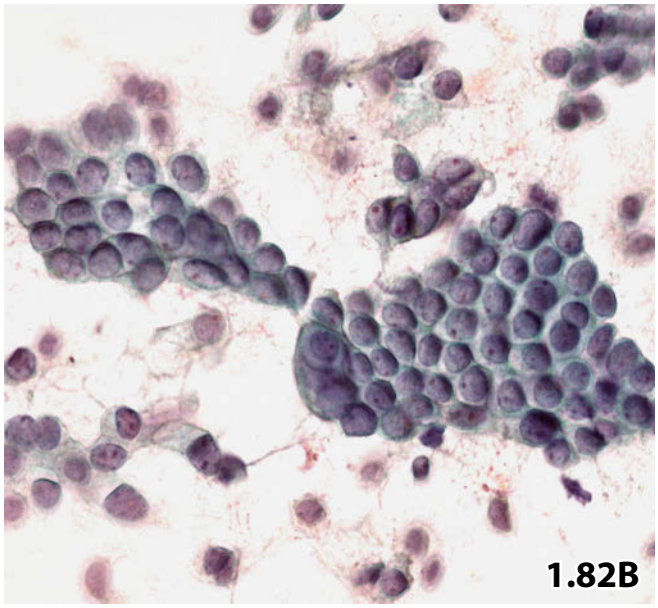
1.82B

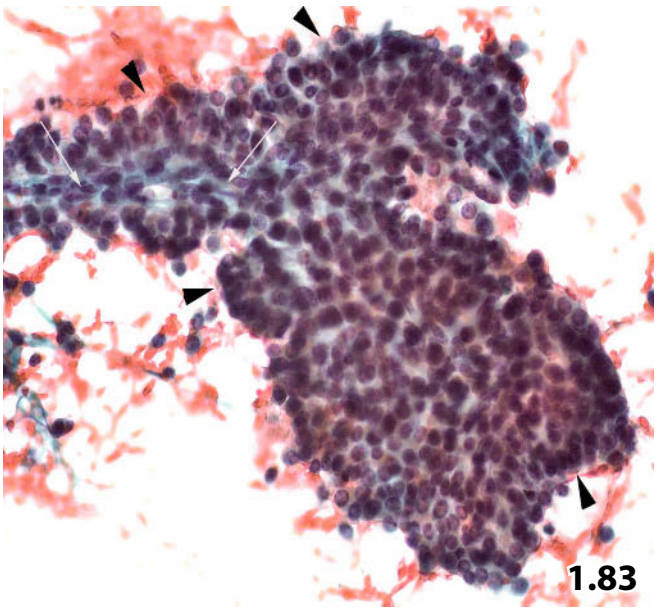
1.83

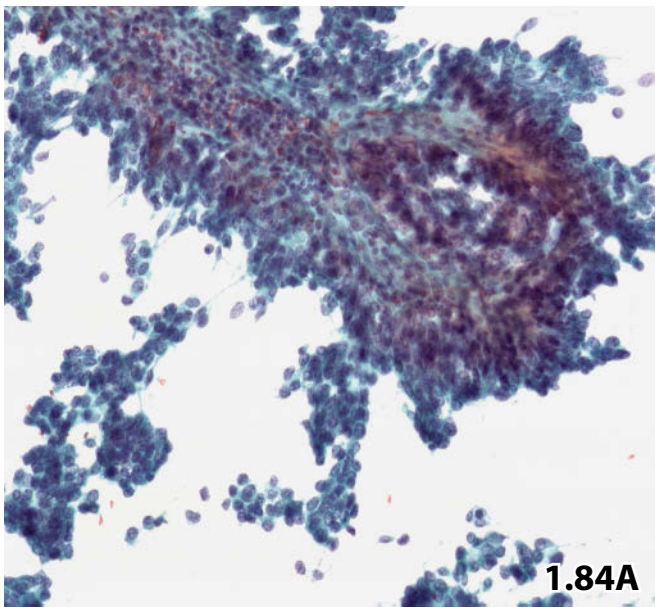
1.84A

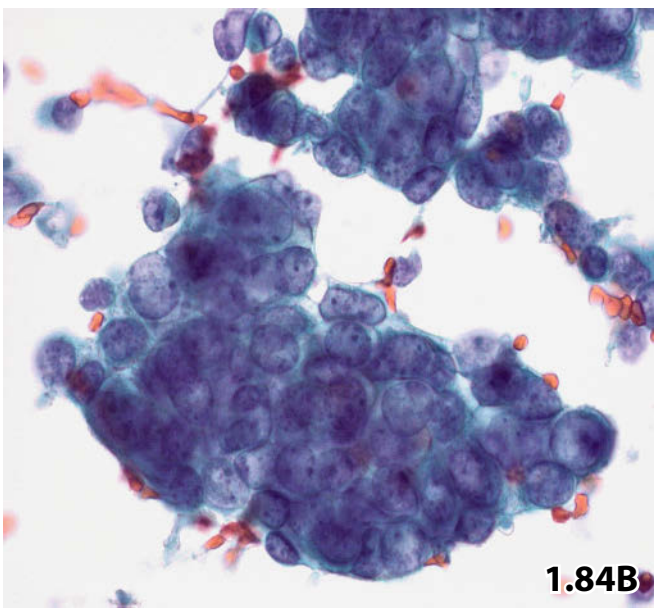
1.84B

1

**Figs. 1.85 and 1.86 Mucinous carcinoma.**
Two examples of a mucinous breast carcinoma. Both women presented with a palpable nodular breast lesion clinically suggestive of carcinoma. FNABs were performed and direct smears were prepared (Pap stain).

**Fig. 1.85** (case #1) Low magnification shows a background of abundant thick (usually concentrically structured) mucinous material interspersed with numerous cohesive three-dimensional epithelial clusters.

**Fig. 1.86** (case #2) High magnification of an epithelial cluster reveals a homogeneous population of small and medium-sized cells. Single tumor cells are available (not depicted), while bare bipolar nuclei (myoepithelial cells) are absent. Note nuclear overlapping, dense granular and coarse chromatin, and occasional highly irregular nuclear contours (arrow).

**Figs. 1.87 and 1.88 Medullary carcinoma.**
FNAB of medullary carcinoma usually provides highly cellular smears. An example exhibits the characteristic cytologic features of this tumor entity.

**Fig. 1.87** Large malignant cells are mainly arranged in syncytial sheets, cytoplasmic borders are ill defined. The pleomorphic and hyperchromatic nuclei contain very prominent nucleoli. The background contains numerous small lymphocytes (direct smear, Pap stain, high magnification).

**Fig. 1.88** The typically admixture of lymphocytes and carcinoma cells is visualized best by immunocytochemical staining using leukocytic marker CD45.

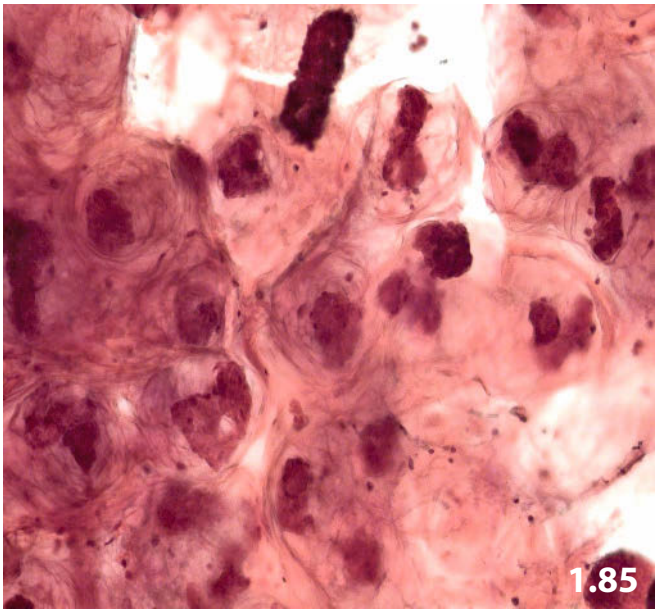
1.85

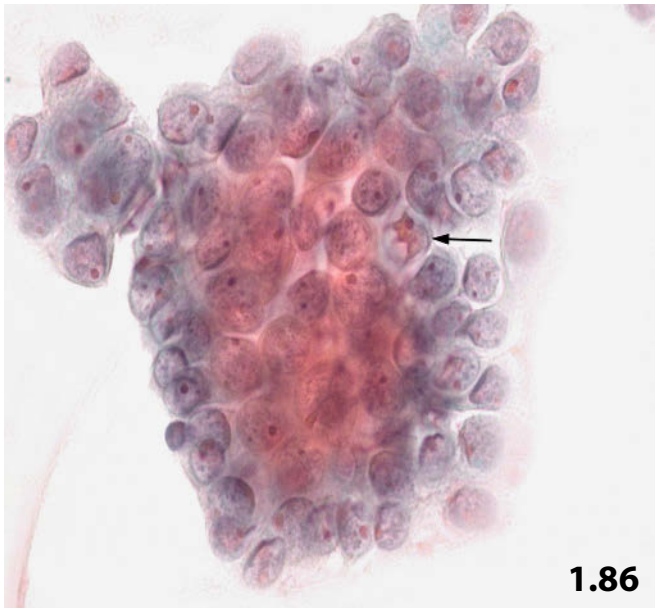
1.86

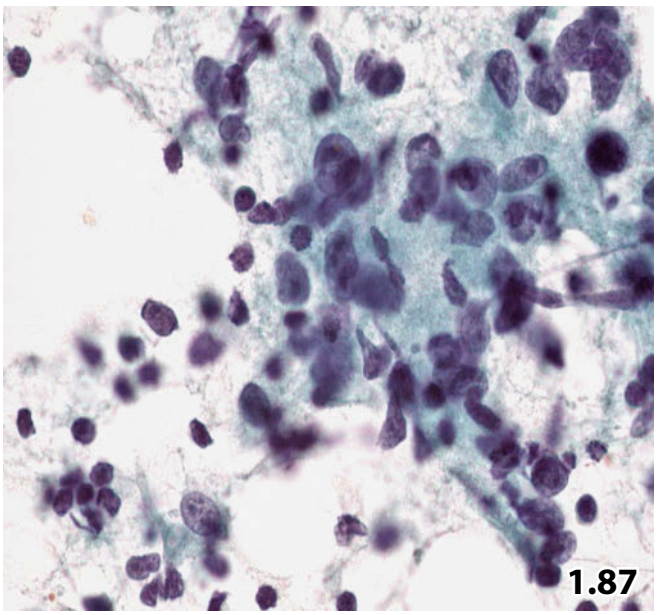
1.87

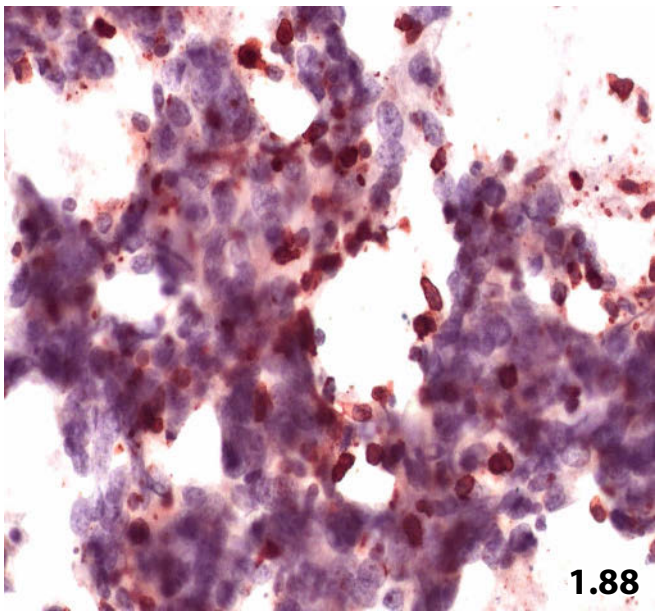
1.88

1

**Fig. 1.89 Apocrine carcinoma.**
A 46-year-old woman presents with a nodular lesion in her left breast having a history of surgical excision at the same location two years ago (histologic diagnosis at that time: fibrocystic disease). Fine-needle aspirate contains cohesive flat sheets (cobblestone cell arrangement) consisting of tumor cells exhibiting abundant dense eosinophilic cytoplasm with distinct borders (rarely in focus). The varying nuclear spacing and the variability in nuclear and nucleolar size and shape are the most important discriminatory features against a benign apocrine lesion (Pap stain, low magnification).
*Cytologic and subsequent tissue diagnosis:* invasive breast carcinoma, apocrine variant (apocrine carcinoma).

**Figs. 1.90 and 1.91 Lipid-rich carcinoma.**
Two examples of lipid-rich carcinoma; the potential diagnostic dilemma is discussed.

**Fig. 1.90** (case #1) A 64-year-old woman with a palpable tumor mass in her right breast. FNAB revealed the classic cytologic features of a lipid-rich carcinoma. A homogeneous epithelial cell population showing several single tumor cells with rounded nuclei and abundant rounded cytoplasm containing small and medium-sized well-defined vacuoles (Pap stain, high magnification).
*Cytologic diagnosis:* breast carcinoma of the large-cell variant, most likely lipid-rich carcinoma.
*Comment*: it may be a challenge to distinguish the current tumor cell pattern from metastatic clear cell carcinomas and activated foamy histiocytes.
*Histologic sections* revealed Sudan-positive staining fat droplets in the cytoplasmic of the tumor cells confirming the diagnosis of lipid-rich carcinoma. The freshly excised tissue was tender and showed a yellow-white cut surface.

**Fig. 1.91** (case #2) 56-year-old woman. Follow-up imaging studies revealed abnormalities in the left mammary gland, confirming a long-standing mastopathic lesion. An US-guided FNAB was routinely performed. Direct smears were Pap-stained (high magnification).
*Cytologic diagnosis with erroneous typing:* the initial diagnosis was apocrine carcinoma. The misinterpretation was caused by the notedly granulated cytoplasm and the large nucleoli.
*Tissue diagnosis:* invasive carcinoma of lipid-rich variant.

**Fig. 1.92 Adenoid cystic carcinoma.**
High magnification shows the typical arrangement of the neoplastic cells around cores of translucent hyaline bodies. A biphasic cell population surrounding the hyaline material is evident: small cells with dark bipolar nuclei and larger cells with clear nuclei are distinguishable (FNAB, direct smear, Pap stain).

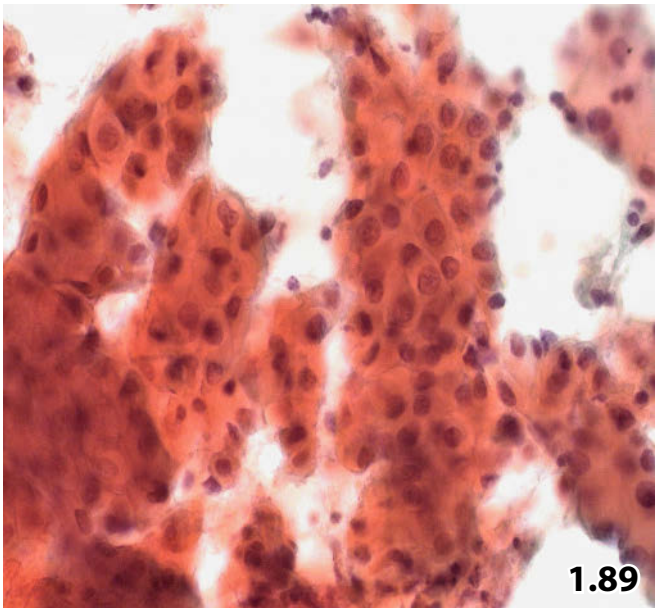
1.89

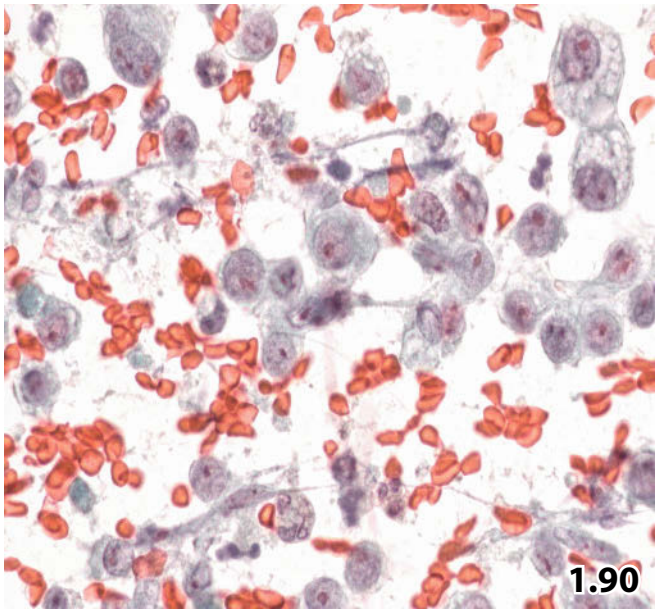
1.90

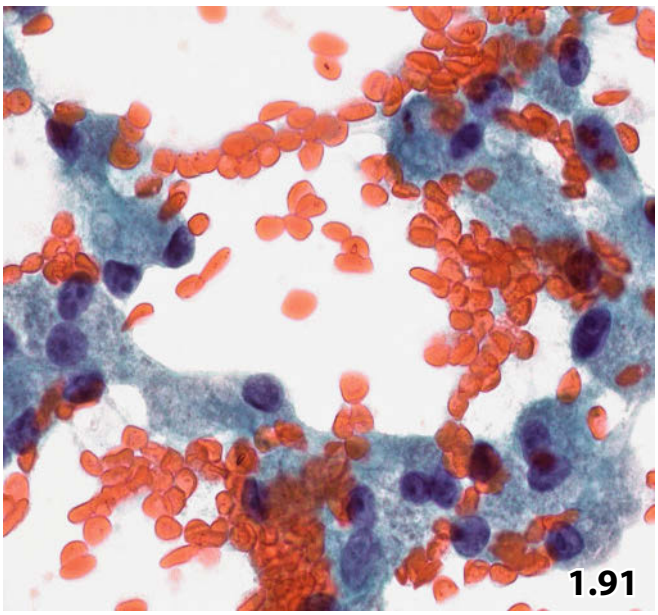
1.91

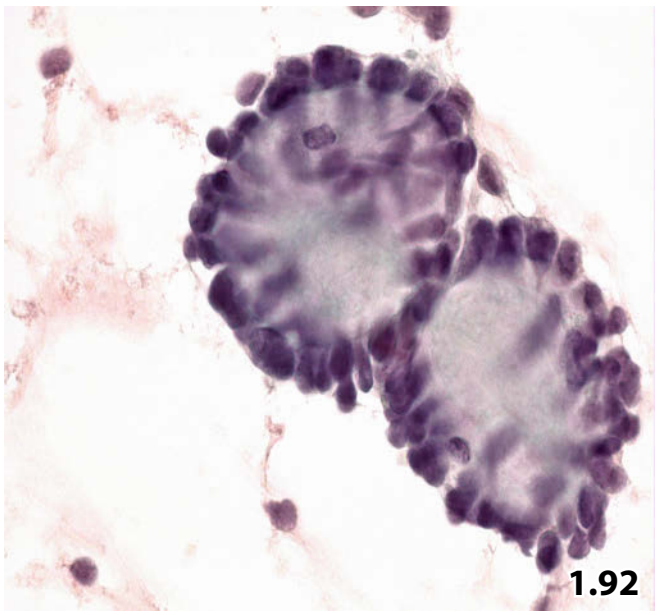
1.92

1

**Fig. 1.93 and 1.94 Metaplastic carcinoma.**
Two different phenotypes of metaplastic breast carcinoma are presented.

**Fig. 1.93** (case #1) A 57-year-old woman presented with fibrocystic breast disease, well established by imaging studies over a 2-year period. FNAB yielded numerous cell clusters consistent with common type breast cancer. Both bundles of atypical elongated cells (arrow) and superimposed cells exhibiting red-stained cytoplasm (arrowheads) are present (Pap stain, low magnification).
*Tentative cytologic diagnosis:* metaplastic carcinoma of squamous type.
*Tissue diagnosis:* metaplastic carcinoma with squamous and spindle cell differentiation.

**Fig. 1.94** (case #2) Example of a metaplastic sarcomatoid carcinoma. Small clusters of carcinoma cells are embedded in a highly cellular sarcomatoid stroma. The malignant epithelial cells demonstrate positive immunoreaction for pancytokeratin (Lu-5), whereas the pseudosarcomatous metaplastic spindle cells show a negative staining result (FNAB, immunostain Lu-5, high magnification).

**Fig. 1.95A, B Breast carcinoma with osteoclastic giant cells.**
FNAB of a rare breast carcinoma with osteoclast-like giant cells in a 59-year-old woman. There was no clinical information available. Direct smears were Pap-stained.
*Cytologic and subsequent histologic diagnosis:* carcinoma with osteoclastic giant cells.
**A** Low magnification revealing a cellular aspirate composed of a biphasic cell population: dissociating small to medium-sized carcinoma cells and large multinucleated giant cells. **B** High magnification exhibits clearly malignant pleomorphic epithelial cells with high mitotic activity (one mitosis: arrow). The giant cells are morphologically different from the malignant epithelial cells: the nuclei of giant cells are crowded to one side of the voluminous cytoplasm, they are round to oval in shape showing osteoclastic features comprising smooth contour, evenly dispersed fine-granular chromatin, and a centrally positioned prominent nucleolus.

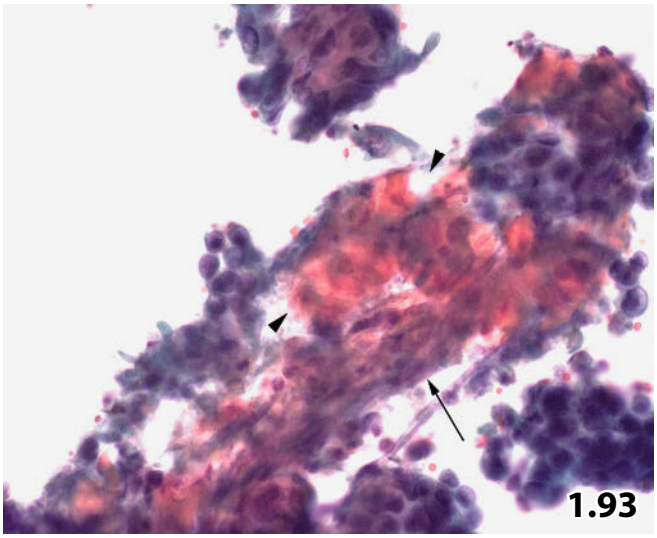
1.93

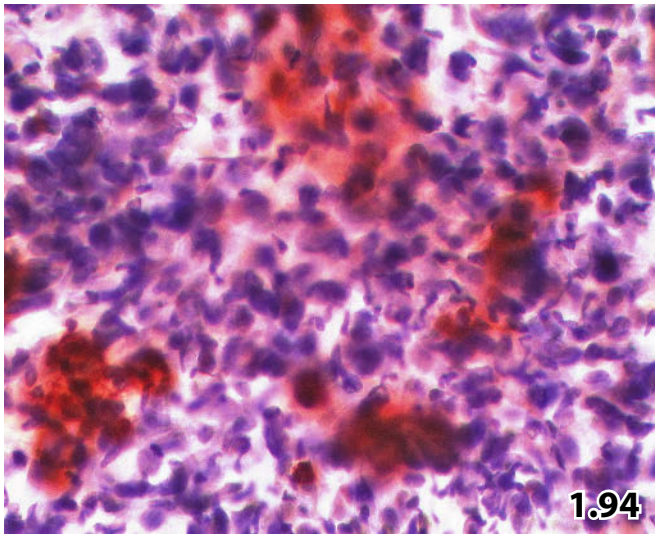
1.94

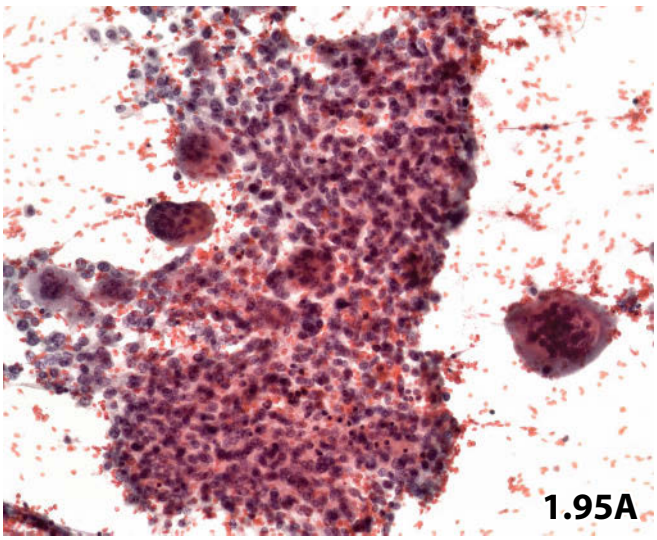
1.95A

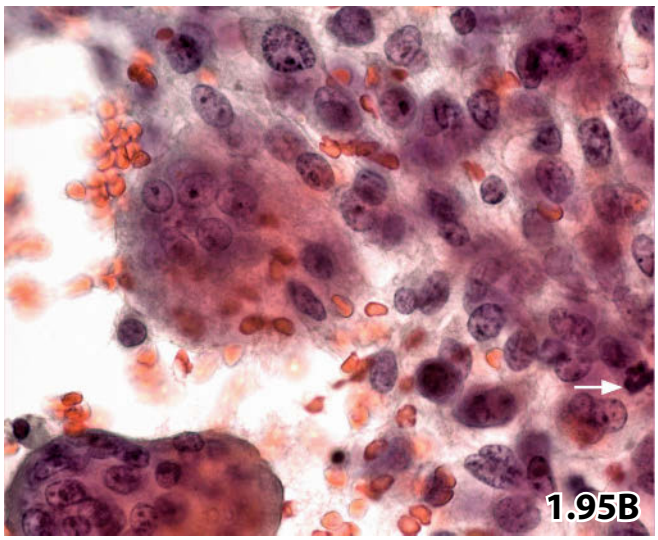
1.95B

1

**Figs. 1.96 and 1.97 Inflammatory carcinoma.**
Both typical cytology and histology are shown.

**Fig. 1.96** A 36-year-old woman presenting with a refractory mastitis puerperalis was referred to FNAB in order to confirm the clinical diagnosis. A direct smear was Pap-stained. The cytologic specimen was paucicellular containing a few clusters of a poorly differentiated malignant epithelial cells. Note the benign single cell (adjacent to the upper margin of the cell cluster) originating from a sebaceous gland of the skin (high magnification)
*Cytologic finding* and clinical signs were suggestive of an inflammatory carcinoma. The diagnosis was histologically verified by tissue diagnosis (surgical excision of mammary cutaneous tissue) (see Fig. 1.97).

**Fig. 1.97** Lymphangiosis carcinomatosa cutis is readily apparent in the histologic section (arrows).

**Fig. 1.98 Paget disease.**
Imprint cytology (cut surface of excisional biopsy of the areola) disclosed a few large malignant cells and an inflammatory background. One epithelial tumor cell is shown (arrow) (Pap stain, low magnification).

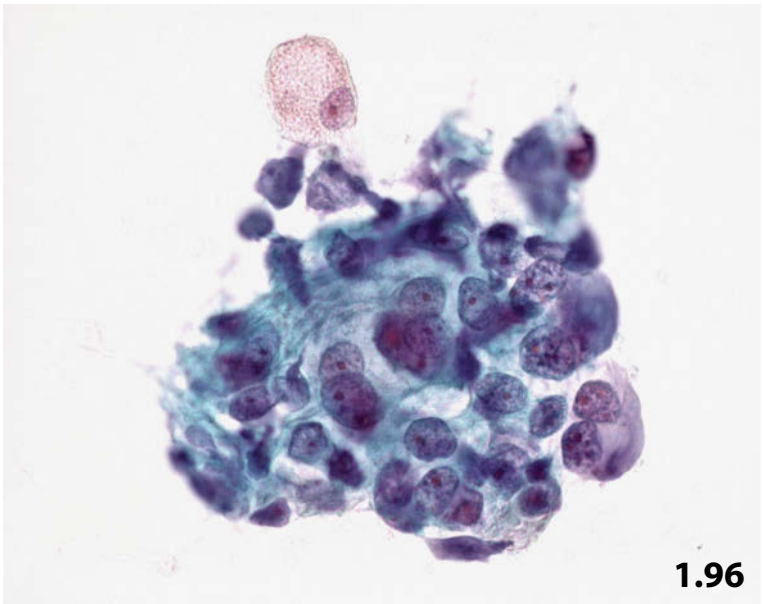

1.96

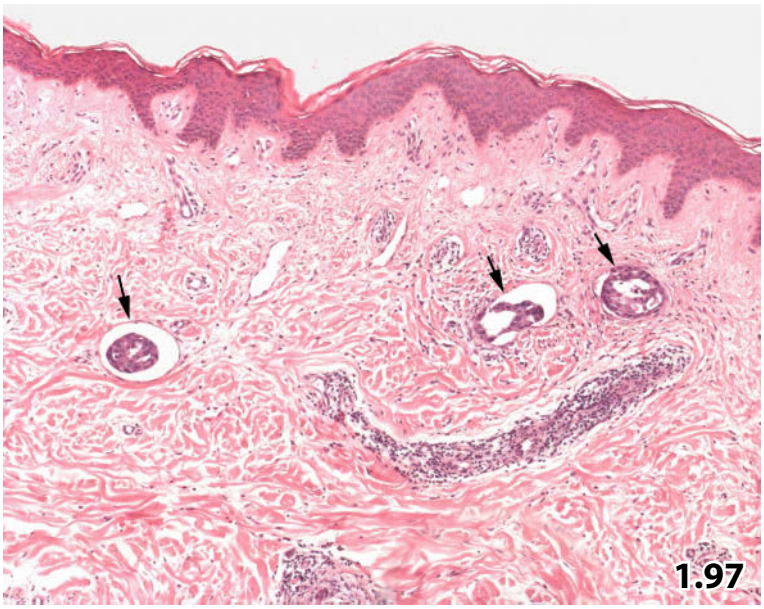

1.97

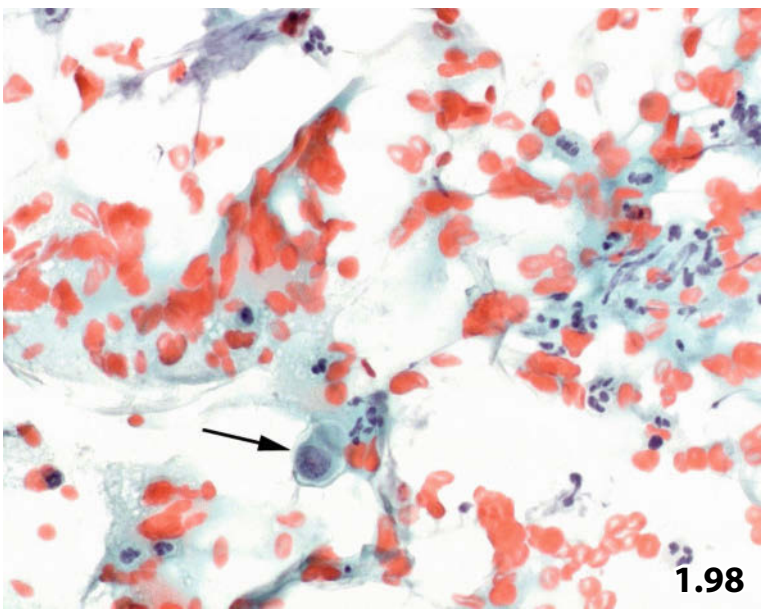

1.98

**Fig. 1.99 Acute lymphoblastic leukemia (ALL).**
A 17-year-old woman presented with masses in both breasts (up to 6 cm in size). Diagnosis of ALL with successful treatment prior to the manifestation of breast masses 18 months before. FNAB of a breast mass shows tight aggregates and rows of small malignant lymphoblastic cells (MGG stain, low magnification).
*Comment:* lack of appropriate clinical information will give rise to a major diagnostic dilemma (lymphoma versus small-cell carcinoma versus neoplasia of the small round cell tumor group).

**Fig. 1.100A, B Large blastic non-Hodgkin lymphoma.**
A 75-year-old woman presented with a tumor mass in her right breast suggestive of mastitis. Ultrasound-guided FNAB was done. Direct smears were stained according to the Papanicolaou technique. **A** High magnification shows large neoplastic cells and background necrosis. Epithelial-like cell clustering and dense cytoplasm are suggestive of a poorly differentiated breast carcinoma. On the other hand, small and intermediate lymphocytes may be an indicator for malignant lymphoma (arrows). **B** Immunocytochemical staining for CD45 decorates both large malignant cells and small lymphocytes. Note the strong immunoreaction of background material characteristic in conventional smears. (Pap-prestained direct smear, no nuclear counterstaining).

Epithelial-like aggregation of malignant lymphoid cells represents a major diagnostic challenge (versus carcinoma) in standard cytology.

**Fig. 1.101A–C Burkitt lymphoma.**
A 45-year-old woman presented with a tumor at the periphery of her left breast associated with enlarged axillary lymph nodes. **A** Initial examination by aspiration biopsy provided the typical monotonous cell pattern of Burkitt lymphoma associated with tingible body macrophages (center); only vague cellular aggregation (direct smear, Pap stain, high magnification). **B** Immunostaining shows positive cytoplasmic reaction of the tumor cells for the B-cell marker CD20 (Pap-prestained ThinPrep specimen). Note the complete absence of background-immunoreactivity in liquid-based specimen. **C** Nuclear immunopositivity for MIB-1 (proliferation index: 94%) (Pap-prestained conventional smear).

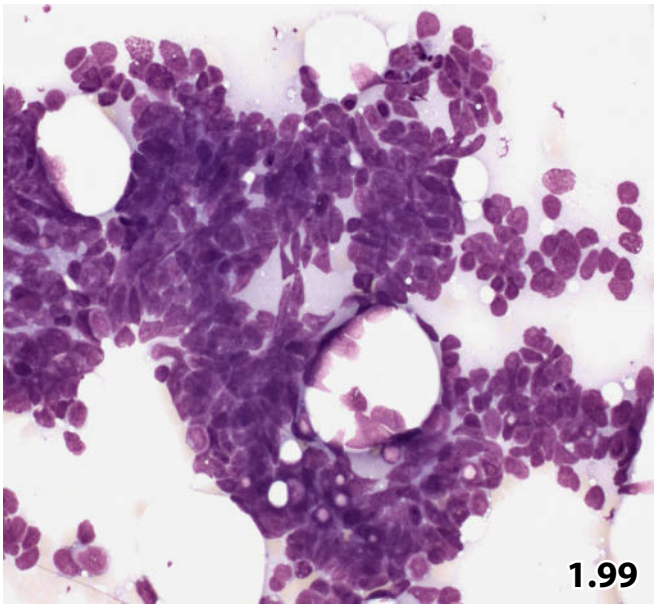
1.99

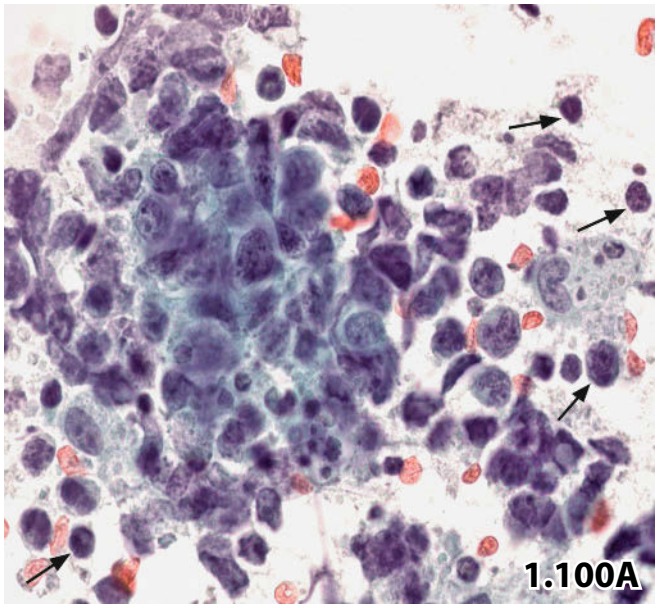
1.100A

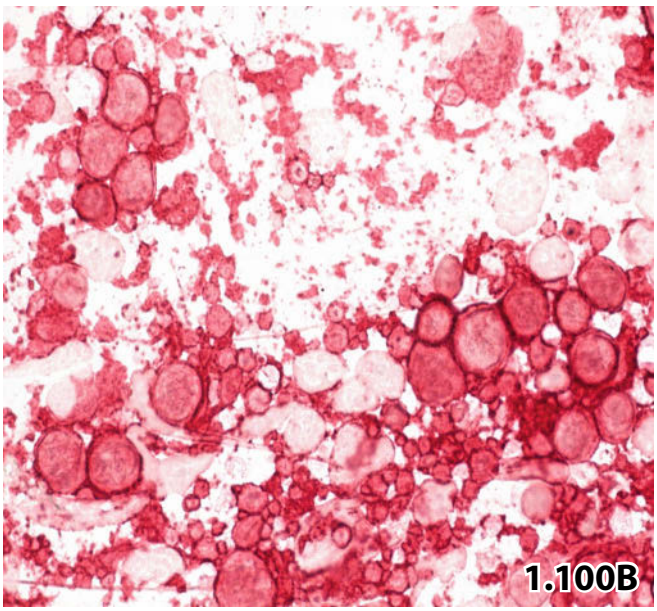
1.100B

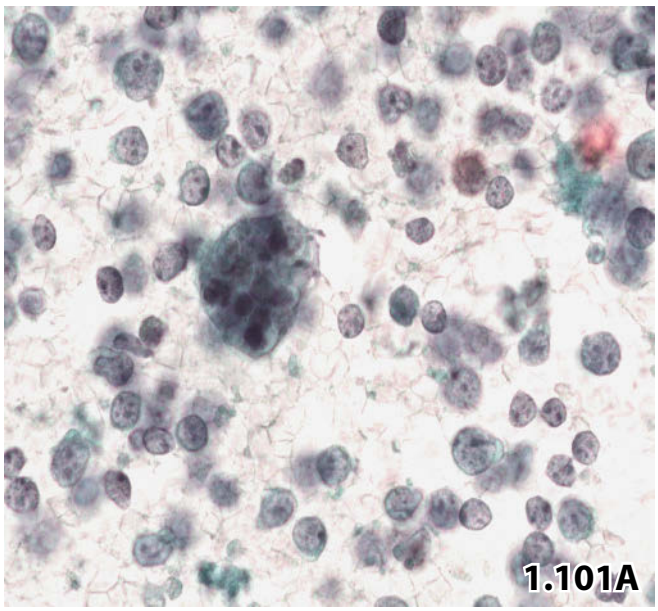
1.101A

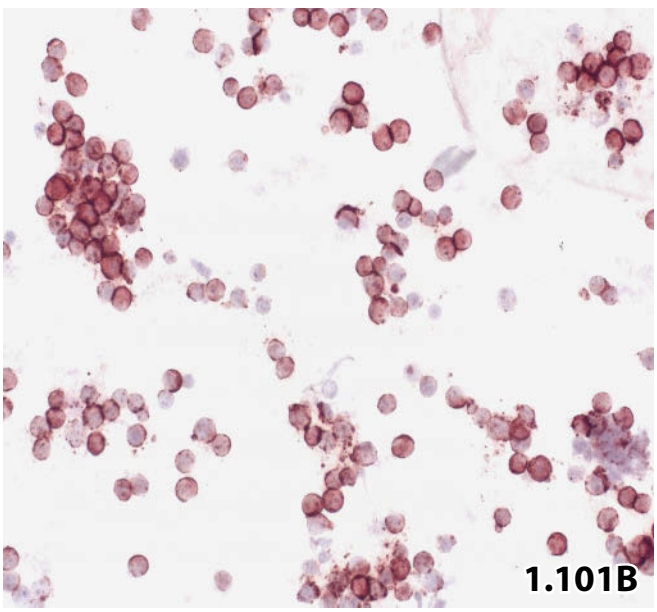
1.101B

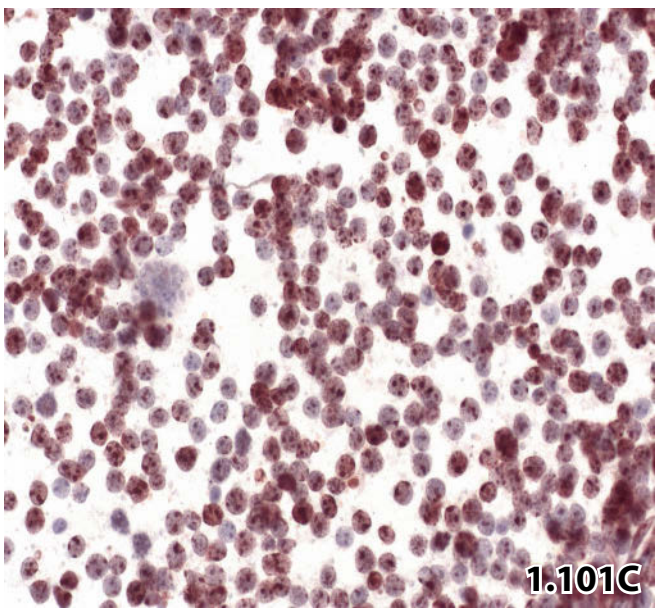
1.101C

**Fig. 1.102 Plasmacytoma.**
An elderly woman with a positive history of relapsing plasmocytoma presented with a mass in her right breast. FNAB of the breast lesion shows manifestation of a lymphoid neoplasm consisting of atypical mature and immature (upper left) plasma cells (direct smear, MGG stain, high magnification).

**Fig. 1.103 Epithelioid monophasic synovial sarcoma.**
A 77-year-old man presented with a mass in the area of his left mammary gland. US-guided FNAB was performed. A lower magnification shows a heterogeneous pattern composed of round and elongated malignant cells that are difficult to classify: carcinoma versus sarcoma versus lymphoma? Immunocytochemical workup (not shown) rendered negative reaction for pancytokeratin and leukocyte common antigen (direct smears, Pap stain).
*Tentative cytologic diagnosis:* most likely malignant mesenchymal tumor. An anaplastic carcinoma with negative expression of epithelial immunomarkers cannot be excluded.
*Tissue diagnosis:* epithelioid monophasic synovial sarcoma.

**Fig. 1.104 Relapsing angiosarcoma of the breast.**
Imprint cytology of the cut surface of an excisional biopsy reveals pleomorphic malignant spindle cells and necrosis. Histology correlated well with the cytologic findings enabling the diagnosis of angiosarcoma of the breast (Pap stain, high magnification).

**Fig. 1.105 Malignant schwannoma.**
FNAB reveals a homogeneous population of highly atypical cells characterized by pale nuclei with prominent irregularities. These features together with cytoplasmic granules suggested breast carcinoma or metastasis of a thyroid neoplasm. The negative immunoreactions for pancytokeratin and thyroglobulin (not shown), however, excluded the targeted neoplasms (direct smear, Pap stain, high magnification).
*Tentative cytologic diagnosis:* pleomorphic malignant neoplasia, most likely of mesenchymal origin. Cytologic and immunocytochemical findings require tissue diagnosis.
*Tissue diagnosis:* malignant schwannoma, epithelioid variant.

**Fig. 1.106 Malignant melanoma.**
Positive history of a metastatic pigmented melanoma in a 48-year-old woman. FNAB of a lump in the left breast shows a malignant tumor. The tumor cell population may mimic breast carcinoma of the large-cell type, but the conclusive diagnosis in the current case is based on strong pigmentation of the tumor cells (direct smear, Pap stain, high magnification).

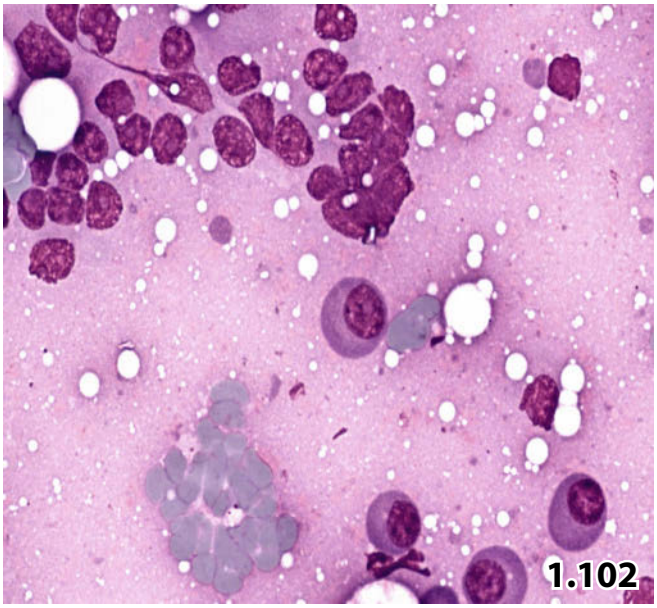
1.102

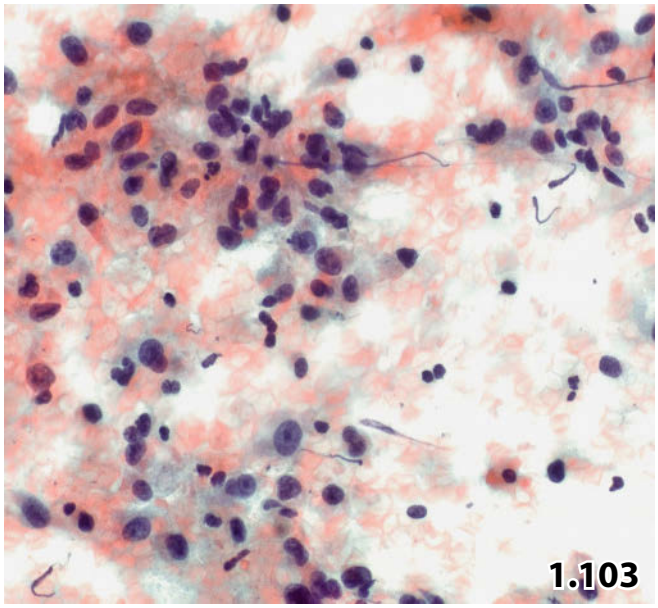
1.103

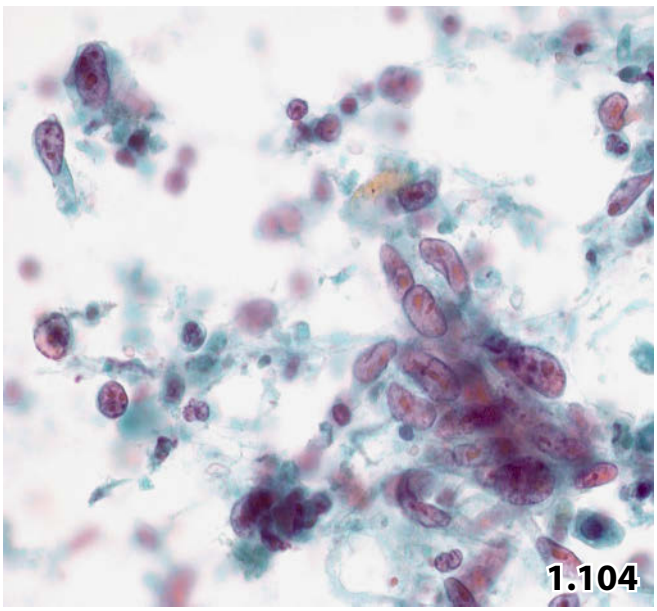
1.104

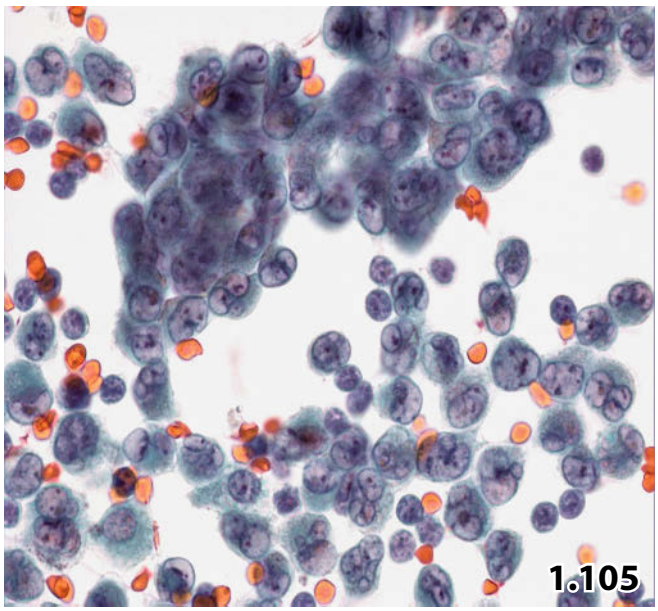
1.105

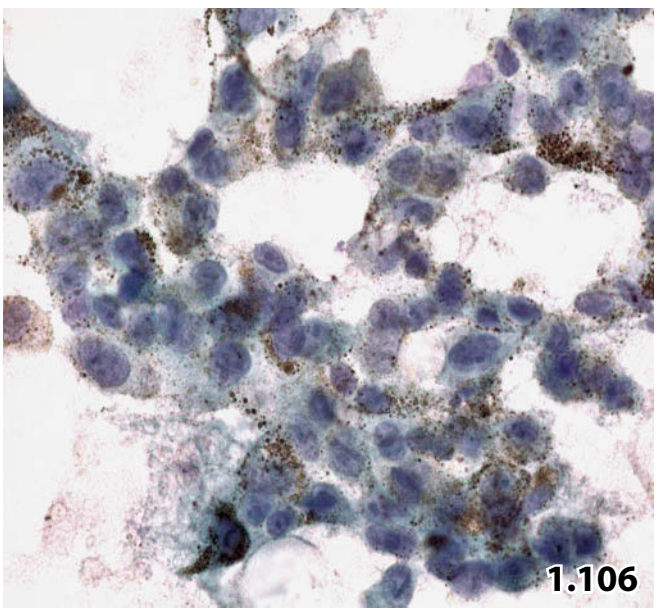
1.106

**Fig. 107A,B Non-small cell lung cancer.**
Positive history of a non-small-cell lung cancer in a 49-year-old woman presenting with a nodular mass (2 cm in diameter) in her left breast. **A** FNAB of the breast lesion yields a cellular specimen consisting of undifferentiated large carcinoma cells of the unclear type (direct smear, Pap stain, high magnification). **B** Immunostaining for TTF-1 (strong nuclear positivity) proved to be helpful in determining a definitive diagnosis of lung cancer metastasis (poorly differentiated adenocarcinoma).

**Fig. 108 Prostatic carcinoma.**
Positive history of a prostatic adenocarcinoma in a 78-year-old man presenting with a mass (4 cm in size) in his left breast. FNAB of the breast tumor showed characteristic cytomorphologic features of a moderately differentiated prostatic adenocarcinoma comprising regularly arranged sheets of monomorphic tumor cells, nuclei exhibiting densely packed granular chromatin, barely visible nuclear membranes, prominent nucleoli, and well-defined cytoplasmic bodies The malignant tumor cells showed a strong positive immunoreaction for prostate acid phosphatase (not shown) (direct smear, Pap stain, high magnification).

**Fig. 109 Small-cell lung cancer.**
Breast metastasis of a small-cell carcinoma of the lung in a 48-year-old woman. The breast lump was detected during preoperative diagnostic evaluations. Tentative clinical diagnosis was fibroma or solitary cyst. FNAB revealed the classic architectural and cellular features of an oat cell carcinoma displaying single-file rows (lower left), typical chromatin texture (salt and pepper), both indistinct nucleoli and indistinct cytoplasmic rims (direct smear, Pap stain, high magnification).

**Fig. 1.110A,B Medullary thyroid carcinoma.**
A 23-year-old woman with a positive history of a medullary carcinoma of the thyroid presenting with a nodule (15 mm in diameter) in her left breast. **A** US-guided FNAB reveals a monomorphic relatively bland cell population comprising three-dimensional irregular cell clustering. The cytoplasm is pale and ill-defined or spindle shaped. The cytoplasmic granules are faintly visible (arrows) (direct smear, Pap stain, low magnification). **B** Immunostaining was crucial in determining the primary tumor site: positive cytoplasmic reaction for calcitonin confirmed the metastatic nature of the mammary tumor.

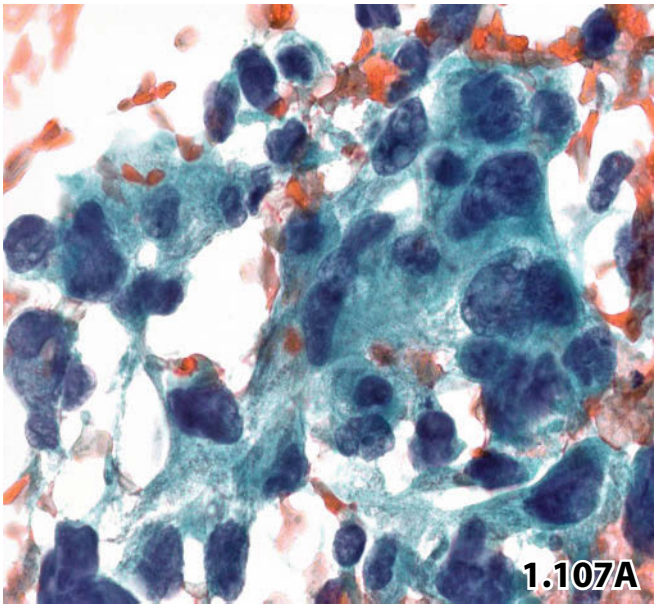
1.107A

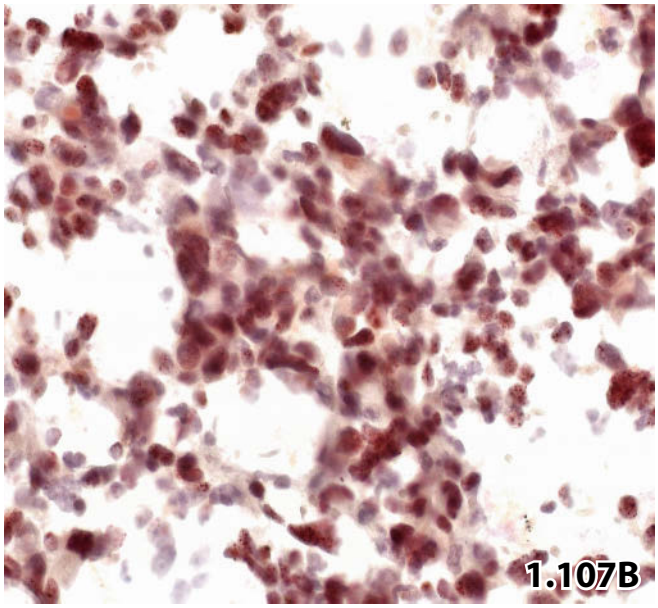
1.107B

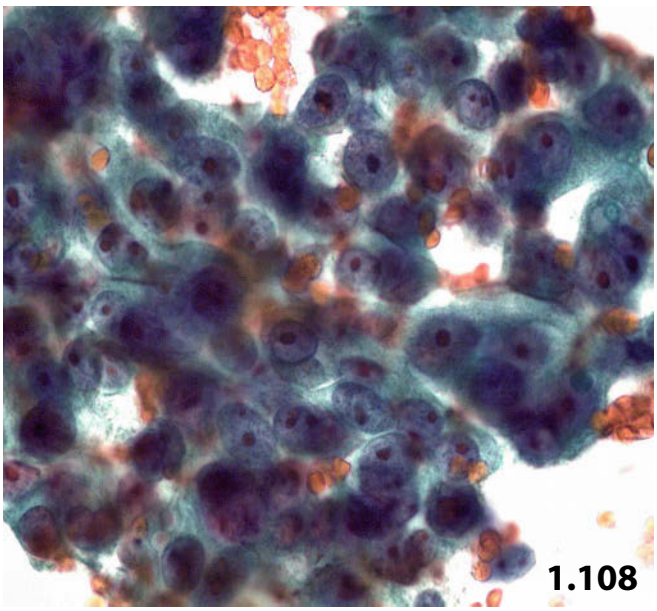
1.108

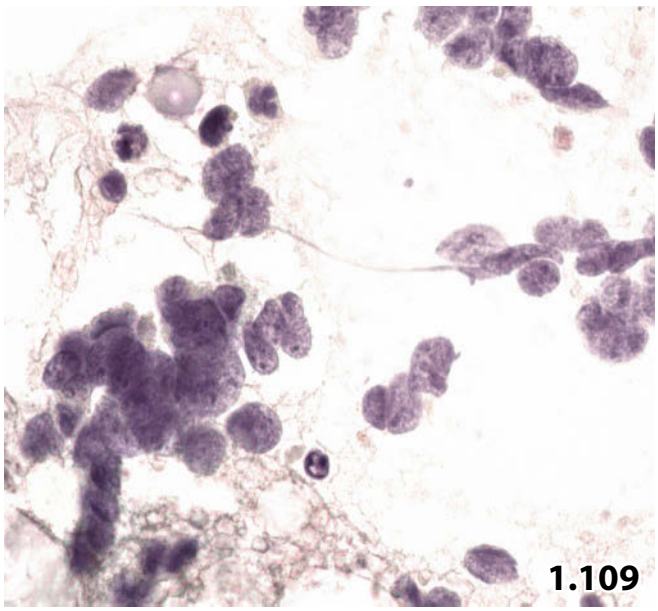
1.109


1.110A

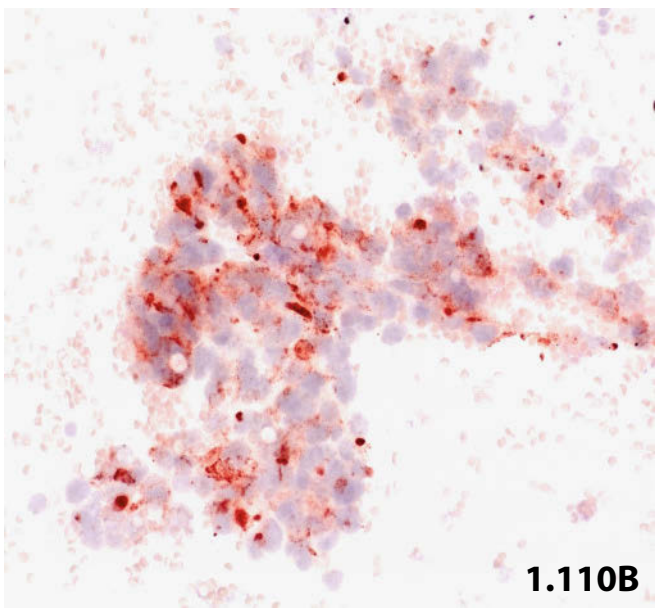
1.110B

# Section 1.4
# Breast

## Nipple Discharge

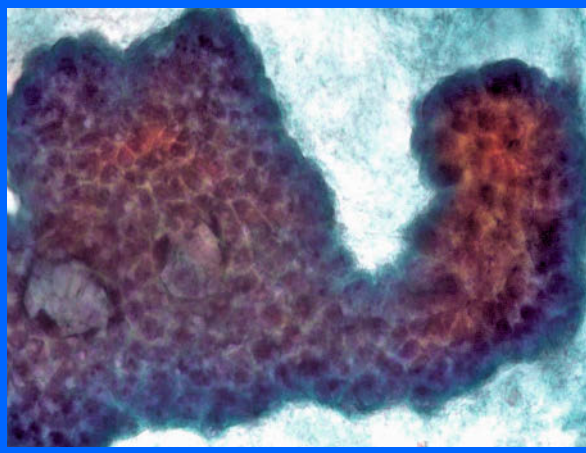

### 1.4.1 Introduction

#### 1.4.1.1 General Comments

- Nipple discharge (ND) is uncomfortable for the patients, although the cause of it is usually benign [1, 3].
- ND cytology is highly specific but not sensitive in the presence of cancer. Exfoliative cytology is only useful when yielding a positive result. The rate of false-negative results is high, because most breast cancers are not associated with nipple secretion. Accuracy of benign and malignant diagnoses in ND is high compared with histopathologic results [1, 3].
- Epithelial cells in cytologic samples of ND show slight to severe degenerative alterations in a high percentage of cases. Therefore, a proper evaluation and an exact diagnosis are often difficult, particularly in hypocellular smears.

#### 1.4.1.2 Sanguineous Nipple Discharge

Sanguineous ND is not a sign of malignancy and is often caused by benign breast disorders (fibrocystic disease/fibroadenosis, duct ectasia, lactation) or benign tumors (e.g., papilloma) [14, 23, 25, 26]. However, Das and coauthors observed more epithelial abnormalities in sanguineous ND than in other types of secretion [1]. A bloody secretion raises a greater suspicion of an association with malignancy compared to other appearances of ND [13].

#### 1.4.1.3 Nipple Discharge of the Male Breast

ND is also observed in men, with gynecomastia the most common cause. Sanguineous ND in men should raise the possibility of breast carcinoma. Florid gynecomastia may easily lead to the misdiagnosis of carcinoma in ND due to a high cellularity and epithelial abnormalities [3, 6] (Fig. 1.111).

#### 1.4.1.4 Imaging and Sampling Techniques Related to Nipple Discharge

- The following techniques are commonly used to evaluate patients who have ND in order to assess a tumorous lesion and to gain an adequate fluid specimen for cytological investigation [12, 15]: mammography, ultrasound, MRI, MR-ductography [4], galactography/ductography [21, 22], ductoscopy and ductal lavage [2, 24], ductal lavage and nipple aspiration [7]. A tumorous process recorded by imaging should immediately be followed by image-guided FNAB.
- Imprint of drops of the fluid onto one or multiple glass slides, obtained directly from the surface of the nipple, is the most simple sampling method. The drops are immediately smeared and fixed with a fixative medium or air dried. Larger amounts of fluid may be encountered in cases with abundant secretion following ductal lavage and/or nipple aspiration. The fluid is centrifuged and direct smears or preparations by means of special techniques are standardly produced and processed.

## 1.4.2 Pathogenesis of Nipple Discharge

### 1.4.2.1 Abnormal Nipple Discharge

Abnormal ND is associated with a wide range of benign disorders primary or secondary to the mammary gland.

- Abnormal milk secretion (galactorrhea) may be caused by:
  - Brain lesions and pathologic conditions of endocrine organs [19].
  - Drugs such as oral contraceptives and psychopharmaca, among others.
  - Mechanical stimulation of the nipple and sexual activities [11].
- Milky discharge in newborns is a well-known phenomenon.
- Bloody ND in infants has been frequently reported in the literature, in the past and recently [5].
- In many patients the cause of discharge remains obscure.

### 1.4.2.2 Pathologic Nipple Discharge

Genuine pathologic ND is usually unilateral and may come from a single duct. Discharge occurs spontaneously and is either persistent or intermittent.

The most common causes of pathologic nipple discharge are inflammatory disease, fibrocystic lesion, and ductal ectasia followed by benign papilloma, and finally invasive carcinoma. The cytologic detection rate of invasive breast carcinoma in nipple aspirate fluid seems to be dependent on the extent of coexistent ductal carcinoma in situ [9].

## 1.4.3 Macroscopic and Microscopic Features in Correlation with Etiology

### 1.4.3.1 Bland Smear

Bland smears may be encountered together with a large number of primary and secondary benign and malignant breast disorders.

- Macroscopy: Yellow (serous) / grey / green-black.
- Microscopy: Proteinaceous background in an acellular smear or together with a few foam cells and/or bland ductal epithelial cells is most often observed in ND cytology.

### 1.4.3.2 Duct Ectasia (Fig. 1.112)

Duct ectasia is a focal dilatation of collecting ducts caused by obstruction and followed by an accumulation of secretions. Sonography visualizes duct dilatation without difficulty.

- Macroscopy: Multicolored sticky discharge is most characteristically (clear / green / brown /green-black), bloody aspect occurs occasionally [13].
- Microscopy: Large amounts of proteinaceous material and possibly cellular debris in the background of the smear. Large numbers of activated foam cells partly multinucleated and a few bland duct cells.

### 1.4.3.3 Galactorrhea

- Macroscopy: Characteristic milky fluid.
- Microscopy: Abundant lipoproteinaceous material, the background masses are interspersed with clear droplets of varying size. Many foam cells are present. Epithelial cells may be sparse or absent. Distinction of secretory active isolated epithelial cells from the foam cells may be difficult, immunostaining for CD68 (histiocytes +) is helpful in determining a definite diagnosis.

### 1.4.3.4 Infection / Inflammation

A variety of bacteria, viruses, parasites, and fungi are causative agents of an inflammatory process [8, 10, 16]. Organisms may be identified by special stainings (e.g., Gram, Giemsa, PAS, Crocott, immunocytochemistry) and by DNA analyses [8]. Acid-fast bacilli may be identified by Ziehl-Neelsen staining, auramine fluorescence, or DNA analysis [18].

- Macroscopy: ND can be serous, dirty-grey, sanguineous, sticky / purulent depending on cellularity.
- Microscopy: Neutrophils in varying numbers correlate with clinical mastitis. Foam cells and macrophages may also be present. Purulent discharge is caused by abscess, the cytologic samples show a vast amount of detritic neutrophils. Epithelioid histiocytes, giant cells, neutrophils, and necrosis can be a sign of tuberculosis.

### 1.4.3.5 Intraductal Papillomatous Neoplasia

Distinguishing between benign papilloma, low-grade papillary carcinoma, benign florid ductal epithelial hyperplasia, and proliferative breast lesion with atypia is very difficult or impossible due to overlapping cytologic characteristics in benign and malignant papillary and papilliform proliferations [17] (Figs. 1.113–1.117). Definitive therapy is based on histopathologic results.

However, sonography can visualize circumscribed intraductal papillomatous lesions; together with corresponding cytology, a selective duct excision can be curative unless the lesions turns out to be invasive by histology.

- Macroscopy: Pink or serosanguineous and brown or reddish-brown secretions suggest bloody discharge.

Bloody discharge is frequently observed together with papillomatous neoplasia.

- Microscopy: Tight papilliform clusters of ductal cells in a hemorrhagic and at least in an inflammatory background are pathognomonic for this lesion. A benign tumor may be suggested when apocrine cells are present. The cellularity of the smears changes in individual patients. Slight nuclear pleomorphism (cleaved and wrinkled membrane) may be observed. Small nucleoli are common.

### 1.4.3.6 Intraductal and Invasive Carcinoma

(Figs. 1.117–1.120)

- Microscopy of low-grade DCIS: This tumor type may exhibit a bland cell pattern mimicking that of papillomatous neoplasia. Differential diagnosis from other types of low-grade neoplasia and benign proliferative ductal lesions is extremely difficult.
- Microscopy of high-grade DCIS: Cytologic preparations show discohesive cell groups and single cells. Malignant cells are enlarged. The nuclei are pleomorphic and hyperchromatic with an irregular outline, grooves, folds, coarse chromatin, and prominent irregular nucleoli. The background is variable but hemorrhagic and necrotic in most cases. Calcifications may be observed. Strong cellular degeneration is frequent [20]. Discrimination between invasive and noninvasive high-grade lesions is not possible by cytology alone.

### 1.4.3.7 Discharge from Lactiferous Ducts

Unlike columnar epithelial lining in collecting ducts of the mammary gland, the terminal portion of the lactiferous sinus and lactiferous ducts are lined by stratified epithelium. Disorders in this area, particularly inflammatory lesions, often produce a secretion that may contain degenerate and/or activated squames. Clinical and repeated cytological examinations are required; tissue biopsy is indispensable in cases with an equivocal follow-up.

- Microscopy: The cytologic sample is associated with squamous cells, squamoid detritus, histiocytic giant cells, and variable numbers of neutrophils. Regressive and regenerative changes of the squamous cells may raise possibility of squamous cell carcinoma (Fig. 1.120).

### 1.4.3.8 Paget Disease

Paget disease is discussed in Sect. 1.3.14.2, p. 65 (Fig. 1.98).

**Caution**

- A bland smear from ND, with or without a few benign cellular elements does not exclude malignancy.
- It is all but impossible to assign papilliform and papillary clusters without distinct cellular atypias to a benign or malignant lesion.
- Epithelial cells in smears from nipple fluids may exhibit strong degeneration:
  - They may look like activated histiocytes or poorly preserved carcinoma cells.
  - Beware of malignant overdiagnosis based on cellular elements with pronounced cytoplasmic and nuclear polymorphism due to regressive changes.
  - Sporadic large, polymorphic single cells with distinct nuclear irregularities, a dense chromatin-structure, and dark staining nucleoplasm should always raise the possibility of malignancy (irrespective of the grade of overall cell degeneration). Such findings have to be emphasized in the cytology report in order to trigger further investigations or complete excision with consecutive histology.

## 1.4.4 Further Reading


1. Das DK, Al-Ayadhy B, Ajrawi MT, et al. Cytodiagnosis of nipple discharge: a study of 602 samples from 484 cases. Diagn Cytopathol 2001;25:25-37.
2. Grunwald S, Heyer H, Paepke S, et al. Diagnostic value of ductoscopy in the diagnosis of nipple discharge and intraductal proliferations in comparison to standard methods. Onkologie 2007;30:243-248.
3. Gupta RK, Gaskell D, Dowle CS, et al. The role of nipple discharge cytology in the diagnosis of breast disease: a study of 1948 nipple discharge smears from 1530 patients. Cytopathology 2004;15:326-330.
4. Hirose M, Nobusawa H, Gokan T. MR ductography: comparison with conventional ductography as a diagnostic method in patients with nipple discharge. Radiographics 2007;27 Suppl 1:S183-196.
5. Imamoglu M, Cay A, Reis A, et al. Bloody nipple discharge in children: possible etiologies and selection of appropriate therapy. Pediatr Surg Int 2006;22:158-163.
6. Kapila K, Verma K. Cytology of nipple discharge in florid gynecomastia. Acta Cytol 2003;47:36-40.
7. Klein PM, Lawrence JA. Lavage and nipple aspiration of breast ductal fluids: a source of biomarkers for environmental mutagenesis. Environ Mol Mutagen 2002;39:127-133.
8. Kobayashi TK, Okamoto H, Yakushiji M. Cytologic detection of Herpes simplex virus DNA in nipple discharge by in situ hybridisation: report of two cases. Diagn Cytopathol 1993;9:296-299.
9. Krishnamurthy S, Sneige N, Thompson PA et al. Nipple aspirate fluid cytology in breast carcinoma. Cancer 2003;99:97-104.

10. Lahiri VL. Microfilariae in nipple secretion. Acta Cytol 1975;19: 154.
11. Lancet. Discharge from the nipple. Lancet (i) 1983;1405.
12. Lang JE, Kuerer HM. Breast ductal secretions: clinical features, potential uses, and possible applications. Cancer Control 2007;14:350-359.
13. Leis HP Jr, Greene FL, Cammarata A, Hilfer SE. Nipple discharge: surgical significance. South Med J 1988;81:20-26.
14. Lorenzen JR, Gravdal JA. Bloody nipple discharge. Am Fam Physician 1986;34:151-154.
15. Masood S, Khalbuss WE. Nipple fluid cytology. Clin Lab Med 2005;25:787-794.
16. Masukawa T. Discovery of psammoma bodies and fungus organism in the nipple secretion with improved breast cytology technique. Acta Cytol 1972;16:408-415.
17. Meherbano KM, Jaywant M, Girish J, et al. Solitary intraductal papilloma of the breast – a diagnostic dilemma and the role of conferencing between surgeons and cytologist. Indian J Pathol Microbiol 2006;49:582-585.
18. Nayar M, Saxena HMK. Tuberculosis of the breast: A cytomorphologic study of needle aspirates and nipple discharges. Acta Cytol 1984;28:325-328.
19. Newman HF, Klein M, Northrup JD, et al. Nipple Discharge: Frequency and pathogenesis in an ambulatory population. NY State J Med 1983;83:928-933.
20. Pritt B, Pang Y, Kellogg M, et al. Diagnostic value of nipple cytology: study of 466 cases. Cancer 2004;102:233-238.
21. Rissanen T, Reinikainen H, Apaja-Sarkkinen M. Breast sonography in localizing the cause of nipple discharge: comparison with galactography in 52 patients. J Ultrasound Med 2007;26:1031-1039.
22. Rongione AJ, Evans BD, Kling KM, McFadden DW. Ductography is a useful technique in evaluation of abnormal nipple discharge. Am Surg 1996;62:785-788.
23. Sauter ER, Schlatter L, Liniger J, Hewett JE. The association of bloody nipple discharge with breast pathology. Surgery 2004;136:780-785.
24. Shen KW, Wu J, Lu JS, et al. Fiberoptic ductoscopy for breast cancer patients with nipple discharge. Surg Endosc 2001;15:1340-1345.
25. Tetirick JE. Nipple discharge. Am Fam Physician 1980;22:101-103.
26. Vargas HI, Romero L, Chlebowski RT. Management of bloody nipple discharge. Curr Treat Options Oncol 2002;3:157-161.

**Fig. 1.111 Gynecomastia.**
A 19-year-old man presenting with diffuse enlargement of his right breast associated with nipple discharge. Imprints directly from the surface of the nipple revealed numerous irregular clusters composed of atypical epithelial cells (Pap stain, high magnification).
*Cytology* cannot rule out carcinoma despite the patient's young age. Note the irregular cell clustering, cell arrangement in rows, nuclear irregularities, hyperchromasia, and high N/C ratio.
*Tissue diagnosis:* Gynecomastia.

Degenerative and/or reactive cell changes may mislead one to overdiagnosis in nipple discharge caused by gynecomastia.

**Fig. 1.112 Duct ectasia.**
A 16-year-old woman presented with a yellow-gray discharge from the nipple of both breasts. There was no palpable lesion and sonography was normal. Cytologic imprint of the nipple microscopically shows dense proteinaceous secretory material and numerous foamy histiocytes frequently occurring in tight aggregates as depicted (Pap stain, high magnification).

Clumping of activated histiocytes in duct ectasia may lead to a false-positive diagnosis of cancer. One should always pay attention to the clinical manifestation/information!

**Figs. 1.113–1.115 Ductal papilloma.**
Examples from three different patient.

**Fig. 1.113** (case #1) A 63-year-old woman presented with hemorrhagic nipple discharge from her right breast. Cytologic imprints from the surface of the nipple reveal papilliform clusters with features of extensive epithelial proliferation(irregular cell arrangement, nuclear overlapping, varied nuclear size and shape). Clear signs of malignancy, however, are absent (bland chromatin pattern and bland nucleoli) (high magnification).
*Tentative cytologic diagnosis:* microscopic findings are highly suggestive of papilloma or low-grade (intraductal) papillary carcinoma.
*Tissue diagnosis:* (excisional biopsy of the retromammilar area): intraductal papilloma.

**Fig. 1.114** (case #2) A 43-year-old woman presented with similar clinical symptoms to the previous case. Imprint cytology from the surface of the nipple shows irregular papilliform clusters of epithelial cells associated with irregularity in their nuclear shape. Cytoplasmic vacuolization is due to degeneration. The background shows debris and inflammation. While myoepithelial cells are not clearly present, the low N/C ratio, bland chromatin pattern, and prominent nucleoli argue more in favor of a benign proliferative papillary lesion. However, the cytologic features do not allow a conclusive diagnosis in this case (high magnification).
*Tentative cytologic diagnosis:* papillary breast tumor of uncertain malignancy status.
*Tissue diagnosis:* intraductal papilloma associated with duct ectasia.

**Fig. 1.115** (case #3) Imprint cytology of hemorrhagic nipple discharge illustrates another phenotype of a benign intraductal papilloma: dense, three-dimensional papilliform clusters are composed of exceptionally small cells (in comparison with red blood cells) with inconspicuous nuclei (low magnification).
*Tentative cytologic diagnosis:* papillary breast tumor, most likely intraductal papilloma.
*Tissue diagnosis:* intraductal papilloma associated with intraductal epithelial hyperplasia (usual ductal hyperplasia).

Papilloma composed of small epithelial cells can masquerade as low-grade DCIS and vice-versa. (Compare with the cytomorphologic pattern in Fig. 1.116).

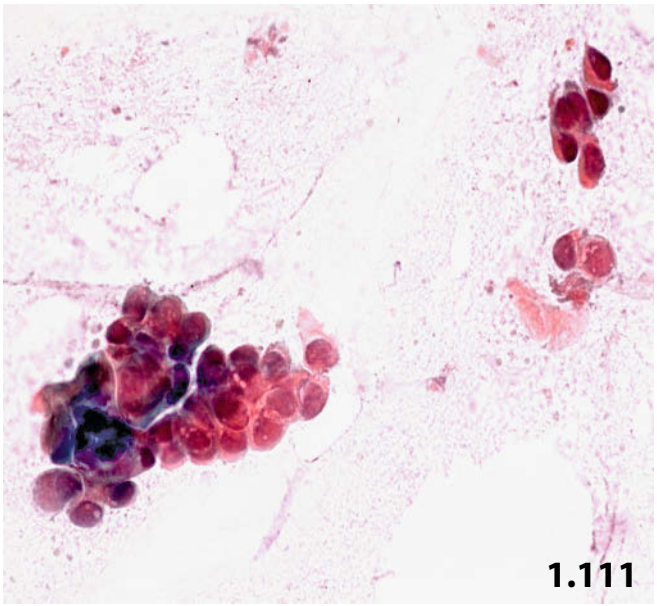
1.111

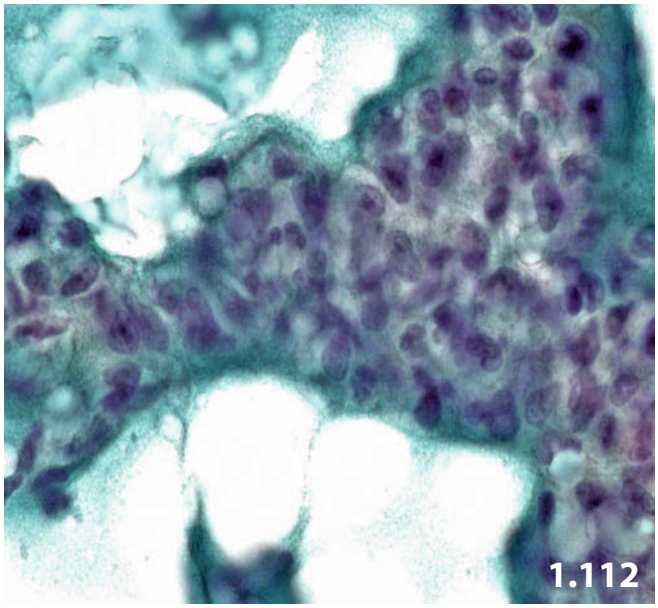
1.112

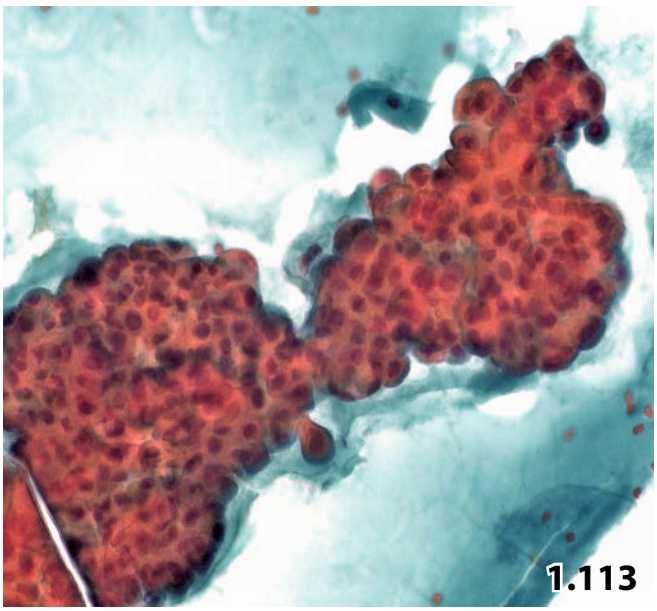
1.113

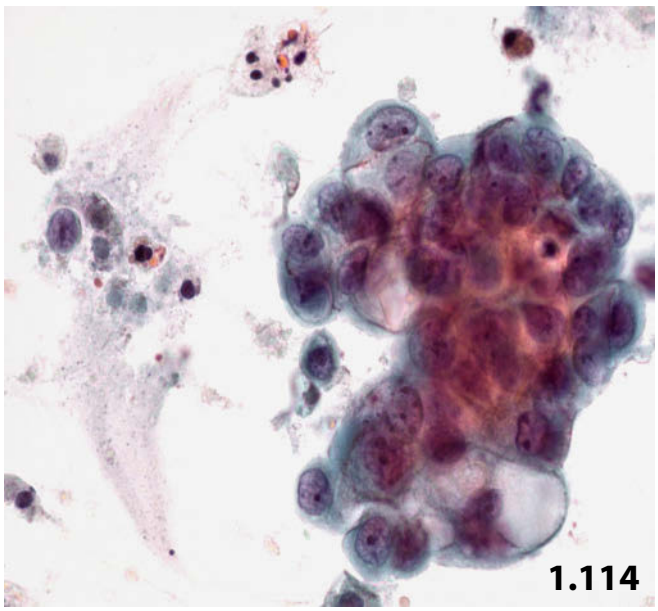
1.114

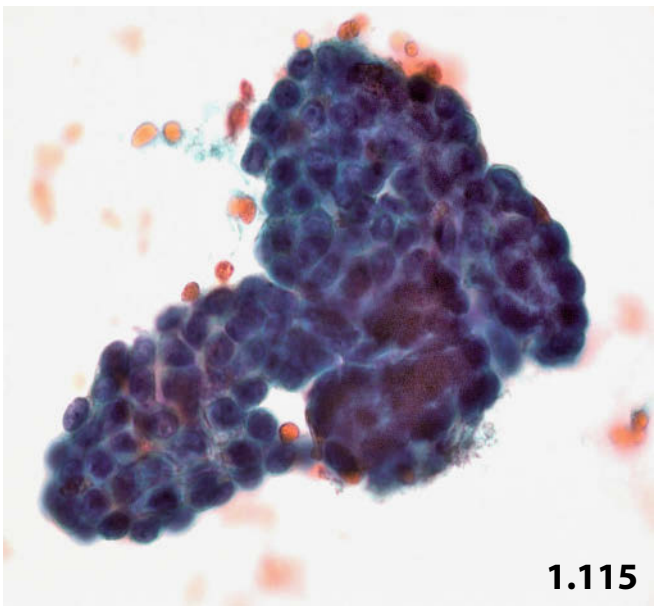
1.115

**Fig. 1.116 Low-grade DCIS versus papilloma.**
Imprint cytology of a hemorrhagic nipple discharge: the papilliform clusters of this and the previous case (Fig. 1.115) look similar. Indeed, both cases show bland nuclei (Pap stain, low magnification).
*Tentative cytologic diagnosis:* benign intraductal papillomatous epithelial proliferation.
*Comment:* compared to Fig. 1.115, this cell cluster is tighter, the nuclei showing marked overlapping and more depolarization.
*Tissue diagnosis:* Low-grade DCIS, micropapillary variant.

**Fig. 1.117 Papillary intraductal carcinoma.**
Liquid-based cytology (ThinPrep) of hemorrhagic nipple discharge. A single cell cluster is depicted from an otherwise hypercellular Thin-layer specimen. Each cluster (compact, three-dimensional, and focally sharply outlined) is composed of epithelial cells showing distinct malignant features such as loss of polarization, high N/C ratio, nuclear irregularities, granular and coarse chromatin, nucleoli (Pap stain).
*Cytologic diagnosis:* carcinoma, papillary growth pattern might be presumed. Cytology cannot distinguish between intraductal and invasive carcinoma.
*Tissue diagnosis:* intraductal papillary carcinoma.

**Fig. 1.118 Low-grade DCIS.**
A 66-year-old woman presented with hemorrhagic nipple discharge from her right breast shortly after excisional biopsy of a low-grade DCIS. Imprint cytology of the nipple shows a few ball-like clusters of atypical epithelial cells consistent with low-grade DCIS (Pap stain, high magnification).
*Cytology:* the microscopic findings are highly suggestive of an incompletely resected intraductal neoplastic lesion. The scarce cell clusters hamper a conclusive diagnosis.
Follow-up is not available.

**Fig. 1.119 High-grade DCIS.**
Imprint cytology of hemorrhagic nipple discharge in a 42-year-old woman.
High magnification reveals pleomorphic malignant epithelial cells associated with necrotic background (Pap stain).
*Cytologic diagnosis:* poorly differentiated carcinoma. Cytology cannot distinguish between high-grade intraductal comedo-type carcinoma and invasive cancer.
*Tissue diagnosis* (core needle biopsy): high-grade DCIS of comedo variant.

**Fig. 1.120 Atypical epithelial cells associated with severe inflammation: a diagnostic challenge.**
A 39-year-old woman presented with hemorrhagic nipple discharge from her left breast. Further clinical information is not available. Imprint cytology from the nipple surface provides a mixed cell pattern (Pap stain, low magnification):
– Strong inflammatory component and both squamous cells with bland nuclei (left) and with mild polymorphism of their nuclei and cytoplasm (arrows).
– Few small ball-like clusters of ductal cells showing mild atypia and degeneration (red staining of the cytoplasm, homogeneous and pycnotic nuclei) (lower right).
*Indeterminate cytologic report:* epithelial atypia associated with severe inflammation; cellular atypia may be caused by the inflammatory process, but a concomitant neoplastic ductal proliferation cannot be excluded.
*Tissue diagnosis* (mastectomy): widespread high-grade DCIS associated with foci of invasive ductal carcinoma and Paget disease of the nipple

On nipple discharge, one should consistently render an indeterminate cytologic diagnosis if atypical epithelial cells of any grade are associated with an inflammatory background.

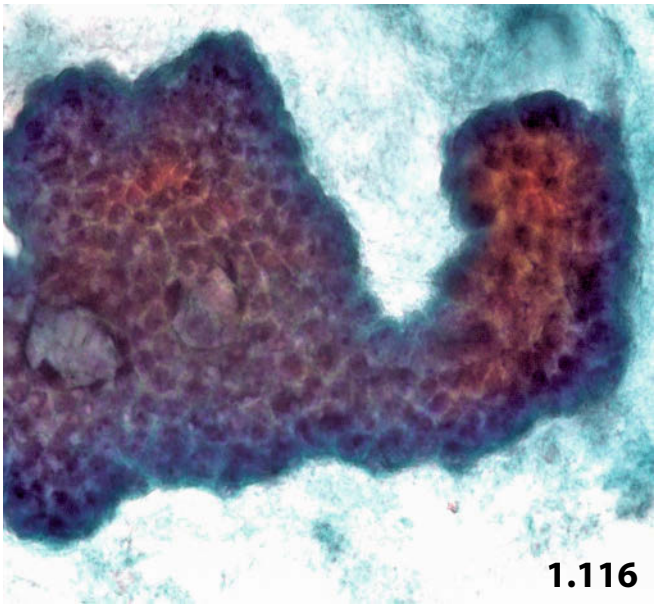
1.116

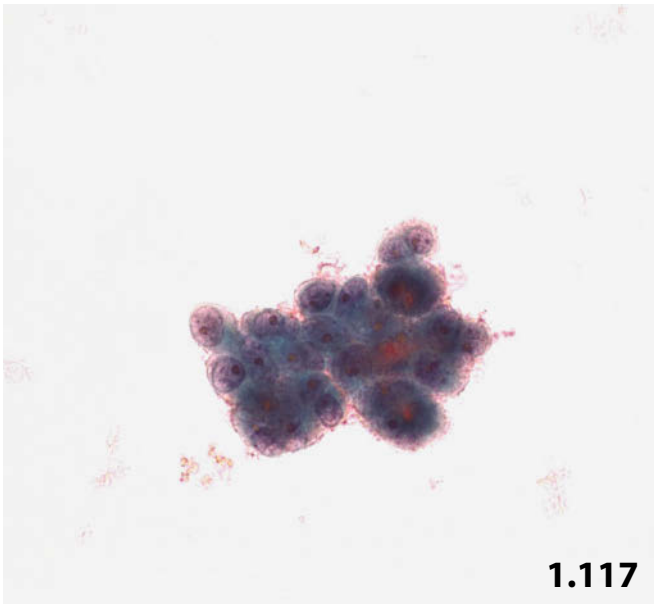
1.117

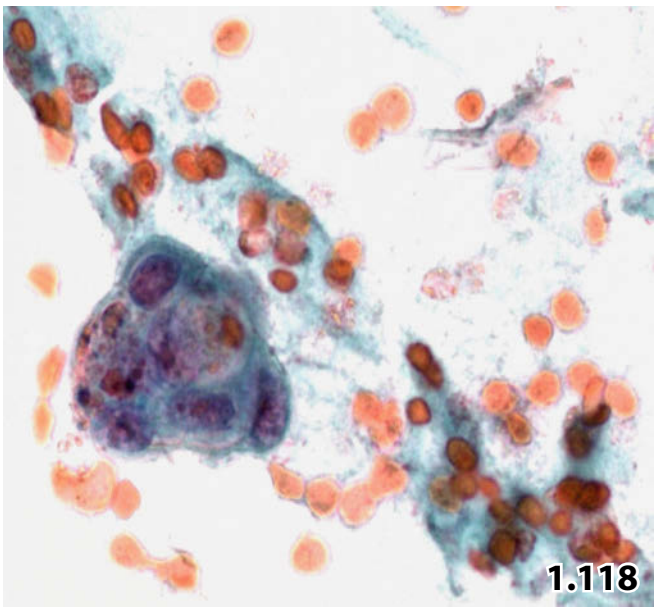
1.118

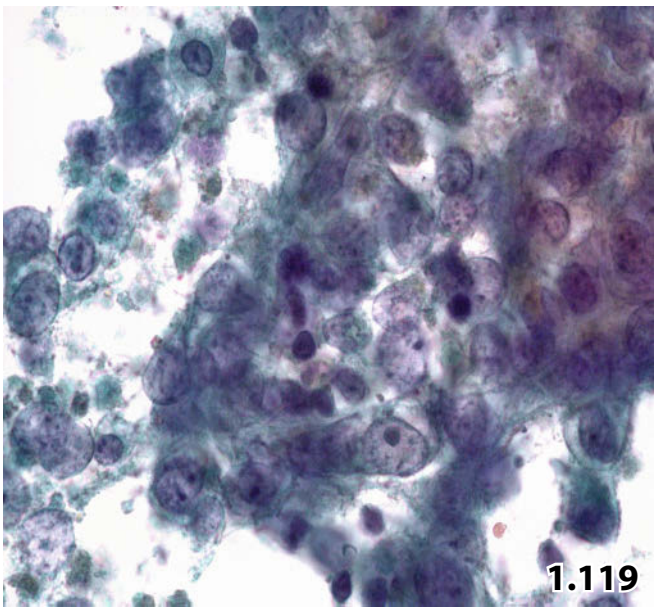
1.119

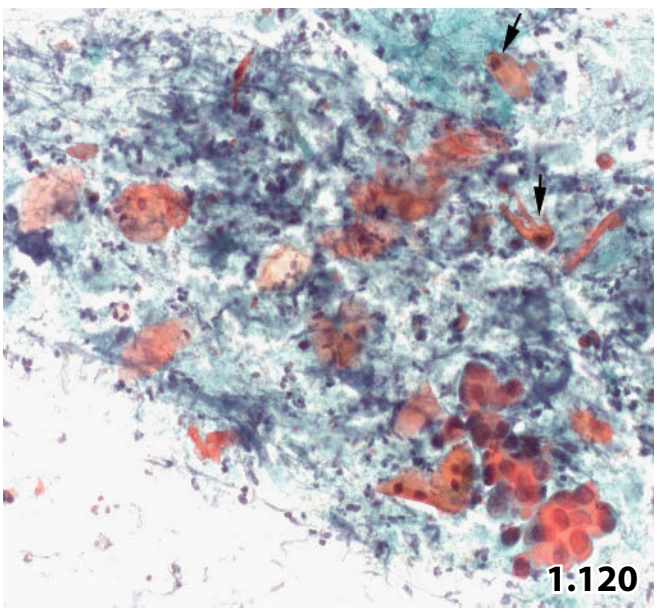
1.120

# Respiratory Tract and Mediastinum 2



Spieler/Rössle, *Nongynecologic Cytopathology. A Practical Guide. Essentials of Diagnostic Pathology*,
DOI 10.1007/978-3-642-24719-4_2, 

## Synopsis and Algorithms

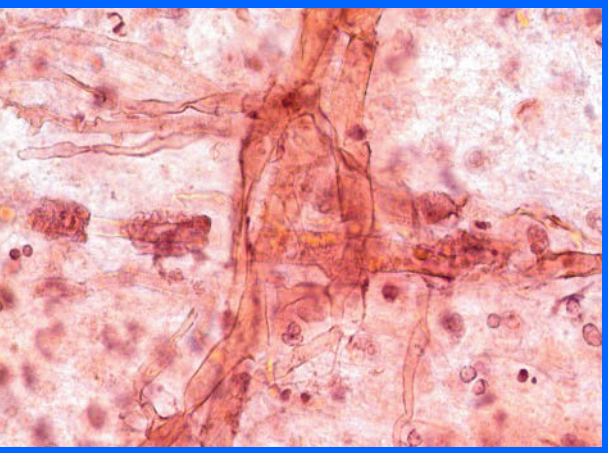

# Section 2.1
# Respiratory Tract: FNAB and Exfoliative Cytology



## 2.1.1 Introduction

**General Comments**

- During the past few decades, the investigation of cytologic samples from the lower respiratory tract has been established in major hospitals, pulmonary clinics, and together with chest physicians' offices throughout the world.
- It has become a common tool in diagnostic evaluation of any patient with suspected lung cancer, particular infectious diseases, and interstitial lung disorders. Furthermore, in recent years fine-needle aspiration biopsy (FNAB) has greatly enhanced the impact of cytology on primary lung cancer diagnosis and tumor staging.
- This section covers:
  (1) The important technical aspects of pulmonary cytology.
  (2) The cytology of exfoliative bronchial and alveolar samples.
  (3) Transthoracic, transbronchial, transesophageal FNAB for diagnosing primary and metastatic lung tumors, and mediastinal lesions.
  (4) Cytologically relevant primary mediastinal pathologic conditions.
- Numerous reviews, monographs, and textbooks are available covering all aspects pertaining to pulmonary cytology.

### 2.1.1.1 Cytopreparatory Methods

#### 2.1.1.1.1 Paraffin Embedding

Paraffin embedding of sputum [110] for histologic work-up was abandoned many years ago. However, the method known as the cell-block technique is still in use for cell material sampled by FNAB and, sporadically, for tissue fragments or clots from exfoliative specimens as well.

#### 2.1.1.1.2 Cell-Freeing Techniques

Techniques for cell freeing and tumor cell concentrating by mucolysis are valuable methods, but they appear to be too laborious and time-consuming in daily practice [11, 53].

#### 2.1.1.1.3 Major Techniques

The major techniques include: the wet-film preparation, the pick-and-smear technique from fresh or prefixed respiratory exfoliative material, the Saccomanno blender technique, and the membrane filtration techniques [14, 23, 94]. These four methods may be used for spontaneously produced or induced sputum, bronchial washings and brushings, bronchoalveolar lavage, and fine-needle aspirates.

*Pick-and-smear from fresh unfixed respiratory material.* This technique generally yields sufficient diagnostic material along with excellent preservation and staining of the cells. The method is highly appreciated at our institution. Fresh early-morning deep-cough specimen of sputum is collected and submitted in a wide-mouthed jar. In the laboratory the specimen is poured into a Petri dish and dispersed for inspection. The mass is examined for grey-white smooth strings of mucus and blood-tinged areas that have been found to most

likely harbor tumor cells. Samples are picked from the selected areas and gently crush-smeared between two glass slides. The smears are immediately placed in 95% ethyl alcohol or Delauney's solution for 15–30 min.

**Caution**

The selection of blood-tinged and/or gray-white mucus strings is critical in correct processing of fresh deep-cough sputum specimens

*Pick-and-smear from prefixed respiratory material*. Prefixed sputum may be obtained in situations where it is not possible to transmit fresh, unfixed material to the laboratory. The patient expectorates into a jar partially filled with 70% ethyl alcohol. The disadvantage of this procedure is insufficient preservation and poor staining quality of the cells trapped in masses of mucus that is penetrated by the fixative and dye with difficulty.

*Saccomanno blender technique*. This technique for homogenization and cell concentration is used for sputum specimens collected in Saccomanno fixative [81]. While in Europe the technique is less accepted, it has gained wide popularity particularly in the United States and on other continents. The method produces artifacts on tumor cells that may impair diagnostic accuracy compared to slide preparations from unfixed sputum samples [73].

#### 2.1.1.1.4 Special Techniques

*The bronchial brush direct smear preparation*. The mucus-rich material adherent to a brush is smeared by rolling the brush over one or more glass slides followed by immediate fixation. This method should only be used by skilled bronchoscopists or an attendant cytotechnologist.

*Cytocentrifugation* is particularly applied to process lavage fluids.

*Liquid-based cytology* is increasingly used for the processing of FNAB material [103]. The advantages and interpretative cautions concerning the liquid-based preparation are reported in the literature [75] and in various chapters of this work (e.g., Sect. 10.1.2.2, p. 634).

#### 2.1.1.1.5 Staining

The Papanicolaou (Pap) method is the most widely accepted staining method for cytologic preparations of respiratory specimens.

### 2.1.1.2 Sampling Modalities

The accuracy of the different modalities as to cancer diagnosis has recently been summarized from published data by Schreiber and McCrory [84].

Sputum has been the most frequently examined sample from the respiratory tract for many decades. Since the introduction of fiberoptic bronchoscopy and the wide use of FNAB, sputum cytology has diminished [58]. Pulmonologists and institutions specialized in lung diseases prefer primary investigation using invasive and more directed methods based upon imaging results and supported by auxiliary device.

#### 2.1.1.2.1 Sputum: Spontaneous and Induced, and Postbronchoscopy Sputum

Sputum specimens are prepared as described. In patients who cannot produce sputum by deep coughing, a sputum sample may be induced by inhalation of an aerosolized solution [72, 80]. The vapor stimulates mucus production and may enhance the coughing stimulus. Another useful physical technique for provoked expectoration is the external percussion and vibration of the chest wall [96]. Postbronchoscopy sputum is an approach used to increase diagnostic accuracy. However, from our experience, a high percentage of postbronchoscopy samples are extremely sanguineous and difficult to evaluate.

**Caution**

Deep-cough specimens and their immediate transfer to the cytology laboratory after collecting are of utmost importance for reliable diagnostic results.

#### 2.1.1.2.2 Bronchial Aspirates, Washings, and Brushing

The development of the flexible fiberoptic bronchoscope has enabled the operator to reach much smaller bronchi compared to those formerly attained by the rigid bronchoscope.

Specimens are obtained from the periphery of the bronchial tree by:

- Aspiration of localized secretions.
- Instilling a few milliliters of a saline solution through the bronchoscope and re-aspiration of the fluid together with the exfoliated cells.
- Brushing a conspicuous lesion with a brush inserted through the endoscope.

Laboratory procedures and technical aspects concerning bronchoalveolar lavage (BAL) are discussed in Sect. 2.3.2, p. 176.

Aspirates and washings, and brush samples rinsed in an appropriate solution (balanced salt solution or cell medium) are to be centrifuged. Subsequently, smears are prepared from the cell button. The different preparation techniques including bronchial brush direct smear preparation have been described above.

Presence of blood in aspirates and brushings is frequent and found most particularly in patients with primary lung cancer involving the bronchial system. Vigorous brushing may provide large tissue fragments from the bronchial wall composed of connective tissue and smooth muscle bundles (Fig. 2.1).

**Caution**

It frequently occurs that cancer cells are included in thick masses of erythrocytes; accordingly target cells become obscured. A careful evaluation of such cytologic specimens is important. Complete absence of tumor cells in extremely sanguineous bronchial material from cancer patients is possible, such that additional cytologic specimens should be prepared from selected areas containing less blood.

#### 2.1.1.2.3 Fine-Needle Aspiration Biopsy Methods

FNAB has led to a revolutionary input to the cytology of the lung. The evolution of sophisticated radiologic and sonographic imaging techniques and improved endoscopic instruments made this progress possible [6].

A variety of techniques exist to visualize and aspirate intrapulmonary lesions, mediastinally located masses, and lymph nodes:

- *Transthoracic FNAB:* A lung mass can be visualized by radiography, computed tomography, or transcutaneous ultrasound. A fine needle attached to a syringe (best attached in a pistol-type holder) is passed through the chest wall into the lesion [28, 34, 87].
- *Transbronchial FNAB:* Modern fiberoptic equipment enables the operator to visualize peripherally located intrabronchial lesions and enlarged peribronchial nodules. The needle is passed through the fiberendoscope and precisely inserted through the bronchial or tracheal wall into the primary pulmonary lesion or peribronchial, hilar, and paratracheal lymph nodes [37, 78].
- *Endoscopic ultrasound-guided FNAB (EUS-FNAB):* In these days, fiberendoscopes can be equipped with highly sophisticated, tiny ultrasound transducers attached to the tip of the instrument. Transbronchial and transtracheal endoscopic ultrasound allows the operator to visualize intramural/submucosal lesions and lesions in adjacent mediastinal compartments that are not detected and not accessible by other techniques, due to their location or their size [78]. Most of these lesions can reliably be evaluated by EUS-FNAB.

  The same technique is applied for transesophageal ultrasound-based minimally invasive morphologic investigation of disorders located adjacent to the esophagus, in the dorsal mediastinal space, and in dorsal regions and the upper lobes of the lung [22, 99, 109].

  Transbronchial, transtracheal and transesophageal EUS-FNAB has become an important tool for staging lung cancer at the time of diagnosis and for assessing diagnosis on otherwise undiagnosed pulmonary and mediastinal masses. [2, 35, 47, 54, 65, 101]. With this procedure, numerous invasive surgical interventions (mediastinoscopy, thoracotomy, thoracoscopy) can be avoided [115].

## 2.1.2 Cell Lining of the Respiratory System and Cell Function

### 2.1.2.1 Ciliated Epithelium

Major portions of the upper and lower respiratory tract are lined by a pseudostratified cuboidal and columnar ciliated epithelium. The function of these cells is the proximal transport of the mucus stream. For this reason, each cell carries approximately 300 cilia (average length 6 $\mu$m) anchored in an apical terminal plate.

### 2.1.2.2 Nonkeratinizing Squamous Epithelium

Nonkeratinizing squamous epithelium predominantly makes up the lining of the oral cavity, throat, and voice box, which represent the main compartments of the upper respiratory tract.

### 2.1.2.3 Mucus-Producing Goblet Cells

Mucus-producing goblet cells are found between ciliated bronchial lining cells; their mucoid glycoprotein is discharged apically. Goblet cells are more numerous proximally in the bronchial tract and increase in number when irritations or certain bronchial disorders occur.

### 2.1.2.4 Basal or Reserve Cells

Adjacent to the basement membrane are small round to polygonal-shaped cells with dark nuclei and scant cytoplasm. These cells are basal or reserve cells and are precursors of the two types of bronchial lining epithelial cells.

### 2.1.2.5 Kulchitsky Cells

Kulchitsky cells are considered part of the diffuse neuroendocrine system. The cells are basally located, occur singly or in groups, and contain cytoplasmic granules.

### 2.1.2.6 Clara Cells

Clara cells are nonmucous and nonciliated secretory, dome-shaped cells found in the bronchioles of the lungs (bronchioles represent the transition from the conducting portion to the respiratory portion of the lung system) and account for the majority of nonciliated bronchiolar cells. They protect the bronchiolar epithelium secreting mucoid and nonmucinous products and contribute to surfactant production. They can also multiply and differentiate into ciliated cells.

#### 2.1.2.7 Alveolar Pneumocytes

Alveolar pneumocytes line the alveoli in the periphery of the lung. The alveolar epithelium comprises two cell types with completely different functions [105]:

- *Type 1* alveolar pneumocytes are very large, flat cells that cover more than 90% of the alveolar surface performing efficient gas exchange. Type 1 pneumocytes are incapable of replication.
- *Type 2* alveolar pneumocytes are small cuboidal to columnar cells comprising about 10% of the alveolar cell lining, ultrastructurally they show prominent microvilli. The cells are responsible for the production and secretion of surfactant that reduces tension of alveolar fluids and maintain alveolar stability (see also Sect. 2.3.4.10, p. 186). Type 2 pneumocytes can replicate and may replace damaged type 1 pneumocytes as well.

### 2.1.3 Normal Cytology and Benign Cellular Components

#### 2.1.3.1 Normal Epithelial Cells (Fig. 2.2)

The normal epithelial components of sputum consist of squamous epithelial cells, usually ciliated columnar cells, bronchiolar cells, and alveolar pneumocytes. The morphology of benign cellular components of respiratory material has repeatedly been described in the literature. References are indicated in the textbook by Johnston and Frable [40] and elsewhere.

##### 2.1.3.1.1 Squamous Cells

These cells exfoliate mainly from the oral cavity and the pharyngeal area. They are generally numerous in sputum but less common in bronchial specimens and are absent in the majority of BALs and FNABs.

- Intermediate squamous cells are characterized by round to oval monomorphic nuclei with smooth membrane and fine loose chromatin. They have a low N/C ratio. The cytoplasm is transparent and cyanophilic.
- Superficial squames have small pyknotic nuclei and broad orangeophilic cytoplasm.

##### 2.1.3.1.2 Columnar Cells

Ciliated columnar cells exfoliate most frequently from the tracheobronchial tree, less frequently from the upper respiratory tract (nasal cavity, sinuses, larynx). Nonciliated cuboidal to columnar cells mainly originate from the bronchioles. Ciliated columnar cells are constantly present in exfoliative respiratory samples. They occur numerously in specimens of induced sputum, in postbronchoscopy sputum, in bronchial aspirates and brushings. They are uncommon in BAL and FNAB specimens.

- The bronchial epithelial cell is characterized by a columnar shape, which at one end tapers off to terminate in a tail-like process. At the opposite or luminal end of the cell, there is a flat terminal plate, anchoring the cilia. The nucleus is located toward the cytoplasmic tail exhibiting a round to oval shape, smooth outline, conspicuous membrane, loose chromatin, and one or multiple small nucleoli.

##### 2.1.3.1.3 Ciliocytophthoria (Fig. 2.3)

Ciliocytophthoria is a specific form of degeneration of ciliated columnar epithelium of the respiratory tract. It was first described by Papanicolaou in 1956 [71]. The cellular alteration has been regarded as a common finding in viral infection.

- Cellular changes include detached ciliary tufts (remnants of ciliated epithelium) and degenerating cytoplasmic fragments with a pyknotic nucleus. Additional round eosinophilic cytoplasmic inclusions may be present. Look-alikes may be seen in body fluids, especially of peritoneal origin and in washings of the pouch of Douglas. They can cause confusion with ciliated protozoa.

##### 2.1.3.1.4 Goblet Cells

Cells of the bronchial lining with extreme mucus production are called goblet cells. They increase in number when irritants interact, and in patients with chronic tracheobronchial disease.

- The nuclei are molded or flattened and displaced to the periphery of the cells. Cytoplasmic mucoid inclusions stain light pink and are translucent in the Papanicolaou staining procedure.

##### 2.1.3.1.5 Parabasal and Basal Cells, Reserve Cell Hyperplasia (Fig. 2.4)

Basal cells (reserve cells) are adherent to the basement membrane of bronchi and bronchioli and are generally covered by the overlying respiratory epithelium. They do not spontaneously exfoliate unless damage occurs to the bronchial lining epithelium. Reserve cells are hardly ever encountered in sputum probes, but they are frequently present in aspirates, bronchial lavages, and particularly in brush specimens. Brushing uncovers deep cell layers enabling an active sampling of the basal cells.

- Basal cells are extremely small (smaller than a small lymphocyte) and round to polygonal. The cytoplasm appears as a scant, densely structured rim and often has a polygonal shape, similar to bronchial metaplastic squamous cells. The nuclei are tiny, darkly stained, and homogeneously structured.
- Reserve cell hyperplasia: Hyperplastic basal cells are mostly grouped in cohesive sheets of variable size. The small cell size and the arrangement in regular sheets exclude a small-cell carcinoma (Fig. 2.4).

**Caution**

Densely clustered basal cells with their deeply stained nuclei may simulate small-cell carcinoma. This is particularly true for bronchial specimens where the cells are entrapped in thick blood masses. However, small cellular and nuclear size together with orderly arrangement are not compatible with any malignant neoplasia.

### 2.1.3.2 Cells of Nonepithelial Origin

#### 2.1.3.2.1 Pulmonary Alveolar Macrophages

(Fig. 2.2)

Alveolar macrophages (AM) are derived from precursor cells called monocytes that first develop in the bone marrow [100]. Monocytes travel throughout the body in the circulatory system of blood. When needed, circulatory monocytes move into tissue, where they become macrophages. Another mechanism of accumulation of alveolar macrophages is hypothesized by increased local proliferation [90]. Alveolar macrophages serve as the front line of cellular defense against respiratory pathogens, clearing the air spaces of infectious, toxic, or allergic particles and ingesting carbon and other inhaled substances [88].

An alveolar macrophage is a mononuclear cell with a high phagocytic capacity on the epithelial surface of lung alveoli. The presence of this cell type in sputum indicates adequacy of the specimen submitted for microscopic evaluation.

- Apart from squamous cells, AMs are the second largest normal cells occurring in bronchial material. Their nuclei are eccentrically positioned, typically bean-shaped, showing a pale thinly dispersed chromatin. One or more small but distinct nucleoli are common. The cytoplasm is abundant and foamy, and includes various types of phagocytized material. Bi- and multinucleation (giant cells) are frequent.

Phagocytized material in the cytoplasm of AMs: The most common material is carbon. In cases of lipid pneumonia, however, AMs exhibit large sharply outlined vacuoles containing fat [50]. The startling cell size and cytoplasmic structure of fat-laden macrophages may overlap with cytologic features of clear cell adenocarcinoma or liposarcoma. However, the AM nuclei are bland and mucus cannot be identified either. Immunocytochemical studies can confirm the cell type in cases with ambiguous cytomorphology (CD68 positivity versus negativity for cytokeratins and other epithelial markers). Phagocytosis of hemosiderin is a sign of previous blood discharge into the alveolar space. Hemosiderin pigments appear as large roundish or square aggregates that are refractile and greenish or rusty colored. For greater detail on hemosiderin pigment, see Sect. 2.3.4.8, "Alveolar Hemorrhage Syndrome," p. 184.

Other noncellular elements are discussed in Sect. 2.1.5, p. 115

**Caution**

The presence of hemosiderin should be confirmed in any critical situation using a special stain for iron.

#### 2.1.3.2.2 Granuloma Cells and Sarcoidosis

Granulomatous diseases of various etiologies may be associated with the presence of characteristic histiocytoid cells in respiratory samples submitted for cytologic testing [79]. Common histiocytes, foam cells, macrophages, leukocytes, small tissue fragments, and detritus may be present in variable amounts.

- Histiocytic giant cells of the foreign-body type show multiple nuclei irregularly distributed within the cytoplasm.
- Nuclei of Langhans-type giant cells are crowded at the periphery, frequently in a horseshoe-like arrangement; the cytoplasm may contain asteroid bodies (Figs. 2.5 and 2.89B).
- Epithelioid cells are elongated mononucleated histiocytoid cells of variable size. The nuclei of Langhans-type cells and epithelioid cells have a bland chromatin structure and a typically elongated nucleus with one end broader than the other. Nucleoli depend on the cellular activity (Fig. 2.6).

*Sarcoidosis*. Langhans-type giant cells together with densely crowded activated epithelioid cells and benign small lymphocytes are highly suggestive of sarcoidosis. Activated epithelioid cells are characterized by enlargement and a more spherical configuration, nucleoli are obvious. Necrosis is absent with few exceptions. More information on sarcoidosis is provided in the Sects. 2.3.4.1, p. 179 and 15.2.5.6, p. 933. Characteristic cellular components of sarcoidosis are rarely encountered in respiratory exfoliative samples. Yet induced sputum, as a noninvasive technique, may be of diagnostic help in pulmonary sarcoidosis regarding the lymphocyte counts [19, 66]. In contrast, EUS-FNAB has been shown to be an extremely accurate method for diagnosing sarcoidosis in patients affected by mediastinal disease [55, 111].

*Mycobacterial granulomatosis* is discussed in Sect. 2.1.6.1, p. 116.

#### 2.1.3.2.3 Neutrophilic Granulocytes

Neutrophils are omnipresent in exfoliative cytologic specimens from the bronchial tree. Abundant polymorphonuclear leukocytes suggest infectious disease. Organisms may be recognized in conventionally stained cytologic specimens, but they are detected with higher accuracy using special stains such as Gram, Ziehl-Neelsen, periodic acid-Schiff reaction (PAS), and silver stains.

**Caution**

Purulent exudates are likely to accompany a mycotic infection. Fungi may be obscured by the inflammatory background and are solely detected using PAS reaction or methenamine silver stain.

#### 2.1.3.2.4 Eosinophilic Granulocytes (Fig. 2.73)

The presence of eosinophilic granulocytes in pulmonary material is often an indicator of a disorder with an allergic component and is most frequently associated with bronchial asthma (see also Sect. 2.1.5, "Charcot-Leyden Crystals," p. 115). A wide variety of etiologies may be responsible for allergic reactions, including inhaled particles, vapor, gases, ingested food, drugs, infectious agents (fungi, parasites), and endogenous processes (intrinsic asthma).

- A characteristic feature of the eosinophilic granulocyte is the bilobed nucleus. This attribute is a diagnostic key feature because the cytoplasmic granules may be faintly visible in Papanicolaou-stained specimens.

#### 2.1.3.2.5 Lymphocytes

These cells are associated with chronic inflammatory processes, granulomatous disease, or acute viral infections. Numerous lymphocytes in a circumscribed area in a smear preparation of sputum and other bronchial material most likely originate from a ruptured lymphoid infiltrate/lymph node located in the bronchial mucosa. Transformed lymphoid cells and starry-sky cells may occasionally be encountered, which makes it easy to exclude small-cell malignant lymphoma (chronic lymphocytic leukemia) and small-cell carcinoma.

- Benign lymphocytes are smaller than cells from a lymphoid or epithelial neoplasia. Nuclear texture of benign lymphocytes is bland, and nucleoli are rare and inconspicuous.

## 2.1.4 Abnormal and Atypical Epithelial Cells

### 2.1.4.1 Etiology

Numerous environmental irritants, various microbiological agents, drugs, chronic lung disorders, embolism [9], bronchial tumors, destructive granulomatous lesions, injuries due to instrumentation, and infarction [41] may induce hyperplastic processes including reactive (atypical) cell changes in the epithelium of the respiratory tract [40].

### 2.1.4.2 Squamous Metaplasia and Abnormal Squamous Cells

**Caution**

Squamous cells that exhibit atypical or frankly malignant features may originate from a regenerative, dysplastic, or neoplastic lesion in the oral/pharyngeal/laryngeal area. In general, only a small number of such cells will be present in exfoliative respiratory specimens [52].

#### 2.1.4.2.1 Squamous Metaplasia (Fig. 2.7)

Squamous metaplasia in reference to the tracheobronchial system means replacement of the ciliated epithelium with a stratified epithelium that resembles immature squamous epithelium. Squamous metaplasia occurs as an abnormal repair response to irritations and to a multitude of environmental toxic agents and organisms [98]. Cigarette smoking is one of the most frequently cited causes responsible for the development of squamous metaplasia [4].

- Metaplastic squamous cells may appear discrete, but typically in small and larger cell groups. The monomorphic cells are arranged in monolayered sheets, whereas the polygonal cell shape gives the sheets a cobblestone-like appearance.
- The cytoplasm is dense and cyanophilic with a smooth outline. Maturing squamous cells become larger with incipient cytoplasmic keratinization (Fig. 2.7).
- Most of the nuclei are dense and patternless with smooth membrane and exhibit a light-blue or gray color with Pap staining. Perinuclear cytoplasmic clearing and karyopyknosis are frequently encountered.

#### 2.1.4.2.2 Atypical Squamous Metaplasia (Figs. 2.8 and 2.9)

Metaplastic squames may undergo changes that should classify them as atypical cells.

- The cells show an increased N/C ratio. The nuclei are slightly irregular in outline and exhibit granular chromatin, hyperchromasia, and nucleoli.

These cellular changes can be associated with prolonged nonneoplastic abnormal conditions of the bronchi and lung, or with carcinoma. It is virtually impossible to differentiate between different grades of atypia and to exclude premalignant epithelial lesions (dysplasia) by light microscopy [12] (Fig. 2.31).

#### 2.1.4.2.3 Abnormal Squamous Cells

Abnormal squamous cells may exfoliate from the oral mucosa. Various diseases such as inflammation, ulceration, infection, chronic mucosal irritation, and others may be responsible for atypical squames, particularly in sputum probes. Cytologic features of the most common disorders of the oral mucosa and adjuvant diagnostic procedures that

could help clarify equivocal cell changes are detailed in Sects. 8.4–8.6, pp. 565.

**Additional Analyses**

Ploidy analysis can be applied to atypical nuclei of mature and immature squamous cells in order to assess their malignant potential more reliably. DNA aneuploidy is a strong indicator for cellular malignancy and its precursors [5, 62, 69]. DNA cytometry on atypical squames is discussed in several chapters of this book, e.g., Sect. 8.4 "DNA Image Cytometry," p. 565.

Computerized cell imaging analyzing morphometric markers may also be helpful for the evaluation of preneoplastic lesions [31].

**Caution**

- Atypical squamous metaplasia is frequently encountered in respiratory samples from patients with lung cancer. Therefore, repeated exfoliative cytology and advanced imaging studies are necessary in patients without an apparent lung lesion [7].
- Image cytometric DNA ploidy assessment can distinguish between reactive atypia and atypical squamous cells with preneoplastic potential. The latter provide DNA aneuploidy, which requires further investigations; a diploid DNA histogram indicates reactive atypia, which should result in monitoring the patient by repeated cytology over a long period.
- Both the progression rate and the regression rate of dysplastic lesions of various morphologic grades should not be disregarded [12]. Both severe cytologic atypia and DNA aneuploidy do not necessarily imply progression to invasive growth.

### 2.1.4.3 Abnormalities in Cells of Bronchial, Terminal Bronchiolar, and Alveolar Epithelium

#### 2.1.4.3.1 Abnormalities in Bronchial Lining Cells

Reactive forms of bronchial epithelial cells cover a wide spectrum ranging from mild cellular changes with inconspicuous nuclear atypias and attached cilia to marked cellular/nuclear alterations that simulate adenocarcinoma [27, 49, 60].

*Multinucleation*

This is a common alteration, most frequently encountered following instrumentation. The cellular shape, terminal plate, and cilia are well preserved, whereas cellular size varies depending on the number of nuclei. The N/C ratio and nuclear features are bland.

*Mild Reactive Cell Changes* (Fig. 2.10A).

Mild irritation of the bronchial epithelium may occur in a number of chronic lung diseases including bronchial asthma, chronic bronchitis, bronchiectasis [43, 64, 82] and tuberculosis. In the majority of cases, the exfoliated single cells and hyperplastic mucosa fragments with mild atypias are accurately recognized as benign, if the cytologic features as indicated below are taken into consideration.

- Mild reactive hyperplasia of the bronchial epithelium is characterized by cohesive cell clusters composed of regularly arranged cells.
- Nuclear structure (pale and reticular) and nuclear shape (slight irregularities but smooth outlines) reveal minor changes. Nucleoli are enlarged but uniform and round.
- Focal preservation of ciliated respiratory cells on the surface of the cell clusters is the most important key as to their benignity.
- Small clusters of tightly grouped cells exhibit some molding of the cytoplasm and occasionally of the nuclei as well.
- Large three-dimensional clusters, the so-called Creola bodies, are papilliform and composed of tightly packed cells. Nuclear details are obscured in large areas and should be carefully evaluated using cells that are not superimposed.
- Highly vacuolated and mucus-producing cells are frequently present in such cell clusters.

*Severe Reactive Cell Changes* (Figs. 2.10B, 2.11–2.13)

Severe atypias due to irritation and proliferation of the bronchial epithelium are easily mistaken for adenocarcinoma. Based on our experience, such changes are mainly caused by viral infections, pulmonary infarction, chronic lung disease with recurrent infections (e.g., bronchiectasis), instrumentation, and toxic chemical agents (e.g., oxygen inhalation) [17, 42]. They may also be observed after radiation therapy [108] and chemotherapy [15, 97].

- The cell clusters may be loose or tight; irregular cellular arrangement, loss of nuclear polarity, and cellular/nuclear overlapping are pronounced.
- Isolated atypical cells may be numerous or completely absent.
- Three-dimensional acinar cell groups as in adenocarcinomas are often encountered. They are characterized by central nuclear clustering and clear vacuolated cytoplasm protruding to the periphery, resembling hobnails. The contour of the clusters may be sharply delineated or knobby.
- All atypical cells are enlarged. The N/C ratio may be normal or slightly increased compared to normal epithelial cells.
- The nuclear outline tends to be smooth but molding and cleaving are possible. The chromatin structure varies from loose or finely granular to coarsely granular and clumping.

- The nucleoplasm may be pale or deep blue in color. The nucleoli occur alone or in groups; they are significantly enlarged and may show pleomorphism.
- Terminal plates and cilia are hardly ever observed together with severe reactive cell atypias.
- The cytoplasm ranges from normal-sized (finely vacuolized) to enlarged (due to large vacuoles).
- Atypical squamous metaplastic cells may appear concomitantly with glandular cell hyperplasia.

#### 2.1.4.3.2 Hyperplasia of Terminal Bronchiolar and Alveolar Epithelium (Figs. 2.72 and 2.84)

- Hyperplastic epithelial components from the terminal bronchioles and alveoli are infrequently encountered, both in sputum and bronchial samples. However, if such cells and cell clusters are present they often pose a major diagnostic challenge as to bronchioloalveolar carcinoma, particularly in bronchoalveolar lavage [8, 32, 91].
- Reactive and proliferative changes of terminal bronchiolar epithelial cells and type II pneumocytes occur with respiratory disorders such as interstitial pneumopathy, organizing pulmonary fibrosis, pulmonary embolism [9], pulmonary infarction, infections particularly of viral origin, and others. Furthermore, radiation and chemotherapy may irritate not only tracheobronchial epithelial cells, but also alveolar epithelium and cells lining the terminal bronchioli.

**Microscopic Features and Differential Diagnosis**

A large spectrum of cellular changes from small cells to pronounced hyperplastic large cells may be seen, frequently mimicking adenocarcinoma. Cell changes share many features with those described for hyperplastic bronchial epithelial cells (Sect. 2.1.4.3.1, p. 113).

*Large hyperplastic type II pneumocytes* can usually be separated from cells of adenocarcinoma by:

- A transient mode with respect to a varying cell amount in subsequent specimens.
- Diverse cytomorphologic manifestations in the same preparation, e.g., wide ranges in the N/C ratio, pale versus hyperchromatic nucleoplasm.
- Their sparse number.
- Their degenerative features.

Epithelial hyperplasia composed of abnormal large cells appearing singly and in atypical cell groups may strongly mimic adenocarcinoma. Furthermore, predominance of atypical single cells may pose difficulties distinguishing benign epithelial proliferation from both malignant lymphoma of the large cell type and malignant melanoma.Stanley and coauthors [91] and numerous related reports deal with the cytologic features of reactive type II pneumocytes and differential diagnostic considerations.

*Small atypical cells:* Small-cell type atypical proliferation resembles bronchioloalveolar carcinoma.

- The cells occur individually, or may be grouped in small papilliform or alveolar tissue fragments.
- The N/C ratio varies widely but is often high.
- The nuclei exhibit membrane irregularities and prominent nucleoli.
- Other than that, the cytologic features are identical, as described for proliferating bronchial lining cells.

**Caution**

- Diagnosis of adenocarcinoma in respiratory exfoliative cytology must be based on large numbers of atypical cells and cell clusters that exhibit unequivocal features of malignancy, in order to avoid false-positive diagnoses. Sparse solitary cells with severe atypias more likely suggest a reactive disorder.
- Bronchoalveolar lavage may contain numerous clusters with severe regenerative cell changes indistinguishable from adenocarcinoma and bronchioloalveolar carcinoma, respectively.
- Clinical information, laboratory results, and image findings are invaluable in order to prevent a false-positive or false-negative cytologic diagnosis [16, 91]. Reactive atypical proliferation appears transient and should disappear within a few days to a few weeks. Thus, repeated cytological tests may be a prudent approach in equivocal situations.
- Adenomatous atypical hyperplasia is believed to have a potential to progress to peripheral lung adenocarcinoma (see Sect. 2.2.2.1, "Preinvasive Lesions," p. 138).

#### 2.1.4.3.3 Peculiar Cellular Response to Irradiation and Chemotherapy (Figs. 2.13 and 2.72)

Reactive cell changes induced by irradiation and chemotherapy can be easily recognized by experienced microscopists.

**Microscopic Features**

- The atypical cells are markedly enlarged, many of them show multinucleation.
- The N/C ratio is preserved; cytoplasmic vacuoles are numerous and prominent.
- The nuclei are pleomorphic; they frequently show indentations and grooves. Occasional nuclear vacuolization.
- The chromatin texture is characterized by fine and coarse granules; and chromatin strands outlining nuclear areas give the nucleus a peculiar empty look.
- Macronucleoli.

**Caution**

Carcinoma cells and benign epithelial cells showing strong degenerative changes induced by ionizing radiation are difficult to distinguish from each other.

### Additional Analyses

#### Immunocytochemistry

Guzman and coworkers showed that proliferative type II pneumocytes share many antigens with epithelial tumor cells, including keratins and TTF-1. Thus, immunocytochemical tests are of little help to differentiate between reactive pneumocytes and malignant cells [33].

#### DNA Ploidy

Several reports suggest DNA analysis on cytologic respiratory samples to be a reliable tool for the detection of early lung cancer and of high-risk patients with cellular atypias [5, 70, 95, 112]. Automated DNA quantitation by image cytometry on cells in sputum and bronchial washings appears to be a sensitive method for the detection of malignancy and therefore also seems suited for screening procedures [44, 51]; DNA aneuploidy serves as a marker for malignancy [113].

DNA flow cytometry has also been applied to various respiratory cytology specimens as an adjunct in cancer diagnosis; diagnostic accuracy is expected to increase [116].

**Caution**

As stated earlier, carcinoma cells are difficult to separate from benign epithelial cells showing marked ionizing radiation-induced degenerative changes. Since radiotherapy can cause major quantitative and structural alterations to the nuclear chromatin, DNA quantification will also be of little help in this setting and may contribute to enhanced confusion in assessing malignancy.

#### Cytomorphometric Analysis

A few reports discuss the significance of morphometric criteria distinguishing between benign reactive epithelial proliferations and bronchioloalveolar carcinoma [24, 117].

#### Molecular Genetics

Recent studies indicate that different genetic analyses using PCR and fluorescence in situ hybridization (FISH) assay yield valuable results for the detection of precancerous lesions and early-stage cancer [36, 45, 48, 89]. On that score, we recently contributed to a bi-institutional study that showed that a commercially available multitarget FISH assay (LA Vysion; Abbott/Vysis; Downers Grove, IL, USA) simultaneously analyzing chromosome 6 and the 5p15, 7p12 (*EGFR* gene), and 8q24 (*MYC* gene) loci, is very helpful in elucidating equivocal lung cytology, differentiating between regenerative-benign and neoplastic cell changes [83].

## 2.1.5 Endogenous and Exogenous Noncellular Elements and Nonhuman Cellular Components

Numerous noncellular structures may be present in cytologic samples from the respiratory tract. Some of them may indicate a specific pulmonary disorder, some are derived from the patient, some may have been inhaled, and some are contaminants from the environment to the cytologic specimen. Some of these elements may be confusing and may lead the less experienced cytologist to incorrect diagnoses.

*Curschmann spirals* are casts of mucus showing varying degrees of inspissation. They are frequently associated with bronchial asthma and heavy smoking, but the common cause is bronchial obstruction [102].

*Mucus spheres* with a pseudo-organoid appearance or with deep staining should not be misinterpreted as cells or nuclei.

*Alveolar proteinosis* may deliver amorphous masses into bronchial canaliculi. Their morphologic characteristics are discussed in Sect. 2.3.4.10, "Alveolar Proteinosis," p. 186 (Figs. 2.78 and 2.79).

*Charcot-Leyden crystals* may be found together with eosinophils in people who suffer from any form of allergic disease; however, in respiratory material they constitute a distinct sign of bronchial asthma. The crystals are derived from disintegrated eosinophils. Charcot-Leyden crystals vary in size and reach a length up to 50 $\mu$m. They are composed of two slender pyramids joining at their bases and tapering into pointed ends, they stain purplish-red with the Papanicolaou method (Fig. 2.14).

*Corpora amylacea* are rounded, hyaline bodies presenting with striations and concentric rings; they are condensates of glycoproteins. Corpora amylacea are formed in the bronchial tubes and in the alveolar spaces. Association with chronic lung disorders is well known.

*Calcospherites* (synonym: psammoma body) appear like corpora amylacea but they contain various anorganic compounds and are calcified. Calcospherites are related to lithiasis of the lung and to primary and secondary adenomatous cancers.

*Ferruginous bodies* (Figs. 2.15 and 2.75) result from inhalation of diverse mineral fibers that become coated with varying substances; ferroprotein is the fraction that yields the typical golden-brown color in Papanicolaou-stained specimens and the positive reaction with iron stains (e.g., Prussian Blue).

A high percentage of ferruginous bodies are seen together with one or more stimulated macrophages, which interact in the forming of these structures and try to ingest the foreign particles [20].

The encrustation of the fibers is extremely irregular, giving them the characteristic beaded bamboo shape segmentation of the shaft and blebs and buds on the branching and bulbous protrusions at both ends. Beaded slender rods with a smooth surface of the protrusions at both ends are most likely associated with asbestos bodies. Asbestos fibers, in interaction with other toxic elements, are responsible for asbestosis (and pulmonary fibrosis) of the lung, lung cancer, and mesothelioma. See also Sect. 2.3.4.9, "Pneumoconioses,." p. 184.

*Plant cells* (Fig. 2.16) disclose a typical morphology and a characteristic layering; in general they are much larger than human cells. Experienced examiners will not mistake these cells for malignancy.

*Microspores of pollen* (Fig. 2.17) show indentations and a thick outer membrane. They should not be confused with yeast cells, vermicular eggs, or even atypical/malignant cells.

## 2.1.6 Infectious Diseases

### 2.1.6.1 Mycobacterial Infection [63, 79]

Components of granulomatous tubercles may be encountered both in exfoliated bronchial material and in FNAB. The occurrence of Langhans-type giant cells and epithelioid cells, together with caseous detritus and neutrophils, is highly suggestive of pulmonary tuberculosis. Atypical mycobacterial disease may present identical cytologic features but is caused by different type species of acid-fast bacilli and has completely different epidemiologic implications.

**Microscopic Features**

- The cytomorphology of Langhans-type giant cells and epithelioid cells is described in Sect. 2.1.3.2.2, "Granuloma Cells and Sarcoidosis," p. 111.
- Hallmarks: Compared to epithelioid cells in sarcoidosis, epithelioid cells in mycobacterial infection are more elongated and more slender, disclosing thinly elongated nuclei that are frequently pyknotic. Caseous necrosis consists of finely granular material in an opaque background (Fig. 2.18A).
- Epithelioid cells and detritus are frequently enmeshed in mucoid strands.

Searching for acid-fast bacilli in cytologic material by means of Ziehl-Neelsen stain is rarely effective (Fig. 2.18B). Bacteriologic procedures in a specialized laboratory are recommended for an accurate diagnosis including mycobacterial typing.

**Differential Diagnosis**

- As a rare exception, sarcoid granulomas may include caseation.
- Epithelioid granulomatosis is also encountered in other types of chronic inflammatory processes of the lung and may occur adjacent to malignant lesions [79].
- Caseous necrosis should not be misinterpreted as tumor necrosis.
- Elongated and somewhat pleomorphic epithelioid cells including dense cytoplasm and deeply stained pyknotic nuclei may mimic malignant squamous cells.

**Caution**

- Beware of cancer diagnosis in exfoliated bronchial material containing great amounts of degenerating epithelioid cells and coarse-type caseous detritus!
- Tuberculoid granulomas may occur in the immediate proximity of lung cancers as a nonspecific reactive process; on the other hand, lung cancer may also coincide with tuberculosis [56].

### 2.1.6.2 Viral Infections

Bronchial epithelial cells seem to be primarily affected in viral lung disorders; various types of cell changes are encountered in response to viral respiratory tract infections [25, 59].

#### 2.1.6.2.1 Nonspecific Virus-Induced Cell Changes (Fig. 2.19)

These alterations are particularly observed in patients with parainfluenza and adenovirus infections:

- Atypias are that of regeneration and repair of the respiratory epithelium. The enlarged cells show hyperchromatic nuclei and prominent nucleoli. Occasional multinucleation, pale nucleoplasm, and nuclear inclusions may occur. The chromatin texture is bland. Nuclear irregularities are variable and the N/C ratio is normal compared with benign bronchial epithelial cells (see also Sect. 2.1.4.3, p. 113). False-positive diagnosis of adenocarcinoma is possible.
- A common finding in viral infections, especially induced by the adenovirus, is the degenerative cell change termed ciliocytophthoria. The morphologic description is given in Sect. 2.1.3.1.3, p. 110.

#### 2.1.6.2.2 Specific Virus-Induced Cell Changes

The cytomorphologic recognition of certain viral infections with their specific cellular alterations has a practical significance not only in samples derived from the respiratory tract, but also from many other organs of the human the body, e.g., in cervical smears, cerebrospinal fluid, and esophageal and skin brushes.

**Herpes Simplex Virus** [29, 61] (Fig. 2.20)

Cellular changes induced by herpes simplex virus are distinctive:

- Bronchial epithelial cells are enlarged and rounded showing mono- or multinucleation and a distinct narrow cytoplasmic rim. The nuclei exhibit characteristic ground-glass texture, cyanophilic or eosinophilic inclusions, and granular condensation of the chromatin to the nuclear periphery. Nuclear molding frequently occurs.

**Cytomegalovirus** [1, 39, 106] (Fig. 2.83)
This is a virus of the herpesvirus group. Infection with cytomegalovirus is found in all geographic locations and can be life-threatening for patients who are immunocompromised (e.g., AIDS patients, organ-transplant recipients):

- Cytomegalic inclusion disease is characterized by striking enlargement of the affected cells, which contain a huge nucleus. Only a few cells may show multinucleation.
- The nuclei include a single deeply basophilic inclusion with inhomogeneous areas. The sharply demarcated inclusion is surrounded by a clear halo separating it from the nuclear membrane, resulting in an owl eye appearance (Fig. 2.83).
- The condensed chromatin is compressed against the inner surface of the nuclear membrane. A pearl necklace-like configuration may be observed.
- Intracytoplasmic, orangeophilic inclusions may be present, in addition to the classical intranuclear inclusion.

**Caution**

- Particularly cytomegalic cell changes, but also other phenotypes of cell alteration caused by viral infestation could mislead the inexperienced cytologist to an erroneous diagnosis of carcinoma.
- A careful search for individual cells with signs of cytomegalovirus infection is essential in any cytologic sample from immunocompromised patients.
- Cytomegalic inclusion disease is occasionally combined with other infectious diseases, particularly with protozoa (e.g., *Pneumocystis jirovecii* infection) [104] and mycoses.

**Respiratory Syncytial Virus** [59] (Fig. 2.21)

- This infection is characterized by formation of enormous syncytial cell aggregates. The cytoplasm contains darkly stained inclusions with clear halos.

**Measles**

- Large multinucleated giant cells show small cytoplasmic and nuclear inclusion bodies, as indicated by Naib [59].

### 2.1.6.3 Pulmonary Mycoses

Mycotic infections have significantly increased:

- Since the implementation of chemotherapeutic and immunosuppressive drugs in therapeutic regimes.
- Because of the obvious increase in malignancies and longer patient survival.
- Because of higher incidence of immunocompromising viral infections.
- The majority of mycotic organisms can be identified in cytologic preparations from the respiratory tract. Routine cytological stains are usually adequate for identification. Special staining procedures are helpful in samples containing only a few fungi and in samples with concomitant acute florid inflammatory infiltrates that obscure the organisms. Grocott-Gomori methenamine-silver stain is the best stain to use, but periodic acid-Schiff may also be effective.

#### 2.1.6.3.1 Primary Pathogenic Fungi

(Figs. 2.81 and 2.82)
The primary pathogenic fungi constitute a large group of variable organisms.The most common organisms of importance in routine cytology are *Cryptococcus neoformans*, *Blastomyces dermatitidis*, *Coccidioides*, and *Histoplasma capsulatum*. We refer the reader to distinguished textbooks, directed publications, and internet data bases for detailed information and morphologic descriptions of mycotic pathogens.

#### 2.1.6.3.2 Most Common Opportunistic Fungi

Opportunistic organisms are saprophytes that contribute to the normal flora in different body sites, but that may become pathogenic in immunosuppressed individuals. Sputum specimens, endoscopically sampled respiratory material, and fine-needle aspirates exhibiting fungi of any opportunistic type together with a purulent inflammation should raise suspicion of a mycosis.

**Candida albicans**
*Candida albicans* can be found in a high percentage of the sputum probes, but its presence most often has no clinical significance. *Candida albicans* in lavages and brushings from the respiratory system suggests true infectious disease, provided that a contamination from oropharyngeal sites is excluded.

- *Candida albicans* appears by light microscopy as round to oval single yeast cells, in groups of two, and as chains called pseudohyphae (Fig. 2.22).

**Aspergillosis**
Aspergillosis may present as diffuse pulmonary infection or may occur as a solitary lung lesion by colonization with *Aspergillus* species of a preexisting cavity in the lung (aspergilloma). A third form of aspergillosis are the Aspergillus-associated hypersensitivity respiratory disorders [86]; allergic bronchopulmonary aspergillosis can be suspected if bronchial secretions and brushings reveal aspergillus hyphae intermingled with eosinophilic granulocytes.

- *Aspergilli* are easily recognized by the uniformly wide and septate hyphae with their rectangular branching (Figs. 2.23 and 2.24).
- A key feature of allergic bronchopulmonary aspergillosis is the additional presence of eosinophils.

Mucormycosis is caused by inhalation of *Mucor spores*. The disorder most commonly affects the nose and the brain (rhinocerebral mucormycosis) and is a severe and potentially fatal infection. Widespread extension and invasion of the blood vessels is pathognomonic for this fungus.

- The morphology of *Mucor* is similar to *Aspergillus* with branching of the hyphae at a 90° angle. Contrary to *Aspergillus*, the hyphae are nonseptate and show great variability in width. The presence of conidiophores is a distinctive feature (Fig. 2.25).
- Neutrophilic infiltrates and detritus are usually pronounced.

### Pneumocystis

*Pneumocystis* (*Pneumocystis jirovecii*, formerly known as *Pneumocystis carinii*)

- Phylogenetic reclassifications of *Pneumocystis* as a fungus resulted in a nomenclatural shift from the Zoological Code to the International Code of Botanical Nomenclature [77]. The correctness of the newly proposed names is controversial [26]. The nomenclature of *Pneumocystis* has recently been reviewed by Redhead and colleagues [77].
- Pneumocystis pneumonia (PCP) is a potentially lifethreatening opportunistic infection in organ-transplant recipients and in patients suffering from acquired immune deficiency syndrome (AIDS).
- In certain areas of the world and in poor environmental conditions, *Pneumocystis* is still considered an important cause of pneumonia in children.

**Microscopic features** (Figs. 2.26 and 2.80)

The organism is found in three distinct morphologic stages: the trophozoite or trophic form, the sporozoite as a precystic form, and the cyst, which contains several intracystic bodies also known as spores [74].

- Hallmarks: The organisms are tiny and more or less spherical, measuring 4–5 $\mu$m in diameter. The capsule is smooth and deeply stained. Disintegrated cysts show a single deep groove or may be crescent shaped or crinkled. Focal thickening of the cyst wall is easily recognized by light microscopy. This phenomenon has been reported as an important diagnostic criterion for the identification of *Pneumocystis* and to differentiate them from yeast-form fungi [107]. Organisms presenting as a dense, foamy mass with irregular margins on Pap-stained smears is characteristic in such a manner that an accurate diagnosis even without special stains can be rendered [30, 85].
- The different morphologic stages of the organism with their intracystic bodies are more easily identified by Giemsa stain than by the Papanicolaou staining method.
- Restaining of Pap preparations with methenamine silver immediately accentuates the pathognomonic diagnostic features of *Pneumocystis* (Fig. 2.26). Toluidine blue O is also suitable for quick identification of the agents.
- Small numbers of organisms that are haphazardly arranged can only be recognized by use of special stain (methenamine silver).

The diagnostically reliable dense foamy masses of organisms generally occur in bronchoalveolar lavage and in lavage and brushing from the very peripheral areas of the bronchial system, as well as in fine-needle aspirations. Induced or postbronchoscopy sputum specimens may have an acceptable diagnostic accuracy as well [10]. Spontaneous sputum has a low sensitivity in detecting *Pneumocystes*; therefore this method should not be applied in the routine evaluation of patients with AIDS and pulmonary complaints [18].

**Differential Diagnosis**

*Pneumocystes* should not be confused with non-living elements such as degenerating and leached out erythrocytes clustering together. Furthermore, it is difficult to separate *Pneumocystis* from other organisms, in particular from yeast-form fungi such as *Candida* species and *Histoplasma* [13, 107].

## 2.1.6.4 Parasitic Infections

A number of parasites can be detected cytologically in respiratory material and have been reported in the medical literature including *Strongyloides stercoralis* [46, 114], *Echinococcus* (pulmonary echinococcosis) [68] (Figs. 9.7, 9.8, 12.5), *Trichomonas* [21, 67], *Microfilaria* [38, 57], *Toxoplasma gondii*, *Cryptosporidia* [92, 93] , and others.

## 2.1.7 Further Reading


1. An-Foraker SH, Haesaert S. Cytomegalic virus inclusion body in bronchial brushing material. Acta Cytol 1977;21:181-182.
2. Ang TL, Tee AK, Fock KM, et al. Endoscopic ultrasound-guided fine needle aspiration in the evaluation of suspected lung cancer. Respir Med 2007;101:1299-1304.
3. Armbruster C, Bernhardt K, Setinek U. Pulmonary tumorlet. A case report of a diagnostic pitfall in cytology. Acta Cytol 2008;52:223-227.
4. Auerbach O, Hammond EC, Garfinkel L. Changes in bronchial epithelium in relation to cigarette smoking 1955-1960 vs 1970-1977. N Engl J Med 1979;300:381-386.
5. Auffermann W, Böcking A. Early detection of precancerous lesions in dysplasias of the lung by rapid DNA image cytometry. Anal Quant Cytol Histol 1985;7:218-226.
6. Baba M, Iyoda A, Yasufuku K, et al. Preoperative cytodiagnosis of very small-sized peripheral-type primary lung cancer. Lung Cancer 2002;37:277-280.
7. Baky AA, Winkler DG, Hunter NR, et al. Atypia status index of respiratory cells: a measurement for the detection and monitoring of neoplastic changes in squamous cell carcinogenesis. Anal Quant Cytol 1980;2:175-185.
8. Beskow CO, Drachenberg CB, Bourquin PM, et al. Diffuse alveolar damage. Morphologic features in bronchoalveolar lavage fluid. Acta Cytol 2000;44:640-646.

9. Bewtra C, Dewan N, O'Donahue WJ Jr. Exfoliative sputum cytology in pulmonary embolism. Acta Cytol 1983;27:489-496.
10. Bigby TD, Margolskee D, Curtis JL, et al. The usefulness of induced sputum in the diagnosis of *Pneumocystis carinii* pneumonia in patients with the acquired immunodeficiency syndrome. Am Rev Respir Dis 1986;133:515-518.
11. Bonime RG. Improved procedure for the preparation of pulmonary cytology smears. Acta Cytol 1972;16:543-545.
12. Breuer RH, Pasic A, Smit EF, et al. The natural course of preneoplastic lesions in bronchial epithelium. Clin Cancer Res 2005;11:537-543.
13. Chan JK, Tsang DN, Wong DK. Penicillium marneffei in bronchoalveolar lavage fluid. Acta cytol 1989;33:523-526.
14. Chang JP, Aken M, Russell WO. Sputum cell concentration by membrane filtration for cancer diagnosis: a preliminary report. Acta Cytol 1961;5:168-172.
15. Collis CH. Lung damage from cytotoxic drugs. Cancer Chemother Pharmacol 1980;4:17-27.
16. Crapanzano JP, Zakowski MF. Diagnostic dilemmas in pulmonary cytology. Cancer 2001;93:364-375.
17. Crapo JD. Morphologic changes in pulmonary oxygen toxicity. Annu Rev Physiol 1986;48:721-731.
18. del Rio C, Guarner J, Honig EG, Slade BA. Sputum examination in the diagnosis of *Pneumocystis carinii* pneumonia in the acquired immunodeficiency syndrome. Arch Pathol Lab Med 1988;112:1229-1232.
19. D'Ippolito R, Foresi A, Chetta A, et al. Induced sputum in patients with newly diagnosed sarcoidosis: comparison with bronchial wash and BAL. Chest 1999;115:1611-1615.
20. Dodson RF, Atkinson MA, O'sullivan M. Stability of ferruginous bodies in human lung tissue following death, embalmment, and burial. Inhal Toxicol 2005;17:789-795.
21. Duboucher C, Caby S, Chabé M, et al. Human pulmonary trichomonoses. Presse Med 2007;36:835-839.
22. Fernandez-Esparrach G, Gines A, Belda J, et al. Transesophageal ultrasound-guided fine needle aspiration imprroves mediastinal staging in patients with non-small cell lung cancer and normal mediastinum on computed tomography. Lung Cancer 2006;54:35-40.
23. Fields MJ, Martin WF, Young BL, Tweeddale DN. Application of the Nedelkoff-Christopherson millipore method to sputum cytology Acta Cytol 1966;10:220-222.
24. Fiorella RM, Gurley SD, Dubey S. Cytologic distinction between bronchioloalveolar carcinoma and reactive/reparative respiratory epithelium: a cytomorphometric analysis. Diagn Cytopathol 1998;19:270-273.
25. Frable WJ, Frable MA, Seney FD. Viral infections of the respiratory tract . Cytopathologic and clinical analysis. Acta Cytol 1977;21:32-36.
26. Gigliotti F. *Pneumocystis carinii*: has the name really been changed? Clin Infect Dis 2005;41:1752-1755.
27. Glatz K, Savic S, Glatz D, et al. An Online Quiz uncovers limitations of morphology in equivocal lung cytology. Cancer(Cancer Cytopathol) 2006;108:480-487.
28. Gouliamos AD, Giannopoulos DH, Panagi GM, et al. Computed tomography-guided fine needle aspiration of peripheral lung opacities. An initial diagnostic procedure? Acta Cytol 2000;44:344-348.
29. Graham BS, Snell JD Jr. Herpes simplex virus infection of the adult lower respiratory tract. Medicine(Baltimore) 1983;62:384-393.
30. Greaves TS, Strigle SM. The recognition of *Pneumocystis carinii* in routine Papanicolaou-stained smears. Acta Cytol 1985;29:714-720.
31. Greenberg SD, Spjut HJ, Estrada RG, et al. Morphometric markers for the evaluation of preneoplastic lesions in the lung. Diagnostic evaluation by high-resolution image analysis of atypical cells in sputum specimens. Anal Quant Cytol Histol 1987;9:49-54.
32. Grotte D, Stanlery MW, Swanson PE, et al. Reactive type II pneumocytes in bronchoalveolar lavage fluid from adult respiratory distress syndrome can be mistaken for cells of adenocarcinoma. Diagn Cytopathol 1990;6:317-322.
33. Guzman J, Izumi T, Nagai S, Costabel U. Immunocytochemical characterization of isolated human type II pneumocytes. Acta Cytol 1994;38:539-542.
34. Halloush RA, Khasawneh FA, Saleh HA, et al. Fine needle aspiration cytology of lung lesions: a clinicopathological and cytopathological review of 150 cases with emphasis on the relation between the number of passes and the incidence of pneumothorax. Cytopathology 2007;18:44-51.
35. Herth FJ, Eberhardt R, Vilmann P, et al. Real-time endobronchial ultrasound guided transbronchial needle aspiration for sampling mediastinal lymph nodes. Thorax 2006;61:795-798.
36. Hsu HS, Chen TP, Wen CK, et al. Multiple genetic and epigenetic biomarkers for lung cancer detection in cytologically negative sputum and a nested case-control study for risk assessment. J Pathol 2007;213:412-419.
37. Iyoda A, Baba M, Shibuya K, et al. Transbronchial fine needle aspiration cytological examination: a useful tool for diagnosing primary lung cancer. Thorac Cardiovasc Surg 2006;54:117-119.
38. Jain S, Sodhani P, Gupta S, et al. Cytomorphology of filariasis revisited. Expansion of the morphologic spectrum and coexistence with other lesions. Acta Cytol 2001;45:186-191.
39. Jain U, Mani K, Frable WJ. Cytomegalic inclusion disease: Cytologic diagnosis from bronchial brushing material. Acta Cytol 1973;17:467-468.
40. Johnston WW, Frable WJ. Diagnostic respiratory cytopathology. Masson Publishing USA, Inc. 1979.
41. Kaminsky DA, Leiman G. False-positive sputum cytology in a case of pulmonary infarction. Respir Care 2004;49:186-188.
42. Katzenstein AL, Bloor CM, Leibow AA. Diffuse alveolar damage – the role of oxygen, shock, and related factors. A review. Am J Pathol 1976;85:209-228.
43. Kawecka M. Cytological evaluation of sputum in patients with bronchiectasis and the possibilities of erroneous diagnosis of cancer. Acta Unio Int Contra Cancrum 1959;15:469-473.
44. Kemp RA, Reinders DM, Turic B. Detection of lung cancer by automated sputum cytometry. J Thorac Oncol 2007;2:993-1000.
45. Kim H, Kwon YM, Kim JS, et al. Tumor-specific methylation in bronchial lavage for the early detection of non-small-cell lung cancer. J Clin Oncol 2004;22:2363-2370.
46. Kramer MR, Gregg PA, Goldstein M, et al. Disseminated strongyloidiasis in AIDS and non-AIDS immunocompromised hosts: diagnosis by sputum and bronchoalveolar lavage. South Med J 1990;83:1226-1229.
47. Lai R. Endoscopic ultrasound-guided fine needle aspiration for diagnosis of recurrent nonsmall cell lung cancer. Ann Thorac Surg 2005;80:2346-2349.
48. Li R, Todd NW, Qiu Q, et al. Genetic deletions in sputum as diagnostic markers for early detection of stage I non-small cell lung cancer. Clin Cancer Res 2007;13:482-487.
49. Linder J. Errors and pitfalls in lung and pleural cytology. Monogr Pathol 1997;39:40-59.
50. Losner S, Volk BW, Slade WR, et al. Diagnosis of lipid pneumonia by examination of sputum. Am J Clin Pathol 1950;20:539-545.
51. Marek W, Krampe S, Dickgreber NJ, et al. Automated quantitative image cytometry of bronchial washings in suspected lung cancer: comparison with cytology, histology and clinical diagnosis. Pneumologie 1999;53:583-595.
52. Matsuda M, Nagumo S, Horai T, Yoshino K. Cytologic diagnosis of laryngeal and hypopharyngeal squamous cell carcinoma in sputum. Acta Cytol 1988;32:655-657.
53. McCarty SA. Solving the cytopreparation problem of mucoid specimens with a mucoliquefying agent (Mucolexx) and Nuclepore filters. Acta Cytol 1972;16:221-223.
54. Micames CG, McCrory DC, Pavey DA, et al. Endoscopic ultrasound-guided fine-needle aspiration for non-small cell lung cancer staging: A systematic review and metaanalysis. Chest 2007;131:539-548.

55. Michael H, Ho S, Pollack B, et al. Diagnosis of intraabdominal and mediastinal sarcoidosis with EUS-guided FNA. Gastrointest Endosc 2008;67:28-34.
56. Morell R, Bardaji O, Delon J, et al. Cytopathological study of the sputum in cases of pulmonary cancer-tuberculosis association. Mars Med 1972;109:724-726.
57. Munjal S, Gupta JC, Munjal KR. Microfilariae in laryngeal and pharyngeal brushing smears from a case of carcinoma of the pharynx. Acta Cytol 1985;29:1009-1010.
58. Murray KL, Duvall E, Salter DM, Monaghan H. Efficacy and pattern of use of sputum cytology as a diagnostic test. Cytopathology 2002;13:350-354.
59. Naib ZM, Stewart JA, Dowdle WR, et al. Cytological features of viral respiratory tract infections. Acta Cytol 1968;12:162-171.
60. Naryshkin S, Young NA. Respiratory cytology: A review of non-neoplastic mimics of malignancy. Diagn Cytopathol 1993;9:89-97. .
61. Nash G, Foley FD. Herpetic infection of the middle and lower respiratory tract. Amer J Clin Pathol 1970;54:857-863.
62. Nasiell M, Kato H, Auer G, et al. Cytomorphological grading and Feulgen DNA analysis of metaplastic and neoplastic bronchial cells. Cancer 1978;41:1511-1521.
63. Nasiell M, Roger V, Nasiell K, et al. Cytologic findings indicating pulmonary tuberculosis. I. The diagnostic significance of epithelioid cells and Langhans giant cells found in sputum or bronchial secretions. Acta Cytol 1972;16:146-151.
64. Naylor B, Railey C. A pitfall in the cytodiagnosis of sputum of asthmatics. J Clin Pathol 1964;17:84-89.
65. Ogita S, Robbins DH, Blum RH, Harris LJ. Endoscopic ultrasound fine-needle aspiration in the staging of non-small-cell lung cancer. Oncology(Williston Park) 2006;20:1419-1425.
66. Olivieri D, D'Ippolito R, Chetta A. Induced sputum: diagnostic value in interstitial lung disease. Curr Opin Pulm Med 2000;6:411-414.
67. Osborne PT, Giltman LI, Uthman EO. Trichomonads in the respiratory tract. A case report and literature review. Acta Cytol 1984;28:136-138.
68. Oztek I, Baloglu H, Demirel D, et al. Cytologic diagnosis of complicated pulmonary unilocular cystic hydatosis. A study of 131 cases. Acta Cytol 1997;41:1159-1166.
69. Pak HY, Ashdjian V, Yokota SB, Teplitz RL. Quantitative DNA determinations by image analysis. I. Application to human pulmonary cytology. Anal Quant Cytol 1982;4:95-104.
70. Palcic B, Garner DM, Beveridge J, et al. Increase of sensitivity of sputum cytology using high-resolution image cytometry: field study results. Cytometry 2002;50:168-176.
71. Papanicolaou GN. Degenerative changes in ciliated cells exfoliating from the bronchial epithelium as a cytologic criterion in the diagnosis of diseases of the lung. NY State J Med 1956;56:2647-2650.
72. Pedersen B, Brons M, Holm K, et al. The value of provoked expectoration in obtaining sputum samples for cytologic investigation. A prospective, consecutive and controlled investigation of 134 patients. Acta Cytol 1985;29:750-752.
73. Perlman EJ, Erozan YS, Howdon A. The role of the Saccomanno technique in sputum cytopathologic diagnosis of lung cancer. Am J Clin Pathol 1989;91:57-60.
74. Pintozzi RL, Blecka LJ, Nanos S. The morphologic identification of *Pneumocystis carinii*. Acta Cytol 1979;23:35-39.
75. Rana DN, O'Donnell M, Malkin A, Griffin M. A comparative study: conventional preparation and ThinPrep 2000 in respiratory cytology. Cytopathology 2001;12:390-398.
76. Ranchod M. The histogenesis and development of pulmonary tumorlets. Cancer 1977;39:1135-1145.
77. Redhead SA, Cushion MT, Frenkel JK, Stringer JR. *Pneumocystis* and *Trypanosoma cruzi*: nomenclature and typifications. J Eukaryot Microbiol 2006;53:2-11.
78. Rintoul RC, Skwarski KM, Murchison JT, et al. Endobronchial and endoscopic ultrasound-guided real-time fine-needle aspiration for mediastinal staging. Eur Respir J 2005;25:416-421.
79. Rogers V, Nasiell M, Nasiell K, et al. Cytologic findings indicating pulmonary tuberculosis. II. The occurrence in sputum of epithelioid cells and multinucleated giant cells in pulmonary tuberculosis, chronic non-tuberculosis inflammatory lung disease and bronchogenic carcinoma. found in sputum or bronchial secretions. Acta Cytol 1972;16:538-541.
80. Rome DS, Olson KB. A direct comparison of natural and aerosol produced sputum collected from 776 asymptomatic men. Acta Cytol 1961;5:173-176.
81. Saccomanno G, Saunders RP, Ellis H, et al. Concentration of carcinoma or atypical cells in sputum. Acta Cytol 1963;7:305-310.
82. Sanerkin NG, Evans DMD. The sputum in bronchial asthma: Pathognomonic patterns. J Pathol Bacteriol 1965;89:535-541.
83. Savic S, Glatz K, Schoenegg R, Spieler P, et al. Multitarget fluorescence in situ hybridization elucidates equivocal lung cytology. Chest 2006;129:1629-1635.
84. Schreiber G, McCrory DC. Performance characteristics of different modalities for diagnosis of suspected lung cancer: summary of published evidence. Chest 2003;123(1 Suppl):115S-128S.
85. Schumann GB, Swensen JJ. Comparison of Papanicolaou's stain with the Gomori methenamine silver (GMS) stain for the cytodiagnosis of *Pneumocystis carinii* in bronchoalveolar lavage (BAL) fluid. Am J Clin Pathol 1991;95:583-586.
86. Shah A. *Aspergillus*-associated hypersensitivity respiratory disorders. Indian J Chest Dis Allied Sci 2008;50:117-128.
87. Shah S, Shukla K, Patel P. Role of fine needle aspiration cytology in diagnosis of lung tumours – a study of 100 cases. Indian J Pathol Microbiol 2007;50:56-58.
88. Sibille Y, Reynolds HY. Macrophages and polymorphonuclear neutrophils in lung defense and injury. Am Rev Respir Dis 1990;141:471-501.
89. Sozzi G, Pastorino U, MoiraghiL, et al. Loss of FHIT function in lung cancer and preinvasive bronchial lesions. Cancer Res 1998;58:5032-5037.
90. Spurzem JR, Saltini C, Rom W, et al. Mechanisms of macrophage accumulation in the lungs of as best-exposed subjects. Am Rev Respir Dis 1987;136:276-280.
91. Stanley MW, Henry-Stanley MJ, Gajl-Peczalska KJ, Bitterman PB. Hyperplasia of type II pneumocytes in acute lung injury. Cytologic findings of sequential bronchoalveolar lavage. Am J Clin Pathol 1992;97:669-677.
92. Strigle SM, Gal AA. A review of pulmonary cytopathology in the acquired immunodeficiency syndrome. Diagn Cytopathol 1989;5:44-54.
93. Sun T, Teichberg S. Protozoal infections in the acquired immunodeficiency syndrome. Electron Microsc Tech 1988;8:79-103.
94. Suprun H. A comparative filter technique study and the relative efficiency of these sieves as applied in sputum cytology for pulmonary cancer cytodiagnosis. Acta Cytol 1974;18:248-251.
95. Thunnissen FB. Sputum examination for early detection of lung cancer. J Clin Pathol 2003;56:805-810.
96. Tweeddale DN, Harbord RP, , Nuzum CT, et al. A new technique to obtain sputum for cytologic study: External percussion and vibration of the chest wall. Acta Cytol 1966;10:214-219.
97. Twohig KJ, Matthay RA. Pulmonary effects of cytotoxic agents other than bleomycin. Clin Chest Med 1990;11:31-54.
98. Valentine EH. Squamous metaplasia of the bronchus. A study of metaplastic changes occurring in epithelium of the major bronchi in cancerous and noncancerous cases. Cancer 1957;10:272-279.
99. van Beek FT, Maas KW, Timmer R, et al. Oesophageal endoscopic ultrasound with fine-needle aspiration biopsy in the staging of non-small-cell lung carcinoma; results from 43 patients. Ned Tijdschr Geneeskd 2006;150:144-150.

100. Velo GP, Spector WG. The origin and turnover of alveolar macrophages in experimental pneumonia. J Pathol 1973;109:7-19.
101. Vilmann P, Puri R. The complete "medical" mediastinoscopy (EUS-FNA + EBUS-TBNA). Minerva Med 2007;98:331-338.
102. Walker KR, Fullmer CD. Progress report on study of respiratory spirals. Acta Cytol 1970;14:396-398.
103. Wallace WA, Monaghan HM, Salter DM, et al. Endobronchial ultrasound-guided fine-needle aspiration and liquid-based thin-layer cytology. J Clin Pathol 2007;60:388-391.
104. Wang NS, Huang SN, Thurlbeck WM. Combined *Pneumocystis carinii* and cytomegalovirus infection. Arch Pathol 1970;90:529-535.
105. Ward HE, Nicholas TE. Alveolar type I and type II cells. Aust N Z J Med 1984;14(5 Suppl 3):731-734.
106. Warner NE, McGrew EA, Nanos S. Cytologic study of the sputum in cytomegalic inclusion disease. Acta Cytol 1964;8:311-315.
107. Watts JC, Chandler FW. *Pneumocystis carinii* pneumonitis. The nature and diagnostic significance of the methenamine silver-positive "intracystic bodies." Am J Surg Pathol 1985;9:744-751.
108. White DC. Chapter 4, lung. in: An Atlas of Radiation Histopathology. USERDA Technical Information Center, Oak Ridge; Tennessee USA. 1975
109. Wiersema MJ, Kochman ML, Cramer HM, Wiersema LM. Preoperative staging of non-small cell lung cancer: transesophageal US-guided fine-needle aspiration biopsy of mediastinal lymph nodes. Radiology 1994;190:239-242.
110. Wihman G, Bergstrom J. Histological technique for the examination of the cell content of sputum. Acta Med Scand (Stockh) 1952;142:433-440.
111. Wildi SM, Judson MA, Fraig M, et al. Is endosonography-guided fine needle aspiration (EUS-FNA) for sarcoidosis as good as we think? Thorax 2004;59;794-799.
112. Xing S, Khanavkar B, Nakhosteen JA, et al. Predictive value of image cytometry for diagnosis of lung cancer in heavy smokers. Eur Respir J 2005;25:956-963.
113. Yang J, Zhou Y. Detection of DNA aneuploidy in exfoliated airway epithelia cells of sputum specimens by the automated image cytometry and its clinical value in the identification of lung cancer. J Huazhong Univ Sci Technolog Med Sci 2004;24:407-410.
114. Yassin SM, Garret M. Parasites in cytodiagnosis: a case report of *Strongyloides stercoralis* in Papanicolaou smears of gastric aspirate, with a review of the literature. Acta Cytol 1980;24:539-544.
115. Yasufuku K, Chiyo M, Koh E, et al. Endobronchial ultrasound-guided transbronchial needle aspiration for staging of lung cancer. Lung Cancer 2005;50:347-354.
116. Yoss EB, Berd D, Cohn JR, Peters SP. Flow cytometric evaluation of bronchoscopic washings and lavage fluid for DNA aneuploidy as an adjunct in the diagnosis of lung cancer and tumors metastatic to the lung. Chest 1989;96:54-59.
117. Zaman SS, van Hoeven KH, Slott S, Gupta PK. Distinction between bronchioloalveolar carcinoma and hyperplastic pulmonary proliferations: a cytologic and morphometric analysis. Diagn Cytopathol 1997;16:396-401.

**Fig. 2.1 Tissue fragment of the bronchial wall in cytologic material.**
Low magnification reveals connective tissue and smooth muscle bundles (arrows) in bronchial brush cytology (from the right lower pulmonary lobe) (Pap stain).

**Fig. 2.2 Common cell content of a sputum probe.**
The specimen is stained according to Papanicolaou (high magnification).
Individual ciliated bronchial epithelial cells.
Goblet cells (arrow), nuclei are displaced to the periphery of the cell, mucoid inclusions appear foamy and stain pinkish.
Carbon-laden (anthracotic pigment) macrophages (upper right), nuclei show features indicating reactive changes (rounded shape, prominent nucleolus).
Degenerating epithelial cells (arrowhead).

**Fig. 2.3 Ciliocytophthoria.**
Ciliocytophthoria is characterized by the presence of:
Cellular debris representing degenerate cytoplasmic fragments with or without pyknotic nuclei. Note the cytoplasm revealing homogeneous eosinophilic staining quality (arrows) and/or eosinophilic inclusions (arrowhead).
Detached ciliary tufts.
Amorphous detritus.
Elements are depicted from a bronchial washing (Pap stain, lower magnification).

Cytologic appearance may mimic tumor necrosis in samples where detached ciliary tufts are absent.

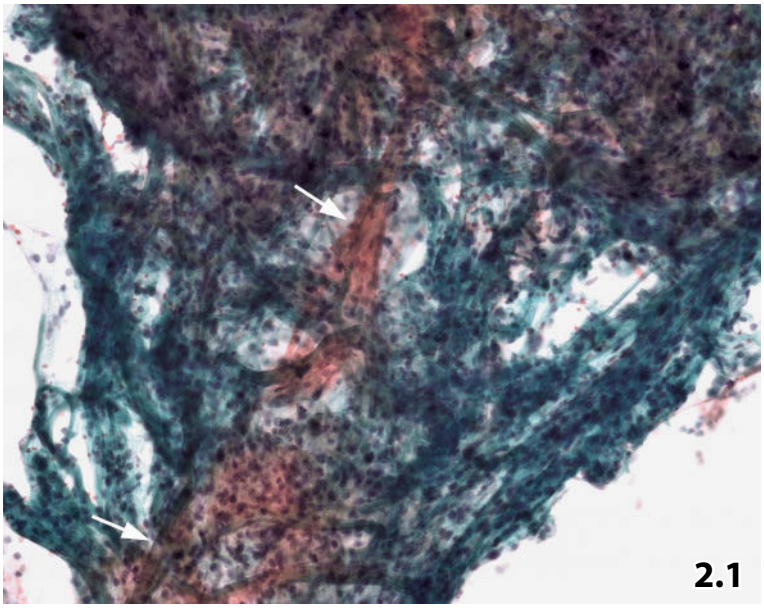
2.1

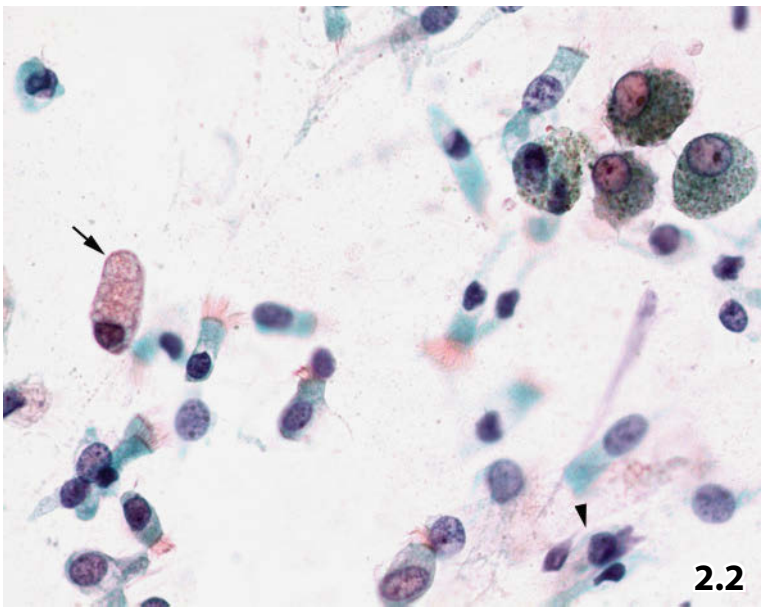
2.2

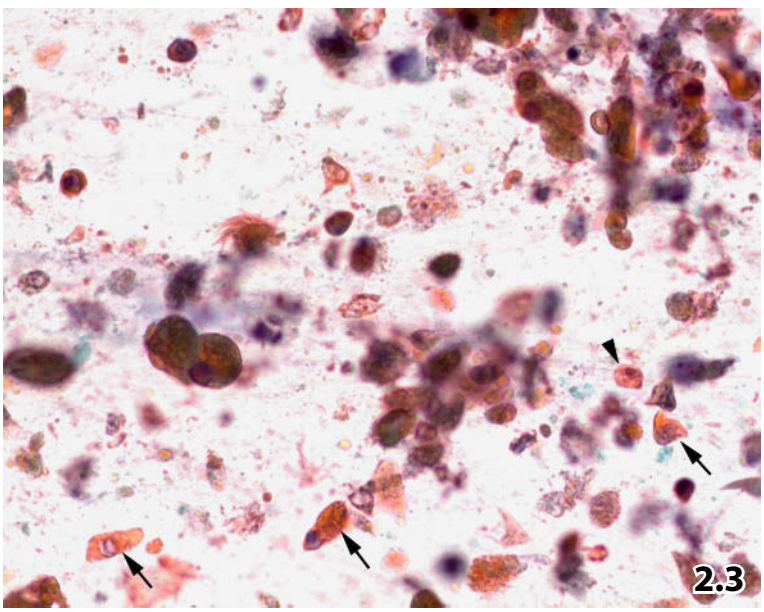
2.3

**Fig. 2.4 Reserve cell hyperplasia.**
A compact cluster of reserve cells. Note the small size of cells and nuclei in comparison to nuclei of the blurred columnar epithelial cells(bottom), the deep-blue-stained nuclei, occasional nuclear molding, and the small rims of homogeneous cyanophilic cytoplasm (bronchial aspirate, Pap stain, lower magnification).

**Fig. 2.5 Langhans-type giant cells.**
Three Langhans-type giant cells presenting in varied positions (FNAB of lung, low magnification, Pap stain):
(1) The multinuclear cell at the right side of the field gives an impression of three-dimensionality of the cell.
(2) Horseshoe-like arrangement of the nuclei is best recognized in profile (centrally located cell).
(3) The same nuclear arrangement is seen top-down (cell on left).
Cytology is highly suspicious for mycobacterial granulomatosis. Ziehl-Neelsen staining for acid-fast bacteria was negative (no information as to further investigations).

**Fig. 2.6 Epithelioid histiocytes.**
Two aggregates of loosely arranged activated epithelioid cells are shown (arrows). Enlarged nuclei exhibiting loose reticular chromatin and usually distinct nucleoli. Interspersed small lymphocytes and absence of debris raise suspicion of sarcoidosis (no further diagnostic evaluation) (sputum probe, Pap stain, lower magnification).

**Fig. 2.7 Squamous metaplasia.**
A flat sheet composed of metaplastic squamous cells is depicted at high magnification. The polygonal shape of the cytoplasm and sharp cytoplasmic borders show a cobblestone-like aspect. Few cells exhibit keratinization. Note patternless or shadowy nuclei and occasional perinuclear cytoplasmic clearing (arrows) (sputum probe, Pap stain).

**Figs. 2.8 and 2.9 Atypical squamous metaplasia.**
Two examples of atypical squamous metaplastic epithelium are presented. The cytologic specimens have been stained with the Papanicolaou method.

**Fig. 2.8** (case #1) A sputum probe of a 55-year-old smoker suffering from COPD shows numerous sheets of abnormal squamous metaplastic epithelium. High magnification of loosely arranged cells discloses characteristics of squamous metaplasia (sharply delineated cyanophilic cytoplasm, partly intact cobblestone-like cell arrangement, perinuclear clearing). Still, variability in cell size, irregular chromatin texture, and distinct nucleolar pleomorphism indicate atypia.
*Follow-up*: Clinical and cytologic long-term follow-up revealed no malignancy.

**Fig. 2.9** (case #2) FNAB of the lung in a 54-year-old woman reveals an inflammatory infiltrate and few highly atypical squamous cells (low N/C ratio, severe nuclear irregularity, hyaline cyanophilic and concentrically laminated cytoplasm, intercellular bridges marked by an arrow) (high magnification). Apparent degenerative nuclear changes (nuclear vacuoles, patternless clear nuclear areas, and absence of nucleoli) do not permit a conclusive diagnosis of malignancy.
*Tissue diagnosis*: Open thoracotomy followed by microscopic evaluation of excised tissue rendered a diagnosis of an abscess accompanied by severe reactive change of the bronchial and alveolar lining cells.

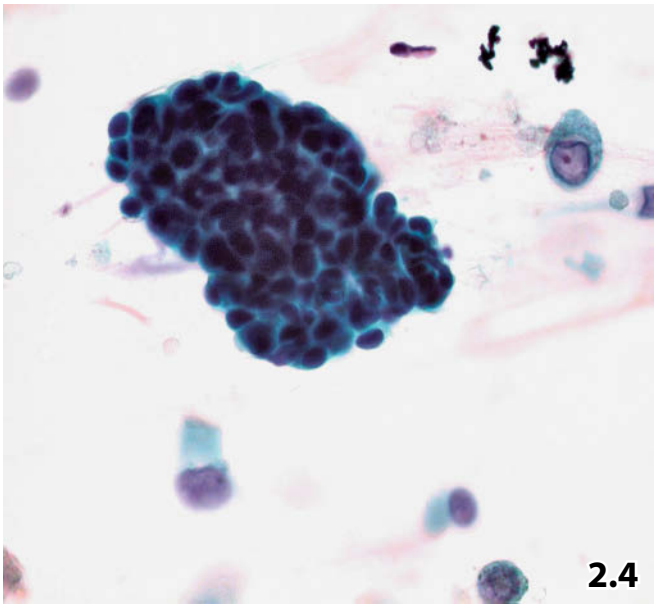
2.4

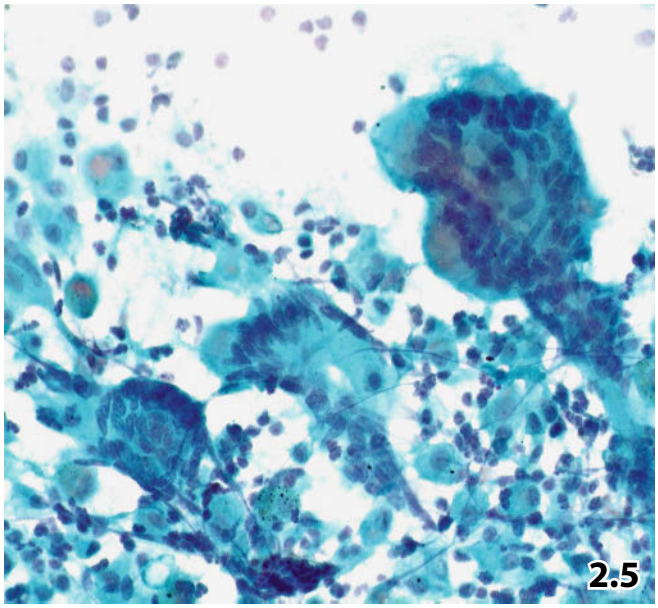
2.5

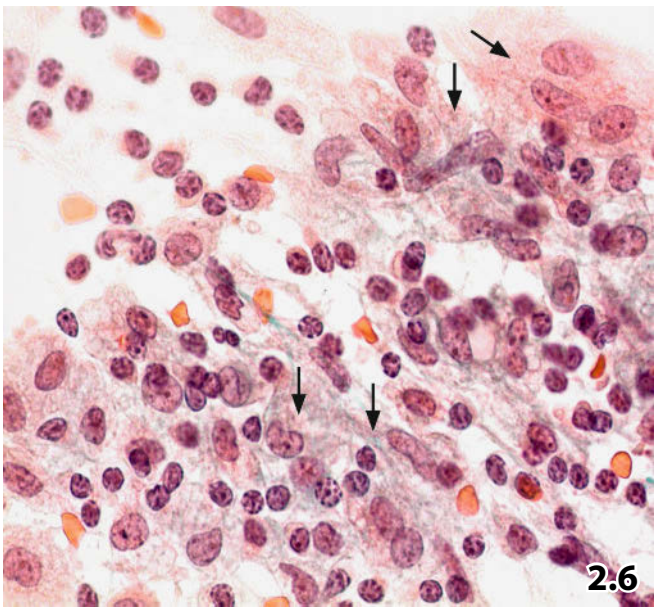
2.6

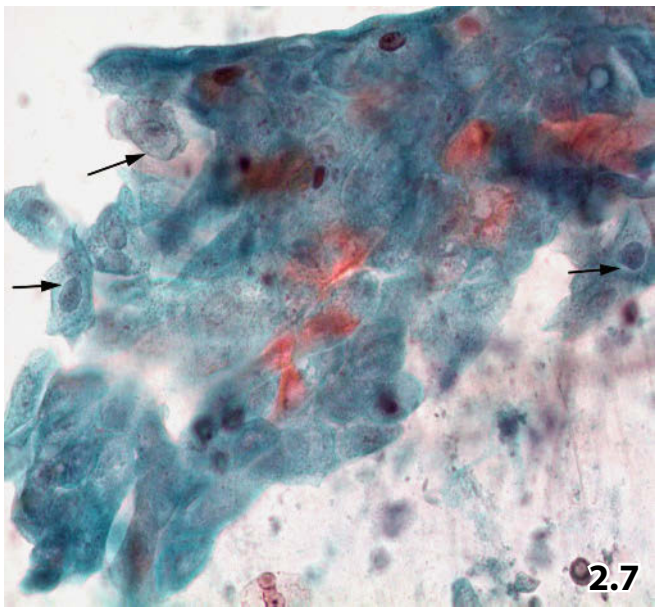
2.7

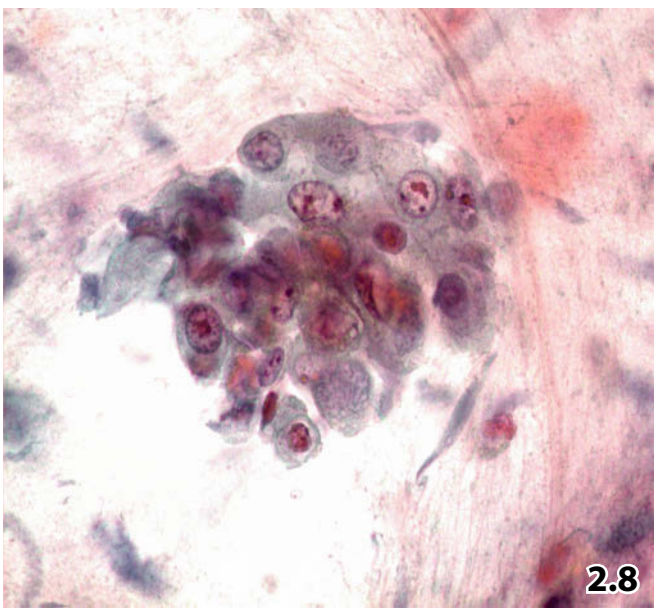
2.8

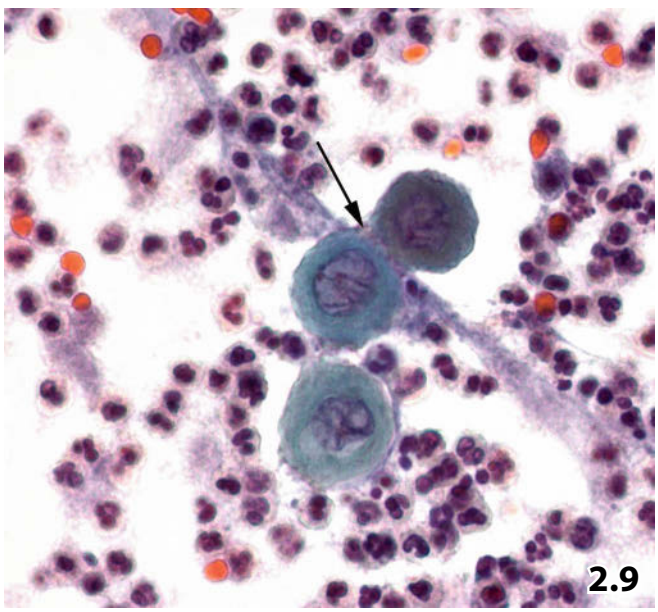
2.9

**Fig. 2.10A Hyperplastic bronchial epithelium.**
A patient suffering from bronchial asthma. Hyperplastic bronchial epithelial cells are depicted (sputum probe, lower magnification, Pap stain). Note regular loose cell arrangement, bland monomorphous nuclei containing centrally located nucleoli, terminal bars, and occasional cilia. A creola body (upper left) is composed of tightly packed reactive epithelial cells. The background shows cellular debris and eosinophils.

**Figs. 2.10B, 2.11, and 2.12 Bronchial epithelial cells exhibiting severe atypia: diagnostic dilemma.**
Examples from different patients have been selected (exfoliative cytology, Pap stain). Diagnostic challenge in standard cytology is emphasized.

**Fig. 2.10B** (case #1) A 57-year-old man presented with pneumonia in the left lung. Sputum cytology revealed three-dimensional cell clusters, loss of nuclear polarity, nuclear irregularity, foamy cytoplasm.
*Tentative cytologic diagnosis*: Epithelial clusters suspicious of a monomorphic adenocarcinoma (possibly bronchioloalveolar carcinoma).
*Follow-up*: Clinical and radiographic symptoms disappeared within 6 months, no further evidence of cancer.
*Cytologic reevaluation*: Focally monolayered cell arrangement (arrowheads) and ciliated cells – cilia are not completely in focus (arrow) – should have favored a benign proliferative lesion. Occurrence and size of the nucleoli do not distinguish between regenerative and malignant lesions.

**Fig. 2.11** (case #2) A 68-year-old man presenting with pulmonary edema and a history of breast carcinoma. Imaging studies suggested neoplastic lung disease. A sputum sample yielded a few small clusters of highly atypical bronchial epithelial cells: nuclear molding, cleaving, and grooving together with pale chromatin texture (high magnification).
*Cytology* suspected bronchioloalveolar carcinoma or metastasis of breast carcinoma.
*Clinical course* revealed no malignant lung disorder.

**Fig. 2.12** (case #3) The bronchial aspirate from an 82-year-old woman with a history of pneumonia showed numerous atypical single cells and atypical cell clusters (higher magnification).
*Tentative cytologic diagnosis:* Most probably reactive bronchial epithelium than adenocarcinoma.
*Tissue diagnosis* (endobronchial biopsy): Adenocarcinoma.

Comment on case #3:
- Sparse nuclear irregularities and loose chromatin suggest a benign reactive lesion.
- However, the large number of atypical single cells and cell clusters comprising virtually absence of nucleoli should be considered as indicator for malignancy.

**Fig. 2.13 Radiation-induced cell changes.**
Bronchial aspirate in the follow-up of a lung cancer patient, status postpneumonectomy and irradiation.
Low N/C ratio, well-demarcated round nuclei, bland nuclear texture punctuated by clear areas or vacuoles (arrows), huge nucleoli, bi(multi)nucleation are intrinsic postirradiation features (Pap stain, high magnification).

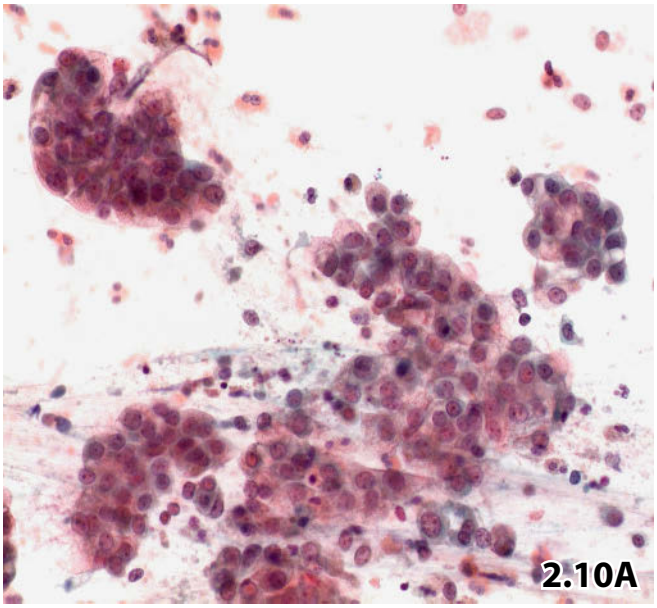
2.10A

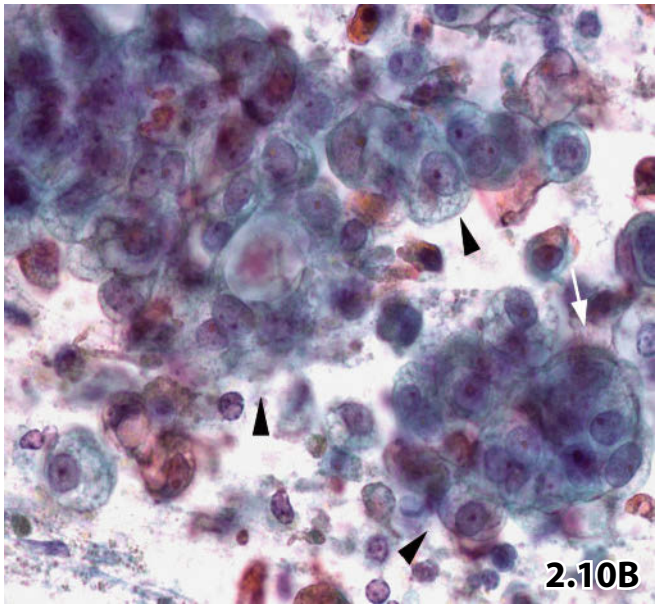
2.10B

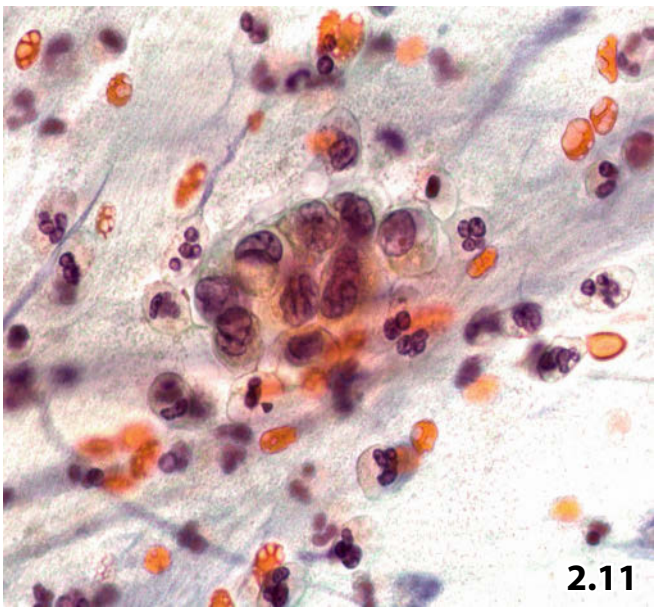
2.11

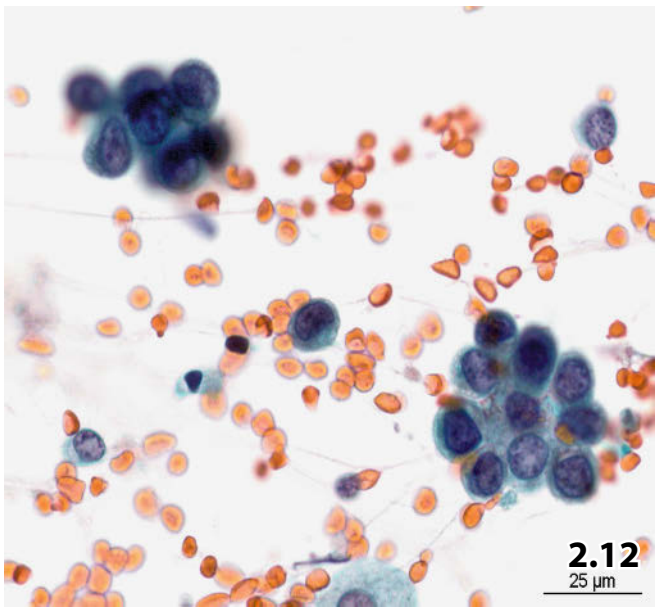

2.12

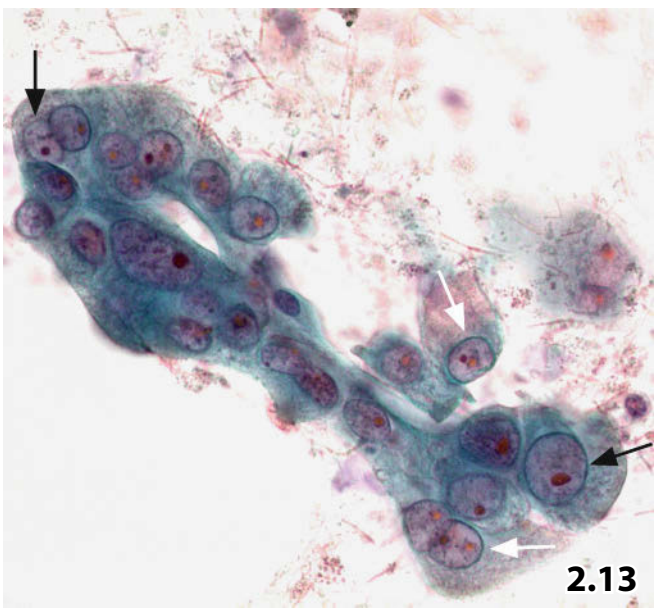
2.13

**Fig. 2.14 Charcot-Leyden crystals.**
A patient with bronchial asthma underwent bronchoscopy.
The bronchial aspirate contains crystalloid elements. Note typical shape, staining quality, and distinct variation in size of the Charcot-Leyden crystals (arrows). Background usually comprises degenerating eosinophils (Pap stain, high magnification).

**Fig. 2.15 Ferruginous bodies.**
Image-guided FNAB of a nodular lesion in a male patient's right lung. Squamous cell carcinoma was found in a subsequent sputum probe.
Asbestos bodies of varied size (lower right) and a large pseudo-asbestos body (upper left) are seen. Both ferruginous body variants are partly engulfed by macrophages (Pap stain, high magnification).

**Fig. 2.16 Plant cells.**
Material depicted from a sputum sample: histogenetic variants of plant cells with marked variation in size, shape, and arrangement (Pap stain, low magnification).

**Fig. 2.17 Microspores of pollen.**
Bronchial aspirate specimen sampled in spring. Microspores may originate from the respiratory tract or may occur as a contaminant from the laboratory environment. Beware of erroneous interpretation! (Pap stain, high magnification).

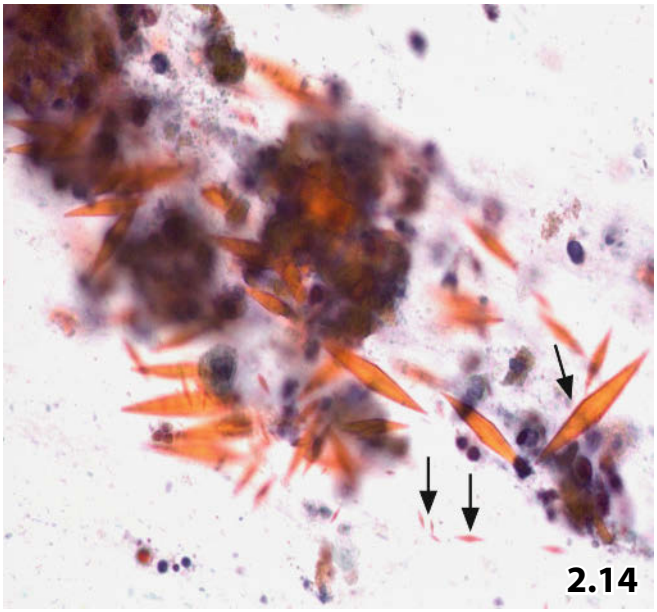
2.14

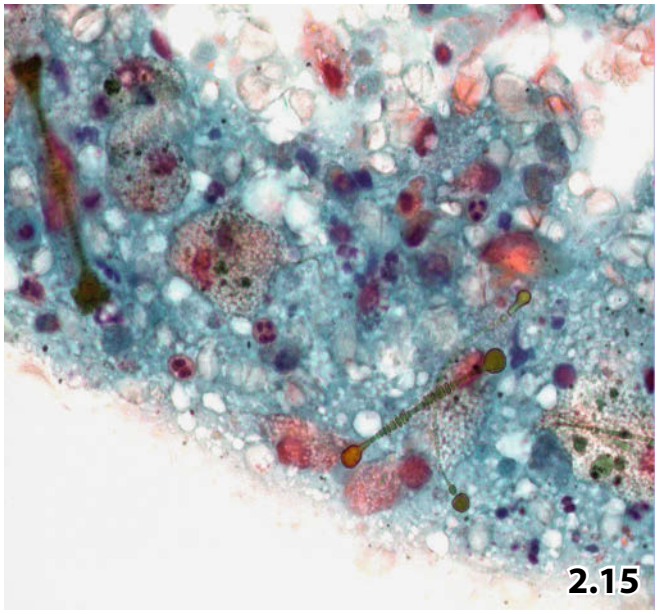
2.15

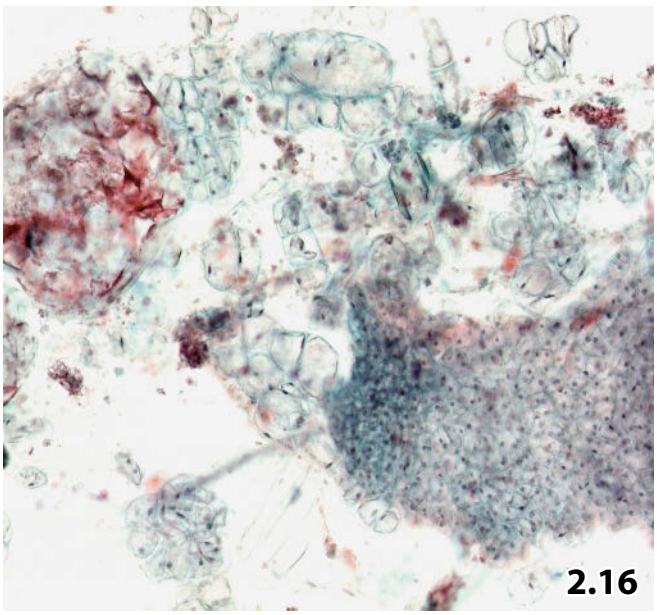
2.16

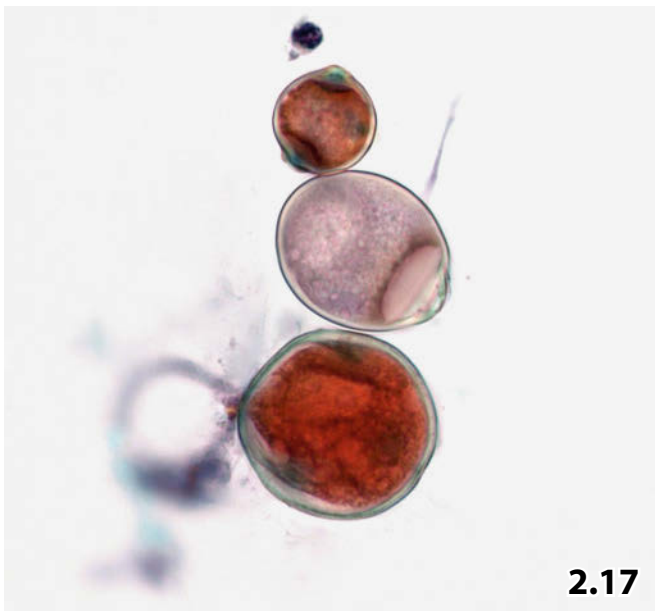
2.17

**Fig. 2.18A, B Mycobacteriosis.**
A sputum specimen showing morphologic characteristics of mycobacterial infection. **A** Lower magnification reveals key features of mycobacterial infection: three-dimensional aggregates of epithelioid cells partially exhibiting extremely slender and pyknotic nuclei (arrows), caseous detritus and tiny calcified deposits (Pap stain). Compare current epithelioid cells with those in a case of probable sarcoidosis (Fig. 2.6). **B** Strong positive reaction of acid-fast bacilli with Ziehl-Neelsen staining (oil immersion, Pap-prestained smear, objective ×100).

**Fig. 2.19 Nonspecific virus-induced cell changes.**
Bronchial brushing containing numerous columnar bronchial epithelial cells, which occasionally show cilia. Abnormal cells exhibit virus-associated changes such as cellular enlargement, multinucleation, and pale nucleoplasm ; cell shape and N/C ratio are usually within normal range. (Pap stain, high magnification).
*Viral culture* tests (undertaken from cytologic material) provided a positive result for poliovirus type 1.

**Fig. 2.20 *Herpes simplex.***
Smears of a sputum sample present epithelial cells exhibiting characteristic *herpes simplex* features: nuclear ground-glass appearance, nuclear inclusions, marginalization of the chromatin (arrow), and a small to medium-sized cytoplasmic rim. The selected cell cluster may lead the inexperienced examiner to a false diagnosis of adenocarcinoma. (Pap stain, high magnification).

**Fig. 2.21 *Respiratory syncytial virus (RSV).***
Key features of cellular alterations caused by *RSV*: syncytial clusters of epithelial cells showing virus-induced nuclear features (marginalization of the chromatin, ground-glass-like nucleoplasm), and few sharply outlined cytoplasmic halos (the commonly associated dark-stained inclusions are not in focus) (bronchial aspirate, Pap stain high magnification).

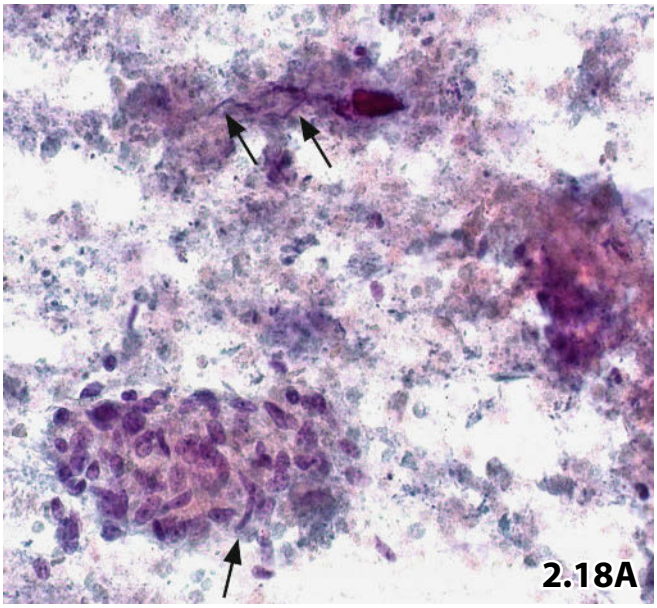
2.18A

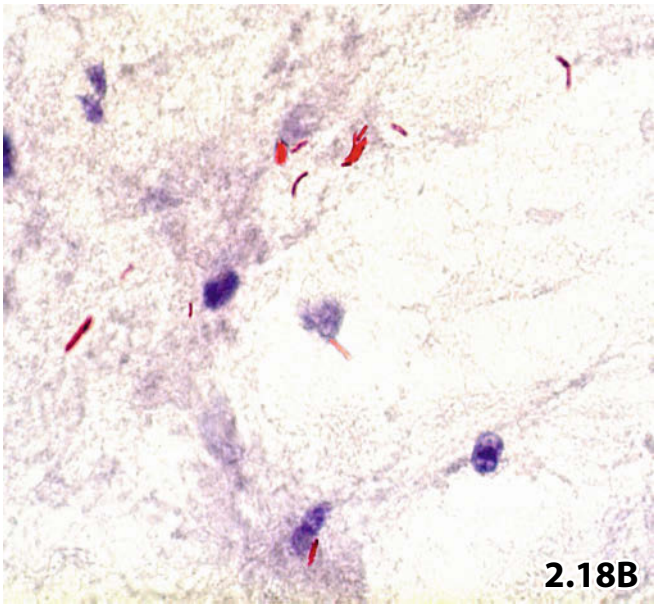
2.18B

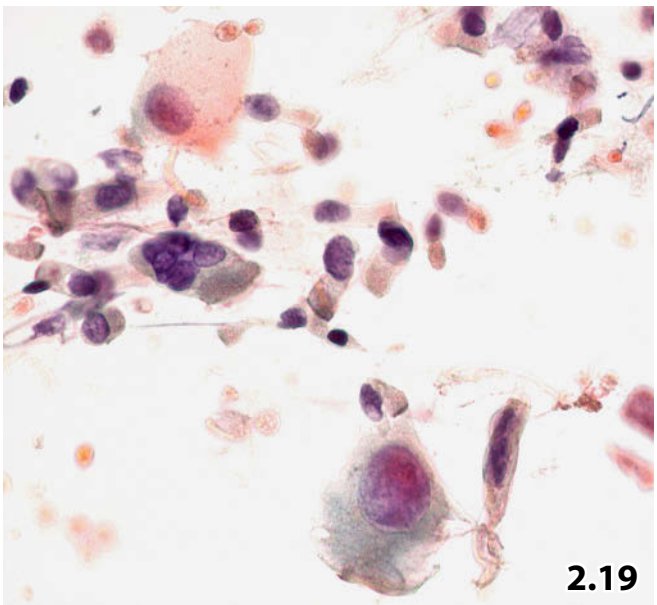
2.19


2.20

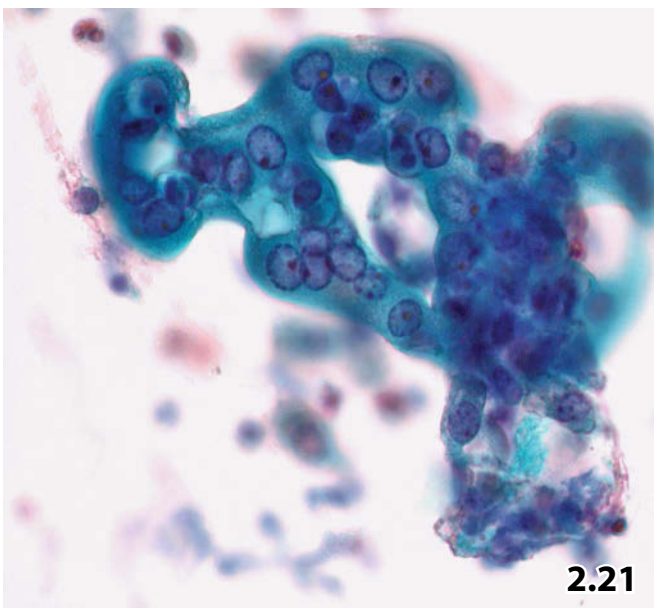
2.21

**Fig. 2.22** ***Candida albicans.***
Single round to oval yeast cells of variable size, dyads of yeast cells, and pseudohyphae are shown against a background of acute inflammation (sputum sample, Pap stain, higher magnification).

**Figs. 2.23 and 2.24** ***Aspergillus.***
Pulmonary aspergillosis that was detected in both exfoliative bronchial material and fine needle aspirate of the lung.

**Fig. 2.23** Many branching septate hyphae that are characterized by prominent cell walls and steady width are embedded in an acute inflammatory background (sputum probe, Pap stain lower magnification).

**Fig. 2.24** Post-therapeutic follow-up of the aspergillus pneumonia by means of FNAB of the lung and silver stain: small fungal fragments and degenerating hyphae are much more easily identified by methenamine silver staining than by conventional cytologic staining methods (high magnification).

**Fig. 2.25** **Mucormycosis.**
Hyphae of mucor species are characterized by absence of septae and great variability in width. The typical morphologic features are readily recognized in a sputum sample ( Pap stain, high magnification).

**Fig. 2.26** **Pneumocystis.**
Methenamine silver stain enhances the typical appearance of the cyst form: folding and dot-like thickening of the membrane and intracystic inclusions. Please compare the appearance of pneumocysts using Pap-staining method (Fig. 2.80) (bronchial aspirate, lower magnification, Pap-prestained smear).

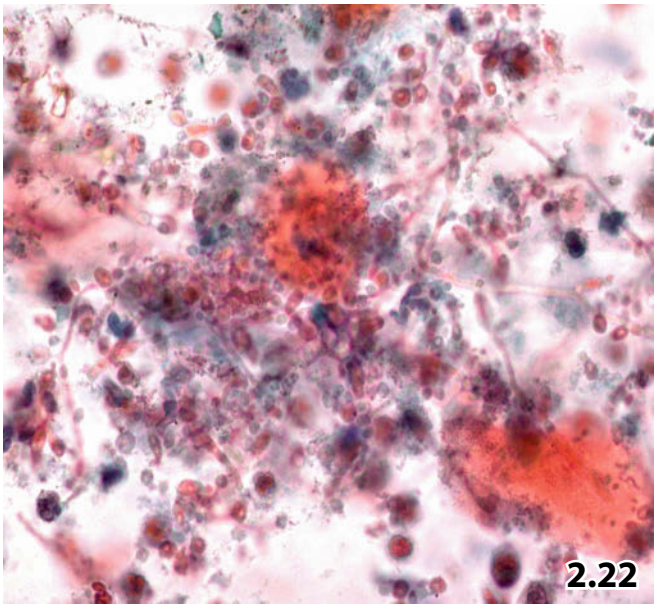
2.22

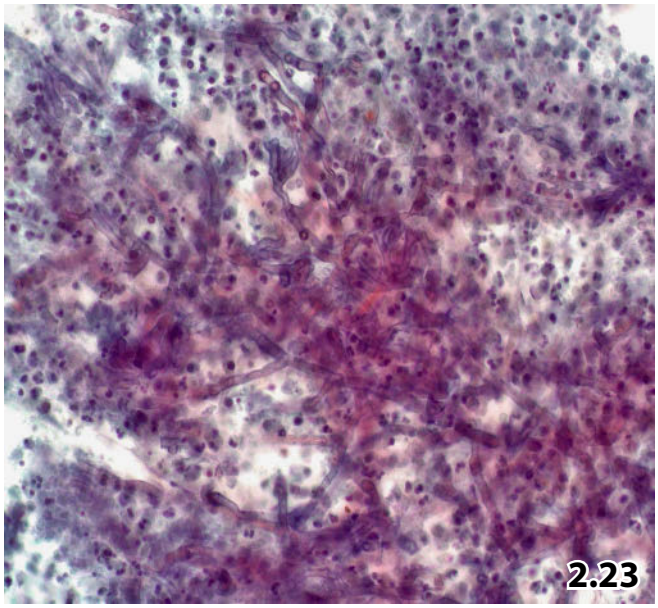
2.23

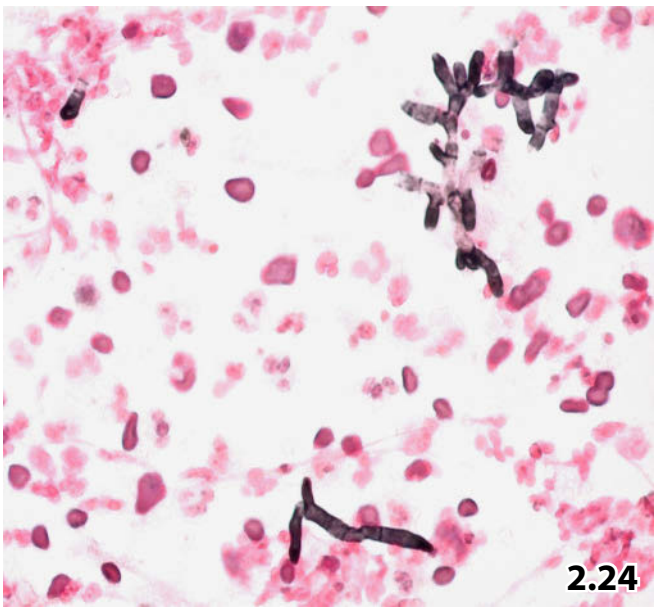
2.24

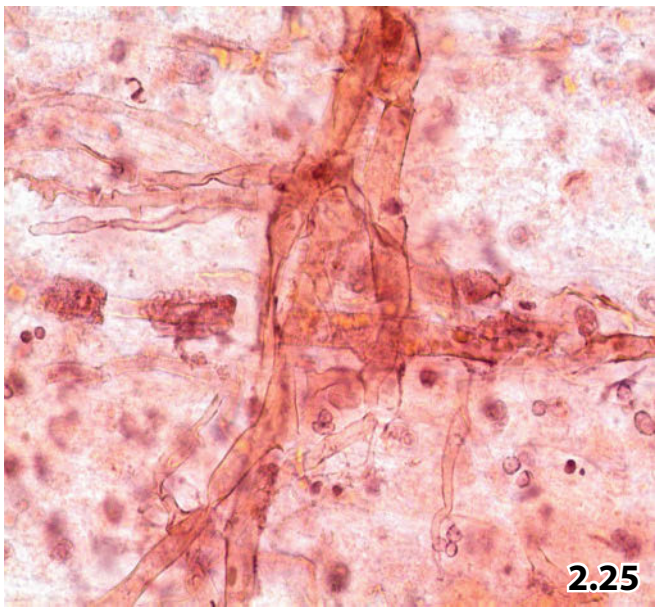
2.25

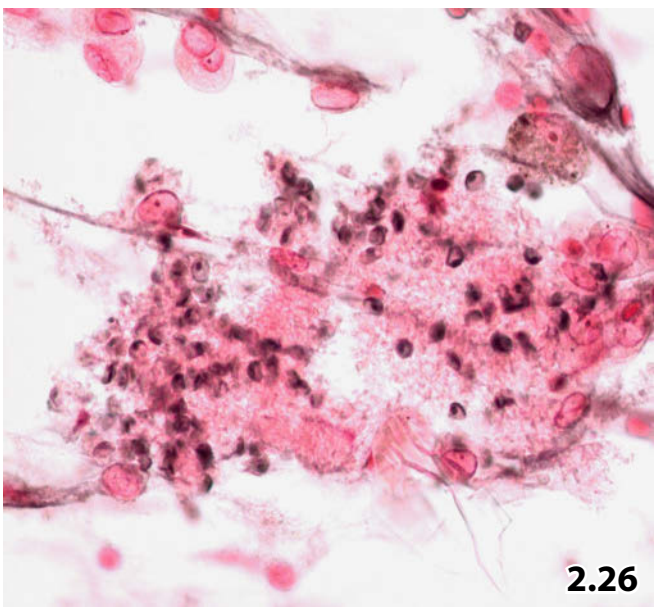
2.26

# Section 2.2
# Respiratory Tract: FNAB and Exfoliative Cytology

## Tumor-Like Lesions
## Benign and Malignant Tumors

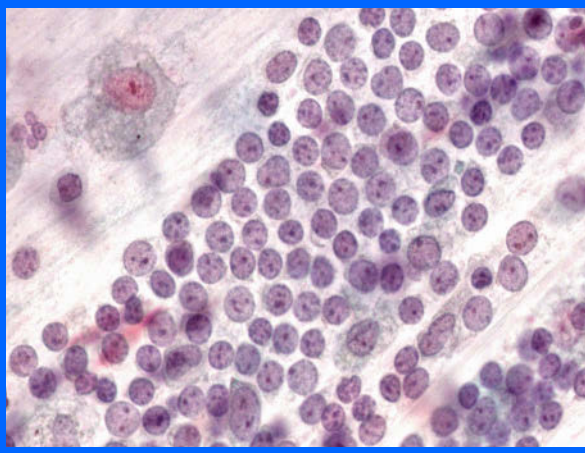

## 2.2.1 Benign Tumors and Pseudotumorous Lesions of the Lung (Selected Entities)

**General Comments**

- Tissue fragments of benign epithelial, mesenchymal, or biphasic lung tumors are uncommonly seen in exfoliative cytologic specimens. Single cells cannot be assigned to normal or neoplastic tissue.
- Benign tumorous lesions may be recorded with success in transthoracic fine-needle aspirates (FNAB) and, with increasing frequency, in endoscopic ultrasound-guided fine-needle aspirates.
- Benign disorders with a strong fibrotic component are unlikely to provide adequate cell yield, whichever sampling method is used.
- Our practical knowledge of diagnosing benign tumors is poor, but a number of such lesions have been described in the cytologic literature. Benign disorders of major interest to cytologic practice are discussed in the following.

### 2.2.1.1 Squamous Cell Papilloma

[98, 101, 122] (Fig. 2.27)

Most papillomas are exophytic but inverted papillomas may occur as well. The tumors exhibit papillary fronds composed of a delicate fibrovascular core and squamous epithelial surface. Squamous papillomas may be solitary or multiple; multiple tumors are referred to as papillomatosis. Papillomas and papillomatosis occur in the upper respiratory tract and in the bronchi, both in adults and in children. Bronchial papillomatosis may progress to dysplasia and in the course occasionally to invasive carcinoma [48].

**Microscopic Features and Differential Diagnosis**

- Regular squamous cells of the superficial and intermediate type. Small basal cells may be present as well.
- Minor cytoplasmic and nuclear irregularities may be observed.
- Nonkeratinizing squamous cells usually are arranged in regular compact groups.
- Koilocytosis may be present as a sign of human papilloma virus-associated etiology of the lesion [101, 119, 120].

Anucleated squames and atypias of nucleated squamous cells may suggest well-differentiated squamous cell carcinoma.

### 2.2.1.2 Various Benign Adenomatous Lesions

Mucinous cystic lesions (adenoma and papilloma arising from bronchial epithelium or tracheobronchial glands), which are composed of mucus producing cells, goblet cells, and any squamous components, should be distinguished from low-grade mucoepidermoid carcinoma (see Sect. 2.2.2.7.2, p. 146). Hamartoma that harbor a pronounced chondromyxoid matrix is difficult to distinguish from mucinous cystadenoma.

### 2.2.1.3 Hamartoma [124, 127 ] (Figs. 2.28 and 2.29)

Pulmonary hamartoma is an uncommon diagnosis in FNAB practice, and the lesion can provoke a variety of erroneous diagnoses. The histologic pattern is that of an abnormal mixture of tissues normally found in the lung. The volume of aspirated material is often small. Tumors including large amounts of fibrotic connective tissue can prevent adequate cell sampling.

#### Microscopic Features

- The mesenchymal component is characterized by fibrous tissue, fibromyxoid stroma, and chondroid masses. A cellular component in a fibromyxoid background is that of stellate cells. Smooth muscle cells and lipomatous components are sporadically present.
- Epithelium is present in the majority of cytologic samples in terms of ciliated and nonciliated columnar cells. Sporadic tumors solely composed of mucin-producing cells have been reported.

#### Immunocytochemistry

Staining with an antibody against the S100 protein is helpful in making a correct diagnosis. The product comprises brown-colored granules in the cytoplasm of stellate cells [124].

#### Differential Diagnosis

- A large epithelial component raises suspicions of low-grade epithelial tumors.
- Hamartomas composed of numerous mucinous epithelial cells and a distinct myxoid background can be misinterpreted as mucinous cystadenoma [54].
- In cases with cellular atypias and detritus background, a false diagnosis of carcinoma can be made.
- Predominance of chondroid material mimics:
  - Normal costochondral or bronchial cartilage.
  - Bronchial chondroma.
  - Tumors containing cartilage such as pleomorphic adenoma of bronchial glands.
  - Teratoma.
- Additional abundant fibrous tissue might raise suspicion of a benign or low-grade spindle cell tumor, fibrotic granulomatous pseudotumor, or peritumoral fibrosis [127].

### 2.2.1.4 Chondroma (Fig. 5.70)

Chondroma is a benign encapsulated cartilaginous tumor, which has a characteristic lobular growth pattern.

#### Microscopic Features and Differential Diagnosis

- Tumor cells resemble normal cartilaginous cells (chondrocytes) and produce cartilaginous matrix. The latter consists of amorphous, basophilic material.
- The cartilaginous cells occur singly and in groups. They contain small round, deeply stained, pyknotic nuclei. The cytoplasm is pale and vacuolated, surrounded by cartilaginous matrix.

Differential diagnosis considerations are much the same as discussed for pulmonary hamartomas (see previous section).

### 2.2.1.5 Granular Cell Tumor

[73, 117] (Figs. 1.63 and 1.64)

Granular cell tumor is a benign mesenchymal tumor assumed to be of Schwann cell origin.

The tumors occur in many organs of the human body. Granular cell tumors of bronchial and tracheal [49] origin protrude into the bronchial/tracheal lumen and may mimic carcinoma. Thus, abundant granular cells can be found not only in FNABs but likewise in brushings and washings obtained during endoscopy. Granular cell tumor has a distinct microscopic appearance that should permit diagnosis in cytologic specimens.

#### Microscopic Features

- Uniform large cells with ill-defined borders and abundant, finely granular cytoplasm. Cells are single or grouped and fragile, leading to a background of granular material.
- The nuclei are small and may be eccentrically positioned with bland granular chromatin. The nucleoli are inconspicuous.

#### Immunocytochemistry and Cytochemistry

(Figs. 1.63B and 1.63C)

Tumor cells stain immunocytochemically positive for the S100 protein, neuron-specific enolase, and vimentin.

The cytoplasmic granules are PAS-positive and diastase-resistant [57].

#### Differential Diagnosis

Granular tumor cells may be misinterpreted as foamy alveolar macrophages, as cells from primary or metastatic low-grade oxyphilic lesions, or as cells from malignant melanoma.

### 2.2.1.6 Germ Cell Tumors [93]

Primary lung teratoma is defined as having no evidence of a gonadal or extragonadal teratomatous neoplasm, including mediastinum. Most pulmonary teratomas are composed of mature elements and are cystic; however, atypical and malignant tissue may occur. Investigation of lung teratoma by FNAB is an exception.

**Microscopic Features and Differential Diagnosis**

- Most intrapulmonary teratomas have a cystic phenotype with the inner surface of the cystic cavity lined with mature squamous cells, comparable to dermoid cysts of the ovary. Other types of tissue may be encountered such as pancreatic, cutaneous, chondroid, and neural tissue, among others.

Low-grade squamous cell carcinoma may be suspected if atypical squames are encountered.

**Caution**

Lung metastasis from a primary germ-cell malignancy in an extrapulmonary location with previous successful therapy may mimic mature teratoma.

### 2.2.1.7 Clear Cell Tumor

Synonym: PEComa.
Clear cell sugar tumor is a rare benign tumor of uncertain histogenesis, usually located in the periphery of the lungs. Single reports suspect clear cell tumors of stemming from perivascular epithelioid cells because the tumor cells exhibit features of pericytes at ultrastructural and immunocytochemical investigations [64]. A few cases diagnosed by FNAB are documented in the literature [31, 79, 91].

**Microscopic Features**

- Polygonal and spindle-shaped cells occur either single or arranged in irregular cohesive clusters. Stripped nuclei are frequently observed in the background of a smear.
- The nuclei, oval to elongated, show bland features comprising thin dispersed chromatin and smooth contour. The nucleoli are indistinct. The N/C ratio is low. The cytoplasm is abundant, finely vacuolated, and granular.
- Cell clusters occasionally contain delicate small vessels.

**Cytochemistry**

A characteristic, but inconstant feature of clear cell tumors is the presence of abundant cytoplasmic glycogen reliably verified by a positive periodic-acid Schiff reaction [64].

**Immunocytochemistry**

Most tumor cells demonstrate strong positivity for HMB-45 and Melan-A. Immunoreactivity with antibodies for CD34 points out the endothelial cells of blood vessels. Negative immunostaining has been established for epithelial antigens, keratins, factor VIII, smooth muscle actin, S100, and for RCCMa (renal cell carcinoma-associated cell marker) [64, 91].

**Differential Diagnosis** [91]

- The differential diagnosis includes primary bronchogenic carcinoma of the clear cell variant, the extremely rare primary acinic cell carcinoma, and secondary clear cell tumors.
- Clear cell variant lung carcinoma should exhibit squamous or glandular differentiation and positive immunoreactivity with antibodies to cytokeratins, epithelial antigens. TTF-1 is likely positive in cells from glandular portions.
- Metastatic tumors with clear cell features may originate from a number of organs, the most important are kidney, breast, liver, and female genital organs. A definitive diagnosis of the primary tumor site should be possible considering the morphologic features, clinical history, and the results from an appropriate immunocytochemical panel.
- Occasionally, bronchogenic clear cell tumors may raise diagnostic problems with mesenchymal tumors [79].

### 2.2.1.8 Pulmonary Oncocytoma [28, 24]

Oncocytomas in bronchial glands are usually small and occur extremely rarely. They are incidentally found in bronchial brushings and secretions after endoscopy.

**Microscopic Features**

- The tumor cells are similar to oncocytes in benign and malignant lesions of various organs. The cells are round to ovoid, showing granular eosinophilic cytoplasm and small bland nuclei.
- Cytoplasmic features correspond ultrastructurally to mitochondrial hyperplasia. Abundance of mitochondria may also lead to a condensed deeply eosinophilic stained cytoplasm.

**Differential Diagnosis**

- Due to the bronchial location of oncocytoma, oncocytic neuroendocrine tumor (oncocytic carcinoid tumor) must be considered first. Endocrine markers are valuable to achieve a correct diagnosis.
- Metastasis of a well-differentiated renal cell carcinoma of granular or chromophobe cell type may masquerade primary lung oncocytoma. Immunocytochemical work-up could possibly be helpful in this setting (see Sect. 12.1.8.1.3, p. 740).

### 2.2.1.9 Tumor-Like Lesions

#### 2.2.1.9.1 Amyloid Tumor [89, 90] (Fig. 4.62)

Amyloid tumor is a tumor-like accumulation of amorphous amyloid protein in the lung parenchyma. Pathogenesis of nodular pulmonary amyloidosis is not clearly understood. In contrast, diffuse amyloidosis is usually part of systemic amy-

loid disease or caused by lymphoid neoplasms [65]. Lung deposits may occur alone or as multiple foci in both lungs [115].

**Microscopic Features**

- Congo-red stain positivity by light microscopy and apple-green birefringence upon polarization are reliable diagnostic criteria. Protein masses may be accompanied by a lymphoproliferative infiltrate and foreign body giant cells.

### 2.2.1.9.2 Endometriosis (Fig. 16.19)

- The term "thoracic endometriosis" refers to the respiratory manifestations that result from the presence of endometrial tissue in thoracic structures. The pathogenesis of thoracic endometriosis is still unclear. Hematogenous and lymphatic embolization of endometrial tissue and other mechanisms have been discussed [9, 131]. In cases with pleuropulmonary nodules, FNAB may be used to establish a definitive diagnosis [39].
- The clinical manifestations consisting of pneumothorax, hemothorax, and hemoptysis classically recur in accordance with the menstrual cycle [9, 82].

**Microscopic Features**

Characteristic cytomorphologic properties in FNAB specimens are also presented in several chapters of this book, for instance in Sect. 16.4.3 (p. 1035), together with general remarks and a list of references.

- Hallmarks: The smears are usually cellular. The background is hemorrhagic composed of detritus and hemosiderin-laden macrophages. A varied number of epithelial cell groups (in a honeycomb pattern, in a syncytial or tubular formation) may be present, in addition to aggregates of fusiform stromal cells.
- Endometrial glandular cells are small to medium-sized, the cytoplasm is scant and cyanophilic. Distinct nuclear membranes are wrinkled. The nucleoli are usually inconspicuous and the chromatin is granular and evenly distributed. Mild to moderate epithelial atypia may be observed depending on hormonal cell activation.
- A tendency to squamous metaplasia may be detected: glandular cells transform into immature squamous cells comprising large polygonal cytoplasm and cobblestone arrangement.
- The nuclei of stromal cells show crowding with varied degrees of overlap.
- Endometrial decidualization may rarely develop, characterized by tall stromal cells embedded in a distinctive myxoid background.

**Differential Diagnosis and Immunocytochemistry**

- Cellular detritus and hemosiderophages in combination with the absence of glandular cells in aspirates from thoracic endometriosis may lead to a diagnosis of granulomatosis, infarct, or tumor necrosis.
- Glandular endometrial cell groups composed of enlarged reactive cells comprising nuclear hyperchromasia, irregular nuclear outline, and nuclear overlapping could lead to a misdiagnosis of primary or metastatic carcinoma.
- Immunocytochemistry is an important tool to reach a final morphological diagnosis. Epithelial endometrial cells should reliably demonstrate positivity for hormone receptors.

### 2.2.1.9.3 Inflammatory Pseudotumor

[70] (Fig. 2.30)

Synonyms include (pseudosarcomatous) inflammatory myofibroblastic tumor, plasma cell granuloma, fibroxanthoma, fibrous histiocytoma, and invasive fibrous tumor of the tracheobronchial tree.

The tumor can occur at any age, but it is one of the most common lung tumors in children. The nature of this disorder (reactive versus neoplastic) has not been completely elucidated yet.

**Microscopic Features**

Histology shows a wide spectrum of fibroblastic/myofibroblastic proliferation and varying infiltrates of histiocytes, lymphoid cells, and mature plasma cells. There is a considerable overlap of multiple phenotypes of this lesion.

The cytologic pattern has repeatedly been described in the current literature:

- Proliferation of spindle cells and histiocytes intermixed with varying numbers of lymphoid cells and typical plasma cells. Small and large tissue fragments may occur [36, 45, 118].

**Differential Diagnosis and Immunocytochemistry**

- Inflammatory pseudotumor is usually diagnosed accurately by FNAB, but the cytologic findings are rather suggestive and nonspecific [45]. A tumor subtype with a lack of plasma cells and aggressive forms of the disorder comprising atypical mesenchymal cells may raise diagnostic difficulties with benign and malignant spindle cell lesions [47] (Fig. 2.30).
- Spindle cells are immunoreactive for vimentin and smooth muscle actin [45].
- ALK1 positivity either by immunocytochemistry or by rearrangement tests such as FISH allows the diagnosis of the neoplastic subtype of inflammatory pseudotumor [112A].

### 2.2.1.9.4 Other Tumor-Like Lesions

- *Langerhans cell histiocytosis* is described in Sect. 2.3.7.1, p. 189.
- *The tumorlet* is discussed together with endocrine tumors in Sect. 2.2.3.5, p. 151.

## 2.2.2 Malignant Tumors of the Lung

**General Comments**

- Lung cancer is currently the most commonly diagnosed noncutaneous malignancy in the world and the most common cause for cancer mortality worldwide. Clinical, epidemiologic, and experimental evidence exists that cigarette smoke has strong carcinogenic effects. Thus, future smoking habits will greatly influence incidence and mortality of lung cancer and will also have an impact upon the histologic tumor types. Other factors that are contributing to the development of lung cancer include asbestos exposure, ionizing, and chemical agents of which environmental pollution supports a synergistic effect [87, 105].
- Although the World Health Organization (WHO) classification [119], in contrast to the recently published IASLC/ATS/ERS lung adenocarcinoma classification [119A], does not address cytology, the authors prefer the WHO nomenclature for practical reasons as well as cytologic purposes. From cytology alone, it is possible to diagnose the major tumor categories and certain tumor subtypes of lung cancers, but it is definitely not possible to identify each tumor type within the WHO nomenclature [8] or the IASLC/ATS/ERS lung adenocarcinoma classification.
- A definitive treatment of lung cancer is feasible, solely on the basis of cytological findings [14].
- Examination of one or repeated sputa will detect the more centrally located neoplasms, whereas washings, brushings, and FNAB will collect adequate samples from tumors in the periphery of the bronchial system and from subpleural lesions. Combined application of multiple sampling methods in the same session can considerably enhance the impact of cytology on primary lung cancer diagnosis and tumor staging.
- The heterogeneity of lung cancers is less frequently detectable in cytologic specimens compared to histologic sections from multiple tumor areas. For cytologic diagnosis of adenosquamous carcinoma, respiratory material or fine-needle aspirates must exhibit malignant cells with evidence of both keratinization and mucus secretion. In our cytologic practice over three decades, we could only sporadically find a combination of small-cell/large-cell carcinoma. Tumor heterogeneity versus synchronous primary tumors of different localization within the respiratory tract has to be considered using exfoliative cytologic methods [125].
- Due to possible therapeutic consequences, the diagnostic term "non-small-cell carcinoma" should be avoided also for cytologic specimens. Additional immunocytological and molecular genetic testing further differentiates adenocarcinoma and squamous cell carcinoma in most cases [119A, 119B, 106A]. Molecular diagnostic methods detecting tumor specific genes in lung cancer specimens for diagnostic and therapeutic purposes (e.g., *EGFR* or *KRAS* mutation, *ALK*-rearrangement) may also be performed on a cytological specimen [2, 119B]. Most particularly, minimally invasive FNAB should provide enough cellular material for such supplementary studies.

### 2.2.2.1 Preinvasive Lesions

- A preinvasive (in situ) lesion of squamous cell carcinoma was postulated by Black and Ackerman in 1953 [10]. The progression of dysplastic changes in squamous metaplastic epithelium to carcinoma in situ and invasive cancer has been documented in the past and is currently accepted [22, 103]. Furthermore, it could be shown that increasing degrees of atypical DNA distribution patterns can serve as an additional biomarker indicating progression toward neoplasia. Further details and references concerning DNA ploidy analysis are provided in Sect. 2.1.4.2, "Additional Analyses," p. 113.
- Two major categories have been added to the group of preinvasive pulmonary lesions in recent years. Atypical adenomatous hyperplasia and diffuse idiopathic pulmonary neuroendocrine cell hyperplasia are believed to progress into adenocarcinoma and carcinoid tumor, respectively [62, 119].
- Many molecular changes in the gradual development of invasive cancer have been observed in recent years. These molecular characteristics may in the future not only provide a useful tool for diagnosis but possibly even for treatment of preneoplastic disorders [26, 62, 88,126].

**Caution**

- Many epithelial atypias are cytomorphologically delicate to assess and the reproducibility of the system is not well established (see Sect. 2.1.4, p. 112). Exfoliated cells from severe dysplasia and in situ carcinoma, both squamous and adenomatous, do not permit a reliable separation from invasive cancer (Fig. 2.31). Proliferation of type II pneumocytes may be indistinguishable from adenocarcinoma and bronchioloalveolar carcinoma, and peripheral squamous cell carcinoma of the lung may shed cells that strongly mimic tumor cells from squamous in situ cancer [60].
- Positive bronchial respiratory cytology in combination with negative imaging results is no proof for in situ cancer; an occult (early) invasive cancer may exist. Endoscopic localization of the cytologically detected disorder is necessary by systematic endoscopic brushings and other targeted procedures.

**Microscopic Features of In-Situ Squamous Cell Carcinoma** (Fig. 2.32)

A number of reports have documented in detail the cytologic appearance of in situ squamous cancer [56]. Morphologic key features include:

- Single small cells of round to oval shape; the N/C ratio is notedly increased.

- The nuclei exhibit obvious malignant features including a dense granular chromatin structure, hyperchromasia, and irregularities of the membrane. Nucleoli variably occur.
- The cytoplasm of the majority of cells is densely keratinized.
- Necrosis and inflammatory infiltrates are rarely encountered.

**Differential Diagnosis**

Distinction of in situ squamous carcinoma from invasive cancer is difficult if not impossible (Fig. 2.32). Diagnostic considerations include:

– Invasive squamous cancer of the early type.
– Squamous cancer from the lung periphery [60].
– Squamous cancer of the oropharyngeal region.

In contrast, invasive squamous cell carcinoma of the common type includes larger cells with pronounced polymorphism, necrosis, and an inflammatory background.

### 2.2.2.2 Invasive Squamous Cell Carcinoma

**General Comments**

- Squamous cell carcinoma (SCC) is still the most frequent histologic type among lung cancers and highly attributed to cigarette smoking. This tumor type accounts for approximately 50% of lung cancers in males and 20% in females. Epidermoid carcinoma is known as a neoplasm of the major bronchi, but a large number of these tumors may start in a small peripheral bronchus followed by a usually centripetal extent into the larger bronchi [34].
- Histological variants of SCC include tumors with papillary, clear cell, small-cell, and basaloid features. In rare cases, such features are present throughout the whole tumor mass; more commonly they occur focally.
- SCCs are graded histologically in well-differentiated (extensive keratinization), moderately differentiated (keratinized tumor cells but not widespread), and poorly differentiated (focal signs of keratinization) tumors. Histological grading may reliably be used on highly cellular FNAB samples but to a lesser extent on exfoliative respiratory cytology.
- Generally, neoplastic squamous cells occur singly and in loose groups except for FNAB and brushings where tissue fragments are common.

**Caution**

- A key feature of squamous cell carcinoma in sputum cytology is the occurrence of the characteristic triad: tumor cells, tumor necrosis, and red blood cells, enmeshed in mucoid masses and mucus strands (Fig. 2.33).
- Thus, specimens of sputa that contain only a few small mucoid strands with the typical cellular entrapments are reliably diagnostic for SCC. In contrast, SCCs exfoliate their cells in washings and brushings in a stochastic distribution pattern.
- Paucity of squamous carcinoma cells may raise difficulties for proper diagnostic assessment, especially in samples where the cells are hidden due to a sanguineous background.
- SCCs composed of tumor cells exhibiting large lucid cytoplasm, bright vesicular nuclei, inconspicuous chromatin texture, variable nucleoli, and indistinct membrane irregularities are difficult to classify as malignant (Fig. 2.36).
- Malignant squamous cells in sputum specimens can originate from extrabronchial sites. SCC of the trachea, larynx, pharynx, oral cavity, and even esophagus may be source for a positive sputum probe.
- Squamous cells and metaplastic squamous cells that display strong nuclear hyperchromasia, focal nucleoplasmic clearing, and a tendency toward degeneration raise diagnostic difficulties with (incomplete list):
  – Degenerating cells of SCC.
  – Severe actinic alterations on malignant or benign squamous cells.
  – Dysplastic changes in squamous metaplastic epithelium (Fig. 2.31).
  – Atypical metaplastic squames due to long-standing lung disorders.
  – Atypical metaplastic squames in specimens obtained by aspiration through a tracheostoma, or from patients with endotracheal intubation.
- Carcinomas composed of small tumor cells do not always mean classic small cell carcinoma. The latter must be distinguished from undifferentiated SCC of the small-cell variant and from combined small-cell carcinoma/squamous cell carcinoma. Please note the characteristic morphology of cells from true small-cell carcinoma (Sect. 2.2.2.6, p. 144)!

#### 2.2.2.2.1 Keratinizing Squamous Cell Carcinoma

(Fig. 2.34)

**Microscopic Features**

- Hallmarks: Obviously malignant cells include:
  – Extreme cellular polymorphism with varying cytoplasmic shape, ranging from small round cells to huge spindle or caudated cells, so-called tadpole cells.
  – The N/C ratio ranges from extremely high to extremely low depending on the amount of cytoplasm of individual cells.

- The nuclei show marked hyperchromasia. The chromatin is homogenized or clumped together; areas of nucleoplasmic clearing are frequent (Fig. 2.34B). The nucleoli are difficult to recognize as a result of the deeply stained chromatin.
- Keratinization of the cytoplasm is obvious, characterized by an intense eosinophilia and orangeophilia or a deep cyanophilic staining. The hyaline appearance of the cytoplasm and concentric lamination are other striking features of keratinized squamous carcinoma cells. The latter is particularly observed in tumor cells with cyanophilic stained cytoplasm(Fig. 2.34).
- Keratin pearls and intercellular bridges are occasionally observed in compact cell clusters.

○ Absence of tumor necrosis and a sanguineous background is extremely rare in cytologic specimens that contain SCC cells, independent of the sampling method.

**Differential Diagnosis**

Differential diagnosis considerations include a variety of benign and malignant conditions.

- Squamous cell carcinomas composed of predominantly small rounded malignant squamous cells may more likely originate from the periphery of the bronchial tree or from the upper aerodigestive tract [60]. As specified above, in situ squamous cell carcinoma may exhibit a quite similar appearance (Fig. 2.32).
- Squamous carcinoma cells with strong nuclear hyperchromasia in combination with a tendency toward pyknosis and areas of cleared nucleoplasm are difficult to distinguish from benign squamous cells with severe actinic changes (Fig. 2.13). Additive DNA ploidy analysis will be of little help in assessing malignancy since radiotherapy can cause major quantitative and structural alterations to the genome.
- Squamous metaplasia with reactive-reparative changes and true dysplastic squamous metaplasia generally comprise, although to a lesser degree, nuclear atypia and smaller cells (Fig. 2.8); benign sheets of metaplastic phenotype are usually present as well. Individual squamous metaplastic cells with severe atypia may be indistinguishable from cancer cells (Figs. 2.9 and 2.31).
- Atypical squamoid cells with severely degenerated nuclei should not lead to a false-positive diagnosis. Such cells may occur in respiratory samples from patients with longstanding lung disorders, from patients with endotracheal intubation, and in specimens obtained by aspiration through a tracheostoma [83].
- Highly elongated, slender malignant squamous cells bearing a small darkly stained, elongated nucleus with a smooth contour may lead to diagnostic confusion with hyperplastic mesenchymal cells, particularly smooth muscle fibers. Spindle-shaped cells are encountered particularly in verrucous SCCs of the upper respiratory tract (trachea, larynx, oropharynx) (Fig. 2.35).
- Plant cells may be misinterpreted as squamous cell carcinoma by inexperienced interpreters (Fig. 2.16).

#### 2.2.2.2.2 Keratinizing Squamous Cell Carcinoma with Clear Nuclei (Figs. 2.36 and 2.37)

Scattered tumor cells with extremely clear nuclei may occasionally be observed in squamous cell carcinoma; however, SCC that is thoroughly composed of cells with clear-type nuclei rarely occurs.

**Microscopic Features**

○ Clear vesicular nuclei with inconspicuous chromatin texture, variably sized nucleoli, and indistinct membrane irregularities.

○ The cells are large, usually comprising broad lucid, eosinophilic, or cyanophilic stained cytoplasm of hyaline appearance.

○ Necrosis is usually not pronounced.

**Differential Diagnosis**

Malignancy is difficult to assess in samples containing only a few tumor cells.

Clear-nuclear variant of SCC is most frequently encountered as a primary tumor from the oropharyngeal area (Fig. 2.37).

#### 2.2.2.2.3 Poorly Differentiated Squamous Cell Carcinoma (Fig. 2.38)

As malignant degeneration of the tumor increases, nuclear and cytoplasmic features of squamous differentiation are less pronounced.

**Microscopic Features**

○ Tumor cells with cytoplasmic keratinization are sparse or completely absent. Dense and concentrically structured, cyanophilic cytoplasm with sharp outlines may be the only reliable morphological criterion of squamous differentiation (Fig. 2.34B). Generally, cytoplasm shows highly varied vacuolization.

○ Clusters of poorly differentiated squamous cells frequently exhibit a focal streaming pattern (Fig. 2.38A).

○ The nuclei are pleomorphic including pronounced irregular outlines (indentations, cleaving), irregular and coarse chromatin clumping, and conspicuous polymorphous nucleoli.

○ Marked necrotic debris.

**Differential Diagnosis and Immunocytochemistry**

- Poorly differentiated SCCs lacking clear signs of squamous differentiation can potentially be misinterpreted as poorly differentiated adenocarcinoma or large-cell undifferentiated carcinoma.
- Regeneration and repair within the epithelium of the respiratory tract may produce large atypical single cells

mimicking nonkeratinizing SCC; however, differential diagnosis problems of proliferative bronchial/alveolar lining cells are much more accentuated against adenocarcinoma.

- Proliferating histiocytes and fibroblasts shed from a florid granulomatous process into the bronchial system may look like poorly differentiated carcinoma cells, in particular in specimens with a tendency toward dense epithelioid clustering of the mesenchymal cells. Immunocytochemical positivity for CD68 and negativity for cytokeratins indicate a histiocytic origin of morphologically equivocal cells.
- An appropriate panel of antibodies proved to be helpful in determining a definite diagnosis: pulmonary squamous cell carcinoma stains positively for CK5/6 [30, 51]. CK20 and CK7 are rarely expressed in malignant squamous cells of the lung, and TTF-1 and leukocyte antigen are never expressed.
- The following primary and secondary neoplasms should primarily be included in the differential diagnosis of nonkeratinizing SCC:
  - Poorly differentiated adenocarcinomas of the lung show positive immunoreactivity for CK7 and TTF-1 [30]. However, CK7 has a low specificity since it is also expressed in pulmonary SCC, in large-cell carcinoma NOS (not otherwise specified), in large-cell neuroendocrine carcinoma, and in a variety of adenocarcinomas secondary to the lung [51].
  - Transitional cell carcinoma demonstrates immunopositivity for CK7 and CK20.
  - Mesothelioma of the undifferentiated epithelial or sarcomatoid variant. Immunocytochemistry, see Sect. 3.2.1.3, "Additional Analyses," p. 262.
  - Melanoma is characterized by positive immunostaining for melanoma-specific antigens (e.g., Melan A, HMB45).
  - Large-cell malignant lymphoma is determined by positive immunostaining with antibodies against leukocyte antigen and lymphocytic markers.

**Caution**

A minimal marker panel of p63 and TTF-1 has been proposed, differentiating pulmonary squamous carcinomas from pulmonary adenocarcinoma, while other markers such as CK5/6 or CK7 could be added [119A]. However, many types of nonpulmonary adenocarcinomas may be positive for CK5/6 [20].

#### 2.2.2.2.4 Squamous Cell Carcinoma: Small-Cell Variant (Fig. 2.39)

The small-cell variant of SCC is composed of cells lacking the typical nuclear morphology of true small-cell carcinoma (see Sect. 2.2.2.6, p. 144).

**Microscopic Features**

- The tumor cell population includes small tumor cells that retain certain properties of malignant squamous cells and cells with obvious squamous differentiation.
- The nuclei exhibit coarse chromatin and prominent nucleoli.
- The cytoplasm is conspicuous, elongated, and sharply outlined. Intercellular bridges may be found in loose tumor cell clusters.

**Differential Diagnosis**

Small-cell variant SCC, a mixture of small-cell carcinoma and squamous cell carcinoma, and true small-cell carcinoma may show similar cytologic patterns. But true small-cell carcinoma has characteristic cell features that are not shared with other carcinomas of the small-cell type.

### 2.2.2.3 Adenocarcinoma

**General Comments**

- The frequency of adenocarcinoma is increasing worldwide. The increase in lung cancer in women is attended by a parallel increase in adenocarcinomas. Females are thought to be predisposed to adenocarcinoma due to a specific determination of the pulmonary epithelial cells to inhaled cigarette smoke [55, 87, 105].
- Adenocarcinoma is a malignant epithelial tumor with glandular differentiation, with or without mucin production. Adenocarcinoma is further classified histologically into the main subtypes: acinar, papillary, solid, and bronchioloalveolar. However, a mixture of the four patterns is common and the mixed subtype is most frequently encountered in routine practice.
- Adenocarcinomas are usually situated more peripherally in the lung compared to SCCs. Thus, adenocarcinoma may shed small numbers of cells or no cells at all into the bronchial system. The yield of exfoliation mainly depends on tumor site and tumor size.
- The differences in cytologic presentation of the varied subtypes of adenocarcinoma have been studied by numerous authors [43, 97, 109]. The studies mainly focused on the cytologic properties and differential diagnosis challenges of bronchioloalveolar carcinoma related to different sampling modalities [85, 104, 108, 110, 116].

**Caution**

- In order to avoid false-positive results, diagnosis of adenocarcinoma in sputum, washings, and brushings must be based on a large number of atypical cells and clusters that exhibit unequivocal features of malignancy. Sparse cells with severe atypia are more likely to be shed from a reactive disorder (Figs. 2.11 and 2.40).

- In contrast, bronchoalveolar lavage may contain numerous atypical clusters with severe regenerative cell changes that are indistinguishable from bronchial adenocarcinoma and bronchioloalveolar carcinoma (Fig. 2.84).
- The presence of micropapillary patterns in adenocarcinomas of the lung and of various other organs has been established to be associated with a poor prognosis. Small papilliform fragments resembling micropapillary tufts in cytologic specimens are not specific and should not render a final diagnosis of adenocarcinoma with micropapillary features [102].

#### 2.2.2.3.1 Adenocarcinoma of the Conventional Type (Predominant Acinar) (Figs. 2.41–2.43)

**Microscopic Features**

- Hallmarks: malignant morphologic cell features are evident, at least in specimens with numerous tumor cells:
  Both single cells and clusters are encountered. Cell groups may consist of syncytial cell arrangement, compact balls, true acini, or papillary fragments.
  A radiating flower petal pattern is obvious in well-differentiated carcinomas.
  The nuclei are eccentrically placed; they are vesicular in appearance and may be lobulated. The nuclear membranes show varying degrees of irregularity. The chromatin is regularly dispersed and finely granular or powdery.
  A centrally placed macronucleolus is a distinct feature for this tumor type.
- The cytoplasm can vary extremely in structure and size. It can appear homogeneous, foamy, or vacuolated; huge vacuoles may lead to a margination of the nucleus.

The cytology varies considerably with the degree of differentiation. A high N/C ratio, nuclear pleomorphism, hyperchromasia, and chromatin coarsening are more prominent the less differentiated the tumor is.

**Differential Diagnosis**

- Well-differentiated adenocarcinoma may be extremely difficult to discriminate against proliferating bronchial and alveolar epithelium (type II pneumocytes). Bronchial and alveolar epithelial hyperplasia has been described in detail in Sect. 2.1.4.3, "Abnormalities of Bronchial and Alveolar Epithelium," p. 113 (Figs. 2.10B, 2.11 and 2.12).
- Poorly differentiated adenocarcinomas share cytological features with several primary and metastatic malignancies of the large-cell type such as poorly differentiated lung carcinoma (squamous and undifferentiated cell type), amelanotic melanoma, large-cell malignant lymphoma, among others. See also Sect. 2.2.2.2.3, p. 140, including immunocytochemical panels.

**Caution**

Proliferative type II pneumocytes share many antigens with epithelial tumor cells including keratins and TTF-1. Thus, immunocytochemical tests are of little help in differentiating between reactive and malignant pneumocytes

#### 2.2.2.3.2 Papillary Adenocarcinoma (Fig. 2.44)

Adenocarcinoma with a predominance of papillary structures is rarely encountered in respiratory cytopathology, but single papillary fragments are occasionally seen.

- Branching papillary fragments consist of fibrovascular cores, layered either by a low-columnar nonmucinous epithelium or by tall cuboid to columnar cells with or without mucin production. Papillary adenocarcinoma shares many criteria with bronchioloalveolar carcinoma.

#### 2.2.2.3.3 Bronchioloalveolar Carcinoma (Figs. 2.45, 2.46, 2.85)

Bronchioloalveolar carcinoma (BAC) may arise from cells of the terminal bronchioles and from the alveolar type II pneumocytes [55]. Pure BAC is characterized by a distinct histological growth pattern: tumor cells are growing along preexistent alveolar and fibrovascular septa lacking parenchymatous, vascular, or pleural invasion. The histological architecture is virtually not reproducible in cytologic material; nevertheless, a number of cytologic features exist that may suggest BAC.

**Microscopic Features**

A number of studies have been published over the last decades as well as in recent years, contributing to the cytological diagnosis and differential diagnosis of BAC [43, 85, 97, 104, 108, 110, 116]. However, for many cases it will not be possible to establish a final diagnosis.

- Cell groups and single cells are present, but the latter are sparse compared with cytologic specimens from bronchial adenocarcinoma
- Hallmarks:
  Cells are small to medium-sized and uniform.
  They occur in tightly packed spherical or papilliform clusters and in flat sheets. Many cell groups show a striking radiating flower petal pattern. Some authors have emphasized the distinct depth of focus for the cells in three-dimensional clusters and the lack of nuclear overlapping.
  The round to oval nuclei are extremely uniform in size, but nuclear grooves are commonly observed together with occasional cytoplasmic invaginations.
  The chromatin is finely granular or powdery and evenly distributed.

The nucleoli are indistinct, but exceptions may occur.
The cytoplasm varies in volume from modest to abundant. It may be homogeneous, granular, foamy, or coarsely vacuolated.
A clean background in cytologic preparations is pathognomonic of BAC.

- Psammoma bodies are present in a minority of tumor cases [42, 108] (Fig. 2.46).
- Bronchioloalveolar tumors of the mucinous type exhibit more abundant cytoplasm with the nuclei pushed to the periphery (Fig. 2.45).
- A small number of BACs are poorly differentiated. These tumors show morphologic features that are very similar to those present in common adenocarcinoma of the bronchial type (Fig. 2.41).
- The morphologic characteristics of BAC vary somewhat with the type of cytologic preparation. Clusters of tumor cells may be prominent, particularly in FNABs comprising intact alveolar septa intersecting tumor fragments [67, 108, 116].

**Caution**

- It is a fact that adenocarcinomas of the lung frequently include a mixture of acinar, papillary, and bronchioloalveolar patterns. Accordingly, a reliable distinction of BAC from other adenocarcinomas is often impossible from cytology alone.
- However, it is of utmost importance to be aware of the bland morphologic features that BACs may exhibit in respiratory cytologic specimens.

### Differential Diagnosis

- Confusion of BAC with proliferative epithelium of terminal bronchioli and reactive type II pneumocytes has been reported elsewhere in the lung chapter (see Sect. 2.1.4.3.2, "Hyperplasia of Terminal Bronchiolar and Alveolar Epithelium," p. 114) (Figs. 2.84–2.86).
- BAC shares many morphological criteria with papillary adenocarcinoma. It is difficult to separate pseudopapillary tumor clusters of BAC from those of papillary bronchial adenocarcinoma.
- BAC of the mucinous type is likely to be overlooked or misinterpreted as mucinous cell hyperplasia: nuclei are pushed to the periphery, and their morphology is obscured by nuclear molding.
- Isolated tumor cells may express a macrophage-like phenotype, which makes it extremely difficult to determine the histogenesis of these elements. On the other hand, clumps of highly atypical (activated) histiocytes/macrophages may mimic adenocarcinoma. Immunocytochemical tests with antibodies against CD68 and cytokeratins can be helpful in cases with uncertain cytology.
- Metastatic carcinoma composed of monomorphic cells may share distinct nuclear features with BAC tumor cells, such as grooving, pseudo-inclusions, chromatin texture, and inconspicuous nucleoli. Most diagnostic difficulties cause breast carcinoma [25], renal cell carcinoma, papillary transitional cell carcinoma, and papillary thyroid carcinoma [16]. In such cases, clinical correlation and appropriate immunostains will be contributory to the diagnosis.
- Poorly differentiated bronchioloalveolar carcinomas share many features with common adenocarcinoma of the bronchial epithelium.

### Immunocytochemistry

- Hormone receptors: Breast carcinoma is one of the most common secondary malignancies to the lung encountered in respiratory cytology. Diagnosis of metastatic breast carcinoma is usually based on the nuclear presence of estrogen (ER) and progesterone (PR) receptors detected by immunocytochemical assay. A few studies revealed the presence of ER in lung carcinoma as well, but the results are conflicting [11, 114]. Dabbs and associates suggest that the detection of ER in pulmonary adenocarcinomas is dependent upon the antibody clone that has been used (e.g., clone 6F11) [25].
- Thyroid transcription factor 1 (TTF-1) (Fig. 2.42): TTF-1 distinguishes primary adenocarcinomas of the lung from the majority of nonadenomatous primary and metastatic neoplasms, excluding metastatic carcinoma of the thyroid.
- Cytokeratin 7 reliably yields positive immunoreactivity in cells of pulmonary adenocarcinomas. However, the marker has a low specificity since it is also expressed in SCC, large-cell carcinoma, and large-cell neuroendocrine carcinoma of the lung, and in a variety of adenocarcinomas metastatic to the lung [51].
- p53 reactivity may be helpful in separating BAC from common lung adenocarcinoma [104].
- Immunocytochemistry in general provides significant information in addition to morphological diagnosis in a high percentage of neoplastic lung disorders [86]. Appropriate panels of immunocytochemical stains have to be used according to the morphological and clinical findings. They enable cytopathologists to differentiate between various types of primary large-cell tumors of the lung and to assess the site of origin of metastatic neoplasms.

**Caution**

- Immunocytochemical positivity of tumor cell nuclei against estrogen receptors may not be absolutely specific for metastatic breast carcinoma (or other sex-hormone-producing tumors). ER may also be present in cells of pulmonary adenocarcinomas.
- TTF-1 immunocytochemical staining cannot distinguish between primary adenocarcinoma of the lung, metastatic thyroid cancer, and proliferative type II pneumocytes mimicking adenocarcinoma.

- CK7 provides high sensitivity for primary pulmonary adenocarcinomas, but the marker has a low specificity.

**Additional Analyses**

DNA ploidy, cytophotometry, and molecular genetics have been discussed in Sect. 2.1.4.3, "Additional Analyses", p. 115.

### 2.2.2.4 Large-Cell Carcinoma (Fig. 2.47)

Undifferentiated large-cell pulmonary carcinoma is composed of highly malignant anaplastic cells that lack morphologic features of squamous or glandular differentiation. The tumor comprises about 10% of all lung carcinomas.

Diagnosis of large-cell undifferentiated carcinoma does not exclude a tumor with focally more differentiated areas of specific morphology whose cells are currently absent in the cytologic specimen.

**Microscopic Features**

- Hallmarks:
  Preponderance of very large single cells.
  Cellular grouping occurs in a syncytial modality.
  The N/C ratio is high.
  The nuclear contour is highly abnormal, cleaved, and lobulated. The chromatin is irregularly dispersed exhibiting strands and clusters. The parachromatin may be hyperchromatic or lucid. The nucleoli are large and pleomorphic and their number varies from cell to cell.
- The cytoplasm is frequently ill defined, and the configuration and staining are variable.
- Giant tumor cells and tumor necrosis are common.

**Differential Diagnosis**

Differential diagnosis considerations are similar to those of poorly differentiated SCC and poorly differentiated adenocarcinoma including: metastatic undifferentiated carcinoma, pulmonary invasive mesothelioma (undifferentiated epithelial or sarcomatoid type), amelanotic melanoma, sarcoma, large-cell lymphoma, cellular alterations due to chemotherapy and irradiation.

Other tumor entities presenting with large tumor cells are discussed in subsequent sections of this chapter.

### 2.2.2.5 Adenosquamous Carcinoma

Adenosquamous carcinoma is a histologically heterogeneous neoplasia due to dual differentiation into squamous cell carcinoma and adenocarcinoma.

Adenosquamous carcinoma is generally easily recognized as malignant neoplasia in cytologic routine practice, but proper subtyping is often not possible: the cytological diagnosis of this tumor entity requires unequivocal evidence of malignant keratinized squamous cells and mucin-secreting cells of the adenocarcinoma type.

### 2.2.2.6 Small-Cell Carcinoma

**General Comments**

- Small-cell carcinoma belongs to the group of neuroendocrine tumors of the lung (see Sect. 2.2.3, p. 149). A majority of small-cell carcinomas demonstrate neuroendocrine differentiation by immunocytochemical staining for neuroendocrine markers (see "Immunocytochemistry" below), both on tissue sections and cytologic specimens [72].
- Small-cell carcinoma is a highly aggressive tumor with a high mitotic activity; they are known to have a poor clinical course [13, 32, 119].
- Cytology, especially FNAB, has proved to be an excellent method to distinguish small-cell carcinoma from other lung cancers [15, 29]. Fundamental and specific cytologic features of small-cell carcinoma include cellular/nuclear molding and fine, smudgy chromatin.

**Caution**

- We emphasize a careful evaluation of all respiratory cytologic specimens from patients with clinically suspected lung cancer. In so doing, a very few well-preserved individual and grouped small undifferentiated tumor cells can be detected and generally allow a correct diagnosis (Fig. 2.48).
- Nuclear hyperchromasia and dyschromasia in small carcinoma cells appear deep blue to black and dark pink to bright pink, respectively.
- Tumor cells of small-cell carcinoma entrapped in blood may be obscured and easily missed.
- Dense clusters of hyperplastic basal cells entrapped in thick blood masses may be misinterpreted as tumor cell clusters from a small-cell carcinoma of the oat cell type.

**Classification of Small-Cell Carcinomas**

The 1981 WHO classification scheme differentiated three subtypes of small-cell carcinoma: oat cell carcinoma, small-cell carcinoma of the intermediate cell type, and combined small-cell carcinoma [128]. Later on, the terms "oat cell carcinoma" and "intermediate cell type" were dropped. The 1999 and 2004 WHO classification [119] propose the terms:

(1) "Small-cell carcinoma" to be used for tumors with a pure small-cell pattern lacking a non-small-cell component.
(2) "Combined small-cell carcinoma" for tumors that show a mixture of small-cell carcinoma and any other non-small-cell component [132].

**Caution**

For cytodiagnostic purposes, it is highly recommended to remember the two small-cell types: oat cell and intermediate. These two cell types contribute to diversified differential diagnostic considerations.

**Microscopic Features** [6, 96, 132]

The cytologic pattern and cellular morphology are pathognomonic in such a manner that a determinate diagnosis should be possible even on single cells.

(1) Cytologic appearance affected by sampling and preparatory modalities:
- *Freshly prepared sputum:* the tumor cells may be entrapped in strands of mucus or arranged along mucus streaks. Tumor cells occur singly but also arranged in small round aggregates and in linear fashion (single-file cellular arrangement), exhibiting the characteristic nuclear molding and focally marked compression of the nuclei (Fig. 2.49).
- *Bronchial washing* producing a similar cytologic appearance as fresh sputum. Obscuration of individual tumor cells and small dense tumor cell clusters by blood masses may offer a tentative diagnosis (Fig. 2.50).
- *Bronchial brushing and FNAB* usually provide cell-rich cytologic smears. Tissue fragments are common, but nuclear molding may be less pronounced, and the tumor cells usually appear larger compared to those in sputum probes or washings.
- *Liquid-based cytology* is increasingly used for the processing material sampled by transthoracic or transbronchial FNAB from lung lesions or mediastinal lymph nodes. Advantages and interpretative cautions concerning liquid-based preparation are reported in the literature [92]. The most distracting morphologic changes of tumor cells processed by means of liquid-based methods include:
  - Cell aggregates that may be crowded and tight.
  - Cell shrinkage and disruption of the cytoplasm that are usually more pronounced compared to direct smearing.
  - More distinct nucleoli.

(2) Pathognomonic cytologic features: cells of the oat cell type (Figs. 2.48B, 2.49, 2.51)
- Tumor cells of the oat cell type are approximately one-and-a-half to two times the size of a lymphocyte.
- The nuclei may appear round with a wrinkled membrane or very irregular in shape and outline.
- The chromatin is very dense and evenly distributed. Hyperchromasia (deep-blue staining) or dyschromasia (dark-pink to bright-pink staining) are invariably present.
- Nucleoli are frequently absent; if present they are inconspicuous.
- The cytoplasm is recognized as a thin cyanophilic rim.
- Intercellular molding of cells and nuclei together with nuclear compression are of the most conspicuous diagnostic features.
- The tumor cells are individually distributed, arranged in small dense clusters or in single files.
- Apoptosis and tumor necrosis are frequent.

(3) Pathognomonic cytologic features: cells of the intermediate cell type (Fig. 2.52)
- In comparison to the oat cell tumor type, the cells of the intermediate subtype are slightly larger in size and the nucleoli are frequently conspicuous.
- The cytoplasmic rim is larger and the cytoplasm tends to be elongated.
- However, the basic features for the diagnosis of small-cell carcinoma are the same as listed above in terms of nuclear shape, nuclear border, chromatin texture, and staining properties.

**Immunocytochemistry**
- Small-cell carcinoma stain most frequently with epithelial markers (e.g., EMA, BerEp-4) [41]. Cytokeratin staining is more variable but a dot-like cytoplasmic positivity is characteristic for small-cell carcinoma.
- Immunocytochemistry for neuroendocrine markers such as CD56, chromogranin, synaptophysin, and neuron-specific enolase shows a positive reaction in a high percentage of small-cell carcinomas [41].
- Immunocytochemical staining for TTF-1 provides a positive reaction in up to 90% of cases [18].

**Caution**
- Negative staining for neuroendocrine markers occurs in about 25% of small-cell carcinomas.
- The immunoprofile TTF-1/ CK20 cannot reliably distinguish between pulmonary and extrapulmonary small-cell carcinoma [18].

**Differential Diagnosis**
- Basal cell hyperplasia (Fig. 2.4): Densely clustered hyperplastic basal cells with their darkly stained nuclei may simulate small-cell carcinoma (oat cell type), but basal cells are usually extremely small (smaller than cells of small-cell carcinoma or even lymphocytes) and show round to polygonal shapes.
  - The cytoplasm appears as small, densely structured cyanophilic rim and often has a polygonal shape. The nuclei are tiny, darkly stained, and homogeneously structured. Hyperplastic basal cells are arranged in cohesive flat sheets.

  Hyperplastic basal cells show highly significant difference in proliferative activity in comparison to small-cell carcinoma, which may be helpful in discriminating the

two entities by application of an immunoassay using antibodies against Ki-67 antigen [40].

- Carcinoid tumors: Typical carcinoid tumors should rarely cause problems discriminating from small-cell carcinoma. However, cases with numerous small and large spindle-shaped cells, pronounced variation in cellular size and shape, and nuclear features of small-cell carcinoma (color, chromatin structure, shape) may easily be misclassified as small cell carcinoma. Still, carcinoid tumors do not produce tumor diathesis and have a mitosis index much lower than small-cell carcinomas. Renshaw and colleagues have studied in detail the cellular features provoking confusion of carcinoid tumors with small cell carcinoma of the lung [95].
- Merkel cell carcinoma: Merkel cell carcinoma shares many cytologic features with small-cell carcinoma. Immunostaining for CK20 and TTF-1 are helpful in distinguishing between these two entities: Merkel cell carcinoma is CK20-positive (often in a dot-like pattern), and TTF-1-negative, and vice versa [18].
- Poorly differentiated squamous cell carcinoma: Small cell carcinoma predominantly composed of cells of the intermediate subtype may be suggestive of poorly differentiated squamous cell carcinoma of the small-cell variant. Immunocytochemical stains for p63 and TTF-1 were shown to reliably distinguish between small-cell carcinoma of the lung and small-cell SCC [59].
- Malignant lymphoma (Figs. 2.53 and 2.56): Distinguishing small-cell carcinoma from malignant lymphoma can be difficult, particularly in bronchial washings and brushings. Problems arise when (1) all carcinoma cells occur isolated and (2) malignant lymphocytes are small to medium-sized, lacking distinct nucleoli, appearing as cohesive clusters, and exhibiting degenerative changes. Nuclear irregularities and tumor debris are not helpful in separating the two tumor entities. Immunoreactivity for leukocyte antigen (CD45) and various lymphocytic markers reliably indicate the lymphatic nature of a tumor. Lymphomas are negative for cytokeratins, neuroendocrine markers, and TTF-1.

**Caution**

There are various reasons for a biphasic small-cell / large-cell tumor pattern:

- Combined small-cell carcinoma shows a distinct mixture of cells of small-cell carcinoma and any other malignant non-small-cell component such as squamous cells, glandular cells, and large cells of neuroendocrine origin.
- Atypical/ malignant squamous cells may originate from dysplastic squamous epithelium and carcinoma in situ of the bronchial epithelium, adjacent to small-cell carcinoma.
- Concomitant squamous cell carcinoma from varying sites of the respiratory tract, oropharynx, and esophagus should always be kept in mind.

### 2.2.2.7 Carcinomas of the Salivary Gland Type

This tumor group comprises neoplasms that are probably of bronchial gland origin. The morphology of these tumors is similar to their counterparts in the salivary glands and in other organs. They are described in more detail in Sect. 5.1.5, p. 414. Several reports in the literature indicate cytomorphologic features and diagnostic problems of the various tumor entities (references are provided in Sect 5.1 together with the various tumor types, p. 401).

#### 2.2.2.7.1 Adenoid Cystic Carcinoma (Fig. 2.54)

Adenoid cystic carcinomas usually arise in large bronchi and in the trachea. Distinction from well-differentiated pulmonary adenocarcinoma and mucin-producing adenocarcinomas with a histologically pronounced cribriform architecture may be difficult [21, 27, 77, 107]. A pure epithelial component can lead to a misdiagnosis of carcinoid tumors.

#### 2.2.2.7.2 Mucoepidermoid Carcinoma (Fig. 2.55)

Mucoepidermoid carcinoma usually arises in the periphery of the bronchial tree. An admixture of neoplastic squamoid cells and mucin-containing tumor cells together with variable amounts of extracellular mucus will definitely provide a correct diagnosis. However, epidermoid features of the malignant squamous cells may be poor and are likely to be overlooked; their cytoplasm may be dense or finely vacuolated.

- Low-grade mucoepidermoid carcinoma is composed of a monotonous tumor cell population with lack of unambiguous evidence of malignancy; the diagnosis will more frequently be suggestive than definite. Differential diagnoses include mucous gland adenoma, bronchioloalveolar carcinoma, mucinous adenocarcinomas (primary and metastatic), among others [77, 99, 107].
- High-grade mucoepidermoid carcinoma is difficult to separate from adenosquamous carcinoma, as keratinized epidermoid cancer cells frequently occur.

#### 2.2.2.7.3 Other Rare Tumors

The group of salivary-gland-type carcinomas further includes epithelial-myoepithelial carcinoma.

### 2.2.2.8 Other Primary Neoplasms of the Lung Rarely Seen in Cytologic Practice

#### 2.2.2.8.1 Clear Cell Carcinoma

Clear cell carcinoma is composed of large polygonal tumor cells with clear foamy cytoplasm whose glycogen content is highly variable. It is important to emphasize a number of secondary lung lesions that highly resemble pulmonary clear cell carcinoma: Extrapulmonary clear cell carcinoma may be situated in the kidney, thyroid, salivary gland, female genital organs, or breast. Benign clear cell tumor of the lung – sugar tumor – has to be excluded as well.

#### 2.2.2.8.2 Lymphoepithelioma-Like Carcinoma

Lymphoepithelial carcinoma is an undifferentiated epithelial neoplasia of the large-cell type associated with prominent benign lymphoid infiltration. This tumor entity is typically located in the nasopharynx and occurs extremely rarely in other sites including the lung. The cytomorphologic features of this tumor are provided in Sect. 8.7.3, p. 568.

Pulmonary lymphoepithelioma-like carcinoma has to be distinguished from benign and malignant lung disorders that are accompanied by pronounced lymphatic hyperplasia such as granulomatous disorders (abundant lymphocytosis and activated histiocytes that mimic carcinoma cells), malignant lymphoma (large-cell blastic type accompanied by benign lymphoid hyperplasia), melanoma, or sarcoma [19].

#### 2.2.2.8.3 Sarcomatoid Carcinoma

Sarcomatoid carcinomas are poorly differentiated non-small-cell lung cancers that are accompanied by spindle cells, giant cells (or a mixture of both cell types), or a sarcomatous component [1, 74, 75, 100, 119].

- *Giant cell carcinomas* are composed of mono- and/or multinucleated large polygonal cells with distinct malignant cytological features. Pure giant cell carcinoma is very rare.
- *Spindle cell carcinomas* consisting exclusively of spindle-shaped tumor cells are rare; an admixture of giant elements is frequently observed. Spindle cell areas display a sarcoma-like growth pattern, but the cells show epithelial differentiation in immunocytochemistry for epithelial markers [75]. If immunostaining for cytokeratins is negative, separation from true sarcoma is practically impossible from cytomorphology alone.
- *Carcinosarcoma* [23] is a highly malignant tumor with carcinomatous and sarcomatous areas. The latter should include heterologous elements such as cartilage, bone, and skeletal muscle. Rhabdomyoid cells together with carcinomatous elements have been reported by Ishizuka and coauthors in a sputum probe [50].
- *Pulmonary blastoma* is a biphasic tumor containing a primitive epithelial component and primitive stroma; the latter show areas of heterologous mesenchymal tissue. The classic pulmonary blastoma is usually encountered in adults [76], whereas pleuropulmonary blastoma is a tumor of early childhood [37, 81].
  - Stromal cells show scant cytoplasm containing ovoid to elongated nuclei with coarse chromatin and irregular nucleoli. Epithelial cells are arranged in sheets, the cytoplasm is vacuolated or foamy and ill defined. The nuclei are eccentrically located and contain irregularly shaped nucleoli [76].

#### 2.2.2.8.4 Soft Tissue Tumors

Sarcomas rarely occur in the lung and a diagnosis from cytology is rather ambivalent. They are more likely encountered in fine-needle aspirates than in exfoliative cytologic samples; stromal tumors rarely exfoliate their cells into the bronchial tree. Only a few cases are on record in the literature, leiomyosarcoma [3, 84, 129], chondrosarcoma [71], synovial sarcoma, fibrosarcoma [66], and malignant fibrous histiocytoma [35, 46]. Leiomyosarcoma is most frequently reported.

Hummel and coauthors recently reviewed a large number of pulmonary spindle cell and mesenchymal lesions in transthoracic FNABs with respect to cytomorphologic features, differential diagnosis, and pitfalls [47]; Wakely studied the features and limitations of FNAB in the analysis of pulmonary spindle cell lesions [121].

#### 2.2.2.8.5 Germ Cell Tumors

Malignant germ cell tumors of the lung are extremely rare. In suspicious cases, an anaplastic primary lung carcinoma should always be excluded.

As known from other body sites (e.g., mediastinum, retroperitoneum), metastatic germ cell neoplasms to the lung may be solely composed of mature tumor elements after successful chemotherapy and radiotherapy of the remote primary tumor.

### 2.2.2.9 Malignant Lymphoid and Myelogenic Tumors

#### 2.2.2.9.1 Non-Hodgkin Lymphoma and Leukemia

[7, 68] (Figs. 2.53, 2.56 and 2.57)

- The prognosis of patients with malignant lymphoma has dramatically improved over the last few decades under new therapeutic regimes, and the tumors are given additional time for recurrence and dissemination. Accordingly, the lung becomes more frequently involved with malignant lymphoid lesions and cytopathologists are more frequently confronted with such cases.
- Differential diagnosis with small-cell carcinoma may be crucial, particularly in cases when small-cell carcinomas are composed of a predominant intermediate cell population. Considerations to distinguish between these two entities are discussed in Sect. 2.2.2.6, p. 144 (Figs. 2.53, 2.56 and 2.57).
- Acute lymphoid and myeloid leukemia share many cytomorphologic features; discrimination may be difficult unless immunocytochemical tests are used. Both tumor entities have to be distinguished from pulmonary and nonpulmonary large-cell neoplasia, particularly large-cell carcinoma and amelanotic melanoma.

#### 2.2.2.9.2 Hodgkin Lymphoma

[33, 38, 111] (Fig. 2.58)

- Hodgkin lymphoma (HL) in the lung can develop during the course of the disease. Pulmonary Hodgkin disease without lymph node involvement is extremely rare [17].

- Cytologic specimens reveal a polymorphous lymphohistiocytic background pattern:
  - Small and large benign mononuclear lymphoid and histiocytoid cells are intermingled with atypical lymphocytes. The latter comprise enlarged nuclei with irregular outlines and conspicuous nucleoli. This cell pattern is not specific for HL; malignant non-Hodgkin lymphoma, various benign lymphoproliferative pulmonary disorders, and small-cell carcinoma should be taken into consideration.
  - Cytology is diagnostic of Hodgkin disease solely in the presence of classic Hodgkin- and Reed-Sternberg cells.

**Caution**

- Large-cell malignant lymphoma and acute myelomonocytic leukemias may simulate large-cell cancer.
- Malignant lymphoma composed of small to medium-sized cells together with features of cell degeneration may lead to a misdiagnosis of small-cell carcinoma.
- The classic pleomorphic lymphoid-histiocytic background of Hodgkin lymphomas is nonspecific; unequivocal Reed-Sternberg cells must be present for a conclusive cytologic diagnosis.

### 2.2.2.10 Secondary Tumors (Metastatic and Invading from Adjacent Organs and Structures)

- The lung is the most common site of metastatic tumor implants. Approximately 50% of all metastatic tumors to the lung shed their cells into the pulmonary airways [61]. Numerous metastatic neoplasms mimic primary lung cancer morphologically, clinically, and on imaging studies. Cavitation, interstitial growth, and an alveolar wall-lining pattern may be marked in varied secondary tumors.
- Adenocarcinoma is by far the most common metastatic tumor detected in exfoliative bronchial specimens. Among these, adenocarcinoma from the colon and breast are the most frequently encountered cancers, both in the past and in current practice [4]. Other relatively frequently encountered metastases and invasive lung tumors from adjacent sites are renal cell carcinoma, transitional cell carcinoma, squamous cell carcinoma, malignant melanoma, and malignant lymphoma.
- Immunocytochemical studies are extremely helpful to establish the primary tumor site for the majority of suspected metastatic tumors with indistinct cytologic findings [86]. Further help may be provided by a positive clinical history and correlative studies with relevant histologic material from the same patient.
- The cytomorphologic pattern of the majority of secondary tumors is relatively nonspecific. Still, a definite or at least peculiar cell pattern in exfoliative specimens may raise suspicions of a neoplasm from a particular extrapulmonary origin.

Selected entities are discussed:

#### 2.2.2.10.1 Breast Carcinoma (Fig. 2.59)

Some breast cancers exhibit small monomorphic tumor cells.

- The nuclei are irregular including deep grooves, the chromatin is fine and pale, and nucleoli may be inconspicuous. In addition, many cases will reveal a single-file tumor cell arrangement.

Thus, the resemblance to bronchioloalveolar carcinoma is striking, as it is to other secondary tumors that exhibit similar nuclear features such as renal cell carcinoma, papillary thyroid carcinoma, and papillary transitional cell carcinoma.

Immunocytochemistry: Breast carcinoma (hormone receptors **+**) and lung adenocarcinoma (TTF-1**+**) show an opposite immunoprofile (please see “Cautions”, p. 149).

#### 2.2.2.10.2 Colonic Carcinoma (Fig. 2.60)

Lung metastases of colonic adenocarcinoma are commonly associated with small and large tight cell clusters.

- Less poorly differentiated tumors exhibit a palisade-like arrangement of columnar cells. The nuclei are hyperchromatic and coarsely structured. Pleomorphic tumor detritus is frequently observed.

Immunocytochemistry: CDX2 and CK20 positivity and CK7 negativity are reliable indicators for metastatic colonic carcinoma.

#### 2.2.2.10.3 Transitional Cell Carcinoma

Cells of poorly differentiated urothelial carcinoma metastatic to the lung may look like those exfoliating from a poorly differentiated squamous cell carcinoma.

- Both tumor entities may contain large cells with pleomorphic nuclei, large nucleoli, and dense cyanophilic cytoplasm; the latter may show vague concentric lamellation. Pronounced necrotic debris raises suspicions of transitional cell carcinoma.

Immunocytochemistry: An immunocytochemical profile including positivity for CK7, CK20, and CK13 raises suspicions of transitional cell carcinoma. CK20 usually show no positive reaction on malignant squamous cells of primary lung origin.

#### 2.2.2.10.4 Adenocarcinoma of the Prostate

This tumor is composed of rather monomorphic medium-sized to large cells showing a characteristic round nucleus, a single pronounced nucleolus, and evenly distributed granular chromatin. The tumor cells are arranged in compact and regular sheets and clusters.

Immunocytochemistry: Positivity for specific prostatic cellular antigens (e.g., PSA) helps to provide a final diagnosis.

#### 2.2.2.10.5 Malignant Melanoma (Fig. 2.61)

Pigmented melanoma should raise no diagnostic problems except in rare cases of carcinoid tumors that exhibit nuclear polymorphism and melanin production. However, nonpigmented melanoma may be difficult to differentiate from poorly differentiated squamous cell carcinoma, poorly differentiated adenocarcinoma, and undifferentiated carcinoma of the lung. All these tumors are characterized by large cells, pleomorphic nuclei, huge nucleoli, clumped chromatin, and cytoplasm of varying shape, size, and structure. Absence of cell clustering is pathognomonic for large-cell neoplasms.

Immunocytochemistry: Reactivity for melanoma-typical markers (HMB-45, Melan A) together with a strong positivity for S100 are indicators for the presence of amelanotic melanoma.

#### 2.2.2.10.6 Malignant Mesothelioma

Pleural mesothelioma is a diffusely spreading tumor involving primarily parietal and visceral surfaces of the thoracic cavity and lung. Mesothelioma, mainly of the sarcomatoid type, may infiltrate beyond the pleura visceralis into the lung parenchyma. Infiltrates may mimic a peripheral lung tumor and can be investigated by FNAB. Mesothelioma cells may rarely be encountered in exfoliative samples from the bronchial system.

Immunocytochemistry: Calretinin-positive epithelioid tumor cells that show negative reactivity for TTF-1 raise high suspicions of a mesothelioma invading the lung.

#### 2.2.2.10.7 Malignant Mesenchymal Tumors (Fig. 2.62)

A distinct tendency exists for sarcomas to metastasize into the lung parenchyma. Spindle cell pulmonary carcinoma, undifferentiated carcinoma, and mesothelioma of the sarcomatoid type have to be excluded by immunocytochemical testing (Fig. 2.62)

**Caution**

- Patients with a long-standing tumor-free interval, whose primary tumor had been successfully treated several years before are most likely to get a diagnosis of primary lung cancer at the time of pulmonary recurrence if the exact clinical history is not available.
- *Breast carcinoma:* Isolated cells from monomorphic breast carcinoma in exfoliative material are likely to be overlooked unless a clinical history of breast cancer is kept in the medical records. Estrogen receptors may be detected in pulmonary adenocarcinomas as well [25].
- *Colonic carcinoma* may be strongly suspected in the presence of clearly malignant columnar carcinoma cells in a palisade arrangement.
- *Transitional cell carcinoma:* Cells of poorly differentiated urothelial carcinoma may look like cells of poorly differentiated squamous cell carcinoma of the lung.
- *Malignant melanoma:* Amelanotic melanoma mimics poorly differentiated and undifferentiated primary cancers of the lung.

## 2.2.3 Neuroendocrine Tumors

### 2.2.3.1 Introduction

- Lung tumors with neuroendocrine tumor (NET) differentiation include four entities that are different in their epidemiologic, clinical, (cyto)morphologic and molecular properties [32]. The two main groups of NET include:
  (1) Typical and atypical carcinoid tumors that are considered low-grade and intermediate-grade carcinomas having a moderate to good prognosis;
  (2) Large-cell neuroendocrine carcinoma and small-cell carcinoma, known to have a poor clinical course [13, 32].

  Typical and atypical carcinoid tumors are distinguished from each other by their appearance under the light microscope (see below).
- Immunocytochemical reactivity for neuroendocrine markers (chromogranin, synaptophysin, and CD56) acts as an indicator for neuroendocrine differentiation. Immunostaining reveals no crucial differences between the four subtypes of neuroendocrine tumors.
- Carcinoids typically appear as nodular exophytic lesions protruding into the bronchial lumen, but tumor cells are rarely observed in sputum and bronchial secretion due to the intact covering mucosa. In contrast, carcinoids generally provide a large number of cells in specimens sampled by brushing and fine-needle aspiration.
- Neuroendocrine differentiation has been found to be an attribute not only of NET but also of a proportion of non-small-cell lung carcinomas. Detection of focal neuroendocrine features in the latter depends on a spectrum of technical approaches and biological properties (antibodies used, nature of tissue specimen, etc.) [12, 112].

### 2.2.3.2 Typical Carcinoid Tumors

[13, 78, 80] (Figs. 2.63 and 2.64)

Typical carcinoid tumors grow slowly and rarely spread beyond the lungs. They are nine times as common as atypical carcinoids. Nearly all central carcinoid tumors are typical carcinoids located in the walls of large bronchi near the lung center.

**Microscopic Features**

- Hallmarks: Uniformity of the neoplastic cells is a pathognomonic feature of this tumor.
  The tumor cells occur singly, in loose sheets, or as three-dimensional cohesive clusters. Cell clusters may show an acinus-like and rosette formation.
  The cells and nuclei are small to medium-sized, round to ovoid. The nucleus is usually displaced to the periphery of the cytoplasm, giving the cell a plasma cell-like appearance.
  The chromatin pattern is finely granular and the nucleoli are inconspicuous.
  Basophilic or eosinophilic cytoplasm is moderate in size and contains fine granules.
  Very few mitoses.
- The N/C ratio is variable.
- On occasion one can observe nests of small spindle cells.
- The background of cytologic specimens is clean, necrosis is absent.

**Caution**

Sputum probes that contain typical carcinoid cells may likely be attended by pronounced cell detritus and necrosis derived from the traumatized mucosal surface area and not from the tumor parenchyma itself.

**Differential Diagnosis**

- A solid epithelial component of adenoid cystic carcinoma that is composed of small monomorphic cells may be mistaken for carcinoid cells. Cells of adenoid cystic carcinoma are immunocytochemically negative for neuroendocrine markers.
- Low-grade non-Hodgkin lymphoma may mimic carcinoid tumors in cases exfoliating numerous isolated monomorphic tumor cells (Fig. 2.56).
- Metastases of monomorphic small-cell adenocarcinomas (e.g., breast carcinoma) exhibiting fine granular chromatin, inconspicuous nucleoli, and variably granular cytoplasm must be eliminated. Immunocytochemically, hormone receptors are not expressed in cells of carcinoid tumors, but cells of breast carcinoma may coexpress neuroendocrine markers.

### 2.2.3.3 Atypical Carcinoid Tumors

[13, 80, 95] (Figs. 2.65 and 2.66)

Atypical carcinoids account for about 10% in the carcinoid tumor group. They grow slightly faster and are more likely to spread to other organs. They have more cells in the process of dividing.

**Microscopic Features**

- The same cytological features appear as described for typical carcinoids, but the neoplastic cells exhibit greater cellular polymorphism. In particular, they are more frequently spindle-shaped.
- The nuclei are more irregular in shape and occasionally molded. The chromatin is coarse. Hyperchromasia and nucleoli are distinct.
- Mitotic figures and necrosis are common.

**Differential Diagnosis**

- Generally, nuclear size and nucleoli are important diagnostic features distinguishing typical carcinoids from atypical carcinoid tumors and large cell neuroendocrine carcinoma.
- Small-cell lung carcinoma [95] and large-cell neuroendocrine carcinoma are distinguished from atypical carcinoid by a notably higher mitotic rate and extensive necrotic background.
- Adenocarcinoma and mucoepidermoid carcinoma with absence of mucin and immunocytochemical positivity for neuroendocrine markers raise suspicions of atypical carcinoid tumor.
- Mesenchymal neoplasms, particularly smooth muscle tumor, are the most frequent lesions, which have to be separated from atypical carcinoids with spindle cell features. An appropriate panel of antibodies generally resolves the problem.
- Rare melanin-producing carcinoids of the spindle cell type share features with fusiform, small-cell pigmented melanoma.
- Prostate carcinoma is characterized by a finely granular chromatin texture, large nucleoli, and occasionally granular cytoplasm. Tumors composed of small to medium-sized cells may resemble atypical carcinoid tumors. An immunocytochemical panel comprising prostate-typical and neuroendocrine antibodies will provide the correct diagnosis.
- Paraganglioma composed of epithelioid cells with carcinoid-like nuclear features is difficult to separate from atypical carcinoid cells [63]. However, pulmonary paraganglioma is extremely rare and cytokeratins are not expressed by use of immunocytochemistry.

### 2.2.3.4 Large-Cell Neuroendocrine Carcinoma

[52, 53, 69, 80, 123] (Fig. 2.67)

The WHO 2004 nomenclature categorizes large-cell neuroendocrine carcinoma (LCNC) as large-cell pulmonary carcinoma [119]. LCNCs may appear in a pure form, but occasionally they are combined with fractions of small-cell carcinoma or non-small-cell carcinoma. LCNCs have a poor clinical outcome.

#### Microscopic Features

- Hallmarks:
  Hypercellular smears containing numerous single tumor cells and stripped nuclei.
  Three-dimensional tumor cell clusters may display distinct peripheral palisading and rosette-like structures.
  The cells are of medium to large size with variable-size cytoplasm.
  The nuclei are pleomorphic comprising irregular contours, molding, and finely or coarsely granular chromatin.
  The prominent nucleoli most often occur singly, but tumors have been observed containing small and inconspicuous nucleoli.
  Necrosis and mitotic figures are common.
- Giant cells may be present.
- A single-file cell arrangement may be encountered.
- Apoptotic changes are frequently observed.

#### Immunocytochemistry

Clear positivity with one neuroendocrine marker is sufficient for a definite diagnosis of LCNC. Synaptophysin seems to be the perfect neuroendocrine marker for this particular tumor entity. Synaptophysin is highly specific and more sensitive than chromogranin [44, 123].

About 50% of the large-cell neuroendocrine carcinomas show nuclear positivity for TTF-1 antigen [53, 113].

#### Differential Diagnosis

- LCNC comprising pronounced nucleolar polymorphism and large cytoplasm may be confused with poorly differentiated primary lung carcinoma of squamous or glandular origin [58] (Fig. 2.67).
- Rarely, LCNC can be misdiagnosed as small-cell carcinoma; even so, single-file cell arrangement, small nuclear size, nuclear molding, and absence of nucleoli are important differential features typically occurring in small-cell carcinoma [58, 130].
- Large-cell-type prostatic carcinoma (large nucleoli, finely granular chromatin, cytoplasmic similarity) may mimic LCNC. Immunocytochemical reactivity for prostate-specific markers and negative immunostaining for neuroendocrine antigens exclude LCNC, and vice versa.

**Caution**

Fifty percent of LCNCs show immunocytochemical positivity for TTF-1. Distinction from poorly differentiated pulmonary adenocarcinoma may be difficult.

### 2.2.3.5 Pulmonary Tumorlet

- Pulmonary tumorlets are evidenced to originate from pulmonary Kulchitsky-type cells. Therefore, tumorlets can be defined as benign localized neuroendocrine cell proliferations looking like tiny peripheral carcinoids (less than 5 mm in diameter). Tumorlets are frequently associated with neuroendocrine cell hyperplasia in the adjacent bronchiolar mucosa [94].
- Nodules with an exceptional protrusion into the bronchial lumen are visualized by endoscopy and may be followed by brushing or transbronchial FNAB.
- Tumorlets are usually composed of spindle cells or epithelial-type cells; therefore, their morphology is indistinguishable from typical or atypical carcinoid tumors.
- The cell pattern of tumorlets can occasionally mimic small-cell carcinoma, well-differentiated adenocarcinoma, or a nonepithelial malignant neoplasm [5, 106]. However, the regularity of the tumorlet nuclei and a very low mitotic activity should exclude malignancy.
- The neuroendocrine origin of the aspirated cells can immunocytochemically be confirmed using antibodies to synaptophysin, chromogranin, and NSE.

## 2.2.4 Further Reading


1. Alasio TM, Sun W, Yang GC. Giant cell carcinoma of the lung impact of diagnosis and review of cytological features. Diagn Cytopathol 2007;35:555-559.
2. Al-Haddad M, Wallace MB. Molecular diagnostics of non-small cell lung cancer using mediastinal lymph nodes sampled by endoscopic ultrasound-guided needle aspiration. Cytopathology 2006;17:3-9.
3. Ali SZ, Kronz JD, Plowden KM, Erozan YS. Metastatic pulmonary leiomyosarcoma: cytopathologic diagnosis on sputum examination. Diagn Cytopathol 1998;18:280-283.
4. Ali TZ, Zakowski MF, Yung RC, et al. Exfoliative sputum cytology of cancers metastatic to the lung. Diagn Cytopathol 2005;33:147-151.
5. Armbruster C, Bernhardt K, Setinek U. Pulmonary tumorlet. A case report of a diagnostic pitfall in cytology. Acta Cytol 2008;52:223-227.
6. Arora VK, Singh N, Chaturvedi S, Bhatia A. Significance of cytologic criteria in distinguishing small cell from non-small cell carcinoma of the lung. Acta cytol 2003;47:216-220.
7. Bardales RH, Powers CN, Frierson HF Jr, et al. Exfoliative respiratory cytology in the diagnosis of leukemias and lymphomas in the lung. Diagn Cytopathol 1996;14:108-113.
8. Berg J, Aase S, Soland TH, et al. The value of cytology in the diagnostics of lung cancer. APMIS 2005;113:208-212.
9. Berwanger I, Bonnet R, Jacobsen JP, et al. Thoracic endometriosis – 2 case reports and review of the literature. Pneumologie 1992;46:236-238.
10. Black H, Ackerman LV. The importance of epidermoid carcinomas in situ in the histogenesis of carcinoma of the lung. Ann Surg 1953;136:44-55.
11. Canver CC, Memoli V A, et al. Sex hormone receptors in non-small-cell lung cancer in human beings. J Thorac Cardiovasc Surg 1994;108:153-157.
12. Carey FA, Save VE. Neuroendocrine differentiation in lung cancer. J Pathol 1997;182:9-10.
13. Carter D, Yesner R. Carcinomas of the lung with neuroendocrine differentiation. Semin Diagn Pathol 1985;2:235-254.
14. Caya JG, Gilles L, Tieu TM, et al. Lung cancer treated on the basis of cytologic findings: an analysis of 112 patients. Diagn Cytopathol 1990;6:313-316.
15. Caya JG, Wollenberg NJ, Clowry LJ, Tieu TM. The diagnosis of pulmonary small-cell anaplastic carcinoma by cytologic means: a 13-year experience. Diagn Cytopathol 1988;4:202-205.
16. Chen C, Hoda RS, Hoda SA. Intranuclear cytoplasmic inclusions in the differential diagnosis of papillary thyroid carcinoma and bronchioloalveolar carcinoma. Diagn Cytopathol 1998;18:384-386.
17. Chetty R, Slavin JL, O'Leary JJ, et al. Primary Hodgkin's disease of the lung. Pathology 1995;27:111-114.
18. Cheuk W, Kwan MY, Suster S, Chan JK. Immunostaining for thyroid transcription factor 1 and cytokeratin 20 aids the distinction of small cell carcinoma from Merkel cell carcinoma, but not pulmonary from extrapulmonary small cell carcinomas. Arch Pathol Lab Med 2001;125:228-231.
19. Chow LT, Chow WH, Tsui WM, et al. Fine-needle aspiration cytologic diagnosis of lymphoepithelioma-like carcinoma of the lung. Report of two cases with immunohistochemical study. Am J Clin Pathol 1995;103:35-40.
20. Chu PG, Weiss LM. Expression of cytokeratin 5/6 in epithelial neoplasms: an immunocytochemical study of 509 cases. Mod Pathol 2002;15:6-10.
21. Chuah KL, Lim KH, Koh MS, et al. Diagnosis of adenoid cystic carcinoma of the lung by bronchial brushing: a case report. Acta Cytol 2007;51:563-566.
22. Cohen MH. Guest Editorial. Lung Cancer: A status report. J Natl Cancer Inst 1975;55:505-511.
23. Cohen-Salmon D, Michel RP, Wang NS, et al. Pulmonary carcinosarcoma and carcinoma: report of a case studied by electron microscopy, with critical review of the literature. Ann Pathol 1985;5:115-124.
24. Cwierzyk TA, Glasberg SS, Virshup MA, Cranmer JC. Pulmonary oncocytoma. Report of a case with cytologic, histologic and electron microscopic study. Acta Cytol 1985;29:620-623.
25. Dabbs DJ, Landreneau RJ, Liu Y, et al. Detection of estrogen receptor by immunohistrochemistry in pulmonary adenocarcinoma. Ann Thorac Surg 2002;73:403-405.
26. Dacic S. Pulmonary preneoplasia. Arch Pathol Lab Med 2008;132:1073--1078.
27. Daneshbod Y, Modjtahedi E, Atefi S, et al. Exfoliative cytologic findings of primary pulmonary adenoid cystic carcinoma: a report of 2 cases with a review of the cytologic features. Acta Cytol 2007;51:558-562.
28. de Aquino RT, Magliari ME, Saad R Jr, et al. Bronchial oncocytoma. Sao Paulo Med J 2000;118:195-197.
29. Delgado PI, Jorda M, Ganjei-Azar P. Small cell carcinoma versus other lung malignancies: diagnosis by fine-needle aspiration cytology. Cancer 2000;90:279-285.
30. Downey P, Cummins R, Moran M, Gulmann C. If it's not CK5/6 positive, TTF-1 negative it's not a squamous cell carcinoma of the lung. APMIS 2008;116:526-529.
31. Edelweiss M, Gupta N, Resetkova E. Preoperative diagnosis of clear cell „sugar" tumor of the lung by computed tomography-guided fine-needle biopsy and core-needle biopsy. Ann Diagn Pathol 2007;11:421-426.
32. Flieder DB. Neuroendocrine tumors of the lung: recent developments in histopathology. Curr Opin Pulm Med 2002;8:275-280.
33. Flint A, Kumar NB, Naylor B. Pulmonary Hodgkin'disease. Diagnosis by fine needle aspiration. Acta Cytol 1988;32:221-225.
34. Fontana RS, Sanderson DR, Woolner LB, et al. The Mayo lung project for early detection and localization of bronchogenic carcinoma: A status report. Chest 1975;67:511-522.
35. Fujita Y, Shimizu T, Yamazaki K, et al. Bronchial brushing cytology features of primary malignant fibrous histiocytoma of the lung. A case report. Acta Cytol 2000;44:227-231.
36. Fulciniti F, Vetrani A, Cozzolino I, et al. Fine-needle cytology of inflammatory myofibroblastic tumor of the lung. Report of a case. Pathologica 2004;96:430-432.
37. Gelven PL, Hopkins MA, Green CA, et al. Fine-needle aspiration cytology of pleuropulmonary blastoma: case report and review of the literature. Diagn Cytopathol 1997;16:336-340.
38. Giangreco A, Ettinger DS, Dragon LH, et al. Sputum cytologic diagnosis of Hodgkin's disease involving the lung. Arch Intern Med 1980;140:910-913.
39. Granberg I, Willems JS. Endometriosis of lung and pleura diagnosed by aspiration biopsy. Acta Cytol 1977;21:295-297.
40. Grefte JM, Salet-van de Pol MR, Gemmink JH, et al. Quantitation of Ki-67 expression in the differential diagnosis of reserve cell hyperplasia vs. small cell lung carcinoma. Acta Cytol 2004;48:608-612.
41. Guinee DG Jr, Fishback NF, Koss MN, et al. The spectrum of immunohistochemical staining of small-cell lung carcinoma in specimens from transbronchial and open-lung biopsies. Am J Clin Pathol 1994;102:406-414.
42. Gupta PK, Verma K. Calcified (Psammoma) bodies in alveolar cell carcinoma of the lung. Acta Cytol 1972;16:59-62.
43. Gupta RK. Value of sputum cytology in the differential diagnosis of alveolar cell carcinoma from bronchogenic adenocarcinoma. Acta Cytol 1981;25:255-258.

44. Hammar SP. Immunohistology of lung and pleural neoplasms. In: Dabbs D, ed. Diagnostic immunohistochemistry. 2nd ed. Churchill Livingston Elsevier; 2006: 329-403.
45. Hannah CD, Oliver DH, Liu J. Fine needle aspiration biopsy and immunostaining findings in an aggressive inflammatory myofibroblastic tumor of the lung: a case report. Acta Cytol 2007;51:239-243.
46. Hoshi R, Satoh Y, Tsuzuku M, Horai T, Ishikawa Y. Fine needle aspiration cytology of fibrous histiocytomas of the lung. Acta Cytol 2004;48:290-292.
47. Hummel P, Cangiarella JF, Cohen JM, et al. Transthoracic fine-needle aspiration biopsy of pulmonary spindle cell and mesenchymal lesions: a study of 61 cases. Cancer 2001;93:187-198.
48. Inoue Y, Oka M, Ishii H, et al. A solitary bronchial papilloma with malignant changes. Intern Med 2001;40:56-60.
49. Ipakchi R, Zager WH, de Baca ME, et al. Granular cell tumor of the trachea in pregnancy: a case report and review of literature. Laryngoscope 2004;114:143-147.
50. Ishizuka T, Yoshitake J, Yamada T, et al. Diagnosis of a case of pulmonary carcinosarcoma by detection of rhabdomyosarcoma cells in sputum. Acta Cytol 1988;32:658-662.
51. Jerome Marson V, Mazieres J, Groussard O, et al. Expression of TTF-1 and cytokeratins in primary and secondary epithelial lung tumours: correlation with histological type and grade. Histopathology 2004;45:125-134.
52. Jiang SX, Kameya T, Shoji M, et al. Large cell neuroendocrine carcinoma of the lung: a histologic and immunohistochemical study of 22 cases. Am J Surg Pathol 1998;22:526-537.
53. Jimenez-Heffernan JA, Lopez-Ferre P, Vicandi B, et al. Fine-needle aspiration cytology of large cell neuroendocrine carcinoma of the lung. A cytohistologic correlation study of 11 cases. Cancer(Cancer Cytopathol) 2008;114:180-186.
54. Jin M-S, Ha H-J, Baek HJ, et al. Adenomyomatous hamartoma of lung mimicking benign mucinous tumor in fine needle aspiration biopsy. A case report. Acta Cytol 2008;52:357-360.
55. Johnston WW, Frable WJ. Diagnostic respiratory cytopathology. Masson Publishing USA, Inc. 1979.
56. Johnston WW, Elson CE. Chapter 14, Respiratory Tract. in:Comprehensive Cytopathology, ed. M.Bibbo. WB.Saunders Company,1991.
57. Junquera LM, de Vicente JC, Vega JA, et al. Granular-cell tumours: an immunohistochemical study. Br J Oral Maxillofac Surg 1997;35:180-184.
58. Kakinuma H, Mikami T, Iwabuchi K, et al. Diagnostic findings of bronchial brush cytology for pulmonary large cell neuroendocrine carcinomas: comparison with poorly differentiated adenocarcinomas, squamous cell carcinomas, and small cell carcinomas. Cancer 2003;99:247-254.
59. Kalhor N, Zander DS, Liu J. TTF-1 and p63 for distinguishing pulmonary small-cell carcinoma from poorly differentiated squamous cell carcinoma in previously pap-stained cytologic material. Mod Pathol 2006;19:1117-1123.
60. Kamiya M, Uei Y, Shimosato Y. Cytologic features of peripheral squamous cell carcinoma of the lung. Acta Cytol 1995;39:61-68.
61. Kern WH, Schweizer C. Sputum cytology of metastatic carcinoma of the lung. Acta Cytol 1976;20:514-520.
62. Kerr KM. Pulmonary preinvasive neoplasia. J Clin Pathol 2001;54:257-271.
63. Kim MK, Park SH, Cho HD, et al. Fine needle aspiration cytology of primary pulmonary paraganglioma. A case report. Acta Cytol 2001;45:459-464.
64. Lantuejoul Clear cell tumor of the lung: an immunohistochemical and ultrastructural study supporting a pericytic differentiation. Mod Pathol 1997;10:1001-1008.
65. Lee SC, Johnson H. Multiple nodular pulmonary amyloidosis. A case report and comparison with diffuse alveolar-septal pulmonary amyloidosis. Thorax 1975;30:178-185.
66. Logrono R, Filipowicz EA, Eyzaguirre EJ, Sawh RN. Diagnosis of primary fibrosarcoma of the lung by fine-needle aspiration and core biopsy. Arch Pathol Lab Med 1999;123:731-735.
67. MacDonald LL, Yazdi HM. Fine-needle aspiration biopsy of bronchioloalveolar carcinoma. Cancer 2001;93:29-34.
68. Manoharan A, Ford J, Hill J, et al. Sputum cytology in the diagnosis of pulmonary non-Hodgkin's lymphoma. Thorax 1984;39:392-393.
69. Marmor S, KorenR, Halpern M, et al. Transthoracic needle biopsy in the diagnosis of large-cell neuroendocrine carcinoma of the lung. Diagn Cytopathol 2005;33:238-243.
70. Matsubara O, Tan-Liu NS, Kenney RM, Mark EJ. Inflammatory pseudotumors of the lung: progression from organizing pneumonia to fibrous histiocytoma or to plasma cell granuloma in 32 cases. Hum Pathol 1988;19:807-814.
71. Matsuo T, Kinoshita S, Iwasaki K, et al. Chondrosarcoma of the trachea. A case report and literature review. Acta Cytol 1988;32:908-912.
72. McCalip B, Reading C, Krishnamurthy S. Diagnosis of small cell carcinoma of the lung on fine needle aspiration samples. Cancer(Cancer Cytopathol 2007; Suppl 111:411-412.
73. Mermolja M, Rott T. Cytology of endobronchial granular cell tumor. Diagn Cytopathol 1991;7:524-526.
74. Mochizuki T, Ishii G, Nagai K, et al. Pleomorphic carcinoma of the lung: Clinicopathologic characteristics of 70 cases. Am J Surg Pathol 2008;32:1727-1735.
75. Nakajima M, Kasai T, Hashimoto T, et al. Sarcomatoid carcinoma of the lung: a clinicopathologic study of 37 cases. Cancer 1999;86:608-616.
76. Nakashima M, Inagaki T, Kunimura T, et al. Cytopathologic and histologic features of biphasic pulmonary blastoma: a case report. Acta Cytol 2005;49:87-91.
77. Nguyen GK. Cytology of bronchial gland carcinoma. Acta Cytol 1988;32:235-239.
78. Nguyen GK. Cytopathology of pulmonary carcinoid tumors in sputum and bronchial brushings. Acta Cytol 1995;39:1152-1160.
79. Nguyen GK. Aspiration biopsy cytology of benign clear cell („sugar") tumor of the lung. Acta Cytol 1989;33:511-515.
80. Nicholson SA, Ryan MR. A review of cytologic findings in neuroendocrine carcinomas including carcinoid tumors with histologic correlation. Cancer 2000;90:148-161.
81. Nicol KK, Geisinger KR. The cytomorphology of pleuropulmonary blastoma. Arch Pathol Lab Med 2000;124:416-418.
82. Nunes H, Bagan P, Kambouchner M, Martinod E. Thoracic endometriosis. Rev Mal Respir 2007;24:1329-1340.
83. Nunez V. Melamed MR, Cahan W. Tracheo-bronchial cytology after laryngectomy for carcinoma of larynx. II. Benign atypias. Acta Cytol 1966;10:38-48.
84. Odashiro AN, Miiji LO, Nguyen GK. Primary lung leiomyosarcoma detected by bronchoscopy cytology. Diagn Cytopathol 2005;33:220-222.
85. Ohori NP, Santa Maria EL. Cytopathologic diagnosis of bronchioloalveolar carcinoma: does it correlate with the 1999 World Health Organization definition? Am J Clin Pathol 2004;122:44-50.
86. O'Reilly PE, Brueckner J, Silverman JF. Value of ancillary studies in fine needle aspiration cytology of the lung. Acta Cytol 1994;38:144-150.
87. Osann KE. Epidemiology of lung cancer. Curr Opin Pulm Med 1998;4:198-204.
88. Pankiewicz W, Minarowski L, Niklinska W, et al. Immunohistochemical markers of cancerogenesis in the lung. Folia Histochem Cytobiol 2007;45:65-74.

89. Papla B, Rudnicka L. Primary amyloid tumors of the lungs – six cases. Pol J Pathol 2005;56:197-202.
90. Pitz MW, Gibson IW, Johnston JB. Isolated pulmonary amyloidosis: case report and review of the literature. Am J Hematol 2006;81:212-213.
91. Policarpio-Nicolas ML, Covell J, Bregman S, Atkins K. Fine needle aspiration cytology of clear cell „sugar“ tumor (PEComa) of the lung: report of a case. Diagn Cytopathol 2008;36:89-93.
92. Rana DN, O'Donnell M, Malkin A, Griffin M. A comparative study: conventional preparation and ThinPrep 2000 in respiratory cytology. Cytopathology 2001;12:390-398.
93. Rana SS, Swami N, Mehta S, et al. intrapulmonary teratoma: an exceptional disease. Ann Thorac Surg 2007;83:1194-1196.
94. Ranchod M. The histogenesis and development of pulmonary tumorlets. Cancer 1977;39:1135-1145.
95. Renshaw AA, Haja J, Lozano RL, et al. Distinguishing carcinoid tumor from small cell carcinoma of the lung: correlating cytological features and performance in the College of American Pathologists Non-Gynecologic Cytology Program. Arch Pathol Lab Med 2005;129: 614-618
96. Renshaw AA (2), Voytek TM, Haja J, et al. Distinguishing small cell carcinoma from non-small cell carcinoma of the lung: correlating cytologic features and performance in the College of American Pathologists Non-Gynecologic Cytology Program. Arch Pathol Lab Med 2005;129: . 619-623.
97. Roger V, Nasiell M, Linden M, Enstad I. Cytologic differential diagnosis of bronchiolo-alveolar carcinoma and bronchogenic adenocarcinoma. Acta Cytol 1976;20:303-307.
98. Roglic M, Jukic S, Damjanov I. Cytology of the solitary papilloma of the bronchus. Acta Cytol 1975;19:11-3.
99. Romagosa C, Morente V, Ramirez JF, et al. Intranuclear inclusions in fine needle aspirates of bronchial low grade mucoepidermoid carcinoma with clear cell change: a report of two cases. Acta Cytol 2002;46:57-60.
100. Rossi G, Cavazza A, Sturm N, et al. Pulmonary carcinomas with pleomorphic, sarcomatoid, or sarcomatous elements: a clinicopathologic and immunohistochemical study of 75 cases. Am J Surg Pathol 2003;27:311-324.
101. Rubel L, Reynolds RE. Cytologic description of squamous cell papilloma of the respiratory tract. Acta Cytol 1979;23:227-231.
102. Rudomina DE, Gatscha RM, Moreira AL. Cytologic diagnosis of pulmonary adenocarcinoma with micropapillary pattern (MPP). Does it correlate with the histologic findings? Cancer(Cancer Cytopathology) 2007;111 (Suppl):407-408.
103. Saccomanno G, Saunders RP, Archer VE, et al. Cancer of the lung: the cytology of sputum prior to the development of carcinoma. Acta Cytol 1965;9:413-423.
104. Saleh HA, Haapaniemi J, Khatib G, Sakr W. Bronchioloalveolar carcinoma: diagnostic pitfalls and immunocytochemical contribution. Diagn Cytopathol 1998;18:301-306.
105. Santos-Martinez MJ, Curull V, Blanco ML, et al. Lung cancer at a university hospital: epidemiological and histological characteristics of a recent and a historical series. Arch Broncopneumol 2005;41:307-312.
106. Satoh Y, Fujiyama J, Ueno M, Ishikawa Y. High cellular atypia in a pulmonary tumorlet. Report of a case with cytologic findings. Acta Cytol 2000;44:242-246.
106A. Schramm M, Wrobel C, Born I, Kazimirek M, Pomjanski N, William M, et al. Equivocal cytology in lung cancer diagnosis:improvement of diagnostic accuracy using adjuvant multicolor FISH, DNA-image cytometry, and quantitative promoter hypermethylation analysis. Cancer Cytopathology 2011; 119:177–192.
107. Segletes LA, Steffee CH, Geisinger KR. Cytology of primary pulmonary mucoepidermoid and adenoid cystic carcinoma. A report of four cases. Acta Cytol 1999;43:1091-1097.
108. Silverman JF, Finley JL, Park HK, et al. Fine needle aspiration cytology of bronchioloalveolar-cell carcinoma of the lung. Acta Cytol 1985;29:887-894.
109. Smith JH, Frable WJ. Adenocarcinoma of the lung. Cytologic correlation with histologic types. Acta Cytol 1974;18:316-320.
110. Spriggs AI, Cole M, Dunnill MS. Alveolar-cell carcinoma: a problem in sputum cytodiagnosis. J Clin Pathol 1982;35:1370-1379.
111. Stanley C, Wolf P, Haghighi P. Reed-Sternberg cells in sputum from a patient with Hodgkin's disease. A case report. Acta Cytol 1993;37:90-92.
112. Stodkowska J. The value of immunohistochemical identification of neuroendocrine differentiation in non small cell lung carcinoma. Rocz Akad Med Bialymst 1997;42 Suppl 1:23-27.
112A. Stoll LM, Li QK. Cytology of fine-needle aspiration of inflammatory myofibroblastic tumor. Diagnostic Cytopathology 2011;39(9):663-672.
113. Sturm N, Rossi G, Lantuejoul S, et al. Expression of thyroid transcription factor-1 in the spectrum of neuroendocrine cell lung proliferations with special interest in carcinoids. Hum Pathol 2002;33:175-182.
114. Su JM, Hsu HK, Chang H, et al. Expression of estrogen and progesterone receptors in non-small-cell lung cancer: immunohistochemical study. Anticancer Research 1996;16:3803-3806.
115. Tamura K, Nakajima N, Makino S, et al. Primary pulmonary amyloidosis with multiple nodules. Eur J Radiol 1988;8:128-130.
116. Tao LC, Weisbrod GL, Pearson FG, et al. Cytologic diagnosis of bronchioloalveolar carcinoma by fine-needle aspiration biopsy. Cancer 1986;57:1565-1570.
117. Thomas L, Risbud M, Gabriel JB, et al. Cytomorphology of granular-cell tumor of the bronchus. A case report. Acta Cytol 1984;28:129-132.
118. Thunnissen FB, Arends JW, Buchholtz RT, ten Velde G. Fine needle aspiration cytology of inflammatory pseudotumor of the lung (plasma cell granuloma). Report of four cases. Acta Cytol 1989;33:917-921.
119. Travis WD, Brambilla E, Muller-Hermelink HK, Harris CC. (Eds.): World Health Organization Classification of Tumours. Pathology and Genetics of Tumours of the Lung, Pleura, Thymus and Heart. IARC Press: Lyon 2004.
119A. Travis WD, Brambilla E, Noguchi M, Nicholson A, Geisinger K, Yatabe Y, et al. International association for the study of lung cancer/american thoracic society/european respiratory society international multidisciplinary classification of lung adenocarcinoma. Journal of Thoracic Oncology 2011;6(2):244-285.
119B. Travis WD, Rekhtman N. Pathological Diagnosis and Classification of Lung Cancer in Small Biopsies and Cytology: Strategic Management of Tissue for Molecular Testing. Semin Respir Crit Care Med 2011;32(01):022,031.
120. Trillo A, Guha A. Solitary condylomatous papilloma of the bronchus. Arch Pathol Lab Med 1988;112:731-733.
121. Wakely P Jr. Pulmonary spindle cell lesions: correlation of aspiration cytopathology and histopathology. Ann Diagn Pathol 2001;5:216-228.
122. Weingarten J. Cytologic and histologic findings in a case of tracheobronchial papillomatosis. Acta Cytol 1981;25:167-170.
123. Wiatrowska BA, Krol J, Zakowski MF. Large-cell neuroendocrine carcinoma of the lung: proposed criteria for cytologic diagnosis. Diagn Cytopathol 2001;24:58-64.

124. Wiatrowska BA, Yazdi HM, Matzinger FR, Mac Donald LL. Fine needle aspiration biopsy of pulmonary hamartomas. Radiologic, cytologic and immunocytochemical study of 15 cases. Acta Cytol 1995;39:1167-1174.
125. Willett GD, Schumann GB, Genack L. Primary cytodiagnosis of synchronous small-cell cancer and squamous-cell carcinoma of the respiratory tract. Acta Cytol 1984;28:610-613.
126. Wistuba II, Gazdar AF. Lung cancer preneoplasia. Annu Rev Pathol 2006;1:331-348.
127. Wood B, Swarbrick N, Frost F. Diagnosis of pulmonary hamartoma by fine needle biopsy. Acta Cytol 2008;52:412-417.
128. World Health Organization. Histological typing of lung tumors, 2nd edn. WHO, Geneva, 1981.
129. Yamaguchi T, Imamura Y, Nakayama K, et al. Primary pulmonary leiomyosarcoma. Report of a case diagnosed by fine needle aspiration cytology. Acta Cytol 2002;46:912-916.
130. Yang Yj, Steele CT, OU XL, et al. Diagnosis of high-grade pulmonary neuroendocrine carcinoma by fine-needle aspiration biopsy: nonsmall-cell or small-cell type? Diagn Cytopathol 2001;25:292-300.
131. Yeh TJ. Endometriosis within the thorax: metaplasia, implantation, or metastasis? J Thorac Cardiovasc Surg 1967;53:201-205.
132. Zaharopoulos P, Wong JY, Stewart GD. Cytomorphology of the variants of small-cell carcinoma of the lung. Acta Cytol 1982;26:800-808.

**Fig. 2.27 Squamous cell papilloma.**
An intrabronchial exophytic papillary tumor was detected by bronchoscopy in a 59-year-old man. Intra/transbronchial FNAB revealed papilliform microfragments composed of metaplastic-like squamous cells of small and intermediate size. Loss of cellular polarity and nuclear irregularities are distinct (direct smear, Pap stain, higher magnification).
*Tentative cytologic diagnosis*: Suggestive of squamous cell carcinoma (papillary neoplasm was not taken into consideration).
*Tissue diagnosis* (excisional biopsy): Squamous cell papilloma exhibiting focal epithelial dysplasia.

**Figs. 2.28 and 2.29 Hamartoma.**
Two examples of intrapulmonary hamartoma presenting with different tissue components.

**Fig. 2.28** (case #1) Transcutaneous FNAB of a long-standing nodular lesion in a 64-year-old man's right lung. Low magnification reveals large fragments of loose but cellular fibrous tissue, myxoid stroma (upper right), and a few groups of glandular cells (lower right) (direct smear, Pap stain).

**Fig. 2.29** (case #2) Transbronchial FNAB of parabronchial situated small nodules (middle-aged male patient). Low magnification shows large sheets of ciliated columnar cells (upper left) and numerous chondroid fragments (lower right). Morphologic findings are consistent with a cartilaginous hamartoma (direct smear, Pap stain).

**Fig. 2.30 Inflammatory pseudotumor.**
A 69-year-old man presented with a small nodule in the periphery of his right lung. Transcutaneous FNAB was performed. The morphology is presented using a specimen immunostained for pancytokeratin-Lu-5 (Pap-prestained direct smear).
The aspirate included numerous compact heterogeneous cell clusters. High magnification disclosed Lu-5-positive staining of mesothelial cells, which are surrounded by clustered round and elongated immunonegative cells (fibroblasts/myofibroblasts, histiocytes, lymphoid cells).
*Cytology* assumed to be benign or malignant stromal tumor.
*Histologic examination* of the excised nodule provided a diagnosis of an inflammatory pseudotumor of the lung.

**Fig. 2.31 Severe dysplasia.**
Bronchial aspirate from a 59-year-old man giving rise to diagnostic dilemmas.
High magnification shows malignant epithelial cells of adenocarcinoma type (arrows) and keratinized squamous cells with severe atypia (direct smear, Pap stain).
*Cytologic evaluation*: The initial cytologic diagnosis from exfoliative respiratory material was adenocarcinoma accompanied by atypical squamous cells originating from adjoining dysplastic squamous metaplasia.
Subsequent mediastinal FNAB confirmed the diagnosis of adenocarcinoma (immunocytochemical TTF-1 positivity of the tumor cells).
The additional diagnosis of dysplastic squamous metaplasia of the bronchial epithelium is assumed to be correct.
*Histologic results* are not available.

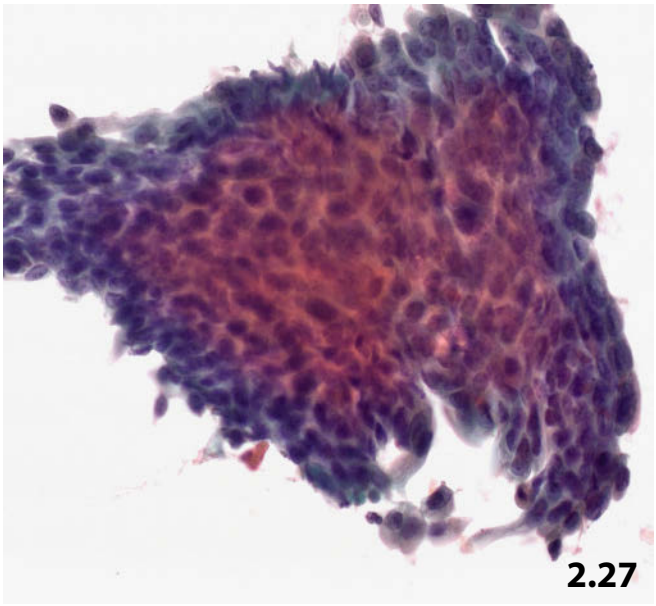
2.27

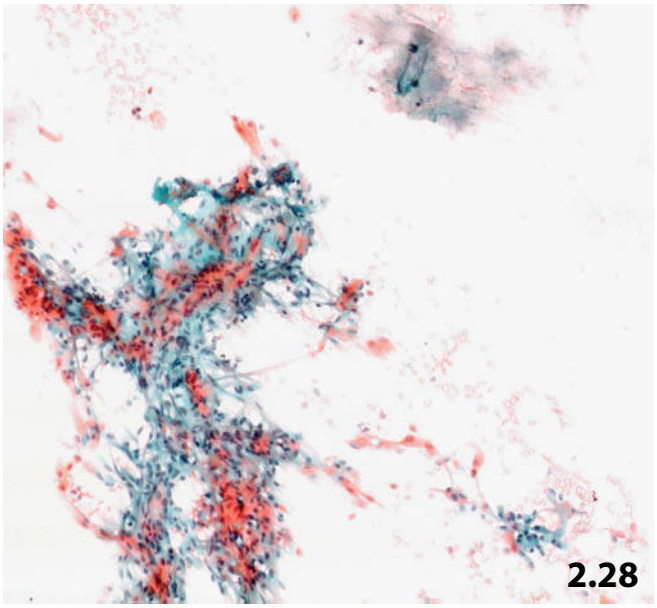
2.28

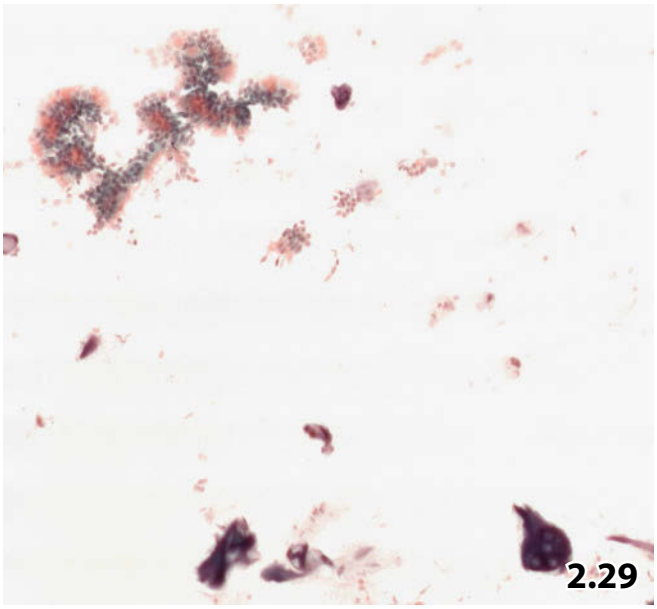
2.29

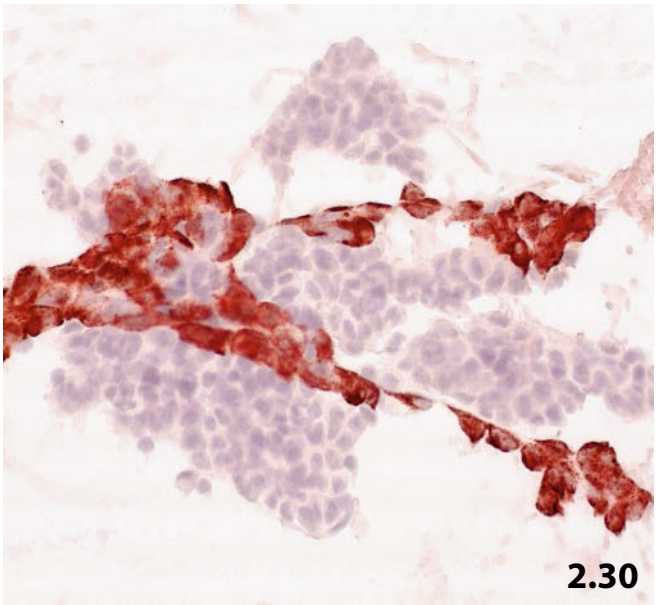
2.30

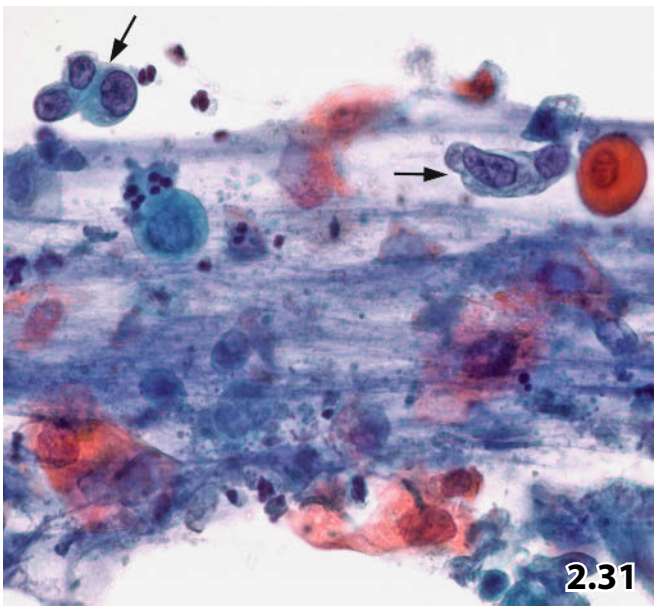
2.31

**Fig. 2.32 In situ squamous cell carcinoma.**
Sputum sample of a 75-year-old man without positive clinical history. Lower magnification shows numerous atypical/malignant squamous cells intermingled with necrotic tumor tissue (Pap stain). The squamous cells are exceptionally small.
*Cytologic (over)diagnosis*: Necrotizing keratinized squamous cell carcinoma.
*Tissue diagnosis* (endobronchial biopsy): Severe dysplastic squamous epithelium/in situ squamous cell carcinoma. Subsequent multiple tissue specimens from the bronchial tree did not reveal any invasive neoplasm.

**Fig. 2.33 Invasive squamous cell carcinoma.**
Very low magnification reveals the appearance of invasive squamous cell carcinoma as it used to be in sputum specimens. There is a triad of:
– Isolated neoplastic cells.
– Necrosis.
– Red blood cells.
All these elements are partly enmeshed in mucoid strands (Pap-stained direct smear).

**Fig. 2.34A, B Keratinizing squamous cell carcinoma.**
The two images demonstrate cells showing all characteristics of common squamous cell carcinoma (bronchial brushing, direct smears, Pap stain, high magnification). **A** Note the keratinized tadpole-like cells (two cells upper left), the marked nuclear hyperchromasia, and concentric lamination of the cytoplasm (arrows). **B** Note in particular the extreme variability of N/C ratio and the occasional pronounced nuclear clearing (arrows).

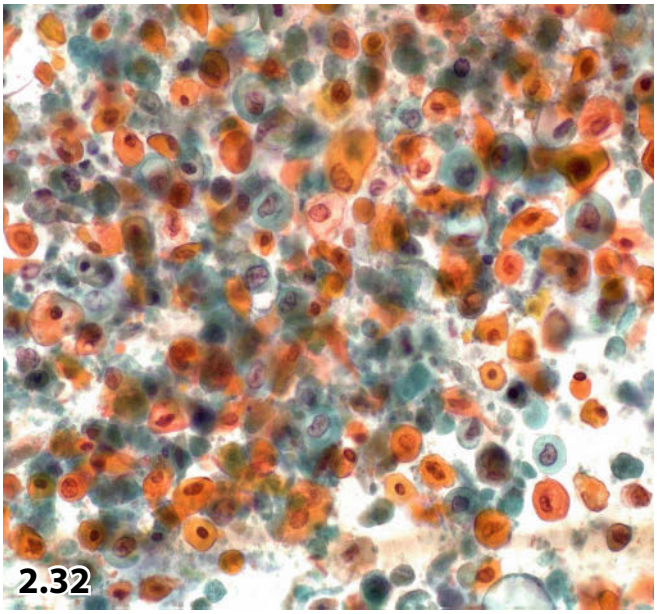
2.32

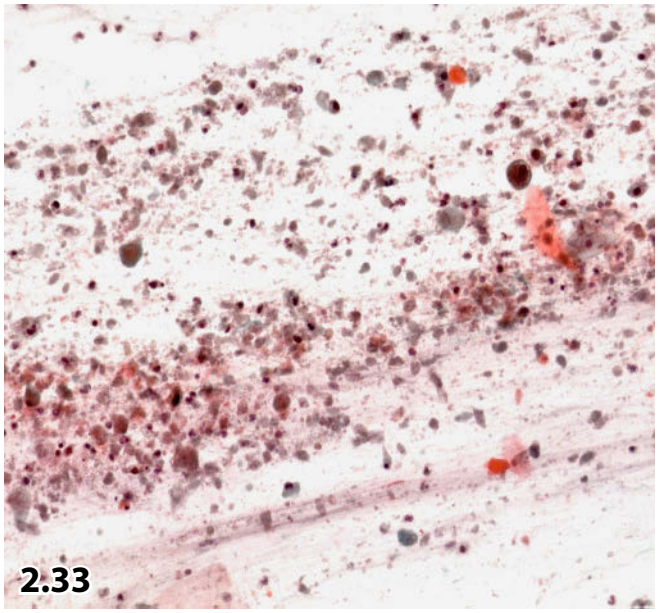
2.33

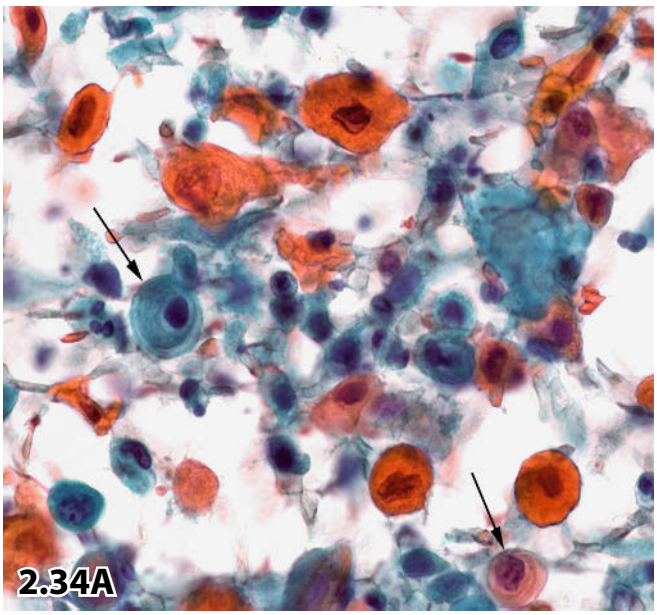
2.34A

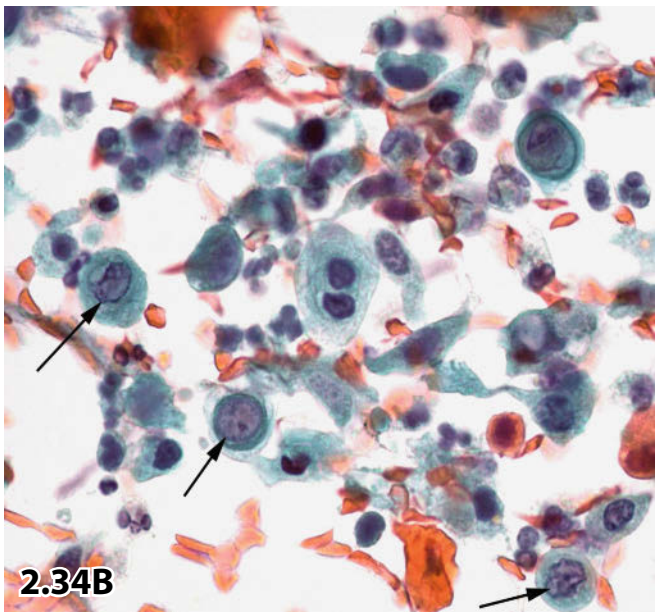
2.34B

**Fig. 2.35 Keratinizing squamous cell carcinoma: spindle cell variant.**
Bronchial aspirate showing clusters of a keratinizing squamous cell carcinoma (upper half of the field). Numerous neoplastic spindle cells exhibit merely minor nuclear atypias (direct smear, Pap stain, lower magnification).

**Figs. 2.36 and 2.37 Keratinizing squamous cell carcinoma: variant with clear nuclei.**
Two examples of keratinizing SCC are presented from a sputum probe and from a fine needle aspirate (see also Fig. 2.34B).

**Fig. 2.36** (case #1) Smears of a sputum sample contained predominantly dispersed single carcinoma cells. Neoplastic cells show extremely clear nucleoplasm frequently associated with a few chromatin clots. It is nearly impossible to differentiate between single tumor cells exhibiting broad vacuolated cytoplasm and activated histiocytes (both supposed cancer cells and supposed activated histiocytes are designated by the arrows). (Pap stain, high magnification).

**Fig. 2.37** (case #2) Transbronchial FNAB revealed an endobronchial metastasis of a keratinizing squamous cell carcinoma (site of origin was the tongue). Note the extremely clear nuclei in a few carcinoma cells partially not completely in focus (arrows) (direct smear, Pap stain, high magnification).

**Fig. 2.38A, B Poorly differentiated squamous cell carcinoma.**
Bronchial brushing in a 59-year-old man presenting with an endobronchial tumor mass that has been detected on the occasion of a fiberscopic examination. Direct brush smears were stained using the Papanicolaou technique**. A** Lower magnification shows dense clustering of elongated carcinoma cells focally providing a pronounced streaming pattern (asterisks)**. B** High magnification exhibits obvious malignant nuclear features. The cytoplasm may be vacuolated or densely structured. Intercellular bridges can be identified (arrow). Cytoplasmic features of nonkeratinized malignant squamous cells are also illustrated in Fig. 2.34B.

**Fig. 2.39 Squamous cell carcinoma: small-cell variant.**
Bronchial brushing in an elderly man presenting with a tumor in his left lung. Direct brush smears were stained using the Papanicolaou technique. Coarse chromatin, prominent nucleoli, occasional sharp cytoplasmic outlines, and a few small keratinizing atypical cells (arrows; cytoplasm is not completely in focus) distinguish small-cell squamous cell carcinoma from classic small-cell carcinoma of the lung.

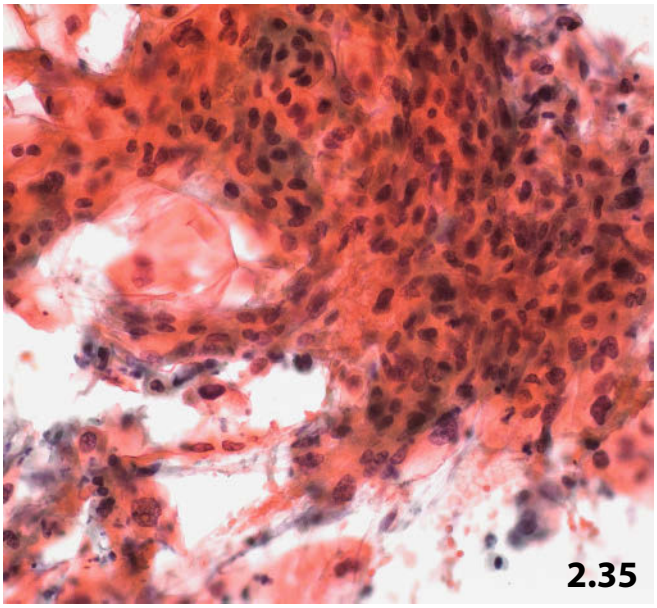
2.35


2.36

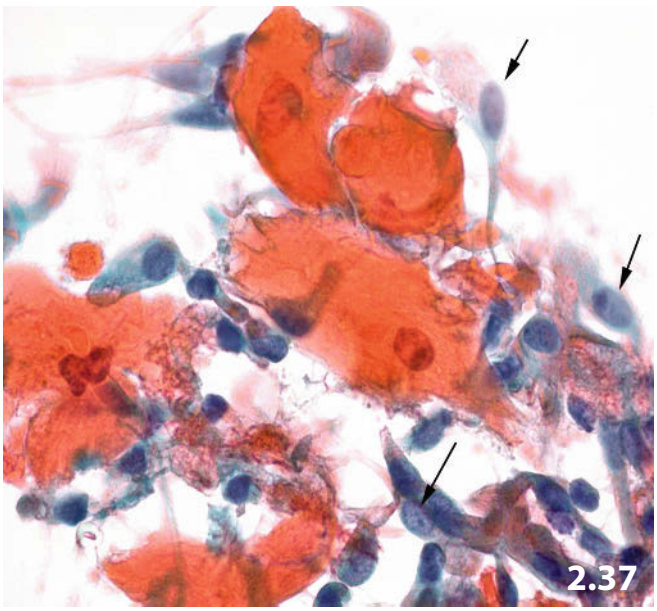
2.37

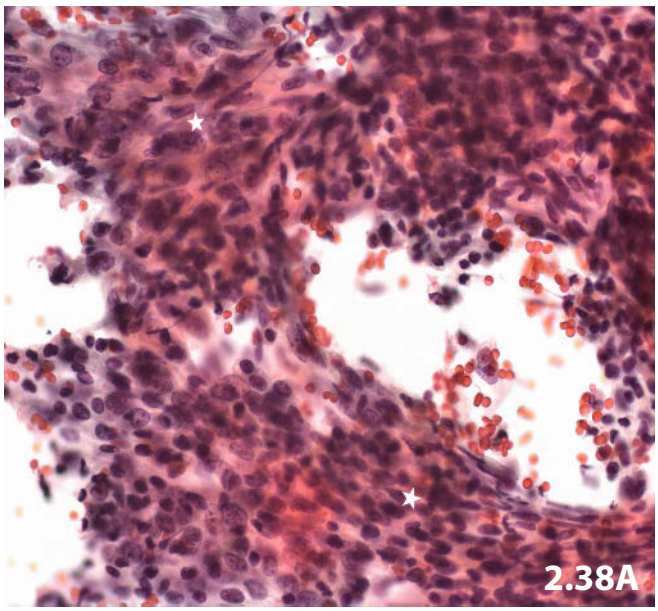
2.38A

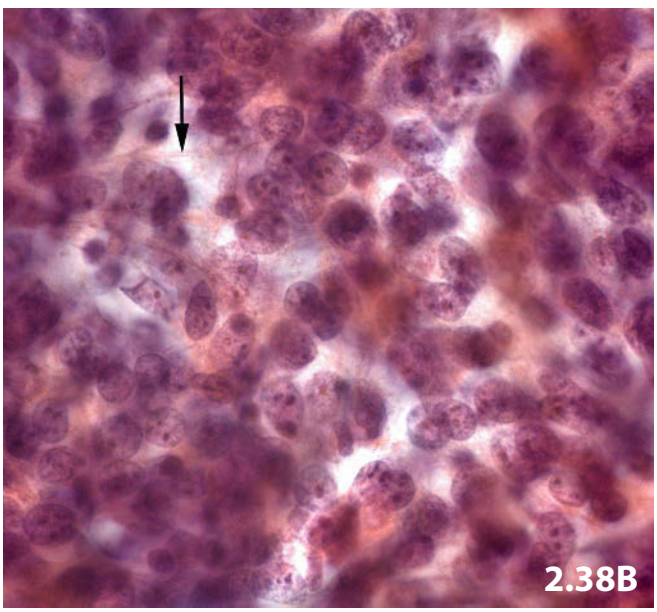
2.38B

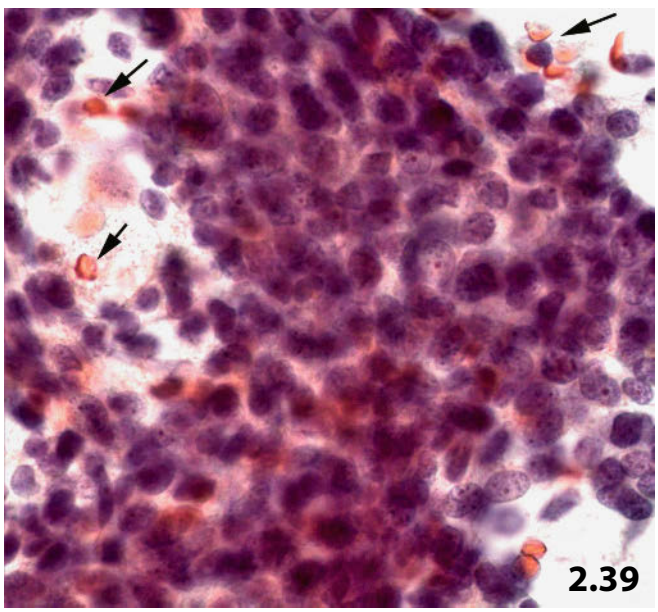
2.39

**Fig. 2.40 Adenocarcinoma versus severe reactive cell changes.**
A small cell cluster from a monomorphic adenocarcinoma of the lung. Take into consideration that severe reactive changes of glandular pulmonary cells may exhibit an identical cell pattern! Compare with the cell cluster depicted in Fig. 2.11 (bronchial aspirate, Pap stain, high magnification).

Diagnosis of adenocarcinoma requires a large number of atypical single cells and cell clusters partly exhibiting unequivocal features of malignancy.

**Figs. 2.41 and 2.42 Adenocarcinoma: conventional type.**
Typical cell features of adenocarcinomas from two patients (bronchial aspirates, Pap stain).

**Fig. 2.41A, B** (case #1) Clusters and cells depicted from the same case showing the characteristic cytologic features of adenocarcinomas. **A** Three-dimensional cell clusters mainly papilliform (lower left) or of acinar type (upper right) (lower magnification). **B** Tumor cell cluster exhibiting radiating flower petal pattern (arrow). Note the cellular characteristics: irregular nuclear outline, powdery chromatin, centrally placed macronucleoli, distinctly outlined cytoplasm tha is eccentric and vacuolated (high magnification).

**Fig. 2.42A, B** (case #2) The classic cellular morphology of adenocarcinoma and its immunocytochemical properties. **A** High-powered view demonstrates dense finely granular chromatin texture, the typical nucleoli, and abundant vacuolated cytoplasm (oil immersion, magnification, ×100). **B** Positive nuclear immunostaining for TTF-1 is helpful in determining a definite diagnosis of pulmonary adenocarcinoma in equivocal cases.

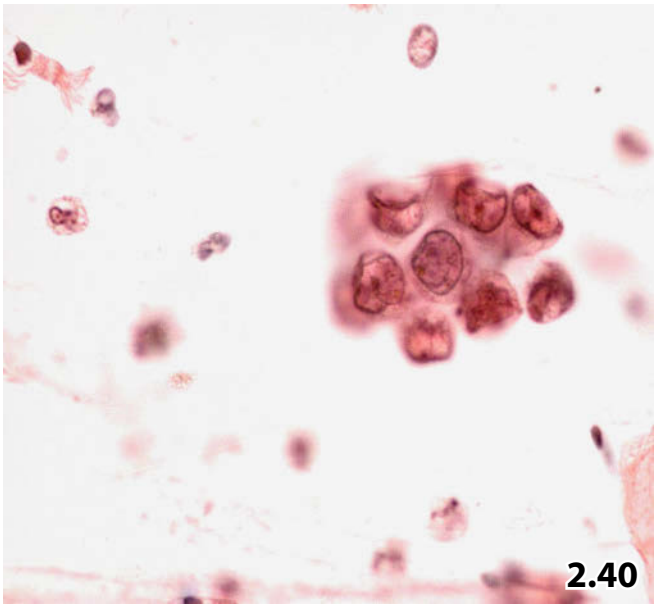
2.40

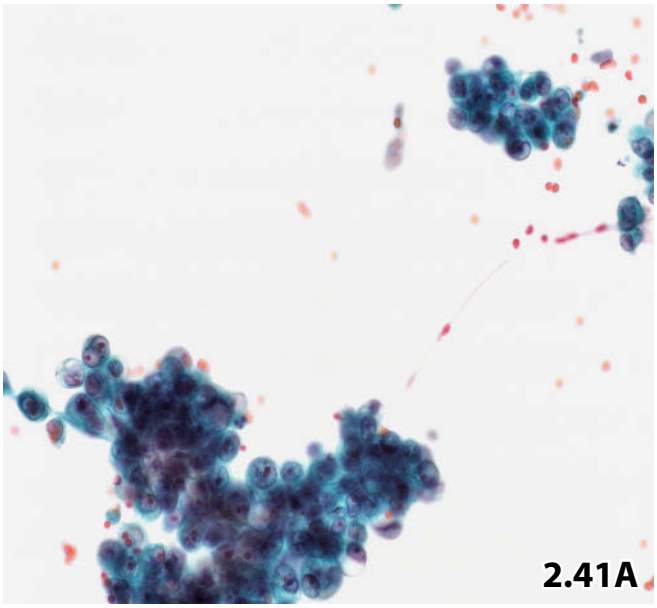
2.41A

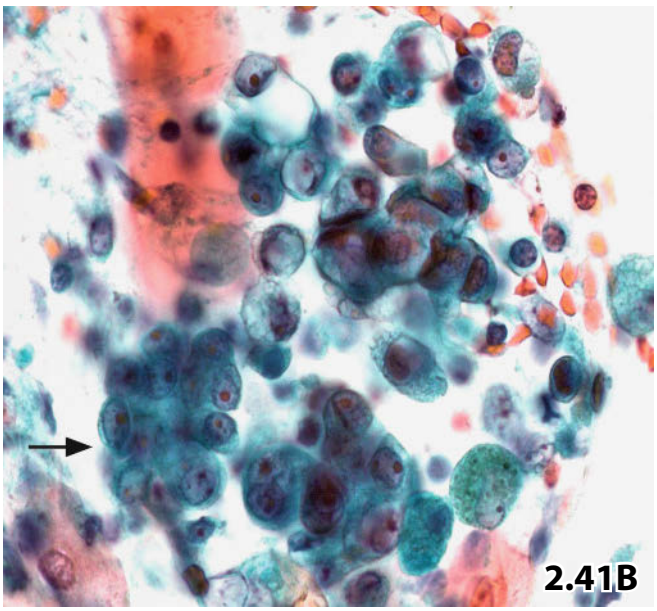
2.41B

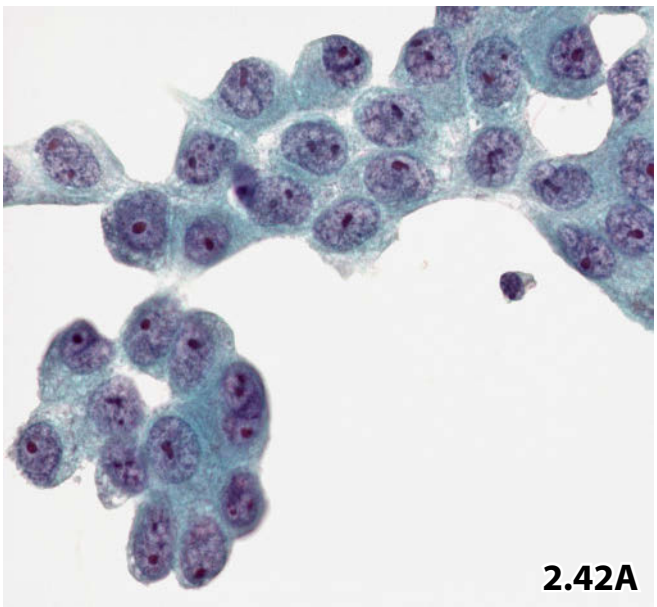
2.42A

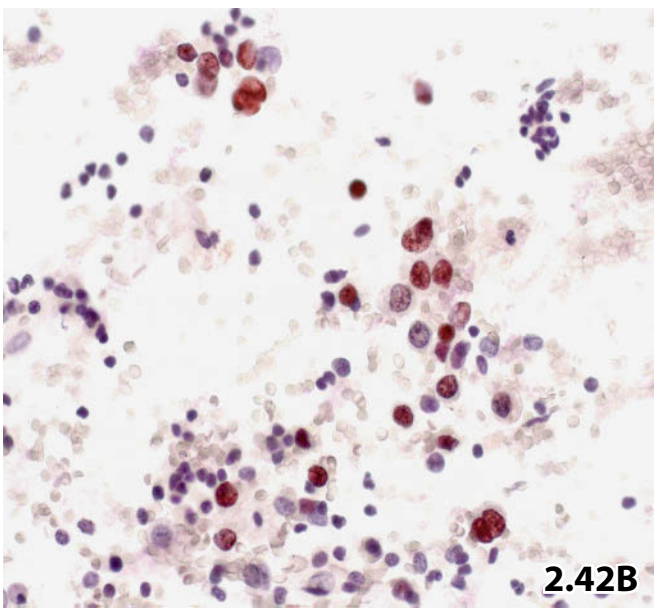
2.42B

**Fig. 2.43 Monomorphic adenocarcinoma versus benign bronchial epithelial cluster.**
Note the striking similarity of the crescent carcinomatous cluster compared to the benign epithelial cluster (arrow): identical cellular and nuclear shape, identical nuclear texture and color, and an identical cytoplasmic structure. A major difference however, is observed regarding cellular arrangement, cellular size, and nucleoli (bronchial brushing, direct smear, Pap stain, high magnification).

**Fig. 2.44 Papillary adenocarcinoma.**
Transcutaneous FNAB of a lung tumor in the upper right lobe of an elderly male patient presenting with metastatic lung cancer. Subtyping of the lung neoplasm was not known at this stage. High magnification shows part of a papillary cluster composed of palisading, elongated atypical columnar cells (direct smear, Pap stain).
*Cytologic findings* are consistent with well differentiated mucinous papillary adenocarcinoma. The attending physicians abstained from histology.

**Figs. 2.45 and 2.46 Bronchioloalveolar carcinoma.**
Bronchial aspirates from two different patients, both suffering from bronchioloalveolar carcinoma. Pap-stained direct smears were performed. Additional figures are presented in Chap. 2.3. "Bronchoalveolar Lavage," Sect. 2.3.6 "Malignancies".

**Fig.2.45** (case #1) Lower magnification reveals a flat sheet (upper right) and three-dimensional compact clusters originating from an adenocarcinoma composed of small to medium-sized cells. Papilliform and acinus-like cell (arrows) arrangement and intracytoplasmic pinkish mucin (arrowheads) are overt. Nuclear irregularities (folds, molding) and loss of polarity indicate a malignant neoplastic lesion.

**Fig. 2.46** (case #2) High magnification focuses on bland chromatin, prominent nuclear irregularities, and occasional distinct nucleoli. Numerous psammoma bodies are encased within a neoplastic cell cluster (upper left).
Note single cells with histiocytoid nuclei and abundant vacuolated cytoplasm (arrows); distinguishing these cells from activated histiocytes is very difficult using conventional cytology alone.

**Fig. 2.47 Large-cell undifferentiated carcinoma.**
Dissociating clusters composed of large pleomorphic tumor cells exhibiting highly variable N/C ratio; strands of chromatin occur centrifugally (arrows). Exceptionally clear nucleoplasm and polyhedral cytoplasmic bodies are striking (bronchial brushing, direct brush smear, Pap stain, higher magnification).

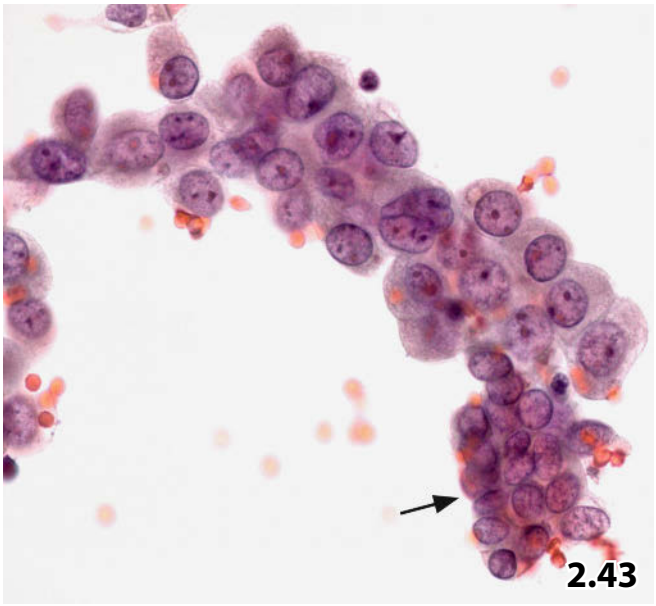
2.43

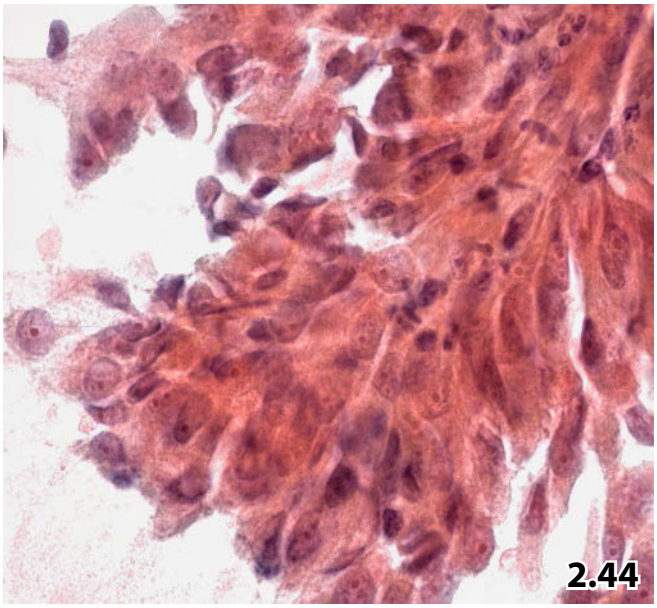
2.44

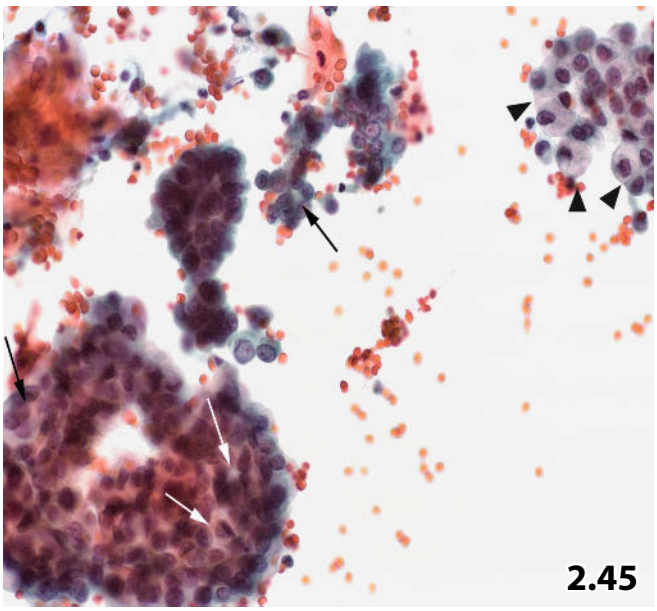
2.45

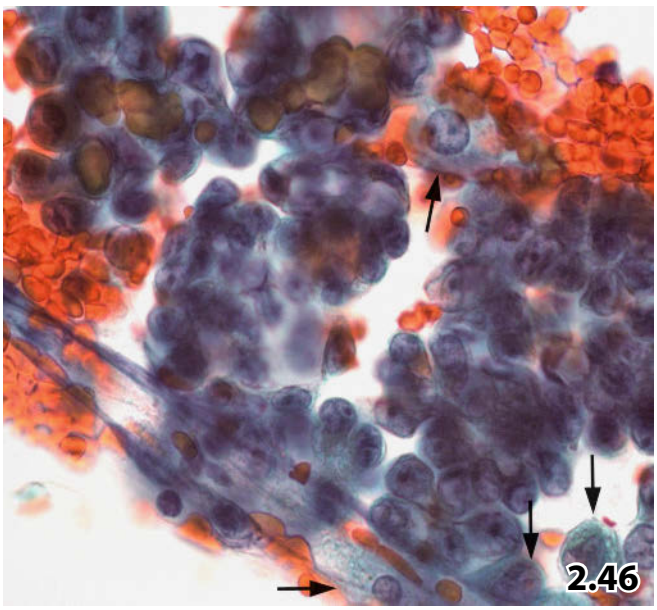
2.46

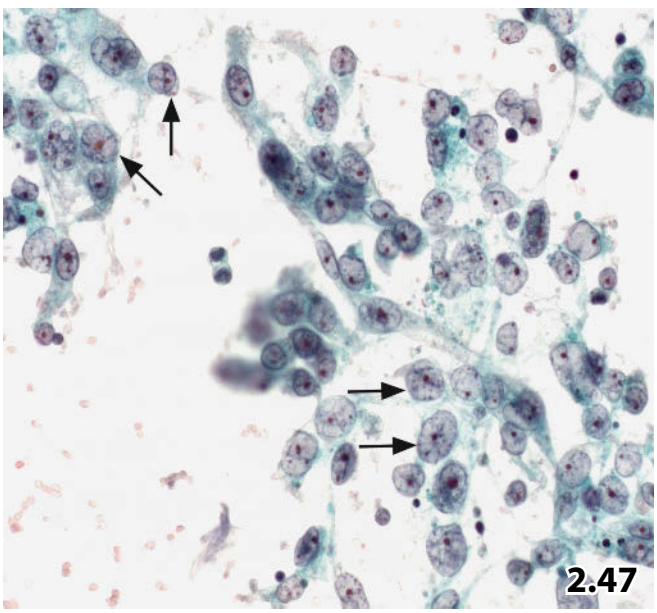
2.47

**Fig. 2.48A, B Small-cell carcinoma: paucicellular exfoliative sample.**
The cells depicted in these two images come from the same sputum probe (Pap stain). The examples emphasize the particular importance of careful microscopic screening in patients with small-cell carcinoma. **A** Very low magnification displays a single tumor cell cluster (arrow) that meets all criteria of small-cell carcinoma**. B** High magnification demonstrates a few single carcinoma cells (arrows) and a dyad of small carcinoma cells (arrowhead) amid benign lymphocytes. Attention should be paid to the size and chromatin texture of the neoplastic cells as compared to lymphocytes.

**Fig. 2.49 Small-cell carcinoma in sputum.**
Note the characteristic morphologic features: cell arrangement along mucus streaks, mainly in a linear fashion. The nuclei show pronounced variability in size, molding, indentations, and thin dispersed or glassy chromatin (Pap stain, high magnification).

**Fig. 2.50 Small-cell carcinoma in bronchial aspirate/washing**
Blood mass frequently masks individual neoplastic cells and small-cell clusters exfoliated from small-cell carcinomas. Unlike bronchial lining epithelial cells (arrows), the neoplastic cells (arrowheads) exhibit enlarged nuclei and irregular nuclear membranes (direct smear, Pap stain, lower magnification).

**Fig. 2.51 Small-cell carcinoma, oat cell type.**
Neoplastic cells from a sputum sample exhibit characteristic features of oat cell carcinoma. Identical features can be observed in Fig. 2.49. However, a few tumor cells in the current field are of the intermediate cell type (see Fig. 2.52) (Pap stain, high magnification).

**Fig. 2.52 Small-cell carcinoma, intermediate cell type.**
Neoplastic cells of small-cell carcinoma of the intermediate cell type are larger than the oat cell type. Multiple nucleoli and an enlarged but often indistinct cytoplasmic body are key features of the intermediate tumor variant. A few cells exhibit elongated cytoplasm (arrows) (bronchial aspirate, high magnification, Pap stain, direct smear).

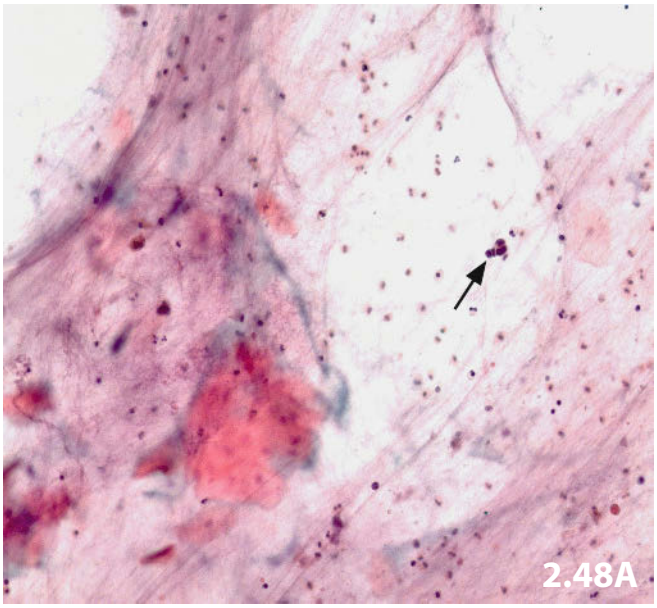
2.48A

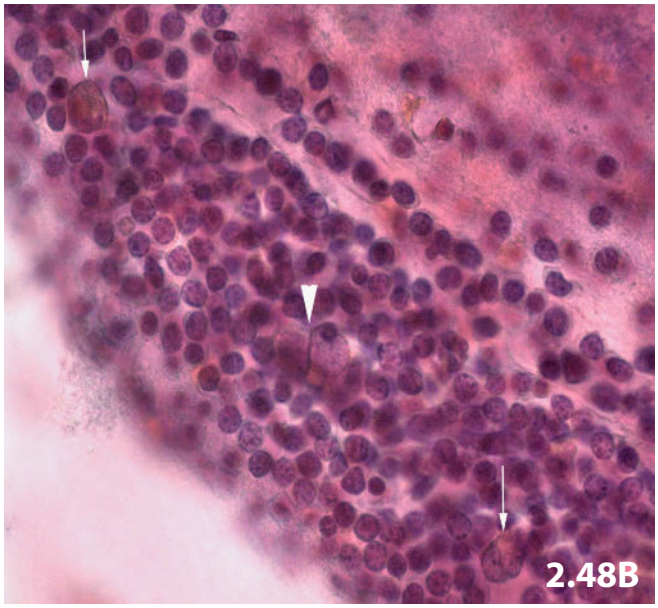
2.48B

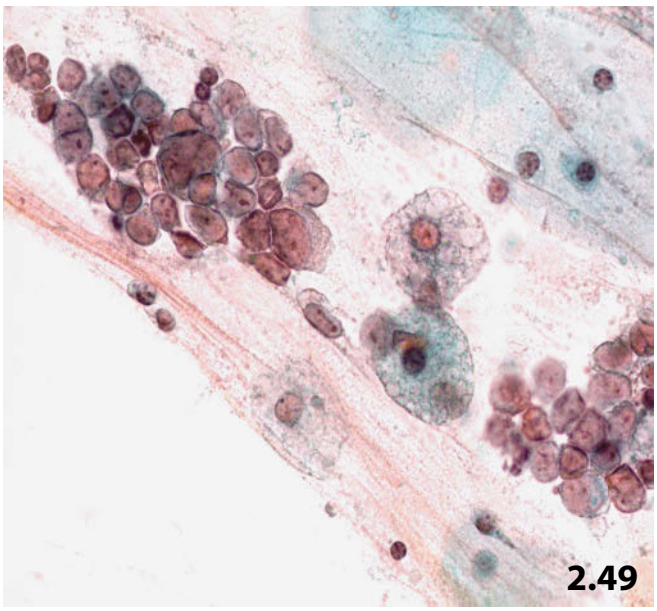
2.49

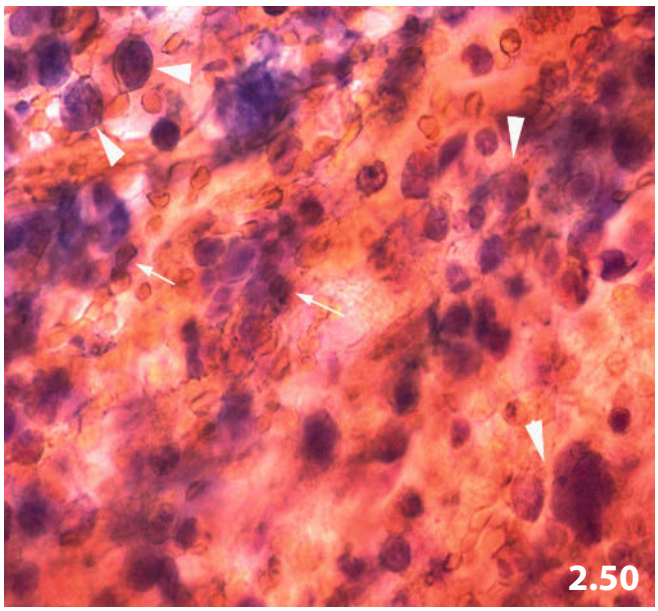
2.50

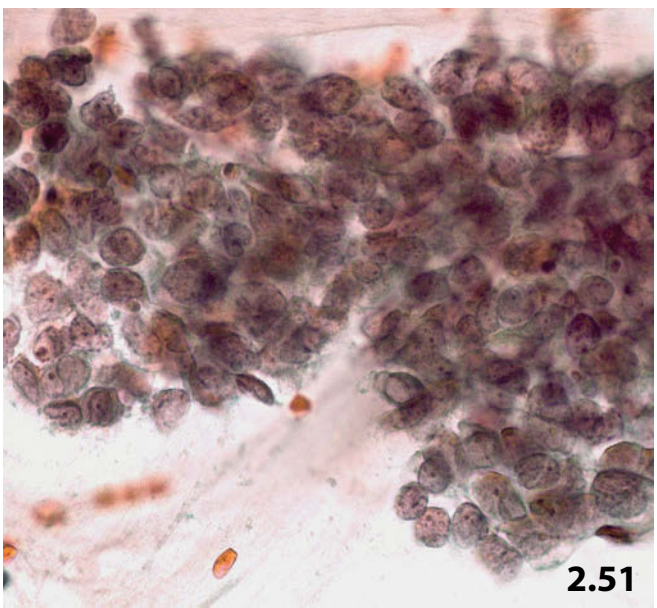
2.51

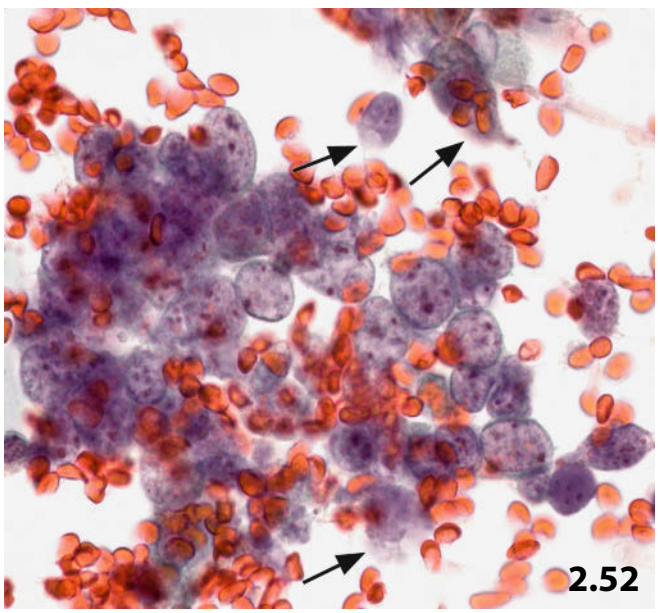
2.52

**Fig. 2.53 Small-cell carcinoma versus malignant non-Hodgkin lymphoma.**
Tumor cells of small-cell carcinoma (mainly of the oat cell type) occurring completely dissociated in a smear from a bronchial aspirate. Therefore, distinguishing between small-cell carcinoma and malignant lymphoma is difficult. Still, absence of unequivocal lymphoid cells, absence of cytoplasmic rims, and absence of nucleoli in the majority of the nuclei favor the diagnosis of small-cell carcinoma (direct smear, Pap stain, higher magnification).

**Fig. 2.54 Adenoid cystic carcinoma.**
Classic appearance of adenoid cystic carcinoma: three-dimensional clusters composed of small monomorphic tumor cells surrounding cores of pinkish hyaline material (bronchial aspirate, direct smear, Pap stain, lower magnification).

**Fig. 2.55 Mucoepidermoid carcinoma.**
A 63-year-old man presented with a tumor in his right lung. Antecedent exfoliative cytologic and histologic investigations yielded no conclusive diagnosis. Transbronchial FNAB revealed a heterogeneous cell pattern composed of metaplasia-like sheets of immature squamous cells interspersed with mucinous glandular cells and goblet cells (arrows) (direct smear, Pap stain, lower magnification). A few keratinizing squamous cells were also present (not shown).
*Cytologic diagnosis* of a mucoepidermoid carcinoma was later verified with histology.

**Fig. 2.56 Follicular non-Hodgkin lymphoma.**
A 63-year-old man presented with a diffuse infiltrate in his right lung. Sputum cytology revealed a neoplasia consisting of atypical monomorphous cells characterized by conspicuous nucleoli, and mostly ill-defined cytoplasm; cytoplasmic vacuolization is overt, unlike the fuzzy granularity (Pap stain, high magnification).
*Cytologic differential diagnosis*: Malignant non-Hodgkin lymphoma, carcinoid tumor, and small-cell carcinoma of intermediate cell type.
*Comments*: The latter diagnosis seems rather unlikely due to the nuclear monomorphism, unfitting chromatin texture, and cytoplasmic features. Clarifying the histogenesis of this tumor requires immunocytochemical workup (not performed by cytology because of technical problems).
*Tissue diagnosis* (open lung biopsy): Follicular non-Hodgkin lymphoma, grade 2.

**Fig. 2.57A, B Burkitt lymphoma: diagnostic challenge.**
A 10-year-old boy presented with an intraabdominal tumor mass and a single subpleural node in his left lung. To investigate the nature of the lesion in the left lung, transcutaneous FNAB was performed as first-line diagnostic approach (direct smears).
*Cytologic diagnosis*: Non-Hodgkin lymphoma, blastic type.
*Tissue diagnosis*: Burkitt lymphoma.
**A** The deeply basophilic cytoplasm with the characteristic vacuoles (arrows) in MGG stain may indicate Burkitt lymphoma (high magnification). **B** Note single-file like tumor cell arrangement in the Pap-stained FNAB-specimen, which may give rise to diagnostic dilemmas, particularly with small-cell carcinoma (arrows) (lower magnification).

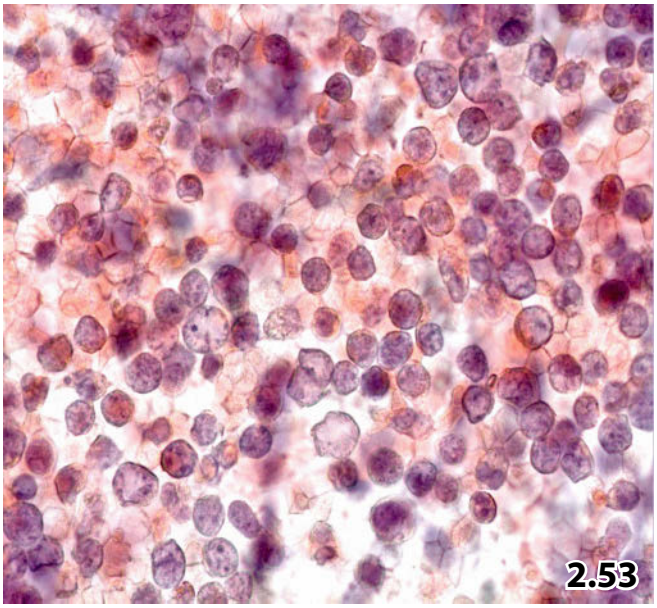
2.53

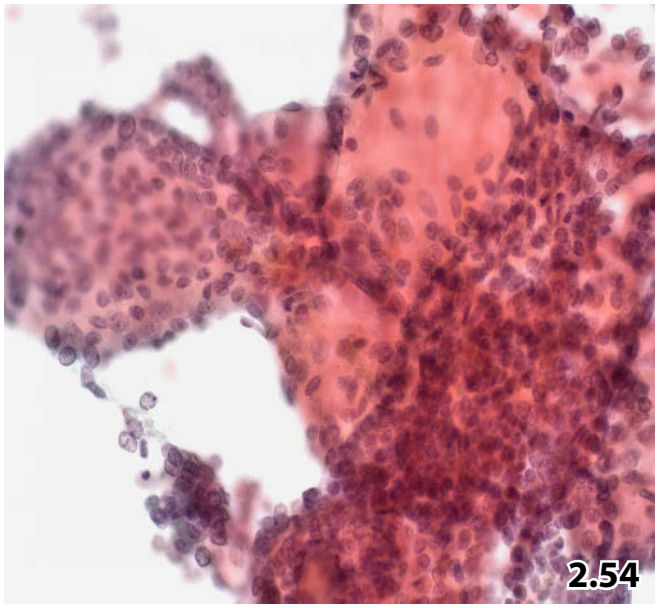
2.54

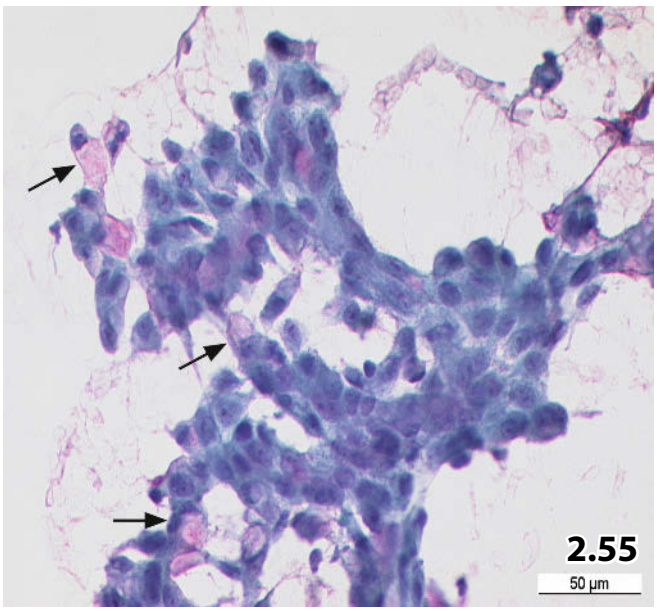

2.55

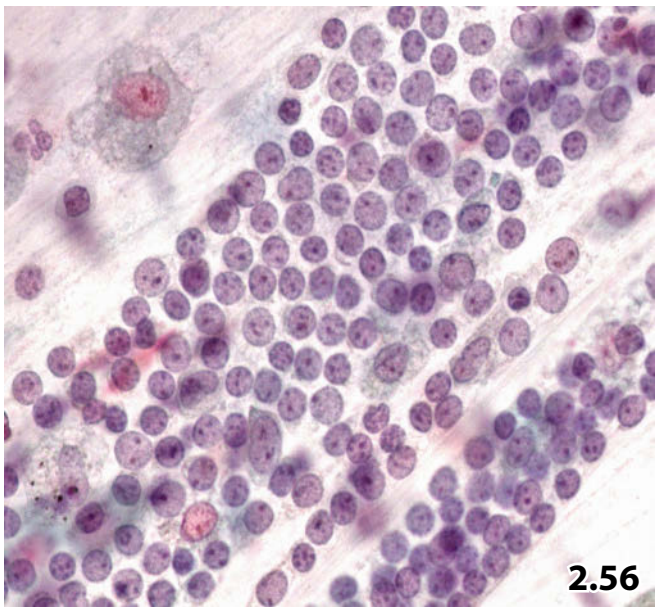
2.56

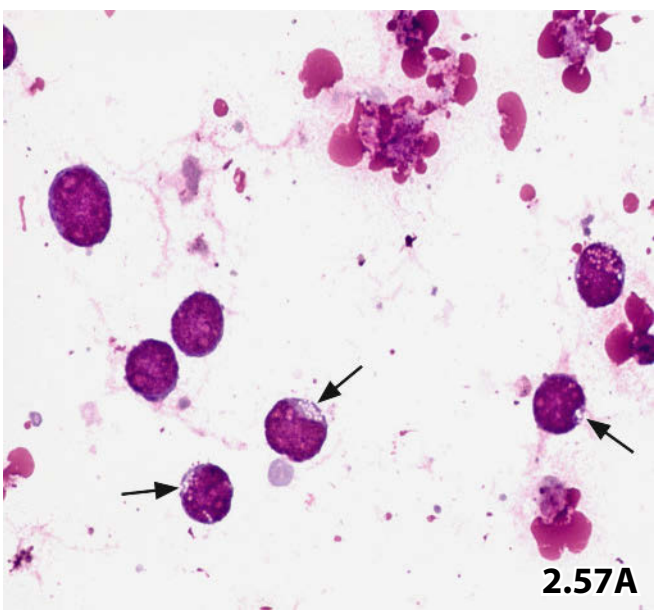
2.57A

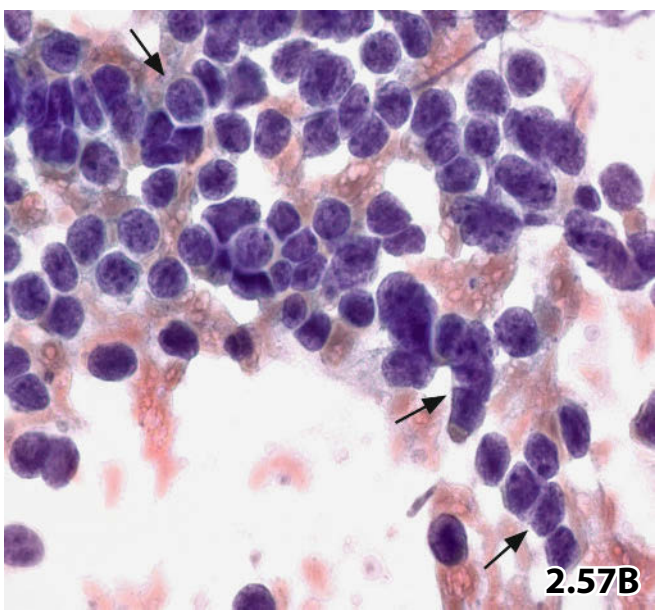
2.57B

**Fig. 2.58 Hodgkin lymphoma.**
A female patient with a positive history of Hodgkin lymphoma; clinical findings suggest tumor dissemination into the lung. Numerous distinct Reed-Sternberg cells (arrow) and mononuclear Hodgkin cells were seen in the first sputum sample (Pap stain, higher magnification).
*Cytologic diagnosis*: Hodgkin lymphoma.
*Comment*: The diagnosis of Hodgkin disease was easy in this case due to patient's history. However, distinguishing RSH cells from cells of anaplastic carcinoma would be very difficult without an appropriate clinical history.

**Fig. 2.59A–C Breast carcinoma.**
A 72-year-old woman with positive history of breast carcinoma (lumpectomy and irradiation 12 years before) presented with a tumorous lesion in her right lung. **A** Bronchial aspirates and bronchial brushings showed numerous isolated and clustered tumor cells consistent with a monomorphous well-differentiated adenocarcinoma (direct smears, Pap stain, high magnification). An appropriate immunopanel is essential in order to assess the primary site of the neoplasia (lung cancer versus metastasis of breast carcinoma).
**B** Nuclear positivity for estrogen receptors (Pap-prestained direct smears). **C** Negative immunoreactivity for TTF-1 (Pap-prestained direct smears).
*Cytologic diagnosis*: Selected immunostains established correct diagnosis of breast cancer.

**Fig. 2.60 Colonic carcinoma.**
A 53-year-old man presenting with lung disorders and a positive history of colonic carcinoma. **A** Compact cell clusters from a poorly differentiated adenocarcinoma were encountered in bronchial brushings (Pap stain, high magnification). **B** Positive immunostaining for CK20 proved helpful in determining a definite diagnosis of metastatic colonic carcinoma.

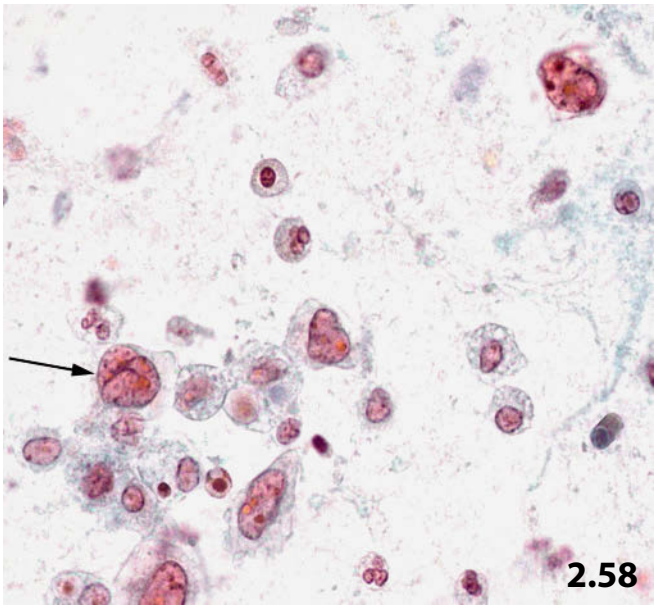
2.58

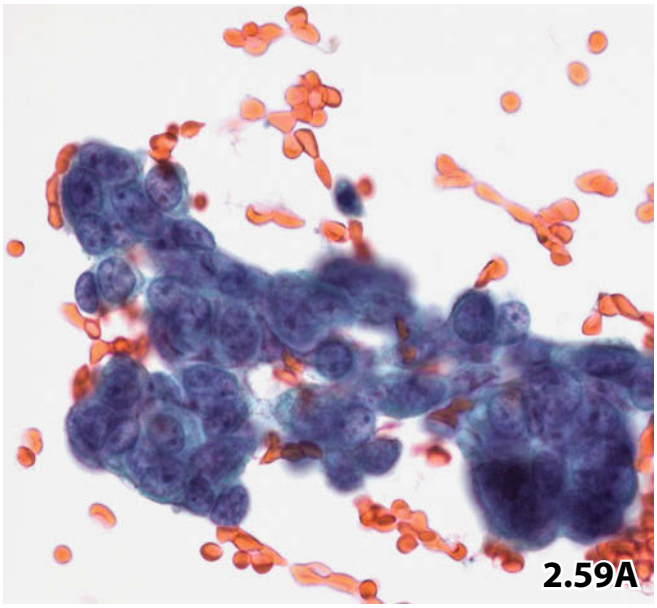
2.59A

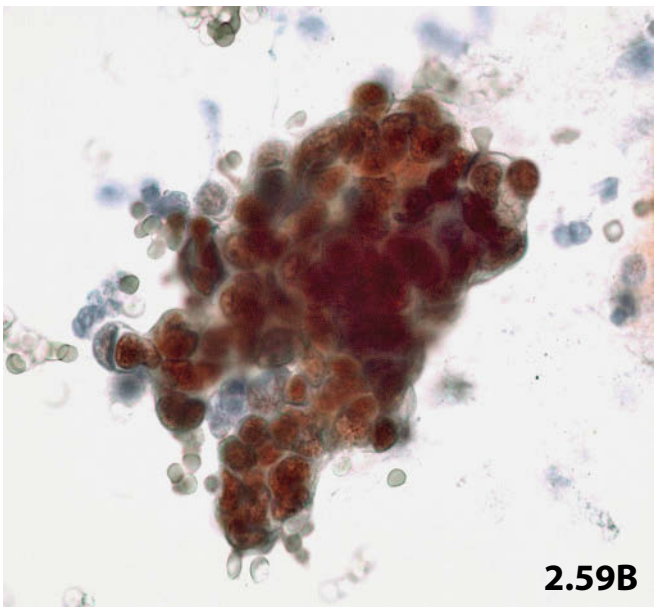
2.59B

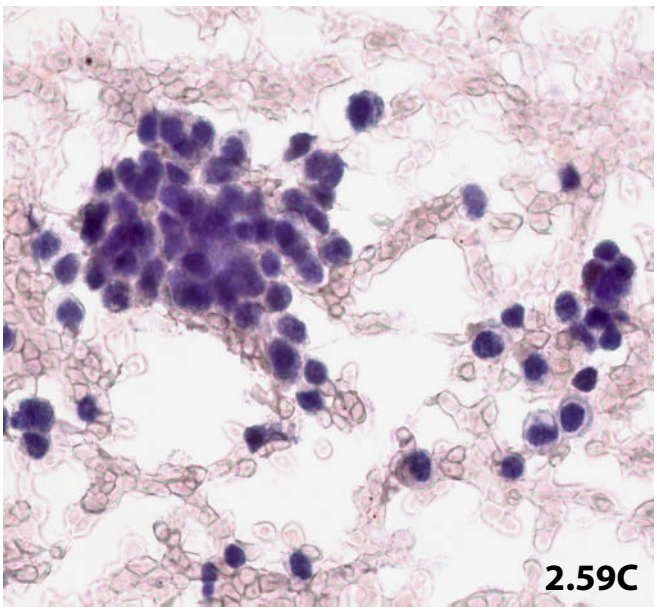
2.59C

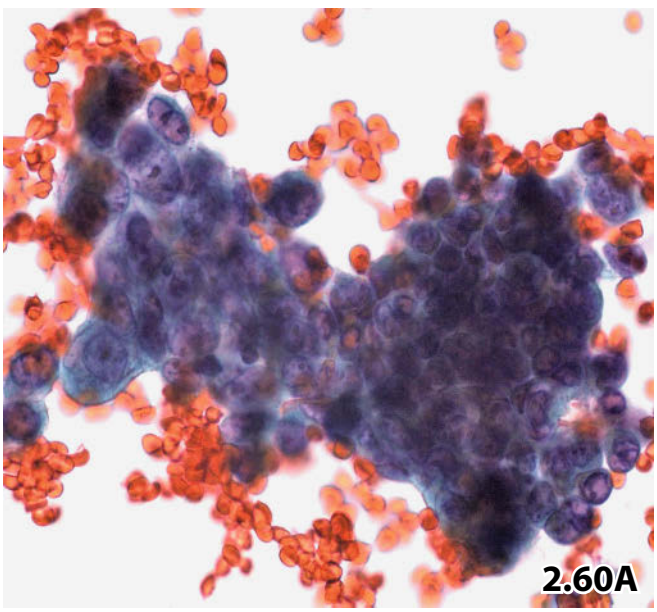
2.60A

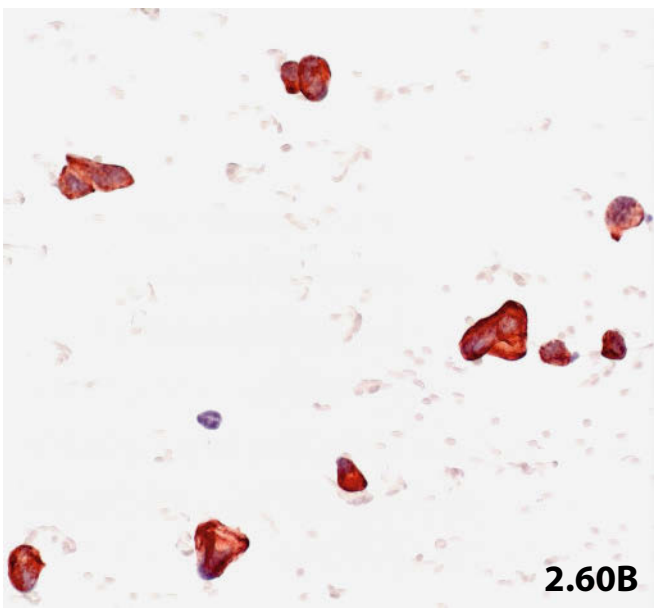
2.60B

**Fig. 2.61A, B Malignant melanoma.**
A 91-year-old man presented with a nodular lesion in the upper lobe of his left lung, there was no further information available. **A** Bronchial brushing revealed mainly isolated large neoplastic cells exhibiting vulnerable vacuolated and granular cytoplasm. A macrophage (arrow) shows coarse granular cytoplasmic inclusions suspicious of melanin, but hemosiderin cannot be excluded by routine staining methods (direct smear, Pap stain, high magnification). **B** Positive immunostaining for HMB-45 (Pap-prestained direct smear).
*Cytology*: Cytomorphologic features and suspected melanophores favor the diagnosis of malignant melanoma (versus another undifferentiated nonepithelial tumor or anaplastic large-cell carcinoma). Immunocytochemical work-up provided the correct diagnosis.

**Fig. 2.62A–C Leiomyosarcoma.**
A 73-year-old woman presenting with a complex clinical history: (1) leiomyosarcoma of the uterus 25 years before (hysterectomy), (2) metastatic breast carcinoma, (3) recent neoplastic process in the upper lobe of the left lung.
*Cytologic diagnosis* (confirmed by histology): Metastasis of a leiomyosarcoma.
**A** Transcutaneous FNAB of lung revealed isolated and aggregated undifferentiated neoplastic cells scattered in a background of proteinaceous material and debris (direct smear, Pap stain, high magnification). Immunocytochemical workup was required to determine the nature of the tumor cells. **B** Cells express strong immunopositivity for alpha smooth muscle actin (Pap-prestained specimen). **C** Negative immunostaining for pancytokeratin (MNF-116). Note the internal positive control using a bronchial epithelial cell (lower right) (Pap-prestained direct smear).

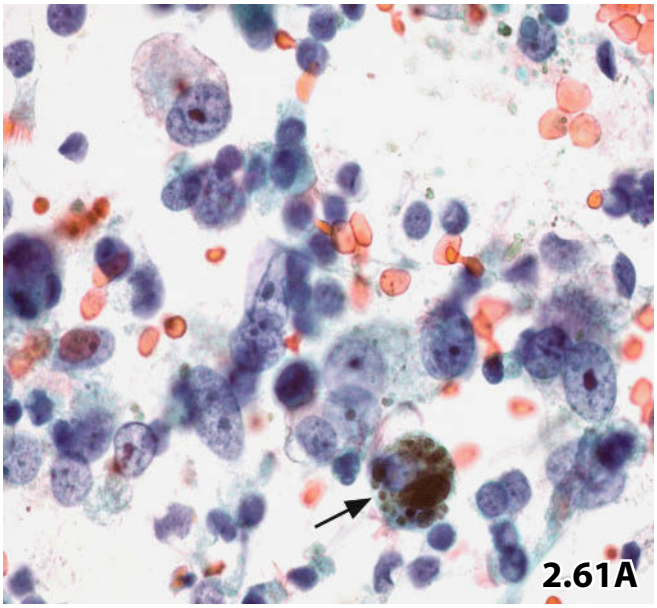
2.61A

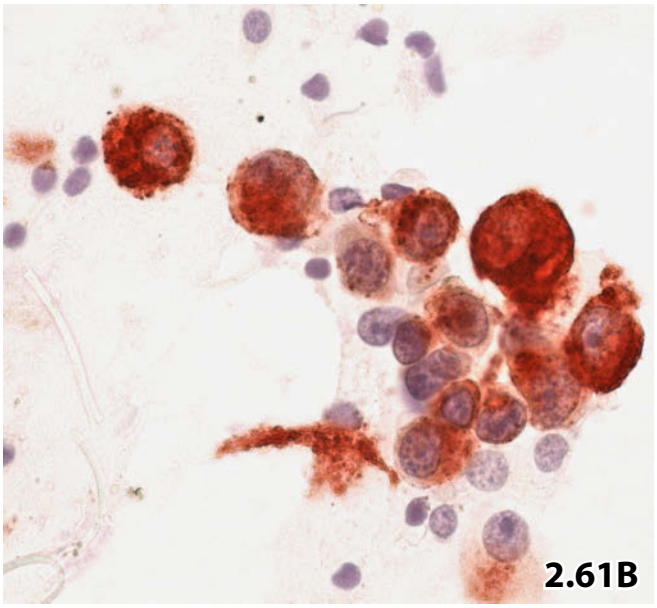
2.61B

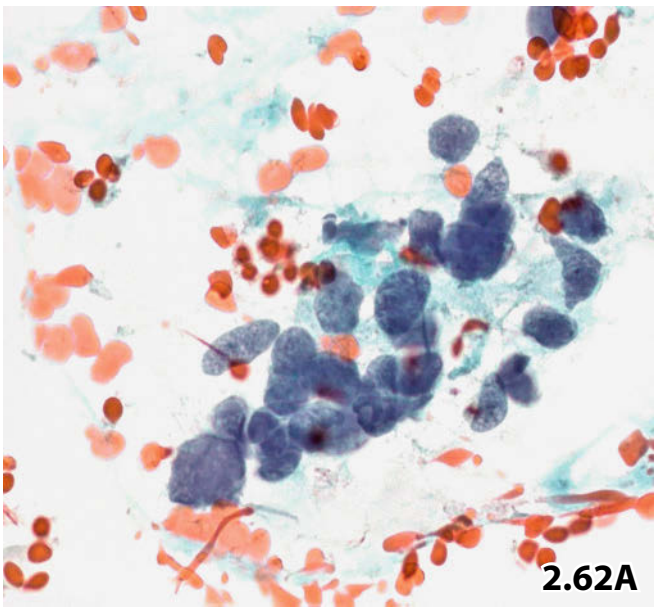
2.62A

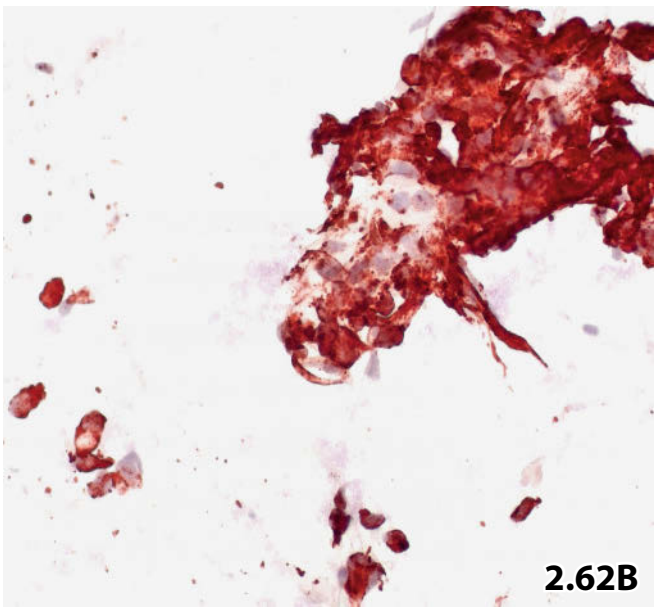
2.62B

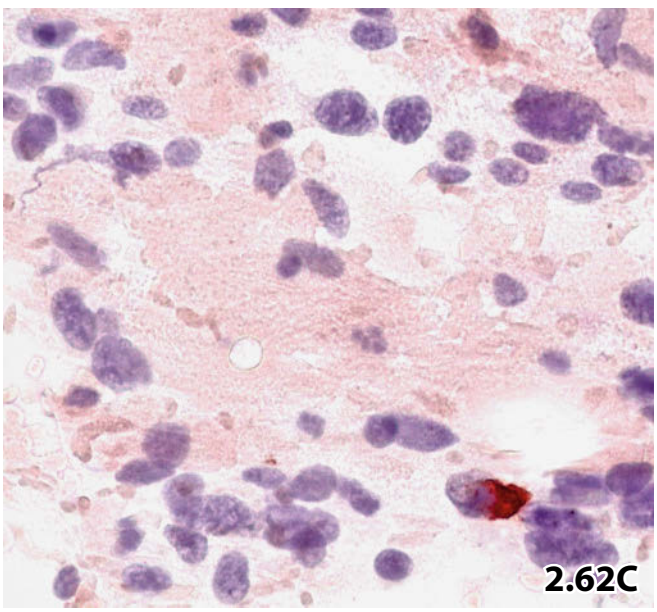
2.62C

**Figs. 2.63 and 2.64 Typical carcinoid tumor.**
Classic cytologic features depicted from a fine needle aspirate and from exfoliated material.



**Fig. 2.63A, B** Carcinoid tumor: appearance in fine needle aspirates. Transbronchial FNAB providing the pathognomonic uniform appearance of the cell pattern (direct smear, Pap stain). **A** Note cohesive cell clusters combined with flat sheets, acini-like formations (arrows), and the plasma cell-like appearance of the majority of tumor cells (lower magnification). **B** Nuclear morphology of the neoplastic cells is bland compared to that of benign ciliated bronchial-lining cells (high magnification).

**Fig. 2.64** Carcinoid tumor: appearance in exfoliative cytologic specimens. Bronchial aspirate from an elderly man containing cells of a neuroendocrine lung tumor. Tumor cells usually occur more crowded and occasionally spindle-shaped (arrows) in comparison with the cells in fine-needle aspirates (direct smear, Pap stain, lower magnification).

**Figs. 2.65 and 2.66 Atypical carcinoid.**
Cytomorphology and immunocytochemistry are shown.

**Fig. 2.65** Atypical carcinoid.
Example of an atypical carcinoid in a transbronchial FNAB of the lung. Note similarity of the cytoarchitecture to that of small cell carcinoma. However, the monotonous pattern and nuclear features simulate those of common carcinoid tumor (direct smear, Pap stain, high magnification).

**Fig. 2.66** Atypical carcinoid: immunocytochemistry.
Example of an endocrine immunodiagnostic marker. Bronchial aspirate containing numerous cells from an atypical carcinoid: immunocytochemical chromogranin A positivity (among other endocrine markers which are not shown) is a key feature in the diagnosis of all grades of neuroendocrine neoplasms ranging from well-differentiated to highly malignant (Pap-prestained direct smear, no nuclear counterstaining).

**Fig. 2.67 Large-cell neuroendocrine carcinoma.**
A 56-year-old man clinically presented with a bronchial carcinoma in the upper lobe of his left lung. Bronchial brushing revealed clearly malignant fusiform cells arranged in clusters exhibiting distinct streaming pattern (Pap stain, high magnification).
*(False) cytologic diagnosis*: Poorly differentiated nonkeratinizing squamous cell carcinoma.
*Comment*: the cytologic diagnosis was established due to the cellular pleomorphism, coarse granular chromatin, and streaming pattern (we failed to perform immunocytochemical studies).
*Tissue diagnosis*: Large-cell neuroendocrine carcinoma; the tumor cells showed strong immunopositivity for NSE, chromogranin A, and synaptophysin.

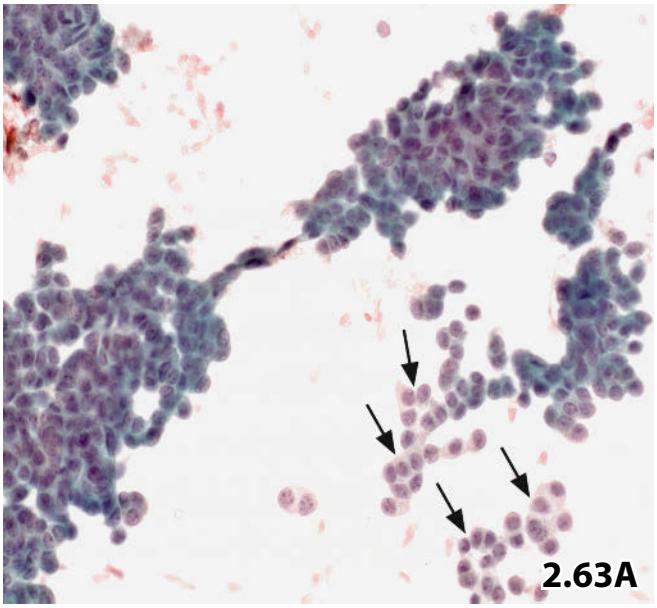
2.63A

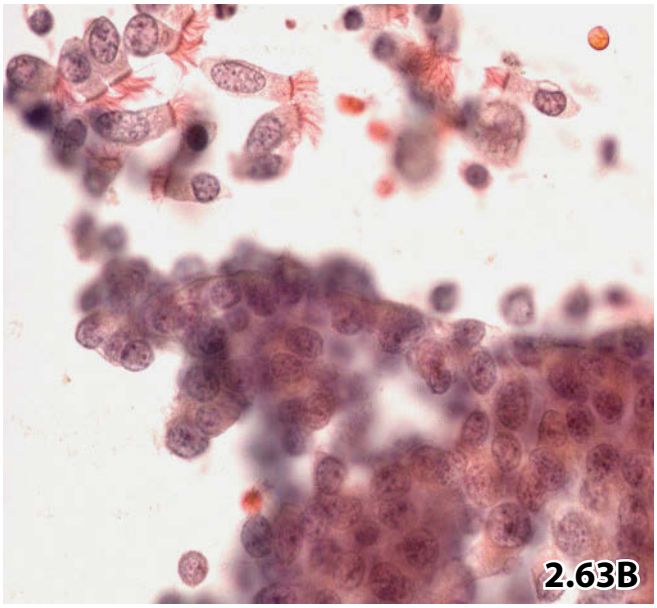
2.63B

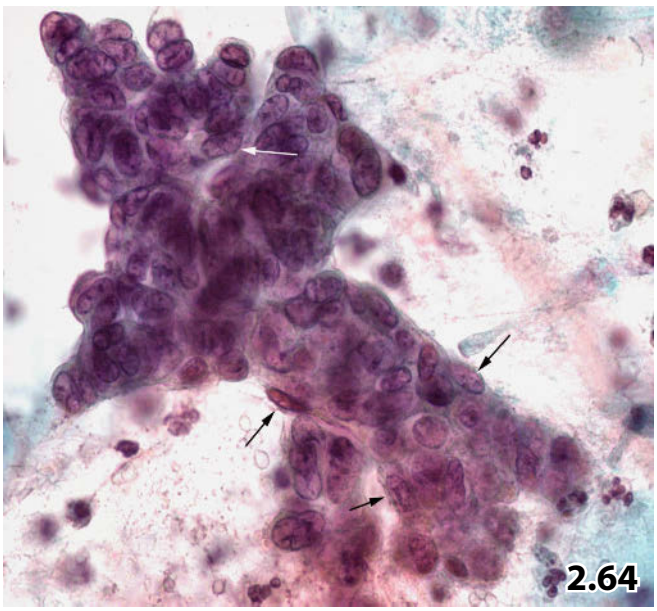
2.64

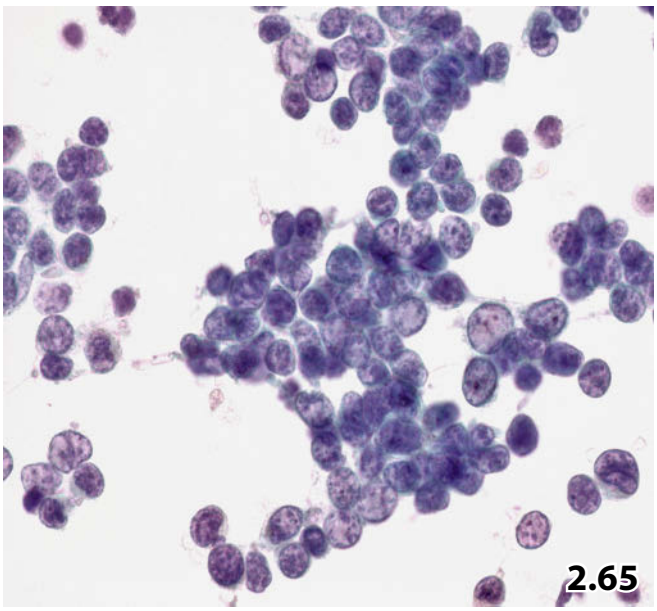
2.65

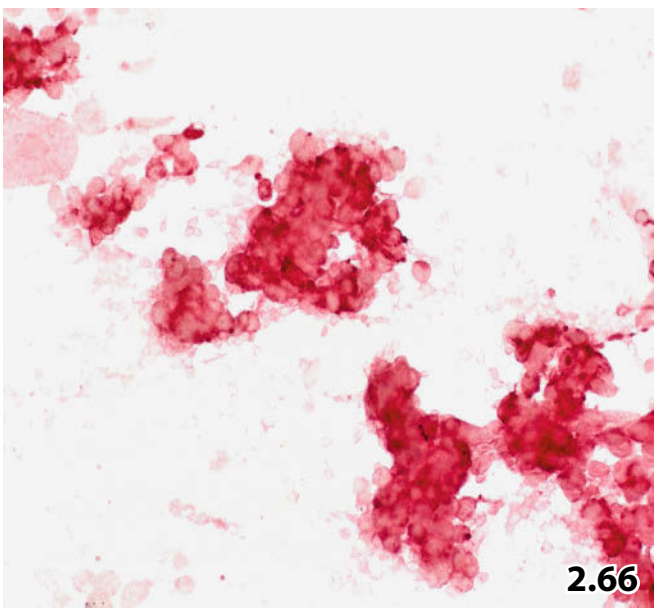
2.66

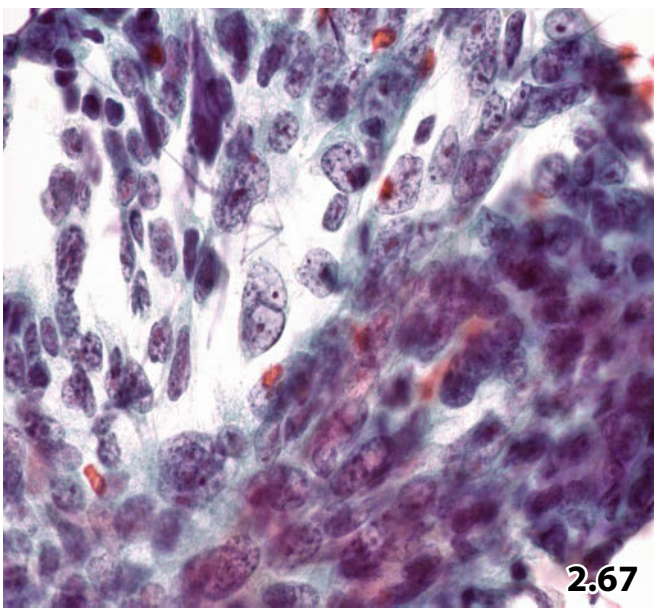
2.67

# Section 2.3
# Respiratory Tract: Bronchoalveolar Lavage

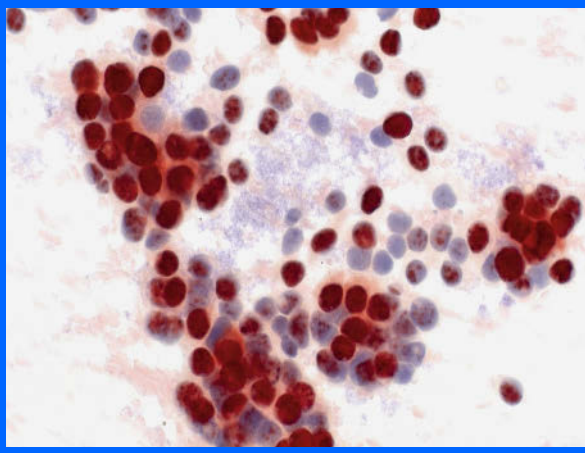

## 2.3.1 Introduction

- Diagnostic bronchoalveolar lavage (BAL) is a minimally invasive and highly cost-effective standard procedure that can contribute significantly to establishing a diagnosis in patients with uncertain interstitial lung disease or alveolar/pneumonic infiltration and may be helpful in monitoring lung allografts. Whether the cell composition in BAL can act as an indicator for activity and prognosis in interstitial lung disorders is still open. BAL complements clinical history, serologic results, biochemical assays, lung function tests, imaging results, and transbronchial lung biopsy.
- The clinical indications for BAL cover three groups of lung disorders:
  - Interstitial infiltrates (indicating granulomatoses, fibrosis, pneumoconiosis, tumor lymphangiosis, among others).
  - Alveolar infiltration (indicating pneumonias, hemorrhage, alveolar proteinosis, among others).
  - Lung infiltration in immunocompromised hosts (e.g. AIDS, post lung transplantation, immunocompromising therapy regimens).
- BAL seems to be a promising tool for research in combination with new technologies [49].
- BAL samples are obtained by wedging a subsegmental bronchus using a flexible bronchoscope and lavaging a defined alveolar area with saline or another appropriate solution. The great advantage of BAL is that diagnostic material is obtained from a whole lung segment, whereas transbronchial lung biopsy provides only a small piece of tissue measuring a few millimeters from a circumscribed lung area.
- Risks of BAL mainly hinge on the bronchoscopic procedure; complications are of minor significance and usually transient [10].
- Information on the use of the BAL technique, clinical indications, technical lavage procedures [3], and diagnostic potential are provided next. Standard textbooks [10] and specialized sources from the literature [8, 30, 36, and other papers] are also available.

## 2.3.2 Laboratory Procedures, Technical Aspects, Reporting

### General Comments

- At our institution, BAL fluid processing has followed standardized rules based on 15 years of experience with a total number of roughly 6,000 specimens. More than half of these BAL samples have been adequate for differential cell count and determination of the lymphocyte subset. Adequacy of the specimens was determined by the volume of the aspirate, by the amount of bronchial/bronchiolar cell admixture, by total cell count, and/or by the limitation of analyses as requested by the attending physician. The nonadequate specimens underwent routine screening for cellular composite, tumor cells, quality of histiocytes/macrophages, dust particles, virus-induced cell changes, and organisms.

- The following clinical informations should necessarily be transferred on the enclosed order form:
  - Main clinical symptoms and/or diagnostic considerations.
  - Issues concerning cytologic investigation.
  - Previous treatment, in particular chemotherapy and irradiation.
  - Smoking habits.
  - Immunodeficiency and its direct cause.
  - Total lavage fluid instillation; recovery of the instillate (ml); and aliquots (ml) of the recovered instillate removed for noncytologic laboratory tests.
  - Date and time of the BAL fluid sampling.
- The management options as performed at our institution are presented in the following.

### 2.3.2.1 Material Transfer and Processing

#### 2.3.2.1.1 Material Transfer to the Cytologic Laboratory

The BAL fluid is transported and processed as quickly as possible, i.e., within 6 h after sampling. Specimens from the hospital-based lung department are supplied immediately after completing the endoscopic investigation. BAL samples from county hospitals and community-based clinicians are supplied individually or by a pick-up service, both within 6 h. In this setting, the samples are delivered in native condition.

Each analysis is announced at least 2 h before the sample arrives at our laboratory.

#### 2.3.2.1.2 Material Processing

1. The first aspirate, the contents of the bronchus segmentalis and bronchioli, is referred separately to our cytology laboratory. This sample generally has cellular and mucus content of the bronchial/bronchiolar system and is suitable for measuring the adequacy of the BAL specimen.
2. Delay of the procedure [14]. Samples arriving at the laboratory too late in the evening for complete routine processing are centrifuged with the sediment transferred to a suitable cell medium (we use MEM HBS without L-glutamine, Amimed BioConcept, Allschwil, Switzerland). Cell suspensions can be stored in the refrigerator (4°C) and all routine BAL examinations are reliable for at least 24 h.
3. Routine processing of BAL fluid and basic evaluation.
   The principle steps are described as performed at our laboratory. Technical details and conditions tailored to our particular needs are disregarded.
   - Amount and gross appearance of the lavage fluid obtained are noted. Portions of the recovered instillation for supplemental noncytologic analyses, such as culture, viral analyses, biochemical tests, etc. have already been submitted to specialized laboratories by the endoscopist.
   - The total amount of liquid is centrifuged (2800 rpm, 10 min). The supernatant is decanted by aspiration and may be deep-frozen for long-term storage. It can be used for subsequent noncellular analyses.
   - Mucus from the sediment is liquefied by adding Shandon Mucolexx ™ (Thermo Fisher Scientific Inc., Waltham, MA, USA); individual exposure is up to 10 min. Afterwards, the resuspended cell pellet with the above-mentioned cell medium (2–3 ml), is again centrifuged (4000 rpm, 2 min).
   - Total cell counts are made in a Neubauer Cell Chamber. The result is reported per liter of recovery fluid.
   - For differential cytology, a routine air-dried smear is stained according to the May-Grünwald-Giemsa (MGG) staining procedure. Differential cytology includes the percentage of macrophages, lymphocytes, neutrophils and eosinophils, mast cells, and plasma cells.

**Caution**

Pay attention to the fact that mast cell granules are faintly or not at all stained by the DiffQuik staining procedure.

   - Two wet-fixed smears are routinely stained with the Papanicolaou method (Pap) and screened for entire cellular composite, tumor cells, quality of histiocytes/macrophages, dust particles, virus-induced cell changes, and organisms. Further slides (wet fixed or/and air-dried) are prepared as simple smears or by cytocentrifugation according to the clinical requirements. Common additional analyses include special stains for iron and fat, Gram and Ziehl-Neelsen staining for bacteria, PAS and silver staining methods for fungi/pneumocysts, and immunostains to identify Langerhans cells, as indicated in Sect. 2.3.7.1.2, p. 189.
   - The remaining sediment is resuspended and refrigerated at 4° C for 1 week as a reserve for potential subsequent analyses on cells and search for noncellular elements.
4. Rapid diagnosis can be performed within 20 min using a DiffQuik-rapid stain method, or rapid and ultrafast Pap-staining techniques (see Sect. 1.1.4.4, "Rapid-Staining and Quick-Read, p. 5).

#### 2.3.2.1.3 Analysis of Lymphocyte Subpopulations

Lymphocyte subpopulations can be identified using immunocytochemical methods on wet-fixed and air-dried cytospin preparations or alternatively by fluorescence-activated cell sorting (FACS® Becton Dickinson, San Jose, CA, USA), a specialized type of flow cytometry. The latter method, which we prefer, is based upon the specific light scattering

and fluorescent characteristics of each cell and in particular lymphocytes (T-helper cells, T-suppressor cells, B cells, among others). Viability tests of lymphocytes are also possible by flow cytometry; at our laboratory, cellular viability is not routinely checked but utilized at random as quality control and in selected cases. Immunocytochemical lymphocyte subtyping is still used as a control method in specific cases.

#### 2.3.2.1.4 Documentation of the Cytologic Analyses

- Diagnostic assessment ends in a written report including a summing up of the decisive cytologic findings, differential diagnostic considerations, and if feasible, a tentative or conclusive diagnosis.
- The written report is completed by a separate form that records:
  - The volume lavage fluid obtained.
  - The total cell count.
  - The differential cytology.
  - The lymphocyte subpopulations (per liter of recovery fluid) including activated lymphocyte subtypes.
  - The CD4/CD8 ratio.
  - The normal values for each cell type.
- Data files with the flow cytometric histograms are individually provided upon request.

## 2.3.3 Normal Cytology in BAL Specimens

### 2.3.3.1 Nonsmokers (Fig. 2.68A)

Differing normal values for differential cytology have been reported in the literature. Guidelines of a Task Group of the European Society of Pneumology recommend the following values as normal [29]:

| | |
|---|---|
| Macrophages | > 80%. |
| Lymphocytes | ≤ 15%. |
| Neutrophils | ≤ 3%. |
| Eosinophils | ≤ 0.5%. |
| Mast cells | ≤ 0.5%. |

The values can be applied to both cytocentrifuged specimens and direct smears.

**Microscopic Features**

- Macrophages are uniform, the nuclei exhibit a characteristic kidney shape, bland chromatin, and a cyanophilic /basophilic cytoplasm. Cytoplasmic vacuoles and particle inclusions are rare. Multinucleation is a normal finding in a small percentage of macrophages.
- The number of epithelial cells in an adequate BAL sample should not exceed 5%.
- The background is completely clean.

### 2.3.3.2 Smokers (Fig. 2.68B)

Total cell counts are markedly increased in otherwise healthy smokers, in the first instance due to the macrophage cell component [16]. Macrophages may show up as clearly increased and irregular cytoplasm bearing round inclusions (MGG stain: blue-black). These so-called smoker's inclusions consist of ingested particles from the inhaled smoke [17, 34].

The percentage of lymphocytes is reduced and that of granulocytes is the same as in nonsmokers.

### 2.3.3.3 CD4/CD8 Ratio

The determination of the lymphocyte subsets, T-helper cells (CD4), and T-suppressor cells (CD8) may be of substantial help in the diagnostic management of patients presenting with alveolar lymphocytosis. Changes in the CD4/CD8 ratio are quite typical for certain peripheral lung diseases.

The CD4/CD8 ratio of the normal lymphocytic population in BALs of healthy individuals and nonsmokers achieves a median value of 2.0 (range, 1.1–3.5), that of smokers is halved [33].

**Caution**

- Normal cellular composite of the BAL definitely excludes active sarcoidosis, active extrinsic allergic alveolitis, common and eosinophilic pneumonia, alveolar hemorrhage syndrome, and alveolar proteinosis.
- Abnormal components in a BAL that are interspersed between numerous normal bronchial epithelial cells call for careful diagnostic interpretation. These elements may originate exclusively from the bronchial and bronchiolar system.

## 2.3.4 Diagnostic Findings in BAL Specimens

Few pathologic lung conditions can be diagnosed by BAL alone. However, in many cases BAL serves as an important adjunct leading to a conclusive diagnosis in the context of clinical, radiologic, and biochemical findings. For other clinical entities, BAL cannot replace lung biopsy, hence a supplemental histologic evaluation is unavoidable.

A synopsis of the most significant findings in BAL specimens is provided in Table 2.3.1, below.

The cytologically most important lung disorders are subsequently focused in connection with diagnostic findings in bronchoalveolar lavage and differential diagnoses. For detailed information, we refer the readers to distinguished books and relevant publications [8, 10, 12, 37]. Several literature reports related to the various entities are cited.

**Table 2.3.1** A general view of significant findings in bronchoalveolar lavage and their related diseases

| Cellular and noncellular abnormalities | Differential diagnosis |
|---|---|
| **Lymphocytosis** | Sarcoidosis (Sect. 2.3.4.1, p. 179)<br>Extrinsic allergic alveolitis (Sect. 2.3.4.2, p. 180)<br>Drug-induced alveolitis (Sect. 2.3.4.4, p. 181)<br>Pneumoconiosis (Sect. 2.3.4.9, p. 184)<br>Berylliosis (Sect. 2.3.4.9.3, p. 186)<br>Neoplastic disease:<br>– Malignant lymphoma<br>– Lymphangiosis carcinomatosa |
| **Neutrophilia**<br>**frequently together with lymphocytosis of varied degree and/or eosinophilia** | Bacterial pneumonia<br>Idiopathic pulmonary fibrosis (Sect. 2.3.4.5, p. 182)<br>Cryptogenic organizing pneumonia (COP) (Sect. 2.3.4.3, p. 181)<br>Collagen / autoimmune disease (Sect. 2.3.4.6, p. 182): Lupus erythematosus, Sjögren syndrome, Crohn disease, rheumatoid arthritis, and others<br>Acute respiratory distress syndrome (ARDS) |
| **Eosinophilia** | Eosinophilic lung disease (Sect. 2.3.4.7, p. 183):<br>– Eosinophilic pneumonias<br>– Drugs<br>– Hypereosinophilia syndrome<br>– Allergic bronchopulmonary aspergillosis<br>– Asthma<br>– Churg-Strauss syndrome |
| **Admixture of plasma cells** | Virtually exclusive with:<br>– Extrinsic allergic alveolitis<br>– Cryptogenic organizing pneumonia<br>– Chronic eosinophilic pneumonia<br>– Aspiration pneumonia (Sects. 2.3.7.2, p. 190, and 2.3.7.3, p. 190) |
| **Increase of mast cells** | Extrinsic allergic alveolitis<br>Cryptogenic organizing pneumonia<br>Sarcoidosis<br>Chronic eosinophilic pneumonia<br>Idiopathic pulmonary fibrosis |
| **Dust particles**<br>**as inclusions in macrophages and in the background** | Pneumoconiosis (Sect. 2.3.4.9, p. 184)<br>Asbestosis (Sect. 2.3.4.9.1, p. 185) |
| **Acellular corpuscles + cellular debris** | Alveolar proteinosis (Sect. 2.3.4.10, p. 186) |
| **Hemosiderin and (degenerate) erythrocytes** | Alveolar hemorrhage syndrome (Sect. 2.3.4.8, p. 184) |
| **Infectious agents (Sect. 2.3.5, p. 187)** | Opportunistic infections with:<br>– Pneumocystis jirovecii<br>– Other fungi<br>– Cytomegalovirus<br>Infectious diseases:<br>– Tuberculosis<br>– Viral pneumonia |
| **Malignant neoplastic cells (Sect. 2.3.6, p. 188)** | Bronchioloalveolar carcinoma<br>Lymphangiosis carcinomatosa of the lung parenchyma<br>Malignant lymphoma / leukemia |
| **Increased number of Langerhans cells** | Langerhans cell histiocytosis (Histiocytosis X) (Sect. 2.3.7.1, p. 189) |

### 2.3.4.1 Sarcoidosis (Tab. 2.3.2)

Sarcoidosis is a multisystem disorder commonly arising in young adults, characterized by noncaseating granulomas with typical cellular features. The cause of the disease is still unknown. Granulomas most often appear in the lungs or in the lymph nodes, but virtually any organ can be affected. The clinical course generally varies and ranges from an asymptomatic disorder to chronic debilitating disease.

**Table 2.3.2** Sarcoidosis: morphologic features and cautions

| Bronchoalveolar lavage | | Caution see also "Differential Diagnosis" |
|---|---|---|
| **Morphologic key features** | **Additional morphology** | |
| – Lymphocytosis: 30–60%<br>– Elevated CD4/CD8 ratio ≥ 3.5 | – Elevated total cell count<br>– Normal percentage of eosinophils and neutrophils<br>– Mast cells, variable<br>– No plasma cells<br>– Epithelioid histiocytes and small fragments of noncaseating granuloma | – Lower percentage quotation for lymphocytosis in inactive sarcoidosis<br>– CD4/CD8 ratio is highly variable<br>– Minor specificity of noncaseating granuloma cell components |

### Additional Comments

- The finding of lymphocytosis in BAL specimens is not specific and the CD4/CD8 ratio values vary considerably [27], but an increased proportion of T-helper lymphocytes is an important finding in the diagnostic evaluation of sarcoidosis. A CD4/CD8 ratio of 4.0 and greater has a high positive predictive value for the diagnosis of sarcoidosis, and ratios between 3.5 and 5 are diagnostic if clinical findings support this diagnosis (Fig. 2.69).
- Moderate lymphocytosis with a normal CD4/CD8 ratio is not uncommon in inactive sarcoidosis.
- Sarcoidosis can be reliably distinguished from most common interstitial lung diseases taking all BAL-cell populations into account (as listed above) [18, 67].
- Advanced disease with fibrotic changes may be associated with an increased number of neutrophils [32]. Neutrophilia together with an increase in NK cells may mean a higher probability of poor outcome [63].
- The presence of epithelioid histiocytes, giant cells of the Langhans type, and fragments of noncaseating granulomas (morphologic details, see Sect. 2.1.3.2.2, "Granuloma Cells and Sarcoidosis," p. 111) in BAL fluid is a strong indicator for sarcoidosis but not at all specific for this diagnosis (Figs. 2.5 and 2.6).

### Differential Diagnosis

Berylliosis may show high CD4/CD8 ratios as well. Increased ratios are also valid for extrinsic allergic alveolitis, nonspecific interstitial pneumonia, idiopathic pulmonary fibrosis, pneumoconiosis, and other disorders. However, the nonlymphoid cell features differ from those in sarcoidosis.

## 2.3.4.2 Extrinsic Allergic Alveolitis (Tab. 2.3.3)

Extrinsic allergic alveolitis (EAA) is an immunologically mediated interstitial lung disease. Many airborne organic antigens in the form of fungal spores, bacteria, aerosolized proteins (predominantly from birds) can cause hypersensitivity pneumonitis after repeated inhalational exposure [26]. A wide variety of hypersensitivity lung diseases with their correspondent antigens are tabulated in Costabel's BAL Atlas [10]. Many people who are exposed to allergens and become sensitized can remain asymptomatic but may show characteristic abnormal BAL morphology. Ongoing alveolitis may progress in chronic illness with evidence of lymphocytic alveolitis, granulomatous reaction, and finally fibrotic interstitial changes.

### Additional Comments

- EAA is associated with the highest total cell count and the highest number of lymphocytes in BAL compared with other interstitial lung disorders.
- Abnormalities in the bronchoalveolar lavage fluid cell counts are almost always seen in patients with EAA according to different phases of the disease: at an early stage of allergen exposure the number of neutrophils increases and returns to a normal range within 1 week. The pathognomonic BAL findings become apparent in the subacute and chronic phase of the disease.
- Mast cells have been reported to occur in higher rates in BAL of EAA compared to other interstitial lung diseases [25, 38].

**Table 2.3.3** EAA: morphologic features and cautions

| Bronchoalveolar lavage | | Caution see also "Differential Diagnosis" |
|---|---|---|
| **Morphologic key features** | **Additional morphology** | |
| – Pronounced lymphocytosis: > 50%<br>– Normal or reduced CD4/CD8 ratio<br>– Increase in CD57+ NK cells (in about two-thirds of all cases)<br>– Presence of mast cells in nearly all cases | – Marked increase in total cell count<br>– Increase of activated HLA-DR+ T lymphocytes<br>– Plasma cell range: up to 2% (in about two-thirds of all cases)<br>– Slight increase in neutrophils<br>– Macrophages often with foamy cytoplasm | – Lymphocytes may be activated<br>– Epithelioid histiocytes and granuloma fragments may be present |

- Plasma cells are fairly characteristic of EAA, as they are observed in only a few other lung disorders such as cryptogenic organizing pneumonia, chronic eosinophilic pneumonia, and aspiration pneumonia [10].

**Differential Diagnosis**

- An activated lymphocytic population in EAA should not lead to a misdiagnosis of malignant lymphoma.
- In the course of EAA, the CD4 T-helper cell fraction and subsequently the CD4/CD8 ratio may increase, a finding that may be misinterpreted as sarcoidosis.
- Granulomatous reaction in chronic stages of EAA can also be encountered in BAL fluids, i.e., granulomatosis is not a specific sign of sarcoidosis. Evaluation of the lymphocyte surface antigen phenotypes provides a correct diagnosis.

### 2.3.4.3 Cryptogenic Organizing Pneumonia

(Fig. 2.70) (Tab. 2.3.4)

Synonym: Bronchiolitis obliterans with organizing pneumonia (BOOP)

Cryptogenic organizing pneumonia (COP) is an inflammatory lung disease with distinct clinical, radiological, and histopathological features. The latter consist of intraalveolar buds of granulation tissue, rich in active fibroblasts and myofibroblasts. COP may be triggered by infectious agents as well as by drugs and toxic fumes. The disease usually begins between the ages of 40 and 60 and affects men and women equally.

**Additional Comments**

- The lymphocyte rate is relatively high and the CD4/CD8 ratio is reduced to a degree barely observed in BAL fluids of other interstitial lung disorders.
- The proportion of $CD57^+$ NK cells is not increased.
- Plasma cells are a common feature in both COP and EAA.
- Mast cells can be significantly increased in individual cases of COP [52].

**Differential Diagnosis**

- COP differs from EAA in a normal $CD57^+$ NK cell number and in a lower CD4/CD8 ratio.
- Low lymphocyte percentage of less than 20% makes the diagnosis of COP quite unlikely; however, idiopathic pulmonary fibrosis should primarily be taken into consideration.
- Chronic eosinophilic pneumonia exhibits a high percentage of eosinophils exceeding 20% of the total cell count, a rate that has rarely been encountered in COP. Compared to BAL results in patients with COP, most patients with eosinophilic pneumonia show a higher eosinophil percentage than lymphocyte percentage [13].

### 2.3.4.4 Drug-Induced Alveolitis (Tab. 2.3.5)

Drug-induced lung damage induces a wide range of BAL cellular changes comprising lymphocytic, neutrophilic, or eosinophilic predominance. Still, lymphocytosis associated with a low CD4/CD8 ratio is most commonly seen.

Numerous drugs with their cytologic patterns observed in BAL fluids have been presented in table form by Costabel [10] and Tötsch and coauthors [59].

**Additional Comments**

- Alveolar hemorrhage syndrome may sometimes be linked with drug-related lung damage.
- A characteristic but not specific cell feature is observed in amiodarone lung (Fig. 2.71): macrophages displaying extremely pronounced cytoplasmic vacuolization. Ultrastructurally, the cytoplasmic deposits occur in lamellar arrangement similar to surfactant lamellar bodies [60]. The characteristic macrophages may also be found in BALs of patients taking amiodarone but lacking pneumopathy [4].
- Hyperplastic type II pneumocytes seem to occur mainly in combination with interstitial fibrosis [4].

**Differential Diagnosis**

- Differential cytology may sometimes mimic the cell constellation seen in EAA or COP.
- Amiodarone-induced foamy vacuolization in the cytoplasm of macrophages is not a specific feature but vacuolization of macrophages in EAA and COP is usually less pronounced.

**Table 2.3.4** COP: morphologic features and cautions

| Bronchoalveolar lavage | | Caution see also "Differential Diagnosis" |
|---|---|---|
| Morphologic key features | Additional morphology | |
| – Lymphocytosis and Increase in neutrophils and eosinophils and Presence of mast cells and plasma cells<br>– Markedly reduced CD4/CD8 ratio < 1.0 | – Increase in total cell count<br>– Macrophages often with foamy cytoplasm<br>– Mast cells, variable | – Cell pattern in BAL may mimic EAA<br>– BAL findings can closely resemble those of EAA |

**Table 2.3.5** Drug-induced alveolitis: differential cytology and cautions

| Bronchoalveolar lavage<br>Differential cytology | Caution<br>see also "Differential Diagnosis" |
|---|---|
| – Predominant:<br>Lymphocytosis and decreased CD4/CD8 ratio | – Pronounced lymphocytosis together with distinct decrease of the T-lymphocyte ratio may provoke misinterpretation (check clinical history!) |
| – Rather uncommon:<br>Neutrophilia, eosinophilia, or mixed cell pattern | |
| – Rarely seen:<br>Alveolar hemorrhage syndrome | |
| – Amiodarone lung (Fig. 2.71):<br>Macrophages with abundant foamy cytoplasm | – Typical foamy macrophages indicate amiodarone intake even if lung disease is absent |
| – Drug-induced cellular atypia<br>– Hyperplastic type II pneumocytes (Fig. 2.72) | – Cytotoxic reaction may be pronounced to such a degree that cellular atypia is mistaken for malignancy |

- Reactive cell changes induced by chemotherapy (and irradiation) can reliably be recognized by experienced microscopists, even though substantial degenerative changes of atypical cells may raise differential diagnostic problems. A drug-induced hyperplastic process of the epithelium of the bronchi, terminal bronchioli, and alveoli (type II pneumocytes) may simulate adenocarcinoma, both on exfoliated single cells and cell clusters (Fig. 2.84). The varied morphologic characteristics, differential diagnostic considerations, cautions, and potential auxiliary analyses regarding hyperplastic cell alterations are discussed in Sect. 2.1.4, "Abnormal and Atypical Epithelial Cells," p. 112.
- Activated macrophages may closely mimic proliferating type II pneumocytes. Immunocytochemistry can separate the two histogenetically different cell types: macrophages are positive for lysozyme (and other histiocytic markers) and negative for EMA, CEA, and cytokeratins [4].

### 2.3.4.5 Idiopathic Pulmonary Fibrosis

[10] (Tab. 2.3.6)

Idiopathic interstitial pneumonia (IIP) is an alveolar disorder of unknown etiology. A primary alveolitis is followed by chronic inflammation and progressive fibrosis of the pulmonary alveolar walls with steady progressive dyspnea as a striking clinical symptom. The disease usually affects males and females aged between 40 and 70 years.

#### Additional Comments

- An increased number of neutrophils is observed in up to 90% of all cases with idiopathic pulmonary fibrosis. Many of the cases (up to 60%) show a parallel increase in eosinophilic granulocytes [43].
- Lymphocytosis may be observed in up to 20% of all cases.
- Differential cytology in BAL can be helpful in assessing the degree of activity of the disease and may act as prognostic indicator. In this respect, an increased percentage of lymphocytes is presumed to be an indicator of a better prognosis [51, 62].

#### Differential Diagnosis

- A normal cell distribution in BAL makes idiopathic pulmonary fibrosis an improbable diagnosis; in contrast, any abnormal BAL cell pattern caused by IIP has a large variety of differential diagnoses.
- Several reports in the literature deal with the subject of discrimination between different types of interstitial pneumonia using cell counts in BAL: the results have not been consistent [17, 51, 64].

### 2.3.4.6 Systemic Connective Tissue Disorders

These disorders encompass an inhomogeneous group of inflammatory immune diseases with a progressive course, involving connective tissue, joints, blood vessels, and other

**Table 2.3.6** IIP: morphologic features and cautions

| Bronchoalveolar lavage<br>Morphologic key features | Additional morphology | Caution<br>see also "Differential Diagnosis" |
|---|---|---|
| – Neutrophilia (± 20%) | – Lymphocytosis with CD4/CD8 ratio in normal or slightly decreased range | – Cell distribution pattern is not reliably diagnostic |
| – Eosinophilia (± 5%) | – Mast cells, variable<br>– Macrophages with variable cytoplasmic vacuolization | – Reactive cell changes: type II pneumocyte hyperplasia versus carcinoma! (see Sect. 2.1.4.3.2, p. 114) |

organs with alternating intensity. The lung is not always affected.

BAL findings are similar to those in idiopathic pulmonary fibrosis. Lymphocytosis seems to be more common in immune conditioned inflammatory processes indicating a more favorable prognosis. Specialized sources in the literature should be consulted for further information [10, 31, 42, and others].

### 2.3.4.7 Eosinophilic Lung Disease

(Fig. 2.73) (Tab. 2.3.7)

Eosinophilic lung diseases are characterized by pulmonary eosinophilia that is an accumulation of abnormal quantities of eosinophils in air spaces and interstitial tissue of the lung.

**Additional Comments and Differential Diagnosis** [10]

- Infectious agents: Pulmonary eosinophilia includes parasitic infections, particularly ascariasis in children. Löffler syndrome is frequently associated with helminthic infections, but about one-third of the cases are idiopathic. Fungal pulmonary eosinophilia is in most cases caused by an aspergillus-associated hypersensitivity respiratory disorder referred to as allergic bronchopulmonary aspergillosis.
- Drugs: Crack, cocaine, and heroin inhalation have been reported to induce acute eosinophilic lung disorder [61].
- Vasculitis/systemic diseases:

  Churg-Strauss syndrome (CSS) is characterized by clinical and pathological manifestations, which separate the condition from other eosinophilic disorders: blood eosinophilia, asthma, and organ-specific disorders effected by vasculitis; the diagnostic relevance of antineutrophil cytoplasmic autoantibodies (ANCA) is under debate. Histopathological findings include epithelioid granuloma, tissue eosinophilia, and necrotizing vasculitis [23]. Marked eosinophilia in BAL fluid is a hallmark of CSS.

  In contrast, Wegener granulomatosis is not associated with asthma bronchiale and exhibits mild eosinophilia together with a definite higher percentage of neutrophils [53].
- Hypereosinophilic syndrome is not associated with vasculitis.
- Idiopathic acute and chronic eosinophilic pneumonia [15, 43]:

  Alveolar eosinophilia is generally combined with peripheral blood eosinophilia. The proportion of alveolar eosinophiles always predominates in contrast to other pneumonic disorders such as ARDS or bacterial pneumonia.

  Chronic eosinophilic pneumonia is almost always associated with the alveolar presence of plasma cells, but the neutrophil count is in normal range (in contrast to Wegener granulomatosis). Chronic idiopathic eosinophilic pneumonia is very sensitive to corticosteroids.

**Table 2.3.7** Eosinophilic lung disease: causes, morphologic features, and cautions

| Causes | Bronchoalveolar lavage | | Caution see also "Additional Comments and Differential Diagnosis" |
|---|---|---|---|
| | Morphologic key feature | Additional morphology see also "Additional Comments and Differential Diagnosis" | |
| **Infectious diseases**<br>– Parasites (Löffler syndrome, tropical) | Generally prominent hypereosinophilia | Usually increased number of lymphocytes and neutrophils | |
| – Mycobacterium tuberculosis<br>– Fungi | | | |
| **Drugs**<br>– Penicillin, etc.<br>– Illegal drugs! | | Eosinophilia variable | |
| **Vasculitis /systemic diseases**<br>– Churg-Strauss syndrome<br>– Wegener granulomatosis<br>– Hypereosinophilia syndrome | | – Marked eosinophilia > 20%<br>– Varying lymphocytosis<br>– Low eosinophilia/neutrophilia ratio | |
| **No etiological agent / idiopathic**<br>– Acute and chronic eosinophilic pneumonia | | Neutrophils are normal to mildly increased | Idiopathic disease is not established before all possible causes can be excluded |
| **Bronchial asthma** | | | |
| **Malignancies** | | | |

- Bronchial asthma is commonly found in patients with Churg-Strauss syndrome, chronic eosinophilic pneumonia, and in most of the interstitial lung disorders caused by specific respiratory allergens. BAL cytology reveals mild to moderate eosinophilia and an occasional increase in neutrophils and mast cells. In general clinical practice, the cytologic examination of BAL fluids in patients with bronchial asthma is of little significance.

### 2.3.4.8 Alveolar Hemorrhage Syndrome

(Fig. 2.74) (Tab. 2.3.8)

Lung hemosiderosis may be caused by unknown factors (idiopathic hemosiderosis). However, many underlying disorders exist for hemorrhage syndromes of the alveolar space such as autoimmune disease, vasculitis, cardiovascular diseases, drugs, hematological diseases, or post-transplantation conditions. The most common causes for alveolar hemorrhage have been compiled and tabulated by Costabel [10].

#### Additional Comments

- The characteristic hemosiderin-relevant greenish or green-brown color of the cytoplasm of macrophages is not always clearly apparent on routine staining procedures (Papanicolaou and May-Grünwald-Giemsa). Therefore, iron staining (e.g., the Prussian-blue method) should always be performed in morphologically doubtful cases and in all cases with clinical doubt.
- The phenotype of hemosiderin content in macrophages appears variably (after Prussian-blue staining) (Fig. 2.74):
  1. Faint blue coloring of a part of the cytoplasm.
  2. Slight to moderate blue coloring of the whole cytoplasm.
  3. In addition, deep blue granules occurring sporadically, or in variable quantities, or that are densely packed throughout the whole cytoplasm.
- Different scoring systems have been applied to create hemosiderin scores, but differential diagnostic conclusions on the basis of a semiquantitative assessment of the cytoplasmic hemosiderin deposits are limited. Grebski and coauthors found the highest hemosiderin scores in patients suffering from immunomediated diseases known to cause alveolar hemorrhage, and in selected groups of patient who had undergone heart transplantation [24].
- Chronic hemorrhage syndrome may show a cytologic appearance, as observed in idiopathic pulmonary fibrosis comprising increases in neutrophils and eosinophils.
- Certain occupational categories such as metal workers or welders are exposed to iron uptake from exogenous sources. Iron-laden macrophages are usually larger with more polymorphic cytoplasm and dust inclusions; iron-containing particles are often bizarre and irregular in shape and size.
- In general, the overall pattern of severe endogenous and exogenous siderosis is not very different: up to 100% of the macrophages exhibit strong positivity to iron stains.

### 2.3.4.9 Pneumoconiosis

- Bronchoalveolar lavage in occupational lung diseases have been broadly covered by Costabel [10] and recently by Cordeiro and coauthors [7].
- Pneumoconiosis is an occupational lung disease caused by inhalation of inorganic dust particles. The disease usually runs a chronic course ending in generalized interstitial lung disease. Dust particles may be permanently but not completely removed from the alveolar space by uptake in the interstitium (elimination through the lymphatic system) and by proximal transport of the mucus stream. Dust particles may be found trapped in macrophages decades after exposure to dust.
- More information on alveolar macrophages and their morphology is provided in Sect. 2.1.3.2.1 “Pulmonary Alveolar Macrophages,” p. 111.

**Table 2.3.8** Alveolar hemorrhage syndrome: macroscopic features, microscopic features, and cautions

| Bronchoalveolar lavage | | Caution see also “Additional Comments” |
|---|---|---|
| **Macroscopic features** | **Microscopy** | |
| **Fresh bleeding**: Dark red coloring | Red blood cells substantially increased | Bronchoscopy-related traumatic mucosal lesion with bleeding has to be excluded |
| **Within 2 days**: Orange-red staining | Macrophages with intracytoplasmic erythrocytes and Ec-fragments | |
| **More than 48 h after onset of bleeding**: Red-brown staining<br>**Older bleeding**: Dark and rust-brown staining | – Macrophages with intracytoplasmic hemosiderin.<br>– In severe disorders, nearly all macrophages show hemosiderin inclusions | – Exogenous iron contamination should always be considered and is most often distinguishable from endogenous hemorrhage<br>– Routine staining procedures may miss intracytoplasmic hemosiderin load |

#### 2.3.4.9.1 Asbestos-Related Disease

- Inhalation of asbestos dust can induce variable occupational diseases such as pulmonary fibrosis (asbestosis), malignant mesothelioma, benign pleural fibrotic disorders, and bronchial carcinoma. Therefore, asbestos use has been banned in most developed countries but exposure still occurs, and asbestosis deaths are not expected to decrease sharply in the United States during the next couple of years [2].
- Pathogenesis, including associated immunological mechanisms of asbestosis, quantitation using the asbestos body filtration technique, and its clinical implication are highlighted in Costabel's atlas [10].

**Phenotype of Asbestos Bodies** (Fig. 2.75)

Asbestos bodies are easily recognized on light microscopy if they are surrounded by a proteinaceous iron-containing coat (ferruginous bodies).

- The classic asbestos body appears as an elongated, slender beaded rod that may display a translucent center and ends on both sides in protrusions exhibiting a smooth surface. The asbestos bodies are surrounded by histiocytic cells and usually phagocytized by one or several macrophages. Asbestos bodies can reach lengths of 20–200 $\mu$m and widths of about 5 $\mu$m.
- The ferroprotein in the fiber coat yields the typical golden-brown color in Papanicolaou-stained specimens and a positive reaction with iron stains (e.g., Prussian blue).

**Asbestos and Alveolitis, microscopic features in BAL**

Early reaction to asbestos inhalation may consist of a mild lymphogranulocytic inflammatory process. Early asbestosis induces a marked inflammatory process that is easily recognized in BAL specimens. Ongoing development of the fibrotic process results in a decrease in the percentage of inflammatory cells. Lymphocytosis may reach 15% with an increased CD4/CD8 ratio. Lymphocytosis is presumed to be associated with a less aggressive course [10, 48, 65].

#### 2.3.4.9.2 Pseudo-asbestos Bodies (Fig. 2.75)

True asbestos bodies have to be distinguished from pseudo-asbestos bodies. The latter are inhaled fibers with a mineralogical composition unlike asbestos but a related iron-containing coat. Such fibers can be made up of carbon, aluminum, glass fibers, and other biological and artificial fiber types [10].

- Compared to classic asbestos bodies, pseudo-asbestos bodies lack the slender beaded shape, and the smooth surface of the terminal protrusions. The elements are more polymorphous and plump.

**Caution**

The term "ferruginous body" is commonly applied to asbestos bodies but can be used for each iron-coated fusiform element regardless of the nature of the central fiber.

#### 2.3.4.9.3 Other Pneumoconioses and Mixed-Dust Disorders (Figs. 2.76 and 2.77)

**Silicosis**

Silicosis (also known as grinder's disease) is caused by inhalation of crystalline silica (quartz crystals) dust and characterized by marked inflammation and scarring nodular lesions in the upper lobes of the lungs.

- Macrophages in BAL fluids show cytoplasmic inclusions of small spicular elements that are birefringent upon polarization. Depending on the degree of contamination, the histiocytic cells may be enlarged with evidence of nuclear activation.
- Cell counts are usually markedly increased reflecting the high proportion of macrophages. Mild inflammation is represented by a mixture of granulocytes and lymphocytes.

**Anthracosilicosis/Coal Miner's Lung**

These are mixed forms of pneumoconioses caused by inhalation of coal dust, stone dust, and other minerals in which the degree of lung injury depends on the composition of the dust and the amount of quartz crystals.

- Carbon particles appear as dark-brown (MGG stain) to black (Pap stain) large and polyhedral cytoplasmic inclusions in macrophages; the elements occur singly or densely clustered. Coal dust inclusions do not stain with the iron-staining method. Quartz crystals, coated pseudo-asbestos fibers, and sporadic asbestos bodies may be encountered as well.

**Metal Worker Lung**

Metal workers are usually exposed to mixed dust inhalation; accordingly, the macrophages may strongly vary in their morphologic aspect. Fully mixed inclusion patterns are referred to as anthraco-sidero-silicosis:

- Cytoplasmic iron load is usually high; the cytoplasm shows blue coloring and varying numbers of deep blue granules. Siderosis results from exposure to inert metallic iron or iron oxides.
- Anthracotic pigment exhibits as small to moderately sized heavy, black, rough deposits.
- Crystalline silica dust particles (specified above).
- Other inclusions exhibit various sizes, shapes, and colors.

**Welder's Lung** (Fig. 2.77)

Welder's lung is a specific presentation of pulmonary siderosis caused by smoke inhalation during welding. Welding dust usually contains metallic iron and iron oxide, which are inert to the human lung. Large amounts of iron dust are ingested in macrophages and settle in lung parenchyma without distinct fibrosis unless crystalline silica is also present [28, 56].

**Table 2.3.9** Berylliosis: morphologic features and cautions

| Bronchoalveolar lavage | | Caution |
|---|---|---|
| **Morphologic key features** | **Additional morphology** | |
| Similar to those in sarcoidosis:<br>– Lymphocytosis<br>– Elevated CD4/CD8 ratio | Activated lymphocytes (HLA-DR+ T lymphocytes) | Granuloma cell components are very similar to those in sarcoidosis and mycobacteriosis |

- Alveolar macrophages are heavily laden with iron-positive particles. The particles are coarser compared to those packed in macrophages due to alveolar bleeding. But in general, the overall pattern of severe endogenous and exogenous siderosis is not very different: up to 100% of the macrophages exhibit strong positivity to iron stains.

### Chronic Berylliosis (Tab. 2.3.9)

This is a chronic lung disease caused by exposure to beryllium and its compounds. In 1–3% of workers with single or prolonged exposure by inhalation, the lungs become hypersensitive to beryllium and develop generalized inflammatory nodules. These granulomas are hard to distinguish from granulomas in tuberculosis and sarcoidosis. The similarities and disparities between sarcoidosis and chronic berylliosis have been reviewed by Rossman and Kreider [50].

### Other Work-Related Lung Diseases

Hard metal lung: Specific elements such as cobalt, titanium, nickel, and others can be traced, for example through radiochemical analysis.

Antimony lung: Typical crystalline elements are found as cytoplasmic inclusions in BAL macrophages and as background material in BAL sediments.

## 2.3.4.10 Alveolar Proteinosis

[21] (Figs. 2.78 and 2.79) (Tab. 2.3.10))

- More than 15 years ago, idiopathic alveolar proteinosis (AP) was recognized as an autoimmune disease caused by neutralizing anti-granulocyte-macrophage colony-stimulating autoantibodies (anti-GM-CSF) [9, 54].
- Secondary AP can occur in patients with pulmonary infections, malignant diseases, particular hematologic malignancies, particular occupational exposures, and as a reaction to drugs.
- Impaired pulmonary surfactant homeostasis is regarded as an additional mechanism in the pathogenesis of AP. There is a strong association between incidence of alveolar proteinosis and tobacco use.
- BAL specimens with the characteristic macroscopic, cytologic and ultrastructural features provide a reliable diagnosis of alveolar proteinosis [6, 35, 55].

### Additional Comments

- The homogeneous granular material is typically PAS-positive and diastase-resistant (Fig. 2.78).
- Ultrastructural analysis with electron microscopy provides a more definitive diagnosis than cytomorphology alone: whorled myelin-like figures that resemble surfactant (Fig. 2.79). They are usually accumulated in the background of the smears, less frequently intracytoplas-

**Table 2.3.10** AP: morphologic features and cautions

| Bronchoalveolar lavage | | Caution<br>see also "Additional Comments" and "Differential Diagnosis" |
|---|---|---|
| **Morphologic key features**<br>see also "Additional Comments" | **Additional morphology** | |
| **Gross inspection:**<br>Fluid with milky-white appearance<br><br>**Microscopy**:<br>– Dirty background<br>– Proteinaceous amorphous globules (MGG: basophilic / Pap: pale eosinophilic)<br>– Cellular debris<br>– Foamy macrophages, variable<br><br>**Electron microscopy**:<br>– Characteristic lamellar bodies | – Globules may be included in macrophages<br>– Few inflammatory cells<br>– Occasional cholesterol crystals<br>– Lymphocytosis and mildly elevated CD4/CD8 ratio | – Less characteristic background and cell pattern after therapeutic lavage<br>– Atypical background features and/or quality of macrophages, together with particular lymphocytic quantification and phenotyping may raise diagnostic confusion |

mic in macrophages. Surfactant is a complex substance containing phospholipids and a number of proteins. The substance is produced by the type II pneumocytes and lines the alveoli and smallest bronchioles. Surfactant reduces surface tension throughout the lung and stabilizes the alveoli.

- Treatment of alveolar proteinosis by lavage eliminates the majority of lipoproteins. The morphologic changes of BAL fluid in a patient with alveolar proteinosis successfully treated with GM-CSF has been reported by Schoch and coauthors [54].

**Differential Diagnosis**

- Lung disorders, other than alveolar proteinosis, which include a dirty background in cytologic preparations of BAL fluid should be diagnostically approached with caution. Such lesions include pulmonary edema, radiation pneumonitis, *Pneumocystis jiroveci* pneumonia, acute respiratory distress syndrome, among others [35].
- Persisting lymphocytosis and increased CD4/CD8 ratio, notably observed after successful treatment of alveolar proteinosis, may mimic other pulmonary disorders such as sarcoidosis, extrinsic allergic alveolitis, nonspecific interstitial pneumonia, idiopathic pulmonary fibrosis, and pneumoconiosis [54].
- AP lavage specimens containing the following elements may mimic lipid pneumonia [35]: lipoid background substance, large numbers of foamy macrophages with droplet-like cytoplasmic fat inclusions, and scant PAS-positive globular material.

## 2.3.5 Infectious Diseases

BAL is the method of choice for the detection of opportunistic pulmonary infection in immunocompromised patients, particularly in patients with HIV infection and after organ transplantation.

BAL may sporadically be applied in immunocompetent patients in conjunction with hospital-acquired (nosocomial) infections.

**Caution**

Whether an organism found in a BAL sample is pathogenic and responsible for the current lung disease must be considered in each individual case. Organisms in BAL fluids may be of no pathologic significance, in the sense of simple colonization of the mucosa, or of extraneous contamination.

Diagnostic relevance for infectious disease indicates:

- Bacteria included in the cytoplasm of neutrophils and macrophages
- Fungi associated with marked neutrophilia and/or eosinophilia (particularly allergic bronchopulmonary aspergillosis).

### 2.3.5.1 Bacterial Infection

Acute bacterial pneumonia is associated with masses of neutrophils. Bacteria are ingested in the cytoplasm of neutrophils and/or macrophages. Bacteria are easily recognized in May-Grünwald-Giemsa-stained specimens and with the Gram staining procedure.

### 2.3.5.2 Tuberculosis (Tab. 2.3.11)

- Search for acid-fast bacilli in cytologic material by means of the Ziehl-Neelsen stain is not always effective. Culture and/or the PCR method in specialized laboratories are recommended for an accurate diagnosis including mycobacterial typing.
- More information is provided in Sect. 2.1.6.1, "Mycobacterial Infection," p. 116.

### 2.3.5.3 Mycoses

#### 2.3.5.3.1 *Pneumocystis jirovecii*

(Figs. 2.26 and 2.80) (Tab. 2.3.12)

- This is the most common pulmonary infection in patients with AIDS. Pneumocystis should be considered as pathogenic whenever it has been identified.

**Table 2.3.11** Tuberculosis: morphologic features and cautions

| Bronchoalveolar lavage | |
|---|---|
| **Typic cell content** | **Caution** |
| – Cavitating tuberculosis → neutrophilia<br>– Noncavitating tuberculosis → lymphocytosis | ○ Increased ratio of T lymphocytes may lead to an erroneous interpretation (sarcoidosis, EAA, idiopathic pulmonary fibrosis and others) |
| – CD4/CD8 ratio is sometimes increased | |
| – Occasionally present:<br>○ Epithelioid histiocytes, Langhans-type giant cells, and caseous detritus<br>○ Eosinophils | ○ Granuloma components are not diagnostic; bacteriologic confirmation is mandatory |

**Table 2.3.12** Pneumocystis pneumonia: Typical cell content of BAL and cautions

| Bronchoalveolar lavage: | |
|---|---|
| **Typic cell content** | **Caution** |
| – Frequently: increased number of lymphocytes and granulocytes | – Pronounced hyperplasia of pneumocytes should not lead to an erroneous diagnosis of malignancy |
| – Hyperplastic type II pneumocytes, variable | – Concomitant cancer should be excluded |

**Table 2.3.13** Viral infections: Typical cell content of BAL and cautions

| Bronchoalveolar lavage: | |
|---|---|
| **Typic cell content in viral infections** | **Caution** |
| – Neutrophilia, mainly during first stages of viral pneumonia<br>– Lymphocytosis is common (mainly CD8 lymphocyte phenotype)<br>– Nonspecific and specific virus-induced cell changes (bronchial epithelial cells are typically affected) | Any type of virus-induced cell change may be mistaken for malignant cell alteration |

- Usually, this pathogen is detected in light microscopy by routine staining procedures (Papanicolaou and Giemsa) or by direct fluorescence stains of bronchoalveolar lavage fluids. The BAL processing mode has been shown not to affect detection of the organism, and silver staining has minor added value in the identification of pneumocysts [1, 40].
- New molecular diagnosis using a real-time PCR assay, performed on a LightCycler system, is potentially more sensitive compared with the use of conventional cytochemical stains and light microscopy. The technique may discriminate as well between colonization and infection with pneumocysts [20].
- Differential cytology in BAL of AIDS patients usually shows an increased number of lymphocytes and granulocytes [10]. Hyperplastic type II pneumocytes may be present.
- More information including morphologic appearance of this organism is provided in Sect. 2.1.6.3.2, "*Pneumocystis*," p. 118.

#### 2.3.5.3.2 Other Fungi

(see also Sect. 2.1.6.3, "Pulmonary Mycoses," p. 117)

- *Candida* and *Aspergillus* are frequently identified in cytologic samples of the lung periphery, but they often indicate a nonpathogenic colonization. These two types of fungi have been shown to be pathogens in only a low percentage of all positive cytologic findings [44].
- *Cryptococcus neoformans* (Fig. 2.81) and *Histoplasma* (Fig. 2.82) should always be considered pathogenic whenever they are identified in BAL specimens

### 2.3.5.4 Viral Infections (Tab. 2.3.13)

Morphologic descriptions of the varied viral induced cell changes and additional information are given in Sect. 2.1.6.2, "Viral Infections," p. 116.

#### 2.3.5.4.1 Cytomegalovirus (Fig. 2.83)

- Cytomegalovirus (CMV) belongs to the herpesvirus group. CMV is responsible for the most common viral infection in organ transplant recipients and may often be life-threatening.
- Cytologic findings of cytomegalic inclusion disease is highly specific; however, cytology is not very sensitive for this type of viral pneumonia. Other laboratory techniques such as culture, immunocytochemistry, in situ hybridization, as well as new developments in PCR technology are much more sensitive [19].
- It is a fact that highly sensitive methods may lead to overdiagnosis of CMV pneumonia because CMV is found worldwide and throughout all socioeconomic groups and infects a high proportion of the adult population without apparent illness [44].

#### 2.3.5.4.2 Other Viruses

Herpes simplex virus, respiratory syncytial virus, or adenovirus, among others can be responsible for viral pneumonia, particularly after organ transplantation.

## 2.3.6 Malignancies [45]

### 2.3.6.1 Carcinomas

- Bronchoalveolar lavage is an extremely valuable tool in the diagnosis of diffusely spreading bronchioloalveolar carcinoma and suspected metastatic lung disease, particularly in cases with pronounced carcinomatous lymphangitis. Diagnostic accuracy ranges from 93% (bronchioloalveolar carcinoma) to 83% (lymphangiosis carcinomatosa due to metastatic cancer) [46].
- Unlike bronchioloalveolar carcinoma, carcinomatous lymphangitis is usually accompanied by a lymphocytosis in BAL [11].

- BAL has turned out to be a minor help in the diagnosis of primary bronchial cancer since this type of cytologic investigation yields no additional information compared to bronchoscopy.
- Tumor markers are helpful to ascertain the primary site of a metastatic neoplasm (see Sect. 2.2.2.3.3, "Bronchioloalveolar Carcinoma," p. 142).

**Differential Diagnosis**

Reactive cell changes due to hyperplasia of terminal bronchiolar epithelial cells and type II pneumocytes occur in acute respiratory disorders such as acute interstitial pneumopathy, acute exacerbation of idiopathic pulmonary fibrosis, and ARDS [45]. We have experienced additional pathologic lung conditions causing severe benign hyperplastic processes in bronchiolar and alveolar epithelium, for instance organizing pulmonary fibrosis, pulmonary embolism, pulmonary infarct, and infections, particularly with viruses.

Benign epithelial hyperplasia can easily be confused with a malignant neoplastic process. To date, no reliable auxiliary analysis exists differentiating reactive pneumocytes from malignant cells (Figs. 2.84–2.86).

Diagnostic and differential diagnostic considerations concerning hyperplasia of terminal bronchiolar and alveolar epithelium versus adenocarcinoma are extensively discussed in Sect. 2.1.4.3.2, "Hyperplasia of Alveolar Epithelium," p. 114, and Sect. 2.2.2.3.3 "Bronchioloalveolar Carcinoma,", p. 142.

**Caution**

- Carcinoma cells are frequently sparse and haphazardly dispersed in cytologic preparations of BAL fluid. Single adenocarcinoma cells are very difficult to distinguish from activated type II pneumocytes.
- Malignant cell clusters of adenocarcinomas share many cytomorphologic and architectural features with cell groups of activated and hyperplastic type II pneumocytes.
- Numerous acute lung disorders and interstitial lung diseases (mentioned above) may induce pronounced hyperplasia of terminal bronchiolar epithelium and type II pneumocytes.

### 2.3.6.2 Hematologic Malignancies

The diagnostic yield of BAL in lung involvement by leukemia or malignant lymphoma ranges from about 40 to 60% [46]. Final diagnosis is reliably reached by immunocytochemical or flow cytometric phenotyping of the lymphoid cells and/or establishing clonality of the lymphoid population by immunocytochemistry or molecular tests. Lung-infiltrating Hodgkin lymphoma can reliably be diagnosed in BAL cytology if the pathognomonic tumor cells (Hodgkin and Reed-Sternberg cells) are present [39].

**Caution**

- It may be difficult to distinguish between inflammatory BAL lymphocytosis with evidence of reactive cell alterations and low-grade malignant non-Hodgkin lymphoma. However, the distinction should pose no major problems using differential cytology and additional analyses in order to assess monoclonality.
- It is impossible to distinguish between inflammatory BAL lymphocytosis with evidence of reactive cell alterations and the lymphoid population of lung-infiltrating Hodgkin lymphoma lacking the pathognomonic Hodgkin and Reed-Sternberg cells, neither by morphology nor by auxiliary analyses.

## 2.3.7 Other Pulmonary Disorders with Particular BAL Cytology

### 2.3.7.1 Langerhans Cell Histiocytosis

#### 2.3.7.1.1 Introduction

The terms formerly used are "histiocytosis X" and "dendritic cell histiocytosis."

- Langerhans cells are derived from specific monocytes and contain large granules called Birbeck granules. The differentiation of the monocytes requires stimulation by colony-stimulating factor-1. The cells are similar in morphology and function to macrophages. Large quantities of Langerhans cells occur in the epidermis and are normally present in lymph nodes.
- Langerhans cell histiocytosis (LCH) is a rare disease caused by a clonal proliferation of Langerhans cells.
  The disorder may present as
  1. Unifocal progressive disease (unifocal eosinophilic granuloma).
  2. Multifocal unisystem disease (Hand-Schüller-Christian disease).
  3. Multifocal multisystemic disease (Letterer-Siwe disease). Multifocal multisystem LCH is a rapidly progressing disease where Langerhans cells proliferate in many tissues. It is mostly seen in children during the 1st and 2nd year of life and is considered a true neoplasm; the 5-year survival rate is only 50%.
- Langerhans cell histiocytosis is also discussed in Sect. 17.1.13.2, "Langerhans Cell Histiocytosis," , p. 1068.

#### 2.3.7.1.2 Pulmonary Langerhans Cell Histiocytosis

[57] (Fig. 2.87)

Pulmonary Langerhans cell histiocytosis (PLCH) of adults is a rare, diffuse interstitial lung disease of unknown etiology that occurs foremost in young smokers. PLCH is believed to be a reactive process associated with Langerhans cell hyperplasia. Only a very small proportion of the patients have extrapulmonary affections. Characteristic high-resolution com-

puted tomography (CT) findings together with distinctive clinical symptoms frequently allow a conclusive diagnosis. In patients with ambiguous imaging and clinical results, further diagnostic procedures may be needed such as surgical lung biopsies in order to confirm the diagnosis on tissue sections [5, 68]. The diagnostic impact of BAL cytology is agreed to be low.

**Microscopic Features, Immunocytochemistry, and Electron Microscopy**

Histology: Tissue sections reveal Langerhans cell granulomas that are infiltrating and destroy distal bronchioles.

Cytology: Typical Langerhans cells may be detected in BAL fluids of patients suffering from active Langerhans cell histiocytosis. An increase in Langerhans cells greater than 4% of the total cell count is assumed to be reliably diagnostic for PLCH [12]. The total cell count in BAL fluids of patients with PLCH is increased due to proliferating Langerhans cells, and large numbers of histiocytes and macrophages.

- Langerhans cells may be larger in comparison to macrophages and they frequently show multinucleation. The nuclei are oval to kidney-shaped including deep grooves and indentations. Their chromatin is vesicular and distinct nucleoli are sometimes present. The cytoplasm is wide with neat margins and eosinophilic staining quality.
- A mild inflammatory background composed of granulocytes and lymphocytes may be seen.
- Macrophages are often present and exhibit the typical smoker's inclusions.

Immunocytochemistry and electron microscopy: Langerhans cells are easily identified by the immunocytochemical or flow cytometric positivity for the monoclonal antigen CD1a and for cytoplasmic S100 protein.

Birbeck granules are intracytoplasmic organelles specific to Langerhans cells. They are detected by electron microscopy showing the characteristic shape of a tennis racket or rod shape. Their function is still being debated.

**Caution**

- An increase in Langerhans cells greater than 4% in BALs should be diagnostic for PLCH in combination with the characteristic CT results and clinical symptoms.
- Sarcoidosis and other pulmonary disorders may be accompanied by a lower percentage of Langerhans cells in BAL fluids; a reliable diagnosis will not be possible in such cases. Therefore, a surgical lung biopsy is necessary in a high percentage of equivocal cases.

#### 2.3.7.2 Lipoid Pneumonia

Lipoid pneumonia together with inflammatory and fibrotic changes in the lungs are caused by inhalation of various fatty substances or provoked by accumulation of endogenous lipid material in the lungs.

Exogenous fatty material from outside the body includes, for example, inhaled nose drops with an oil base or accidental inhalation of cosmetic oil. Endogenous lipid pneumonia occurs when an airway is obstructed or following the fracture of a bone.

- A great number of macrophages showing abundant foamy cytoplasm together with droplet-like fat inclusions. Lipid-laden giant cells are common. Lipid inclusions stain positively with fat stains (e.g., Sudan III).

#### 2.3.7.3 Aspiration Pneumonia

This is a pneumonia induced by aspiration of foreign material into the lungs. The extraneous material includes fat, proteolytic and toxic substances, as well as plant cells and muscle fibers accidentally breathed into the respiratory system instead of being swallowed into the stomach.

- Plant cells are in general much larger compared to human cells occurring in the alveolar space, and they disclose typical morphology and arrangement. Muscle fibers exhibit characteristic red staining and distinct transverse striations.
- Plasma cells are fairly characteristic of aspiration pneumonia as they are observed in only a few other lung disorders such as extrinsic allergic alveolitis, cryptogenic organizing pneumonia, or chronic eosinophilic pneumonia.
- Secondary bacterial infection and abscess formation is common.

### 2.3.8 Bronchoalveolar Lavage in Lung Transplant Recipients

BAL in transplantation patients may be effective for the detection of pulmonary infectious pathogens and rare disorders complicating the course after lung transplantation, such as alveolar proteinosis [22] and obliterative bronchiolitis [47]. Whether a surveillance of BAL cell profiles has additive diagnostic value in routine lung transplant monitoring and in patients in whom rejection is suggested, is highly controversial and more often refused than accepted [47, 58, 66].

**Caution**

Occasional atypias of epithelial cells in BAL specimens from lung (heart-lung) transplant recipients may demonstrate significant resemblance to carcinoma cells [41].

## 2.3.9 Further Reading


1. Al-Za'abi AM, MacDonald S, Geddie W, Boerner SL. Cytologic examination of bronchoalveolar lavage fluid from immunosuppressed patients. Diagn Cytopathol 2007;35:710-714.
2. Antao VC, Pinheiro GA, Wassell JT. Asbestosis mortality in the United States: Facts and predictions. Occup Environ Med 2009;66:335-338.
3. Baughman RP. Technical aspects of bronchoalveolar lavage: recommendations for a standard procedure. Semin Respir Crit Care Med 2007;28:475-485.
4. Bedrossian CWM, Warren CJ, Ohar J, Bhan R. Amiodarone pulmonary toxicity: Cytopathology, Ultrastructure, and Immunocytochemistry. Ann Diagn Pathol 1997;1:47-56.
5. Bianchi M, Cataldi M. Pneumothorax secondary to pulmonary histiocytosis X. Minerva Chir 1999;54:531-536.
6. Burkhalter A, Silverman JF, Hopkins MB 3rd, Geisinger KR. Bronchoalveolar lavage cytology in pulmonary alveolar proteinosis. Am J Clin Pathol 1996;106:504-510.
7. Cordeiro CR, Jones JC, Alfaro T, Ferreira AJ. Bronchoalveolar lavage in occupational lung diseases. Semin Respir Crit Care Med 2007;28:504-513.
8. Costabel U, Guzman J. Bronchoalveolar lavage in interstitial lung disease. Curr Opin Pulm Med 2001;7:255-261.
9. Costabel U, Guzman J. Pulmonary alveolar proteinosis: a new autoimmune disease. Sarcoidosis Vasc Diffuse Lung Dis 2005;22 Suppl 1:S67-73.
10. Costabel U, Mitchell JN. Atlas of Bronchoalveolar Lavage. Chapman&Hall London 1998.
11. Costabel U, Bross KJ, Guzman J, Matthys H. Bronchoalveoläre Lavage bei diffusen malignen Lungenveränderungen. Atemw Lungenkr 1987;13:S79-S82.
12. Costabel U, Guzman J, Bonella F, Oshimo S. Bronchoalveolar lavage in other interstitial lung diseases. Semin Respir Crit Care Med 2007;28:514-524.
13. Costabel U, Teschler H, Guzman J. Bronchiolitis obliterans organizing pneumonia (BOOP): The cytological and immunocytological profile of bronchoalveolar lavage. Eur Respir J 1992;5:791-797.
14. Costabel U, Teschler H, Ziesche R, et al. Transport of bronchoalveolar lavage cells in appropriate medium for 24 hours does not affect cell differentials and lymphocyte subsets (abstract). Am Rev Respir Dis 1989;139:A472.
15. Cottin V, Cordier JF. Eosinophilic pneumonias. Allergy 2005;60:841-857.
16. DeShazo RD, Banks DE, Diem JE, et al. Broncho-alveolar lavage cell-lymphocyte interactions in normal non smokers and smokers. Am Rev Respir Dis 1983;127:545-548.
17. Domagala-Kulawik J. BAL in the diagnosis of smoking-related interstitial lung disease: review of literature and analysis of our experience. Diagn Cytopathol 2008;36:909-915.
18. Drent M, Mansour K, Linssen C. Bronchoalveolar lavage in sarcoidosis. Semin Respir Crit Care Med 2007;28:486-495.
19. Drew WL. Laboratory diagnosis of cytomegalovirus infection and disease in immunocompromised patients. Curr Opin Infect Dis 2007;20:408-411.
20. Fillaux J, Malvy S, Alvarez M, et al. Accuracy of a routine real-time PCR assay for the diagnosis of *Pneumocystis jirovecii* pneumonia. J Microbiol Methods 2008;75:258-261.
21. Frazier AA, Franks TJ, Cooke EO, et al. From the archives of the AFIP: pulmonary alveolar proteinosis. Radiographics 2008;28:883-899.
22. Gal AA, Bryan JA, Kanter KR, Lawrence EC. Cytopathology of pulmonary alveolar proteinosis complicating lung transplantation. J Heart Lung Transplant 2004;23:135-138.
23. Grau RG. Churg-Strauss syndrome: 2005-2008 update. Curr Rheumatol Rep 2008;10:453-458.
24. Grebski E, Hess T, Hold G, et al. Diagnostic value of hemosiderin-containing macrophages in bronchoalveolar lavage. Chest 1992; 102:1794-179.
25. Haslam PL, Dewar A, Butchers P, et al. Mast cells, atypical lymphocytes and neutrophils in bronchoalveolar lavage in extrinsic allergic alveolitis. Am Rev Respir Dis 1987;135:35-47.
26. Ismail T, McSharry C, Boyd G. Extrinsic allergic alveolitis. Respirology 2006;11:262-268.
27. Kantrow SP, Meyer KC, Kidd P, Raghu G. The CD4/CD8 ratio in BAL fluid is highly variable in sarcoidosis. Eur Respir J 1997;10:2716-2721.
28. Kayser K, Hagemeyer O. Natural and synthetic mineral fibers affecting man. Zürich: BI-Wiss.-Verl., 1994; pp:182-184.
29. Klech H, Hutter C. Clinical guidelines and indications for bronchoalveolar lavage (BAL): Report of the European Society of Pneumology Task Group on BAL. Eur Respir J 1990;3:937-974.
30. Klech H, Hutter C, Costabel U. Clinical guidelines and indications for bronchoalveolar lavage (BAL): Report of the European Society of Pneumology Task Group on BAL. Eur Respir Rev 1992;2:47-127.
31. König G, Behr J. Bronchoalveoläre Lavage be pulmonaler Beteiligung systemischer Erkrankungen. Atemw Lungenkr 1989;15:605-609.
32. Lin YH, Haslam PL, Turner-Warwick M. Chronic pulmonary sarcoidosis: Relationship between lung lavage cell counts, chest radiograph, and results of standard lung function tests. Thorax 1985;40:501-507.
33. Mancini NM, Béné MC, Gérard H, et al. Early effects of short-time cigarette smoking on the human lung: a study of bronchoalveolar lavage fluids. Lung 1993;171:277-291.
34. Marques LJ, Teschler H, Guzman J, Costabel U. Smoker's lung transplanted to a nonsmoker. Long-term detection of smoker's macrophages. Am J Respir Crit Care Med 1997;156:1700-1702.
35. Maygarden SJ, Iacocca MV, Funkhouser WK, Novotny DB. Pulmonary alveolar proteinosis: a spectrum of cytologic, histochemical, and ultrastructural findings in bronchoalveolar lavage fluid. Diagn Cytopathol 2001;24:389-395.
36. Meyer KC. Bronchoalveolar lavage as a diagnostic tool. Semin Respir Crit Care Med 2007;28:546-560.
37. Mikuz G, Gschwendtner A. Value of bronchoalveolar lavage in the diagnosis of lung disease. Verh Dtsch Ges Pathol 2000;84:129-135.
38. Moises JA, Xaubet A, Agusti C, et al. Significance of the presence of mastocytes in bronchoalveolar lavage in the diagnostic evaluation of diffuse interstitial lung disease. Med Clin (Barc) 1989;92: 454-456.
39. Morales FM, Matthews JI. Diagnosis of parenchymal Hodgkin's disease using bronchoalveolar lavage. Chest 1987;91:785-787.
40. Nassar A, Zapata M, Little JV, Siddiqui MT. Utility of reflex Gomori methenamine silver staining for *Pneumocystis jirovecii* on bronchoalveolar lavage cytologic specimens: a review. Diagn Cytopathol 2006;34:719-723.
41. Ohori NP. Epithelial cell atypia in bronchoalveolar lavage specimens from lung transplant recipients. Am J Clin Pathol 1999;112:204-210.
42. Owens GR, Paradis I, Gryzan S, et al. Role of inflammation in the lung disease of systemic sclerosis: Comparison with idiopathic pulmonary fibrosis. J Lab Clin Med 1986;107:253-260.
43. Pesci A, Bertorelli G, Manganelli P, et al. Bronchoalveolar lavage in chronic eosinophilic pneumonia. Analysis of six cases in comparison with other interstitial lung diseases. Respiration 1988;54 Suppl 1:16-22.
44. Pisani RJ, Wrigt AJ. Clinical utility of bronchoalveolar lavage in immunocompromised hosts. Mayo Clin Proc 1992;67:221-227.
45. Poletti V, Poletti G, Murer B, et al. Bronchoalveolar lavage in malignancy. Semin Respir Crit Care Med 2007;28:534-545.
46. Poletti V, Romagna M, Allen KA, et al. Bronchoalveolar lavage in the diagnosis of disseminated lung tumors. Acta Cytol 1995;39:472-477.

47. Reynaud-Gaubert M, Thomas P, Gregoire R, et al. Clinical utility of bronchoalveolar lavage cell phenotype analyses in the postoperative monitoring of lung transplant recipients. Eur J Cardiothorac Surg 2002;21:60-66.
48. Robinson BWS, Rose AH, James A, Whitaker D. Alveolitis of pulmonary asbestosis. Chest 1986;90:396-402.
49. Rose AS, Knox KS. Bronchoalveolar lavage as a research tool. Semin Respir Crit Care Med 2007;28:561-573.
50. Rossman MD, Kreider ME. Is chronic beryllium disease sarcoidosis of known etiology? Sarcoidosis Vasc Diffuse Lung Dis 2003;20:104-109.
51. Ryu YJ, Chung MP, Han J, et al. Bronchoalveolar lavage in fibrotic idiopathic interstitial pneumonias. Respir Med 2007;101:655-660.
52. Schildge J, Klar B, Hardung-Backes M. Mast cells in bronchoalveolar lavage fluid of patients with interstitial lung disease. Pneumologie 2003;57:202-207.
53. Schnabel A, Reuter M, Gloeckner K, et al. Bronchoalveolar lavage cell profiles in Wegener's granulomatosis. Respir Med 1999;93:498-506.
54. Schoch OD, Schanz U, Koller M, et al. BAL findings in a patient with pulmonary alveolar proteinosis successfully treated with GM-CSF. Thorax 2002;57:277-280.
55. Sosolik RC, Gammon RR, Julius CJ, Ayers LW. Pulmonary alveolar proteinosis. A report of two cases with diagnostic features in bronchoalveolar lavage specimens. Acta Cytol 1998;42:377-383.
56. Strobel SL. Pathologic quiz case: Recurrent spontaneous pneumothorax in an industrial worker. Arch Pathol Lab Med 2002;126:749-750.
57. Tazi A. Adult pulmonary Langerhans cell histiocytosis. Eur Respir J 2006;27:1272-1285.
58. Tiroke AH, Bewig B, Haverich A. Bronchoalveolar lavage in lung transplantation. State of the art. Clin Transplant 1999;13:131-157.
59. Tötsch M, Guzman J, Theegarten D, et al. Bronchoalveoläre Lavage Pathologe 2007;28:346-353.
60. Trzpuc TD, Shidham VB, Nagarjun Rao R. Pathologic Quiz Case. Pulmonary infiltrates with characteristic light and electron microscopic features. Arch Pathol Lab Med 2002;126:745-746.
61. Tsapas A, Paletas K, Vlachaki E, et al. Eosinophilic pneumonia associated with heroin inhalation: a case report. Wien Klin Wochenschr 2008;120:178-180.
62. Turner-Warwick M, Haslam PL. The value of serial bronchoalveolar lavages in assessing the clinical progress of patients with cryptogenic fibrosing alveolitis. Am Rev Respir Dis 1987;135:26-34.
63. Tutor-Ureta P, Citores MJ, Castejon R, et al. Prognostic value of neutrophils and NK cells in bronchoalveolar lavage of sarcoidosis. Cytometry B Clin Cytom 2006;70:416-422.
64. Veeraraghavan S, Latsi PI, Wells AU, et al. BAL findings in idiopathic nonspecific interstitial pneumonia and usual interstitial pneumonia. Eur Respir J 2003;22:239-244.
65. Wallace JM, Oishi JS, Barbers RG, et al. Bronchoalveolar lavage cell and lymphocyte phenotype profiles in healthy asbestos-exposed shipyard workers. Am Rev Respir Dis 1989;139:22-38. 66. Wanner TJ, Gerhardt SG, Diette GB, et al. The utility of cytopathology testing in lung transplantation recipients. J Heart Lung Transplant 2005;24:870-874.
67. Winterbauer RH, Lammert J, Selland M, et al. Bronchoalveolar lavage cell populations in the diagnosis of sarcoidosis. Chest 1993;104:352-361.
68. Zeppa P, Cozzolino I, Russo M, et al. Pulmonary Langerhans cell histiocytosis (Histiocytosis X) on bronchoalveolar lavage. A report of 2 cases. Acta Cytol 2007;51:480-482.

**Fig. 2.68A, B BAL Normal findings in non-smokers and smokers.**
**A** Findings in nonsmokers. The majority of cells are macrophages exhibiting isolated intracytoplasmic carbon particles. Occasional lymphocytes and ciliated epithelial cells (lower left) are also present (direct sediment smear, Pap stain, lower magnification). **B** BAL: Findings in a smoker. Less monotonous appearance of the macrophage population. Macrophages exhibit so-called cytoplasmic smoker's inclusions (arrows). A few lymphocytes and eosinophils are seen at the top end of the field (direct sediment smear, MGG stain, high magnification).

**Fig. 2.69 Flow cytometry histograms in sarcoidosis from a bronchoalveolar lavage.**
The framed dotplot in the upper histogram shows the selection of lymphocytes of the T phenotype. The lower histogram shows a dense plotting of a T-cell subpopulation (upper left) according to T4 lymphocytes (89%), while a few dots matching T8 lymphocytes (11%) appear in the lower right gate.

**Fig. 2.70 Cryptogenic organizing pneumonia (synonym: BOOP).**
Pronounced cytoplasmic vacuolization of the macrophages, marked lymphocytosis, increased numbers of eosinophils (arrows), and mast cells (arrowheads) are characteristic features of cryptogenic organizing pneumonia in BAL (direct sediment smear, MGG stain, high magnification). Both exogenous allergic alveolitis and drug-induced alveolitis may exhibit a similar cell pattern.

**Fig. 2.71 Amiodarone lung.**
Note the extremely pronounced cytoplasmic vacuolization of the macrophages (direct sediment smear, MGG stain, high magnification).

**Fig. 2.72 Activated type II pneumocytes.**
A 62-year-old man suffering from long-standing Behçet disease treated with cytostatic drugs (Endoxan). Drug-induced reactive hyperplasia of terminal bronchiolar epithelial cells (type II pneumocytes). Cellular arrangement, low N/C ratio, round nuclei, smooth nuclear outline, bland chromatin, and uniform centrally positioned nucleoli exclude malignancy (direct sediment smear, Pap stain, lower magnification).

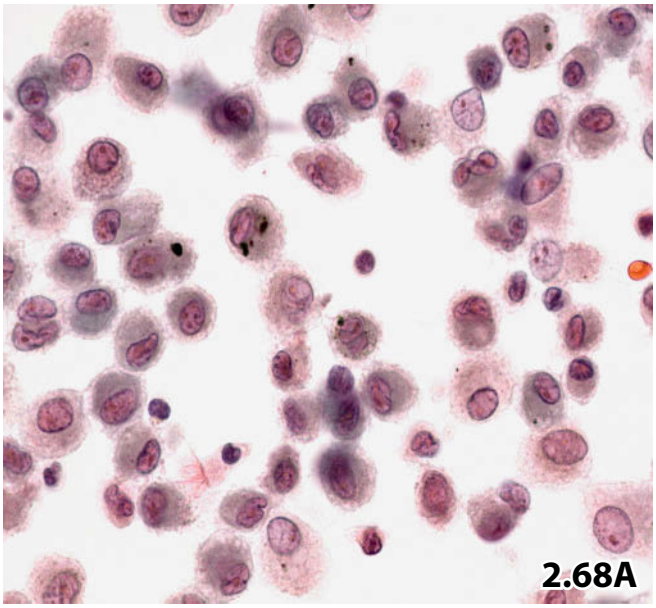
2.68A

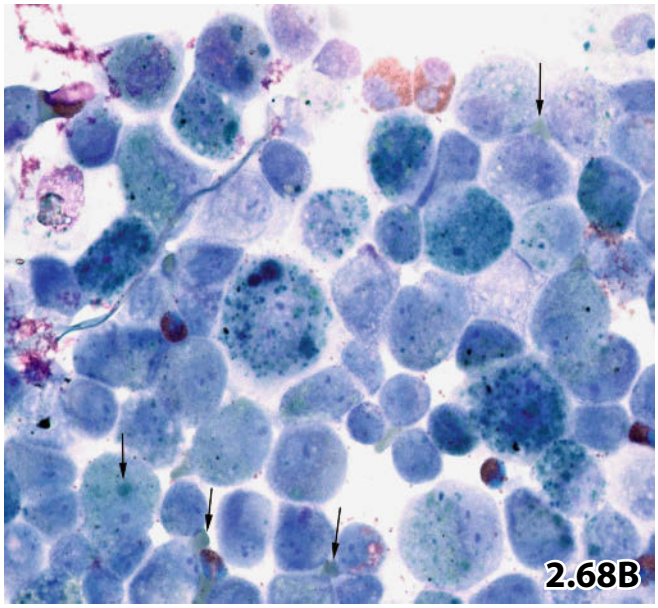
2.68B

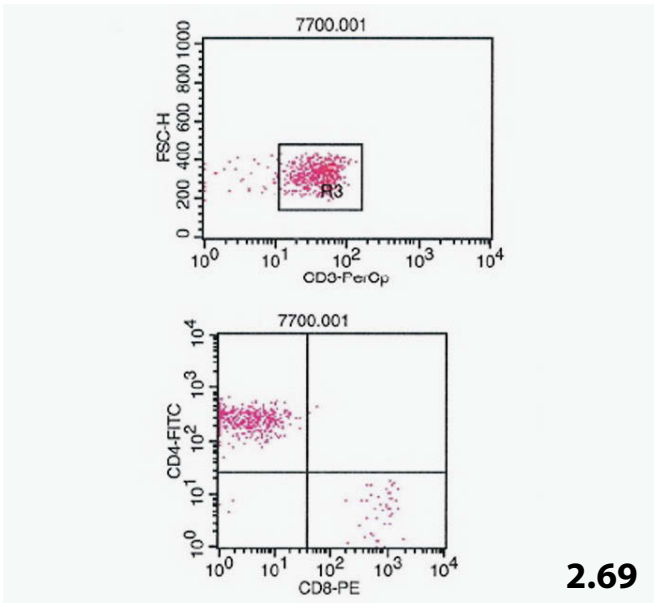

2.69

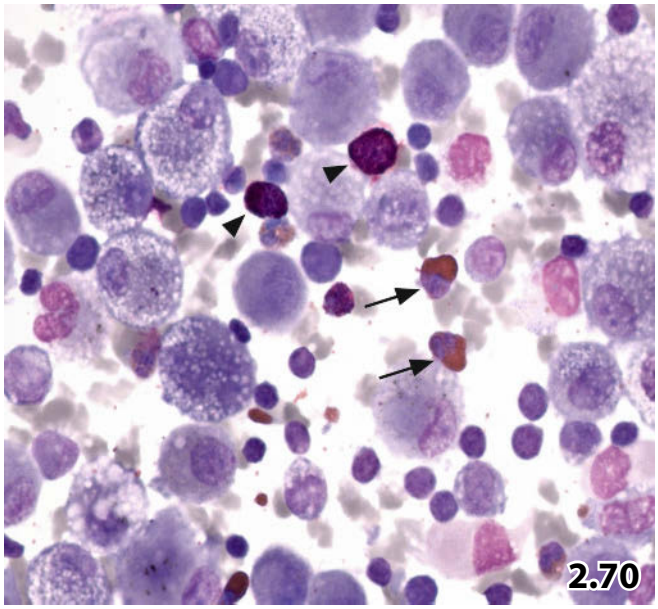
2.70

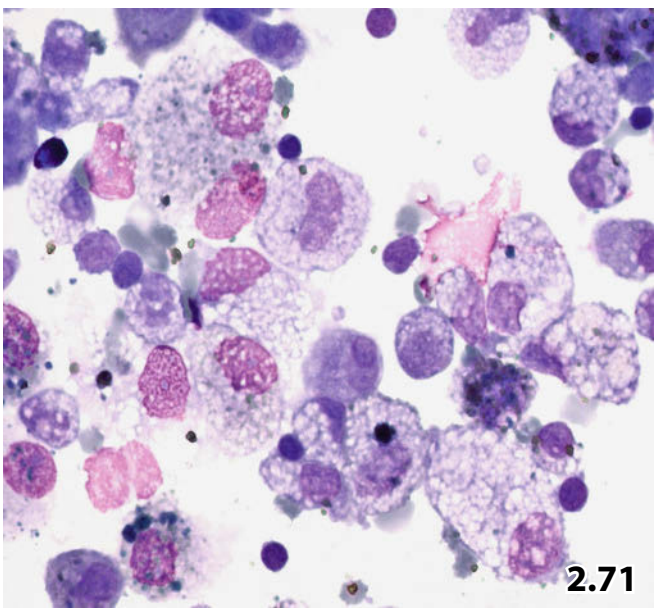
2.71

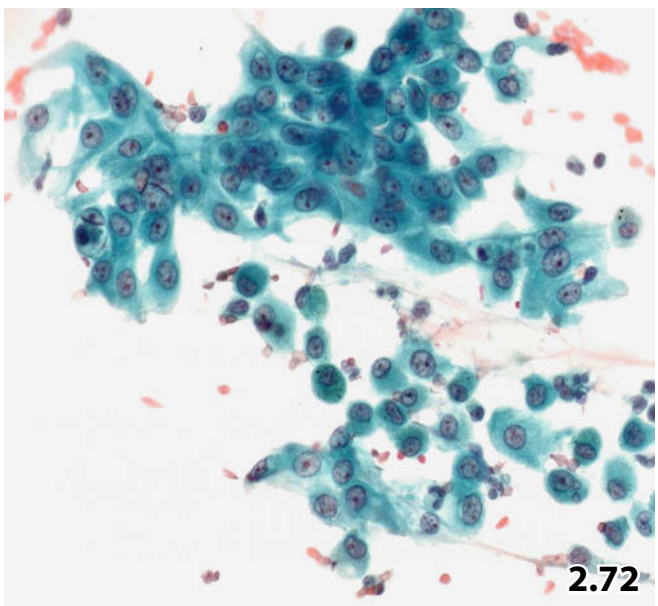
2.72

**Fig. 2.73 Eosinophilic lung disease.**
A middle aged woman presented with clinical symptoms of bronchial asthma. Direct smears from BAL sediment reveal mainly eosinophilic granulocytes (87%) interspersed with macrophages and a few mast cells (arrows) (MGG stain, lower magnification).

**Fig. 2.74 Alveolar hemorrhage syndrome.**
Iron staining (Prussian blue) of a Pap-prestained direct smear of BAL sediment displays the variable phenotype of cytoplasmic hemosiderin inclusions in macrophages (higher magnification):
- Blue coloring of part of the cytoplasm (arrow).
- Blue coloring of the entire cytoplasm (arrowheads).
- Deep-blue coarse intracytoplasmic granules (large macrophage, lower right).

**Fig. 2.75 Ferruginous bodies.**
High magnification reveals the varied phenotypes of ferruginous bodies (direct sediment smear, Pap stain):
- Asbestos body (lower left): slender rod showing marked segmentation ending on both sides in Pprotrusions with smooth contours
- Pseudo-asbestos body (upper right): gross irregularly structured rod, ending with ridged protrusions on both sides (not completely in focus).

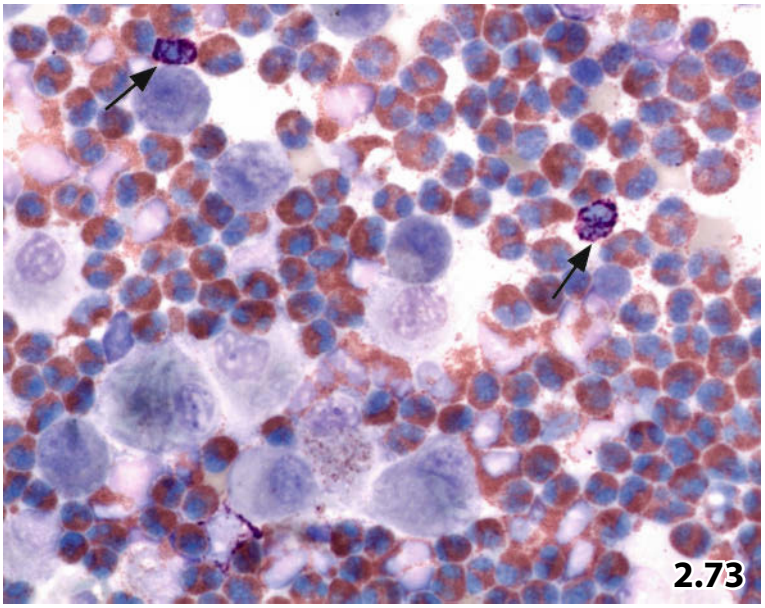
2.73

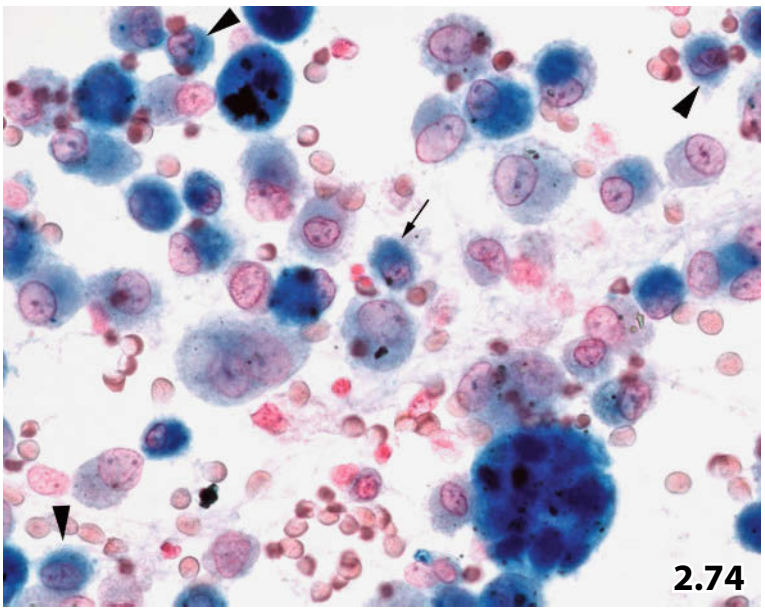
2.74

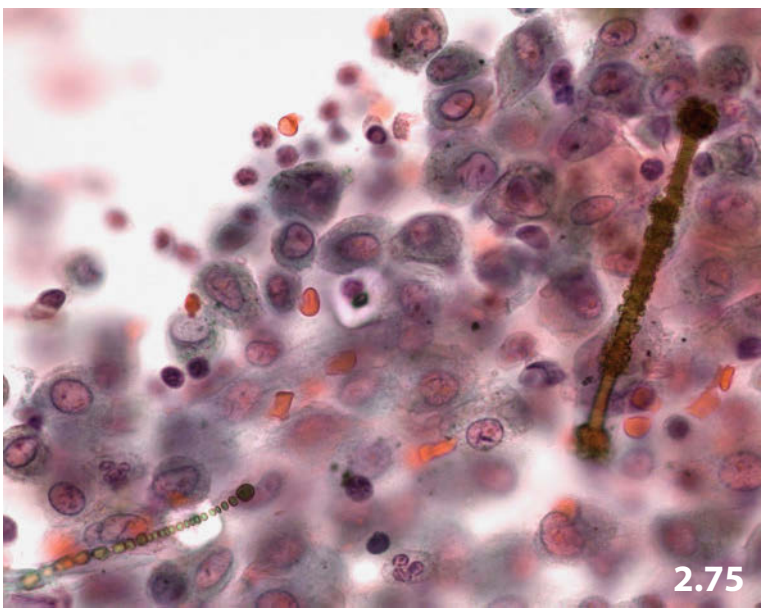
2.75

**Fig. 2.76 Graphite dust exposure.**
An elderly male patient with a positive history of graphite dust exposure. Numerous macrophages exhibit black-stained inclusions of variable size and shape (direct sediment smear, Pap stain, higher magnification).

**Fig. 2.77 Mixed dust exposure.**
Sidero-silico-anthracosis (Welder's lung) in a metal worker's BAL. The 52-year old man is welder by profession. Virtually all macrophages exhibit a blue staining cytoplasm. Coarse cytoplasmic deposits are deep blue (iron particles) or black (carbon particles). Quartz crystals could be visualized using the polarization microscope (not shown) (direct sediment smear, iron stain, higher magnification).

**Figs. 2.78 and 2.79 Alveolar proteinosis..**
Alveolar proteinosis is shown by conventional and electron microscopy.

**Fig. 2.78** Characteristic dirty background in a smear of BAL from a patient with alveolar proteinosis: PAS-positive acellular amorphous globules and cellular debris. Two foamy macrophages are present in this field (arrows) (direct sediment smear, periodic-acid-Schiff stain, lower magnification).

**Fig. 2.79** The BAL material was used for electron microscopic studies as well: myelin-like figures resembling lamellar bodies of surfactant are characteristic for alveolar proteinosis.

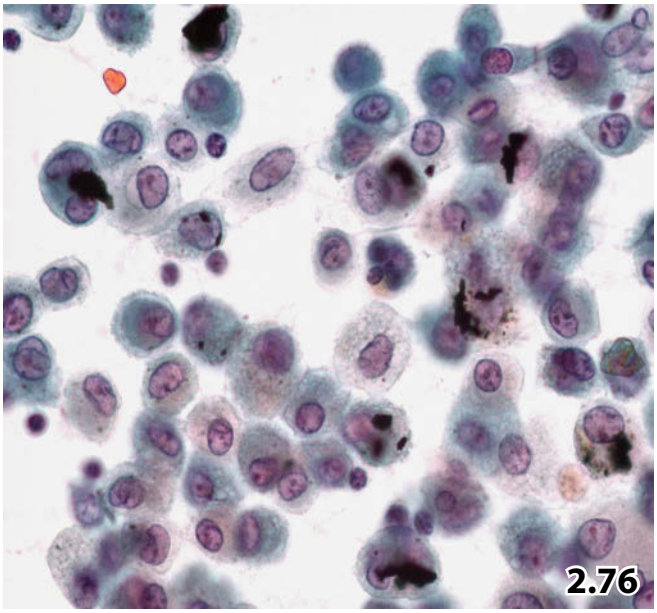
2.76

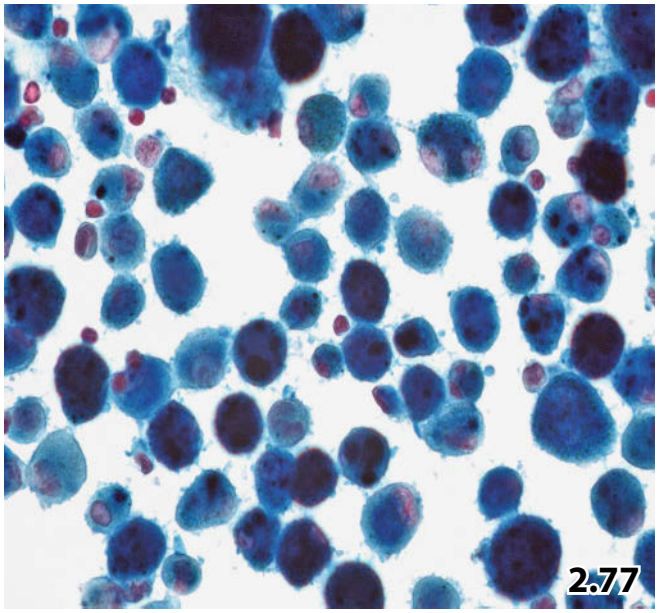
2.77

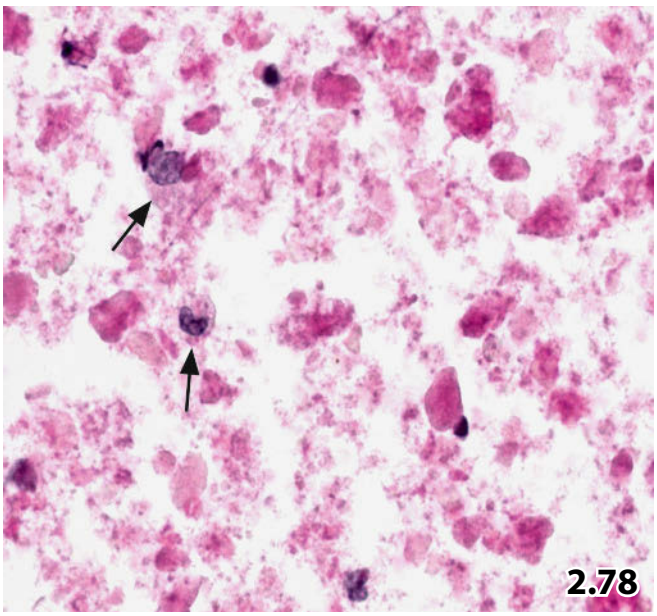
2.78

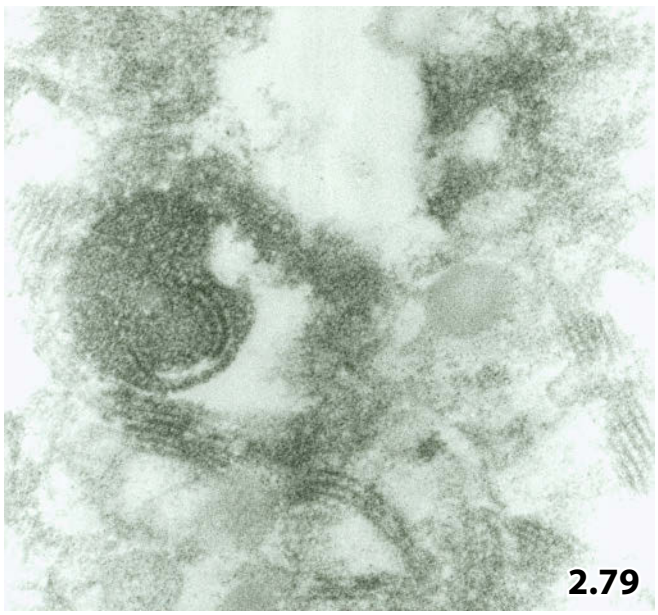
2.79

**Fig. 2.80A, B** ***Pneumocystis jirovecii.***
Cytomorphologic appearance of the pathogen is demonstrated at low and high magnification from Pap-stained direct sediment smears. **A** Low magnification: Compact accumulation of pneumocysts presenting as a foamy mass with irregular outlines (arrow). The appearance is so characteristic that an accurate diagnosis can be established using conventional staining procedures. **B** High magnification shows sharply demarcated cysts, focal thickening of the cystic membranes, and grey-brown intracystic bodies (arrows).

**Fig. 2.81** ***Cryptococcus neoformans.***
Numerous intra- and extracellular yeast cells of varying size. Note the thick sharply demarcated capsule (arrow) (direct sediment smear, periodic-acid-Schiff stain, high magnification).

**Fig. 2.82** ***Histoplasma capsulatum.***
Accumulation of yeast cells in the cytoplasm of an activated multinucleated macrophage (direct sediment smear, Pap stain, high magnification).

**Fig. 2.83** **Cytomegalovirus.**
A younger male patient suffering from AIDS presenting with cytomegalic inclusion disease in a BAL sample. Three affected epithelial cells are shown: two cells on the *left* exhibit the characteristic owl eye appearance; the cell at the right (arrow) seems to be in an earlier state of viral infestation (direct sediment smear, Pap stain, high magnification).

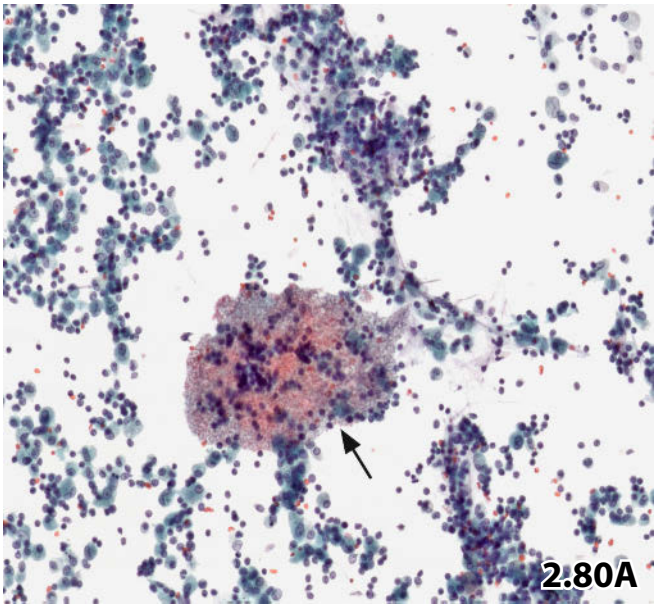
2.80A

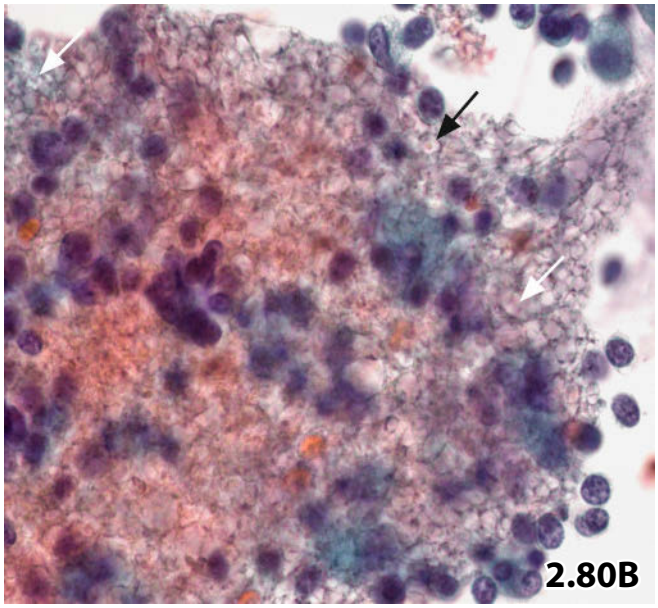
2.80B

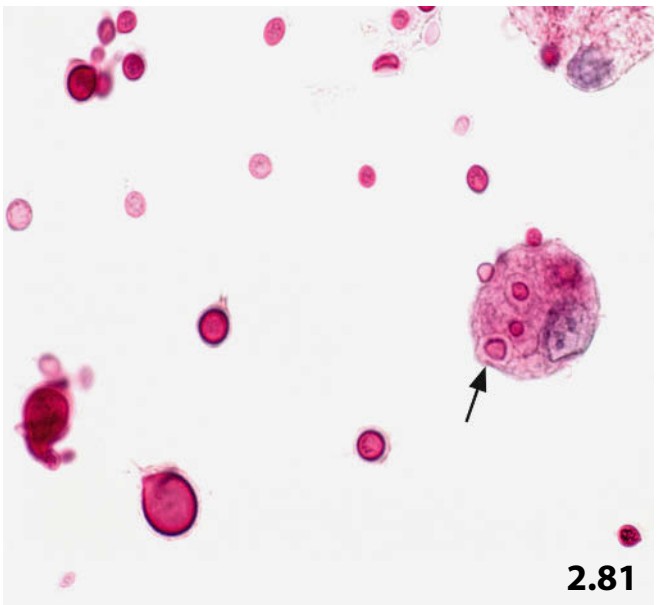
2.81

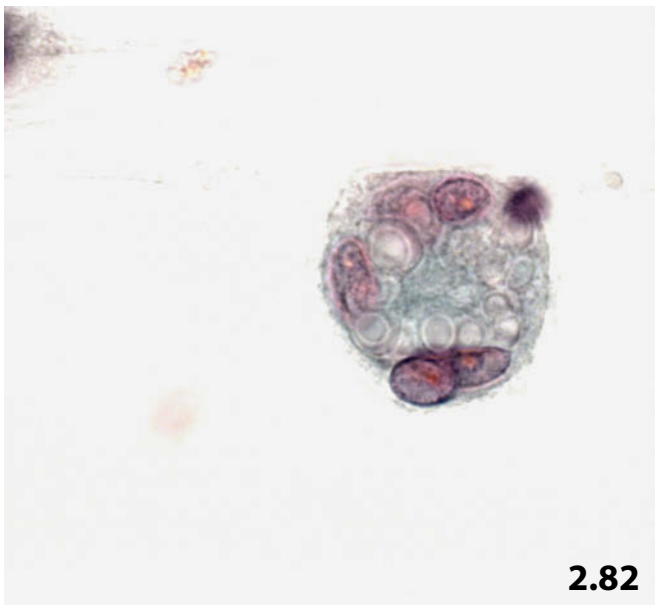
2.82

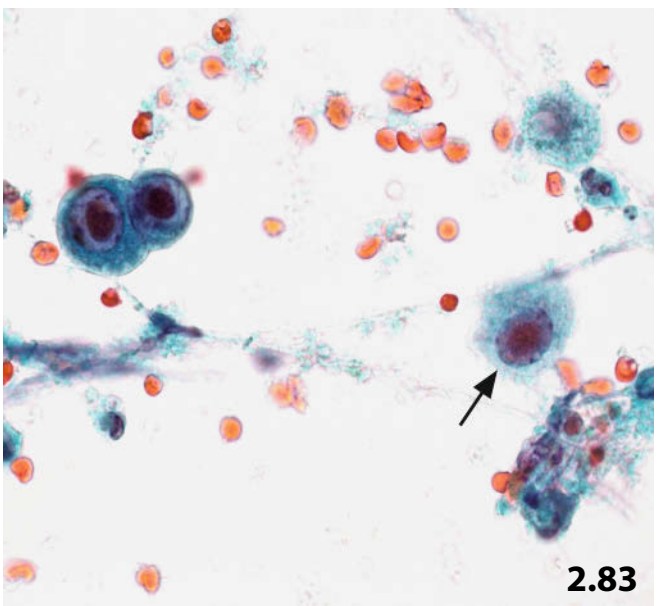
2.83

**Fig. 2.84 Activated type II pneumocytes.**
A 56-year-old man presenting with multiple infiltrates in the right lung. Direct smears from a BAL sediment show numerous small and medium-sized compact three-dimensional clusters of epithelial cells with minor atypias. The papilliform cluster shown displays acini-like formations and monomorphic cell appearance Pap stain, (high magnification).
*Cytology*: Cell changes are indeterminate between benign (hyperplastic type II pneumocytes) and malignant (bronchioloalveolar carcinoma).
*Comment*: Compare cell features with those of a bronchioloalveolar carcinoma presented in Fig. 2.85 for the distinct differences in nuclear texture and nuclear contour.
*Final diagnosis* was *Chlamydia* pneumonia.

**Fig. 2.85 Bronchioloalveolar carcinoma.**
A 36-year-old man presented with nodular infiltrates in both lungs. Direct smears were performed from the sediment of a BAL fluid (Pap stain).
*Cytology and histologic diagnosis*: Bronchioloalveolar carcinoma.
Note similarities and differences of the malignant tumor cells in comparison with hyperplastic type II pneumocytes as shown in Fig. 2.84 (same magnification).

**Fig. 2.86 Pulmonary lymphangiosis carcinomatosa secondary to breast carcinoma**
BAL in a 57-year-old woman with a history of breast carcinoma presenting with diffuse pulmonary infiltrates. Direct sediment smears reveal numerous loose clusters composed of malignant cells. Tumor cells exhibit distinct features of common type breast carcinoma: monomorphous cell population, eccentric nuclei, homogeneous cyanophilic cytoplasm, occasional lucid cytoplasmic inclusions, nuclear molding and cleaving, both finely granular and focally patternless chromatin (Pap stain, high magnification).
*Cytologic diagnosis*: Adenocarcinoma. The overall cell pattern in comparison with the previous histomorphology is consistent with metastatic breast carcinoma.
*Comment*: In cases with equivocal clinical history and absence of a preceding histologic/cytologic investigation, the differential diagnosis must also consider hyperplasia of type II histiocytes and bronchioloalveolar carcinoma. An appropriate immunopanel is helpful to solve the diagnostic problems.

**Fig. 2.87 Langerhans cell histiocytosis.**
BAL of a 38-year-old woman presenting with an uneventful history. Bronchoscopy revealed nonspecific inflammatory changes of the bronchial mucosa. Extremely cellular bronchoalveolar lavage fluids from the lung periphery showed a heterogeneous histiocytic population. Abnormal histiocytes exhibit multinucleation, nuclear cleaves and grooves, and vesicular chromatin (arrows). Positive immunostaining for S-100 and CD1 (immunocytochemistry not shown) classified the atypical cells as Langerhans cells accounting for 64% of the total number of histiocytic elements (direct sediment smear, MGG stain, high magnification).

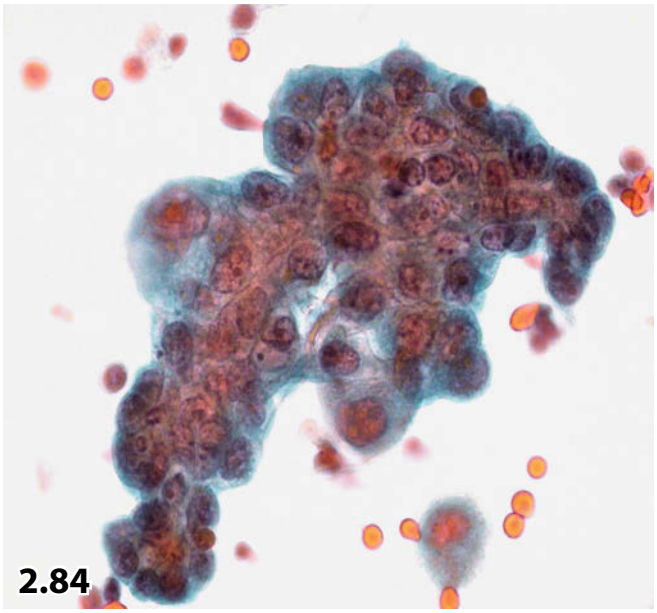
2.84

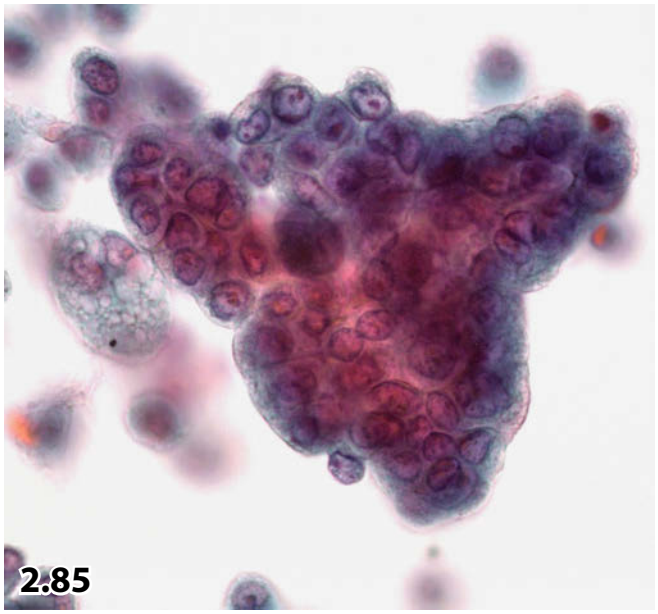
2.85

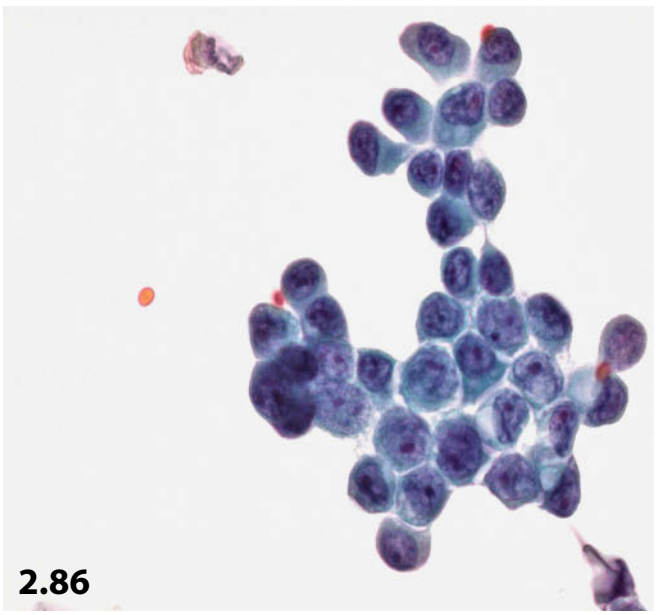
2.86

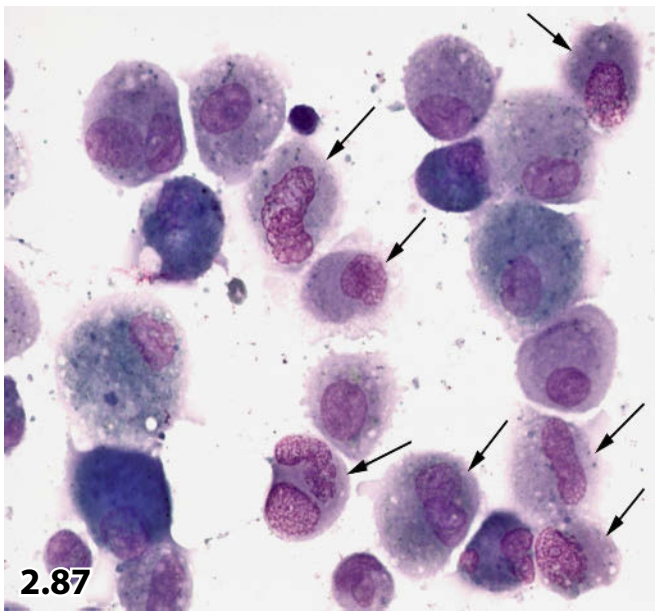
2.87

# Section 2.4
# Mediastinum

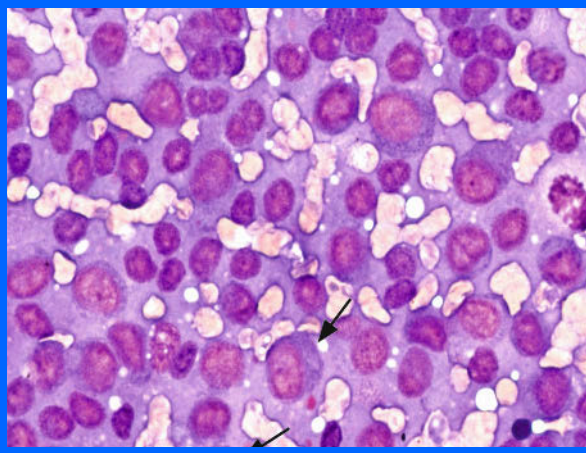

## Introduction

## Non-tumorous and Neoplastic Mediastinal Disorders

## Thymus Gland and its Diseases

### 2.4.1 Introduction

**General Comments**

- The mediastinum is a part of the chest cavity that extends anteroposteriorly from the posterior surface of the sternum to the spine and sagittally from the thoracic aperture to the diaphragm. The most widely used scheme to divide the mediastinum uses four compartments: superior, anterior, middle, and posterior.
- The mediastinum is an area of great interest, because it is a site of numerous organs that can become involved in various pathologic disorders (thymus, lymph nodes, ganglia, soft tissue), apart from lesions spreading from organs that are located in the mediastinum or border this space (heart, esophagus, major vessels, vertebral column, and the membranes confining the heart and lungs).
- The development of new radiologic techniques such as computerized tomography, sonography, or endoscopic ultrasound allows the chest physician extensive use of invasive preoperative diagnostic procedures such as mediastinoscopy, limited thoracotomy, transthoracic fine-needle aspiration biopsy (FNAB), and endoscopic ultrasound-guided fine-needle aspiration (EUS-FNAB). Tumorous mediastinal lesions such as tumors of the thymus, lymph nodes, ganglia, soft tissue, and others have gained interest in recent years not only to surgical pathologists, but also, to a great extent, to cytopathologists.
- Metastases are the largest category of mediastinal neoplasms diagnosed by FNAB followed by primary mediastinal tumors. Metastases usually present minor cytodiagnostic difficulties and ancillary immunocytochemical studies are helpful in assessing primary tumor location. In contrast, many primary neoplasms such as malignant lymphoma, thymoma, and germ cell tumors implicitly call for additional analyses, in order to achieve a reliable cytologic diagnosis and subclassification, or surgical biopsies [80].
- An excellent review of the various entities of mediastinal lesions in FNABs has been published by Geisinger [28].

#### 2.4.1.1 Fine-Needle Aspiration Biopsy Techniques

- Varied FNAB techniques have made the morphologic investigation of mediastinal masses not only possible, but also safe. Complications are rare including pneumothorax, hemorrhage, and hemoptysis. Pneumothorax has been reported as the most common complication [1, 34. 81]. Image-guided FNAB is becoming increasingly accepted as a diagnostic tool and as a substitute for core biopsy. This method can prevent a substantial number of more invasive surgeries, for instance mediastinoscopy and open thoracotomy. Furthermore, FNAB has been shown to be an excellent tool in diagnosing mediastinal lesions in correlation with clinical history, imaging studies, laboratory features, and with excellent team work with interventional radiologists or chest physicians performing the needle aspirations [80].
- Diagnostic accuracy ranges from about 80% to 100% [10, 29, 41, 80]. Diagnostic yield for tumors has been shown to be roughly equal in FNAB and punch biopsies, but his-

topathologic examination of core-needle biopsies seems to be more accurate for tumor typing [11].

- Inadequate aspirates have been reported constituting a rate between 10 and 20% [29, 80]. Proximity of major vessels and deep-seated small lesions are major technical reasons for inadequate sampling, whereas necrosis and fibrosis are biological factors responsible for limited cellularity in aspirate smears. Bloody specimens are a third reason for inadequate cytological results.
- High specificity and sensitivity have been achieved when an experienced cytopathologist or cytotechnologist is on site to ensure the adequacy of the sample [5, 20]. Immediate on-site cytologic interpretation is an additional factor that can improve diagnostic outcome [20, 92], but this setting is very time-consuming for cytopathologists and impracticable in a majority of institutions.
- Ancillary tests such as cytochemical staining, immunocytochemistry, and molecular pathology are helpful in increasing the diagnostic accuracy of FNAB samples. Scant cellularity, poor preservation of cellular material, and blood-rich specimens are limiting factors in this respect. Special stains are particularly useful in the presence of inflammatory lesions in order to visualize organisms, such as bacteria (Gram), mycobacteria (Ziehl-Neelsen), and fungi (periodic acid-Schiff and Crocott-Gomori methenamine-silver stain). Immunocytochemical work-up of neoplastic mediastinal masses is essential in order to confirm and subclassify primary neoplasms, and to assess the primary origin of metastases [80]. FNAB may also provide material for microbiological tests (including culture) and molecular genetic analyses.
- Ancillary laboratory techniques including liquid-based cytology and cell block preparations [6] can be extremely helpful in certain diagnostic settings. At our institution, the liquid-based technique has recently been successfully implemented for endoscopic transbronchial FNAB of hilar, parabronchial, paratracheal, and mediastinal lymph nodes.

#### 2.4.1.1.1 Transthoracic FNAB [6, 29, 80, 81]

Most FNABs today are performed under radiologic guidance using computed tomography. Ultrasound can also be used to guide a fine needle into lesions located in the different compartments of the mediastinum. Masses located in the superior mediastinum may reliably be targeted by ultrasound-guided FNAB using retroclavicular and retrosternal needle passes. A fine needle attached to a syringe (best attached in a pistol-type holder) is passed through the chest wall into the lesion (references are indicated in Sect. 2.1.1.2.3, "FNAB Methods," p. 109).

#### 2.4.1.1.2 Transbronchial FNAB [85]

Modern fiberoptic equipment enables the operator to visualize parabronchial-situated nodules molding the wall of the tracheobronchial tree. The needle is passed through the fiberendoscope and precisely inserted through the bronchial or tracheal wall into enlarged parabronchial, hilar, and paratracheal lymph nodes.

#### 2.4.1.1.3 Endoscopic Ultrasound-Guided FNAB

Endoscopic ultrasound-guided FNAB (EUS-FNAB) has proved to be a highly accurate diagnostic test for suspected tumorous lesions at various sites of the body, therefore avoiding numerous invasive surgical interventions [113]. Transesophageal and transbronchial EUS-FNABs are used with a high degree of sensitivity and specificity for staging of lung cancers and for primary diagnoses of mediastinal lesions. EUS-FNAB is a highly valuable method for diagnostic evaluation of lesions, especially when other modalities have failed [21, 42, 53, 68, 106]. The intervention is usually well tolerated [10].

*Transbronchial EUS-FNAB* allows the operator to visualize and evaluate small intramural/submucosal-situated lesions of the bronchi, and tumors within the lung parenchyma, as well as lymph nodes and abnormal findings located in the mediastinal space [5, 35, 85].

*Transesophageal EUS-FNAB* has become an important tool for staging lung cancer at the time of diagnosis and for assessing diagnoses on otherwise undiagnosed pulmonary and mediastinal masses. Such lesions are usually located in the posterior areas of the mediastinum and in the upper lobes of the lung [10, 13, 21, 42, 103, 111].

**Caution**

The passing of the needle into the mediastinal lesion causes contamination of cells from the bronchial/esophageal inner layers and from bronchial glands (Fig. 2.88).
Beware of erroneous diagnostic conclusions!

### 2.4.1.2 Liquid-Based Cytology for FNAB Samples [108]

At our institution, we prefer the use of liquid-based thin-layer technology (Cytospin, ThinPrep) for endoscopic image-guided FNAB of mediastinal disorders. The reasons for this procedure are the following:

- The entire amount of FNAB material can be preserved.
- The thin-layer method has proved to be a perfect procedure for clinicians who are not familiar with the proper preparation and fixation technique for the aspirated material, or when a cytotechnologist is not available on site during the intervention.
- In many circumstances, the liquid-based method is superior to conventional smears with regard to clear background, monolayer cell preparation, and cell preservation.
- An optimal preparation can be achieved for special investigations, in particular for immunocytochemistry, FISH,

or static DNA cytometry (Figs. 2.108 and 2.112). In addition, the rinse from needle and syringe may be used for immunolabeled flow cytometry.

- Regardless of operator, hemolyzing fixatives (Cytolyt and others) have shown to be indispensable as initial transport medium for highly sanguineous FNAB material. Combined with thin-layer preparation, hemolyzing fixatives are a useful modality for blood-rich aspirates providing well-preserved cells and a clean background.
- In our experience, which is in agreement with the results reported in the literature, smear preparation and fixation is improved and artifacts are reduced using the thin-layer technique. However, morphologic features may be altered and cell interpretation may need modification. The most challenging morphologic changes compared with conventional smears are (Figs. 2.114 and 2.115):
  - Cell aggregates may be crowded and tight.
  - Cell shrinkage and disruption of the cytoplasm may be more pronounced.
  - Nucleoli are more distinct.
  - Background material such as mucin or detritus may be scant or completely lost.

Practically all recent reports in the literature indicate that liquid-based cytology is an accurate and feasible method in the FNAB investigation from lesions of various sites, comparable with conventional smear preparation (references are provided in Sect. 10.1.2.2, "Liquid-Based Cytology," p. 634, and elsewhere). The liquid-based technique has rarely been applied on FNAB samples for the diagnosis of thymic lesions [74].

### 2.4.1.3 Mediastinal Compartments with Their Organs and Principal Lesions

Dividing the mediastinum into four compartments is not only useful for clinical purposes, but also for pathologists, because many lesions are restricted to certain compartments and related to the individual organs:

#### 2.4.1.3.1 Superior Mediastinum

- Thymus: cysts, thymoma, carcinoid, lymphoma.
- Thyroid: goiter and neoplasms, originating from ectopic tissue or primary thyroid lesions extending into the mediastinal space [88].
- Parathyroid glands: cysts, tumors.
- Lymph node: inflammatory disease, lymphoma, metastases.
- Generally: cysts, aneurysm.

#### 2.4.1.3.2 Anterior Mediastinum

- Lesions of the superior mediastinum.
- Germ cell tumors.
- Paraganglioma.
- Mesenchymal tumors such as lipoma, angioma, and others.

#### 2.4.1.3.3 Middle Mediastinum

- Heart and pericardium: cysts and tumors.
- Lung hilus: bronchogenic cyst.
- Hilar and broncho-pulmonary lymph nodes: inflammatory disease, lymphoma, metastases.

#### 2.4.1.3.4 Posterior Mediastinum

- Neurogenic system, also sympathetic: schwannoma, ganglioneuroma/blastoma, neuroblastoma, paraganglioma, and others.
- Lymph nodes: inflammatory disease, lymphoma, metastases.
- Development defect: gastroenteric cysts.
- Esophagus: carcinoma and other lesions.
- Spinal column: osseous and chondroid tumors, lymphoma (plasmacytoma), hypostatic abscess, meningocele.
- Major vessels: aneurysm.

## 2.4.2 Cytology of Nontumorous Mediastinal Disorders

### 2.4.2.1 Inflammatory Diseases

#### 2.4.2.1.1 Acute Mediastinitis [82]

Esophageal perforation is the most common cause for this uncommon but severe clinical condition frequently resulting from postoperative dehiscence of intrathoracic esophageal anastomoses. Perforation can also follow endoscopy, dilatation of the esophagus, trauma, ingestion of foreign bodies, irradiation, erosion of the esophageal wall by malignant tumors, etc. Mediastinitis may exceptionally result from lymphatic spread of infections located in tissues and organs adjacent to the mediastinum such as deep neck infections, lung abscess, subphrenic abscess, or vertebral osteomyelitis.

- Cytologic specimens contain abundant neutrophils and signs of abscess formation (degenerating neutrophils and debris). It is recommended to submit a portion of the aspirated material for microbiological studies.

#### 2.4.2.1.2 Chronic Mediastinitis [24, 50, 55, 90]

Synonyms: Granulomatous mediastinitis, fibrous and sclerosing mediastinitis, and others.

Infectious and noninfectious diseases may lead to the development of a chronic mediastinal inflammatory process frequently associated with granulomatosis and fibrosis. Histoplasmosis and tuberculosis are the most common etiologic factors for granulomatous mediastinitis. A noninfectious etiology is assumed to be associated with sarcoidosis (Figs. 2.89 and 2.90), autoimmune diseases, drugs, trauma, cancer, and coexistent with similar fibrotic processes in the retroperitoneum, thyroid, orbita, and other

parts of the body. Sclerosing mediastinitis is usually self-limiting.

**Microscopic features**

- The inflammatory process shows various morphologic patterns [24]. Cellular fibromyxoid tissue, leukocytes, and plasma cells mark the florid stage, whereas sclerosis with collagen and dystrophic calcification represents the final stage of the disorder.
- FNAB samples are likely to be hypocellular, comprising a few stromal cells and fragments of fibrotic tissue unless a florid inflammatory process provides characteristic elements of granulomatous tissue.
- Epithelioid cells and giant cells of the Langhans type raise suspicions of sarcoidosis, tuberculosis, or atypical mycobacteriosis. Additional caseating necrosis is a strong indication of mycobacterial infection. Detection of mycobacteria by Ziehl-Neelsen stain or microbiological studies supports the morphologic diagnosis [31].

**Differential Diagnosis**

- Granulomatous inflammation may be associated with malignant neoplasms such as germ cell neoplasia, Hodgkin lymphoma and non-Hodgkin lymphoma [94].
- Malignant neoplasms with a strong sclerotic component such as sarcoma, Hodgkin lymphoma of the nodular sclerosing type [23], or sclerosing non-Hodgkin lymphoma may simulate chronic sclerosing mediastinitis.

### 2.4.2.2 Uncommon Mediastinal Deposits

#### 2.4.2.2.1 Pronounced Anthracosis

Pronounced anthracosis in mediastinal lymph nodes may induce unorthodox proliferative activity of histiocytes and enlargement of the lymph node. Aspirated material appears as a black stained mass.

- Microscopy: masses of extracellular anthracotic pigment is also included in the cytoplasm of macrophages as well as a few lymphocytes.

#### 2.4.2.2.2 Mediastinal Amyloidosis

Amyloid deposits within the mediastinal space may give rise to reactive cell changes. Cellular atypias should not lead to a misdiagnosis of cancer [80]. Morphologic features and other attributes of amyloid are covered elsewhere in this book (Sect. 2.2.1.9.1, "Amyloid Tumor," p. 136).

### 2.4.2.3 Mediastinal Cysts

Mediastinal cysts comprise 10–27% of all mediastinal tumorous disorders [50]. A variety of mediastinal cysts exist, which can be divided into two main categories:

1. Congenital cysts resulting from developmental anomalies of the foregut or related embryonal structures.
2. Acquired cysts including benign cyst-like lesions and secondary cystic changes in neoplastic disorders.

Transthoracic or endoscopically guided FNAB is an effective method for diagnosing cystic lesions [19, 32]. Their nature can be assessed or suspected in a number of cases as a result of the cytologic features in the aspirated cyst content.

#### 2.4.2.3.1 Congenital Cysts [19, 32, 87]

Most of these cysts are spherical and usually unilocular, and show a strong variability in size, up to several centimeters.

**Cystic mature teratoma** (Fig. 2.91)

More information is available in Sect. 2.4.3.6.1, "Benign Teratoma," p. 213.

**Bronchogenic cyst**

Bronchogenic cysts result from abnormal branching of the tracheobronchial tree during embryonic development. They are the most common variety of all congenital cysts found in the mediastinum and occur at any age. Bronchogenic cysts are located in the anterior mediastinum but may be present elsewhere in the mediastinal space and also within the lung parenchyma.

The cyst fluid may be clear, turbid, or mucoid.

**Microscopic Features and Differential Diagnosis**

- Sediment smears contain ciliated columnar cells of the respiratory type and usually sheets of metaplastic squamous cells. A few detached ciliary tufts may be the only remnants of ciliated columnar cells [19] (Fig. 2.92).
- Other elements that are normally present in bronchial walls may be found as well such as cartilage, smooth muscles, and bronchial glands.
- Calcium deposits occasionally occur. Birefringent, needle-shaped crystals have been described in many cases [43, 44, 91].

Esophageal cysts contain cellular elements equal to bronchogenic cysts, except cartilage tissue and chondrocytes.

**Esophageal cyst**

Esophageal cysts arise from noncoalescing vacuoles in the wall of the foregut during development of the esophagus. These cysts are most frequently found in children and young men.

**Microscopic Features and Differential diagnosis**

- Nonkeratinized stratified epithelium is most likely encountered, but varying amounts of ciliated columnar epithelial cells and ciliary tufts may be present as well.

- Other elements as mentioned for bronchogenic cysts may also be encountered.

Distinction from bronchogenic cyst is difficult. However, cartilage is definitely no component in fluids of esophageal cysts.

#### Gastroenteric cyst

Gastroenteric cysts develop in the posterior mediastinum. They are usually associated with vertebral anomalies [87]. Gastroenteric cysts may be reported under various terms: gastric cyst, enterogenous cyst, foregut duplications, esophageal duplications, etc.

- The epithelial cells may be of the gastric type, intestinal type, or both, including mucin-secreting cells. Ciliated columnar cells and squamous cells are frequently observed.

#### Pericardial and Mesothelial cyst

Pericardial and mesothelial cysts result from developmental abnormalities of the pericardial or pleuroperitoneal coelom. They are typically located close to the pericardium and adjacent to the diaphragm, they are usually found in adult patients.

The cystic fluid is watery, clear, and frequently acellular.

- Mesothelial cells may occur, arranged in regular flattened sheets. The mesothelial cytoplasm is wide, nuclei are monomorphic with bland chromatin and smooth borders, and the N/C ratio is low. An inflammatory component is usually absent.

#### Cysts containing pancreatic tissue

These cystic lesions have been rarely reported [110]. Ectopic pancreatic tissue associated with cystic changes generally includes ducts, acini, and islets of Langerhans.

**Differential diagnosis**

Mediastinal teratoma containing pancreatic tissue and pancreatic pseudocysts extending into the mediastinum have to be taken into consideration.

Other congenital cystic disorders of the mediastinum that have to be included in differential diagnosis considerations are thymic cysts (described in Sect. 2.4.3.3, p. 209) and meningoceles.

#### 2.4.2.3.2 Acquired Cysts (Fig. 2.93)

#### Thoracic duct cyst

Thoracic duct cysts are probably caused by degenerative changes or congenital harm of the thoracic duct wall followed by duct dilatation and aneurysm formation [50].

A macroscopically milky chylous fluid is a diagnostic key feature.

- A few spindle-shaped or flattened endothelial cells and a variable number of mature lymphocytes may be present in smear preparations.

#### Parasitic cysts

Hydatid cysts are most common in the mediastinum are hydatid cysts. They are caused by the larval stage of the dog tapeworm. The cystic lesion appears unilocular and multilocular, characteristically with focal areas of calcification in the cyst wall.

Microscopic features, general comments, and cautions are given in several chapters of this book, e.g. Sect. 9.1.7.3, "Hydatid Cyst," p. 590.

#### Neoplastic cyst

Neoplastic cysts are frequent. Many mediastinal tumors are primarily cystic or have a cystic component: thymoma (see Sect. 2.4.3.4, p. 209), thymus lymphoma, teratogenous tumors, thyroid and parathyroidal tumors, nerve sheath tumors, and metastatic neoplasms (Fig. 2.94).

#### Other cystic formations

They can occur in the regressive course of hematomas and inflammatory process. Mediastinal pancreatic pseudocyst has been mentioned in the context of mediastinal cystic pancreatic tissue. Normal thymus in adults can show extensive cystic degeneration.

**Caution**

Contaminating cells from organs penetrated by the needle on its way into the cyst may cause erroneous typing of the cystic lesion (Fig. 2 .88)

## 2.4.3 Thymus Gland and Its Diseases

### 2.4.3.1 Normal Thymus Gland [50]

- The thymus is a pure epithelial organ during the first stages of its evolution. By the end of the second month of intrauterine life, the epithelial tissue becomes secondarily infiltrated by bone marrow-derived lymphocytes and mesenchymal elements.
- The thymus gland reaches the maximum weight during puberty followed by a gradual process of fatty involution. However, the organ never completely disappears but commonly becomes cystic.
- The thymus plays an important role for the immune system and produces several hormones. Primarily undifferentiated lymphocytes – migrated from bone marrow – acquire characteristics of T cells in close contact with thymic epithelium and its microenvironment. After migration to peripheral lymphoid organs the post-thymic precursor T cells finally acquire the characteristics of mature immunocompetent T cells. The process is triggered by thymic hormones.
- The thymus is located in the anterior mediastinum but small ectopic islands of thymic tissue are found throughout the mediastinal space and are extramediastinal as well.

- The encapsulated organ consists of two lobes and is divided into lobules by fibrous strands. The peripheral portion of the thymic lobes is the cortex, it appears darker than the central area, which is called the medulla.
- Parathyroid tissue is commonly found in the anterior mediastinum adjacent to the thymus gland or surrounded by thymic parenchyma.

**Histology and Immunocytochemistry**

*The cortex* is almost entirely composed of lymphocytes. The lymphoid population is best analyzed by flow cytometric analysis, which predominantly demonstrates T cells coexpressing CD4 and CD8 and staining positive for the early T-cell markers CD1a and TdT. A few small lymphoid follicles and rare plasma cells represent the B-cell lymphoid population. A few scattered cortical epithelial cells are difficult to distinguish from large histiocytes.

*The medulla* (Fig. 2.95) chiefly contains epithelial cells occurring in small groups. Squamous differentiation and formation of keratin pearls (called Hassall corpuscles) are obvious. Lymphocytes of the medulla mainly represent the inducer phenotype T4. Myoid cells are also found.

### 2.4.3.2 Thymic Hyperplasia (Fig. 2.96)

#### 2.4.3.2.1 True Thymic Hyperplasia

True thymic hyperplasia is characterized by an increase in the size and weight of the whole gland without changes in normal architecture and morphology for age. Common hyperplasia has to be separated from a true neoplastic disorder (thymoma). Massive benign enlargement of the thymus gland is rare. It has been described in children treated for malignancies and in conjunction with other pathological conditions [50].

#### 2.4.3.2.2 Reactive Lymphoid Hyperplasia

Follicular hyperplasia is characterized by the presence of germinal centers in the medullary area of the thymus gland. Follicular hyperplasia of lymphocytes of the B phenotype is often associated with myasthenia gravis and various autoimmune disorders [30]. Morphologic features of follicular hyperplasia are provided in Sect. 15.2.2, "Common Reactive Lymphadenopathy," p. 926.

### 2.4.3.3 Thymic Cysts [50] (Fig. 2.97)

Thymic cysts are particular lesions. Most of them are probably congenital and derived from tubular remnants of the thymus anlage. Distention occurs by fluid accumulation or hemorrhage.

The cyst fluid is serous but may also be sanguineous.

- The background of the smears may contain inflammatory cells, erythrocytes, debris, calcium deposits, and particularly cholesterol crystals.
- If present, epithelial cells are cuboid, columnar, ciliated columnar, or squamous.

Differential diagnosis: Various types of congenital mediastinal cysts show a similar fluid cell pattern in comparison to thymic cysts (see Sect. 2.4.2.3.1, p. 207). Other cystic disorders should be considered as well such as cystic thymoma, cystic germ cell tumor,lymphangioma, and cystic lymphoma of the thymus gland.

### 2.4.3.4 Thymoma

In the past, the term "thymoma" has generally been applied to any type of tumor originating in the thymus gland: thymic neoplasms included tumors arising from thymic epithelium, neuroendocrine cells, germ cells, lymphoid cell populations, and various mesenchymal cell types, particularly adipose cells.

Today, the term "thymoma" is restricted to tumors originating from the thymic epithelial cells [50]; therefore, thymomas should be separated from other neoplasms that have their origin in the thymic gland such as carcinoid, germ cell tumors, and malignant lymphomas.

There have been several varied classifications of thymic tumors up to the end of the last century. Nowadays, the most widely used classing is the 2004 WHO histological typing system [102].

#### 2.4.3.4.1 Tumors of the Thymic Epithelium: Common Type Thymoma (Fig. 2.98)

**General Comments**

- Thymoma is the most common primary tumor in the superior/anterior mediastinum and one of the most frequent tumors of the entire mediastinal space.
- Most tumors are observed in patients in the fifth and sixth decades of life. There is no predilection for sex, race, and geographic area [48].
- Thymoma can sporadically be found in unusual sites according to its particular embryologic development, descending through the neck into the mediastinum. Tumors may be located in the neck area [105], lung [60], pleura, and mediastinal areas other than the anterior compartment.
- A unique feature of the tumor is its association with paraneoplastic syndromes, and in particular myasthenia gravis.
- Thymomas may be roughly categorized into a noninvasive stage and invasive stage, whereas prognosis depends on the invasive status of the individual tumor. The vast majority of the thymomas are completely encapsulated and behave clinically benign. The 2004 WHO typing system classifies thymomas into five types according to the morphology and the atypical features of the tumor cells as well as the proportion of epithelial cells and lymphocytes.

Invasiveness and prognosis of the thymomas were shown to correlate with this classification system. Other prognostic factors include the tumor stage, tumor size, and the presence of clinical symptoms. Surgery is the principal treatment for thymomas [39, 46, 71].

- Extrathoracic metastases are rare; the most important sites include cervical lymph nodes and liver parenchyma [48].

### Histology

- Most thymomas are well encapsulated, reaching a diameter of up to several centimeters. Calcification of the tumor capsule is uncommon but presumed to be a characteristic of thymomas. The tumors exhibit variable degrees of cyst formation as well as areas of hemorrhage and necrosis.
- Basically, thymomas are composed of a biphasic cell population, namely neoplastic epithelial cells and lymphocytes of the T-cell phenotype.
- Thymoma can be evaluated from two different perspectives:
  1. Related to the relative proportions of epithelial cells and lymphocytes:
     - In epithelial thymomas, the epithelial cell population predominates. Epithelial cells represent more than two-thirds of all cells.
     - In lymphocytic thymomas, lymphocytes predominate.
     - In mixed thymomas, the number of epithelial tumor cells and lymphocytes is almost equal.
  2. Based on cortical and medullary differentiation of the epithelial cells:
     - Cortical thymomas show epithelioid thymocytes. These are tumors having a more aggressive behavior belonging to the mixed thymoma variant [14].
     - Medullary thymomas are composed of spindle epithelial cells.
     - Mixed thymomas contain both cell types.

Epithelioid tumor cells show epithelial clustering, clearly distinguishing these tumor cells from histiocytes/mesenchymal cells. Spindle epithelial cells may mimic fibroblasts; their growth pattern is manifold such as whorls or bundles. Epithelial cells in benign thymomas may be very large and pleomorphic but lack clear signs of malignancy. Architectural features include rosettes, glandular and papillary structures, perivascular spaces, and Hassall corpuscles. Squamous epithelial cells and myoid cells may also be observed and glands may be lined by goblet cells or ciliated epithelium.

### Cytologic Features

[4, 14, 28, 97, 98, 107] (Fig. 2.98)

A biphasic population of epithelial cells and lymphocytes in varying proportions is a key feature for the cytologic diagnosis of thymoma.

- *Epithelioid epithelial cells* (Fig. 2.95B) are round to oval in shape and variable in size. The nuclei are bland in appearance, showing a smooth outline, pale chromatin, and distinct but small nucleoli. The nuclei may sometimes be crowded and cytoplasmic invaginations may be observed.
  The cytoplasm is typically round or polygonal, varying from scant to moderate in size and has indistinct borders. It may be clear and delicate or densely structured and squamoid.
  Identical architectural features, as seen in histologic sections, including Hassall corpuscles, may be detected (Fig. 2.95A)
- *Spindle epithelial cells* are commonly seen in fine-needle aspiration of thymomas, but predominance of this cell type is less common. The cells are arranged in loose groups or bundles. Both cytoplasm and nuclei are elongated. Regular nuclei show evenly distributed chromatin.
- *Lymphoid cells* vary in number and phenotype, depending of the thymoma type. Type A thymomas show only a few mature T-cell lymphocytes. The number of T cells and the fraction of immature T cells increase within the type B thymoma group. Activated lymphocytes show increased size, nuclear irregularities, and nucleoli. Plasma cells are extremely rare.
- Thymoma cells that have accumulated glycogen in their cytoplasm stand out as clear cells with abundant pale cytoplasm.
- Benign thymoma can exhibit distinctive atypias of the epithelial cells including pronounced cellular enlargement, cellular and nuclear pleomorphism, and large nucleoli. Unequivocal malignant cell features together with necrosis and high mitotic activity may suggest a diagnosis of thymic carcinoma.
- Calcification, fibrotic tissue fragments, and cystic degeneration with foam cells vary depending on the tumor subtype. No mitotic activity.

**Caution**

- Cytologic examination alone cannot reliably discriminate among the various subtypes of thymomas.
- Cytologic diagnosis of thymoma is challenging if a pronounced population of lymphocytes is obscuring the epithelial component.
- Cytologic features alone are not adequate to determine invasive growth of thymoma into surrounding structures. Absence of atypias and necrosis do not exclude an aggressive tumor behavior [14].
- Pronounced cytological atypias, necrosis, and mitoses raise suspicions of thymic carcinoma.

#### 2.4.3.4.2 Tumors of the Thymic Epithelium: Invasive Thymoma (Figs. 2.99 and 2.100)

- Invasiveness of thymomas is invariably established by histologic examination of the periphery of the tumors, demonstrating invasion through the capsule and into surrounding tissues (vessels, nerves, pericardium, pleura, and lung).
- A considerable number of invasive thymomas goes along with a bland cytologic pattern. Such tumors rarely show metastases in distant organs.
- Neither cytological features nor histological classification and paraneoplastic clinical symptoms are reliable parameters for the biological behavior of an individual tumor. However, Baba and coauthors have emphasized cytological features as well as morphometric results that are useful in distinguishing between low-stage and high-stage thymomas [7].

**Microscopic Features**

- Microscopic patterns, in particular the characteristic biphasic cell population and cytologic features, are the same as described above [22,107]
- Features that may suggest invasive growth (as compared to common thymoma type) are:
  - Predominant epithelioid cell pattern.
  - Nuclear enlargement.
  - Pronounced nucleoli.
  - Enhanced mitotic activity.

**Caution**

Presence of focal cellular atypias, cellular pleomorphism, and increased mitotic activity is of limited value for estimating invasive behavior and prognosis of thymomas by cytology [14, 84, 107].

#### 2.4.3.4.3 Tumors of the Thymic Epithelium: Thymic Carcinoma [33, 56]

- Thymic neoplasms that exhibit unequivocal cytologic features of malignancy should be classified as thymic carcinoma. They have all the characteristics of malignant behavior, both histologically and clinically. Thymic carcinomas account for only a small group of the mediastinal neoplasms. A great number of morphologic variants have been reported [102], whereas squamous cell carcinoma has proved to be the most common entity among thymic carcinomas. The histologic and cytologic features of thymic carcinoma variants as listed below are indistinguishable from corresponding tumors arising in a variety of other organs throughout the body.

**Microscopic Features and Immunocytochemistry**

- General cytological and background features include pronounced cellular and nuclear pleomorphism, prominent nucleoli, numerous and bizarre mitotic figures, tumor necrosis, inflammatory infiltrate [7].
- We refer to other chapters of this book regarding the cytologic pattern of particular tumor types and ordinary differential diagnosis considerations:
  - *Squamous cell carcinoma* (Fig. 2.101). Intercellular bridges and keratotic pearls are usually present (cytomorphology and others see Sect. 2.2.2.2, "Squamous Cell Carcinoma," p. 139). A combination of immunocytochemical staining for CD117(KIT) and CD5 indicates the thymic origin of the tumor and has been shown to be extremely helpful in distinguishing between thymic squamous cell carcinoma and metastatic squamous cell carcinoma [61].
  - *Lymphoepithelioma-like carcinoma* (cytomorphology and other information are given in Sect. 8.7.3, "Lymphoepithelial Carcinoma," p. 568). Mediastinal seminoma/dysgerminoma may closely resemble this particular subtype of thymic carcinoma.
  - *Basaloid carcinoma* [79] (cytomorphology and others see Sect. 16.2.7, "Basal Cell Carcinoma," p. 1029).
  - *Small-cell carcinoma* (cytomorphology and others see Sect. 2.2.2.6, "Small-Cell Carcinoma," p. 144). Pure and mixed tumors (combined small-cell carcinoma) have been reported. Neuroendocrine features of thymic small-cell carcinoma have been confirmed by immunohistochemical studies for chromogranin and CD56 [101]. Differential diagnosis with metastatic small-cell carcinoma of the lung is very difficult if not impossible.
  - *Clear cell carcinoma* (cytomorphology and others see Sect. 12.1.8.1.1, "Clear Cell Renal Cell Carcinoma," p. 739).
  - *Other high-grade thymic carcinomas* include mucoepidermoid carcinoma, adenosquamous carcinoma, and carcinosarcoma

#### 2.4.3.4.4 Additional Analyses on Tumors of Thymic Epithelium

Immunocytochemistry [18, 99] (Figs. 2.99B–E)

The thymocytic tumor cell exhibit a bilineage pattern of epithelial and lymphocytic antigens. On the one hand, they show varied epithelial markers such as EMA and different cytokeratins (e.g., AE1/AE3, Cam 5.2, CK5/6, CK7, CK14, CK19), and on the other hand CD20 or CD57.

The accompanying lymphocytes usually express an immature T-cell phenotype showing variable reactivity for several T-cell antigens (e.g., CD1a, CD3, CD5, CD4, CD8, CD99, TdT).

CD5 and CD117 have been reported to express positive immunoreactivity in a high percentage of thymic carcinoma cells in contrast to thymoma cells. Furthermore, CD205 and Foxn1 have been proposed as a sensitive and specific marker for benign and malignant thymoma. The sensitivity of CD205 seems to be lower than CD5 and CD117 for thymic carcinoma, and Foxn1 was found to be superior

to CD5 and CD117 as a marker for thymic carcinomas [61, 66].

Flow Cytometry

Flow cytometric immunophenotyping of the lymphoid cell population may be helpful in preoperative diagnosis of thymomas, excluding benign thymic tissue and other types of thymic tumors [78]. CD4/CD8 coexpression on the lymphocytes in thymic tumors assessed by fluorescence-activated cell sorting analysis is an additional indicator for the diagnosis of thymoma [27, 28, 70, 114]. Furthermore, flow cytometric analysis on the lymphocytic population appears to be useful to determine the malignant potential of thymomas [62, 114].

Enzyme Immunoassay in Cystic Fluids

Elevated CA-125 content in the fluid obtained from a cystic mediastinal tumor may be helpful in classifying the lesion as thymoma [76].

**Differential Diagnosis** [28, 80]

The most frequent differential diagnoses of thymomas are listed next, together with immunocytochemical markers proved to be the most helpful:

- Thymomas with a dominant epithelioid component may be confused with
  - Primary mediastinal neoplasms: germinomas, embryonal carcinoma (placental alkaline phosphatase +), thymic carcinoid (neuroendocrine markers +); admixture of a lymphoid cell population may occur, particularly with germ cell tumors (seminoma/dysgerminoma).
  - Any metastatic carcinoma and melanoma (melanoma-typical markers +) to the mediastinum. TTF-1 may be expressed immunocytochemically in pulmonary adenocarcinomas but not in thymoma cells [77].
  - Thyroid papillary carcinoma (TTF-1 and thyroglobulin +) if the nuclei of a thymoma exhibit pale chromatin, small nucleoli, nuclear crowding and cytoplasmic invaginations [51, 67].
- Thymomas composed of an epithelioid population of predominant small cells have to be differentiated from non-Hodgkin lymphoma (CD45 +) , small-cell carcinoma, and carcinoid of the lung (neuroendocrine markers + and TTF-1 +), and paraganglioma in adult patients (see Sect. 5.2.6.2, "Carotid Body Paraganglioma," p. 467).
  Tumors of the small blue round cell tumor group, in particular neuroblastoma (see Sect. 12.1.10.2.2, "Wilms Tumor," p. 743) and malignant lymphoma should be considered in the pediatric patient group.
- Thymomas with intense admixture of lymphocytes to the epithelioid cell component may mimic lymphoma. Various adjuvant techniques are available on FNAB material to establish monoclonality of a malignant lymphoid cell population (see Sect. 3.2.3.2, "Malignant Lymphoma," p. 267, and Sect. 15.1.4, "Ancillary Techniques," p. 910):
  - Lymphocyte-rich thymoma that contains numerous transformed lymphoid elements of the B phenotype (benign lymphoblasts) may be mistaken for large-cell B-type non-Hodgkin lymphoma infiltrating the thymus gland [25, 115].
  - A small-cell lymphoid infiltrate may simulate lymphoblastic non-Hodgkin lymphoma, which is a disease that affects predominantly children and young adults. The vast majority of these tumors are of T-cell lineage.
- Thymomas associated with a significant spindle cell component have a wide variety of benign and malignant counterparts [94]:
  - Granulomatous inflammation and cellular fibrous tissue. Monocytes, histiocytes, and macrophages express CD68 +.
  - Granulomatosis and cellular fibrous tissue may also occur as a reactive component or genuine proportion of epithelial and lymphoid neoplasias, e.g., Hodgkin lymphoma.
  - Benign and malignant mesenchymal tumors such as sarcoma and nerve sheath tumors (cell line-typical mesenchymal immunmarkers).
  - Spindle cell squamous carcinoma.
  - Spindle cell melanoma, nonpigmented [8] (melanoma-typical markers +).
  - Spindle cell carcinoid (neuroendocrine markers +).

**Caution**

- Primaries in remote organs metastasizing to the thymic gland and mediastinum must be unambiguously excluded before assessing a diagnosis of primary thymic carcinoma by cytology.
- Remember germinoma (seminoma/dysgerminoma) as another potential mediastinal tumor entity with a biphasic appearance exhibiting epithelioid cells and lymphoid cells !
- Thymoma and thymic carcinoid [72] exhibit negative immunoreactivity for TTF-1.
- Thymomas presenting as a palpable tumor of the neck are easily mistaken as a primary disorder of the thyroid [54]. Immunocytochemically, TTF-1 [77] and thyroglobulin should reliably differentiate thymic tumors from benign and malignant thyroid tissue.

### 2.4.3.5 Thymic Carcinoid (Figs. 2.102 and 2.103)

- Thymic carcinoid is a rare tumor accounting for about 2% of all neoplasms of this organ. Carcinoid tumors are of neural crest origin but commonly develop in endodermal organs including the thymus gland, lung, and gastrointestinal tract.

- The peak incidence of thymic carcinoids is in the fifth decade and is more frequent in male patients. Endocrine disorders are observed in about half of the patients afflicted with thymic carcinoid [50].
- In contrast to thymomas, thymic carcinoids do not present with an explicit encapsulation, they are frequently invasive to adjacent structures, and show frequent metastases to regional lymph nodes and distant organs. Thymic carcinoid has an overall poor prognosis [65]. Focal hemorrhage and necrosis, but not cystic degeneration, may be present.
- Thymic carcinoid is very rarely encountered in FNABs of the mediastinum.

**Microscopic Features** [65, 83, 109]

- Hallmarks: Cellular smears are composed of cell clusters and numerous single tumor cells. Cells have round to oval nuclei, finely granular chromatin, and a scant granular cytoplasm. Dispersed large-tumor cells are usually present showing abundant granular cytoplasm and macronucleoli. Occasionally, spindle-shaped tumor cells can be found.
- Predominance of spindle cells has been reported [47].
- Numerous small pyknotic tumor cells may mimic lymphocytes.

**Differential Diagnosis and Immunocytochemistry**

- Thymoma has been reported as the most frequent misdiagnosis in the presence of a carcinoid tumor of the thymus (Fig. 2.102). Cells of carcinoid tumors may share morphologic features with epithelioid cells of thymomas, but the frequent occurrence of pyknotic cells in carcinoids mimicking lymphocytes seems to be the main reason for misdiagnosis between carcinoid tumor and thymoma [83]. Immunocytochemical reactivity for neuroendocrine markers (synaptophysin, chromogranin, CD56) should help in the correct assignment of a thymic carcinoid tumor [101]; however, positivity for neuroendocrine markers is occasionally achieved in thymic carcinomas as well. Further immunostainings that may be helpful to distinguish thymoma from carcinoid tumor are p63 and CK5/6 (positive on thymoma and thymic carcinoma, negative on carcinoids) and CD5. CD5 yields a positive reaction in half of the thymic carcinomas and is suitable in distinguishing poorly differentiated carcinoids [83].
- Malignant lymphoma usually demonstrates a pattern composed of noncohesive cells with typical morphologic features. An immunocytochemical panel with antibodies directed against epithelial, leukocytic/lymphoid, and neuroendocrine markers provides a correct diagnosis.
- Adenocarcinomas represent characteristic cytomorphologic features including single cells, compact spherical and acinar clusters, large eccentric nuclei, prominent nucleoli, thinly dispersed chromatin, and usually a low N/C ratio. Certain monomorphic adenocarcinomas of the granular cell type may provoke differential diagnosis problems, such as metastasis of renal cell carcinoma and thyroid carcinoma (among others).
- Small-cell carcinomas show characteristic cell clustering and cellular features on single cells (see Sect. 2.2.2.6, "Small-Cell Carcinoma," p. 144). However, the differential diagnosis between thymic carcinoid tumor and metastatic small-cell carcinoma can be difficult in individual cases from cytology alone (Fig. 2.103). Immunocytochemistry cannot distinguish between thymic carcinoid tumor and small-cell carcinoma of the thymus or between small-cell neuroendocrine carcinoma of the thymus and small cell carcinoma secondary to the mediastinum.
- Spindle cell tumors must be differentiated from thymic carcinoid with a pronounced spindle cell pattern (see also Sect. 2.4.3.4.4 "Additional Analyses," p. 211, and Sect. 2.4.4, "Neurogenic and Mesenchymal Tumors," p. 216).

### 2.4.3.6 Germ Cell Tumors [17, 112]

**General Comments**

- The mediastinum is the most common site of extragonadal germ cell tumors in adults: approximately 15% of all primary mediastinal tumors in adults are germ cell tumors.
- Twenty-five percent of all primary mediastinal tumors in the pediatric age group are germ cell tumors [64].
- Most germ cell tumors arise in the anterior mediastinum near the thymus gland.
- Most patients with mediastinal germ cell tumors are male and in the third decade of their life, except for mature teratomas (benign germ cell tumors) whose male:female ratio is about equal.
- The majority of all mediastinal germ cell tumors are benign teratomas. The prognosis for malignant nonseminomatous germ cell tumors is poor.
- Morphologically, primary mediastinal germ cell tumors are practically identical to their counterparts in the male and female gonads.

**Caution**

Mediastinal metastases from a primary germ cell tumor of the gonads must always be excluded by clinical and radiographic examination of the testes/ovaries and retroperitoneal lymph nodes, and the patient's history.

#### 2.4.3.6.1 Teratoma

- Mature teratomas are predominantly cystic (Fig. 2.91). They are composed of tissue elements usually derived from all three germ layers.
- Immature teratomas occur extremely rarely in the mediastinum and are particularly characterized by the presence of immature squamous cells and mesenchymal cells.

- Fine-needle aspiration usually contains cells of ectodermal origin (squamous cells, sebaceous cells, squamous epithelium detritus). Calcification and a granulomatous response to keratin including foreign body giant cells are common.

#### 2.4.3.6.2 Seminoma (Germinoma)

[3, 15, 45, 58] (Fig. 12.38)

Seminoma in the mediastinum occurs nearly exclusively in men and is the most common malignant germ cell tumor at this site. Seminomas have a better prognosis compared to other malignant germ cell tumors of the mediastinum because they are highly sensitive to radiation therapy.

**Microscopic Features**

- Highly cellular smears are composed of a dual cell population. Large monomorphic tumor cells are obviously malignant with minor evidence of intercellular cohesion. They are interspersed with mature and reactive lymphocytes including mature plasma cells.
- Malignant cells show large vesicular, hyperchromatic nuclei with membrane irregularities and one or multiple prominent nucleoli.
- The cytoplasm is usually scant, comprising a well-defined border and intermittent double-contour and thickenings.
- Naked nuclei and necrosis are rather frequent. The latter effects a so-called tigroid background.
- The granulomatous tissue reaction including histiocytic multinucleated giant cells may be present.

**Caution**

Syncytiotrophoblast-like multinucleated giant cells of histiocytic origin should not mislead the cytopathologist to a diagnosis of choriocarcinoma. Syncytiotrophoblasts are immunocytochemically positive for β-human chorionic gonadotropin and giant cells of histiocytic origin exhibit CD68 antigen.

**Differential Diagnosis and Immunocytochemistry**

[15, 28, 45]

- Placental alkaline phosphatase (PLAP) is a reliable immunomarker for germinoma on cytological preparations (Fig. 12.38D).
- The dual cell component of seminoma may give the impression of thymoma as well as of undifferentiated large-cell carcinomas metastatic to mediastinal lymph nodes. Thymoma cells generally exhibit a completely different morphology compared with seminoma cells, and their lymphoid component lacks plasma cells.
  Immunocytochemistry: thymoma as well as metastatic carcinoma cells show positivity for cytokeratins, but antibodies against cytokeratins rarely stain seminomatous cells positive. PLAP is definitely not expressed in neoplastic thymoma and carcinoma cells.
- Non-Hodgkin lymphoma of the large-cell type is a major challenge in the differential diagnosis with seminoma, particularly in cases of lymphoma with a tendency to cellular cohesion. Large-cell lymphoma with a reactive hyperplastic population of T-lineage lymphocytes should not exhibit plasma cells.
  In cytomorphologically equivocal cases, immunocytochemistry is of major help: large-cell lymphoma cells are usually positive for CD45 and in most cases for B-cell markers. Positive immunoreaction for leukocyte/lymphocytic markers is definitely absent in germinomatous cells.

#### 2.4.3.6.3 Embryonal Carcinoma, Yolk Sac Tumor, Choriocarcinoma [2, 15, 57, 58]

These variants of germ cell tumors rarely arise in the mediastinum. Microscopic and immunocytochemical characteristics of these entities are provided in Sect. 12.3.7, "Germ Cell Tumors," p. 784, and Table 12.3.2, respectively (Figs. 2.104, 12.39, 12.40).

### 2.4.3.7. Benign and Malignant Lymphoid Disorders in Mediastinal Lymph Nodes and Thymus (see also Chap. 15, p. 905)

#### 2.4.3.7.1 Angiofollicular Hyperplasia (Castleman Disease) (Fig. 15.38)

- Angiofollicular hyperplasia is a benign lesion that may develop at a single site (in particular in the mediastinum) or throughout the body.
- The lesion in the mediastinum usually presents as a large single mass and may resemble thymoma to a certain extent.
- Castleman disease occurs in lymphoid organs and involves hyperproliferation of B lymphocytes including plasma cells, vessels, and endothelial cells [12, 40, 63].
- The hyaline vascular variant of this lymphoid hyperplastic process is much more common compared to the plasma cell variant. The latter accounts for only about 10% of all cases.

**Microscopic Features and Differential Diagnosis**

- A polymorphous lymphoid population is encountered: predominantly small mature lymphocytes (B and T phenotype) as well as eosinophils, follicle center cells (including immunoblasts), and plasma cells.
- Furthermore, large atypical histiocytoid cells (follicular dendritic cells) are encountered, showing ill-defined cytoplasm and enlarged nuclei with a distinctly irregular outline or crumpled appearance, granular to coarse chromatin, and nucleoli [49, 52, 100]. These cells may be clustered and concentrically arranged, resembling Hassall thymoma corpuscles. Occurring in an isolated

manner, they may cause confusion with Hodgkin or Reed-Sternberg cells. Immunocytochemical stains demonstrate no positivity for cytokeratins.

- The plasma cell type of angiofollicular hyperplasia may be characterized by sheets of plasma cells and many follicle center cells originating from large germinal centers. Plasmacytoma has to be excluded in this morphologic setting.

#### 2.4.3.7.2 Hodgkin Lymphoma

[9, 28] (Figs. 2.105 and 2.106)

Hodgkin lymphoma may arise in the thymus or in mediastinal lymph nodes. The lesion most frequently affects young female patients.

**Histologic and Cytologic Features**

Hodgkin lymphoma may exhibit particular histological features characteristic for Hodgkin lymphoma at this site [50]:

1. Cystic changes occasionally occur, and in rare instances cysts predominate.
2. Areas of the lymphoid tumor tissue may be interspersed with hyperplastic remnants of the thymus gland (squamous epithelial cells, ciliated epithelium, Hassall corpuscles).
3. Most cases of mediastinal Hodgkin lymphoma are of the nodular sclerosing subtype (Fig. 2.106).

Cytology

- Cytological specimens are frequently sparsely cellular due to tumor sclerosis.
- The lymphoid cell population is polymorphous. The vast majority of cells are small lymphocytes intermingled with atypical lymphoid elements comprising enlarged irregular nuclei (wrinkled and molded), hyperchromasia, pronounced nucleoli, and indistinct cytoplasm. These atypical lymphoid cells may be difficult to separate from true mononuclear Hodgkin cells.
- Reed-Sternberg cells establish a definite diagnosis for Hodgkin lymphoma. However, the cells may occur extremely rarely and need to be carefully searched for. Typical Reed-Sternberg cells are huge and present with two large, mirror-image nuclei that contain red-colored, comma-shaped nucleoli. The chromatin is slightly hyperchromatic, finely granular, densely packed, and evenly distributed throughout the whole nucleus.
- Plasma cells, eosinophils, and histiocytes commonly occur together with the lymphoid population.
- Epithelioid cell granulomatosis occasionally is marked.

**Differential Diagnosis and Immunocytochemistry**

- Hodgkin cells and Reed-Sternberg cells show pathognomonic immunopositivity for CD30, CD15, and PAX5.
- Malignant germ cell tumors and metastatic pleomorphic carcinoma are two neoplasms composed of huge tumor cells mimicking Hodgkin cells and Reed-Sternberg cells. Syncytiotrophoblasts from choriocarcinomatous components in germ cell tumors generally show multiple nuclei and are immunocytochemically positive for human chorionic gonadotropin. Carcinoma cells show positivity for cytokeratins and epithelial antigens.

**Caution**

- Cyst fluid from cystic degenerating Hodgkin lymphomas is usually clear and contains a nonspecific cell population. Distinguishing them from other cystic lesions of the mediastinum is difficult.
- Reed-Sternberg cells may be rare in aspirates from mediastinal Hodgkin lymphoma, they have to be searched for carefully in all cytologic smears.
- Furthermore, an overall pattern corresponding to an inflammatory infiltrate may indicate Hodgkin disease; but the finding is definitely not diagnostic if the specific HRS cells are absent.
- Aspirates from a mediastinal mass showing only a granulomatous component including a loose infiltrate of mixed and polymorphous lymphoid cells should always raise suspicions of Hodgkin lymphoma and call for advanced investigations.

#### 2.4.3.7.3 Non-Hodgkin Lymphomas

Lymphoblastic Lymphoma (Fig. 15.43)

Cells of this high-grade malignant lymphoma usually exhibit the T-cell immunophenotype. Lymphoblastic lymphoma is the most common malignant lymphoma in children and young adults (particularly in males) and concomitantly a rather common cause of mediastinal mass in this age group [95]. A majority of the tumors arises in the thymus. Acute T-cell leukemia may occur during the course of the disease.

**Microscopic Features**

- Cellular smears are composed of monotonous-appearing lymphoblasts. The tumor cells are about twice the size of small benign lymphocytes.
- Hallmarks: Nuclei usually show characteristic indentations and grooves and a granular and powdery chromatin. Small blasts have inconspicuous nucleoli, whereas medium-sized blasts show variably prominent nucleoli. The cytoplasm displays a small but distinct rim.
- The mitotic rate is high.
- Background necrosis and a focal starry-sky pattern may occasionally be pronounced.
- Epithelial thymic fragments including residual Hassall corpuscles may be encountered in fine-needle aspirates, especially in lymphomas infiltrating the thymus [115].

**Differential Diagnosis**

Lymphocyte-rich thymoma could be misdiagnosed as lymphoblastic lymphoma. This is a challenging differential diag-

nosis, particularly in cases where the tumor cells are intermingled with residual thymic epithelial components. But the typical appearance of the neoplastic lymphoblasts and the clinical features should provide enough evidence for a correct diagnosis.

### Large-Cell Non-Hodgkin Lymphoma

[89, 96] (Figs. 2.107 and 2.108)

Large-cell non-Hodgkin lymphoma of the mediastinum represents in most cases a distinct tumor entity arising from a native thymic B-cell population, unless mediastinal involvement is part of a systemic malignant lymphoid disorder. The primary mediastinal disorder occurs typically in a young adult patient group with a female preponderance [95] and suggests a more favorable course than that of diffuse large B-cell lymphoma [89].

**Microscopic Features** [36, 37, 93]

- The aspirates are usually highly cellular, composed of predominantly large atypical lymphocytes scattered throughout the smear; small cleaved atypical lymphocytes tend to be intermingled in a varying number.
- The nuclei are often cleaved and lobulated. Hyperlobulation may be pronounced.
- The chromatin is vesicular.
- The nucleoli are prominent and sporadically huge, occurring singly or multiply.
- The N/C ratio varies strongly within the same tumor. The cytoplasms often display basophilia using the May-Grünwald-Giemsa staining procedure and related staining methods.
- Fragments of sclerotic tissue and spindle mesenchymal cells are observed in cases associated with pronounced tumor sclerosis. Accordingly, the specimens tend to paucity of cells.

**Differential Diagnosis and Immunocytochemistry** [28, 93, 115]

- Paucity of cells due to strong tumor sclerosis may:
  - lead to a false-negative diagnosis.
  - suspect spindle cell neoplasia such as soft tissue sarcoma, nerve sheath tumors, spindle-cell thymoma, spindle-cell melanoma. All these tumor entities express tissue-typical markers but not CD45.
  - lead to erroneous interpretation of individual large lymphoid tumor cells as (1) large epithelial cells from a thymoma (immunocytochemistry of neoplastic thymic epithelium: see Sect. 2.4.3.4.4, p. 211), (2) undifferentiated carcinoma cells (CKs **+**), or (3) Hodgkin/Reed-Sternberg cells (CD15, CD30, and PAX5 **+**).
- The immunoblastic-like variant of large-cell lymphoma can appear quite similar to Hodgkin lymphoma. However, the background of small lymphocytes is different when comparing the two entities. Hodgkin lymphoma yields much fewer large tumor cells on FNAB samples compared to large cell non-Hodgkin lymphoma.
- A pseudo-dual cell pattern composed of large and small malignant lymphoma cells may be misinterpreted as germinoma. However, the morphological features of small lymphoid cells and immunocytochemical reactivities are completely different between the two tumor entities: germinoma cells exhibit PLAP, large lymphoid tumor cells are positive for CD45.
- Cohesive cell grouping in specimens of non-Hodgkin lymphoma may be confused with thymic carcinoma or metastatic carcinoma (Fig. 2.107).
- Residual thymic epithelial tissue enmeshed in a malignant lymphoid cell population can lead to a false diagnosis of thymoma.
- Immunocytochemical and flow cytometric immunophenotyping have been shown to be helpful as an ancillary investigation supporting the diagnosis of malignant lymphoma. Cytogenetic studies are mandatory when morphologic and immunophenotyping results are not conclusive.

**Caution**

Cytomorphology and immunophenotyping are complemental investigations in order to distinguish between reactive lymphoid lesions and malignant lymphomas of the mediastinum. But the limitations of these two basic tests should always be remembered regarding:

- FNAB samples with limited cellularity.
- Partial tumor infiltration of a lymph node or of an organ with an important benign lymphoid proportion.
- Hodgkin lymphoma comprising a strong reactive lymphoid background together with a poor specific tumor cell fraction.
- Malignant lymphomas of the T-cell phenotype.

## 2.4.4 Neurogenic Tumors and Mesenchymal Tumors

- *Neurogenic tumors* are the most common neoplasias arising in the posterior mediastinum. Nerve sheath tumors and paragangliomas are more frequent in the adult patient group, whereas tumors of the sympathetic nervous system are frequently encountered in children.
- Any *mesenchymal tumor* may arise in the mediastinal soft tissue (Fig. 2.109). Only a few cases are on record concerning cytological investigation using fine needle aspirates. Benign mesenchymal lesions comprise, among others, lipomas, hemangiomas, and lymphangiomas [16]. Primary sarcomas are rare; however, a few case reports on FNAB of liposarcoma are available in the literature [28, 59, 73, 94].

- A variety of information on diagnosis, differential diagnoses, and ancillary studies of the varied spindle cell lesions in FNAB samples are given in comprehensive publications by Geisinger [28], and Slagel and coauthors [94].

#### 2.4.4.1 Tumors of the Peripheral Nervous System (Figs. 17.14–17.17)

The tumor group includes neurofibroma as well as benign and malignant schwannoma. The tumors are characterized by spindle-shaped cells; hence, the differential diagnosis includes a wide variety of benign and neoplastic conditions known to occur as primary or secondary tumors in the mediastinum. The morphologic features and immunocytochemical markers for schwannomas are reported in Sects. 12.3.4.3, "Schwannoma," p. 781, and 12.3.5.1.3, "Malignant Nerve Sheath Tumor," p. 783, respectively.

#### 2.4.4.2 Paraganglioma (Figs. 5.73 and 12.28)

Paraganglia are clusters of neuroendocrine cells associated with the sympathetic and parasympathetic nervous system. They are located throughout the body at various sites. Tumors arising from these cells are referred to as paraganglioma, pheochromocytoma, carotid body tumor, and others. Adrenal medulla is one of the major locations of this neoplasm. Cytomorphology and differential diagnosis challenges of pheochromocytoma (Fig. 12.28) and carotid body paraganglioma (Fig. 5.73) are highlighted in Sects. 12.2.3.3.1, p. 769, and 5.2.6.2, p. 467, of this book, and in a recent study by Varma and coauthors [104].

#### 2.4.4.3 Tumors of the Sympathetic Nervous System

The tumors are derived from non-chromaffin cells and include neuroblastoma, ganglioneuroblastoma (Fig. 2.110), and ganglioneuroma (Fig. 2.111). The three tumor entities together with differential diagnosis considerations are described in Sects. 12.2.3.3.2, p. 769, and 12.1.10.2.2, "Wilms Tumor," p. 743, respectively.

### 2.4.5 Miscellaneous Lesions

#### 2.4.5.1 Thymolipoma

Thymolipoma usually appears as a large anterior mediastinal mass with a predilection in adolescents and young adults. The histogenesis of this benign disorder is not yet clear; it may possibly be caused by a precedent thymic hyperplasia.

- FNAB specimens contain normal thymic cells, tissue fragments of epithelial (including Hassall corpuscles) and lymphatic origin, and mature adipose tissue.

The lesions must be distinguished from true lipomatous tumors [86].

#### 2.4.5.2 Thyroid and Parathyroid Tissue (Fig. 2.94)

Thyroid and parathyroid tissue may be found in the superior/anterior mediastinum as a primary ectopic lesion, a lesion extending from the cervical area into the mediastinal space, or a metastatic neoplasm. Goiters [88], thyroid cysts, parathyroid cyst [75], and parathyroid neoplasms [69] are among the most frequently diagnosed disorders on FNAB samples.

### 2.4.6 Metastases to the Thymus and Mediastinum (Figs. 2.112–2.115)

The thymus gland, mediastinal lymph nodes, and the mediastinal space can be affected by metastatic cancer. Metastases are the most common intrathoracic/extrapulmonary lesions diagnosed by FNAB. Tumor dissemination may occur by lymphogenic and hematogenic spreading, or by direct extension from adjacent structures and organs. Thymic and mediastinal metastasis is an indicator for generalized malignant disease. The most common source of mediastinal metastases is the lung, particularly small-cell carcinoma [28]. Breast, thyroid, head and neck tumors, malignant melanoma, and others are additional sources.

**Caution**

Trivial solid ectopic epithelial tissue should not be misinterpreted as metastasis in FNAB samples.

## 2.4.7 Further Reading


1. Adler OB, Rosenberger A, Peleg H. Fine-needle aspiration biopsy of mediastinal masses: evaluation of 136 experiences. AJR 1983;140:893-896.
2. Afroz N, Khan N, Chana RS. Cytodiagnosis of yolk sac tumor. Indian J Pediatr 2004;71:939-942.
3. Akhtar M, Ali MA, Hug M, Bakry M. Fine-needle aspiration biopsy of seminoma and dysgerminoma: cytologic, histologic, and electron microscopic correlations. Diagn Cytopathol 1990;6:99-105.
4. Ali SZ, Erozan YS. Thymoma. Cytopathologic features and differential diagnosis on fine needle aspiration. Acta Cytol 1998;42:845-854.
5. Alsharif M, Andrade RS, Stelow EB, et al. Endobronchial ultrasound-guided (EBUS) transbronchial fine needle aspiration (FNA): The University of Minnesota initial experience. Cancer(Cancer Cytopathol) 2007; Suppl 111:408-409.
6. Assaad MW, Pantanowitz L, Otis CN. Diagnostic accuracy of image-guided percutaneous fine needle aspiration biopsy of the mediastinum. Diagn Cytopathol 2007;35:705-709.
7. Baba M, Nomoto Y, Iyoda A, et al. Cytomorphologic features characteristic of tumor stages of thymomas. Oncol Rep 2001;8:1139-1143.
8. Bavi P, Shet T, Gujral S. Malignant melanoma of mediastinum misdiagnosed as a spindle cell thymoma in a fine needle aspirate: a case report. Acta Cytol 2005;49:424-426.
9. Bergh NP, Gatzinsky P, Larsson S, et al. Tumors of the thymus and thymic region: II Clinicopathological studies on Hodgkin's disease of the thymus. Ann Thorac Surg 1978;25:99-106.
10. Binek J, Abraham D, Borovicka J , Spieler P, et al. Endosonographic guided fine needle aspiration (EUS-FNA) in mediastinal and abdominal lesions: accuracy and patients tolerance. Gut 2004;53 (Suppl VI):A42.
11. Boecking A, Klose KC, Kyll HJ, Hauptmann S. Cytologic versus histologic evaluation of needle biopsy of the lung, hilum and mediastinum: sensitivity, specificity and typing accuracy. Acta Cytol 1995;39:463-471.
12. Castleman B, Iverson L, Menendez VP. Localized mediastinal lymph node hyperplasia resembling thymoma. Cancer 1956;9: 822–30.
13. Catalano MF, Rosenblatt ML, Chak A, et al. Endoscopic ultrasound-guided fine needle aspiration in the diagnosis of mediastinal masses of unknown origin. Am J Gastroenterol 2002;97:2559-2565.
14. Chhieng DC, Rose D, Ludwig ME, Zakowski MF. Cytology of thymomas: emphasis on morphology and correlation with histologic subtypes. Cancer 2000;25:90:24-32.
15. Chhieng DC, Lin O, Moran CA, et al. Fine-needle aspiration biopsy of nonteratomatous germ cell tumors of the mediastinum. Am J Clin Pathol 2002;118:418-424.
16. Coffing B, Gutmann EJ. Lymphangioma of the posterior mediastinum in an adult: diagnosis via cytopathologist-assisted fine-needle aspiration biopsy with cell block. Diagn Cytopathol 2005;33:412-415.
17. Dehner LP. Germ cell tumors of the mediastinum. Semin Diagn Pathol 1990;7:266-284.
18. Dorfman DM, Shahsafaei A, Chan JK. Thymic carcinomas, but not thymomas and carcinomas of other sites, show CD5 immunoreactivity. Am J Surg Pathol 1997;21:936-940.
19. Eloubeidi MA, Cohn M, Cerfolio RJ, et al. Endoscopic ultrasound-guided fine-needle aspiration in the diagnosis of foregut duplication cysts: the value of demonstrating detached ciliary tufts in cyst fluid. Cancer 2004;102:253-258.
20. Emery SC, Savides TJ, Behling CA. Utility of immediate evaluation of endoscopic ultrasound-guided transesophageal fine needle aspiration of mediastinal lymph nodes. Acta Cytol 2004;48:630-634.
21. Fernandez-Esparrach G, Gines A, Belda J, et al. Transesophageal ultrasound-guided fine needle aspiration improves mediastinal staging in patients with non-small cell lung cancer and normal mediastinum on computed tomography. Lung Cancer 2006;54:35-40.
22. Finley JL, Silverman JF, Strausbauch PH, et al. Malignant thymic neoplasms: diagnosis by fine-needle aspiration biopsy with histologic, immunocytochemical, and ultrastructural confirmation. Diagn Cytopathol 1986;2:118-125.
23. Flannery MT, Espino M, Altus P, et al. Hodgkin's disease masquerading as sclerosing mediastinitis. South Med J 1994;87:921-923.
24. Flieder DB, Suster S, Moran CA. Idiopathic fibroinflammatory (fibrosing/sclerosing) lesions of the mediastinum: a study of 30 cases with emphasis on morphologic heterogeneity. Mod Pathol 1999;12:257-264.
25. Friedman HD, Hutchison RE, Kohman LJ, Powers CN. Thymoma mimicking lymphoblastic lymphoma: a pitfall in fine-needle aspiration biopsy interpretation. Diagn Cytopathol 1996;14:165-169.
26. Fujii Y, Okumura M, Yamamoto S. Flow cytometric study of lymphocytes associated with thymoma and other thymic tumors. J Surg Res 1999;82:312-318.
27. Geisinger KR. Differential diagnostic considerations and potential pitfalls in fine-needle aspiration biopsies of the mediastinum. Diagn Cytopathol 1995;13:436-442.
28. Gatzimos KR, Moriarty AT, Pingleton JM, Mc Closkey DW. Diagnosis of metastatic thymoma using flow cytometry. Pathobiology 1992;60:168-172.
29. Goel D, Prayaga AK, Sundaram Challa, et al. Utility of fine needle aspiration cytology in mediastinal lesions. A clinicopathologic study of 161 cases from a single institution. Acta Cytol 2008;52:404-411.
30. Goldstein G, Abbot A, Mackay IR. An electron microscopic study of the human thymus: Normal appearances and findings in myasthenia gravis and systemic lupus erythematosus. J Pathol 1968;95:211-215.
31. Gulati M, Venkataramu NK, Gupta S, et al. Ultrasound guided fine needle aspiration biopsy in mediastinal tuberculosis. Int J Tuberc Lung Dis 2000;4:1164-1168.
32. Hall DA, Pu RT, Pang Y. Diagnosis of foregut and tailgut cysts by endosonographically guided fine-needle aspiration. Diagn Cytopathol 2007;35:43-46.
33. Hartmann CA, Roth C, Minck C, Niedobitek G. Thymic carcinoma. Report of five cases and review of the literature. J Cancer Res Clin Oncol 1990;116:69-82.
34. Herman SJ, Holub RV, Weisbrod GL, et al. Anterior mediastinal masses: Utility of transthoracic needle biopsy. Radiology 1991;180:167-170.
35. Herth FJ, Eberhardt R, Vilmann P, et al. Real-time endobronchial ultrasound guided transbronchial needle aspiration for sampling mediastinal lymph nodes. Thorax 2006;61:795-798.
36. Hoda RS, Picklesimer L, Green KM, Self S. Fine-needle aspiration of a primary mediastinal large B-cell lymphoma: a case report with cytologic, histologic, and flow cytometric considerations. Diagn Cytopathol 2005;32:370-373.
37. Hughes JH, Katz RL, Fonseca GA, Cabanillas FF. Fine-needle aspiration cytology of mediastinal non-Hodgkin's nonlymphoblastic lymphoma. Cancer 1998;84:26-35.
38. Inoue M, Starostik P, Zettl A, et al. Correlating genetic aberrations with World Health Organization-defined histology and stage across the spectrum of thymomas. Cancer Res 2003;63:3708-3715.
39. Johnson S, Eng TY, Giaccone G, Thomas CR Jr. Thymoma: update for the new millennium. Oncologist 2001;6:239-246.
40. Kardziev B, Hotzel B, Jachmann M. The angiofollicular lymph node hyperplasia Castleman – casuistic and review of the literature. Pneumologie 2006;60:229-234.
41. Kramer H, Sanders J, Post WJ, et al. Analysis of cytological specimens from mediastinal lesions obtained by endoscopic ultrasound-guided fine-needle aspiration. Cancer(Cancer Cytopathol) 2006;108:206-211.

42. Kramer H, van Putten JW, Post WJ, et al. Oesophageal endoscopic ultrasound with fine needle aspiration improves and simplifies the staging of lung cancer. Thorax 2004;59:596-601.
43. Kuhlman JE, Fishman EK, Wang KP, et al. Mediastinal cysts: diagnosis by CT and needle aspiration. Am J Roentgenol 1988;150:75-78.
44. Kumar PV, Ashraf MJ, Safaei A, et al. Fine needle aspiration diagnosis of bronchogenic cysts. Acta Cytol 2001;45:656-658.
45. Kwon MS. Aspiration cytology of mediastinal seminoma: report of a case with emphasis on the diagnostic role of aspiration cytology, cell block and immunocytochemistry. Acta Cytol 2005;49:669-672.
46. Lara PN Jr. Malignant thymoma: current status and future directions. Cancer Treat Rev 2000;26:127-131.
47. Levine GD, Rosai J. A spindle cell variant of thymic carcinoid. A clinical, histologic and fine structural study with emphasis on its distinction from spindle cell thymoma. Arch Pathol 1976;100:293-300.
48. Lewis JE, Wick MR, Scheithauer BW, et al. Thymoma: A clinicopathologic review. Cancer 1987;60:2727-2743.
49. Mallik MK, Kapila K, Das DK, et al. Cytomorphology of hyaline-vascular Castleman's disease: a diagnostic challenge. Cytopathology 2007;18:168-174.
50. Marchevsky AM, Kaneko M. Surgical Pathology of the Mediastinum. Raven Press, New York 1984.
51. Matsuura B, Tokunaga H, Miyake T, et al. A case of malignant thymoma mimicking thyroid carcinoma: a pitfall in fine-needle aspiration. Endocr J 2004;51:237-241.
52. Meyer L, Gibbons D, Ashfaq R, et al. Fine-needle aspiration findings in Castleman's disease. Diagn Cytopathol 1999;21:57-60.
53. Micames CG, McCrory DC, Pavey DA, et al. Endoscopic ultrasound-guided fine-needle aspiration for non-small cell lung cancer staging: A systematic review and metaanalysis. Chest 2007;131:539-548.
54. Milde P, Sidawy MK. Thymoma presenting as a palpable thyroid nodule: a pitfall in fine needle aspiration (FNA) of the neck. Cytopathology 1999;10:415-419.
55. Mole TM, Glover J, Sheppard MN. Sclerosing mediastinitis: a report on 18 cases. Thorax 1995;50:280-283.
56. Moran CA, Suster S. Thymic carcinoma: current concepts and histologic features. Hematol Oncol Clin North Am 2008;22:393-407.
57. Moran CA, Suster S, Koss MN. Primary germ cell tumors of the mediastinum: III. Yolk sac tumor, embryonal carcinoma, choriocarcinoma, and combined nonteratomatous germ cell tumors of the mediastinum – a clinicopathologic and immunohistochemical study of 64 cases. Cancer 1997;80:699-707.
58. Motoyama T, Yamamoto O, Iwamoto H, Watanabe H. Fine needle aspiration cytology of primary mediastinal germ cell tumors. Acta Cytol 1995;39:725-732.
59. Munjal K, Pancholi V, Rege J, et al. Fine needle aspiration cytology in mediastinal myxoid liposarcoma: a case report. Acta Cytol 2007;51:456-458.
60. Myers PO, Kritikos N, Bongiovanni M, et al. Primary intrapulmonary thymoma: a systematic review. Eur J Surg Oncol 2007;33:1137-1141.
61. Nakagawa K, Matsuno Y, Kunitoh H, et al. Immunohistochemical KIT (CD117) expression in thymic epithelial tumors. Chest 2005;128:140-144.
62. Nakajima J, Takamoto S, Oka T, et al. Flow cytometric analysis of lymphoid cells in thymic epithelial neoplasms. Eur J Cardiothorac Surg 2000;18:287-292.
63. Newlon JL, Couch M, Brennan J. Castleman's disease: three case reports and a review of the literature. Ear Nose Throat J 2007;86:414-418.
64. Nichols CR. Mediastinal germ cell tumors: Clinical features and biological correlates. Chest 1991;99:472-479.
65. Nichols GL Jr., Hopkins III MB, Geisinger KR. Thymic carcinoid. Report of a case with diagnosis by fine needle aspiration biopsy. Acta Cytol 1997;41:1839-1844.
66. Nonaka D, Henley JD, Chiriboga L, Yee H. Diagnostic utility of thymic epithelial markers CD205 (DEC205) and Foxn1 in thymic epithelial neoplasms. Am J Surg Pathol 2007;31:1038-1044.
67. Oertel YC. Thymoma mimicking thyroid papillary carcinoma: another pitfall in fine-needle aspiration. Diagn Cytopathol 1997;17:61-63.
68. Ogita S, Robbins DH, Blum RH, Harris LJ. Endoscopic ultrasound fine-needle aspiration in the staging of non-small-cell lung cancer. Oncology(Williston Park) 2006;20:1419-1425.
69. Okazaki M, Matsumoto H, Tomioka H, et al. A case of mediastinal parathyroid adenoma diagnosed by transtracheal needle aspiration. Nihon Kyobu Shikkan Gakkai Zasshi 1994;32:1104-1108.
70. Okumura M, Fujii Y, Miyoshi S, et al. Three-color flow cytometric study on lymphocytes derived from thymic diseases. J Surg Res 2001;101:130-137.
71. Okumura M, Shiono H, Minami M, et al. Clinical and pathological aspects of thymic epithelial tumors. Gen Thorac Cardiovasc Surg 2008;56:10-16.
72. Oliveira AM, Tazelaar HD, Myers JL, et al. Thyroid transcription factor- distinguishes metastatic pulmonary from well-differentiated neuroendocrine tumors of other sites. Am J Surg Pathol 2001;25:815-819.
73. Pant I, Kaur G, Joshi SC, Khalid IA. Myxoid liposarcoma of the breast in a 25-year-old female as a diagnostic pitfall in fine needle aspiration cytology: report of a rare case. Diagn Cytopathol 2008;36:674-677.
74. Pantidou A, Kiziridou A, Antoniadis T, et al. Mediastinum thymoma diagnosed by FNA and ThinPrep technique: a case report. Diagn Cytopathol 2006;34:37-40.
75. Petri N, Holten I. Parathyroid cyst: Report of a case in the mediastinum. J Laryngol Otol 1990;104:56-57.
76. Pinto MM, Dovgan D, Kaye AD, Chinniah A. Fine needle aspiration for diagnosing a thymoma producing CA-125. A case report. Acta Cytol 1993;37:929-932.
77. Pomplun S, Wotherspoon AC, Shah G, et al. Immunohistochemical markers in the differentiation of thymic and pulmonary neoplasms. Histopathology 2002;40:152-158.
78. Ponder TB, Collins BT, Bee CS, et al. Diagnosis of cervical thymoma by fine needle aspiration biopsy with flow cytometry. A case report. Acta Cytol 2002;46:1129-1132.
79. Posligua L, Ylagan L. Fine-needle aspiration cytology of thymic basaloid carcinoma: case studies and review of the literature. Diagn Cytopathol 2006;34:358-366.
80. Powers CN, Silverman JF, Geisinger KR, Frable WJ. Fine-needle aspiration biopsy of the mediastinum. A multi-institutional analysis. Am J Clin Pathol 1996;105:168-173.
81. Priola AM, Priola SM, Cataldi A, et al. CT-guided percutaneous transthoracic biopsy in the diagnosis of mediastinal masses: evaluation of 73 procedures. Radiol Med(Torino) 2008;113:3-15.
82. Ragusa M, Avenia N, Fedeli C, et al. Acute mediastinitis: clinical features and review of a case load. Chir Ital 2003;55:519-524.
83. Renshaw AA, Haja JC, Neal MH, et al. Distinguishing carcinoid tumor of the mediastinum from thymoma. Correlating cytologic features and performance in the College of American Pathologists Interlaboratory Comparison Program in Nongynecologic Cytopathology. Arch Pathol Lab Med 2006;130:1612-1615.
84. Riazmontazer N, Bedayat C, Izadi B. Epithelial cytologic atypia in fine needle aspirate of an invasive thymoma. A case report. Acta Cytol 1992;36:387-390.
85. Rintoul RC, Skwarski KM, Murchison JT, et al. Endobronchial and endoscopic ultrasound-guided real-time fine-needle aspiration for mediastinal staging. Eur Respir J 2005;25:416-421.

86. Romero-Guadarrama MB, Duran-Padilla MA, Cruz-Ortiz H, et al. Diagnosis of thymolipoma with fine needle aspiration biopsy. Report of a case initially misdiagnosed as liposarcoma. Acta Cytol 2004;48:441-446.
87. Salyer DC, Salyer WR, Eggleston JC. Benign developmental cysts of the mediastinum. Arch Pathol Lab Med 1977;101:136-139.
88. Sanders LE, Rossi RL, Shahian DM, et al. Mediastinal goiters: The need for an aggressive approach. Arch Surg 1992;127:609-613.
89. Savage KJ. Primary mediastinal large B-cell lymphoma. Oncologist 2006;11:488-495.
90. Schowengerdt CG, Suyemoto R, Main FB. Granulomatous and fibrous mediastinitis: A review and analysis of 180 cases. J Thorac Cardiovasc Surg 1969;57:365-379.
91. Schwartz AR, Fishman EK, Wang KP. Diagnosis and treatment of a bronchogenic cyst using transbronchial needle aspiration. Thorax 1986;41:326-327.
92. Silverman JF, Finley JL, O'Brien KF, et al. Diagnostic accuracy and role of immediate interpretation of fine-needle aspiration biopsy specimens from various sites. Acta Cytol 1989;33:791-796.
93. Silverman JF, Raab SS, Park HK. Fine-needle aspiration cytology of primary large-cell lymphoma of the mediastinum: cytomorphologic findings with potential pitfalls in diagnosis. Diagn Cytopathol 1993;9:209-214.
94. Slagel DD, Powers CN, Melaragno MJ, et al. Spindle cell lesions of the mediastinum: Diagnosis by fine-needle aspiration biopsy. Diagn Cytopathol 1997;17:167-176.
95. Strickler JG, Kurtin PJ. Mediastinal lymphoma. Semin Diagn Pathol 1991;8:2-13.
96. Suster S. Primary large-cell lymphomas of the mediastinum. Semin Diagn Pathol 1999;16:51-64.
97. Tangthangtham A, Chonmaitri I, Subhannachart P, Tungsagunwattana S. Fine needle aspiration cytology of thymoma. J Med Assoc Thai 1999;82:1226-1229.
98. Tao LC, Pearson FG, Cooper JD, et al. Cytopathology of thymoma. Acta Cytol 1984;28:165-170.
99. Tateyama H, Eimoto T, Tada T, et al. Immunoreactivity of new CD5 antibody with normal epithelium and malignant tumors including thymic carcinoma. Am J Clin Pathol 1999;111:235-240.
100. Taylor GB, Smeeton IW. Cytologic demonstration of "dysplastic" follicular dendritic cells in a case of hyaline-vascular Castleman's disease. Diagn Cytopathol 2000;22:230-234.
101. Tiffet O, Nicholson AG, Ladas G, et al. A clinicopathologic study of 12 neuroendocrine tumors arising in the thymus. Chest 2004;125:2368-2369.
102. Travis WD, Brambilla E, Muller-Hermelink HK, Harris CC. (Eds.): World Health Organization Classification of Tumours. Pathology and Genetics of Tumours of the Lung, Pleura, Thymus and Heart. IARC Press: Lyon 2004.
103. van Beek FT, Maas KW, Timmer R, et al. Oesophageal endoscopic ultrasound with fine-needle aspiration biopsy in the staging of non-small-cell lung carcinoma; results from 43 patients. Ned Tijdschr Geneeskd 2006;150:144-150.
104. Varma K, Jain S, Mandal S. Cytomorphologic spectrum in paraganglioma. Acta Cytol 2008;52:549-556.
105. Vengrove MA, Schimmel M, Atkinson BF, et al. Invasive cervical thymoma masquerading as a solitary thyroid nodule: Report of a case studied by fine needle aspiration. Acta Cytol 1991;35:431-433.
106. Vilmann P, Puri R. The complete "medical" mediastinoscopy (EUS-FNA + EBUS-TBNA). Minerva Med 2007;98:331-338.
107. Wakely PE Jr. Fine needle aspiration in the diagnosis of thymic epithelial neoplasms. Hematol Oncol Clin North Am 2008;22:433-442.
108. Wallace WA, Monaghan HM, Salter DM, et al. Endobronchial ultrasound-guided fine-needle aspiration and liquid-based thin-layer cytology. J Clin Pathol 2007;60:388-391.
109. Wang DY, Kuo SH, Chang DB, et al. Fine needle aspiration cytology of thymic carcinoid tumor. Acta Cytol 1995;39:423-427.
110. Wang W, Li K, Qin W, et al. Ectopic pancreas in mediastinum: report of 2 cases and review of the literature. J Thorac Imaging 2007;22:256-258.
111. Wiersema MJ, Kochman ML, Cramer HM, Wiersema LM. Preoperative staging of non-small cell lung cancer: transesophageal US-guided fine-needle aspiration biopsy of mediastinal lymph nodes. Radiology 1994;190:239-242.
112. Yang CJ, Cheng MS, Chou SH, et al. Primary germ cell tumors of the mediastinum: 10 years of experience in a tertiary teaching hospital. Kaohsiung J Med Sci 2005;21:395-400.
113. Yasufuku K, Chiyo M, Koh E, et al. Endobronchial ultrasound-guided transbronchial needle aspiration for staging of lung cancer. Lung Cancer 2005;50:347-354.
114. Yokoyama T, Tanahashi M,Tateyama H, et al. Flow-cytometric diagnosis of thymoma using needle biopsy specimens. Surg Today 2003;33:163-168.
115. Yu GH, Salhany KE, Gokaslan ST, et al. Thymic epithelial cells as a diagnostic pitfall in the fine-needle aspiration diagnosis of primary mediastinal lymphoma. Diagn Cytopathol 1997;16:460-465.

**Fig. 2.88 Contaminant glandular cells from the needle track.**
A 73-year-old woman with a history of both Hodgkin lymphoma and breast carcinoma presented with enlarged mediastinal lymph nodes. Ultrasound-guided transtracheal FNAB of a mediastinal lymph node yielded single cells and clusters from a seromucinous tracheal gland (direct smear, Pap stain, high magnification). There were no malignant cells present.

Erroneous interpretation of benign but activated tracheal/bronchial gland cells may lead to a false diagnosis of carcinoma, such as the clear cell variant, oncocytic variant, or mucoepidermoid variant.

**Figs. 2.89 and 2.90 Sarcoidosis.**
Transtracheal FNAB in two patients presenting with enlarged mediastinal lymph nodes. The cytologic samples provided a diagnosis of a granulomatous inflammatory disorder consistent with sarcoidosis.

**Fig. 2.89A, B** (case #1) Sarcoidosis in a conventional smear. Cytologic appearance in a direct aspirate smear is demonstrated (Pap stain). **A** Lower magnification shows a large fragment of granulomatous tissue composed of histiocytes, epithelioid cells, and lymphocytes. Isolated epithelioid cells (bottom) and mucosal goblet cells (arrows) are encountered as well. **B** High magnification focuses on an asteroid body enclosed in a giant cell of the Langhans type.

**Fig. 2.90** (case #2) Sarcoidosis in a liquid-based specimen. Liquid-based preparation (ThinPrep) of a fine-needle aspirate exhibiting identical morphologic characteristics of an epithelioid granulomatous fragment compared to the conventional smear (Pap stain, higher magnification).

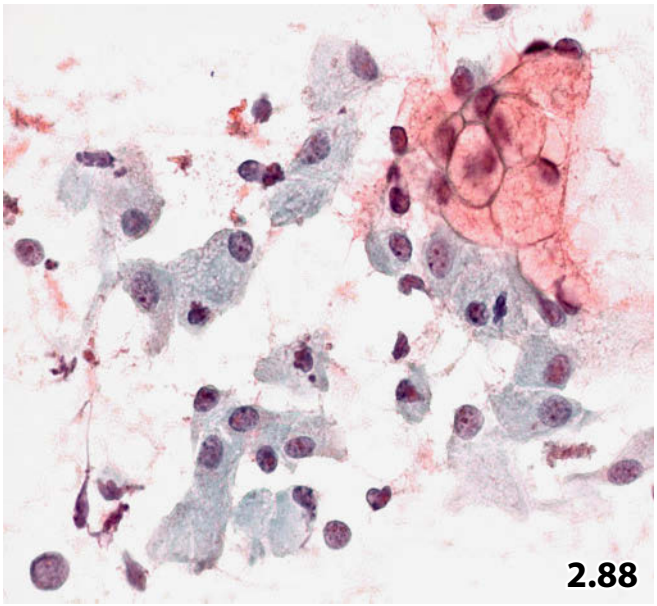
2.88

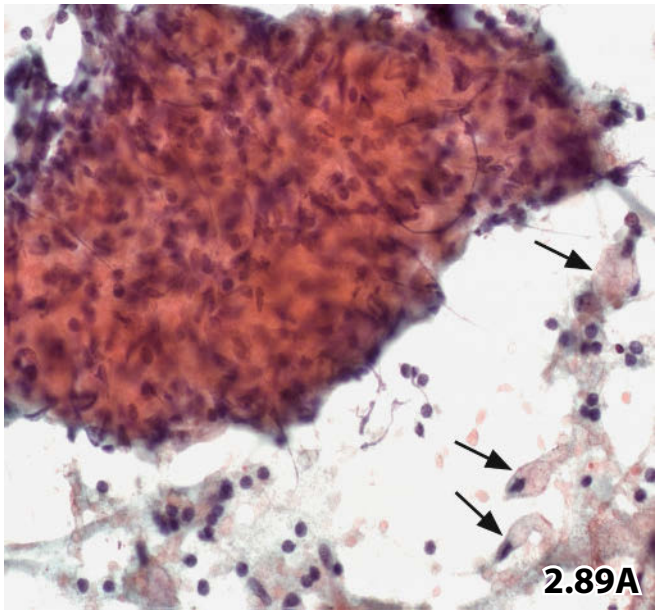
2.89A

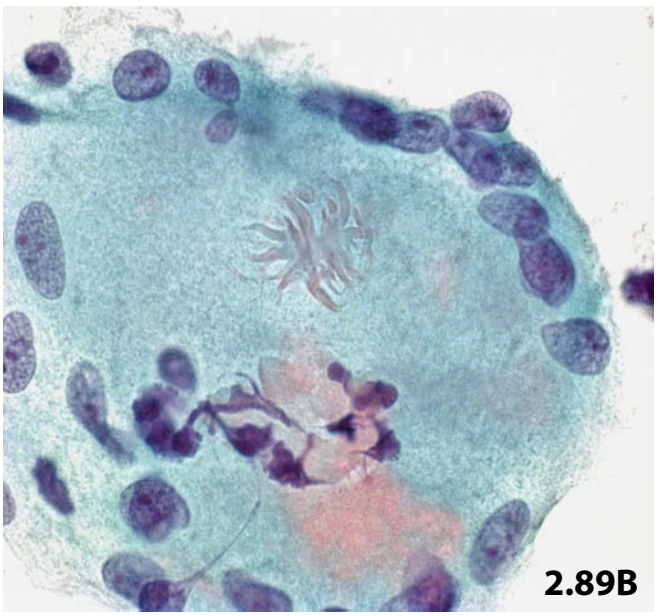
2.89B

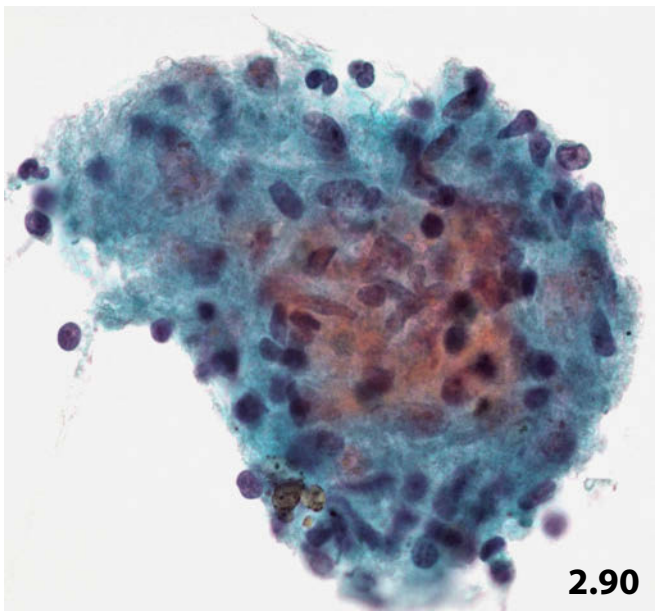
2.90

**Fig. 2.91 Cystic mature teratoma.**
CT-guided transthoracic FNAB of a mediastinal mass in an 11-year-old girl. The aspirated fluid originated from an inflammatory cystic lesion containing a few degenerating keratinized squamous cells (arrows) (direct sediment smear, Pap stain, low magnification).
*Cytology*: A descriptive diagnosis was made. A more specific diagnosis was not possible.
*Tissue diagnosis* (excision of the cystic mass): Cystic mature teratoma.

**Fig. 2.92 Bronchogenic cyst.**
Transbronchial FNAB of a tumorous lesion located in the posterior mediastinum of a 66-year-old man. Fine-needle aspirate reveals proteinaceous cystic background, well preserved and degenerating columnar cells of the respiratory type, detached ciliary tufts (incompletely focused; arrows), and a few degenerating squamous cells (direct sediment smear, Pap stain, lower magnification).
*Tentative cytologic diagnosis*: Bronchogenic cyst (confirmed by histology).

**Fig. 2.93 Cystic lesion of unclear origin.**
Transtracheal FNAB of a mediastinal cystic lesion in a 62-year-old man. Image studies provided no further information. Cyst fluid containing hemosiderophages (arrow) and benign lymphocytes sporadically exhibiting reactive changes (arrowhead). Absence of epithelial cells (direct sediment smear, Pap stain, higher magnification).
*Tentative cytologic diagnosis*: Cyst content from a nonspecific cystic lesion.
*Comment*: Lymphocytosis may suspect thoracic duct cyst, but reactive lymphocytes and macrophages do not necessarily support this diagnosis.
*Tissue diagnosis* (surgical excision of the mediastinal cyst): Benign epithelial cyst.

Caution: reactive lymphoid cells should not lead to an erroneous diagnosis of malignant lymphoma.

**Fig. 2.94 Cystic changes in a mediastinal goiter.**
Transthoracic FNAB of a tumor located in the anterior/superior mediastinum of a 48-year-old man. Low magnification shows the classical appearance of a cystic goiter: thyroidal parenchymatous tissue containing small follicles and a background with hemosiderophages (arrows) and colloid masses (direct smear, Pap stain).

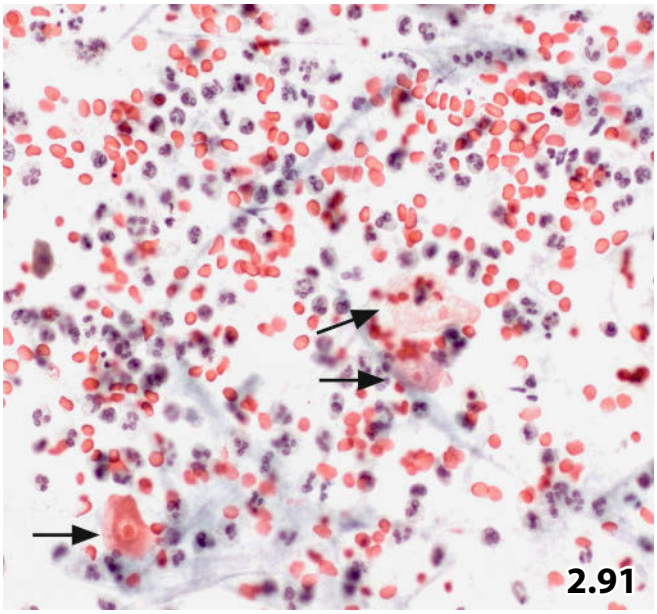
2.91

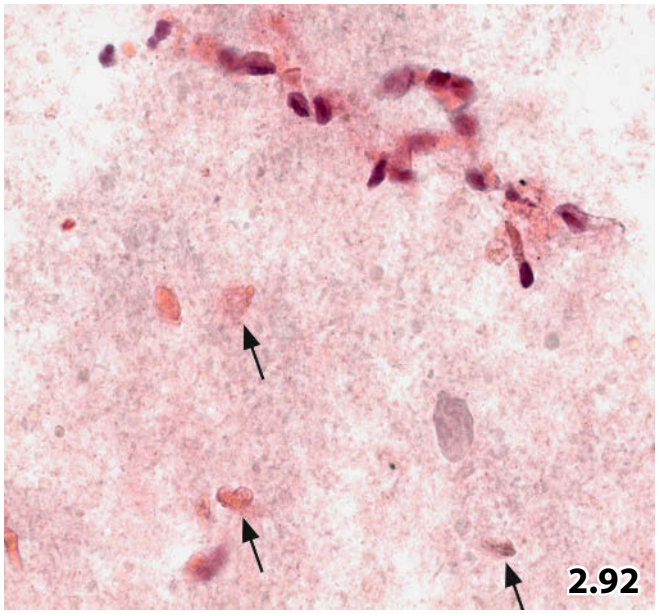
2.92

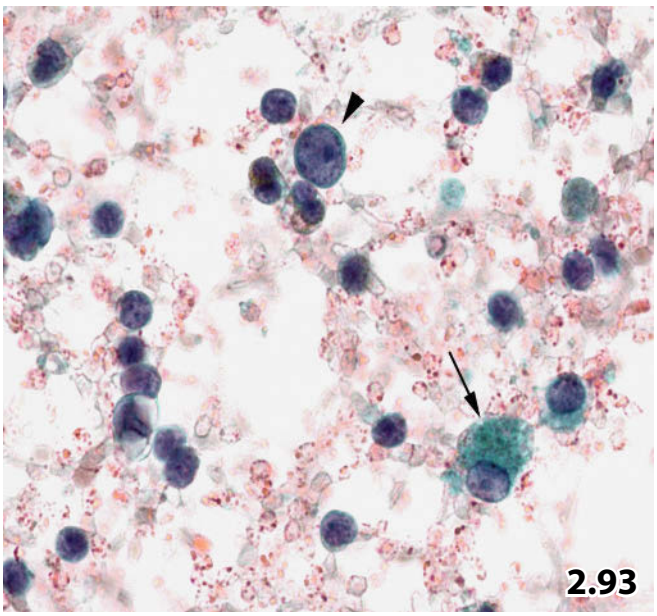
2.93

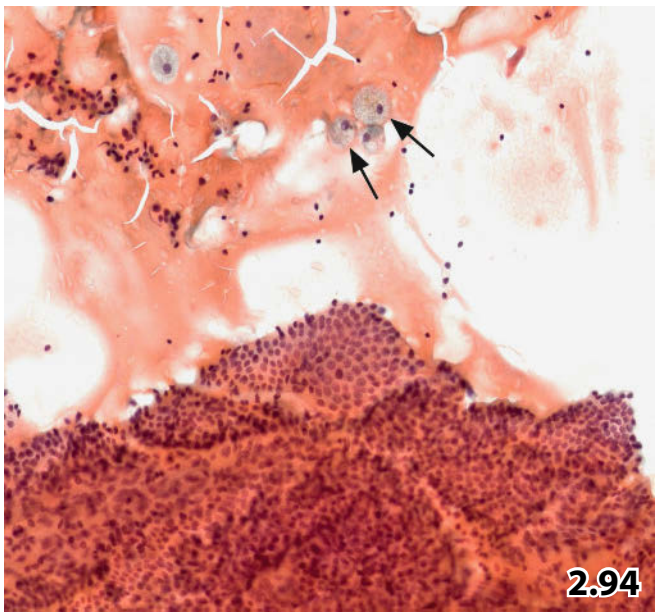
2.94

**Fig. 2.95A, B Normal thymic gland**
Scraping from the medullary zone of the cut surface of a normal thymic gland (Pap stain). **A** A keratin pearl, so-called Hassall corpuscle is embedded in a lymphoid cell population (high magnification). **B** Sparsely dispersed and grouped (not in view) epithelial thymocytes; note single thymocytes exhibiting prominent nucleoli and a foamy cytoplasm of variable size (arrows) (lower magnification).

**Fig. 2.96A, B Thymic hyperplasia.**
Image-guided (CT) FNAB of a retrosternal tumorous lesion in a 35-year-old man. Direct smears were stained with the Papanicolaou method.
*Initial cytologic diagnosis* in combination with clinical information was thymic hyperplasia.
*Tissue diagnosis* (subsequent surgical biopsy): Thymus hyperplasia.
**A** Numerous epithelial cells (arrows) intermingled with lymphocytes (high magnification).
**B** Epithelial thymocytes are highlighted by positive immunostaining for pancytokeratin (Lu-5). Negative-staining lymphocytes are seen in the background (note their faint nuclear pseudopositivity) (Pap-prestained specimen).

**Fig. 2.97 Thymic cyst.**
Transthoracic FNAB of a voluminous cystic lesion (10 cm) in the anterior/superior mediastinum of a 5-year-old boy. Sediment preparations from the fluid revealed a sanguineous cystic background together with squamoid cells (arrows and asterisk), lymphocytes, and histiocytes (Pap stain, low magnification).
*Cytology* suggested a thymic cyst.
*Histology*: The cytologic diagnosis was confirmed by subsequent histologic examination of the excised tumor mass.

**Fig. 2.98 Common type thymoma.**
A 55-year-old man presented with a lesion in the anterior mediastinum; clinical and radiological findings suggested metastatic manifestation of a lung cancer. Image-guided transthoracic FNAB revealed a biphasic pattern comprising lymphocytes (showing deep-staining nuclei) and epithelial cells. The latter exhibit irregularly outlined nuclei, usually blurred nucleoli, and cytoplasmic bodies that are highly variable in size (direct smear, MGG stain, higher magnification). Epithelial thymocytes stained immunocytochemically positive for pancytokeratin Lu-5 (not shown).
*Cytologic diagnosis*: Thymoma.
*Tissue diagnosis* (tumor excision): Cortical thymoma.

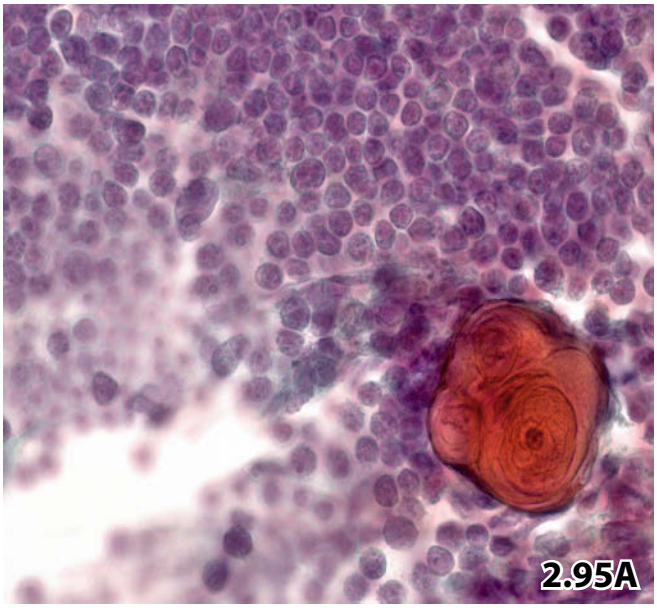
2.95A

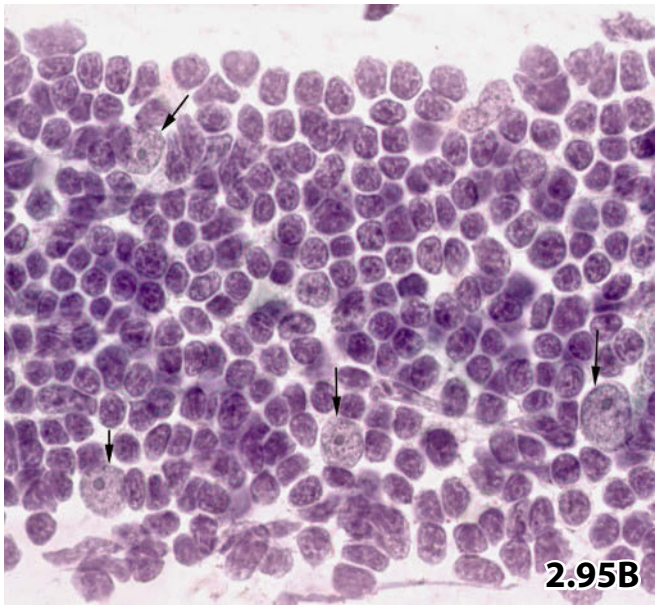
2.95B

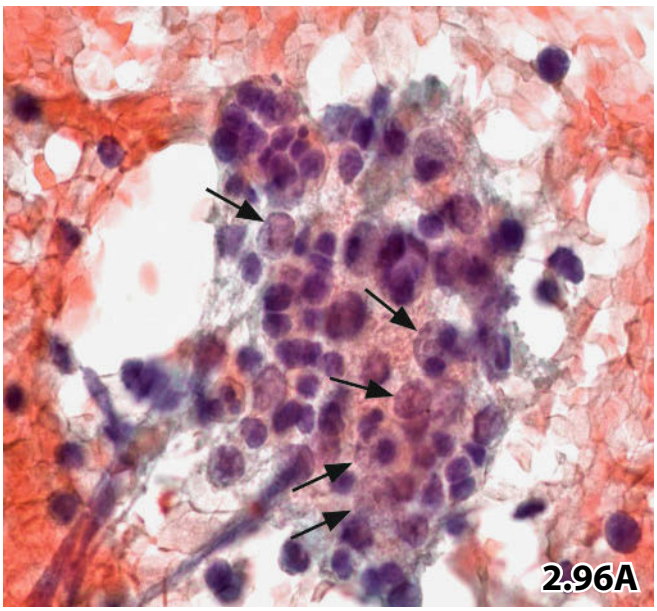
2.96A

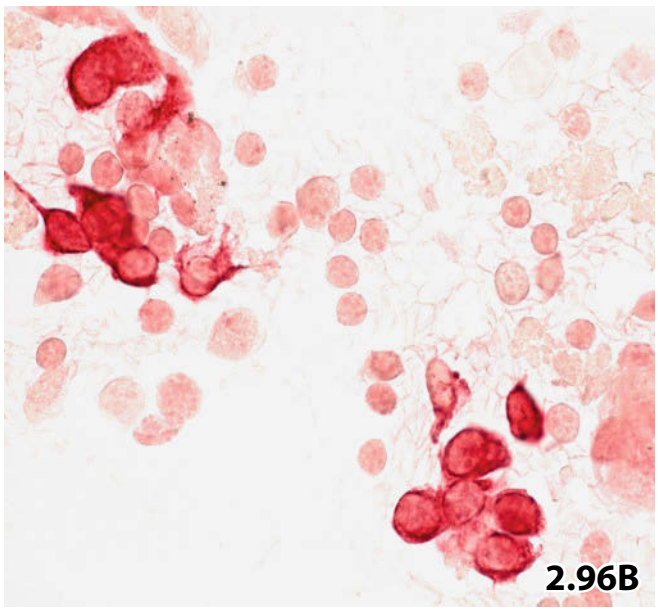
2.96B

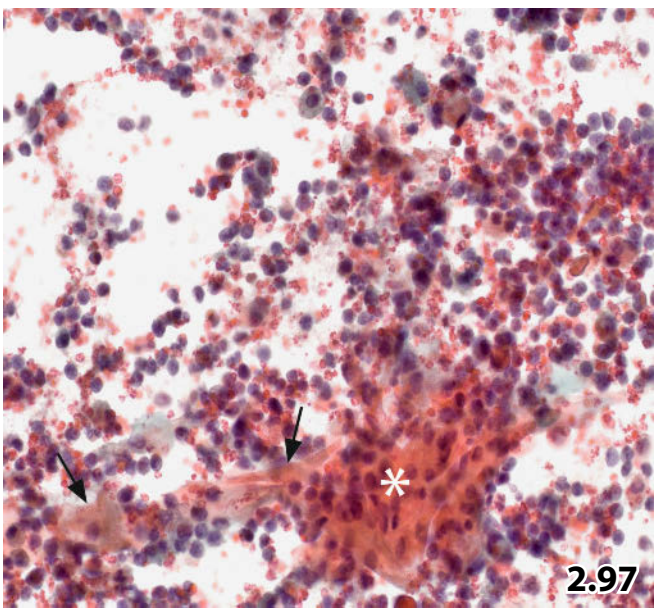
2.97

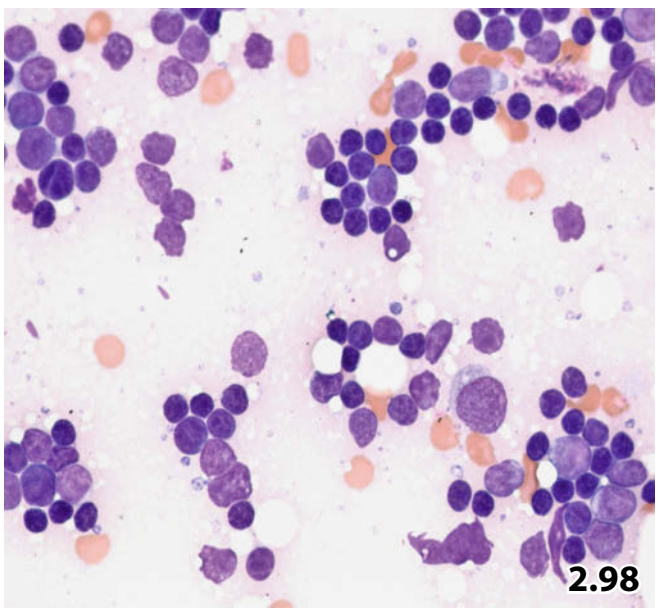
2.98

**Figs. 2.99 and 2.100 Invasive thymoma.**
Two examples refer to cytomorphologic and immunocytochemical features of invasive thymoma.

**Fig. 2.99A–E** (case #1) A 71-year-old woman presented with a solid tumor mass in the anterior mediastinal compartment. Endoscopic transtracheal FNAB was performed. Direct smears were Pap-stained. All immunostains were performed using Pap-prestained smears.
*Tentative cytologic diagnosis*: Morphology and immunocytochemical results suggest invasive thymoma.
*Tissue diagnosis* (tumor excision): Invasive epithelial thymoma rich in lymphocytes (type B1-2).
**A** High magnification discloses a predominant epithelioid pattern consistent with epithelial thymocytes. A few lymphoid cells are also present. The irregularly grouped epithelial cells show mild nuclear atypias with varied size, irregular contours, and coarse chromatin. **B** Epithelioid cells demonstrate strong immunopositivity for pancytokeratin, MNF-116. **C** Epithelioid cells occasionally showing positivity for CD20. **D** Note immunoreactivity of the lymphocytes for CD3, in contrast to negative staining of the epithelial cells (arrows) and histiocytes. **E** Nuclear immunopositivity for MIB-1 of the thymocytes, indicating high proliferation index.

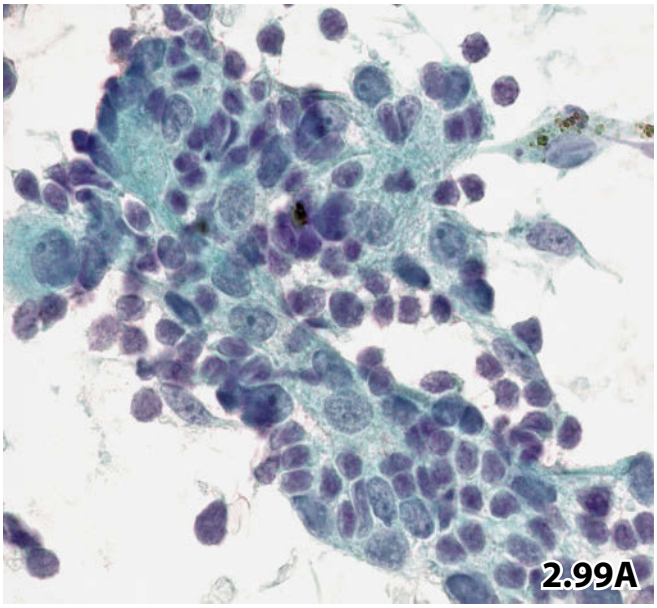
2.99A

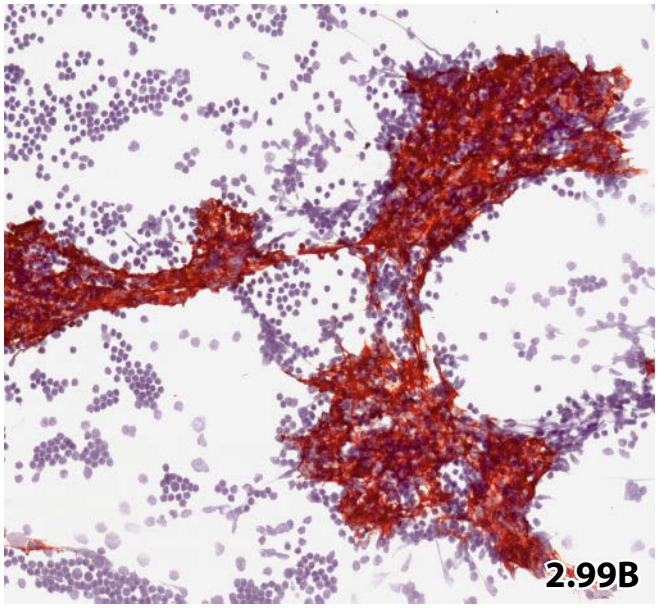
2.99B

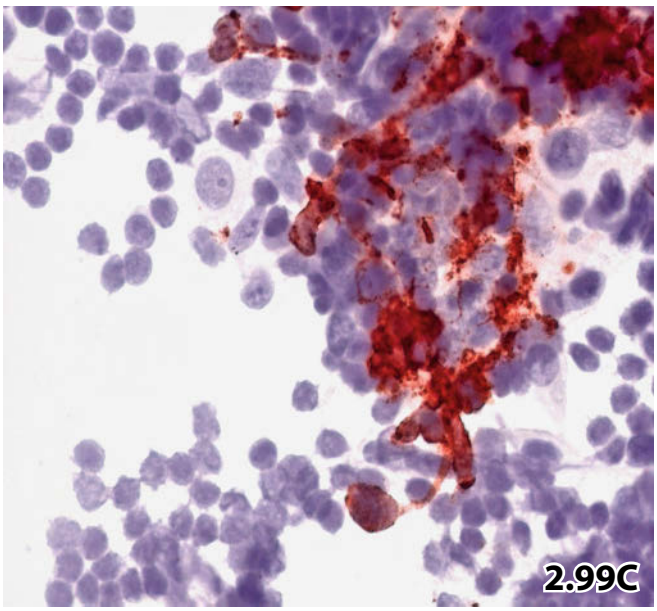
2.99C

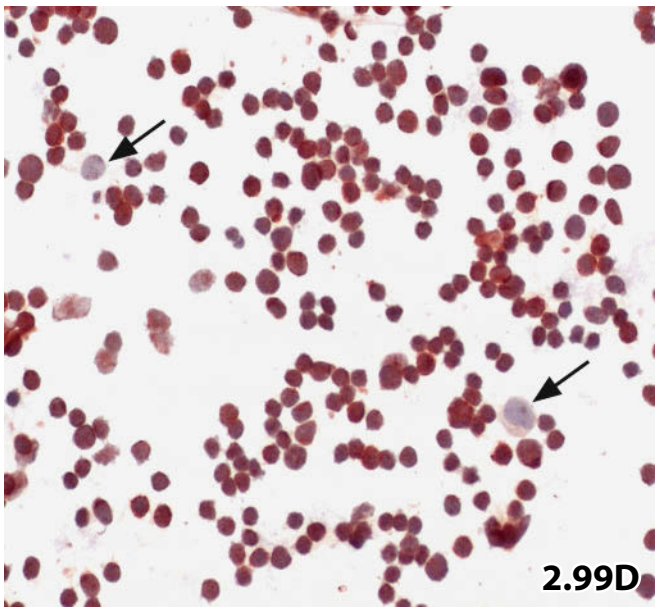
2.99D

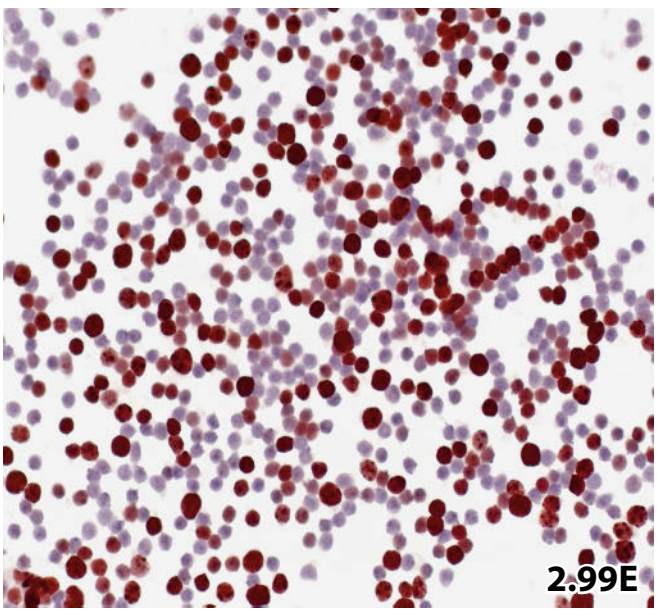
2.99E

**Fig. 2.100A, B** (case #2) Another example of invasive thymoma: CT-guided transthoracic FNAB of a mediastinal mass in a 58-year-old woman. Direct smears were Pap-stained.
*Cytologic diagnosis*: Epithelial spindle-cell thymoma.
*Tissue diagnosis*: Invasive epithelial thymoma.
**A** Low magnification reveals bundles and compact clusters of epithelioid thymocytes. The cells of this case exhibit mainly elongated and spindle-shaped cytoplasm. **B** High magnification: nuclear features are virtually identical compared to those depicted in A.

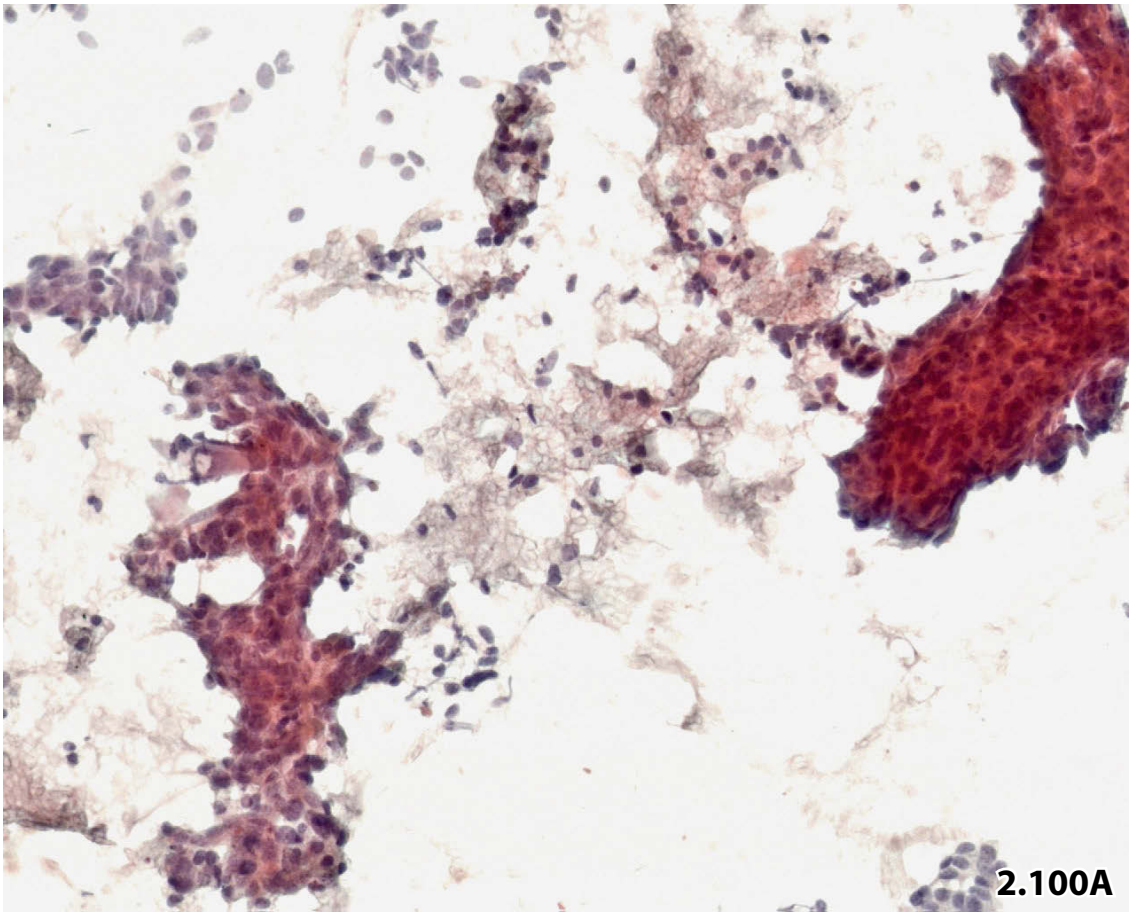

2.100A

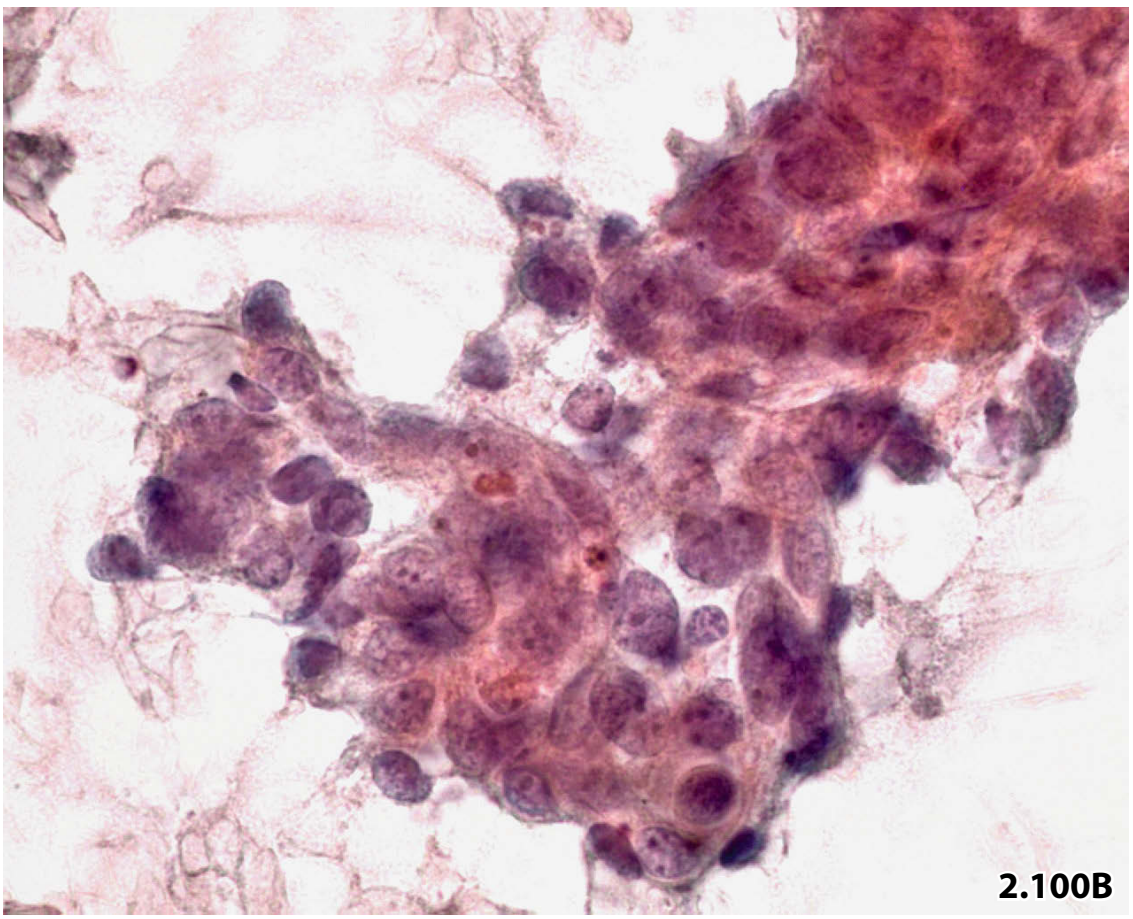

2.100B

**Fig. 2.101 Thymic carcinoma: squamous cell variant.**
A 49-year-old man presented with a retrosternal tumor mass (anterior/superior mediastinum) associated with pleural and pericardial effusion. Image-guided transthoracic FNAB was performed. Direct smears were stained using the Papanicolaou procedure. Lower magnification reveals clusters composed of malignant spindle cells together with degenerating keratinized squamous cells in the background (right). Tumor cell nuclei showing dense and thinly dispersed chromatin may indicate thymic cell origin.
*Cytology and histology* suggested squamous cell carcinoma of thymic origin, a secondary squamoid neoplasia to the mediastinum could not be excluded.
*Final diagnosis*: Thymic squamous cell carcinoma.

**Fig. 2.102 and 2.103 Thymic carcinoid.**
Two different patients underwent image-guided transthoracic fine needle aspiration biopsy of a thymic carcinoid. Cytomorphology and diagnostic challenge are discussed.
**Fig. 2.102** (case #1) Dissociated atypical cells exhibiting distinct variation in nuclear and cytoplasmic size (direct smear, MGG stain, high magnification).
*Cytology* as a first-line diagnostic procedure established a diagnosis of epithelial thymoma, which turned out to be wrong. Absence of lymphocytes, pronounced variation of cell size, occasional plasmacytoid cell appearance (arrows), conspicuous granularity of the cytoplasm, frequent absence of nucleoli, and minor cellular clustering indicate endocrine origin of the neoplastic cells.
*Tissue diagnosis* (extirpation of the tumor): Thymic carcinoid tumor.
**Fig. 2.103** (case #2) The current case of thymic carcinoid mimics the cytoarchitecture of an undifferentiated small-cell carcinoma (e.g., single-file cell arrangement and dense cell clustering; left). However, the tumor cell sheet (arrow) displays the characteristic features of a neuroendocrine tumors: eccentrically located nuclei, relatively bland nuclear texture, and granular cytoplasm (direct smear, Pap stain, lower magnification).
*Cytologic and subsequent histologic diagnosis*: Thymic carcinoid.

**Fig. 2.104 Embryonal carcinoma.**
A 26-year-old man presenting with a voluminous mediastinal mass and nodular lesions in the liver. Transthoracic FNAB reveals the characteristic cumulative cell pattern of embryonal carcinoma: syncytial arrangement of pleomorphic neoplastic cells, abundant cytoplasms showing indistinct borders, variable N/C ratio, and varying nuclear size and shape. The chromatin tends to be coarse and clumped. Occasional prominent nucleoli. Multinucleation is frequent (direct smear, Pap stain, lower magnification). Immunocytochemistry revealed strong expression of pancytokeratin-Lu-5 (not shown).
*Cytologic diagnosis*: Undifferentiated pleomorphic carcinoma, most likely embryonal carcinoma.
*Final diagnosis* (extended pneumonectomy including tumor mass and imaging results): Undifferentiated embryonal carcinoma of the mediastinum infiltrating into the right lung, secondary liver tumors.

**Fig. 2.105 Hodgkin lymphoma: mixed cellularity.**
A 21-year-old man presented with a tumor mass in the anterior superior mediastinal space. Direct smears from a CT-guided transthoracic FNAB disclosed the classical cytologic pattern of mixed cellular variant Hodgkin lymphoma. Note the mixed cellular background (lymphocytes, neutrophils, eosinophils, histiocytes), Reed-Sternberg cells, and Hodgkin cells (MGG stain, lower magnification).

**Fig. 2.106 Hodgkin lymphoma: nodular sclerosis.**
A 26-year-old woman presented with a mediastinal-parasternal tumor mass with evidence of sternal bone and rib erosion. Image-guided transthoracic FNAB was performed. A direct smear of the paucicellular aspirate was prepared and Pap-stained. Microscopy revealed sporadic HRS cells (one Reed-Sternberg cell is depicted) together with scarce inflammatory background (low magnification). The smear with a paucity of cells may indicate a lesion comprising a high proportion of fibrosclerotic tissue.
*Tentative cytologic diagnosis*: Malignant lesion comprising giant cells, most likely Hodgkin lymphoma. The FNA specimen is too paucicellular to provide a conclusive diagnosis.
*Tissue diagnosis*: Hodgkin lymphoma, nodular sclerosis, G1.

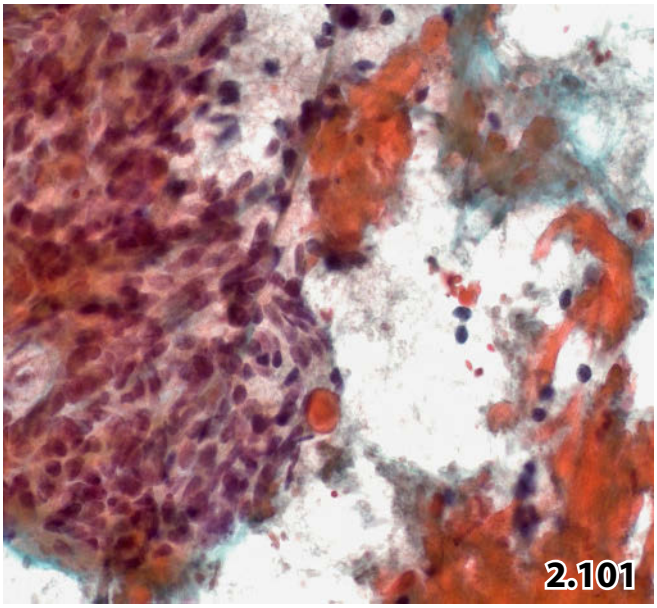
2.101

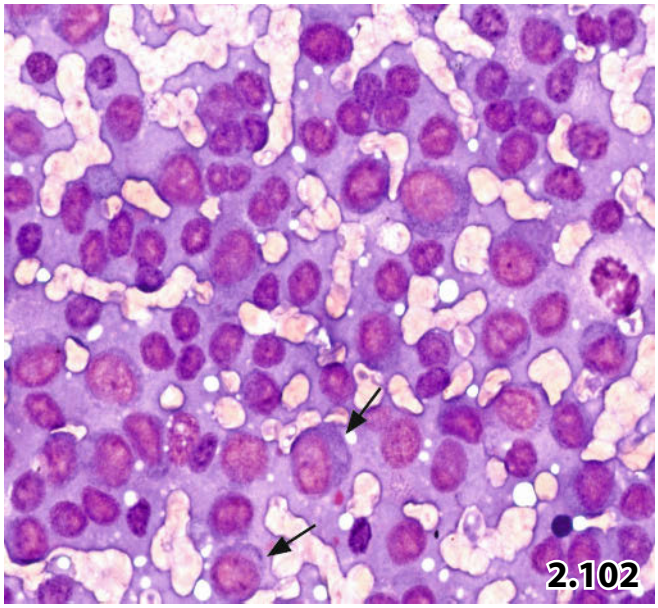
2.102

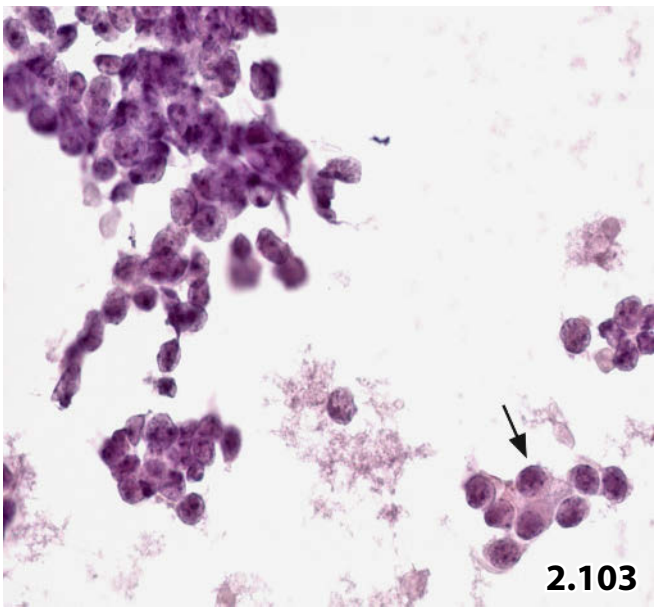
2.103

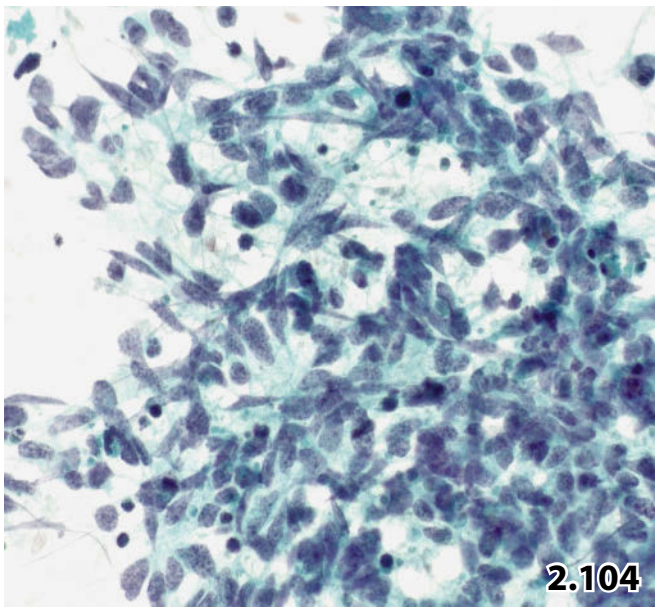
2.104

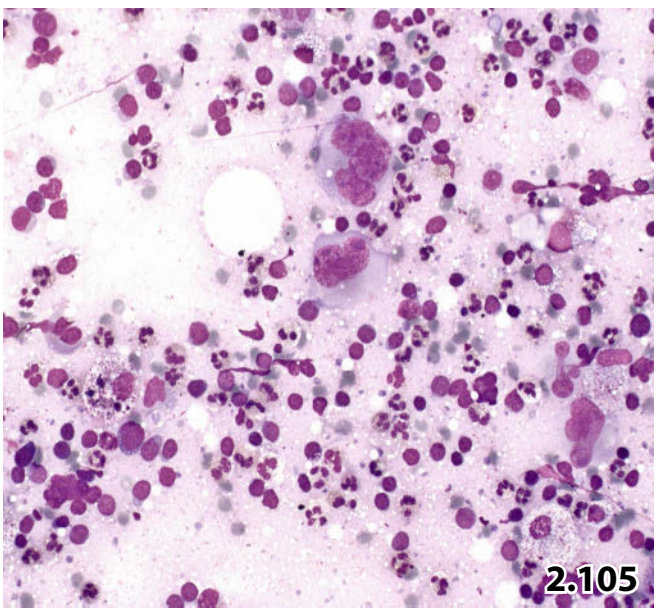
2.105

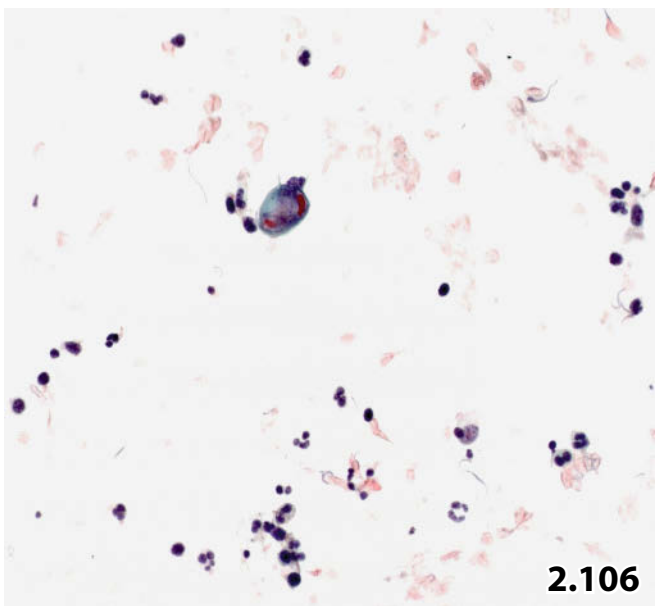
2.106

**Fig. 2.107 Mediastinal large-cell non-Hodgkin lymphoma.**
Transthoracic FNAB of a mediastinal tumor in a young woman. Direct smears revealed small and large malignant cells sometimes arranged in compact clusters (Pap stain, higher magnification).
*Cytology*: Differential diagnostic considerations included high-grade malignant lymphoma, poorly differentiated carcinoma, and invasive thymoma (immunocytochemical analyses were not performed for technical reasons).
*Histologic diagnosis* (surgical biopsy): Highly malignant sclerosing large-cell mediastinal lymphoma of the B-cell phenotype.

**Fig. 2.108A, B High-grade follicular non-Hodgkin lymphoma of the mediastinum.**
A transtracheal FNAB was performed in an elderly woman presenting with a mediastinal mass. Imaging and clinical data suggested metastatic lung carcinoma. The sanguineous but paucicellular aspirate was processed by the liquid-based ThinPrep method.
*Initial diagnosis by cytology*: High-grade non-Hodgkin lymphoma.
*Tissue diagnosis*: Follicular lymphoma, G2/G3a.
**A** ThinPrep specimen contains blood and few large individual cells of atypical blast type (Pap stain, lower magnification). **B** CD45 immunostaining confirmed lymphoid origin of the large atypical cells (ThinPrep preparation, low magnification).

**Fig. 2.109 Synovial sarcoma of the mediastinum.**
A 29-year-old man presented with a mediastinal tumor. Transbronchial aspirates were performed, direct smears were Pap-stained. Highly cellular smears revealed a uniform population of medium-sized tumor cells appearing solitary and in compact clusters (lower magnification).
*Cytology*: The overall cell pattern caused diagnostic dilemma; a tentative cytologic diagnosis of epithelial thymoma was established.
*Tissue diagnosis* including immunohistochemical investigations: mediastinal synovial sarcoma.

**Figs. 2.110 and 2.111 Ganglioneuroblastoma and ganglioneuroma.**
Two tumors of the sympathetic nervous system are demonstrated. Both lesions occurred in young patients‘ posterior mediastinum. Image-guided transthoracic FNABs were performed in order to reach an initial morphologic result. Direct smears were Pap-stained.

**Fig. 2.110** (case #1) A 17-year-old woman presented with a tumor in the posterior mediastinum.
*Cytologic diagnosis*: Ganglioneuroblastoma.
*Comment*: Aspirates revealed a heterogeneous cellular population consistent with ganglioneuroblastoma (higher magnification):
– Irregularly clustered small cells exhibiting small cytoplasmic rims (bottom) represent neuroblasts.
– Medium-sized cells with eccentric nuclei (arrows) represent differentiating neuroblasts.
– Mature ganglion cells are readily identified by their large nucleoli, and abundant cytoplasm with vague processes (arrowheads).
*Tissue diagnosis* (extirpation of the tumor): Ganglioneuroma associated with ganglioneuroblastoma.

**Fig.2.111** (case #2) The second patient was a 16-year-old woman.
Cytologic specimens showed mature ganglion cells (lower left) enclosed in bundles of nerve fibers (low magnification).
*Cytologic and subsequent histologic diagnosis*: Ganglioneuroma.

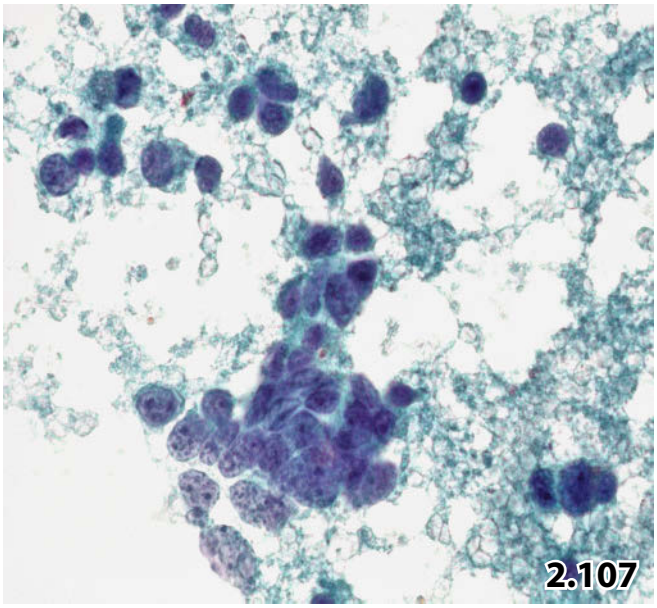
2.107

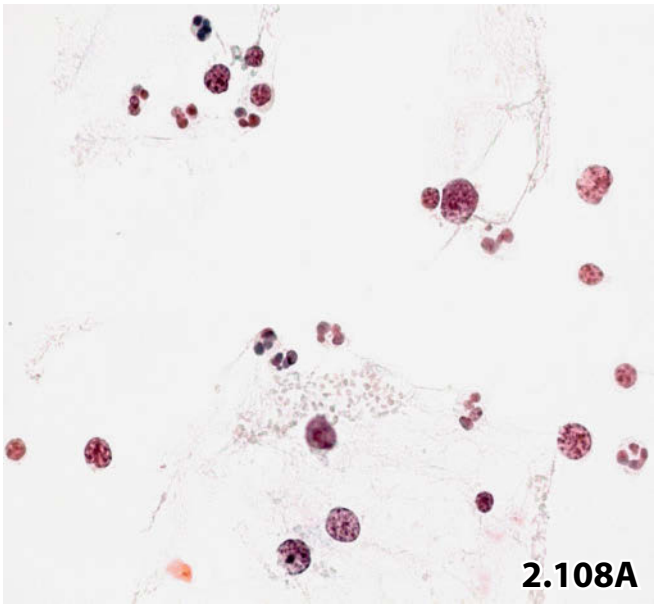
2.108A

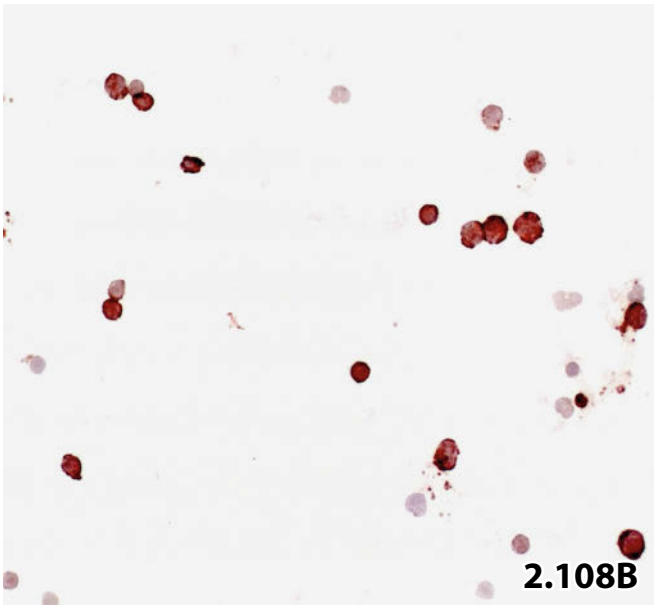
2.108B

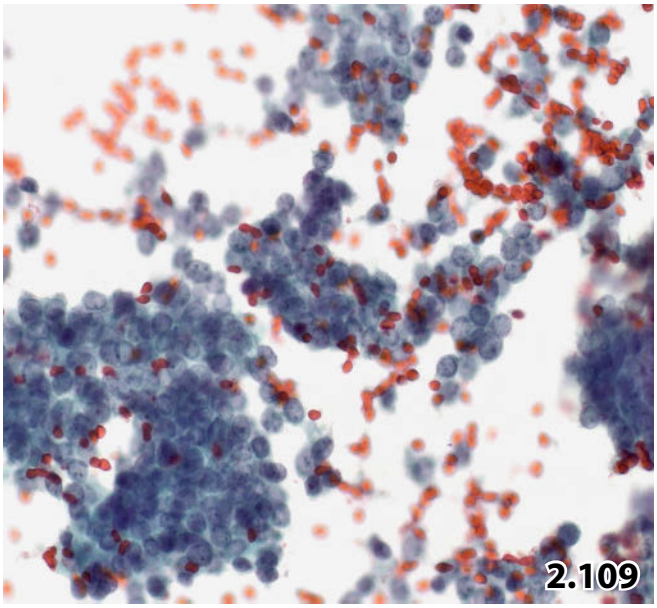
2.109

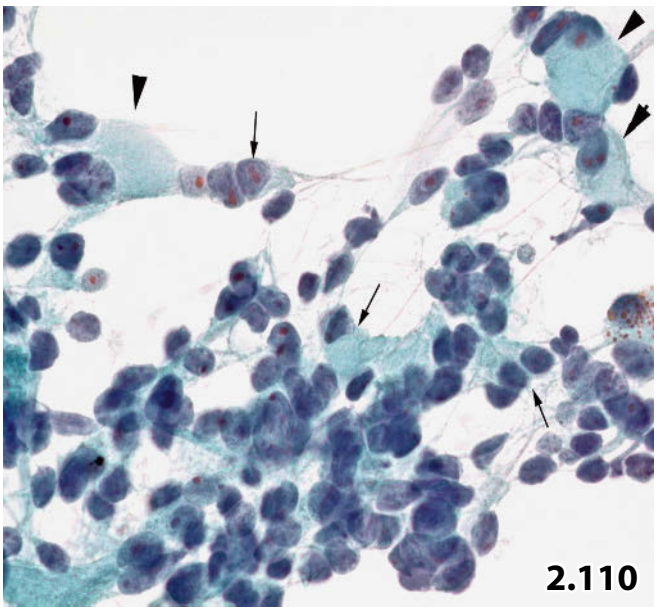
2.110

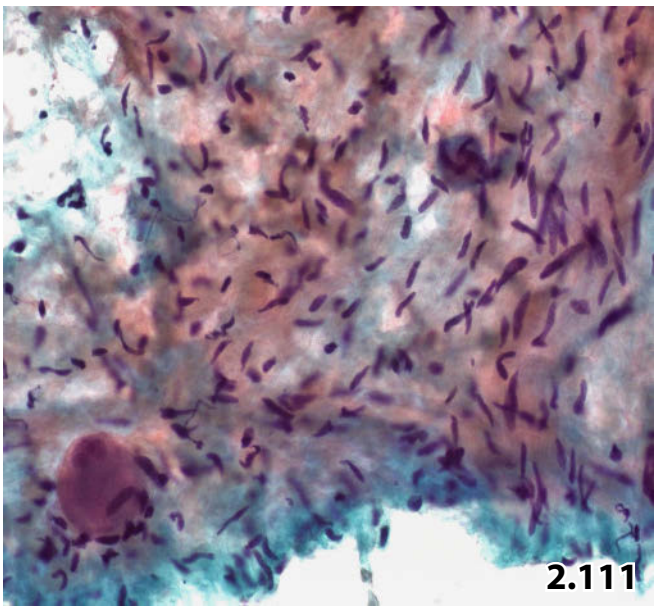
2.111

**Fig. 2.112A–C Mediastinal metastasis of uncertain clinical assessment.**
A transtracheal aspirate from an enlarged mediastinal lymph node in a 74-year-old woman was processed using the cytospin technique.
*Cytologic and immunocytochemical diagnosis*: Metastatic ovarian carcinoma, serous type (confirmed by postmortem examination).
**A** Thin-layer specimens contained numerous cells of a poorly differentiated non-small-cell carcinoma (Pap stain, high magnification). **B** A panel of selected immunocytochemical markers established the aforementioned conclusive diagnosis: strong immunopositivity for CK7. **C** Positive immunoreaction for CK5/6. Negative immunoreaction for CK20 is not shown.

**Fig. 2.113 Transitional cell carcinoma.**
A 63-year-old man with a history of bladder cancer presented with enlarged mediastinal lymph nodes. The sanguineous transtracheal mediastinal aspirates were transferred to a hemolyzing fixative (Cytolyt) and subsequently processed using the cytospin technique. Tumor cells exhibiting polymorphic deep-staining nuclei and squamoid cytoplasm were strong indicators for transitional cell carcinoma (Pap stain, high magnification).
*Cytologic diagnosis*: Metastatic transitional cell carcinoma. Neither surgical intervention nor histologic examinations were performed.

**Fig. 2.114 Small-cell carcinoma of lung.**
A 66-year-old man presented with a nonspecific lung disorder and enlarged mediastinal lymph nodes. The sanguineous transbronchial mediastinal aspirate was transferred to a hemolyzing fixative (Cytolyt) and subsequently processed by cytospin technique.
*Liquid-based cytology* exhibits characteristic cell arrangement (short single-file rows, arrows), dense granular chromatin, and necrosis, indicating small-cell carcinoma (Pap stain, higher magnification).
*Simultaneous bronchial brushing* yielded the same diagnosis. No tissue examination.

**Fig. 2.115 Adenocarcinoma of lung.**
A 69-year-old man presented with a lung tumor and enlarged paratracheal lymph nodes. Transtracheal aspirates of the lymph nodes were processed using the the cytospin technique.
*Cytologic findings*: Rather monomorphic malignant cells showing large foamy cytoplasm, evenly distributed granular chromatin, and prominent nucleoli. Background with histiocytes and trachea lining epithelial cells (Pap stain, high magnification).
*Cytologic and synchronous histologic diagnosis (bronchial biopsy)*: Poorly differentiated mucinous adenocarcinoma.

Note the cellular shrinking associated with deeply stained nuclei in Figs. 2.112A, 2.114, 2.115. This is an artifact resulting from the liquid-based processing.

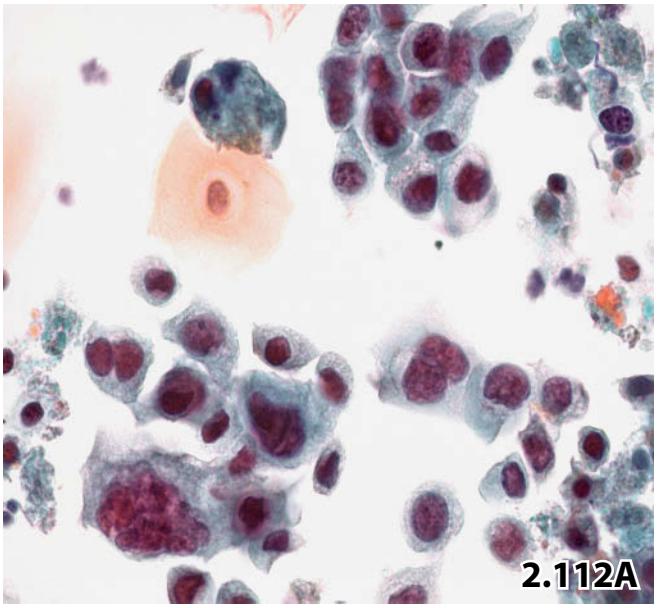
2.112A

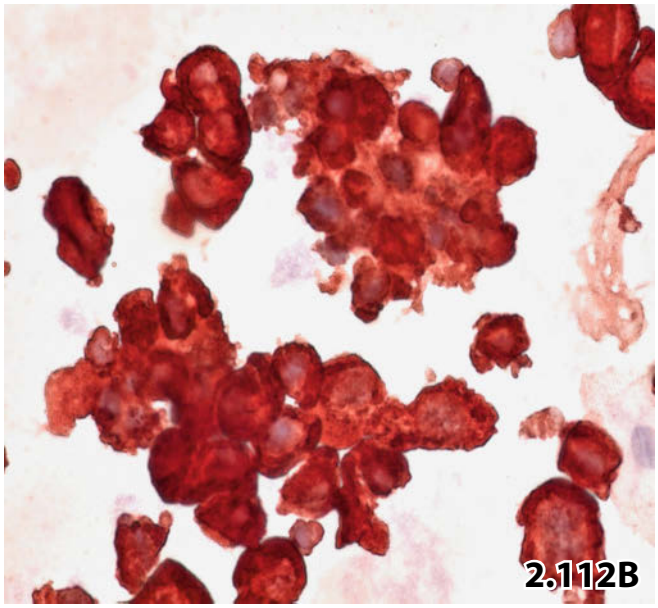
2.112B

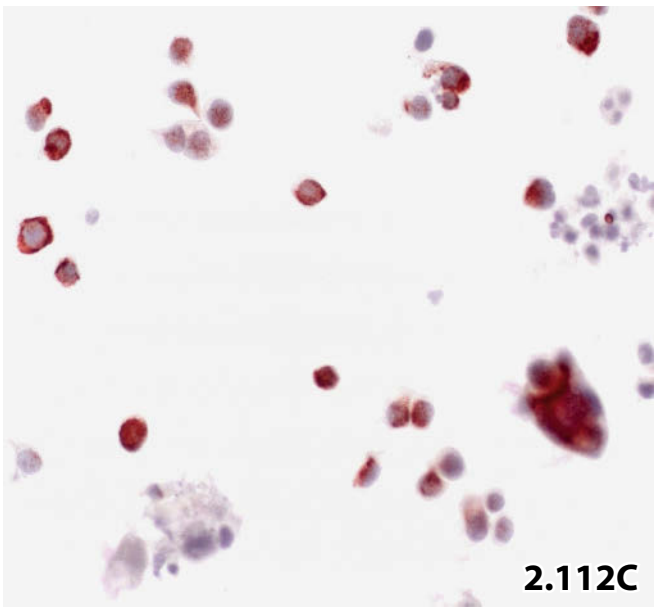
2.112C

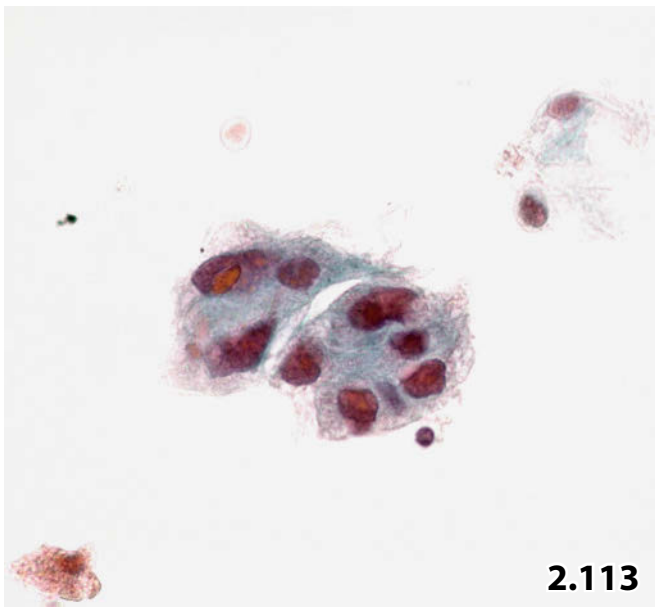
2.113

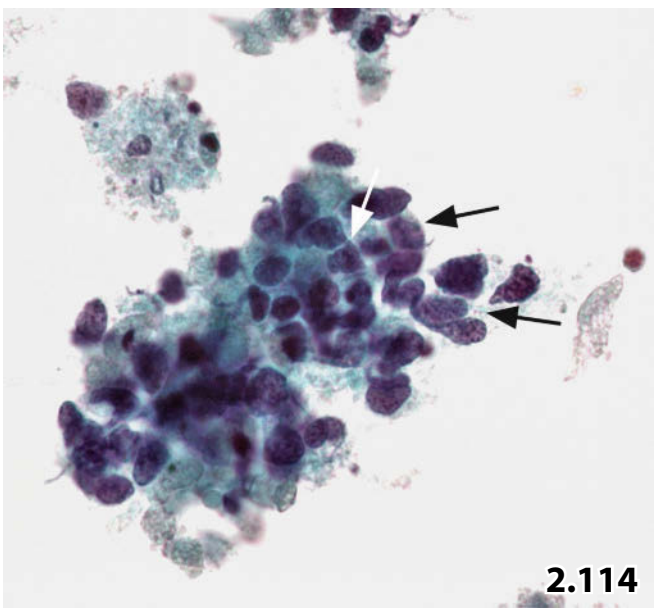
2.114

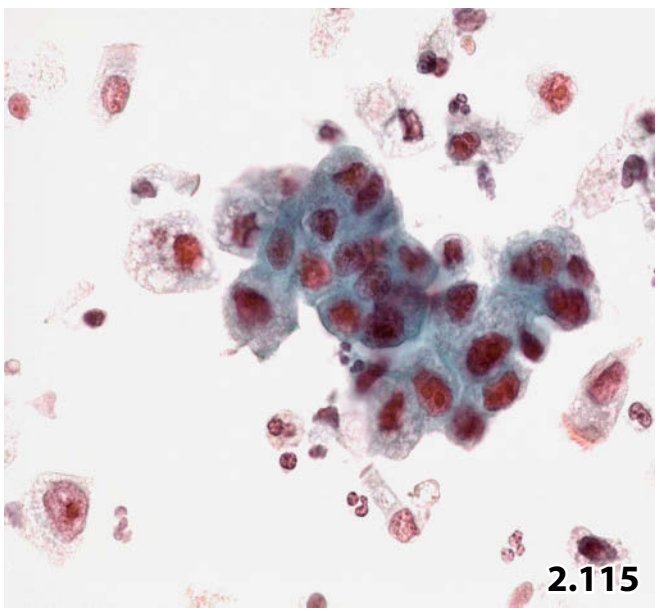
2.115

# 3 Effusions



Spieler/Rössle, *Nongynecologic Cytopathology. A Practical Guide. Essentials of Diagnostic Pathology*,
DOI 10.1007/978-3-642-24719-4_3, 

## Synopsis and Algorithms

# Section 3.1
# Effusions

## Pleural
## Pericardial
## Peritoneal
## Tunica Vaginalis Testis

## Benign and Equivocal Lesions

### 3.1.1 Introduction

**General Comments**

- Transudates are an accumulation of fluid in serous cavities, in most cases due to circulatory disturbances.
- Exudates can be produced:
  - By inflammatory processes.
  - By primary and metastatic tumors in serous membranes or serous cavities.
  - Following a trauma, surgery, or other invasive diagnostic procedures.
- Each abnormal fluid accumulation in a body cavity should be investigated cytologically.
- It must be emphasized that large amounts of liquid have to be supplied for cytologic investigations. The more fluid there is, the greater the chance of detecting malignant elements. A sample with less than 30 ml liquid often lacks malignant cells in spite of tumor spread beyond serous membranes; a larger sample has to be taken for a repeat cytologic investigation.
- Macroscopically turbid and milky liquids are most likely to raise suspicions of chyle admixture and a malignant process, chiefly a malignant lymphoma.
- It is important to carefully read the overall cell pattern in low magnification, which will give a first impression of the cell mixture, the proportion of the individual cell types, the architecture of cell clusters, the different nuclear staining qualities, and the background features.
- In cytologic preparations of body cavity fluids, the size and shape of cells and nuclear chromasia are difficult to assess compared to the corresponding cells in FNABs or histologic sections. Depending on the time between sampling and laboratory processing, the cytoplasm and nucleus of vital cells may balloon together with cytoplasmic vacuolization.

**Caution**

It must be emphasized that cellular morphology of target cells should be evaluated in comparison with all other cells in the same preparation.

#### 3.1.1.1 Processing of Cytologic Material

##### 3.1.1.1.1 Transfer and Storage

If the sample cannot be transferred to the cytology laboratory within 12 hours, it must be stored in a refrigerator at 4° Celsius, a recommendation which is better than prefixation with alcohol. Stored in this way, cytological preparations are still suitable after a delay of 1 to 2 days before the first degenerative changes become apparent.

##### 3.1.1.1.2 Conventional Smear and Staining

- Wet fixed direct smears are prepared from the aspirated material after centrifugation and discarding the supernatant. Two or three slides are fixed immediately to prevent cell degeneration. We prefer Delaney solution as fixative; 95% ethyl alcohol pure or mixed with ether is also frequently used.
- Papanicolaou (Pap) is a highly suitable staining method also for sediment preparations from fluids. It offers a great

advantage with regard to comparative cell studies in histologic sections. However, in many institutions, hematoxylin-eosin, May-Grünwald-Giemsa, Diff-Quik, and other staining methods are preferred.

3

#### 3.1.1.1.3 Cytocentrifuge Preparation

Cytocentrifuge preparation is recommended for small amounts of fluid with sparse cellular content.

#### 3.1.1.1.4 Thin Layer Preparation

Thin layer preparation (cytospin, ThinPrep, and others) is becoming more and more popular. The method may be preferred for adjacent analyses. The remaining cellular material should be retained and stored at 4° Celsius, mixed up with a certain amount of the supernatant.

#### 3.1.1.1.5 Cell Block Technique

- The value of cell-blocks produced from cytologic specimens depends on the type and amount of cytologic material that is available and is a matter of individual preference in this technique.
- The cell block technique applied to body fluid cytology can be recommended most particularly in cases in which the cell load is abundant. The great advantage of this method is the possibility of extra slides to be cut for ancillary tests, especially for a large battery of immunocytochemical stains.
- Preservation of architectural features equivalent to conventional histologic sections is of minor relevance, because the cytoarchitectural features in well-preserved and well-stained smear preparations are of singular diagnostic value, which should not be underestimated.

**Caution**

- Reading the slides in low magnification is very important for a first impression of the overall cell pattern.
- Cytologic preparations of small amounts of liquid are frequently negative for malignant cells; repeated investigations with larger fluid samples will become diagnostic in many cases.

## 3.1.2 Benign Effusion, Not Otherwise Specified (Figs. 3.1 and 3.2)

**Microscopic Features**

Benign effusions (not otherwise specified, NOS) exhibit a pathognomonic mixed cell pattern with typical mesothelial cells, histiocytes, lymphocytes, neutrophils, and a few eosinophilic granulocytes. The amount of the different cell types and blood content vary greatly.

- *Benign mesothelial cells* exhibit a dense cytoplasm with a fading finely vacuolated periphery. The nucleus is often positioned eccentrically with a distinct smooth membrane, loose and evenly distributed chromatin, and a typical kidney shape. The number of distinct rounded nucleoli with peculiar variations in size depends on cellular activity. Mesothelial cells, forming a pair and short chains with empty "windows" between cells, are a typical feature in cytologic preparations (Fig. 3.1). Smoothly contoured three-dimensional clusters enclosing a core of homogeneous collagen could raise the suspicion of well-differentiated mesothelioma; however, these elements are exceptional and the cells are small and completely benign.
- A hallmark of *degenerated mesothelial cells* is the red cytoplasm in Pap stains. Large irregular cytoplasm bodies with dark-red staining may lead to diagnostic confusion with malignant cells of squamous cancer (Fig. 3.2). In these cases, one has to pay close attention to the nuclear morphology and background of the smear. Strong cytoplasmic vacuolization as a sign of degeneration is mainly observed in delayed unprocessed fluids. Large cytoplasmic vacuoles with sharply defined margins may generate pseudo signet ring cells (Fig. 3.1), which must be distinguished from true malignant signet ring cells containing mucus.
- *Histiocytes* compared to mesothelial cells exhibit finer chromatin, more pronounced nuclear polymorphism, and small nucleoli (Fig. 3.1), although it is often impossible to differentiate between large histiocytes and activated mesothelial cells.

**Caution**

- Marked vacuolization of the cytoplasm is a sign of delayed unprocessed material, degeneration, or glycogen storage. The cells should not be misinterpreted as mucin-containing carcinoma cells or even signet ring cells.
- Degenerate mesothelial cells with large eosinophilic cytoplasm may look similar to squamous carcinoma cells.

## 3.1.3 Hyperplastic Mesothelial Cells, Uniform and Polymorph Cell Pattern (Figs. 3.2–3.5)

In many disorders accompanied by effusions, stimulated mesothelial cells and mesothelial tissue exfoliate into the fluid. The cytologic smears exhibit a predominance of hyperplastic single cells, papillary clusters, and three-dimensional spheres.

**Microscopic Features**

- The cells show enlargement, rounded nuclei, multinucleation, and huge nucleoli.
- It can be difficult to differentiate between mesothelial and carcinoma cells in cases in which carcinoma cells

exhibit chromatin and nuclear staining patterns comparable to hyperplastic mesothelial cells in the same smear.
- Sometimes, papillary clusters and three-dimensional spheres of activated benign mesothelial cells occur. An irregular blackberry-like outline together with benign nuclear characteristics may help to distinguish reactive mesothelial cells from malignant cells. In single cases, this differentiation may be impossible.

#### 3.1.3.1 Pronounced Cellular Atypia

- Important reasons for pronounced mesothelial proliferation are repeated centeses, surgery, instillation, irradiation, chemotherapeutic agents, chronic peritoneal dialysis, and uremia (Fig. 3.5).
- In many of these instances – especially after radio- and/or chemotherapy – cellular atypia is so strong that the difference between reactive mesothelial and malignant cell changes is reduced to a minimum. The mesothelial and histiocytic cells become substantially enlarged and vacuolized and exhibit bizarre shapes. A high N/C ratio and the bizarrely cleaved and folded nuclei with enlarged polymorphous nucleoli are striking. Differential diagnostic considerations concern large-cell carcinoma, large-cell anaplastic lymphoma, and sarcoma.
- Compared to malignant cells, the nuclei of atypical but benign mesothelial or histiocytic cells generally miss distinct hyperchromasia, showing thinly dispersed or patternless dense chromatin.
- Diagnostic assessment is highly dependent upon auxiliary clinical information.

**Caution**
- Cells and clusters from hyperplastic mesothelium may be difficult to assess against adenocarcinoma.
- Extremely stimulated mesothelial cells may be observed, particularly in pericardial fluids after surgery and radiation.
- Single bizarre reactive cells match the cytomorphology of malignant cells.

**Additional Analyses**

Immunocytochemistry (Figs. 3.3B, 3.24B, 3.24C):
- Desmin and epithelial membrane antigen (EMA) have been shown to be most useful to distinguish between benign and malignant pleural disease [13]. Desmin seems to be a useful marker differentiating reactive mesothelial cells (positive) from mesothelioma (negative) [1, 9].
- p53 could have potential in the differentiation of malignant cells (carcinoma or mesothelioma) from benign mesothelial cells [13].
- In cases with equivocal cytodiagnostic assessment, the differentiation between mesothelial and carcinoma cells is reliably achieved by applying two antibodies (AB) in the first instance, namely ABs against Ber-Ep4 and calretinin. The former are present in all epithelial cells and in a large number of adenocarcinomas. The latter is a reliable mesothelial cell marker.

Cytogenetics and DNA Ploidy

See Sect. 3.2.1.3 “Additional Analyses,” p. 262.

### 3.1.4 Acute Inflammation and Empyema

(Fig. 3.6)

Specimens of serous fluid always contain neutrophil leukocytes in a varying number. Highly cellular fluids, containing almost exclusively neutrophils, are consistent with acute inflammation. Purulent fluids, also referred to as empyema, caused by infection, exhibit strongly degenerated and detritic neutrophils. Gram, Giemsa, PAS, and Grocott stains are adequate for identification of bacteria, parasites, and fungi. Pneumonia, infarction, rupture of an organ, and surgery are the principal causes of inflammatory and infectious disorders.

### 3.1.5 Eosinophilic Effusions

**General Comments**
- Eosinophilic effusions are defined as those containing more than 10% eosinophilic leukocytes in smears of body cavity fluids. The pathogenesis of this entity is poorly understood [11]. Association with air in the pleural cavity seems to be common [25].
- Characteristic slender rhomboid Charcot-Leyden crystals of variable size can be detected, particularly in cases with degenerate eosinophilic leukocytes [2].
- Eosinophilic pericardial effusion is extremely rare.

#### 3.1.5.1 Eosinophilic Pleural Effusion

Eosinophilic pleural effusions have been reported in a wide variety of disorders: pulmonary infarct, pneumothoraces, repeated pleurocentesis, trauma, allergy, drugs, various forms of pneumonia, tuberculosis, parasitic and mycotic infection, echinococcosis, cancer including malignant lymphoma, and various lung disorders [4, 15, 28]. The most common causes for the increase in eosinophils in pleural fluids seem to be pulmonary infarct, pneumonia, and cancer.

#### 3.1.5.2 Eosinophilic Peritoneal Effusion

This is a rare disorder induced by some of the potential agents described above. Gastroenteropathies and chronic peritoneal dialysis are worth mentioning as additional causes.

## 3.1.6 Lymphocytic Effusions

### Definition and General Comments

- Each collection of benign serous fluid contains lymphoid cells with a high percentage of T-cell origin.
  Those effusions containing more than 50% lymphoid cells are defined as lymphocytic or lymphocyte-rich effusions. A majority of the benign lymphocytic effusions develop in the pleural cavity.
- Serous effusions containing numerous lymphoid cells may be caused by benign noninfectious disorders but can also be an expression of specific infections or lymphoid malignancies. In many cases, a proper diagnosis is not possible on cytomorphologic features alone.
- Clinical information is indispensable for selective evaluation: B- and T-cell enumeration using immunophenotyping, flow cytometry (FCM) and molecular tests are basically important as adjacent analytic methods in equivocal cases [5]. Mono- and polyclonality, respectively, may be assessed immunocytochemically or by in-situ hybridization (immunoglobulin light chain restriction).

### 3.1.6.1 Mixed Lymphoid Cell Pattern

#### 3.1.6.1.1 Etiology of Benign Lymphocytosis and Microscopic Features (Figs. 3.7 and 3.8)

A variety of benign disorders are responsible for mixed lymphoid cell patterns in pleural and pericardial fluids: pulmonary infarct, pneumothorax, repeated pleurocentesis, cardial disorders, chronic inflammation, viral infection, submesothelial carcinosis, trauma, and surgery.

- The smear is dominated by small mature lymphocytes with the cytoplasm scant or not visible. Nuclei are round with a few indentations, indicating T-cell lineage. Chromatin structure is granular to coarse. Small and centrally located nucleoli frequently appear when applying a proper Pap stain.
- Less mature lymphoid cells are present in various amounts. Cytoplasm may be distinct and stain cyanophilic. The chromatin is pale and loose; nucleoli are common (Fig. 3.8).
- Plasma cells may be found.
- In rare cases, viral infections in the lung or abdominal organs may be associated with a highly immature lymphocytic population. Large polymorphic immunocytes, immunoblasts, cell degeneration, and debris dominate the cytologic preparations of these effusions.

**Caution**

Viral infections may generate a polymorphic blast cell pattern with cellular degeneration and debris. Exclusion of a blastic variant of non-Hodgkin lymphoma is practically impossible by light microscopy.

### Differential Diagnosis

- In most cases, the assessment of a benign lymphocytosis is no problem, but a benign lymphocytic population containing large immature cells may be difficult to classify (Fig. 3.8). In the first step, epithelial cancer cells should be excluded immunocytochemically; it is well known that serous carcinomatosis is accompanied by pronounced reactive lymphocytosis. Immunostaining with ABs against BerEp-4 antigen can reliably confirm the epithelial nature of atypical cells.
- Various types of malignant lymphoma may appear with strongly atypical blast cells along with a population of small lymphoid cells (see Sect. 3.2.3.2.2 “Mixed Lymphoid Pattern with a Varying number of Large Blast Cells,” p. 268):
  - Non-Hodgkin lymphomas (NHL) may exfoliate a mixed lymphoid cell population (mature, maturing, and immature lymphocytes, immature plasma cells and plasmablasts) mimicking benign lymphocytosis. Cytology alone cannot differentiate between benign and malignant lymphoid lesions, and B- and T-cell enumeration frequently fails to distinguish reactive from neoplastic lymphoproliferative lesions as well. Only molecular genetic methods are able to establish clonality of the lymphoid population (see Sect. 3.2.3.2 “Malignant Lymphoma and Myeloid Lesions: Additional Analyses,” p. ).
  - Hodgkin lymphoma. The cell component in cytologic preparations of serous effusions caused by Hodgkin lymphoma is nonspecific in most cases. Smears exhibit a mixed lymphoid cell pattern together with histiocytes and mesothelial cells. Plasma cells may be present. Eosinophils have no diagnostic relevance. The only reliable diagnostic features are multinucleated Reed-Sternberg cells and mononuclear Hodgkin cells; however, these pathognomonic cells are rarely present in Hodgkin-related effusions [19].

### 3.1.6.2 Pure Lymphocytic Pattern: Uniform (Fig. 3.9)

Pure lymphocytic effusions are characterized by huge numbers of small lymphocytes, densely packed but clearly separated from each other. Mesothelial cells and histiocytes rarely appear or are completely absent.

#### 3.1.6.2.1 Florid Pleural Tuberculosis

Florid pleural tuberculosis is virtually the sole benign serosal disorder that causes a smear pattern exclusively composed of small lymphocytes [26, 22] (Fig. 3.9).

### Microscopic Features

- The pleural effusions caused by florid pleural tuberculosis exhibit a stunning monotonous cell pattern.

- Lymphoid cells are uniform, slightly enlarged, and display a benign nuclear morphology.
- Small centrally placed nucleoli occur in about 50% of all nuclei.
- A few authors have recorded giant macrophages and epithelioid cells, a phenomenon that should be considered an extreme rarity. These cells may have been collected when the needle passes hit a tuberculoid granuloma.

**Caution**

The presence of a variable proportion of mesothelial cells should be regarded as evidence that the effusion is not caused by tuberculosis.

**Differential Diagnosis and Immunocytochemistry** [24]

- Immunocytochemical B- and T-cell enumeration is very helpful to exclude lymphocytic non-Hodgkin lymphoma of the B-cell phenotype because a lymphoid cell population accompanying serosal tuberculosis is positive for the T-cell marker CD3. Analyzing T-cell subsets and activation markers on T cells has revealed poor relevance for further diagnostic outcome [10].
- NHL of the T-cell phenotype is practically excluded because cellular attributes of tuberculosis rarely match the morphology of T-cell lymphoma. Diagnosis of T-cell NHL can be assessed with molecular genetic analyses.

**Caution**

In tuberculous effusions, no acid-fast organisms may be detected using Ziehl-Neelsen staining or additional molecular genetic tests.

## 3.1.7 Effusions with Peculiar Histiocytic Background

### 3.1.7.1 Liver Cirrhosis (Fig. 3.10)

Ascitic fluid with small histiocytic cells or macrophages accounting for more than 50% of all nuclear elements in cytologic smears could be caused by cirrhotic liver disease, a suspicion that should be communicated to the clinicians. A definite diagnosis of cirrhosis is not possible by cytology.

**Microscopic Features**

- Histiocytes are smaller than mesothelial cells in the same preparation. Nuclei are wrinkled or folded with fine indistinct chromatin.
- A large foamy cytoplasm shows phagocytic activity and hyaline cyanophilic inclusions.
- In most cases, mesothelial cells exhibit hyperplastic activity, as described in Sect. 3.1.3, p. 242.
- Smears from fluids caused by liver cirrhosis are less likely to be rich in blood.
- Varying amounts of lymphocytes, neutrophils, and eosinophilic granulocytes.

### 3.1.7.2 Cyst Content (Fig. 3.11)

In females, large ovarian cysts expanding without restraint in the abdominal cavity can be misinterpreted clinically and radiographically as to be ascitic fluid filling the entire abdomen.

It is important to diagnose cystic content; otherwise patients will be subjected to more invasive investigations [21].

A pure histiocytic cell content frequently causes diagnostic confusion and is often misinterpreted as ascitic fluid with degenerate mesothelial cells.

**Microscopic Features and Immunocytochemistry**

- Many large foam cells exhibit a typical histiocytic nucleus.
- The background of the smear contains varying amounts of cellular debris and inflammatory cells.
- Cholesterol crystals may be apparent in slowly growing cysts. Together with a foam cell pattern, this finding is pathognomonic for cyst content. Cholesterol is readily recognizable under the light microscope as refractile glassy plates, usually laminated, demonstrating birefringence upon polarization.

To differentiate between serous effusion and cystic fluid, see Table 3.1.1, below.

The histiocytic nature of the cells can be determined by immunoreactivity for CD68.

**Table 3.1.1** Differing cellular content of serous effusion and of cystic fluid from the abdominal cavity

| Features | Serous or chylous effusion | Cyst content |
|---|---|---|
| Cellularity | Large cell amount | Rather poor cellularity |
| Typical mesothelial cells | Various amount of mesothelial cells | Absence of mesothelial cells<br>Typical foam cells! |
| Leukocytes | Various amount | Absent or sporadic |
| Debris | Absent | Mainly granular detritus |

### 3.1.7.3 Langerhans Cell Histiocytosis [16, 20, 30 ]

Cytologic appearance of Langerhans cells in effusions is observed extremely rarely and most often in children. Cells may exfoliate from a tumor manifestation within the serous membranes or from a ruptured tumor into a body cavity. Pleural manifestation is most common.

#### Microscopic Features

- The small to medium-sized histiocytoid cells resemble benign macrophages with indented and twisted nuclei and a finely granular chromatin pattern. The clear cytoplasm frequently marginalizes the nucleus. Eosinophilic granulocytes may be abundant.

#### Additional Analyses

Immunocytochemistry

The cells show positivity for S100 protein and CD1a.

Electron Microscopy

Electron microscopic evaluation reveals the diagnostic Birbeck granules.

### 3.1.7.4 Rheumatoid Serositis

[7, 12, 18, 23] (Figs. 3.12 and 3.13)

#### Etiology

Necrotizing granulomas as present in synovial tissue of rheumatoid inflamed joints may develop in pleural or pericardial serosa as well. Granulomas exfoliate their cellular component into the serous cavity, resulting in an effusion. The cytologic picture of rheumatoid serositis is pathognomonic.

#### Microscopic Features

- Hallmarks
  - Elongated spindle-shaped histiocytes. The cytoplasm is clear and dense. Nuclei are small and elongated, resulting in a low N/C ratio. The chromatin texture is often dense and patternless, resulting in darkly staining nucleoplasm. The cells may resemble epithelioid histiocytes as observed in tuberculoid granulomatous disease (Fig. 3.13).
  - Multinucleated giant macrophages are round with up to a tenfold diameter of erythrocytes and may contain varied numbers of nuclei.
  - Necrotic background material, resulting from disintegration of histiocytic cells, is granular. The granules show a broad spectrum of size, varying from eosinophilia to cyanophilia in Pap-stained smears.
- In addition, various types of inflammatory cells may be present.
- Cholesterol crescents and plates may be present in cases with chronic relapsing serosal rheumatoid inflammation accompanied by persistent effusions.

**Caution**

In rheumatoid effusions, the number of spindle-shaped and multinucleated histiocytes varies.

#### Differential Diagnosis

In absence of the key features described above, a correct cytologic diagnosis is difficult. Necrotic background may mislead to a false diagnosis of necrotic cancer of epithelial or lymphocytic origin, and the presence of polymorphous spindle cells with dark nuclei and irregular outlines may raise the suspicion of sarcoma or sarcomatous mesothelioma (Fig. 3.12B).

#### Additional Comments

- Neutrophils with small spheric cytoplasmic inclusions are called ragocytes, a term introduced by Delbarre and colleagues. These cells are common in rheumatoid effusions, but they have a low diagnostic impact because they may be present in a variety of other disorders. We refer to the comments in Chap. 22 of *Comprehensive Cytopathology* by M. Bibbo [17].
- Almost all patients with rheumatoid effusions diagnosed by cytology have clear evidence of rheumatoid arthritis.
- However, pleural or pericardial manifestation of rheumatoid disease may rarely precede joint disorder [3, 29], a fact that has to be kept in mind in cases where an adequate cytologic pattern is present but accompanying clinical information is incomplete or arthralgia is not yet apparent.
- As mentioned above, rheumatoid granulomas exfoliate their cellular components into serous cavities. In contrast, tuberculous nodules in serous membranes are unable to release granulomatous elements, because they are encased by a thick wall of lymphocytes resulting in typical lymphocytic effusions.

### 3.1.7.5 Granuloma Fragments

In rare cases, small fragments of granulomas composed of activated histiocytes and a fibrous component may be encountered in smears from effusions. The most common source is postoperative exfoliation of cells from fresh granular scar tissue into the body cavity fluid. However, epithelioid features of the histiocytes could suggest sarcoidosis.

## 3.1.8 Crystalline Deposits

### 3.1.8.1 Intracytoplasmic Immunoglobulin Deposits [8, 14] (Fig. 3.14)

**Etiology**

- Based on a few studies, it has been concluded that the crystalline inclusions are probably abnormal paraproteins and immunoglobulins produced by plasma cells. The mechanism for immunoglobulin crystal storing in tissues of various organs and in effusions is unclear.
- Crystalline inclusions have been observed in patients with multiple myeloma, isolated plasma cell tumors, transient plasma cell hyperplasia, monoclonal gammopathy, non-Hodgkin lymphoma, and after bone marrow transplantation. Immunoglobulin deposits are overwhelmingly associated with tumors expressing kappa light chain immunoglobulins.
- The disorder may precede the clinical diagnosis of plasma cell dyscrasia or one of the above-mentioned diseases.

**Microscopic Features and Immunocytochemistry**

- Cytoplasmic immunoglobulin storage is mainly observed in histiocytes but also in mesothelial cells and plasma cells. The deposits may also occur as background material.
- In the Pap stain, the refractile inclusions are bright green-yellow, made up of bar-like and needle-like elements. The bars are irregularly laminated. Lack of birefringence.

Galed-Placed and contributors [8] could show immunopositivity of the inclusions for selected heavy- and light-chain immunoglobulins.

**Additional Comments**

Other inclusions forming concentric lamellar bodies of phospholipid type in distended cytoplasm have been described by Zaharopoulos et al. [31].

### 3.1.8.2 Cholesterol (Fig. 3.15)

Cholesterol crescents and plates may be present in cases of chronic relapsing effusions of nontumorous and tumorous origin. In the vast majority of cases, cholesterol deposits are due to chronic pleural tuberculosis and rheumatoid pleuritis and can be observed in relapsing postobliteration effusion. Fluid from the abdominal cavity containing cholesterol deposits is strongly indicative of a large cystic tumor (see Sect. 3.1.7.2 “Cyst Content,” p. 245).

### 3.1.8.3 Psammoma Bodies

Psammoma bodies are described in Sect. 3.2.4.1, p. 271.

## 3.1.9 Effusion with Necrotic Background

- Elements from *benign cellular debris* are uniform and round, granular and finely vacuolated. Large intra-abdominal cysts or tuberculous and rheumatoid serositis (pleural and pericardial fluids) mainly provide cell detritus.
- *Tumor necrosis* is characterized by polymorphic small to large elements partly maintaining cellular shapes. Those elements may still contain pyknotic nuclei. Using the Pap stain, the cytoplasm is cyanophilic to eosinophilic and focally vacuolated. Necrotic background material is indicative of undifferentiated large-cell carcinoma or high-grade NHL.

## 3.1.10 Effusions and Mucus

- The Pap method stains mucus pink. Mucinous cytoplasmic inclusions appear as homogeneous globules of various sizes; the nucleus is excentrically positioned. Mucinous background material in cytologic preparations exhibits as streaks that may be stained cyanophilic.
- Mucin containing cells with or without nuclear atypia and background mucus are highly suggestive of a malignant mucinous neoplasia.
- See also Sects. 3.2.3.3.1 “Pseudomyxoma Peritonei,” p. 269, 3.2.4.2 “Mucus,” p. 271, and 3.2.4.3 “Cytoplasmic Vacuolization,” p. 271.

**Caution**

- Background mucus and complete absence of malignant cells does not argue against malignancy.
- Extremely well-differentiated adenocarcinomas attended with background mucus (e.g., pseudomyxoma peritonei) may completely lack nuclear atypia and other cytologic signs of malignancy.
- Background mucus attended by “activated histiocytes” is an important diagnostic indicator for discohesive adenocarcinomas with histiocytoid features.
- It should be emphasized that most background features, including mucus, are readily recognized in low magnification.

## 3.1.11 Rare Events

When practicing cytodiagnostics of effusion, it is important to keep in mind the following issues:

#### 3.1.11.1 Right-Side Pleurocentesis in Patients with Diaphragmatic Elevation

Right-side pleurocentesis in patients with diaphragmatic elevation may yield normal hepatocytes, content of a hepatic hydatid cyst, or fluid from a huge abdominal cystic lesion.

- *Normal hepatocytes* (Fig. 3.16) should not be misinterpreted as metastasis of an oncocytic neoplasia.
- The typical basic pattern of *hydatid cysts* (Fig. 3.17) should always be present: smears that contain opaque debris and lack nucleated cellular elements. Subsequently, one has to search carefully for hooklets (see Sect. 9.1.7.3, p. 590).
- Right-side pleurocentesis may accidentally yield *cystic content* in patients with diaphragmatic elevation caused by a large abdomen-filling cystic mass and concomitant pleural effusion (further information is given in Sect. 3.1.7.2 "Cyst Content," p. 245 including Table 3.1.1).

#### 3.1.11.2 Puncture of a Rib (Fig. 3.18)

Immature myeloid cells and megakaryocytes have to be accurately identified. Misdiagnosis of a malignant tumor is easily possible.

#### 3.1.11.3 Accidental Puncture of Adjacent Organs

Besides hepatic parenchyma cells, components from other organs may be aspirated when an effusion is removed by inserting a large-bore needle: cells from cardiac muscle, cells from the lung periphery, and epithelial clusters from the bowel mucosa. The latter could cause diagnostic problems with adenocarcinoma.

#### 3.1.11.4 Rare Benign Lesions and Tumors

- Selected localized mesothelial and submesothelial entities are documented in the literature: pleural plaques, benign multicystic mesothelioma (peritoneal inclusion cysts), adenomatoid tumor, localized and diffuse fibrosis of serous membranes, and lymphangioleiomyomatosis [27]. However, these disorders are hardly ever encountered in cytologic specimens.
- Benign and equivocal disorders encountered in peritoneal washings are discussed in the corresponding Chap. 3.3 "Effusions, Aspiration and Washing from Cul-de-Sac, Douglas Pouch, Peritoneal Cavity" (p. 300).

### 3.1.12 Further Reading


1. Afify AM, Al-Khafaji BM, Paulino AF, Davila RM. Diagnostic use of muscle markers in the cytologic evaluation of serous fluids. Appl Immunohistochem Mol Morphol 2002;10:178-82.
2. BeesonPB, Bass DA. The Eosinophil. Philadephia, WB Saunders, 1977.
3. Boddington MM,Spriggs AI, Morton Ja, Mowat AG. Cytodiagnosis of rheumatoid pleural effusion. J Clin Pathol 1971;24:95-106.
4. Chang CJ, Cheng JH, Lin MS, et al. J Formos Med Assoc 2007;106:156-160.
5. Das DK. Serous effusions in malignant lymphomas: a review. Diagn Cytopathol 2006;34:335-347.
6. Domfeh AB, Nodit L, Gradowski JF, Bastacky S. *Mycobacterium kansasii* infection diagnosed by pleural fluid cytology. a case report. Acta Cytol 2007;51:627-630.
7. Ellman Ph, Cudkowics L, Elwood JS. Widespread serous membrane involvement by rheumatoid nodules. J Clin Path 1954;7:239-244.
8. Galed-Placed I. Immunoglobulin Crystal-Storing histiocytosis in a Pleural Effusion from a woman with Iga kappa Multiple Myeloma. A case report. Acta Cytol 2006;50:539-541.
9. Gill SA, Meier P A, Kendall BS. Use of desmin immunohistochemistry to distinguish between mesothelial cells and carcinoma in serous fluid cell block preparations. Acta Cytol 2000;44:976-80.
10. Guzman J, Bross KJ, Wurtemberger G, et al. Tuberculous pleural effusions: Lymphocyte phenotypes in comparison with other lymphocyte-rich effusions. Diagn Cytopathol 1989;5:139.
11. Kalomenidis I, Light RW. Pathogenesis of the eosinophilic pleural effusions. Curr Opin Pulm Med 2004;10:289-293.
12. Keagle M, Marcks KA, Kaiser JS. Cytologic manifestation of rheumatoid arthritis in pleural effusion. Acta Cytol 1981;25:33-36.
13. King J, Thatcher N, Pickering C, Hasleton P. Sensitivity and specificity of immunohistochemical antibodies used to distinguish between benign and malignant pleural disease: a systematic review of published reports. Histopathology 2006;49:561-568.
14. Martin AW, Carstens PHB, Yam LT. Crystalline deposits in ascites in a case of cryoglobulinemia. Acta Cytol 1987;31:631-636.
15. Matthai SM, Kini U. Diagnostic value of eosinophils in pleural effusion: a prospective study of 26 cases. Diagn Cytopathol 2003;28:96-99.
16. Nagaoka S, Maruyama R, Koike M, et al. Cytology of Langerhans cell histiocytosis in effusions: a case report. Acta Cytol 1996;40:563-566.
17. Naylor B. Pleural, Peritoneal and Pericardial fluids. In: Bibbo M. (ed). Comprehensive Cytopathology. W.B. Saunders Company, Philadelphia, 1991,p.569.
18. Nosanchuk JS, Naylor B. A unique cytologic picture in pleural fluid from patients with rheumatoid arthritis. Amer J Clin Pathol 1968;50:330-335.
19. Olson PR, Silverman JF, Powers CN. Pleural fluid cytology of Hodgkin's disease: Cytomorphologic features and the value of immunohistochemical studies. Diagn Cytopathol 2000,22:21-24.
20. Pappas CA, Rheinlander HF, Stadecker MJ. Pleural effusion as a complication of solitary eosinophilic granuloma of the rib. Hum Pathol 1980;11:675-677.
21. Spieler P. Beurteilung und Bedeutung cholesterinhaltiger Punktionsflüssigkeiten aus dem Abdomen. Schweiz med Wschr 1976;106:1510-1513.
22. Spieler P. The cytologic diagnosis of tuberculosis in pleural effusion. Acta Cytol 1979;23:374-379.
23. Spieler P, Hell M. Serous rheumatoid disease following chronic polyarthritis. Five cases with special regard to cytopathology. Schweiz med Wschr 1984;114:1110-1117.

24. Spieler P, Kradolfer D, Schmid U. Immunocytochemical characterization of lymphocytes in benign and malignant lymphocyte-rich serous effusions. Virchows Arch Pathol Anat 1986;409:211-221.
25. Spriggs AI. Pleural eosinophilia due to pneumothorax. Acta Cytol 1979;23:425.
26. Spriggs AI, Boddington MM. Absence of mesothelial cells from tuberculous pleural effusions. Thorax 1960;15:169-171.
27. Tynski Z, Eisenberg R. Cytologic findings of lymphangioleiomyomatosis in pleural effusions. Acta Cytol 2007;51:578-580.
28. Veress JF, Koss LG, Schreiber K. Eosinophilic pleural effusions. Acta Cytol 1979;23:40-44.
29. Ward R. Pleural effusion and rheumatoid disease. Lancet 1961;2:1336-1338.
30. Winkler CF, Yam LT. Pleural effusion in histiocytosis X. Arch Intern Med 1980;140:988.
31. Zaharopoulos P, Wen JW, Wong D. Membranous lamellar cytoplasmic inclusions in histiocytes and mesothelial cells of serous fluids. Their relationship to phagocytosis of red blood cells. Acta Cytol 1998;42:607-613.

## Figs. 3.1 and 3.2 Common benign effusion cytology.

**Fig. 3.1** Peritoneal fluid exhibiting a few lymphocytes, a few histiocytes, and numerous benign mesothelial cells. Mesothelial cytoplasm is typically biphasic: dense cyanophilic perinuclear rim and fine vacuolation at the periphery. Cytoplasm comprising foamy appearance (short arrow) and empty inclusions, giving the cell a signet ring aspect (long arrow). Mesothelial cells forming pairs, with one pair shows an empty window between the cells (tall arrowheads), are also present. Note cytomorphology of typical histiocytes (small arrowheads) (direct sediment smear, Pap stain, higher magnification).

**Fig. 3.2** Direct sediment smear of a pleural effusion showing activated mesothelial cells. The cells are irregularly arranged and enlarged exhibiting rounded nuclei and prominent nucleoli. Note a degenerating mesothelial cell with a homogeneous dark nucleus and eosinophilic cytoplasm (arrow); degenerative mesothelial cell changes should not lead to a misdiagnosis of squamous cell carcinoma (Pap stain, high magnification).

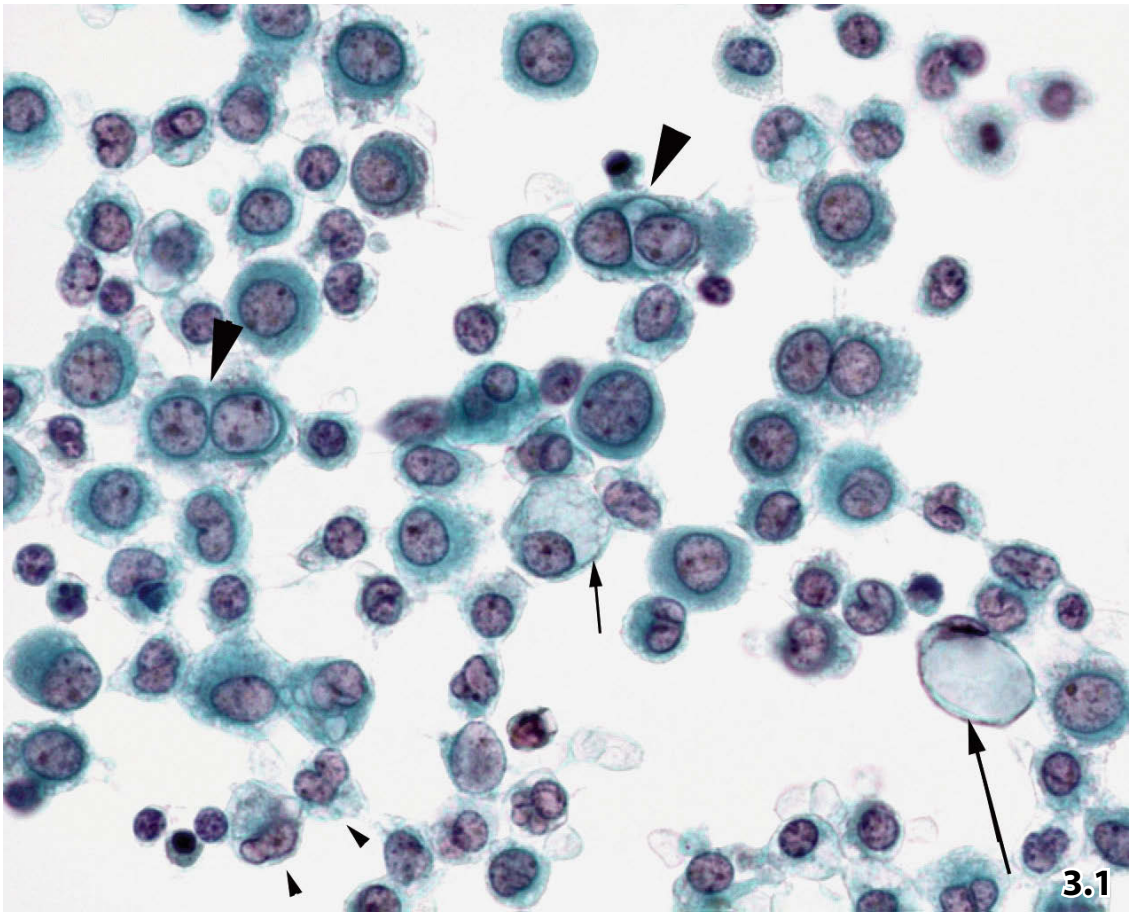

3.1

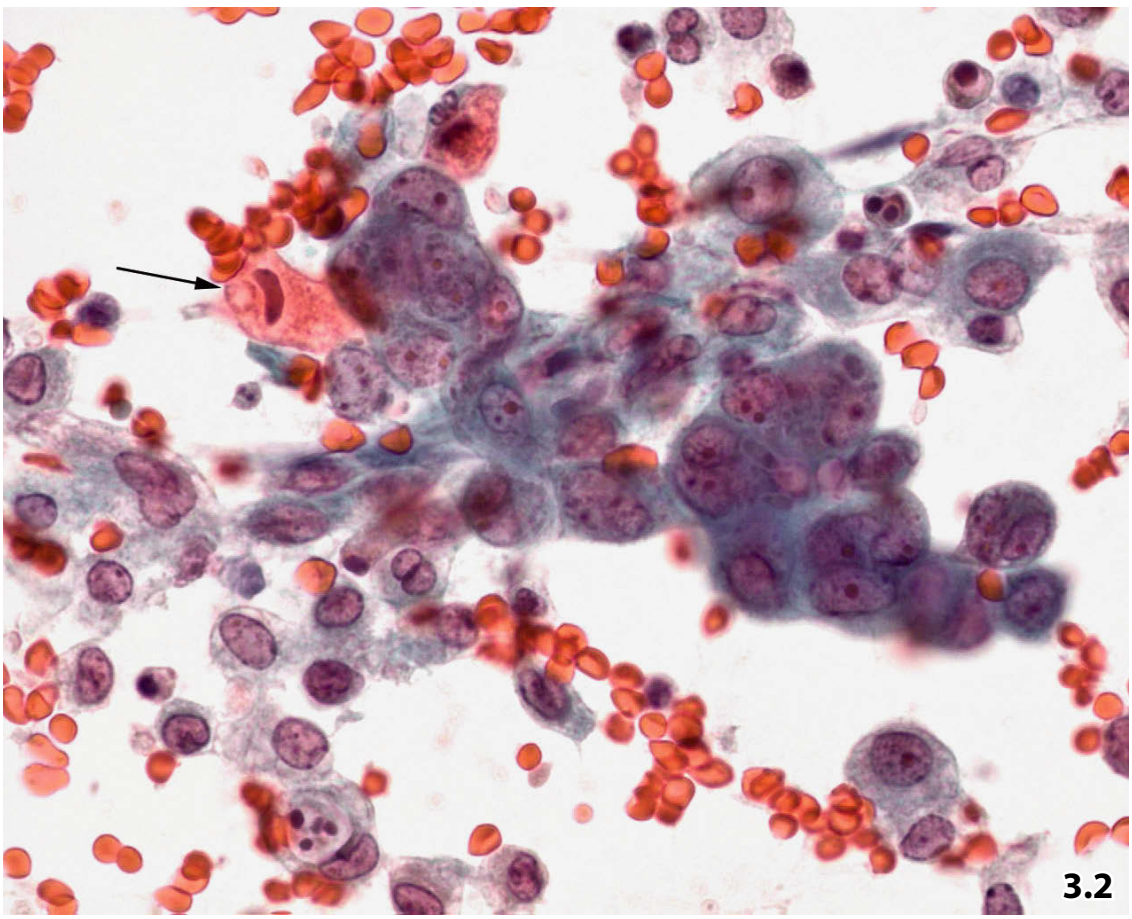

3.2

**Fig. 3.3A, B Hyperplastic mesothelial cells versus carcinoma.**
A 77-year-old woman with a history of metastatic breast cancer presented with a very recent pleural effusion. **A** Compact cell clustering, loss of cellular polarization, and pronounced nuclear irregularity give rise to diagnostic dilemma between activated mesothelial cells and breast cancer (direct sediment smear, Pap stain, high magnification). **B** Immunostaining using calretinin affirmed the mesothelial nature of the atypical cell clusters (Pap-prestained smear).

**Fig. 3.4A, B Metastatic endocrine tumor versus hyperplastic mesothelial cells.**
A 59-year-old man presented with a parapancreatic tumor (by ultrasound) and ascites. **A** *Cytologic diagnosis* of ascitic fluid was proliferating mesothelial cells, even though tight ball-like cell clustering with smooth outline (arrows) is generally accepted to be an unusual feature of mesothelial hyperplasia in effusion (direct sediment smear, Pap stain, higher magnification). **B** A consecutive FNAB of the abdominal tumor mass yielded the diagnosis of an endocrine tumor, likewise subsequent immunostaining of the mesothelial cell clusters in the peritoneal fluid (Pap-prestained smear, chromogranin A).
*Final diagnosis:* Abdominal endocrine carcinoma metastatic to the abdominal cavity.

**Fig. 3.5 Hyperplastic mesothelial cells in uremia.**
Certain metabolic disorders such as uremia may give rise to severe atypias of the mesothelial cells (pleural effusion, direct sediment smear, Pap stain, lower magnification).

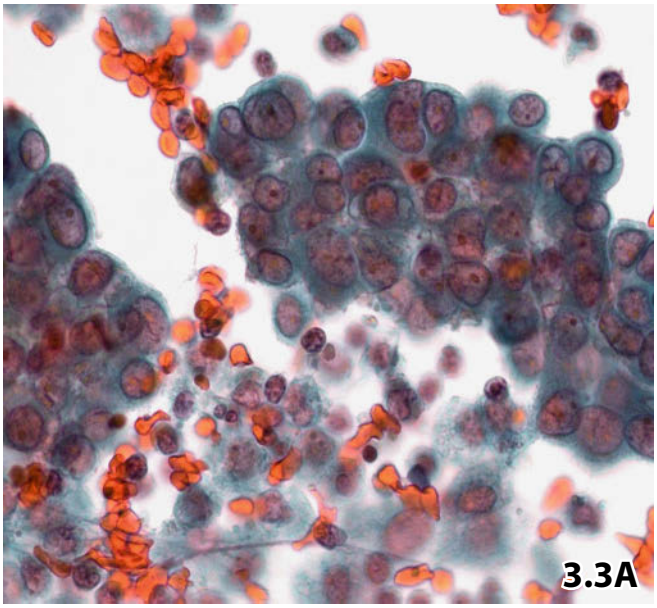
3.3A

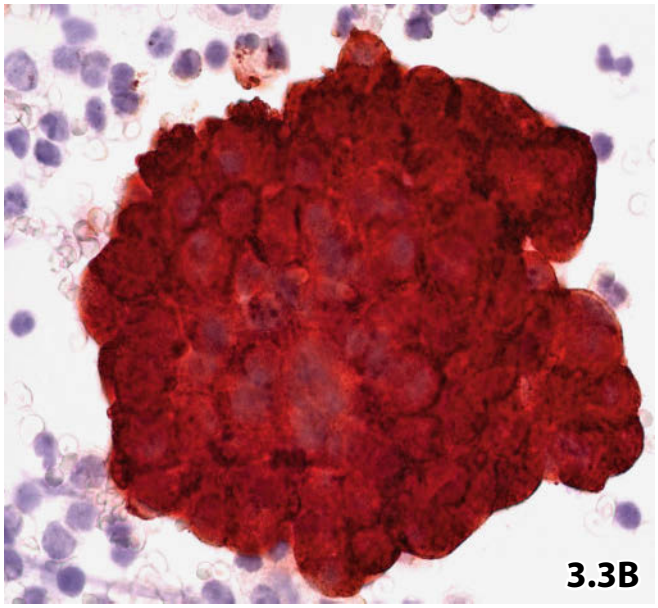
3.3B

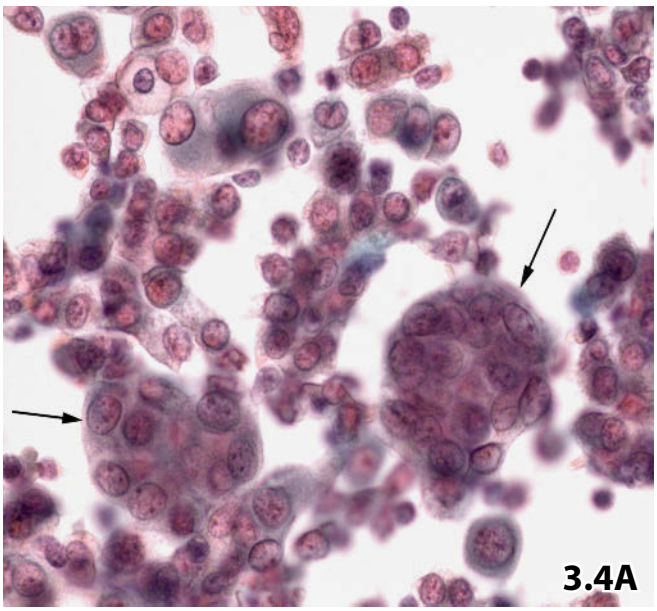
3.4A

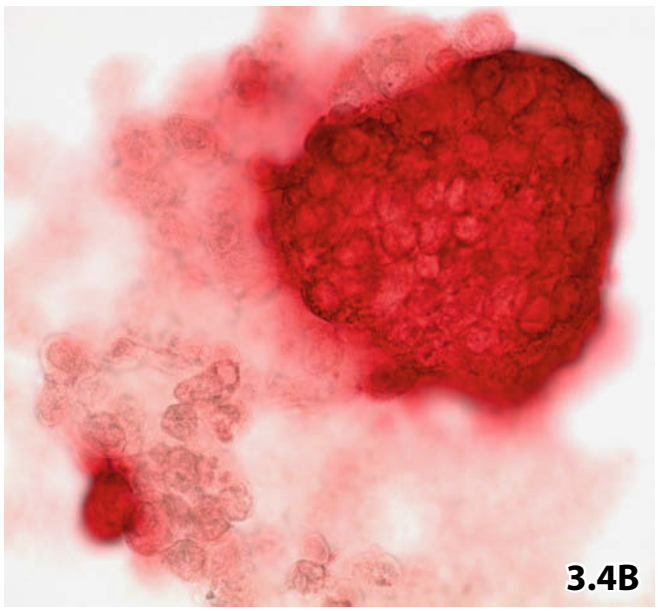
3.4B

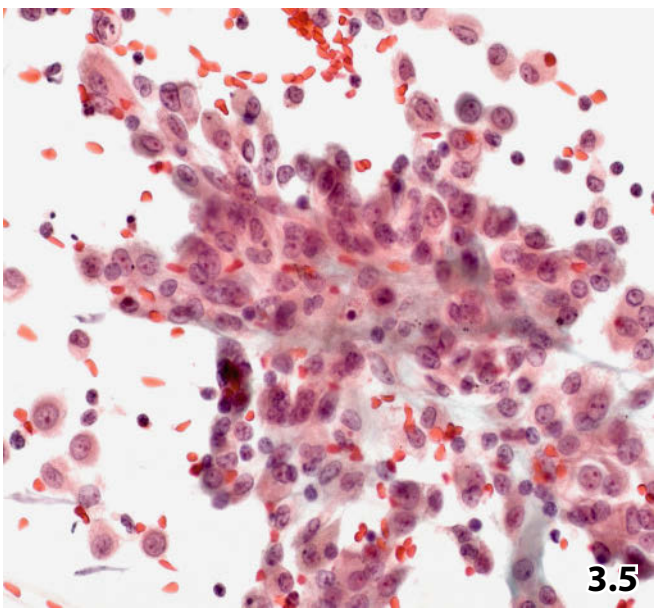
3.5

**Fig. 3.6 Empyema.**
Example of a purulent pleural effusion comprising hyphae of aspergillus species (arrow). Detritic neutrophils should not be mistaken for tumor necrosis (direct sediment smear, Pap stain, low magnification).



## Figs. 3.7 and 3.8 Benign reactive lymphocytosis.

**Fig. 3.7** An elderly woman presented with a pleural effusion. There was no specific clinical history available. The microscopic picture at high magnification reveals three mesothelial cells and numerous lymphocytes, the latter exhibiting sporadic prominent nucleoli. Nuclear molding, nuclear indentations (arrows), and the loose coarse chromatin texture indicate benign T lymphocytes (direct sediment smear, Pap stain).

**Fig. 3.8** Severe reactive lymphocytosis developing after surgical implantation of an epimyocardial pacemaker (old case from the 1970s). Note the distinct blastic transformation of the lymphoid cells and high mitotic activity (one mitosis, arrow). Monomorphic appearance of the cell population and overall bland nuclear features exclude malignant lymphoma (pericardial effusion, direct sediment smear, Pap stain, high magnification).

**Fig. 3.9A, B Lymphocytosis in florid pleural tuberculosis.**
A 61-year-old man suffering from open pulmonary tuberculosis confirmed by microbiologic tests. A pleural effusion sample revealed the classical cell features of florid pleural tuberculosis (direct sediment smear, Pap stain). **A** At very low magnification, the sample shows a monotonous lymphoid cell pattern. Note complete absence of histiocytes and mesothelial cells. **B** The benign nature of the lymphocytes is characterized by their nuclear shape (indicating T lymphocytes) and the chromatin texture. Still, to some extent mild nuclear enlargement and distinct nucleoli are evident (high magnification).

**Fig. 3.10 Liver cirrhosis.**
Abdominal transudates in the course of liver cirrhosis may show distinct cytologic characteristics: lower magnification reveals a mixed cell pattern mainly consisting of small to medium-sized histiocytes. Histiocytic nuclei are wrinkled and folded. The cytoplasm has a foamy appearance; both phagocytic activity and hyaline cyanophil inclusions (arrows) are striking. Activated mesothelial cells rarely appear compared to the number of histiocytes, neutrophils, and lymphocytes (direct sediment smear, Pap stain).

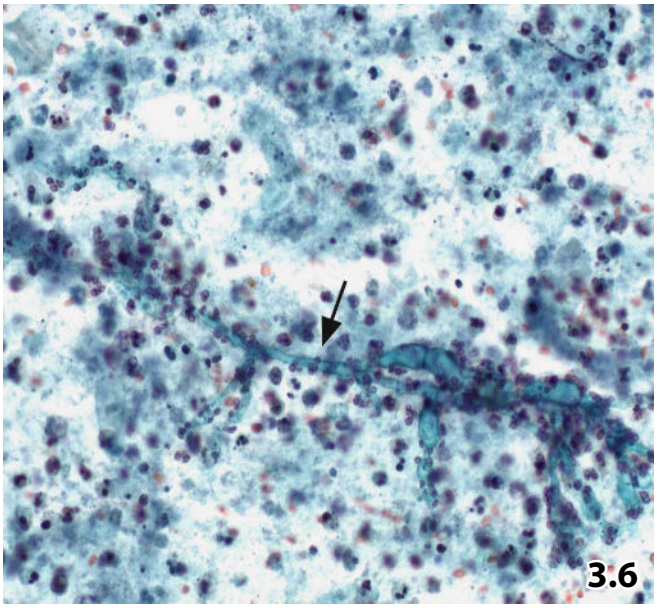
3.6

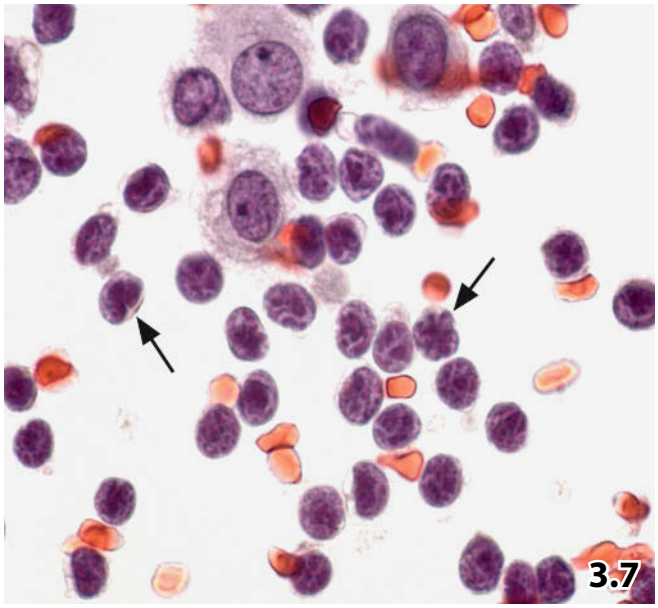
3.7

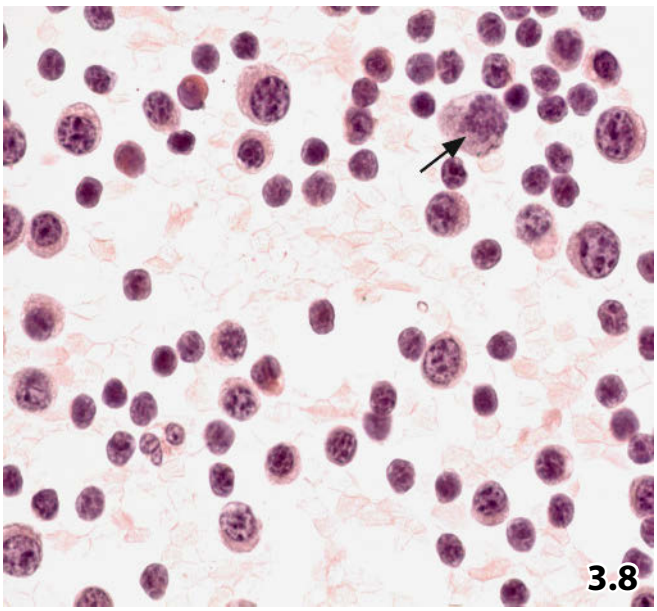
3.8

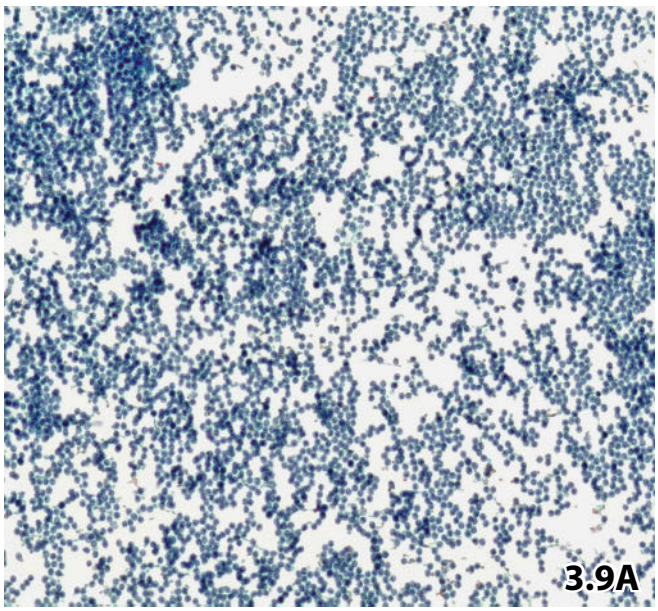
3.9A

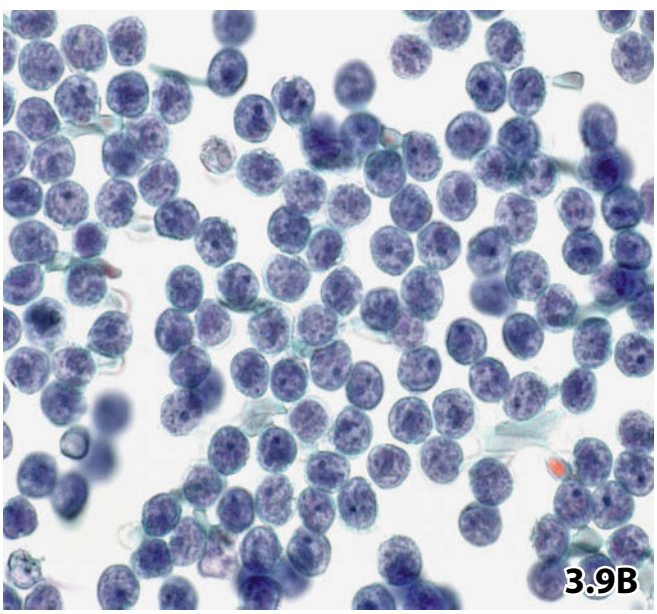
3.9B

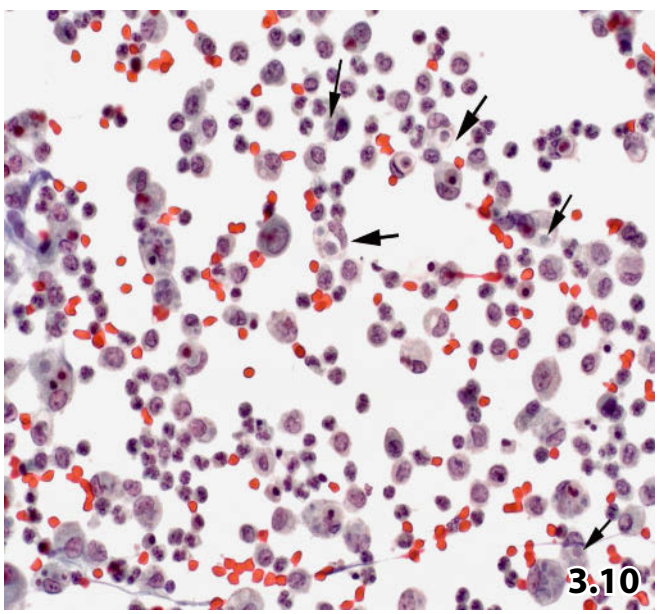
3.10

**Fig. 3.11 Cyst content.**
An elderly woman presented with a gigantically swollen belly at the emergency unit; the patient had never consulted a physician before. Voluminous ascites caused by ovarian cancer was the initial clinical diagnosis.
*Cytologic examination* of the ascitic sediment could not confirm the clinical diagnosis: microscopy revealed cyst content displaying large histiocytes with abundant foamy cytoplasm scattered in a hemorrhagic and proteinaceous background comprising detritic material (direct sediment smear, Pap stain, high magnification).
*Final diagnosis* (surgical exploration and histology): Abdomen-filling monstrous benign ovarian cyst embodying several liters of serous fluid.

**Figs. 3.12 and 3.13 Rheumatoid serositis.**
Two different patients suffering from rheumatoid disorders.

**Fig. 3.12A, B** The microphotographs from a sediment smear of a pericardial effusion exhibit the unique appearance of rheumatoid serositis. Direct sediment smears are Pap-stained. **A** Spindle-shaped histiocytes occasionally multinucleated and histiocytic giant cells exhibiting polygonal cytoplasm (arrows). Background of the smear exhibiting degenerating cells and amorphous granular debris (lower magnification). **B** Pronounced nuclear irregularities in combination with a clear nucleoplasm are readily recognized at high magnification. Irregularly shaped pyknotic dark nuclei should not mislead one to a false-positive diagnosis of malignancy such as sarcoma (arrows).

**Fig. 3.13** A 50-year-old woman presented with a pleural effusion. Direct sediment smears were stained with the Papanicolaou method. Well preserved fragments of rheumatoid granulomatous tissue may occasionally appear in sediment smears of effusions from patients with rheumatoid serositis: activated histiocytes, epithelioid histiocytes, granular debris (high magnification)

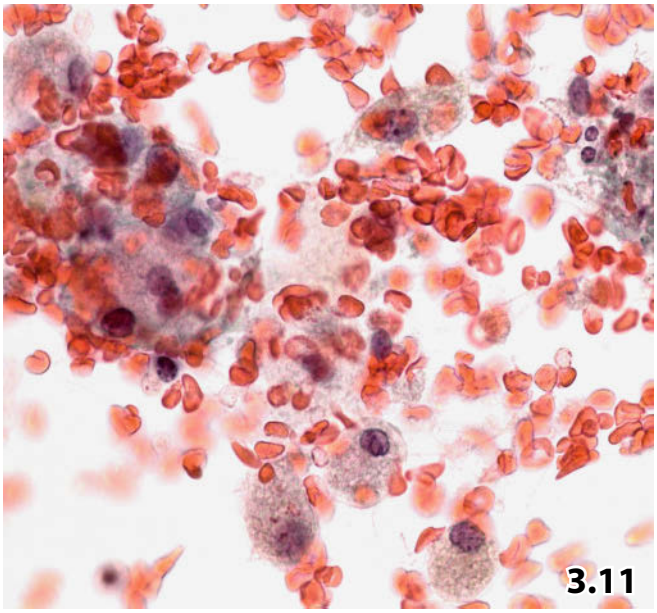
3.11

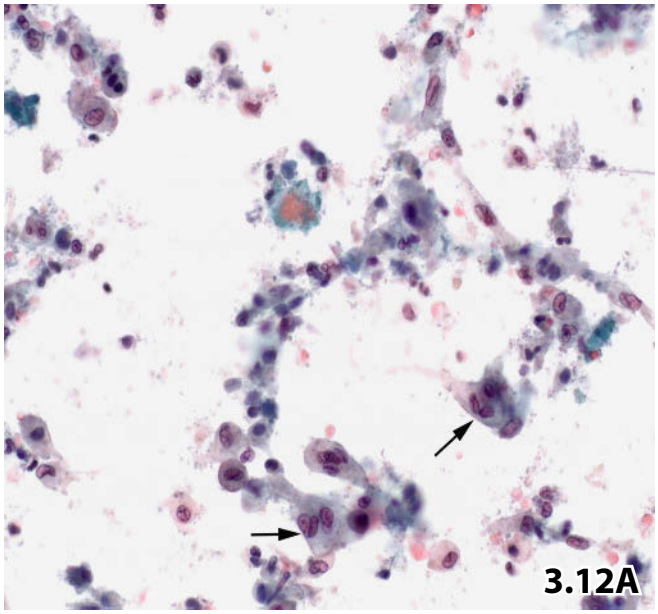
3.12A

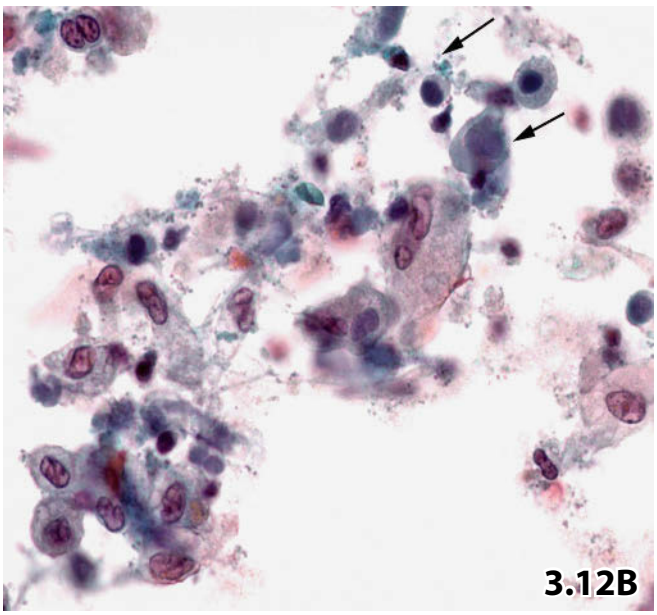
3.12B

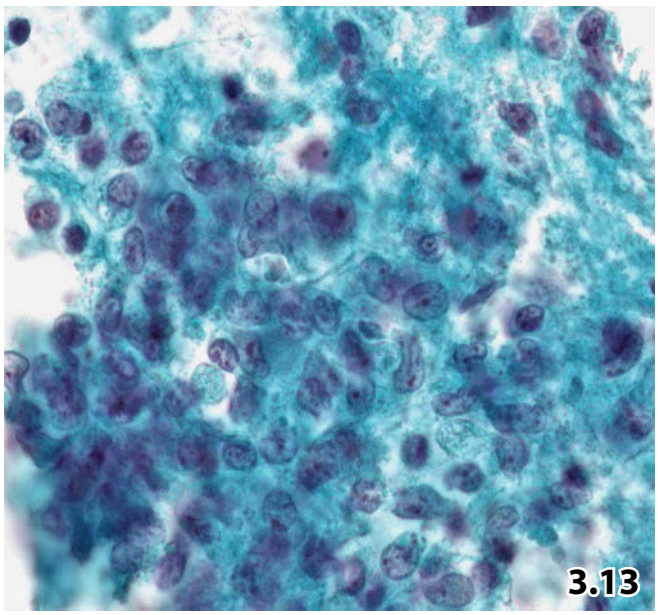
3.13

**Fig. 3.14 Intracytoplasmic immunoglobulin deposits.**
A 74-year-old man suffering from heart failure and dyspnea. Transitional cell carcinoma of the bladder had been diagnosed 2 years before. The patient presented with right-sided pleural effusion. Cytologic sediment smears were extremely cellular. They exhibited mesothelial cells and histiocytes occasionally loaded with bar-like refractile elements (center). The latter are consistent with proteinaceous condensates. Absence of malignant cells. Subsequent laboratory tests did not detect any lymphoid or hematopoietic disorder (Pap stain, high magnification).

**Fig. 3.15 Cholesterol deposits.**
Cytologic diagnosis of cholesterol pleuritis was established in a patient with long-lasting pleural effusion. Sediment smears exclusively contain cholesterol plates and cholesterol needles being birefringent upon polarization (native specimen, high magnification).

**Fig. 3.16 Right side pleurocentesis and diaphragmatic elevation: accidental liver puncture.**
Hepatocytes occurring in pleural fluid may easily mislead one to a diagnosis of oncocytic neoplasia (direct sediment smear, Pap stain, high magnification).

**Fig. 3.17 Right-sided pleurocentesis and diaphragmatic elevation: accidental puncture of a hepatic hydatid cyst.**
Characteristic background material of hydatid cystic fluid with scattered hooklets (upper and lower left). Please note that hooklets that are not presented in profile (arrow) may easily be ignored (direct sediment smear, Pap stain, high magnification).

**Fig. 3.18 Pleurocentesis and accidental puncture of a rib.**
Heterogeneous cellular appearance: erythroblasts, immature myeloid cells and a few megakaryocytes (upper left). It is important to be aware of the possibility of accidental aspiration of bone marrow during thoracal and transthoracic needle punctures. Otherwise, there are chances that a misdiagnosis of a myeloproliferative disorder or another malignant neoplasia is rendered (direct smear, Pap stain, high magnification).

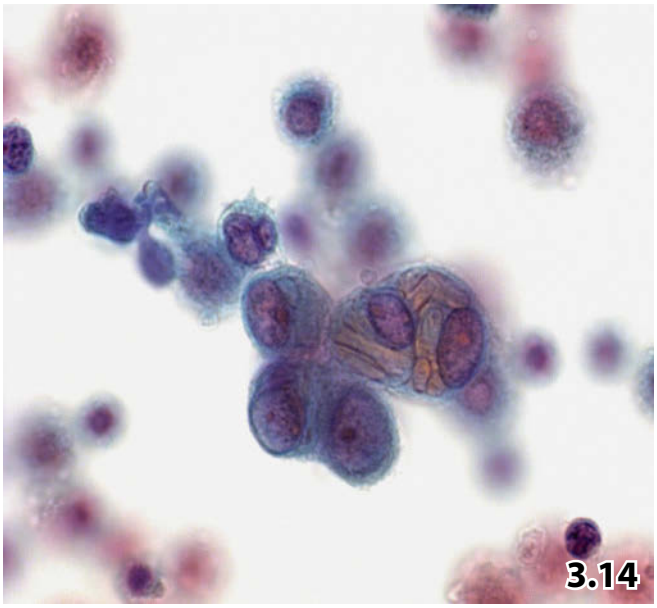
3.14


3.15

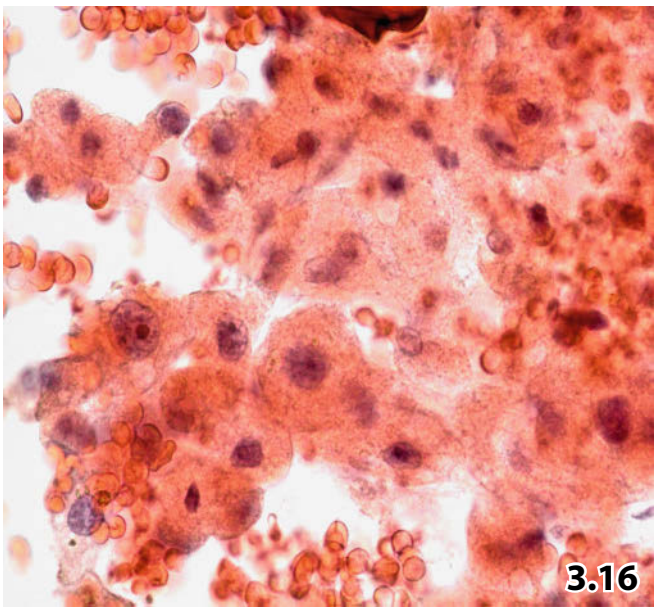
3.16

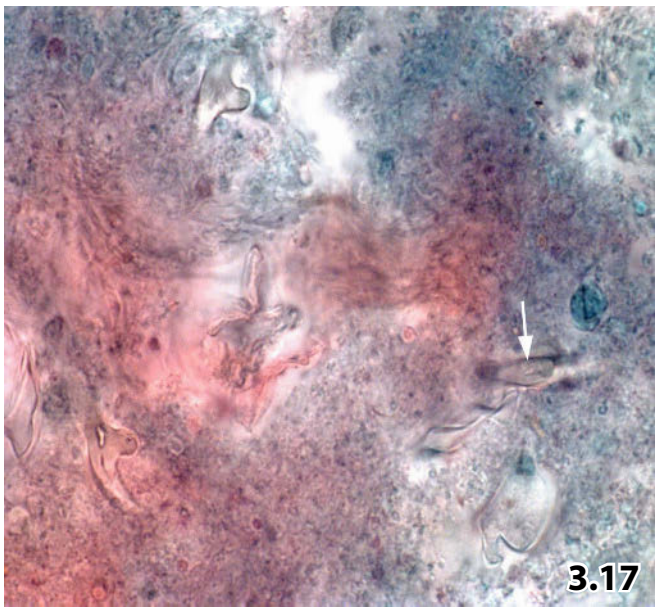
3.17

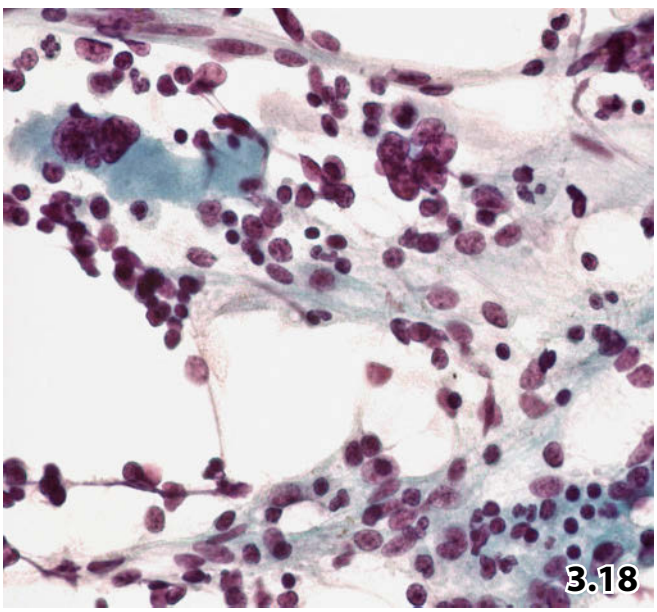
3.18

# Section 3.2
# Effusions

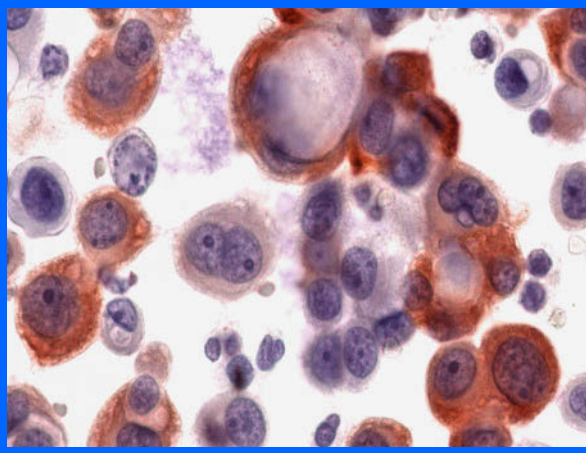

## Pleural
## Pericardial
## Peritoneal
## Tunica Vaginalis Testis

## Malignant Lesions

### 3.2.1 Primary Neoplasm: Diffuse Malignant Mesothelioma

**Etiology, Pathogenesis, General Comments** [15]

- In 1960, Wagner and contributors provided the first significant evidence of the relationship between asbestos and pleural mesothelioma [64]. Other studies confirmed this link on the basis of clinical findings and animal experiments. An association between asbestos and diffuse peritoneal mesothelioma, pericardial mesothelioma, and mesothelial tumors of the tunica vaginalis testis was established later.
- The carcinogenic effect of asbestos fibers is due to the physical interaction of fibers with the target cells, and the production of chemical mediators at the area of asbestos deposits.
- Pleural mesotheliomas are common. Peritoneal mesothelioma accounts for roughly 25% of these tumors, and 2% of mesotheliomas arise in the pericardium. Malignant mesothelioma of the tunica vaginalis testis are rare and predominantly of the papillary type.
- Large bloody effusions lacking nucleated cells in cytologic preparations are sometimes observed with mesothelioma. It could be hypothesized that the absence of tumor cells is particularly observed in the desmoplastic and sarcomatous variants of mesothelioma, which are unable to release the tightly enclosed epithelial tumor cells.
- Malignant mesothelioma exhibit a wide spectrum of subtypes ranging from entirely epithelial to entirely mesenchymal, and well differentiated to anaplastic.
- 50% of pleural and 75% of peritoneal malignant mesothelioma are of the epithelial type; 25% and 15%, respectively, are of the biphasic and sarcomatous type.

#### 3.2.1.1 Epithelial Mesothelioma (Figs. 3.19–3.24)

**General Comments**

- The mesothelial origin of epithelial mesothelioma is supported by tissue culture and electron microscopy studies, and by the close resemblance between reactive and malignant mesothelial cells. Most mesotheliomas initially exhibit with an effusion on clinical and radiographic examination. In many cases, cytologic examination of the aspirated fluid yields the first firm or at least tentative diagnosis with minimal trauma for the patient. In experienced hands, a reliable cytodiagnosis is rendered in 60–80% of epithelial mesotheliomas [58].
- Radiographic tests of the chest may show nodular or irregular thickened pleura as a strong hint of mesothelioma, information which may be helpful for cytologic evaluation.
- Extension of *pleural mesotheliomas* to the opposite pleural cavity, into the pericardial and peritoneal cavity, is common in advanced tumors.
- *Pericardial mesothelioma* often spreads to the adjacent pleura and the mediastinum.
- *Malignant mesotheliomas of the tunica vaginalis testis* may grow as solid nodules but may also form papillary excrescences.

**Microscopic Features**

- Cytomorphology of single cells and the cytoarchitectural pattern are often highly specific, because mesothelial characteristics are preserved. In other cases, the distinction from secondary adenocarcinoma is not possible at all. Auxiliary analyses are required in many cases.
- Epithelial mesotheliomas exhibit mainly a solid or tubulopapillary pattern.
- It is difficult to differentiate between well-differentiated mesothelioma and hyperplastic mesothelial cells. However, the cytologic preparations are mostly cellular and the monomorphic tumor cells are intermingled with less well-differentiated cells and typical clusters, indicating malignancy.

Criteria of malignancy of the epithelial tumor form include:

- Enlargement of the malignant mesothelial cells compared to the benign counterparts in the same smear.
- Irregular outlined nuclei with a dense granular and coarse chromatin texture.
- Hyperchromasia, even though often discrete.
- Prominent nucleolus.
- Heavily stained abundant cytoplasm with a foamy appearance at the periphery.
- Malignant mesothelial cell clusters may predominate and are larger than those of hyperplastic mesothelium. The former are ball- or morula-like with a hobnail contour; the outer cell layers frequently enclose a core of homogeneous material.
- The central cores are an important diagnostic feature because their frequency is much higher in mesothelioma than in clusters of hyperplastic mesothelial cells or in aggregates of adenocarcinomas [66] (Fig. 3.21).
- The cytoplasm of degenerate malignant mesothelial cells may sometimes stain acidophilic with the Papanicolaou method. Mesothelioma with squamous differentiation, although rare, is a possible diagnosis in those cases. However, large irregular dark-red-stained cytoplasmic bodies combined with nuclear irregularity may lead to diagnostic confusion with malignant cells of squamous cancer.
- Effusions caused by epithelial mesothelioma may contain high concentrations of hyaluronic acid, giving rise to high viscosity of the fluid sample and are recognizable as acidophilic or cyanophilic background material in the cytologic specimens. Masses of hyaluronic acid cannot be differentiated from mucus by visual microscopic impression.

**Caution**

- Large cytoplasm vacuoles in mesothelioma cells may stain pink with Pap. A false diagnosis of signet ring cells accompanying mucinous adenocarcinoma is possible (Fig. 3.24A).
- Acidophilic or cyanophilic background material matches hyaluronic acid and mucus by light microscopy.
- Degenerating mesothelioma cells with large irregular eosinophilic cytoplasm and hyperchromatic nuclei may closely resemble squamous carcinoma cells (Fig. 3.22).
- Morphologic differences between benign and malignant mesothelial cells have been analyzed quantitatively by Kwee et al. [38].

**Differential Diagnosis**

- Epithelial mesotheliomas may resemble adenocarcinomas in various stages of differentiation, which can originate from various organs (see Sect. 3.2.3.1, "Most Frequent Metastatic Carcinomas," p. 263).
- Three different primary origins should be considered in cases with papillary tumors in peritoneal effusions in women: serous papillary carcinoma of the ovary, primary serous papillary carcinoma of the peritoneum, and the rare well-differentiated peritoneal papillary malignant mesothelioma [20]. However, the third tumor type presents only in rare instances with ascites.
- A small-cell variant of mesothelioma [31, 42] has rarely been reported and resembles small-cell carcinoma in other organs: monomorphic small cells with a high N/C ratio and hyperchromatic wrinkled nuclei. Sometimes small malignant cells appear along with more typical mesothelioma cells. Small-cell lung cancer with a pleural invasion may be difficult to exclude.

### 3.2.1.2 Mesothelioma with Sarcomatous Component (Fig. 3.25)

Malignant mesotheliomas can partly or completely exhibit sarcomatous features. Mixed tumors are referred to as biphasic malignant mesothelioma and pure spindle cell tumors as sarcomatous malignant mesothelioma.

**Microscopic Features**

- The sarcomatoid mesothelioma cells are mainly plump and polymorphic, oval to spindle-shaped; however, sarcomatous tumors can exhibit a wide range of appearances.
- Irregular hyperchromatic nuclei typically adapt to the form of the cytoplasm.
- Occasionally prominent giant cells.
- Rare metaplastic osteoid or cartilage components are barely detectable in smear preparations.

**Differential Diagnosis**

- The sarcomatous pattern of mesothelial neoplasia overlap with that of soft tissue tumors such as malignant fibrous histiocytoma, fibrous sarcoma, and rhabdomyosarcoma. Cytologic determination of these entities is difficult in most cases.
- A biphasic pattern could also be caused by carcinoma with atypical cellular stromal reaction and by spindle cell carcinoma.

### 3.2.1.3 Additional Analyses in the Diagnosis of Mesothelioma

Immunocytochemistry

In cytologic cases with equivocal diagnostic assessment, differentiation between mesothelial and epithelial cells is reliably achieved by applying an antibody panel; we prefer, in the first instance, the two antibodies (AB) for Ber-Ep4 and calretinin.

- Ber-EP4 is present in all epithelial cells and a large number of adenocarcinomas but stains a few mesothelial/mesthelioma cells as well [4, 21] (Fig. 3.24C).
- Calretinin is a reliable marker for mesothelial cells [59] (Fig. 3.24B).
- WT1 (Wilms tumor gene 1) is present in most mesothelial cells but absent in many epithelial cells.
- Cytokeratin 5/6 is also a useful mesothelial marker, but it is of low specificity; immunoreactivity is also documented on cells of pulmonary and nonpulmonary adenocarcinomas, non-small-cell lung carcinomas, and squamous cell carcinoma [22, 59].
- Cytokeratin 5/6 and calretinin may also be positive in sarcomatous mesothelioma.
- CEA has a high specificity for carcinoma cells but a low sensitivity.
- Thyroid transcription factor 1 (TTF1) shows nuclear staining only in cells of lung or thyroid origin; TTF1 is therefore very useful in discriminating mesothelioma from lung carcinoma.

The value of immunocytochemistry in differentiating benign and malignant mesothelial cells has been controversial:

- In some studies [9, 43], p53 and EMA (epithelial membrane antigen) positivity was more often observed in mesothelioma cells than in reactive mesothelial cells. These findings could not be confirmed in other studies [40, 54].
- Similarly, there exist equivocal study results for the role of desmin in differentiating between reactive mesothelial cells (desmin-positive), mesothelioma (desmin-negative), and carcinoma (desmin-negative) [2, 19, 28, 33, 37].
- There are no firmly established guidelines for the use of immunostaining to discern between mesothelial cells, reactive mesothelial cells, and carcinoma cells. Therefore, cytopathologists should develop their own immunocytochemical algorithms for their individual diagnostic practice [41].
- In equivocal cases, a definite cytologic diagnosis is frequently only possible after the investigation of repeated effusion samples.

Cytogenetics

- Homozygous deletion of the *CDKN2A/ARF* (gene locus 9p21), encoding for tumor suppressor genes $p16^{INK4a}$ and $p14^{ARF}$, is one of the best-known genetic abnormalities in mesothelioma. Detection of this deletion by fluorescence in situ hybridization(FISH) has been established [34, 50].
- Detection of numerical chromosomal aberrations of chromosomes 7 and 9 seems to have a valuable potential for improving diagnostic accuracy in effusion cytology [60]. The Multi-target Uro Vysion FISH assay has been reported to be a helpful adjunct in rendering a final diagnosis of malignant mesothelioma by cytology [57].

DNA Ploidy: Flow and Image Cytometry

The potential usefulness of DNA ploidy analysis to distinguish between benign effusion, mesothelioma, and certain types of adenocarcinoma has been reported in several publications [24, 25, 36, 45, 51]. All cases with reactive mesothelial proliferation have been reported as diploid. In contrast, all aneuploid results correspond to malignancy. Still, up to 50% of malignant mesothelioma are reported to express diploid DNA profiles.

## 3.2.2 Primary Neoplasm: Primary Effusion Lymphoma [3, 8, 10, 11, 12, 18, 23, 26, 39, 47, 65]

**Pathogenesis and Etiology**

- Primary effusion lymphoma (PEL) occurs almost exclusively in patients with HIV infection and is consistently associated with the presence of DNA from the human herpes virus 8 (HHV8) [10, 11, 12, 47, 65], which is also known as an etiologic factor in Kaposi sarcoma and Castleman disease.
- The expression of viral interleukin 6 (vIL-6) seems to play an important role in the pathogenesis of PEL [3, 23].

**General Comments**

- The small group of lymphomas called primary effusion lymphomas (PEL) exhibit exclusive or dominant involvement of serous cavities, without a detectable solid tumor mass. Together with the pathognomonic biological marker panel, it is suggested that these tumors are a distinct clinicopathologic entity.
- A PEL-analog malignant lymphoma exclusively involving the pericardium and heart is referred to as primary cardiac lymphoma.
- The diagnosis of PEL depends on distinct results from immunocytochemical and molecular genetic tests (see "Additional Analyses" below).

- PEL is a large-cell lymphoma with morphologic features of large-cell immunoblastic and anaplastic lymphoma.

**Microscopic Features**

- Large and highly polymorphic lymphoid blastic cells with high N/C ratio.
- Irregular nuclear outline, coarse chromatin, hyperchromasia.
- Polymorphic multiple nucleoli.
- Small rims of cytoplasm – vacuolated or densely structured.

**Additional Analyses**

Immunocytochemistry [8]

Tumor cells express leukocyte antigen CD45.

In contrast, B-cell-associated antigens are almost invariably absent.

Plasma cell markers such as CD38 and CD138 should be positive in most cases [26].

HHV8-immunohistochemistry shows a nuclear positivity in virtually all cases.

Molecular Genetics [65]

Exhibition of clonal immunoglobulin gene rearrangements (kappa monoclonal light chains).

HHV8 identification by DNA extraction or in situ polymerase chain reaction (PCR).

Positivity for Epstein-Barr virus by in-situ hybridization in most cases.

**Differential Diagnosis**

PEL should be differentiated from pyothorax-associated lymphoma (PAL), which is strongly associated with Ebstein-Barr virus (EBV) infection but not with HHV8. The tumor cells of PAL typically express B-cell antigens such as CD20 or CD79a, which are usually not detectable in PEL.

**Additional Comments**

Years ago in our institution, we observed two cases of primary cardiac lymphoma with the pathognomonic cytomorphologic features of PEL including an aneuploid DNA profile [39]. Immunocytochemical staining revealed CD45 positivity and in one case positivity for B-cell marker CD20. Immunocytochemistry with a broad marker panel, PCR, and studies for EBV, HHV 8, and HIV could not be performed in those days. Both patients were free of cancer after 9 and 10 years. Despite an unequivocal diagnosis of malignancy based on morphologic and DNA-cytometric findings, the long-term survival rate suggests a pronounced reactive lymphocytic disorder, possibly due to viral pericarditis.

## 3.2.3 Secondary Tumors / Metastases to Serous Membranes

**General Comments**

- Cytomorphologic features and suggestions for auxiliary diagnostic methods are discussed in numerous books and pertinent publications. Therefore, we refer to the literature only for special issues.
- Serosal metastases may be followed by direct extension from adjacent viscera, by vascular tumor-cell spread, or transcoelomic dissemination.
- A wide range of malignant tumors may spread to serous membranes, but adenocarcinomas still account for the majority of malignant effusions. Malignant pleural effusions are caused by adenocarcinomas in about 70% of cases [53]. Papillary cell clustering is an unequivocal characteristic of adenocarcinoma. Cell clusters are elongated, exhibiting branching and budding (Figs. 3.26 and 3.27A).
- A stepwise cytodiagnostic procedure is recommended:
  - Assessment of malignancy on target cells in fluid preparations.
  - Attempt to relate the cellular and cytoarchitectural characteristics to a histogenetic entity.
  - Reflexion to ascertain the primary origin of the tumor.
- Adjacent analyses are essential to help ascertain malignancy, type, and primary site of neoplasms.
- The greatest challenge is to distinguish between adenocarcinoma and mesothelioma.
- A cytologic specimen that is negative for neoplastic cells does not exclude a neoplasm as a cause of the effusion. Effusions may result from subserosal tumor growth, or neoplastic occlusion of vascular channels. Repeated samples from the same patient will present with malignant cells in most cases.
- DNA aneuploidy was found to be a diagnostic marker for malignant cells in serous effusions. Sensitivity depends on the applied cytometric method and histogram interpretation in the respective institutions [46].
- Pay attention to general comments on metastatic neoplasms, including their immunocytochemical attributes provided in Table 15.3.3 (Sect. 15.3.24, p. 978).

### 3.2.3.1 Most Frequent Metastatic Carcinomas

#### 3.2.3.1.1 Lung Primaries

- Carcinoma of the lung is the most common cause of malignant pleural effusion (in about 40% of all cases) and adenocarcinoma is the most common tumor type.
- Tumor dissemination beyond the diaphragm is rare.
- A malignant pleural effusion as the first clinical evidence of nonmesothelial neoplastic disease is due to lung cancer in almost 100% of cases. Primary lung tumor can be tiny and may only be detected with difficulty on radiographic studies.

**Adenocarcinoma** (Figs. 3.26 and 3.27)
The range of morphologic variations is striking with monomorphic bronchioalveolar carcinoma, at one extreme, and poorly differentiated large-cell adenocarcinoma at the other.

- Cytomorphologic hallmarks for common adenocarcinoma: Multinucleation of tumor cells, extreme cytoplasmic vacuolization, mucin content, three-dimensional morulae, and papillary clusters.
- Besides the common criteria of malignancy, tumors are also characterized by large malignant cells with varying N/C ratio, clear foamy cytoplasm with an irregular outline, and large nucleoli.
- Cell size, polymorphism, and a finely granular to clumped chromatin reflect the grade of differentiation.

- Cytomorphologic hallmarks for bronchioloalveolar carcinoma:
  - Small monomorphic cells with a low N/C ratio frequently clustered in papillary formations.
  - Fine granular chromatin, and indistinct hyperchromasia.
  - Occasional psammoma bodies.

### Differential Diagnosis and Immunocytochemistry

- Expression of CK7 and negativity for CK20 is characteristic of adenocarcinomas of the lung. These two antibodies are helpful to distinguish between adenomatous lung cancer and adenocarcinoma of the colon.
- Nuclear TTF-1 staining is usually present with high specificity, particularly in better differentiated tumors (Fig. 3.27B). Negative immunoreactivity for thyroglobulin excludes thyroid carcinoma.
- Expression of epithelial markers and CEA yields a result with high sensitivity but very low specificity.
- Mucinous tumors may exhibit an atypical immuno-pattern expressing TTF-1 negativity and CK20 positivity.
- For morphologic and immunocytochemical differentiation between adenocarcinoma and mesothelioma, see Sect. 3.2.1.3, “Additional Analyses,” p. 262.
- Poorly differentiated adenocarcinoma shares morphologic features with many other epithelial neoplasms (Fig. 3.28).
- Tumors composed of small and monomorphic cells share features with cancer of the breast, endometrium, and neuroendocrine system. To help ascertain the primary site of a neoplasm, appropriate panels of antibodies are mandatory.

**Small-Cell Carcinoma** (Figs. 3.29–3.33)

- Small-cell carcinoma of the lung may show widespread dissemination, including pleural serosal invasion previous to primary tumor diagnosis.
- Small carcinoma cells in cytologic preparations of fluids are frequently available in small numbers only (Fig. 3.29). It is important to read the smear carefully; however, the key features of this tumor (see below) are striking. Special attention must be paid in lymphocytic effusions interspersed with a few carcinoma cells of the small-cell type (Fig. 3.30).
- In rare cases, an additional component of large-cell carcinoma may be observed in smears with typical elements of small-cell carcinoma.

Cytomorphologic hallmarks of small-cell carcinoma:

- Small cells, but larger compared to lymphocytes in the same sample.
- Scant or absent cytoplasm.
- Nuclei are round, oval, or elongated: wrinkled nuclear membranes.
- Hyperchromasia is evident, but the nucleoplasm may exhibit a dirty blue-grey or pinkish color instead of the usual deep-blue staining.
- Finely granular chromatin, larger nuclei may display a salt-and-pepper chromatin pattern.
- Small inconspicuous or absent nucleoli.
- Tumor cell arrangement in small densely packed balls or in single lines, combined with nuclear molding.
- The nuclei are extremely fragile that so-called crush-artifacts, consistent with streaks and smudges of nuclear material, can often be observed.

### Differential Diagnosis and Immunocytochemistry

(Fig. 3.33)

- Expression of endocrine markers such as CD56, chromogranin A, and synaptophysin in most cases.
- TTF-1 positivity can be observed in up to 90% of cases.
- Differential diagnoses include other neuroendocrine tumors and so-called small blue round cell tumors:
  - Malignant lymphoma: lymphocytic surface antigens (CD3, CD20, CD45, and others +), cytokeratins (negative), neuroendocrine markers (negative), and TTF-1 (negative) are helpful to reach a diagnostic conclusion.
  - Primitive neuroectodermal tumor (PNET) shows positive immunoreaction for CD99 but negative reaction for cytokeratin and TTF-1 [30].
  - Merkel cell carcinoma can be differentiated from pulmonary small-cell carcinoma with positive dot-like cytoplasmic staining for CK20, but negativity for CK7 or TTF-1 [13].

**Caution**

Do not overlook sporadic cells of the small-cell carcinoma type, particularly in fluid smears with an abundant reactive lymphocytic background.

**Squamous Cell Carcinoma** (Figs. 3.28, 3.34–3.36)

- The finding of malignant squamous cells in effusions is an uncommon event. The cells are mainly found in pleural fluids, originating from primary neoplasms of the lung.
- The diagnosis is easy in cases with clear evidence of cytoplasmic keratinization. Otherwise the squamous origin of the tumor cells can be easily overlooked.
- Intercellular bridges are helpful in assessing the diagnosis and may be recognized if the cell borders of clustered cells are exactly evaluated.

Cytomorphologic hallmarks for keratinizing squamous cell carcinoma (Fig. 3.34):

- Large polygonal orangeophilic or eosinophilic cytoplasm, sharply defined cellular borders.
- Anucleated squamous cells.
- The nuclei are irregular and darkly stained, the chromatin is coarse. Apoptotic nuclei frequently occur.

Cytomorphologic hallmarks for nonkeratinizing squamous cell carcinoma:

- Key features for nonkeratinizing tumors are compact cell balls with sharply outlined edges and concentric lamination of the outermost cells. The cytoplasm is densely structured and cyanophilic, and the cell boundaries are well defined (Figs. 3.35 and 3.36). Strong variation of nuclear polymorphism and nuclear staining characteristics.
- Large single tumor cells with densely structured or vacuolated cytoplasm may readily be misinterpreted as cells from undifferentiated carcinoma or poorly differentiated adenocarcinoma (Fig. 3.28).

**Differential Diagnosis and Immunocytochemistry**

- Immunostaining for CK5/6 is helpful for recognizing squamous carcinoma cells with a high sensitivity but low specificity.
- BerEP4 and TTF-1 are usually not expressed by this cell type.
- Degenerate mesothelial cells may masquerade as malignant keratinizing squames.
- Polygonal squamous cells, nucleated or anucleated, may have other rare sources: metastatic or ruptured teratoma, biphasic carcinoma with a squamous component (e.g., urothelial carcinoma), fistula between a serous cavity and an organ with a squamous epithelial layer.
- Contaminant benign squamous cells should readily be recognized. They reveal large polygonal cytoplasm, a pale staining reaction, and a small smooth nucleus [48].

### 3.2.3.1.2 Carcinoma of the Breast (Figs. 3.37–3.41)

- Breast carcinoma has a high incident rate and metastasizes with a high frequency to serous membranes. Breast carcinoma cells are frequently found in pleural effusions.
- In many cases, pleural effusion is the first manifestation of recurrent breast cancer. The gap between primary therapy and manifestation of recurrence as malignant effusion may be up to two or three decades.
- Characteristic nuclear features of malignancy may be difficult to discern. They must be carefully searched for on isolated tumor cells.

Cytomorphologic hallmarks:

- The common type of breast carcinoma, 80% of all epithelial breast tumors exhibit small to medium-sized monomorphic cells. A high percentage of the tumor cells may occur in isolation. The cytoplasm is distinct and sharply outlined.
- The classic presentation is a compact, three-dimensional, round or gently papilliform cell cluster with a smooth or slightly knobby contour. Due to the tight overlapping of the nuclei, the cytologic features may only be evaluated on the outermost cells of the spheres.
- Cytoplasmic vacuoles with target-like dark central droplets of mucus.
- Nuclei reveal smooth margins and granular chromatin, but many nuclei appear dense and patternless.
- Discrete or no hyperchromasia.
- If at all, small nucleoli.
- Nuclear features indicating malignancy are: dense finely granular chromatin that is evenly distributed, discrete focally wrinkled membranes or deep indentations, and slight hyperchromasia or at least a change in staining quality compared to normal cells.
- Lobular carcinomas of the breast conventionally manifest with numerous, small single cells and target-like cytoplasmic mucin inclusions; however, these morphologic features are not specific and may appear as well in ductal breast carcinomas (Fig. 3.41).

**Differential Diagnosis**

- Spheres composed of tumor cells may be seen in effusions containing carcinoma cells from other sources. Yet, the morphology of individual cells and the configuration of the clusters are different (in this respect compare cytomorphologic descriptions of nonkeratinizing squamous cell carcinoma, small-cell carcinoma, endometrial carcinoma, and ovarian carcinoma, as well as mesothelioma).
- The well-differentiated neuroendocrine carcinoma is a neoplasm rarely found in effusions, but it can share morphologic features with breast carcinoma, differentiated epithelial mesothelioma, or benign hyperplastic mesothelium (Fig. 3.4).
- Abundant isolated monomorphic breast carcinoma cells suggest lobular carcinoma and may be mistaken for small mesothelial cells (Fig. 3.41). A careful search for distinctive morphologic signs and an appropriate immunopanel render a correct diagnosis.

**Additional analyses**

Immunocytochemistry

- CK7 positivity is highly sensitive for carcinoma of the breast but has a rather poor specificity. Simultaneous negative staining for CK20 excludes many look-alikes, except for adenocarcinoma of the lung.
- Immunoreactivity for estrogen and progesterone receptors (Fig. 3.39B) strongly supports diagnosis of breast carcinoma, has an additional predictive value, and may influence therapeutic decision making.
- Positive mammaglobin stain has a high specificity but the marker is not very sensitive.
- E-cadherin can differentiate between ductal and lobular breast carcinoma. It shows positive immunostaining in ductal carcinoma while lobular carcinomas are negative.

Molecular Genetics

Amplification of the Her2/neu oncogen using fluorescence in situ hybridization (FISH) has a strong influence on the therapeutic regime in patients undergoing presurgical neoadjuvant therapy and in recurrent breast carcinoma.

In cytologic specimens, the uncut nuclei are well preserved in a three-dimensional fashion and therefore the whole genome is perfectly available for the FISH technique. Isolated cells must be selected for genetic analysis; they should not be covered by blood.

#### 3.2.3.1.3 Adenocarcinoma of the Pancreas and Bile Duct System (Figs. 3.42–3.44)

- Carcinomas from the two different sources yield an identical cytomorphologic pattern.
- Adenocarcinoma of the pancreas is frequently encountered in fluids from the abdominal cavity but infrequently in pleural effusions. Malignant effusion as a primary manifestation of this tumor type may occur.
- Intracytoplasmic and background mucus is commonly observed.

Cytomorphologic hallmarks:

- Small and large slender papillary clusters made up of small glandular cells that are focally distinctly palisaded.
- Bright nuclei with bizarre shapes: cleaving and folding.
- Thinly dispersed and sometimes patternless chromatin.
- Single large, rounded malignant cells with unambiguous nuclear malignancy.

**Differential Diagnosis and Immunocytochemistry**

- The key features mentioned above disappear in poorly differentiated pancreas and bile duct neoplasms. The cytologic presentation may be similar to colonic and gastric carcinoma. A positive immunoreaction for CK7 may exclude colonic adenocarcinoma.
- CA 19-9 is recommended as an additional marker for pancreatic and bile duct cancer, but the low specificity of this marker provides only poor differential diagnostic value in cytologic practice.
- Smears from ascitic fluid with slender papillae and small cylindric cells but indistinct cytoplasmic mucus may be indicative of a neoplasia of other primary origin, namely low-grade papillary carcinoma of the ovary or peritoneum and papillary mesothelioma:
  - CA 125 positivity may argue for ovarian cancer, and hormone receptor positivity would be helpful in determining a definite diagnosis of carcinoma of the ovary.
  - Calretinin has been proved to be a reliable marker for mesothelial tumors (see Sect. 3.2.1.3, “Mesothelioma: Additional Analyses,” p. 262).

#### 3.2.3.1.4 Gastric Carcinoma (Figs. 3.45 and 3.46)

The cytologic presentation of gastric cancer is, in many cases, similar to mucinous adenocarcinoma from other sources.

The following cytomorphologic peculiarities may be suggestive of gastric carcinoma:

- Cytoplasm with a large mucin-filled vacuole compressing the nucleus to one margin, the so-called signet ring cell.
- Large number of small or large histiocytoid or mesothelial discohesive cells with the cytoplasm wide and foamy. Nuclei are frequently kidney-shaped and irregularly outlined. The chromatin is thinly dispersed or coarsely granular.
- Absence of unequivocal criteria of malignancy may lead to a misdiagnosis of activated histiocytes or of a histiocytic neoplasm. Positive immunostaining for CD68 (histiocytes) or cytokeratins / Ber-Ep4 (carcinoma cells) is helpful to differentiate between the different cell lines.

#### 3.2.3.1.5 Colonic Carcinoma

Adenocarcinoma of the large bowel may be suggested in cases exhibiting small and large compact irregular papillary clusters. The epithelial glandular cells are large and cylindrical, and show a palisade arrangement. Immunostains for CK7 and CK20 yield a negative and a positive staining result, respectively.

#### 3.2.3.1.6 Carcinoma of the Ovary (Figs. 3.47–3.49)

- Ovarian carcinoma is a common cause of ascites. Cytologic examination of ascitic fluid frequently yields the first morphologic diagnosis of an ovarian carcinoma.
- A diagnosis of ovarian adenocarcinoma is not difficult if clinical information is available.
- Invasive ovarian carcinoma shows a wide range of differentiation, from tumors with low malignant potential to poorly differentiated neoplasms.

**Microscopic Features and Immunocytochemistry**

Cytomorphologic hallmarks for less well-differentiated ovarian carcinoma are as follows:

- Moderately and poorly differentiated adenocarcinoma of the ovary present an extreme form of cytoplasmic vacuolization.
- Tumor cells are heavily enlarged with a low N/C ratio, extremely polymorphous, folded and multilobated nuclei, and coarsely clumped chromatin.
- Multiple large nucleoli.
- Irregular crowded and diffuse cell sheets. Papillary tumor cell clusters frequently occur.
- Psammoma bodies are frequently encountered.

A positive reaction for CA 125 and hormone receptors may help in problematic cases.

#### 3.2.3.1.7 Endometrial Adenocarcinoma

(Figs. 3.50 and 3.51)

**Cytomorphology and Immunocytochemistry**

- *Poorly differentiated endometrial adenocarcinomas* (Fig. 3.50) share cytomorphologic features with many other carcinomas of different origin such as ovary, colon, stomach, and lung.
- *Well-differentiated endometrial carcinomas* (Fig. 3.51) are rarely found in ascitic fluid. Their appearance is similar to monomorphic carcinoma of the breast and the lung, and tumors of neuroendocrine origin: monomorphic tumor cells with distinct cytoplasm, medium-sized nuclei with smooth margins, small nucleoli, granular chromatin, and discrete or missing hyperchromasia. Compact cell balls with a distinct outer edge but also papillary fragments may be identified.

Immunocytochemical hormone receptor positivity is helpful for a correct diagnosis, but breast and low-grade ovarian carcinoma cannot be excluded.

#### 3.2.3.1.8 Low-Grade Serous and Papillary Tumors of the Ovary and Peritoneum

Diagnosis and differential diagnostic considerations are provided in a separate section (Sect. 3.3.7, p. 303), together with selected literature.

### 3.2.3.2 Malignant Lymphoma and Myeloid Lesions

**General Comments**

- Serosal membranes are frequently involved in the course of a malignant lymphoma.
- In rare cases, effusion is the first distinct clinical manifestation of lymphoma and cytology yields the first morphologic diagnosis from the fluid sample. Peritoneal serosa is more often involved in lymphoma infiltration than pleural serosa or the pericardial sac [35].
- Malignant lymphomas have been reported to be the commonest cause of chylous effusions.
- Proper classification of lymphoma from effusions is rarely demanded because the type of neoplasm is already known in most cases.
- More important is the recognition of a possible upgrade of the tumor by cytology, which may influence further therapeutic modalities. In CD20-positive B-cell non-Hodgkin-lymphomas (NHL), cytomorphology and an immunocytochemical test (assessing proliferation index) are adequate to solve this problem (see "Additional Analyses" below).
- Only lymphoma variants that occur with a higher frequency in serous effusions are described below.

**Additional Analyses**

Different techniques are available to assess monoclonality, tumor type, proliferative activity, and genetic properties of lymphoid cells in effusions.

Immunocytochemistry

- B-cell lymphoma is characterized by immunopositivity of the B-cell marker CD20 in a high percentage of the tumor cells, but the proportion of benign lymphocytes (CD3-positive) varies from case to case. The threshold for a definite diagnosis of a lymphoid malignancy of the B phenotype is a CD20 positivity on more than 70% of all lymphoid cells present in the cytologic smear (see also Sect. 3.1.6, p. 244) [5, 56, 62].
- Monoclonality, proved by immunoglobulin light chain restriction, can be assessed immunocytochemically or with in situ hybridization. The kappa:lambda ratio approving malignant lymphoma must be notably high or low dependent on the properties of the cell clone.
- The proliferation index of a cell population is defined by the percentage of tumor cell nuclei stained positive with antibodies against Ki67/MIB-1.
- Immunocytochemistry may be helpful to classify selected non-Hodgkin lymphomas:
  - Chronic lymphatic leukemia: CD5**+** / C23**+** / CD10**–**
  - Follicular lymphoma: CD5**–** / CD19**+** / CD10**+**
  - Mantle cell lymphoma: CD5**+** / cyclin D1_nuclear **+**
  - Plasmacytoma CD38**+** / CD138**+**; CD45 and CD20 negativity!
- Multiparameter flow cytometric analysis is a reliable and approved method for immunophenotyping of lymphoid cells in lymphomatous effusions [16, 17].

Molecular Genetics

- Polymerase gene amplification either followed by gel electrophoresis or fragment analysis using DNA, extracted from cytological samples is a safe method to assess clonal rearrangement of heavy and light Ig chain genes in B-cell lymphoma, and of T-cell receptor genes in T-cell populations [44, 18].

- Southern blot analysis has been shown to be a reliable tool for detection of a monoclonal B-cell and T-cell gene rearrangement [44]. However, the method requires unfixed material in large amounts.
- Fluorescence in situ hybridization (FISH) detecting specific translocation is an excellent tool for lymphoma subtyping. Among others, the method is routinely applied for assessing lymphoma of follicle center cell origin, t(14;18) and mantle cell lymphoma, t(11;14) [7].
- Additional information is available in Sect. 15.1.4.3, "Molecular Genetics," p. 911.

#### 3.2.3.2.1 Small Lymphocytic Lymphoma / Chronic Lymphatic Leukemia (Fig. 3.52)

Lymphocytic NHL / chronic lymphatic leukemia (CLL) exhibit a pure lymphocytic morphology on sediment smears. The tumor cells are monomorphous but more irregularly shaped and larger in size than the benign lymphoid cells in tuberculous effusion (Fig. 3.9) or in smears containing many benign T lymphocytes.

Hallmarks:

- Tumor cells are monomorphic.
- The nuclear membranes are wrinkled.
- The chromatin is granular and densely packed.
- A distinct nucleolus is obvious in a high percentage of the nuclei.

**Caution**

- It may be difficult to distinguish between detached cells of small-cell epithelial tumors and cells from CLL (Fig. 3.33).
- It is impossible to detect cells from a monomorphic low-grade NHL interspersed with numerous reactive T lymphocytes.
- Lymphoblastic lymphoma may appear as a monomorphic lymphoid smear pattern, and the immature blast cells are small to medium-sized. Unlike CLL, the cells of lymphoblastic lymphomas usually exhibit considerable nuclear irregularities, coarse granular chromatin, and a large nucleolus in each nucleus (Fig. 3.53).

#### 3.2.3.2.2 Mixed Lymphoid Pattern with a Varying Number of Large Atypical/Blast Cells

Many benign and malignant disorders are responsible for a predominantly mixed lymphoid cell pattern in serosal fluids (see also Sect. 3.1.6, p. 244). In this setting, it is often difficult to distinguish between benign lymphoproliferative lesions, malignant lymphoma, and a mixture of benign and malignant cells. A conclusive diagnosis can be extremely difficult in cases exhibiting less mature and immature lymphocytes, and immature plasmacytoid cells and plasmablasts.

The most frequently encountered diagnostic challenges are discussed together with additional analyses:

- *Malignant B-cell NHL with a predominance of small to medium-sized lymphocytes and only a few large blast cells* (e.g., follicular lymphoma).
  In contrast to benign lymphocytes, small tumorous lymphocytes are angulated with cleaved nuclei and conspicuous nucleoli. Blast cells are polymorphous. B- and T-cell enumeration with marked preponderance of B cells should be diagnostic in many cases, except in cases with a predominate admixture of a benign T-cell population. Molecular genetic methods can establish clonality of the lymphoid cell population unless only a small quantity of DNA is available due to sparse neoplastic lymphoid cells.
- *Immunoblastic and anaplastic large-cell lymphoma with benign T-lymphocyte hyperplasia*. Reactive T-cell hyperplasia may occur together with serosal infiltration of a large-cell NHL. Isolated malignant large cells should be recognized in cytologic sediment smears by careful screening, but an accurate classification and diagnosis is not possible in the vast majority of cases. Limitation of ancillary techniques may depend on the scarcity of target cells and of nuclear DNA. Neither immunocytochemical nor molecular genetic analyses may be able to prove the presence of neoplastic lymphoid B cells in such cases [14]. However, a carcinomatous lesion can still be excluded by immunostaining for epithelial markers.
- *Serous carcinomatosis* is well known to be accompanied by pronounced lymphocytosis; note that individual cancer cells may be barely visible. Immunostaining with ABs for BerEp-4 and cytokeratins can reliably confirm the epithelial nature of sporadic neoplastic cells. Clinical information is indispensable.
- *Hodgkin lymphoma* [49] (Fig. 3.54):
  - The occurrence of pleural effusions in Hodgkin lymphoma is reported in up to 25% of all cases.
  - The cell component in cytologic preparations is in most cases not diagnostic of Hodgkin lymphoma: smears exhibit a mixed lymphoid cell pattern together with histiocytes and mesothelial cells; plasma cells and eosinophils may be present.
  - The only reliable diagnostic features are multinucleated Reed-Sternberg cells and mononuclear Hodgkin cells with their typical size, nuclear shape, and distinct nucleolus. However, these pathognomonic cells are often sparsely distributed, or not at all present in effusions.
  - In a high percentage of the effusions accompanying Hodgkin lymphoma, the diagnosis has already been established, and mediastinal irradiation has already been performed. Therefore, it is difficult to decide whether effusion is due to irradiation or to tumor involvement of the serosal membranes. Furthermore, irradiation

may induce strong mesothelial hyperplasia with cellular atypias, in which nuclei may exhibit bizarre cleaving and folding as well as enlarged polymorphous nucleoli. In those cases, it is virtually impossible to distinguish between reactive mesothelial atypia and Hodgkin or Reed-Sternberg cells.

– Reed-Sternberg and Hodgkin cells show negative immunoreactivity for CD45 (leukocyte common antigen) and a positive reaction for CD15, CD30, and PAX5. PAX5 nuclear immunoreactivity is generally weak.

#### 3.2.3.2.3 Numerous Malignant Blast Cells

Compared to their low-grade counterpart, high-grade NHL are more frequently observed as secondary tumor manifestation in effusions, in the main affecting the abdominal cavity. Rapidly growing large-cell anaplastic lymphoma with huge intraabdominal and retroperitoneal masses may give rise to an initial cytologic tumor diagnosis.

**Microscopic Features and Differential Diagnosis**

Blastic B-cell lymphoma and T-cell counterparts such as lymphoblastic NHL (Fig. 3.53) and diffuse large B-cell lymphoma (Fig. 3.55) exhibit numerous overtly malignant individual cells.

Hallmarks:

- Pronounced polymorphism of the cytoplasm and the nucleus.
- Bizarre nucleoli and multinucleation are key features of these tumors.
- Blastic large-cell lymphoma may produce a necrotic background, which is exceptional in cases with serosal carcinosis.

Other neoplasms must be taken into consideration:

- Highly immature plasmacytoma with absence of the typical plasmacytoid features. The tumor cells exhibit criteria of malignant blast cells with heterogeneous cytologic findings, but abundant eccentric and foamy cytoplasm is common (Fig. 3.56).
  Immunocytochemistry: Positivity for CD38 and CD138. Negative for CD20 and CD45.
- Hodgkin lymphoma with a distinct component of Hodgkin and Reed-Sternberg cells.
  Immunocytochemistry: HRS cells are positive for CD30, CD15, and PAX5. Negativity for CD45.
- Malignant lymphoma of the T-cell phenotype.
  Immunocytochemistry: Positivity for T-cell markers CD3, CD7, CD 4, CD5, CD8.
  Diagnosis should be confirmed by molecular genetic investigations [1].
- Anaplastic carcinoma.
  Immunocytochemistry: Positivity for cytokeratins, BerEp4, and CEA
- Malignant histiocytosis.
  Immunocytochemistry: Positivity for CD68
- Primary effusion lymphoma (PEL). For details, see Sect. 3.2.2, p. 262.

#### 3.2.3.2.4 Myeloid Lesion (Fig. 3.57)

Foci of so-called myelogenic sarcoma (chloroma) may develop beneath as well as in the serous membranes. These lesions rarely occur; note that solid tumor masses may accompany or even precede myelomonocytic leukemias. Tumor cells are large and mostly reveal lobated pale nuclei and vacuolated cytoplasm. It is difficult to discriminate between a myeloid tumor cell population and large-cell malignant lymphoma.

Immunocytochemistry: positivity for myeloid markers such as myeloperoxidase (Fig. 3.57B), CD15, CD117, lysozyme, chloracetate esterase, and CD43. Negative expression of lymphocytic antigens such as CD3 and CD79a.

**Caution**

- Myeloid tumor cells in a blood-rich cytologic sample:
  1. May originate from a cell spreading solid myelogenic tumor or
  2. Are genuine blood components in a course of a pure leukemic disorders.
- Myelogenic sarcoma, located in serosal membranes, may accompany or even precede myelomonocytic leukemia.

### 3.2.3.3 Rare Secondary Neoplasia

Check also differential diagnostic considerations noted above.

#### 3.2.3.3.1 Pseudomyxoma Peritonei

See Fig. 3.58.

**Etiology and Cytomorphology**

- Pseudomyxoma peritonei (PMP) is a rare tumor most frequently originating from the appendix. It gives rise to extensive mucus accumulation in the abdominal and pelvic cavity.
- PMP associated with a primary ovarian lesion is rare and probably restricted to mucinous disorders arising in mature cystic teratomas [55, 63].
- A mucus-secreting cystic tumor may rupture, spilling its contents into the abdominal cavity. The tumor cells continually proliferate within the mucoid masses and themselves produce mucus.
- Ascitic fluid has a thick mucoid consistency and is difficult to aspirate and to smear.
  Hallmarks:
  - Abundant background mucus; lucid and thick mucinous masses.
  - Cytologic preparations can completely lack malignant cells.

- In other cases, sporadic epithelial cells and small cell clusters may be detected.
- The tumor cells are benign or may show discrete nuclear atypias, unequivocal cellular criteria of malignancy are rare.

#### 3.2.3.3.2 Malignant Melanoma (Figs. 3.59–3.61)

Malignant melanoma is characterized by distinct morphologic features, which enables a correct diagnosis in nonpigmented neoplasms as well.

**Cytomorphology**

- Cells are larger than reactive mesothelial cells, and binucleation is found in up to 20% of all tumor cells [61].
- The cytoplasm is abundant.
- The melanoma cells may contain densely packed small, dirty greenish-brown stained pigment granules or there is a light brownish dusting of the cytoplasm.
- A common characteristic are centrally located round nuclei with wrinkled membrane and distinct empty vacuoles caused by cytoplasmic invagination.
- The chromatin appears as discrete densely packed granulation.
- Nucleoli are large and often bizarrely shaped.
- Pigment-loaded macrophages (melanophages) may outnumber pigmented melanoma cells (Fig. 3.61). Heavily pigmented cells are difficult to classify as macrophages or tumor cells.

**Differential Diagnosis**

- The diagnosis may become uncertain in malignant melanoma composed of small tumor cells with indistinct nucleoli, and absence of melanin pigment and/or nuclear inclusions. Consequently, these cells may resemble hyperplastic mesothelial cells, cells of a well-differentiated mesothelioma, cells from breast carcinoma exfoliating exclusively individual cells, or cells from gastric carcinoma of the small-cell type.
- It is important to be aware of melanoma cells displaying a tendency toward a spindle cell shape. Spindle-shaped neuroendocrine tumors and soft tissue tumors have to be taken into consideration.

**Immunocytochemistry** (Fig. 3.60)

Characterization of melanoma cells is almost always successful with melanoma-typical markers such as HMB-45, Melan A and tyrosinase.

S100 protein staining usually yields a strong positivity in all tumor cells.

**Caution**

- Malignant melanoma has a strong tendency to metastasize into serous membranes. Therefore, it is mandatory to include melanoma markers in immunocytochemical panels for each case with equivocal tumor typing.
- Spindle-shaped cells must arouse suspicion of malignant melanoma.

#### 3.2.3.3.3 Other Rare Neoplasms

Neoplasms of this category include sarcoma, thymoma, germ cell tumors, tumors of the small round cell category, and others.

Rare tumor types exhibiting particular cytomorphologic features of diagnostic and differential diagnostic potential are mentioned below, including differential diagnoses and immunocytochemical characteristics:

- *Large-cell carcinoma with distinct granular eosinophilic cytoplasm* should raise the possibility of hepatocellular carcinoma (HCC). Shrinking of the cytoplasm may conceal granulation. Contamination with benign hepatocytes should always be excluded (see also Sect. 3.1.11.1 "Right-Side Pleurocentesis in Patients with Diaphragmatic Elevation," p. 248).
  Immunocytochemical characteristics for HCC: Diffuse cytoplasmic immunoreactivity for alpha fetoprotein (AFP) and HepPar 1/human hepatocyte antigen (see Sect. 9.2.7 "Immunocytochemistry," p. 610).
- *Renal clear cell carcinoma* (Fig. 3.62). Large clear cytoplasm and bright nuclei. The chromatin texture may be indistinct or finely granular. Cellular enlargement (in comparison with benign mesothelial cells and histiocytes), typical chromatin pattern, and casual sheet formation are features indicating renal cell carcinoma.
  Immunocytochemical characteristics: Tumor cells are positive for the renal cell carcinoma marker (RCC Ma). Unfortunately, the sensitivity of this marker is low for metastatic renal cell carcinoma, and breast carcinoma cells may also be positive.
- *Papillary thyroid carcinoma* may occur in pleural and pericardial effusions. Cytomorphologic features are of minor value for differential diagnostic considerations.
  Immunocytochemical characteristics: TTF-1 and thyroglobulin are reliable markers for thyroid neoplasms. Papillary carcinoma of the lung and of the endocrine system cannot be excluded with TTF-1-positive immunoreaction alone.
- *Adenocarcinoma of the prostate* exhibits typical dense, usually monolayered sheets of large malignant cells. The uniformity of the tumor cells is striking. The cytoplasm is extended and foamy. A rounded nucleus with a dense, granular chromatin pattern exhibits one large, centrally placed nucleolus.

Immunocytochemical characteristics: Positive immunostaining for prostate-specific antigen (PSA) and prostatic acid phosphatase (PAP) is highly specific and sensitive for this tumor type.

- *Well-differentiated endocrine carcinoma* (Fig. 3.4.) may exhibit compact, sharply delineated cell balls and single cells as well. Well-differentiated endocrine neoplasms particularly mimic breast carcinoma of the monomorphic subtype and proliferating mesothelial cells.
  Immunocytochemical characteristics: Endocrine markers are diagnostic, they include synaptophysin, chromogranins, NSE, and Leu7.
- *Seminoma* (Fig. 3.63) in fluids from the tunica vaginalis testis may mimic high-grade malignant lymphoma or anaplastic carcinoma.
  Immunocytochemical characteristics: Placental alkaline phosphatase (PLAP) is sensitive and highly specific for germ cell tumors. Negative immunocytochemical stainings for CD45 and cytokeratins exclude malignant lymphoma and epithelial tumors, respectively.
- Description of particular cases and reviews referring to rare tumor entities are reported in various publications. A comprehensive description of rare neoplasms in effusions is published in the book by Hajdu and Hajdu [29].

## 3.2.4 Noncellular Components related to Malignant Cells and Neoplasms

### 3.2.4.1 Psammoma Bodies [52] (Figs. 3.48 and 3.74)

- Laminated, calcified debris is known as psammoma bodies. Generally they are dark-stained, rounded bodies with concentric rings. A possible pathogenic link between the development of psammoma bodies and nanobacterial infection has recently been described [32].
- Psammoma bodies are typically incorporated into epithelial clusters or into the fibrovascular core of true papillae.
- The psammoma body is a well-known morphological feature of ovarian adenocarcinomas, but they may also be encountered in other human malignancies. The most relevant malignancies presenting with varying amounts of psammoma bodies are: carcinoma of ovary, thyroid, endometrium, lung, breast, pancreas, and stomach. Psammoma bodies most frequently occur in ovarian neoplasia and may be numerous. Massive psammoma body formation is observed in serous psammocarcinoma of the ovary [27].
- Psammoma bodies as a background element in sediment smears from peritoneal fluids generally indicate a benign lesion of the peritoneal serosal membranes (e.g., endosalpingiosis). See also Sect. 3.3.5, “Endosalpingiosis,” p. 302 (Fig. 3.72).

### 3.2.4.2 Mucus

- Mucus stains pink or light green and is lucid using Pap stain (Fig. 3.58). Cells with intracytoplasmic mucoid inclusions exhibit round homogeneous globules. Rounded cells with a large mucin-filled vacuole displacing the nucleus to one margin are called signet ring cells (Fig. 3.45). Background mucus forms streaks and opaque masses, which are Pap-stained eosinophilic or cyanophilic.
- Mucoid masses in the background of a cytology preparation, regardless of the presence of malignant cells, raise high suspicion of mucinous adenocarcinoma.
- Very-well-differentiated adenocarcinoma and pseudomyxoma peritonei may exclusively display free mucus. In other cases, few isolated tumor cells and small-cell clusters may be encountered, but the tumor cells rarely meet obvious criteria of malignancy.
- Strong cytoplasmic vacuolization without the typical staining features described above should not mislead the cytopathologist to a diagnosis of intracytoplasmic mucus; see Sect. 3.2.4.3 below.

### 3.2.4.3 Cytoplasmic Vacuolization

Vacuolization may be due to degenerative changes, uptake of fluid in long-standing liquids, or glycogen.

Large cytoplasmic vacuoles with sharply defined margins may imitate signet ring cells. They should not be mistaken for true malignant signet ring cells containing mucus. Coarse vacuolization does not necessarily mean mucinous inclusions.

## 3.2.5 Further Reading

1. Abraham MG, Levin KA, Balasubramanian M, et al. Diagnosis of T-cell lymphoma in body fluids. Cytologic features and unusual flow cytometric findings. Anal Quant Cytol Histol 2007;29:333-338.
2. Afify AM, Al-Khafaji BM, Paulino AF, Davila RM. Diagnostic use of muscle markers in the cytologic evaluation of serous fluids. Appl Immunohistochem Mol Morphol 2002;10:178-82.
3. Aoki Y, Yarchoan R, Braun J, et al. Viral and cellular cytokines in AIDS-related malignant lymphomatous effusions. Blood 2000;96:1599-1601.
4. Bailey ME, Brown RW, Mody DR, et al. Ber-Ep4 for differentiating adenocarcinoma from reactive and neoplastic mesothelial cells in serous effusions. Comparison with carcinoembryonic antigen, B72.3 and Leu-M1. Acta Cytol 1996;40:1212-1216.
5. Bangerter M, Hildebrand A, Griesshammer M. Combined cytomorphologic and immunophenotypic analysis in the diagnostic workup of lymphomatous effusions. Acta Cytol 2001;45:307-312.
6. Battifora H, McCaughey WTE. Atlas of tumor pathology, Tumors of the serosal membranes. 3rd series,fascicle 15, Juan Rosai (ed.) Armed Forces Institute of pathology, Washington D.C., 1995 pp. 17-23 / 31.

7. Bentz JS, Rowe LR, Anderson SR, et al. Rapid detection of the t(11;14) translocation in mantle cell lymphoma by interphase fluorescence in situ hybridization on archival cytopathologic material. Cancer 2004;102:124-131.
8. Brimo F, Michel RP, Khetani K, Auger M. Primary effusion lymphoma: a series of 4 cases and review of the literature with emphasis on cytomorphologic and immunocytochemical differential diagnosis. Cancer 2007;111:224-233.
9. Cagle PT, Brown RW, Lebovitz RM. p53 immunostaining in the differentiation of reactive processes from malignancy in pleural biopsy specimens. Hum Pathol 1994;25:443-448.
10. Carbone A, Gloghini A. HHV-8-associated lymphoma: state-of-the-art review. Acta Haematol 2007;117:129-131.
11. Carbone A, Gloghini A. PEL and HHV8-unrelated effusion lymphomas. Classification and diagnosis. Cancer (Cancer Cytopathol) 2008;114:225-227.
12. Cesarman E, Chang Y, Moore PS, et al. Kaposi's sarcoma-associated herpesvirus-like DNA sequences in AIDS-related body-cavity-based lymphomas. N Engl J Med 1995;332:1186-1191.
13. Chan JK, Suster S, Wenig BM, et al. Cytokeratin 20 immunoreactivity distinguishes Merkel cell (primary cutaneous neuroendocrine) carcinomas and salivary gland small cell carcinomas from small cell carcinomas of various sites. Am J Surg Pathol 1997;21:226-234.
14. Chang H, Sun C-F. Detection of B-cell lymphoma involvement in T cell-rich serous fluid by immunoglobulin Gene rearrangement. A report of 2 cases. Acta Cytol 2008;52:231-234.
15. Churg A, , Cagle PT, , Roggli VL. AFIP Atlas of Tumor Pathology, fourth series, fasc 3. AFIP, Tumors of the serosal membranes. ed. Silverberg SG. American Registry of Pathology, Washington DC, 2006.
16. Craig FE, Foon KA. Flow cytometric immunophenotyping for hematologic neoplasms. Blood 2008;111:3941-3967.
17. Czader M, Ali SZ. Flow Cytometry as an adjunct to cytomorphologic analysis of serous effusions. Diagn Cytopathol 2003;29:74-78.
18. Das DK. Serous effusions in malignant lymphomas: a review. Diagn Cytopathol 2006;34:335-347.
19. Davidson B, Nielsen S, Christensen J, et al. The role of desmin and N-cadherin in effusion cytology: a comparative study using established markers of mesothelial and epithelial cells. Am J Surg Pathol. 2001;25:1405-1412.
20. Daya D, Mc Caughey WT. Well-differentiated papillary mesothelioma of the peritoneum. A clinicopathologic study of 22 cases. Cancer 1990;65:292-296.
21. De Angelis M, Buley ID, Heryet A, Gray W. Immunocytochemical staining of serous effusions with the monoclonal antibody Ber-Ep4. Cytopathology 1992;3:111-117.
22. Dejmek A. CK 5/6 in effusions. No difference between mesothelioma and pulmonary and nonpulmonary adenocarcinoma. Acta Cytol 2008;52:579-583.
23. Drexler HG, Meyer C, Gaidano G, Carbone A. Constitutive cytokine production by primary effusion (body cavity-based) lymphoma-derived cell lines. Leukemia 1999;13:634-640.
24. Esteban JM, Sheibani K. DNA ploidy analysis of pleural mesotheliomas: its usefulness for their distinction from lung adenocarcinomas. Modern pathol 1992;5:626-630.
25. Friedman MT, Gentile P, Tarectecan A, Fuchs A. Malignant mesothelioma: Immunohistochemistry and DNA ploidy analysis as methods to differentiate mesothelioma from benign reactive mesothelial cell proliferation and adenocarcinoma in pleural and peritoneal effusions. Arch Pathol Lab Med 1996;120:959-966.
26. Gaidano G, Gloghini A, Gattei V, et al. Association of Kaposi's sarcoma-associated herpesvirus-positive primary effusion lymphoma with expression of the CD138/syndecan-1 antigen. Blood 1997;90:4894-4900.
27. Giordano G, Gnetti L, Milione M, et al. Serous psammocarcinoma of the ovary: a case report and review of the literature. Gynecol Oncol 2005;96:259-262.
28. Gonzalez-Lois C, Ballestin C, Sotelo MT, et al. Combined use of novel epithelial (MOC-31) and mesothelial (HBME-1) immunohistochemical markers for optimal first line diagnostic distinction between mesothelioma and metastatic carcinoma in pleura. Histopathology 2001;38:528-534.
29. Hajdu SI, Hajdu EO. Cytopathology of sarcomas and other nonepithelial malignant tumors. Philadelphia, WB Saunders, 1976.
30. Halliday BE, Slagel DD, Elsheikh TE, Siverman JF. Diagnostic utility of MIC-2 immunocytochemical staining in the differential diagnosis of small blue cell tumors. Diagn Cytopathol 1998;19:410-416.
31. Hoekman K, Tognon G, Risse EK et al. Well-differentiated papillary mesothelioma of the peritoneum: a separate entity. Eur J Cancer 1996;32A:255-258.
32. Hudelist G, Singer CF,Kubista E, et al. Presence of nanobacteria in psammoma bodies of ovarian cancer: evidence for pathogenetic role in intratumoral biomineralization. Histopathology 2004;45:633-637.
33. Hurlimann J. Desmin and neural marker expression in mesothelial cells and mesotheliomas. Hum Pathol 1994;25:753-757.
34. Illei PB, Ladanyi M, Rusch VW, Zakowski MF: The use of CDK-N2A deletion as a diagnostic marker for malignant mesothelioma in body cavity effusions. Cancer Cytopathol 2003;99:51-56.
35. Izban KF, Pooley RJ, Selvaggi SM, Alkan S. Cytologic diagnosis of peripheral T-cell lymphoma manifesting as ascites. A case report. Acta Cytol 2001;45:385-392.
36. Joseph MG, Banerjee D, Harris P, et al. Multiparameter flow cytometric DNA analysis of effusions: a prospective study of 36 cases compared with routine cytology and immunohistochemistry. Mod Pathol 1995;8:686-693.
37. King J, Thatcher N, Pickering C, Hasleton P. Sensitivity and specificity of immunohistochemical antibodies used to distinguish between benign and malignant pleural disease: a systematic review of published reports. Histopathology 2006;49:561-568
38. Kwee WS, Veldhuizen RW, Alons CA, et al. Quantitative and qualitative differences between benign and malignant mesothelial cells in pleural fluid. Acta Cytol 1982;26:401-406.
39. Maeder M, Spieler P, Krapf R, Diethelm M. Cytologically malignant lymphoid pericardial effusion with benign clinical outcome. Report of two cases. Swiss Med Wkly 2005;135:377-381.
40. Mangano WE, Cagle PT, Churg A, et al. The diagnosis of desmoplastic malignant mesothelioma and its distinction from fibrous pleurisy: a histologic and immunohistological analysis of 31 cases including p53 immunostaining. Am J Clin Pathol 1998;110:191-199.
41. Marchevsky AM, Wick MR. Evidence-based guidelines for the utilization of immunostains in diagnostic pathology: pulmonary adenocarcinoma versus mesothelioma. Appl Immunohistochem Mol Morphol 2007;15:140-144.
42. Mayall FG, Gibbs AR. The histology and immunohistochemistry of small cell mesothelioma. Histopathology 1992;20:47-51.
43. Mayall FG, Goddard H, Gibbs AR. p53 immunostaining in the distinction between benign and malignant mesothelial proliferations using formalin-fixed paraffin sections. J Pathol 1992;168:377-381.
44. Mihaescu A, Gebhard S, Chaubert P, et al. Application of molecular genetics to the diagnosis of lymphoid-rich effusions: study of 95 cases with concomitant immunophenotyping. Diagn Cytopathol 2002;27:90-95.
45. Motherby H, Kube M, Friedrichs N, et al. Immunocytochemistry and DNA-image cytometry in diagnostic effusion cytology I. Prevalence of markers in tumour cell positive and negative smears. Anal Cell Pathol 1999;19:7-20.
46. Motherby H, Pomjanski N, Kube M, et al. Diagnostic DNA-flow-vs. image-cytometry in effusion cytology. Anal Cell Pathol 2002;24:5-15.
47. Nador RG, Cesarman E, Chadburn A, et al. Primary effusion lymphoma: A distinct clinicopathologic entity associated with the Kaposi's sarcoma-associated herpes virus. Blood 1996;88:645-656.

48. Naylor B. Pleural, Peritoneal and Pericardial fluids. In: Bibbo M. (ed). Comprehensive Cytopathology. W.B. Saunders Company, Philadelphia, 1991,pp.585-587.
49. Olson PR, Silverman JF, Powers CN. Pleural fluid cytology of Hodgkin's disease: Cytomorphologic features and the value of immunohistochemical studies. Diagn Cytopathol 2000,22:21-24.
50. Onofre FB, Onofre AS, Pomjanski N, et al. 9p21 deletion in the diagnosis of malignant mesothelioma in serous effusions additional to immunocytochemistry, DNA-ICM and AgNOR analysis. Cancer(Cancer Cytopathol) 2008;114:204-215.
51. Osterheld MC, Liette C, Anca M. Image Cytometry: An aid for cytological diagnosis of pleural effusions. Diagn Cytopathol 2005;32:173-176.
52. Parwani AV, Chan Ty, Ali SZ. Significance of psammoma bodies in serous cavity fluid: a cytopathologic analysis. Cancer 2004;102:87-91.
53. Pokieser L. et al. Klinische Zytologie der Lunge und Pleura. Springer-Verlag Wien, 2001.
54. Roberts F, McCall AE, Burnett RA. Malignant mesothelioma: a comparison of biopsy and postmortem material by light microscopy and immunohistochemistry. J Clin Pathol 2001;54:766-770.
55. Rojo Sebastian A, Fernandez Morejon FJ, Bretcha Boix P, et al. Controversial origin of pseudomyxoma peritonei. Clin Transl Oncol 2006;8:767-769.
56. Santos GC, Longatti-Filho A, de Carvalho LV, et al. Immunocytochemical study of malignant lymphoma in serous effusions. Acta Cytol 2000;44:539-542.
57. Savic S, Franco N, Grilli B, Barascud Ade V, Herzog M, Bode B, Loosli H, Spieler P, et al. Fluorescence in situ hybridization in the definitive diagnosis of malignant mesothelioma in effusion cytology. Chest 2010;138:137-44.
58. Sherman ME, Mark EJ. Effusion cytology in the diagnosis of malignant epithelioid and biphasic pleural mesothelioma. Arch Pathol Lab Med 1990;114:845-851.
59. Shield PW, Koivurinne K. The value of calretinin and cytokeratin 5/6 as markers for mesothelioma in cell block preparations of serous effusions. Cytopathology 2008;19:218-223.
60. Shin HJ, Shin DM, Tarco E, Sneige N. Detection of numerical aberrations of chromosomes 7 and 9 in cytologic specimens of pleural malignant mesothelioma. Cancer 2003;99:233-239.
61. Spieler P, Gloor F. Identification of Types and primary sites of malignant Tumors by examination of exfoliated tumor cells in serous fluids. Comparison with the diagnostic accuracy on small histologic biopsies. Acta Cytol 1985;29:753-767.
62. Spieler P, Kradolfer D, Schmid U. Immunocytochemical characterization of lymphocytes in benign and malignant lymphocyte-rich serous effusions. Virchows Arch Pathol Anat 1986;409:211-221.
63. Stewart CJ, Tsukamoto T, Cooke B, et al. Ovarian mucinous tumour arising in mature cystic teratoma and associated with pseudomyxoma peritonei. Pathology 2006;38:534-538.
64. Wagner JC, Sleggs CA, Marchand P. Diffuse pleural mesothelioma and asbestos exposure in the North Western Cape Province. Br J Ind Med 1960;17:260-271.
65. Wakely PE Jr, Menezes G, Nuovo GJ. Primary effusion lymphoma: Cytopathologic diagnosis using in situ molecular genetic analysis for human herpesvirus 8. Mod Pathol 2002;15:944-950.
66. Whitaker D. Cell aggregates in malignant mesothelioma. Acta Cytol 1977;21:236-239.

**Figs. 3.19 and 3.20 Epithelial mesothelioma versus hyperplastic mesothelial cells.** Two patients suffering from malignant mesothelioma. Cytology displays minor cellular atypias that are intermediate between those of mesothelioma and hyperplastic mesothelial cells. In such cases, the cytologic diagnosis will frequently remain inconclusive.

**Fig. 3.19** A case of well-differentiated pleural malignant mesothelioma highlights striking resemblance between benign and malignant mesothelial cells. Still, neoplastic cells can be suggested on the basis of cellular and nuclear enlargement, and huge nucleoli (arrow) (direct sediment smear, Pap stain, high magnification).
*Tissue diagnosis* (surgical biopsy): Well-differentiated epithelial mesothelioma.

**Fig. 3.20** A second example of pleural mesothelioma its cells exhibit similar morphologic features as compared with benign mesothelial cells. The malignant cell cluster depicted shows at least vague features indicating malignancy: high N/C ratio, nuclear marginalization, nuclear variability in size and shape, inhomogeneous chromatin texture, and large nucleoli (direct sediment smear, Pap stain, high magnification).
*Tissue diagnosis* (surgical biopsy): Biphasic mesothelioma.

**Figs. 3.21 and 3.22 Cytologically unequivocal malignant epithelial mesothelioma.**

**Fig. 3.21** A 60-year-old man presenting with left-sided pleural effusion. Lower magnification shows sharply delineated spheres that are composed of atypical mesothelial cells enclosing slightly pink stained cores of hyaline material (arrows). By immunocytochemistry, the tumor cells expressed strong positivity for calretinin and negativity for the epithelial marker Ber-Ep4 (not shown) (direct sediment smear, Pap stain).
*Cytologic diagnosis:* Monomorphic epithelial mesothelioma.
*Tissue diagnosis:* Epithelial mesothelioma.

**Fig. 3.22** Cellular details from another case of pleural epithelial mesothelioma (confirmed by histology) are demonstrated in relation to benign mesothelial cells (lower right) and histiocytes (bottom): enlarged mesothelial cells (note the typical mesothelial texture of the cytoplasm!) exhibit nuclei displaced to the basal border of the cytoplasm; nuclei show cleaves and grooves and occasional prominent nucleoli (arrows). Note degenerating neoplastic cells (top) with their homogeneous darkly stained nuclei and eosinophilic cytoplasm. (Pap stain, high magnification).

Degenerating cells of both benign mesothelium and malignant mesothelial tumors may come along with eosinophilic cytoplasm and dark-staining nuclei; these changes should not be mistaken for metastatic squamous cell carcinoma.

**Fig. 3.23A, B Well-differentiated papillary malignant mesothelioma.**
Physical examination of a 47-year-old man revealed a large-sized hydrocele comprising firm nodular tumor masses. After centrifugation, the fluid sediment was processed providing Pap-stained conventional smears.
*Cytologic diagnosis:* malignant well-differentiated papillary mesothelioma (the cytologic diagnosis was confirmed by histologic tissue examination after semilateral orchiectomy).
**A** A sanguineous fluid sample from the tunica vaginalis testis contained numerous papilliform clusters showing a knobby contour and cores of homogeneous material (bottom) (lower magnification). **B** High magnification shows mild cellular atypias, lucid hyaline material, and psammoma bodies encased in the tumor cell clusters (right).

Psammoma bodies encased in clusters of atypical mesothelial cells should not be considered as an absolute indicator of malignancy.

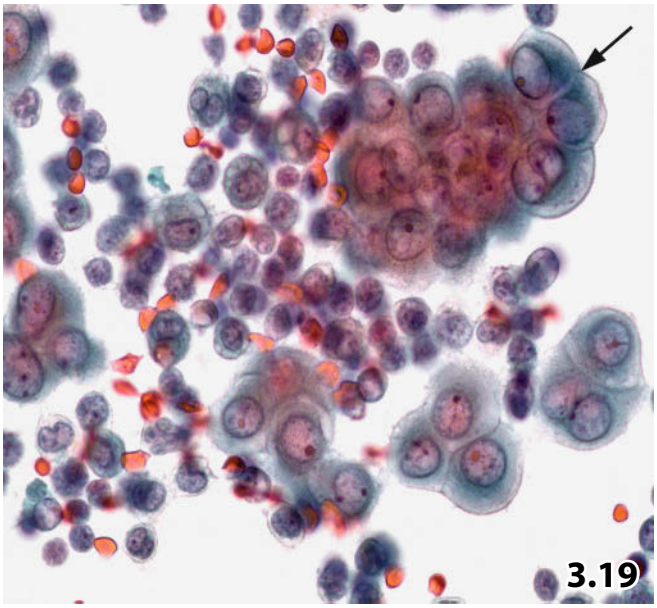
3.19

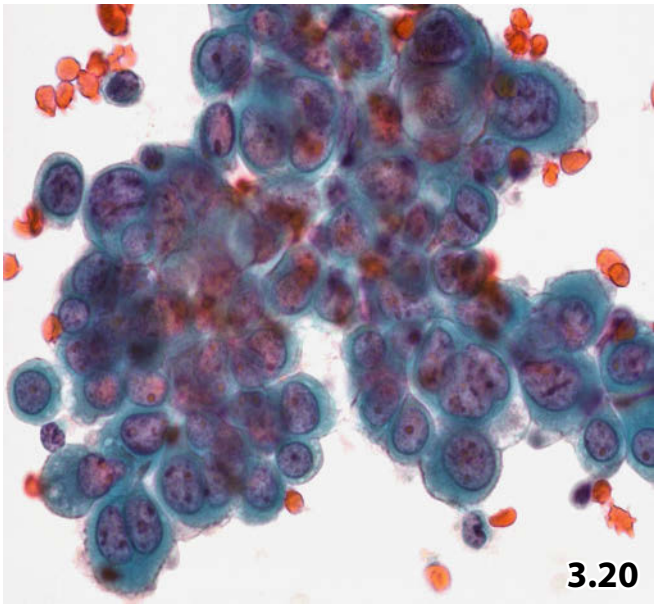
3.20

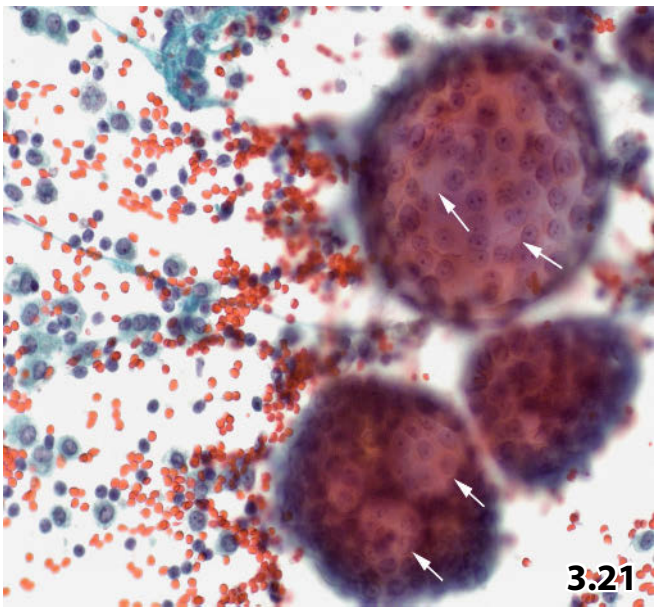
3.21

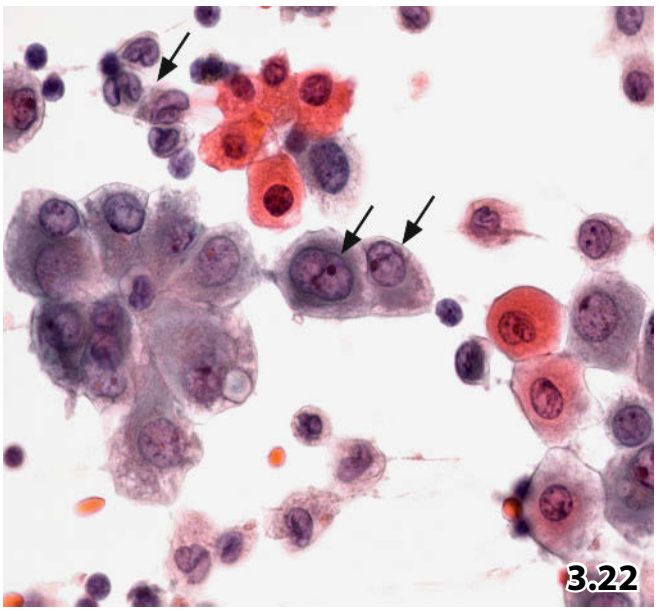
3.22

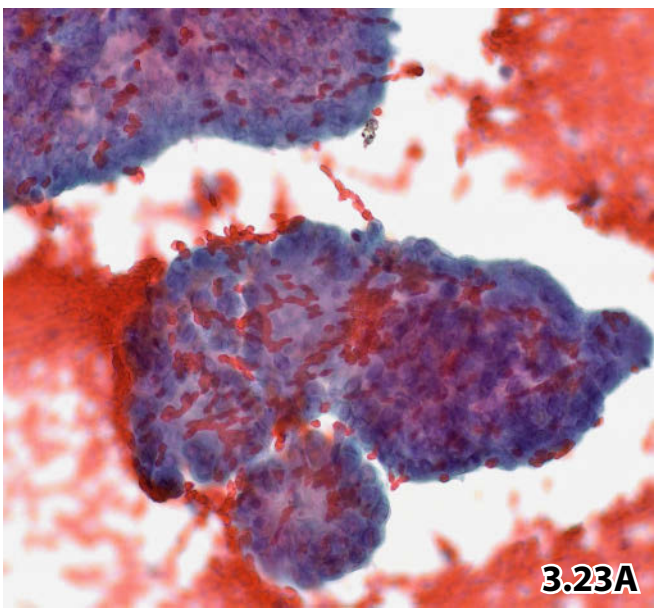
3.23A

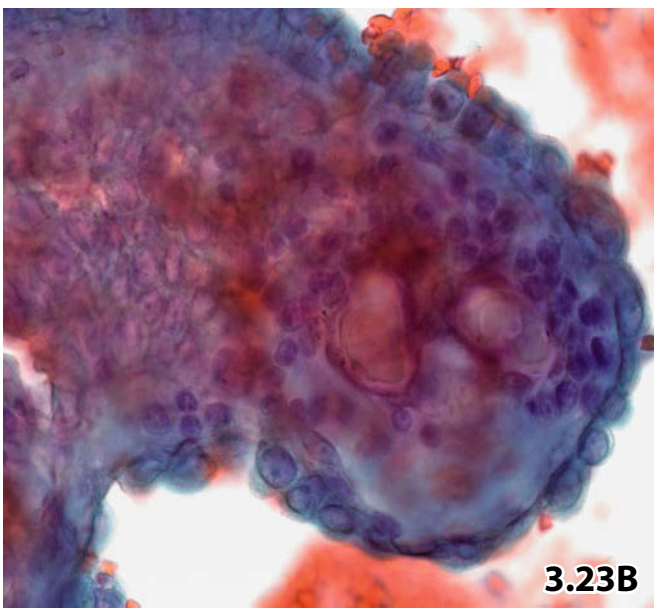
3.23B

**Fig. 3.24A–C Epithelial mesothelioma versus metastatic carcinoma.**
A 69-year-old man presenting with dyspnea was found to have a right-sided pleural effusion with an otherwise uneventful clinical history. Direct sediment smears were stained with the Papanicolaou technique.
*Tissue diagnosis* (surgical biopsy): Epithelial mesothelioma.
**A** Cytologic detail: atypical epithelioid cells exhibiting nuclear cleaving and coarse chromatin were accompanied by large signet-ring-like cells (arrows) and degenerating squamoid mesothelial cells (upper right).
*Tentative cytologic diagnosis* was malignant mesothelioma. Metastatic adenocarcinoma could not be excluded by standard cytology, immunostains were useful to separate mesothelioma from adenocarcinoma. **B** The vast majority of nonvacuolated and vacuolated atypical mesothelial cells showed unequivocal positivity for calretinin. **C** Only a few mesothelial cells expressed the epithelial marker Ber-Ep4.

**Fig. 3.25 Mesothelioma with sarcomatous component.**
An elderly male patient presented with a positive history of asbestos exposure. Cytology of a pleural fluid showed large pleomorphic malignant cells associated with abundant ill-defined and occasional fusiform cytoplasm (direct sediment smear, Pap stain, lower magnification).
*Tentative cytologic diagnosis:* Sarcomatous mesothelioma.
*Tissue diagnosis by necropsy:* Sarcomatous mesothelioma infiltrating pleural and abdominal cavity.

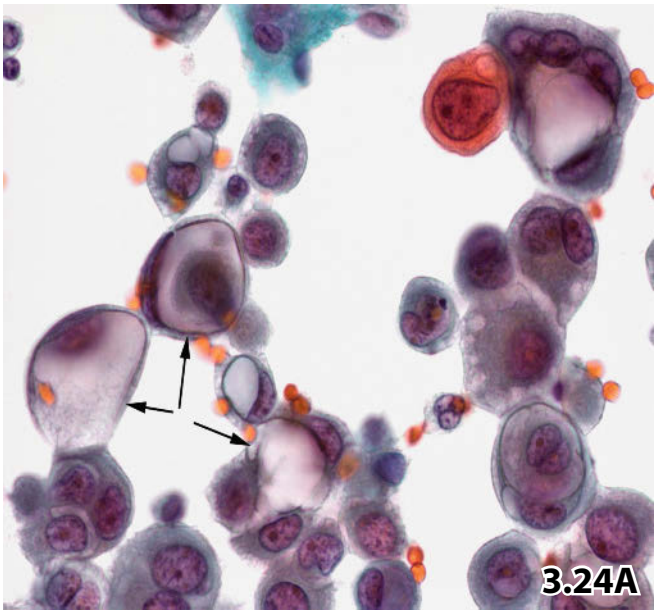
3.24A

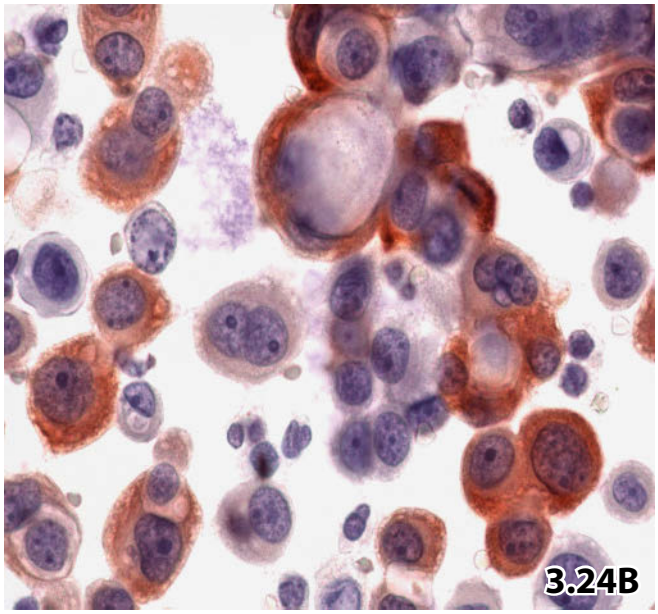
3.24B

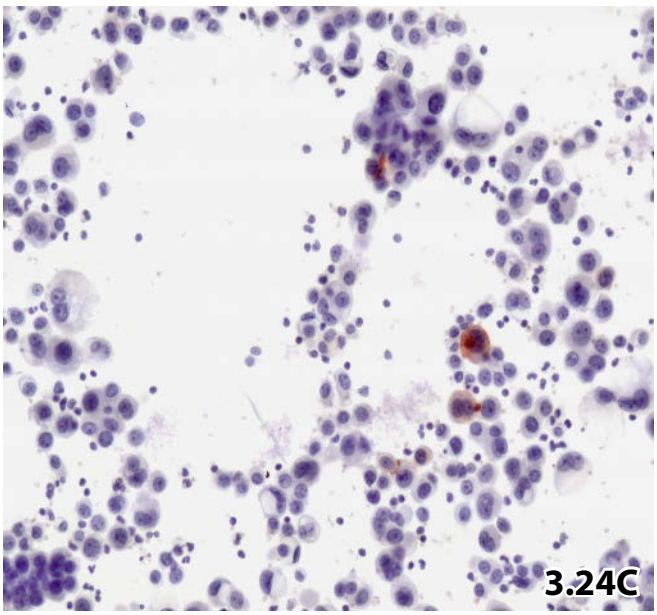
3.24C

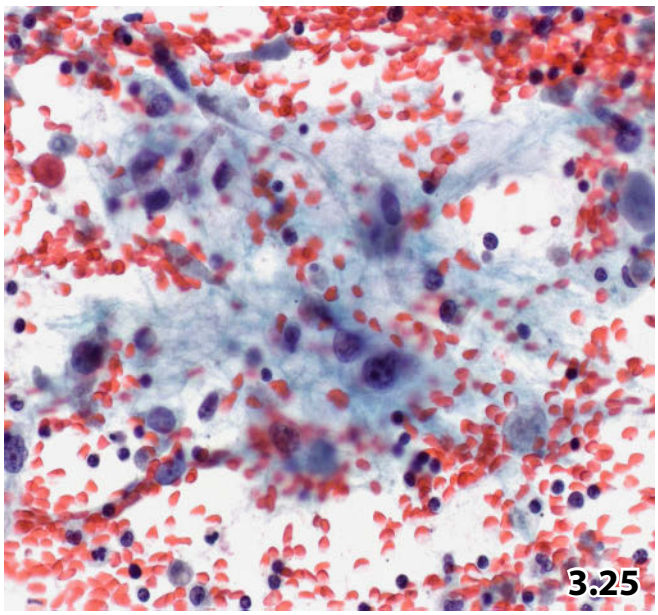
3.25

## Figs. 3.26 and 3.27 Adenocarcinoma.

**Fig. 3.26** Common aspect of adenocarcinomas: at very low magnification, adenocarcinomas are characterized by compact three-dimensional cell balls and papilliform clusters exhibiting fairly smooth border (pleural fluid, direct sediment smear, Pap stain).

**Fig. 3.27A, B** Adenocarcinoma of lung. Picture detail focuses on cytomorphologic features of common adenocarcinoma. Immunocytochemistry is helpful in ascertaining the primary site of metastatic adenocarcinoma. **A** Monotonous population of adenocarcinoma cells occurring both in papilliform clusters and isolated. Tumor cells show vacuolated cytoplasm and pronounced nucleoli. Malignant transformation is readily recognized by a high N/C ratio, irregular nuclear borders, dense and coarse chromatin. Compare the morphology of carcinoma cells with that of benign mesothelial cells (arrows) (pleural fluid, direct sediment smear, Pap stain). **B** Positive nuclear immunostaining for TTF-1 proved pulmonary origin of the neoplastic cells (Pap-prestained direct smear).

**Fig. 3.28 Undifferentiated squamous cell carcinoma versus poorly differentiated adenocarcinoma.**
This case focuses on cytologic diagnostic dilemma between poorly differentiated neoplasms of different histogenesis. High magnification shows cell features that are indicative of a poorly differentiated adenocarcinoma rather than of a poorly differentiated squamous cell carcinoma: abundant vacuolated cytoplasm, coarse but loose atypical chromatin texture, huge nucleoli (pleural effusion, direct sediment smear, Pap stain).
*Tentative cytologic diagnosis:* Poorly differentiated carcinoma of the large-cell type, most likely poorly differentiated adenocarcinoma.
*Tissue diagnosis by necropsy:* Metastatic nonkeratinizing squamous cell carcinoma of lung.

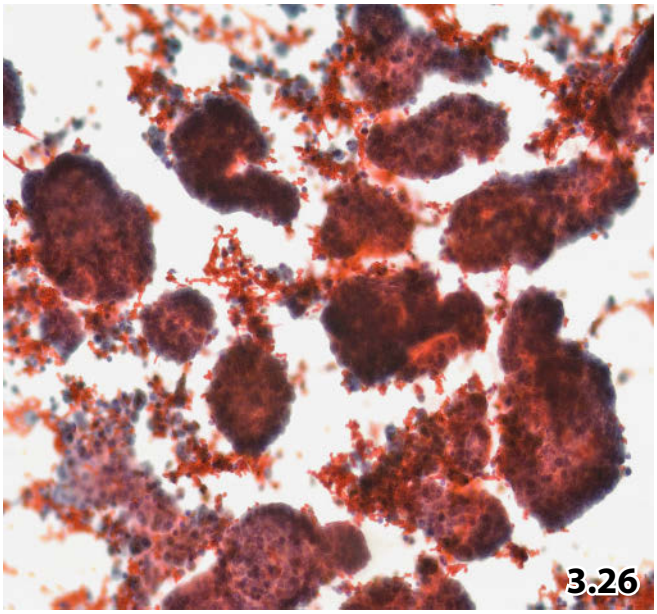
3.26

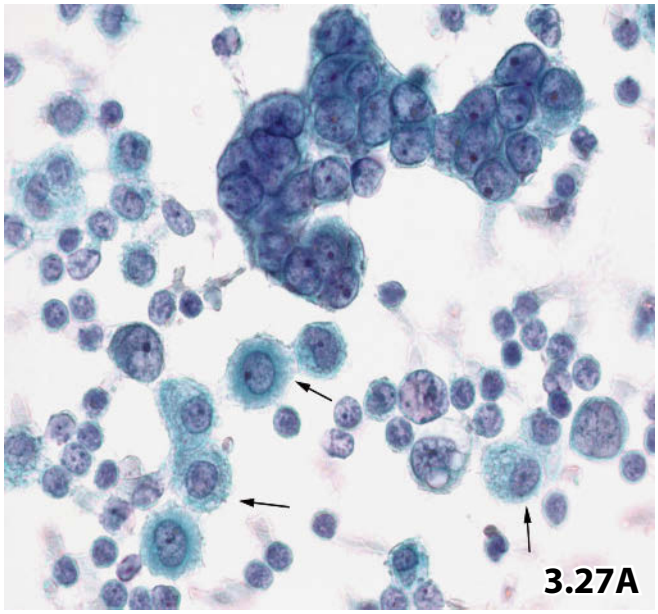
3.27A

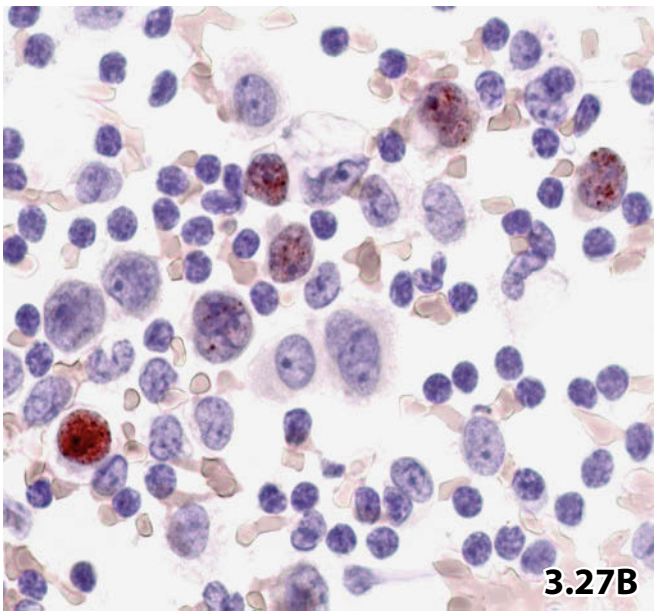
3.27B

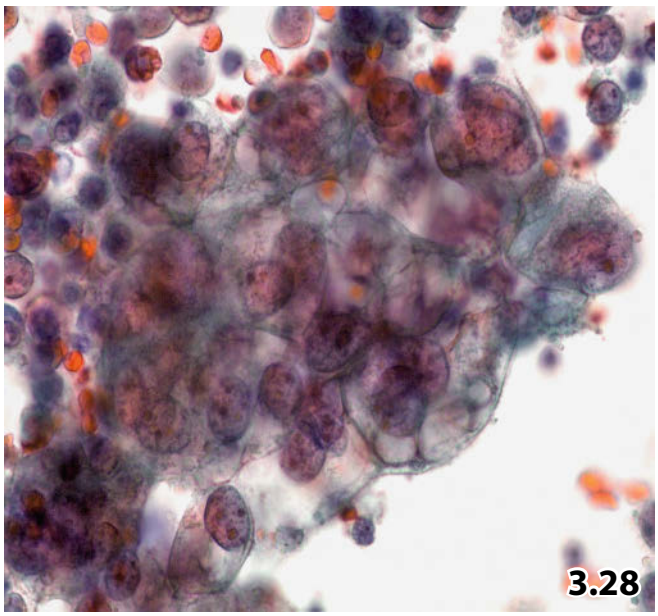
3.28

**Figs. 3.29–3.32 Small-cell carcinoma.**
Small-cell carcinoma of lung from three different patients: each tumor was metastatic to the pleural serosa or invading the pleural cavity. Direct smears from the three fluid sediments were Pap-stained.



**Fig.3.29** (case #1) Low magnification emphasizes that small-cell carcinoma may exfoliate extremely few cells into serous fluids, which are easily overlooked (arrows). Therefore, we recommend careful cytologic evaluation of any serous fluid specimen from patients found to have a small-cell carcinoma of the lung or lung cancer of undetermined histogenesis.

**Fig. 3.30** (case #2) Pleural fluid from a second patient containing mainly isolated tumor cells exfoliated from an invading small-cell carcinoma (large arrows.). Higher magnification reveals numerous activated lymphocytes (small arrows) and occasional mesothelial cells (arrowheads) as well. Cellular characteristics of small-cell carcinoma of the lung are overt (see Figs. 3.31 and 3.32). Please compare the tumor cells with lymphocytes and mesothelial cells regarding nuclear shape, size, chromatin, and cytoplasm.

**Fig. 3.31** (case #3) High magnification focuses on a small single-file arrangement of the tumor cells (arrow). Note features of small-cell carcinoma of the oat cell variant: pronounced nuclear molding, nuclear membrane irregularities, dense finely granular chromatin, scant cytoplasm.

**Fig. 3.32** (case #3) A last picture once again presenting the pathognomonic cell features of small-cell carcinoma of the oat cell variant, at very high magnification. Please keep in mind nuclear shape, salt-and-pepper chromatin, indistinct nucleoli, and scant cytoplasm (oil immersion, magnification ×100).

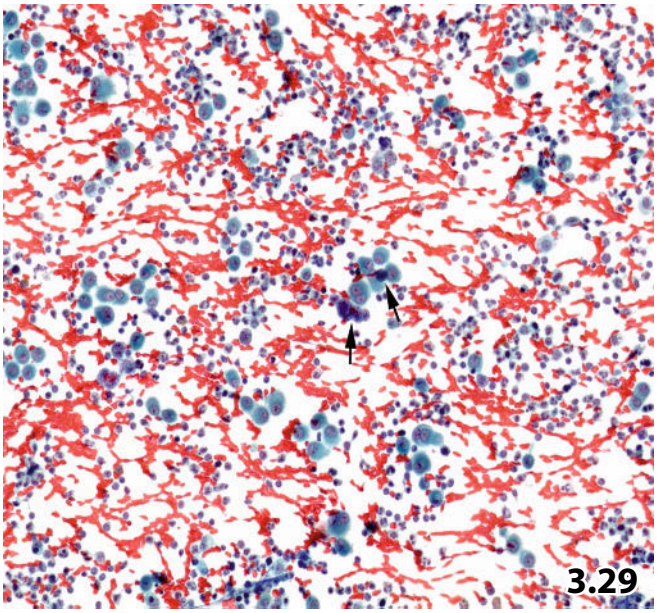
3.29

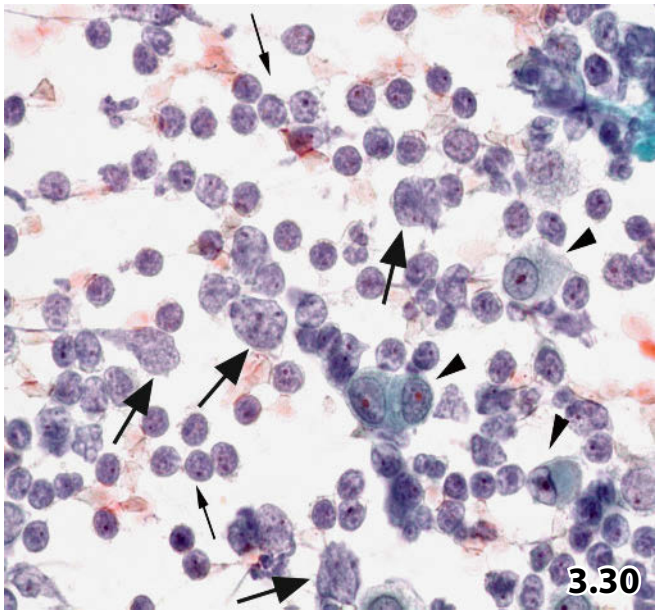
3.30

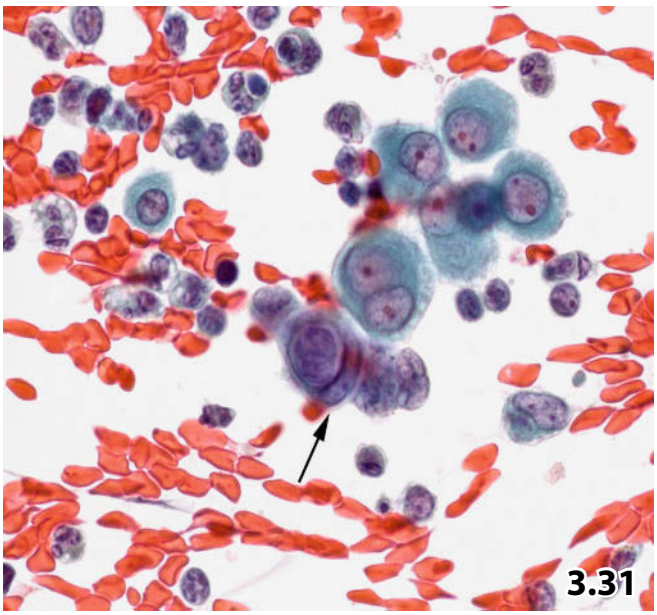
3.31

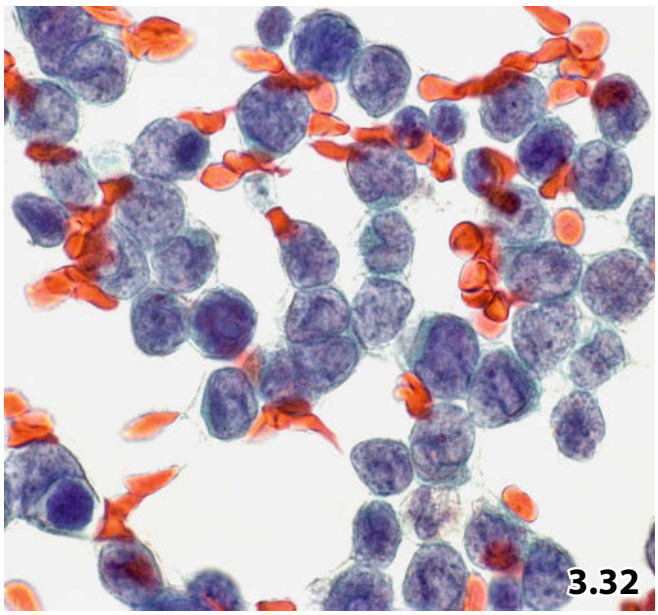
3.32

**Fig. 3.33A–C Small-cell carcinoma versus malignant lymphoma.**
An 83-year-old man with a history of B-CLL presented with ascites and pleural effusion. Image studies revealed a tumor mass in the lower abdomen. Direct smears were prepared from a pleural fluid sediment, and the specimens were Pap-stained. **A** The smears exhibited high cellularity but cytomorphology alone failed to differentiate between non-Hodgkin lymphoma and another small blue round cell tumor (higher magnification). Immunocytochemical stainings using Pap-prestained sediment smears were helpful in assessing the nature of the neoplasm. **B** Positive immunoreactivity of the tumor cells for CK8. **C** Positive nuclear immunoreactivity of the tumor cells for MIB-1 (proliferation index: 45%). Additional positive immunoreactivity of the tumor cells for CK18 and neuroendocrine markers is not shown.
*Final diagnosis* (FNAB of the abdominal mass and additional laboratory investigations): Metastatic undifferentiated small-cell carcinoma with neuroendocrine differentiation.
*Discussion:* Negative immunostaining for CD20, CD3, and CD5 (not shown) excluded intrathoracic spreading B-CLL. Furthermore, small lymphocytic lymphoma would express neither cytokeratins nor endocrine markers and usually exhibit a very low proliferation index.

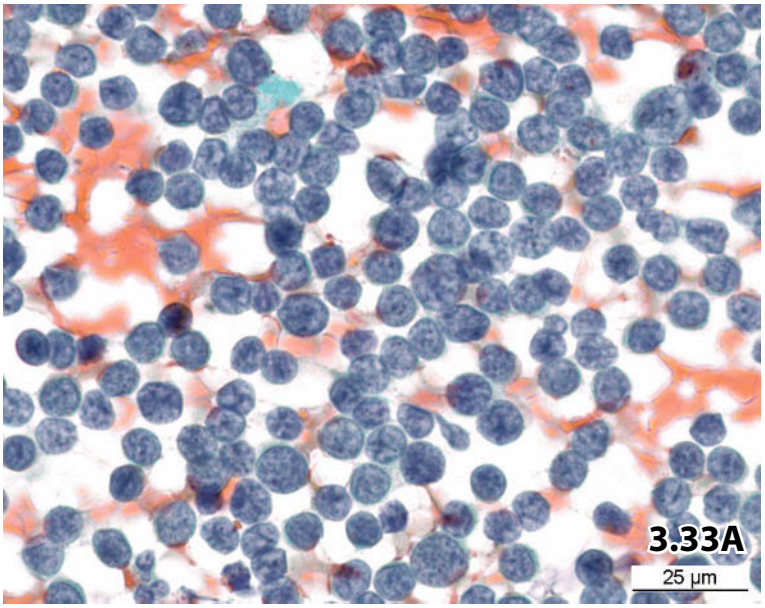
3.33A
25 µm

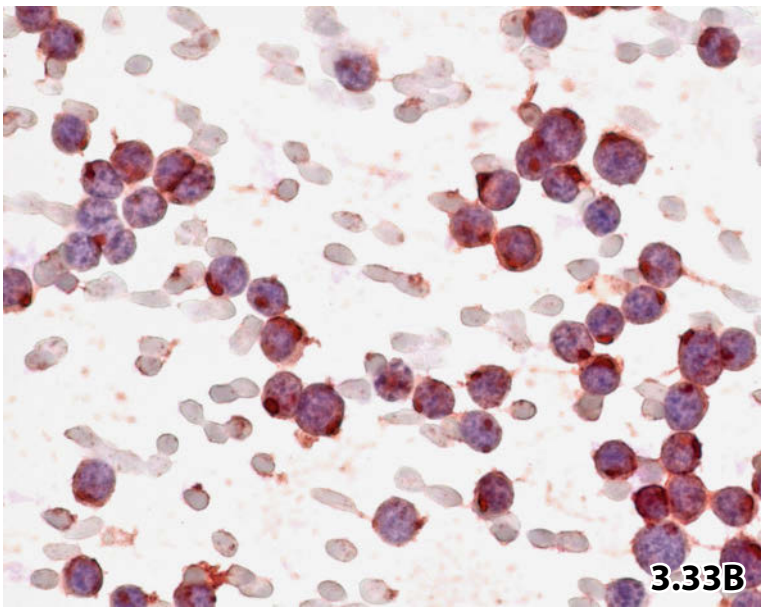
3.33B

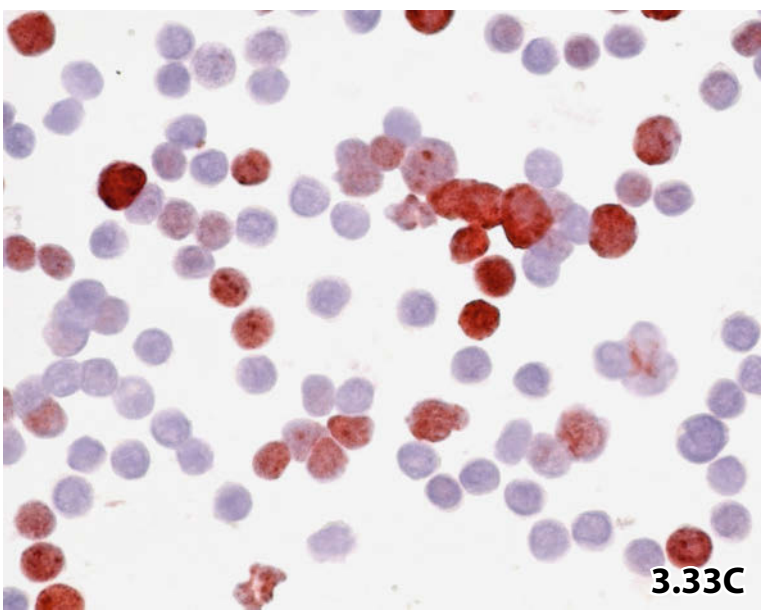
3.33C

**Fig. 3.34 Keratinizing squamous cell carcinoma.**
Isolated highly atypical keratinized cells (lower right) occur together with laminated cell clusters (upper left) and necrosis (direct sediment smear from pleural fluid, Pap stain, higher magnification).

3

Please check the appearance of isolated malignant squamous cells as compared with degenerating benign and malignant mesothelial cells (Figs. 3.2 and 3.22).

### Figs. 3.35 and 3.36 Nonkeratinizing squamous cell carcinoma.

A 54-year-old woman with a history of squamous cell carcinoma of the uterine cervix presented with pleural and pericardial effusions. Direct sediment smears were performed and Pap-stained.

**Fig. 3.35** Cytologic specimens of the pleural and pericardial fluid contained compact three-dimensional ball-like and papilliform cell clusters exhibiting sharp outlines and concentric lamination of the outermost cells (lower magnification).

**Fig. 3.36** High magnification (same case) emphasizes the characteristic peripheral cell arrangement and the well-defined cell boundaries. Note fairly bland nuclear morphology in the clustered tumor cells, still malignant nuclear features become evident on isolated tumor cells (arrow).

Sharply outlined tumor cell balls of squamoid origin should not be confused with the cell balls in malignant exudates caused by breast carcinoma (see Fig. 3.37). The homogeneously structured sharply defined cytoplasm and distinct cell lamination are key features of squamous cell carcinoma.

### Figs. 3.37 and 3.38 Carcinoma of the breast: cytologic key features.

**Fig. 3.37** (case #1) Lower magnification shows the characteristic knobby contour of three-dimensional spheres and papilliform clusters, indicating metastatic breast carcinoma (pleural fluid, direct sediment smear, Pap stain).

**Fig. 3.38** (case #2) High magnification highlights cellular morphology of breast carcinoma with particular emphasis on finely dispersed chromatin, nuclear molding and grooving, frequently triangular cytoplasm, intracytoplasmic vacuoles and targetoid cells (arrows) (ascitic fluid, direct sediment smear, Pap stain).

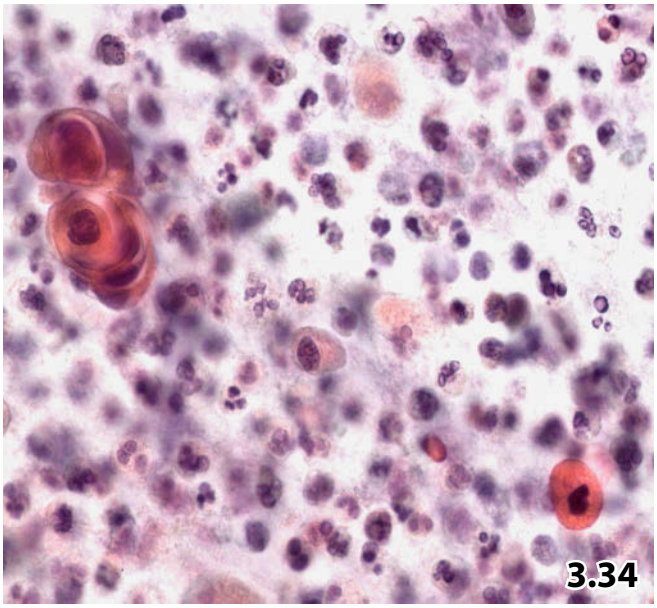
3.34

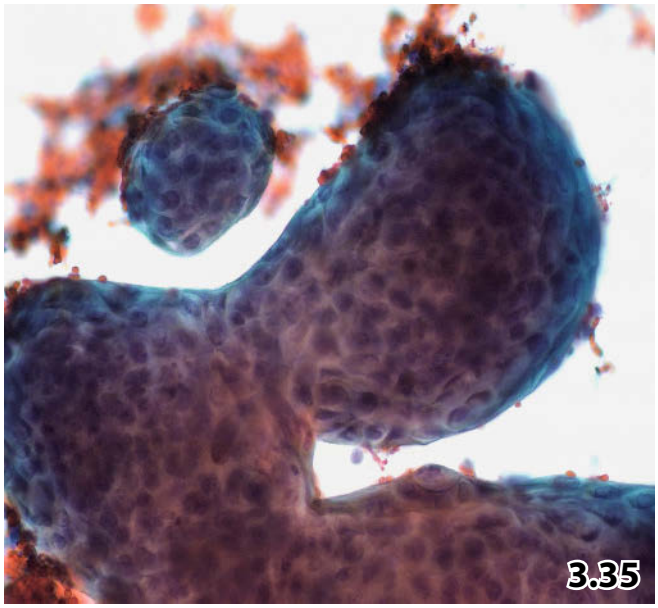
3.35


3.36

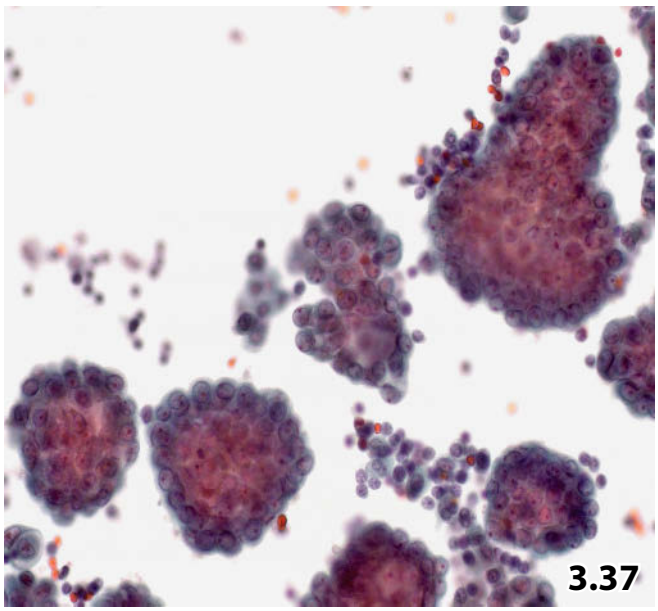
3.37

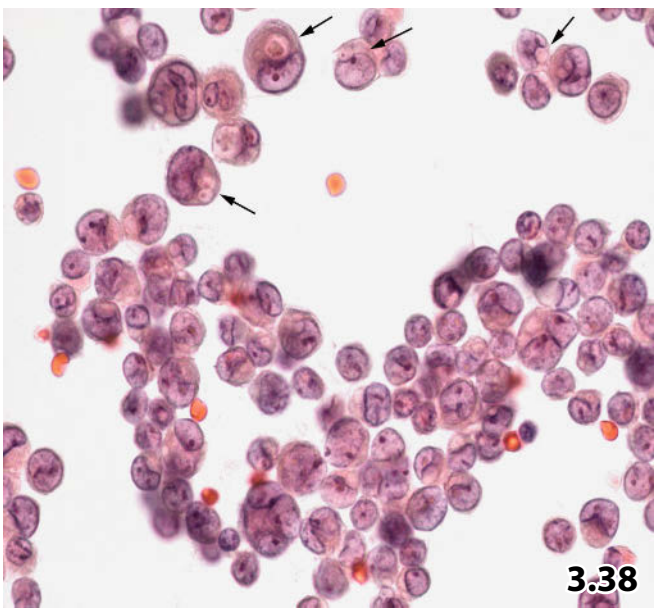
3.38

**Fig. 3.39A, B Carcinoma of the breast versus activated mesothelial cells.**
Peritoneal manifestation of a breast carcinoma in a 60-year-old woman. Ascitic fluid was processed using a conventional centrifuge, direct sediment smears were Pap-stained. **A** Compare carcinoma cells (arrows) with interspersed mesothelial cells/histiocytes (arrowheads) with respect to N/C ratio, nuclear staining quality, and chromatin texture (high magnification). **B** Conclusive diagnosis frequently depends on immunostaining. In the present case, nuclear positivity for estrogen receptor and progesterone receptor (the latter immunostain is not shown) confirmed mammary origin of the neoplastic cells (Pap-prestained smears).

**Fig. 3.40 Carcinoma of the breast versus adenocarcinoma of the gastrointestinal tract.**
Laparoscopy in a 74-year-old woman suggested infiltrates of the peritoneal surfaces due to gallbladder cancer. Ascites sediment was directly smeared, specimens were Pap-stained. All cellular features, except for pronounced nucleoli and cytoplasmic vacuolization, indicated breast carcinoma in cytology. Further investigations of the gallbladder, including FNAB, provided no evidence of a gallbladder neoplasia (high magnification).
*Final diagnosis:* Metastatic breast carcinoma.

**Fig. 3.41A, B Lobular carcinoma of the breast.**
A 63-year-old woman with a history of metastatic lobular breast carcinoma presented with ascites. Direct sediment smears from ascitic fluid were Pap-stained. **A** The monomorphic appearance of the small-cell epithelial population is compatible with lobular mammary carcinoma (low magnification). **B** High magnification shows that features of individual lobular-type carcinoma cells are akin to those of ductal breast carcinomas. Compare with Fig. 3.38: note the equivocal diagnostic value of mucoid cytoplasmic inclusions (left) and targetoid cells (not shown) distinguishing between the two breast cancer variants.

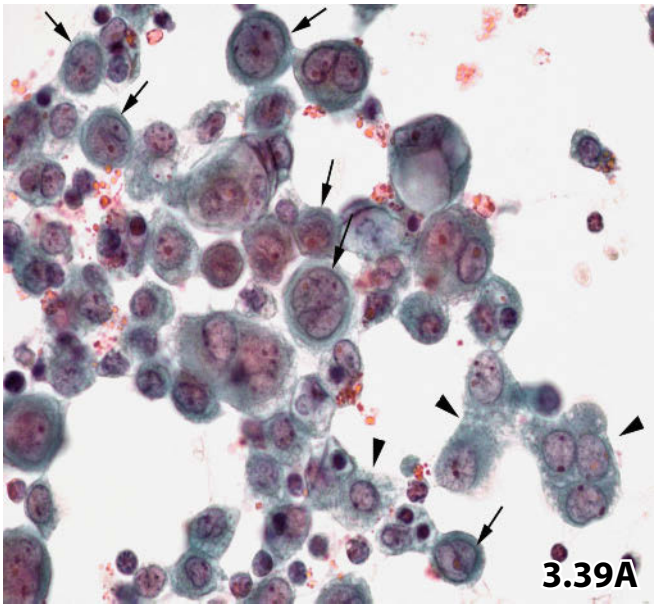
3.39A

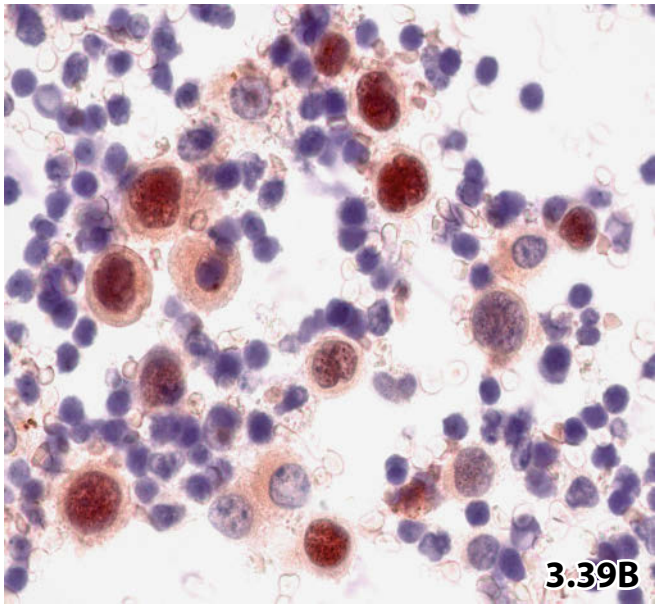
3.39B

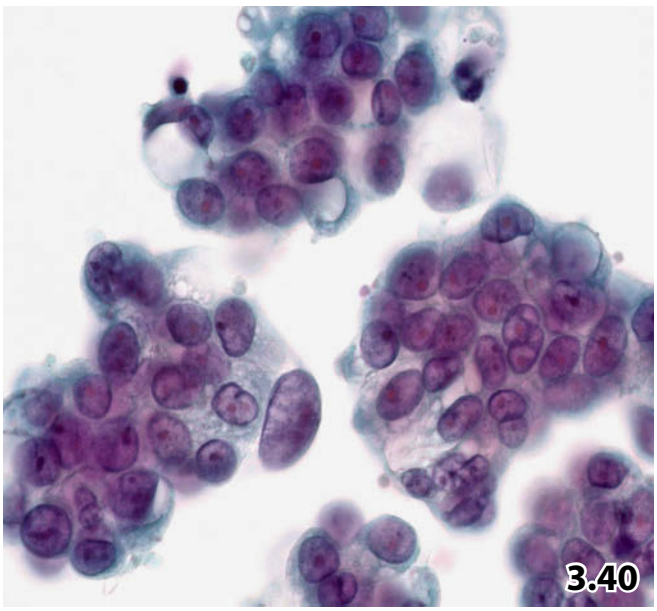
3.40

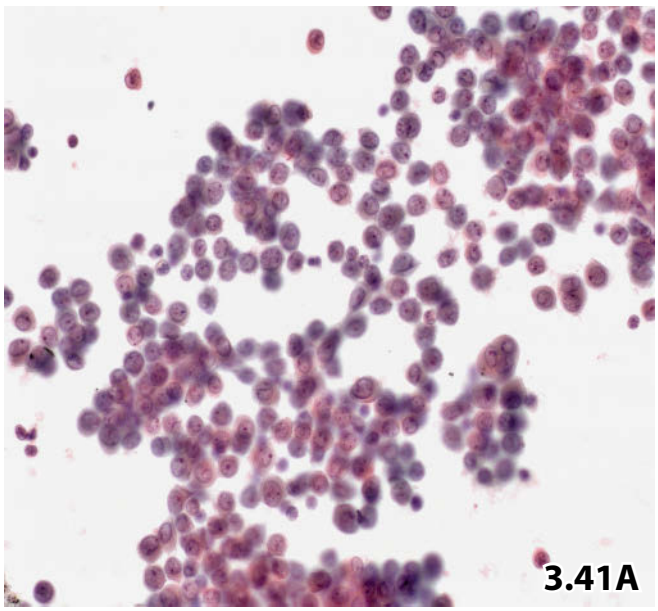
3.41A

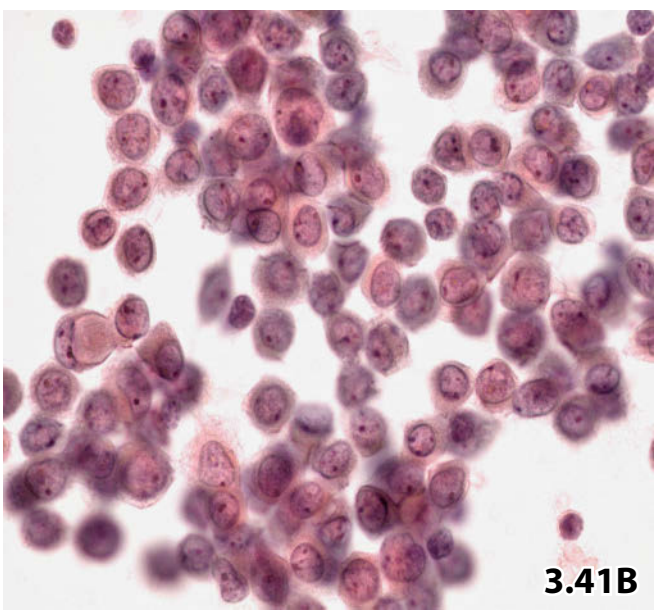
3.41B

**Figs. 3.42–3.44 Pancreatic adenocarcinoma.**
Three different cases of pancreatic adenocarcinoma with their characteristic cell features in effusion cytology. Direct sediment smears of peritoneal fluids were Pap-stained.



**Fig. 3.42** (case #1) Low magnification displays characteristic small to medium-sized papilliform and spherical tumor cell clusters; frequently distinct cellular palisading (center). Note isolated large tumor cells in the background (arrows).

**Fig. 3.43** (case #2) Higher magnification emphasizes the monomorphism and the small size of the cuboid and columnar neoplastic cells. Note distinct cellular palisading (bottom) and the cytoplasmic mucus (arrows)

**Fig. 3.44** (case #3) High magnification demonstrates nuclear clearing, bland chromatin, and bizarre nuclear shape (cleaving and folding) of the neoplastic cells. Note pink staining intracytoplasmic mucus and thin mucoid strands in the background of the smear (arrowheads). Compare the morphology of the carcinoma cells with that of benign mesothelial cells (arrow).

**Figs. 3.45 and 3.46 Gastric carcinoma.**
Effusion cytology of gastric carcinoma. Two different morphologic phenotypes are demonstrated by direct sediment smears, Pap-stained specimens.

**Fig. 3.45** (case #1) Admixture of signet-ring-like cells (arrow) is a characteristic feature of gastric carcinomas. The majority of the tumor cells appear solitary (pleural fluid, high magnification).

**Fig. 3.46** (case #2) Another case from a patient with a history of gastric cancer shows the histiocytoid variant of gastric carcinoma in ascitic fluid cytology. The discrete carcinoma cells exhibiting vacuolated cytoplasm and histiocytoid nuclear features may be misinterpreted as activated or neoplastic histiocytes. Histology of the primary tumor correlated with the current cytologic findings (high magnification).

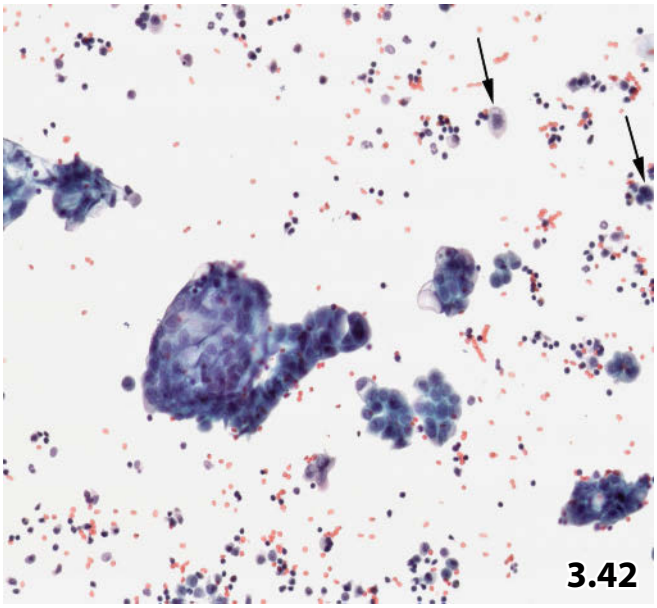
3.42

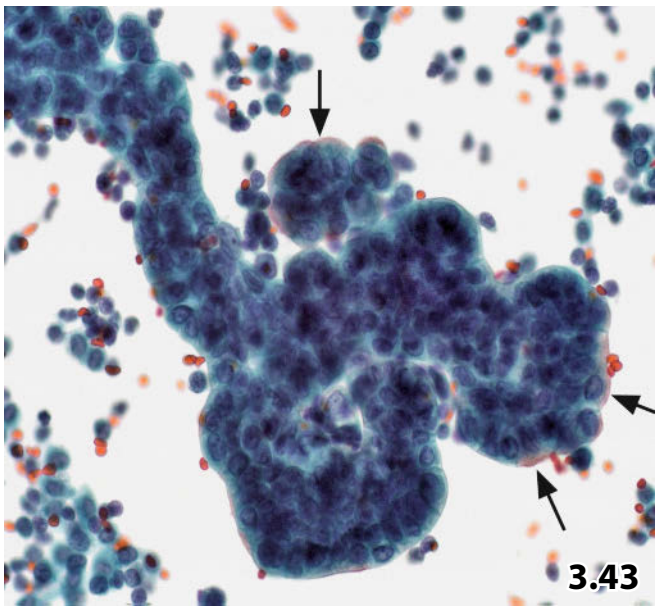
3.43

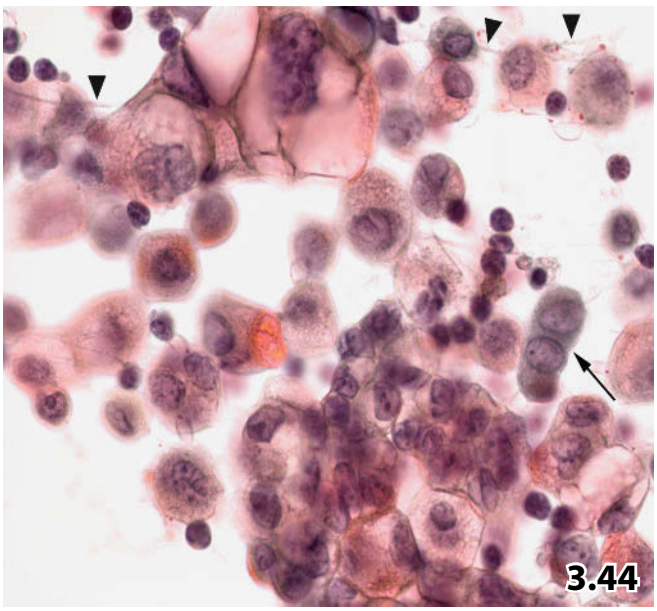
3.44

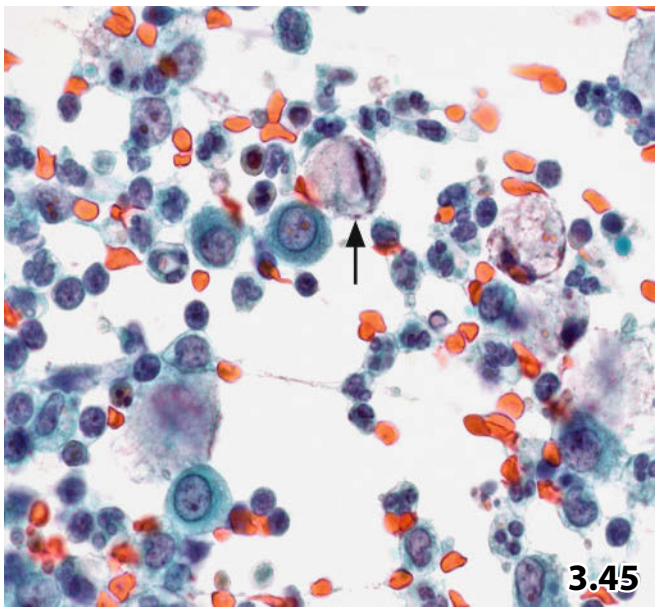
3.45

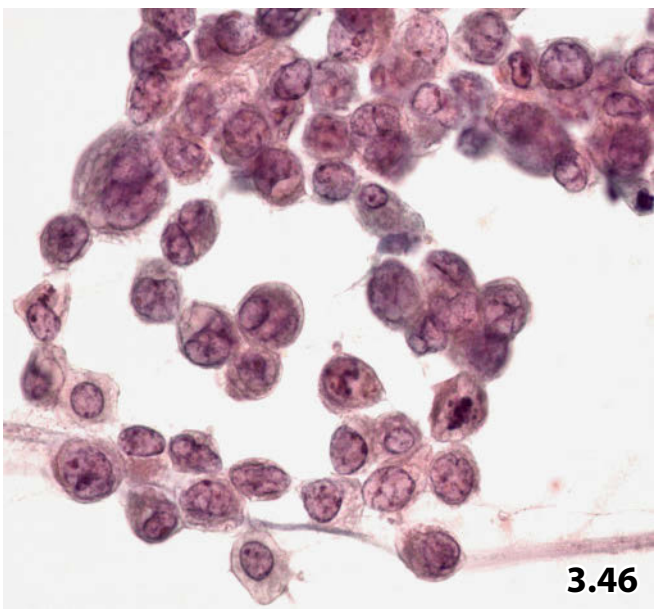
3.46

**Figs. 3.47 and 3.48: Ovarian carcinoma: poorly differentiated.**
Two examples of high-grade ovarian adenocarcinoma from two patients. Direct sediment smears were Pap-stained.



**Fig. 3.47** (case #1) Lower magnification exhibits characteristic tumor cell clusters: complex three-dimensional cellular clustering, abundant cytoplasm showing coarse vacuolization, and pronounced variability of nuclear size and shape.

**Fig. 3.48** (case #2) High magnification shows nuclear pleomorphism, coarse clumping chromatin, and multiple large nucleoli. Psammoma bodies concealed between tumor cells are also present (lower left and bottom).

**Fig. 3.49A, B Ovarian adenocarcinoma: low-grade, papillary variant.**
An 88-year-old woman with a history of well-differentiated serous papillary ovarian carcinoma (pT1, G1) presented with a pleural effusion. Cytology and immunocytochemical properties are demonstrated using direct sediment smears (Pap stain). **A** Medium-sized monomorphic tumor cells are arranged in small papilliform clusters. The nuclei exhibit loose chromatin and clearing. Cytoplasmic vacuoles and nucleoli occur to a minor degree as compared with poorly differentiated ovarian carcinoma (high magnification).
*Comment:* Other metastatic carcinomas, such as adenocarcinoma of lung or endometrium may share architectural and cellular features of low-grade ovarian carcinoma. **B** Strong positive immunoreaction for CA-125 and negativity for TTF-1 (the latter staining is not shown) indicate ovarian origin of the tumor (Pap-prestained smear).

**Fig. 3.50 Endometrial adenocarcinoma: poorly differentiated.**
Monomorphic cell appearance, dense fine granular chromatin, faint hyperchromasia, and small nucleoli are hallmarks of adenocarcinomas of endometrial origin. The pleomorphic variant of endometrial carcinoma would share cellular features with many other adenocarcinomas spreading into serous cavities (pleural effusion, direct sediment smear, Pap stain, high magnification).

**Fig. 3.51 Endometrial adenocarcinoma: well-differentiated.**
A 66-year-old woman presented with a history of endometrial carcinoma and recent pleural effusion. Direct sediment smears exhibited unambiguous tumor fragments of an adenocarcinoma. Nuclear features are comparable with those of poorly differentiated endometrial neoplasia as described above (higher magnification, Pap stain)

**Caution**

The lucid nucleoplasm, indistinct chromatin texture, nuclear indentations, dense cyanophilic cytoplasm, and compact papilliform clusters and spheres simulate breast carcinoma.

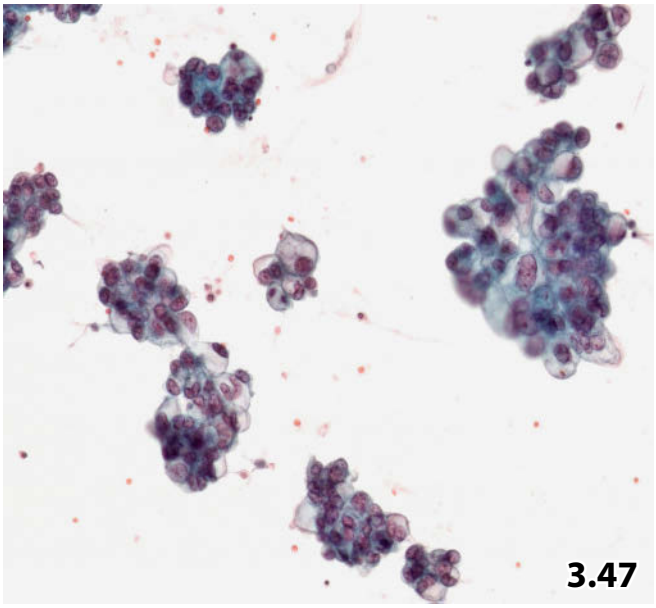
3.47

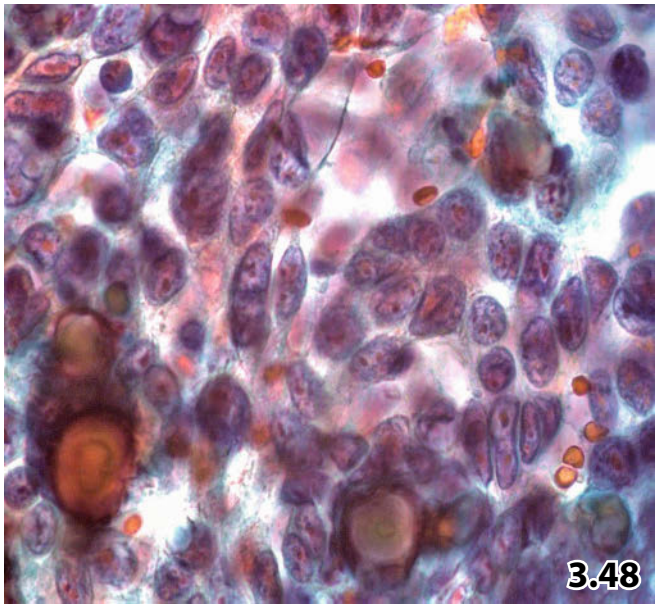
3.48

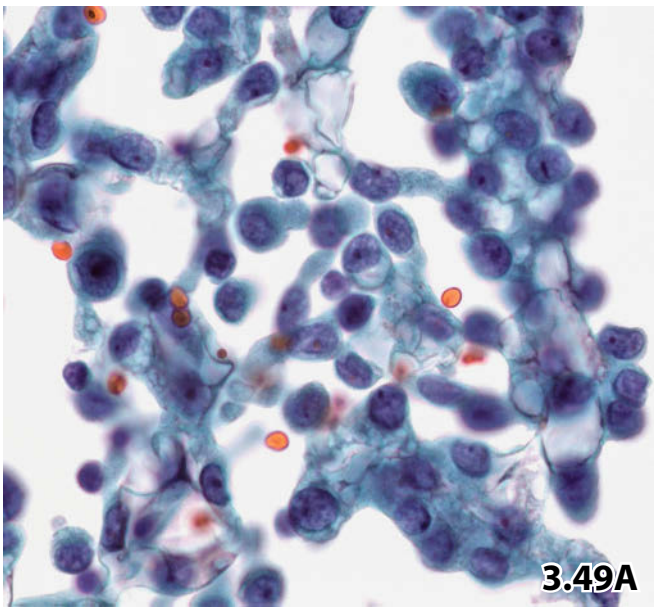
3.49A

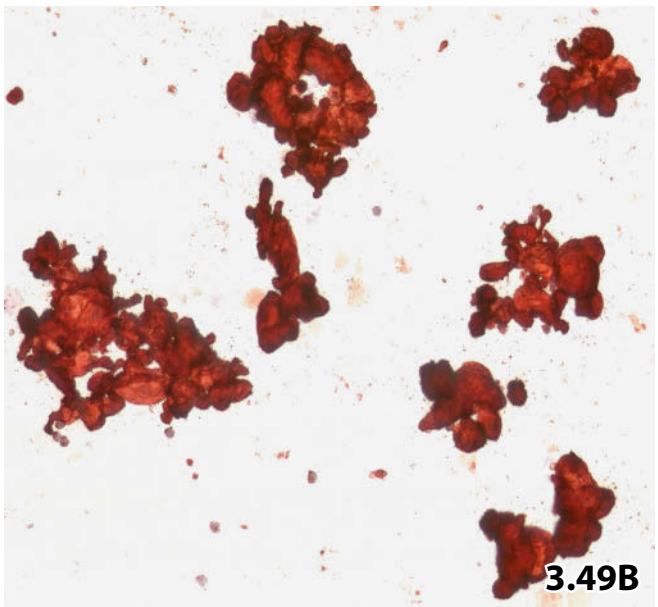
3.49B

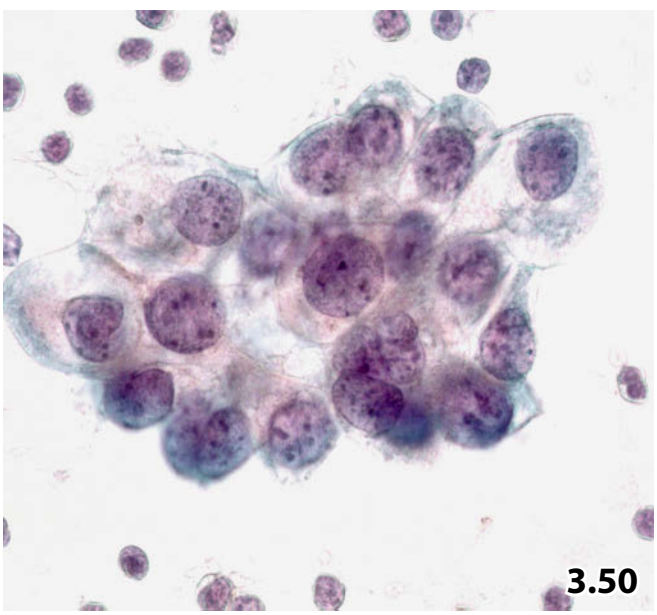
3.50

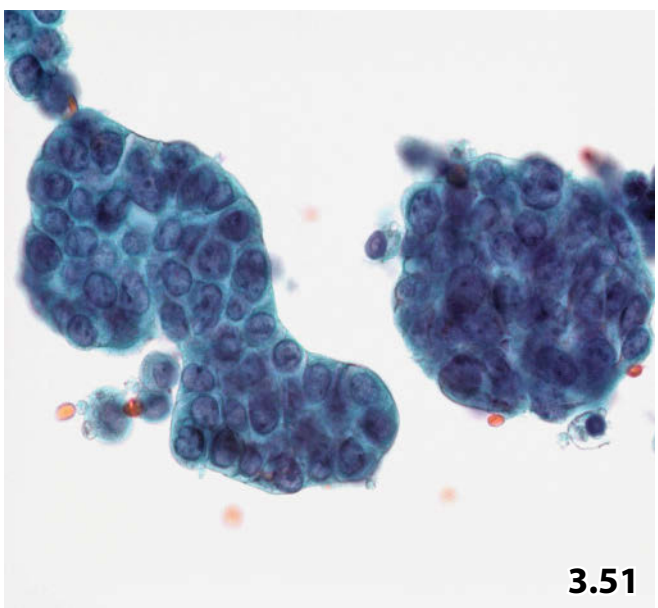
3.51

**Fig. 3.52A, B Small lymphocytic lymphoma/B-CLL.**
An 89-year-old woman with a history of chronic lymphatic leukemia diagnosed 3 years before presents with relapsing right-sided pleural effusions. Effusion cytology is required prior to readministering chemotherapy. Direct sediment smears are Pap-stained. **A** Overall cell pattern of low-grade lymphocytic lymphoma may masquerade that of benign lymphocytosis in florid pleural tuberculosis (compare with Fig. 3.9). Still, neoplastic lymphocytes as presented show increased nuclear irregularities and a dense smudged chromatin as compared to benign lymphocytosis (higher magnification). **B** Immunostaining for the B-cell marker CD20 was very helpful in determining a correct diagnosis: all cells showed a positive reaction, indicating B-CLL (Pap-prestained smears).

**Fig. 3.53A, B Lymphoblastic non-Hodgkin lymphoma.**
A 9-year-old boy presented with a mediastinal tumor and a pleural effusion. Clinical and imaging results suspected malignant lymphoma. Pleurocentesis was performed initially in order to reach a preliminary diagnosis (direct sediment smears, Papanicolaou staining method). **A** Cytologic smears displayed small and medium-sized blastic cells exhibiting a small but distinct cytoplasmic rim, irregular nuclear shape, and large pleomorphic nucleoli (arrows) (lower magnification).

> Small malignant lymphoblasts share many features with benign small immature blast cells.

**B** A conclusive cytologic diagnosis of a T-lymphoblastic lymphoma could be established due to positive nuclear immunoreaction for TdT and for CD3 (the latter immunostaining is not shown). Note absent nuclear immunopositivity on small benign lymphocytes.

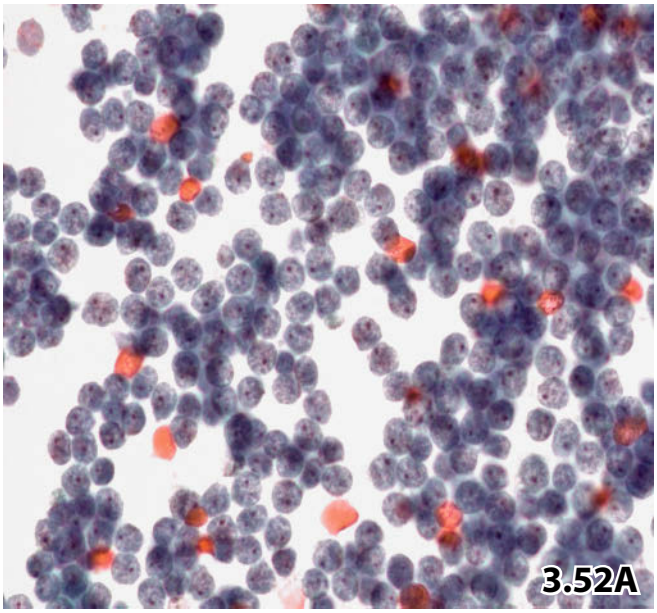
3.52A

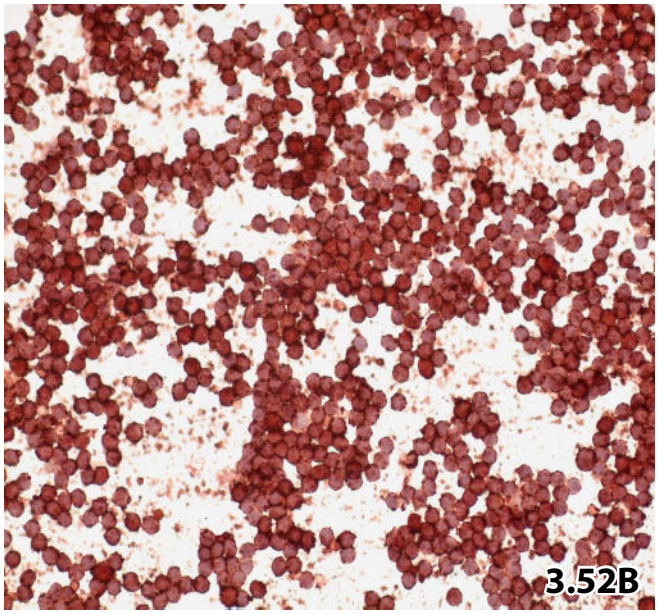
3.52B

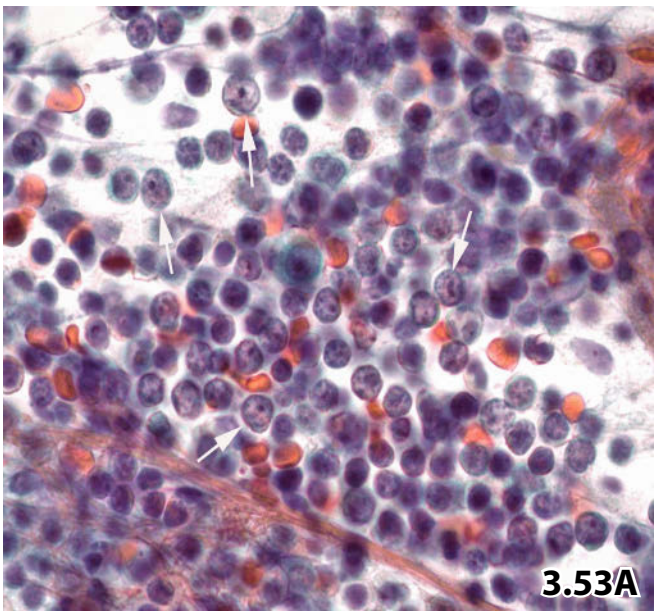
3.53A

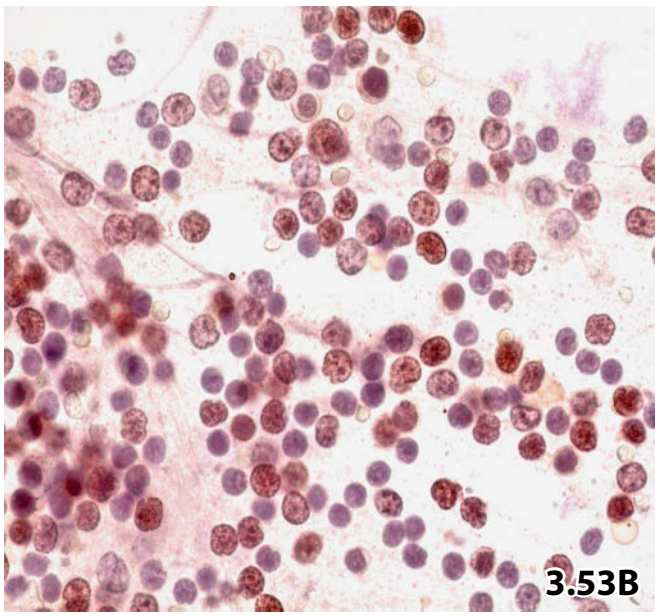
3.53B

**Fig. 3.54 Hodgkin lymphoma.**
The lymphocytic population in a pericardial fluid of a patient with a clinical history of Morbus Hodgkin showed a heterogeneous appearance in direct sediment smears. Highly atypical small to medium-sized lymphocytes are numerous. A few Reed-Sternberg cells (one is located at the right) enable a definite diagnosis of pericardial infiltration from Hodgkin disease (Pap stain, high magnification).

**Fig. 3.55A, B Blastic non-Hodgkin lymphoma: large-cell type.**
A 52-year-old man presented with a right-sided pleural effusion. Direct sediment smears were Pap-stained.
*Cytologic / immunocytochemical diagnosis:* Blastic B non-Hodgkin lymphoma.
*Histologic diagnosis* from an excised lymph node: Diffuse large B cell lymphoma, centroblastic variant.
**A** High magnification illustrates a highly pleomorphic discohesive cell population. The N/C ratio of the tumor cells is high and the nuclear lobulation is striking. Compare the tumor cells with a pair of benign mesothelial cells (arrow). **B** Strong immunopositivity for CD20. Mesothelial cells (paracentral left) remain unstained.

**Fig. 3.56 Plasmacytoma: immature variant.**
Recent pleural effusion in an elderly woman suffering from multiple myeloma. Immature plasmacytoid cells display eccentrically positioned nuclei surrounded by a strongly basophilic cytoplasm; dense granular chromatin, and very prominent nucleoli. Vague paranuclear clearing is occasionally detected (arrows) (direct sediment smear, MGG stain, high magnification).

**Fig. 3.57A, B Pleural myelogenic sarcoma in a patient suffering from chronic myeloic leukemia.**
Pleural fluid of a patient with a history of chronic myeloic leukemia yielded cellular direct sediment smears, which were stained according to MGG. **A** Cytologic specimens exhibiting a variegated cell pattern composed of myeloic cells in different stages of maturation. Note dense and partly vacuolated cytoplasms and pleomorphic nuclei exhibiting a coarse chromatin texture (higher magnification). **B** Positive immunostaining for myeloperoxidase is useful in distinguishing between myeloid neoplasm and malignant lymphoma.

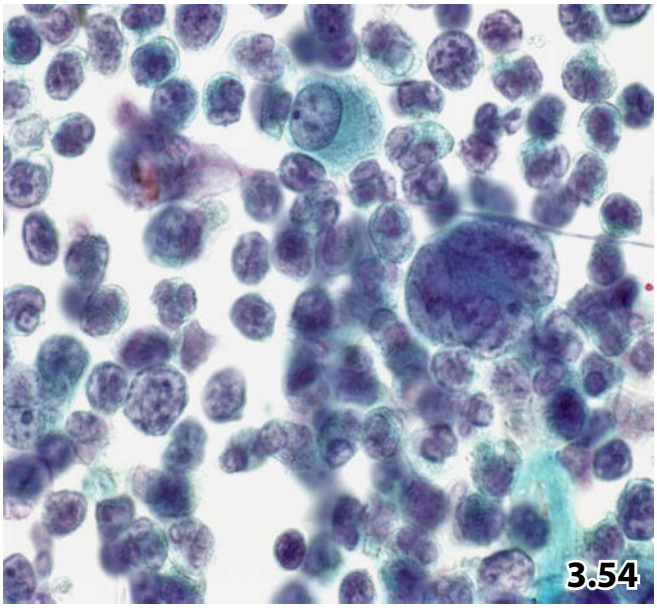
3.54

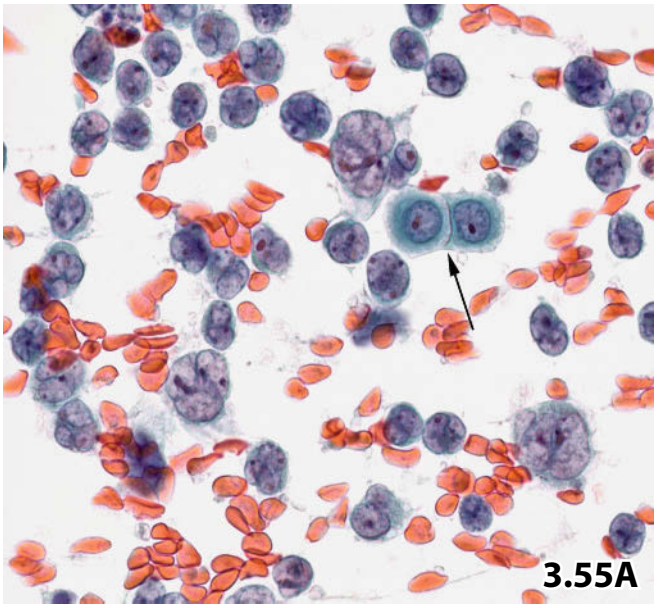
3.55A

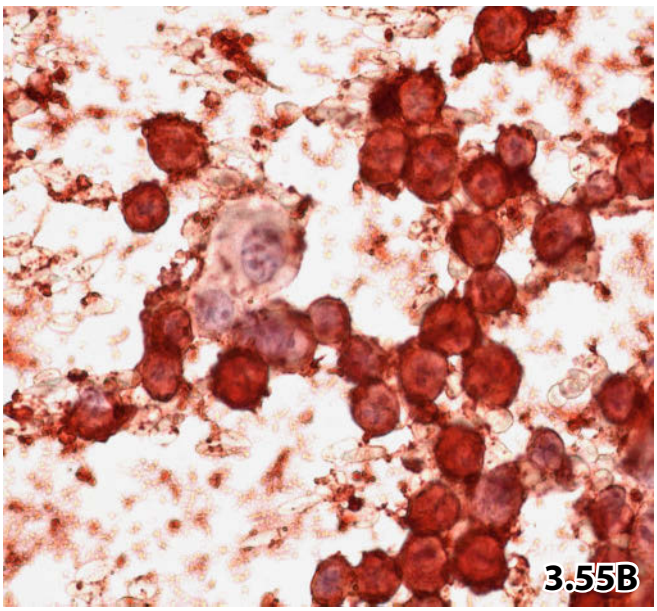
3.55B

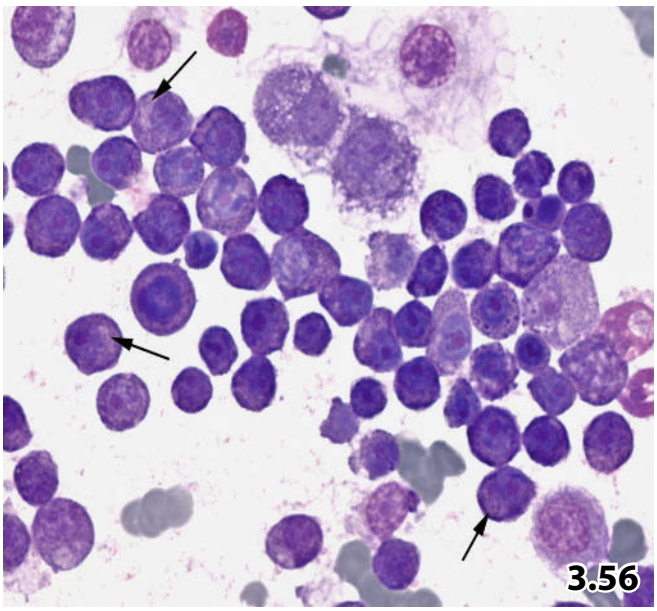
3.56

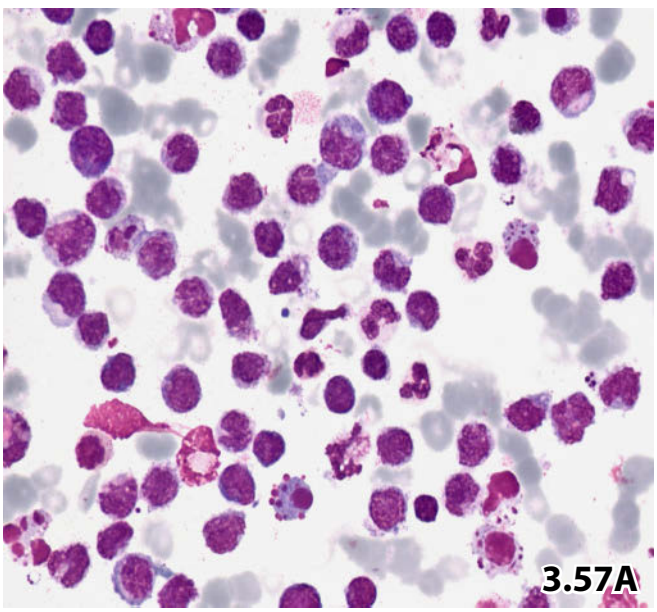
3.57A

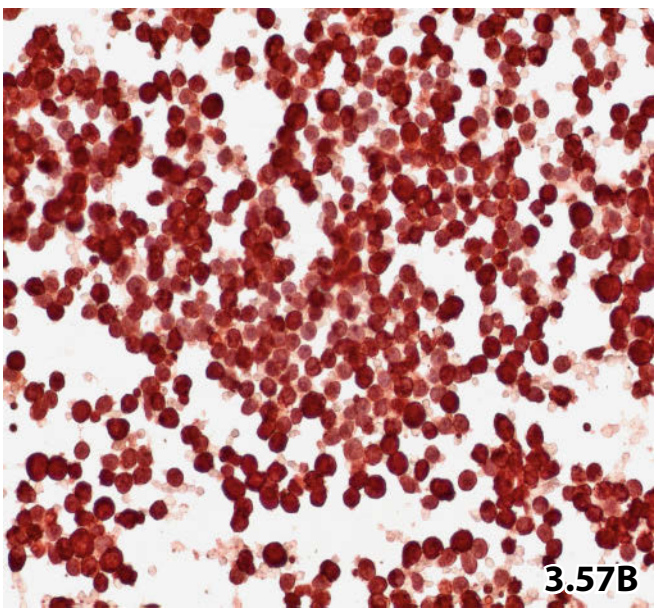
3.57B

**Fig. 3.58A, B Pseudomyxoma peritonei.**
A 48-year-old man presented with a swollen belly caused by intraperitoneal fluid. The patient did not complain of any additional discomfort. The viscous aspirate was directly smeared onto glass slides and Pap-stained.
*Cytologic diagnosis:* Pseudomyxoma peritonei: low-grade mucinous adenocarcinoma.
*Final diagnosis* (subsequent to laparotomy and microscopic tissue examination): Pseudomyxoma peritonei evolved by dissemination of a well-differentiated mucin-producing cystadenocarcinoma of the appendix.
**A** The micro-photograph at low magnification shows a few epithelial cells with abundant foamy cytoplasm (arrows) embedded in mucinous masses. **B** High magnification focuses on the morphology of isolated well-differentiated tumor cells exhibiting vacuolated cytoplasm and minor nuclear irregularities. One small tumor cell cluster is also present (arrow).

**Figs. 3.59 and 3.60 Amelanotic malignant melanoma: cytologic key features.**
Metastatic malignant melanoma in an elderly man. Cytology of a pleural fluid reveals tumor involvement of the serous membranes (direct sediment smears, Pap stain).

**Fig. 3.59** High magnification demonstrates cytologic hallmarks of malignant melanoma cells: draw your attention to cellular size, abundant eccentric cytoplasm, prominent nucleoli, nuclear grooves, nuclear inclusions (arrowheads), and compare with unequivocal benign histiocytes (arrows).

**Fig. 3.60** The neoplastic cells show strong positive immunoreaction for melanoma-typical markers; HMB-45 is actually demonstrated (Pap-prestained smear).

**Fig. 3.61 Melanophages versus pigmented malignant melanoma cells.**
A female patient with a history of malignant melanoma presented with ascites. Until then, there was no evidence of tumor spread. Cellular ascitic fluid exhibited exclusively discohesive cells loaded with pigment granules; its structure and color suggested melanin pigment, and Prussian blue staining for iron on a Pap-prestained smear provided a negative reaction (higher magnification).
*Cytology:* All cells are assumed to be melanin-loaded macrophages. Scattered malignant melanoma cells of histiocytoid appearance may be present as well but cannot be visualized by standard microscopy. However, the particular cytologic findings suggest melanoma invasion into the abdominal cavity.

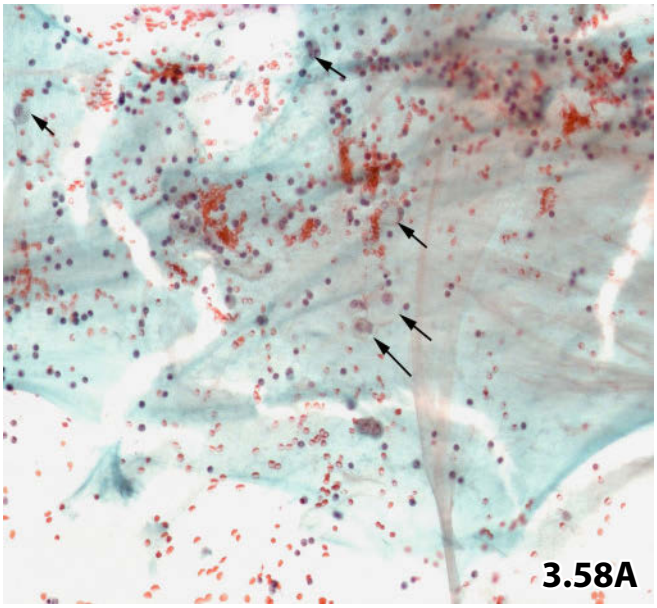
3.58A

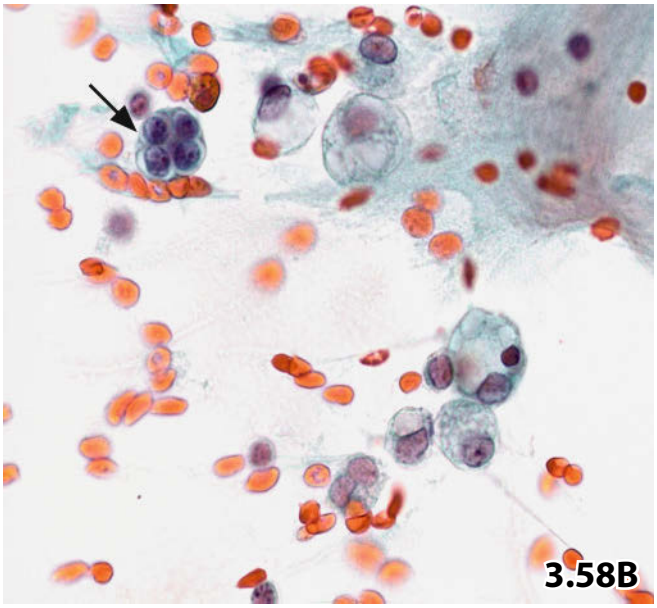
3.58B

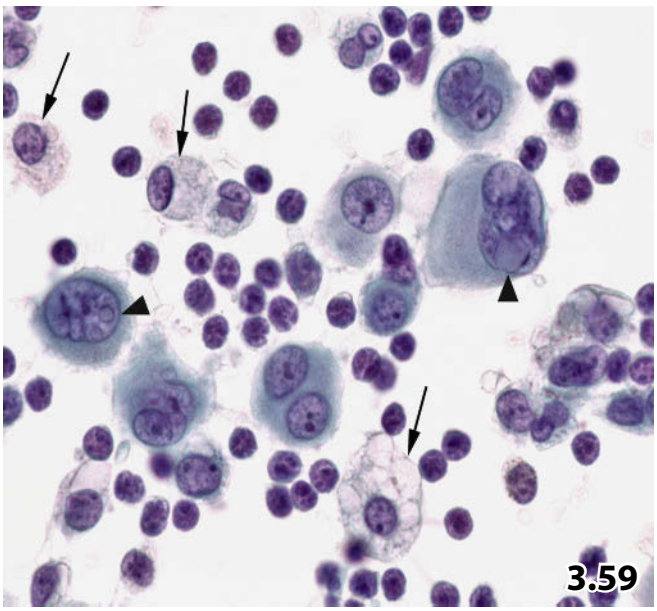
3.59

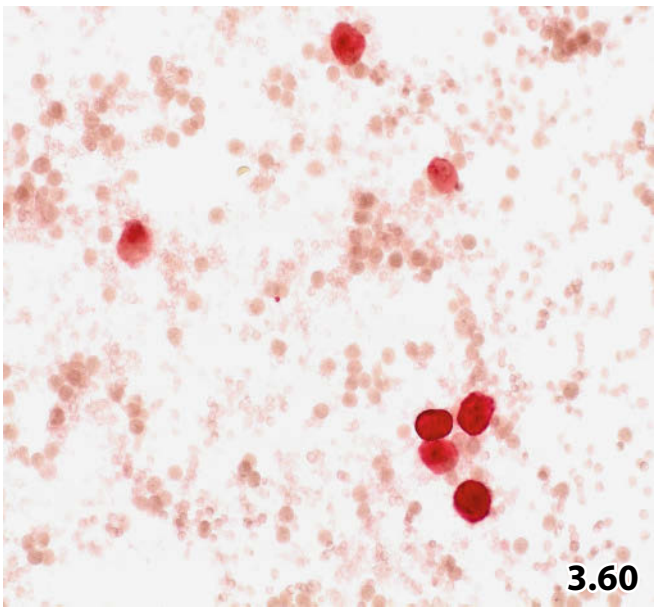
3.60

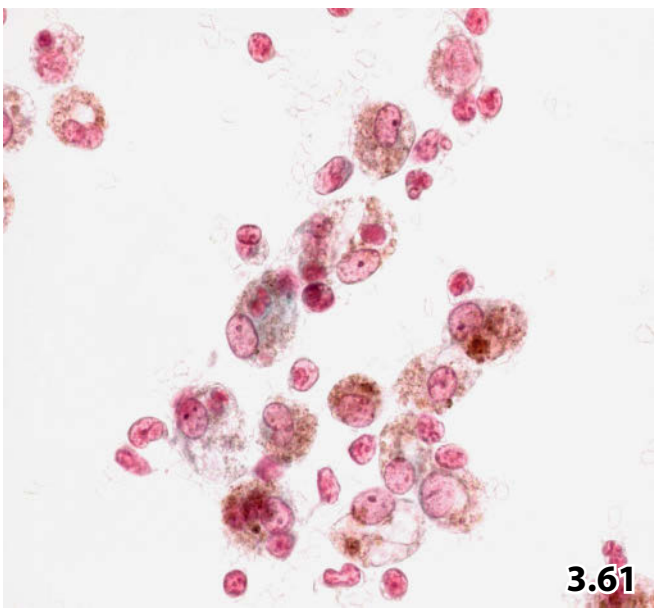
3.61

**Fig. 3.62 Renal clear cell carcinoma versus histiocytes.**
A 72-year-old man presented with a history of renal adenocarcinoma and ascites. Tumor cells, isolated and arranged in loose sheets, occur in direct sediment smears from ascitic fluid. Cellular grouping, pronounced nuclear cleaving, and finely granular chromatin are consistent with a well-differentiated clear cell renal cell carcinoma. Previous histology of the primary tumor correlates well with these cytologic findings (Pap stain, lower magnification)

One should keep clearly in mind that it is practically impossible to differentiate between clear carcinoma cells and activated histiocytes using ordinary microscopy.

**Fig. 3.63 Seminoma.**
Undifferentiated large tumor cells in a fluid from the tunica vaginalis testis. Distinguishing seminoma from blastic lymphoma and undifferentiated large-cell carcinoma is very difficult based on cytology of serous exudates unless an appropriate panel of antibodies is applied (higher magnification, Pap stain).
*Final diagnosis* in the current case: Seminoma of testis.

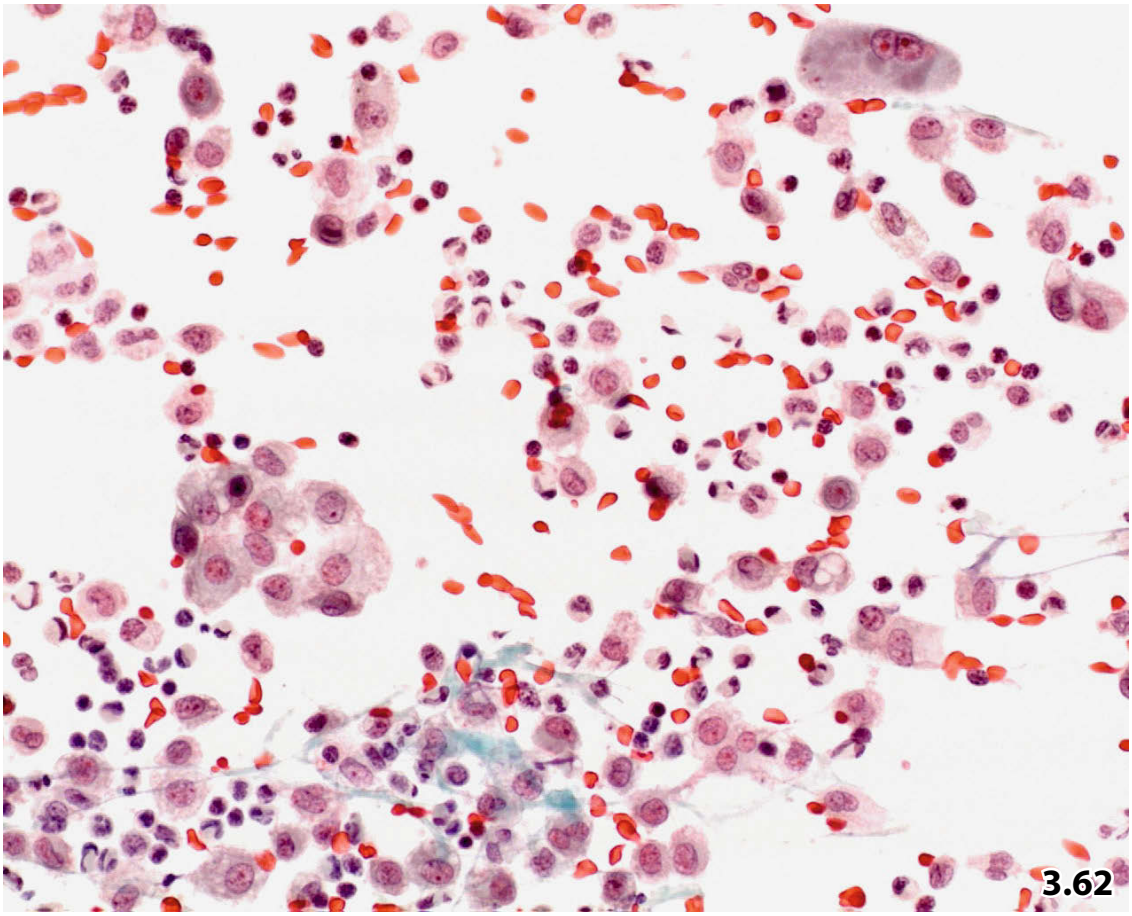

3.62

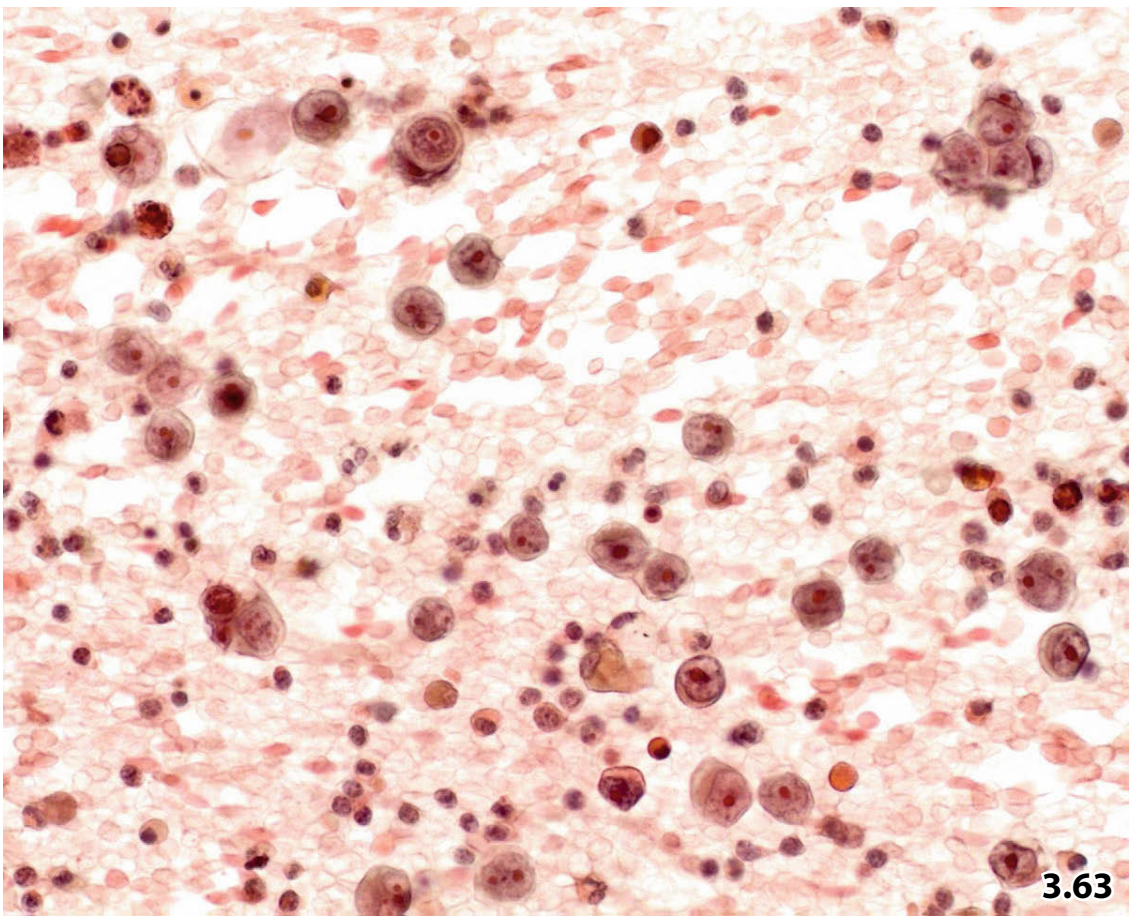

3.63

# Section 3.3
# Effusions, Aspiration and Washing

Peritoneal Cavity

Cul-de-Sac

Douglas Pouch

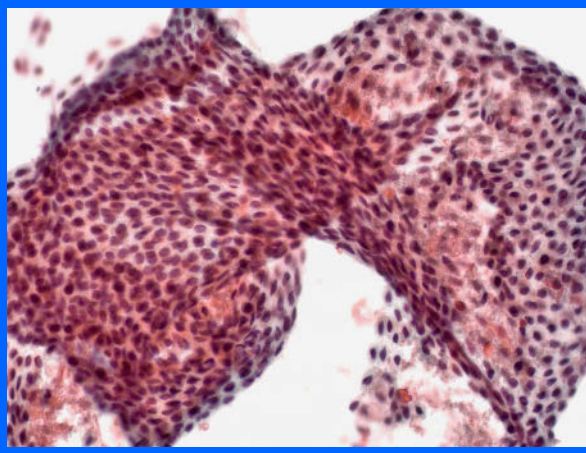

## 3.3.1 Introduction

Several comprehensive and pertinent publications on peritoneal washing cytology are available [3, 14, 20, 23, 26, 27, 28].

### 3.3.1.1 Purpose of Peritoneal Fluid Examination

- Cytologic examination of peritoneal fluids is regarded as an useful adjunct to multiple peritoneal biopsies at primary and second-look surgical procedures.
- Detection of microscopic peritoneal spread of primaries from different organs, particularly of gynecologic malignancies.
- Staging and classification of ovarian carcinoma, particularly in addition to initial surgical staging in patients with presumed stage I and II ovarian cancer.
- Evaluation of the effect of a previous treatment in patients with ovarian malignancy, in line with second-look operations. If the patient is disease-free in peritoneal fluid cytology, chemotherapy may be discontinued.

### 3.3.1.2 Sampling Techniques [12]

- Collection of free ascitic fluid as an adjunct to laparoscopy or laparotomy.
- Culdocentesis means needle aspiration of fluid from the cul-de-sac by transvaginal puncture.
- Saline lavage of the pouch of Douglas or of selected areas of the peritoneal surface after the abdomen has been opened. Samples for cytologic examination should be taken prior to surgical biopsies and resections.
- Direct peritoneal scraping or brushing during laparoscopy allows targeted sampling from the peritoneal surface.
- Laparoscopic cytology has high sensitivity and specificity [4].

**Caution**

Technical procedure at diagnostic hysteroscopy may be responsible for contamination of the peritoneal cavity with malignant cells when tumor cells are squeezed through the lumen of the fallopian tubes, sporadic atypical or frankly malignant cells may be encountered in abdominal fluid specimens.

### 3.3.1.3 Processing of Cytologic Material

Various methods are used in order to process fluid specimens. The advantages, disadvantages, and comparative studies of the various methods are described in many studies in the literature. Specific methods may be individually preferred for subsequent analyses. A few selected reports have been cited [25, 21, 22].

We have already described the different laboratory methods in Sect. 3.1.1.1 “Processing of Cytologic Material,” p. 241.

#### 3.3.1.4 Psammoma Bodies

Laminated, calcified debris is known as psammoma body. The elements appear as rounded bodies with concentric rings and are generally stained deep blue. They are found in peritoneal fluids produced by many different benign and malignant lesions [18] (see also Sects. 3.3.5, p. 302, 3.3.7, p. 303 and 3.2.4.1, p. 271).

**Caution**

Psammoma bodies – isolated or as epithelial inclusions – should not be considered diagnostic for malignancy

### 3.3.2 Benign Sheets from the Mesothelial Layer (Figs. 3.64 and 3.65)

Accelerated peritoneal washing may cause detachment of large mesothelial cell sheets.

**Microscopic Features**

Hallmarks:

- The cohesive sheets composed of flattened cells may reach an impressive size.
- The low N/C ratio is caused by an abundant polygonal clear cytoplasm.
- Centrally placed pale nuclei, bizarrely cleaved and folded, reveal an accentuated nuclear membrane, an indistinct chromatin pattern, and a distinct nucleolus. Some authors refer these cells to as daisy cells.

**Differential Diagnosis**

- Large sheets may fold and resemble papillary structures.
- In most cytologic preparations from peritoneal fluids, degenerate cellular elements with smeared nuclei are present. The condensed chromatin is darkly stained and tightly packed together. The chromatin cords should not be misread as a manifestation of small-cell cancer (Fig. 3.66).
- Intermediate and superficial squamous cells may originate from vaginal epithelium aspirated by culdocentesis. Content from a dermoid cyst harboring squamous cells would additionally be characterized by cystic background with foam cells and debris.

**Caution**

- Degenerate mesothelial cells in combination with eosinophilic cytoplasm may mimic atypical squamous cells.
- Hyaline globules surrounded by activated histiocytes/mesothelial cells may give rise to diagnostic confusion with low-grade adenocarcinoma or adenoid cystic carcinoma (Fig. 3.67).

### 3.3.3 Epithelial Cells Derived from the Fallopian Tube and Fimbriae (Fig. 3.68)

- Ciliary tufts are anucleated fragments of ciliated cells originating from the fallopian tube.
- Detached ciliary tufts occur more frequently in peritoneal washings than in fluids from the pouch of Douglas. The shedding of ciliated cells from the fallopian tubes is most likely to occur during the luteal phase of the menstrual cycle [24].
- In rare cases, ciliary tufts may originate from a ruptured hydrosalpinx or ectopic pregnancy.
- Well-preserved large columnar cells lying discretely or in small clusters with tight palisading derive from the epithelium of the fallopian tube and especially the fimbriae. Suspicion or misdiagnosis of a well-differentiated papillary neoplasm is possible if these cells lack cilia and exhibit large activated nuclei including nucleoli (Fig. 3.68).

**Caution**

- Well-preserved and palisading cells from epithelium of the fallopian tubes and fimbriae in tightly packed clusters could mislead to a tumor diagnosis of papillary variant.
- Ciliated carcinoma cells have been described as an extreme rarity [7].

### 3.3.4 Spillage of Cyst Content into the Abdominal Cavity

**Pathogenesis and Microscopic Features**

- Peritoneal aspirates and washings may occasionally contain cystic properties, due to spillage of cyst content into the abdominal cavity. Abdominal cystic lesions may undergo spontaneous rupture or may be accidentally damaged during surgical intervention.
  - Cystic content is characterized by large foamy histiocytes with phagocytosis, and cellular debris.
  - The typical mixed cell pattern of a genuine body cavity fluid is not present (see Sect. 3.1.2 “Benign Effusion: NOS,” p. 242) (Fig. 3.11).
- In sediment smears with a mixture of cells from cyst content and numerous cells from common ascitic fluid, it is impossible to establish a proper cytologic diagnosis of a cystic lesion.
- Besides peritoneal cysts without epithelial content and of uncertain etiology, cystic fluids may be encountered that present a distinct epithelial cell population allowing a precise classification of the cystic lesion:
  - *Follicle cyst/secondary follicle* (Fig. 3.69). Crowded follicular epithelial cells, occasionally encasing an egg cell.
  - *Simple serosal cyst* of adnexa. Detached ciliary tufts.

- *Serous cystadenoma*. Regular epithelial clusters of cuboidal cells with bland nuclei. The cells exhibit BerEp-4 immunopositivity.
- *Mucinous cystadenoma* (Fig. 3.70). Regular epithelial clusters of mucinous cells, basally located nuclei, distinct cellular palisading.
- *Dermoid cyst*. Benign squamous cells of the intermediate and superficial type. Differential diagnosis: culdocentesis may be contaminated with squamous cells from the vaginal epithelium.
- *Endometriotic cyst*. Huge amount of debris intermingled with hemosiderophages is the most distinctive finding in cystic endometriotic lesions. A well-preserved epithelial component is rarely present: densely and three-dimensionally clustered small to medium-sized cells exhibit irregular nuclei with an indistinct chromatin pattern. Immunocytochemical expression of BerEp-4 and hormone receptors on well-preserved epithelial cells.
- *Mesothelial cyst*. Single cells and a few clusters of typical mesothelial cells, immunocytochemically positive for calretinin.
- *Hydatid cyst* (Fig. 3.71). Characteristic hooklets, scolices, and chitin masses may been countered in peritoneal washings/aspirates after spontaneous or inadvertent disintegration of an abdominal echinococcal cyst.

## 3.3.5 Endosalpingiosis (Fig. 3.72)

Synonyms: Benign müllerian inclusions, inclusion cysts, benign glandular inclusions.

### Pathogenesis and Microscopic Features

The pathogenesis of this entity is unclear; the two mechanisms most often cited include mesothelial metaplasia and secondary implantation of tubal mucosa on the serosal surface [27]. Macroscopically, the lesions are seen as small cysts or protrusions on the surface of the ovary, uterus, and the pelvic and omental serosa.

Peritoneal mesothelium covering the ovaries includes the germinal epithelium, which retains the embryonic potentialities of müllerian epithelium and is capable of differentiating into many diversified structures [3]. Batt and colleagues interpret the lesion as choristoma composed of müllerian remains incorporated within otherwise normal organs during organogenesis [2].

- Hallmarks: Microcalcifications and definite psammoma bodies mostly incorporated into small cohesive rounded aggregates or papillary clusters of mesothelial cells.
- The cells are uniform but vary in size from cluster to cluster, and are more likely to show a high N/C ratio.
- The nuclei are round and smooth with occasional indentations.
- The chromatin is fine and evenly distributed.
- Large nucleoli may be observed in activated cells.

### Differential Diagnosis

- Groups of hyperplastic mesothelial cells sealing psammoma bodies are morphologically identical to endosalpingiosis.
- Endosalpingiosis with strongly reactive cells forming distinct papillary cell clusters may lead to an erroneous positive diagnosis of low-grade papillary neoplasm.
- Making a definite diagnosis is often a problem due to the scarcity of the target cell groups.

### Immunocytochemistry

Cells of endosalpingiosis may stain positively for the mesothelial marker calretinin and for the epithelial cell marker BerEp-4.

## 3.3.6 Endometriosis (Fig. 3.73)

### Definition

Endometriosis is the ectopic endometrium most frequently implanted in the pelvic serosa and on the surface of pelvic organs but also involves adjacent connective tissue.

### Microscopic Features and Differential Diagnosis

- Hallmarks: Hemosiderophages are the most distinctive finding, in most cases along with cellular debris.
- It is unusual to find endometrial epithelial cells or even stromal cells in peritoneal washings. If present, these cellular elements are safely diagnostic. Endometrial glandular cells appear as tight clusters of small or medium-sized cells with scant cyanophilic cytoplasm. The nuclei are wrinkled and show a distinct membrane and a tiny nucleolus. The chromatin is granular and evenly distributed.
- A tendency to squamous metaplasia may be detected: glandular cells transform into immature squamous cells with large polygonal cytoplasm, they are arranged in cobblestone fashion.

Glandular endometrial cell groups composed of enlarged reactive cells could lead to a false-positive diagnosis of low-grade endometrial adenocarcinoma. However, well-differentiated endometrial carcinoma are unlikely to spread into the abdominal cavity. Obtaining the whole clinical history and a review of histologic material is essential in such cases (Fig. 3.76). A large-scale study on endometrial carcinoma in peritoneal washings was published in 2000 by Mai Gu and coauthors [6].

**Caution**

Many conditions with previous leakage of blood into the peritoneal cavity must be expected to yield hemosiderin-laden histiocytes. Thus, the finding of hemosiderophages in cytologic preparations of peritoneal fluids is nonspecific but may indicate endometriosis.

## 3.3.7 Low-Grade Serous (Papillary) Tumors of the Ovary and Peritoneum

### General Comments

- Borderline serous tumors (Figs. 3.74 and 3.75) of ovary and peritoneum are tumors of low malignant potential; they are histologically noninvasive and behave in a benign fashion. However, pelvic recurrence and occasional transformation into invasive carcinoma may occur.
- Well-differentiated adenocarcinomas (Fig. 3.77) are histologically invasive and have an unfavorable outcome [19].
- In general, the definite assessment of the biological behavior of a low-grade tumor is dependent on histologic investigations after complete surgical staging.
- The content of accidentally punctured or ruptured cysts with benign serous or mucinous epithelium gives rise to diagnostic problems with well-differentiated ovarian carcinoma (Fig. 3.70).
- Tumors with innumerable psammomatous calcifications are referred to as psammocarcinoma. It is a rare subset of serous carcinomas that can easily be recognized in cytologic preparations although the cellular morphology is bland. These tumors have a favorable prognosis.
- A large-scale study on endometrial carcinoma in peritoneal washings was published in 2000 by Mai Gu and coauthors [6].

### Microscopic Features and Differential Diagnosis

- Borderline serous tumors (Figs. 3.74, 3.75A, 3.75B) are cytologically characterized by large cohesive rounded, pseudopapillary, or branching papillary clusters with smooth borders. Cells exhibit variable degrees of atypia with nuclear molding, finely granular chromatin, indistinct hyperchromasia, and variable nucleoli.
- Reactive mesothelial disorders and their distinction from low-grade noninvasive and invasive serous tumors is often impossible from cytomorphologic features alone because the cells are morphologically and embryologically similar.
- However, the cytoarchitecture and single cell morphology may aid in differentiating borderline tumor from invasive neoplasm [5]. Serous adenocarcinomas (Fig. 3.77), compared to borderline tumors, show cell clusters and papillae that are smaller and less cohesive, exhibiting irregular outlines. More single cells can be found. The cells are more pleomorphic, the nuclei exhibit various shapes and sizes, coarser chromatin, and larger nucleoli.
- Low-grade ovarian carcinoma is also difficult to differentiate from low grade endometrial carcinoma (Fig. 3.76).

### Additional Analyses

#### Immunocytochemistry

- A panel of antibodies against calretinin, epithelial marker BerEp-4, estrogen, and progesterone receptor has a high sensitivity and specificity in discriminating peritoneal mesothelioma from ovarian carcinoma, primary papillary neoplasm of the peritoneum, and metastatic cancer [1].
- Well-differentiated endometrial carcinomas have no discriminatory immunopattern against ovarian carcinoma.

#### DNA Ploidy

- DNA ploidy by image cytometry (ICM-DNA) may provide important information on the biological behavior of low-grade neoplasms cytologically diagnosed from peritoneal fluids. ICM-DNA is of prognostic significance, particularly for peritoneal implants.
- Aneuploidy has been shown to be common in invasive ovarian adenocarcinoma but rare in borderline tumors (Fig. 3.75C). Aneuploidy in a low-grade tumor of cytologically equivocal malignancy could be considered an indicator of invasion or at least increased malignant potential [8, 10, 11, 15].

**Caution**

In many of the low-grade neoplasms, the tumor cells occur unfortunately in tightly packed aggregates and nuclei are superimposed. Isolated tumor cells are often too sparse for a reliable quantitative DNA assessment by ICM.

#### Molecular Genetics

Osterberg and coauthors report distinct chromosomal aberrations that might characterize a subgroup of borderline ovarian tumors with increased malignant potential [16].

## 3.3.8 Rare Gynecologic Tumors

Uterine neoplasms of endometrial and nonendometrial origin, carcinoma of the fallopian tube, sex cord-stromal tumors, germ cell tumors, soft tissue tumors, lymphoma, and others are rarely encountered in aspirations and washings of the Douglas pouch.

#### 3.3.8.1 Squamous Cell Carcinoma

Cytomorphologic properties of squamous cell carcinoma, as a rare event of metastatic cervical cancer, are described in Sect. 3.2.3.1.1, "Squamous Cell Carcinoma," p. 265 and in a paper by Zuna and coworkers [28].

#### 3.3.8.2 Malignant Mixed Mesodermal Tumor

Malignant mixed mesodermal tumors (Fig. 3.78) originate mainly from the endometrium but may also be observed as primary ovarian neoplasm. In many patients, the müllerian tumors exfoliate adenocarcinoma cells into the peritoneal cavity, in a minority together with sarcomatous cells, and in rare cases sarcomatous cells alone.

- The adenomatous components appear as high-grade carcinoma composed of large polymorphic cells including coarse chromatin and pleomorphic nucleoli. Sarcoma cells are large, elongated, and loosely clustered.

#### 3.3.8.3 Granulosa Cell Tumor

Granulosa cell tumors (Fig. 3.79), as a special entity of sex cord-stromal tumors, may have a pseudopapillary pattern that can be confused with papillary ovarian tumors.
However, identification of cellular characteristics of this tumor type can resolve most cases.

- Hallmarks: The cells of adult granulosa cell tumors exhibit pale and folded nuclei, and a longitudinal groove along the length of the nucleus is characteristic. The cytoplasm may be vaguely visible.
  Rosettes and glandular structures containing globular, amorphous material correspond to Call-Exner bodies [17].

### 3.3.9 Cancers in Peritoneal Washings Originating from Various Extragenital Organs

The cytology of gastrointestinal malignant lesions in peritoneal washings is discussed in a report by Martin and Goellner [13].

Cytomorphologic descriptions relating to the most frequent tumors encountered in abdominal fluids are given in Section 3.2.3 "Metastases into Serous Membranes," p. 263.

### 3.3.10 Further Reading


1. Barnetson RJ, Burnett RA, Downie I, et al. Immunohistochemical analysis of peritoneal mesothelioma and primary and secondary serous carcinoma of the peritoneum. Am J Clin Pathol 2006;125:67-76.
2. Batt RE, Smith RA, Buck Louis GM, et al. Müllerianosis. Histol Histopathol. 2007;22:1161-1166.
3. Covell JL, Carry JB, Feldman PS. Peritoneal washings in ovarian tumors. Potential sources of errors in cytologic diagnosis. Acta Cytol 1985;29:310-316.
4. Cusso X,Marti-Vincente A,Mones-Xiol J,Vilardell F. Laparoscopic cytology – an evaluation. Endoscopy 1988;20:102-103.
5. DeMay RM. The Art and Science of Cytopathology, Exfoliative Cytology. Amer Soc of Clinical Pathologists. 1996; p.288.
6. Gu M, Shi W, Barakat RR, et al. Peritoneal washings in endometrial carcinoma. A study of 298 patients with histopathologic correlation. Acta Cytol 2000;44:783-789.
7. Gupta PK, Albritton N, Erozan YS, Frost JK. Occurrence of cilia in exfoliated ovarian adenocarcinoma cells. Diagn Cytopathol 1985:1:228-231.
8. Gurley AM, Hidvegi DF, Cajulis RS, Bacus S. Morphologic and morphometric features of low grade serous tumours of the ovary. Diagn Cytopathol 1994;11:220-225.
9. Hudelist G, Singer CF,Kubista E, et al. Presence of nanobacteria in psammoma bodies of ovarian cancer: evidence for pathogenetic role in intratumoral biomineralization. Histopathology 2004;45:633-637.
10. Ioakim-Liossi A, Karakitsos P, Aroni K, et al. P53 protein expression and DNA ploidy in common epithelial tumors of the ovary. Acta Cytol 1997;41:1714-1718.
11. Korabiowska M, Brinck U, Skubis J, et al. Application of new ploidy-related parameters for the diagnosis of ovarian tumors. Anticancer Res 2004;24:4191-4194.
12. Luesley DM, Williams DR, Ward K, et al. Prospective comparative cytologic study of direct peritoneal smears and lavage fluids in patients with epithelial ovarian cancer and benign gynecologic disease. Acta Cytol 1990;34:539-544.
13. Martin JK, Goellner JR. Abdominal fluid cytology in patients with gastrointestinal malignant lesions. Mayo Clin Proc 1986;61:467-471.
14. Mulvany N. Cytohistologic correlation in malignant peritoneal washings. Analysis of 75 malignant fluids. Acta Cytol 1996;40:1231-1239.
15. Nagai N, Oshita T, Fujii T, et al. Are DNA ploidy and epidermal growth factor receptor prognostic factors for untreated ovarian cancer? A prospective study. Am J Clin Oncol 2001;24:215-221.
16. Osterberg L, Akeson M, Levan K, et al. Genetic alterations of serous borderline tumors of the ovary compared to stage I serous ovarian carcinomas. Cancer Genet Cytogenet 2006;167:103-108.
17. Özkara SK, Turan G. Cystic fluid and fine needle aspiration cytopathology of cystic adult granulosa cell tumor of the ovary. A case report. Acta Cytol 2008;52:247-250.
18. Parwani AV, Chan Ty, Ali SZ. Significance of psammoma bodies in serous cavity fluid: a cytopathologic analysis. Cancer 2004;102:87-91.
19. Prat J, De Nictolis M. Serous borderline tumors of the ovary: A long-term follow-up study of 137 cases, including 18 with a micropapillary pattern and 20 with microinvasion. Am J Surg Pathol 2002;26:1111-1128.
20. Ravinsky E. Cytology of Peritoneal Washings in gynecologic patients. Diagnostic criteria and pitfalls. Acta Cytol 1986;30:8-16.
21. Sadeghi S, Ylagan LR. Pelvic washing cytology in serous borderline tumors of the ovary using ThinPrep: are there cytologic clues to detecting tumor cells? Diagn Cytopathol 2004;30:313-319.

22. Selvaggi SM. Diagnostic pitfalls of peritoneal washing cytology and the role of cell blocks in their diagnosis. Diagn Cytopathol 2003;28:335-341.
23. Shield P. Peritoneal washing cytology. Cytopathology 2004;15:131-141.
24. Sidawy MK, Chandra P, Oertel YC. Detached ciliary tufts in female peritoneal washings. A common finding. Acta cytol 1987;31:841-844.
25. Yun Gong, Xiaoping Sun, Michael CW, et al. Immunocytochemistry of serous effusion specimens: a comparison of ThinPrep® vs. cell block. Diagn Cytopathol 2003;28:1-5.
26. Ziselman EM, Harkavy SE, Hogan M, et al. Peritoneal washing cytology. Uses and diagnostic criteria in gynecologic neoplasms. Acta Cytol 1984;28:105-110.
27. Zuna RE, Mitchell ML. Cytologic findings in peritoneal washings associated with benign gynecologic disease. Acta Cytol 1988;32:139-147.
28. Zuna RE, Mitchell ML, Mulick KA, Weijchert WM. Cytohistologic correlation of peritoneal washing cytology in gynecologic disease. Acta Cytol 1989;33:327-336.

**Figs. 3.64 and 3.65 Sheets of normal mesothelial layer.**
Cytologic appearance of mesothelial sheets in Douglas lavage, the cytologic specimens originate from two separate patients (direct sediment smears, Pap stain).



**Fig. 3.64** (case #1) Lower magnification: a large-cell sheet of mesothelial origin exhibiting typical folding.

**Fig. 3.65** (case #2) High magnification highlights cellular morphology: bland chromatin, pronounced nuclear membrane exhibiting marked cleaving and folding, usually distinct nucleoli. Mesothelial cells are called daisy cells if the nuclei are bizarrely folded (arrow).

**Fig. 3.66 Poorly preserved mesothelial cells versus malignant neoplasia.**
Degenerating mesothelial cells in Douglas lavage frequently get smeared and/or tightly clustered during sediment processing. Dense cytoplasm and deeply stained nuclei should not lead to an incorrect diagnosis of malignancy (direct sediment smear, Pap stain, lower magnification).

**Fig. 3.67 Mesothelial spheres including hyaline globules versus adenocarcinoma.**
Fluid from cul-de-sac. Direct sediment smears were Pap-stained. A compact, sharply outlined sphere is composed of activated mesothelial cells enclosing a hyaline globule (left). Focusing the center reveals planes of cells. The ball-like cluster could be misinterpreted as a microfragment from a well-differentiated adenocarcinoma; however, the nuclei show completely bland morphology (high magnification).

**Fig. 3.68 Cells from fallopian tubes and fimbriae.**
A 76-year-old woman with a history of well-differentiated endometrial adenocarcinoma was referred to the hospital for a second-look laparoscopy. Direct sediment smears from peritoneal washing contained few compact papilliform clusters composed of regularly arranged cuboid to columnar cells. Note squeezed and overlapping nuclei comprising prominent nucleoli (high magnification, Pap stain).
*Comments:* Key feature for a correct diagnosis are the cilia on the free surface of the superficial lining cells (arrows). Misdiagnosing a low-grade papillary neoplasm must be avoided. In this case, benign ciliated epithelial clusters were completely absent in the primary well-differentiated adenocarcinoma of endometrium.

**Fig. 3.69 Human egg cell in a Douglas lavage.**
The oosphere, escaped from a secondary follicle, is surrounded by a pale corona and by an outer coat of densely packed follicular epithelial cells. The nucleus and nucleolus of the egg cell are marked with short arrows and an elongated arrow, respectively. Mesothelial cells in the background are numerous (direct sediment smear, Pap stain, high magnification).

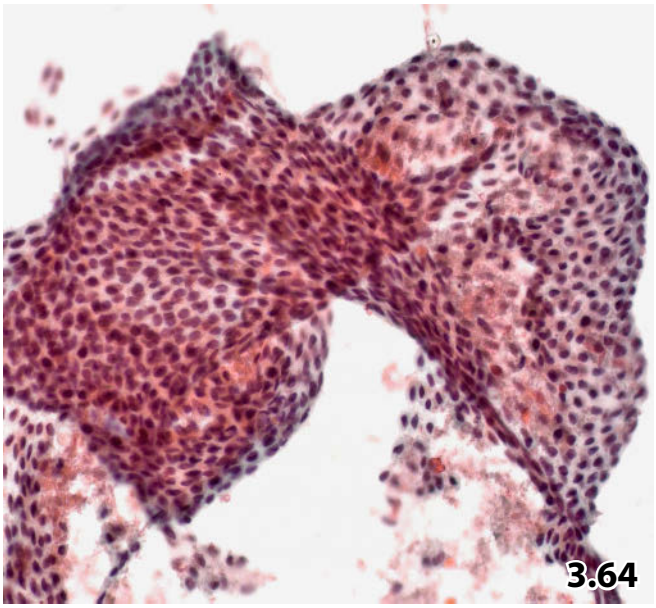
3.64

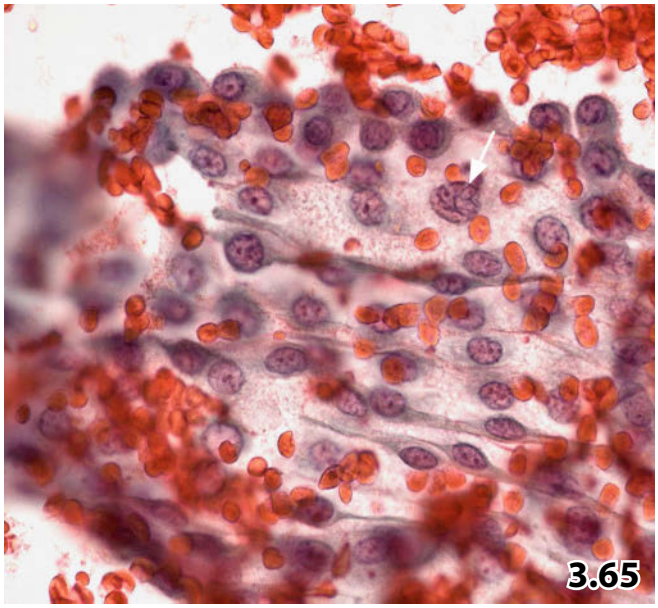
3.65

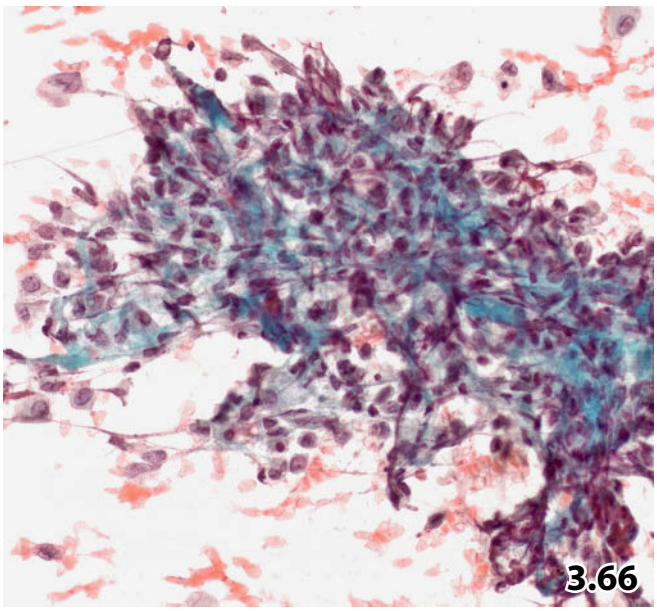
3.66

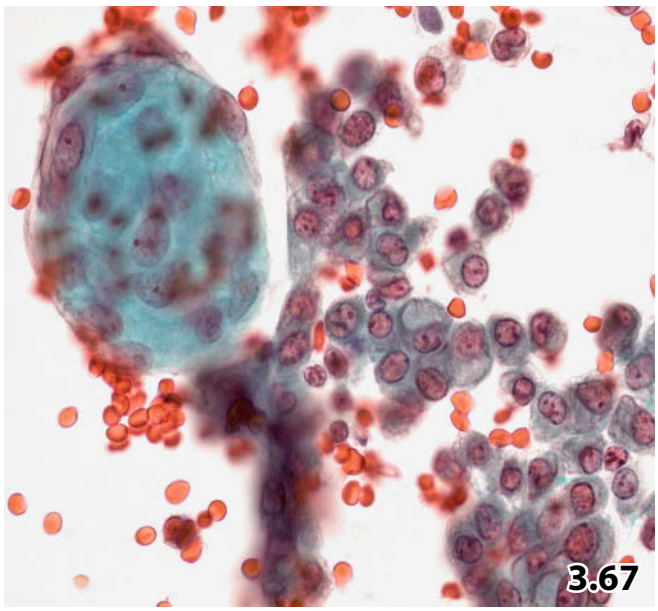
3.67

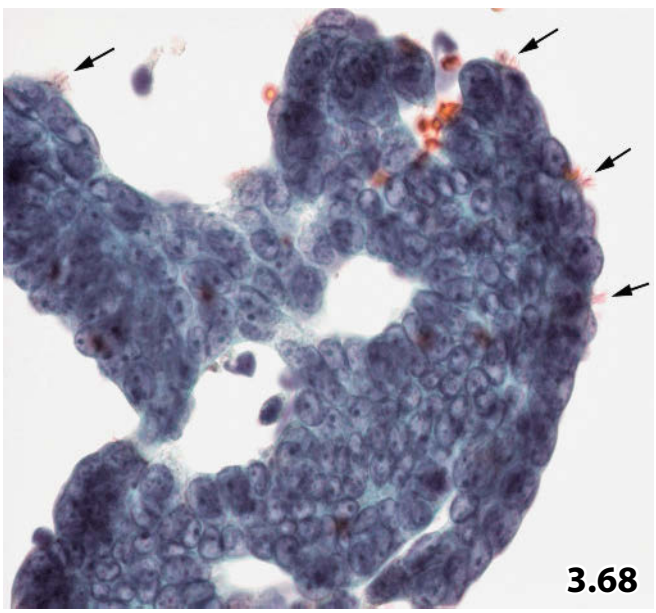
3.68


3.69

**Fig. 3.70 Ruptured ovarian mucinous cystadenoma.**
An elderly woman underwent laparoscopic investigation for a unilocular adnexal cystic lesion. Cytology from the sanguineous Douglas lavage revealed several clusters composed of palisading mucinous columnar cells and goblet cells. Foam cells in the background (arrow) indicate spillage of cyst content into the peritoneal cavity (Pap stain, high magnification).
*Comment on cytologic findings:* Efficient communication between surgeon and cytologist is of utmost importance to eliminate a potential false diagnosis of low-grade mucinous adenocarcinoma with peritoneal spread.
*Tissue diagnosis* (extirpation of the cystic mass): Mucinous cystadenoma of the ovary.

**Fig. 3.71A, B Ruptured hydatid cyst located at the liver periphery.**
Peritoneal fluid intermingled with the content of a disintegrated cystic lesion located at the liver periphery was obtained during laparoscopy in a 20-year-old woman. Pap-stained direct sediment smears were available for microscopy. **A** Lower magnification shows chitin masses (upper right) in a background composed of histiocytes and mesothelial cells. **B** Multiple scolices (high magnification) confirm the diagnosis of hydatid cyst (of liver).

Spontaneous or inadvertent rupture of cystic lesions during intraabdominal surgical intervention may cause major cytodiagnostic pitfalls if operating surgeons fail in prompt interdisciplinary communication.

**Fig. 3.72 Endosalpingiosis.**
A compact papilliform cluster composed of activated mesothelial cells and several concentrically laminated psammoma bodies indicate endosalpingiosis. The nuclei are bland; however, it may be difficult to exclude a low-grade papillary neoplasm (fluid from cul-de-sac, direct sediment smear Pap stain, high magnification).
*Follow-up:* Both cytologic and histologic evaluations of the uterus and adnexa revealed no malignant disorder.

**Fig. 3.73 Endometriosis.**
A 26-year-old woman presenting with a history of endometriosis. Cytology of a Douglas fluid disclosed further manifestation of extrauterine spreading endometrial tissue. The picture illustrates a cluster of degenerating endometrial cells, both fresh and long-standing red blood cells, and degenerating macrophages (upper right) containing coarse granules (most likely hemosiderin; iron staining was not performed) (direct sediment smears, Pap stain, high magnification).

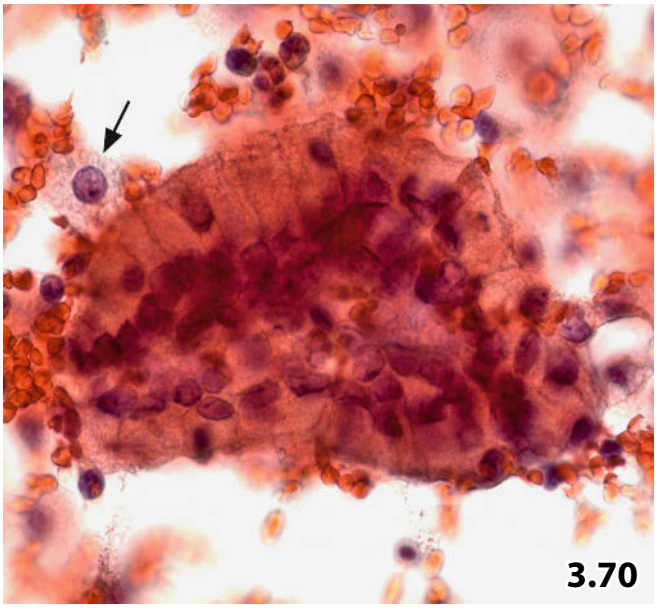
3.70

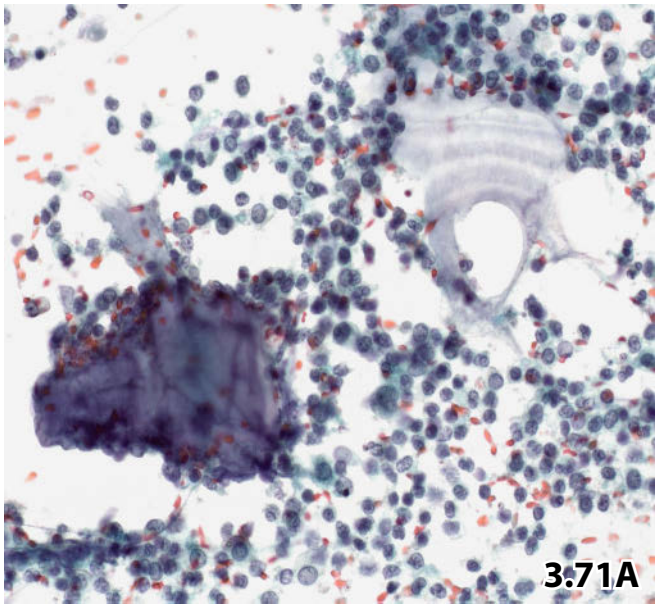
3.71A

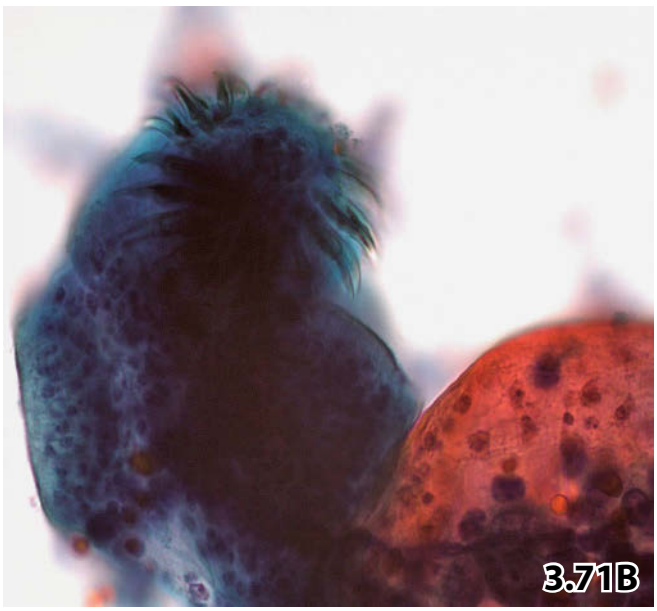
3.71B

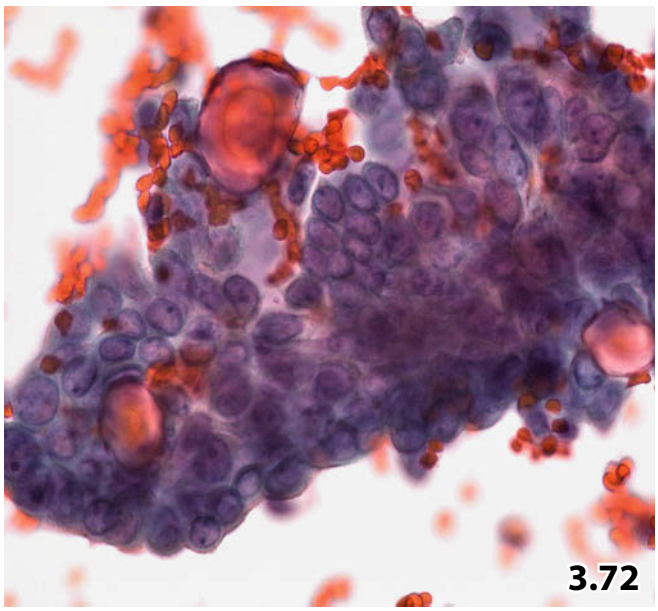
3.72

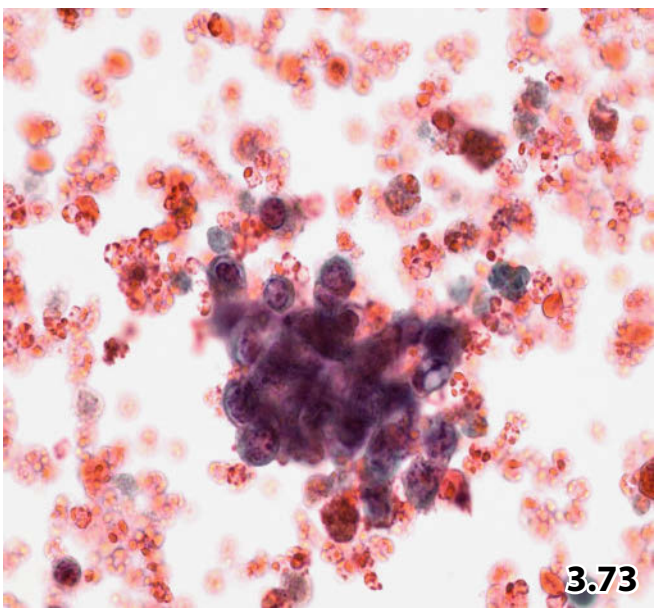
3.73

**Figs. 3.74 and 3.75 Borderline serous tumor of the ovary.**
Two cytologic examples of borderline serous ovarian tumors are presented.



**Fig. 3.74** (case #1) Lower magnification shows numerous small papilliform clusters composed of monomorphous epithelial cells with minor atypias. The tumor clusters contain a great many psammoma bodies (peritoneal washing, direct sediment smear, Pap stain).
*Cytology:* Monomorphic cell appearance, bland chromatin, small but distinct nucleoli, cytoplasmic vacuoles, and psammoma bodies cytologically suggest low-grade serous neoplasia of the ovary or peritoneum.
*Final diagnosis* (laparotomy and tissue examination): Borderline serous tumor of the ovary.

**Fig. 3.75A–C** (case #2) The second borderline tumor of the ovary was initially detected in the fluid from cul-de-sac of a 47-year-old woman. Laparoscopic investigation disclosed a cystic adnexal disorder. Direct sediment smears produced from the aspirate were Pap-stained. **A** The serous ovarian borderline tumor shows a very similar cytoarchitecture to that of the first patient (low magnification). **B** A picture in extremely high magnification illustrates cellular details of this tumor type. Note the fine granular and dense chromatin texture, and the distinct nucleoli (oil immersion, magnification ×100). **C** ICM-DNA of case #2: The diploid DNA distribution pattern of the tumor cell population may be indicative of a benign course of the disease (Pap-prestained Feulgen stain, Ahrens Cytometrie-System).

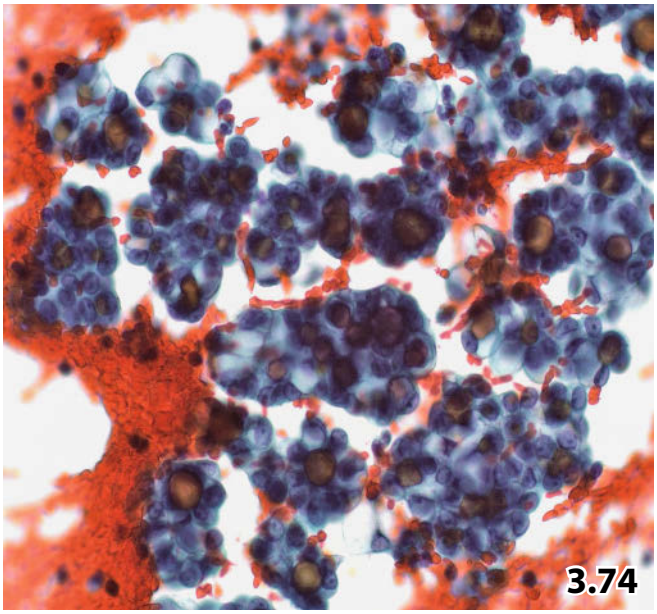
3.74

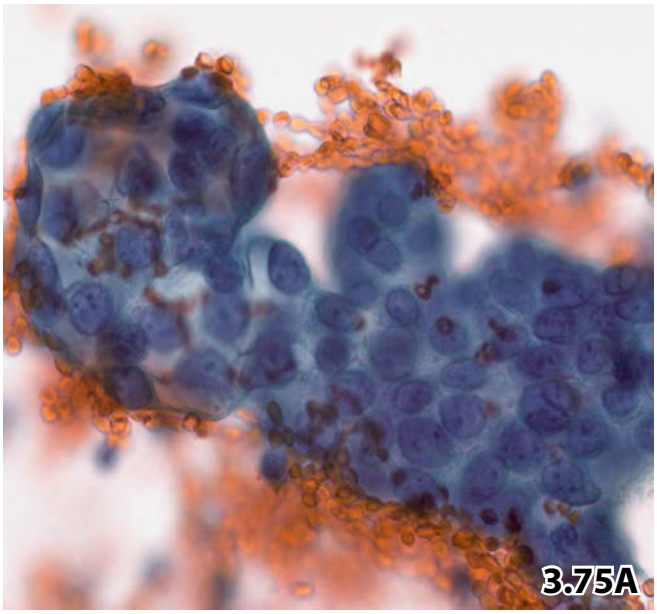
3.75A

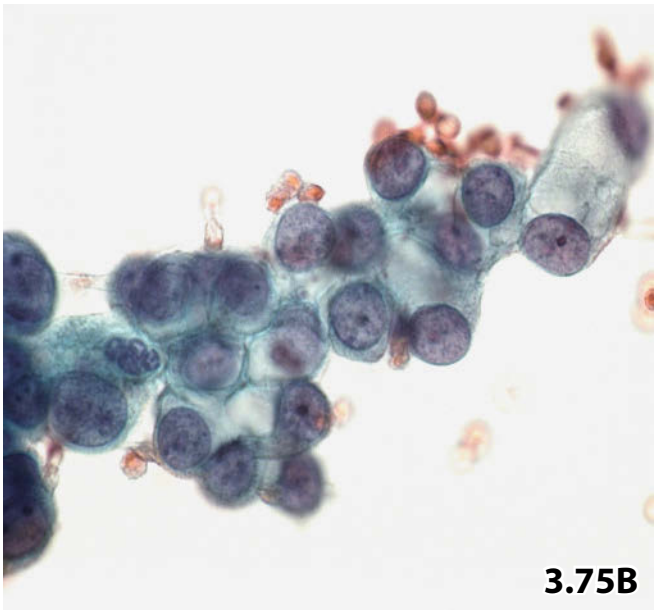
3.75B

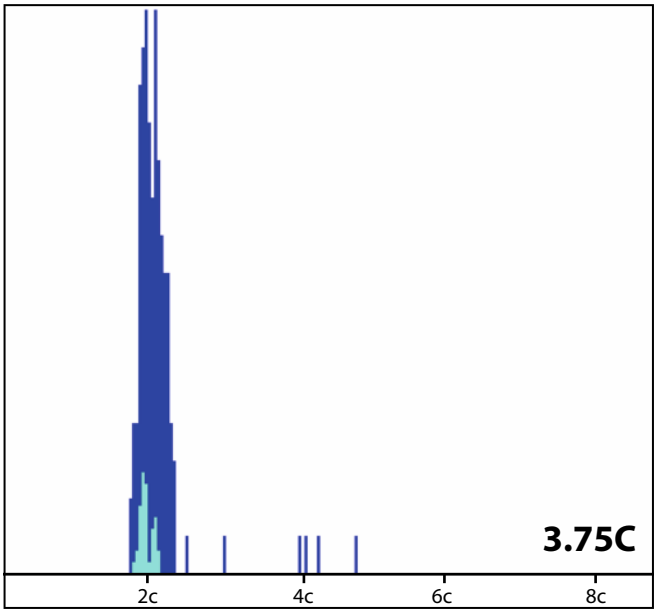

3.75C

**Fig. 3.76 Low-grade adenocarcinoma: ovarian versus endometrial origin.**
Douglas fluid from an elderly woman was referred to cytology without clinical information. High magnification from a direct sediment smear (Pap stain) displays papilliform clusters consisting of slightly atypical epithelial cells: loss of nuclear polarity, varying nuclear size, occasional highly irregular nuclear outline (arrow), and dyschromasia of the nucleoplasm. Additional psammoma bodies are not shown. Compare tumor cell morphology with that of benign mesothelial cells (arrowhead) in particular noting the different staining quality of benign and malignant nuclei!
*Tentative cytologic diagnosis:* Ovarian borderline tumor or low-grade adenocarcinoma of the ovary.
*Tissue diagnosis:* Well-differentiated adenocarcinoma of the endometrium.

Low-grade epithelial neoplasms originating from the ovary and endometrium may share the same cellular features.

**Fig. 3.77 Metastatic adenocarcinoma of the ovary, clear cell variant.**
High magnification shows a discohesive tumor cell population predominantly composed of large cells exhibiting enlarged nuclei, prominent and pleomorphic nucleoli, and distinct clear cytoplasm (Douglas lavage, direct sediment smear, Pap stain).
*Tentative cytologic diagnosis:* Adenocarcinoma, clear cell variant. The abundant clear cytoplasm may raise suspicion of another primary tumor site than the ovary, such as renal cell carcinoma.
*Final diagnosis* (histology, clinical and imaging results): Metastatic adenocarcinoma of the ovary, clear cell variant.

**Fig. 3.78 Malignant mixed mesodermal tumor.**
Peritoneal lavage of an elderly woman contained crowded aggregates of pleomorphic neoplastic cells (direct sediment smears, Pap stain, lower magnification).
*Tentative cytologic diagnosis:* Undifferentiated carcinoma of unclear primary origin.
*Histology* from a large ovarian mass revealed a müllerian tumor of heterologous variant.
*Comment:* Rescreening of the cytologic specimens provided no evidence of a sarcomatous component.

**Fig. 3.79 Granulosa cell tumor.**
Long-term tumor follow-up using periodical peritoneal washings in an elderly woman with a clinical history of granulosa cell tumor. Direct sediment smears from the latest washing display the typical cytologic features of granulosa cell tumor: pale nuclei exhibiting wrinkling and folding occasionally combined with longitudinal grooves. The cytoplasm is clear and peripherally fading (Pap stain, high magnification).

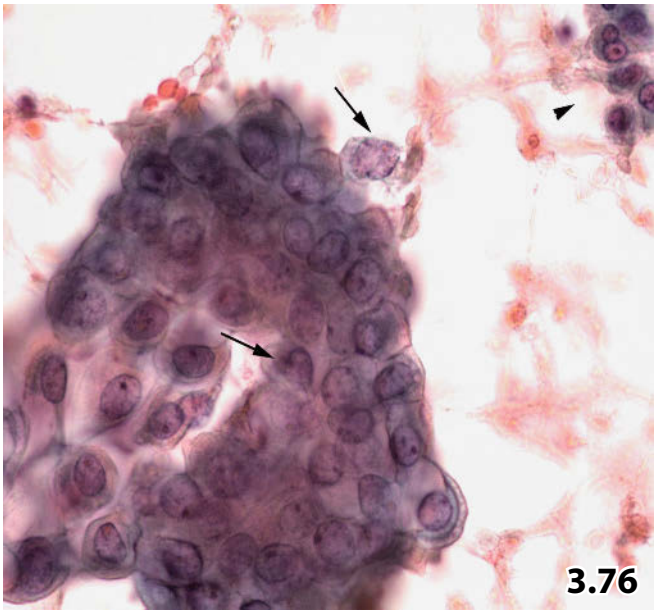
3.76

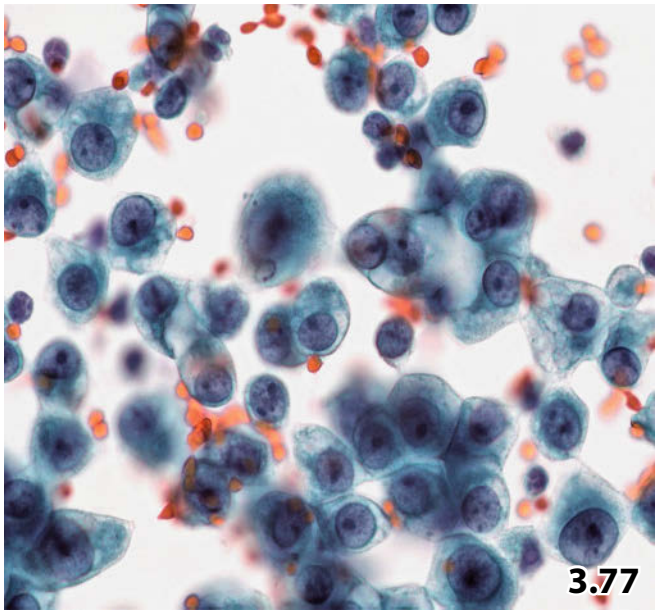
3.77

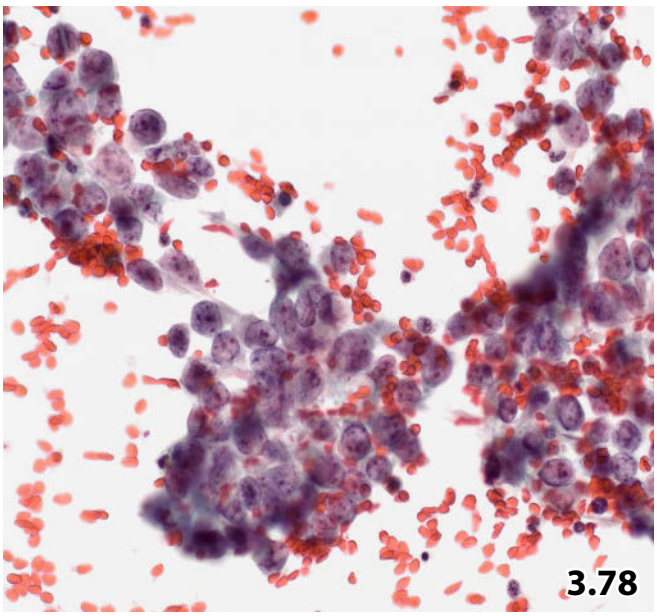
3.78

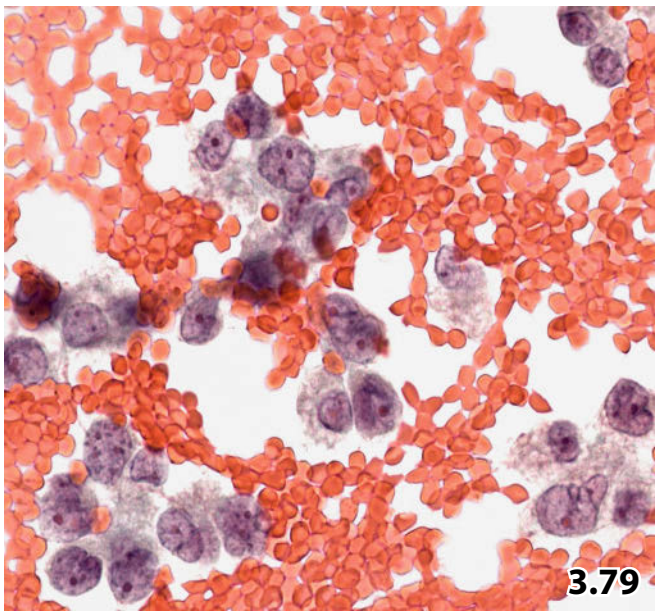
3.79

# Section 3.4
# Effusions

## Synovial Fluids

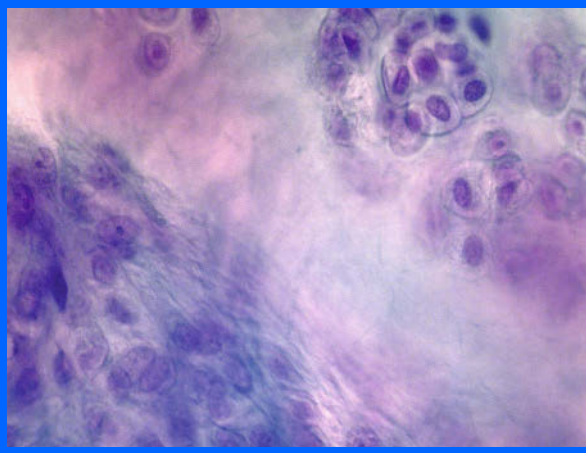

**General Comments**

- Synovial fluid functions as a lubricant for joints but is also responsible for nutrient supply to the articular cartilage. Normally, synovial fluid accumulates only a film coating the cartilaginous surface of the joints. Increased fluid is always sign of a pathologic process.
- Cytologic findings in fluid microscopy may render definitive diagnosis in a variety of joint diseases such as malignancies, infections, or pathogenic crystalloid deposits. Osteosarcoma (Fig. 3.80) is presented as representative of a small group of malignant neoplasms that may occur in synovial fluids.
- Examination of native preparations (wet cover-slipped) from fresh fluid sediments should always be performed as an initial test for the detection or exclusion of crystals by means of birefringence and polarized light microscopy.
- Synovial fluid leukocyte count is considered to be of potential help as a discriminator of certain types of arthritis [12].
- Several reports in the literature document the value of cytologic evaluation of synovial fluids and suggest guidelines accordingly [5, 7, 9, 11, 15, 24].

### 3.4.1 Normal and Pathologic Synovial Fluid: Macroscopy and Microscopic Features

#### 3.4.1.1 Normal Synovial Fluid (Fig. 3.81)

Normal synovial fluid is highly viscous, transparent, and amber in color.

- It contains a small number of leukocytes, histiocytes, and synovial-lining cells. The latter resemble mesothelial cells, their morphology is described in Sect. 3.1.2, p. 242.
- The background of the cytologic preparations is flimsy, exhibiting eosinophilic or cyanophilic staining with the Pap method.

#### 3.4.1.2 Osteoarthritis and Trauma: Mature Cartilage Cells (Figs. 3.82 and 3.83)

Chondrocytes may be encountered in fluids from joints with degenerate cartilage of various etiologies. The cartilage cells occur singly or in small groups and are frequently embedded in cartilaginous matrix.

- Chondrocytes contain small, round, dark-stained, pyknotic nuclei. The nuclei are often multiple.
- The cytoplasm is pale and vacuolated surrounded by a capsule-like dense rim of cartilage.
- An inflammatory infiltrate may occur.
- Debris, proteinaceous background and hemosiderophages may be seen particularly in patients suffering from traumatic arthritis.

#### 3.4.1.3 Inflammation and Infection

##### 3.4.1.3.1 Aseptic Inflammatory Process

An aseptic inflammatory process shows greatly increased number of neutrophils and sporadic eosinophils, lymphocytes and histiocytes. The cellular composite in chronic inflammatory disorders is similar to that in effusions of other body cavities; synovial lining cells, leukocytes and histiocytes are evident.

##### 3.4.1.3.2 Infectious Arthritis

Infectious arthritis is caused by different microbiologic agents such as bacteria, virus, fungi, and worms. Organisms are readily identifiable by special staining methods (Gram, periodic acid Schiff, Grocott).

- *Septic arthritis* is associated with a gray or purulent aspirate comprising abundant neutrophilic granulocytes, granulocytic detritus, and degenerating synovial cells.
- *Tuberculous arthritis* may be characterized by a mixed leukocytic cell pattern including a variable number of lymphocytes, caseous necrotic debris, and occasional epithelioid cells [20]. Acid-fast bacilli are rarely detected in cytologic smears stained with the Ziehl-Neelsen method.
- *Chlamydial polyarthritis* is referred to as Reiter syndrome. Chlamydial cytoplasmic inclusions may be found in activated synovial cells [15]. The inflammatory infiltrate consists of lymphocytes and histiocytic cells, and is at a later stage completed by neutrophils. T-lymphocyte enumeration is considered to be useful to distinguish inflammatory joint effusion in chlamydial infection from that in rheumatoid arthritis [16].
- *Hydatid disease* rarely shows joint involvement; however, it is occasionally observed in countries with endemic Echinococcosis. The articular disorder is caused by secondary extension from the adjacent bone but hematogenous spread may also occur [2, 19, 25]. For morphologic features and diagnostic cautions, see Sect. 9.1.7.3, p. 590.

#### 3.4.1.4 Rheumatoid Arthritis

Rheumatoid arthritis is traditionally considered a systemic chronic, inflammatory autoimmune disorder affecting extra-articular tissues throughout the body as well as the joints. The articular disease can lead to substantial loss of mobility due to pain and joint destruction. It is usually diagnosed by clinical history and laboratory data and not by cytomorphologic features of synovial fluids.

- Numerous neutrophils are present in the acute phase of the inflammatory process. At later stages, mature and immature lymphocytes may emerge [4, 8].
- Scattered synovial cells are present as well, usually together with debris, proteinaceous precipitate and cholesterol crystals.

A significant number of ragocytes is considered diagnostic for rheumatoid arthritis by some cytologists. Ragocytes are neutrophilic granulocytes containing dark blue basophilic (in Pap stain), round cytoplasmic inclusions most likely reflecting abnormal immunoglobulin. The presence of ragocytes is not specific for the diagnosis of rheumatoid joint disorder. The cells have been observed in other disorders such as rheumatic arthritis and pseudogout [15].

#### 3.4.1.5 Villonodular Synovitis [6, 10] (Fig. 3.84)

Pigmented villonodular synovitis (PVNS) is a benign proliferative disorder of uncertain etiology that affects synovium-lined joints, bursae, and tendon sheaths. Localized (nodular) PVNS is less common than the diffuse form, the former typically occurs in smaller joints, e.g., of the hands and feet. The diffuse form typically affects the knee of young adult males. The fluid aspirate is macroscopically pink or brown.

- The microscopic pattern includes hemosiderin-laden macrophages and multinucleated giant cells. The latter are quite characteristic but they may also be observed in other forms of arthritis and in giant cell tumors of the bone involving joints.
- Single synovial cells as well as papillary cell clusters may be seen.
- Red blood cells and proteinaceous material are present in the background of cytologic smears.

### 3.4.2 Crystal Arthropathies [3, 13, 26]

#### 3.4.2.1 Gout [17, 18, 23] (Figs. 3.85 and 3.86)

Gout is a genetically determined metabolic disorder. It is characterized by deposition of monosodium urate crystals in joints and adjacent tissue.

Gouty synovitis may produce yellow and cloudy fluid, but fluid aspirate can also present as a thick and milky-white mass in cases with many urate crystals [22].

- Needle-shaped urate crystals either free or phagocytosed by neutrophils are diagnostic. The crystals are 5–10 $\mu$m long and birefringent.
- Synovial cells, cartilage cells, and neutrophils are usually degenerated. Neutrophils occur typically in recurring synovitis (Fig. 3.86).

Fine-needle aspiration of periarticular infiltrates is a reliable alternative to joint fluid analysis in patients presenting with gouty tophi.

#### 3.4.2.2 Chondrocalcinosis / Pseudogout

[14, 15, 20] (Fig. 3.87)

Pseudogout is also a genetically determined metabolic disorder, resulting in deposition of calcium pyrophosphate dihydrate crystals in the matrix of cartilage tissue of major joints. The aspirated fluid is yellow and cloudy, similar to that from gouty joints.

- The characteristic calcium pyrophosphate crystals are smaller (about 5 $\mu$m) than urate crystals. The former are rhomboid or rod-shaped with blunt ends and birefringent upon polarization.
- The number of inflammatory cells varies depending on the stage of the disorder.
- Degenerate synovial cells, cartilage cells, and ragocytes may be present.

#### 3.4.2.3 Wear-Particle Disease (Fig. 3.88)

Particle disease is a lesion following arthroplasty. It refers to the host's adverse biologic response to wear debris generated from the prosthesis. Particulate wear debris causes periprosthetic bone destruction (aseptic osteolysis) that results in an inflammatory response comprising macrophage activation and phagocytosis [1]. Debris from several materials can generate an inflammatory process, such as polymethylmethacrylate (cement disease), polyethylene, or metal components (metallosis). Some of the particles may be birefringent upon polarization.

For more information, cytopathological findings, and references, see Sect. 16.4.4, p. 1035.

### 3.4.3 Bursae and Ganglia

#### 3.4.3.1 Bursae and Herniation of the Synovial Membrane

- *Bursae synovialis* exist where muscles, tendons, and skin are in proximate contact with bony prominences. They contain synovial fluid. Formation of cysts and accumulation of fluid result in a palpable subcutaneous mass.
- *Baker cyst* is located in the popliteal space; it occurs from herniation of the synovial membrane through the posterior part of the joint capsule.
  - Fluids from bursae and Baker cyst exhibit the same cellular composite as described in normal and pathological synovial fluid, respectively (see Sect. 3.4.1, p. 314).

#### 3.4.3.2 Ganglia (Fig. 3.89)

Ganglia develop from myxoid and cystic degeneration of the soft tissue of joint capsule or tendon sheath. Ganglia are not lined by synovia and do not communicate with the joint cavity.

Ganglia are usually removed by surgical excision, but lesions presenting as small and firm subcutaneous nodules may afford an opportunity to be discharged by fine-needle aspiration biopsy.

- The aspirate shows scant cellularity with a small number of leukocytes and mesenchymal cells. The background of the smear is flimsy and eosinophilic or cyanophilic stained (Pap method).

### 3.4.4 Further Reading


1. Amstutz HC, Campbell P, Kossovsky N, Clarke IC. Mechanism and clinical significance of wear debris-induced osteolysis. Clin Orthop Relat Res 1992;276:7-18.
2. Belzunegui J, Maiz O, Lopez L, et al. Hydatid disease of bone with adjacent joint involvement. A radiological follow-up of 12 years. Br J Rheumatol 1997 ;36 :133-135.
3. Bjelle A, Crocker PR, Huskisson EC. Crystal arthroplasties in osteo-arthritis - clinical aspects and laboratory techniques for crystal identification. Scand J Rheumatol Suppl. 1982 ;43 :23-33.
4. Bjelle A, Norberg B, Sjögren G. The cytology of joint exudates in rheumatoid arthritis. Morphology and preparation techniques. Scand J Rheumatol 1982 ;11 :124-128.
5. Broderick PA, Corvese N, Pierik MG, et al. Exfoliative cytology interpretation of synovial fluid in joint disease. J Bone Joint Surg Am 1976 ;58 :396-399.
6. Chhieng DC, Boguniewicz A, McKenna BJ. Pigmented villonodular synovitis. Report of a case with diagnostic synovial fluid cytologic features. Acta Cytol 1997 ;41 :1811-1814.
7. Dougados M. Synovial fluid cell analysis. Baillieres Clin Rheumatol 1996 ;10 :519-534.
8. Dzisiow F. Cytological picture of synovial fluid in rheumatoid arthritis. Pol Med J 1966 ;5 :997-1003
9. Freemont AJ, Denton J, Chuck A, et al. Diagnostic value of synovial fluid microscopy: a reassessment and rationalisation. Ann Rheum Dis 1991 ;50 :101-107.
10. Gupta S, Mishra RS. Cytologic appearance of pigmented villonodular synovitis. A case report. Acta Cytol 2002 ;46 :728-730.
11. Kellner G, KleinG. Guidelines for synovial cytology. Z Rheumatol 1976 ;35 :141-153.
12. Kortekangas P, Aro HT, Tuominen J, Toivanen A. Synovial fluid leukocytosis in bacterial arthritis vs. reactive arthritis and rheumatoid arthritis in the adult knee. Scand J Rheumatol 1992 ;21 :283-288.
13. McCarty DJ. Crystal identification in human synovial fluids. Methods and interpretation. Rheum Dis Clin North Am 1988 ;14 :253-267.
14. McLaughlin RE, Davis JS. Gout and pseudogout established by polarized light microscopy of synovial fluid. Methods and two case reports. Va Med Mon (1918) 1970 ;97 :345-349.
15. Naib ZM. Cytology of synovial fluids. Acta Cytol 1973 ;17 :299-309.

16. Nordström D, Konttinen YT, Bergroth V, et al. Synovial fluid cells in Reiter's syndrome. Ann Rheum Dis 1985 ;44 :852-856.
17. Rege J, Shet T, Naik L. Fine needle aspiration of tophi for crystal identification in problematic cases of gout. A report of two cases. Acta Cytol 2000 ;44 :433-436.
18. Sah SP, Rani S, Mahto R. Fine Needle aspiration of gouty tophi: a report of two cases. Acta Cytol 2002 ;46 :784-785.
19. Sapkas GS, Stathakopoulos DP, Babis GC, Tsarouchas JK. Hydatid disease of bones and joints. 8 cases followed for 4-16 years. Acta Orthop Scand 1998 ;69 :89-94.
20. Selvi E, Manganelli S, Catenaccio M, et al. Diff Quik staining method for detection and identification of monosodium urate and calcium pyrophosphate crystals in synovial fluids. Ann Rheum Dis 2001 ;60 :194-198.
21. Siddaraju N, Bundele MM. Caseous, necrotic material and epithelioid cell granulomas in synovial fluid from a patient with tuberculous infection: a case report. Acta Cytol 2007 ;51 :597-598.
22. Siddaraju N, Aier M, Yaranal PJ, Basu D. Cytology of urate milk in gouty arthritis: a case report. Acta Cytol 2007 ;51 :586-588.
23. Suprun H, Mansoor I. An aspiration cytodiagnostic test for gouty arthritis: a case report. Acta Cytol 1973 ;17 :198-199.
24. Villanueva TG, Schumacher HR Jr. Cytologic examination of synovial fluid. Diagn Cytopathol 1987 ;3 :141-147.
25. Wahane RN, Pangarkar MA, Bobhate SK. Fine needle aspiration cytology of a hydatid cyst of the pelvis and hip joint. Acta Cytol 2008 ;52 :381-384.
26. Zaharopoulos P, Wong JY. Identification of crystals in joint fluids. Acta Cytol 1980 ;24 :197-202.

**Fig. 3.80 Osteosarcoma.**
Cytology of a knee joint aspirate of a 14-year-old male shows typical features of osteosarcoma. Note a giant cell of the osteoclast type (arrows) (direct sediment smear, Pap stain, high magnification).
*Tissue diagnosis:* Osteosarcoma, grade 3.



**Fig. 3.81 Cytology of normal synovial fluid.**
Few mesothelial synovial lining cells scattered on a flimsy cyanophilic background (knee joint effusion (direct sediment smear, Pap stain, lower magnification).

**Figs. 3.82 and 3.83 Variants of cartilage cells occurring in synovial fluid.**
Joint effusions of two patients are demonstrated.

**Fig. 3.82** (case #1) Synovial fluid sampled from an arthritic hip joint contains detritic material, foam cells, and groups of mature chondrocytes (upper right) embedded in cartilaginous matrix (direct sediment smear, Pap stain, high magnification).

**Fig. 3.83** (case #2) A second synovial sample from an arthritic knee joint. High magnification exhibits tissue fragments of immature cartilage (direct sediment smear, Pap stain).

**Fig. 3.84 Villonodular synovitis.**
Fluid obtained from a joint of the left middle finger. Histiocytes, macrophages, and multinucleated giant cells embedded in a sanguineous and proteinaceous background are a characteristic but nonspecific feature of villonodular synovitis. Coarse cytoplasmic inclusions represent hemosiderin (arrow); positive iron staining is not shown (direct sediment smear, Pap stain, high magnification).

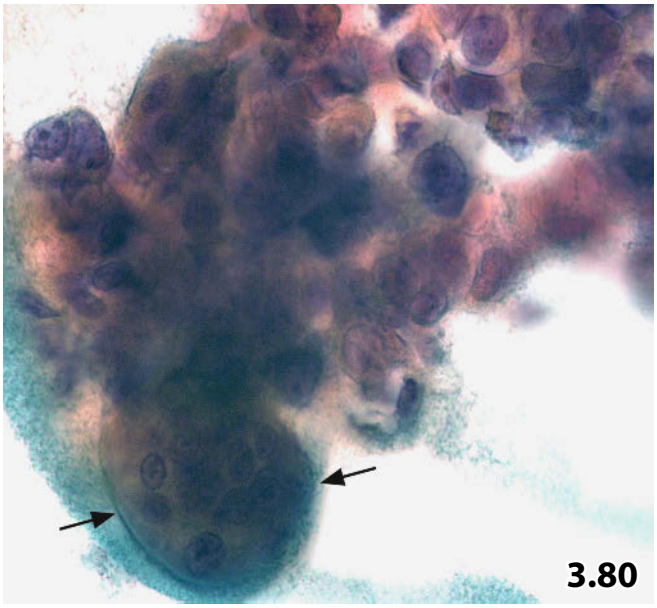
3.80

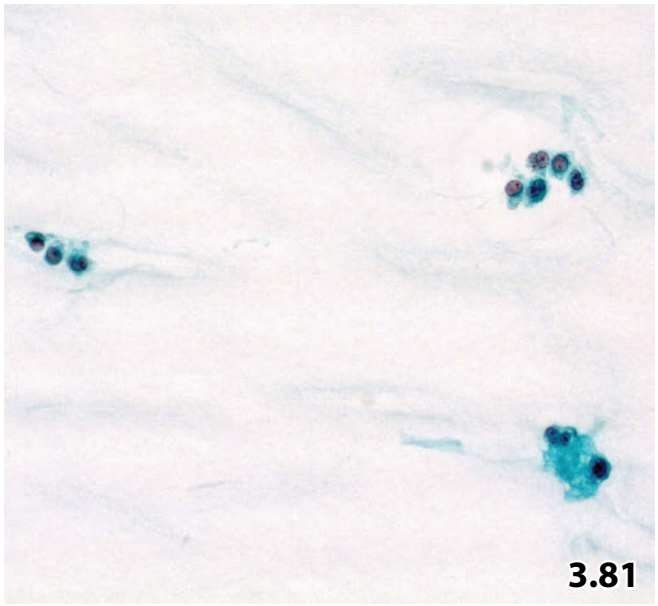
3.81

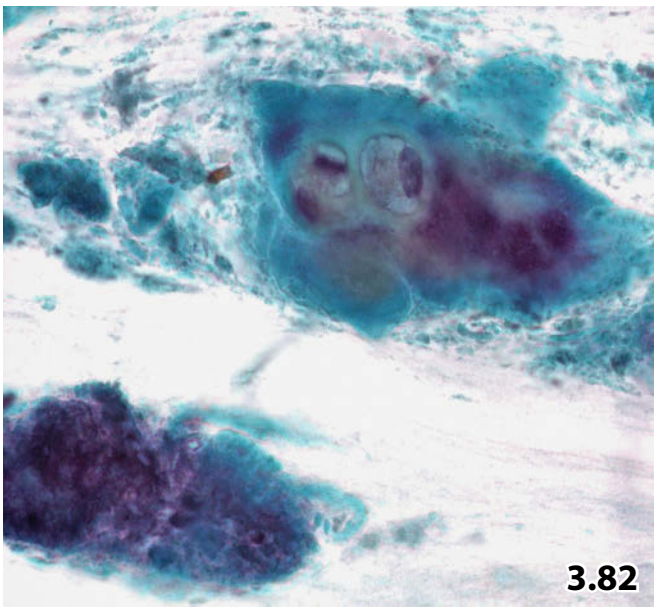
3.82

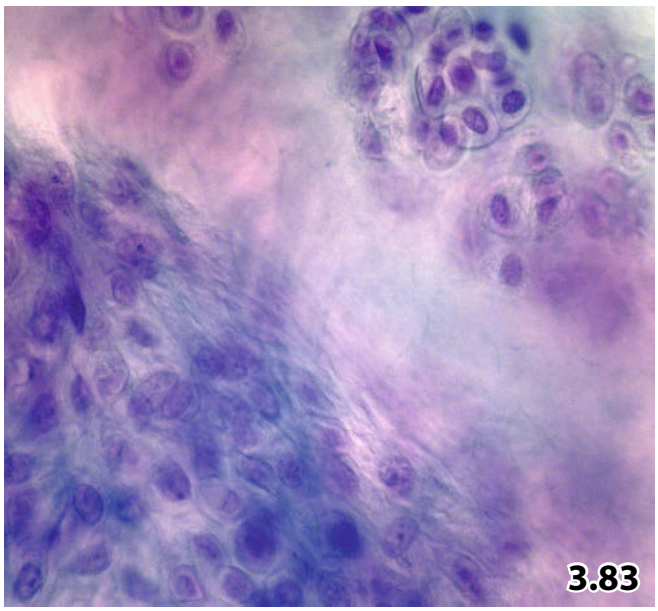
3.83

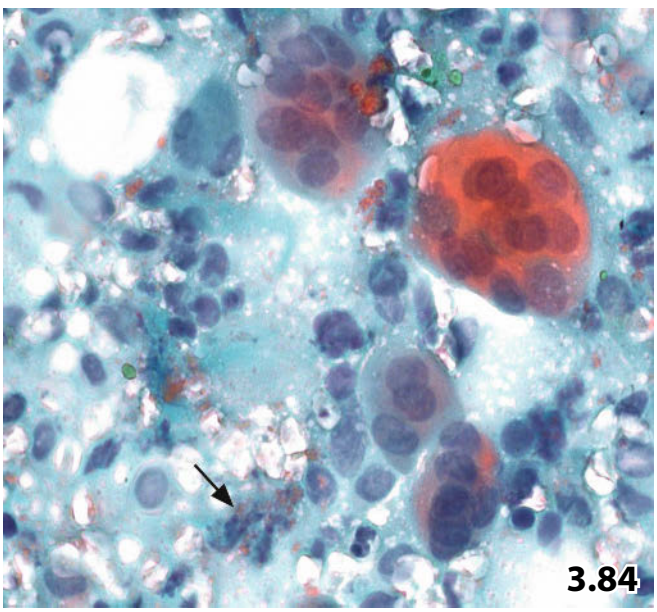
3.84

**Figs. 3.85 and 3.86 Gout.**
Two examples of how to recognize best urate crystals in direct sediment smears.

**Fig. 3.85** (case #1) Birefringent urate crystals in a direct fluid smear. Material was obtained from the metacarpophalangeal joint of the fifth toe (native preparation, polarized light microscopy).

**Fig. 3.86** (case #2) Fluid obtained from a knee joint. The microscopic field at lower magnification shows large amounts of refractile urate crystals (lowered substage condenser). Neutrophils and chondroid cells in the background indicate an acute gout attack (direct sediment smear, Pap stain).

**Fig. 3.87A, B Chondrocalcinosis/pseudogout.**
Microscopic features of pseudogout and varied phenotypes of pyrophosphate crystals are presented using direct sediment smears. **A** Fluid from a knee joint reveals a few fragments of chondroid tissue (top) and a background composed of histiocytoid cells and neutrophils. Cellular appearance together with intra- and extracellular refractile pyrophosphate crystals (arrows) indicate pseudogout (lowered substage condenser, Pap stain, high magnification). **B** Birefringence upon polarization focuses on varying shape and size of the crystals (native specimen preparation).

**Fig. 3.88 Wear-particle disease.**
A 77-year-old woman presented with fluid accumulation in her left knee joint after partial artificial replacement. Cytology of the fluid shows uni- and multinucleated macrophages embedded in hyaline and granular background material. Cytoplasm of the macrophages contains plump birefringent crystalloid elements (Pap-stained direct sediment smear under polarization, high magnification).

**Fig. 3.89 Ganglion.**
FNAB of a ganglion located in the area of a tendon sheath from a middle finger yielded a paucicellular direct smear. The smear contains a few mesothelial sheets originating from the synovial lining. The cells are embedded in a flimsy mucoid cyanophilic-stained background (Pap stain, lower magnification).

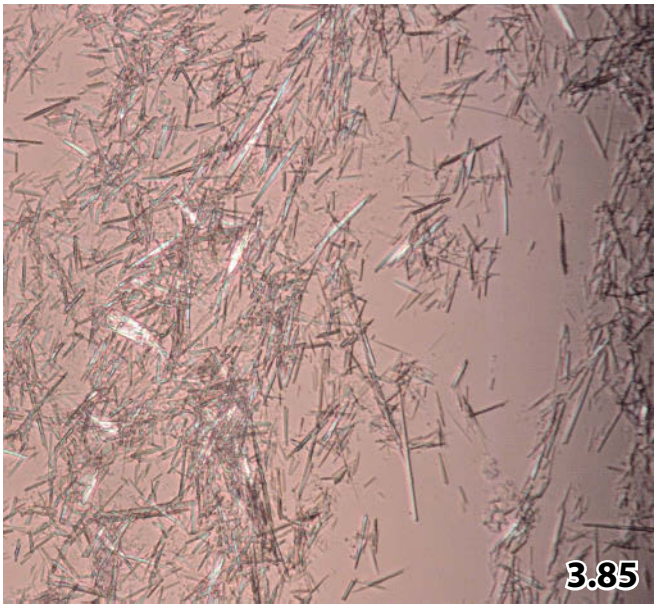
3.85

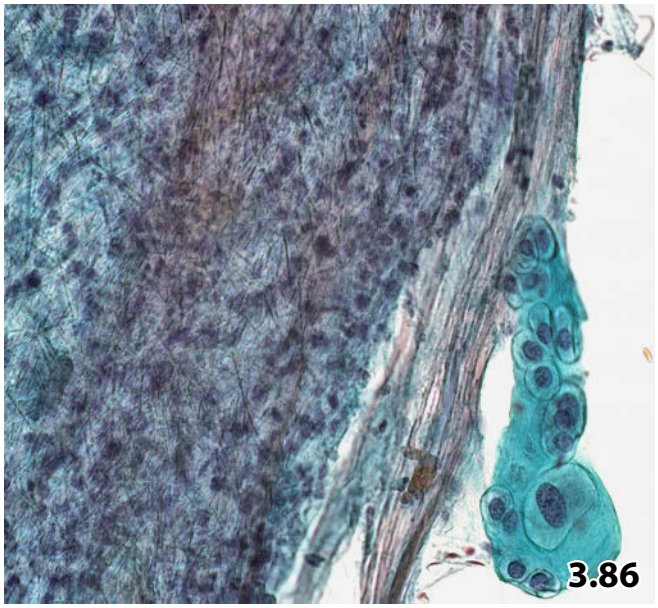
3.86

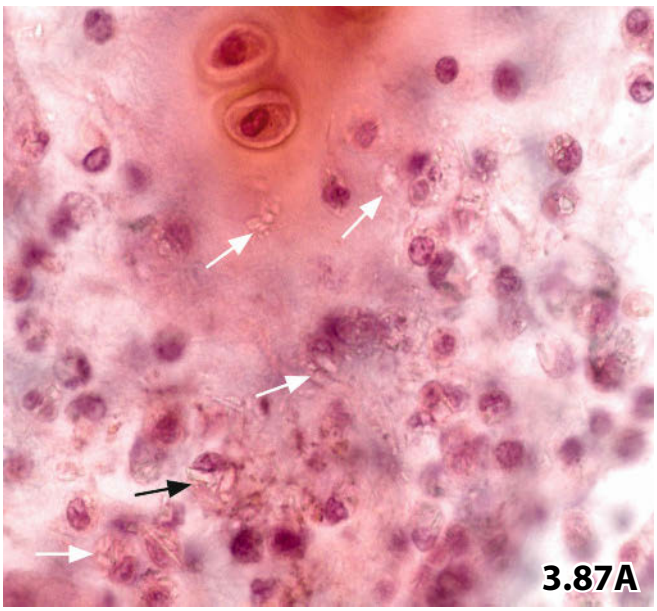
3.87A

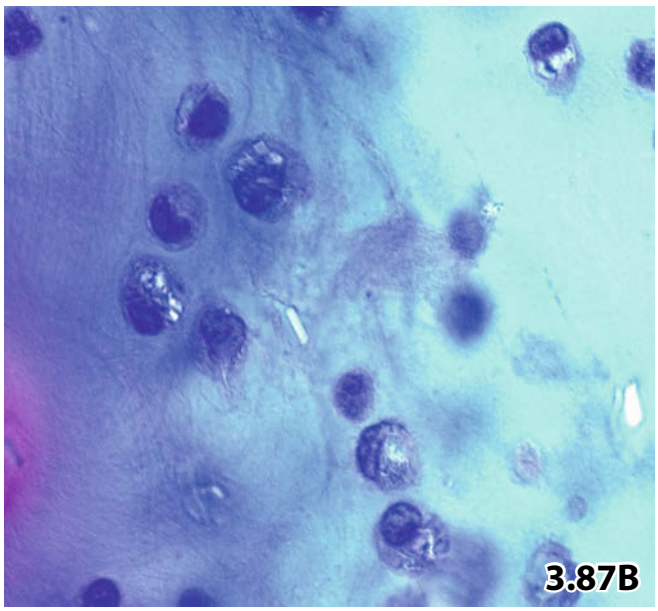
3.87B

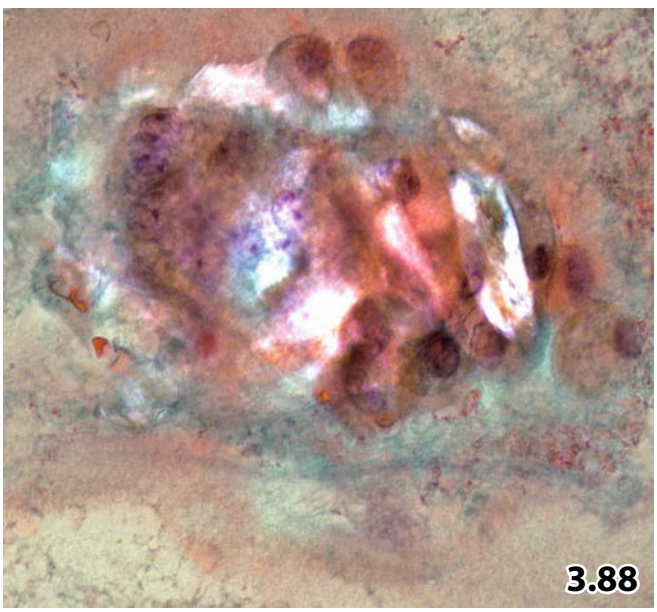
3.88

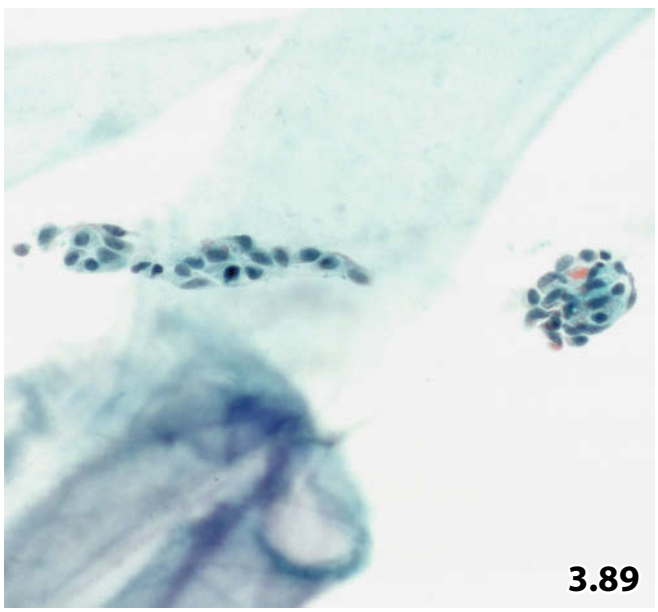
3.89

# Thyroid and Parathyroid Glands 4



## Synopsis and Algorithms




Spieler/Rössle, *Nongynecologic Cytopathology. A Practical Guide. Essentials of Diagnostic Pathology*,
DOI 10.1007/978-3-642-24719-4_4, © Springer-Verlag Berlin Heidelberg 2012

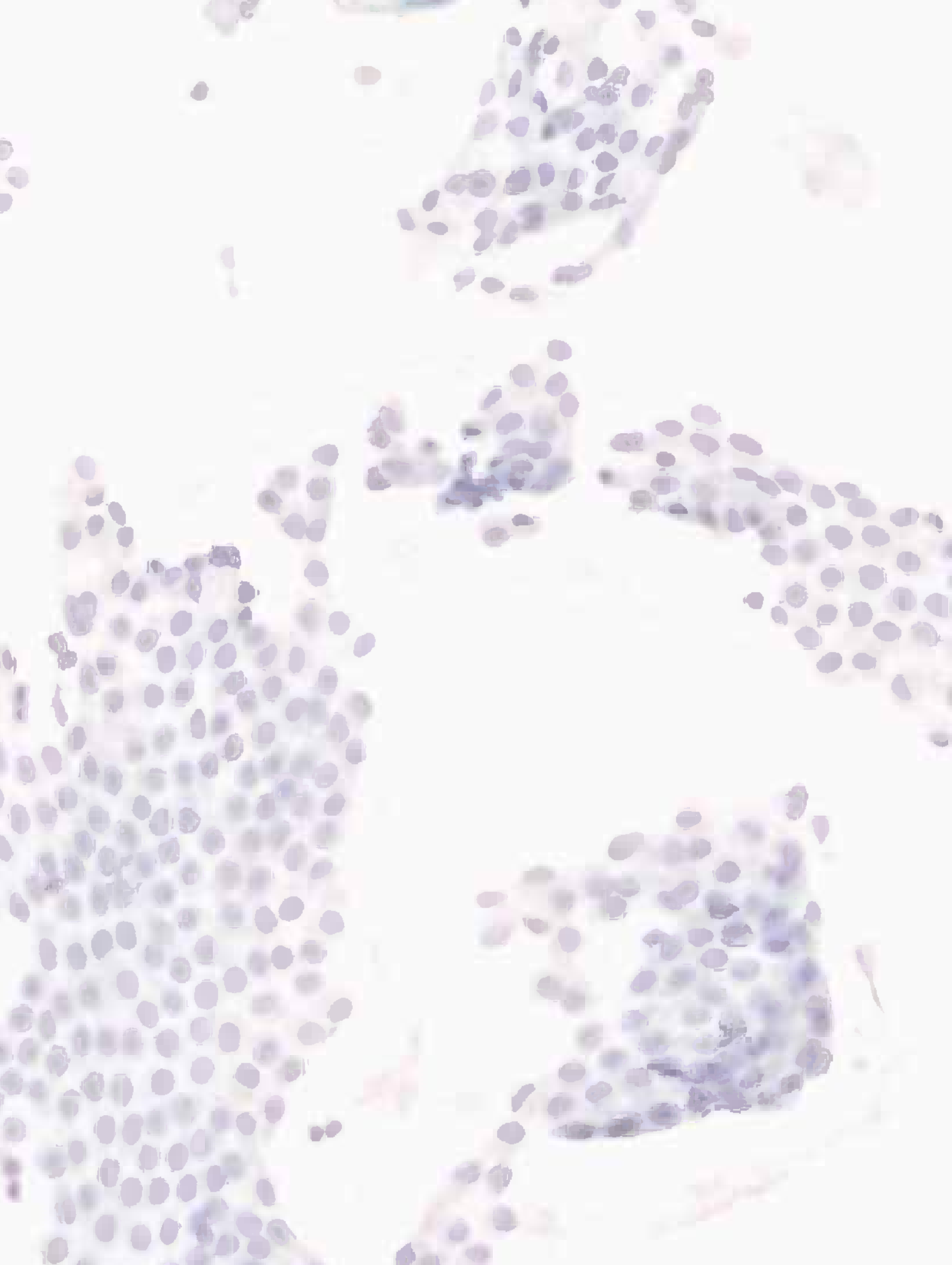

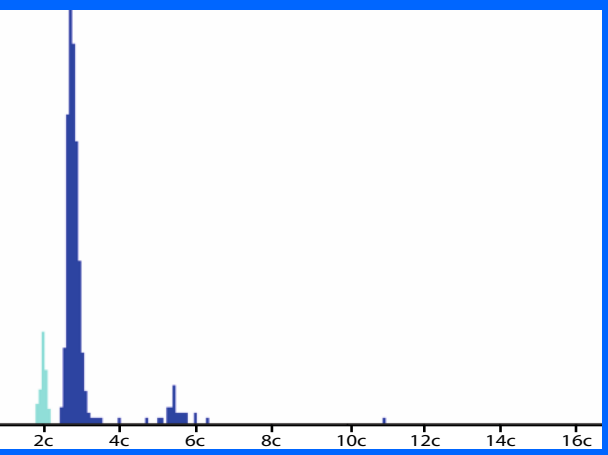


# Section 4.1
# Thyroid



## 4.1.1 Introduction

- Nodular thyroid disease is very common. The prevalence of thyroid nodules ranges from 4 to 7% in the adult population, but thyroid cancer is only found in 5–17% of all thyroid nodules [56, 71]. The purpose of fine-needle aspiration (FNAB) of the thyroid is to decrease the number of unnecessary surgical interventions and to increase the percentage of cancers identified on the total of surgical specimens.
- FNAB is currently the most accurate method for improving preoperative diagnosis of nodular thyroid lesions [4, 75, 84, 93, 94, 107]. FNA cytology of the thyroid is able to detect malignancy at an earlier stage and to identify cancers that have been classified as a benign condition clinically and by imaging studies. The method is simple, safe, easy to perform, and cost-effective. It is also well accepted by patients, and severe complications are rare [48]. Core biopsy and histologic assessment have sporadically been reported as an alternative to FNAB [45, 57, 91], but the technique has not widespread in clinical practice.
- Drawing a comparison between FNAB results of different institutions relative to the sample adequacy, sensitivity, specificity, and negative and positive predictive value is very difficult. Furthermore, terminology, inclusion or exclusion criteria, and criteria comparing histological and cytological findings are inconsistent for many thyroid disorders. Nevertheless, a huge number of publications highlight thyroid FNAB to be an effective screening test in the evaluation of thyroid nodules and also for determining the appropriate therapeutic approach for the treatment of thyroid lesions. We refer to a few more recent reports with large-scale patient cohorts. [5, 61, 80, 109, 111].
- Consensus has been achieved on clinical aspects of thyroid FNAB by various professional associations. The results on this issue have subsequently been published as guidelines for clinicians and cytopathologists [1, 40, 102].

**Caution**

Thyroid lesions in patients with a history of radiation exposure or radiotherapeutic intervention to the neck area are likely to be malignant (in particular papillary carcinoma).
Occult thyroid cancer has been reported to have accumulated more in this patient group than in nonirradiated patients [59].

## 4.1.2 Aspiration Techniques: FNAB and Its Facilities

### General Comments

- The thyroid gland and a majority of its nodular disorders harbor a richly vascularized stroma. A small needle should be used in order to prevent bloody aspirates; at our institution, we prefer the 24-gauge needle. One should realize that the larger the needle the greater the possibility of a large volume of aspirated blood and the fewer the number of cells and tissue fragments. It is important to emphasize that the negative pressure in the syringe should be built up

cautiously and that the process should be stopped if suction is immediately followed by blood masses filling the barrel of the syringe. Intensity of the needling should be measured individually on each lesion.

- Aspirations should be avoided in central zones of large nodules due to frequent regenerative changes in this area. In contrast, the periphery of the nodule must be needled at different locations.
- In our own experience, thyroid FNAB yields the best results when all the following steps are performed by a skilled cytopathologist:
  - Assessment of the clinical history and the image appearance of the target lesion.
  - Selection of the interventional procedure (with or without image control).
  - Selection of the specimen processing (conventional smears versus liquid based-method versus cell block technique).
  - Microscopic evaluation and making a diagnosis considering ancillary test results.

  The cytopathologist has to be experienced in ultrasound (technical handling and image assessment) and in ultrasound-guided FNAB. The sonographic examination method and sonographic findings are described in distinguished textbooks and publications [20]. Inexperienced operators and physicians without adequate training reduce diagnostic sensitivity; their aspirates often provide inadequate material that is inconclusive for diagnostic assessment and potentially misleading.

#### 4.1.2.1 Directed FNAB / Freehand Aspiration

For freehand aspiration, a 10- or 20-cc syringe should be mounted on a pistol-like device. This makes the aspiration easier and the targeting of small lesions more precise. The second hand must be used to immobilize the nodule.

#### 4.1.2.2 Nonaspiration FNAB

The size of the needle, number of needle passes, and the number of aspirations may induce worrisome histologic alterations leading to misinterpretation of thyroidectomy specimens [12, 21, 30, 77]. The less traumatic technique of nonaspiration FNAB (needle sampling without suctioning) has therefore been suggested [30, 87, 112]. Our own experience with the nonaspiration technique applied by a few colleagues is ambivalent; a few of the samples have been cellular enough for a proper diagnosis, but a majority of the samples contained only blood.

#### 4.1.2.3 Ultrasound-Guided FNAB

- According to data in literature, the frequency of palpable thyroid nodules varies from 4% to 7% in adults, whereas additional ultrasound investigation reveals that about 30% of the adult population has thyroid nodules [33, 56].
- At our institution, ultrasound-guided (US-FNAB) has become obligatory not only for detecting nonpalpable lesions, but also in the work-up of palpable thyroid disorders.

  The benefits of US-FNAB are manifold:
  - Diagnostic evaluation of nonpalpable nodules.
  - Diagnostic evaluation of small nodules measuring less than 2 cm in greatest dimension, and more reliable cell sampling from small lesions.
  - Investigation of multiple nodules during the same session [13, 41].
  - Optimal diagnostic work-up in out-patient settings.
  - Diagnostic evaluation of suspected nodules and areas within large, nonspecific hyperplastic disorders and multinodular goiters by a selective use of multiple targeted aspirations.

Data reported in the literature demonstrate an increased diagnostic accuracy for thyroid nodules sampled using US-FNAB [14, 74, 110]. Lin and colleagues conclude an earlier detection of well-differentiated thyroid cancer by combined sonography and US-FNAB; the results are based on a retrospective large-scale study that includes 21 748 patients comparing previous series [63].

#### 4.1.2.4 On-site Assistance at the Time of Aspiration

On-site assessment of specimen adequacy and on-site interpretation has been widely discussed.

The results are divergent with respect to the FNAB adequacy rate with and without on-site evaluation by cytopathologists or cytotechnologists. On-site FNAB interpretation demands the skill of an experienced cytopathologist; one great advantage of this approach is the chance for immediate reaspiration if required. On-site interpretation is costly and time-consuming, meaning that each institution has to evaluate the advantages and disadvantages of the diagnostic on-site service individually [81]. Finally, the benefit of on-site evaluations depends above all on the experience of the operators [43].

### 4.1.3 Sample Processing

#### 4.1.3.1 Conventional Smear

- Both wet-fixed and air-dried direct smears are convenient for a reliable cytodiagnostic performance. Generally, cyto-

pathologists prefer wet fixed specimens followed by Papanicolaou staining because cytologic details are well preserved and match nuclear and cytoplasmic structures observed in histologic paraffin sections. Direct smears for wet fixation must be fixed immediately within 1–3 s after spreading the material. Slides can be dropped into a pot with alcohol-based fixative, or a spray fixative can be used.

- Air-dried slides stained with the May-Grünwald-Giemsa method (or a related staining procedure) accentuate colloidal background and cytoplasmic features of the thyrocytes, therefore this method is preferred by many cytologists.

#### 4.1.3.2 Liquid-Based Cytology (cytospin, ThinPrep and others)

- FNAB material is rinsed in a vial containing a cell medium. Thin layer preparations can be performed as instructed by the manufacturer. Direct-to-vial methods are best used by clinical operators that are not familiar with proper preparation and fixation technique. In addition, the liquid-based technique seems to be an appropriate tool to lower the proportion of inadequate specimens and false-negative rates [67, 92].
- Optimal preparation can be achieved using the liquid-based procedure with regard to ancillary techniques such as immunocytochemistry, fluorescence in situ hybridization, static image cytometry, or flow cytometry [28, 67, 97] (Figs. 4.15 and 4.67).
- Many reports in the literature emphasize that the ThinPrep technique is a valid method for cytologic diagnosis of thyroid lesions. It is superior to conventional smears with regard to clear background, thin-layer cell preparation and cell preservation; and it reduces the screening workload of the cytologic staff. Cellular morphology and architectural pattern show only minor differences as compared to conventional smears [19, 92, 97, 104]; ThinPrep method enhances nuclear details and the nucleoli appear more prominent [28, 19, 67].

  However, our own experience corresponding with reports in the literature show that liquid based preparation (particularly Thin Prep method) should call for awareness of certain morphologic peculiarities:
  - Slides contain less free colloid and the colloid occur as a few droplets rather than as a diffuse pattern; in this setting missing the diagnosis of a colloid nodule most likely occurs [19, 67] (Figs. 4.1 and 4.2).
  - Cell aggregates may be crowded and tight, cell shrinkage and disruption of the cytoplasm may be more pronounced than with conventional smears [3] (Figs. 4.45, 4.46, 4.51).
  - Occasionally, the nuclear hallmarks of papillary carcinomas may be vague.
  - Immediate assessment of adequacy of the sampled material is not possible [65].
- The following procedure is routinely performed at our institution: direct smears are made using the needle content and if present, thin-layer specimens are prepared from the bloody material in the syringe barrel (see also Sect. 4.1.3.3, below).

#### 4.1.3.3 Grossly Sanguinous Aspirates

(Figs. 4.15, 4.26, 4.27)

Regardless of the operator, hemolyzing fixatives (Cytolyt and others) have been shown to be extremely useful as initial transport medium if FNAB of the thyroid provides grossly bloody specimens. Cytolyt is an accurate medium in combination with the ThinPrep modality for sanguineous aspirates. It lyses red blood cells and yields well-preserved thin-layered cell material and a clear background.

In many cases, we have obtained inadequate direct smears from the needle content and highly cellular Cytolyt/ThinPrep smears by adequate processing of the blood masses from the syringe barrel.

#### 4.1.3.4 Cell-Block Technique

Application of the cell-block technique depends on the type and the amount of cytologic material that has been aspirated. The preparation of cell blocks has been found diagnostically helpful in cases where tissue fragments or clots are present.

### 4.1.4 Ancillary Studies

Immunocytochemistry [16, 64, 98]

Immunocytochemical characteristics of the cells coming from primary thyroid tumors and cells from benign parathyroid tissue including their cross-reactions are tabulated in Table 4.1.1, p. 328. Immunoprofiles of neoplasms metastasizing to the thyroid gland are indicated in Sect. 4.2.11, "Metastases," p. 350.

- Thyroglobulin and calcitonin indicate follicular thyroid cells and parafollicular cells, respectively, with high specificity.
- Thyroglobulin positivity is observed in the large majority of follicular neoplasms of the thyroid, except for the clear cell areas in follicular tumors [86] and for the columnar cell variant of papillary carcinoma (see also Sect. 4.2.6.1.3, p. 345). The cells of oncocytic (Hürthle cell) neoplasms show immunopositivity for thyroglobulin and for low-molecular-weight keratin. The anaplastic type of thyroid cancer shows inconsistent positive reactivity.
- Thyroid transcription factor-1 (TTF-1) shows positive immunoreactivity in thyroid neoplasms of follicular origin. TTF-1 seems to be a more sensitive marker for poorly differentiated carcinomas and metastatic follicular tumors [16].

**Table 4.1.1** Immunocytochemistry of cells originating from the thyroid and parathyroid gland

| Immunomarkers | Thyroid tumors of follicular cell origin | Thyroid tumors of parafollicular cell origin | Parathyroid gland cells | Cross-reactions<br>Positive reaction in: |
|---|---|---|---|---|
| **Thyroglobulin** | Positive | Negative | Negative | |
| **TTF-1** [ 64] | Positive | Negative | Negative | Metastases of:<br>– Pulmonary adenocarcinoma<br>– Small-cell carcinoma with neuroendocrine features of various primary sites |
| **Calcitonin** | Negative | Positive | Rarely positive | |
| **Parathyroid hormone-related protein** | Negative | Negative | Positive | |
| **Chromogranin** | Negative | Positive | Positive | – Benign and neoplastic neuroendocrine cells |
| **Synaptophysin** | Negative | Positive | Positive | |
| **Cytokeratin 7** | Positive | Positive | | – A large number of benign and malignant secondary lesions |
| **Cytokeratin 20** | Negative | Negative | | |
| **CEA** | | Positive | | |

- The selective panel of antibodies against thyroglobulin, TTF-1, CK7, and CK20 is useful to differentiate tumors of thyroid origin from neoplasms metastatic to the thyroid gland.
- Immunocytochemical demonstration of calcitonin and carcinoembryonic antigen (CEA) is appropriate for the diagnosis of medullary carcinoma of the thyroid [101].
- Parathyroid hormone-related protein is present in cells of the parathyroid glands but not in thyroid follicular cells. An immunopanel comprising thyroglobulin, TTF-1, and parathormone is very helpful to distinguish cells of thyroid origin from those of parathyroid origin [2, 29, 108].
- CK19 and CD44 immunostaining have been reported to be of value on FNAB samples distinguishing between thyroid papillary carcinoma and lesions exhibiting cytologic overlap (nuclear grooves and nuclear cytoplasmic inclusions) [31, 72].
- Other immunomarkers, galectin-3 and metalloproteinases, may serve for the recognition of follicular carcinoma (particularly minimally invasive tumors) and are suitable for the application on histologic material [15].

## DNA Ploidy

*DNA Ploidy and Malignancy Assessment*

Several pertinent publications revealed that DNA distribution patterns assessed by digital image analysis (ICM-DNA) or flow cytometry (FCM) were not useful in distinguishing between benign and malignant thyroid follicular neoplasia of the nonoxyphilic and oxyphilic variant. Furthermore, there is no conclusive evidence for noneuploid DNA patterns indicating premalignancy or having prognostic significance in histologically benign neoplasia [26, 35, 49, 68, 70, 71, 78, 90, 100, 113]. Our own unpublished data of a retrospective study (301 consecutive cases between 1994 and 2001) support these findings: 36% of the diploid, 60% of the polyploid, 41% of the triploid, and 66% of the aneuploid follicular neoplasms were diagnosed as atypical adenoma (12 cases) or cancer (120 cases) by histology. Still, our results show that thyroidal adenomatous lesions exhibiting an aneuploid DNA distribution pattern of any type are more frequently associated with malignancy compared to those showing DNA diploidy; and several authors [17, 58, 62, 82, 88] emphasized that DNA aneuploidy is strongly indicative for malignancy or should at least be considered as being premalignant.

*DNA Ploidy and Prognosis*

The biological impact of numerical and structural chromosomal changes are difficult to assess mainly due to an extremely slow evolution of many thyroid neoplasms. Histologically benign euploid and aneuploid neoplasms have an excellent prognosis after complete surgical resection, yet little is known about progression of aneuploid neoplasms into malignant tumors if the lesions are left in place. One may hypothesize that histologically benign encapsulated aneuploid follicular adenomas should be regarded as a potentially malignant equivalent to the encapsulated papillary neoplasms of the thyroid.

Literature results have shown that DNA aneuploidy of differentiated oxyphilic and nonoxyphilic malignant neoplasia seems to be associated with a higher probability of invasiveness but lack prognostic potential [17, 22, 39, 42, 62, 68, 79, 88, 113]. However, retrospective series with long follow-up periods indicate that patients with nondiploid/aneuploid follicular, papillary, and medullary cancer had a significantly worse outcome after surgical treatment [7, 8, 10, 18, 23, 24, 25, 34, 36, 46, 47, 50, 54, 73, 76, 83, 85, 89, 105], developed more distant metastatic disease [73, 99], or were seen only in

the lethal group [68, 95]. On the other hand, it was shown that nonaneuploid tumors exhibiting poor clinical and histologic parameters may have a favorable course [24].

The strongest correlation between quantitative nuclear DNA content and survival was reported for papillary carcinoma followed by follicular and medullary carcinoma [47]. Well-differentiated aneuploid cancers in children and adolescents have a poor prognosis [69]. The agreement between ploidy status and biologic aggressiveness is unequivocally best for high-grade thyroid carcinomas expressing aneuploidy [9, 37, 60, 66, 76]. Varying noneuploid DNA patterns of anaplastic carcinomas do not seem to provide additional prognostic information, nor can they explain the longer survival of individual patients [37].

*DNA Ploidy on Oxyphilic Thyroid Lesions*

The rate of DNA aneuploidy seems to be higher in oxyphilic adenoma and low-grade oncocytic carcinoma compared to their nonoxyphilic counterparts [47, 52, 53, 55, 71, 79]. A few papers suggest a significant relation between aneuploidy and histologic malignancy of oxyphilic neoplasia [22, 39,42]. The findings are supported by the results of our own prospective study showing at least a tendency to a higher rate of malignancy in nondiploid oxyphilic neoplasms in comparison with all oxyphilic and nonoxyphilic tumors.

*Clinical Utility of Cytometric DNA Ploidy Analysis*

- An euploid DNA distribution pattern does not exclude malignancy, but DNA aneuploidy seems to be more frequently associated with tumor invasion, especially in oxyphilic neoplasia.
- Polyploidy may indicate malignancy, though it is frequently observed in cases exhibiting activated follicular cells, such as thyroiditis and hyperplastic epithelial disorders (Figs. 4.3 and 4.4).
- Aneuploidy generally excludes non-neoplastic follicular lesions. Therefore, the preoperative assessment of DNA aneuploidy by means of FNAB may act as an important factor in clinical decision making about surgery.
- In differentiated follicular carcinoma and medullary cancer, a correlation exists between DNA content and prognosis. Therefore, preoperative assessment of DNA ploidy using FNAB samples could be helpful for selecting the most appropriate surgical approach.
- After successful surgery, standardized cytometric DNA measurements on any relapsing tumor may be of practical value for further therapeutic decision making, follow-up strategies, and weighing the clinical outcome.

Molecular Genetics

In summary, it can be stated that the cytogenetic findings show good correlation with the cytometric DNA ploidy results. It has been shown that today structural chromosomal analysis offers no decisive additional information on malignancy assessment or on the behavior of thyroid neoplasms [96, 103]. Still, promising molecular investigations have recently been communicated [27, 51].

## 4.1.5 Reporting System

- Many different guidelines covering cytologic terminology and other issues related to FNAB of the thyroid gland have been developed within the past few years [e.g., 6, 11, 32, 38, 44, 106].
- The following eight-category diagnostic scheme represents our own in-house classification used for thyroid FNA cytology:
  1. Nondiagnostic: only blood or inadequate cellularity [1]
  2. Negative for malignancy: well-preserved epithelial cells but no specific diagnostic pattern [2]
  3. Thyroiditis [3]
  4. Benign cystic lesions [4]
  5. Hyperplastic lesion: diffuse or nodular goiter [4]
  6. Hyperplastic lesion: oncocytic or nononcocytic follicular proliferation and neoplasia respectively, with or without mild atypias [5]
  7. Atypical cells suggestive of carcinoma, or malignancy cannot be excluded by cytology [5]
  8. Malignant disorder [3]

*Procedures generally recommended by our cytopathologists:*

[1] Repeated FNAB
[2] Repeated FNAB or clinical and sonographic follow-up
[3] Appropriate therapy
[4] Clinical and sonographic follow-up
[5] ICM-DNA, excision and histology

## 4.1.6 Further Reading


1. AACE/AME Task force on thyroid nodules. American Association of Clinical Endocrinologists and Associazione Medici Endocrinologi: medical guidelines for clinical practice for the diagnosis and management of thyroid nodules. Endocr Pract 2006;12:63-101.
2. Abati A, Skarulis MC, Shawker T, Solomon D. Ultrasound-guided fine-needle aspiration of para-thyroid lesions: a morphological and immunocytochemical approach. Hum Pathol 1995;26:338-343.
3. Afify AM, Liu J, Al-Khafaji BM. Cytologic artifacts and pitfalls of thyroid fine-needle aspiration using ThinPrep: a comparative retrospective review. Cancer 2001;93:179-186.
4. Altavilla G, Pascale M, Nenci I. Fine needle aspiration cytology of thyroid gland diseases. Acta Cytol 1990;34:251-256.
5. Amrikachi M, Ramzy I, Rubenfeld S, Wheeler TM. Accuracy of fine-needle aspiration of thyroid Arch Pathol Lab Med 2001;125:484-488.
6. Anderson CE, McLaren KM,. Best practice in thyroid pathology. J Clin Pathol 2003;56:401-405.
7. Auer GU, Backdahl M, Forsslund GM, Askensten UG . Ploidy levels in nonneoplastic and neoplastic thyroid cells. Anal Quant Cytol Histol 1985;7:97-106.
8. Backdahl M, Auer G, Forsslund G, et al. Prognostic value of nuclear DNA content in follicular thyroid tumours. Acta Chir Scand 1986a;152:1-7.
9. Backdahl M, Carstensen J, Auer G, Tallroth E. Statistical evaluation of the prognostic value of nuclear DNA content in papillary, follicular, and medullary thyroid tumors. World J Surg 1986b;10:974-980.
10. Backdahl M, Tallroth E, Auer G, et al. Prognostic value of nuclear DNA content in medullary thyroid carcinoma. World J Surg 1985a;9:980-987.
11. Baloch ZW, Cibas ES, Clark DP, Layfield LJ, Ljung B, Pitman MB, Abati A. The National Cancer Institute Thyroid fine needle aspiration state of the science conference: A summation. CytoJournal 2008;5:6
12. Baloch ZW, LiVolsi VA. Post fine needle aspiration histologic alteration of thyroid revisited. Am J Clin Pathol 1999;112:311-316.
13. Barroeta JE, Wang H, Shiina N, et al. Is fine-needle aspiration (FNA) of multiple thyroid nodules justified? Endocr Pathol 2006;17:61-65.
14. Baskin HJ. Ultrasound-guided fine-needle aspiration biopsy of thyroid nodules and multinodular goiters. Endocr Pract 2004;10:242-245.
15. Beesley MF, McLaren KM. Cytokeratin 19 and galectin-3 immunohistochemistry in the differential diagnosis of solitary thyroid nodules. Histopathology 2002;41:236-243.
16. Bejarano PA, Nikiforov YE, Swenson ES, Biddinger PW. Thyroid transcription factor-1, thyroglobulin, cytokeratin 7 and cytokeratin 20 in thyroid neoplasms. Appl Immunohistochem Mol Morphol 2000;8:189-194.
17. Bengtsson A, Malmaeus J, Grimelius L, et al. Measurement of nuclear DNA content in thyroid diagnosis. World J Surg 1984;8:481-486.
18. Bergholm U, Adami HO, Auer G, et al. Histopathologic characteristics and nuclear DNA content as prognostic factors in medullary thyroid carcinoma. A nationwide study in Sweden. The Swedish MTC Study Group. Cancer 1989;64:135-142.
19. Biscotti CV, Hollow JA, Toddy SM, et al. ThinPrep versus conventional smear cytologic preparations in the analysis of thyroid fine-needle aspiration specimens. Am J Clin Pathol 1995;104:150-153.
20. Blank W, Braun B. Sonography of the thyroid – Part 1. Ultraschall in Med 2007;28:554-575.
21. Bolat F, Kayaselcuk F, Nursal TZ, et al. Histopathologic changes in thyroid tissue after fine needle aspiration biopsy. Pathol Res Pract 2007;203:641-645.
22. Bondeson L, Azavedo E, Bondeson AG, et al. Nuclear DNA content and behavior of oxyphil thyroid tumors. Cancer 1986;58:672-675.
23. Bottger T, Gabbert H, Stockle M, et al. Initial results of image cytometric DNA analysis in the evaluation of prognosis in papillary thyroid cancer. Langenbecks Arch Chir 1991;376:158-162.
24. Bottger T, Potratz D, Gabbert H, et al. Image analysis DNA cytometry in medullary thyroid gland cancer. Comparison with histomorphologic parameters and prognostic effect. Chirurg 1993;64:122-129.
25. Bottger T, Potratz D, Schernus B, et al. The value of quantitative DNA analysis in evaluating the prognosis of differentiated thyroid cancer. Chirurg 1994;65:190-193.
26. Cannon CR, Hayne ST . DNA ploidy of thyroid lesions. J Miss State Med Assoc 1995;36:237-240.
27. Carroll NM, Carty SE. Promising molecular techniques for discriminating among follicular thyroid neoplasms. Surg Oncol 2006;15:59-64.
28. Chan-Kwon J, Ahwon L, Eun-Sun J, Yeong-Jin Choi, et al. Split sample comparison of a liquid-based method and conventional smears in thyroid fine needle aspiration. Acta Cytol 2008;52:313-319.
29. Chang TC, Tung CC, Hsiao YL, Chen MH. Immunoperoxidase staining in the differential diagnosis of parathyroid from thyroid origin in fine needle aspirates of suspected parathyroid lesions. Acta Cytol 1998;42:619-624.
30. Chetna S, Geeta K. Histologic analysis and comparison of techniques in fine needle aspiration-induced alterations in thyroid. Acta Cytol 2008;52:56-64.
31. Chhieng DC, Ross JS, McKenna BJ. CD44 immunostaining of thyroid fine-needle aspirates differentiates thyroid papillary carcinoma from other lesions with nuclear grooves and inclusions. Cancer 1997;81:157-162.
32. Cibas ES, Sanchez MA. The National Cancer Institute Thyroid fine-needle aspiration State-of-the-Science Conference. Cancer(Cancer Cytopathol) 2008;114:71-73.
33. Cochand-Priollet B, Guillausseau PJ, Chagnon S, et al. The diagnostic value of fine-needle aspiration biopsy under ultrasonography in nonfunctional thyroid nodules: a prospective study comparing cytologic and histologic findings. Am J Med 1994;97:152-157.
34. Cohn K, Backdahl M, Forsslund G, et al. Prognostic value of nuclear DNA content in papillary thyroid carcinoma. World J Surg 1984;8:474-480.
35. Cusick EL, Ewen SW, Krukowski ZH, Matheson NA. DNA aneuploidy in follicular thyroid neoplasia. Br J Surg 1991;78:94-96.
36. Ekman ET, Bergholm U, Backdahl M, et al. Nuclear DNA content and survival in medullary thyroid carcinoma. Swedish Medullary Thyroid Cancer Study Group. Cancer 1990;65:511-517.
37. Ekman ET, Wallin G, Backdahl M, et al. Nuclear DNA content in anaplastic giant-cell thyroid carcinoma. Am J Clin Oncol 1989;12:442-446.
38. Fine needle aspiration cytology (FNAC). In: Guidelines for the management of thyroid cancer in adults. London: British Thyroid Association and Royal College of Physicians; 2002; pp:7-8.
39. Flint A, Davenport RD, Lloyd RV, et al. Cytophotometric measurements of Hürthle cell tumors of the thyroid gland. Correlation with pathologic features and clinical behavior. Cancer 1988;61:110-113.
40. Frates MC, Benson CB, Charboneau JW, et al. Management of thyroid nodules detected at US: Society of Radiologists in Ultrasound Consensus Conference Statement. Radiology 2005;237:794-800.

41. Frates MC, Benson CB, Doubilet PM, et al. Prevalence and distribution of carcinoma in patients with solitary and multiple thyroid nodules on sonography. J Clin Endocrinol Metab 2006;91:3411-3417.
42. Galera-Davidson H, Bibbo M, Bartels PH, et al. Correlation between automated DNA ploidy measurements of Hürthle-cell tumors and their histopathologic and clinical features. Anal Quant Cytol Histol 1986;8:158-167.
43. Ghofrani M, Beckman D, Rimm DL. The value of on site adequacy assessment of thyroid fine-needle aspirations is a function of operator experience. Cancer 2006;108:110-113.
44. Guidelines of the Papanicolaou Society of Cytopathology for the examination of fine-needle aspiration specimens from thyroid nodules. The Papanicolaou Society of Cytopathology Task Force on Standards of Practice. Mod Pathol 1996;9:710-715.
45. Harvey JN, Parker D, De P, et al. Sonographically guided core biopsy in the assessment of thyroid nodules. J Clin Ultrasound 2005;33:57-62.
46. Hay ID. Papillary thyroid carcinoma. Endocrinol Metab Clin North Am 1990;19:545-576.
47. Hay ID, Ryan JJ, Grant CS, et al. Prognostic significance of nondiploid DNA determined by flow cytometry in sporadic and familial medullary thyroid carcinoma. Surgery 1990;108:972-979.
48. Hor T, Lahiri SW. Bilateral thyroid hematomas after fine-needle aspiration causing acute airway obstruction. Thyroid 2008;18:567-569.
49. Hostetter AL, Hrafnkelsson J, Wingren SO, et al. A comparative study of DNA cytometry methods for benign and malignant thyroid tissue. Am J Clin Pathol 1988;89:760-763.
50. Hrafnkelsson J, Stal O, Enestrom S, et al. Cellular DNA pattern, S-phase frequency and survival in papillary thyroid cancer. Acta Oncol 1988;27:329-333.
51. Hunt J. Understanding the genotype of follicular thyroid tumors. Endocr Pathol 2005;16:311-321.
52. Joensuu H, Klemi PJ. DNA aneuploidy in adenomas of endocrine organs. Am J Pathol 1988a;132:145-151.
53. Joensuu H, Klemi P, Eerola E. DNA aneuploidy in follicular adenomas of the thyroid gland. Am J Pathol 1986b;124:373-376.
54. Joensuu H, Klemi P, Eerola E, Tuominen J. Influence of cellular DNA content on survival in differentiated thyroid cancer. Cancer 1986a;58:2462-2467.
55. Johannessen JV, Sobrinho-Simoes M, Tangen KO, Lindmo T. A flow cytometric deoxyribonucleic acid analysis of papillary thyroid carcinoma. Lab Invest 1981;45:336-341.
56. Karakitsos P, Cochand-Priollet B, Pouliakis A, Guillausseau PJ, and Ioakim-Liossi A (1999). Learning vector quantizer in the investigation of thyroid lesions. Anal Quant Cytol Histol 1999;21:201-208.
57. Karstrup S,Balslev E, Juul N, et al. US-guided fine needle aspiration versus coarse needle biopsy of thyroid nodules. Eur J Ultrasound 2001;13:1-5.
58. Kashyap V, Kaushik N, Bhambhani S, et al. Supportive role of image analysis and DNA ploidy pattern in the diagnosis of thyroid tumors. Diagn Cytopathol 1992;8:228-230.
59. Kikuchi S, Perrier ND, Ituarte PH, et al. Accuracy of fine-needle aspiration cytology in patients with radiation-induced thyroid neoplasms. Br J Surg 2003;90:755-758.
60. Klemi PJ, Joensuu H, Eerola E. DNA aneuploidy in anaplastic carcinoma of the thyroid gland. Am J Clin Pathol 1988a;89:154-159.
61. Ko HM, Jhu IK, Yang SH, et al. Clinicopathologic analysis of fine needle aspiration cytology of the thyroid. A review of 1613 cases and correlation with histopathologic diagnoses. Acta Cytol 2003;47:727-732.
62. Liautaud-Roger F, Dufer J, Pluot M, et al. Contribution of quantitative cytology to the cytological diagnosis of thyroid neoplasms. Anticancer Res 1989;9:231-234.
63. Lin JD, Chao TC, Huang BY, et al. Thyroid cancer in the thyroid nodules evaluated by ultrasonography and fine-needle aspiration cytology. Thyroid 2005;15:708-717.
64. Liu J, Farhood A. Immunostaining for thyroid transcription factor-1 on fine-needle aspiration specimens of lung tumors: a comparison of direct smears and cell block preparations. Cancer 2004;102:109-114.
65. Ljung B-M. Thyroid fine-needle aspiration: Smears versus liquid-based preparations. Cancer(Cancer Cytopathol) 2008;114:144-148.
66. Lukacs G, Balazs G, Nagy I, Juhasz F. Prognostic significance of nuclear DNA content in highly malignant thyroid tumors. Wien Klin Wochenschr 1990;102:253-256.
67. Malle D, Valeri RM, Pazaitou-Panajiotou K, et al. Use of thin-layer technique in thyroid fine needle aspiration. Acta Cytol 2006;50:23-27.
68. McLeod MK. The measurement of DNA content and ploidy analysis in thyroid neoplasms. Otolaryngol Clin North Am 1990;23:271-290.
69. Mizukami Y, Michigishi T, Nonomura A, et al. Carcinoma of the thyroid at a young age--a review of 23 patients. Histopathology 1992;20:63-66.
70. Montironi R, Alberti R, Sisti S, et al. Discrimination between follicular adenoma and follicular carcinoma of the thyroid: preoperative validity of cytometry on aspiration smears. Appl Pathol 1989a;7:367-374.
71. Nadjari B, Motherby H, Pooschke T, et al. DNA aneuploidy as a specific marker of neoplastic cells in FNAB of the thyroid. Anal Quant Cytol Histol 1999;21:481-488.
72. Nasser SM, Pitman MB, Pilch BZ, Faquin WC. Fine-needle aspiration biopsy of papillary thyroid carcinoma: diagnostic utility of cytokeratin 19 immunostaining. Cancer 2000;90:307-311.
73. Nishida T, Nakao K, Hamaji M, et al. Overexpression of p53 protein and DNA content are important biologic prognostic factors for thyroid cancer. Surgery 1996;119:568-575.
74. Ogawa Y, Kato Y, Ikeda K, et al. The value of ultrasound-guided fine-needle aspiration cytology for thyroid nodules: an assessment of its diagnostic potential and pitfalls. Surg Today 2001;31:97-101.
75. Ogilvie JB, Piatigorsky EJ, Clark OH. Current status of fine needle aspiration for thyroid nodules. Adv Surg 2006;40:223-238.
76. Onaran Y, Tezelman S, Gurel N, et al. The value of DNA content in predicting the prognosis of thyroid carcinoma in an endemic iodine deficiency region. Acta Chir Belg 1999;99:30-35.
77. Pandit AA, Phulpagar MD. Worrisome histologic alterations following fine needle aspiration of thyroid. Acta Cytol 2001;45:173-179.
78. Perigli G, Cicchi P, Cianchi F, et al. Diagnostic value of preoperative DNA measurement on FNA in benign and malignant thyroid neoplasm. J Exp Clin Cancer Res 1998;17:113-116.
79. Pilch H, Back W, Winter J. DNA cytophotometry of oxyphilic thyroid tumors. Zentralbl Pathol 1994; 139:433-436.
80. Piromalli D, Martelli G, Del Prato I, et al. The role of fine needle aspiration in the diagnosis of thyroid nodules: analysis of 795 consecutive cases. J Surg Oncol 1992;50:247-250.
81. Poller DN, Stelow EB, Yiangou C. Thyroid FNAC cytology: can we do it better? Cytopathology 2008;19:4-10.
82. Rabenhorst G. The diagnostic value of the DNA content of fine needle biopsies of the thyroid gland. Virchows Arch B Cell Pathol 1974;16:379-383.

83. Rainwater LM, Farrow GM, Hay ID, Lieber MM. Oncocytic tumours of the salivary gland, kidney, and thyroid: nuclear DNA patterns studied by flow cytometry. Br J Cancer 1986;53:799-804.
84. Ravetto C, Colombo L, Dottorini ME. Usefulness of fine-needle aspiration in the diagnosis of thyroid carcinoma: a retrospective study in 37,895 patients. Cancer 2000;90:357-363.
85. Riddell DA, Lampe HB, Cramer H, Troster M. Medullary thyroid carcinoma: prognostic factors. J Otolaryngol 1993;22:180-183.
86. Ropp BG, Solomides C, Palazzo J, Bibbo M. Follicular carcinoma of the thyroid with extensive clear-cell differentiation: a potential diagnostic pitfall. Diagn Cytopathol 2000;23:222-223.
87. Santos JEC, Leiman G. Non-aspirational fine needle cytology. Acta Cytol 1988;32:353-356.
88. Schelfhout LJ, Cornelisse CJ, Goslings BM, et al. Frequency and degree of aneuploidy in benign and malignant thyroid neoplasms. Int J Cancer 1990;45:16-20.
89. Schroder S, Bocker W, Baisch H, et al. Prognostic factors in medullary thyroid carcinomas. Survival in relation to age, sex, stage, histology, immunocytochemistry, and DNA content. Cancer 1988;61:806-816.
90. Schurmann G, Mattfeldt T, Feichter G, Buhr HJ. Differential diagnosis of follicular neoplasm of the thyroid. Langenbecks Arch Chir 1990;375:95-101.
91. Screaton NJ, Berman LH, Grant JW: US guided core needle biopsy of the thyroid gland. Radiology 2003;226:827-832.
92. Scurry JP, Duggan MA. Thin layer compared to direct smear in thyroid fine needle aspiration. Cytopathology 2000;11:104-115.
93. Settakorn J, Chaiwun B, Thamprasert K, et al. Fine needle aspiration of the thyroid gland. J Med Assoc Thai 2001;84:1401-1406.
94. Sidoti M, Marino G, Resmini E, et al. The rational use of fine needle aspiration biopsy (FNAB) in diagnosing thyroid nodules. Minerva Endocrinol 2006;31:159-172.
95. Smith SA, Hay ID, Goellner JR, et al. Mortality from papillary thyroid carcinoma. A case-control study of 56 lethal cases. Cancer 1988;62:1381-1388.
96. Soares P,Sobrinho-Simoes M. Recent advances in cytometry, cytogenetics and molecular genetics of thyroid tumours and tumour-like lesions. Pathol Res Pract 1995;191:304-317.
97. Stamataki M, Anninos D, Brountzos E, et al. The role of liquid-based cytology in the investigation of thyroid lesions. Cytopathology 2008;19:11-18.
98. Stevenson JC, Hillyard CJ. Thyroid cancer: tumour markers. Recent Results Cancer Res 1980;73:60-67.
99. Sturgis CD, Caraway NP, Johnston DA, et al. Image analysis of papillary thyroid carcinoma fine-needle aspirates: significant association between aneuploidy and death from disease. Cancer 1999;87:155-160.
100. Suissa J, Hoang C, Soubrane C, et al. Flow cytometry of thyroid tumors. Study of fresh tissue in 50 patients. Presse Med 1994;23:159-163.
101. Talerman A, Lindeman J, Kievit-Tyson PA, Dröge-Droppert C. Demonstration of calcitonin and carcinoembryonic antigen (CEA) in medullary carcinoma of the Thyroid (MCT) by immunoperoxidase technique. Histopathology 1979;3:503-510.
102. The American Thyroid Association Guidelines Task Force. Management guidelines for patients with thyroid nodules and differentiated thyroid cancer. Thyroid 2006;16:1-33.
103. Treseler PA, Clark OH. Prognostic factors in thyroid carcinoma. Surg Oncol Clin N Am 1997;6:555-598.
104. Tulecke MA, Wang HH. ThinPrep for cytologic evaluation of follicular thyroid lesions: correlation with histologic findings. Diagn Cytopathol 2004;30:7-13.
105. Wallin G, Backdahl M, Lundell G, et al. Nuclear DNA content and prognosis in Hürthle cell tumours of the thyroid gland. Acta Chir Scand 1988;154:501-504.
106. Wang HH. Reporting thyroid fine-needle aspiration: literature review and a proposal. Diagn Cytopathol 2006;34:67-76.
107. Werga P, WallinG, Skoog L, et al. Expanding role of fine-needle aspiration cytology in thyroid diagnosis and management. World J Surg 2000;24:907-912.
108. Winkler B, Gooding GA, Montgomery CK, et al. Immunoperoxidase confirmation of parathyroid origin of ultrasound-guided fine needle aspirates of the parathyroid glands Acta Cytol 1987;31:40-44.
109. Yang J, Schnadig V, Logrono R, Wasserman PG. Fine-needle aspiration of thyroid nodules: a study of 4703 patients with histologic and clinical correlations. Cancer 2007;111:306-315.
110. Yassa L, Cibas ES, Benson CB, et al. Long-term assessment of a multidisciplinary approach to thyroid nodule diagnostic evaluation. Cancer(Cancer Cytopathology) 2007;111:508-516.
111. Zagorianakou P, Malamou-Mitsi V, Zagorianakou N, et al. The role of fine-needle aspiration biopsy in the management of patients with thyroid Winkler Acta Cytol 1987nodules. In Vivo 2005;19:605-609.
112. Zajdela A, Zillhardt P, Voillemot N. Cytological diagnosis by fine needle sampling without aspiration. Cancer 1987;59:1201-1205.
113. Zedenius J, Auer G, Backdahl M, et al. Follicular tumors of the thyroid gland: diagnosis, clinical aspects and nuclear DNA analysis. World J Surg 1992;16:589-594.

**Figs. 4.1 and 4.2 Conventional smear versus liquid-based preparation.**
Fine-needle aspirate of a nodular goiter. Comparison between two preparation techniques reveals distinct differences in cytologic appearance (Pap stain, same low magnification).

**Fig. 4.1** Conventional smear showing background of colloid, a few hemosiderophages (arrow), and sheets composed of follicular cells.



**Fig. 4.2** Cytospin preparation exhibits only a few condensed blobs of colloid (lower right), a few macrophages (upper left), and a slight increase in epithelial cell sheets (arrows) as compared to the conventional specimen.

**Figs. 4.3 and 4.4 Activated thyrocytes revealing a polyploid DNA histogram.**
.

**Fig. 4.3** High magnification shows an oncocytic cell sheet loosely interspersed with lymphocytes indicating chronic lymphocytic thyroiditis. Reactive cell changes are striking, including irregular nuclear spacing and nuclear irregularities (FNAB, direct smear, Pap stain).

**Fig. 4.4** ICM DNA of the activated nuclei demonstrates a euploid-polyploid histogram (Pap-prestained Feulgen stain, Zeiss-Kontron/Cires 3.1).

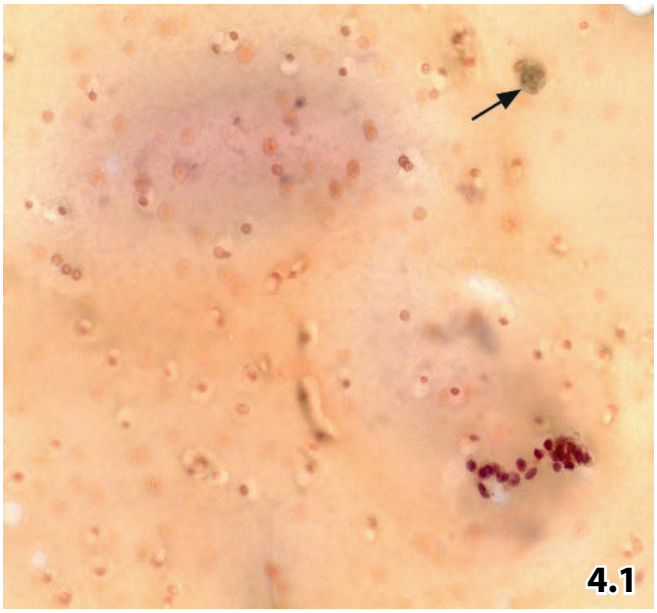

4.1

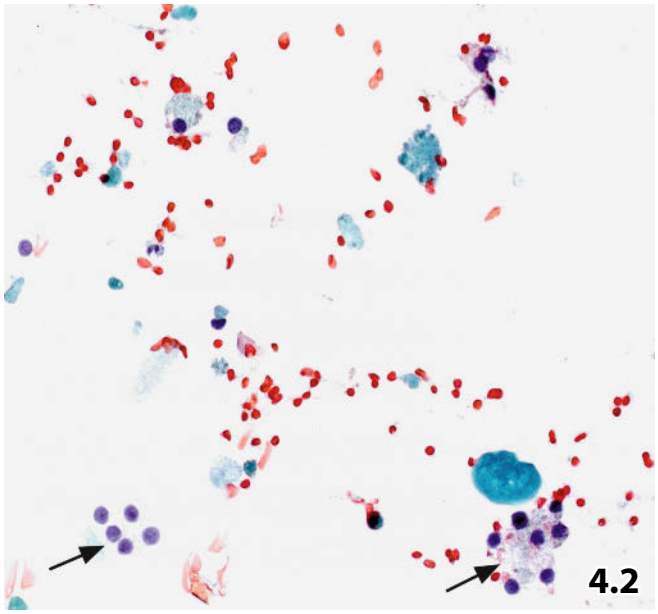

4.2

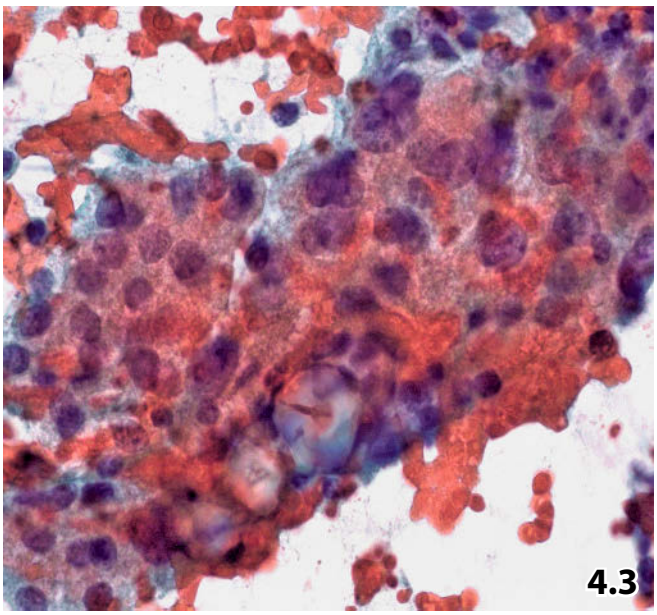

4.3

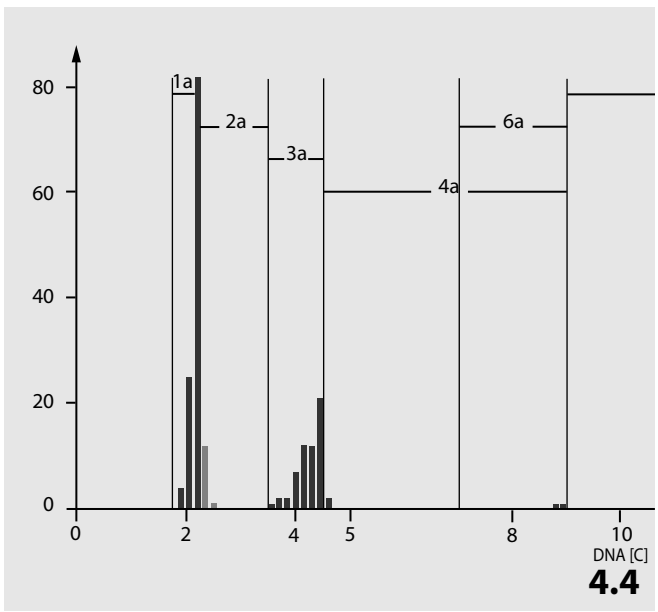


4.4

# Section 4.2
# Thyroid and Parathyroid Glands

## Benign and Malignant Lesions

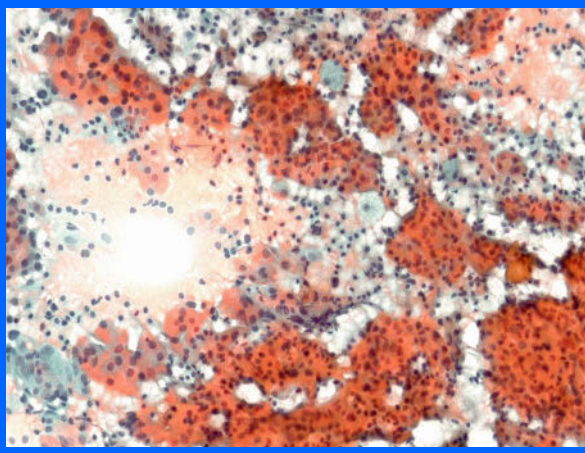

### 4.2.1 Thyroiditis

Inflammatory processes in the thyroid gland can clinically be mistaken for a tumor. The patient's general clinical symptoms and serological results together with aspiration biopsy confirm the diagnosis in the majority of the cases.

#### 4.2.1.1 Acute Suppurative Thyroiditis (Fig. 4.5)

Suppurative thyroiditis is a rare acute inflammatory condition of the thyroid occurring predominantly in immunosuppressed patients. It develops locally and hematogenically in septicemia and is caused by bacteria, fungi, or parasites.

Microscopy

- Masses of degenerating neutrophils and debris are basically diagnostic.
- Extensive search for causative organisms is demanded, if necessary by application of appropriate special stainings (Gram, periodic-acid-Schiff reaction (PAS), Crocott) (Fig. 4.5B).

#### 4.2.1.2 Subacute and Chronic Thyroiditis

##### 4.2.1.2.1 Granulomatous Thyroiditis de Quervain (Figs. 4.6–4.9)

**General Comments**

- Synonyms for this inflammatory disorder include subacute thyroiditis, pseudotuberculous thyroiditis, viral thyroiditis, nonsuppurative thyroiditis, struma granulomatosa, and giant cell thyroiditis.
- It is a self-limited inflammation, probably of viral origin, and occurs most frequently in middle-aged women. The disorder generally resolves spontaneously after 2–3 months.
- Gland involvement can be diffuse or nodular. The destruction of the parenchyma is followed by inflammatory infiltrates and granulomatosis, the latter has morphologically a pathognomonic appearance.

**Microscopic Features**

Cytologic findings vary depending on the stage of the disease:

- *In the early stages*, a cellular aspirate is obtained with follicular epithelium, various inflammatory cells, a granulomatous component with giant cells, debris, and masses of colloid.
- *In advanced stages*, the aspirate is poor of cells; active fibroblasts and inflammatory cells dominate (Fig. 4.9).
  - Hallmarks: Aggregation of epithelioid cells and multinucleated giant cells of the Langhans type. The nuclei are large and appear pale.
    The chromatin is fine and loose. Conspicuous nucleoli vary in size.
    Not only lymphocytes and neutrophils, but also eosinophils and plasma cells may be observed. Debris and abundant colloid may be present.
    The cytoplasm of giant cells may contain masses of condensed colloid (Fig. 4.7).

- Sheets of follicular cells are usually present. The nuclei are bland or shrunken and degenerated Fig. 4.8).

**Caution**

Cytologic findings are highly variable depending on the stage of inflammation. It is recommended to rely upon clinical history in patients with indistinct cytologic findings.

#### 4.2.1.2.2 Subacute Lymphocytic Thyroiditis

**Sporadic Form** [104]

This rare disorder, also referred to as painless thyroiditis, occurs sporadically and shows spontaneous remission within a few months.

**Postpartum Thyroiditis** [94, 138] (Fig. 4.10)

Postpartum thyroiditis is a special form of autoimmune thyroiditis with an incidence estimated at 1–16% in normal pregnancy. Slight hyperthyroidism becomes apparent postpartum and is followed by hypothyroidism over a period of several months. The disease is self-limiting. Inflammatory infiltrates may be observed within a period of 1 year postpartum in FNAB material.

**Microscopic Features**

- The few cases observed at our institution revealed infiltration of mature lymphocytes and sheets of bland or slightly activated follicular cells. Degenerative changes were not found.

**Caution**

Sporadic mature lymphocytes interspersed between clustered follicular cells are a reliable indicator for lymphocytic thyroiditis. Final diagnosis may be reached using repeated FNAB.

#### 4.2.1.2.3 Chronic Lymphocytic Thyroiditis (Hashimoto Autoimmune Thyroiditis)

[13, 58, 109] (Figs. 4.11–4.15, 4.36)

Three different stages of Hashimoto thyroiditis (HT) have been identified:

- *Early stage HT* (Fig. 4.15). Cytologic samples are mainly composed of mature lymphocytes. The number of follicular cells is variable and oncocytic features are rarely observed. The FNAB result is equivalent to Basedow (Graves) disease. The correct diagnosis can be achieved serologically with a high titer of antibodies against thyroid peroxidase and no evidence of elevated TSH-receptor antibodies [13].
- *Atrophic HT* presents with hypothyroidism and fibrosis. Aspiration yields sparse cellularity comprising leukocytes, fibroblasts, and follicular cells, occasionally with oncocytic features. FNAB is rarely performed in this stage of disease.
- *The hypertrophic or florid form of HT* (Figs. 4.11 and 4.12) yields aspirates with abundant cellularity.

**Microscopic Features of Florid HT**

- Hallmarks. Large numbers of mature lymphocytes, plasma cells, and lymphoid follicle center cells including starry sky cells.
  Considerable numbers of small and large regular sheets composed of oncocytes. Oncocytes (synonyms: Hürthle cells, oxyphilic cells) are large polygonal cells with well-defined borders and dense eosinophilic cytoplasmic granularity. The centrally placed nuclei are round and deeply stained, containing finely granular, evenly distributed chromatin and a prominent central nucleolus.
  Scant colloid.
- Activated mesenchymal cells, giant cells, and rare psammoma bodies may be interspersed.

**Differential Diagnosis** [99, 109] (Figs. 4.16–4.18)

- A pure lymphocyte population has to be differentiated from malignant lymphoma using immunocytochemical or molecular techniques in order to establish clonality of the lymphoid population (Fig. 4.16).
- A predominance of Hürthle cells may lead to a misdiagnosis of an oncocytic neoplasia, especially in HT cases presenting with irregular clustering of the oncocytes and increased cellular polymorphism (Figs. 4.17 and 4.18).

**Caution**

- Malignant lymphoma has to be excluded using adjuvant tests in all cases with aspirates presenting an ambiguous lymphoid pattern.
- Take account of the possible coexistence of Hashimoto thyroiditis and malignant lymphoma or thyroid carcinoma! [11, 74, 120]

#### 4.2.1.2.4 Focal Chronic Lymphocytic Thyroiditis

Focal lymphoid infiltrates may be encountered in association with various thyroid disorders:

- Thyroid hyperplasia.
- Thyroid malignancies.
- Autoimmune diseases (diabetes mellitus, pernicious anemia, and others).
- Iatrogenic hypothyroidism provoked by surgery, radioiodine therapy, or drug administration.

**Microscopic Features**

FNABs may exhibit varied numbers of lymphocytes with or without a substantial proportion of thyroid tissue.

#### 4.2.1.2.5 Chronic Fibrotic and Granulomatous Thyroiditis

##### Riedel Thyroiditis

Riedel thyroiditis [118] is a rare chronic fibrosing disorder of undetermined origin. Intense fibrosis and sclerosis destroy the thyroid parenchyma and spread into the adjacent soft tissue. Fine-needle aspirate is usually poor in cells and inadequate for selective diagnosis [67].

##### Chronic Granulomatous Thyroiditis

This inflammation is characterized by disseminated or confluent granulomas that may show degeneration and necrosis. In the first instance, the etiology of the lesion is tuberculotic or mycotic.

## 4.2.2 Thyroid Cysts [84, pp. 371–386]

### General Comments

Most of the thyroid cystic lesions are pseudocysts developed following degeneration, necrosis, and hemorrhage within the parenchyma. Large nodular or diffuse goiters are the most common disorders going along with cystic degeneration. Cystic changes may sonographically appear singly round and sharply outlined, or multifocal as hypoechogenic areas with indistinct borders and bizarrely shaped.

### Types of Cystic Lesions in the Thyroid Gland and their Microscopic Features

- *Simple cyst.*
- *Colloid cyst or colloid-filled giant follicle* (Fig. 4.19)
  - The aspirate is viscous. The smears exhibit abundant dense colloid, which is often cracked, forming a mosaic pattern. A few monolayer sheets composed of small cuboid follicular cells containing pyknotic nuclei can be detected in most cases. Sparse foam cells, if any.
- *Cysts in lymphocytic thyroiditis*
- *Cystic changes in goiters* (Fig. 4.20)
  - Cystic fluids from adenomatous goiters may be clear, translucent brown, or sanguineous. Smears show variable numbers of histiocytes, frequently with cytoplasmic hemosiderin pigment. Foreign-body giant cells and diverse inflammatory cells are variably present. Red-colored fluids of long-standing cysts contain cholesterol crystals, calcified particles, rarely psammoma bodies, small connective tissue fragments, and fibroblasts.
- *Cystic degeneration of neoplastic disorders*
  - Adenoma: Cystic fluids from benign tumorous lesions may be nonspecific or contain cells that may fit in with the background lesion.
  - Malignant disease: Cystic change in the group of malignant thyroid lesions is most frequently encountered in papillary carcinomas. False-negative tumor diagnosis is frequently due to low cellularity of the fluid, the absence of typical cellular features and cytoarchitecture, or pronounced cell degeneration (see Sect. 4.2.6.1.6, "Cystic Papillary Carcinoma," p. 346).

**Caution**

- Rapid enlargement of a thyroid nodule is in most cases caused by sudden intracystic hemorrhage.
- Successfully drained cysts may immediately refill with blood after fine-needle aspiration; this should not be regarded as a sign of malignancy.
- The cyst wall should always be checked sonographically before and after complete emptying of the cyst by aspiration, with regard to irregular outline, nodular protrusions, or luminal excrescences. These changes have to be punctured selectively (at first or secondary) under ultrasound guidance in order to exclude a small malignant neoplasm.
- Cystic changes in thyroid nodules, particularly in younger patients, are suggestive of papillary carcinoma; see Sect. 4.2.6.1.6, p. 346.

### Differential Diagnosis and Equivocal Findings

- The differential diagnosis includes thyroglossal duct cyst, branchial cleft cyst, and parathyroid cyst.
- Cystic formations originating in remnants of embryonic structures yield columnar and squamous cells, the latter of which are sometimes keratinized (Fig. 4.21). The background may disclose inflammation, squamous debris, and histiocytes.
- Epithelial cells in parathyroid cystic fluids are practically indistinguishable from thyroid follicular epithelium [2, 90]. Immunocytochemical confirmation of the cell type with an antibody against parathyroid hormone-related protein and measurement of parathyroid hormone concentration in the fluid is most helpful to differentiate parathyroid from a thyroidal cystic process [47, 143].
- Histiocytes in cystic fluid may be strongly activated, comprising pleomorphism of cytoplasm and nuclei, the latter exhibiting prominent nucleoli and coarse clumping chromatin. Grossly enlarged and degenerated follicular cells and atypical cyst-lining cells can mimic reactive histiocytes as described. Cellular changes may be pronounced in such a manner that misdiagnosis of malignancy is possible [43] (Fig. 4.22).
- Pseudocysts may partially be lined with metaplastic squamous cells (Fig. 4.21).

**Caution**

- Squamous cells may also occur as lining of pseudocysts in hyperplastic thyroid tissue.
- Regenerative and degenerative changes of both histiocytes and follicular epithelial cells in cystic fluids can lead to a false-positive diagnosis of cancer.

## 4.2.3 Hyperplastic Thyroid Lesions

### 4.2.3.1 Diffuse and Nodular Hyperplasia (Goiter)

[34] (Figs. 4.23–4.31)

#### Definition and Synonyms

- Clinically, the term "goiter" indicates any chronic enlargement of the thyroid gland caused by hormonal stimulation related to both various well-known factors (iodine deficiency, environmental goitrogens, and others) and unknown factors. Nodular goiter can mimic true thyroid neoplasia. For this reason, such lesions are frequently referred for FNAB as the most appropriate tool for quick and reliable diagnostic evaluation.
- Synonyms: Struma, nontoxic nodular goiter, multinodular goiter.

#### Microscopic Features

- Hallmarks: The smears are cellular and show a mixture of colloid and benign follicular cells. The latter occur isolated or in small sheets, but can also be grouped in large regular tissue fragments with or without micro- and mediofollicular pattern. The amount of epithelial fragments varies depending on the proliferative activity of the struma.
- Background-colloid appears as a crumpled or mosaic-like cracked film that is thin and lucid.
- Follicles incorporated into large tissue fragments retain their three-dimensional form and are composed of uniform cuboid cells; colloid is generally accumulated in their lumina.
- Papilliform and even papillary tissue fragments are observed in cytologic specimens from pronounced hyperplastic goitrous lesions.
- The cellular arrangement is regular, in both the monolayered honeycomb-like sheets and large tissue fragments. The nuclei are small with neat margins and they are regularly spaced. Chromatin is finely granular and evenly distributed. Enlarged but otherwise bland nuclei with centrally placed, pronounced nucleoli are observed in activated cells. The cytoplasm is distinct, pale and well defined.
- Goiter involution may yield numbers of stripped small pyknotic, dark-staining nuclei that mimic small mature lymphocytes.
- Focal Hürthle cell metaplasia is frequently present in goiters, cytologic description of oncocytes is provided in Sect. 4.2.1.2.3, "Chronic Lymphocytic Thyroiditis," p. 337.
- The following elements may be encountered as well, depending on stage and regressive changes in nodular goiters:
  - Large tissue fragments harboring stromal cells and areas of granulomatous and fibrous tissue (Fig. 4.24).
  - Degeneration of follicular cells: large vacuolated cytoplasm, hemosiderin inclusions, polymorphic nuclei comprising conspicuous nucleoli.
  - Recent and old hemorrhage, histiocytes, hemosiderophages, foreign body-type giant cells, calcification, sporadic psammoma bodies, inflammatory cell component.

**Caution**

- Hyperplastic papilliform and papillary tissue fragments should not be misinterpreted as originating from thyroid papillary carcinoma (Fig. 4.29). Take into consideration both the differing cytoarchitecture of papillae and the nuclear morphology in goiters compared to that in papillary carcinoma! Even so, cytology of reactive and degenerating follicular cells in goiters may overlap that of cancer cells (Figs. 4.30 and 4.31).
- Large numbers of single follicular cells with small, pyknotic, dark-staining nuclei should not be misinterpreted as lymphocytes leading to a misdiagnosis of lymphocytic thyroiditis.
- Occasional psammoma bodies scattered in the background of a smear without additional signs of a papillary neoplasia should be considered with caution in respect of their association with malignancy [29, 40,132]. The further procedure is different for each patient and has to be discussed with the clinicians (see also Sect. 4.2.6, "Other Microscopic Features," p. 344).
- Condensed and rounded colloid globes presenting with concentric lamination may look like psammoma bodies, but their color is akin to colloid masses in the same preparation. In contrast, psammoma bodies generally stain purple to deep-blue with the Papanicolaou method.

### 4.2.3.2 Hyperplasia in Line of Thyroid Hyperfunction (Figs. 4.32–4.36)

#### General Comments

- Morphologic changes are very similar in all forms of hyperthyroidism including toxic diffuse hyperplasia (Graves

disease), toxic adenoma, and primary hyperthyroidism. The diagnosis of hyperthyroidism is made on the basis of clinical symptoms and laboratory data.

- FNAB is generally not performed for diagnostic reasons but in order to exclude an accessory thyroid neoplasia.
- Cytomorphologic appearance, and in particular the cytoplasmic features, are suggestive of toxic goiter but not specific at all.

**Microscopic Features**

- Hallmark: Abundant pale and finely granular cytoplasm, fading away against the background due to marginal vacuoles. These vacuoles stain pink with the May-Grünwald-Giemsa method and contain granular material; as a result the periphery of the cells they look like fire flares (flare cells) [33, 111].
- In fine-needle aspirates, cellular material is scant to moderate.
- The follicular cells are dispersed or arranged in loose syncytial sheets, nuclei are widely spaced and follicular formations may possibly be supposed. Hürthle cells are an inconstant finding.
- Colloid rarely occurs if at all, as thin and pale slightly eosinophilic film.
- Activated nuclei are frequent; they are eccentrically positioned, showing variable shape and size and small nucleoli.
- Multinucleation, epithelioid granulomatous component, and focal lymphocytic infiltrates may be encountered.

**Differential Diagnosis** [4, 18, 45]

The following entities demonstrate overlapping cytologic features in FNAB samples:

- Thyroid hyperplasia versus adenomatous nodules, well-differentiated follicular carcinoma and papillary carcinoma.
- Toxic goiter with a large Hürthle cell population accompanied by a pronounced lymphoid infiltration versus Hashimoto thyroiditis.
- Involuted goiter with large numbers of degenerated follicular cells exhibiting small, deeply stained nuclei versus lymphocytic thyroiditis.
- Thyroid hyperplasia comprising a large number of degenerating follicular cells with nuclear pleomorphism should not be mistaken for carcinoma (Figs. 4.35 and 4.36). Spindle cells should not be misdiagnosed as anaplastic carcinoma or medullary carcinoma of the thyroid. The latter demonstrate immunocytochemical positivity for calcitonin.

**Caution**

- Differentiation between nonneoplastic hyperplastic thyroid nodules and follicular adenoma is rarely possible with cytology. The same is true of follicular adenoma and well-differentiated follicular carcinoma (see Sect. 4.2.4, below), and of the follicular variant of papillary carcinoma.
- Excision of the whole nodule followed by histologic examination is mandatory in order to obtain a definite diagnosis.

## 4.2.4 Follicular Neoplasia: Benign and Malignant

**General Comments**

- By definition, follicular adenoma is microscopically encapsulated and the surrounding thyroid parenchyma is compressed. This feature differentiates the true neoplasms from non-neoplastic hyperplastic nodules in goiters.
- Confusion and controversy exist over the histologic criteria that assess malignancy. Widely accepted criteria include capsular and/or vascular invasion (and of course metastases). However, capsular invasion ranges from minimal nibbling of the capsule to broad penetration of the full thickness of the capsule; therefore, interpretation and diagnosis of malignancy remains subjective.
- Benign and malignant thyroid tumors can cytologically masquerade as hyperplastic follicular lesions [8, 27, 51, 77, 78, 80, 86, 140]. The most important entities of this group include:
  - Follicular adenoma (see Sect. 4.2.4.1, p. 341).
  - Follicular carcinoma (see Sect. 4.2.4.4, p. 342).
  - Follicular variant of papillary carcinoma (see Sect. 4.2.6.1.1, p. 345).

**Proposed Diagnostic Procedure and Additional Analyses**

At our institution, the diagnosis of follicular neoplasia is rendered if an FNAB specimen is composed of:

- High cellularity.
- Microfollicular features.
- Lack of colloid.
- No or marginal nuclear atypia. Cytologic criteria of cellular atypia are indeterminate and debatable in this setting.

- Any diagnosis of follicular neoplasm results in quantitative DNA (DNA ploidy) assessment by means of digital image analysis. The results on our own FNAB material have shown that follicular neoplasms with a nondiploid DNA distribution pattern of any type are more frequently associated with malignancy than diploid tumors. Several authors have emphasized that DNA aneuploidy is strongly

indicative for malignancy or should at least be considered as being premalignant. Therefore, preoperative assessment of DNA ploidy on fine-needle aspirates was accepted by our endocrinologists and surgeons to be of practical value as a decisive procedure for surgical intervention, immediately after its implementation in diagnostics.
It should once more be pointed out that the DNA pattern alone permits neither assessment nor exclusion of malignancy. Still, DNA aneuploidy seems to be more frequently associated with tumor invasion and generally excludes nonneoplastic thyroid hyperplasia. Details and references are provided in Sect. 4.1.4, "DNA ploidy," p. 328.

- Promising results have also been reported in order to distinguish between varied follicular thyroid lesions using morphometric parameters [36, 68, 150].

#### 4.2.4.1 Conventional Adenomas

Unusual variants of follicular adenoma are not described in this section. More information may be obtained from individual publications and distinguished textbooks [84].

##### 4.2.4.1.1 Colloid Adenoma

Colloid adenoma is cytologically identical to macrofollicular areas in a goiter, except for encapsulation (only identifiable on histologic sections!). Malignancy is rarely if ever observed.

##### 4.2.4.1.2 Simple (Follicular) Adenoma

Simple adenoma is composed of well-developed follicles as seen in normal thyroid glands and nodular goiters; it additionally exhibits microfollicular areas. The lesion may usually be interpreted as nodular goiter or follicular adenoma by cytology.

##### 4.2.4.1.3 Microfollicular Adenoma

(Figs. 4.37 and 4.38)
The aspirates of microfollicular adenoma present a cell pattern that is difficult to distinguish from well-differentiated follicular carcinoma. Overlap of cytologic features of benign and malignant neoplastic disease is strong, an issue which is repeatedly discussed in Chap. 4 (Fig. 4.41).

In accordance with the varying histologic architecture, aspirates of trabecular and solid tumor areas may yield nests and trabeculae of follicular cells lacking a microfollicular pattern.

- Cytologic hallmarks: Abundance of monomorphic follicle cells occurring singly, in loose clusters, or in three-dimensional arrangement.
  Microfollicles are more or less distinct. The majority of the follicles are empty, but a few of them contain pale staining colloid.
  The nuclei are round to oval and smooth. They show a slight increase in size compared with nonneoplastic follicle cells. Granular chromatin is evenly distributed. The nucleoli are small, round, and not consistent.
  The cytoplasm is variable in size and pale. Background colloid is absent.
- Minor variations in nuclear size, a certain loss of nuclear polarity, and focal nuclear crowding and overlapping may be classified as atypical.

**Caution**

- Distinguishing between follicular adenoma and well-differentiated follicular carcinoma, and follicular variant of papillary carcinoma is rarely possible by cytology.
- Follicular adenoma may present with papillary hyperplasia mostly together with cyst formation. This follicular tumor variant is considered to be more frequent in young adolescents [95]. Exact interpretation of cellular and nuclear details can prevent misinterpretation as papillary carcinoma.

#### 4.2.4.2 Hyalinizing Trabecular Adenoma

[3, 21, 87]

Hyalinizing trabecular adenoma is an uncommon subtype of thyroid adenomas. The tumor generally behaves in a benign fashion.

**Microscopic Features and Differential Diagnosis**

- The cells are isolated or grouped in loose aggregates and syncytial clusters. They are oval to spindle-shaped and frequently radially oriented surrounding a central hyaline core.
- The cytoplasm is huge and elongated, containing round, pale inclusion bodies.
- The nuclei are oval to spindle-shaped and mildly pleomorphic. Nuclear longitudinal grooves and cytoplasmic nuclear inclusions are distinct and frequently observed.
- The chromatin is thinly dispersed.
- The nucleoli are small and inconspicuous.
- Hyaline background material is usually present.

Hyalinized trabecular adenomas are frequently diagnosed as papillary or medullary carcinoma because of mutual cytologic features. The cells stain immunocytochemically positive for thyroglobulin and TTF-1 but negative for calcitonin and consequently medullary carcinoma can be excluded based on its opposite immunoprofile; but papillary carcinoma cannot be differentiated by immunocytochemistry.

#### 4.2.4.3 Atypical Adenoma (Fig. 4.39)

Atypical adenoma is a highly cellular tumor with microfollicular, trabecular, and solid architecture. The cells are pleomorphic and spindle-shaped with bizarre nuclei and mitotic activity. In spite of distinct cellular atypias, the lesion is histologically completely encapsulated and lacks invasive features.

**Microscopic Features and Differential Diagnosis**

- Aspirates demonstrate marked cellularity.
- Syncytial cellular aggregates forming empty microfollicles are loose or crowded, and exhibit areas with marked cellular overlapping.
- The nuclei are polymorphous and their membranes show bizarre indentations and folds.
- Large nucleoli.
- Irregular chromatin distribution and hyperchromasia.

The cytological pattern often presents diagnostic dilemmas, possibly leading to an erroneous diagnosis of follicular carcinoma.

### 4.2.4.4 Follicular Carcinoma [136]

**General Comments**

- Definition: A malignant epithelial tumor with clear evidence of follicular differentiation, lacking pathognomonic cellular features of other thyroid malignancies.
- The frequency of follicular carcinoma among thyroid malignancies ranges from 5 to 15%. A high incidence is reported in iodine-deficient areas, where follicular carcinoma accounts for 40% of all thyroid cancers. They occur frequently in middle-aged and older age groups.
- Follicular carcinoma metastasizes rarely to cervical lymph nodes, contrary to papillary carcinoma. Distant metastases are commonly observed in bones and lung. The prognosis is less favorable in comparison to papillary carcinomas.

**Classification**

Classification may be based on tumor differentiation (suitable for cytologic diagnostic procedure) or on the extent of invasion (a useful feature for the histopathologic evaluation). The majority of well-differentiated tumors go along with minimally invasive growth. Carcinomas with a worse differentiation show extensive areas of invasion in most cases.

#### 4.2.4.4.1 Well-Differentiated Follicular Carcinomas (Figs. 4.40 and 4.41)

These tumors exhibit a micro-, normo-, or macrofollicular pattern admixed with trabecular and solid areas and roughly resemble their benign counterparts. This carcinoma subtype is usually minimally invasive. Their differential diagnostic properties and cytologic features have been discussed in the introduction to Sect. 4.2.4, p. 340, and in Sect. 4.2.4.1.3, "Microfollicular Adenoma," p. 341.

#### 4.2.4.4.2 Poorly Differentiated Follicular Carcinomas (Fig. 4.42)

These tumors show a follicular architecture including clear cellular features of malignancy. Distinguishing between poorly differentiated follicular carcinoma and atypical adenoma is very difficult with cytology (see also Sect. 4.2.4.3, p. 342).

**Microscopic Features**

- Aspirates are cellular.
- The syncytial tissue fragments are loose or dense comprising irregularly formed follicles.
- Colloid is infrequently observed in the follicular lumina.
- Nuclear crowding and overlapping is variably pronounced in different areas of the cytologic smear. The nuclear size is increased and variable. The nuclei are round, wrinkled, or folded.
- The chromatin is coarse granular and irregularly distributed. Distinct hyperchromasia.
- Nucleoli are always present and vary in size.
- Background colloid is sparse.
- Necrosis is common.

#### 4.2.4.4.3 Insular Carcinoma [20, 60, 124, 136, 146]

This term has been proposed for a morphologically distinctive form of poorly differentiated thyroid carcinoma arising from follicular cells. It is suggested that this tumor type is an intermediate form between follicular/papillary carcinoma and anaplastic carcinoma [20, 136].

**Microscopic Features**

- The tumor exhibits predominantly single cells. A variable degree of cellular polymorphism, microfollicular and papillary cell arrangement, and necrosis occurs.

## 4.2.5 Oncocytic Neoplasia [39, 84, 110, 158]

Synonyms: Oncocytes are also called Hürthle cells , oxyphil cells, or Askanazy cells.

**General Comments**

- Oncocytes are altered follicular cells. Alteration (in the sense of metaplasia) occurs not only in carcinomas of the follicular and papillary type, but also in adenomas, adenomatous goiters, Hashimoto thyroiditis, Graves disease, and in other disorders affecting the thyroid gland.
- Oncocytic tumors account for 5% of all thyroid tumors. The biological behavior of oncocytic tumors seems to be

more aggressive than differentiated follicular cell tumors, especially in males and older patients [52, 56, 127, 158].

- Distinction of benign from malignant oncocytes, and benign from malignant oncocytic neoplasms (Figs. 4.43 and 4.44) may be difficult. Benign and malignant tumors usually appear distinctly monomorphic in cytologic smears; but many oncocytic carcinomas exhibit cytologic features that lead to a definite malignant diagnosis or being at least suggestive of malignancy.
- An increase in the malignant potential in tumors with oncocytic features may also be supported by the results of DNA ploidy assessment: the aneuploidy rate seems to be higher in oxyphilic adenoma and low-grade oncocytic carcinoma compared to their nonoxyphilic counterparts. A few papers suggest a significant association between aneuploidy and histologic malignancy of oxyphilic neoplasia (for more information and references, see Sect. 4.1.4, "DNA Ploidy," p. 328).

### Microscopic Features

- *The oncocyte*
  - Oncocytes are large polygonal cells with abundant granular cytoplasm and well-defined margins. Granularity is the result of an accumulation of abundant mitochondria.
  - The cytoplasmic body is either packed with clearly distinguishable granules, or extremely dense in structure; staining is eosinophilic, cyanophilic, or amphophilic with the Papanicolaou method.
  - The nucleus is large and round, occurring in a central or eccentric position.
  - The nucleoli are prominent and red in color.
- *Oncocytic adenoma* (Fig. 4.43)
  - Single cells and loosely cohesive cell groups occasionally embodying follicles. Typical oxyphil cells having a low N/C ratio.
  - The nuclei are round, smooth, and uniform in size; they contain a single round nucleolus.
  - Finely granular chromatin pattern.
  - Individual large oxyphil cells with deep-staining polymorphous nuclei should not mislead to diagnosis of malignancy.
  - The presence of colloid and lymphocytes favors a benign lesion.
- *Oncocytic carcinoma (synonym: oncocytic variant of follicular carcinoma)* [131] (Figs. 4.44–4.46)
  - Large numbers of isolated cells and syncytial-type tissue fragments with areas of nuclear crowding. The cells are smaller compared with those of adenomatous lesions and have an increased N/C ratio.
  - Variation in nuclear size and shape is distinct.
  - Macronucleoli are frequently multiple and may exhibit irregular shapes.
  - Occasional psammoma bodies and cellular debris.
  - No colloid.
  - A papillary growth pattern may be observed, but the nuclei are devoid of ground-glass structure and grooves; the latter are a key feature for the diagnosis of papillary carcinomas. The presence of psammoma bodies is on its own not diagnostic for papillary carcinoma with oncocytic transformation [14].

### Differential Diagnosis

- Differential diagnoses include nodular goiter with oncocytic metaplasia, Hashimoto thyroiditis, Graves disease, and papillary and medullary carcinoma.
- Transgressing vessels and intracytoplasmic vacuoles have sporadically been reported as useful criteria to separate nonneoplastic from neoplastic oncocytic lesions [161].
- The oncocytic varieties of parathyroid tumors can be distinguished from thyroidal Hürthle cell lesions solely by immunocytochemical tests.

**Caution**

- Gross enlargement and pleomorphism of oncocytes in thyroid aspirates should not lead to a false-positive diagnosis of malignancy. Oncocytes from Hashimoto thyroiditis may display much greater pleomorphism as compared with oncocytic tumor cells.
- A particular monomorphic cell pattern is a key feature for a neoplastic oncocytic lesion.
- Distinguishing between oncocytic parathyroid lesions and oncocytic thyroid lesions is only possible using immunocytochemistry.

## 4.2.6 Papillary Thyroid Carcinoma

[128, 136] (Figs. 4.47–4.52)

### General Comments

- Papillary carcinoma is the most common subtype of thyroid carcinoma occurring more commonly in women than in men. The tumor is frequently diagnosed in adolescents and young females.
- The tumor has a predilection to multicentricity, uni- or bilaterality, and lymphatic dissemination. Regional cervical lymph node metastases have been reported in more than 50% of all tumor patients at the time of surgery. Distant metastases are observed in approximately 10% of the cases.
- The overall long-term survival of patients with papillary carcinoma is excellent [102].
- There exists a repeatedly documented association between irradiation of the neck and development of subsequent thyroid papillary carcinoma [16, 69]. If radiation has been applied during childhood, an interval of up to 20 years until development of malignancy has been observed. However, administration of high-dose radiation to

the neck area may give rise to tumor development shortly after completion of the therapy.

- CK19 and CD44 immunostaining has been reported to be valuable on FNAB samples in the differentiation between thyroid papillary carcinoma and other lesions of the thyroid exhibiting overlapping cytologic features (e.g., nuclear grooves and inclusions) [25, 107].
- Additional molecular genetics such as *BRAF and RAS mutational analysis or RET/PTC* and *PAX8/PPAR* rearrangement tests might be useful in cases with an indeterminate cytology [28A, 110A].

### Microscopic Features

Key features: Three morphologic features are pathognomonic for papillary carcinoma: papillae, monolayer sheets, and nuclear characteristic:

- Papillary formations can vary greatly in size and may show various degrees of architectural complexity. The vascular component within the fibrous core is prominent; capillaries are frequently dilated and filled with red blood cells. Branched papillary fragments are lined with multiple layers of tumor cells in loose or dense syncytial arrangements.
- Cells have a cuboidal or columnar shape. Nuclei are palisaded at the periphery and show pronounced overlapping.
- Monolayered cohesive sheets of enlarged thyrocytes perfectly visualize the diagnostically important nuclear features.
- The nuclei are round to oval, normo-, or even hypochromatic.
  - The usually irregular nuclear contour is caused by grooves and longitudinal folds. Grooves are best identified on Pap-stained smears. However, sporadic nuclear grooves are observed in nonpapillary carcinoma lesions as well [144, 148]. Yang and Demirci propose a semiquantitative approach that may help to improve the diagnostic relevance of nuclear grooves for papillary thyroid carcinoma lacking other nuclear characteristics [160].
  - Nuclear cytoplasmic invaginations presenting as sharply outlined intranuclear inclusions are common. Nuclear inclusion is not specific and encountered in primary neoplastic and nonneoplastic lesions of the thyroid as well as in secondary tumors. Nuclear inclusions may also be observed in adenoma, follicular neoplasms, oncocytic carcinoma, medullary carcinoma, anaplastic carcinoma, and metastases of breast carcinoma, renal cell carcinoma, pulmonary adenocarcinoma, among others [14, 54, 92].
  - The chromatin is finely granular or dusty. Ground-glass appearance of the nucleus – a hallmark in histologic sections – may rarely be articulate in cytologic preparations.
  - The nucleolus is small.

In summary, the following four nuclear features are definitely of high value for the diagnosis of papillary carcinoma: light-colored nuclei, multiple nuclear grooves, intranuclear cytoplasmic inclusions, and small nucleoli.

Other microscopic features:

- Cellularity: Aspirates are highly cellular and they contain scant colloid. Isolated tumor cells occasionally occur. Cells are larger than those in hyperplastic follicular lesions.
- Cytoplasm: The cytoplasm is generally polygonal and wide and its structure varies from dense and homogeneous (squamoid appearance) to granular (oncocytoid) and vacuolated (mainly in cystic tumor variant). The nucleus is centrally placed.
- Psammoma bodies: Psammoma bodies – calcified concentrically laminated structures – may be identified. Psammoma bodies are a highly characteristic feature but not specific for papillary carcinoma; they may also be encountered in benign hyperplastic thyroid lesions [40, 132] and in lymphocytic or Hashimoto thyroiditis [38]. However, we must refer to a report by Hunt and Barnes, who identified 27 of 29 patients with "non-tumor associated" psammoma bodies who finally had a tumor in their thyroid gland or in perithyroidal lymph nodes; most of these tumors appeared to be of the papillary variant [72].
- Colloid: Colloid is absent in the majority of cases or is scant with a characteristic appearance. It is viscous and may exhibit a peculiar smearing effect like bubblegum, which is best seen in May-Grünwald-Giemsa stain.
- Foamy/vacuolated histiocytes and multinucleated giant cells may be numerous, particularly in cystic forms of the tumor.
- Lymphocytes may be present. Nuclear characteristics of the epithelial tumor cells should prevent confusion with Hashimoto thyroiditis.

### Differential Diagnosis

- Rare single tumor cells from papillary carcinomas encountered in direct smears or in cystic fluid aspirates may be mistaken for activated histiocytes, due to nuclear shape, structure, color, and cytoplasmic vacuolation. Still, a focus on sporadic squamoid cytoplasmic features and distinct nuclear characteristics suggests papillary cancer.
- Mutual existence of cellular features in both papillary and nonpapillary thyroid disorders and nonthyroid neoplasms have been discussed above in "Microscopic Features."
- Immunoreactivity for typical cellular/tissue antigens should indicate the correct nature of the cells, distinguishing between primary thyroid lesions and nonthyroid lesions.

**Caution**

Architectural and cellular hallmarks of papillary carcinoma may be found only focally in the smear or only on individual cells. The cytologic criteria must be searched for systematically in cases suggestive of papillary neoplasm but lacking unequivocal morphologic features by routine screening.

**Caution**

In FNA specimens, papillary carcinoma with a pure or predominantly follicular pattern often yields a diagnosis of follicular neoplasm, unless the cytologic hallmarks are systematically searched for by meticulous screening.

### 4.2.6.1 Variants of Papillary Carcinoma

[61, 84 (pp. 148–176), 91]

**General Comments**

- Several histologic subtypes of papillary carcinoma have been described [136]. All variants disclose the same pathognomonic nuclear features with the exception of the columnar cell variant. That is, nearly all papillary thyroid tumors are cytologically recognized and should be referred to thyroidectomy regardless of their correct morphologic classification.
- Some of the tumor variants that are easily recognized by histology cannot be identified in cytologic samples; but again, they represent cytomorphologic characteristics of common papillary carcinoma:
  - Papillary microcarcinoma [123].
  - Encapsulated papillary carcinoma.
  - Papillary carcinoma with distinct stromal properties (diffuse sclerosis, fasciitis-like stroma).
  - Solid and trabecular variant of papillary carcinoma.
  - Diffuse follicular variant of papillary carcinoma.
- The term "occult papillary (micro)carcinoma" is used for tumors with regional lymph node metastases in the absence of a palpable tumor in the thyroid gland.

#### 4.2.6.1.1 Follicular Variant

[6, 49, 65, 96, 103, 126, 159] (Fig. 4.53)

**General Comments and Microscopic Features**

The follicular variant comprises roughly 12% of all thyroid papillary carcinomas.

- This tumor entity shows predominantly or exclusively a follicular architecture. The follicles are small or medium-sized and filled with colloid that may be thick and abundant.
- The characteristic cellular features of papillary carcinoma together with lack of a papillary pattern, follicular cell arrangement, dense colloid, and a large number of histiocytes are the strongest signs for the diagnosis of the follicular subtype of papillary carcinoma.
- On the other hand, chromatin clearing, nuclear grooves, and syncytial clusters exclude other thyroid lesions.

**Differential Diagnosis**

Absence of tumor-typical cell features in large tumor areas, privileged presence of macrofollicles, and abundant colloid can lead to a false cytologic diagnosis of goiter [26].

#### 4.2.6.1.2 Tall Cell Variant

[42, 50, 66, 79]

**General Comments and Microscopic Features**

The tall cell variant comprises about 10% of the thyroid papillary carcinoma. The biological behavior is more aggressive with a high incidence of regional lymph node involvement and distant metastases.

- The tumor is composed of large cells of polygonal to columnar shape.
- The abundant cytoplasm is dense, shows sharply defined margins and either cyanophilic or eosinophilic staining. The cells should not be misinterpreted as oncocytes.
- Papillary fronds and lymphoid infiltrates may be present.
- Nuclear details and additional characteristic features should permit a diagnosis of papillary carcinoma.

**Differential Diagnosis**

- Pronounced oncocytoid cell features give rise to suspicion of the oxyphilic cell variant of papillary carcinoma.
- The lymphoid infiltrates may mimic Hashimoto disease.
- Metastasis of a breast carcinoma subtype can closely mimic the tall cell variant of thyroid cancer due to the overlapping nuclear features (see Sect. 4.2.11.1.2, p. 350) [17, 42, 149].

#### 4.2.6.1.3 Columnar Cell Variant

[71, 75, 122, 162]

**General Comments and Microscopic Features**

This variant of thyroid papillary carcinoma is extremely rare; the tumor is known to have a poor prognosis.

- Complete lack of nuclear grooves and intranuclear cytoplasmic inclusions!
- Cells are grouped in syncytial tissue fragments occasionally showing a papillary configuration; true papillae show fibrovascular cores.
- The cells are monomorphic with palisade arrangement.
- The nuclei are elongated, overlapping, and pseudostratified.
- Chromatin is described as finely granular, or dusty, and nucleoli as small or inconspicuous.
- The cytoplasm is pale and clear.

**Differential Diagnosis**

- The tall cell variant can be distinguished from columnar cell variant of papillary carcinoma. The former shows dense cytoplasm, lack of nuclear pseudostratification and typical nuclear features.

- Difficulties in differentiating columnar cell papillary carcinoma from metastatic adenocarcinoma are emphasized by Jayaram and contributors [75].

**Caution**

- The columnar cell variant of papillary carcinoma is the sole papillary tumor variant of the thyroid with absence of the characteristic nuclear grooves and cytoplasmic inclusions.
- Furthermore, the tumor cells demonstrate negative immunoreactivity for thyroglobulin.

#### 4.2.6.1.4 Oncocytic Variant

[9, 37, 100, 154] (Fig. 4.54)

**General Comments and Microscopic Features**

The oncocytic variant of papillary carcinoma is uncommon and seems frequently to be associated with the tall cell variant. The aggressive behavior appears to be intermediate between that of conventional papillary carcinoma and oncocytic carcinoma.

- Cytologic samples present a pure oncocytic population.
- The cells are large and variable in size, occurring in loose groups and syncytial fragments; papillary fronds are common.
- The nuclei are eccentrically placed, their chromatin is dense and granular. Nuclear grooves and nuclear cytoplasmic inclusions are variably present. Nucleoli are prominent and centrally located.
- The cytoplasm is abundant and granular.
- Psammoma bodies are rarely encountered.

**Differential Diagnosis**

- The cytoplasmic features of papillary tall cell variant are very similar in comparison to those of the oxyphilic variant of papillary carcinoma. Both subtypes occasionally occur together [100].
- Nuclear inclusions are also observed in nonpapillary oncocytic tumors. That is, they are of poor differential diagnostic value in distinguishing papillary from nonpapillary oxyphilic neoplasia.
- A pronounced lymphoplasmacytic background together with an epithelial cell population lacking typical nuclear features of papillary carcinoma may lead to a misdiagnosis of Hashimoto thyroiditis.

#### 4.2.6.1.5 Papillary Carcinoma with Clear Cell Change

**General Comments and Microscopic Features**

Clear cell change has been considered as a rare morphologic variant of thyroid papillary carcinoma [136]. A few reports emphasize that clear cell change also occurs in follicular carcinoma [108, 135] and adenoma of the thyroid [113].

- Cells in cytologic samples are characterized by poorly defined cell borders and frequently stripped nuclei, which are enlarged and present the typical features of papillary carcinoma. The cytoplasm is barely visible.

**Differential Diagnosis**

An overall pattern of single cells may lead to a misdiagnosis of thyroid medullary carcinoma, but it can also mimic mesenchymal lesions and metastatic tumors. Clear cell areas of thyroid neoplasms may not react with thyroglobulin on immunocytochemical work-up [135].

#### 4.2.6.1.6 Cystic Papillary Carcinoma

[22, 43, 84, p. 171, 156] (Figs. 4.55 and 4.56)

**Interpretation Problems**

Aspirates from thyroid lesions with marked cystic changes are generally difficult to interpret:

- The aspirated fluid is often of low cellularity and inadequate for cytologic interpretation.
- Distinguishing between sporadic and degenerating papillary tumor cells and activated histiocytes is challenging.
- Inflammatory background, debris, and hemorrhage may obscure morphologic features of individual tumor cells. Nonthyroid lesions such as branchial-cleft cysts or metastases of squamous cell carcinoma should always be included in the diagnostic consideration.
- Cyst-lining cells (Fig. 4.57) may disclose regenerative atypia comprising pleomorphic and elongated cytoplasm, densely structured and squamoid cytoplasmic features, and distinct nucleoli. However, the crucial nuclear criteria typical of papillary thyroid cancer are absent in nontumorous atypical cells.

**Caution**

- Papillary carcinoma with cystic degeneration can pose major problems in a proper diagnosis. Aspirates may be composed of foamy macrophages, lymphocytes, and few or no tumor cells at all.
- Isolated histiocytoid tumor cells lacking nuclear grooves and inclusions may easily be misinterpreted as reactive or degenerating histiocytes [130].
- On the other hand, histiocytic aggregates in aspirates from goiters and nonpapillary cystic neoplasms can mimic papillary thyroid carcinoma [106].
- Immunostaining for thyroglobulin, TTF-1, and CD68 may at least be helpful in separating cells of thyroidal origin from those of histiocytic origin.

## 4.2.7 Medullary Carcinoma

[12, 35, 85,117, 151] (Figs. 4.58–4.61)

### General Comments

- Medullary carcinoma arises from the calcitonin-producing cells of the thyroid gland. The cells are called C-cells, clear cells, or parafollicular cells. The biological behavior of medullary carcinoma is more aggressive than the differentiated follicular thyroid cancers.
- The incidence of medullary carcinoma is reported at roughly 10% of all thyroid carcinomas.
- The tumor can occur sporadically or is genetically transmitted. The latter comprises up to 30% of all medullary carcinomas and can appear as an isolated lesion or associated with other endocrine tumors, often in the context of multiple endocrine neoplasia (MEN) syndrome.
- Medullary carcinoma is characterized by high levels of serum calcitonin.
- Corresponding calcitonin expression in the cytoplasm of tumor cells, demonstrated by immunocytochemical staining, is an important diagnostic tool for the pathomorphologic tumor typing. An immunocytochemically positive reaction is specific and reliable on cytologic specimens; even so, cases with negative immunoreactivity for calcitonin have been reported [12, 15, 35].

**Caution**

Calcitonin positivity by immunocytochemistry may occasionally occur in cells of benign and tumorous parathyroid lesions [30]

### Microscopic Features

- Hallmarks: Abundant isolated cells that show marked variation in size and shape and granular cytoplasm. Plasmacytoid cell appearance and cytoplasmic processes are most helpful to achieve a correct diagnosis. Amyloid may be observed between the cells as acellular, cloudy material.
- The pattern of medullary carcinoma varies widely in cytologic specimens. The most common tumor variant is characterized by polygonal and fusiform cells. The overall cell pattern may be polymorphic, disclosing a mixture of tumor cells of different shapes and sizes, or monomorphic comprising only one cell type.
- Groups of loosely arranged cells are observed beside the isolated tumor cells. Dense clusters are rarely seen. Papillary and follicular patterns are not present.
- Nuclei in tumor cells of medullary carcinoma are always eccentrically positioned. Extreme nuclear bordering yields a plasmacytoid aspect to the cells. Nuclei appearing round to oval in polyhedral cells and spindle-shaped in combination with elongated cytoplasm. Bi- and multinucleation are frequently observed.
- Intranuclear cytoplasmic inclusions are frequent.
- The presence of nucleoli is not consistent.
- The chromatin is coarse and scattered throughout the nucleus.
- The cytoplasm is moderately dense and frequently contains small granules best seen in air-dried smears stained according to the Romanowsky method. One or multiple cytoplasmic processes may be present in cells displaying fusiform, large polyhedral, and triangular cytoplasm.
- Dense acellular and cloudy material in the background, occasionally associated with mesenchymal cells, is a characteristic feature of medullary carcinoma representing amyloid. Amyloid has similar staining qualities as compared to colloid in Pap-stained smears, but it demonstrates characteristic bottle-green birefringence under polarized light after staining with Congo red.

### Differential Diagnosis [46].

- A monomorphic cell pattern (Fig. 4.60) may be mistaken for the follicular variant of thyroid carcinoma or for adenoma or – together with distinct cytoplasmic granularity and large nucleoli – for oncocytic carcinoma.
- Spindle cell pattern (Fig. 4.61):
  - Spindle-cell papillary thyroid carcinoma lacking typical nuclear features can be indistinguishable from medullary carcinoma. Intranuclear cytoplasmic inclusions are observed in both tumor types and are not helpful in differentiating the two entities.
  - Spindle cell patterns comprising pleomorphic nuclei are difficult to assign to the medullary or anaplastic type of thyroid carcinoma [129], or to spindle cell malignant melanoma. Again, nuclear inclusions may be observed in cells of any tumor entity.
  - Extremely proliferating mesenchymal cells from granulation tissue may disclose nuclear and cytoplasmic pleomorphism including large nucleoli and prominent coarse chromatin texture. Misdiagnosis of medullary (or anaplastic) carcinoma is possible. But benign atypical fibroblasts/histiocytes differ from malignant spindle cells in the low N/C ratio, loose chromatin arrangement, and the few pleomorphic nucleoli [84, p. 387–403] (Fig. 4.62A).
- Amyloid deposits that involve the thyroid gland in systemic amyloidosis [116] can potentially be misinterpreted as a diagnostic element of medullary carcinoma [64, 76] (Fig. 4.62).

**Caution**

Diagnosis of medullary carcinoma is ultimately based on both demonstration of intracytoplasmic calcitonin storage by immunocytochemical tests and elevated serum calcitonin levels.

## 4.2.8 Anaplastic Carcinoma

[23, 59, 98, 152] (Figs. 4.63–4.66)

### General Comments

- Anaplastic carcinoma comprises 5–15% of all thyroid carcinomas.
- It is a highly aggressive tumor in an older age group of patients generally appearing in the seventh decade of life. The tumors behave both in a locally invasive manner and spreading to distant sites.
- Many patients have a previous history of thyroid enlargement due to a benign hyperplastic process or a benign or a malignant thyroid tumor [19]. Anaplastic carcinoma is a rapidly growing tumorous disorder often having a negative effect on the function of the esophagus, trachea, and larynx.

### Microscopic Features

Hallmarks:

- A pure form of spindle cell tumors may occur, but most tumors showing a mixture of fusiform, polygonal, rounded, and giant cells.
- The aspirates are cellular and exhibit pleomorphic neoplastic cells in a background of necrosis and blood. Most of the tumor cells are dispersed, but loose grouping and dense clustering may also occur.
- Malignant cells of any type show extreme pleomorphism in size and shape. Polygonal cells can be small to large and are occasionally multinucleated.
- Nuclei show highly irregular contours, irregularly distributed bizarre chromatin clumps, and multiple irregular nucleoli. Nuclear lobulation and cytoplasmic inclusions also appear. Mitoses are present.
- The cytoplasm is usually abundant and dense but sometimes vacuolated. Cells with extremely dense cytoplasmic bodies and sharply outlined cell borders share features with malignant squamous cells.
- Multinucleated osteoclast-like giant cells may be observed [10, 88].
- The inflammatory background is variable and may be combined with neutrophilic cannibalism in cancer cells.
- In a small number of anaplastic carcinomas, areas of differentiated thyroid carcinoma may be detected.

### Differential Diagnosis [152]

- Fusiform cell pattern (Fig. 4.65):
  - Extremely proliferating mesenchymal cells originating from granulation tissue and regressive histiocytes may disclose nuclear and cytoplasmic pleomorphism including large nucleoli and prominent coarse chromatin texture. Misdiagnosis of undifferentiated carcinoma NOS or medullary thyroid carcinoma is possible. The benign atypical fibroblasts/histiocytes, however, differ from malignant spindle cells in the low N/C ratio, loose chromatin arrangement, and less pleomorphic nucleoli [84, pp. 387–403].
  - Spindle cell medullary carcinoma with marked pleomorphism may simulate anaplastic carcinoma. Intranuclear cytoplasmic inclusions are observed in both tumor types and are not helpful in the differential diagnosis.
  - Other tumors with fusiform cells arrayed in fascicles comprise fibrosarcoma, hemangiopericytoma, and angiosarcoma.
- Polygonal/ round cell pattern (Fig. 4.66):
  - Malignant lymphoma of the blastic type and poorly differentiated carcinoma of varied origin may masquerade as anaplastic thyroid carcinoma. Immunocytochemical studies are helpful in identifying malignant lymphoma, which are CD45-positive and thyroglobulin-negative (and vice-versa).
  - Severe atypias of follicular thyroid cells caused by radioiodine therapy and irradiation can lead to a false diagnosis of anaplastic cancer.
- Mixed cell pattern:
  A mixed cell pattern composed of fusiform and polyhedral tumor cells can be misinterpreted as squamous cell carcinoma, malignant fibrohistiocytoma, angiosarcoma, or malignant hemangioendothelioma [98]. Resemblance may be striking in cases exhibiting additional inflammatory infiltrates.

**Caution**

- Cytologic features of anaplastic thyroid carcinoma are highly specific. A correct diagnosis is possible in most of the cases unless sampling provides inadequate material.
- Bear in mind particularly the following look-alikes:
  - Severe changes on mesenchymal/histiocytic cells due to proliferation and regression.
  - Malignant lymphoma of the large-cell type.
  - Changes in thyroid cells due to radioiodine ablation and radiation therapy.
- A small percentage of the anaplastic thyroid cancers is well known for being negative for all immunomarkers [145].

## 4.2.9 Uncommon Thyroid Neoplasms

Clear cell, squamous, mucinous, and mucoepidermoid features may occasionally be observed in otherwise typical thyroid neoplasms. Bear in mind that true primary thyroidal mucinous, squamous, or mucoepidermoid cancers are exceptionally rare. A few reports present cytologic pictures of selected neoplastic entities of epithelial [63, 89, 155] or mesenchymal origin [70, 82, 125, 163]. For rare neoplastic disorders of the thyroid, we also refer to distinguished cytologic textbooks [84] and to the histologic literature [32, 136].

## 4.2.10 Malignant Lymphoma

[7, 28, 101, 121, 141]

### General Comments

- Malignant lymphoma with primary involvement of the thyroid is considered to be rare. The incidence reported in the literature varies from 1% up to 10% [28, 141] with a preponderance in females. Systemic malignant lymphoma affecting the thyroid gland must be excluded in each case.
- On large histologic series, Pedersen and Pedersen [121] reported a considerable preponderance of high-grade lymphoma (83% high-grade versus 17% low-grade lymphomas), almost exclusively of the B-cell phenotype (98%).
- Primary thyroid high-grade lymphomas appear to evolve from low-grade B-cell lymphoma of the MALT type (marginal-zone B-cell lymphoma of mucosa-associated lymphoid tissue); Hashimoto thyroiditis seems to play an important role in the etiology of primary thyroid lymphoma [5, 73, 121]. More than the half of primary thyroid lymphomas are assumed to be preceded by Hashimoto thyroiditis.
- Other lymphoma types than those of non-Hodgkin B-cell lineage have been reported sporadically: T-cell lymphoma [105] and primary thyroid Hodgkin disease [153].

**Caution**

Thyroid lesions in patients with a history of radiation exposure or radiotherapeutic intervention to the neck area are likely to turn out to be papillary carcinoma or less frequently malignant lymphoma.

### Differential Diagnosis

- MALT lymphoma usually coexists with Hashimoto thyroiditis. In this setting, a diagnosis of benign lymphocytic thyroiditis is not uncommon due to underdiagnosis of the slightly atypical mixed lymphoid population or due to sampling error [141] (see also "Additional Analyses" below).
- Malignant lymphoma of the large-cell (blastic) type may be mistaken for carcinoma, in particular for anaplastic carcinoma of thyroid origin.
- Malignant lymphoma of the small-cell type should not be misdiagnosed as thyroid small-cell anaplastic carcinoma or metastatic small-cell carcinoma [101].

### Additional Analyses

- Immunophenotyping of lymphoma versus carcinoma: An appropriate set of immunodiagnostic markers is in most cases successful in determining a definite diagnosis: CD45, CD20 (B lymphocytes), CD3 (T lymphocytes), among others, indicate a lymphoid origin of the cell population, while cytokeratins demonstrate positivity in epithelial/carcinoma cells. TTF-1 positivity and expression of neuroendocrine markers may be helpful in recognizing metastatic small-cell carcinoma.
- Demonstrating the neoplastic nature of lymphocytes requires:
  - Immunocytochemical T- and B-cell enumeration or flow cytometric analysis (FCM) in order to identify monoclonality of the lymphoid population.
  - Polymerase chain amplification (PCR) using DNA, extracted from cytologic samples, is a reliable method to assess clonal rearrangement, particularly in lymphoid proliferations where immunocytochemical analyses are not diagnostic.
  - Southern blot analysis may be another reliable tool for detection of a monoclonal B-cell and T-cell gene rearrangement. However, the method requires unfixed material in large amounts.
- Lymphoma subtyping: Fluorescence in situ hybridization (FISH) detecting specific translocation of gene loci is an excellent tool for lymphoma subtyping. Among others, the method is routinely applied for assessing lymphoma of follicle center cell origin, t(14;18); mantle cell lymphoma, t(11;14); and MALT-type lymphoma, t(11;18).
- Further information is available in Sect. 15.1.4, "Ancillary Techniques," p. 910.

### 4.2.10.1 Selected Subtypes of Malignant Lymphomas

Characteristic immunocytochemical and molecular features of selected lymphoma subtypes that may be encountered in thyroid aspirates are listed below. A comprehensive synopsis on lymphoma diagnostics is given in Sect. 15.3, "Lymph Nodes: Malignant Lymphomas," p. 950.

- *Lymphoma of MALT-type:* Positive staining for B-cell markers (e.g., CD20,CD79a); CD5**–**; CD10**–**; CD23**–**; translocation t(11;18).
- *Diffuse large B-cell lymphoma* (Fig. 4.67): Variable positivity for B-cell markers (CD79a and others); BCL-6**+** nuclear positivity in a high proportion of cases; MIB-1**+** high proliferative index; CD30**+** in anaplastic variants; translocation t(14;18) in a minority of cases.
- *Anaplastic large-cell lymphoma:* CD30**+**; variable staining for CD45, T-cell markers, EMA and ALK; translocation t(2;5) in a majority of the cases.
- *Burkitt lymphoma:* CD20**+**; CD10**+**; BCL-6**+**; MIB-1**+** proliferative index nearly 100%; CD5**–**; BCL-2**–**; Characteristic cytoplasmic vacuolization and large numbers of starry-sky cells.
- *Plasmablastic lymphoma:* CD38**+**; CD138**+**; CD45 and CD20 negative!
- *Multilobated T-cell lymphoma:* T-cell NHL is identified by a strong positive reaction of the tumor cells for CD45 (LCA) and T-cell antibodies (CD3 and others); variable CD30 positivity.

- *Hodgkin lymphoma:* Hodgkin and Reed-Sternberg cells, if present, yield positive immunostaining for CD15, CD30, and PAX5; and negativity for CD45.

## 4.2.11 Metastases



### General Comments

- The thyroid gland is a rare site for secondary malignancy. Involvement by direct spread from neighboring organs such as the pharynx, larynx, and esophagus (Fig. 4.68) may be observed in the majority of secondary tumor manifestations.
- The thyroid gland can harbor secondary tumors from many different organs, but the most common primary sites have been reported to be kidney, breast, lung, colon, supplemented by malignant melanoma (Fig. 4.69) [83, 84, pp. 361–370]. In recent years, several reports in the cytologic literature have investigated this issue [83, 93]. Selected case reports are indicated below.

### Basic Microscopic Pattern

Cytologic samples may show a mixture of benign thyroidal follicular cells and malignant cells (Fig. 4.69), or a monomorphic pattern purely composed of cancer cells. Large secondary tumors frequently present with necrotic debris. The overall cell pattern mainly depends on the size and type of growth.

**Caution**

Tumor-to-tumor metastasis of a remote cancer into a primary thyroid neoplasm has repeatedly been reported. Diagnostic problems on FNAB specimens should not be underestimated [81, 139].

#### 4.2.11.1 Metastatic Cancers Masquerading as Primary Thyroid Tumor

Metastases masquerading as primary thyroid cancer are rare. The most common metastatic tumors mimicking primary thyroid carcinoma are briefly discussed with their related morphologic features and immunocytochemical differentiators.

Remember immunocytochemistry for thyroid tumors (see also Sect. 4.1.4, "Immunocytochemistry," p. 327):

- The selective panel of immunocytochemical stains for thyroglobulin, thyroid transcription factor-1 (TTF-1), CK7, and CK20 is useful to differentiate tumors of thyroid follicular origin from many neoplasms of remote sites.

**Caution**

Thyroglobulin does not show positive immunoreaction in clear cell areas of follicular tumors and in cells of the columnar cell papillary carcinoma variant.

- K19 and CD44 immunostaining have been reported to be of value in FNAB samples in order to differentiate between thyroid papillary carcinoma and other lesions, with overlap in cytologic features (nuclear grooves and inclusions).
- The cells of oncocytic thyroid neoplasms react positively to thyroglobulin and to low-molecular-weight keratin as well.

An overview of immunomarkers for differentiation of metastatic neoplasms is given in chapter Sect. 15.3.24, p. 978, Table 15.3.3.

##### 4.2.11.1.1 Renal Cell Carcinomas

[57, 62, 133, 142] (Fig. 4.70)

Metastasis of clear cell renal cell carcinoma (CRCC) may strongly mimic primary follicular carcinoma of the thyroid due to intranuclear inclusions.

Papillary renal carcinoma may share nuclear indentations, grooves, and inclusions with papillary thyroid cancer.

Chromophobe renal cell carcinoma with their oncocytic features may mimic oncocytic thyroid neoplasia.

#### Immunocytochemistry

- CRCC: Renal cell carcinoma-associated marker (RCCMa) demonstrates positivity in about 90% of all cases. CK13 and CK7 are usually negative.
- Papillary renal cell carcinoma: RCCMa and CD10 are strongly positive; CK13 and CK7 usually reveal positive immunoreaction.
- Chromophobe renal cell carcinoma: Usually positive for CK13 and CK7.

All cytologic and immunocytochemical properties are broadly discussed in Sect. 12.1.8.1, "Renal Cell Carcinoma,", p. 738.

##### 4.2.11.1.2 Breast Carcinoma (Fig. 4.71)

- Metastases of typical breast carcinoma show the well-established cellular features [114].
- Poorly differentiated breast carcinoma may pose differential diagnostic problems against medullary and anaplastic carcinoma of the thyroid [44].
- Metastasis of a metaplastic breast carcinoma is difficult to categorize properly [55].
- Neuroendocrine differentiated breast carcinoma should be separated from endocrine carcinoma of various sites and in particular from a parathyroid gland tumor [97].
- A few recent reports emphasize a particular type of breast cancer having similar cytohistological features of the tall

cell variant of papillary thyroid carcinoma including papillary architecture, clear chromatin, nuclear grooves, nuclear pseudo-inclusions, and dense eosinophilic cytoplasm [17, 42, 149].

**Immunocytochemistry**

Positivity for hormone receptors, CK7 and mammaglobin should make it possible to render a correct diagnosis of metastatic breast carcinoma in most cases.

#### 4.2.11.1.3 Varied Adenocarcinomas [31]

- Problems differentiating columnar cell papillary carcinoma from metastatic adenocarcinoma of colonic or endometrial origin are emphasized by Jayaram and coauthors [75].
- Marked mucinous and mucoepidermoid features in otherwise typical thyroid neoplasms and even true mucinous cancer of primary thyroid origin could give rise to diagnostic problems against metastatic mucinous adenocarcinomas.

**Immunocytochemistry**

CK20 positivity distinguishes colonic cancer from thyroid tumors and positive staining for hormone receptors helps determine endometrial carcinoma.

## 4.2.12 Parathyroid Glands

**General Comments**

- Nodular disorders of the parathyroid glands are often mistaken for thyroid tumors clinically and on imaging studies, especially when these lesions are incorporated in, or in close vicinity to the thyroid gland. Enlarged parathyroid glands in the submandibular area may be considered as neck tumors from other sources, such as enlarged lymph nodes or branchiogenic cysts.
- Cytologists should always be aware of unforeseen parathyroid sampling. Cellular patterns of parathyroidal tissue strongly mimic those from thyroid tissue.
- Immunocytochemistry on cytologic specimens and biochemical analysis of parathyroid hormone levels in aspirates reliably serve as differentiating tools.

### 4.2.12.1 Benign Parathyroidal Lesions and Differential Diagnosis Considerations

[2, 48, 53, 90, 137]

#### 4.2.12.1.1 Parathyroid Cyst [90]

Aspirated fluids are watery clear and generally free of cells. Elevated parathormone level in cyst fluid clarifies the origin of the lesion.

In contrast, cysts from other origins present with colored, amber, hemorrhagic, or thick fluid. Cellular debris, epithelial, histiocytic cells, and macrophages with and without hemosiderin are also frequently present.

#### 4.2.12.1.2 Parathyroid Hyperplasia and Adenoma

(Figs. 4.72 and 4.73)

These two conditions cannot be distinguished from each other due to practically identical cytologic features.

**Microscopic Features**

- The aspirates are cellular, cells appear dissociated, in loose syncytial groups or in cohesive clusters including vague microfollicular structures. Stripped nuclei are frequent.
- The cells are slightly smaller compared to thyroid follicle cells.
- Their nuclei are smooth, the chromatin is coarsely granular and evenly distributed. Micronucleoli may be observed.
- The cytoplasm is pale with ill-defined borders or exhibit pronounced eosinophilic granularity.
- The overall pattern is generally monomorphic but polymorphism in size and shape can be pronounced.
- Background material consists of proteinaceous fluid but colloid is completely absent.
- A clear cell component may focally occur; however, pure clear cell adenomas rarely occur.

**Differential Diagnosis**

- The most frequent misdiagnoses of hyperplastic parathyroid lesions include hyperplastic goiter, follicular thyroid adenoma/well-differentiated carcinoma, and papillary thyroid carcinoma [48].
- Pleomorphic parathyroid adenoma may exhibit a cell pattern mimicking that of carotid body tumors.
- Parathyroidal lesions with a prominent oxyphilic component have to be separated from a number of thyroidal lesions with oncocytic features such as Hashimoto thyroiditis, oncocytic thyroid neoplasms, oxyphilic papillary and medullary carcinoma, and others [53].
- Pure clear cell adenoma may mimic metastasis of well-differentiated clear cell carcinoma, e.g., from the kidney (Fig. 4.73)

**Immunocytochemistry and Biochemical Assay**

Each of these lesions has its distinct nuclear and cellular characteristics described in the corresponding sections of Chapter 4 and other chapters of this book.

Still, diagnostic problems can be resolved by a selective panel of immunocytochemical stains including parathormone-related protein, thyroglobulin, and TTF-1 [1, 24, 157]. Owens and coauthors postulate routine use of biochemical analysis of parathyroid hormone in rinsed FNAB material of thyroid and neck lesions with equivocal morphologic findings [115]. Parathyroid lesions and paraganglioma contradict each other only in an opposite immunoprofile for parathormone.

#### 4.2.12.2 Parathyroid Carcinoma

The authors have not found any report as to the cytologic features and differential diagnosis of this extremely rare neoplasm. Therefore, we refer to selected papers that address the clinical and histopathologic features of parathyroid carcinoma in updates and reviews [41, 112, 119, 134, 147].

4

## 4.2.13 Further Reading


1. Abati A, Skarulis MC, Shawker T, Solomon D. Ultrasound-guided fine-needle aspiration of para-thyroid lesions: a morphological and immunocytochemical approach. Hum Pathol 1995;26:338-343.
2. Absher KJ, Truong LD, Khurana KK, Ramzy I. Parathyroid cytology: avoiding diagnostic pitfalls. Head Neck 2002;24:157-164.
3. Akin MR, Nguyen GK. Fine-needle aspiration biopsy cytology of hyalinizing trabecular adenomas of the thyroid. Diagn Cytopathol 1999;20:90-94.
4. Anderson RJ, Pragasam PJ, Nazar T. Atypical, retrogressive and metaplastic changes in nodular goiters. Potential pitfalls in aspiration cytology of the thyroid. Acta Cytol 1990;34:715-716(A).
5. Aozasa K. Hashimoto's thyroiditis as a risk factor of thyroid lymphoma. Acta Pathol Jpn 1990;40:459-468.
6. Aron M, Mallik A, Verma K. Fine needle aspiration cytology of follicular variant of papillary carcinoma of the thyroid: morphologic pointers to its diagnosis. Acta Cytol 2006;50:663-668.
7. Babu N, Dey P. Fine needle aspiration cytology of non-Hodgkin's lymphoma of thyroid. Cytopathology 2002;13:188.
8. Baloch ZW, Fleisher S, LiVolsi VA, Gupta PK. Diagnosis of "follicular neoplasm": a gray zone in thyroid fine-needle aspiration cytology. Diagn Cytopathol 2002;26:41-44.
9. Berho M, Suster S. The oncocytic variant of papillary carcinoma of the thyroid: a clinicopathologic study of 15 cases. Hum Pathol 1997;28:47-53.
10. Berry B, MacFarlane J, Chan N. Osteoclastoma-like anaplastic carcinoma of the thyroid. Diagnosis by fine needle aspiration cytology. Acta Cytol 1990;34:248-250.
11. Beyan C, Kaptan K, Ifran A. Coexistence of chronic lymphocytic leukemia and Hashimoto's thyroiditis. Ann Hematol 2006;85:811-812.
12. Bhanot P, Yang J, Schnadig VJ, Logrono R. Role of FNA cytology and immunochemistry in the diagnosis and management of medullary thyroid carcinoma: report of six cases and review of the literature. Diagn Cytopathol 2007;35:285-292.
13. Blank W, Braun B. Sonography of the thyroid – Part 2: thyroid inflammation, impairment of thyroid function and interventions. Ultraschall in Med 2008;29:128-155.
14. Blumenfeld W, Nair R, Mir R. Diagnostic significance of papillary structures and intranuclear inclusions in Hürthle-cell neoplasms of the thyroid. Diagn Cytopathol 1999;20:185-189.
15. Bose S, Kapila K, Verma K. Medullary carcinoma of the thyroid: a cytological immunocytochemical, and ultrastructural study. Diagn Cytopathol 1992;8:28-32.
16. Calandra DB, Shah KH, Lawrence AM, et al. Total thyroidectomy in irradiated patients. A twenty-year experience in 206 patients. Ann Surg 1985;202:356-360.
17. Cameselle-Teijeiro J, Abdulkader I, Barreiro-Morandeira F, et al. Breast tumor resembling the tall cell variant of papillary thyroid carcinoma: a case report. Int J Surg Pathol 2006;14:79-84.
18. Caraway NP, Sneige N, Samaan NA. Diagnostic pitfalls in thyroid fine-needle aspiration. A review of 394 cases. Diagn Cytopathol 1993;9:345-350.
19. Carcangiu ML, Steeder T, Zampi G, Rosai J. Anaplastic thyroid carcinoma. A study of 70 cases. Am J Clin Pathol 1985;83:135-158.
20. Carcangiu ML, Zampi G, Rosai J. Poorly differentiated ("insular") thyroid carcinoma. A reinterpretation of Langhans "wuchernde Struma". Am J Surg Pathol 1984;8:655-668.
21. Casey MB, Sebo TJ, Carney JA. Hyalinizing trabecular adenoma of the thyroid gland: cytologic features in 29 cases. Am J Surg Pathol 2004;28:859-867.
22. Castro-Gomez L, Cordova-Ramirez S, Duarte-Torres R, et al. Cytologic criteria of cystic papillary carcinoma of the thyroid. Acta Cytol 2003;47:590-594.
23. Chang TC, Liaw KY, Kuo SH, et al. Anaplastic thyroid carcinoma: review of 24 cases, with emphasis on cytodiagnosis and leukocytosis. Taiwan Yi Xue Hui Za Zhi 1989;88:551-556.
24. Chang TC, Tung CC, Hsiao YL, Chen MH. Immunoperoxidase staining in the differential diagnosis of parathyroid from thyroid origin in fine needle aspirates of suspected parathyroid lesions. Acta Cytol 1998;42:619-624.
25. Chhieng DC, Ross JS, McKenna BJ. CD44 immunostaining of thyroid fine-needle aspirates differentiates thyroid papillary carcinoma from other lesions with nuclear grooves and inclusions. Cancer 1997;81:157-162.
26. Chung D, Ghossien RA, Lin O. Macrofollicular variant of papillary carcinoma: a potential thyroid FNA pitfall. Diagn Cytopathol 2007;35:560-564.
27. Clary KM, Condel JL, Liu Y, et al. Interobserver variability in the fine needle aspiration biopsy diagnosis of follicular lesions of the thyroid gland. Acta Cytol 2005;49:378-382.
28. Compagno J, Oertel JE. Malignant lymphoma and other lymphoproliferative disorders of the thyroid gland. A clinicopathologic study of 245 cases. Am J Clin Pathol 1980;74:1-11.

28A. Cooper D, Doherty G, Haugen B, Hauger B, Kloos R, Lee S, et al. Revised American Thyroid Association management guidelines for patients with thyroid nodules and differentiated thyroid cancer. Thyroid 2009;19(11):1167-1214.

29. Cooper DS, Tiamson E, Ladenson PW. Psammoma bodies in fine needle aspiration biopsies of benign thyroid nodules. Thyroidology 1988;1:55-59.
30. Copp DH, Cameron EC, Cheney BA, et al. Evidence for calcitonin – a new hormone from the parathyroid that lowers blood calcium. Endocrinology 1962;70:638-649.
31. Cristallini EG, Bolis GB, Francucci M. Diagnosis of thyroid metastasis of colonic adenocarcinoma by fine needle aspiration biopsy. Acta Cytol 1990;34:363-365.
32. D'Antonio A, Adesso M, De Dominicis G, et al. Mucinous carcinoma of thyroid gland. Report of a primary and a metastatic mucinous tumor from ovarian adenocarcinoma with immunohistochemical study and review of literature. Virchows Arch 2007;451:847-851.
33. Das DK. Marginal vacuoles (fire-flare appearance) in fine needle aspiration smears of thyroid lesions: does it represent diffusing out of thyroid hormones at the base of follicular cells? Diagn Cytopathol 2006;34:277-283.
34. Das DK, Khanna CM, Tripathi RP, et al. Solitary nodular goiter. Review of cytomorphologic features in 441 cases. Acta Cytol 1999;43:563-574.
35. Das DK, Mallik MK, George SS, et al. Secretory activity in medullary thyroid carcinoma: a cytomorphological and immunocytochemical study. Diagn Cytopathol 2007;35:329-337.
36. Deshpande V, Kapila K, Sai KS, Verma K. Follicular neoplasms of the thyroid. Decision tree approach using morphologic and morphometric parameters. Acta Cytol 1997;41:369-376.
37. Doria MI Jr, Attal H, Wang HH, et al. Fine needle aspiration cytology of the oxyphilic variant of papillary carcinoma of the thyroid. A report of three cases. Acta Cytol 1996;40:1007-1011.
38. Dugan JM, Atkinson BF, Avitabile A, et al. Psammoma bodies in fine needle aspirate of the thyroid in lymphocytic thyroiditis. Acta Cytol 1987;31:330-334.

39. Elliott DD, Pitman MB, Bloom L, Faquin WC. Fine-needle aspiration biopsy of Hürthle cell lesions of the thyroid gland: a cytomorphologic study of 139 cases with statistical analysis. Cancer 2006;108:102-109.
40. Ellison E, Lapuerta P, Martin SE. Psammoma bodies in fine-needle aspirates of the thyroid: predictive value for papillary carcinoma. Cancer 1998;84:169-175.
41. Erickson LA, Jin L, Papotti M, Lloyd RV. Oxyphil parathyroid carcinomas: a clinicopathologic and immunohistochemical study of 10 cases. Am J Surg Pathol 2002;26:344-349.
42. Eusebi V, Damiani S, Ellis IO, et al. Breast tumor resembling the tall cell variant of papillary thyroid carcinoma: report of 5 cases. Am J Surg Pathol 2003;27:1114-1118.
43. Faquin WC, Cibas ES, Renshaw AA. "Atypical" cells in fine-needle aspiration biopsy specimens of benign thyroid cysts. Cancer 2005;105:71-79.
44. Ferrara G, Ianniello GP, Nappi O. Thyroid metastases from a ductal carcinoma of the breast. A case report. Tumori 1997;83:783-787.
45. Fiorella RM, Isky W, Miller L, et al. Multinodular goiter of the thyroid mimicking malignancy. Diagnostic pitfalls in fine-needle aspiration biopsy. Diagn Cytopathol 1993;9:351-354.
46. Forrest CH, Frost FA, de Boer WB, et al. Medullary carcinoma of the thyroid: accuracy of diagnosis of fine-needle aspiration cytology. Cancer 1998;84:295-302.
47. Fortson JK, Patel VG, Henderson VJ. Parathyroid cysts: a case report and review of literature. Laryngoscope 2001;111:1726-1728.
48. Friedman M, Shimaoka K, Lopez CA, Shedd DP. Parathyroid adenoma diagnosed as papillary carcinoma of thyroid on needle aspiration smears. Acta Cytol 1983;27:337-340.
49. Fulciniti F, Benincasa G, Vetrani A, Palombini L. Follicular variant of papillary carcinoma: cytologic findings on FNAB samples – experience with 16 cases. Diagn Cytopathol 2001;25:86-93.
50. Gamboa-Dominguez A, Candanedo-Gonzalez F, Uribe-Uribe NO, et al. Tall cell variant of papillary thyroid carcinoma. A cytohistologic correlation. Acta Cytol 1997;41:672-676.
51. Gharib H, Goellner JR, Zinsmeister AR, et al. Fine needle aspiration biopsy of the thyroid. The problem of suspicious cytologic findings. Ann Intern Med 1984;101:25-28.
52. Giorgadze T, Rossi ED, Fadda G, et al. Does the fine-needle aspiration diagnosis of "Hürthle-cell neoplasm/follicular neoplasm with oncocytic features" denote increased risk of malignancy? Diagn Cytopathol 2004;31:307-312.
53. Giorgadze T, Stratton B, Baloch ZW, LiVolsi VA. Oncocytic parathyroid adenoma: problem in cytological diagnosis. Diagn Cytopathol 2004;31:276-280.
54. Glant MD, Berger EK, Davey DD. Intranuclear cytoplasmic inclusions in aspirates of follicular neoplasms of the thyroid. A report of two cases. Acta Cytol 1984;28:576-580.
55. Gong Y, Jalali M, Staerkel G. Fine needle aspiration cytology of a thyroid metastasis of metaplastic breast carcinoma: a case report. Acta Cytol 2005;49:327-330.
56. Gonzalez-Campora R, Herrero-Zapatero A, Lerma E, et al. Hürthle cell and mitochondrion-rich cell tumors. A clinicopathologic study. Cancer 1986;57:1154-1163.
57. Gritsman AY, Popok SM, Ro JY, et al. Renal-cell carcinoma with intranuclear inclusions metastatic to thyroid: a diagnostic problem in aspiration cytology. Diagn Cytopathol 1988;4:125-129.
58. Guarda LA, Baskin HJ. Inflammatory and lymphoid lesions of the thyroid gland. Cytopathology by fine-needle aspiration. Am J Clin Pathol 1987;87:14-22.
59. Guarda LA, Peterson CE,Hall W, Baskin HJ. Anaplastic thyroid carcinoma: cytomorphology and clinical implications of fine-needle aspiration. Diagn Cytopathol 1991;7:63-67.
60. Guiter GE, Auger M, Ali SZ, et al. Cytopathology of insular carcinoma of the thyroid. Cancer 1999;87:196-202.
61. Gupta S, Sodhani P, Jain S, Kumar N. Morphologic spectrum of papillary carcinoma of the thyroid: role of cytology in identifying the variants. Acta cytol 2004;48:795-800.
62. Halbauer M, Kardum-Skelin I, Vranesic D, Crepinko I. Aspiration cytology of renal-cell carcinoma metastatic to the thyroid. Acta Cytol 1991;35:443-446.
63. Haleem A, Akhtar M, Ali MA, Iqbal Z. Fine-needle aspiration biopsy of mucus-producing medullary carcinoma of thyroid: report of a case with cytologic, histologic, and ultrastructural correlations. Diagn Cytopathol 1990;6:112-117.
64. Halliday BE, Silverman JF, Finley JL. Fine-needle aspiration cytology of amyloid associated with nonneoplastic and malignant lesions. Diagn Cytopathol 1998;18:270-275.
65. Harach HR, Zusman SB. Cytologic findings in the follicular variant of papillary carcinoma of the thyroid. Acta Cytol 1992;36:142-146.
66. Harach (2) HR, Zusman SB. Cytopathology of the tall cell variant of thyroid papillary carcinoma. Acta Cytol 1992;36:895-899.
67. Harigopal M, Sahoo S, Recant WM, DeMay RM. Fine-needle aspiration of Riedel's disease: report of a case and review of the literature. Diagn Cytopathol 2004;30:193-197.
68. Harms H, Hofmann M, Ruschenburg I. Fine needle aspiration of the thyroid: can an image processing system improve differentiation? Anal Quant Cytol Histol 2002;24:147-153.
69. Hempelmann LH, Hall WJ, Phillips M, et al. Neoplasms in persons treated with x-rays in infancy: fourth survey in 20 years. J Natl Cancer Inst 1975;55:519-530.
70. Hsu KF, Lin YS, Hsieh CB, et al. Primary malignant fibrous histiocytoma of the thyroid: review of the literature with two new cases. Thyroid 2008;18:51-55.
71. Hui PK, Chan JKC, Cheung PSY, et al. Columnar cell carcinoma of the thyroid: fine needle aspiration findings in a case. Acta Cytol 1990;34:355-358.
72. Hunt JL, Barnes EL. Non-tumor-associated psammoma bodies in the thyroid. Am J Clin Pathol 2003;119:90-94.
73. Hyjek E, Isaacson PG. Primary B cell lymphoma of the thyroid and its relationship to Hashimoto's thyroiditis. Hum Pathol 1988;19:1315-1326.
74. Intidhar Labidi S, Chaabouni AM, Kraiem T, et al. Thyroid carcinoma and Hashimoto thyroiditis. Ann Otolaryngol Chir Cervicofac 2006;123:175-178.
75. Jayaram G. Cytology of columnar-cell variant of papillary thyroid carcinoma. Diagn Cytopathol 2000;22:227-229.
76. Kapila K, Verma K. Amyloid goiter in fine needle aspirates. Acta Cytol 1993;37:256-257.
77. Kapur U, Wojcik EM. Follicular neoplasm of the thyroid – vanishing cytologic diagnosis? Diagn Cytopathol 2007;35:525-528.
78. Kaur A, Jayaram G. Thyroid tumors: cytomorphology of follicular neoplasms. Diagn Cytopathol 1991;7:469-472.
79. Kaw YT. Fine needle aspiration cytology of the tall cell variant of papillary carcinoma of the thyroid. Acta Cytol 1994;38:282-283.
80. Kelman AS, Rathan A, Leibowitz J, et al. Thyroid cytology and the risk of malignancy in thyroid nodules: importance of nuclear atypia in indeterminate specimens. Thyroid 2001;11:271-277.
81. Khurana KK, Powers CN. Basaloid squamous carcinoma metastatic to renal-cell carcinoma: fine-needle aspiration cytology of tumor-to-tumor metastasis. Diagn Cytopathol 1997;17:379-382.
82. Kikuchi I, Anbo J, Nakamura S, et al. Synovial sarcoma of the thyroid. Report of a case with aspiration cytology findings and gene analysis. Acta Cytol 2003;47:495-500.
83. Kim TY, Kim WB, Gong G, et al. Metastasis to the thyroid diagnosed by fine-needle aspiration biopsy. Clin Endocrinol (Oxf) 2005;62:236-241.
84. Kini SR. Thyroid 2nd ed. Guides to Clinical Aspiration Biopsy. ed: Kline TS. New York Igaku-Shoin. 1996.
85. Kini SR, Miller JM, Hamburger JI, Smith MJ. Cytopathologic features of medullary carcinoma of the thyroid. Arch Pathol Lab Med 1984;108:156-159.
86. Kini SR, Miller JM, Hamburger JI, Smith-Purlow MJ. Cytopathology of follicular lesions of the thyroid gland. Diagn Cytopathol 1985;1:123-132.

87. Kuma S, Hirokawa M, Miyauchi A, et al. Cytologic features of hyalinizing trabecular adenoma of the thyroid. Acta Cytol 2003;47:399-404.
88. Kumar PV, Torabinejad S, Omrani GH. Osteoclastoma-like anaplastic carcinoma of the thyroid gland diagnosed by fine needle aspiration cytology. Report of two cases. Acta Cytol 1997;41:1345-1348.
89. Larson RS, Wick MR Primary mucoepidermoid carcinoma of the thyroid: diagnosis by fine-needle aspiration biopsy. Diagn Cytopathol 1993;9:438-443.
90. Layfield LJ. Fine needle aspiration cytology of cystic parathyroid lesions. A cytomorphologic overlap with cystic lesions of the thyroid. Acta Cytol 1991;35:447-450.
91. Leung C-S, Hartwick RW, Bedard YC. Correlation of cytologic and histologic features in variants of papillary carcinoma of the thyroid. Acta Cytol 1993;37:645-650.
92. Lew W, Orell S, Henderson DW. Intranuclear vacuoles in non-papillary carcinoma of the thyroid. Acta Cytol 1984;28:581-586.
93. Lin SY, Sheu WH, Chang MC, et al. Diagnosis of thyroid metastasis in cancer patients with thyroid mass by fine needle aspiration cytology and ultrasonography. Zhonghua Yi Xue Za Zhi (Taipei) 2002;65:101-105.
94. LiVolsi VA. Postpartum thyroiditis. The pathology slowly unravels. Am J Clin Pathol 1993;100:193-194.
95. LiVolsi VA. Surgical Pathology of the Thyroid. Philadelphia, Saunders, 1990.
96. Logani S, Gupta PK, LiVolsi VA, Mandel S, Baloch ZW. Thyroid nodules with FNA cytology suspicious for follicular variant of papillary thyroid carcinoma: follow-up and management. Diagn Cytopathol 2000;23:380-385.
97. Loo CK, Burchett IJ. Fine needle aspiration biopsy of neuroendocrine breast carcinoma metastatic to the thyroid. A case report. Acta Cytol 2003;47:83-87.
98. Luze T, Tötsch M, Bangerl I, et al. Fine needle aspiration cytodiagnosis of anaplastic carcinoma and malignant haemangioendothelioma of the thyroid in endemic goitre area. Cytopathology 1990;1:305-310.
99. MacDonald L, Yazdi HM. Fine needle aspiration biopsy of Hashimoto's thyroiditis. Sources of diagnostic error. Acta Cytol 1999;43:400-406.
100. Mai KT, Thomas J, Yazdi HM, et al. Pathologic study and clinical significance of Hürthle cell papillary thyroid carcinoma. Appl Immunohistochem Mol Morphol 2004;12:329-337.
101. Matsuda M, Sone H, Koyama H, Ishiguro S. Fine-needle aspiration cytology of malignant lymphoma of the thyroid. Diagn Cytopathol 1987;3:244-249.
102. McConahey WM, Hay ID, Woolner LB, et al. Papillary thyroid cancer treated at the Mayo clinic, 1946 through 1970: initial manifestations, pathologic findings, therapy and outcome. Mayo Clin Proc 1986;61:978-996.
103. Mesonero CE, Jugle JE, Wilbur DC, Nayar R. Fine-needle aspiration of the macrofollicular and microfollicular subtypes of the follicular variant of papillary carcinoma of the thyroid. Cancer 1998;84:235-244.
104. Mittra ES, McDougall IR. Recurrent silent thyroiditis: a report of four patients and review of the literature. Thyroid 2007;17:671-675.
105. Motoi N, Ozawa Y. Malignant T-cell lymphoma of the thyroid gland associated with Hashimoto's thyroiditis. Pathol Int 2005;55:425-430.
106. Nassar A, Gupta P, LiVolsi VA, Baloch Z. Histiocytic aggregates in benign nodular goiters mimicking cytologic features of papillary thyroid carcinoma (PTC). Diagn Cytopathol 2003;29:243-245.
107. Nasser SM, Pitman MB, Pilch BZ, Faquin WC. Fine-needle aspiration biopsy of papillary thyroid carcinoma: diagnostic utility of cytokeratin 19 immunostaining. Cancer 2000;90:307-311.
108. Ng WK, Tang V, Poon CS. Fine needle aspiration cytology of follicular carcinoma with clear cell change. A case report. Acta Cytol 2002;46:757-761.
109. Nguyen GK, Ginsberg J, Crockford PM, et al. Hashimoto's thyroiditis: Cytodiagnostic accuracy and pitfalls. Diagn Cytopathol 1997;16:531-536.
110. Nguyen GK, Husain M, Akin MR. Cytodiagnosis of benign and malignant Hürthle cell lesions of the thyroid by fine-needle aspiration biopsy. Diagn Cytopathol 1999;20:261-265.
110A. Nikiforov YE, Steward DL, Robinson-Smith TM, Haugen BR, Klopper JP, Zhu Z, et al. Molecular Testing for Mutations in Improving the Fine-Needle Aspiration Diagnosis of Thyroid Nodules. J Clin Endocrinol Metab 2009;94(6):2092-2098.
111. Nilsson G. Marginal vacuoles in fine needle aspiration biopsy smears of toxic goiters. Acta Pathol Microbiol Scand Sect A 1972;80:289-293.
112. Obara T, Fujimoto Y. Diagnosis and treatment of patients with parathyroid carcinoma: an update and review. World J Surg 1991;15:738-744.
113. Orlando CA, Salman K, Miller JL, Naryshkin S. Clear-cell change in follicular adenoma mimicking Hürthle-cell tumor on thyroid aspiration biopsy cytology. Diagn Cytopathol 1991;7:273-276.
114. Owens CL, Basaria S, Nicol TL. Metastatic breast carcinoma involving the thyroid gland diagnosed by fine-needle aspiration: a case report. Diagn Cytopathol 2005;33:110-115.
115. Owens CL, Rekhtman N, Sokoll L, Ali SZ. Parathyroid hormone assay in fine-needle aspirate is useful in differentiating inadvertently sampled parathyroid tissue from thyroid lesions. Diagn Cytopathol 2008;36:227-231.
116. Ozdemir BH, Uyar P, Ozdemir FN. Diagnosing amyloid goiter with thyroid aspiration biopsy. Cytopathology 2006;17:262-266.
117. Papaparaskeva K, Nagel H, Droese M. Cytologic diagnosis of medullary carcinoma of the thyroid gland. Diagn Cytopathol 2000;22:351-358.
118. Papi G, LiVolsi VA. Current concepts on Riedel thyroiditis. Am J Clin Pathol 2004;121 Suppl:S50-63.
119. Park ST, Condemi G, Shakir KM, et al. Parathyroid carcinoma: report of three cases and review of the literature. Mil Med 1998;163:246-249.
120. Patil PV, Godhi AS, Sant AN. Fine needle aspiration cytology of papillary carcinoma thyroid with Hashimoto's thyroiditis - report of two cases. Indian J Pathol Microbiol 1997;40:165-168.
121. Pedersen RK, Pedersen NT. Primary non-Hodgkin's lymphoma of the thyroid gland: a population based study. Histopathology 1996;28:25-32.
122. Perez F, Llobet M, Garijo G, et al. Fine-needle aspiration cytology of columnar-cell carcinoma of the thyroid: report of two cases with cytohistologic correlation. Diagn Cytopathol 1998:352-356.
123. Perez LA, Gupta PK, Mandel SJ, et al. Thyroid papillary microcarcinoma. Is it really a pitfall of fine needle aspiration cytology? Acta Cytol 2001;45:341-346.
124. Pietribiasi F, Sapino A, Papotti M, et al. Cytologic features of poorly differentiated "insular" carcinoma of the thyroid, as revealed by fine-needle aspiration biopsy. Am J Clin Pathol 1990;94:687-692.
125. Poniecka A, Ghorab Z, Arnold D, et al. Kaposi's sarcoma of the thyroid gland in an HIV-negative woman: a case report. Acta Cytol 2007;51:421-423.
126. Powari M, Dey P, Saikia UN. Fine needle aspiration cytology of follicular variant of papillary carcinoma of thyroid. Cytopathology 2003;14:212-215.
127. Pu RT, Yang J, Wasserman PG, et al. Does Hürthle cell lesion/neoplasm predict malignancy more than follicular lesion/neoplasm on thyroid fine-needle aspiration. Diagn Cytopathol 2006;34:330-334.
128. Punthakee X, Palme CE, Franklin JH, et al. Fine-needle aspiration biopsy findings suspicious of papillary thyroid carcinoma: a

review of cytopathological features. Laryngoscope 2005;115:433-436.
129. Rekhi B, Kane SV, D'Cruz A. Cytomorphology of anaplastic giant cell type of medullary thyroid carcinoma – a diagnostic dilemma in an elderly female: a case report. Diagn Cytopathol 2008;36:136-138.
130. Renshaw AA. "Histiocytoid" cells in fine-needle aspirations of papillary carcinoma of the thyroid: frequency and significance of an under-recognized cytologic pattern. Cancer 2002;96:240-243.
131. Renshaw AA. Hürthle cell carcinoma is a better gold standard than Hürthle cell neoplasm for fine-needle aspiration of the thyroid: defining more consistent and specific cytologic criteria. Cancer 2002;96:261-266.
132. Riazmontazer N, BedayatG. Psammoma bodies in fine needles aspirates from thyroids containing nontoxic hyperplastic goiters. Acta Cytol 1991;35:563-566.
133. Rikabi AC, Young AE, Wilson C. Metastatic renal cell carcinoma in the thyroid gland diagnosed by fine needle aspiration cytology. Cytopathology 1991;2:47-49.
134. Rodgers SE, Perrier ND. Parathyroid carcinoma. Curr Opin Oncol 2006;18:16-22.
135. Ropp BG, Solomides C, Palazzo J, Bibbo M. Follicular carcinoma of the thyroid with extensive clear-cell differentiation: a potential diagnostic pitfall. Diagn Cytopathol 2000;23:222-223.
136. Rosai J, Carcangiu ML, DeLellis RA. Tumors of the thyroid gland. Atlas of Tumor Pathology, 3rd Series, Fascicle 5. Washington, D.C.: Armed Forces Institute of Pathology, 1992.
137. Rossi ED, Mule A, Zannoni GF, Fadda G. Asymptomatic intrathyroidal adenoma. Report of a case with a cytologic differential diagnosis including thyroid neoplasms. Acta Cytol 2004;48:437-440.
138. Roti E, Uberti E. Post-partum thyroiditis – a clinical update. Eur J Endocrinol 2002;146:275-279.
139. Ryska A, Cap J. Tumor-to-tumor metastasis of renal cell carcinoma into oncocytic carcinoma of the thyroid. Report of a case and review of the literature. Pathol Res Pract 2003;199:101-106.
140. Sahin M, Gursoy A, Tutuncu NB, Guvener DN. Prevalence and prediction of malignancy in cytologically indeterminate thyroid nodules. Clin Endocrinol (Oxf) 2006;65:514-518.
141. Sangalli G, Serio G, Zampatti C, et al. Fine needle aspiration cytology of primary lymphoma of the thyroid. a report of 17 cases. Cytopathology 2001;12:257-263.
142. Sant F, Moysset I, Badal JM, et al. Fine-needle aspiration of chromophobe renal-cell carcinoma metastatic to the thyroid gland. Diagn Cytopathol 2001;24:193-194.
143. Sardi A, Bolton JS, Mitchell WT Jr, Merritt CR. Immunoperoxidase confirmation of ultrasonically guided fine needle aspirates in patients with recurrent hyperparathyroidism. Surg Gynecol Obstet 1992;175:563-568.
144. Shurbaji MS, Gupta PK, Frost JK. Nuclear grooves: a useful criterion in the cytopathologic diagnosis of papillary thyroid carcinoma. Diagn Cytopathol 1988;4:91-94.
145. Shvero J, Gal R, Avidor I, et al. Anaplastic thyroid carcinoma. A clinical, histologic and immunohistochemical study. Cancer 1988;62:319-325.
146. Sironi M, Collini P, Cantaboni A. Fine needle aspiration cytology of insular thyroid carcinoma. A report of four cases. Acta Cytol 1992;36:435-439.
147. Smith JF, Coombs RR. Histologic diagnosis of carcinoma of the parathyroid gland. J Clin Pathol 1984;37:1370-1378.
148. Tahlan A, Dey P. Nuclear grooves. How specific are they? Acta Cytol 2001;45:48-50.
149. Tosi AL, Ragazzi M, Asioli S, et al. Breast tumor resembling the tall cell variant of papillary thyroid carcinoma: report of 4 cases with evidence of malignant potential. Int J Surg Pathol 2007;15:14-19.
150. Tseleni-Balafouta S, Kavantzas N, Paraskevakou H, Davaris P. Computerized morphometric study on fine needle aspirates of cellular follicular lesions of the thyroid. Anal Quant Cytol Histol 2000;22:323-326.
151. Us-Krasovec M, Auersperg M, Bergant D, et al. Medullary carcinoma of the thyroid gland: diagnostic cytopathological characteristics. Pathologica 1998;90:5-13.
152. Us-Krasovec M, Golouh R, Auersperg M, et al. Anaplastic thyroid carcinoma in fine needle aspirates. Acta Cytol 1996;40:953-958.
153. Vailati A, Marena C, Aristia L, et al. Primary Hodgkin's disease of the thyroid: report of a case and a review of the literature. Haematologica 1991;76:69-71.
154. Vasei M, Kumar PV, Malekhoseini SA, Kadivar M. Papillary Hürthle cell carcinoma (Warthin-like tumor of the thyroid). Report of a case with fine needle aspiration findings. Acta Cytol 1998;42:1437-1440.
155. Vazquez Ramirez F, Otal Salaverri C, Argueta Manzano O, et al. Fine needle aspiration cytology of high grade mucoepidermoid carcinoma of the thyroid. A case report. Acta Cytol 2000;44:259-264.
156. Weber D, Brainard J, Chen L. Atypical epithelial cells, cannot exclude papillary carcinoma, in fine needle aspiration of the thyroid. Acta Cytol 2008;52:320-324.
157. Winkler B, Gooding GA, Montgomery CK, et al. Immunoperoxidase confirmation of parathyroid origin of ultrasound-guided fine needle aspirates of the parathyroid glands. Acta Cytol 1987;31:40-44.
158. Wu HH, Clouse J, Ren R. Fine-needle aspiration cytology of Hürthle cell carcinoma of the thyroid. Diagn Cytopathol 2008;36:149-154.
159. Wu HH, Jones JN, Grzybicki DM, Elsheikh TM. Sensitive cytologic criteria for the identification of follicular variant of papillary thyroid carcinoma in fine-needle aspiration biopsy. Diagn Cytopathol 2003;29:262-266.
160. Yang YJ, Demirci SS. Evaluating the diagnostic significance of nuclear grooves in thyroid fine needle aspirates with a semiquantitative approach. Acta Cytol 2003;47:563-570.
161. Yang YJ, Khurana KK. Diagnostic utility of intracytoplasmic lumen and transgressing vessels in evaluation of Hürthle cell lesions by fine-needle aspiration. Arch Pathol Lab Med 2001;125:1031-1035.
162. Ylagan LR, Dehner LP, Huettner PC, Lu D. Columnar cell variant of papillary thyroid carcinoma. Report of a case with cytologic findings. Acta Cytol 2004;48:73-77.
163. Zhu H, Hu DX. Langerhans cell histiocytosis of the thyroid diagnosed by fine needle aspiration cytology. A case report. Acta Cytol 2004;48:278-28.

**Fig. 4.5A, B Acute suppurative thyroiditis.**
A 14-year-old boy with a history of T-lymphoblastic lymphoma and Aspergillus pneumonia exhibited a positive thyroid focus on PET scan. Image-guided FNAB of the thyroidal lesion (direct smear, Pap stain). **A** Inflammatory pattern composed of detritic neutrophils and histiocytes. Naked activated thyreocytes (nucleoli!, arrowheads) are present as well. Note the single blurred hyphae (arrow) (lower magnification). **B**: Silver stain strongly accentuates hyphae of *Aspergillus* species as the causative organism of thyroiditis (high magnification).



**Figs. 4.6–4.9 Granulomatous de Quervain thyroiditis.**
Thyroid FNABs were performed in different patients affected by de Quervain thyroiditis. Pap-stained direct smears.

**Fig. 4.6** (case #1) Low magnification demonstrates the classical microscopic appearance of subacute thyroiditis: multinucleated giant cells of the Langhans type (small arrow), aggregations of epitheloid cells (arrowheads), and sheets of follicular cells (center). Condensed colloid, a soft tissue fragment (large arrow), lymphocytes, and neutrophils are also present.

**Fig. 4.7** (case #2) Higher magnification image showing activated epitheloid cells (note cellular crowding and distinct nucleoli) and Langhans giant cells containing intracytoplasmic blobs of colloid (arrow).

**Fig. 4.8** (case #3) Numerous sheets are composed of monomorphic follicular cells, in parts with pyknotic nuclei (upper right); the latter are frequently encountered in cytologic specimens of de Quervain thyroiditis. Multinucleated giant cells are also present (upper left) (high magnification).

**Fig. 4.9** (case #4) The image is taken at low magnification from a case of thyroiditis in an advanced stage. A compact tissue fragment composed of histiocytes, epitheloid cells, fibroblasts, and fibrocytes indicate fibrosclerotic transformation. Small groups of thyreocytes may be encased (arrow).

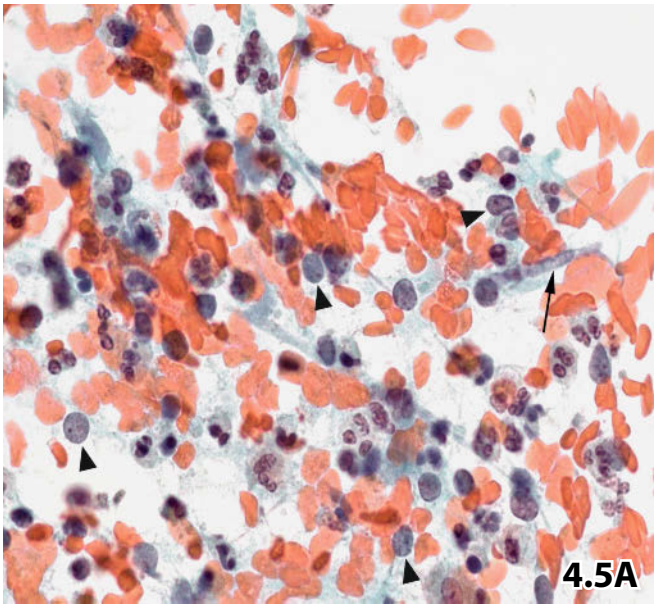
4.5A

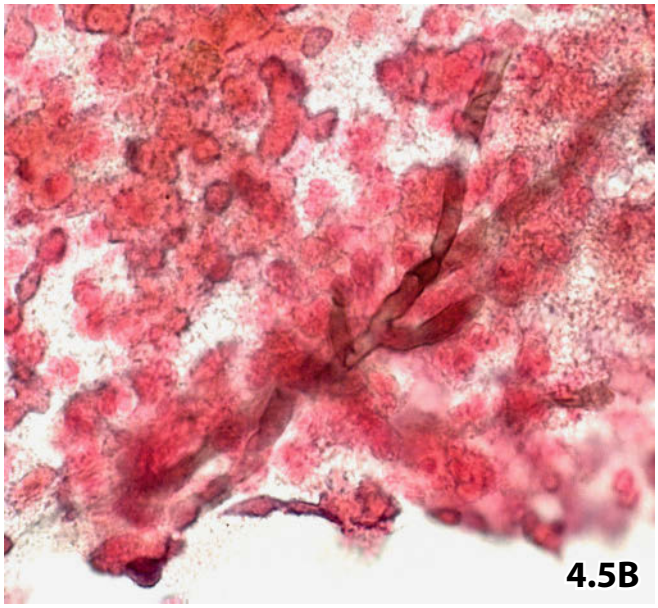
4.5B

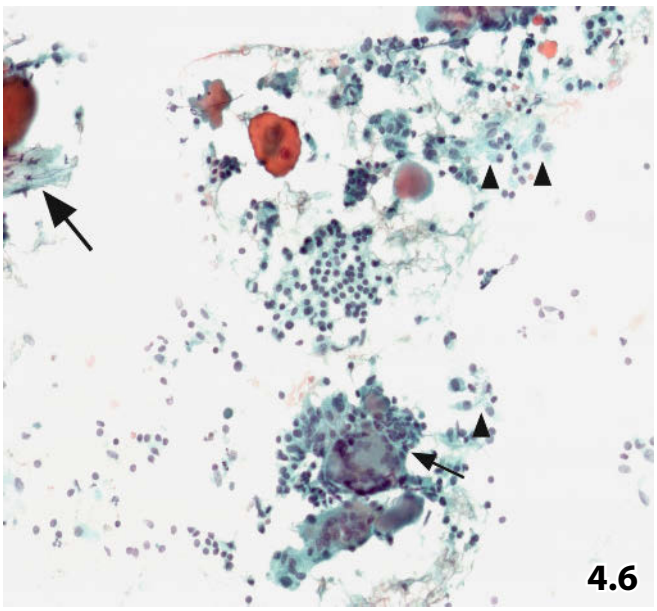
4.6

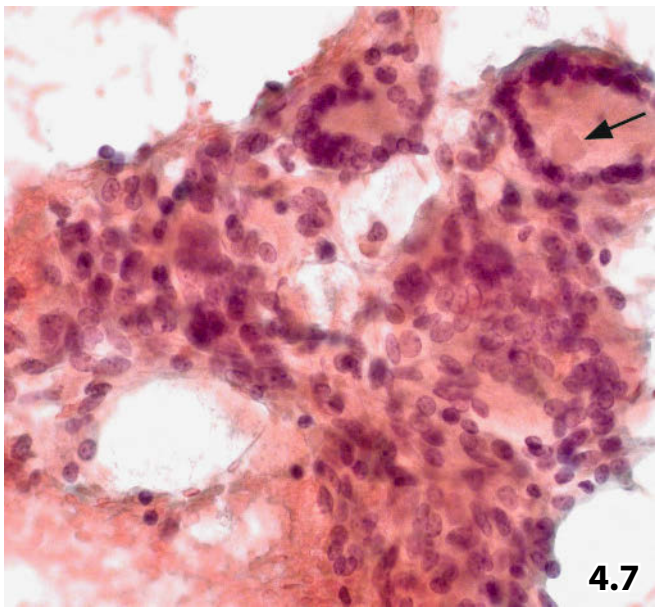
4.7

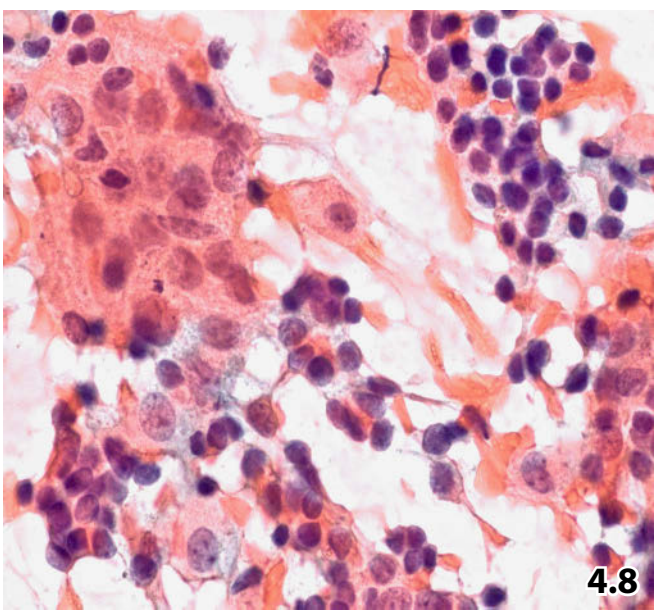
4.8

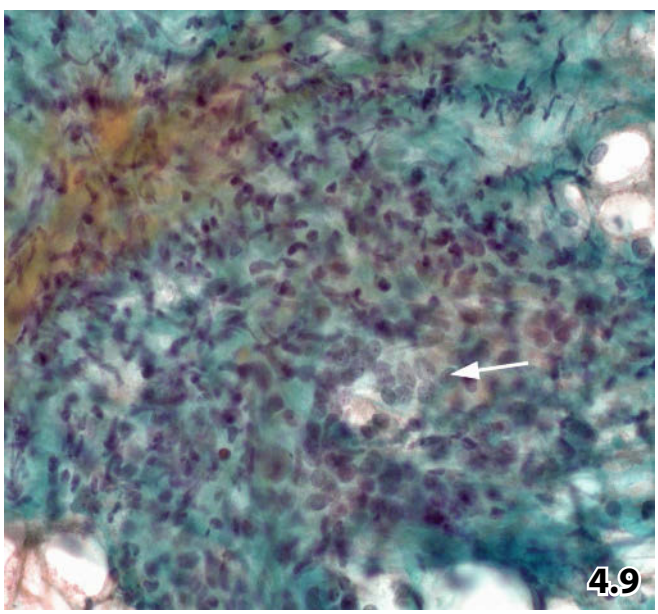
4.9

**Fig. 4.10 Postpartum thyroiditis.**
Physical and laboratory investigations in a 23-year-old woman, 6 months postpartum, revealed diffuse enlargement of her thyroid gland and high blood serum level of thyroid-stimulating hormone (TSH). FNABs from the thyroid yielded sheets and clusters of activated thyreocytes focally arranged in follicles (arrows). Numerous discrete lymphocytes (arrowheads) both scattered in the background and adjacent to follicular cells (direct smear, Pap stain, lower magnification).



**Figs. 4.11–4.14 Hashimoto thyroiditis: classic features.**
FNAB of different patients suffering from chronic lymphocytic thyroiditis. All cytologic specimens (direct smears) are Pap-stained.

**Fig. 4.11** (case #1) Low magnification shows flat sheets composed of oncocytes against a background rich in lymphocytes. Pale colloid, foam cells, epithelioid cells, and giant cells (arrow) are also present.

**Fig. 4.12** (case #2) Higher magnification exhibiting classical morphologic features of oncocytes and the heterogeneous appearance of the lymphoid population including a tingible-body macrophage (arrow).

**Fig. 4.13** (case #3) Large aggregates of lymphocytes may occasionally mimic papilliform formations (arrows). The picture has been taken from a smear containing an otherwise typical population of chronic lymphocytic thyroiditis.

Pseudopapillary grouping of lymphocytes should not mislead to a diagnosis of a papillary epithelial tumor.

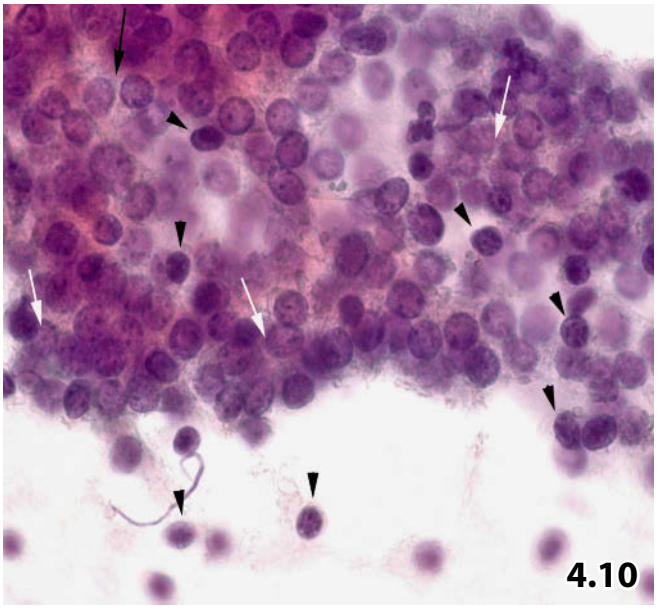
4.10

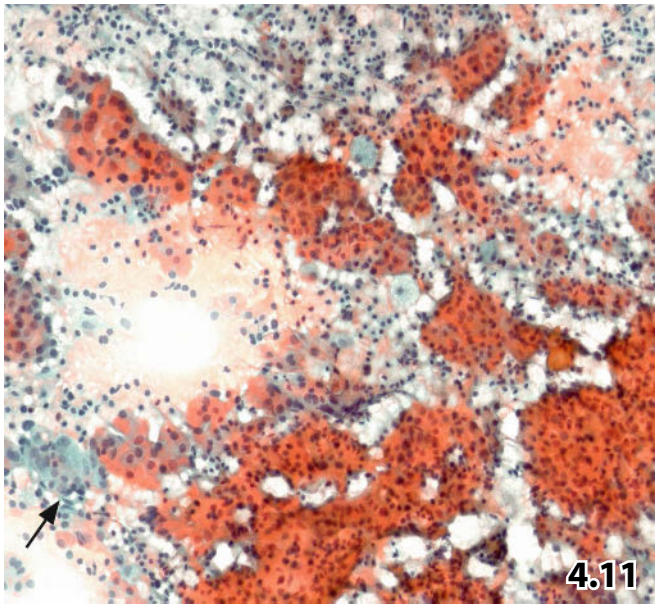
4.11

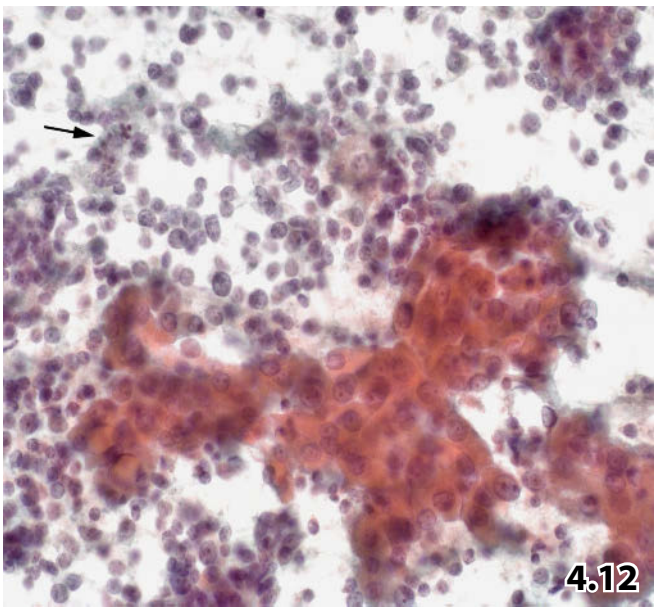
4.12

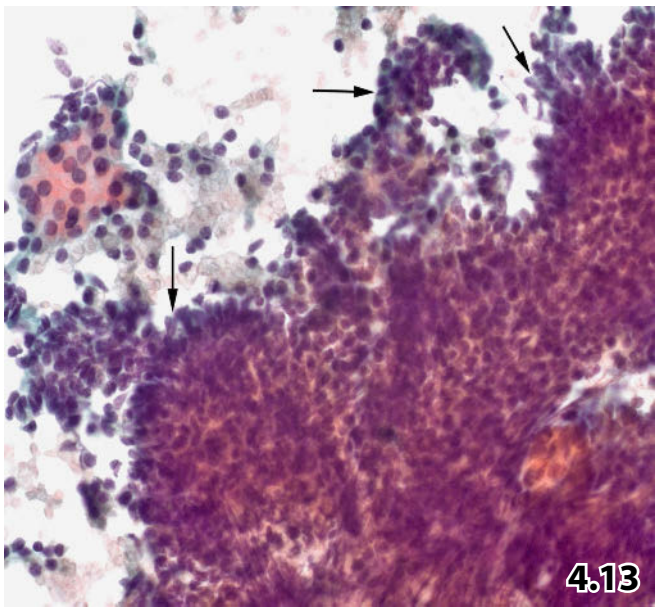
4.13

**Fig. 4.14** (case #4) Sheets of oncocytes (top and lower right), an increased number of lymphocytes, numerous clusters composed of epitheloid cells (arrows), and giant cells of the Langhans type (arrowhead) may occasionally be encountered. Such a heterogeneous cytologic appearance may give rise to diagnostic confusion.
*Tentative cytologic diagnosis:* Hashimoto thyroiditis associated with of a granulomatous component.
*Serologic tests:* Serum thyroid antibody titers were high.

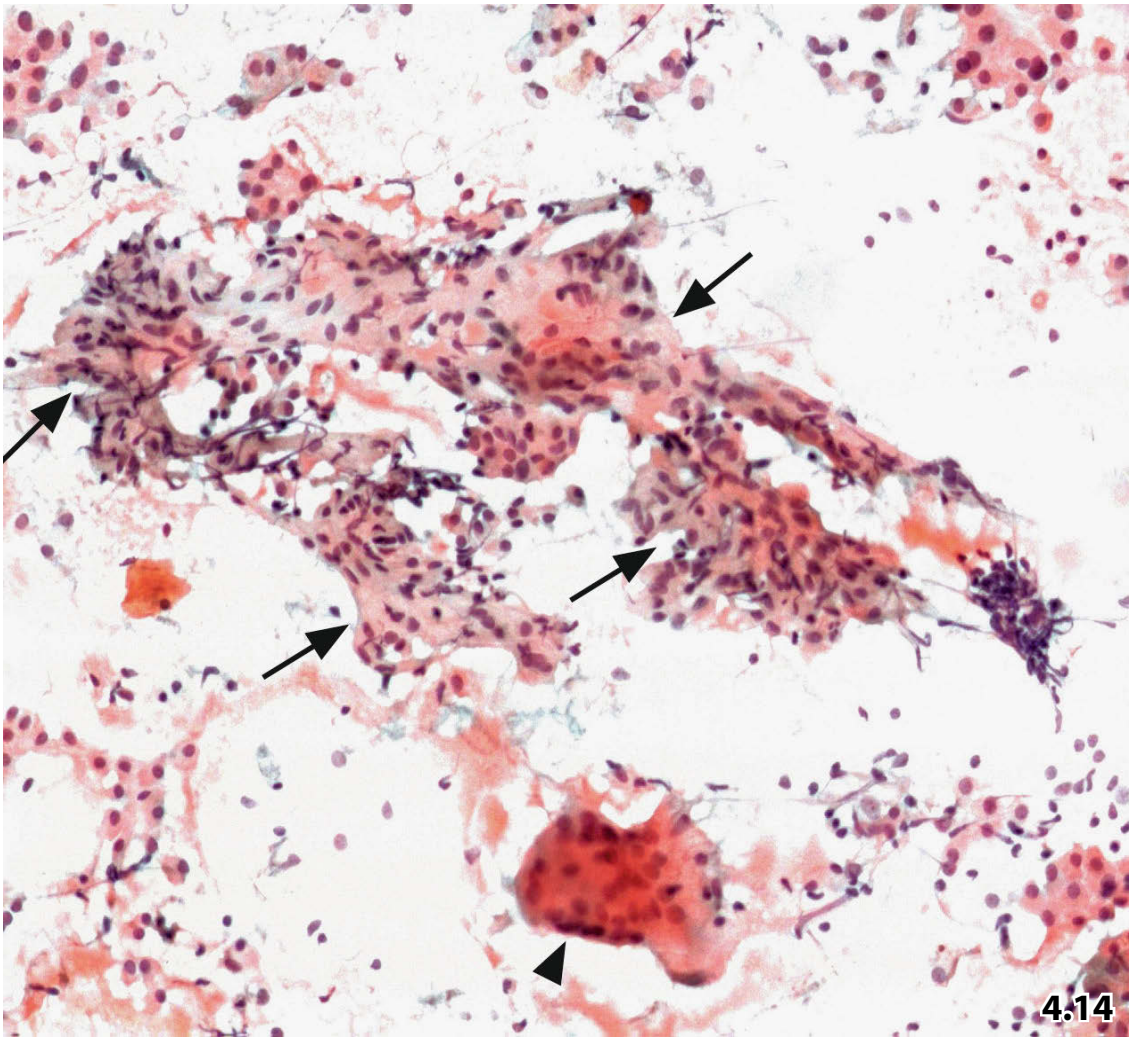
4.14

**Fig. 4.15A, B Hashimoto thyroiditis: conventional smear versus liquid-based method (ThinPrep).**
**A** The extremely sanguineous conventionally prepared smears hampered an accurate cytologic diagnosis (Pap stain, lower magnification). **B** Immunocytochemical reaction on a Pap-prestained ThinPrep specimen shows a clean background and well-preserved three-dimensional clusters of follicle cells interspersed with lymphocytes. The latter are positive for CD45. Adequate liquid-based specimens enabled an appropriate diagnosis.



**Fig. 4.16 Hashimoto thyroiditis versus malignant lymphoma.**
FNAB revealed sparse sheets composed of oncocytes (lower right) embedded in a background that was rich in polymorphous lymphoid cells (direct smear, MGG stain, high magnification). The mixed lymphoid cell pattern indicated benign proliferative lesion. Yet occasionally it may be difficult to exclude malignant lymphoma by cytology alone.
*Serologic tests and follow-up:* The level of the antibody titer against thyroid peroxidase (TPO) was high and long-term follow-up yielded no malignant disorder.

**Figs. 4.17 and 4.18 Hashimoto thyroiditis versus oncocytic neoplasia.**
FNAB of a thyroid nodule of two different patients revealed numerous oncocytic sheets and three-dimensional epithelial clusters (direct smears, Pap stain). Both cases exhibited only sporadic lymphocytes (note arrows in Fig. 4.17).
*Tentative cytologic diagnoses:* Chronic lymphocytic thyroiditis or oncocytic adenoma with perifocal lymphocytosis.
*Serological tests:* Testing for elevated levels of thyroid antibodies was positive in both cases.

**Fig. 4.17** (case #1) The first case shows obviously well-developped colloid-filled follicles and a few lymphocytes (arrows) (higher magnification).

**Fig. 4.18** (case #2) The second case is characterized by a considerable cell dissociation and many stripped nuclei originating from oncocytes (arrows) (low magnification).

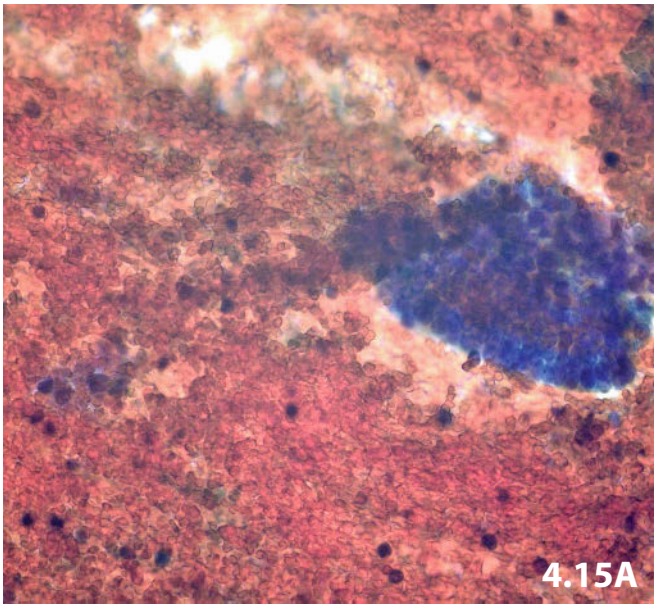
4.15A

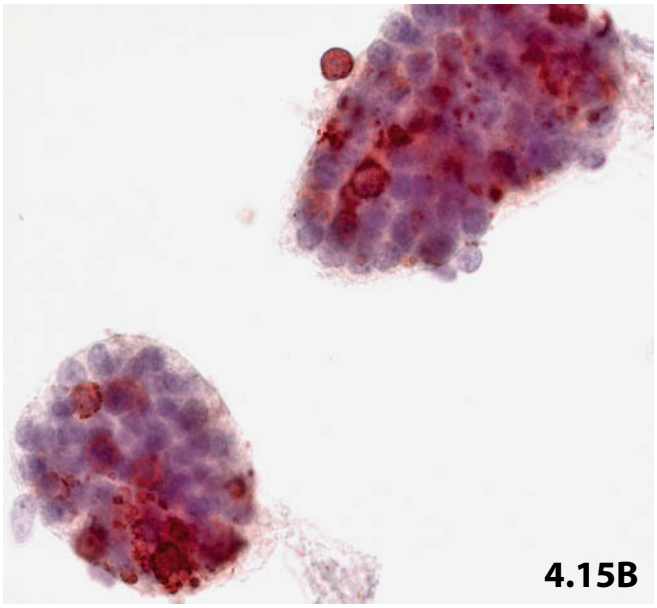
4.15B

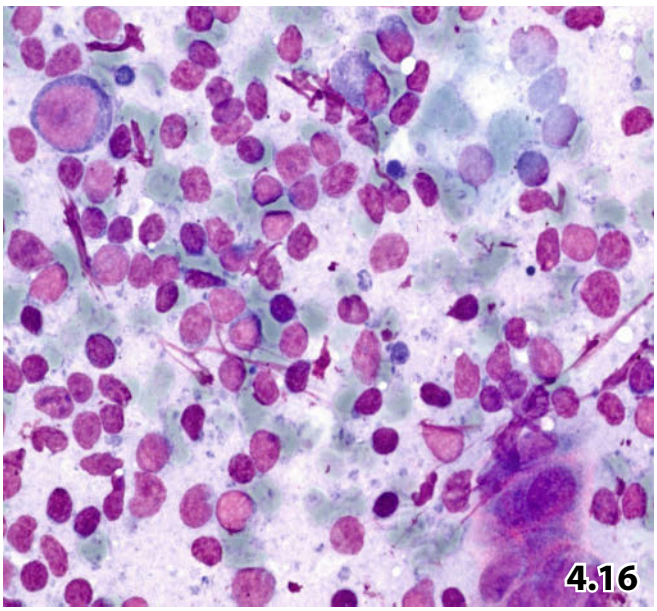
4.16

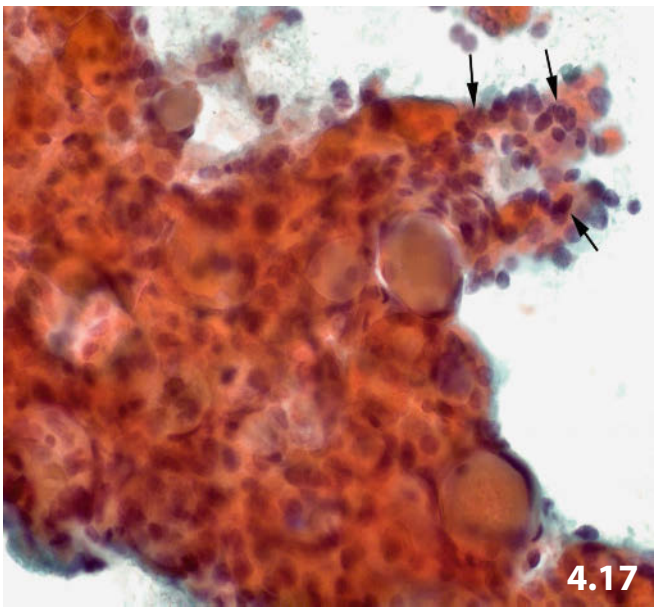
4.17

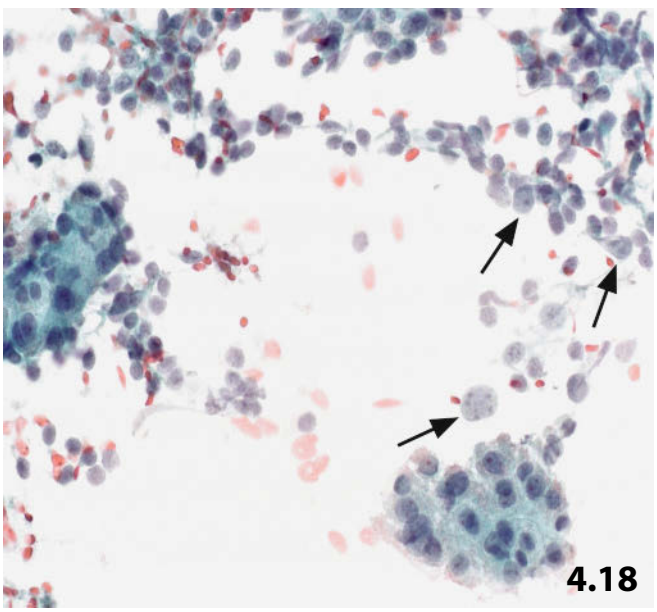
4.18

**Fig. 4.19 Colloid cyst.**
FNAB from a thyroid cysts of the colloid variant providing abundant dense , frequently cracked colloid, forming a mosaic pattern. Note isolated detritic cells, red blood cells, and a single barely recognizable foam cell (upper right). One should keep in mind that a great amount of the aspirated colloid gets lost using liquid-based methods (as shown in Figs. 4.1 and 4.2) (direct smear, Pap stain,low magnification).



**Fig. 4.20 Cystic change in goiters.**
Elements depicted in this figure represent fluid from a long-standing hemorrhagic cyst. Large amount of background debris, uni- and multinucleated histiocytes showing phagocytosis of red blood cells (arrowhead), extracellular erythrocytes, inflammatory cells, and refractile crystalloid bars (arrow). Additional siderophages and calcium deposits are not shown (direct sediment smear, Pap stain, high magnification).

**Fig. 4.21 Squamous cells in thyroid cystic fluid.**
The aspirate from a 45-year-old man's thyroid cyst exhibits polymporphous, keratinized squamous cells along with a sanguineous and inflammatory background (direct sediment smear, Pap stain, low magnification).
*Cytology:* A broad differential diagnosis of well-differentiated keratinizing squamous cell carcinoma should be considered.
*Tissue diagnosis* (excision of a conglomerate of cysts): Cystic degeneration of a goiter, the pseudocysts are partially lined with metaplastic squamous cells.

**Fig. 4.22 Cyst-lining cells with regenerative changes.**
A 60-year-old woman presented with a cystic goiter. Detail of a conventional FNAB smear reveals a compact three-dimensional cluster composed of polymorphous cells (Pap stain).
*Tentative cytologic diagnosis:* Low N/C ratio and patternless lucid nuclei containing vacuoles suggest severe regenerative and degenerative alterations of cyst-lining cells.
*Histology* established a similar diagnosis; signs of malignant transformation were absent.

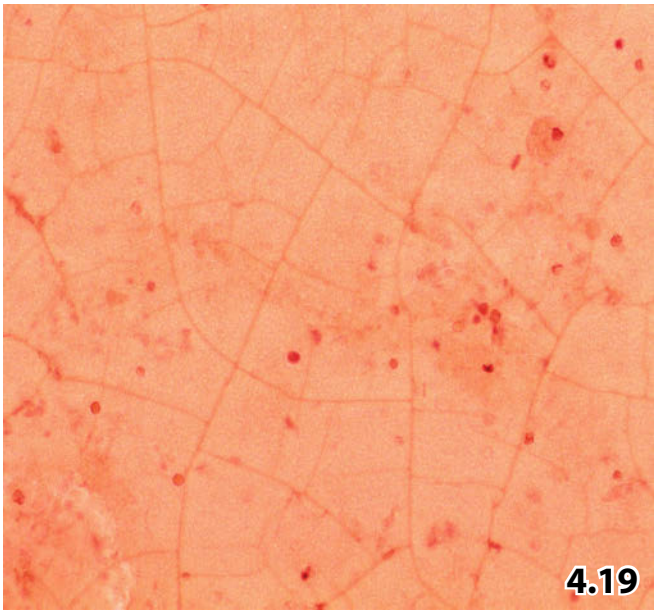
4.19

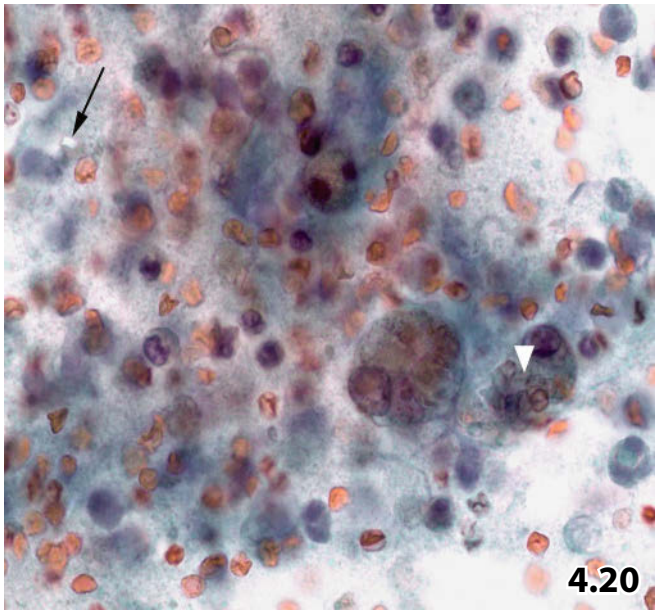
4.20

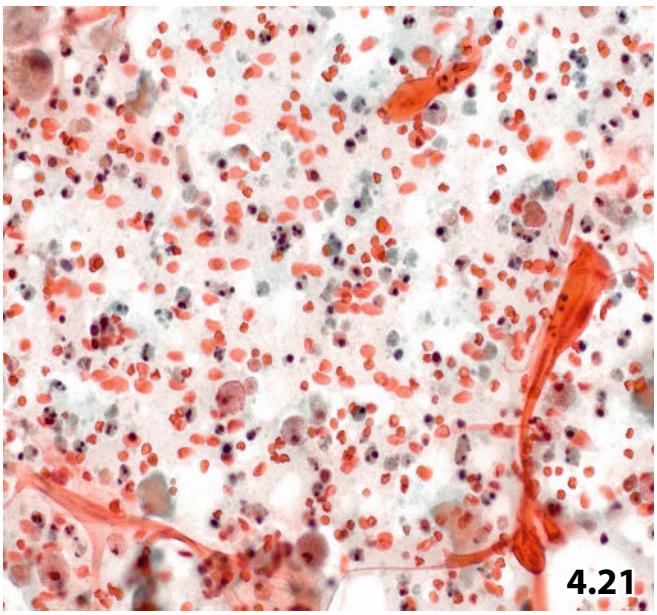
4.21

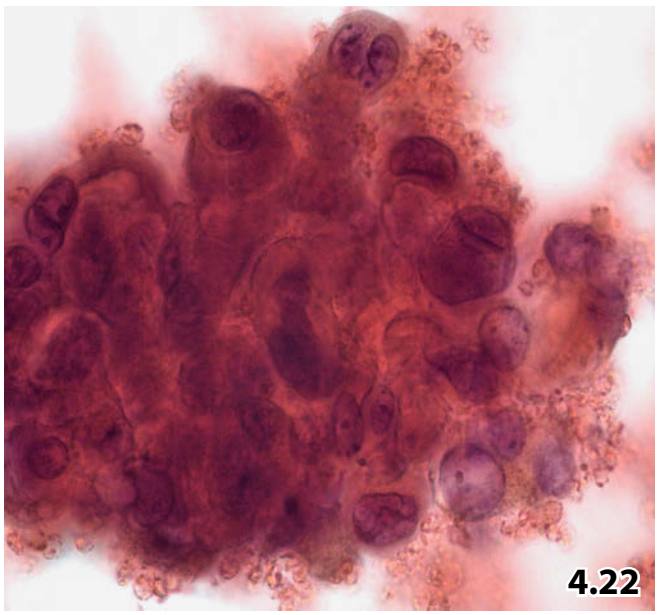
4.22

**Figs. 4.23–4.25 Diffuse and nodular thyroid hyperplasia (goiter).**
Classic cytologic features are presented under varied magnifications, and different types of staining methods are used. FNA material originates from three patients. Aspirated cells were conventionally prepared.

**Fig. 4.23** (case #1) Classical goiters are characterized by both dense colloid and abundant follicular cells forming regular sheets and follicles of varied size. Note numerous bare nuclei in the background of the smear mimicking lymphocytes (Pap stain, low magnification).

**Fig. 4.24** (case #2) MGG staining additionally shows focal oncocytic transformation of follicle cells (upper left) and strands of stromal cells (upper right) (low magnification).

**Fig. 4.25** (case #3) The morphologic features of follicle cells are presented at high magnification (Pap stain).

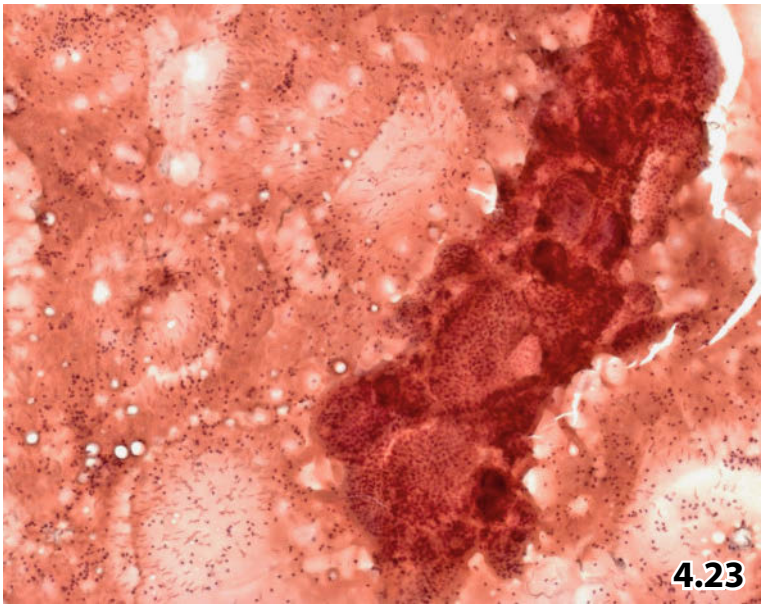
4.23

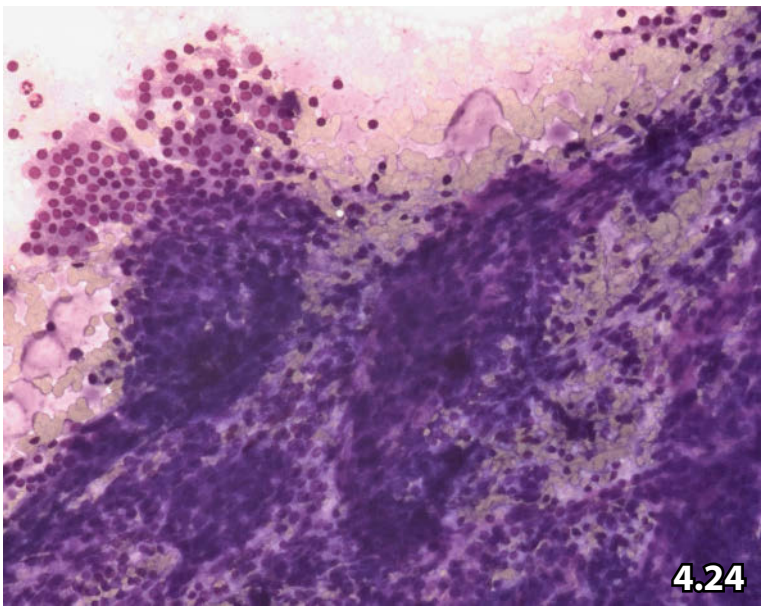
4.24

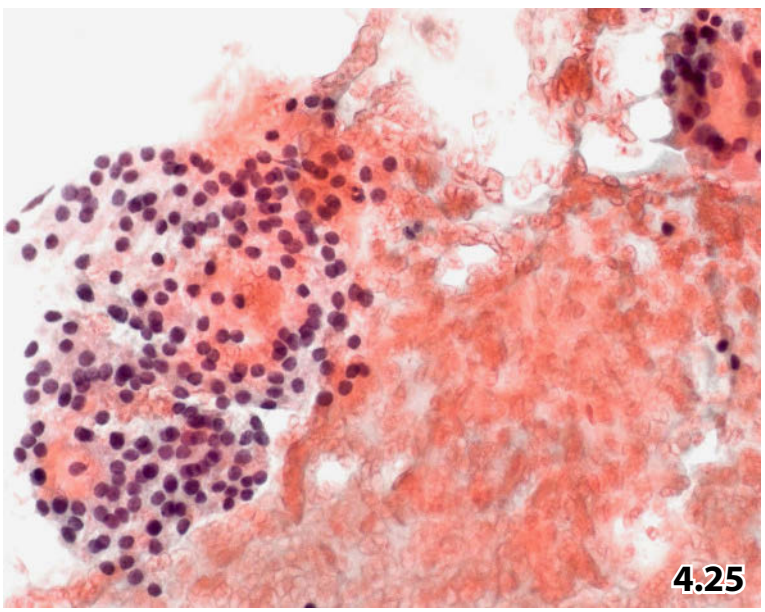
4.25

**Figs. 4.26 and 4.27 A Goiter: conventional smear versus liquid-based preparation.** Cells from an aspirate of a goiter were processed using different laboratory methods (Pap stain, high magnification).

**Fig. 4.26** Blurring of the cellular elements in conventional smears is caused by the bloody background.



**Fig. 4.27A** In contrast, liquid-based preparations (Cytospin) showing well-preserved cells and a clean background.

Liquid-based processing alters some cellular features and often produces shrunken and crumpled epithelial nuclei. The latter may mimic those in cells of papillary thyroid carcinoma.

**Figs. 4.27B and 4.28 Goiter: liquid-based preparation, Cytospin versus ThinPrep.** Both methods provide identical morphologic results (Pap stain, lower magnifications)

**Fig. 4.27** B Cytospin: Foam cells and well-preserved thyrocytes, the latter forming follicles occasionally filled with colloid. The background is clean except for granular detritus due to degenerating erythrocytes.

**Fig. 4.28** ThinPrep: Identical cellular appearance.

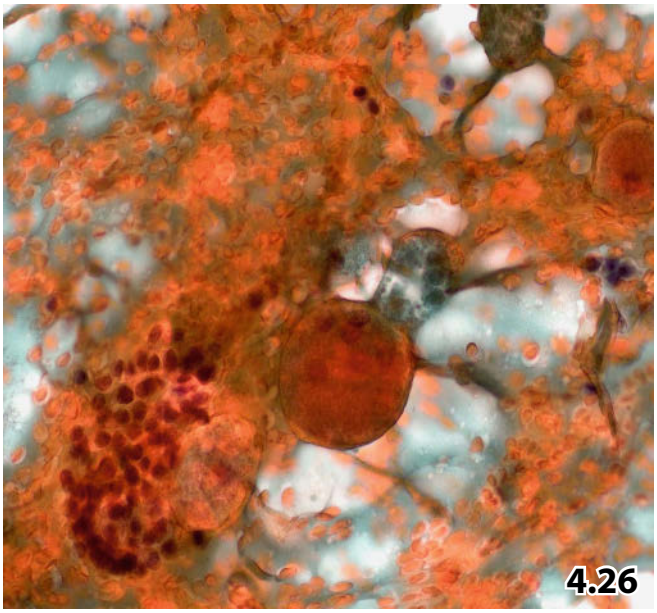
4.26

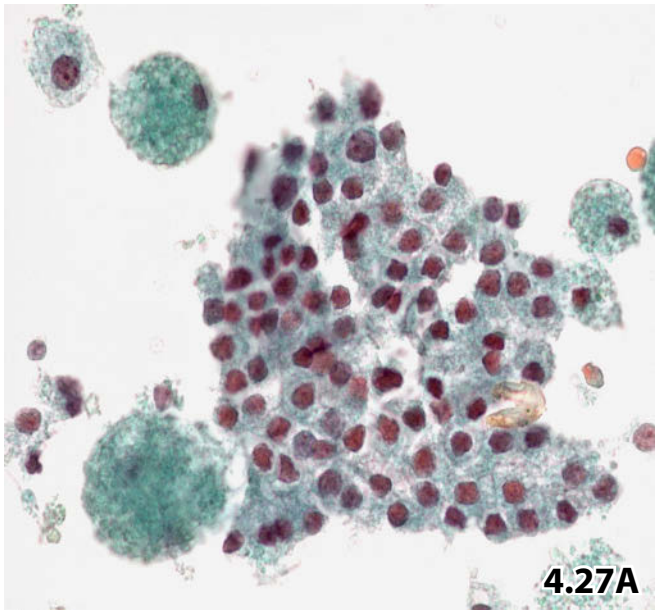
4.27A

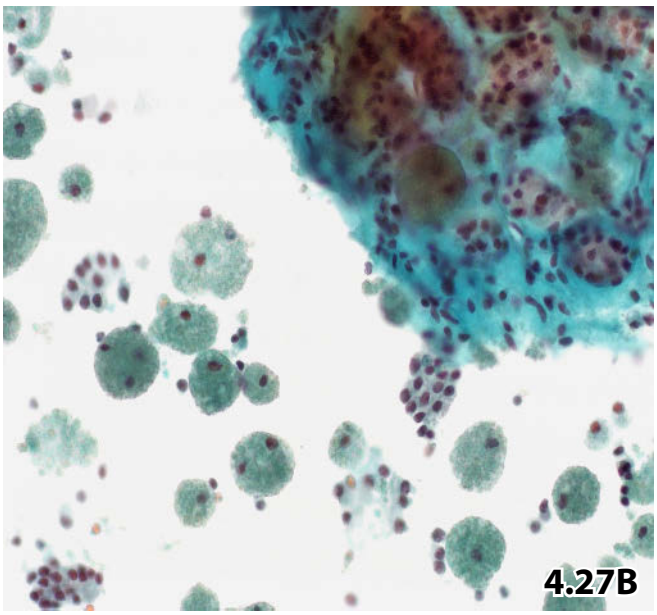
4.27B

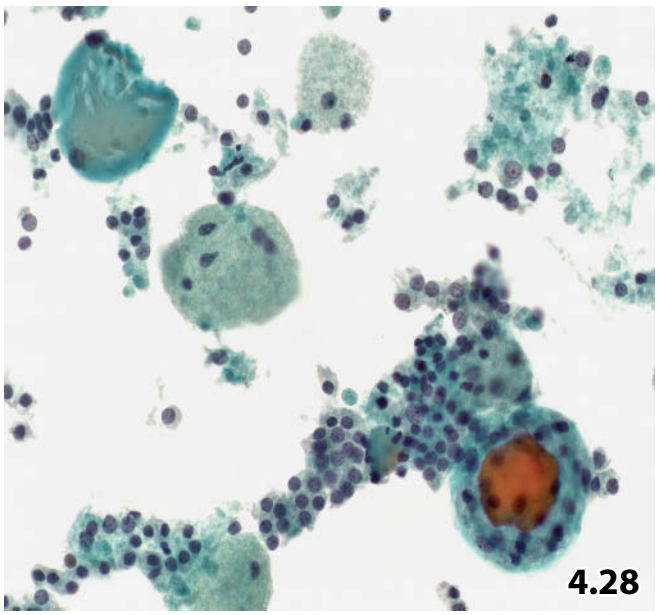
4.28

**Fig. 4.29 Papillary epithelial hyperplasia versus papillary carcinoma.**
High magnification shows a detail of a papillary cluster originating from hyperplastic epithelium of a goiter (FNAB direct smear, Pap stain).
*Cytology:* Distinguishing between benign papillary hyperplastic proliferation and papillary thyroid carcinoma can be very difficult. Still, the benign activated nuclei are bland and the typical grooves characteristic of papillary carcinoma are lacking (best seen upper right).
*Tissue diagnosis* (thyroidectomy): Multinodular goiter comprising hyperplastic epithelium and macropapillae.



**Figs. 4.30 and 4.31 Hyperplastic follicular cells: diagnostic considerations.**
FNAB of two patients' struma showing regenerative epithelial cell changes (conventional smears, Pap stain).

**Fig. 4.30** (case #1) Low N/C ratio and bland nuclear features allow a diagnosis of benign reactive follicle cells. Comparison with benign normal thyrocytes (bottom) reveal identical nuclear morphology (lower magnification).

**Fig. 4.31** (case #2) In this case, the reactive cells reveal enhanced nuclear polymorphism including occasional nuclear grooves (arrows) (high magnification). Differentiating from papillary thyroid carcinoma may be impossible by cytology. Accurate cytologic diagnosis is based on overall cell pattern, clinical history, and follow-up unless the diagnosis is ascertained by histologic tissue examination.

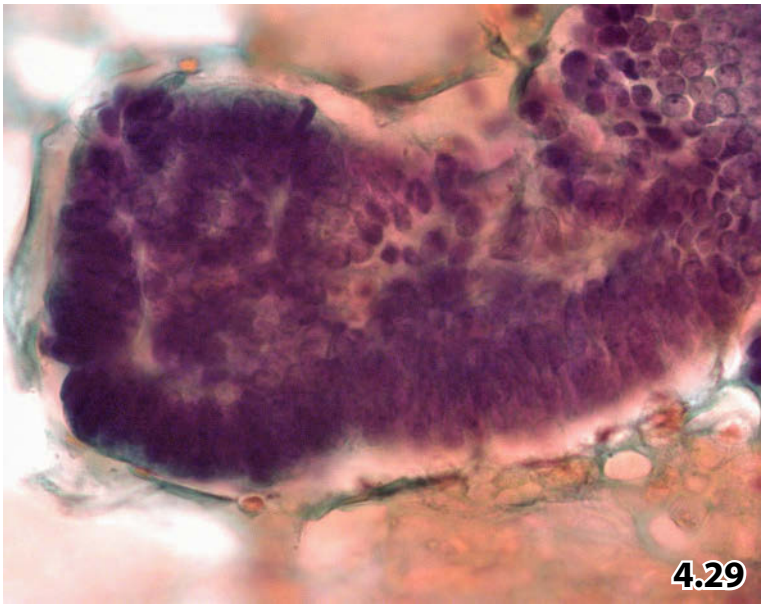
4.29

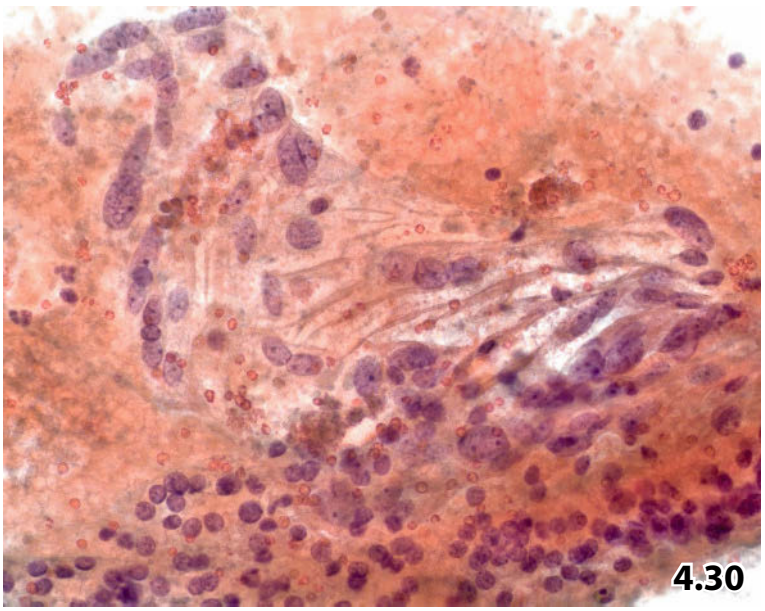
4.30

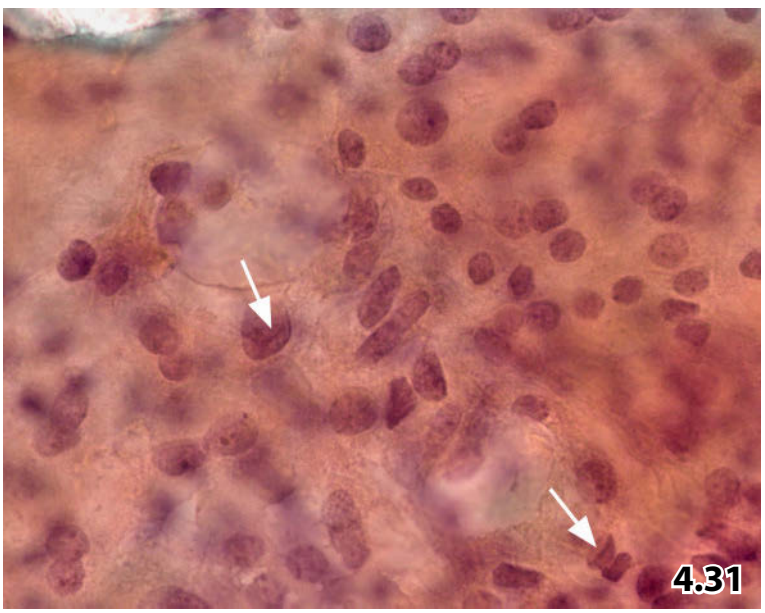
4.31

**Figs. 4.32 and 4.33 Epithelial hyperplasia in toxic goiter.**
FNAB of the thyroid gland of two patients presenting with primary hyperthyroidism. Direct smears were Pap-stained.

**Fig. 4.32** (case #1) FNAB in a 65-year-old woman. Follicular cells depicted in this figure exhibit characteristic cytoarchitectural and cytoplasmic features of thyroid hyperfunction (lower magnification).



**Fig. 4.33** (case #2) FNAB in a 15-year-old woman. Higher magnification focuses on activated nuclei showing variability in size and shape including prominent nucleoli. Please note cytoplasmic granularity of the follicular cells and a small group of epithelioid cells (upper left).

**Fig. 4.34 Epithelial regenerative atypias caused by antithyroid drugs.**
A 17-year-old young man being under antithyroid drug treatment for Basedow disease. FNAB from the thyroid shows pronounced alterations of the follicular cells: irregular grouping of enlarged follicular cells, excentrically positioned nuclei in large foamy and granular cytoplasm, marked variation of nucleolar size, and multinucleated epithelial giant cells (upper right). A low N/C ratio, regular nuclear shape, bland chromatin, and interspersed lymphocytes (arrows) are leading indicators of a benign reactive lesion (direct smear, Pap stain, higher magnification).

**Figs. 4.35 and 4.36 Extremely hyperplastic cell changes.**
This is an impressive cytologic and histologic example of highly confusing reactive cell changes from two patients.

**Fig. 4.35** FNAB of a toxic goiter shows extremely pronounced variations in cell size, chromatin texture, and in nucleolar features. Degenerative nuclear changes are frequently encountered comprising apoptosis and nuclear vacuolization (arrows) (Pap stain, high magnification).

**Fig. 4.36** A histologic section of Hashimoto thyroiditis shows extreme alterations of the follicle cells (HE stain, lower magnification).

Extreme regenerative cellular alterations caused by varied disorders may occasionally be encountered. Discriminating between benign and malignant lesions is challenging.

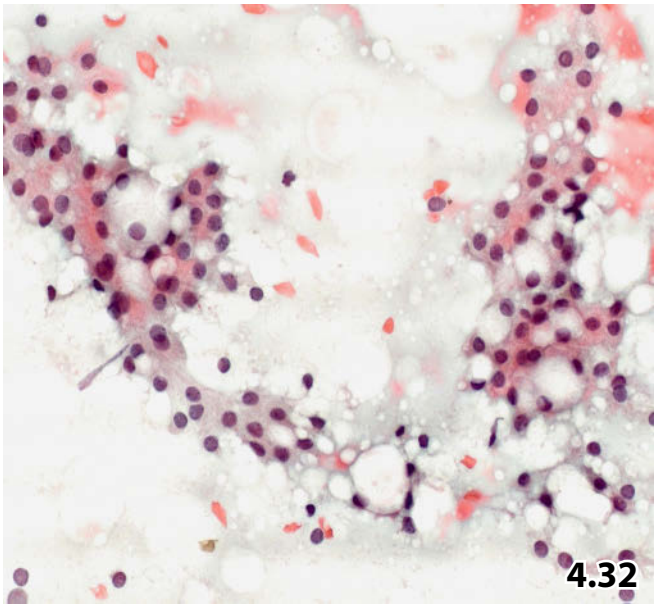
4.32

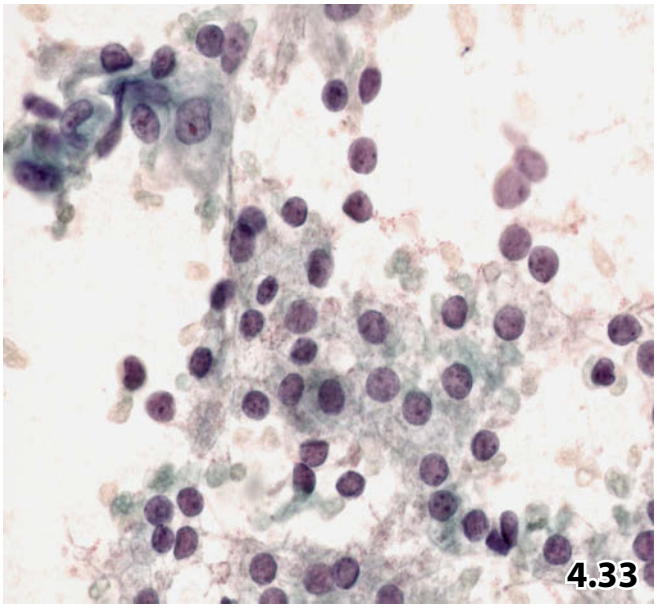
4.33

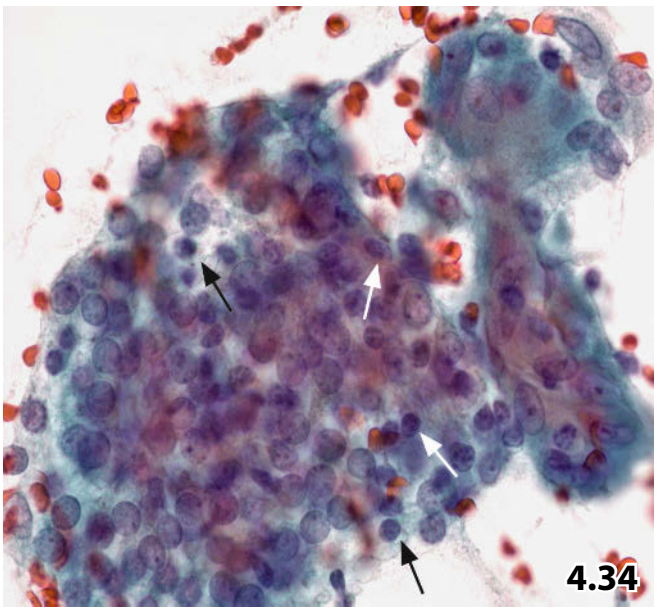
4.34

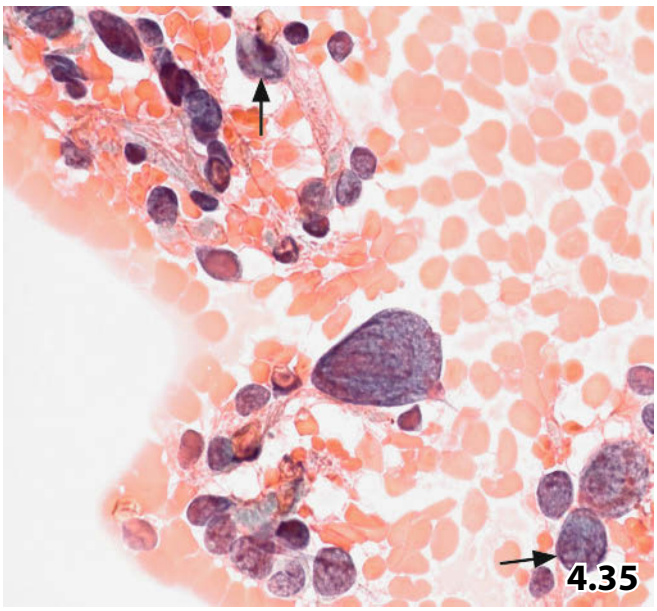
4.35

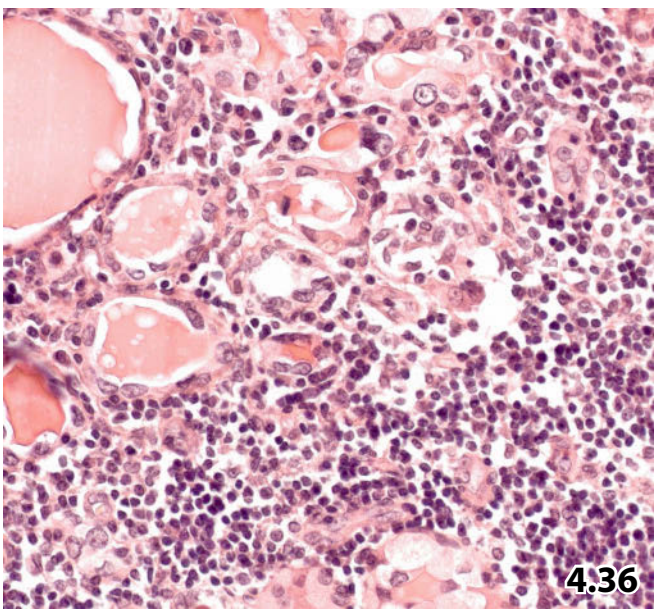
4.36

**Figs. 4.37 and 4.38 Microfollicular adenoma.**
Two examples of a microfollicular adenoma with different processing of the aspirates and completed by ICM DNA studies are presented.

**Fig. 4.37A–C** (case #1) FNAB of a thyroid nodule in a younger woman.
*Cytomorphologic and cytometric features* suggested well-differentiated follicular carcinoma.
*Tissue diagnosis:* Microfollicular adenoma.



**A** A conventional smear shows numerous small aggregates of epithelial cells forming small follicles rarely filled with colloid (direct smear, Pap stain, low magnification). **B** High magnification indicates irregular cellular grouping, irregular nuclear contours, and pronounced nucleoli. **C** Digital single cell DNA analysis provides a triploid histogram (Pap-prestained Feulgen stain, Ahrens Cytometrie System).

**Fig. 4.38** (case #2) A 49-year-old man presented with a thyroid nodule. Liquid-based preparation (ThinPrep) revealed cell features akin to those depicted from conventional smears of the previous case (Pap stain, higher magnification).
*ICM DNA study:* Diploid DNA distribution pattern (not shown).
*Tentative cytologic/cytometric diagnosis:* Microfollicular thyroid neoplasia with nuclear atypia. Cytometric result suggested adenoma or well-differentiated follicular carcinoma of low malignant potential.
*Follow-up* (clinical, cytological, and ultrasound): There was no evidence of malignancy over a period of 3 years. Surgical exploration was not performed.

**Fig. 4.39A, B Atypical adenoma.**
Physical examination of a 46-year-old man revealed a sharply defined thyroid nodule (2.5 cm in diameter). **A** FNAB displayed marked pleomorphism of follicular cells including multinucleation and compact cell clustering. Abnormal dense granular chromatin texture is obvious (direct smear, Pap stain, high magnification). **B** Image cytometry (Pap-prestained Feulgen stain, AutoCyte) yielded a clearly atypical DNA histogram: aneuploid polyploid stemlines in the 1.25c and 2.5c area and numerous aneuploid single cells, even >9c.
*Cytology/cytometry:* Follicular carcinoma was suggested from cytologic and cytometric studies.
*Tissue diagnosis:* Atypical follicular adenoma.

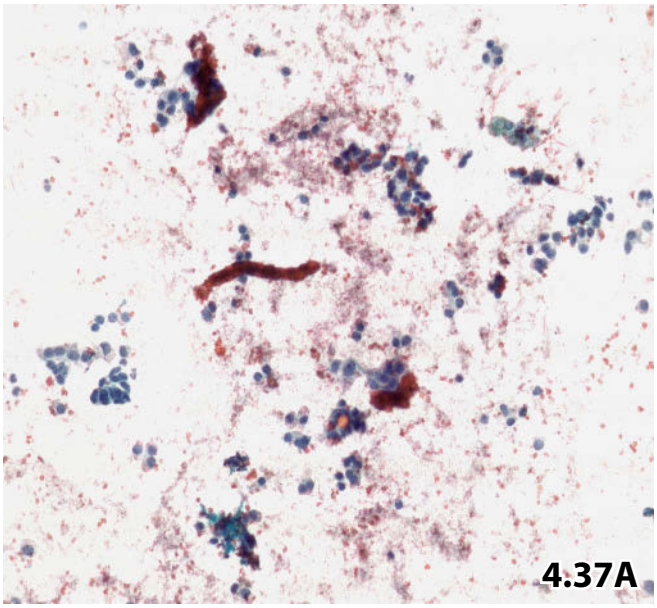
4.37A

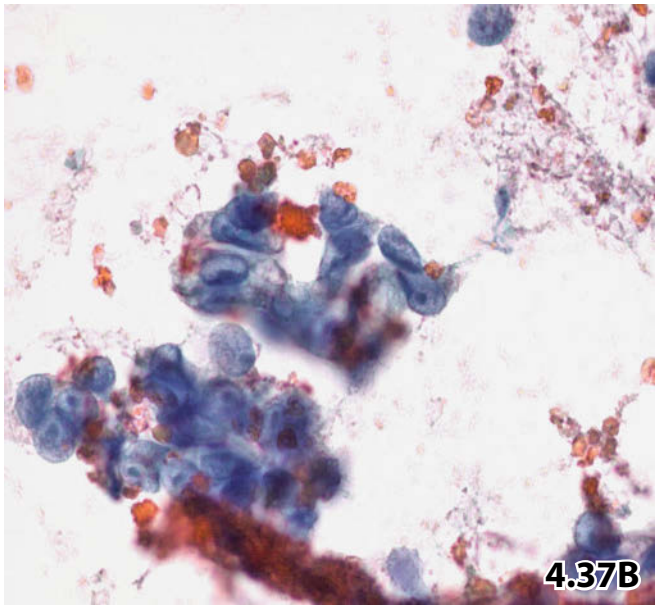
4.37B

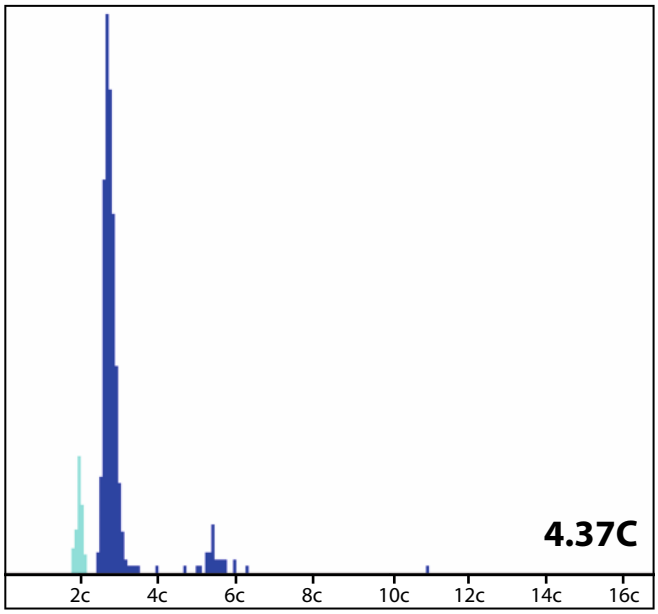

4.37C

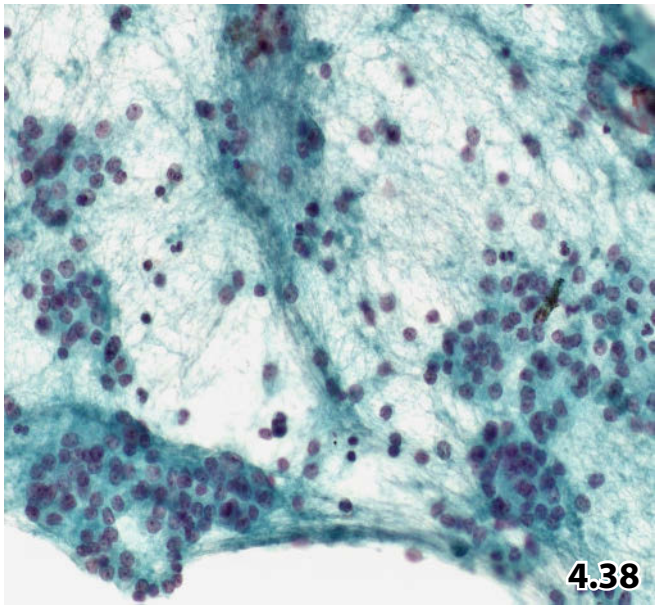
4.38

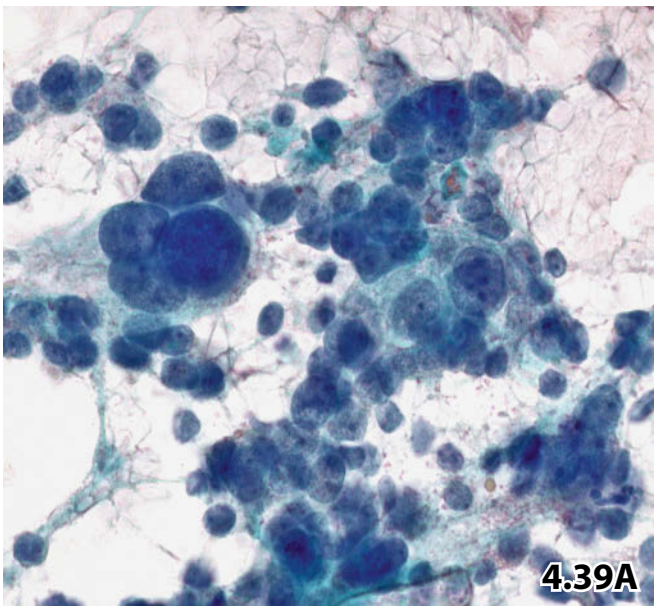
4.39A

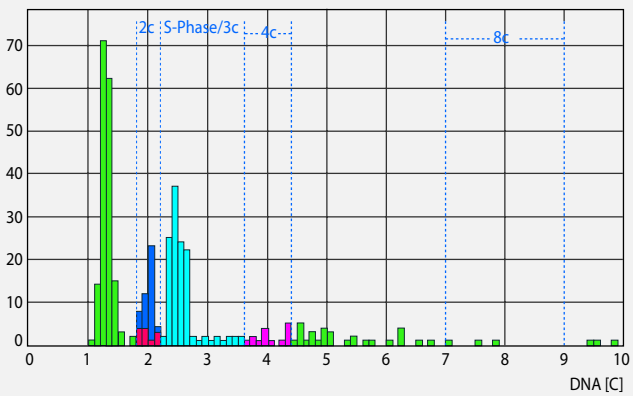

4.39B

**Figs. 4.40 and 4.41 Well-differentiated follicular carcinoma.**
Two examples of well-differentiated follicular carcinoma verified in tissue sections. Varied cytologic phenotypes in the fine-needle aspirates, quantitiative DNA analysis, and diagnostic dilemmas are presented.

**Fig. 4.40** (case #1) A 72-year-old man presenting with hyperthyroidism and myastenia gravis.
High magnification of a direct smear (Pap stain) reveals monomorphic appearance of the thyrocytes forming follicles with and without colloid. Irregular nuclear overlapping and eccentrically positioned nucleoli suggest malignancy. ICM DNA was not performed.
*Tentative cytologic diagnosis:* Suspicious of well-differentiated follicular carcinoma.
*Histology* (excisional biopsy): Microscopic tissue examination detected a predominantly capsulated well-differentiated follicular carcinoma.

**Fig. 4.41** (case #2) A 41-year-old woman presented with a recently increasing thyroid nodule (5×4×3 cm). FNAB was performed, direct smears were Pap-stained.
*Cytology and cytometric results* (DNA diploidy, not shown) were suggestive of microfollicular adenoma.
*Tumorectomy and subsequent histology* detected a well-differentiated follicular carcinoma.
**A** Low magnification exhibits a monotonous appearance of grouped epithelial cells predominantly forming small follicles. Follicular colloid is flimsy and barely visible (arrows).
**B** High magnification also shows striking uniform appearance; nuclear atypia does not seem of paramount importance.

**Fig. 4.42 Poorly differentiated follicular carcinoma.**
High magnification exhibits a large cell cluster of a follicular neoplasia with evidence of severe atypias. Dense cell clustering, a high N/C ratio, nuclear irregularities, and huge nucleoli are hallmarks of malignancy (FNAB, direct smear, Pap stain).
*Image cytometric study* detected an aneuploid DNA distribution pattern (not shown).
*Cytologic diagnosis* (supported by cytometric result): follicular carcinoma.
*Tissue diagnosis* (total thyroidectomy and lymphadenectomy): locally invasive and metastatic follicular carcinoma.

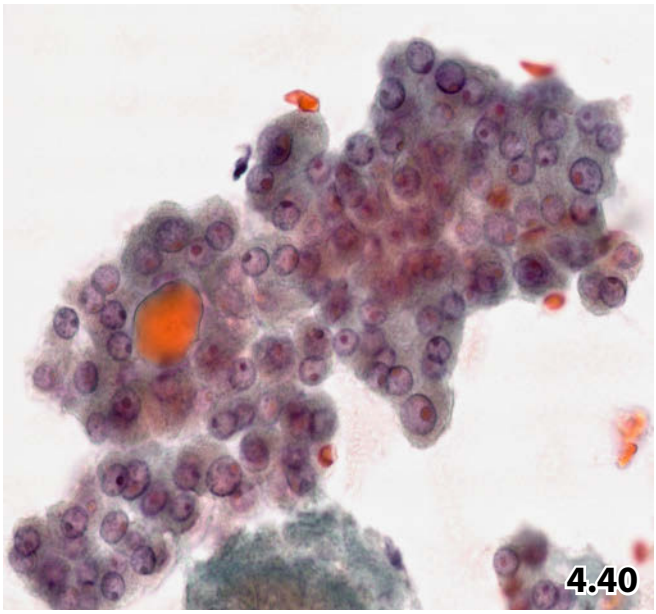
4.40

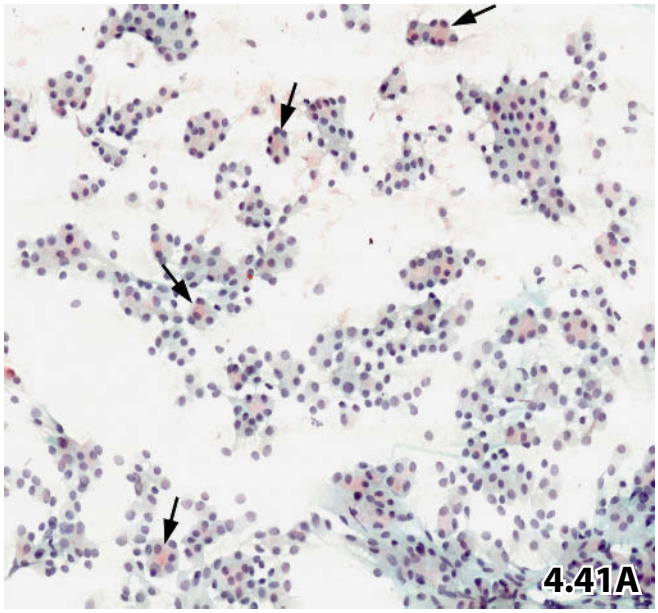
4.41A

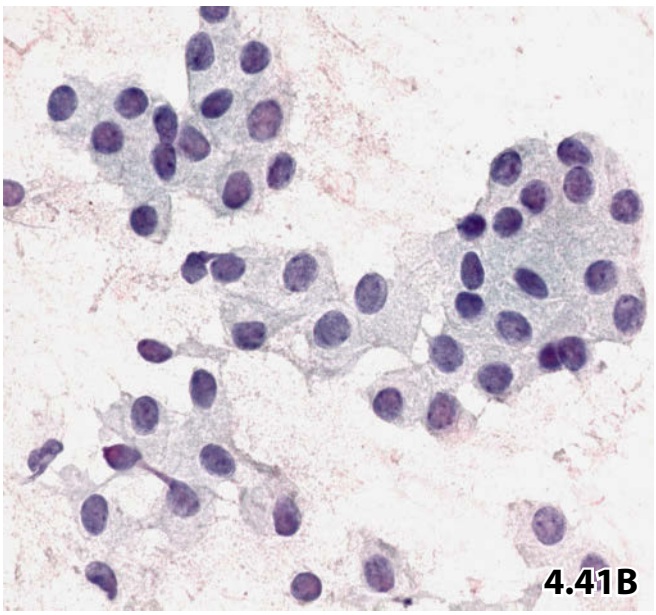
4.41B

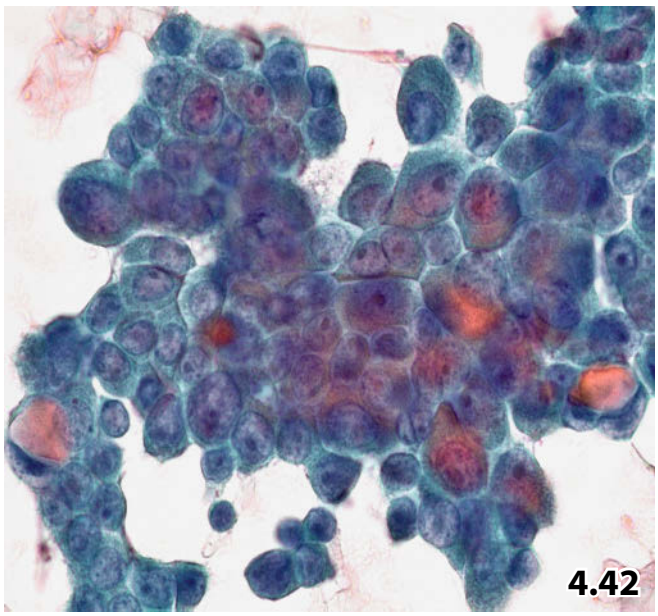
4.42

**Figs. 4.43 and 4.44 Low-grade oncocytic neoplasia.**
Two examples of low-grade oncocytic neoplasms are demonstrated by fine-needle aspiration cytology using different laboratory processes.

**Fig. 4.43** (case #1) During the course of routine physical examination, a 66-year-old woman was found to have a firm nodule in her left thyroid. Initial FNAB was performed. Cobblestone arrangement of the follicular cells associated with dense polygonal amphophilic cytoplasm indicates low-grade oncocytic follicular neoplasia. Note the small follicular formation lower right (conventional smears, Pap stain, low magnification).
*Tentative cytologic diagnosis:* Oncocytic follicular neoplasia with mild atypias.
*Tissue diagnosis* (tumorectomy): Oncocytic adenoma.

**Fig. 4.44** (case #2) Struma uninodosa in a middle-aged woman. Aspirated material was processed using ThinPrep technology. High magnification focuses on oncocytic cell features. Eccentrically located nuclei and certain variations in nuclear shape may suggest a low-grade malignant lesion. Digital quantitative DNA analysis detected a polyploidizing hypodiploid-aneuploid stem line (not shown).
*Tentative cytologic diagnosis and discussion:* Oncocytic low-grade neoplasia. DNA aneuploidy may indicate increased malignant potential or a well-differentiated invasive carcinoma.
*Tissue diagnosis:* Total thyroidectomy was performed, histologic examination revealed a focally invasive atypical oncocytic adenoma (only minor invasive growth).

**Figs. 4.45 and 4.46 Oncocytic carcinoma: routine smear versus liquid-based preparation.**
FNABs are derived from two patients suffering from invasive and relapsing oncocytic follicular carcinoma of the thyroid. If the following features are present in thyroid aspirates, a cytologic diagnosis of oncocytic carcinoma can be assessed or at least suggested:

**Fig. 4.45** (case #1) Discohesive oncocytes with eccentrically positioned nuclei, varying N/C ratio, slight nuclear irregularities, irregular coarse chromatin, polymorphous macronucleoli (conventional smear, Pap stain).

**Fig. 4.46** (case #2) Similar malignant cell characteristics can be observed in liquid-based specimens (ThinPrep). In liquid-based preparations, nuclei of the neoplastic cells often exhibit increased polymorphism, shrinkage and crumpling as compared to conventional smears.

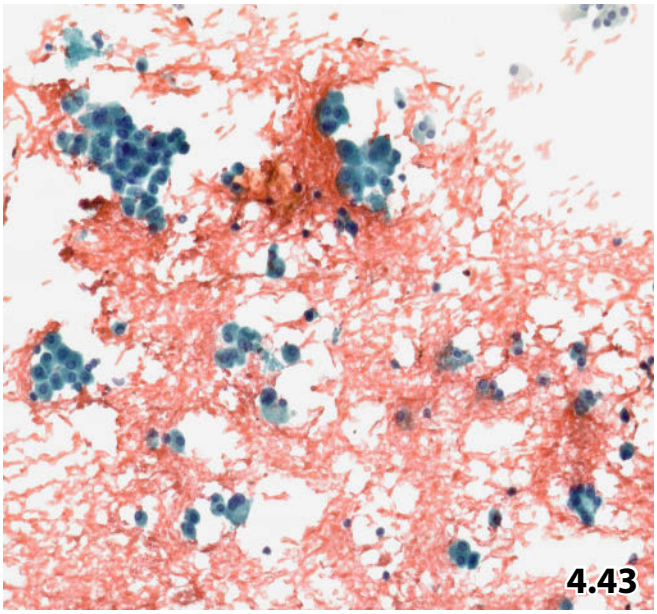
4.43

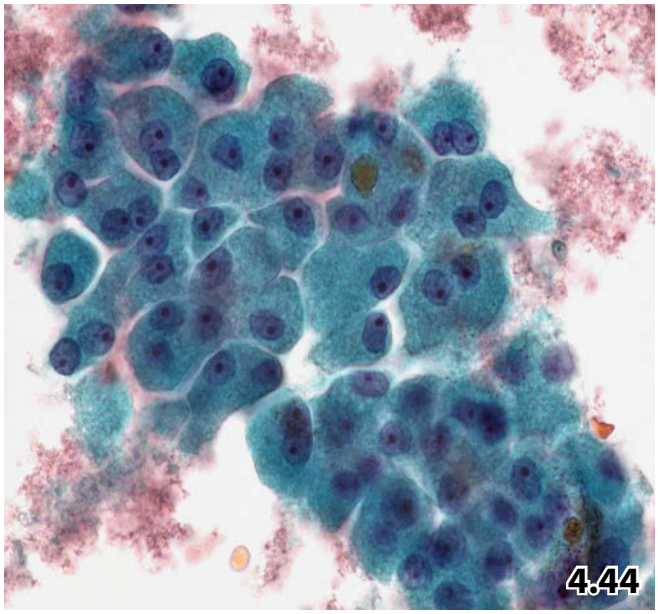
4.44

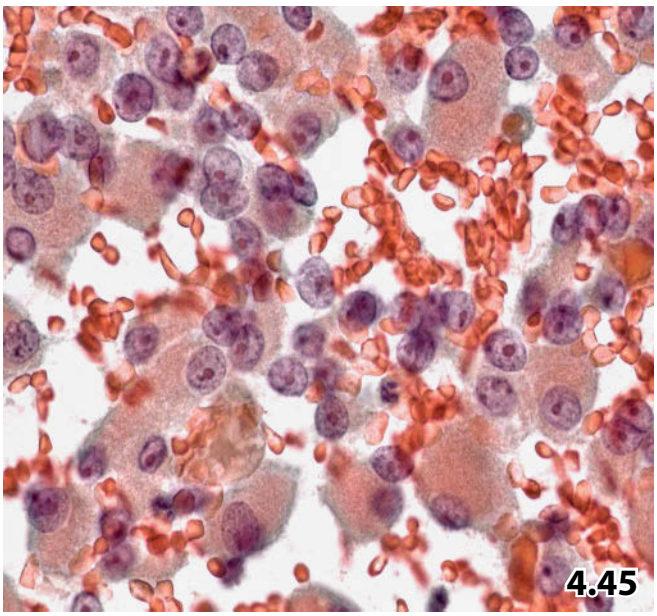
4.45

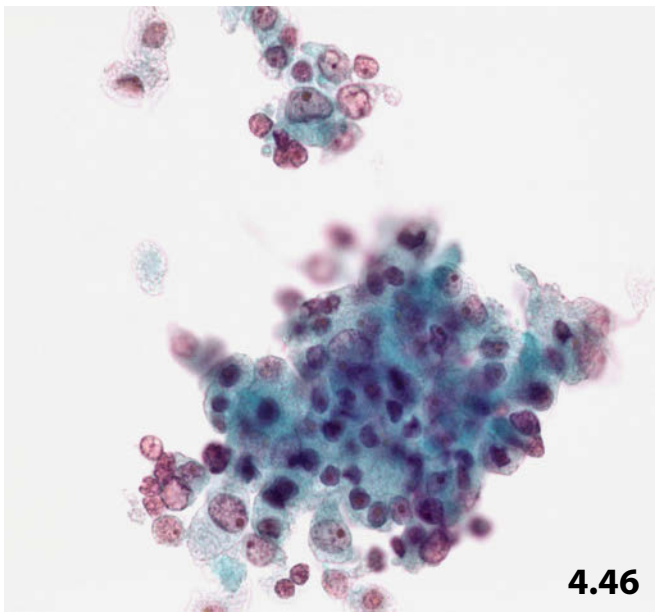
4.46

**Figs. 4.47–4.50 Cytoarchitecture of papillary carcinoma.**
Cytoarchitecture is demonstrated by direct smears of fine-needle aspirates using different staining methods and varied magnification.

**Fig. 4.47** (case #1) Papillary formations comprising fibrovascular cores and cellular palisading at the periphery (arrows). Cohesive monolayered sheets (arrowheads) are also highly characteristic for papillary thyroid carcinoma (MGG stain, low magnification).



**Fig. 4.48** (case #2) Pap-stained smear. Note (1) distinct cellular palisading, (2) mesenchymal cores containing subepithelial-located wide capillaries (arrows), and (3) isolated columnar tumor cells (higher magnification).

**Fig. 4.49** (case#3) Psammoma bodies are embedded in the stromal and/or epithelial compartment of the tumor papillae, a feature that is observed in the majority of thyroidal papillary carcinomas (Pap stain, high magnification).

**Fig. 4.50 A** (case #4) The fourth case of papillary carcinoma exclusively presented flat tumor cell sheets in the aspirate smears (Pap stain, low magnification). **B** (case #4) Neoplastic nuclear key features (lower right) become readily apparent at higher magnification (see Fig. 4.51).

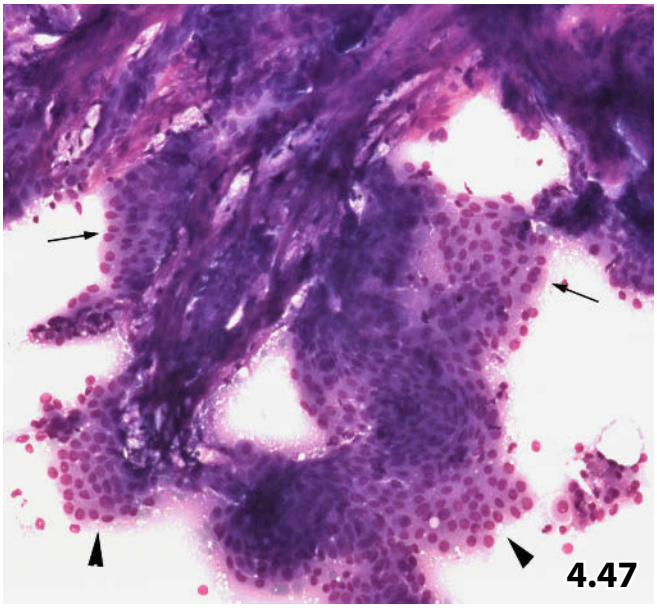
4.47

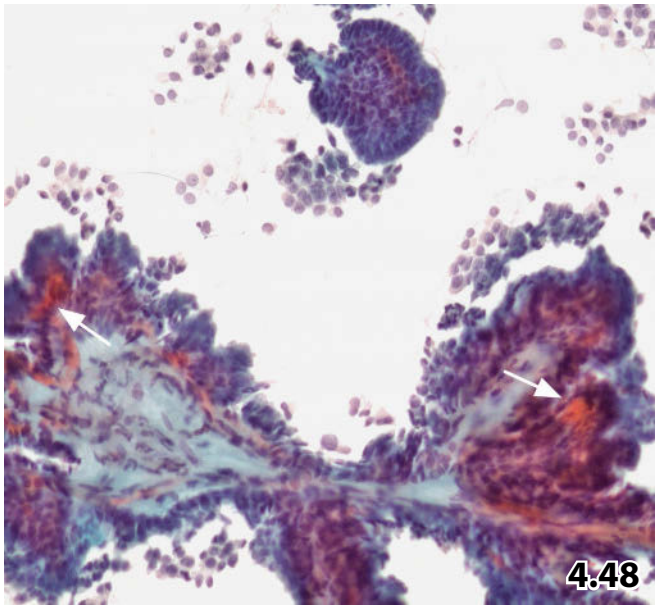
4.48

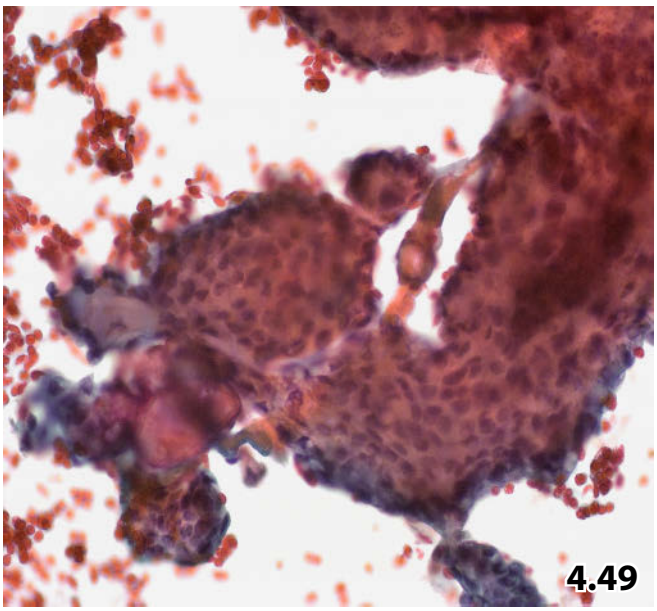
4.49

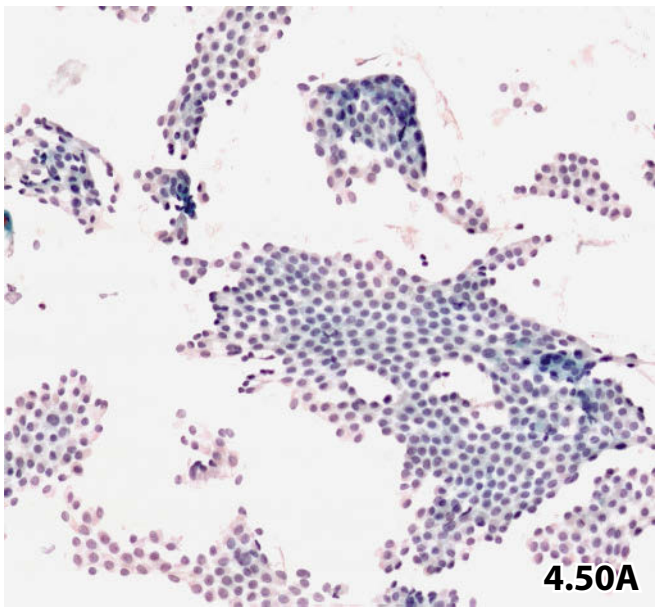
4.50A

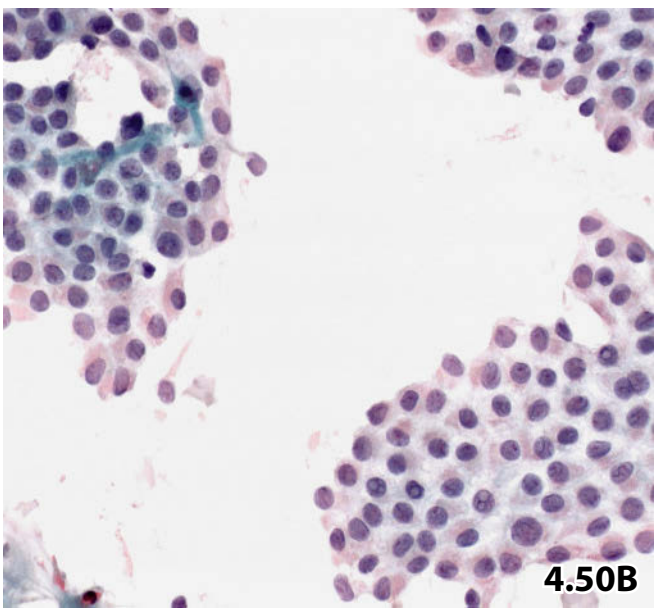
4.50B

**Fig. 4.51 A, B Nuclear hallmarks of papillary carcinoma.**
Typical nuclear features are displayed both in conventional smear and liquid-based preparation from a thyroid FNAB (same nodule, Pap stain, high magnification). **A** Conventional smear: Irregular nuclei with grooves and longitudinal folds including nuclear cytoplasmic inclusions (see also Fig. 4.50B). Dusty chromatin and/or nuclear clearing are distinct. **B** Liquid-based preparation (ThinPrep): Nuclear folding and nucleoli are definitely more pronounced in the ThinPrep specimen as compared with direct smears. Various shrunken nuclei are identifiable.

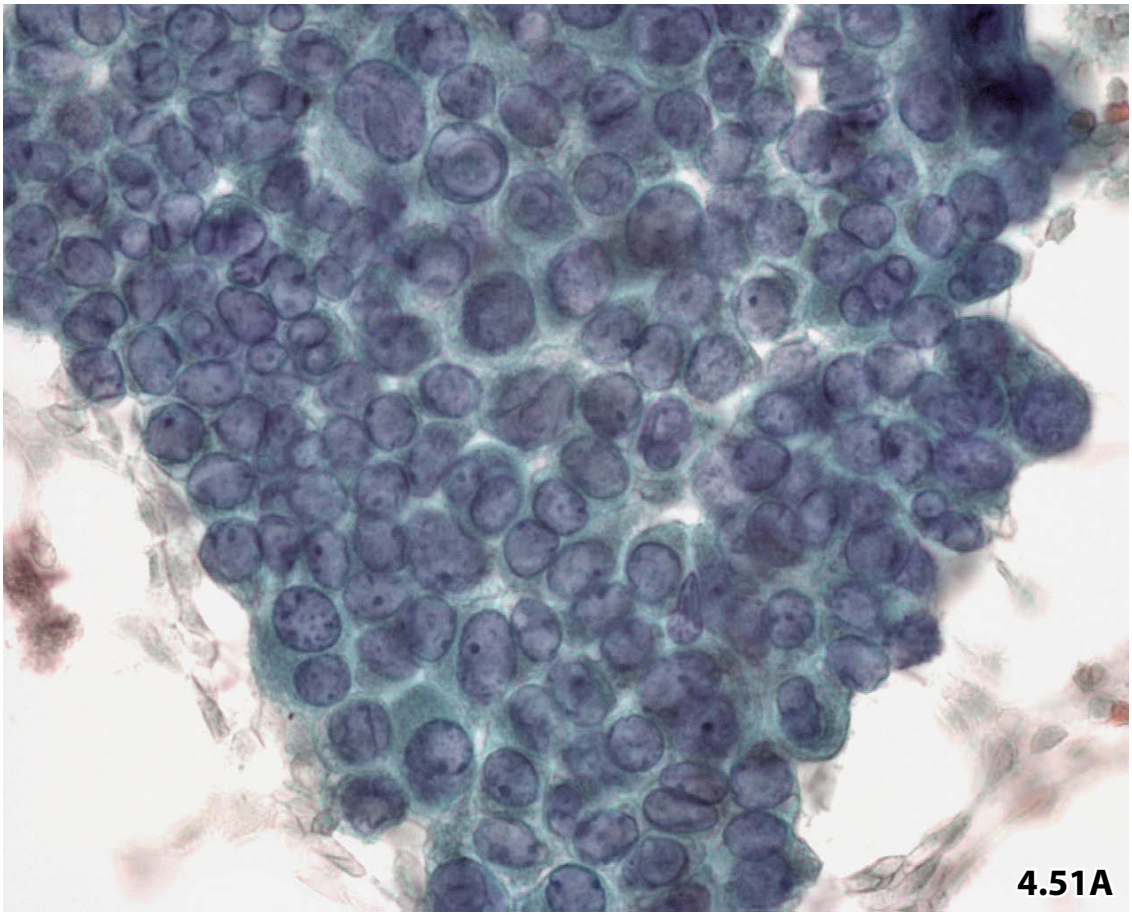

4.51A

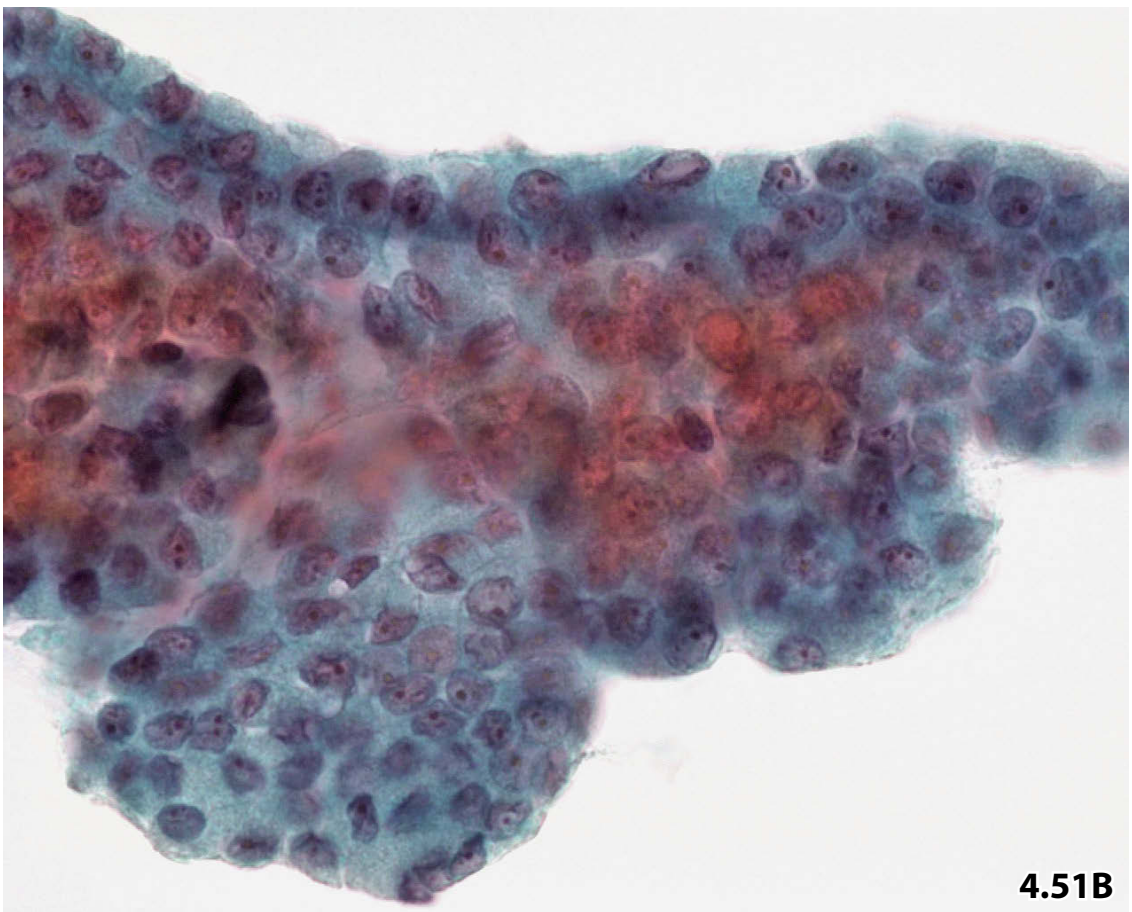

4.51B

**Fig. 4.52 Papillary carcinoma: small-cell variant.**
Morphologic nuclear features can be obscured due to small size and dense structure of the nuclei. But careful microscopic evaluation will elucidate the characteristic nuclear features. Please note the small palisaded epithelial cell group (lower left) (FNAB, direct smear, Pap stain, high magnification).



**Fig. 4.53A, B Papillary carcinoma: follicular variant.**
A 24-year-old man presenting with a solitary, sonographically complex thyroid lesion comprising cystic formations and microcalcification. US-guided FNAB provided hypercellular direct Pap-stained smears.
*Cytologic diagnosis:* Cystic papillary thyroid carcinoma.
*Comment:* Neoplastic follicular formations were scarce, preventing an accurate tumor subtyping (compare histologic diagnosis).
*Tissue diagnosis* (hemithyroidectomy): Mostly encapsulated papillary thyroid carcinoma, follicular variant.
**A** Lower magnification presents a rare microfragment composed of densely packed cells forming colloid-filled follicles of varied size (arrows). Nuclei are atypical showing irregular borders. Chromatin is cleared (lower right) or granular (upper left). **B** At high magnification, nuclear key features indicating thyroid papillary carcinoma are readily identified in selected papilliform cell clusters.

**Fig. 4.54 Papillary carcinoma: oncocytic variant.**
A pure oncocytic population of a histologically verified oncocytic papillary carcinoma is shown at high magnification. The neoplastic nuclei exhibit wrinkling, cleaving, and longitudinal grooves (these features are not detectable in the nuclei of other oncocytic tumor entities). Unequivocal papillary formations are lacking (FNAB, direct smear, Pap stain).

**Figs. 4.55 and 4.56 Cystic papillary carcinoma.**
Two younger women presented with cystic lesions in their thyroid. The aspirated fluids were processed by conventional centrifugation; direct sediment smears were Pap-stained.
*Cytology:* Cystic papillary carcinoma was suspected from fine-needle aspiration cytology in both cases, and the diagnosis was confirmed by histology.

**Fig. 4.55** (case #1) High magnification shows a small compact epithelial cluster and the classical nuclear features associated with thyroid papillary carcinoma. The background of the smears was composed of debris.

**Fig. 4.56** (case #2) Lower magnification shows similar atypical cell cluster as described above including a psammoma body (enclosed in the cell cluster, upper right) and foam cells in the background.

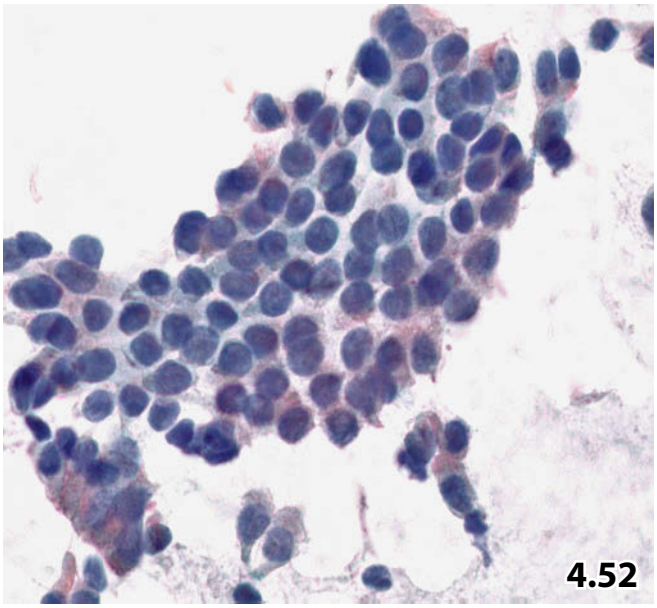
4.52

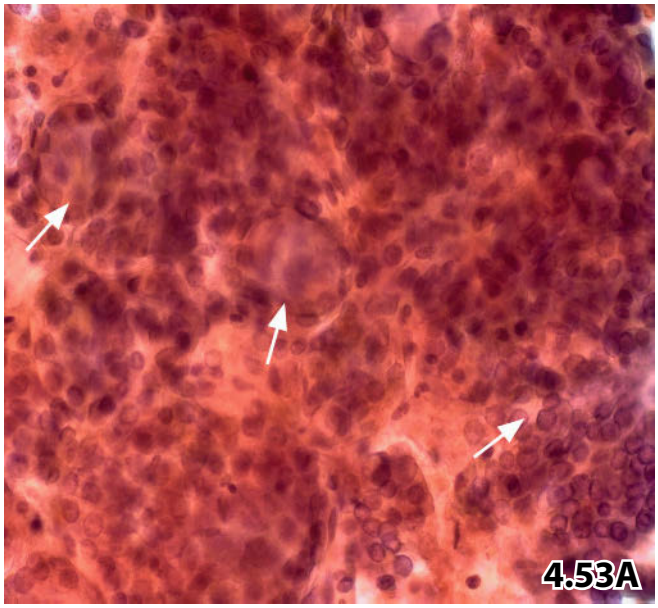
4.53A

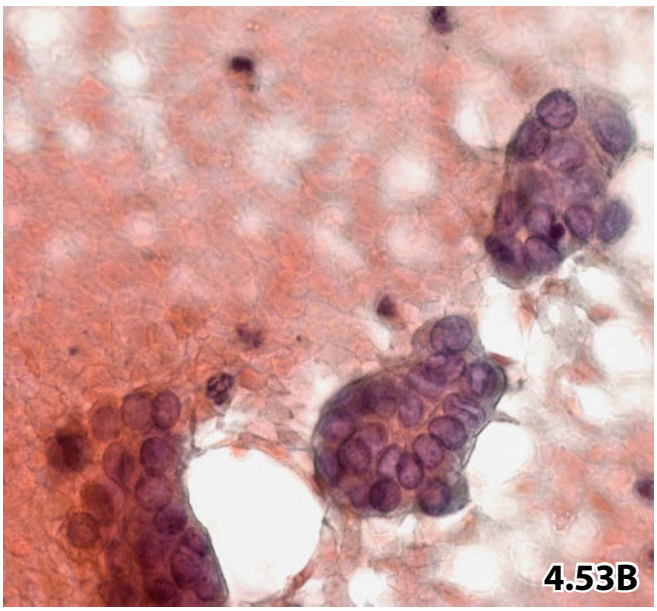
4.53B

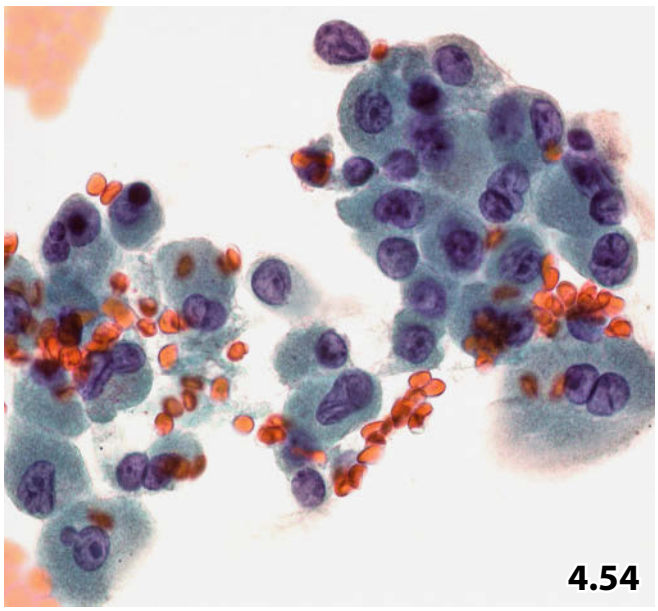
4.54

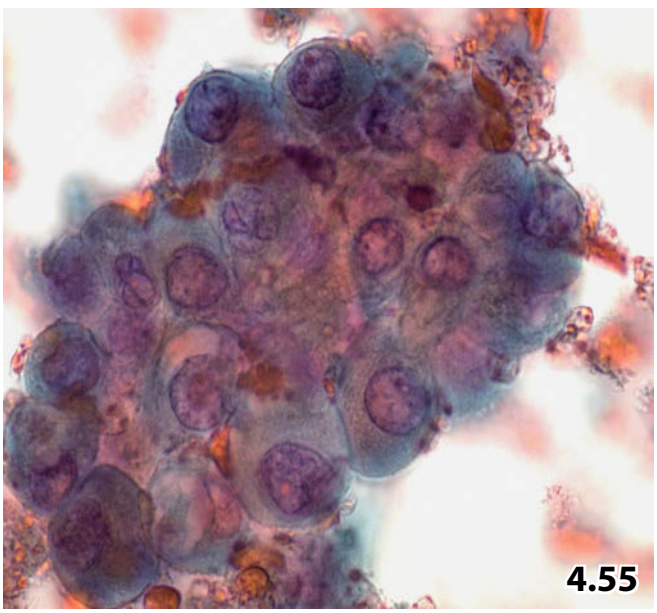
4.55

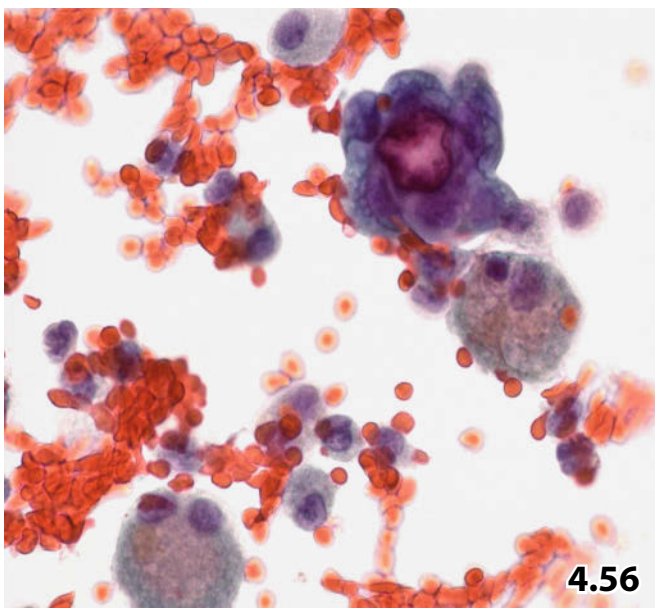
4.56

**Fig. 4.57 Hyperplasia of cyst-lining epithelial cells versus cystic papillary carcinoma.** A 16-year-old man presented with a relapsing cystic goiter. A previous right-sided subtotal thyroidectomy did not reveal any suggestion of a neoplastic disorder. FNAB from the left thyroid lobe yielded sanguineous cystic fluid containing large papilliform clusters composed of follicular cells. Microscopy at lower magnification displays nuclear crowding, mild nuclear atypia, and cellular palisading (e.g., lower right) (direct smear, Pap stain, lower magnification).
*Tentative cytologic diagnosis:* Very likely cystic papillary carcinoma.
*Tissue diagnosis:* Left-sided thyroidectomy and subsequent histologic examination found a cystic goiter presenting with hyperplasia of the cyst-lining epithelium including macropapillae. Meticulous search for invasive growth gave a negative result.

**Figs. 4.58 and 4.59 Medullary thyroid carcinoma: classic variant.**
Cytomorphology and immunocytochemistry of classic medullary thyroid carcinoma are presented using direct smears of fine-needle aspirates from two different patients. Conventional smears were Pap-stained.

**Fig. 4.58A–C** (case#1) Medullary thyroid carcinoma relapsing 8 years after the primary diagnosis and a successful therapy in a 54-year-old woman. Initial FNAB was performed for the preliminary diagnosis. **A** Cellular direct smears exhibiting the distinct appearance of medullary carcinomas: cohesive cell groups and syncytial type of tissue fragments are composed of monomorphic polygonal to spindle-shaped cells; isolated cells are common (Pap stain, low magnification). **B** Detail focuses on cellular features: (1) the plasmacytoid and fusiform appearance of isolated cells, (2) granular cytoplasm, (3) nuclear grooves (arrows), (4) nuclear inclusions (arrowheads), and (5) dense and coarse chromatin. **C** With positive immunostaining for calcitonin, a conclusive diagnosis of medullary carcinoma can be established (Pap-prestained conventional smear).

**Fig. 4.59** (case #2) Primary medullary thyroid carcinoma in a 32-year-old woman. The cell-rich sample is mainly composed of spindle cells with interspersed neoplastic giant cells. Hyaline material representing amyloid protein are both surrounded by tumor cells and isolated in the background (arrows) (FNAB, direct smear, Pap stain, lower magnification).
Amyloid staining properties are presented in Fig. 4.62B.

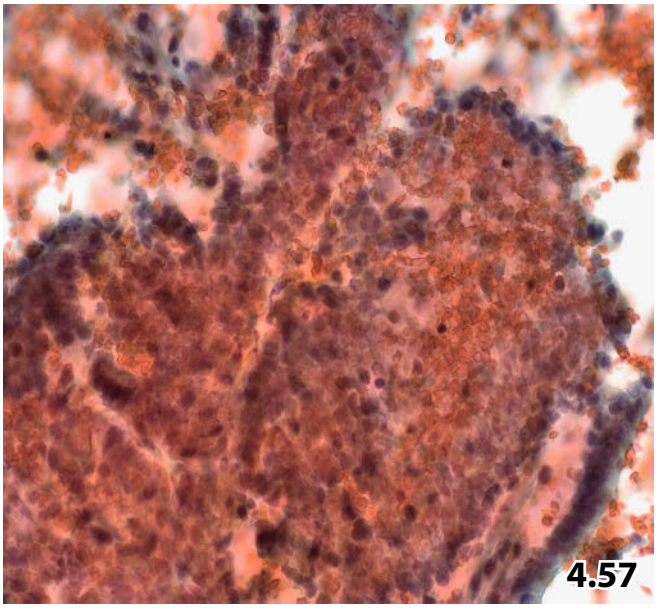
4.57

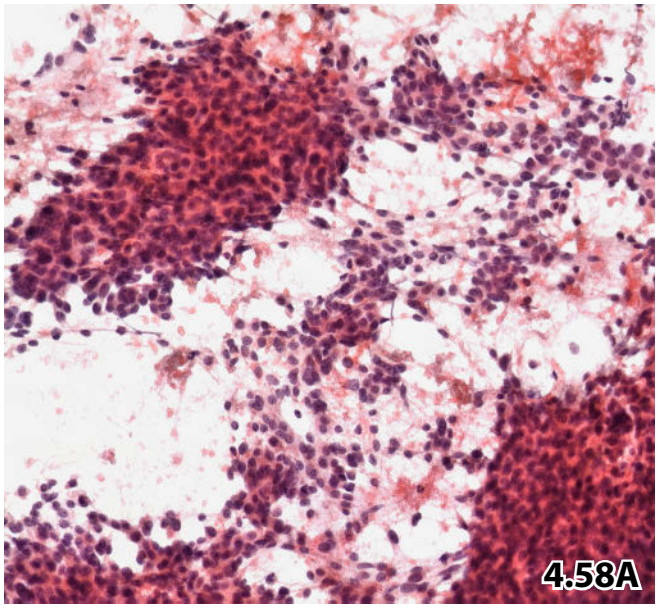
4.58A

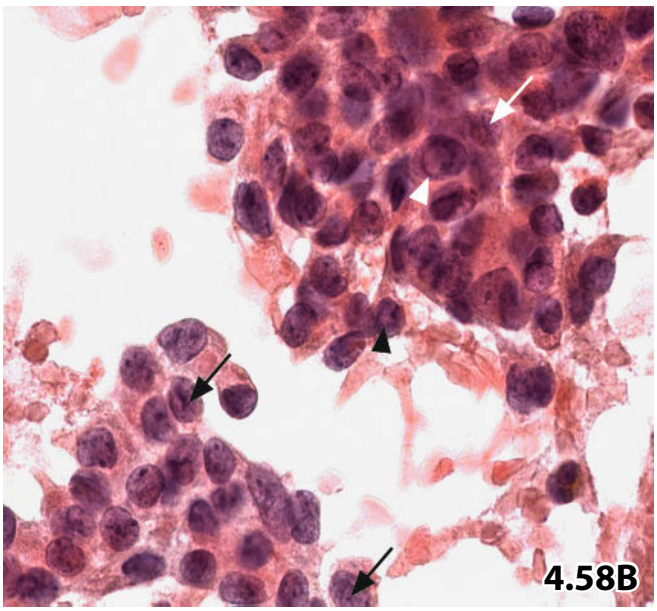
4.58B

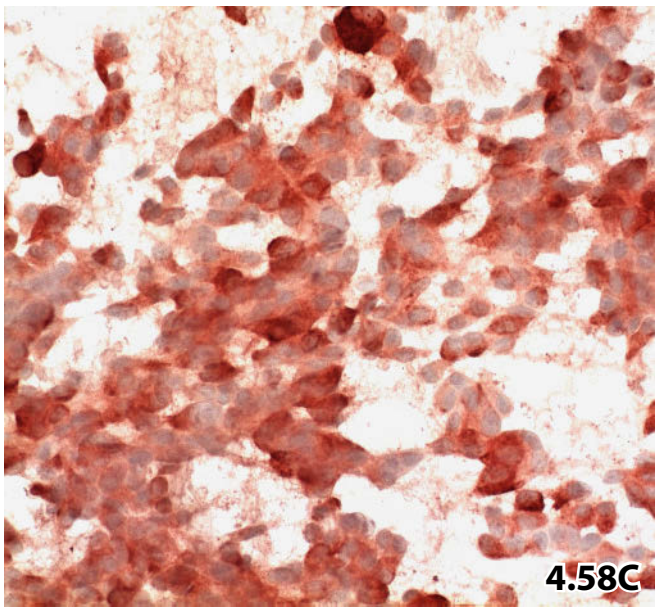
4.58C

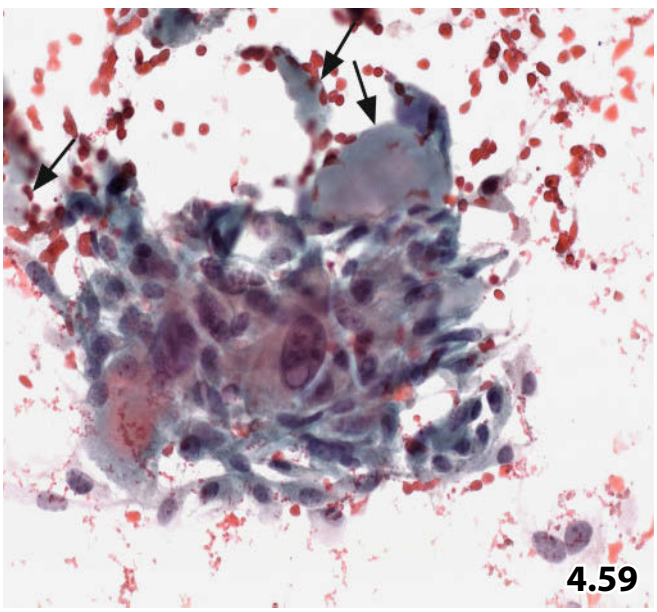
4.59

**Fig. 4.60 Medullary carcinoma versus follicular thyroid carcinoma.**
Lower magnification displays a medullary carcinoma composed of exclusively round shaped cells. Nuclear atypias together with follicle-like structures (arrows) primarily suggested follicular carcinoma. Strong immunocytochemical positivity for calcitonin (not shown) provided a correct cytologic diagnosis (FNAB, direct smears, Pap stain).
*Tissue diagnosis:* Medullary thyroid carcinoma, follicular variant.



**Fig. 4.61A, B Medullary carcinoma versus papillary thyroid carcinoma.**
Medullary carcinomas exhibiting a distinct spindle cell pattern may give rise to diagnostic confusion. FNAB of a large nodule (sonographic measures 6×4×4 cm) performed from the left thyroid of a 33-year-old man. Direct smears were Pap-stained. **A** Low magnification showing distinct fusiform cells arranged in papillary clusters and palisades. The overall pattern may be indistinguishable from papillary thyroid carcinoma by cytology alone. **B** Positive immunostaining for calcitonin demonstrates the true nature of the neoplastic cells (Pap-prestained smear).

**Fig. 4.62A, B Amyloid tumor of the thyroid versus medullary carcinoma.**
*Final diagnosis in this case:* Systemic amyloidosis including nodular amyloid deposits in the thyroid gland.
**A** Thyroid amyloid deposits occurring together with activated fibroblasts and histiocytes may mimic medullary carcinoma. However, the spindle-shaped mesenchymal cells exhibit histiocytoid nuclear features, bland chromatin, and indistinct cytoplasm unlike neoplastic cells of medullary carcinoma. Note interspersed single thyrocytes and small epithelial cell clusters (arrows) (thyroid FNAB, Congo red stain, lower magnification). **B** Amyloid masses demonstrate bottle-green birefringence upon polarization after staining with Congo red. White birefringence represents fibrous connective tissue.

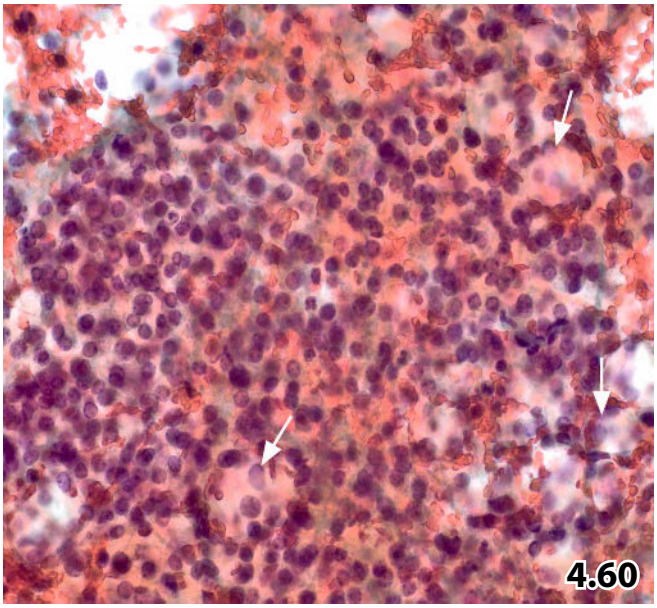
4.60

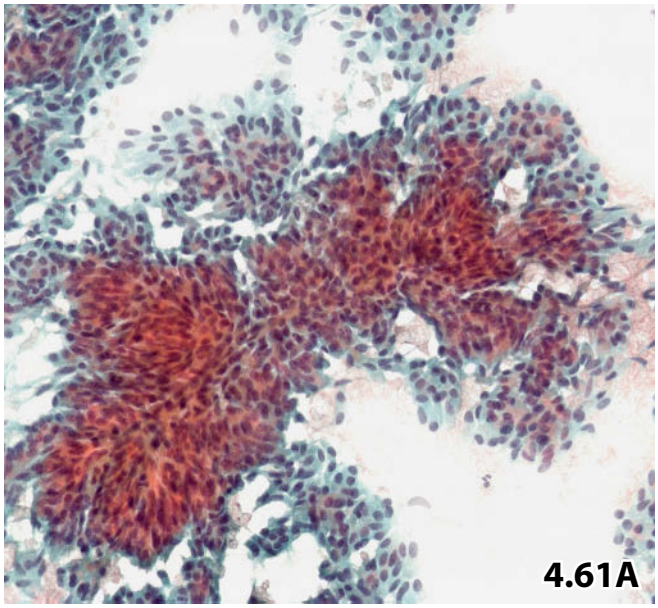
4.61A

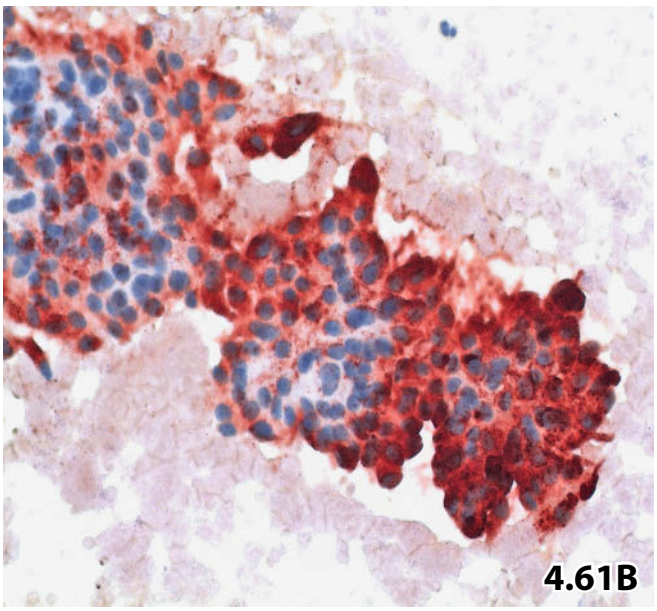
4.61B

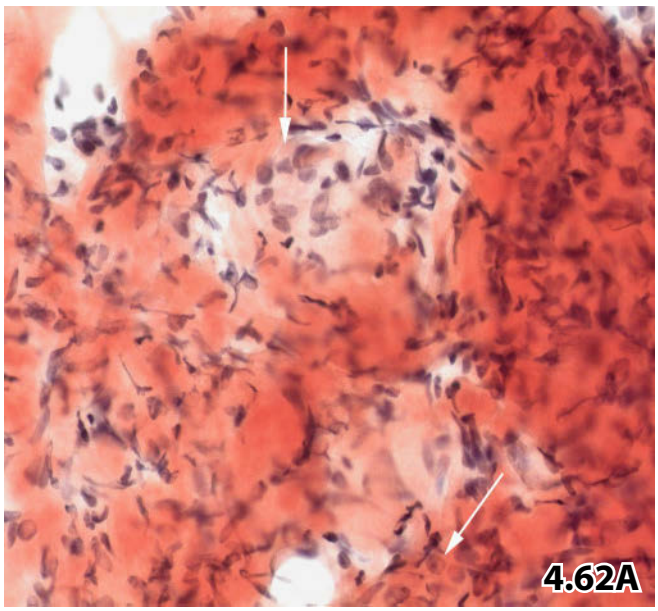
4.62A

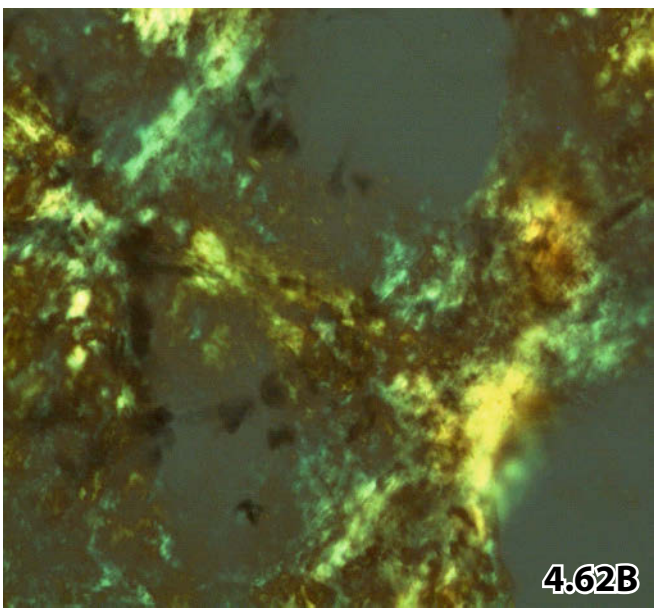
4.62B

**Figs. 4.63 and 4.64 Anaplastic carcinoma: classic cell features.**
Thyroid FNABs from two different patients exhibiting multinodular goiter. FNABs provided cell-rich direct smears (Pap stain).

**Fig. 4.63** (case #1) Highly pleomorphic large neoplastic cells occur isolated or arranged in dense aggregates. Pleomorphic nuclei, giant cells, multiple prominent nucleoli, and detritus are characteristic features of anaplastic carcinoma (high magnification).



**Fig. 4.64** (case #2) Note additional inflammatory component and phagocytic activity of the tumor cells (upper right) depicted in this figure (high magnification).

**Fig. 4.65 Anaplastic carcinoma: fusiform pattern.**
An 80-year-old woman presented with a tumor mass occupying the lower neck area and anterior mediastinal space. FNAB was performed of the mediastinal tumor fraction. Direct smears were Pap-stained. Pleomorphic spindle cells exhibit unambiguous malignant features (higher magnification). Cell detritus is also present.
*Cytologic diagnosis:* Malignant spindle cell neoplasia, most likely anaplastic thyroid carcinoma.
*Comment:* Immunolabeling is of major practical value in separating fusiform anaplastic carcinoma from other tumors composed of spindle cells. (Immunohistochemistry was only applied to paraffin sections).
*Tissue diagnosis* (surgical biopsies of the tumor): Anaplastic thyroid carcinoma.

**Fig. 4.66A, B Anaplastic carcinoma: polygonal/round cell pattern.**
Clinical and imaging studies suggested metastatic thyroid carcinoma in a 70-year-old woman. The fine-needle aspirate was processed for conventional smears and Pap staining.
*Cytologic/immunocytochemical diagnosis:* Anaplastic thyroid carcinoma (no further investigations were undertaken).
**A** The undifferentiated malignant neoplasm presented with a few isolated malignant cells, clearly standing out from an inflammatory and necrotic background (lower magnification). Standard cytology cannot differentiate between undifferentiated carcinoma and blastic non-Hodgkin lymphoma in the current setting. **B** Immunocytochemical workup resulted in negative staining for both pancytokeratin (Lu-5) (not shown) and CD45. Negative CD45 immunoreaction of the tumor cells (upper left) in combination with internal positive control cells (a normal lymphocyte is seen lower right) was indicative of anaplastic carcinoma (Pap-prestained conventional smear). Keep in mind that a number of anaplastic carcinomas will show negative immunoreactivity for Lu-5.

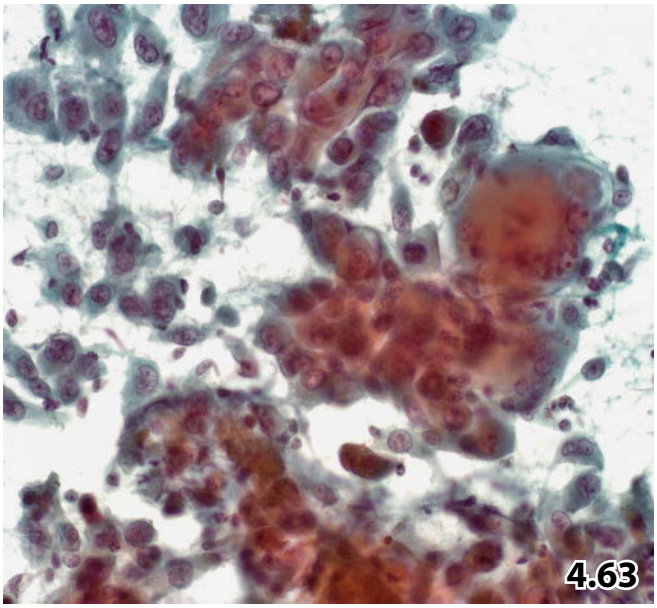
4.63

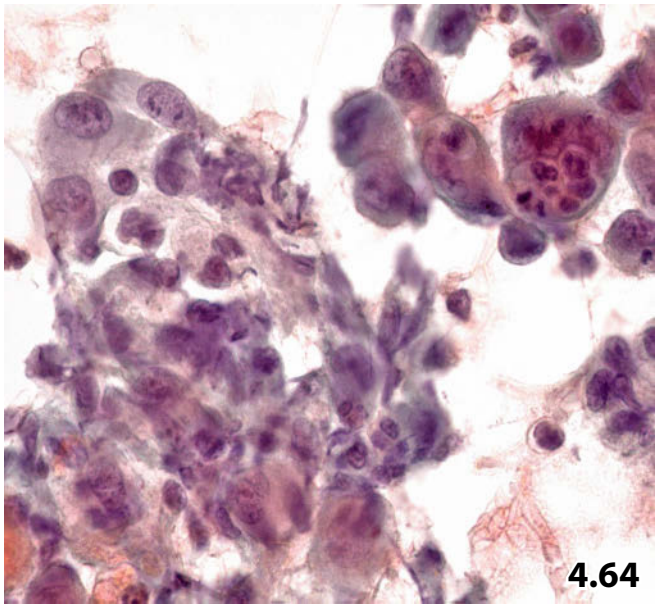
4.64

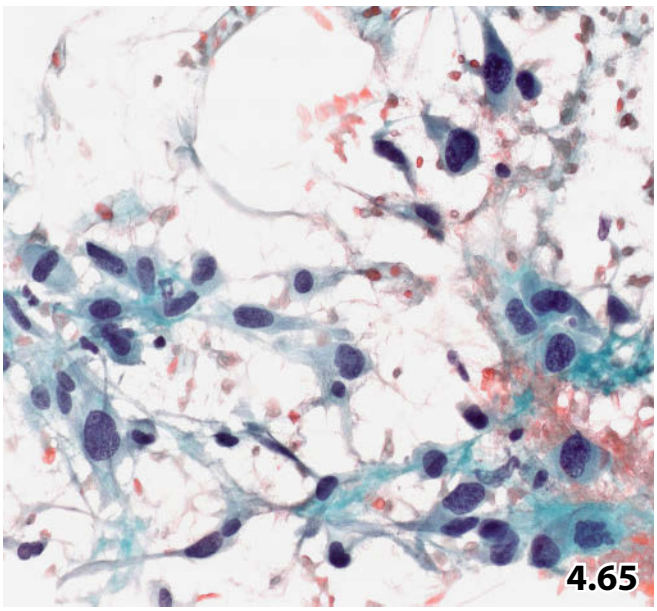
4.65

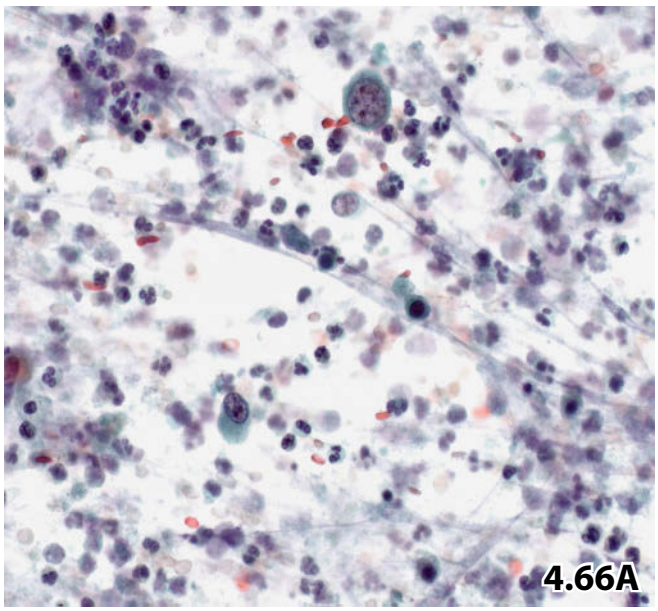
4.66A

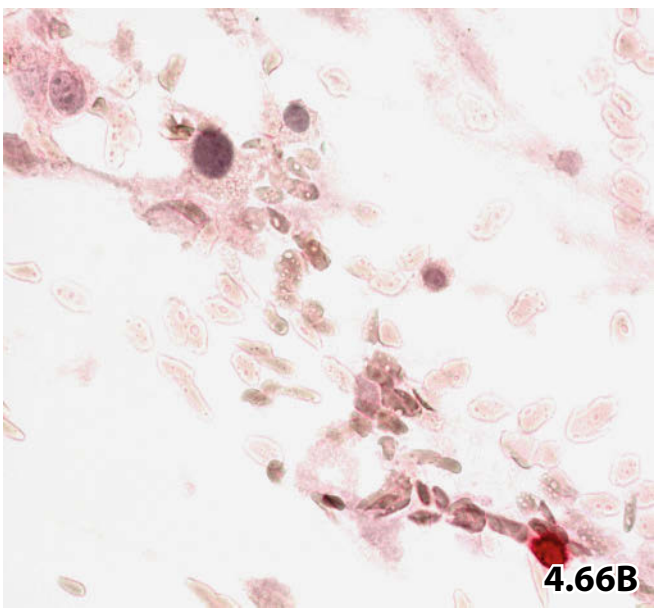
4.66B

**Fig. 4.67A–D Blastic non-Hodgkin lymphoma.**
A 77-year-old woman presented with a huge firm mass in her thyroid. FNAB provided hypercellular direct smears as well as cell-rich liquid-based preparations. A panel of antibodies was helpful to establish a conclusive diagnosis and the critically ill patient was spared surgical intervention. Immunostains were performed on liquid-based preparations (Figs. 4.67B–D).
*Cytologic/ immunocytochemical diagnosis:* Blastic B-cell non-Hodgkin lymphoma (consistent with diffuse large B-cell lymphoma).
*Follow-up:* No other manifestation of the malignant lymphoid tumor was detected. Tumor-free bone marrow biopsies.
**A** An MGG-stained conventional smear exhibits classic blastic cells with atypical nuclei that are surrounded by a rim of basophilic cytoplasm. Sharply demarcated cytoplasmic vacuoles are striking (arrows) (high magnification). **B** CD20 positive blasts (liquid-based ThinPrep preparation). **C** CD3 positive normal lymphocytes, blastic cells stained negative (liquid-based ThinPrep preparation). **D** Nuclear positivity for MIB-1 of virtually all blastic cells indicate high proliferation index (liquid-based ThinPrep preparation).

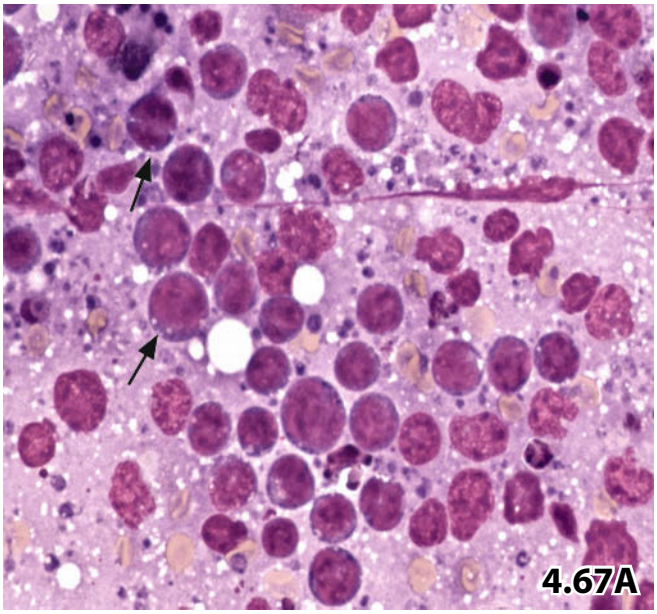
4.67A

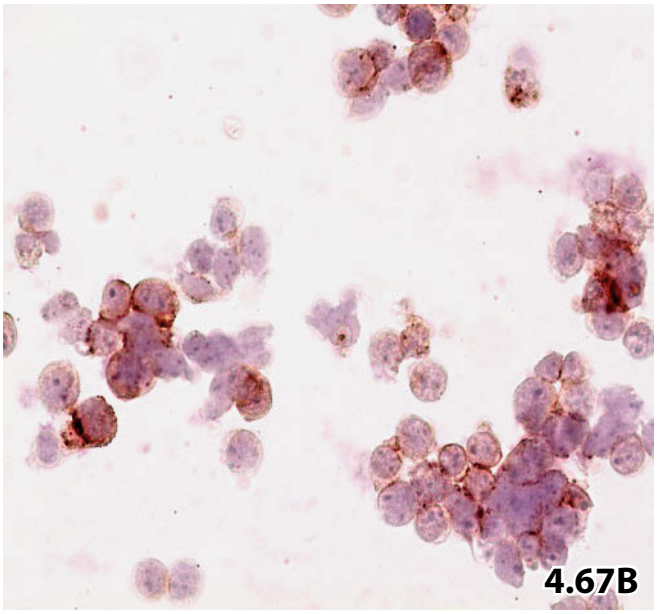
4.67B

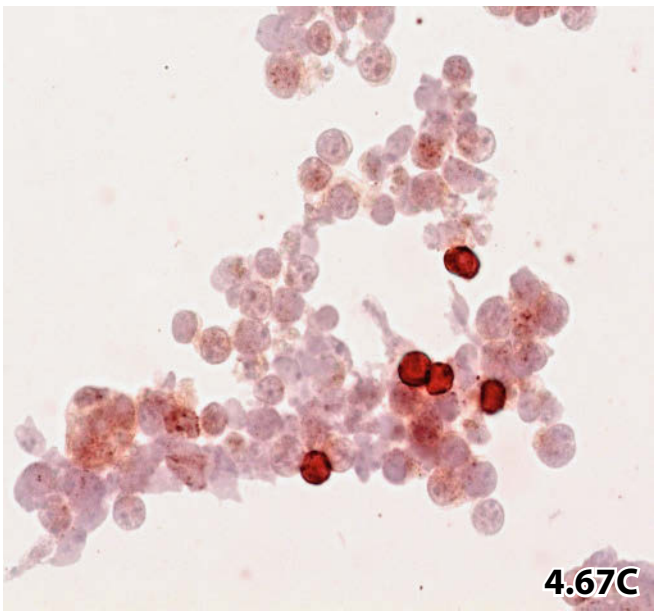
4.67C

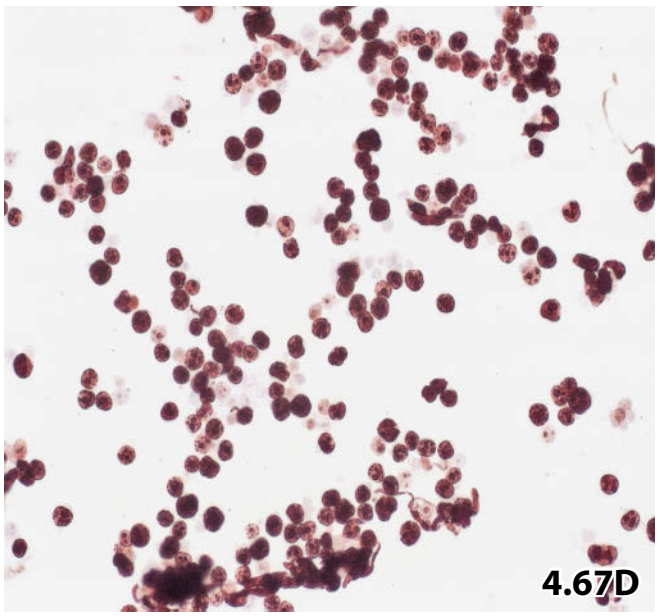
4.67D

**Fig. 4.68 Poorly differentiated squamous cell carcinoma spreading into the thyroid.**
A 68-year-old man presented with a tumor in the thyroid area. Imaging studies concluded parathyroid carcinoma spreading into the thyroid gland. FNAB mainly revealed fusiform and loosely arranged undifferentiated malignant cells (direct smear, Pap stain, high magnification). Immunostaining results (not shown: cytokeratins **+**, neuroendocrine markers negative) suggested carcinoma, excluding neuroendocrine differentiation.
*Tentative cytologic diagnosis:* Anaplastic thyroid carcinoma or metastatic undifferentiated carcinoma.
*Final diagnosis* (clinical, imaging, and histologic work-up): Poorly differentiated squamous cell carcinoma of the esophagus.

**Fig. 4.69 Metastatic malignant melanoma.**
An old woman with a positive clinical history of melanoma was referred to FNAB for a voluminous thyroid left lobe. Direct smears were prepared and Pap-stained. Cytology revealed numerous large discohesive malignant cells with elongated cytoplasm (high magnification). Numerous small sheets composed of benign follicular cells were embedded between the tumor cells (arrow).
*Cytologic diagnosis* of malignant melanoma was established from morphologic features and immunocytochemical stainings (not shown: S100 **+**, pancytokeratin-negative). Medullary carcinoma was excluded.

**Fig. 4.70A–C Metastatic renal cell adenocarcinoma.**
An 80-year-old woman presented with a thyroid tumor and multiple nodules in her lung. Thyroid FNAB was performed as initial diagnostic intervention (Pap-stained direct smears).
*Cytologic diagnosis* (supported by immunocytochemistry): Renal cell adenocarcinoma (verified by nephrectomy and subsequent histologic examination).
**A** Lower magnification showing papilliform clusters composed of monomorphic tumor cells. Note the prominent nucleoli and abundant cytoplasm indicating hypernephroma. **B** High magnification exhibits nuclear details such as loose chromatin, absence of hyperchromasia, nuclear wrinkling and grooves. Bear in mind that the nuclear features listed above are usually shared by both hypernephroma and papillary thyroid carcinoma. **C** Immunocytochemical workup was necessary to distinguish metastatic renal cell carcinoma from primary papillary thyroid carcinoma: antibodies against renal cell carcinoma associated cell marker (RCCMa) decorated most of the neoplastic cells (Pap-prestained conventional smear); antibodies against TTF-1 provided a negative staining result (not shown).

**Fig. 4.71 Metastatic lobular breast carcinoma.**
A 51-year-old woman presented with diffuse metastatic tumor disease of unknown primary origin. Physical examination revealed a firm thyroid nodule, referring the patient to FNAB. Direct smears were Pap-stained. High magnification of a loose tumor cell group shows typical features of breast carcinoma of the monomorphic subtype: eccentric cytoplasm, cytoplasmic vacuoles, and targetoid eosinophilic inclusions (arrow), indistinct irregularities of nuclear outline, nuclear folds and inclusions (arrowheads), and dense granular chromatin.
*Tentative cytologic diagnosis:* Probably thyroidal metastasis of a breast carcinoma.
*Final diagnosis* (effusion cytology, imaging studies, histology): Lobular breast carcinoma, metastatic into the abdominal cavity, skin, thyroid, and other organs.

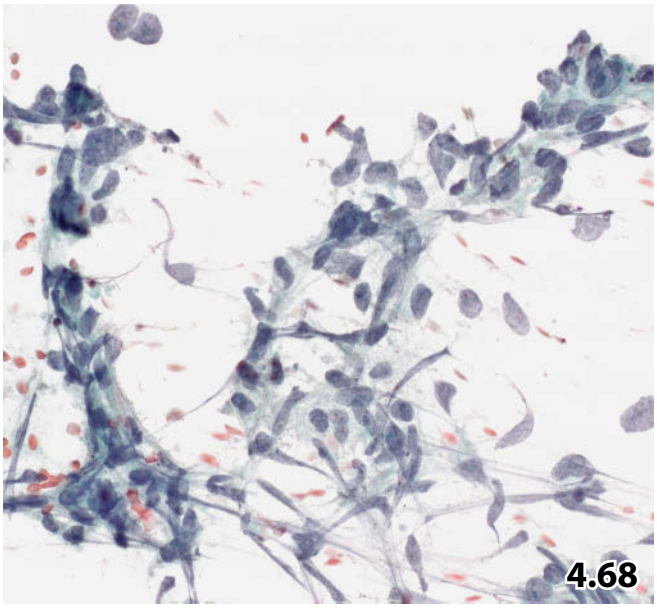
4.68

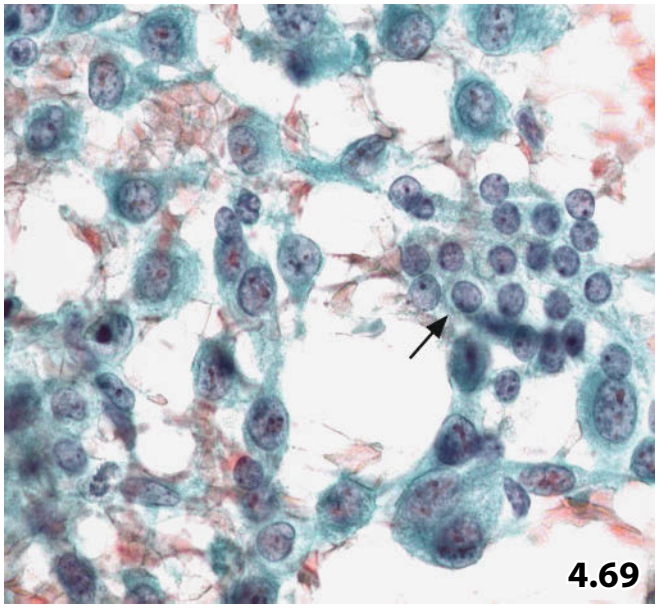
4.69

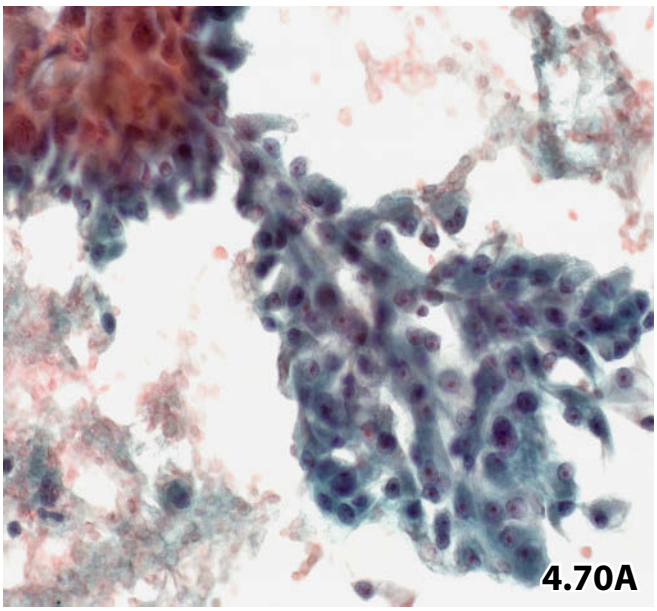
4.70A

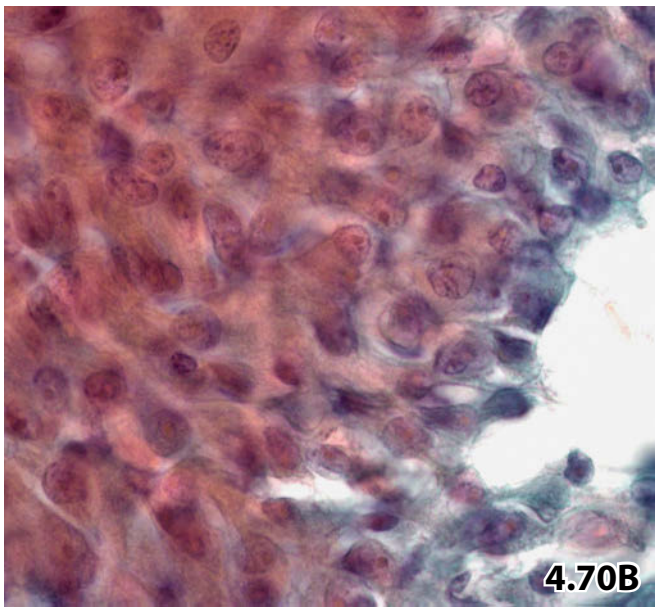
4.70B

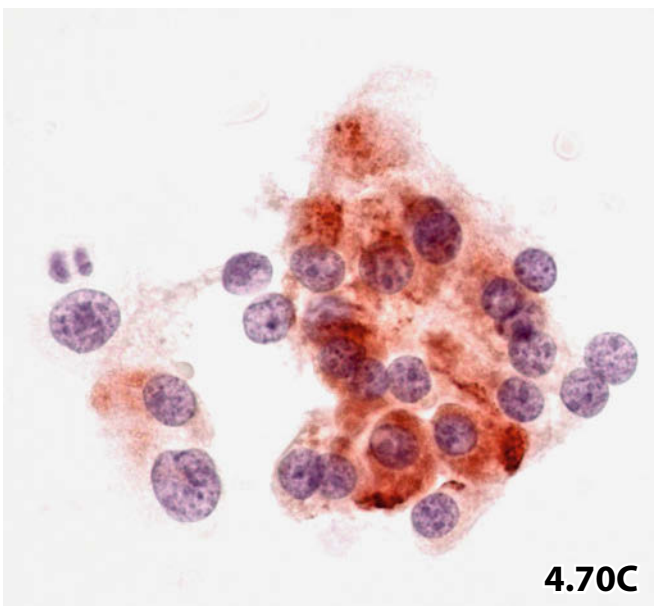
4.70C

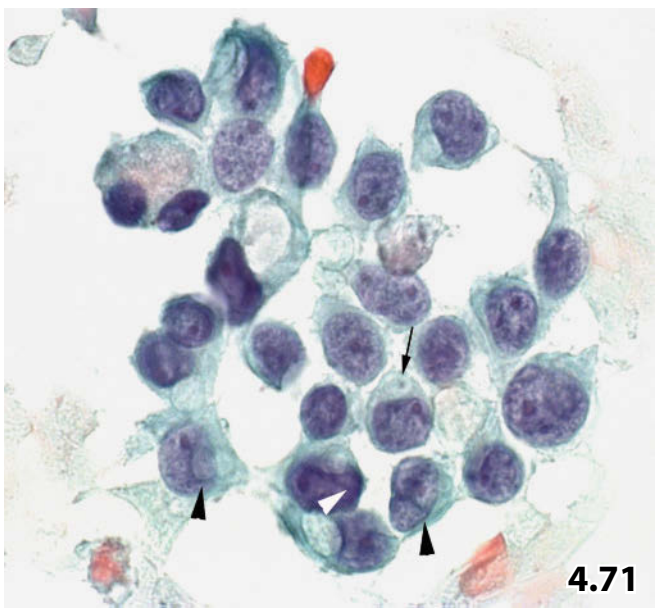
4.71

**Figs. 4.72A, B Parathyroid hyperplasia and parathyroid adenoma.**
A 62-year-old male patient with a nodule in the thyroid region and a positive history of hyperparathyroidism was subjected to FNAB.
*Cytologic diagnosis:* Hyperplastic/adenomatous parathyroid parenchyma. Immunostaining with antibodies against parathormone-related protein yielded a positive result contrary to the immunostaining for thyroglobulin (immunoreactions are not shown).
**A** Low magnification discloses a cellular smear composed of large, compact, frequently folded sheets. The monomorphous nuclei are small as compared to red blood cells; an obvious follicular differentiation is not observed. Stripped nuclei are often encountered in the background but colloid masses are completely missing (direct smear, Pap stain). **B** High magnification exhibits cellular details and colloid-free microfollicular structures throughout the cell cluster (arrows).

**Fig. 4.73 Parathyroid adenoma: clear cell variant.**
FNAB from an enlarged parathyroid gland (sonographically 15 mm in diameter) represents the clear cell variant of parathyroid adenoma. High magnification shows abundant clear and foamy cytoplasm in combination with relatively pronounced nuclear irregularities concerning size and shape (direct smear, Pap stain). Excluding a secondary well-differentiated clear cell carcinoma may be impossible unless an appropriate immunopanel is used.
*Cytologic diagnosis:* Parathyroid adenoma.
*Excisional biopsy* and subsequent tissue examination confirmed the cytologic diagnosis of parathyroid adenoma, subtyping: clear cell type adenoma.

Pronounced nuclear irregularities may be encountered in any type of parathyroid adenoma.

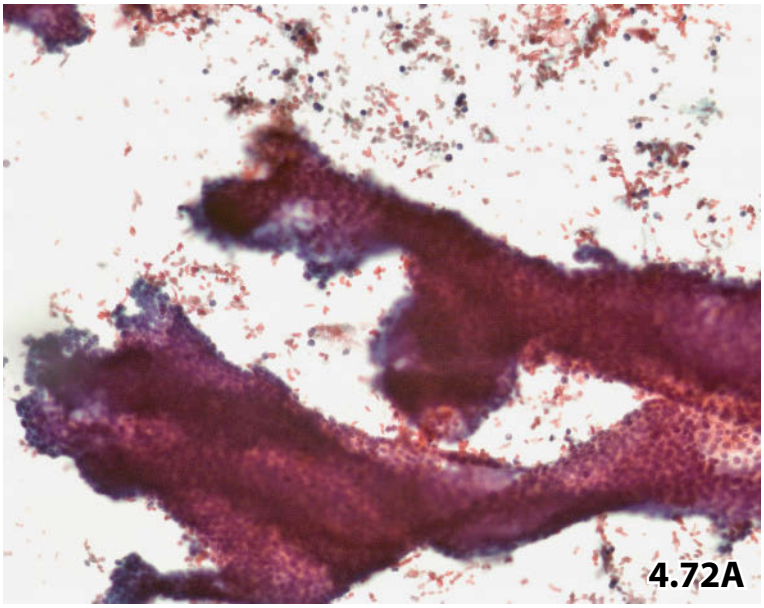

4.72A

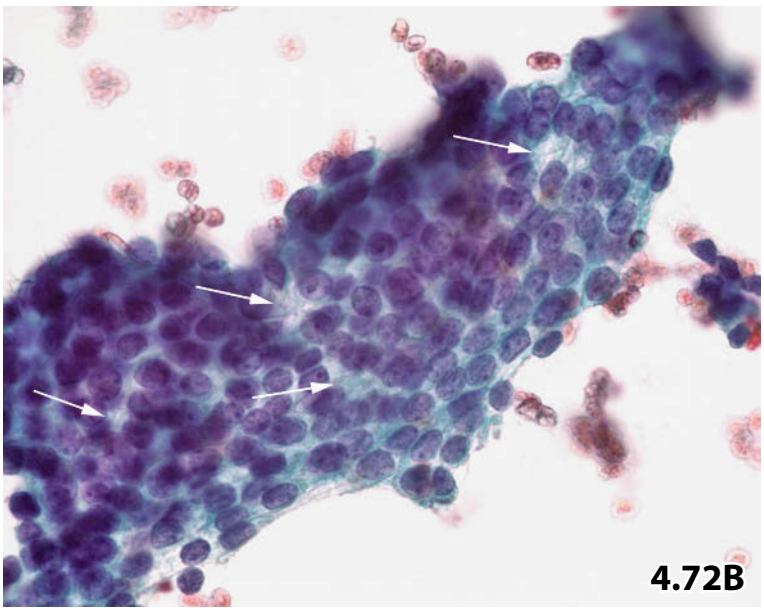

4.72B

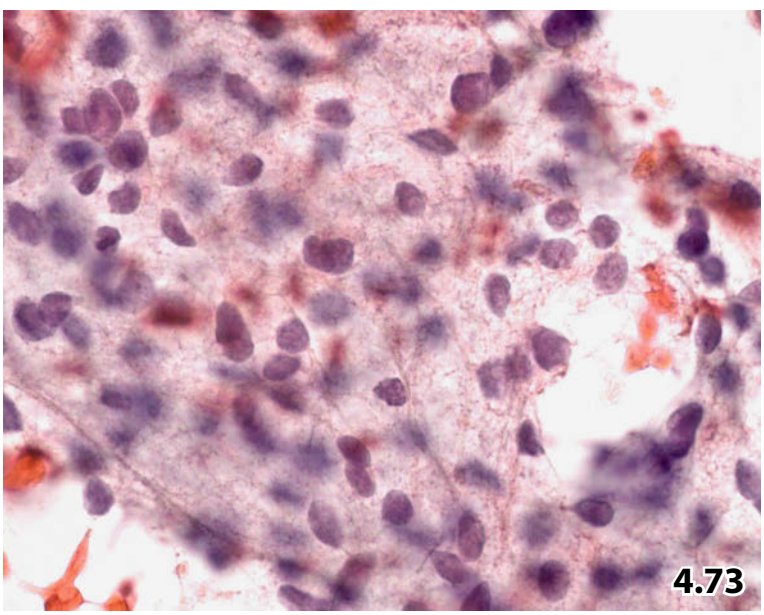

4.73

# Salivary Glands, Head and Neck 5



## Synopsis and Algorithms



Spieler/Rössle, *Nongynecologic Cytopathology. A Practical Guide. Essentials of Diagnostic Pathology*,
DOI 10.1007/978-3-642-24719-4_5, 

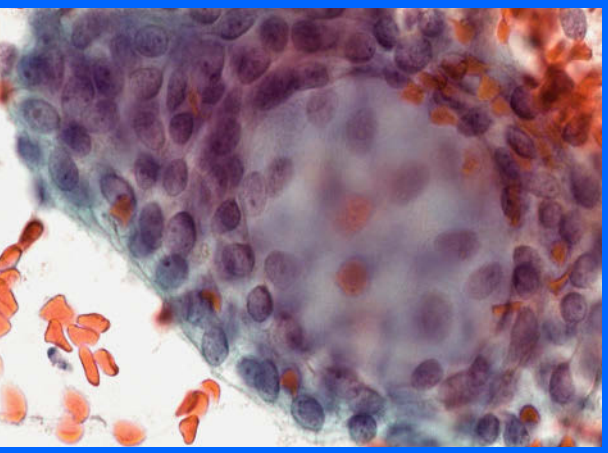

# Section 5.1
# Salivary Glands

## 5.1.1 Introduction

### General Comments

- Incisional biopsy and large-needle biopsy are not generally accepted as the procedure of choice to obtain cellular material and tissue for pathological investigation of salivary gland swelling due to major complications. In contrast, fine-needle aspiration biopsy (FNAB) has been widely accepted as a useful, safe, and cost-effective tool for the preoperative diagnostic assessment of salivary gland masses. The technique can be safely performed as an outpatient procedure. There are no contraindications, and complications are minimal. At our institution, we have rarely observed acute intraglandular infections following discharging a cyst.
- The majority of the salivary gland lesions are benign nonneoplastic disorders. Inflammatory processes are more frequently encountered in submandibular glands than in parotids [41].
- Benign and malignant salivary gland neoplasms together have a male-to-female ratio of 0.7 to 1 [90].
- FNAB and cytological examination are most commonly used to investigate disorders of the parotid glands and submandibular glands, but cytologic investigation is much less frequently applied to enlarged minor salivary glands.
- The high value of fine-needle aspiration cytology has been demonstrated in quite a few studies carried out over the past few decades. We refer herein merely to a small number of selected studies that have been conducted in recent years [2, 14, 31, 34, 41, 49, 65, 87, 165]. The results of these investigations emphasize the high negative predictive value, the high sensitivity for benign and malignant lesions (range: 74–98%), and varied specificity (range: 75–100%). In addition, preoperative FNAB allows better management of the patient and an optimal technical planning and timing of surgical interventions.
- Established diagnostic criteria should allow an initial cytologic diagnosis of the current variants of both nonneoplastic disorders and true salivary gland neoplasms with a high level of accuracy [82]. Rare salivary gland lesions, salivary gland disorders composed of a complex histologic pattern with cyst formation, and tumors exhibiting focal cellular atypia may lead to dubious cytological results, leaving the definite diagnosis open. In such cases, a histological investigation is indispensable [14]. Cytological FNAB results must in any case be considered in conjunction with the patient's clinical history and imaging findings [43].
- A few studies investigated the liquid-based procedure relevant to FNAB of salivary glands [3, 138]. To the best of our knowledge and experience from other organs, the methodological cellular artifacts and poor presentation of the crucial noncellular background material may frequently lead to vague cytodiagnoses on thin layer preparations.
- Tissue alterations caused by previous fine-needle aspiration biopsy may so extensive that misdiagnoses are possible by histologic examination of subsequent parotidectomy specimens [108].

**Caution**

Common variants of nonneoplastic and neoplastic lesions of the salivary glands are easily diagnosed with FNAB. However, benign and malignant disorders that are rarely encountered on cytologic specimens, tumors exhibiting complex histologic patterns, lesions with pronounced cystic changes, and neoplasms bearing focal cellular atypias may raise considerable diagnostic problems.



### 5.1.1.1 Regarding Minor Salivary Glands

- The vast majority of the minor salivary glands are located throughout the oral cavity. Minor salivary gland tumors occur most frequently in the palate; with an average rate of 50%. Benign tumors of the intraoral salivary glands are slightly more frequent than malignant lesions [19, 181]. Neoplasms of labial salivary glands of the upper lip are more often benign than those in the glands of the lower lip [181].
- The distribution characteristics of the epithelial tumors of the minor salivary glands in a Chinese population were studied by Wang and coauthors [179].
- FNABs of the minor salivary glands are rarely documented in the literature [133], but an experienced operator can easily perform intraoral FNABs on large tumorous masses as well as on tiny nodules exceeding 5 mm in diameter. The procedure is highly cost-effective and helpful in the diagnostic workup of intraoral lesions.

### 5.1.1.2 Particular Technical Aspects of Salivary Gland FNAB

The technique of aspiration is quite similar to that recommended for superficial lesions anywhere on the body (see Sect. 1.1.2, "Aspiration Technique" p. 4, and other chapters), but a few basic essentials should be considered:

**Table 5.1.1** Both common lesions and selected rare disorders of the salivary glands are listed with respect to their preferred location

| Entities | Preferred salivary gland type | | | |
|---|---|---|---|---|
| | Major | Minor | Predominant parotid | Predominant submandibular |
| Sialadenosis | + | | + | |
| Lipomatosis | + | | + | |
| Sialadenitis acute and chronic | + | | | |
| Chronic sclerosing sialadenitis, Küttner tumor | + | | | + |
| Sarcoidosis and tuberculosis | + | | | |
| Necrotizing sialometaplasia | | + Palate | | |
| Extravasation mucocele | | + Lower lip | | |
| Mucus retention cyst | | + | | |
| Retention cyst | + | + Lower lip | | |
| Lymphoepithelial cyst HIV-associated | + | | + | |
| Branchial cleft cyst, intraglandular | + | + | + | |
| Benign lymphoepithelial lesion | + | | + | |
| Pleomorphic adenoma | + | | + | |
| Warthin tumor | + | | + Lower pole | |
| Oncocytoma | + | | + | |
| Basal cell adenoma | + | | + | |
| Canalicular adenoma | | + Upper lip | | |
| Sebaceous (lymph)adenoma | + | + | + | |
| Myoepithelioma | + | + Palate | + | |
| Mucoepidermoid carcinoma | + | + Palate | + | |
| Adenoid cystic carcinoma | + | + Palate | | |
| Acinic cell carcinoma | + | | + | |
| Polymorphous low-grade adenocarcinoma | | + Palate | | |
| Basal cell adenocarcinoma | + | + | + | |
| Clear cell carcinoma | | + Palate | | |
| Malignant lymphomas | + | | + | |
| Metastases | + | | + | |

- Invasive procedures on salivary glands may frequently be painful for the patient. Using a notedly thin needle (23–27 gauge) can reduce discomfort to a tolerable degree and enables the operator to collect enough cellular material by multiple needle passes.
- A large needle diameter (21 gauge) is convenient to empty a cyst with thick content.
- FNAB of intraoral nodules is reliably performed using a thin needle (between 23 and 25 gauge), and a syringe linked to a syringe-holder that suits the intraoral intervention (be careful of the teeth!) [133]. A longer needle is required for lesions located at the rear palate. The needle should be guided by the free hand into the target lesion; the guiding hand should be protected by an abacterial glove.

### 5.1.1.3 Salivary Glands and Ultrasound

[102, 107, 161]

A combination of ultrasound and ultrasound-guided fine-needle aspiration biopsy (US-FNAB) is an investigative method to improve sampling and diagnostic accuracy in comparison to blindly performed FNAB:

- First of all, sonography can identify the target lesion as a true salivary gland lesion or assign it to another tissue.
- Ultrasound imaging reveals the shape of the lesion and its demarcation from the normal gland tissue, and detects adjacent or regional lymph node abnormality.
- US-FNAB offers the advantage of selected diagnostic evaluation of areas within the same lesion exhibiting varied tissue characteristics.
- US-FNAB enables reliable evaluation of enlarged glands and tumors that are barely palpable.
- US-FNAB provides access to midget lesions.
- It could be shown that 40–50% of the patients affected by a nonneoplastic lesion are spared from a surgical intervention by applying initial US-FNAB [161].
- Adequacy of the sampled material is high using US-FNAB.

**Caution**

- The caudal lobe of the parotid gland may be blurred by the mandible.
- Minor salivary glands in the mucosa of the oral cavity and in other sites of the upper respiratory tract are not amenable to conventional sonography.
- From our experience, ultrasound-guided FNAB on salivary gland swellings improves the result of sampling as well as diagnostic accuracy. Hence, the method is highly recommended in the diagnostic workup of salivary gland lesions.

### 5.1.1.4 Additional Analyses

#### Immunocytochemistry

Immunocytochemistry is of minor help distinguishing between varied primary salivary gland tumors of epithelial origin and secondary neoplasms.

- In contrast to mixed salivary gland tumors, squamous cell carcinomas and their variants exhibit positive immunoreaction for high-molecular-weight CKs.
- *Myoepithelial cells:*
  - Myoepithelial cells are best identified using alpha-smooth muscle actin (SMA) and calponin. However, calponin should always be used together with SMA or vimentin, because calponin shares positivity with epithelioid and plasmacytoid cells of pleomorphic adenoma and with cells of adenoid cystic carcinoma.
  - Myoepithelial cells demonstrate both nuclear and cytoplasmic positivity for S100 protein. However, this marker is of uncertain value because ductal cells may also provide a positive reaction, especially those of pleomorphic adenomas [63].
  - Immunocytochemical positivity for cytokeratins has been demonstrated in different types of myoepithelial cells.
  - Antibodies against glial fibrillary acid protein (GFAP) may render positivity in up to 50% of myoepithelial cells [4].
  - Jäkel and Löning [85] propose an immunopanel to differentiate between ductal epithelial cells and myoepithelial cells: CK5/6 or high molecular-weight CK34βE12 in combination with vimentin (predominantly or exclusively positive on myoepithelial cells) versus CK7 (predominantly positive on ductal epithelial cells).

**Caution**

A low sensitivity for muscle-specific actin and smooth-muscle actin in myoepithelial tumors has been demonstrated by Alos and associates [4].

#### DNA Ploidy

DNA aneuploidy has recently been shown to be a distinct indicator of malignant salivary gland disorders, by both flow cytometry [4, 47] and image cytometry [124, 174]. Whether the method is helpful in identifying a population of atypical cells as malignant within an otherwise benign salivary gland lesion remains unclear [174].

## 5.1.2 Crystalloids (Figs. 5.1 and 5.2)

Crystalline deposits in FNAB of cystic salivary gland disorders are mainly encountered in benign lesions. The various biochemically differing elements are usually detected by light microscopy due to differences in structural appearance.

The group of crystalloids commonly occurring in salivary gland lesions include [89, 147, 162]:
- Amylase crystalloids.
- Tyrosine-rich crystalloids.
- Collagen-rich crystalloids.
- Other crystalloid elements occasionally seen in malignant tumors.

**Caution**

- Amylase crystalloids are an indicator for benign salivary gland cyst disease of various histogenesis; they have never been found in malignant lesions associated with cystic changes.
- In contrast, other morphologically and chemically differing crystalloids may occasionally accompany both chronic inflammatory disorders and malignant salivary gland lesions.



#### 5.1.2.1 Amylase Crystalloids (Nontyrosine Crystalloids) (Fig. 5.1)

Amylase crystalloids can be associated with nonneoplastic and neoplastic salivary gland diseases including sialolithiasis [130], sialadenitis [150], lymphoepithelial cyst [113], and various benign salivary gland tumors [130].

Amylase crystalloids are preferentially localized in sialocysts that are lined with an oncocytic epithelium; therefore it has been speculated that they may be a secondary product of oncocytic secretion [130].

Crystalloids of salivary alpha-amylase can easily be identified by routine staining methods such as May-Grünwald-Giemsa and Papanicolaou (Pap) stain. High amylase activity in cystic fluids can be assessed using biochemical methods [15].

**Microscopic Features** [15, 72, 130, 162]
- Smears show large numbers of nonbirefringent polyhedral crystalloids of varying size and shape. They are predominantly needle-shaped with pointed ends ranging from 10 to 500 $\mu$m in length and around 20 $\mu$m in width. Smaller crystalloids are tabular in shape.
- May-Grünwald-Giemsa stains the elements in a deep-blue fashion, and in Pap staining they appear bright orange.
- The inflammatory background is variable.

#### 5.1.2.2 Tyrosine Crystalloids (Fig. 5.2)

Tyrosine crystalloids are most frequently encountered in tumors comprising a predominant myxochondroid component such as pleomorphic adenoma, where they are embedded in the myxoid areas. An increased occurrence of this phenomenon has been confirmed in black patients.

Tyrosine crystalloids are not only associated with benign salivary gland tumors, they have also been encountered in carcinoma ex adenoma [171] and in other malignancies [30].

**Microscopic Features** [162, 171]
- Irregular crystals in floral or rosette arrangement.
- They usually stain pink with the Pap staining method.
- The Millon reaction is suggested to be specific for tyrosine [171].

#### 5.1.2.3 Collagen-Rich Crystalloids [162, 166]

Collagen-rich crystalloids are reported to occur in pleomorphic adenomas.
- They form sunburst-like structures with radially arranged collagen fibers around a clear central area.

#### 5.1.2.4 Cholesterol Crystals and Plates

They are diagnostically nonspecific and a result of long-standing cystic changes. Cholesterol deposits may typically occur in Warthin tumors.

### 5.1.3 Normal Salivary Gland and Nonneoplastic Disorders [118]

#### 5.1.3.1 Cytology of Normal Salivary Glands

##### 5.1.3.1.1 Major Salivary Glands (Figs. 5.3–5.5)

The group of major salivary glands comprises the parotid, submandibular, and sublingual glands. The parotid gland produces serous secretion. Secretions of the other glands are mixed, predominantly serous from submandibular glands and predominantly mucoid from sublingual organs.

**Microscopic Features**
- Aspirates of normal salivary glands contain a few small parenchymatous tissue fragments together with scattered cells and stripped nuclei.
- Acinar cells are loosely grouped in spherical formations with a small round nucleus frequently displaced toward the basal border of the cytoplasm. The chromatin is loose, the nuclear membrane pronounced, and the nucleolus indistinct.
- The abundant cytoplasm of the serous gland cells is granular and foamy, that of mucous gland cells is clear.
- Epithelial clusters of the secretory ducts appear as regular tubular structures of varying size composed of cuboid and columnar cells interspersed with myoepithelial cells. The latter show a typical small deeply stained elongated nucleus.

- Benign lymphoid cells are usually present originating from intrasalivary lymphoid tissue or small intrasalivary lymph nodes.

#### 5.1.3.1.2 Minor Salivary Glands

Minor salivary glands are composed of aggregates of mucous glands or mixed mucous-serous glands. They are most frequently located in the mucosa of the oral cavity.

Cells of normal minor salivary gland tissue are only exceptionally encountered in FNAB samples.

### 5.1.3.2 Cellular Components Causing Diagnostic Confusion

#### 5.1.3.2.1 Squamous Cells

Various nonneoplastic and neoplastic entities of the salivary glands may contain benign and/or atypical squamous cells in FNAB specimens [10, 170, 125]:

- Salivary duct cyst.
- Lymphoepithelial cyst.
- Chronic inflammatory process.
- Necrotizing sialometaplasia.
- Pleomorphic adenoma.
- Warthin tumor.
- Mucoepidermoid carcinoma.
- Squamous cell carcinoma.
- Other disorders.

#### 5.1.3.2.2 Mucinous Metaplasia

Warthin tumors and much less frequent oncocytomas can be associated with mucinous (and squamous) metaplasia.

#### 5.1.3.2.3 Oncocytic Metaplasia

Warthin tumor and oncocytoma yield oncocyte-predominant aspirates. However, a variety of other salivary gland lesions may present with varying degrees of oncocytic differentiation [38]:

- Oncocytic adenomatous hyperplasia.
- Basal cell adenoma.
- Pleomorphic adenoma.
- Myoepithelioma.
- Polymorphous low-grade adenocarcinoma.
- Mucoepidermoid carcinoma.
- Acinic and ductal cells exhibiting oncocytic features may occur, particularly in elderly patients.

#### 5.1.3.2.4 Clear Cell Predominance and Sebaceous Cytoplasmic Features

Salivary gland lesions commonly characterized by a distinct clear cell component include:

- Pleomorphic adenoma.
- Oncocytic lesion.
- Benign and malignant (epithelial-) myoepithelial tumors.
- Clear cell carcinoma.

One should always take into account metastases of the classic clear cell tumors from the kidney, thyroid, lung, and malignant melanoma.

A special group of clear cell tumors are those with sebaceous cytoplasmic features.

#### 5.1.3.2.5 Prominent Lymphoid Infiltrate

Salivary gland lesions associated with a substantial lymphoid component include:

- Large intraparotid lymph nodes.
- Intra- and paraglandular reactive lymphoid hyperplasia caused by various benign and malignant disorders.
- Lymphoepithelial cyst.
- Chronic sialadenitis.
- Mucosa-associated lymphoid tissue or chronic immunosialadenitis (MESA).
- Warthin tumor.
- Mucoepidermoid carcinoma.
- Malignant lymphoma including Hodgkin lymphoma [45, 22, 26, 79, 122].

#### 5.1.3.2.6 Necrosis

Benign salivary gland lesions may occasionally be associated with extensive necrosis, suggesting malignancy [170].

**Caution**

It is highly important to be aware of variations in the cellular pattern due to metaplastic cell changes or the admixture of an unusual cell population in otherwise typical salivary gland disorders, constituting a high potential for false cytologic diagnoses. The unusual smear components can also appear coincidentally.
Histologic examination is necessary unless the overall features on cytologic specimens permit a conclusive diagnosis.

### 5.1.3.3 Salivary Gland Cysts

**Caution**

- A major proportion of benign and malignant salivary gland lesions (nonneoplastic disorders, epithelial and myoepithelial tumors) disclose a cystic component [48, 76, 106, 131]. Aspirates may contain cellular debris, metaplastic squames, mucus-producing cells, or cellular atypias to such an extent that major diagnostic pitfalls may arise.
- Evacuation of the cyst cavity alone often remains a significant risk of initial nondiagnostic cytology. Therefore, persisting and recurrent cysts demand repeat FNAB and US-FNAB, respectively; the latter should include the cyst wall at sonographically ominous areas.

#### 5.1.3.3.1 Retention Cysts [163] (Fig. 5.6)

The most common cystic disorder in salivary glands is a ductal retention cyst due to obstruction of the duct system. Obstruction is usually caused by sialolithiasis or sclerosis.

**Microscopic Features**

- Watery fluid and foamy cells, or viscous mucoid fluid.
- Varying degree of inflammation.
- Sparse epithelial cells of cuboid and columnar shape are generally present.
- Metaplastic squamous cells and/or mucoid background are common.
- Concrements may sporadically occur.

**Differential Diagnosis**

- A combination of metaplastic squamous cells and mucoid background simulates low-grade mucoepidermoid carcinoma [48, 163].
- Atypical squamous metaplasia, however unusual, may mimic cystic squamous cell carcinoma [88, 106]. The presence of calcifications may be helpful to reach a correct diagnosis.
  Baschinsky and associates reported two patients with parotid masses whose aspirates revealed nucleated and anucleated squames and keratin debris (referred to as dermoid cyst) [12]. The cellular pattern may be easily confused with necrotic squamous cell carcinoma.

#### 5.1.3.3.2 Mucus Retention Cysts (Fig. 5.7)

The retention mucocele comprises small superficial mucinous cysts that originate from minor salivary glands in all areas of the oral cavity [157].

- The FNAB sample contains mucous material enclosing a few epithelial cells.
- There is no inflammatory infiltrate.

#### 5.1.3.3.3 Branchial Cleft Cyst (Figs. 5.63 and 5.64)

Branchial cleft cysts can appear near to or in the anterior compartment of the parotid gland and can be mistaken clinically and sonographically for a parotid disorder [121]. Inflammatory changes occur frequently in these cysts.

#### 5.1.3.3.4 Polycystic Disease [46, 105]

Polycystic disease of the parotid gland is a very rare disorder resembling polycystic anomalies in other organs (kidney, pancreas), but it is not associated with these disorders. The etiology of the disorder is unclear.

**Microscopic Features**

- A microscopic key feature of the secretions are eosinophilic, laminated spheroliths.
- In addition, the smears show a clean or bloody background, histiocytes, and clusters of bland cuboidal or polygonal cells with slender nongranular cytoplasm.
- Inflammatory change or lymphocytic infiltration is practically absent.

**Differential Diagnosis**

Differential diagnosis should consider various benign nonmucinous cystic lesions and cystic neoplasms.

#### 5.1.3.3.5 Lymphoepithelial Cyst (Fig. 5.8)

The development of unilateral, bilateral, or multiple lymphoepithelial cysts in major salivary glands is considered a precursor of acquired immunodeficiency syndrome (AIDS) occurring in the early stages of human immunodeficiency virus (HIV) infection. Associated opportunistic infections or malignant neoplasms might not be present in this early stage of the disease [120]. Parotid glands are in particular affected. The disorder accounts for an estimated 3–6% of all HIV-infected patients [60].

**Microscopic Features** [50, 169]

- Proteinaceous background.
- Epithelial cells are of metaplastic squamous origin. Numerous anucleated squames are additionally present.
- A mixed population of small lymphocytes, follicle center cells (centrocytes, centroblasts, immunoblasts), plasma cells, and histiocytes is pathognomonic.
- Lymphoepithelial cysts may contain amylase crystalloids [113].

**Caution**

- Aspiration has to be performed both from the cyst compartment and the paracystic areas in order to obtain the characteristic dual cell pattern.
- In the case of morphological features suggesting a lymphoepithelial lesion in a salivary gland aspirate, the patient should be tested for HIV in order to detect an early stage of this infection.
- Lymphoepithelial cysts of the parotid gland are likewise observed in the pediatric HIV population [42].

**Differential Diagnosis**

Differential diagnosis comprises a number of lymphoproliferative salivary gland lesions along with squamous metaplastic changes of the ductal epithelium, such as salivary duct cysts, chronic inflammatory process, pleomorphic adenoma, Warthin tumor, malignant lymphoma, and others.

#### 5.1.3.3.6 Hematoma

Fluids containing numerous hemosiderin-laden macrophages may first and foremost be aspirated from hematomas.

### 5.1.3.4 Nontumorous, Noncystic Disorders

#### 5.1.3.4.1 Sialadenosis

The term "sialadenosis" stands for diffuse bilateral swelling of major salivary glands, particularly of the parotid glands, due to metabolic and secretory dysfunction [129].

- Aspirates contain large amounts of normally structured parenchymatous tissue fragments occurring in an edematous background; inflammatory infiltrates are lacking. The acini are swollen and their cells may be enlarged.

#### 5.1.3.4.2 Oncocytic Hyperplasia

Diffuse oncocytosis is an exceedingly rare lesion, the rarest among all oncocytic lesions in the parotid gland. The lesion encompasses complete oncocytic metaplasia of the glandular lobules.

One case with FNAB has recently been reported in the literature [71]:

- Typical oncocytic cells appearing singly or arranged in clusters showing moderate nuclear pleomorphism. Overdiagnosis of a true benign or malignant oncocytic neoplasm is more than likely.

#### 5.1.3.4.3 Fatty Infiltration: Lipomatosis

[152] (Fig. 5.9)

Tumorous lipomatosis in the parotid gland is well recognized but infrequently encountered.

The disorder is rarely seen in children, both in the parotid gland and in minor salivary glands. A true neoplastic lipoma is barely distinguishable by cytology.

### 5.1.3.5 Inflammatory and Infectious Lesions

#### 5.1.3.5.1 Acute Sialadenitis

Acute sialadenitis is an infectious disease that is mainly encountered in elderly patients. Poor oral hygiene, sialolithiasis, or immunodeficiency syndromes may strongly contribute to the disorder.

- Aspirate specimens contain large quantities of neutrophils, cellular debris, fibrin, and a varying number of lymphocytes and histiocytes/macrophages.
  Fragments of calculi may be encountered.
- Abscess formation yields masses of degenerating neutrophils.

#### 5.1.3.5.2 Chronic Sialadenitis and Granulomatous Disease

**Chronic Sialadenitis** (Figs. 5.10 and 5.11)

Nonspecific chronic sialadenitis is in the majority of cases caused by various types of duct obstruction. The epithelium may undergo squamous and mucoid metaplasia, and the dilatated ducts are filled with mucoid material.

**Microscopic Features and Differential Diagnosis**

- *Nonobstructive inflammatory disorders:* These represent chronic disease and provide specimens of low cellularity: predominantly small duct fragments and a few atrophic acinic cells are encountered in addition to scattered fibroblasts and a mixed population of inflammatory cells.
- *Disorders with ductal obstruction:* Chronic sialadenitis comprising ductal obstruction contains masses originating from dilatated ducts: mucoid background and ductal epithelial cells with evidence of squamous and mucoid metaplasia. Histiocytes, macrophages, lymphocytes, granulocytes, and miscellaneous crystalloid elements are additionally present.
  Atypical squamous cell metaplasia and mucoid metaplasia are difficult to distinguish from keratinized squamous cell carcinoma and low-grade mucoepidermoid carcinoma, respectively (Fig. 5.12).

**Chronic Sclerosing Sialadenitis (Küttner Tumor)**

(Figs. 5.13 and 5.14)

Küttner tumor is a chronic inflammatory process to the submandibular glands clinically mimicking malignant neoplasm due to the firm consistency of the affected gland. The process tends to be painful. An abnormal immune process is suspected to be a main pathogenetic factor in this disorder. Unusual presentations of this inflammatory entity have been reported comprising bilateral involvement of salivary glands, and involvement of both minor salivary glands and lacrimal glands [13, 149].

**Microscopic Features** [23, 29, 91]

- Dense lymphocytic infiltrate consisting of a mixture of small lymphocytes and cells originating from secondary lymph follicles.
- Clusters of ductal cells surrounded by collagen (corresponding to periductal sclerosis in histology) and infiltrated by lymphocytes.
- Paucity or absence of acinic cells.
- Fibroblasts and fragments of sclerotic tissue are present in various amounts.
- FNAB samples of low cellularity occur in cases with progressed fibrosis.

**Differential Diagnosis**

Nonspecific chronic inflammation and malignant lymphoma should be considered.

**Extravasation Mucocele** [136, 157]

Synonym: Mucus granuloma.

Initial mucus spreading into surrounding tissue forming interstitial lakes is followed by a granulomatous reaction. Microtrauma and congestion play a key role in the development of extravasation mucocele. This disorder is practically limited to minor salivary glands with the predominant location at the lower lip.

**Microscopic Features**

- Mucoid masses inducing a granulomatous reaction: foam cells, foreign-body giant cells, and macrophages incorporating mucus.

**Differential Diagnosis**

Other granulomatous disorders of the salivary glands.

### Necrotizing Sialometaplasia [61]

Synonym: Salivary gland infarction.

This lesion has an ischemic etiology with evidence of parenchyma necrosis comparable to identical processes in other glandular organs. The lesion affects mostly palatine salivary glands.

**Microscopic Features**

- Necrotic acini.
- Salivary gland ducts showing squamous cell metaplasia interspersed with goblet cells.
- Mixed inflammatory infiltrate.

**Differential Diagnosis**

Concomitance of squamous cell metaplasia and goblet cells may mimic low-grade mucoepidermoid carcinoma.

**Caution**

Infarction of major salivary glands may be observed as a result of previous trauma or fine-needle aspiration biopsy.

Reactive changes in metaplastic squamous cells together with cellular debris may mislead to a positive tumor diagnosis such as squamous cell carcinoma.

### Sarcoidosis [1, 156] (Fig. 5.15)

Sarcoidosis is a granulomatous multisystemic disease of indistinct origin that can occur in varied organs of the human body. The most common sites of manifestation include the lung, peripheral and mediastinal lymph nodes, liver, and eye. The incidence of major salivary gland sarcoidosis is very low.

**Microscopic Features**

- FNAB comprising fragments of noncaseating epithelioid cell granulomas interspersed with lymphocytes, with or without Langhans-type giant cells, may indicate sarcoidosis.
- The microscopic details are given in Sect. 15.2.5.6, p. 933.

Heerfordt syndrome is an acute presentation of sarcoidosis presenting a classical triad: involvement of parotid and other salivary glands, involvement of lacrimal glands, and involvement of the eyes (uveitis) along with episodes of fever.

**Differential Diagnosis**

Other nonspecific and specific (tuberculosis) granulomatous lesions must be excluded.

## 5.1.3.5.3 Other Infectious Diseases

### Mycobacterial Infection

Major salivary glands are rarely affected by *Mycobacterium tuberculosis* [96]. Salivary gland tuberculosis usually presents as swelling of the gland that is clinically often misinterpreted as a neoplasm. A review of documented cases in the literature reveals that a majority of the patients presenting with tuberculosis of the parotid gland originate from Asian or African countries [62].

- Cytomorphologic hallmarks of tuberculosis are described in Sect. 2.1.6.1, p. 116, and are documented in literature [8, 96].
- Caseous necrosis is not specific but strongly suggestive of tuberculosis.

Additional investigations such as PCR or culture are necessary to render the correct diagnosis. Ancillary tests from FNAB material strongly contribute to the recognition and definitive typing of various organisms having a substantial impact on rapid therapeutic decision making [73].

**Differential Diagnosis**

Tuberculosis may mimic simple chronic inflammation if the typical necrotic fraction is absent [96]. Many other chronic inflammatory and granulomatous disorders should be taken into consideration.

### HIV-Related Salivary Gland Lesions

HIV-infected patients frequently exhibit swelling of salivary glands. Benign lymphoepithelial lesion, inflammation, and neoplasm are the three main categories of disorders encountered in this particular patient group. An evaluation of FNAB performance on a large series of salivary gland lesions in HIV-infected patients has been made by Chhieng and coauthors [25].

Concerning HIV infection and lymphoepithelial cyst, we refer to Sect. 5.1.3.3.5, p. 406.

### Fungal Infections

Only single case reports of salivary gland mycotic disease diagnosed by FNAB are available in literature [128, 145].

### 5.1.3.6 Benign Lymphoproliferative Lesions
(Figs. 5.20 and 5.21)

- Benign lymphoproliferative lesions include primary salivary gland disorders associated with a prominent lymphocytic component, the most common lesion in this group is the Warthin tumor.
  Differential diagnostic considerations concerning various hyperplastic lymphoid salivary gland disorders are listed in Sect. 5.1.3.2.5, "Prominent Lymphoid Infiltrate," p. 405.
- The cytomorphology of the lymphoid infiltrate overlaps within the various categories, hampering a reliable recognition of the underlying lesion unless an additional specific tissue component is found such as oncocytes indicating Warthin tumor, cystic background comprising squamous cells indicating lymphoepithelial cyst, epimyoepithelial cell islands indicating MESA, carcinoma cells indicating peritumoral lymphatic hyperplasia, etc.

#### 5.1.3.6.1 Benign Lymphoepithelial Lesion
(Fig. 5.16)

Benign lymphoepithelial lesion is regarded as an autoimmune disease of the salivary glands and constitutes one of the most prevalent autoimmune disorders, local disorder of the salivary gland is referred to as myoepithelial sialadenitis (MESA). The systemic disease affecting many organs (including salivary and lacrimal glands) is called Sjögren syndrome. Clinical key symptoms are dry mouth and dry eyes.

Histopathologic features include parenchymatous atrophy, interstitial lymphocytic infiltration, and the pathognomonic epimyoepithelial cell islands. The latter run through different phases of development ending in hyaline transformation.

**Microscopic Features** [22]

- Cytologic specimens are composed of cellular components according to the histology pattern: mixed lymphoid infiltrate including follicle center cells as well as maturing and mature plasma cells. In addition, tingible body macrophages are present. The epimyoepithelial elements are large polygonal cells showing abundant pale cytoplasm and bland round nuclei with well-defined nucleoli. The three-dimensional epimyoepithelial cell clusters are closely associated with small lymphocytes (Fig. 5.16A).

**Caution**

According to our cytologic experience, epimyoepithelial cell islands are rarely available or obscured by abundant lymphoid infiltrates.

#### 5.1.3.6.2 Lymphoepithelial Lesion and Malignant Lymphoma (Figs. 5.17–5.19)

The risk of malignant lymphoma development in salivary glands of patients with Sjögren syndrome is highly increased as compared with the normal population. Heterogeneity of the lymphoid cell population in cytologic specimens may indicate transition from chronic inflammatory condition to malignant lymphoma (extranodal marginal zone lymphoma of mucosa-associated lymphoid tissue, MALT lymphoma), but the distinction from a reactive condition is practically impossible with cytology alone. A reliable diagnosis of myoepithelial sialadenitis and the recognition of its transition to malignant lymphoma are beyond the scope of cytology (see also Sect. 5.1.5.7, p. 419). An unequivocal diagnosis of MALT lymphoma requires biopsies (often multiple during long-term follow-up), immunohistochemical, and molecular information [7, 115, 178].

**Caution**

Using molecular genetic methods, a monoclonal B-cell population is detected in over 50% of the patients affected by lymphoepithelial sialadenitis but lacking clinical and histologic evidence of malignant transformation [9, 18, 172]. Accordingly, establishing the clonality of a lymphoid population on cytologic material using immunocytochemistry, flow cytometry, or molecular-genetic methods may provoke a false-positive diagnosis

#### 5.1.3.6.3 Castleman Disease (Fig. 15.38)

Castleman disease is a benign condition of the lymphatic tissue, the most common site of involvement is the mediastinum. However, sporadic cases of the disorder have recently been reported affecting the parotid gland in children [57, 139].

Detailed information and advanced literature are provided in Sects. 2.4.3.7.1, p. 214 and 15.2.5.4, p. 932.

## 5.1.4 Benign Tumors

**General Comments**

- A large-scale demographic study of salivary gland tumors in a European population (UK) has recently been published by Jones and associates [90], and the distribution characteristics of epithelial tumors of minor salivary glands in a Chinese population have been studied in a similar design by Wang and coauthors [179].
- About two-thirds of all salivary gland tumors are benign.
- The parotid gland is more frequently affected by neoplasms compared to the submandibular gland regions. Among benign tumors, pleomorphic adenoma is the most common neoplasm in major salivary glands followed by Warthin tumor [41, 90].
- Minor salivary glands: more than 90% of the tumors of the minor salivary glands are benign and their preferential site is the hard palate. The most common benign tumor variant is pleomorphic adenoma, accounting for 50–80% of all benign tumors in the minor salivary glands [143, 179].

- The cytological criteria of common and rare salivary gland tumors have been described in numerous publications and distinguished text books [82].

### 5.1.4.1 Pleomorphic Adenoma (Mixed Tumor of the Salivary Gland Type) (Figs. 5.22–5.30)



#### General Comments

Pleomorphic adenoma is by far the most common type of all salivary gland tumors and the most common tumor of the parotid glands [90, 111]. About 85% of mixed salivary gland tumors are found in the parotid glands; but they also occur in minor salivary glands as a majority of all neoplasms at that site, accounting for about 50% of all minor salivary gland tumors [143]. Women are predominantly affected, with a female-to-male ratio of 3:2.

The tumor derives its name from the architectural heterogeneity comprising an epithelial, myoepithelial, and a chondromyxoid component. Yet, considerable histologic and cytologic variations are seen within the same tumor and between individual neoplasms.

#### Microscopic Features

- Hallmarks:
  - Aspirates provide a thick, gelatinous mass representing myxoid, mucoid, chondroid, and hyaline material. The background appears as a red to dark purple substance in May-Grünwald-Giemsa stained smears, and gray-greenish to pale pink in Pap-stained specimens. There is clear evidence of a fibrillar structure.
  - Numerous monomorphous medium-sized epithelial cells, which are rounded or plasmacytoid in appearance, the latter exhibiting eccentrically placed nuclei. The nuclei are bland, showing finely reticular chromatin and inconspicuous nucleoli. The cytoplasm is sharply demarcated, dense, and cyanophilic (Pap stain). The epithelial cell clusters may be entrapped in stromal tissue or separate.
  - Epithelial cells occur together with spindle-shaped myoepithelial cells. In some areas, the latter stream into the stroma from the periphery of the epithelial cell clusters.
- Enlarged single cells containing atypical nuclei are occasionally interspersed in tissue fragments of otherwise typical pleomorphic adenoma.
- The epithelial component may show variable architectural patterns such as glandular or adenoid-cystic patterns.
- A clear cell component may occasionally be prominent.
- Oncocytic metaplasia or a sebaceous cell component rarely occur.
- Cystic change may occur, frequently including squamous metaplasia, mucus-producing cells, and detritus.
- The ratio of the different epithelial cell types and the ratio of epithelial and mesenchymal components vary widely within the same tumor and among tumors from different patients.

**Caution**

Great variability of the ratio of epithelial cell types and epithelial and mesenchymal components within the same tumor demands broad needling of the whole tumor mass and of various tumor areas, best achieved by means of ultrasound guidance.

#### 5.1.4.1.1 Variety of Cytological Patterns Causing Diagnostic Errors

- By cytology, the diagnostic accuracy of pleomorphic adenoma of the salivary gland is high. Klijanienko and Viehl reported approximately 90% concordant cytologic and histologic results on a large series of pleomorphic adenomas.
- Difficulties may arise in cases with inadequate FNAB sampling and in cases with the presence of various uncommon cytological patterns, which usually reflect the predominant histological differentiation of the individual tumors [97]:
  - *Chondromyxoid pattern* (Fig. 5.27): Poor presence or the complete absence of epithelial tissue can lead to a misdiagnosis of benign or malignant mesenchymal tumor.
  - *Cylindromatous pattern:* A large amount of cohesive clusters composed of basaloid cells surrounding mucoid globules can mimic adenoid cystic carcinoma [20, 52, 93, 175, 177]. The globules may represent hyalinized stroma [97].
  - *Cellular variant* (Fig. 5.28): Tumors composed almost entirely of epithelial cells raise suspicions of monophasic benign or malignant epithelial neoplasms of salivary glands. The tentative cytologic diagnosis depends on the predominant cell type, the cellular size, cellular pleomorphism, and the pattern of tumor cell clustering. The differential diagnosis includes myoepithelioma, monomorphic adenoma, basal cell adenocarcinoma, adenoid cystic carcinoma, small-cell carcinoma, and others.
  - *Myoepithelial variant:* Excessive proliferation of spindle-shaped myoepithelial cells must be differentiated from myoepithelial-cell rich adenoma, benign and malignant myoepithelial tumor, and epithelial-myoepithelial carcinoma (immunocytochemical discrimination, see Sect. 5.1.1.4, p. 403). Malignant myoepithelial proliferation is characterized by distinct cellular pleomorphism, increased mitotic rates and necrosis [39].

– *Clear cell variant* (Fig. 5.29A): A variant of pleomorphic adenoma bearing resemblance to other benign primary salivary gland lesions that are usually characterized by clear cells (myoepithelioma, oncocytic disorders), and to analogous malignant tumors (clear cell carcinoma, carcinomas that are completely or partially composed of myoepithelial cells). Metastatic malignancies with evidence of a distinct clear cell component particularly encompass carcinomas of the kidney, thyroid, and melanoma.
– *Oncocytic metaplasia:* A pronounced proportion of oncocytes may primarily lead to confusion with oncocytic adenoma and Warthin tumor.
– *Squamous metaplasia* (Fig. 5.29B): This tumor component is rarely predominant and may lead to a misdiagnosis of mucoepidermoid carcinoma (possibly ex pleomorphic adenoma). It is important to pay attention to the residual tissue components.
– *Cystic transformation:* Large cysts with an inner layer of squamous metaplastic or mucus-producing epithelium combined with cellular debris may simulate keratin cyst, squamous cell carcinoma, or mucoepidermoid carcinoma.
– *Cellular atypias* (Fig. 5.30): Occasional isolated or grouped cells showing carcinoma-like cellular atypias should not be overestimated (for malignancy) if the basic pattern of the aspirate is typical of pleomorphic adenoma [54, 97, 114]. The definite diagnosis rests upon excision of the tumor and diagnostic evaluation by histology [135], because the sole indicator of malignancy is an infiltrative and destructive tumor growth. However, the absence of a mesenchymal background associated with numerous markedly atypical tumor cells should lead to the tentative cytologic diagnosis of malignancy [54].

#### 5.1.4.1.2 Metastatic Pleomorphic Adenoma

Metastatic pleomorphic adenoma is a curiosity, only sporadically reported. Primary and secondary tumors usually display the identical morphological features of a classical benign mixed tumor [148].

**Caution**

Tumor cell seeding along the needle tract (using a fine needle or a core needle), or in the area of previous surgical intervention has to be excluded [167].

#### 5.1.4.1.3 Carcinoma ex pleomorphic adenoma

- Malignant transformation within a pleomorphic adenoma occurs infrequently. Cytologically, the neoplasia usually presents as an undifferentiated carcinoma with unequivocal cellular features of malignancy. In general, carcinoma ex pleomorphic adenoma is difficult to identify on preoperative FNAB specimens [100, 135, 184].
- Other types of carcinomas arising from pleomorphic adenoma, located in major and minor salivary glands, have been reported including cytologic findings. FNAB sampling of cells and tissue fragments from both tumor entities will result in a heterogeneous and complex smear pattern that is difficult to interpret. These tumors include clear cell carcinoma [132], mucoepidermoid carcinoma [84, 100], salivary duct carcinoma [5], sebaceous carcinoma [33], epithelial-myoepithelial carcinoma [37, 39], myoepithelial carcinoma [140, 39], and carcinosarcoma [95].

**Caution**

FNAB of varied carcinomas arising in pleomorphic adenomas may provide an extremely complex cell pattern giving rise to cytodiagnostic dilemmas.

### 5.1.4.2 Warthin Tumor (Adenolymphoma)

(Figs. 5.31–5.36)

**General Comments**

- The gland most likely affected is the parotid gland with its lower pole, and Warthin tumor is the second most common benign parotid tumor. The patient group most often afflicted is between 60 and 70 years old.
- Warthin tumor is the most common salivary gland lesion that is characterized by a prominent lymphoid component. The tumor is assumed to arise from salivary gland inclusions in lymph nodes situated in or adjacent to the parotid gland. Adenolymphoma will only exceptionally present diagnostic dilemmas.

**Microscopic Features** [22, 53, 176]

- Hallmarks: The protein-rich background of the smears has a dirty and granular appearance.
  A dual population of lymphocytes and regular flat sheets consisting of typical oncocytes are scattered throughout the background. The oncocytic sheets vary greatly in size and number.
- Squamous metaplasia is frequently identified and atypical squamous cells are occasionally encountered [176].
- Cholesterol deposits may be observed.
- Occasionally, the aspirated viscous material contains only scattered mature lymphocytes in a typical background, as described above. The assumed lack of oncocytic cells can frequently not be substantiated if a careful evaluation of the cytologic specimen is performed; few degenerating oncocytes are found in most cases.
  Degenerating oncocytes show a characteristic morphology and support the diagnosis of Warthin tumor:
  – Sharply outlined anuclear particles correspond to cytoplasmic remnants of epithelial oncocytes.

– Their shape may be polygonal, columnar, or pyramidal, and the size is variable.
– The cytoplasm is rarely granular but dense and homogeneous exhibiting the pathognomonic salmon staining characteristics of well-preserved oncocytic granules.

**Differential Diagnosis** [176]

- In cases with minimal lymphocytic and necrotic background, Warthin tumor can be confused with oncocytoma. But the latter is composed of oncocytic epithelial cells forming papillary fragments and acini; and a significant proportion of the cells tend to occur in isolation.
- Oncocyte-predominant benign lesions of the salivary glands (see Sect. 5.1.3.2.3, "Oncocytic metaplasia," p. 405) may mimic Warthin tumor.
- The lymphoid background of sebaceous adenoma is very similar to Warthin tumor, but the epithelial cells of the former lesion exhibit the characteristic sebaceous-type cytoplasm.
- Warthin tumor accompanied by accentuated squamous cell and/or mucinous metaplasia together with cellular atypia and extensive necrosis can give rise to diagnostic difficulties against squamous cell carcinoma, mucoepidermoid carcinoma, or benign sialometaplasia, the latter being confined to minor salivary glands [10, 170] (Fig. 5.36).

**Caution**

Aspirates from Warthin tumor may exhibit dirty and granular background with scattered lymphocytes lacking well-preserved oncocytic epithelial cells. However, remnants of degenerating oncocytes (Fig. 5.34) can be detected by careful evaluation of the cytologic smears, permitting an accurate diagnosis in most cases.

### 5.1.4.3 Oncocytoma [53, 176] (Figs. 5.37 and 5.38)

**Microscopic Features**

- Cellular aspirates contain numerous oncocytic epithelial cells appearing as scattered single cells, in clusters, and in papillary fragments.
- A clear cell variant can occur. The large clear cytoplasm is due to artifacts and intracytoplasmic glycogen deposits [51].
- Proteinaceous background material and lymphocytes may be encountered, but they occur in minor quantities. Cholesterol crystals are variably present.
- Mucinous and squamous metaplastic changes including cellular atypia are rarely seen.

**Differential Diagnosis**

- Oncocytomas with evidence of pronounced lymphoid infiltration and dirty background in cytologic smears may raise suspicions of Warthin tumor.
- Oncocytomas can meet mucinous and squamous metaplasia, cellular atypia, and necrosis (but much less frequent than Warthin tumors). In this setting, a misdiagnosis of squamous cell carcinoma, low-grade mucoepidermoid carcinoma, or necrotizing sialometaplasia (the latter is confined to minor salivary glands) is possible [170].
- Furthermore, certain benign salivary disorders along with oncocytic or clear cell predominance can be confused with oncocytoma (see Sects. 5.1.3.2.3 and 5.1.3.2.4, p. 405).

### 5.1.4.4 Basal Cell Adenoma

[68] (Figs. 5.39 and 5.40)

Basal cell adenoma is an uncommon type of monomorphous adenoma (accounting for about 2% of all primary salivary gland tumors). It is most frequently located in the parotid gland and tends to be multiple. Histologically the tumor is characterized by monomorphic basaloid cells with a prominent basal cell layer and distinct basement membrane-like substance; but the architecture can show considerable variations comprising solid, trabecular, tubular, and papillary features.

**Microscopic Features** [77, 182]

- The smears are cellular containing numerous cohesive cell clusters and branching cords.
- The individual cells are monomorphous and have round to ovoid nuclei showing granular chromatin and occasionally a distinct nucleolus. The cytoplasm appears as a small pale rim.
- Single cells are rarely seen; they frequently appear as naked nuclei.
- Stromal fragments are sparse, staining bright red in MGG-stained slides and are almost translucent in Pap stain. The matrix appears hyaline and homogeneous, usually attached to the border of the cell clusters, in contrast to the myxoid-mucous background in pleomorphic adenomas. Basically, the myxoid-chondroid stroma of pleomorphic adenoma is completely absent in basal cell adenoma.
- Cystic changes are possible: the smears show a watery proteinaceous background with scattered bland epithelial cells that may appear singly, densely clustered, or in papillary fragments.

**Differential Diagnosis and Immunocytochemistry** [24, 85] (Fig. 5.40)

- Basal cell adenoma should be differentiated from both other basaloid tumors of the salivary gland and predomi-

nantly basaloid-type tumor variants: basal cell adenocarcinoma, the cellular variant of pleomorphic adenoma, the solid form of adenoid-cystic carcinoma, basaloid squamous cell carcinoma, small-cell carcinoma, and other primary and secondary tumors of epithelial and nonepithelial origin. The cytomorphologic differentiation between these look-alikes can be very difficult.

- However, basal cell adenocarcinomas may show increased cellular dissociation and coarse chromatin texture; immunocytochemical investigation (see Sect. 5.1.1.4, p. 403) can help to exclude certain tumor entities such as myoepithelial neoplasms or basaloid squamous cell carcinoma.

### 5.1.4.5 Other Rare Benign Salivary Gland Tumors

#### 5.1.4.5.1 Cystadenoma (Figs. 5.41 and 5.42) and Papillary Cystadenoma

- *Nonpapillary cystadenomas:* Aspirates yield mucinous masses and bland goblet cells. The cytologic features are bland. Cystadenomas exhibiting pronounced mucinous features may be difficult to distinguish from their malignant counterpart (mucinous adenocarcinoma) and from other mucinous lesions such as well-differentiated cystic mucoepidermoid carcinoma.
- *Papillary cystadenoma* is characterized by papillae protruding into cystic spaces. Papillary cystadenoma (and papillary cystadenocarcinoma) share many cytological characteristics with other papillary tumors, e.g., the papillary cystic type of acinic cell carcinoma, metastasis of papillary thyroid carcinoma, and others. Differentiation between the malignant tumor type with minor cellular atypias and the benign variant of papillary cystic neoplasia depends upon the evidence of infiltrative growth. However, malignancy should be overt cytologically in carcinomas composed of papillary fronds disclosing unequivocal malignant features [64].
- A single case has been reported with psammoma bodies sampled by FNAB [109].

#### 5.1.4.5.2 Clear Cell Adenoma [51, 117]

The group of clear cell tumors of salivary glands include first and foremost two benign lesions, namely clear cell oncocytoma and myoepithelioma.

#### 5.1.4.5.3 Canalicular Adenoma [83]

This is a benign tumor of the salivary glands typically located in the upper lip, composed of bland columnar epithelial cells and loose highly vascular stroma. The tumor particularly simulates the trabecular type of basal cell adenoma. Only a single case report exists regarding cytologic findings.

#### 5.1.4.5.4 Sebaceous (Lymph)adenoma [11, 16, 80]

- *Sebaceous adenoma* is a rare benign neoplasm most often diagnosed in the parotid gland; it is composed of benign sebaceous cells.
  - Clusters of glandular epithelium showing sebaceous metaplastic changes with the characteristic finely vacuolated cytoplasm, and individual cells with pyknotic nuclei.
  - Occasional basaloid cells adhere to the periphery of the epithelial clusters.
- The *lymphadenomatous variety of sebaceous adenoma* exhibits a very similar cell pattern to Warthin tumor, suggesting a comparable pathogenesis. Cytology has been described in single case reports:
  - The epithelial cells are scattered among a lymphocytic infiltrate comprising follicle center cells, plasma cells, and tingible body macrophages.

#### 5.1.4.5.5 Myoepithelioma (Myoepithelial Adenoma) (Figs. 5.43 and 5.44)

Myoepithelioma is a rare salivary gland neoplasm with preferential site in the parotid glands and in minor salivary glands of the palate. Myoepitheliomas show a more aggressive behavior including occasional malignant transformation.

**Microscopic Features and Differential Diagnosis**

  - Various growth patterns can be encountered: solid, mixed, and reticular as well as cystic patterns [76]. The cellular components may be spindle-shaped, plasmacytoid, epithelioid, and of the clear cell type.

- A broad differential diagnostic palette must be regarded. A particularly close similarity to pleomorphic adenoma exists since both tumors go along with myoepithelial proliferation; nevertheless, cell clusters in myoepithelioma are sharply demarcated from the myxoid stroma, contrary to those in pleomorphic adenoma.
- The best approach for a reliable identification of myoepithelial cells is the immunocytochemical staining for alpha smooth muscle actin or calponin in combination with vimentin (see also Sect. 5.1.1.4, p. 403) [63].

**Caution**

A low immunocytochemical sensitivity of the myoepithelial cellsfor muscle-specific actin and smooth-muscle actin has been demonstrated by Alos and associates[4].

- The cytologic features of various types of parotid myoepithelioma and diagnostic considerations are documented in a few single case reports:
  - Myoepithelioma of the spindle-cell type has to be differentiated from various types of spindle cell tumors, in particular low-grade spindle cell sarcoma and schwannoma [104, 159].

– Plasmacytoid-cell type may be confused with pleomorphic adenoma and plasmacytoma [104, 112].
– Epithelioid variant [146].
– Mixed type [40, 104].
– Clear cell type myoepitheliomas are repeatedly mentioned in this chapter in the differential diagnosis of a number of primary and secondary salivary gland tumors.

#### 5.1.4.5.6 Nonepithelial Tumors [27, 28]

- Nonepithelial tumors account for about 5% of all tumors of the salivary glands, 90% are benign. The most common type of mesenchymal tumor is *angioma* (hemangioma or lymphangioma), most frequently occurring in children. FNAB rarely succeeds in rendering a reliable preoperative diagnosis [21].
- *Lipomas and neural tumors* encompass another group of mesenchymal tumors of primary salivary gland origin. Neural tumors include schwannoma, neurofibroma, and neurofibromatosis. Cytologic findings have rarely been reported [119].
- *Salivary gland disorders exhibiting a significant spindle cell component,* such as pleomorphic adenoma and granulomatosis, must be distinguished from true stromal lesions [27].
- General cytologic and immunocytochemical features of benign mesenchymal and neural tumors are provided in Sect. 17.1, "Soft Tissue and Bone: Benign Lesions," p. 1055.

### 5.1.5 Malignant Tumors

- Malignant tumors of the salivary glands are less frequent than benign neoplastic disorders, the ratio is approximately 1:2 in a European population [90]. The most common malignant tumor is mucoepidermoid carcinoma.
- Both the submandibular glands and the minor salivary glands are more commonly affected by malignant neoplasms than the parotid gland [41, 58]. About 50% of the lesions in minor salivary glands have been shown to be malignant.
- Several reports have pointed out the utility of preoperative FNAB of malignant salivary gland lesions, particularly with regard to preoperative management of the patients, improvement of the surgical treatment, and overall therapy [32, 110].
- Carcinoma ex pleomorphic adenoma has briefly been discussed in Sect. 5.1.4.1.3, p. 411.

#### 5.1.5.1 Mucoepidermoid Carcinoma

[32, 99, 103, 106, 183] (Figs. 5.45–5.48)

**General Comments**

- Although comprising less than 10% of all salivary gland tumors, mucoepidermoid carcinoma is the most common entity among malignant salivary gland neoplasms, accounting for about 30% [90, 111]. Approximately 60% of the neoplasms occur in the parotid gland and 30% in the minor salivary glands, with the palate being the most frequent site [141].
- All mucoepidermoid carcinomas should be regarded as malignant, though their biologic behavior is in correlation with the histological grade of the tumor.
- The diagnostic usefulness of the recently detected *MEC1/MAML2*-translocation (t(11;19)(q21;p13)), which seems to be rather exclusive in mucoepidermoid carcinoma [155A], needs further investigation in FNABs.

**Microscopic Features**

- *Mucin-producing cells* vary in shape, exhibiting a large polyhedral cytoplasm that is well defined and finely vacuolated. The nuclei are small with bland shape and structure. The mucus can be visualized using an appropriate stain (periodic-acid Schiff stain and others). Individual mucin-producing cells may imitate histiocytes. In low-grade mucoepidermoid carcinoma, cell clusters may exhibit glandular differentiation.
- *Intermediate epidermoid cells* appear as multilayered tightly packed clusters. Individual intermediate cells may occur, but in fact these cells are neither simply nor safely identifiable. The cells show a moderate N/C ratio and a homogeneous, sharply outlined cytoplasm. Cytoplasmic vacuoles may indicate transition to mucus secreting cells. Distinct keratinization is rarely encountered in well-differentiated mucoepidermoid carcinoma. The nuclei are bland and small, round to oval, and deeply staining, presenting with a small nucleolus.
- *Squamous cells* are readily identified by their keratinized cytoplasm. Nuclear atypia is usually minimal unless tumor cells originate from a high-grade mucoepidermoid carcinoma. Squamous cells are much more frequently encountered in high-grade than in low-grade tumors.
- Cystic changes, mucoid material, cellular debris, inflammatory infiltrate, and accumulation of lymphocytes are variable features, mainly depending on the tumor grade.
- Hallmarks of low-grade mucoepidermoid carcinoma (Figs. 5.45 and 5.46): Low-grade tumors are predominantly cystic. On histologic sections, cysts are filled with mucoid masses and lined by both mucus-secreting cells and intermediate cells showing varied degree of epidermoid differentiation.
  – A mucin-rich background in cytologic smears is pathognomonic for the low-grade tumor variant comprising a varying number of mucinous epithelial cells, intermediate cells, and well-defined squamous cells. The latter are usually scarce.
  – Minor cellular atypias are a leading feature.
- Hallmarks of high-grade mucoepidermoid carcinoma (Figs. 5.47 and 5.48): High-grade tumors are predominantly solid, composed of atypical intermediate cells,

atypical/malignant epidermoid cells, and scanty mucin-producing cells.
  - Highly atypical epidermoid cells with keratinized cytoplasm (intercellular bridges may be observed), a low number of mucus-producing cells, cellular and nuclear polymorphism, increased mitotic activity, and minor cystic changes are characteristic features on cytology.

**Differential Diagnosis**

Many morphologic features of mucoepidermoid carcinoma can be observed in other salivary gland lesions as well.

- Squamous and glandular cells, mucus, debris, and inflammatory infiltrates are present in aspirates from retention cysts, sialadenitis, Warthin tumor, and other lesions.
- Warthin tumor and well-differentiated mucoepidermoid carcinoma can give rise to a differential diagnosis challenge: free mucus and intracellular mucus may occur in both tumor types [70]; an admixture of large numbers of lymphocytes in mucoepidermoid carcinoma may mimic Warthin tumor. Even so, comparison between the two tumor entities reveals a completely different cytoarchitecture of the cell sheets and clusters.
- Cystic pleomorphic adenoma exhibiting mucoid masses, metaplastic epithelial changes (squamous, mucinous, sebaceous), and absence of myxoid background is difficult to separate from mucoepidermoid carcinoma [160].
- High-grade mucoepidermoid carcinoma may masquerade as primary or metastatic salivary gland cancer such as salivary duct carcinoma, poorly differentiated squamous cell carcinoma, or adenosquamous carcinoma.
- An isolated case report is available in the literature, discussing the cytologic features of the rare sebaceous variant of mucoepidermoid carcinoma [81].

**Caution**

- An accurate cytological diagnosis of mucoepidermoid carcinoma is possible in cases exhibiting the three characteristic cellular components: (1) epidermoid cells, (2) intermediate cells, and (3) mucus-producing cells.
- Tight clustering of the tumor cells, nuclear overlapping, no or minimal atypias, and characteristic cell features are highly indicative for low-grade mucoepidermoid carcinoma. But remember that cytologic investigation of low-grade mucoepidermoid carcinomas frequently provides unsatisfactory diagnostic results.
- The presence of cells exhibiting finely vacuolated cytoplasm (often perinuclear) is frequently observed in FNAB smears from mucoepidermoid carcinomas, but the phenomenon has turned out to be not completely specific for the diagnosis of this tumor entity [32].
- Cytologic specimens of mucoepidermoid carcinomas containing mucoid masses but lacking epithelial cells often provoke a false-negative diagnosis of a mucoid cystic lesions of varying pathogenesis [106].
- Squamous cells, mucin-producing cells, and free mucus may appear as contaminants from the skin, oral mucosa, and benign glandular tissue, respectively.

### 5.1.5.2 Adenoid Cystic Carcinoma

[55, 78, 98, 133, 180] (Figs. 5.49–5.51)

**General Comments**

- The tumor was formerly known as cylindroma. It is the second most common malignant salivary gland tumor and involves the minor and major salivary glands with a preponderance of intraoral glands and the submandibular gland. Adenoid cystic carcinoma (ACC) accounts for approximately 5% of all salivary gland tumors.
- ACC is a slow-growing malignant tumor with a high tendency for perineural and perivascular invasion; therefore, the tumor shows a high recurrence rate after surgical removal; but it can also give rise to metastases.
- Histologically, ACC exhibit three different growth patterns that may coexist in the same tumor:
  1. Glandular or cribriform type where solid epithelial cell nests are interspersed with spaces filled with homogeneous globular material.
  2. Tubular type consisting of ducts surrounded by hyaline stroma.
  3. The solid type is composed of solid epithelial tumor parenchyma and cell nests are separated by subtle stromal cords (Fig. 5.51).

**Microscopic Features**

In FNA specimens, the cribriform variant of ACC is characterized by the typical histologic architecture, which is highly reliable and important in the cytodiagnostic workup.

- Hallmarks: small polyhedral cells showing minor variation in cell size. The nuclei are round to oval and hyperchromatic, the cytoplasm appears as a small rim. The chromatin is coarse and the nucleoli are irregular. Generally, tumor cells show a high degree of intercellular cohesion and are tightly clustered.
  The characteristic extracellular globular material appears as homogeneous spherical bodies surrounded by carcinoma cells (translucent in Pap stain and pink when May-Grünwald-Giemsa-stained) [94]. Isolated hyaline globules frequently occur.

**Caution**

It must be emphasized that only around 50% of the tumor aspirates exhibit the characteristic globules [36]. The diagnostic assessment of the other half of ACCs is solely based on cellular and structural features.

### Differential Diagnosis

FNA specimens composed of cells with monotonous small nuclei and/or including significant tight clusters with mucoid globules may give rise to difficulties distinguishing between ACC and other benign and malignant salivary gland tumors. Such entities include:

- Basal cell adenoma (Fig. 5.50): Basal cell adenoma and ACC are barely distinguishable, in particular when the former exhibits a solid pleomorphic pattern or when adenoid cystic carcinoma exhibits only a few typical globules [164]. However, the cells of basal cell adenoma show larger cytoplasm, smaller nuclei, and minor atypia among other tumor-typical features [133, 180].
- Pleomorphic adenoma [78, 133, 164, 180] (Fig. 5.51): Pleomorphic adenoma (PA) is the second most frequent tumor causing differential diagnosis problems with ACC, because the former shows the most frequent variation of cytologic findings. However, globules rarely occur in PA and PA cells are less monotonous including plasmacytoid appearance, spindle shape, as well as dense and abundant cytoplasm. The spreading of tumor cells into the myxoid background tissue is typical for PA, whereas the demarcation between tumor cell clusters and interstitial globular substance is distinct in ACC. The nuclei of cells from PAs show a fine granular chromatin, indistinct nucleoli, and absence of hyperchromasia. The background matrix in aspirates from PAs is more fibrillar and irregular than the homogeneous spheres in ACC.
- Polymorphous low-grade adenocarcinoma of intraoral minor salivary glands can give rise to major problems distinguishing ACC, but a reliable distinction is essential because of the differences in the clinical behavior, treatment, and prognosis of the two neoplasms. In polymorphous low-grade adenocarcinoma, the cells show more abundant cytoplasm, the nuclei are more irregular, and the hyaline globules are more scattered as compared to ACC [133].
- Myoepithelioma and epithelial-myoepithelial carcinoma may mimic ACC by cytology (Fig. 5.51, compare with Fig. 5.43A).

### Immunocytochemistry

A few reports in the literature suggest the utility of certain immunocytochemical markers in distinguishing pleomorphic adenoma and polymorphous low-grade adenocarcinoma from ACC. The markers include cytokeratins, vimentin, glial fibrillary acid protein, and integrins [6].

## 5.1.5.3 Acinic Cell Carcinoma (Acinar / Acinous Cell Carcinoma) [56, 126, 144] (Figs. 5.52–5.56)

### General Comments

- Acinic cell carcinoma is a rare salivary gland tumor, comprising approximately 6–10% of all salivary gland cancers; however, some studies report a much lower percentage. Acinic cell carcinomas account for approximately 3–13% of all malignancies of the parotid gland, and are rarely seen elsewhere.
- Most of the acinic cell carcinomas are slow-growing low-grade malignant neoplasms bearing a high potential for recurrence. Recurrence and metastases many years after primary surgical removal are common.
- The histologic appearance includes an acinar, solid, microcystic, papillary-cystic, intercalated duct-like, and follicular growth pattern. The individual cells also show a broad morphologic spectrum, they may appear vacuolated, clear, columnar, etc. Any of these tissue and cell variants may be seen in an individual tumor, yet the acinar cell component enables histologists and cytopathologists to assess the correct tumor typing.

### Microscopic Features

- Hallmarks of well-differentiated acinic cell carcinoma: The aspirated cellular material is a distinctly monotonous admixture of ductal elements, mesenchymal cells are absent. The smears contain abundant tumor cells, frequently aggregated in cohesive clusters, but stripped nuclei are found in most cases.
  More or less well-formed acinic formations are encountered in various amounts. The nuclei are monomorphic, round, or oval with granular chromatin and a central nucleolus. Slight atypias may be seen (irregular nuclear shape, chromatin coarsening, increased nucleolar size). The cytoplasm appears foamy, often supplemented with eosinophilic granules; thus the tumor cells strongly resemble benign acinic cells. Occasionally, a predominance of tumor cells with dense cytoplasm (homogeneous grey in MGG stain) may occur resembling oncocytes.
- Papillary clusters with fibrovascular cores indicate a papillary growth pattern (Fig. 5.54).
- A lymphocytic component may occasionally be encountered originating from lymphocytic infiltrates and/or lymphatic tissue adjacent to the tumor.
- Calcifications, possibly psammoma body-like, are rarely seen.
- Hallmarks of poorly differentiated acinic cell carcinoma (Fig. 5.55) displays a clearly malignant cell population comprising polymorphic cells and nuclei, irregular chromatin, and enlarged polymorphic nucleoli.

**Caution**

- Acinar cell formation is the morphologic key feature for an accurate cytologic tumor typing. This component tends to be unequally developed, but it can be detected in nearly all acinic cell carcinomas.
- Well-developed tumorous acini with minimal cell atypias may mislead to a diagnosis of nonneoplastic salivary gland tissue; individual tumor cells originating from well-differentiated acinic cell carcinoma may look like benign acinic cells
- Stripped nuclei should not be misinterpreted as lymphocytes.

**Differential Diagnosis**

- Well-differentiated monomorphic tumor cells and well-formed tumorous acini may have a strong resemblance to cells and tissue fragments of the normal salivary gland (Fig. 5.53). However, the basket-like cell arrangement of benign acinic cells, ductal structures, and loose interstitial tissue are absent in aspirates from acinic cell carcinomas.
- Acinic cell carcinoma composed of numerous tumor cells with abundant clear and foamy cytoplasm may mimic clear cell carcinoma, myoepithelial carcinoma, or mucoepidermoid carcinoma (Fig. 5.56), but intracellular mucus is completely absent in acinic cell carcinomas, and myoepithelial tumor cells are well characterized by their particular immunoreactivity.
- Tumor cells showing homogeneous and dense cytoplasm may present diagnostic confusion with oncocytic tumors.
- Cytologic specimens from a papillary-cystic acinic cell carcinoma variant may raise suspicions of cystic lesions of various etiologies. A correct tumor typing is often not possible [126, 158].
- Isolated vacuolated tumor cells in an otherwise hypocellular specimen are difficult to differentiate from histiocytes/macrophages
- Naked nuclei of acinic-type tumor cells are of lymphocyte size; they may mimic lymphocytic infiltrate and (together with oncocytoid cells) Warthin tumor. Lymphoid infiltrates can lead to a misdiagnosis of a lymph node with metastatic carcinoma.
- Poorly differentiated acinic cell carcinoma is very difficult to ascertain, differential diagnosis includes primary and metastatic undifferentiated pleomorphic carcinoma.
- Dedifferentiated acinic cell carcinoma has been reported; the tumor is composed of both a typical acinic tumor component and dedifferentiated tumor areas [69].

### 5.1.5.4 Polymorphous Low-Grade Adenocarcinoma [66, 137, 151, 168] (Fig. 5.57)

Polymorphous low-grade adenocarcinoma (PLGA) predominantly occurs in minor salivary glands where it is the second most malignant neoplasm. The primary location is usually the palate. Its occurrence in major salivary glands is extremely rare [127, 168]. PLGA is a slow-growing tumor showing local invasion but extremely low metastatic potential [142].

The pathognomonic feature of the neoplasm is the variety of histologic patterns in combination with bland monomorphic tumor cells and low mitotic activity.

**Microscopic Features and Differential Diagnosis**

- The hypercellular smears contain uniform cells forming a variety of papillae, sheets, and clusters.
- The cells are small to medium-sized, exhibiting bland chromatin texture and occasional nucleoli.
- The cytoplasm is dense and eosinophilic stained.

The solid tumor variant imitates monomorphic adenoma. Occasional tubular structures containing hyaline globules suggest adenoid cystic carcinoma, and cases with myxoid matrix mimic pleomorphic adenoma. In general, a definite diagnosis is difficult to establish with cytology alone.

### 5.1.5.5 Other Rare Malignant Salivary Gland Neoplasms of Epithelial and Myoepithelial Origin

#### 5.1.5.5.1 Epithelial-Myoepithelial Carcinoma

Epithelial-myoepithelial carcinoma is a low-grade malignant tumor of the salivary glands with the cells showing biphasic cellularity. Histologically, the duct-like structures are formed by an inner layer of duct lining cuboidal cells and an outer layer of clear cells.

- The peculiar biphasic pattern consisting of small ductal cells and large clear myoepithelial cells results in a rather typical cytologic appearance. However, the biphasic pattern is often difficult to identify due to the fragile cytoplasm of the clear cells, which appear as naked nuclei. The myoepithelial cells usually stain immunocytochemically positive for S100, p63, smooth muscle actin, and myosin.
- The differential diagnosis includes in particular varied carcinomas of the clear cell type, adenoid cystic carcinoma, pleomorphic adenoma, and polymorphous low-grade adenocarcinoma. Cytological features and cytodiagnostic considerations regarding epithelial-myoepithelial carcinoma have been reviewed in the literature [44, 123, 134].

#### 5.1.5.5.2 Basal Cell Adenocarcinoma [24, 59, 74]

Basal cell adenocarcinoma is a low-grade adenocarcinoma. It is encountered in minor and major salivary glands. Invasive tumor growth distinguishes basal cell adenocarcinoma

from basal cell adenoma. It is often impossible to differentiate between malignant and benign tumors solely on the basis of cytologic features (for cellular features and differential diagnosis, see Sect. 5.1.4.4, "Basal Cell Adenoma" p. 412).

#### 5.1.5.5.3 Clear Cell Carcinoma [117]

Clear cell carcinoma is a rare salivary gland tumor, most frequently found in minor salivary glands. Sporadic tumors have been reported arising from pleomorphic adenoma [132].



**Microscopic Features and Differential Diagnosis**

- Tumor cells comprise moderate to abundant foamy and vacuolated cytoplasm as well as bland nuclear features.
- Cell clusters may show a diverse architecture. Glandular and acinic structures may include hyaline-homogeneous globular material [101, 132].

- Numerous neoplasms located in the salivary glands – primary in origin or lymphogenous/hematogenous metastatic or invasive from adjacent areas – may be characterized by a predominant clear cell component.
  This heterogenous tumor group most particularly includes: oncocytoma; myoepithelial tumors; mucoepidermoid carcinoma; metastases of clear cell carcinomas from different sites such as kidney, thyroid, and liver; and metastatic melanoma.
- In minor salivary glands, metastatic or directly invasive odontogenic neoplasms should be considered against clear cell carcinoma [117].

#### 5.1.5.5.4 Sebaceous Carcinoma [35, 67]

Sebaceous carcinoma is an extremely rare variety of low-grade salivary gland tumors, characterized by sebaceous-type cells of varying degrees of maturation. The tumor represents the malignant transformation of sebaceous (lymph-) adenoma (see also Sect. 5.1.4.5.4, p. 413).

#### 5.1.5.5.5 Lymphoepithelial Carcinoma

An association between benign lymphoepithelial lesions and lymphoepithelial carcinoma has recently been reviewed by Schneider and Rizzardi [155].

FNA findings of malignant lymphoepithelial lesions have rarely been reported [75, 92]:

- Cohesive and isolated obviously malignant epithelial cells are intermingled with mature lymphocytes.

Differential diagnosis includes benign lymphoepithelial lesions and malignant lymphoma respectively (see Sects. 5.1.3.6.1, p. 409 and 5.1.5.7, p. 419), large-cell malignant lymphoma associated with benign lymphoid hyperplasia of the T-cell phenotype, lymphoepithelioma-like carcinoma metastatic to the salivary glands, and lymph node metastasis of a pleomorphic carcinoma.

#### 5.1.5.5.6 Papillary Cystadenocarcinoma (Fig. 5.58)

- Microscopic evaluation of cytologic smears shows a watery proteinaceous background and papillary clusters composed of cuboidal and columnar cells.
- The epithelial cells to a certain extent show loss of polarization and pseudostratification.
- Psammoma bodies are occasionally encountered.

Distinction of benign from malignant papillary cystic salivary gland tumors can be very difficult based on cytology alone unless the individual cells are pleomorphic with clear evidence of nuclear malignancy (see also Sect. 5.1.4.5.1, p. 413). Other papillary neoplasms should also be considered.

#### 5.1.5.5.7 Salivary Duct Carcinoma [86] (Fig. 5.59)

This is an extremely rare and highly malignant neoplasm comparable with comedocarcinoma of the breast. Salivary duct carcinoma has a much worse prognosis as compared with primary salivary gland tumors sharing similar morphology. The latter include high-grade mucoepidermoid carcinoma with minor squamous cell fraction, and polymorphous low-grade adenocarcinoma.

#### 5.1.5.5.8 Myoepithelial Carcinoma [153] (Fig. 5.60)

Myoepithelial carcinomas show a wide spectrum of histoarchitectural and cytomorphological features, so this particular malignancy can easily be confused with many other benign and malignant tumors. Cytologic peculiarities, differential diagnostic problems, reliability of immunocytochemistry, and selected references regarding myoepithelial tumors are provided in Sects. 5.1.1.4, "Immunocytochemistry", p. 403 and 5.1.4.5.5 "Myoepithelioma", p. 413.

#### 5.1.5.5.9 Other Epithelial Malignancies

Other Epithelial malignancies exhibiting a practically identical cytomorphology as known from primary sites other than the salivary glands include squamous cell carcinoma, adenosquamous carcinoma, small-cell carcinoma, undifferentiated carcinoma, and carcinosarcoma. Correct assessment of the primary tumor site may more often than not rest on clinical data and the patient's history.

### 5.1.5.6 Malignant Mesenchymal Neoplasms of the Salivary Glands

- As already mentioned, nonepithelial salivary gland tumors are rare, accounting for only 10% of all salivary gland neoplasms.
- The most frequent primary sarcomas that have been found are malignant fibrous histiocytoma (MFH) and malignant neural tumors. The histologic pattern of dermatofibrosarcoma protuberans, synovial sarcoma, leiomyosarcoma, liposarcoma, small round cell tumor, and the cytologic features of MFH and osteoclastoma-like giant cell tumor have been reported in the literature [27, 28, 173].

- Salivary gland malignant melanoma occurs more frequently as a secondary lesion [27] than as a primary tumor [116]. Cytologic features are generally accepted and described in various chapters in this book.

### 5.1.5.7 Malignant Lymphomas and Myeloid Sarcoma

#### General Comments

- Malignant lymphoma in salivary glands can occur primarily, and secondarily in the course of systemic tumor dissemination. Primary salivary gland lymphomas are usually associated with autoimmune diseases such as immunologically induced (myoepithelial) sialadenitis, i.e., MESA with or without Sjögren syndrome. The risk for developing malignant lymphoma in salivary glands of patients with Sjögren syndrome is high.
- The prototype of primary salivary gland lymphoma is the extranodal marginal zone B-cell lymphoma of the mucosa-associated lymphoid tissue (MALT) type [9, 18,154].
- Approximately one-third of salivary gland non-Hodgkin lymphomas are high-grade lymphomas; Hodgkin lymphomas account for only 10% of all malignant lymphomas.
- Discriminating between benign myoepithelial sialadenitis and subsequent early-stage malignant lymphoma is crucial, but usually beyond the scope of FNA cytology.

**Caution**

- Using cytology, it is not possible to differentiate between malignant lymphoma originating from salivary gland tissue and lymphoma with the primary source in intra-/paraparotid lymph nodes.
- The diagnostic assessment of malignant lymphoma arising in the background of a benign MESA is beyond the scope of cytology in most of the cases. Accurate diagnosis of MALT lymphoma requires histologic examination, immunohistochemical tests, and molecular genetic evaluation [7, 115,178].
- MESA-associated monoclonal B-cell populations may be detected by molecular genetic methods in the absence of clinical and histologic evidence of malignant lymphoma [9, 18,172].

#### Microscopic Features and Differential Diagnosis

The reader is referred to Sects. 15.3.2–15.3.18, p. 955 for detailed cytomorphologic information as to various types of non-Hodgkin lymphomas.

A few selected entities of importance in standard cytology are briefly mentioned below:

- *Marginal zone B-cell lymphoma of the MALT type* [22, 115] (Figs. 5.17–5.19):
  - A heterogeneous population of lymphocytes with a predominance of enlarged lymphoid cells and absence of both tingible body macrophages and typical follicle center cells may be suggestive of a marginal zone B-cell lymphoma.

  The mixed lymphoid cell pattern may lead to a misdiagnosis of benign lymphoproliferation or myoepithelial sialadenitis. Furthermore, the cellular background of mixed cellularity classical Hodgkin lymphoma may mimic the tumor cell population of MALT lymphoma.
- *Non-Hodgkin lymphoma of the common low-grade type* (primary and secondary to the salivary gland) [22]:
  - Cytologically, a monotonous lymphoid cell population is highly suspicious of non-Hodgkin lymphoma (NHL), a reactive lymphoid hyperplasia is practically excluded.
  - Lymphoid cells are enlarged, comprising darkly stained nuclei, irregular nuclear outline, nuclear indentations, and nucleoli. Small mature lymphocytes are rarely encountered and never encountered as a major component.
  - Starry-sky histiocytes and epimyoepithelial cell groups are absent.

  Primary and secondary small-cell malignant tumors have to be distinguished from monomorphic low-grade malignant lymphoma.
- *Myeloid sarcoma* (Fig. 5.61):
  Involvement of salivary glands by myelogenous leukemia (myeloid sarcoma) is extremely rare. In most cases, patients having a history of myeloid neoplasia. The clinical history together with the immunocytochemical identification of the myeloic lineage (myeloperoxidase positivity of the tumor cells) provides the correct diagnosis. A few cases that were diagnosed by FNAB are on record [17].
  - Tumor cells are medium-sized and large, usually showing a clear and lobated nucleus with a histiocytoid aspect, and large vacuolated or granular cytoplasm.

  Malignant neoplasms of the large-cell type such as acute myeloid leukemia of monoblastic/monocytic lineage (positive immunostaining for CD68), large-cell NHL, carcinoma, and melanoma have to be excluded.
- *Extramedullary hemopoiesis* including normoblasts, myeloid precursors, immature granulocytes and megakaryocytes should usually present no diagnostic dilemmas (Fig. 15.102).

### 5.1.5.8 Metastases

- Metastases account for about 20% of the malignant neoplasms affecting major salivary glands with the most common site of tumor origin in the parotid glands. Secondary tumors are localized in the parenchyma of the salivary glands (40%), or in lymph nodes enclosed in the glandular parenchyma, or in lymph nodes adjacent to the gland (60%).
- Metastases caused by lymphatic spread may predominantly originate from primary squamous cell carcinoma of the skin, or regional malignant melanomas, and very rarely from nasopharyngeal carcinoma or thyroid carcinoma.
- Primary salivary gland tumors showing particular morphologic features such as (A) cystic spaces containing papillary projections or (B) clear cells with nuclear lobulation may simulate secondary invasion by:
  - Papillary thyroid carcinoma and pulmonary adenocarcinoma (A + B) (Fig. 5.58).
  - Breast carcinoma, renal cell carcinoma, or melanoma (B) (Fig. 5.62).

  These tumors metastasize hematogenously into salivary glands.
- Immunocytochemistry can correctly classify most of the tumors with cytologically equivocal findings: thyroid carcinoma (TTF-1 +/thyroglobulin +), lung carcinoma (CK7+/TTF-1 +), breast carcinoma (hormone receptors +), renal cell carcinoma (renal cell marker +), malignant melanoma (melanoma-typical antigens +).
- A larger series addressing FNAB of secondary neoplasms involving the salivary glands has been published by Zhang and co-authors [185].

## 5.1.6 Further Reading


1. Aggarwal AP, Jayaram G, Mandal AK. Sarcoidosis diagnosed on fine-needle aspiration cytology of salivary glands: a report of three cases. Diagn Cytopathol 1989;5:289-292.
2. Akhter J, Hirachand S, Lakhey M. Role of FNAC in the diagnosis of salivary gland swellings. Kathmandu Univ Med J 2008;6:204-208.
3. Al-Khafaji BM, Afify AM. Salivary gland fine needle aspiration using the ThinPrep technique: diagnostic accuracy, cytologic artifacts and pitfalls. Acta Cytol 2001;45:567-574.
4. Alos L, Cardesa A, Bombi JA, et al. Myoepithelial tumors of salivary glands: a clinicopathologic, immunohistochemical, ultrastructural, and flow-cytometric study. Semin Diagn Pathol 1996;13:138-147.
5. Anand A, Brockie ES. Cytomorphological features of salivary duct carcinoma ex pleomorphic adenoma: diagnosis by fine-needle aspiration biopsy with histologic correlation. Diagn Cytopathol 1999;20:375-378.
6. Araujo VC, Loducca SV, Sousa SO, et al. The cribriform features of adenoid cystic carcinoma and polymorphous low-grade adenocarcinoma: cytokeratin and integrin expression. Ann Diagn Pathol 2001;5:330-334.
7. Bacon CM, Du MQ, Dogan A. Mucosa-associated lymphoid tissue (MALT) lymphoma: a practical guide for pathologists. J Clin Pathol 2007;60:361-372.
8. Bagga P, Pandey P, Shahi M, et al. Parotid gland tuberculosis diagnosed on FNAC: a case report. Cytopathology 2008;Epub Aug 7.
9. Bahler DW, Swerdlow SH. Clonal salivary gland infiltrates associated with myoepithelial sialadenitis (Sjögren's syndrome) begin as nonmalignant antigen-selected expansions. Blood 1998;91:1864-1872.
10. Ballo MS, Shin HJ, Sneige N. Sources of diagnostic error in the fine-needle aspiration diagnosis of Warthin's tumor and clues to a correct diagnosis. Diagn Cytopathol 1997;17:230-234.
11. Banich J, Reyes CV, Bier-Laning C. Sebaceous lymphadenoma identified by fine needle aspiration biopsy: a case report. Acta Cytol 2007;51:211-213.
12. Baschinsky D, Hameed A, Keyhani-Rofagha S. Fine-needle aspiration cytological features of dermoid cyst of the parotid gland: a report of two cases. Diagn Cytopathol 1999;20:387-388.
13. Bianco M, Mesko T, Cura M, Cabello-Inchausti B. Chronic sclerosing sialadenitis (Kuttner's tumor): unusual presentation with bilateral involvement of major and minor salivary glands. Ann Diagn Pathol 2003;7:25-30.
14. Boccato P, Altavilla G, Blandamura S. Fine needle aspiration biopsy of salivary gland lesions. A reappraisal of pitfalls and problems. Acta Cytol 1998;42:888-898.
15. Boutonnat J, Ducros V, Pinel C, et al. Identification of amylase crystalloids in cystic lesions of the parotid gland. Acta Cytol 2000;44:51-56.
16. Boyle JL, Meschter SC. Fine needle aspiration cytology of a sebaceous lymphadenoma: a case report. Acta Cytol 2004;48:551-554.
17. Cai G, Levine P, Sen F. Diagnosis of myeloid sarcoma involving salivary glands by fine-needle aspiration cytology and flow cytometry: report of four cases. Diagn Cytopathology 2008;36:124-127.
18. Carbone A, Gloghini A, Ferlito A. Pathological features of lymphoid proliferations of the salivary glands: lymphoepithelial sialadenitis versus low-grade B-cell lymphoma of the malt type. Ann Otol Rhinol Laryngol 2000;109:1170-1175.

19. Carino S, Cabrini RL. Meta-analysis of the literature on 1946 cases of minor salivary gland tumors of the palate. Acta Odontol Latinoam 2007;20:23-31.
20. Cerulli G, Renzi G, Perugini M, Becelli R. Differential diagnosis between adenoid cystic carcinoma and pleomorphic adenoma of the minor salivary glands of palate. J Craniofac Surg 2004;15:1056-1060.
21. Chahine KN, Tohme SM, Chouairy CJ. Cavernous hemangioma of the parotid gland. J Med Liban 2007;55:165-166.
22. Chai C, Dodd LG, Glasgow BJ, Layfield LJ. Salivary gland lesions with a prominent lymphoid component: cytologic findings and differential diagnosis by fine-needle aspiration biopsy. Diagn Cytopathol 1997;17:183-190.
23. Cheuk W, Chan JK. Kuttner tumor of the submandibular gland: fine-needle aspiration cytologic findings of seven cases. Am J Clin Pathol 2002;117:103-108.
24. Chhieng DC, Paulino AF. Basaloid tumors of the salivary glands. Ann Diagn Pathol 2002;6:364-372.
25. Chhieng DC, Argosino R, McKenna BJ, et al. Utility of fine-needle aspiration in the diagnosis of salivary gland lesions in patients infected with human immunodeficiency virus. Diagn Cytopathol 1999;21:260-264.
26. Chhieng DC, Cangiarella JF, Cohen JM. Fine-needle aspiration cytology of lymphoproliferative lesions involving the major salivary glands. Am J Clin Pathol 2000;113:563-571.
27. Chhieng DC, Cohen JM, Cangiarella JF. Fine-needle aspiration of spindle cell and mesenchymal lesions of the salivary glands. Diagn Cytopathol 2000;23:253-259.
28. Cho KJ, Ro JY, Choi J, et al. Mesenchymal neoplasms of the major salivary glands: clinicopathological features of 18 cases. Eur Arch Otorhinolaryngol 2008;265 Suppl 1:S47-56.
29. Chow TL, Chan TT, Choi CY, Lam SH. Kuttner's tumour (chronic sclerosing sialadenitis) of the submandibular gland: a clinical perspective. Hong Kong Med J 2008;14:46-49.
30. Cleveland DB, Cosgrove MM, Martin SE. Tyrosine-rich crystalloids in a fine needle aspirate of a polymorphous low grade adenocarcinoma of a minor salivary gland. Acta Cytol 1994;38:347-351.
31. Cohen EG, Patel SG, Lin O, et al. Fine-needle aspiration biopsy of salivary gland lesions in a selected patient population. Arch Otolaryngol Head Neck Surg 2004;130:773-778.
32. Cohen MB, Fisher PE, Holly EA, et al. Fine needle aspiration biopsy diagnosis of mucoepidermoid carcinoma. Statistical analysis. Acta Cytol 1990;34:43-49.
33. Cohn ML, Callender DL, El-Naggar AK. Sebaceous carcinoma ex-pleomorphic adenoma: a rare phenotypic occurence. Ann Diagn Pathol 2004;8:224-226.
34. Cristallini EG, Ascani S, Farabi R, et al. Fine needle aspiration biopsy of salivary gland, 1985-1995. Acta Cytol 1997;41:1421-1425.
35. Croitoru CM, Mooney JE, Luna MA. Sebaceous lymphadenocarcinoma of salivary glands. Ann Diagn Pathol 2003;7:236-239.
36. Da Cruz Perez DE, de Abreu Alves F, Nobuko Nishimoto I, et al. Prognostic factors in head and neck adenoid cystic carcinoma. Oral Oncol 2006;42:139-146.
37. Daneshbod Y, Negahban S, Khademi B, Daneshbod K. Epithelial myoepithelial carcinoma of the parotid gland with malignant ductal and myoepithelial components arising in a pleomorphic adenoma: a case report with cytologic, histologic and immunohistochemical correlation. Acta Cytol 2007;51:807-813.
38. Dardick I, Birek C, Lingen MW, Rowe PE. Differentiation and the cytomorphology of salivary gland tumors with specific reference to oncocytic metaplasia. Oral Surg Oral Med Oral Pathol Oral Radiol Endod 1999;88:691-701.
39. Darvishian F, Lin O. Myoepithelial cell-rich neoplasms: cytologic features of benign and malignant lesions. Cancer 2004;102:355-361.
40. Das DK, Haji BE, Ahmed MS, Hossain MN. Myoepithelioma of the parotid gland initially diagnosed by fine needle aspiration cytology and immunocytochemistry: a case report. Acta Cytol 2005;49:65-70.
41. Das DK, Petkar MA, Al-Mane NM, et al. Role of fine needle aspiration cytology in the diagnosis of swellings in the salivary gland regions: a study of 712 cases. Med Princ Pract 2004;13:95-106.
42. Dave SP, Pernas FG, Roy S. The benign lymphoepithelial cyst and a classification system for lymphocytic parotid gland enlargement in the pediatric HIV population. Laryngoscope 2007;117:106-113.
43. David O, Blaney S, Hearp M. Parotid gland fine-needle aspiration cytology: an approach to differential diagnosis. Diagn Cytopathol 2007;35:47-56.
44. Deere H, Hore I, McDermott N, Levine T. Epithelial-myoepithelial carcinoma of the parotid gland: a case report and review of the cytological and histological features. J Laryngol Otol 2001;115:434-436.
45. DiGuiseppe JA, Corio RL, Westra WH. Lymphoid infiltrates of the salivary glands: pathology, biology and clinical significance. Curr Opin Oncol 1996;8:232-237.
46. Dobson CM, Ellis HA. Polycystic disease of the parotid glands: case report of a rare entity and review of the literature. Histopathology 1987;11:953-961.
47. Driemel O, Kraft K, Hemmer J. DNA ploidy and proliferative activity in salivary gland tumours. Mund Kiefer Gesichtschir 2007;11:139-144.
48. Edwards PC, Wasserman P. Evaluation of cystic salivary gland lesions by fine needle aspiration: an analysis of 21 cases. Acta Cytol 2005;49:489-494.
49. Elagoz S, Gulluoglu M, Yilmazbayhan D, et al. The value of fine-needle aspiration cytology in salivary gland lesions, 1994-2004. ORL J Otorhinolaryngol Relat Spec 2007;69:51-56.
50. Elliott JN, Oertel YC. Lymphoepithelial cysts of the salivary glands. Histologic and cytologic features. Am J Clin Pathol 1990;93:39-43.
51. Ellis GL. "Clear cell" oncocytoma of salivary gland. Hum Pathol 1988;19:862-867.
52. Elsheikh TM, Bernacki EG. Fine needle aspiration cytology of cellular pleomorphic adenoma. Acta Cytol 1996;40:1165-1175.
53. Eneroth CM , Zajicek J. Aspiration biopsy of salivary gland tumors. II. Morphologic studies on smears and histologic sections from oncocytic tumors (45 cases of papillary cystadenoma lymphomatosum and 4 cases of oncocytoma) . Acta Cytol 1965;9:355-361.
54. Eneroth CM, Zajicek J. Aspiration biopsy of salivary gland tumors. III. Morphologic studies on smears and histologic sections from 368 mixed tumors. Acta Cytol 1966;10:440-454.
55. Eneroth CM, Zajicek J. Aspiration biopsy of salivary gland tumors. IV. Morphologic studies on smear and histologic sections from 45 cases of adenoid cystic carcinoma. Acta Cytol 1969;13:59-63.
56. Eneroth CM, Hamberger CA, Jakobsson P. Malignancy of acinic cell carcinoma. Ann Otol Rhinol Laryngol 1966;75:780-793.
57. Erdogan F, Altas S, Altas E, et al. A rare location of Castleman's disease: parotid region. N Z Med J 2008;121:86-90.
58. Eveson JW, Cawson RA. Salivary gland tumors: a review of 2,410 cases with particular reference to histological types, site, age, and sex distribution. J Pathol 1985;146:51-58.
59. Farrell T, Chang YL. Basal cell adenocarcinoma of minor salivary glands. Arch Pathol Lab Med 2007;131:1602-1604.

60. Favia G, Capodiferro S, Scivetti M, et al. Multiple parotid lymphoepithelial cysts in patients with HIV-infection: report of two cases. Oral Dis 2004;10:151-154.
61. Flint SR. Necrotizing sialometaplasia: an important diagnosis – review of the literature and spectrum of clinical presentation. J Ir Dent Assoc 2005;51:26-28.
62. Franzen A, Franzen CK, Koegel K. Tuberculosis of the parotid gland: a rare differential diagnosis of parotid tumor. Laryngorhinootologie 1997;76:308-311.
63. Furuse C, Sousa SO, Nunes FD, et al. Myoepithelial cell markers in salivary gland neoplasms. Int J Surg Pathol 2005;13:57-65.
64. Gallego L, Junquera L, Fresno MF, de Vicente JC. Papillary cystadenoma and cystadenocarcinoma of salivary glands: two unusual entities. Med Oral Patol Oral Bucal 2008;13:E460-463.
65. Gete Garcia P, Almodovar Alvarez C, Garcia Alvarez G, et al. Parotid tumours: correlation between fine needle aspiration biopsy and histological findings. Acta Otorrinolaringol Esp 2006;57:279-282.
66. Gibbons D, Saboorian MH, Vuitch, et al. Fine-needle aspiration findings in patients with polymorphous low grade adenocarcinoma of the salivary glands. Cancer 1999;87:31-36.
67. Gnepp DR, Brannon R. Sebaceous neoplasms of salivary gland origin. Report of 21 cases. Cancer 1984;53:2155-2170.
68. Gonzalez-Garcia R, Nam-Cha SH, Munoz-Guerra MF, et al. Basal cell adenoma of the parotid gland. Case report and review of the literature. Med Oral Patol Oral Cir Bucal 2006;11:E206-209.
69. Gonzalez-Peramato P, Jimenez-Heffernan JA, Lopez-Ferrer P, et al. Fine needle aspiration cytology of dedifferentiated acinic cell carcinoma of the parotid gland: a case report. Acta Cytol 2006;50:105-108.
70. Goonewardene SA, Nasuti JF. Value of mucin detection in distinguishing mucoepidermoid carcinoma from Warthin's tumor on fine needle aspiration. Acta Cytol 2002;46:704-708.
71. Goyal R, Ahuja A, Gupta N, et al. Multifocal nodular oncocytic hyperplasia in parotid gland: a case report. Acta Cytol 2007;51:621-623.
72. Granter SR, Renshaw AA, Cibas ES. Nontyrosine crystalloids in fine-needle aspiration specimens of the parotid gland: a report of two cases and review of the literature. Diagn Cytopathol 1999;20:44-46.
73. Granville LA, Laucirica R, Verstovsek G. Clinical significance of cultures collected from fine-needle aspiration biopsy. Diagn Cytopathol 2008;36:85-88.
74. Gross M, Maly B, Goldfarb A, Eliashar R. Basal cell adenocarcinoma in a buccal minor salivary gland. Acta Otolaryngol 2004;124:213-216.
75. Günhan O, Celasun B, Safali M, et al. Fine needle aspiration cytology of malignant lymphoepithelial lesion of the salivary gland. A report of two cases. Acta Cytol 1994;38:751-754
76. Hansen T, Hilka MB, Hansen I, et al. Cystic myoepithelioma. A rare differential diagnosis of a cystic lesion of the parotid gland. HNO 2004;52:1001-1003.
77. Hara H, Oyama T, Saku T. Fine needle aspiration cytology of basal cell adenoma of the salivary gland. Acta Cytol 2007;51:685-691.
78. Hara H, Oyama T, Suda K. New criteria for cytologic diagnosis of adenoid cystic carcinoma. Acta Cytol 2005;49:43-50.
79. Harris NL. Lymphoid proliferations of the salivary glands. Am J Clin Pathol 1999;111(1 Suppl 1): S94-103.
80. Hayashi D, Tysome JR, Boyei E, et al. Sebaceous lymphadenoma of the parotid gland: report of two cases and review of the literature. Acta Otorhinolaryngol Ital 2007;27:144-146.
81. Hayes MM, Cameron RD, Jones EA. Sebaceous variant of mucoepidermoid carcinoma of the salivary gland. A case report with cytohistologic correlation. Acta Cytol 1993;37:237-241.
82. Höbling W, Balon R. Cytological diagnosis of salivary gland tumours. Pathologe 2007;28:360-367.
83. Hruban RH, Erozan YS, Zinreich SJ, Kashima HK. Fine-needle aspiration cytology of monomorphic adenomas. Am J Clin Pathol 1988;90:46-51.
84. Jacobs JC. Low grade mucoepidermoid carcinoma ex pleomorphic adenoma. A diagnostic problem in fine needle aspiration biopsy. Acta Cytol 1994;38:93-97.
85. Jäkel KT, Löning T. Differential diagnosis of basaloid salivary gland tumors. Pathologe 2004;25:46-55.
86. Jamal AM, Sun ZJ, Chen XM, Zhao YF. Salivary duct carcinoma of the parotid gland: case report and review of the literature. J Oral Maxillofac Surg 2008;66:1708-1713.
87. Jan IS, Chung PF, Weng MH, et al. Analysis of fine-needle aspiration cytology of the salivary gland. J Formos Med Assoc 2008;107:364-370.
88. Jayaram G, Pathmanathan R, Khanijow V. Cystic lesion of the parotid gland with squamous metaplasia mistaken for squamous cell carcinoma. A case report. Acta Cytol 1998;42:1468-1472.
89. Johnson FB, Oertel YC, Ammann K. Sialadenitis with crystalloid formation: a report of six cases diagnosed by fine needle aspiration. Diagn Cytopathol 1995;12:76-80.
90. Jones AV, Craig GT, Speight PM, Franklin CD. The range and demographics of salivary gland tumours diagnosed in a UK population. Oral Oncol 2008;44:407-417.
91. Kaba S, Kojima M, Matsuda H, et al. Küttner's tumor of the submandibular glands: report of five cases with fine-needle aspiration cytology. Diagn Cytopathol 2006;34:631-635.
92. Kanjanavirojkul N, Kularbkaew C, Yutanawiboonchai W. Fine needle aspiration in a malignant lymphoepithelial lesion. A case report. Acta Cytol 2008;52:369-372.
93. Kapadia SB, Dusenbery D, Dekker A. Fine needle aspiration of pleomorphic adenoma and adenoid cystic carcinoma of salivary gland origin. Acta Cytol 1997;41:487-492.
94. Kawahara A, Harada H, Kage M, et al. Extracellular material in adenoid cystic carcinoma of the salivary glands: a comparative cytological study with other salivary myoepithelial tumors. Diagn Cytopathol 2004;31:14-18.
95. Kim T, Yoon GS, Kim O, Gong G. Fine needle aspiration diagnosis of malignant mixed tumor (carcinosarcoma) arising in pleomorphic adenoma of the salivary gland. A case report. Acta Cytol 1998;42:1027-1031.
96. Kim YH, Jeong WJ, Jung KY, et al. Diagnosis of major salivary gland tuberculosis: experience of eight cases and review of the literature. Acta Otolaryngol 2005;125:1318-1322.
97. Klijanienko J, Vielh P. Fine-needle sampling of salivary gland lesions. I. Cytology and histology correlation of 412 cases of pleomorphic adenoma. Diagn Cytopathol 1996;14:195-200.
98. Klijanienko J, Vielh P. Fine-needle sampling of salivary gland lesions. III. Cytologic and histologic correlation of 75 cases of adenoid cystic carcinoma: review and experience at the Institute Curie with emphasis on cytologic pitfalls. Diagn Cytopathol 1997;17:36-41.
99. Klijanienko J, Vielh P. Fine-needle sampling of salivary gland lesions. IV. Review of 50 cases of mucoepidermoid carcinoma with histologic correlation. Diagn Cytopathol 1997;17:92-98.

100. Klijanienko J, El-Naggar AK, Servois V, et al. Mucoepidermoid carcinoma ex pleomorphic adenoma: nonspecific preoperative cytologic findings in six cases. Cancer 1998;84:231-234.
101. Kobayashi M, Hattori M, Miyamoto T, et al. Basement membrane-like substance in cytologic diagnosis in clear cell adenocarcinoma of the minor salivary gland of the palate. A case report Acta Cytol 2007;51:916-920.
102. Kraft M, Lang F, Mihaescu A, Wolfensberger M. Evaluation of clinician-operated sonography and fine-needle aspiration in the assessment of salivary gland tumours. Clin Otolaryngol 2008;33:18-24.
103. Kumar N, Kapila K, Verma K. Fine needle aspiration cytology of mucoepidermoid carcinoma. A diagnostic problem. Acta Cytol 1991;35:357-359.
104. Kumar PV, Sobhani SA, Monabati A, et al. Myoepithelioma of the salivary glands. Fine needle aspiration biopsy findings. Acta Cytol 2004;48:302-308.
105. Layfield LJ, Gopez EV. Cystic lesions of the salivary glands: cytologic features in fine-needle aspiration biopsies. Diagn Cytopathol 2002;27:197-204.
106. Layfield LJ, Gopez EV. Histologic and fine-needle aspiration cytologic features of polycystic disease of the parotid glands: case report and review of the literature. Diagn Cytopathol 2002;26:324-328.
107. Lee YY, Wong KT, King AD, Ahuja AT. Imaging of salivary gland tumours. Eur J Radiol 2008;66:419-436.
108. Li S, Baloch ZW, Tomaszewski JE, LiVolsi VA. Worrisome histologic alterations following fine-needle aspiration of benign parotid lesions. Arch Pathol Lab Med 2000;124:87-91.
109. Lim CS, Ngu I, Collins AP, McKellar GM. Papillary cystadenoma of a minor salivary gland: report of a case involving cytological analysis and review of the literature. Oral Surg Oral Med Oral Pathol Oral Radiol Endod 2008;105:e28-33.
110. Lin AC, Bhattacharyya N. The utility of fine needle aspiration in parotid malignancy. Otolaryngol Head Neck Surg 2007;136:793-798.
111. Lin CC, Tsai MH, Huang CC, et al. Parotid tumors: a 10-year experience. Am J Otolaryngol 2008;29:94-100.
112. Lopez JI, Ugalde A, Arostegui J, Bilbao FJ. Plasmacytoid myoepithelioma of the soft palate. Report of a case with cytologic, immunohistochemical and electron microscopic studies. Acta Cytol 2000;44:647-652.
113. Lopez-Rios F, Ballestin C, Martinez-Gonzalez MA, et al. Lymphoepithelial cyst with crystalloid formation. Cytologic features of two cases. Acta Cytol 1999;43:277-280.
114. Löwhagen T, Tani EM, Skoog L. Salivary glands and rare head and neck lesions. In: Comprehensive Cytopathology, ed: M. Bibbo. WB. Saunders Company. 1991; p:226-227.
115. Maes B, De Wolf-Peeters C. Marginal zone cell lymphoma - an update on recent advances. Histopathology 2002;40:117-126.
116. Maier H, Mühlmeier G, Kraft K, et al. Primary malignant melanoma of the parotid gland: a case report and review of the literature. HNO 2008;56:627-632.
117. Maiorano E, Altini M, Favia G. Clear cell tumors of the salivary glands, jaws, and oral mucosa. Semin Diagn Pathol 1997;14:203-212.
118. Malhotra P, Arora VK, Singh N, Bhatia A. Algorithm for cytological diagnosis of nonneoplastic lesions of the salivary glands. Diagn Cytopathol 2005;33:90-94.
119. Maly B, Maly A, Doviner V, et al. Fine needle aspiration biopsy of intraparotid schwannoma. A case report. Acta Cytol 2003;47:1131-1134.
120. Mandel L, Reich R. HIV parotid gland lymphoepithelial cysts: Review and case reports. Oral Surg Oral Med Oral Pathol 1992;74:273-278.
121. Martinez del Pero M, Majumdar S, Bateman N, Bull PD. Presentation of first branchial cleft anomalies: the Sheffield experience. J Laryngol Otol 2007;121:455-459.
122. McCallum PL, Lampe HB, Cramer H, Matthews TW. Fine-needle aspiration cytology of lymphoid lesions of the salivary gland: a review of 35 cases. J Otolaryngol 1996;25:300-304.
123. Miliauskas JR, Orell SR. Fine-needle aspiration cytological findings in five cases of epithelial-myoepithelial carcinoma in salivary glands. Diagn Cytopathol 2003;28:163-167.
124. Milroy CM, Ferlito A, Devaney KO, Rinaldo A. Role of DNA measurements of head and neck tumors. Ann Otol Rhinol Laryngol 1997;106:801-804.
125. Mooney EE, Dodd LG, Layfield LJ. Squamous cells in fine-needle aspiration biopsies of salivary gland lesions: potential pitfalls in cytologic diagnosis. Diagn Cytopathol 1996;15:447-452.
126. Mosunjac MB, Siddiqui MT, Tadros T. Acinic cell carcinoma-papillary variant. Pitfalls of fine needle aspiration diagnosis: study of five cases and review of literature. Cytopathology 2009;20:96-102.
127. Nagao T, Gaffey TA, Kay PA, et al. Polymorphous low-grade adenocarcinoma of the major salivary glands: report of three cases in an unusual location. Histopathology 2004;44:164-171.
128. Namiq AL, Tollefson T, Fan F. Cryptococcal parotitis presenting as a cystic parotid mass: report of a case diagnosed by fine-needle aspiration cytology. Diagn Cytopathol 2005;33:36-38.
129. Nassour DN, Patel SV, Kosseifi SG, et al. Marked bilateral parotid enlargement in metabolic syndrome: a case report and review of the literature. Tenn Med 2007;100:39-41.
130. Nasuti JF, Gupta PK, Fleisher SR, LiVolsi VA. Nontyrosine crystalloids in salivary gland lesions: report of seven cases with fine-needle aspiration cytology and follow-up surgical pathology. Diagn Cytopathol 2000;22:167-171.
131. Nasuti JF, Yu GH, Gupta PK. Fine-needle aspiration of cystic parotid glands lesions: an institutional review of 46 cases with histologic correlation. Cancer 2000;90:111-116.
132. Negahban S, Daneshbod Y, Shishegar M. Clear cell carcinoma arising from pleomorphic adenoma of a minor salivary gland: Report of a case with fine needle aspiration, histologic and immunohistochemical findings. Acta Cytol 2006;50:687-690.
133. Netto Jde N, Miranda AM, da Silveira HM, et al. Fine-needle aspiration biopsy as an auxiliary diagnostic tool on intraoral minor salivary gland adenoid cystic carcinoma. Oral Surg Oral Med Oral Pathol Oral Radiol Endod 2008;106:242-245.
134. Ng WK, Choy C, Ip P, et al. Fine needle aspiration cytology of epithelial-myoepithelial carcinoma of salivary glands. A report of three cases. Acta Cytol 1999;43:675-680.
135. Nigam S, Kumar N, Jain S. Cytomorphologic spectrum of carcinoma ex pleomorphic adenoma. Acta Cytol 2004;48:309-314.
136. Oliveira DTConlar A, Freias FJ. Histopathological spectrum of 112 cases of mucocele. Braz Dent J 1993;4:29-36.
137. Paleri V, Robinson M, Bradley P. Polymorphous low-grade adenocarcinoma of the head and neck. Curr Opin Otolaryngol Head Neck Surg 2008;16:163-169.

138. Parfitt JR, McLachlin CM, Weir MM. Comparison of ThinPrep and conventional smears in salivary gland fine-needle aspiration biopsies. Cancer 2007;111:123-129.
139. Park JH, Lee SW, Koh YW. Castleman disease of the parotid gland in childhood: an unusual entity. Auris Nasus Larynx 2008;35:451-454.
140. Parwani AV, Lujan G, Ali SZ. Myoepithelial carcinoma arising in a pleomorphic adenoma of the parotid gland: report of a case with cytopathologic findings. Acta Cytol 2006;50:93-96.
141. Peel RL, Gnepp DR. Diseases of the salivary glands. In: Surgical Pathology of the Head and Neck. Ed: L.Barnes, Marcel Dekker, Inc.1985: 533-645.
142. Pogodzinski MS, Sabri AN, Lewis JE, Olsen KD. Retrospective study and review of polymorphous low-grade adenocarcinoma. Laryngoscope 2006;116:2145-2149.
143. Pons Vicente O, Almendros Marques N, Berini Aytes L, Gay Escoda C. Minor salivary gland tumors: A clinicopathological study of 18 cases. Med Oral Patol Oral Cir Bucal 2008;13:E582-588.
144. Prieto-Rodriguez M, Artes-Martinez MJ, Navarro-Hervas M, et al. Cytological characteristics of acinic cell carcinoma (ACC) diagnosed by fine-needle aspiration biopsy (FNAB). A study of four cases. Med Oral Patol Oral Cir Bucal 2005;10:103-108.
145. Raab SS, Thomas PA, Cohen MB. Fine-needle aspiration biopsy of salivary gland mycoses. Diagn Cytopathol 1994;11:286-290.
146. Ramdall RB, Cai G, Levine PH, et al. Fine-needle aspiration biopsy findings in epithelioid myoepithelioma of the parotid gland: a case report. Diagn Cytopathol 2006;34:776-779.
147. Ro JY, Mackay B, Batsakis JG, Cartwright J Jr. Intraluminal crystalloids in malignant salivary gland tumors (electron microscopy and X-ray microanalytic studies). J Laryngol Otol 1987;101:1175-1181.
148. Rodriguez-Fernandez J, Mateos-Micas M, Martinez-Tello FJ, et al. Metastatic benign pleomorphic adenoma. Report of a case and review of the literature. Med Oral Patol Oral Cir Bucal 2008;13:E193-196.
149. Roh JL, Kim JM. Küttner's tumor: unusual presentation with bilateral involvement of the lacrimal and submandibular glands. Acta Otolaryngol 2005;125:792-796.
150. Saenz-Santamaria J, Catalina-Fernandez I, Fernandez-Mera JJ. Sialadenitis with crystalloid formation. Fine needle aspiration cytodiagnosis of 15 cases. Acta Cytol 2003;47:1-4.
151. Saenz-Santamaria J, Catalina-Fernandez I. Polymorphous low grade adenocarcinoma of the salivary gland. Diagnosis by fine needle aspiration cytology. Acta Cytol 2004;48:52-56.
152. Saleh HA, Ram B, Harmse JL, et al. Lipomatosis of the minor salivary glands. J Laryngol Otol 1998;112:895-897.
153. Savera AT, Sloman A, Huvos AG, Klimstra DS. Myoepithelial carcinoma of the salivary glands: a clinicopathologic study of 25 patients. Am J Surg Pathol 2000;24:761-774.
154. Schmid U, Helbron D, Lennert K. Development of malignant lymphomas in myoepithelial sialadenitis (Sjögren's syndrome). Virchows Arch (Pathol Anat) 1981;;395:11-43.
155. Schneider M, Rizzardi C. Lymphoepithelial carcinoma of the parotid glands and its relationship with benign lymphoepithelial lesions. Arch Pathol Lab Med 2008;132:278-282.
155A. Seethala RR, Dacic S, Cieply K, Kelly LM, Nikiforova MN. A Reappraisal of the MECT1/MAML2 translocation in salivary mucoepidermoid carcinomas. The American Journal of Surgical Pathology 2010;34(8):1106-1121.
156. Seichter A, Szymanski L, Warchol R. Parotid gland sarcoidosis. Otolaryngol Pol 2007;61:491-496.
157. Seifert G, Donath K, von Gumberz C. Mucoceles of the minor salivary glands. Extravasation mucoceles (mucus granulomas) and retention mucoceles (mucus retention cysts). HNO 1981;29:179-191.
158. Shet T, Ghodke R, Kane S, Chinoy RN. Cytomorphologic patterns in papillary cystic variant of acinic cell carcinoma of the salivary gland. Acta Cytol 2006;50:388-392.
159. Siddaraju N, Badhe BA, Goneppanavar M, Mishra MM. Preoperative fine needle aspiration cytologic diagnosis of spindle cell myoepithelioma of the parotid gland: a case report. Acta Cytol 2008;52:495-499.
160. Siddiqui NH, Wu SJ. Fine-needle aspiration biopsy of cystic pleomorphic adenoma with adnexa-like differentiation mimicking mucoepidermoid carcinoma: a case report. Diagn Cytopathol 2005;32:229-232.
161. Siewert B, Kruskal JB, Kelly D, et al. Utility and safety of ultrasound-guided fine-needle aspiration of salivary gland masses including a cytologist's review. J Ultrasound Med 2004;23:777-783.
162. Singh G, Iyer VK. Amylase crystalloids in a cystic lesion of the parotid salivary gland diagnosed by fine needle aspiration cytology. J Cytol 2008;25:77-78.
163. Stanley MW, Bardales RH, Beneke J, et al. Sialolithiasis. Differential diagnostic problems in fine-needle aspiration cytology. Am J Clin Pathol 1996;106:229-233.
164. Stanley MW. Selected problems in fine needle aspiration of head and neck masses. Mod Pathol 2002;15:342-350.
165. Stewart CJ, MacKenzie K, McGarry GW, Mowat A. Fine-needle aspiration cytology of salivary gland: a review of 341 cases. Diagn Cytopathol 2000;22:139-146.
166. Sugihara K, Hirokawa M, Shimizu M, et al. Collagenous crystalloids in a fine needle aspirate of a pleomorphic adenoma of the minor salivary gland. A case report. Acta Cytol 1998;42:751-753.
167. Supriya M, Denholm S, Palmer T. Seeding of tumor cells after fine needle aspiration cytology in benign parotid tumor: a case report and literature review. Laryngoscope 2008;118:263-265.
168. Tamiolakis D, Thomaidis V, Tsamis I, et al. Polymorphous low grade adenocarcinoma of the parotid gland. Cytological, histological and immunohistochemical features and review of the literature. Acta Medica (Hradec Kralove) 2004;47:3-6..
169. Tao LC, Gullane PJ. HIV infection-associated lymphoepithelial lesions of the parotid gland: aspiration biopsy cytology, histology, and pathogenesis. Diagn Cytopathol 1991;7:158-162.
170. Taxy JB. Necrotizing squamous/mucinous metaplasia in oncocytic salivary gland tumors. A potential diagnostic problem. Am J Clin Pathol 1992;97:40-45.
171. Thomas K, Hutt MSR. Tyrosine crystals in salivary gland tumours. J Clin Pathol 1981;34:1003-1005.
172. Tiemann M, Asbeck R, Wacker HH. Clonal B-cell reaction in Sjögren disease and Hashimoto autoimmune thyroiditis. Pathologe 1996;17:289-295.
173. Torabinezad S, Kumar PV, Hashemi SB, Rahimi A. Osteoclastoma-like giant cell tumor of the parotid gland: report of a case with fine needle aspiration diagnosis. Acta Cytol 2006;50:80-83.
174. Vargas PA, Torres-Rendon A, Speight PM. DNA ploidy analysis in salivary gland tumours by image cytometry. J Oral Pathol Med 2007;36:371-376.
175. Verma K, Kapila K. Role of fine needle aspiration cytology in diagnosis of pleomorphic adenomas. Cytopathology 2002;13:121-127.

176. Verma K, Kapila K. Salivary gland tumor with a prominent oncocytic component. Cytologic findings and differential diagnosis of oncocytomas and Warthin's tumor on fine needle aspirates. Acta Cytol 2003;47:221-226.
177. Viguer JM, Vicandi B, Jimenez-Heffernan JA, et al. Fine needle aspiration cytology of pleomorphic adenoma. An analysis of 212 cases. Acta Cytol 1997;41:786-794.
178. Voulgarelis M, Skopouli FN. Clinical, immunologic, and molecular factors predicting lymphoma development in Sjögren's syndrome patients. Clin Rev Allergy Immunol 2007;32:265-274.
179. Wang D, Li Y, He H, et al. Intraoral minor salivary gland tumors in a Chinese population: a retrospective study on 737 cases. Oral Surg Oral Med Oral Pathol Oral Radiol Endod 2007;104:94-100.
180. Yang GC, Waisman J. Distinguishing adenoid cystic carcinoma from cylindromatous adenomas in salivary fine-needle aspirates: the cytologic clues and their ultrastructural basis. Diagn Cytopathol 2006;34:284-288.
181. Yih WY, Kratochvil FJ, Stewart JC. Intraoral minor salivary gland neoplasms: review of 213 cases. J Oral Maxillofac Surg 2005;63:805-810.
182. Zajicek J. Aspiration biopsy cytology. I. Cytology of supradiaphragmatic organs. Monogr Clin Cytol 1974;4:37-39.
183. Zajicek J, Eneroth CM, Jakobsson P. Aspiration biopsy of salivary gland tumors. VI. Morphologic studies on smears and histologic sections from mucoepidermoid carcinoma. Acta Cytol 1976;20:35-41.
184. Zbären P, Zbären S, Caversaccio MD, Stauffer E. Carcinoma ex pleomorphic adenoma: diagnostic difficulty and outcome. Otolaryngol Head Neck Surg 2008;138:601-605.
185. Zhang C, Cohen JM, Cangiarella JF, et al. Fine-needle aspiration of secondary neoplasms involving the salivary glands. A report of 36 cases. Am J Clin Pathol 2000;113:21-28.

**Fig. 5.1 Amylase crystalloids.**
Direct sediment smears of a fluid aspirate from the left parotid gland reveal clearly refractile, but nonbirefringent, polyhedral crystalloids corresponding to cristalloids of salivary alpha-amylase. The elements are embedded in a background of cystic debris and inflammation (FNAB, Pap stain, higher magnification).

**Fig. 5.2 Crystalline elements suggesting tyrosine crystalloids.**
Ultrasound-guided FNAB of a complex, partly cystic lesion localized in the left parotid gland. Direct smears showed abundant bar-like and polyhedral crystalloids against a clean background (Pap stain, high magnification). The elements are refractile, but nonbirefringent by polarized light microscopy.
*Cytology:* A definite classification was not possible. Overall appearance suggests tyrosine crystalloids.



**Figs. 5.3, 5.4, and 5.5 Benign cells and tissue fragments aspirated from major salivary glands.**

**Fig. 5.3** Low magnification of an FNAB specimen shows large fragments of normal salivary gland tissue of serous type (direct smear, Pap stain). The ball-like formations and protrusions are acini. Small ducts are occasionally present (arrow).

**Fig. 5.4** Detail of the same smear shows a duct composed of regularly arranged cuboid to columnar cells (lower left). The duct is surrounded by loose mesenchymal stroma and acinar cells. The latter exhibit abundant foamy and granular cytoplasm. Smooth nuclear contour, indistinct nucleoli, and nearly patternless chromatin are hallmarks for normal ductal and acinar cells.

**Fig. 5.5** FNAB of a slightly enlarged submandibular gland. The smears include elements of a mixed mucous and serous salivary gland: serous-type foamy acinar cells (upper left) and mucinous-type pale acinar cells (arrow) embedded in a mucoid background. Stripped nuclei are numerous (direct smear, Pap stain, high magnification).

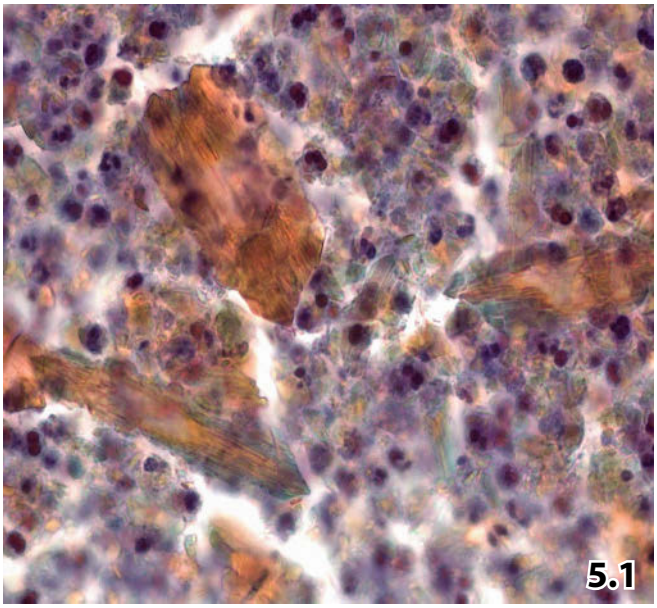
5.1


5.2

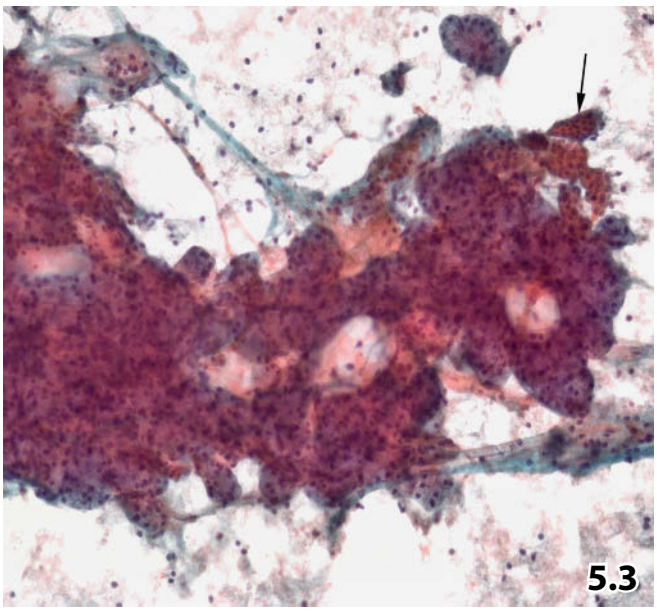
5.3

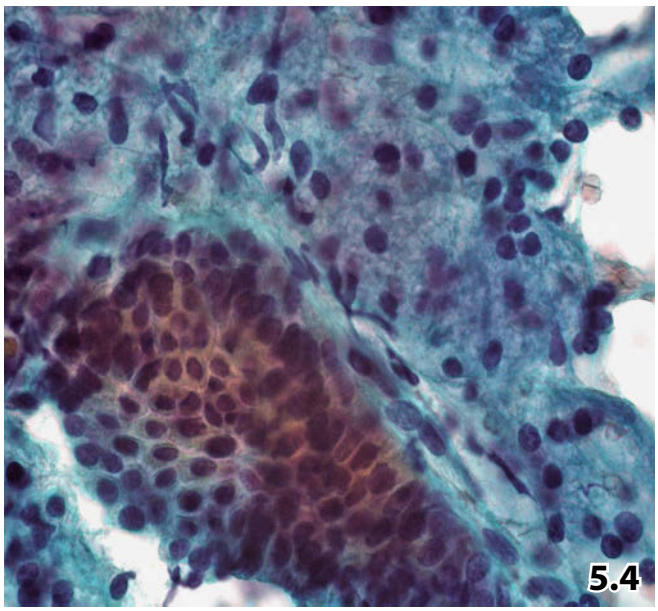
5.4

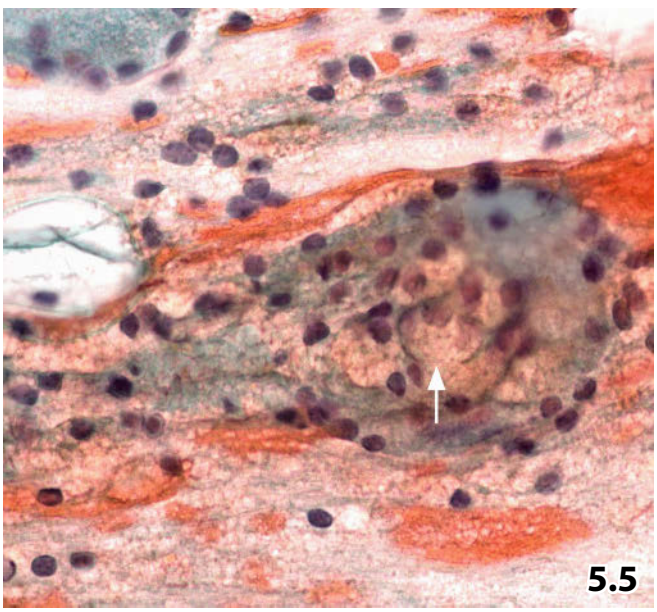
5.5

**Fig. 5.6 Retention cyst.**
A 66-year-old man was referred to FNAB presenting with a cystic nodule in the right submandibular gland. Processing of the aspirated fluid provided cellular specimens containing degenerate keratinized squames (arrows) and degenerate foam cells in a background with strands of mucus (arrowheads) and detritus (direct sediment smear, Pap stain, high magnification).
*Tentative cytologic diagnosis:* cyst content comprising squamous cells with mild atypia. To arrive to a definite diagnosis, histopathologic examination is required.
*Tissue diagnosis:* ectatic and cystic main duct of salivary gland lined with metaplastic squamous epithelium.



**Fig. 5.7 Mucus retention cyst.**
FNAB of a firm tumor in a 21-year-old man's lower lip yielded a gelatinous substance. Direct smears contained mucoid masses enclosing small mucin-producing epithelial cells with dense and pale cytoplasm (arrows), and histiocytes with large foamy cytoplasm (arrowheads) (Pap stain, lower magnification).
*Cytologic diagnosis:* Mucocele (no subsequent surgical excision).

**Fig. 5.8 Lymphoepithelial cyst.**
A 27-year-old man with positive history of HIV infection presented with a swelling in the left parotid area. FNAB revealed degenerate keratinized and nonkeratinized squamous cells devoid of any nuclear atypia, neutrophils, and histiocytes; sparse lymphocytes (direct sediment smear, Pap stain, high magnification).
*Cytology:* diagnostic considerations included atheroma and lymphoepithelial cyst of the parotid gland.
*Final diagnosis:* Lymphoepithelial cyst.

> Any patient with AIDS presenting with a tumorous lesion in the parotid region and with squamous cells in its aspirate is suggestive of a lymphoepithelial cyst even if lymphocytes are absent in the cytologic specimens.

**Fig. 5.9 Lipomatosis of the parotid gland.**
FNAB of a markedly enlarged parotid gland (imaging studies and sialography without further abnormalities) provided normal salivary gland tissue embedded in mature adipose tissue (direct smear, Pap stain, low magnification).
*Final diagnosis:* Consideration and integration of the clinical results to the cytology findings resulted in the diagnosis of parotid lipomatosis.

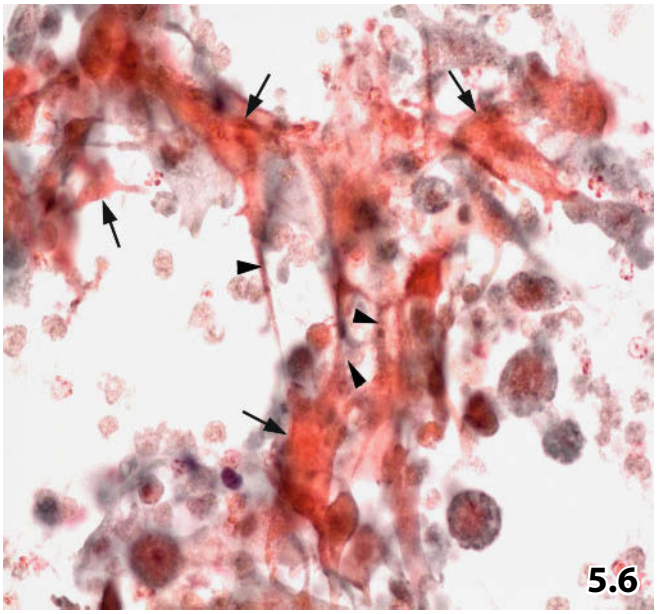
5.6

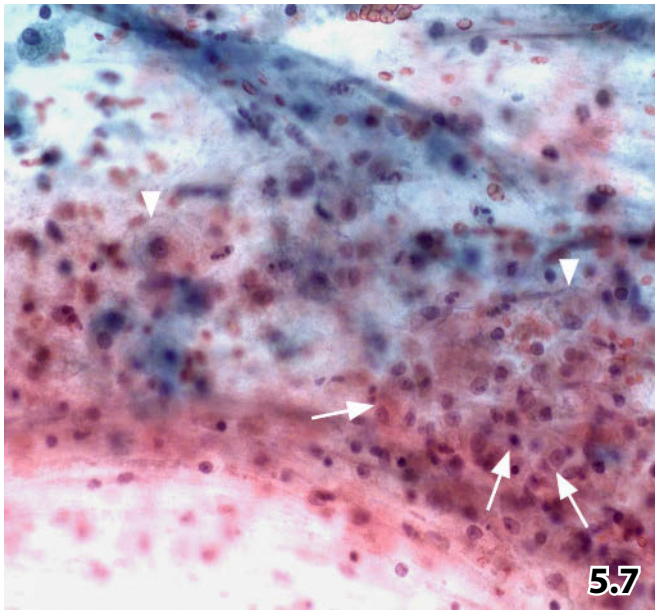
5.7

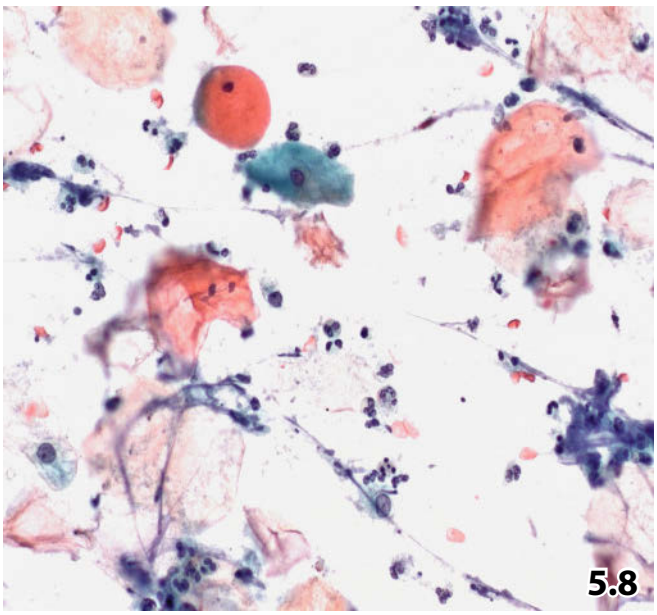
5.8

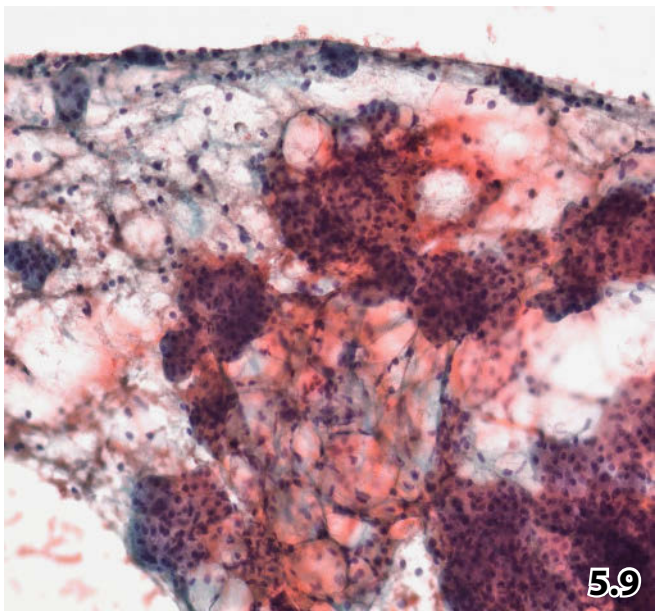
5.9

**Figs. 5.10 and 5.11 Chronic sialadenitis.**
FNAB of abnormal submandibular glands from two different patients. The direct smears were Pap-stained.

**Fig. 5.10A, B** (case #1) A 48-year-old man presented with a history of bilateral squamous cell carcinoma in the floor of his mouth, treated with laser technique. **A** Low magnification reveals clusters of ductal cells (right); the acinic tissue fraction is almost absent. The background of the smear consists of red blood cells, lymphocytes, and small fragments of loose stromal and granulomatous tissue (arrows). **B** High magnification of the same case highlights a sheet of ductal cells showing mucoid metaplasia comprising fully developed goblet cells. Note that the activated nuclei show variable sizes and distinct nucleoli.
*Cytologic diagnosis:* Chronic sialadenitis including mucoid metaplasia.

**Fig. 5.11** (case #2) High magnification of another case (56-year-old man) displays squamous metaplasia of the ductal epithelium. Note typical shape, sharp outline, and dense structure of the cytoplasm. Intercellular bridges may be suspected but they are not evident.
*Cytologic diagnosis:* Chronic relapsing sialadenitis including squamous and mucoid metaplasia.
*Tissue diagnosis:* Chronic sialadenitis associated with severe sclerotic change.

**Figs. 5.12A, B Chronic sialadenitis: atypical epithelial metaplasia versus low-grade malignant neoplasia.**
A 73-year-old woman with a history of squamous cell carcinoma of the tongue treated with laser technique, presents with a subsequent tumorous lesion in her right submandibular gland. FNAB was the initial diagnostic procedure. Direct smears were Pap-stained.
*Tentative cytologic diagnosis:* Chronic sialadenitis including severe metaplastic changes of the ductal epithelium. FNAB is not efficient in excluding additional keratinizing squamous cell carcinoma or mucoepidermoid carcinoma.
*Tissue diagnosis:* Finally, excisional biopsy of the submandibular tumor and histologic examination revealed chronic sialadenitis with evidence of severe metaplastic changes in combination with a metastasis of a well-differentiated squamous cell carcinoma.
**A** Lower magnification shows a heterogeneous cell population: ductal cell clusters (upper left) and squamous cells with mild nuclear atypias (arrows), granulomatosis (center) and histiocytoid giant cells (lower left). The background of the smears contains inflammatory cells and thin streaks of mucus. It was difficult to differentiate pronounced squamous/mucoid metaplasia from low-grade mucoepidermoid/squamous cell carcinoma. **B** Highly atypical squamous cells (nuclear indentations and nuclear clearing) and polymorphous anuclear keratinizing squames are shown in detail.

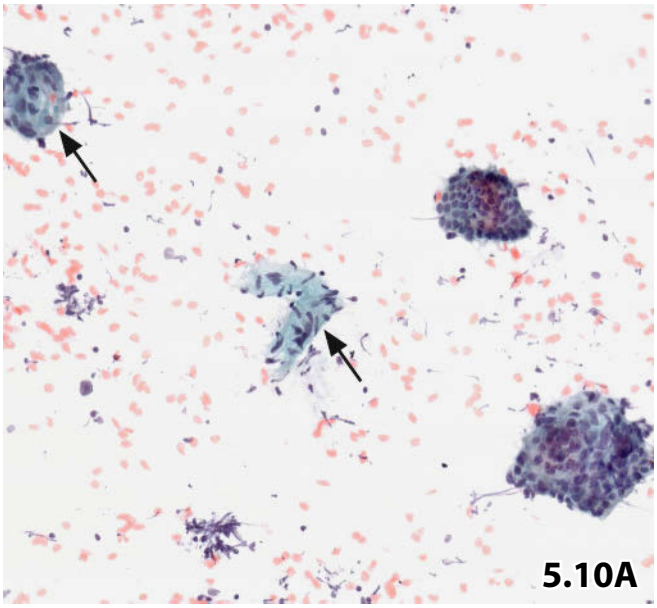

5.10A

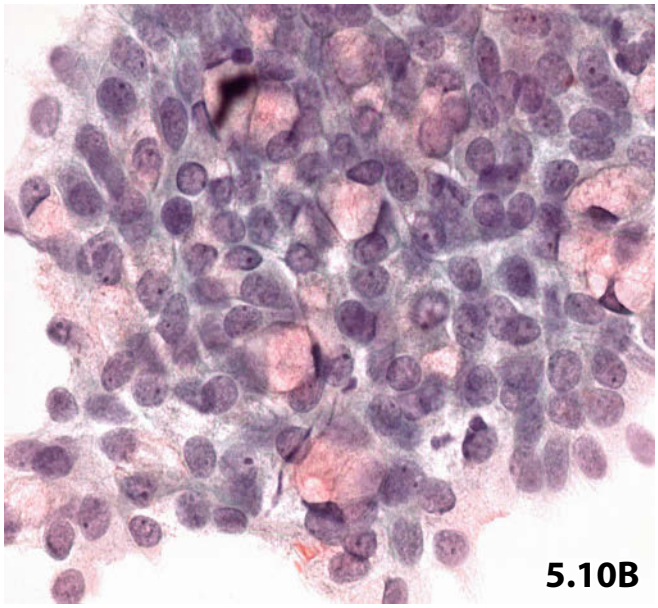

5.10B

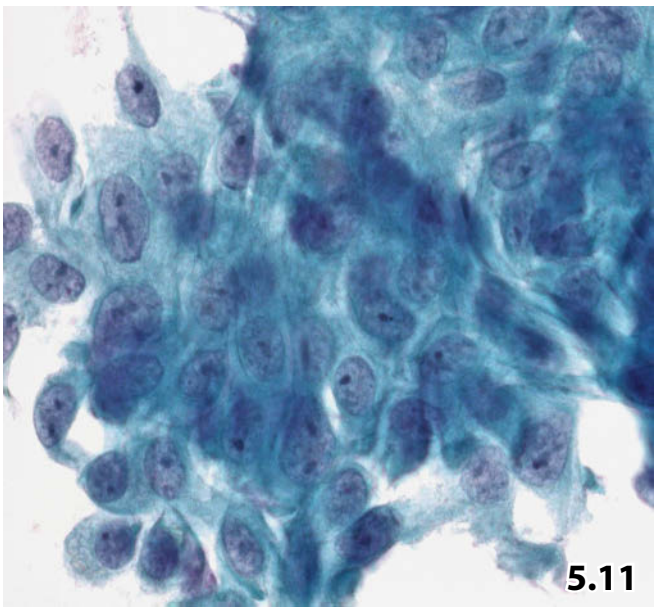

5.11

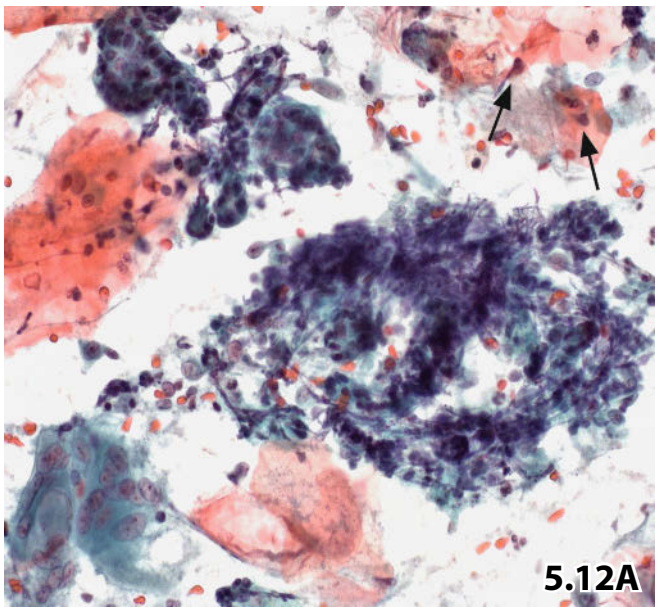

5.12A

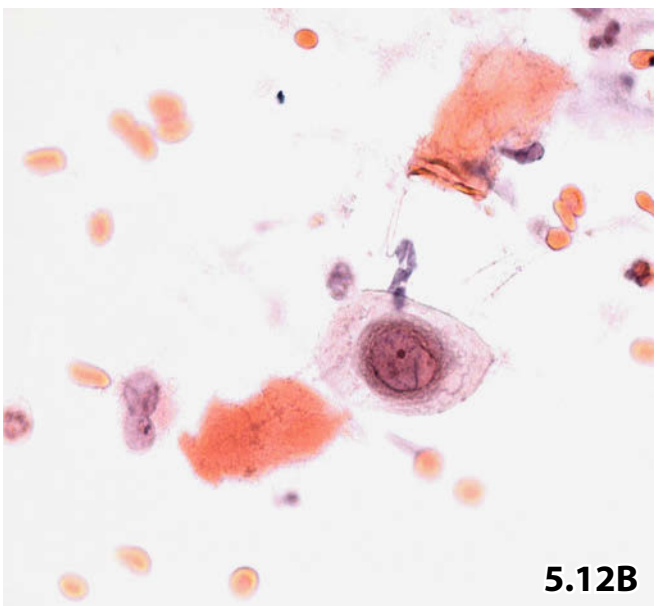

5.12B

**Figs. 5.13 and 5.14 Küttner tumor.**
FNAB of firm nodule located in the submandibular gland. Due to painfulness of the intervention, the aspirated cell material was scanty. Pap-stained direct smears.

**Fig. 5.13** Low magnification shows ductal cell clusters encased in fibrous and sclerotic tissue. Blood and lymphocytes dominate in the background of the field.

**Fig. 5.14** Higher magnification shows a single large three dimensional fragment of cellular fibrotic tissue interspersed with numerous lymphocytes.



**Fig. 5.15 Sarcoidosis.**
A 66-year-old man presenting with diffuse enlargement of both parotid glands. FNAB from one side revealed characteristic morphologic features of sarcoidosis: loose aggregates of activated epithelioid cells (right), Langhans-type giant cell (center), absence of necrosis. Acinar cell clusters embedded in granulomatous tissue are seen at the left (direct smear, Pap stain, higher magnification).

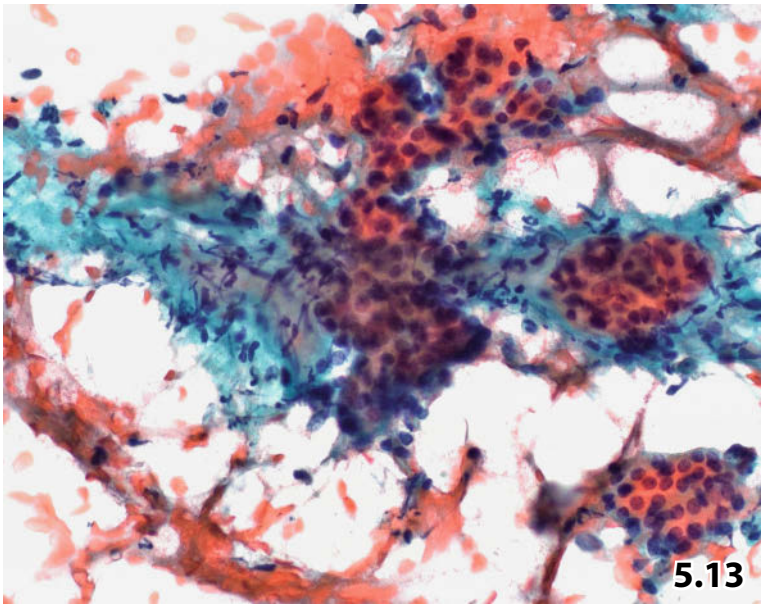

5.13

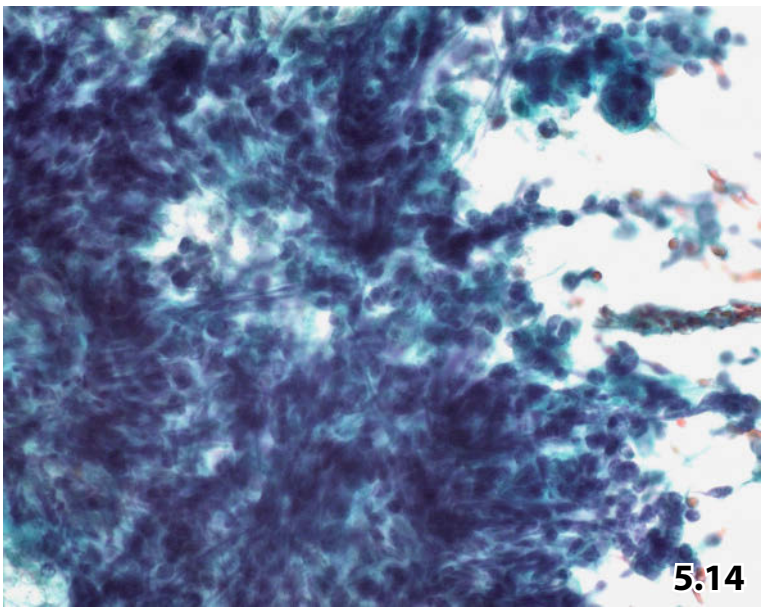

5.14

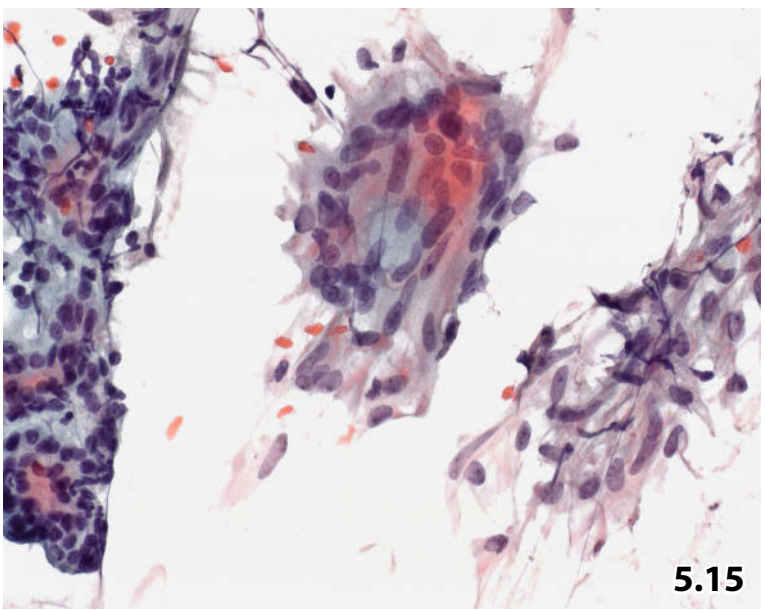

5.15

**Fig. 5.16A–D Cytology of benign lymphoepithelial lesions.**
A 74-year-old female patient with positive history of Sjögren syndrome presented for FNAB of her left parotid gland. Cytomorphology is demonstrated under high magnification on direct smears and various staining methods. **A** A small cluster of typical epimyoepithelial cells in close association with lymphocytes (MGG stain). **B** Same mixed cell population as pictured in A, but this smear was Pap-stained. **C** A loose aggregate of activated epithelioid histiocytes in association with lymphocytes. Note the morphologic varieties as compared with epimyoepithelial cells (Pap stain). **D** The cells depicted here show the characteristic benign heterogeneous lymphoid population of lymphoepithelial lesions (MGG stain). Tingible body macrophages were rarely encountered but absent in this field.

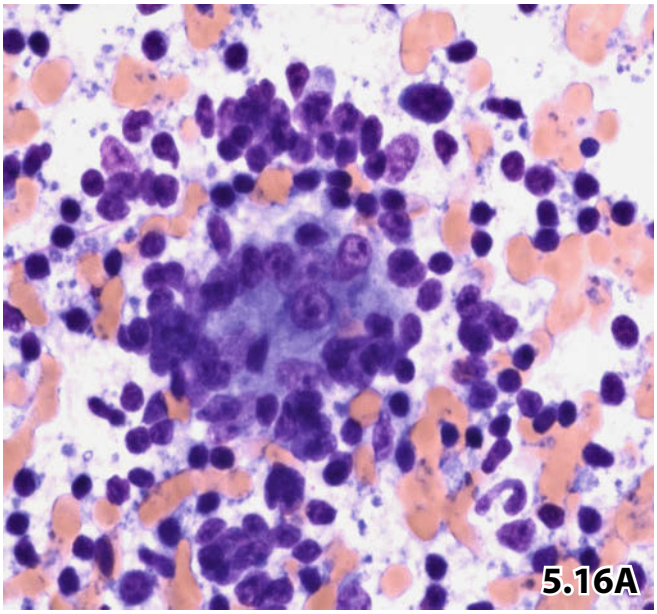
5.16A

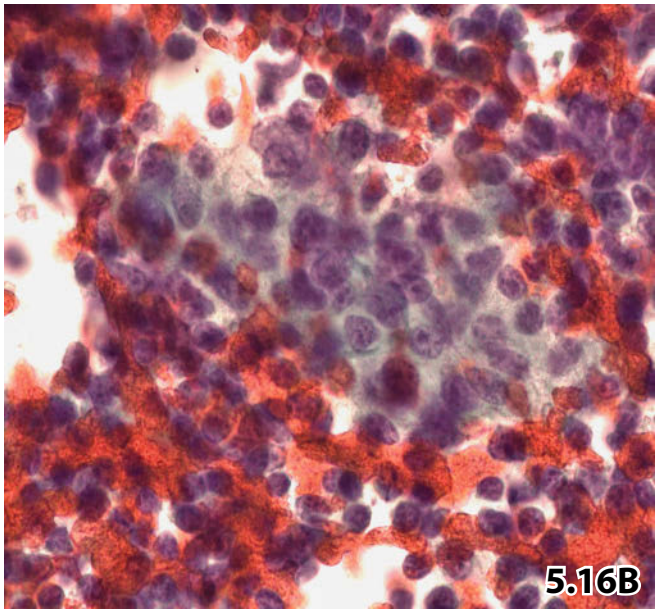
5.16B

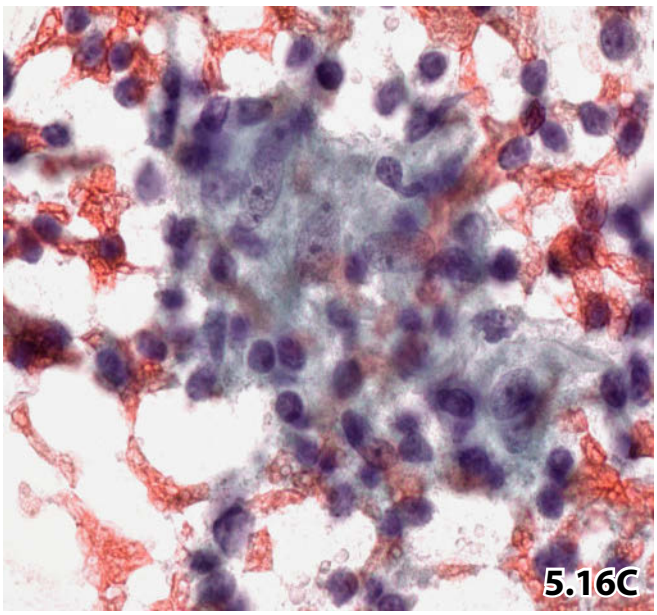
5.16C

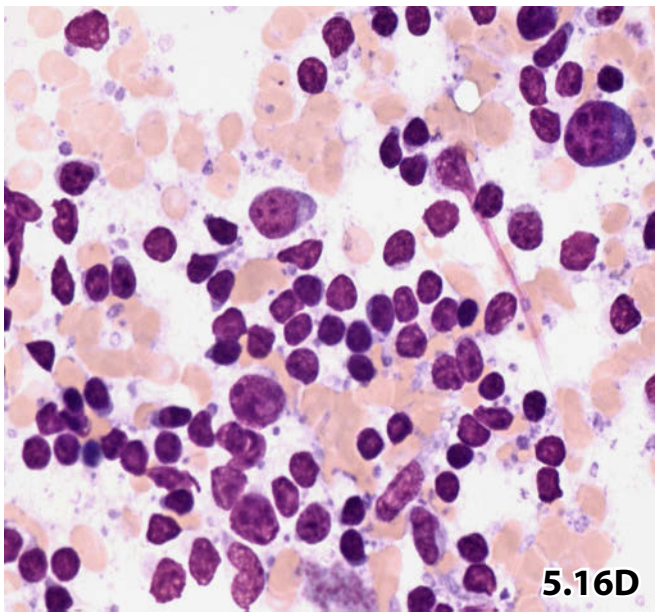
5.16D

**Figs. 5.17–5.19 Lymphoepithelial lesion and malignant lymphoma.**
Transition of lymphoepithelial lesion into malignant lymphoma always presents diagnostic dilemmas in FNAB cytology. Three examples of FNAB with direct smear preparation are presented.

**Fig. 5.17** (case #1) An 81-year-old man presented with a tumorous lesion of the right parotid gland. FNAB provided an atypical lymphoid cell population with distinct variation of cell size. Heterogeneity may suggest reactive lymphoproliferative disorder; however, note nuclear irregularities, pronounced and multiple nucleoli, and the small rims of cytoplasm (Pap stain, high magnification).
*Tentative cytologic diagnosis:* Most likely non-Hodgkin lymphoma.
*Tissue diagnosis* (surgical biopsy): MALT lymphoma ex myoepithelial sialadenitis.

**Fig. 5.18** (case #2) A 58-year-old woman presents with a personal clinical history of enlargement of her parotid and submandibular glands. The patient was referred to FNAB for initial diagnostic procedure. Direct smears from the parotid aspirate contained a heterogeneous lymphoid cell population together with small dense aggregates of atypical blast cells (lower right). The latter showed features suggestive of malignant lymphoma: distinct nuclear indentations, polymorphous nucleoli, and thin dispersed chromatin (MGG stain, high magnification).
*Tentative cytologic diagnosis:* lymphoepithelial lesion and non-Hodgkin lymphoma.
*Tissue diagnosis* (surgical biopsies): MALT lymphoma ex myoepithelial sialadenitis; MALT lymphoma showing evidence of focal transformation to high-grade NHL.

**Fig. 5.19** A 77-year-old woman presenting with a tumor in her right parotid gland. FNAB specimens disclosed numerous individual medium-sized to large atypical blasts, morphologically similar to those presented in the previous case (Fig. 5.18) (Pap stain, high magnification).
*Tentative cytologic diagnosis:* atypical blasts consistent with high-grade non-Hodgkin lymphoma.
*Tissue diagnosis* (surgical biopsy): MALT lymphoma ex myoepithelial sialadenitis; MALT lymphoma with secondary transformation to high-grade B-NHL, centroblastic variant.

**Figs. 5.20 and 5.21 Benign lymphoproliferative disorder: intraparotid lymph node.**
Physical examination of a 40-year-old man revealed a firm nodule in the left parotid gland. Clinical diagnosis was pleomorphic adenoma. FNAB was performed, direct smears were Pap-stained. Definite diagnosis was achieved by histologic examination of the removed tissue.

**Fig. 5.20** Cytology showed a mixed lymphoid cell population comprising small and large cells from germinal centers. Fragments of normal salivary gland tissue were also present, but not seen in this field (high magnification). Please compare the benign large blast cells with atypical blasts in Figs. 5.18 and 5.19 regarding nuclear shape, chromatin texture and size of nucleoli.
*Cytologic differential diagnosis* includes (1) myoepithelial sialadenitis, transformation to low-grade non-Hodgkin lymphoma cannot be excluded, (2) nonspecific chronic sialadenitis, (3) intraparotid lymph node.

**Fig. 5.21** Definite diagnosis was achieved by histologic examination of the removed tissue, revealing a normal parotid gland embodying a reactive lymph node with germinal centers (HE stain).

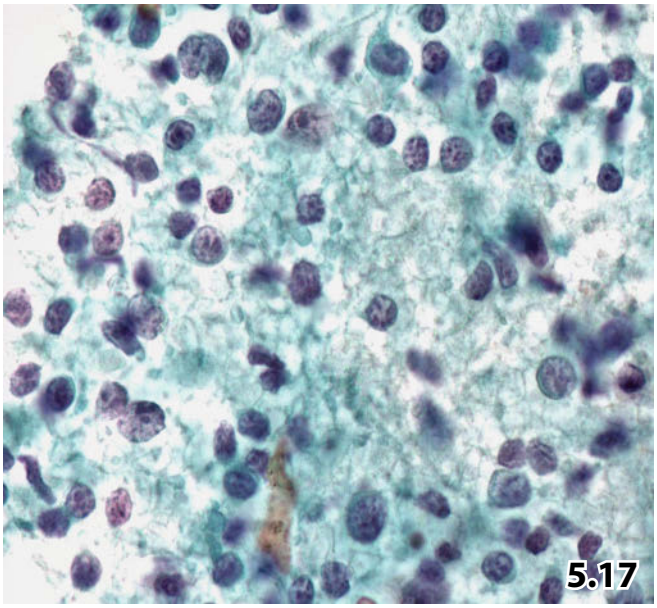
5.17

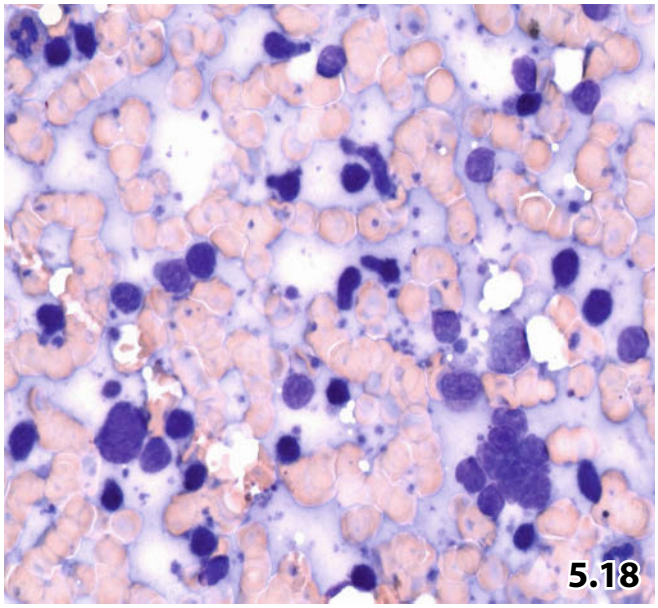
5.18

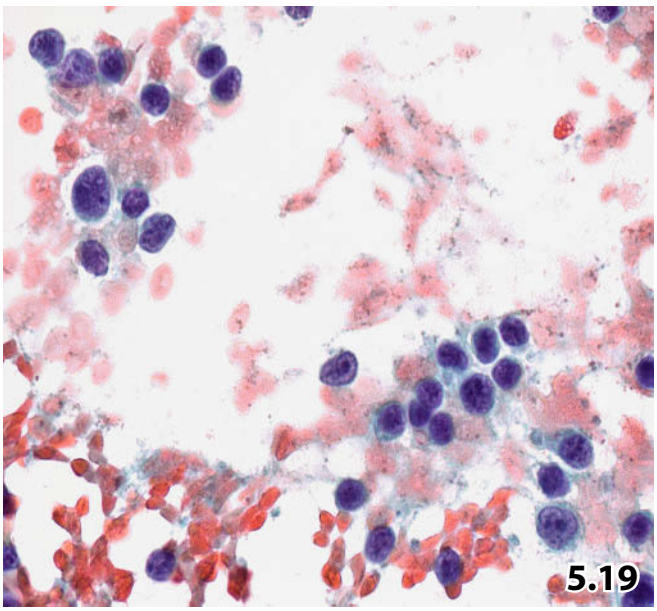
5.19

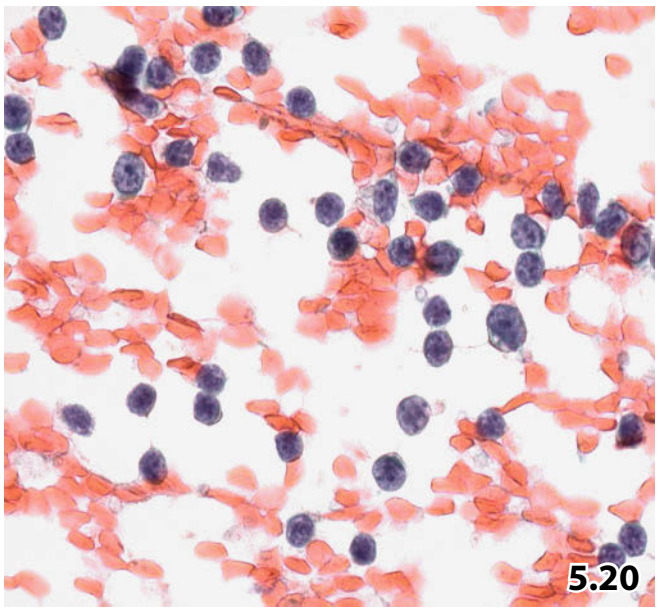
5.20

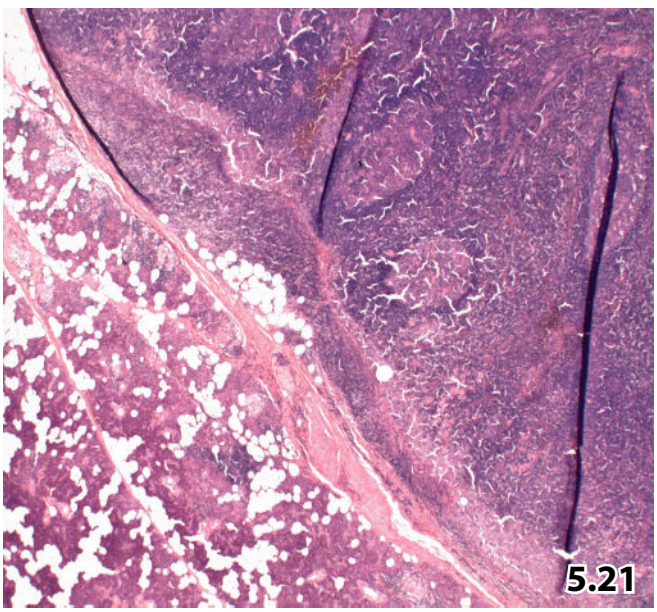
5.21

**Figs. 5.22–5.26 Pleomorphic adenoma: classic cytologic features.**
Classic cytologic features of pleomorphic adenoma are presented in FNAB specimens (direct smears) from different patients.

**Fig. 5.22** (case #1) MGG stain showing hyaline myxoid material and loosely arranged monomorphic epithelial cells (high magnification).

**Fig. 5.23** (case #2) Very low magnification showing greyish-green to pale-pink staining myxoid background with the Papanicolaou method. Epithelial cells are clustered or isolated.



**Fig. 5.24** (case #3) A mixed tumor from another patient containing large amounts of hyaline material, with the epithelial cells located in a marginal position (lower magnification, Pap stain). Fibrillary elements embedded in hyaline masses could be discerned under very high magnification.

**Fig. 5.25** (case #4) An example of pleomorphic adenoma showing a heterogeneous epithelial cell population. In addition to typical epithelial cells, oncocytes (arrow) and immature metaplastic squamous cells (arrowheads) may occur (Pap stain, low magnification).

**Fig. 5.26** (case #5) A pleomorphic adenoma containing sheets of monomorphic epithelial cells exhibiting pronounced plasmacytoid appearance (Pap stain, high magnification).

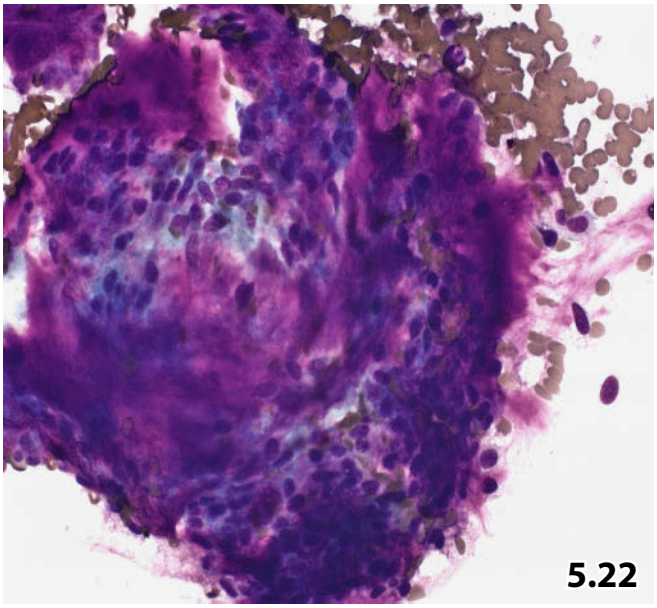
5.22

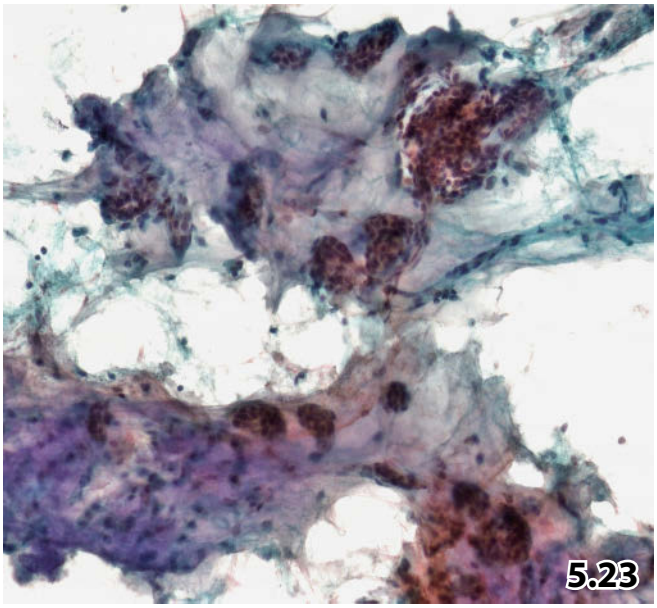
5.23

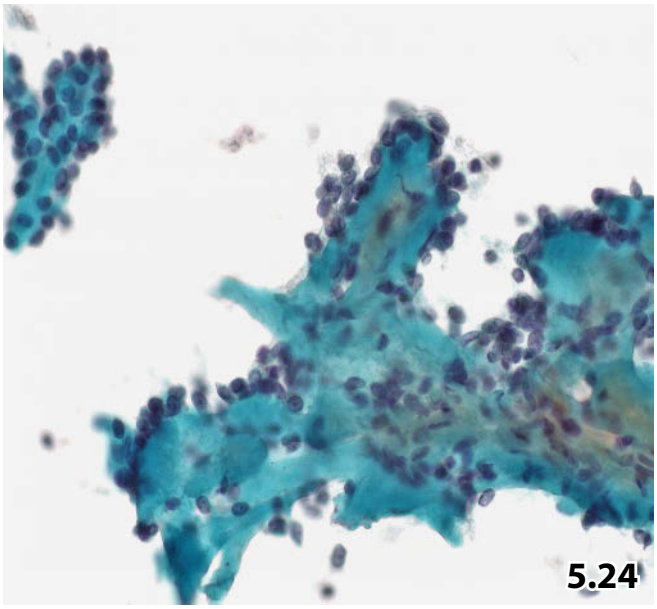
5.24

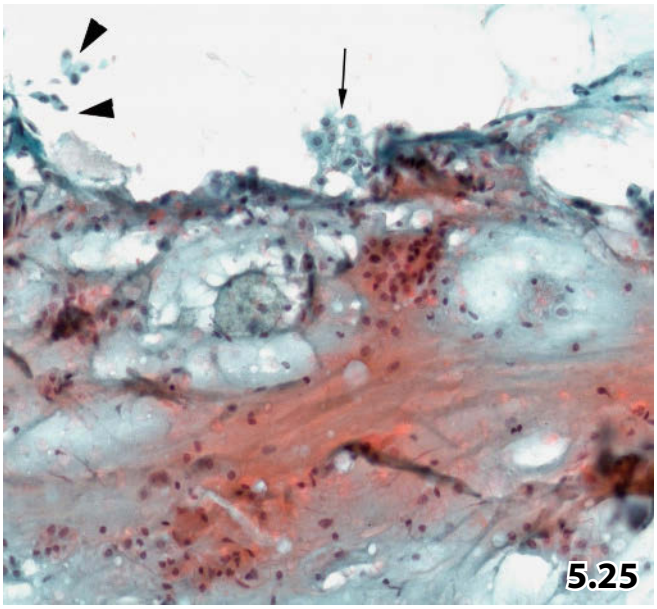
5.25

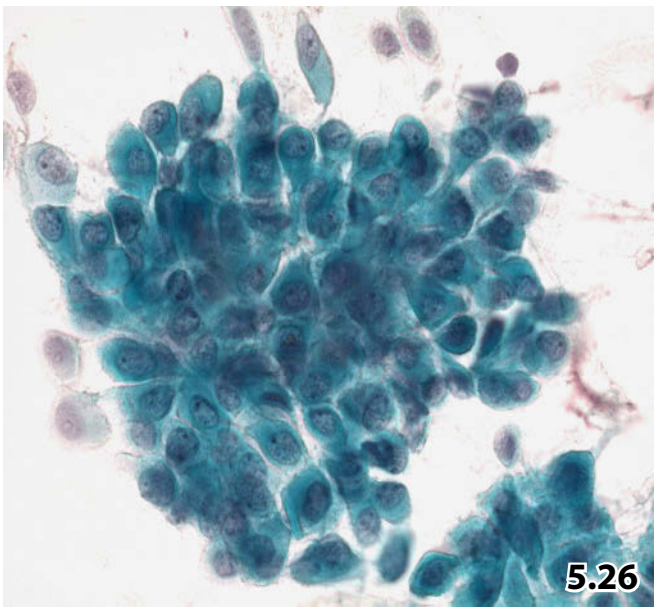
5.26

**Figs. 5.27–5.30 Pleomorphic adenoma: selected variants.**
Five subtypes of pleomorphic adenoma are discussed. FNAB direct smear, Pap-stained. These variants are frequently encountered in standard cytology presenting diagnostic dilemmas.

**Fig. 5.27** (case #1) Pleomorphic adenoma: chondromyxoid pattern.
Lower magnification shows a mixed tumor of the salivary gland type comprising a pronounced chondromyxoid component and a few dispersed epithelial cells (arrows).



**Fig. 5.28A, B** (case #2) Pleomorphic adenoma: cellular variant.
**A** A tumor almost entirely composed of epithelial cells. The epithelial nature of the cells is clearly identified by positive immunostaining for CK1, 5, 10, 14 (Pap-prestained smear, lower magnification). The sparse myxoid component is not shown. **B** Immunostaining for alpha smooth muscle actin also shows a meshwork of elongated myoepithelial cells pervading a large epithelial cell cluster (arrows) (Pap-prestained smear, lower magnification).

**Fig. 5.29A** (case #3) Pleomorphic adenoma: clear cell variant.
Example of a pleomorphic adenoma with its epithelial component composed of predominantly sebaceous-like clear cells (higher magnification).
**B** (case #4) Pleomorphic adenoma: pronounced squamous metaplastic component
An otherwise typical pleomorphic adenoma containing numerous sheets and pearl formations (upper right) composed of metaplastic squamous cells. Strong keratinization may be observed (high magnification).

**Fig. 5.30** (case #5) Pleomorphic adenoma associated with cellular atypia.
High magnification shows a cellular composite characteristic of pleomorphic adenoma (epithelial cells with their plasmacytoid features, myoepithelial cells with their elongated dark nuclei, myxoid material). However, irregularities of the epithelial nuclei are seen such as variation in size, molding, grooves, and coarse chromatin.
*Tentative cytologic diagnosis:* Pleomorphic adenoma. Cytology cannot effectively exclude malignant degeneration.
*Tissue diagnosis:* Pleomorphic adenoma with chondroid component.

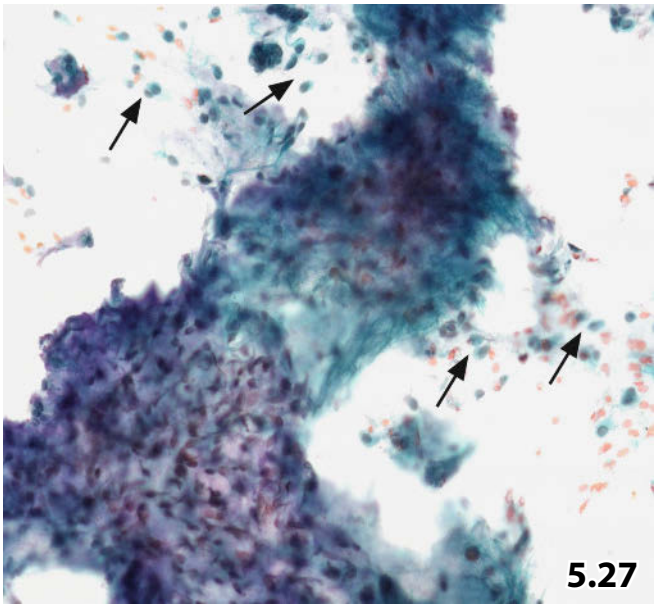
5.27

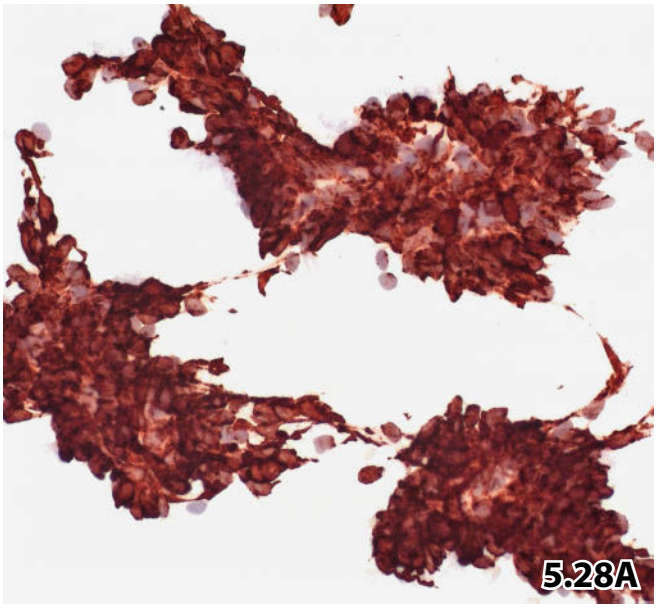
5.28A

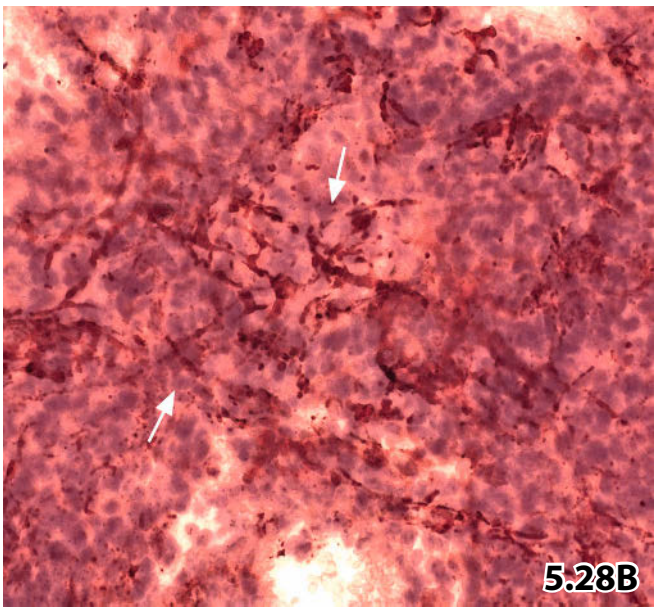
5.28B

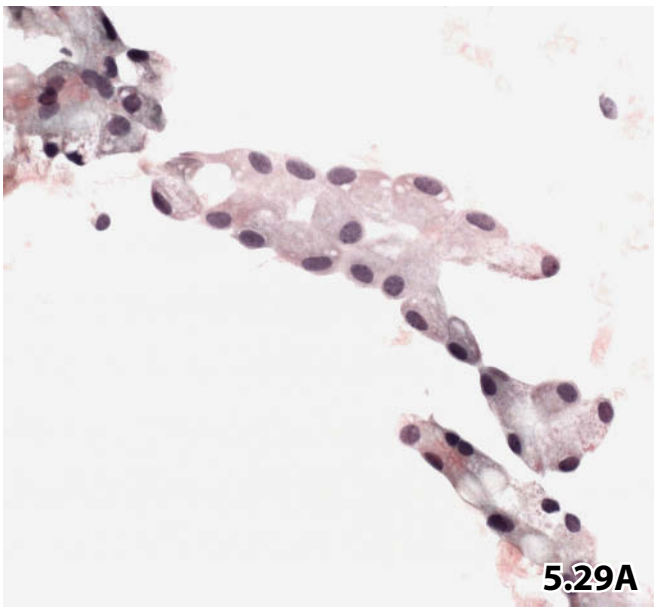
5.29A

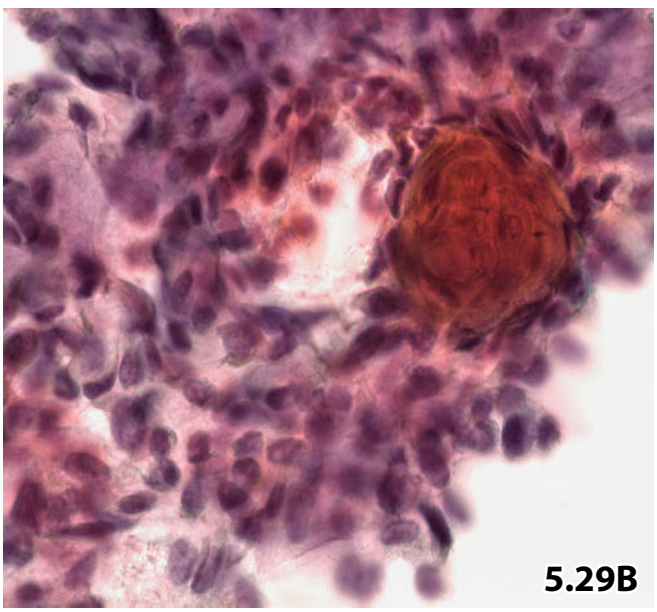
5.29B

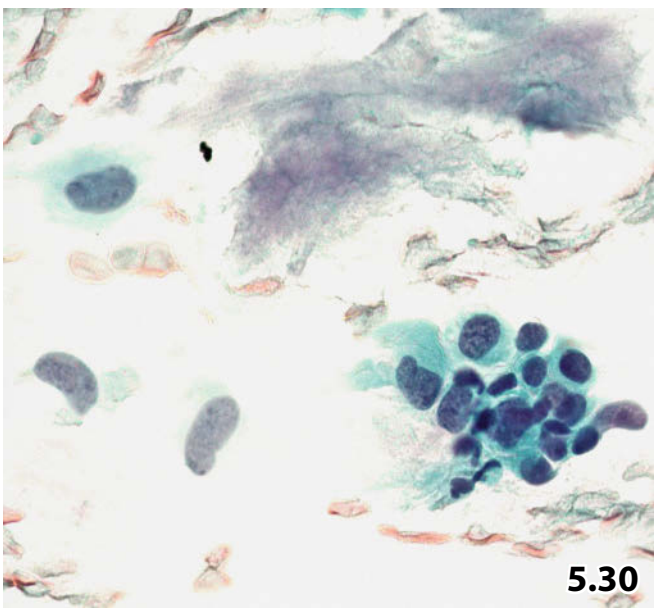
5.30

**Figs. 5.31–5.35 Adenolymphoma: classic cytologic features.**
Classic cytologic features of adenolymphoma are presented from FNAB specimens from different patients. The aspirated material has been processed in various ways. All specimens are Pap-stained.

**Fig. 5.31** (case #1) Low magnification points out the key features of adenolymphoma: flat sheets of oncocytes varying greatly in size, against a background of granular proteinaceous material and lymphocytes. Note several discohesive oncocytes (arrows) (direct smear).



**Fig. 5.32** (case #2) The same heterogeneous cell pattern is readily observed in liquid-based preparation (ThinPrep technique, lower magnification). Note the comparatively clean background.

**Fig. 5.33** (case #3) A Warthin tumor exhibiting a particular morphology: crowds of crushed lymphocytes adhering to sheets of oncocytes. The single foam cell (upper right) indicates cystic degeneration of the tumor (direct smear, lower magnification).

**Fig.5.34** (case #4) Aspirates from adenolymphomas containing only degenerate material in most cases allow an accurate diagnosis provided that the cytologic smears have been carefully evaluated. Well-preserved cells, remnants, and background depicted here indicate the most important clues for a correct cytologic diagnosis: (1) degenerate anuclear oncocytes presenting with typical cytoplasmic features such as shape, structure, color (arrows), (2) typical granular background including a few single lymphocytes (upper right), (3) well-preserved and degenerate foam cells. Stripped nuclei that are difficult to assign to a specific cell type may be encountered (arrowhead) (direct sediment smear of a cyst aspirate, higher magnification).

One should always keep in mind that remnants of degenerating oncocytes may occur in large numbers or only sporadically.

**Fig. 5.35** (case #5) Cells depicted in this figure represent the typical polymorphic lymphoid cell population occurring in Warthin tumors. Tingible body macrophages are usually present (bottom). Note the single degenerate oncocyte with preserved cytoplasmic characteristics (arrow) (direct smear, high magnification).

**Fig. 5.36 Warthin tumor associated with accentuated mucinous metaplasia.**
A 73-year-old woman presented with a cystic tumor in her right parotid gland. FNAB provided a gelatinous sample. Direct smears of the aspirate were performed and Pap-stained. Cytology shows large quantities of mucoid mass, debris, and epithelial cells of the clear cell type; the latter are arranged in cohesive sheets. The clear cells exhibit rounded or elongated foamy cytoplasm, the cytoplasmic borders are accentuated, imitating intermediate epidermoid cells (high magnification).
*Cytologic consideration:* in this setting, it is not possible to differentiate between adenolymphoma associated with mucinous metaplasia and low-grade mucoepidermoid carcinoma.
*Tissue diagnosis* (excisional biopsy): Adenolymphoma.

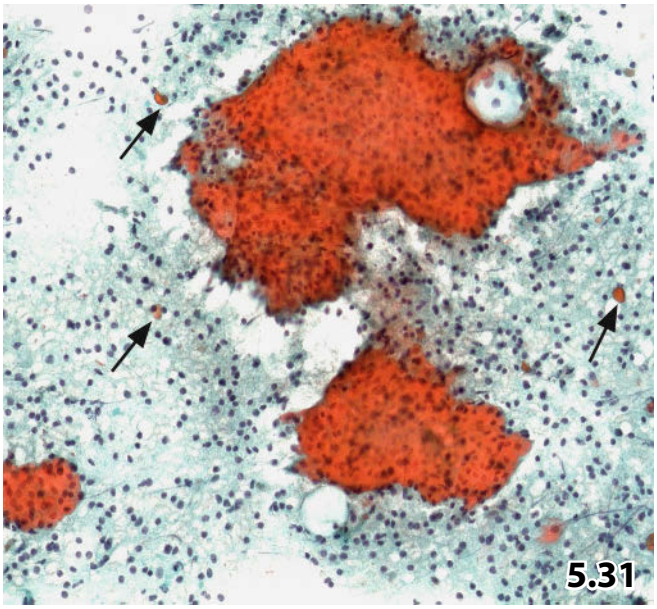
5.31

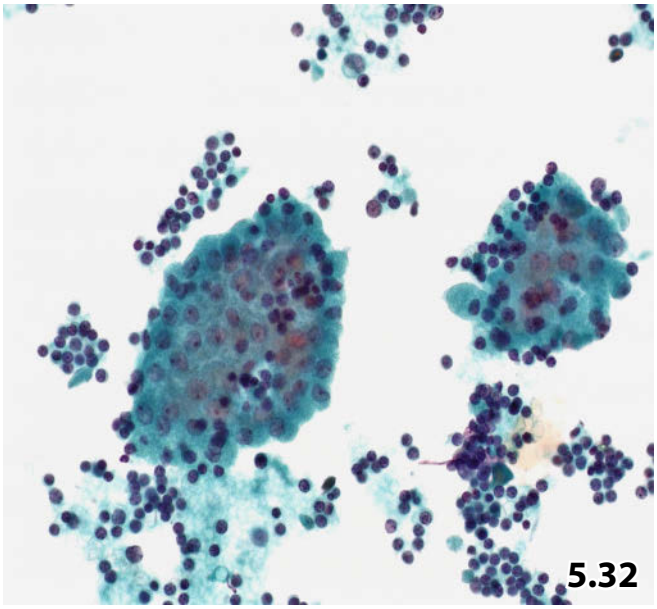
5.32

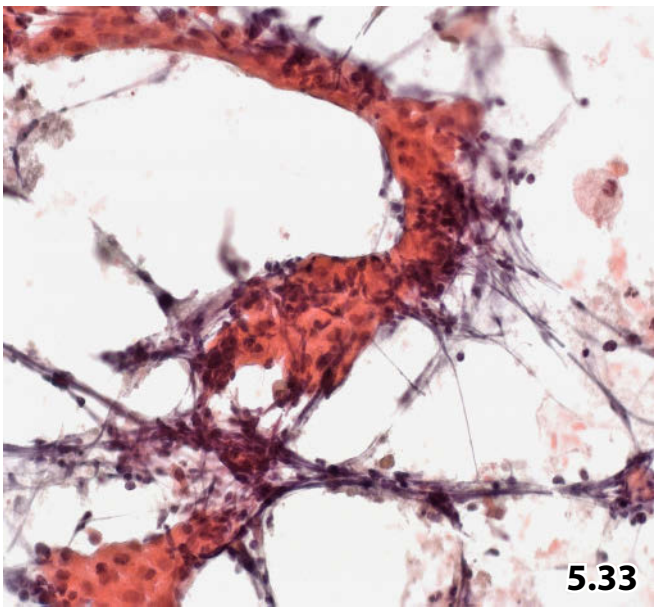
5.33

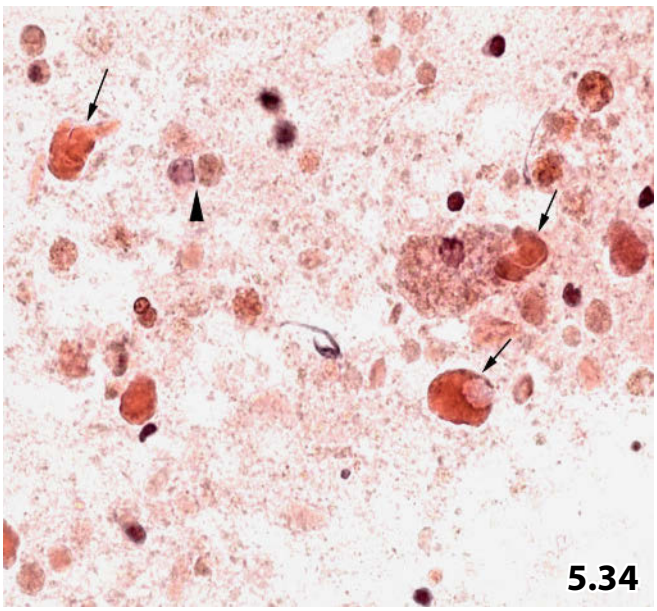
5.34

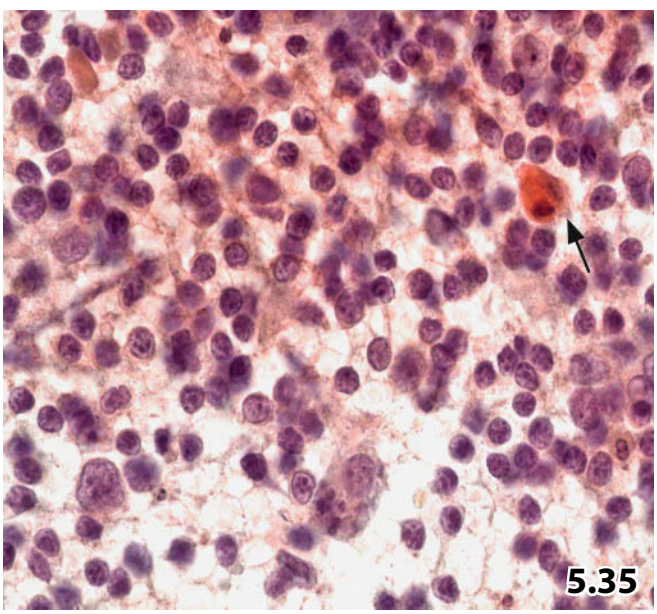
5.35

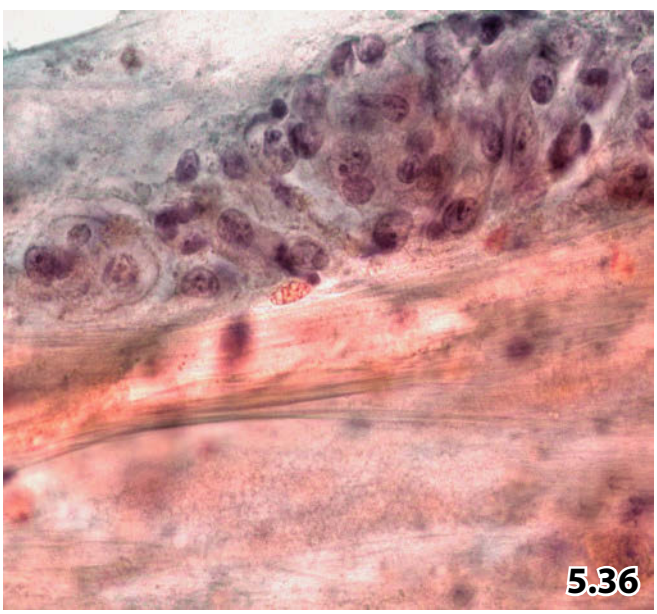
5.36

**Figs. 5.37 and 5.38 Oncocytoma**
Salivary gland FNABs from two different patients demonstrating cytologic features of oncocytomas (direct smears, Pap stain). In both patients, the lesion was assumed to be an enlarged lymph node due to clinical and imaging results.

**Fig. 5.37A, B** (case #1) A 67-year-old woman with a positive history of breast carcinoma and lymph node tuberculosis presented with a left-sided submandibular nodule. **A** Lower magnification reveals clusters of oxyphilic cells against a clean background devoid of lymphocytes. Contrary to adenolymphoma, the epithelial cells of oncocytomas occur in papilliform and three-dimensional arrangement, and their nuclei are eccentrically positioned. **B** High magnification of the same case exhibits bland oncocytes, yet irregular nuclear spacing and enlarged nucleoli are obvious.



**Fig. 5.38** (case #2) Oncocytoma from another patient (parotid nodule in an 80-year-old woman) represents the papillary variant of this tumor entity. Oncocytic clusters show identical features within the range specified above. Papillary formations are composed of fibrovascular cores and oncocytes focally coating the surface (low magnification).

**Figs. 5.39 and 5.40 Basal cell adenoma: diagnostic challenge.**
Two examples emphasize the potential confusion between basal cell adenoma and adenoid cystic carcinoma.

**Fig. 5.39A, B** (case #1) A 33-year-old woman with a long-standing nodular lesion on the left side of her neck. Direct FNA smears were Pap-stained.
*Cytology diagnostic consideration:* monomorphic adenoma of a salivary gland or adenoid cystic carcinoma. Definite diagnosis requires histologic examination of the lesion.
*Tissue diagnosis:* Monomorphic adenoma of basal cell variant.
**A** Basaloid cells are tightly packed in small and large three-dimensional clusters. The tumor cells are focally arranged in distinct basal cell layers (arrows). Note the cell clusters bounded by basement membrane-like substance (low magnification). **B** High magnification of the same case shows the monomorphic small tumor cell nuclei with bland chromatin and distinct nucleoli. Typical hyaline homogeneous matrix coating the cell clusters. Embedded hyaline globules may be assumed (arrows). Compare the nuclear size of the tumor cells with the size of red blood cells.

**Fig. 5.40** (case #2) Nodular lesion in the right parotid gland of an 82-year-old woman. FNAB from the intraparotid nodule revealed basaloid-type tumor cells often arranged around hyaline masses (direct smear, Pap stain, lower magnification).
*Cytology* suspected basal cell adenoma, adenoid-cystic carcinoma, or a combination of both entities. Enclosed hyaline globules and numerous discohesive epithelial cells suggested adenoid-cystic carcinoma.
*Tissue diagnosis:* Basal cell adenoma.

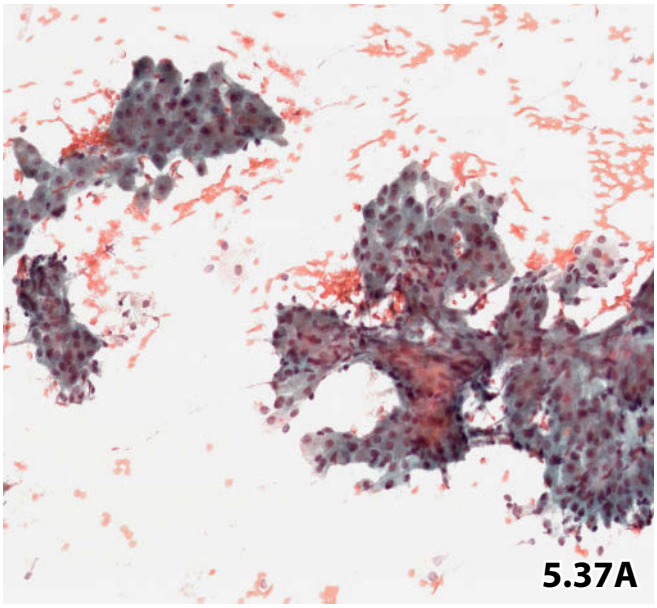
5.37A

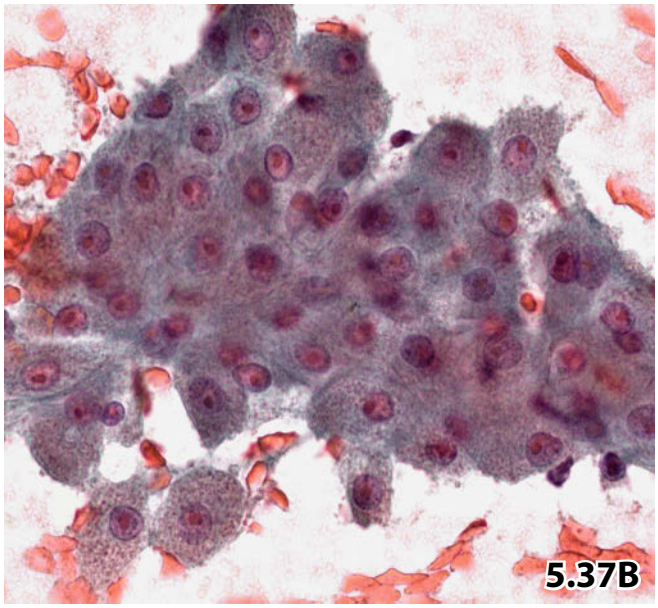
5.37B

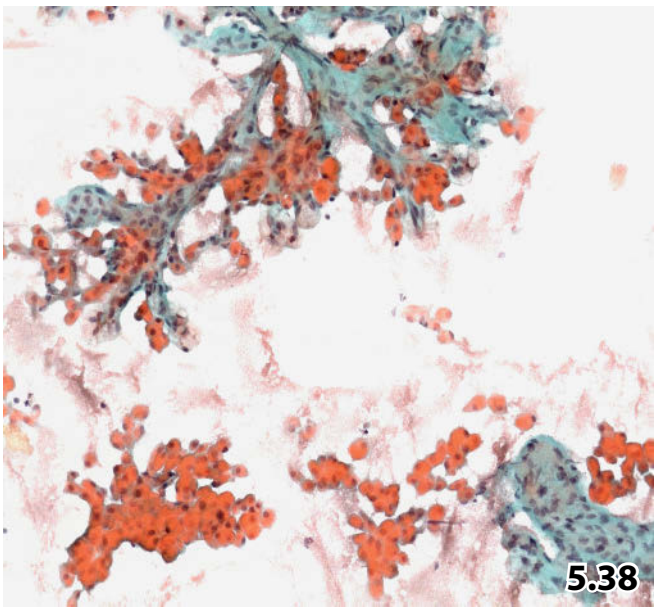
5.38

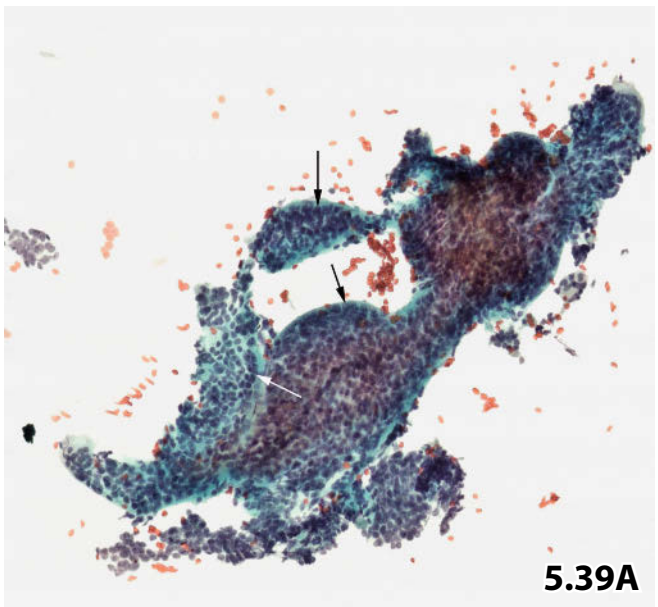
5.39A

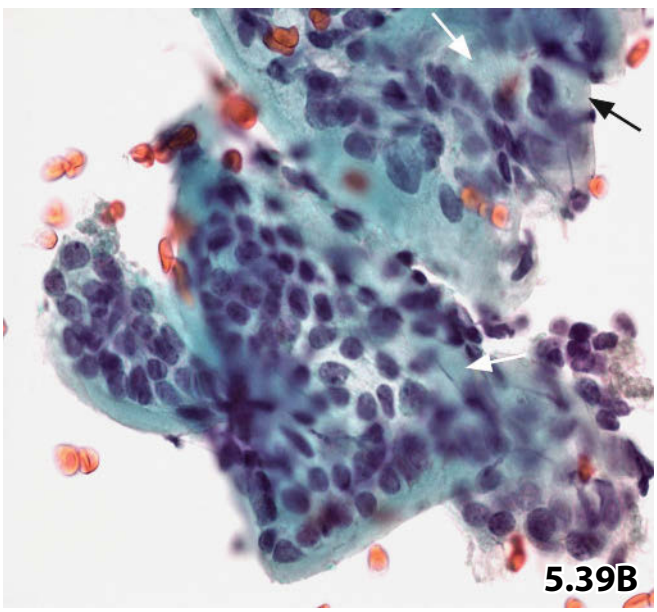
5.39B

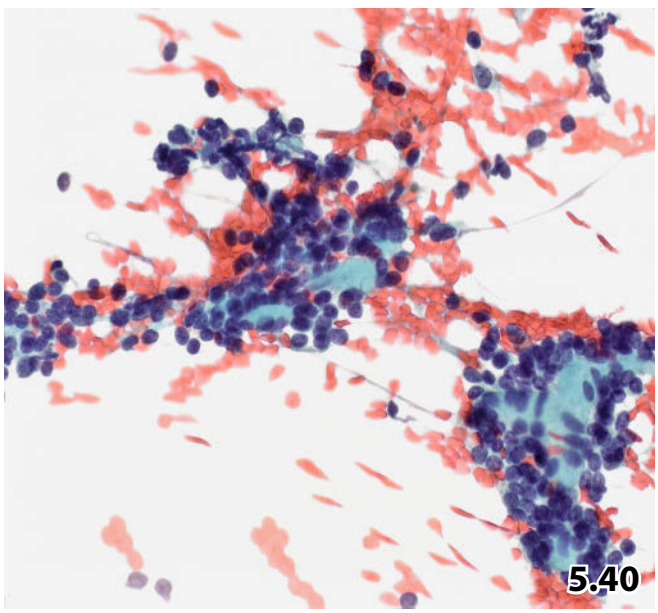
5.40

**Figs. 5.41 and 5.42 Cystadenoma: diagnostic difficulties.**
Cystadenomas of the parotid gland. The two selected cases (middle-aged women) demonstrate the diagnostic difficulties that may arise in aspiration cytology. Direct smears were Pap-stained.

**Fig. 5.41** (case #1) Low magnification shows regular papilliform clusters composed of uniform cells. Background material is indicative of a cystic alteration of the lesion: amorphous granular debris and foamy histiocytes (arrow).
*Cytologic diagnosis:* monomorphous adenoma.
*Tissue diagnosis:* cystadenoma.



**Fig. 5.42** (case #2) An example of the mucinous variant of cystadenoma: high magnification shows a cluster composed of bland tumor cells and goblet cells (Alcian blue-PAS stain). Mucinous tumor variant as presented here may be difficult to separate from low-grade mucoepidermoid carcinoma.
*Cytologic differential diagnosis:* (1) monomorphic epithelial neoplasm (NOS) or (2) pleomorphic adenoma associated with mucinous differentiation or (3) well-differentiated mucoepidermoid carcinoma.
*Tissue diagnosis* (excisional biopsy): ductal adenoma in combination with cystic duct dilatation.

**Figs. 5.43 and 5.44 Myoepithelioma: diagnostic challenge.**
Two myoepitheliomas of separate parotid glands demonstrate the diagnostic dilemmas in fine-needle aspiration cytology. Numerous tumor-microfragments were obtained by FNABs. Immunocytochemical stainings were not performed.

**Fig. 5.43A, B** (case #1) A 70-year-old man presented with a firm nodule in his right parotid gland.
*Cytologic differential diagnosis:* (1) cellular variant of pleomorphic adenoma comprising a distinct fusiform cell component, (2) myoepithelioma, and (3) other particular tumor entities going along with spindle cells cannot be excluded.
*Tissue diagnosis:* myoepithelioma, no signs of malignancy.
**A** The tumor fragment presented here in lower magnification exhibits a biphasic pattern: aggregates of elongated cells in a streaming pattern accompanied by clusters of rounded epithelioid cells (arrows). Both cell types show monomorphous and bland nuclei (direct smear, Pap stain). **B** High magnification shows a fraction of myoepithelial cells exhibiting plasmacytoid features (lower right), a feature highly indicative of pleomorphic adenoma.

**Fig. 5.44** (case #2) Same clinical situation as the previous case (62-year-old woman). Cellular composite of a cluster substantiates the diagnostic difficulties between myoepithelioma, cellular variant of pleomorphic adenoma, and acinus cell tumor. Note the acinic-like structures (arrows) that may mislead to a diagnosis of acinic cell carcinoma! (direct smear, Pap stain, lower magnification).
*Cytologic differential diagnosis:* (1) Pleomorphic adenoma, cellular variant, and (2) acinus cell carcinoma. Myoepithelioma was not taken into consideration.
*Tissue diagnosis:* Encapsulated myoepithelioma.

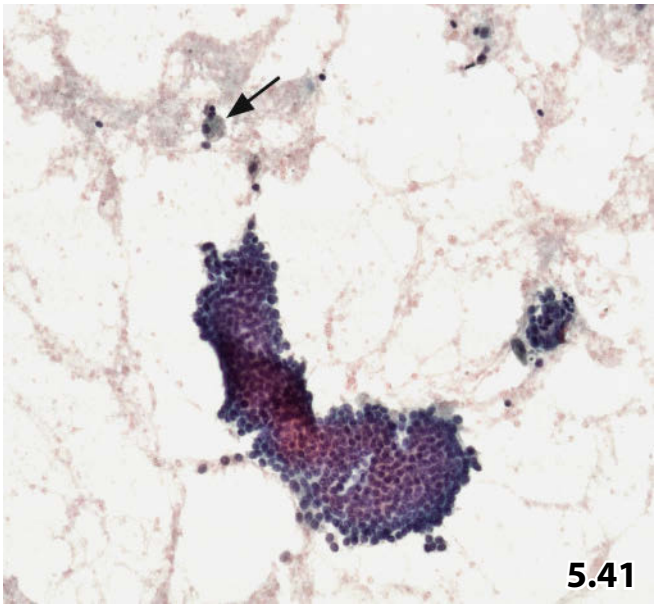
5.41

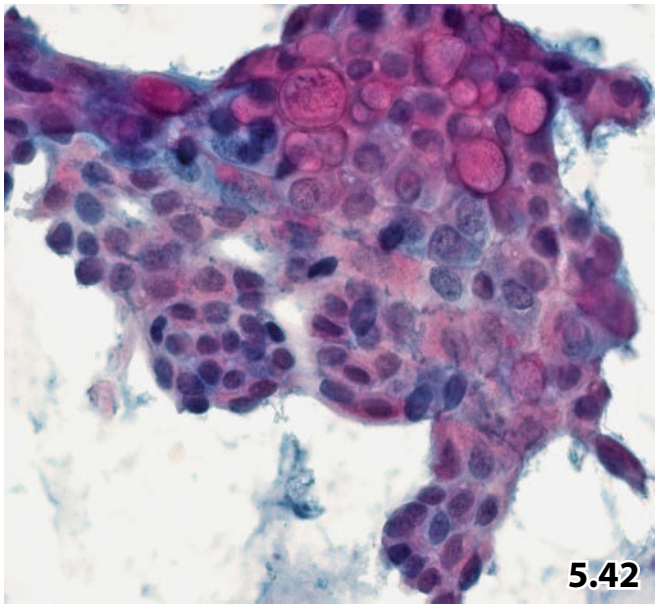
5.42

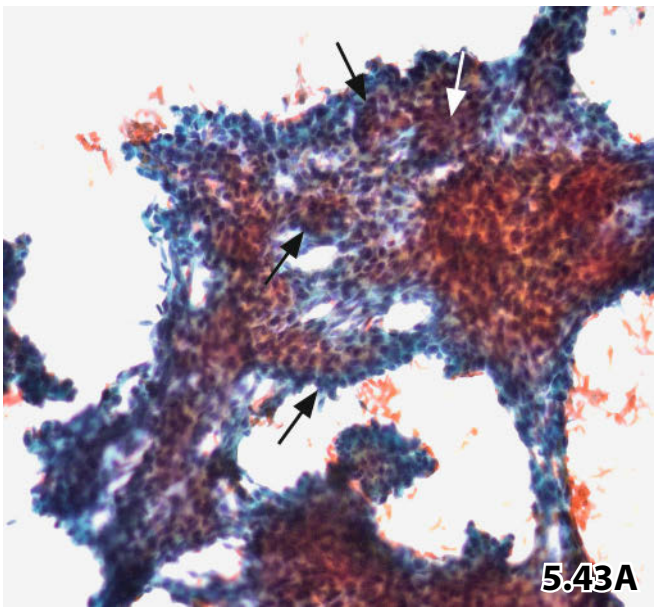
5.43A

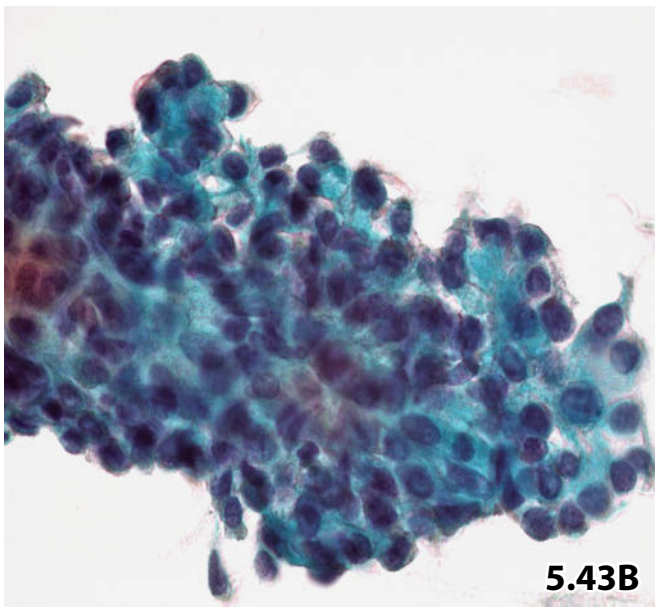
5.43B

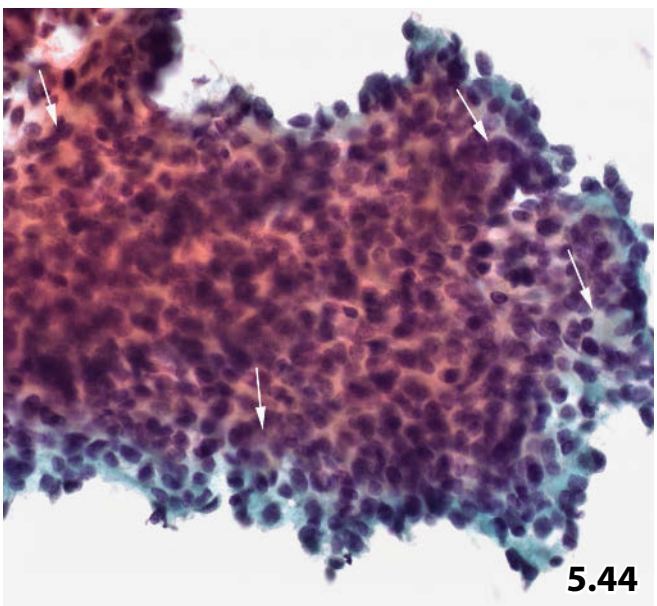
5.44

**Figs. 5.45 and 5.46 Low-grade mucoepidermoid carcinoma.**
Low-grade mucoepidermoid carcinoma located in the parotid gland of two different patients. Direct smears (FNAB), Pap-stained, elucidate the cytologic hallmarks.
*Tissue diagnosis in both cases:* Locally metastatic low-grade mucoepidermoid carcinoma.

**Fig. 5.45A, B** (case #1) A 24-year-old man presenting with a nodular lesion in his left parotid gland. Clinical examinations suggested pleomorphic adenoma.
*Cytologic diagnosis:* Mucoepidermoid carcinoma.
**A** Lower magnification shows mucin-rich background and a biphasic epithelial cell population: mucinous cells and clusters of cells showing epidermoid nature due to homogeneous cyanophilic cytoplasm (arrows). Epidermoid-like cells (cobblestone-like arrangement of cells with sharply defined cytoplasm) showing vacuolated cytoplasm indicate transition to mucus-producing cells (arrowheads). Compare the sheets of intermediate epidermoid cells with the three-dimensional clusters of mucinous cells. **B** Detail shows an aggregate of mucinous cells including a small sheet of most likely intermediate epidermoid cells (arrows). Note minor nuclear atypias – molding and nucleolar irregularities – displayed in both cell types.

**Fig. 5.46A, B** (case #2) A 64-year-old woman presented with a nodule in her right parotid gland with a swollen neck lymph node. FNAB was performed of both lesions.
*Cytologic diagnosis:* low-grade mucoepidermoid carcinoma.
**A** Direct smear preparation reveals numerous dense clusters of squamous metaplastic and intermediate epidermoid cells (low magnification). **B** Detail meets cytologic criteria of intermediate epidermoid cells exhibiting (1) distinct squamous metaplastic features (lower right) and (2) signs of transition to mucus-secreting cells (arrows).

**Figs. 5.47 and 5.48 High-grade mucoepidermoid carcinoma.**
Two examples are presented. One of the two cases presenting severe diagnostic problems in standard cytology.

**Fig. 5.47** (case #1) A 59-year-old man presenting with a firm nodule in his left parotid gland and hemifacial weakness. FNAB was performed (direct smears, Pap stain). Aspirates from high-grade mucoepidermoid carcinomas are dominated by marked atypical intermediate epidermoid cells and distinctive malignant keratinized squamous cells (upper right) (high magnification).
*Cytology and tissue diagnosis:* high-grade mucoepidermoid carcinoma (histologically grade 2–3).

**Fig. 5.48** (case #2) The aspirate of another parotid high-grade mucoepidermoid carcinoma (48-year-old woman) revealed cobblestone cell arrangement and polyhedral shape of the atypical intermediate epidermoid cells.
*Comment:* These features gave rise to an erroneous interpretation of an oncocytic tumor. Still, a careful examination of the cells fails to establish a distinct cytoplasmic granularity. In fact the cells display the presence of intercellular bridges (arrows) (direct smear, Pap stain, high magnification).
*Tentative cytologic diagnosis:* oncocytic neoplasia of the glandula parotis (cystic adenolymphoma or oncocytic adenoma).
*Tissue diagnosis:* mucoepidermoid carcinoma, grade 2.

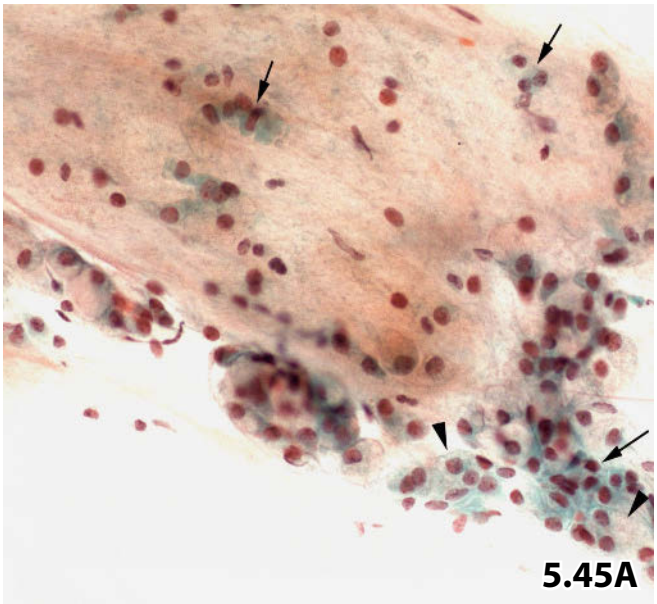
5.45A

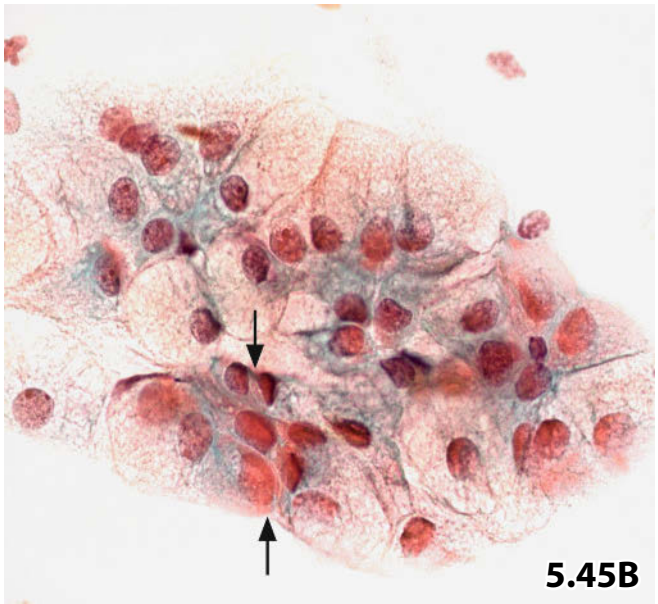
5.45B

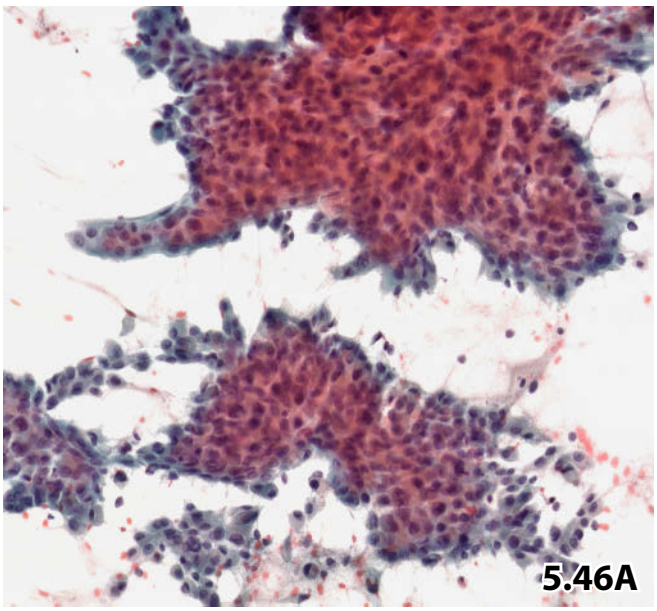
5.46A


5.46B

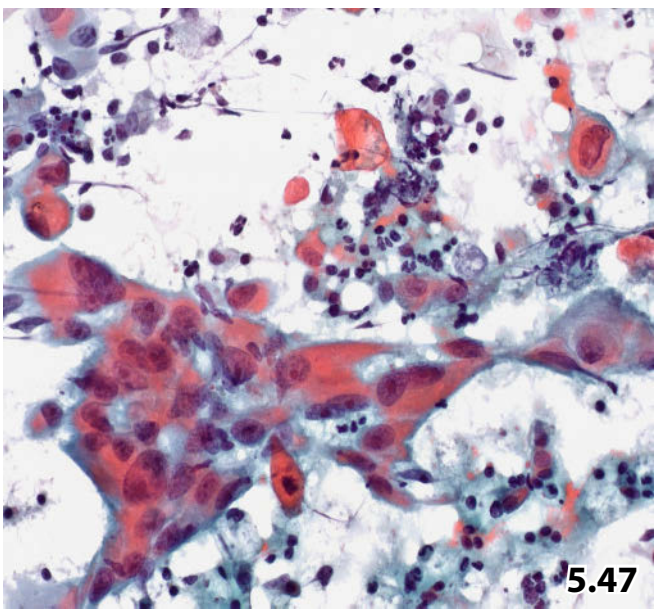
5.47

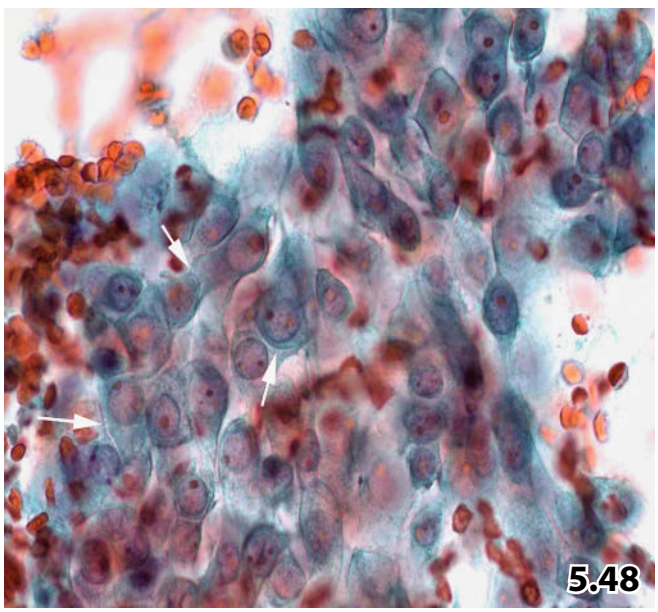
5.48

**Fig. 5.49A, B Adenoid cystic carcinoma, cribriform variant: classic cytologic features.** FNAB of a small tumor located in an older man's floor of the mouth. Direct smears, Pap stain. *Cytologic and histologic diagnosis:* adenoid cystic carcinoma.
**A** Clusters of small uniform epithelial cells surrounding translucent homogeneous globules. Globules of acellular material may also appear isolated in the background of cytologic smears (arrows) (low magnification). **B** Spheric globule exhibits characteristic sharp borders against surrounding epithelial cells. The latter show mild nuclear irregularities, granular chromatin, and variation of nucleolar size (high magnification).



**Figs. 5.50 and 5.51 Adenoid cystic carcinoma: diagnostic challenge.**
FNAB of two different adenoid cystic carcinomas presenting diagnostic confusion (direct smears, Pap stain). Diagnosis was verified by histologic examination in both cases.

**Fig. 5.50** (case #1) During the course of routine physical examination of a 61-year-old woman, a nodular lesion was found at her left cheek; FNAB was perfomed. Lower magnification shows compact three-dimensional epithelial clusters. Epithelial cells are focally arranged in distinct basal cell layers. Translucent globules are present but poorly visible.
*Tentative cytologic diagnosis:* adenoid cystic carcinoma.
*Comment:* translucent globules are present but poorly visible, thus the tumor could be mistaken for basal cell neoplasm (compare with Fig. 5.40). Globules can be better visualized by focusing on different plains.

**Fig. 5.51** (case #2) An example of the solid variant of adenoid cystic carcinoma located in the cheek of an elderly woman. Low magnification shows tightly packed fusiform epithelial cells and complete absence of spheric globules.
*Cytologic diagnosis* remained vague: cellular variant of pleomorphic adenoma versus myoepithelial neoplasm versus other tumor entity.

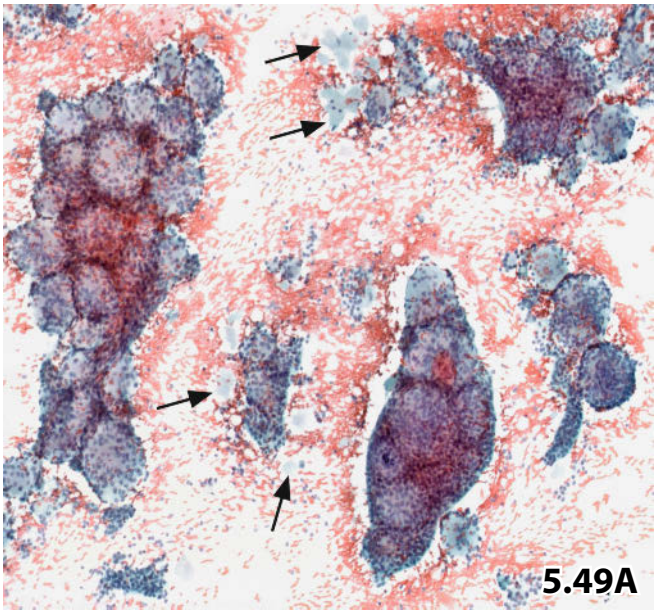
5.49A

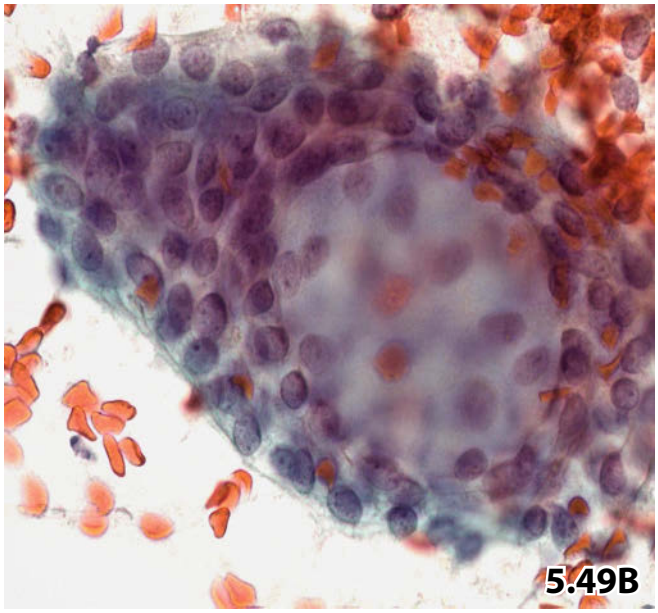
5.49B

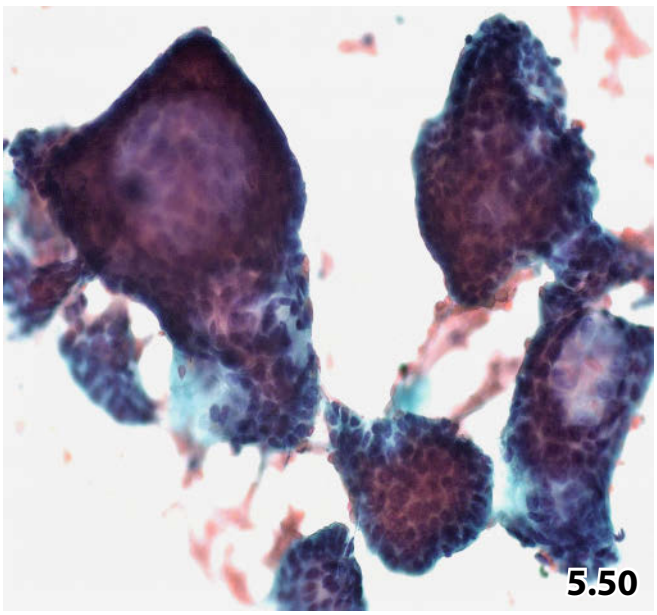
5.50

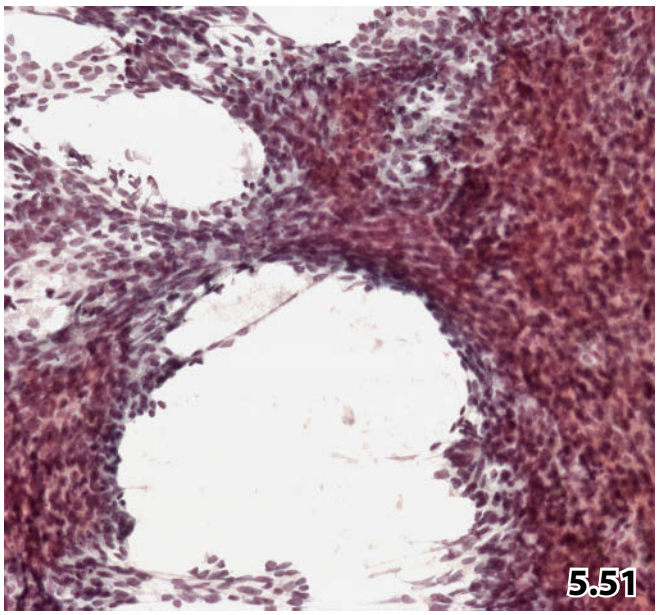
5.51

**Figs. 5.52–5.54 Well-differentiated acinic cell carcinoma.**
Cytologic features of acinic cell carcinoma are shown by means of FNAB specimens of three different well-differentiated neoplasms. Direct smears were Pap- or MGG-stained.

**Fig. 5.52A, B** (case #1) A 77-year-old woman presented with relapsing parotid acinic cell carcinoma following radical neck dissection. The patient detected a submandibular tumor mass that was referred to FNAB. **A** Three-dimensional clusters exhibit acini. Small acinic formations are present in the background as well (arrows), together with bare epithelial nuclei (MGG stain, low magnification). **B** High magnification of the same case shows monomorphic tumor cells with round nuclei and a foamy granular cytoplasm. The nucleoli are frequently obscured due to a very dense chromatin texture.



**Fig. 5.53** (case #2) High magnification of a tissue fragment from an acinic cell carcinoma composed of extremely monomorphic and small cells focuses on the diagnostic dilemma between low-grade neoplasia and benign salivary gland tissue (FNAB, Pap stain).

**Fig. 5.54** (case #3) The papillary variant of low-grade acinic cell carcinoma is composed of papillary fragments with evidence of fibrovascular cores and numerous small acinic formations (lower left) (Pap stain, higher magnification).

**Fig. 5.55 Poorly differentiated acinic cell carcinoma.**
Enlarged left parotid gland in a 70-year-old man referred to FNAB. Cytology shows both tightly packed and dissociating epithelial cells showing moderate to severe nuclear atypias. The cells are irregularly arranged including nuclear overlapping. Note the frequent acinar or acinic-like formations (arrows) (direct smear, Pap stain, higher magnification).
*Tentative cytologic diagnosis:* acinic cell carcinoma, most likely high-grade.
*Tissue diagnosis:* acinic cell carcinoma composed of low-grade and high-grade fractions, metastasizing into local lymph node.

**Fig. 5.56 Acinic cell carcinoma: clear cell variant.**
An elderly woman presenting with a nodular lesion at the left side of the neck. FNAB was initially performed. Acinic cell carcinoma of the clear cell type shares morphologic features with many other clear cell neoplasias such as mucoepidermoid carcinoma, myoepithelial neoplasia, oncocytic tumor, and varied metastatic carcinomas of the clear cell type. The tumor cell cluster depicted in this figure is composed of clear cells showing distinct acinic formations (arrows), suggesting acinic cell carcinoma of the clear cell type (direct smear, Pap stain, higher magnification).
*Tentative cytologic diagnosis:* most likely acinic cell carcinoma of a salivary gland.
*Tissue diagnosis:* Acinic cell carcinoma of the parotid gland.

Acinic formations may occur scantily in acinic cell carcinoma of the clear cell type.

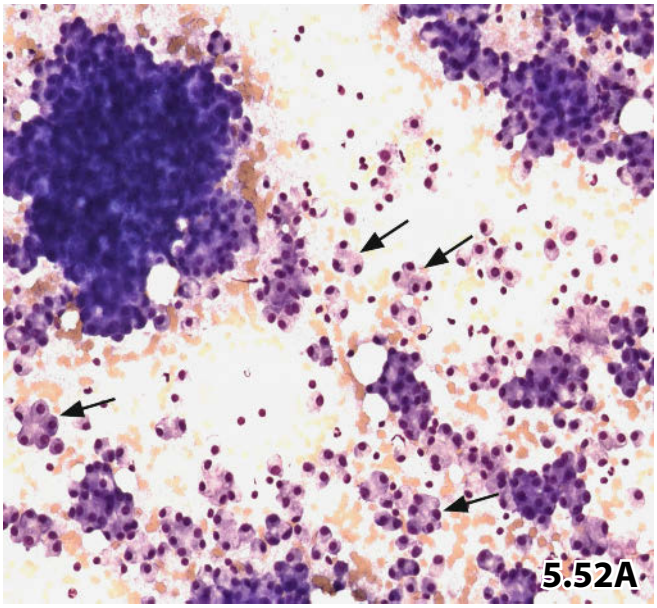
5.52A

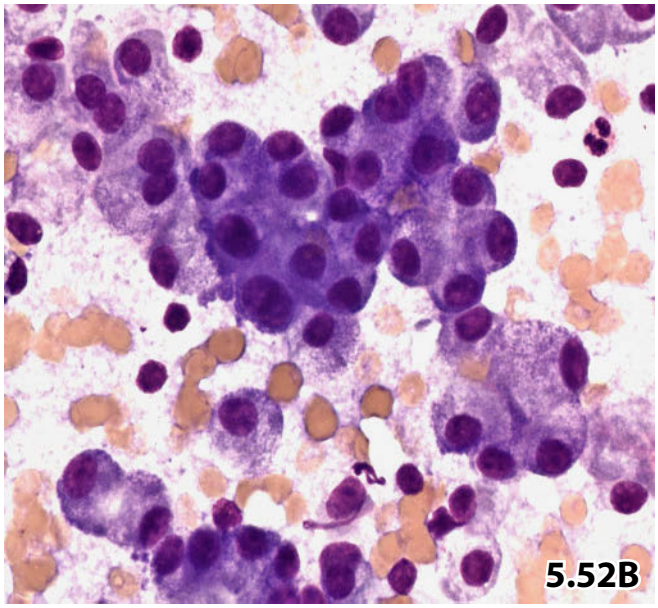
5.52B

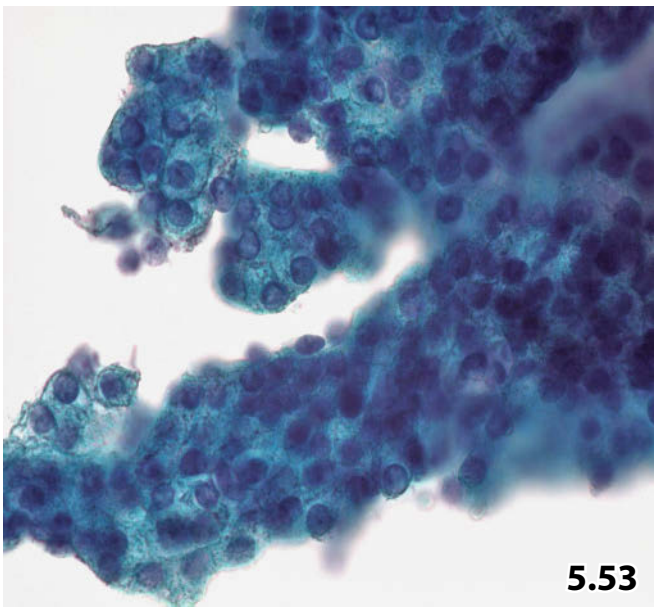
5.53

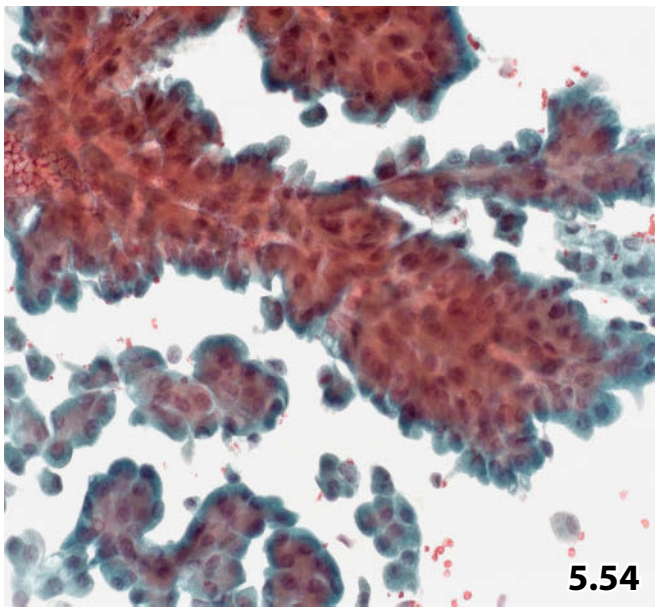
5.54

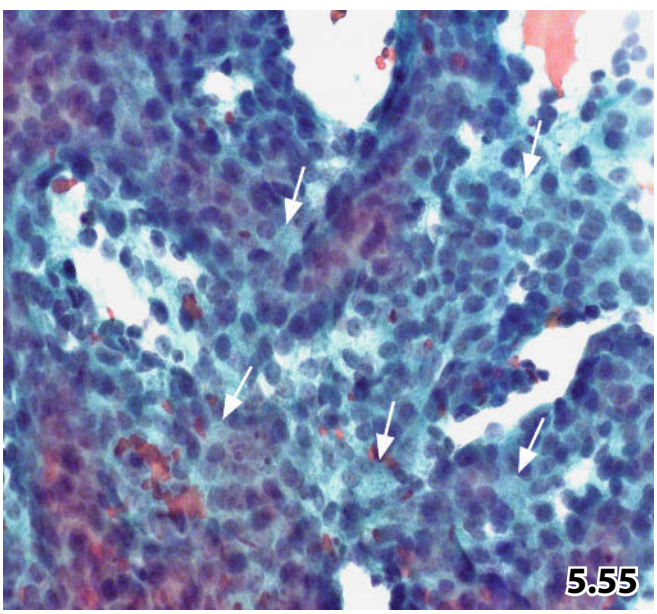
5.55

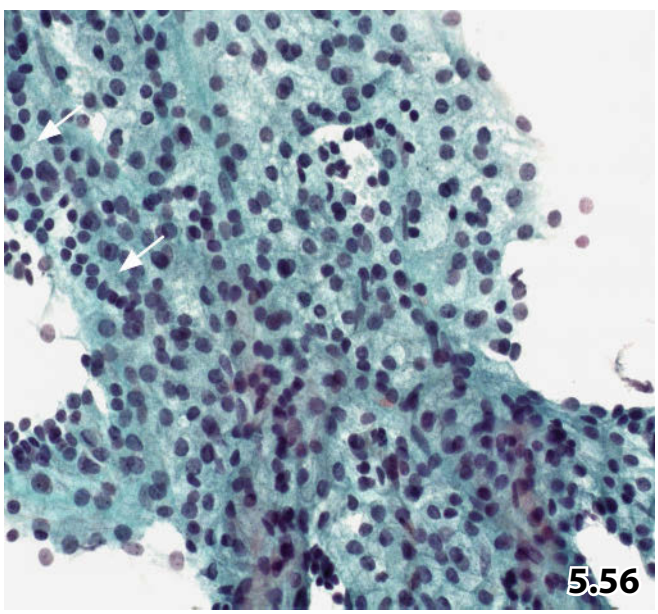
5.56

**Fig. 5.57A, B Polymorphous low-grade adenocarcinoma.**
Physical examination of a 69-year-old woman provided a voluminous intraoral nodular disorder located at the left side of the palate. Direct-guided peroral fine-needle aspiration was performed. Direct smears were Pap-stained.
*Tentative cytologic diagnosis:* polymorphous low-grade adenocarcinoma.
*Comment:* Together the patient's age, tumor location, local tumor growth pattern, and cytologic features suggested polymorphous low-grade adenocarcinoma, but one has to keep in mind that cytomorphologic features of polymorphous low-grade adenocarcinoma may mimic various other tumor entities of salivary gland origin.
*Tissue diagnosis:* Polymorphous low-grade adenocarcinoma originating from an oral salivary gland.
**A** Lower magnification shows a compact three-dimensional papilliform cluster composed of uniform epithelial cells. **B** Detail highlights bland nuclear morphology with mostly absent nucleoli. The cytoplasm tends to be dense and homogeneously structured. Note the sharply outlined hyaline bodies surrounded by tumor cells, which occasionally occur (lower left).

**Fig. 5.58A, B Papillary cystadenocarcinoma of the salivary gland type.**
A 65-year-old man presenting with a cystic lesion in the right parotid gland. Clinical diagnosis was Warthin tumor. FNAB of the parotid cyst was the initial investigation. Sediment smears were Pap-stained.
*Cytologic diagnosis* was uncertain due to morphologic overlap with other tumor entities.
*Tissue diagnosis:* minimally invasive low-grade cystadenocarcinoma of the parotid gland.
**A** Huge compact true papillary and papilliform clusters composed of uniform epithelial cells. The cell shape is cuboid to columnar. Cystic background features are indistinct (low magnification). **B** Detail reveals nuclear atypias in terms of clearing, sharply defined inclusions (arrows), and grooves (arrowheads). These nuclear alterations are shared by other carcinomas such as papillary thyroid carcinoma, renal cell adenocarcinoma, and breast carcinoma. Thus, metastatic cancer has to be excluded.

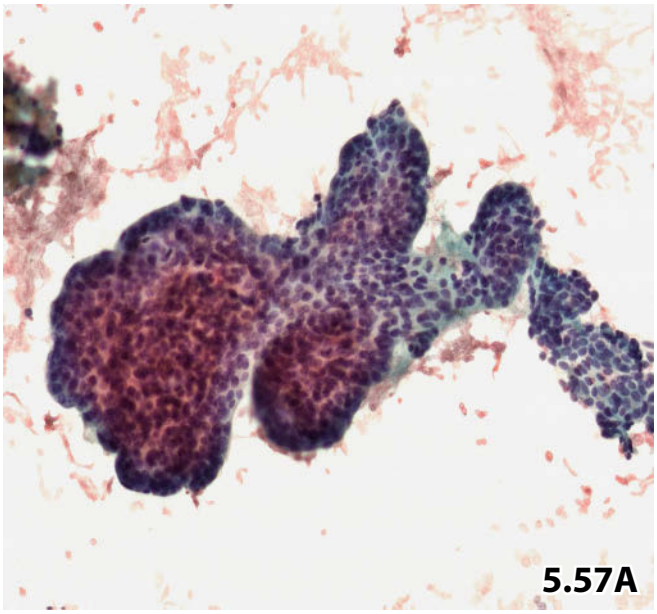
5.57A

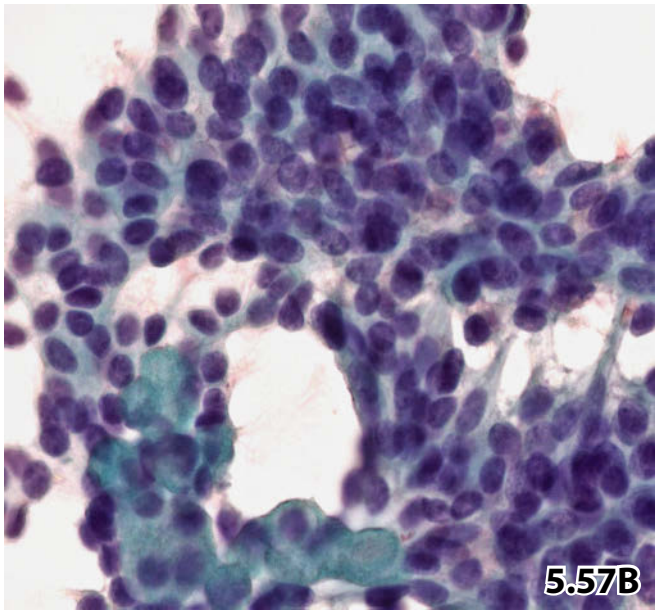
5.57B

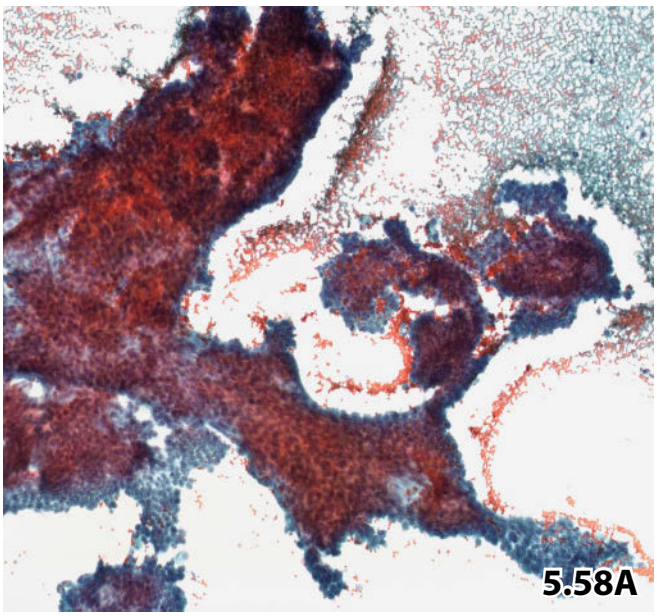
5.58A

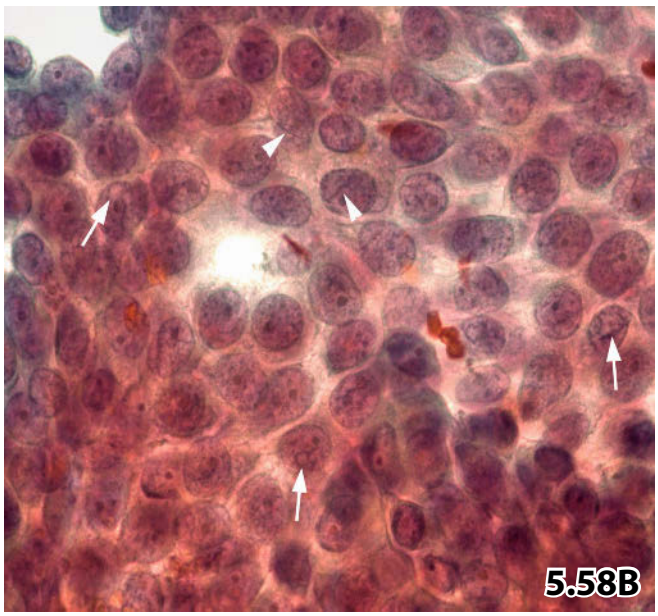
5.58B

**Fig. 5.59 Salivary duct carcinoma.**
A 42-year-old woman presented with relapsing salivary duct carcinoma originally located in a salivary gland of the sinus piriformis. FNAB of a nodule in the area of previous excision. Direct smears were Pap-stained. The cellular pattern of salivary duct carcinoma resembles that of comedocarcinoma of the breast: homogeneous appearance of an obvious malignant epithelial cell population forming glandular structures (arrow), accompanied by apoptosis and necrotic debris (high magnification).

**Fig. 5.60 Myoepithelial carcinoma.**
This case of a myoepithelial carcinoma (confirmed by histology) appeared cytologically as large cell carcinoma, not otherwise specified, associated with necrosis. Immunostainings were not applied to cytologic specimens (direct smear, Pap stain, higher magnification).

**Fig. 5.61A, B Granulocytic sarcoma.**
An elderly male patient with positive history of chronic myeloid leukemia underwent FNAB due to a tumor formation in his parotid gland. **A** Aspirated cell material of the parotid lesion exhibits numerous myeloid blasts. The blast cells are large, showing rounded and lobulated nuclei usually mimicking activated histiocytes. The chromatin is finely dispersed and the nucleoli are usually prominent. The N/C ratio is medium to high. The cytoplasm is cyanophilic and agranular (direct smear, Pap stain, high magnification). **B** Positive immunocytochemical staining for myeloperoxidase is useful to differentiate myelogenic neoplasms from malignant lymphoproliferative disorders and other malignancies.

**Fig. 5.62 Metastatic renal cell carcinoma.**
Metastasis in the parotid gland of a 72-year-old man with a positive history of metastatic hypernephroma. Tumor cells with their clear cytoplasm and atypical nuclear features (molding, grooves, loose chromatin) may also be an integral part of primary tumors of salivary glands (e.g., cystadenocarcinoma) and of other secondary cancer. An appropriate panel of antibodies is usually helpful to determine definite diagnosis.

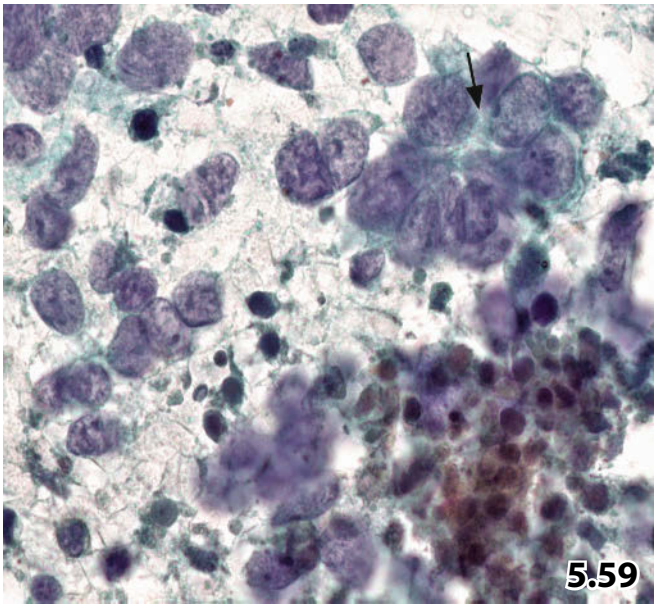
5.59

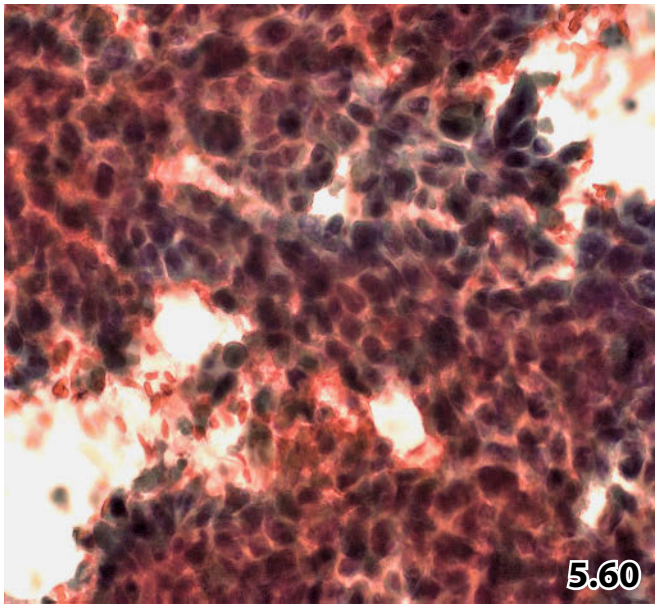
5.60

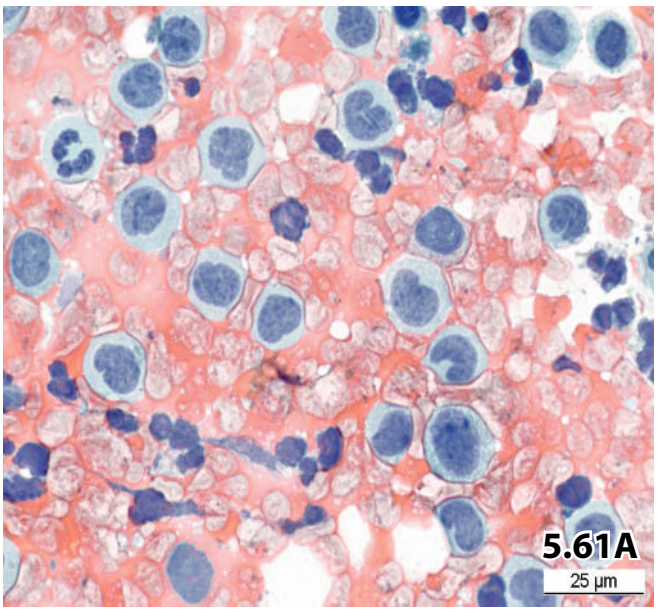

5.61A

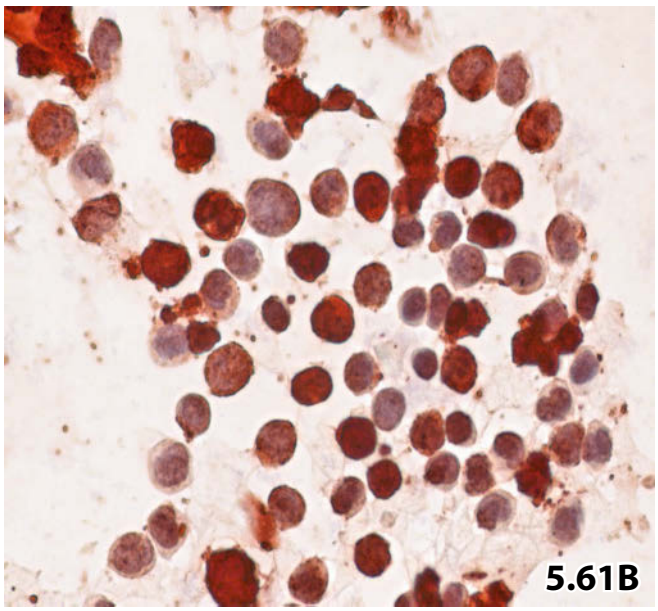
5.61B

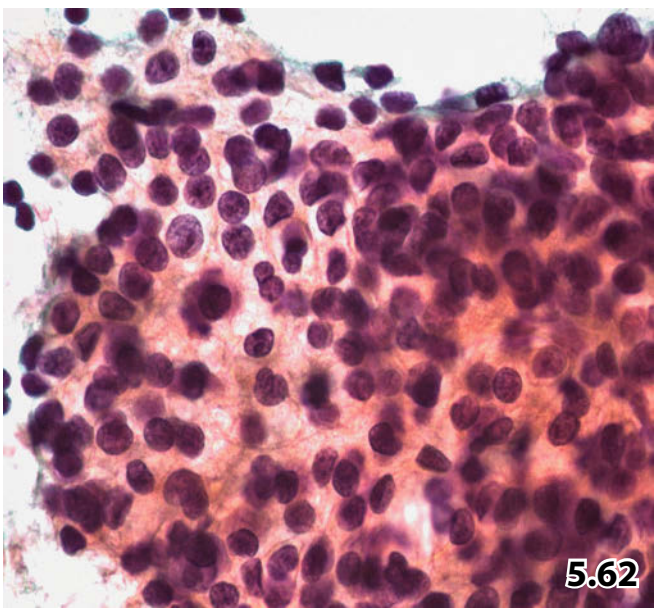
5.62

# Section 5.2
# Head and Neck Lesions

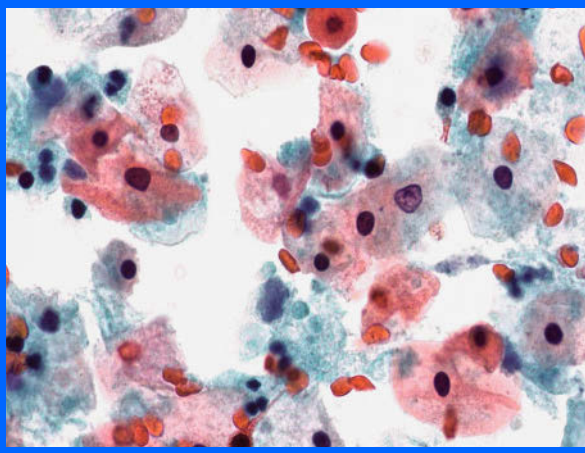

## 5.2.1 Introduction

The role of cytopathology in the management of head and neck cancer in the UK has recently been discussed by Kocjan and coauthors [48].

### 5.2.1.1 Contents of the Section

- This section focuses on tumorous masses of the head and neck as listed below:
  - All congenital neck masses and their differential diagnoses are summarized.
  - Special attention is given to cystic lesions.
  - Both common and rare head and neck lesions that have relevance in cytologic practice are presented.
- Disorders of the thyroid and salivary glands are disregarded in this section except for differential diagnostic considerations.
- The cytomorphology of reactive and malignant disorders of the lymphoid tissues is covered in Chap. 15, "Lymph Nodes."
- Many of the topics discussed herein are based on our clinical and diagnostic experience. Fine-needle aspiration biopsy (FNAB), sonographic imaging, and ultrasound-guided FNAB (US-FNAB) have been performed at our institution by cytopathologists over the course of three decades.

### 5.2.1.2 Morphologic Appearance of Head and Neck Lesions

The lesions can present as a:
- Mono- or multicystic mass.
- Infectious or inflammatory mass.
- Solid tumor.
- Sinuses or fistulae.

A cystic lesion is by far the most frequently encountered tumor type in the pediatric and young adult age group. In elderly patients, both benign cystic neck lesions and cystic formation within primary or metastatic neoplastic processes are rather common; in this age group, any cervical cystic disorder should be presumed to be a cystic malignant tumor – in particular cystic squamous cell carcinoma – until proven otherwise.

**Caution**

- It is commonly accepted that head and neck cysts often result in diagnostic dilemmas for cytopathologists and are a major cause of diagnostic pitfalls [34].
- Cystic change within a malignant tumor is one of the most common causes for a false-negative cytologic result [86]. In this respect, we highly recommend the use of sonographic imaging and US-FNAB as an initial approach, paying special attention to the border of the cyst and cyst-surrounding tissues at any spot providing an equivocal imaging result.

### 5.2.1.3 FNAB and Additional Procedures

#### 5.2.1.3.1 Fine-Needle Aspiration Biopsy

[2, 28, 53, 69, 87]

- Fine-needle aspiration biopsy is a tool gaining increasing acceptance in the diagnostic work-up of tumorous lesions of the head and neck region. In children and young adults, a high percentage of neck masses are caused by inflammation and misguided development of embryonal structures, respectively. In this age group, preoperative management is likely restricted to laboratory tests and imaging studies, FNAB is less frequently used. The role of FNAB in the diagnosis of pediatric head and neck masses has been illustrated in the literature many times [3, 20, 76]. The likelihood of malignancy rapidly increases in older patients; therefore pathomorphologic workup of neck masses in this age group should be mandatory prior to an excisional biopsy [68].
- FNA cytology on masses of the head and neck is a simple, rapid, reliable, and cost-effective technique [35, 66]. The complication rate after FNAB of head and neck masses is extremely low. The technique has a high degree of accuracy for the diagnosis of benign and malignant disorders as well as for primary and secondary neoplasms.
- The diagnostic performance is notably enhanced by application of auxiliary methods on aspirated cell material including immunocytochemistry, image cytometry, flow cytometry, and molecular genetic assays.
- The clinical utility of FNABs first means confirmation or exclusion of a malignant tumor. Initial surgical biopsy of a cervical lymphadenopathy should by all means be avoided if the nature of the process is not established. Establishing a benign lesion avoids the need for more invasive diagnostic procedures.
- Preoperative FNAB providing rapid first-line diagnoses is a valuable approach in the work-up of head and neck masses. Such methods have proven to be extremely helpful not only with respect to dedicated head and neck clinics, but also to secondary care hospitals with limited resources and to developing countries with limited public health service [28, 61]. Intraoperative FNAB and intraoperative touch preparation have been recommended as an additional approach to the diagnosis of head and neck masses [4].

#### 5.2.1.3.2 Sonography and Ultrasound-Guided FNAB

FNA sampling errors are unacceptable from lumps of the head and neck area. Sampling error is almost completely eliminated by initial sonographic investigation of the lesion, including surrounding tissues, and subsequent image-guided aspiration biopsy [9, 43, 56, 91]. The methodological, diagnostic, and clinical benefits of this procedure are evident:

1. Using sonography, most lesions can reliably be assigned to the subcutaneous/interstitial space, or to a decisive organ such as thyroid gland, salivary gland, lymph node, and others.
2. The needle can be placed exactly in the target lesion using US-FNAB.
3. US-FNAB offers the chance for repeated cell sampling from multiple areas of inhomogeneous lesions, to the best advantage in cystic lesions! [96].
4. Avoidance of inadequate cell sampling.
5. Enhancing the cytodiagnostic approach for one-stop head and neck clinics. Wherever possible, FNAB/US-FNAB should be conducted by a skilled cytopathologist or at least attended by an experienced cytopathologist or cytotechnologist for on-site diagnostic assessment or sample adequacy assessment, respectively [95].
6. Both palpable and nonpalpable disorders can be evaluated reliably [77].
7. Slightly swollen lymph nodes, especially those with unsuspicious imaging findings, can easily be investigated.
8. The technique facilitates complete tumor staging in the neck area [78, 91] and detection of nodal recurrence [56].

#### 5.2.1.3.3 Technical Procedures

The FNAB, US-FNAB technique for head and neck tumors and the laboratory techniques are the same as those we use for lesions in other organs. The procedures have been described in many chapters of this book: Sect. 1.1.1, p. 3, Sect. 1.1.2, p. 4, and Sects. 4.1.2 and 4.1.3, p. 325. They are also documented in review articles [87] and distinguished textbooks.

#### 5.2.1.3.4 DNA Ploidy [12, 58, 65]

- Cytological limitations in distinguishing reactive atypical squamous cells from premalignant/malignant squamous cells can be outweighed by determination of DNA ploidy, at least to a certain degree. DNA ploidy can be assessed by both image cytometric analysis or flow cytometry. DNA aneuploidy is established as an early event in developing malignancy of squamous cells and as a reliable marker for squamous cell carcinoma.
- DNA ploidy is particularly helpful in differentiating between benign and malignant cystic lesions whose atypical squamous cells have provided ambiguous results by conventional cytology.
- DNA aneuploidy and the proliferation index can be used as biological parameters for improved estimating the potential malignant behavior of squamous cell carcinomas of the head and neck [40].
- At our institution, histogram algorithms have been applied in accordance to ploidy evaluation of squamous cell lesions located in other organs of the human body. The DNA histogram has solely been determined by image cytometric measurements on Feulgen-stained atypical nuclei.
- Ploidy algorithms for squamous cells and advanced information are documented in Sect. 8.4, "DNA image cytometry", p. 565.

**Table 5.2.1** Topographical areas and types of congenital neck masses

| Favored neck area | Entity |
|---|---|
| Lateral | Branchial cleft cysts |
| | Congenital muscular torticollis |
| Midline | Ectopic thyroid tissue<br>Thyroglossal duct cyst |
| | Dermoid cyst |
| | Teratoma |
| | Plunging ranula |
| Any neck region | Ectopic thymic tissue<br>Thymic cyst<br>Cervical thymoma |
| | Cystic hygroma |
| | Cervical bronchogenic cyst |

## 5.2.2 Congenital Neck Masses [1, 49, 89]

- Congenital disorders of the neck show varied manifestations and may present at any age. Even so, the greatest proportion of congenital lesions in the neck has been found in the first and second decade of life accounting for between 38% and 32% [1, 55]. The vast majority of congenital neck masses in children and young adults appear as cystic disorder, with occasional infection.
- The diagnosis of congenital neck disorders is based on histologic examinations in a large percentage of the reported cases. But FNAB is gaining more and more acceptance in primary evaluation of neck masses; therefore we wish to present the most important features of the varied entities and their cytomorphologic peculiarities.

### 5.2.2.1 Congenital Lateral Neck Masses

#### 5.2.2.1.1 Branchial Anomalies (Figs. 5.63–5.66)

- Synonyms: The terms "lateral neck cyst" "branchial cyst," and "cervical lymphoepithelial cyst" are often used for branchial cleft cysts.
- Branchial anomalies are the most common congenital malformations on the side of the neck comprising cysts, sinuses, and fistulae. They occur regularly in the right and left lateral sector of the neck anterior to the sternocleidomastoid muscle. The vast majority of branchial cleft cysts arise from incomplete obliteration of the second pharyngeal cleft and pouch during embryogenesis [55].
- Branchial cleft cysts may also appear near the parotid gland or in the anterior compartment of the parotid gland and can be mistaken clinically and even sonographically for a parotid disorder. Misinterpretation as a tumor of the submandibular gland may occur as well. A history of infection is quite frequent.
- Malignant transformation of the cyst lining epithelium is an extremely rare event. Both, in situ squamous cell carcinoma and invasive squamous cell carcinoma have been observed with histology, as reported by Bhanote and Yang [11].

**Microscopic Features**

A limited number of studies are available on the cellular content of branchial cleft cyst fluids [31, 75].

- Benign squamous cells line the inner surface of the cyst. Superficial squamous cells may show mild nuclear irregularities and distinct but small nucleoli may be observed.
- Occasionally, the cyst is lined with respiratory (ciliated columnar) epithelium.
- Lymphocytes originate from lymphoid tissue surrounding the cyst.
- Mixed inflammatory infiltrates (neutrophils, histiocytes, macrophages) may result from secondary infections.
- Cholesterol crystals are occasionally encountered.
- In a minority of branchial cyst aspirates, the smears are devoid of cells, or merely show abundant inflammatory infiltrates.

**Differential Diagnosis**

- Any swelling in the patient's lateral aspect of the neck should include the differential diagnosis of a branchial cleft anomaly regardless of the clinical presentation [22].
- Inflamed branchial cysts, especially in the absence of epithelial elements, mimic inflammatory disorders such as abscess related to the parotid or submandibular gland, cystic granuloma, and odontogenic infection.
- Cystic fluid exhibiting squamous cells may be collected from a dermoid cyst, epidermal inclusion cyst, or an odontogenic neoplasm. Furthermore, squamous elements may be found in aspirates of various salivary gland lesions such as salivary duct cysts, chronic sialadenitis, pleomorphic adenoma, Warthin tumor, mucoepidermoid carcinoma [75] (see also Sect. 5.1.3.2.1, p. 405).
- Metastatic to a cervical lymph node, squamous cell carcinoma showing inflammation and cystic degeneration may imitate inflammatory branchial cyst; both lesions usually exhibit atypical squamous cells. Malignant aspirates usually contain squames with more pronounced atypias, more polymorphous necrotic debris, and increased tissue fragments [14, 62]. Severity of background inflammation and anucleated squames are minor discriminators between benign and malignant squamous-lined cysts.

- Atypical squamous cells may indicate a premalignant lesion or an invasive neoplasm emerging from a branchial cyst.
- Lymphoepithelial cysts of the parotids may exhibit a histologic architecture and cytologic pattern close to branchial cleft cysts. Compare morphologic features in Sect. 5.1.3.3.5, p. 406 (Fig. 5.8).
- Fluids from a mass of the lateral neck that contain nothing but lymphocytes may derive from a branchial cyst, cystic hygroma, thoracic duct ectasia, or lymphangioma.

**Caution**

- It is well known that differentiated squamous cell carcinomas and their metastases can be characterized by minimal cellular atypia. Thus, aspirates from neck metastases may occasionally contain squamous neoplastic cells without obvious signs of malignancy [31]. Such tumors concern in particular primaries of the skin, oral cavity, pharynx, and larynx (see also Sects. 8.7.1. and 8.7.2, p. 568, and Sect. 16.2.8, p. 1030).
- Do not under-diagnose mildly atypical squamous cells in a branchial cyst aspirate, particularly in association with an inflammatory process! Also avoid regenerative atypical squamous cell over-diagnosis! [11] (Figs. 5.65 and 5.66).
- Premalignant and malignant squamous cells may be reliably recognized and excluded, respectively, using DNA ploidy analysis (see also Sect. 5.2.1.3.4, p. 459).
- Always remember that atypical squamous cells may also occur in aspirates from previously treated patients (possibly many years ago) by radiotherapy in the neck area!

#### 5.2.2.1.2 Congenital Muscular Torticollis

- Congenital muscular torticollis may occur due to a defect in the development of the sternocleidomastoid muscle, an abnormal fetal position in the uterus, or following a difficult birth. The injured muscle develops scar tissue that causes the muscle to shorten and tighten. The fibrotic process occasionally forms a palpable mass or lump on the side of the neck.
- An early noninvasive diagnosis is most desirable in order to avoid surgery at a very early age. FNAB is useful in cases where the diagnosis cannot be established on clinical and imaging findings alone. Numerous cases are documented in the literature where FNAB has been used in patients affected by this peculiar fibrotic pseudotumor [37, 70, 81, 85].

**Microscopic Features**

- Hallmarks: Benign slender and spindle fibroblasts appearing as single cells or arranged in parallel clusters of varied size. The nuclei are ovoid with bland morphologic features.
- Atrophic skeletal muscle is present together with multinucleated cells, showing abundant cytoplasm (corresponding to degenerating muscle fibers). Collagen is invariably found.
- Inflammatory infiltrates may be observed but generally they are not pronounced.
- The cells may be scattered in a clean or pink granular background.

**Differential Diagnosis**

Differential diagnosis includes other childhood fibrous neck disorders including fibromatosis colli, infantile desmoid fibromatosis, and calcifying aponeurotic fibrosis. These entities present in neonates in the first weeks of life and in older children. Infantile fibromatosis is a more infiltrative process than the relatively circumscribed congenital torticollis, and calcifying aponeurotic fibrosis is characterized by multiple calcium deposits.

### 5.2.2.2 Congenital Midline Neck Masses

These lesions are usually located in a line drawn from the middle of the forehead to the bottom of the neck [33].

#### 5.2.2.2.1 Thyroglossal Duct Cyst [83, 84] (Fig. 5.67)

- Thyroglossal duct cyst or fistula is the most common congenital neck lesion accounting for approximately 50% of congenital neck disorders. The maximum frequency occurs during the second or third decade of life [1].
- The thyroglossal duct is a connection between the primary thyroid anlage at the base of the tongue and the definite positioning of the thyroid gland at the anterior aspect of the neck. This duct normally disappears during gestation. If it persists, thyroglossal duct cyst, fistula, thyroglossal sinus, or ectopic thyroid tissue may develop anywhere along the duct. Thyroglossal duct cysts may become infected.
- Thyroid carcinoma of the papillary and follicular variant has rarely been reported within thyroglossal duct cysts [92]. Morphologic and immunocytochemical properties of these tumors are described in the thyroid chapter (see Sect. 4.2, p. 336).

**Microscopic Features**

- Hallmarks: the aspirates are usually paucicellular containing colloid with different structural aspects. The epithelial cells are of the columnar type and mostly ciliated, of the metaplastic squamous type, or of the normal-looking superficial squamous type.
- A possible inflammatory cell pattern is composed of macrophages, lymphocytes, and neutrophils; the latter are usually dominant.

**Differential Diagnosis**

- Aspirates devoid of squamous cells and ciliated columnar cells strongly mimic intrathyroid thyroglossal duct cyst and common cystic thyroid nodule [41].
- Cystic fluids containing only squamous cells may suggest an intrathyroidal or parathyroidal cystic lesion of teratomatous histogenesis or an epidermal inclusion cyst.
- Cystic fluid including (ciliated) columnar cells may originate from a bronchogenic cyst. However, the presence of metaplastic squamous cells, cartilage, smooth muscle cells, and cells of bronchial gland-type would exclude thyroglossal duct cyst.

#### 5.2.2.2.2 Ectopic Thyroid Tissue

Ectopic thyroid tissue is the result of abnormal migration and abnormal settling of portions of the gland. Ectopic tissue can be encountered along the midline of the neck, paramedian, and in the upper and anterior mediastinal space. The prevalence of ectopic thyroid tissue ranges from 7 to 10%.

#### 5.2.2.2.3 Dermoid Cyst

A dermoid cyst is a mass containing skin and epithelial appendages (hair, hair follicles, and skin glands) within the cyst wall. The lesion results from an inaccurate closure of the midline during development followed by entrapment of epithelial elements [1, 33].

**Differential Diagnosis**

Other cystic midline neck lesions lined by squamous cells concern the thyroglossal duct cyst, cystic teratoma, and the epidermoid cyst. The epidermoid cyst differs from the dermoid cyst in the absence of hair, hair follicle, and glandular elements.

#### 5.2.2.2.4 Teratoma

- Congenital cervical teratomas are rare, constituting only 3% of the teratomas in childhood, but they account for about 10% of all cervical tumors in this age group [1]. Teratomas usually comprise tissue from the three germ layers but ratios and the degree of differentiation vary considerably [39].
- The lesions are usually benign, but if they become apparent during adulthood they are noted for a high potential of malignant degeneration [30, 51].
- Cervical teratomas are diagnosed during the neonatal period and increasingly by prenatal sonography tests [30, 39]. At this age, imaging is essential for a conclusive diagnosis and cytological investigation is extremely uncommon.

**Differential Diagnosis**

- Cystic teratoma should be included in the differential diagnosis of other congenital midline cysts lined with squamous cells or (ciliated) glandular cells, e.g., thyroglossal duct cyst, epidermal inclusion cyst, and cervical bronchogenic cyst.
- Other tissue components originating from different germ layers may lead to a misdiagnosis of ectopic thyroid, neural tumor, chondroma, among others.

**Caution**

Cervical teratomas in adult patients are rare but have a high potential of malignant transformation. One should pay attention to atypical squamous cells in aspirates suggesting premalignant disorder or early carcinoma.

#### 5.2.2.2.5 Plunging Ranula

Ranulas are cysts resulting from retention or extravasation of saliva from the sublingual gland. The cervical ranula is referred to as plunging ranula. The disorder may present as a swelling, generally located in the upper part of the neck.

To the best of our knowledge, no reports are available in the literature dealing with FNAB of ranulas. According to the histologic appearance [52], cytologic features seem likely to match the mucus retention cyst and the extravasation mucocele described in Sects. 5.1.3.3.2, p. 406 and 5.1.3.5.2, p. 407, respectively (Fig. 5.7):

### 5.2.2.3 Congenital Masses in Any Neck Area

#### 5.2.2.3.1 Ectopic Thymic Tissue, Cervical Thymoma and Thymic Cyst

Congenital anomalies of thymic origin in the neck may be encountered anywhere on the path from the embryonic origin of the gland (pharyngeal/branchial pouches at the angle of the jaw) to the superior and anterior mediastinum. Morphology, adjuvant analyses, and differential diagnostic considerations concerning thymus gland tissue and its disorders are discussed in extenso in Sect. 2.4.3, p. 208.

**General Comments and Microscopic Features**

1. *Ectopic thymic tissue* [88]: Thymic remnants located in the neck area and in the thyroid gland may form an ectopic thymus. Ectopic thymic tissue is an infrequent clinical finding but its occurrence seems to be fairly common. Therefore, this lesion should always be included in the differential diagnosis of neck masses, especially in children. About 60% of all patients with ectopic cervical thymic tissue are children under 10 years of age. In contrast, ectopic cervical thymic tissue rarely occurs in patients more than 20 years old and the disorder is commonly found in males. The lesion is cystic in the majority of cases [80]. Histologic features of normal and hyperplastic thymus tissue are listed in Sects. 2.4.3.1 and 2.4.3.2, p. 208.
2. *Cervical thymoma* [13, 88]: Cervical thymomas are characteristically found in females and appear as a solid mass.

- Microscopy: The smears are cellular, composed of small mature lymphocytes, large lymphocytes, monocytes, and a few thymocytes. Studies for B- and T-cell subsets demonstrate the thymic lymphocytic phenotype.
  Cervical thymomas exhibiting a predominant epithelial component are extremely rare [13]. The detailed cytomorphology of thymomas is provided in Sect. 2.4.3.4, p. 209

3. *Thymic cysts:* These cysts develop from remnants of the thymopharyngeal duct.
   Congenital thymic cysts are clinically often misdiagnosed as thyroid lesion, branchial cleft cyst, or cystic hygromas. The cytologic features are similar to thymic cysts of the mediastinum (Fig. 2.97).
   - Macroscopic and microscopic features: The cyst fluid is serous but may also be sanguineous. The background of the smears may contain inflammatory cells, erythrocytes, debris, calcium deposits, and frequently cholesterol crystals. If present, epithelial cells can appear cuboidal, columnar, ciliated-columnar, or squamous.

**Differential Diagnosis** [13]

- Distinguishing between ectopic cervical thymic tissue and cervical thymoma may not be possible with cytology and enumeration of lymphocytes alone. Clinical and other information should help reach an accurate diagnosis.
- Epithelial thymoma may mimic metastatic carcinoma, melanoma, and invasive mesothelioma. Thymomas within or adjacent to the thyroid gland could most likely lead to an erroneous diagnosis of follicular or medullar thyroid carcinoma. Lymphocyte-predominant thymomas may give rise to a false diagnosis of malignant lymphoma or lymphocytic thyroiditis [57, 93]. Appropriate immunocytochemical studies of the epithelial and lymphocytic components are helpful in establishing a correct diagnosis.
- Comparing the cystic fluids, various congenital cysts and thymic cysts show a similar cell pattern. Other cystic disorders should also be considered such as cystic thymoma, cystic teratoma, and lymphangioma.

#### 5.2.2.3.2 Cystic Hygroma (Cavernous Lymphangioma / Lymphocele) (Fig. 5.68)

Lymphangiomatous cystic disorders can readily be diagnosed preoperatively using FNAB, providing a yellowish-white chylous fluid.

- *Cystic hygroma* is a congenital lymphatic malformation. It is the more common type of lymphangioma, compared with its capillary counterpart. It usually presents early in life. A cystic hygroma can arise anywhere but is classically found in the left posterior triangle of the neck [36].
- *Lymphocele* of the thoracic duct (thoracic duct cyst) can present as a cervical mass occurring in an older age group. It is a rare lesion that is mainly caused by surgical injury and blunt trauma [54].

**Microscopic Features**

- The cystic fluid contains various amounts of small mature lymphocytes. A few spindle-shaped or flattened endothelial cells may be present. Positive immunoreactivity to factor VIII and/or lymphoendothelial markers (D2-40, podoplanin) will demonstrate the nature of the nonlymphoid cells [15].

#### 5.2.2.3.3 Cervical Bronchogenic Cyst [63] (Fig. 2.92)

Bronchogenic cysts are rare congenital malformations of the primitive foregut, most of which are located in the chest. Cervical bronchogenic cysts are usually diagnosed in a pediatric population, with only a limited number of reports in the literature commenting on such lesions among adults. The bronchogenic cyst may present as a midline lesion (usually located in the suprasternal notch) but also as a lateral neck mass.

**Microscopic Features and Differential Diagnosis**

Cytologic components of aspirates from bronchogenic cysts are listed in Sect. 2.4.2.3.1, p. 207.

- Key features are ciliated columnar cells of the respiratory type, sheets of squamous metaplastic cells, ciliary tufts, and elements typically present in the bronchial wall such as cartilage, smooth muscles, and bronchial glands.

Branchial cleft cysts and thyroglossal duct cysts are most commonly confused with bronchogenic cyst due to a similar epithelial lining. However, the presence of cartilage, smooth muscles, and cells of bronchial glands make diagnosis of bronchogenic cyst most likely. The cytomorphology of tracheal diverticula looks similar to bronchogenic cysts; by the way, the latter may be referred to as a tracheal diverticula that has lost connection to the tracheobronchial tree.

### 5.2.2.4 Other Rare Congenital Neck Disorders

- *Hemangioma* may be suspected in sanguineous fine-needle aspirates comprising endothelial cells. The clinical and image results should be adequate.
- *Laryngocele* refers to a congenital anomalous sac filled with air; the lesion may protrude into the neck area.
- *Heterotopic salivary gland tissue* usually occurs along the lower anterior aspect of the sternocleidomastoid muscle. FNAB may detect normal salivary gland tissue or tumorous lesions of salivary gland type [5].

## 5.2.3 Pseudotumors and Neoplasms from Adjacent Structures

### 5.2.3.1 Cervical Rib (Fig. 3.18)

A congenital overdevelopment of the lateral process of cerebral vertebrae (the seventh cervical vertebra is usually affected) can produce a hard cervical lump that is easily detected on physical examination. Patients are mostly referred to FNAB with the suspected diagnosis of malignancy. Needling will readily disclose the bony nature of the lesion.

- In cases with thin cortical zoning, the aspirates will yield typical bone marrow cells. Still, the aspirate tends to be rather dry including a few stromal cells.

### 5.2.3.2 Tietze Syndrome (Fig. 1.65)

Tietze syndrome is a painful parasternal swelling of the costochondral junction due to microfractures of the upper ribs.

The lesion is located close, but not directly linked, to the neck area. The clinical impression is that of a process originating from the upper ventral-thoracal bony structures, or of the extension of an upper mediastinal/cervical tumor, or of a disorder in parasternal mammary gland tissue.

- The paucicellular aspirate specimen contains small fragments of edematous mesenchymal tissue and activated fibroblasts.

### 5.2.3.3 Mycotic Aneurysm of the Carotid Artery (Fig. 5.69)

Clinically and with imaging, mycotic aneurysm may imitate a necrotic cervical metastasis. In this setting, cytologic aspirates containing neutrophils and debris should not mislead to a diagnosis of an inflammatory or necrotic neoplasm.

### 5.2.3.4 Chondroma (Fig. 5.70)

Rare chondroma of the hyoid bone can appear as a firm mass in the submandibular space. Clinically, the lesion is practically indistinguishable from a primary salivary gland tumor.

- Varied amounts of chondroid fragments are present in the aspirate smears, occasionally along with scattered chondrocytes.

The distinction of chondroma from "pleomorphic adenoma with a large proportion of chondroid tissue" may be impossible.

### 5.2.3.5 Chordoma [46, 94] (Figs. 5.71 and 11.33)

- Chordomas arise from remnants of the primitive notochord; the notochord forms the early spine in the early stages of fetal development. Chordomas are slow-growing locally aggressive tumors predominantly found in people between 40 and 70 years of age. Spread to other organs is possible, in particular to the lungs. Chordomas are most often found in the sacrococcygeal or skull base area but can unusually occur throughout the spine.
- Cervical chordoma is rare and may initially be detected as a neck mass. The tumor is slow-growing, reaching a considerable size before the patient becomes symptomatic [42].
- Many case reports and a few series describe cytologic features and adjuvant diagnostic tools of chordomas at various sites of the spine [46, 94] .

#### Microscopic Features

- Hallmarks: The smears exhibit a conspicuous myxoid background matrix. The pathognomonic physaliferous cells are medium-sized to large cells with a bubbly cytoplasm; occasionally, physaliferous cells occur only sporadically. Matrix and cytoplasmic vacuoles are visualized best with the May-Grünwald-Giemsa staining procedure. The nuclei are relatively uniform but may exhibit a considerable pleomorphism. The chromatin texture is bland.
- Small epithelial-like cells and spindle-shaped cells may dominate the cellular fraction; the cytoplasm may be eosinophilic, mimicking oncocytes
- The chondroid chordoma variant contains cartilaginous areas that are indistinguishable from hyaline-type chondrosarcoma [60].
- Anaplastic cellular components may be observed, in most cases along with the classic features of chordoma [64].

#### Differential Diagnosis and Immunocytochemistry

[ 46, 60, 73, 94]

- Overlapping cytologic features occur between chordoma, chondrosarcoma, myxoid liposarcoma, and metastatic carcinomas such as clear cell carcinoma, mucinous carcinoma, poorly differentiated carcinoma, thyroid carcinoma, and malignant salivary gland tumors.
- Cellular features (physaliferous cells) and diffuse strong S100 protein immunoreactivity distinguish chordoma cells from carcinoma cells.
- Marked immunopositivity for a spectrum of cytokeratin subtypes and epithelial membrane antigen distinguishes between chondrogenic tumors (in particular chondrosarcoma) and chordoma [42].

## 5.2.4 Benign Noncongenital, Nonneoplastic Lesions of the Head and Neck

### 5.2.4.1 Inflammation and Infections

#### 5.2.4.1.1 Cervical Lymphadenopathy

Lymphadenopathy is the most common cause for an inflammatory neck mass. Enlargement of the lymph nodes occurs in response to infection or inflammation. Lymph nodes of the whole neck can be affected, comprising the nodes of the posterior triangle (between sternocleidomastoid and trapezius muscle) and the nuchal nodes, which are usually located at the hairline.

Cytomorphologic features of various forms of reactive lymphadenopathy and potential pitfalls are discussed in Sect. 15.2 "Lymph Nodes: Benign Lesions," p. 926.

**Caution**

- Lymphadenopathy in young children often presents as a large and very painful tumor mass. It may only slowly resolve over a period of weeks and months.
- At any age, enlargement of nuchal lymph nodes is most unlikely caused by a malignant infiltrate unless the patient's history reveals an adequate tumor.
- Enlarged supraclavicular and retroclavicular lymph nodes are more likely affected by a metastatic tumor than by an inflammatory process.

#### 5.2.4.1.2 Kimura Disease

Kimura disease as seen in Asia is an immune-mediated inflammatory lesion presenting as subcutaneous masses, especially in the periauricular area and in neighboring muscles, accompanied by a regional lymphadenopathy. The disorder was initially described by Kimura and associates [47]. Kimura disease may be difficult to distinguish from angiolymphoid hyperplasia with eosinophilia, both clinically and with cytology. Cytologic features [26] and differential diagnostic considerations are provided in Sect. 5.2.4.2.3, "Angiolymphoid Hyperplasia with Eosinophilia," p. 466.

#### 5.2.4.1.3 Infectious Diseases

**Cervicofacial Actinomycosis** [23] (Fig. 5.72)

Actinomycosis is caused by the anaerobic bacterium *Actinomyces israelii*. The organism is a Gram-positive bacterium occasionally staining positive with Gomori silver methenamine.

Cervicofacial actinomycosis may appear as a mass simulating lymphadenopathy. Microscopically, nonspecific lymphadenitis is a common under-diagnosis.

**Microscopic Features**

- Aspirates show a cell-rich inflammatory infiltrate predominantly composed of neutrophils interspersed with histiocytes and a few lymphocytes.
- Actinomycosis comprises cotton ball-like colonies with radiating and protruding mycelial filaments that may be branching.
- Sporadic bacteria are easily ignored.

**Other Infections**

We refer to Sect. 15.2, p. 926 and to Table 5.2.2 below for other pathognomonic cell patterns associated with particular pathogenic organisms observed in fine-needle aspirates. The key cytomorphological features of mycobacterial and fungal infection, and hydatid cyst are presented on several occasions in this book.

### 5.2.4.2 Nonneoplastic Disorders of the Soft Tissues

A category of disorders includes nodular fasciitis, proliferative fasciitis, desmoid-type fibromatosis, and proliferative myositis, which exhibit a common cytomorphologic basepattern.

**Table 5.2.2** Selected variants of benign lymphoid disorders and infections in the neck area that should be kept in mind for cytologic practice

| Entities | Reference to chapters with related information |
|---|---|
| Angiofollicular hyperplasia: Castleman disease | Lymph nodes: Sect. 15.2.5.4, p. 932 |
| Sarcoidosis | Respiratory tract: Sect. 2.1.3.2.2, p. 111<br>Lymph nodes: Sect. 15.2.5.6, p. 933 |
| Mycobacterial infections | Respiratory tract: Sect. 2.1.6.1, p. 116 |
| Infectious mononucleosis | Lymph nodes and malignant lymphoma: Sect. 15.2.4.1, p. 930 |
| Cat-scratch disease | Lymph nodes and malignant lymphoma: Sect. 15.2.3.3, p. 929 |
| HIV-associated lymphadenopathy | Lymph nodes and malignant lymphoma: Sect. 15.2.4.2, p. 931 |
| Toxoplasmosis | Lymph nodes and malignant lymphoma: Sect. 15.2.3.4, p. 929 |
| Fungal infections | Respiratory tract: Sect. 2.1.6.3, p. 117 |
| Hydatid cyst [10] | Liver: Sect. 9.1.7.3, p. 590; Pancreas: Sect. 10.1.5.5, p. 638 |

#### 5.2.4.2.1 Nodular Fasciitis (Figs. 17.5–17.7)

- Nodular fasciitis is much more common than proliferative fasciitis/myositis. A benign proliferation of fibroblasts and myofibroblasts in the subcutaneous tissues is frequently associated with fascial attachment. The cause of this reactive disorder is unknown, but it may be triggered by a local injury or inflammatory process. Spontaneous resolution generally happens within a few months.
- The lesions are solid and generally less than 5 cm in size. The head and neck region is particularly involved in infants and children; rare sites of nodular fasciitis are found in the immediate vicinity of salivary glands, the face, and the oral cavity. Nodular fasciitis arising in the upper extremities is most commonly seen in adults between the ages of 30 and 40.

**Microscopic Features**

Pseudosarcomatous reactive soft tissue lesions are cytologically characterized by a mixed and often polymorphic cellular pattern of proliferating cells [21, 74, 97]. In most instances, the cytologic pattern provides a definitive diagnosis:

- Hallmarks: Cytologic smears are usually cellular and composed of slender and plump fusiform fibroblasts/myofibroblasts bearing bland nuclei. Cells may be grouped in aggregates or occur in isolation. The overall cell pattern may appear polymorphic with articulate variations in cellular size and shape.
- Varying proportions of inflammatory cells are present and small drops of hyalin and myxoid masses may be observed.
- Specimens of *proliferative fasciitis (and myositis)* also include large plump cells with a rounded eccentrically positioned nucleus, a prominent nucleolus, and abundant amphophilic cytoplasm with long slender and interdigitating processes. The cells display morphologic similarities to ganglion cells and have been described as ganglion-like cells. The chromatin is fine, granular, and evenly distributed.

**Immunocytochemistry**

Immunocytochemical studies will aid in the final diagnosis: vimentin, smooth muscle actin (SMA), and muscle-specific actin decorate myofibroblasts. Antibodies against CD68 identify scattered histiocytes.

**Differential Diagnosis** [24, 27]

- Rich cellularity including dense clustering of spindle cells frequently lead to a misdiagnosis of schwannoma or other spindle cell lesions, mainly fibrous histiocytoma, solitary fibrous tumor, fibrosarcoma, leiomyoma, angiomyolipoma, and myofibroma. The immunocytochemical profile of nodular fasciitis differs from benign peripheral nerve sheath tumor (Schwannoma: S100 **+**, SMA –) and is helpful in reaching a conclusive diagnosis [50].
- Aggregates of spindle cells embedded in a myxoid background and pronounced plasmacytoid features of the epithelioid component may raise suspicions of pleomorphic adenoma [79].

#### 5.2.4.2.2 Proliferative Myositis [44] (Fig. 17.8)

This lesion also belongs to the group of pseudosarcomatous proliferative lesions of the soft tissue representing the intramuscular counterpart of proliferative fasciitis. Muscles of the trunk are normally affected, but the sternocleidomastoid muscle is rarely involved.

Pseudosarcomatous fibromatosis of the neck and neck muscles occurring in early childhood and older children may be a cause of pediatric torticollis; in many patients the lesion may be a late consequence of muscle injury during difficult delivery.

- The cytologic appearance is characteristic: proliferative myositis exhibits atrophic muscle fibers in addition to the typical morphologic features of nodular fasciitis.

Differential diagnoses are the same as discussed for proliferative fasciitis (see Sect. 5.2.4.2.1, above).

#### 5.2.4.2.3 Angiolymphoid Hyperplasia with Eosinophilia [6, 71]

- Synonyms: Angiofollicular hyperplasia with eosinophilia, epithelioid hemangioma, histiocytoid hemangioma, pseudopyogenic granuloma, papular angioplasia, inflammatory angiomatous nodule, among others.
- Angiolymphoid hyperplasia with eosinophilia (ALHE) is a condition that manifests in adults as plaques or nodules in the skin of the head and neck. Most patients present with lesions in the periauricular region, forehead, or scalp. The disorder is rarely observed in other sites of the body.
- It is controversial whether ALHE and Kimura disease represent the same entity. Recent studies argue that ALHE is an arteriovenous malformation with secondary inflammation, whereas Kimura disease may be a primary inflammatory process with secondary vascular proliferation [17].

**Microscopic Features and Immunocytochemistry**

- The smears are hypercellular and are composed of a mixed lymphoid population (small and intermediate lymphocytes, and immunoblasts) and eosinophilic infiltrates.
- Spindle-shaped and polygonal cells representing proliferative endothelial cells. Their nuclei are vesicular and the cytoplasm deeply eosinophilic. The endothelial nature of these cells can be demonstrated by positive factor VIII and CD31 immunoreactivity.
- Fragments of collagenous tissue may occur.

**Differential Diagnosis** [6]

- ALHE shares cytomorphologic characteristics with Kimura disease as well as low- and high-grade angiomatous tumors such as hemangioendothelioma and angiosarcoma.
  - Epithelioid endothelial cells may be misinterpreted as undifferentiated carcinoma cells. A combination of endothelial cell markers and cytokeratins can easily solve the problem using immunocytochemistry (endothelial cells: factor VIII and other endothelial markers **+**; cytokeratins **–** , carcinoma cells: factor VIII and other endothelial markers **–** ; cytokeratins **+**).
- An almost pure polymorphic lymphoid background may lead to a false diagnosis of reactive lymphadenopathy; scattered endothelial cells may mimic activated histiocytes.
- A pronounced mixed lymphoid cell population with a background of eosinophils and a few polyhedral mono- and binucleated endothelial cells may suggest Hodgkin lymphoma. In this setting, immunocytochemistry should provide a reliable diagnosis: CD15 and CD30 are specific immunomarkers for Hodgkin and Reed-Sternberg cells simultaneously exhibiting negative immunoreactivity for endothelial cell markers.
- Non-Hodgkin lymphoma is readily excluded by immunocytochemical or molecular clonality assessment.
- Langerhans cell histiocytosis (histiocytosis X) comprising dense lymphocytic infiltrates may be confused with ALHE. However, Langerhans cells showing abundant clear cytoplasm and pale nuclei with distinct indentations and grooves. CD1a and S100 protein are antigens typically presented by Langerhans cells and easily demonstrated by immunocytochemistry. Characteristic Birbeck granules included in the cytoplasm of Langerhans cells can be detected by electron microscopy.

## 5.2.5 Parathyroid Lesions (Figs. 4.72 and 4.73)

Nodular disorders of the parathyroid glands are often mistaken for thyroid tumors clinically and on imaging studies, especially when enlarged parathyroidal tissue is incorporated in, or in close vicinity to the thyroid gland. Enlarged parathyroid glands in the submandibular area may be considered as neck tumors of another origin, such as an enlarged lymph node or branchiogenic cyst.

Disorders of the parathyroid gland, its cytologic features, and differential diagnostic problems are extensively discussed in Sect. 4.2.12, p. 351.

**Caution**

- Cytologists should always be prepared for unforeseen parathyroid sampling. Cellular patterns of parathyroidal tissue strongly mimic those of thyroid tissue. The absence of colloid may be helpful in suggesting parathyroid tissue.
- Immunocytochemical staining of cytologic smears and biochemical analysis of parathyroid hormone levels in aspirates reliably serve as differentiating tools.

## 5.2.6 Benign and Malignant Neoplasms

### 5.2.6.1 Pilomatrixoma (Calcifying Epithelioma of Malherbe) (Figs. 16.5 and 16.6)

- Pilomatrixoma is a benign tumor of the hair follicle frequently seen in young people with a predilection for the head and neck area [18, 29] and the upper extremity. The tumor's cellular composition is highly characteristic, concurrently implying a high risk for misinterpretation.
- Cytology with its hallmarks, differential diagnostic challenges, and attendant references are highlighted in Sect. 16.2.6, p. 1028.

**Caution**

- A number of reports in the literature emphasize the high potential of pilomatrixoma masquerading as a malignant neoplasm, especially if tumors are located in unusual sites and present with exceptional clinical features (Fig. 16.7).
- A tentative cytodiagnosis of a subcutaneous small-cell malignant tumor should always include pilomatrixoma.
- A few cases of pilomatrix carcinoma of the head and neck have been reported in the literature [16]

### 5.2.6.2 Carotid Body Paraganglioma [32, 59] (Fig. 5.73)

Synonyms: Carotid body tumor, glomus tumor, chemodectoma, nonchromaffin paraganglioma.

- Carotid body tumors originate from the carotid glomus (a cluster of chemoreceptors and concomitant cells located near the bifurcation of the carotid artery). Pulsation of the nodule may suggest carotid body tumor.
- Several reports in the literature caution against aspiration of a suspected carotid body tumor presenting as a neck nodule. Local severe hemorrhage resulting from the aspiration may compress the artery followed by serious cerebral injury. We have no experience in this field, but we

agree with M.W. Stanley [87] that complications can be eliminated to a large extent by performing fine-needle aspiration using very thin needles, beyond 24-gauge.

**Microscopic Features and Immunocytochemistry**

The overall cellular pattern is considered to be most helpful in establishing a conclusive diagnosis; unfortunately the aspiration often fails to recover cellular material with the smears containing only blood.

- The smears reveal a sanguineous background and usually hypercellularity. They are composed of single cells, loose cell groups, and pseudorosettes including acinar structures.
- The cells vary in shape from round to fusiform:
  - *Chief cells* are polyhedral exhibiting moderate anisokaryocytosis. Considerable anisonucleosis and huge nuclei may be present in a number of cases.
  - *Supporting cells* are usually sparsely present and are distinctly spindle-shaped and small.
- The nuclei are round, ovoid, or crescent-shaped.
- The abundant cytoplasm is pale and poorly outlined, occasionally exhibiting variable granularity (eosinophilic in May-Grünwald-Giemsa stain).

- The cells of carotid body tumors immunocytochemically express vimentin and smooth muscle actin, and they are usually negative for cytokeratins, CD31, CD34, chromogranin, synaptophysin, neuron-specific enolase (NSE), and S100 protein.
- Supporting cells express S100 protein and glial fibrillary acidic protein.

**Differential Diagnosis**

- Carotid body tumors predominantly composed of a spindle cells may mimic fibrous and neural neoplasms as well as amelanotic spindle cell melanoma.
- Carotid body tumors showing epithelioid cell features and distinct cell clustering including microfollicular structures mimic thyroid carcinoma (immunostaining: TTF-1 **+**, thyroglobulin **+**), medullary variant of thyroid carcinoma (immunostaining: calcitonin **+**), neuroendocrine tumors, metastases of various large-cell carcinomas comprising clear cell features (immunostaining: cytokeratins **+**, if necessary tumor-typical markers **+**), and malignant melanoma (immunostaining: melanoma-typical markers **+**).

### 5.2.6.3 Merkel Cell Carcinoma (Fig. 16.16)

- Merkel cell carcinoma is a malignant cutaneous neoplasm showing neuroendocrine and epithelial differentiation. The tumor usually occurs in the dermis but sometimes in the subcutaneous tissue. Most frequent localization of the tumor is the skin of the face, neck, and extremities; an elderly population is affected by this lesion.
- The tumor has a striking tendency for local recurrence and spreading into regional lymph nodes, but distant metastases may occur as well.
- Cytomorphologic hallmarks, immunocytochemical properties, and differential diagnostic considerations are presented in Sect. 16.2.10, p. 1032.

**Caution**

- The cells of most Merkel cell carcinomas show intense immunocytochemical staining for cytokeratins and positive reactivity for neuroendocrine markers.
- Dot-like immunoreaction for CK20 is a characteristic feature of this tumor entity.
- In cytologic specimens, the following neoplasms may closely resemble Merkel cell carcinoma: metastatic small-cell carcinoma, neoplasms of the small round blue cell malignant tumor group, basal cell carcinoma, small-cell malignant melanoma, and malignant lymphoma.

## 5.2.7 Metastases in the Head and Neck Area (Selected Entities)

Common nonlymphoid immunocytochemical tumor cell markers having major diagnostic relevance are listed in Table 15.3.3 (Sect. 15.3.24, p. 978).

### 5.2.7.1 Cystic Neck Metastases

- Clinically, it is difficult to distinguish between a congenital cystic neck lesion and a cystic neck metastasis.
- Cystic degeneration of secondary malignancies located in head and neck lymph nodes is frequently encountered. The most frequent metastases with cystic alterations include squamous cell carcinoma, carcinoma of the thyroid, carcinoma of the salivary glands, and melanoma [19, 90].

**Caution**

Preoperative cytologic investigation of any cystic lesion in the neck area is of utmost importance in order to prevent inopportune primary surgical interventions. FNAB and US-FNAB is strongly recommended in this setting.

### 5.2.7.2 Squamous Cell Carcinoma and Its Variants

In most publications, squamous cell carcinoma (SCC) is stated to be the most frequent malignant diagnosis in FNABs obtained from head and neck masses. It is widely accepted that FNAB and not open biopsy should be used as initial in-

vestigation for SCCs in the neck area. Diagnostic sensitivity and specificity for this tumor type achieved between 90% and nearly 100% [72]. Most tumors are of the common types, namely keratinized SCC and poorly differentiated (nonkeratinizing) SCC, but occasional SCC variants can be a source of problems in proper tumor typing and grading [72]:

- *Nonkeratinizing SCC* cells (Fig. 5.74) can closely mimic the cells of poorly differentiated adenocarcinoma, large cell malignant lymphoma, malignant melanoma, and other more uncommon tumors. Appropriate immunocytochemical panels will solve the diagnostic problem in most cases. Differentiating immunocytochemical panels are provided in several chapters of this book. Of special interest might be p16-immunocytochemistry, whose positivity strongly indicates a HPV-associated SCC of the tonsils or oropharyngeal region.
- *Cystic SCC lymph node metastases* can lead to a misdiagnosis of benign cystic disease [14, 38, 62]:
  - In cases with hypocellularity of the cyst fluid.
  - In cases where unambiguously atypical cells, abnormal keratinization, and the characteristic necrotic debris are sparse or absent.
  - In cases where few scattered carcinoma cells are obscured by dense inflammatory infiltrates.

  More information on this subject and differential diagnoses are provided in Sect. 5.2.2.1.1, "Branchial Anomalies," p. 460.
- Metastases of two SCC variants whose primaries are typically located in the head and neck area may be responsible for diagnostic pitfalls:
  - *Well-differentiated SCC* (Figs. 5.75 and 5.76) may exhibit minimal cellular pleomorphism and merely squamous cells of the parakeratotic type (elongated densely keratinized cytoplasm and small darkly stained nuclei). See also Sects. 8.7.1 and 8.7.2, p. 568, and 16.2.8.2.1, p. 1030.
  - *SCCs with clear nuclei* (Fig. 2.37) comprising minor atypias and large, slightly eosinophilic cytoplasm may lack clear signs of malignancy. Paucity of cells will hamper a correct diagnosis of malignancy.
- *Spindle-cell squamous carcinoma* (Fig. 5.77) may foremost mimic mesenchymal spindle cell neoplasm and unpigmented spindle cell melanoma. Immunocytochemical staining is usually helpful in differentiating between the three entities; further information is given elsewhere in this book.
- *SCC associated with a strong granulomatous and foreign-body reaction* can be misinterpreted as benign reactive granulomatous pseudotumor or pilomatrixoma. Immunocytochemical staining for cytokeratins and CD68 can reliably assess the nature of isolated and loosely clustered polymorphous cells, respectively. The morphologic features of pilomatrixoma are highlighted inSect. 16.2.6, p. 1028.

**Caution**

- Benign cystic neck disorders may mimic squamous cell carcinoma if the aspirate provides atypical metaplastic squamous cells, extensive cellular debris, and inflammatory infiltrate [7, 8] (Figs. 5.65 and 5.66).
- Cystic fluid with abnormal squamous cells can be collected from a dermoid cyst, epidermal inclusion cyst, or an odontogenic neoplasm.
- Furthermore, squamous elements morphologically overlapping with SCC cells may be found in various cystic and solid salivary gland lesions [75] (see Sect. 5.1.3.2.1 "Squamous Cells," p. 405.).

### 5.2.7.3 Thyroid Carcinoma (Figs. 5.78 and 5.79)

A notable trend for regional lymphatic dissemination is well known in papillary carcinoma of the thyroid. In up to 50% of patients, affected regional lymph nodes can be found at the time of surgery.

Cervical lymph node metastases can be the initial sign of papillary thyroid carcinoma in patients with an occult small primary tumor.

Metastases of papillary thyroid carcinoma frequently show cystic changes.

#### Differential Diagnosis and Immunocytochemistry

- Some metastatic tumors can display overlapping cytomorphologic features with carcinoma of the thyroid (immunocytochemistry: TTF-1 **+**, thyroglobulin **+**), such as clear cell carcinoma of the kidney (immunocytochemistry: RCC Ma **+**, CD10 **+**), clear cell variant of breast carcinoma (immunocytochemistry: hormone receptors **+**), adenocarcinoma and bronchioloalveolar carcinoma of the lung (immunocytochemistry: lack of a particular immunopanel distinguishing thyroid carcinoma) and nonmelanotic malignant melanoma (immunocytochemistry: melanoma-typical markers **+**) (Figs. 5.79).
- On the other hand, histiocytic aggregates in cystic fluids of nonneoplastic lesions can mimic papillary thyroid carcinoma (immunocytochemistry: histiocytes are identified by CD68 immunostaining).

### 5.2.7.4 Breast Carcinoma

During the tumor progression of breast carcinoma, supraclavicular and retroclavicular lymph nodes are preferentially affected. Lymph node metastasis of breast cancer usually appears as a solid firm nodule. Cystic metastases may be confused with other secondary neoplasms, as specified above.

### 5.2.7.5 Lung Carcinoma (Other than Squamous Cell Carcinoma)

Small-cell carcinoma, poorly differentiated adenocarcinoma, and undifferentiated carcinoma of the lung may spread into both cervical lymph nodes and soft tissue spaces of the head and neck. The primary tumor diagnosis is established in a high percentage of the patients at the time of apparent metastases.

**Caution**

- Coincident subcutaneous pilomatrixoma should not be misinterpreted as soft tissue metastasis of an established small-cell carcinoma.
- Metastases of poorly differentiated lung carcinoma of the large-cell type may most of all be mistaken for nonpigmented malignant melanoma or large-cell malignant lymphoma (Fig. 5.74).

### 5.2.7.6 Malignant Melanoma (Figs. 5.80 and 5.81)

We emphasize the wide variability of cytologic patterns of malignant melanoma; the diagnostic challenge is substantial in amelanotic melanoma:

– Tumor cells may appear small or large, monomorphic or polymorphic, round, polygonal, polyhedral or fusiform.
– The cytoplasm can be small and densely structured, plasmacytoid, abundant and vacuolated, sharply outlined, or fading away.

**Microscopic Features**

Cytologic features supporting diagnosis of melanoma include:

- Mostly isolated tumor cells.
- Pale nuclei showing dense fine granular chromatin.
- Pronounced nuclear lobulation, and intranuclear cytoplasmic inclusions.
- Huge pleomorphic nucleoli.
- Few melanophores scattered in the background.

**Differential Diagnosis and Immunocytochemistry**

(Figs. 5.74, 5.77, 5.79, 5.81)

- Melan A, HMB-45, and tyrosinase supplemented by S100 protein are reliable immunocytochemical markers for the melanoma cell.
- A large variety of epithelial, mesenchymal, and lymphoid tumors must be taken into consideration. Differential diagnostic aspects are frequently discussed in this book. Common nonlymphoid immunocytochemical tumor cell markers having major diagnostic relevance are listed in Table 15.3.3 (Sect. 15.3.24, p. 978).

### 5.2.7.7 Lymphoepithelial Carcinoma

(Figs. 5.82–5.84)

Lymphoepithelial carcinoma (LEC) is an undifferentiated squamous cell carcinoma accompanied by a prominent lymphoplasmacytic infiltrate.

LEC typically is a primary tumor of the nasopharynx. Outside this area the tumor occurs rarely, but cervical lymph node metastases from overt or occult LEC are quite frequent and can easily be missed. See also Sect. 8.7.3, p. 568.

- Hallmarks of the epithelial tumor cells: Large undifferentiated malignant cells comprising vesicular lucid nuclei with marked irregular borders. The chromatin structure is indistinct. The nucleoli are variable in size and shape. The cytoplasm tends to be wide, clear, and delicate.
- Tumor cells can strongly mimic activated histiocytes and lymphoid/myeloid blasts.

**Caution**

Nodal metastasis of lymphoepithelial carcinoma is frequently difficult to ascertain in cytologic specimens: isolated histiocytoid and blast-like carcinoma cells scattered in a reactive lymphocytic background strongly mimic activated histiocytes and lymphoid blasts, respectively.

### 5.2.7.8 Occult Head and Neck Carcinoma with Cervical Lymph Node Metastases

Unknown primary cancer presenting as cervical lymph node metastasis accounts for around 5% of all head and neck neoplasms. More than 90% of these tumors are poorly differentiated squamous cell carcinoma originating in the nasopharyngeal area or the oral cavity [82]. Positive p16-immunocytochemistry strongly indicates a HPV-associated SCC of the tonsils or oropharyngeal region. The remaining tumors include adenocarcinoma of the thyroid and lung, malignant melanoma, and other rare entities.

Careful evaluation of the head and neck area, the oropharynx, and the lung by multiple diagnostic procedures (fiberoptic endoscopy, targeted biopsies from suspicious sites, and blind biopsies from areas known to be possible sites of primaries, imaging studies including positron emission tomography) will uncover many of the occult primaries [25, 45, 67].

**Caution**

Primary squamous cell carcinoma of the neck originating from a teratoma or branchial cleft cyst should not be disregarded.

## 5.2.8 Further Reading


1. Al-Khateeb TH, Al Zoubi F. Congenital neck masses: A descriptive retrospective study of 252 cases. J Oral Maxillofac Surg 2007;65:2242-2247.
2. Alvi A, Johnson JT. The neck mass. A challenging differential diagnosis. Postgrad Med 1995;97:87-90.
3. Anne S, Teot LA, Mandell DL. Fine needle aspiration biopsy: Role in diagnosis of pediatric head and neck masses. Int J Pediatr Otorhinolaryngol 2008;72:1547-1553.
4. Arabi H, Yousef N, Bandyopadhyay S, et al. Fine needle aspiration of head and neck masses in the operating room: accuracy and potential benefits. Diagn Cytopathol 2008;36:369-374.
5. Ashraf MJ, Azarpira N, Khademi B. Diagnosis of pleomorphic adenoma in a heterotopic salivary gland: a case report. Acta Cytol 2007;51:197-199.
6. Azarpira N, Ashraf MJ, Shishegar M. Fine needle aspiration findings in angiofollicular hyperplasia with eosinophilia. A case report. Acta Cytol 2008;52:220-222.
7. Babb MJ, Rasgon BM, Cruz RM, Rumore GJ. Submandibular gland squamous metaplasia mimicking recurrent squamous cell carcinoma: A diagnostic dilemma. Arch Otolaryngol Head Neck Surg 2002;128:1201-1203.
8. Ballo MS, Shin HJ, Sneige N. Sources of diagnostic error in the fine-needle aspiration diagnosis of Warthin's tumor and clues to a correct diagnosis. Diagn Cytopathol 1997;17:230-234.
9. Beatenburg de Jong RJ, Rongen RJ, Lameris JS, et al. Metastatic neck disease. Palpation vs. ultrasound examination. Arch Otolaryngol Head Neck Surg 1989;115:689-690.
10. Benhammou A, Benbouzid MA, Bencheikh R, et al. Hydatid cyst of the neck. B-ENT 2007;3:201-203.
11. Bhanote M, Yang GC. Malignant first branchial cleft cysts presented as submandibular abscess in fine-needle aspiration: Report of three cases and review of literature. Diagn Cytopathol 2008;36:876-881.
12. Bockmühl U, Petersen I. DNA ploidy and chromosomal alterations in head and neck squamous cell carcinoma. Virchows Arch 2002;441:541-550.
13. Brent Ponder T, Collins BT, Bee CS, et al. Diagnosis of cervical thymoma by fine needle aspiration biopsy with flow cytometry. A case report. Acta Cytol 2002;46:1129-1132.
14. Burgess KL, Hartwick RW, Bedard YC. Metastatic squamous carcinoma presenting as a neck cyst. Differential diagnosis from inflamed branchial cleft cyst in fine needle aspirates. Acta Cytol 1993;37:494-498.
15. Carson HJ, Taxy JB. Role of the autopsy in congenital cystic hygroma. Pediatr Pathol 1994;14:183-189.
16. Caubet Biayna J, Santiago Juan C, Ramos Asensio R, et al. Pilomatrix carcinoma of the face. Two case reports. Ann Otorhinolaringol Ibero Am 2000;27:137-143.
17. Chong WS, Thomas A, Goh CL. Kimura's disease and angiolymphoid hyperplasia with eosinophilia: two disease entities in the same patient: case report and review of the literature. Int J Dermatol 2006;45:139-145.
18. Chuang CC, Lin HC. Pilomatrixoma of the head and neck. J Chin Med Assoc 2004;67:633-636.
19. Cinberg J, Silver CE, Molnar JJ, Vogl SE. Cervical cysts: cancer until proven otherwise? Laryngoscope 1982;92:27-30.
20. Connolly AA, MacKenzie K. Pediatric neck masses – a diagnostic dilemma. J Laryngol Otol 1997;111:541-545.
21. Dahl I, Akerman M. Nodular fasciitis: a correlative cytologic and histologic study of 13 cases. Acta cytol 1981;25:215-223.
22. Daoud FS. Branchial cyst: an often forgotten diagnosis. Asian J Surg 2005;28:174-178.
23. Das DK. Cervicofacial Actinomycosis: Diagnosis by fine needle aspiration cytology. Acta Cytol 1989;33:278-280.
24. Dayan D, Nasrallah V, Vered M. Clinico-pathologic correlations of myofibroblastic tumors of the oral cavity: 1. Nodular fasciitis. J Oral Pathol Med 2005;34:426-435.
25. de Brand F, al-Sarraf M. Diagnosis and management of squamous cell carcinoma of unknown primary tumor site of the neck. Semin Oncol 1993;20:273-278.
26. Deshpande AH, Nayak S, Munshi MM, Bobhate SK. Kimura's disease: Diagnosis by aspiration cytology. Acta Cytol 2002;46:357-363.
27. Dodd LG, Martinez S. Fine-needle aspiration cytology of pseudosarcomatous lesions of soft tissue. Diagn Cytopathol 2001;24:28-35.
28. El Hag IA, Chiedozi LC, Al Reyees FA,Kollur SM. Fine needle aspiration cytology of head and neck masses. Seven years' experience in a secondary care hospital. Acta Cytol 2003;47:387-392.
29. El Hag IA, Kollur SM. Fine needle aspiration cytology of pilomatrixoma of the neck region: differentiation from metastatic undifferentiated nasopharyngeal carcinoma. Acta Cytol 2003;47:526-528.
30. Elmasalme F, Giacomantonio M, Clarke KD, et al. Congenital cervical teratoma in neonates. Case report and review. Eur J Pediatr Surg 2000;10:252-257.
31. Engzell U, Zajicek J. Aspiration biopsy of tumors of the neck I. Aspiration biopsy and cytologic findings in 100 cases of congenital cysts. Acta Cytol 1970;14:51-57.
32. Engzell U, Franzen S, Zajicek J. Aspiration biopsy of tumors of the neck. II. Cytologic findings in 13 cases of carotid body tumor. Acta Cytol 1971;15:25-30.
33. Foley DS, Fallat ME. Thyroglossal duct and other congenital midline cervical anomalies. Semin Pediatr Surg 2006;15:70-74.
34. Frierson HF Jr. Cysts of the head and neck sampled by fine-needle aspiration. Sources of diagnostic difficulty. Am J Clin Pathol 1996;106:559-560.
35. Fulciniti F, Califano L, Zupi A, Vetrani A. Accuracy of fine needle aspiration biopsy in head and neck tumors. J Oral Maxillofac Surg 1997;55:1094-1097.
36. Gidvani VK, Bhowmick SK. Midline posterior cervical cystic hygroma. South Med J 1999;92:340-343.
37. Gonzales J, Ljung BM, Guerry T, Schoenrock LD. Congenital torticollis: evaluation by fine-needle aspiration biopsy. Laryngoscope 1989;99:651-654.
38. Gourin CG, Johnson JT. Incidence of unsuspected metastases in lateral cervical cysts. Laryngoscope 2000;110:1637-1641.
39. Hasiotou M, Vakaki M, Pitsoulakis G, et al. Congenital cervical teratomas. Int J Pediatr Otorhinolaryngol 2004;68:1133-1139.
40. Hass HG, Schmidt A, Nehls O, Kaiser S. DNA ploidy, proliferative capacity and intratumoral heterogeneity in primary and recurrent head and neck squamous cell carcinomas (HNSCC) – potential implications for clinical management and treatment decisions. Oral Oncol 2008;44:78-85.
41. Hatada T, Ichii S, Sagayama K, et al. Intrathyroid thyroglossal duct cyst simulating a thyroid nodule. Tumori 2000;86:250-252.
42. Horn KD, Fowler JC, Carrau R, et al. Cytokeratin immunophenotyping of an unusual cervical vertebral chordoma with extensive chondroid foci and perilaryngeal recurrence: a case report with review of the literature. Am J Otolaryngol 2001;22:428-434.
43. Howlett DC, Harper B, Quante M, et al. Diagnostic adequacy and accuracy of fine needle aspiration cytology in neck lump assessment: results from a regional cancer network over a one year period. J Laryngol Otol 2007;121:571-579.
44. Jacobs JC. Aspiration cytology of proliferative myositis. A case report. Acta Cytol 1995;39:535-538.
45. Jereczek-Fossa BA, Jassem J, Orecchia R. Cervical lymph node metastases of squamous cell carcinoma from unknown primary. Cancer Treat Rev 2004;30:153-164.
46. Kay PA, Nascimento AG, Unni KK; Salomao DR. Chordoma. Cytomorphologic findings in 14 cases diagnosed by fine needle aspiration. Acta Cytol 2003;47:202-208.

47. Kimura T, Yoshimura S, Ishikawa E. On the unusual granulation combined with hyperplastic changes of lymphatic tissue. Trans Soc Pathol Jpn 1948;37:179-180.
48. Kocjan G, Ramsay A, Beale T, O'Flynn P. Head and Neck cancer in the UK: what is expected of cytopathology. Cytopathol 2009;20:69-77.
49. Koeller KK, Alamo L, Adair CF, Smirniotopoulos JG. Congenital cystic masses of the neck: radiologic-pathologic correlation. Radiographics 1999;19:121-146.
50. Kong CS, Cha I. Nodular fasciitis: diagnosis by fine needle aspiration biopsy. Acta Cytol 2004;48:473-477.
51. Kountakis SE, Minotti AM, Maillard A, Stiernberg CM. Teratomas of the head and neck. Am J Otolaryngol 1994;15:292-296.
52. Langlois NE, Kolhe P. Plunging ranula: a case report and literature review. Hum Pathol 1992;23:1306-1308.
53. Layfield LJ. Fine-needle aspiration of the head and neck. Pathology (Phila) 1996;4:409-438.
54. Lecanu JB, Gallas D, Biacabe B, Bonfils P. Lymphocele of the thoracic duct presenting as a left supraclavicular mass: a case report and review of the literature. Auris Nasus Larynx 2001
55. Marsot-Dupuch K, Levret N, Pharaboz C, et al. Congenital neck masses: Embryonic origin and diagnosis. Report of the CIREOL. J Radiol 1995;76:405.
56. McIvor NP, Freeman JL; Salem S, et al. Ultrasonography and ultrasound-guided fine-needle aspiration biopsy of head and neck lesions: a surgical perspective. Laryngoscope 1994;104:669-674.
57. Milde P, Sidawy MK. Thymoma presenting as a palpable thyroid nodule: a pitfall in fine needle aspiration (FNA) of the neck. Cytopathology 1999;10:415-419.
58. Milroy CM, Ferlito A, Devaney KO, Rinaldo A. Role of DNA measurements of head and neck tumors. Ann Otol Rhinol Laryngol 1997;106:801-804.
59. Monabati A, Hodjati H, Kumar PV. Cytologic findings in carotid body tumors. Acta Cytol 2002;46:1101-1104.
60. Moriki T, Takahashi T, Wada M, et al. Chondroid chordoma: fine-needle aspiration cytology with histopathological, immunohistochemical, and ultrastructural study of two cases. Diagn Cytopathol 1999;21:335-339.
61. Mueller JS, Schultenover S, Simpson J, et al. Value of rapid assessment cytology in the surgical management of head and neck tumors in a Nigerian mission hospital. Head Neck 2008;30:1083-1085.
62. Nasuti JF, Braccia MG, Roberts S, Baloch ZW. Utility of cytomorphologic criteria and p53 immunolocalization in distinguishing benign from malignant cystic squamous-lined lesions of the neck on fine-needle aspiration. Diagn Cytopathol 2002;27:10-14.
63. Newkirk KA, Tassler AB, Krowiak EJ, Deeb ZE. Bronchogenic cysts of the neck in adults. Ann Otol Rhinol Laryngol 2004;113:691-695.
64. Nijhawan VS, Rajwanshi A, Das A, et al. Fine needle aspiration cytology of sacrococcygeal chordoma. Diagn Cytopathol 1989;5:404-407.
65. Nordemar S, Tani E, Högmo A, et al. Image cytometric DNA-analysis of fine needle aspiration cytology to aid cytomorphology in the distinction of branchial cleft cyst from cystic metastasis of squamous cell carcinoma: a prospective study. Laryngoscope 2004;114:1997-2000.
66. O'Donnell ME, Salem A, Badger SA, et al. Fine needle aspiration at a Regional Head and Neck Clinic: A clinically beneficial and cost-effective service. Cytopathology 2009;20:81-86.
67. O'Mara W, Butler NN, Nemechek AJ. Carcinomas of unknown primary in the head and neck. J La State Med Soc 2001;153:341-346.
68. Otto RA, Bowes AK. Neck masses: benign or malignant? Sorting out the causes by age-group. Postgrad Med 1990;88:199-204.
69. Oyafuso MS, Longatto Filho A, Ikeda MK. The role of fine needle aspiration cytology in the diagnosis of lesions of the head and neck excluding the thyroid and salivary glands. Tumori 1992;78:134-136.
70. Pereira S, Tani E, Skoog L. Diagnosis of fibromatosis colli by fine needle aspiration (FNA) cytology. Cytopathology 1999;10:25-29.
71. Pettinato G, Insabato L, De Chiara A, et al. Fine-needle aspiration cytology of angiolymphoid hyperplasia with eosinophilia: a case report with electron microscopy and immunohistochemistry. Diagn Cytopathol 1989;5:88-94.
72. Pisharodi LR. False negative diagnosis in fine-needle aspirations of squamous-cell carcinoma of head and neck. Diagn Cytopathol 1997;17:70-73.
73. Plaza JA, Ballestin C, Perez-Barrios A, et al. Cytologic, cytochemical, immunocytochemical and ultrastructural diagnosis of a sacrococcygeal chordoma in a fine needle aspiration biopsy specimen. Acta Cytol 1989;33:89-92.
74. Raab SS, Silverman JF, McLeod DL, et al. Fine needle aspiration biopsy of fibromatoses. Acta Cytol 1993;37:323-328.
75. Ramzy I, Rone R, Schantz D. Squamous cells in needle aspirates of subcutaneous lesions: A diagnostic problem. Am J Clin Pathol 1986;85:319-324.
76. Rapkiewicz A, Thuy Le B, Simsir A, et al. Spectrum of head and neck lesions diagnosed by fine-needle aspiration cytology in the pediatric population. Cancer 2007;111:242-251.
77. Robbins KT, van Sonnenberg E, Casola G, Varney RR. Image-guided needle biopsy of inaccessible head and neck lesions. Arch Otolaryngol Head Neck Surg 1990;116:957-961.
78. Rottey S, Petrovic M, Bauters W, et al. Evaluation of metastatic lymph nodes in head and neck cancer: a comparative study between palpation, sonography, ultrasound-guided fine needle aspiration cytology and computed tomography. Acta Clin Belg 2006;61:236-241.
79. Saad RS, Takei H, Lipscomb J, Ruiz B. Nodular fasciitis of parotid region: a pitfall in the diagnosis of pleomorphic adenomas on fine-needle aspiration cytology. Diagn Cytopathol 2005;33:191-194.
80. Saggese D, Ceroni Compadretti G, Cartaroni C. Cervical ectopic thymus: a case report and review of the literature. Int J Pediatr Otorhinolaryngol 2002;66:77-80.
81. Sauer T, Selmer L, Freng A. Cytologic features of fibromatosis colli of infancy. Acta Cytol 1997;41:633-635.
82. Schmalbach CE, Miller FR. Occult primary head and neck carcinoma. Curr Oncol Rep 2007;9:139-146.
83. Shaffer MM, Oertel YC, Oertel JE. Thyroglossal duct cysts: diagnostic criteria by fine-needle aspiration. Arch Pathol Lab Med 1996;120:1039-1043.
84. Shahin A, Burroughs FH, Kirby JP, Ali SZ. Thyroglossal duct cyst: a cytopathologic study of 26 cases. Diagn Cytopathol 2005;33:365-369.
85. Sharma S, Mishra K, Khanna G. Fibromatosis colli in infants. A cytologic study of eight cases. Acta Cytol 2003;47:359-362.
86. Sheahan P, Fitzgibbon J, O'Leary G, Lee G. Efficacy and pitfalls of fine needle aspiration in the diagnosis of neck masses. Surgeon 2004;2:152-156.
87. Stanley MW. Selected problems in fine needle aspiration of head and neck masses. Mod Pathol 2002;15:342-350.
88. Tunkel DE, Erozan YS, Weir EG. Ectopic cervical thymic tissue: diagnosis by fine needle aspiration. Arch Pathol Lab Med 2001;125:278-281.
89. Turkyilmaz Z, Karabulut R, Bayazit YA, et al. Congenital neck masses in children and their embryologic and clinical features. B-Ent 2008;4:7-18.
90. Ustün M, Risberg B, Davidson B, Berner A. Cystic change in metastatic lymph nodes: a common diagnostic pitfall in fine-needle aspiration cytology. Diagn Cytopathol 2002;27:387-392.
91. van den Brekel MW, Castelijns JA, Stel HV, et al. Modern imaging techniques and ultrasound-guided aspiration cytology for the assessment of neck metastases: a prospective comparative study. Eur Arch Otorhinolaryngol 1993;250:11-17.
92. Van Vuuren PA, Balm AJ, Gregor RT, et al. Carcinoma arising in thyroglossal remnants. Clin Otolaryngol Allied Sci 1994;19:509-515.

93. Vengrove MA, Schimmel M, Atkinson BF, et al. Invasive cervical thymoma masquerading as a solitary thyroid nodule. Report of a case studied by fine needle aspiration. Acta Cytol 1991;35:431-433.
94. Walaas L, Kindblom LG. Fine-needle aspiration biopsy in the preoperative diagnosis of chordoma: a study of 17 cases with application of electron microscopic, histochemical, and immunocytochemical examination. Hum Pathol 1991;22:22-28.
95. Witcher TP, Williams MD, Howlett DC. "One-stop" clinics in the investigation and diagnosis of head and neck lumps. Brit J Oral Maxillofac Surg 2007;45:19-22.
96. Wong KT, Lee YY, King AD, Ahuja AT. Imaging of cystic or cystlike neck masses. Clin Radiol 2008;63:613-622.
97. Wong NL. Fine needle aspiration cytology of pseudosarcomatous reactive proliferative lesions of soft tissue. Acta Cytol 2002; 46:1049-1055.

**Figs. 5.63 and 5.64 Branchial cleft cyst.**
Two patients presenting with a cystic lesion on the side of their neck. Direct smears were prepared from the sediment of centrifuged aspirated fluid and then Pap-stained.
*Cytologic and histologic diagnoses:* branchial cleft cyst.

**Fig. 5.63** (case #1) Keratinized and nonkeratinized superficial squamous cells originating from the innermost layer of the cyst. Note mild nuclear irregularities and occasional nucleoli. Epithelial cells are scattered in a cystic background composed of debris and foam cells (higher magnification).



**Fig. 5.64** (case #2) The second aspirate originates from a lateral neck cyst lined with ciliated columnar epithelium (arrows). Foam cells, inflammatory cells, and a few squames (not shown) are embedded in a proteinaceous granular background (higher magnification).

**Figs. 5.65 and 5.66 Branchial cleft cyst versus differentiated squamous cell carcinoma.**
FNABs of two cystic neck lesions presenting with atypical squamous cells. Direct smears were prepared from the fluid sediment and Pap-stained.
*Tissue diagnosis in both cases:* branchial cleft cyst lined with regenerative squamous epithelium.

**Fig. 5.65** (case #1) Aspirates from the first patient show numerous nonkeratinized and keratinized atypical squamous cells. Nuclei and cytoplasm are irregular in shape, but chromatin is loose. Small but indistinct nucleoli are present. Background showing an increased number of neutrophils (high magnification).
*Tentative cytologic diagnosis:* most likely inflammatory branchial cleft cyst accompanied by reactive epithelial atypias. Well-differentiated squamous cell carcinoma cannot be completely excluded.

**Fig. 5.66** (case #2) The second aspirate showed numerous pleomorphic squames markedly keratinized and usually anucleated. Background contained many neutrophilic granulocytes. Note occasional squamous cells showing clear nucleoplasm, wrinkled nuclear membranes (arrows), and concentrically laminated cyanophilic cytoplasm (arrowheads) (high magnification). All these cell features may be indicative of low-grade squamous neoplasia.
*Cytology* suggested well-differentiated squamous cell carcinoma. We restrained from rendering a conclusive diagnosis due to the strong concomitant acute inflammatory process.

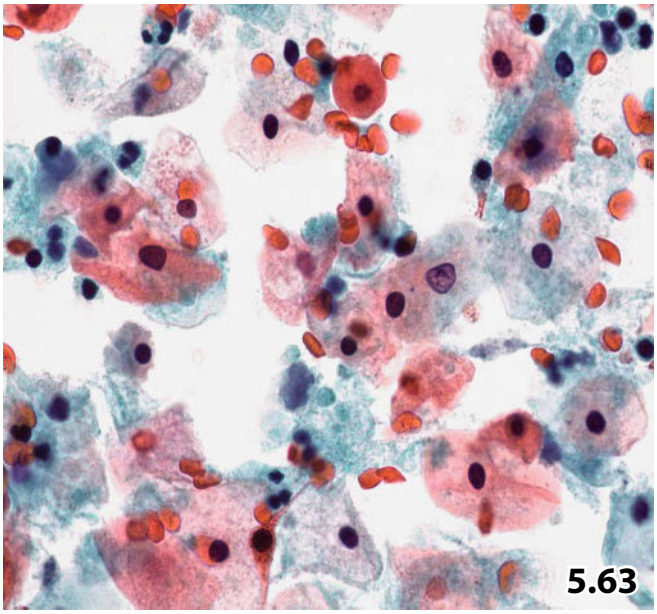
5.63

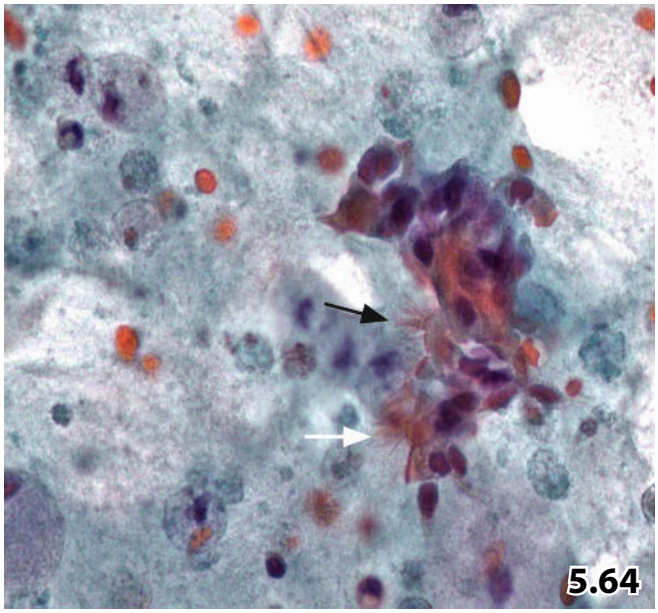
5.64

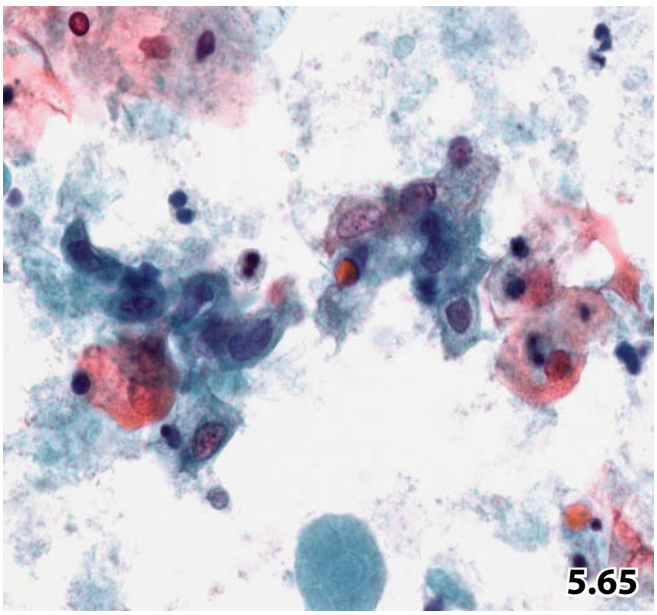
5.65

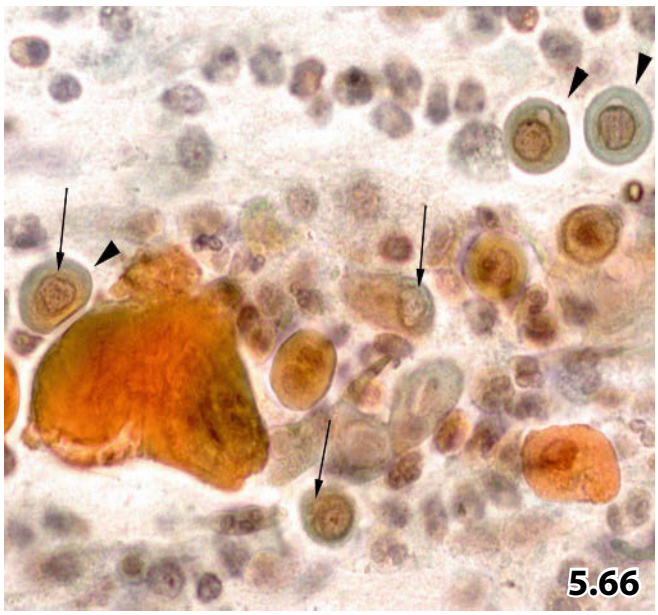
5.66

**Fig. 5.67 Thyroglossal duct cyst.**
Aspirated fluid from a cyst in the midline of the neck of a middle-aged woman contains numerous ciliary tufts (arrows), degenerating ciliated columnar cells, and foam cells scattered in a granular background. Squamous cells may occasionally be encountered (direct sediment smear, Pap stain, high magnification). There is no histology available.

**Fig. 5.68 Lymphocele/lymphangioma.**
A 79-year-old man presented with a voluminous cystic lesion on the left side of his neck. Direct sediment smears of the aspirate exhibited numerous monomorphic benign lymphocytes (Pap stain, higher magnification). Pay attention to occasional pronounced nucleoli (arrows) being a common feature of lymphoid cells that are stored in liquid medium. Nuclear irregularities and delicate cytoplasms are caused by degeneration. No endothelial cells could be observed.
*Cytologic and histologic diagnosis:* lymphangioma.

**Fig. 5.69 Mycotic aneurysm.**
A 63-year-old man presented with a voluminous tumor mass on the right side of his neck. Physical examination and imaging supported the diagnosis of a necrotic metastasis obviously caused by an occult primary tumor elsewhere. FNAB was performed as an initial diagnostic test. Direct sediment smears from the aspirated fluid were composed of degenerating neutrophils, detritus, and erythrocytes (MGG stain, lower magnification). Atypical cells of both epithelial and mesenchymal origin were completely absent.
*Tentative cytologic diagnosis:* tumor necrosis accompanied by an inflammatory component.
*Tissue diagnosis:* mycotic aneurysm of the carotid artery.

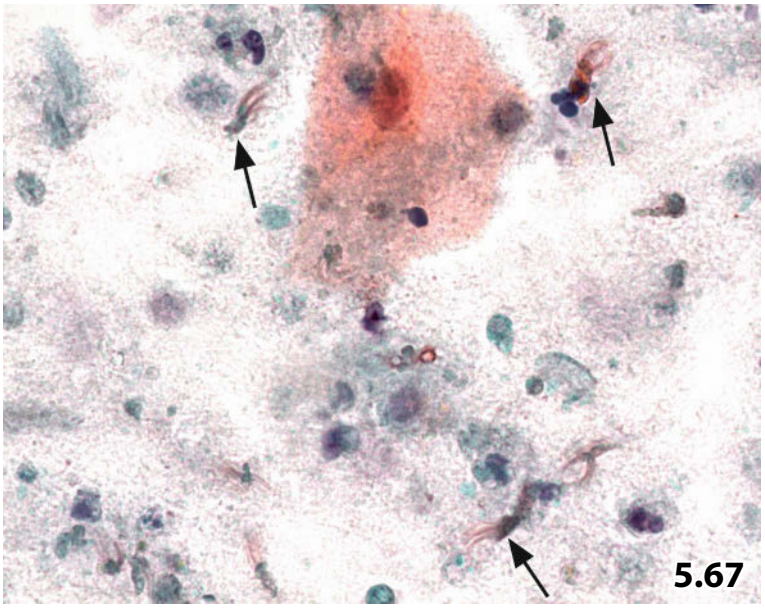
5.67

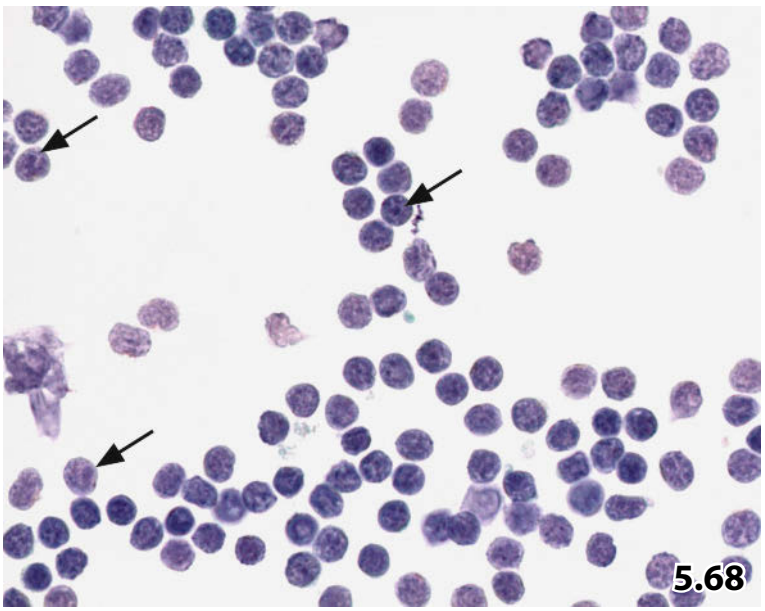
5.68

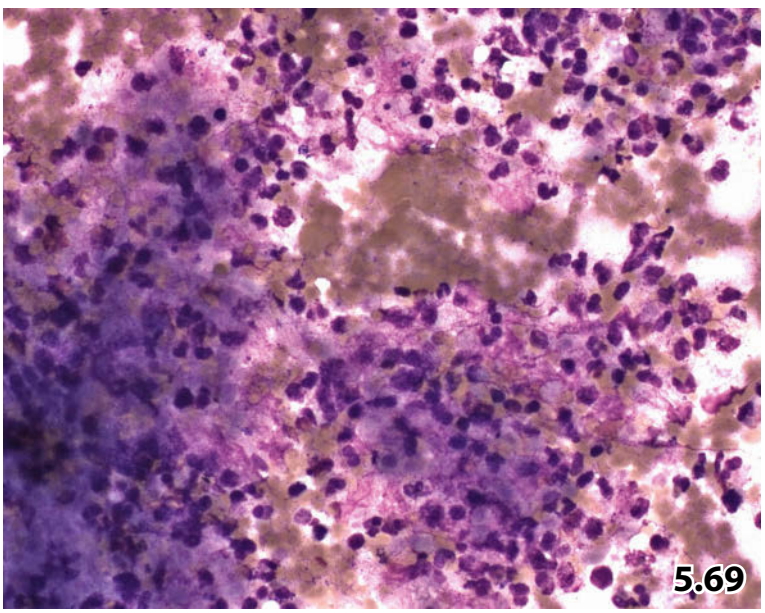
5.69

**Fig. 5.70 Chondroma.**
A firm nodule of the neck in a 55-year-old man was explored with FNAB. Aspirates of chondromas usually yield few fragments of hyaline chondroid tissue and scattered chondrocytes (direct smear, Pap stain, high magnification).

**Fig. 5.71A–C Chordoma.**
Computed tomography in a 58-year-old man revealed a deeply located cervical tumor (10 cm in its greatest diameter) associated with disintegration of the cervical spine. CT-guided FNAB was performed. Direct smears were Pap-stained.
*Cytologic and histologic diagnosis:* chordoma.
**A** High magnification highlights the typical physaliferous cells frequently exhibiting a finely vacuolated cytoplasm. The nuclei are irregular in size and shape but their chromatin is bland. Myxoid background is not shown. **B** Strong immunoreactivity for pancytokeratin: MNF116 (Pap-prestained direct smear). Only a small percentage of the physaliferous cells exhibited positive immunoreaction for CK5/6 (not shown). **C** Coexpression of Vimentin (Pap-prestained direct smear).

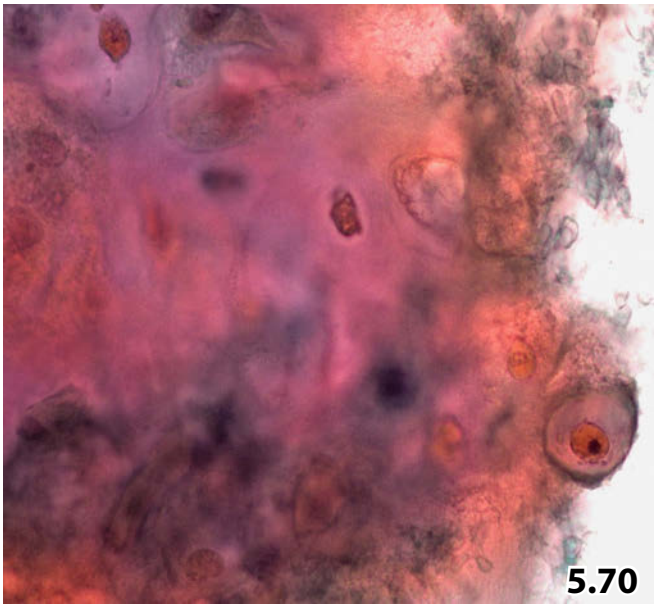
5.70

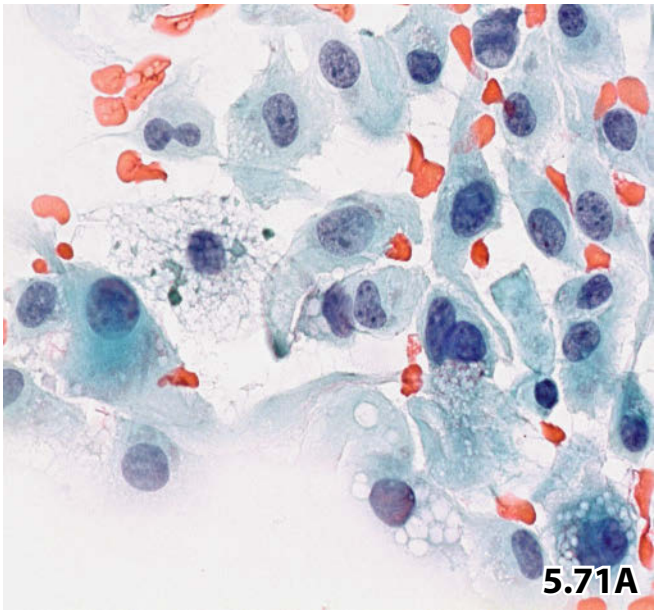
5.71A

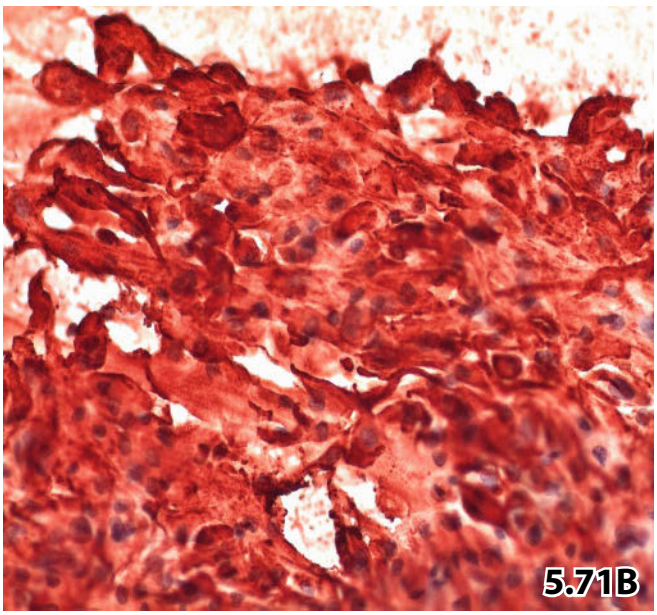
5.71B

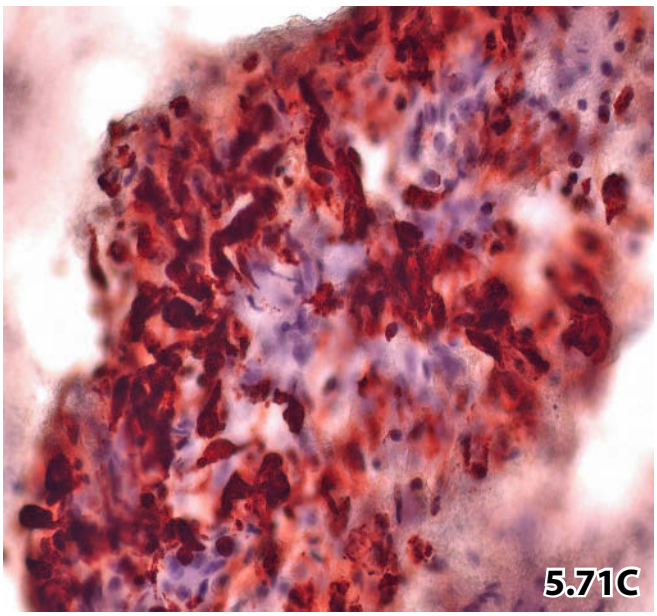
5.71C

**Fig. 5.72 Actinomycosis.**
A 55-year-old woman presented with a steadily increasing swelling in her right neck area. Image studies revealed invasive growth. FNAB showed balls of actinomyces embedded in a purulent inflammatory background. Radiating delicate filaments are seen at the lower periphery of the bacterial cluster (direct smear, Pap stain, high magnification).

**Fig. 5.73A, B Paraganglioma.**
A 71-year-old man presented with a tumorous lesion in the left parotid gland steadily increasing in size over the past few years. Strong vascularization of the lesion in combination with recent palsy of the vagus nerve led to clinical suspicion of paraganglioma. FNAB was performed. Direct smears were Pap-stained. **A** Low magnification shows the classic heterogeneous appearance of paraganglioma: loose cell clustering, pronounced anisokariocytosis, round and spindle-shaped cells. **B** Cytologic key features are presented at high magnification. Note in particular the abundant and distinct granular cytoplasm and the huge tumor cells.

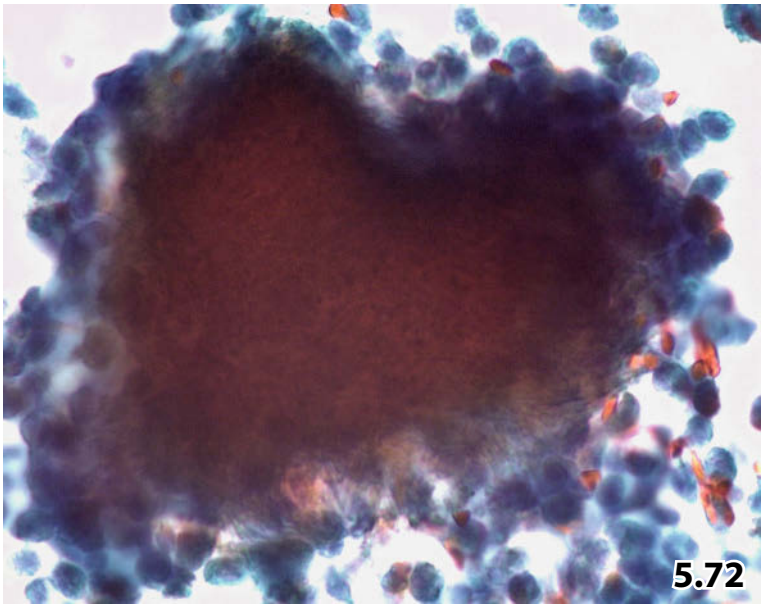

5.72

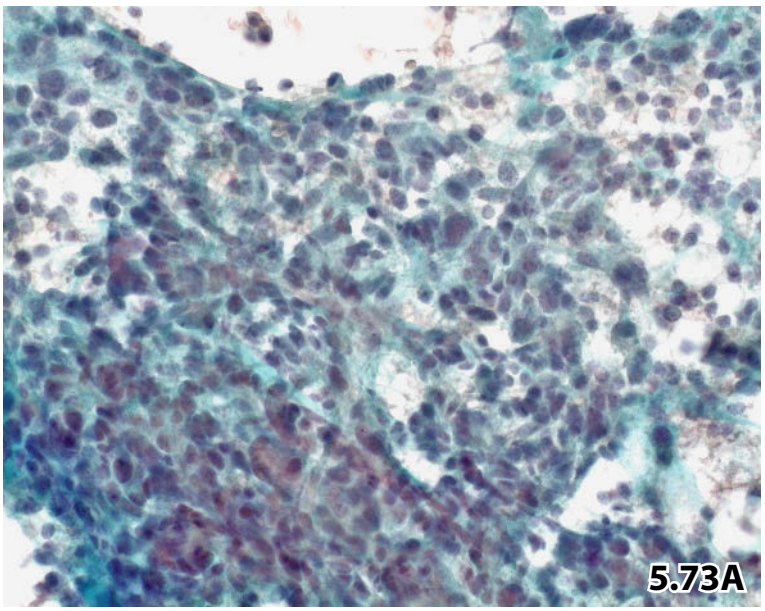

5.73A

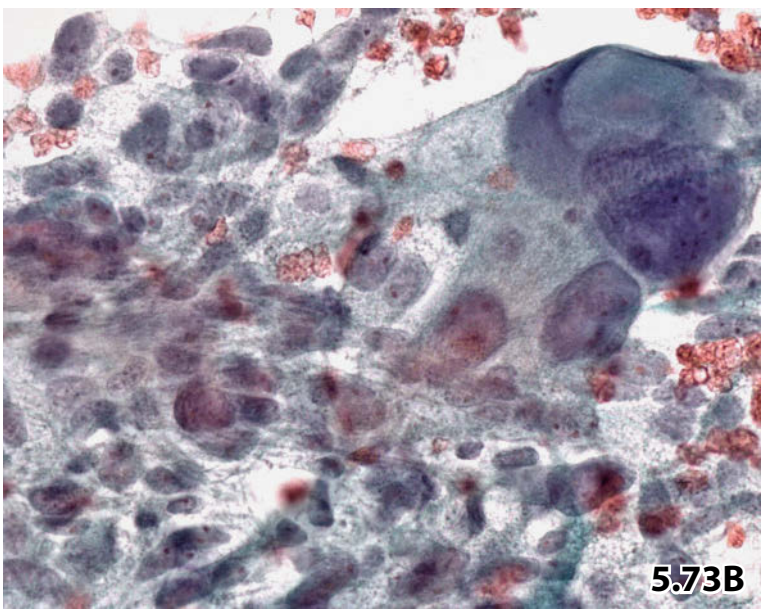

5.73B

**Figs. 5.74–5.77 Variants of squamous cell carcinoma.**
Certain variants of squamous cell carcinoma (SCC) can present diagnostic dilemmas. Various SCC subtypes (four different patients) are presented below. All direct smears were Pap-stained. In each case, diagnosis of SCC was confirmed by histology.

**Fig. 5.74** (case #1) Poorly differentiated nonkeratinized SCC.
FNAB of an enlarged lymph node in the neck area of an elderly woman. High magnification shows pleomorphic malignant cells, which usually are dissociated. Tumor cells exhibit both rounded and fusiform cytoplasm of varying size.
*Tentative cytologic diagnosis:* anaplastic large-cell carcinoma, possibly nonkeratinized SCC.
*Differential diagnostic consideration:* undifferentiated carcinoma, malignant melanoma, blastic non-Hodgkin lymphoma (note interspersed small lymphocytes as a potential indicator of malignant lymphoma! (arrows)). The epithelial nature of the tumor cells was verified by positive immunostaining for pancytokeratin-Lu-5 (not shown).
*Tissue diagnosis* (surgical biopsy of a pharyngeal lesion): poorly differentiated, nonkeratinizing SCC.

**Fig. 5.75** (case #2) Keratinized SCC.
FNAB of a relapsing swelling in the left submandibular region in a 71-year-old woman. Lower magnification exhibits numerous anucleated and occasional nucleated squames, mostly with keratinized cytoplasm. The cells are scattered in a cystic background composed of foam cells and debris. Cellular atypias are mild (polymorphous cytoplasm and slightly enlarged dark nuclei). Distinct malignant features are not encountered.
A *cytologic report* of squamoid lesion indeterminate for malignancy was provided.
*Differential diagnostic consideration:* branchial cleft cyst versus well-differentiated SCC.
*Tissue diagnosis* (excisional biopsy): keratinized SCC. Site of the primary tumor remained unclear.

**Fig. 5.76** (case #3) Keratinized SCC.
FNAB of a supraclavicular lymph node in a 62-year-old man. Abundant keratinized anucleated and nucleated cells revealing pronounced cytoplasmic pleomorphism. Pearl formation is also present. A few squamous cells with minor nuclear atypias such as irregular nuclear border, variation in size, and hyperchromasia (high magnification).
*Tentative cytologic diagnosis:* first and foremost suspicion of well-differentiated SCC.
*Differential diagnostic consideration:* branchial cleft cyst is most unlikely due to the absence of cystic background.
*Tissue diagnosis* (autopsy result): keratinized SCC metastatic to cervical lymph nodes. The primary tumor site could not be assessed.

**Fig. 5.77** (case #4) Spindle cell SCC.
FNAB of a right lateral neck mass in a middle-aged male patient. Spindle-shaped cells occur dissociated or grouped in tight clusters. Nuclear shape and chromatin texture are comparatively bland (higher magnification).
*Tentative cytologic diagnosis:* most likely variant of a primary salivary gland neoplasm composed of fusiform cells.
*Differential diagnostic consideration:* salivary gland tumor variants such as cellular type of pleomorphic adenoma, mucoepidermoid carcinoma, myoepithelial tumor, and others; and secondary neoplasms (spindle cell SCC, nonpigmented spindle cell malignant melanoma, and others). SCC may be suspected due to clusters composed of spindle cells showing well-defined cytoplasmic margins and streaming pattern arrangement (arrows).
*Tissue diagnosis* (excision of a lymph node): poorly differentiated SCC.

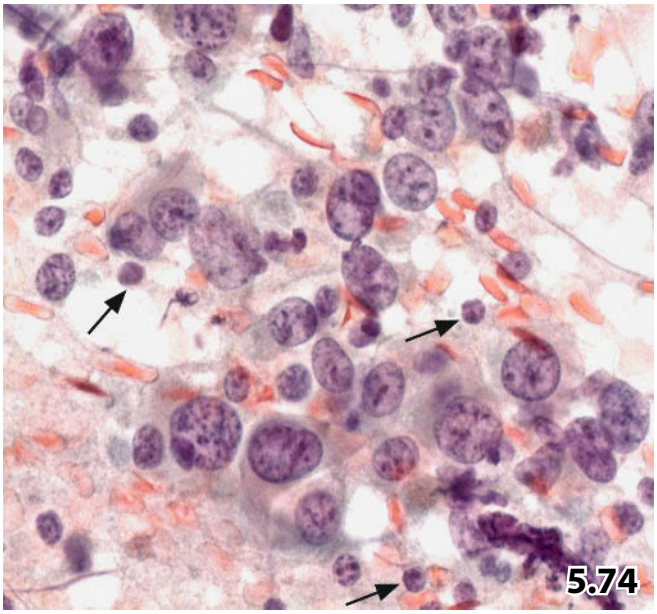
5.74

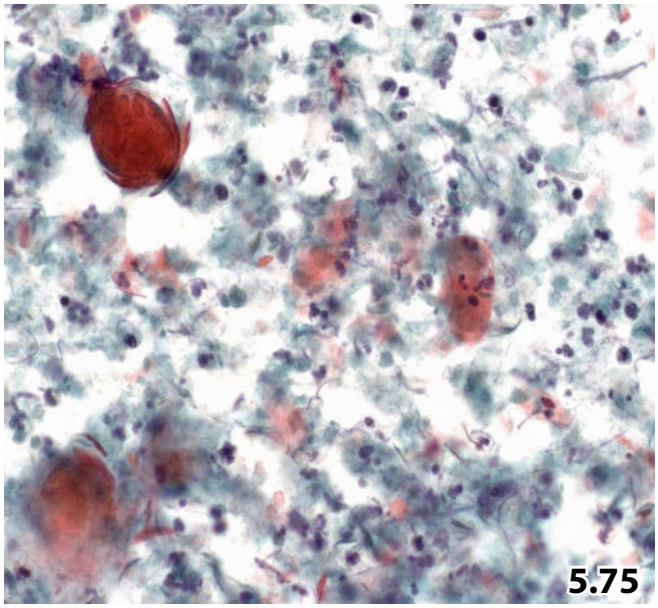
5.75

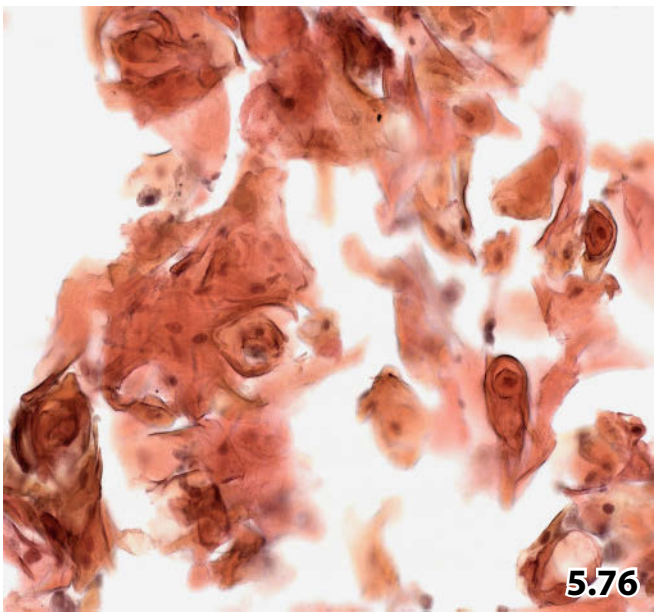
5.76

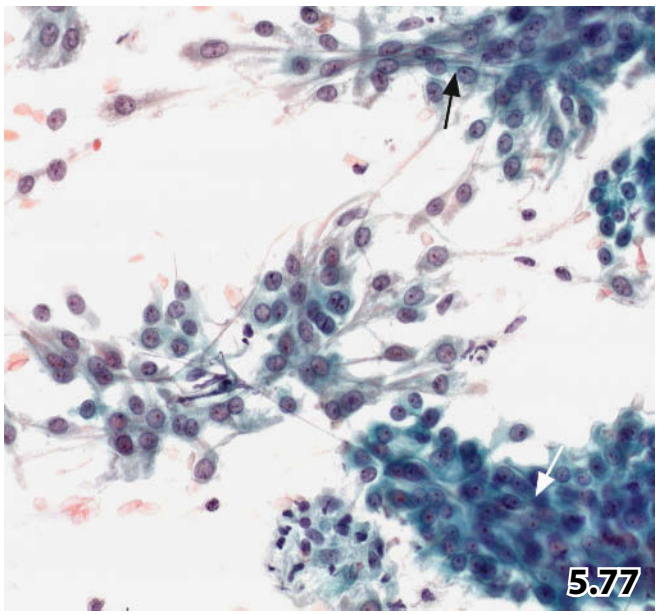
5.77

**Fig. 5.78 Papillary thyroid carcinoma.**
Positron emission tomographic (PET) examination showed multiple positive nodules in a variety of anatomical sites in an 81-year-old woman with no history of malignancy. US-guided FNAB of a PET-positive cervical lesion was performed. Aspiration material was prepared using the liquid-based (ThinPrep) technique. High magnification shows a compact papilliform sheet. The epithelial cells exhibit (1) eccentrically located nuclei, (2) nuclear molding, cleaving and grooves, and (3) a loose chromatin pattern (Pap stain).
*Cytologic diagnosis:* metastasis of a papillary thyroid carcinoma. The thyroid origin of the tumor cells was verified by positive immunostaining for TTF-1 (not shown).
*Comment:* similar cytologic features may be found in breast carcinomas (TTF-1 negative).
*Tissue diagnosis:* thyroid tissue examination revealed a small papillary thyroid carcinoma.



**Fig. 5.79A, B Medullary thyroid carcinoma.**
A 40-year-old man with no particular clinical history presenting with enlarged cervical lymph nodes. FNAB was performed. Direct smears were Pap- and MGG-stained. **A** High magnification shows mainly dissociated large malignant cells with polyhedral cytoplasm. The latter exhibits granular features to some extent (arrows) (MGG stain). **B** Specific cell type was verified by positive immunostaining for calcitonin on a Pap-prestained conventional smear.
*Cytologic diagnosis:* metastasis of a medullary thyroid carcinoma.
*Comment:* medullary thyroid carcinoma may mimic undifferentiated large-cell neoplasms (epithelial or mesenchymal) and malignant melanoma.

**Figs. 5.80 Malignant melanoma: classic cytologic features.**
FNAB of an enlarged cervical lymph node from a patient with a positive history of malignant melanoma. Direct smears are Pap-stained. Classical features of malignant melanoma cells are highlighted: low N/C ratio, granular chromatin, nuclear cytoplasmic inclusions, pronounced nucleoli, multinucleation, spindle-shaped tumor cells, melanin pigment (arrows) (higher magnification).

**Fig. 5.81A, B Spindle cell malignant melanoma: diagnostic challenge.**
A 54-year-old man with a positive history of malignant melanoma presented with a nodular lesion of the neck. Direct smears from aspirates were Pap-stained. **A** Lower magnification reveals numerous isolated polyhedral medium-sized cells in a dirty background. **B** At high magnification, a majority of fusiform cells meet the cytologic criteria of epithelioid histiocytes.
*Tentative cytologic diagnosis:* most likely florid epithelioid cell granulomatosis.
*Comments:* definitive diagnosis requires histopathologic examination of the lesion. Immunocytochemistry was not initially performed; a subsequent S100 immunostaining yielded strong positivity, indicating melanoma cells.
*Tissue diagnosis* (lymph node excision): amelanotic malignant melanoma, spindle cell variant.

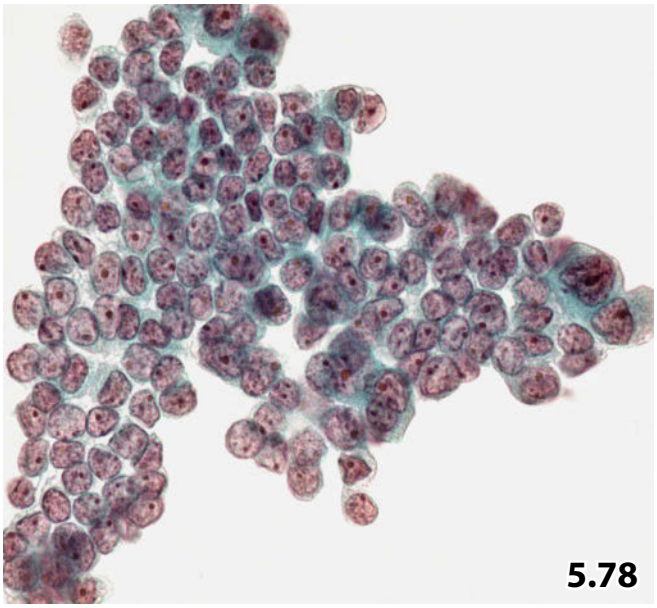
5.78

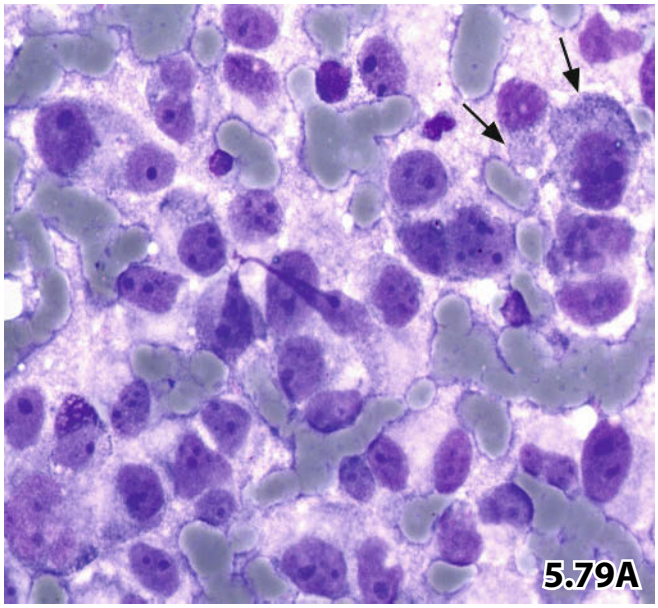
5.79A

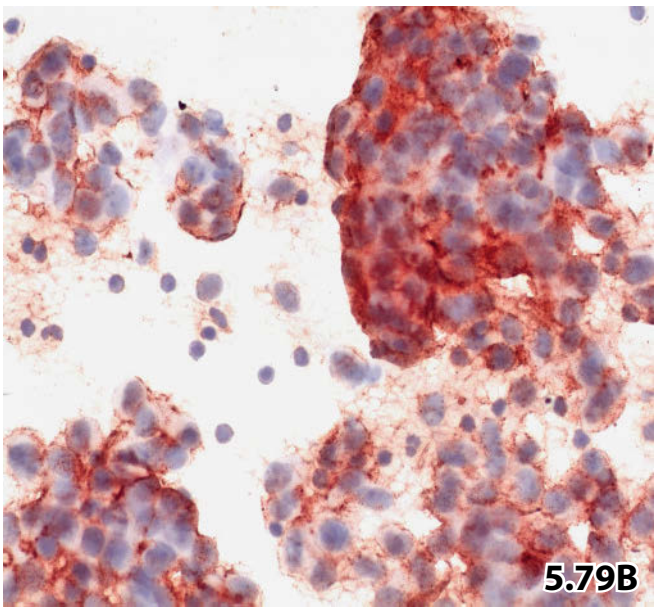
5.79B

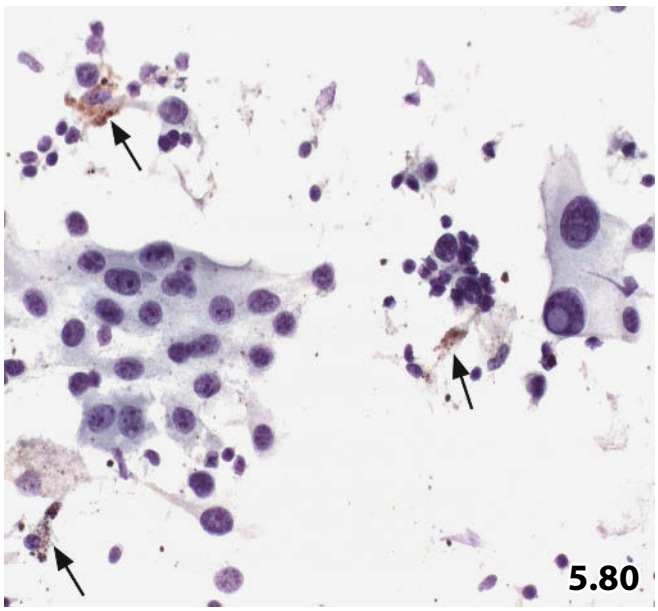
5.80

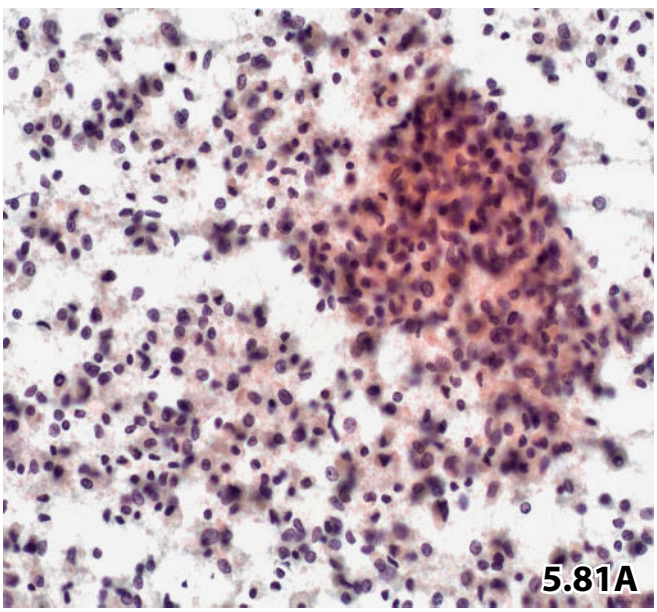
5.81A

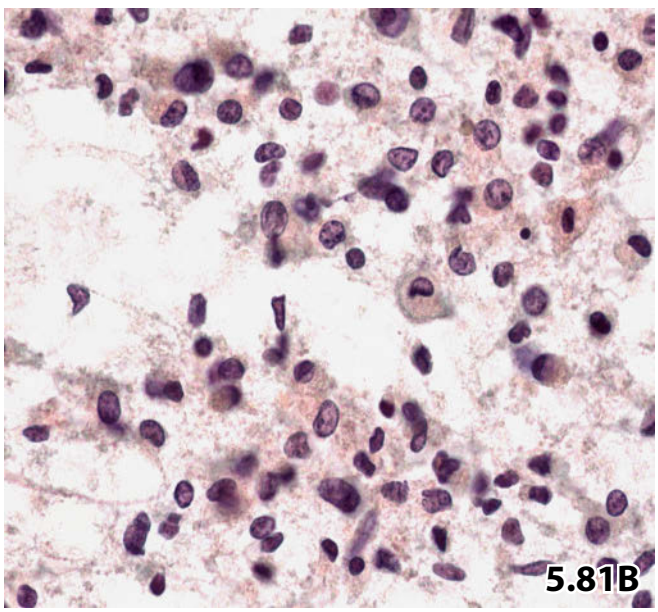
5.81B

**Fig. 5.82 Lymphoepithelial carcinoma: cytologic detail.**
A 36-year-old man with a positive history of lymphoepithelial carcinoma. FNAB demonstrates loose tumor cell clusters (lower right) in combination with histiocytes and lymphocytes. Pay attention to the morphologic similarities of the carcinoma cells as compared to activated histiocytes (arrows); but the tumor cell nuclei exceed the size of histiocytic nuclei showing a more dense granular chromatin, and prominent nucleoli (direct smear, Pap stain, high magnification). Immunocytochemical staining for pancytokeratin-Lu-5 (not shown) strongly decorated the neoplastic cells.



**Figs. 5.83 and 5.84 Lymphoepithelial carcinoma: diagnostic challenge.**
A 41-year-old man presented with an enlarged lymph node at the right side of his neck. Physical examination, imaging, and serologic tests did not provide any clarifying results. FNAB and subsequent excisional biopsy of the lymph node were performed.
*Initial (false) cytologic diagnosis:* benign reactive lymphoproliferative lesion.
*Comment:* cytologic misinterpretation was caused by scattered carcinoma cells imitating large lymphoid blasts or reactive histiocytes.
*Tissue diagnosis* (lymph node excision):Lymphoepithelial carcinoma.

**Fig. 5.83A** Variegated reactive lymphocytic population including germinal center cells and tingible-body macrophages. The large polymorphous nucleus (or clustered atypical nuclei?) on the right (arrow) and the cell at the bottom (arrow) may represent carcinoma cells (direct smear, MGG stain, high magnification). **B** A direct smear obtained from the same aspirate but Pap-stained shows an identical reactive lymphocytic background. Two cells (arrows) may suggest neoplasia due to their size, the huge polymorphous nucleoli, and the abundant pale cytoplasm (high magnification). **C** Delayed immunostaining for pancytokeratin Lu-5 (Pap-prestained ThinPrep specimen) highlights scattered scarce carcinoma cells (arrow).

**Fig. 5.84** In histologic sections of the same lymph node (HE stain), scattered carcinoma cells (arrows) could be detected in the interfollicular area. Neoplastic cells are morphologically akin to those in cytologic specimens and are also difficult to separate from large lymphoid blasts.

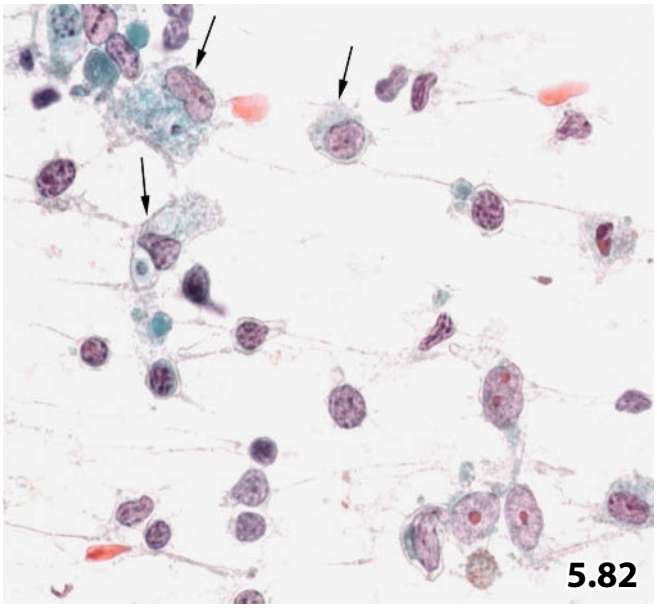
5.82

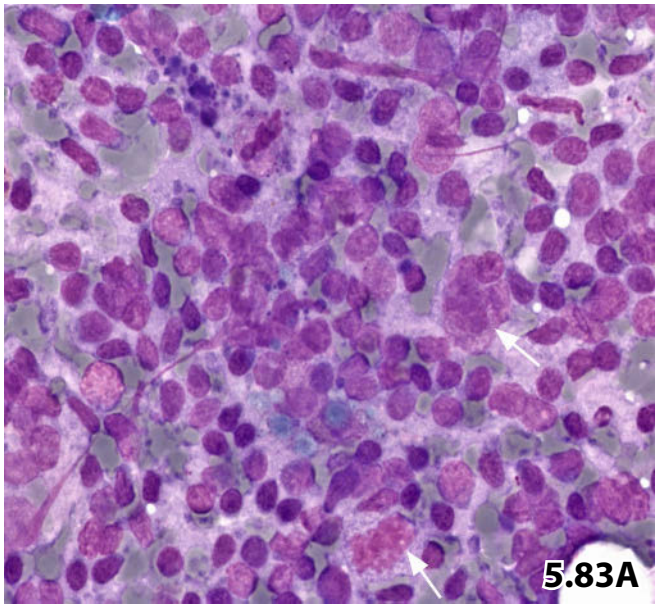
5.83A

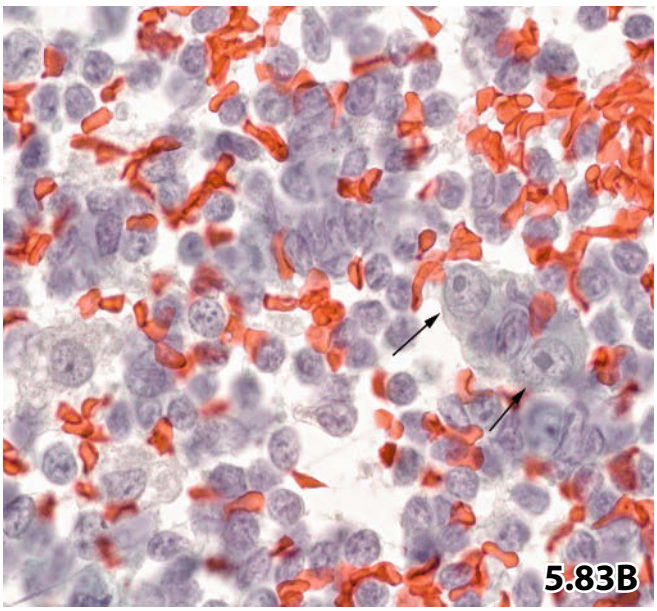
5.83B

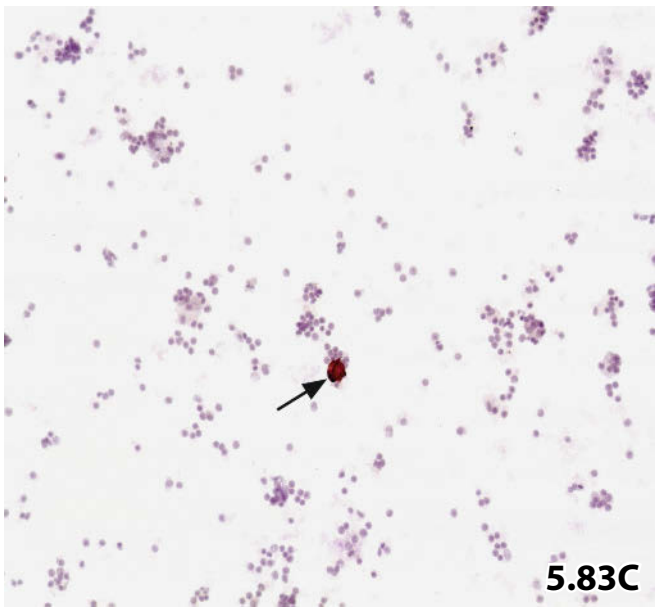
5.83C

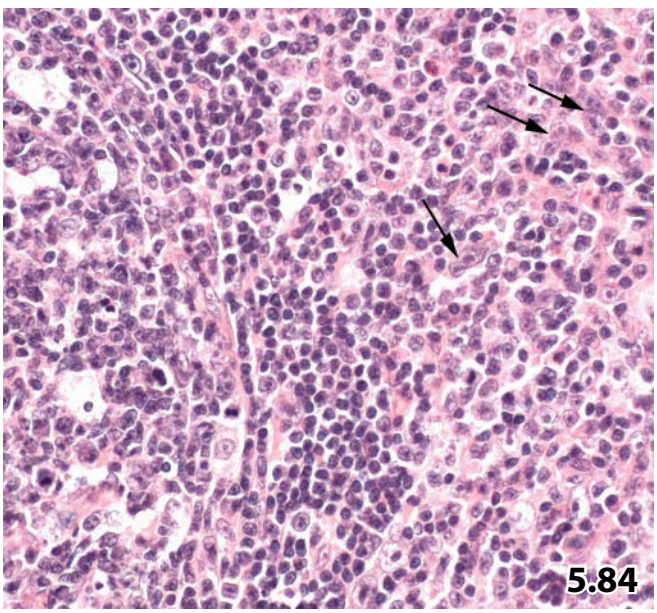
5.84

# Central Nervous System 6



## Synopsis and Algorithms




Spieler/Rössle, *Nongynecologic Cytopathology. A Practical Guide. Essentials of Diagnostic Pathology*,
DOI 10.1007/978-3-642-24719-4_6, © Springer-Verlag Berlin Heidelberg 2012

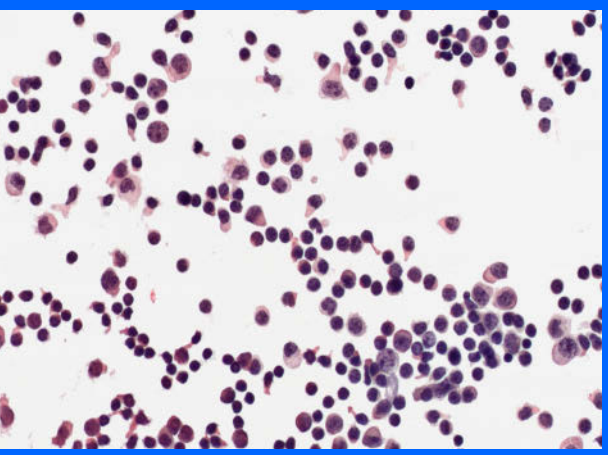

# Section 6.1
# Central Nervous System

## Cerebrospinal Fluid

### 6.1.1 Introduction

**General Comments**

- Choroid plexus and ependymal lining of the ventricles and cerebral subarachnoid space produce cerebrospinal fluid by ultrafiltration of blood plasma. The reabsorption is effected by the arachnoid villi. The cerebral spinal fluid (CSF) compartment is composed of the ventricle areas and the subarachnoid space.
- Cytologic evaluation of CSF is a part of complete neurologic evaluation in patients who have symptoms due to central nervous system (CNS) disorders. Diagnostic application comprises a wide spectrum of lesions and findings [5, 58, 66].
- CSF is also useful in monitoring intrathecal chemotherapy, mainly for patients with malignant lymphoma/leukemia and irradiation to the brain. CSF specimens often provide the first pathomorphologic diagnosis of a CNS disease, particularly in metastatic cancer patients. Thus, prognosis and therapeutic modalities are based upon the cytologic diagnosis.
- Cytology of cerebrospinal fluid is challenging for several reasons. Repeated CSF sampling and other strategies may be necessary to establish a diagnosis and to minimize false-negative results [30]:
  - Generally, only a small volume of fluid is obtained and the sample usually has to be split and distributed to various laboratories (cytology, hematology, biochemistry, microbiology etc.).
  - In many cases, the fluid contains only a few cells.
  - CSF is unlikely to be an appropriate cell medium, so degeneration of the fragile cells may cause diagnostic difficulties. Rapid delivery of the aspirate to the cytologic laboratory and immediate processing are of utmost importance.
  - The CSF may be contaminated with blood or extraneous cell material such as nucleus pulposus/chondroid substance, bone marrow, or cells from soft mesenchymal tissue. Contamination is likely to occur when the collector is not skilled enough in tapping cerebrospinal fluid spaces.
  - Invasive diagnostic and therapeutic procedures could affect the CNS causing reactive changes such as previous CSF sampling, previous surgery, myelography, pneumoencephalography, intrathecal medication, shunts, reservoirs, irradiation to the brain or cord, and others. A window of several days between the first and subsequent material collection should be conceded in order to avoid diagnostic difficulties.
- Ancillary studies (such as cytochemistry, immunocytochemistry, DNA quantification, molecular analyses) on cells in CSF samples can be performed without difficulty [5, 20, 33, 40, 54, 78] (Fig. 6.1).
- Direct contact of a tumor mass with the cerebrospinal fluid compartment is a precondition for cell-shedding and consequently for tumor cell recovery by lumbar or ventricular puncture. Leptomeningeal infiltration most likely ensures cell exfoliation; while tumors situated within the brain parenchyma may enter the CSF compartment by direct infiltration, perivascular spread, or via the arterial route [43].

The following tumors are most likely exfoliating cells into cerebrospinal fluids:
- Metastatic carcinomas and melanoma.
- Medulloblastoma.
- Ependymoma.
- Malignant lymphoma and leukemia.

Strong cohesiveness of the tumor cells prevents exfoliation, e.g., from meningioma of the subarachnoid space.

**Specimen Preparation**

Total cell recovery and optimal preservation of morphological details are the two prime requirements for any preparatory method.

- *Cytocentrifugation* has become the method of choice in the majority of cytology laboratories. It is a simple and rapid method, and the least time-consuming for screening. The technique provides specimens for wet fixation (any adequate fixative may be used) as well as for air-drying followed by either Papanicolaou or May-Grünwald-Giemsa/Diff-Quik staining procedures. The latter staining techniques are advantageous in diagnosing malignant lymphoma/leukemia and identifying hematopoietic cells.
  Similar to other thin-layer methods, cytocentrifugation may produce certain cellular artifacts including cellular crowding, irregular nuclear outlines, pronounced nucleoli and cytoplasmic vacuolization.
- *Liquid-based technology* (ThinPrep, SurePath, etc.) is less commonly used with CSF samples. A limited number of studies have shown that this technique yields appropriate results in everyday cytology practice [6, 74].
- *Membrane filter methods*. Maximum cell yield can be reached using membrane filter methods including Gellman, Millipore, and Nuclepore filters, but cellular details may be altered due to fixation-induced shrinkage. Other disadvantages of filters are the limitation to the Papanicolaou staining technique and the need for skilled personal for optimal preparation [4, 6, 51].
- *Conventional smears* from the sediment after ordinary centrifugation are recommended only for highly cellular CSF samples. For wet fixation, direct smears must be fixed immediately within 1–3 s after slide preparation. Slides can be placed in a jar with alcohol-based fixative or a spray fixative can be used.

## 6.1.2 Cytology of Normal CSF and Contaminants [6]

### 6.1.2.1 Basic Cell Pattern of Normal CSF

Normal cerebrospinal fluid is colorless and looks like water. The specimen contains scarce cellular material with few lymphocytes and monocytes.

**Microscopic Features**

- The lymphocytes are small, characterized by round nuclei with a smooth outline, dense granular chromatin, practically invisible nucleoli, and a slight cytoplasmic rim.
- Monocytes usually have eccentrically placed nuclei exhibiting a distinct bean or horseshoe shape. The chromatin is bland and the nucleoli are barely visible.
- Neutrophils are virtually absent in normal specimens, but they may be encountered together with red blood cells [35].
- Eosinophils and plasma cells are not seen in cerebrospinal fluids of healthy people.

**Caution**

Benign normal lymphocytes in thin-layer preparations (cytocentrifuge, ThinPrep, and others) may exhibit pronounced nucleoli.

### 6.1.2.2 Lumbar Cerebrospinal Fluid

- Cells from normal brain and spinal cord tissues are hardly ever detected; the normal neuroglial cells should not mislead to a diagnosis of neoplasia. However, papilliform fragments of cuboidal cells may sporadically appear, probably originating from the choroid plexus; isolated choroid plexus cells strongly mimic ependymal cells. Above all choroid plexus is assumed to be a formation composed of modified ependymal cells.
- *Benign spindle-shaped cells* are rarely observed; they most likely originate from loose connective tissue of the leptomeninx. They may closely resemble astrocytes.
- *Immature hematopoietic cells* appear in CSF, if an unintentional sampling of bone marrow occurs (usually from vertebral bodies). The presence of immature cells of all hematopoietic cell lines including megakaryocytes results in a rather heterogeneous pattern that should prevent a false diagnosis of lymphoma/leukemia in most cases [23] (Fig. 3.18).
- *Chondrocytes* and nucleus pulposus cells may be sampled from the intervertebral space during needling. They frequently occur in CSF preparations [18].
  - The cartilage cells occur singly and on occasion in groups of two to three cells. Chondrocytes contain small, round, deeply stained, pyknotic nuclei. The cytoplasm is pale and vacuolated surrounded by a capsule-like dense rim of cartilage. Multiple nuclei may occur (Fig. 3.82).

### 6.1.2.3 Ventricular Cerebrospinal Fluid (Fig. 6.2)

Ventricular fluids obtained through a shunt or by needle frequently contain fragments with choroid plexus cells, occasionally in large numbers. Brain tissue fragments are fre-

quently seen in cytologic specimens at the time of ventricular shunt placement. They are composed of gray and white brain matter containing neurons, loosely arranged glial cells, and small capillary networks (Fig. 6.2).

#### 6.1.2.4 CSF and Numerous Red Blood Cells

A problem in the cytologic evaluation of a sanguineous CSF specimen lies in distinguishing between a traumatic tap and a true vascular disorder [14].

Generally, puncture of a traumatic event shows well-preserved red blood cells, whereas pathologic bleeding gives rise to a xanthochromic fluid and degenerating erythrocytes. The appearance of erythrocytes incorporated into macrophages (red blood cell phagocytosis begins within a few hours after appearance of blood in CSF), and later hemosiderin-laden macrophages (within a few days), occurs irregardless of the etiology of the bleeding (Fig. 6.3).

#### 6.1.2.5 CSF and Melanin Pigment

Melanin pigment and melanin-laden macrophages do not necessarily refer to a malignant melanoma. This condition can be generated by various benign and malignant lesions of the CNS, such as neurocutaneous melanosis [13], melanotic progonoma of the brain [63], Vogt-Koyanagi-Harada syndrome [53], melanotic medulloblastoma [25], and others.

### 6.1.3 Reactive and Atypical Cell Change

**General Comments**

A wide variety of disorders affecting the central nervous system and various diagnostic/therapeutic procedures may cause quantitative and qualitative cell alterations in the CSF.

In general, increased numbers of leptomeningeal cells, monocytes (the two cell types are difficult to distinguish), and lymphocytes are observed, less commonly glial elements. Polymorphonuclear leukocytes may be present early in the course of any pathological condition.

Reactive changes may be encountered as a result of:

- CNS investigation (myelography, previous puncture, and others) and CNS therapy (irradiation, intrathecal chemotherapy).
- Shunts, trauma, and surgery.
- Demyelinating disease.
- Neoplasms.
- Infection.
- Hemorrhage.
- Infarct.
- Hydrocephalus.

**Microscopic Features and Differential Diagnosis**

The most irritating reactive cell features concern:

- *Monocytes* (Fig. 6.4A) often exhibit pronounced enlargement. The nuclei usually retain a horseshoe shape and smooth membrane, but they can be bizarrely indented or multilobated. The chromatin is pale and thinly dispersed. A prominent nucleolus may be present in individual cells. The cytoplasm is wide, polyhedral, and focally vacuolated. Cell degeneration including nuclear pyknosis may be observed.
- *Fibroblasts and astrocytes* may show elongated nuclei with indentations, granular chromatin, and signs of beginning degeneration.
- *Lymphocytes* (Fig. 6.4B) generally show atypical features including coarse chromatin texture, prominent nucleoli, and nuclear membrane irregularities.

- Stimulated lymphocytes and monocytes are frequently observed due to radiation and chemotherapy.
- The distinction between reactive changes and malignant lymphoma can be difficult, but a heterogeneous lymphocytic population will suggest a reactive infiltrate.
- Many destructive disorders are associated with histiocytic proliferation and phagocytic activity. Distinct clustering of histiocytes may be seen in multiple sclerosis. Activated macrophages forming dense clusters can be misinterpreted as carcinoma.
- Hemorrhage into the subarachnoidal space leads to erythrophagocytosis followed later by hemosiderin-laden macrophages (Fig. 6.3.).
- Degenerating glial cells are usually observed in pathologic conditions associated with necrosis of brain tissue, such as encephalomalacia. In later stages, the CSF displays enlarged reactive glial cells and lipophages. Detritus should not be confused with tumor necrosis.

**Caution**

- The composition of the cellular infiltrate together with the morphology of individual cells define whether the cellular atypias are reactive-benign or neoplastic.
- The patient's clinical history has great impact on an accurate cytologic diagnosis.
- Cellular contamination from intervertebral disk and reactive histiocytic/ fibroblastic cells from the subarachnoidal space and from granulomatous lesions may present diagnostic confusion [77].

## 6.1.4 CSF in Nontumorous Conditions (Selected Disorders) [6]

### 6.1.4.1 Inflammation and Infections

**General Comments**

- *Acute inflammatory disorders*. The hallmark of acute inflammation in CSF specimens is a huge number of polymorphonuclear leukocytes. This infiltrate is not specific for bacterial meningitis. Likewise, it may occur in the course of various infections and noninfectious disorders such as brain infarcts.
- *A subacute inflammatory pattern* is composed of a variety of polymorphonuclear and mononuclear cells, the latter associated with reactive features, as described above.
- *Chronic inflammatory disorders* provide a predominance of lymphoid cells. The infiltrate may be composed of numerous small, mature lymphocytes or of a mixture of mature lymphoid cells, immunocytes, immunoblasts, and plasma cells. The latter suggests immune response, e.g., attendant viral infection.
- *Granulomatous lesions*. Granulomatous tissue fragments are infrequently encountered in CSF cytology. A granulomatous lesion of the foreign-body type characterized by foreign-body giant histiocytes is most likely seen as a reaction to shunts and reservoirs.
- *Sarcoidosis*. The CSF of patients with sarcoidosis involving the meninges shows normal and atypical lymphocytes, mostly of T-cell origin [46].
- *CSF and eosinophilic granulocytes*. Eosinophilia may occur in the context of various disorders such as parasitic disease, inflammatory leptomeningeal disorders, cerebral hemorrhage, ischemia, hydrocephalus, and tumors. Bosch and Oehmichen have reported a larger series of cases together with a review of the literature [10].

#### 6.1.4.1.1 Bacterial and Viral Infections

##### Bacterial Meningitis

Bacterial meningitis (Fig. 6.5) in the acute phase shows excessive cell counts with more than 90% neutrophils. The remaining cells are lymphocytes and monocytes/histiocytes. Numerous neutrophils are degenerating, and the background of the samples contains debris and fibrin. Microorganisms may be detected by standard staining methods. Special stains (Gram, Ziehl-Neelsen, silver stains) are adequate for identification of bacteria and other pathogens.

##### Tuberculous Meningitis

Tuberculous meningitis shows no specific cytologic pattern. The disorder may present as an acute, subacute, or chronic infection. Characteristic cytologic and biochemical CSF findings are reported in the majority of the cases: lymphoid pleocytosis, low glucose level, and elevated protein level [42].

- Neutrophilic granulocytes predominate the early stage of the disease.
- Lymphocytes, reactive lymphoid cells, and monocytes become predominant in a later stage of the disease; plasma cells can be observed in about 30% of cases [39].
- Nevertheless, pleocytosis consisting mainly of neutrophils has been described throughout the course of the infection and during therapy [79].

Nontuberculous mycobacteria is a rare causative agent of infectious disease of the CNS [42].

##### Lyme Disease (Lymphocytic Meningoradiculitis)

[45, 61, 76] (Fig. 6.6)

This disease results from infection by the tick-borne spirochete *Borrelia burgdorferi* and is a multisystem disorder. The CSF cell pattern is indicated by lymphocytic pleocytosis, composed mainly of immunoblasts and plasma cells in association with numerous foamy macrophages. The infiltrate may simulate malignant lymphoma [76]; similar CSF findings have been described in individual cases of multiple sclerosis and herpes zoster.

##### Viral Meningoencephalitis

- An infection usually results in an increased number of lymphocytes in the CSF. The infection is usually caused by enteroviruses. Other viral pathogens that involve the CNS parenchyma and the leptomeninx include viruses of the herpes group, cytomegalovirus, and others.
  - Lymphocytes are of the small mature type but transformed and atypical lymphoid cells also occur.
  - Plasma cells and histiocytic cells are present as well.
  - Neutrophils may be predominant in the very early stage of infection.
  - Eosinophils and basophils are occasionally encountered.
- Viral-induced lymphocytosis may mimic large-cell malignant lymphoma. In particular, an Epstein-Barr virus infection has to be considered [48].
- The characteristic nuclear inclusions caused by certain viruses (such as herpetic virus and cytomegalovirus) are rarely identified in CSF [32, 41].

##### Acquired Immune Deficiency Syndrome

Human immunodeficiency virus (HIV) is the causative agent of acquired immune deficiency syndrome (AIDS). It is a retrovirus and the HIV-1 type is usually responsible for immunodeficiency infectious disorders in the human population.

Three types of CNS manifestations are seen in patients with AIDS:

1. AIDS encephalopathy [34, 41] caused by HIV affecting cells within the parenchyma of the brain and spinal cord.
   - Pleocytotic CSF is characterized by a nonspecific chronic inflammatory infiltrate comprising macrophages, activated monocytes, and rarely multinucleated giant cells.

2. Opportunistic infections [21, 83] involving the brain are numerous. The four most frequent conditions are cytomegalovirus infection, toxoplasmosis, progressive multifocal leukoencephalopathy viral infection, and cryptococcosis.
   - CSF findings are usually nonspecific; but CSF cytology remains helpful in diagnosing cryptococcosis in most AIDS patients affected by this pathogen (Fig. 6.7).
3. Malignant neoplasia involving the CNS. Malignant lymphoma is the most frequent tumoral disorder of the CNS in patients with AIDS, either by primary lymphoma or secondarily by widespread tumor disease. Lymphoma is often a challenge to differentiate from reactive lymphoid infiltrates and undifferentiated nonlymphoid tumors. Selective panels of immunocytochemical stains including cytokeratins, CD45, as well as B-cell and T-cell markers are qualified for tumor classification and immunophenotyping of the lymphocytic population.

**Caution**

- Regenerative atypical lymphoid cell populations in the CSF can be overinterpreted as malignant lymphoma. Lyme disease and viral infections (e.g., Epstein-Barr virus) are most likely to produce equivocal lymphoid cell patterns. Final diagnosis is reliably established by immunocytochemical or flow cytometric phenotyping of the lymphoid cells and/or by clonality assessment of the lymphoid CSF population using immunocytochemistry or molecular tests [31, 62, 65].
- Information on hematologic and other laboratory test results is inevitable.

#### 6.1.4.1.2 Fungal Infections and Parasitic Disease

**Cryptococcosis** [3, 67] (Fig. 6.7)

Cryptococcus is the fungal agent most commonly encountered in CSF. Normally, it is found in immunosuppressed transplantation patients, in patients on immunosuppressive therapy, in patients suffering from lymphoma/leukemias, and in AIDS patients.

- The yeasts are frequently identified with the light microscope due to a refractile appearance. They have a round shape, vary in diameter (5–15 $\mu$m), and produce thin-necked buds. Cryptococci are often surrounded by a mucopolysaccharide capsule that stains positive with a special dye such as mucicarmine, Alcian blue, or colloidal iron. The capsule and buds, as described, are characteristic of cryptococcus.
- Yeasts without a prominent capsule are difficult to distinguish from nonfungal elements such as erythrocytes and small bubbles of air and water. Cellular reaction is frequently marginal or lacking, particularly in immunosuppressed patients, but reactive lymphocytosis can occur during the course of cryptococcal meningitis. Reactive lymphocytosis can simulate malignant lymphoma.

**Caution**

- Mucopolysaccharide capsule and thin-necked buds are characteristic of *Cryptococcus*.
- *Cryptococcus* may be overlooked, especially in Pap-stained specimens.
- In the CSF of AIDS patients, malignant lymphoma, cryptococcosis, and a cellular response to another infectious agent can occur simultaneously.

**Other Fungi**

Other fungi [52] may occur in CSF including *Blastomyces dermatitidis*, *Histoplasma capsulatum*, *Coccidioides*, *Actinomyces*, *Aspergillus*, *Mucor*, and *Penicillium*. We refer to individual publications and distinguished textbooks.

**Toxoplasmosis** [11, 24, 26]

*Toxoplasma gondii* can be identified in CSF preparations. Extracellular tachyzoite, phagocytosed tachyzoite, and cystic elements may be identified best with Romanowsky stains (Wright staining, Diff-Quik, among others). Toxoplasmic CSF initially exhibits a mixed inflammatory pattern and subsequently a distinct mononuclear pleocytosis. It is suggested that parasites are likely to be found in CSF from patients in the acute stage of infection [26]. Furthermore, it has been reported that in patients with obstructive hydrocephalus, tachyzoites are more often detected in ventricular than in lumbar samples [11].

**Other Parasitic Disease**

CSF findings in other parasitic diseases (e.g., *Trichomonas*) have rarely been reported [49].

### 6.1.4.2 Demyelinating Diseases

**General Comments**

This group of CNS disorders includes multiple sclerosis and other neuroimmunological disorders, such as Guillain-Barré syndrome and chronic inflammatory demyelinating polyneuropathy. The cellular pattern in CSF is variable, depending on the specific type, the phase, and the extent of the disease. In many patients, the CSF conditions are normal during quiescent stages of the disease.

*Multiple Sclerosis*

Multiple sclerosis (MS) generally reveals a T-lymphocyte predominance with mature T cells of either the helper (T4) or suppressor (T8) phenotype. Whether different T4:T8 ratios are diagnostic for the course of the disease and can distinguish between multiple sclerosis and other neurological dis-

eases is the subject of contradictory discussion in the literature [1, 44, 57]. MS-CSF may also contain activated lymphocytes, lymphoplasmacytoid cells, and mature plasma cells [56, 22, 82, 84]. A dominating monocytic cell reaction may suggest chronic or progressive disease [15, 71]. Distinct clustering of activated monocytes should not lead to a false-positive diagnosis of carcinoma.

Diagnosis of MS is supported by clinical symptoms, the typical findings in magnet resonance imaging, and properties of CSF analysis. However, today a specific diagnostic CSF test does not exist [47].



## 6.1.5 CSF and Neoplastic Lesions in the Central Nervous System

### 6.1.5.1 Introduction

- Roughly two-thirds of neoplasms occurring in the central nervous system are primary CNS tumors, but the majority of tumors involving CSF are secondary neoplasms.
- Distribution of tumor cell-positive CSF is as follows [19, 27]:
  - About 10% are caused by primary CNS tumors.
  - About 30% tumor cell positivity results from lymphoma/leukemia.
  - About 60% are caused by metastatic neoplasms.
- Only a few patients presenting with malignant cells in the CSF have no history of neoplastic disease.
- An inflammatory background is frequently observed interspersed with malignant cells, the latter may be fuzzy and easily overlooked; single carcinoma cells are reliably recognized by application of anticytokeratin antibodies.
- CSF is frequently abnormal in the presence of a brain tumor, including changes in biochemical levels and abnormal cell counts, whereas neoplastic cells are absent. Thus, a lack of tumor cells does not exclude a malignant lesion within the CNS. Glantz and colleagues proposed a practical policy to minimize false-negative results, including an increase in the CSF sample volume, optimizing fluid processing, obtaining CSF from different sites (lumbar and ventricular), and repeated investigations [30].
- One of the most important circumstances in cancer detection based on CSF cytology is tumor location. Tumors that are confined to the parenchyma of the brain and spinal cord, the bones, the dura mater, or the extradural space of the skull and spine only occasionally shed cells into the CSF. The compactness and cohesiveness of the tumor cells are other factors that determine the exfoliation of neoplastic cells. Tumor involvement of the leptomeninges usually ensures a high detection rate with CSF cytology.
- Use of immunocytochemical and molecular biological techniques in CSF practice enables one to distinguish between the most common tumor types such as lymphoma/leukemia, carcinoma, melanoma, and primary CNS tumors. Assessment of the site of origin of metastatic tumors is limited.

**Caution**

- Location of the tumor within the CNS and its possible access to the subarachnoidal space are the most important preconditions for a positive exfoliation into CSF.
- A lumbar tap may be nondiagnostic for tumor cells, whereas cisternal/ventricular puncture yields a positive result and vice-versa. CSF should be sampled most particularly from the site that clinically and radiologically presents pathologic findings [16, 64].

### 6.1.5.2 Metastases to the Central Nervous System

**General Comments**

- Only up to 20% of all tumors metastatic to the CNS preoperatively yield positive CSF [2]. Brain metastases may occur as multifocal lesions or less frequently as subarachnoidal infiltration, termed carcinomatous meningitis. The latter may be difficult to diagnose clinically and with imaging, but CSF cytology provides a high detection rate.
- Most patients with neoplastic cells in the CSF present with a previous tumor diagnosis. An immunocytochemical panel of adequate antibodies can distinguish between the most frequent tumor entities including carcinoma, malignant lymphoma, malignant melanoma, and primary CNS tumor in patients with an occult primary neoplasm.
- Occult primary tumors of the lung most frequently yield a positive CSF cytology result [8].
- The characteristic morphology of cells of various tumor types is generally the same as displayed in cytologic samples from the counterparts in other organs. However, in CSF exfoliated carcinoma cells appear singly rather than in dense clusters, which makes the distinction more difficult between epithelial tumor cells, lymphoid tumor cells, and activated lymphocytes and histiocytes (Figs. 6.8–6.13).
- Application of selective immunostains is extremely helpful in assessing tumor type and less frequently primary tumor origin. The diagnostic relevant cytomorphologic features and the immunopatterns of various neoplasms are provided in the respective chapters of this book and in the literature [7, 33, 78].

#### 6.1.5.2.1 Special Notes on Melanoma and Selected Carcinomas

Tumor cells of lung and breast cancers and of malignant melanoma are most frequently encountered in CSF, but numerous other sources for CNS metastases exist [7].

*Melanoma*. Cutaneous melanoma is one of the tumors with a high frequency of dissemination to the CNS. Rare primary meningeal melanoma has to be taken into consideration in patients with no identified primary tumor in extracranial sites [55, 70, 81]. Cytoplasmic melanin pigment in tumor cells allows a definite diagnosis of melanoma, but in the absence of pigment the diagnosis may be difficult. Undifferentiated large-cell neoplasms, in particular large-cell carcinoma and large-cell lymphoma, have to be excluded by means of a selective panel of immunomarkers composed of antimelanoma antibodies, antibodies against cytokeratins and epithelial antigens, and antileukocyte antibodies.

**Caution**

In CSF sediments, macrophages and cells of other malignant tumors may sporadically contain melanin pigment [7].

*Lung carcinoma* (Figs. 6.8 and 6.9). Cells of lung carcinomas (especially small-cell carcinoma) are most frequently seen in CSF and the most frequent occult primary tumors with positive CSF exfoliative cytology are situated in the lung.

*Breast carcinoma* (Figs. 6.10 and 6.14). Tumor cells occur most often singly and the primary tumor has been already diagnosed in almost all patients [8]. Cytoplasmic protrusions and blebs, giving the tumor cells a toothed wheel-like appearance are a characteristic feature of individual breast cancer cells in CSF specimens. However, the phenomenon is not completely specific for mammary carcinoma cells but may be observed on tumor cells from other primary origin as well (Fig. 6.11A).

*Gastric carcinoma* (Figs. 6.12 and 6.13) may produce meningeal carcinomatosis in the presence of an occult primary tumor [8].

*Squamous cell carcinoma* arising in the head area and paranasal sinuses may exceptionally spread into the subarachnoidal space by direct invasion or spreading along cranial nerves. Atypical squamous cells originating from craniopharyngioma should not mislead to an overdiagnosis of malignancy [77].

*Transitional-cell carcinoma* is rarely encountered in CSF; only a few cases are documented in the literature [37, 75].

*Renal cell carcinoma*. A high frequency of brain metastases has recently been reported for patients with renal cell carcinoma [72].

**Caution**

The majority of epithelial tumors metastasizing into the CNS belong to the group of adenocarcinomas [27].

### 6.1.5.3 Lymphoid and Myeloid Neoplasms [5, 6]

#### General Comments

- Leukemia and systemic lymphoma are among the tumor types that frequently involve the CNS. These tumors shed their cells into cerebrospinal fluid due to pronounced subarachnoidal dissemination.
- Assessment of the exact diagnosis and phenotyping on primary and secondary lymphoma and myeloid lesions is difficult in CNS cytology [9, 69]; it is necessary to refer to tumor properties demonstrated in the lymph nodes of the same patient. Immunocytochemical investigations are helpful in distinguishing nonlymphoid neoplasms from reactive and malignant lymphoid populations in CSF specimens. Clonality assessment by means of flow cytometry or molecular methods provides final lymphoma diagnosis in cases with immunocytochemically equivocal results (see Sects. 3.2.3.2, "Additional Analyses", p. 267, and 15.1.4, "Ancillary Techniques", p. 910) [31, 65, 62, 78].
- Chronic leukemia and small-cell lymphomas rarely involve the CNS as compared to the acute forms of leukemia and large-cell lymphomas.

#### 6.1.5.3.1 Acute Leukemias

Acute forms include acute lymphocytic leukemia and nonlymphocytic leukemia (acute myelogenous, acute myelomonocytic, and undifferentiated leukemia). In contrast to the acute form of leukemia, involvement of the CNS rarely occurs in chronic leukemias, yet patients with chronic myelogenous tumors in an accelerated phase can be affected by CNS infiltration.

#### Microscopic Features and Differential Diagnosis

- CSF preparations of *lymphoblastic* leukemia disclose a fairly monomorphic single-cell pattern. The N/C ratio is high. The nuclei exhibit finely granular chromatin and large nucleoli as well as irregular nuclear membrane (Fig. 6.15).
- Many of the *large-cell* type lymphoid leukemias exhibit nuclear convolutions and grooves, especially the lymphatic neoplasias of the T-cell phenotype. Differential diagnosis consideration should include metastatic CNS involvement by large-cell tumors that are composed of cells displaying nuclear convolutions such as adenocarcinoma and undifferentiated carcinoma of the lung, breast, kidney, and malignant melanoma.
- Cells of *acute nonlymphocytic (myeloid/monocytic) leukemia* frequently disclose cytoplasmic granules. The granules are best recognized in Romanowsky stains (MayGrünwald-Giemsa or Diff-Quik) (Figs. 6.16–6.18).

**Caution**

- Chronic leukemia rarely involves CNS compartments. A reactive inflammatory process has to be excluded in CSF presenting few tumor cells, numerous small monomorphic tumor cells, or a mixed lymphoid cellular pattern.
- Diagnostic difficulties arise in CSF containing:
  - Few abnormal cells within a mixed lymphoid/histiocytic cell population
  - Few abnormal cells in specimens exhibiting extremely low cell counts

  Immunocytochemical and molecular genetic tests often fail or provide untrustworthy results in such situations. Repeated CSF examination may lead to an accurate diagnosis.
- In case of traumatic sanguineous taps in patients affected with leukemia, leukemic cells that are accumulated in the peripheral blood may give a false impression of a positive CSF

#### 6.1.5.3.2 Primary and Secondary Lymphoma

(Figs. 6.19 and 6.20)

- *Primary central nervous system lymphoma* generally presents as parenchymal mass, but dissemination occurs not infrequently during the course of the disease. Hence the diagnosis is best achieved by stereotactic biopsy and histologic examination in early tumor manifestation. Cerebrospinal fluid cytology may help in a later stage of the disease [28, 38, 50].
- *Disseminating extracranial malignant lymphomas* may occur involving part of the subarachnoidal space. The vast majority of these lymphoid tumors are large-cell blast-type lymphoma of the B-cell phenotype such as lymphoblastic lymphoma, Burkitt lymphoma, and undifferentiated lymphomas (Fig. 6.19), but T-cell lymphoma may occur as well. Distinguishing between tumorous and reactive lymphoid populations should be easy, due to presence of cellular monomorphism, overt malignant cell characteristics, and monoclonality (proven by immunophenotyping or molecular properties of the cell population) (Fig. 6.1).

  Small-cell (low-grade) malignant lymphoma and Hodgkin disease (Fig. 6.20) infrequently involve the central nervous system. Infectious etiology should always be considered when patients show small lymphocytic or mixed lymphoid infiltrates.

### 6.1.5.4 Primary Tumors of the Central Nervous System [7, 17]

Roughly 15% of the primary CNS neoplasms are preoperatively detected by CSF cytology [2]. Corresponding to metastatic tumors, solely primary CNS neoplasms that involve ventricles and the subarachnoidal space may shed their cells into the CSF.

The most important primary CNS tumors exfoliating their cells into the CSF are briefly discussed below.

#### 6.1.5.4.1 Glial Neoplasms [12, 19, 60]

- *High-grade gliomas:* Glioblastoma multiforme most commonly disseminates widely shedding cells into the CSF followed by other types of highly malignant gliomas such as anaplastic oligodendroglioma and anaplastic ependymoma.
  - CSF from anaplastic glial tumors (Fig. 6.21) is composed of fairly nonspecific highly pleomorphic cells of variable size comprising irregular nuclear membranes, coarse chromatin, and large nucleoli. The tumor cells are scattered or grouped in loose clusters.
  - CSF in patients with ependymoma (Fig. 6.22) is usually cellular, and the tumor cells are loosely aggregated. The cells have epithelioid characteristics with a cuboidal to columnar shape. The variations of this tumor entity provide pronounced differences in nuclear pleomorphism and cytoplasmic appearance [60].
  - Most of the poorly differentiated gliomas seem to retain an immunocytochemical expression of glial fibrillary acidic protein (GFAP) [5, 80].
- *Low-grade gliomas* (astrocytoma, ependymoma, oligodendroglioma) may spread into the cerebrospinal liquor space, but their cells are rarely encountered in cytologic CSF samples due to poor exfoliation. Furthermore, the cells look cytologically benign; they can be distinguished from macrophages and monocytes with specific antibodies [36].
- Immunocytochemical expression of cytoplasmic GFAP allows at least a specific diagnosis of glial tumor origin; an advanced subtyping is not possible using immunocytochemical tests [5, 80].

#### 6.1.5.4.2 Choroid Plexus Tumors [5]

These tumors occur most often in childhood. They virtually always exhibit a papillary architecture. See also Sect. 6.2.3.10, "Choroid Plexus Papilloma and Choroid Plexus Carcinoma," p. 517.

- *Choroid plexus papilloma* is composed of monomorphic cells with bland nuclei. The individual tumor cells are indistinguishable from cells exfoliated from normal choroid plexus.

**Caution**

Papillary fragments of a normal choroid plexus in ventricular CSF specimens are difficult to differentiate from tumoral fragments.

- *Choroid plexus carcinomas* generally shed unambiguous malignant cells into the CSF. Nuclear pleomorphism, irregular chromatin pattern and nucleoli are prominent. The

only differential diagnosis on cytologic specimens includes papillary adenocarcinoma.

Since CSF positivity for adenocarcinoma is extremely rare in the traditional age group affected by choroid plexus carcinoma, the age of the patient together with the diagnosis of an intraventricular malignant papillary lesion may be sufficiently specific to establish a conclusive cytologic diagnosis.

#### 6.1.5.4.3 Medulloblastoma [5, 19]

Medulloblastoma is the most common malignant primary brain tumor of childhood; the tumor is located in the cerebellum.

- CSF specimens are highly cellular.
- The anaplastic cells are small (about the size of a large lymphocyte), showing a high N/C-ratio, pleomorphic nucleus, irregular nuclear outline, and hyperchromasia. Cells occur either in isolation or clustered together.
- Rosette formation and necrosis have occasionally been reported.

The morphology of this entity is virtually indistinguishable from tumors of the small round cell tumor group which includes small-cell carcinoma of the lung, retinoblastoma, neuroblastoma, among others. The age of the patient and tumor localization is helpful in order to render a correct diagnosis.

#### 6.1.5.4.4 Germ Cell Tumors and Pineal Tumors [5, 19, 68, 73]

This is an uncommon group of childhood tumors that develop from the pineal gland and hypothalamic region and therefore shed their cells into the spinal fluid compartment.

Positive immunocytochemical staining of the tumor cells for placental alkaline phosphatase is helpful to establish a firm diagnosis [19].

#### 6.1.5.4.5 Langerhans Cell Histiocytosis [6, 29] (Fig. 6.23)

Langerhans cell histiocytosis (LCH) is characterized by a proliferation of particular histiocytic cells referred to as Langerhans cells. LCH can be unifocal or multifocal, with single-organ or multiple-organ involvement including the CNS. The presence of Birbeck granules detected by electron microscopy and immunocytochemical positivity for CD1a are quite specific.

At our institution, we have seen a young patient whose clinical investigations raised suspicion of LCH in the pituitary region. The diagnosis was confirmed by cytology: the CSF sample showed isolated highly atypical histiocytoid cells that were immunocytochemically decorated with antibodies for CD1a [59] (Fig. 6.23).

## 6.1.6 Further Reading


1. Antonen J, Syrjälä P, Oikarinen R, et al. Acute multiple sclerosis exacerbations are characterized by low cerebrospinal fluid suppressor/cytotoxic T-cells. Acta Neurol Scand 1987;75:156-160.
2. Balhuizen JC, Bots GT, Schaberg A, Bosman FT. Value of cerebrospinal fluid cytology for the diagnosis of malignancies in the central nervous system. J Neurosurg 1978;48:747-753.
3. Bernad PG, Szyfelbein WM, Weiss HD, Richardson EP Jr. Diagnosis of cryptococcal meningitis by cytologic methods: an old technique revisited. Neurology 1980;30:102-105.
4. Bernhardt H, Gourley RD, Young JM, et al. A modified membrane-filter technique for detection of cancer cells in body fluids. Am J Clin Pathol 1961;36:462-464.
5. Bigner SH. Cerebrospinal fluid (CSF) cytology: current status and diagnostic applications. J Neuropathol Exp Neurol 1992;51:235-245.
6. Bigner SH, Johnston WW. The cytopathology of cerebrospinal fluid I. Nonneoplastic conditions, lymphoma and leukemia. Acta Cytol 1981;25:335-353.
7. Bigner SH, Johnston WW. The cytopathology of cerebrospinal fluid II. Meningeal carcinomatosis and primary central nervous system neoplasms. Acta Cytol 1981;25:461-479.
8. Bigner SH, Johnston WW. The diagnostic challenge of tumors manifested initially by the shedding of cells into cerebrospinal fluid. Acta Cytol 1984;28:29-36.
9. Borowitz M, Bigner SH, Johnston WW. Diagnostic problems in the cytologic evaluation of cerebrospinal fluid for lymphoma and leukemia. Acta Cytol 1981;25:665-674.
10. Bosch I, Oehmichen M. Eosinophilic granulocytes in cerebrospinal fluid: analysis of 94 cerebrospinal fluid specimens and review of the literature. J Neurol 1978;219:93-105.
11. Brogi E, Cibas ES. Cytologic detection of *Toxoplasma gondii* tachyzoites in cerebrospinal fluid. Am J Clin Pathol 2000;114:951-955.
12. Browne TJ, Goumnerova LC, De Girolami U, Cibas ES. Cytologic features of pilocytic astrocytoma in cerebrospinal fluid specimens. Acta Cytol 2004;48:3-8.
13. Burstein F, Seier H, Hudgins PA, Zapiach L. Neurocutaneous melanosis. J Craniofac Surg 2005;16:874-876.
14. Buruma OJ, Janson HL, Den Bergh FA, Bots GT. Blood-stained cerebrospinal fluid: traumatic puncture or hemorrhage? J Neurol Neurosurg Psychiatry 1981;44:144-147.
15. Cepok S, Jacobsen M, Schock S, et al. Pattern of cerebrospinal fluid pathology correlates with disease progression in multiple sclerosis. Brain 2001;124:2169-2176.
16. Chamberlain MC, Kormanik PA, Glantz MJ. A comparison between ventricular and lumbar cerebrospinal fluid cytology in adult patients with leptomeningeal metastases. Neuro Oncol 2001;3:42-45.
17. Chaudhry RJ, Ali SZ. Primary central nervous system tumors involving cerebrospinal fluid: cytomorphologic characteristics and clinicopathologic correlates. Cancer(Cancer Cytopathol) Suppl 2007;111:403-404.
18. Chen KT, Moseley D. Cartilage cells in cerebrospinal fluid. Arch Pathol Lab Med 1990;114:212.
19. Chhieng DC, Elgert P,Cohen J-M, et al. Cytology of primary central nervous system neoplasms in cerebrospinal fluid specimens. Diagn Cytopathol 2002;26:209-212.
20. Cibas ES, Malkin MG, Posner JB, Melamed MR. Detection of DNA abnormalities by flow cytometry in cells from cerebrospinal fluid. Am J Clin Pathol 1987;88:570-577.
21. Collazos J. Opportunistic infections of the CNS in patients with AIDS: diagnosis and management. CNS Drugs 2003;17:869-887.
22. Confavreux C, Caudie C, Touraine F, et al. Plasma cells in cerebrospinal fluid and multiple sclerosis: diagnostic yield and clinicobiological correlations. Acta Neurol Scand 1986;74:432-438.

23. Craver RD, Carson TH. Hematopoietic elements in cerebrospinal fluid in children. Am J Clin Pathol 1991;95:532-535.
24. DeMent SH, Cox MC, Gupta PK. Diagnosis of central nervous system *Toxoplasma gondii* from the cerebrospinal fluid in a patient with acquired immunodeficiency syndrome. Diagn Cytopathol 1987;3:148-151.
25. Dolman CL. Melanotic medulloblastoma. A case report with immunohistochemical and ultrastructural examination. Acta Neuropathol 1988;76:528-531.
26. Eggers C, Gross U, Klinker H, et al. Limited value of cerebrospinal fluid for direct detection of *Toxoplasma gondii* in toxoplasmic encephalitis associated with AIDS. J Neurol 1995;242:644-649.
27. Ehya H, Hajdu SI, Melamed MR. Cytopathology of nonlymphoreticular neoplasms metastatic to the central nervous system. Acta Cytol 1981;25:599-610.
28. Feiden W, Milutinovic S. Primary CNS lymphomas. Morphology and diagnosis. Pathologe 2002;23:284-291.
29. Ghosal N, Kapila K, Kakkar S, et al. Langerhans cell histiocytosis infiltration in cerebrospinal fluid: A case report. Diagn Cytopathol 2001;24:123-125.
30. Glantz MJ, Cole BF, Glantz LK, et al. Cerebrospinal fluid cytology in patients with cancer: minimizing false-negative results. Cancer 1998;82:733-739.
31. Gleissner B, Siehl J, Korfel A, et al. CSF evaluation in primary CNS lymphoma patients by PCR of the CDR III IgH genes. Neurology 2002;58:390-396.
32. Gupta PK, Gupta PC, Roy S, Banerji AK. Herpes simplex encephalitis, cerebrospinal fluid cytology studies. Two case reports. Acta Cytol 1972;16:563-565.
33. Gupta RK, Naran S, Lallu S, Fauck R. Cytodiagnosis of neoplasms of the central nervous system in cerebrospinal fluid samples with an application of selective immunostains in differentiation. Cytopathology 2004;15:38-43.
34. Hagberg L, Forsman A, Norkrans G, et al. Cytological and immunoglobulin findings in cerebrospinal fluid of symptomatic and asymptomatic human immunodeficiency virus (HIV) seropositive patients. Infection 1988;16:13-18.
35. Hayward RA, Oye RK. Are polymorphonuclear leukocytes an abnormal finding in cerebrospinal fluid? Results from 225 normal cerebrospinal fluid specimens. Arch Intern Med 1988;148:1623-1624.
36. Ho KL, Hoschner JA,Wolfe DE. Primary leptomeningeal gliomatosis. Arch Neurol 1981;38:662-666.
37. Hust MH, Pfitzer P. Cerebrospinal fluid and metastasis of transitional cell carcinoma of the bladder. Acta Cytol 1982;26:217-223.
38. Jellinger KA, Paulus W. Primary central nervous system lymphomas – an update. J Cancer Res Clin Oncol 1992;119:7-27.
39. Jeren T, Beus I. Characteristics of cerebrospinal fluid in tuberculous meningitis. Acta Cytol 1982;26:678-680.
40. Jorda M, Ganjei-Azar P, Nadji M. Cytologic characteristics of meningeal carcinomatosis: increased diagnostic accuracy using carcinoembryonic antigen and epithelial membrane antigen immunocytochemistry. Arch Neurol 1998;55:181-184.
41. Katz RL, Alappattu C, Glass JP, Bruner JM. Cerebrospinal fluid manifestations of the neurologic complications of human immunodeficiency virus infection. Acta Cytol 1989;33:233-244.
42. Klein NC, Damsker B, Hirschman SZ. Mycobacterial meningitis. Retrospective analysis from 1970 to 1983. Am J Med 1985;79:29-34.
43. Kokkoris CP. Leptomeningeal carcinomatosis. How does cancer reach the pia-arachnoid? Cancer 1983;51:154-160.
44. Kölmel HW, Sudau C. Cell count and ratio of helper/inducer to suppressor/cytotoxic T-cells in the cerebrospinal fluid of patients with multiple sclerosis. J Neurol 1989;236:424-426.
45. Kraft R, Altermatt HJ, Nguyen-Tran Q. Differential diagnosis of atypical plasma cells in the cerebrospinal fluid. Dtsch Med Wochenschr 1989;114:1729-1733.
46. Li CY, Yam LT. Cytologic and immunocytochemical studies of cerebrospinal fluid in meningeal sarcoidosis. A case report. Acta Cytol 1992;36:963-967.
47. Luque FA, Jaffe SL. Cerebrospinal fluid analysis in multiple sclerosis. Int Rev Neurobiol 2007;79:341-356.
48. Manucha V, Zhao F, Rodgers W. Atypical lymphoid cells in cerebrospinal fluid in acute Epstein Barr virus infection. A case report demonstrating a pitfall in cerebrospinal fluid cytology. Acta Cytol 2008;52:334-336.
49. Masur H, Hook E 3rd, Armstrong D. A *Trichomonas* species in a mixed microbial meningitis. JAMA 1976;236:1978-1979.
50. McAllister LD. Primary central nervous system lymphoma: a review. Curr Neurol Neurosci Rep 2002;2:210-215.
51. McAlpine LL, Ellsworth B. A modified membrane filter technique for cytodiagnosis. Tech Bull Regist Med Technol 1969;39:154-156.
52. McGinnis MR. Detection of fungi in cerebrospinal fluid. Am J Med 1983;75(1B):129-138.
53. Nakamura S, Nakazawa M, Yoshioka M, et al. Melanin-laden macrophages in cerebrospinal fluid in Vogt-Koyanagi-Harada syndrome. Arch Ophthalmol 1996;114:1184-1188.
54. Oschmann P, Kaps M, Völker J, Dorndorf W. Meningeal carcinomatosis: CSF cytology, immunocytochemistry and biochemical tumor markers. Acta Neurol Scand 1994;89:395-399.
55. Pasquier B, Couderc P, Pasquier D, et al. Primary malignant melanoma of the cerebellum: a case with metastases outside the nervous system Cancer 1978;41:344-351.
56. Pilz P. Cerebrospinal fluid and multiple sclerosis. Wien Med Wochenschr 1985;135:22-25.
57. Polman CH, de Groot CJ, Koetsier JC, et al. Cerebrospinal fluid cells in multiple sclerosis and other neurological diseases: an immunocytochemical study. J Neurol 1987;234:19-22.
58. Prayson RA, Fischler DF. Cerebrospinal fluid cytology: an 11-year experience with 5951 specimens. Arch Pathol Lab Med 1998;122:47-51.
59. Prosch H, Feldges A, Grois N, Fretz C, Spieler P, et al. Demonstration of CD1a positive cells in the cerebrospinal fluid – A clue to diagnosis of isolated Langerhans Cell Histiocytosis of the hypothalamic-pituitary axis? Med Pediatr Oncol 2003;41:474-476.
60. Qian X, Goumnerova LC, De Girolami U, Cibas ES. Cerebrospinal fluid cytology in patients with ependymoma: a bi-institutional retrospective study. Cancer 2008;114:307-314.
61. Razavi-Encha F, Fleury-Feith J, Gherardi R, Bernaudin JF. Cytologic features of cerebrospinal fluid in Lyme disease. Acta Cytol 1987;31:439-440.
62. Rhodes CH, Glantz MJ, Glantz L, et al. A comparison of polymerase chain reaction examination of cerebrospinal fluid and conventional cytology in the diagnosis of lymphomatous meningitis. Cancer 1996;77:543-548.
63. Rickert CH, Probst-Cousin S, Blasius S, Gullotta F. Melanotic progonoma of the brain: a case report and review. Childs Nerv Syst 1998;14:389-393.
64. Rogers LR, Duchesneau PM, Nunez C, et al. Comparison of cisternal and lumbar CSF examination in leptomeningeal metastasis. Neurology 1992;42:1239-1241.
65. Roma AA, Garcia A, Avagnina A, et al. Lymphoid and myeloid neoplasms involving cerebrospinal fluid: comparison of morphologic examination and immunophenotyping by flow cytometry. Diagn Cytopathol 2002;27:271-275.
66. Rosenthal DL. Cytology of the Central Nervous System. in: Monographs in clinical cytology, Vol.8. G.L. Wied ed. S.Karger Basel München. 1984.
67. Saigo P, Rosen PP, Kaplan MH, et al. Identification of *Cryptococcus neoformans* in cytologic preparations of cerebrospinal fluid. Am J Clin Pathol 1977;67:141-145.
68. Schild SE, Scheithauer BW, Haddock MG, et al. Histologically confirmed pineal tumors and other germ cell tumors of the brain. Cancer 1996;78:2564-2571.

69. Schinstine M, Filie AC, Wilson W, et al. Detection of malignant hematopoietic cells in cerebral spinal fluid previously diagnosed as atypical or suspicious. Cancer 2006;108:157-162.
70. Schmidt P, Neuen-Jacob E, Blanke M, et al. Primary malignant melanoblastosis of the meninges. Clinical, cytologic and neuropathologic findings in a case. Acta Cytol 1988;32713-717.
71. Schmidt RM, Neumann V. Liquor-cytological investigations in multiple sclerosis. Schweiz Arch Neurol Neurochir Psychiatr 1980;127:237-242.
72. Schouten LJ, Rutten J, Huveneers HA, Twijnstra A. Incidence of brain metastases in a cohort of patients with carcinoma of the breast, colon, kidney, and lung and melanoma. Cancer 2002;94:2698-2705.
73. Schulte FJ, Herrmann HD, Müller D, et al. Pineal region tumours of childhood. Eur J Pediatr 1987;146:233-245.
74. Sioutopoulou DO, Kampas LI, Gerasimidou D, et al. Diagnosis of metastatic tumors in cerebrospinal fluid samples using thin-layer cytology. Acta Cytol 2008;52:304-308.
75. Stastny JF, Sprague RI, Frable WJ. Transitional-cell carcinoma metastatic to cerebrospinal fluid: presentation of two cases. Diagn Cytopathol 1996;15:338-340.
76. Szyfelbein WM, Ross JS. Lyme disease meningopolyneuritis simulating malignant lymphoma. Mod Pathol 1988;1:464-468.
77. Takeda M, King DE, Choi HY, et al. Diagnostic pitfalls in cerebrospinal fluid cytology. Acta Cytol 1981;25:245-250.
78. Tani E, Costa I, Svedmyr E, Skoog L. Diagnosis of lymphoma, leukemia, and metastatic tumor involvement of the cerebrospinal fluid by cytology and immunocytochemistry. Diagn Cytopathol 1995;12:14-22.
79. Teoh R, O'Mahony G, Yeung VT. Polymorphonuclear pleocytosis in the cerebrospinal fluid during chemotherapy for tuberculous meningitis. J Neurol 1986;233:237-241.
80. Vick WW, Wikstrand CJ, Bullard DE, et al. The use of a panel of monoclonal antibodies in the evaluation of cytologic specimens from the central nervous system. Acta Cytol 1987;31:815-824.
81. Whinney D, Kitchen N, Revesz T, Brookes G. Primary malignant melanoma of the cerebellopontine angle. Otol Neurotol 2001;22:218-222.
82. Winges KM, Gilden DH, Bennett JL, et al. Analysis of multiple sclerosis cerebrospinal fluid reveals a continuum of clonally related antibody-secreting cells that are predominantly plasma blasts. J Neuroimmunol 2007;192:226-234.
83. Zelman IB, Mossakowski MJ. Opportunistic infections of the central nervous system in the course of acquired immune deficiency syndrome (AIDS). Morphological analysis of 172 cases. Folia Neuropathol 1998;36:129-144.
84. Zeman D, Adam P, Kalistova H, et al. Cerebrospinal fluid cytologic findings in multiple sclerosis. A comparison between patient subgroups. Acta Cytol 2001;45:51-59.

**Fig. 6.1 Molecular analysis: FISH study.**
A 72-year-old man presented with meningeal symptoms and a positive history of mantle cell lymphoma. Lumbar puncture was performed. Cytologic analysis of CSF revealed numerous atypical lymphoid cells (Cytospin preparation, Pap stain) suggestive of meningeal infiltration by mantle cell lymphoma. The diagnosis was verified by a t(11;14) (q13;q32) translocation FISH study, using an orange probe against gene locus 11q13 and a green probe against gene locus 14q32; two fusion genes appeared as yellow signals (arrows) in 12% of all nuclei.

**Fig. 6.2A, B Common cytologic findings in ventricular CSF.**
Direct smears of fluid sediment, Pap-stained. **A** Small fragments of brain tissue composed of neurons, glial fibers, and loosely arranged glial cells (low magnification). A few well-preserved red blood cells stemming from the traumatic tap. **B** Detail shows blood-filled (top) thin capillaries and ganglion cells (arrows). Some of the latter are out of focus. The background is composed of disintegrated brain tissue.



**Fig. 6.3 CSF and pathologic bleeding.**
An older patient with a history of trepanation of the skull for cerebellar meningioma. Lumbar puncture yields CSF containing reactive lymphocytosis, hemosiderophages (right and upper left) and anuclear squames as a contaminant (Pap stain, high magnification).

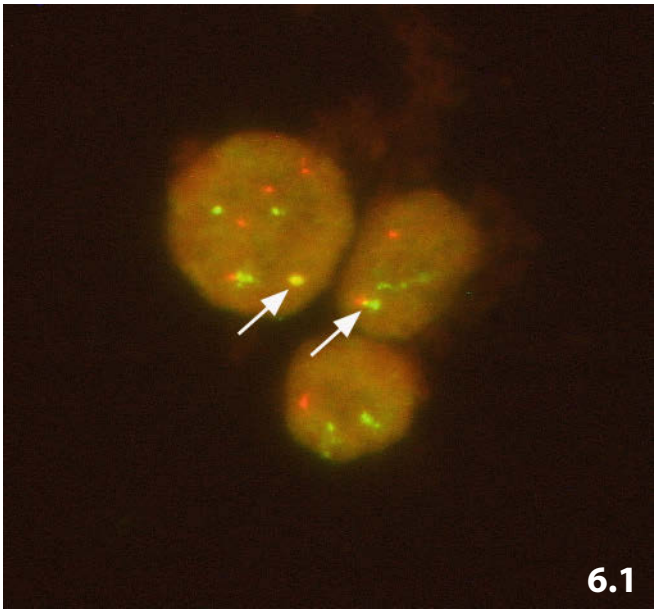
6.1

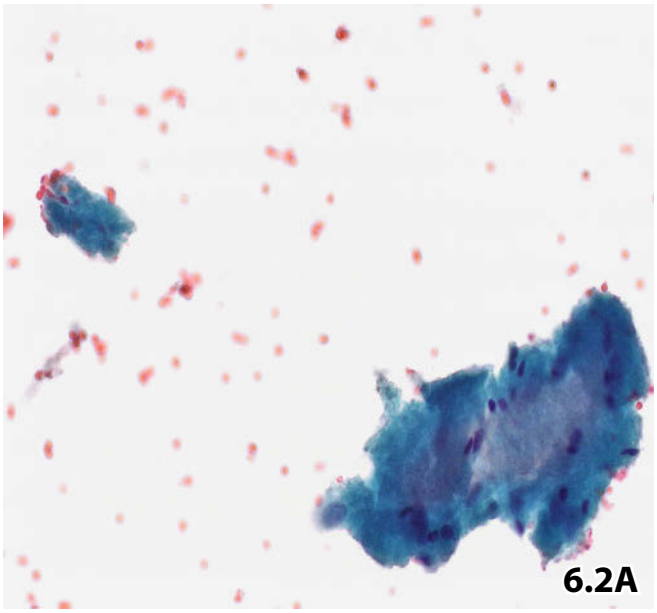
6.2A

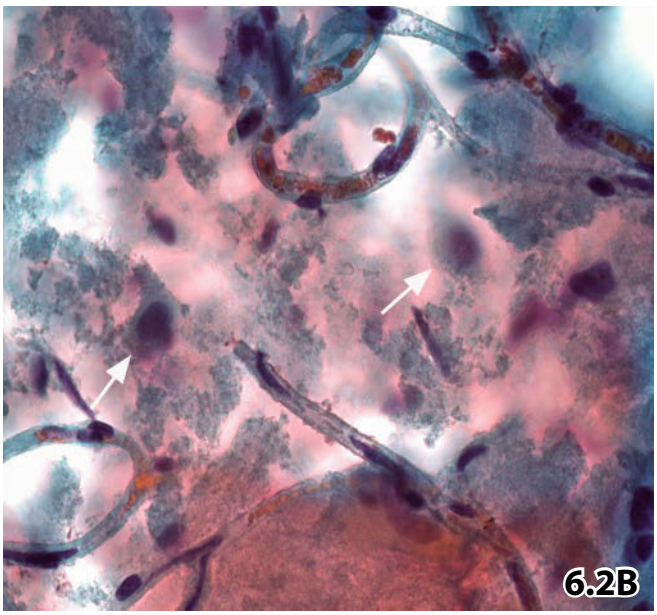
6.2B

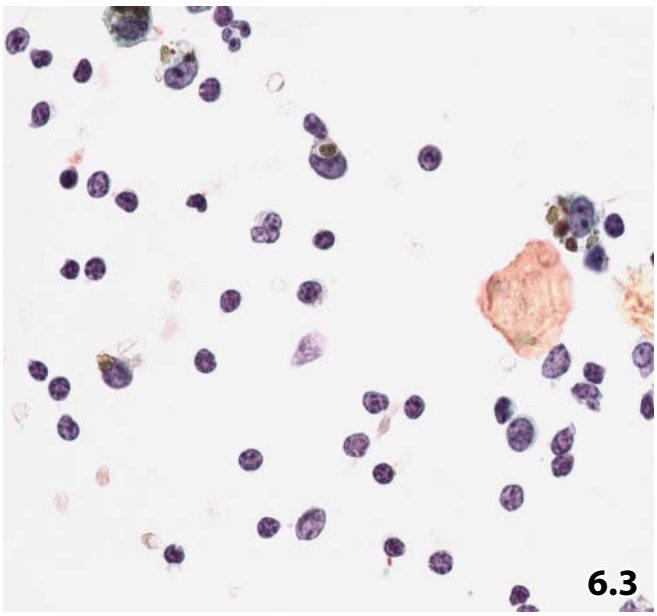
6.3

**Fig. 6.4A, B Nonspecific reactive cellular atypias.**
Lyme borreliosis involving central nervous system was clinically suggested in a 39-year-old man, but the diagnosis could not be validated by repeated serologic tests. Lumbar puncture was performed. Direct sediment smears from the CSF sediment (Pap stain). **A** Detail shows loose aggregation of activated histiocytes/monocytes. Note pronounced nuclear polymorphism, coarse chromatin, and multiple small and large nucleoli. Distinct eccentric position of the nuclei within a polyhedral cytoplasm. A few normal lymphocytes are also present (arrows). **B** Lower magnification exhibits a mixed, typically reactive lymphoid cell population including small lymphocytes, plasmacytoid cells, and lymphoid blasts. A few histiocytes are observed as well.



**Fig. 6.5 Bacterial meningitis.**
A considerable number of neutrophils and activated histiocytes in a sample of lumbar CSF. Note the coccoid bacteria frequently arranged in files (arrows) (Cytospin preparation, Pap stain, high magnification).
*Final diagnosis:* Streptococcal meningitis.

**Fig. 6.6 Lyme disease.**
A 68-year-old woman presented with headache and abnormal laboratory CSF values. Serologic and clinical tests revealed Lyme borreliosis attending by myelomeningoradiculitis.
High magnification of the hypercellular lumbar CFS shows small and enlarged reactive lymphocytes, plasmacytoid cells (arrows), blast cells (arrowhead), and activated histiocytes (right margin) (Cytospin specimen, Pap stain). Mitotic activity of monocytes and lymphocytes is present as well (not shown).

**Fig. 6.7 Cryptococcosis.**
Lumbar CSF from a patient with AIDS contains multiple small groups of yeasts showing a prominent capsule and buds. Enhanced refractivity of the fungi is best recognized by lowering the substage condenser of the light microscope. The background of the smear is completely clean (direct sediment smear, Pap stain, high magnification).

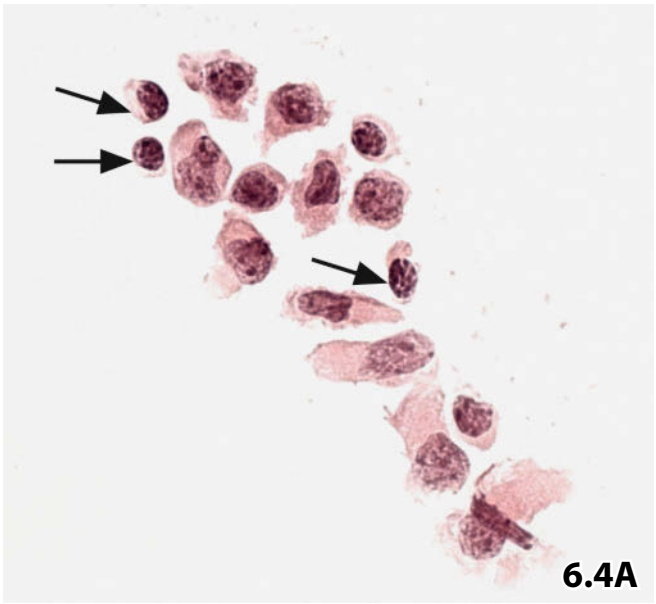
6.4A

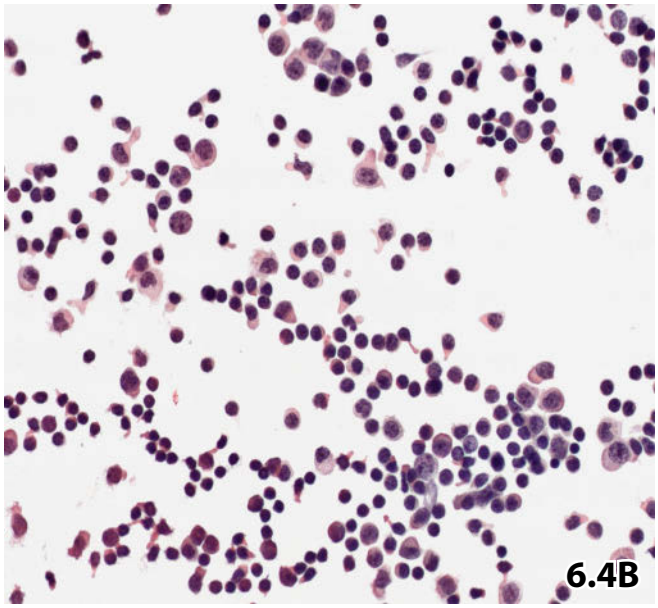
6.4B

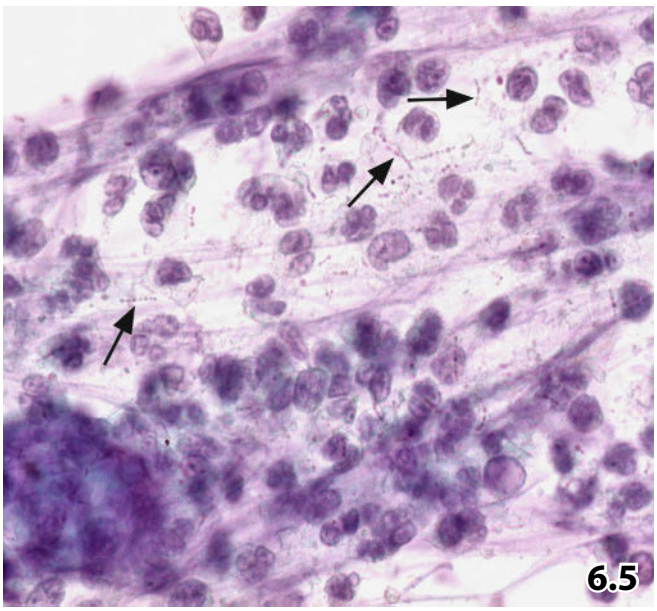
6.5

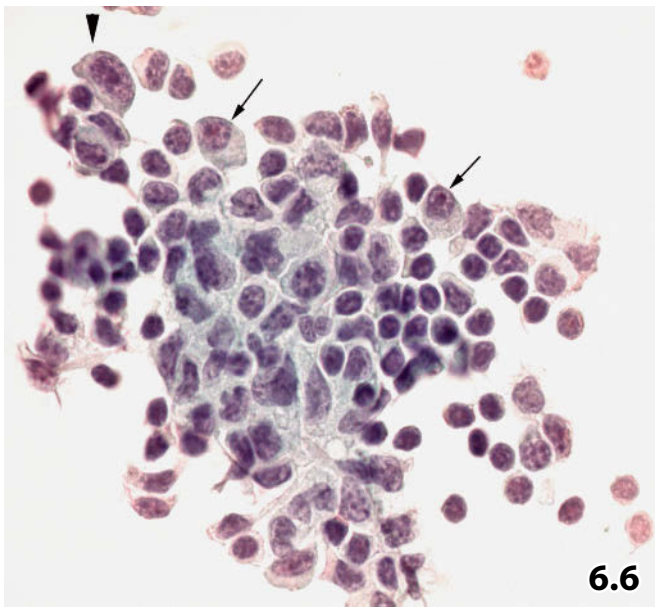
6.6


6.7

**Figs. 6.8–6.13 Diagnostic dilemmas concerning typing of metastatic tumors.**
Differential diagnosis considerations are shown through five different neoplasms. We would like to emphasize that an appropriate immunocytochemical panel of antibodies is extremely helpful in achieving an accurate cytologic diagnosis.

**Fig. 6.8** (case #1) Bronchioloalveolar carcinoma versus. . .
A female patient presented with a history of metastatic bronchioloalveolar carcinoma. High magnification shows discrete carcinoma cells in a direct sediment smear of lumbar CSF. Carcinoma cells share morphologic features with both activated monocytes and malignant lymphoid blasts (Pap stain).



**Fig. 6.9** (case #2) Small-cell pulmonary carcinoma versus. . .
High magnification shows a cluster of cells that originate from a small-cell carcinoma of the lung. Cell dissociation and degenerative changes may cause major problems distinguishing between carcinoma, malignant lymphoma, and poorly preserved activated histiocytes (lumbar CSF, conventional sediment smear, Pap stain).

**Fig. 6.10** (case #3) Breast carcinoma cells: toothed wheel-like cell appearance.
Carcinomatous meningitis in a woman with a positive history of breast carcinoma. Direct sediment smears (Pap stain) show only a few malignant cells with typical but nonspecific toothed wheel-like appearance (high magnification). Compare with tumor cells presented in Fig. 6.11A.

**Fig. 6.11A, B** (case #4) Cells of poorly differentiated squamous cell carcinoma: toothed wheel-like appearance.
Carcinomatous meningitis in a woman with a history of metastatic, poorly differentiated squamous cell carcinoma of the cervix. **A** Lumbar CSF contains numerous malignant cells showing cytoplasmic protrusions and blebs, which are similar to the alterations on breast carcinoma cells (Fig. 6.10). Note that mitotic tumor cells may have a toothed wheel-like appearance as well (arrow). The cells from metastatic breast neoplasia and cervical carcinoma differ in the chromatin texture and in the immune pattern (Cytospin preparation, Pap stain, high magnification). **B** Immunocytochemical positivity of the squamous carcinoma cells for CK5/6 (Pap-prestained Cytospin preparation).

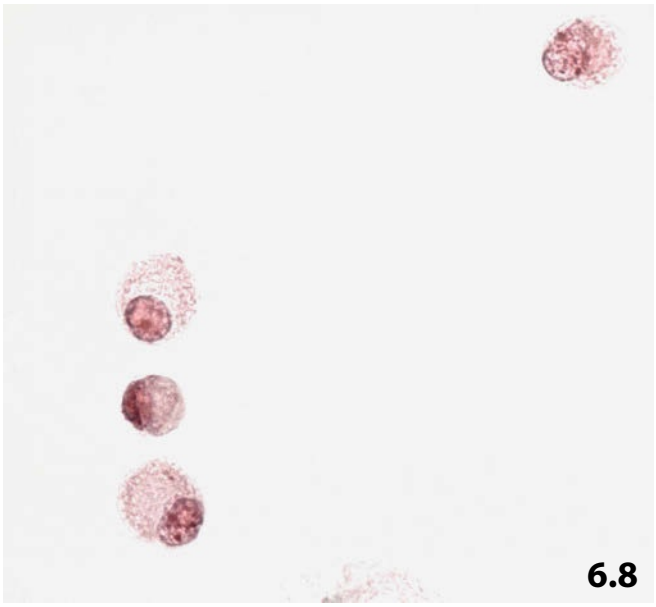

6.8

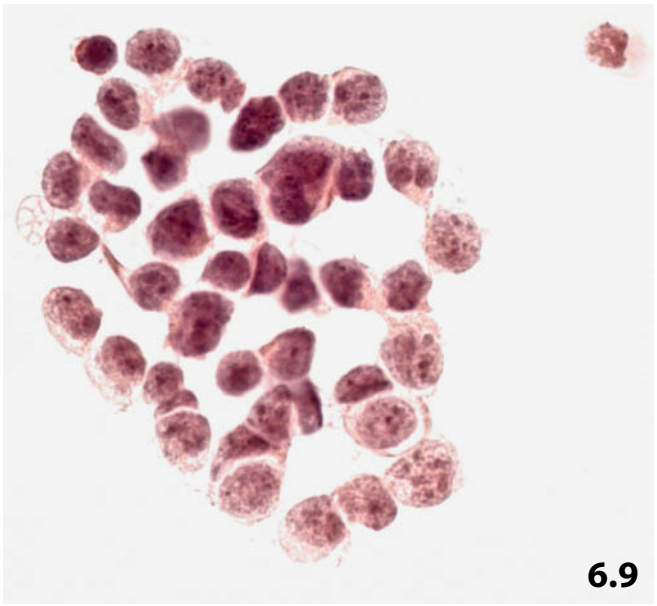

6.9

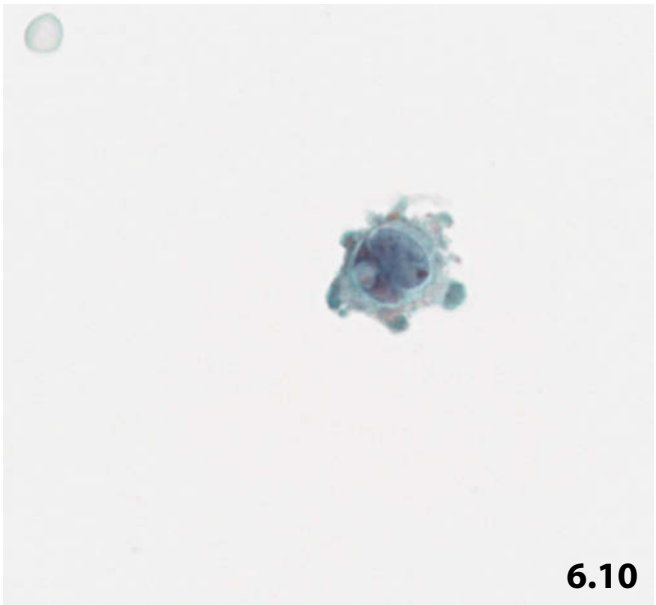

6.10

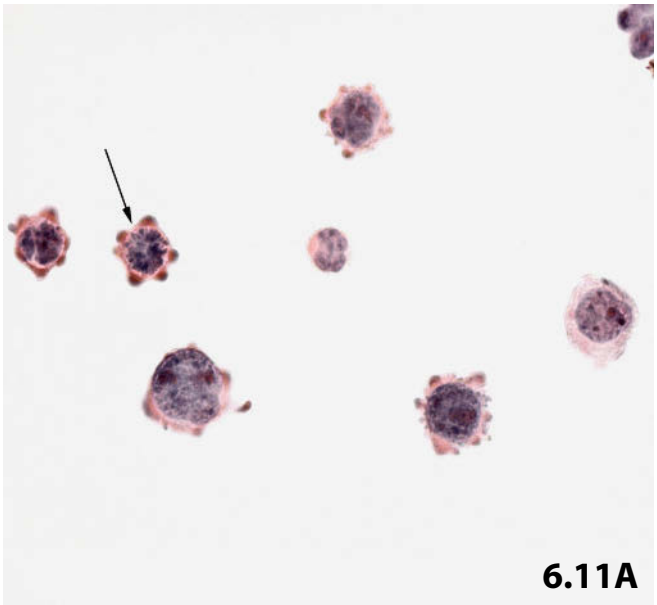

6.11A

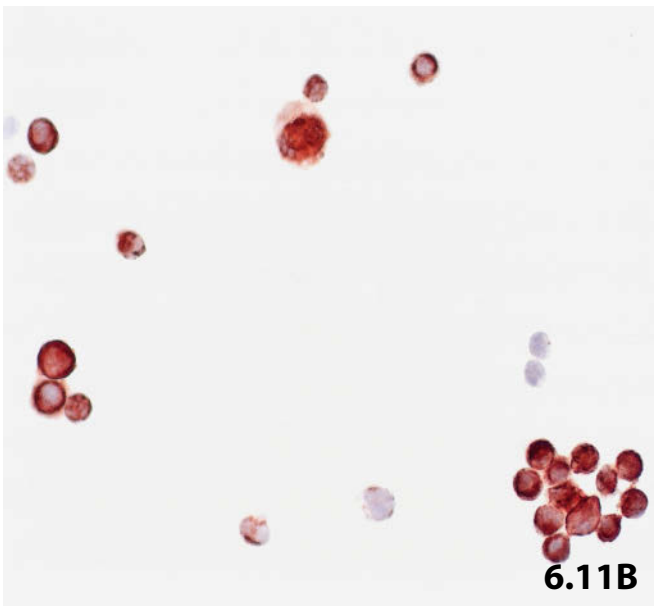

6.11B

**Figs. 6.12 and Fig. 6.13** (case #5) Gastric adenocarcinoma versus activated histiocytes/monocytes.
A 53-year-old man presented with indistinct cerebral symptoms. First of all, lumbar and ventricular liquor was sampled.
*Cytologic diagnosis:* Mucinous adenocarcinoma.
*Postmortem diagnosis:* Metastatic gastric adenocarcinoma of the signet ring cell variant, carcinomatous meningitis.

**Fig. 6.12** Lumbar CSF: Cytospin preparations revealed abundant histiocytoid/monocytoid cells (lower left) but signet ring-like cells containing pink-staining mucus were also present (upper right) (Pap stain, high magnification).



**Fig. 6.13** Ventricular CSF: Cytologic diagnosis of a mucus-producing adenocarcinoma was made by positive immunostaining of both cell types described above for pancytokeratin-MNF116, proving the carcinomatous origin of the histiocyte-like cells (Pap-prestained direct sediment smear).

**Fig. 6.14 Breast carcinoma.**
Breast carcinoma cells in direct sediment smears of lumbar CSF show distinct morphologic characteristics: Cell arrangement in rows, eccentrically positioned clear nuclei, fine granular chromatin, cleaved membranes, dense and focally granular cytoplasm, and cytoplasmic mucus inclusion (arrow) (Pap stain, high magnification).

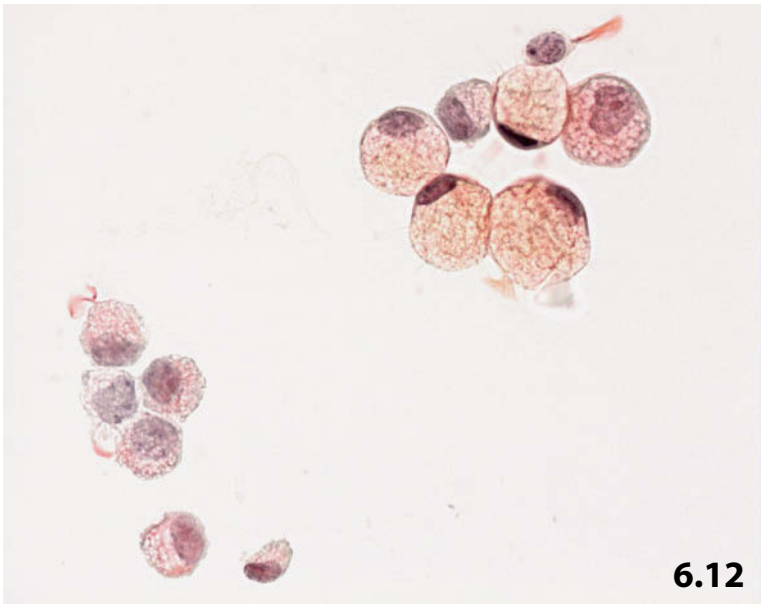

6.12

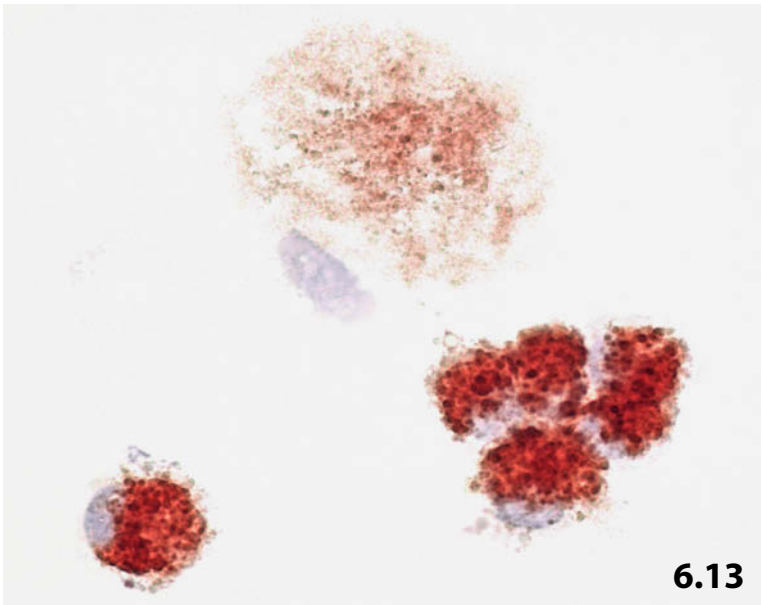

6.13

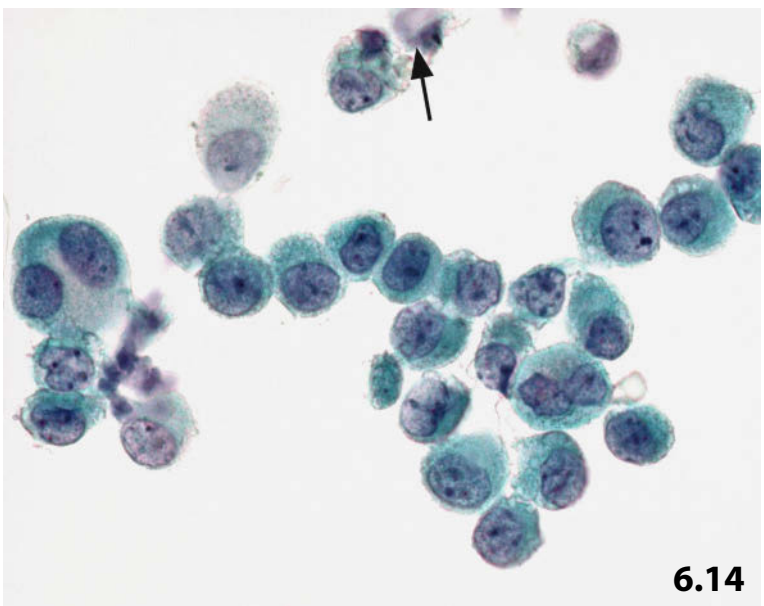

6.14

**Fig. 6.15 B lymphoblastic leukemia.**
A 69-year-old male with a positive history of B-ALL. Lumbar CSF contains numerous medium-sized pleomorphic lymphoid blasts. Cell pattern obviously appears monomorphous (direct sediment smear, Pap stain, lower magnification).

**Figs. 6.16–6.18 Acute myeloid leukemia.**
Three examples of acute myeloid leukemia. Varied preparation techniques and staining methods were applied to the cytologic specimens.

**Fig. 6.16** (case #1) A 44-year-old woman presented with a history of acute myeloid leukemia complaining of headache. Cytospin preparations from a lumbar CSF were composed of myeloid precursors and myeloblasts (Pap stain, high magnification). Cytologic findings were consistent with AML.



**Fig. 6.17** (case #2) Tumor cells from another case immunocytochemically express myeloperoxidase, confirming the morphologic diagnosis of myeloid malignancy (Pap-prestained direct smear).

**Fig. 6.18** (case #3) Direct sediment smear of CSF from a third patient with AML was MGG-stained (high magnification). A similar overall cell pattern can be observed comparing with Fig. 6.16; however, cytoplasmic details are more explicit compared to those in the Pap-stained specimen.

**Fig. 6.19 High-grade non-Hodgkin lymphoma.**
An 48-year-old man with a positive history of malignant lymphoma presented with diffuse neural disorders. Direct sediment smears from lumbar CSF are rich in malignant lymphoid blasts of the centroblast type. Large tumor cells contain pleomorphic nuclei, mostly with cleaved contours, and multiple distinct nucleoli typically located close to the nuclear membrane (Pap stain, higher magnification).
*Previous histologic diagnosis from a lymph node:* Follicular lymphoma, grade 3b.

**Fig. 6.20 Hodgkin lymphoma.**
A rare occurrence of Hodgkin disease in a 33-year-old woman who presented with tumor invasion of the spinal cord subsequent to repeated chemotherapy. High magnification shows a heterogeneous inflammatory cell pattern predominantly composed of activated (atypical) lymphocytes and histiocytes (lumbar CSF, Cytospin preparation, Pap stain, high magnification).
*Indeterminate cytology:* Reed-Sternberg cells and Hodgkin cells are completely absent; therefore cytology cannot distinguish between nonspecific inflammation and the reactive cellular component of Hodgkin lymphoma.

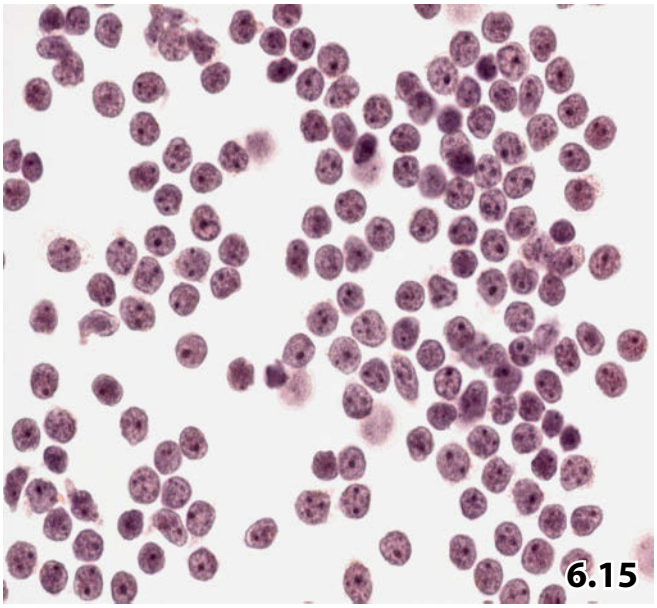
6.15

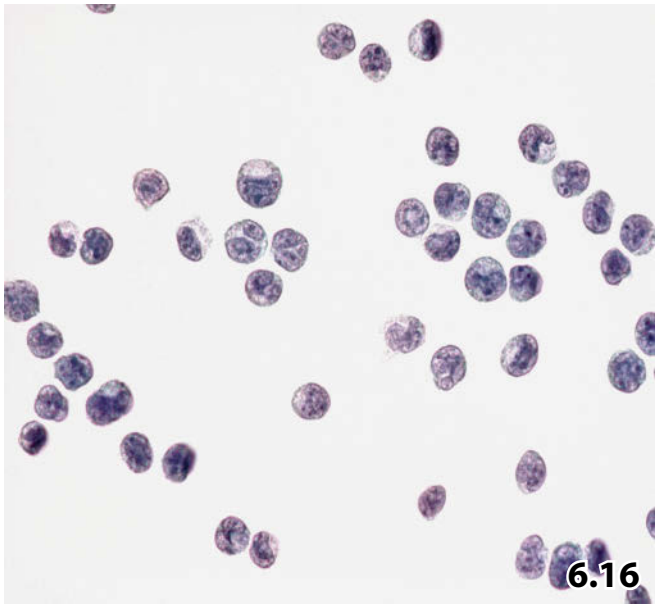
6.16

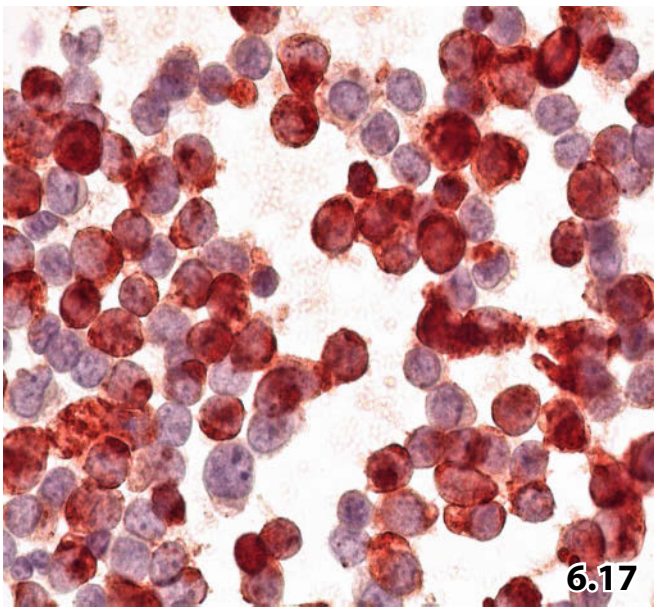
6.17

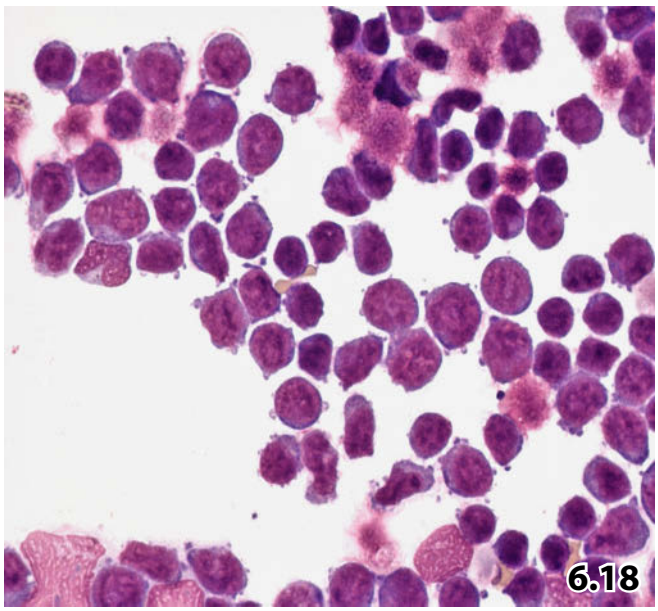
6.18

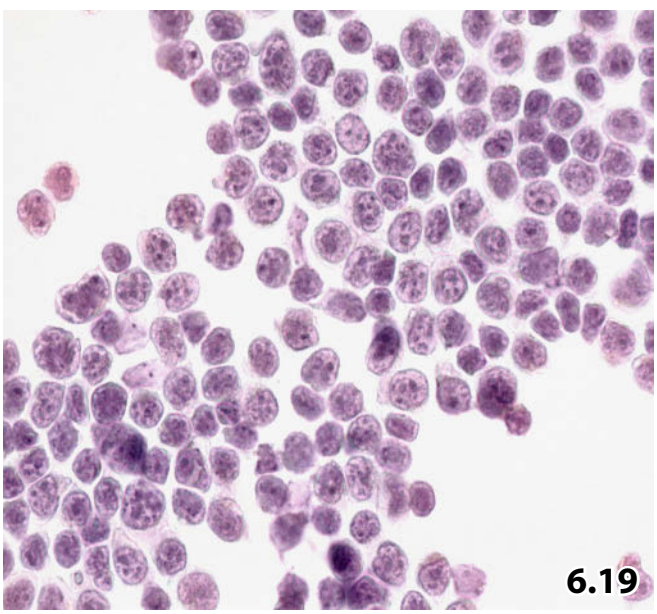
6.19

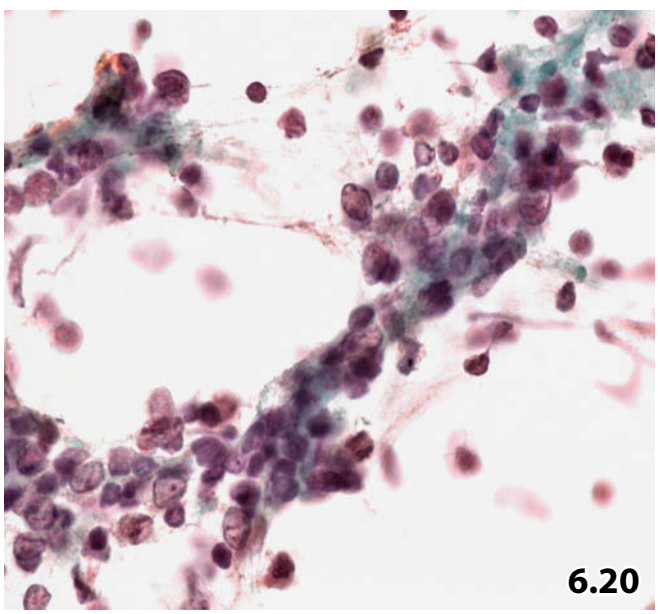
6.20

**Fig. 6.21 Glial neoplasms: high-grade astrocytoma.**
A younger woman with a positive history of anaplastic astrocytoma presented with tumor relapse. Ventricular CSF reveals compact clusters of large malignant cells (direct sediment smear, Pap stain, high magnification).

Malignant glial cells occurring in epithelioid aggregates strongly mimic undifferentiated carcinoma

**Figs. 6.22 Glial neoplasm: ependymoma.**
A 45-year-old man presented with increasing cerebrospinal symptoms after incomplete surgical excision of a low-grade ependymoma. Cytology of lumbar CSF showed heterogeneous aggregations of histiocyte-like tumor cells. Note bland chromatin texture in contrast to moderate and high N/C ratios, and pleomorphic nuclei (direct sediment smear, Pap stain, high magnification). Positive immunocytochemical staining of the tumor cells for vimentin is not shown.



**Fig. 6.23 Langerhans cell histiocytosis.**
A 3-year-old boy with clinical suspicion of Langerhans cell histiocytosis involving the pituitary stalk is presented. The direct sediment smear from a lumbar CSF sample reveals a few atypical histiocytoid cells, which are compatible with neoplastic Langerhans cells, which are larger than macrophages. The nuclei are kidney-shaped, showing additional deep grooves and indentations. Chromatin is vesicular and the cytoplasm wide with neat margins (Pap-restained smear after having established positive immunoreactivity for CD1a, high magnification).
*Cytologic and immunocytochemical diagnosis:* Langerhans cell histiocytosis. Positive immunoreaction of the atypical cells for CD1a cannot be shown. Electron microscopic investigation for Birbeck granules could not be carried out due to the extreme low number of atypical cells.
*Final diagnosis:* Langerhans cell histiocytosis in the area of the pituitary stalk.

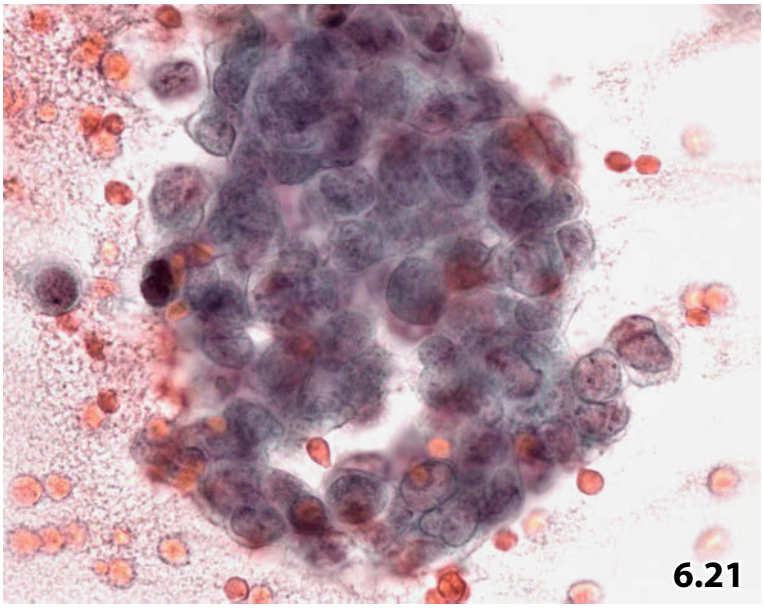

6.21

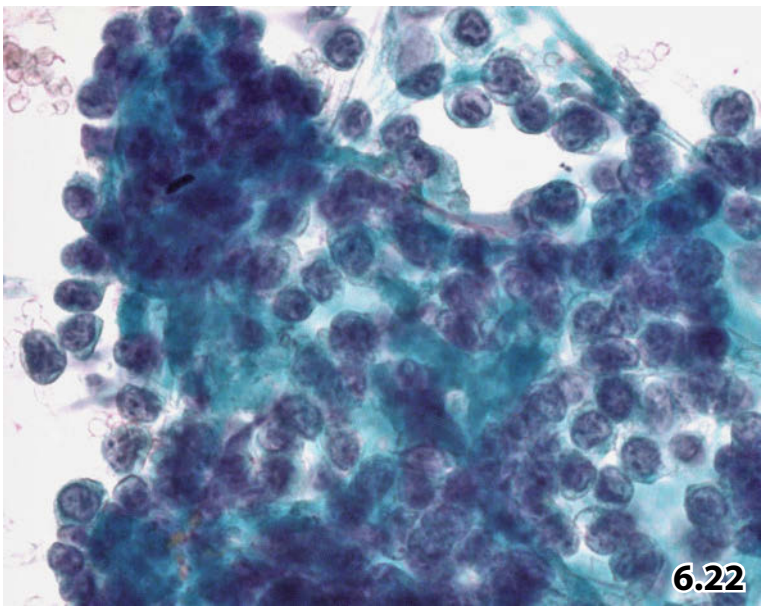

6.22

6.23

# Section 6.2
# Central Nervous System: FNAB and Imprints

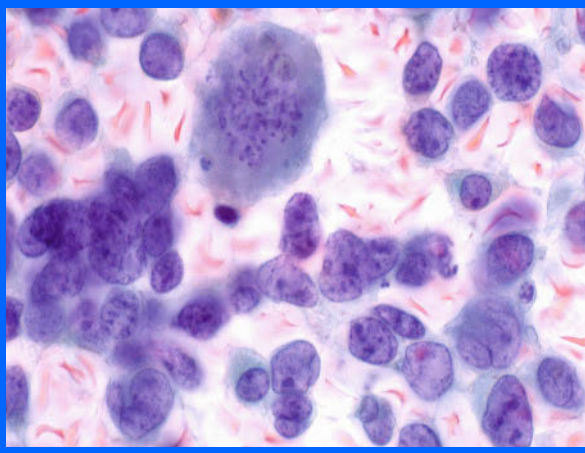

## Intracranial Lesions

### 6.2.1 Introduction

- Cytologic examination on tissue obtained from the central nervous system (CNS) usually is performed in the context of intraoperative examination of stereotactic biopsies or tumor resections. In this case, squash or crush preparations, stained with various methods such as H&E, May-Grünwald-Giemsa, or Toluidine blue are made of fresh tissue samples, often simultaneously with frozen sections.
- Several studies have shown that the diagnostic accuracy by cytology, compared with the definite histological diagnosis, reaches 85–90% [6, 25, 31, 33]. The highest rates (up to 96%) are usually reached in the diagnosis of meningiomas, metastases, and glioblastomas, whereas intraoperative diagnostic accuracy of lesions such as oligodendroglioma or ependymoma is about 80%.
- The morphological advantage of cytologic smear preparations over frozen sections is obvious in tumors, in which the evaluation of fibrillary background or cytoplasmic processes plays an important role in establishing the diagnosis.

**Caution**

- The clinical and radiological findings are crucial for an accurate cytological and histological diagnosis.
- Especially the patient's age and his or her relevant history, the location of the lesion, symptoms such as seizures or vomiting, and the imaging results should be known at the time of pathomorphological diagnosis. All this information may strongly influence the differential diagnostic considerations.

- The diagnostic value of additional methods such as immunocytochemistry, in situ hybridization, and molecular genetics strongly depends on the differential diagnostic considerations and is therefore discussed in the particular sections.
- As our experience with neuropathological specimen is limited, we present here only a short overview considering the cytological features of the most common and a few rare nontumoral and tumoral lesions of the CNS.
- Regarding special diagnostic problems we refer to neuropathological standard textbooks or to the references listed at the end of this chapter.

### 6.2.2 Normal Brain and Benign Nontumoral Lesions

#### 6.2.2.1 Normal Anatomy

As the center of the human nervous system, the brain is protected by skin and skull and surrounded by fibrous membranes called the dura mater, the arachnoid membrane, and the delicate innermost pia mater. Between the pia mater and the arachnoid membrane lies the subarachnoid space, which is filled with cerebrospinal fluid. The brain itself is composed of the cerebral hemispheres, the cerebellum and the brain stem. These compartments enclose the four ventricles (lateral ventricles in the hemispheres, the third ventricle in the central midline, and the fourth ventricle in the brain stem and cerebellum).

Particular parts of the brain harbor the pineal gland and the pituitary gland.

### 6.2.2.2 Cellular Components

The two main cell types of the brain are the neurons (or ganglion cells) and the glial cells.

*Ganglion cell* (Figs. 2.110, 2.111, 6.24)

- Ganglion cells strongly vary in size, but usually they are large cells measuring up to 40 $\mu$m in diameter with one or multiple cytoplasmic processes of different length, called dendrites. The most prominent protrusions that arise from the cell body are also known as axons, the usual mechanism for transmitting signals.
- The nuclei of the ganglion cells are large, usually centrally or paracentrally located, showing prominent nucleoli.
- The often very prominent rough endoplasmic reticulum (Nissl substance) in the cytoplasm is a typical feature of neurons. It stains brown using the Papanicolaou staining procedure and blue with the May-Grünwald-Giemsa (MGG) or DiffQuik stain and can occasionally obscure the nucleus.

The glial cells (Fig. 6.24) can be subdivided into astrocytes, oligodendroglial cells (microglia), and ependymal cells:

- The *astrocytes*, named after their star-like silhouette, show a small cytoplasmic rim with multiple processes. The nucleus is small with an inconspicuous or absent nucleolus.
- The *oligodendrocytes* are usually small and round with a lymphocyte-like appearance. They sometimes attend neurons, especially in tumoral lesions (referred to as satellitosis).
- *Ependymal cells* are small epithelial cells, lining the ventricular system, showing a cuboidal to columnar shape. The nucleus is centrally located and the cytoplasm frequently has a granular appearance.
- *Choroid plexus cells*. Another cell type, which can be seen in cytologic brain specimens, are cells of the choroid plexus, which produces the cerebrospinal fluid. Their morphology is comparable to ependymal cells, meningeal cells, and certain blood vessel cells.

### 6.2.2.3 Inflammatory Changes

Abscess, infarct and hemorrhage show a very similar morphological pattern, but are caused by many different factors (e.g., bacteria, viruses, vascular obliteration, trauma).

- Microscopically, a variable mixture of cellular debris and inflammatory background is present.
- A few small fragments of brain tissue and normal brain cells may sometimes occur.
- Infectious agents such as bacteria or protozoa are rarely detected in cytological smears. *Toxoplasma gondii* and fungi will most frequently be encountered. Typical virus-associated cellular changes such as enlarged nuclei, multinucleation, nuclear inclusions or perinuclear halos may sometimes be observed.

According to cytomorphology, appropriate immunocytochemical stains, or PCR-based investigations may identify bacteria and certain viral types (e.g., mycobacteria, JC virus, Herpes simplex, cytomegaly virus, rabies virus, and others).

### 6.2.2.4 Cysts

Cysts in the CNS are observed under different conditions. Most often, they are part of primary neoplastic or metastatic lesions or are residual conditions after infarcts or intracranial hemorrhage. In the latter case, degenerate red blood cells, iron-laden macrophages, foamy histiocytes, reactive inflammatory cells, and cellular debris typically occur depending on the age of lesion.

For an overview of cystic lesions of the sellar and suprasellar region, we refer to the article of Smith and colleagues [26].

#### 6.2.2.4.1 Colloid Cyst

A colloid cyst [22] of the brain is typically located at the foramen of Monroe in the anterosuperior part of the third ventricle. It usually occurs in adults and presents with headaches. Radiologically, these lesions are smooth, round and well demarcated. The material, which is obtained by a stereotactic procedure, has a viscous consistence on gross examination and often adheres inside the lumen of the needle.

- The smears show a thick proteinaceous material, which is akin to thyroidal colloid.
- The cellular composite includes foamy macrophages and epithelial cells. The latter are small uniform cuboidal cells, with round nuclei and clear cytoplasm. In most cases, numerous goblet cells can be found, and columnar cells with ciliated surface are sometimes present.

#### 6.2.2.4.2 Rathke Cleft Cyst

- Cytologic smears show cellular aggregates and single cells of benign-appearing squamous cells or columnar cells (occasionally ciliated) as well as various amounts of iron-laden macrophages.
- A proteinaceous or mucinous background is also present [26].

#### 6.2.2.4.3 Epidermoid Cyst

Fluid from epidermoid cysts usually contains benign squamous cells and lamellated keratin.

#### 6.2.2.4.4 Arachnoid Cyst

Smears of arachnoid cyst fluid are usually acellular [26].

#### 6.2.2.4.5 Parasitic Cyst

Parasitic cysts are mostly caused by the larval form of pork tapeworm (*Taenia solium*). Cytologic smears can be completely acellular and clean or show transparent background material, hooklets, and scolices [14].

## 6.2.3 Primary Tumors of the CNS (Selected Entities)

### 6.2.3.1 Pilocytic Astrocytoma (WHO Grade 1)

[3, 8, 30]

- Cytologic smears show scattered small cells in a clear, sometimes myxoid background.
- The nuclei are spindle-shaped with fine chromatin.
- The cytoplasm shows many small fibrillary hair-like processes.

The occurrence of Rosenthal fibers and eosinophilic granular bodies is helpful in distinguishing between pilocytic astrocytoma and diffuse astrocytoma.

### 6.2.3.2 Diffuse Astrocytoma (WHO Grade 2) [3, 8]

- Cytologic preparations show unevenly distributed cells in a clear background. The tumor cells have filamentous cytoplasmic processes and small, mildly pleomorphic nuclei with fine granular chromatin. Small inconspicuous nucleoli sometimes occur.
- Mitoses and necrotic debris are absent.
- In some areas, thin-walled capillaries can be observed forming a loose network between the tumor cells; the endothelial lining consists of one to two cell layers.

### 6.2.3.3 Pleomorphic Xanthoastrocytoma (WHO Grade 2) [1]

Pleomorphic xanthoastrocytoma (PXA) usually presents as a superficial cerebral mass in adolescents and young adults and causes symptoms such as seizures and vomiting.

- Cytological smears show numerous pleomorphic giant cells on a fibrillary background. The nuclei are bizarre and polymorphous with irregular borders.
- Eosinophilic granular bodies, which are common in histological sections of PXA, are usually absent in cytological smears.
- Hallmarks: The most important cytologic diagnostic factor, in combination with the clinical and radiological findings, is the distinct nuclear and cellular pleomorphism combined with the absence of mitosis, necrosis, and prominent vascular endothelial proliferation.

For differential diagnosis of CNS lesions presenting with giant cells in cytological specimens, see also the article by Bleggi-Torres and colleagues [1].

### 6.2.3.4 Anaplastic Astrocytoma (WHO Grade 3)

[8] (Fig. 6.25)

- Cytologic smears are more cellular than those of diffuse astrocytoma and the tumor cells are disseminated in a hemorrhagic background.
- The neoplastic cells have oval irregular and pleomorphic nuclei, and a small cytoplasmic rim with short and thick processes (Fig. 6.25B). The chromatin is coarse.
- A few mitoses can be encountered.
- The inner layer of the blood vessels is composed of two to three endothelial cell layers, and the plump endothelial cells show a coarser and more granular chromatin than in diffuse astrocytomas (Fig. 6.25A).

### 6.2.3.5 Glioblastoma (WHO Grade 4)

[3, 8] (Fig. 6.26)

- In cytologic specimens of glioblastomas, many obviously malignant cells are densely spread in a necrotic background and admixed with thick-walled blood vessels with up to ten or more endothelial cell layers (Fig. 6.26A).
- The tumor cells show short and blunt cytoplasmic processes, whereas the hyperchromatic nuclei are large, irregularly shaped, and of variable size. The chromatin is dense and coarse, and the nucleoli may be very prominent with an irregular shape (Figs. 6.26B and 6.26C).
- Mitoses are numerous (Fig. 6.26C).

#### 6.2.3.5.1 Gliosarcoma

An additional mesenchymal cell population can be observed in a subgroup of glioblastoma (so-called gliosarcoma). These cells usually predominate the cytologic smears. The mesenchymal cells are extremely polymorphic, spindle-shaped to fusiform cells including hyperchromatic, pleomorphic, and sometimes bizarre nuclei. Multinucleated giant cells and/or cells with a rhabdoid appearance may be observed. In some cases a chondroid, osteoid, or leiomyomatous differentiation may be observed [21].

### 6.2.3.6 Oligodendroglioma (WHO Grade 2)

[3, 8] (Fig. 6.27)

- In cytological smears, the tumor cells are sparsely scattered and usually appear slim with many filamentous cytoplasmic processes. The nuclei are small and round with uniform, finely granular chromatin.

- The cells are intermingled with a fine capillary network.
- The background is clean; mitoses and necrotic debris are absent.

### 6.2.3.7 Anaplastic Oligodendroglioma (WHO Grade 3) [7, 8] (Figs. 6.28–6.30)

**Microscopy**

- Tumor cells are densely distributed in a partially necrotic background with a vacuolated appearance.
- Cells show a large polymorphous nucleus, the chromatin is coarse and granular, and mitotic figures are common.
- The cytoplasm is distinct and its processes, if available at all, are somewhat plumper compared to those in G2 oligodendrogliomas; they are frequently arranged adjacent to blood vessels.
- The blood vessels are more crowded and the endothelial cells have larger nuclei in comparison to those in G2 oligodendroglioma.

**Molecular Genetics**

Differentiating these tumors from other, especially astrocytic, lesions can be difficult. A FISH test may help, since a deletion of the short arm of chromosome 1 (1p) and a deletion of the long arm of chromosome 19 (19q) occur exclusively in oligodendroglial cells (Fig. 6.30).

### 6.2.3.8 Oligoastrocytoma [8]

- In cytologic preparations of oligoastrocytomas, a mixture of small round oligodendroglial cells and large astrocytic cells can be observed.

A subdivision into G2 or G3 oligoastrocytoma can be made dependent on the grade of cellular atypia, endothelial cell proliferation, and the presence of necrotic debris and mitoses.

### 6.2.3.9 Ependymoma (WHO Grade 2) [3, 15, 29]

Ependymomas are the most common neoplasms of the spinal cord.

- Cytologic smears are usually cellular and composed of monomorphous small cells.
- The round-to-oval nuclei often exhibit grooves, and the cytoplasm may extend to glial fibrils.
- A perivascular arrangement of the tumor cells (pseudorosettes) and hyaline globules are common features in cytological and histological specimens.

#### 6.2.3.9.1 Myxopapillary Ependymomas (WHO Grade 1)

Myxopapillary ependymomas are usually located in the conus-cauda-filum terminale region.

- In cytological smears, an abundant myxoid background is frequently present, whereas papillary formations are rarely observed.

### 6.2.3.10 Choroid Plexus Papilloma (WHO Grade 1) and Choroid Plexus Carcinoma (WHO Grade 3) [3, 19]

Choroid plexus tumors are papillary neoplasms derived from choroid plexus epithelium. They occur in children and are usually located in the third and lateral ventricle of the brain. Clinically, they present with hydrocephalus by producing large amounts of CSF simultaneously obstructing its flow. Radiologically and macroscopically, the lesions are usually cystic with a solid, sometimes papillary or lobulated fraction. The tumor is highly vascularized.

- Cytologic specimens contain single cells, cohesive cell clusters, papillae with fibrovascular cores, and scattered psammoma bodies.
- The tumor cells exhibit cuboidal to cylindric shape and round to oval, sometimes elongated nuclei. Small inconspicuous nuclei can be seen embedded in a fine chromatin texture.
  - In choroid plexus papillomas, cellular atypia, if present at all, is very discrete and mitoses are absent.
  - Cells of choroid plexus carcinoma are more atypical, less well organized, and may show some mitoses.

**Differential Diagnosis and Immunocytochemistry**

The most important differential diagnoses include normal choroid plexus tissue and papillary ependymoma.

- Compared to normal choroid plexus epithelium, the smears from papillomas are more cellular with somehow disordered papillae, and the tumour cells have a slightly increased nucleus/cytoplasm ratio.
- In contrast to choroid plexus papillomas, papillary ependymomas usually show fibrillated cells forming perivascular pseudorosettes and ependymal rosettes. The papillary formations usually lack fibrovascular cores.
- Immunocytochemically, ependymoma cells strongly express GFAP positivity and they show weak reactivity for cytokeratin 7. The cells of choroid plexus papilloma show an opposite immunoprofile.

### 6.2.3.11 Angiocentric Glioma (WHO Grade 1) [17, 32]

Angiocentric glioma (ACG) typically occurs in younger people, with refractory epilepsy as the main symptom. The most common locations are the temporal lobes, followed by the temporoparietal, parietal, and frontal lobes.

**Microscopy and Immunocytochemistry**

- Histologically, ACGs are poorly demarcated tumors in the grey and white matter of the brain. The tumor cells show a distinct perivascular arrangement.
- Cytologically, the spindle-shaped neoplastic cells are embedded in a fibrillary background. They are monomorphic, showing elongated oval nuclei and speckled chromatin. The cytoplasm is focally reddish to pink and may reveal a long astrocytic process. Rosenthal fibers, eosinophilic granular bodies, mitoses, necrosis, myxoid background, and vascular proliferation are virtually never observed.
- Immunocytochemically, the tumor cells show a strong positivity for GFAP, S100, and synaptophysin. A dot-like EMA-positivity is quite characteristic.

### 6.2.3.12 Chordoid Glioma of the Third Ventricle (WHO Grade 2) [28]

These tumors exclusively occur in the third ventricle/hypothalamic region and are categorized in the group of other neuroepithelial tumors according to the current WHO classification [17].

- The cytological smears of these tumors are usually cellular.
- As Takei and colleagues [28] report, the epithelioid tumor cells are mostly arranged in cohesive sheets, nests, and strands, while some three-dimensional, papillary-like fronds can also be seen.
- The tumor cells show round to oval, partly eccentrically positioned nuclei showing finely granular chromatin and sporadic small nucleoli. A slight variation in the nuclear size, binucleation, a few mitotic figures, and rare intranuclear pseudoinclusions can be seen.
- The polygonal or elongated cytoplasm shows rare vacuolation and long but flimsy processes.
- The tumor cells are intermingled with a lymphoplasmacytic population, sometimes forming lymphoglandula bodies.
- Slight basophilic, mucinous material and some debris-like substance might be observed in the background of the smears.

**Differential Diagnosis and Immunocytochemistry**

- Immunocytochemically, the tumor cells strongly express GFAP, cytokeratin 7, vimentin, EMA, CD34, and NSE.
- The most important differential diagnosis is the chordoid variant of meningioma; its cells are cytologically very similar to chordoid glioma cells, but GFAP expression is usually absent in meningiomas.

### 6.2.3.13 Dysembryoplastic Neuroepithelial Tumor (WHO Grade 1) [2, 3, 20]

Dysembryoplastic neuroepithelial tumor (DNET) is a glia-neuronal neoplasm, usually supratentorially located. It occurs most often in children and young adults in the first two decades of life and presents with partial seizures.

- Cytologic smears and squash preparations are cellular showing single cells and/or cell clusters; small cell aggregates may occasionally be arranged around small capillaries. A myxoid or partly fibrillary background is almost always present.
- The tumor cells are rather small and often appear round to oval: they are referred to as OLCs (oligodendroglia-like cells). Multinuclear giant cells may occur.
- Elongated naked nuclei sometimes occur. The nuclei have irregular contours with indentations or grooves, showing a fine granular chromatin and multiple small nucleoli. Intranuclear eosinophilic pseudoinclusions may be present.
- Note that mature neurons can be found in most cases.

**Differential Diagnosis**

The presence of eosinophilic granular bodies may be helpful in distinguishing this entity from oligodendroglioma.

### 6.2.3.14 Central Neurocytoma (WHO Grade 2) [27]

Central neurocytomas typically occur in young adults and grow in the ventricles.

- Cytologic smears are usually cellular revealing isomorphous, round cells with small, ill-defined cytoplasm. The nuclei are round to oval with finely dispersed chromatin and small nucleoli. Mitotic figures, nuclear polymorphism, and necrotic debris are usually absent.
- A fibrillary background with neuropil matter can generally be observed, although the tumour cells lack processes. Sometimes, hemosiderin-laden macrophages and histiocytic giant cells can be found.

**Differential Diagnosis**

Cytological preparations of oligodendroglioma virtually never contain a fibrillary background and often show gemistocytic or astrocytic cells, which cannot be found in smears of central neurocytoma.

### 6.2.3.15 Papillary Glioneural Tumor (WHO Grade 1) [13, 17, 32]

Papillary glioneural tumor is a rare low-grade neoplasm, usually located in the cerebral hemisphere with a predilection for the temporal lobe and periventricular area. It was described first by Komori et al. [13] and sometimes considered a variant of ganglioglioma. Due to its good prognosis and histological appearance, it is recognized as a separate entity in the fourth edition of the WHO classification of CNS tumors.

- Histology: These tumors show a biphasic appearance. The neuronal component consists of ganglion cells, ganglioid cells, and mature neurocytes embedded in a neuropil-rich background. Flat-to-cuboidal spindle-shaped astrocytes with round nuclei forming single-layer and three-dimensional pseudo-papillae demonstrate the glial component. The cells occasionally show reactive changes.
- Cytology: Depending on the histologic pattern, the cytological specimens show both pseudo-papillary formations composed of centrally located hyalinized vessels surrounded by cuboidal tumor cells and dispersed small round cells; the latter having neuroendocrine nuclear features and small to moderate cytoplasm. Some ganglion cells can occasionally be seen. The background usually contains neuropils.

#### Immunocytochemistry

The neuronal component is positive for neuronal markers such as synaptophysin or neuron-specific enolase, whereas the glial cells express GFAP. The proliferation fraction, assessed by the immunomarker Ki67, is usually 2–3%, mainly confined to the neuronal cell component.

### 6.2.3.16 Papillary Tumor of the Pineal Region (WHO Grade 2 or 3) [10, 17, 32]

This rare neuroepithelial tumor, first described by Jouvet et al. [10], is solely localized in the pineal region.

- Histologic paraffin sections show a papillary tumor including multilayered perivascular pseudo-rosettes.
- Cytology: depending on the histology, cytologic specimens display papillae with central fibrovascular cores, numerous single cells, and a clear background. The round to oval cells have a plasmacytoid appearance and cytoplasmic vacuoles and nuclear grooves may be encountered.
- An anaplastic variant with more pronounced cellular atypia may occur.

#### Immunocytochemistry

Immunocytochemistry shows positivity for broad-spectrum cytokeratins, S100 protein, and neuron-specific enolase. A weak GFAP expression and a weak dot-like cytoplasmic staining for epithelial membrane antigen can be seen.

### 6.2.3.17 Medulloblastoma (WHO Grade 4) [3, 16]

Medulloblastoma is a malignant small-cell tumor of the cerebellum, usually affecting children and young adults in the first two decades of life.

- Cytologically, medulloblastoma is composed of cells that reveal scanty to broad cytoplasm and nuclear pleomorphism of varying degrees.
- Two tumor types can be differentiated cytologically:
  1. The differentiated variant exhibits neuroblastic differentiation and a distinct hypercellularity indicated by small monomorphic cells and frequent Homer-Wright rosettes.
  2. The cells of the undifferentiated type exhibit nuclear pleomorphism to variable degrees, granular chromatin, and prominent nucleoli. Mitotic and apoptotic figures, target inclusions, and cell phagocytosis are common incidents. Rosettes occur rarely and appear vague.

#### Differential Diagnosis and Immunocytochemistry

Immunocytochemically, the tumor cells are positive for synaptophysin and sometimes for GFAP.

The differential diagnoses include atypical teratoid/rhabdoid tumor of the brain (usually INI1-negative), neuroblastoma, retinoblastoma, pinealoblastoma (tumors that are rarely located in the cerebellum), lymphoma (positive for lymphocytic markers such as CD45), metastatic carcinoma (positive for cytokeratins), ependymoma (pseudorosettes are GFAP-positive and synaptophysin-negative, with increased calcification), and high-grade astrocytoma (usually strong GFAP positivity).

### 6.2.3.18 Atypical Teratoid/Rhabdoid Tumor of the Brain (WHO Grade 4) [3, 23]

Atypical teratoid/rhabdoid tumour (AT/RT) is a highly aggressive neoplasm in the CNS in young children. It is most frequently localized in the intracranial posterior fossa.

- Cytological smears usually are strongly hypercellular made up of large tissue fragments. The latter are composed of tumor cells surrounding capillaries and/or fibrovascular cores, resulting in a papillary appearance.
- The large, round, and pleomorphic tumor cells may exhibit plasmacytoid features with dense amphophilic cytoplasm and eccentric nuclei or a rhabdoid appearance with a broad, eosinophilic cytoplasm (sometimes with globoid inclusions).
- Large eccentrically placed nuclei exhibit prominent nucleoli.

- Another cellular component, which may be very prominent, comprises primitive, small, round cells characterized by a small cytoplasmic rim, speckled chromatin, and small nucleoli.
- Extremely pleomorphic multinucleated cells can also be observed. Mitoses, necrosis, calcifications, and apoptotic bodies are numerous.

**Immunocytochemistry**

The tumor cells are variably positive for GFAP, EMA, cytokeratins, smooth muscle actin, and vimentin. The most helpful marker is INI1, whose nuclear immunoreactivity is lost in AT/RT cells.



### 6.2.3.19 Schwannoma (WHO Grade 1) [3, 5]

Schwannoma of the CNS may occur as conventional, cellular, or melanotic Schwannoma. The most affected sites are the spinal nerve roots and (intracranially) the region around the vestibular ganglion of the eighth cranial nerve, but schwannoma may also arise inside the brain.

- Cytological specimens are usually cellular, containing large clusters of spindle cells, which may show some nuclear palisading.
- The nuclei are club-shaped or elongated with mild pleomorphism and finely granular chromatin, whereas the cytoplasm is fibrillary and ill defined.
- In other areas, the cells are more dissociated with round to oval nuclei and a plump cytoplasm.
- In melanotic schwannoma, the cytoplasm contains melanotic pigment in a varying proportion of the tumor cells.

**Differential Diagnosis and Immunocytochemistry**

- Immunocytochemically, the schwannoma cells are positive for S100 protein and show variable positive staining for GFAP. Positivity for HMB45 may be observed in cells of melanocytic schwannoma.
- Meningioma is the most frequent differential diagnosis with schwannoma. Smears from meningioma show more cell dissociation and the nuclei usually appear more distinct, exhibiting a round to oval shape. EMA positivity of meningioma cells may be helpful for diagnosis. In general, schwannoma cells are EMA-negative.

### 6.2.3.20 Meningioma (WHO Grades 1–3)

Among the meningiomas there are several subtypes with various biological behaviors and distinct cytologic features:

- *Meningioma grade 1*. In smear preparations, the tumor cells occur in clusters as well as singly. Psammoma bodies and meningothelial whorls may be found. The nuclei are round to oval with finely distributed chromatin and overt intranuclear inclusions. Mitoses or necrosis are usually absent.
- *Chordoid meningioma (WHO grade 2)*. In addition to the above-mentioned cellular features of conventional meningioma, cells of chordoid meningioma are often arranged in a cord-like pattern. The background of the smears is composed of mucoid masses and inflammatory infiltrates [9].
- *Rhabdoid meningioma (WHO grade 3)*. This entity frequently shows huge cells with mild nuclear pleomorphism and broad eosinophilic cytoplasm; the latter may exhibit short processes [12]. Individual mitoses may occur.

**Immunocytochemistry**

Meningioma cells are usually positive for vimentin and EMA. Immunostaining for GFAP and S100 protein is negative, while cytokeratins vary in their staining results. Myogenic antigens such as desmin, actin, and myogenin are usually not expressed.

### 6.2.3.21 Hemangioblastoma (WHO Grade 1) [4]

Hemangioblastoma may be associated with the von Hippel-Lindau syndrome or occur sporadically. The tumor is composed of a capillary network enclosing tumor cells, which show a broad pale and sometimes foamy cytoplasm.

- Cytological smears of these tumors characteristically show very cohesive large-cell clusters. Details of the tumor cells are best identified at the marginal areas of the clusters.
- The hyperchromatic round to oval nuclei exhibit evenly distributed chromatin, mild polymorphism, and sporadic nuclear grooves.
- The cytoplasm is usually pale or foamy.
- Hemosiderin may be present.

**Differential Diagnosis**

Distinguishing between metastatic renal cell carcinoma, anaplastic astrocytoma, and meningioma is discussed in the article by Commins and Hinton [4].

### 6.2.3.22 Craniopharyngioma (WHO Grade 1) [3, 26]

Craniopharyngioma (CP) can be divided into an adamantinomatous and a papillary type. The adamantinomatous type is more often seen in children and young adults and usually affects the sellar region, whereas the papillary type occurs more often in elderly adults presenting as a suprasellar tumor. In imaging studies, both tumor types may present as a cystic or solid mass.

- The yellow-brown machinery-oil-like fluid, obtained from adamantinomatous CP, contains cholesterol crystals, which can be seen best in unfixed/unstained smears using polarized light microscopy.
- *Common craniopharyngioma*. The stained smears contain sheets and clusters of basaloid cells, plump anucleate squamous cells (wet keratin), macrophages, and debris.
- *Adamantinomatous CP-type*. Calcifications are virtually always seen in this tumor type.
- *Papillary CP-type*. Nucleated squamous cells dominate the cytological picture, while wet keratin and calcifications are usually absent.

### 6.2.3.23 Granular Cell Tumor of the Neurohypophysis (WHO Grade 1) [24]

Granular cell tumors (GCT) of the neurohypophysis generally show the same cytomorphological features as GCTs in other body regions (Figs. 1.63 and 1.64) (see Sect. 1.2.18, p. 26):

- In a granular background, the ovoid to polygonal cells occur individually or in loose clusters. The cells usually exhibit a low nuclear/cytoplasmic ratio, round uniform nuclei, and eosinophilic granular cytoplasm.

#### Immunocytochemistry

Positivity for S100 protein and a diffuse membranous staining for CD68 (occasionally weak) can be observed.

### 6.2.3.24 Pituitary Adenoma [14, 18]

#### Microscopic Features

- In comparison to normal pituitary gland tissue, the direct smear preparations of pituitary adenomas are more cellular and exhibit a more monotonous cell pattern. There are small to medium-sized, usually round cells, which are arranged in small clusters and trabeculae. Papillary and acinic formations may be observed. The background is clear or contains pale mucoid masses.
- In nonsecreting tumors, the nuclear polymorphism is mild to moderate, the chromatin slightly coarse, and the nucleoli are indistinct. The cytoplasm is clear containing fine vacuoles.
- Nuclear polymorphism, multinucleation, so-called fibrous bodies (paranuclear eosinophilic inclusions), and acidophilic granular cytoplasm typically occur in growth hormone- and prolactin-producing tumors.

#### Differential Diagnosis

Important differential diagnoses are:

- Oligodendrogliomas, which lack the epithelial and glandular architecture of pituitary adenoma.
- Germinomas, which contain a mixed population of small lymphocytes and large atypical germ cells.
- Meningiomas, which usually show meningothelial whorls, uniform spindle cells, and psammoma bodies.

#### Immunocytochemistry

Pituitary adenomas are immunocytochemically positive for neuroendocrine markers (e.g., chromogranin, synaptophysin) and pituitary peptide hormones.

### 6.2.3.25 Chordoma [3, 11] (Figs. 5.71 and 11.33)

Chordoma is a malignant notochordal neoplasm occurring along the axial skeleton, especially in its cranial and sacral areas. Usually adults in their fifth or sixth decade of life are affected, but these tumors also occur in children. In cranial lesions, headaches and nerve palsies are clinical symptoms, whereas sacral tumors produce pain, sphincter disturbances, and neurological symptoms belonging to compressed nerve roots.

More information is provided in Sect. 5.2.3.5, p. 464.

- The smear preparations of these tumors show single cells and sheets of round or cuboidal cells scattered in a mucoid and myxoid-fibrillary background.
- The presence of multivacuolated, large, physaliferous cells is almost pathognomonic for this tumor entity.

#### Differential Diagnosis and Immunocytochemistry

The tumor cells are usually positive for EMA, cytokeratins, and S100 protein.

Myxoid chondrosarcoma and myxoid liposarcoma may present diagnostic dilemma, but absence of physaliferous cells and negative immunoreaction for cytokeratins exclude chordoma. Metastatic adenocarcinomas are usually negative for S100 protein.

### 6.2.3.26 Soft Tissue Tumors

Soft tissue tumors in the CNS are exceptionally diagnosed by cytology alone. They present the same cytomorphological features as stromal tumors from any other body site. For greater detail and cytomorphologic descriptions, we refer the reader to Chap. 17, "Soft Tissue and Bone," p. 1053.

### 6.2.3.27 Lymphoma

Primary lymphomas of the CNS are usually large-cell lymphomas of the B-cell type, but also other lymphomatous entities such as mantle cell lymphoma, marginal zone lymphoma, or T-cell lymphoma may occur. For more information as to cytomorphology, subtyping, differential diagnosis, references, and figures see Sect. 15.3, "Lymph Nodes: Malignant Lymphomas, " p. 950.

## 6.2.4 Metastases (Selected Entities)

(Figs. 6.31 and 6.32)

Carcinoma and melanoma are the most frequently encountered secondary neoplasms within the CNS.

- Smear preparations of carcinomatous lesions show single cells and cohesive clusters of obviously atypical and malignant cells; cell alterations strongly vary between different tumor types. In metastatic adenocarcinoma (Figs. 6.31 and 6.32), some mucin-containing cells and signet-ring-like cells may be seen.
- Melanoma cells are usually discohesive, showing a spindle or epithelioid configuration and optionally pigmented cytoplasm. Nuclear chromatin is variably granular and prominent nucleoli are obvious.



### Immunocytochemistry

Metastatic cells usually express the typical immunocytochemical pattern of their primary tumor. Metastatic carcinomas together with their most important immunocytochemical attributes for cytodiagnostic purpose are discussed in Sect. 15.3.24, p. 978, Table 15.3.3.

*Melanoma* cells variably express melanocytic markers such as Melan A, HMB45, tyrosinase, or S100 protein.

*Pulmonary adenocarcinomas* are usually positive for cytokeratin 7 and TTF-1.

*Thyroid cancer* cells express thyroglobulin and TTF-1.

*Metastatic small-cell* cancers are immunoreactive for cytokeratins, neuroendocrine markers such as chromogranin A or synaptophysin, and frequently for TTF-1.

*Renal cell cancer* usually exhibits CD10, renal cell cancer antigen (RCCMa), EMA, vimentin, and cytokeratins.

*Prostatic cancer* metastases show immunoreactivity for prostate-specific antigen (PSA) and prostatic acid phosphatase (PAP).

*Breast carcinoma:* Positivity for estrogen or progesterone receptor is highly indicative for this neoplasm.

*Metastases of gastrointestinal carcinoma* are usually positive for cytokeratin 20 and CDX2.

## 6.2.5 Further Reading


1. Bleggi-Torres LF, Gasparetto EL, Faoro LN, et al. Pleomorphic xanthoastrocytoma: report of a case diagnosed by intraoperative cytopathological examination. Diagn Cytopathol 2001;24:120-122.
2. Bleggi-Torres LF, Netto MR, Gasparetto EL et al. Dysembryoplastic neuroepithelial tumor: cytological diagnosis by intraoperative smear preparation. Diagn Cytopathol 2002;26:92-94.
3. Burger PC, Scheithauer BW. Tumors of the central nervous system. Washington, DC: American Registry of Pathology, 2007.
4. Commins D L, Hinton DR. Cytologic features of hemangioblastoma: comparison with meningioma, anaplastic astrocytoma and renal cell carcinoma. Acta Cytol 1998;42: 1104-1110.
5. Galant C, Mazy S, Berliere M, et al. Two schwannomas presenting as lumps in the same breast. Diagnostic Cytopathology 1997;16: 281-284.
6. Goel D, Sundaram C, Paul TR, et al. Intraoperative cytology (squash smear) in neurosurgical practice - pitfalls in diagnosis experience based on 3057 samples from a single institution. Cytopathology 2007;18:300-308.
7. Goh SG, Chuah KL. Role of intraoperative smear cytology in the diagnosis of anaplastic oligodendroglioma. A case report. Acta Cytol 2003;47:293-298.
8. Inagawa H, Ishizawa K, Hirose T. Qualitative and quantitative analysis of cytologic assessment of astrocytoma, oligodendroglioma and oligoastrocytoma. Acta Cytol 2007;51:900-906.
9. Inagawa H, Ishizawa K, Shimada S, et al. Cytologic features of chordoid meningioma. A case report. Acta Cytol 2004;48:397-401.
10. Jouvet A, Fauchon F, Liberski P, Saint-Pierre G. Didier-Bazes M, et al. Papillary tumor of the pineal region. Am J Surg Pathol 2003; 27:505-512.
11. Kfoury H, Haleem A, Burgess A. Fine-needle aspiration biopsy of metastatic chordoma: case report and review of the literature. Diagnostic Cytopathology 2000;22:104-106.
12. Kirby PA Rhabdoid meningioma: intraoperative diagnosis using smear preparation. Diagn Cytopathol 2003;29:292-296.
13. Komori T, Scheithauer BW, Anthony DC, et al. Papillary glioneuronal tumor: a new variant of mixed neuronal-glial neoplasm. Am J Surg Pathol 1998;22:1171-1183.
14. Koss LG, Rodriguez CA. The Central Nervous System. In L. G. Koss (Ed.), 'Diagnostic cytology and its histopathologic bases' (5th ed., pp. 1523-1543). Philadelphia: Lippincott Williams & Wilkins, 2006.
15. Kumar PV. Nuclear grooves in ependymoma. Cytologic study of 21 cases. Acta Cytol 1997;41:1726-1731.
16. Kumar PV, Hosseinzadeh M, Bedayat GR. Cytologic findings of medulloblastoma in crush smears. Acta Cytol 2001;45:542-546.
17. Louis DN, Ohgaki H, Wiestler OD, Cavenee WK. WHO Classification of Tumours of the central nervous system. Lyon: International Agency for Research on Cancer, 2007.
18. Ng HK. Smears in the diagnosis of pituitary adenomas. Acta Cytol 1998;42:614-618.
19. Pai RR, Kini H, Rao VS, Naik R. Choroid plexus papilloma diagnosed by crush cytology. Diagnostic Cytopathology 2001;25:165-167.
20. Park JY, Suh YL, Han J. Dysembryoplastic neuroepithelial tumor. Features distinguishing it from oligodendroglioma on cytologic squash preparations. Acta Cytol 2003;47:624-629.
21. Parwani AV, Berman D, Burger PC, Ali SZ. Gliosarcoma: cytopathologic characteristics on fine-needle aspiration (FNA) and intraoperative touch imprint. Diagn Cytopathol 2004;30:77-81.

22. Parwani AV, Fatani IY, Burger PC, et al. Colloid cyst of the third ventricle: cytomorphologic features on stereotactic fine-needle aspiration. Diagn Cytopathol 2002;27:27-31.
23. Parwani AV, Stelow EB, Pambuccian SE, et al. Atypical teratoid/rhabdoid tumor of the brain: cytopathologic characteristics and differential diagnosis. Cancer 2005;105:65-70.
24. Policarpio-Nicolas ML, Le BH, Mandell JW, Lopes MB. Granular cell tumor of the neurohypophysis: report of a case with intraoperative cytologic diagnosis. Diagn Cytopathol 2008;36:58-63.
25. Roessler K, Dietrich W, Kitz K. High diagnostic accuracy of cytologic smears of central nervous system tumors. A 15-year experience based on 4,172 patients. Acta Cytol 2002;46:667-674.
26. Smith AR, Elsheikh TM, Silverman JF. Intraoperative cytologic diagnosis of suprasellar and sellar cystic lesions. Diagnostic Cytopathology 1999;20:137-147.
27. Sugita Y, Tokunaga O, Morimatsu M, Abe H. Cytodiagnosis of central neurocytoma in intraoperative preparations. Acta Cytol 2004;48:194-198.
28. Takei H, Bhattacharjee MB, Adesina AM. Chordoid glioma of the third ventricle: report of a case with cytologic features and utility during intraoperative consultation. Acta Cytol 2006;50:691-696.
29. Takei H, Kosarac O, Powell SZ. Cytomorphologic features of myxopapillary ependymoma: a review of 13 cases. Acta Cytol 2009;53:297-302.
30. Teo JG, Ng HK. Cytodiagnosis of pilocytic astrocytoma in smear preparations. Acta Cytol 1998;42:673-678.
31. Tilgner J, Herr M, Ostertag C, Volk B. Validation of intraoperative diagnoses using smear preparations from stereotactic brain biopsies: intraoperative versus final diagnosis--influence of clinical factors. Neurosurgery 2005;56:257-265; discussion 257-265.
32. Varikatt W, Dexter M, Mahajan H, et al. Usefulness of smears in intra-operative diagnosis of newly described entities of CNS. Neuropathology Epub 2009 Jun 25.
33. Winkler D, Lindner D, Richter A, et al. The value of intraoperative smear examination of stereotaxic brain specimens. Minim Invasive Neurosurg 2006;49:353-356.

**Fig. 6.24 Cytology of normal brain.**
Imprint cytology of a normal brain shows large triangular neurons (ganglion cells) with one thick axon (the so-called dendrite). The neurons are surrounded by different types of glial cells. On one hand, special attention is paid to the astrocytes with small and dark nuclei, and on the other hand to the oligodendrocytes with somewhat larger and more lucid nuclei (arrows) (Pap stain, low magnification).

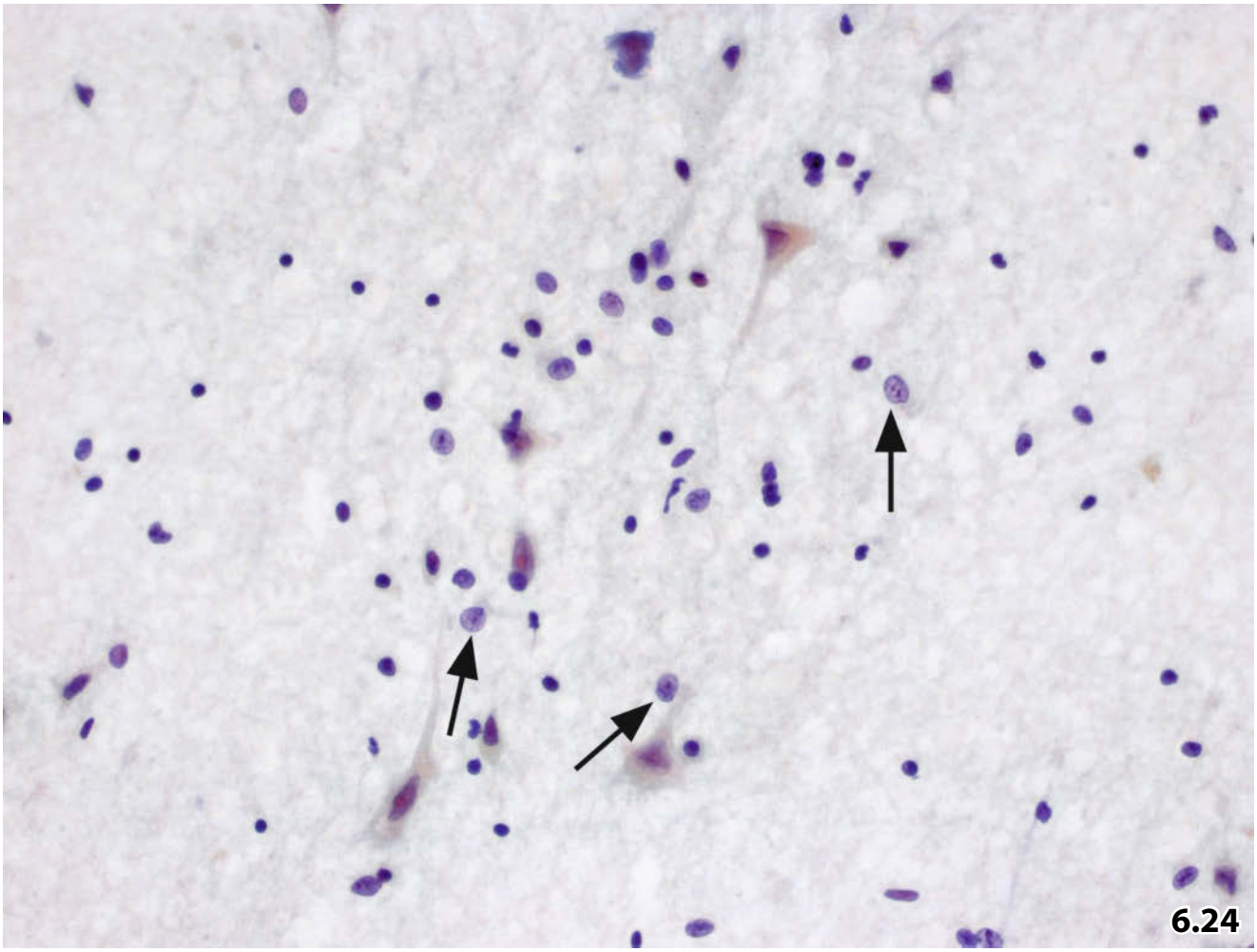

6.24

**Fig. 6.25A, B Anaplastic astrocytoma.**
Direct smears, Pap stain. **A** Low magnification of an anaplastic astrocytoma shows a network of branching capillaries without increased endothelial proliferation. The vessels are surrounded by polymorphous glial cells with fibrillary processes. **B** High magnification: The irregular nuclei show grooves and indentations, sporadic nucleoli can be seen accompanied by clumps of chromatin. Short and thick cytoplasmic processes are obvious.

**Fig. 6.26A–C Glioblastoma.**
Squash smear preparations of a glioblastoma, Pap-stained. **A** High magnification shows a marked endothelial proliferation in a glomeruloid vascular conglomerate. **B** In other parts of the slides, a distinct hypercellularity with increased cellular polymorphism could be found. The obvious malignant cells show a small cytoplasmic rim with only a few abortive processes (low magnification). **C** Detail shows the variability of nuclear morphology, which is much more pronounced compared to smears of anaplastic astrocytoma (Fig. 6.25). Indentations, grooves, and prominent nucleoli are common; hyperchromasia and clumping of the chromatin are increased. An atypical mitosis can also be seen.

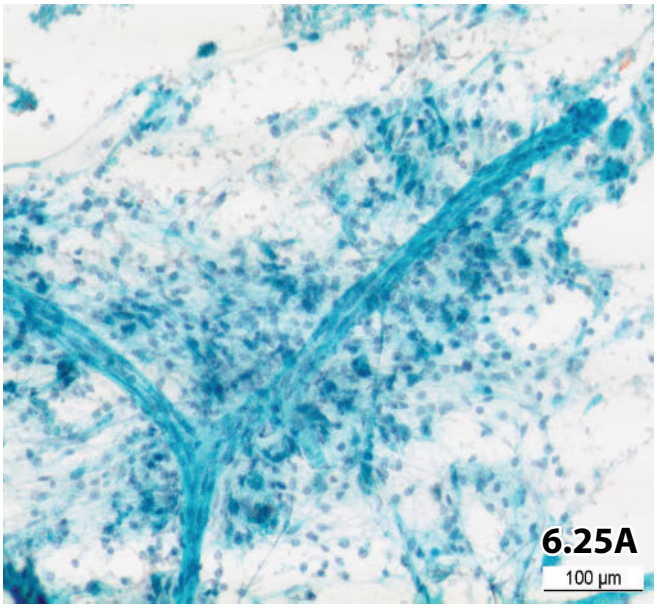
6.25A
100 µm

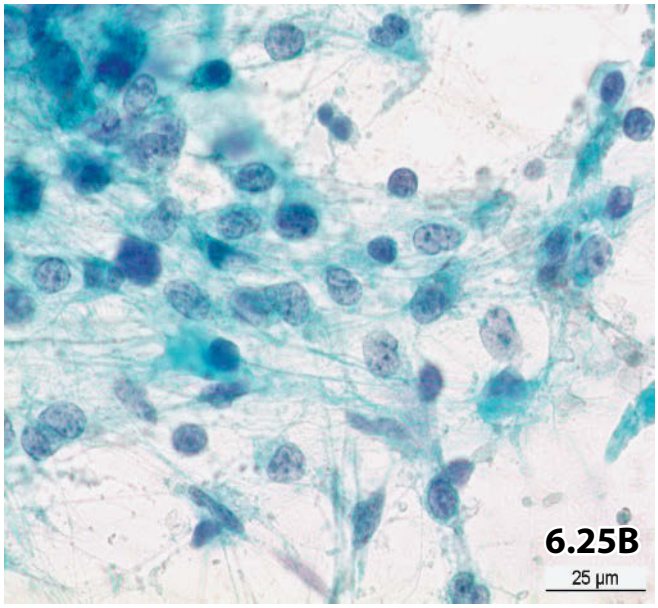
6.25B
25 µm

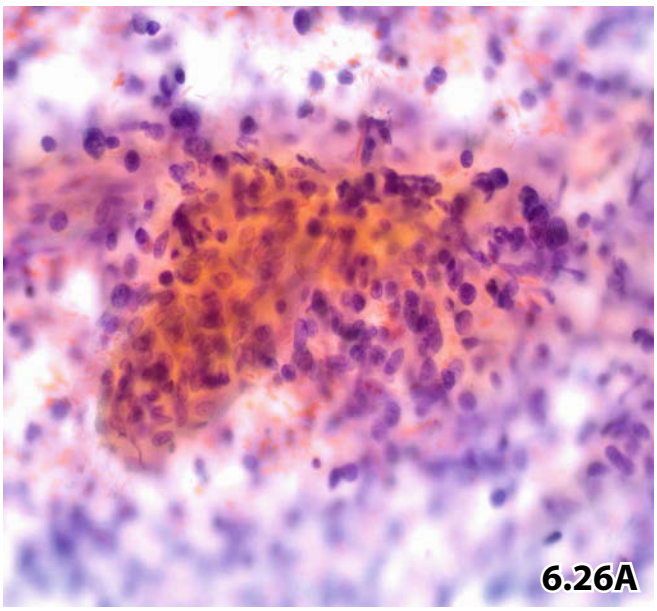
6.26A

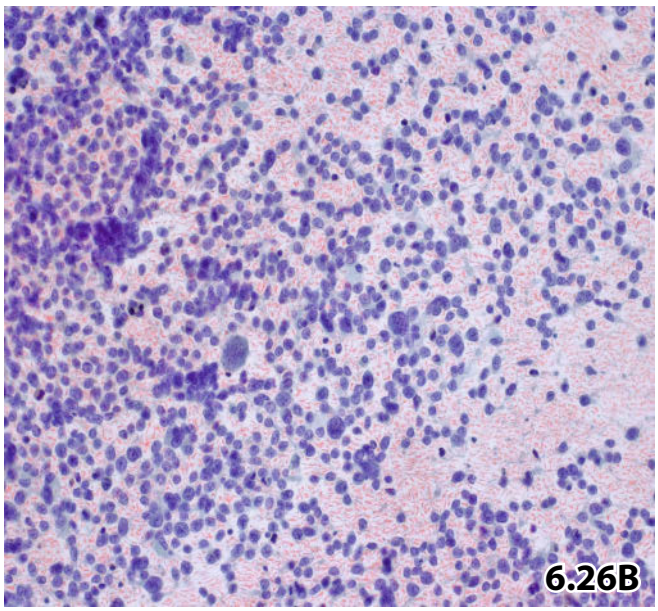
6.26B

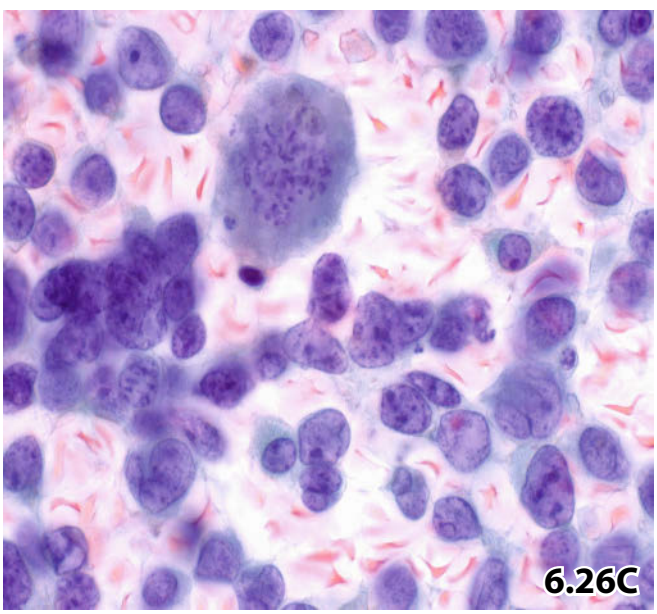
6.26C

**Fig. 6.27A, B Oligodendroglioma (WHO grade 2).**
Smear preparations of an oligodendroglioma, Pap stain. The grade of cellular pleomorphism is mild, grade 2 according to WHO. **A** Lower magnification shows a rather monotonous population of neoplastic oligodendrocytes. The round to oval nuclei appear naked, but a small cytoplasmic rim may occasionally be visible. The chromatin is lucid, whereas some small inconspicuous nucleoli can be seen. **B** Psammomatous calcifications may also occur (lower magnification).

**Figs. 6.28–6.30 Anaplastic oligodendroglioma (WHO grade 3).**
Cytology, histology, and molecular genetic analysis of a case of anaplastic oligodendroglioma are presented.



**Fig. 6.28A, B** Direct cytologic smear, Pap stain. **A** Compared with the tumor cell features in Fig. 6.27, the neoplastic cells of an anaplastic oligodendroglioma (WHO grade 3) show pronounced atypia (low magnification). **B** High magnification reveals enlarged nuclei with a slightly irregular shape, the chromatin is conspicuously granular, and one to two prominent nucleoli can be observed.

**Fig. 6.29** An H&E stained histologic section of the same tumor shows the perinuclear halo that is typical of neoplastic oligodendroglial cells.

**Fig. 6.30** A heterozygous deletion of the long arm of chromosome 19 (19q) was detected by fluorescence-in-situ-hybridization (FISH). The picture illustrates blue nuclei containing two green signals (short arm of chromosome 19 = 19p) and only one red signal (19q) (observed in most of the tumoral nuclei).

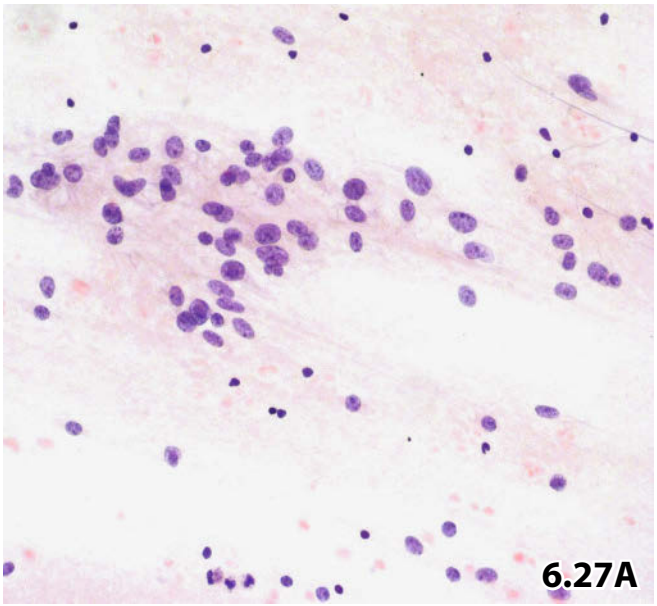
6.27A

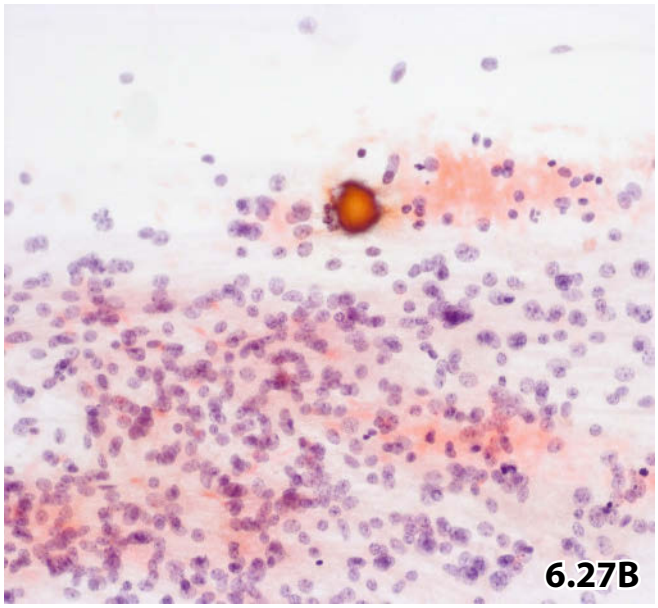
6.27B

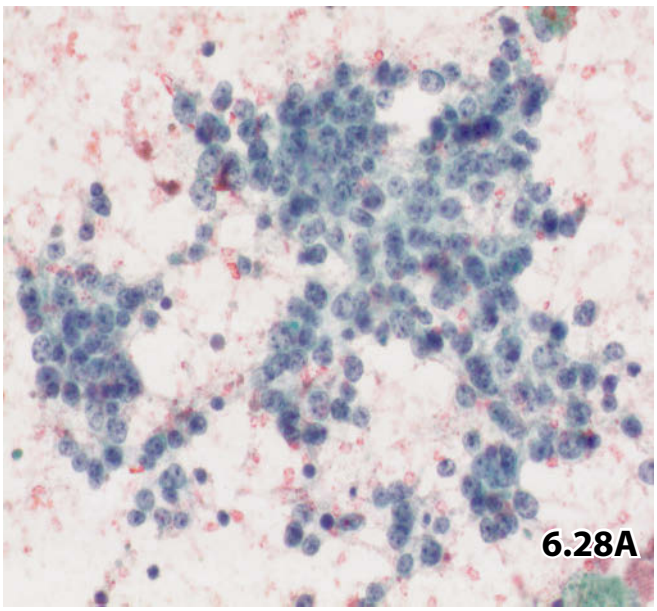
6.28A

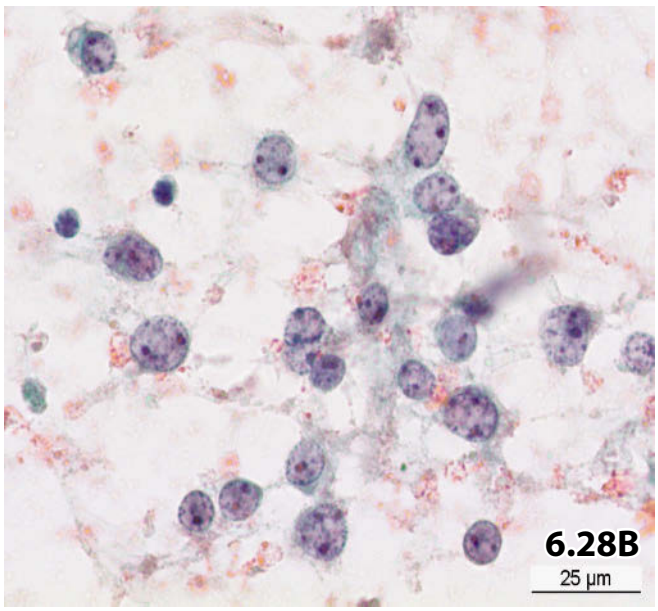

6.28B

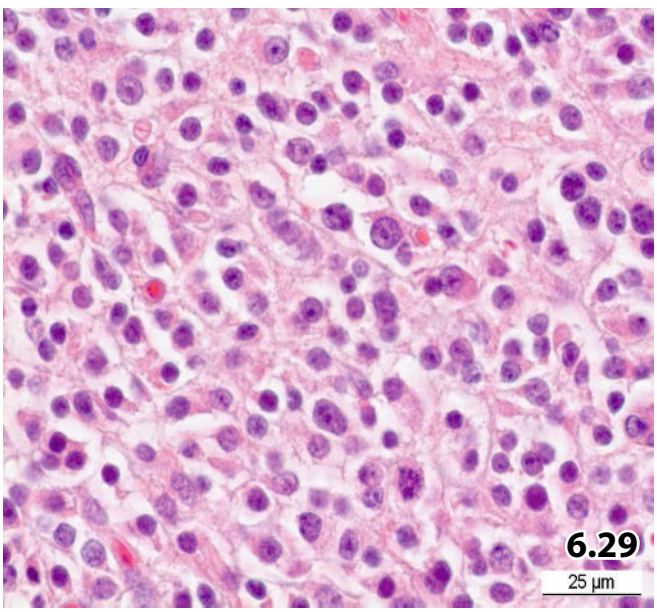

6.29

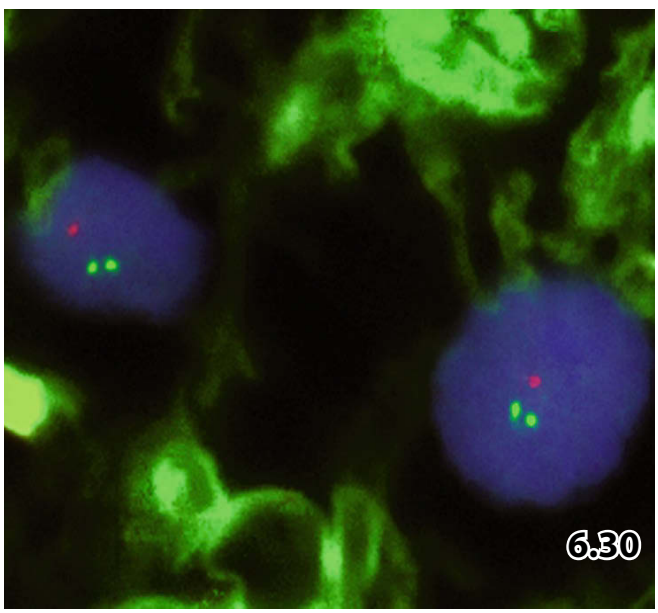
6.30

**Fig. 6.31 Metastasis of a colorectal carcinoma.**
Two years after a left-sided hemicolectomy for colorectal adenocarcinoma, a 63-year-old male patient complained of increasing headache. A computed tomography showed a lesion in the right temporal lobe. Direct smears from tissue obtained by means of stereotactic biopsies were Pap-stained. Cytologic specimens were hypocellular with pronounced necrotic debris in the background. A few atypical cells with an increased N/C-ratio and some cytoplasmic vacuoles can be seen. The pleomorphic nuclei with irregular borders contain dense chromatin and sporadic nucleoli (high magnification). Together with the immunocytochemical results (positivity for cytokeratin 20 and CDX-2, negativity for GFAP, not shown) the diagnosis of a brain metastasis of colorectal carcinoma could be established.



**Fig. 6.32 Metastasis of a breast carcinoma.**
A 57-year-old female patient developed seizures 5 years after resection of a mammary carcinoma of the invasive ductal type. A CT scan showed a single lesion in the right cerebral hemisphere. Subsequently, a stereotactic biopsy was performed. Imprint smears were prepared and Pap-stained.
High magnification shows a cell population composed of atypical single cells and clusters against an almost clear background. The cytoplasm is dense with irregular contours, whereas the round to oval nuclei are variable in size and usually eccentrically placed. The chromatin is patternless or sometimes coarse (arrows), nuclei contain one or two prominent eosinophilic nucleoli. Rare mitotic figures can be observed. Based on additional immunohistochemical findings (positivity for estrogen and progesterone receptors, negativity for GFAP, not shown), and the patient's history, the diagnosis of breast carcinoma metastatic to the brain was made.

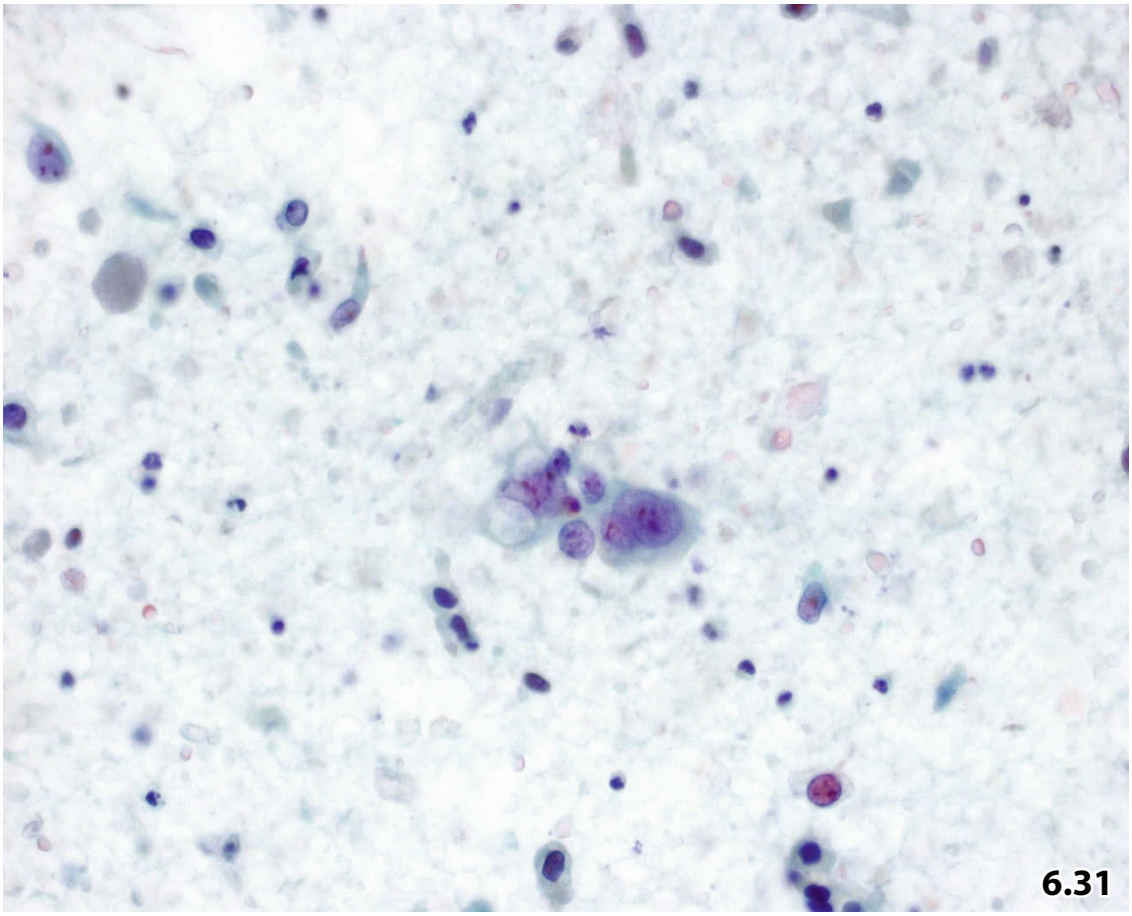

6.31

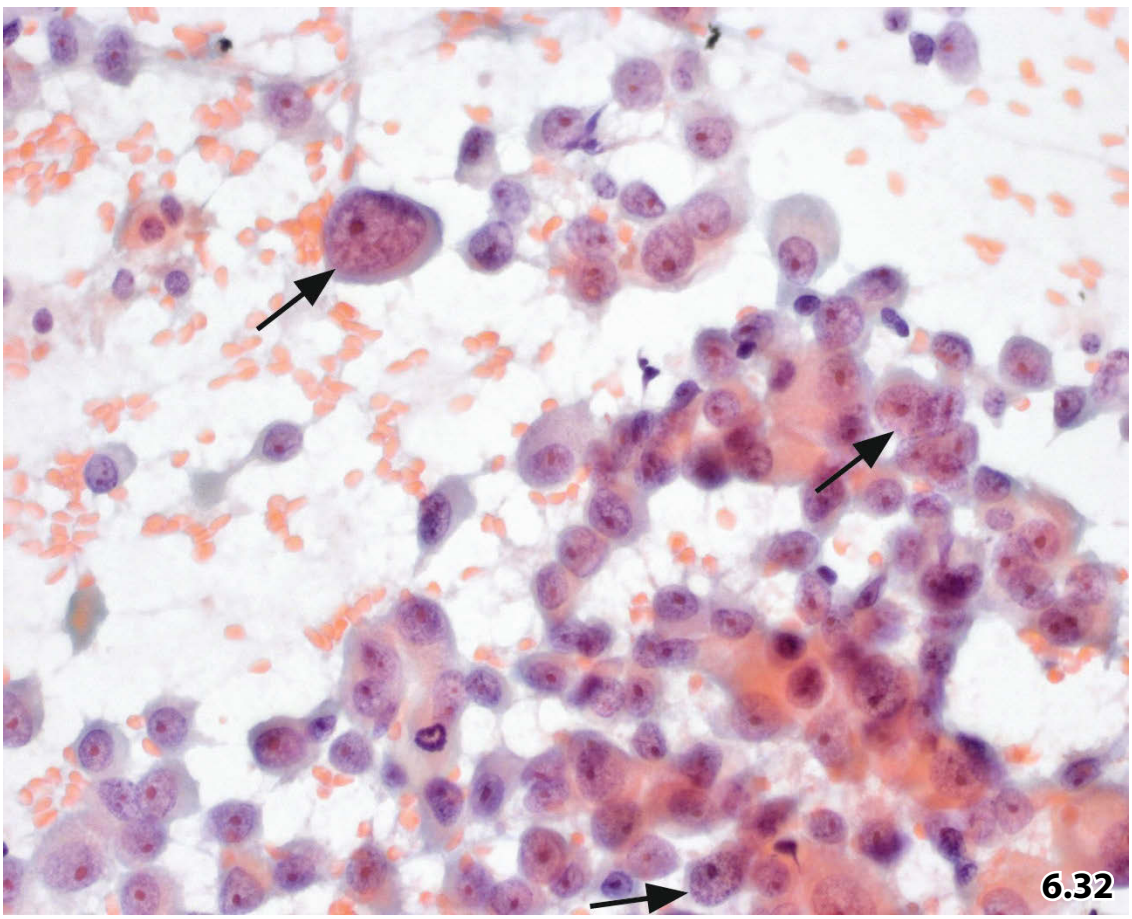

6.32

# 7 Eye



Spieler/Rössle, *Nongynecologic Cytopathology. A Practical Guide*. *Essentials of Diagnostic Pathology*,
DOI 10.1007/978-3-642-24719-4_7, 

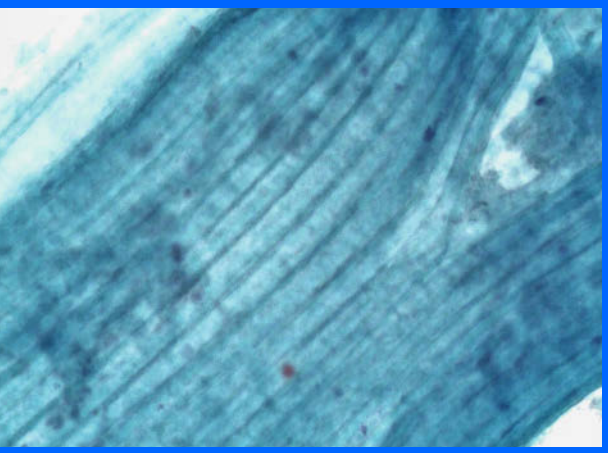

# Eye

## Introduction, Sampling Techniques, Processing, Adjuvant Techniques

## Globe: Cornea and Conjunctiva, Anterior Chamber and Uvea, Vitreous Body, Retina

## Orbit and Lacrimal Glands

## Eyelid

## 7.1 Introduction

**General Comments**

- The central unit of the eye is the globe (eyeball) encased by eyelids, conjunctiva, and orbit (orbital cavity). Paired lacrimal glands are situated in the upper laterofrontal area of each orbit.
- The reader is referred to distinguished textbooks for further information on anatomic details of the different compartments of the globe, their correlation to the surrounding tissues, and histologic features.
- At our institution, we have limited experience with cytologic samples from the eye, mainly confined to vitreous aspirates and fine-needle aspiration biopsies from the orbit; therefore, we restrict our explanations to selected disorders. Lesions that may rarely be found in cytologic samples from globe compartments, eyelids, lacrimal gland, and orbit can be found in distinguished case reports and publications, for instance, "*2006 AFIP Atlas of Tumor Pathology. Tumors of the Eye and Ocular Adnexa*" [46].
- In certain situations, cytologic examination is the gold standard in ocular pathomorphologic diagnostics.
- Many eye-nonspecific lesions and their cytological appearance brought up in this chapter are basically discussed elsewhere in this book. We refer in each case to corresponding chapters and sections.

### 7.1.1 Sampling Techniques [21, 51]

#### 7.1.1.1 Impression Smear and Scrape Technique

Superficial lesions that are readily visible can cytologically be managed using a scraping or impression technique. Such lesions include ulcerations, exophytic tissue growth, and flat disorders of the cornea, conjunctiva, and eyelid. The impression methods are more simply performed and less traumatic in comparison to scraping techniques. Any adjuvant analyses such as DNA cytometry, immunocytochemistry, or PCR may be performed on cells sampled by impression or scrape techniques [104].

- Scrapings may be performed with a spatula or cytobrush. Transfer of the cellular material for microscopy is made by rolling or smearing the device onto a glass slide. Immediate fixation in an alcohol-based fixative or with a spray fixative is of particular importance.
- Impression cytology using a cellulose-acetate-filter preparation technique has been widely used as a research tool. In cytologic practice, direct-to-the-glass-slide impression smears are recommended from lesions showing an overt loose and wet tissue fraction at the surface. Furthermore the technique is suitable for the evaluation of the ocular surface epithelium in trachoma, avitaminosis A, and other disorders.

#### 7.1.1.2 Fine-Needle Aspiration [4, 33, 99]

- *Palpable lesions* at the ocular surface and in the frontal periphery of the orbit can be aspirated by a direct approach to the tumor using the device and techniques repeatedly described in this book.
- *Nonpalpable intraocular lesions* can be aspirated under direct visualization using specialized ophthalmologic instrumentation, the methods include transscleral and transvitreal FNAB. Instrumentation and techniques that may be used, and potential complications are presented in detail in the literature [3, 21, 51]. Sampling by ultrasonographic guided FNAB (US-FNAB) is another approach for deep-seated intraocular lesions. Any guided aspiration procedure allows a precise hit of the target and an adequate sampling of cellular material [62]. FNAB of solid intraocular tumors should be reserved for a highly selected group of patients including suspected intraocular metastasis, dubious clinical and imaging results, the patient's insistence on preliminary diagnosis [3], and tumors demanding precise initial typing in order to decide on the optimal treatment protocol [30]. FNABs of intraocular lesions have to be undertaken by skilled ophthalmologic surgeons. Experienced cytopathologists are a requirement for accurate diagnoses.
- At our hospital, numerous nonpalpable masses within the orbit space have been reliably managed by fine-needle aspiration based on computed tomographic localization. Localization and needling of orbital lesions by ultrasound and US guidance have also been effective in experienced hands.

#### 7.1.1.3 Vitreous Sampling

- Most intraocular cytologic specimens come from the vitreous body and are obtained by intraocular washing/vitrectomy. Various specialized ophthalmologic techniques are utilized to remove the vitreous and the additional fluid. The material is saved and submitted for cytologic evaluation.
- At our institution, the aspirated material has either been left undiluted or has been diluted prior to delivery to the cytology laboratory, but fixatives have not been added. Vitreous specimens can be refrigerated at 4°C; cellular components stay well preserved for 12 h after the removal.

### 7.1.2 Sample Processing and Staining Techniques as Performed at Our Institute

#### 7.1.2.1 Conventional Smear

Cellular aspirates are directly smeared onto a glass slide and immediately wet-fixed in Delaney solution or using a spray fixative. Additional air-dried smears are advantageous in special cases. Fluids are centrifuged and two or three slides are prepared from the cell button after the supernatant has been discarded.

#### 7.1.2.2 Cytocentrifuge Preparation

Cytospin preparations may be used as a cell-concentrating method. It is recommended for small amounts of fluid with sparse cellular content and for hypocellular FNAB samples (after rinsing the needle and syringe in saline or in a cell medium).

#### 7.1.2.3 Liquid-Based Cytology

We have no experience with thin-layer technique in ocular cytology, but there should be no contraindication for this method if the staff is familiar with the diagnostic specifics [7]. The most commonly used methods include ThinPrep (Hologic, Marlborough, MA, USA), and SurePath (Becton Dickinson, Franklin Lake, NJ, USA).

#### 7.1.2.4 Cell Block Technique

Application of the cell block technique to cytologic samples from the eye may depend on the type of the sample and the amount of material obtained. Tissue fragments and clots are well suited for a cell block.

#### 7.1.2.5 Staining Methods

Papanicolaou and May-Grünwald-Giemsa staining procedures have been routinely applied to wet-fixed and air-dried smears, respectively.

### 7.1.3 Adjuvant Technologies

Special Staining (Figs. 7.5B, 7.12, 7.13B)
Special stains are sometimes helpful to verify suspicious findings:
– Iron stain to prove the presence of hemosiderin.
– Gram stain to distinguish bacteria.
– Silver stain for fungi.
Immunocytochemistry (Figs. 7.11 and 7.16)
Immunocytochemical investigation is a requisite for tumor typing, to ascertain the primary site of a neoplasm, for B-/T-cell enumeration, and to assess monoclonality of a lymphoid cell population.
Flow Cytometry
Multiparameter flow cytometry (FCM) analysis is a reliable method for immunophenotyping and the evaluation of clo-

nality of a lymphoid cell population [35]. FCM may also be used for DNA quantitation.

DNA Ploidy by Image Analysis

The scope of DNA quantitation by ICM-DNA in ocular cytology is confined to squamous lesions of the ocular surface and to estimating the biological behavior of selected malignant tumors [73, 75]. This biological marker may be helpful to resolve equivocal alterations of squamous cell nuclei and can distinguish premalignant and malignant cell changes from reparative nuclear atypia [73]. DNA aneuploidy is a safe marker for malignant transformation of squamous cells.

Molecular Genetics

Polymerase chain amplification (PCR) gene amplification followed either by gel electrophoresis or fragment analysis using DNA extracted from cytologic samples is a reliable assay to assess clonal lymphoid cell proliferation. PCR is more sensitive in detecting clonality compared with immunocytochemical and flow cytometric tests (see references Sect. 7.2.2.3.4, "Malignant Lymphoma," p. 542).

Furthermore, molecular genetic methods on cells from impressions, scrapings, or FNABs may be used to evaluate chromosomal alterations in selected malignancies [116], and for quick detection of bacterial and fungal pathogens [76, 89].

## 7.2 Globe (Eyeball)

### 7.2.1 Normal Cytology (Figs. 7.1–7.3)

### 7.2.2 Nontumoral Disorders and Neoplasms of the Different Compartments

#### 7.2.2.1 Cornea and Conjunctiva

*The cornea* is the transparent front part of the eye that covers the iris, pupil, and anterior chamber. The cornea refracts light together with the lens.

*Conjunctiva* is the protective membrane that lines the inner surface of the eyelids and covers exposed areas of the sclera (also referred to as the white of the eye).

##### 7.2.2.1.1 Strongly Keratinized Cells

Strongly keratinized but otherwise normal squamous cells without atypical nuclear features could be caused by keratoconjunctivitis sicca and vitamin A deficiency.

**Caution**

Exfoliative material from the ocular surface that solely exhibits keratinized anucleated squames may indicate an underlying dysplastic or invasive neoplastic squamous cell lesion.

##### 7.2.2.1.2 Keratitis and Ulceration of the Cornea

The cornea is sometimes damaged by a foreign object penetrating the tissue, or bacteria and fungi (e.g., from a contaminated contact lens) can pass into the cornea. Such disor-

**Table 7.1** Normal cells from areas of the globe accessible for cytologic investigation

| Compartment of the globe | Common sampling technique / cell presentation | Normal cytologic features and components |
|---|---|---|
| **Cornea** | Scraping<br>Impression smear | Squamous cells, intermediate type, nonkeratinized |
| **Conjunctiva of the eyelid**<br><br>**Conjunctiva bulbi** | Scraping<br>Impression smear | Squamous cells, intermediate type<br><br>Columnar cells and interspersed goblet cells |
| **Anterior ocular chamber** | FNAB | – Clear fluid<br>– Few lymphocytes and monocytes |
| **Vitreous body** (Fig.7.1) | FNAB<br>Vitrectomy and washing | – Watery to mucoid fluid<br>– Few lymphocytes and monocytes |
| **Uvea:**<br>**Iris**<br>**Ciliary body**<br><br>**Choroid** | FNAB | – Delicate vascular stroma<br>– Strongly pigmented epithelial cells<br>– Smooth muscles variable<br><br>– Dense vascular stroma and pigmented stromal cells |
| **Retina** (Fig. 7.2) | Cells are occasionally encountered in vitreous washings and aspirates | – Cuboid polygonal cells from the retinal pigment epithelium fully loaded by brown pigment granules<br>– Clustered small dark nuclei from rods and cones<br>– Possibly nerve fibers and ganglion cells |
| **Lens** (Fig. 7.3) | Lens material may occur in:<br>– Anterior chamber aspirate<br>– Vitreous fluid | – Plump, well-demarcated, transparent bar-like elements, discohesive and in bundles<br>– Lens epithelium is characterized by small dark nuclei |

ders can result in painful inflammation and infections called keratitis, possibly followed by ulceration.

Microscopic hallmarks:

- Scraping from corneal ulcerations provides intermediate squamous cells, which usually exhibit features of cellular repair comprising enlarged nuclei, minor nuclear irregularities, pronounced nucleoli, irregular cytoplasmic shape, and keratinization.
- The N/C ratio and nuclear texture are bland.
- Varying amounts of inflammatory cells and histiocytes.
- Vigorous scraping often removes parabasal squamous cells and less frequently basal cells.

#### 7.2.2.1.3 Allergic Conjunctivitis

Allergic conjunctivitis encompasses a variety of disorders that cause identical clinical symptoms [14]. Allergic conjunctivitis is not a common object for cytologic investigation, but it may be performed in patients with suspicion of other causes of a red eye than allergens.

- The smears contain inflammatory cells including eosinophils, mast cells or basophils, and lymphocytes [13].
- Eosinophilic granulocytes are not always present.

#### 7.2.2.1.4 Infectious Keratitis and Conjunctivitis [57]

Keratoconjunctivitis is a widespread disease. It can spread from one person to another and affects millions of people at any given time. Infectious conjunctivitis can be caused by bacteria, viruses, fungi, or vermin.

**Bacterial Infections**

Routinely stained (May-Grünwald-Giemsa) cytologic specimens and auxiliary Gram staining can detect bacterial pathogens. This procedure is essential for a rapid diagnosis and for starting empirical therapy.

The cytologic findings indicate an acute inflammatory disorder irrespective of the causal agent.

- Cytologic smears show squamous cells and/or glandular cells and numerous neutrophils.
- The epithelial cells may exhibit reactive changes and neutrophils may be degenerated.
- A chronic process is accompanied by numerous goblet cells.

Conventional culture technique to isolate organisms is increasingly substituted by molecular diagnostic techniques such as PCR technology. The latter increases the rate of identified specific pathogens and provides a result in less time [92].

*Trachoma* is caused by the bacterium *Chlamydia trachomatis* and affects millions of people every year, particularly in developing countries. This infectious eye disease is the leading cause of the world's infectious blindness. In addition, genital chlamydial infection is recognized as the world's most common sexually transmitted disease. The high prevalence in women of child-bearing age results in exposure of a large number of neonates. Many of these children develop conjunctivitis or pneumonia (or both) in the first months of life [31].

Few studies in the literature report cytologic findings from proven conjunctival chlamydia infections. Specimens have been collected by scraping or imprint of the ocular surface and were stained using the Giemsa or Papanicolaou method [29, 38, 110]:

- Characteristic cytoplasmic chlamydial inclusions are rarely found in conjunctival smears [110]. If present, the initial body stains basophilic with the Giemsa method and is helmet-shaped.
- The inflammatory pattern is not consistent but neutrophils are reported to be predominant in most cases. Lymphocytes, plasma cells, and multinucleated giant cells complete the overall pattern.
- Goblet cells in great numbers and the amount of squamous metaplasia in cytologic preparations from the conjunctival surface may be helpful in predicting the clinical severity of trachoma [1].

Culture, direct immunofluorescence using monoclonal antibodies, in-situ hybridization, DNA-based nucleic acid amplification tests, and rRNA-based tests have one by one replaced cytologic diagnosis of chlamydia. The rRNA-based nucleic acid amplification test appears to have a very high sensitivity for the detection of ocular chlamydial infections [113].

**Fungal Infections** [54]

Fungal keratitis is established as a major ophthalmological problem in tropical regions all over the world. Keratomycosis is predominant in the young adult group and trauma is the main predisposing factor [54]. Routine cytologic staining methods such as May-Grünwald-Giemsa, Papanicolaou, and others applied to scrape and impression smears detect fungi with high accuracy and may be useful for a tentative typing of the organism. Potassium hydroxide with calcofluor white stain (KOH+CFW) is highly recommended in the literature for a reliable diagnosis of fungal keratitis. *Aspergillus* species is predominant in the clinical setting of keratomycoses [61, 92].

PCR has been found to be a rapid and sensitive method for specific typing of fungi in infectious keratitis [41].

**Viral Infections**

If viral identification is needed, scraping material can directly be transferred into a special virus transport medium in patients with suspected viral keratoconjunctivitis.

- Cytologic preparations from eyes affected by a viral infection usually show a mixed lymphoid cell pattern, histiocytes, and degenerate epithelial cells.
- Pathognomonic viral inclusions may be detected in conjunctival epithelial cells.

*Ocular herpes* is a recurrent viral infection that is caused by the herpes simplex virus and is the most common infectious cause of corneal blindness. Prompt treatment with antiviral drugs is important to stop the herpes virus from destroying epithelial cells and spreading deeper into the cornea. Viral invasion would lead to a severe disorder, so-called stromal keratitis.

- Herpes simplex virus gives rise to specific cellular alterations, which are described in several chapters of this book (e.g., Sect. 2.1.6.2, "Viral Infections, " p. 116).

*Adenovirus* infection may cause a red eye and watery discharge.

- Impression smears from the watery discharge are composed of a lymphoid population and occasionally epithelial cells showing nuclear enlargement and rare intranuclear inclusions.

*Varicella-zoster virus* is another virus involving the eye and frequently the cornea.

#### 7.2.2.1.5 Ocular Surface Squamous Neoplasia [12, 67]

Surface squamous neoplasia mainly occurs in the older male population.

Ocular surface squamous neoplasia encompasses the whole cascade of mild dysplasia to carcinoma in situ to invasive squamous cell carcinoma. Isolated corneal squamous neoplastic lesions rarely occur; corneal squamous neoplasia is usually associated with a process at the limbus (sclerocorneal junction) and in the adjoining conjunctiva. A high recurrence rate can be expected after simple surgical excision.

**Microscopic Features and Additional Analysis**

- Strongly keratinizing squamous cells including the pleomorphic shape of the cytoplasm and varying N/C ratios indicate dysplastic change.
- The severity of nuclear atypias indicates the grade of dysplasia.
- Invasiveness of the tumor cannot be assessed by cytology unless abundant necrotic debris and unequivocal cellular criteria of malignancy are available.

DNA ploidy analysis using abnormal squamous cell nuclei may be helpful to separate stimulated atypical but benign squamous cells from precancerous/ malignant squames (see Sect. 8.4, "DNA Image Cytometry", p. 565).

**Caution**

- Exfoliative material from the ocular surface that exhibits solely keratinized anucleated squames may indicate an underlying dysplastic or invasive neoplastic squamous cell lesion!
- Squamous cell carcinoma in situ of the conjunctiva may occasionally present as a pigmented tumor simulating melanoma [96].

### 7.2.2.2 Anterior Ocular Chamber and Uvea

*Anterior ocular chamber* is the space between the posterior corneal surface and the iris and lens.

*Anterior uvea* is part of the pigmented middle layer of the three concentric layers that make up the orbit. It is composed of the iris and the ciliary body.

*Posterior uvea* is called choroid (choroidea) and means the vascular layer of the eye lying between the retina and the sclera.

#### 7.2.2.2.1 Anterior Ocular Chamber

Due to mechanical and degenerative injuries of the frontal area of the globe, the following elements can be seen in aspirates from the anterior ocular chamber:

- Proteinaceous debris.
- Histiocytes and macrophages with engulfed lens material, iron, and melanin pigment (Fig. 7.4).
- Free lens fragments (Fig. 7.3).
- Inflammatory cells.

Inflammatory and infectious processes and neoplastic disorders originating in the cornea, iris, and the anterior chamber angles may be detected cytologically in aspirated fluid specimens. Infectious diseases presenting as endophthalmitis are briefly discussed in Sect. 7.2.2.3.3, p. 542. Neoplastic entities are listed in Sect. 7.2.2.2.2, below.

#### 7.2.2.2.2 Benign and Malignant Tumors of the Uvea [4]

FNAB of a ciliary body tumor seems to be relatively save, but needle aspiration of posterior uveal tumors requires wide experience and skill on the part of the operator [2].

**Coronal Adenoma** [50, 51]

Coronal adenoma is the most common intraocular tumor. The tumors occur most often in middle-aged patients with a mean age of 50 years.

Synonyms include ciliary body adenoma of nonpigmented epithelium, Fuchs adenoma, Fuchs epithelioma, and hyperplasia of the nonpigmented ciliary epithelium.

**Microscopic Features**

Aspiration biopsy will readily distinguish coronal adenoma from malignant neoplasms based on the characteristic morphologic features. FNAB helps to avoid unnecessary surgery.

- Cohesive clusters of nonpigmented epithelial cells.
- The nuclei are bland and the cytoplasm abundant.
- Epithelial cell groups are surrounded by a characteristic extracellular matrix.

**Additional Comments and Differential Diagnosis**
Rare cases of locally invasive low-grade adenocarcinoma originating from the nonpigmented ciliary body epithelium have been reported. Malignancy can exclusively be confirmed by histologic examination of the surgically removed lesion [87, 94].

It is well known from the literature that coronal adenoma may clinically be mistaken for malignant amelanotic melanoma or metastatic carcinoma [25].

### Melanocytoma [69]

Melanocytoma is a benign lesion that can be found in any area of the uvea. It occasionally occurs in the ciliary body.



**Microscopic Features** [40, 69, 85] **and Differential Diagnosis**

- Large numbers of cohesive melanocytes.
- The large cells are round or elongated. The nuclei are round and uniform showing bland chromatin and small but distinct nucleoli.
- The cytoplasm is abundant and densely pigmented.

Differential diagnosis should include malignant melanoma and benign and malignant tumors of the pigmented ciliary epithelium [22, 69].

### Adenoma of the Iris/Ciliary Pigmented Epithelium [101]

The pigmented adenoma is a rare lesion. It is a benign tumor that has a certain tendency for local invasion. The patient's mean age is 60 years.

**Microscopic Features** [22] **and Differential Diagnosis**

- Large cells exhibit abundant intra- and extracellular pigment accumulation.
- The nuclei are round showing inconspicuous nucleoli and bland chromatin texture (at least in cells where morphologic details are not concealed with heavy pigmentation).

Pigmented adenoma has to be differentiated from malignant melanoma, melanocytoma, and iris cyst.

### Leiomyoma [98]

Leiomyoma of the ciliary body is rare. The tumor is assumed to arise from ciliary muscle. Isolated case reports on FNAB findings exist [51].

**Microscopic Features and Differential Diagnosis**

- Tight clusters of spindle cells and more oval cells incorporated in a fibrillary background.
- The nuclei appear bland.

Leiomyoma mimics spindle cell amelanotic melanoma and neural tumors such as schwannoma. Immunostains are useful in separating leiomyoma from other spindle cell tumors. Leiomyoma cells show immunoreactivity for smooth muscle markers and stain negative with antibodies against melanoma-typical and neural antigens [98].

### Uveal Malignant Melanoma [18]

- Ocular melanomas can occur in the eyelid, conjunctiva, within the globe, and in the orbit. Melanomas are the most common intraocular malignant neoplasms in adults.
- Uveal melanomas account for 10% of all melanomas, and the majority are choroidal melanomas. Approximately 10% of the ocular melanomas arise in areas of the anterior uvea. Iris melanomas have a different clinical behavior compared with their counterparts in the ciliary body and choroid [51].
- Several studies have shown that FNAB is a useful tool in establishing a precise preoperative diagnosis of uveal melanomas; however, the technique should be restricted to a selected patient group only [24, 97, 115].
- FNAB can also provide cells for adjunct molecular pathological analyses [6].

**Microscopic Features**

- Common cytomorphologic features and immunocytochemical properties of melanoma are detailed in the literature [24, 30] and in various chapters of this book, e.g., Sect. 16.2.9, p. 1030.

**Differential Diagnoses** [22]

- Distinguishing between pigmented ocular malignant melanoma, melanocytoma, and iris/ciliary pigmented adenoma; furthermore, distinguishing between benign and malignant tumors of the pigmented ciliary epithelium may be difficult. If the nuclear details are visible under normal light-microscopic conditions, the cells should be reliably classified in most cases.
- Nonpigmented ocular malignant melanoma may mimic coronal adenoma and metastatic carcinoma.
- Spindle cell malignant melanoma lacking pigmentation may mimic leiomyoma or neural tumors.
- Diagnostic problems and biological categorization of small pigmented choroidal tumors in samples of transvitreal FNABs have been highlighted by Augsburger and associates [5].

### Malignant Lymphoma and Leukemia [81, 82]

Ocular manifestations in leukemic processes occur fairly frequent, usually as an infiltration of the choroid. Leukemic ophthalmopathy may be observed together with both lymphocytic and myelogenous leukemias.

### Extremely Unusual Neoplasms of the Anterior Uvea

This tumor group includes the few entities listed below; FNAB results are available from sporadic cases:

– Nonpigmented/pigmented malignant medulloepithelioma [53, 95]
– Nonpigmented/pigmented pleomorphic adenoma [66]
– Acquired pleomorphic adenocarcinoma [56]

**Metastases** [2]
- Suspicion of intraocular metastasis is a major indication for FNAB.
- The most common malignant tumors metastasizing to the ciliary body and choroid are breast carcinoma in the female population and bronchogenic carcinoma in males [37, 105]. Single case reports of other secondary uveal tumors are available in the literature [8].
- Neuroblastoma in the pediatric age group may directly spread into the eye; the tumor masquerades as retinoblastoma. It is practically impossible to make the distinction between these two neoplasms by cytology alone.
- Immunocytochemistry can be helpful to identify the primary tumor site of metastatic neoplasms.

### 7.2.2.3 Vitreous Body

- Vitreous samples can be obtained as part of a therapeutic procedure and/or for diagnostic purposes. The objective of vitrectomy is to remove vitreous opacities such as hemorrhage and fibrovascular streaks and to rule out intraocular malignant lymphoma and metastatic neoplasms.
- Routine cytologic processing of all vitrectomy specimens is strongly recommended, particularly to exclude endophthalmitis and primary intraocular lymphoma, and to identify unforeseen vitreous pathologic conditions.
- Cytologic results from a large series of diagnostic vitrectomies have recently been reported by Wittenberg and associates [111].

#### 7.2.2.3.1 Vitreous Hemorrhage (Fig. 7.5)

Vitreous hemorrhage may be caused by trauma and obliterative vasculopathy.

Cytologic findings in vitrectomy and fluid samples are characteristic:
- Degenerating erythrocytes appear as small rings with clear inner area. Hemolyzed red blood cells with small fragments of hemoglobin attached to the inner surface of the cellular membrane are referred to as ghost erythrocytes [16].
- Extracellular hemoglobin spherules may vary greatly in size. The spheres stain eosinophilic with different staining methods [55].
- Hemosiderin-laden macrophages.

#### 7.2.2.3.2 Vitreous Fibrous Tissue and Nonspecific Granulomatosis (Figs. 7.6–7.11)

Various etiologic factors of soft tissue deposits include:
– Inflammatory disease.
– Trauma.
– Therapeutic intervention.
– Proliferative vitreoretinopathy and proliferative diabetic retinopathy (usually at the posterior vitreous surface). Diabetic retinopathy and proliferative vitreoretinopathy account for the majority of intraocular washings with evidence of fibrous tissue.
– Congenitally persistent hyperplastic primary vitreous [79, 84].

Histologically, fibrovascular proliferation and granulomatosis in the vitreous cavity is composed of fibrocytes, fibroblasts, macrophages, retinal pigment epithelial cells, and glial cells [63]. However, cellular composition changes according to various etiologic factors.

**Microscopic Features**

Cytologic specimens reveal a large range of characteristic components [83]:
- Spindle cells are isolated or embedded in a fibrovascular background. The cells show elongated cytoplasm. The nuclei are small and deeply stained, or large with a clear nucleoplasm. Nuclear shape is round to bean-shaped to crescent. Activated nuclei contain a small but distinct nucleolus.
- Retinal pigmented epithelial cells appear as cuboidal cells containing masses of melanin granules in their cytoplasmic body.
- Photoreceptive retinal cells are slender and elongated. The nuclei are small and deep-stained, and positioned at one end of the ill-defined cytoplasmic body. Retinal cells may occur singly, in groups, or arranged in parallel rows.
- Melanin pigment can be randomly distributed in the background of the smear; or it appears enclosed in the cytoplasm of retinal pigment epithelium and/or macrophages.
- Primitive mesenchymal tissue of a persistent and hyperplastic primary vitreous can mature to adipose tissue, cartilage, and smooth muscle tissue [47, 114].
- Lens fragments are a common occurrence in vitreous samples (the morphology is highlighted in Table 7.1, p. 537).
- Signs of vitreous hemorrhage may be present.
- Varying numbers of scattered lymphocytes, histiocytes, neutrophilic granulocytes, and a variable amount of amorphous debris.

**Caution**
- Aggregation of activated fibrohistiocytic spindle cells showing epithelioid features and intermingled lymphocytes may reflect sarcoidosis. However, sarcoidosis should only be considered in cases with tight grouping of epithelioid histiocytes, enclosed lymphocytes, and absence of overt background material (particularly caseous detritus).

- Both paucicellular specimens containing sporadic mature and immature lymphocytes and cell-rich smears containing a pure lymphoid cell population predominantly composed of blast cells give rise to severe diagnostic problems in differentiating between inflammatory disorder and malignant lymphoma (see Sect. 7.2.2.3.4, below) (Fig. 7.11A)

#### 7.2.2.3.3 Endophthalmitis (Figs. 7.12 and 7.13 )

- Endophthalmitis is characterized by neutrophils and debris (acute inflammation), and lymphocytes and histiocytes (chronic inflammation). Distinguishing between bacterial endophthalmitis and a reactive inflammatory process may be difficult, particularly after ocular surgery.
- Infectious endophthalmitis requires immediate antibiotic therapy; therefore, rapid recognition of infectious organisms in cytologic smears and subsequent specific microbiological or molecular tests from the remaining aspirate are highly important. Note that the sensitivity for detection of infectious agents in cytologic routine preparations is rather low [45]. Vitreoretinal infectious diseases that are important regarding ocular cytology are presented in distinguished textbooks [51].

#### 7.2.2.3.4 Malignant Lymphoma [21, 34, 42, 65, 68]

- Ocular lymphomas rarely occur. They are usually associated with extraocular lymphomas infiltrating the central nervous system.
- Single cases of primary ocular low-grade lymphoma (mucosa-associated lymphoid tissue lymphoma [MALT lymphoma]) [80, 86], and lymphoma of the T-cell type [26] have been reported.
- Most intraocular non-Hodgkin lymphomas (NHL) are large-cell tumors of B-cell origin, and immunophenotyping suggests a germinal center origin [27].

**Microscopic Features** [42, 68]

- Malignant ocular lymphomas are usually characterized by greatly enlarged abnormal lymphoid cells showing a high N/C ratio. The morphologic characteristics include a dense granular to coarse chromatin, nuclear dyschromasia compared with the color of normal lymphocytic nuclei, an irregular nuclear outline, and pronounced nucleoli.
- Rare lymphoma variants such as low-grade (MALT-type-) NHL, or NHL of the T-cell phenotype exhibit different cell features. The cytomorphology of the various lymphoma variants is described in detail in Sect. 15.3, "Lymph Nodes: Malignant Lesions," p. 950.

**Additional Analyses**

Limitation in cytologic diagnostics of malignant lymphoma requires auxiliary analyses. These tests encompass an immunocytochemical panel for T- and B-cell subsets [27] and immunophenotyping of the lymphocytes by flow cytometry [36, 117]. Furthermore, monoclonal gene amplification can be demonstrated using polymerase chain reaction (PCR) for rearrangement of the immunoglobulin heavy chain gene and T-cell receptor gamma gene as well as DNA sequencing [26, 109].

**Caution**

Immunophenotyping and molecular clonality assessment may fail to diagnose lymphoma in cases with paucicellular samples or in cytologic samples composed of few malignant cells accompanied by a hyperplastic benign lymphoid population.

**Differential Diagnosis**

- Diagnosis of primary intraocular malignant lymphoma based on cytomorphologic features alone can be extremely difficult. Scanty enlarged atypical lymphoid cells, reactive lymphocytosis exhibiting a predominantly blastic component, and poorly preserved cellular material in vitreous aspirates or vitrectomy specimens frequently lead to unequivocal diagnoses [42] (Fig. 7.11).
- Malignant lymphoid cells of the large-cell type may share morphologic features with those of myelogenous leukemia, undifferentiated carcinoma, and nonpigmented malignant melanoma. Appropriate immunocytochemical marker panels and clinical history can solve the diagnostic problems to a large extent.

#### 7.2.2.3.5 Other Rare Abnormalities of the Vitreous Body Recognized by Cytology

*Asteroid hyalosis* is a rare degenerative disorder of the vitreous.

- Cytologic preparations reveal amorphous round bodies that are birefringent upon polarization. A foreign body reaction may be associated [108].

*Amyloidosis* (Figs. 4.62B and 7.14) of the vitreous is usually associated with familial amyloidosis.

- The amorphous mass stains positive with Congo red and reveals characteristic bottle-green birefringence by polarized light microscopy [51].

### 7.2.2.4 Retina

#### 7.2.2.4.1 Nonneoplastic Diseases

- Cytologic preparations from intraocular washings occasionally reveal retinal fragments. In most cases, neither retinal fragments nor the cellular pattern of the vitreous fluid allow the diagnosis of a specific retinal disease. Most of the nonneoplastic retinal disorders result in vascularization and vitreous hemorrhage.
- Diabetic retinopathy and proliferative vitreoretinopathy have been mentioned in Sect. 7.2.2.3.2, p. 541.

- Other pathologic conditions of the retina include Coats disease, Eales disease, retinal vein occlusion, sickle cell retinopathy, occlusive syndrome of the large vessels, and hyperviscosity syndromes [51].

#### 7.2.2.4.2 Retinal Neoplasms

Primary malignant intraocular tumors are rare, metastatic tumors are more common. Both tumor types usually affect the choroid and retina.

Melanoma together with choroidal neoplasms are presented in Sect. 7.2.2.2.2, "Benign and Malignant Tumors of the Uvea," p. 539. Malignant lymphoma is discussed in Sect. 7.2.2.3.4, p. 542.

**Retinoblastoma** [19, 64, 88, 91]

Retinoblastoma bears morphologic resemblance to the cancers of the small round cell tumor group. Retinoblastoma develops in the light-sensitive cells of the retina and becomes apparent in early childhood. Retinoblastoma is a treatable cancer and has one of the best cure rates of all childhood neoplasms.

Intraocular FNABs of retinoblastoma have been repeatedly reported in the literature. Whether a preoperative diagnosis should be sought is a controversial issue (due to potential tumor cell seeding).

**Microscopic Features and Differential Diagnosis**

- Cytologic specimens exhibit small cells that have hyperchromatic nuclei as well as scanty and poorly defined cytoplasm, and rare distinct nucleoli.
- The tumor cells appear in cohesive aggregates forming clusters and strands. Rosettes are rarely encountered [88].
- The background of the smears is composed of abundant necrotic debris and nuclear smearing. Calcific deposits are obvious.

Retinoblastoma may mimic neuroblastoma spreading in and around the eye. Other small round cell tumors in the young pediatric group (before the age of 5 years) should be excluded (see Sect. 12.1.10 "Pediatric Renal Tumors," p. 743, including Table 12.1.1).

**Retinal Pigment Epithelium Neoplasm** [44, 100]

These tumors are rare and predominantly seen in women. Most of the tumors are benign but a few adenocarcinomas have been reported. Clinically, retinal pigment epithelium neoplasm may strongly simulate melanoma.

Other benign pigmented tumors have been reported to share cytologic features with retinal pigment epithelium neoplasm.

**Metastases**

The choroid is the most common site for ocular metastases and melanoma, and the retina is often secondarily involved by tumor spreading [10] (see also Sect. 7.2.2.2.2, "Tumors of the Uvea," p. 539). A solitary well-circumscribed metastasis of a large-cell carcinoma may easily be confused with primary amelanotic melanoma.

## 7.3 Orbit (Orbital Cavity [102]

Orbital fine-needle aspiration has proved to be helpful in confirming a clinical and radiologic diagnosis:

- FNAB may spare patients the need for more extensive surgical interventions if the lesion can be treated without surgery.
- FNAB (together with additional analyses) can establish a diagnosis in cases of suspected metastatic neoplasia.
- Initial FNAB is useful in planning therapy modalities.
- Application of FNAB to orbital masses has repeatedly been described in the literature [17, 32]

### 7.3.1 Orbital Pseudotumor [20]

Orbital pseudotumor is a benign idiopathic inflammatory disorder that involves the entire orbit or presents in a localized mode in various organs and compartments of the orbital cavity. It may present as an acute, subacute, or chronic inflammation. The lesion usually responds well to corticosteroid treatment. Fine-needle aspiration may be useful in clarifying clinically ambiguous cases.

**Microscopic Features and Differential Diagnosis**

- The *lymphocytic type* of orbital pseudotumor is composed of large numbers of small and enlarged activated lymphocytes. Only a small amount of collagen may be found.
- The *mixed type* presents with lymphoid cells and an admixture of neutrophils, chronic inflammatory cells, and fibrotic tissue fragments.
- In contrast, the *fibrotic type* is composed of large amounts of fibrotic tissue; only a few inflammatory cells are encountered. The aspirates are usually paucicellular, composed of small fragments of sclerotic tissue, histiocytes, fibroblasts, and leukocytes. Cytologic investigations frequently provide no conclusive diagnosis.

Distinguishing between the lymphocytic variant of pseudotumor and common reactive lymphocytosis, Rosai-Dorfman disease [70], pseudolymphoma, and malignant lymphoma is difficult by cytology alone. Immunocytochemical investigations, flow cytometric immunophenotyping and clonality assessment using various methods may permit a conclusive diagnosis.

### 7.3.2 Meningioma

Meningioma may arise from the arachnoid tissue covering the optic nerve or it penetrates the orbit from a primary brain-lining meningeal area close to the eye.

Fine-needle aspiration biopsy has been reported to be useful in diagnosing meningioma [28, 53, 71].

**Microscopic Features**

- Hallmarks: Small cells with round to oval nuclei and scant cytoplasm. The cells are tightly clustered and occasionally organized in whorls. Nucleoli are indistinct and the chromatin is fine and evenly distributed. Occasional nuclear pseudoinclusions and psammoma bodies are diagnostic key features.



### 7.3.3 Malignant Melanoma (Fig. 7.15)

Primary orbital melanomas are rare. Most tumors are secondary to the orbital cavity originating from the choroid, conjunctiva, the skin of the eyelid, and from paranasal sinuses [77, 78].

Immunocytochemistry should be used to establish the diagnosis of amelanotic melanoma, which may simulate metastatic large-cell carcinoma and spindle cell tumors.

More information is provided in Sect. 7.2.2.2.2, "Uveal Malignant Melanoma," p. 540.

### 7.3.4 Malignant Lymphoma (Fig. 7.16)

Lymphoid proliferations are among the most commonly diagnosed disorders affecting the orbital cavity.

- Cytologic distinction between benign and malignant orbital lymphoid lesions is difficult [74, 107]. Diagnostic features, adjuvant analyses, and differential diagnostic dilemmas have been discussed in Sect. 7.2.2.3.4,"Vitreous Body: Malignant Lymphoma," p. 542 and Sect. 7.3.1, Orbital Pseudotumor," p. 543, and in several chapters of this book.
- Plasmacytoma [74, 112] may rarely be encountered in orbital aspirates (Fig. 7.16).
- A large series of malignant lymphomas of the ocular adnexa has recently been reported by Ferry and coworkers [43].

**Caution**

Immature plasmocytoma may be confused with a variety of large-cell malignancies such as undifferentiated carcinoma, amelanotic melanoma, soft tissue neoplasm, and others.

### 7.3.5 Other Benign and Malignant Lesions that Might Be Observed in Orbital FNAB

The cytomorphology of many of the lesions as listed below is described in different chapters of this book. We refer the reader to distinguished textbooks and publications providing details on their occurrence within the orbit.

- Inflammation and miscellaneous infections.
- Granulomatoses (e.g., foreign-body granuloma, sarcoidosis, Wegener granulomatosis).
- Vascular lesions (e.g., lymphangioma, hemangioma, hemangiopericytoma).
- Cystic lesions (e.g., dermoid cyst, mucocele).
- Langerhans cell histiocytosis (e.g., eosinophilic granuloma) (Fig. 17.27).
- Benign tumors of neurogenic origin (e.g., schwannoma, granular cell tumor).
- Paraganglioma.
- Benign mesenchymal disorders (e.g., nodular fasciitis, xanthogranuloma, fibrous histiocytoma).
- Sarcoma (e.g., rhabdomyosarcoma, several variants of sarcoma).

### 7.3.6 Orbital Metastases [23, 59]

- Orbital metastasis as primary manifestation of a patient's tumor is extremely rare.
- The most common sites of remote primary tumors are breast and lung [59].
- Tumors invading the orbital space spreading from adjacent structures are:
  - Squamous cell carcinoma in adults, originating in sinus adjacent to the orbit.
  - Malignancies of the eyelid such as sebaceous gland carcinoma.
  - Neuroblastoma and Ewing sarcoma [58] in the pediatric patient group.
- Other remote primary neoplasms with secondary manifestation in the orbital cavity have been found in the prostate, gastrointestinal tract, urinary bladder, oropharynx [59], and neuroendocrine system [72].

**Differential Diagnoses**

- Small round cell tumors in children and young adults presenting diagnostic dilemmas include Ewing sarcoma, neuroblastoma, embryonal rhabdomyosarcoma, lymphoma, and retinoblastoma.
- Metastatic small-cell carcinoma of the lung can be confused both with malignant lymphoma and small-cell tumors of the skin or lacrimal glands. We refer to Sect. 16.2, "Variety of Skin Lesions," p. 1026.
- Immunocytochemical work-up may be helpful in assessing the primary origin of orbital metastases.

**Caution**

Ectopic lacrimal gland tissue in the orbital cavity may simulate an epithelial neoplasia, primary or metastatic [11].

### 7.3.7 Lacrimal Glands (Figs. 7.17 and 7.18)

- FNAB may be extremely helpful in rapidly differentiating between inflammatory and neoplastic enlargement of the lacrimal glands (Fig. 7.17).
- The most common primary tumors of the lacrimal glands include pleomorphic adenoma and adenoid cystic carcinoma. FNAB results have most commonly been reported for these two entities [103, 106]. It is generally acknowledged that tumors of the lacrimal glands are comparable with their counterparts originating in the major salivary glands. Therefore, diagnostic cytologic criteria for lacrimal tumoral lesions match those of salivary gland-type tumors [9, 106] (see Sects. 5.1.4, "Benign Tumors", p. 409 and 5.1.5, "Malignant Tumors", p. 414) (Fig. 7.18).
- Bernardini and colleagues have recently presented a comprehensive update on diagnosis and classification of lacrimal gland tumors [9]; and results from a large series of ocular adnexal lymphomas were reported by Ferry and coauthors in 2007 [43].

## 7.4 Eyelid

### 7.4.1 Common Skin Lesions

- Most lesions affecting the eyelids are comparable with the corresponding skin disorders; the cytologic diagnosis is based upon the same morphologic features as described in Chap. 16, "Skin lesions and Unusual Subcutaneous Lesions," p. 1023.
- Depending on the clinical appearance, the eyelid lesions may be evaluated by scraping or FNAB.
- The most common nonneoplastic and neoplastic disorders in the lid include:
  - Amyloid deposits.
  - Viral infections.
  - Pilomatrixoma/ pilomatrix carcinoma [15, 90].
  - Adenocarcinoma [60].
  - Skin adnexal tumors [60].
  - Melanoma.

### 7.4.2 Particular Disorders of the Lids

#### 7.4.2.1 Xanthelasma

This lesion is a sharply demarcated yellowish collection of cholesterol underneath the skin. FNAB is rarely performed; lipid filled macrophages may be collected.

#### 7.4.2.2 Chalazion (Meibomian Gland Lipogranuloma)

Chalazion is caused by retention of secretions due to a blockage of the meibomian gland ducts.

- Cytologic smears demonstrate a mixture of lipid laden macrophages and granulomatous components comprising neutrophils, lymphocytes, plasma cells, histiocytes, fibroblasts, and giant cells. Suppuration or granuloma fragments are variably present.

The inflammatory component and absence of cellular atypia exclude sebaceous carcinoma [39].

#### 7.4.2.3 Sebaceous Carcinoma

This tumor originates from meibomian glands and Zeis glands located in the eyelid [93]. Clinically, the lesion is easily misinterpreted as chalazion.

**Microscopic Features and Differential Diagnoses**

- The aspirates are cellular comprising isolated large pale cells with a vacuolated cytoplasm dispersed in a bubbly background. Cytoplasmic vacuoles contain lipids.
- The sebaceous-type cells exhibit varying degrees of maturation, including irregular nuclear shape and hyperchromasia. Basaloid or squamous features may also be present.

In contrast to the sebaceous carcinoma is the chalazion accompanied by an inflammatory and granulomatous background, and cellular atypias are absent.

Other eyelid neoplasms such as pilomatrixoma and basal cell carcinoma should provide minor differential diagnosis problems [48, 49].

#### 7.4.2.4 Basal Cell Carcinoma

This is the most common malignant epithelial tumor of the eyelid. Morphologic characteristics of this tumor are provided in Sect. 16.2.7, p. 1029.

## 7.5 Further Reading


1. Aksünger A, Unlü K, Karakas N, et al. Impression cytology, tear film break up, and Schirmer test in patients with inactive trachoma. Jpn J Ophthalmol 1997;41:305-307.
2. Augsburger JJ. Fine needle aspiration biopsy of suspected metastatic cancers to the posterior uvea. Trans Am Ophtalmol Soc 1988;86:499-560.
3. Augsburger JJ, Shields JA. Fine needle aspiration biopsy of solid intraocular tumors: indications, instrumentation and techniques. Ophthalmic Surg 1984;15:34-40.
4. Augsburger JJ, Shields JA, Folberg R, et al. Fine needle aspiration biopsy in the diagnosis of intraocular cancer. Cytologic-histologic correlations. Ophthalmology 1985;92:39-49.
5. Augsburger JJ, Correa ZM, Schneider S, et al. Diagnostic transvitreal fine-needle aspiration biopsy of small melanocytic choroidal tumors in nevus versus melanoma category. Trans Am Ophtalmol Soc 2002;100:225-232.
6. Baggetto LG, Gambrelle J, Dayan G, et al. Major cytogenetic aberrations and typical multidrug resistance phenotype of uveal melanoma: current views and new therapeutic prospects. Cancer Treat Rev 2005;31:361-379.
7. Baker SE, Singh AD, Fu E, et al. The role of fine needle aspiration in the evaluation of uveal tumors: A clinicopathologic analysis of 26 consecutive cases. Cancer Cytopathol 2008;114:357-358.
8. Bardenstein DS, Char DH, Jones C, et al. Metastatic ciliary body carcinoid tumor. Arch Ophthalmol 1990;108:1590-1594.
9. Bernardini FP, Devoto MH, Croxatto JO. Epithelial tumors of the lacrimal gland: an update. Curr Opin Ophthalmol 2008;19:409-413.
10. Block RS, Gartner S. The incidence of ocular metastatic carcinoma. Arch Opthalmol 1971;85:673-675.
11. Boccato P, Blandamura S, Midena E, Carollo C. Orbital ectopic lacrimal gland tissue simulating a neoplasm. Report of a case with fine needle aspiration biopsy diagnosis. Acta Cytol 1992;36:737-743.
12. Brown HH, Glasgow BJ, Holland GN, Foos RY. Keratinizing corneal intraepithelial neoplasia. Cornea 1989;8:220-224.
13. Butrus SI, Abelson MP. Laboratory evaluation of ocular allergy. Int Ophthalmol Clin 1988;28:324-328.
14. Butrus S, Portela R. Ocular allergy: diagnosis and treatment. Ophthalmol Clin North Am 2005;18:485-492.
15. Cahill MT, Moriarty PM, Mooney DJ, Kennedy SM. Pilomatrix carcinoma of the eyelid. Am J Ophthalmol 1999;127:463-464.
16. Campbell DG, Essigmann EM. Hemolytic ghost cell glaucoma. Arch Ophthalmol 1979;97:2141-2146.
17. Cangiarella JF, Cajigas A, Savala E, et al. Fine needle aspiration cytology of orbital masses. Acta Cytol 1996;40:1205-1211.
18. Char DH. Ocular melanoma. Surg Clin North Am 2003;83:253-274, vii.
19. Char DH, Miller TR. Fine needle biopsy in retinoblastoma. Am J Ophthalmol 1984;97:686-690.
20. Char DH, Miller T. Orbital pseudotumor. Fine-needle aspiration biopsy and response to therapy. Ophthalmology 1993;100:1702-1710.
21. Char DH, Kemlitz AE, Miller T. Intraocular biopsy. Ophthalmol Clin N Am 2005;18:177-185.
22. Char DH, Miller TR, Crawford JB. Cytopathologic diagnosis of benign lesions simulating choroidal melanomas. Am J Ophthalmol 1991;112:70-75.
23. Char DH, Miller T, Kroll S. Orbital metastases: diagnosis and course. Br J Ophthalmol 1997;81:386-390.
24. Char DH, Miller TR, Ljung BM, et al. Fine needle aspiration biopsy in uveal melanoma. Acta Cytol 1989;33:599-605.
25. Chen ZQ, Fang XY. Adenoma of nonpigmented epithelium in ciliary body: literature review and case report. J Zhejiang Univ Sci B 2007;8:612-615.
26. Coupland SE, Anastassiou G, Bornfeld N, et al. Primary intraocular lymphoma of T-cell type: report of a case and review of the literature. Graefes Arch Clin Exp Ophthalmol 2005;243:189-197.
27. Coupland SE, Bechrakis NE, Anastassiou G, et al. Evaluation of vitrectomy specimens and chorioretinal biopsies in the diagnosis of primary intraocular lymphoma in patients with Masquerade syndrome. Graefes Arch Clin Exp Ophthalmol 2003;241:860-870.
28. Cristallini EG, Bolis GB, Ottaviano P. Fine-needle aspiration biopsy of orbital meningioma. Acta cytol 1990;34:236-238.
29. Cvenkel B, Globocnik M. Conjunctival scrapings and impression cytology in chronic conjunctivitis. Correlation with microbiology. Eur J Ophthalmol 1997;7:19-23.
30. Czerniak B, Woyke S, Domagala W, Krzysztolik Z. Fine needle aspiration cytology of intraocular malignant melanoma. Acta Cytol 1983;27:157-165.
31. Darville T. Chlamydia trachomatis infections in neonates and young children. Semin Pediatr Infect Dis 2005;16:235-244.
32. Das DK, Das J, Bhatt NC, et al. Orbital lesions. Diagnosis by fine needle aspiration cytology. Acta Cytol 1994;38:158-164.
33. Davila RM, Miranda MC, Smith ME. Role of cytopathology in the diagnosis of ocular malignancies. Acta Cytol 1998;42:362-366.
34. Davis JL. Diagnosis of intraocular lymphoma. Ocul Immunol Inflamm 2004;12:7-16.
35. Davis JL, Miller DM, Ruiz P. Diagnostic testing of vitrectomy specimens. Am J Ophthalmol 2005;140:822-829.
36. Davis JL, Viciana AL, Ruiz P. Diagnosis of intraocular lymphoma by flow cytometry. Am J Ophthalmol 1997;124:362-372.
37. de Rivas P, Marti T, Andreu D, et al. Metastatic bronchogenic carcinoma of the iris and ciliary body. Arch Ophthalmol 1991;109:470.
38. Dewan S, Mittal S, D'Souza, Logani KB. Cytological evaluation of conjunctival scrape smears in cases of conjunctivitis. Indian J Pathol Microbiol 1992;35:118-124.
39. Dhaliwal U, Arora VK, Singh N, Bhatia A. Cytopathology of chalazia. Diagn Cytopathol 2004;31:118-122.
40. El-Harazi SM, Kellaway J, Font RL. Melanocytoma of the ciliary body diagnosed by fine-needle aspiration biopsy. Diagn Cytopathol 2000;22:394-397.
41. Embong Z, Wan Hitam WH, Yean CY, et al. Specific detection of fungal pathogens by 18S rRNA gene PCR in microbial keratitis. BMC Ophthalmol 2008;8:7.
42. Farkas T, Harbour JW, Davila RM. Cytologic diagnosis of intraocular lymphoma in vitreous aspirates. Acta Cytol 2004;48:487-491.
43. Ferry JA, Fung CY, Zukerberg L, et al. Lymphoma of the Ocular Adnexa: A study of 353 cases. Am J Surg Pathol 2007;31:170-184.
44. Finger PT, McCormick SA, Davidian M, Walsh JB. Adenocarcinoma of the retinal pigment epithelium: a diagnostic and therapeutic challenge. Graefes Arch Clin Exp Ophthalmol 1996;234 Suppl 1:S22-27.
45. Fischler DF, Prayson RA. Cytologic specimens from the eye: a clinicopathologic study of 33 patients. Diagn Cytopathol 1997;17:262-266.
46. Font RL, Croxato JO, Rao NA. AFIP Atlas of Tumor Pathology, fourth series, Fasc 5. Tumors of the Eye and Ocular Adnexa. 2006.
47. Font RL, Yanoff M, Zimmerman LE. Intraocular adipose tissue and persistent hyperplastic primary vitreous. Arch Ophthalmol 1969;82:43-50.
48. Gao L, Lin WH, Gong ZJ, et al. Fine needle aspiration cytology of eyelid sebaceous gland carcinoma and its differential diagnosis. Zhonghua Bing Li Xue Za Zhi 2004;33:36-39.
49. Garbyal RS, Gupta P, Kumar M, et al. A cytologic perspective on meibomian gland carcinoma. Acta Cytol 2007;51:171-177.
50. Glasgow BJ. Intraocular fine-needle aspiration biopsy of coronal adenomas. Diagn Cytopathol 1991;7:239-242.
51. Glasgow BJ, Foos RY. Ocular Cytopathology. Butterworth-Heinemann Boston, 1993.
52. Glasgow BJ, Layfield LJ. Fine-needle aspiration biopsy of orbital and periorbital masses. Diagn Cytopathol 1991;7:132-141.

53. Gopal L, Babu EK, Gupta S, et al. Pigmented malignant medulloepithelioma of the ciliary body. J Pediatr Ophthalmol Strabismus 2004;41:364-366.
54. Gopinathan U, Garg P, Fernandes M, et al. The epidemiological features and laboratory results of fungal keratitis: a 10-year review at a referral eye care center in South India. Cornea 2002;21:555-559.
55. Grossniklaus HE, Frank KE, Farhi DC, et al. Hemoglobin spherulosis in the vitreous cavity. Arch Ophthalmol 1988;106:961-962.
56. Grossniklaus HE, Zimmermann LE, Kachmer ML. Pleomorphic adenocarcinoma of the ciliary body. Immunohistochemical and electron microscopic features. Ophthalmology 1990;97:763-768.
57. Gupta N, Tandon R. Investigative modalities in infectious keratitis. Indian J Ophthalmol 2008;56:209-213.
58. Gupta N, Bansal D, Saxena AK, et al. Primary orbital Ewing's sarcoma presenting with unilateral proptosis. Cytopathology 2008;19:124-126.
59. Holland D, Maune S, Kovacs G, Behrendt S. Metastatic tumors of the orbit. a retrospective study. Orbit 2003;22:15-24.
60. Huerva V, Sanchez MC, Egido RM, Matias-Guiu X. Pleomorphic adenoma with extensive myoepithelial component (myoepithelioma) of the lower eyelid. Ophthal Plast Reconstr Surg 2008;24:223-225.
61. Jain AK, Bansal R, Felcida V, Rajwanshi A. Evaluation of impression smear in the diagnosis of fungal keratitis. Indian J Ophthalmol 2007;55:33-36.
62. Jakobiec FA, Coleman DJ, Chattock A, Smith M. Ultrasonically guided needle biopsy and cytologic diagnosis of solid intraocular tumors. Ophthalmology 1979;86:1662-1681.
63. Kampik A, Kenyon KR, Michels RG, et al. Epiretinal and vitreous membranes. Comparative study of 56 cases. Arch Ophthalmol 1981;99:1445-1454.
64. Karcioglu ZA. Fine needle aspiration biopsy (FNAB) for retinoblastoma. Retina 2002;22:707-710.
65. Karma A, von Willebrand EO, Tommila PV, et al. Primary intraocular lymphoma: Improving the diagnostic procedure. Ophthalmology 2007;114:1372-1377.
66. Laver NV, Rubinfeld RS, Baum M, de Brito PA. Cytomorphology of a mixed pigmented/nonpigmented pleomorphic adenoma of the ciliary body: a diagnostic pitfall in the evaluation of intraocular tumors. Diagn Cytopathol 1996;14:259-262.
67. Lee GA, Hirst LW. Retrospective study of ocular surface squamous neoplasia. Aust N Z J Ophthalmol 1997;269-276.
68. Ljung BM, Char D, Miller TR, Deschenes J. Intraocular lymphoma. Cytologic diagnosis and the role of immunologic markers. Acta Cytol 1988;32:840-847.
69. LoRusso FJ, Boniuk M, Font RL. Melanocytoma (magnocellular nevus) of the ciliary body: report of 10 cases and review of the literature. Ophthalmology 2000;107:795-800.
70. Malur PR, Bannur HB, Kodkany SB. Orbital Rosai-Dorfman disease: report of a case with fine needle aspiration cytology and histopathology. Acta Cytol 2007;51:581-582.
71. Mehrotra R, Kumar S, Singh K, et al. Fine needle aspiration biopsy of orbital meningioma. Diagn Cytopathol 1999;21:402-404.
72. Mehta JS, Abou-Rayyah Y, Rose GE. Orbital carcinoid metastases. Ophthalmology 2006;113:466-472.
73. Nadjari B, Kersten A, Ross B, et al. A cytologic and DNA cytometric diagnosis and therapy monitoring of squamous cell carcinoma in situ and malignant melanoma of the cornea and conjunctiva. Anal Quant Cytol Histol 1999;21:387-396.
74. Nassar DL, Raab SS, Silverman JF, et al. Fine-needle aspiration for the diagnosis of orbital hematolymphoid lesions. Diagn Cytopathol 2000;23:314-317.
75. Nicolo M, Nicolo G, Zingirian M. Pleomorphic adenocarcinoma of the ciliary epithelium: a clinicopathological, immunohistochemical, ultrastructural, DNA-ploidy and comparative genomic hybridization analysis of an unusual case. Eur J Ophthalmol 2002 ;12:319-323.
76. Okhravi N, Adamson P, Lightman S. Use of PCR in endophthalmitis. Ocul Immunol Inflamm 2000;8:189-200.
77. Poli T, Mora P, Reichegger V, et al. Surgical management of orbital malignant melanoma: our experience and a report of three cases. Klin Monatsbl Augenheilkd 2007;224:794-798.
78. Polito E, Leccisotti A. Primary and secondary orbital melanomas: a clinical and prognostic study. Ophthal Plast Reconstr Surg 1995;11:169-181.
79. Pollard ZF. Persistent hyperplastic primary vitreous: diagnosis, treatment and results. Trans Am Ophthalmol Soc 1997;95:487-549.
80. Ramulu P, Iliff NT, Green WR, Kuo IC. Asymptomatic conjunctival mucosa-associated lymphoid tissue-type lymphoma with presumed intraocular involvement. Cornea 2007;26:484-486.
81. Reddy SC, Jackson N, Menon BS. Ocular involvement in leukemia - a study of 288 cases. Ophthalmologica 2003;217:441-445.
82. Rosenthal AR. Ocular manifestations of leukemia. A review. Ophthalmology 1983;90:899-905.
83. Rosenthal DL, Mandell DB, Glasgow BJ. 'Eye, chapter 19' , In: Comprehensive Cytopathology, ed: M.Bibbo, WB.Saunders Company Philadelphia. 1991.
84. Roussat B, Barbat V, Cantaloube C, et al. Persistent and hyperplastic primary vitreous syndrome. Clinical and therapeutic aspects. J Fr Ophthalmol 1998;21:501-507.
85. Saro F, Clua A, Esteva E, et al. Cytologic diagnosis of ocular melanocytoma. A case report. Acta Cytol 2008;52:87-90.
86. Sarraf D, Jain A, Dubovy S, et al. Mucosa-associated lymphoid tissue lymphoma with intraocular involvement. Retina 2005;25:94-98.
87. Schalenbourg A, Uffer S, Chamot L, et al. Adenocarcinoma of the nonpigmented ciliary body epithelium: report of a rare case. Bull Soc Belge Ophthalmol 1999;271:29-35.
88. Scroggs MW, Johnston WW, Klintworth GK. Intraocular tumors. A cytopathologic study. Acta Cytol 1990;34:401-408.
89. Seal D, Reischl U, Behr A, et al. Laboratory diagnosis of endophthalmitis: comparison of microbiology and molecular methods in the European Society of Cataract & Refractive Surgeons multicenter study and susceptibility testing. J Cataract Refract Surg 2008;34:1439-1450.
90. Seitz B, Holbach LM, Naumann GO. Pilomatrixoma of the eyelids – clinical differential diagnosis and follow-up. Report of 17 patients. Ophthalmologe 1993;90:746-749.
91. Sen S, Singha U, Kumar H, et al. Diagnostic intraocular fine-needle aspiration biopsy - An experience in three cases of retinoblastoma. Diagn Cytopathol 1999;21:331-334.
92. Sharma S, Kunimoto DY, Gopinathan U, et al. Evaluation of corneal scraping smear examination methods in the diagnosis of bacterial and fungal keratitis: a survey of eight years of laboratory experience. Cornea 2002;21:643-647.
93. Shields JA, Demirci H, Marr BP, et al. Sebaceous carcinoma of the eyelids: personal experience with 60 cases. Ophthalmology 2004;111:2151-2157.
94. Shields JA, Eagle RC Jr, Shields CL, De Potter P. Acquired neoplasms of the nonpigmented ciliary epithelium (adenoma and adenocarcinoma). Ophthalmology 1996;103:2007-2016.
95. Shields JA, Eagle RC, Shields CL, Potter PD. Congenital neoplasms of the nonpigmented ciliary epithelium (medulloepithelioma). Ophthalmology 1996;103:1998-2006.
96. Shields CL, Manchandia A, Subbiah R, et al. Pigmented squamous cell carcinoma in situ of the conjunctiva in 5 cases. Ophthalmology 2008;115:1673-1678.
97. Shields JA, Shields CL, De Potter P, Singh AD. Diagnosis and treatment of uveal melanoma. Semin Oncol 1996;23:763-767.
98. Shields JA, Shields CL, Eagle RC Jr, De Potter P. Observations on seven cases of intraocular leiomyoma. The 1993 Byron Demorest Lecture. Arch Ophthalmol 1994;112:521-528.

99. Shields JA, Shields CL, Ehya H, et al. Fine-needle aspiration biopsy of suspected intraocular tumors. The 1992 Urwick Lecture. Ophthalmology 1993;100:1677-1684.
100. Shields JA, Shields CL, Gündüz K, Eagle RC Jr. Neoplasms of the retinal pigment epithelium: the 1998 Albert Ruedemann, Sr, memorial lecture, Part 2. Arch Ophthalmol 1999;117:601-608.
101. Shields JA, Shields CL, Mercado G, et al. Adenoma of the iris pigment epithelium: a report of 20 cases: the 1998 Pan-American Lecture. Arch Ophthalmol 1999;117:736-741.
102. Shields JA, Shields CL, Scartozzi R. Survey of 1264 patients with orbital tumors and simulating lesions: The 2002 Montgomery Lecture, part 1. Ophthalmology 2004;111:997-1008.
103. Siddaraju N, Solo S, Soundararaghavan J, Srinivasan R. Fine needle aspiration biopsy of pleomorphic adenoma and adenoid cystic carcinoma of the lacrimal gland. Acta Cytol 2008;52:515-517.
104. Singh R, Joseph A, Umapathy T, et al. Impression cytology of the ocular surface. Br J Ophthalmol 2005;89:1655-1659.
105. Sternberg P Jr, Tiedman J, Hickingbotham D, et al. Controlled aspiration of subretinal fluid in the diagnosis of carcinoma metastatic to the choroid. Arch Ophthalmol 1984;102:1622-1625.
106. Sturgis CD, Silverman JF, Kennerdell JS, Raab SS. Fine-needle aspiration for the diagnosis of primary epithelial tumors of the lacrimal gland and ocular adnexa. Diagn Cytopathol 2001;24:86-89.
107. Subramanian R, Solo S, Mishra MM, et al. Fine needle aspiration cytology of primary lymphoid lesions of the orbit: report of four cases. Acta Cytol 2007;51:417-420.
108. Wafi M, Rais L, Lahbil D, et al. A case of a retinitis pigmentosa and asteroid hyalosis. J Fr Ophthalmol 2004;27:801-804.
109. White VA, Gascoyne RD, Paton KE. Use of the polymerase chain reaction to detect B- and T-cell gene rearrangements in vitreous specimens from patients with intraocular lymphoma. Arch Ophthalmol 1999;117:761-765.
110. Wilhelmus KR, Robinson NM, Tredici LL, Jones DB. Conjunctival cytology of adult chlamydial conjunctivitis. Arch Ophthalmol 1986;104:691-693.
111. Wittenberg LA, Maberley DA, Ma PE, et al. Contribution of vitreous cytology to final clinical diagnosis. Fifteen-year review of vitreous cytology specimens from one institution. Ophthalmology 2008;115:1944-1950.
112. Yakulis R, Dawson RR, Wang SE, Kennerdell JS. Fine needle aspiration diagnosis of orbital plasmacytoma with amyloidosis. A case report. Acta Cytol 1995;39:104-110.
113. Yang JL, Schachter J, Moncada J, et al. Comparison of an rRNA-based and DNA-based nucleic acid amplification test for the detection of Chlamydia trachomatis in trachoma. Br J Ophthalmol 2007;91:293-295.
114. Yanoff M, Font RL. Intraocular cartilage in a microphthalmic eye of an otherwise healthy girl. Arch Ophthalmol 1969;81:238-240.
115. Young TA, Burgess BL, Rao NP, et al. Transscleral fine-needle aspiration biopsy of macular choroidal melanoma. Am J Ophthalmol 2008;145:297-302.
116. Young TA, Rao NP, Glasgow BJ, et al. Fluorescent in situ hybridization for monosomy 3 via 30-gauge fine-needle aspiration biopsy of choroidal melanoma in vivo. Ophthalmology 2007;114:142-146.
117. Zaldivar RA, Martin DF, Holden JT, Grossniklaus HE. Primary intraocular lymphoma: clinical, cytologic, and flow cytometric analysis. Ophthalmology 2004;111:1762-1767.

**Fig. 7.1 Normal vitreous fluid.**
Few histiocytes and lymphocytes entrapped in strands of mucoid material (direct sediment smear, Pap stain, high magnification).

**Fig. 7.2 Melanin pigment in vitreous fluid.**
Numerous melanin-laden cells occur in a vitrectomy fluid. It is difficult to differentiate degenerate melanophages associated with apoptotic nuclei from retinal pigment epithelium (conventional sediment smear, Pap stain, higher magnification).

**Fig. 7.3A–C Lens fragments and lens epithelium.**
Material originating from vitrectomy washing. Direct sediment smears are Pap-stained. **A** Several lens fragments both in bundles and discohesive (low magnification). **B** Morphology of a lens fragment in high magnification. **C** A sheet of lens epithelial cells and dissociated lens cells showing characteristic small dark nuclei (lower magnification).



**Fig. 7.4 Melanin pigment in fluid removed from the anterior chamber.**
A 74-year-old woman complained of vague symptoms in her left eye. Normal cytology was found in vitrectomy washing. Fluid aspirate from the anterior chamber shows red blood cells and numerous histiocytes packed with melanin granules (Cytospin preparation, Pap stain, high magnification). Abnormal cytology is most likely caused by prior trauma or degenerative process.

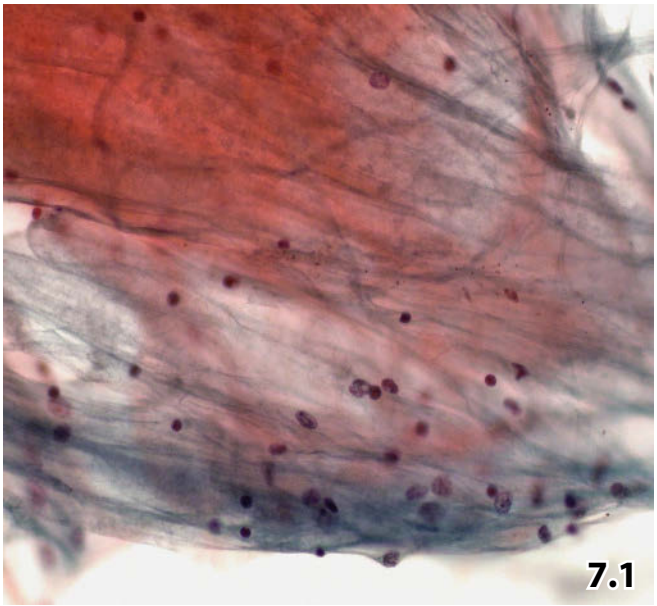
7.1

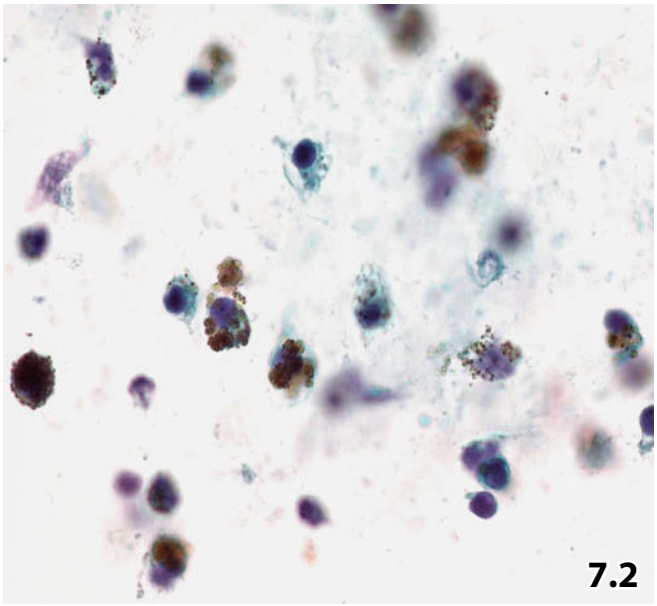
7.2

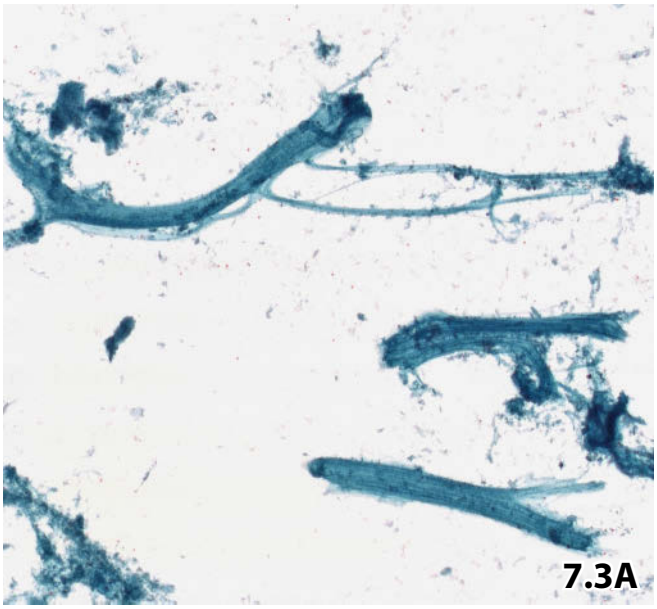
7.3A

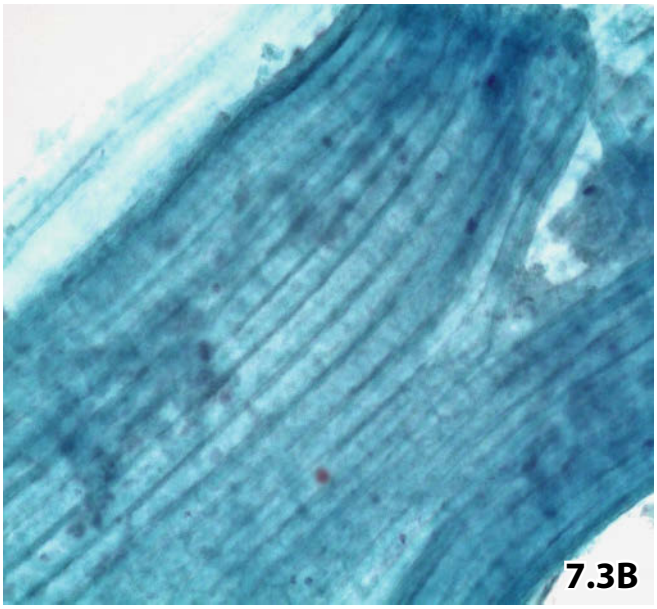
7.3B

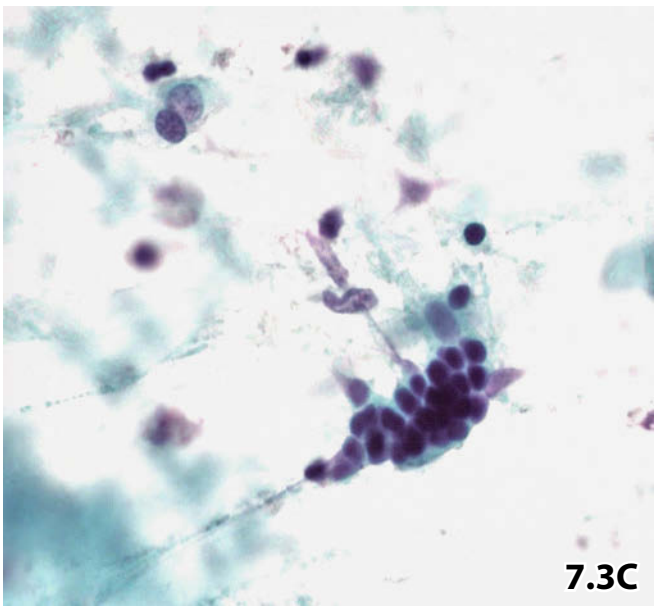
7.3C

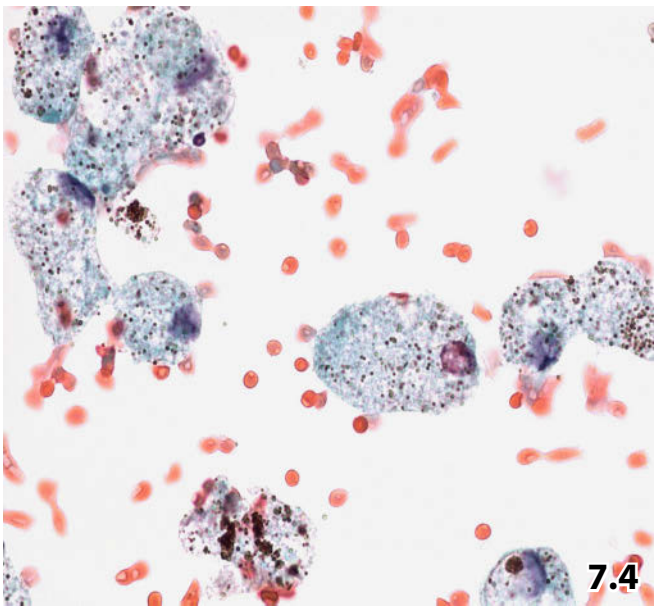
7.4

**Fig. 7.5A, B Vitreous hemorrhage.**
Ocular vasculitis was suggested in a 29-year-old man. Vitreous aspirate was performed. **A** Pap-stained direct sediment smears revealed lymphocytosis, debris, and scattered degenerating macrophages with cytoplasmic erythrocyte incorporation (arrows), together with several refractile amorphous elements (arrowhead) (low magnification). A definite diagnosis of iron substance is not possible in routinely stained specimens. **B** Special stain for iron (Prussian blue reaction) confirmed intracytoplasmic and free-floating hemosiderin.

**Figs. 7.6–7.11 Nonspecific granulomatosis, fibrosclerotic lesion, and inflammatory infiltrates in vitreous body.**
Various inflammatory lesions of the vitreous body are demonstrated by vitrectomy washing samples from different patients. All sediment smears were of high cellularity and were Pap-stained.

**Fig. 7.6** (case #1) Lower magnification: large fragments of granulomatous mesenchymal tissue. Loose fibrous matrix is interspersed with fibroblasts, histiocytes, and lymphocytes.



**Fig. 7.7** (case #2) Detail shows fibrosclerotic connective tissue encasing fibroblasts and fibrocytes (cells with elongated, slender, and dark nuclei) (arrows).

**Fig. 7.8** (case #3) Another detail reveals activated fibroblasts embedded in a meshwork of reticular fibers. Note the activated fibroblasts, which can mimic neoplastic cells.

**Fig. 7.9** (case #4) A 6-year-old girl presented with long-standing bilateral uveitis. High magnification shows typical epithelioid cells of histiocytic origin and a multinucleated giant cell of the Langhans type (arrow) embedded in a fibrous matrix. Scattered lymphocytes are also present.
*Comment:* Cytology suspected sarcoidosis, which could not be verified; the etiology of the ocular disorder remained open.

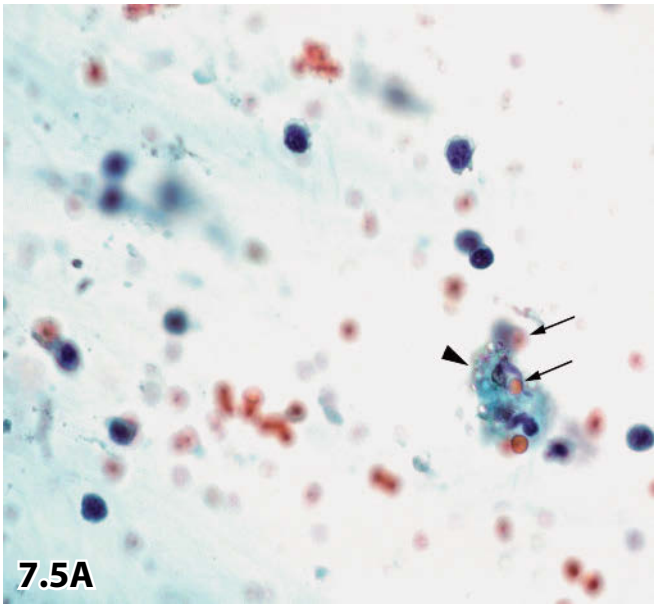
7.5A

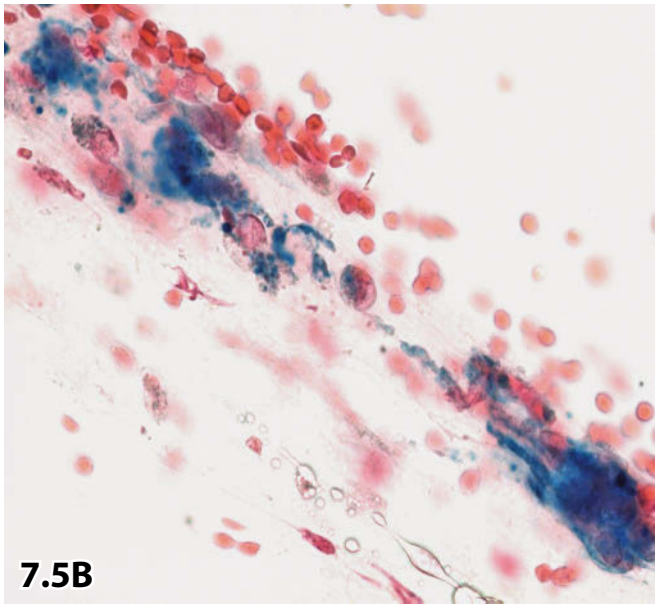
7.5B

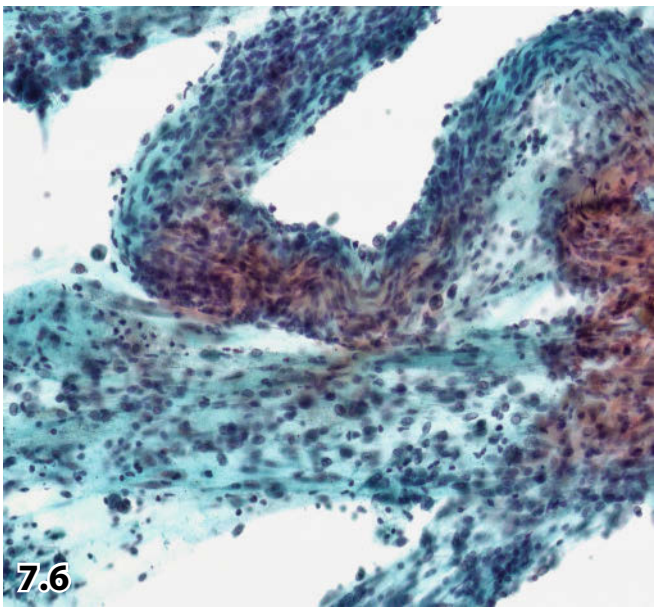
7.6

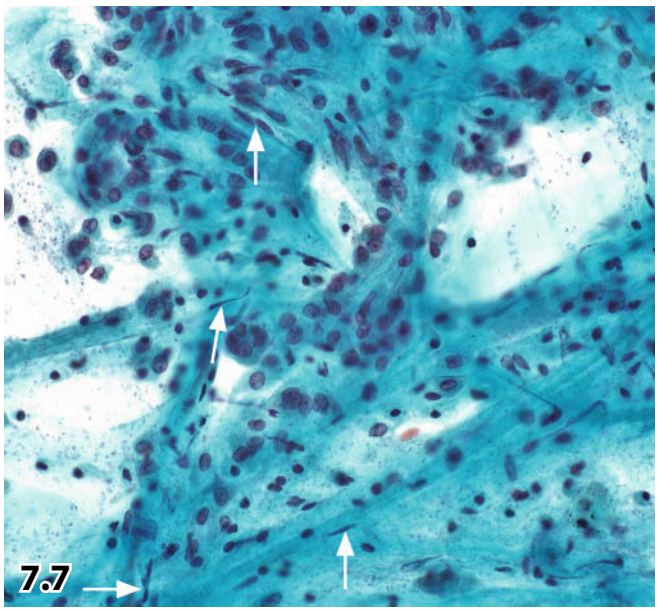
7.7

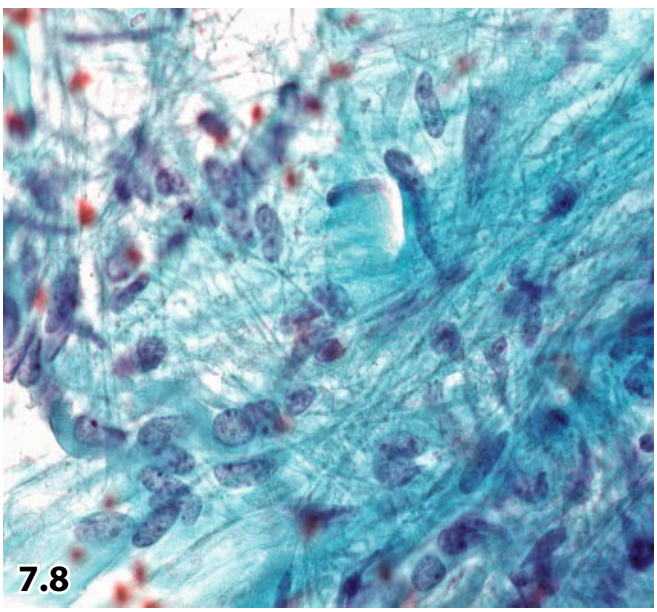
7.8

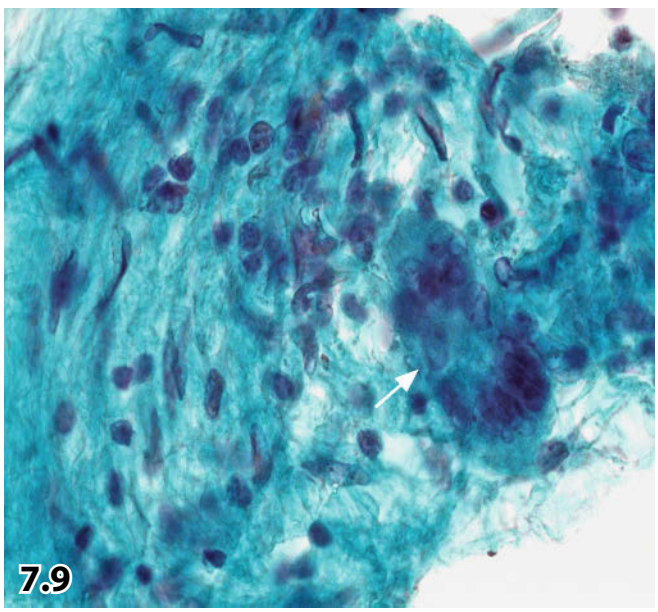
7.9

**Fig. 7.10** (case #5) High magnification shows a small fragment of florid granulomatous tissue (left), amorphous debris, and multiple lens fragments (arrows). The elderly patient suffered from long-standing granulomatous uveitis.

**Fig. 7.11A, B** (case #6) A 70-year-old man presented with ocular disorder that was clinically suspicious for malignant lymphoma. Vitrectomy was performed. **A** Vitrectomy specimen exhibiting pronounced reactive lymphocytosis: predominantly blast-like cells showing nuclear irregularities and multiple polymorphic nucleoli. Note the considerable necrotic background. Polymerase chain reaction using DNA extracted from a prestained cytologic smear excluded clonal rearrangement of both heavy immunoglobulin chain genes (in favor of B-NHL) and of T-cell receptor genes (in favor of T-NHL); PCR results are not shown. **B** Blast cells immunocytochemically expressed strong positivity for CD45, thus a nonlymphoid neoplasm could be excluded (sediment smear, Pap stain, lower magnification).
*Cytology:* An indeterminate cytologic report was rendered (most probably benign lymphoproliferative lesion).
*Final diagnosis:* Severe reactive lymphoproliferative lesion of unknown origin. There was no evidence of an extraocular lymphoid disorder.

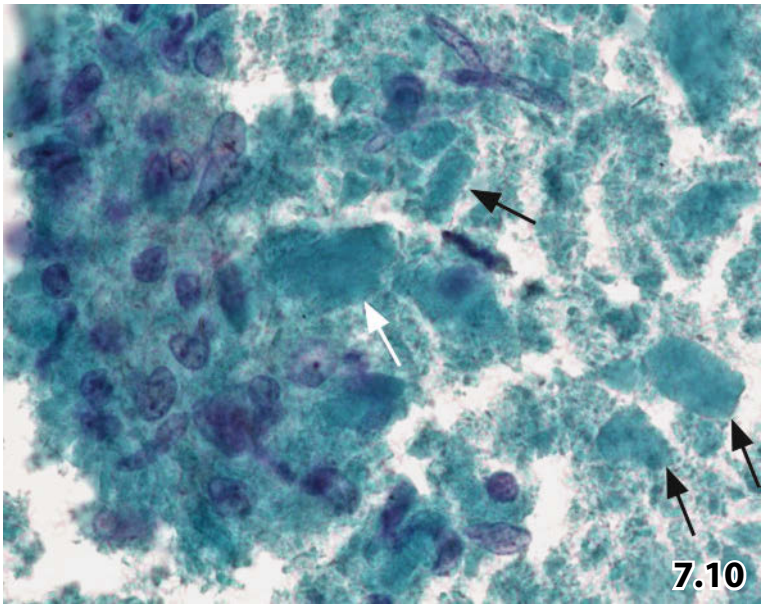

7.10

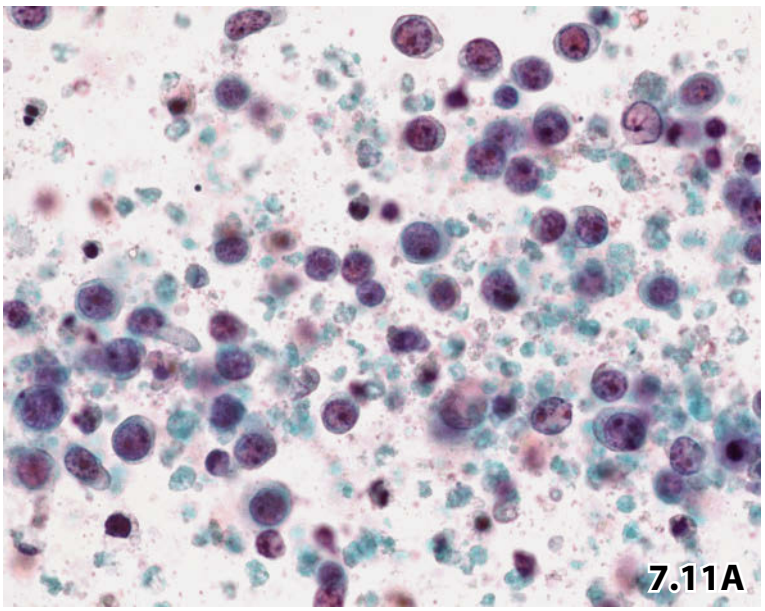

7.11A

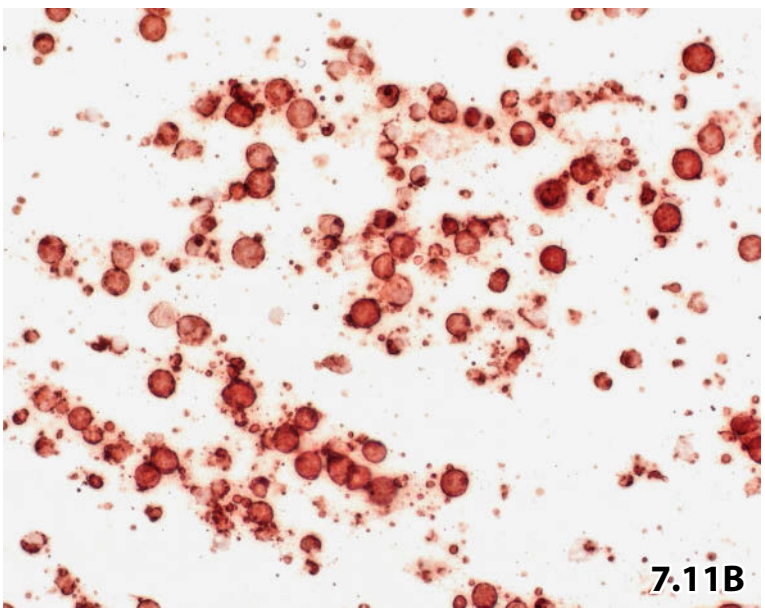

7.11B

**Figs. 7.12 and 7.13 Endophthalmitis.**
Two cases of postsurgical vitreous infection.

**Fig. 7.12** (case #1) A local bacterial infection occurred in a 78-year-old man 5 days after replacing the lens. Vitreous cytology revealed a purulent infiltrate and coccoid bacteria. Gram stain indicated Gram-positive cocci (direct sediment smear, Gram stain, high magnification).

**Fig. 7.13A, B** (case #2) A 69-year-old woman presented with endophthalmitis a few days after local surgical intervention (further details were not communicated). **A** High magnification shows densely packed granular background material, histiocytes, sparse neutrophil granulocytes (not present in this field), and pigment (Cytospin preparation, Pap stain). **B** Fungi were not recognizable in Pap-stained specimens but became clearly visible using a silver stain method (Cytospin preparation, Crocott, lower magnification).



**Fig. 7.14 Amyloidosis.**
The initial diagnosis of amyloidosis in a 51-year-old man was made by cytologic investigation of a vitreous aspirate. Generalized amyloidosis was found later on, using FNABs of subcutaneous abdominal fat and multiple histologic biopsies from different locations. Vitreous fluid sediment contains cloudy amyloid deposits staining red using Congo red (direct sediment smear, low magnification). Amyloid masses demonstrate bottle-green birefringence upon polarization in specimens stained with Congo red; see Fig. 4.62B.

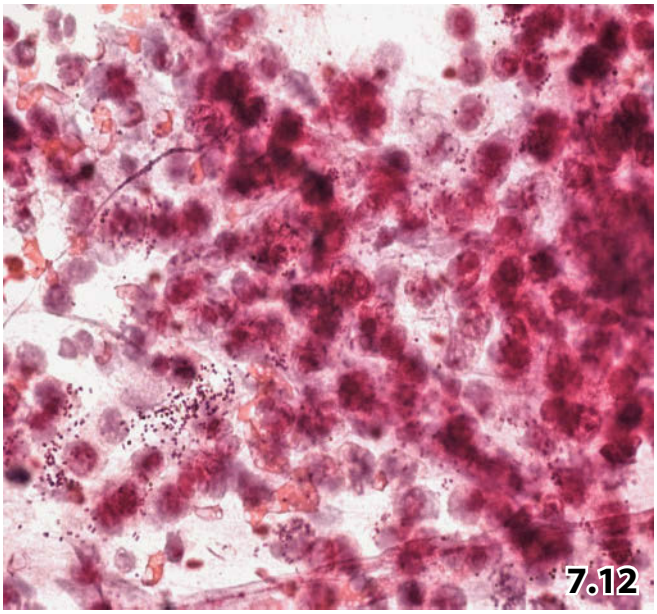
7.12

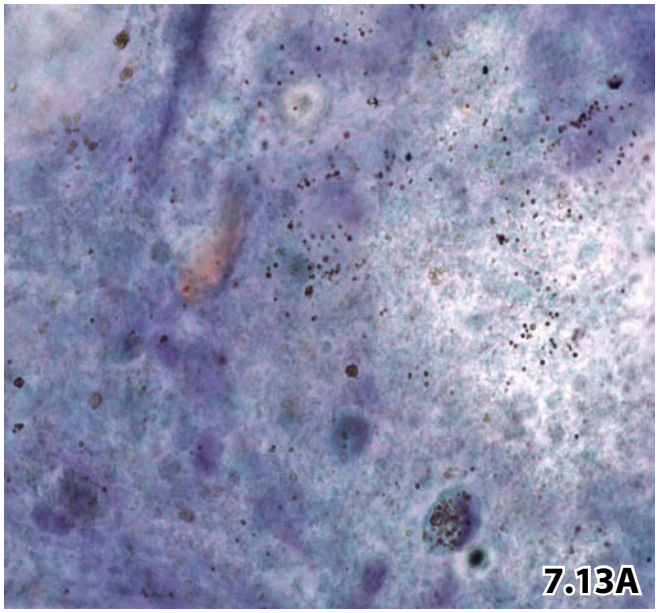
7.13A

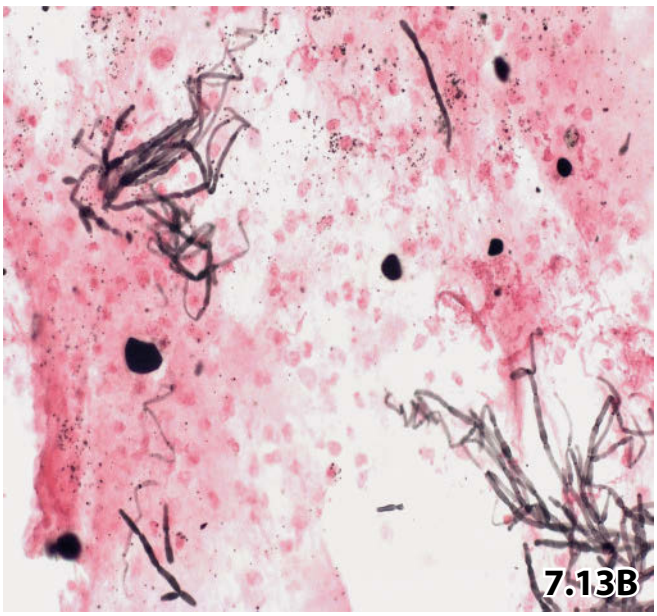
7.13B

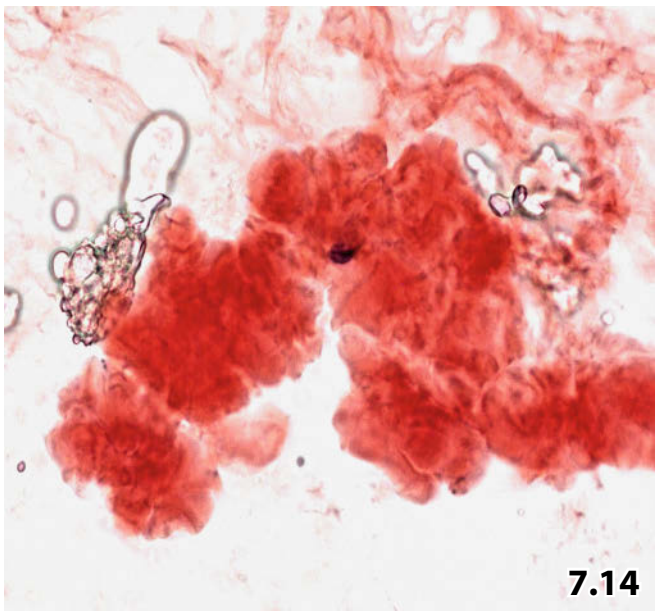
7.14

**Fig. 7.15 Malignant melanoma.**
An intraorbital tumoral mass was recently detected in a 78-year-old man who had a previous exenteration of the orbit for orbital malignant melanoma. FNAB revealed a neoplastic process of the spindle cell type consistent with histologic pattern of the primary tumor (direct smear, Pap stain, high magnification). A granulomatous inflammatory process was excluded. Appropriate immunostainings failed due to inadequate technical processing of the aspirate.

**Fig. 7.16A–C Plasmacytoma.**
A 73-year-old man with a history of invasive plasmacytoma in the neck area, presented with a mass in the right orbit. **A** FNAB of the orbital tumor mass showed immature tumor form of plasmacytoma (direct smear, MGG stain, high magnification). **B** Monoclonal expression of light-chain immunoglobulin (kappa) (ThinPrep preparation) by immunocytochemistry. **C** Monoclonal expression of heavy-chain immunoglobulin (IgA) (ThinPrep preparation) by immunocytochemistry.



**Fig. 7.17 Lacrimal gland: inflammatory disorder.**
Swelling of the lacrimal gland in the right orbit of a 64-year-old woman. FNAB shows regular sheets of ductal-type epithelial cuboid cells. The small, round to oval nuclei exhibit a smooth outline and dense chromatin. Background of the direct smear is composed of a mixed inflammatory cell population and mucoid strands (direct smear, Pap stain, higher magnification).
*Cytologic diagnosis:* Chronic relapsing inflammation of the lacrimal gland. No further investigations were performed.

**Fig. 7.18 Lacrimal gland: neoplastic lesion.**
A 44-year-old man with a history of metastatic adenocarcinoma of unknown primary origin. Advanced investigations revealed a tumor mass in the right lacrimal gland, which was assumed to represent the primary tumor. FNAB from lacrimal gland of the right orbita was performed. Conventional smears were Pap-stained.
*An indeterminate cytologic report* was rendered: acinic cell carcinoma (multiple small acinic-like formations: arrowheads) versus adenoid-cystic carcinoma (lucid, sharply bordered hyaline globules: arrow, upper left) (lower magnification). Endocrine nature of the tumor was immunocytochemically excluded (not shown). No information available concerning further investigations.

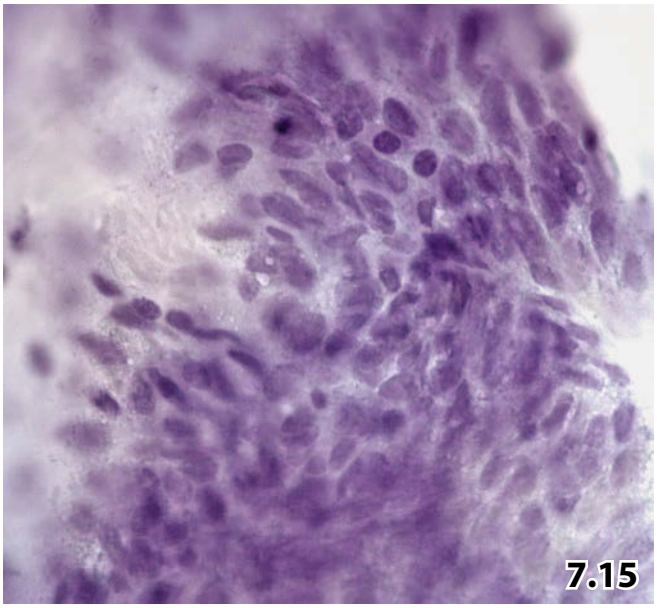
7.15

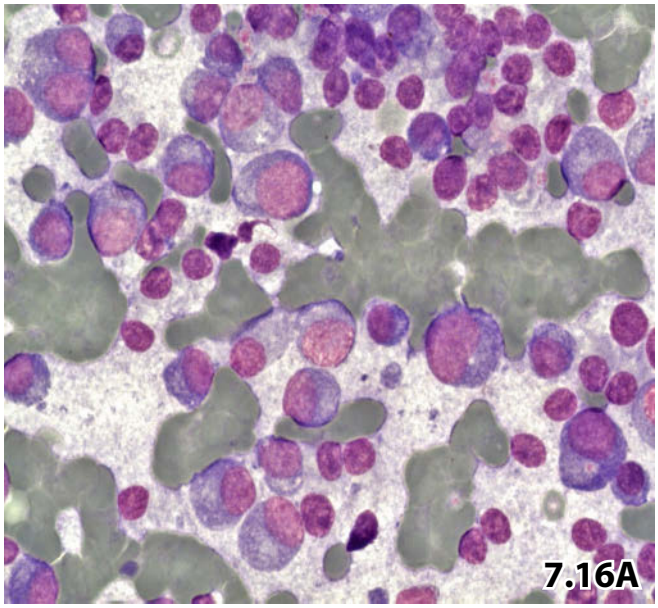
7.16A

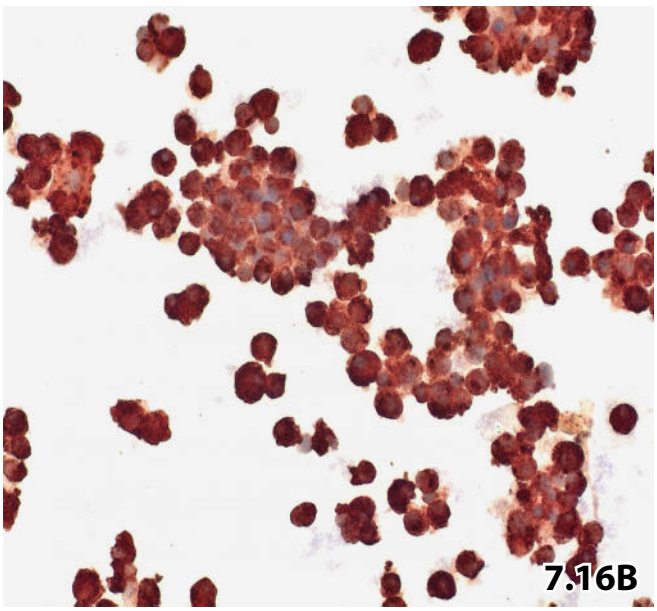
7.16B

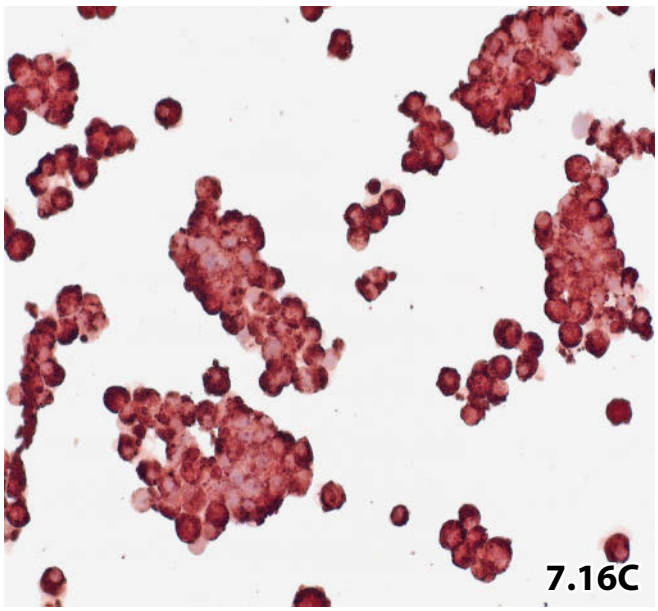
7.16C

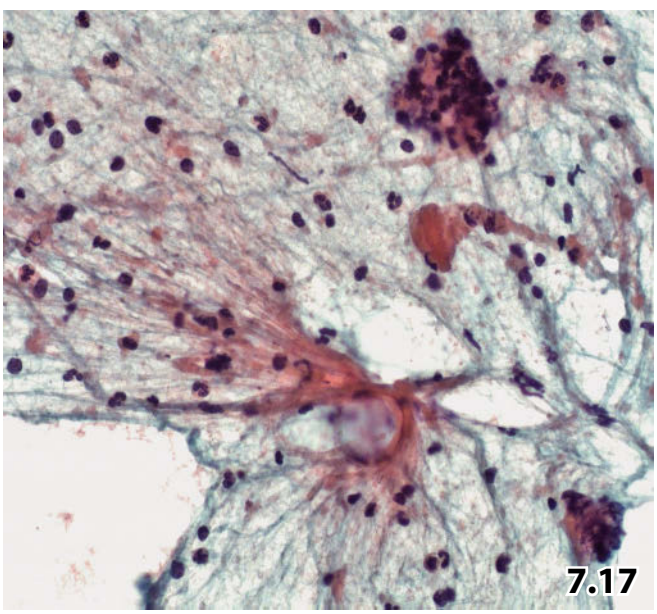
7.17

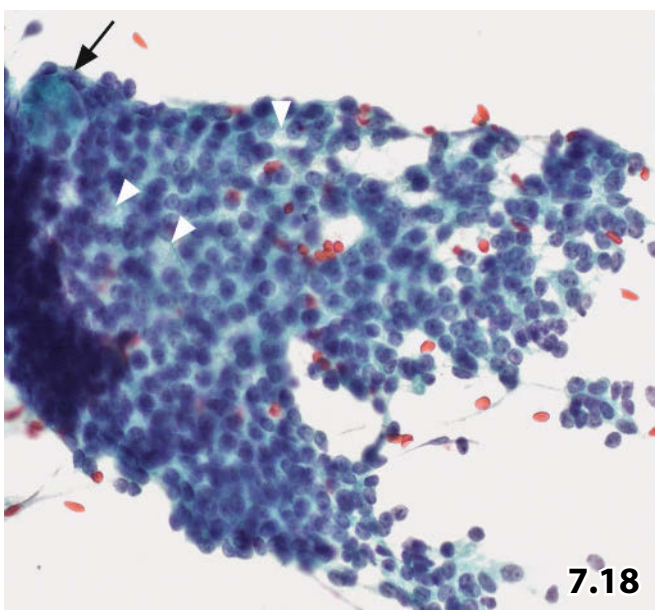
7.18

# Oral Cavity and Oropharynx 8



Spieler/Rössle, *Nongynecologic Cytopathology. A Practical Guide. Essentials of Diagnostic Pathology*,
DOI 10.1007/978-3-642-24719-4_8, 

## Synopsis and Algorithms

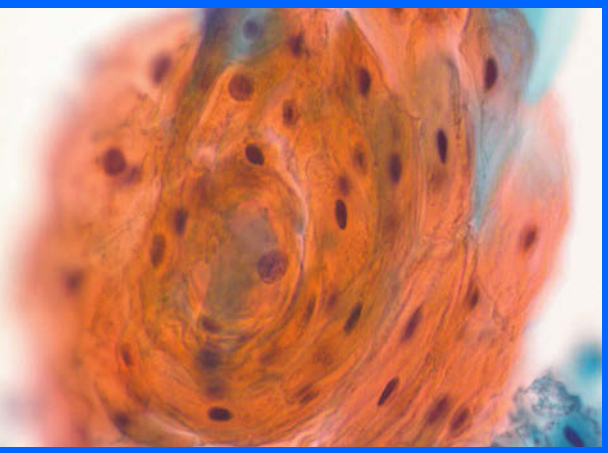

# Oral Cavity and Oropharynx

## 8.1 Introduction

### 8.1.1 Epidemiology and Tumor Characteristics

- Squamous cell carcinoma (SCC) of the oral cavity accounts for 3–5% of all squamous malignancies of the human body [83]. This tumor type accounts for more than 90% of the malignant neoplasms of the oral cavity and oropharynx. Its prognosis is very poor, up to 50% of the patients will die within a 5-year period after primary tumor diagnosis.
- Early and correct identification of both squamous cell carcinoma and SCC precursors in these regions is of great importance in reducing the high morbidity and mortality.
- Dominant risk factors of oral squamous cell carcinoma are tobacco and alcohol habits in a strongly synergistic manner [3, 5].
- Recent studies suggest that human papilloma viruses play an etiologic role in a small subgroup of cancers of the oral cavity and in many cancers of the oropharynx [24].

### 8.1.2 High-Risk Tumor Sites

Squamous cell carcinoma may arise in any area of the oral cavity and oropharynx but high-risk tumor locations are well-known:

- The lower lip is the preferred site for lip squamous cell carcinoma.
- Oral cavity cancers show the highest frequency on the floor of the mouth, the ventrolateral tongue, and the soft palate.
- The base of the tongue is the most common localization for oropharyngeal carcinoma.

### 8.1.3 Tumor Multiplicity

It is important to be aware of the fact that patients with squamous cell carcinoma of the oral cavity and oropharynx have an increased risk of synchronous or metachronous tumors in the pharynx, larynx, and esophagus as well as in the tracheobronchial area.

Panendoscopy may be indicated in many of the tumor patients after initial tumor diagnosis.

### 8.1.4 Oral Cancer Screening

Visual examination, toluidine blue test, brush cytology, computer-assisted cytologic analysis, and other tests are proposed for population-based oral cancer screening programs. No consistent opinion exists as to whether a nation-wide screening program would have a positive impact on the morbidity and mortality of oral cancer [15, 31, 37, 38].

### 8.1.5 Fine-Needle Aspiration Biopsy [11, 21]

- In general, diagnosis of a large tumor mass in the oral cavity is confirmed by one or multiple biopsies. In special situations, FNAB may be the preferred tool to evaluate tumors at this site. Both apparent large lesions and small tumors accessible for palpation may be aspirated successfully. An adequate device and a needle of effective length and gauge have to be chosen for each individual lesion. It is important to perform vigorous needling in a fan-like

modality and substantial suction to obtain ample cell material.
- FNAB of enlarged cervical lymph nodes is a helpful tool for staging patients with an obvious primary tumor in the oral cavity.
- FNAB may help to establish a preliminary diagnosis in patients presenting with enlarged neck lymph nodes but with absence of an obvious primary lesion in the oral cavity and oropharynx.
- Excisional lymph node biopsy on the neck should not be performed as long as:
  - FNABs have shown to be nondiagnostic.
  - FNABs are suggestive of malignant lymphoma.
  - The search for an occult primary tumor provides a negative result.



### 8.1.6 Tumors of Small Salivary Glands

Oral cavity tumors which are derived from salivary gland tissue are covered in Sect. 5.1, "Salivary Glands," p. 401.

## 8.2 Brush Cytology [20, 28]

#### Indications and General Comments

- Oral brush biopsy as a noninvasive diagnostic method can be helpful in early detection of oral mucosal lesions and may be used as a method for population-based screening in the oral cavity. Brush cytology may be applied to all visible oral lesions, ranging from small spots to large ulcerated lesions. However, oral brush biopsy has been shown to be most effective for detection of small cancers, precancerous lesions, and lesions clinically considered benign by mistake. Many of these lesions appear as visible white, red-white, or red patches (leukoplakia or erythroplakia).
- Large unsuspicious mucosal areas can be evaluated by brushing for screening purposes or the brush technique may be applied in addition to a targeted biopsy. One should be aware that the brush technique covers expanded surface areas, whereas a small-needle biopsy or small surgical biopsies may miss relevant foci [43].
- Positive cytologic results despite negative clinical findings is an indication to refer the patient to a specialized clinic where surgical biopsies are performed, followed by histopathological analysis. Histopathology remains the gold standard for a definitive diagnosis.
- Adjunctive methods have proved successful in increasing the diagnostic sensitivity of oral brush biopsies up to 100% (see Sect. 8.4, "Additional Analyses," p. 565).

### 8.2.1 False-Negative Diagnoses [14, 54, 55]

Reasons for a false-negative cancer diagnosis by brushing include:
- The cell material may originate from nonrepresentative areas (sampling error).
- The slides have not been screened carefully enough by both cytotechnologists and cytopathologists.
- Underestimation of cellular changes as being within normal limits or of reparative regenerative nature.
- Borderline cell changes that are not sufficiently distinct for a definite diagnosis of malignancy. These cases demand further clarification using adjuvant analytical methods on cytologic material or by surgical biopsy.

False-negative results in histology are mainly caused by sampling error and incomplete work-up such as a lack of serial sections.

### 8.2.2 Practice and Collection of Cells

- Brush biopsy is easily practicable, inexpensive, noninvasive, accurate, and safe. It can be used by dentists in their daily practice to clarify the nature of common small oral spots that many people occasionally have in their mouth. The method requires no anesthesia, causes no pain and minimal or no bleeding.
- A specially designed brush (cytobrush), a wood spatula, or a cotton-tipped applicator may be used for collection of the specimen [30]. A cotton-tipped device is less recommended and unfeasible in cases where liquid-based processing is intended.
- If cell material is collected by scraping, pseudomembranes, masses of thick saliva, and bleeding can be responsible for inadequate samples.
- Lavage of the mouth and oropharynx followed by digital DNA measurement on squamous cells from the rinsing fluid has been proposed as a minimally invasive screening tool in patients who are at high risk, or for follow-up of patients with successful initial tumor surgery [26].

## 8.3 Processing of the Cell Material

### 8.3.1 Conventional Smear

Wet-fixed smears are convenient for cytodiagnostic purposes on squamous cells. Nuclear details are well preserved and Pap-stained cells match nuclear and cytoplasmic structures observed in paraffin sections.

Scraped cell material must immediately be smeared on a slide and the smears must be fixed within 1–3 s. Slides can be dropped into a pot with alcohol-based fixative or a commer-

cial spray fixative can be used. The smears are routinely Pap-stained.

### 8.3.2 Liquid-Based Cytology (Cytospin, ThinPrep, SurePath, etc.)

[ 23, 45] (Figs. 8.1 and 8.11)

The device with the collected cell material is rinsed in a vial containing a cell medium. Thin-layer preparations can be performed as instructed by the manufacturer. The thin layer method is best used by operators who are not familiar with proper preparation and fixation of direct smears [77].

In comparison to conventional smears, liquid-based oral cytology has minor advantages with regard to clear background, monolayer cell preparation, and cell preservation. Still, the technique guarantees quantitatively and qualitatively optimal specimens for special investigations, in particular for immunocytochemistry, fluorescence in situ hybridization, or static DNA cytometry [45].

### 8.3.3 Microbiopsies

Application of a dermatological curette may allow collection of small tissue fragments. These can be used for cytologic processing, and as microbiopsies for additional histological investigation [46].

## 8.4 Additional Analyses

DNA Image Cytometry

- DNA image cytometry (ICM-DNA) is an adjuvant diagnostic procedure to conventional oral cytology having a high level of standardization, high objectivity, and high diagnostic accuracy.
  DNA ploidy is a biological marker that:
  - Increases sensitivity and specificity of oral brush biopsies.
  - –. Improves early detection of precancerous and cancerous oral lesions.
  - Can confirm a sole cytological diagnosis of malignancy (Figs. 8.13 and 8.14).
  - Is exquisitely helpful in clarifying the nature of cytologically equivocal changes on squamous cells, distinguishing with high accuracy between premalignant (dysplasia) or malignant degeneration and reparative atypia (Figs. 8.7–8.12).
  - May also be helpful in assessing a local relapse of squamous cell carcinoma after successful surgical resection with tumor-free margins [22].
  - Eliminates false-negative diagnosis possibly rendered by conventional cytology.
  - Avoids false-positive light microscopic diagnoses [39, 41, 54, 57, 59, 66, 76, 79].
- DNA aneuploidy is a reliable (early) marker for malignant transformation of oral squamous cells.
- DNA ploidy has been reported to be a trustworthy prognostic indicator, superior to histological grading [75].
- Cytometric DNA quantification may be combined with additional morphometric data [51].
- ICM-DNA standards should be in accordance with consensus statements of the European Society of Analytical Cellular Pathology (ESACP) [22A]. At our institution, the histogram algorithms have been applied according to the ploidy evaluation of other lesions composed of squamous epithelium (tumors of the uterine cervix, esophagus, and others) [18, 29]:

> **DNA diploidy:**
> 1.8c ≤ DNA index of the stemline (SL) ≤ 2.2c
> **DNA polyploidy:**
> 1.8c ≤ SL ≤ 2.2.c and 3.6c ≤ SL ≤ 4.4c. No 9c exceeding events
> **DNA aneuploidy:**
> Aneuploid Stemline: SL < 0.9c , or 1.1c < SL < 1.8c, or 2.2c < SL < 3.6c, or SL > 4.4c, or at least 2 cells > 9c

- Several reports in the literature refer to flow cytometric DNA analysis of cells from oral squamous carcinoma [2, 47, 69, 80] and leukoplakias [33, 63, 64, 70] regarding various biological aspects.

Computer-Assisted Brush Biopsy

Based on various studies, a computer-assisted method has recently been proposed as an accurate method to detect malignant and premalignant oral lesions. Samples of brush biopsies are operated at a specialized laboratory where specially-trained pathologists use highly sophisticated computers to help detect abnormal cells. The most widely used technique is known as OralCDX analysis [9, 15, 54, 67].

Molecular Genetics

In the future, molecular biological analyses (fluorescence in situ hybridization, comparative genomic hybridization, and others) may not only enhance early detection of potentially malignant cells but also predict the development of recurrent oral malignancy. It may further elucidate the relationship between aberration and biological behavior of oral SCCs and may have an impact on therapeutic modalities [6, 25, 44, 48, 49, 60, 61, 65].

Immunocytochemistry

- Antibodies against laminin-5 and MCMs (minichromosome maintenance proteins) have recently been reported to be promising immunomarkers for early detection of oral squamous cell carcinoma and dysplasia on a cytologic platform [13, 28, 68].
- Immunocytochemical analysis of p53 protein seems to yield disappointing results concerning assessment of oral precancerous and malignant lesions, and immunocyto-

chemical results of the p53 protein are reported to have relatively poor correlation with p53 gene mutation [27, 60].

AgNOR Analysis

According to the results of multiple studies, argyrophilic nucleolar organizer regions (AgNORs) appear to be of diagnostic value in distinguishing between oral dysplastic and nondysplastic lesions. AgNOR count appears to also have prognostic significance and may influence treatment planning [7, 50, 53].

It has been shown that AgNOR analysis is applicable to routine brush specimens in cytologically doubtful cases in addition to other methods [58].

## 8.5 Cytology of Benign Oral Lesions



### 8.5.1 Normal Epithelial Cells (Fig. 8.1)

- Normal squamous epithelial cells lining the oral cavity closely resemble those found in samples of sputa and the cervix/vagina, but oral squamous cells do not exhibit nuclear pyknosis. Keratinized squamous cells and their intermediate stages are commonly encountered and must not necessarily stand for epithelial abnormalities (Fig. 8.1).
- Parabasal and possibly basal squamous cells may occur if scraping has been vigorously carried out or performed on superficially damaged epithelium.
- Columnar cells with or without mucus secretion originate from the nasopharynx area or from salivary glands.
- Well-preserved acini from salivary gland tissue may sporadically be observed.
- Lymphocytes may be shed from the tonsillae or from sub- or intraepithelial hyperplastic lymph nodes.

### 8.5.2 Enlargement of Oral Squamous Cells

Enlarged squamous cells are frequently observed in cytologic specimens from the oral cavity due to a mucosal response to different agents. Significant enlargement of both the cytoplasm and nucleus is observed in deficiency diseases such as pernicious anemia, iron-deficiency anemia, and in tropical sprue [12, 19, 74]. Cell enlargement is also observed in patients receiving certain drugs including chemotherapeutics, in patients with mucosal irritations (e.g., from dentures), and after local radiation therapy.

Drug- and radiation-induced cell changes may include bi- or multinucleation, slight to pronounced nuclear pleomorphism, nuclear pseudoinclusions, giant nucleoli, and cytoplasmic vacuolization.

### 8.5.3 Inflammation, Infections, and Cell Alterations

- Oral mucosa is frequently affected by inflammatory disorders caused by various physical, chemical, and other agents. The presence of cells from lower epithelial layers, neutrophils, lymphocytes, and histiocytes in cytologic specimens supports the presence of an ulcerative process.
- Epithelial atypias in line with an inflammatory process are a common challenge for cytopathologists. The cell changes should not be overestimated as dysplastic (Fig. 8.5). ICM-DNA is accepted as an effective method to differentiate between reactive and dysplastic cellular atypia (see Sect. 8.4, "DNA Image Cytometry," p. 565).
- Infections with bacteria and fungi can be detected on cytologic smears by means of selective staining methods such as Gram, PAS, Crocott, and Ziehl-Neelsen stain for acid-fast bacilli (Fig. 8.3B).
- Morphologic changes in herpes virus-infected cells are pathognomonic but, in combination with hyperkeratinization, they may be misinterpreted as sign of malignancy by unexperienced interpreters (Fig. 8.2 and Fig. 11.3). Cellular changes are described in Sect. 11.2.2.2.5, "Viral Infections," p. 703. As for current cytologic practice, one should remember that herpetic stomatitis varies widely in its clinical appearance.

**Microscopic Features** (Figs. 8.3–8.5)

- Hallmarks: The cytoplasm is characterized by abnormal acidophilia and irregularities in shape.
  Nuclei are enlarged but their borders tend to be smooth; chromatin pattern is loose but abnormalities may occur.
  Prominent and multiple nucleoli are infrequent.
  The N/C ratio is frequently increased.

**Caution**

- Cellular atypias together with an inflammatory pattern should never be judged as dysplasia or malignancy solely on light microscopic evaluation. Auxiliary methods may contribute to an accurate diagnosis. Static DNA cytometry is helpful in assessing or excluding a precancerous or malignant lesion.
- Repeated brush biopsies or surgical excision are mandatory after an initial ineffective therapeutic approach.

### 8.5.4 Pemphigus Vulgaris [35, 42, 62, 71]

- Pemphigus vulgaris is a group of mucocutaneous diseases of unclear, possibly autoimmune etiology. Pemphigus vulgaris is characterized by formation of bullae within the epithelium. Involvement of the oral mucosa is common, in most patients secondary to skin disorders, but it may occur as a primary manifestation as well.
- Loss of intercellular connections in the stratum spinosum of the squamous epithelium (acantholysis) results in decreased cellular cohesiveness. Ruptured bullae shed abundant parabasal and basal cells, which can clinically be misinterpreted as a malignant lesion.
  - Microscopic hallmarks: High cellularity of the cytologic samples. Uniform cell pattern composed of small squamous cells that exhibit an increased N/C ratio and nuclei with distinct individual or multiple irregular nucleoli.
  - Occasional cell-in-cell arrangement may be seen.
  - Chromatin texture is generally loose and fairly even; irregularities may occur.
  - Hyperchromasia is exceptional.

**Caution**

- Acantholytic changes within the squamous epithelium generate activated immature squamous cells desquamating in large numbers from the ruptured bullae. Erroneous diagnosis of carcinoma is possible. Reevaluation of the patient's clinical history is helpful to avoid a misdiagnosis.

## 8.6 Leukoplakia: The Cytodiagnostic Challenge

- Leukoplakia is defined as a visible white patch that cannot be removed by scrapping. The clinical appearance of common leukoplakia and leukoplakia caused by premalignant cell changes is almost identical. Detection of leukoplakia should be followed by histologic biopsy and/or cytologic brushing.
- The key features of leukoplakia in histologic sections are hyperkeratosis and parakeratosis (formation of a thick stratum corneum with focal preservation of the nuclei).

#### Microscopic Features and Differential Diagnosis

The cytological evaluation of brush biopsies from leukoplakias is a challenge. The various cell patterns are listed below, including differential diagnostic considerations and suggestions for further proceeding:

1. *Keratinized red-, orange-, or yellow-stained anucleated, uniform squamous cells*. Occasional bland and regular formed nuclei (Fig. 8.6).
   *Conclusion:* The lesion is most likely benign but requires clinical observation with cytologic follow-up or surgical excision
2. *Markedly keratinized anucleated cells* reveal some pleomorphism and sporadic pearl formation may be observed. A few squamous cells contain nuclei with slight irregularities but bland chromatin texture and coloring (Figs. 8.7–8.10).
   *Conclusion:* Such lesions should not simply be regarded as benign. Differential diagnoses range from keratinizing squamous cell papilloma or verruca vulgaris to dysplastic epithelium, and well-differentiated squamous cell carcinoma. Proliferative verrucous leukoplakia shows a strong predilection for malignant transformation [4]. Nuclear dysplasia or malignancy may be assessed or excluded by additive analyses (ICM-DNA and others; see Sect. 8.4, p. 565) in cases where enough well-preserved cells and nuclei allow additional tests. Otherwise, a surgical biopsy followed by histologic examination is inevitable.
3. *Distinct cytoplasmic and nuclear pleomorphism*. Nuclei show indentations and cleaving, the chromatin pattern is dense, finely granular or coarse, and hyperchromasia is articulate. Nucleoli are variable in size and shape. The N/C ratio is increased. The cytoplasm exhibits varying degrees of keratinization (Figs. 8.11–8.14) .
   *Conclusion:* Dysplastic premalignant lesion or carcinoma in situ; moderately differentiated invasive squamous cell carcinoma cannot be excluded. The cytologic diagnosis can be verified using a biological marker such as DNA ploidy status (see Sect. 8.4, p. 565). Cytomorphologic findings demand immediate biopsy or a complete excision of the lesion.

#### Additional Comments

- Areas in the oral mucosa harboring premalignant or malignant cells occur not only as leukoplakia, but may also occur as white-red plaques –erythroleukoplakia – or red plaques – erythroplakia [78].
- Distinct oral lesions, which may resemble leukoplakia, are the white sponge nevus (Fig. 8.7), Darier disease, and hereditary benign intraepithelial dyskeratosis. Cell changes of these lesions have been reported to be characteristic; however, they are not specific [36].
- A small number of selected papers reporting leukoplakia and premalignant oral mucosal lesions are cited [1, 10, 56, 72, 73, 82]. We also refer the reader to the references given in Sect. 8.4 "Additional Analyses," p. 565.

**Caution**

Any grade of nuclear and cytoplasmic atypia in brush samples from leukoplakic lesions demands further investigations, either analysis of nuclear biological properties or a surgical intervention followed by histologic analysis .

## 8.7 Squamous Cell Carcinoma and Its Variants

### 8.7.1 Common Squamous Cell Carcinoma

SCC may present as a flat plaque or polypoid excrescence that is usually ulcerated.

Microscopic features match those in SCCs from other sites of the human body such as esophagus, bronchus, cervix/vagina, penis, etc.

#### 8.7.1.1 Keratinized SCC: Well-Differentiated

[1] (Fig. 8.15)

It is difficult to separate this malignant neoplasm from strongly keratinized benign or dysplastic leukoplakic lesions. Cytology alone often miss a conclusive diagnosis.

**Microscopic Features**

- Abundantly keratinized anucleated cells reveal minor pleomorphism.
- Pearl formation may be observed.
- The cytoplasm generally exhibits bright red and orange staining.
- Few squamous cells contain nuclei with minor irregularities of their outline but bland texture and coloring.

#### 8.7.1.2 SCC: Moderately to Poorly Differentiated

**Microscopic Features**

- Keratinization is much less prominent. The shape of individual cancer cells and their degree of maturation are extremely variable.
- Nuclei are enlarged and exhibit marked pleomorphism. Nuclear borders are prominent and irregular.
- Increased N/C ratio.
- Hyperchromasia is distinct. Chromatin texture and chromatin distribution are irregular.
- One or multiple prominent nucleoli.
- Anucleated strongly keratinized cells, necrotic debris, red blood cells, and leukocytes are found in most of the cases.

### 8.7.2. Verrucous Carcinoma (Fig. 14.57)

Verrucous carcinoma is a well-differentiated, exophytically growing squamous cell carcinoma with wart-like configuration. Verrucous carcinoma has the lowest progressive potential of all oral SCC subtypes [52]. Cytologically, verrucous carcinoma strongly shares morphologic features with the common well-differentiated SCC (Sect. 8.7.1.1, above).

**Microscopic Features**

- Like other types of hyperkeratinized SSCs, verrucous carcinoma shows abundant keratinized anucleated cells comprising some pleomorphism.
- Pearl formation may be observed.
- A few squamous cells contain nuclei with minor irregularities of their outline but bland texture and coloring.

**Caution**

Keratinizing squamous cell papilloma, keratoacanthoma and verruca vulgaris are difficult to differentiate from keratinized SCC using cytopathological features alone. DNA ploidy measurement may be helpful in assessing the biological potential of the disorder [34, 40].

### 8.7.3 Lymphoepithelial Carcinoma

[8, 16, 17] (Fig. 5.82)

Lymphoepithelial carcinoma (LEC) is an undifferentiated squamous cell carcinoma accompanied by a prominent lymphoplasmacytic infiltrate.

LEC was initially described in the nasopharynx; outside this typical site the tumor is extremely rare. The cytomorphology of the tumor is identical to those arising in other organs.

**Microscopic Features**

- Hallmarks: Syncytial sheets of large undifferentiated malignant cells comprising vesicular and lucid nuclei with marked irregular borders. The chromatin structure is indistinct. Nucleoli are variable in size and shape. The cytoplasm tend to be wide, clear and delicate.
  The background is characterized by a dense lymphoplasmacytic infiltrate.

**Differential Diagnosis**

- Non-Hodgkin lymphoma of the blastic type combined with benign lymphoplasmacytic hyperplasia may strongly mimic LEC.
- Single large carcinoma cells with clear nuclei scattered among lymphocytes and plasma cells may be misinterpreted as benign follicle-center blasts or as activated histiocytes.

## 8.8 Other Primary Tumors and Metastases

### 8.8.1 Granular Cell Tumor (Figs. 1.63 and 1.64)

- Granular cell tumor is a benign mesenchymal tumor assumed to be of Schwann cell origin. Granular cell tumors may arise in many sites of the body, but 50% of these tu-

mors involve the head and neck region, and the tongue is the commonest single site (see also Sect. 1.2.18, p. 26).
- Congenital gingival granular cell tumor of the newborn is a rare benign tumor, also referred to as congenital epulis.
- Granular cell tumor has a distinctive cytomorphologic appearance that permits a definite diagnosis [32, 81].

#### Microscopic Features, Immunocytochemistry, and Cytochemistry

- Hallmarks: Cytologic specimens are highly cellular, composed of uniform large cells with ill-defined borders and abundant, finely granular cytoplasm.
  Cells are single or grouped, and are fragile with a background of granular material.
  The nuclei are small and may be eccentrically positioned with bland granular chromatin. Nucleoli are inconspicuous.

Tumor cells stain immunocytochemically positive for S100 protein, neuron-specific enolase, and vimentin. Cytoplasmic granules are PAS-positive and diastase-resistant [32].

#### Differential Diagnosis

Granular tumor cells may be misinterpreted as foamy cells from cystic fluid, cells from metastatic renal cell carcinoma, or malignant melanoma.

### 8.8.2 Rare Primary Tumors of the Oral Cavity and Oropharynx

- Cytologic features and differential diagnostic aspects of basaloid squamous cell carcinoma and spindle cell SCC are presented in Sect. 14.2.6, "SCC and Its Variants," p. 899, and elsewhere in this book.
- Adenosquamous carcinoma, giant cell carcinoma, and small-cell carcinoma are rare entities; their pathomorphologic features are discussed elsewhere.
- Primary malignant melanoma, primary extranodal malignant lymphoma, and benign and malignant soft tissue tumors are exceptionally encountered in routine cytologic practice.

### 8.8.3 Metastases

Metastases to oral soft tissues are extremely rare. Most common primary tumor sites have been reported to be the lung, kidney, and skin in males and the breast in females. The commonest site of secondary tumors is the gingiva.

## 8.9 Further Reading


1. Banoczy J, Rigo O. Comparative cytologic and histologic studies in oral leukoplakia. Acta Cytol 1976;20:308-312.
2. Baretton G, Li X, Stoll C, et al. Prognostic significance of DNA ploidy in oral squamous cell carcinomas. A retrospective flow and image cytometric study with comparison of DNA ploidy in excisional biopsy specimens and resection specimens, primary tumors and lymph node metastases. Oral Surg Oral Med Oral Pathol Oral Radiol Endod 1995;79:68-76.
3. Barnes L, Eveson JW, Reichart P, Sidransky D. World Health Organization Classification of Tumours. Pathology and Genetics of Head and Neck Tumours. IARC Press: Lyon 2005.
4. Batsakis JG, Suarez P, El Naggar AK. Proliferative verrucous leukoplakia and its related lesions. Oral Oncol 1999;35:354-359.
5. Blot WJ, McLaughlin JK, Winn DM, et al. Smoking and drinking in relation to oral and pharyngeal cancer. Cancer Res 1988;48:3282-3287.
6. Bremmer JF, Braakhuis BJ, Ruijter-Schippers HJ, et al. A noninvasive genetic screening test to detect oral preneoplastic lesions. Lab Invest 2005;85:1481-1488.
7. Chattopadhyay A, Ray JG, Caplan DJ. AgNOR count as objective marker for dysplastic features in oral leukoplakia. J Oral Pathol Med 2002;31:512-517.
8. Chow TL, Chow TK, Lui YH, et al. Lymphoepithelioma-like carcinoma of oral cavity: report of three cases and literature review. Int J Oral Maxillofac Surg 2002;31:212-218.
9. Christian DC. Computer-assisted analysis of oral brush biopsies at an oral cancer screening program. J Am Dent Assoc 2002;133:357-362.
10. Dabelsteen E, Roed-Petersen B, Smith CJ, Pindborg JJ. The limitation of exfoliative cytology for the detection of epithelial atypia in oral leukoplakias. Br J Cancer 1971;25:21-24.
11. Daskalopoulou D, Rapidis AD, Maounis N, Markidou S. Fine-needle aspiration cytology in tumors and tumor-like conditions of the oral and maxillofacial region: diagnostic reliability and limitations. Cancer 1997;81:238-252.
12. Diversi HL, Griffin JW, Payne T. Correlation of cytologic nuclear changes to anemias. Oral Surg Oral med Oral Pathol 1966;21:341-346.
13. Driemel O, Dahse R, Hakim SG, et al. Laminin-5 immunocytochemistry: a new tool for identifying dysplastic cells in oral brush biopsies. Cytopathology 2007;18:348-355.
14. Driemel O, Kunkel M, Hullmann M, et al. Performance of conventional oral brush biopsies. HNO 2008;56:205-210.
15. Drinnan AJ. Screening for oral cancer and precancer – a valuable new technique. Gen Dent 2000;48:656-660.
16. Ferlito A. Primary lymphoepithelial carcinoma of the hypopharynx. J Laryngol Otol 1977;91:361-367.
17. Frank DK, Cheron F, Cho H, et al. Nonnasopharyngeal lymphoepitheliomas (undifferentiated carcinomas) of the upper aerodigestive tract. Ann Otol Rhinol Laryngol 1995;104:305-310.
18. Gockel I, Kammerer P, Brieger J, et al. Image cytometric analysis of mucosal biopsies in patients with primary achalasia. World J Gastroenterol 2006;12:3020-3025.
19. Graham RM, Rheault MH. Characteristic cellular changes in epithelial cells in pernicious anemia. J Lab Clin Med 1954;43:235-245.
20. Grayson R. Oral cancer, early detection by cytology report of 1000 cases from a group of dentists in New Jersey. Acta Cytol 1969;13:502-506.
21. Günhan Ö, Dogan N, Celasun B, et al. Fine needle aspiration cytology of oral cavity and jaw bone lesions. A report of 102 cases. Acta Cytol 1993;37:135-141.
22. Handschel J, Oz D, Pomjanski N, et al. Additional use of DNA cytometry improves the assessment of resection margins. J Oral Pathol Med 2007;36:472-475.

22A. Haroske G, Baak JP, Danielsen H, Giroud F, Gschwendtner A, Oberholzer M, Reith A, Spieler P, Böcking A. Fourth updated ESACP consensus report on diagnostic DNA image cytometry. Anal Cell Pathol 2001;23:89-95.
23. Hayama FH, Motta AC, Silva Ade P, Maigliari DA. Liquid-based preparations versus conventional cytology: specimen adequacy and diagnostic agreement in oral lesions. Med Oral Patol Oral Cir Bucal 2005;10:115-122.
24. Herrero R, Castellsagué X, Pawlita M, et al. The viral etiology of oral cancer: evidence from the IARC multicentric-study. J Natl Cancer Inst 2003:47-51.
25. Hirshberg A, Yarom N, Amariglio N, et al. Detection of non-diploid cells in premalignant and malignant oral lesions using combined morphological and FISH analysis - a new method for early detection of suspicious oral lesions. Cancer Lett 2007;253:282-290.
26. Höfken F, Welkoborsky HJ, Jacob R, Mann W. Examination with DNA cytometry of mouth and oropharyngeal lavage fluid as a screening method in diagnosis of malignancies of the mouth cavity and oropharynx. Laryngorhinootologie 1995;74:678-683.
27. Högmo A, Lindskog S, Lindholm J, et al. Preneoplastic oral lesions: the clinical value of image cytometry DNA analysis, p53 and p21/WAF1 expression. Anticancer Res 1998;18(5B):3645-3650.
28. Hullmann M, Reichert TE, Dahse R, et al. Oral cytology: historical development, current status, and perspectives. Mund Kiefer Gesichtschirurgie 2007;11:1-9.
29. Itakura Y. Sasano H, Mori S, Nagura H. DNA ploidy in human esophageal squamous dysplasias and squamous cell carcinomas as determined by image analysis. Mod Pathol 1994;7:867-873.
30. Jones AC, Pink FE, Sandow PL, et al. The cytobrush Plus cell collector in oral cytology. Oral Surg Oral Med Oral Pathol 1994;77:95-99.
31. Joseph BK. Oral cancer: prevention and detection. Med Princ Pract 2002;11 Suppl 1:32-35.
32. Junquera LM, de Vicente JC, Vega JA, et al. Granular-cell tumours: an immunohistochemical study. Br J Oral Maxillofac Surg 1997;35:180-184.
33. Kahn MA, Dockter ME, Hermann-Petrin JM. Proliferative verrucous leukoplakia. Four cases with flow cytometric analysis. Oral Surg Oral Med Oral Pathol 1994;78:469-475.
34. Klanrit P, Sperandio M, Brown AL, et al. DNA ploidy in proliferative verrucous leukoplakia. Oral Oncol 2007;43:310-316.
35. Kobayashi TK, Kaneko C, Sugishima S, et al. Scrape cytology of oral pemphigus. Report of a case with immunocytochemistry and light, scanning electron and transmission electron microscopy. Acta Cytol 1999;43:289-294.
36. Koss LG. The oral cavity, larynx, trachea, nasopharynx, and paranasal sinuses (chapter 21), In: Koss' Diagnostic Cytology, 5th edition. Lippincott Williams & Wilkins 2006; p.714 - 725
37. Kujan O, Duxbury AJ, Glenny AM, et al. Opinions and attitudes of the UK's GDPs and specialists in oral surgery, oral medicine and surgical dentistry on oral cancer screening. Oral Dis 2006;12:194-199.
38. Lingen MW, Kalmar JR, Karrison T, Speight PM. Critical evaluation of diagnostic aids for the detection of oral cancer. Oral Oncol 2008;44:10-22.
39. Maraki D, Becker J, Boecking A. Cytologic and DNA-cytometric very early diagnosis of oral cancer. J Oral Pathol Med 2004;33:398-404.
40. Maraki D, Boecking A, Pomjanski N, et al. Verrucous carcinoma of the buccal mucosa: histopathological, cytological and DNA-cytometric features. J Oral Pathol Med 2006;35:633-635.
41. Maraki D, Yalcinkaya S, Pomjanski N, et al. Cytologic and DNA-cytometric examination of oral lesions in lichen planus. J Oral Pathol Med 2006;35:227-232.
42. Medak H, Burlakow P, McGrew EA, Tiecke R. The cytology of vesicular conditions affecting the oral mucosa: pemphigus vulgaris. Acta Cytol 1970;14:11-21.
43. Moralis A, Kunkel M, Reichert TE, et al. Identification of a recurrent oral squamous cell carcinoma by brush cytology. Mund Kiefer Gesichtschir 2007;11:355-358.
44. Nagler RM. Molecular aspects of oral cancer. Anticancer Res 2002;22:2977-2980.
45. Navone R, Burlo P, Pich A, et al. The impact of liquid-based oral cytology on the diagnosis of oral squamous dysplasia and carcinoma. Cytopathology 2007;18:356-360.
46. Navone R, Pentenero M, Rostan I, et al. Oral potentially malignant lesions: first-level micro-histological diagnosis from tissue fragments sampled in liquid-based diagnostic cytology. J Oral Pathol Med 2008;37:358-363.
47. Noguchi M, Kinjyo H, Kohama GI, Nakamori K. Invasive front in oral squamous cell carcinoma: Image and flow cytometric analysis with clinicopathologic correlation. Oral Surg Oral Med Oral Pathol Oral Radiol Endod 2002;93:682-687.
48. Noutomi Y, Oga A, Uchida K, et al. Comparative genomic hybridization reveals genetic progression of oral squamous cell carcinoma from dysplasia via two different tumourigenic pathways. J Pathol 2006;210:67-74.
49. Ogden GR. The future role for oral exfoliative cytology - bleak or bright? Oral Oncol 1997;33:2-4.
50. Pandit S, Aithal D. A qualitative and quantitative estimation of AgNORs in dysplastic and non-dysplastic leukoplakias. Indian J Dent Res 2002;13:27-30.
51. Pektas ZO, Keskin A, Günhan O, Karslioglu Y. Evaluation of nuclear morphometry and DNA ploidy status for detection of malignant and premalignant oral lesions: quantitative cytologic assessment and review of methods for cytomorphometric measurements. Oral Maxillofac Surg 2006;64:628-635.
52. Pereira MC, Oliveira DT, Landman G, Kowalski LP. Histologic subtypes of oral squamous cell carcinoma: prognostic relevance. J Can Dent Assoc 2007;73:339-344.
53. Pillai KR, Sujathan K, Madhavan J, Abraham EK. Significance of silver-stained nucleolar organizer regions in early diagnosis and prognosis of oral squamous cell carcinoma: a multivariate analysis. In Vivo 2005;19:807-812.
54. Poate TW, Buchanan JA, Hodgson TA, et al. An audit of the efficacy of the oral brush biopsy technique in a specialist oral medicine unit. Oral Oncol 2004;40:829-834.
55. Potter TJ, Summerlin DJ, Campbell JH. Oral malignancies associated with negative transepithelial brush biopsy J Oral Maxillofac Surg 2003;61:674-677.
56. Ramaesh T, Ratnatunga N, Mendis BR, Rajapaksa S. Exfoliative cytology in screening for malignant and premalignant lesions in the buccal mucosa. Ceylon Med J 1998;43:206-209.
57. Remmerbach TW, Weidenbach H, Hemprich A, Böcking A. Earliest detection of oral cancer using non-invasive brush biopsy including DNA-image-cytometry: report on four cases. Anal Cell Pathol 2003;25:159-166.
58. Remmerbach TW, Weidenbach H, Müller C, et al. Diagnostic value of nucleolar organizer regions (AgNORs) in brush biopsies of suspicious lesions of the oral cavity. Anal Cell Pathol 2003;25:139-146.
59. Remmerbach TW, Weidenbach H, Pomjanski N et al. Cytologic and DNA-cytometry early diagnosis of oral cancer. Anal Cell Pathol 2001;22:211-221.
60. Ries JC, Schreiner D, Steininger H, Girod SC. p53 mutation and detection of p53 protein expression in oral leukoplakia and oral squamous cell carcinoma. Anticancer Res 1998;18(3B):2031-2036.
61. Rosin MP, Lam WL, Poh C, et al. 3p14 and 9p21 loss is a simple tool for predicting second oral malignancy at previously treated oral cancer sites. Cancer Res 2002;62:6447-6450.
62. Ruocco V, Coscia-Porrazzi L, Pisani M. Reliability of cytodiagnosis in oral pemphigus vulgaris. A study of 30 cases. J Dermatol 1984;11:535-540.

63. Saito T, Mizuno S, Notani K, et al. Flow cytometric analysis of cell cycle fractions in oral leukoplakia. Int J Oral Maxillofac Surg 1998;27:217-221.
64. Saito T, Yamashita T, Notani K, et al. Flow cytometric analysis of nuclear DNA content in oral leukoplakia: relation to clinicopathologic findings. Int J Oral Maxillofac Surg 1995;24:44-47.
65. Scheifele C, Schlechte H, Bethke G, Reichart PA. Detection of TP53-mutations in brush biopsies from oral leukoplakias. Mund Kiefer Gesichtschir 2002;6:410-414.
66. Schulte EK, Joos U, Kasper M, Eckert HM. Cytological detection of epithelial dysplasia in the oral mucosa using Feulgen-DNA-image cytometry. Diagn Cytopathol 1991;7:436-441.
67. Sciubba JJ. Improving detection of precancerous and cancerous oral lesions. Computer-assisted analysis of the oral brush biopsy. U.S. Collaborative Oral CDx Study Group. J Am Dent Assoc 1999;130:1445-1457.
68. Scott IS, Odell E, Chatrath P, et al. A minimally invasive immunocytochemical approach to early detection of oral squamous cell carcinoma and dysplasia. Br J Cancer 2006;94:1170-1175.
69. Seoane J, Asenjo JA, Bascones A, et al. Flow cytometric DNA ploidy analysis of oral cancer comparison with histologic grading. Oral Oncol 1999;35:266-272.
70. Seoane J, Bascones A, Asenjo JA, et al. Flow cytometric analysis of nuclear DNA content in oral leukoplakia. Clin Otolaryngol Allied Sci 1998;23:136-140.
71. Shah RM, Nirmal NJ, Doshi JJ, Bilimoria KF. Cyto-diagnosis of oral pemphigus vulgaris. J Oral Med 1982;37:98-101.
72. Silverman S Jr. Early diagnosis of oral cancer . Cancer 1988;62:1796-1799.
73. Silverman S, Bilimoria KF, Bhargava K, et al. Cytologic, histologic and clinical correlations of precancerous and cancerous oral lesions in 57,518 industrial workers of Gujarat, India. Acta Cytol 1977;21:196-198.
74. Staats OJ, Robinson LH, Butterworth CE Jr. The effect of systemic therapy on nuclear size of oral epithelial cells in folate-related anemias. Acta Cytol 1969;13:84.
75. Sudbo J, Bryne M, Johannessen AC, et al. Comparison of histological grading and large-scale genomic status (DNA ploidy) as prognostic tool in oral dysplasia. J Pathol 2001;194:303-310.
76. Sudbo J, Ried T, Bryne M, et al. Abnormal DNA content predicts the occurrence of carcinomas in non-dysplastic oral white patches. Oral Oncol 2001;37:558-565.
77. Suen KC, et al. The Papanicolaou Society of Cytopathology Task Force on standards of practice. Guidelines of the Papanicolaou Society of Cytopathology for fine-needle aspiration procedure and reporting. Modern Pathol 1997;10:739-747.
78. Suter VGA, Morger R, Altermatt HJ, Spieler P, Bornstein MM. Oral erythroplakia and erythroleukoplakia: red and red-white epithelial precursor lesions of the oral mucosa. – part 1: Epidemiology, etiology, histopathology and differential diagnosis. Schweiz Monatschr Zahnmed 2008;118:1-8
79. Suter VGA, Morger R, Altermatt HJ, Spieler P, Bornstein MM. Oral erythroplakia and erythroleukoplakia: red and red-white epithelial precursor lesions of the oral mucosa. – part 2: cytopathology, pathogenesis, therapy, and prognostic aspects. Schweiz Monatsschr Zahnmed 2008;118:510-518.
80. Tytor M, Wingren S, Olofsson J. Heterogeneity of squamous cell carcinomas of the oral cavity studied by flow cytometry. Pathol Res Pract 1991;187:30-35.
81. Ugras S, Demirtas I, Bekerecioglu M, et al. Immunohistochemical study on histogenesis of congenital epulis and review of the literature. Pathol Int 1997;47:627-632.
82. Waldron CA, Shafer WG. Leukoplakia revisited. A clinico-pathologic study of 3256 oral leukoplakias. Cancer 1975;36:1386.
83. Weir JC, Davenport WD, Skinner RL. A diagnostic and epidemiologic survey of 15,783 oral lesions. J Am Dent Assoc 1987;115:439-442.

**Fig. 8.1 Squamous cells exfoliated from normal buccal mucosa.**
Benign nonkeratinized and keratinized squamous cells against a clean background (brush cytology, ThinPrep preparation, Pap stain, lower magnification).

**Fig. 8.2 Herpes virus-infected cells versus squamous cell carcinoma.**
A 21-year-old woman presented with oral leukoplakia suggestive of candidiasis. Targeted brushing of a buccal-palatine lesion reveals cell changes due to herpes virus infection: multinucleated squamous cells exhibit characteristic nuclear features (arrows). Herpetic stomatitis may be attended by marked hyperkeratinization (right), which can mislead to a diagnosis of squamous cell carcinoma (oral brush smear, Pap stain, high magnification). See also Fig. 11.3B.

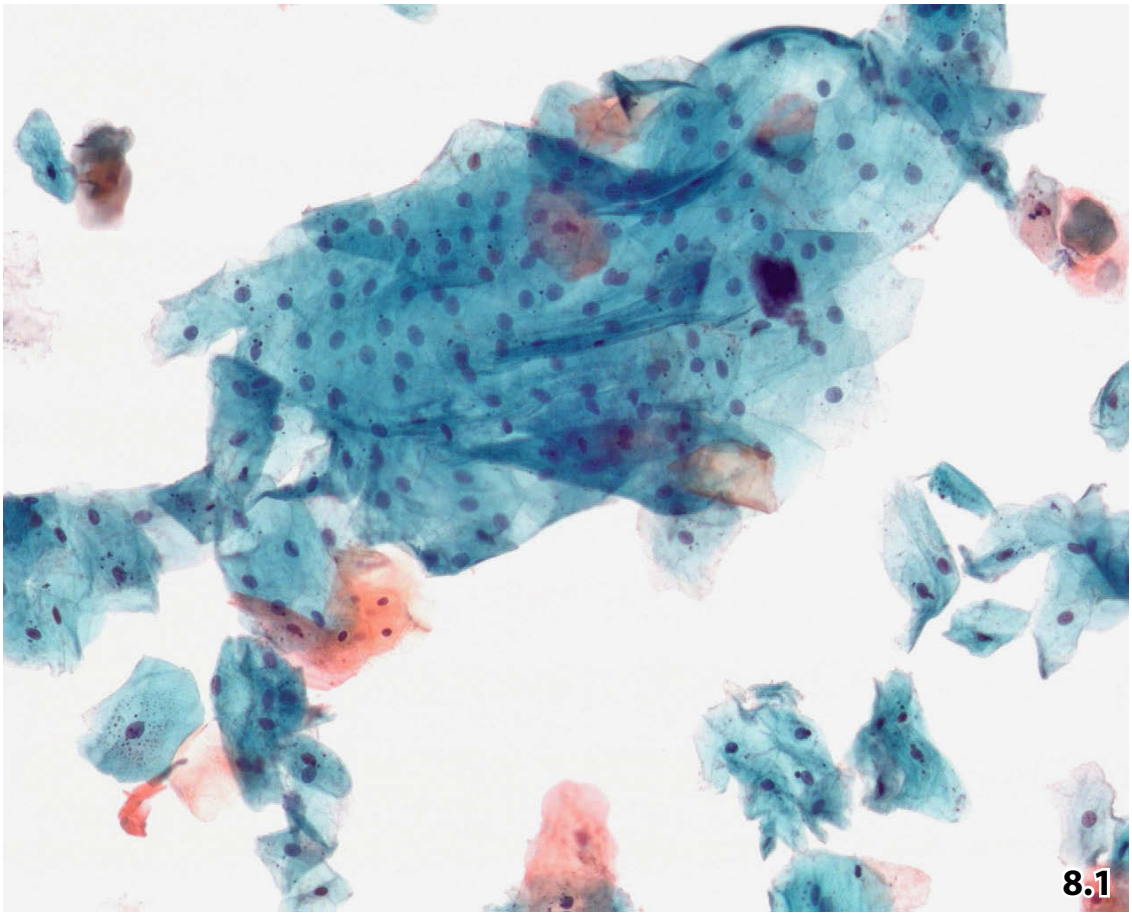

8.1

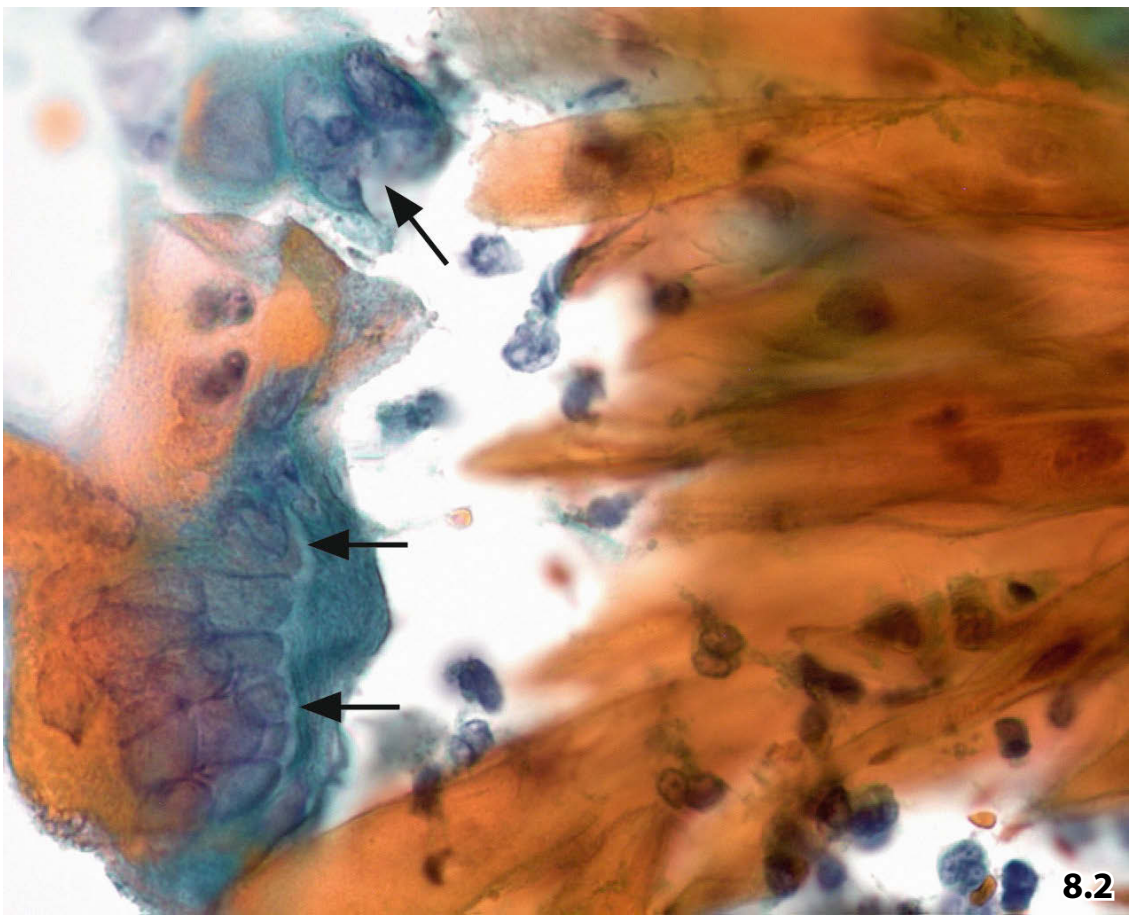

8.2

**Figs. 8.3–8.5 Reactive/reparative cell changes in squamous cells.**
Oral brush biopsies of three patients with oral infections with bacteria and/or fungi. Brushing material was directly smeared and Pap-stained.

**Fig. 8.3A, B** (case #1) A patient with oral candidiasis yields slightly abnormal cytology. **A** Irregularly shaped squamous cells. The cytoplasm shows abnormal acidophilia and perinuclear clearing (arrows), but nuclei have bland appearance (low magnification). It is very difficult to identify fungi on routinely stained smears. **B** Silver stain (Grocott) unveils hyphae close to squamous cells.

**Fig. 8.4** (case #2) Another patient presents with an oral infection of mixed type (bacteria and fungi). The background of the smear contains neutrophils. Squamous cells show discoloration, enlarged and notedly degenerated nuclei (shadowy appearance, vacuoles, karyorrhexis) (high magnification).

**Fig. 8.5** (case #3) A third patient with acute oral infection of the mixed type. Detail of squamous cells shows mild nuclear irregularities, perinuclear clearing (arrows), and occasionally enlarged nuclei (upper right). Background (not shown) is composed of neutrophils, bacteria, and fungi.

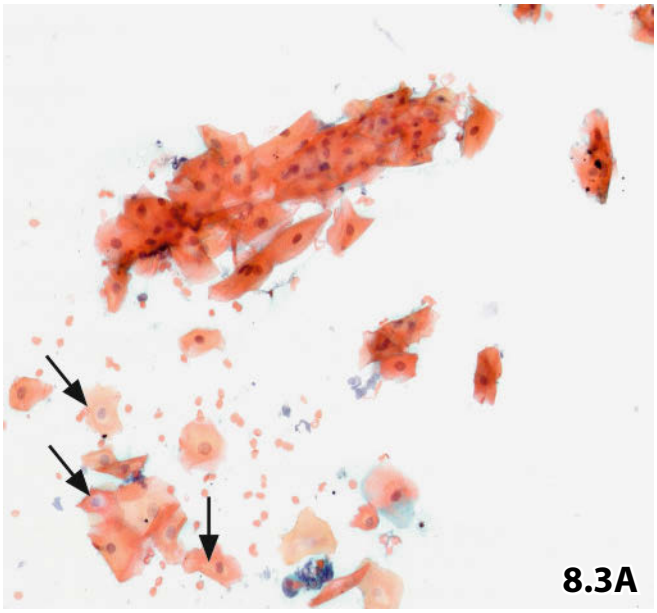
8.3A

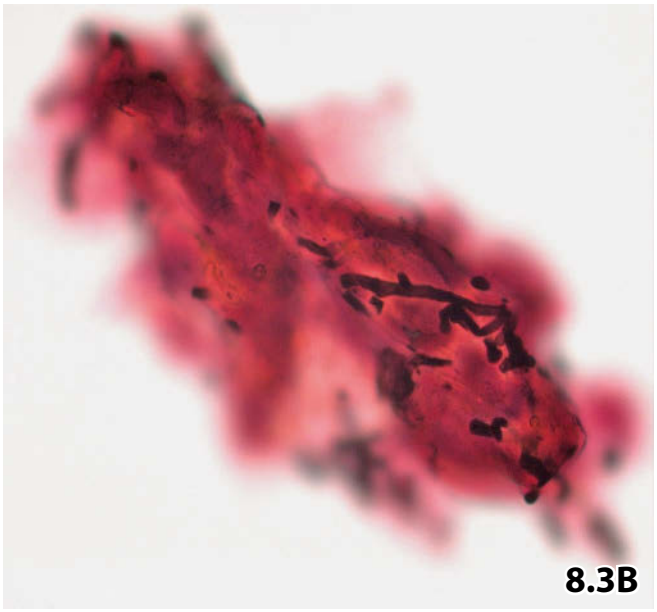
8.3B

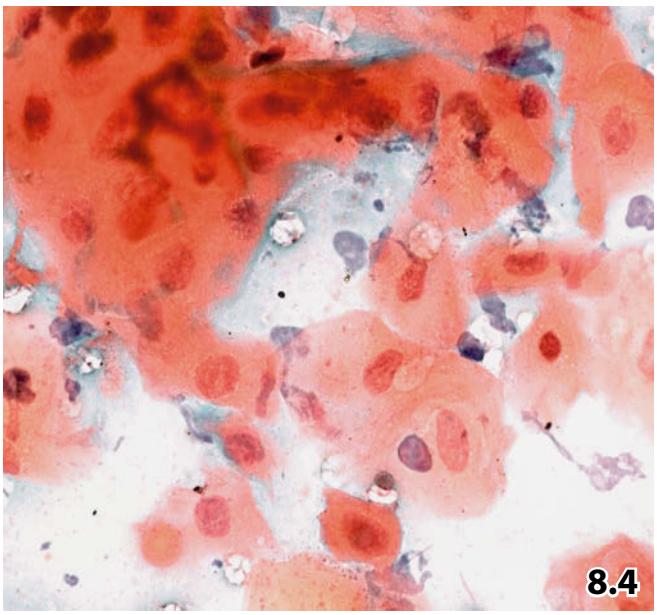
8.4

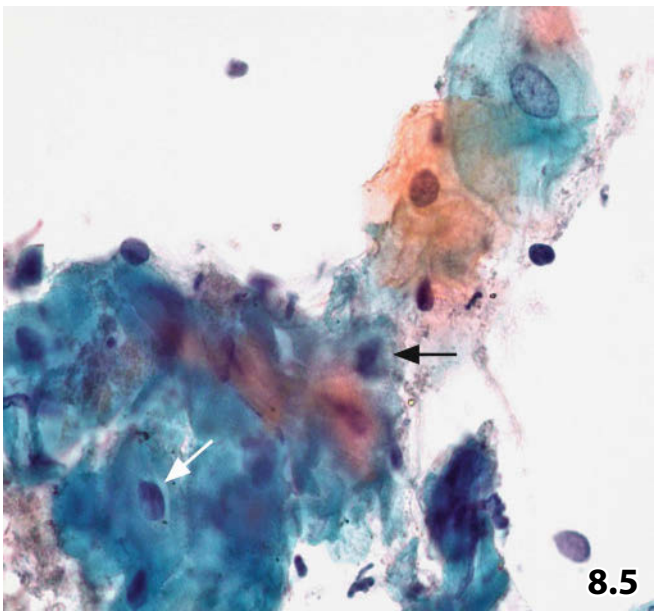
8.5

**Figs. 8.6–8.15 Leukoplakia: cytologic challenge and ICM-DNA as an adjuvant diagnostic tool.**
Oral brush biopsies originating from different leukoplakic lesions in six patients. Cytologic features are demonstrated by means of direct brush smears and liquid-based specimens that have been Pap-stained. Cytology, cytometric results, and the final diagnoses are presented.

**Fig. 8.6** (case #1) Numerous anucleated squamous cells. A minority of squames reveal bland nuclei (high magnification).
*Cytologic diagnosis:* Hyperkeratosis.
*Final diagnosis:* Benign hyperkeratosis.

**Figs. 8.7 and 8.8** (case #2) Clinical diagnosis of white sponge nevus was established in a 21-year-old man. Hypercellular direct smears and ThinPrep specimens could be obtained by brushing.

**Fig. 8.7A** Lower magnification reveals numerous strongly keratinized squamous cells. Transition to parakeratosis and mild nuclear atypia are also present. **B** A pearl formation of keratinized squames is shown in detail. C Sporadic clearly atypical nuclei (irregular outline, deep staining, high N/C ratio) are detected in extremely high magnification (lower left) (oil immersion, ×100).

**Fig. 8.8** Image cytometric DNA analysis provides a diploid histogram (Pap-prestained Feulgen stain, AutoCyte).
*Cytologic diagnosis supported by DNA cytometric result:* Hyperplastic oral mucosal epithelium (acanthosis) including reactive changes of the squamous cells.
*Excisional biopsy:* White sponge nevus.

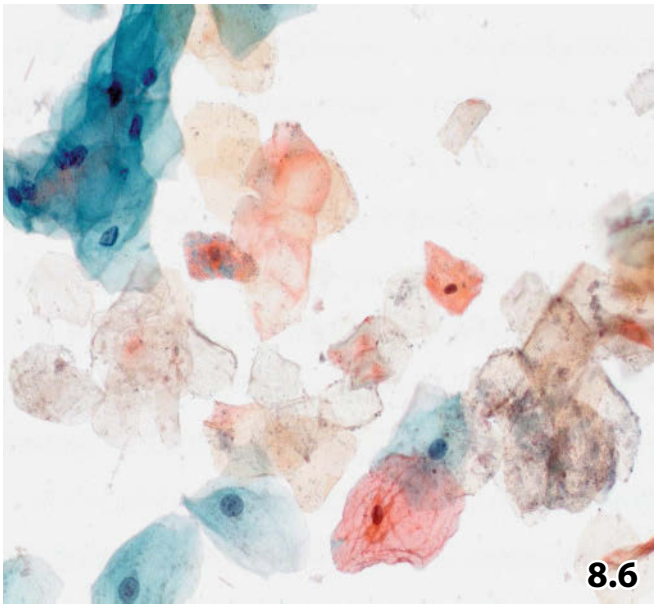

8.6

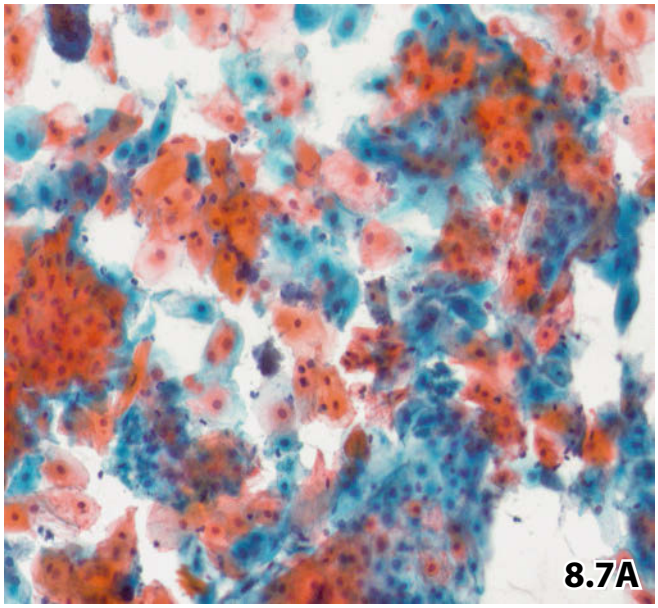

8.7A

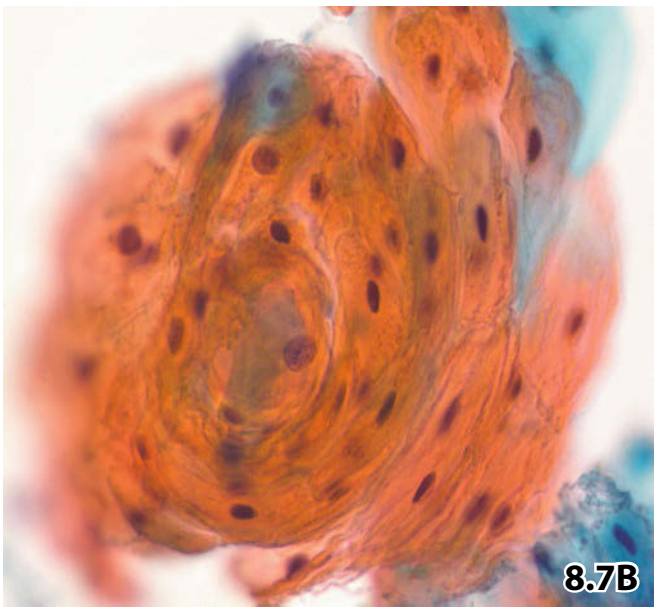

8.7B

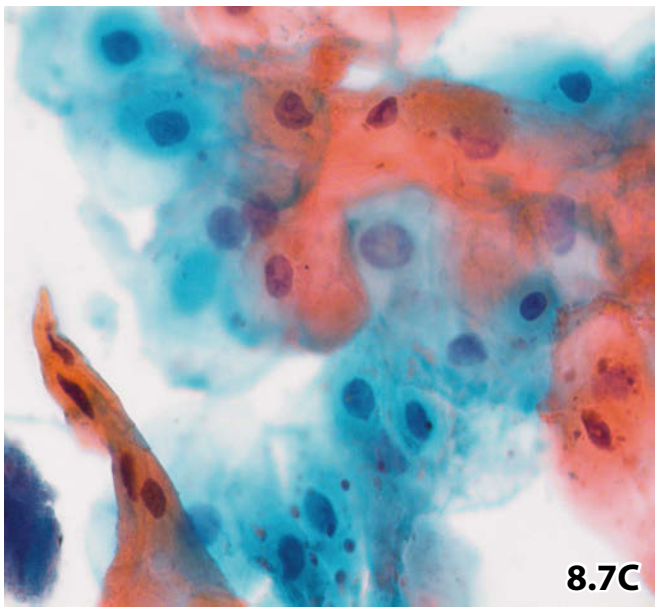

8.7C

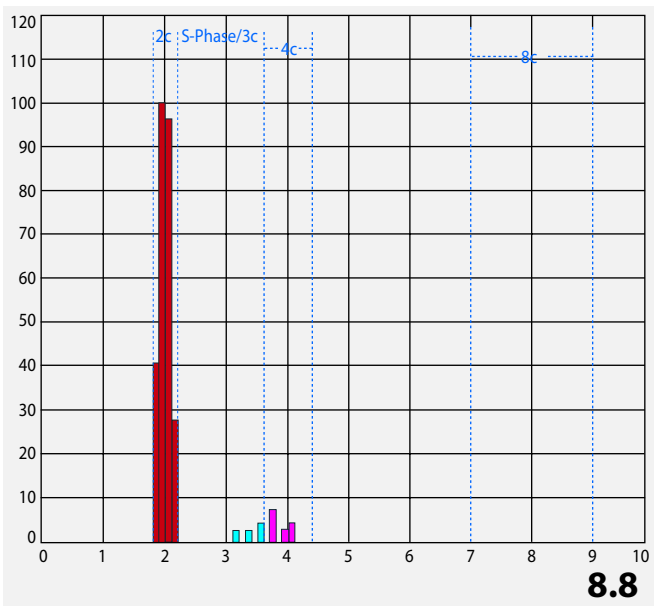


8.8

**Figs. 8.9 and 8.10** (case #3) Leukoplakia detected in the buccal mucosa of a middle-aged man.

**Fig. 8.9A** Lower magnification displays numerous nucleated and anucleated squames exhibiting abnormal polyhedral cytoplasm; keratinization is frequently encountered. **B** High magnification shows irregular nuclear outline, nuclear hyperchromasia, and higher N/C ratio (arrows).

**Fig. 8.10** Image cytometric evaluation of DNA ploidy provided aneuploidy. A considerable number of aneuploid single cells (particularly in the 3c area) and two cells > 9c (Papprestained Feulgen stain, Ahrens Cytometrie-System).
*Cytologic diagnosis* supported by DNA cytometric result: Dysplastic squamous epithelium.
*Follow-up:* No histologic examination. The patient was lost to further follow-up.

Cellular atypias in Fig. 8.7C (benign lesion) are less pronounced than those in Fig. 8.9B (dysplastic lesion), which contains more anucleated cells, more pronounced nuclear irregularities, and more cells with evidence of a high N/C ratio.

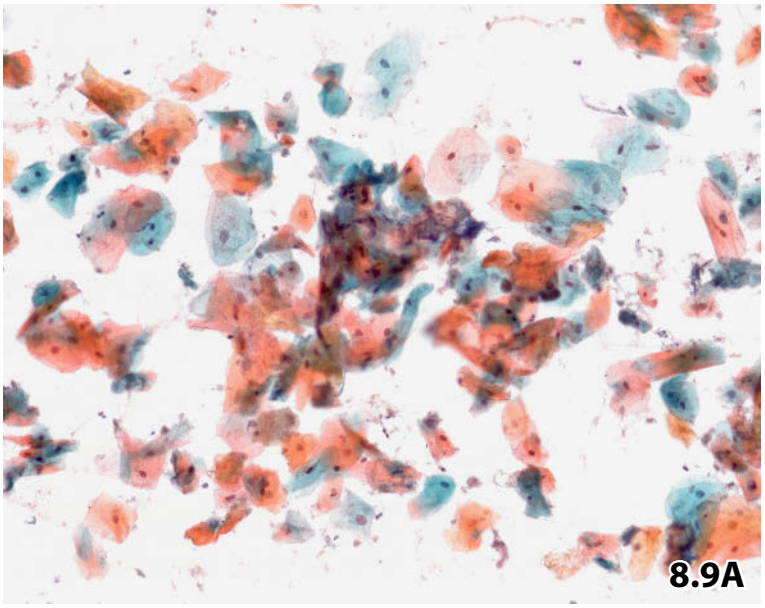

8.9A

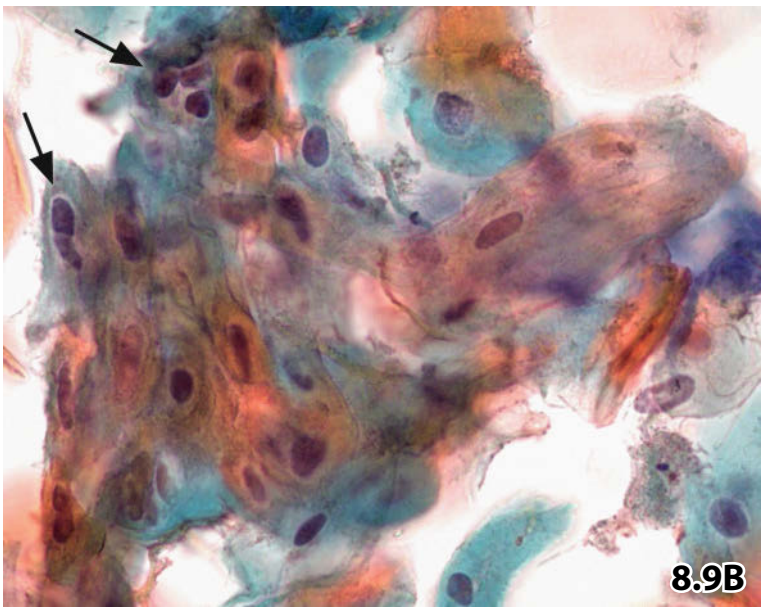

8.9B

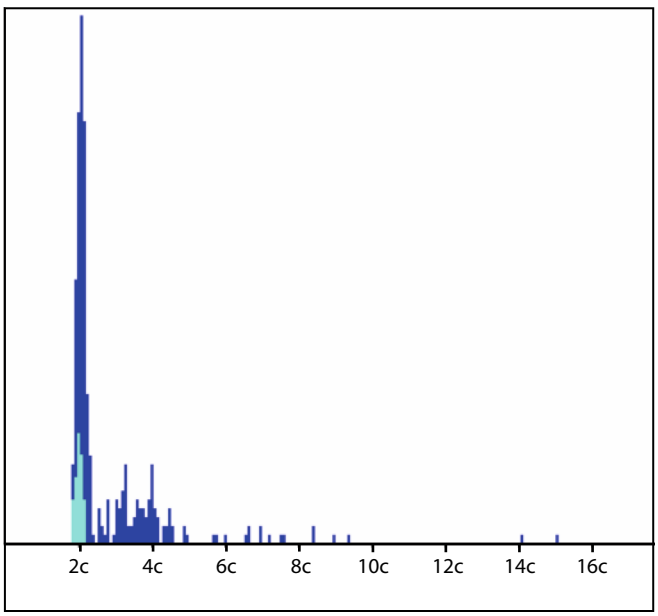


8.10

**Figs. 8.11 and 8.12** (case #4) A 34-year-old man with an excessive consumption of tobacco and alcohol presented with leukoplakia at the root of the tongue. Cytomorphology is shown in detail (ThinPrep method).

**Fig. 8.11A** Strongly atypical nuclei in keratinized squamous cells. **B** Strongly atypical nuclei in nonkeratinized squamous cells. **C** Pleomorphic keratinized anucleated squames.

**Fig. 8.12** Aneuploid DNA distribution pattern. Two aneuploid stemlines in the 3c and 5c area, three nuclei with a DNA content > 9c (Pap-prestained Feulgen stain, AutoCyte).
*Standard cytology and DNA image cytometry* established severe dysplasia of squamous epithelium. Still, both these methods are not efficient to exclude invasive SCC.
*Tissue diagnosis* (excisional biopsy): Severe dysplasia.

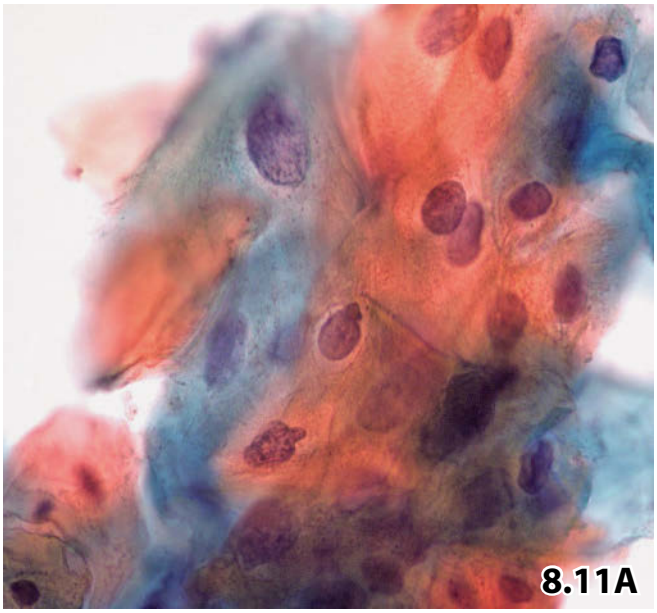

8.11A

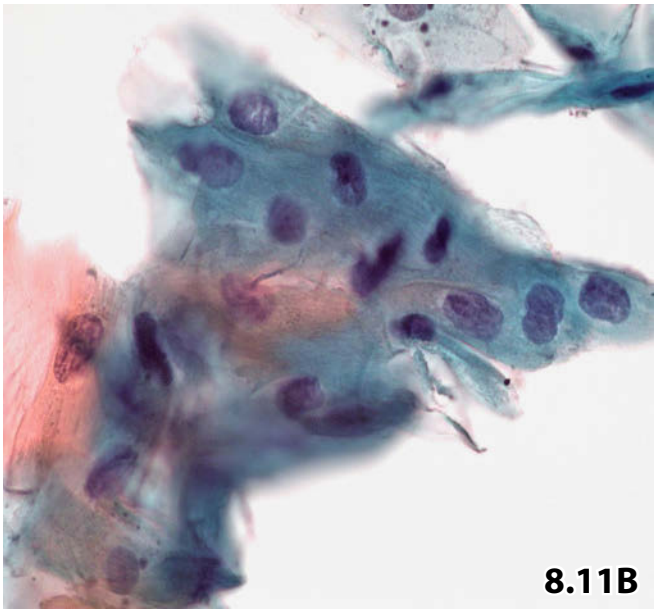

8.11B

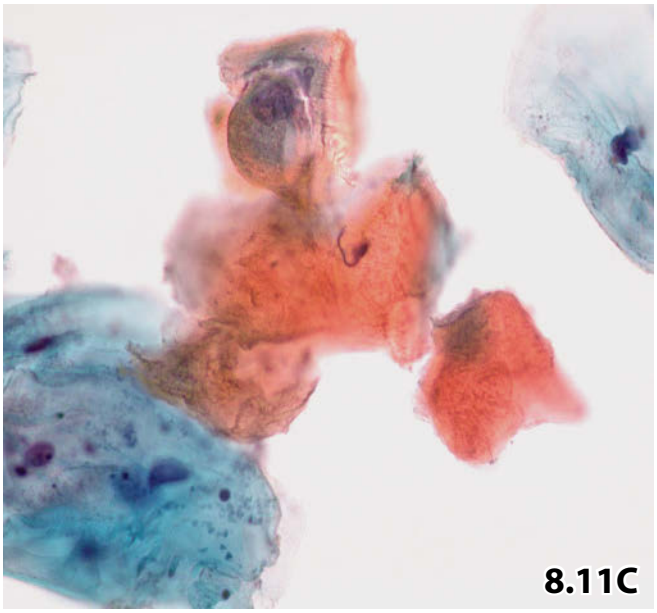

8.11C

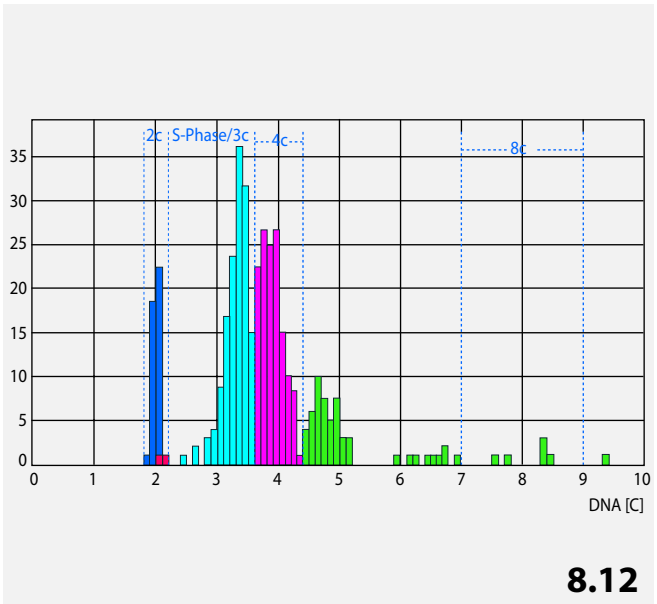


8.12

**Figs. 8.13 and 8.14** (case #5) A 73-year-old man presented with a focal whitish lesion in the oral mucosa combined with a nodular submucous swelling.

**Fig. 8.13A** Parakeratotic, strongly keratinized squames showing atypical dark staining nuclei (high magnification). **B** Irregular compact cluster composed of highly atypical immature squamous cells (high magnification). Attention should be paid to more pronounced cellular atypias and more disordered cytoarchitecture compared to the cell pattern depicted in Fig. 8.11B.

**Fig. 8.14** Aneuploid DNA distribution pattern. Aneuploid stemline in the 3c area and between 5c and 6c (Pap-prestained Feulgen stain, AutoCyte).

*Standard cytology* suggested squamous cell carcinoma. Results from DNA image cytometry are consistent with both dysplastic and invasive malignant squamous lesion.

*Tissue diagnosis* (excisional biopsy): Squamous cell carcinoma.

**Fig. 8.15A, B** (case #6) An 87-year-old man presented with a single leukoplakia at his tongue. **A** Extremely keratinizing and pleomorphic anucleated squames suggest keratinized squamous cell carcinoma (high magnification). **B** But mild nuclear atypias depicted in this figure make a cytologic diagnosis challenging (high magnification).

*Tentative cytologic diagnosis:* Most likely well-differentiated keratinized squamous cell carcinoma.

*Tissue diagnosis* (excisional biopsy): Squamous cell carcinoma, moderately differentiated.

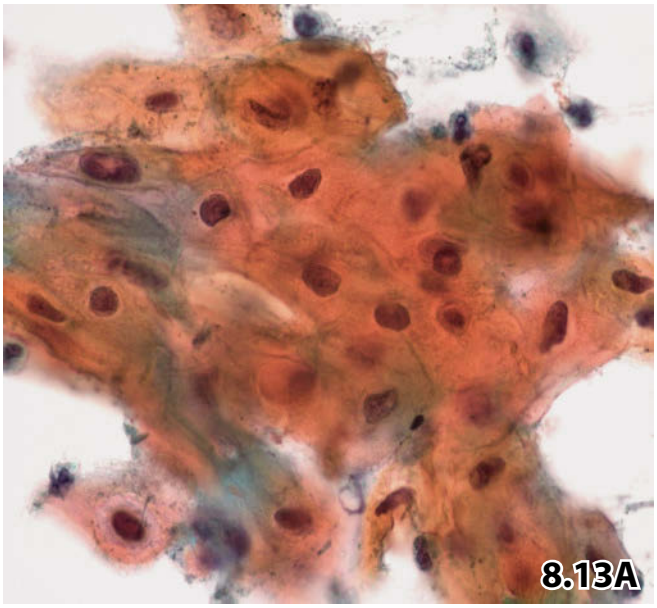

8.13A

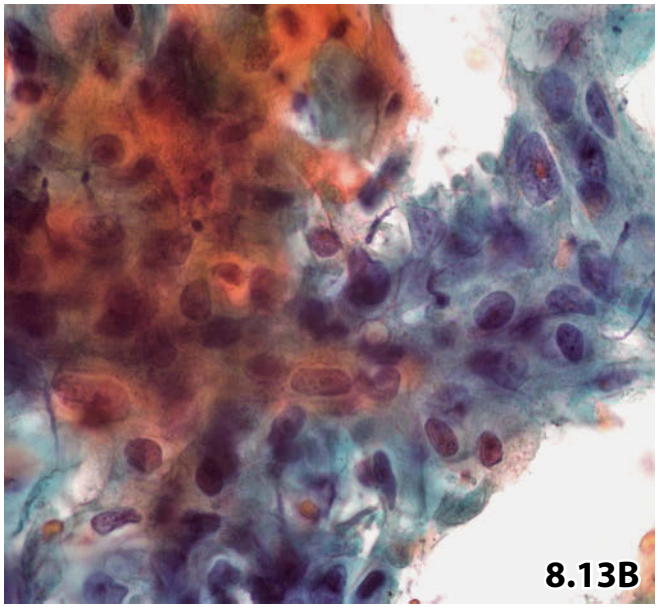

8.13B

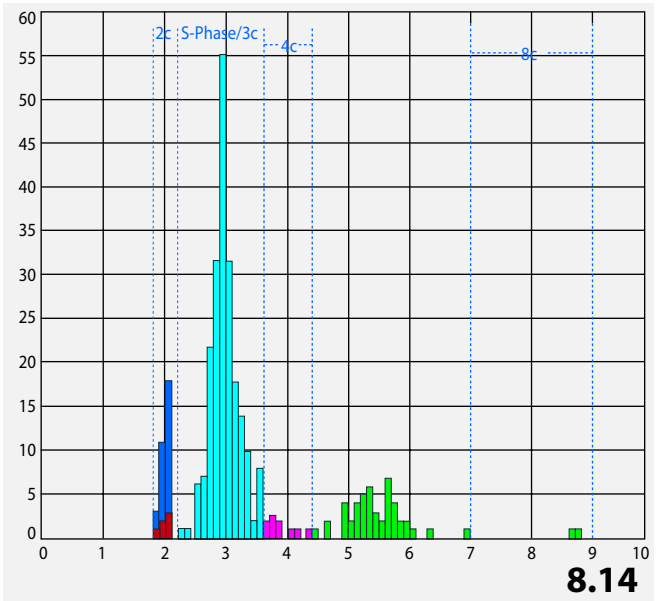


8.14

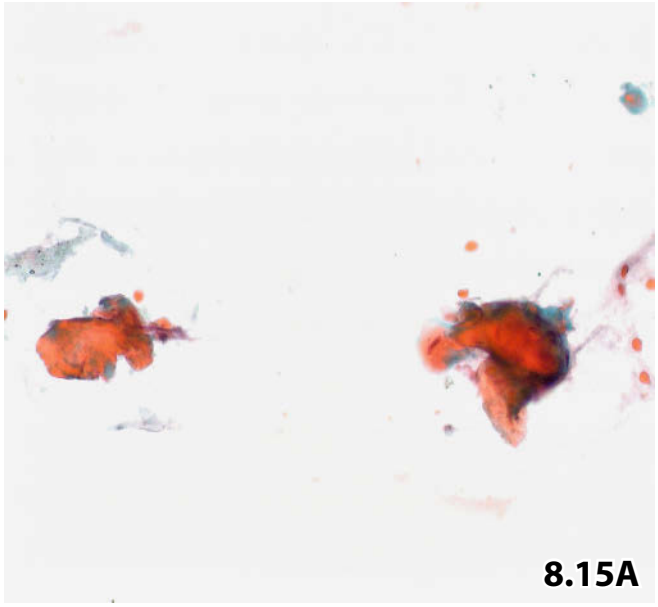

8.15A

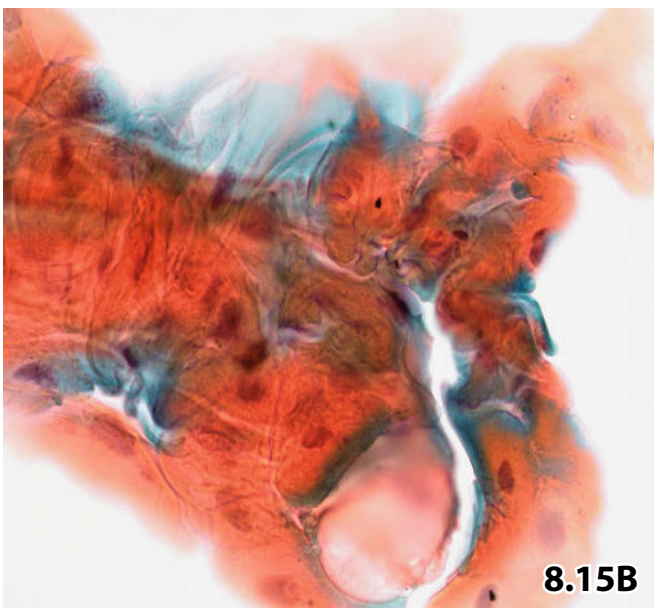

8.15B

# 9 Liver



## Synopsis and Algorithms




Spieler/Rössle, *Nongynecologic Cytopathology. A Practical Guide. Essentials of Diagnostic Pathology*,
DOI 10.1007/978-3-642-24719-4_9, © Springer-Verlag Berlin Heidelberg 2012

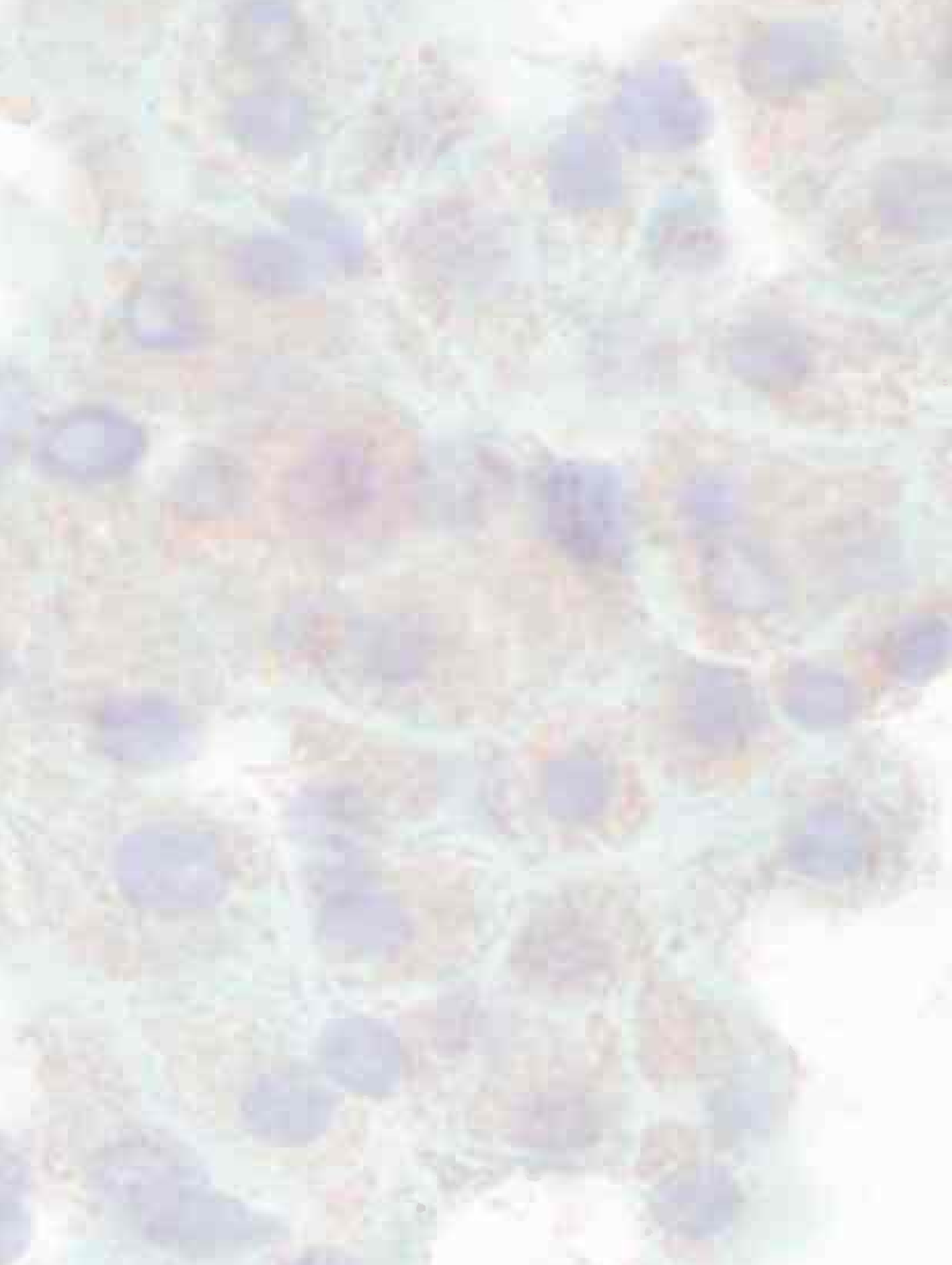

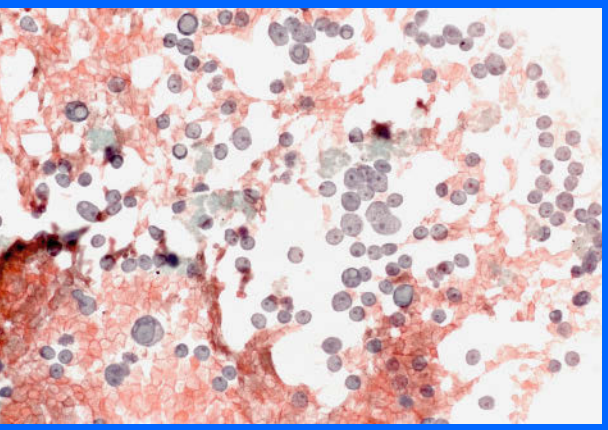

# Section 9.1
# Liver



## 9.1.1 Introduction

**General Comments**

- Naked nuclei are hardly ever encountered in nonneoplastic liver lesions as compared with liver cell adenoma (Sect. 9.1.9.1, p. 591) and malignant liver disorders (Sect. 9.2, p. 604).
- Kupffer cells appear as macrophages exhibiting variable size and varying phagocytic activity.
- Groups of mesothelial cells from the peritoneal or pleural coat may sometimes be admixed in liver FNA samples. The mesothelial sheets are monolayered and the nuclei are widely spaced with evenly and finely dispersed chromatin. The N/C ratio is low (Figs. 9.1 and 9.2).
- An overview of aspiration cytology of the liver is presented by Guy and Ballo [17].

**Caution**

Sheets of activated mesothelial cells exhibiting large irregular nuclei with distinct nucleoli could possibly lead to an erroneous diagnosis of cancer.

### 9.1.1.1 Laboratory and Diagnostic Techniques (Selected Items)

Different methods to prepare the aspirated cell sample are available in addition to the conventional direct smear technique. The various techniques are described in several chapters of this book, e.g., Sects. 1.1.2, and 1.1.4, p. 4.

#### 9.1.1.1.1 Liquid-Based Cytology (Cytospin, ThinPrep, SurePath, and Others)

- The processing of FNAB liver specimens using liquid-based methodology offers an ideal diagnostic tool especially for bloody aspirates by providing a solution lysing erythrocytes.
- Liquid-based technology is superior to conventional smears with respect to the adequacy of the sample, cell preservation, cell recognition, absence of red blood cells, and background quality. Furthermore, liquid-based cytology, with the advantage of additional cell preparations for ancillary techniques, renders superior results in terms of immunohistochemistry, ploidy analysis (ICM-DNA), and molecular biology.
- Microscopic screening is easier and less time-consuming.
- Comparing liquid-based and conventional cytology, diagnostic accuracy is equal even though certain tumors yield a pathognomonic cell pattern in conventional smears that may be vague or missing in liquid-based preparations.

#### 9.1.1.1.2 Cell-Block Technique

The value of cell blocks produced from cytologic specimens depends on the type and amount of cytologic material that is available and is a matter of individual preference for this technique. The cell-block technique may be recommended for all the liver aspirates providing extremely cellular material such as hepatocellular carcinoma and metastatic tumors.

#### 9.1.1.1.3 Imaging and Endosonographic FNAB of Hepatic Lesions

- Endosonography increases the chance of discerning small liver lesions, which is reported to be important information in patients being considered for liver transplantation [51], and endosonography-guided aspiration is an adequate method to resolve small hepatic lesions. In contrast, current diagnostic imaging modalities such as computed tomography and magnetic resonance imaging often miss small lesions.
- Percutaneous and endosonographic FNAB samples from very small lesions may constitute a particular challenge for cytopathologists due to scarcity of the aspirated cellular material.

### 9.1.2 Normal Liver Parenchyma (Fig. 9.3)



**Microscopic Features**

- Normal hepatocytes usually occur as polygonal cells that are arranged in monolayered sheets.
- The nuclei are round, showing distinct smooth membrane and variation in size. Binucleation and nuclear inclusions frequently occur.
- Frequent conspicuous nucleoli.
- Fine and loose chromatin pattern.
- Abundant well-defined granular cytoplasm contains variable amounts of lipofuscin pigment.
- Fragments of bile ductules appear as tightly packed tubular clusters composed of small cuboid and columnar cells, occasionally palisading.

**Caution**

- Variable nuclear size and deep nuclear staining of benign hepatocytes are due to DNA polyploidization (repeated doubling of euploid DNA amounts).
- With the Pap staining procedure, the typical cytoplasmic granulation may appear eosinophilic, cyanophilic, or grey-blue depending on the technical and chemical prerequisites of the staining process.
- Sinusoidal endothelial cells are difficult to distinguish in FNAB samples from normal liver parenchyma.

### 9.1.3 Fatty Liver / Steatosis (Fig. 9.4)

Sharply demarcated steatotic liver areas may mimic a neoplastic lesion in routine imaging studies. Such findings are often followed by FNAB in order to reach morphologic clarification. In unfixed smears, hepatocytes contain variably sized empty cytoplasmic vacuoles staining red using the oil red staining technique.

**Microscopic Features**

- Enlarged hepatocytes show medium-sized and large cytoplasmic vacuoles.
- The nuclei are marginalized.

### 9.1.4 Pigments in Benign Hepatocytes (Fig. 9.3B)

- *Lipofuscin* (Fig. 9.3B) is a pale golden brown finely granular pigment existing in nearly all hepatocytes. It is considered one of the aging pigments with deposits in many organs; but impressing amounts of lipofuscin both in parenchyma cells and prominent Kupffer cells may be observed in combination with different hepatic lesions.
- *Bile*. Intracytoplasmic bile deposits can be identified in cytologic preparations. Large amounts of bile plugs may suggest a mechanical obstruction of the biliary tree.
- *Hemosiderin*. Small numbers of hemosiderin granules are found in hepatocytes of many normal livers and in a variety of hepatic disorders.
  Hemosiderin storage is readily discernible in MGG- and Pap-stained smears: the elements are large and coarse, exhibiting a polymorphous shape. They stain browner than bile pigment using the MGG technique and appear as a prominent dirty greenish-brown conglomerate with the Pap staining method.
  A specific iron stain is definitely necessary for proper identification.
  Hemochromatosis may be suggested in cases exhibiting large numbers of hemosiderin-laden hepatocytes.

### 9.1.5 Myeloid Metaplasia (Fig. 15.102)

**General Comments**

Myeloid metaplasia belongs to the list of potential pitfalls in FNAB of the liver. Myeloid metaplasia should be recognized and communicated to clinicians because this finding may refer to a predisposing hematologic abnormality or a preexistent pathologic condition of the bone marrow. Myeloid metaplasia is more reliably recognized in MGG- or Diff-Quik-stained smears than in Pap staining.

**Microscopic Features and Differential Diagnosis** [5]

- A hallmark of myelogenic metaplasia is the megakaryocyte, unfortunately available in a minority of cytologic samples. Megakaryocytes appear as large cells with multilobated or multisegmented dark nuclei and abundant cytoplasm. The chromatin is thinly dispersed. Nucleoli are practically absent.

Even though megakaryocytes show distinct polymorphism, the overall cellular characteristics should prevent a misinterpretation of malignancy.

The atypical immature cells of metaplastic myeloid disorders could lead to a false diagnosis of carcinoma or myelogenic sarcoma. However, both carcinoma and sarcoma present with distinct malignant cellular features.We refer the reader to Sects. 15.3.22 and 15.3.23, "Myeloproliferative Disorders," p. 975.

## 9.1.6 Inflammation / Infection (Fig. 9.5)

### 9.1.6.1 Abscess

- Varying inflammatory infiltrates composed of granulocytes, lymphocytes, and histiocytes are interspersed with detritus and necrotic material.

Gram, Giemsa, PAS, and Crocott stains are appropriate in order to visualize bacteria, parasites, and fungi, although hyphae may also be clearly recognizable using the Papanicolaou staining procedure (Fig. 9.5).

#### Amebic Liver Disease

Amebic liver disease is usually diagnosed in patients with a history of exposure in an endemic area. Abscess results mainly from primary infection in the colon by *Entamoeba histolytica*. From the circulation, protozoa are filtered in the liver forming abscesses.

Based on our experience, there is little chance of detecting trophozoites of *Entamoeba histolytica* in cytologic samples from the abscess cavity where the parasites are completely destroyed, i.e., the fine-needle aspirate should be carried out on the peripheral areas of the lesion. In either case, a careful search for trophozoites is indispensable.

**Microscopic Features**

- The pathogens display pretty typical morphologic features: large, round, foamy elements with ingested red blood cells.
- Eccentric round nuclei are sporadically observed, exhibiting a small dark center that stains positive with periodic acid-Schiff reagent [1].

### 9.1.6.2 Chronic and Viral Hepatitis (Fig. 9.6)

FNAB is rarely used with patients suffering from chronic or viral hepatitis.

Both a monomorphic or polymorphic population of lymphoid cells must raise suspicion of low-grade malignant non-Hodgkin lymphoma (NHL). If enumeration of B and T lymphocytes (Fig. 9.6B and 9.6C) is not diagnostic, PCR in combination with fragment analysis of nuclear DNA extracted from cells of a cytologic sample is essential to establish clonality (benign versus malignant lymphoid cell population).

### 9.1.6.3 Granulomas

Granulomas in the liver may have different etiologies:
- Infections.
- Drug sensitivity.
- Foreign-body reaction due to talc crystals and other foreign bodies.
- Neoplasms.
- Immunodeficiency.
- Sarcoidosis [37].

**Microscopic Features**

- The basic cell pattern consists of histiocytes/epithelioid cells, multinucleated histiocytes/Langhans giant cells, lymphocytes, and microfragments of granulomatous tissue.

#### 9.1.6.3.1 Infection

Cytologic diagnosis of infectious granulomas is based on the identification of organisms using special staining methods.

#### 9.1.6.3.2 Caseating Granulomatosis

Most cases of caseating granulomatosis are due to *Mycobacterium tuberculosis*, morphologically characterized by granular debris. Epithelioid cells are usually present as well (Fig. 15.20) (for further information, see Sect. 2.1.6.1, p. 116). If mycobacteriosis is suspected a search for acid-fast bacilli by Ziehl-Neelsen staining can contribute to a positive cytologic diagnosis (Fig. 2.18B). In each case, medically important species of mycobacteria should be typed by molecular methods.

#### 9.1.6.3.3 Foreign-Body Reactions

- A reaction in the absence of identifiable foreign bodies may sporadically be encountered.
- Homogeneous and glassy cytoplasmic inclusions in histiocytes/macrophages, optionally refractile, may attract attention as the cause of a foreign-body reaction.
- Talc crystals are composed of magnesium silicate showing strong birefringence under polarized light and are often ingested by histiocytic giant cells.

#### 9.1.6.3.4 Sarcoidosis

Sarcoidosis is hardly ever accompanied by debris (for further information, see Sect. 2.1.3.2.2, p. 111).

## 9.1.7 Cystic Lesions

### 9.1.7.1 Congenital Benign Cysts

- Congenital cysts may appear singly or multiply (grouped or disseminated throughout the liver) and are usually of the simple type.

- Proteinaceous fluid and foamy histiocytic cells are pathognomonic for benign simple liver cysts.

- Aspirates from cysts with a well-preserved epithelial layer are unusual. A tentative diagnosis as to the histogenetic type of such lesions depends on the cell features detected:
  - *Columnar, cuboidal, or flat glandular cells:* cystic disorder of the bile duct system or cystically dilated biliary microhamartoma (von Meyenburg complexes).
  - *Ciliated cylindric cells:* foregut cyst, representing a remnant of the cephalic portion of the primitive digestive tube in the embryo [56].
  - *Mesothelial cell sheets:* mesothelial cyst, frequently originating from the liver surface. It is important to avoid an erroneous diagnosis of cancer. Sheets of activated mesothelial cells exhibiting large irregular nuclei with distinct nucleoli could possibly lead to an erroneous diagnosis of cancer.



### 9.1.7.2 Secondary Cysts: Necrotic Malignancy

Central necrotic transformation is a typical outcome of large secondary tumors of the liver. Experienced operators are used to aspirating material both from the central and marginal areas of the lesion using image guiding.

#### Microscopic Features and Differential Diagnosis

- Tumor necrosis is characterized by polymorphic eosinophilic and cyanophilic elements strongly varying in shape, interspersed with cellular elements exhibiting homogeneous apoptotic nuclei.
- An inflammatory component is common.

Caseating tuberculosis (see Sect. 9.1.6.3.2, p. 589) must always be kept in mind, though caseous necrosis differs in quality from tumor necrosis.

#### Additional Comment

The measurement of CEA levels by enzyme immunoassay in the supernatant after centrifugation of the aspirated fluid is helpful in distinguishing between benign and malignant cystic liver lesions [40].

**Caution**

Large amounts of mucous masses should raise suspicion of a cystic tumor of equivocal malignant potential (see Sect. 9.1.10, p. 592) or a malignant neoplasm (see Sect. 9.2.4, "Intrahepatic Cholangiocarcinoma," p. 609).

### 9.1.7.3 Hydatid Cyst (Echinococcosis)

(Figs. 3.17, 9.7, 9.8)

#### General Comments

- The larvae of the animal tapeworm *Echinococcus* reside mainly in liver and lungs and produce multiloculated fluid-filled cysts.
- *Echinococcus multilocularis* produces multilocular alveolar cysts with exogenous proliferation invading the adjacent parenchyma and tissues. Calcifications are frequent and an important attribute in imaging diagnosis.
- Single, unilocular cyst or multiseptated cysts are caused by *Echinococcus granulosus*.
- In North America, the classic hydatid disease is caused by *Echinococcus granulosus*, a parasite of dogs and wolfs. The fox tapeworm is probably the worst parasite in Central Europe, increasingly causing echinococcosis of the alveolar type.
- Hydatid disease is frequently diagnosed in immigrants.
- In most cases, a specific diagnosis of echinococcosis is made by imaging techniques. However, guided fine-needle aspiration is the method of choice to assess the nature of small obscure cystic lesions devoid of calcium deposits.
- Cystic lesions caused by other mycotic, protozoal, and helminth infections are not further discussed in this setting. Single cases are described in many pertinent papers and distinguished textbooks, for example in McSween's *Pathology of the Liver* (2007) [31].

#### Microscopic Features

- The finding of hooks and scolices is diagnostic for hydatid disease.
- Also pathognomonic is a bloodless sediment smear exhibiting opaque masses in the background, sparse cellular elements, and sporadic hooks. The latter may be completely absent (Fig. 9.8).

**Caution**

- In cytologic samples with only sparse diagnostic elements, it is very important to read the smear carefully, if necessary even at high magnification in order to identify single small hooks.
- Furthermore, one has to search for hooks viewed on edge (positioned upright on their narrow border), masking the tiny barbed hook (Fig. 3.17).
- Minimal closing of the microscope diaphragm can be helpful in detecting sporadic hooks.

## 9.1.8 Nonneoplastic Epithelial Lesions Presenting as a Mass

### 9.1.8.1 Cirrhosis (Fig. 9.9)

**General Comments**

- Nonneoplastic liver lesions such as liver cirrhosis are frequently accompanied by proliferating hepatocytes forming hyperplastic nodules. The reactive cellular atypias may be pronounced, causing serious diagnostic problems to an extent that a neoplastic or at least preneoplastic lesion cannot be safely excluded. Note that marked variation of the cellular activity is a strong indicator for a benign regenerative lesion of the liver parenchyma.
- Active liver cirrhosis can be suspected in cytologic specimens that present with small bile duct fragments and stromal components.

**Microscopic Features**

Regenerative nodules are characterized by activated hepatocytes:

- The cells are often binucleated, exhibiting marked variation in size and shape.
- The chromatin is loosely arranged, but occasionally it may appear coarsely.
- The nucleoli are large, irregular, and distinct.
- Fragments of stromal tissue are obvious, from case to case occurring in varying amounts.
- Proliferating bile ducts, inflammatory infiltrates, and an active fibroblastic component are encountered, particularly in active cirrhosis.

### 9.1.8.2 Focal Nodular Hyperplasia

(Figs. 9.10 and 9.11)

**Etiology and General Comments**

- Focal nodular hyperplasia (FNH) is a benign pseudotumor. The association of FNH with the use of oral contraceptives has been postulated in many reports [30].
- FNH can occur in anyone at any age; however, it occurs most commonly in women between the forth and the sixth decade of life.
- The lesion is increasingly being diagnosed through widespread screening using sonography, computed tomography, and magnetic resonance imaging in patients with nonspecific abdominal symptoms. Since many of the image findings are presumed to be malignant, FNAB is frequently used in daily practice as an initial diagnostic tool.

**Microscopic Features and Differential Diagnosis**

- Hallmark: Small sheets of normal-appearing hepatocytes intermingled with fibrous tissue and activated fibroblasts.
- Tubular fragments or small clusters of bile duct epithelium revealing activated nuclei.
- Mitotic activity is absent.

**Caution**

- The diagnosis of FNH will be difficult in cases where the mesenchymal elements are underrepresented; the overall cell pattern may mimic normal liver parenchyma.
- The classic cell pattern of FNH shares many cytologic features with liver cirrhosis.

## 9.1.9 Benign Epithelial Tumors

### 9.1.9.1 Liver Cell Adenoma / Hepatocellular Adenoma [30] (Fig. 9.12)

**Etiology and General Comments**

- Hepatocellular adenoma (HCA) is a rare benign tumor of the liver that appears almost exclusively in women over 30 years of age with oral contraceptive intake longer than 5 years [46].
- Malignant alteration of the tumor has been reported in rare instances [4].
- Distinguishing between a benign hepatocellular neoplasia and well-differentiated hepatocellular carcinoma (HCC) is a well-known diagnostic problem (see also "Additional Analyses", below).

**Microscopic Features**

- Hallmarks: Cell-rich aspirate. Three-dimensional clustering of benign hepatocytes and numerous single stripped nuclei. The nuclei are regular and round showing smooth borders; they are frequently patternless and pale. The nucleoli are round appearing distinct.
  Bile ducts are definitely not a component of liver cell adenomas.
- Thin walled vascular channels and sinusoids may appear within the epithelial fragments, but they are difficult to identify in cytologic preparations. However, the immunocytochemically positive endothelial cell pattern contrasts strongly with that of HCCs (see chapter 9.2."Liver - malignant lesions", section 9.2.7, p. 610).
- Cytoplasmic pigmentation may sporadically be observed.
- Degenerative changes may be present, including apoptotic bodies, necrosis, hemorrhages, and scar tissue containing hemosiderin-laden macrophages.

**Differential Diagnosis**

- Cytologically, the distinction between HCA exhibiting a certain polymorphism of the hepatocytes and regenerative parenchymal nodules is not possible.

**Table 9.1.1** Cytologic differential diagnosis of liver cell adenoma and hepatocellular carcinoma

| Feature | HCA | Well-differentiated HCC |
|---|---|---|
| **Sheets** | Mono- or multilayered | – Trabecular, acinar, pseudoglandular<br>– Sheets with antler-horn structure |
| **Nuclei** | Round, regular, smooth-bordered, and pale | – Irregular in size and shape,<br>– Indentations |
| **Chromatin** | – Finely granular<br>– Occasionally patternless | Dense, granular, irregular |
| **Nucleoli** | Round but variable in size | Prominent and often irregular |
| **N/C ratio** | Low | Moderate to high |
| **Mitoses** | Absent | Often present |
| **Endothelial cells** | | Typical endothelial cell pattern |



- On the other hand, hepatocytes showing any nuclear polymorphism, a high N/C ratio, and irregular prominent pleomorphic nucleoli should raise the possibility of liver cell dysplasia or well-differentiated HHC (see also "Additional Analyses", below and Sect. 9.2.1, "HCC," p. 604).
  A differential diagnostic synopsis on this subject is given in Table 9.1.1.

**Caution**

HCA exhibiting pleomorphic cells and dysplastic nuclei can be seen in patients using oral contraceptives over a long period of time [53].

#### Additional Analyses

Immunocytochemistry

A few reports in the literature emphasize the difference in immunoreactivity of sinusoids in various benign and malignant hepatocellular lesions using different antibodies. Anti-CD34 has proved to be a valuable antibody in distinguishing well-differentiated HCC from nonneoplastic and regenerative lesions [12, 48].

Molecular Genetics

A few recent reports combine genotype (mutation of hepatocyte-related genes) and phenotype of hepatocellular adenoma in order to create a new histologic/molecular classification, which should identify adenomas at an increased risk of malignant transformation [2, 66].

Enzyme Immunoassay

In cases of a cystic adenomatous lesion, the measurement of CEA levels by enzyme immunoassay in the supernatant after centrifugation of the aspirated fluid is helpful in distinguishing between benign and malignant cystic liver lesions [40].

### 9.1.9.2 Noncystic Benign Cholangiocellular Tumors (Fig. 9.13)

This tumor group includes bile duct adenoma, biliary microhamartoma (von Meyenburg complex), biliary adenofibroma, and biliary papillomatosis.

#### Microscopic Features and Comments

- Hallmarks: Benign cuboidal to columnar epithelial cells with uniform nuclei and absence of mitoses.
- Focal mucin production and polypoid or papillary formations may be encountered.
- Varying amounts of stromal tissue.

Marked stromal tissue components could prevent successful aspiration of an ample number of cells.

**Caution**

Both mucin production and papillary elements should definitely raise suspicion of malignancy; further investigations are necessary (see Sect. 9.1.10).

## 9.1.10 Cholangiocellular Tumors of Equivocal Malignant Potential: Biliary Mucinous Cystadenoma and Biliary Papillomatosis

The malignant transformation of mucinous cystadenoma [10, 63] and biliary papillomatosis [14, 55] is a well-known complication. These tumors should be considered low-grade malignancies and therefore a correct interpretation in cytologic samples is of utmost importance; just a few atypical cells may indicate an increased malignant potential.

Few reports are found in the literature concerning FNAB of intrahepatic borderline tumors [54] (see also Sect. 10.1.7, "Neoplastic Cysts," p. 640).

**Microscopic Features**

- Cuboidal and columnar cells occur singly or grouped in dense clusters.
- Benign round to oval nuclei of varying size with distinct nucleoli is an indicator of proliferative activity.
- Cellular degeneration and hemorrhage combined with cystic background and an inflammatory component may be encountered.
- *Mucinous cystadenomas* exhibit abundant mucinous background material and scattered single cells showing mucin-laden cytoplasm.
- *Biliary papillomatosis:* Slender papillae with delicate fibrovascular stalks and palisade arrangement of the columnar epithelial cells allow an unequivocal diagnosis.
- Epithelial atypia/dysplasia is characterized by cellular enlargement, nuclear polymorphism, nuclear hyperchromasia, multilayers, loss of cellular polarity, pseudostratification, and mitoses.

**Additional Comments**

- Malignant transformation is supported by atypical/dysplastic changes in parts of the epithelial cell component. True dysplastic cell changes emphasizing malignant transformation are difficult to assess by light microscopy alone; assessing a quantitative DNA distribution pattern may be helpful in this respect [16].
- Individual degenerative epithelial cells comprising indistinct nuclei and large vacuolized cytoplasm may resemble histiocytes.
- The abnormal cell features closely resemble those of mucinous neoplasms of the pancreatic duct system. Zen et al. concluded that at least biliary papillary tumors may be the counterpart of intraductal papillary mucinous neoplasm of the pancreas [65].

**Additional Analyses**

Immunocytochemistry

Immunocytochemical analysis with antibodies for pancytokeratin (epithelial cells) and CD68 (histiocytes) can easily elucidate the nature of degenerating cellular elements, provided that degeneration has not progressed considerably.

ICM-DNA

DNA aneuploidy is associated with dysplastic cell changes suggesting increasing malignant potential. More information is provided in Sect. 10.2.3.2, p. 681.

Enzyme Immunoassay

A simultaneous measurement of CEA levels in the centrifuged supernatant by an enzyme immunoassay enhances the sensitivity of FNAB in the detection of (pre)malignant cystic lesions [40].

**Caution**

Proper classification of degenerate cellular elements may be a challenge, especially in lesions with cystic changes. Degenerating epithelial cells exhibiting large vacuolated cytoplasm and an irregular nuclear outline may resemble histiocytes.

## 9.1.11 Liver Cell Dysplasia (Fig. 9.14)

By aspiration cytology, it is difficult to distinguish between regenerative liver parenchyma, liver cell dysplasia, and hepatocellular carcinoma. In this regard, Lin et al. proposed a cytologic scoring system using the resulting score to distinguish dysplasia from hepatocellular carcinoma.

**Microscopic Features and Differential Diagnosis**

- *Dysplasia of the large-cell type:* Medium-sized and large hepatocytes exhibiting nuclear pleomorphism, a high N/C ratio, dense irregular chromatin, and pleomorphic nucleoli are intermingled with benign and regenerative hepatocytes. Differential diagnostic considerations include regenerative hepatic nodule, polymorphic liver cell adenoma, and well-differentiated HCC (see Sect. 9.2.1.1, p. 605).
- *Dysplasia of the small-cell type:* Atypical small hepatocytes appear in microtrabecular and acinar arrangement. The morphology of the atypical hepatocytes resembles that of small-cell malignant tumors. An accurate diagnosis based on cytologic features alone is very difficult (see also Sect. 9.2.2.2, "HCC of the Small-Cell Type," p. 607).

**Additional Comments and DNA Ploidy**

- Liver cell dysplasia of both types mentioned above is one of the risk factors for HCC development [25, 27].
- Determination of the DNA ploidy pattern may be helpful in defining dysplastic cell changes. It has been shown that true liver cell dysplasia is associated with an aneuploid DNA distribution pattern [11].

## 9.1.12 Rare Benign Primary Liver Tumors

- It is expected that more exceptional benign tumor entities will be encountered in the future due to increased use of image-guided FNAB of the liver. Some of these lesions are worth mentioning because aspiration cytology may be helpful as an initial diagnostic tool. A few selected entities are briefly discussed below.
- A first-line cytologic diagnosis would be important, allowing conservative clinical management in asymptomatic patients and in surgical high-risk patients.

- A comprehensive overview of the histomorphology of rare hepatic lesions is available in the corresponding *Atlas of the Armed Forces Institute of Pathology* [20].

#### 9.1.12.1 Cavernous Hemangioma

**Microscopic Features**

- Bloody aspirates.
- Groups of stromal cells occasionally showing nuclear pleomorphism.
- Rare endothelial cells.

A definite cytologic diagnosis is only possible in the context of imaging study results.

#### 9.1.12.2 Angiomyolipoma [22, 47, 49]

**Microscopic Features**

- Cytologic aspirates contain clusters of cells with arborizing intersecting endothelium.
- Smooth muscle cells: atypical cells exhibit enlarged nuclei, macronucleoli, and usually.
- Intranuclear cytoplasmic inclusions.
- No mitotic figures.

**Immunocytochemistry**

Staining for HMB-45 and smooth muscle actin (SMA) exhibits strong positivity.

#### 9.1.12.3 Myelolipoma

- The cellular specimen demonstrating trilineage hematopoiesis and a variable amount of mature adipose tissue.

#### 9.1.12.4 Dermoid Cyst

- The aspirate consists of scanty keratinous material and anucleated squamous cells.

### 9.1.13 Further Reading

The references are listed at the end of Sect. 9.2, p. 611.

**Figs. 9.1 and 9.2 Mesothelial cells: contaminant from the needle track.**

**Fig. 9.1** (case #1) A dissociating flat sheet of activated mesothelial cells in a patient with a history of long-standing cirrhosis. Note some mesothelial cells exhibiting bar-like intracytoplasmic refractile immunoglobulin deposits (arrows) (transcutaneous FNAB of liver, conventional smear, Pap stain, high magnification).

**Fig. 9.2** (case #2) Almost identical appearance of an aspirated mesothelial cell sheet in liquid-based preparation. Lymphocytes in the background (upper left and top) (transcutaneous FNAB of liver, ThinPrep, Pap stain, high magnification).

**Fig. 9.3A, B Normal liver parenchyma.**
FNAB of a 75-year-old woman's liver (direct smear, Pap stain). **A** Low magnification reveals numerous sheets of benign hepatocytes, variation in nuclear size and abundance of cytoplasm are obvious. An epithelial sheet originating from a small bile duct (arrows) and loose connective tissue (arrowhead) are also present. **B** Benign liver cells in detail. Variable nuclear size and abundant heavily granulated cytoplasm. Centrally placed nuclei show loose chromatin, sharply delineated inclusions, and prominent nucleoli. Binucleation is common. Nuclear enlargement and dark staining are due to DNA polyploidization. Bright golden cytoplasmic granules (e.g., lower left) represent lipofuscin.



**Fig. 9.4 Liver steatosis.**
Sheets of benign hepatocytes. Nuclei are displaced to the cellular margin by well-defined empty cytoplasmic vacuoles of varying size (FNAB of liver, direct smear, Pap stain, lower magnification).

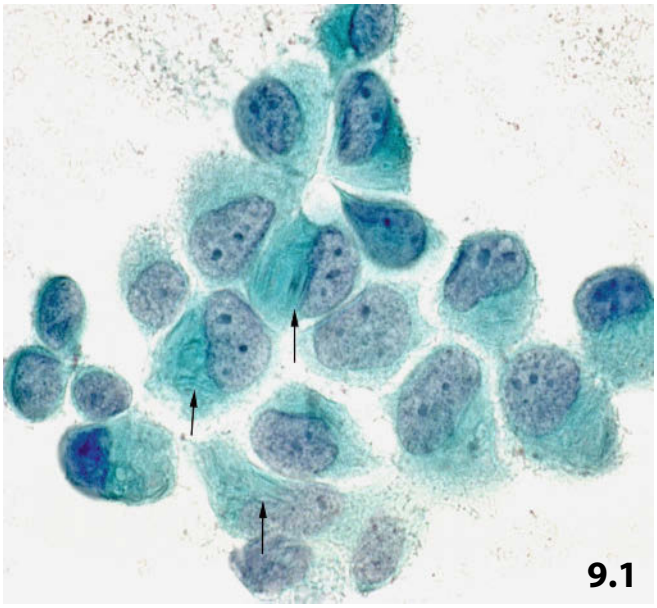
9.1

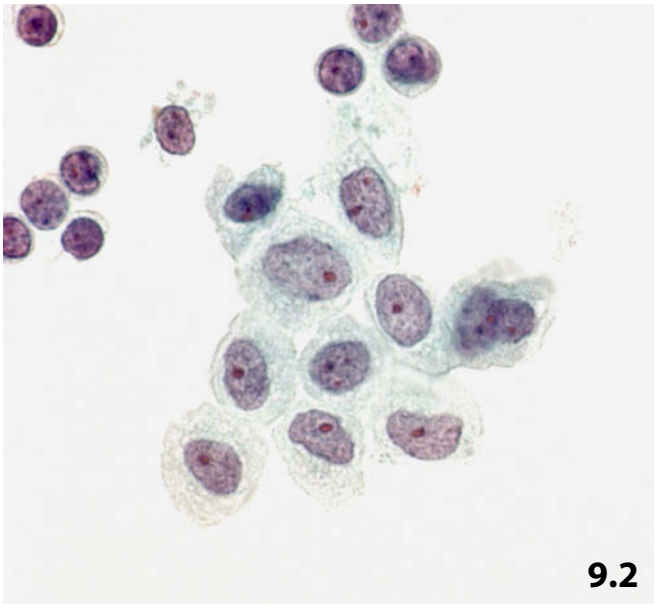
9.2

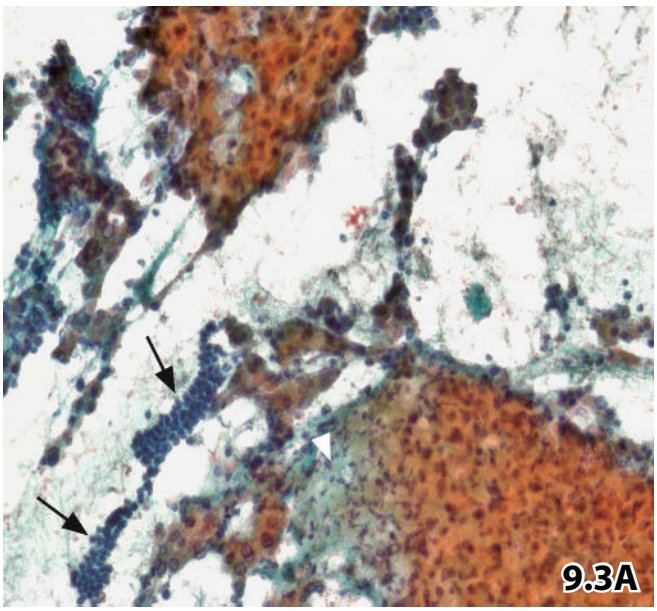
9.3A

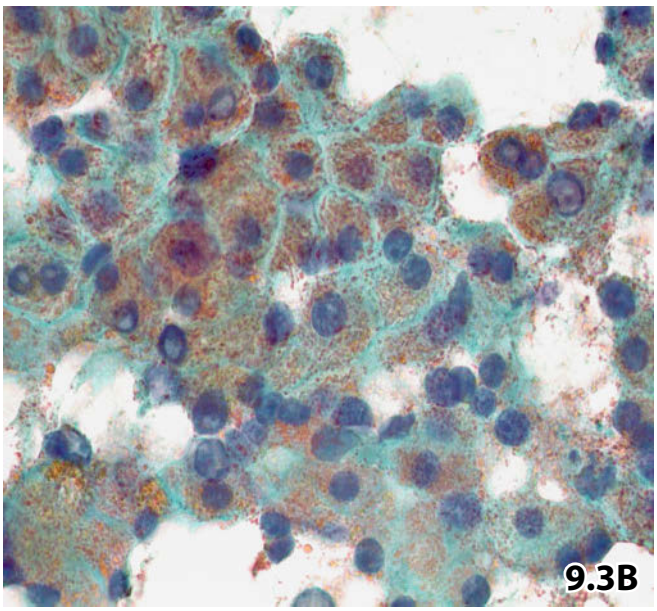
9.3B

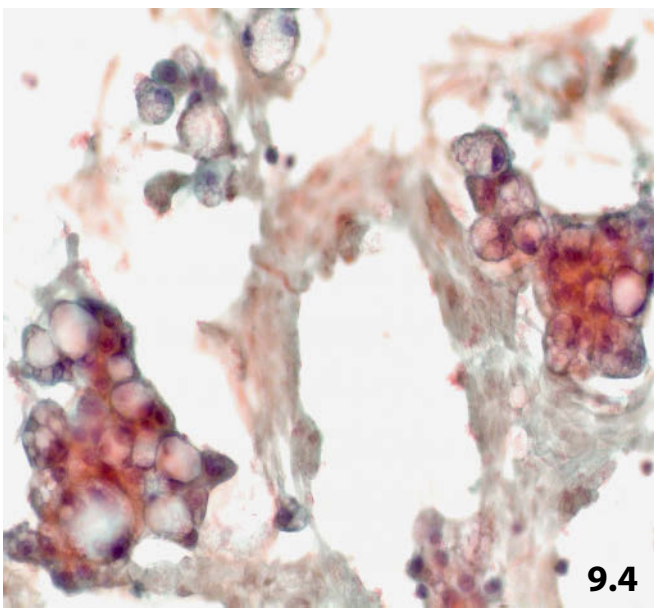
9.4

**Fig. 9.5 Abscess.**
A 17-year-old man presenting with a history of aplasia of his bone marrow and a recently detected hepatic mass. Transcutaneous FNAB was performed. Hyphae scattered in a purulent background are readily distinguishable using the Papnicolaou staining technique (direct smear, higher magnification).

**Fig. 9.6A–C Lymphocytosis.**
Imaging provided a vague hepatic lesion in the liver of an elderly woman. US-guided transcutaneous FNAB of the liver was performed. Aspirated material was processed using liquid-based method (ThinPrep) and the Pap staining technique. **A** Liquid-based specimens show numerous small and medium-sized lymphocytes. Note that the large nucleus associated with a prominent nucleolus (top) belongs to a degenerating hepatocyte. Immunocytochemical characterization of the lymphocytes can exclude a B-cell non-Hodgkin lymphoma. **B** Enumeration of T lymphocytes (CD3: 88% positive cells) (ThinPrep specimen, higher magnification). **C** Enumeration of B lymphocytes (CD20: 12% positive cells) (ThinPrep specimen, lower magnification).

**Figs. 9.7 and 9.8 Hydatid cyst.**
Hepatic echinococcosis in two patients presenting with voluminous cystic liver lesions. Hydatid disease was not ranked first in clinical diagnostic consideration. The two fine-needle aspirates provided completely different cytologic appearance (direct sediment smears, Pap stain).

**Fig. 9.7** (case #1) Smears containing numerous scolices (the larval stage of the parasite) that exhibit characteristic wreath of hooklets (higher magnification).
*Cytologic diagnosis:* Hydatid cyst.

**Fig. 9.8** (case #2) Bloodless and paucicellular fluid sediment containing opaque masses (chitin). Epithelioid cells and histiocytic giant cells were also present (not shown).
*Tentative cytologic diagnosis:* Necrotizing epithelioid cell granulomatosis comprising histiocytic giant cells. Definite diagnosis requires histologic examination.
*Tissue diagnosis: Echinococcus alveolaris* associated with pronounced granulomatous inflammation.
*Comment:* The cytologic specimens were completely devoid of pieces from the tapeworm.

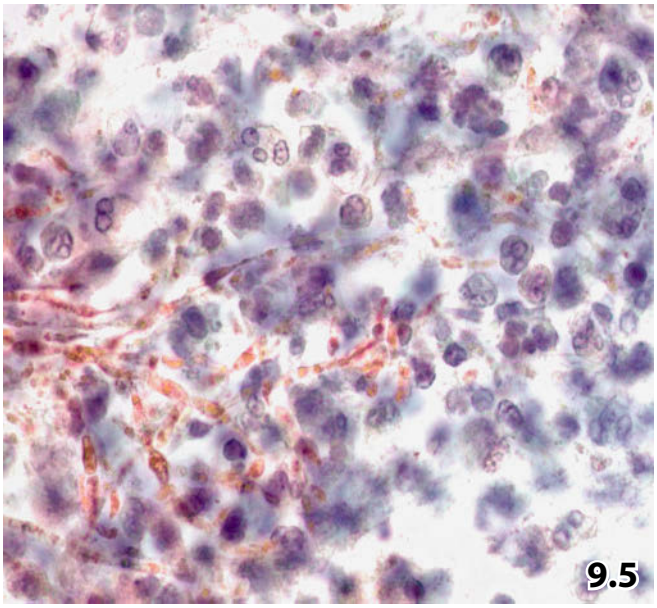
9.5

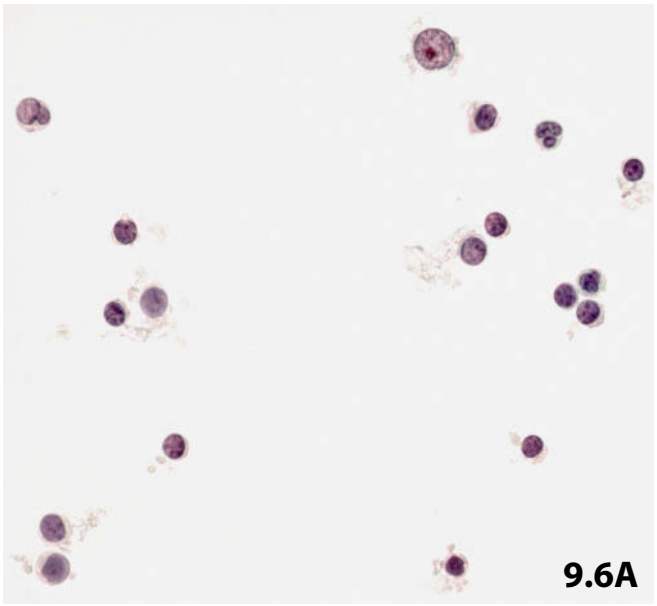
9.6A

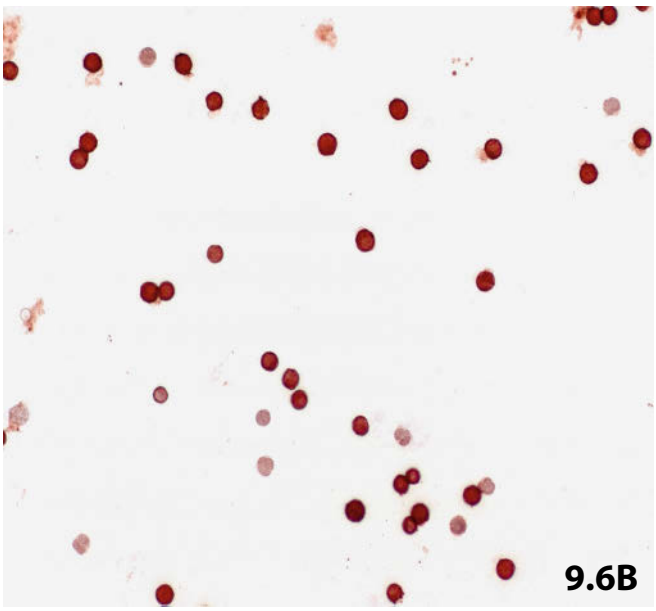
9.6B

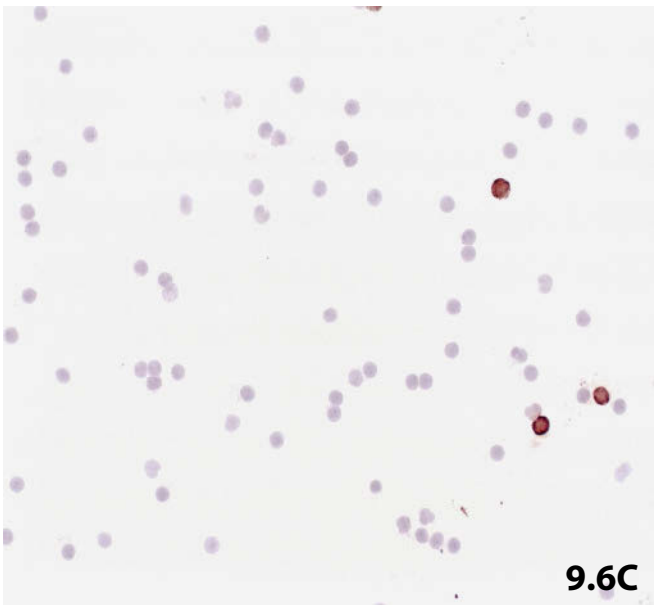
9.6C

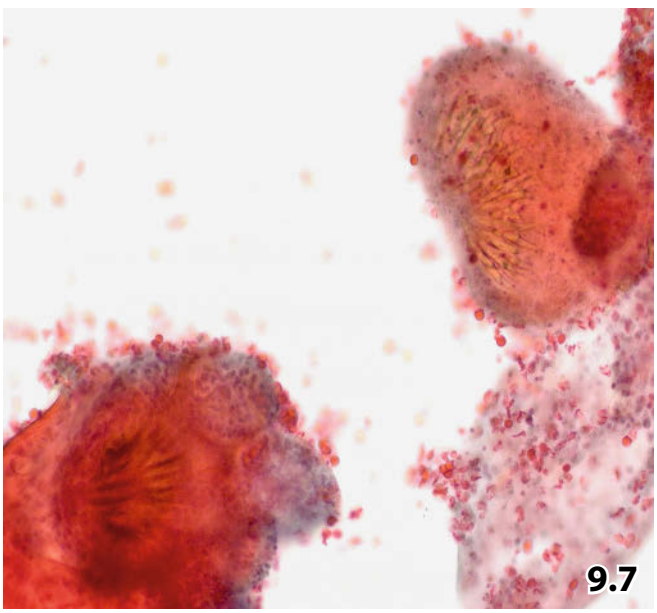
9.7

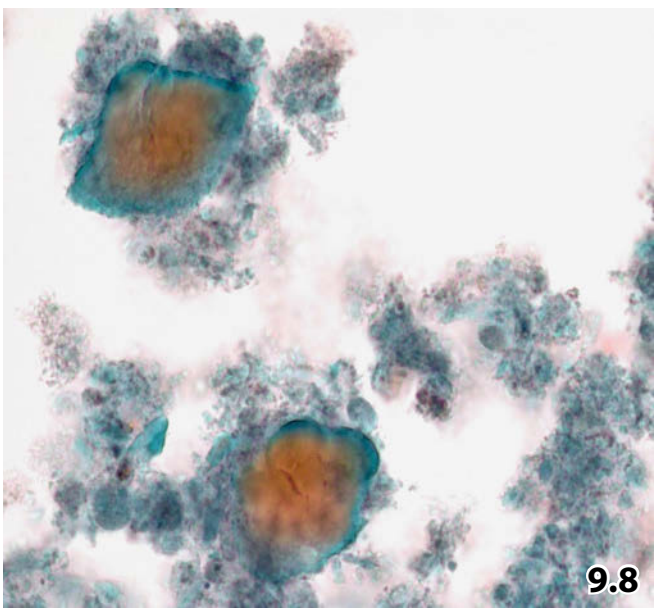
9.8

**Fig. 9.9A, B Cirrhosis.**
FNAB of a cirrhotic liver. Characteristic microscopic appearance at low- and high-power magnification (direct smears, Pap stain). **A** Low magnification: Polymorphic liver cells (upper left) and proliferating bile ductules (arrow) adherent to fragments of fibrotic and sclerotic stromal tissue (right). **B** High magnification: Hepatocytes originating from regenerative parenchyma nodules exhibit marked variation in cell size and nuclear shape. In addition, extreme variability of the nucleoli in size, shape, and number. Small-sized cell clusters, marked disparity of the hepatocytes, and the loose chromatin texture are indicators of a benign lesion.

**Figs. 9.10 and 9.11 Focal nodular hyperplasia.**
Focal nodular hyperplasia in liver aspirates of two patients, both of whom were middle-aged women. Direct smears were Pap-stained. The diagnosis was verified in both cases by histologic tissue examination.

**Fig. 9.10** (case #1) Very low magnification shows a large fragment of fibrous tissue encasing sheets of liver cells and clusters of bile duct cells (the epithelial cells being not in focus or obscured).



**Fig. 9.11** (case #2) Higher magnification reveals minor irregularities of the hepatocytes as compared with the marked cellular polymorphism in cirrhotic livers (compare with Fig. 9.9B). A strand of fibroblasts and fibrocytes crosses the liver parenchyma (bottom). A small ball-like cluster of bile duct cells is encountered at the top (arrow); distinct nucleoli are present but can barely be visualized.

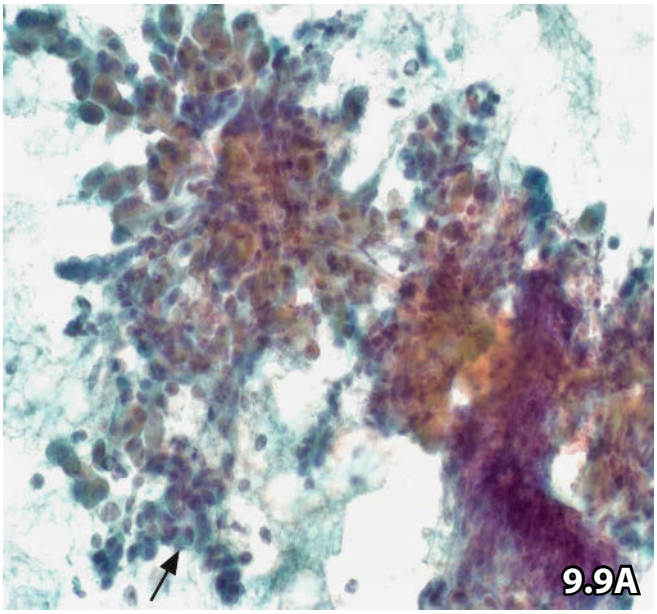
9.9A

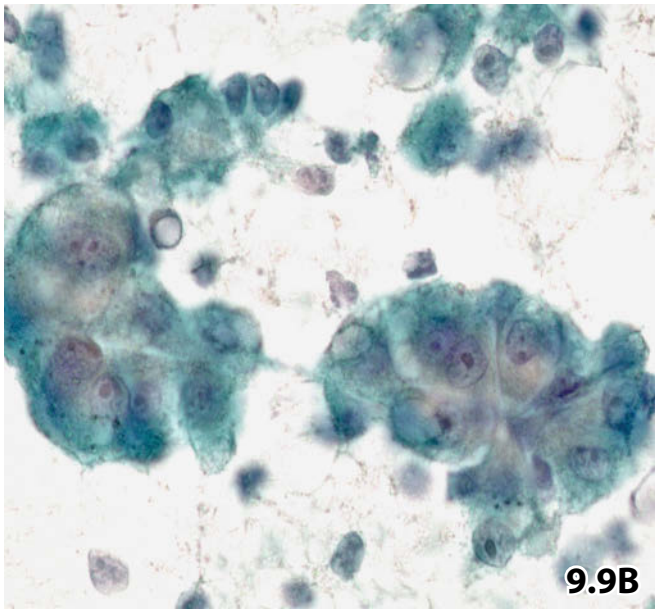
9.9B

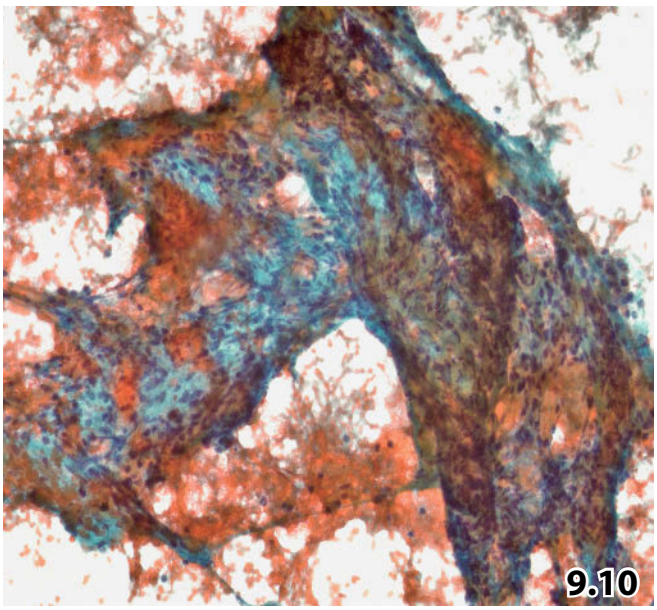
9.10

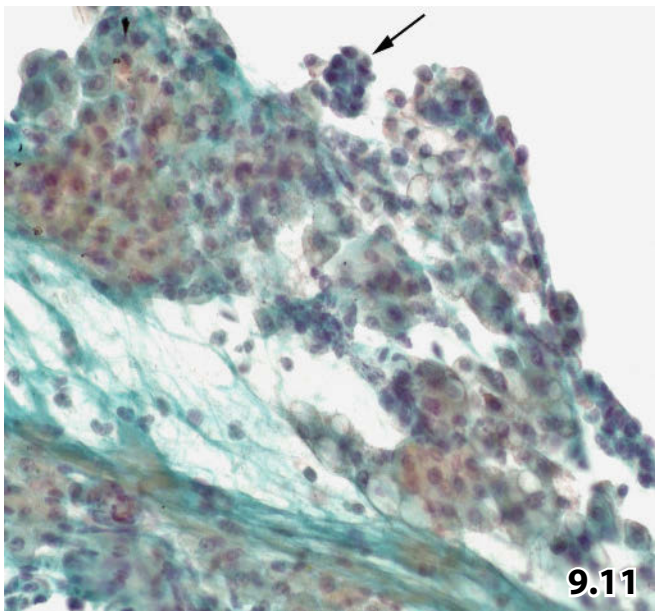
9.11

**Fig. 9.12 Liver cell adenoma.**
A 77-year-old woman had repeated FNAB of a nodule situated in the right lobe of her liver. Direct smears are rich in benign-looking hepatocytes and in a substantial number of stripped nuclei. The latter frequently are patternless and pale, sporadically occurring in aggregates. Occasional apoptotic changes (Pap stain, higher magnification). Both c*linical and cytologic findings* are consistent with liver cell adenoma. Surgical excision was not performed.

**Fig. 9.13 Tumor-forming hyperplasia of bile ductules.**
A 69-year-old man presented with a sharply defined nodular lesion in his liver (5 cm in diameter). Computed tomography suggested genuine liver tissue. Fine-needle aspirate provides numerous large sheets composed of benign uniform cuboidal and columnar epithelial cells in regular arrangement. The cell sheets occasionally exhibit papillary features. The nuclei show smooth margins and bland chromatin (direct smears, Pap stain, higher magnification).
*Cytology* suspected biliary adenoma or hamartoma. Exact tumor typing by cytology alone was not possible.
Neither histologic examination of liver tissue nor surgery were performed.

**Fig. 9.14 Liver cell dysplasia.**
FNAB of a nodule located in a 46-year-old woman's liver. Clinical examination and imaging studies suggested adenoma or hepatocellular carcinoma. Cellular direct smears exhibit a heterogeneous appearance of the hepatocyte population. Cells depicted in the figure represent normal hepatocytes, hepatocytes with reactive changes, and dysplastic cells (upper right). The latter show nuclear enlargement, irregular outline, and dense chromatin (Pap stain, high magnification).
*Cytology:* A definite cytologic diagnosis is not possible. Regenerative hepatic nodule, liver cell adenoma with atypias, and hepatocellular carcinoma are considered in the differential diagnosis.
*Tissue diagnosis* after liver resection: Liver cell adenoma exhibiting foci of dysplastic epithelium.

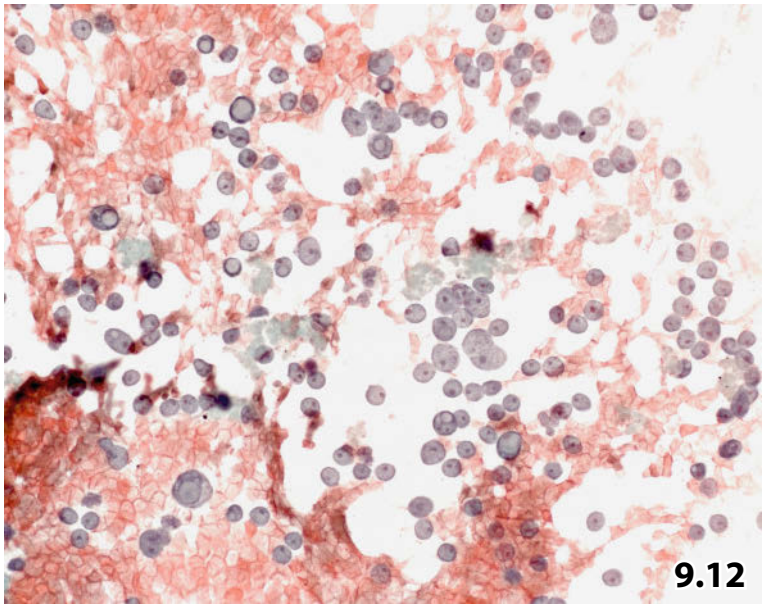
9.12

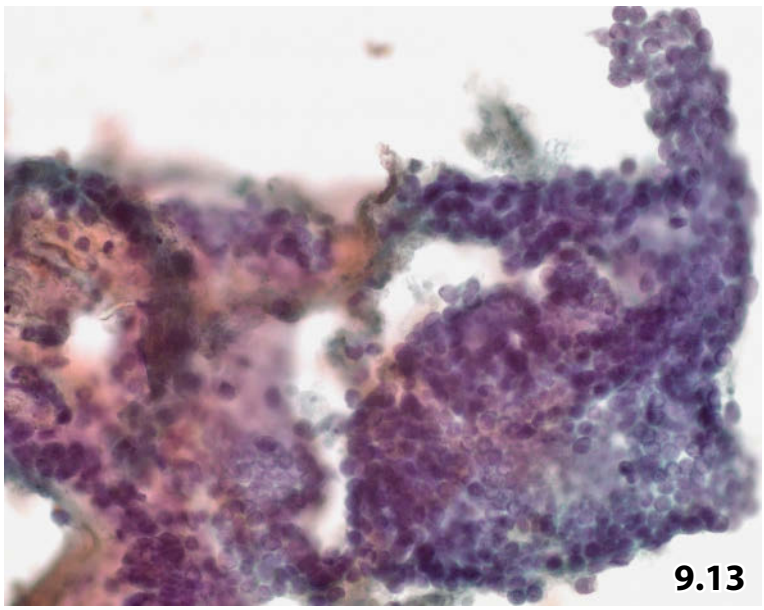
9.13

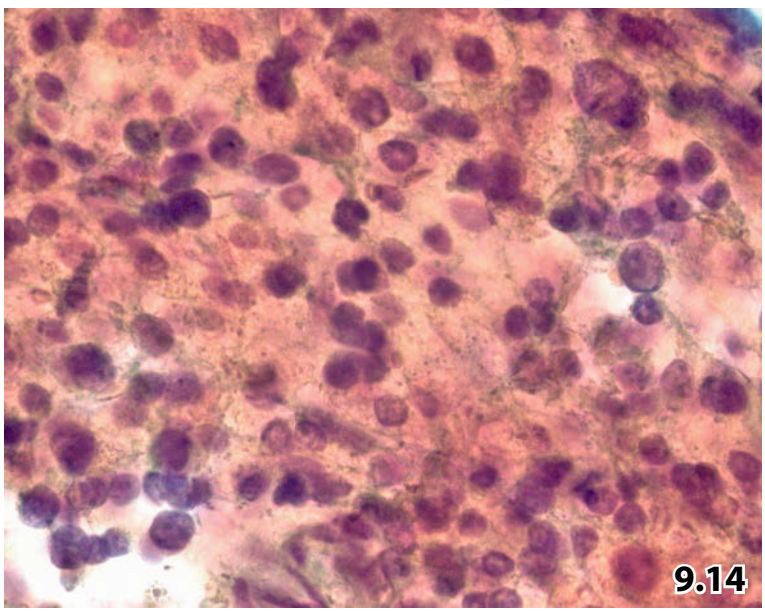
9.14

# Section 9.2
# Liver

## Malignant Lesions
## Corresponding Additional Analyses

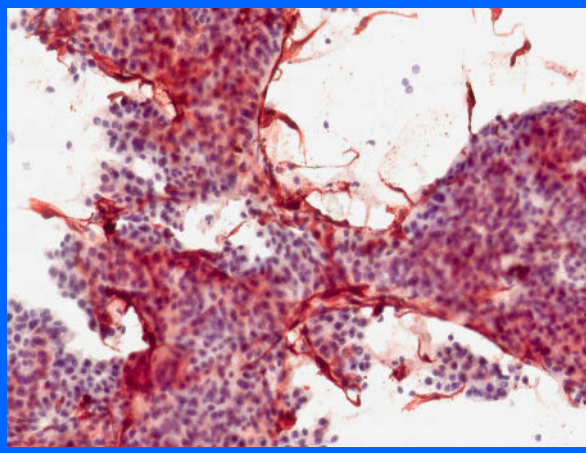

### 9.2.1 Hepatocellular Carcinoma (Figs. 9.15–9.21)

#### Etiology

- Various etiologies have been linked to the development of hepatocellular carcinoma (HCC): the most prominent are chronic hepatitis B and C virus infections, chronic alcohol consumption, and dietary ingestion of high levels of aflatoxin. In approximately 10% of all HCCs, the etiology remains unclear.
- However, epidemiologic data suggest that most of the cryptogenic HCCs develop due to nonalcoholic steatohepatitis.
- Cirrhosis from any cause is a predisposing factor for HCC and could be considered a premalignant condition. HCC is almost exclusively found in cirrhotic hepatitis C virus patients, while HCC may be found in hepatitis B virus patients with mild or absent cirrhosis [3].

#### General Comments

- The prevalence in FNAB specimens of the liver is roughly 40% for HCC, 10% for cholangiocarcinoma, and 50% for secondary tumors.
- Large tumors may comprise areas that are easier to recognize as malignant than others, an indication for extensive sampling (performing a high number of needle passes) and for the exact reading of all available smears, particularly in cases suggestive of well-differentiated HCC.
- The fairly specific serum alpha-fetoprotein (AFP) provides poor sensitivity for the diagnosis of HCC, especially in small well-differentiated tumors. Significant AFP elevation is expected in about 50–60% of all HCC cases.
- Hepatic neoplasms rarely occur in children and adolescents; however, primary malignant tumors such as hepatoblastoma are distinctly more frequent than benign lesions. Regarding cancers, most of them are metastatic: Wilms tumor, leukemias, and germ cell tumors.
- Multifocal growth of HCC is rather frequently encountered.
- Comprehensive overviews pertaining to neoplasms of the liver, algorithmic approach, and cytologic diagnosis of HCC have been published [15, 58, 59].

#### Microscopic Features

The microscopic features in cytologic smears listed below apply to HCCs of any grade of malignancy.

- Hallmarks of malignant hepatocellular tumors:
  - Excessive cellularity, the atypical/malignant cells are of the hepatocyte type.
  - Fingerlike ramification of large tumor cell sheets (Fig. 9.15).
  - Markedly enlarged nucleoli as compared with benign hepatocytes.
  - Atypical stripped nuclei. Stripped nuclei are hardly ever discerned in nonneoplastic liver lesions. The presence of atypical naked nuclei is almost conclusive for the diagnosis of HCC. In conventional smears, stripped nuclei exhibit a cauliflower shape and may typically be arranged in stripes (Fig. 9.18).
  - Endothelial cells: (1) coating smooth bordered tumor cell clusters or (2) outlining cellular trabeculae of irregular thickness or (3) accompanying sinusoi-

dal capillarization of tumor cell sheets [43] (Figs. 9.16 and 9.19).

- Cell-rich smears with large ramified clusters are highly suggestive of HCC; they are best seen at low magnification and macroscopically.
- Excessive nuclear pseudoinclusions may obscure both the typical malignant chromatin pattern and the nucleoli, hampering a correct diagnosis (Fig. 9.20).
- Clear cell change is due to cytoplasmic glycogen or lipid storage. Diffuse clear cell change occurs in about 10% of all HCC cases [59] (Fig. 9.21).
- Cytoplasmic fatty change producing large empty vacuoles can mislead to a diagnosis of benign hepatocytes from a liver with focal steatosis.
- Intracytoplasmic bodies and inclusions may be helpful in the diagnostic assessment of HCC:
  - Mallory bodies: Irregular in shape, eosinophilic, periodic acid-Schiff stain (PAS)-negative. Immunocytochemistry: Positivity with anti-ubiquitin antibodies.
  - Globular hyaline bodies: Round and homogeneous, PAS-positive. Immunocytochemistry: positive for alpha-1-antitrypsin.
  - Pale bodies: Round and amorphous. Immunocytochemistry: Positivity with anti-fibrinogen antibodies.
  - Ground glass inclusions: Rarely observed in tumors of HbsAg-positive patients.
    Immunocytochemistry: Positivity with anti-HbsAg antibodies.
- Bile pigment is encountered in both HCC and benign hepatocytic lesions but not in metastatic tumors. Bile appears as plugs or as cytoplasmic inclusions (Figs. 9.21B and 9.22).

Overviews as to HCC diagnostic features are presented in several publications [52, 59, 62].

**Caution**

- Diffuse clear-cell change of the cytoplasm of malignant hepatocytes occurs only sporadically, presenting diagnostic dilemmas; misinterpretation of non-hepatic neoplasms is possible (Fig. 9.21).
- Clinical and image-based data of multifocal liver lesions are often interpreted and reported as metastatic disease, an information that may affect objective pathology reporting. Therefore, the interpreter should rely strictly upon cytomorphologic features and immunocytochemical patterns for decision making.
- The appearance of intracytoplasmic inclusions and bile pigment may be dependent on the type of staining method used. Therefore, absence of these features cannot reliably be used for cytologic decision making.

#### 9.2.1.1 Well-Differentiated HCC (Figs. 9.23–9.25)

**Microscopic Features**

- Hallmarks:
  - Very well-differentiated HCC exhibit pronounced cellular monotony.
  - Hypercellular smears are dominated by large cohesive regular sheets and a three or more cell layer-thick trabecular meshwork, both sporadically delimited by a single layer of endothelial cells. Microacinar structures are present as well.
  - Features of sinusoidal capillaries [64].
  - Minimal nuclear atypia.
  - The malignant cells exhibit distinct hepatoid features, they are minimally enlarged compared to normal hepatocytes.
  - The nucleus is round, showing finely dispersed chromatin and one conspicuous, centrally located nucleolus.
  - Bile duct cells are completely absent.

**Differential Diagnosis**

It is difficult to separate well-differentiated HCC from:

- Regenerative liver parenchyma.
- Liver cell adenoma.
- Liver cell dysplasia of the large-cell type (see Sect. 9.1.11, p. 593).
- Well-differentiated neuroendocrine neoplasms exhibiting distinct granular cytoplasm, eccentric nuclei with indistinct atypias, inconspicuous nucleoli, and microacinar cell arrangement (see also Sect. 9.2.3, p. 607).

**Caution**

- Possible limitations for the cytologic diagnosis of very-well-differentiated HCC should always be kept in mind, especially in cases with interspersed slightly abnormal cells.
- Atypical small hepatocytes arranged in a microtrabecular or acinar smear pattern may refer to small-cell dysplasia, a diagnosis that is beyond the cytodiagnostic potential. Among other features, the size of the lesion gives direction to a conclusive diagnosis (see also Sect. 9.1.11, p. 593).

#### 9.2.1.2 Well- to Moderately Differentiated HCC

An accurate cytologic diagnosis can be rendered in almost all cases provided that a representative sampling is available.

**Microscopic Features**

- Hallmarks are the indispensable atypical or malignant cells of the hepatoid type comprising nuclear enlargement, densely packed granular chromatin, cleaved nuc-

lear membrane, and conspicuous polymorphous nucleoli that are centrally located.
- Further cytologic features diagnostic of HCC include large sheets with papillary fronds and to some extent trabecular architecture (more than two cells thick), smooth bordered tumor cell clusters focally delimited by endothelial cells, sinusoidal capillarization of tumor cell sheets, focal nuclear crowding, polymorphous stripped nuclei, and bile pigment.

#### 9.2.1.3 Poorly Differentiated HCC (Fig. 9.26)

**Microscopic Features and Differential Diagnosis**

Distinguishing poorly differentiated HCC from metastatic carcinoma and from nonmucinous cholangiocarcinoma is a well-recognized diagnostic problem. Poorly differentiated liver tumors are metastatic lesions in a high percentage of cases [52].

Therefore, it is important to search for and rely upon typical hepatocytic characteristics, clinical information, and serologic results.
- Intranuclear cytoplasmic inclusions are recognized in a high percentage of HCC cases but sporadically as well in patients with metastatic tumors such as in malignant melanoma, thyroid cancer, breast carcinoma, neuroendocrine tumors, and in adrenocortical carcinoma.
- Bile formation and the characteristic atypical naked nuclei (see Sect. 9.2.1, "Microscopic Features," p. 604) support the diagnosis of HCC.
- High levels of serum AFP are rarely observed in patients with liver metastases but in over 75% of patients suffering from HCC.

**Additional Comments**
- Obvious hepatoid cell characteristics may be rarely encountered in undifferentiated HCCs.
- HCC of the giant cell variant and spindle cell type is very rare. Spindle cells may represent a sarcomatous transformation of HCC [32].
- Tumor necrosis is rather frequent in the group of poorly differentiated HCC.

**Caution**
- Detection of bile pigment may also depend on the staining method applied in routine work-up [52].
- Large fat vacuoles in the cytoplasm of poorly differentiated HCC cells should not mislead to a diagnosis of signet ring cell adenocarcinoma. Mucin stains pink using the Papanicolaou staining method.
- Serum AFP can reach high levels in viral hepatitis and other benign liver disorders, but also in cancers of the intestinal compartment, the lung, and in a majority of germ cell tumors.

#### 9.2.1.4 Fibrolamellar Variant of HCC (Figs. 9.27 and 9.28)

**General Comments**
- Fibrolamellar HCC occurs in the liver of young patients with a more favorable outcome than the conventional HCC variants. Fibrolamellar HCC is rare and accounts for 1–2% of all HCCs.
- Morphologic key features, described below, together with clinical and radiographic data (the latter showing a well-demarcated tumor with a central scar on the CT scan) are very distinct and permit a specific diagnosis in most FNAB samples.

**Microscopic Features**
- Usually paucicellular cytologic specimens.
- Very large dispersed atypical hepatoid cells with abundant oncocytic cytoplasm and normal N/C ratio (at least three times the size of normal hepatocytes).
- Huge centrally located nucleus exhibiting the characteristic atypical, dense granular chromatin pattern.
- A solitary giant nucleolus.
- Cytoplasmic invaginations (pale bodies) and hyaline globules.
- Individual tumor cells and cell aggregates are separated by bands of fibrous tissue and bundles of collagen fibers along with activated fibroblasts.

Comprehensive overviews of fibrolamellar HCC have been reported by different authors [8, 21, 38].

**Differential Diagnosis**
- Differential diagnostic considerations should include benign hepatic lesions (hepatocellular adenoma and focal nodular hyperplasia) with pronounced reactive cell changes.
- The cytologic features may overlap those of a variety of metastatic malignancies exhibiting oncocytic features. However, cytomorphologic qualities of fibrolamellar HCC are sufficiently distinct in most cases.

### 9.2.2 Special Variants of HCC

#### 9.2.2.1 HCC of the Clear Cell Type [18, 50] (Fig. 9.21)

A diffuse clear cell pattern occurs in about 1% of all HCC cases [59].

**Microscopic Features and Differential Diagnosis**
- The cells are characterized by clear appearance of the cytoplasm due to the glycogen or lipid content.
- Nuclear features match those of common HCC variants.

Clear cell metastatic tumors from different distant primary sites often have a striking similar appearance and may morphologically be indistinguishable. The anatomic site of origin has to be established with immunocytochemical studies. Clear cell renal cell carcinoma seems to be by far the most frequent lesion giving rise to metastatic clear cell tumor in the liver. Immunocytochemistry using the monoclonal antibody for the renal cell carcinoma marker (RCCMa) is able to establish the majority of renal cell neoplasms (see also Sect. 9.2.7, p. 610). Clear cell carcinomas of other primary sites occur sporadically.

#### 9.2.2.2 HCC of the Small-Cell Type (Fig. 9.25)

**Microscopic Features**

- The typical trabecular-sinusoidal pattern of conventional HCCs is missing, but microtrabecular and microacinar cell arrangement of the hepatoid tumor cells may be observed.
- The cell-rich smears exhibit clusters of small uniform neoplastic cells.
- The nuclei are round to oval with irregular granular chromatin.
- Nucleoli are inconspicuous or even absent.
- The cytoplasm is usually indistinct.
- Sheets of normal bile duct epithelium may be encountered.

**Differential Diagnosis**

- Small-cell tumors in the liver can basically be classified into five groups [41]:
  - Small-cell liver primaries.
  - Neuroendocrine lesions, particularly small-cell variants.
  - Secondary small-cell carcinomas.
  - Nonepithelial small cell tumors.
  - Small round cell tumors including non-Hodgkin lymphoma, neuroblastoma, retinoblastoma, hepatoblastoma, nephroblastoma, rhabdomyosarcoma, small-cell anaplastic carcinoma, Ewing sarcoma, peripheral neuroectodermal tumor, and desmoplastic round cell tumor.
- Ancillary techniques are mandatory in order to establish a correct diagnosis.
- Fairly well-differentiated HCC of the small-cell type with scanty cytoplasm and microacinar cell pattern may resemble well-differentiated endocrine neoplasms (Fig. 9.25). Primary small-cell HCC can be elucidated by immunocytochemistry, the marker profile being consistent with HCC while neuroendocrine epitopes (see Sect. 9.2.3.4, "Immunocytochemistry," p. 608) are not expressed. Auxiliary information includes high serum AFP level and absence of extrahepatic tumoral lesions [39].
- Atypical small hepatocytes arranged in a microtrabecular or acinar smear pattern may refer to small-cell liver dysplasia, a diagnosis that is beyond cytodiagnostic potential. Among cytometric, clinical, and serologic features, a definite diagnosis is usually determined by the size of the tumoral lesion (see also Sect. 9.1.11, p. 593) [64].
- Differential diagnosis considerations of small-cell tumors of the liver have been emphasized in a recent report [23].

**Caution**

One has to keep in mind that neuroendocrine differentiation of liver cell carcinomas may occasionally occur.

### 9.2.3 Neuroendocrine Tumor

**General Comments**

- Neuroendocrine tumors (NET) in the liver may occur as solitary or multiple lesions. The overwhelming majority of these lesions represent metastatic involvement from a primary tumor located elsewhere, usually in the gastrointestinal tract (stomach, duodenum, small and large intestine, appendix, pancreas, and extrahepatic biliary system including gallbladder) or in endocrine glands (e.g., metastasis of a thyroid medullary carcinoma) (Fig. 9.34).
- On some occasions, typical endocrine tumors are seen in the liver in the absence of a neoplasm in any other site of the body. In this situation, it is appropriate to take the endocrine tumor for a hepatic primary. However, endocrine tumors in the gastrointestinal tract can be extremely small and may be missed during clinical and imaging investigation.
- In aspiration smears, well-differentiated neuroendocrine tumor and well-differentiated neuroendocrine carcinoma provide identical cytologic patterns. Therefore it is not possible to reliably assess malignancy or aggressiveness by cytology alone.
- Small-cell endocrine carcinoma represents the poorly differentiated end of the spectrum of neuroendocrine neoplasms.
- Neuroendocrine tumors are also discussed in Sect. 10.1.10, p. 646.

#### 9.2.3.1 Neuroendocrine Neoplasia of the Common Type (Figs. 9.29–9.33)

**Microscopic Features**

Hallmarks of common NET:

- Cell-rich samples with predominantly isolated monomorphic epithelial cells and loose cell clusters.
- The cells have a moderate amount of cytoplasm with more or less distinct reddish granulation and eccentrically placed nuclei. The tumor cells often exhibit plasmacytoid features.
- Conspicuous rosette-like and acinar formations.
- Stripped huge single nuclei are frequently interspersed (Fig. 9.30).

**Differential Diagnosis**

- Common NET may exhibit features similar to HCC. Immunocytochemical staining provides reliable help in confusing cases [45], see Sects. 9.2.3.4, "Immunocytochemistry", below and 9.2.7, p. 610 (Figs. 9.32 and 9.33).
- Hepatic metastases of breast cancer are common. Metastatic breast cancer consisting of monomorphous small to medium-sized tumor cells exhibiting eccentrically placed nuclei, a plasmacytoid cytoplasm, and granular cytoplasmic inclusions may strongly mimic neuroendocrine tumors (Figs. 1.68 and 1.70).

**Caution**

- Patients with established primary breast cancer and malignant cells in aspirates of their liver require the whole battery of appropriate immunocytochemical stains such as neuroendocrine markers, CK7, CK19, BRST2, mammaglobin, and hormone receptors, in order reach a correct diagnosis.
- One should always bear in mind that breast carcinomas may partially exhibit neuroendocrine differentiation.



### 9.2.3.2 Neuroendocrine Neoplasia of the Large-Cell Type (Fig. 9.31)

NET of the large-cell variant is a rare neoplasm; it is exclusively composed of large tumor cells.

**Microscopic Features**

- The cytologic specimens usually include branching sheets composed of large atypical hepatoid cells with a polygonal shape.
- The nuclei exhibit the characteristic dense granular chromatin and a prominent nucleolus.
- Eosinophilic granulation of the cytoplasm may be absent.

**Differential Diagnosis**

- Similar to common NET, the large-cell variant may exhibit morphologic features mimicking HCC (Fig. 9.31).
- Large-cell malignant NET is difficult to distinguish from metastatic carcinoma of the large-cell type, such as peripheral neuroectodermal tumor and in particular metastatic breast carcinoma (Fig. 9.34).

### 9.2.3.3 Poorly Differentiated Small-Cell Neuroendocrine Carcinoma

Poorly differentiated NET belongs to the group of small round cell tumors and is characterized by predominantly small round undifferentiated malignant cells posing differential diagnostic problems in cytologic and histologic practice. Cytomorphologic features along with ancillary tests are essential for the diagnostic accuracy [7] (see also Sect. 9.2.2.2, "HCC of the Small-Cell Type," p. 607).

**Microscopic Features**

The cytologic hallmarks are the same as described for small-cell anaplastic carcinoma in many different organs:

- Small rounded and fusiform cells are scattered throughout a cell-rich smear.
- The cells appear clumped, arranged in single files and in small tight balls.
- Cytoplasm is entirely absent or may appear as a narrow rim.
- Prominent nuclear hyperchromasia is not mandatory, but dyschromasia (in comparison with benign nuclei) is always present.
- The chromatin is densely granular or exhibits the typical salt and pepper pattern.

**Caution**

Neuroendocrine carcinomas with distinct spindle cell features are frequently encountered. A conclusive diagnosis can be reached using immunocytochemical studies.

### 9.2.3.4 Immunocytochemistry of NET (Figs. 9.31B, 9.32B, 9.32C)

- In most cases, the cytomorphologic features are sufficient to distinguish the endocrine nature of the cells under study. However, it is highly recommended to verify the endocrine nature of a tumor by immunocytochemical staining in each case.
- In ambiguous cases, an immunocytochemical panel consisting of antibodies for neuroendocrine antigens and other markers is needed for proper tumor identification.
- Immunocytochemical staining for hormones to verify specific hormonal cell products that may provide information as to the biological behavior of a tumor go beyond the scope of common cytologic practice.
- Generally approved neuroendocrine markers include:
  - Chromogranin A (CgA): CgA known as a component of the matrix of neurosecretory granules is a highly specific epitope for neuroendocrine tumors. However, CgA may provide negative immunoreactions in tumors with sparse or absent neurosecretory granules.
  - Synaptophysin: Synaptophysin also exhibits high specificity and additionally provides a better sensitivity than CgA.
  - Neuron-specific enolases (NSE).
  - TTF-1: TTF-1 nuclear positivity strongly indicating pulmonary origin of both small-cell cancer and differentiated NETs.

NETs of most other primary origins including those of the intestinal tract are reported to show negative TTF-1 expression. However, a nuclear positivity for TTF-1 may occur in approximately one-third of extrapulmonary small-cell cancers. Therefore, it is important to apply a panel of immunostains in order to determine the primary site of neuroendocrine tumors [29, 33].

– CD 56 (NCAM): NCAM is positive in most small-cell cancers and in NETs of the foregut. Tumors expressing CD56 positivity may show a more aggressive progress.

**Caution**

- It is well established that epithelial neoplasm originating from many different organs may express neuroendocrine differentiation. These tumors should be differentiated from true neuroendocrine lesions (Fig. 9.35).
- Besides pulmonary small-cell carcinoma, nuclear positivity for TTF-1 may also occur in approximately one-third of extrapulmonary small-cell cancers.

## 9.2.4 Intrahepatic Cholangiocarcinoma

(Figs. 9.36 and 9.37)

**General Comments**

- Predisposing factors for cholangiocarcinoma (CC) may include hepatolithiasis, sclerosing cholangitis, hemochromatosis, and liver fluke infection.
- Multifocality of CC is frequently encountered.

**Microscopic Features and Immunocytochemistry**

- Hallmark: FNAB of a liver lesion displaying typical features of adenocarcinoma combined with abundant mucus production is first and foremost suggestive of CC.
- CC usually appears as typical adenocarcinoma comprising a variable mucinous component.
- Besides the tubular component, a papillary pattern may be observed. Squamous component is rare.
- Other rare variants of CC such as spindle cell carcinoma have been reported [34].

The immunocytochemical workup may be helpful as CC cells stain positive for CK7 (stronger), CK20 (weaker), CA19-9, and p-carcinoembryonic antigen (pCEA). Unfortunately, the suggested panel cannot distinguish between CC and adenocarcinomas of the pancreas, the stomach, and the small intestine.

## 9.2.5 Uncommon Primary Liver Neoplasia in FNAB

### 9.2.5.1 Combined Hepatocellular Carcinoma and Cholangiocarcinoma

- This combined liver neoplasm is rare, accounting for 1–2% of all primary liver tumors. The question of whether the neoplastic populations originate from common progenitor cells or represent a synchronous tumor occurrence cannot be elucidated with certainty.
- A recent report on the clinicopathologic features and prognosis of these tumors is given by Koh et al. [24].

**Microscopic Features**

- For a conclusive cytologic diagnosis, unequivocal cell and tissue elements of HCC together with atypical mucin-producing columnar cells must be present. The latter show nuclear palisading, forming acinar and papillary structures. Intracytoplasmic and intratubular mucin production is variable.
- Intermediate cells that express equivocal morphologic characteristics of hepatoid and glandular cells are difficult to classify [13, 61].

**Caution**

True collision of HCC with a cholangiocarcinoma or with a metastatic adenocarcinoma is possible.

### 9.2.5.2 Hepatoblastoma

Hepatoblastoma is the most common primary malignant hepatic tumor in children and is affiliated with the group of small round cell tumors. Cytological findings and differential diagnoses are discussed in a study of 20 cases by Parikh et al. [36].

### 9.2.5.3 Angiosarcoma (Fig. 9.38)

Angiosarcoma is a rare primary malignant neoplasm of the liver with a poor prognosis. The etiology is unknown, but some cases are linked to the exposure of vinyl chloride monomer or inorganic arsenic, and the extensive use of androgenic anabolic steroids. The neoplasm accounts for 0.1% of primary liver malignancies.

The neoplastic cells may exhibit factor VIII and/or CD34, indicating an endothelial origin [26].

### 9.2.5.4 Other Rare Primary Tumors

- Other primary sarcomas, except for those mentioned above, have been reported as singular cases including primary hepatic malignant lymphoma. They are reviewed in the respective literature.

**Table 9.2.1** Most frequent liver metastases and their immunocytochemical features determining histogenesis and primary site of origin

| Tumor type | | Recommended immunopanels |
|---|---|---|
| Cancer of the large bowel | | **CK20, CDX-2,** CK7 |
| Pancreatic cancer<br>Bile duct cancer | | **CK7, CK20 (weak), CA19-9** |
| Lung cancer | Adenocarcinoma | **CK7, TTF-1,** CK20 |
| | Squamous cell carcinoma | **CK 5/6** |
| | Small-cell carcinoma | **TTF-1, endocrine AGs** |
| Breast cancer | | **CK7**, CK20<br>**Mammaglobin**<br>**Hormone receptors** |
| Gastric cancer | | No specific epitopes |
| Endocrine neoplasia<br>Endocrine carcinoma | | **Endocrine AGs** (for details see Sect. 9.2.3.4, "Immunocytochemistry," p. 608. |
| Malignant melanoma, pigmented and nonpigmented | | **Melan A, HMB-45, S100** |
| Hepatic manifestation of malignant lymphoma | | **CD45*, CD20, CD3, PCR / fragment analysis**<br>Pan-cytokeratin (e.g., MNF116)* |
| Other neoplasms | | Dependent on differential diagnostic considerations; see also Sect. 9.2.7, below. |

AG = Antigen

**Bold text**: immunopanel reliably diagnostic for the referred tumor entity.

* Differentiate anaplastic large-cell carcinoma from large-cell anaplastic NHL and vice versa.



- Sporadically, a primary hepatic squamous cell carcinoma may originate in congenital liver cysts or from an intrahepatic tumor of the germ cell type [44]. The need to search for another primary tumor site is self-evident.

## 9.2.6 Metastatic Tumors

### General Comments

- The assessment of the primary tumor site requires a reliable clinicopathologic correlation and the whole battery of immunocytochemical stains. Initial careful microscopic evaluation of the cell morphology is essential in the work-up of a lesion. Applying an adequate immunopanel may be difficult in those cases providing either too few smears or specimens with too few cells for auxiliary analyses.
- Secondary liver lesions are frequently necrotic in the central areas, a condition that should oblige radiologists and gastroenterologists to needle both the central part and multiple marginal areas of the tumor mass, whenever possible with image guidance.
- Completely necrotic metastasis of a pigmented malignant melanoma can for once be properly identified based on pronounced aggregation of the pathognomonic melanin pigment (Fig. 9.39).
- Several reports deal with diagnostic dilemmas of malignant lesions of different types in liver aspirates [6, 23, 42].

### Immunocytochemistry

The most frequent cancers metastasizing to the liver and their immunocytochemical characteristics are shown in Table 9.2.1.

**Caution**

- HCC, endocrine neoplasia, and intrahepatic cholangiocarcinoma must always be taken into consideration in cases where clinical and imaging investigations report a multifocal liver lesion.
- Clinical and image-based findings should not interfere with the cytomorphologic considerations.
- In cases with an established extrahepatic primary tumor, an additional primary liver neoplasia and an additional secondary cancer metastasizing to the liver must always be considered.

## 9.2.7 Comments on Additional Analyses for Malignant Liver Lesions (Selected Topics)

### Immunocytochemistry

- *Hepatocyte markers:* Cells of HCC may exhibit diffuse cytoplasmic immunoreactivity for both AFP and Hep Par 1/human hepatocyte AG. AFP is fairly specific for HCC but provides low sensitivity (immunopositivity in about 50% of all cases). At our institution, a better sensitivity for cytology was achieved with HepPar 1, which is reported

in the literature to be the most sensitive marker for HCC [57].

- *pCEA* may be helpful to distinguish clear and small-cell variants of HCC from neuroendocrine tumors and metastasis of renal cell carcinoma, respectively [60].
- *Neuroendocrine markers:* S100, neuron-specific enolase (NSE), chromogranin A, and synaptophysin are negative in HCC but positive in neuroendocrine tumors with strong reliability.
- *CD34 and factor VIII* expose endothelial cells and basement membrane deposits coating tumor cell clusters and reveal sinusoidal capillarization. A diffuse or focal reaction can be observed in HCC [9, 43]. A specific immunopositive endothelial cell pattern is highly sensitive and specific for HCC; it is helpful to differentiate between HCC and benign hepatocytic lesions such as liver cell adenoma and focal nodular hyperplasia, which express endothelial cells as well [12, 43, 48].
- *TTF-1* is considered a reliable marker for metastatic adenocarcinoma of the lung and the thyroid. Small-cell carcinoma with neuroendocrine features may also exhibit nuclear TTF-1 positivity, in particular primary lung NETs.
- *Renal cell carcinoma marker (RCC Ma)* is a monoclonal antibody with a high specificity for renal cell carcinoma, particularly in its clear cell and papillary variant. However, its sensitivity is reported to be higher in primary (80%) than in secondary (67%) tumors. It is essential to keep in mind that breast carcinoma is the most important tumor within which RCC Ma immunoreactive tumor cells may arise.
- *Lymphocytic markers:* Enumeration of B lymphocytes (CD20) and T lymphocytes (CD3) frequently facilitate distinguishing between reactive lymphoproliferative lesions and malignant lymphoma.
- *CD10* is useful distinguishing between HCC and non-HCC malignancies. The sensitivity for HCC is reported to reach more than 50%.
- Further selective immunopanels are suggested by different authors [19, 35].
- A comprehensive list including immunomarkers for the differentiation of nonlymphoid tumors is presented in Sect. 15.3.24 Table 15.3.3, p. 978.

### Molecular Genetics

If B- and T-lymphocyte enumeration is not diagnostic, polymerase gene amplification in combination with fragment analysis using nuclear DNA obtained from cells scraped off the cytologic smears can establish the clonality of a lymphoid population in most cases (for details see Sect. 15.1.4.3, “Molecular Genetics,” p. 911).

### DNA Ploidy

Cytophotometric ploidy analysis may be convenient to assess dysplastic or malignant cell change in hepatocytic tumors and in equivocal epithelial cell populations of the pancreas and biliary duct system (see Sect. 10.1.3.2, “DNA Ploidy Analysis”, p. 635).

**Caution**

- Pancytokeratin immunostaining is indispensable in distinguishing between large-cell carcinoma and blastic NHL on aspirates from liver malignancies providing just a few poorly differentiated malignant cells.
- Be aware that poorly differentiated tumor cells may lack immunocytochemical expression of certain tumor markers.
- Pronounced degenerative changes of liver metastases are well known. Consequently, immunocytochemical results on degenerate cytologic material should be interpreted with caution.

## 9.2.8 Further Reading


1. Bhat DM, Pangarkar MA, Gadkari RU, et al. Ameboma in Ultrasound-Guided Fine-Needle Aspiration. Acta Cytol 2004;48:873-874.
2. Bioulac-Sage P, Rebouissou S, Thomas C, et al. Hepatocellular adenoma subtype classification using molecular markers and immunohistochemistry. Hepatology 2007;46:740-748.
3. But DY, Lai CL, Yuen MF. Natural history of hepatitis-related hepatocellular carcinoma. World J Gastroenterol 2008;14:1652-1656.
4. Colovic R, Grubor N, Micev M, Radak V. Hepatocellular adenoma with malignant alteration. Hepatogastroenterology 2007;54:386-388.
5. Dardi LE, Marzano M,Froula E. Fine Needle Aspiration Cytologic Diagnosis of Focal Intrahepatic Extramedullary Hematopoiesis. Acta Cytol 1990;34:567-569.
6. Das DK. Cytodiagnosis of Hepatocellular Carcinoma in Fine-Needle Aspirates of the Liver: Its differentiation from Reactive Hepatocytes and Metastatic Adenocarcinoma. Diagn Cytopathol 1999;21:309-318.
7. Das DK. Fine-needle aspiration (FNA) cytology diagnosis of small round cell tumors: value and limitations. Indian J Pathol Microbiol 2004;47:331-336.
8. Davenport RD. Cytologic Diagnosis of Fibrolamellar Carcinoma of the Liver by Fine-Needle Aspiration. Diagn Cytopathol 1990;6:275-279.
9. de BoerWB, Segal A, Frost FA,Sterrett GF. Can CD 34 discriminate between benign and malignant hepatocytic lesions in fine-needle aspirates and thin core biopsies. Cancer Cancer Cytopathol 2000;90:273-278.
10. Devaney K, Goodman ZD, Ishak KG. Hepatobiliary cystadenoma and cystadenocarcinoma. A light microscopic and immunohistochemical study of 70 patients. Am J Surg Pathol 1994;18: 1078-1091.
11. El-Sayed SS, El-Sadany M, Tabll AA, et al. DNA ploidy and liver cell dysplasia in liver biopsies from patients with liver cirrhosis. Can J Gastroenterol 2004;18:87-91.
12. Fischer HP,Flucke U, Zhou H. Pathology along the liver sinusoids: endothelial and perisinusoidal findings. Pathologe 2008;29:37-46.
13. Gibbons D, de las Morenas A. Fine needle aspiration diagnosis of combined hepatocellular carcinoma and cholangiocarcinoma. A case report. Acta Cytol 1997;41:1269-1272.
14. Gigot JF, Geubel A,Haot J, et al. Papillomatose des voies biliares. Acta Endoscopica 1989;19:345-366.

15. Goodman ZD. Neoplasms of the liver. Mod Pathol 2007;20 Suppl 1:S49-60.
16. Gunven P, Auer G, Gerdes U, et al. Molecular and virological studies on a rare case of biliary papillomatosis. Anticancer Res 2006;26:2205-2208.
17. Guy CD, Ballo MS. Fine needle aspiration biopsy of the liver. Adv Anat Pathol 1999;6:303-316.
18. Hughes JH, Jensen CS, Donnelly AD, et al. The role of fine-needle aspiration cytology in the evaluation of metastatic clear cell tumors. Cancer 1999;87:380-389.
19. Hurlimann J,Gardiol D. Immunohistochemistry in the differential diagnosis of liver carcinomas. Am J Surg Pathol 1991;15:280-288.
20. Ishak KG, Goodman ZD, Stocker JT. In Atlas of Tumor Pathology. Tumors of the liver and intrahepatic Bile Ducts 3rd series, fascicle 31, Juan Rosai (ed.) Armed Forces Institute of Pathology, Washington D.C., 2001, pp. 271-323.
21. Jain M, Niveditha SR, Bharadwaj M, Pathania OP. Cytological features of fibrolamellar variant of hepatocellular carcinoma with review of literature. Cytopathology 2002;13:175-188.
22. Kha I, Cartwright D, Guis M, et al. Angiomyolipoma of the liver in Fine-Needle Aspiration Biopsies. Its distinction from hepatocellular carcinoma. Cancer (Cancer Cytopathol) 1999;87:25-30.
23. Khalbuss WE, Grigorian S, Bui MM,Elhosseiny A. Small-cell tumors of the liver:a cytologic study of 91 cases and a review of the literature. Diagn Cytopathol 2005;33:8-14.
24. Koh KC, Choi MS, Lee Jh, et al. Clinicopathologic features and prognosis of combined hepatocellular cholangiocarcinoma. Am J Surg 2005;189:120-125.
25. Koo JS, Kim H, Park BK, et al. Predictive value of liver cell dysplasia for development of hepatocellular carcinoma in patients with chronic hepatitis B. J Clin Gastroenterol 2008;42:738-743.
26. Liang-Che Tao. Liver and Pancreas. In: Bibbo M. (ed). Comprehensive Cytopathology. W.B. Saunders Company, Philadelphia, 1991,pp.839-840.
27. Libbrecht L, Craninx M, Nevens F, et al. Predictive value of liver cell dysplasia for development of hepatocellular carcinoma in patients with non-cirrhotic and cirrhotic chronic viral hepatitis. Histopathology 2001;39:66-73.
28. Lin CC, Lin CJ, Hsu CW, et al. Fine-needle aspiration cytology to distinguish dysplasia from hepatocellular carcinoma with different grades. J Gastroenterol Hepatol 2007;23: e 146-152.
29. Lin X, Saad RS, Luckasevic TM, Silverman Jf, Liu Y. Diagnostic value of CDX-2 and TTF-1 expressions in separating metastatic neuroendocrine neoplasms of unknown origin. Appl Immunohistochem Mol Morphol 2007;15:407-414.
30. Lizardi-Cervera J, Cuéllar-Gamboa L, Motola-Kuba D. Focal nodular hyperplasia and hepatic adenoma. a review. Ann Hepatol 2006;5:206-211.
31. Lucas SB. Other viral and infectious diseases and HIV-related liver disease. in: MacSween's Pathology of the liver 5th edition, ed. by AD Burt, Churchill Livingston Elsevier, 2007; pp:455-472.
32. Maeda T, Adachi E, Kajiyama K, et al. Spindle cell hepatocellular carcinoma. Cancer 1996;77:51-57
33. McCluggage WG, Sargent A, Bailey A, Wilson GE. Large cell neuroendocrine carcinoma of the uterine cervix exhibiting TTF-1 immunoreactivity. Histopathology 2007;51:405-407.
34. Ng CS, Suen MWM, Mok SD, Li AKC. Spindle cell carcinoma of bile duct origin. Histopathology 1988;12:329-340.
35. Onofre AS, Pomjanski N, Buckstegge B, Böcking A. Immunocytochemical diagnosis of hepatocellular carcinoma and identification of carcinomas of unknown primary metastatic to the liver on fine-needle aspiration cytologies. Cancer 2007;111:259.268.
36. Parikh B, Jojo A, Shah B, et al. Fine needle aspiration cytology of hepatoblastoma: a study of 20 cases. Indian J Pathol Microbiol 2005;48:331-336.
37. Pavic M, Le Pape E, Debourdeau P, et al. Non-tuberculous sytemic granulomatosis mimicking sarcoidosis but related to a specific etiology.Study of 67 cases. Rev Med Intern 2008;29:5-14.
38. Pérez-Guillermo M, Masgrau NA, Garcia-Solano J, et al. Cytologic aspect of fibrolamellar hepatocellular carcinoma in Fine-Needle Aspirates. Diagn Cytopathol 1999;21:180-187.
39. Piatti B, Caspani B, Giudici C, Ferrario D. Fine Needle Aspiration Biopsy of Hepatocellular Carcinoma resembling Neuroendocrine Tumor. A case report. Acta Cytol 1997;41:583-586.
40. Pinto MM, Kaye AD. Fine needle aspirate of cystic liver lesions. Cytologic examination and carcinoembryonic antigen assay of cyst contents. Acta Cytol 1989;33:852-856.
41. Pisharodi LR, Lavoie R, Bedrossian C. Differential Diagnostic Dilemmas in Malignant Fine-Needle Aspirates of Liver: A Practical Approach to Final Diagnosis. Diagn Cytopathol 1995;12:364-371.
42. Pisharodi LR, Bedrossian C. Diagnosis and Differential Diagnosis of small-cell lesions of the liver. Diagn Cytopathol 1998;19:29-32.
43. Pitman MB, Szyfelbein WM. Significance of endothelium in the fine-needle aspiration biopsy diagnosis of hepatocellular carcinoma. Diagn Cytopathol 1995;12:208-214
44. Pliskin A, Cualing H, Stenger RJ. Primary squamous cell carcinoma originating in congenital cysts of the liver. Report of a case and review of the literature. Arch Pathol Lab Med 1992;116:105-107.
45. Prosser JM, Dusenbery D. Histocytologic diagnosis of neuroendocrine tumors in the liver: a retrospective study of 23 cases. Diagn Cytopathol 1997;16:383-391.
46. Rooks JB, Ory HW, Ishak KG, et al. Epidemiology of hepatocellular adenoma. The role of oral contraceptive use. JAMA 1979;242:644-648.
47. Rouquie D, Eggenspieler P, Algayres JP, et al. Malignant-like angiomyolipoma of the liver: report of one case and review of the literature. Ann Chir 2006;131:338-341.
48. Ruck P, Xiao JC, Kaiserling E. Immunoreactivity of sinusoids in hepatocellular carcinoma. An immunohistochemical study using lectin UEA-1 and antibodies against endothelial markers, including CD 34. Arch Pathol Lab Med 1995;119:173-178.
49. Sawai H, Manabe T, Yamanaka Y, et al. Angiomyolipoma of the liver: case report and collective review of cases diagnosed from fine needle aspiration biopsy specimens. Hepatobiliary Pancreat Surg 1998;5:333-338.,
50. Singh HK, Silverman JF, Geisinger KR. Fine-Needle Aspiration Cytomorphology of Clear-Cell Hepatocellular Carcinoma. Diagn Cytopathol 1997;17:306-310.
51. Singh P, Erickson RA, Mukhopadhyay P, et al. EUS for detection of the hepatocellular carcinoma: results of a prospective study. Gastrointest Endosc 2007;66:265-273.
52. Soyuer I, Ekinci C, Kaya M, et al. Diagnosis of Hepatocellular carcinoma by Fine Needle Aspiration Cytology. Cellular features. Acta Cytol 2003;47:581-589.
53. Tao L-C. Are oral conceptive – associated Liver Cell Adenomas premalignant? Acta Cytol 1992;36:338-344.
54. Tsui WM, Lam PW, Mak CK, Pay KH. Fine-needle aspiration cytology diagnosis of intrahepatic biliary papillomatosis(intraductal papillary tumor): report of three cases and comparative study with cholangiocarcinoma. Diagn Cytopathol 2000;22:293-298.
55. Vassiliou I, Kairi-Vassilatou E,Marinis A, et al. Malignant potential of intrahepatic biliary papillomatosis: a case report and review of the literature. World J Surg Oncol 2006;4:71.
56. Vick DJ, Goodman ZD, Deavers MT, et al. Ciliated hepatic foregut cyst: a study of 6 cases and review of the literature. Am J Surg Pathol 1999;23:671-677.
57. Wang L, Vuolo M, Suhrland MJ, Schlesinger K. HepPar1, MOC-31, pCEA, mCEA and CD10 for distinguishing hepatocellular carcinoma vs. metastatic adenocarcinoma in liver fine needle aspirates. Acta Cytol 2006;50:257-262.
58. Wang P, Meng ZQ, Chen Z, et al. Diagnostic value and complications of fine needle aspiration for primary liver cancer and its influence on the treatment outcome. a study based on 3011 patients in China. Eur J Surg Oncol 2008;34:541-546.
59. Wee A, Nilsson B, Tan LKA, Yap Ivy. Fine Needle Aspiration Biopsy of Hepatocellular Carcinoma. Acta Cyto 1994;38:347-354.

60. Wee A, Nilsson B. pCEA canalicular immunostaining in fine needle aspiration biopsy diagnosis of hepatocellular carcinoma. Acta Cytol 1997;41:1147-1155.
61. Wee A, Nilsson B. Combined hepatocellular-cholangiocarcinoma. Diagnostic challenge in hepatic fine needle aspiration biopsy. Acta Cytol 1999;43:131-138.
62. Wee A. Fine needle aspiration biopsy of the liver: Algorithmic approach and current issues in the diagnosis of hepatocellular carcinoma. CytoJournal 2005;2:7.
63. Wheeler DA, Edmondson HA. Cystadenoma with mesenchymal stroma(CMS) in the liver and bile ducts. A clinicopathologic study of 17 cases, 4 with malignant change. Cancer 1985;56:1434-1445.
64. Yang GCH, Yang G-Y, Tao L-C. Cytologic features and histologic correlations of microacinar and microtrabecular Types of well-differentiated Hepatocellular Carcinoma in Fine-Needle Aspiration Biopsy. Cancer (Cancer Cytopathol) 2004;102:27-33.
65. Zen Y, Fujii T,Itatsu K, et al. Biliary papillary tumors share pathological features with intraductal papillary mucinous neoplasm of the pancreas. Hepatology 2006;44:1333-1343.
66. Zucman-Rossi J, Jeannot E, Nhieu JT, et al. Genotype-phenotype correlation in hepatocellular adenoma: new classification and relationship with HCC. Hepatology 2006;43:515-524.

**Figs. 9.15–9.22 Common cytologic features of hepatocellular carcinoma and possible diagnostic pitfalls.**
Basic cytomorphology of hepatocellular carcinoma (HCC) is presented by use of FNAB material from different patients having verified hepatocellular carcinoma by histology or clinical follow-up. Conventional smear preparation was performed except in one case. All specimens were Pap-stained.

**Fig. 9.15** (case #1) Very low magnification exhibits typical fingerlike ramification of the tumor cell clusters.

**Fig. 9.16A, B** (case #2) Cytoarchitecture and endothelial cells are brought into focus. **A** Higher magnification shows three-dimensional papilliform and ball-like arrangement of the tumor cells. Note loss of nuclear polarity and clearly visible endothelial cells (often incompletely in focus) coating the tumor cell clusters (arrows). **B** CD34 immunostain is very useful to visualize endothelial cells (Pap-prestained smear).

**Figs. 9.17 and 9.18** (case #3) Image details highlighting the cellular morphology of HCC.



**Fig. 9.17** Tumor cells basically exhibit hepatoid features. Nuclei show eccentric position, loss of polarization, overlapping, and irregular outline. Nucleoli are larger in size and may occur multiply, unlike in benign hepatocytes. The chromatin is dense but unevenly distributed and coarsely clumped.

**Fig. 9.18** Naked tumor cell nuclei may exhibit pronounced cleaving and lobulation resulting in cauliflower-like appearance.

**Fig. 9.19** (case#4) Liquid-based preparation.
Detail of a tumor cell cluster depicted from a liquid-based preparation (ThinPrep®). Cytoarchitecture and cellular details, in particular the peripheral layer of endothelial cells are immediately recognized. A substantial number of cells show nuclear shrinking caused by liquid-based processing of the aspirate (arrows).

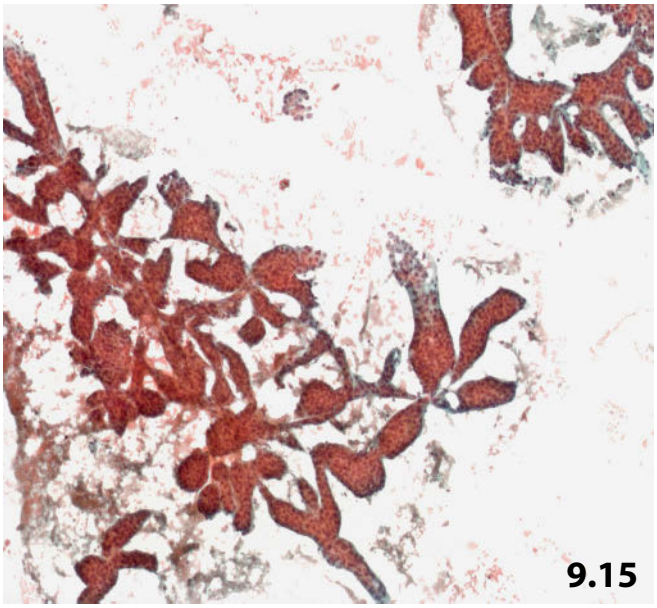
9.15

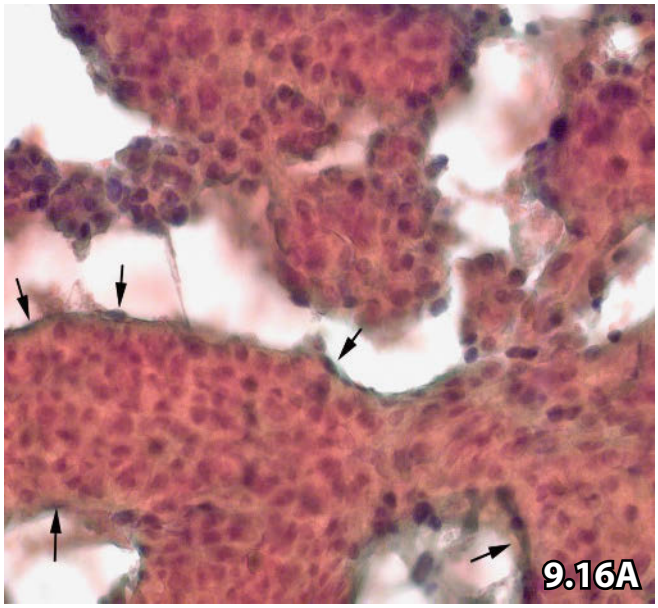
9.16A

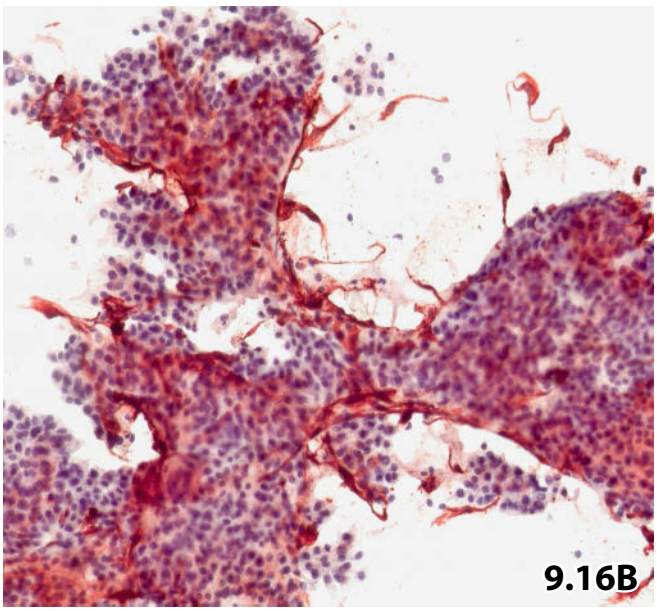
9.16B

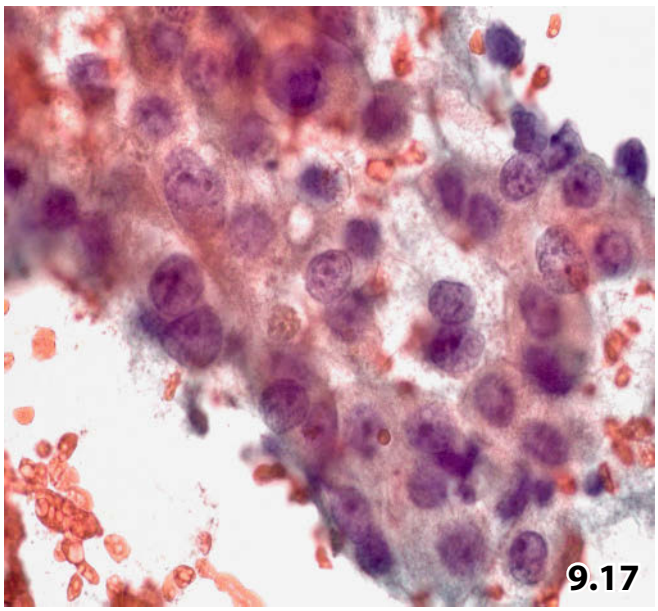
9.17

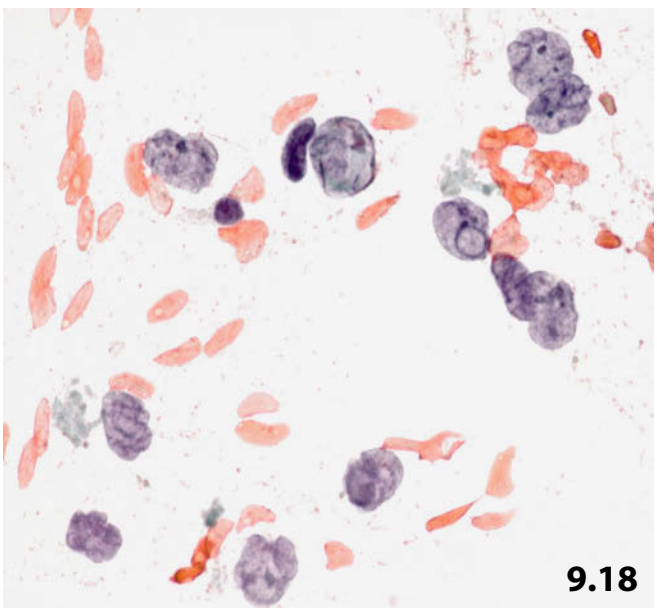
9.18

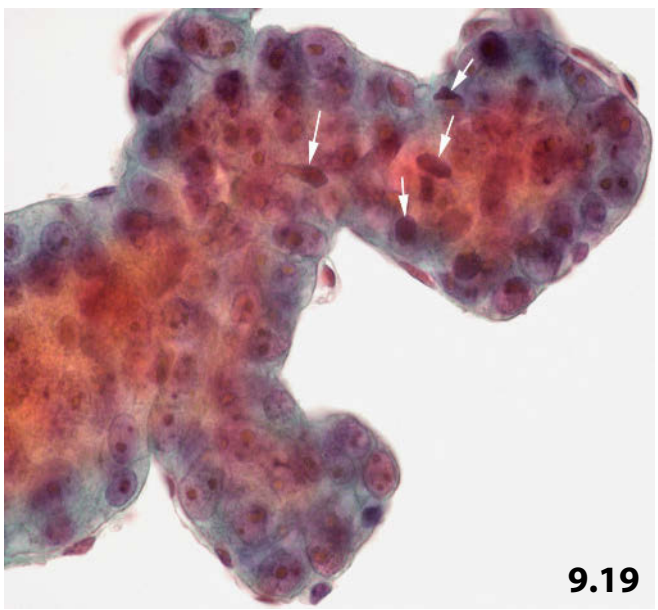
9.19

**Fig. 9.20** (case #5) Possible diagnostic pitfall (1).
Higher magnification reveals typical cytoarchitecture of HCC including nuclear polymorphism and endothelial cells (arrow). But pronounced nuclear inclusions obscuring intranuclear details may hamper an accurate diagnosis.

**Fig. 9.21A, B** (case #6) HCC of clear cell variant: possible diagnostic pitfall (2).
**A** Flat sheets composed of tumor cells with broad vacuolated and foamy cytoplasm are characteristic of HCC of the clear cell variant. Note also the monomorphic and rather small nuclei exhibiting indistinct nucleoli (lower magnification). The differential diagnosis should consider clear cell carcinomas of various primary origins (e.g., renal cell adenocarcinoma).
**B** High magnification shows intracytoplasmic eosinophilic granules in the non-vacuolated areas of the cytoplasm, and bile (center). The latter is a feature favoring HCC. Scarce inclusions of bile can only be detected by careful screening of each available smear.

**Fig. 9.22** (case #7) Bile.
Intercellular bile plugs and intracytoplasmic bile droplets stain brownish-yellow (arrows) and green (see also Fig. 9.21B) with Pap stain. Depending on staining methods and staining quality, bile deposits may be difficult to detect (high magnification).

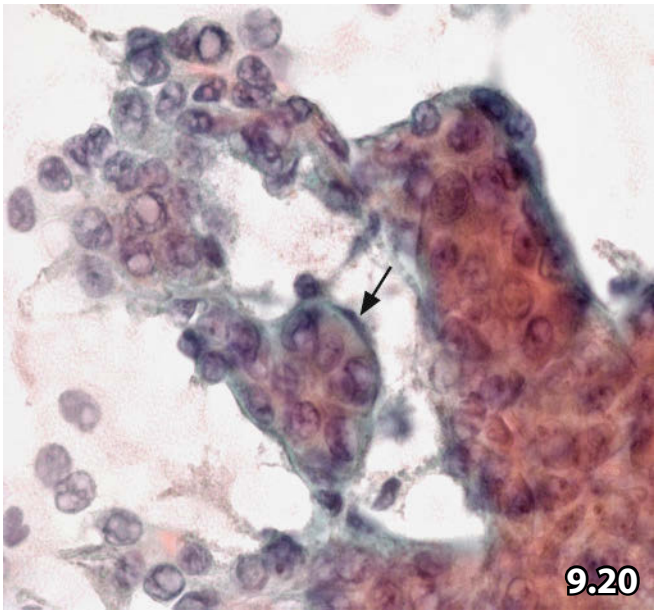
9.20

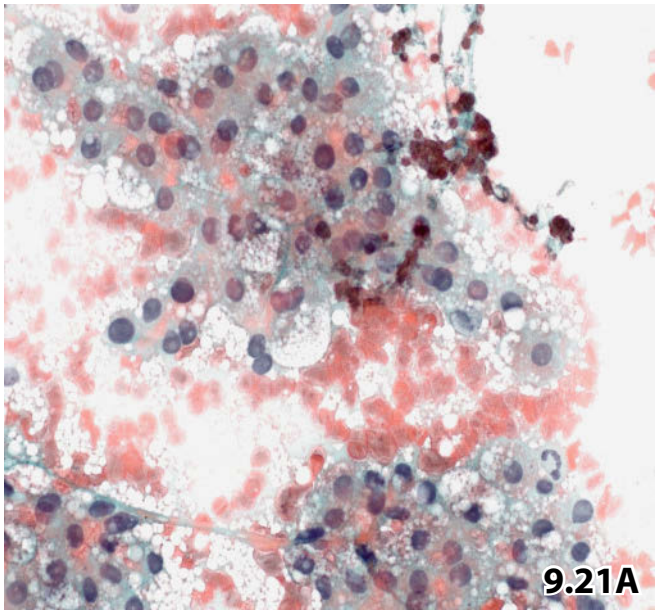
9.21A

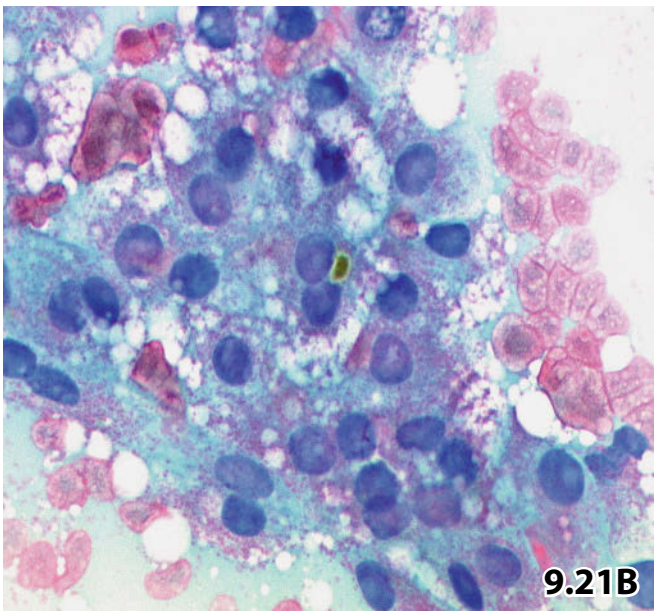
9.21B

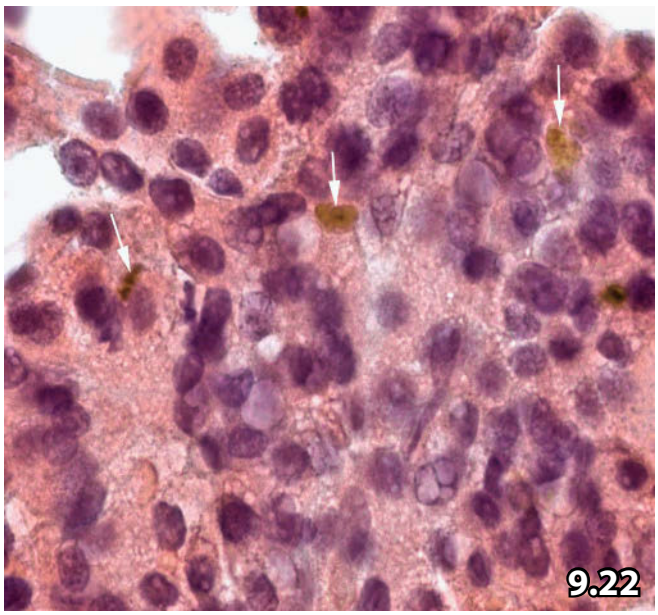
9.22

**Figs. 9.23–9.25 Well-differentiated hepatocellular carcinoma.**
FNAB from three patients presenting with well-differentiated HCC. Tumor type has been confirmed by histology in each case. The current pictures emphasize cytologic features of malignancy (conventional smears, Pap stain).

**Fig. 9.23** (case #1) Clusters are composed of uniform small cells showing minimal atypias. Nevertheless, there are many features favoring malignancy already detected at low magnification: compact multi-layering of epithelial tumor cells, sharply outlined cell clusters, superficial endothelial cell lining (arrows), loss of nuclear polarity, high N/C ratio.

**Fig. 9.24** (case #2) High magnification shows uniformity of well-differentiated hepatic tumor cells. Cytoarchitecture comprising huge pleomorphic nucleoli, higher N/C ratio as compared to benign hepatocytes, and slightly atypical chromatin (granular and clumping) indicate a malignant neoplastic lesion.

**Fig. 9.25A, B** (case #3) Possible diagnostic dilemma and impact of immunocytochemistry. **A** Uniform small tumor cells occur alone and in loose clusters. The latter comprise acini (bottom), suggesting low-grade endocrine neoplasia. Note the abundant foamy and granular cytoplasm (higher magnification). **B** Strong positive immunoreactivity for alpha-fetoprotein affirm primary hepatic origin of the tumor cells (Pap-prestained conventional smear).

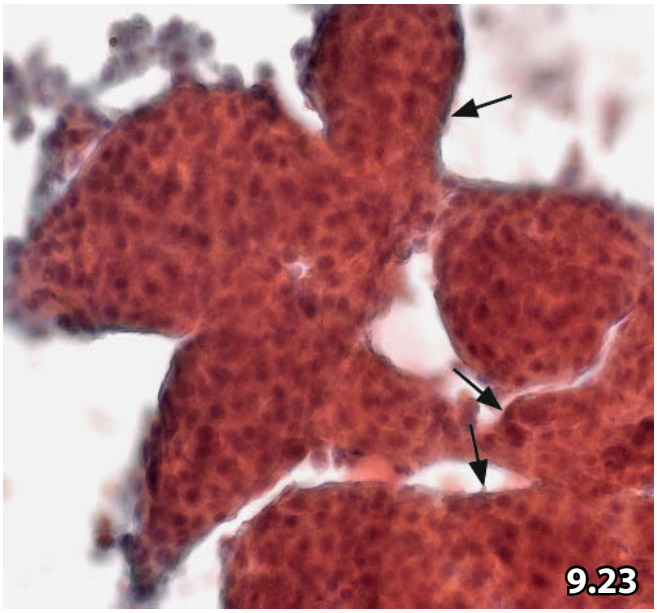
9.23

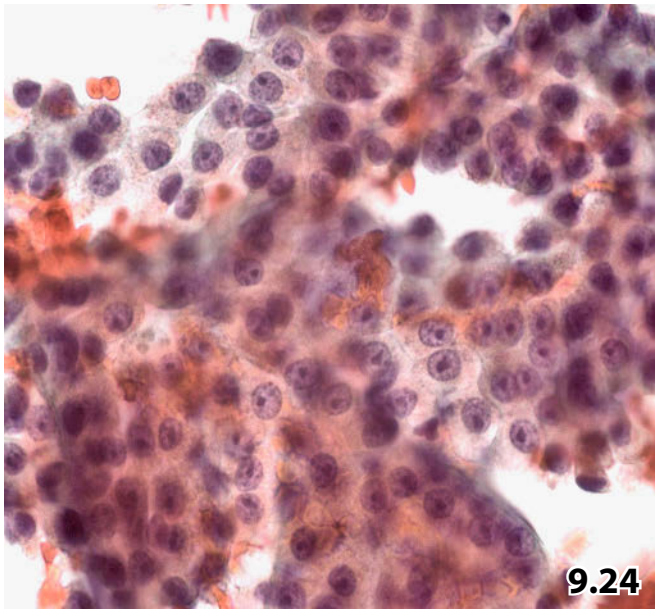
9.24

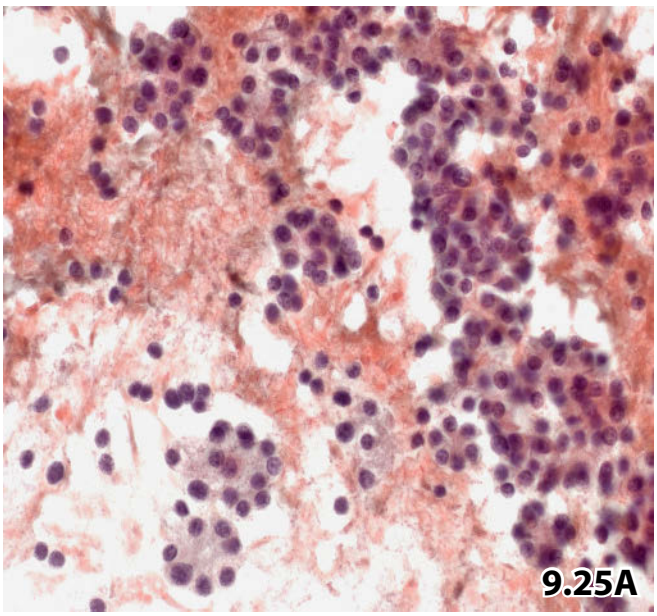
9.25A

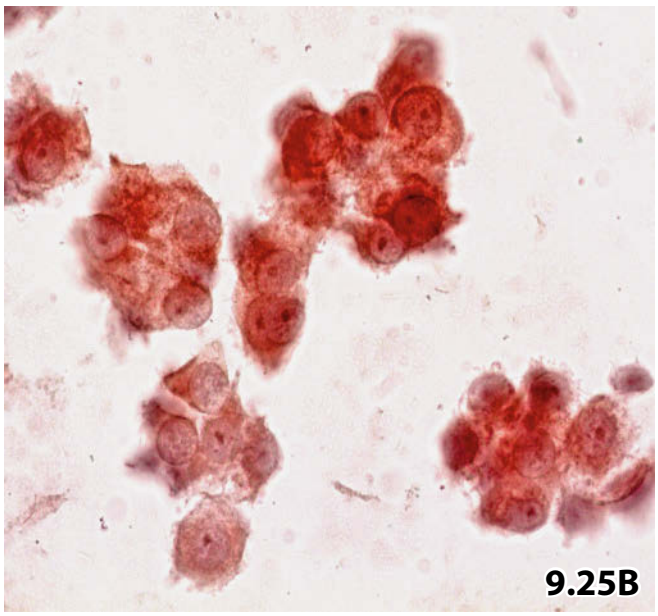
9.25B

**Fig. 9.26 Poorly differentiated hepatocellular carcinoma.**
Dissociating irregular clusters of pleomorphic hepatoid cells together with bile plugs (arrow) support the diagnosis of high-grade HCC (lower magnification).

**Figs. 9.27 and 9.28 Hepatocellular carcinoma: fibrolamellar variant.**
Figures reveal typical cytologic and histologic features of this tumor entity.

**Fig. 9.27A, B** Liver FNAB, direct Pap-stained smears. **A** Giant hepatoid cells along with huge nucleoli and dense granular chromatin indicate fibrolamellar HCC (high magnification). **B** Low magnification shows a broad band of cellular fibrotic and sclerotic tissue encasing isolated atypical giant liver cells (arrows), which exhibit identical morphology as specified above.

**Fig. 9.28** Liver resection was performed. The histologic section shows huge hepatoid tumor cells embedded in fibrotic and collagen tissue (lower magnification, HE stain).

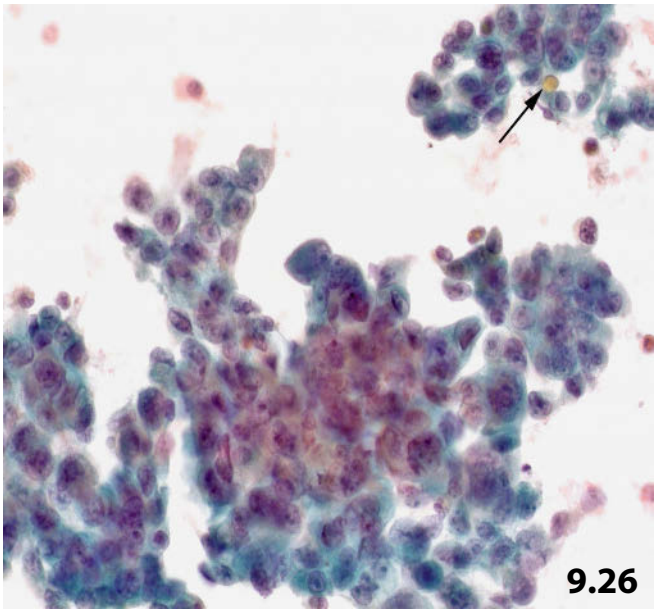
9.26

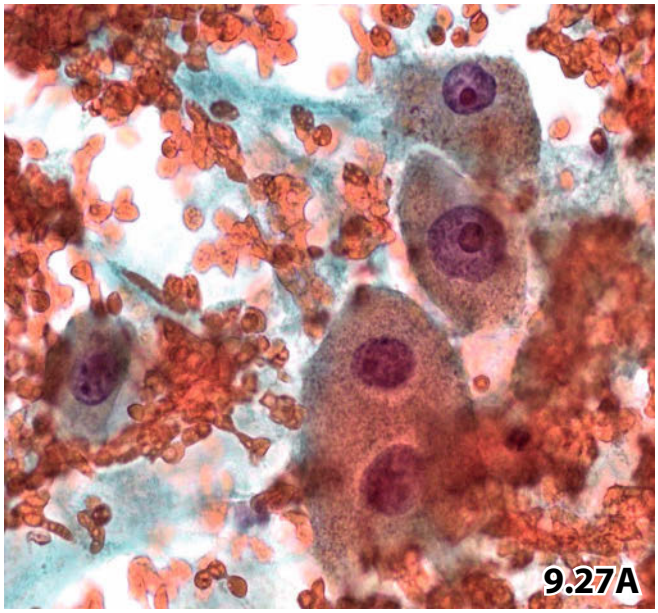
9.27A

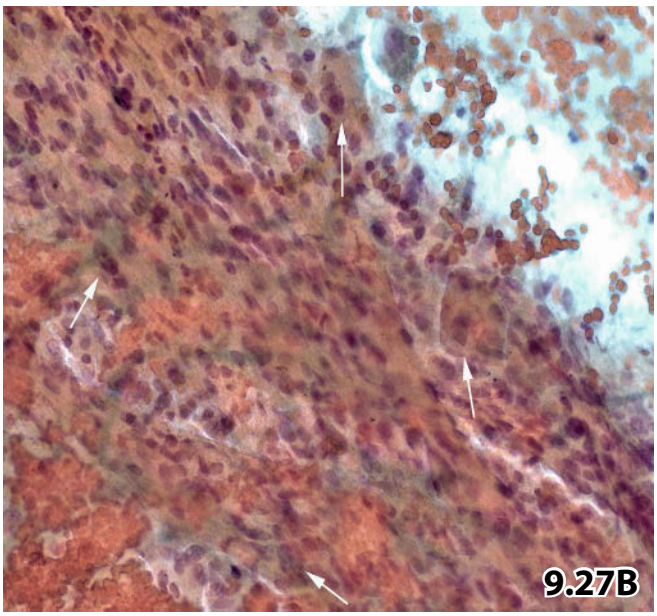
9.27B

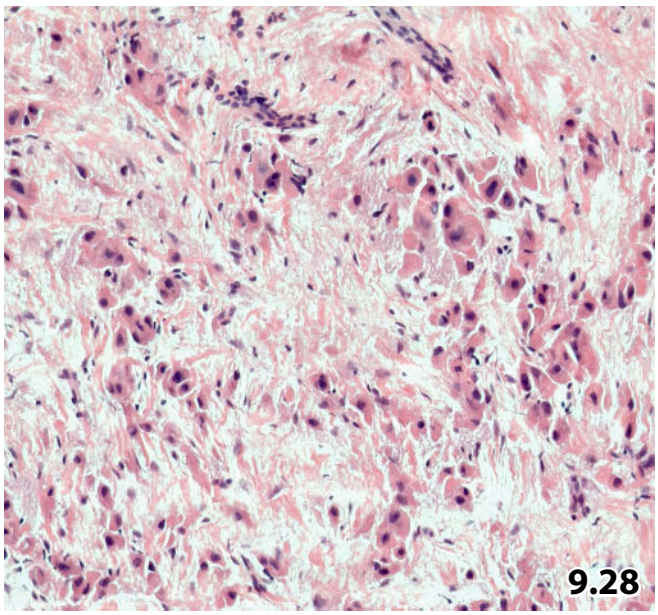
9.28

**Figs. 9.29–9.35 Primary and metastatic neuroendocrine neoplasms (NET) in the liver including differential diagnostic considerations.**
Characteristic cytologic features, immunocytochemistry, and differential diagnostic problems of NET are discussed based on selected cases. Aspirated cell material has been processed using direct smears and liquid-based technique in one case.

**Fig. 9.29** (case #1) Common cytologic features of NET.
Image-guided FNAB of a liver metastasis from a low-grade pancreatic NET in a 76-year-old man. Liquid-based preparation (ThinPrep) yielded a cellular specimen composed of dispersed and clustered monotypic cells. Eccentrically placed nuclei, plasmacytoid cell features, variation in cell size, and acini-like cell formations (arrows) are key features of the endocrine nature of this neoplasm. Strong immunocytochemical positivity for chromogranin A (not shown) (Pap stain, higher magnification).

**Fig. 9.30** (case #2) Extreme variation in cell size in NET.
Image-guided FNAB of a metastasizing primary endocrine tumor of the liver in a 26-year-old man (postmortem histologic diagnosis). Mono- and multinucleated giant cells and bare giant nuclei are encountered at low magnification (arrows). Such cells usually occur in endocrine tumors and do not serve as a reliable indicator of malignancy; note the bland chromatin texture. Strong immunocytochemical positivity for chromogranin A (not shown) (Pap stain).



**Fig. 9.31A, B** (case #3) NET: large-cell type.
A 45-year-old man presenting with nodular lesions in his liver and a mass in the pancreatic tail. Image findings suggested neuroendocrine tumor or hepatoma. FNAB of the liver was performed. Direct smears were prepared and Pap-stained.
*Cytologic/immunocytochemical diagnosis:* Endocrine tumor of the large-cell type.
*Follow-up:* No histologic diagnosis was achieved. The site of the primary tumor remained open in spite of repeated imaging studies.
**A** High magnification reveals large tumor cells with eccentrically placed nuclei in an abundant pale cytoplasm. Compare the tumor cells with small sheets of benign hepatocytes (arrows). Cytomorphology alone presented diagnostic confusion concerning tumor typing. **B** Positive immunocytochemical staining for chromogranin A rendered a conclusive diagnosis of NET. A negative immunoreaction for AFP is not shown (Pap-prestained conventional smear).

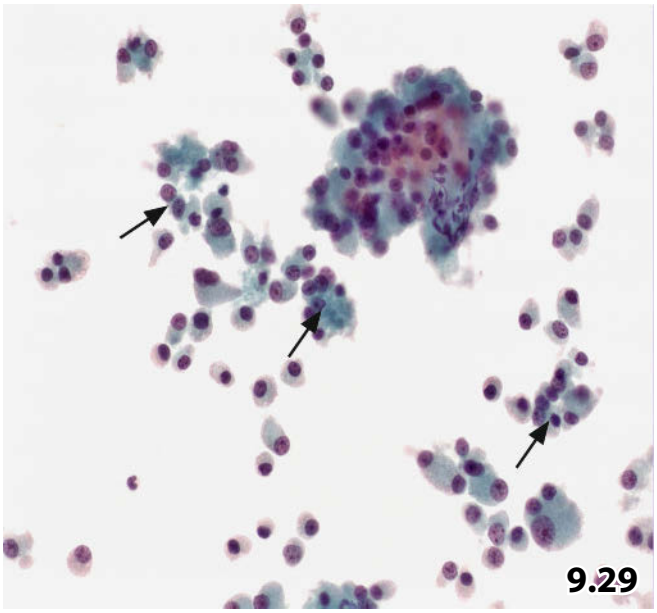
9.29

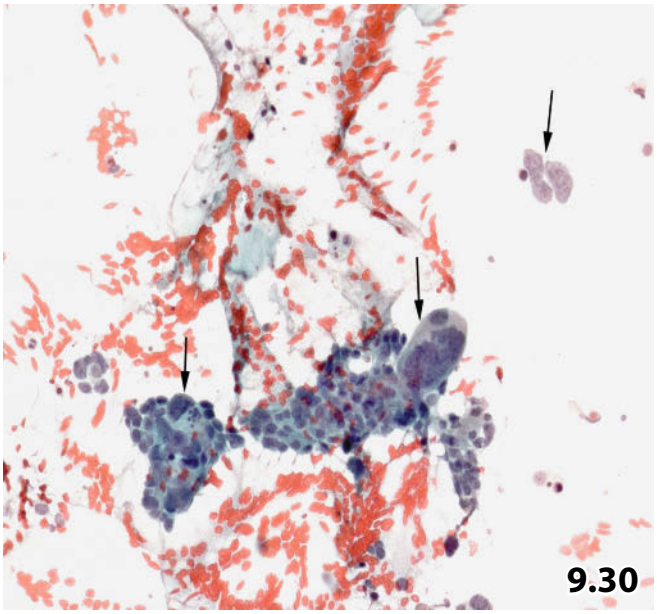
9.30

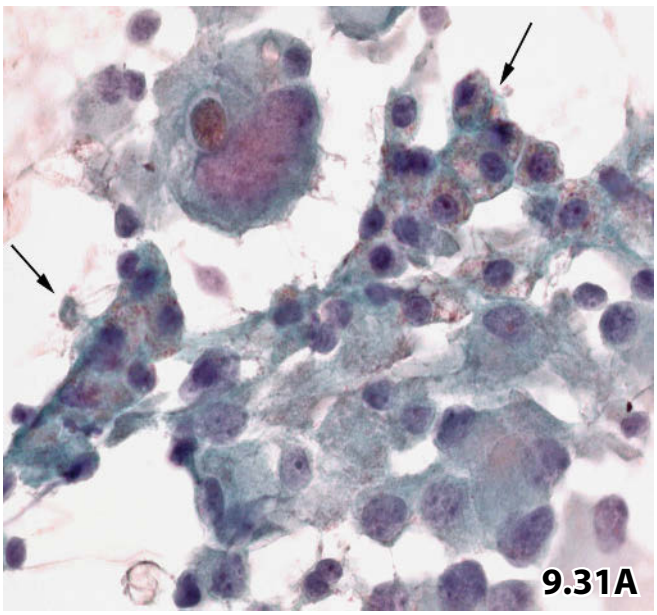
9.31A

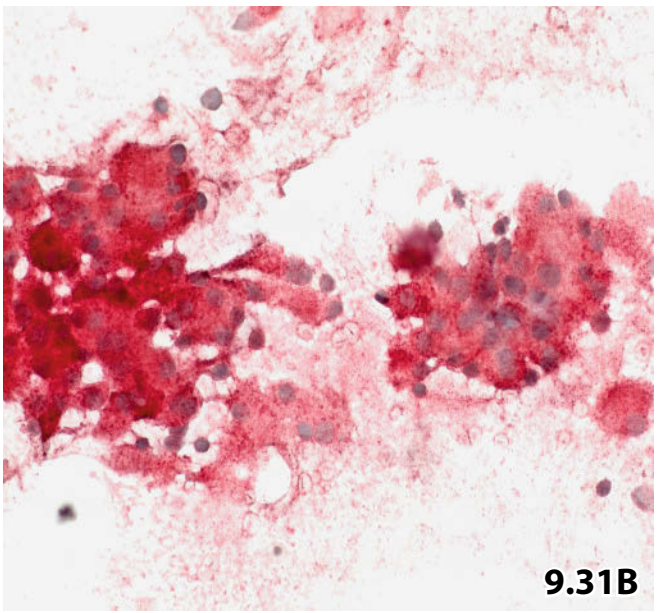
9.31B

**Figs. 9.32A–C** (case #4) NET versus well differentiated hepatocellular carcinoma.
A 71-year-old man with a positive history of lung carcinoid presented with a tumor mass in the right lobe of his liver. FNAB of the hepatic lesion was performed (direct smears, Pap stain).
*Cytologic/ immunocytochemical diagnosis:* Endocrine tumor.
*Tissue diagnosis* after partial hepatectomy: Hepatic metastases from pulmonary carcinoid tumor.
**A** Lower magnification showed compact tumor cell clusters composed of uniform epithelial cells. Eccentrically placed nuclei, plasmacytoid cell features, and small acinic-like formations suggested endocrine tumor but diagnostic consideration also included well-differentiated hepatocellular carcinoma. Immunocytochemical staining was performed using Pap-prestained conventional smears. **B** Positivity for chromogranin A. **C** Positivity for synaptophysin.

**Fig. 9.33** (case #5) NET versus well-differentiated hepatocellular carcinoma.
A 63-year-old woman presenting with a tumorous mass in her liver and in the retroperitoneal space was referred to image-guided FNAB of her hepatic disorder. Cytology showed sheets composed of uniform tumor cells. The epithelial cells exhibited minor nuclear irregularities, dense and coarse chromatin, and granular cytoplasm (direct smear, Pap stain, high magnification).
*Cytologic diagnosis:* Cytology alone was inadequate as a tool for the distinction between NET and hepatocellular carcinoma, but positive immunocytochemical reaction for chromogranin A (not shown) indicated neuroendocrine origin of the tumor cells.
*Final diagnosis* after laparotomy and microscopic evaluation of multiple biopsies: Metastatic endocrine neoplasia of the ileum.

**Fig. 9.34A, B** (case #6) NET versus breast carcinoma.
A 76-year-old woman with a history of well-differentiated breast carcinoma of the ductal type presented with a hepatic nodule. FNAB of the liver lesion was performed.
*Initial cytologic diagnosis:* Metastasis of breast carcinoma.
*Revised cytologic diagnosis* together with immunocytochemical results: Medullary thyroid carcinoma.
*Final diagnosis* of a metastatic medullary thyroid carcinoma was reached based on US-guided FNAB of a small thyroid nodule (1 cm in diameter).
**A** Cytologic details suggested metastasis of breast carcinoma: small to medium-sized cells, finely granular and lucid chromatin, wrinkled nuclear membranes, dense trapezoid cytoplasm (direct smear, Pap stain). **B** Immunocytochemistry was ordered because clinical symptoms and laboratory tests suggested an endocrine disorder. Subsequent immunoreaction for calcitonin revealed strong positivity of the tumor cells obtained from the liver. Immunostaining for chromogranin A-decorated tumor cells as well (not shown) (Pap-prestained conventional smear).

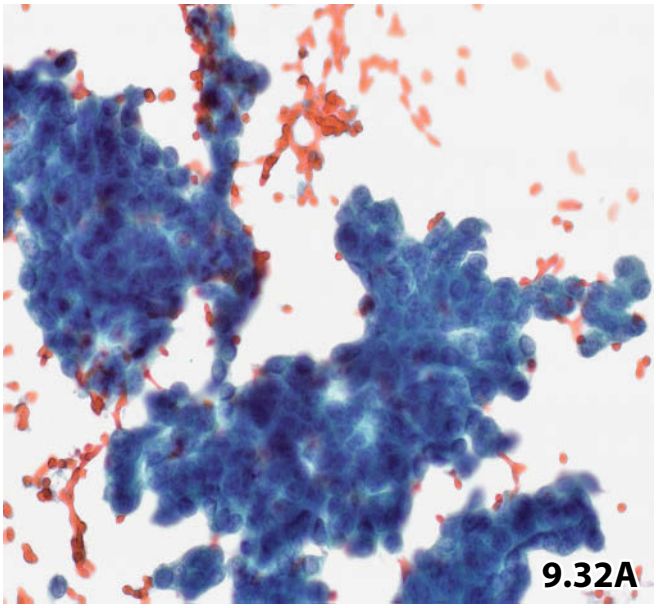
9.32A

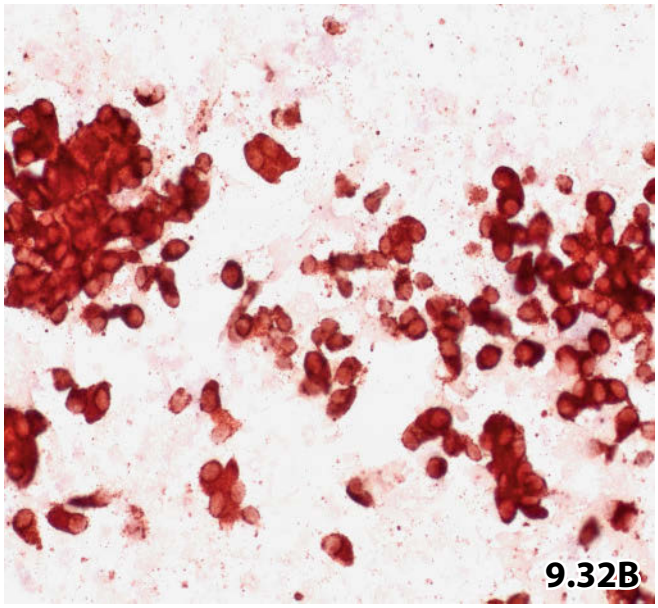
9.32B

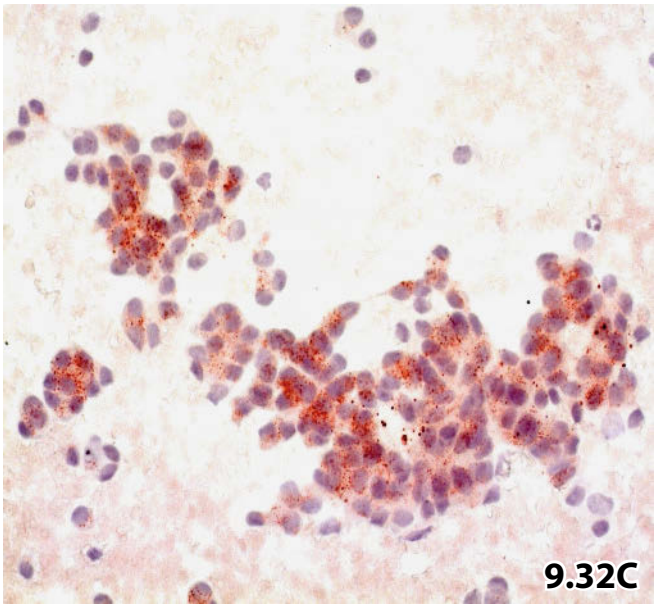
9.32C

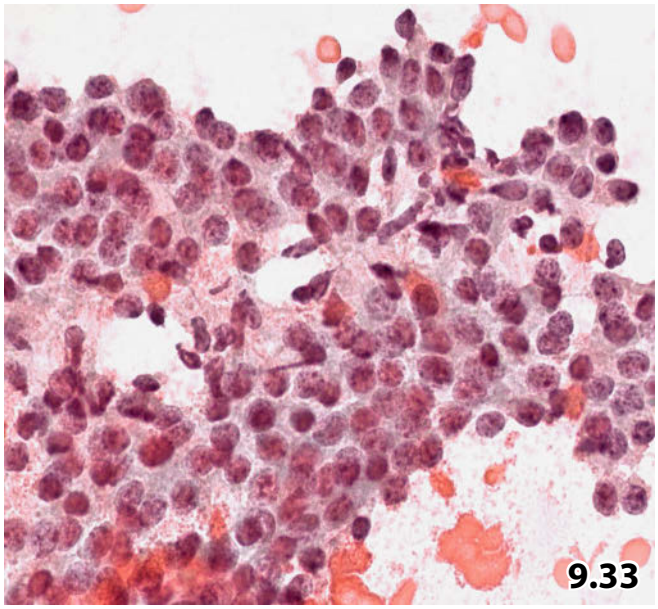
9.33

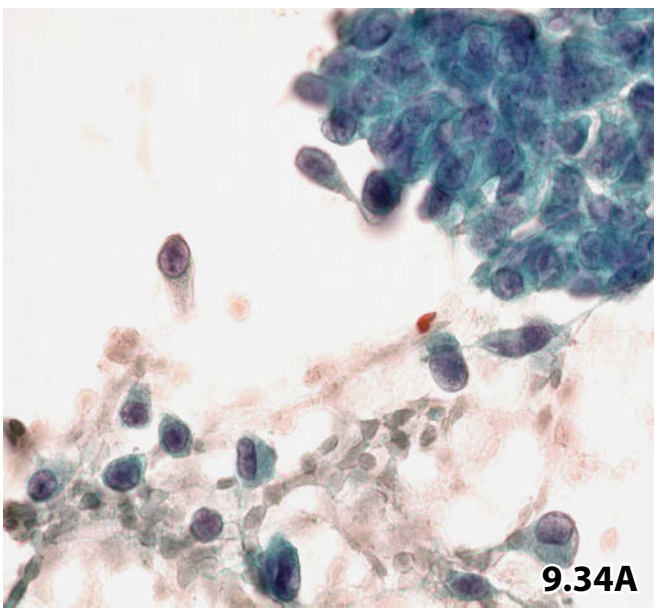
9.34A

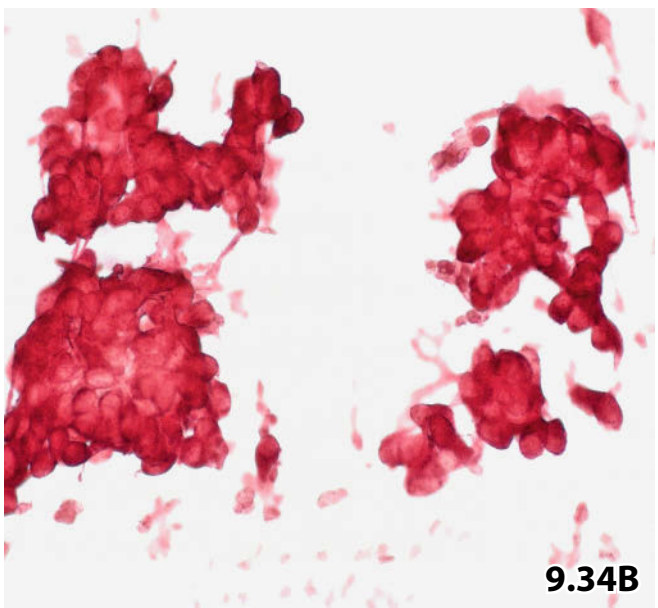
9.34B

**Fig. 9.35** (case #7) NET versus hepatocellular carcinoma with neuroendocrine differentiation.
FNAB of a hepatic lesion in an elderly patient provided a cell population that gave rise to diagnostic difficulties between NET and hepatocellular carcinoma. Immunocytochemical staining shows positivity for chromogranin A in the majority of the tumor cells (not shown) (direct smear, Pap stain, higher magnification).
*Cytologic/immunocytochemical diagnosis:* Neuroendocrine tumor in the liver.
*Tissue diagnosis* (right hepatic lobectomy): Hepatocellular carcinoma with endocrine differentiation (immunohistochemical positivity for both neuroendocrine markers and alpha-feto protein).

**Figs. 9.36 and 9.37 Intrahepatic cholangiocarcinoma.**
Primary cholangiocarcinoma of the liver in two different patients. Transcutaneous hepatic FNAB shows characteristic morphologic features (direct smears, Pap stain).
*Histology* has confirmed the cytologic diagnosis in both patients.

**Fig. 9.36** (case #1) Lower magnification shows isolated and densely clustered carcinoma cells (upper right). Polymorphous nuclei are embedded in distinct cyanophilic or vacuolated cytoplasm. Note faint strands of pink-stained mucus (arrows) in the background of the smear. Compare morphology of the tumor cells with that of benign liver cells (arrowhead).
*Tentative cytologic diagnosis:* Poorly differentiated mucinous adenocarcinoma, most likely intrahepatic cholangiocarcinoma.

**Fig. 9.37** (case #2) Imaging studies suggest cholangiocarcinoma of the liver in a 76-year-old woman. Microscopy (high magnification) exhibits typical morphologic features of cholangiocarcinoma: loss of nuclear polarity, intracytoplasmic storage of mucus, bland chromatin, and pale nucleoplasm combined with distinct nuclear grooves and lobulation. Indistinct nucleoli. Cells of cholangiocarcinoma share most of the cytologic features with cells of pancreatic adenocarcinoma.
*Cytologic diagnosis:* Intrahepatic cholangiocarcinoma.

**Fig. 9.38A, B Angiosarcoma.**
Computed tomography revealed a hypodense area in the liver of a 75-year-old man. CT-guided FNAB was performed (direct smears, Pap stain).
*Cytologic/immunocytochemical diagnosis:* Angiosarcoma. Hepatic wedge resection followed by histologic examination confirmed the cytologic diagnosis.
**A** Epithelial-like aggregation of large malignant cells is shown at high magnification. The type of cell clusters give rise to diagnostic confusion between carcinoma and sarcoma.
**B** Immunocytochemistry was helpful in differentiating carcinoma from sarcomatous neoplasia: cells stained positive for factor VIII indicating angiomatous malignancy (Pap-prestained direct smear).

**Fig. 9.39 Malignant melanoma.**
A 50-year-old woman presented with nodular lesions both in her liver and in the abdominal cavity. The patient's history was positive for a malignant melanoma at the shoulder successfully treated 19 years before. Image-guided FNAB of a liver lesion was performed. Cytology revealed large amounts of melanin pigment (dirty-green granules and clumps) stored in cytoplasm of degenerated cells and scattered in the background. There were no well-preserved cells available (direct smears, Pap stain, lower magnification).
*Cytologic diagnosis:* Completely necrotic metastasis of a malignant melanoma.
*Tissue diagnosis* (resection of a tumor mass located in the small bowel): The morphologic criteria for the histologic diagnosis were basically the same as described in the liver aspirate.

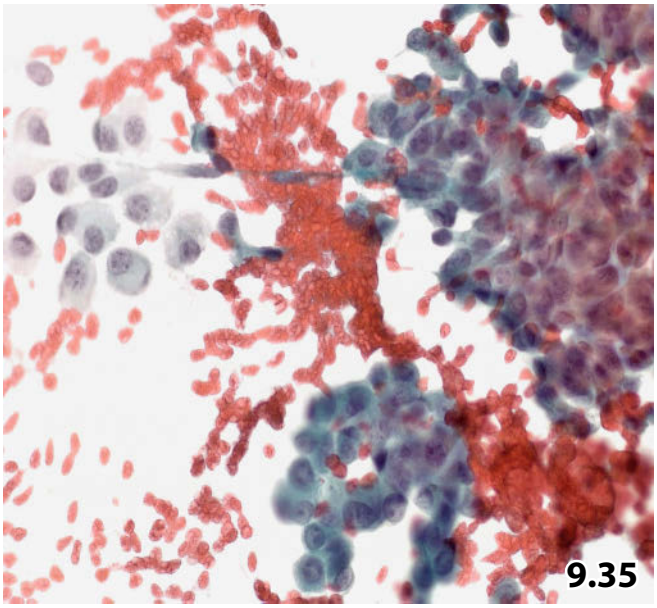
9.35

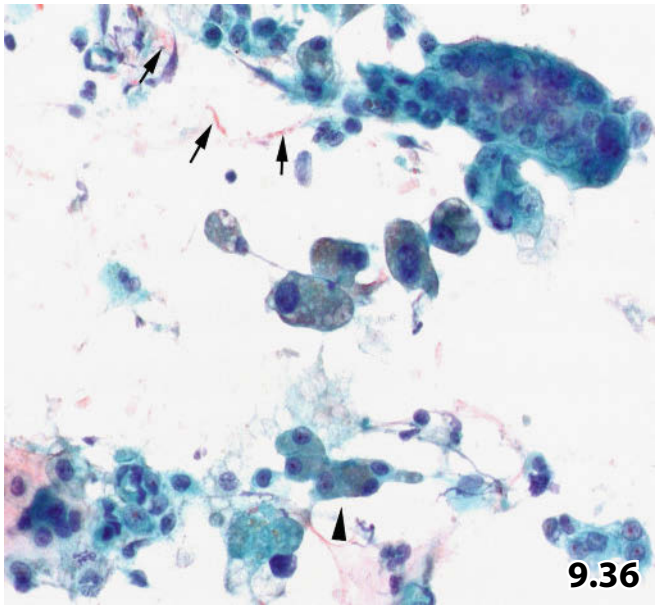
9.36

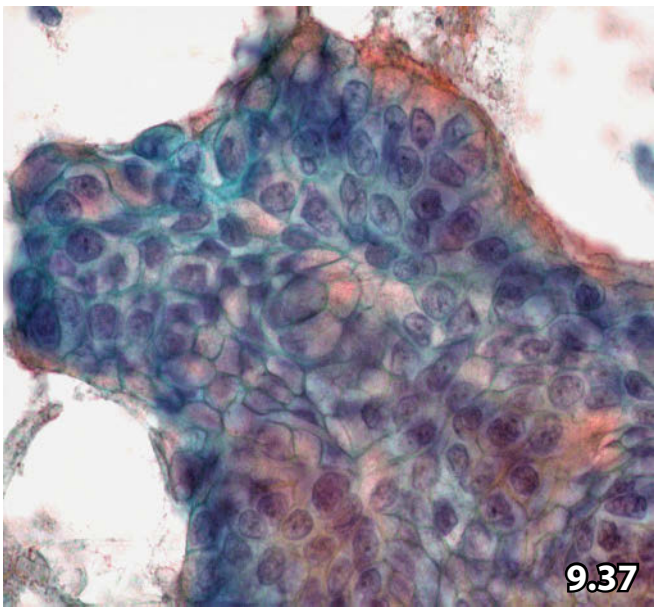
9.37

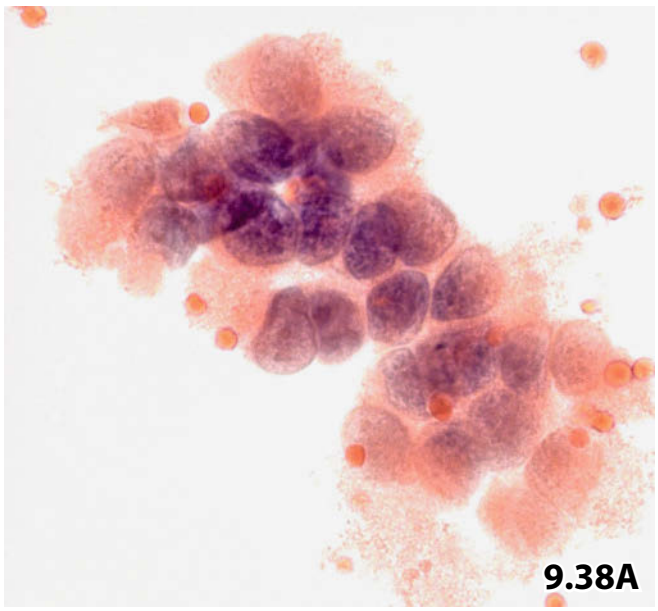
9.38A

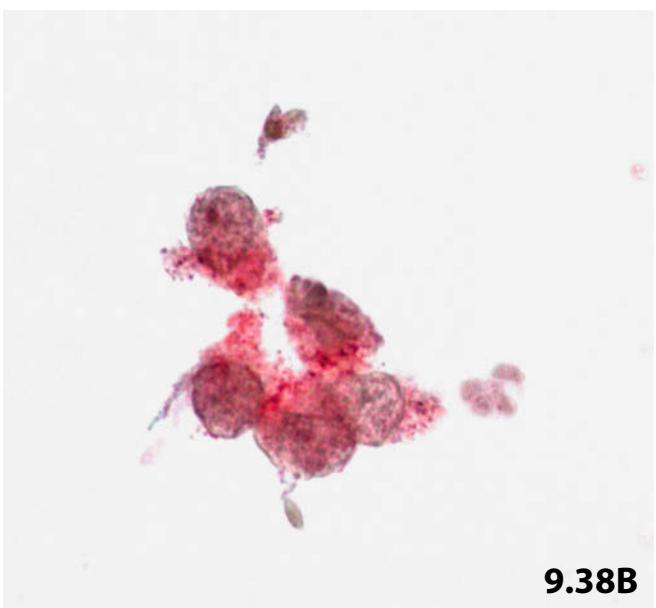
9.38B

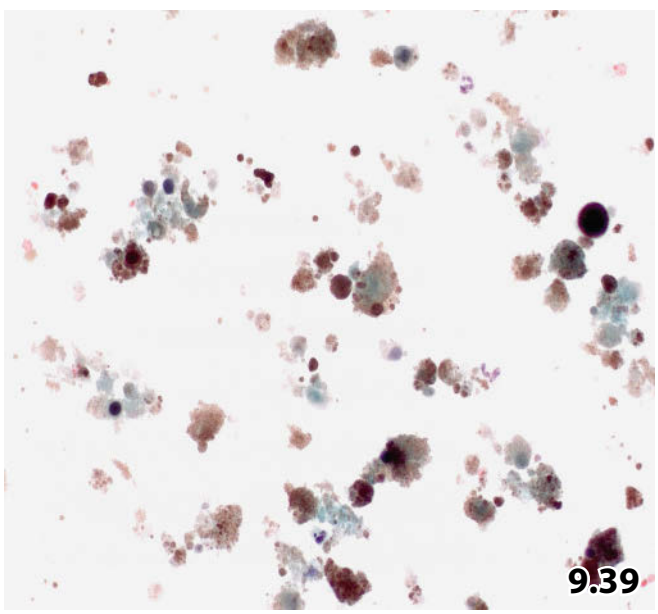
9.39

# 10 Pancreas, Extrahepatic Bile Ducts, Ampullary Region



## Synopsis and Algorithms



Spieler/Rössle, *Nongynecologic Cytopathology. A Practical Guide. Essentials of Diagnostic Pathology*,
DOI 10.1007/978-3-642-24719-4_10, 

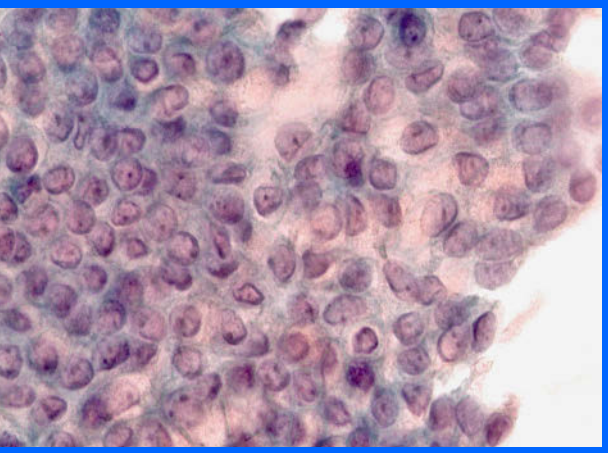

# Section 10.1
# Pancreas

## 10.1.1 Introduction and Diagnostic Procedures

- The pancreas is difficult to investigate because of its deep, retroperitoneal localization and the complex and immediate vicinity to other organs of the upper abdomen.
- *Pancreatic carcinoma:* Pancreatic carcinoma is a neoplasm of the elderly population, 80% of the cases manifest in patients aged between 60 and 80 years. Pancreas carcinoma is a highly aggressive neoplasm with a poor prognosis. A strong association is assumed between cigarette smoking and pancreatic carcinoma; additional etiological factors remain to be established. Ductal adenocarcinoma is the most frequent type of pancreatic cancer accounting for 75% and up to 90% of all primary malignancies of the pancreas [104].
  Imaging findings can be diagnostically misleading in patients with a mass-forming inflammatory pancreatic process, which may look like a neoplastic disorder.
  A triple diagnosis combining cytologic, radiologic/sonographic, and clinical findings can greatly enhance the diagnostic reliability.
- *Pancreatic cystic lesions:* Cystic mass lesions of the pancreas have a high prevalence in the human population. They comprise a pathologically heterogenous group of lesions that share many clinical, radiologic, and sonographic features. Cystic lesions can be classified into three main groups: congenital, inflammatory, and neoplastic. The vast majority are pseudocysts, accounting for 75–90% of the pancreatic cysts. Cystic pancreatic neoplasms constitute approximately 5–15% of all pancreatic cystic lesions [33, 67]. They are increasingly identified, often as incidental findings due to increasing practice of abdominal imaging techniques and their continuing refinement.
  The cardinal purpose of preoperative diagnostic evaluation is to distinguish nontumoral cystic lesions (such as pseudocyst, retention cyst) and benign cystic tumor (serous cystadenoma) from mucinous neoplasms. The former do not necessarily demand surgical intervention; the latter are established to have at least potential for malignant behavior demanding excision in any case. An approach in the preoperative diagnosis of pancreatic cysts combining cytology with different imaging modalities along with cyst fluid analysis [12, 116] is essential to increase the sensitivity of FNAB diagnosis of neoplastic cystic lesions of the pancreas [8, 10, 28, 45, 67, 68, 79, 148, 212].
- In transplantation medicine, ultrasound-guided FNAB may be used to monitor pancreatic graft status. The cytologic method allows more accelerated control and a number of needle passes at multiple sites of the allograft. The percentage of leukocytes, immature lymphocytes, and histiocytic cells are calculated on cytologic specimens [168]. The experience of pancreatic graft monitoring by cytology is still relatively poor.

### 10.1.1.1 Comments on Diagnostic Procedures

- Cytology has achieved wide acceptance in the evaluation of patients with suspected pancreatic malignancy due to improved imaging techniques, the application of a variety of diagnostic FNAB techniques, and other cytologic pro-

cedures. Furthermore, newer radiography and biopsy techniques can detect and examine smaller pancreatic lesions, increasing the number of pancreatic tumor diagnoses.

- Endoscopic ultrasonography-guided FNAB (EUS-FNAB) or brushing during endoscopic retrograde cholangiopancreatography (ERCP) should be exclusively performed in patients estimated to have resectable cancer disease, unless a primary pancreaticoduodenectomy without previous bioptic intervention is indicated. Cytologic investigations can be performed on patients with an unresectable tumoral lesion regardless of the methods used [127].
- FNAB differentiates between benign and malignant disorders and recognizes different types of primary pancreatic neoplasms to a reasonable degree of diagnostic accuracy. FNAB appears to be safe and is associated with a low complication rate [26, 49].
- Percutaneous FNAB of the pancreas guided by fluoroscopy, angiography, or cholangiography remains a valuable but now infrequently used technique [189, 197].
- The exfoliative methods may likewise detect early and potentially curable pancreatic cancer [137, 138], and contribute to a reliable identification of malignant intraductal papillary mucinous neoplasms of the pancreas [207].



### 10.1.1.2 Fine-Needle Aspiration Biopsy

#### 10.1.1.2.1 Transcutaneous FNAB

Pancreatic lesions are aspirated using image-guided procedures such as transabdominal ultrasound (US), computed tomography (CT), or magnetic resonance imaging (MRI). Nowadays, FNAB using ultrasound guidance is the most commonly performed procedure; CT guidance of the needle is preferred in smaller lesions and in patients who undergo a repeat biopsy [189]. MRI-guided biopsy is performed in few institutions because the technique is cost-intensive and its value still uncertain.

Transcutaneous FNAB of the pancreas is a diagnostic procedure that provides high sensitivity and specificity in the detection of malignancy. In selected studies between 1990 and 1998, the sensitivity was reported to range from 79% to 98% and the specificity from 92% to 100% [26, 44, 49, 86, 97, 192].

#### 10.1.1.2.2 Endoscopic Ultrasonography-Guided FNAB [148]

- Directed endoscopic biopsy has been replaced over the past few years by techniques with image guidance. EUS-FNAB of pancreatic lesions is a safe and effective method for experienced endosonographers and skilled cytopathologists [8]. The method provides accurate diagnoses with high predictive values and a high overall accuracy. Reported sensitivity and specificity for malignant disease range from 82% to 100% in the most recent papers [41, 56, 152, 160, 204].
- Diagnostic sensitivity for focal pancreatic lesions in the presence of chronic pancreatitis has been found to be much lower than lesions located within normal pancreatic parenchyma. Increasing the number of needle passes in EUS-FNAB may be an appropriate means to improve the diagnostic accuracy [65, 198].
- Adequate specimens are obtained in over 90% of the samplings done by EUS-FNAB [160, 205]. The highest sample adequacy has been reported for lesions measuring 20–40 mm in diameter [152], and the lowest in both small lesions (<20 mm) and enormous solid lesions (≥ 40 mm). On the other hand, diagnostic results seem to be better for small solid lesions compared with larger tumors in terms of sensitivity, negative predictive value, and diagnostic accuracy [10]. The combination of two sampling modalities, such as EUS-FNAB and Tru-Cut needle biopsy seems to have a positive effect on the sample adequacy and the diagnostic accuracy of larger lesions (> 20 mm) [205]. The safety of EUS-FNAB is reported to be acceptable. Several studies have found no complications using EUS-FNAB for solid pancreatic lesions, but a few complications occurred in patients having cystic lesions [23, 145].

##### EUS-FNAB and Solid Pancreatic Lesions

The diagnostic approach by EUS-FNAB for solid pancreatic lesions has a sizeable clinical impact:

- It avoids the need for further investigations (such as surgical biopsies and additional imaging studies) in patients with inoperable disease.
- It allows conservative management of patients with benign disease.
- It is cost-saving [34].
- It permits primary diagnosis and staging during the same procedure [147].
- It improves resolution of small lesions in comparison with other imaging techniques and allows subsequent cell or tissue sampling [148].
- Repeated EUS-FNAB may be performed in patients with inadequate sampling or indeterminate or negative diagnosis at initial FNAB [57], or other biopsy methods (forceps biopsy, CT-guided biopsy, or ERCP brush sampling) [73].
- The methodology is safely performed on an outpatient basis [8].
- The intervention is well tolerated [23].

##### EUS-FNAB and Cystic Mass Lesions

- EUS-FNAB is also a valuable tool in the diagnostic assessment of cystic pancreas lesions. Additionally, completion of EUS findings and cytologic fluid evaluation is highly recommended by means of ancillary analyses in order to distinguish reliably between mucinous cystic neoplasms (MCNs) and nonmucinous cystic neoplasms, and to differentiate malignant from benign MCNs.

- Contamination of cytologic specimens with gastric and duodenal epithelium may be critical for an accurate interpretation of EUS-FNABs.
- Further information as to diagnostic problems of pancreatic cystic lesions, their differing microscopic features, the clinical impact of a reliable diagnosis, as well as references from the literature are provided in Sects. 10.1.6, p. 639 and 10.1.7, p. 640.

**Caution**

Contamination of transgastric and transduodenal EUS aspirates with intestinal epithelium can be a great challenge for less experienced cytologists, leading to misdiagnoses.

#### EUS-FNAB and Implications on Peritoneal Seeding

[91, 127]

EUS-FNAB is assumed to have a lower risk of peritoneal tumor seeding than percutaneous FNAB. Therefore, the former should be the preferred method to obtain a cytologic diagnosis in patients with localized cancer and potentially resectable neoplastic lesions.

#### 10.1.1.2.3 Intraoperative FNAB

Intraoperative FNAB of the pancreas has been shown to be a highly accurate diagnostic tool. The results are comparable with those achieved by other aspiration techniques [52, 126, 162]. Malberger and coworkers recommend an intraoperative procedure in patients with pancreatic masses incidentally found at laparotomy and in patients with pancreatic lesions unsuccessfully clarified preoperatively by repeated biopsy procedures [126].

### 10.1.1.3 Pancreaticobiliary Duct Brushing

- Cytologic material is obtained via endoscopic retrograde cholangiopancreatography (ERCP) by brushing biliary and/or pancreatic ducts. False-negative diagnoses occur most frequently due to erroneous sampling, followed by reader error and technical sampling problems [54].
- Pancreatic duct brushing seems to be an accurate method to identify ductal pancreas carcinoma but has its limitations, especially in patients with mucinous cystic lesions [18].
- The diagnostic sensitivity of brush cytology from biliary strictures is reported to be significantly higher in patients with cholangiocarcinoma than those presenting with a pancreatic carcinoma [70].
- Negative, inconclusive, and atypical or dysplastic findings frequently occur in the cytologic work-up of brush samples leading to an overall poor diagnostic sensitivity for carcinoma. Sensitivity has been cited at less than 70% [54, 71, 119, 185, 201]. In this setting, it is essential to maintain a high degree of specificity.
- A very low sensitivity of 33.3% and a low diagnostic accuracy of 46.7% have been found using brush cytology during ERCP in patients with pancreatic masses lacking evidence of a biliary stricture [202].
- Percutaneous transhepatic cholangiodrainage offers the possibility of endobiliary brushings or biliary fluid collection for cytologic evaluation. Brushing of biliary strictures at cholangiodrainage seems to be a useful method to establish malignant disorders [206].

### 10.1.1.4 Pancreatic Juice Cytology

[136, 137, 138, 177, 207] (Fig. 10.1)

Pancreatic juice cytology is an additive method to ascertain malignancy in ductal pancreatic disorders.

- Pure pancreatic juice for cytologic examination may be collected by direct suction, washing of the duct system, aspiration after secretin stimulation, or by fluid collection from the orifice of the ampulla of Vater. Furthermore, a variety of refined sampling methods exist for helping collect pancreatic juice from the pancreatic duct such as endoscopic cannulation using a duodenoscope or endoscopic retrograde intraductal catheter aspiration after intravenous administration of secretin (Fig. 10.38).
- Pancreatic carcinoma cells may also be detected in duodenal secretion [92].
- Positive results depend on the anatomic site of the carcinoma (head, body, or tail of the pancreas), character of underlying fibrotic restriction of the duct, size of the neoplastic lesion, applied sampling technique, and cellularity of the cytologic aliquot. Positive results have been reported in 38–76% of patients with pancreatic carcinoma [136, 177].
- The CEA levels in the pancreatic juice may provide useful information to distinguish between pancreatic cancer and chronic pancreatitis, and raise the diagnostic rate of malignancy in comparison to microscopic evaluation alone. Molecular analysis of *K-RAS* point mutation status has been shown to be potentially useful in identifying patients at high risk for the development of pancreatic cancer [139, 150].

## 10.1.2 Processing the Cell Material

### 10.1.2.1 Conventional Smears

- *Cyst fluid and pancreatic juice* are collected in a clean vial and transferred to the cytology laboratory as soon as possible. After centrifugation, direct smears are prepared from the sediment. The remaining cellular material should be retained and stored at 4°C mixed with a certain amount of the supernatant. Cytocentrifuge preparation is recommended for small amounts of fluid with sparse cellular content.

- *Aspirated cell material* in the needle and syringe cone or cells from *brush samples* are smeared directly on glass slides and either fixed or air dried. Fixation has to occur immediately to prevent cell degeneration. We prefer wet fixation with Delauney solution; 95% ethyl alcohol pure or mixed with ether is also frequently used. Residual contents in the needle and syringe may be rinsed with a tissue culture solution if cytospin smears, thin-layer preparation, cell block preparation, or flow cytometric analyses are required.
- *Staining:* Papanicolaou and hematoxylin-eosin are highly suitable staining methods for fixed samples. They offer great advantages for comparative cell studies in paraffin tissue sections and are suitable for all common immunocytochemical markers.

#### 10.1.2.2 Liquid-Based Cytology

(Figs. 10.3, 10.30, 10.33, 10.35)



- The current techniques being used in standard cytology are: Cytospin, ThinPrep, SurePath, and others.
- The whole amount of FNAB and brush material is rinsed in a vial containing a cell medium. Thin-layer preparations can be processed as instructed by the manufacturer. Thin-layer methods are strongly recommended if the FNA operator is not familiar with proper conventional preparation and fixation techniques. In many circumstances, a liquid-based method is superior to conventional smears with regard to clear background, monolayer cell preparation, and cell preservation.
- With this procedure an optimal preparation can be achieved for special investigations, in particular for immunocytochemistry, fluorescence in situ hybridization, or static DNA cytometry. In addition, the rinsing liquid from the needle and syringe may be used for immunolabeled flow cytometry.
- In our experience, which is in accordance with the results reported in the literature, specimen preparation and fixation is improved and artifacts are reduced by the thin-layer technique. However, morphologic features may be altered using liquid-based methods and cell interpretation may need modification. The most challenging morphologic changes compared with conventional smears are (Fig. 10.33) :
  - Cell aggregates may be crowded and tight.
  - Cell shrinkage and disruption of the cytoplasm may be more pronounced.
  - Nucleoli are distinct.
  - Background material such as mucus may be scant or completely absent.
- Practically all recent reports in the literature indicate that liquid-based cytology is an accurate and feasible method for the investigation of pancreatic FNABs, and brush specimens from the pancreaticobiliary area respectively, and comparable with conventional preparations [47, 51, 171, 172, 201]. Combining direct brush smears with a liquid-based method seems to enhance the diagnostic accuracy [201].
- Regardless of the operator, hemolyzing fixatives (Cytolyt and others) have been shown to be indispensable as initial transport medium for blood-rich FNABs of intraabdominal lesions and brush samples in combination with thin-layer preparation. By lyzing blood cells, the method yields well-preserved cellular material and a clear background. FNABs of the pancreas frequently provide bloody material.

#### 10.1.2.3 Cell-Block Technique (Fig. 10.45A)

Application of cell-block production depends on the type and the amount of cytologic material that is available. The preparation of cell blocks has been found to aid mainly in diagnostic situations where tissue fragments or clots are present in the original cytologic specimen, especially in the liquid-based setting.

### 10.1.3 Additional Analyses

#### 10.1.3.1 Immunocytochemistry [101] (Fig. 10.2)

No immunocytochemical marker is known that can reliably distinguish between pancreatic and extrapancreatic adenocarcinoma.

- Routinely applied immunocytochemical markers providing a positive staining reaction for cells of ductal pancreatic adenocarcinoma are CA19-9 and MUC (Fig. 10.2B). Specificity of CA19-9 is rather low, because this antigen is also expressed in benign pancreatic duct cells and in epithelial cells of benign cystic tumors. MUC4 and clusterin-β can be helpful in separating reactive ductal epithelial cells from malignant cells of pancreatic adenocarcinoma in FNAB samples [89].
- Cytokeratins do not distinguish benign pancreatic cells and cells of ductal adenocarcinoma, but the latter may be separated from nonductal-type pancreatic cancers by different cytokeratin profiles.
- Cells of ductal pancreatic adenocarcinomas usually do not express vimentin and endocrine markers.
- Monospecific antibodies against carcinoembryonic antigen (CEA) may be helpful to separate certain types of pancreas neoplasms from nonneoplastic disorders. Other markers that could help distinguish between benign and malignant pancreatic cells in cytologic specimens have recently been evaluated [13, 209].
- p53 immunostaining in brush specimens of patients with extrahepatic bile duct stenosis may be helpful in the diag-

nosis of bile duct carcinoma, but the marker is less valuable in the assessment of pancreatic carcinoma [188].

### 10.1.3.2 DNA Ploidy Analysis

#### 10.1.3.2.1 DNA Image Cytometry

[17, 24, 25, 102, 110, 130, 158, 159]
(Figs. 10.5, 10.24, 10.26)

- Ploidy assessment by DNA image cytometry (ICM DNA) is a valuable adjunct to routine cytology for detecting malignant or potentially malignant disorders in FNAB of mucinous cystic tumors and in brush cytology performed on strictures of the biliary and pancreatic ducts (see also Sect. 10.2.8, "Dysplastic and Reactive/Regenerative Biliary Epithelium," p. 685).
- Quantitative DNA results are helpful in distinguishing between benign and malignant cell populations (Figs. 10.3–10.5):
  - Increasing diagnostic sensitivity as compared to cytology alone.
  - Rectification of false-negative results based on prior cytologic evaluations.
  - An abnormal DNA histogram selects patients with negative and atypical cytology for stringent evaluation of malignancy and continuous follow-up, respectively.
  - Quantitative DNA analysis can verify the majority of benign and malignant cytologic diagnoses or can reassure the cytopathologist in cases with an uncertain cytodiagnosis. In this setting, performance of the DNA test is of particular importance in patients with positive cytology and simultaneous negative or equivocal clinical and histologic-bioptic findings.

**Caution**

- The very high specificity for malignancy in conventional cytology may be reduced by DNA image analysis (for the same patient group) . Hence, the results of DNA measurement need to be interpreted together with the patient's history, endoscopic and clinical findings, and imaging results [17, 102, 159] .
- The extent of specificity reduction is determined by the individual histogram classification.

- For digital DNA analysis, routine cytologic specimens are restained with the Feulgen method.
- Histogram interpretation at our institution has been refined with increasing practical experience over a long period. The purpose has been to achieve as high as possible a grade of diagnostic sensitivity and specificity for atypical epithelial cells of undetermined significance originating from biliary strictures (related to a pancreatic or primary bile duct process) and from the epithelial lining of cystic lesions of the pancreas. The currently applied histogram algorithm is listed below.

**DNA diploidy:**
1.8c ≤ DNA index of the stemline (SL) ≤ 2.2c
**DNA intermediate profile:**
diploid SL and more than 10% single cells < 4.4c,
or high S-phase fraction (lacking distinct SL in the 3c area),
or single cells in the octoploid area
**DNA aneuploidy:**
1. aneuploid SL: SL < 0.9c, **or** 1.1c < SL < 1.8c, **or** 2.2c < SL < 3.6c, **or** SL > 4.4c
2. tetraploid SL and ≥ 15% of all cells measured in noneuploid regions
3. 15% noneuploid cells (of all cells measured) > 4.4c
4. 9c exceeding events more than three cells

A stemline contains more than 20% of all cells measured.

- Aneuploidy indicates severe epithelial dysplasia (preneoplasia) or malignancy and is in general a marker of poor prognosis in patients with malignant biliary strictures related to a pancreatic cancer, whereas an intermediate DNA profile has been shown to be indeterminant for malignancy (Figs. 10.66 and 10.67). In our series, we have found sporadic pancreatic cancers presenting with a diploid DNA profile in accordance with the algorithm stated above.
- The histogram interpretation may be equally applied for malignancy assessment of epithelial cells of intestinal origin such as cells from intestinal metaplasia of the esophagus (Barrett esophagus), gastric epithelial cells, and epithelial cells of small and large bowel mucosa.

#### 10.1.3.2.2 DNA Flow Cytometry

Quantitative DNA studies using the flow cytometry (FCM) method yield similar results and conclusions to those reported for ICM DNA [115, 159].

### 10.1.3.3 Molecular Genetics

- *KRAS* point mutation and mutations of tumor suppressor genes *p16*, *TP53* and *DPC4* have been identified as the most frequent genetic changes in ductal pancreatic carcinomas. Both the specificity and impact of these chromosomal abnormalities for pancreatic carcinogenesis is not yet determined [11, 74, 90, 104, 117, 150].
- Recent studies indicate that the fluorescence in situ hybridization (FISH) test has increased sensitivity while preserving the specificity of cytologic diagnosis in the detection of malignant bile duct strictures. The UroVysion multiprobe assay has been used, which detects abnormal signal copy numbers of chromosomes 3, 7, and 17 and deletion in the 9p21 gene locus [98, 110, 130].

#### 10.1.3.4 Cyst Fluid Analysis (Enzymes, Tumor Markers)

Biochemical cyst fluid analysis may significantly enhance the diagnostic accuracy for pancreatic cystic neoplasms distinguishing between neoplastic cysts and nontumoral pancreatic cystic lesions in a substantial number of cases.

*Enzymes:* Amylase content and amylase isoenzyme level aids differentiation of pseudocysts from cystic tumors. Insulin-content, among other hormones, has been reported to be helpful in the preoperative differentiation of cystic endocrine tumors from other cystic pancreatic neoplasms [203].

*Tumor markers:* Various sets of tumor markers have been evaluated regarding their potential for preoperative classification of morphologically indeterminate cystic lesions of the pancreas. The most frequently investigated markers are carcinoembryonic antigen (CEA), CA 19-9, CA 125, CA 15-3, pancreatitis-associated protein, and tumor-associated glycoprotein 72 (TAG-72).

We refer to the literature (selected papers cited) for standardization of individual enzyme levels and marker profiles, for difficulties and pitfalls, and for further information [6, 12, 33, 112, 116, 167, 203].



### 10.1.4 Normal Cytology of the Pancreas and Contaminants

#### 10.1.4.1 Benign Pancreatic Cells

(Figs. 10.6 and 10.7)

Acinar and ductal cells originate from the exocrine portion of the pancreas.

- *Acinar cells* (Fig. 10.6A) appear in FNA preparations in small acinar groupings.
  - The small nuclei are uniform, round to ovoid, with slight variation in size showing a smooth distinct membrane.
  - Most nuclei are excentrically and basally placed. Nucleoli are small, round, and conspicuous.
  - The chromatin is finely granular and evenly distributed.
  - The cytoplasm is abundant and finely granular, though granularity may appear vaguely in the Papanicolaou stain.
  - Small and large tissue fragments of acini may be encountered, arranged in lobules and separated by loose fibrovascular tissue.
- *Cells of small pancreatic ducts* (Fig. 10.6B) in FNAB specimens are arranged in regular, flat sheets.
  - The cells are cuboid to columnar.
  - The small round nuclei exhibit regularly distributed granular chromatin and occasionally a tiny nucleolus.
  - The cytoplasm is relatively scant and poorly defined.
- *Cells of large pancreatic ducts* (Fig. 10.6C) rarely turn up in FNAB samples. The cells are a typical finding in pancreatic duct samples collected by brushing or direct juice aspiration.
  - Epithelial cells lining large pancreatic ducts are in general slightly smaller than epithelial cells originating from the bile duct system.
  - The cells are small to medium-sized and of cuboid or columnar shape. They occur singly, in palisades, or in a regular flat honeycomb-like arrangement.
  - The nuclei are round and distinctly outlined.
  - The chromatin is evenly dispersed and granular.
  - Nucleoli may be distinct, suggesting cellular activity.
  - The cytoplasm is well defined, densely structured, or vacuolated.
  - Variable numbers of degenerating epithelial cells are usually present.
- *Islet cells* (Fig. 10.7) are cells forming the endocrine fraction of the pancreas. The endocrine fraction of the pancreas consists of numerous dispersed islets of Langerhans with the highest concentration in the body and the tail of the organ.
  - Islet cells appear very infrequently in pancreatic aspirates or are simply not identifiable.
  - The cells occur singly or in loose aggregation and are larger than exocrine acinar cells.
  - The nuclei are very similar to those of acinar cells; the N/C ratio is low. Assignment of stripped nuclei to islet cells or exocrine acinar cells is not possible.
  - The cytoplasm may appear either pale or flimsy, or is not recognizable at all.

#### 10.1.4.2 Contaminants in FNAB (Figs. 10.8–10.10)

- *Mesothelial cells* are encountered mainly in percutaneous aspirates.
  - The large mesothelial sheets are composed of flattened cells, the sheets are occasionally folded.
  - The nuclei are widely spaced, frequently exhibiting indentations. The nucleoplasm is clear and the chromatin texture indistinct; nucleoli may be conspicuous.
  - Reactive-reparative changes of the mesothelium can enhance nuclear polymorphism and nucleolar size. Additional nuclear overlapping, hyperchromasia, and coarsening of the chromatin could lead to an erroneous diagnosis of malignancy (Fig. 10.8).
- *Gastrointestinal epithelium* (Figs. 10.9 and 10.10) is a major contaminant in FNABs performed during routine endoscopic examination. Distinguishing between gastrointestinal epithelium and pancreatic ductal epithelium may be challenging; misdiagnosis of a mucinous cystic tumor of the pancreas is possible (see also Sect. 10.1.7.2, p. 640) (Fig. 10.10).
- *Hepatocytes* may sporadically be encountered.

### 10.1.4.3 Contaminants in Pancreatic Juice
(Figs. 10.11–10.14)

Cells from bile duct lining epithelium and from the superficial duodenal mucosa are admixed in cases where the pancreatic juice is collected from the ampulla or together with duodenal secretion.
Distinction of bile duct lining cells from pancreatic ductal epithelial cells is not always possible.

- *Epithelial cells from the bile duct system*
  - They appear as slender elongated columnar cells with small round basally located nuclei; the cells are commonly referred to as matchsticks. However, not all cells of biliary tract origin are necessarily elongated, they may also appear cuboidal (Fig. 10.11).
- *Cells from the duodenal lining epithelium* (Figs. 10.12 and 10.13A)
  - They have a cuboid to cylindrical shape, usually displaying a well-preserved prominent brush border. They are typically arranged in flat sheets that are interspersed with goblet cells.
- *Degenerating epithelial cells*
  - Large numbers of degenerating epithelial cells (debris) (Fig. 10.13B), particularly originating from gastrointestinal epithelium, should not be misinterpreted as tumor necrosis.
- *Cells of intramural duodenal/ampullary glands.*
  Harm of the duodenal/ampullary surface epithelium by mechanical manipulation may shed clusters of intramural glands into pancreatic juice and duodenal fluid aspirates (Fig. 10.14).
  - Cells of intramural glands are more voluminous and polygon-shaped compared to duct lining cells. Their nuclei exhibit loose chromatin, focally irregular outline, and distinct nucleoli of variable size.
  - The cytoplasm is clear and coarsely vacuolated and tends to be abundant.
  - Pronounced irregular cell clustering and nuclear crowding can potentially be misinterpreted as adenocarcinoma of the clear cell type.

**Caution**

- Reactive-reparative changes in mesothelial cell clusters may be misinterpreted as malignant.
- Activated clusters of duodenal/ampullary intramural glandular cells may be misinterpreted as clear cell adenocarcinoma.
- Large amounts of gastrointestinal cellular debris should not lead to an erroneous interpretation of necrotic cancer.

## 10.1.5 Inflammation, Infection, and Infectious Cysts

### 10.1.5.1 Acute Pancreatitis [33]

Most cases of acute pancreatitis are caused by proteolytic destruction of the gland and the fatty tissue, whereas an infectious etiology is rare. Acute pancreatitis may lead to complications such as hemorrhage, necrosis, and development of pseudocysts and abscess; complications that are associated with a high mortality. In survivors, a considerable proportion of acute disorders progress to chronic pancreatitis.

**Microscopic Features**

*Early form of acute pancreatitis*

- Degenerated fat cells (fat necrosis), foam cells, lipid-laden vacuolated macrophages, numerous neutrophils, and granular debris. Degenerating and necrotic acinar and ductal cells; the nuclei are pyknotic, small, and deeply stained.

*Healing form of pancreatitis*

- In addition to cellular components as described above, the smears contain granulation tissue comprising reactive immature fibroblasts, activated histiocytes, numerous leukocytes of various types, and proliferating capillaries. Granular calcium deposits are frequent (Fig. 10.15).

**Caution**

Well-preserved activated and regenerative cells can present diagnostic dilemmas:
- Reactive immature fibroblasts and histiocytes/macrophages may exhibit distinct nuclear atypia overlapping the atypia of malignant cells.
- Nuclear features of activated mesenchymal cells can match those of pancreatic carcinoma cells (pleomorphic nucleus with clear nucleoplasm, irregularities of the nuclear membrane, indistinct chromatin texture, pronounced nucleoli).

### 10.1.5.2 Chronic Pancreatitis
[33, 46, 124] (Fig. 10.16)

Cellularity of the smears in chronic pancreatitis depends on the degree of fibrosis in the needle pass areas. FNAB samples of a chronic inflammatory lesion should contain an inflammatory cell component and/or fragments of fibrous tissue. An additional epithelial component with indeterminate cellular atypias should raise suspicion of adenocarcinoma of the pancreas.

**Microscopic Features**

- Hallmarks: Minor acinar cell component, with the ductal cells predominating. The latter are usually arranged in small, cohesive, slightly irregular sheets.

- Numerous ductal cells display atypical features varying in their characters:
  - Focally nuclear overlapping may be observed in the cell sheets.
  - The nuclei are somewhat larger as compared to those of completely normal cells varying in size and shape. Nuclear wrinkles and indentations are infrequent and not pronounced.
  - The N/C ratio is within normal range or slightly increased.
  - The nucleoli are conspicuous and variable in size.
  - The chromatin distribution in the nuclei is loose and regular.
  - The cytoplasm is frequently vacuolated. Squamoid cytoplasmic features characterized by a dense structure and sharp outlines are observed in aspirates from ductal squamous metaplastic areas.
  - The background of the smears reveals lymphocytes, plasma cells, and fragments of fibrotic tissue.

**Differential Diagnosis** (Fig. 10.16B)

Reactive epithelial atypia in a background of chronic inflammation can give rise to considerable difficulties in diagnosis.

- Monolayered sheets of the ductal cell type exhibiting focal nuclear crowding, distinct abnormalities of nuclear shape (bizarre molding and cleaving), chromatin clearing, and prominent nucleoli should be considered as diagnostic for well-differentiated pancreatic adenocarcinoma. Histologic evaluation is frequently inevitable in such cases in order to exclude severe reactive cell changes in the course of chronic pancreatitis.
- Cell groups of the ductal type characterized by marked nuclear overlapping, nuclear crowding, cellular discohesion, pronounced nuclear pleomorphism (folds and grooves), nuclear hyperchromasia, increased N/C ratio, mitoses, and necrosis are strongly indicative of poorly differentiated adenocarcinoma, but cytology alone cannot completely exclude severe reactive atypias provoked by chronic pancreatitis.
- Pronounced membrane irregularities and anisonucleosis are the most specific indicators of an adenocarcinoma.

Cytologic features of cellular atypia in chronic pancreatitis versus pancreatic adenocarcinoma of various grades are tabulated in the textbook by Centeno and Pitman, pp. 45–47 [33] and discussed in individual publications [44, 84, 119]

**Caution**

Aspirates of chronic pancreatitis, comprising ductal cells with regenerative and reparative changes and nuclear atypia, lacking a concomitant morphologic background are difficult to distinguish from pancreatic adenocarcinoma.

### 10.1.5.3 Autoimmune Pancreatitis

Autoimmune pancreatitis (AIP) is a new entity among chronic pancreatic inflammatory disorders. AIP has been identified as pancreatic manifestation of a systemic fibroinflammatory disease (IgG4-related systemic disease). Affected pancreas demonstrate a dense lymphoplasmacytic infiltration, and numerous cells are IgG4-positive [69]. Studies of AIP in cytologic FNAB samples are very limited [111].

### 10.1.5.4 Pancreatic Tuberculosis [78, 96, 121]

Pancreatic tuberculosis is considered a rare disease. It usually occurs as a complication of miliary tuberculosis, especially in immunosuppressed individuals. Pancreatic tuberculosis is often misinterpreted as a neoplastic mass or nonspecific pancreatitis by imaging procedures.

- The pathognomonic cytologic pattern is composed of caseous necrosis, epithelioid histiocytes, Langhans giant cells along with neutrophilic and/or lymphoplasmacytic infiltrates.

Ziehl-Neelsen staining for acid-fast bacilli should be performed on cytologic preparations to prove a suspected mycobacterial infection. Mycotic infectious disease can be excluded using Grocott and PAS staining.

**Caution**

Pure caseous debris with absence of typical histiocytic elements may mimic cancer necrosis. A misdiagnosis of malignancy is easily made in patients known to be immunocompetent.

### 10.1.5.5 Infectious Cysts

- *Secondary infected pseudocysts and abscesses* are characterized by abundance of neutrophils, degenerating neutrophils, and debris. Application of special stains (Giemsa, Gram, periodic acid-Schiff reaction, Grocott) will identify infectious organisms, such as bacteria, fungi, or protozoa. Additional microbiologic analyses from a fraction of the aspirate will enable the classification of the nature and type of the pathogen.
- *Hydatid cyst (echinococcosis)* (Figs. 3.17, 9.7, 9.8) is rarely encountered in the pancreas. A specific diagnosis of echinococcosis is usually made by imaging techniques. However, guided fine-needle aspiration is a safe method to assess the nature of obscure cystic lesions suggestive of a hydatid cyst but lacking calcification by imaging.
  - The finding of hooklets and scoleces is diagnostic for hydatid disease (Figs. 3.17 and 9.7).

- A bloodless fluid sediment having opaque debris in the background, only a few cellular elements, and sporadic hooklets, if any, is also pathognomonic (Fig. 9.8).

**Caution**

It is highly important to read smears from poorly cellular cystic fluids carefully, if necessary in high magnification. Minimal closing of the microscope diaphragm can be helpful in detecting single and tiny hooklets.

- Cystic lesions caused by other protozoal and helminthic infections are not further discussed in this section. They are described in pertinent papers and distinguished textbooks [104].

## 10.1.6 Nontumoral Cystic Lesions: Findings in Aspirates [33]

### 10.1.6.1 Pseudocysts (Fig. 10.17)

Pseudocysts are the most common type of cystic lesions, accounting for 75–90% of all pancreatic cysts. In general, they follow acute pancreatitis, trauma, and surgery, and may result from acute episodes of chronic relapsing pancreatitis. Pseudocysts are cavities following the rupture of ducts; they are filled with fluid subsequently producing an inflammatory reaction. Pseudocysts occur most often as unilocular lesions.

- The mixed inflammatory component varies, hemosiderin-laden macrophages are usually present.
- Furthermore, the smear background is composed of debris, blood, and hemosiderin. Bile pigment may be observed.
- Cyst-lining epithelium is practically absent.
- Occasional normal pancreatic parenchyma cells originate from the needle passes through normal gland tissue.

Analysis of amylase content in aspirated cystic fluids is useful in identifying pseudocysts [112].

**Caution**

Presence of mucin with or without mucinous epithelial cells is highly suspicious of a mucinous cystic neoplasm.

### 10.1.6.2 Retention Cysts

They result from an obstruction of the pancreatic duct system. The wall of small cysts is lined by genuine ductal epithelium, which undergoes degeneration and vanishes during cyst enlargement by pressure and inflammation.

- Overlap of the cytologic features of retention cysts with those of pseudocysts is striking.
- Cyst-lining epithelial cells – even with mucin inclusions – may be present.
- Islet cells from neighboring pancreatic tissue have been observed.

**Caution**

- A few endocrine cells in the fluid of retention cysts should not mislead to a diagnosis of a cystic islet cell tumor (see Sects. 10.1.6.5, p. 640 and 10.1.7.5.1, p. 642).
- Endoscopy and imaging are crucial tests to distinguish mucinous retention cysts from mucinous cystic neoplasia.

### 10.1.6.3 Congenital Cysts

Cytologic experience with fluids from congenital pancreatic cysts obtained by fine-needle aspiration is limited to reports of single cases [33, 181, 187]. Biochemical analysis of cyst fluid and correspondent immunocytochemical findings for the lining epithelial cells are reported in the indicated literature.

- The sediment smears of the cystic fluid show scant cellularity.
- Single cuboidal epithelial cells have bland nuclei and usually sharply outlined basophilic cytoplasm. Squamous cells as the cyst's inner lining have been found in histologic sections [187].

### 10.1.6.4 Lymphoepithelial Cysts

[2, 3, 35, 194, 195] (Fig. 10.18)

#### General Comments and Histologic Appearance

- Lymphoepithelial cyst (LEC) is an unusual and benign entity among the cystic disorders of the pancreas. Its common location is the tail of the pancreas. The most accepted theory of histogenesis of LEC is epithelial inclusion in a pancreatic lymph node or ectopic pancreatic tissue in a peripancreatic lymph node [194]. LECs occur as unilocular and multilocular entities.
- No pancreas LEC patients have been found in the course of immunosuppression. In contrast, lymphoepithelial cystic disorder in salivary glands is a typical lesion of immunocompromised hosts.
- Histologically, the cysts are lined with mature stratified squamous epithelium surrounded by lymphoid tissue usually including prominent follicles. Areas in the lining epithelium display transitional or cuboidal appearance; mucinous cells are infrequently observed.

#### Microscopic Features, Differential Diagnosis, and Immunocytochemistry

- Cytologic samples [3, 35] are cellular, mainly composed of benign superficial squamous cells and anucleated squames.

- Mucin-secreting cells may rarely be encountered.
- Histiocytes, lymphocytes, and cholesterol crystals are commonly present.

Differential diagnosis includes dermoid cyst, congenital cyst, and other squamous cysts located in the neighborhood of the pancreas. Mucin-producing epithelial cells could lead to a false diagnosis of retention cyst or mucinous cystic neoplasia. The squamous cells of LEC are completely benign making a false diagnosis of squamous cell carcinoma extremely unlikely.

Cyst-lining glandular cells are immunocytochemically positive for CEA [35] and CA19-9. The latter marker has also been found in cyst contents using a biochemical assay [195].

### 10.1.6.5 Extremely Rare Pancreatic Cystic Lesions

Single cases have been described in the clinical, cytologic, and histologic literature:

- *Dermoid cyst* [61, 199] is not really a simple cyst but a cystic neoplasm. It evolves from remnants of embryonic tissue located in the pancreas. The cytologic features are very similar to those of dermoid cysts at anatomic sites other than pancreas: anucleated and nucleated squames, keratinized debris, and inflammatory infiltrates. Other squamous cell-lined cysts should be considered in the differential diagnosis.
- *Mesothelial cyst* [141]: The lining epithelium is similar to the mesothelial layer of the body cavities. Immunocytochemical positivity for vimentin, calretinin, and CK5/6 confirms the histogenetic nature of the cells.
- *Cystic islet cell tumor* [85] should be considered in cases with overt endocrine cells in fluid aspirates (see also Sect. 10.1.7.5.1, p. 642). Differential diagnosis is islet cell contamination from adjacent pancreatic tissue caused by the needle passes.

## 10.1.7 Neoplastic Cysts: Findings in Aspirates

- Differentiating the morphologic features of the various pancreatic cystic lesions is discussed in several sections of Chapter 10. For further information, we refer to references listed in the corresponding sections of this chapter.
- For biochemical cyst fluid analysis see Sect. 10.1.3.4, p. 636.

### 10.1.7.1 Serous Cystadenoma

[80, 105, 118, 140] (Figs. 10.19 and 10.20)

#### General Comments

- Synonyms for serous cystadenoma (SCA) are microcystic adenoma and glycogen-rich cystadenoma.
- SCA is an invariably benign tumor occurring in older patients, usually in females. The tumors present with innumerable small cysts resulting in a classic radiologic picture, but macrocystic variants have also been described [83, 95]. Immunocytochemical and ultrastructural properties of the tumor cells resemble centroacinar cells [7, 95].

#### Microscopic Features

- The aspirated fluid is clear and cytologic preparations comprise scarce epithelial cells and a proteinaceous background.
- The cells are cuboid or small, columnar in shape, and arranged in small regular sheets. Their nuclei are round and smooth with a bland chromatin texture and indistinct nucleoli.
- The cytoplasm is clear, vacuolated, and sharply outlined. Intracytoplasmic glycogen can be demonstrated by the PAS stain.
- Foamy macrophages, small fragments of fibrous stroma, and calcification may be present.

**Caution**

- It should be emphasized that FNAB of SCAs in general have markedly scant cellularity or are even devoid of epithelial cells, with the result that the aspirate is often nondiagnostic or not suitable for classifying the tumor [64].
- Gastrointestinal-contaminating epithelium in endoscopic ultrasonography-guided aspirates from SCA is a major reason for an erroneous diagnosis of a cystic mucinous tumor [20].

### 10.1.7.2 Mucinous Cystic Neoplasms

[29, 43] (Figs. 10.21–10.27)

#### General Comments and Histologic Classification

- Mucinous cystic neoplasms occur particularly in middle-aged women. Most of these tumors are multiloculated with a site predilection in the body and tail of the pancreas.
- Pancreatic duct epithelial cells are assumed to be the precursor cells of these tumors.
- Histologic classification: Depending on the grade of cellular atypia/dysplasia in the cyst-lining epithelium, tumors should be classified histologically as adenoma, borderline tumor (dysplastic epithelium), carcinoma in situ (noninvasive malignant epithelium), or carcinoma (invasive behavior) [211]. The distinction between benign, bor-

derline, and malignant tumors is not always obvious. Intraepithelial neoplasia (dysplasia, carcinoma in situ) usually occurs focally. The abnormal epithelial foci may be detected only after intensive searches in multiple histologic sections from different regions of the cyst wall.

- A progression from adenoma to carcinoma is widely accepted. Any mucinous tumor should be regarded as a potentially malignant disorder, regardless of the morphology of the epithelial cells [29, 43].
- The term "mucinous cystadenocarcinoma" is exclusively used for neoplasms showing unequivocal invasion beyond the cyst wall, or distant metastases.
- Elevated levels of certain biomarkers in cyst fluids may have a strong correlation with a mucinous cystic neoplasm (see also Sect. 10.1.3.4, "Cyst Fluid Analysis: Enzymes, Tumor Markers," p. 636).

### Microscopic Features

- Basic attributes of cystic neoplasms: The aspirates usually show moderate to high cellularity, but adenomas and borderline tumors with mild dysplastic changes may exhibit paucity of cells. The presence of background mucin is pathognomonic.
  The epithelial cells have a columnar shape and contain mucin. They may be arranged in flat sheets with a honeycomb pattern, in palisading rows, and in small papillary formations; or they occur in isolation, often appearing as goblet cells. Numerous foamy histiocytes and mucin-containing macrophages are usually admixed.
  - *Mucinous cystic adenoma:* The nuclei are round with bland chromatin and small nucleoli (Figs. 10.21–10.23).
  - *Mucinous cystic borderline tumor:* Dysplastic cells are larger than those originating from benign epithelium, and the N/C ratio is increased. Their nuclei exhibit variable size, irregularities of the membrane, granular or coarse chromatin, and distinct nucleoli. Pronounced cellular palisading and cell clustering may be observed, giving rise to an enhanced architectural complexity (Fig. 10.25).
  - *Mucinous cystadenocarcinoma (invasive cystic carcinoma):* Aspirates are highly cellular. Cell clusters are three-dimensional acinic-like or papilliform and cellular dyshesion is prominent. Cells are highly abnormal with unambiguous features of malignancy, such as a high N/C ratio, wrinkled and folded nuclei, irregularly distributed granular and coarse chromatin, and dark nucleoplasm. The nucleoli are prominent and frequently multiple. Mitoses and necrosis are distinct (Fig. 10.27).

### Differential Diagnosis

Any pancreatic cystic lesion containing mucin is highly suspicious of a cystic mucinous neoplasia. But there are occurrences one has to be aware of:

- Retention cysts may be layered with mucin-producing epithelium, but retention cysts are small and occur rarely.
- Activated mucin-laden macrophages may mimic dysplastic/malignant mucin-producing epithelial cells. Such cases require immunocytochemical work-up using antibodies against cytokeratins (positivity in epithelial cells) and histiocytic markers such as CD68 (Fig. 10.25).
- Distinguishing noninvasive from invasive mucinous cystadenocarcinoma and distinction between mucinous cystadenocarcinoma and ductal adenocarcinoma with secondary cystic changes is not possible by cytology.
- Gastrointestinal-contaminating epithelium in endoscopic ultrasonography-guided aspirates may lead to a misdiagnosis of cystic mucinous neoplasia (Figs. 10.9 and 10.10).
- Marked degeneration of individual epithelial cells in smear preparations sets limitations on the cytodiagnostic work-up. Such cells may easily be misinterpreted as degenerating histiocytes (Fig. 10.25A).

**Caution**

- High fluid viscosity may prevent successful aspiration of cyst content in mucinous cystic neoplasms.
- Cytology alone does not allow a distinction of intracystic carcinoma in situ from invasive cystic carcinoma.
- Pronounced degeneration of numerous single epithelial cells may present diagnostic dilemmas.
- Activated mucin-laden macrophages can lead to an erroneous diagnosis of mucin-producing carcinoma cells.
- Gastrointestinal-contaminating epithelium in endoscopic ultrasonography-guided aspirates from otherwise nonmucinous cystic lesions is a major reason for the misdiagnosis of a mucinous cystic neoplasm. We would like to emphasize that only the triad of typical cyst fluid debris, background mucus, and mucin-forming epithelial cells is a reliable indication for the diagnosis of mucinous cystic neoplasia.

## 10.1.7.3 Intraductal Papillary Mucinous Neoplasm

[15, 59, 107, 120, 165, 170, 179, 184] (Fig. 10.28)

### General Comments

- Synonyms for intraductal papillary mucinous neoplasm (IPMN) are intraductal mucinous hypersecreting neoplasm, mucinous ductal ectasia, ductectatic mucinous cystadenoma, intraductal papillary neoplasm, papillary cystadenoma, and cystadenocarcinoma.
- IPMN is an entity with a clinicopathologic presentation distinct from that of mucinous cystic neoplasms. The neoplasms affect elderly patients, particularly males.

- The majority of IPMNs occur in the main pancreatic duct and its branches in the head and body of the organ. Extension to the ampulla of Vater and into the common bile ducts has been observed. The tumors are divided into benign, borderline, and malignant lesions.

**Microscopic Features and Tumor Grading**

Cytologic experience in the preoperative diagnosis of IPMN had long been limited. In recent years, the cytomorphologic features of this entity have been described by means of single cases and larger series with the aim of standardization for diagnostic purposes. Cytology was found to be helpful in confirming suspected IPMN diagnosis preoperatively. Cytological specimens were sampled in most patients by EUS-guided FNAB. In a few cases, pancreatic juice was investigated, sampled by pancreatoscopy or pancreatic duct lavage [53, 163, 207].

- Hallmarks: Abundant extracellular viscous mucin. Cohesive sheets of mucinous epithelial cells, frequently of the goblet cell type, are entrapped in pools of mucin or in the background. Papillary clusters occur only in a small proportion of all cases.
- Histiocytes and mucin-laden macrophages may be present.
- Inflammatory infiltrates are rarely observed.

The degree of cellular atypia, cellular crowding, nuclear pleomorphism, and nucleolar size may vary in cytologic preparations of the same case, and accurate tumor grading is considered to be difficult [107, 170]. However, irregular clusters, nonmucinous epithelial cells, numerous single cells, severe nuclear atypia comprising nuclear clearing, and necrosis indicate a high probability of malignancy [128, 179].

### 10.1.7.4 Solid Pseudopapillary Tumor

[16, 22, 87, 164] (Fig. 10.29)

**General Comments**

- Synonyms for solid pseudopapillary tumor (SPPT) are papillary cystic neoplasm, solid and cystic tumor of the pancreas, papillary cystic tumor of the pancreas, and papillary epithelial neoplasm of the pancreas.
- This is a rare neoplasm of low malignant potential, mainly occurring in young women.
- The gross tumor is well encapsulated and composed of solid and cystic areas, focal hemorrhage, and necrosis.
- The patient is usually cured after complete surgical resection.

**Microscopic Features and Immunocytochemistry**

- Hallmarks: The cytologic smears are highly cellular. They are composed of numerous branching papillary fragments disclosing characteristic delicate fibrovascular cores surrounded by myxoid stroma and superficial monolayered or multilayered neoplastic cell lining. Myxoid or mucoid tissue fragments free of cell cover may also occur. The cells are monomorphic, exhibiting an amphophilic ill-defined occasionally granular cytoplasm. The nuclei are usually oval and clear with finely granular chromatin. Distinct nuclear grooves and inclusions are pathognomonic for this tumor entity but may not be encountered in each individual case. The nucleoli are small but conspicuous.
- Macrophages and necrosis frequently occur.

No differential diagnosis problems should arise if the key features of SPPT are overt.

Constant immunohistochemical positivity has been described for vimentin, alpha1-antitrypsin, and alpha1-antichymotrypsin. Positive immunoreaction for synaptophysin and neuron-specific enolase has variably been reported [16, 22, 164].

### 10.1.7.5 Rare Cystic Tumors and Tumors with Variable Cystic Components

#### 10.1.7.5.1 Cystic Pancreatic Endocrine Tumor

(Fig. 10.30)

Cystic degeneration of pancreatic endocrine tumors seems to be relatively common among nonhyperfunctioning large islet cell tumors [30]. Cytologic examination of cyst fluid reveals neuroendocrine-type cells. Cytomorphology of the specific epithelial cell component meets that of its solid counterparts (see Sect. 10.1.10, p. 646).

The biochemical fluid analysis results in low levels for CEA, CA-125, and CA-15-3, and variable levels for amylase. Insulin levels have been reported to be elevated and may be helpful in the preoperative differentiation between endocrine tumor cysts and other cystic entities [203].

#### 10.1.7.5.2 Acinar Cell Cystadenocarcinoma

This variant of the classic solid type of acinar cell carcinoma is extremely rare; reports on cytomorphologic findings are lacking. Histologically, the cyst lining cells are described to form acinar formations; the immunohistochemical pattern confirms the acinar origin (cytoplasmic expression of alpha1-antitrypsin, trypsin, and lipase) [42] (see also Sect. 10.1.9.2, p. 645).

#### 10.1.7.5.3 Other Cystic Tumors (Fig. 10.31)

Vascular tumors (hemangioma, lymphangioma) in the pancreas and varied cystic tumors in the peripancreatic and retroperitoneal space should always be included in the differential diagnosis of pancreatic cysts. Such lesions have been compiled from various sources and are listed in Centeno's textbook *Fine-Needle Aspiration Biopsy of the Pancreas*, p. 99. [33].

## 10.1.8 Invasive Carcinoma and Precursor Lesions of the Pancreatic Duct System

### 10.1.8.1 Ductal Adenocarcinoma

(Figs. 10.32–10.36, 10.38)

- Primary ductal adenocarcinoma accounts for 80–90% of all malignant neoplasms of the pancreas. About two-thirds of the neoplasms occur in the head of the pancreas. Most patients are in the fifth to seventh decade of their life. Tumors of the head of the pancreas generally produce early symptoms, in contrast to cancers of the body and tail. The latter grow symptomless over a longer period and are correspondingly larger in size at the time of diagnosis. The overall 5-year survival rate of pancreatic ductal adenocarcinoma with or without conservative therapy and after resection is extremely poor [60].
- Reported specificity of FNAB for ductal pancreatic adenocarcinoma is in most series 100%, whereas sensitivity ranges from 50 to 100%. Strict application of well-defined cellular criteria can clearly improve the accuracy of the cytologic diagnosis [39, 113, 129, 157].
- Transcutaneous ultrasound-guided [26, 49, 180], computed tomography-guided [182], and endoscopic ultrasound-guided FNABs [55, 210] are highly accurate tools for the diagnosis of adenocarcinomas of the pancreas, with comparable results regarding sensitivity and specificity. False-negative results have been found to be caused particularly by interventional technical problems, the size and nature of the lesion, and the cellularity of the aspirate.
- On-site cytologic evaluation by a skilled cytopathologist may reduce the problem of sample inadequacy due to the possibility of immediate repeat aspiration.

#### 10.1.8.1.1 Well-Differentiated Ductal Adenocarcinoma [113] (Figs. 10.32, 10.33, 10.38)

**Microscopic Features**

- Hallmarks:
  - Small and large cohesive sheets with striking sharply defined outer edges, no peripheral dissociation of cells. Sheets are flat, occasionally with a honeycomb appearance as a result of abundant cytoplasmic mucin.
  - The cells are usually tightly packed with nuclear crowding and overlapping.
  - The nuclei show considerable variations in size and might be smaller than benign ductal pancreatic cells. Nuclear membrane irregularity is a key feature for the diagnosis of well-differentiated adenocarcinoma: tiny wrinkles, folds, or subtle lobulation are detectable on each malignant nucleus with thorough cell study.
  - Chromatin clearing is pathognomic for this type of adenocarcinoma unless the chromatin texture is finely granular and irregular. Conspicuous small nucleoli are present in some of the nuclei.
  - The cytoplasm is clear, vacuolated, or mucinous, and sharply outlined.
- The smears are usually cellular with mitotic activity present in most cases to a lesser extent.
- Necrosis is rarely observed.

**Differential Diagnosis**

Biliary duct adenocarcinomas mimic ductal pancreatic adenocarcinomas. Metastases of adenocarcinomas from distant sites must also be excluded.

**Caution**

Careful search for the pathognomonic nuclear features (tiny wrinkles, folds or lobulation, and chromatin clearing) allows a definite diagnosis in the vast majority of well-differentiated carcinomas of the pancreas.

#### 10.1.8.1.2 Moderately Differentiated Ductal Adenocarcinoma (Fig. 10.34)

**Microscopic Features**

These tumors exhibit the same basic cytological features as stated for the well-differentiated carcinoma variant, but atypias are more pronounced and the tumors are easily recognized as malignant:

- Cellular groupings and three-dimensional clusters exhibiting increased irregularities.
- Overt nuclear pleomorphism comprising indentations, cleaving, and lobulation.
- Coarse chromatin and hyperchromasia.
- Micronucleoli and occasional macronucleoli.
- Mitoses and necrosis.

**Differential Diagnosis**

As specified above.

**Caution**

Cytologic features of well- and moderately differentiated adenocarcinomas of bile ducts are virtually identical compared to their pancreatic duct counterparts. Adenocarcinomas with extensive mucin production most likely indicate bile duct origin.

#### 10.1.8.1.3 Poorly Differentiated Ductal Adenocarcinoma (Figs. 10.35 and 10.36)

**Microscopic Features**

- Numerous single cells and irregular three-dimensional cell clusters with marked cell dissociation. The cell clusters show acinic-like or micropapillary features; nuclear overlapping, and loss of polarity are pronounced.
- Marked cellular and nuclear pleomorphism.

- High N/C ratio.
- Coarse chromatin and articulate hyperchromasia.
- Numerous mitoses and extensive necrosis.

**Differential Diagnosis**

Undifferentiated secondary carcinoma and high-grade non-Hodgkin lymphoma of the blastic type have to be excluded. Immunocytochemical positivity for leukocyte common antigen (CD45) and other lymphocyte markers (e.g., against B-cell and T-cell epitopes) indicate cells of lymphoid origin.

**Caution**

- Marked cell dissociation of undifferentiated carcinoma cells and conversely loose and tight clustering of lymphoid blasts in cytologic preparations may lead to erroneous tumor typing with severe consequences for the patient in terms of additional investigations or primary therapeutic schemes which are not suitable.
- Tumor cells with clear cytoplasm and conspicuous vacuolization may mimic macrophages, especially in specimens with numerous degenerating isolated tumor cells, though the pathognomonic malignant nuclear features should easily be recognized at high magnification [88].



### 10.1.8.2 Variants of Ductal Carcinoma

#### 10.1.8.2.1 Adenosquamous Carcinoma and Squamous Cell Carcinoma

*Adenosquamous carcinoma* [94, 134, 151, 176] (Fig. 10.37) is a rare neoplasm constituting 3–4% of all pancreatic exocrine carcinomas. It is defined as a biphasic tumor composed of mucinous adenocarcinoma and a minimum of 30% of squamoid elements with keratinization; the latter are thought to be of metaplastic origin. The degree of differentiation and the proportion of squamous to glandular component varies from case to case.

*Pure primary squamous cell carcinoma* of the pancreas is an extremely rare tumor. Differential diagnosis includes adenosquamous carcinoma with a very scanty adenomatous component and squamous cell carcinoma of nonpancreatic origin.

**Caution**

- Adenosquamous carcinoma may present with a virtually exclusive squamous component; careful microscopic evaluation may disclose single mucinous carcinoma cells as the only evidence of glandular differentiation.
- Squamous cell carcinoma of the pancreas is a very rare primary entity.
- Metastatic squamous or adenosquamous carcinoma has to be excluded [108].

#### 10.1.8.2.2 Clear Cell Carcinoma [93, 154, 155]

Immunohistochemical findings and *KRAS* gene mutation provide evidence of the ductal phenotype of this rare type of pancreatic carcinoma [123, 155].

**Microscopic Features and Differential Diagnosis**

- The tumor is predominantly composed of cells having abundant clear cytoplasm (>90% clear cells) expressing PAS positivity for intracytoplasmic mucin [93, 155].

- Clear cell endocrine pancreatic tumor may mimic the ductal pancreatic counterpart but immunostaining for endocrine markers such as synaptophysin and chromogranin shows a positive reaction. The endocrine pancreatic tumor variant occurs predominantly in patients affected by Hippel-Lindau disease [81, 142].
- Metastatic clear cell carcinoma, which closely resemble pancreatic tumor of the clear cell type, predominantly includes renal clear cell carcinoma, adrenocortical carcinoma, tumors of the female genital tract, and lung cancers.
- Tumor cells with clear cytoplasm may mimic macrophages, especially in cytologic smears that are primarily composed of degenerating individual tumor cells.

#### 10.1.8.2.3 Oncocytic Neoplasia

The tumors are composed of oncocytes with their characteristic cytomorphologic features described in many other organs.

Low- and high-grade oncocytic tumors of the pancreas have been reported as intraductal lesions [1, 143], but also as variants of pancreatic endocrine tumors [146, 161, 200]. Differential diagnosis considerations concern other types of pancreatic carcinoma since cells with oncocytic features and granular cytoplasm may frequently be encountered, e.g., in acinar cell carcinoma [27]. Secondary tumors have to be excluded.

#### 10.1.8.2.4 Other Variants of Ductal Carcinoma

These include papillary carcinoma (Fig. 10.38), mucinous noncystic carcinoma and signet ring cell carcinoma, undifferentiated pleomorphic giant cell carcinoma [173], ciliated cell carcinoma [131], and mixed ductal-endocrine neoplasm [14, 190, 191]. For these extremely rare tumors, we refer to specialized sources in the literature, textbooks [33, 196], and individual publications.

### 10.1.8.3 Precursor Lesions of Invasive Ductal Pancreatic Adenocarcinoma [125]

**General Comments**

- Several noninvasive pancreatic lesions have been recognized as precursors for invasive adenocarcinoma of the pancreas. These lesions include: pancreatic intraepithelial

neoplasias (PanIN), intraductal papillary mucinous neoplasm (IPMN), and mucinous cystic neoplasms [125]. Consensus on the classification of the precursor lesions PanIN and IPMN including definitions and diagnostic guidelines for histologists have recently been developed [82].

- Pancreatic intraepithelial neoplasms are histologically classified into different grades: PanIN-1A, PanIN-1B, PanIN-2, and PanIN-3.
  PanIN-1 and PanIN-2 lesions are of unproved clinical significance and can develop in glands without cancer. It may be difficult to separate these lesions from reactive epithelial cell changes.
  In contrast, PanIN-3 has a high progressive potential for invasion [9, 82].
- In the future, precursors of invasive pancreatic ductal adenocarcinoma may be more often encountered in cytologic samples by increasing application of imaging, FNAB, and exfoliative cytological methods to the pancreatic duct system. Cytologic evaluation in combination with molecular methods (such as ploidy assessment by ICM DNA) offers the chance to detect preinvasive ductal lesions at an asymptomatic stage, consequently improving the prognosis in pancreatic carcinoma disease [31, 128, 139]. In recent years, it has become evident that molecular analyses could be helpful in defining a progression model for pancreatic neoplastic lesions [100, 144]. Hence, high-risk individuals could benefit from future screening programs [31]. The number of reports on this issue is still rare.

#### 10.1.8.3.1 Cytology and Ductal Precursor Lesions

A few attempts have been undertaken to evaluate cytologic features that may be useful to distinguish between intraductal dysplastic and malignant in situ lesions and invasive cancer:

- Small papillary cohesive clusters, presence of goblet cells, and sharply defined cell borders are reported to be main features of noninvasive IPMN [77] and PanIN-3 [76, 128].
- In contrast, loss of cellular cohesiveness, irregular chromatin texture, chromatin clearance, and conspicuous nucleoli are highly suggestive of invasive carcinoma.

## 10.1.9 Other Exocrine Pancreatic Cancers

### 10.1.9.1 Undifferentiated Small-Cell Carcinoma

[21, 37, 132, 156]

These are rare pancreatic primaries and their morphologic features are akin to small-cell carcinomas encountered in different organs, especially in small-cell carcinoma of the lung. Few reports in the literature presume an exocrine origin of this pancreatic tumor variant [132, 156].

### 10.1.9.2 Acinar Cell Carcinoma

[33, 103, 166, 183] (Fig. 10.39)

An incidence of approximately 1–2% has been reported for this rare pancreatic neoplasm with a higher survival rate than ductal pancreatic carcinoma. The predilection site of acinar cell carcinoma (ACC) is the head of the pancreas.

**Microscopic Features**

- Hallmarks: The microscopic hallmark of ACC is the presence of distinct acinar structures, albeit in many of the tumors in focal distribution.
  Highly cellular smears with large and small loosely cohesive clusters, prominent acinar formations, and numerous single cells.
  Monomorphic tumor cells showing one or two prominent nucleoli, and granular cytoplasm.
- In contrast to aspirated material from benign pancreatic tissue, the acini of ACC are characterized by an irregular arrangement of the tumor cells; the cells are slightly enlarged and the cytoplasm is scant to moderate in size.
- Isolated tumor cells are frequently stripped of their cytoplasm.

**Immunocytochemistry and Cytochemistry**

Immunocytochemical/cytochemical stainings show positivity for trypsin and chymotrypsin [103] and the cytoplasmic granules are periodically acid-Schiff-positive and resistant to diastase [166].

**Differential Diagnosis** [183]

- Cytomorphologic features of ACC overlap with those of endocrine tumors of the pancreas, particularly in ACCs with a prominent trabecular growth pattern. Endocrine tumors are readily distinguishable from ACC by their opposite immunoprofile (trypsin-negative, chromogranin-positive, and synaptophysin-positive).
- Solid pseudopapillary tumors may disclose cytologic features in common with ACCs, but the latter lack branching papillary fragments with fibrovascular cores.
- Benign pancreatic acini are more regular and exhibit an articulate organoid aspect that is less distinctive in tumorous acinic formations.

### 10.1.9.3 Osteoclastic Giant Cell Tumor

[38, 63, 75, 106, 135, 174]

The histogenesis of this tumor is controversial: a number of studies support an epithelial and others a mesenchymal origin.

**Microscopic Features**

Cytologically, three cell types can be observed:

- The characteristic *multinucleated giant cells* of the osteoclast type with bland-appearing nuclei comprising distinct nucleoli.

- *Mononuclear cells*. Conspicuous nuclear pleomorphism is usually absent.
- *Pleomorphic spindle cells* may be present as well.

**Differential Diagnosis**

Pleomorphic giant cell carcinoma should first of all be excluded. This tumor may also contain osteoclastic giant cells, and a combination of both components within an individual tumor has been reported [122]. Reports in the literature assume that osteoclastic giant cell tumor and pleomorphic giant cell carcinoma represent a morphologic spectrum of a common tumor entity with osteoclastic giant cell tumor at one end and pleomorphic carcinoma at the other [106].

### 10.1.9.4 Pancreatoblastoma [33, 149, 175, 213]

Pancreatoblastoma is an exceedingly rare malignant epithelial tumor generally occurring in young children. Pancreatoblastoma is a highly aggressive tumor, and patients with metastases have a poor prognosis. The head of the pancreas is a predilection site for this tumor.



**Microscopic Features**

Cytologic descriptions of this tumor entity are infrequent:

- The cytologic preparations are cellular; they are composed of a biphasic cell pattern including cohesive sheets and loose grouping of epithelial cells, and primitive spindle cell mesenchymal tissue. The nuclei of the epithelial tumor cells are round to oval and vesicular with fine chromatin and small nucleoli.
- Cell-block preparation is reported to be most suitable for both the detection of acinar differentiation and the squamoid corpuscles. The latter together with heterologous elements such as cartilage are considered diagnostic key features of pancreatoblastoma.

**Immunocytochemistry**

Immunocytochemical tests show positivity of the epithelial cells for cytokeratins, carcinoembryonic antigen, trypsin, and chymotrypsin. Focal positive immunostaining is also achieved in about 50% of the cases with chromogranin, synaptophysin, and neuron-specific enolase (NSE).

**Differential Diagnosis**

Acinar cell carcinoma is most difficult to separate from pancreatoblastoma. Other exocrine pancreatic neoplasms and endocrine tumors should also be taken into consideration.

## 10.1.10 Endocrine Tumors of the Pancreas [5, 19, 32, 36, 40]

### 10.1.10.1 General Comments

- Endocrine pancreatic tumors (EPT), also referred to as islet cell tumors, account for up to 5% of all pancreatic neoplasms. The most common site of these tumors is the body or tail of the pancreas. Most endocrine neoplasms occur in adults.
- Functional neoplasms are classified according to the primary hormone being produced. Tumors producing multiple hormones and consisting of more than one cell type have been communicated. EPTs that do not cause hormone-induced clinical symptoms and show no elevation of serum hormone levels are referred to as nonfunctioning. Nonfunctioning tumors account for 1–40% of all EPTs [99].
- Sophisticated radiographic and sonographic methods and image-guided biopsy techniques will detect more endocrine tumors and an increasing number of small EPTs [32].
- There is no chance to assess malignancy of EPTs based on cytomorphologic features alone. Definitive signs of malignancy are gross invasion of the surrounding tissue, regional or distant metastases, or blood vessel invasion; the latter is a histological criterion of malignant tumor behavior. Many other parameters associated with clinical outcome have been discussed [178]. Nuclear DNA ploidy analyses have provided equivocal results as to prognostication of tumor outcome [4, 72, 109, 186].

### 10.1.10.2 Islet Cell Hyperplasia

Islet cell hyperplasia of the pancreas may disclose as a nodular lesion and may be hormonally active or inactive. This benign nontumorous disorder is generally indistinguishable from true endocrine tumors by cytology alone.

### 10.1.10.3 Common Type of Endocrine Pancreatic Tumor (Figs. 2.63, 9.29, 10.40–10.42)

**Microscopic Features**

Distinct cytological features and specific endocrine cell markers make it easy to render a final diagnosis of EPT using fine-needle aspirates [5, 19, 32, 36, 40].

- Hallmarks: The smears are very cellular, composed of a homogeneous cell population. Isolated cells dominate the overall pattern but loose cell groups and rosette-like structures are also present.
  The nuclei are eccentrically placed, giving the cells a striking plasmacytoid appearance. The nuclei are round to oval and monomorphic. Their chromatin pattern is

finely granular and evenly distributed, and the membranes are smooth.
Tumor cells have either an ill-defined vacuolated or a large, dense, and sharply outlined cytoplasm.
Fibrovascular stromal fragments with focally loosely attached epithelial cells are usually present.

- A spindle cell component may outweigh the common endocrine cells exhibiting a round and triangular shape (Fig. 10.42).
- Multiple nuclei as well as nuclear hyperchromasia, nuclear pleomorphism, inconspicuous nucleoli, and mitoses may occur (Fig. 9.30).

**Caution**

Particular cytomorphologic features have no predictive value with respect to the malignant potential of endocrine tumors; isolated enlarged tumor cells with pleomorphic and deep-staining nuclei, mitoses, multinucleation, and small nucleoli cannot be accepted as indicators of malignancy.

**Differential Diagnosis**

- Cells originating from normal pancreatic acini.
- Islet cell hyperplasia (Sect. 10.1.10.2, p. 646).
- The differential diagnosis versus acinar cell carcinoma is discussed in Sect. 10.1.9.2, p. 645.
- Solid pseudopapillary tumor of the pancreas (SPPT) may present diagnostic confusion. The pathognomonic cell features of SPPT are listed in Sect. 10.1.7.4, p. 642.
- Malignant lymphoma may be suggested in EPTs showing marked cellular dyshesion.
- Pronounced plasmacytoid features of the endocrine tumor cells may mimic extramedullary plasmacytoma [50]. (see also Sect. 10.1.11.2, p. 648).
- Malignant melanoma of the monomorphic small-cell type or the spindle cell type is another tumor giving rise to diagnostic dilemmas. Immunocytochemical expression of melanoma cell markers should permit straightforward confirmation of tumor origin.

Additional use of suitable immunostains to cytologic smears can reliably differentiate between endocrine tumors and most of the nonendocrine tumors listed above.

### 10.1.10.4 Variants of Endocrine Pancreatic Tumors

- *Poorly differentiated large cell neuroendocrine carcinoma* (Fig. 9.31A) is composed of large pleomorphic tumor cells comprising pleomorphic nuclei, large nucleoli, dense granular chromatin, variable eosinophilic cytoplasmic granularity, and mitotic figures. Necrotic debris is usually present.
- *Poorly differentiated small-cell carcinomas of neuroendocrine origin* are morphologically identical to small-cell carcinomas of the lung. Most neuroendocrine tumors of other than pulmonary origin, including those of the intestinal tract, are reported to show negative TTF-1 expression. However, in approximately one-third of extrapulmonary small-cell cancers, a nuclear positivity of TTF-1 may occur. It is important to use an appropriate panel of antibodies to ascertain the primary site of neuroendocrine tumors (see also Sect. 9.2.3.4, p. 608).
- The *clear cell variant of neuroendocrine tumors* shows abundant clear and vacuolated cytoplasm caused by lipid deposition. This tumor variant occurs predominantly in patients with clinical symptoms of Hippel-Lindau disease [81, 142].
- The *oncocytic variant* (Fig. 10.43) is characterized by oxyphilic cells with a large polygonal or round cytoplasm densely packed with granules. The nuclei are round and deeply stained, showing a centrally placed large nucleolus [146, 161, 200].
- A *mucinous variant* including goblet cells [193] and a variant with *sarcomatous differentiation* [58, 62] has rarely been reported in the histologic literature.
- The *mixed ductal-endocrine neoplasm* shows features of both ductal and endocrine differentiation [14, 190, 191].

### 10.1.10.5 Immunocytochemistry of Endocrine Tumors

Cell markers indicating neuroendocrine differentiation are essential for a conclusive cytologic assessment of the tumor entity. They include synaptophysin, chromogranins, neuron-specific enolase (NSE), and Leu7.

On request, immunocytochemical stainings for insulin, glucagon, gastrin, and other hormones produced by functional neoplasms may easily be applied to cytologic smears [5, 36].

## 10.1.11 Other Pancreatic Tumors and Metastases

### 10.1.11.1 Mesenchymal Lesions of the Pancreas

- Primary mesenchymal tumors of the pancreas are exceedingly rare [153]. Leiomyosarcoma and gastrointestinal stromal tumor are reported to be the most common neoplasms in this tumor group. Yan and coauthors recently described the cytologic and immunocytochemical findings in a FNAB sample from a gastrointestinal stromal tumor [208].
- An intrapancreatic accessory spleen may mimic pancreatic neoplasia by imaging studies, predominantly pancreatic endocrine tumor. A characteristic cell pattern in cyto-

logic smears should allow a conclusive diagnosis: the specimens are composed of large numbers of lymphocytes as well as histiocytes, granulocytes, plasma cells, and splenic sinus-lining endothelial cells [169].

### 10.1.11.2 Malignant Lymphoma of the Pancreas

(Fig. 10.44)

Primary lymphoma of the pancreas is considered to be rare, accounting for less than 1% of all pancreatic tumors. The pancreas is more frequently involved by local spreading of a lymphatic tumor with its origin in peripancreatic lymph nodes. Primary pancreatic lymphomas are mainly of B-cell phenotype. Lymphomas of various types have been histologically described [114, 133]. Cytological subtyping of the most frequently observed lymphomas in FNAB samples is discussed in other chapters of this book; see Sect. 15.3, "Lymph Nodes: Malignant Lesions," p. 950.

**Differential Diagnosis**

- The distinction of plasmacytoma from neuroendocrine neoplasms that are solely composed of single cells may be challenging on cytologic smears [50].
- Malignant lymphoma of the large-cell (blastic) type may be mistaken for primary or metastatic undifferentiated nonmucinous carcinoma, in particular in cytologic specimens with lymphoid tumor cells arranged in loose groups and clusters; even so, intermingled small lymphocytes may be suggestive of a lymphoid disorder. Immunocytochemical (cytokeratins versus CD45 and phenotypic lymphoid markers) and/or molecular tests are indispensable in all cases with doubtful morphologic results (Fig. 10.44B).
- Other malignant and benign disorders comprising a predominant mixed lymphoid background in cytologic specimens may mimic malignant lymphoma, including undifferentiated carcinoma of the small-cell type, lymphoepithelial cyst, and pancreatitis (such as autoimmune pancreatitis).

**Caution**

- Distinguishing between neuroendocrine neoplasm and plasmacytoma may be problematic. Remember, plasmacytoma usually lacks immunocytochemical expression of common leukocyte antigen (CD45) and B-cell marker CD20, whereas antibodies against CD38 and CD138 yield a positive reaction!
- Malignant lymphoma of the large-cell (blastic) type can mimic primary or metastatic undifferentiated, nonmucinous carcinoma. Loose or dense grouping of high-grade lymphoid tumor cells should not be misinterpreted as a sign of an epithelial disorder. Intermingled small lymphocytes may be suggestive of a lymphoid tumor.

### 10.1.11.3 Metastases to the Pancreas

(Figs. 10.45–10.47)

- Epithelial and nonepithelial secondary tumors occur in the pancreas, either by spread from contiguous tissues and organs or by lymphatic or hematogenous spread.
- Secondary epithelial tumors giving rise to major differential diagnosis problems against primary pancreatic cancer include renal cell carcinoma and undifferentiated small-cell carcinoma. Renal cell carcinoma seems to be one of the most frequent epithelial cancers metastasizing to the pancreas [48, 66]. Immunocytochemistry is most helpful in assessing a final diagnosis in the majority of cases and self-evident together with clinicopathologic correlation. Tumor markers for the most frequent malignancies are indicated in several chapters of this book; see Sect. 15.3.24, p. 978, and Table 15.3.3.

## 10.1.12 Further Reading


1. Adsay NV, Adair CF, Heffess CS, Klimstra DS. Intraductal oncocytic papillary neoplasms of the pancreas. Am J Surg Pathol 1996;20:980-994.
2. Adsay NV, Hasteh F, Cheng JD, et al. Lymphoepithelial cysts of the pancreas: a report of 12 cases and a review of the literature. Mod Pathol 2002;15:492-501.
3. Ahlawat SK, Lymphoepithelial cyst of pancreas. Role of endoscopic ultrasound guided fine needle aspiration. JOP 2008;9:230-234.
4. Alanen KA, Joensuu H, Klemi PJ, et al. DNA ploidy in pancreatic neuroendocrine tumors. Am J Clin Pathol 1990;93:784-788.
5. Al-Kaisi N, Weaver MG, Abdul KFW, et al. Fine needle aspiration cytology of neuroendocrine tumors of the pancreas. Acta Cytol 1992;36:655-660.
6. Alles AJ, Warshaw AL, Southern JF, et al. Expression of CA 72-4 (TAG-72) in the fluid contents of pancreatic cysts. A new marker to distinguish malignant pancreatic cystic tumors from benign neoplasms and pseudocysts. Ann Surg 1994;219:131-134.
7. Alpert LC, Truong LD, Bosart MI, et al. Microcystic adenoma (serous cystadenoma) of the pancreas. A study of 14 cases with immunohistochemical and electron microscopic correlation. Am J Surg Pathol 1988;12:251-263.
8. Alsibai KD, Denis B, Bottlaender J, et al. Impact of cytopathologist expert on diagnosis and treatment of pancreatic lesions in current clinical practice. A series of 106 endoscopic ultrasound-guided fine needle aspirations. Cytopathology 2006;17:18-26.
9. Andea A, Sarkar F, Adsay NV. Clinicopathologic correlates of pancreatic intraepithelial neoplasia: a comparative analysis of 82 cases with and 152 cases without pancreatic ductal adenocarcinoma. Mod Pathol 2003;16:996-1006.
10. Ardengh JC, Lopes CV, de Lima LF; et al. Diagnosis of pancreatic tumors by endoscopic ultrasound-guided fine-needle aspiration. World J Gastroenterol 2007;13:3112-3116.
11. Arvanitakis M, Van Laethem JL, Parma J, et al. Predictive factors for pancreatic cancer in patients with chronic pancreatitis in association with K-ras gene mutation. Endoscopy 2004;36:535-542.
12. Attasaranya S, Pais S, LeBlanc J, et al. Endoscopic ultrasound-guided fine needle aspiration and cyst fluid analysis for pancreatic cysts. JOP 2007;8:553-563.
13. Awadallah NS, Shroyer KR, Langer DA, et al. Detection of B7-H4 and p53 in pancreatic cancer: potential role as a cytological diagnostic adjunct. Pancreas 2008;36:200-206.

14. Ballas KD, Rafailidis SF, Demertzidis C, et al. Mixed exocrine-endocrine tumor of the pancreas. JOP 2005;6:449-454.
15. Barabino M, Santambrogio P, Pisani A, et al. Endoscopic ultrasonography coupled with fine needle aspiration biopsy of intraductal papillary–mucinous tumours of the pancreas. Tool or gadget? A report of three cases. Chir Ital 2007;59:489-494.
16. Bardales RH, Centeno B, Mallery JS, et al. Endoscopic ultrasound-guided fine-needle aspiration cytology diagnosis of solid-pseudopapillary tumor of the pancreas: a rare neoplasm of elusive origin but characteristic cytomorphologic features. Am J Clin Pathol 2004;121:654-662.
17. Baron TH, Harewood GC, Rumalla A, et al. A prospective comparison of digital image analysis and routine cytology for the identification of malignancy in biliary tract strictures. Clin Gastroenterol Hepatol 2004;2:214-219.
18. Basir Z, Pello N, Dayer AM, et al. Accuracy of cytologic interpretation of pancreatic neoplasms by fine needle aspiration and pancreatic duct brushings. Acta Cytol 2003;47:733-738.
19. Bell DA. Cytologic features of islet-cell tumors. Acta Cytol 1987;31:485-492.
20. Belsley NA, Pitman MB, Lauwers GY, et al. Serous cystadenoma of the pancreas. Limitations and pitfalls of endoscopic ultrasound-guided fine-needle aspiration biopsy. Cancer(Cancer Cytopathol) 2008;114:102-110.
21. Berkel S, Hummel F, Gaa J, et al. Poorly differentiated small cell carcinoma of the pancreas. A case report and review of the literature. Pancreatology 2004;4:521-526.
22. Bhanot P, Nealon WH, Walser EM, et al. Clinical, imaging, and cytopathological features of solid pseudopapillary tumor of the pancreas: a clinicopathologic study of three cases and review of the literature. Diagn Cytopathol 2005;33:421-428.
23. Binek J, Abraham D, Borovicka J , Spieler P, et al. Endosonographic guided fine needle aspiration (EUS-FNA) in mediastinal and abdominal lesions: accuracy and patient tolerance. Gut 2004;53 (Suppl VI):A42.
24. Binek J, Lindenmann N, Meyenberger CM, Spieler P, et al. Malignant biliary stenosis: Conventional cytology versus DNA image cytometry. Surg Endosc 2011;25:1808-1813.
25. Binek J, Meyenberger C, Spieler P, et al. DNA-Image-Cytometry (ICM-DNA) of brush cytology for the diagnosis of malignant biliary tumors. Gastroenterology, Suppl1 2001;120:A-573.
26. Binek J, Spieler P, Hürlimann R, et al. Ultrasound-guided fine-needle aspiration of abdominal masses: accuracy and short-term complications. European Journal of Ultrasound 1995;2:199-203.
27. Bondeson L, Bondeson A-G, Grimelius L, Kjellström U. Oncocytic tumor of the pancreas. Report of a case with aspiration cytology. Acta Cytol 1990;34:425-428.
28. Brandwein SL, Farrell JJ, Centeno BA, Brugge WR. Detection and tumor staging of malignancy in cystic, intraductal, and solid tumors of the pancreas by EUS. Gastrointest Endosc 2001;53:722-727.
29. Bret PM, Nicolet V. Percutaneous fine-needle aspiration biopsy of the pancreas. Diagn Cytopathol 1986;2:221-227.
30. Buetow PC, Parrino TV, Buck Jl, et al. Islet cell tumors of the pancreas: Pathologic-imaging correlation among size, necrosis and cysts, calcification, malignant behaviour, and functional status. Am J Roentgenol 1995;165:1175.
31. Canto MI, Goggins M, Hruban RH, et al. Screening for early pancreatic neoplasia in high risk individuals: a prospective controlled study. Clin Gastroenterol Hepatol 2006 ;4:766-781.
32. Caudill JL, Humphrey SK, Salomao DR. Islet cell tumor of the pancreas. Increasing diagnosis after instituting ultrasonography-guided fine needle aspiration. Acta Cytol 2008;52:45-51.
33. Centeno BA, Pitman MB. Fine needle aspiration biopsy of the pancreas. Butterworth-Heinemann Boston Oxford 1999.
34. Chang KJ, Nguyen P, Erickson RA, et al. The clinical utility of endoscopic ultrasound-guided fine-needle aspiration in the diagnosis and staging of pancreatic carcinoma. Gastrointest Endosc 1997;45:387-393.
35. Chatelain D, Couvelard A, Hammel P, et al. Lympho-epithelial cyst of the pancreas: a difficult diagnosis. About two cases. Gastroenterol Clin Biol 2002;26:935-938.
36. Chatzipantelis P, Salla C, Konstantinou P, et al. Endoscopic ultrasound-guided Fine-needle aspiration cytology of pancreatic neuroendocrine tumors. A study of 48 cases. Cancer(Cancer Cytopathol) 2008;114:255-262.
37. Chetty R, Clark SP, Pitson GA. Primary small cell carcinoma of the pancreas. Pathology 1993;25:240-242.
38. Chopra S, Wu ML, Imagawa DK, et al. Endoscopic ultrasound-guided fine-needle aspiration of undifferentiated carcinoma with osteoclast-like giant cells of the pancreas: a report of 2 cases with literature review. Diagn Cytopathol 2007;35:601-606.
39. Cohen MB, Egerter DP, Holly EA, et al. Pancreatic adenocarcinoma: regression analysis to identify improved cytologic criteria. Diagn Cytopathol 1991;7:341-345.
40. Collins BT, Cramer HM. Fine-needle aspiration cytology of islet cell tumors (review) Diagn Cytopathol 1996;15:37-45.
41. Collins BT, Agarwal B, Krishna NB, et al. Diagnostic value of endoscopic ultrasound fine needle aspiration in suspected pancreatic cancer patients with focal lesion on CT/MRI without obstructive jaundice. Cancer(Cancer Cytopathol) Suppl. 2007;111:418-419.
42. Colombo P, Arizzi C, Roncalli M. Acinar cell cystadenocarcinoma of the pancreas: report of rare cases and review of the literature. Hum Pathol 2004 ;35:1568-1571.
43. Compagno J, Oertel JE. Mucinous cystic neoplasms of the pancreas with overt and latent malignancy (cystadenocarcinoma and cystadenoma). A clinicopathologic study of 41 cases. Am J Clin Pathol 1978;69:573-580.
44. David O, Green L, Reddy V, et al. Pancreatic masses: a multi-institutional study of 364 fine-needle aspiration biopsies with histopathologic correlation. Diagn Cytopathol 1998;19:423-427.
45. Delatour NR, Policarpio-Nicolas MLC, Yazdi H, Islam S. Fine needle aspiration biopsy for preoperative workup of pancreatic cystic neoplasms. Report of 4 cases. Acta Cytol 2007;51:925-933.
46. DelMaschio A, Vanzulli A, Sironi S, et al. Pancreatic cancer versus chronic pancreatitis: diagnosis with CA 19-9 assessment, US, CT, and CT-guided fine-needle biopsy. Radiology 1991;178:95-99.
47. de Luna R, Eloubeidi MA, Sheffield MV, et al. Comparison of ThinPrep and conventional preparations in pancreatic fine-needle aspiration biopsy. Diagn Cytopathol 2004;30:71-76.
48. DeWitt J, Jowell P, Leblanc J, et al. EUS-guided FNA of pancreatic metastases: a multicenter experience. Gastrointest Endosc 2005;61:689-696.
49. Di Stasi M, Lencioni R, Solmi L, et al. Ultrasound-guided fine needle biopsy of pancreatic masses: results of a multicenter study. Am J Gastroenterol 1998;93:1329-1333.
50. Dodd LG, Evans DB, Symmans F, Katz RL. Fine-needle aspiration of pancreatic extramedullary plasmacytoma: possible confusion with islet cell tumor. Diagn Cytopathol 1994;10:371-374.
51. Duggan MA, Brasher P, Medlicott SA. ERCP-directed brush cytology prepared by the ThinPrep method: test performance and morphology of 149 cases. Cytopathology 2004;15:80-86.
52. Edoute Y, Lemberg S, Malberger E. Preoperative and intraoperative fine needle aspiration cytology of pancreatic lesions. Am J Gastroenterol 1991;86:1015-1019.
53. Eguchi H, Ishikawa O, Ohigashi H, et al. Role of intraoperative cytology combined with histology in detecting continuous and skip type intraductal cancer existence for intraductal papillary mucinous carcinoma of the pancreas. Cancer 2006;107:2567-2575.
54. Elek G, Gyökeres T, Schäfer E, et al. Early diagnosis of pancreatobiliary duct malignancies by brush cytology and biopsy. Pathol Oncol Res 2005;11:145-155.
55. Eloubeidi MA, Jhala D, Chhieng DC, et al. Yield of endoscopic ultrasound-guided fine-needle aspiration biopsy in patients with suspected pancreatic carcinoma. Cancer 2003;99:285-292.

56. Eloubeidi MA, Varadarajulu S, Desai S, et al. A prospective evaluation of an algorithm incorporating routine preoperative endoscopic ultrasound-guided fine needle aspiration in suspected pancreatic cancer. J Gastrointest Surg 2007;11:813-819.
57. Eloubeidi MA, Varadarajulu S, Desai S, Wilcox CM. Value of repeat endoscopic ultrasound-guided fine needle aspiration for suspected pancreatic cancer. J Gastroenterol Hepatol 2008;23:567-570.
58. Emerson L, Layfield LJ, Reiss R, et al. Malignant islet cell tumor with sarcomatous differentiation. Mod Pathol 2001;14:1187-1191.
59. Emerson RE, Randolph ML, Cramer HM. Endoscopic ultrasound-guided fine-needle aspiration cytology diagnosis of intraductal papillary mucinous neoplasm of the pancreas is highly predictive of pancreatic neoplasia. Diagn Cytopathol 2006;34:457-462.
60. Ettinghausen SE, Schwartzentruber DJ, Sindelar WF. Evolving strategies for the treatment of adenocarcinoma of the pancreas. A review. J Clin Gastroenterol 1995;21:48-60.
61. Fernandez-Cebrian JM, Carda P, Morales V, Galindo J. Dermoid cyst of the pancreas: a rare cystic neoplasm. Hepatogastroenterology 1998;45:1874-1876.
62. Ferreiro J, Lewin K, Herron RM, et al. Malignant islet cell tumor with rhabdomyosarcomatous differentiation. Am J Surg Pathol 1989;13:422-427.
63. Fischer HP, Altmannsberger M, Kracht J. Osteoclast-type giant cell tumor of the pancreas (review). Virchows Arch A 1988;412:247.
64. Fitzhugh VA, Mirani N, Aisner S, et al. Preoperative fine needle aspiration cytology diagnosis of microcystic adenoma of the pancreas: fact or fiction? A report of 2 cases. Acta Cytol 2008;52:240-246.
65. Fritscher-Ravens A, Brand L, Knöfel WT, et al. Comparison of endoscopic ultrasound-guided fine needle aspiration for focal pancreatic lesions in patients with normal parenchyma and chronic pancreatitis. Am J Gastroenterol 2002;97:2768-2775.
66. Fritscher-Ravens A, Sriram PVJ, Krause C, et al. Detection of pancreatic metastases by EUS-guided fine-needle aspiration. Gastrointest Endosc 2001;53:65-70.
67. Frossard JL, Amouyal P, Amouyal G, et al. Performance of endosonography-guided fine needle aspiration and biopsy in the diagnosis of pancreatic cystic lesions. Am J Gastroenterol 2003;98:1516-1524.
68. Garcea G, Ong SL, Rajesh A, et al. Cystic lesions of the pancreas. A diagnostic and management dilemma Pancreatology 2008;8:236-251.
69. Ghazale AH, Chari ST, Vege SS. Update on the diagnosis and treatment of autoimmune pancreatitis. Curr Gastroenterol Rep 2008;10:115-121.
70. Glasbrenner B, Ardan M, Boeck W, et al. Prospective evaluation of brush cytology of biliary strictures during endoscopic retrograde cholangiopancreatography. Endoscopy 1999;31:712-717.
71. Govil H, Reddy V, Kluskens L, et al. Brush cytology of the biliary tract: retrospective study of 278 cases with histopathologic correlation. Diagn Cytopathol 2002;26:273-277.
72. Graeme-Cook F, Bell DA, Flotte TJ, et al. Aneuploidy in pancreatic insulinomas does not predict malignancy. Cancer 1990;66:2365-2368.
73. Gress F, Gottlieb K, Sherman S, Lehman G. Endoscopic ultrasonography-guided fine-needle aspiration biopsy of suspected pancreatic cancer. Ann Intern Med 2001;134:459-464.
74. Griffin CA, Hruban RH, Morsberger LA, et al. Consistent chromosomal abnormalities in adenocarcinoma of the pancreas. Cancer Res 1995;55:2394-2399.
75. Hansen T, Burg J, Kirkpatrick CJ, et al. Osteoclast-like giant cell tumor of the pancreas with ductal adenocarcinoma: case report with novel data on histogenesis. Pancreas 2002;;25:317-319.
76. Hara H, Suda K. Review of the cytologic features of noninvasive ductal carcinomas of the pancreas: differences from invasive ductal carcinoma. Am J Clin Pathol 2008;129:115-129.
77. Hara H, Suda K, Oyama T. Cytologic study of noninvasive intraductal papillary-mucinous carcinoma of the pancreas. Acta Cytol 2002;46:519-526.
78. Hari S, Seith A, Srivastava DN, Makharia G, Pal S. Isolated tuberculosis of the pancreas diagnosed with needle aspiration: a case report and review of the literature. Trop Gastroenterol 2005;26:141-143.
79. Hernandez LV, Mishra G, Forsmark C, et al. Role of endoscopic ultrasound (EUS) and EUS-guided fine needle aspiration in the diagnosis and treatment of cystic lesions of the pancreas. Pancreas 2002;25:222-228.
80. Hittmair A, Pernthaler H, Totsch M, et al. Preoperative fine needle aspiration cytology of a microcystic adenoma of the pancreas. Acta Cytol 1991;35:546-548.
81. Hoang MP, Hruban RH, Albores-Saavedra J. Clear cell endocrine pancreatic tumor mimicking renal cell carcinoma: a distinctive neoplasm of von Hippel-Lindau disease. Am J Surg Pathol 2001;25:602-609.
82. Hruban RH, Takaori K, Klimstra DS, et al. An illustrated consensus on the classification of pancreatic intraepithelial neoplasia and intraductal papillary mucinous neoplasms. Am J Surg Pathol 2004;28:977-987.
83. Huh JR, Chi JG, Jung KC, et al. Macrocystic serous cystadenoma of pancreas – a case report. J Korean Med Sci 1994;9:78.
84. Hysell C, Belsley N, Deshpande V. EUS guided fine needle aspiration biopsies of solid ductal adenocarcinomas of the pancreas: a critical look at the atypical and suspicious categories. Cancer(Cancer Cytopathol) Suppl 2007;111:351-352.
85. Iacono C, Serio G, Fugazzola C, et al. Cystic islet cell tumors of the pancreas. A clinico-pathological report of two nonfunctioning cases and review of the literature. Int J Pancreatol 1992;11:199-208.
86. Itani KM, Taylor TV, Green LK. Needle biopsy for suspicious lesions of the head of the pancreas: pit falls and implications for therapy. J Gastrointest Surg 1997;1:337-341.
87. Jani N, Dewitt J, Eloubeidi M, et al. Endoscopic ultrasound-guided fine-needle aspiration for diagnosis of solid pseudopapillary tumors of the pancreas: a multicenter experience. Endoscopy 2008;40:200-203.
88. Jhala D, Grizzle WE, Jhala N. Clear cells with cytoplasmic vacuolization mimicking macrophages in pancreatic adenocarcinoma in fine needle aspirates obtained by EUS-FNA: a diagnostic caveat. Cancer(Cancer Cytopathol) Suppl 2007;111:416.
89. Jhala N, Jhala D, Vickers SM, et al. Biomarkers in diagnosis of pancreatic carcinoma in fine-needle aspirates. A translational research application. Am J Clin Pathol 2006;126:572-579.
90. Johansson B, Bardi G, Heim S, et al. Nonrandom chromosomal rearrangements in pancreatic carcinoma. Cancer 1992;69:1674-1681.
91. Johnson DE, Pendurthi TK, Balshem AM, et al. Implications of fine-needle aspiration in patients with resectable pancreatic cancer. Am Surg 1997;63:675-679.
92. Kameya S, Kuno N, Kasugai T. The diagnosis of pancreatic cancer by pancreatic juice cytology. Acta Cytol 1981;25:354-360.
93. Kanai N, Nagaki S, Tanaka T. Clear cell carcinoma of the pancreas. Acta Pathol Jpn 1987;37:1521-1526.
94. Kardon DE, Thompson LD, Przygodzki RM, Heffess CS. Adenosquamous carcinoma of the pancreas: a clinicopathologic series of 25 cases. Mod Pathol 2001;14:443-451.
95. Khadaroo R, Knetman N, Joy S, Nguyen GK. Macrocystic serous adenoma of the pancreas. Pathol Res Pract 2002;198:485-491.
96. Khurana A, Rekhi B, Kane SV, et al. Pancreatic tuberculosis masquerading as pancreatic carcinoma in two cases: role of fine needle aspiration cytology in diagnosis. Cytopathology 2007;18:380-383.
97. Kim K, Booth R, Myles J. Transcutaneous fine-needle aspiration biopsy of pancreatic cancer. Int J Pancreatol 1990;7:61-69.

98. Kipp BR, Stadheim LM, Halling SA, et al. A comparison of routine cytology and fluorescence in situ hybridization for the detection of malignant bile duct strictures. Am J Gastroenterol 2004;99:1675-1681
99. Klöppel G, Heitz PU. Pancreatic endocrine tumors. Pathol Res Pract 1988;183:155-168.
100. Klöppel G, Lüttges J. The pathology of ductal-type pancreatic carcinomas and pancreatic intraepithelial neoplasia: insights for clinicians. Curr Gastroenterol Rep 2004;6:111-118.
101. Klöppel G, Hruban RH, Longnecker DS. Ductal adenocarcinoma of the pancreas, in: Hamilton SR, Aaltonen LA (Eds.): World Health Organization Classification of Tumours. Pathology and Genetics of tumours of the digestive system. IARC Press:Lyon 2000
102. Krishnamurthy S, Katz RL, Shumate A, et al. DNA image analysis combined with routine cytology improves diagnostic sensitivity of common bile duct brushing. Cancer 2001;93:229-235.
103. Labate AM, Klimstra DL, Zakowski MF. Comparative cytologic features of pancreatic acinar cell carcinoma and islet cell tumor. Diagn Cytopathol 1997;16:112-116.
104. Lack EE. Pathology of the pancreas, gallbladder, extrahepatic biliary tract, and ampullary region. Oxford University Press, Inc. 2003.
105. Lal A, Bourtsos EP, DeFrias DV, et al. Microcystic adenoma of the pancreas: clinical, radiologic, and cytologic features. Cancer 2004;102:288-294.
106. Layfield LJ, Bentz J. Giant-cell containing neoplasms of the pancreas: an aspiration cytology study. Diagn Cytopathol 2008;36:238-244.
107. Layfield LJ, Cramer H. Fine-needle aspiration cytology of intraductal papillary-mucinous tumors: a retrospective analysis. Diagn Cytopathol 2005;32:16-20.
108. Layfield LJ, Cramer H, Madden J, et al. Atypical squamous epithelium in cytologic specimens from the pancreas: cytological differential diagnosis and clinical implications. Diagn Cytopathol 2001;25:38-42.
109. Lee CS, Charlton IG, Williams RA, et al. Malignant potential of aneuploid pancreatic endocrine tumors. J Pathol 1993;169:451-456.
110. Levy MJ, Baron TH, Clayton AC, et al. Prospective evaluation of advanced molecular markers and imaging techniques in patients with indeterminate bile duct strictures. Am J Gastroenterol 2008;103:1263-1273.
111. Levy MJ, Wiersema MJ, Chari ST. Chronic pancreatitis: focal pancreatitis or cancer? Is there a role for FNA/biopsy? Autoimmune pancreatitis. Endoscopy 2006;38 Suppl 1:S30-35.
112. Lewandrowski KB, Southern JF, Pins MR, et al. Cyst fluid in the differential diagnosis of pancreatic cysts. A comparison of pseudocysts, serous cystadenomas, mucinous cystic neoplasms, and mucinous cystadenocarcinoma. Ann Surg 1993;217:41-47.
113. Lin F, Staerkel G. Cytologic criteria for well differentiated adenocarcinoma of the pancreas in fine-needle aspiration biopsy specimens. Cancer 2003;99:44-50.
114. Lin H, Li SD, Hu XG, Li ZS. Primary pancreatic lymphoma: report of six cases. World J Gastroenterol 2006;12:5064-5067.
115. Lindberg B, Enochsson L, Tribukait B, et al. Diagnostic and prognostic implications of DNA ploidy and S-phase evaluation in the assessment of malignancy in biliary strictures. Endoscopy 2006;38:561-565.
116. Linder JD, Geenen JE, Catalano MF. Cyst fluid analysis obtained by EUS-guided FNA in the evaluation of discrete cystic neoplasms of the pancreas: a prospective single-center experience. Gastrointest Endoscop 2006;64:697-702.
117. Liu F, Li ZS, Xu GM, et al. Detection of K-ras gene mutation at codon 12 by pancreatic duct brushing for pancreatic cancer. Hepatobiliary Pancreat Dis Int 2003;2:313-317.
118. Logrono R, Vyas SH, Molina CP, Waxman I. Microcystic adenoma of the pancreas: cytologic appearance on percutaneous and endoscopic ultrasound-guided fine-needle aspiration: report of a case. Diagn Cytopathol 1999;20:298-301.
119. Logrono R, Wong JY. Reporting the presence of significant epithelial atypia in pancreaticobiliary brush cytology specimens lacking evidence of obvious carcinoma: impact on performance measures. Acta Cytol 2004;48:613-621.
120. Longnecker DS, Adler G. Intraductal papillary-mucinous neoplasms of the pancreas. in: Hamilton SR, Aaltonen LA. (Eds.): World Health Organization Classification of Tumours: Pathology and Genetics of Tumours of the Digestive Sytem. IARC Press:Lyon 2000.
121. Loya AC, Prayaga AK, Sundaram C, et al. Cytologic diagnosis of pancreatic tuberculosis in immunocompetent and immunocompromised patients: a report of 2 cases. Acta Cytol 2005;49:97-100.
122. Loya AC, Ratnakar KS, Shastry RA. Combined osteoclastic giant cell and pleomorphic giant cell tumor of the pancreas: a rarity. An immunohistochemical analysis and review of the literature. JOP 2004;5:220-224.
123. Lüttges J, Vogel I, Menke M, et al. Clear cell carcinoma of the pancreas: an adenocarcinoma with ductal phenotype. Histopathology 1998;32:444-448.
124. Mackie CR, Cooper MJ, Lewis MH, Moossa AR. Non-operative differentiation between pancreatic cancer and chronic pancreatitis. Ann Surg 1979;189:480-487.
125. Maitra A, Fukushima N, Takaori K, Hruban RH. Precursors to invasive pancreatic cancer. Adv Anat Pathol 2005;12:81-91.
126. Malberger E, Lemberg S, Edoute Y. Intraoperative fine needle aspiration cytology of pancreatic lesions. J Surg Oncol 1991;46:241-245.
127. Micames C, Jowell PS, White ChBR, et al. Lower frequency of peritoneal carcinomatosis in patients with pancreatic cancer diagnosed by EUS-guided FNA vs. percutaneous FNA. Gastrointest Endosc 2003;58:690-695.
128. Michaels PJ, Brachtel EF, Bounds BC, et al. Intraductal papillary mucinous neoplasm of the pancreas: cytologic features predict histologic grade. Cancer 2006;108:163-173.
129. Mitchell ML, Carney CN. Cytologic criteria for the diagnosis of pancreatic carcinoma. Am J Clin Pathol 1985;83:171-176.
130. Morena Luna LE, Kipp B, Halling KC, et al. Advanced cytologic techniques for the detection of malignant pancreatobiliary strictures. Gastroenterology 2006;131:1064-1072.
131. Morinaga S, Tsumuraya M, Nakajima T, et al. Ciliated-cell adenocarcinoma of the pancreas. Acta Pathol Jpn 1986;36:1905-1910.
132. Motojima K, Furui J, Terada M, et al. Small cell carcinoma of the pancreas and biliary tract. J Surg Oncol 1990;45:164-168.
133. Müller-Hermelink HK, Chott A, Gascoyne RD, Wotherspoon A. Lymphoma of the pancreas. in: HamiltonSR, Aaltonen LA (Eds.): World Health Organization Classification of Tumours. Pathology and Genetics of tumours of the digestive system. IARC Press:Lyon 2000.
134. Murakami Y, Yokoyama T, Yokoyama Y, et al. Adenosquamous carcinoma of the pancreas: preoperative diagnosis and molecular alterations. J Gastroenterol 2003;38:1171-1175.
135. Nai GA, Amico E, Gimenez VR, Guilmar M. Osteoclast-like giant cell tumor of the pancreas associated with mucus-secreting adenocarcinoma. Case report and discussion of the histogenesis. Pancreatology 2005;5:279-284.
136. Nakaizumi A, Tatsuta M, Uehara H, et al. Cytologic examination of pure pancreatic juice in the diagnosis of pancreatic carcinoma. The endoscopic retrograde intraductal catheter aspiration cytology technique. Cancer 1992;70:2610-2614.
137. Nakaizumi A, Tatsuta M, Uehara H, et al. Effectiveness of the cytologic examination of pure pancreatic juice in the diagnosis of early neoplasia of the pancreas. Cancer 1995;76:750-757.

138. Nakaizumi A, Tatsuta M, Uehara H, et al. Usefulness of simple endoscopic aspiration cytology of pancreatic juice for diagnosis of early pancreatic neoplasm. A prospective study. Dig Dis Sci 1997;42:1796-1803.
139. Nakaizumi A, Uehara H, Takenaka A, et al. Diagnosis of pancreatic cancer by cytology and measurement of oncogene and tumor markers in pure pancreatic juice aspirated by endoscopy. Hepatogastroenterology 1999;46:31-37.
140. Nguyen GK, Vogelsang PJ. Microcystic adenoma of the pancreas. A report of two cases with fine needle aspiration cytology and differential diagnosis. Acta Cytol 1993;37:908-912.
141. Nicolas MM, Talamonti M, Rao MS. Mesothelial cyst of the pancreas. Ann Diagn Pathol 2006;10:371-373.
142. Nunobe S, Fukushima N, Yachida S, et al. Clear cell endocrine tumor of the pancreas which is not associated with von Hippel-Lindau disease: report of a case. Surg Today 2003;33:470-474.
143. Oku T, Maeda M, Wada Y, et al. Intraductal oncocytic papillary neoplasm having clinical characteristics of mucinous cystic neoplasm and a benign histology. JOP 2007;8:206-213.
144. Ott C, Heinmöller E, Gaumann A, et al. Intraepithelial neoplasms (PanIN) and intraductal papillary-mucinous neoplasms (IPMN) of the pancreas as precursor lesions of pancreatic carcinoma. Med Klin (Munich) 2007;102:127-135.
145. O'Toole D, Palazzo L, Arotcarena R, et al. Assessment of complications of EUS-guided fine-needle aspiration. Gastrointest Endosc 2001;53:470-474.
146. Pacchioni D, Papotti M, Macri L, et al. Pancreatic oncocytic endocrine tumors. Cytologic features of two cases. Acta Cytol 1996;40:742-746.
147. Peng HQ, Greenwald BD, Tavora FR, et al. Evaluation of performance of EUS-FNA in preoperative lymph node staging of cancers of esophagus, lung, and pancreas. Diagn Cytopathol 2008;36:290-296.
148. Pitman MB, Deshpande V. Endoscopic ultrasound-guided fine needle aspiration cytology of the pancreas: a morphological and multimodal approach to the diagnosis of solid and cystic mass lesions. Cytopathology 2007;18:331-347.
149. Pitman MB, Faquin WC. The fine-needle aspiration biopsy cytology of pancreatoblastoma. Diagn Cytopathol 2004;31:402-406.
150. Pugliese V, Pujic N, Saccomanno S, et al. Pancreatic intraductal sampling during ERCP in patients with chronic pancreatitis and pancreatic cancer: cytologic studies and k-ras-2 codon 12 molecular analysis in 47 cases. Gastrointest Endosc 2001;54:595-599.
151. Rahemtullah A, Misdraji J, Pitman MB. Adenosquamous carcinoma of the pancreas: cytologic features in 14 cases. Cancer 2003;99:372-378.
152. Ramirez-Luna MA, Zepeda-Gomez S, Chavez-TapiaNC, Tellez-Avila FI. Diagnostic yield and therapeutic impact of fine-needle aspiration biopsies guided by endoscopic ultrasound in pancreatic lesions. Rev Invest Clin 2008;60:11-14.
153. Raut CP, Fernandez-Del Castillo C. Giant lipoma of the pancreas: Case report and review of lipomatous lesions of the pancreas. Pancreas 2003;26:97-99.
154. Ray B, New NE, Wedgwood KR. Clear cell carcinoma of exocrine pancreas: a rare tumor with an unusual presentation. Pancreas 2005;30:184-185.
155. Ray S, Lu Z, Rajendiran S. Clear cell ductal adenocarcinoma of pancreas: a case report and review of the literature. Arch Pathol Lab Med 2004;128:693-696.
156. Reyes CV, Wang T. Undifferentiated small cell carcinoma of the pancreas: a report of five cases. Cancer 1981;47:2500-2502.
157. Robins DB, Katz RL, Evans DB, et al. Fine needle aspiration of the pancreas. In quest of accuracy. Acta Cytol 1995;39:1-10.
158. Rumalla A, Baron TH, Leontovich O, et al. Improved diagnostic yield of endoscopic biliary brush cytology by digital image analysis. Mayo Clin Proc 2001;76:29-33.
159. Ryan ME, Baldauf MC. Comparison of flow cytometry for DNA content and brush cytology for detection of malignancy in pancreaticobiliary strictures. Gastrointest Endosc 1994;40:133-139.
160. Ryozawa S, Kitoh H, Gondo T, et al. Usefulness of endoscopic ultrasound-guided fine-needle aspiration biopsy for the diagnosis of pancreatic cancer. J Gastroenterol 2005;40:907-911.
161. Sadoul JL, Saint-Paul MC, Hoffman P, et al. Malignant pancreatic oncocytoma. An unusual cause of organic hypoglycemia. J Endocrinol Invest 1992;15:211-217.
162. Saez A, Catala I, Brossa R, et al. Intraoperative fine needle aspiration cytology of pancreatic lesions. A study of 90 cases. Acta Cytol 1995;39:485-488.
163. Sai JK, Suyama M, Kubokawa Y, Watanabe S. Pancreatic duct lavage cytology for the diagnosis of branch duct-type intraductal papillary mucinous neoplasm of the pancreas. Pancreas 2008;36:216-217
164. Salla C, Chatzipantelis P, Konstantinou P, et al. Endoscopic ultrasound-guided fine-needle aspiration cytology diagnosis of solid pseudopapillary tumor of the pancreas: a case report and literature review. World J Gastroenterol 2007;13:5158-5163.
165. Salla C, Chatzipantelis P, Konstantinou P, et al. Endoscopic ultrasound-guided fine-needle aspiration cytology in the diagnosis of intraductal papillary mucinous neoplasms of the pancreas. A study of 8 cases. JOP 2007;8:715-724.
166. Samuel LH, Frierson HF Jr. Fine needle aspiration cytology of acinar cell carcinoma of the pancreas: a report of two cases. Acta Cytol 1996;40:585-591.
167. Sand JA, Hyoty MK, Mattila J, et al. Clinical assessment compared with cyst fluid analysis in the differential diagnosis of cystic lesions in the pancreas. Surgery 1996;119:275-280.
168. Sariya D, Kluskens L, Assad L, et al. Diagnostic role of fine-needle aspiration of pancreatic allograft to detect rejection. Diagn Cytopathol 2002;27:266-270.
169. Schreiner AM, Mansoor A, Faigel DO, Morgan TK. Intrapancreatic accessory spleen: mimic of pancreatic endocrine tumor diagnosed by endoscopic ultrasound-guided fine-needle aspiration biopsy. Diagn Cytopathol 2008;36:262-265.
170. Shabaik A. Endoscopic ultrasound-guided fine needle aspiration cytology of intraductal papillary mucinous tumor of the pancreas. A case report. Acta Cytol 2003;47:657-662.
171. Sheehan MM, Fraser A, Ravindran R, McAteer D. Bile duct brushings cytology – improving sensitivity of diagnosis using the ThinPrep technique: a review of 113 cases. Cytopathology 2007;18:225-233.
172. Siddiqui MT, Gokasian ST, Saboorian MH, et al. Comparison of ThinPrep and conventional smears in detecting carcinoma in bile duct brushings. Cancer 2003;99:205-210.
173. Silverman JF, Dabbs DJ, Finley JL, Geisinger KR. Fine needle aspiration biopsy of pleomorphic (giant cell) carcinoma of the pancreas. Cytologic, immunocytochemical, and ultrastructural findings. Am J Clin Pathol 1988;89:714-720.
174. Silverman JF, Finley JL, MacDonald KG Jr. Fine-needle aspiration cytology of osteoclastic giant-cell tumor of the pancreas. Diagn Cytopathol 1990;6:336-340.
175. Silverman JF, Holbrook CT, Pories WJ, et al. Fine needle aspiration cytology of pancreatoblastoma with immunocytochemical and ultrastructural studies. Acta Cytol 1990;34:632-640.
176. Smit W, Mathy JP, Donaldson E. Pancreatic cytology and adenosquamous carcinoma of the pancreas. Pathology 1993;25:420-422.
177. Smithies A, Hatfield ARW, Brown BE. The cytodiagnostic aspects of pure pancreatic juice obtained at the time of endoscopic retrograde cholangio-pancreatography (E.R.C.P.) Acta Cytol 1977;21:191-195.
178. Solcia E, Capella C, Klöppel G. Tumors of the endocrine pancreas. in E Socia, C Capella, G Klöppel (eds), Atlas of Tumor Pathology: Tumors of the Pancreas (3rd ed). Washington, DC: Armed Forces Institute of Pathology, 1997.

179. Solé M, Iglesias C, Fernandez-Esparrach G, et al. Fine-needle aspiration cytology of intraductal papillary mucinous tumors of the pancreas. Cancer 2005;105:298-303.
180. Solmi L, Gandolfi L, Muratori R, et al. Echo-guided fine-needle biopsy of pancreatic masses. Am J Gastroenterol 1987;82:744-748.
181. Sperti C, Pasquali C, Costantino V, et al. Solitary true cyst of the pancreas in adults. Report of three cases and review of the literature. Int J Pancreatol 1995;18:161-167.
182. Sperti C, Pasquali C, Di Prima F, et al. Percutaneous CT-guided fine needle aspiration cytology in the differential diagnosis of pancreatic lesions. Ital J Gastroenterol 1994;26:126-131.
183. Stelow EB, Bardales RH, Shami VM, et al. Cytology of pancreatic acinar cell carcinoma. Diagn Cytopathol 2006;34:367-372.
184. Stelow EB, Stanley MW, Bardales RH, et al. Intraductal papillary – mucinous neoplasm of the pancreas. The findings and limitations of cytologic samples obtained by endoscopic ultrasound-guided fine-needle aspiration. Am J Clin Pathol 2003;120:398-404.
185. Stewart CJ, Mills PR, Carter R, et al. Brush cytology in the assessment of pancreatico-biliary strictures: a review of 406 cases. J Clin Pathol 2001;54:449-455.
186. Stipa F, Arganini M, Bibbo M, et al. Nuclear DNA analysis of insulinomas and gastrinomas. Surgery 1987;102:988-998.
187. Tanno S, Obara T, Izawa T, et al. Solitary true cyst of the pancreas in two adults: analysis of cyst fluid and review of the literature. Am J Gastroenterol 1998;93:1972-1975.
188. Tascilar M, Sturm PD, Caspers E, et al. Diagnostic p53 immunostaining of endobiliary brush cytology: preoperative cytology compared with the surgical specimen. Cancer 1999;87:306-311.
189. Teplick SK, Haskin PH, Kline TS, et al. Percutaneous pancreaticobiliary biopsies in 173 patients using primarily ultrasound or fluoroscopic guidance. Cardiovasc Intervent Radiol 1988;11:26-28.
190. Terada T, Kawaguchi M, Furukawa K, et al. Minute mixed ductal-endocrine carcinoma of the pancreas with predominant intraductal growth. Pathol Int 2002;52:740-746.
191. Terada T, Matsunaga Y, Maeta H, et al. Mixed ductal-endocrine carcinoma of the pancreas presenting as gastrinoma with Zollinger-Ellison syndrome. An autopsy case with a 24-year survival period. Virchows Arch 1999;435:606-611.
192. Tikkakoski T, Siniluoto T, Päivänsalo M, et al. Diagnostic accuracy of ultrasound-guided fine-needle-aspiration pancreatic biopsy. Rofo 1992;156:178-181.
193. Tomita T, Bhatia P, Gourley W. Mucin producing islet cell adenoma. Hum Pathol 1981;12:850-853.
194. Truong LD, Stewart MG; Hao H, et al. A comprehensive characterization of lymphoepithelial cyst associated with the pancreas. Am J Surg 1995;170:27.
195. Tsuchiya Y, Suzuki S, Sakaguchi T, et al. Lymphoepithelial cyst of the pancreas: report of a case. Surg Today 2000;30:856-860.
196. Tumors of the exocrine pancreas. in: HamiltonSR, Aaltonen LA (Eds.): World Health Organization Classification of Tumours. Pathology and Genetics of tumours of the digestive system. IARC Press:Lyon 2000
197. Tylen U, Arnesjö B, Lindberg LG, et al. Percutaneous biopsy of carcinoma of the pancreas guided by angiography. Surgery, Gynec Obstet 1976;142:737-739.
198. Varadarajulu S, Tamhane A, Eloubeidi MA. Yield of EUS-guided FNA of pancreatic masses in the presence or the absence of chronic pancreatitis. Gastrointest Endoscop 2005;62:728-736.
199. Vermeulen BJ, Widgren S, Gur V, et al. Dermoid cyst of the pancreas. Case report and review of the literature. Gastroenterol Clin Biol 1990;14:1023-1025.
200. Volante M, La Rosa S, Castellano I, et al. Clinico-pathological features of a series of 11 oncocytic endocrine tumours of the pancreas. Virchows Arch 2006;448:545-551.
201. Volmar KE, Vollmer RT, Routbort MJ, Creager AJ. Pancreatic and bile duct brushing cytology in 1000 cases: review of findings and comparison of preparation methods. Cancer 2006;108:231-238.
202. Wakatsuki T, Irisawa A, Bhutani MS, et al. Comparative study of diagnostic value of cytologic sampling by endoscopic ultrasonography-guided fine-needle aspiration and that by endoscopic retrograde pancreatography for the management of pancreatic mass without biliary stricture. J Gastroenterol Hepatol 2005;20:1707-1711.
203. Weissmann D, Lewandrowski K, Godine J, et al. Pancreatic cystic islet-cell tumors. Clinical and pathologic features in two cases with cystic fluid analysis. Int J Pancreatol 1994;15:75-79.
204. Wilson JL, Kalade A, Prasad S, et al. Diagnosis of solid pancreatic masses by endoscopic ultrasound-guided fine-needle aspiration. Intern Med J 2009;39:32-37.
205. Wittmann J, Kocjan G, Sgouros SN, et al. Endoscopic ultrasound-guided tissue sampling by combined fine needle aspiration and trucut needle biopsy: a prospective study. Cytopathology 2006;17:27-33.
206. Xing GS, Geng JC, Han XW, et al. Endobiliary brush cytology during percutaneous transhepatic cholangiodrainage in patients with obstructive jaundice. Hepatobiliary Pancreat Dis Int 2005;4:98-103.
207. Yamaguchi T, Shirai Y, Ishihara T. Pancreatic juice cytology in the diagnosis of intraductal papillary mucinous neoplasm of the pancreas: significance of sampling by peroral pancreatoscopy. Cancer 2005;104:2830-2836.
208. Yan BM, Pai RK, Van Dam J. Diagnosis of pancreatic gastrointestinal stromal tumor by EUS guided FNA. JOP 2008;9:192-196.
209. Yantiss RK, Cosar E, Fischer AH. Use of IMP3 in identification of carcinoma in fine needle aspiration of pancreas. Acta Cytol 2008;52:133-138.
210. Ylagan LR, Edmundowicz S, Kasal K, et al. Endoscopic ultrasound guided fine-needle aspiration cytology of pancreatic carcinoma: a 3-year experience and review of the literature. Cancer 2002;96:362-369.
211. Zamboni G, Klöppel G, Hruban RH et al. Mucinous cystic neoplasms of the pancreas. in: Hamilton SR, Aaltonen LA. (Eds.): World Health Organization Classification of Tumours: Pathology and Genetics of Tumours of the Digestive Sytem. IARC Press:Lyon 2000
212. Zhang S, Luzadder R, Ramos MC, et al. Using EUS-FNA in the evaluation of pancreatic cystic lesions: five years experience from Northwestern University, Feinberg School of Medicine. Cancer(Cancer Cytopathol) Suppl 2007;111:415-416.
213. Zhu LC, Sidhu GS, Cassai ND, Yang GC. Fine-needle aspiration cytology of pancreatoblastoma in a young woman: report of a case and review of the literature. Diagn Cytopathol 2005;33:258-262.

**Fig. 10.1 Pancreatic juice after secretin stimulation.**
Pancreatic juice aspirate (selected example) showing dispersed carcinoma cells and a compact cluster of tumor cells (upper right), originating from adenocarcinoma of the pancreatic main duct. Background typically comprises large amounts of degenerating cells and necrosis (conventional sediment smear after centrifugation, Pap stain, high magnification).

**Fig. 10.2A, B CA19-9 and ductal pancreatic carcinoma.**
A 60-year-old man with a positive history of pancreatic carcinoma. Rectal palpation revealed a firm mass located in the wall of the rectum outside the prostate. Differential diagnoses were metastasis of the pancreatic cancer, prostatic carcinoma, adenocarcinoma of the rectum. Transrectal FNAB was performed, direct smears were prepared from the aspirate and Pap-stained.
*Cytologic/immunocytochemical diagnosis:* Metastasis of pancreatic carcinoma.
*Follow-up:* No further investigations.
**A** Detail shows a sheet of mucin-forming carcinoma cells (arrows: faintly pink staining vacuolated cytoplasmic bodies). Nuclei displaying grooves and clear or thin dispersed chromatin indicate adenocarcinoma of pancreatic origin. **B** Strong immunocytochemical expression of CA-19-9 proved helpful in determining a definite diagnosis of metastatic pancreatic carcinoma. Note strong immunopositive background due to the large amount of tumor necrosis (Pap-prestained smear, low magnification).

10

**Figs. 10.3–10.5 ICM DNA as an adjunct to routine cytology.**
Two examples emphasize the diagnostic impact of static DNA cytometry on pancreatic cytology results.

**Fig. 10.3** (case #1) Liquid-based specimens (Cytospin) prepared from pancreas duct brushings. High magnification reveals a regular sheet composed of slightly atypical ductal cells: irregular nuclear outlines, variation in size and shape of the nucleoli, and intracytoplasmic mucin (arrows). However, loose chromatin texture and the pronounced nucleoli suggest benign reactive cell changes (Pap stain). Diagnosis could be affirmed by a diploid DNA distribution pattern (not shown).
*Cytologic/cytometric diagnosis:* Reactive-regenerative atypias.
*Tissue diagnosis* (pancreas resection): Chronic pancreatitis, focal regenerative duct epithelium.

**Fig. 10.4** (case #2) Pancreas duct brushing yielded benign ductal cell sheets and few atypical cell clusters. The latter were composed of relatively uniform abnormal ductal cells characterized by dense crowding, loss of nuclear polarity, nuclear clearing, occasional deep nuclear indentations, and high N/C ratio, features suggesting pancreatic carcinoma (direct smear, Pap stain, lower magnification).

**Fig. 10.5** (case #2) DNA aneuploidy(hypotetraploid-aneuploid stemline and aneuploid single cells in the 5c and 6c area) confirmed cytologic diagnosis (Pap-prestained Feulgen stain, AutoCyte).
*Definite diagnosis* assessed by image-guided FNAB of the pancreatic tumor: mucinous pancreatic adenocarcinoma.

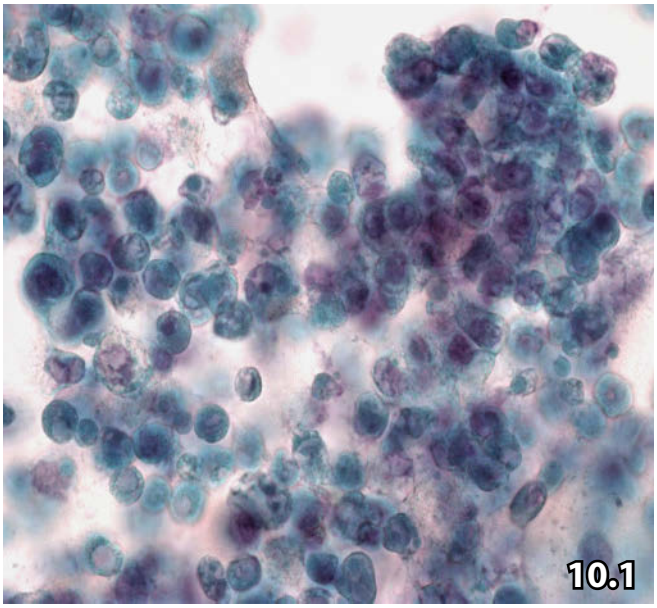
10.1

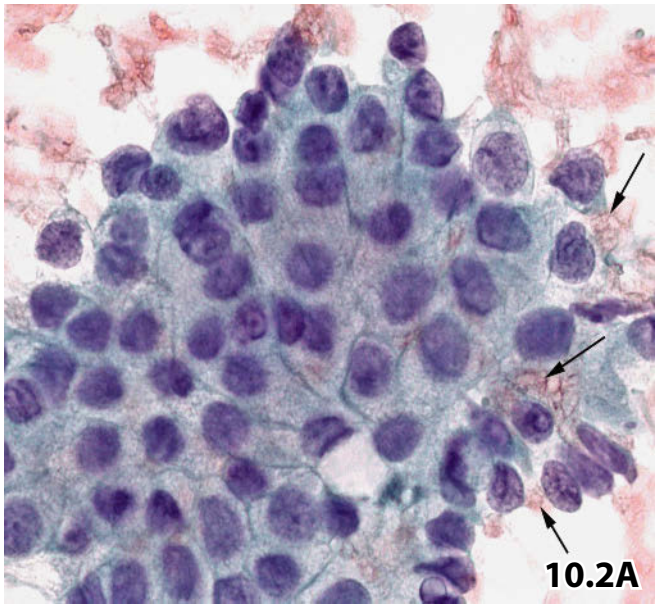
10.2A

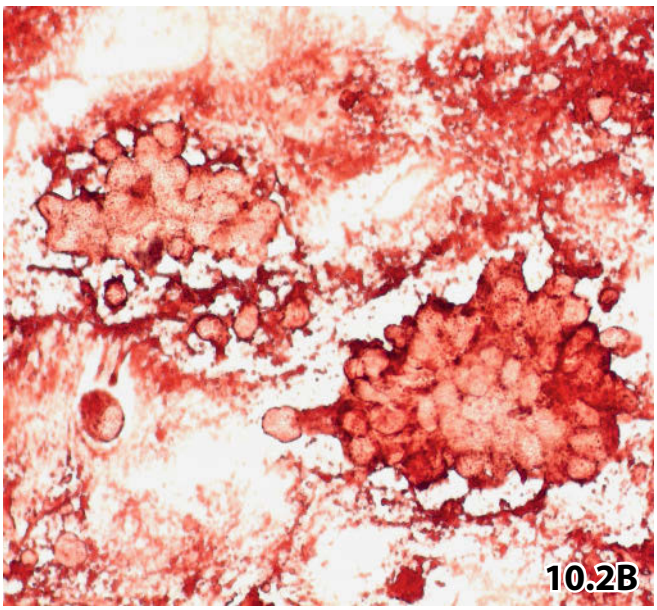
10.2B

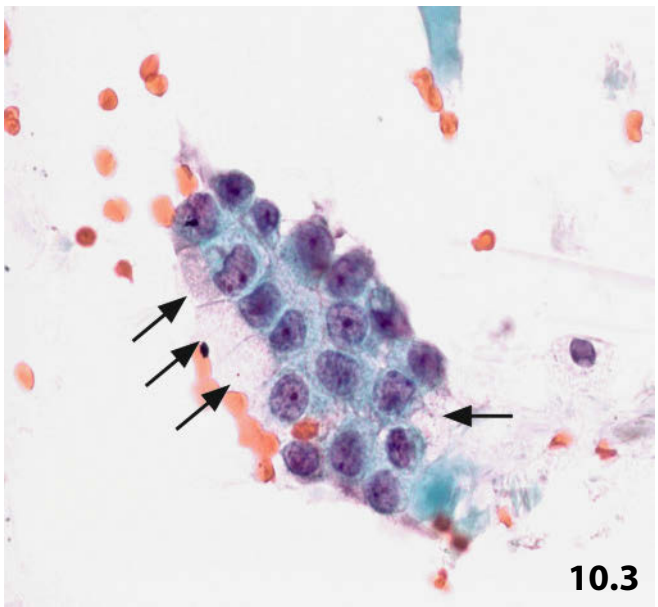
10.3

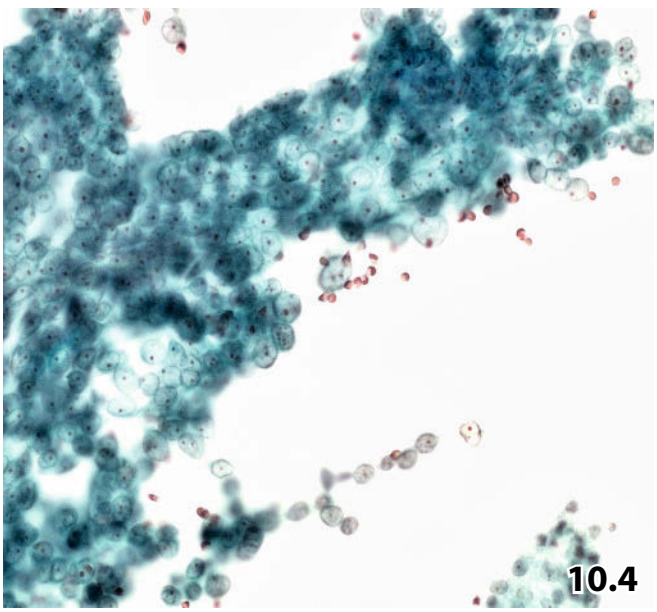
10.4

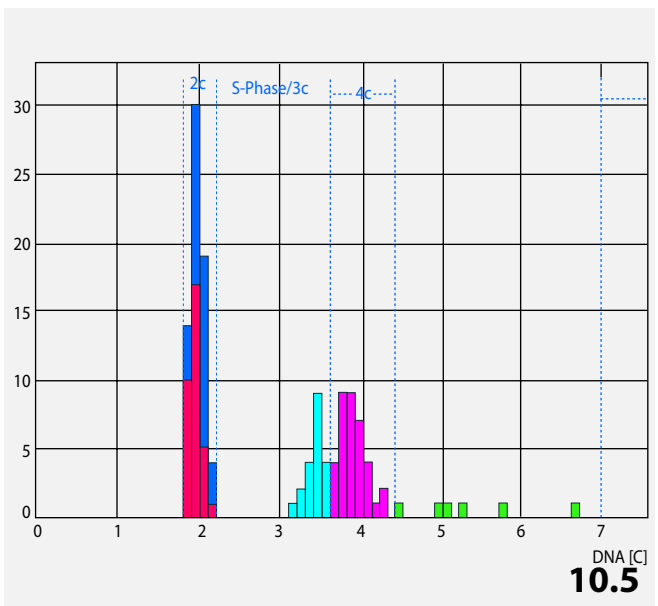

10.5

**Fig. 10.6A–C Benign pancreatic cells in FNAB and Brushing.**
Conventional smears were Pap-stained.
**A** A fragment of benign parenchymal pancreatic tissue composed of exocrine acini and crossing strands of loose stromal tissue (lower magnification). **B** A regular sheet of ductal epithelium originating from a small pancreatic duct is composed of small cuboidal to columnar cells (high magnification). **C** Benign pancreas duct cells collected by brushing. A majority of ductal cells originating from large pancreatic ducts are evidently columnar in shape and occur in palisade arrangement (direct sediment smear after rinsing the brush in an appropriate solution and centrifugation, Pap stain, high magnification).

**Fig. 10.7 Islet cell.**
Detail shows a single benign acinar cluster and an endocrine islet cell (arrow) (transcutaneous pancreatic FNAB, direct smear, Pap stain).

**Fig. 10.8 Mesothelial cells in FNAB sample.**
Transcutaneous FNAB of the pancreas. Proliferating mesothelial cells are grouped in sheets and clusters. Nuclear polymorphism, irregular cell arrangement, and pseudoglandular formation (upper right) may lead to an erroneous diagnosis of well-differentiated adenocarcinoma. However, the overall architecture, loose granular chromatin, and the cytoplasmic features do not really correspond to pancreatic carcinoma (direct smear, Pap stain, high magnification).

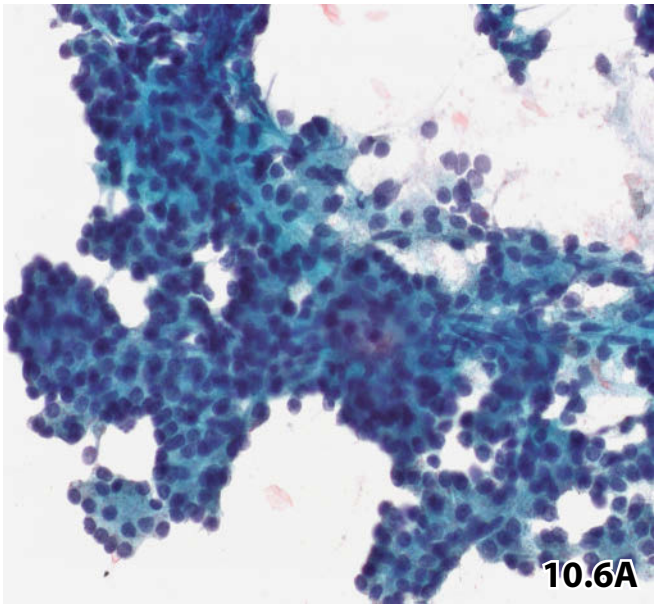
10.6A

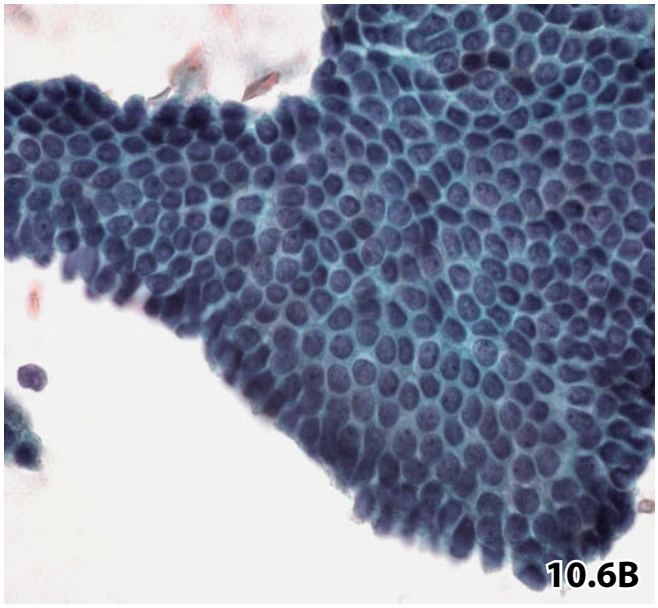
10.6B

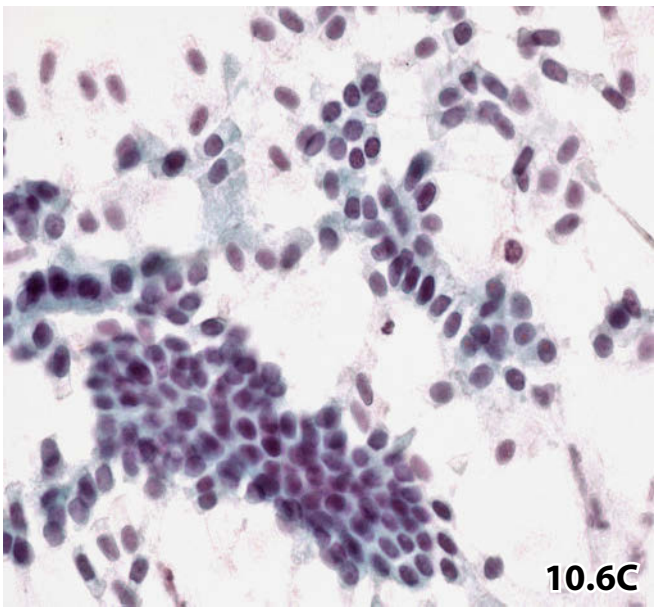
10.6C

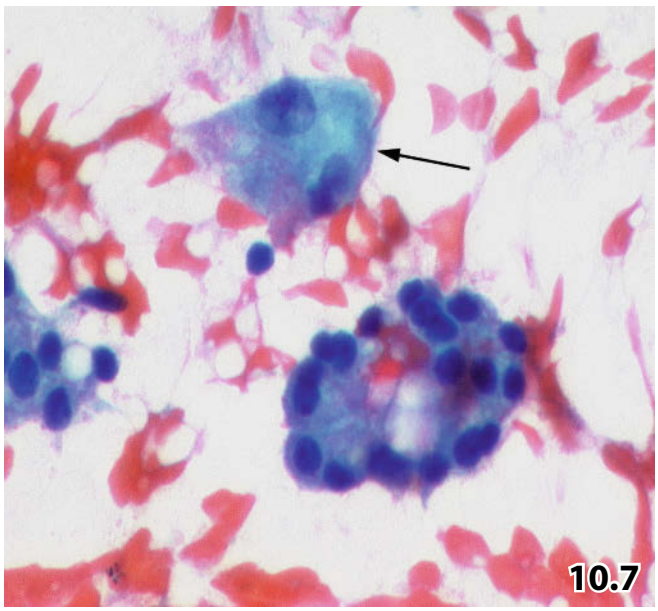
10.7

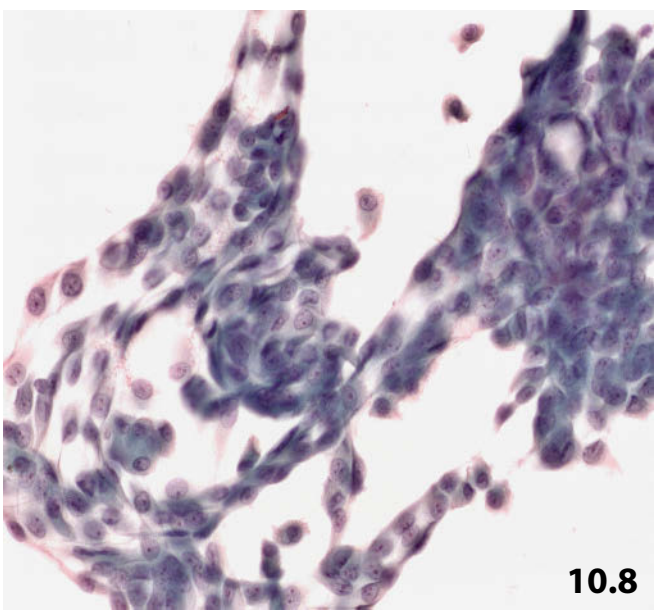
10.8

**Figs. 10.9 and 10.10 Gastric epithelium in FNAB: morphology and diagnostic dilemma.**
Transgastric FNAB of a pancreatic lesion in two different patients. Direct smears were prepared and the specimens were Pap-stained.

**Fig. 10.9** (case #1) Lower magnification shows honeycomb-like sheets of gastric epithelial cells against a background containing masses of free mucus.

**Fig. 10.10** (case #2) Gastric epithelial cells exhibiting distinct nuclear polymorphism (cleaved membrane, grooves, lobation), nuclear crowding, and intracytoplasmic mucin strongly mimic mucinous cystadenoma or well-differentiated pancreatic carcinoma (high magnification).

**Fig. 10.11 Bile duct epithelium in an exfoliative sample of the pancreatic duct.**
Brushing of the pancreatic duct. A benign epithelial sheet assumed to originate from bile duct epithelium based on nuclear features (pronounced membrane and small nucleoli), though the cytoplasm mainly exhibits a cuboidal and not the typical slender shape of bile duct-lining cells (direct sediment smears after rinsing the brush in an appropriate solution and centrifugation, Pap stain, higher magnification). For comparison see Fig. 10.6B and 10.6C.

We would like to emphasize that bile duct-lining epithelial cells may be indistinguishable from pancreatic ductal cells.



**Figs. 10.12 and 10.13 Duodenal epithelium in pancreatic juice aspirate.**
Duodenal epithelial cells are frequently encountered in pancreatic juice sampled by duct cannulation or in duodenal secretion. Two samples from different patients demonstrate cytologic key features of duodenal mucosal lining. In both patients, pancreatic juice was aspirated after secretin stimulation. Direct smears of the sediment (after conventional centrifugation) were performed and Pap-stained.

**Fig. 10.12** (case #1) Large flat sheets composed of monomorphic cuboidal and columnar cells are typically interspersed with goblet cells (arrows) (low magnification).

**Fig. 10.13A, B** (case #2) Demonstration of morphologic details. **A** Another key feature of duodenal mucosal cells is the prominent brush border (arrows) often appearing out of focus. **B** The background of the smear contains numerous degenerating gastrointestinal epithelial cells, histiocytes, and amorphous material.

Degenerated epithelial cells in duodenal secretions must never be misinterpreted as poorly preserved hepatocytes or tumor necrosis.

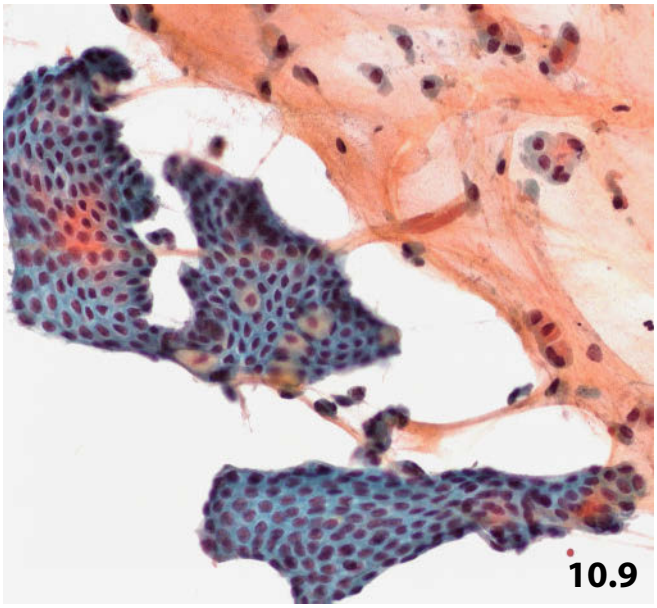
10.9

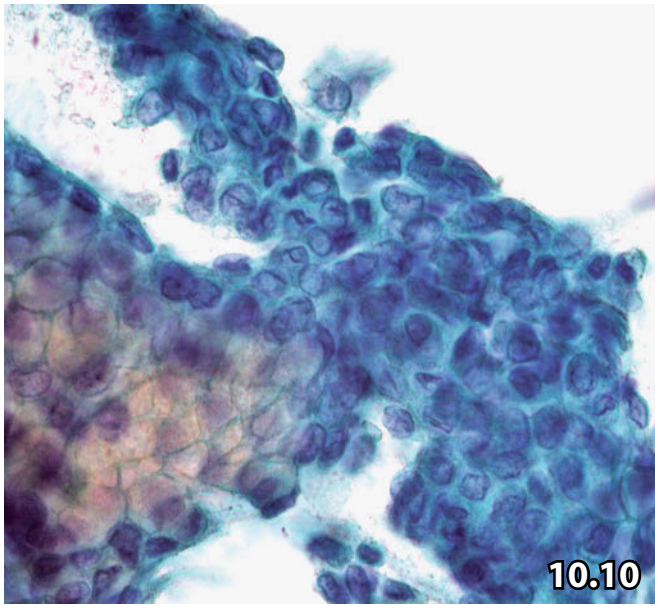
10.10

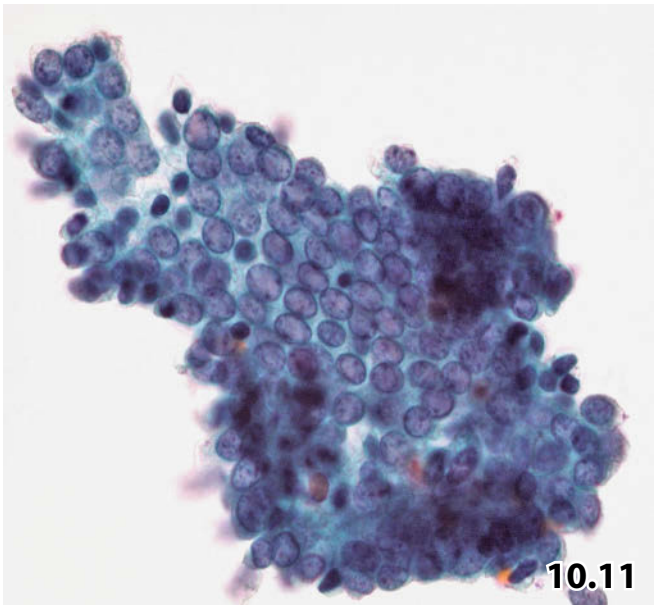
10.11

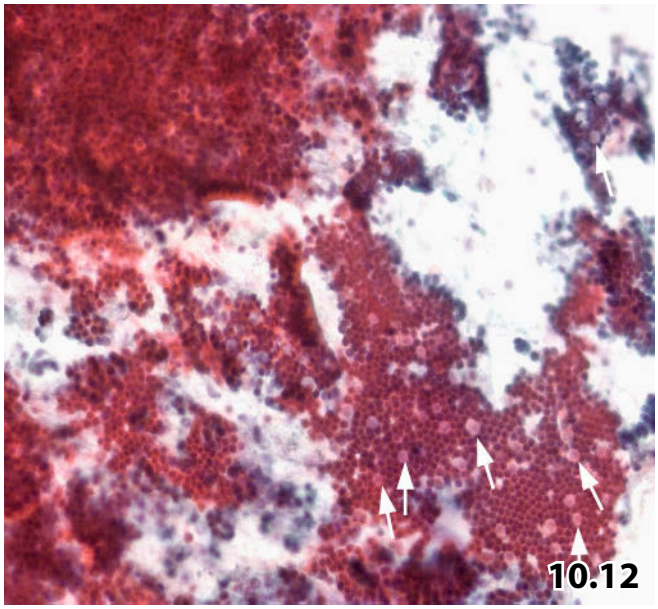
10.12

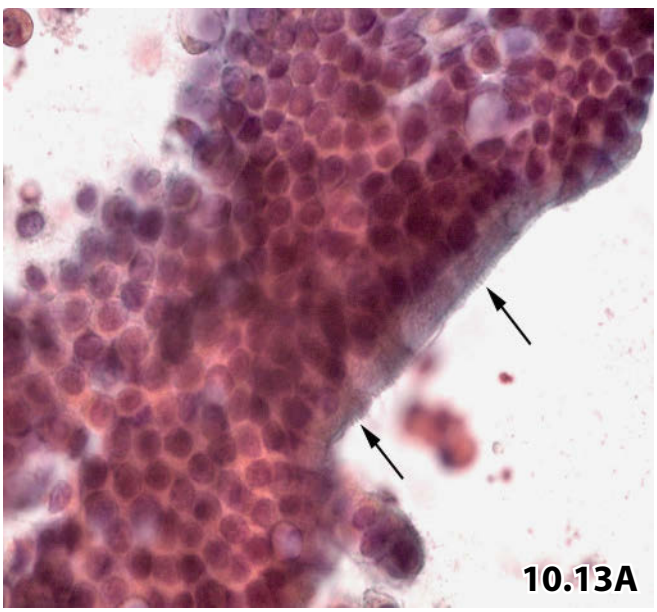
10.13A

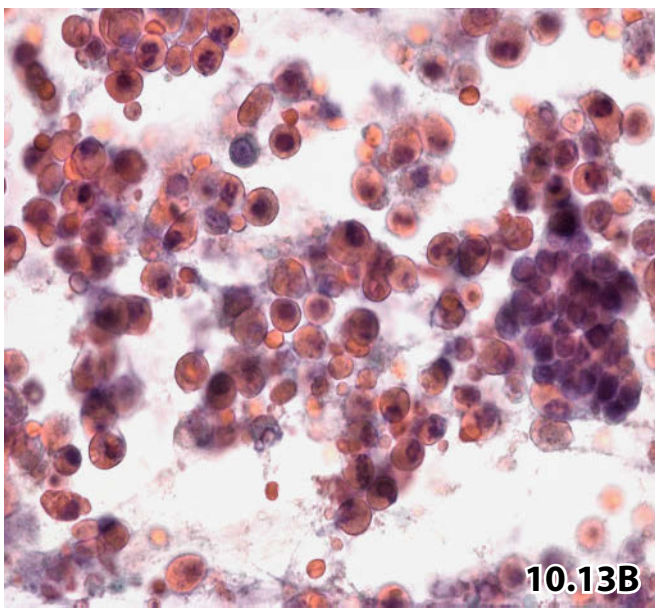
10.13B

**Fig. 10.14 Cells from duodenal glands in brush cytology.**
Fragments of intramural duodenal glands may be obtained by vigorously brushing the distal segment of the ductus choledochus and the ampullary area. High magnification shows activated secretory duodenal glandular cells exhibiting distinct atypias (brush specimen of the distal ductus choledochus, direct sediment smears after rinsing the brush in an appropriate solution and centrifugation, Pap stain).

Strongly activated glandular cells together with the peculiar cytoarchitecture may mislead to a diagnosis of adenocarcinoma of the clear cell type.

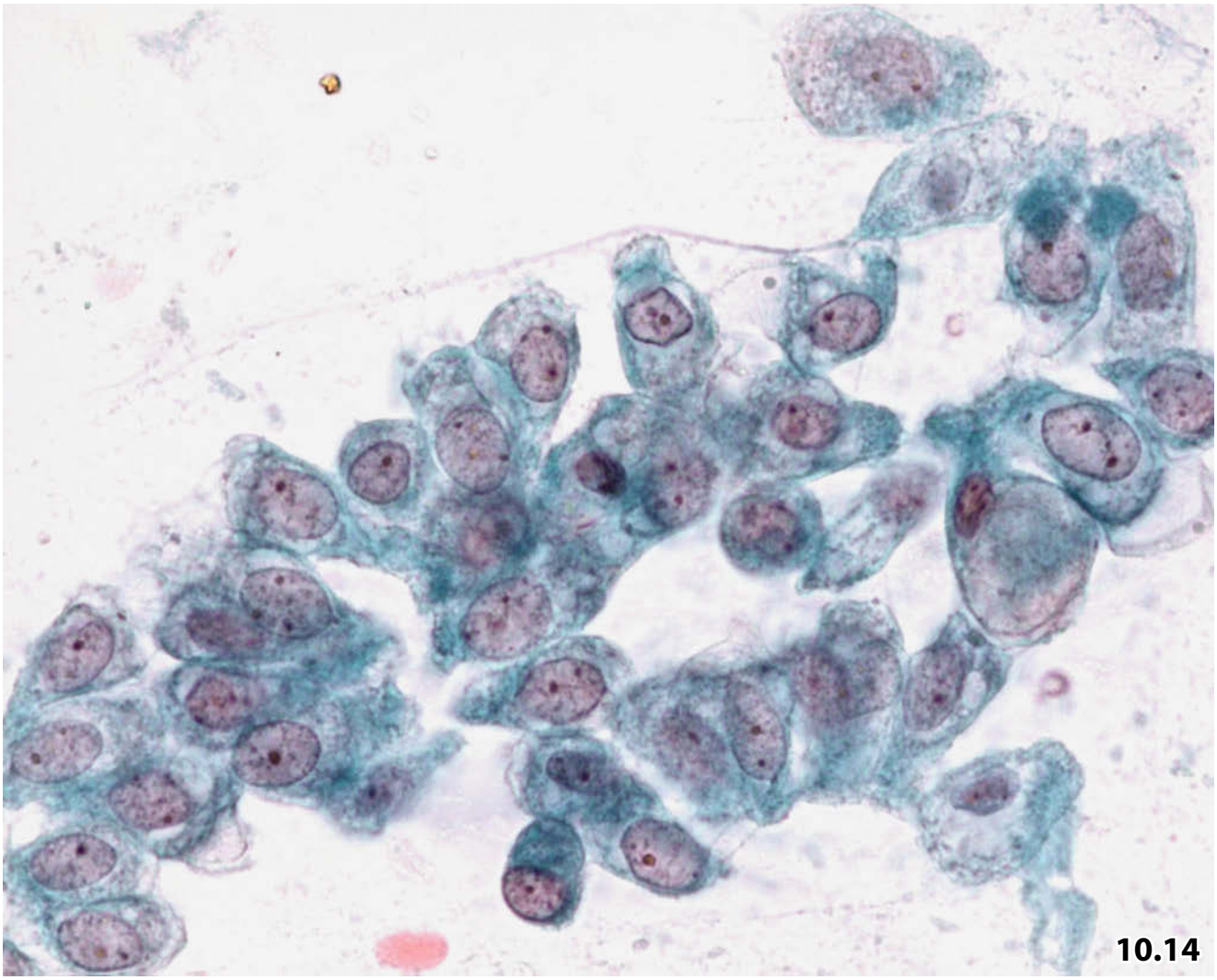

10.14

**Fig. 10.15 Acute pancreatitis, healing form.**
A 48-year-old man presented with diffuse enlargement of his pancreas. Image-guided transcutaneous FNAB yielded a viscous aspirate. Direct smears exhibiting degenerating epithelial cells, neutrophils, debris, and calcific deposits. Benign pancreatic tissue fragments were also present (not shown) (Pap stain, higher magnification).
*Cytology* is compatible with the healing form of pancreatitis. Excisional biopsy and resection were not performed.

**Fig. 10.16A, B Chronic relapsing pancreatitis.**
Intraoperative FNAB of an unexpected pancreatic lesion in a 59-year-old man; laparatomy was performed for excision of a gastric ulcer. On-site rapid cytologic interpretation was provided using ultrarapid Pap stain.
*Cytologic diagnosis:* Purulent pancreatitis (histologic-bioptic investigation was not performed).
**A** A compact cluster of ductal cells exhibiting reactive changes: varying nuclear size, nucleoli, nuclear overlapping. Background of the direct smear shows neutrophils and debris. Epithelial cell clusters are also interspersed with neutrophils (high magnification). **B** Another cell cluster from the same smear points to an important fact: epithelial sheets aspirated from an inflammatory pancreatic process may express features that mimic well-differentiated pancreatic adenocarcinoma such as small monomorphic cells, loss of nuclear polarity, wrinkled and folded nuclear membranes (arrows), and conspicuous but small nucleoli (high magnification).



**Fig. 10.17 Pseudocyst.**
Imaging revealed a pancreatic pseudocyst in a 46-year-old man. Sediment of the aspirated cyst fluid is composed of degenerated histiocytes, neutrophils, and detritus. Yellow-brown pigment deposits (arrows) may represent hemosiderin and/or hematoidin. Well preserved epithelial cells are absent (sediment direct smear, Pap stain, higher magnification).

**Fig. 10.18 Lymphoepithelial cyst.**
A 45-year-old man presented with a tumoral lesion in the head of his pancreas. EUS-FNAB was performed. Cytology revealed nucleated and anucleated markedly keratinized squamous cells scattered in a background of blood and debris. Sporadic lymphocytes were also present.
*Tentative cytologic diagnosis:* Dermoid cyst.
*Discussion:* An extremely well-differentiated squamous cell carcinoma was included in the diagnostic considerations due to the irregularity of the nuclei, nuclear deep staining, marked cytoplasmic keratinization, and polymorphism. Lymphoepithelial cyst, however, was erroneously disregarded due to scantiness of lymphoid cells.
*Tissue diagnosis* (partial removal of the pancreas): Lymphoepithelial cyst.

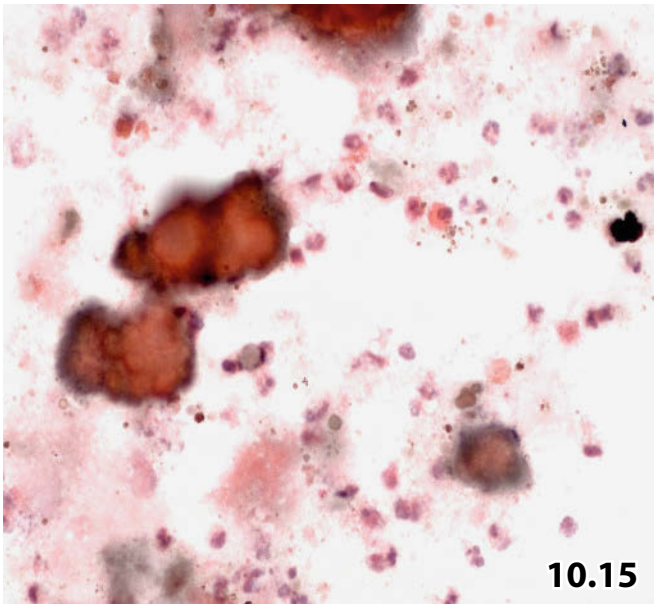
10.15

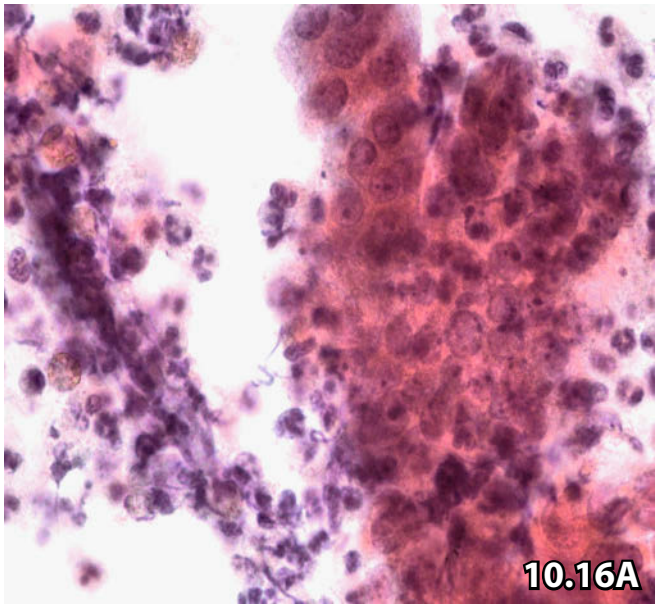
10.16A

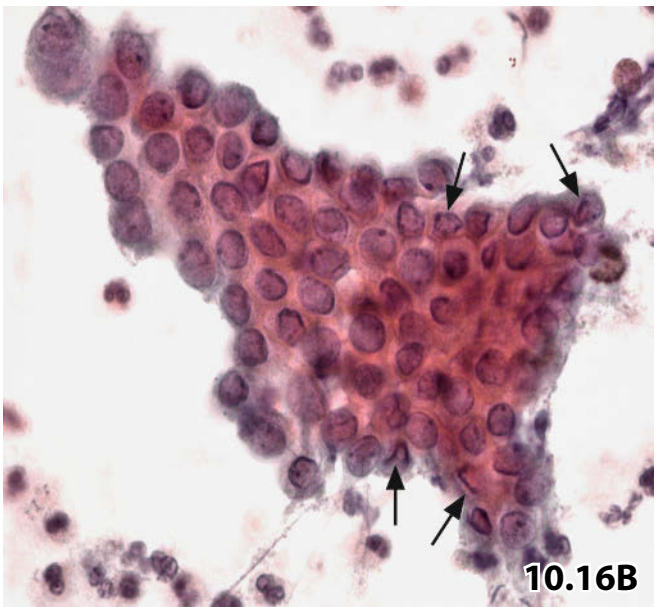
10.16B

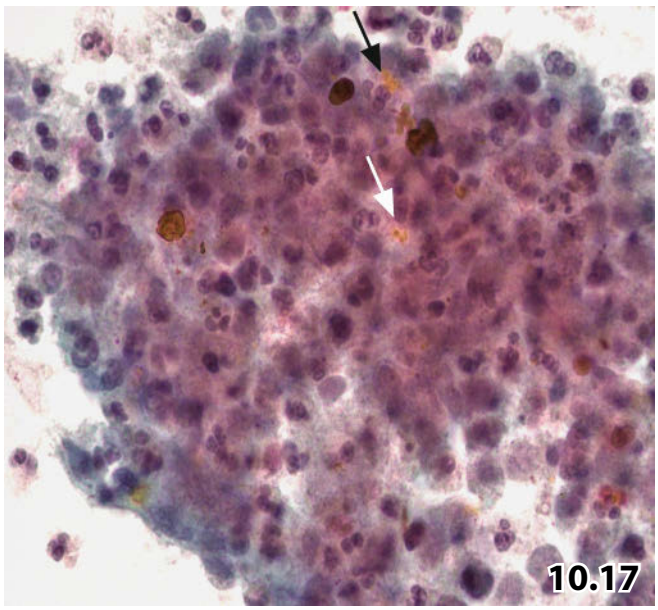
10.17

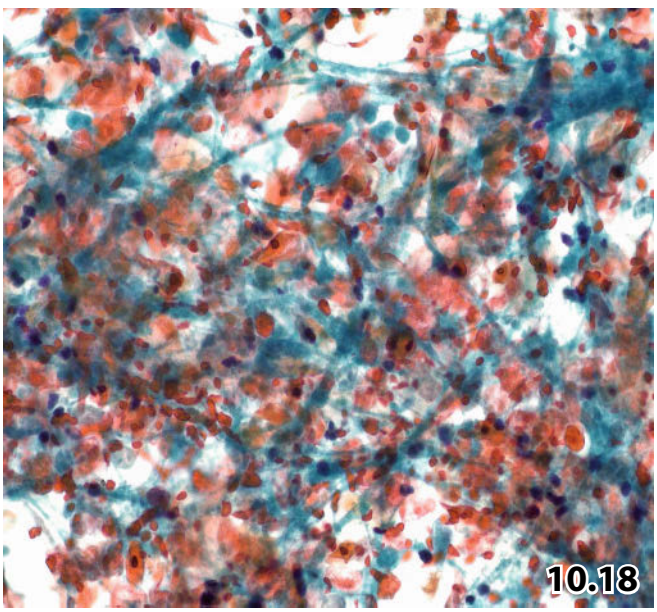
10.18

**Figs. 10.19 and 10.20 Serous cystadenoma.**
Primary transcutaneous US-guided FNAB was performed in a 69-year-old man presenting with a tumoral lesion (5 cm in diameter) in the head of his pancreas. Cytology and histology is presented.

**Fig.10.19** Direct smears are extremely paucicellular. Low magnification shows a few sheets of benign cuboid to columnar epithelial cells as well as a few histiocytes (bottom) and proteinaceous material in the background (Pap stain).
*Tentative cytologic diagnosis:* Cytologic findings are consistent with serous cystadenoma.

**Fig. 10.20** *Histologic examination* of the pancreas (Whipple resection) confirmed cytologic diagnosis of serous cystadenoma (HE stain, low magnification).

**Figs. 10.21–10.27 Mucinous cystic neoplasms: adenoma, borderline tumor, adenocarcinoma.**
Cytologic features and diagnostic challenge of mucinous cystic neoplasms are demonstrated by means of tumor aspirates from different patients. The diagnostic impact of DNA image cytometry and the value of immunocytochemistry are pointed out. Each aspirated cyst fluid was processed using a conventional centrifuge; direct smears of the sediments were Pap-stained.



**Figs.10.21 and 10.22** (case #1) Ultrasound revealed a well-delineated cystic lesion (2 cm in diameter) in the pancreas of an otherwise healthy 57-year-old man. US-guided FNAB was performed.
*Tentative cytologic diagnosis:* Mucinous neoplasia, most likely mucinous cystadenoma of the pancreas. Tissue diagnosis is mandatory as cytology cannot exclude preneoplastic cell changes and focal invasive growth.

**Fig.10.21A** Lower magnification shows flat sheets of cuboid to columnar cells (often mucin-forming) embedded in a mucinous background. Note substantial nuclear irregularities. **B** High magnification demonstrates nuclear polymorphism and hyperchromasia. A few single cells are clearly atypical and exhibit goblet-cell-like features (left).

**Fig. 10.22** *Histologic examination* (pancreas resection) confirmed cytologic diagnosis; no evidence of invasiveness (HE stain).

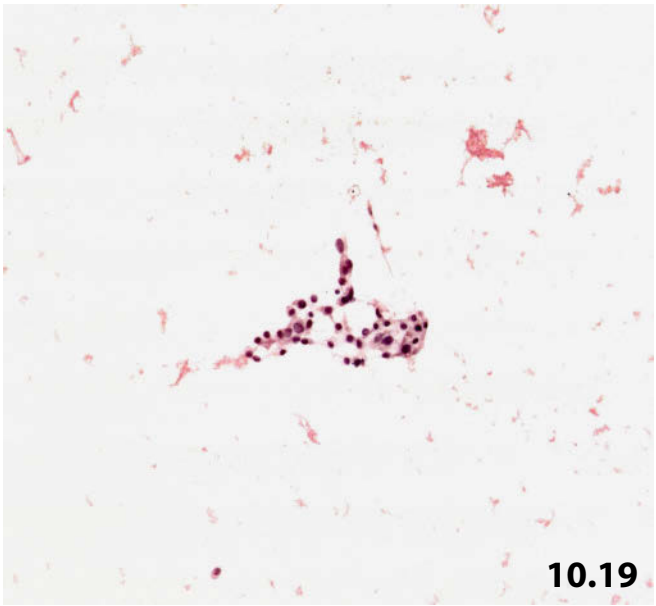
10.19

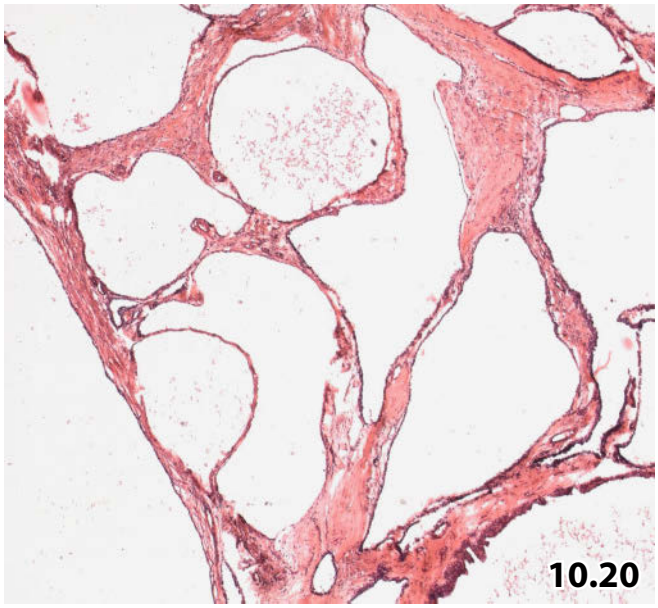
10.20

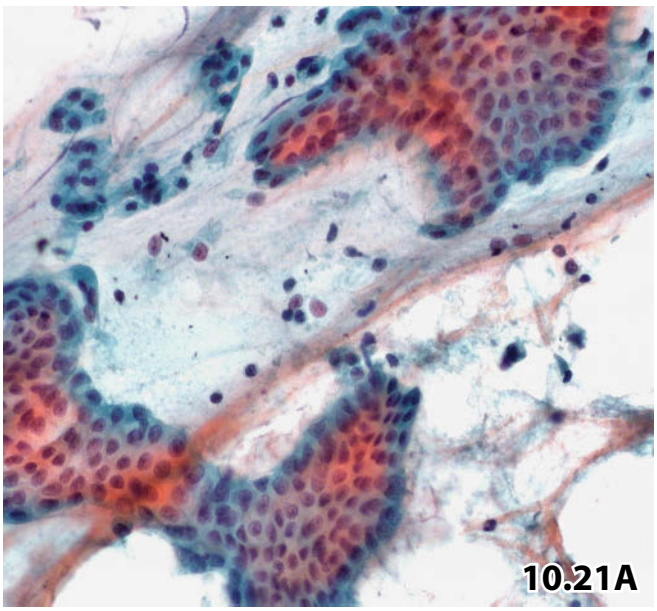
10.21A

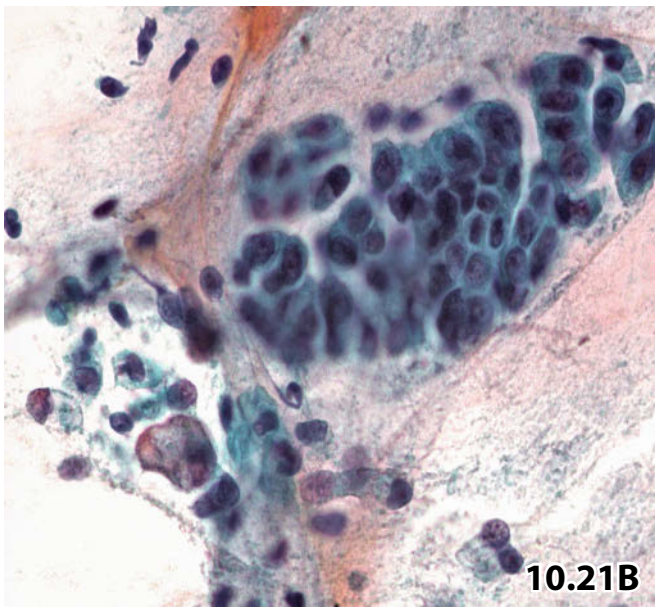
10.21B

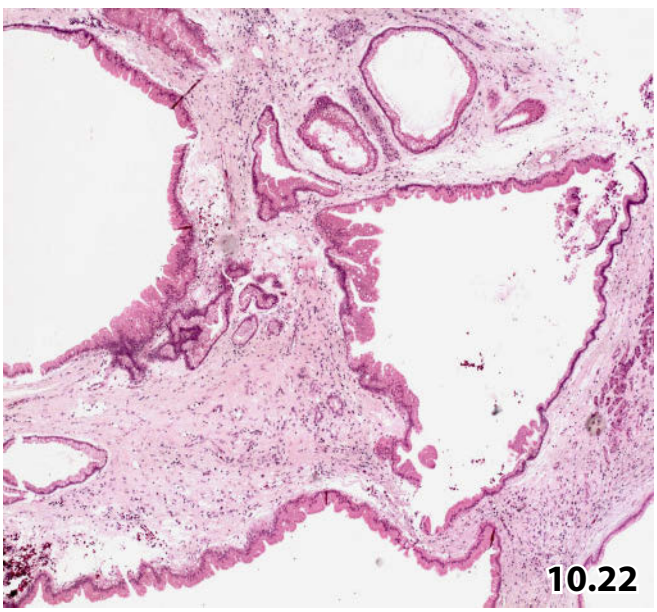
10.22

**Fig. 10.23 and 10.24** (case #2) US-guided FNAB of a cystic lesion in the pancreas of an elderly woman provided fairly cellular cytologic smears.
*Cytologic diagnosis* supported by ICM DNA: Mucinous neoplasia of the pancreas, most likely mucinous cystadenoma (low progressive potential).
*Tissue diagnosis:* Cytologic diagnosis was confirmed by histology (pancreas resection), no invasive growth could be detected.

**Fig. 10.23A** Low magnification shows sheets of mucinous epithelial cells, the nuclei exhibiting striking irregularities in their shape. Dispersed atypical cells are also present (center). **B** High magnification focuses on nuclear atypias: cleaving, indentations, longitudinal grooves, and occasional coarse granular chromatin (arrows).

**Fig. 10.24** DNA ploidy assessment using image cytometry (Pap-prestained Feulgen stain, AutoCyte): Diploidy indicates a benign lesion or a borderline tumor associated with minor progressive behavior.

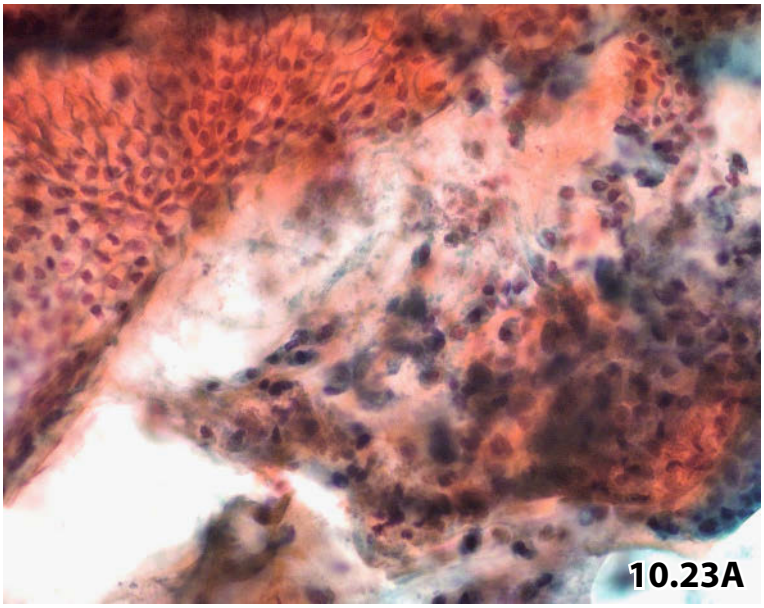

10.23A

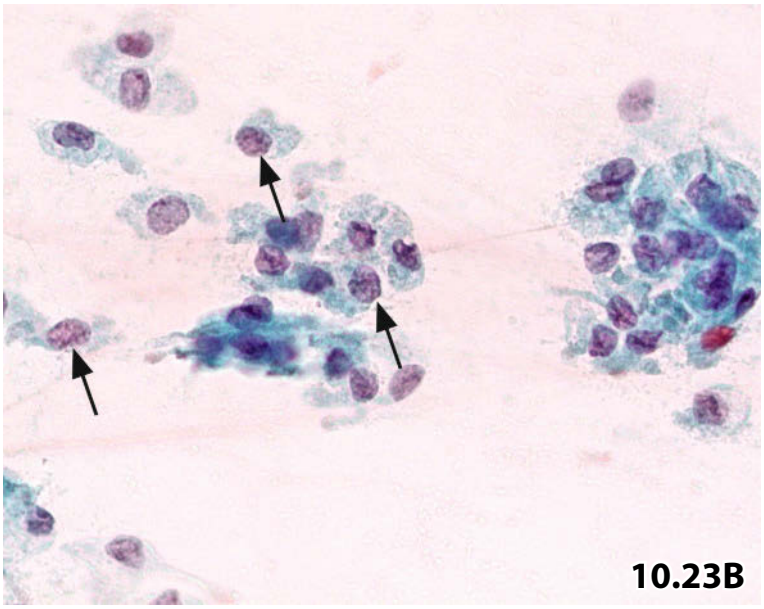

10.23B

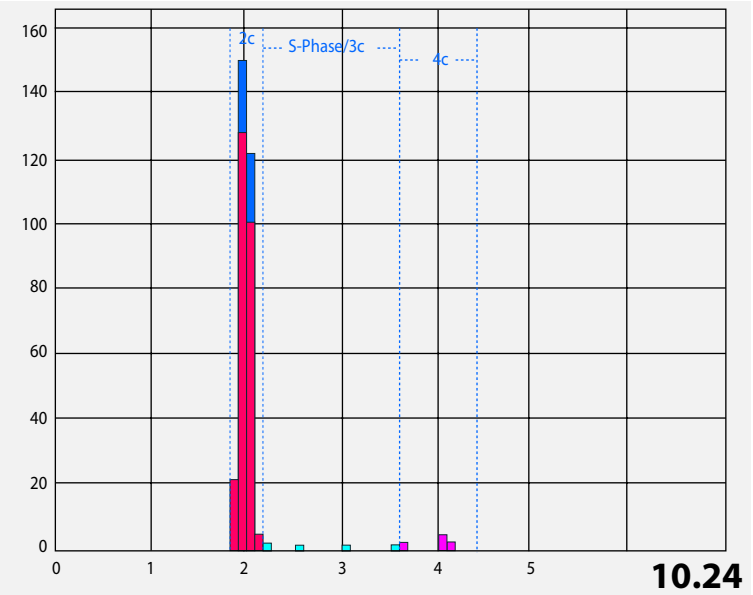


10.24

**Figs. 10.25 and 10.26** (case # 3) An 80-year-old male patient presented with a cystic tumor in the tail of his pancreas.
*Cytologic diagnosis* supported by ICM DNA: Mucinous cystic neoplasia of the pancreas: mucinous borderline tumor with distinct progressive potential or invasive carcinoma. Neither histologic diagnosis nor clinical follow-up are available. Surgery was not performed due to the patient's poor general condition.

**Fig. 10.25A** High magnification reveals pleomorphic cells scattered in a background of old blood, debris, and mucus (left margin). The varying size of cells together with dark-staining nuclei suggest epithelial cells rather than activated histiocytes; proper discrimination is difficult by light microscopy alone. **B** Immunocytochemical staining for pancytokeratin (MNF-116) solved the diagnostic confusion: large cells represent atypical epithelial cells (MNF-116 positivity) and small cells correspond to activated histiocytes (Pap-prestained direct smear).

**Fig. 10.26** The malignant potential of the lesion was estimated by DNA ploidy assessment using image cytometry (Pap-prestained Feulgen stain, Ahrens Cytometrie-System). Aneuploidy indicates a borderline tumor with major progressive potential or a malignant invasive lesion.

**Fig. 10.27** (case #4) A 55-year-old man presented with a voluminous cystic lesion in the tail of his pancreas. Dysplastic mucin-forming epithelial cells occurring in isolation or in three-dimensional clusters, the latter exhibiting scalloped contour. Free mucus and numerous signet ring-like tumor cells are also present (high magnification).
*Cytology* suggests intracystic carcinoma in situ or cystadenocarcinoma of the mucinous variant.
*Tissue diagnosis* (pancreas resection): Mucinous cystadenocarcinoma.

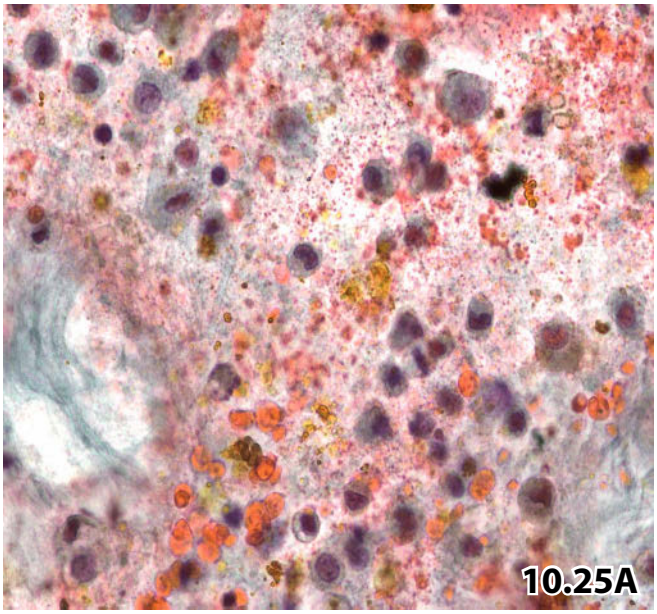
10.25A

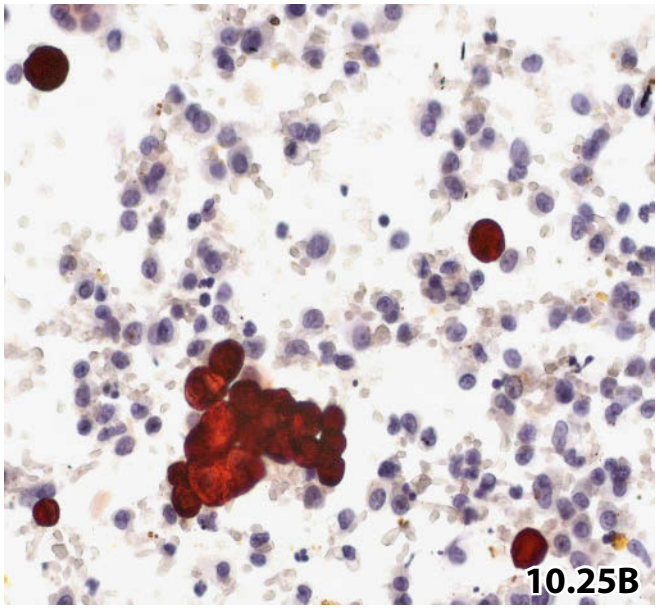
10.25B

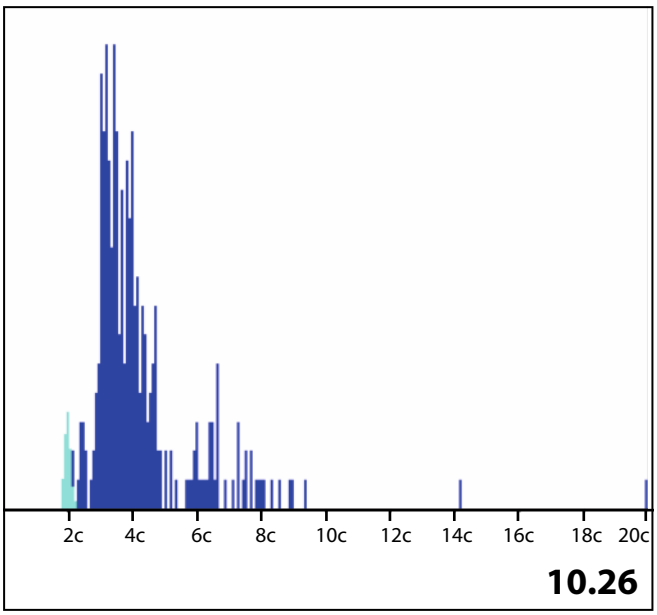

10.26

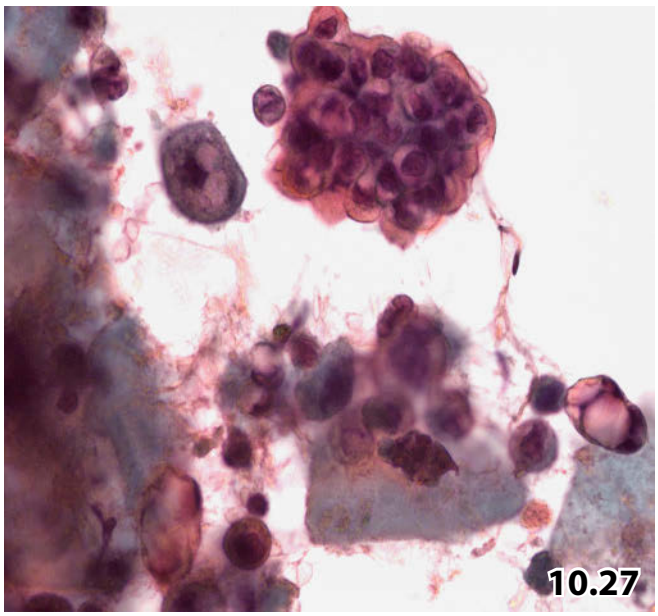
10.27

**Fig. 10.28 Intraductal papillary-mucinous neoplasia.**
A 71-year-old woman presented with a cystic disorder in her pancreas. Sediment smears from the aspirated cyst fluid revealed numerous isolated atypical epithelial cells and goblet cells (arrows) scattered in a mucinous background. Cell clusters were not encountered (direct sediment smear, Pap stain, lower magnification).
*Tentative cytologic diagnosis:* Mucinous cystic neoplasia; further subtyping is not possible.
*Tissue diagnosis* (pancreas resection): Intraductal papillary-mucinous neoplasia.

**Figs. 10.29A, B Solid pseudopapillary tumor.**
Imaging studies revealed a well-delineated pancreatic tumor (7 cm in diameter) in a 14-year-old female. Image-guided FNAB was performed. Direct smears were Pap-stained.
*Cytologic diagnosis:* Solid pseudopapillary tumor of the pancreas. Diagnosis was confirmed by histologic examination of the tumor.
**A** A branching papillary tissue fragment is shown at lower magnification. Note the delicate fibrovascular core (arrow). **B** High magnification highlights the characteristic nuclear features: clear or finely granular chromatin, deep nuclear indentations, longitudinal nuclear grooves (arrows), and conspicuous small to medium-sized nucleoli. The typical nuclear inclusions cannot be demonstrated in this field. The cytoplasm is rather abundant, vacuolated or granular. Quantitative DNA analysis by image cytometry provided a diploid histogram (not shown).



**Fig. 10.30 Cystic endocrine tumor.**
EUS-FNAB was used to aspirate 12 ml of a turbid fluid from a cystic pancreatic lesion in a young female patient. The aspirated material was processed using a liquid-based method (Cytospin) and the specimens were Pap-stained. Numerous clustered and isolated uniform cells with eccentric vacuolated and granular cytoplasm suggested endocrine tumor. Mild nuclear atypias are overt (higher magnification). Note the cells with a tendency to be fusiform in shape! Positive immunostaining for synaptophysin (not shown).
*Cytologic diagnosis* determined by immunocytochemistry: Cystic endocrine tumor (bioptic histology verified a cystic endocrine tumor of the low-grade variant).

**Fig. 10.31 Lymphangioma.**
A cystic pancreatic/parapancreatic lesion in a 64-year-old man with a history of gastric surgery turned out to be a lymphangioma (image-guided transcutaneous FNAB). Direct sediment smears exhibit a clean background and numerous benign lymphoid cells. A few transformed lymphocytes (arrows) and histiocytes (arrowhead) are also present (Pap stain, lower magnification).

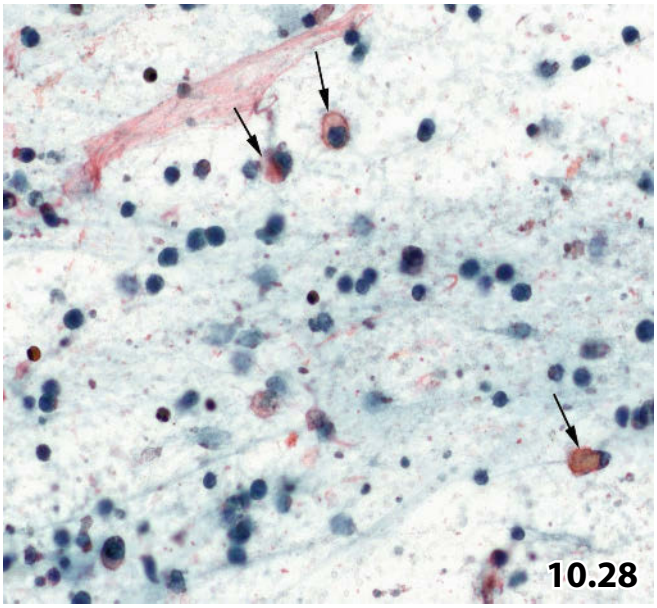
10.28

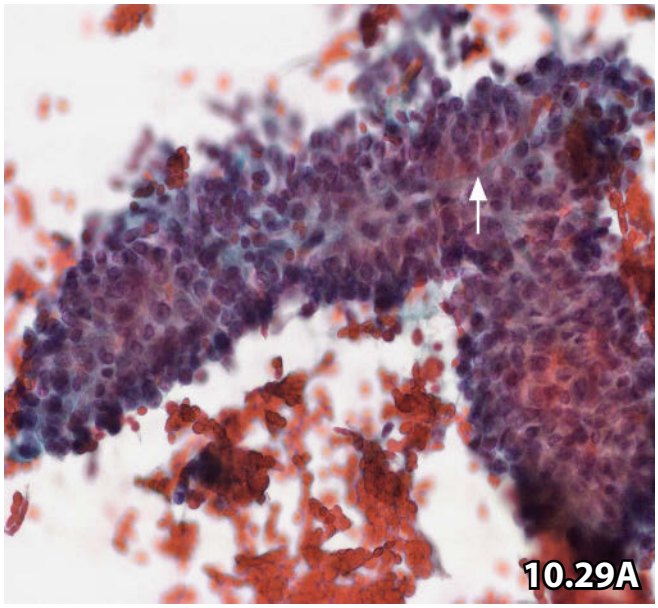
10.29A

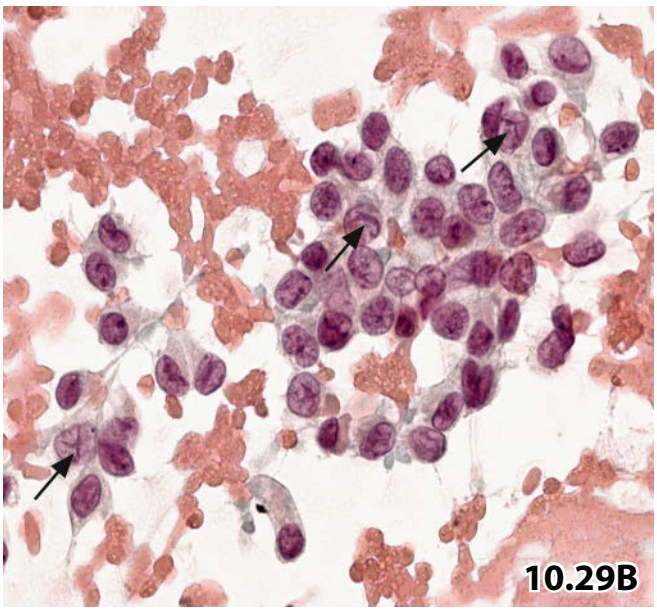
10.29B

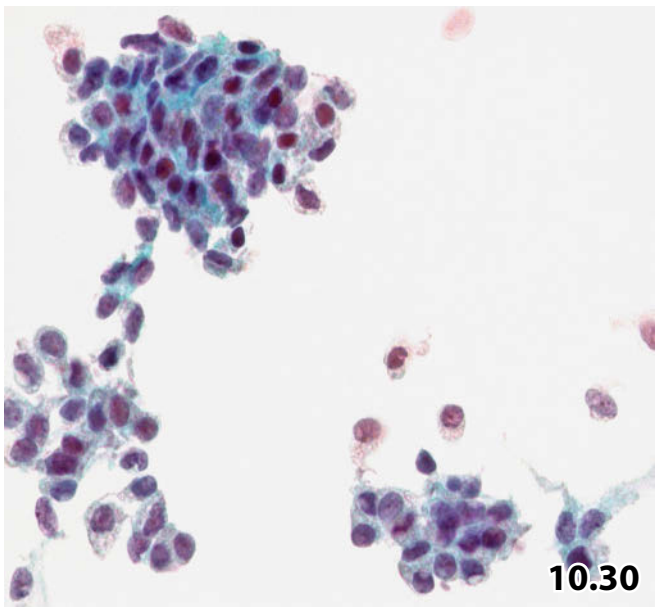
10.30

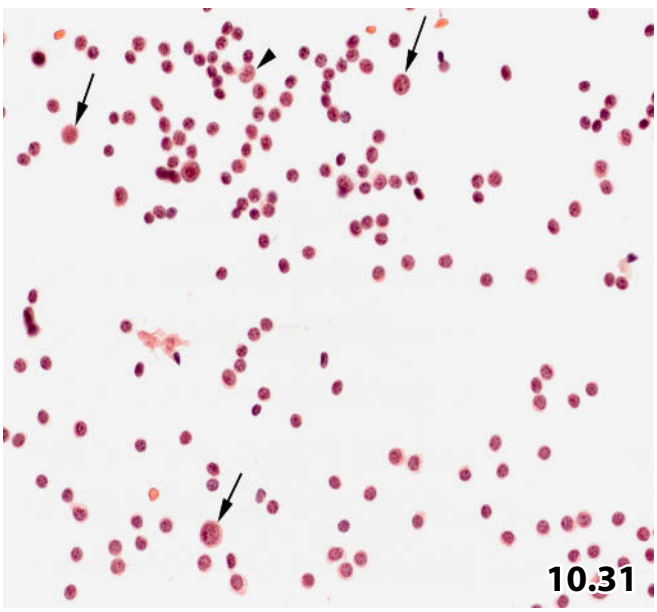
10.31

**Figs. 10.32 and 10.33 Well-differentiated ductal adenocarcinoma of the pancreas.** Two examples. Aspirates are processed using both direct smears and liquid-based method. No tissue examination was performed during the patients' life time.

**Fig. 10.32A, B** (case #1) CT-guided FNAB of a pancreatic tumor mass in an elderly woman. Direct smears were Pap-stained. **A** Sharply delineated small and large flat sheets with honeycomb-like appearance. Note nuclear polymorphism and intracytoplasmic mucin (pink-colored), which are recognized even at low magnification. Compare malignant cell sheets with benign pancreatic parenchyma composed of acini (arrows). **B** High magnification highlights cytologic key features of well-differentiated adenocarcinoma of the pancreas.

**Fig. 10.33** (case #2) Liquid-based preparations (ThinPrep) of an aspirate from a pancreatic mass (image-guided transcutaneous FNAB). High magnification once again emphasizes the cytologic characteristics of well-differentiated pancreatic cancer.

Liquid-based specimens exhibit particular cell criteria that are more pronounced than in conventional smears: nuclear wrinkling, nuclear shrinking, nuclear crowding, and prominent nucleoli (please compare with Fig. 10.32B).

**Fig. 10.34 Moderately differentiated ductal adenocarcinoma of the pancreas.** EUS-FNAB of a tumor in the head of the pancreas in an elderly woman. Direct smears, Pap stain. Basic cell features of less well-differentiated adenocarcinoma match those of well-differentiated tumors. Moderately differentiated cancers are composed of large pleomorphic cells, more granular chromatin, and more pronounced nucleoli as compared to well-differentiated cancer (high magnification). Please compare with Fig. 10.32B. No tissue diagnosis was available.

**Figs. 10.35 and 10.36 Poorly differentiated ductal adenocarcinoma of the pancreas.** Two examples. Except for FNA cytology, no further diagnostic evaluation was carried out.

**Fig. 10.35** (case #1) 70-year-old woman. The aspirated carcinoma cells are presented on Cytospin preparation (EUS-guided FNAB, Pap-stained specimens). Pleomorphic carcinoma cells mainly dispersed against a background containing neutrophils, degenerate cells, and necrosis (high magnification).

**Fig. 10.36** (case #2) Image-guided transcutaneous FNAB of the pancreas in a 45-year-old man. A second example exhibits many isolated poorly differentiated tumor cells and sporadic small tumor cell aggregates. The diagnostic consideration of the monotonous appearance of the cell population should include blastic lymphoma. Still, abundant cytoplasm and notable variation in cell size favor carcinoma (direct smear, Pap stain, lower magnification). Please compare with Fig. 10.44A.

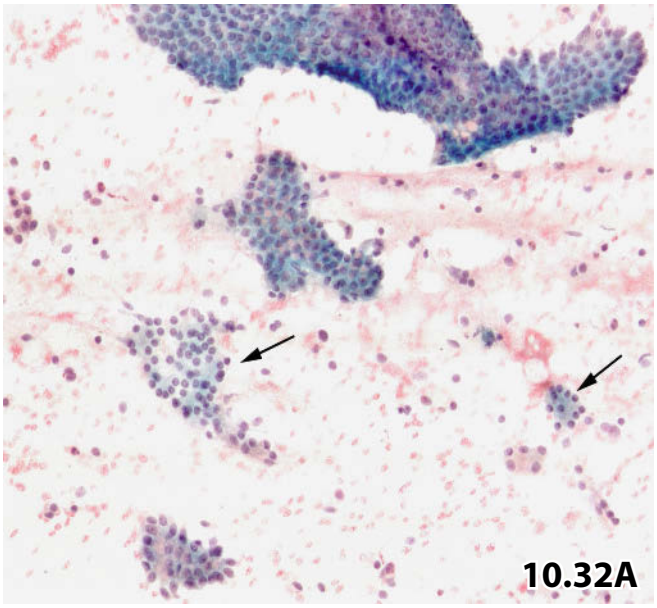
10.32A

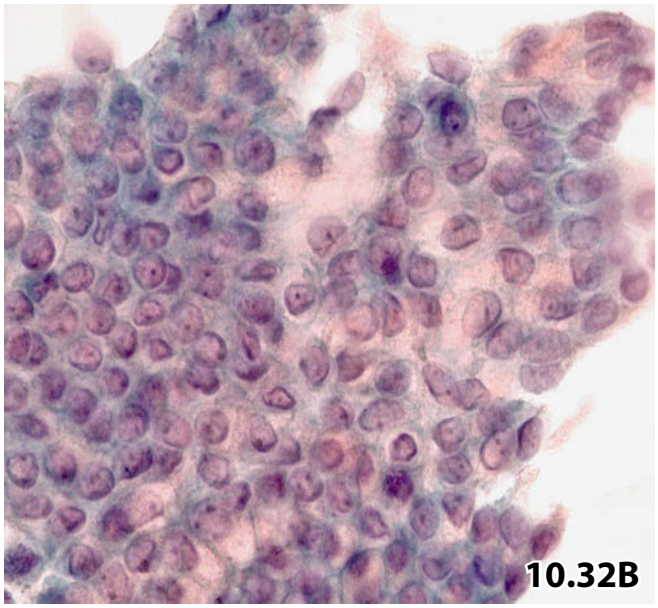
10.32B

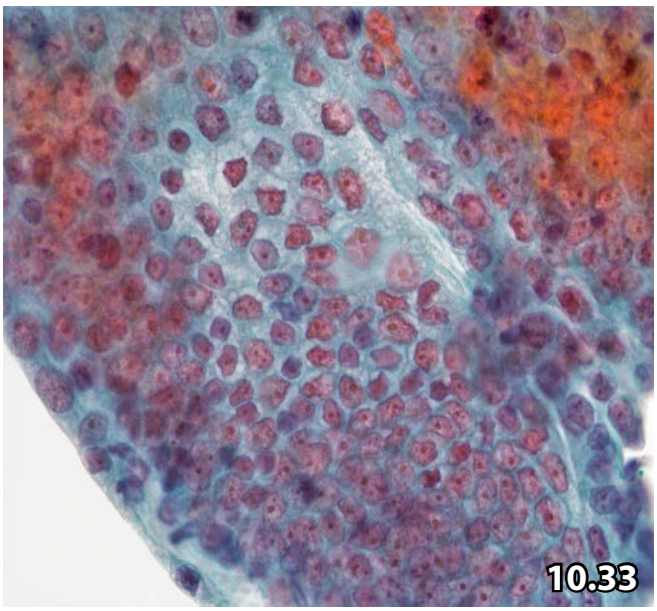
10.33

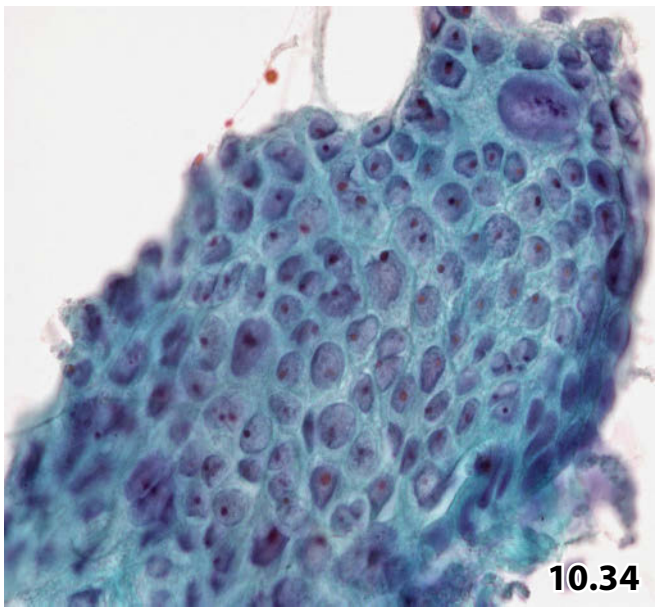
10.34

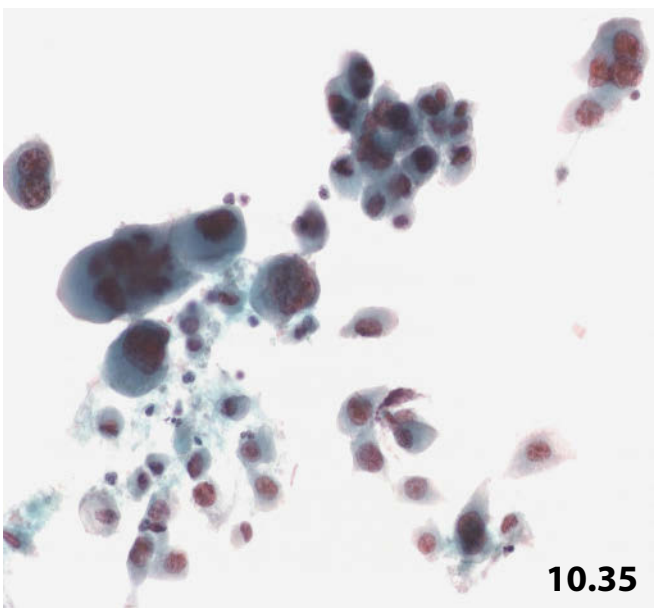
10.35

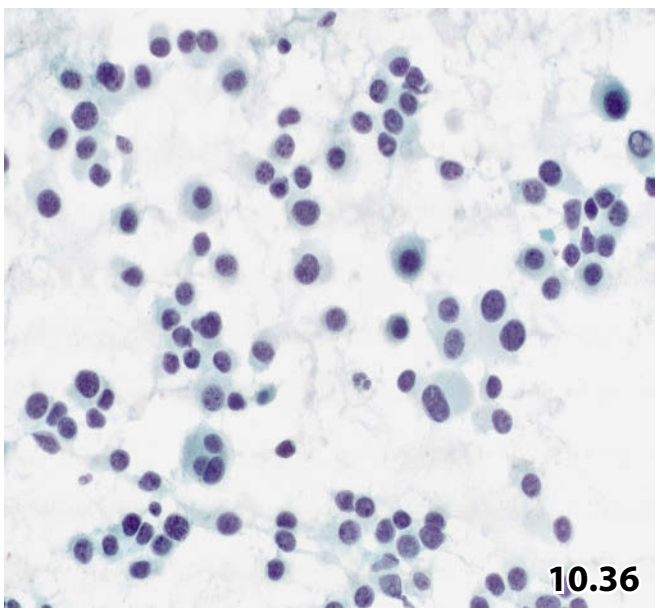
10.36

**Figs. 10.37A, B Adenosquamous carcinoma of the pancreas.**
Image-guided FNAB of a pancreatic lesion in a 74-year-old woman. Conventional smears were Pap-stained.
*Tentative cytologic diagnosis:* Adenosquamous carcinoma; primary or secondary?
*Tissue diagnosis* (pancreatectomy): Adenosquamous carcinoma of the pancreas, grade 2–3.
**A** High magnification showing the malignant adenomatous proportion of adenosquamous carcinoma. Cellular features match those of pancreatic ductal adenocarcinoma. **B** Lower magnification reveals frankly malignant squamous cells and pleomorphic keratinized cell detritus. Numerous degenerating elements exhibit abnormal nuclear features. Squamous carcinoma cells embedded in strands of mucus are not shown.

**Fig. 10.38A, B Papillary adenocarcinoma of the pancreas.**
Pancreatic juice aspirate by endoscopic retrograde cannulation yields an extremely cellular sediment. Direct smears were prepared from the sediment after conventional centrifugation; smears were Pap-stained.
*Tentative cytologic diagnosis:* Low-grade papillary lesion, most likely well-differentiated papillary adenocarcinoma originating from duct epithelium.
*Tissue diagnosis* (pancreas resection): Well-differentiated papillary adenocarcinoma, measuring 5 mm, invading the wall of the main pancreatic duct, and distinct severe dysplasia/carcinoma in situ of the adjacent duct epithelium.
**A** Low magnification exhibits microfragments of papillary projections. Note fibrovascular cores and distinct palisading (arrows) of the epithelial cells. **B** High magnification of the epithelial proportion of the tumor reveals the typical cell features of a moderately differentiated pancreatic adenocarcinoma.



**Fig. 10.39A, B Acinar cell carcinoma of the pancreas.**
A 70-year-old man presented with a tumoral lesion in the head of his pancreas. Differential diagnoses based on imaging results were cystadenoma, endocrine tumor, and carcinoma. US-guided FNAB was performed. Direct smears were Pap-stained.
*Tentative cytologic diagnosis:* Moderately differentiated pancreatic adenocarcinoma, possibly acinar cell variant.
*Tissue diagnosis* (pancreatectomy): Moderately differentiated acinar cell carcinoma of the pancreas.
**A** Compact three-dimensional clusters exhibit monomorphic cells frequently arranged in small acinic-like formations (arrows). Occasional stripped nuclei in the background of the specimen (low magnification). **B** High magnification reveals irregular arrangement of the tumor cells and nuclear polymorphism. Occasional acinic formations (upper right) are present.

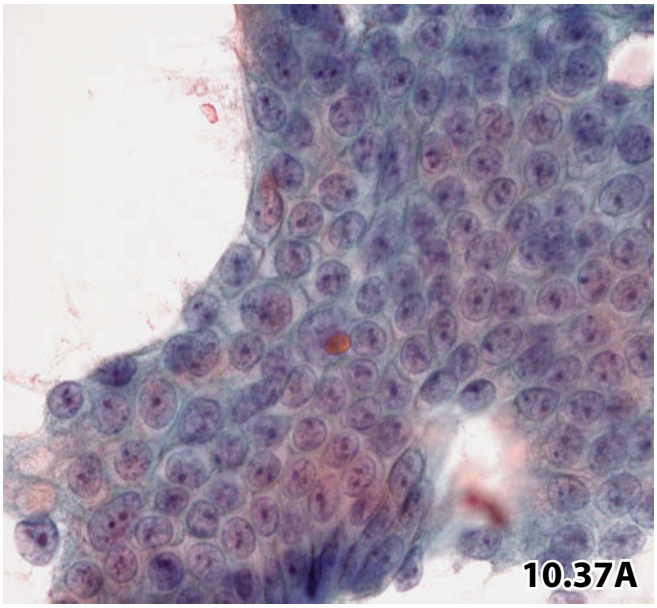
10.37A

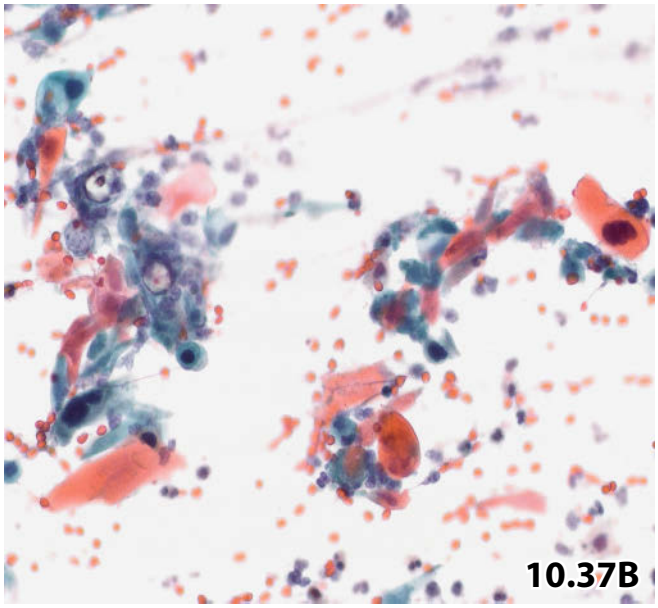
10.37B

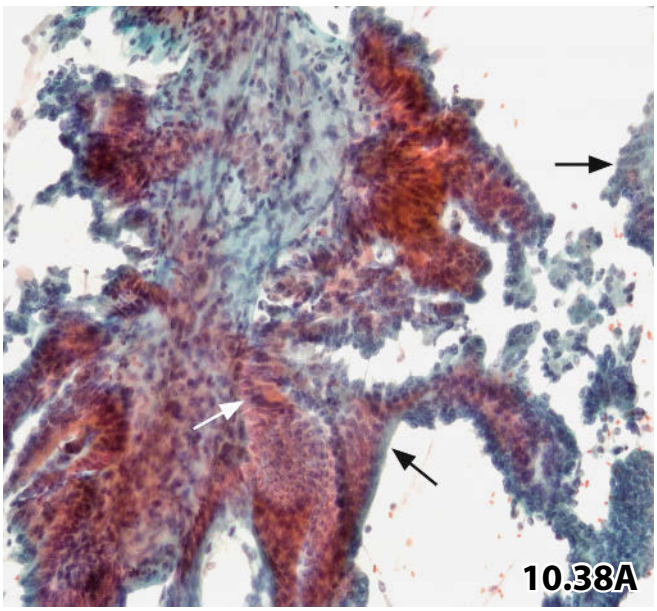
10.38A

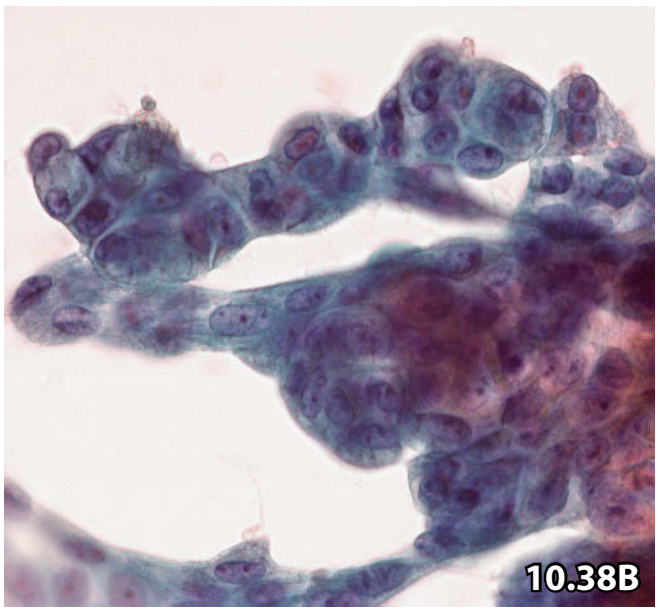
10.38B

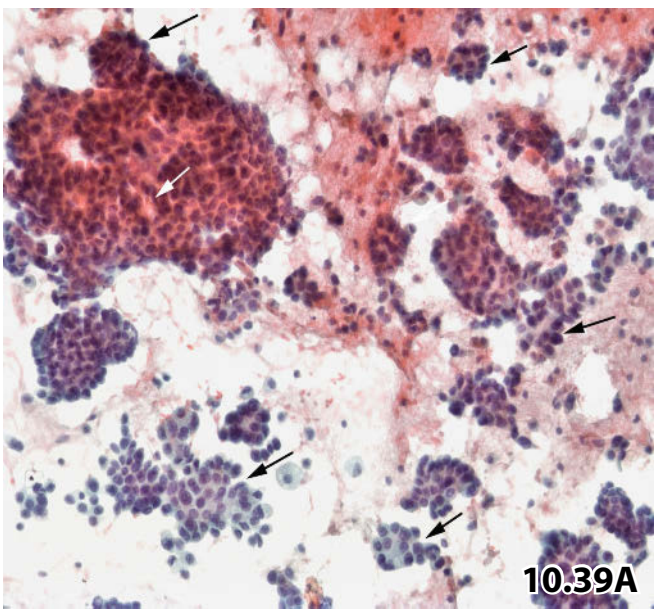
10.39A

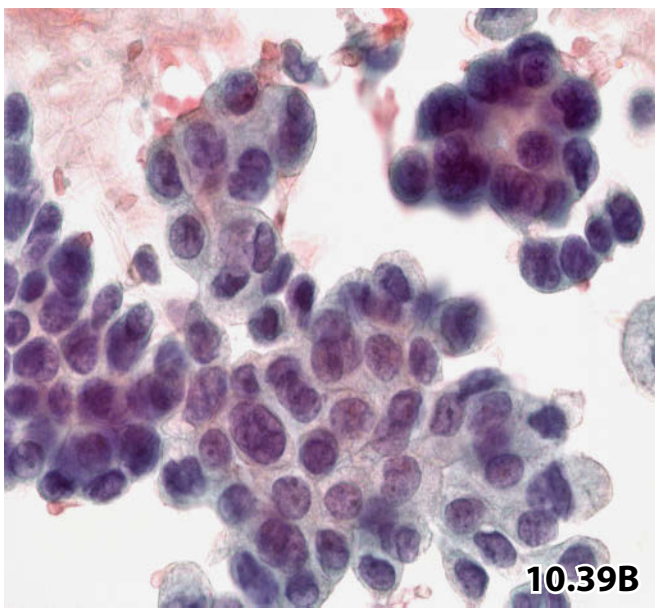
10.39B

**Fig. 10.40A, B Extremely well-differentiated endocrine tumor.**
Imaging studies detect a nodule in the pancreas of an elderly male patient. Image-guided transcutaneous FNAB was performed. Conventional smears were Pap-stained.
*Cytologic diagnosis* supported by immunocytochemistry: Well-differentiated neuroendocrine tumor. No further diagnostic evaluation.
**A** At low magnification, compact ball-like and papilliform tissue fragments are composed of uniform small tumor cells often arranged in acinar-like formations. Overall cell pattern may be suggestive of normal pancreatic tissue. However, tight cell clustering, absence of individual cells (in the current setting), and absence of connective tissue crossing cell aggregates indicate a tumoral lesion. Differential diagnosis should consider acinar cell carcinoma, neuroendocrine tumor, and other lesions. **B** Immunostaining revealed positivity for the endocrine marker chromogranin A (Pap-prestained direct smear).

**Fig. 10.41 Classic cell features of endocrine tumors.**
The distinct plasmacytoid features of isolated tumor cells are primarily suggestive of endocrine tumor. Positive immunocytochemical reaction for chromogranin A and synaptophysin confirmed the cytologic diagnosis (not shown) (FNAB, direct smear, Pap stain high magnification).
*Postmortem histologic diagnosis*: Metastatic neuroendocrine tumor of the pancreas.



**Fig. 10.42 Endocrine tumor of the pancreas: spindle cell variant.**
From the archives, a single immunocytochemically stained smear (Pap-prestained) is available from the current case. Rather polymorphic elongated cells present diagnostic dilemmas (right). Note ill-defined granular cytoplasm indicating the endocrine nature of the cells. Immunopositivity for synaptophysin confirmed the light-microscopically suspected endocrine tumor.
*Cytologic diagnosis* supported by immunocytochemistry: Spindle cell endocrine tumor.
*Final diagnosis:* MEN-1 comprising parathyroid adenoma in a 47-year-old woman.

**Fig. 10.43 Endocrine tumor of the pancreas: oncocytic variant.**
Intraoperative FNAB of a nodular pancreatic lesion was performed in a 44-year-old man.
*Preliminary cytologic diagnosis:* Endocrine tumor with mild atypias or oncocytic neoplasm. Note low and high N/C ratio, irregular cell arrangement, and nuclear overlapping. Eosinophilic granules are densely packed, giving rise to a homogeneous brownish-red appearance of the cytoplasm (direct smear, ultra-fast Pap stain, higher magnification).
*Final cytologic/immunocytochemical diagnosis:* Diagnosis of endocrine tumor of the oncocytic variant was established using an appropriate panel of immunocytochemical stains including neuron specific enolase and neuroendocrine markers (positive staining results are not shown).
*Postmortem evaluation* revealed endocrine tumor of the pancreas with multiple metastases in the liver (no further subtyping available).

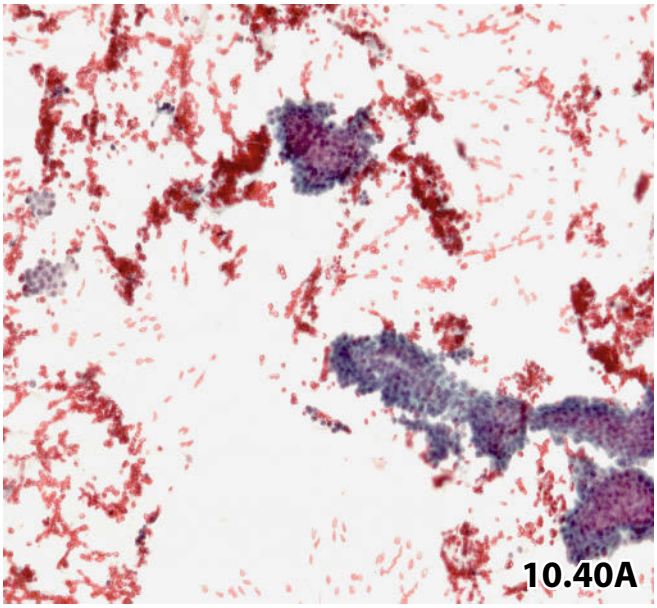
10.40A

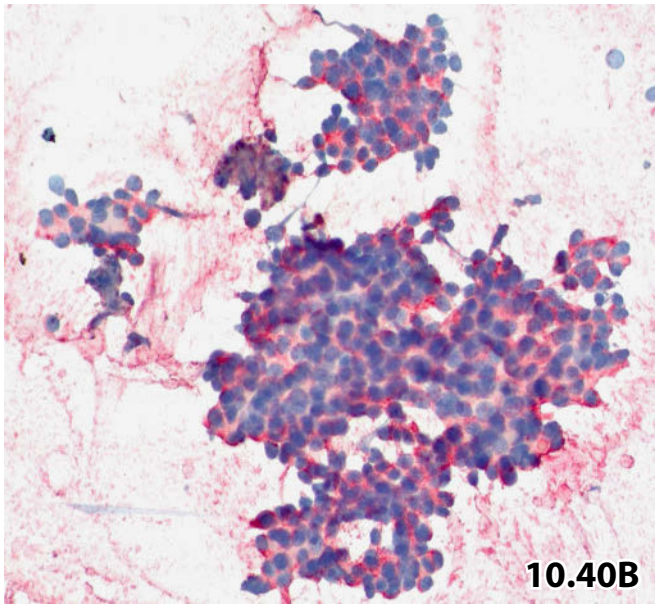
10.40B

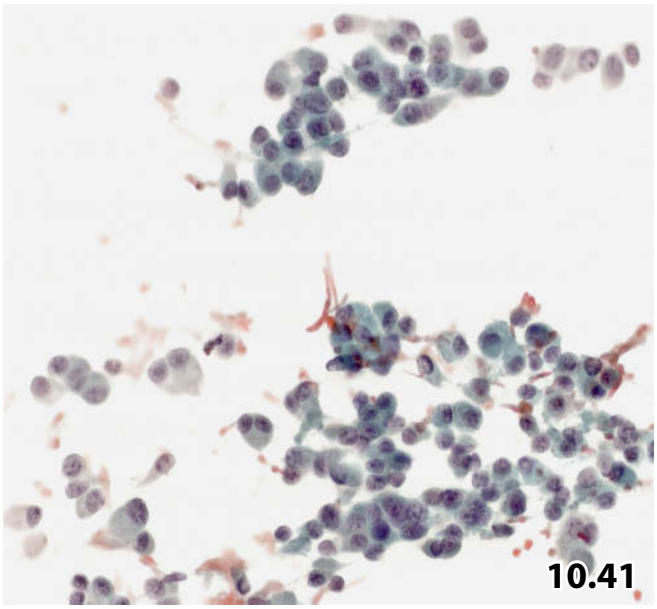
10.41

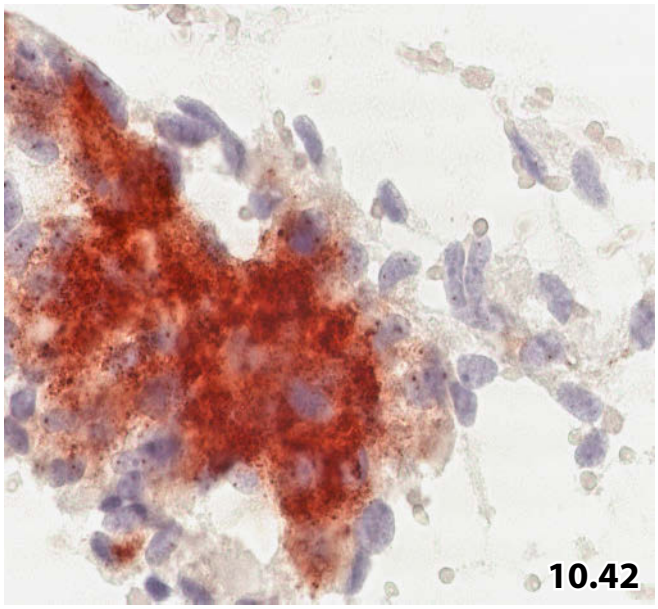
10.42

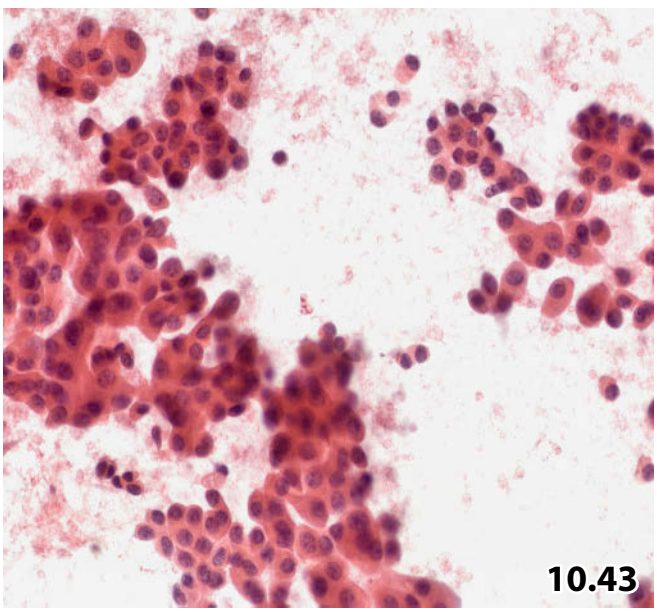
10.43

**Fig. 10.44A, B Blastic non-Hodgkin lymphoma.**
A 77-year-old woman with a positive history of adenocarcinoma of the cervix uteri presented with a tumoral lesion in her pancreas. Image-guided FNAB was performed. Direct smears were MGG- and Pap-stained.
*Cytologic diagnosis* supported by immunocytochemistry: High-grade blastic non-Hodgkin lymphoma.
*Tissue diagnosis* (extirpation of a lymph node): Diffuse large B-cell lymphoma, centroblastic variant.
**A** MGG-stained smear reveals blastic cells often arranged in dense small clusters or rows (arrows) (lower magnification). Narrow rims of deeply basophilic stained cytoplasm suggest malignant lymphoma; but a malignant epithelial disorder must definitely be excluded by additional analyses. **B** Neoplastic cells show distinct positive immunocytochemical reaction for CD45, indicating malignant non-Hodgkin lymphoma.

**Fig. 10.45A, B Pancreatic metastasis of renal cell adenocarcinoma.**
Aspirated material from an elderly man was prepared as cellblock (image-guided transcutaneous FNAB of a nodule in the pancreas).
*Cellblock diagnosis and immunohistochemistry:* Renal cell carcinoma, clear cell variant.
**A** Cellblock sections revealed sheets of a well-differentiated carcinoma of the clear cell type (HE stain, high magnification). **B** Renal cell carcinoma associated cell marker (RCCMa) was immunohistochemically clearly expressed in the cytoplasm of tumor cells.



**Fig. 10.46 Pancreatic metastasis of a classic small-cell carcinoma of the lung.**
A 56-year-old man presented with a metastatic tumor of unknown primary origin. On imaging, a voluminous mass was found in the pancreas. US-guided FNAB was performed. Direct smears prepared from the aspirates were Pap-stained. Classic cytologic features of small-cell carcinoma become overt at high magnification: a secondary pancreatic tumor was supposed.
*Final diagnosis:* Sputum and bronchial brushing revealed small-cell carcinoma of the intermediate variant.

**Fig. 10.47 Pancreatic metastasis of primary prostatic adenocarcinoma.**
An elderly male patient presented with enlarged retroperitoneal lymph nodes and a tumor convolute involving the head of the pancreas. An FNAB of the pancreatic mass was initially performed (direct smears, Pap stain). Lower magnification showed large fragments of epithelial tumor tissue composed of uniform small to medium-sized cells often arranged in acinic formations (arrows). Nucleoli are fairly indistinct.
*Cytodiagnostic consideration* included primary pancreatic neoplasia, most likely acinic cell carcinoma among other tumors.
*Further evaluations and final diagnosis:* Routine rectal palpation of the prostate suggested prostatic carcinoma, and transrectal prostatic FNAB confirmed the diagnosis. Subsequent immunocytochemical staining of a Pap-prestained FNAB smear of the pancreas revealed strong cellular positivity for prostate acid phosphatase (not shown).

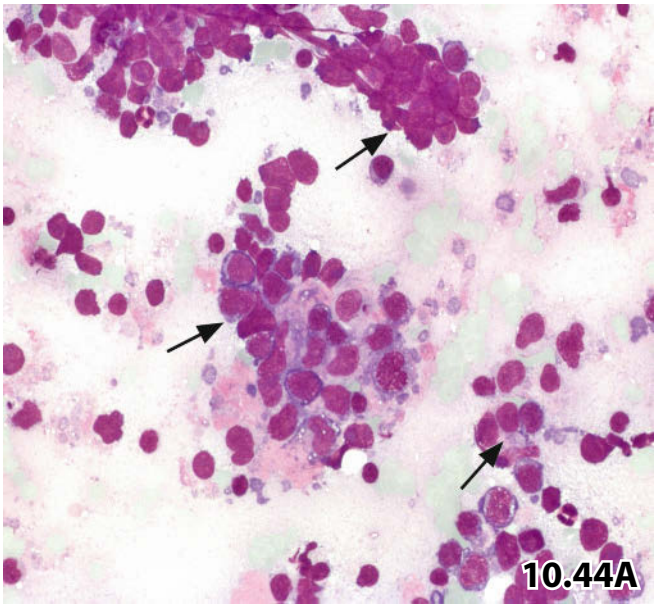
10.44A

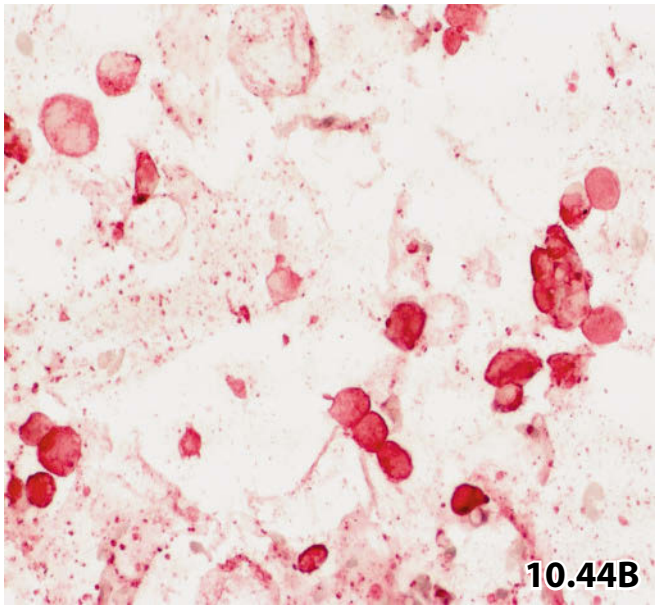
10.44B

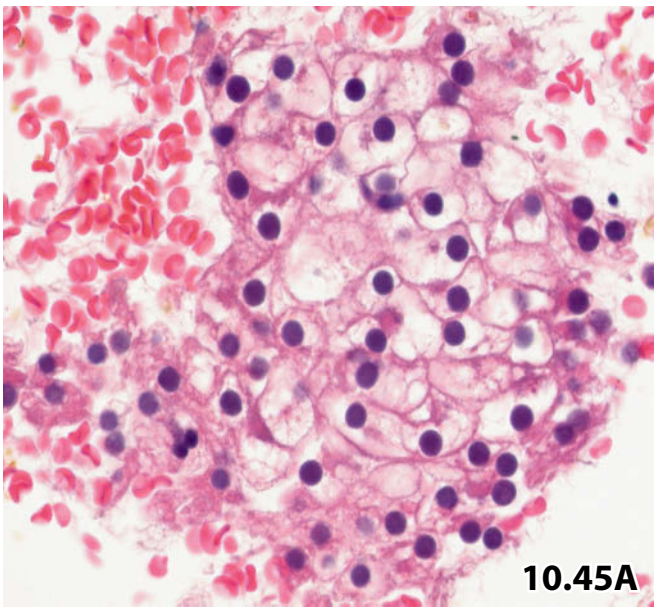
10.45A

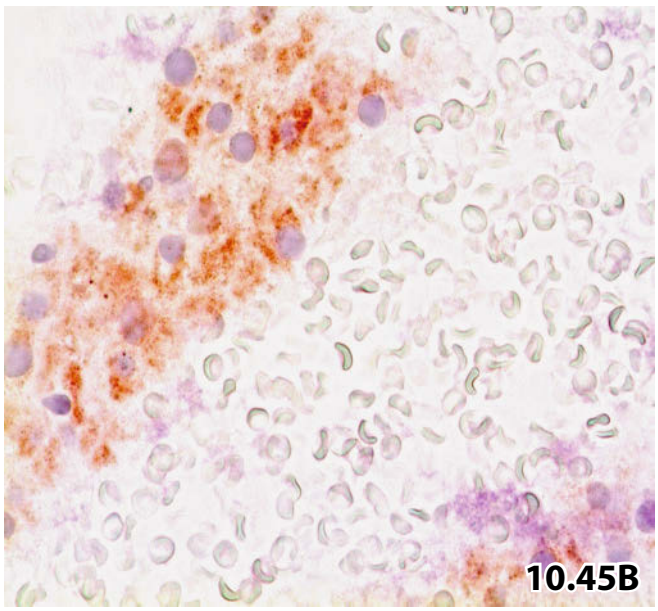
10.45B

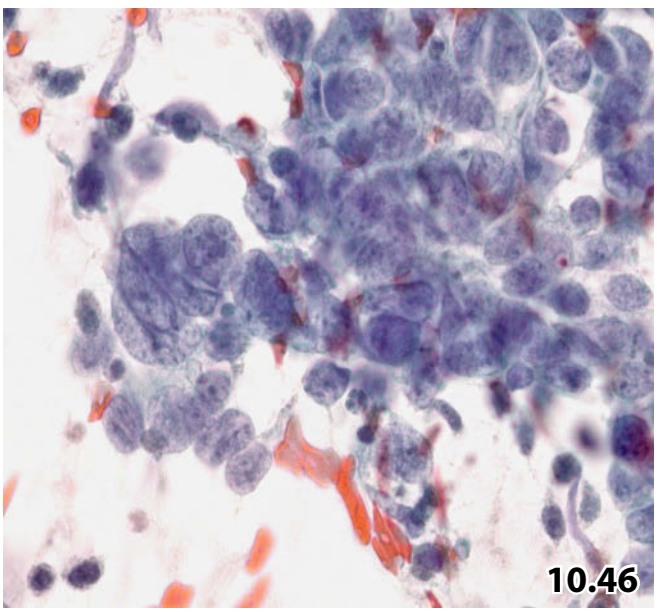
10.46

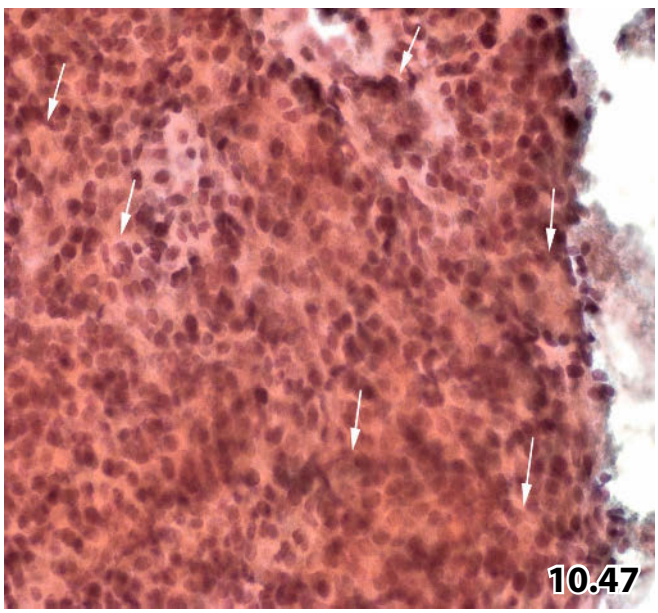
10.47

# Section 10.2
# Extrahepatic Bile Ducts and Ampullary Region

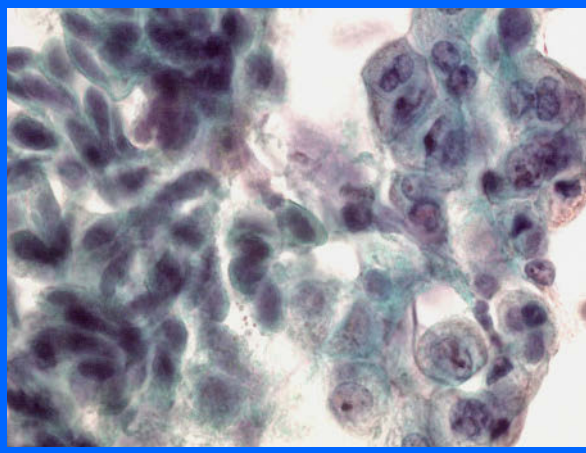

## 10.2.1 Introduction and Diagnostic Procedures [68]

- Adenocarcinomas are the most common epithelial malignancies of the extrahepatic bile ducts and the ampullary region, accounting for more than 95% of all biliary cancers [28]. The distribution of biliary tract carcinomas has been recorded as perihilar (67%), distal including the ampulla of Vater (27%), and intrahepatic (6%) [52]; the latter is generally referred to as cholangiocarcinoma.
- Imaging procedures have a high impact on the preoperative evaluation of patients with suspected or overt biliary tract cancer.
- Primary tools and cornerstones for a preoperative pathomorphologic diagnosis of malignancy are:
  - Forceps biopsy.
  - Cytologic brushing during cholangiographic studies such as endoscopic retrograde cholangiopancreatography (ERCP).
  - Endoscopic ultrasound-guided fine needle aspiration biopsy (EUS-FNAB).

  Tissue biopsies are routinely less frequently performed because of their higher morbidity rates such as bile leakage, hemorrhage, and scar formation with subsequent stricture. In addition, intraductal biopsies miss the target lesion more frequently than brush biopsy, and tissue artifacts are reported in a considerable number of specimens [4]. Combination of brush cytology and forceps biopsy may enhance the diagnostic results in cases with malignant bile duct strictures [56, 59].
- Biliary duct strictures may be caused by both biliary and pancreatic disorders. The main purpose of preoperative cytological evaluation of the bile duct system is to confirm the presence of biliary or pancreatic cancer by noninvasive procedures.
- Cytology of the gallbladder: Experience with preoperative cytologic diagnosis by means of image-guided FNAB, bile collection using an endoscopic approach, or direct puncture of the gallbladder is limited [1, 49]. EUS-FNAB seems to be a promising new approach in patients with a suspected gallbladder malignancy [50].

### 10.2.1.1 Exfoliative Cytology

(see also Sect. 10.1.1.3, “Pancreaticobiliary Duct Brushing,” p. 633)

- The primary tool for a preoperative cytological diagnosis of malignancy in the biliary tract and in the ampullary area [6, 22, 62] is brushing during cholangiographic studies, such as ERCP [12, 22, 26, 48, 57, 60, 64, 67].
- Supplementary methods for the collection of exfoliated ductal cells are washing of the bile canaliculi, aspiration of pure bile from the bile ducts, directed collection of secreted bile, endobiliary brush cytology during percutaneous transhepatic cholangiodrainage (PTCD) [70], and the aspiration of duodenal secretion [37, 53].
- A great variety of benign and/or abnormal cells originating from different duct systems (biliary tract, pancreatic duct, duodenal compartment) should always be respected in the cytological evaluation of fluids. Additionally, vari-

ous degrees of cellular degeneration may pose problems in the assessment of a conclusive diagnosis.

*Bile Duct Brushing*

Bile duct brushing appears to be a more sensitive method to detect malignancy than duct washing or pure bile sampling. The adequacy of the sample is of primary importance for a reliable diagnostic result [12]. Bile duct brushing has modest sensitivity: the reported sensitivities were on average between 33% and 80%. Still, a high degree of specificity for a definite carcinoma diagnosis is reached in all studies and false-positive cancer diagnoses are rare [12, 26, 48, 57, 60, 64, 67]. Sensitivity of bile duct brush cytology is reported to be significantly higher for bile duct carcinoma as compared with pancreatic carcinoma [25], and the diagnostic efficacy is best for ampullary and parapapillary tumors [22]. Athanassiadou and Grapsa have comprehensively compiled sources from previous reports that elucidate the low sensitivity of brushings [4]:

1. Poor sampling is reported to be the most important reason for indeterminate cytologic reports. It is primarily caused by lack of skill and experience on the part of the endoscopist, an unsatisfactory sampling device, location of the disorder, and from the size of the tumor.
2. Poor technical preparation of the smears (smearing and fixation).
3. Interpretation errors.

*Brushing of Ampulla of Vater*

The terminal portion of the main bile duct (ductus choledochus) forms a dilatation prior to its entry into the duodenum, called the ampulla of Vater. The main pancreatic duct usually discharges into the ampulla but may have a separate entrance into the duodenum. Diagnostic efficacy of brush cytology was rated better for ampullary and parapapillary tumors in comparison with brushing in patients having duct strictures [22].

#### 10.2.1.2 Fine-Needle Aspiration

- The utility of endoscopic fine-needle aspiration biopsy at ERCP for sampling bile duct strictures suspicious of malignancy has repeatedly been studied [17, 19]. The technique has become refined by sphincterectomy and secondary cannulation using an endoscopic FNA device [30].
- Currently, EUS-FNAB is the favored aspiration method for patients with suspected cholangiocarcinoma in both the distal bile duct/ampullary area [14, 20, 23] and the proximal/hilar biliary tree [21, 24]. The results suggest EUS-FNAB to be valuable as a less invasive method to clarify the cause of bile duct strictures at any site of the biliary tree. This technology provides accurate and safe results and has been shown to be feasible without significant risks, especially when other methods fail.
- Transcutaneous FNAB guided by ultrasound or computed tomography is a minimally invasive supplementary diagnostic method for large tumorous lesions in the biliary tract region.

### 10.2.2 Processing the Cell Material

- Processing cell samples from fine-needle aspirates, brushings, duct washings, and secretions follows basically the same criteria as indicated in Sect. 10.1.2, p. 633.
- Several studies argue that better diagnostic performance is obtained from bile duct brushings prepared by liquid-based techniques (ThinPrep, Cytospin, and others) compared with direct brush smears [54, 61, 72]. Combining the ThinPrep technique and direct smearing is reported to provide superior sensitivity and accuracy relative to cytospin and direct smear alone [67]. The comments in Sect. 10.1.2.2, "Liquid-Based Cytology," p. 634, emphasize the advantages and disadvantages of the liquid-based methods in clinical and diagnostic practice.

### 10.2.3 Additional Analyses

#### 10.2.3.1 Immunocytochemistry

- There is no single immunocytochemical marker or marker panel that reliably distinguishes between adenocarcinomas of pancreatic and biliary origin, or between cancer of biliary duct cell lining and secondary neoplasia from distant organs (see also Sect. 10.1.3.1, p. 634).
- Bile duct carcinoma cells are reactive for CEA and CA 19-9. p53 immunostaining using biliary brush preparations from patients with extrahepatic bile duct stenosis may have an additive value for the diagnosis of bile duct carcinoma [63].
- Immunocytochemical loss of DPC4 expression has been reported in a number of ampullary carcinomas but has not been observed in adenomas.

#### 10.2.3.2 DNA Ploidy Analysis

DNA Image Cytometry

[7, 11, 12, 38, 43, 44, 46, 51, 55, 58]

- Ploidy assessment by ICM DNA is a valuable adjunct to routine biliary cytology:
  - Detecting malignant or potentially malignant disorders of the biliary tract .
  - Improving sensitivity and accuracy for malignant neoplasms in comparison with cytology alone (Figs. 10.64 and 10.65).
  - Confirming a benign or malignant cytologic diagnosis (Figs. 10.60–10.63).

- DNA histogram interpretation discerns aneuploidy as a reliable marker for chromosomal aberrations in premalignant and malignant lesions. Cautions are discussed in Sect. 10.1.3.2, "DNA Ploidy Analysis," p. 635.
- An intermediate DNA profile has shown to be undetermined as to malignancy (Figs. 10.66 and 10.67).
- Explanations for false-negative and false-positive ICM results are discussed in a recent study that was conducted in cooperation with the department of gastroenterology at the Kantonsspital St. Gallen. We would like to emphasize that we did not have any concordance of false-positive results regarding conventional cytology and simultaneous ICM-DNA studies [12].

DNA Flow Cytometry

Quantitative DNA analysis by flow cytometry (after enzymatic treatment of formalin-fixed brush biopsies of the biliary tree) as a diagnostic marker for cancer has been shown as an adjunct to routine cytologic assessment [11].

#### 10.2.3.3 Molecular Genetics

Molecular pathologic findings are summarized in detail in Lack's textbook *Pathology of the Pancreas, Gallbladder, Extrahepatic Biliary Tract, and Ampullary Region* [39] together with other specialized sources:

- Mutations in the p53 gene were reported in most neoplasms of the extrahepatic biliary tract comprising tumors of the ampulla of Vater. Conclusions regarding biological tumor behavior are inconsistent.
- DPC4 tumor suppressor gene product is presumed to be a specific marker for extrahepatic bile duct carcinoma. Immunocytochemical loss of DPC4 expression was reported in a number of ampullary carcinomas but has not been observed in adenomas.
- Frequency of *KRAS* mutations and the relative proportion involving each codon were shown to vary with the anatomic location of the carcinoma.
- Overexpression of growth factors was reported in both carcinomas and periampullary adenomas exhibiting increasing dysplasia.
- Recent studies indicate that both fluorescence in situ hybridization (FISH test) and the results of DNA image cytometry analysis increase diagnostic sensitivity while preserving the specificity of the cytologic diagnosis for biliary carcinomatous lesions. The UroVysion multiprobe assay detects abnormal signal copy numbers of chromosomes 3, 7, 17 and deletions in the *9p21* gene locus [35, 43, 44, 51].

### 10.2.4 Normal Cytology of Bile Ducts and Ampulla of Vater

#### 10.2.4.1 Epithelial Cells of the Large Bile Ducts

(Figs. 10.11 and 10.48)

- Slender, elongated columnar cells with a basally located small round nucleus; they are referred to as matchsticks.
- However, not all cells of biliary tract origin are necessarily elongated; they may also appear cuboidal. Cuboidal epithelial bile duct cells cannot be clearly separated from epithelial cells of the pancreatic duct.
- The nuclei are bland and show an articulate and regular membrane, and occasionally a small and round nucleolus.
- The regularly outlined cytoplasm is pale, and it may be vacuolated.

A variety of metaplastic lesions in the epithelial lining of large biliary ducts have been reported, including pyloric gland, intestinal, and squamous metaplasia [29]. Metaplastic changes may be associated with bile duct cysts, chronic inflammation, cancer of the biliary tract, and others.

#### 10.2.4.2 Cells from the Duodenal Lining Epithelium (Figs. 10.12 and 10.13A)

- They exhibit cuboid to cylindric shape and usually a well-preserved and prominent brush border.
- Duodenal epithelial cells usually are arranged in flat sheets interspersed with goblet cells. The appearance of the sheets has been described as having a honeycomb appearance.

Cells occurring singly cannot unequivocally be differentiated from cells of biliary or pancreatic duct origin.

**Caution**

Epithelial cells of the bile ducts are occasionally difficult to separate from superficial lining cells of pancreatic ducts or duodenal mucosa.

#### 10.2.4.3 Contaminants in Brushings of Biliary Ducts and Ampulla of Vater

##### 10.2.4.3.1 Pancreatic Duct Epithelial Cells

These have been presented in Sect. 10.1.4.1, p. 636 (Fig. 10.6C)

##### 10.2.4.3.2 Gastrointestinal Epithelium

(Figs. 10.9. and 10.10)

Gastrointestinal epithelium is occasionally admixed to brush samples taken during ERCP. Well-preserved epithelial sheets rarely provide major diagnostic difficulties. Substantial

amounts of debris due to rapid enzymatic digestion of gastrointestinal epithelial cells should not be misinterpreted as tumor necrosis (Fig. 10.13B).

#### 10.2.4.3.3 Intramural Ampullary/Duodenal Glands

(Fig. 10.14)

Vigorous brushing the ampullary area may damage the surface of the mucosa, resulting in sampling of clusters of intramural glands.

- Cells of intramural ampullary/duodenal glands are more voluminous and polygonal than duct lining cells.
- Their nuclei focally exhibit irregular outline, loose chromatin, and distinct nucleoli of variable size.
- The cytoplasm is clear with coarse vacuolation and tends to be abundant.
- Pronounced irregular cell clustering and nuclear crowding may occur, leading to a false diagnosis of adenocarcinoma of the clear cell type.

#### 10.2.4.3.4 Cell Damage Due to Thermal Cautery

(Fig. 10.49)

Thermal cautery is used for sphincterotomy of the papilla of Vater during endoscopic retrograde cholangiography. Thermal artifacts induced by current devices appear as degenerative changes of the mucosal epithelial cells:

- Both isolated and clustered cells show pronounced elongation of their cytoplasm and nuclei; the latter are darkly stained and homogeneous.

Degenerated single cells and tissue fragments may lead to an erroneous diagnosis of spindle cell neoplasia.

**Caution**

- Gastrointestinal cell debris should not mislead to a diagnosis of cancer necrosis.
- Irregular cell clusters comprising nuclear atypia and crowding originating from duodenal/ampullary intramural glands may be misinterpreted as clear cell adenocarcinoma.
- Cell degeneration due to thermal cautery should not be overdiagnosed as spindle cell neoplasia.

### 10.2.5 Inflammation and Infection

#### 10.2.5.1 Nonspecific Inflammations and Infections (Fig. 10.50)

Inflammatory changes in cytologic specimens of the biliary tree and ampullary area may be caused by duodenitis, peptic duodenal ulceration, cholangitis, or pancreatitis. Partial or complete obstruction of the common bile duct is the main reason for cholangitis. Obstruction is commonly due to choledocholithiasis, but other lesions such as stent placement, neoplasms, parasites, pancreatitis, etc. may be causative as well.

- Cytologic smears are usually highly cellular, composed of a mixture of inflammatory cells and epithelial cells. Poor preservation of the epithelial cells usually occurs both in fine-needle aspirates and in brush specimens.
- Numerous nuclei are stripped; degenerated cells show cytoplasmic vacuolization or shrinkage together with chromatin clumping and karyorrhexis.
- Bile pigment is usually present.

#### 10.2.5.2 Primary Sclerosing Cholangitis

- Primary sclerosing cholangitis (PSC) is a chronic progressive cholestatic liver disease of unknown etiology. The disorder is characterized by inflammation, fibrosis, and obliteration of intrahepatic and extrahepatic bile ducts. Bile duct scarring leads to a characteristic beaded pattern seen on cholangiogram and endoscopy by ERCP [45]. Approximately 70% of patients with PSC are males, and the mean age at diagnosis is 39 years [15].
- The impact of brush cytology in PSC can be significant [13, 40, 41] because patients with PSC have an increased risk of both carcinoma in the biliary tree and hepatocellular carcinoma [40]. Therefore, biliary brush cytology is an important screening tool for continuous evaluation of the bile duct epithelium with the objective of early detection of dysplastic changes and cholangiocarcinoma in situ. Early neoplastic changes can be treated by liver transplantation. Patients with liver transplantation prior to development of bile duct cancer have a significantly better prognosis than patients with a liver transplant in the presence of cholangiocarcinoma [27].
- Ancillary studies such as molecular tests can improve diagnostic accuracy. More information is provided in Sect. 10.2.8, "Dysplastic and Reactive/Regenerative Biliary Epithelium," p. 685.

#### 10.2.5.3 Protozoal Infections, *Giardia Lamblia*, and Helminthic Infections

Infections of this type occasionally occur in patients who are immunosuppressed for various reasons.

- *Giardia lamblia* (Fig. 10.51) may exceptionally be observed in duodenal aspirates. *Giardia lamblia* is the most common enteric protozoan worldwide; finding it in duodenal biopsies is suggested to be coincidental, at least in the European population [16].
  - *Giardia lamblia* is a flagellated protozoan parasite. Under a normal light microscope, the stained parasite has a characteristic appearance, looking like a smiley face. Distinguishing features of the trophozoites are large karyosomes; the lack of peripheral chromatin giving the two nuclei a halo appearance.

- *Helminths* afflicting the biliary tract include several types. The authors refer to comprehensive books dealing with the pathology of infectious diseases, for sophisticated morphologic descriptions, and other specific information,

## 10.2.6 Benign Tumors of the Extrahepatic Biliary Tract and Ampullary Region

### 10.2.6.1 Benign Epithelial Tumors

Cytologic investigation has rarely been applied to benign tumors arising from the bile duct lining epithelium. Yet these tumors may be encountered more frequently in the future due to increased use of cytological methods for primary diagnostic purposes.

#### 10.2.6.1.1 Adenoma and Cystadenoma of the Bile Ducts (Fig. 10.52)

Cystadenomas seem to closely resemble its counterparts in the pancreas regarding cytologic features and clinical behavior (see Sect. 10.1.7, p. 640).

#### 10.2.6.1.2 Papillomatosis of the Biliary Tract

Again, an analogy has been discussed with intraductal papillary mucinous neoplasms of the pancreas [33] (see Section 10.1.7.3, p. 641). A small series of this tumor entity including FNAB-results has been reported [65].

#### 10.2.6.1.3 Ampullary Adenomas

These tumors are considered to be premalignant lesions [71]. Histologically, various degrees of epithelial atypia, epithelial dysplasia, or carcinoma in situ may be present, and foci with invasive carcinoma may be found in tumors investigated thoroughly by histology. Endoscopy will usually identify the polypoid-appearing tumors and permit biopsy.

Cytological sampling should be avoided since the morphologic complexity of this lesion is virtually a contraindication for cytologic diagnostics.

### 10.2.6.2 Benign Mesenchymal Tumors

#### 10.2.6.2.1 Granular Cell Tumor

[32] (Figs. 1.63 and 1.64)

This is a benign tumor most probably originating from Schwann cells and is also found in many organs outside the biliary tract. Granular cell tumors can arise at various sites of the biliary tree; most of the reported tumors involve the common bile duct and most patients are young women. Little is known about the cytological diagnosis of granular cell tumors that are located in the biliary tree.

The tumor has a distinctive cytomorphologic appearance and shows characteristic cytochemical and immunocytochemical reactivity that permits a conclusive cytological diagnosis.

Differential diagnosis considerations include foam cells, apocrine tumors, clear cell tumors, and malignant lymphoma. This tumor entity is described in Sect. 1.2.18, p. 26, together with all relevant items.

#### 10.2.6.2.2 Other Rare Benign Mesenchymal Neoplasms

These include leiomyoma, lipoma, angioma, and tumors of neural origin. Gastrointestinal stromal tumors are discussed in Sect. 11.3.3.2, p. 708.

## 10.2.7 Malignant Tumors of the Extrahepatic Biliary Tract and Ampullary Region

### 10.2.7.1 Adenocarcinoma

- Adenocarcinomas are the most common epithelial malignancy of the extrahepatic bile ducts and ampullary region, accounting for more than 95% of all biliary cancers [28]. The distribution of biliary tract carcinoma has been recorded as perihilar (67%), distal included the ampulla of Vater (27%), and intrahepatic (6%) [52].
- Adenocarcinomas that are located in the area of bifurcation of the hepatic ducts are referred to as Klatskin tumor [36], showing poor differentiation in the majority of the cases. Proximal bile duct adenocarcinomas are usually well or moderately differentiated [3], and the growth pattern is polypoid and/or papillary.
- Extension of carcinomas into the ampullary region gives rise to difficulties in assessing the precise anatomic point of the origin of the tumor. The potential primary sites include the distal area of the common bile duct, main pancreatic duct, (peri-)ampullary mucosa, and duodenal mucosa.

**Microscopic Features of Bile Duct Adenocarcinoma**

(Figs. 10.53–10.56)

- Adenocarcinomas of the distal bile duct may be cytomorphologically indistinguishable from their perihilar counterparts and from ductal pancreatic adenocarcinomas. Still, bile duct adenocarcinomas may exhibit an increased number of mucin-producing cells and focal intestinal epithelial differentiation, including goblet cells and endocrine cells, unlike pancreatic carcinoma.
- Several studies have analyzed the diagnostic cytomorphologic criteria in brush cytology of pancreaticobiliary strictures and FNAB of tumorous biliary lesions [4, 18, 20, 47, 57, 66].

  Based on the reported features in the literature and on personal experience, the following criteria provide an accurate diagnosis of malignancy or at least suspicion of adenocarcinoma:
  - A high cellularity of the cytologic sample is common.
  - Single cells along with small three-dimensional clusters are a key feature. The cell clusters are variably

dense, showing acinic-like or micropapillary features, nuclear overlapping, and pronounced loss of polarity. The N/C ratio is high.
- The nuclei disclose irregularities of the nuclear membrane, in particular wrinkling and molding, and prominent irregularly shaped nucleoli.
- The chromatin is coarse and unevenly distributed, but chromatin clearing may be distinct.
- Necrosis and severe inflammatory infiltrate may obscure the malignant cell population.
- The presence of necrotic debris is generally an important sign of invasive cancer.

Comparison of benign epithelium with atypical cells in the same smear is of high value in establishing an accurate diagnosis.

**Microscopic Features of Ampullary Carcinoma**
(Fig. 10.57)
Ampullary adenocarcinoma and adenocarcinomas of the bile ducts are for the most part morphologically similar to each other, but the former may mimic primary adenocarcinomas of the intestinal tract and may have a predominantly villous pattern or at least a papillary component [69].
- Cellular cytologic samples may show branching papillary fronds and a more or less complex papillary architecture.
- Nuclear polymorphism and overlapping, pseudostratification of the superficial lining cells, mitotic activity, and columnar cytoplasm suggest ampullary papillary carcinoma.

Papillary tissue fragments of invasive carcinoma may appear akin to in-situ adenocarcinoma.

#### 10.2.7.1.1 Variants of Bile Duct Adenocarcinoma
Varieties include adenosquamous carcinoma [31], squamous cell carcinoma, clear cell carcinoma, mucinous adenocarcinoma, small-cell carcinoma, and others. Some of these lesions are covered in Sect. 10.1.8.2, "Variants of Ductal Carcinoma," p. 644.

#### 10.2.7.1.2 Adenocarcinomas of the Gallbladder
(Fig. 10.58)
These tumors are morphologically very similar to primary carcinomas of the intrahepatic and extrahepatic biliary ducts, but the latter tend to be better differentiated; and abundant dense cyanophilic cytoplasm is characteristic of gallbladder adenocarcinoma. We do not further dwell on cytologic diagnosis of gallbladder tumors.

#### 10.2.7.2 Sarcoma, Melanoma, and Malignant Lymphoma
- Sarcomas of the extrahepatic biliary tract have been described histologically, most often as single case reports. Embryonal rhabdomyosarcoma is reported to be the most common malignant neoplasm of the biliary tract in childhood.
- Primary non-Hodgkin lymphoma has been reported involving not only the ampulla of Vater and the gallbladder, but also the extrahepatic biliary tract [34]. Still, involvement of the biliary tree may more frequently be a secondary manifestation of lymphoma at an advanced stage.
- Primary malignant melanoma is extremely rare; the tumor occurs exclusively in the gallbladder.

### 10.2.8 Dysplastic and Reactive/Regenerative Biliary Epithelium
- Various degrees of *epithelial dysplasia* (Fig. 10.59) may be present in the extrahepatic biliary tree adjacent to invasive carcinomas. The finding is consistent with a dysplasia-to-carcinoma sequence that has been acknowledged for bile duct cancers. High-grade dysplasia and carcinoma in situ are rarely diagnosed in the absence of carcinoma. The cytological differentiation between severe dysplasia and carcinoma in situ is virtually impossible, but this is not really important because the two lesions are biologically closely related. It is much more important to differentiate between dysplasia with premalignant potential and benign reparative/inflammatory cell alteration.
- *Reactive/regenerative cell changes* (Figs. 10.60 and 10.61) may in particular be caused by bile duct stones, stent placement, and degenerating processes. The cytological criteria that distinguish between reactive cellular atypia and dysplastic changes are subjective and not accurately reproducible. Ultimately, applying these criteria is highly dependent on the cytopathologist's experience.
- Application of strict morphologic criteria is essential in biliary tract cytology, applying these criteria is highly dependent on the cytopathologist's experience. Several studies have evaluated cytologic features that may be helpful in the diagnosis of dysplasia and malignancy in bile duct brushings [4, 42, 57]. Brush cytology is associated with a relatively low sensitivity but high specificity concerning dysplastic lesions; anyhow marked reactive cell changes may cause false-positive diagnoses [41]. Overinterpretation may particularly occur with stent placement. Close communication with gastroenterologists is of high importance [40].
- DNA ploidy assessment has been shown to be a valuable adjunct to routine cytology in order to ascertain or exclude the potential malignant behavior of atypical/dysplastic changes of bile duct epithelium [4, 10, 46] (Figs. 10.60–

10.67). Further comments and references on this issue are given in Sect. 10.2.3.2, "DNA Ploidy Analysis," p. 681.

- Advanced molecular diagnostic methods may in the future also contribute to categorizing the atypical cell cohort [4].

## 10.2.9 Endocrine Tumors of the Extrahepatic Biliary Tract and Ampullary Region

Endocrine tumors of the extrahepatic bile tract are exceedingly rare and unlikely to be encountered in cytologic samples. Still, endocrine tumors commonly occur in the duodenum, ampullary region, and gallbladder [39]. The tumors show a characteristic morphologic pattern as compared to their counterparts at other anatomic sites, and the endocrine nature of the lesions can be confirmed by immunocytochemical stains. Cytological and immunocytochemical features, differential diagnoses, and cautions of common endocrine tumors and their variants are provided in Sect. 10.1.10, "Endocrine Tumors of the Pancreas", p. 646.

10

## 10.2.10 Secondary Tumors (Figs. 10.68 and 10.69)

Reported extrahepatic bile duct and gallbladder metastases comprise primary carcinoma of the kidney, lung, breast, ovary, prostate, carcinomas of the digestive tract, and sarcoma [2, 8]. Yet, malignant melanoma accounts for approximately 50% of all reported cases of biliary and gallbladder metastases [5]. Barr Fritcher and colleagues recently reported 11 metastatic cancers presenting as pancreatobiliary stricture. The lesions were detected using ERCP cell sampling, routine cytology, and advanced techniques [8].

## 10.2.11 Further Reading


1. Akosa AB, Barker F, Desa L, et al. Cytologic diagnosis in the management of gallbladder carcinoma. Acta Cytol 1995;39:494-498.
2. Albores-Saavedra J, Henson DE, Klimstra D. Tumors of the Gallbladder and Extrahepatic Bile Ducts. Atlas of Tumor Pathology. Third series. AFIP: Washington D.C. 1999.
3. Albores-Saavedra J, Scoazec JC, Wittekind C, et al. Carcinoma of the gallbladder and extrahepatic bile ducts. In:Hamilton SR, AaltonenLA (Eds.): World Health classification of tumors. Pathology and Genetics of tumours of the digestive system. IARC Press:Lyon 2000.
4. Athanassiadou P, Grapsa D. Value of endoscopic retrograde cholangiopancreatography-guided brushings in preoperative assessment of pancreaticobiliary strictures. What's new? Acta Cytol 2008;52:24-34.
5. Backman H. Metastases of malignant melanoma in the gastrointestinal tract. Geriatrics 1969;24:112-120.
6. Bardales RH, Stanley MW, Simpson DD, et al. Diagnostic value of brush cytology in the diagnosis of duodenal, biliary, and ampullary neoplasms. Am J Clin Pathol 1998;109:540-548.
7. Baron TH, Harewood GC, Rumalla A, et al. A prospective comparison of digital image analysis and routine cytology for the identification of malignancy in biliary tract strictures. Clin Gastroenterol Hepatol 2004;2:214-219.
8. Barr Fritcher E, Kipp B, Oberg T, et al. Advanced cytologic techniques for the detection of metastatic malignancy in pancreatobiliary tract strictures. Cancer(Cancer Cytopathol) Suppl. 2007;111:415.
9. Bergquist A, Lindberg B, Castro J, Tribukait B. Methodologic aspects of evaluating brush samples from biliary strictures by cytology and DNA flow cytometry. Acta Cytol 2004;48:341-347.
10. Bergquist A, Tribukait B, Glaumann H, Broome U. Can DNA cytometry be used for evaluation of malignancy and premalignancy in bile duct strictures in primary sclerosing cholangitis? J Hepatol 2000;33:873-877.
11. Binek J, Lindenmann N, Meyenberger CM, Spieler P, et al. Malignant biliary stenosis: Conventional cytology versus DNA image cytometry. Surg Endosc 2011;25:1808-1813.
12. Binek JS, Meyenberger C, Spieler P, et al. DNA-image-cytometry (ICM-DNA) of brush cytology for the diagnosis of malignant biliary tumors. Gastroenterology, Suppl 1 2001;120:A-573.
13. Boberg KM, Jebsen P, Clausen OP, et al. Diagnostic benefit of biliary brush cytology in cholangiocarcinoma in primary sclerosing cholangitis. J Hepatol 2006;45:568-574.
14. Byrne MF, Gerke H, Mitchell RM, et al. Yield of endoscopic ultrasound-guided fine-needle aspiration of bile duct lesions. Endoscopy 2004;36:715-719.
15. Case records of the Massachusetts General Hospital. Case 3-2002. 2002;346:271-276.
16. Chew TS, Hopper AD, Sanders DS. Is there a role for routine biopsy in diagnosing giardiasis in a European population? Scand J Gastroenterol 2008;8:1-5.
17. Cohan RH, Illescas FF, Braun SD, et al. Fine needle aspiration biopsy in malignant obstructive jaundice. Gastrointest Radiol 1986;11:145-150.
18. Cohen MB, Wittchow RJ, Johlin FC, et al. Brush cytology of the extrahepatic biliary tract: comparison of cytologic features of adenocarcinoma and benign biliary strictures. Mod Pathol 1995;8:498-502.
19. de Bellis M, Sherman S, Fogel EL, et al. Tissue sampling at ERCP in suspected malignant biliary strictures (Part 1). Gastrointest Endosc 2002;56:552-561.
20. Defrain C, Chang CY, Srikureja W, et al. Cytologic features and diagnostic pitfalls of primary ampullary tumors by endoscopic ultrasound-guided fine-needle aspiration biopsy. Cancer 2005;105:289-297.
21. DeWitt J, Misra VL, Leblanc JK, et al. EUS-guided FNA of proximal biliary strictures after negative ERCP brush cytology results. Gastrointest Endosc 2006;64:325-333.
22. Elek G, Gyökeres T, Schäfer E, et al. Early diagnosis of pancreatobiliary duct malignancies by brush cytology and biopsy. Pathol Oncol Res 2005;11:145-155.
23. Eloubeidi MA, Chen VK, Jhala NC, et al. Endoscopic ultrasound-guided fine-needle aspiration biopsy of suspected cholangiocarcinoma. Clin Gastroenterol Hepatol 2004;2:209-213.
24. Fritscher-Ravens A, Broering DC, Knoepfel WT, et al. EUS-guided fine-needle aspiration of suspected hilar cholangiocarcinoma in potentially operable patients with negative brush cytology. Am J Gastroenterol 2004;99:45-51.
25. Glasbrenner B, Ardan M, Boeck W, et al. Prospective evaluation of brush cytology of biliary strictures during endoscopic retrograde cholangiopancreatography. Endoscopy 1999;31:712-717.
26. Govil H, Reddy V, Kluskens L, et al. Brush cytology of the biliary tract: retrospective study of 278 cases with histopathologic correlation. Diagn Cytopathol 2002;26:273-277.
27. Harrison PM. Prevention of bile duct cancer in primary sclerosing cholangitis. Ann Oncol 1999;10:208-211.
28. Henson DE, Albores-Saavedra J, Corle D. Carcinoma of the extrahepatic bile ducts. Cancer 1992;70:1498-1501.
29. Hoang MP, Murakata LA, Padilla-Rodriguez AL, et al. Metaplastic lesions of the extrahepatic bile ducts: a morphologic and immunohistochemical study. Mod Pathol 2001;14:1119-1125.

30. Howell DA, Beveridge RP, Bosco J, Jones M. Endoscopic needle aspiration biopsy at ERCP in the diagnosis of biliary strictures. Gastrointest Endosc 1992;38:531-535.
31. Hughes JH, Niemann TH. Adenosquamous carcinoma of the bile duct: cytologic features of brush specimens from two cases. Diagn Cytopathol 1996;15:322-324.
32. Jain KM, Hastings OM, Rickert RR, et al. Granular cell tumor of the common bile duct. Case report and review of literature. Am J Gastroenterol 1979;71:401-407.
33. Ji Y, Zhou J, Wang BS, et al. Intraductal papillary neoplasms of bile duct. A distinct entity like its counterpart in pancreas. Histol Histopathol 2008;23:41-50.
34. Joo YE, Park CH, Lee WS, et al. Primary non-Hodgkin's lymphoma of the common bile duct presenting as obstructive jaundice. J Gastroenterol 2004;39:692-696.
35. Kipp BR, Stadheim LM, Halling SA, et al. A comparison of routine cytology and fluorescence in situ hybridization for the detection of malignant bile duct strictures. Am J Gastroenterol 2004;99:1675-1681.
36. Klatskin G. Adenocarcinoma of the hepatic duct at its bifurcation within the porta hepatis: an unusual tumor with distinctive clinical and pathological features. Am J Med 1965;38:241-256.
37. Kline TS, Joshi LP, Goldstein F. Preoperative diagnosis of pancreatic malignancy by the cytologic examination of duodenal secretions. Am J Clin Pathol 1978;70:851-854.
38. Krishnamurthy S, Katz RL, Shumate A, et al. DNA image analysis combined with routine cytology improves diagnostic sensitivity of common bile duct brushing. Cancer 2001;93:229-235.
39. Lack EE. Pathology of the extrahepatic biliary tract and ampullary region. in: Pathology of the Pancreas, Gallbladder, Extrahepatic Biliary Tract, and Ampullary Region. Oxford University Press, Inc. 2003.
40. Lal A, Okonkwo A, Schindler S, et al. Role of biliary brush cytology in primary sclerosing cholangitis. Acta Cytol 2004;48:9-12.
41. Layfield LJ, Cramer H. Primary sclerosing cholangitis as a cause of false positive bile duct brushing cytology: report of two cases. Diagn Cytopathol 2005;32:119-124.
42. Layfield LJ, Wax TD, Lee JG, Cotton PB. Accuracy and morphologic aspects of pancreatic and biliary duct brushings. Acta Cytol 1995;39:11-18.
43. Levy MJ, Baron TH, Clayton AC, et al. Prospective evaluation of advanced molecular markers and imaging techniques in patients with indeterminate bile duct strictures. Am J Gastroenterol 2008;103:1263-1273.
44. Levy MJ, Clain JE, Clayton A, et al. Preliminary experience comparing routine cytology results with the composite results of digital image analysis and fluorescence in situ hybridization in patients undergoing EUS-guided FNA: Gastrointest Endosc 2007;66:483-490.
45. Lindberg B, Arnelo U, Bergquist A, et al. Diagnosis of biliary strictures in conjunction with endoscopic retrograde cholangiopancreaticography, with special reference to patients with primary sclerosing cholangitis. Endoscopy 2002;34:909-916.
46. Lindberg B, Enochsson L, Tribukait B, et al. Diagnostic and prognostic implications of DNA ploidy and S-phase evaluation in the assessment of malignancy in biliary strictures. Endoscopy 2006;38:561-565.
47. Logrono R, Kurtycz DF, Molina CP, et al. Analysis of false negative diagnosis on endoscopic brush cytology of biliary and pancreatic duct strictures: the experience at 2 university hospitals. Arch Pathol Lab Med 2000;124:387-392.
48. Mahmoudi N, Enns R, Amar J, et al. Biliary brush cytology: factors associated with positive yields on biliary brush cytology. World J Gastroenterol 2008;14:569-573.
49. Matsubara S, Arizumi T, Togawa O, et al. Endoscopic transpapillary approach to the gallbladder for diagnosing gallbladder cancer. Can J Gastroenterol 2007;21:809-813.
50. Meara RS, Jhala D, Eloubeidi MA, et al. Endoscopic ultrasound-guided FNA biopsy of bile duct and gallbladder: analysis of 53 cases. Cytopathology 2006;17:42-49.
51. Moreno Luna LE, Kipp B, Halling KC, et al. Advanced cytologic techniques for the detection of malignant pancreatobiliary strictures. Gastroenterology 2006;131:1064-1072.
52. Nakeeb A, Pitt HA, Sohn TA, et al. Cholangiocarcinoma: a spectrum of intrahepatic, perihilar and distal tumors. Ann Surg 1996;224:463-475.
53. Nieburgs HE, Dreiling DA, Rubio C, Reisman H. The morphology of cells in duodenal-drainage smears: histologic origin and pathologic significance. Amer J Dig Dis 1962;7:489-505.
54. Okonkwo AM, De Frias DV, Gunn R, et al. Reclassification of "atypical" diagnoses in endoscopic retrograde cholangio-pancreatography-guided biliary brushings. Acta Cytol 2003;47:435-442.
55. Osterheld MC, Andrejevic Blant S, Caron L, et al. Digital image DNA cytometry: a useful tool for the evaluation of malignancy in biliary strictures. Cell Oncol 2005;27:255-260.
56. Ponchon T, Gagnon P, Berger F, et al. Value of endobiliary brush cytology and biopsies for the diagnosis of malignant bile duct stenosis: results of a prospective study. Gastrointest Endoscop 1995;42:565-572.
57. Renshaw AA, Madge R, Jiroutek M, Granter SR. Bile duct brushing cytology. Statistical analysis of proposed diagnostic criteria. Am J Clin Pathol 1998;110:635-640.
58. Rumalla A, Baron TH, Leontovich O, et al. Improved diagnostic yield of endoscopic biliary brush cytology by digital image analysis. Mayo Clin Proc 2001;76:29-33.
59. Schoefl R, Haefner M, Wrba F, et al. Forceps biopsy and brush cytology during endoscopic retrograde cholangiopancreatography for the diagnosis of biliary stenoses. Scand J Gastroenterol 1997;32:363-368.
60. Selvaggi SM. Biliary brushing cytology. Cytopathology 2004;15:74-79.
61. Sheehan MM, Fraser A, Ravindran R, McAteer D. Bile duct brushings cytology – improving sensitivity of diagnosis using the ThinPrep technique: a review of 113 cases. Cytopathology 2007;18:225-233.
62. Stewart CJ, Mills PR, Carter R, et al. Brush cytology in the assessment of pancreatico-biliary strictures: a review of 406 cases. J Clin Pathol 2001;54:449-455.
63. Tascilar M, Sturm PD, Caspers E, et al. Diagnostic p53 immunostaining of endobiliary brush cytology: preoperative cytology compared with the surgical specimen. Cancer 1999;87:306-311.
64. Trent V, Khurana KK, Pisharodi LR. Diagnostic accuracy and clinical utility of endoscopic bile duct brushing in the evaluation of biliary strictures. Arch Pathol Lab Med 1999;123:712-715.
65. Tsui WMS, Lam PWY, Mak CKL, Pay KH. Fine-needle aspiration cytologic diagnosis of intrahepatic biliary papillomatosis (intraductal papillary tumor): report of three cases and comparative study with cholangiocarcinoma. Diagn Cytopathol 2000;22:293-298.
66. Vadmal MS, Byrne-Semmelmeier S, Smilari TF, Haidu SI. Biliary brush cytology. Acta Cytol 2000;44:533-538.
67. Volmar KE, Vollmer RT, Routbort MJ, Creager AJ. Pancreatic and bile duct brushing cytology in 1000 cases: review of findings and comparison of preparation methods. Cancer 2006;108:231-238.
68. Weber A, Schmid RM, Prinz C. Diagnostic approaches for cholangiocarcinoma. World J Gastroenterol 2008;14:4131-4136.
69. Wise L, Pizzimbono C, Dehner LP. Periampullary cancer: a clinicopathologic study of sixty-two patients. Am J Surg 1976;131:141-148.
70. Xing GS, Geng JC, Han XW, et al. Endobiliary brush cytology during percutaneous transhepatic cholangiodrainage in patients with obstructive jaundice. Hepatobiliary Pancreat Dis Int 2005;4:98-103.
71. Yamaguchi K, Enjoji M. Adenoma of the ampulla of Vater: putative precancerous lesion. Gut 1991;32:1558-1561.
72. Ylagan LR, Liu LH, Maluf HM. Endoscopic bile duct brushing of malignant pancreatic biliary strictures: retrospective study with comparison of conventional smear and ThinPrep® techniques. Diagn Cytopathol 2003;28:196-204.

**Fig. 10.48 Normal epithelial cells lining large bile ducts.**
Elongated columnar epithelial cells in direct smears of bile duct brushings: slender vacuolated cytoplasm with the nucleus basally located (matchstick cells). Small nucleoli may be present (Pap stain, high magnification). See also Fig. 10.11.

**Fig. 10.49 Thermal cell changes in the context of sphincterotomy.**
Thermal cautery usually gives rise to thermal artifacts of the mucosa involved. Individual cells and cell clusters exhibit pronounced elongation of the nuclei and cytoplasm as shown in the lower half of the field. Note pale and lucid nuclear chromatin. In contrast, aggregates of rounded cells showing homogeneous dark nuclei (arrows) belong to malignant cells originating from a bile duct carcinoma (brushing of the distal portion of the choledochal duct, direct smear, Pap stain, higher magnification).

**Fig. 10.50 Acute cholangitis.**
Degenerating clusters of bile duct-lining cells (lower left and upper right) are embedded in a background of mucoid masses and neutrophils. Bile droplets may be present as well (bile duct brushing, direct smear, Pap stain, low magnification).

**Fig. 10.51 Lambliasis.**
Pancreatic juice after secretin stimulation contains numerous protozoan parasites. *Gardia lamblia* are characterized by smiley face and tail-like flagella (arrows) (direct sediment smear after centrifugation, Pap stain, high magnification).



**Fig. 10.52 Bile duct adenoma associated with epithelial dysplasia.**
A 64-year-old woman with a positive history of obstruction of the choledochal duct. Sediment smears of bile fluid contain papillary tissue fragments. Detail of a papillary frond is presented at higher magnification: fibrovascular tissue is coated with multilayered spindle-formed atypical epithelial cells. Note pronounced palisading and nuclear overlapping (Pap stain).
*Tentative cytologic diagnosis:* Papillary adenocarcinoma of the bile duct.
*Excisional biopsy and histology* revealed villous adenoma associated with focally strong epithelial atypia.
*Postmortem histologic examination:* Papillary adenomatous tumor lacking evidence of invasive growth.

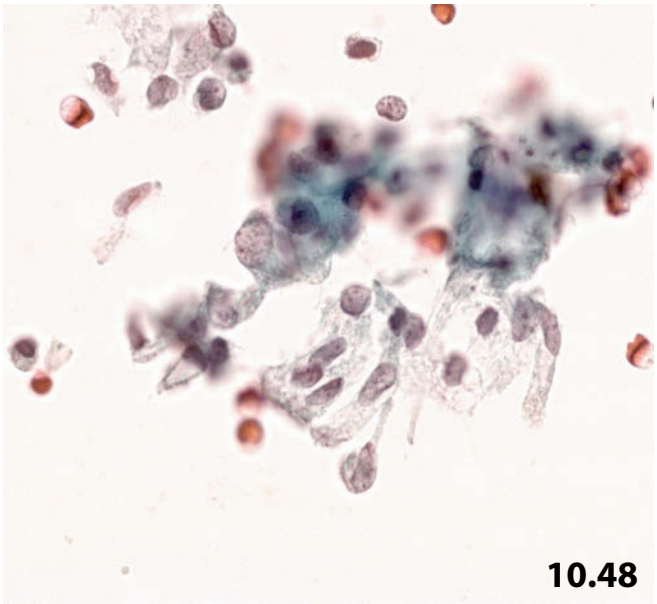
10.48

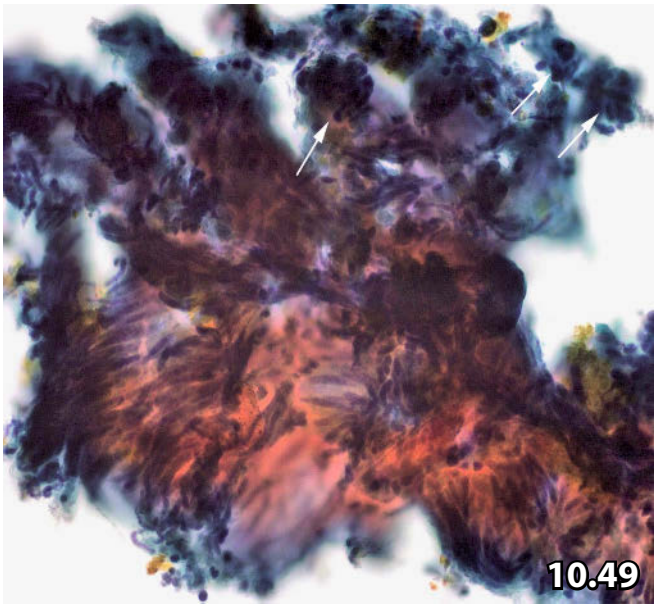
10.49

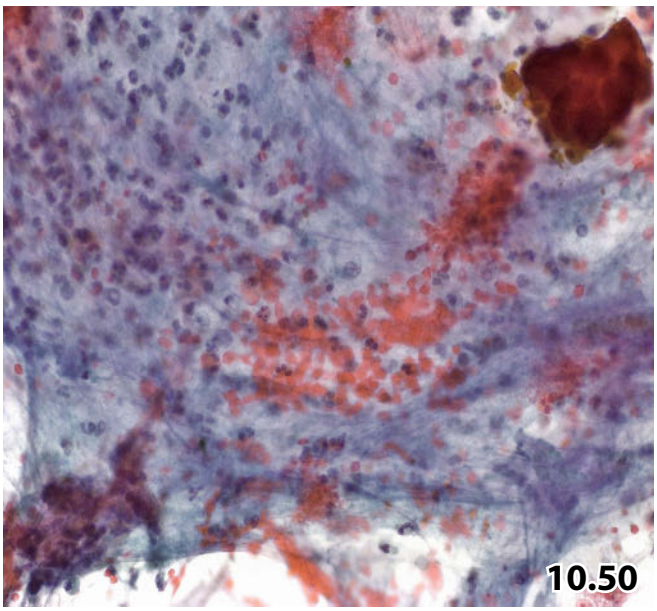
10.50

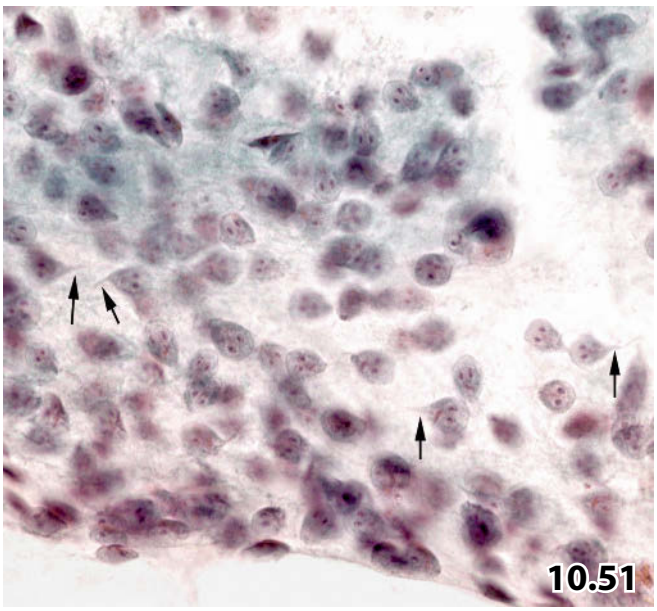
10.51

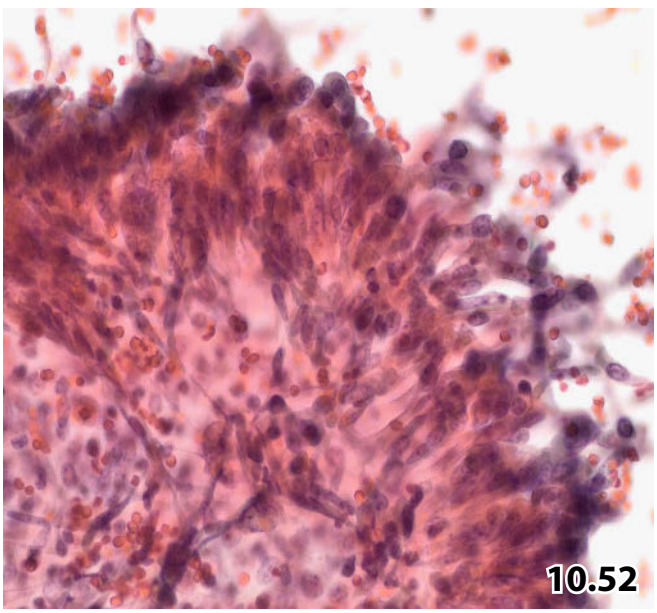
10.52

**Figs. 10.53–10.56 Adenocarcinomas in bile duct brushing.**
Characteristic cytologic features indicating malignancy are presented in brush material sampled from large bile ducts in four patients suffering from cancer of a varying degree of differentiation and varying location. All cytologic specimens were Pap-stained.

It is practically impossible to discriminate bile duct-invasive pancreatic carcinoma from primary adenocarcinoma of the bile duct by cytomorphology alone. Cytologic features of both neoplasms strongly overlap.

**Fig. 10.53** (case #1) Well-differentiated adenocarcinoma of bile duct origin.
A 61-year-old man presented with clinical symptoms suggestive of cholangiocarcinoma. Direct sediment smears (after rinsing the brush in an appropriate solution and centrifugation) were prepared from choledochal brush material. Higher magnification shows the typical cytoarchitecture and single-cell morphology of bile duct adenocarcinoma. However, absence of tumor necrosis may suggest severe dysplasia of bile duct lining epithelium. ICM DNA: aneuploid histogram (not shown).
*Tentative cytologic diagnosis:* Severe epithelial dysplasia or invasive well- to moderately differentiated adenocarcinoma.
*Histology* found a well-differentiated adenocarcinoma of bile duct origin and severe dysplasia of the adjacent bile duct epithelium.



**Fig. 10.54** (case #2) Poorly differentiated adenocarcinoma of bile duct origin.
A 57-year-old woman presented with a stenotic papilla of Vater. Direct sediment smears (after rinsing the brush in an appropriate solution and centrifugation) were prepared from brush material sampled from the distal segment of ductus choledochus. High magnification shows frank malignant cells usually occurring in isolation against a background of blood and detritus. ICM DNA: aneuploid histogram (not shown).
*Cytologic and histologic diagnosis:* Poorly differentiated adenocarcinoma of the common bile duct.

**Fig. 10.55** (case #3) Pancreatic adenocarcinoma in bile duct brushing.
A 62-year-old woman presented with pancreatic carcinoma, based on clinical and imaging findings. Brush material from the choledochal duct was processed using the Cytospin technique. Two different cell sheets are presented at high magnification: (1) the cell sheet upper right exhibits malignant cell features; (2) the cellular aggregate lower left does not show unequivocal malignant cell alterations, but cells are characterized by loss of nuclear polarization, sporadic irregular nuclear outline, and dense granular chromatin.
*Cytodiagnostic consideration:* It is impossible to distinguish severe reactive cell changes from severe dysplasia and invasive malignancy by cytology alone.
*Tissue diagnosis* (pancreatectomy): Choledochal duct-invasive pancreatic adenocarcinoma. Adjacent choledochal duct epithelium exhibits both regenerative and dysplastic cell changes.

**Fig. 10.56** (case #4) Klatskin tumor.
A 66-year-old woman. Endoscopic sampling of cells from the bile duct was not possible due to a firm stenotic lesion in the ampullary area. Thus, bile fluid was obtained using percutaneous transhepatic biliary drainage. Direct sediment smears after conventional centrifugation were prepared. Higher magnification shows large and small tightly cohesive sheets and clusters composed of strongly mucin-producing carcinoma cells. Tumor cells exhibit the characteristic malignant nuclear features. Dispersed carcinoma cells and necrotic debris are sporadically present (lower right). A benign cluster of bile duct-lining cells is also present (arrow).
*Cytologic diagnosis:* Mucinous adenocarcinoma.
*Tissue diagnosis:* Mucinous adenocarcinoma located at the confluence of the right and left hepatic duct, so-called Klatskin tumor.

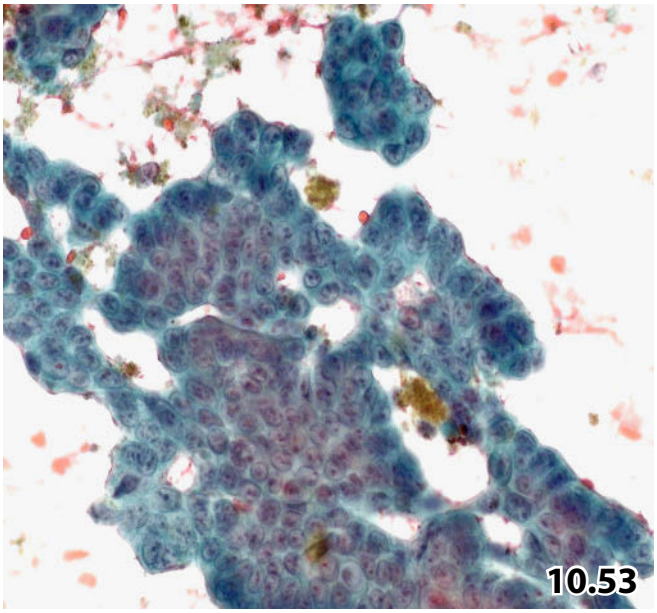
10.53

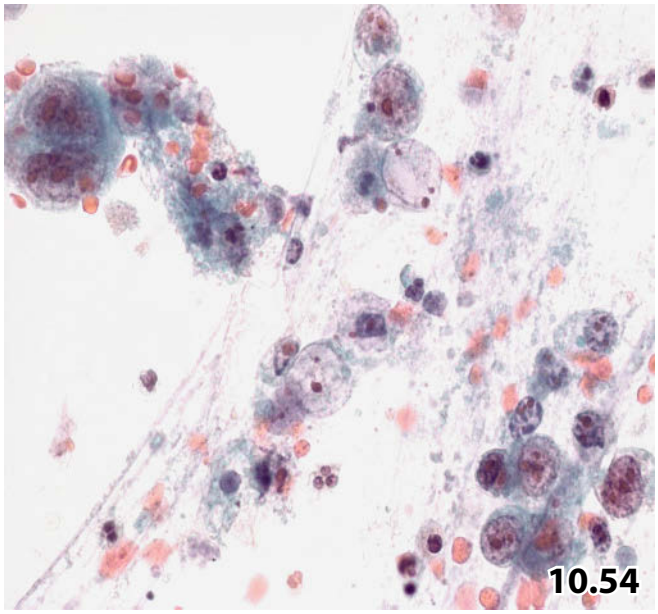
10.54

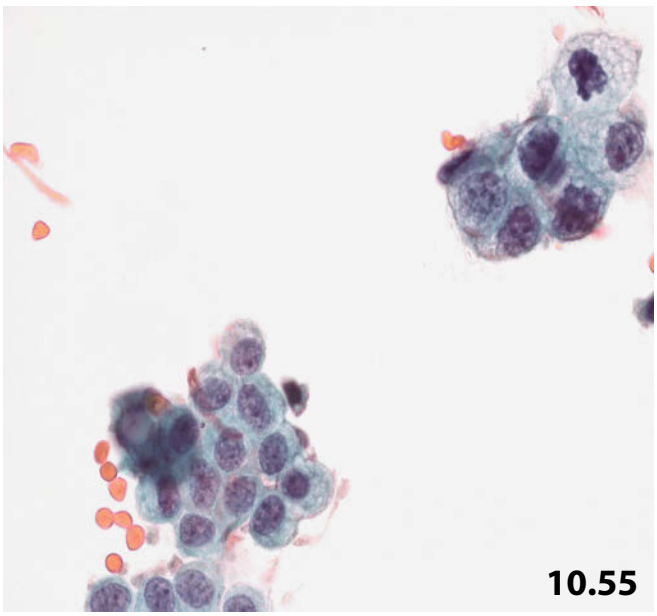
10.55

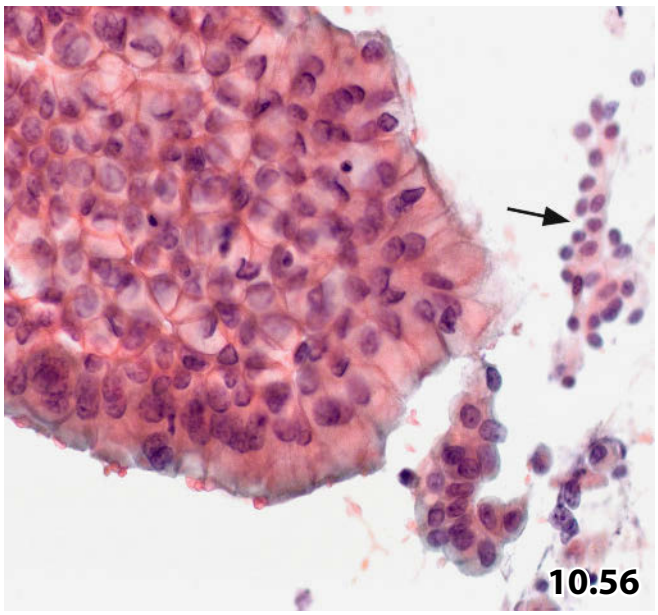
10.56

**Fig. 10.57 Ampullary carcinoma.**
An elderly woman with a history of adenoma of papilla Vater (5 years before) presented with a tumor at the same location. Brushing of the ampulla was performed and direct smears were prepared (Pap stain). Higher magnification shows atypical and malignant epithelial cells crowded in complex papilliform clusters. Cells are usually elongated or columnar-shaped. Nuclear features match those of bile duct/pancreatic adenocarcinomas. ICM DNA: aneuploid histogram (not shown).
*Cytologic diagnosis:* Poorly differentiated adenocarcinoma.
*Tissue diagnosis:* Moderately differentiated adenocarcinoma of the papilla of Vater.

**Fig. 10.58 Adenocarcinoma of the gallbladder.**
Image-guided transcutaneous FNAB of a large tumor mass situated in the upper abdominal cavity beneath the liver (80-year-old woman). High magnification shows discohesive pleomorphic malignant cells. Note homogeneous cyanophilic cytoplasm (direct smears, Pap stain). Immunostains for specific melanoma markers yielded negative result (not shown).
*Cytologic diagnosis* (in accord with clinical findings): Poorly differentiated adenocarcinoma, most likely gallbladder primary.
*Comment:* The abundant dense cyanophilic cytoplasm is a characteristic feature of adenocarcinoma of gallbladder.
*Tissue diagnosis:* Poorly differentiated adenocarcinoma of the gallbladder.



**Fig. 10.59 Dysplastic bile duct epithelial cells.**
Endoscopy detected stenotic choledochal duct in an elderly male patient. High magnification shows a sheet of atypical epithelial cells partly covered with bile (choledochal brushing, Cytospin specimen, Pap stain). Loose chromatin, lack of nuclear clearing, absence of necrosis, and overall monomorphic appearance of the cytoarchitecture (not shown) may favor severe dysplasia.
*Cytodiagnostic consideration:* Most likely severe dysplasia; invasive carcinoma cannot be excluded.
*Comments:* Aneuploid DNA distribution pattern (ICM DNA, not shown) excludes reactive cell changes. An invasive malignant tumor is actually not excluded by cytology or DNA cytometric results.
*Tissue diagnosis* (pancreas resection): Multifocal severe dysplasia of the choledochal epithelium. No invasive neoplasia detectable.

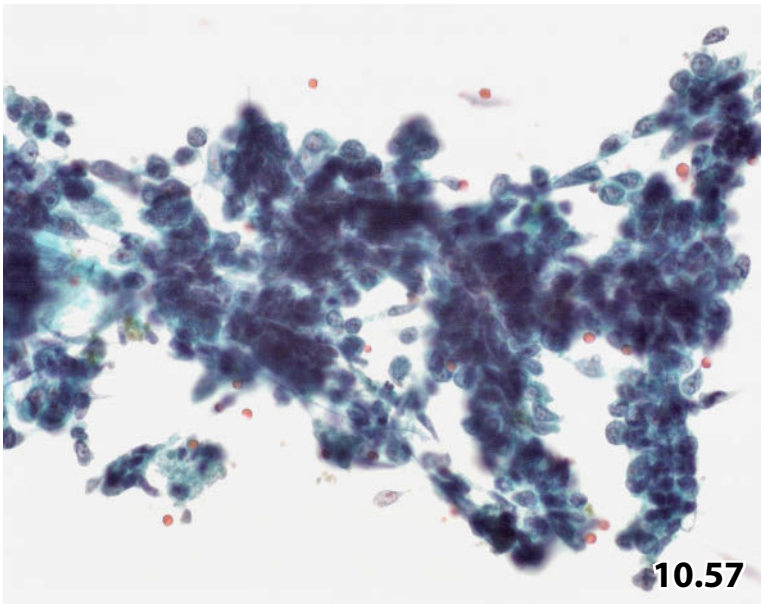
10.57

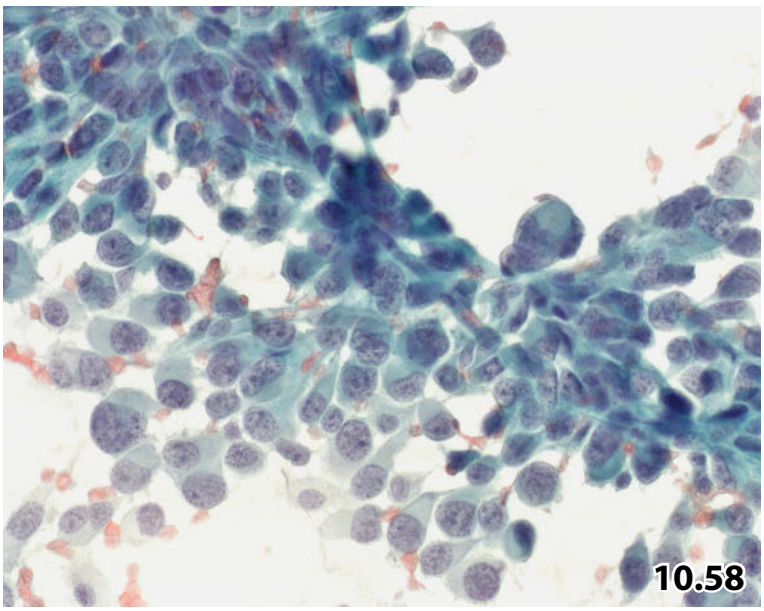
10.58

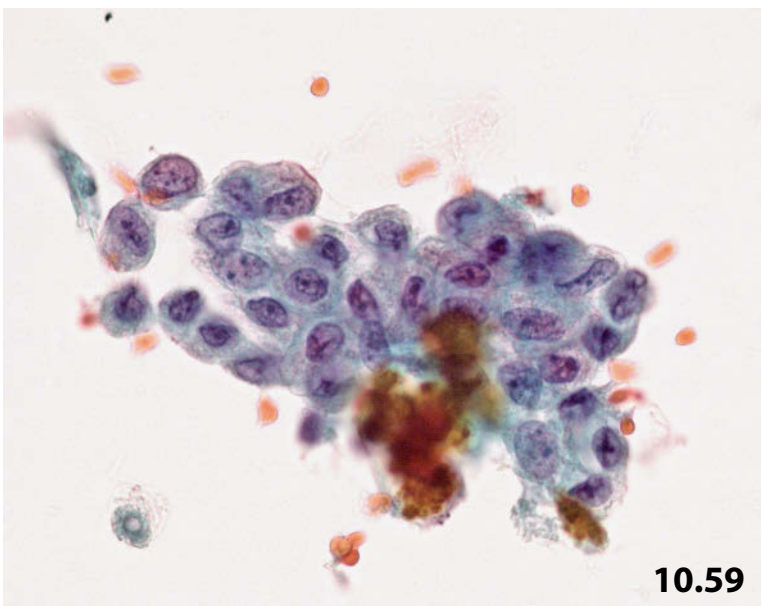
10.59

**Figs. 10.60–10.67 Reactive cellular atypia versus dysplasia: ICM DNA as a helpful diagnostic adjunct.**
Cytologic features, diagnostic challenge, and impact of DNA cytometry distinguishing reactive cell changes and dysplasia are emphasized by means of bile duct brushings in four patients. Each patient had brushing of the bile ducts. Cytologic specimens (direct smear or Cytospin preparation) were Pap-stained. Quantitative DNA analyses using image cytometry were applied to Pap-prestained Feulgen stained specimens.

**Fig. 10.60** (case #1) A 41-year-old man with a positive history of gallstones in the common bile duct presented with a sclerotic papilla of Vater. Cytology was performed in order to exclude a neoplastic lesion. High magnification shows discohesive flat sheets composed of atypical epithelial cells. Cytoarchitecture, loose chromatin, and pronounced nucleoli favor severe reactive cell changes (Cytospin specimen).

**Fig. 10.61** (case #1) DNA-euploid polyploidization (Ahrens Cytometrie-System).
*Cytologic diagnosis* (considering ICM DNA result): Benign regenerative cell changes.
*Tissue diagnosis* (endoscopic biopsy): No malignant lesion detectable.

**Fig. 10.62** (case #2) An 80-year-old man with findings suggestive of a neoplastic disorder in the bile duct system. The patient underwent several bile duct brushings within a period of 12 months. High magnification shows ball-like clusters composed of dysplastic (arrows) and malignant cells (Cytospin preparation).



**Fig. 10.63** (case #2) DNA-aneuploidy: SL in the 4c area, and >15% of all cells measured in noneuploid regions (AutoCyte).
*Cytology* repeatedly provided diagnoses of severe dysplasia, invasive tumor not excluded, which were twice confirmed by DNA-aneuploidy, but histology from endoscopic biopsies revealed benign tissue.
*Histologic examination* of another endoscopic biopsy finally established the diagnosis of invasive cancer.

**Fig. 10.64** (case #3) Pancreatic cancer was suspected based on clinical symptoms and imaging studies in an elderly woman. Bile duct brushing was performed followed by direct smearing of the sampled cell material.
Detail shows a sheet composed of atypical ductal epithelial cells.

**Fig. 10.65** (case #3) DNA-aneuploidy supported the tentative cytologic diagnosis (AutoCyte).
*Cytodiagnostic considerations and tentative diagnosis:* Distinguishing between reactive cellular atypia and malignant cell changes is very difficult on the basis of the selected cell sheet presented herein.
However, pronounced variability in nuclear size and shape together with a high N/C ratio and frequent absence of nucleoli favor a neoplastic lesion (in situ carcinoma or invasive cancer).
*Tissue diagnosis* (surgical resection of the head of the pancreas): Poorly differentiated adenocarcinoma of the pancreas, locally invasive including the bile duct system.

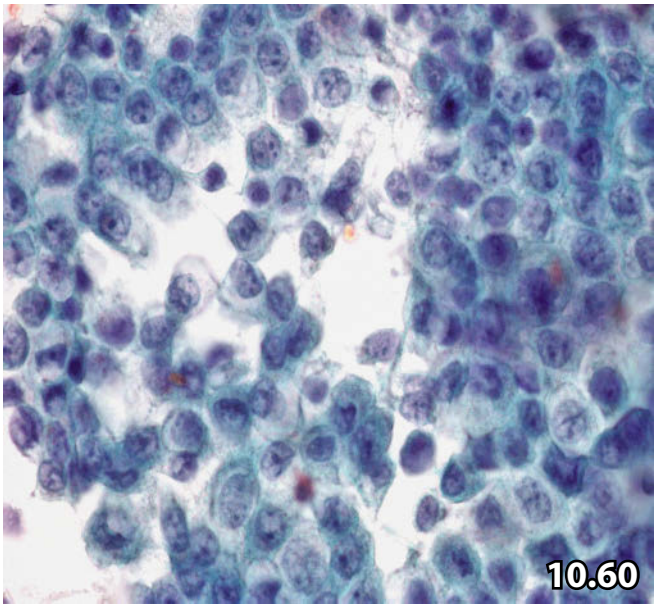
10.60

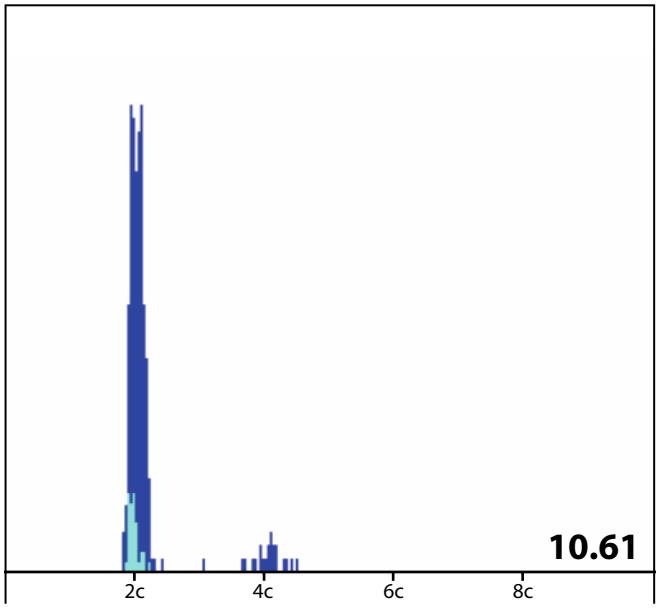

10.61

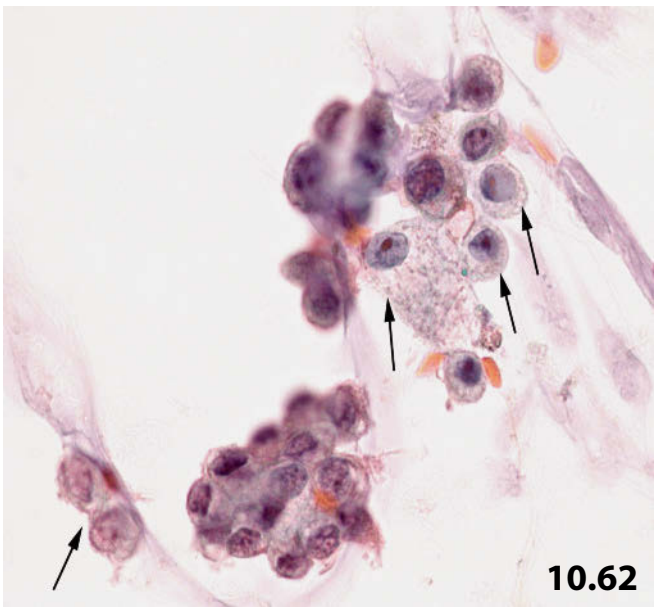
10.62

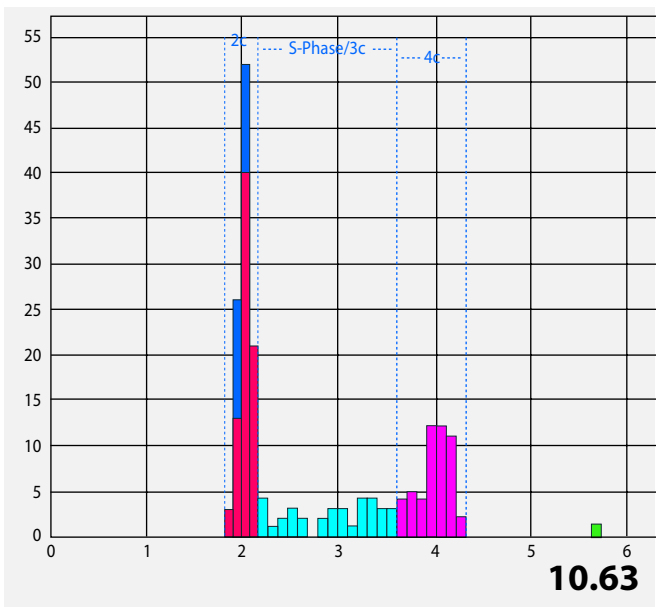

10.63

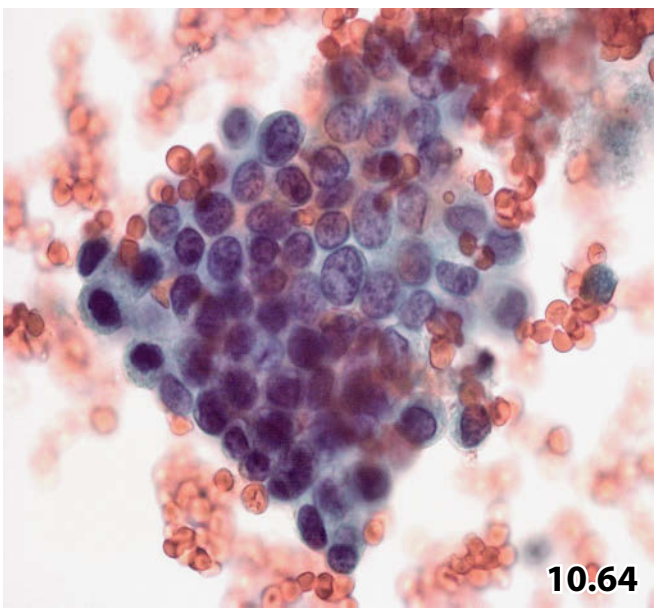
10.64

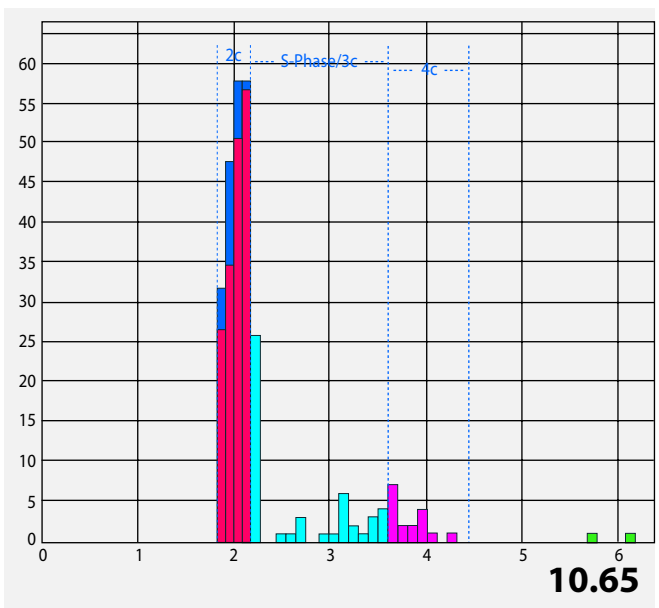

10.65

**Fig. 10.66** (case #4) Clinical diagnosis in an elderly female patient was pancreatic or choledochal carcinoma. High magnification exhibits irregular cell clusters composed of frankly dysplastic epithelial cells. Note irregular tight cell clustering, nuclear polymorphism and nuclear clearing (Cytospin preparation).

**Fig. 10.67** (case #4) Intermediate DNA profile (high S-phase fraction), undetermined as to malignancy.
*Tentative cytologic diagnosis:* Severe epithelial dysplasia of the bile duct-lining epithelium or invasive carcinoma (originating from bile ducts or pancreas).
*Final diagnosis* (clinical/imaging findings and surgical biopsies): Metastatic adenocarcinoma of the pancreas invading the bile duct system.

Distinguishing between reactive and dysplastic/malignant cell changes may be impossible by standard cytology alone.
Irregularities of the nuclear margin comprising wrinkles, cleaves, and longitudinal grooves are unreliable diagnostic features. They may occur in both reactive/regenerative and malignant cells sampled from the bile ducts.

**Fig. 10.68 Metastasis of colon carcinoma to the bile duct system.**
A 64-year-old man with a clinical history of metastatic adenocarcinoma of the large intestine was investigated for biliary duct stenosis. Choledochal duct brushing revealed tight clusters of pleomorphic carcinoma cells and necrosis. Cellular palisading (arrows), intracytoplasmic mucus (not in focus), and degeneration are reliable features indicating carcinoma of the bowel (direct smear, Pap stain, high magnification).

**Fig. 10.69 Metastatic malignant melanoma to the bile duct system.**
Brushing of bile duct system. Direct sediment smears were performed for Pap staining, after rinsing the brush in an appropriate solution and centrifugation. Lower magnification shows malignant melanoma cells exhibiting the characteristic morphologic features (between arrows). Pigmented melanoma cells are also present but not shown. Please compare melanoma cells with a sheet of benign activated bile duct epithelial cells (left of the malignant cells).

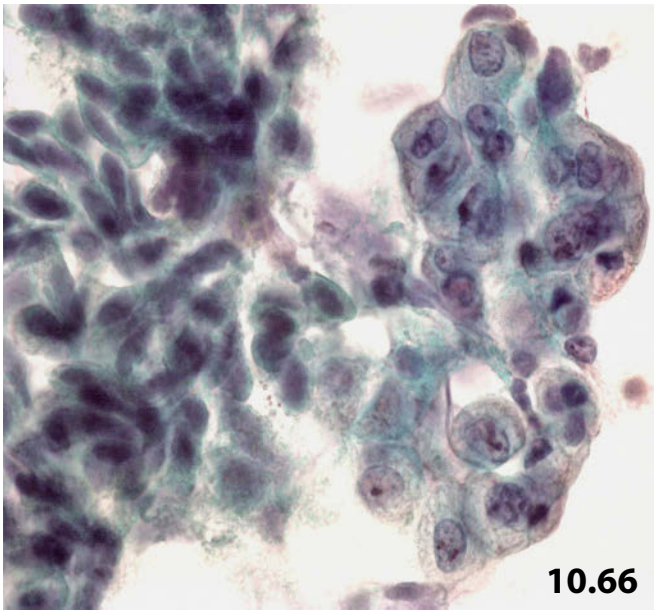

10.66

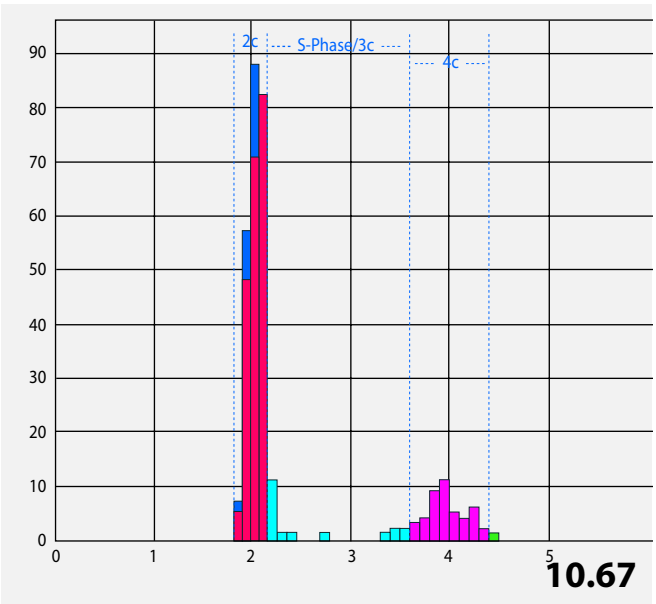


10.67

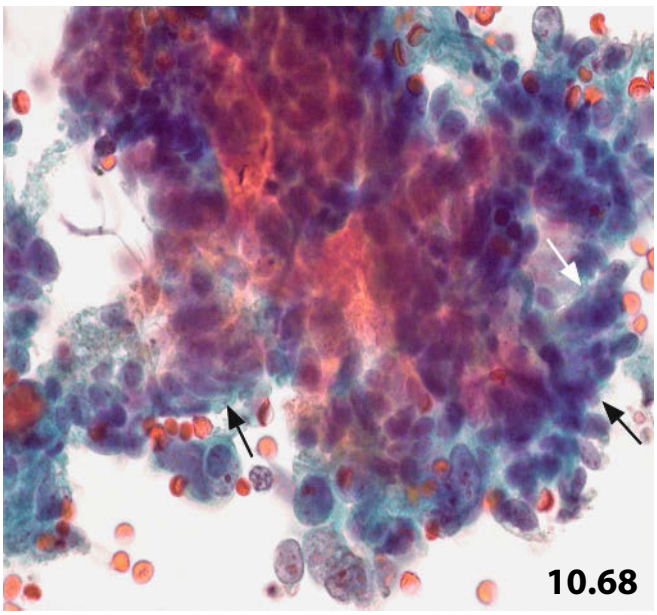

10.68

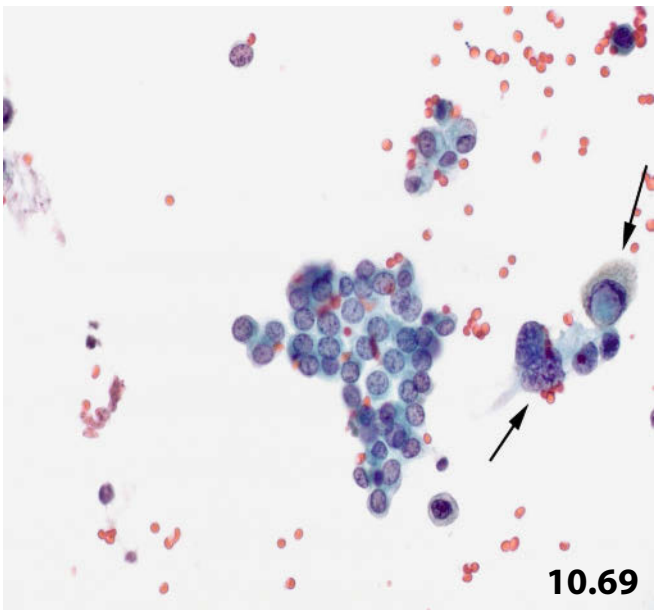

10.69

# Gastrointestinal Tract 11



## Synopsis and Algorithms



Spieler/Rössle, *Nongynecologic Cytopathology. A Practical Guide. Essentials of Diagnostic Pathology*,
DOI 10.1007/978-3-642-24719-4_11, © Springer-Verlag Berlin Heidelberg 2012

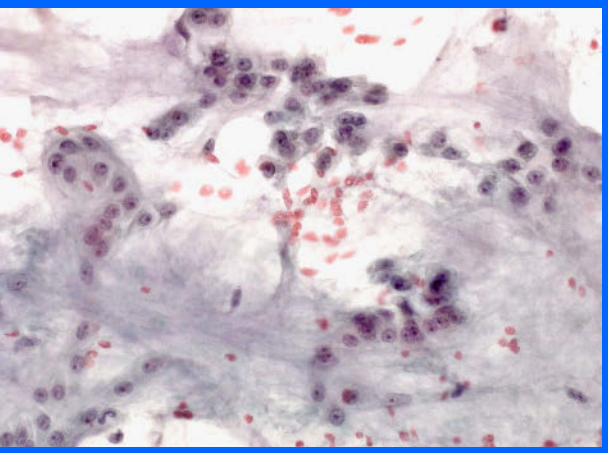

# Gastrointestinal Tract

Esophagus
Stomach
Small Bowel
Colon/Rectum
Anal Canal
Perirectal Area

## 11.1 Introduction

### General Comments

- A large number of methods have been applied for cell collection in gastrointestinal diagnostic cytology since the 1940s and 1950s. Many of these sampling techniques, in particular related to esophageal and gastric lesions are of historic interest only. They comprise blind lavage methods using solutions such as buffered saline solution, blind mechanical abrasive methods by means of "Zelltupfsonde" brushing, and other abrasive techniques. Balloon cytology has been shown to still be a helpful method for esophageal cancer screening in China, its population having particularly high rates of esophageal cancer [65, 90].
  These sampling techniques together with details regarding preparation and staining methods, etc., are described in distinguished textbooks and specialized sections of comprehensive books on cytopathology [41, 68].
- Availability of fiberendoscopes since the 1970s increased the use of intestinal endoscopy tremendously and facilitated the collection of cells under direct vision. In recent years, a variety of new diagnostic procedures have been established for patients with suspected malignant lesions in the esophagus and gastrointestinal tract, first of all in combination with highly advanced imaging techniques. Cytologic specimens are provided by endoscopy in combination with washings or brushings, transcutaneous FNAB, and endoscopic ultrasonography-guided FNAB (EUS-FNAB). Common endoscopic biopsy techniques have been replaced over the past few years by aspiration techniques with image guidance.

### Sampling Methods and Sample Processing

- *Washing*. Direct vision cytology may be accomplished by washing where a forceful jet of a solution is directed at the lesion under visual control and afterward the lavage fluid is recovered with a collection tube.
- *Brushing*. There is no doubt that brush sampling is superior to wash collection as the lesion can be accurately reached and cell waste tends to be minimal. Chromoendoscopy detects small multifocal lesions with high accuracy, permitting well-directed brush sampling and biopsy [8].
- *Transcutaneous FNAB* [5, 82]. Direct aspiration may be applied on large palpable abdominal masses wherever the tumor has originated or is located. Image guidance procedures such as transabdominal ultrasound and computed tomography scan are commonly used to evaluate intraabdominal masses in patients where endoscopic investigations failed or have not been feasible.
  All FNAB methodologies have shown accurate diagnostic utility and safe performance on an outpatient basis.
- *EUS-FNAB* [1, 16, 17, 45, 64, 85, 88] is a safe and effective diagnostic method for experienced endosonographers and skilled cytopathologists. The method permits primary clarification of intramural and extramural abnormal findings as well as tumor staging during the same procedure. In many cases it avoids the need for more invasive procedures to obtain a pathomorphologic diagnosis. Compared with other imaging techniques, it improves the resolution of small lesions (< 3 cm) [45]. Repeat EUS-FNAB may be performed in patients with inadequate sampling, indeterminate findings, surprisingly negative findings at initial

FNAB, or previously unsuccessful endoscopic forceps biopsy. Diagnostic sensitivity, specificity, and accuracy are reported to be high [1, 16, 17, 85, 88].

- *Intraoperative aspiration* by palpation is a supplemental but exceptionally used tool for the management of intestinal and abdominal masses.
- *Wireless capsule endoscopy* [30, 69, 86] is an innovative technique in diagnostic gastrointestinal endoscopy. The device consists of a pill that contains a color video camera and a wireless radiofrequency transmitter. Capsule endoscopy has been developed to access areas of the intestinal tract that are difficult to meet with push enteroscopy. Over the past few years, it has become an established tool for evaluating various pathologies of the small bowel, especially obscure gastrointestinal blood loss and inflammatory bowel disease. The future will show whether capsule endoscopy can replace conventional endoscopy in the first-line diagnosis and reach the expected clinical significance. Furthermore, it will be interesting to learn whether this technology will emerge with brushing and fluid aspiration for cytological tests and with biopsy for histological investigation.
- *Sample processing*. The variably sampled cytologic specimens from the alimentary tract are processed according to the usual practice as described in this book, such as in Sect. 10.1.2, p. 633. The liquid-based method is best used by operators who are not familiar with proper preparation and fixation technique. The technique guarantees quantitatively and qualitatively optimal specimens for special investigations, in particular for immunocytochemistry, fluorescence in situ hybridization, or static DNA cytometry [65].



## 11.2 Esophagus

### 11.2.1 Topography, Histology, and Cell Collection Methods

- The esophagus is a hollow muscular tube (length, approximately 25 cm), which connects the pharynx with the stomach. It runs through the chest traversing the mediastinal tissue in front of the spine and behind the trachea. At the distal ending, a smooth muscle system forms the esophageal sphincter that prevents the regurgitation of food from the stomach.
- The bulk of the esophagus is composed of nonkeratinizing stratified squamous epithelium. A basal lamina separates the epithelial layer from the fibrous lamina propria mucosae. There are cardiac-type glands in the lamina propria that discharge secretion onto the esophageal mucosal surface. Scattered melanoblasts are interspersed among the squamous cells.
- Intramural esophageal disorders may be evaluated cytologically by means of washing, directed brush sampling, and EUS-FNAB. Transcutaneous FNAB methodologies are hardly ever applied to primary lesions of the esophagus.
- The EUS-FNAB procedure for the management of extramural lesions located in the mediastinal space is discussed in Sects. 2.1.1.2.3, p. 109, and 2.4.1.1.3, p. 205. Cytodiagnostic features and diagnostic dilemmas of mediastinal nonneoplastic and neoplastic lesions are exemplified in Sect. 2.4, "Mediastinum," p. 204.

### 11.2.2 Normal Cytology and Esophagitis/Infections

#### 11.2.2.1 Normal Cytology (Fig. 11.1)

- Cytological features: mature squamous cells of superficial and intermediate type. Nuclear pyknosis may occur but keratinization of the cytoplasm is unusual. Parabasal and possibly basal squamous cells may occur as a result of vigorous scraping.
- The round to oval nuclei have a smooth contour and a vesicular chromatin pattern.
- Glandular cells with or without mucus secretion may originate from glands embedded in the esophageal mucosa or from the gastric mucosa as a result of brushing reaching the stomach. Replacement of the normal squamous epithelium lining the esophagus by metaplastic columnar epithelium (Barrett esophagus) should always to be taken into account.

#### 11.2.2.2 Inflammation and Infections

##### 11.2.2.2.1 Chronic Granulomatous Esophagitis

- A variety of chronic inflammatory disorders may affect the esophageal mucosa such as tuberculosis, syphilis, and granulomatous lesions in Crohn disease patients [63, 79], together with nonspecific conditions. Patients' clinical history and special stains (Gram, Ziehl-Neelsen stain for acid-fast bacilli, and others) together with microbiological investigations are usually needed to reach a reliable diagnosis.
  - Neutrophils, lymphocytes, and epithelioid histiocytes, giant cells and microgranulomas indicate a granulomatous lesion in cytological specimens. Squamous cells may show reactive/regenerative changes (see Sect. 11.2.3, p. 703).

##### 11.2.2.2.2 Reflux Esophagitis

Gastroesophageal reflux disease can result in an erosion of the squamous epithelium of the lower esophagus by hydrochloric acid, pepsin, and/or bile.

- Cell-rich cytologic specimens are composed of a mixed inflammatory pattern and squamous cells from all epi-

thelial layers. Deep-seated immature squamous cells occur in cohesive and regular sheets, the nuclei are round and dark-stained with bland chromatin.

**Caution**

Possible parabasal and basal squames should not be confused with undifferentiated cancer cells. Cell grouping and chromatin pattern contrast distinctly with those of carcinoma cells.

#### 11.2.2.2.3 Eosinophilic Esophagitis [15, 35]

Eosinophilic esophagitis is a relatively new disease in which evidence of etiology has not yet been established and its prevalence is continuously growing. It is a chronic allergy-like inflammation of the esophagus affecting children as well as adults. The disorder is characterized by eosinophilic infiltration of the esophageal mucosa. Histopathological diagnosis is based upon the presence of 15 or more eosinophils per high power field.

#### 11.2.2.2.4 Fungal Infections (Fig. 11.2)

*Candida* species are the most frequent causative organisms, followed by *Aspergillus*. Fungi can be identified in cytologic smears by means of selective staining methods: periodic acid-Schiff (PAS), and silver stains.

- A purulent exudate characterized by numerous neutrophils mostly with severe degeneration and cell debris should raise strong suspicion of a mycotic infection. Squamous cells may include all degrees of differentiation and reactive changes (see Sect. 11.2.3, below).

#### 11.2.2.2.5 Viral Infections (Figs. 11.3 and 11.4)

The most common viral infection is that of the *herpes simplex virus* (Fig. 11.3).

- Hallmarks: Immature squamous cells show considerable enlargement and a peculiar narrow rim of cytoplasm. The nuclei, presenting in a three-dimensional fashion (ballooned), have smooth margins and show either pale ground glass plasma or a single eosinophilic inclusion surrounded by a halo. The chromatin is arranged at the inner surface of the nuclear membrane as small but distinct granules. Multinucleated giant cells occur frequently.
- Concomitant nonspecific atypias of superficial squamous cells frequently occur (Fig. 11.4).

The morphologic changes of herpes virus-infected cells are pathognomonic, but they may be mistaken for malignant cells by inexperienced interpreters.

### 11.2.3 Reactive/Reparative Squamous Cell Changes (Figs. 11.2B, 11.3B, 11.4, 11.5)

- Hallmarks: The cytoplasm is characterized by an abnormal acidophilia and irregular shape. The nuclei are enlarged but their borders tend to be smooth. The chromatin pattern is loose but abnormalities may occur. Variably prominent and multiple nucleoli are present. The N/C ratio is within normal limits or slightly increased.

Epithelial atypias caused by an inflammatory process are a common challenge for cytopathologists. The cell changes should not be overestimated as dysplastic or even malignant. Preoperative DNA ploidy assessment is believed to be an effective and reliable method to differentiate between reactive cell change and premalignant/malignant cellular degeneration (see Sect. 11.2.6, p. 704).

**Caution**

- Cellular atypias together with an inflammatory pattern should never be judged as dysplasia by light microscopy alone. Additional staining methods for infectious organisms may contribute to an accurate diagnosis, and static DNA cytometry is helpful to ascertain or exclude a precancerous or malignant lesion.
- An ineffective initial therapy requires repeated brush biopsies or surgical excisional biopsy.

### 11.2.4 Benign Tumors of the Esophagus

A comprehensive documentation of benign esophageal tumors has been compiled by Choong and Meyers [18].

#### 11.2.4.1 Squamous Papilloma

True benign papillary squamous tumors exist but an accurate cytologic diagnosis is not possible unless papillary fragments are present in smears or cell-bloc preparations. Most of the papilliform lesions in the esophagus are of inflammatory origin. They exhibit either a bland epithelial cell layer or reactive cell changes of varied degrees.

#### 11.2.4.2 Granular Cell Tumor

[12] (Figs. 1.63 and 1.64)

In the majority of cases, granular cell tumor is a benign lesion that can be found in many organs. Only 2% of these tumors are of esophageal origin; they usually are found accidentally. Cytologic and immunocytochemical features are

discussed in Sect. 8.8.1, p. 568 and 1.2.18, p. 26, and in other sections of this book.

## 11.2.5 Premalignant Lesions of Esophageal Squamous Epithelium

White patches in the mucosa of the esophagus may be harmless (e.g., glycogenic acanthosis), but they may also indicate a precancerous lesion. Some investigators consider leukoplakia and esophageal lichen planus to have malignant potential after longstanding existence [13].
The cytologic appearance of mild and severe dysplasia is not really specific.

**Microscopic Features and Differential Diagnosis**

- *Mild dysplasia:* Keratinized superficial squames are either anucleated or contain pyknotic nuclei. Parakeratotic squamous cells are present as well. The cytoplasm shows orangeophilic or eosinophilic staining. These features together with mild cytoplasmic and nuclear polymorphism suggest mild dysplasia.

In this setting, distinction of dyspasia from reactive cell changes is not possible by cytology alone, and only histologic tissue sampling can detect severe dysplasia confined to the middle and lower part of the epithelium.

- *High-grade dysplasia:* Distinct cytoplasmic and nuclear pleomorphism, coarse chromatin, increased N/C ratio, and mitotic activity are characteristics of high-grade dysplasia.

In this setting, a cytology-based distinction from invasive squamous cell carcinoma is difficult if not impossible.

For further information and related pictures, we refer the reader to Sect. 8.6, "Leukoplakia," p. 567.

## 11.2.6 Additional Analyses on Squamous Lesions

Lugol Chromoendoscopy
Lugol chromoendoscopy enhances the detection rate of high-grade squamous lesions using targeted brushing and biopsies from unstained mucosal areas [8].
DNA Image Cytometry
ICM DNA is an adjuvant diagnostic procedure to conventional cytology of the esophagus with a high level of standardization, objectivity, and diagnostic accuracy [6, 7, 9, 10, 42].
DNA ploidy is a biological marker:

1. That confirms a cytological diagnosis of malignancy.
2. That predicts or excludes the occurrence of squamous cell carcinoma.
3. That is exquisitely helpful in clarifying the nature of cytologically equivocal changes of squamous cells; premalignant change (dysplasia) can be distinguished from reparative atypia with high accuracy; aneuploidy correlates with invasive cancer, and severe dysplasia/carcinoma in situ having progressive potential to invasion.
4. For tumor staging and predicting tumor prognosis.
5. That eliminates false-negative cytologic results obtained with the conventional brush biopsy technique, and false-positive diagnoses can be avoided.

Histogram algorithms have been applied at our institution according to ploidy evaluation on squamous epithelium from other organs: see Sect. 8.4, "DNA Image Cytometry," p. 565.
DNA Flow Cytometry
Several reports in the literature refer to flow cytometric DNA analyses of esophageal squamous cell carcinoma [6, 22, 74, 76] regarding various biological aspects of the tumor. A comparative study has shown digital image cytometry to be superior to flow cytometry (the latter using formalin fixed paraffin embedded tissue) [24].
Fluorescence In Situ Hybridization
We conducted a study together with the department of gastroenterology at the Kantonsspital St. Gallen to assess the risk of esophageal carcinogenesis by means of a two-color FISH test using a locus-specific probe for the p53 gene and a probe for chromosome 17 [7]. Larger biomarker studies are necessary to elucidate whether p53 LOH (loss of heterozygosity) may be a marker for early detection of potentially malignant cells.

## 11.2.7 Malignant Neoplasms of the Esophagus

### 11.2.7.1 Squamous Cell Carcinoma (Fig. 11.6)

- Squamous cell carcinoma (SCC) is the most common malignant tumor of the esophagus and accounts for up to 95% of all esophageal tumors. The growth pattern may be polypoid or ulcerative.
- Cytologically, SCCs reflect good, moderate, or poor differentiation. Verrucous carcinoma of the esophagus rarely occurs. Microscopic features match those of SCCs at other sites such as bronchus, cervix/vagina, penis, and others. Morphologic features of the three tumor grades are listed in Chap. 11, "Synopsis and Algorithms," p. 1199, in Sect. 8.7, p. 568, and in other sections of this book.
- Poorly differentiated SCCs composed of polymorphous rounded cells devoid of keratin, disseminated, or grouped in compact spheric clusters are difficult to distinguish from poorly differentiated adenocarcinoma (Fig. 11.7). The term "large-cell undifferentiated carcinoma" may best be applied to such undifferentiated tumors. Predominantly dissociated undifferentiated carcinoma cells share features with anaplastic large-cell non-Hodgkin lymphoma. Immunocytochemical work-up including antibodies against cytokeratins (MNF-116 and others), leukocyte common antigen (CD45), and B-/ T-cell epitopes is mandatory as a first step.

#### 11.2.7.2 Adenocarcinoma (Fig. 11.7)

The incidence of adenocarcinoma in the upper and middle thirds of the esophagus is low (accounting for around 2% of all malignancies). The lower third of the esophagus reveals much more frequent adenocarcinomas, either by extension from the stomach or arising in metaplastic epithelium of Barrett esophagus. The cytologic pattern of adenocarcinomas will be described in Sect. 11.2.8, "Barrett esophagus," below.

#### 11.2.7.3 Other Malignancies

They rarely occur and are hardly ever referred for cytologic evaluation. The WHO histological classification presents the complete list of esophageal tumors [39]. Many of these entities are discussed elsewhere in this book.

### 11.2.8 Barrett Esophagus (Intestinal Metaplasia)

#### 11.2.8.1 Introduction and General Comments

- Barrett esophagus (BE) is the abnormal intraepithelial growth of intestinal-type cells (referred to as intestinal metaplasia) above the squamocolumnar epithelial junction. Chronic gastroesophageal reflux is the common cause for development of BE, which is the precursor of most esophageal adenocarcinomas. BE cells may develop abnormal changes known as dysplasia (synonym: intraepithelial neoplasia). In approximately 5% of patients with Barrett esophagus, dysplasia progresses over a period of several years to cancer [19, 25]. This means that the early diagnosis of intraepithelial precursor lesions or adenocarcinoma is the primary objective of surveillance of patients with BE.
- Unlike histological biopsy, brush cytology allows the sampling of large surface areas of Barrett mucosa. The procedure is readily available in gastroenterology practice. Cells in routinely processed cytologic specimens may be referred to digital image cytometry and FISH subsequently to cytomorphologic evaluation.

**Caution**

Intestinal metaplasia of Barrett type per se cannot be diagnosed cytologically.
In smears presenting with intestinal-type glandular cells, Barrett lesion may be assumed if the brush has not passed through the gastroesophageal sphincter during the sampling process.

#### 11.2.8.2 Benign and Reactive Barrett Epithelium

*Benign cells* from Barrett mucosa are characterized by two different types (Fig. 11.8):

- Columnar cells and goblet cells; the latter stain positive with Alcian blue. The cells occur singly, in palisade alignment closely attached to each other when seen in profile, or tightly cohesive in regular sheets.
- Nuclear spacing is uniform, nuclear overlapping is absent. The nuclei are small, round to oval, and situated at the base of the cell.
- The chromatin structure is loose, the nucleoplasm clear, and the nucleoli are indistinct.
- The N/C ratio is low.

*Reactive/regenerative cell changes* are a feature of intestinal metaplasia (Figs. 11.9–11.13):

- The N/C ratio, chromatin pattern, and nuclear color are the same as in benign glandular cells, but the cells and nuclei tend to be slightly enlarged, exhibiting inconspicuous outline irregularities and distinct round centrally placed nucleoli. Mucus production is poor.

Diagnosis of reactive cell changes should be limited to cases in which the changes are too pronounced for normal cells but not sufficient for diagnosis of dysplasia.

**Caution**

Distinguishing between reactive and dysplastic cell changes is particularly difficult on cells originating from areas adjacent to erosions and ulcerations.

#### 11.2.8.3 Intraepithelial Neoplasia and Adenocarcinoma (Figs. 11.14–11.22)

Intraepithelial neoplasia should be classified as low grade and high grade according to the histological nomenclature. Low-grade dysplasia is synonymous with mild to moderate dysplasia, whereas high-grade dysplasia includes severe dysplasia and carcinoma in situ.

Cellular and architectural features for the cytologic classification of dysplastic lesions and adenocarcinoma are listed in Table 11.1, p. 706.

#### 11.2.8.4 Additional Analyses on Cells Originating from Barrett Mucosa

- Histologically assessed dysplasia grade is the approved means of risk stratification in patients with BE. However, the problems of this method include poor reproducibility of dysplasia interpretation, poor predictive value for pa-

**Table 11.1** Barrett mucosa: cytological criteria of dysplasia and adenocarcinoma

| | Cytological features | |
|---|---|---|
| | **Architectural** | **In single cells** |
| **Low-grade dysplasia** | Mild changes:<br>– Indistinct irregularities of sheets and palisades | Enlarged nuclei:<br>– Moderate membrane irregularities<br>– Faint hyperchromasia<br>– Fine granular or reticular chromatin<br>– Rare coarse chromatin clots<br>Distinct single or multiple nucleoli<br>Cuboid to cylindric cytoplasm, occasionally rounded<br>Abnormal basal position of the nuclei |
| **High-grade dysplasia** | Irregular cell clusters of variable size and shape:<br>– Three-dimensional<br>– Frequently smooth borders<br>– Loss of cellular palisading and loss of nuclear polarity | Variations in cell size and shape<br>Strongly enlarged nuclei:<br>– Variable size and shape<br>– Distinct nuclear pleomorphism: wrinkled and cleaved prominent membranes<br>– Pronounced hyperchromasia<br>– Chromatin occurring as finely granular and densely packed, or coarsely clumped<br>Grossly enlarged round or bizarre nucleoli<br>Polygonal cytoplasm |
| **Adenocarcinoma** | Features favoring invasive cancer:<br>Clusters having complex architecture<br>- Three-dimensional<br>- Irregular cellular crowding and nuclear overlapping<br>- Disaggregation of the cell clusters | All cellular characteristics of high-grade dysplasia and additionally:<br>– Mucus secretion<br>– Signet-ring cells<br>– Necrotic debris |
| **Caution**<br>Differentiation between high-grade dysplasia, carcinoma in situ, and invasive adenocarcinoma is often impossible by standard cytology (Figs. 11.14, 11.17–11.19, 11.21 and 11.22). | | |

11

tients affected by indefinite cell changes, low-grade dysplasia, and other challenging points.

- In the future, biomarkers appear to be useful for detecting:
  - Subsets of patients with BE having an increased risk of cancer progression but showing no correlation in baseline histology.
  - Patients who do not suffer from high-grade dysplasia whilst histologically supposed.

Currently, ploidy status as well as p16 and p53 gene abnormalities are most extensively evaluated [11, 31, 50, 71].

DNA Ploidy

Histograms and corresponding figures and legends are shown on pages 718-723.

- *DNA flow cytometry* (FCM) analyses of biopsy specimens have previously been shown to be able to identify BE patients at high progressive cancer risk and to have impact on prognosticating the survival of BE patients afflicted with adenocarcinoma [59, 70, 71, 72].
- Using endoscopic brush cytology, we evaluated the additional diagnostic benefit of *digital image cytometry (ICM DNA)* for BE patients in comparison to histologic workup. The results of a cohort study of 164 patients at the Kantonsspital St. Gallen showed that the combination of brush cytology and ICM DNA can:
  - Confirm benign and malignant cytologic diagnoses.
  - Classify dubious cytologic findings.
  - Identify additional high risk patients.

  The data suggest that brush cytology combined with ICM DNA testing is helpful in detecting individuals with Barrett esophagus at increased risk of malignancy with surveillance over a long period of time [11].
- Only a few studies have addressed the predictive value of DNA abnormalities in BE using digital image cytometry and brush specimens. Most studies took measurements on Feulgen-stained tissue sections [27, 43, 96] or imprints [83].
- The histogram algorithm for ploidy assessment in BE used at our institution are identical with that currently used to test intestinal glandular cells from other organs. The distinguished algorithm and the interpretative features are presented in Sect. 10.1.3.2, "DNA Ploidy Analysis," p. 635.

Molecular Genetics (Fig. 11.19)

- A variety of molecular genetic modifications have been detected in the course of development of intestinal metaplasia to adenocarcinoma. p16 and p53 gene abnormalities are at present the most extensively documented. It has been shown that patients with 17p (p53) loss of heterozygosity (LOH) are at increased risk for development of adenocarcinoma [73]. A combination of 17p LOH, 9p

LOH, and quantitative DNA abnormalities seems to provide better risk prediction in patients with BE than analysis of the three biomarkers on their own [36].

- There is a good correlation between ploidy pattern and p16/p53 LOH. A prerequisite is however, that reliable quantitative cut-offs for LOH have to be determined in order to minimizing false-positive results.
- A recent study by Barr Fritcher and associates [3] showed that polysomy of 8q24 (C-MYC), 9p21 (P16), 17q12 (HER2), and 20q13 implies a high risk factor for high-grade dysplasia and development of adenocarcinoma. Furthermore, the study revealed that FISH analysis may have a higher sensitivity for low-grade dysplasia, high-grade dysplasia, as well as esophageal adenocarcinoma compared with DNA ploidy results.

## 11.3 Stomach, Duodenum, Small Bowel, Large Bowel, Anal Canal, and Perirectal Area

### 11.3.1 Exfoliative Cytology

Gastrointestinal exfoliative cytology has occasionally been performed by our gastroenterologists over the last few years; Therefore, our diagnostic experience in this field is limited. We recommend referring to the information available in distinguished textbooks, review articles, individual publications, and internet databases.

A few items of general interest are worth mentioning.

- *Normal cytologic patterns* should be readily recognizable. The variable cell components and the varying architecture of tissue fragments reflect (micro)anatomic and functional features of the mucosa in the different intestinal segments (Figs. 10.9, 10.10, 10.12–10.14, 11.23, 11.24).
- *Inflammatory diseases* (various types of gastritis, colitis, diverticulitis, and ulcerative disorders) may produce a cytologic pattern comprising variable inflammatory background and epithelial cells with varying degrees of reactive, metaplastic, and degenerative changes. Distinguishing between reactive cell changes, preneoplastic intraepithelial disorders, and invasive carcinoma has been discussed in different chapters of this book, including the application of adjunct analyses, which are helpful in solving the diagnostic problems.
- *Giardia lamblia* (Fig. 10.51) may be encountered in brushings and fluids obtained from the bowel; the morphology of the protozoa has been described in Sect. 10.2.5.3, p. 683.
- *Benign epithelial tumors* generally do not reflect any morphological details that could separate them from other benign lesions.
- *Superficial (early) carcinoma of the stomach* is a well-known entity. The Japanese have the largest experience with this type of tumor and related cytologic techniques. Usually, there is no difference in the cytologic pattern of superficial carcinoma and invasive cancer.
- *Colorectal dysplasia* may be difficult to distinguish from severe regenerative atypia, particularly in cases accompanying chronic inflammatory disease. Gross genetic analysis (ploidy analysis) and structural genetic analyses (gene mutations, loss and amplification of gene loci, and others) may be helpful in identifying a premalignant condition that can progress to adenocarcinoma.
- *Adenocarcinoma* (Figs. 11.25 and 11.26) from any site of the gastrointestinal tract meet the cytological criteria of malignancy that are basically the same as encountered in adenocarcinomas at other sites, such as bronchus, lung, uterine cervix, esophagus.

  The most important cytologic features include:
  - Cellular enlargement, anisocytosis, nuclear pleomorphism, hyperchromatic nucleoplasm, densely granular or coarse chromatin texture, and variable N/C ratio.

  CK20 and CDX-2 are appropriate immunocytochemical markers indicating intestinal adenocarcinoma.
- *Nonepithelial tumors* have been recorded elsewhere in this work. Numerous variants of malignant lymphomas that are of interest to cytopathologists are described in detail in Sect. 15.3, “Lymph Nodes: Malignant Lesions,” p. 950.

### 11.3.2 Endoscopic Ultrasound-Guided Fine-Needle Aspiration Biopsy

- Endoscopic ultrasound-guided fine-needle aspiration biopsy (EUS-FNAB) is considered a reliable method for the evaluation of intramural/submucosal lesions of the gastrointestinal tract. Diagnostic sensitivity, specificity, and accuracy are reported to be high [16, 88]. Vander Noot and coauthors emphasize false-negative and false-positive diagnoses of lesions from various sites of the gastrointestinal tract [88]. EUS-FNAB allows direct visualization of tumoral lesions and adequate sampling of cellular specimens for cytologic, immunocytochemical, and molecular diagnosis. EUS-FNAB will significantly reduce the need for more invasive procedures aimed at obtaining a primary tissue diagnosis and reliable results of tumor stage.
- Furthermore, EUS-FNAB offers an accurate morphologic diagnosis in a wide variety of extraintestinal mass lesions such as intraabdominal tumors, pelvic tumors, retroperitoneal masses, and lymph nodes in close proximity to the gut wall [1, 16, 17]. Diagnostic utility of transintestinal EUS-FNAB for the detection of lesions located in abdominal organs is discussed in the respective chapters.
- Cytologic appearance, diagnostic challenge, and immunocytochemical features of intraabdominal metastases are similar to their primary counterparts. They are documented in the literature or in distinguished textbooks, and dis-

cussed in varied chapters of this book (see Sects. 12.3.8, p. 785, 9.2.6, Table 9.2.1, p. 610, and 15.3.24, Table 15.3.3, p. 978)

- Transesophageal EUS-FNAB has become an important tool for assessing primary diagnoses of abnormal structures located in the mediastinum adjacent to the esophagus and in the dorsal areas of the lung. Today, preoperative staging of pulmonary carcinomas is barely conceivable without this method [28, 38, 40]. EUS-FNAB procedure for the management of lesions located in the mediastinal space are discussed in Sect. 2.1.1.2.3, p. 109, and 2.4.1.1.3, p. 205. Cytodiagnostic features and diagnostic difficulties of mediastinal nonneoplastic and neoplastic lesions are explained in Sect. 2.4, "Mediastinum," p. 204.

## 11.3.3 Cytology of Selected Disorders of the Gastrointestinal Tract

### 11.3.3.1 Extraneous Cells and Material

(Figs. 2.16, 2.17, 11.27)



1. Extraneous material will frequently appear in esophageal and gastric exfoliative-cytologic samples but sporadically also in transenteral FNABs. This is swallowed material originating from the respiratory tract and from the buccopharyngeal cavity:
   - Buccal and tracheal mature squamous cells predominantly of the superficial and intermediate type.
   - Bronchial columnar cells, ciliated columnar cells, and mucus-producing cells.
   - Pulmonary macrophages containing anthracotic and blood pigment.
2. Well-preserved foreign epithelial cells in exfoliative samples from the colorectal area should raise suspicions of a fistula. In addition, fistulas are frequently responsible for secondary acute inflammation:
   - Squamous cells occur together with a rectovaginal fistula.
   - Urothelial cells occur together with a rectovesical fistula.
3. Food contaminants may disturb the cytological evaluation:
   - Vegetables: vegetable cells can mimic tumor cells or vermicular eggs (Figs. 2.16 and 11.27).
   - Other ingested foreign material such as microspores of pollen (Fig. 2.17).

### 11.3.3.2 Gastrointestinal Stromal Tumor

(Figs. 11.30–11.32)

- Gastrointestinal stromal tumor (GIST) is the most common mesenchymal neoplasm of the gastrointestinal tract, mostly encountered in the stomach. It is now thought that GISTs originate from the interstitial cells of Cajal acting as pacemakers for peristalsis [60].
- Differentiating from other mesenchymal tumors is very important because of prognostic differences and targeted therapeutic strategies. An overview of different aspects of GIST has been provided by Miettinen and Lasotta [60].
- The malignant potential of GIST depends on the site of origin (gastric tumors have a more favorable outcome than intestinal GISTs), the tumor size, and the mitotic activity [60, 75, 87].
- EUS-FNAB from GISTs generally provides adequate samples both for tissue diagnosis and immunocytochemical and molecular analyses. Immunoreactivity may yield more reliable results on cell block preparations compared to smear specimens [2, 14, 34, 78].

**Microscopic Features** [26, 54, 57]

- Most cytologic specimens contain abundant cellular material.
- A *pure spindle cell pattern* consists of uniform spindle cells arranged in fascicles or whorls and exhibits focal nuclear palisading. The nuclei are bland and the cytoplasmic borders are ill defined. Myxoid stroma is obvious.
- A *pure epithelioid tumor variant* [23, 52] is almost exclusively composed of epithelioid cells, variably with plasmacytoid features. The tumor cells are arranged singly or in small clusters. The nuclei are round; they usually show irregular outlines and small nucleoli. Multinucleated cells are often encountered. The cytoplasm is well defined, appearing as a condensed eosinophilic to clear rim. Collagenous stromal fragments are frequently encountered.
- A biphasic tumor pattern is standard.

Cytological features cannot reliably distinguish between benign and malignant tumors. The presence of mitoses and necrosis seem to correlate best with malignant degeneration [26].

**Molecular Genetics and Immunocytochemistry**

(Figs. 11.28 and 11.29)

- GIST is associated with mutations of the c-kit proto-oncogene, or PDGFRA. Other genetic aberrations are assumed to be responsible for tumor genesis of GIST [94]. In the future, molecular characterization of GISTs may gain increasing significance both for patient´s prognosis and the increase in the effectiveness of targeted therapies [91].
- CD117, the c-kit proto-oncogene product (Fig. 11.28) in GISTs is usually expressed in the majority of cells in both the spindle cell and epithelioid tumor variants, in benign and malignant GISTs, and in tumors of any site of origin. Results of numerous studies indicate that CD117 is a relatively specific immunomarker for GIST [48, 77].
  However, in a small subgroup of GISTs CD117 immunopostivity is absent [49]; and tumors exhibiting variable

CD117 positivity include clear cell sarcoma, metastatic melanoma, and malignant fibrous histiocytoma; a few other mesenchymal tumors occasionally express the c-kit product [77].

A few cells exhibiting positivity for CD117 intermingling with spindle cell tumors are most likely mast cells [4].

- CD34 (hematopoietic progenitor cell antigen) (Fig. 11.29) is a immunomarker for GIST having lower specificity than CD117. CD117 may be positive in some CD34-negative tumors. CD34 has been reported to be also present in many fibroblastic and endothelial cell tumors [77].
- Smooth muscle actins show coexpression with CD117 in up to one-third of all GISTs. [77].
- Desmin is sporadically coexpressed in gastric GISTs [61].

**Differential Diagnosis**

Various types of mesenchymal tumors can cause diagnostic confusion with GIST when using light microscopy. Immunophenotyping is the primary tool to identify the different entities (the immunocytochemistry of GIST is stated above).

- Classic spindle cell GIST exhibiting cellular polymorphism may resemble nonkeratinizing squamous cell carcinoma (Fig. 11.32).
- Epithelioid-type GIST exhibiting certain pleomorphisms may mimic adenocarcinoma [54] (Fig. 11.31).
- Benign tissue fragments from the gastrointestinal wall should not lead to a misinterpretation of GIST and vice-versa [34].
- The following nonepithelial tumor entities have been identified as showing consistent negativity for CD117: peripheral nerve-sheath tumors, leiomyomatous tumors, fibrous tumors, and Kaposi sarcoma [77].
- Strong immunoreactivity for smooth muscle actin and/or desmin is a reliable indicator of leiomyoma [84] and leiomyosarcoma [92].
- Intraabdominal fibrosis and GIST unfortunately overlap notably in their immunoprofiles [95].

**Caution** [77]

- Solitary fibrous tumors and Kaposi sarcoma exhibit CD34 positivity.
- Occasional CD117 positivity can be observed in CD34-positive non-GIST tumors, such as dermatofibrosarcoma protuberans, hemangiopericytoma, clear cell sarcoma, melanoma, and malignant fibrous histiocytoma.

### 11.3.3.3 Primary Ampullary Tumors [20]

See also Sect. 10.2, "Extrahepatic Bile Ducts and Ampullary Region," p. 680.

- Ampullary masses represent a large variety of benign and malignant disorders such as adenocarcinomas developing from various anatomic sites (common bile duct, main pancreatic duct, (peri-)ampullary mucosa, or duodenal mucosa), adenoma, endocrine tumors, and eventually a voluminous head of the pancreas extending into the ampullary region.
- Both vigorous brushing of the ampullary area damaging the surface of the mucosa and FNAB may result in sampling cell clusters from intramural ampullary and duodenal glands. Pronounced irregular cell clustering and nuclear crowding of the glandular cells caused by reactive changes may lead to a misdiagnosis of adenocarcinoma of clear cell type (see Sect. 10.2.4.3, "Contaminants in Brushings," p. 682) (Fig. 10.14).
- Gastrointestinal cell debris should not be confused with cancer necrosis (Fig. 10.13B).
- *Ampullary cancer* and carcinomas of the bile and pancreatic ducts are, for the most part, cytologically similar to each other. The consistent cytomorphologic features of malignancy are listed in Sect. 10.2.7, p. 684 (Fig. 10.57).
- *Ampullary adenomas* are considered to be premalignant lesions [93]. Histologically, various degrees of atypia, epithelial dysplasia, or carcinoma in situ may be present, and foci with invasive carcinoma may be found in tumors investigated thoroughly by light microscopy. Cytological sampling should be avoided since the morphologic complexity of this lesion is virtually a contraindication for cytologic diagnostics.

### 11.3.3.4 Endocrine Tumors

(Figs. 2.63–2.67, 9.29–9.31, 10.40–10.43)

Endocrine tumors of the gastrointestinal tract are most commonly located in the duodenum, ampullary region, or gallbladder [51].

They include:

- Well-differentiated neoplasms of the diffuse endocrine system (carcinoid tumors)
- Poorly differentiated endocrine neoplasms (small-cell carcinomas)
- Large-cell neuroendocrine carcinomas

As in other anatomic sites of the human body, the tumors show typical morphologic patterns, and the endocrine nature of the lesions can be confirmed by immunocytochemical work-up. Cytological and immunocytochemical features, differential diagnoses, and cautions of common endocrine tumors and their variants are recorded in Sect. 10.1.10, p. 646.

### 11.3.3.5 Ulcerative Colitis

Patients with long-standing ulcerative colitis have an increased risk of colorectal adenocarcinoma. Colonic lavage together with DNA ploidy assessment may be useful in surveillance of colitis patients in order to improve the early de-

tection of individuals at high risk for cancer [47, 53, 55, 56, 58]. DNA aneuploidy is a marker for (potential) malignant transformation complying with the biological behavior of atypical glandular cells in other organs (see Sect. 10.1.3.2, "DNA Ploidy Analysis", p. 635).

### 11.3.3.6 Lesions Located in or Adjacent to the Terminal Rectum and the Anal Canal

#### 11.3.3.6.1 General Comments and Tools

A tumorous mass located in the area of the terminal part of the large intestine is usually palpable and easily visualized by direct inspection or by endoscopy. These lesions are in general confirmed by tissue biopsy and histological examination; but FNAB or brush cytology may be used in particular situations to establish a diagnosis.

Transrectal FNAB may be a reliable tool for accurate preoperative nodal staging in patients with rectal carcinoma [81]; and to clarify suspected secondary lesions in the wall of the bowel and in the pelvic space. Adenocarcinoma of the rectum and uterus and squamous cell carcinoma of the uterine cervix and the anal canal are the most frequently encountered tumor types.

- *Digitally guided transrectal fine-needle aspiration biopsy.* The tool can be applied for cytologic study of circumscribed nodular lesions that are unequivocally recognized by palpatory examination. The most commonly used instrument and technique for digitally guided transrectal aspiration of the prostate was developed by Sixten Franzén in the 1950s [33] (see Sect. 14.1.1, p. 853). This procedure may also be recommended for other transrectally palpable tumors located outside the prostatic gland.
- *Endoscopic ultrasound-guided fine-needle aspiration biopsy.* EUS-FNAB is appropriate for pelvic lymph nodes and tumor masses in patients for whom an excisional biopsy is difficult to perform or inadvisable. The method has also been applied for preoperative staging of rectal adenocarcinoma [81].
- *Cytology brushing* is sporadically used, particularly in patients with erosive disorders in the epithelium of the anal canal and in the perianal area.

#### 11.3.3.6.2 Chordoma

[29, 46, 62, 66, 67, 89] (Figs. 5.71, 11.33)

**General Comments**

Chordomas are rare tumors originating from the remnants of the notochord. They have a predilection for the ends of the axial skeleton and occupy most frequently the sacral area. Chordoma is thought to be a locally invasive tumor but metastases may occur in 10–40% of tumors; most of them are reported to be clinically occult [44]. Nonpalpable presacral chordomas are detected by radiologic and ultrasound methods and can consecutively be evaluated by means of percutaneous FNAB [46, 89] or EUS-FNAB [37]. Accurate preoperative diagnosis is important for an optimal management of these tumors.

**Microscopic Features**

- Hallmarks are physaliferous cells having vacuolated and blistered cytoplasm; the cells are large, showing mono- or binucleation.
- The spectrum of cellular variants also includes uniform small rounded epithelial-like cells, fusiform cells, and bi- and multinucleated giant cells.
- Intranuclear inclusions and mitotic figures may occur.
- The cytoplasm is clear and vacuolated in a high proportion of the tumor cells. Cells occur dissociated and in small groups.
- Chondroid extracellular matrix is readily recognizable in May-Gruenwald-Giemsa staining (superior to Papanicolaou staining).
- Physaliferous cells may be absent in some chordomas. These tumors usually exhibit areas composed of bizarre anaplastic cells [46, 62, 66].

Histochemical ultrastructural findings may also be helpful to reach a proper diagnosis.

**Immunocytochemistry** [29, 67, 89]

Each cell type shows marked positivity for keratins, S100 protein, epithelial membrane antigen (EMA), and vimentin. Absence of S100 immunopositivity has been observed.

Absent expression of carcinoembryonic antigen (CEA) and glial fibrillary acidic protein (GFAP) is of value in distinguishing between chordoma and other mesenchymal tumors and mucus-producing carcinoma, respectively.

**Differential Diagnosis** [46, 29, 67, 89]

Overlapping cytologic features have been observed between chordoma and:

- Chondrogenic tumors, myxoid liposarcoma (no immunoreactivity for cytokeratins and EMA).
- Ependymoma (immunocytochemical expression of GFAP and usually immunonegative for cytokeratins).
- Metastatic clear cell carcinoma and mucin-producing adenocarcinoma (immunopositive for CEA).

#### 11.3.3.6.3 Intraepithelial Neoplasia (HPV infection)

Precancerous intraepithelial neoplasia in the anal canal and the perianal skin is most often an incidental finding. These neoplastic lesions presenting as eczematoid areas or plaques may occasionally be evaluated by brush cytology. Anal cytology is assumed to be a useful technique for diagnosis, screening, and follow-up of at-risk individuals such as HIV-positive homosexual men and women with genital intraepithelial neoplasia [21, 32, 80].

Anal intraepithelial neoplasias share morphologic features with their counterparts at other sites (esophagus, oral cavity, uterine cervix).

Keratinized surface may hamper a conclusive diagnosis. However, koilocytic changes should be searched for by carefully reading all available smears.

#### 11.3.3.6.4 Other Disorders Rarely Encountered in Cytologic Specimens

*Squamous cell carcinoma with pronounced basaloid features* may pose problems in distinguishing from other primary and secondary tumors (basal cell carcinoma, metastases of small-cell carcinoma from various sites, endocrine tumor, and others).

- The tumors are composed of small malignant cells that are focally palisaded.

*Malignant melanoma* rarely develops in the anal mucosa.

- Cellular features resemble those of cutaneous melanoma. Cytology and a specific immunopanel are recorded elsewhere (e.g., in Sect. 16.2.9, p. 1030).

*Malakoplakia* is a pseudogranulomatous histiocytic disease characterized by concentrically laminated cytoplasmic inclusions known as Michaelis-Gutmann bodies or calcospherites (see Sect. 13.2.4.3, p. 814).

## 11.4 Further Reading


1. Anand D, Barroeta JE, Gupta PK, et al. Endoscopic ultrasound-guided fine-needle aspiration of non-pancreatic lesions: an institutional experience. J Clin Pathol 2007;60:1254-1262.
2. Ando N, Goto H, Niwa Y, et al. The diagnosis of GI stromal tumors with EUS-guided fine needle aspiration with immunohistochemical analysis. Gastrointest Endosc 2002;55:37-43.
3. Barr Fritcher EG, Brankley SM, Kipp BR et al. A comparison of conventional cytology, DNA ploidy analysis, and fluorescence in situ hybridization for the detection of dysplasia and adenocarcinoma in patients with Barrett's esophagus Human Pathology 2008; 39:1128–1135.
4. Berman J, O'Leary TJ. Gastrointestinal tumor workshop. Human Pathol 2001;32:578-582.
5. Binek J, Spieler P, Hürlimann R, et al. Ultrasound-guided fine-needle aspiration of abdominal masses: Accuracy and short-term complications. Europ J Ultrasound 1995;2:199-203.
6. Blant SA, Ballini JP, Caron CT, et al. Evolution of DNA ploidy during squamous cell carcinogenesis in the esophagus. Dis Esophagus 2001;14:178-184.
7. Boller DA, Borovicka J, Spieler P, et al. Lugol chromoendoscopy combined with image cytometry and p53 LOH in patients at risk for esophageal squamous cell carcinoma. Gastrointest Endosc 2006;63:S1520.
8. Boller D, Spieler P, Schoenegg R, et al. Lugol chromoendoscopy combined with brush cytology in patients at risk for esophageal squamous cell carcinoma. Surg Endoscop 2009;23:2748-2754.
9. Boettger T, Störkel S, Stöckle M, et al. DNA image cytometry. A prognostic tool in squamous cell carcinoma of the esophagus? Cancer 1991;67:2290-2294.
10. Boettger T, Dutkowski P, Kirkpatrick CJ, et al. Prognostic relevance of histomorphological parameters and DNA content and their therapeutic consequences in esophageal carcinoma: a multivariate approach. Hepatogastroenterology 1998;45:994-1004.
11. Borovicka J, Schoenegg R, Hell M, Spieler P. et al. Is there an advantage to be gained from adding digital image cytometry of brush cytology to a standard biopsy protocol in patients with Barrett's esophagus? Endoscopy 2009;41:409-414.
12. Buratti S, Savides TJ, Newbury RO, Dohil R. Granular cell tumor of the esophagus: report of a pediatric case and literature review. J Pediatr Gastroenterol Nutr 2004;38:97-101.
13. Chandan VS, Murray JA, Abraham SC. Esophageal lichen planus. Arch Pathol Lab Med 2008;132:1026-1029.
14. Chatzipantelis P, Salla C, Karoumpalis I, et al. Endoscopic ultrasound-guided fine needle aspiration biopsy in the diagnosis of gastrointestinal stromal tumors of the stomach. A study of 17 cases. J Gastrointestin Liver Dis 2008;17:15-20.
15. Chehade M, Sampson HA. Epidemiology and etiology of eosinophilic esophagitis. Gastrointest Endosc Clin N Am 2008;18:33-44;viii.
16. Chen VK, Eloubeidi MA. Endoscopic ultrasound guided fine needle aspiration of intramural and extraintestinal mass lesions: diagnostic accuracy, complication assessment, and impact on management. Endoscopy 2005;37:984-989.
17. Chhieng DC, Jhala D, Jhala N, et al. Endoscopic ultrasound-guided fine-needle aspiration biopsy: a study of 103 cases. Cancer 2002;96:232-239.
18. Choong CK, Meyers BF. Benign esophageal tumors: introduction, incidence, classification, and clinical features. Semin Thorac Cardiovasc Surg 2003;15:3-8.
19. Conio M, Bianchi S, Lapertosa G, et al. Long-term endoscopic surveillance of patients with Barrett's esophagus. Incidence of dysplasia and adenocarcinoma: a prospective study. Am J Gastroenterol 2003;98:1931-1939.
20. Defrain C, Chang CY, Srikureja W, et al. Cytologic features and diagnostic pitfalls of primary ampullary tumors by endoscopic ultrasound-guided fine-needle aspiration biopsy. Cancer 2005;105:289-297.
21. de Ruiter A, Carter P, Katz DR, et al. A comparison between cytology and histology to detect anal intraepithelial neoplasia. Genitourin Med 1994;70:22-25.
22. Doki Y, Shiozaki H, Tahara H, et al. Prognostic value of DNA ploidy in squamous cell carcinoma of esophagus. Analyzed with improved flow cytometric measurement. Cancer 1993;72:1813-1818.
23. Dong Q, McKee G, Pitman M, et al. Epithelioid variant of gastrointestinal stromal tumor: diagnosis by fine needle aspiration. Diagn Cytopathol 2003;29:55-60.
24. Dorman AM, Walsh TN, Droogan O, et al. DNA quantification of squamous cell carcinoma of the esophagus by flow cytometry and cytophotometric image analysis using formalin fixed paraffin embedded tissue. Cytometry 1992;13:886-892.
25. Drewitz DJ, Sampliner RE, Garewal HS. The incidence of adenocarcinoma in Barrett's esophagus: a prospective study of 170 patients followed 4.8 years. Am J Gastroenterol 1997;92:212-215.
26. Elliott DD, Fanning CV, Caraway NP. The utility of fine-needle aspiration in the diagnosis of gastrointestinal stromal tumors: a cytomorphologic and immunohistochemical analysis with emphasis on malignant tumors. Cancer 2006;108:49-55.
27. Fang M, Lew E, Klein M, et al. DNA abnormalities as marker of risk for progression of Barrett's esophagus to adenocarcinoma: image cytometric DNA analysis in formalin-fixed tissues. Am J Gastroenterol 2004;99:1887-1894.
28. Fernandez-Esparrach G, Gines A, Belda J, et al. Transesophageal ultrasound-guided fine needle aspiration improves mediastinal staging in patients with non-small cell lung cancer and normal mediastinum on computed tomography. Lung Cancer 2006;54:35-40.

29. Finley JL, Silverman JF; Dabbs DJ, et al. Chordoma: diagnosis by fine-needle aspiration biopsy with histologic, immunocytochemical, and ultrastructural confirmation. Diagn Cytopathol 1986;2:330-337.
30. Fireman Z, Kopelman Y. New frontiers in capsule endoscopy. J Gastroenterol Hepatol 2007;22:1174-1177.
31. Fléjou JF Barrett's oesophagus: from metaplasia to dysplasia and cancer. Gut 2005;54 Suppl 1:i6-12.
32. Fox PA, Seet JE, Stebbing J, et al. The value of anal cytology and human papilloma virus typing in the detection of anal intraepithelial neoplasia: a review of cases from an anoscopy clinic. Sex Transm Infect 2005;81:142-146.
33. Franzén S, Giertz G, Zajicek J. Cytological diagnosis of prostatic tumours by transrectal aspiration biopsy: a preliminary report. Br J Urol 1960;32:193-196.
34. Fu K, Eloubeidi MA, Jhala NC, et al. Diagnosis of gastrointestinal stromal tumor by endoscopic ultrasound-guided fine needle aspiration biopsy - a potential pitfall. Ann Diagn Pathol 2002;6:294-301.
35. Furuta GT, Liacouras CA, Collins MH, et al. Eosinophilic esophagitis in children and adults: a systematic review and consensus recommendations for diagnosis and treatment. Gastroenterology 2007;133:1342-1363.
36. Galipeau PC, Li X, Blount PL, et al. NSAIDs modulate CDKN2A, TP53, and DNA content risk for progression to esophageal adenocarcinoma. PloS Med 2007;4:e67.
37. Gottlieb K, Lin PH, Liu DM, Anders K. Transrectal EUS-guided FNA biopsy of a presacral chordoma - report of a case and review of the literature. World J Gastroenterol 2008;14:2586-2589.
38. Günter E. Transesophageal ultrasonography for mediastinum diagnostics. Chirurg 2008;79:56-60.
39. Hamilton SR, Aaltonen LA. World Health Organization Classification of Tumours. Pathology and Genetics of Tumours of the Digestive System. IARC Press:Lyon 2000.
40. Herth FJ, Rabe KF, Gasparini S, Annema JT. Transbronchial and transoesophageal (ultrasound-guided) needle aspirations for the analysis of mediastinal lesions. Eur Respir J 2006;28:1264-1275.
41. Husain OAN. Alimentary tract (esophagus, stomach, colon, rectum) In: M.Bibbo (Ed) Comprehensive Cytopathology . W.B. Saunders Comp, 1991.
42. Ikebe M, Kitamura K, Baba K, et al. DNA ploidy as a prognostic factor in early esophageal carcinoma. Hepatogastroenterology 1993;40:232-235.
43. James PD, Atkinson M. Value of DNA image cytometry in the prediction of malignant change in Barrett's oesophagus. Gut 1989;30:899-905.
44. Jenkins CN, Colquhoun IR. Case report: symptomatic metastasis from a sacrococcygeal chordoma. Clin Radiol 1995;50:416-417.
45. Jhala NC, Jhala D, Eltoum I, et al. Endoscopic ultrasound-guided fine-needle aspiration biopsy: a powerful tool to obtain samples from small lesions. Cancer 2004;102:203-206.
46. Kay PA, Nascimento AG, Unni KK, Salomao DR. Chordoma. Cytomorphologic findings in 14 cases diagnosed by fine needle aspiration. Acta Cytol 2003;47:202-208.
47. Keller R, Brandt B, Terpe HJ, et al. Cytology and image cytometry after colonic lavage: a complementary diagnostic tool in patients with ulcerative colitis. Dig Liver Dis 2003;35:24-31.
48. Koh JS, Trent J, Chen L, et al. Gastrointestinal stromal tumors: overview of pathologic features, molecular biology, and therapy with imatinib mesylate. Histol Histopathol 2004;19:565-574.
49. Kontogianni-Katsarou K, Lariou C, Tsompanaki E, et al. KIT-negative gastrointestinal stromal tumors with a long term follow-up: a new subgroup does exist. World J Gastroenterol 2007;13:1098-1102.
50. Krishnadath KK, Reid BJ, Wang KK. Biomarkers in Barrett esophagus Mayo Clin Proc 2001;76:438-446.
51. Lack EE. Pathology of the extrahepatic biliary tract and ampullary region. in: Pathology of the Pancreas, Gallbladder, Extrahepatic Biliary Tract, and Ampullary Region. Oxford University Press, Inc. 2003.
52. Laforga JB. Malignant epithelioid gastrointestinal stromal tumors: report of a case with cytologic and immunohistochemical studies. Acta Cytol 2005;49:435-440.
53. Levine DS, Rabinovitch PS, Haggitt RC, et al. Distribution of aneuploid cell populations in ulcerative colitis with dysplasia or cancer. Gastroenterology 1991;101:1198-1210.
54. Li SQ, O'Leary TJ, Buchner SB, et al. Fine needle aspiration of gastrointestinal stromal tumors. Acta Cytol 2001;45:9-17.
55. Lindberg JO, Stenling RB, Rutegard JN. DNA aneuploidy as a marker of premalignancy in surveillance of patients with ulcerative colitis. Br J Surg 1999;86:947-950.
56. Löfberg R. Studies in longstanding ulcerative colitis with special reference to malignant transformation of the colorectal mucosa. Acta Chir Scand Suppl 1989;552:1-45.
57. Logrono R, Bhanot P, Chaya C, et al. Imaging, morphologic, and immunohistochemical correlation in gastrointestinal stromal tumors. Cancer 2006;108:257-266.
58. Markowitz J, McKinley M, Kahn E, et al. Endoscopic screening for dysplasia and mucosal aneuploidy in adolescents and young adults with childhood onset colitis. Am J Gastroenterol 1997;92:2001-2006.
59. Menke-Pluymers MB, Hop WC, Mulder AH, Tilanus HW. DNA ploidy as a prognostic factor for patients with an adenocarcinoma in Barrett's esophagus. Hepatogastroenterology 1995;42:786-788.
60. Miettinen M, Lasota J. Gastrointestinal stromal tumors review on morphology, molecular pathology, prognosis, and differential diagnosis. Arch Pathol Lab Med 2006;130:1466–1478.
61. Miettinen M, Sobin LH, Lasota J. Gastrointestinal stromal tumor of the stomach: a clinicopathologic, immunohistochemical, and molecular genetic study of 1765 cases with long-term follow-up. Am J Surg Pathol 2005;29:52-68.
62. Nijhawan VS, Rajwanshi A, Das A, et al. Fine-needle aspiration cytology of sacrococcygeal chordoma. Diagn Cytopathol 1989;5:404-407.
63. Oberhuber G. Histology of Crohn disease-type lesions in the upper gastrointestinal tract. Pathologe 2001;22:91-96.
64. O'Toole D, Palazzo L, Arotcarena R, et al. Assessment of complications of EUS-guided fine-needle aspiration. Gastrointest Endosc 2001;53:470-474.
65. Pan Q-J, Roth MJ, Guo H-Q, et al. Cytologic detection of esophageal squamous cell carcinoma and its precursor lesions using balloon samplers and liquid-based cytology in asymptomatic adults in Linxian, China. Acta Cytol 2008;52:14-23.
66. Perasole A, Infantolino D, Spigariol F. Aspiration cytology and immunocytochemistry of sacral chordoma with liver metastases: a case report. Diagn Cytopathol 1991;7:277-281.
67. Plazza JA, Ballestin C, Perez-Barrios A, et al. Cytologic, cytochemical, immunocytochemical and ultrastructural diagnosis of a sacrococcygeal chordoma in a fine needle aspiration biopsy specimen. Acta Cytol 1989;33:89-92.
68. Prolla JC, Kirsner JB. Handbook and Atlas of Gastrointestinal Exfoliative Cytology. The University of Chicago Press, Chicago. 1972.
69. Rabenstein T, Krauss N, Hahn EG, Konturek P. Wireless capsule endoscopy – beyond the frontiers of flexible gastrointestinal endoscopy. Med Sci Monit 2002;8:RA128-132.
70. Reid BJ, Blount PL, Rubin CE, et al. Flow-cytometric and histological progression to malignancy in Barrett's esophagus: prospective endoscopic surveillance of a cohort. Gastroenterology 1992;102:1212-1219.
71. Reid BJ, Blount PL, Rabinovitch PS. Biomarkers in Barrett's esophagus. Gastrointest Endosc Clin N Am 2003;13:369-397.
72. Reid BJ, Levine DS, Longton G, et al. Predictors of progression to cancer in Barrett's esophagus: baseline histology and flow cytometry identify low- and high-risk subsets. Am J Gastroenterol 2000;95:1669-1676.

73. Reid BJ, Prevo LJ, Galipeau PC, et al. Predictors of progression in Barrett's esophagus II: baseline 17p (p53) loss of heterozygosity identifies a patient subset at increased risk for neoplastic progression. Am J Gastroenterol 2001;96:2839-2848.
74. Rickes S, Hauptmann S, Flath B, et al. Development of a flow cytometric method to determine DNA ploidy of esophageal cancer cells obtained by forceps biopsy samples during esophago-gastroduodenoscopy. Onkologie 2003;26:32-37.
75. Rubin BP, Heinrich MC, Corless CL. Gastrointestinal stromal tumour. Lancet 2007; 369:1731–1741.
76. Ruol A, Segalin A, Panozzo M, et al. Flow cytometric DNA analysis of squamous cell carcinoma of the esophagus. Cancer 1990;65:1185-1188.
77. Sarlomo-Rikala M, Kovatich AJ, Barusevicius A, Miettinen M. CD117: a sensitive marker for gastrointestinal stromal tumors that is more specific than CD34. Mod Pathol 1998;11:728-734.
78. Scarpa M, Bertin M, Ruffolo C, et al. A systematic review on the clinical diagnosis of gastrointestinal stromal tumors. J Surg Oncol 2008;98:384-392.
79. Schmitz-Moormann P, Malchow H, Pittner PM. Endoscopic and bioptic study of the upper gastrointestinal tract in Crohn's disease patients. Pathol Res Pract 1985;179:377-387.
80. Scholefield JH, Johnson J, Hitchcock A, et al. Guidelines for anal cytology – to make cytologic diagnosis and follow-up much more reliable. Cytopathology 1998;9:15-22.
81. Shami VM, Parmar KS, Waxman I. Clinical impact of endoscopic ultrasound and endoscopic ultrasound-guided fine-needle aspiration in the management of rectal carcinoma. Dis Colon Rectum 2004;47:59-65.
82. Smith C, Butler JA. Efficacy of directed percutaneous fine-needle aspiration cytology in the diagnosis of intra-abdominal masses. Arch Surg 1988;123:820-824.
83. Spiethoff A, Kakobs R, Martin WR, et al. DNA cytometric studies of Barrett mucosa. Med Klin (Munich) 2001;96:208-211.
84. Stelow EB, Murad FM, Debol SM, et al. A limited immunocytochemical panel for the distinction of subepithelial gastrointestinal mesenchymal neoplasms sampled by endoscopic ultrasound-guided fine-needle aspiration. Am J Clin Pathol 2008;129: 219-225.
85. Südhoff T, Hollerbach S, Wilhelms I, et al. Clinical utility of EUS-FNA in upper gastrointestinal and mediastinal disease. Dtsch med Wochenschr 2004;129:2227-2232.
86. Swain P. The future of wireless capsule endoscopy. World J Gastroenterol 2008;14:4142-4145.
87. Trupiano JK, Stewart RE, Misick C, et al. Gastric stromal tumors: a clinicopathologic study of 77 cases with correlation of features with nonaggressive and aggressive clinical behaviors. Am J Surg Pathol 2002;26:705-714.
88. Vander Noot MR 3rd , Eloubeidi MA, Chen VK, et al. Diagnosis of gastrointestinal tract lesions by endoscopic ultrasound-guided fine-needle aspiration biopsy. Cancer 2004;102:157-163.
89. Walaas L, Kindblom LG. Fine-needle aspiration biopsy in the preoperative diagnosis of chordoma: a study of 17 cases with application of electron microscopic, histochemical, and immunocytochemical examination. Hum Pathol 1991;22:22-28.
90. Wang LD, Yang HH, Fan ZM, et al. Cytological screening and 15 years' follow-up (1986–2001) for early esophageal squamous cell carcinoma and precancerous lesions in a high-risk population in Anyang County, Henan province, Northern China. Cancer Detect Prev 2005;29:317-322.
91. Wardelmann E, Büttner R, Merkelbach-Bruse S, Schildhaus H-U. Mutation analysis of gastrointestinal stromal tumors: increasing significance for risk assessment and effective targeted therapy. Virchows Arch 2007;451:743-749.
92. Wieczorek TJ, Faquin WC, Rubin BP, Cibas ES. Cytologic diagnosis of gastrointestinal stromal tumor with emphasis on the differential diagnosis with leiomyosarcoma. Cancer 2001;93:276-287.
93. Yamaguchi K, Enjoji M. Adenoma of the ampulla of Vater: putative precancerous lesion. Gut 1991;32:1558-1561.
94. Yang J, Du X, Lazar AJ, et al. Genetic aberrations of gastrointestinal stromal tumors. Cancer 2008;113:1532-1543.
95. Yantiss RK, Spiro IJ, Compton CC, Rosenberg AE. Gastrointestinal stromal tumor versus intra-abdominal fibromatosis of the bowel wall: a clinically important differential diagnosis. Am J Surg Pathol 2000;24:947-957.
96. Yu C, Zhang X, Huang Q, et al. High-fidelity DNA histograms in neoplastic progression in Barrett's esophagus. Lab Invest 2007;87:466-472.

**Fig. 11.1 Esophageal brushing: Normal cytology.**
Liquid-based cytologic slides (ThinPrep) made from cell samples collected during esophageal brushing reveal keratinized and nonkeratinized superficial squamous cells (Pap stain, high magnification).

**Fig. 11.2A, B Esophagitis: fungal infection.**
An 82-year-old man presenting with gastrointestinal bleeding revealed erosion of his proximal esophagus by endoscopic evaluation. Brushing was performed. Direct sediment smears (after rinsing the brush in an appropriate solution and centrifugation) were stained according to the Papanicolaou method. **A** Inflammatory background and squamous cells exhibiting nuclear irregularity (left) (low magnification). **B** Detail is focused on considerable atypias of the squamous cells; nuclei showing irregular arrangement, varying size and shape, and membrane irregularities.
*Cytology:* It was not possible to render a determinate report. The differential diagnosis was severe regenerative cell changes or neoplastic lesion.
*Tissue diagnosis* (endoscopic biopsy): Ulcerative esophagitis caused by *Candida* species. No neoplastic lesion.

*Comments:* Few hyphae were subsequently detected by careful re-evaluation of the cytologic specimen. Primary silver staining is strongly advocated in every case presenting with similar cytologic features as demonstrated here.



**Fig. 11.3A, B Herpetic esophagitis.**
Endoscopic examination of an elderly woman's esophagus revealed severe ulcerative esophagitis. Findings were suggestive of candidiasis. Esophageal brushing was performed. Direct sediment smears (after rinsing the brush in an appropriate solution and centrifugation) were Pap-stained. **A** Cell changes due to herpes virus infection are readily recognizable at higher magnification: multinucleation and pale ground glass nucleoplasm (arrows). **B** High magnification reveals heterogeneous appearance of the cell pattern: (1) Nonkeratinized squamous cells showing characteristic nuclear features of viral infection and (2) slightly keratinized polymorphous squamous cells with dark staining nuclei (top). The latter should not be misinterpreted as malignant.

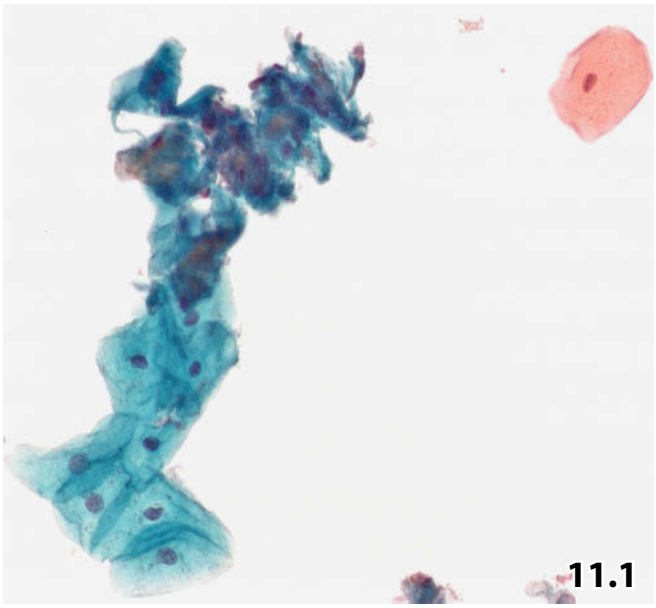

11.1

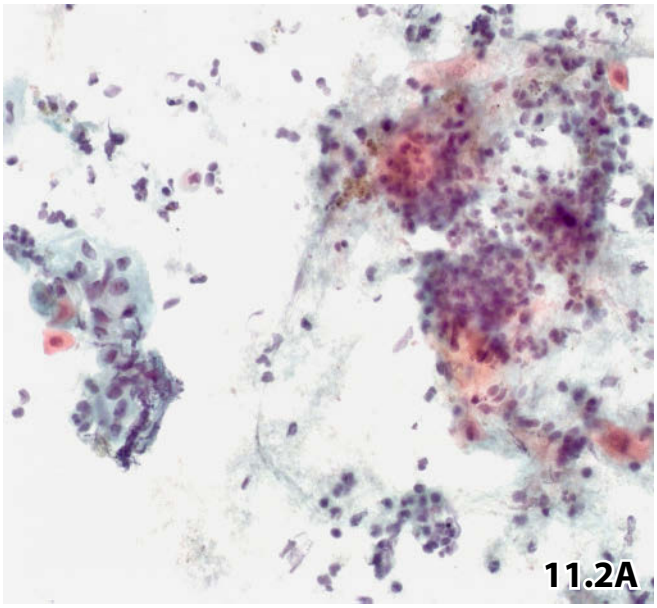

11.2A

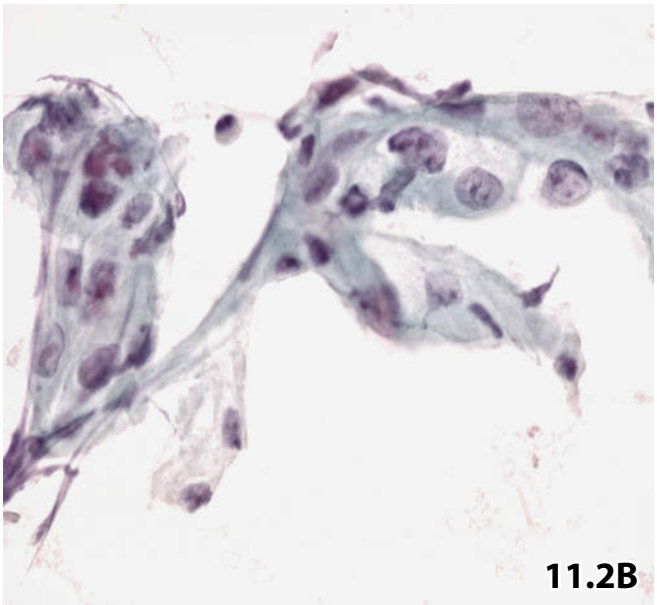

11.2B

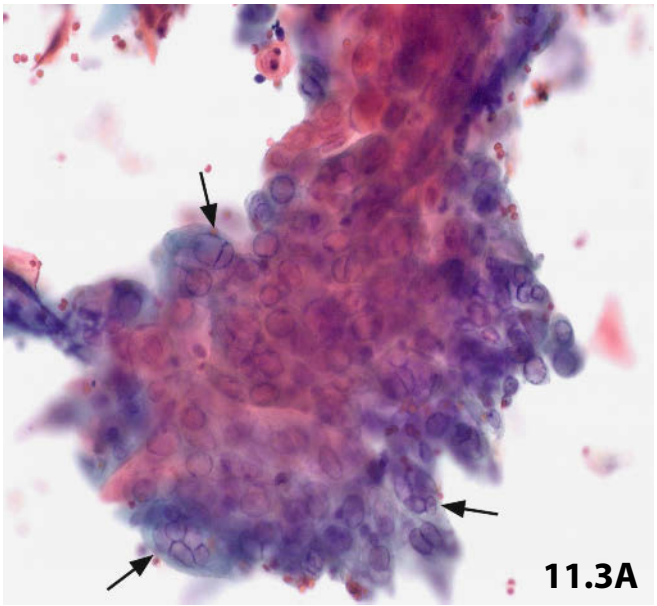

11.3A

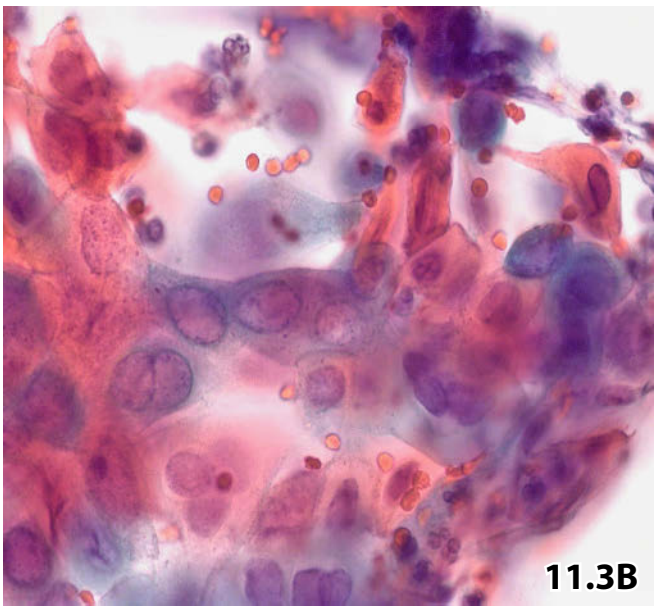

11.3B

**Figs. 11.4 and 11.5 Reactive/reparative changes on squamous epithelial cells.**
Two additional examples are displayed in Figs. 11.2B and 11.3B.

**Fig. 11.4** (case #1) Squamous cells showing mild nuclear atypia are arranged in pearl-like formation (esophageal brushing, direct smear, Pap stain, high magnification).
*Cytologic diagnosis:* Herpes virus esophagitis (typical cell changes are not present in this field) associated with reactive atypia of squamous cells.

**Fig. 11.5** (case #2) Esophageal brushing in a young woman suffering from esophageal burn. Large tightly cohesive clusters composed of nonkeratinizing squamous cells occur in direct smears. Variation in cellular size and shape, nuclear irregularities, distinct nucleoli, and absence of inflammatory background present diagnostic dilemmas (Pap stain, lower magnification).
*Cytologic diagnostic consideration:* Differential diagnosis included severe regenerative atypia of squamous cells, squamous cell dysplasia, and squamous cell carcinoma. ICM DNA could not be applied for technical reasons.
*Final diagnosis* (clinical follow-up and histiologic examinations): Nonspecific esophagitis.

**Fig. 11.6A, B Well-differentiated keratinizing squamous cell carcinoma.**
Endoscopy revealed a tumorous stenosis of the esophagus in a 74-year-old man. Cell material was sampled by brushing and processed using the Cytospin technique (Pap stain). **A** High magnification shows clusters of polymorphous, markedly keratinized anucleated squamous cells. Occasional nuclei are atypical and deeply stained (lower right). **B** Discohesive aggregates of undifferentiated carcinoma cells (high magnification).
*Cytologic diagnosis:* Squamous cell carcinoma exhibiting strong superficial cornification (Bioptic procedures for histology were unsuccessful).
*Clinical follow up:* Squamous cell carcinoma of the esophagus.

**Fig. 11.7 Poorly differentiated adenocarcinoma.**
A 56-year-old woman presented with a carcinoma of the esophagus. Cytospin specimens from mid-esophageal brushings exhibited cells of an undifferentiated malignant neoplasm (Pap stain, higher magnification).
*Tentative cytological diagnosis:* Undifferentiated large cell carcinoma. Immunocytochemical positivity for CK5/6 (not shown) suggests poorly differentiated squamous cell carcinoma.
*Tissue diagnosis* (synchronous endoscopic esophageal biopsy): Poorly differentiated adenocarcinoma associated with glandular formations and signet ring-like mucin-producing cells.
*Comment:* The pinkish foamy cytoplasm (top) and large pinkish vacuoles (arrows) have falsely been taken for signs of degeneration instead of mucus.

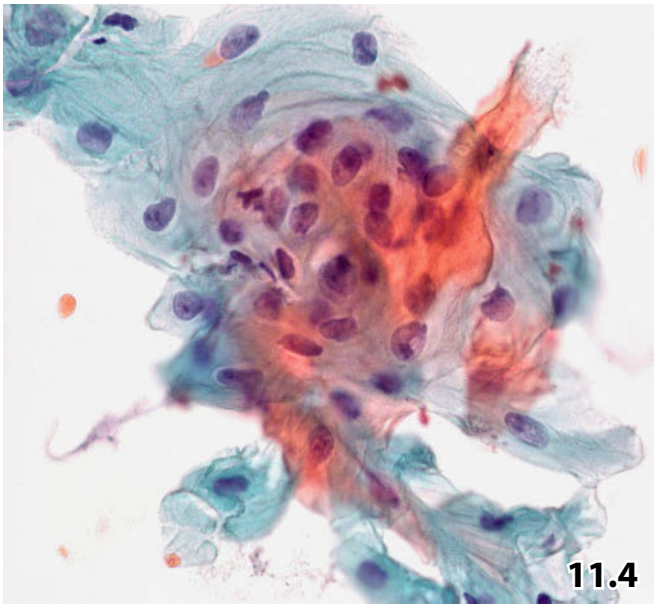
11.4

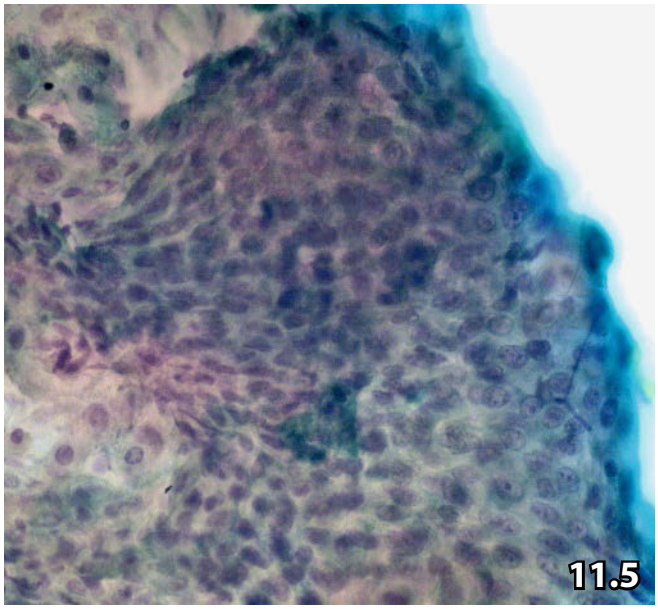
11.5

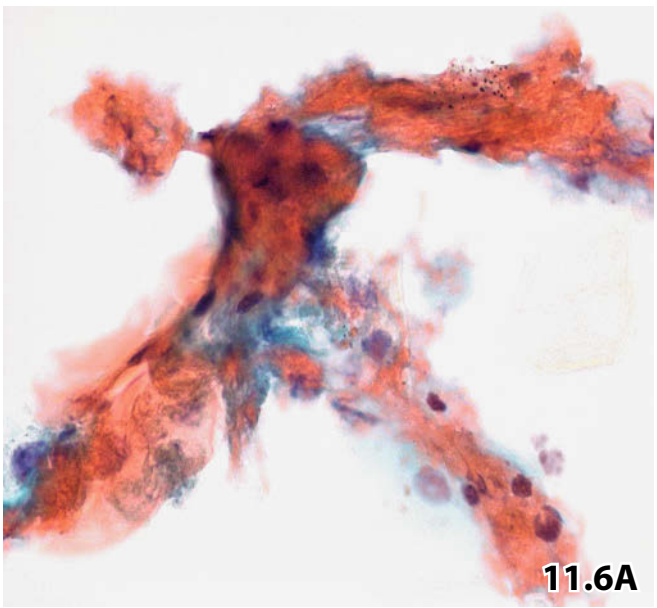
11.6A

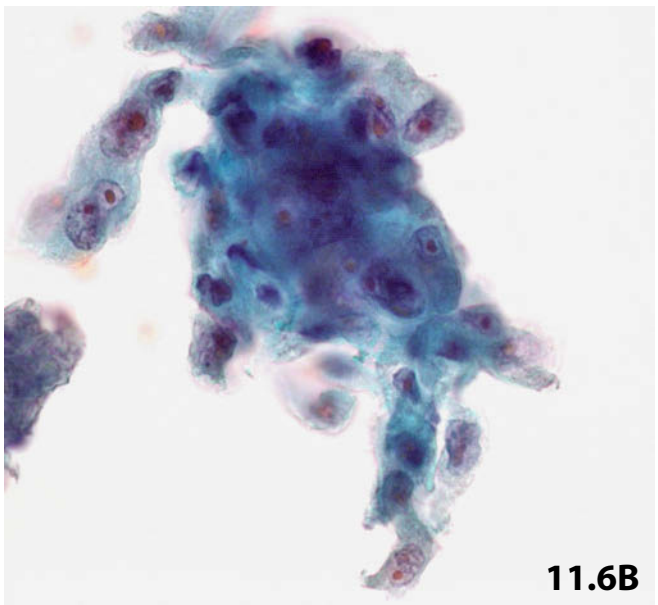
11.6B

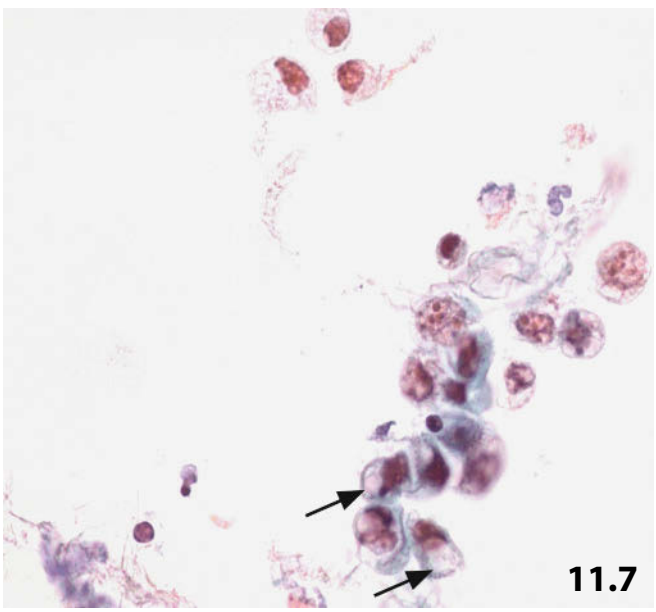
11.7

**Fig. 11.8 Benign Barrett epithelium.**
Brush cytology from a Barrett lesion. Removed cell sample was processed by the liquid-based ThinPrep method. A large sheet is composed of uniform glandular cells revealing classic features of metaplastic intestinal epithelium: regular cell arrangement, palisading of the superficial mucinous columnar cells, small uniform nuclei (Pap stain, low magnification). Squamous cells originate from the inner lining of the upper esophagus.

**Figs. 11.9–11.13 Reactive/regenerative Barrett epithelium.**
Three patients suffering from long-lasting Barrett esophagus. Endoscopic biopsy and/or cytologic brushings were used for the controls at regular intervals. Cell material was processed using liquid-based methods (ThinPrep or Cytospin), the slides were Pap-stained. Potential diagnostic dilemmas and diagnostic impact of static DNA cytometry are presented.

**Fig. 11.9** (case #1) A sheet is composed of irregularly arranged cuboidal to columnar cells including loss of nuclear polarization, nuclear overlapping, mild nuclear irregularities, pale chromatin, and occasional pronounced nucleoli (ThinPrep, high magnification). Note neutrophils scattered between epithelial cells (arrows) indicating reactive cell changes in Barrett mucosa.
*Follow-up:* 8 years of follow-up by cytology and histology revealed no malignant degeneration.

**Fig. 11.10** (case #2) In contrast to case #1, the compact cell clusters reveal sharp delineation, and the chromatin is comparatively coarser (ThinPrep, high magnification). It is difficult to distinguish between reactive cell alterations and mild dysplasia. Note a few interspersed neutrophils.

**Fig. 11.11** (case #2) Image cytometric DNA analysis proved helpful to assess a benign diagnosis. DNA measurement provided a diploid DNA histogram (Pap-prestained liquid-based specimen restained with the Feulgen method, Ahrens Cytometrie-System).
*Cytologic/ cytometric diagnosis:* Reactive cell changes of Barrett mucosa. No biopsies were taken for histologic examination.
*Comments:* Low-grade Barrett-related dysplasia is not completely excluded. However, the unambiguous diploid DNA distribution pattern and the scattered neutrophilic granulocytes suggest a reactive lesion.

**Fig. 11.12** case #3) Cytospin specimens containing numerous ball-like clusters composed of rounded atypical glandular cells. Distinct nuclear polymorphism (cleaves and wrinkles) is in contrast to the clear nucleoplasm and loose chromatin texture (high magnification).

**Fig. 11.13** (case #3) Image cytometry showed an intermediate DNA profile (DNA stemline [SL] in the hyperdiploid area, but no distinct aneuploid SL) that was undetermined as for malignancy (Pap-prestained liquid-based specimen restained with Feulgen method, Ahrens Cytometrie-System).
*Tentative cytologic diagnosis:* Severe regenerative Barrett mucosa; a dysplastic lesion is not excluded. Further investigations by histology are indispensable.
*Tissue diagnosis* (a single endoscopic biopsy was taken): No dysplastic Barrett epithelium detectable. The patient was lost to further follow-up.

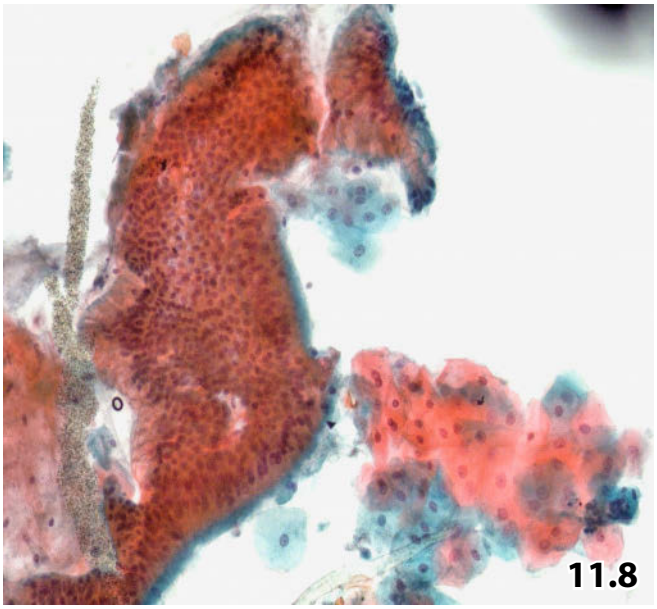
11.8

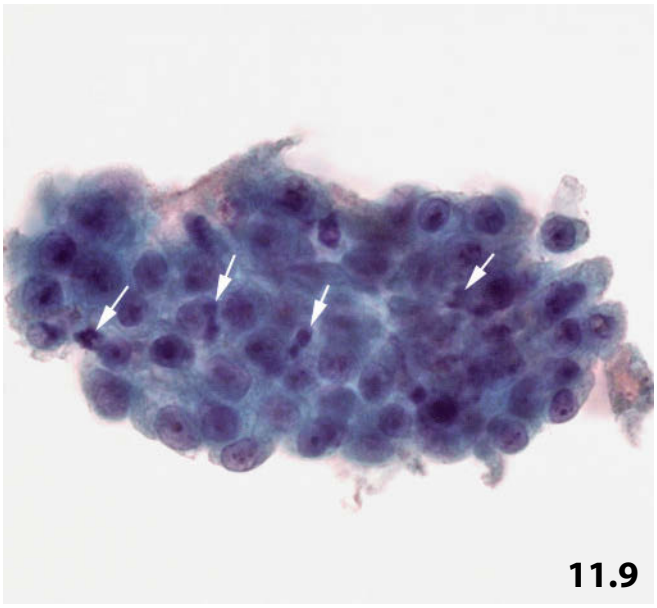
11.9


11.10

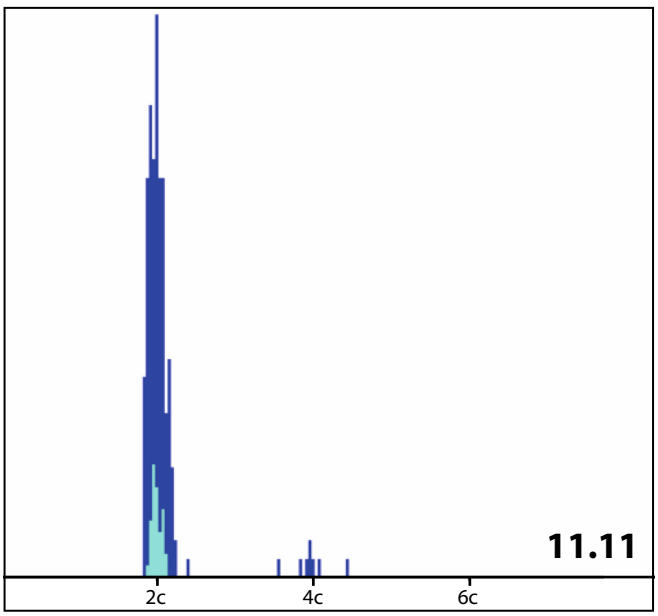

11.11

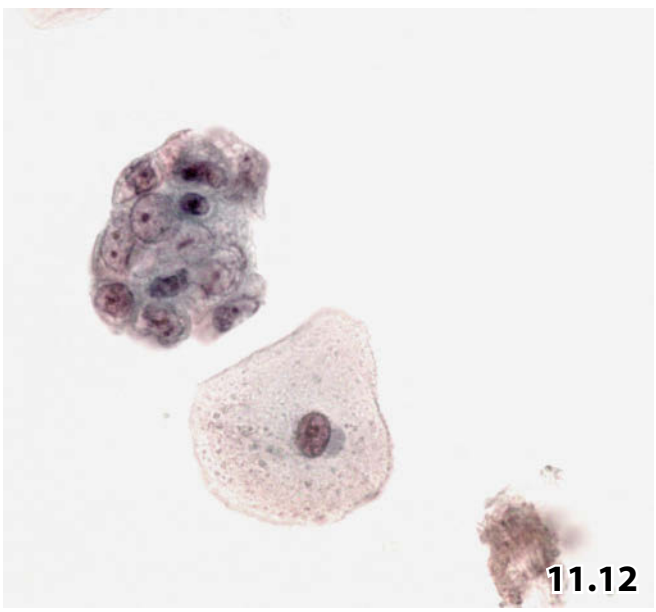
11.12

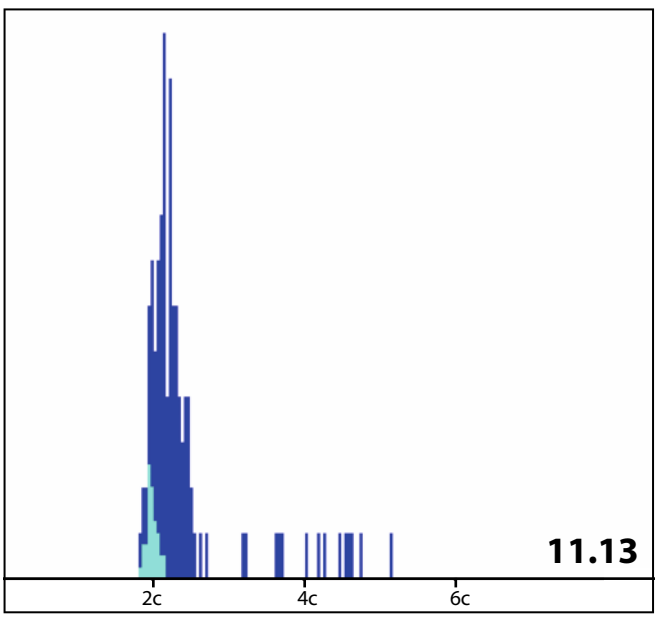

11.13

**Figs. 11.14–11.22: Barrett esophagus: dysplasia versus carcinoma. ICM DNA and FISH analysis as a helpful diagnostic adjunct.**

Brush cytology from five patients suffering from a Barrett lesion. The following cases demonstrate the diagnostic challenge, possible value of accessory analyses, and follow-up results. All cytologic specimens were Pap-stained.

**Fig. 11.14** (case #1) A 77-year-old man presenting with a positive history of high-grade dysplasia of the Barrett mucosa. Small dissociating clusters of pleomorphic cells, frequently degenerating. Densely packed dark chromatin. Absence of distinct necrosis (Cytospin, high magnification).
*Cytologic diagnosis:* High-grade Barrett-related dysplasia, possibly invasive adenocarcinoma.
*Comment:* Highly pleomorphic epithelial cells and absence of necrosis favor high-grade dysplasia versus invasive adenocarcinoma. In addition, ICM DNA provided an aneuploid histogram (not shown).
*Histologic diagnosis* (endoscopic biopsy): High-grade dysplasia of Barrett mucosa.

**Fig. 11.15** (case #2) A 57-year-old man with a positive history of high-grade dysplasia of Barrett mucosa and current local fungal infection. High magnification shows an irregular sheet of atypical glandular cells. Loss of nuclear polarity, nuclear variability in size and shape, densely packed fine granular chromatin, and polymorphous nucleoli indicate high-grade dysplasia, possibly invasive carcinoma (ThinPrep specimen). Neutrophils are scattered between dysplastic cells (arrow).

**Fig. 11.16** (case #2) Intermediate DNA histogram type is not really helpful in establishing a conclusive diagnosis (Pap-prestained liquid-based specimen restained with Feulgen method, AutoCyto).
*Tentative cytologic diagnosis:* Overall cell pattern highly suggestive of a severe Barrett-related dysplastic lesion.
*Discussion:* The additional inflammatory component prevents a definite grading. Absence of necrosis in ThinPrep specimens does not necessarily favor dysplasia versus invasive carcinoma, since ThinPrep processing usually completely eliminates background necrosis.
*Histologic diagnosis* (endoscopic biopsy): Dysplasia of Barrett mucosa, grades 2 and 3.

**Fig. 11.17** (case #3) A 71-year-old man suffering from a long-lasting Barrett lesion. Within the last 4 years the patient had several cytologic diagnoses of Barrett-related dysplasia, including aneuploid DNA profiles. Morphology and ICM DNA results are shown from the most recent brush sample: High magnification exhibits polymorphic cuboid to columnar cells with nuclei showing extreme variability in size and shape, including large nucleoli. A few neutrophils are scattered both between epithelial cells and in the background (Cytospin).

**Fig. 11.18** (case #3) Aneuploid DNA distribution pattern (Pap-prestained liquid-based specimen was stained with the Feulgen method, Ahrens Cytometrie-System).

**Fig. 11.19** (case #3) Clinicians additionally required evaluation of the p53 status. p53 LOH (loss of heterozygosity) was evaluated by FISH analysis using a green probe for chromosome 17 (CEP17) and a locus-specific red probe for 17p13.1 (p53 gene). The chromosomes appear as a twin signal in each nucleus while evidence of LOH in two nuclei (arrows) appears as a single red dot (present in 15% of all nuclei).
*Cytologic diagnosis:* Barrett-related dysplasia of high-grade type with increased malignant potential. Reactive cell changes can be excluded.
*Comment:* Patient's history, cytologic appearance, pathologic result of DNA analysis, and p53 LOH call at least for a diagnosis of severe dysplasia.
*Histologic diagnoses:* Numerous biopsies provided benign Barrett mucosa except for a few fragments lined with epithelium exhibiting "low-grade dysplasia" or "changes indefinite for dysplasia." Follow-up continues.

Note that the pronounced nuclear cleaving may partially be caused by the liquid-based preparation

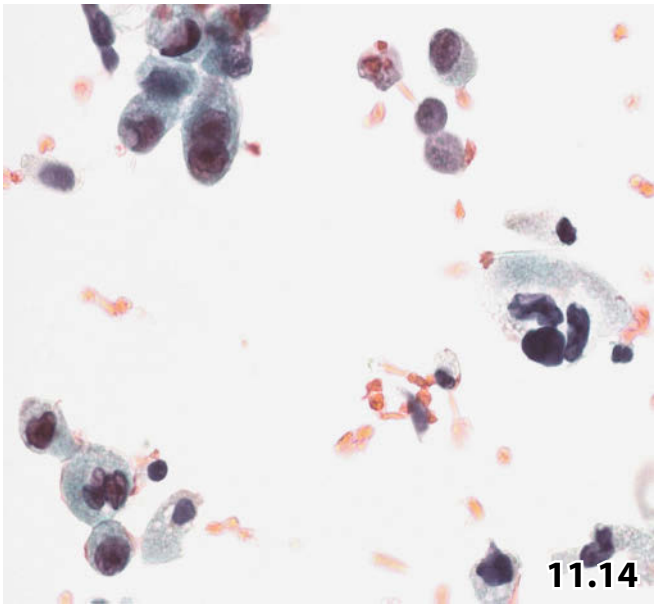
11.14

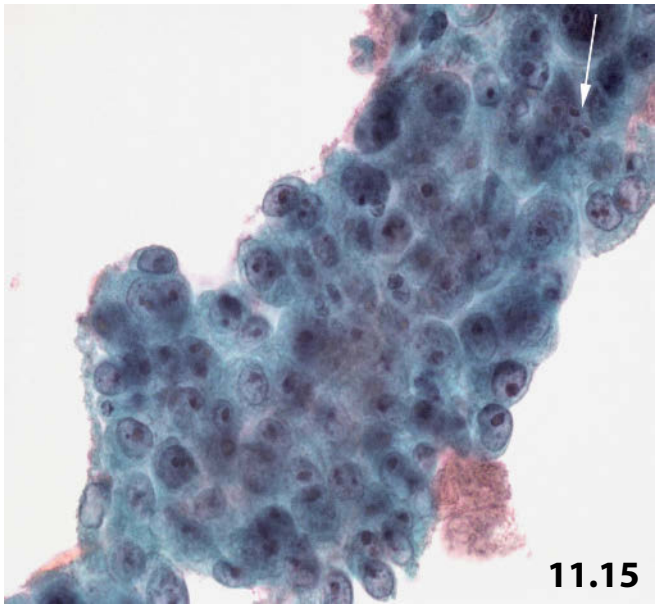
11.15

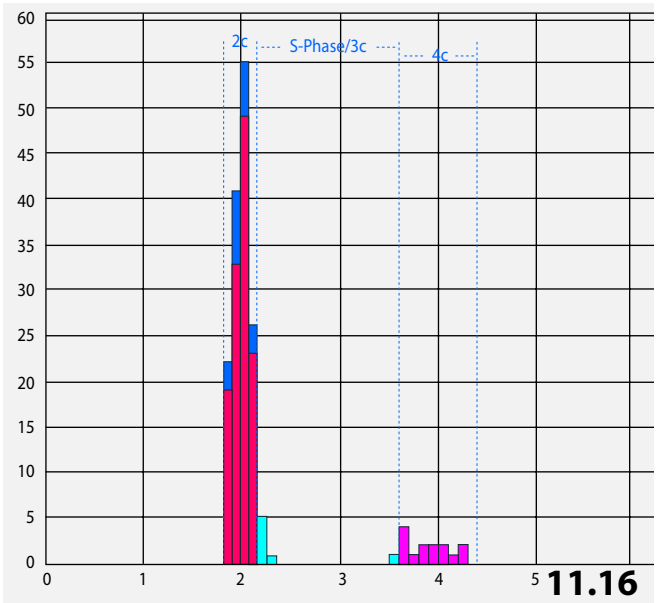

11.16

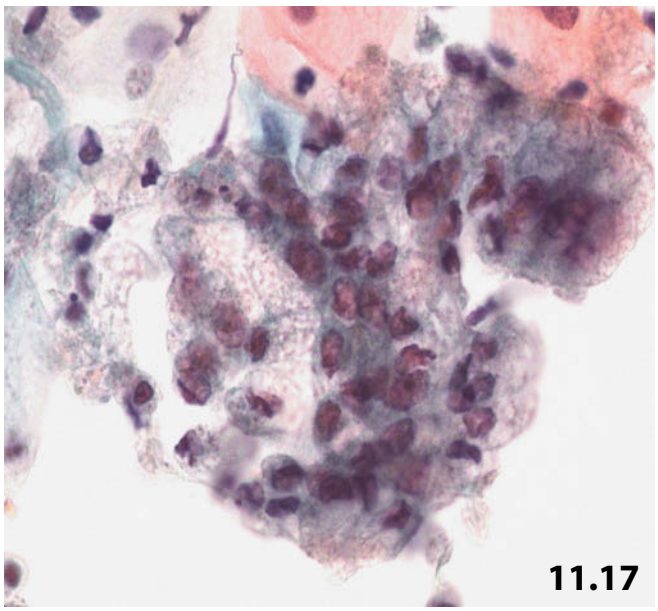
11.17

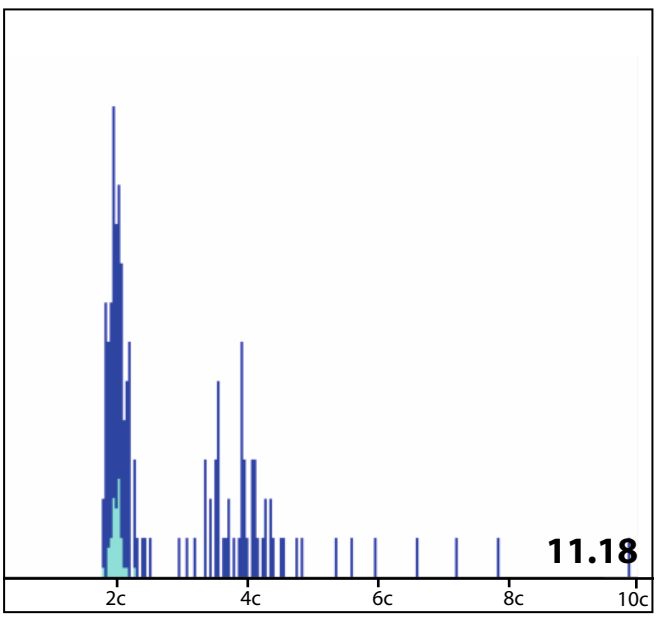

11.18

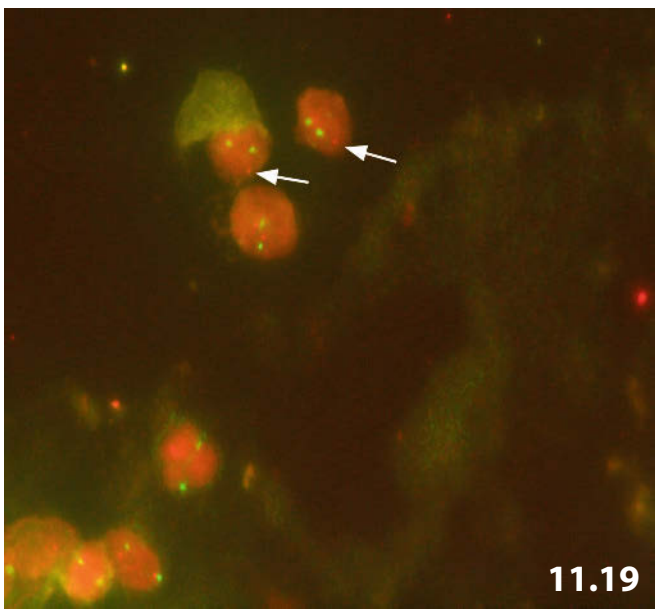
11.19

**Fig. 11.20** (case #4) A 64-year-old man with long-standing Barrett esophagus. Increasing severity of the grade of dysplasia has been assessed by both multiple brushings and biopsies extending over several years. Lower magnification shows pleomorphic malignant cells (bottom) scattered in a background of detritus and inflammation (conventional sediment smear after rinsing the brush and conventional centrifugation).
*Cytologic diagnosis:* Poorly differentiated adenocarcinoma.
*Tissue diagnosis* (esophageal resection): Large areas exhibiting severe dysplastic Barrett epithelium associated with multifocal microinvasion.

**Fig. 11.21** (case #5) A 54-year-old man presented with a long-lasting history of Barrett esophagus. Cytologic and histologic investigation during follow-up reported benign metaplastic epithelium. However, recent brush cytology showed atypical cells: High magnification shows an irregular and dissociating cluster composed of highly atypical epithelial cells. Note high N/C ratio, variability of nuclear size and shape, and multiple nucleoli.

**Fig. 11.22** (case #5) Clear evidence of DNA aneuploidy (Pap-prestained direct smear was stained with Feulgen, Zeiss-Contron/Cires).
*Cytologic diagnosis:* Severe Barrett-related dysplasia or poorly differentiated adenocarcinoma.
*Histologic diagnosis* (endoscopic biopsy 19 months after the initial abnormal cytologic/cytometric findings!): Poorly differentiated adenocarcinoma.

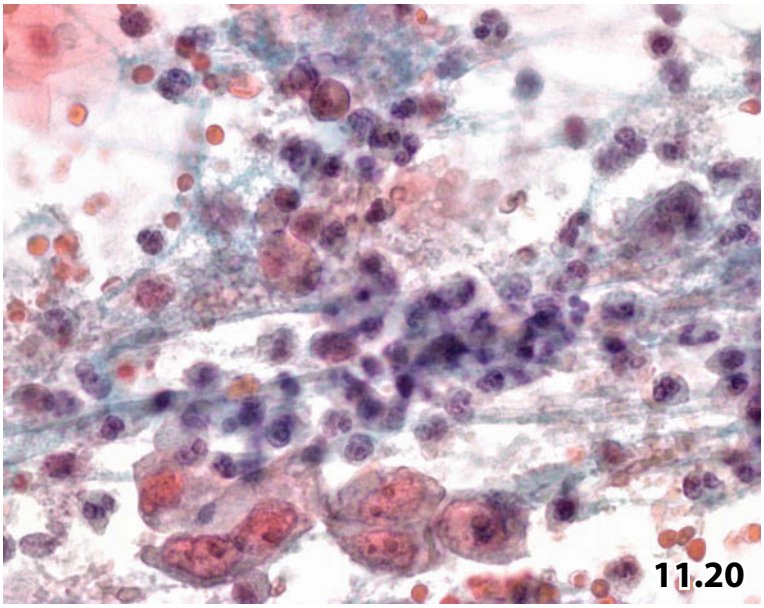

11.20

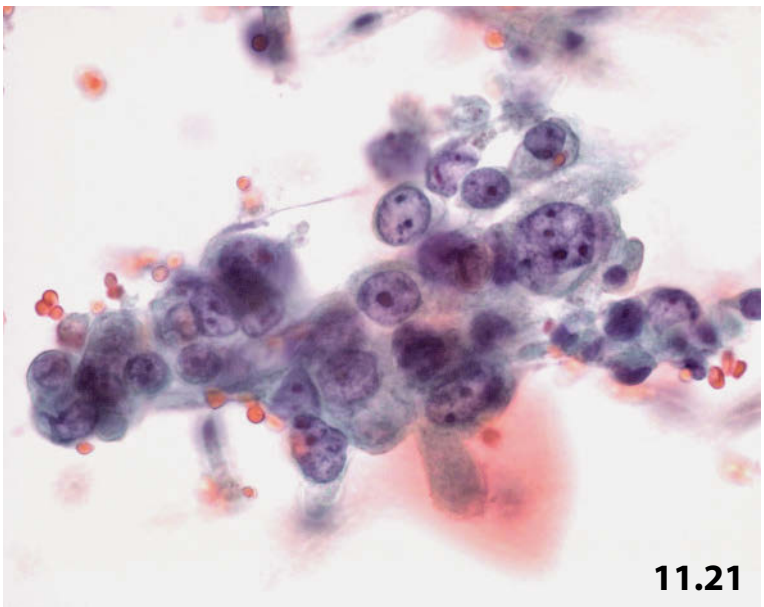

11.21

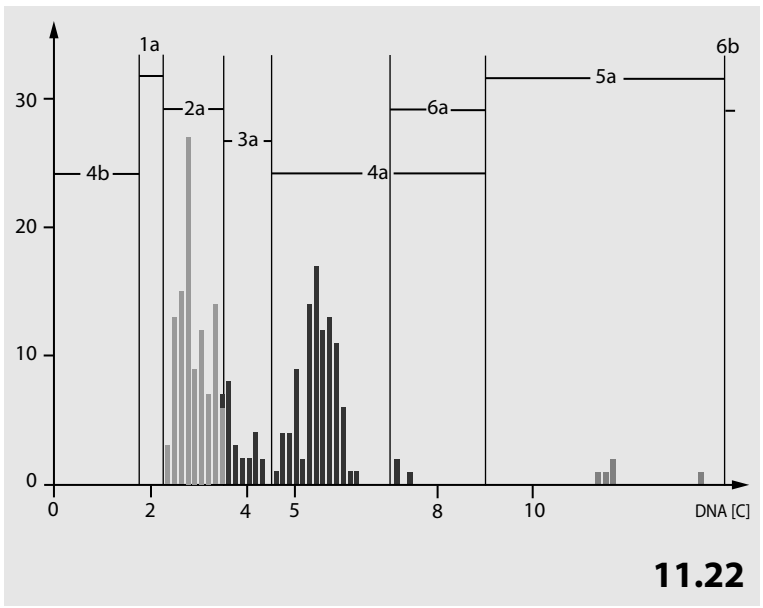


11.22

**Fig. 11.23 Benign gastric mucosa.**
High magnification shows crowded activated epithelial cells originating from gastric cardia mucosa. Note smooth nuclear contours, fine reticular chromatin, and distinct small nucleoli (gastric brushing, ThinPrep specimen, Pap stain).

**Fig. 11.24 Benign rectal mucosa and feces.**
High magnification shows a benign epithelial fragment of the rectal mucosa. Note characteristics of these cells: columnar-shaped cytoplasm, glandular formations, pink staining intracytoplasmic mucus, and sharply defined nuclear margins. Feces (bottom) containing anucleated squames are seen adjacent to epithelium (transrectal FNAB, ThinPrep specimen, Pap stain).

**Fig. 11.25 Gastric carcinoma, diffuse variant.**
Image-guided transcutaneous FNAB of a large intraabdominal tumor mass in a 40-year-old woman shows malignant cell clusters exhibiting pronounced nuclear irregularities, loose and clear chromatin, foamy vacuolated or mucinous cytoplasm, marked variation in N/C ratio, and goblet cell-like and signet ring-like tumor cells (direct smear, Pap stain, high magnification).
*Cytologic diagnosis:* Poorly differentiated adenocarcinoma associated with signet ring-like malignant cells. Cytologic features favor primary gastric carcinoma.
*Tissue diagnosis* (gastroscopic biopsy): Poorly differentiated mucinous gastric adenocarcinoma.



**Fig. 11.26 Adenocarcinoma of colon.**
Transcutaneous FNAB of a large tumor located in the upper right abdominal area of an elderly man. Contrary to gastric carcinoma, cell clusters from colonic adenocarcinoma show columnar-shaped tumor cells, distinct cellular palisading (arrows), and usually coarse granular and clumped chromatin (direct smear, Pap stain, higher magnification). Signet ring-like cells are infrequently encountered unlike cytoplasmic mucin (upper left).

**Fig. 11.27 Food contaminants.**
Image-guided transcutaneous FNAB of a retroperitoneal tumor mass containing large amounts of food contaminants from the intestinal tract: plant cells, vegetable cell clusters, and meat fibers (right) (direct smear, Pap stain, lower magnification). In particular cases, these elements may mimic human neoplastic cells or parasites.

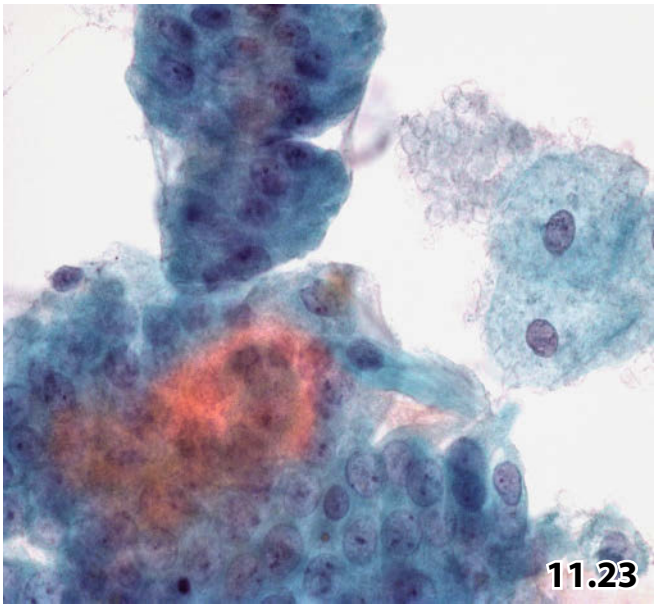
11.23

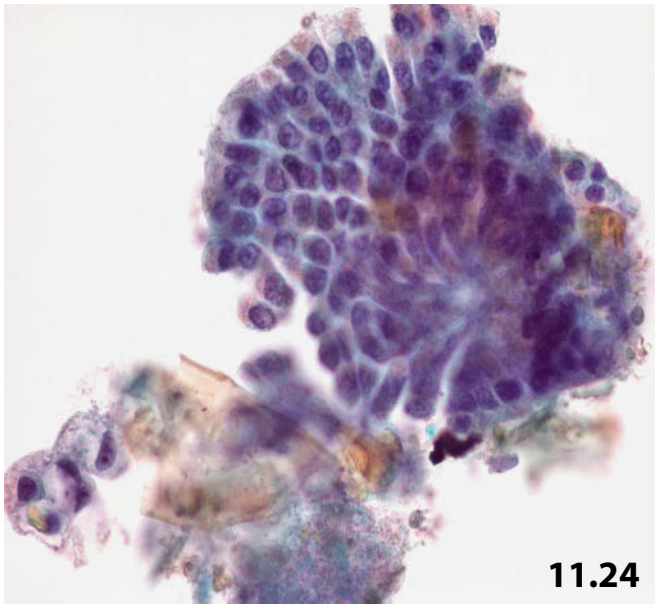
11.24

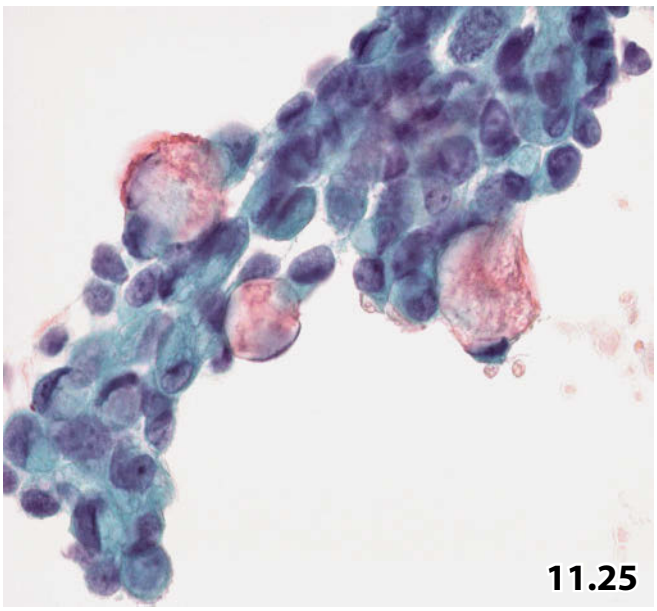
11.25

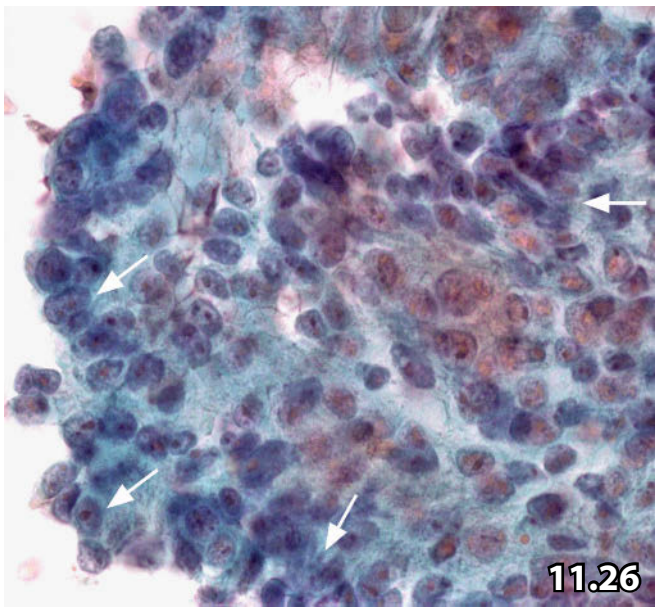
11.26

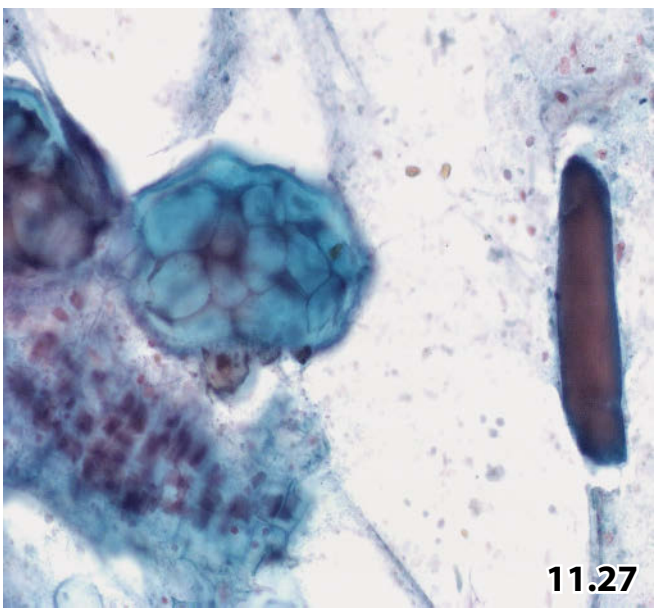
11.27

**Figs. 11.28–11.32 Gastrointestinal stromal tumor (GIST).**
Five selected examples of GIST emphasizing morphologic variants of this tumor entity and immunocytochemical particularities.

**Fig. 11.28** (case #1) GIST, CD117.
A relatively specific and reliable immunomarker for GIST is the c-kit proto-oncogene product CD117. Immunocytochemical positivity is demonstrated using a Pap-prestained conventional smear (FNAB from a tumor of the small intestine).

**Fig. 11.29** (case #2) GIST, CD34.
Strong positive immunoreaction can be demonstrated for CD34 on cells of a GIST of the epithelioid variant (FNAB, Pap-prestained direct smear).

**Fig. 11.30A, B** (case #3) GIST, common spindle cell pattern.
**A** Low magnification shows solitary and densely packed spindle-shaped cells that are focally palisading (lower right). Myxoid background is sparsely present in this field (arrows) (FNAB of an abdominal tumor, direct smear, Pap stain). **B** Detail of the same tumor focuses on morphologic properties of the cytoplasm and nuclei; the latter exhibit fusiform or round shape.

**Fig. 11.31** (case #4) GIST, epithelioid variant.
Higher magnification exhibits spindle cells but also tightly clustered epithelioid tumor cells at the left side of the picture (FNAB of a gastric GIST, direct smear, Pap stain).



**Fig. 11.32** (case #5) GIST, polymorphic pattern.
The nuclei exhibit more irregularities, coarser chromatin, and more pronounced nucleoli in comparison to common tumor variants. The cytoplasm is condensed and well defined (image-guided FNAB of a large abdominal mass, direct smear, high magnification). Overall cell pattern may resemble that of nonkeratinizing squamous spindle cell carcinoma.
*Postmortem diagnosis:* Metastatic GIST. Site of primary tumor: small bowel.

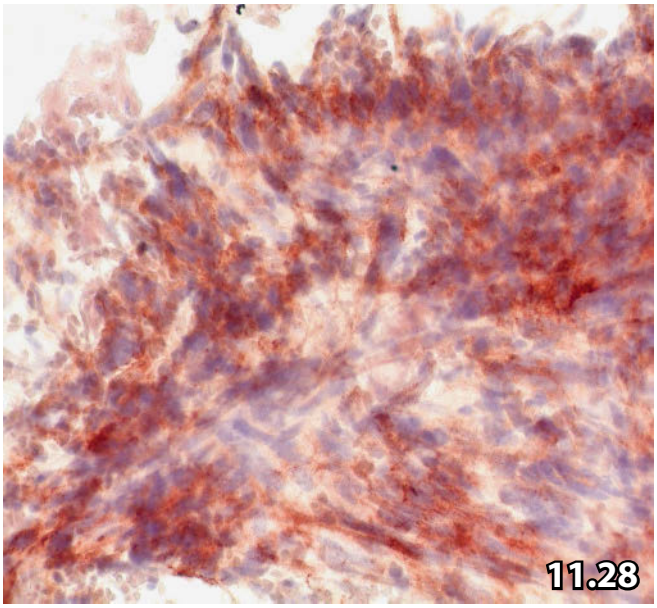
11.28

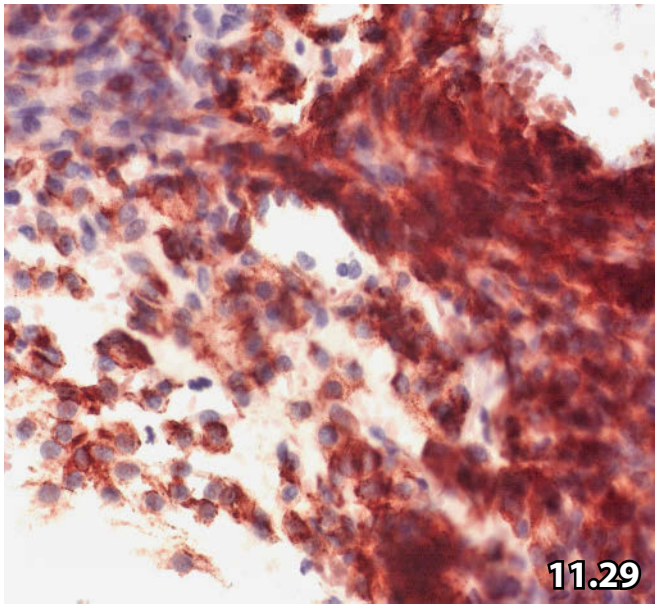
11.29

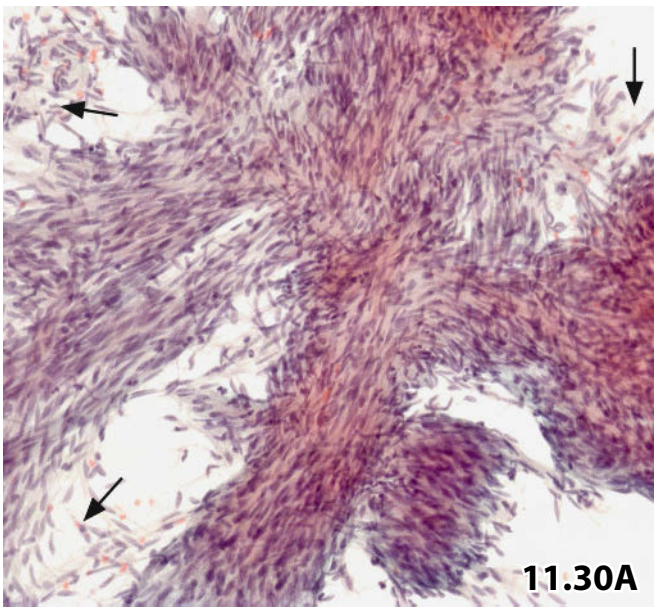
11.30A

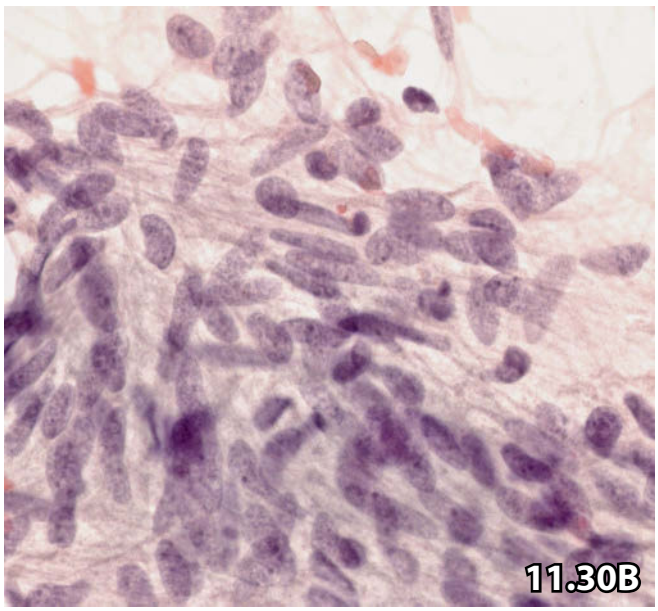
11.30B

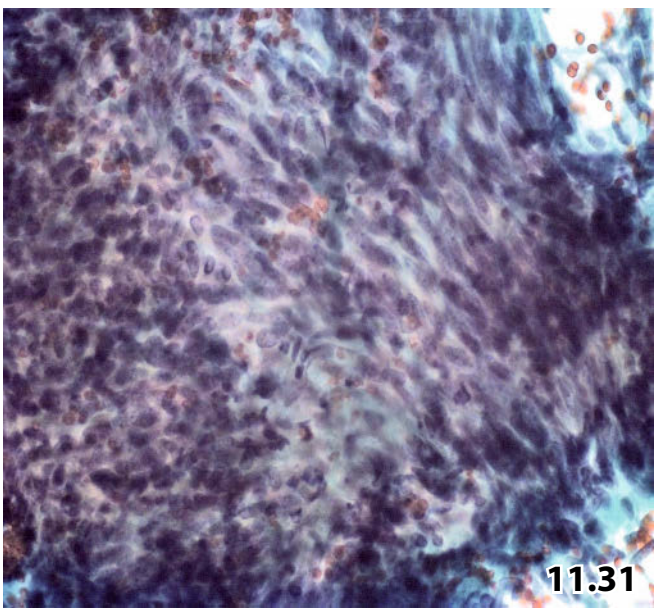
11.31

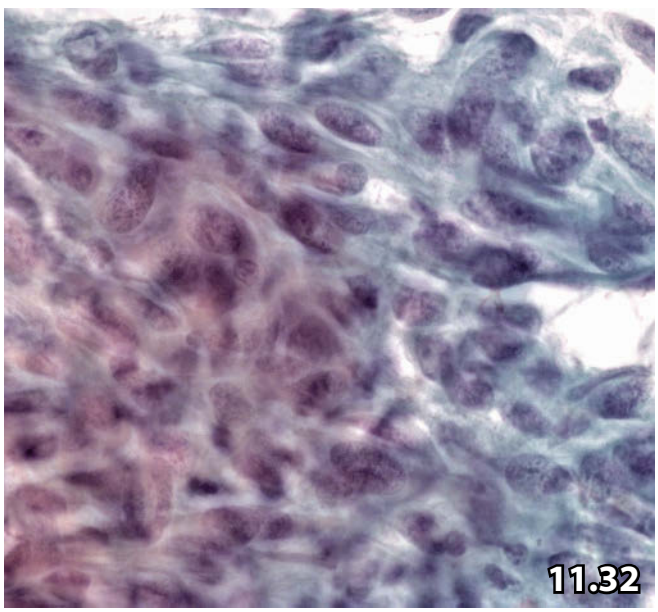
11.32

**Figs. 11.33A, B Presacral chordoma.**
Imaging studies detected a large tumor in the presacral area of a 42-year-old woman. Image-guided transcutaneous FNAB was performed. Direct smears were prepared and Pap-stained. **A** Lower magnification shows chondroid matrix and groups of tumor cells with more chondroid aspect (arrow) and groups of typical blistered cells **B** Detailed morphology of chordoma cells is demonstrated at high magnification. Multinucleated tumor cells occur as well (difficult to visualize). Tumor cells expressed positivity for pancytokeratin (Lu-5), vimentin, and S100 (immunostains are not shown).
*Cytologic and subsequent histologic (surgical excision) diagnosis:* Chordoma.

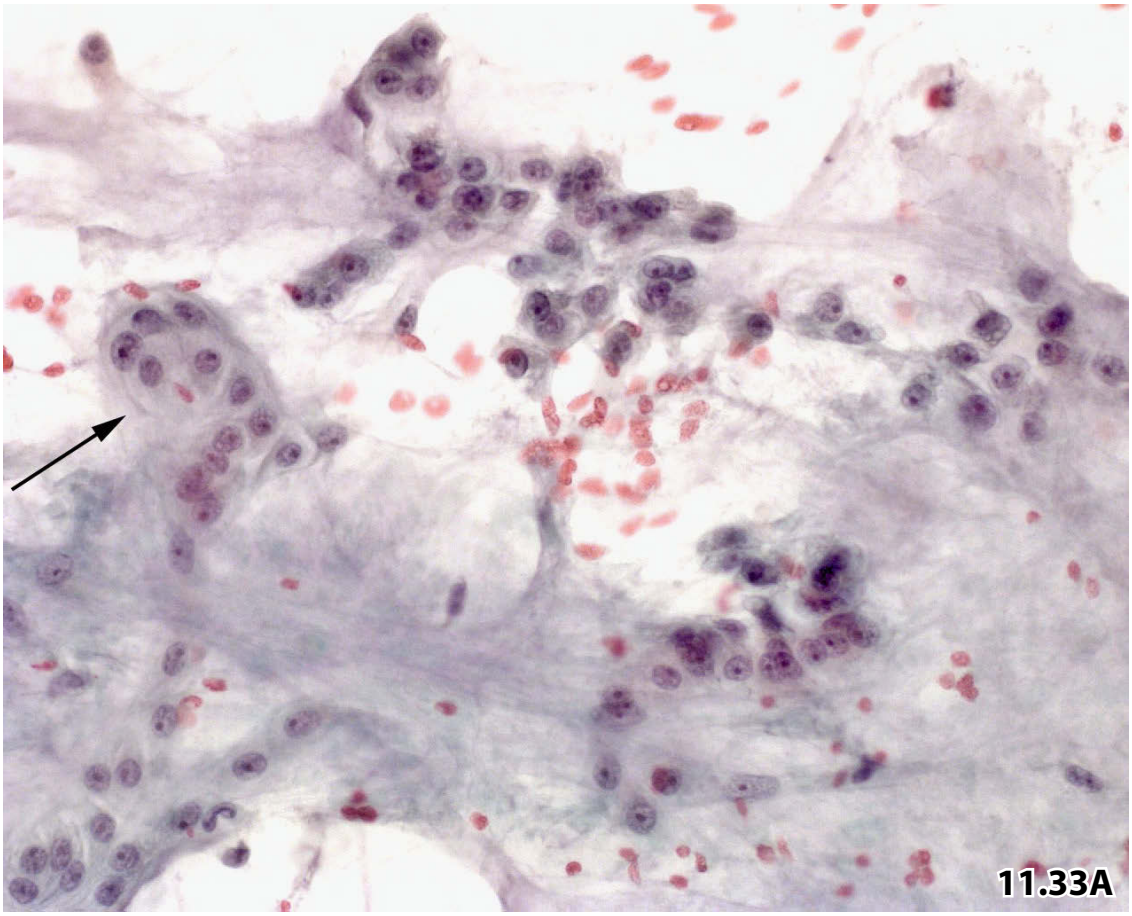

11.33A

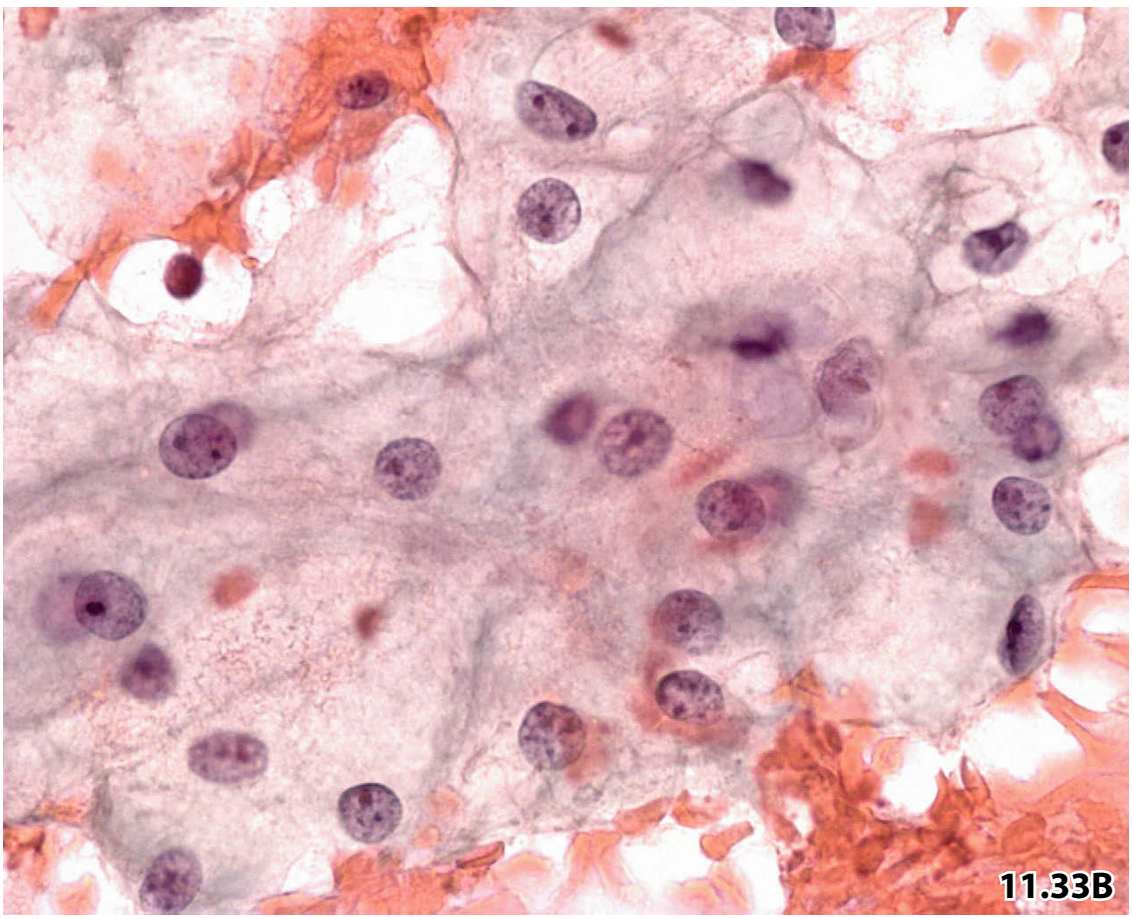

11.33B

# 12 Kidney, Adrenal Glands, Retroperitoneum



Spieler/Rössle, *Nongynecologic Cytopathology. A Practical Guide*. *Essentials of Diagnostic Pathology*,
DOI 10.1007/978-3-642-24719-4_12, 

## Synopsis and Algorithms

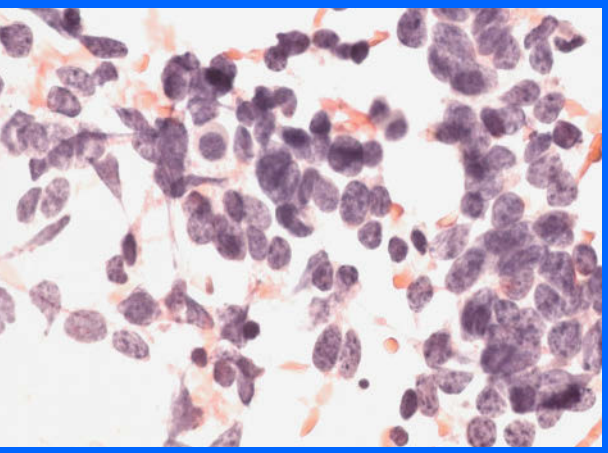

# Section 12.1
# Kidney

## 12.1.1 Introduction

- Urine cytology is not a useful method for detecting tumoral and nontumoral conditions located in the renal parenchyma. Most inflammatory processes and neoplasms do not shed enough cells, if any, into the urinary collecting system for a reliable diagnosis. In addition, cells of renal origin tend to become increasingly degenerated during the long transport period through the excretory duct system.
- Fine-needle sampling (FNAB) of renal lesions has proved to be the most effective method for cytologic diagnostics. The method was introduced into clinical practice more than 50 years ago [85], and its increasing use parallels the technologic advances in image techniques.
- Imaging techniques have recently achieved a high degree of diagnostic accuracy and have likewise proved to be useful in tumor staging. Due to vast extension and improvements in abdominal imaging (sonography, computed tomography, magnetic resonance imaging), an increasing number of renal lesions are incidentally identified. Ultrasound-, and computed tomography-guided FNAB are at present the common approach for obtaining cytologic samples.
- Renal aspiration biopsy cytology has to be accurate and safe:
  Diagnostic accuracy of FNAB has been reported to reach a sensitivity of more than 90% and a specificity of between 90% and 100% [69, 80, 121]. Renal FNAB has a high negative predictive value; but limitations and pitfalls in subclassification of renal cell carcinoma frequently occur, and distinguishing between renal cell carcinoma and benign, foremost cystic lesions can be difficult [67, 77, 102, 114, 115, 121]. Negative FNAB results do not exclude malignancy in sonographically and radiologically suspicious cases. A combined imaging and fine-needle aspiration procedure provides high accuracy in the diagnosis of malignancy; it is well established that the two methods complement each other [40, 121].
  Reported complications of FNAB of the kidney include, among others:
  – Transient hematuria.
  – Painful parenchymatous hemorrhage.
  – Perirenal abscess formation following cyst aspiration [68, 85].
  Cutaneous tumor cell seeding and cell implantation along the needle tract are extremely rare complications [58, 110, 111].
- FNAB has been used to monitor rejection of renal allografts by investigating the cellular components in the aspirated cell samples. Multiple former and more recent studies highlight the value of combined FNAB and immunolabeling compared to other methods [1, 14, 52, 76, 90].
- A general view concerning application of immunocytochemical tests to tumorous lesions of the kidney has recently been given by Hammerich and colleagues [50].

## 12.1.2 Indications for FNAB

A multitude of indications for renal FNAB is proposed in the literature [6, 56, 84, 100, 118] :

- Radiographically indeterminate lesions.
- Small renal lesion suggestive of carcinoma, especially in elderly and weak patients.
- Renal mass and functionally compromised opposite kidney.
- Assessing the diagnosis of renal cell carcinoma avoiding nephrectomy in patients with a renal mass and disseminated metastases.
- Tumorous renal disorder in patients with metastatic disease of unknown primary origin.
- Previous contralateral nephrectomy for a renal cell neoplasm.
- Renal transplant mass.
- Suspected malignant lymphoma confined to the kidney.
- Decrease in unnecessary surgery and enhanced selection of renal tumors for minimally invasive ablative therapies (partial rather than radical nephrectomy).
- Enhanced selection of renal tumors for active surveillance.
- In the future: therapy strategies on the base of molecular tumor characteristics.

## 12.1.3 Processing of the Fine-Needle Aspirates



- *Attendance of cytologic staff* at image-guided FNABs is desirable, particularly for immediate assessment of specimen adequacy.
- *Aspirated cell material* is smeared from the needle and the syringe conus onto slides, which can either be wet-fixed or air-dried. Fixation should immediately occur in order to prevent cell degeneration. We prefer Delauney solution as fixative, 95% ethyl alcohol pure or mixed with ether is also frequently used.
  Residual contents of the needle and syringe are rinsed into a tissue culture solution if thin-layer preparation, cell block preparation, or flow cytometric analyses are required.
- *Liquid-based cytology* is superior to conventional smears with regard to clear background, monolayer cell preparation, and cell preservation. Thin-layer preparations are processed by cytocentrifugation, by means of ThinPrep, or other processors. The thin-layer method should be recommended to clinicians performing FNABs who are not familiar with proper preparation and fixation technique, and when cytologic staff attendance is not available [112]. With thin-layer methods, an optimal specimen can be achieved for special investigations, in particular for immunocytochemistry, fluorescence in situ hybridization, or static DNA cytometry. In addition, needle and syringe rinse may be used for immunolabeled flow cytometry.
  Regardless of the operator, CytoLyt (among other hemolyzing fixatives) has been shown to be indispensable as an initial transport medium for FNABs providing sanguineous aspirates. The medium is best used in combination with the ThinPrep modality for blood-rich aspirates. CytoLyt lyses erythrocytes providing well-preserved cellular material and clear background.
- *Cell blocks* may be prepared from renal aspirates that yield large amounts of sediment or contain tissue fragments and clots.
- *Cyst fluids* are collected into clean vials and transferred to the cytology laboratory as soon as possible. After conventional centrifugation, direct smears are performed from the cell button. The remaining cellular material should be retained and stored at 4°C, mixed with a certain amount of the supernatant. Cytocentrifuge preparation is recommended for small amounts of fluid containing only a few cells.
- *Staining:* Papanicolaou and hematoxylin-eosin are highly suitable staining methods, offering many advantages for comparative cell studies in histologic sections. However, in many institutions May-Grünwald-Giemsa, Diff-Quik, and other staining methods are preferred, applied to air-dried specimens.

## 12.1.4 Histology and Cytology of Normal Renal Parenchyma

### Histology

The functional unit of the kidney comprises two embryologically different units, a secretory portion called the nephron and an excretory duct system.

The *nephron* is composed of:

- The glomerulus, which includes endothelial and epithelial cells, and mesangium.
- The proximal convoluted tubule, which is lined with columnar cells exhibiting microvilli and numerous mitochondria. The latter generate an acidophilic and granular cytoplasm.
- The loop of Henle and the distal convoluted tubule, which is lined with small columnar and cuboidal cells with less conspicuous cytoplasm containing organelles to a lesser extent compared with epithelial cells of the proximal tubules.

*Secretory ducts*

- The cells of small collecting ducts are small and cuboidal, those of the larger ducts are tall and columnar.
- The nuclei are centrally positioned, the cytoplasm is clear and well defined, exhibiting a few organelles and peripheral microvilli.

### Cytology (Figs. 12.1 and 12.2)

In many cases, normal renal parenchyma components are sampled during FNAB of the kidney.

- *The glomeruli* are large, sharply outlined three-dimensional clusters composed of small epithelial and endothelial cells exhibiting a lobule-like appearance. Small blood vessels may be identified by the erythrocytes present (Fig. 12.1A and 12.1B).

- *Cells of proximal convoluted tubules* are medium-sized, appearing singly or in flat sheets with inconspicuous nucleoli. The abundant granular cytoplasm stains typically greenish-blue or eosinophilic with Papanicolaou stain and pinkish-blue with May-Grünwald-Giemsa stain. Microvilli or brush borders are barely identifiable in cytologic preparations (Fig. 12.1C).
- *The cells from the Henle loop and distal convoluted tubules* are small and appear isolated, in flat sheets, or as intact multilayered tubules (Fig. 12.2). They show centrally placed nuclei and much less granular cytoplasm than epithelial cells from the proximal tubules.
- *The cells of collecting ducts* are cuboid and sharply outlined, varying in size.

**Immunocytochemistry**

Distinguishing between epithelial cells of distal convoluted tubules and collecting tubules may be possible only by immunostaining: cells of the collecting ducts reveal strong positivity with antibodies against high-molecular-weight keratins, in contrast to epithelial cells of the proximal and distal tubules.

## 12.1.5 Inflammatory Disorders and Infection

### 12.1.5.1 Abscess of the Kidney

Intrarenal or perinephric abscesses may occur. Accurate localization is usually achieved by ultrasound. Part of the aspirated turbid fluid is directly smeared on multiple glass slides for cytomorphologic investigation and for special stains (Gram, Giemsa, PAS, Grocott) in order to identify bacteria and fungi. The remaining material should be referred to the microbiologic laboratory for cultures, PCR, and other tests.

**Microscopic Features**

- Abundant degenerating neutrophilic granulocytes and histiocytes including debris. Organisms may be identified by light microscopy using a routinely stained specimen.

### 12.1.5.2 Xanthogranulomatous Pyelonephritis

**General Comments**

Xanthogranulomatous pyelonephritis (XPN) is a rare inflammatory kidney disease associated with recurrent infections of the urinary tract and renal calculi. The disorder also occurs in childhood [124]. Only a few cytologic descriptions of XPN exist [122], because the lesion can reliably be recognized by clinical symptoms in combination with laboratory tests and radiological findings [15]; percutaneous biopsy may be indicated in selected cases in order to confirm the diagnosis.

**Microscopic Features**

- Abundant necrosis interspersed with neutrophils and xanthomatous cells presenting as foamy macrophages. Large numbers of multinucleated giant cell histiocytes and activated fibroblasts are seen as well.

**Differential Diagnosis**

- Malakoplakia with an abundance of foamy macrophages that contain scanty Michaelis-Gutmann bodies strongly mimic xanthogranulomatous pyelonephritis (Fig. 12.4).
- XPN, which is dominated by activated foamy macrophages showing a finely vacuolated cytoplasm and enlarged nuclei with irregular outlines and conspicuous nucleoli, can mimic clear cell renal cell adenocarcinoma [70, 77], especially in cases where dense grouping of the histiocytic cells is overt. However, in renal clear cell carcinoma, the cytoplasm is rather clear and not finely vacuolated. Furthermore, an extensive inflammatory component is unusual in primary renal cell carcinoma.
- Activated atypical fibroblasts may mimic features of malignant spindle cell tumors, anaplastic carcinoma, or sarcoma.
- The inflammation, the necrotic background, and the multinucleated giant cells could raise suspicions of tuberculosis. Ziehl-Neelsen stain and specific microbiologic tests resolve the differential diagnostic problem.

**Immunocytochemistry**

- An appropriate immunocytochemical panel can easily differentiate between histiocytes and epithelial cells: CD68 decorates cells of histiocytic origin and pancytokeratins (e.g., MNF116) indicate carcinoma cells.
- Renal cell carcinoma marker (RCC Ma) and CD10 show a positive reaction in renal cell carcinoma of the clear cell type and in the papillary tumor variant; the result is highly specific for the above-mentioned types of cancer.

### 12.1.5.3 Tuberculosis (Fig. 12.3)

Infestation of renal parenchyma with *Mycobacterium tuberculosis* leads to a granulomatous inflammatory process comprising epithelioid histiocytes, histiocytic giant cells of the Langhans type, caseous necrosis, and leukocytes. As described in Sect. 12.1.5.2, above, the distinction between florid tuberculosis from XPN may be difficult. Tuberculous foci in the kidney are most often secondary, and the patients usually present with a corresponding clinical history.

### 12.1.5.4 Malakoplakia (Fig. 12.4)

Malakoplakia is rarely seen in the kidney [63]. The pseudogranulomatous disease occurs much more commonly in the urethra and the urinary bladder but may also involve organs

of the genital system as well as extraurogenital organs. Malakoplakia can be diagnosed by fine-needle aspiration based on the characteristic elements; only a few reports are available in literature[48, 59].

**Microscopic Features**

- Microscopic hallmark of malakoplakia are concentrically laminated cytoplasmic inclusions in epithelioid cells and common histiocytes, known as Michaelis-Gutmann bodies or calcospherites. They stain positive with periodic acid-Schiff reaction and show positive reaction for iron and calcium.
- The inflammatory disease is characterized by accumulation of proliferative epithelioid histiocytes intermingled with foamy cells, giant cells, lymphocytes, plasma cells, and granulocytes.

**Differential Diagnosis**

- Abundance of foamy macrophages together with a rare presence of Michaelis-Gutmann bodies may lead to a nonspecific diagnosis of xanthogranulomatous pyelonephritis (Fig. 12.4A).
- Epithelium-like arrangement of large histiocytes comprising irregular nuclei and vacuolated cytoplasm may lead to a false diagnosis of renal adenocarcinoma (Fig. 12.4B).
- Epithelioid cell proliferation devoid of Michaelis-Gutmann bodies is observed in mycobacterial infections, lues (*Treponema pallidum*), mycotic infections, after surgery, and in other disorders.

### 12.1.5.5 Renal Infarct

Necrosis is abundant. Cytologic samples may exhibit renal epithelial cells, which can show degeneration and reparative atypia. Cellular atypia together with necrotic debris may mimic malignancy.

## 12.1.6 Cystic Lesions

Renal cysts are often discovered incidentally in the course of investigation of urinary tract symptoms. It has been estimated that roughly 50% of the population older than 50 years have some kind of renal cystic disease. Up to 85% of the asymptomatic renal masses detected by imaging investigations are at least partially cystic.

**Caution**

- Cytologic-radiologic correlation is important in patients with renal cysts in order to avoid false-negative cytologic results [114].
- Sanguineous cystic fluid is suspicious of malignancy, but it should not be considered a diagnostic key feature unless polymorphous necrotic debris and distinct cellular atypia are identified. On the other hand, cystic renal cell carcinomas may present with clear cystic fluids [114].
- Occasional Liesegang rings should not be misinterpreted as parasites or algae (see Sect. 12.1.6.2, p. 737).

### 12.1.6.1 Simple Cysts

A simple cyst is one of the most frequently aspirated renal cystic disorders. Imaging studies of simple cysts exhibit a regular, smooth border. Simple renal cysts may be congenital or acquired.

*Congenital cysts* result from disordered embryogenesis. They are frequently multiple and occasionally manifest clinically.

*Acquired cysts* are clinically silent, they may be multiple, and they vary greatly in size.

**Microscopic Features**

- Microscopic examination reveals foamy cells and occasional neutrophilic granulocytes. A few benign variably degenerating epithelial cells may be encountered in fluids of small cysts, unlike fluids of large cysts where epithelial cells are completely absent.
- Bloody fluids containing hemosiderophages are rarely encountered in aspirates from simple cysts.
- Calcified concretions rarely occur.

### 12.1.6.2 Complex Cysts [114]

- In the majority of complex cysts, imaging studies reveal an irregular outline, irregular nodular thickening of the cyst wall, luminal excrescences, or high-density cyst content. FNAB is the procedure of choice for definitive diagnosis of complex cystic lesions that cannot reliably be classified by ultrasound and radiologic investigations alone.
- Unfortunately, the cytologic appearance of complex renal cysts may be tricky as well. Todd and her colleagues discussed the problem of renal cysts providing a cytologic pattern that is not readily classifiable. Diagnoses included varying types of benign and infectious cysts (Fig. 12.5), and benign and malignant cystic tumors [114] (Fig. 12.6).

**Microscopic Features**

- The findings in cytologic specimens vary greatly. Epithelium-containing cystic fluids may show large numbers of tubular cell clusters, high cellularity with indistinct cell features, high cellularity without obvious atypia, or scanty atypical cells.

- Ring-shaped concretions that are concentrically laminated are referred to as *Liesegang rings*. They are sporadically encountered in degenerative chronic lesions of many organs and particularly in FNABs from complex renal cysts and perirenal inflammatory disorders. Liesegang rings can easily be identified in aspirates, but they may be confused with parasites, algae, calcifications, and psammoma bodies (for additional information and references, see Sect. 1.2.8.1, p. 19) (Fig. 1.25).

## 12.1.7 Benign Renal Tumors

Common benign tumors as seen in other organs of the human body are not further mentioned; they include lipomas, fibromas, leiomyomas, and hemangiomas. These tumors may occasionally be encountered in renal FNABs.

### 12.1.7.1 Angiomyolipoma [33, 42, 83, 88, 113]

**General Comments**

- Angiomyolipomas (AML) are rare benign tumors composed of a mixture of mature soft tissues; they are believed to be derived from perivascular epithelioid cells [33]. Thick-walled blood vessels, bundles of smooth muscle, and fatty tissue are the main components of this tumor. Generally, the tumors are large, measuring up to several centimeters in diameter.
- A strong association with tuberous sclerosis is well known, but about half of all cases of AML occur sporadically.
- Renal AML can undergo sarcomatous transformation with local invasion and metastatic spreading [37].

**Microscopic Features**

- Hallmarks:
  Mature adipose tissue fragments may be abundant.
  Smooth muscle cells occur either singly or in groups, cell clustering may be dense. Pleomorphism of smooth muscle cells can be pronounced, the cells exhibit variability of cell size and shape, and varied chromatin patterns from fine to coarse granular.
  Blood vessels are thick-walled and lined by endothelial cells; the lumen may contain erythrocytes.

**Differential Diagnosis**

- Highly cellular areas exhibiting predominantly atypical round cells may be confused with renal cell carcinoma. Numerous fragments of fatty tissue generally argue against carcinoma.
- Pronounced pleomorphic smooth muscle cells of AML share morphologic features with sarcomatous neoplasm or a sarcomatoid component of renal cell carcinoma.

**Immunocytochemistry**

Positive immunocytochemical staining for melanocytic markers (e.g., HMB 45), muscle markers (smooth muscle actin, desmin), and CD117 (c-kit) confirms the diagnosis of AML [88].

### 12.1.7.2 Renal Cortical Adenoma (Fig. 12.6)

**General Comments**

- Tumor size has been used as a criterion for the term "adenoma": well-differentiated tumors of renal cortical origin less than 3 cm in diameter should be regarded as adenomas. Most of these small tumors are found incidentally at autopsy or in surgically removed kidneys.
- Many reports have repeatedly documented that small renal tumors are more likely benign or reveal a lower grade of malignancy as compared to larger tumors of the same type, and that symptomatic lesions show an increased malignant potential [86, 99, 106, 107].
- The renal cortical adenoma should be accepted as small renal cell carcinoma with a low risk of metastasis. Adenoma is indistinguishable from well-differentiated renal cell carcinoma by morphology, immunohistochemistry, or ultrastructural features.

**Microscopic Features**

- The cytologic samples are cellular.
- The cells display an abundant clear cytoplasm.
- The nuclei are small and centrally positioned, showing indistinct irregularities. No mitoses are present.
- Adenomas may have papillary, tubulopapillary, or tubular architecture, and may be accompanied by cyst formation. The latter may rise diagnostic problems (Fig. 12.6).

### 12.1.7.3 Renal Oncocytoma

[7, 72, 74, 120] (Fig. 12.7)

**General Comments**

- Renal oncocytoma is a benign neoplasm regarded as a variant of renal adenoma. It is derived from the inner layer of proximal convoluted tubules. The abundant granular cytoplasm is consistent with the huge amount of mitochondria showing abnormal configuration with the electron microscope.
- The tumors account for about 5% of all renal tumors; they are more common in men than in women [7].
- Tumors are usually solitary but multicentric and bilateral occurrence is well known.
- In a large series, coexistence with renal cell carcinoma (RCC) was found in 10% of all cases [20]. Rare cases with metastases are described [72]. However, cells of malignant neoplasms exhibit more pronounced pleomorphism compared to usual oncocytoma.

### Microscopic Features

- Highly cellular aspirates show a monotonous population of polygonal cells occurring singly or in regular clusters.
- The abundant clearly defined eosinophilic cytoplasm exhibits a homogeneous or granular texture.
- Nuclei occur singly or multiply, they are deeply stained with an evenly distributed chromatin and only slight membrane irregularities. Occasionally, apoptotic or distinctly enlarged hyperchromatic nuclei can be encountered.
- The nucleoli may be prominent.

### Differential Diagnosis

Oncocytomas must be differentiated from:

- Chromophobe renal cell carcinoma whose nuclei are large, explicitly hyperchromatic, more irregular, and grooved.
- Differentiated RCC comprising large numbers of granular cells. But well-differentiated RCCs also harbor the characteristic large clear cells and numerous small blood vessels.

### Additional Analyses

Immunocytochemistry

Several recent reports recommend a panel of antibodies to distinguish reliably between oncocytoma and chromophobe RCC as well as clear cell RCC:

- CD63 was shown to differentiate renal oncocytomas from eosinophilic chromophobe RCCs with high sensitivity and specificity [78].
- All renal oncocytomas were reported to be negative for MOC31 and usually also for CD10. In contrast, a high percentage of chromophobe RCCs is positive for MOC31 [87].
- Epithelial cell adhesion molecule (EpCAM) positivity on individual cells seems to be characteristic of oncocytomas, whereas a homogeneous expression of this marker indicates chromophobe carcinoma of the kidney.
- All oncocytomas were negative for CK7 [75].
- Renal cell carcinoma associated cell marker (RCCMa) demonstrates positivity in about 90% of all clear cell RCCs, while cells of oncocytomas are completely negative [9].

DNA Image Cytometry

In general, renal oncocytomas exhibit a diploid DNA distribution pattern by image cytometry and flow cytometric studies [51, 57, 16].

Molecular Genetics

Chromosomal abnormalities distinguish renal oncocytoma from eosinophilic and chromophobe RCC: both malignant renal cancers exhibit similar genetic abnormalities such as loss of chromosomes 2, 6, 10, or 17, losses that are not expressed in oncocytomas [12A].

## 12.1.8 Malignant Renal Tumors

### 12.1.8.1 Renal Cell Carcinoma

### General Comments

- Renal adenocarcinoma or renal cell carcinoma (RCC) derives from proximal convoluted tubules.
- RCCs occur predominantly in adults with a peak incidence in the sixth decade.
- The majority of RCCs range from 3 to 8 cm.
- Well-differentiated tumors are less than 3 cm in diameter and infrequently metastasize; they are referred to as adenoma, provided that the lesion is encapsulated and lacks hemorrhage and necrosis. (see also Sect. 12.1.7.2, "Renal Cortical Adenoma," p. 737).
- Imaging (ultrasound, computed tomography, magnet resonance imaging) is a method for accurate detection of RCCs. US-guided FNAB is a helpful tool in confirming the diagnosis of this tumor type.
- Four different cell types classify RCCs. As indicated below, these variants are reliably recognized in the majority of FNAB samples [102].
  1. Clear cell renal cell carcinoma.
  2. Papillary renal cell carcinoma.
  3. Chromophobe renal cell carcinoma.
  4. The term "granular cell renal cell carcinoma" should no longer be used because variable numbers of tumor cells with granular and eosinophilic cytoplasm occur in the different renal tumor variants.

**Caution**

Extensive cystic components may prevent the recognition and the proper cytologic typing of RCCs. The quality of the cystic fluid is of little diagnostic value; both sanguineous and clear cystic fluid can be obtained from malignant lesions [114].

### Tumor Grading and DNA Ploidy

- The preferred grading system in histology is the Fuhrman classification [38, 39]. Fuhrman and colleagues have shown that the nuclear grade can predict the tumor outcome after nephrectomy more effectively than the size, cell type, and histologic architecture of the neoplasia.
- Al Nazer and Mourad have proposed a cytologic grading system in correlation with the Fuhrman nuclear grading system: the N/C ratio and the presence or absence of nucleoli have proved to be the most reliable cytologic features distinguishing between low-grade and high-grade tumors [6] (compare Figs. 12.8B, 12.9B, and 12.10).
- Assessment of DNA ploidy both by image and flow cytometric studies is closely related to the nuclear grade of malignancy. DNA ploidy has been established as a significant predictor of progression in patients with organ-confined RCCs [1, 13, 18, 27, 65, 89, 92]. A hypodiploid

DNA profile seems to refer to the worst prognosis for patients with papillary renal cell carcinoma [22]. Intratumoral heterogeneity of DNA content may be an uncertainty factor for prognostication [103].

#### 12.1.8.1.1 Clear Cell Renal Cell Carcinoma

(Figs. 12.8–12.10)

**General Comments**

- Synonyms: the terms "Grawitz tumor" and "hypernephroma" have been used for clear cell renal cell carcinoma in the past.
- Clear cell renal cell carcinoma (CRCC) is the common histologic type (75%). Tumors may occur multiply or bilaterally and are usually well demarcated.
- The lesions are frequently hemorrhagic and necrotic, comprising calcification and cyst formation, the latter of which may be striking.

**Microscopic Features**

The cellularity of the cytologic sample depends on the quality of aspiration and the extensiveness of intratumoral hemorrhage and cyst formation.

- Hallmarks
  - Cells with abundant clear cytoplasm; the latter is caused by a great variety of vacuoles in terms of size and shape.
  - The N/C ratio is low.
  - Branching capillaries are often evident, passing through tumor cell aggregations or detached.
- The nuclei are clear, showing grooves and sporadic pseudoinclusions. They are generally small, exhibiting an accentuated membrane and a finely dispersed chromatin. Nuclear multilobation, irregularity in shape, and enlarged nucleoli may occur depending on the degree of cellular differentiation (compare Figs. 12.8B, 12.9B and 12.10). Occasionally, nuclei may be stripped and are scattered in a vacuolated background.
- The cell borders are well defined or indistinct.
- The cytoplasm may show eosinophilic globules.
- Granular cells occur admixed to the clear cells as a minor population. Granular cells exhibit eosinophilic granular cytoplasm, which is not as densely structured as that of oncocytic cells (the cytoplasm of oncocytes with abundant and tightly packed mitochondria usually shows blurred granularity; the cytoplasm is eosinophilic, very dense, and practically homogeneous).
- The tumor cells may occur singly or they are arranged in loose sheets or in an alveolar pattern. Papilliform clusters and even a few papillary fronds may be observed.
- Hemorrhage and necrosis are particularly common in high-grade tumors.

**Cytochemistry**

The cytoplasm contains lipids that can be visualized using Oil red-O on air-dried slides, and glycogen, which is positive with periodic acid-Schiff stain (PAS) on routinely fixed smears.

**Differential Diagnosis and Immunocytochemistry**

- CRCC cells with a more dense cytoplasm and lobate nuclei may look like cells from transitional cell carcinoma of the renal pelvis (Figs. 12.9A and 12.9B).
  - Immunocytochemistry: RCCMa demonstrates positivity in about 90% of all clear cell RCCs (Fig. 12.9C). In contrast, transitional cell carcinoma shows immunoreactivity for CK7 and CK13. CK7 is usually negative in CRCC but positive in chromophobe and papillary RCC.
- CRCC harboring large numbers of granular cells should be distinguished from oncocytoma because the latter is a benign tumor requiring a different surgical procedure compared to renal cell carcinoma.
  - Immunocytochemistry: RCCMa expresses positivity in about 90% of all clear cell RCCs while oncocytomas are completely negative [9]. CD10 positivity is a strong indicator for RCC but some oncocytomas can also be positive.
- Angiomyolipomas that exhibit highly cellular areas composed of predominantly atypical round cells and rather thin-walled blood vessels may be confused with renal cell carcinoma.
- RCC in children may be confused with Wilms tumor, but blastema is a characteristic feature of Wilms tumor.
- Xanthogranulomatous pyelonephritis can raise problems against CRCC, especially in specimens exhibiting dense aggregation of the histiocytes; but cytoplasmic features of the histiocytes poorly match those of CRCC (Fig. 12.4B). An inflammatory component is unusual in renal cell carcinoma (see also Sect. 12.1.5.2, p. 735).
  - Immunocytochemistry: An appropriate immunocytochemical panel can easily differentiate between histiocytes and epithelial cells: CD68 decorates cells of histiocytic origin, and carcinoma cells exhibit pancytokeratins (e.g., MNF116). RCCMa and CD10 indicate cells of CRCC with high specificity.
- RCCs with focal cellular pleomorphism, spindle-formed cells exhibiting dense cytoplasm, large numbers of clustered naked nuclei, and a vacuolated background have to be differentiated from adrenocortical carcinoma.
- Metastatic or directly invading carcinomas may mimic RCC (Figs. 12.8 and 12.16). The patient's clinical history, imaging studies, and a selective panel of antibodies are helpful in most problematic cases. For further details concerning appropriate immunopanels, see Table 15.3.3 in Sect. 15.3.24, p. 978 and elsewhere in this book.

**Caution**

- Proximal tubular epithelium and CRCC grade 1 may share many cellular features. Misdiagnosis of a tumoral condition is possible in FNABs showing a huge number of clustered benign tubular epithelial cells.
- Accidentally aspirated hepatocytes may be confused with RCCs exhibiting large oncocytic and granular tissue components. Organ-specific immunocytochemical markers can solve the diagnostic problem. RCC Ma shows positivity in cells of RCC, and Hep Par 1 / human hepatocyte AG is positive in liver cells.

### Molecular Genetics

Deletion of chromosome 3p has been reported in the vast majority of sporadic CRCC; the chromosomal anomaly can be assessed by FISH and other genetic analysis techniques [79, 123].

## 12.1.8.1.2 Papillary Renal Cell Carcinoma

[21, 46] (Figs. 12.11 and 12.12)

### General Comments and Definition

- Papillary renal cell carcinomas (PRCC) are usually located in the renal cortex. They are well delineated, often multiple, and associated with renal cortical adenomas or adjacent to cysts.
- In standard cytology, approximately 10% of the renal cell carcinoma are of the papillary type.
- The tumor grade of PRCCs has an effect on survival [91]; the clinical outcome is comparable to that of clear cell renal cell carcinomas.
- Histologically, PRCC is defined as a tumor with papillary or tubulopapillary architecture including at least 50% of the tumor tissue.

### Microscopic Features

Hallmarks:

- Cellular aspirates reveal multiple three-dimensional papillary fragments. The papillae exhibit fibrovascular cores covered with cuboid or columnar cells; papillary clusters lacking fibrovascular cores are rarely encountered.
  - Nuclear grooving is frequently observed.
  - Large numbers of lipid-laden macrophages are present attached to the cell groups or occurring singly.
  - Necrosis is common.
- The nuclear outline may be smooth or irregular; nuclear grooves are typical for PRCC. Distinct nuclear pleomorphism is rare.
- The chromatin is generally finely granular and dense.
- Nucleoli occur singly and are small except in high-grade tumors.
- The N/C ratio is moderate to high, depending on the predominant cell type.
- Intracytoplasmic hemosiderin is common.
- Hemorrhage and cystic change are rather common.
- Variable amounts of psammomatous bodies.

### Differential Diagnosis and Immunocytochemistry

- PRCC composed of columnar cells exhibiting vacuolated cytoplasm and a few papillary clusters may be misdiagnosed as clear cell RCC.
- Renal cell carcinoma of the Bellini collecting ducts is a rare tumor with similar cytologic features compared to those of PRCC. However, cell clusters are predominantly tubular and dilated tubules are lined with a single layer of cuboidal cells; nuclear pleomorphism is indistinct. Collecting duct-type carcinoma is located in the medulla of the kidney.
- In aspirates, low-grade papillary transitional cell carcinoma of the renal pelvis also exhibits papillary clusters sharing cytoplasmic features and nuclear grooves with PRCC (see Sect. 13.3.4.1, p. 834); hence the two neoplasms may easily be confused (Figs. 12.15 and 12.16).
  Higher-grade papillary transitional cell carcinomas show distinct features: the cytoplasm is dense, sharply outlined, and spindle shaped; the nuclei are large, pleomorphic, and hyperchromatic.
  - Immunocytochemistry: PRCCs are strongly positive for RCCMa and CD10. Transitional cell carcinoma shows immunoreactivity for CK13 (negative staining results in PRCC cells). CK7 does not reliably discriminate between PRCC and urothelial neoplasms.
- Secondary malignancies of visceral origin such as gastrointestinal stromal tumor and colonic adenocarcinoma may pose diagnostic dilemmas and pitfalls in PRCC aspirates. Distinct cytologic features of PRCC, the patient's history, and discriminating immunocytochemical tests should provide a correct diagnosis [73].
- Papillary formations, nuclear grooves, and minor nuclear pleomorphism make it virtually impossible to exclude PRCC and papillary thyroid cancer (Figs. 12.8 and 12.12). An appropriate set of immunodiagnostic markers is required to establish a correct diagnosis:
  - RCCMa and CD10 show positivity in PRCCs; thyroglobulin and TTF1 show positivity in papillary thyroid carcinoma [49].

### Molecular Genetics

Trisomy or tetrasomy 7, trisomy 17, and loss of chromosome Y are the most common karyotypic changes in PRCC, detectable by FISH [64].

## 12.1.8.1.3 Renal Cell Carcinoma, Chromophobe Cell Type [44, 104]

Chromophobe renal cell carcinoma accounts for 5% of all renal neoplasms. This tumor has a better prognosis in comparison with the tumor types discussed above.

**Microscopic Features**

- Hallmarks
  - Large polygonal cells with abundant pale or dense eosinophilic(eosinophilic variant) cytoplasm.
  - Conspicuously thickened cell membranes.
  - The characteristic perinuclear halos are caused by aggregation of microvesicles containing mucopolysaccharides.
  - Hale colloidal iron stain provides a positive reaction.
- The tumors do not show hemorrhage, necrosis, or calcification.
- As in other types of renal cell carcinoma, granular eosinophilic cells are commonly admixed to the characteristic basic cell population mentioned above.
- The aspirates are cellular, comprising single cells and cell groups.

**Differential Diagnosis and Immunocytochemistry**

- Cytoplasmic features of the pale tumor cells may raise suspicion of vegetable cells or koilocytes [44].
- The eosinophilic variant of chromophobe cell RCC is completely composed of eosinophilic cells with thickened membranes; the tumor may closely resemble oncocytoma, but the latter shows regular nuclei with smooth borders, and the typical perinuclear halos of chromophobe RCC are absent.
  - Immunocytochemistry: Immunocytochemical stains distinguish between eosinophilic chromophobe RCC and renal oncocytoma.
- Distinction of chromophobe RCC from the granular cell variant of clear cell RCC may be a diagnostic dilemma.
  - Immunocytochemistry: CD117 has been reported to be positive in chromophobe cell RCC but absent in granular cell variants of clear cell RCC; an opposite immunoprofile has been observed using the immunomarker RCCMa [119].

**Molecular Genetics**

Chromophobe RCC and its eosinophilic variant exhibit similar genetic abnormalities including losses of chromosomes 2, 6, 10, or 17. Chromosomal abnormalities differentiate these tumors from oncocytoma [12A].

#### 12.1.8.1.4 Renal Cell Carcinoma with Sarcomatoid Differentiation [16, 23, 60] (Fig. 12.13)

**General Comments**

Sarcomatoid renal cell carcinoma is not a distinct tumor entity. It represents high-grade transformation of tumor cells in different subtypes of RCC, indicating a worse prognosis. A varying mixture of a typical renal cell carcinoma component and a component of high-grade spindle cells is characteristic. Clear cell RCC and chromophobe RCC have been reported as being the most frequent subtypes associated with sarcomatoid transformation [5, 16].

**Microscopic Features, Immunocytochemistry, and Differential Diagnosis** [60]

- The epithelial cell components show variable nuclear grading and either clear or granular cytoplasm.
- The sarcomatoid component morphologically matches sarcoma.

- The cytologic diagnosis will be sarcoma if a pure sarcomatoid tumor component has been aspirated.
- It may be difficult to distinguish between high-grade RCCs and sarcomatoid differentiated RCCs.
- Immunocytochemistry is mandatory in the work-up of equivocal cases: cytokeratins are usually negative in sarcomas, whereas malignant fusiform carcinoma cells provide a positive reaction for epithelial markers.

### 12.1.8.2 Rare Primary and Secondary Tumors of the Kidney

#### 12.1.8.2.1 Malignant Lymphoma [53]

Accurate diagnosis of lymphoma is important in order to avoid unnecessary surgery and to enable immediate therapeutic decisions. Flow cytometric, immunocytochemical, and molecular genetic analyses can be performed on lymphocytes sampled by FNAB, yielding additional information for cytological evaluation. Distinction of malignant lymphoma from carcinoma is achieved by immunostaining for leukocyte antigen (CD45) and cytokeratins. Detailed information on additional analyses is provided in Sects. 15.1 p. 907 and 15.3, p. 950.

#### 12.1.8.2.2 Soft Tissue Tumors and Other Tumor Entities

Benign soft tissue tumors, primary sarcoma [3, 17, 117], neural tumors, endocrine tumors, and others rarely occur in the kidney; they are rarely seen in cytologic practice. We refer to other chapters of this book and to the histologic literature [34, 47] regarding the characteristic cytomorphologic features of selected tumor entities.

#### 12.1.8.2.3 Metastases to the Kidney [41] (Fig. 12.14)

- Secondary tumors to the kidney causing diagnostic problems have been discussed together with the corresponding subtypes of renal cell carcinomas. The patient's history, imaging results, and auxiliary analyses are helpful in gaining an accurate diagnosis.
- Metastatic thyroid carcinoma may strongly mimic primary renal cell carcinoma [105]. Distinguishing between papillary thyroid cancer and papillary renal cell carcinoma [49], between well-differentiated follicular thyroid cancer and clear cell RCC, and between oncocytic thyroid carcinoma and RCC with oncocytic features [36] may be extremely difficult by cytology alone. Immunoreactivity for thyroglobulin and TTF-1 indicate the thyroidal nature of dubious neoplasms.

- Unusual tumor-to-tumor metastasis of a cancer from a remote organ into a carcinoma of the target organ has also been reported for the kidney [62] (Fig. 12.14).

## 12.1.9 Tumors of the Renal Pelvis [28, 60]

### General Comments

- Most common tumors of the renal pelvis are transitional cell carcinomas (TCC). High-grade tumors often present squamous or glandular metaplastic changes. Pure squamous cell carcinoma, adenocarcinoma, and undifferentiated carcinoma are rare.
- With regard to the common cytologic criteria of transitional cell carcinoma, we refer to other chapters of this book (e.g., Sect. 13.3, "Urinary Tract: Precancerous and Malignant Lesions, " p. 830).
- It has been reported that the incidence of TCCs is 7% of all neoplasms of the kidney. TCC of the renal pelvis is frequently associated with synchronous and metachronous transitional cell tumors at other sites of the urinary tract [28].
- Most TCCs show an exophytic and papillary growth pattern and are of low-grade malignancy.
- Cytologically, benign transitional cell papilloma is unlikely to be differentiated from low-grade papillary transitional carcinoma.
- Cytologic classification and grading of TCC by FNA cytology follows the specifications given in Sect. 13.3, "Urinary Tract: Precancerous and Malignant Lesions," p. 830, including additional information.

### 12.1.9.1 Low-Grade Transitional Cell Carcinoma

(Figs. 12.15 and 12.16)

#### Microscopic Features

- Minimally atypical urothelial cells occurring in isolation or in loose aggregates. Papillary clusters with fibrovascular core may also be present.
- The cell pattern is monotonous.
- The nuclei are eccentrically located, slightly irregular, and frequently exhibit grooves along the length of their longer axis. The chromatin is fine, granular and evenly dispersed.
- Small nucleoli are usually present.
- The cytoplasm is homogeneous and slightly cyanophilic.

#### Differential Diagnosis and Immunocytochemistry

- Well-differentiated papillary renal cell carcinoma (PRCC) may easily be confused with papillary TCC of low-grade malignancy. In aspirates, both tumor types show papillary clusters exhibiting related nuclear features, but a more fusiform overall cell pattern of TCC is striking. The cytoplasm is denser and cyanophilic and tends to be sharply outlined. Finally, foamy histiocytes, hemosiderin pigment, and psammoma bodies are exclusively found in PRCC (see Sect. 12.1.8.1.2, p. 740) (Fig. 12.12A).
- Papillary RCCs are strongly positive for RCCMa and CD10. On the other hand, transitional cell carcinoma shows immunoreactivity for CK13. CK7 cannot reliably distinguish between PRCC and urothelial neoplasms.

### 12.1.9.2 High-Grade Transitional Cell Carcinoma

(Fig. 12.17)

#### Microscopic Features

- Large columnar, spindle, or polygonal cells usually occur singly or irregularly grouped. Bizarre cells may be seen as well.
- Papilliform or even papillary clusters, the latter exhibiting fibrovascular cores, may be present.
- The nuclei are hyperchromatic. The chromatin is coarse and clumped.
- Irregular nucleoli.
- High N/C ratio.
- The dense or vacuolated cytoplasm is sharply defined.
- Necrosis is common.

#### Differential Diagnoses and Immunocytochemistry

TCC of high-grade malignancy may share cytomorphologic features with

- Sarcomatoid differentiated RCC: a tumor entity that is usually biphasic, with the epithelial cell component exhibiting typical RCC features.
- High-grade renal cell carcinoma: Malignant cells of renal origin usually present with a lower N/C ratio, less irregular nuclei, and light-colored cytoplasm. Better differentiated RCC areas are helpful in obtaining a conclusive diagnosis.
  Immunocytochemistry: Transitional cell carcinoma shows immunoreactivity for CK7 and CK13. CK7 is usually negative in clear renal cell carcinoma but positive in chromophobe and papillary RCC. RCCMa demonstrates positivity in about 90% of all clear cell RCCs.
- Non-Hodgkin lymphoma of the blastic type.This entity should always be included in the differential diagnostic considerations. Immunostaining for cytokeratins and leukocyte antigens (CD45) is crucial for a definite diagnosis.
- Tumors metastatic to the kidney. TCCs exhibiting marked squamous differentiation can particularly be mistaken for secondary squamous cell carcinoma.

## 12.1.10 Pediatric (and Young Adult) Renal Tumors [108]

A mesenchymal phenotype is the hallmark of renal tumors in the pediatric age group compared with the predominant epithelial-appearing tumors in the adult age group.

### 12.1.10.1 Metanephric Adenoma [45, 54]

Metanephric adenoma is a benign tumor encountered in children and young adults. The tumor is assumed to be histogenetically related to Wilms tumor [8, 81]. Immunocytochemical results are highlighted in the publication of Muir and colleagues [81].

#### Microscopic Features

- The cytologic samples are cellular, composed of small deeply stained cells with scant cytoplasm. Small nucleoli are present. The cells can mimic lymphocytes.
- The cells form tightly packed acinar, tubular, glomeruloid, and occasional papillary structures.
- Psammoma bodies may be encountered.
- Tumors with a fibroblastic component have been referred to as metanephric adenofibroma [109].

#### Differential Diagnosis [94]

- The adenofibromatous variant of metanephric adenoma may particularly mislead to a diagnosis of Wilms tumor. Wilms tumor shows closely packed epithelial cells with faint cell borders. Nuclear overlapping, membrane irregularities, and nucleoli are striking. Mitotic activity is pronounced [61]. A conclusive discrimination of these two tumor entities by cytology and/or immunocytochemistry is not always possible.
- Furthermore, mesoblastic nephroma composed of tightly cohesive fusiform tumour cells with bland appearance may mimic metanephric adenoma.
- Renal clear cell sarcoma can be mistaken for metanephric adenoma. However, clear cell sarcoma is usually composed of cells with moderate to large pale cytoplasm showing immunoreactivity for vimentin.

### 12.1.10.2 Malignant Tumors

#### 12.1.10.2.1 Renal Cell Carcinoma

RCC is a rare tumor in the pediatric age group. The cytologic features of RCC in children are virtually identical to those in adults (see Sect. 12.1.8.1, p. 738). However, Renshaw and coworkers found particular morphologic qualities in RCCs of children and young adults [101].

Well-differentiated renal cell carcinoma is indistinguishable from adenoma. Small RCCs are more likely to be benign or reveal a lower grade of malignancy compared to larger tumors (see also Sect. 12.1.7.2, p. 737).

Distinguishing between RCC and Wilms tumor may be difficult in cases where the typical blastema component of Wilms tumor is scarce or completely absent [95].

#### 12.1.10.2.2 Wilms Tumor [2, 25, 96] (Fig. 12.18)

- Wilms tumor (synonym: nephroblastoma) is responsible for 6% of all pediatric cancers, occurring most frequently between the ages of 1 and 5 years. The tumor is rarely seen in adults [71].
- Wilms tumors may be bilateral and multicentric. They are usually greater than 5 cm in diameter, but sizes of up to 10 cm and more may be encountered.
- Histologically, the tumor is typically composed of stromal tissue, epithelial tissue, and a significant proportion of embryonal blastema (primordial cellular mass).

#### Microscopic Features

The cytologic appearance in FNA samples reflects the trilinear histologic pattern. Three different types of cells are easily distinguished:

- *Blastemal cells*. The cells show extremely scant cytoplasm and small, strongly basophilic, slightly irregular nuclei with granular and coarse chromatin; the latter is evenly distributed. The nucleoli are inconspicuous or absent.
  The cells are haphazardly grouped and smearing artifacts are common due to nuclear fragility.
- *Epithelial cells*. These cells show slightly enlarged nuclei and distinct cytoplasmic rims in comparison to blastemal cells.
  The cells are arranged in rosettes, tubules, and abortive glomerulus-like structures. Epithelial cell clusters may be surrounded by basal lamina material (cyanophilic on Pap-stain preparations).
- *Stromal cells*. They are spindle-shaped and arranged in loose groups together with myxoid material.
  Smooth or skeletal muscle, fat, or cartilage may sporadically occur.
- Hemorrhage, necrosis, and cyst formation are not pronounced.

#### Immunocytochemistry

- WT1 protein is typically expressed (nuclear positivity) in epithelial and blastemal cells of Wilms tumor but not in the stromal component. WT1 is usually not expressed in small round cell tumors such as neuroblastoma.
- Positive immunoreactivity for cytokeratin and vimentin is characteristic of the epithelial cells of Wilms tumor; antibodies against vimentin decorate blastemal cells as well.
- CD56 may decorate the cells of nephroblastoma, but it is more strongly expressed in neuroblastoma cells [93].
- Cells of the tubular and blastemic components of Wilms tumors may express neuron-specific enolases (NSE) [29,

35]. Compare also immunocytochemical staining patterns mentioned under "Differential Diagnosis,".

We refer to the literature for the diagnostic value of other additive analytical tests, such as DNA ploidy and electron microscopy [35].

**Differential Diagnosis** [43, 97]

- Difficulties differentiating Wilms tumor from other neoplasms are caused by:
  - A predominant blastemal component in Wilms tumors.
  - General morphologic similarities between different tumor entities.
  - Absence of a specific immunopattern of neoplasms other than Wilms tumor.
  - Inadequate aspiration of Wilms tumors with heterologous components.
  - Nonrepresentative FNAB samples.
- Small round cell tumors (SRCT). The differential diagnostic challenge of Wilms tumor particularly concerns all childhood small round cell tumors [12, 19, 93, 98]. Distinguishing between Wilms tumor and small round cell tumors usually calls for a broad and appropriate panel of immunocytochemical stains.
  SRCT are summarized in Table 12.1.1 according to a publication by Pohar-Marinsek [93].
- The most common SRCTs with their morphologic and immunocytochemical features are briefly mentioned:
  - Embryonal rhabdomyosarcoma (Fig. 12.19). Absence of a bi- or trilinear component. Rhabdomyoblasts are large cells comprising excentric nuclei and eosinophilic cytoplasm; multinucleation is possible. Single rhabdomyoblasts may be observed in Wilms tumors as well!
    Immunocytochemistry: Tumor cells are positive for myogenic markers (e.g., Desmin) and negative for cytokeratin.
  - Neuroblastoma (Figs. 12.20 and 12.21) in its well-differentiated form shows typical rosettes and a neurofibrillary background (rosette-like structures may also be exhibited in other SRCTs such as nephroblastoma, hepatoblastoma, and others). Individual ganglion cells may be present. Cytologically, undifferentiated neuroblastoma strongly mimics a blastemal-predominant nephroblastoma.
    Immunocytochemistry: CD56 decorates a high percentage of the neuroblastoma cells, but may also be expressed in Wilms tumor cells. In general, immunopositivity for NSE, chromogranin, and synaptophysin is associated with neuroblastoma, but NSE is also expressed in cells of Wilms tumors. Positivity for NB84 may be diagnostically helpful: it is a marker that is not expressed in nephroblastoma [93].
  - Non-Hodgkin lymphomas (NHL) occurring in children are generally high-grade tumors. The most common subtypes are lymphoblastic NHL, Burkitt lymphoma, and anaplastic large-cell lymphoma. Distinction of NHL from Wilms tumor based on cytologic features alone should pose minor problems in most cases (Figs. 15.43A and 15.43B).
    Immunocytochemistry: Lymphoma cells stain reliably positive for leucocyte common antigen(CD45), but cell degeneration may cause a false-negative result, and rare lymphoma subtypes may show negative staining results (Fig. 15.43C).
  - Extraskeletal Ewing sarcoma/PNET (Fig. 12.22) exhibit a uniform cell pattern composed of round cells including varying rosette formation (more in PNET than in Ewing sarcoma) (Figs. 12.22A and 12.22B). Demonstration of abundant intracellular glycogen is helpful for the diagnosis of this tumor entity (Fig. 12.22C).
    Immunocytochemistry: CD99 is usually positive in Ewing sarcoma/PNET and negative in Wilms tumor, whereas WT1 shows an opposite staining pattern.

**Table 12.1.1** Small round cell tumors

| Classic SRCTs | Other SRCT entities |
|---|---|
| – Embryonal rhabdomyosarcoma | – Primitive neuroendocrine tumor (PNET) |
| – Neuroblastoma | – Desmoplastic small round cell tumor |
| – Non-Hodgkin lymphoma | – Nephroblastoma |
| – Ewing sarcoma | – Hepatoblastoma |
| | – Pleuropulmonary blastoma |
| | – Small-cell osteogenic sarcoma |
| | – Rhabdoid tumor of soft tissue |
| | – Mesenchymal chondrosarcoma |
| | – Synovial sarcoma |
| | – Granulocytic sarcoma |

#### 12.1.10.2.3 Other Rare Pediatric Renal Tumors

This tumor group includes benign multilocular cystic nephroma, mesoblastic nephroma, rhabdoid tumor, and clear cell sarcoma. Some of them share morphologic features with Wilms tumor.

These tumor entities are rarely seen in cytologic practice; nevertheless they are briefly discussed:

**Cystic Partially Differentiated Nephroblastoma** [24, 82]

Synonyms of this uncommon renal tumor are cystic nephroma, cystic Wilms tumor, and polycystic nephroblastoma.

The tumor occurs in early infancy and is considered to have no or little metastatic potential. Misdiagnosis of Wilms tumor is possible by cytology alone, but combination with radiologic data may be helpful in the preoperative assessment of a correct diagnosis.

- Predominance of tight cell clusters, rows, tubules, and glomeruloid bodies. Occasional single cells.
- Epithelial cells are round, showing a small cytoplasmic rim and slight nuclear pleomorphism.
- Blastemal and mesenchymal cells may be present.

**Mesoblastic Nephroma** [26, 30, 94, 108]

This is a congenital tumor clinically recognized in the first months of life.

- The tumor is composed of mesenchymal spindle- and tadpole-shaped cells. The cells are arranged in cohesive clusters showing small nuclei with mild atypias. The cytoplasmic body is distinct.
- The cells are embedded in myxoid/fibrillary background material.

**Rhabdoid Tumor** [4, 10, 31]

This tumor has a very poor prognosis.

- The cells are round and polygonal but irregularly shaped; they resemble malignant cells of skeletal muscle tumors. The large vesicular nuclei contain granular chromatin and prominent nucleoli. The cytoplasm is dense, sometimes exhibiting a plasmacytoid appearance.
- A high mitotic rate is common.

**Renal Clear Cell Sarcoma** [32, 55, 66, 94]

Clear cell sarcoma is an aggressive tumor.

- FNAB yields cellular smears.
- The monomorphic cell population is composed of large polygonal cells with abundant pale cytoplasm. The nuclei are round to oval and are eccentrically placed, showing a loose chromatin pattern. Nuclear grooves are a characteristic feature of this tumor entity.
- Fragile cytoplasm leads to large amounts of stripped nuclei. Pronounced cell degeneration and pyknotic nuclei frequently occur.
- Stromal fragments containing branching blood vessels and mucoid background may be encountered.

## 12.1.11 Further Reading


1. Abou-Rebyeh H, Borgmann V, Nagel R, Al-Abadi H. DNA ploidy is a valuable predictor for prognosis of patients with resected renal cell carcinoma. Cancer 2001;92:2280-2285.
2. Akhtar M, Ali MA, Sackey K, et al. Aspiration cytology of Wilms tumor: correlation of cytologic and histologic features. Diagn Cytopathol 1989;5:269-274.
3. Akthar M, Ali MA, Sackey K, Burgess A. Fine-needle aspiration biopsy of clear-cell sarcoma of the kidney: light and electron microscopic features. Diagn Cytopathol 1989;5:181-187.
4. Akhtar M, Ali MA, Sackey K, et al. Fine-needle aspiration biopsy diagnosis of malignant rhabdoid tumor of the kidney. Diagn Cytopathol 1991;7:36-40.
5. Akhtar AM, Tulbah A, Karbar AH, Ali MA. Sarcomatoid renal cell carcinoma: the chromophobe connection. Am J Surg Pathol 1997;21:1188-1195.
6. Al Nazer M, Mourad WA. Successful grading of renal-cell carcinoma in fine-needle aspirates. Diagn Cytopathol 2000;22:223-226.
7. Amin MB, Crotty TB, Tickoo SK, Farrow GM. Renal oncocytoma: a reappraisal of morphologic features with clinicopathologic findings in 80 cases. Am J Surg Pathol 1997;21:1-12.
8. Arroyo MR, Green DM, Perlman EJ, et al. The spectrum of metanephric adenofibroma and related lesions: clinicopathologic study of 25 cases from the National Wilms Tumor Study Group Pathology Center. Am J Surg Pathol 2001;25:433-444.
9. Avery AK, Beckstead J, Renshaw AA, Corless CL. Use of antibodies to RCC and CD10 in the differential diagnosis of renal neoplasms. Am J Surg Pathol 2000;24:203-210.
10. Barroca HM, Costa MJ, Carvalho JL. Cytologic profile of rhabdoid tumor of the kidney. A report of 3 cases. Acta Cytol 2003;47:1055-1058.
11. Bishop GA. Wuagh J, Horvath JS, et al. Diagnosis of renal allograft rejection by analysis of fine-needle aspiration biopsy specimens with immunostains and simple cytology. Lancet 1986;2:645-650.
12. Brahmi U, Rajwanshi A, Joshi K, et al. Role of immunocytochemistry and DNA flow cytometry in the fine-needle aspiration diagnosis of malignant small round cell tumors. Diagn Cytopathology 2001;24:233-239.

12A. Brunelli M, Eble JN, Zhang S, et al. Eosinophilic and classic chromophobe renal cell carcinomas have similar frequent losses of multiple chromosomes from among chromosomes 1, 2, 6, 10, and 17, and this pattern of genetic abnormality is not present in renal oncocytoma. Mod Pathol 2005;18:161-169.

13. Budia Alba A, Gomez Perez L, Bango V, et al. Prognostic factors for disease progression in patients with renal cell carcinoma. Actas Urol Esp 2007;31:831-844.
14. Chandrakar A. Diagnostic techniques in the work-up of renal allograft dysfunction – an update. Curr Opin Nephrol Hypertens 1999;8:723-728.
15. Charrada-Ben Farhat L, Saied W, Dali N, et al. Imaging features of xanthogranulomatous pyelonephritis. J Radiol 2007;88:1171-1177.
16. Cheville JC, Lohse CM, Zincke H, et al. Sarcomatoid renal cell carcinoma: an examination of underlying histologic subtype and an analysis of associations with patient outcome. Am J Surg Pathol 2004;28:435-441.
17. Chow LT, Chen SK, Chow WH. Fine needle aspiration cytodiagnosis of leiomyosarcoma of the renal pelvis. A case report with immunohistochemical study. Acta Cytol 1994;38:759-763.
18. Clark PE, Veys JA, Eskridge MR, et al. Prognostic significance of clinicopathologic and deoxyribonucleic acid flow cytometric variables in non-metastatic renal cell carcinoma in the modern era. Urol Oncol 2005;23:328-332.
19. Das DK. Fine-needle aspiration (FNA) cytology diagnosis of small round cell tumors: value and limitations. Indian J Pathol Microbiol 2004;47:309-318.
20. Dechet CB, Bostwick DG, Blute ML, et al. Renal oncocytoma: multifocality, bilateralism, metachronous tumor development and coexistent renal cell carcinoma. J Urol 1999;162:40-42.
21. Dekmezian R, Sneige N, Shabb N. Papillary renal-cell carcinoma: fine-needle aspiration of 15 cases. Diagn Cytopathol 1991;7:198.203.
22. del Vecchio MT, Lazzi S, Bruni A, et al. DNA ploidy pattern in papillary renal cell carcinoma. Correlation with clinicopathological parameters and survival. Pathol Res Pract 1998;194:325-333.
23. de Peralta-Venturina M, Moch H, Amin M, et al. Sarcomatoid differentiation in renal cell carcinoma: a study of 101 cases. Am J Surg Pathol 2001;25:275-284.
24. Dey P, Das A, Radhika S. Fine needle aspiration cytology of cystic partially differentiated nephroblastoma. A case report. Acta Cytol 1996;40:770-772.
25. Dey P, Radhika S, Rajwanshi A, et al. Aspiration cytology of Wilms tumor. Acta Cytol 1993;37:477-482.
26. Dey P, Srinivasan R, Nijhawan R, et al. Fine needle aspiration cytology of mesoblastic nephroma. A case report. Acta Cytol 1992;36:404-406.
27. Di Silverio F, Casale P, Colella D, et al. Independent value of tumor size and DNA ploidy for the prediction of disease progression in patients with organ-confined renal cell carcinoma. Cancer 2000;88:835-843.
28. Donnelly JD, Koontz WW. Carcinoma of the renal pelvis: a ten year review. South Med J 1975;68:943-946.
29. Drut R. Neuron-specific enolase-positive rosettes in nephroblastoma: a possible diagnostic pitfall in aspiration cytology. Diagn Cytopathol 1987;3:74-76.
30. Drut R. Cytologic characteristics of congenital mesoblastic nephroma in fine-needle aspiration cytology: a case report. Diagn Cytopathol 1992;8:374-376.
31. Drut R, Drut RM. Renal and extrarenal congenital rhabdoid tumor: diagnosis by fine-needle aspiration biopsy and FISH. Diagn Cytopathol 2002;27:32-34.
32. Drut R, Pomar M. Cytologic characteristics of clear cell sarcoma of the kidney in fine-needle aspiration biopsy: a report of 4 cases. Diagn Cytopathol 1991;7:611-614.
33. Eble J. Angiomyolipoma of the kidney. Semin Diagn Pathol 1998;15:21-40.
34. Eble JN, Sauter G, Epstein JI, Sesterhenn IA. (Eds.): World Health Organization Classification of tumors. Pathology and Genetics of tumors of the urinary system and male genital organs. IARC Press: Lyon 2004.; pp:56-87.
35. Ellison DA, Silverman JF, Strausbauch PH, et al. Role of immunocytochemistry, electron microscopy, and DNA analysis in fine-needle aspiration biopsy diagnosis of Wilms tumor. Diagn Cytopathol 1996;14:101-107.
36. Ferrer Garcia JC, Merino Torres JF, Ponce Marco JL, Pinon Selles F. Unusual metastasis of differentiated thyroid carcinoma. An Med Interna 2002;19:579-582.
37. Ferry JA, Malt RA, Zamboni G. Renal angiomyolipoma with sarcomatous transformation and pulmonary metastases. Am J Surg Pathol 1991;15:977-979.
38. Ficarra V, Righetti R, Martignoni G, et al. Prognostic value of renal cell carcinoma nuclear grading: multivariate analysis of 333 cases. Urol Int 2001;67:130-134.
39. Fuhrman SA, Lasky LC, Limas C. Prognostic significance of morphologic parameters in renal cell carcinoma. Surg Pathol 1982;6:655-663.

40. Garcia-Solano J, Acosta-Ortega J, Perez-Guillermo M, et al. Solid renal masses in adults: image-guided fine-needle aspiration cytology and imaging techniques –two heads better than one? Diagn Cytopathol 2008;36:8-12.
41. Giashuddin S, Cangiarella J, Elgert P, Levine PH. Metastases to the kidney: eleven cases diagnosed by aspiration biopsy with histological correlation. Diagn Cytopathology 2005;32:325-329.
42. Glentoj A, Partoft S. Ultrasound-guided percutaneous aspiration of renal angiomyolipoma. Report of two cases diagnosed by cytology. Acta Cytol 1984;28:265-268.
43. Goregaonkar R, Shet T, Ramadwar M, Chinoy R. Critical role of fine needle aspiration cytology and immunocytochemistry in preoperative diagnosis of pediatric renal tumors. Acta Cytol 2007;51:721-729.
44. Granter SR, Renshaw AA. Fine-needle aspiration of chromophobe renal cell carcinoma. Analysis of six cases. Cancer(Cancer Cytopathol) 1997;81:122-128.
45. Granter SR, Fletcher JA, Renshaw AA. Cytologic and cytogenetic analysis of metanephric adenoma of the kidney: a report of 2 cases. Am J Clin Pathol 1997;108:544-549.
46. Granter SR, Perez-Atayde AR, Renshaw AA. Cytologic analysis of papillary renal cell carcinoma. Cancer 1998;84:303-308.
47. Grignon DJ, Ayala AG, Ro JY, et al. Primary sarcomas of the kidney. A clinicopathologic and DNA flow cytometric study of 17 cases. Cancer 1990;65:1611-1618.
48. Gupta M, Venkatesh SK, Kumar A, Pandey R. Fine-needle aspiration cytology of bilateral renal malakoplakia. Diagn Cytopathol 2004;31:116-117.
49. Gupta R, Viswanathan S, D'Cruz A, Kane SV. Metastatic papillary carcinoma of thyroid masquerading as a renal tumor. J Clin Pathol 2008;61:143.
50. Hammerich KH, Gustavo EA, Wheeler TM. Application of immunohistochemistry to the genitourinary system (prostate, urinary bladder, testis, and kidney). Arch Pathol Lab Med 2008;132:432-440.
51. Hartwick RW, el-Naggar AK, Ro JY, et al. Renal oncocytoma and granular renal cell carcinoma. A comparative clinicopathologic and DNA flow cytometric study. Am J Clin Pathol 1992;98:587-593.
52. Hayry P, von Willebrand E, Ahonen J, et al. Monitoring of organ allograft rejection by transplantation aspiration cytology. Ann Clin Res 1981;13:264-287.
53. Hunter S, Samir A, Eisner B, et al. Diagnosis of renal lymphoma by percutaneous image guided biopsy: experience with 11 cases. J Urol 2006;176:1952-1956.
54. Imamoto T, Furuya Y, Ueda T, Ito H. Metanephric adenoma of the kidney. Int J Urol 1999;6:200-202.
55. Iyer VK, Agarwala S, Verma K. Fine-needle aspiration cytology of clear-cell sarcoma of the kidney: study of eight cases. Diagn Cytopathol 2005;33:83-89
56. Johnson PT, nazarian LN, Feld RI, et al. Sonographically guided renal mass biopsy: indications and efficacy. J Ultrasound Med 2001;20:749-753.
57. Jow WW, Zeid MY, Cowan D, et al. Renal oncocytoma: long-term follow-up and flow cytometric DNA analysis. J Surg Oncol 1991;46:53-59.
58. Juul N, Torp-Pedersen S, Gronvall S, et al. Ultrasonically guided fine needle aspiration biopsy of renal masses. J Urol 1985;133:579-581.
59. Kapasi H, Robertson S, Futter N. Diagnosis of renal malakoplakia by fine needle aspiration cytology. A case report. Acta Cytol 1998;42:1419-1423.
60. Katz RL. Kidney, Adrenal and retroperitoneum. In: Bibbo M. (ed). Comprehensive Cytopathology. W.B. Saunders Company, Philadelphia, 1991,pp.781-782.
61. Khayyata S, Grignon DJ, Aulicino MR, Al-Abbadi MA. Metanephric adenoma vs. Wilms tumor: a report of 2 cases with diagnosis by fine needle aspiration and cytologic comparisons. Acta Cytol 2007;51:464-467.
62. Khurana KK, Powers CN. Basaloid squamous carcinoma metastatic to renal-cell carcinoma: fine-needle aspiration cytology of tumor-to-tumor metastasis. Diagn Cytopathol 1997;17:379-382.
63. Kobayashi A, Utsunomiya Y, Kono M, et al. Malakoplakia of the kidney. Am J Kidney Dis 2008;51:326-330.
64. Kovacs G, Fuzesi L, Emanual A, et al. Cytogenetics of papillary renal cell tumors. Genes Chromosomes Cancer 1991;3:249-255.
65. Kramer BA, Gao X, Davis M, et al. Prognostic significance of ploidy, MIB-1 proliferation marker, and p53 in renal cell carcinoma. J Am Coll Surg 2005;201:565-570.
66. Krishnamurthy S, Bharadwaj R. Fine needle aspiration cytology of clear cell sarcoma of the kidney. A case report. Acta Cytol 1998;42:1444-1446.
67. Kümmerlin IP, Smedts F, Ten Kate FJ, et al. Cytological punctures in the diagnosis of renal tumours: a study on accuracy and reproducibility. Eur Urol 2009;55:187-195.
68. Lang EK. Renal cyst puncture and aspiration. A survey of complications. Am J Roentgenol 1997;128:723.
69. Leiman G. Audit of fine needle aspiration cytology of 120 renal lesions. Cytopathol 1990;1:65-72.
70. Leppaniemi A, Wuokko E, Taavitsainen M, et al. Xanthogranulomatous pyelonephritis in a functioning kidney. Ann Chir Gynaecol 1987;76:226-229.
71. Li P, Perle MA, Scholes JV, Yang GC. Wilms tumor in adults: aspiration cytology and cytogenetics. Diagn Cytopathol 2002;26:99-103.
72. Lieber MM, Tomera KM, Farrow GM. Renal oncocytoma. J Urol 1981;125:481-485.
73. Lim JC, Wojcik EM. Fine-needle aspiration cytology of papillary renal cell carcinoma: the association with concomitant secondary malignancies. Diagn Cytopathol 2006;34:797-800.
74. Liu J, Fanning CV. Can renal oncocytomas be distinguished from renal cell carcinoma on fine-needle aspiration specimens? A study of conventional smears in conjunction with ancillary studies. Cancer 2001;93:390-397.
75. Liu L, Qian J, Singh H, et al. Immunohistochemical analysis of chromophobe renal carcinoma, renal oncocytoma and clear cell carcinoma: an optimal and practical panel for differential diagnosis. Arch Pathol Lab Med 2007;131:1290-1297.
76. Manfro RC, Goncalves LF, de Moura LA. Reproducibility of fine-needle aspiration biopsy in the diagnosis of acute rejection of renal allografts. Nephrol Dial Transplant 1995;10:2306-2309.
77. Masoom S, Venkataraman G, Jensen J, et al. Renal FNA-based typing of renal masses remains a useful adjunctive modality: evaluation of 31 renal masses with correlative histology. Cytopathology 2009;20:50-55.
78. Mete O, Kilicasian I, Gulluoglu MG, Uysal V. Can renal oncocytoma be differentiated from its renal mimics? The utility of antimitochondrial, caveolin 1, CD63 and cytokeratin 14 antibodies in the differential diagnosis. Virchows Arch 2005;447:938-946.
79. Moch H, Presti JCJr, Amin MB, et al. Genetic aberrations detected by comparative genomic hybridization are associated with clinical outcome in renal cell carcinoma. Cancer Res 1996;56:27-30.
80. Mondal A, Ghosh E. Fine needle aspiration cytology (FNAC) in the diagnosis of solid renal masses – a study of 92 cases. Indian J Pathol Microbiol 1992;35:333-339.
81. Muir TE, Cheville JC, Lager DJ. Metanephric adenoma, nephrogenic rests, and Wilms tumor: a histologic and immunophenotypic comparison. Am J Surg Pathol 2001;25:1290-1296.

82. Nayak A, Iyer VK, Agarwala S, Verma K. Fine needle aspiration cytology of cystic partially differentiated nephroblastoma of the kidney. Cytopathology 2006;17:145-148.
83. Nguyen GK. Aspiration biopsy cytology of renal angiomyolipoma. Acta Cytol 1984;28:261-268.
84. Niceforo J, Coughlin BF. Diagnosis of renal cell carcinoma: value of fine-needle aspiration cytology in patients with metastases or contraindications to nephrectomy. AJR Am J Roentgenol 1993;161:1303-1305.
85. Orell SR, Langlois SLL, Marshall VR. Fine needle aspiration cytology in the diagnosis of solid renal and adrenal masses. Scand J Urol Nephrol 1985;19:211-216.
86. Pahernik S, Ziegler S, Roos F, et al. Small renal tumors: correlation of clinical and pathological features with tumor size. J Urol 2007;178:414-417.
87. Pan CC, Chen PC, Ho DM. The diagnostic utility of MOC31, BerEp4, RCC marker and CD10 in the classification of renal cell carcinoma and renal oncocytoma: an immunohistochemical analysis of 328 cases. Histopathology 2004;45:452-259.
88. Pancholi V, Munjal K, Jain M, et al. Preoperative diagnosis of renal angiomyolipoma with fine needle aspiration cytology: a report of 3 cases. Acta Cytol 2006;50:466-468.
89. Papadopoulos I, Weichert-Jacobsen K, Nürnberg N, Sprenger E. Quantitative DNA analysis in renal cell carcinoma. Comparison of flow and image cytometry. Anal Quant Cytol Histol 1995;17:272-275.
90. Pasternak A. Fine-needle aspiration biopsy of human renal homografts. Lancet 1968;2:82.
91. Pignot G, Elie C, Conquy S, et al. Survival analysis of 130 patients with papillary renal carcinoma: prognostic utility of type 1 and type 2 subclassification. Urology 2007;69:230-235.
92. Pinto AE, Monteiro P, Silva G, et al. Prognostic biomarkers in renal cell carcinoma: relevance of DNA ploidy in predicting disease-related survival. Int J Biol Markers 2005;20:249-256.
93. Pohar-Marinsek Z. Difficulties in diagnosing small round cell tumors of childhood from fine needle aspiration cytology samples. Cytopathology 2008;19:67-79.
94. Portugal R, Barroca H. Clear cell sarcoma, cellular mesoblastic nephroma and metanephric adenoma: cytological features and differential diagnosis with Wilms tumor. Cytopathology 2008;19:80-85.
95. Pranab D, Srinivasan R, Ashim D, Raje N. Aspiration cytology of renal cell carcinoma and adenoma in childhood. Acta Cytol 1996;40:457-460.
96. Quijano G, Drut R. Cytologic characteristics of Wilms tumors in fine needle aspirates. A study of ten cases. Acta Cytol 1989;33:263-266.
97. Radhika S, Bakshi A, Rajwanshi A, et al. Cytopathology of uncommon malignant renal neoplasms in the pediatric age group. Diagn Cytopathol 2005;32:281-286.
98. Ravindra S, Kini U. Cytomorphology and morphometry of small round-cell tumors in the region of the kidney. Diagn Cytopathol 2005;32:211-216.
99. Remzi M, Ozsoy M, Klingler HC, et al. Are small renal tumors harmless? Analysis of histopathological features according to tumors 4 cm or less in diameter. J Urol 2006;176:896-899.
100. Renshaw AA, Granter SR, Cibas ES. Fine-needle aspiration of the adult kidney. Cancer 1997;81:71-88.
101. Renshaw AA, Granter SR, Fletcher JA, et al. Renal cell carcinomas in children and young adults: increased incidence of papillary architecture and unique subtypes. Am J Surg Pathol 1999;23:795-802.
102. Renshaw AA, Lee KR, Madge R, Granter SR. Accuracy of fine needle aspiration in distinguishing subtypes of renal cell carcinoma. Acta Cytol 1997;41:987-994.
103. Ruiz-Cerda JL, Hernandez M, Sempere A, et al. Intratumoral heterogeneity of DNA content in renal cell carcinoma and its prognostic significance. Cancer 1999;86:664-671.
104. Salamanca J, Alberti N, Lopez-Rios F, et al. Fine needle aspiration of chromophobe renal cell carcinoma. Acta Cytol 2007;51:9-15.
105. Sardi A, Agnone CM, Pellegrini A. Renal metastases from papillary thyroid carcinoma. J La State Med Soc 1992;144:416-420.
106. Schachter LR, Cookson MS, Chang SS, et al. Second prize: frequency of benign renal cortical tumors and histologic subtypes based on size in a contemporary series: what tell to our patients. J Endourol 2007;21:819-823.
107. Schlomer B, Figenshau RS, Yan Y, et al. Pathological features of renal neoplasms classified by size and symptomatology. J Urol 2006;176:1317-1320.
108. Sharifah NA. Fine needle aspiration cytology characteristics of renal tumors in children. Pathology 1994;26:359-364.
109. Shek TW, Luk IS, Peh WC. Metanephric adenofibroma: report of a case and review of the literature. Am J Surg Pathol 1999;23:727-733.
110. Shenoy PD, Lakhkar BN, Ghosh MK, et al. Cutaneous seeding of renal carcinoma by Chiba needle aspiration biopsy. Case report Acta Radiol 1991;32:50-52.
111. Slwotzky C, Maya M. Needle tract seeding of transitional cell carcinoma following fine-needle aspiration of a renal mass. Abdom Imaging 1994;19:174-176.
112. Suen KC, et al. The Papanicolaou Society of Cytopathology Task Force on standards of practice. Guidelines of the Papanicolaou Society of Cytopathology for fine-needle aspiration procedure and reporting. Modern Pathol 1997;10:739-747.
113. Tallada N,Martinez S, Rowentos A. Cytologic study of renal angiomyolipoma by fine-needle aspiration biopsy: report of four cases. Diagn Cytopathol 1994;10:37-40.
114. Todd TD, Dhurandhar B, Mody D, et al. Fine-needle aspiration of cystic lesions of the kidney. Morphologic spectrum and diagnostic problems in 41 cases. Am J Clin Pathol 1999;111:317-328.
115. Truong LD, Todd TD, Dhurandhar B, Ramzy I. Fine-needle aspiration of renal masses in adults: analysis of results and diagnostic problems in 108 cases. Diagn Cytopathol 1999;20:339-349.
116. Veloso JD, Solis OG, Barada JH, et al. DNA ploidy of oncocytic-granular renal cell carcinomas and renal oncocytomas by image analysis. Arch Pathol Lab Med 1992;116;154-158.
117. Villanueva RR, Nguyen-Ho P, Nguyen GK. Leiomyosarcoma of the kidney. Report of a case diagnosed by fine needle aspiration cytology and electron microscopy. Acta Cytol 1994;38:568-572.
118. Volpe A, Kachura JR, Geddie WR, et al. Techniques, safety and accuracy of sampling of renal tumors by fine needle aspiration and core biopsy. J Urol 2007;178:379-386.
119. Wang HY, Mills SE. KIT and RCC are useful in distinguishing chromophobe renal cell carcinoma from the granular variant of clear cell renal cell carcinoma. Am J Surg Pathol 2005;29:640-646.

120. Wiatrowska BA, Zakowski MF. Fine-needle aspiration biopsy of chromophobe renal carcinoma and oncocytoma: comparison of cytomorphologic features. Cancer 1999;87:161-167.
121. Zardawi IM. Renal fine needle aspiration cytology. Acta Cytol 1999;43:184-190.
122. Zajicek J. Aspiration biopsy cytology, II. Cytology of infradiaphragmatic organs. in: Monographs in Clinical Cytology. Basel, S Karger, pp: 1-37, 1987.
123. Zbar B, Brauch H, Talmadge C, Linehan M. Loss of alleles of loci on the short arm of chromosome 3 in renal cell carcinoma. Nature 1987;327:721-724.
124. Zugor V, Schott GE, Labanaris AP. Xanthogranulomatous pyelonephritis in childhood: a critical analysis of 10 cases and of the literature. Urology 2007;70:157-160.

**Figs. 12.1 and 12.2 Cytology of normal renal parenchyma.**
Direct smears from aspirates of the kidney are Pap-stained.

**Fig. 12.1A–C** Glomerule and proximal convoluted tubule.
**A** A whole intact glomerule is presented (lower magnification). **B** Glomerular detail exhibits the difficulty distinguishing between endothelial cells of small capillary vessels and small epithelial cells. **C** Epithelial cells lining proximal convoluted tubules are arranged in flat sheets exhibiting granular cytoplasm (high magnification).

**Fig. 12.2** Henle loop / distal convoluted tubule.
A tubular formation is composed of small to medium-sized cells with no cytoplasmic granulation. Nuclei in focus exhibit prominent nucleoli (high magnification).

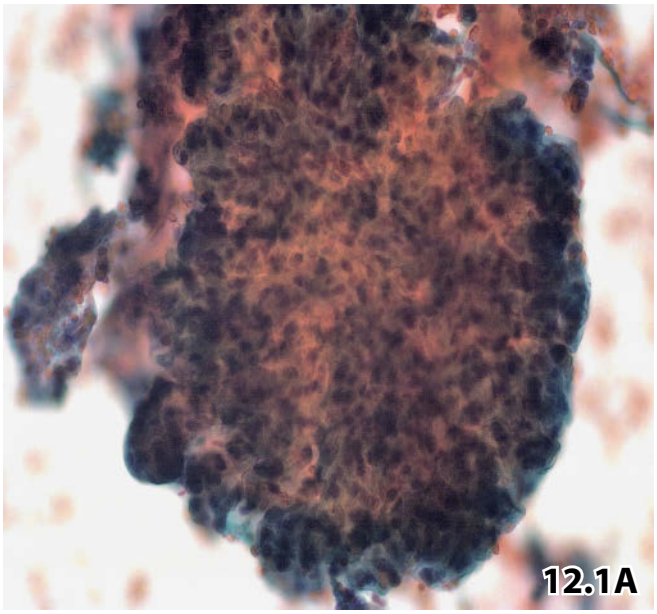
12.1A

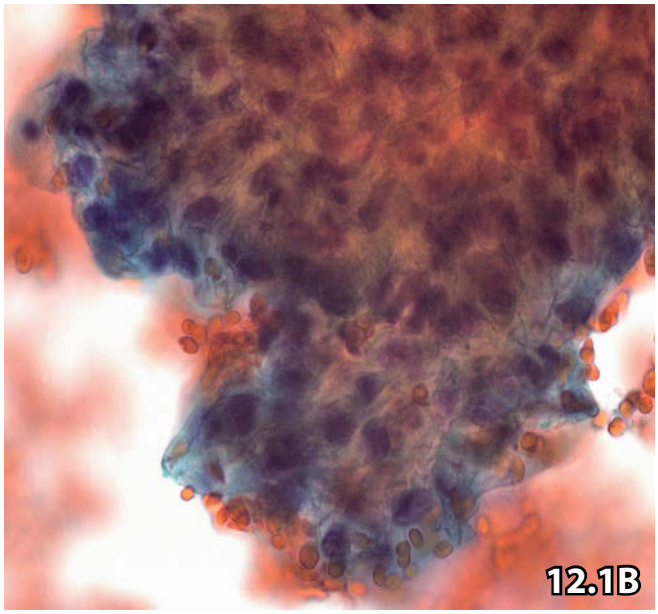
12.1B

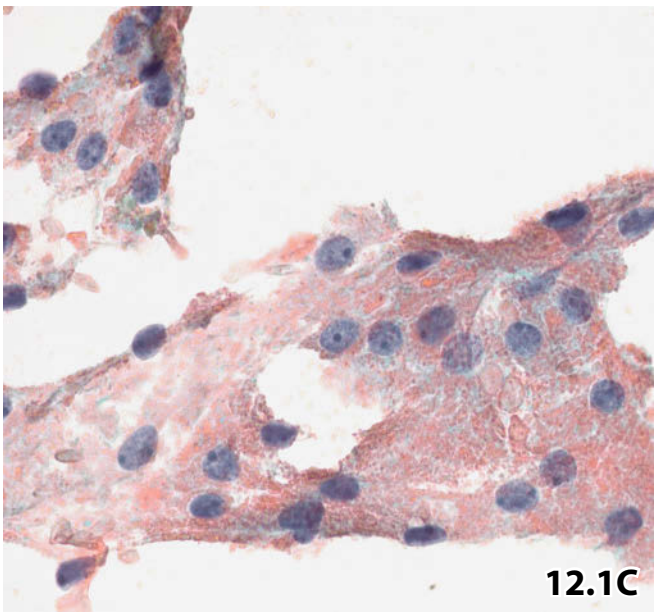
12.1C

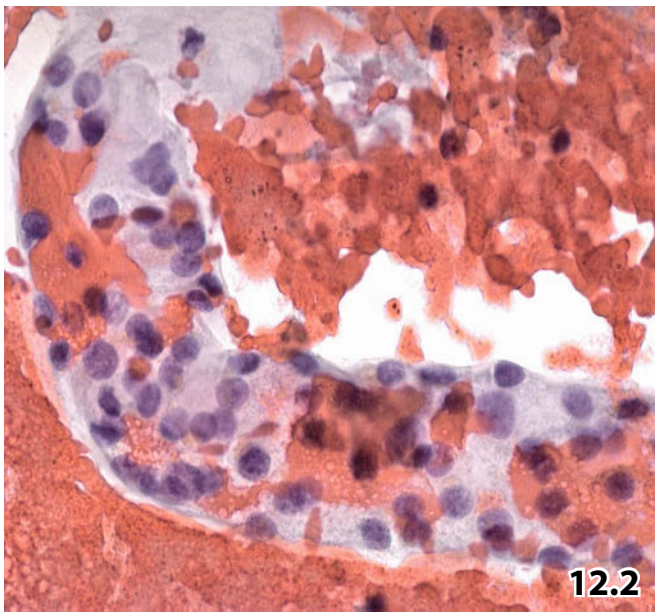
12.2

**Fig. 12.3 Mycobacteriosis.**
Imaging showed a cyst in the right kidney of a young woman. Irregular aggregates of slender epithelioid cells are embedded in a detritic background (image-guided FNAB, direct smear, Pap stain, higher magnification).
*Cytomorphology* suggested mycobacteriosis. Acid-fast bacilli were detected in direct smears (not shown). Typing by culture failed for technical reasons. The patient was lost to follow-up and advanced investigation.

**Fig. 12.4A, B Xanthogranulomatous pyelonephritis versus malakoplakia: diagnostic dilemmas.**
A 70-year-old woman presented with a large palpable tumor mass in her right flank. Clinical and image investigations suggested hypernephroma. FNAB was performed; direct smears were Pap-stained.
*Cytologic diagnosis:* Xanthogranulomatous pyelonephritis.
*Discussion:* Since intracytoplasmic calcospherites were not found, the histologic diagnosis, as stated below, could not be assessed by cytology. Aggregations of xanthomatous macrophages should not be misinterpreted as renal cell carcinoma.
*Histology* supplemented by electron microscopic findings: Malakoplakia.
**A** Large quantities of xanthomatous cells. Cellular degeneration, bi- and multinucleation, as well as phagocytosis of neutrophils (upper right) frequently occur (lower magnification). **B** Another area of the smear exhibits dense aggregation of foam cells. A mesenchymal strand with adherent xanthomatous macrophages mimics true papillary formation and consequently renal cell carcinoma (lower magnification).

**Fig. 12.5 Hydatid cyst.**
Aspirate from a renal cyst of a 37-year-old man mainly revealed debris and opaque masses; cellular elements were absent. Very few hooklets of a tapeworm (arrow) were scattered in the background of the smear (direct smear, Pap stain, low magnification).

Pay close attention to individual hooklets, as they are easily missed.
The refractivity of the hooklets can be accentuated by closing the substage diaphragm during microscopic screening (as demonstrated herein).

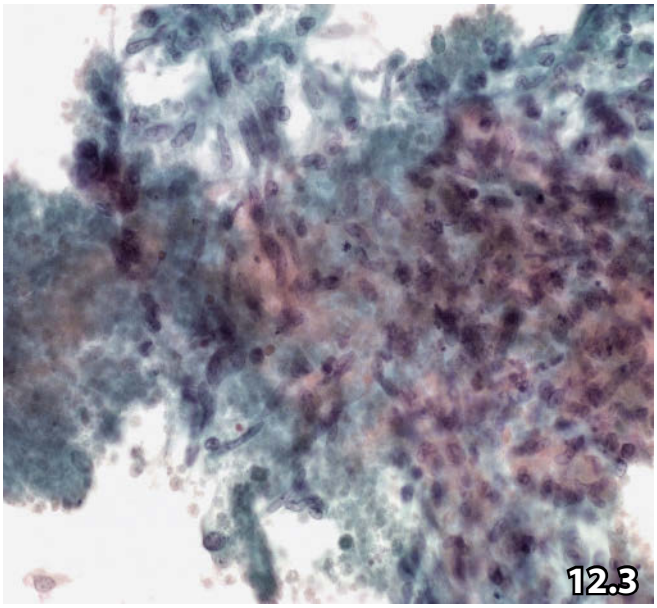
12.3

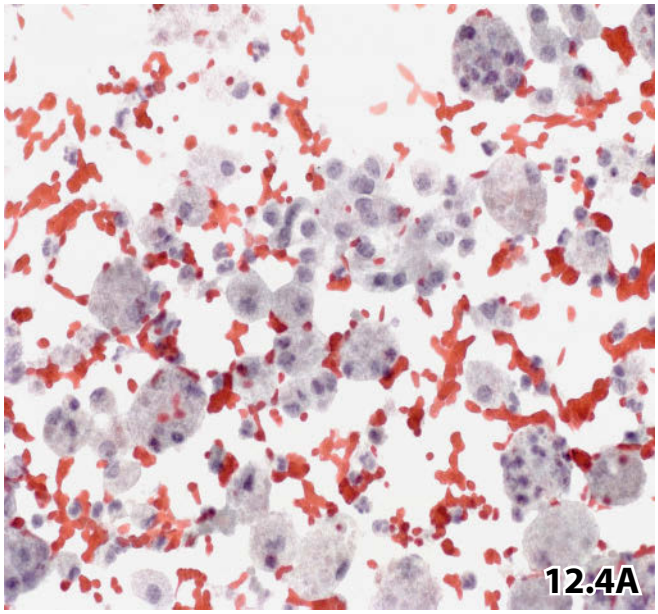
12.4A

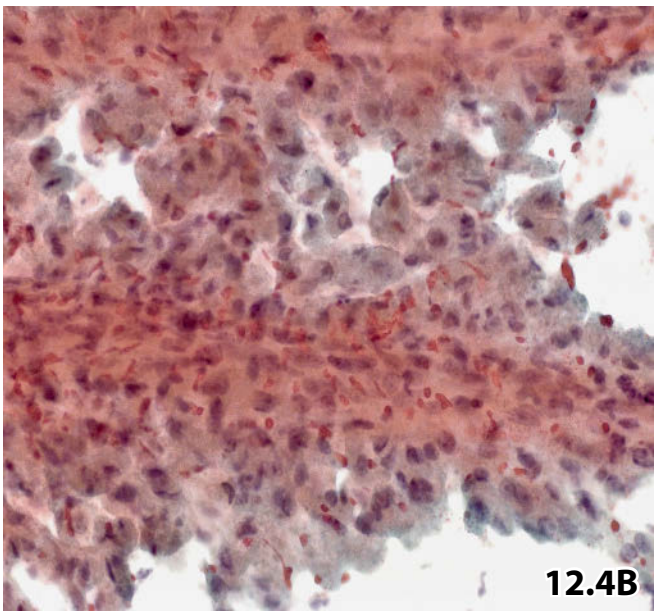
12.4B

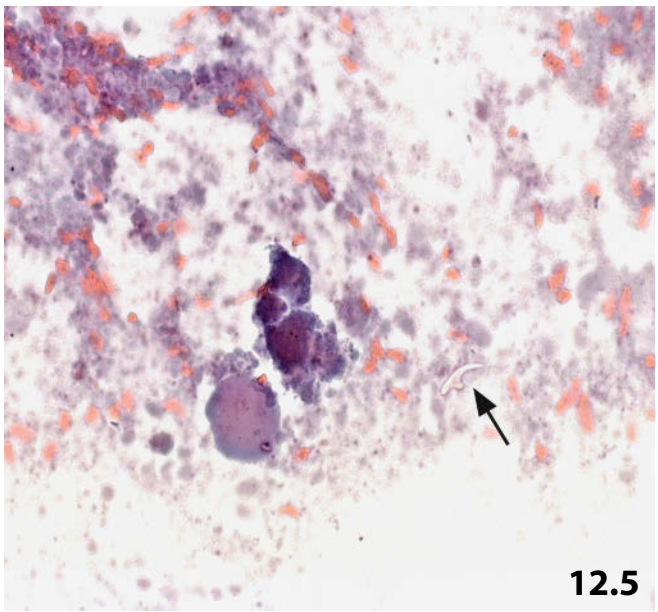
12.5

**Fig. 12.6A, B Cystic renal cortical adenoma.**
A 58-year-old woman with a positive history of both benign adnexal cysts and breast cancer presented with a cyst in her right kidney. Cyst fluid aspirate was processed using a conventional centrifuge, direct sediment smears were Pap-stained.
*Cytologic differential diagnosis*
(1) Severe regenerative cyst-lining epithelial cells.
(2) Cystic low-grade epithelial neoplasia (primary or metastatic).
(3) Metastasis from breast carcinoma (less likely because the cell features sort ill with mammary cancer).
*Tissue diagnosis* (resection of the renal tumor): Cystic renal cortical adenoma.
**A** High magnification shows numerous small lymphocytes and three-dimensional cell clusters with a knobby contour. The nuclei exhibit signs of activation (pronounced nucleoli) and bland chromatin. Distinguishing between activated epithelial cells and clustered activated histiocytes was not possible by light microscopy alone. **B** Immunostaining for epithelial antigen (BerEP4) indicated the epithelial nature of the cell clusters (Pap-prestained direct smear).

**Fig. 12.7A, B Renal oncocytoma.**
Coincidentally detected mass in the left kidney in a 49-year-old woman. Image-guided FNAB was performed. Conventional smears were Pap-stained.
*Tentative cytologic diagnosis:* Oncocytic adenoma or well-differentiated oncocytic carcinoma.
*Tissue diagnosis* (nephrectomy): Renal oncocytoma. Careful evaluation of the tumor periphery revealed no evidence of invasive growth.
**A** Low magnification shows irregular flat sheets composed of oncocytes. **B** Detail is focused on cells and nuclei exhibiting loss of polarity, variability in size and shape, nuclear displacement to the cytoplasmic border, and apoptotic nuclei. All these features suggest malignant degeneration.

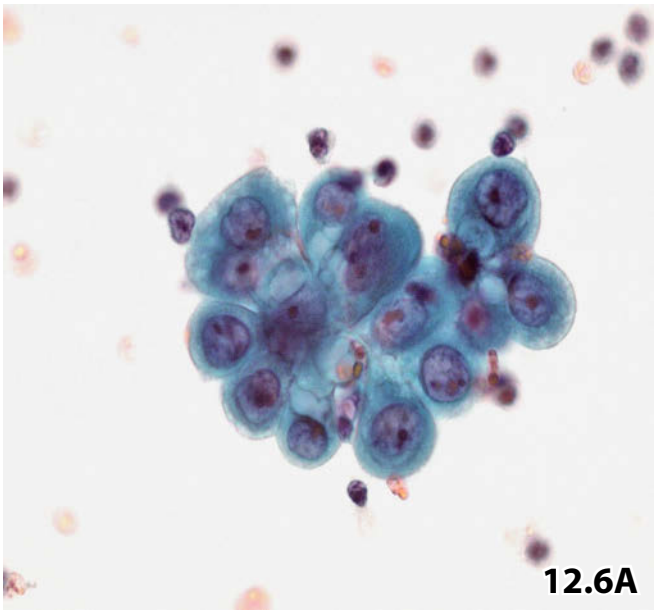

12.6A

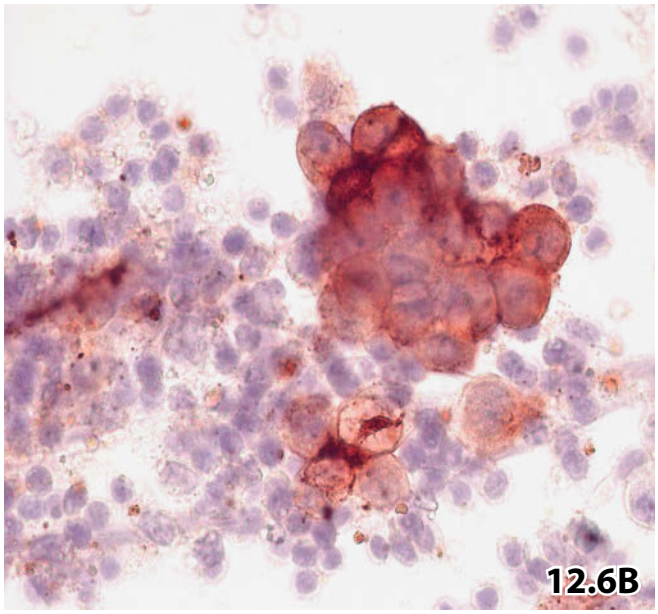

12.6B

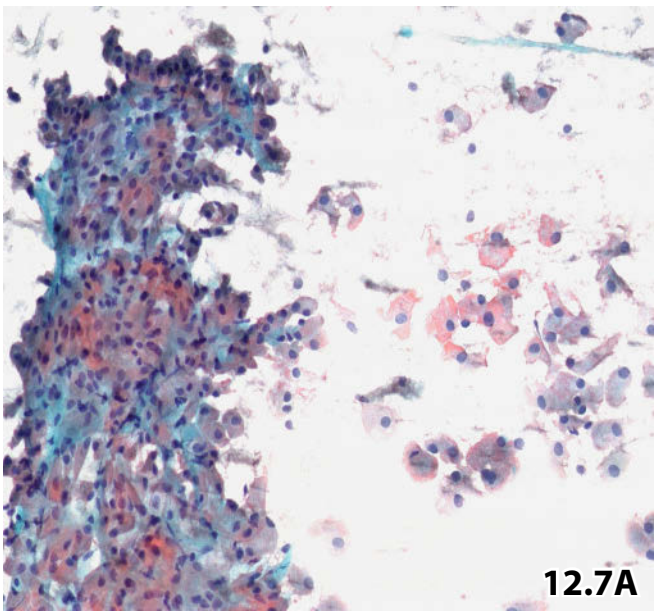

12.7A

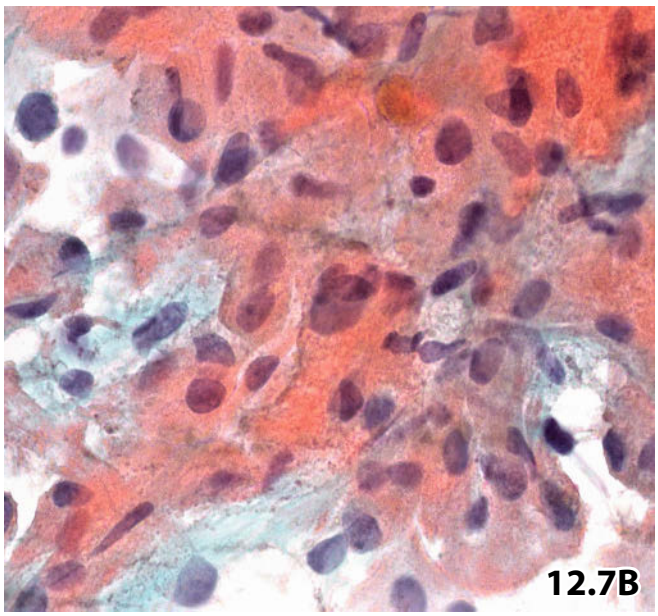

12.7B

**Figs. 12.8–12.10 Clear cell renal cell carcinoma.**
Primary clear cell renal carcinoma (CRCC) of three elderly female patients are demonstrated. Cell material was obtained by image-guided FNAB. Direct smears were Pap-stained.

**Fig. 12.8A, B** (case #1) Well-differentiated CRCC.
A 59-year-old woman presenting with a renal mass highly suspicious for renal cell carcinoma.
*Cytologic diagnosis* (confirmed by histology): Well-differentiated CRCC.
**A** Low magnification shows irregular papilliform clusters composed of monomorphic epithelial cells. The cytoplasm is abundant and clear. **B** High magnification is focused on clear cytoplasm which may be ill-defined (top) as well as sharply outlined, and tumor cell nuclei. Nuclear features of CRCC match those of papillary thyroid carcinoma and well-differentiated breast carcinoma: fine granular chromatin, clear nucleoplasm, small and indistinct nucleoli, nuclear molding, wrinkling, indentations, and grooves. Stripped nuclei are also present (a single nucleus is shown at the upper margin).

**Fig. 12.9A–C** (case #2) Moderately differentiated CRCC.
Follow-up imaging study revealed a large renal tumor mass in a 66-year-old woman with positive history of metastatic breast cancer.
*Cytologic/immunocytochemical diagnosis* (confirmed by histology): Moderately differentiated CRCC.
**A** Less well-differentiated CRCCs reveal the same basic morphologic features as presented for well-differentiated carcinoma. In addition, tumor cells present a denser cyanophilic or eosinophilic cytoplasm and exhibit more variability in size, and loss of polarization (lower magnification). **B** High magnification shows both clear and granular cytoplasm. The nucleoli tend to be larger in size as compared to those in well-differentiated CRCCs. Nuclear cleaving (not completely in focus) along with a dense cytoplasmic body could mislead to a false diagnosis of papillary transitional cell carcinoma. **C** Tumor cells immunocytochemically express renal cell antigen (RCCMa) (Pap-prestained specimen) and show negative reaction for CK13 (not shown).

**Fig. 12.10** (case #3) Poorly differentiated RCC.
An 80-year-old woman presented with a huge renal tumor mass invading the retroperitoneal space. Distinct cellular pleomorphism, large nucleoli, and wide dense or lucid cytoplasmic bodies are features indicating poorly differentiated RCC. Note hemosiderin deposits in the cytoplasm of macrophages and tumor cells (arrows) (high magnification). Further diagnostic evaluation was stopped due to the patient's advanced age and poor general condition.

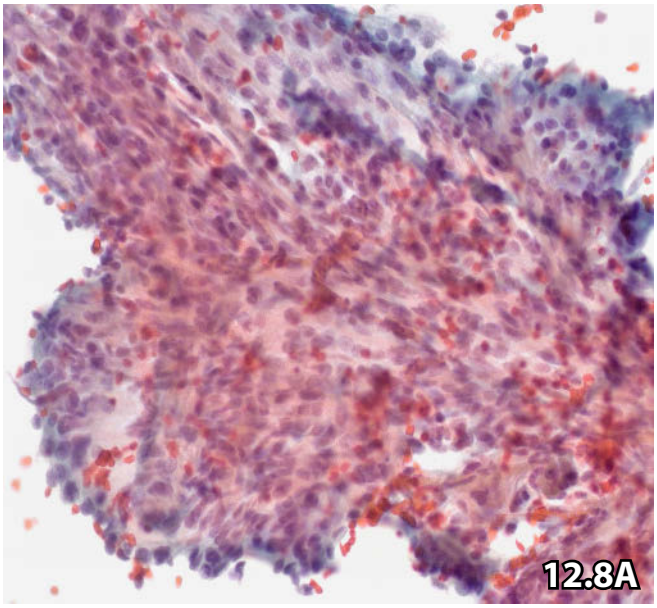
12.8A

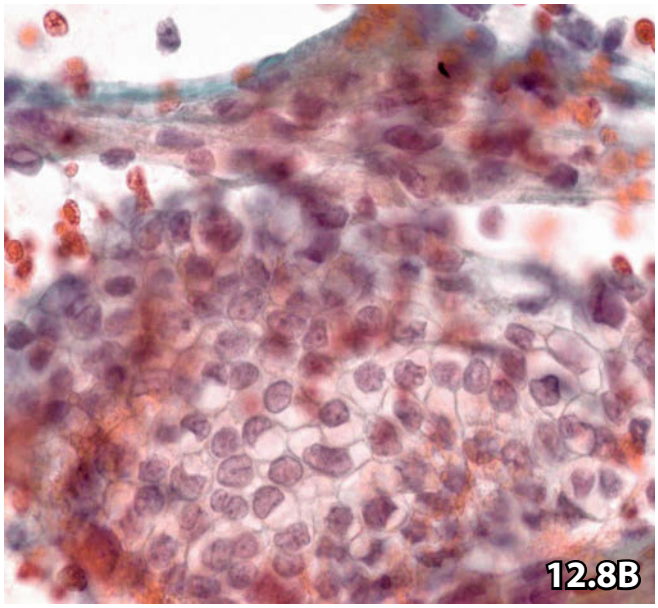
12.8B

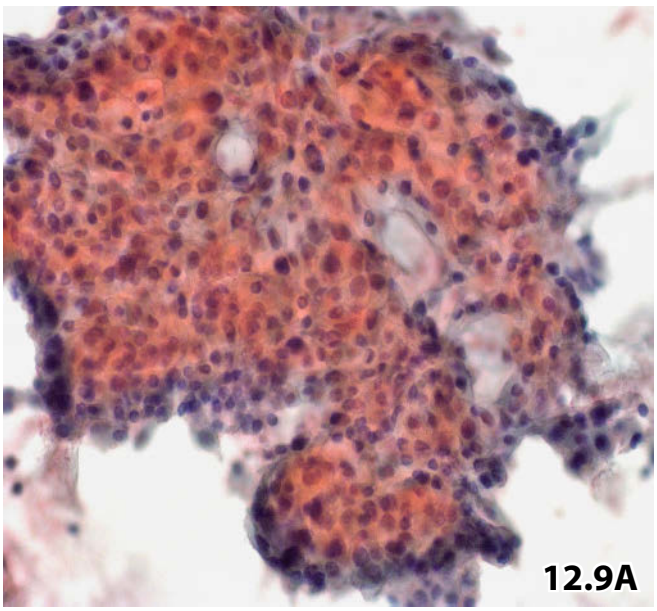
12.9A

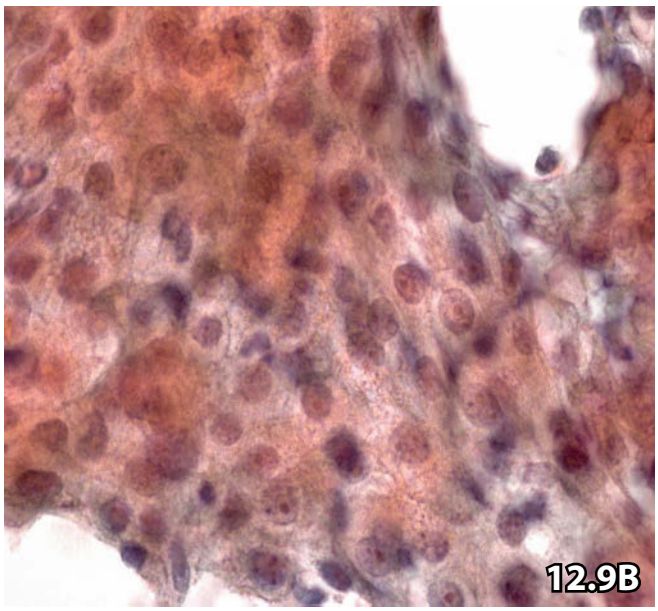
12.9B

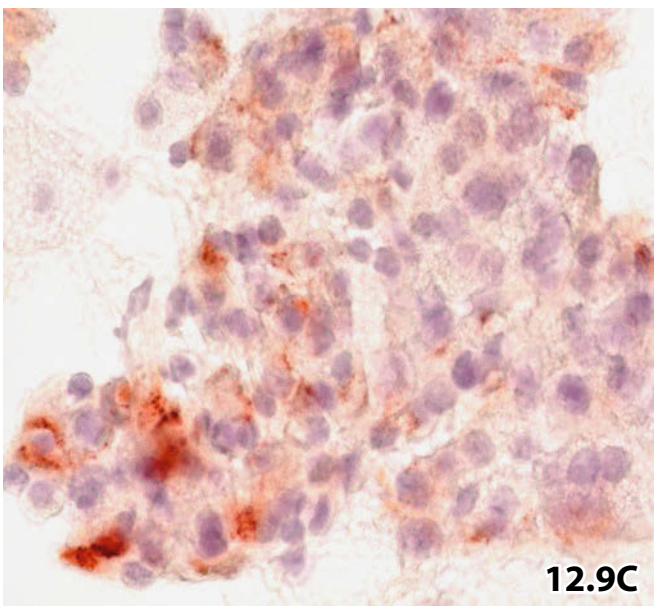
12.9C

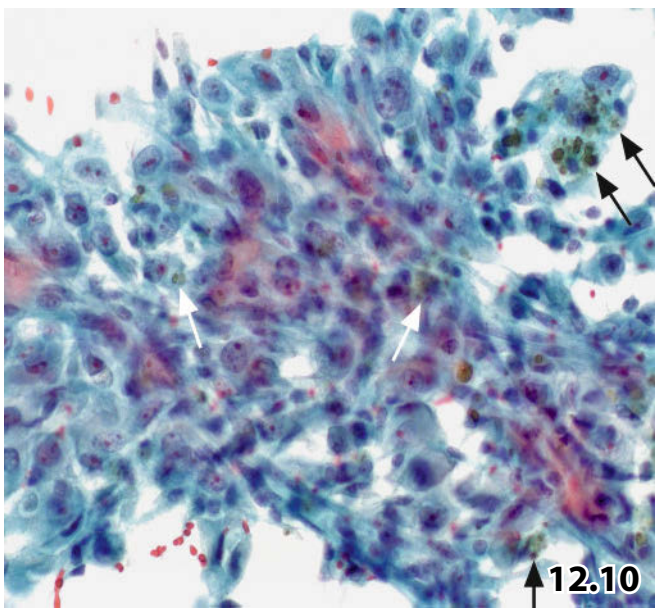
12.10

**Figs. 12.11 and 12.12 Papillary renal cell carcinoma.**
Examples of the papillary RCC variant are demonstrated in renal fine needle aspirates from two men. FNABs of the renal lesions were undertaken as a first-line diagnostic procedure in both patients. Direct smears from the aspirates were Pap-stained.
*Cytologic diagnosis and autopsic results in both cases:* Well-differentiated papillary RCC.

**Fig. 12.11** (case #1):A 79-year-old man presented with a huge renal tumor mass. An overview at low magnification exhibits large papillary tumor convolutes composed of monomorphic epithelial cells.

**Fig. 12.12A, B** (case #2) Sonography showed bilateral renal tumors in a 50-year-old man. **A** Nuclear overlapping and cellular palisading (arrows) are key features of papillary neoplasms shown at higher magnification. Note calcium deposits and psammomatous bodies (upper left). **B** Cleaved nuclear membranes (arrows) and nuclear grooves (arrowheads) are illustrated at high magnification. Foam cells (upper right) may mimic tumor cells.

Cytoarchitecture, cytoplasmic features, nuclear irregularities, psammoma bodies, and scattered foam cells are characteristics of papillary RCC. But the same features may be encountered in thyroid papillary carcinoma and low-grade papillary transitional cell carcinoma.

**Fig. 12.13 Renal cell carcinoma with sarcomatoid features.**
Dissociating tumor cell clusters of either epithelial type (upper left) or stromal type (bottom) represent poorly differentiated RCC with sarcomatoid differentiation. Note the large, clear and granular cytoplasm. Mitotic activity and inflammatory infiltrates are common (CT-guided FNAB of a renal mass, conventional smear, Pap stain, higher magnification).



**Fig. 12.14 Infiltrate of plasmacytoma in well-differentiated clear cell RCC.**
A 64-year-old man with a history of plasmacytoma presented with a mass in his left kidney. Ultrasound studies suspected hypernephroma. US-guided FNAB was performed. Direct smears of the aspirate were Pap-stained. High magnification shows unequivocal cells of plasmacytoma (arrowheads). The remaining cells exhibit abundant clear cytoplasm presenting diagnostic dilemmas, they may represent both immature plasma cells or tumor cells of clear cell RCC (some of the ambiguous cells are marked with arrows).
*Tentative cytologic diagnosis:* Plasmacytoma, immature tumor form.
*Comment:* By standard cytology, it is impossible to assign scattered clear tumor cells to immature portions of plasmacytoma or RCC. Immunostaining was not performed for technical reasons.
*Postmortem tissue diagnosis:* Well-differentiated RCC exhibiting focal infiltrates of plasmacytoma.

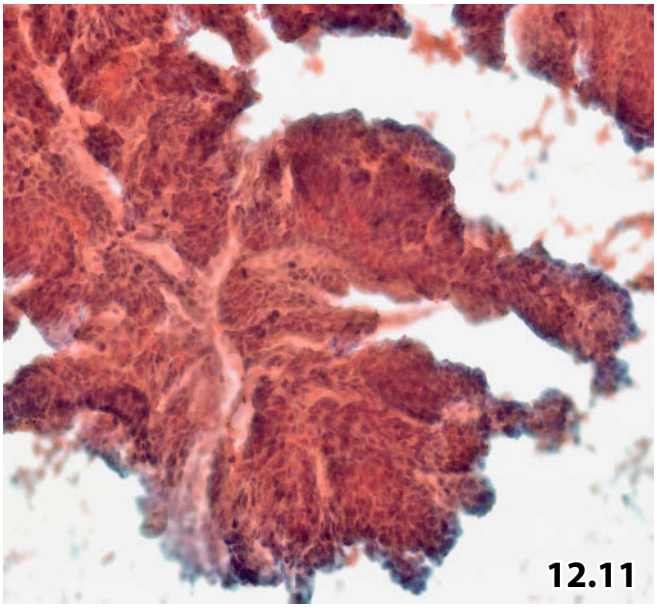
12.11

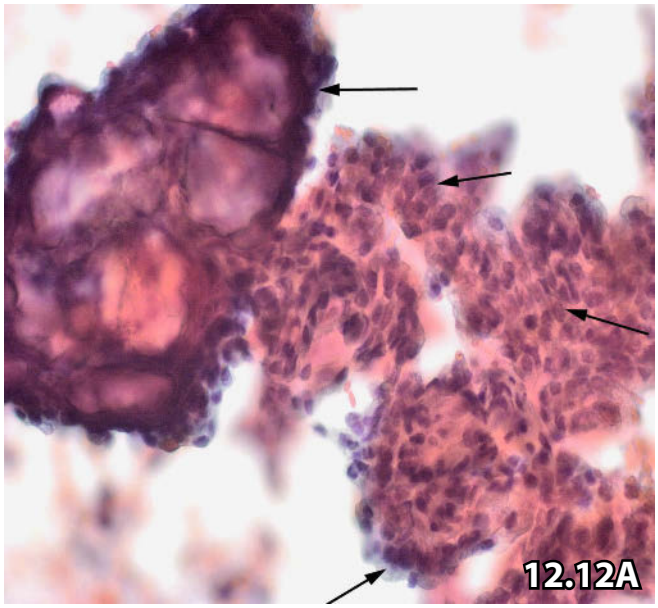
12.12A

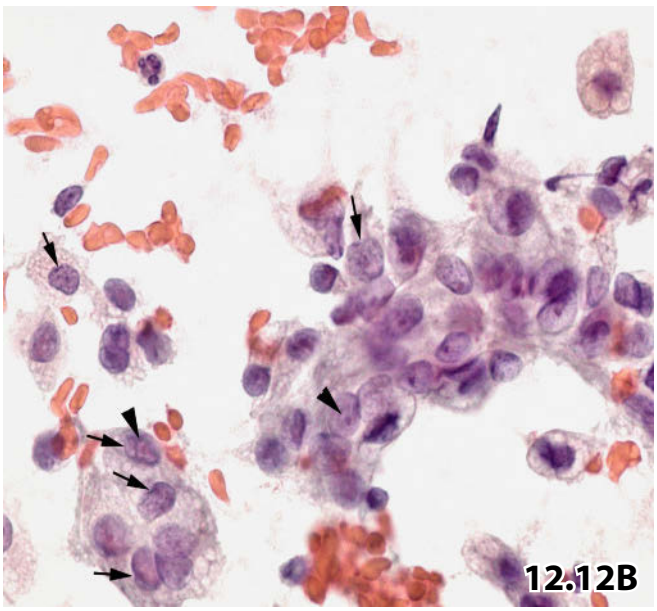
12.12B

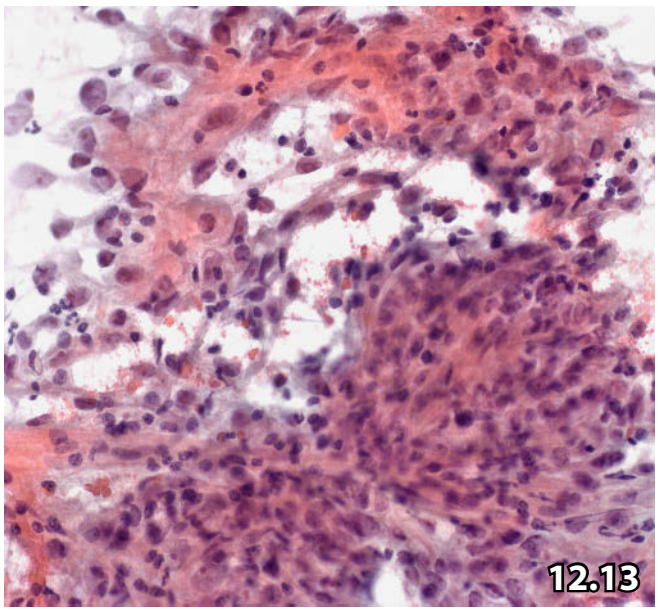
12.13

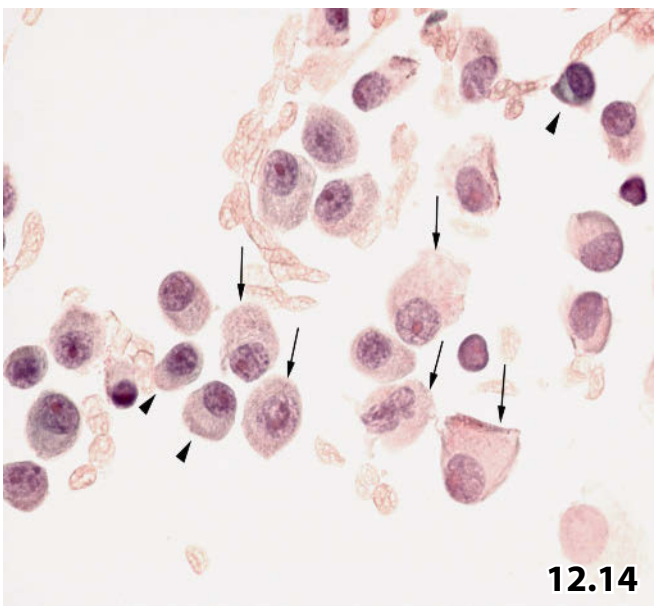
12.14

**Figs. 12.15 and 12.16 Low-grade transitional cell carcinoma versus papillary RCC.**
Two patients with papillary transitional cell carcinoma of the renal pelvis. We would like to emphasize that papillary neoplasms of the kidney may give rise to diagnostic confusion.

**Fig. 12.15** (case #1) A 77-year-old woman presented with hydronephrosis associated with a lesion in the right kidney. Image-guided FNAB was performed (direct smears, Pap stain). Low magnification shows papilliform and papillary cell clusters of uniform appearance (fibrovascular cores are not in focus). Compare architectural features with those of papillary renal cell carcinoma in Figs. 12.11 and 12.12A.
*(False) cytologic diagnosis:* Papillary RCC.
*Comment:* A renal process at the edge of the lower renal pole was localized by imaging. This incorrect information was a crucial factor for mistyping the renal tumor.
*Tissue diagnosis* (nephrectomy): Papillary transitional cell carcinoma of the renal pelvis.

**Fig. 12.16** (case #2) High magnification shows cellular features of another transitional cell carcinoma predominantly composed of clear cells comprising lucid nuclei and nuclear cleaving and grooves (renal FNAB, direct smear, Pap stain).
*Cytologic and metachronous histologic diagnosis:* Papillary transitional cell carcinoma, grade 1.

Distinguishing between papillary transitional cell cancer and papillary renal cell carcinoma and metastatic papillary thyroid carcinoma can be extremely difficult (compare with Fig. 12.12B).

**Fig. 12.17 High-grade transitional cell carcinoma.**
High magnification shows small tumor cell clusters and dispersed malignant cells. High N/C ratio, dense cyanophilic cytoplasm, and nuclear polymorphism are typical features of poorly differentiated transitional cell carcinoma (FNAB of a mass in the right kidney, direct smear, Pap stain).

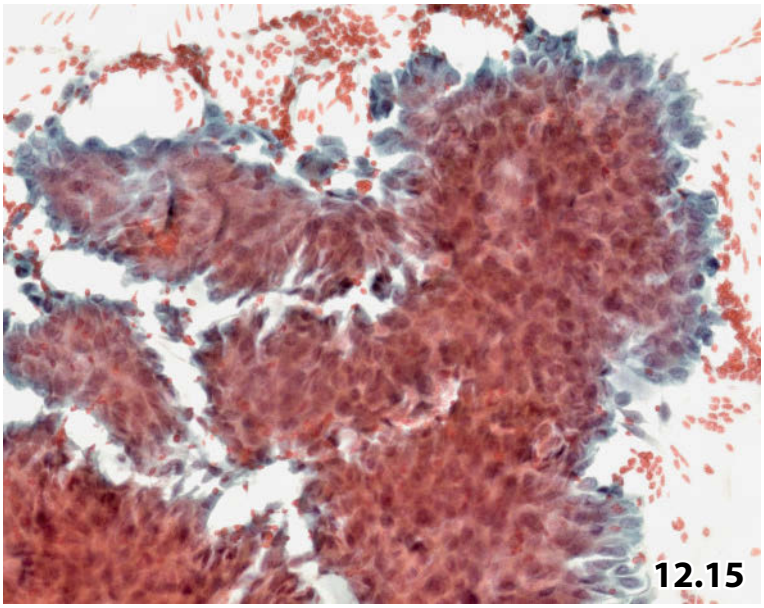
12.15

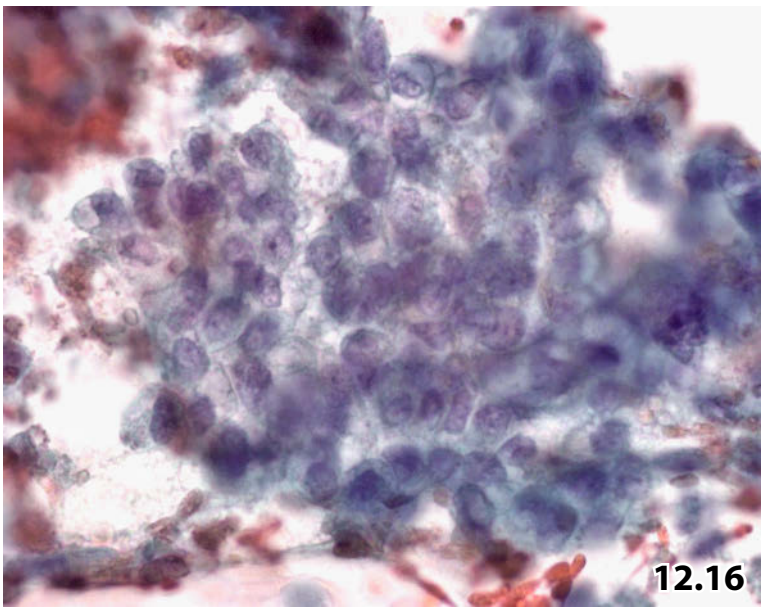
12.16

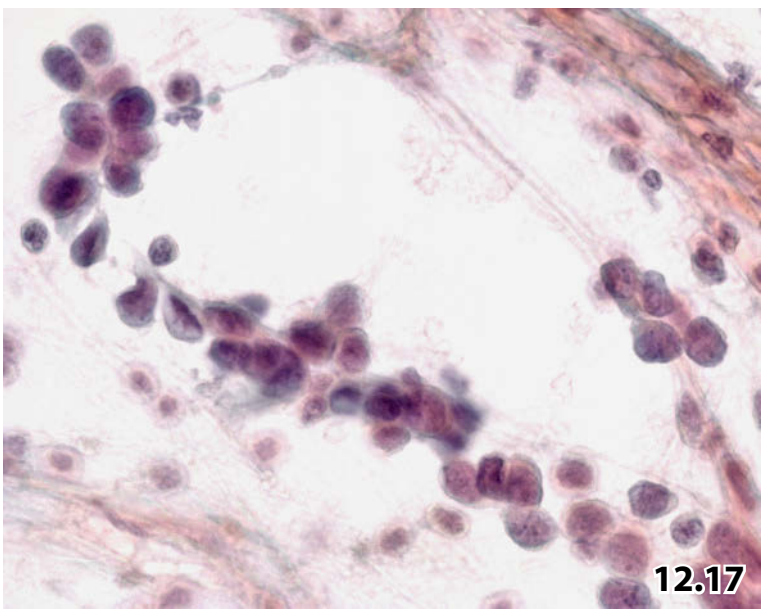
12.17

**Fig. 12.18A, B Wilms tumor (nephroblastoma): classic morphologic features.**
A 17-year-old woman was found to have a mass in her right kidney. Image-guided FNAB was performed. Aspirated cell material was directly smeared and Pap-stained. **A** A sharply circumscribed tubular formation is embedded in embryonal blastema. The epithelial tubular cluster is surrounded by a thin basal lamina (arrows). Haphazard arrangement of blastemal cells (lower magnification). **B** High magnification shows morphologic features of blastemal cells. Cellular elongation together with deep-staining nuclei are smearing artifacts.

**Fig. 12.19 Embryonal rhabdomyosarcoma versus Wilms tumor.**
Cells of embryonal rhabdomyosarcoma differ from cells of nephroblastoma: Cells of rhabdomyosarcoma have eccentrically placed nuclei that are surrounded by lightly staining eosinophilic cytoplasm (FNAB, direct smear, Pap stain, high magnification).

**Figs. 12.20 and 12.21 Neuroblastoma versus Wilms tumor.**
Cellular details and background features of two neuroblastomas are presented by means of an aspirate smear of a 25-year-old man and a scrape specimen from fresh tumor tissue of a 3-month-old baby.

**Fig. 12.20** (case #1) Cellular morphology of Wilms tumor and neuroblastoma can appear to be quite similar. Note the ganglion cell-like element (arrow) acting as a diagnostic indicator for a neuronal neoplasm (FNAB, direct smear, Pap stain, high magnification).

**Fig. 12.21** (case #2) Neurofibrillary background matrix and rosette-like aggregation of the tumor cells (arrows) are demonstrated in a scrape specimen taken from fresh tumor tissue (high magnification, Pap stain).

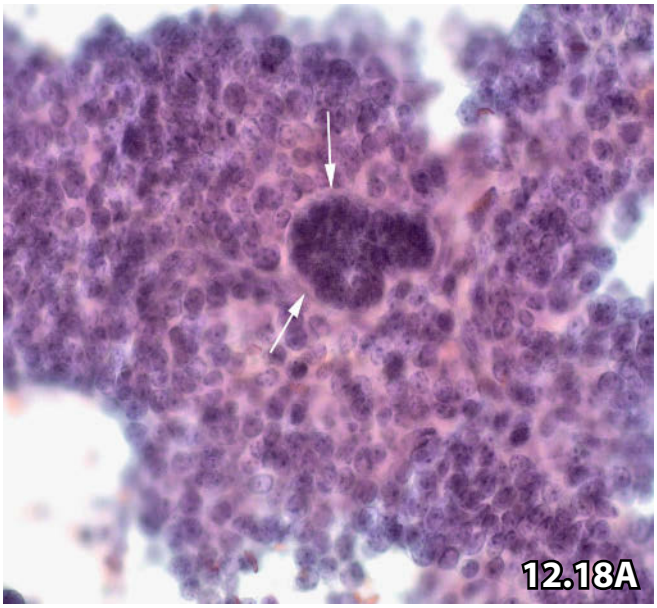
12.18A

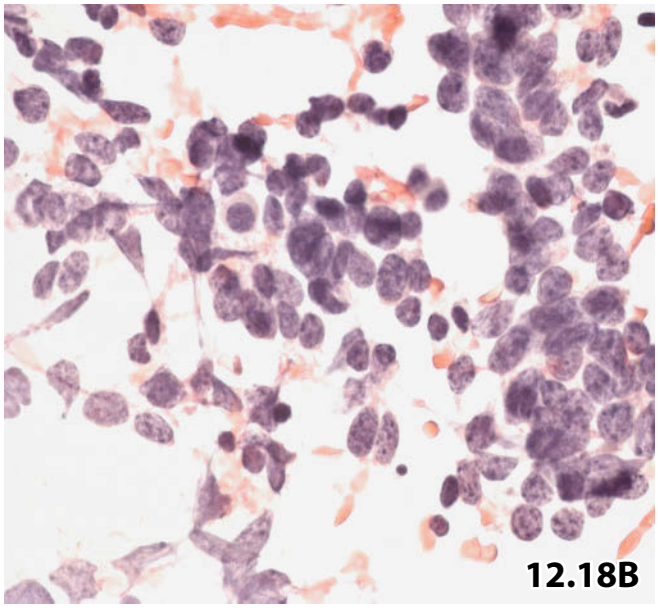
12.18B

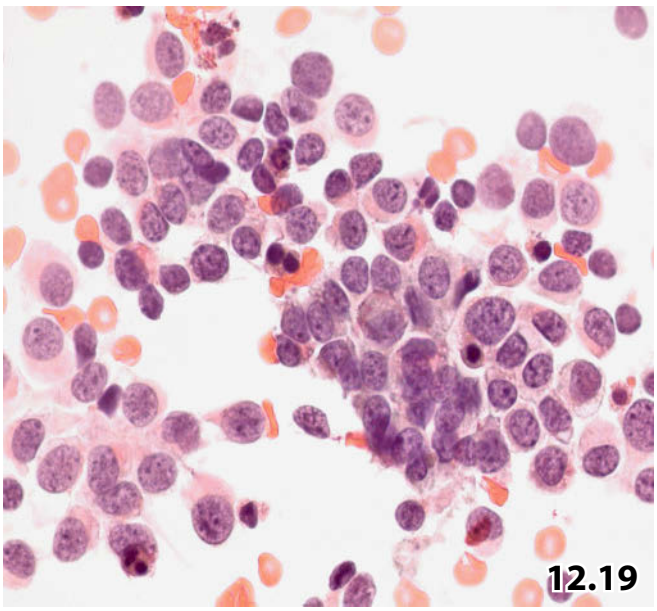
12.19

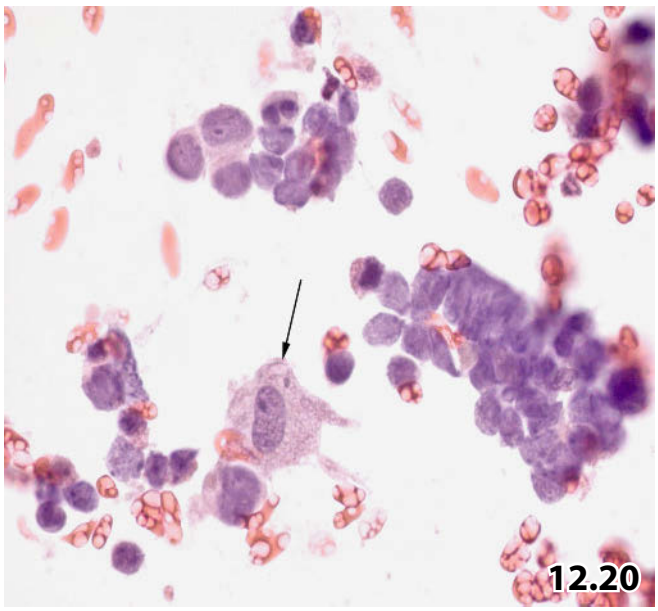
12.20

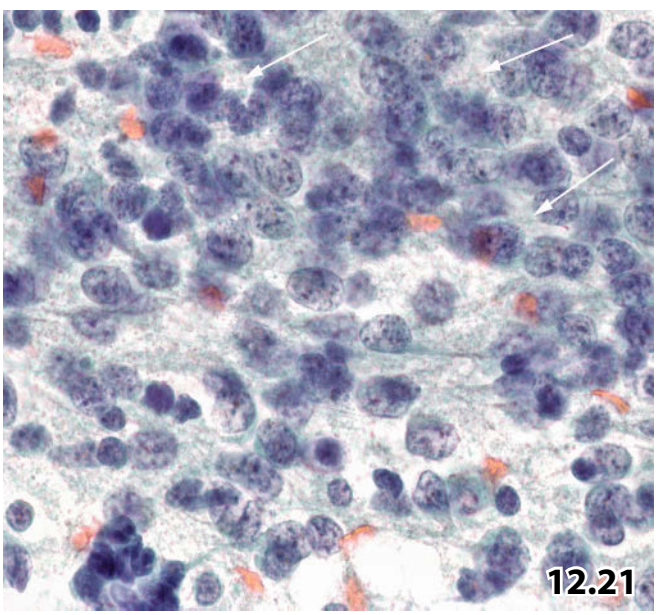
12.21

**Fig. 12.22A–C Ewing sarcoma versus Wilms tumor.**
FNAB of an extraskeletal Ewing sarcoma in a 20-year-old man. Direct smears were Pap-stained. **A** Monomorphic appearance of the cell pattern. The tumor cells are medium-sized, usually showing distinct cytoplasmic rims (low magnification). **B** High magnification exhibits pronounced nucleoli and distinct cytoplasm. Rosette-like formations are present (arrows). **C** Intracytoplasmic glycogen is visualized by periodic-acid Schiff stain (PAS). Glycogen was digested by hydrolyzing enzymes diastase (PAS/diastase reaction is not shown).

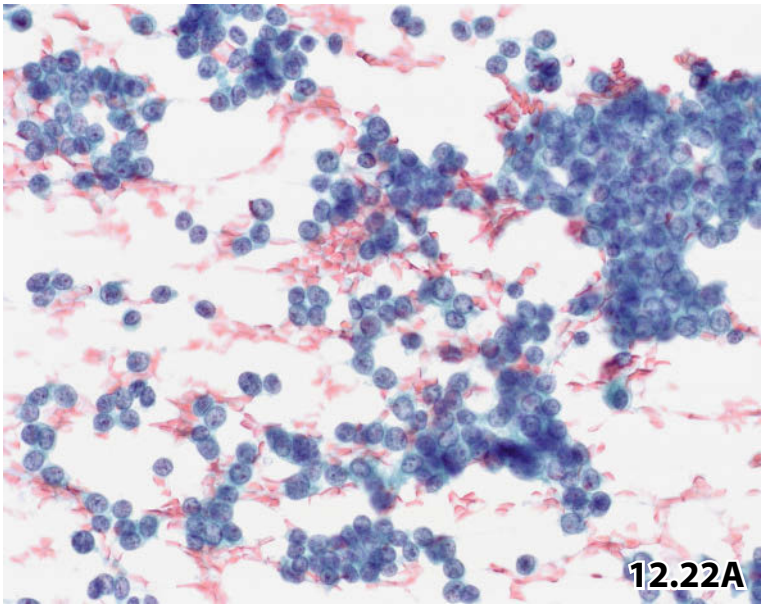
12.22A

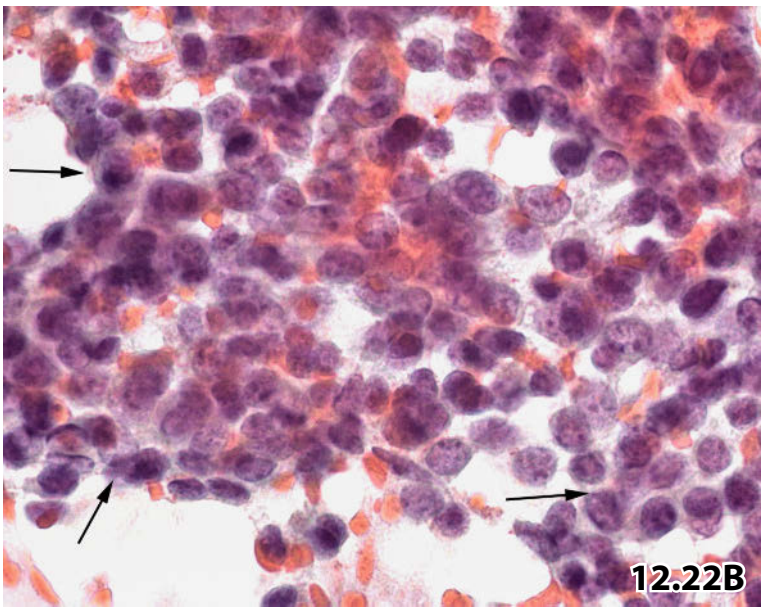
12.22B

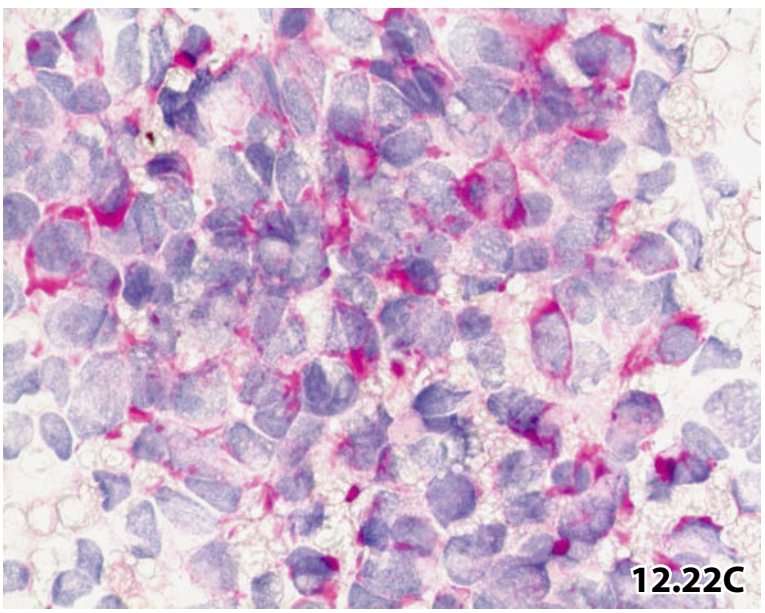
12.22C

# Section 12.2
# Adrenal Glands

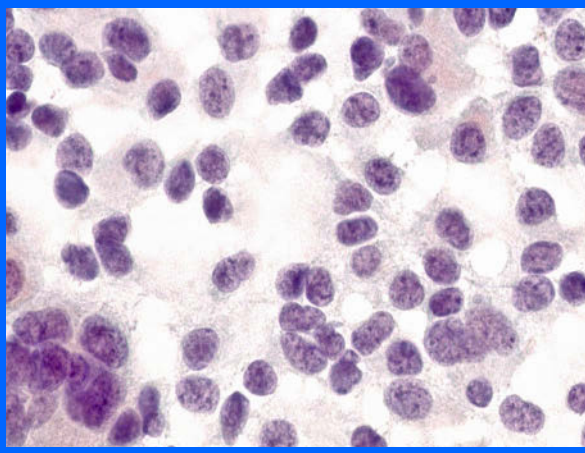

## 12.2.1 Introduction

Large-scale studies have found that FNAB is a highly specific and sensitive procedure for the evaluation of primary and secondary malignancies involving the adrenal glands; but the method seems to be less effective for benign disorders [4, 35, 45]. Sample cellularity has been shown to be adequate in the majority of the cases.

### 12.2.1.1 Imaging and Image-Guided FNAB

- Sonography, computed tomography, and magnet resonance imaging are most useful and well-established imaging procedures. Any method has shown to be appropriate for pathomorphological diagnostics in combination with transcutaneous FNAB [23, 24, 31].
- Endoscopic ultrasound-guided fine-needle aspiration biopsy (EUS-FNAB) is a relatively new tool that has been shown to be extremely helpful in clarifying small and large lesions located in the adrenals. EUS-guided transgastric aspiration offers easy access to the left-sided adrenal gland [2, 7, 11, 17, 39]. A limited number of studies indicate that EUS-FNAB may also be an option for right-sided adrenal masses [6].

### 12.2.1.2 Complications Following FNAB

- Complications following FNAB of adrenal masses have rarely been reported in the literature. However, adrenal and periadrenal hematoma are the most frequent side effects seen.
- Liver hematoma may occur when the needle incidentally pierces the hepar, causing extensive intraabdominal hemorrhage that may lead to a life-threatening situation.
- The dorsal approach can cause pneumothorax/hematothorax when the biopsy needle penetrates the lung.
- In order to prevent a potentially dangerous hypertensive crisis, biochemical testing for pheochromocytoma should be performed prior to aspiration biopsy [22, 25, 31, 33].

### 12.2.1.3 Indications for FNAB

General indications for FNAB of the adrenal glands as have been repeatedly established and reported in literature are as follows:

- Staging in patients with known or suspected malignant disease: a pathologic diagnosis will dictate therapeutic proceedings.
- Suspected lymphoma.
- Large (3- to 5-cm) lesion that is hormonally inactive and shows unequivocal signs of a tumor on imaging studies.
- Disorders of equivocal malignancy in selected cases.
- Incidentalomas.
- Disorders of the adrenals suggestive of an infection.
- Patients refusing surgery.

#### 12.2.1.4 Incidentaloma

Haphazardly discovered lesions greater than 1 cm in diameter that are hormonally inactive are referred to as adrenal incidentaloma. With the widespread application of varied image modalities, the chance of detecting an incidentaloma is close to 6% for all patients with radiographic and ultrasound tests [41].

Inconsistent comments on the value of FNAB in the diagnostic workup of incidentally detected adrenal masses are given in the literature [23, 24, 31, 33, 41]. The following procedure is widely accepted and has been proposed by several experts [ 24,31]:

- Lesion < 3 cm and hormonally inactive: ultrasound follow-up.
- Lesion 3–5 cm: FNAB after previous laboratory testing.
- Lesion > 5 cm and suspected neoplasia: surgery and histologic investigation.

## 12.2.2 Normal Adrenal Gland

### 12.2.2.1 Adrenal Cortex

According to the complex composition of the tripartite cortex (zona glomerulosa, zona fasciculata, zona reticularis), FNAB samples reveal three different cell types characterized by their cytoplasmic features:

- *Outermost layer: zona glomerulosa* (Fig. 12.23A). Small aggregates and rows of cuboidal cells showing faint to intense staining qualities. The cytoplasm is delicate, foamy, and ill defined.
- *Middle zone: zona fasciculata* (Fig. 12.23B). An abundant cytoplasmic body exhibits single or multiple clear vacuoles due to lipid inclusions.
- *Innermost layer: zona reticularis* (Fig. 12.23C). The dense and compact cyanophilic cytoplasm contains fine granular golden-brown lipofuscin pigment.

- The nuclei of all three cell types are broadly similar: they are small and round and sometimes eccentrically located. The chromatin is loose and regularly distributed. Nucleoli are single and mostly inconspicuous. Distinct intranuclear, sharply demarcated cytoplasmic inclusions may be seen.

### 12.2.2.2 Adrenal Medulla

The medulla is located at the center of the gland. It is composed of irregularly shaped large cells that are usually grouped around blood vessels.

## 12.2.3 Benign and Malignant Primary Lesions of the Adrenals

- Cortical tissue fragments or cortical cells indicating a benign nodular cortical disorder, and metastatic neoplasms are by far the most frequently detected lesions.
- Rare primary adrenal lesions are cortical carcinomas, pheochromocytoma, myelolipoma, and inflammation [7, 35, 45].

### 12.2.3.1 Benign Adrenal Disorders

#### 12.2.3.1.1 Adrenal cyst

Endothelial cysts of lymphangiomatous or hemangiomatous origin are the most common subtypes of all adrenal cystic lesions. Pseudocysts secondary to hemorrhage and degeneration in normal or tumoral tissue are less frequent.

Parasitic cysts are rare and frequently of echinococcal origin (see also Sect. 9.1.7.3, p. 590).

**Microscopic Features**

- The cystic fluid is clear, turbid, brown, or bloody comprising foam cells and a few epithelial cells. Leukocytes or hemosiderophages may be admixed in accordance with the nature of the cyst.

**Caution**

- Adrenocortical carcinomas may be associated with benign-appearing cysts [12].
- In order to detect tiny and isolated echinococcal hooklets, careful reading of the cytologic smears is essential, if necessary at high magnification. A minimally closed diaphragm of the microscope can be helpful in detecting this. In smears with sparse hydatid elements, it is recommended to look for hooklets viewed from the edge (positioned upright), masking the tiny barbed hook.

#### 12.2.3.1.2 Adrenal Myelolipoma [17, 46]

Myelolipoma is a rare tumor that can reach a huge size. Association with adrenocortical adenoma is well known. The lesion is thought to be a metaplastic transformation of adrenocortical or primitive stromal cells into adipose and hematopoietic tissue.

**Microscopic Features, Immunocytochemistry, and Differential Diagnosis**

- The aspirates demonstrate mature adipose tissue and immature hematopoietic cells of myeloid and erythroid origin. Megakaryocytes and lymphocytes may also be present.
- Diagnosis is based on a positive immunocytochemical reaction for myeloperoxidase in myeloid cells.

- Tumors extending from the kidney or from the retroperitoneal compartment into the adrenal gland have to be excluded, such as renal angiomyolipoma, lipoma, or liposarcoma.

#### 12.2.3.1.3 Adrenal Adenoma

[3, 19, 24] (Figs. 12.24 and 12.25)

Adrenal adenomas may be functional or nonfunctional, the latter having a high frequency in the general population. The lesion is closely associated with age [3] and optionally with various benign and malignant disorders. Nonfunctioning adenomas are generally small, ranging from 0.5 to 3 cm in diameter. In general, imaging studies cannot discriminate between adrenal adenoma and small metastatic cancer [19, 24].

**Microscopic Features**

Katz gives a comprehensive description of the two distinct cytologic patterns of adrenal adenoma [20]:

- 1. Hypercellular smears composed of numerous small, round, naked nuclei against a granular or bubbly background. No necrosis. Cells with intact lipid-laden cytoplasm rarely occur. Stromal spindle cells may be observed.
- 2. Less cellular specimens composed of cell aggregates; the cells exhibit well-preserved vacuolated cytoplasm; the cell aggregations may comprise sinusoidal endothelial cells [47].
- The nuclei are small and round, exhibiting fine and evenly distributed chromatin, inconspicuous small nucleoli, and rare vacuoles. Atypias comprise nuclear enlargement and polymorphism (Fig. 12.25).

**Differential Diagnosis**

- Cytomorphology alone can rarely distinguish between adrenal adenoma and adrenal hyperplasia.
- FNA passes to the right adrenal gland may penetrate the liver hence, benign hepatocytes should not be confused with adrenal cortical cells; liver cells are large and polygonal, with a sharply defined cytoplasmic margin. The presence of bile pigment contributes to a precise diagnosis.
- The cytologic differentiation between adenoma and well-differentiated adrenocortical carcinoma may be a challenge (Fig. 12.25 vs Fig. 12.26A). However, the large size of the tumors (usually > 6 cm in diameter) as well as cytologic atypias, necrosis, and a high mitotic rate favor carcinoma.
- In adult patients, it may be difficult to differentiate between undifferentiated small-cell carcinoma and adrenal adenoma if the latter presents with degeneration and a preponderance of small naked nuclei [40]. However, nuclear pleomorphism and the typical granularity of chromatin are more pronounced in small-cell carcinoma; furthermore, the indicative single-file cell arrangement is much more pronounced in small-cell carcinoma. The different specimen background (small-cell carcinoma: dirty, necrotic, smudged tumor cells) should also be helpful in distinguishing between these two tumor entities.
- Under certain conditions, the differential diagnosis of renal adenoma may include small round cell tumors (SRCT) of childhood [26]. SRCTs are listed in Sect. 12.1.10.2.2, p. 744, Table 12.1.1 Differential diagnoses are discussed in the same section.

### 12.2.3.2 Adrenocortical Carcinoma

(Figs. 12.26 and 12.27)

**General Comments**

- Adrenocortical carcinoma (ACC) can occur throughout life. Between 80% and 90% of the neoplasms are functional, and patients present with clinical symptoms due to hormone production.
- Most ACCs present as large masses with a maximum size greater than 20 cm. Small lesions are rather benign, whereas large lesions measuring more than 6 cm in diameter are more likely to be malignant. Note: due to the refinement of imaging techniques, adrenal cortical tumors are discovered earlier and they tend to be smaller in size. Still, malignancy cannot reliably be ascertained by imaging techniques alone [14].
- In addition, malignant tumors include areas of hemorrhage and necrosis.
- The phenotype of ACC ranges from well-differentiated to highly anaplastic tumors, and the intratumoral heterogeneity can be marked.

**Microscopic Features** [8, 34, 36]

- Hallmarks. Hypercellular cytologic specimens. Nuclear enlargement and prominent nucleoli are features that go along with each tumor variety irrespective of its tumor grade.
  Mitosis and necrosis are distinct features of ACC even in well-differentiated tumors exhibiting quite bland cytology [34, 36].
- Cells are isolated or aggregated in dense groups.
- *Well-differentiated ACC*. The cytoplasm of is abundant, clear, and lipid-laden. Mitoses are rare.
- *Less well-differentiated ACC*. The cytoplasm may be more granular, and the nuclei show pleomorphism.
- *Poorly differentiated carcinomas* (Fig. 12.27) reveal extremely pleomorphic cells comprising multinucleation, nuclear hyperchromasia, coarse chromatin, and bizarre nucleoli. Giant cells may be found. The cytoplasms vary from spindle-shaped to polyhedral.
- Rare variants of ACC with myxoid [18], oncocytic [16], and adenosquamous [10] differentiation have been reported.

**Differential Diagnosis**

- Well-differentiated ACC share cytologic features with benign cortical lesions, low-grade neuroendocrine tumor, and renal cell carcinoma [38]. Particularly renal cell carcinomas showing dense cytoplasm, focal cellular pleomorphic, and spindle-shaped cells are difficult to differentiate from ACC.
- Cytologically, it may be difficult to differentiate between undifferentiated pleomorphic ACC and poorly differentiated extra-adrenal carcinoma, melanoma, and high-grade sarcoma [34].
- ACC may also mimic pheochromocytoma [1].

**Immunocytochemistry**

A few new immunomarkers have recently been evaluated on histologic material aiming to assess malignancy of cortical adrenal tumors and to distinguish secondary malignancies:

- The Ki-67 index has been proposed as an indicator of malignancy; cut-off values as reported by several authors range from 2.5% to 5% [44].
- Immunocytochemical expression of metalloproteinase type 2 (MMP-2) seems to be reliably restricted to malignant adrenocortical tumors with high specificity, whereas sensitivity seems to be low [43].
- Adrenal 4 binding protein (Ad4BP) or a transcription factor of steroidogenesis (SF-1) have been shown to be valuable immunomarkers differentiating between adrenal cortical tumors and metastatic malignancies [36, 37].

### 12.2.3.3 Tumors of the Adrenal Medulla

#### 12.2.3.3.1 Pheochromocytoma

[20, 21, 29, 30, 42] (Fig. 12.28)

**General Comments**

- Pheochromocytoma is a tumor of the chromaffin cells of the adrenal medulla. A minor proportion of all tumors occur in extra-adrenal sites; they are usually referred to as paraganglioma.
- As a high percentage of all tumors is diagnosed clinically and biochemically, FNAB is considered to be contraindicated due to the risk of hypertensive crises and fatal hemorrhage. FNAB may be used in nonfunctional tumors (up to 20% of all pheochromocytomas) to achieve a preoperative diagnosis.
- Approximately 10% of all pheochromocytomas are malignant. The diagnosis of malignancy is based on invasion beyond the capsule into adjacent tissues and metastases.

**Microscopic Features**

- The smears are hypercellular, composed of single cells, loose cell groups, and pseudorosettes.
- Three different cell types may be encountered, demonstrating varying distribution patterns:
  - *Neuroendocrine cell-type*. Medium-sized polygonal cells showing eccentric round to oval uniform nuclei with granular chromatin and indistinct nucleoli. The cytoplasm is finely granular.
  - *Spindle cells* having abundant cytoplasm, elongated nuclei, and coarse chromatin.
  - *Large cells* comprising eccentric nuclei, pronounced nucleoli, pale and granular cytoplasm. These cells are considered to be most helpful in establishing a correct diagnosis.

**Immunocytochemistry**

Pheochromocytoma exhibits immunocytochemical positivity for chromogranin, synaptophysin, neuron-specific enolase (NSE), CD 65, and S100. Immunostaining for pancytokeratin shows a positive reaction in approximately 30% of all tumors.

**Differential Diagnosis**

- Pheochromocytoma, which is to a large extent composed of small cells with hyperchromatic nuclei showing dense grouping, must be differentiated from small round cell neoplasms. Immunocytochemistry is less useful in establishing a correct diagnosis in this setting [5].
- Adrenocortical tumors may give rise to difficulties in the diagnosis of pheochromocytoma. Immunocytochemical tests should render the correct diagnosis in most cases, though, adrenocortical tumors have been observed immunocytochemically presenting neuroendocrine features [1].
- Pheochromocytoma exhibiting a predominant spindle cell pattern include the following differential diagnoses: spindle cell adrenal cortical carcinoma and secondary desmoplastic malignant melanoma. Applying an appropriate immunocytochemical panel including antibodies against NSE, chromogranin, S100, melanocyte-typical antigens, cytokeratins, muscle-specific actin, and vimentin [28] should be able to differentiate between the three tumor entities.

**Caution**

- Adrenal cortical tumors may share immunocytochemical properties with pheochromocytoma.
- Cells of pheochromocytomas may contain melanin. Misdiagnosis of melanoma based on cytology findings alone is possible in cases with indistinct cell features. The clinical history and an accurate immunopanel are essential for a correct diagnosis [15].

#### 12.2.3.3.2 Neuroblastoma, Ganglioneuroblastoma, Ganglioneuroma [9, 13, 27]

**General Comments and Microscopic Features**

The three tumors are derived from nonchromaffin cells of the sympathetic nervous system, but they may occur extra-adrenally as well. The tumors show a spectrum of different cell

types at various stages of differentiation of neuroblasts into mature ganglion cells.

**Neuroblastoma** (Figs. 12.20 and 12.21)
Neuroblastoma is the most frequent congenital malignant tumor with a peak incidence in the first 2 years of life. It is the most poorly differentiated neoplasm of this tumor group and highly malignant.

**Microscopic Features**

- Small uniform cells with hyperchromatic dense nuclei and coarse chromatin.
- Small cytoplasmic rims.
- Cell clustering and rosette formation may be pronounced.
- The fibrillary matrix in the background of the smears corresponds to neural cell processes.
- Presence of differentiating neuroblasts is a sign of maturation.

**Differential Diagnosis**
Malignant lymphoma and small cell carcinoma should be considered in adult patients; lymphoma and tumors of the small blue cell tumor group in pediatric patients (see also Sect. 12.1.10.2.2, p. 743).

**Ganglioneuroblastoma** (Fig. 2.110)
The tumor is composed of neuroblasts, differentiating neuroblasts, and ganglion cells.

**Ganglioneuroma** [9] (Fig. 2.111)
This tumor consists of differentiated ganglion cells scattered among nerve fibers and fiber bundles. Absence of immature cells and necrosis.

**Microscopic Features**

- Differentiated ganglion cells are huge cells with a low N/C ratio.
- The centrally located nucleus is uniform, pale, or finely granular.
- A single round prominent nucleolus is usually present.
- The cytoplasm exhibits multiple processes that taper off into neuronal fibers. Paranuclear granulation may be distinct.

### 12.2.4 Metastases [17, 35, 45] (Fig. 12.29)

- The adrenal gland is one of the favored target organs for metastatic disease. Tumor size is regarded to be the most important criterion for differentiating between primary and secondary adrenal lesions. However, with improved imaging techniques more and more very small metastases can be detected, which are difficult to distinguish from primary adrenal nodules [19, 24].
- The most important differential diagnosis for small metastatic lesions is the benign adrenal cortical nodule; both lesions can reliably be diagnosed in FNA specimens [47].
- The most common primary site of secondary tumors to the adrenals is the lung (Fig. 12.29). Much less frequently encountered are metastases from cancers of the kidney and carcinomas of the gastrointestinal tract; tumors of other primary sites occur only sporadically. The literature reports regarding the incidence of adrenal metastases due to breast cancer are inconsistent [32, 35].
- The patient's clinical history and a correlation with previous pathomorphological results, together with appropriate immunocytochemical tests, are most helpful for successful tumor typing.
- The morphological and immunocytochemical characteristics of common metastatic tumors are discussed in different chapters of this book. Common nonlymphoid tumor cell markers are tabulated in Sect. 9.2.6, Table 9.2.1, p. 610, and in Sect. 15.3.24, Table 15.3.3, p. 978.

## 12.2.5 Further Reading


1. Alsabeh R, Mazoujian G, Goates J, et al. Adrenal cortical tumors clinically mimicking pheochromocytoma. Am J Clin Pathol 1995;104:382-390.
2. Ang TL, Chua TS, Fock KM, et al. EUS-FNA of the left adrenal gland is safe and useful. Ann Acad Med Singapore 2007;36:954-957.
3. Commons RR, Callaway CP. Adenomas of the adrenal cortex. Arch Intern Med 1948;81:37-41.
4. de Agustin P, Lopez-Rios F, Alberti N, Perez-Barrios A. Fine-needle aspiration biopsy of the adrenal glands: a ten-year experience. Diagn Cytopathol 1999;21:92-97.
5. Deodhare S, Chalvardjian A, Lata A, Marcuzzi D. Adrenal pheochromocytoma mimicking small cell carcinoma on fine needle aspiration biopsy. Acta Cytol 1996;40:1003-1006.
6. DeWitt JM. Endoscopic ultrasound-guided fine-needle aspiration of right adrenal masses: report of 2 cases. J Ultrasound Med 2008;27:261-267.
7. DeWitt J, Alsatie M, LeBlanc J, et al. Endoscopic ultrasound guided fine-needle aspiration of left adrenal gland masses. Endoscopy 2007;39:65-71 .
8. Dhawan SB, Aggarwal R, Mohan H, Bawa AS. Adrenocortical carcinoma: diagnosis by fine needle aspiration cytology. Indian J Pathol Microbiol 2004;47:44-45.
9. Domanski HA. Fine-needle aspiration of ganglioneuroma. Diagn Cytopathol 2005;32:363-366.
10. Drachenberg CB, Lee HK, Gann DS, et al. Adrenal cortical carcinoma with adenosquamous differentiation. Report of a case with immunohistochemical and ultrastructural studies. Arch Pathol Lab Med 1995;119:260-265.
11. Eloubeidi MA, Seewald S, Tamhane A, et al. EUS-guided FNA of the left adrenal gland in patients with thoracic or GI malignancies. Gastrointest Endosc 2004;59:627-633.
12. Erickson LA, Lloyd RV, Hartman R, Thompson G. Cystic adrenal neoplasms. Cancer 2004;101:1537-1544.
13. Fröstad B, Tani E, Kogner P, et al. The clinical use of fine needle aspiration cytology for diagnosis and management of children with neuroblastic tumors. Eur J Cancer 1984:529-536.

14. Hamper UM, Fishman EK, Hartman DS, et al. Primary adrenocortical carcinoma: sonographic evaluation with clinical and pathologic correlation in 26 patients. AJR Am J Roentgenol 1987;148:915-919.
15. Handa U, Khullar U, Mohan H. Pigmented pheochromocytoma: report of a case with diagnosis by fine needle aspiration. Acta Cytol 2005;49:421-423.
16. Hoang MP, Ayala AG, Albores-Saavedra J. Oncocytic adrenocortical carcinoma: a morphologic, immunohistochemical and ultrastructural study of four cases. Mod Pathol 2002;15:973-978.
17. Jhala NC, Jhala D, Eloubeidi MA, et al. Endoscopic ultrasound-guided fine-needle aspiration biopsy of the adrenal gland. Analysis of 24 patients. Cancer(Cancer Cytopathol) 2004;102:308-314.
18. Karim RZ, Wills EJ, McCarthy SW, Scolyer RA. Myxoid variant of adrenocortical carcinoma: report of an unique case. Pathol Int 2006;56:89-94.
19. Katz R, Shirkhoda A. Diagnostic approach to incidental adrenal nodules in the cancer patient. Results of a clinical, radiologic, and fine needle aspiration study. Cancer 1985;55:1995-2000.
20. Katz RL. Kidney, Adrenal and retroperitoneum. In: Bibbo M. (ed). Comprehensive Cytopathology. W.B. Saunders Company, Philadelphia, 1991,pp.792 and 795.
21. Layfield LJ, Glasgow BJ, Du Puis MH, Bhuta S. Aspiration cytology and immunohistochemistry of a pheochromocytoma – ganglioneuroma of the adrenal gland. Acta Cytol 1987;31:33-39.
22. Lumachi F, Borsato S, Brandes AA, et al. Fine-needle aspiration cytology of adrenal masses in non-cancer patients: clinicoradiologic and histologic correlations in functioning and nonfunctioning tumors. Cancer 2001;93:323-329.
23. Lumachi F, Borsato S, Tregnaghi A, et al. CT-scan, MRI and image-guided FNA cytology of incidental adrenal masses. Eur J Surg Oncol 2003;29:689-692.
24. Lumachi F, Borsato S, Tregnaghi A, et al. High risk of malignancy in patients with incidentally discovered adrenal masses: accuracy of adrenal imaging and image-guided fine-needle aspiration cytology. Tumori 2007;3:269-274.
25. McCorkell SJ, Niles NL. Fine needle aspiration of catecholamine-producing adrenal masses: a possible fatal mistake. AJR 1985;145: 113-114
26. Min KW, Song J, Boesenberg M, Acebey J. Adrenal cortical nodule mimicking small round cell malignancy on fine needle aspiration. Acta Cytol 1988;32:543-546.
27. Mondal A. Cytopathology of neuroblastoma, ganglioneuroblastoma and ganglioneuroma. J Indian Med Assoc 1995; 93:340-343.
28. Nance KV, McLeod DL, Silverman JF. Fine needle aspiration cytology of spindle cell neoplasms of the adrenal gland. Diagn Cytopathol 1992;8:235-241.
29. Nguyen GK. Cytopathologic aspects of adrenal pheochromocytoma in a fine needle aspiration biopsy: a case report. Acta Cytol 1982;26:354-358.
30. Niveditha SR, Suguna BV, Krishnamurthy, et al. Cytologic features of malignant cystic pheochromocytoma: a case report. Acta Cytol 2007;51:200-202.
31. Nürnberg D. Ultrasound of adrenal gland tumors and indications for fine needle biopsy (uFNB) Ultraschall Med 2005;26:458-469.
32. Omoigui NA, Cave WTJr., Chang AYC. Adrenal insufficiency: a rare initial sign of metastatic colon carcinoma. J Clin Gastroenterol 1987;9:470-473.
33. Quayle FJ, Spitler JA, Pierce RA, et al. Needle biopsy of incidentally discovered adrenal masses is rarely informative and potentially hazardous. Surgery 2007;142:497-502.
34. Ren R, Guo M, Sneige N, et al. Fine-needle aspiration of adrenal cortical carcinoma: cytologic spectrum and diagnostic challenges. Am J Clin Pathol 2006;126:389-398.
35. Saboorian MH, Katz RL, Charnsangavej C. Fine needle aspiration cytology of primary and metastatic lesions of the adrenal gland. A series of 188 biopsies with radiologic correlation. Acta Cytol 1995;39:843-851.
36. Sasano H, Shizawa S, Nagura H. Adrenocortical cytopathology. Am J Clin Pathol 1995;104:161-166.
37. Sasano H, Suzuki T, Moriya T. Recent advances in histopathology and immunohistochemistry of adrenocortical carcinoma. Endocr Pathol 2006;17:345-354.
38. Sharma S, Singh R, Verma K. Cytomorphology of adrenocortical carcinoma and comparison with renal cell carcinoma. Acta Cytol 1997;41:385-392.
39. Stelow EB, Debol SM, Stanley MW, et al. Sampling of the adrenal glands by endoscopic ultrasound-guided fine-needle aspiration. Diagn Cytopathol 2005;33:26-30.
40. Suen KC, McNeely TB. Adrenal cortical cells mimicking small cell anaplastic carcinoma in fine-needle aspirate. Mod Pathol 1991;4:594-595.
41. Thompson GB, Young WFJr. Adrenal incidentaloma. Curr Opin Oncol 2003;15:84-90.
42. Varma K, Jain S, Mandal S. Cytomorphologic spectrum in paraganglioma. Acta Cytol 2008;52:549-556
43. Volante M, Sperone P, Bollito E, et al. Matrix metalloproteinase type 2 expression in malignant adrenocortical tumors: diagnostic and prognostic significance in a series of 50 adrenocortical carcinomas. Mod Pathol 2006;19:1563-1569.
44. Wachenfeld C, BeuschleinF, Zwermann O, et al. Discerning malignancy in adrenocortical tumors: are molecular markers useful? Eur J Endocrinol 2001;145:335-341.
45. Wadih GE, Nance KV, Silverman JF. Fine-needle aspiration cytology of the adrenal gland. Fifty biopsies in 48 patients. Arch Pathol Lab Med 1992;116:841-846.
46. Wagnerova H, Lazurova I, Bober J, et al. Adrenal myelolipoma. 6 cases and a review of the literature. Neoplasma 2004;51:300-305.
47. Wu HH, Cramer HM, Kho J, Elsheikh TM. Fine needle aspiration cytology of benign adrenal cortical nodules. A comparison of cytologic findings with those of primary and metastatic adrenal malignancies. Acta Cytol 1998;42:1352-1358.

**Fig. 12.23A–C Normal cells from different zones of the adrenal cortex.**
Image-guided FNAB of an adrenal gland in a 62-year-old man. Adrenal hyperplasia was suggested by imaging. Direct smears, Pap staining. **A** Zona glomerulosa: a small sheet of cuboid cells showing intense staining qualities. The cytoplasm is vacuolated (higher magnification). **B** Zona fasciculata: abundant sharply outlined and vacuolated cytoplasm (high magnification). **C** Zona reticularis: abundant granular cytoplasm including lipofuscin pigment. The latter is difficult to discern in the current image detail (high magnification).

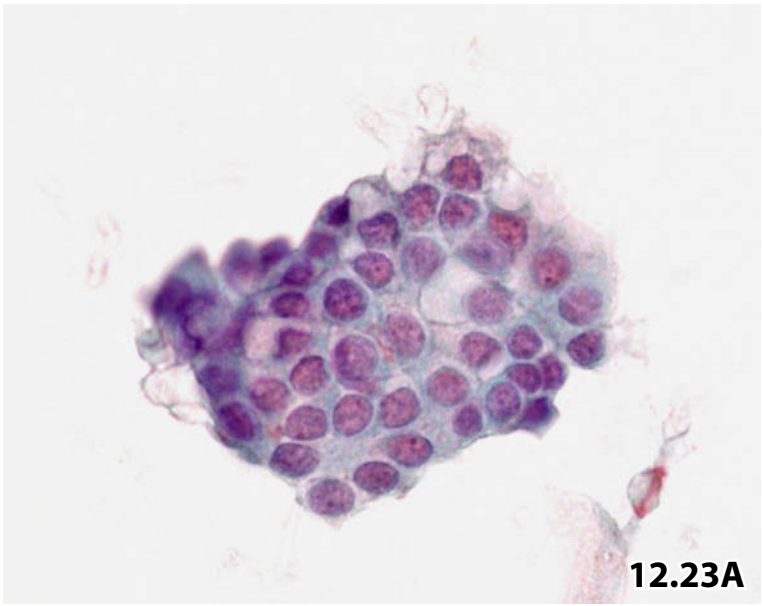

12.23A

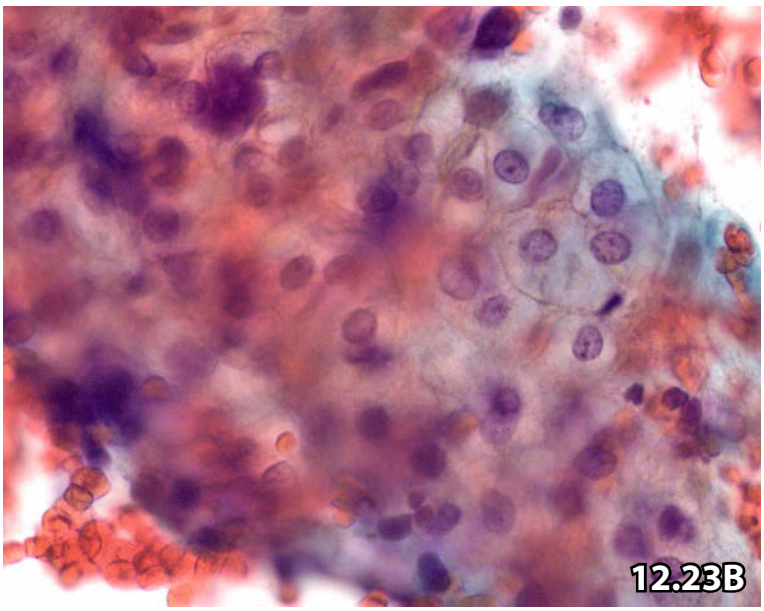

12.23B

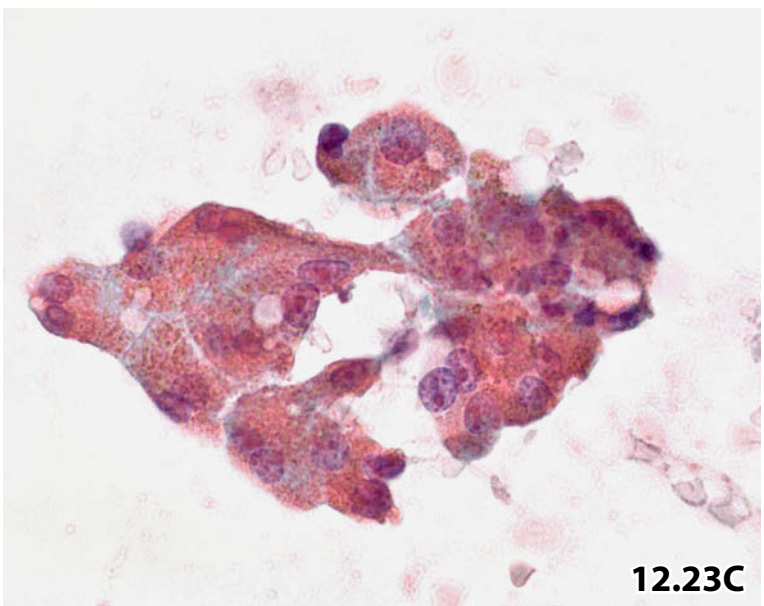

12.23C

**Figs. 12.24 and 12.25 Variants of adrenal adenomas.**
Two types of adrenal adenoma are presented (image-guided FNAB, direct smears, Pap stain).

**Fig. 12.24A, B** (case #1) Classic cytomorphology of adrenal adenoma.
A 52-year-old woman with a history of both breast carcinoma and endometrial carcinoma. Follow-up imaging detected a nodule in the left adrenal gland. **A** Cytology showed the typical aspect of adrenal adenoma at low magnification: numerous small round cells and stripped nuclei together with cells exhibiting vacuolated cytoplasm. **B** The same features are demonstrated in detail. Note lipid-laden bubbly cytoplasm.

**Fig. 12.25** (case #2) Polymorphous adrenal adenoma.
Routine imaging detected a pararenal tumor mass in a 66-year-old woman. Image-guided FNAB was performed. Higher magnification shows an irregular cluster composed of polymorphic cells. Individual cells and stripped nuclei are also present (lower right).
*(False) cytologic diagnosis:* Renal cell carcinoma.
*Comment:* Cellular polymorphism gave rise to an erroneous diagnosis of renal cell adenocarcinoma. Pale and evenly dispersed chromatin and very low N/C ratio should be taken as indicators of a benign endocrine lesion.
*Tissue diagnosis* (excised adrenal lesion): Adrenocortical adenoma exhibiting striking nuclear polymorphism.

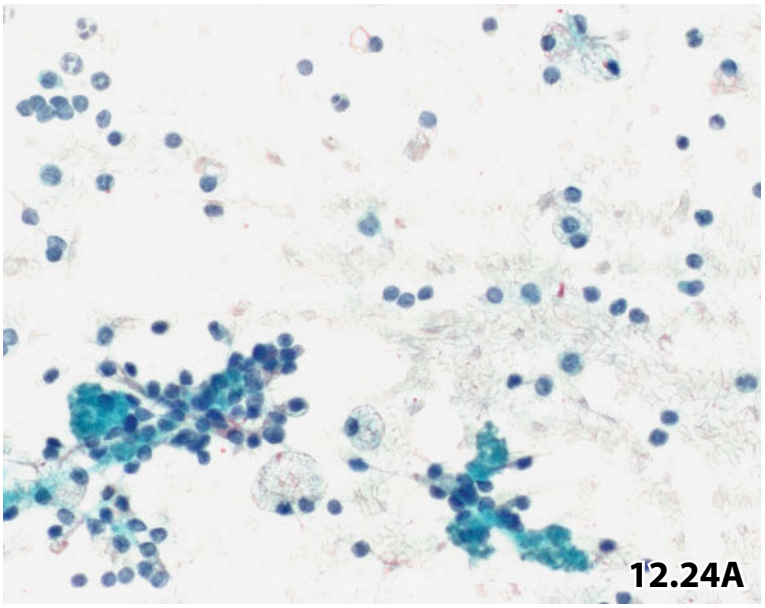

12.24A

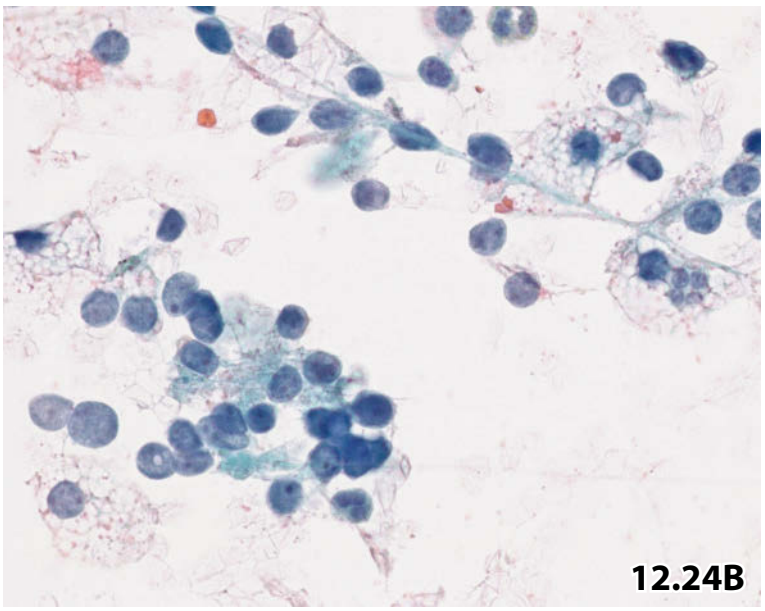

12.24B

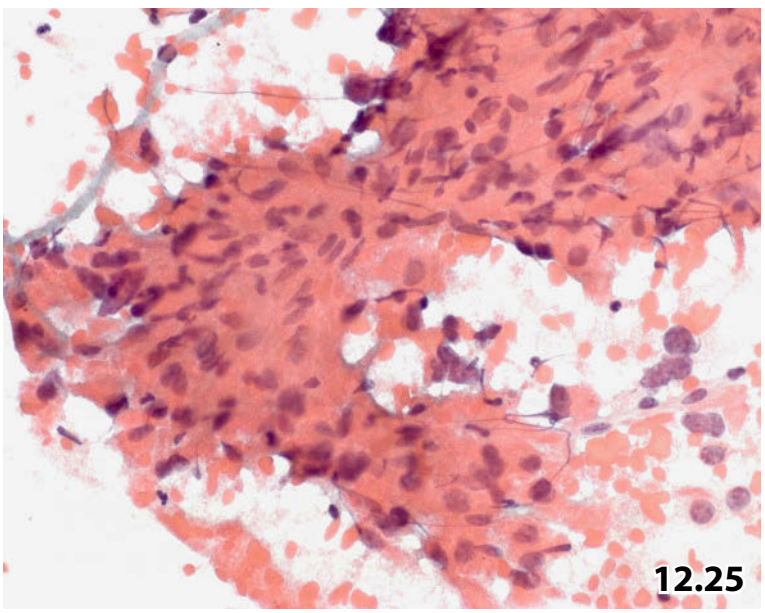

12.25

**Figs. 12.26 and 12.27 Subtypes of adrenocortical carcinomas.**
Example of a well-differentiated and a poorly differentiated adrenocortical carcinoma (image-guided FNAB, conventional smears, Pap stain).

**Fig. 12.26A, B** (case #1) Well-differentiated adrenocortical carcinoma.
A 60-year-old woman presented with a large nodule (11 cm in diameter) in her left adrenal. **A** Discohesive polyhedral cells exhibiting nuclear polymorphism and hyperchromasia (lower magnification). **B** High magnification focusing on nuclear atypias, cytoplasmic features, and multinucleation.
*Tentative cytologic diagnosis:* Adrenocortical neoplasm.
*Comment:* Absence of necrosis and mitotic activity hamper a definite cytologic diagnosis of malignancy.
*Tissue diagnosis* (excision of the tumor): Well-differentiated adrenocortical carcinoma, invasion of the tumor capsule and vessels.

**Fig. 12.27** (case #2) Poorly differentiated adrenocortical carcinoma.
Mass lesion in the abdominal wall of a 60-year-old woman with a positive history of adrenal carcinoma. Successful surgical excision of the primary neoplasm had been performed 9 years before. FNAB of the abdominal tumor (direct smears, Pap stain). The dissociated tumor cells exhibit enhanced pleomorphism compared to cells of the previous case (Fig. 12.26A). In addition, the tumor cells are scattered in a necrotic background (lower magnification).
*Final diagnosis* (cytology, histology, follow-up): Metastatic poorly differentiated adrenocortical carcinoma.

**Fig. 12.28A, B Pheochromocytoma.**
Abdominal sonographic imaging was performed in a 68-year-old woman. Ultrasound studies detected a nodular tumor located at the lower pole of the patient's left kidney. FNAB provided a highly sanguineous aspirate. Direct smears were Pap-stained.
**A** High magnification showing sheets and clusters composed of polygonal and fusiform cells considerably varying in their size. The N/C ratio is low and nuclear chromatin is bland. **B** Cells depicted in this figure exhibit extreme variation in size and shape. Note in particular the pale nuclei, the indistinct chromatin, and the monstrous giant cells at the left (high magnification).
*Tentative cytologic diagnosis:* Renal cell carcinoma; an endocrine neoplasm cannot be ruled out.
*Comment:* Actually, all morphologic features suggest an endocrine neoplasm, but due to the tumor topography that had been communicated to the pathologist (specified above) the diagnosis of an adrenal tumor was unlikely.
*Tissue diagnosis:* Pheochromocytoma (intraoperatively localized at the upper renal pole).

**Fig. 12.29 Metastatic adenocarcinoma of the lung: liquid-based preparation.**
A 69-year-old man with a history of adenocarcinoma of the lung presented with a nodular lesion in his left adrenal. The primary lung tumor had been successfully resected 6 years before. The aspirate from the adrenal gland was processed using the ThinPrep method and Pap staining. Degeneration of the neoplastic cells, in particular the marked nuclear shrinking presented a diagnostic dilemma. The cytopreparatory mode may be the reason for cellular and nuclear shrinkage.
*Cytology:* Primary adrenocortical carcinoma was included in the differential diagnosis together with secondary tumor entities. Immunocytochemical work-up was not performed due to degenerative cell changes and broad nuclear overlapping.
*Final diagnosis:* Adrenal metastasis of a poorly differentiated adenocarcinoma of the lung.

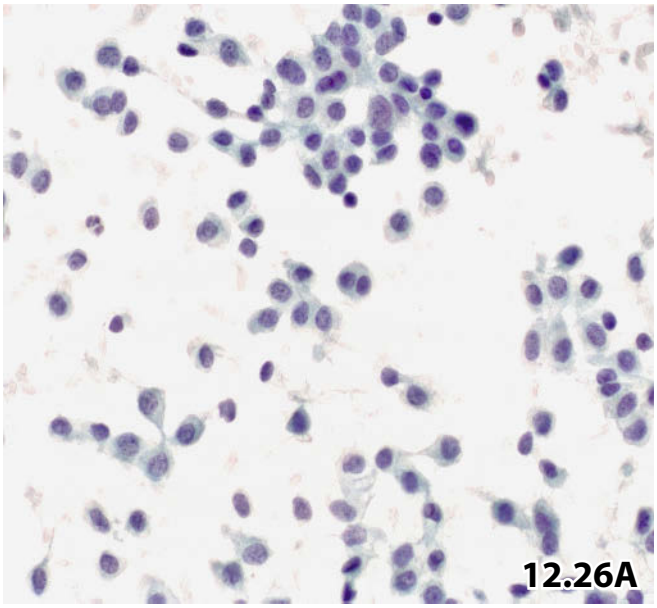
12.26A

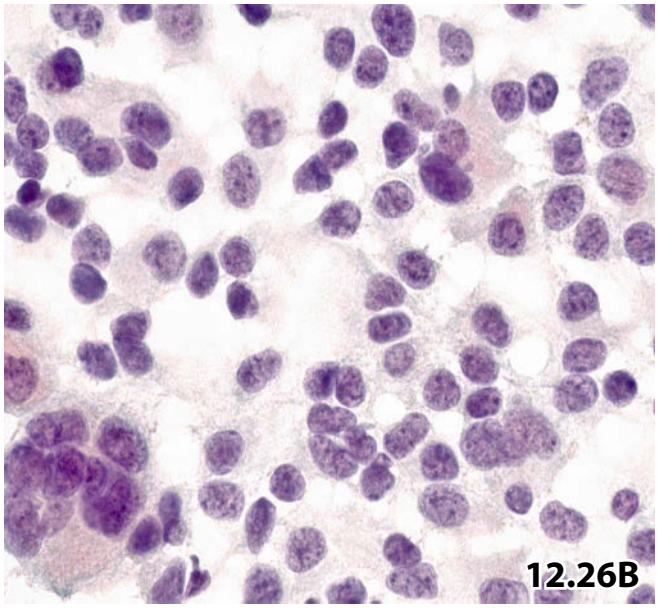
12.26B

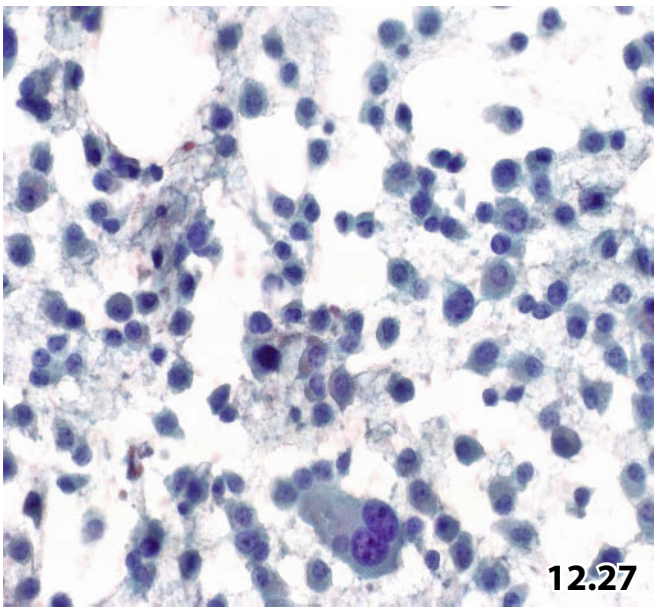
12.27

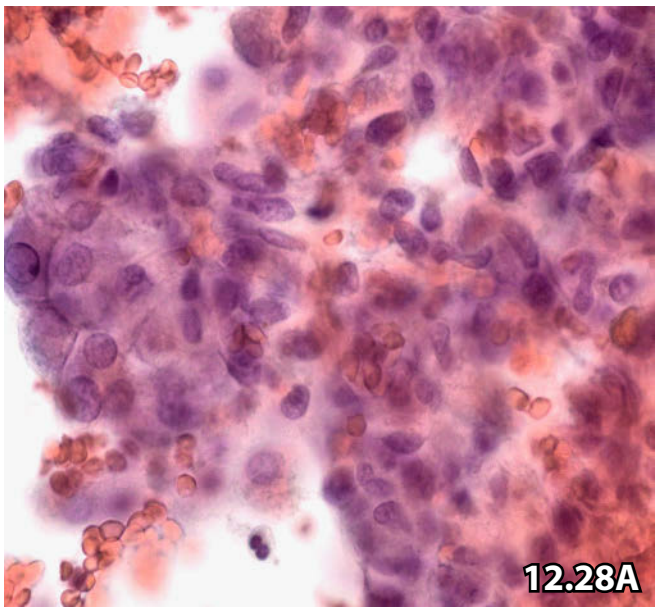
12.28A

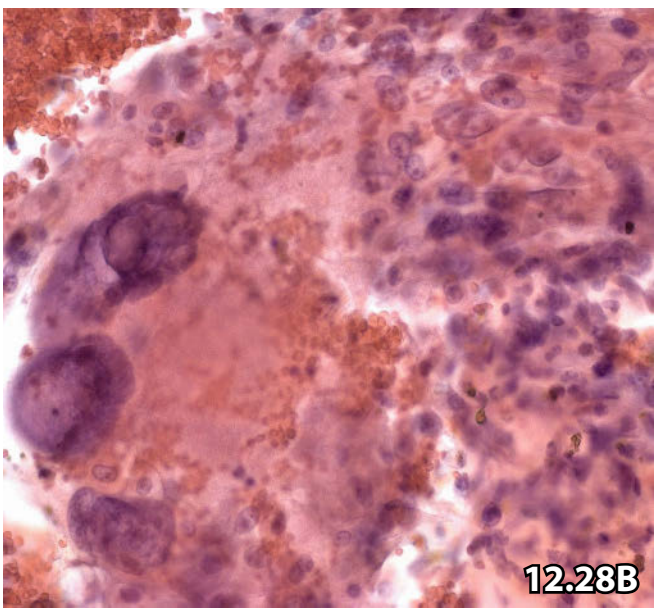
12.28B

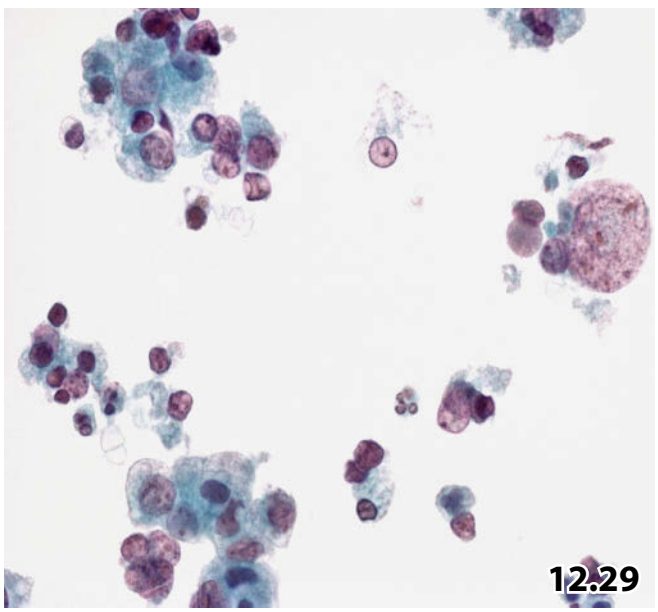
12.29

# Section 12.3
# Retroperitoneum

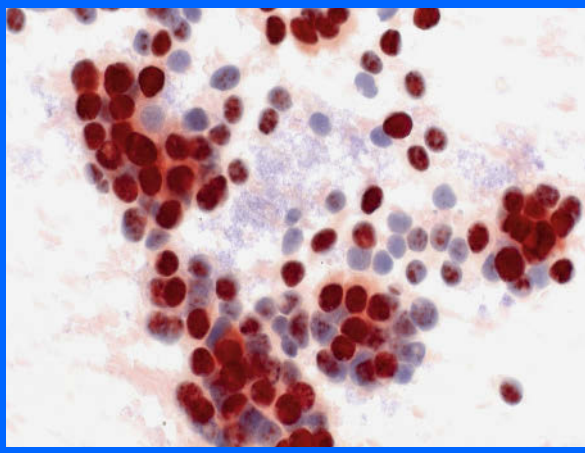

## 12.3.1 Introduction

### 12.3.1.1 Retroperitoneal Space and Retroperitoneal Structures

- The retroperitoneal space is of mesodermal origin. The compartment is defined anteriorly by the posterior layer of the parietal peritoneum, and posteriorly by the spine and the interior back muscles. It extends from the superior diaphragm to the muscles of the pelvic diaphragm. The lateral borders are defined by the quadratus lumborum muscles.
- All organs that are uncovered or partially covered by the peritoneum having no mesenteries are defined as retroperitoneal. Major organs and structures within this area are the pancreas, a segment of the duodenum, the kidneys, the ureters, the adrenals, the abdominal part of the aorta, the vena cava, lymph nodes, a part of the sympathetic nerve system, nerves, and ganglions. The space between is filled with fat, fibrous/connective tissue, blood vessels, lymphatic vessels, and nerves.

### 12.3.1.2 Fine-Needle Aspiration Biopsy and Imaging

- Whereas exploratory laparotomy has formerly been the only available tool to assess the nature of pathologic retroperitoneal findings, image-guided FNAB has made substantial progress in the evaluation of pathologic conditions in the retroperitoneal space.
- Retroperitoneal FNAB offers great advantages for different groups of patients:
  - A diagnosis prior to surgery enables the attending physicians to plan further preoperative evaluations and treatment modalities respectively.
  - Accurate preoperative staging in tumor patients.
  - A strenuous laparotomy can be spared for patients with advanced malignant disease or malignant lymphoma limited to the retroperitoneum.
- Ultrasound and computed tomography are established imaging techniques used for transcutaneous-guided FNAB of a retroperitoneal mass. Results in most of the reported series achieved a sensitivity of between 90% and 95% and a specificity of 100% [13, 28, 50, 51, 61]. A few studies compared diagnostic accuracy of radiologically guided FNAB with that of core-needle biopsy [64].
- A different access for the needle puncture is required depending on the location of the target lesion: from anterior (transperitoneal), from paraspinal, or from a lateral position. Transvaginal access to the pelvic space is an option for gynecologists [48].
- Endoscopic ultrasound-guided fine-needle aspiration biopsy (EUS-FNAB) is a relatively new modality that has been shown to be a safe tool offering easy access to deep-seated and small lesions located adjacent to the gastrointestinal tract. EUS-guided aspiration of retroperitoneal disorders may be performed via transgastric, transduodenal, and transrectal routes [10, 20, 70]. Combined EUS-FNAB and Tru-Cut needle biopsy can improve diagnostic accuracy and sampling adequacy compared with either technique alone [71].

**Caution**

Mesothelial fragments may occur as contaminants from the needle tract. They should not be misinterpreted as well-differentiated adenocarcinoma (Fig. 12.30C).

#### 12.3.1.3 Sample Processing and Additional Analyses

**Sample Processing**

- *Conventional smearing* is the standard procedure for FNA material from retroperitoneal lesions. Direct smears may be wet fixed or air-dried. Fixation has to take place immediately after spreading the cell material in order to prevent cell alteration. We prefer Delauney solution as fixative; 95% ethyl alcohol pure or mixed with ether is also frequently used.
- *Liquid-based method* is a procedure that guarantees optimal preparation for special investigations, in particular for immunocytochemistry, fluorescence in situ hybridization, or static DNA cytometry. This technique is highly recommended in cases with strong suspicion of malignant lymphoma. Residual or whole contents of the needle and syringe are rinsed into a tissue culture solution and processed either with the cytocentrifuge or a suitable processor such as the ThinPrep processor. The thin-layer method is strongly recommended for operators who are not familiar with proper preparation and fixation technique and if cytology staff attendance is not possible.
- *Sanguineous aspirates* require a special procedure. Needle passes through vessels can provide extremely bloody aspirates. In such cases, we recommend CytoLyt (or another hemolyzing fixative) to use as a rinse medium. CytoLyt is an accurate medium for sanguineous aspirates in combination with the ThinPrep technique. It lyses blood cells, yields well-preserved cell material, and warrants a clear background.
- *Cell-block technique*. Aspirates containing large amounts of cellular material, tissue fragments, and clots may be processed using the cell-block technique.
- *Attendance of cytologic staff* at image-guided FNABs is desirable, particularly for immediate assessment of specimen adequacy, and in order to split cell samples for additive analyses.

**Additional analyses**

- Needle/syringe rinse or a repeated cell sampling can be used for DNA flow cytometry or for immunophenotyping of lymphoid cells by multiparameter flow cytometry.
- Polymerase gene amplification can be performed with nuclear DNA obtained from cells scraped off a conventionally stained cytologic smear.

More information on the items mentioned above is provided in different chapters of this book.

### 12.3.2 Nonneoplastic Lesions of the Retroperitoneum

Several benign nonneoplastic disorders may occur in the retroperitoneal space, but they are rare compared to malignant tumors. Descriptions of the commonest lesions are listed below.

#### 12.3.2.1. Cysts

The components of the aspirated fluid reflects the nature of the cyst.

**Microscopic Features**

- Hallmarks of most cystic lesions are foam cells.
- Cysts resulting from organization of a previous hematoma yield no specific cell pattern.
- Lymphatic cysts/lymphocele contain lymphocytes.
- Dermoid cysts are characterized by squamous cells.
- Mucinous cysts contain mucoid masses in abundance [57].
- Cysts associated with infections may present bacteria, fungi, or parasites. Special stains (Gram, Giemsa, PAS, Grocott) can identify the organisms.
- Cysts resulting from degeneration of neoplastic tissues usually exhibit pleomorphic detritus.

**Caution**

Do not miss a hydatid cyst!
See Sect. 9.1.7.3, p. 590, and Figs. 3.17, 9.7, 9.8, 12.5.

#### 12.3.2.2 Lymphangioleiomyomatosis [7, 11, 53]

Lymphangioleiomyomatosis is a disorder caused by abnormal proliferation of smooth muscle cells around lymphatic vessels. The lesion induces occlusion of large lymphatic channels resulting in cyst formation or chylascites/chylothorax. The fluid aspirates are macroscopically clear.

**Microscopic Features**

- The sediment is composed of high numbers of lymphocytes and large monomorphic spindle cells appearing in loose groups or discrete clusters.

#### 12.3.2.3 Abscess

Macroscopically, an abscess yields a characteristic purulent aspirate and microscopically large numbers of degenerated neutrophils.

#### 12.3.2.4 Retroperitoneal Mycobacterial Infection

- A lesion that may occur subsequent to urogenital or vertebral tuberculosis (hypostatic abscess). Cytomorphology of mycobacteriosis is discussed in Sect. 15.2.3.2, p. 928.
- AIDS related 'retroperitoneal lymph node mycobacteriosis' is presented in Fig. 15.31.

**Caution**

A retroperitoneal mass presenting cytologically as inflammatory process comprising epithelioid histiocytes, debris, and large numbers of neutrophils should raise suspicion of tuberculosis. Ziehl-Neelsen staining and microbiological investigations are indispensable.

#### 12.3.2.5. Malakoplakia

Malakoplakia occurs extremely rarely as an autonomous retroperitoneal process. For more details see Sects. 12.1.5.4, p. 735, and 13.2.4.3, p. 814.

#### 12.3.2.6 Idiopathic Retroperitoneal Fibrosis [23, 63] (Fig. 12.30)

This is an inflammatory and fibrosing process that may lead to an encasement of the ureters and subsequent renal failure. Specific diagnosis is only possible together with clinical and radiologic findings.

**Microscopic Features**

- The fibrotic tissue and mixed inflammatory infiltrate include fibroblasts/fibrocytes, histiocytes, lymphocytes, plasma cells, scarce eosinophils, and mast cells.
- Tissue fragments may be hyalinized or composed of tightly packed spindle cells.

#### 12.3.2.7 Extramedullary Hemopoiesis (Fig. 15.102)

Extramedullary hemopoiesis should not be misinterpreted as myeloid neoplasia or undifferentiated malignancy.

#### 12.3.2.8 Endometriosis [9, 12] (Fig. 16.19)

Ectopic endometrium (endometriosis) occurs most often in the pelvis, but unusual occurrence in the retroperitoneal space has likewise been reported.

Endometriosis usually presents as a hemorrhagic cyst; cystic degeneration is caused by cyclic hormonal stimulation of the tissue.

**Microscopic Features**

- Hemosiderophages along with cellular debris are key features of this lesion, but the findings are not specific.
- Endometrial epithelium is a sporadic finding.

Further information and pictures can be seen in Sects. 3.3.6, p. 302, and 16.4.3, p. 1035 (Fig. 16.19).

**Caution**

- Hemosiderophages and debris, per se a common finding in cystic fluids, must always include endometriosis as a potential diagnosis.
- Clusters composed of hormonally activated epithelial cells of endometriotic origin may mimic well-differentiated adenocarcinoma.

### 12.3.3 Tumorous Lesions of the Retroperitoneum

**General Comments**

- Primary retroperitoneal tumor and pseudotumor are considered to originate within the retroperitoneal space, if a primary connection to retroperitoneal organs cannot be ascertained.
- Retroperitoneal neoplasms may be classified into three main groups [16]:
  1. Tumors of mesodermal or neurogenous origin.
  2. Tumors arising from tissue remnants or from heterotopic tissue.
  3. Tumors involving lymph nodes as primary lymphoma or metastasis.
- Neoplasms of the pancreas, duodenum, kidneys, ureters, adrenals, and lymph nodes are documented in separate chapters and sections of this book; cytomorphologic and differential diagnostic properties, and relevant additional techniques are discussed.

#### 12.3.3.1 Synopsis of Retroperitoneal Tumoral Lesions

Table 12.3.1, p. 781 shows a synopsis of primary retroperitoneal disorders, according to Bosniak and coauthors [16].

**Table 12.3.1** Primary retroperitoneal tumors and pseudotumors

| Tissue | Benign lesions | Malignant neoplasms |
|---|---|---|
| **Mesoderm** | | |
| Adipose tissue | Lipoma | Liposarcoma |
| Smooth muscle | Leiomyoma | Leiomyosarcoma |
| Mesenchymal tissue / histiocytes | Fibroma<br>Myxoma<br>Mesenchymoma<br>Xanthogranuloma | Fibrosarcoma<br>Myxosarcoma<br>Sarcoma NOS<br>Xanthosarcoma |
| Vascular tissue | Lymphangioma<br>Hemangioma<br>Hemangiopericytoma | Lymphangiosarcoma<br>Angiosarcoma<br>Malignant hemangiopericytoma |
| **Neurogenous** | | |
| Peripheral nerves | Neurofibroma<br>Neurilemmoma | Neurogenic sarcoma<br>Malignant schwannoma |
| Sympathetic nervous system | Ganglioneuroma | (Ganglio)neuroblastoma |
| Paraganglion system (extra-adrenal) | Paraganglioma<br>Pheochromocytoma | Pheochromocytoma |
| **Congenital tissue remnants** | Benign teratoma | Germ cell tumors<br>Chordoma |
| **Heterotopic tissue** | | |
| Renal blastema | | Wilms tumor |
| Heterotopic adrenal tissue | Benign adrenal tissue / adrenocortical adenoma | Adrenocortical carcinoma |
| **Lymphoid tissue** | Enlarged benign lymph nodes (reactive, infection, and others) | Malignant lymphoma<br>Metastatic neoplasms |

## 12.3.4 Benign Tumors

### 12.3.4.1 Lipomatous Tumors (Figs. 17.1–17.4)

Comprehensive information on benign and malignant adipocytic tumors is provided in Chap. 17, "Soft Tissue and Bone, p. 1053."

#### 12.3.4.1.1 Lipoma and Well-Differentiated Liposarcoma

- Aspirates from lipomas (Fig. 17.1) contain mature fatty tissue. However, deep-seated lipoma are extremely difficult to distinguish from well-differentiated liposarcoma [24, 52] (Fig. 17.4).
- Rare focal nuclear atypia, a varying number of lipoblasts, a stromal spindle cell component [27], and immunostaining exhibiting nuclear positivity for MDM-2 and CDK4 [14] may raise suspicion of malignancy.

#### 12.3.4.1.2 Hibernoma (Fig. 17.3)

Brown fatty tissue tumors, known as hibernoma are rarely encountered in the retroperitoneal space [18]. They should not be misinterpreted as neoplasms with granular/oncocytic features, granular cell tumor, histiocytoma, proliferative myositis, or alveolar soft part sarcoma.

### 12.3.4.2 Leiomyoma (Fig. 12.31)

**Microscopic Features and Immunocytochemistry**

Cytologic specimens of leiomyoma are composed of:

- Single and clustered spindle cells with abundant eosinophilic cytoplasm and indistinct cell borders.
- Nuclei are predominantly cigar-shaped (with blunted ends), containing fine granular chromatin and inconspicuous nucleoli.
- Foci of mildly atypical cells may be encountered.

Cells stain immunocytochemically positive for smooth muscle actin (SMA) and desmin.

### 12.3.4.3 Schwannoma [59] (Figs. 17.14–17.17)

**Microscopic Features and Immunocytochemistry**

Schwannoma (synonym: neurilemmoma) is cytomorphologically characterized by:

- Numerous individual spindle-shaped cells with pale and wavy cytoplasm.
- The nuclei are elongated, usually exhibiting pointed ends, but blunted ends are observed as well.

- Microscopic hallmark: organoid cell arrangement, known as Verocay bodies, may also appear in cytologic smears [60].

S100 and glial fibrillary acidic protein (GFAP) positivity indicate neurogenic origin of the neoplastic cells.

#### 12.3.4.4 Other Rare Benign Tumors

Other rare benign tumors can be diagnosed using FNA cytology. Description and differentiating cytologic characteristics of selected lesions are found in other sections of this book and/or in the literature:
- Myelolipoma (Sect. 12.2.3.1.2, p. 767).
- Angiomyolipoma (Sect. 12.1.7.1, p. 737).
- Hemangiopericytoma [30, 58].
- Paraganglioma [2] (Sect. 5.2.6.2, p. 467).

### 12.3.5 Sarcomas (Selection of the Most Common Entities)

#### General Comments

- The retroperitoneum is one of the most frequent sites of stromal tumors: 13% of all soft tissue sarcomas have been found to develop in the retroperitoneal space [62]. Retroperitoneal sarcomas generally have a poor prognosis.
- Definitive sarcoma classification should be based on surgical resection and histologic investigation combined with a battery of immunostainings. Still, preoperative diagnosis should not be underestimated; it may be of value for further preoperative evaluation and operation planning.
- Only a few cytology case reports are available addressing retroperitoneal sarcomas. A convenient approach to cytologic diagnosis of sarcomas is to group them into three main classes [65]:
  - Spindle cell sarcoma.
  - Pleomorphic sarcoma.
  - Round cell sarcoma.

**Caution**

Limited cell material is usually aspirated from retroperitoneal stromal tumors accompanied by rich fibrotic or collagenous components; hence an accurate diagnosis by cytology is often impossible.

#### 12.3.5.1 Spindle Cell Sarcomas

##### 12.3.5.1.1 Low-Grade Liposarcoma

This is a tumor group comprising a myxoid and a well-differentiated subtype.

**Myxoid Liposarcoma** (Fig. 12.32)

Myxoid liposarcoma is the most common subtype of liposarcoma; the retroperitoneum is the second most common location of this tumor type.

**Microscopic Features and Molecular Genetics**

Hallmarks:
- The cells are spindle-shaped, but they may also occur as stellate or round in shape. The nuclei are small and bland.
- The background of smears is characterized by gelatinous material (myxoid matrix), and branching delicate capillaries.
- Lipoblasts are essential for the diagnosis; they display excentric hyperchromatic and folded nuclei that are surrounded by a fat-laden vacuolated cytoplasm (Fig. 12.32B).

Myxoid liposarcomas carry a specific cytogenetic abnormality that is very helpful in establishing an accurate diagnosis and differentiating between myxoid liposarcoma and other myxoid soft tissue tumors. FISH is a reliable method to detect the specific translocation t(12;16) (q13;p11) FUSDDIT3 in cytologic samples [25, 44].

**Caution**

- Lipoblasts may also be found in benign disorders such as fatty tissue necrosis and common benign lipomas. Lipoblasts in benign lesions exhibit less pronounced atypias.
- Myxoid stroma is a tumor component that can also be found in other benign and malignant stromal tumors: myxoma, schwannoma, myxoid fibrosarcoma, myxoid subtype of low-grade malignant fibrous histiocytoma, chordoma, and others [3, 31, 35, 41, 49].

**Well-Differentiated Liposarcoma**

This entity strongly resembles benign lipoma (see Sects. 12.3.4.1.1, p. 781, 17.1.2.1, p. 1056, and 17.2.3, p. 1094) (Fig. 17.4).

##### 12.3.5.1.2 Leiomyosarcoma

[8, 38] (Figs. 12.33–12.35)

Primary retroperitoneal leiomyosarcoma rarely occurs, but this tumor type frequently invades the retroperitoneal space originating in the uterus. Tumor size is believed to be a good indicator of malignancy.

**Microscopic Features and Differential Diagnosis**

- The tumor is composed of spindle cells that are arranged singly or in clusters. The syncytial cytoplasm is abundant.
- The nuclei are predominantly cigar-shaped and blunt-ended.
- The degree of nuclear atypia and coarseness of chromatin depends on the tumor grade.

Well-differentiated leiomyosarcoma is difficult to distinguish from neurogenic sarcoma and leiomyoma.

High-grade tumors may show notable cellular pleomorphism and large nucleoli (Fig. 12.34) and must be differentiated from malignant fibrous histiocytoma.

**Immunocytochemistry**

Tumor cells stain immunocytochemically positive for smooth muscle actin (SMA) and desmin (Fig. 12.35).

#### 12.3.5.1.3 Malignant Peripheral Nerve Sheath Tumor [32, 39, 42, 54, 65]

Malignant peripheral nerve sheath tumor (MPNST, malignant schwannoma) is uncommon, but up to 10% of these tumors occur in the retroperitoneum.

**Microscopic Features**

- Loose clusters and fascicular arrangement of spindle cells with blunt ends.
- Nuclear polymorphism and distinct nucleoli depend on the histologic tumor grade.
- Mitoses are present in most cases.
- A fibrillary background may be observed.
- The cell pattern as stated above is not specific enough for a firm cytologic diagnosis, unless characteristic Verocay bodies can be observed. Unfortunately, these structures are more often present in benign than in malignant schwannoma.

**Immunocytochemistry**

Positivity for S100 protein may indicate malignant schwannoma differentiating from other spindle cell sarcomas.

### 12.3.5.2 Pleomorphic Sarcomas

#### 12.3.5.2.1 Malignant Fibrous Histiocytoma/ Undifferentiated Pleomorphic Sarcoma

[43, 69] (Fig. 12.36)

- Malignant fibrous histiocytoma (MFH) is a pleomorphic sarcoma, usually composed of spindle cells. It is the most common malignant soft tissue tumor in late adult life. The histogenesis of this tumor is still controversial. In the future, the diagnosis MFH will most likely be replaced by a new tumor classification based on immunocytochemical, molecular biological, and ultrastructural findings [6, 46] (see also Sect. 17.2.5, p. 1095).
- The classic subtypes of MFH that have been described histologically are [26]:
  - Pleomorphic variant.
  - Myxoid variant.
  - Giant cell variant.
  - Inflammatory variant.
  - Angiomatoid variant.

**Microscopic Features**

- The two main cell types of pleomorphic MFH are:
  - The large polymorphic and bizarre histiocyte-like cell type, mono- and multinucleated.
  - The atypical fibroblast-like cell type.
- Phagocytotic activity (ingestion of debris, leukocytes, red blood cells) of the highly atypical histiocytoid tumor cells and multinucleated giant cells is characteristic of pleomorphic MFH.

**Differential Diagnosis**

- MFHs share morphologic patterns with a number of other sarcomas such as pleomorphic liposarcoma, pleomorphic rhabdomyosarcoma, and leiomyosarcoma.
- The tumor may also be confused with Hodgkin disease (Fig. 12.36).
- Myxoid liposarcoma and leiomyosarcoma should be considered in cases of low-grade MFH, which is composed of fibroblast- and histiocyte-like cells scattered in a myxoid background .

#### 12.3.5.2.2 Pleomorphic Liposarcoma [68]

Pleomorphic liposarcomas rarely occur in the retroperitoneal area, unlike the myxoid and well-differentiated variant of liposarcoma.

**Microscopic Features and Differential Diagnosis**

- Lipoblasts with their sharply defined cytoplasmic fat vacuoles and the eccentrically located scalloped nuclei are suggestive of pleomorphic liposarcoma (histiocytoid cells of MFH exhibit a foamy and finely vacuolated cytoplasm as compared to the cells of pleomorphic liposarcoma). But in many cases, it is difficult or impossible to distinguish between pleomorphic liposarcoma and pleomorphic MFH.

According to the subtype, other differential diagnostic considerations include myxoid fibrosarcoma, extraskeletal myxoid chondrosarcoma [37], and chordoma.

### 12.3.5.3 Round Cell Sarcomas

- Round cell liposarcoma occurring in adult patients may be confused with other round cell tumors [67] (Fig. 12.37).
- Two types of round cell sarcoma occurring in infancy and childhood have to be mentioned, namely embryonal rhabdomyosarcoma and extraskeletal Ewing sarcoma. Embryonal rhabdomyosarcoma is infrequently encountered in the retroperitoneal space, whereas Ewing sarcoma chiefly occurs in retroperitoneal and paravertebral areas. Both neoplasms belong to the group of small round cell tumors. Their diagnostic and differential diagnostic features are presented in Sect. 12.1.10.2.2 “Wilms Tumor,” p. 743, including a table with all small cell tumors (Table 12.1.1) and references.

#### 12.3.5.4 Chordoma (Fig. 5.71)

Chordoma arises from remnants of the primitive notochord, the notochord forms the early spine in the early stages of fetal development. These tumors are slow-growing and locally aggressive, predominantly found in people aged between 40 and 70 years. The tumors are most often located in the sacrococcygeal or skull base area, but unusually they can occur throughout the spine. Spreading to other organs is possible, especially to the lungs.

Further information, cytologic features and references are provided in Sect. 5.2.3.5, p. 464.

### 12.3.6 Malignant Lymphoma [17, 55, 72]

- Overt or presumed malignant lymphoma is one of the most frequent indications for FNAB of retroperitoneal masses and enlarged retroperitoneal lymph nodes.
- The majority of retroperitoneal lymphoid tumors are non-Hodgkin lymphomas. The initial retroperitoneal presentation of Hodgkin lymphoma is rare.
- Indications for FNAB of enlarged retroperitoneal lymph nodes are:
  - Initial affirmation or exclusion of a malignant lymphoma as a triage in patients with equivocal clinical and imaging results.
  - Definite lymphoma diagnosis in patients whose condition is too poor for surgical biopsy.
  - Staging of lymphoma.
  - Regrading of lymphoma in relapsing tumors.
  - History of malignant tumor: confirmation or exclusion of recurrence or metastases or of a second primary neoplasm.
  - Residual or recurrent masses, synchronous or metachronous to therapeutic regimes.
- For a detailed description of the cytomorphology of various lymphoma entities, ancillary methods on cytologic material and differential diagnostic considerations see Sect. 15.3, "Lymph Nodes: Malignant Lesions," p. 950.

### 12.3.7 Germ Cell Tumors [4, 22, 40]

- Germ cell tumors are sporadically encountered in FNABs of the retroperitoneum. Most tumors represent metastatic disease of primary germ cell tumors in both testes and ovaries. Primary extragonadal germ cell tumors of the retroperitoneum rarely occur.
- Malignant germ cell tumors may be composed of varied cell types, which are characterized by their immunocytochemical properties.

#### 12.3.7.1 Seminoma [19, 45] (Fig. 12.38)

Seminoma is the most common malignant germ cell tumor. Morphologically identical tumors in the ovaries are denominated dysgerminoma.

**Microscopic Features and Differential Diagnosis**

- Aspirates mainly consist of large single tumor cells interspersed with mature lymphocytes.
- Tumor cells are rounded and characterized by a large single nucleus exhibiting an irregularly wrinkled membrane and a prominent central nucleolus.
- The cytoplasm is clear and the border is well-defined with characteristic intermittent double-contours and thickenings.
- High N/C ratio.
- Frequent necrotic debris and rare epithelioid cells.

Seminoma is most likely confused with large-cell lymphoma of the blastic type. Still, the overall pattern and cytoplasmic features are sufficiently characteristic to render a final diagnosis in virtually all cases (more information is provided in Sect. 2.4.3.6.2, p. 214).

#### 12.3.7.2 Embryonal Carcinoma and Endodermal Sinus Tumor (Yolk Sac Tumor)

[1, 29, 56] (Figs. 2.104 and 12.39)

It may be difficult to separate these two neoplasms from each other in fine-needle aspirates [1].

##### 12.3.7.2.1 Embryonal Carcinoma (Fig. 2.104)

- The tumor cells are very large and anaplastic. The large cytoplasmic bodies are devoid of distinct membranes; thus tumor cell arrangement mainly occurs in syncytial groups.
- Variable nuclear size and shape including multiple prominent nucleoli, coarse and clumped chromatin.
- Multinucleated giant cells may be observed.

##### 12.3.7.2.2 Yolk Sac Tumor

- In comparison to embryonal carcinoma, the tumor cells may exhibit less pronounced pleomorphism, denser clustering into papillary and acinar formations, and minor cytoplasmic vacuolization.
- Intracytoplasmic and extracellular eosinophilic bodies may be found (Fig. 12.39A).

#### 12.3.7.3 Choriocarcinoma [21, 36] (Fig. 12.40)

Choriocarcinoma occurs as a gonadal tumor or as a uterine cancer typically associated with pregnancy. Nongestational tumors are frequently composed of various germ cell elements.

**Table 12.3.2** Immunostains for common types of germ cell tumors

| Tumor entity | PLAP | AFP | HCG | CK | Others |
|---|---|---|---|---|---|
| Seminoma | ++ | | (+) | (+) | CD117 (c-kit) in tumor cells<br>CD 45 +++ in background lymphocytes |
| Embryonal carcinoma | ++ | + | | +++ | |
| Endodermal sinus tumor | + | +++ | | ++ | |
| Choriocarcinoma | ++ | | +++ | ++ | |
| Syncytiotrophoblastic giant cells (admixed to other cell types) | ++ | | +++ | ++ | |
| Teratoma* | (+) | | | + | |

Semiquantitative scoring: + to +++ a variable percentage of cells stain positively

(+) negative, or weak positive staining in a few cells

Abbreviations: PLAP, placental alkaline phosphatase; AFP, alpha-fetoprotein; HCG, human chorionic gonadotropin; CK, cytokeratin; LCA, leukocyte common antigen

* Supplemental immunopositivity is dependent on the germinal tissue components

Organ-specific mature tissue stains positively with corresponding markers (CEA, CKs, TTF1, thyroglobulin, etc.)

Choriocarcinoma is composed of two different cell types:

- *Syncytiotrophoblasts* are pleomorphic multinucleated giant cells. The nuclei are bizarrely shaped and hyperchromatic containing large nucleoli (Fig. 12.40A).
- *Cytotrophoblasts* are large to medium-sized rounded cells. The nuclei are irregular and coarsely structured; the cytoplasm is sharply outlined. High N/C ratio (Figs. 12.40A and 12.40B).

#### 12.3.7.4 Teratomas (Figs. 2.91 and 12.41)

The teratoma is composed of tissue elements derived from the three germ layers. The tissue components and corresponding cells are in various stages of maturation. The potential tumor behavior depends on the grade of cellular dedifferentiation.

**Caution**

- Retroperitoneal metastasis of a successfully treated gonadal germ cell tumor may occur after a long disease-free interval.
- Immature tumor elements of a gonadal teratoma may be destroyed by cytotoxic drugs and irradiation therapy. As a consequence, the well-differentiated tumor fraction – mainly well-differentiated squamous cancer cells – can be the only secondary tumor manifestation.

#### 12.3.7.5 Immunocytochemistry of Germ Cell Tumors (Figs. 12.38D, 12.39B, 12.39C)

Table 12.3.2 shows the appropriate panel of immunocytochemical stains, which has shown to be helpful in differentiating between common germ cell tumors. The cytoplasmic immunoreactivity is typical for each marker indicated. Further immunocytochemical stainings, which could be diagnostically helpful, are discussed in the literature [34, 45].

### 12.3.8 Metastases

**General Comments**

- Transcutaneous- and endosonographic-guided FNAB is in many cases used for staging metastatic disease in the retroperitoneal space. Image-guided aspiration is particularly important in order to avoid invasive diagnostic surgery.
- Malignoma of the pelvic organs predominantly metastasize to pelvic and paraaortic lymph nodes; metastases of carcinoma of the ovary, uterine cervix, endometrium, prostate, and urinary tract are frequently diagnosed by means of FNAB.
- Cytologic appearance and immunocytochemical features of metastases are similar to their primary counterparts. They are documented in the literature or in distinguished textbooks [15, 66], and discussed in varied chapters of this book; see Sects. 9.2.6, Table 9.2.1, p. 610, and 15.3.24, Table 15.3.3, p. 978.

Selected differential diagnostic problems are briefly discussed:

#### 12.3.8.1 Squamous Cell Carcinoma

Secondary retroperitoneal squamous cell carcinoma originates predominantly from uterine and vaginal tumors, less often from lung cancer. The differential diagnostic challenge of nonkeratinizing squamous cell carcinoma comprises malignant melanoma, spindle cell and round cell sarcoma, round cell or spindle cell tumors of the kidney, and other cancers.

#### 12.3.8.2 Adenocarcinoma

Retroperitoneal metastases may derive from tumors of the prostate, endometrium, gastrointestinal tract, ovaries, breast, and others. Most of these metastases will exhibit characteristic cytomorphologic and immunocytochemical features.

#### 12.3.8.3 Large-Cell Tumors

In retroperitoneal FNABs, large-cell tumors presenting with loose cell clusters and abundant single cells should give rise to a suspicion of:

- Dedifferentiated adenocarcinoma or squamous cell carcinoma.
- Transitional cell carcinoma.
- Tumors of the kidney and adrenals.
- Germ cell tumors.
- Poorly differentiated round cell sarcoma.
- Large-cell malignant lymphoma.
- Melanoma.
- Chordoma.
- Other cancers may be a possibility.



#### 12.3.8.4 Tumors with Myxoid / Mucinous Background

This tumor group is challenging, particularly in view of cytologic samples that originate from the sacral bone, perisacral soft tissue, and vertebra [5, 33, 47].

The group includes:

- Metastatic mucinous adenocarcinoma.
- Chordoma (see Sect. 11.3.3.6.2, p. 710).
- Myxoid ependymoma.
- Extraskeletal myxoid chondrosarcoma.
- Other rare primary and secondary tumors with myxoid / mucoid features.

### 12.3.9 Further Reading


1. Afroz N, Khan N, Chana RS. Cytodiagnosis of yolk sac tumor. Indian J Pediatr 2004;71:939-942.
2. Akdamar MK, Eltoum I, Eloubeidi MA. Retroperitoneal paraganglioma: EUS appearance and risk associated with EUS-guided FNA. Gastrointest Endosc 2004;60:1018-1021.
3. Akerman M, Rydholm A. Aspiration cytology of lipomatous tumors: a 10-year experience at an orthopedic oncology center. Diagn Cytopathol 1987;3:295-302.
4. Akhtar M, al Dayel F. Is it feasible to diagnose germ-cell tumors by fine-needle aspiration biopsy? Diagn Cytopathol 1997;16:72-77.
5. Akhtar I, Flowers R, Siddiqi, et al. Fine needle aspiration biopsy of vertebral and paravertebral lesions: retrospective study of 124 cases. Acta Cytol 2006;50:364-371.
6. Al-Agha OM, Igbokwe AA. Malignant fibrous histiocytoma: between the past and the present. Arch Pathol Lab Med 2008;132:1030-1035.
7. Al-Bozom IA, Mujeeb IB, Murad N. Retroperitoneal lymphangiomyomatosis diagnosed by fine needle aspiration: a case report. Acta Cytol 2007;51:594-596.
8. Al-Rikabi A, Hussain AA, Buchler M, et al. Primary leiomyosarcoma of the inferior vena cava: report of a case diagnosed by fine needle aspiration cytology and confirmed by histopathologic examination. Acta Cytol 2007;51:477-479.
9. Artifon EL, Franzini TA, Kumar A, et al. EUS-guided FNA facilitates the diagnosis of retroperitoneal endometriosis. Gastrointest Endosc 2007;66:620-622.
10. Bentz JS, kochman ML, Faigel DO, et al. Endoscopic ultrasound-guided real time fine-needle aspiration: clinicopathologic features of 60 patients. Diagn Cytopathol 1998;18:98-109.
11. Berner A, Franzen S, Heilo A. Fine needle aspiration cytology as a diagnostic approach to lymphangioleiomyomatosis. A case report. Acta Cytol 1997;41:877-879.
12. Bhat SN, Mohanty SP, Kustagi P. Endometriosis presenting like a psoas abscess. Saudi Med J 2007;28:952-954.
13. Binek J, Spieler P, Hürlimann R, et al. Ultrasound-guided fine-needle aspiration of abdominal masses: accuracy and short-term complications. Europ J Ultrasound 1995;2:199-203.
14. Binh MBN, Sastre-Garau X, Guillou L. MDM2 and CDK4 immunostainings are useful adjuncts in diagnosing well-differentiated and dedifferentiated liposarcoma subtypes Am J Surg Pathol 2005;29:1340–1347
15. Bonfiglio TA, MacIntosh PK, Patten SF Jr, et al. Fine needle aspiration cytology of retroperitoneal lymph nodes in the evaluation of metastatic disease. Acta Cytol 1979;23:126-130.
16. Bosniak MA, Siegelman SS, Evans JA. The adrenal retroperitoneum and lower urinary tract. in: Year Book Medical Publishers, Chicago, 1976; pp:232-237.
17. Cafferty LL, Katz RL, Ordonez NG, et al. Fine needle aspiration diagnosis of intraabdominal and retroperitoneal lymphomas by a morphologic and immunocytochemical approach. Cancer 1990;65:72-77.
18. Cantisani V, Mortele KJ, Glickman JN, et al. Large retroperitoneal hibernoma in an adult male: CT imaging findings with pathologic correlation. Abdom Imaging 2003;28:721-724.
19. Caraway NP, Fanning CV, Amato RJ, Sneige N. Fine-needle aspiration cytology of seminoma: a review of 16 cases. Diagn Cytopathol 1995;12:327-333.
20. Chhieng DC, Jhala D, Jhala N, et al. Endoscopic ultrasound-guided fine-needle aspiration biopsy: a study of103 cases. Cancer 2002;96:232-239.
21. Choi HJ, Park IA. Fine needle aspiration cytology of metastatic choriocarcinoma presenting as a breast lump. A case report. Acta Cytol 2004;48:91-94.
22. Collins KA, Geisinger KR, Wakely PE Jr, et al. Extragonadal germ cell tumors: a fine-needle aspiration biopsy study. Diagn Cytopathol 1995;12:223-229.
23. Dash RC, Liu K, Sheafor DH, Dodd LG. Fine-needle aspiration findings in idiopathic retroperitoneal fibrosis. Diagn Cytopathol 1999;21:22-26.
24. DeWeerd JH, Dockerty MB. Lipomatous retroperitoneal tumors. Am J Surg 1952;84:397-407.
25. Downs-Kelly E, Goldblum JR, Patel RM, et al. The utility of fluorescence in situ hybridization (FISH) in the diagnosis of myxoid soft tissue neoplasms. Am J Surg Pathol 2008;32:8-13.
26. Enzinger FM, Weiss SW. Malignant fibrohistiocytic tumors. In: Soft Tissue Tumors. St.Louis, CV Mosby, 1983; pp:166-199.
27. Fukunaga M. Histologically low-grade dedifferentiated liposarcoma of the retroperitoneum. Pathol Int 2001;51:392-395.
28. Garre Sanchez MC, Sola Perez J, Bas Bernal A, et al. Ultrasound-guided fine-needle aspiration biopsy. Study of the cost per patient and comparison with computed tomography-guided biopsy. Rev Esp Enferm Dig 1997;89:297-304.
29. Gilbert KL, Bergman S, Dodd LG, et al. Cytomorphology of yolk sac tumor of the liver in fine-needle aspiration: a pediatric case. Diagn Cytopathol 2006;34:421-423.

30. Goldman SM, Davidson AJ, Neal J. Retroperitoneal and pelvic hemangiopericytomas: clinical, radiologic and pathologic correlation. Radiology 1988;168:13-17.
31. Gonzalez-Campora R, Otal-Salaverri C, Hevia-Vazquez A, et al. Fine needle aspiration in myxoid tumors of the soft tissues. Acta Cytol 1990;34:179-191.
32. Gupta K, Dey P, Vashisht R. Fine-needle aspiration cytology of malignant peripheral nerve sheath tumors. Diagn Cytopathol 2004;31:1-4.
33. Gupta RK, Cheung YK, Al Ansari AG, et al. Diagnostic value of image-guided needle aspiration cytology in the assessment of vertebral and intervertebral lesions. Diagn Cytopathol 2002;27:191-196.
34. Hammerich KH, Gustavo EA, Wheeler TM. Application of immunohistochemistry to the genitourinary system (prostate, urinary bladder, testis, and kidney). Arch Pathol Lab Med 2008;132:432-440.
35. Hisaoka M, Morimitsu Y, Hashimoto H, et al. Retroperitoneal liposarcoma with combined well-differentiated and myxoid malignant fibrous histiocytoma-like myxoid areas. Am J Surg Pathol 1999;23:1480-1492.
36. Hoover LA, Hafiz MA. Fine-needle aspiration diagnosis of extragonadal choriocarcinoma with immunoperoxidase studies. Diagn Cytopathol 1989;5:84-87.
37. Jakowski JD, Wakely PE Jr. Cytopathology of extraskeletal myxoid chondrosarcoma: report of 8 cases. Cancer 2007;111:298-305.
38. Jenssen C, Siebert C, Bartho S. Leiomyosarcoma of the inferior vena cava. Diagnosis using endoscopic ultrasound-guided fine-needle aspiration biopsy. Dtsch Med Wschr 2008;133:769-772.
39. Jimenez-Heffernan JA, Lopez-Ferrer P, Vicandi B, et al. Cytologic features of malignant peripheral nerve sheath tumor. Acta Cytol 1999;43:175-183.
40. Kapila K, Hajdu SI, Whitmore WF Jr, et al. Cytologic diagnosis of metastatic germ cell tumors. Acta Cytol 1983;27:245-251.
41. Kilpatrick SE, Ward WG, Bos GD. The value of fine-needle aspiration biopsy in the differential diagnosis of adult myxoid sarcoma. Cancer 2000;90:167-177.
42. Klijanienko J, Caillaud JM, Lagace R, Viehl P. Cytohistologic correlations of 24 malignant peripheral nerve sheath tumor(MPNST) in 17 patients: the Institute Curie experience. Diagn Cytopathol 2002 ;27:103-108.
43. Klijanienko J, Caillaud JM, Lagacé R, Vielh P. Comparative fine-needle aspiration and pathologic study of malignant fibrous histiocytoma: cytodiagnostic features of 95 tumors in 71 patients. Diagn Cytopathol 2003;29:320-326.
44. Klijanienko J, Caillaud JM, Lagace R. Fine needle aspiration in liposarcoma: cytohistologic correlative study including well-differentiated, myxoid, and pleomorphic variants. Diagn Cytopathol 2004;30:307-312.
45. Kwon MS. Aspiration cytology of mediastinal seminoma: report of a case with emphasis on the diagnostic role of aspiration cytology, cell block and immunocytochemistry. Acta Cytol 2005;49:669-672.
46. Lagacé R, Aurias A. Does malignant fibrous histiocytoma exist? Ann Pathol 2002;22:29-34.
47. Layfield LJ. Cytologic differential diagnosis of myxoid and mucinous neoplasms of the sacrum and parasacral soft tissues. Diagn Cytopathol 2003;28:264-271.
48. Lemieszczuk B, Bidzinski M, Zielinski J, Sikorowa L. Clinical value of transvaginal, sonographically guided fine needle aspiration biopsy of parametria in recurrent cervical carcinoma. Eur J Gynaecol Oncol 1993;14 Suppl:68-76.
49. Lindberg GM, Maitra A, Gokaslan ST, et al. Low grade fibromyxoid sarcoma: fine-needle aspiration cytology with histologic, cytogenetic, immunohistochemical, and ultrastructural correlation. Cancer 1999;87:75-82.
50. Logrono R, Kurtycz DF, Sproat IA, et al. Multidisciplinary approach to deep-seated lesions requiring radiologically-guided fine-needle aspiration. Diagn Cytopathol 1998;18:338-342.
51. Long BW. Image-guided percutaneous needle biopsy: an overview. Radiol technol 2000;71:335-359.
52. Martinez CA, Palma RT, Waisberg J. Giant retroperitoneal lipoma: a case report. Arq Gastroenterol 2003;40:251-255.
53. Matthews LM. Fine needle aspiration diagnosis of lymphangiomyomatosis. a case report. Acta Cytol 1999;43:1155-1158.
54. McGee RS Jr., Ward WG, Kilpatrick SE. Malignant peripheral nerve sheath tumor: a fine-needle aspiration biopsy study. Diagn Cytopathol 1997;17:298-305.
55. Mehra M, Tamhane A, Eloubeidi MA. EUS-guided FNA combined with flow cytometry in the diagnoses of suspected or recurrent intrathoracic or retroperitoneal lymphoma. Gastrointest Endosc 2005;62:508-513.
56. Mizrak B, Ekinci C. Cytologic diagnosis of yolk sac tumor. A report of seven cases. Acta Cytol 1995;39:936-940.
57. Motoyama T, Chida T, Fujiwara T, Watanabe H. Mucinous cystic tumor of the retroperitoneum. A report of two cases. Acta Cytol. 1994;38:261-266.
58. Nguyen GK, Neifer R. The cells of benign and malignant hemangiopericytomas in aspiration biopsy. Diagn Cytopathol 1985;1:327-331.
59. Okada N, Hirooka Y, Itoh A, et al. Retroperitoneal neurilemmoma diagnosed by EUS-guided FNA. Gastrointest Endosc 2003;57:790-792.
60. Ramzy I. Benign schwannoma: demonstration of Verocay bodies using fine needle aspiration. Acta Cytol 1977;21:316-319.
61. Reddy VB, Gattuso P, Abraham KP, et al. Computed tomography-guided fine needle aspiration biopsy of deep-seated lesions. Acta Cytol 1991;35:753-756.
62. Russell WO, Cohen J, Enzinger FM, et al. A clinical and pathological staging system for soft tissue sarcomas. Cancer 1977;40:1562-1570.
63. Stein AL, Bardawil RG, Silverman SG, Cibas ES. Fine needle aspiration biopsy of idiopathic retroperitoneal fibrosis. Acta Cytol 1997;41:461-466.
64. Stewart CJ, Coldewey J, Stewart IS. Comparison of fine needle aspiration cytology and needle core biopsy in the diagnosis of radiologically detected abdominal lesions. J Clin Pathol 2002;55:93-97.
65. Suen KC. Retroperitoneal sarcomas. in: Guides to Clinical Aspiration Biopsy. ed. TS. Kline. Retroperitoneum and Intestine. Igaku-Shoin New York,1987; pp:31-51.
66. Suen KC. Retroperitoneal sarcomas. in: Guides to Clinical Aspiration Biopsy. ed. TS. Kline. Retroperitoneum and Intestine. Igaku-Shoin New York,1987; pp:66-81.
67. Vicandi B, Jimenez-Heffernan J, Lopez-Ferrer P, et al. Cytologic features of round cell liposarcoma: a report on five patients. Cancer 2003;99:28-32.
68. Walaas L, Kindblom L.G. Lipomatous tumors: a correlative cytologic and histologic study of 27 tumors examined by fine needle aspiration cytology. Hum Pathol 1985;16:6-18.
69. Walaas L, Angervall L, Hagmar B et al. A correlative cytologic and histologic study of malignant fibrous histiocytoma: an analysis of 40 cases examined by fine-needle aspiration cytology. Diagn Cytopathol 1986;2:46-54.
70. Williams DB, Sahai AV, Aabakken L, et al. Endoscopic ultrasound guided fine needle aspiration biopsy: a large single center experience. Gut 1999;44:720-726.
71. Wittmann J, Kocjan G, Sgouros SN, et al. Endoscopic ultrasound-guided tissue sampling by combined fine needle aspiration and trucut needle biopsy: a prospective study. Cytopathology 2006;17:27-33.
72. Zornoza J, Jonsson K, Wallace S, Lukeman JM. Fine needle aspiration biopsy of retroperitoneal lymph nodes and abdominal masses: an updated report. Radiology 1977;125:87-88.

**Fig. 12.30A–C Idiopathic retroperitoneal fibrosis.**
A 57-year-old woman presented with bilateral hydronephrosis. Clinical symptoms and laboratory investigations indicated retroperitoneal fibrosis. Image-guided FNAB of the retroperitoneal mass was performed and direct smears were Pap-stained.
*Cytology* substantiated the clinical diagnosis.
**A** Fibroblasts, fibrocytes, histiocytes, and lymphocytes occur within compact fibrosclerotic mesenchymal tissue, indicating active fibrotic disorder (high magnification). **B** Another detail shows thick sclerotic bundles encasing fibrocytes. **C** Mesothelial fragments as a contaminant from the needle tract: transabdominal ventrodorsal needle passes provided tissue fragments from retroperitoneal fibrosis accompanied by numerous mesothelial cell sheets. High microscopic magnification shows a flat but overlapping sheet of activated mesothelial cells that could be misinterpreted as well-differentiated adenocarcinoma.

**Fig. 12.31 Leiomyoma.**
FNAB of a retroperitoneal nodule in an elderly woman provided paucicellular cytologic smears.
*Cytology:* A few tissue microfragments consisting of fusiform cells embedded in a compact fibrillary background suggested a tumor of neurogenic or myogenic origin. Immunocytochemistry was not performed due to lack of adequate cytologic material (direct smear, Pap stain, lower magnification).
*Tissue diagnosis* (surgical biopsy): Leiomyoma.

**Fig. 12.32A, B Myxoid liposarcoma.**
Example of a low-grade myxoid liposarcoma (FNAB, direct smear, Pap stain).
*Cytologic and histologic diagnosis:* Myxoid liposarcoma.
**A** High magnification demonstrates small round and fusiform cells set in a myxoid background. Small lipoblasts (arrow) and large mature adipocytes (arrowheads) are also present. **B** High magnification showing accumulation of lipoblasts, which are characterized by varied size, eccentrically positioned atypical nuclei, and cytoplasmic fat vacuoles (arrows).

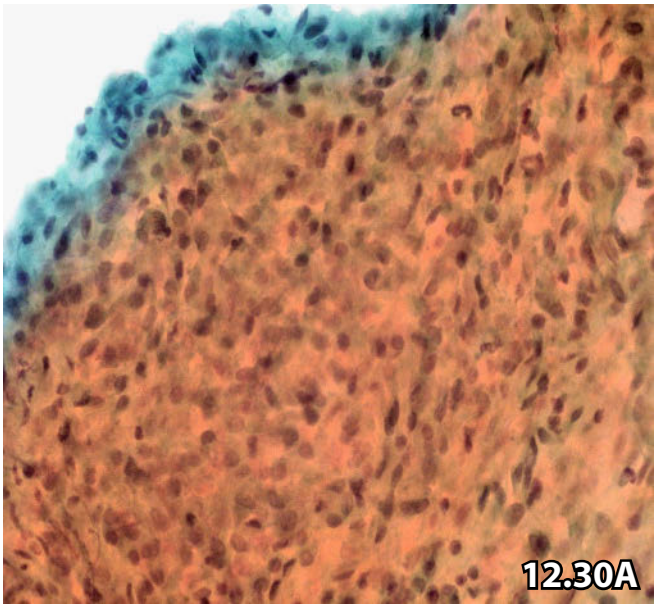
12.30A

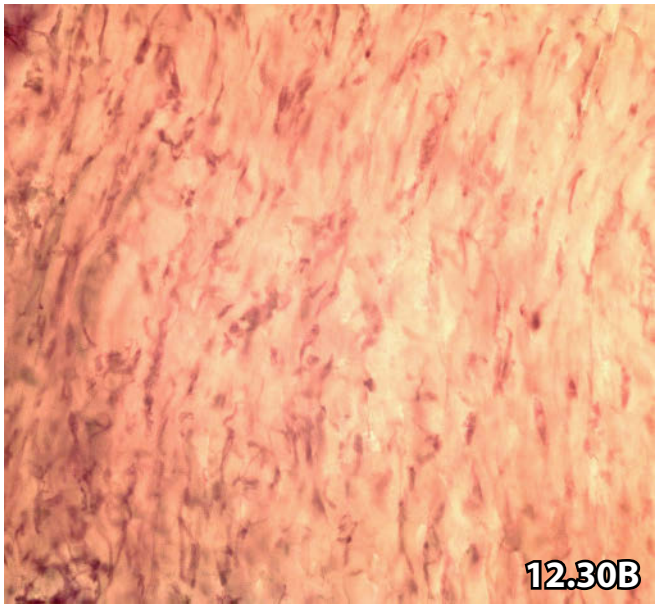
12.30B

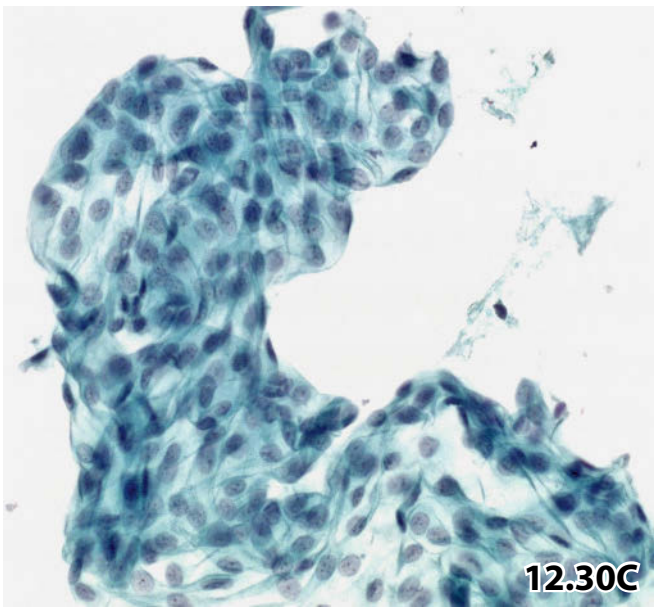
12.30C

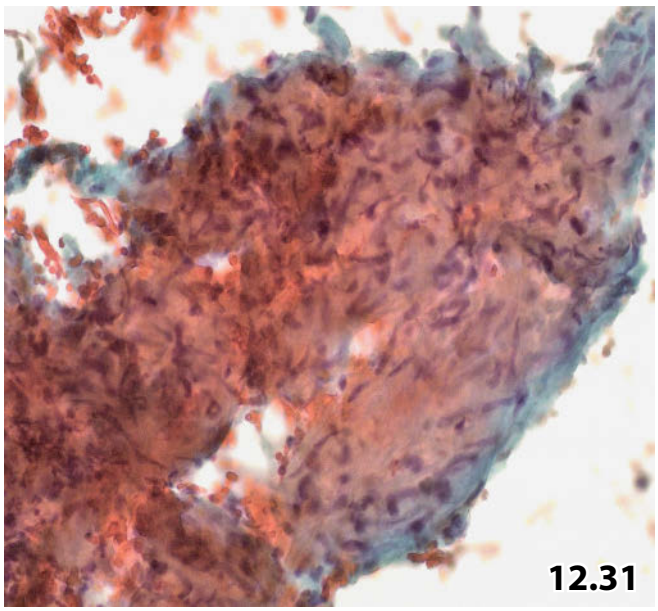
12.31

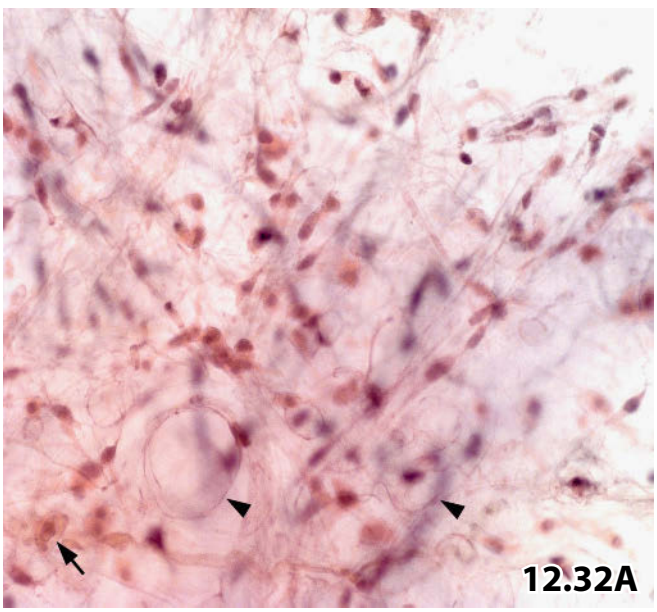
12.32A

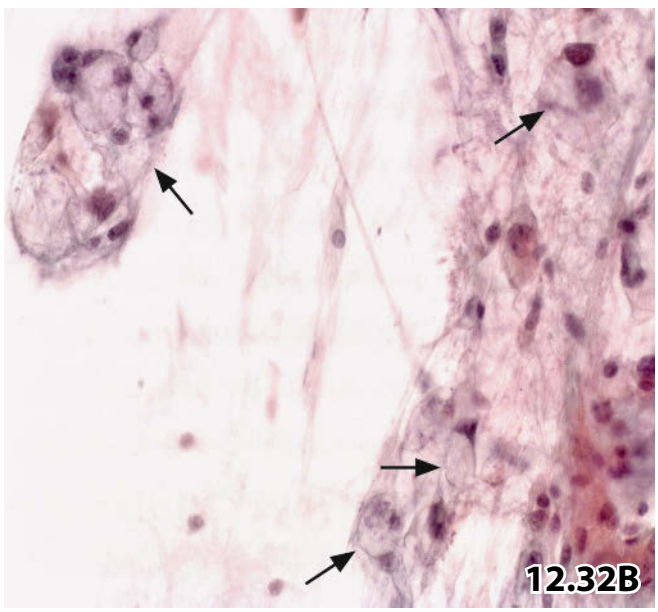
12.32B

**Fig. 12.33 Low-grade leiomyosarcoma.**
Loosely arranged spindle cells showing abundant elongated cytoplasm. Nuclei are blunt ended and monomorphic except for a certain variation in their size, and coarse granular chromatin (FNAB, conventional smear, Pap stain, high magnification).

**Figs. 12.34 and 12.35 High-grade leiomyosarcoma.**
Conventional FNA smears (Pap stain) exhibiting cytologic details and immunocytochemical characteristics.

**Fig. 12.34** (case #1) High magnification shows densely crowded tumor cells and distinct syncytial cytoplasm. The pleomorphic nuclei exhibit coarse chromatin and pronounced nucleoli.

**Fig. 12.35** (case #2) Immunostaining for alpha smooth muscle actin is useful to separate leiomyosarcoma from other spindle cell tumors (Pap-prestained conventional smear).

**Fig. 12.36 Malignant fibrous histiocytoma/undifferentiated pleomorphic sarcoma.**
Fine-needle aspiration cytology of a pleomorphic malignant fibrous histiocytoma (MFH) in an elderly woman shows huge multinucleated giant cells (lower left) and small mononucleated pleomorphic cells (arrows) embedded in a sanguineous background (direct smear, Pap stain, high magnification).
*Tentative cytologic diagnosis:* High-grade sarcomatous neoplasia comprising giant cells.
*Comment:* The giant cells closely resemble Reed-Sternberg cells, giving rise to diagnostic dilemmas. Note the cellular background, which is completely different in MFH as compared to Hodgkin lymphoma.
*Histologic diagnosis:* Pleomorphic MFH.

**Fig. 12.37 Round cell liposarcoma.**
This tumor entity as demonstrated at high magnification (direct smear, Pap stain) should be differentiated from small round blue cell tumors, non-Hodgkin lymphoma, undifferentiated carcinoma, and other neoplastic lesions. Immunocytochemical work-up is indispensable in order to reach a useful diagnosis.
*Cytology:* Lymphoma and carcinoma could be excluded by negative immunoreaction for CD45 and Lu-5 (not shown); nevertheless, the cytologic diagnosis remained inconclusive.
*Tissue diagnosis:* Biphasic liposarcoma, myxoid and round cell variant.

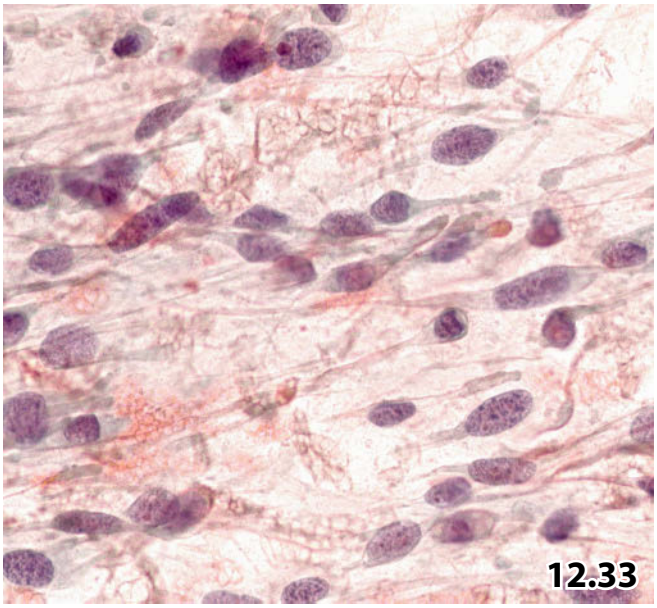
12.33

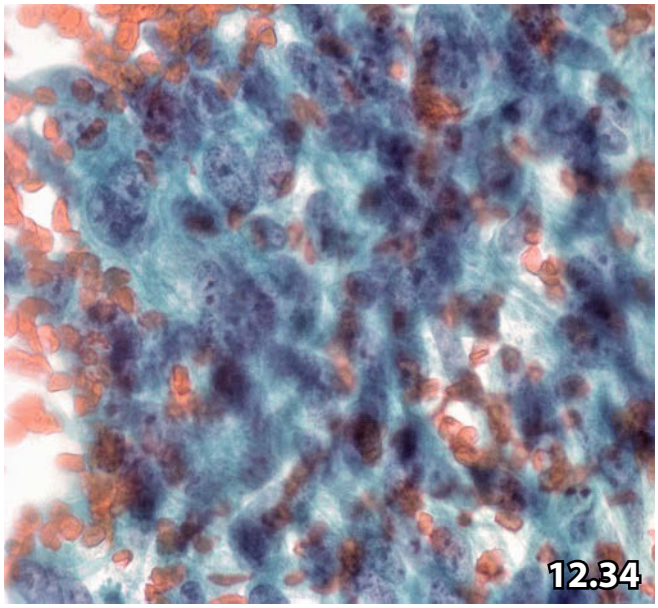
12.34

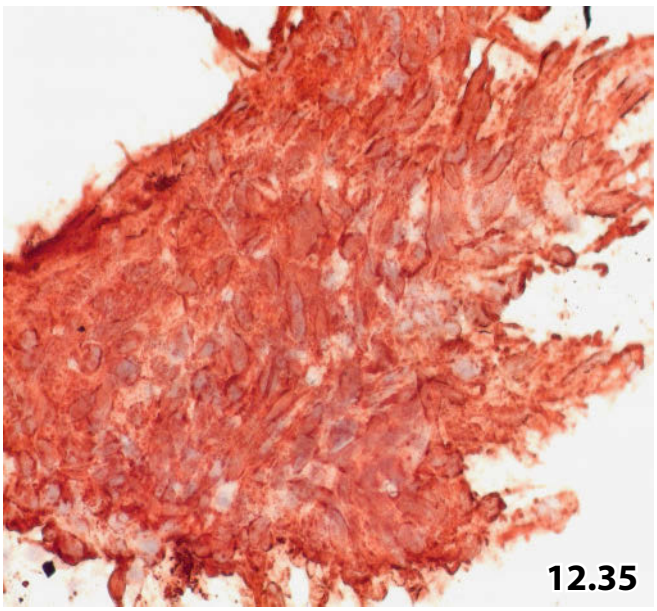
12.35

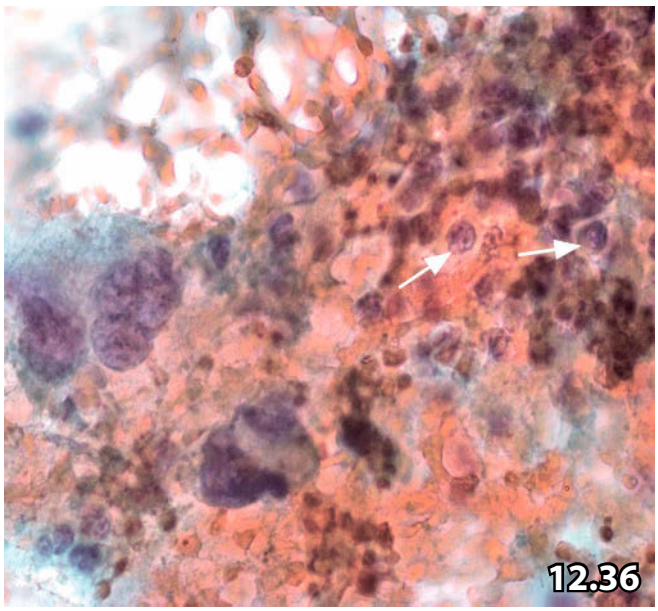
12.36

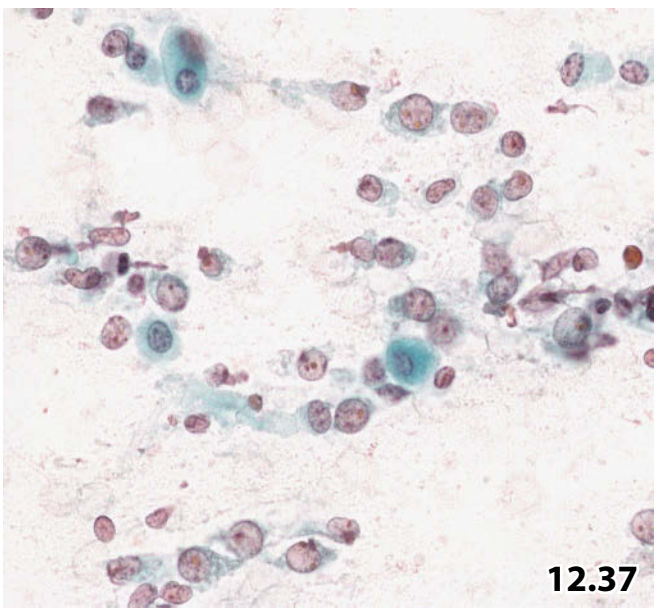
12.37

**Fig. 12.38A–D Seminoma.**
A 48-year-old man with a positive history of testicular seminoma presented with a retroperitoneal tumor mass. Image-guided FNAB was required by the physician in order to exclude a second primary tumor. Direct smears were prepared and Pap-stained. **A** Characteristic dual population depicted at low magnification: isolated large neoplastic cells along with small lymphocytes. Pay attention to degenerating tumor cells with apoptotic nuclei that are difficult to differentiate from small lymphocytes (arrows) by standard cytology (see also C). **B** High magnification is focused on the morphologic key features of single tumor cells. Note sharply defined cytoplasmic margins frequently associated with double contours (arrows). **C** Immunostaining for CD45 highlights the lymphoid population; the procedure is helpful in differentiating between lymphocytes and lymphocyte-mimicking apoptotic tumor cell nuclei (arrows) (Pap-prestained direct smear). **D** Immunocytochemistry: tumor cells are decorated using an antibody for placental alkaline phosphatase (Pap-prestained direct smear).

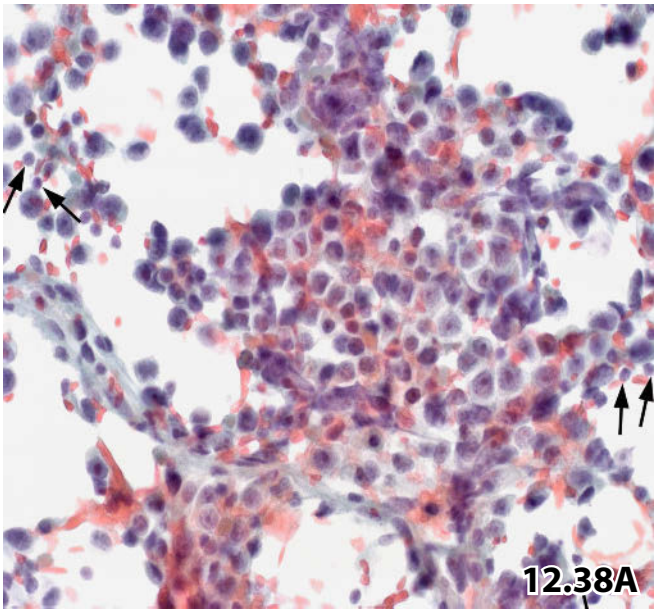

12.38A

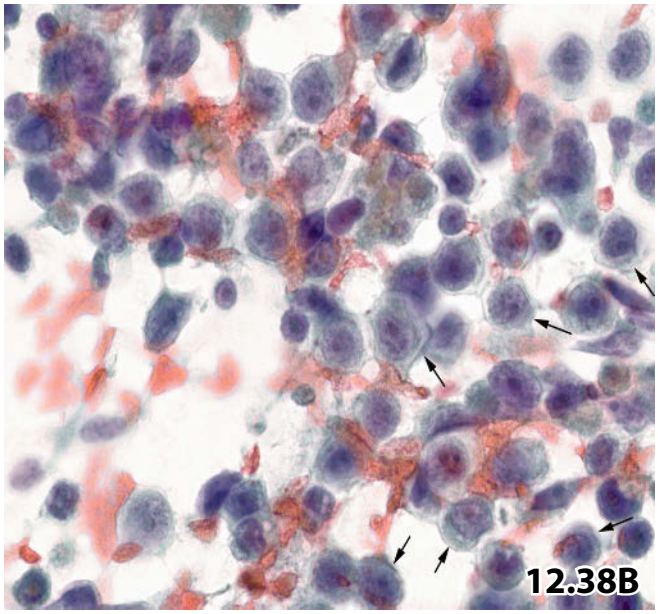

12.38B

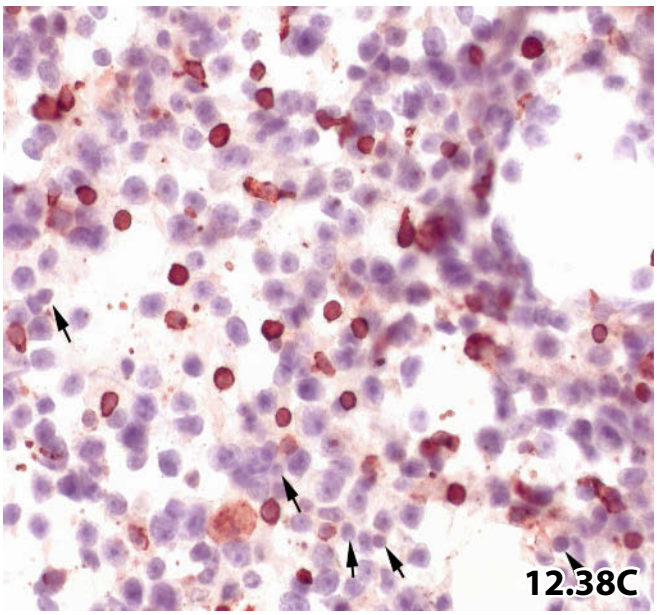

12.38C

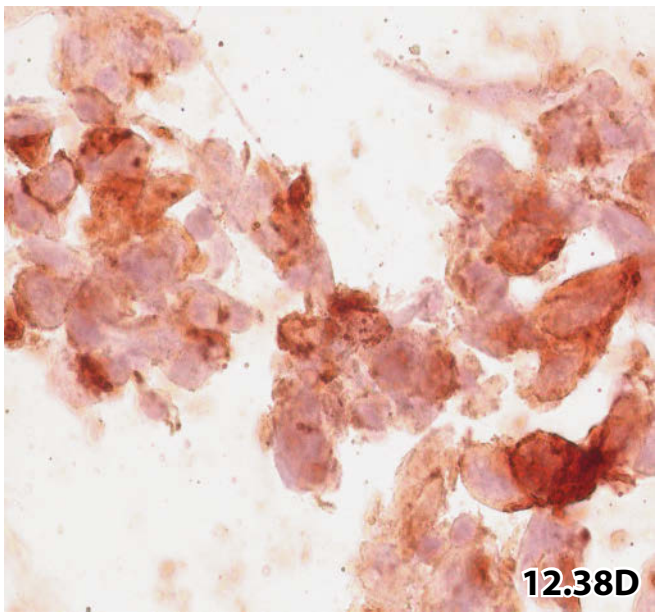

12.38D

**Fig. 12.39A–C Embryonal carcinoma and endodermal sinus tumor.**
FNAB of a tumor located in the retroperitoneal space of a 30-year-old man (conventional smears and liquid-based preparations, ThinPrep).
*Cytologic diagnosis:* Cytomorphology and immunocytochemical results indicate endodermal sinus tumor.
*Histologic diagnosis:* Embryonal carcinoma associated with areas of endodermal sinus tumor.
**A** High magnification shows fairly monomorphic medium-sized to large tumor cells arranged in compact clusters. The nuclei are glassy and the chromatin is unevenly distributed. Tumor cells occasionally surround translucent hyaline globules (direct smear, Pap stain). **B** Tumor cells exhibit strong immunopositivity for pancytokeratin (Lu-5, Pap-prestained ThinPrep specimen). **C** Alpha-fetoprotein is merely exhibited in well-preserved tumor cells (Pap-prestained ThinPrep specimen). The positive staining results for placental alkaline phosphatase is not shown.

**Fig. 12.40A, B Choriocarcinoma.**
A 19-year-old man presented with a large tumor mass in the upper retroperitoneal compartment. Image-guided FNAB was performed in order to achieve a preliminary diagnosis in a concerned young patient in poor condition. Direct smears were Pap-stained.
*Tentative cytologic diagnosis:* Pleomorphic large-cell carcinoma (possibly of germ cell origin). Immunocytochemistry was not performed for technical reasons.
*Tissue diagnosis* on the occasion of an autopsy (the patient died shortly after the initial diagnostic evaluations): Choriocarcinoma.
**A** A multinucleated syncytiotrophoblast (lower left) is shown at high magnification. **B** Cytotrophoblasts are arranged in compact three-dimensional clusters. Note nuclear polymorphism and occasionally sharply defined cytoplasmic margins (high magnification).



Densely clustered cytotrophoblasts exhibiting syncytial cytoplasm (missing sharply outlined borders) are difficult to differentiate from syncytiotrophoblasts (arrows in Fig. 12.40B).

**Fig. 12.41 Teratoma.**
A female newborn presented with a cystic sacrococcygeal teratoma. Cyst content was sampled by FNAB. Direct smears from the sediment were Pap-stained. Higher magnification shows a similar appearance of the cell population as seen in ganglioneuroblastoma: atypical small to medium-sized immature cells and large cells of the immature ganglion cell type exhibiting multiple vague cytoplasmic processes (arrows). DNA quantitation using image cytometry yielded an euploid-polyploid histogram (not shown).
*Cytologic diagnosis:* Cell population originating from immature neuroectodermal tissue consistent with immature teratoma.
*Tissue diagnosis* (tumorectomy): Cystic and solid teratoma – cerebral glial tissue outweighing by far components of other embryonic germ layers.

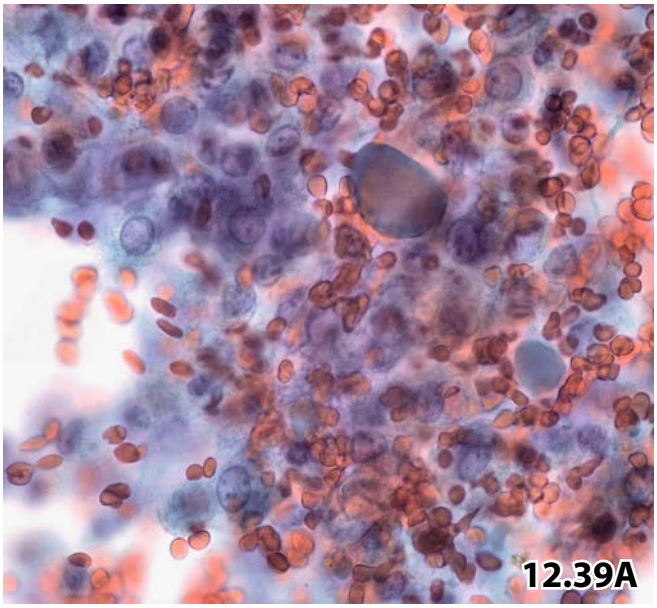
12.39A

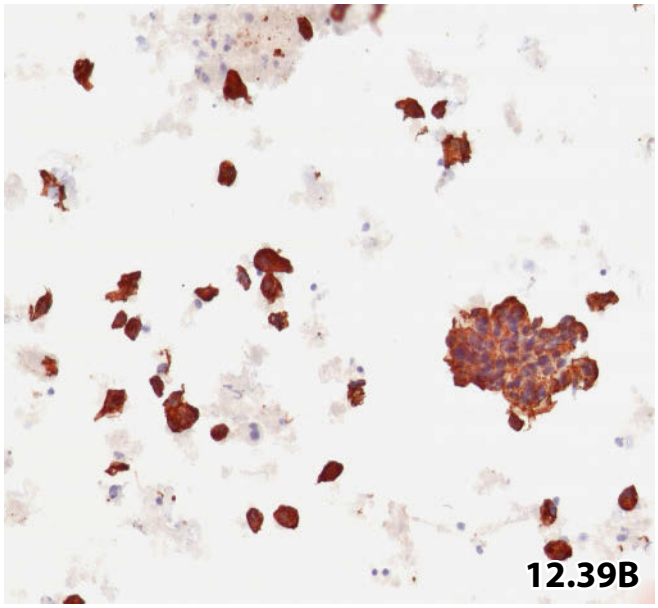
12.39B

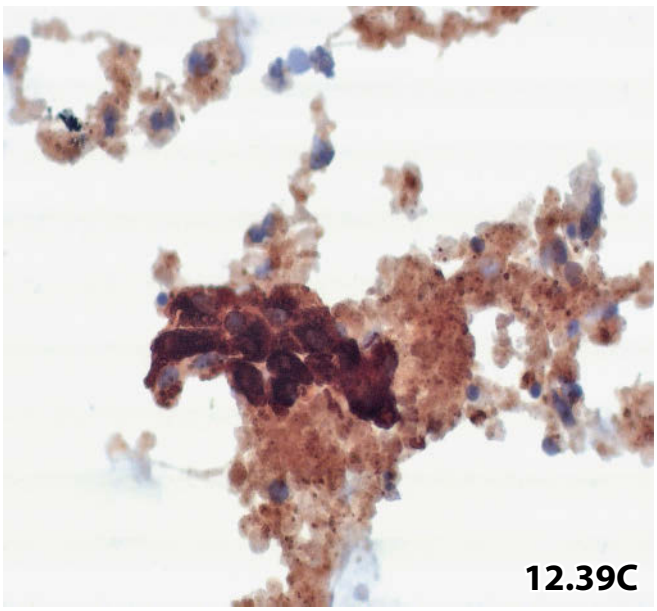
12.39C

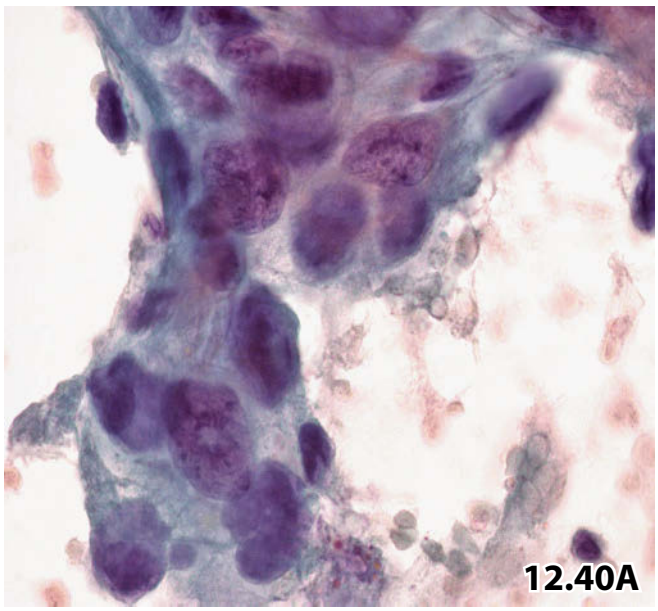
12.40A

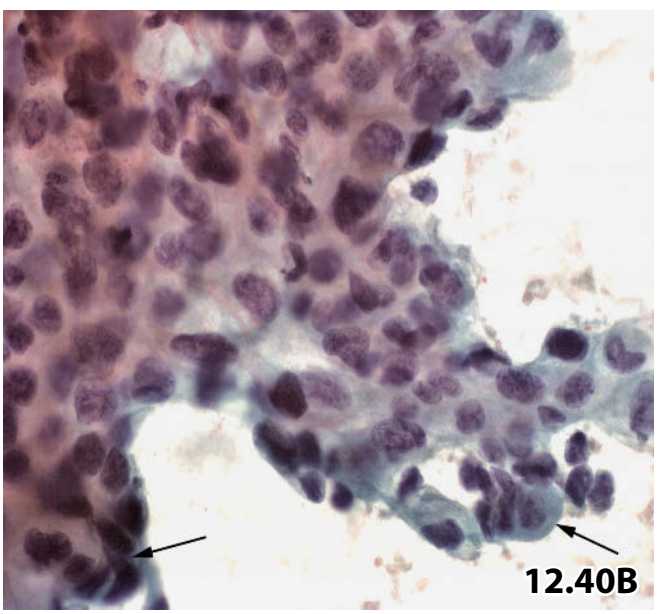
12.40B

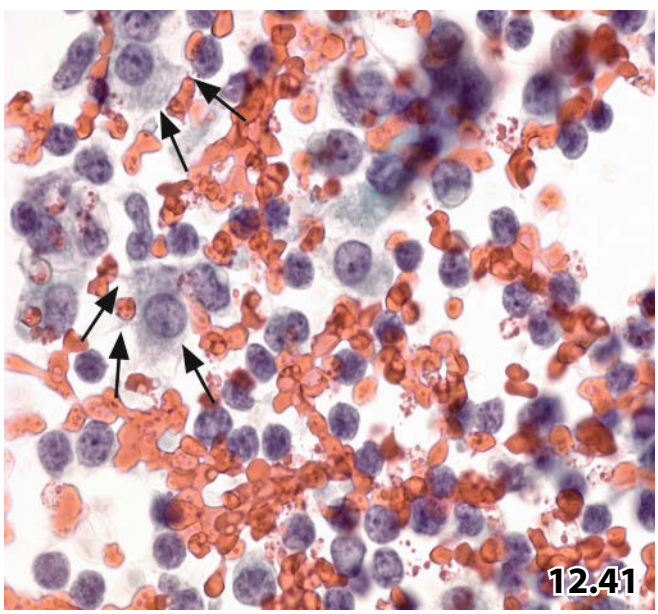
12.41

# 13 Urinary Tract



## Synopsis and Algorithms



Spieler/Rössle, *Nongynecologic Cytopathology. A Practical Guide. Essentials of Diagnostic Pathology*,
DOI 10.1007/978-3-642-24719-4_13, 

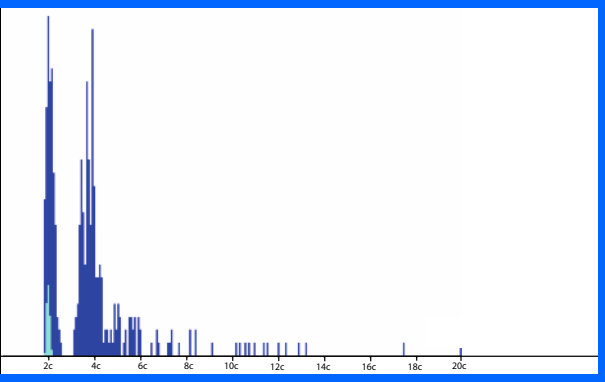


# Section 13.1
# Urinary Tract



## 13.1.1 Introduction

### 13.1.1.1 Screening for Bladder Cancer

Screening programs for bladder cancer and its precursor (dysplasia and carcinoma in situ) by means of urine samples have been infrequently reported in the literature. Programs have been carried out on individuals considered at high risk, such as industrial workers exposed to defined toxic agents, drug abusers, heavy smokers, and populations with high incidence of *Schistosoma hematobium* infections (Bilharziosis) [15, 32, 33, 53]. There is poor evidence that early detection has a considerable impact on the length of survival in screened populations [30].

Cytology screening may become more efficient in combination with molecular analysis (UroVysion FISH test and dip stick urine chemistry analyzers) [53].

### 13.1.1.2 Examination of Symptomatic Patients and Sampling Techniques

- Hematuria is the most common symptom in patients with bladder cancer. All patients with gross hematuria, and patients with microscopic hematuria above 50 years of age need a full investigation [1]. Protocol of investigation may include urine cytology, upper tract imaging, flexible cystoscopy comprising biopsies, cytologic examination of washings and brushings, auxiliary tests such as flow and image cytometry, and molecular pathology.
- Studies suggest that routine urine cytology has poor performance and should not be used routinely in patients with hematuria [13, 58]. Voided urine has a high specificity and sensitivity for nonpapillary and in-situ urothelial carcinoma (up to 100%), but it yields poor diagnostic results for low-grade neoplastic disorders due to sparse cellular shedding and minor cellular atypia [37, 46].

### 13.1.1.3 Tumor Recurrence and Tumor Follow-Up

- Urothelial carcinoma is known to have the highest recurrence rate of any carcinoma type in the urinary system. Continuous cytologic follow-up is mandatory during the entire life span of patients treated for urothelial cancer of the lower and upper urinary tract.
- It has been shown that metachronous urothelial neoplasms frequently occur and that excisional treatment of a low-grade papillary neoplasm does not preclude synchronous intraurothelial precancerous lesions such as urothelial dysplasia and carcinoma in situ [24, 28].
- Both low-grade papillary urothelial tumors and solid carcinoma of the bladder also show a tendency for recurrence in the ureter and renal pelvis.
- Cytology has the great advantage that cell sampling includes the entire urothelium, permitting detection of patients with carcinoma in situ and cystoscopically occult neoplasia. High-grade intraurothelial neoplasia is identified in a high percentage using cytologic techniques.

**Caution**

Positive urinary bladder cytology together with negative cystoscopic and bioptic findings should trigger major investigations for urothelial neoplasia particulary in the upper urinary tract.

## 13.1.2 Sampling Techniques

### 13.1.2.1 Voided Urine

Voided urine is the method of choice for screening programs and for diagnostic purposes in men, whereas catheterized urine is preferred in female patients. Voided urine has a high specificity and sensitivity for nonpapillary and in-situ urothelial carcinoma (up to 100%), but it yields poor diagnostic results for low-grade papillary neoplastic disorders and low-grade dysplasia due to faint cellular shedding [37, 46].

- Voided urine is valuable basic material for cytodiagnostics if the cells are well preserved. Thus, the following approach is recommended:
  - Discard first urine in the morning.
  - Hydration of the patient.
  - Collect second urine.
  - The fresh sample has to be processed within 2 h in the cytologic laboratory. Urine samples may be stored in a refrigerator at 4° for at most 24 h in cases with delayed laboratory processing; in this setting, cells show minor degeneration and are sufficiently well preserved for diagnostic purposes. Prompt fixation of the fresh sample by collecting in an equal amount of fixative, for example 50% alcohol, is another possibility for good preservation of the cellular morphology.
- Collection of multiple successive morning specimens is debatable. A first specimen with satisfactory cellularity will generally be reliably diagnostic.

### 13.1.2.2 Direct Sampling

#### 13.1.2.2.1 Washings of Bladder, Ureter, and Renal Pelvis

- Washings of the bladder is highly recommended whenever cystoscopy is performed. Irrigation cytology specimens contain more single cells and cell clusters than voided urine, and cell degeneration tends to be minimal.
- In addition to bladder irrigation, washings of ureters and renal pelves can be achieved if the primary lesion is suspected in these areas. Patients having undergone surgery for malignant bladder tumor may benefit from periodic examination of ureteral and pelvic washings. The material can be obtained by retrograde catheterization or flexible ureterorenoscopy [5]. Compared to voided urine, cytodiagnostic accuracy is increased using these methods.
- The irrigation fluids from different compartments of the urinary tract should always be separately collected and transferred in discrete vials to the laboratory.

#### 13.1.2.2.2 Washings of the Urethra

- Primary carcinoma of the female and male urethra are exceedingly uncommon; therefore routine cell sampling for early diagnosis is not indicated.
- Patients who have undergone radical cystectomy for malignant bladder tumor are proposed long-term follow-up by periodic examination of urethral washings [52].
  Urethral washing cytology is reported to benefit selected individual patients, but there seems to be no statistical survival difference in patients followed or not followed by urethral washings [35, 40].

#### 13.1.2.2.3 Urinary Conduit (Ileal Bladder)

Tumor patients who have undergone radical cystectomy followed by urinary conduit must be controlled by periodic examination of the neobladder by cytologic evaluation of urine and/or washings. Urothelial carcinoma in situ seems to develop most of all at the neobladder anastomoses [29, 44].

#### 13.1.2.2.4 Urinary Tract Brushing

If circumscribed lesions are endoscopically detected, targeted brushing can be performed. Brush cytology is a more specific sampling method than irrigation or voided urine [6, 20].

## 13.1.3 Sample Preparation

- Direct smears from the cell button are recommended in cases with clearly discernible sediment after centrifugation.
- Samples with low cellularity should instead be processed by cytocentrifugation.
- Thin-layer preparation by means of a special processor is not necessary for urinary samples.
- Routine cell-block preparations are not recommended in urinary cytology because urine cytology specimens rarely contain enough material for preparation of cell blocks. Still, cell blocks may occasionally be prepared from washings and brushings that yield large amounts of sediment or contain tissue fragments and clots.
- Slides are preferably fixed in an alcohol-based fixative; a spray fixative can be used as well. Slides are best stained according to the Papanicolaou (Pap) technique.

## 13.1.4 Ancillary Studies

Ancillary studies can be performed with reliable results on each type of cytologic sample from the urinary collecting system.

- Special studies are particularly useful in order to assess premalignancy and malignancy on cells with undeter-

mined changes at primary investigation and in the follow-up of patients treated for urothelial cancer.

- Furthermore, it is important having appropriate tools available to confirm a positive cytological diagnosis in cases where endoscopic, imaging, and histologic studies provide negative results.
- Metastatic disease from distant organs into the urinary system can be clarified by an appropriate set of immunodiagnostic markers.
- Performance of varied ancillary methods such as morphology-based assays, biochemical tests, and molecular markers has been studied by several authors. Some of the procedures have received acceptance by urologists as a helpful supplement for the management of their patients; however, standardization has not yet been achieved [21, 45, 59].

### 13.1.4.1 Immunocytochemistry

Morphologic features are able to distinguish between poorly differentiated urothelial carcinoma and nonurothelial cancer in most cases. Overlapping cytomorphology may occur, making the determination of the site of origin difficult, particularly against prostate cancer.

In cytologic cases with equivocal diagnostic outcome regarding urothelial versus prostatic cancer, we prefer a primary antibody panel comprising three antibodies (AB):

– PSA (prostate-specific antigen): positive cytoplasmic reactivity in nearly all prostate cancers (PC) and negative in urothelial carcinoma (UC).
– PAP (prostate acid phosphatase): strongly expressed in PCs and negative in UCs.
– Cytokeratin 7: Positive in a majority of UCs. PCs exhibit negative immunoreactivity except for occasional positivity on single carcinoma cells.

Further evaluation of ABs and AB panels and a review of the literature are provided in a recent paper by Hammerich and colleagues [26].

A synopsis of the most useful markers which differentiate UC from PC are shown in Table 13.1.1.

Application of biochemical markers in order to identify other invading tumors (apart from prostate cancer) and rare secondary tumors to the urinary system is discussed in Sects. 13.3.7, p. 836 and 13.3.8, p. 837.

### 13.1.4.2 Quantitative DNA Cytometry

#### General Comments

- Parameters determined by static DNA image cytometry (ICM DNA) appear to be valuable in predicting both overall survival and progression-free survival and may be useful in addition to the classic parameters of stage and grade. DNA image analysis improves diagnostic sensitivity in transitional cell cancer, especially in superficial carcinoma compared with cytodiagnosis alone.
- Complementary to urine cytology (voided urine and washings from lower and upper urinary tract), image cytometric ploidy analysis is a reliable method [2, 3, 7, 9, 11, 12, 36, 39,43, 48, 54, 56]:
  – To differentiate between reactive cell atypia, dysplastic lesions and low-grade papillary transitional cell carcinoma respectively.
  – To confirm a cytologic diagnosis of primary bladder cancer.
  – To predict tumor recurrence.
  – To estimate biological behaviour in recurrent neoplasms.
- In contrast to flow cytometry (FCM), static cytometry has great advantages as to DNA evaluation:
  – It can be performed on routine cytologic smears.

**Table 13.1.1** Immunopanel: urothelial carcinoma versus prostate carcinoma

| | Urothelial carcinoma | Prostate carcinoma |
|---|---|---|
| EMA epithelial membrane antigen | + | – |
| CK7 | + | – |
| P63 | + / – | 0 |
| TM thrombomodulin | + / – | 0 |
| CK5/6 high molecular weight cytokeratin | + / – | 0 |
| EpCam | – / + | + |
| CD57 | – | + |
| PSA | 0 | + / – |
| PAP | 0 | + |
| NKX3.1 | 0 | + |
| Prostein | 0 | + |

+ most tumor cells positive – variable positivity 0 always negative

- Reliable results can be achieved measuring smaller numbers of cells as compared to FCM.
- A relevant ploidy status can be determined in tumors with a low number of aneuploid cells.
- The relevant cells can be discriminated visually and analyzed selectively (Fig. 13.37).
- Individual cells can be relocated and remeasured.

- Several studies refer to the performance of flow cytometric DNA analyses, or compare flow and image cytometry technique in order to find out advantages and disadvantages of each method [3, 8, 19, 22, 42, 43, 55]. Complementary use of ICM and FCM may be suitable in equivocal cases [4]. Image cytometry and flow cytometry may also be applied to single cell suspensions from unfixed and paraffin-embedded tumor tissue [3]. Feulgen-stained imprints are also suited as basic material for cytometric analyses [41, 50].
- Discrepant ploidy patterns can be achieved from cells of the same urothelial cancer using DNA image cytometry. The discrepancy may be due to tumor heterogeneity and is of clinical significance. DNA assessments on both washings and imprints directly obtained from the tumor would solve the problem in many cases [50].
- Diagnostic sensitivity of image cytometry can be increased by a combination of various DNA parameters.
- A state of the art paper of DNA image cytometry on bladder cancers has recently been published by Palmeira and coworkers [42].

13

#### 13.1.4.2.1 Interpretation of DNA Measurement

At our institution, cytometric studies have predominantly been performed on cells obtained from urinary tract washings. The DNA histogram was found to be a stable and reproducible tumor characteristic; the following algorithm has proved to be consistent for DNA interpretation using Feulgen-restained routine smears:

**DNA diploidy:**
1.8c ≤ DNA index of the stemline (SL) ≤ 2.2c
**DNA polyploidy:**
1.8c ≤ SL ≤ 2.2c, and 3.6c ≤ SL ≤ 4.4c, and 7.4c ≤ SL≤ 8.6c. No 9c exceeding events
**DNA tetraploidy:**
3.6c ≤ SL ≤ 4.4c. The remaining nuclei show varied quantitative DNA distribution patterns.
**DNA aneuploidy:**
1. aneuploid SL: SL < 0.9c, **or** 1.1c < SL < 1.8c, **or** 2.2c < SL < 3.6c, **or** SL > 4.4c
2. > 15% of all cells measured exhibit varying aneuploid DNA values.
3. at least two cells with DNA values > 9c

A stemline contains more than 20% of all cells measured.

#### 13.1.4.2.2 Comments on Cytometric DNA Results

- Single-cell and stemline interpretation follow the standards of the 2001 consensus report of the European Society for Analytical Cellular Pathology for ICM DNA [27].
- A diploid stemline corresponds to a benign cell population, but low-grade urothelial neoplasia and dysplasia can not be ruled out.
- A polyploid histogram is consistent with reactive cellular atypias or virus-induced nuclear changes (Figs. 13.19 and 13.20). But again, low-grade urothelial neoplasia is not definitely ruled out. An additional UroVysion FISH test should urgently be applied to clinically and cytologically equivocal cases (see Sect. 13.1.4.3, p. 803).
- Our experience has shown that a pronounced tetraploid DNA stemline along with single cells exhibiting varied quantitative DNA distribution patterns is highly suggestive of malignancy. Generally, such a histogram is associated with superficial and invasive low-grade neoplasms [10, 34] (Figs. 13.22, 13.23, 13.33). However, the phenomenon of DNA tetraploidy should be interpreted with caution, particularly in cytologically negative cases; it may rarely be found in patients without cystoscopic or cytologic/histologic evidence of neoplasia.
- The results of large series show that a high percentage of high-grade transitional cell tumors are aneuploid and that the detection of aneuploidy can usually be accepted as an objective marker for malignancy.

**Caution**

DNA aneuploidy may act as a false-positive indicator of malignancy in cases with genomic alterations that are caused by radiation therapy, chemotherapeutic agents, and viral infection.

#### 13.1.4.2.3 Indications for ICM DNA

We would like to emphasize that DNA ploidy assessment is of great value in routine urinary cytology practice.

At our institution, we have successfully applied the method for more than a decade. The purpose of ICM DNA analysis in primary tumor diagnosis and in tumor follow-up is as follows:

- Conspicuous nuclear atypia but ambiguous features of malignancy (in cases with inflammation, lithiasis, among other disorders) (Figs. 13.22 and 13.23).
- Highly atypical or malignant cells but absence of a cystoscopic and/or clinical correlate (occult carcinoma in situ, cancer located in the upper urinary tract) (Fig. 13.33).

– In addition to conventional cytology as an objective and reproducible tumor feature that may be helpful to predict survival and potential tumor progression.
– Increased DNA ploidy (in comparison to earlier ploidy results) in recurrent tumors generally refers to a higher tumor grade (Figs. 13.1 and 13.2).
– The cytometric result will help urologists and oncologists choose treatment methods with the greatest benefit for their patients.

### 13.1.4.3 Fluorescence In Situ Hybridization

[10, 17, 18, 25, 23, 31, 49, 51, 57] (Figs. 13.31 and 13.33)

- UroVysion fluorescence in situ hybridization (FISH) test is a multiprobe assay for detection of urothelial precancerous lesions and carcinoma in voided urine and bladder washings. The test detects abnormal signal copy numbers of chromosomes 3, 7, 17, and alterations in the 9p21 gene locus (deletion in cells of low-grade tumors and amplification in cells of high-grade neoplasia) (Fig. 13.31).
- FISH is easily performed by specially trained cytotechnologists in routine cytology laboratories.
- FISH may be used as a screening test in patients with clinical suspicion of urothelial carcinoma as well as for follow-up in patients presenting with a history of urothelial carcinoma.

#### 13.1.4.3.1 FISH Versus Conventional Cytology

- A recent review of comparative studies evaluating the role of FISH compared with conventional cytology by Jones [31] showed that FISH outperforms cytology in the diagnosis of urothelial carcinoma across all tumor stages and grades. Many studies showed that FISH detects malignancy-associated chromosomal abnormalities prior to the expression of malignant cell changes in cytologic samples [17, 18, 23, 51, 57].
- In particular, the UroVysion assay is superior in sensitivity to detect grade 1, Ta, and T1 transitional cell carcinoma and mild urothelial dysplasia compared with cytology alone. These results reflect the established knowledge that it is difficult to distinguish low-grade urothelial cancer from reactive cell changes by routine cytology.
- The FISH test is also very helpful in patients with clinically suspected primary or recurrent urothelial carcinoma but cytologically equivocal or negative results.

#### 13.1.4.3.2 FISH Versus DNA Image Cytometry and DNA Flow Cytometry

- FISH and ploidy assessment using ICM DNA are complementary methods in addition to urinary cytology: UroVysion FISH detects more low-grade and low-stage tumors than static cytophotometry; only a relatively small number of low-grade urothelial tumors reveal abnormal DNA distribution patterns and aneuploidy [16, 38]. As a result, the two tools are applied at our institution as follows (using routine cytologic samples):
  – ICM DNA in cases with definite nuclear atypias suggestive of malignancy, and in cases with unequivocal cellular signs of malignancy.
  – UroVysion FISH in cases with equivocal cell changes, with mild nuclear atypias, or with a negative cytologic result but clinical suspicion of bladder tumor; or routinely in the follow up of patients with urothelial tumors (Figs. 13.30 and 13.31).
- The sensitivity of FISH in detecting chromosomal aberrations exceeds FCM's sensitivity; the results are comparable to the ICM technique [14, 47].

## 13.1.5 Further Reading


1. Alishahi S, Byrne D, Goodman CM, Baxby K. Haematuria investigation based on standard protocol: emphasis on the diagnosis of urological malignancy. J R Coll Surg Edinb 2002;47:422-427.
2. Amberson JB, Laino JP. Image cytometric deoxyribonucleic acid analysis of urine specimens as an adjunct to visual cytology in the detection of urothelial cell carcinoma. J Urol 1993;149:42-45.
3. Baak JPA, Bol MGW, van Diermen B, et al. CNA cytometry features in biopsies of TaT1 urothelial cell cancer predict recurrence and stage progression more accurately than stage, grade, or treatment modality. Urology 2003;61:1266-1272.
4. Bertino B, Knape WA, Pytlinska M et al. A comparative study of DNA content as measured by flow cytometry and image analysis in 1864 specimens. Anal Cell Pathol 1994;6:377-394.
5. Bian Y, Ehya H, Bagley DH. Cytologic diagnosis of upper urinary tract neoplasms by ureteroscopic sampling. Acta Cytol 1995;39:733-740.
6. Bibbo M, Gill WB, Harris MJ, et al. Retrograde brushing as a diagnostic procedure of ureteral, renal pelvic and renal calyceal lesions. A preliminary report. Acta Cytol 1974;18:137-141.
7. Biesterfeld S, Borchers H, Jellouschek H, et al. Differential diagnosis and evaluation of the clinical course of transurethrally resected T1G3 urothelial carcinoma of the bladder by DNA image cytometry. Anticancer Res 2005;25:3243-3249.
8. Bol MG, Baak Jp, Diermen B, et al. Correlation of grade of urothelial cell carcinomas and DNA histogram features assessed by flow cytometry and automated image cytometry. Anal Cell Pathol 2003;25:147-153.
9. Boudry C, Herlin P, Coster M, Chermant JL. Influence of sample size on image cytometry of DNA ploidy measurements. Anal Quant Cytol Histol 1999;21:209-215.
10. Bubendorf L, Grilli B, Sauter G, et al. Multiprobe FISH for enhanced detection of bladder cancer in voided urine specimens and bladder washings. Am J Clin Pathol 2001;116:79-86.
11. Cai T, Margallo E, Nesi G, et al. Prognostic value of static cytometry in transitional cell carcinoma of the bladder: recurrence rate and survival in a group of patients at 10 years follow-up. Oncol Rep 2006;15:213-219.
12. Caraway NP, Khanna A, Payne L, et al. Combination of cytologic evaluation and quantitative digital cytometry is reliable in detecting recurrent disease in patients with urinary diversions. Cancer(Cancer Cytopathol) 2007;111:323-329.
13. Chahai R, Gogoi NK, Sundaram SK. Is it necessary to perform urine cytology in screening patients with haematuria? Eur Urol 2001;39:283-286.
14. Cianciulli AM, Bovani R, Leonardo C, et al. DNA aberrations in urinary bladder cancer detected by flow cytometry and FISH: prognostic implications. Eur J Histochem 2001;45:65-71.
15. Cohen SM, Shirai T, Steineck G. Epidemiology and etiology of premalignant and malignant urothelial changes. Scand J Urol Nephrol Suppl. 2000;205:105-115.
16. Dalquen P, Kleiber B, Grilli B, et al. DNA image cytometry and fluorescence in situ hybridization for noninvasive detection of urothelial tumors in voided urine. Cancer 2002;96:374-379.
17. Daniely M, Rona R, Kaplan T, et al. Combined morphologic and fluorescence in situ hybridization analysis of voided urine samples for the detection and follow-up of bladder cancer in patients with benign urine cytology. Cancer(Cancer Cytopathol) 2007;111:517-524.
18. Degtyar P, Neulander E, Zirkin H, et al. fluorescence in situ hybridization performed on exfoliated urothelial cells in patients with transitional cell carcinoma of the bladder. Urology 2004;63:398-401.
19. deVere White RW, Deitch AD. Evaluation of DNA flow cytometry as a screening test for bladder cancer. J Cell Biochem Suppl. 1992;161:80-84
20. Dodd LG, Johnston WW, Robertson CN, et al. Endoscopic brush cytology of the upper urinary tract. Evaluation of its efficacy and potential limitations in diagnosis. Acta Cytol 1997;41:377-384.
21. Eissa S, Kassim S, El-Ahmady O. Detection of bladder tumors: role of cytology, morphology-based assays, biochemical and molecular markers. Curr Opin Obstet Gynecol 2003;15:395-403.
22. Goulandris N, Karakitsos P, Georgoulakis J, et al. Deoxyribonucleic acid measurements in transitional cell carcinomas: comparison of flow and image cytometry techniques. J Urol 1996;156:958-960.
23. Grossman Combined morphologic and fluorescence in situ hybridization analysis of voided urine samples for the detection and follow-up of bladder cancer in patients with benign urine cytology. Urol Oncol 2008;26:332.
24. Habuchi T. Origin of multifocal carcinomas of the bladder and upper urinary tract: molecular analysis and clinical implications. Int J Urol 2005;12:709-716.
25. Halling KC, King W, Sokolova IA, et al. A comparison of cytology and fluorescence in situ hybridization for the detection of urothelial carcinoma. J Urol 2000;164:1768-1775.
26. Hammerich KH, Gustavo EA, Wheeler TM. Application of immunohistochemistry to the genitourinary system (prostate, urinary bladder, testis, and kidney). Arch Pathol Lab Med 2008;132:432-440.
27. Haroske G, Baak JP, Danielsen H, et al. Fourth updated ESACP consensus report on diagnostic DNA image cytometry. Anal Cell Pathol 2001;23:89-95.
28. Höglund M. On the origin of syn- and metachronous urothelial carcinomas. Eur Urol 2007;51:1185-1193.
29. Ide H, Kikuchi E, Shinoda K, et al. Carcinoma in situ developing in an ileal neobladder. Urology 2007;69:576.e9-11. Raica Rom J J Morphol Embryol 1992
30. Jacobs R. A review of the effectiveness of urinary cytology as a screening technique for occupational bladder cancer. J Soc Occup Med 1987;37:24-26.
31. Jones JS. DNA-based molecular cytology for bladder cancer surveillance. Urology 2006;67(3 Suppl 1):35-45.
32. Kälble T. Etiopathology, risk factors, environmental influences and epidemiology of bladder cancer. Urologe A 2001;40:447-450.
33. Kern W. Screening tests for bladder cancer. In: Screening for cancer. ed: Miller AB. Orlando Academic Press, pp 121-140, 1985.
34. Kline MJ, Wilkinson EJ, Askeland R, et al. DNA tetraploidy in Feulgen-stained bladder washings assessed by image cytometry. Anal Quant Cytol Histol 1995;17:129-134.
35. Knapik JA, Murphy WM. Urethral wash cytopathology for monitoring patients after cystoprostatectomy with urinary diversion. Cancer 2003;99:352-356.
36. Koss LG. Urinary cytology: the subjective diagnostic clues and their evaluation by computer. Anal Quant Cytol Histol 1979;1:202-206.
37. Koss LG, Deitch D, Ramanathan R, Sherman AB. Diagnostic value of cytology of voided urine. Acta Cytol 1985;29:810-816.
38. Krause FS, Feil G, Zumbrägel A, Bichler KH. Molecular genetic methods in the diagnosis of invasive bladder cancer. Anticancer Res 2000;20:5015-5021.
39. Krause FS, Feil G, Bichler KH, et al. Clinical aspects for the use of DNA image cytometry in detection of bladder cancer: a valuable tool? DNA Cell Biol 2003;22:721-725.
40. Lin DW, Herr HW, Dalbagni G. Value of urethral wash cytology in the retained male urethra after radical cystoprostatectomy. J Urol 2003;169:961-963.
41. Mainguené C, Choquenet C, Deplano C, et al. DNA ploidy by image cytometry in urothelial carcinomas. Comparison of touch imprints and paraffin-embedded biopsies from 31 patients. Anal Quant Cytol Histol 1997;19:437-442.
42. Palmeira CA, OliveiraPA, Seixas F, et al. DNA image cytometry in bladder cancer: state of the art. Anticancer Research 2008;28:443-450.

43. Planz B, Synek C, Robben J, et al. Diagnostic accuracy of DNA image cytometry and urinary cytology with cells from voided urine in the detection of bladder cancer. Urology 2000;56:782-786.
44. Raica M, Ioiart I Urethral and neobladder cytologic survey in patients with total cystectomy. Rom J Morphol Embryol 1992;38:29-34.
45. Ross JS, Cohen MB. Biomarkers for the detection of bladder cancer. Adv Anat Pathol 2001;8:37-45.
46. Sack MJ, Artymyshyn RL, Tomaszewski, Gupta PK. Diagnostic value of bladder wash cytology, with special reference to low grade urothelial neoplasms. Acta Cytol 1995;39:187-194.
47. Sauter G, Gasser TC, Moch H, et al. DNA aberrations in urinary bladder cancer detected by flow cytometry and FISH. Urol Res 1997;25 Suppl 1:S37-43.
48. Schapers RF, Ploem-Zaaijer JJ, Pauwels RP, et al. Image cytometric DNA analysis in transitional cell carcinoma of the bladder. Cancer 1993;72:182-189.
49. Schwarz S, Rechenmacher M, Filbeck T, et al. Value of muticolour fluorescence in situ hybridisation (UroVysion) in the differential diagnosis of flat urothelial lesions. J Clin Pathol 2008;61:272-277.
50. Seigneurin D, Rambeaud JJ, Bosio C, Louis J. DNA image cytometry of bladder tumors: comparison of washings and tumor imprints from 61 patients. Anal Cell Pathol 1993;5:39-48.
51. Skacel M, Fahmy M, Brainard JA, et al. Multitarget fluorescence in situ hybridization assay detects transitional cell carcinoma in the majority of patients with bladder cancer and atypical or negative urine cytology. J Urol 2003;169:2101-2105.
52. Stein JP, Clark P, Miranda G, et al. Urethral tumor recurrence following cystectomy and urinary diversion: clinical and pathological characteristics in 768 male patients. J Urol 2005;173:1163-1168.
53. Steiner H, Bergmeister M, Verdorfer I, et al. Early results of bladder-cancer screening in a high-risk population of heavy smokers. BJU Int 2008;102:291-296.
54. Stöckle M, Steinbach F, Voges H, Hohenfellner R. Image analysis DNA cytometry of bladder cancer. Recent Results Cancer Res 1993;126:151-163.
55. Tachibana M, Miyakawa A, Miyakawa M, et al. Prognostic significance of flow cytometric deoxyribonucleic acid analysis for patients with superficial bladder cancers: a long-term follow-up study. Cancer Detect Prev 1999;23:155-162.
56. van der Poel HG, Boon ME, van Stratum P, et al. Conventional bladder wash cytology performed by four experts versus quantitative image analysis. Mod Pathol 1997;10:976-982.
57. Veeramachaneni R, Nordberg ML, Shi R, et al. Evaluation of fluorescence in situ hybridization as an ancillary tool to urine cytology in diagnosing urothelial carcinoma. Diagn Cytopathol 2003;28:301-307.
58. Viswanath S, Zelhof B, Ho E, et al. Is routine urine cytology useful in the haematuria clinic? Ann R Coll Surg Engl 2008;90:153-155.
59. Zaher A, Sheridan T. Tumor markers in the detection of recurrent transitional carcinoma of the bladder: a brief review. Acta Cytol 2001;45:575-581.

**Figs. 13.1 and 13.2 Comparative DNA profiles can detect increased risk of tumor progression.**

Cystoscopy detected a papillary tumor in a 79-year-old man's urinary bladder.

(1) *Initial cytologic (bladder washing) and histologic diagnosis:* papillary transitional carcinoma, grade 3.

(2) Eight months after primary diagnosis: cytological follow-up detected highly malignant urothelial cells. Cystoscopy and cytology studies suggested carcinoma in situ.

Comparison of the two DNA profiles, as stated below, suggests a novel highly atypical cell clone indicating an increased potential for progression to invasiveness.

**Fig. 13.1** (1) Primary tumor DNA profile: Digital image analysis of the primary tumor provides an aneuploid DNA histogram, more than 20% of all measured nuclei exhibit an aneuploid DNA content; 14 nuclei having a DNA content greater than 9c, up to 20c (Feulgen-stained Pap-prestained sediment smear, Ahrens Cytometrie-System).

**Fig. 13.2** (2) Follow-up DNA profile: Digital image analysis of cells from the carcinoma in situ provides a highly aneuploid DNA histogram. An aneuploid stemline in the 6c area runs parallel to aneuploid DNA content in the majority of all measured nuclei; 75 nuclei have a DNA content greater than 9c, up to 70c (Feulgen-stained Pap-prestained sediment smear, Ahrens Cytometrie-System).

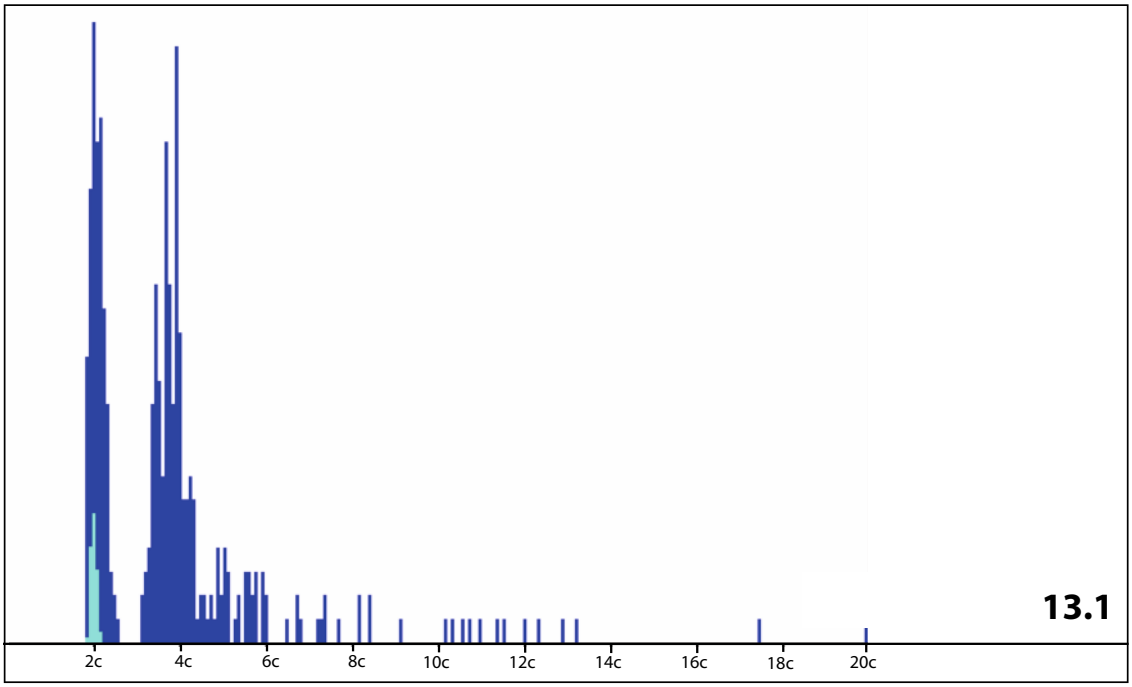
2c
4c
6c
8c
10c
12c
14c
16c
18c
20c

13.1

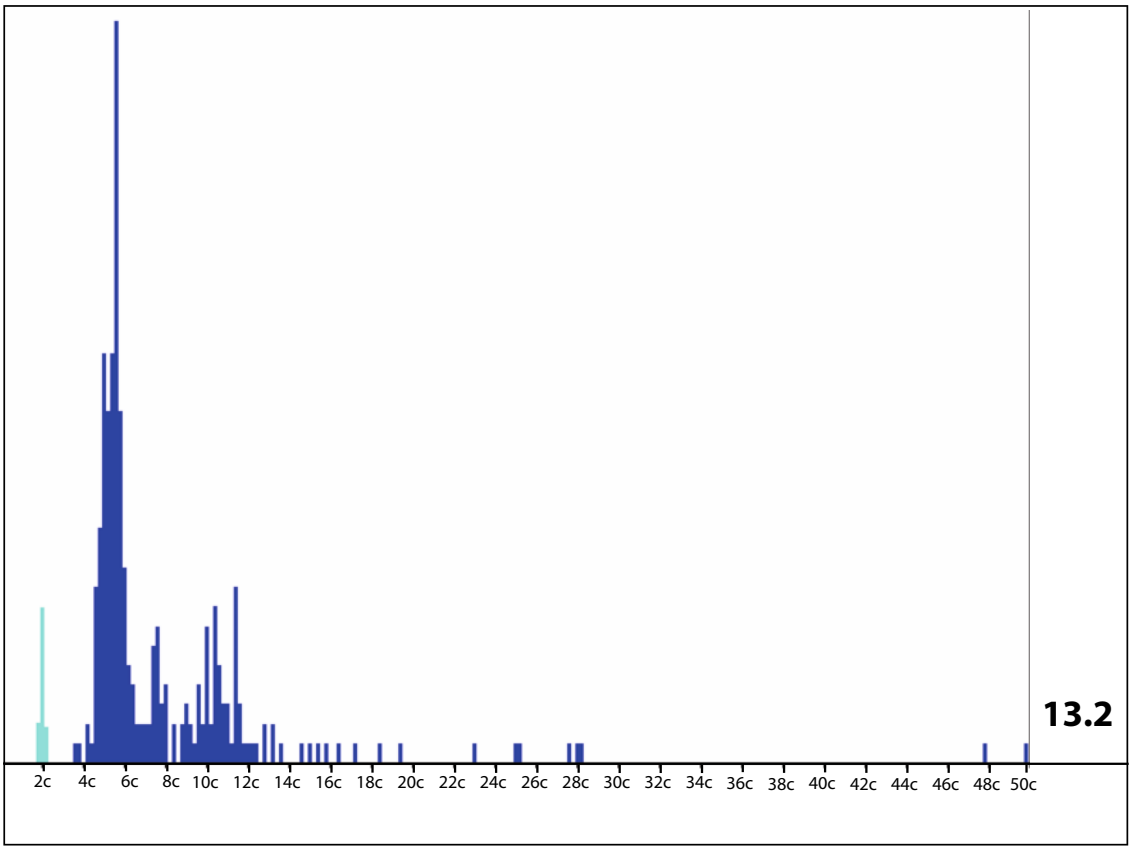
2c
4c
6c
8c
10c
12c
14c
16c
18c
20c
22c
24c
26c
28c
30c
32c
34c
36c
38c
40c
42c
44c
46c
48c
50c

13.2

# Section 13.2
# Urinary Tract

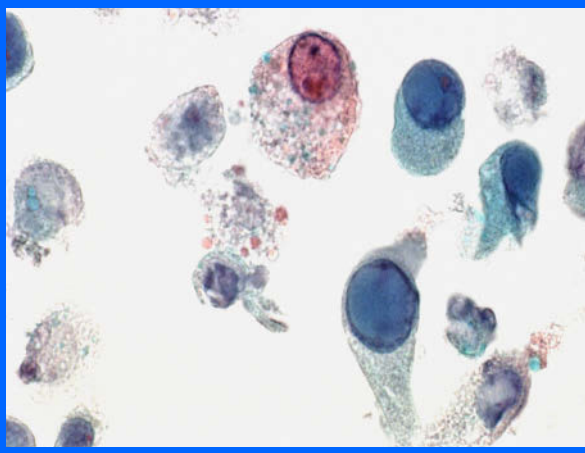

## Normal and Metaplastic Findings
## Degenerative and Reactive Atypias
## Nonneoplastic Lesions, Benign Tumors
## Inflammation/Infections

### 13.2.1 Normal Cytology and Metaplastic Lesions

#### 13.2.1.1 Squamous Cells (Fig. 13.3)

- Squamous cells of the superficial and intermediate type are present in all urinary bladder specimens, whereas samples from the upper urinary tract should exclusively show urothelial cells.
- Squamous cells exfoliate from the distal portion of the urethra and from areas of squamous metaplasia in the bladder mucosa.
- Squamous cells in urine samples of female patients may represent contamination from the vaginal and vulvar epithelium. Mature metaplastic squamous cells of the bladder mucosa cannot be differentiated from cells of other squamous areas.
- In rare cases, superficial metaplastic squamous cells may exhibit marked keratinization, yet the nuclei are bland (Fig. 13.3).

#### 13.2.1.2 Urothelial Cells (Figs. 13.4–13.09)

**General Comments**

- Urothelial cells in voided urine occur singly or in loose groups. In contrast, washing specimens are more cellular and display characteristic dense clusters.
- Large numbers of multinucleated urothelial cells in bladder washing are mainly observed in specimens collected by cystoscopy, samples obtained by retrograde catheterization, and flexible ureterorenoscope.
- Upper urinary tract: Urothelial cells in urine and washings of the upper urinary tract resemble those found in urinary bladder specimens. The fluids are of lower cellularity compared with samples obtained from the bladder unless a proliferative disorder is present. Squamous cells are unusual.

##### 13.2.1.2.1 Morphology of Superficial Urothelial Cells (Figs. 13.4–13.6)

- Cells appear in isolation but may also be arranged in loose groups or tight cohesive clusters of different size with a knobby contour. Cells arranged in compact clusters exhibit characteristic cytoplasmic molding.
- Considerable variability in cell size.
- Frequent bi- and multinucleation.
- Nuclei are bland, showing loosely arranged granular chromatin, chromocenters and an irregular outline.
- Nucleoli are rarely seen in benign, nonreactive cells.
- The wide and pale cytoplasm is sharply defined, its structure changing depending on cellular activity and degeneration.

#### 13.2.1.2.2 Morphology of Intermediate, Basal, and Atrophic Transitional Epithelial Cells (Fig. 13.7)

- These cells are considerably smaller than superficial urothelial cells, they have a pyramidal or round shape and a small dense clearly demarcated cytoplasm. The cells are frequently arranged in compact three-dimensional regular clusters associated with narrow nuclear spacing.
- The cells are usually observed with a single nucleus showing a smooth margin, a dense structure, and deep-blue staining.
- Atrophic transitional cells from elderly male patients show similar morphology.

#### 13.2.1.2.3 Morphology of Elongated or Columnar Urothelial and Nonurothelial Cells

(Figs. 13.8–13.10)

*Elongated and columnar urothelial cells* can be observed in virtually any urinary specimen. A number of samples may present with a high percentage of these cells.

- The nuclei show smooth membranes or irregular outlines; shrunken and darkly stained nuclei are frequently observed.
- The chromatin is granular and thinly dispersed.
- The cytoplasm is clear and sharply defined, showing a fusiform or columnar shape.
- The N/C ratio is in a normal range.
- The nucleoli appear variably prominent.

*Columnar glandular cells* exfoliating from metaplastic glandular epithelium, from epithelium of periurethral glands, or from prostatic epithelium, cannot reliably be differentiated from columnar transitional epithelial cells. Glandular (intestinal) metaplasia of the urothelium is characterized by sheets and clusters of mucin-secreting cylindrical cells interspersed with nonmucinous cells, the latter showing morphologic characteristics of urothelial cells (Fig. 13.10).

Furthermore, each of the cells mentioned above may mimic cells exfoliating from low-grade papillary tumors (see Sect. 13.3.4.1, p. 834).

**Caution**

Columnar cells in urinary samples can originate from different sites and lesions:

- Columnar-shaped urothelial cells.
- Urothelial cells from the intermediate zone.
- Columnar metaplasia of the urothelium (absence of mucus production as an exception) .
- Glandular cells from periurethral glands.
- Glandular cells from the prostate.
- Columnar-shaped neoplastic cells from low-grade papillary transitional cell carcinoma.

### 13.2.1.3 Benign Cells of Nonurothelial Origin

(Figs. 13.11–13.13)

#### 13.2.1.3.1 Cells from Ileal Bladder

[17, 25] (Fig. 13.11)

Ileal bladder (synonym, ileal conduit) is surgically constructed to bypass the natural lower urinary system, most often at the time of cystectomy for bladder cancer. Urine sediments are rich in cells of the intestinal type. The columnar configuration of these cells is mostly well preserved in spite of substantial degeneration.

- Nuclear pyknosis, karyorrhexis, cytoplasmic vacuolization, and cytoplasmic inclusions are signs of cellular degeneration along with background debris.
- Mucoid masses are overt.
- The well-preserved nuclei of intestinal cells are small and regularly outlined, containing thinly dispersed chromatin.
- It is difficult to recognize urothelial cells unless they occur in typical clusters.
- Granulocytes and bacteria may be present.

#### 13.2.1.3.2 Cells of Renal Origin [29]

Cells of renal origin are rarely found in fluids from the urinary tract except in cases of renal disorders, such as renal parenchymal disease and renal transplantation.

The cells showing different morphology depending on their tubular origin include:

- Cells from proximal tubules are medium-sized with abundant granular cytoplasm, but granularity is often difficult to identify.
- Cells from the distal tubular system are smaller than cells of the proximal tubules, and cytoplasmic granulation is missing.
- The nuclei of renal tubular cells are round and show an inconspicuous chromatin texture.

Renal epithelial cells may be accurately identified if they appear in numbers and together with renal casts. However, single renal cells are difficult to distinguish.

#### 13.2.1.3.3 Prostatic and Seminal Vesicle Epithelial Cells (Fig. 13.12)

These cells may rarely be encountered after instrumentation and prostatic massage. Spontaneous exfoliation hardly ever occurs.

#### 13.2.1.3.4 Mature Sperms (Fig. 13.13)

Mature sperms are mainly encountered in elderly male patients with a history of prostatic resection.

- Sperms usually appear clustered in the background of the smears, frequently adjacent to urothelial cells and/or embedded in mucoid masses.

## 13.2.2 Cell Degeneration and Reactive/Reparative Atypia [17]

**General Comments**

- Unfortunately, several pathologic conditions in the urinary tract along with reversible proliferative changes of the urothelium may exhibit cellular signs of severe atypia or even malignancy. The diagnosis of urothelial atypia or suspicious cytology may cause a dilemma for clinicians as to further investigations and therapeutic decisions.
- Atypical cells originating from reactive, premalignant, and malignant lesions are alike in the lower and upper urinary tract, but cytopathologists seem to have a lower threshold for diagnosing the category of urothelial atypia in fluids from the upper urinary tract. The reasons may include the relative lack of broad cytodiagnostic experience at this anatomic site and the fact that definite surgery is often solely based on a positive cytologic diagnosis [22].
- Murphy and colleagues have described cytological features and differential diagnostic considerations regarding urothelial lesions such as reactive conditions, dysplasia, and nonpapillary cancer [26].

**Microscopic Features** (Fig. 13.14)

Atypical degenerating and reactive/reparative urothelial cells can be distinguished from dysplastic/malignant cells if distinct criteria of malignancy are absent:

- Urothelial cells are frequently enlarged with the N/C ratio in a normal range.
- The large cytoplasm is clear or coarsely vacuolated and sharply demarcated.
- The nuclei are irregularly outlined, nuclear membranes are molded and cleaved, and the nucleoplasm shows clear areas and scattered chromatin condensates.
- The nucleoli are prominent; they may be pleomorphic and multiple in grossly activated cells.

### 13.2.2.1 Cause for Reversible Urothelial Atypia and Related Cell Features (Figs. 13.15–13.21)

#### 13.2.2.1.1 Cell Degeneration (Figs. 13.15 and 13.16)

- Pronounced degenerative changes of the cells include disintegration of the cytoplasm, pyknosis of the nuclei, and karyolysis.
- Occasional nucleoli.
- Deep-stained and polymorphous pyknotic nuclei should not be misinterpreted as a sign of malignancy, particularly in cytologic smears exhibiting a great deal of cell detritus.

#### 13.2.2.1.2 Inflammation (Fig. 13.16)

- Atypical reactive cell changes caused by an inflammatory process are easily recognized as nonmalignant due to cytoplasmic phagocytosis of leukocytes and absence of clear nuclear criteria of malignancy.
- Large, regularly shaped nucleoli are frequently present and should not lead to a false-positive diagnosis.

Cytologic urine control after successful antibiotic therapy should be undertaken in every case.

#### 13.2.2.1.3 Calculi [7, 10, 14] (Fig. 13.17)

Lithiasis may be the most important source of false-positive diagnosis in urinary tract cytology due to striking alterations of the lining cells. However, a number of samples from the urinary tract with known lithiasis have unremarkable cytology.

**Microscopic Features**

- Binucleation or multinucleation of urothelial cells and darkly stained nuclei are frequent.
- The nucleoli are prominent.
- The cytoplasm is large and vacuolated but occasionally may display a narrow rim.
- Refractile crystalline deposits in the cytoplasm and birefringent crystals as background material may be observed, as well as neutrophils due to secondary inflammation or infection.
- Small and large three-dimensional cell balls and papillary clusters are shed from the urothelial layer. Unlike in papillary carcinoma, the borders of the clusters appear regular and cellular polarity is maintained.
- Metaplastic squamous cells are increased in a high percentage of cases.
- Mitotic activity may be observed in large fragments of urothelium detached by calculi.

- Coexistence of urothelial cancer and lithiasis is possible. It will be very difficult to separate cells with marked reactive atypia from true malignant cells by cytology alone.
- Stones lodged in the renal pelvis and calices combined with pronounced cellular atypias are a special challenge for cytologists in cases in which the condition is interpreted as a tumoral process by imaging techniques.
- Ploidy analysis and FISH are powerful tools to distinguish between lithiasis-induced cellular atypia and high-grade urothelial carcinoma.

#### 13.2.2.1.4 Radiation Therapy (Fig. 13.18)

Irradiation to organs located in the pelvis may cause marked changes in the urothelial layer of the bladder. Distinguishing between malignancy and actinic changes can be extremely difficult.

Actinic changes in dysplastic and malignant cells can also provoke diagnostic dilemmas.

**Microscopic Features**

- Cellular changes are identical compared with irradiated cells elsewhere in the human body: markedly enlarged cells, mostly bi- or multinucleated. The nuclei appear in a three-dimensional fashion. The nucleoplasm may be homogeneously clear or hyperchromatic, or areas of clear nucleoplasm alternate with chromatin condensates. Pyknosis and karyorrhexis occasionally occur.
- Hallmarks are intranuclear and cytoplasmic vacuoles, huge nucleoli, and the N/C ratio in a normal range.

**Caution**

Abnormal DNA distribution patterns call for critical interpretation because radiation may induce aneuploidy.

#### 13.2.2.1.5 Chemotherapeutic Agents

[17, 18] (Figs. 13.19 and 13.20)

- Metabolic products of chemotherapeutic drugs administered to cancer patients may evoke marked cytotoxic effects on the urothelium. Urinary tract specimens from patients with bladder cancer after either topical or systemic treatment modalities exhibit practically identical cell changes.
- Ploidy assessment is of little differential diagnostic value, as illustrated above (Sect. 13.2.2.1.4).
- As a rule, long-term follow-up including bioptic investigations, is necessary in this patient group.
- The following drugs, among others, induce urothelial cell changes:
  - Alkylating agents (cyclophosphamide, thiotepa).
  - Antitumor antibiotics (mitomycin C).

**Microscopic Features**

- Morphologic cell changes are similar compared to those described above. Yet, nuclear irregularities and hyperchromasia are nearly always present together with coarse chromatin or complete loss of chromatin texture.
- Extremely pronounced chemotherapy-induced cell changes may perfectly imitate severe dysplasia or carcinoma.

#### 13.2.2.1.6 Instrument Artifacts and Artifacts Caused by Other Therapeutic Procedures (Fig. 13.21)

Cytoarchitectural and cellular artifacts as described below may not only be induced by instruments, but also by laser therapy, photodynamic therapy, and other techniques [18].

**Microscopic Features**

- Three-dimensional cell balls and papillary clusters may be removed from the urothelial layer. Papillary neoplasia has to be regarded, although the architecture of the clusters and cellular morphology are bland.
- Cellular alterations as described in the whole Sect. 13.2.2 are variable.

**Differential Diagnosis**

- It is sometimes difficult to distinguish between reactive and reparative urothelial atypias and low-grade flat neoplastic lesions and papillary neoplasms of low and moderate grade.
- Cytotoxic effects on urothelial cells after varied therapeutic interventions may mimic high-grade transitional cell carcinoma.

**DNA Ploidy and FISH Analyses**

(Figs. 13.22, 13.23, 13.30, 13.31, 13.35, 13.36)

Ploidy analysis on atypical cells is notably helpful in patients with lithiasis, persistent inflammation, and ambiguous clinical situations (check comments in the corresponding paragraphs of Sect. 13.2.2) (Figs. 13.22 and 13.23).

In cases exhibiting discrepancies between cytologic and cystoscopic and bioptic findings, it is highly recommended to confirm a positive cytologic diagnosis using a supplementary method. Moderate and high-grade dysplasia or carcinoma in situ is most easily diagnosed by quantitation of nuclear DNA (ICM DNA) (Figs. 13.35 and 13.36). In contrast, low-grade lesions can be detected by UroVysion FISH test (Figs. 13.30 and 13.31) (see also Sects. 13.1.4.2, p. 801, and 13.1.4.3, p. 803).

**Caution**

DNA aneuploidy may act as false-positive indicator of malignancy in cases with nuclear alterations caused by radiation therapy, chemotherapeutic agents, and viral infections

## 13.2.3 Benign Urothelial and Nonurothelial Lesions and Benign Tumors

A general overview of etiology, morphology, and differential diagnosis concerning miscellaneous benign lesions of the urinary tract is given by Borda and coworkers [4].

### 13.2.3.1 Benign Urothelial Disorders

Benign urothelial lesions include diverticulosis, von Brunn nests, papilloma/polyps of the bladder and urethra, among others. These lesions generally exfoliate cells that are morphologically similar or even identical to cells originating from normal urothelial lining.

#### 13.2.3.1.1 Diverticulosis

Urothelial lining in diverticula is often replaced by metaplastic squamous epithelium that may show hyperkeratosis. Diverticulosis may be suspected by cytology when clinical findings support this diagnosis.

#### 13.2.3.1.2 Von Brunn Nests (Fig. 13.24)

Von Brunn nests are buds of transitional urothelium growing into the subepithelial stroma. They frequently form gland-like spaces lined with columnar epithelium. Rarely, we were able to diagnose von Brunn nests from accelerated bladder washings that yielded small urothelial tissue fragments:

- Tissue fragments are composed of aggregates of urothelial cells and loose connective tissue. Epithelial nests are surrounded by basement membrane material and show a central lumen lined with cuboid to columnar-shaped urothelial cells.

#### 13.2.3.1.3 Transitional Cell Papillomas

These are lined with benign urothelium of normal cellular thickness that is composed of elongated and columnar cells. Determinate cytologic diagnosis is not possible unless papillary fragments with fibrovascular cores are detached.

#### 13.2.3.1.4 Papillary Urothelial Neoplasm of Low Malignant Potential [33]

Papillary urothelial neoplasm of low malignant potential (PUNLMP) is a lesion that is histologically similar to exophytic urothelial papilloma but exhibits increased cellular thickness of epithelium and increased proliferative activity, in absence of any significant cytologic atypia. It is unlikely that PUNLMP can be cytologically differentiated from transitional cell papilloma and low-grade exophytic papillary carcinoma [33].

### 13.2.3.2 Benign Nonurothelial Disorders

#### 13.2.3.2.1 Müllerianosis

[1, 5, 12, 16, 23, 34, 36] (Fig. 16.19)

**General Comments**

- The designation "müllerianosis" is presumed to be appropriate for varied coexisting related benign müllerian glandular epithelial proliferations, i.e., endosalpingiosis, endocervicosis, and endometriosis [8A, 34]. The most common site of involvement for endosalpingiosis, endocervicosis, and endometriosis in the urinary tract is the bladder.
- The pathogenesis is still under discussion; implantation-related, metaplastic, and ectopic origin have been suggested.
- Endometrial and stromal cells may be shed into the urinary collecting system in endometriosis involving the surface of the bladder mucosa [12].

**Microscopic Features and Immunocytochemistry**

Characteristic cytologic features and absence of unequivocal signs of malignancy, together with vague urinary tract symptoms, should suggest the correct diagnosis.

*Endosalpingiosis* [34]

- Small cohesive aggregates or papilliform clusters of mesothelial cells or tubal-type epithelium, including ciliated cells.

*Endocervicosis:* This is a very unusual finding. Differentiating this entity from glandular urothelial metaplasia is difficult.

- Endocervical-like mucinous single cells and small epithelial fragments.

*Endometriosis* (Fig. 16.19): Characteristic cytologic features and urinary tract symptoms during menstruation should suggest the correct diagnosis in fertile women.

- The endometrial cells are uniform and generally small with a high N/C ratio.
- The nuclei are round and smooth or show indentations. The chromatin is fine and evenly distributed. Nucleoli are large in activated cells.
- Small deeply stained stromal cells may be adherent to epithelial clusters or to individual cells.
- The cytoarchitecture resembles that of exodus in cervical smears.

Cells of endometriosis show positive nuclear immunoreactivity for estrogen and progesterone receptors.

**Differential Diagnosis**

Urothelial carcinoma, small-cell adenocarcinoma of the low-grade type, and occasionally lymphoma have to be excluded.

#### 13.2.3.2.2 Ectopic Prostatic Tissue and Polyps with Prostatic-Type Epithelium (Fig. 13.12)

- The urothelial mucosa of male urinary bladders is rarely interspersed with hyperplastic prostatic epithelial nests. Cuboid to columnar glandular cells exfoliating from ectopic prostatic epithelium cannot be reliably differentiated from columnar transitional epithelial cells unless the typical honeycomb monolayer sheets are present (see Sect. 14.1.2.1, p. 854).
- Prostatic epithelial cells exfoliating from genuine prostatic parenchyma are rare.
- A few benign polyps with prostatic-type epithelium occurring in the urethra and in the urinary bladder have been described histologically, suspected of being of metaplastic origin [26]. The surface of these polypoid lesions is lined by prostatic epithelial cells intermingled with transitional epithelial cells.
- Prostatic cells show strong positive immunoreactivity for specific prostatic antigens (PSA and PAP).

#### 13.2.3.2.3 Benign Nonurothelial Tumors

We would like to point out that two rare soft tissue tumors that may shed adequate cellular amounts should be remembered in dubious cases.

**Granular Cell Tumor** [20] (Figs. 1.63 and 1.64)

The morphology and special features of this tumor are described in Sect. 1.2.18, p. 26.

**Pheochromocytoma / Paraganglioma**

(Figs. 5.73 and 12.28)

Extraadrenal benign and malignant pheochromocytoma/paraganglioma is a rare neoplasm; 1% of all cases occur in the bladder [13].

The key diagnostic elements are moderately sized polygonal cells with eosinophilic and granular cytoplasm.

Immunocytochemistry (immunoreactivity for chromogranin A and synaptophysin, and S100-protein-positive sustentacular cells), distinct clinical symptoms, and biochemical tests confirm the diagnosis.

Spindle cells together with large polymorphous cells forming groups and clusters could lead to a misdiagnosis of high-grade carcinoma. More information is provided in Sect. 12.2.3.3.1, p. 769.

#### 13.2.3.2.4 Fistulas

Fistulas may be recognized or at least suspected in cytologic specimens of urine and bladder washings.

**Vesicointestinal (Rectal) Fistulas** (Fig. 13.25)

The fistula may discharge masses of feces and vegetable cells into the bladder. In addition, the fistula may be accompanied by an inflammatory process causing reactive changes of the intestinal mucosa. However, atypical regenerative glandular cells should not be mistaken for carcinoma cells.

**Vesicovaginal Fistula**

Squamous cells are discharged into the bladder of female patients suffering from a vesicovaginal fistula. Usually, these cells look like squamous metaplastic cells of the bladder mucosa. However, concomitant normal vaginal bacterial flora (Döderlein bacilli) can be helpful to recognize the source of the squames.

### 13.2.4 Inflammation, Infections, and Granulomatosis

**General Comments**

Inflammation and infection in the urinary tract are a frequent occurrence. Transitional cells may exhibit degeneration, hyperplastic activity, and atypias. Cellular atypias are readily recognized as reactive, in most cases associated with a coexistent inflammatory process (see also Sect. 13.2.2, p. 810) (Figs. 13.14–13.16, 13.27, and others).

Basic microscopic cell features:

- *Degenerating urothelial cells* are frequently enlarged, the large cytoplasm is clear or coarsely vacuolated containing granulocytes. The nuclei may be irregularly outlined, showing alternating areas of clear plasma and chromatin condensates. Nucleoli are infrequent.
  Atypical degenerating urothelial cells are easily differentiated from dysplastic/malignant cells due to phagocytosis of leukocytes and absence of distinct malignant nuclear criteria.
- *Atypical hyperplastic urothelial cells* are enlarged, showing N/C ratios in a normal range. The nuclei may be polymorphous with cleaved and folded membrane. The chromatin is densely granular or coarsely condensed, appearing as loosely arranged. Nucleoli are prominent; they may be pleomorphic and multiple in strongly activated cells. Hyperplastic cells showing severe changes may mimic malignant cells.

**Caution**

Sporadic carcinoma cells in the context of a strong inflammatory process may be missed.

#### 13.2.4.1 Nonspecific Inflammation and Bacterial/Mycotic Infection (Fig. 13.26)

- Inflammation of the urinary bladder is commonly caused by bacteria. The hallmark is the presence of neutrophil granulocytes, necrotic debris, and histiocytes. Transitional cells are either scanty or numerous.
- Mycosis should always be excluded in cases with an offensive purulent sediment by application of appropriate special stainings, such as periodic acid-Schiff reaction and Grocott stain.

#### 13.2.4.2 Epithelioid Cell Granulomatosis

##### 13.2.4.2.1 Tuberculosis

Tuberculosis [24] of the urinary bladder is frequently observed in patients with urogenital tuberculosis. Mycobacteriosis of the urinary bladder occurs in particular as a severe complication of renal tuberculosis.

- The presence of epithelioid cells, giant cells of the Langhans type, caseous-necrotic background material, and large numbers of neutrophils cytologically suggest tuberculosis. Acid-fast bacilli may be detected with the Ziehl-Neelsen staining method.

##### 13.2.4.2.2 Intravesical Bacillus Calmette-Guerin Therapy (Fig. 13.27)

Intravesical bacillus Calmette-Guerin therapy effects immunological reactivity by inhibiting growth of superficial bladder tumors, thereby preventing tumor recurrence.

- Bladder urine after BCG therapy usually shows lymphocytosis of varied extent. In rare cases, fragments of epithelioid granuloma and granular debris are present as well (Fig. 13.27).

#### 13.2.4.3 Malakoplakia

Malakoplakia is a pseudo-granulomatous disease of the urethra, bladder, and upper urinary tract, but the disorder also involves organs of the genital system as well as extraurogenital organs [2, 9]. The inflammatory disease is characterized by an accumulation of proliferative epithelioid histiocytes intermingled with foamy cells, giant cells, lymphocytes, plasma cells, and granulocytes. The diagnostic elements are more likely to be found in FNAB material of tumoral lesions than in exfoliative samples from the urinary tract (see Sect. 12.1.5.4, p. 735)

**Microscopic Features and Differential Diagnosis**

- Microscopic hallmarks of malakoplakia are concentrically laminated cytoplasmic inclusions of epithelioid/histiocytic cells, known as Michaelis-Gutmann bodies or calcospherites. They stain positive with the periodic acid-Schiff reaction and for iron and calcium. The initial stage of calcification is regarded to be deposits of apatite crystals within phagolysosomes in the cytoplasm of histiocytes. Whether the process is related to a bacterial infection is not completely clarified [11, 21].

Epithelioid cell proliferation lacking Michaelis-Gutmann bodies may be caused by mycobacteria, lues, fungi, surgery, or it may be iatrogenic.

Malakoplakia closely resembles xanthogranulomatous cystitis.

#### 13.2.4.4 Xanthogranulomatous Cystitis [8, 31]

Xanthogranulomatous cystitis is a rare chronic inflammatory disease of unknown etiology that has been reported in many anatomical sites of the human body, particularly in the kidney (see Sect. 12.1.5.2, p. 735). It involves the bladder only sporadically and may be associated with benign and malignant tumors.

Morphologically, the lesion resembles malakoplakia but Michaelis-Gutmann bodies are absent; a key feature is large numbers of histiocytic giant cells. Granuloma formation is absent in many cases, similar to malakoplakia.

#### 13.2.4.5 Viral Infections

A number of viral infections cause changes in the lining cells of the renal tubules and in urothelial cells. Varied characteristic alterations in superficial epithelial cells that are caused by viral attack are discussed below.

##### 13.2.4.5.1 Cytomegalovirus (Fig. 2.83)

*Cytomegalovirus* (CMV) is a subtype within the herpesvirus group. Patients at risk are particularly those who are immunosuppressed due to tumor, in association with transplants, or to acquired immunodeficiency syndrome.

Renal tubular cells are affected most frequently.

**Microscopic Features**

- The affected cells are strikingly enlarged and rounded, they contain a single huge nucleus.
- The nuclei contain a single deep-basophilic inclusion that may be inhomogeneous.
- The inclusion is sharply demarcated and surrounded by a clear halo separating the inclusion from the nuclear membrane.
- The chromatin is peripherally condensed as dark small dots, sometimes pearl necklace-like, along the inner rim of the nuclear membrane.

#### 13.2.4.5.2 Papovaviruses

The family of papovaviruses is divided into two groups: polyomaviruses and papillomaviruses.

**Polyomavirus** (Fig. 13.28)

**General Comments**

Humans are natural host species for *Polyomavirus*, mainly BK virus and JC virus. Primary infection occurs during childhood. The DNA virus remains latent in the host and reactivates upon immunosuppressive events [19]. Polyomavirus nephropathy (BKV-type) is a rare but serious complication after renal transplantation in combination with immunosuppressive drugs. It has been recognized as an important cause of renal graft dysfunction and graft loss. As in CMV infection, renal tubular cells are frequently involved but also epithelial cells of the collecting tubules, glomeruli, and the transitional cell layer of the bladder, ureter, and renal pelvis.

Cytologic analysis of the urine is an important diagnostic tool in order to monitor renal transplant patients at risk of BKV nephropathy [3, 15, 30, 35].

**Microscopic Features and Differential Diagnosis**

The morphologic sign of polyomavirus activation is the detection of typical intranuclear viral inclusion-bearing epithelial cells in urine samples, so-called decoy cells.

- The virus-affected cells are enlarged and rounded. The cytoplasm may appear as a small rim or attached like a tag, which is variably preserved.
- Neutrophilic granulocytes and cellular debris are frequently observed.

The type of nuclear inclusion bodies is diagnostic for BKV-type infection, usually differing from cells infected with CMV. The inclusion bodies usually show varied morphology, sometimes the same urine sample.

Four morphologic variants of *decoy cells* are established [30]:

*Type 1 (classic form)* (Fig. 13.28A):
Dense, basophilic, homogeneous inclusion completely filling the nucleus.
Thickened nuclear membrane due to marginal condensation of chromatin substance.

*Type 2* (Fig.13.28B):
Centrally positioned granular inclusions surrounded by an incomplete halo.
**Caution: Type 2 decoy cells may mimic CMV-infected cells!**

*Type 3* (Fig. 13.28C):
Diffusely distributed coarse chromatin, absence of a particular halo. Cells may exhibit two to three nuclei.

*Type 4* (Fig. 13.28D):
Vesicular and polymorphous nuclei showing aggregation of coarse chromatin, hyperchromasia, and a single nucleolus (postinclusion decoy cells).
**Caution: Type 4 cells resemble carcinoma cells!**

**Additional Analyses**

Immunocytochemistry, molecular genetics (FISH and PCR) and electron microscopy are ancillary techniques for virus identification [3, 15, 30, 35].

**Caution**

- Cell changes due to viral infection may lead to a false-positive malignant diagnosis. Misleading cell changes include cellular enlargement, dark stained nuclei, small rims of cytoplasm, background debris.
- It is necessary to take account of the nuclear morphology: virus-induced nuclear inclusions do not match malignant chromatin patterns!
- ICM-DNA is by no means a reliable method to distinguish between virus-induced cell changes and malignant cells: intranuclear deposits of the viral genome may cause aneuploidy!

**Human Papilloma Virus**

Human papilloma virus (HPV) is responsible for condylomatous lesions. These lesions are generally confined to urethra and to mucocutaneous areas of the male and female genital organ. The morphology of koilocytotic cell changes are described elsewhere.

### 13.2.4.6 Parasitic Disease

#### 13.2.4.6.1 Schistosomiasis *(Schistosoma haematobium)*

- Schistosomiasis is an important parasitic infection of the urinary tract because it is one of the most common reasons for urothelial malignancies [6]. It affects about 80 million people in Africa, the Middle East, and India.
- Among immigrants from endemic areas and returning travellers it is still rarely seen, but the risk of introduction could rise in some regions considering the presence of intermediate host and an appropriate climate [27, 28].
- Urinary tract schistosomiasis shows a wide range of clinical manifestations related to mucosal and submucosal granulomatous lesions of the bladder. While clinical symptoms are most important in the early diagnosis of this parasitic disease, ova of *Schistosoma haematobium* are rarely detected in urine probes [32].

#### 13.2.4.6.2 Other Parasitic Diseases

For other parasitic diseases, we refer the reader to information available in individual publications and distinguished textbooks.

## 13.2.5 Further Reading


1. Akhter N, Sohail I, Shah S, et al. Vesical endometriosis. J Coll Physicians Surg Pak 2007;17:702-703.
2. Ballesteros Sampol JJ. Urogenital malakoplakia. Report of 4 cases and review of the literature. Arch Esp Urol 2001;54:768-776.
3. Boldorini R, Brustia M, Veggiani C, et al. Periodic assessment of urine and serum by cytology and molecular biology as a diagnostic tool for BK virus nephropathy in renal transplant patients. Acta Cytol 2005;49:235-243.
4. Borda A, Petrucci MD, Berger N. Miscellaneous benign lesions of the bladder and the urinary tract. Ann Pathol 2004;24:18-30.
5. Chen SS, Hsu YS, Chen KK, Chang LS. Urinary bladder endometriosis: a report of two cases. Zhonghua Yi Xue Za Zhi(Taipei) 1996;58:66-69.
6. Cohen SM, Shirai T, Steineck G. Epidemiology and etiology of premalignant and malignant urothelial changes. Scand J Urol Nephrol Suppl. 2000;205:105-115.
7. de Ruiter F, Beyer-Boon ME, de Voogt HJ. The effect of calculi on transitional epithelium. A clinical and cytological study. Urol Res 1975;3:67-72.
8. Goel R, Kadam G, Devra A, et al. Xanthogranulomatous cystitis. Int Urol Nephrol 2007;39:477-478.

8A. Guan H, Rosenthal DL, Erozan YS. Mullerianosis of the urinary bladder: report of a case with diagnosis suggested in urine cytology and review of literature. Diagn Cytopathol 2011 Apr 28, [Epub ahead of print].

9. Hatzinger M, Vöge D, Häfele J et al. Manifestation of malakoplakia in a urethral diverticulum in a female patient. Aktuelle Urol 2008;39:68-70.
10. Highman W, Wilson E. Urine cytology in patients with calculi. J Clin Pathol 1982;35:350-356.
11. Ho KL. Morphogenesis of Michaelis-Gutmann bodies in cerebral malakoplakia. An ultrastructural study. Arch Pathol Lab Med 1989;113:874-879.
12. Jimenez-Heffernan JA, Sanchez-Piedra D, Bernaldo de Quiros L, Martinez V. Endosalpingiosis (müllerianosis) of the bladder: a potential source of error in urinary cytology. Cytopathology 2000;11:348-353.
13. Jorge AA, Lucon AM, Bloise W, Mendoca BB. Pheochromocytoma of the urinary bladder, report of a case and review of the literature. Rev Hosp Clin Fac Med Sao Paulo 1997;52:28-31.
14. Kannan V, Gupta D. Calculus artifact. A challenge in urinary cytology. Acta Cytol 1999;43:794-800.
15. Kapila K, Nampoory MR, Johny KV, et al. Role of urinary cytology in detecting human polyoma BK virus in kidney transplant recipients. A preliminary report. Med Princ Pract 2007;16:237-239.
16. Koren J, Mensikova J, Mukensnabl P, Zamecnik M. Mullerianosis of the urinary bladder: report of a case with suggested metaplastic origin. Virchows Arch 2006;449:268-271.
17. Koss LG. Diagnostic cytology and its histopathologic bases. Fifth ed. Lippincott Williams & Wilkins, Philadelphia, 2006.
18. Mazzuchelli R, Barbisan F, Tarquini LM, et al. Urothelial changes induced by therapeutic procedures for bladder cancer. A review. Anal Quant Cytol Histol 2005;27:27-34.
19. Medeiros M, Alberu J, Garcia GR, et al. Polyoma virus in transplant recipients. Nefrologia 2008;28:203-211.
20. Mogorovich A, Giannarini G, De Maria M, et al. Granular cell tumor of the urinary bladder: a case report and review of the literature. Arch Ital Urol Androl 2007;79:43-44.
21. Ng KF, Chen TC, Hsueh S. Malakoplakia of urinary tract: report of two cases emphasizing the histologic spectrum and the morphogenesis of Michaelis-Gutmann bodies. Changgeng Yi Xue Za Zhi 1996;19:55-61.
22. Nikolaeva D, BS, Ali SZ. Significance of urothelial atypia in exfoliative cytology of upper urinary tract lesions. Cancer (Cancer Cytopathol) Suppl . 2007;111/Issue 5:424-425.
23. Pastor Navarro H, Donate Moreno MJ, Gimenez Bachs JM, et al. Bladder endometriosis. A report of two cases and bibliographic review, with special focus on Spanish articles. Arch Esp Urol 2006;59:111-122
24. Piscioli F, Pusiol T, Polla E, et al. Urinary cytology of tuberculosis of the bladder. Acta Cytol 1985;29:125-131.
25. Raica M, Ioiart I. Urethral and neobladder cytology survey in patients with total cystectomy. Rom J Morphol Embryol 1992;XXXVIII:29-34.
26. Remick DG, Kumar NB. Benign polyps with prostatic-type epithelium of the urethra and the urinary bladder. Am J Surg Pathol 1984;8:833-839.
27. Salvana EM, King CH. Schistosomiasis in travelers and immigrants. Curr Infect Dis Rep 2008;10:42-49.
28. Scarlata F, Giordano S, Romano A, et al. Urinary schistosomiasis: remarks on a case. Infez Med 2005;13:259-264.
29. Schumann GB, Johnston JL, Weiss MA. Renal epithelial fragments in urine sediment. Acta Cytol 1981;25:147-152.
30. Singh HK, Bubendorf L, Mihatsch MJ, et al. Urine cytology findings of polyomavirus infections. Adv Exp Med Biol 2006;577:201-212.
31. Tan LB, Chiang CP, Huang CH, Chian CH. Xanthogranulomatous cystitis: a case report and review of the literature. Int Urol Nephrol 1994;26:413-417.
32. Waugh MS, Perfect JR, Dash RC. Schistosoma haematobium in urine: morphology with ThinPrep method. Diagn Cytopathol 2007;35:649-650.
33. Whisnant RE, Bastacky SI, Ohori NP. Cytologic diagnosis of low-grade papillary urothelial neoplasms (low malignant potential and low-grade carcinoma) in the context of the 1998 WHO/ISUP classification. Diagn Cytopathol 2003;28:186-190.
34. Young RH, Clement PB. Müllerianosis of the urinary bladder. Mod Pathol 1996;9:731-737.
35. Yuste RS, Frias C, Lopez A, et al. Diagnostic value of JC/BK virus antibody immunohistochemistry staining in urine samples from posttransplant immunosuppressed patients in relation to polyomavirus reactivation. Acta Cytol 2008;52:191-195.
36. Zugor V, Schott GE. Endometriosis involving the ureter. The Erlangen experience exemplified by two case reports. Aktuelle Urol 2007;38:55-58.

**Fig. 13.3 Squamous metaplasia.**
An elderly male patient suffering from repeated relapsing bladder tumors was cystoscopically suspected of having a carcinoma in situ. Pronounced squamous metaplasia associated with marked keratinization simulated intraepithelial neoplasia by cystoscopy. Note squamous cells displaying mild nuclear irregularities but a bland chromatin pattern (direct sediment smear, Pap stain, higher magnification).

**Figs. 13.4–13.6 Superficial urothelial cells, varying phenotypes.**
Bladder washings from three patients. Samples were processed by different laboratory methods, all preparations were Pap-stained.

**Fig. 13.4** (case #1) Classic cytology is demonstrated in a Cytospin specimen at low magnification. Superficial urothelial cells exhibit variation in size and occasional bi-/multinucleation. The tight cell clusters show characteristic knobby contour.

**Fig. 13.5** (case #2) Huge superficial urothelial cells harboring numerous monomorphic but activated nuclei (conventional sediment smear, low magnification).

**Fig. 13.6** (case #3) Classic nuclear features of normal urothelial cells are focused at high magnification: distinct variability of nuclear size, irregular nuclear outline, loose chromatin pattern, and varying nucleolar appearance (conventional sediment smear).

**Fig. 13.7 Intermediate and atrophic urothelial cells.**
Intermediate and atrophic transitional cells of the urinary tract are very similar in appearance. They are much smaller than their superficial counterparts. Note the high N/C ratio and the bland nuclei containing indistinct nucleoli (direct sediment smear, Pap stain, higher magnification).

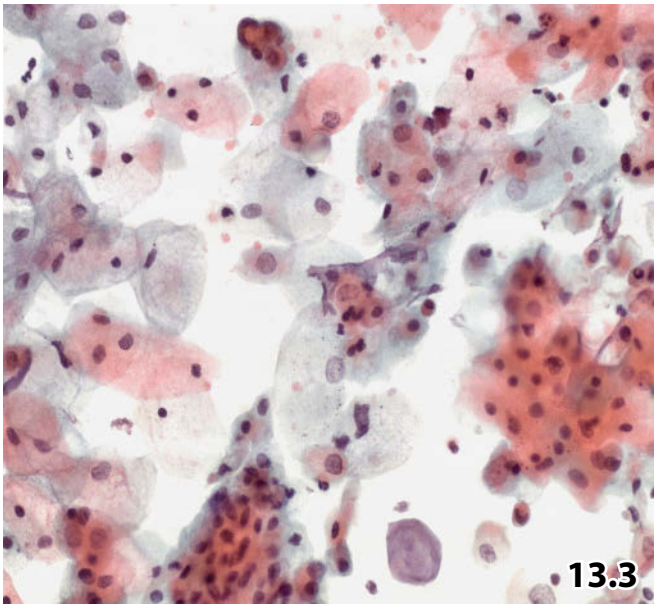
13.3

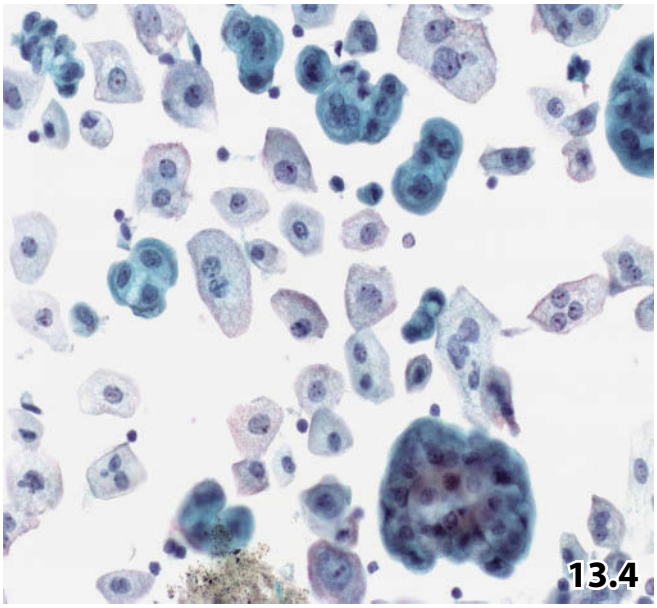
13.4

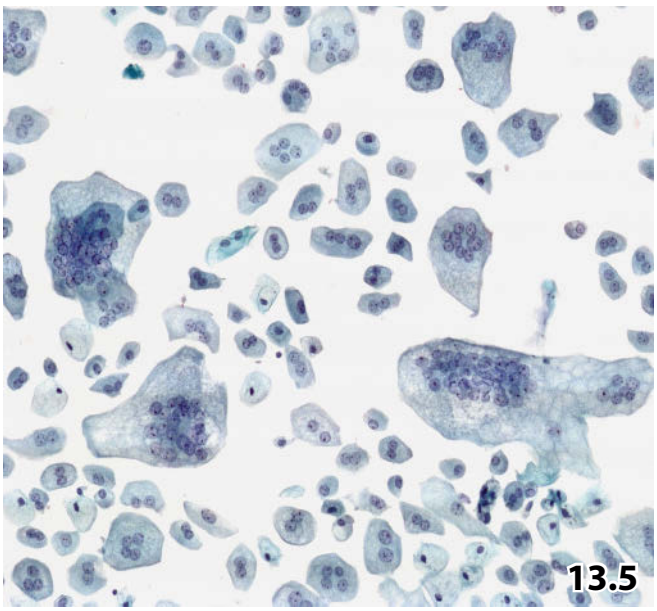
13.5


13.6

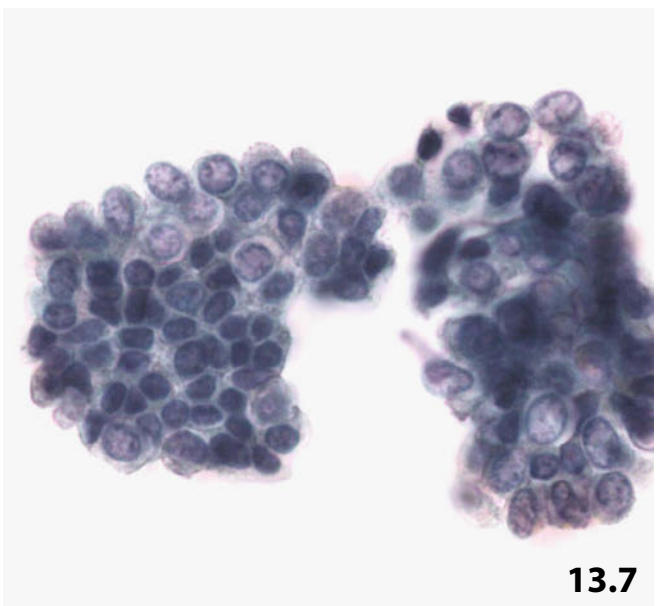
13.7

**Figs. 13.8 and 13.9 Elongated and columnar urothelial cells.**
One has to bear in mind that benign urothelial cells of the fusiform and columnar type may simulate both true glandular cells and cells originating from a low-grade papillary transitional cell carcinoma. Two examples are demonstrated. Both patients did not develop any neoplastic process in their urinary tract during long-term follow-up. Direct smears were prepared from the sediments of the irrigation fluid, and Pap-stained.

**Fig. 13.8** (case #1) Spindle-shaped and columnar-shaped urothelial cells occur in papilliform arrangement simulating papillary transitional cell carcinoma grade 1 (low magnification). The following cytologic features should exclude a neoplastic process:
– Absence of fibrovascular cores.
– Streaming pattern (arrows), but absence of definite cellular palisading.
– The sheets are largely overlapping, but true nuclear overlapping is absent.
– Sharply defined cytoplasm.
– Bland nuclei.

**Fig. 13.9** (case #2) Higher magnification reveals numerous columnar-shaped urothelial cells. Separating these cells from true glandular cells is practically impossible unless a panel of adequate immunostains is applied.

**Fig. 13.10 Glandular (intestinal) metaplasia.**
High magnification shows an aggregate of goblet cells that is a characteristic of glandular metaplasia of the urothelium. Note both cytoplasmic inclusions of mucus and mucus threads in the background of the smear (upper left) (bladder washing, direct sediment smear, Pap stain).

**Fig. 13.11 Cytology of ileal conduit.**
Degenerating columnar cells, apoptotic nuclei, large amounts of cellular debris, and clusters of bacteria (lower left) represent the cytologic appearance of an ileal conduit. A few well-preserved epithelial cells (arrow) may occasionally be encountered (neobladder washing, direct sediment smear, Pap stain, lower magnification).

**Fig. 13.12 Prostatic epithelial cells.**
A large sheet of benign prostatic epithelial cells (left) morphologically differs from the smaller urothelial cell clusters (right): prostatic cells occur in a flat sheet, and their nuclei are mildly activated due to acute inflammation. Note neutrophilic granulocytes scattered between the epithelial cells (arrows). Furthermore, the cytoplasm contains coarse lipofuscin granules, which are barely visible at the current magnification (bladder washing, direct sediment smear, Pap stain, lower magnification). Positive immunocytochemical staining for prostate-specific antigen (not shown) verified the cytologic diagnosis.

**Fig. 13.13 Sperms in voided urine and bladder washing.**
Mature sperms may occur isolated in the background of the smear or enclosed in inspissated proteinaceous secretion, as demonstrated here at higher magnification (arrows) (bladder washing, Cytospin preparation, Pap stain). These findings should not be mistaken for cellular debris or tumor necrosis.

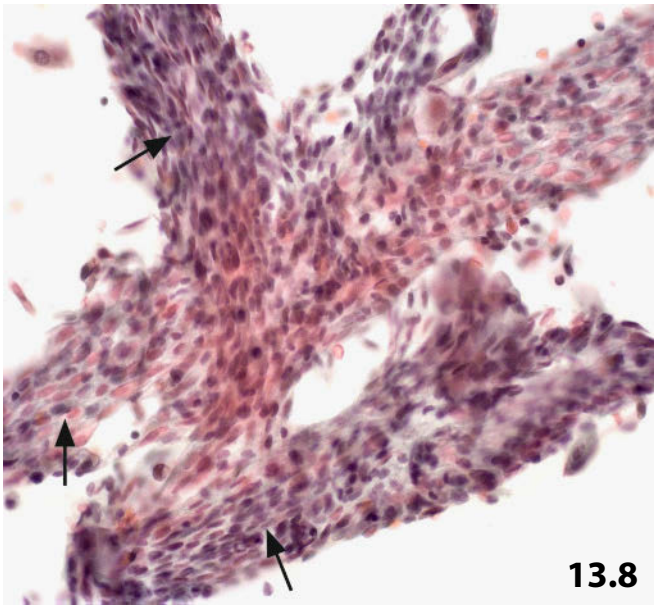
13.8

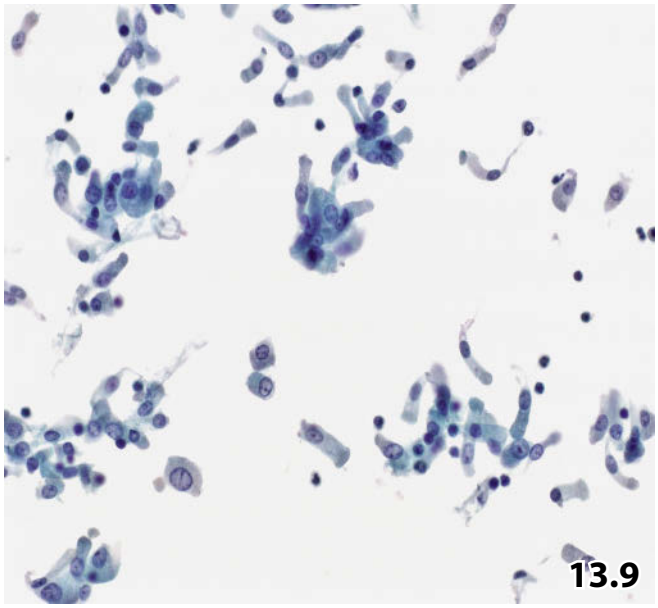
13.9

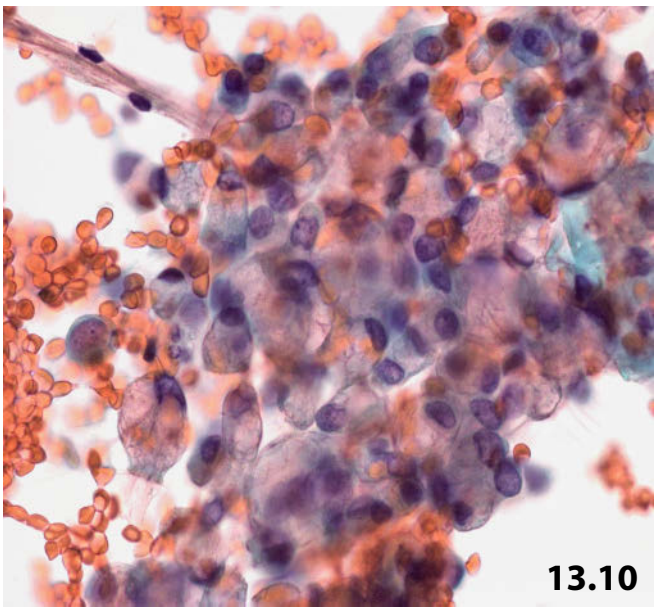
13.10

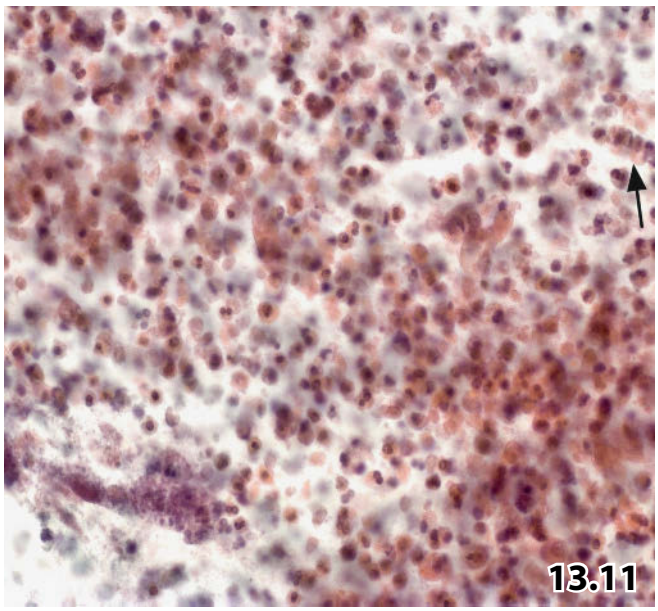
13.11

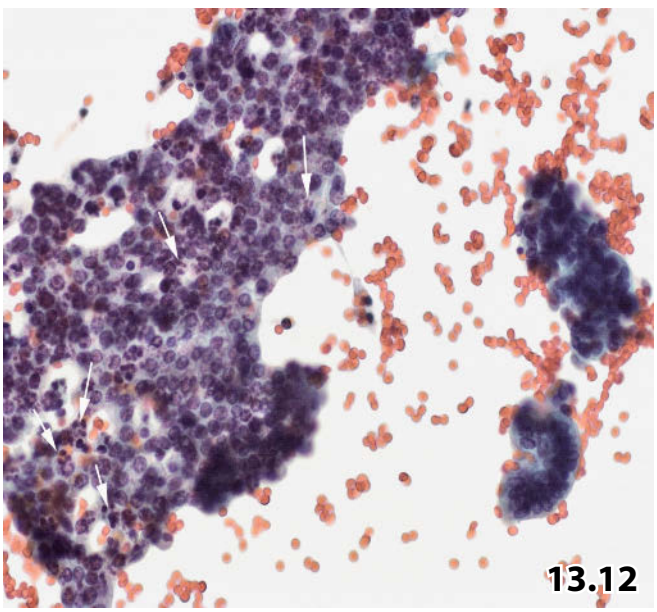
13.12

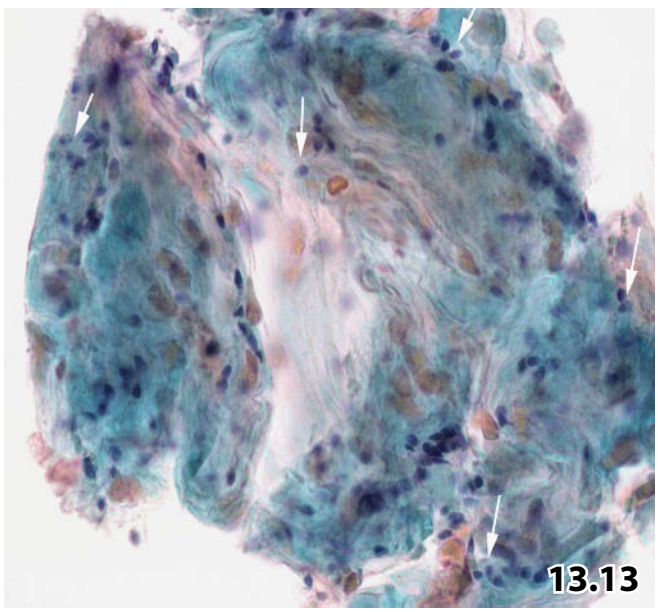
13.13

**Figs. 13.14–13.23 Reversible atypias of transitional cells.**
Several examples address the varied cytologic appearance of reactive/regenerative and degenerative transitional cells, comprising causative agents and diagnostic impact of ICM-DNA.

**Fig. 13.14** (case #1) Classic features of reactive cell change.
Ureteral washing. A cluster composed of atypical but benign urothelial cells is shown in detail: irregular cellular arrangement, pronounced variability of cellular size and shape, varied N/C ratio, increased nuclear irregularities, distinct and polymorphic nucleoli, bland chromatin (Cytospin preparation, Pap stain).

**Fig. 13.15** (case #2) Degenerative cell change.
Ureteral washing. Cytospin specimen contains numerous urothelial cells dispersed and in clusters, exhibiting dark-staining shriveled nuclei (arrow). Nuclear features may suggest malignancy, but architecture of the cell clusters, normal N/C ratios, and bland chromatin differentiate between benign and malignant cells (Pap stain, high magnification).

**Fig. 13.16** (case #3) Reactive cell changes caused by inflammation.
Bladder washing. Neutrophils in the background of a direct sediment smear and inflammatory cells enclosed in the cytoplasm of urothelial cells indicate benign cell alteration. Attention should be paid to individual urothelial cells, which show severe regenerative atypias mimicking malignant cells (arrows) (direct sediment smear, Pap stain, higher magnification).

**Fig. 13.17** (case #4) Reactive cell changes caused by urinary tract lithiasis.
A young male patient with a positive history of urinary tract lithiasis. Bladder washing reveals small and large abnormal transitional cells: occasional multinucleation, marked vacuolization of the cytoplasm, striking glassy chromatin, and homogeneous dark-staining nuclei (arrows). Prominent nucleoli do not appear in this field. Concrements are out of focus due to depth of field (direct sediment smear, Pap stain, lower magnification).



**Fig. 13.18** (case #5) Radiation-induced reactive cell changes.
An 80-year-old man suffering from cystoscopically verified radiation cystitis. Bladder washing displays the characteristic cell alterations: abundant cytoplasm exhibiting small and large vacuoles, multinucleation, polymorphic nuclear shape, clear intranuclear vacuoles of varied size, and macronucleoli (direct sediment smear, Pap stain, high magnification).

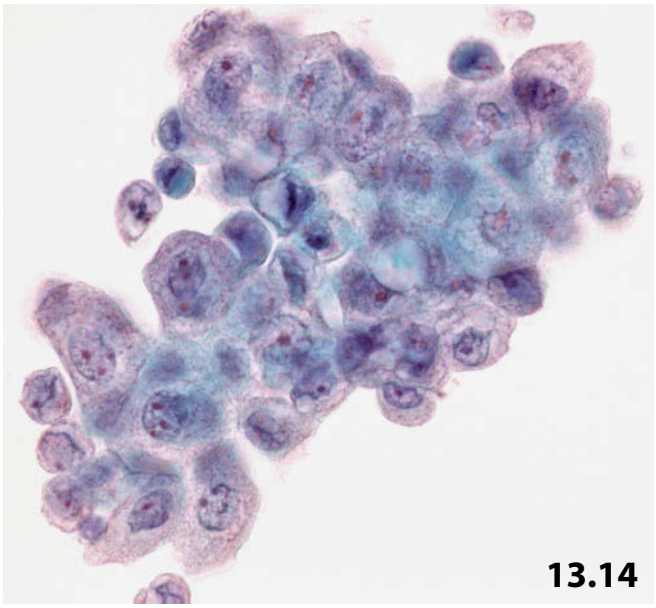
13.14

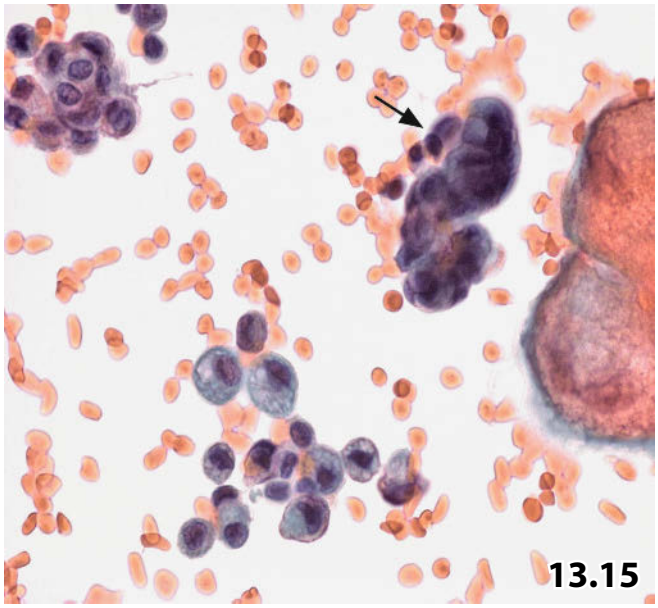
13.15

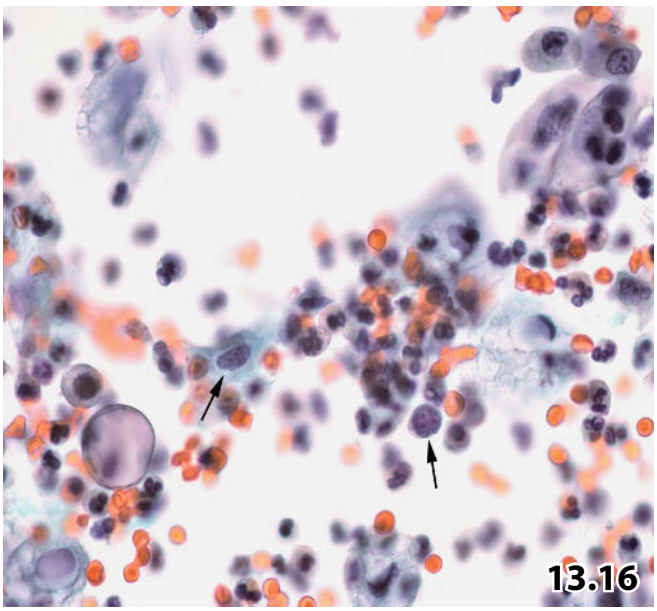
13.16

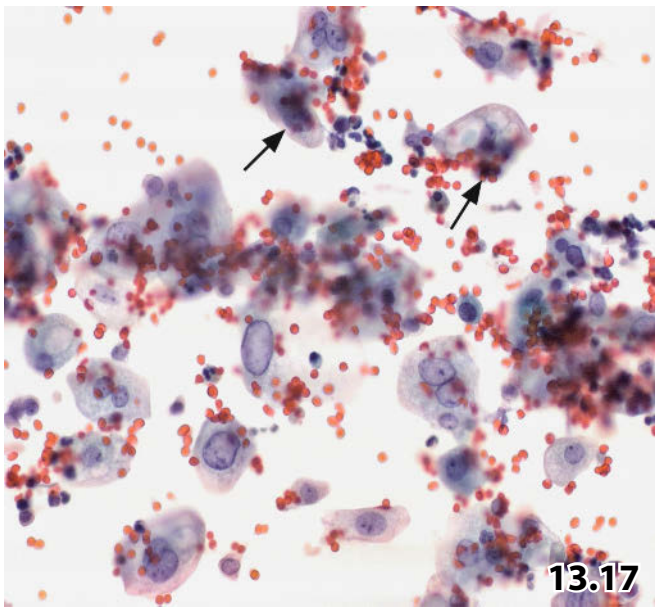
13.17


13.18

**Figs. 13.19 and 13.20** (case #6) Cytotoxic effect caused by chemotherapeutic drugs.
A 48-year-old woman presenting with a positive history of psoriatic arthritis; previous treatment protocols comprising cyclophosphamide. Cystoscopic findings were bland.

**Fig. 13.19** Direct sediment smears (after conventional centrifugation) from a bladder washing display atypical urothelial cells that are difficult to classify as benign or malignant on the basis of standard light microscopy. Several cell features serve as indicators for benign reactive alterations, such as extreme variability of cell size, N/C ratio in normal range, and a large number of nuclei showing loose and pale chromatin (Pap stain, lower magnification).

**Fig. 13.20** ICM-DNA (same case) Euploid-polyploid DNA distribution pattern supports benign regenerative cell population in spite of a single aneuploid nucleus in the 27c area (Pap-prestained Feulgen stain, Zeiss-Kontron/Cires).

**Fig. 13.21** (case #7) Instrument artifact accompanied by particular tissue fragments.
A 46-year-old woman presenting with a catheter placed in her right renal pelvis. Cystourethroscopy revealed reddened mucosal areas in the urinary system. Renal pelvis washing was performed. Direct sediment smears (irrigation fluid after centrifugation) were Pap-stained. Higher magnification shows large papilliform sheets and three-dimensional clusters composed of comparatively monomorphic urothelial cells. Variation in cell shape, varied N/C ratio, nuclear irregularities, and distinct nucleoli may lead to diagnostic confusion. However, bland chromatin favors benign disorder.
*Cytologic follow-up:* 14 months later, completely normal cytologic findings in a renal pelvis washing.

**Figs. 13.22 and 13.23** (case #8) Inflammation and atypical urothelial cells: reactive benign versus dysplastic/malignant cells.
*Cytologic diagnosis supported by DNA cytometric results:* Severe urothelial dysplasia or high-grade neoplasia, accompanied by acute inflammation.
*Tissue diagnosis* (excisional biopsy of a small tumoral lesion at the inner surface of the urinary bladder): Papillary transitional cell carcinoma pTa, grade 2.



**Fig. 13.22** A direct sediment smear from a bladder washing (after centrifugation) exhibits: Two benign urothelial cells (lower left), scattered small atypical cells with deep-staining nuclei (most likely representing degenerating dysplastic/malignant cells), numerous scattered neutrophils, and a transitional cell revealing severe atypia (arrow). High N/C ratio, hyperchromasia, and coarse chromatin of the latter favor an isolated neoplastic cell (Pap stain, lower magnification).

**Fig. 13.23** ICM-DNA (same case) The DNA histogram shows a distinct tetraploid stemline, complete absence of diploid target cells, a smaller fraction of aneuploid cells, and a few aneuploid nuclei exhibiting DNA content > 9c . The DNA distribution pattern is highly suggestive of a neoplastic disorder (Pap-prestained Feulgen stain, Ahrens Cytometrie-System).

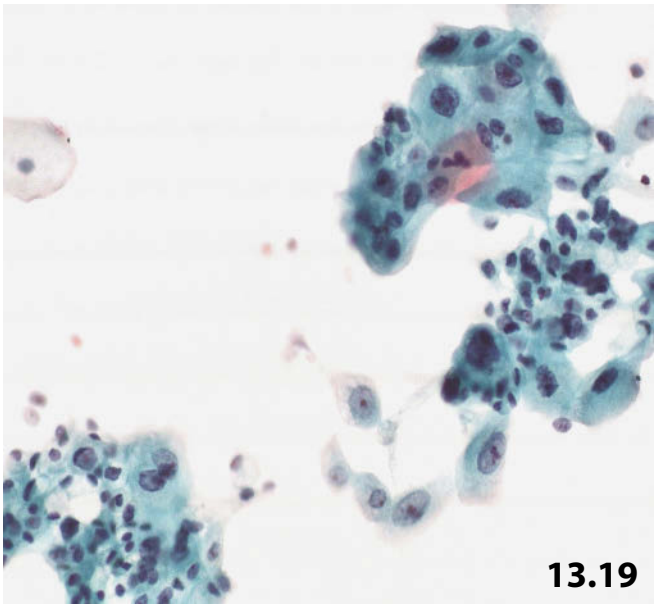

13.19

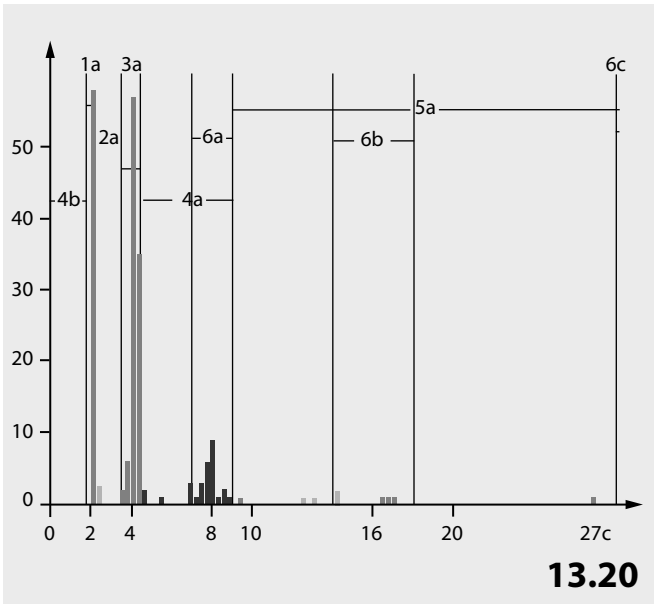


13.20

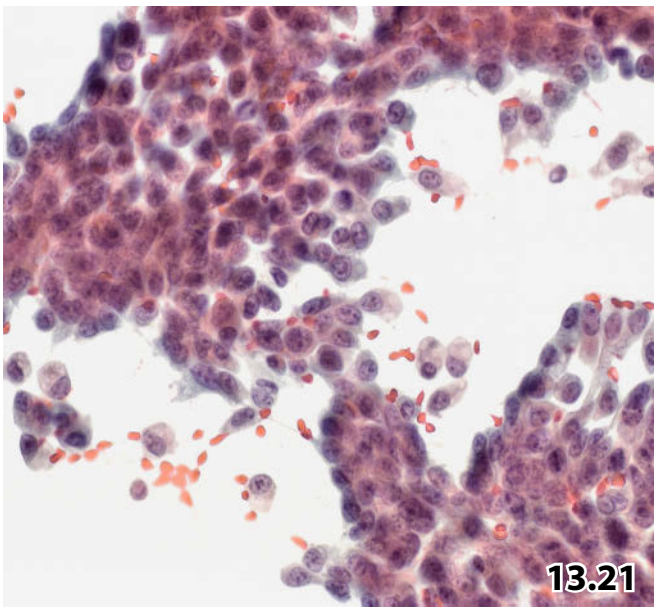

13.21

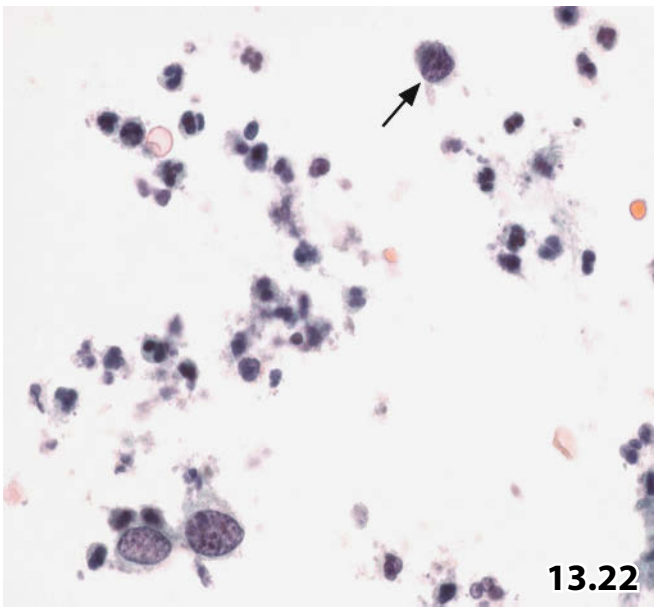

13.22

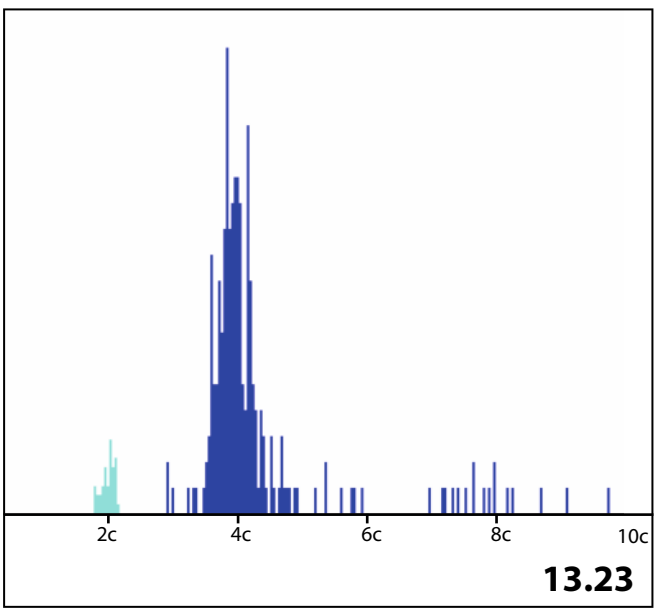


13.23

**Fig. 13.24 Von Brunn Nests.**
A large microfragment exfoliated from the inner bladder wall displays transitional cell nests showing glandular formations, embedded in loose connective tissue (bladder washing, direct sediment smear, Pap stain, low magnification).

**Fig. 13.25 Vesicointestinal fistula.**
The sanguineous bladder washing is contaminated with feces (vegetable cells and crystalloid elements). The material has been discharged through a vesicorectal fistula into the urinary bladder (direct sediment smear, Pap stain, high magnification).

**Fig. 13.26 Candida cystitis.**
Voided urine. The direct smears (after centrifugation) of a urine sediment are hypercellular. High magnification shows reactive urothelial cells and *Candida* spores scattered in a purulent background. Characteristic arrangement of the spores in pairs and triads (arrows) clearly differentiates them from degenerating red blood cells (Pap stain, lower magnification).

**Fig. 13.27 Cytologic findings after intravesical bacillus Calmette-Guerin therapy.**
A 75-year-old man had excision of transitional cell carcinoma of the urinary bladder and metachronous intravesical BCG therapy. Cytologic follow-up by means of bladder washings reveals BCG-itis, which is characterized by pronounced reactive alterations of the urothelial cells, by epithelioid histiocytes, Langhans-type giant cells (lower right), and an inflammatory background composed of lymphocytes and neutrophils (direct sediment smear, Pap stain, lower magnification).

It is difficult to distinguish between fusiform reactive transitional cells and epithelioid histiocytes.

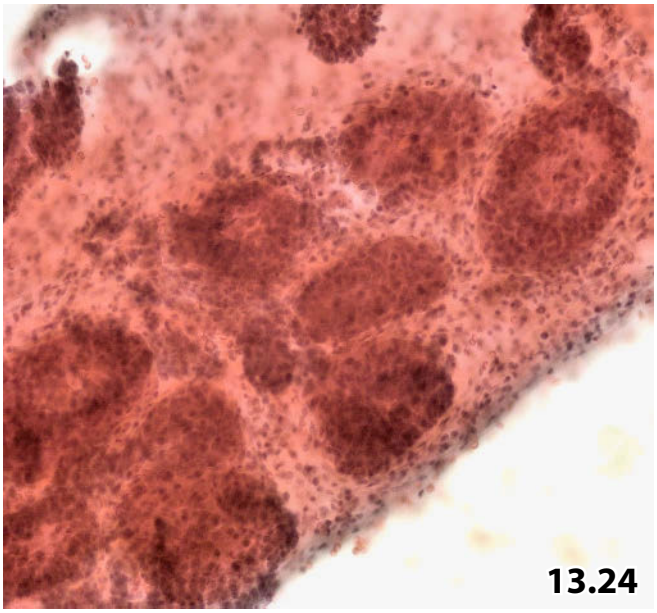
13.24

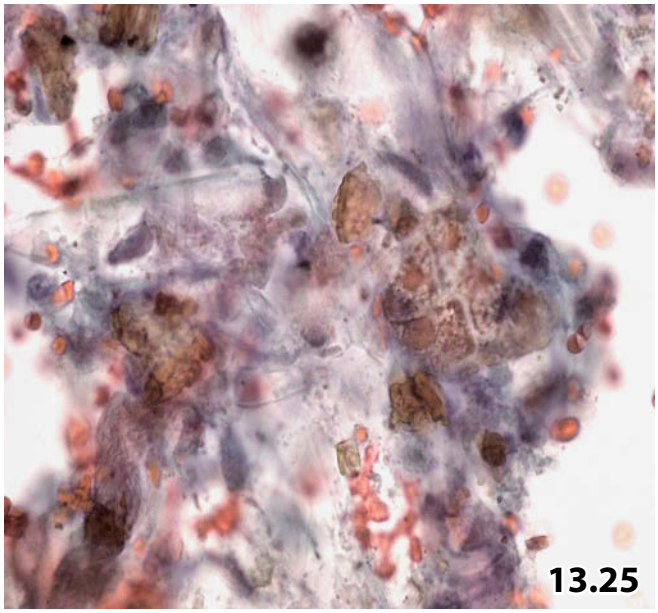
13.25

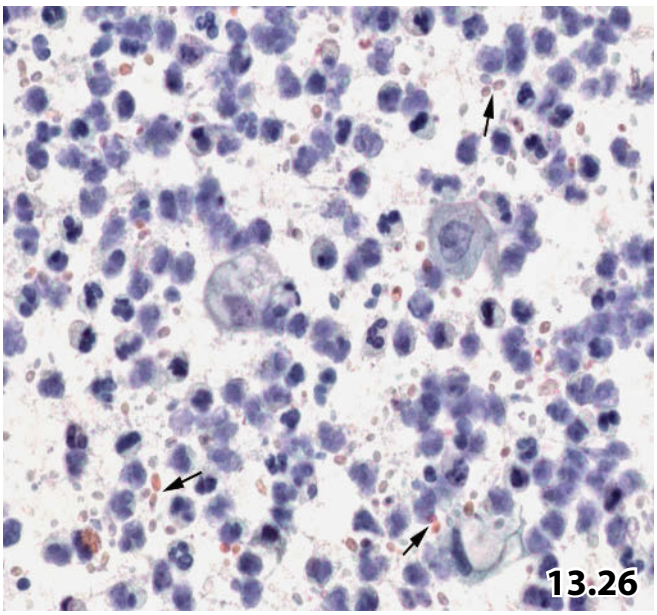
13.26

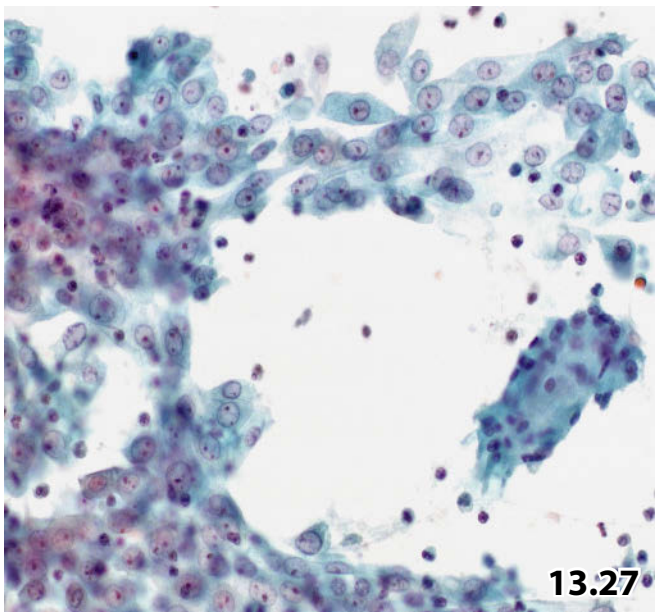
13.27

**Fig. 13.28A–D Morphology of decoy cells caused by *Polyomavirus* infection**
Voided urine of a 26-year-old man after renal transplantation. Urine sediment was processed using the Cytospin method. The four morphologically distinct variants of decoy cells are demonstrated in detail (Pap stain):
**A** Type 1 (classic form): Homogeneous inclusion completely filling the nucleus (arrows). **B** Type 2: Centrally positioned inclusion surrounded by an incomplete halo (arrows). **C** Type 3: Diffusely distributed coarse chromatin (arrows). **D** Type 4: Polymorphous nucleus exhibiting coarse chromatin (arrow) and a single nucleolus (arrowhead).
Details related to microscopic features and differential diagnostic aspects are discussed in Sect. 13.2.4.5.2, "Polyomavirus," p. 815.

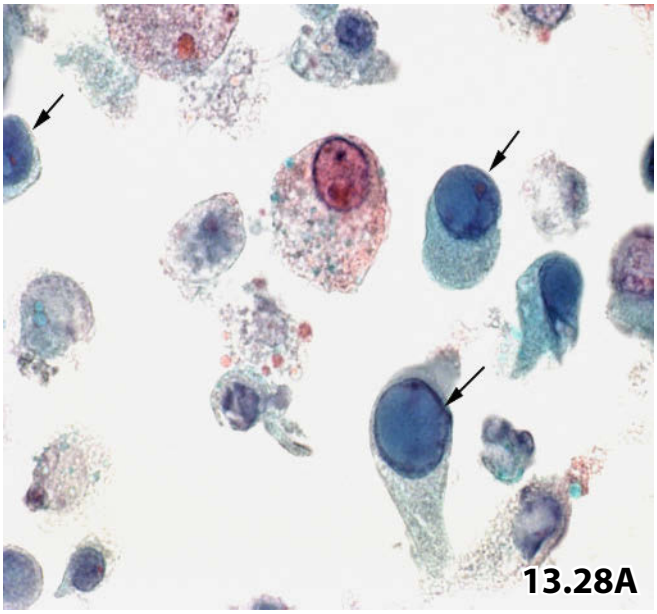
13.28A

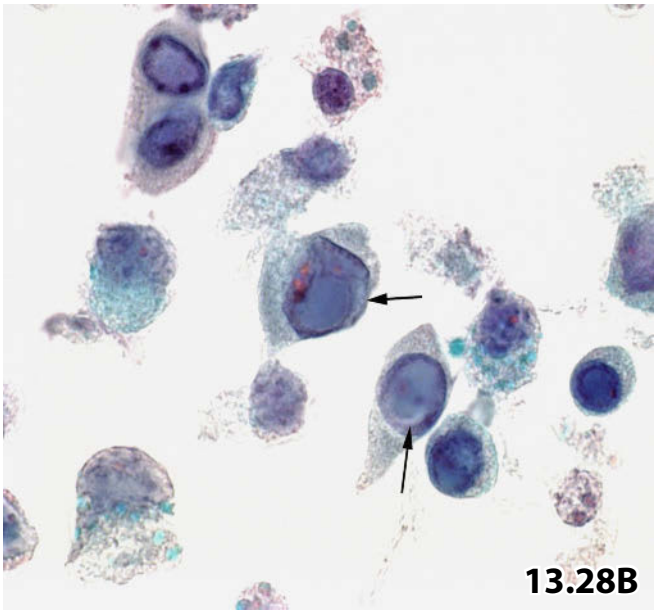
13.28B

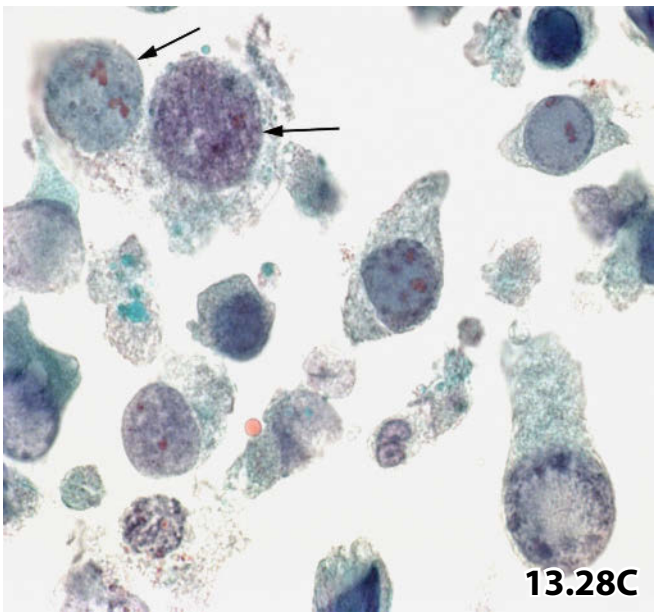
13.28C

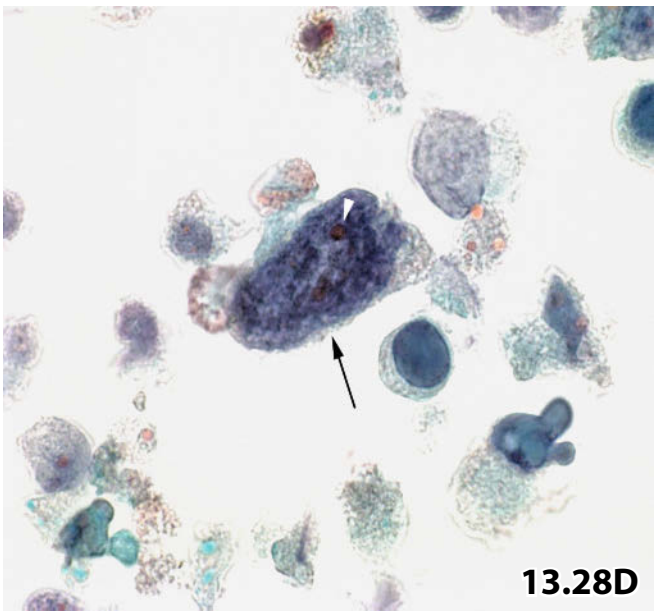
13.28D

# Section 13.3
# Urinary Tract

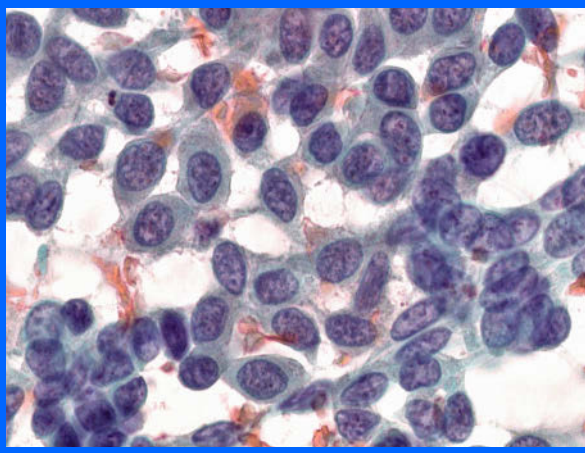

## Precancerous Urothelial Lesions
## Malignant Lesions

### 13.3.1 Urethra: Malignant Neoplasms

#### 13.3.1.1 Primary Malignancies

Urethral carcinoma may be associated with synchronous or metachronous bladder cancer, but primary malignancies of the male and female urethra rarely occur. Squamous cell carcinoma is the most frequent tumor followed by adenocarcinoma (clear cell type) and urothelial cancer.
Primary malignant melanoma has rarely been reported.

##### 13.3.1.1.1 Squamous Cell Carcinoma and Common Adenocarcinoma

Both tumor types present similar cytomorphology as compared to their counterparts in other sites of the human body.

##### 13.3.1.1.2 Clear Cell Adenocarcinoma

Clear cell adenocarcinoma usually occurs in adult women having a particular association with urethral diverticula, but it seems not to be related to the prostatic epithelium in male patients, because the tumor cells stain negative for prostate-specific antigen and prostatic acid phosphatase [27].

**Microscopic Features**

- The microscopic features match those of clear cell carcinoma of the female genital tract.
- Papillary pattern may occur.
- The tumor cells show abundant clear cytoplasm.
- The nuclear pleomorphism is moderate to pronounced, the chromatin is granular to vesicular and prominent, and occasionally there are multiple nucleoli.
- Mitotic activity is distinct.

Differentiating this entity from nephrogenic adenoma should pose no problem [9, 27, 31].

##### 13.3.1.1.3 Urethral Transitional Cell Carcinoma

This is observed infrequently in men as well as in women. The tumors may reveal varying morphologic grade, stage (in-situ or invasive), and architectural pattern (papillary or solid) [15, 28, 39].

The cytomorphology of urothelial carcinomas is described in Sects. 13.3.4, p. 833, and 13.3.5, p. 835.

##### 13.3.1.1.4 Malignant Melanoma

Primary malignant melanoma has rarely been reported in the literature. The tumors are usually encountered in the female urethra [44]. The cytomorphology is identical to melanocytic neoplasias elsewhere in the human body. However, melanoma can mimic solid urothelial carcinoma [33].

#### 13.3.1.2 Prostatic Ductal Adenocarcinoma

[3, 5, 10, 37, 40, 42] (Fig. 13.29)

**Synonyms and General Comments**

- Synonyms: prostatic duct carcinoma, endometrial or endometrioid carcinoma.
- Ductal adenocarcinoma is a rare prostatic tumor, pure ductal adenocarcinoma accounts for less than 1% of all prostate cancers.
- Approximately 50% of all prostatic ductal adenocarcinomas disclose an acinar tissue component.
- The tumor initially involves the male prostatic urethra, generally presenting with polypoid intraurethral masses; therefore, the tumors are typically diagnosed by means of transurethral resection or – depending on the pattern of spread – in bladder washings or voided urine.
- It is important to reach a correct diagnosis because this rare prostatic tumor type pursues a more aggressive clinical course than the common acinar prostate cancer.

**Microscopic Features** (Fig. 13.29A)

- Hallmark is the striking papillary and tubulopapillary growth pattern; tubules and papillae are lined with a single or pseudostratified layer of tall columnar epithelium with elongated nuclei containing large nucleoli. Nuclear grooves are described as characteristic [14, 30, 42].
- Most ductal adenocarcinomas show high-grade atypia and enhanced mitotic activity as compared to conventional prostatic adenocarcinomas.

**Differential Diagnosis**

- The ductal type of prostate adenocarcinoma may mimic high-grade papillary transitional carcinoma, but the latter does not exhibit tubular differentiation and positive immunoreactivity for prostate-specific cell markers.
- With careful reading of the overall cell pattern, a minor component of conventional prostatic acinar adenocarcinoma is detected in up to 50% of the ductal adenocarcinomas.

**Immunocytochemistry** (Fig. 13.29B)

The ductal type of prostate adenocarcinoma mimicking high-grade papillary transitional carcinoma shows positive immunoreactivity for PSA and PAP and negative immunoreaction for CK7, CK20, and CK13.

#### 13.3.1.3 Urethral Washing Cytology in Men After Cystoprostatectomy [6, 18, 21, 38]

- Urethral tumor recurrence occurs in approximately 7% of the men who had cystectomy for transitional bladder cancer [38]. Urethral washing screening cytology detects a substantial proportion of tumor recurrence.
- Poor survival is reported for urethral transitional cell carcinoma following radical cystectomy, but the survival difference in patients with and without cytologic urethral monitoring is a controversial subject [6, 21]. However, urethral washing may benefit individual patients [18].

### 13.3.2 Bladder, Ureter, and Renal Pelvis: Interaction of Precancerous and Invasive Urothelial Lesions

- Recent research on whole-organ mapping of the mucosal genome has provided new information concerning development of bladder cancer. The authors demonstrated genetic alterations of cells from dysplastic mucosal areas as well as of cells from morphologically normal mucosa. These genetic alterations, together with so-called forerunner genes and known tumor suppressor genes (such as *RB1-Retinoblastoma gene 1*) may be responsible for driving development of bladder cancer [7, 23]. However, the association of precancerous lesions with invasive bladder cancer was documented long ago by morphological mapping of the urothelium in bladders resected for invasive tumor by Koss and colleagues and Farrow and associates [12, 19].
- Intraurothelial neoplasia, called dysplasia, precedes or goes together with both carcinoma in situ and invasive cancer. Each class of dysplastic epithelial disorders, ranging from mild dysplasia to severe dysplasia/carcinoma in situ, marks a premalignant condition with increasing biological potential for developing invasive cancer.
- Recent publications in the literature advocate a new histologic classification of the noninvasive bladder neoplasms, which should comprise both morphologic features of the 1973 and 2004 WHO terminology and molecular genetic information [43].
- Tumors occurring in different compartments of the urinary tract reveal very similar morphologic features. Washings from the upper urinary tract are more likely to show low cellularity, especially when a flat-type neoplasia is present.
- A recent publication by Garbar and colleagues [13], among many other papers that are briefly cited in this chapter, emphasizes the high impact and accuracy of urinary cytology in current urological practice.

## 13.3.3 Bladder, Ureter, and Renal Pelvis: Precancerous Urothelial Lesions

### 13.3.3.1 Urothelial Dysplasia [10, 25]

#### Definition and General Comments

- Dysplastic lesions are flat noninvasive areas of urothelium composed of morphologically and genetically abnormal cells with precancerous potential. Dysplasia generally is asymptomatic, but a limited number of patients may present with irritative bladder symptoms and hematuria.
- Dysplasia may precede in situ carcinoma and invasive neoplasia, may occur concomitantly with bladder cancer, or is detected in patients with follow-up care after primary treatment of their transitional cell carcinoma.
- The dysplastic epithelial lesions may be divided into two groups: low-grade and high-grade dysplasia.
- In current-day practice at our institution, we prefer a morphologic subclassification into mild, moderate, and severe dysplasia simultaneously taking into account the results of image cytometric DNA ploidy studies (see Sect. 13.1.4.2,"Quantitative DNA Cytometry," p. 801) .

#### 13.3.3.1.1 Mild Dysplasia (Fig. 13.30)

Mild dysplasia closely resembles benign (reactive) urothelium. A conclusive diagnosis based on cytomorphologic features alone is rarely possible; a tentative cytologic report is common.

#### Microscopic Features

- The cells in cytologic preparations may be slightly enlarged, sometimes crowded and elongated.
- Hallmarks: A major proportion of the cells have longitudinal nuclear grooves and membrane irregularities, characteristic signs of dysplastic changes.
  The chromatin is finely granular but distinct.
  Small nucleoli are usually present.

#### Differential Diagnosis and Additional Analyses

- Mild dysplasia presents diagnostic dilemmas in distinguishing it from both nonspecific reactive cell changes and low-grade papillary carcinoma.
- In most cases, image cytometry provides a diploid or polyploid DNA distribution pattern; therefore cytometry cannot discriminate between a benign transitional cell population, a dysplastic cell population, and a low-grade neoplasia.
- UroVysion FISH is the most suitable routine method establishing a premalignant potential of urothelial cells with marginal alterations (Fig. 13.31).

#### 13.3.3.1.2 Moderate Dysplasia (Fig. 13.32)

Moderate dysplasia represents a diagnostic class with cell features that meet cytologic criteria between the two extremes of mild and severe dysplasia.

#### Microscopic Features

Hallmarks:

- Cellular atypias are overt: cells are enlarged, crowded, and frequently elongated, but the overall pattern is uniform.
- Loss of nuclear polarity is observed in a limited number of the cell groups.
- Nuclei are hyperchromatic showing distinct irregular outline as well as dense and granular chromatin. Nuclear grooves are common.
- The N/C ratio is normal or slightly increased.
- Small to medium-sized nucleoli are distinctly visible in a majority of the nuclei.
- In general, the smears are hypercellular.

#### Differential Diagnosis and Additional Analyses

- Moderate dysplasia exhibit similar morphologic features to transitional papillary carcinoma grade 2 and severe reactive/reparative atypia (see Sect. 13.2.2, p. 810).
- In most cases, moderate dysplasia with cytomorphologic characteristics, as stated above, yields an abnormal quantitative DNA distribution pattern (tetraploidy or aneuploidy).

#### 13.3.3.1.3 Severe Dysplasia (Fig. 13.33)

Severe dysplasia is characterized by distinctly abnormal urothelial cells.

#### Microscopic Features and Differential Diagnosis

- Cells are enlarged, rounded, or elongated.
- Marked loss of polarity is observed in cellular groupings.
- The nuclei are hyperchromatic and polymorphous with granular and coarse chromatin.
- The N/C ratio is increased. Medium-sized and large pleomorphic nucleoli are present.
- Mitotic activity is increased.

Dysplastic cells share morphology with the cells of both urothelial carcinoma in situ and invasive transitional cell cancer.

### 13.3.3.2 Transitional Cell Carcinoma In Situ

(Figs. 13.34–13.37)

Carcinoma in situ (CIS), also called high-grade intraurothelial neoplasia, progresses to invasive bladder cancer in a significant proportion of patients.

Carcinoma in situ is associated with extensive cell exfoliation due to lack of cellular cohesion.

#### Microscopic Features and Additional Analyses

- Key feature of CIS is a clean background of the cytologic smears, lacking detritus and signs of inflammation in spite of abundance of severely atypical cells.
- Urine sediments contain numerous single abnormal cells; cell clustering rarely occurs. The overall cell pattern has a uniform appearance.
- The tumor cells are round or polygonal with a high N/C ratio.
- The cytoplasmic rims are densely structured and focally vacuolated.
- The nuclei are hyperchromatic, wrinkled, and folded. The chromatin texture is coarsely granular and coarsely clumped.
- The nucleoli are large and pleomorphism is common.

Polysomy of at least one of the chromosomes is found in more than 90% of all CIS-cells using the UroVysion FISH test [36]. Correspondingly, most carcinomas in situ exhibit an aneuploid DNA distribution pattern. All cases with carcinoma in situ measured at our institute provided highly aneuploid DNA contents comprising one or multiple stemlines in different non-euploid areas (Fig. 13.36).

**Caution**

- Rare cases of urothelial CIS predominantly composed of cells with clear nuclei may lead to a false-negative tumor diagnosis (Fig.13.35).
- At our institution, we have observed a few cases with synchronous appearance (on the same slide) of both typical CIS and fragments and single cells from a papillary low-grade urothelial neoplasia. DNA ploidy analysis is able to confirm the cytologic diagnosis and to assess the different biological properties of the two cell populations (Fig. 13.37)
- It is important to insist on cytologic diagnoses of severe dysplasia or CIS, even in cases with cystoscopy and biopsies providing negative results:
  - Flat neoplastic intraurothelial alterations of the bladder are often occult and can easily be missed, by cystoscopy and biopsy.
  - CIS, which is located in the upper urinary tract and clinically free of symptoms, must always be excluded in this setting.

## 13.3.4 Bladder, Ureter, and Renal Pelvis: Papillary Transitional Cell Carcinoma

#### General Comments

- A conclusive cytologic diagnosis of papillary transitional cell carcinoma (PTC) is based on:
  1. The evidence of papillary tumor formations comprising fibrovascular cores and corresponding cellular atypias. Elongated and columnar epithelial cells showing palisade arrangement, pseudostratification, and loss of polarity. The atypical cell features are more pronounced the higher the tumor grade.
  2. Highly cellular smears containing large numbers of single cells that are typically arranged in a streaming pattern, and rosette-like or palm frond-like formations.
- The cytologic diagnosis of papillary transitional cell carcinoma of any grade will neither rule out nor confirm an invasive tumor growth.

#### Tumor Grading

- Cytological criteria are not sufficiently refined to reliably differentiate between the three categories of PTC tumor grade considered herein. At our institution, we have implemented a grading system for PTCs based on cytomorphology complemented by ICM ploidy analysis as an objective grading method:
  - Diploid/polyploid DNA distribution pattern is consistent with low-grade lesions.
  - Aneuploidy is consistent with high-grade lesions.
  - Tetraploidy should be rated equivocally (see Sects. 13.1.4.2.1 and 13.1.4.2.2, p. 802).

  As a result, one portion of cytomorphologically grade 2 PTCs fall into the low-grade tumor group, another portion into the high-grade category, and a small number of cases cannot be precisely graded.
- A critical study "The effects of the current WHO/ISUP classification system on urine cytology results" was published in 2002 by Curry and Wojcik [8, 11].
- Exact correlation of the cytologic and histologic grading is not always possible as histologists rely on architectural features rather than distinct cellular and nuclear changes, and image cytometric studies are not acceptable using histologic sections.

### 13.3.4.1 Papillary Transitional Cell Carcinoma, Grade 1 [26, 34] (Figs. 13.38 and 13.39)

#### Microscopic Features

- Grade 1 (low-grade) PTC cells are somewhat larger than normal basal and intermediate urothelial cells.
- The homogeneous, slightly cyanophilic cytoplasm is elongated, fusiform, or columnar.
- Nuclei are eccentrically positioned and slightly irregular, exhibiting wrinkled membranes. Their chromatin is usually denser and more granular than that in nuclei of normal urothelial cells and evenly dispersed. Opaque nucleoplasm frequently occurs.
- Nucleoli are small but distinct and appear in the majority of the tumor cells.
- Hallmarks:
  - A majority of the cells show a flexed groove along the length of the nucleus.
  - Opaque nucleoplasm or evenly distributed fine granular chromatin are distinct.
  - The tumor cells occurring in papillary or papilliform aggregates show nuclear overlapping, focally with vague cellular depolarization.
  - The cytoplasm fades away at the periphery, giving rise to a syncytial-like architecture.
  - Single tumor cells may be close-packed, arranged in a streaming pattern and sometimes in rosette-like or palm frond-like formations.

#### Differential Diagnosis

Differential diagnoses of grade 1 PTC (in cases with or without entire papillary fronds) include:

- Proliferating intermediate urothelial cells.
- Urothelial cells with reactive/reparative changes.
- Benign elongated and columnar transitional cells.
  These benign cells differ from those of low-grade PTC in their sharply outlined cytoplasm, bland nuclear shape, chromatin texture, and nucleolar features (see Sects. 13.2.1.2.3, p. 809, and 13.2.2, p. 810) (Figs. 13.8 and 13.9).
- Flat intraurothelial mild dysplasia, and
  Papillary urothelial neoplasm of low malignant potential (PUNLMP) (Sect. 13.2.3.1.4, p. 812).
  The cellular and nuclear features of the two lesions match those of grade 1 PTC.

**Caution**

- The cytomorphologic criteria are characteristic but often not sufficient for a conclusive diagnosis of grade 1 PTC. Cytodiagnosis of this tumor entity remains challenging.
- Bare fibrovascular cores are occasionally observed in washings from the urinary system affected by PTCs of any grade (Fig. 13.41B).
- The cytologic diagnostic sensitivity increases with advancing malignancy grade of the PTC.
- UroVysion FISH is the most suitable routine laboratory method to assess or rule out premalignant potential of atypical urothelial cells suggestive of low-grade PTC.

### 13.3.4.2 Papillary Transitional Cell Carcinoma, Grade 2 (Fig. 13.40)

#### Microscopic Features

- Sediment smears show high cellularity.
- Cytoarchitecture of papillary and papilliform aggregates and arrangement of single cells are similar compared to grade 1 PTC, but the cells are clearly enlarged, crowded, and frequently elongated, presenting an overall monotonous pattern. Loss of polarity is observed in some of the cellular groupings.
- Nuclear grooves along the length of the nucleus are obvious, and the nuclei are hyperchromatic, exhibiting a distinct irregular outline.
- Dense granular and focally coarse chromatin.
- The N/C ratio is slightly increased.
- Small to medium-sized nucleoli are distinct in the majority of the nuclei.

#### Differential Diagnosis

Differential diagnoses of grade 2 PTC (in cases with or without papillary fragments) include:

- Moderate to severe reactive/reparative atypia, but property of cytoplasm and chromatin is different to those of grade 2 PTC (see also Sect. 13.2.2, p. 810).
- Flat intraurothelial moderate dysplasia that exhibits similar cytomorphologic features compared to grade 2 transitional papillary carcinoma.

#### 13.3.4.3 Papillary Transitional Cell Carcinoma, Grade 3 (Fig. 13.41)

Grade 3 PTC shares cytomorphologic features with transitional cell CIS and invasive solid transitional cell carcinoma (see Sects. 13.3.3.2, p. 833, and 13.3.5, below).

A diagnosis of exophytic high-grade papillary tumor is only possible if true papillae comprising connective tissue cores are encountered in the cytologic specimens.

## 13.3.5 Bladder, Ureter, and Renal Pelvis: Invasive Nonpapillary Transitional Cell Carcinoma

**Microscopic Features** (Fig. 13.42)

- Cellularity of the urine sample is highly increased.
- The tumor cells usually occur singly but three-dimensional irregular clusters may also be seen.
- The large pleomorphic cells present an increased N/C ratio and irregular pleomorphic, hyperchromatic nuclei. The nuclei show irregular borders with wrinkled and folded membranes.
- The chromatin is coarsely granular, clumped, and irregularly distributed.
- The nucleoli are prominent, pleomorphic, and frequently multiple.
- Exhibiting a dense homogeneous cytoplasm, the carcinoma cells retain a distinct transitional cell feature, but vacuolization is frequent.
- Necrotic debris and blood contribute to a diagnosis of invasive cancer.
- Unlike glandular and trophoblastic differentiation, a squamous cell component is frequently observed in urothelial carcinoma. The squamous cells are most often clearly malignant, comprising large polymorphous keratinized or cyanophilic cytoplasm, and a pleomorphic, hyperchromatic densely structured nucleus. Less well-differentiated malignant squames are difficult to distinguish from cancer cells of urothelial origin.

**Additional Comments**

- WHO histological classification [10] describes different subtypes of urothelial cancer: micropapillary, lymphoepithelioma-like, lymphoma-like, sarcomatoid, giant cell, mucoid, and others [22, 35] (Fig. 13.43). Such tumors are rarely encountered in routine cytology, precise subclassification should be left to histology.
- All invasive urothelial carcinoma shows atypical DNA distribution patterns using both flow and static cytometry.
- DNA aneuploid stem lines are associated with the highest recurrence rate.

**Differential Diagnosis**

- Compared to invasive TC, transitional cell carcinoma in situ exhibits a more uniform cell pattern, cell clusters rarely occur, and the background is not necrotic.
- Undifferentiated malignant epithelial, mesenchymal, and lymphatic tumors may masquerade as transitional cell carcinoma, yet these tumors rarely occur (see Sects. 13.3.6–13.3.8, below). Selective panels of antibodies should be applied in order to ascertain a specific tumor type.

**Caution**

- Occurrence of only a few malignant urothelial cells is exceptional but possible in cytologic specimens. This setting is specifically observed in cases associated with marked inflammation. Sporadic tumor cells should not be missed or misdiagnosed as regenerative epithelial cells or activated histiocytes.
- Ploidy analysis by means of image cytometry can accurately categorize single cells: diploidy indicates benign cells, whereas aneuploidy is diagnostic for neoplastic cells originating from high-grade dysplasia/CIS or invasive neoplasia.

## 13.3.6 Bladder, Ureter, and Renal Pelvis: Other Primary Cancers [10]

#### 13.3.6.1 Squamous Cell Carcinoma [20] (Fig. 13.44)

This tumor entity commonly occurs in regions where infestation with *Schistosoma haematobium* is endemic (see also Sect. 13.2.4.6.1, p. 815). In contrast, a squamous cell component in transitional cell cancer is frequently observed throughout the world.

**Tumor Variants, Microscopic Features, and Differential Diagnosis**

- *Common squamous cell bladder carcinoma*. The morphologic characteristics of this cancer are well known from their counterparts in other sites of the body. Description of cytomorphology is provided in other chapters of this book.
- *Verrucous carcinoma*. An uncommon variant of squamous cell carcinoma, but otherwise typically occurring in patients affected by schistosomiasis (Fig. 13.44). The tumor appears as an exophytic warty mass exhibiting pronounced epithelial acanthosis. Cytology is often negative for malignancy; endoscopic biopsy or surgical tumor excision and subsequent histology provide definite diagnosis.

- A verrucous neoplasm may be suggested due to large numbers of polymorphous squames lacking nuclei, and a densely structured eosinophilic and orangeophilic cytoplasm. A few squames may have nuclei exhibiting minimal atypia or apoptotic change.

- *Poorly differentiated nonkeratinizing squamous cancer* is difficult to distinguish from transitional cell cancer.

**Caution**

Squamous cancer spreading to the urinary system or direct extension of squamous cell carcinoma from the anal region or from the female cervix must be ruled out.

### 13.3.6.2 Adenocarcinoma (Fig. 13.45)

**General Comments and Microscopic Features**

- Adenocarcinomas account for less than 2% of all malignant urinary bladder tumors.
- Adenocarcinoma is associated with longstanding intestinal metaplasia of the urothelium. As a rare variant, adenocarcinoma may arise from remnants of the urachus.
- Mucin-secreting tumors may resemble colonic adenocarcinoma. Tumors of the colloid type and signet ring cell type are the most frequently reported variants.
- Cytologic findings are akin to adenocarcinomas in other body sites:
  - Three-dimensional clusters showing a scalloped contour and single cells are encountered. The cells are cuboidal or columnar in shape.
  - The nuclei are large and irregular with hyperchromasia and vesicular and glassy structure. The chromatin appears densely granular or in strands.
  - A large round or pleomorphic nucleolus is always present.
  - The cytoplasm is vacuolated and may contain mucus.

**Differential Diagnosis**

Metastatic disease is generally caused by cancers having their primary site in the colorectal area and in the prostate gland (see Sect. 13.3.7, below).

### 13.3.6.3 Small-Cell Undifferentiated Carcinoma [2, 4]

- Small-cell carcinoma (SCC) of the bladder is a rare entity with a poor prognosis. Proportions of small-cell carcinoma are found together with common transitional cell tumor types in a high percentage of cases. Small tumor cells share morphologic features with small-cell carcinomas in other parts of the body such as the lung.
- The tumors may show positive immunoreactivity for neuroendocrine markers [1], reliable neuroendocrine markers are: chromogranin A, synaptophysin, CD56, and neuron-specific enolases. Whether TTF-1 is a valuable marker for differentiating between primary bladder SCC and secondary SCC from the lung is, to the best of our knowledge, not yet clarified.
- Small-cell carcinoma must be distinguished from malignant lymphoma. SCC cells stain positive for cytokeratins and negative for CD45. Non-Hodgkin lymphomas have an opposite immunoprofile.

## 13.3.7 Carcinoma of Adjacent Organs Invading the Urinary Collecting System

### 13.3.7.1 Prostatic Adenocarcinoma (Fig. 13.46)

- Direct extension of prostatic cancer tissue into the urinary bladder is relatively common. Clinical and cystoscopic findings are sometimes bland; other patients may present with diffuse bleeding from the prostate region.
- Adenocarcinoma of the prostate has a characteristic morphology and should be diagnosed in most cases by routine light microscopy:
  - Small and large sheets of monomorphic cuboidal malignant cells with broad, foamy, or vacuolated cytoplasm.
  - The nuclei are round and swollen, exhibiting faint irregularities.
  - Dense and evenly distributed granular chromatin.
  - A single prominent centrally located nucleolus.
  - Detritus is absent.
- It is recommended to confirm the diagnosis using appropriate immunocytochemical stains; the prostate-specific markers PSA and PAP reveal strong positivity, which is confined to benign and malignant prostatic cells (Fig. 13.46B).

### 13.3.7.2 Colorectal Adenocarcinoma (Fig. 13.47)

These cancers may proceed with direct extension into the urinary bladder or they may exfoliate their cells into the urinary tract through a rectovesical fistula, particularly after therapeutic irradiation.

**Microscopic Features, Differential Diagnosis, and Immunocytochemistry**

- The cells of classic colonic adenocarcinoma are large and columnar-shaped, occurring in palisade arrangement.

- The nuclei are pleomorphic and hyperchromatic, exhibiting a coarse granular chromatin texture.
- Multiple nucleoli are common.
- The wide vacuolated cytoplasm contains variable amounts of mucin.
- Necrosis is present in most cases.

- Differential diagnosis should include primary adenocarcinoma of the urinary bladder mucosa and a variety of rare metastatic adenocarcinomas such as gastric cancer, breast carcinoma, adenocarcinoma of the lung, and others.
- With few exceptions, colorectal adenocarcinoma cells stain immunocytochemically positive for CK20 and CDX-2 but negative for CK7.

#### 13.3.7.3 Cervical Squamous Cell Carcinoma

Squamous cell carcinoma in urine samples from female patients is foremost suggestive of spreading cervical cancer into the urinary bladder. The different tumor subtypes are described in Sect. 13.3.6.1, p. 835.

#### 13.3.7.4 Renal Adenocarcinoma

(Figs. 13.48 and 13.49)

Locally advanced renal cell carcinoma may involve the urinary collecting system exfoliating cells into the urinary tract. A cytological diagnosis of renal adenocarcinoma is rarely made in urine probes.

**Microscopic Features, Differential Diagnosis, and Immunocytochemistry**

- Well-preserved tumor cells rarely occur.
- Tumor cell clustering is very uncommon.
- Renal adenocarcinoma is frequently of the clear cell type. Hence, the nuclei exhibit histiocytoid shape, and the cytoplasm is huge, foamy, and vacuolated.

- Single tumor cells with degenerative changes can rarely be distinguished from activated histiocytes (Fig. 13.49).
- Differential diagnosis should include primary clear cell adenocarcinoma (urethra, urinary bladder) [45], metastasis of clear cell adenocarcinomas, and nephrogenic adenoma/adenosis.
- In cases with enough well-preserved tumor cells, immunostaining for pancytokeratins (e.g., MNF116) and for the renal cell carcinoma marker (RCCMa) is helpful to achieve a conclusive cytologic diagnosis.

### 13.3.8 Rare Nonurothelial Primaries

Our knowledge in cytomorphology of extremely rare urinary tract tumors is based on single histologic and cytologic reports and on special references in textbooks. A comprehensive synopsis of nonurothelial tumors of the urinary tract was described by Mikuz [24].

In brief, selected entities have potential relevance for cytology:

#### 13.3.8.1 Soft Tissue Tumors

Nearly 75% of all primary nonurothelial tumors of the urinary tract belong to the soft tissue tumor group. Cytologic features may show significant overlap with those of sarcomatoid carcinomas, carcinosarcomas, small-cell carcinoma, or inflammatory pseudotumors [24, 29].

#### 13.3.8.2 Melanoma

A few cases of primary malignant melanoma have been reported in the literature. Melanomas occur more frequently in the urethra as compared with the mucosa of the urinary bladder [44]. Cytomorphology is identical to its counterparts elsewhere in the human body; however, melanoma can mimic urothelial carcinoma [33]. Targeted immunocytochemical work-up with antibodies against cytokeratins and specific melanoma antigens will be diagnostic.

#### 13.3.8.3 Malignant Lymphomas

The urinary tract may be affected in patients with generalized malignant lymphoma. Primary localization of lymphoma in the urinary tract is extremely rare and occurs particularly in HIV-positive and otherwise immunosuppressed patients [32, 41]. The most frequent reported lymphoma type is low-grade non-Hodgkin lymphoma (NHL) (Fig. 13.50) [17, 24].

**Differential Diagnosis**

- Lymphocyte-rich specimens of chronic cystitis must be distinguished from low-grade NHL by assessing clonality with immunocytochemical, cytometric, and/or molecular tests.

- NHL with a preponderance of blastic cells may mimic undifferentiated malignancies of varied types, especially transitional cell carcinoma. Differentiation is easily achieved by immunocytochemical staining for cytokeratins, e.g., MNF116 (positive reaction on carcinoma cells) and leukocyte antigen CD45 (positive reaction on lymphoma cells).
- The rare plasmacytoid subtype of transitional cell carcinoma should not be misinterpreted as extramedullary plasmacytoma of the bladder. Plasmacytomas are positive for CD38/CD138 (caution: CD45 and CD20 negativity!) but negative for cytokeratins.

#### 13.3.8.4 Pheochromocytoma

Extraadrenal benign and malignant pheochromocytoma is a rare neoplasm: only 1% of all cases occur in the bladder [16].

Key diagnostic cells are enlarged polygonal elements with eosinophilic, granular cytoplasm. Spindle cells together with large polymorphous cells forming groups and clusters could lead to misdiagnoses. Prominent clinical symptoms and biochemical tests confirm the diagnosis in most cases.

### 13.3.9 Further Reading


1. Ali SZ, Reuter VE, Zakowski MF. Small cell neuroendocrine carcinoma of the urinary bladder. A clinicopathologic study with emphasis on cytologic features. Cancer. 1997;79:356-61.
2. Asami H, Ito Y, Alda JS, et al. Small cell undifferentiated carcinoma of the urinary bladder: a cytodiagnostic case report of its variant type. Pathol Int 1997;47:876-882.
3. Brinker DA, Potter SR, Epstein JI. Ductal adenocarcinoma of the prostate diagnosed on needle biopsy: correlation with clinical and radical prostatectomy findings and progression. Am J Surg Pathol 1999;23:1471-1479.
4. Cheng L, Pan CX, Yang XJ, et al. Small cell carcinoma of the urinary bladder: a clinicopathologic analysis of 64 patients. Cancer 2004;101:957-962.
5. Christensen WN, Steinberg G, Walsh PC, Epstein JI. Prostatic duct adenocarcinoma. Findings at radical prostatectomy. Cancer 1991;67:2118-2124.
6. Clark PE, Stein JP, Groshen SG, et al. The management of urethral transitional cell carcinoma after radical cystectomy for invasive bladder cancer. J Urol 2004;172:1342-1347
7. Crawford JM. The origins of bladder cancer. Lab Invest 2008;88:686-693.
8. Curry JL, Wojcik EM. The effects of the current World Health Organization / International Society of Urologic Pathologists bladder neoplasm classification system on urine cytology results. Cancer(Cancer Cytopathol) 2002;96:140-145.
9. Doria MI Jr, Saint Martin G, Wang HH, et al. Cytologic features of clear cell carcinoma of the urethra and urinary bladder. Diagn Cytopathol 1996;14:150-154.
10. Eble JN, Sauter G, Epstein JI, Sesterhenn IA. (Eds.): World Health Organization Classification of tumors. Pathology and genetics of tumors of the urinary system and male genital organs. IARC Press: Lyon 2004.
11. Epstein J, Amin MB, Reuter VR, Mostofi FK. Bladder consensus conference committee. The World Health Organization / International Society of Urological Pathology consensus classification of urothelial (transitional cell) neoplasms of the urinary bladder. Am J Surg Pathol 1998;22:1435-1448.
12. Farrow GM, Utz DC,Rife CC. Morphological and clinical observations of patients with early bladder cancer treated with total cystectomy. Cancer 1976;36:2495.
13. Garbar C, Mascaux C, Wespes E. Is urinary tract cytology still useful for diagnosis of bladder carcinomas? A large series of 592 bladder washings using a five-category classification of different cytological diagnosis. Cytopathology 2007;18:79-83.
14. Gong Y, Caraway N, Stewart J, Staerkel G. Metastatic ductal adenocarcinoma of the prostate: cytologic features and clinical findings. Am J Clin Pathol 2006;126:302-309.
15. Hayashi Y, Komada S, Maruyama, et al. Primary transitional cell carcinoma of the male urethra: report of a case. Hinyokika Kiyo 1987;33:428-432.
16. Jorge AA, Lucon AM, Bloise W, Mendoca BB. Pheochromocytoma of the urinary bladder, report of a case and review of the literature. Rev Hosp Clin Fac Med Sao Paulo 1997;52:28-31.
17. Kempton CL, Kurtin PJ, Inwards DJ, et al. Malignant lymphoma of the bladder: evidence from 36 cases that low-grade lymphoma of the MALT-type is the most common primary bladder lymphoma. Am J Surg Pathol 1997;21:1324-1333.
18. Knapik JA, Murphy WM. Urethral wash cytopathology for monitoring patients after cystoprostatectomy with urinary diversion. Cancer 2003;99:352-356.
19. Koss LG, Tiamson EM, Robbins MD. Mapping of cancerous and precancerous bladder changes. JAMA 1974;227:281-285.
20. Lagwinski N, Thomas A, Stephenson AJ, et al. Squamous cell carcinoma of the bladder: a clinicopathologic analysis of 45 cases. Am J Surg Pathol 2007;31:1777-1787.
21. Lin DW, Herr HW, Dalbagni G. Value of urethral wash cytology in the retained male urethra after radical cystoprostatectomy. J Urol 2003;169:961-963.
22. Maeda D, Fujii A, Yamaguchi K, et al. Sarcomatoid carcinoma with a predominant basaloid squamous carcinoma component: the first report of an unusual biphasic tumor of the ureter. Jpn J Clin Oncol 2007;37:878-883.
23. Majewski T, Lee S, Jeong J, et al. Understanding the development of human bladder cancer by using a whole-organ genomic mapping strategy. Lab Invest 2008;88:694-721.
24. Mikuz G. Non-urothelial tumors of the urinary tract. Verh Dtsch Ges Pathol 1993;77:180-198.
25. Murphy WM, Soloway MS: Urothelial dysplasia: A review. J Urol 1982;127:849-854.
26. Murphy WM, Soloway MS, Jukkola AF, et al. Urinary cytology and bladder cancer. The cellular features of transitional cell neoplasms. Cancer 1984;53:1555-1565.
27. Oliva E, Young RH. Clear cell adenocarcinoma of the urethra: a clinicopathologic analysis of 19 cases. Mod Pathol 1996;9:513-520.
28. Ono Y, Matsumoto K, Kosaku N, et al. Transitional cell carcinoma in the fossa navicularis of the male urethra: a case report. Int J Urol 1998;5:294-295.
29. Paner GP, McKenney JK, Epstein Ji, Amin MB. Rhabdomyosarcoma of the urinary bladder in adults: predilection for alveolar morphology with anaplasia and significant morphologic overlap with small cell carcinoma. Am J Surg Pathol 2008;32:1022-1028.
30. Pérez-Guillermo M, Acosta-Ortega J, Garcia-Solano J. Pitfalls and infrequent findings in fine-needle aspiration of the prostate gland. Diagn Cytopathol 2005;33:126-137.
31. Peven DR, Hidvegi DF. Clear-cell adenocarcinoma of the female urethra. Acta Cytol 1985;29:142-146.

32. Proca DM, De Renne L, Marsh,Jr. WL, et al. Anaplastic large cell lymphoma in a human immunodeficiency virus-positive patient with cytologic findings in bladder wash. a case report. Acta Cytol 2008;52:83-86.
33. Radhi JM. Urethral malignant melanoma closely mimicking urothelial carcinoma. J Clin Pathol 1997;250-252.
34. Renshaw AA,, Nappi D, Weinberg DS. Cytology grade 1 papillary transitional cell carcinoma. A comparison of cytologic, architectural and morphometric criteria in cystoscopically obtained urine. Acta Cytol 1996;40:676-682.
35. Ro JY, Shen SS, Lee HI, et al. Plasmacytoid transitional cell carcinoma of urinary bladder: a clinicopathologic study of 9 cases. Am J Surg Pathol 2008;32:752-757.
36. Schwarz S, Rechenmacher M, Filbeck T, et al. Value of muticolour fluorescence in situ hybridisation (UroVysion) in the differential diagnosis of flat urothelial lesions. J Clin Pathol 2008;61:272-277.
37. Stamatiou K, Alevizos A, Mariolis A, et al. Adenocarcinomas of the prostatic duct in necropsy material. Can J Urol 2007;14:3502-3506.
38. Stein JP, Clark P, Miranda G, et al. Urethral tumor recurrence following cystectomy and urinary diversion: clinical and pathological characteristics in 768 patients. J Urol 2005;173:1163-1168.
39. Takahashi H, Hirano A, Nakano M, et al. Primary carcinoma of the female urethra. Hinyokika Kiyo 1989;35:1943-1945.
40. Takazawa R, Kawakami S, Yamamoto K, et al. A case of prostatic duct adenocarcinoma: its clinical significance in comparison with typical acinar adenocarcinoma. Hinyokika Kiyo 2008;54:243-247.
41. Tanaka T, Yoshimi N, Sawada K, et al. Ki-1-positive large cell anaplastic lymphoma diagnosed by urinary cytology. A case report. Acta Cytol 1993;37:520-524.
42. Vandersteen DP, Wiemerslage SJ, Cohen MB. Prostatic duct adenocarcinoma: a cytologic and histologic case report with review of the literature. Diagn Cytopathol 1997;17:480-483.
43. Van der Kwast TH, Zlotta AR, Fleshner N, et al. Thirty-five years of noninvasive bladder carcinoma. Anal Quant Cytol Histol 2008;30:309-315.
44. Yoshizawa T, Kawata N, Sato K, et al. Primary malignant melanoma of the female urethra. Urology 2007;70:1222.e13-16.
45. Young RH, Scully RE. Clear cell adenocarcinoma of the bladder and urethra. A report of three cases and review of the literature. Am J Surg Pathol. 1985;9:816-26.

**Fig. 13.29A, B Prostatic ductal adenocarcinoma.**
An 84-year-old man with a positive history of a papillary transitional cell carcinoma of the urinary bladder (pTa, grade 1) presented with an intraurethral papillary tumor. Combined urethral-vesical irrigation was performed. Direct sediment smears (after conventional centrifugation) were Pap-stained.
*Cytologic diagnosis:* Prostatic adenocarcinoma grade 2, consistent with prostatic ductal adenocarcinoma.
*Tissue diagnosis:* Well-differentiated prostatic carcinoma was detected 24 months later by means of prostatic punch biopsies.
**A** High magnification reveals morphologically typical prostatic carcinoma cells arranged in unusual papilliform clusters. Note focal palisading of the neoplastic cells (arrow). Normal urothelial cells (upper left corner). **B** Immunocytochemically, the malignant cells express prostate acid phosphatase (right) unlike adjacent connective tissue fragments at left. Immunopositivity for PSA and opposite immunoprofile for CK7 and CK20 are not shown (Pap-prestained direct sediment smear, low magnification).

**Figs. 13.30 and 13.31 Mild urothelial dysplasia and diagnostic impact of UroVysion FISH test.**
A young male patient with a positive history of low-grade papillary transitional cell carcinoma of the left ureter. Current follow-up cystoscopy and right-side ureteroscopy (post-left-side ureterectomy) provided normal results. Nevertheless, bladder washing was performed for cytologic examination.

**Fig. 13.30** High magnification shows clusters composed of slightly atypical transitional cells: loss of cellular polarization, focal cellular palisading (small arrows), distinct nuclear overlapping (large arrows), nuclear grooves and membrane irregularities (white arrowheads), and occasional small but distinct nucleoli. Dispersed granular chromatin is occasionally encountered as well (direct sediment smear, Pap stain).
*Cytology:* Distinguishing between reactive cell atypia and low-grade transitional cell neoplasia/mild dysplasia is not possible by conventional cytology alone. Thus, a Pap-prestained smear was referred for FISH analysis.

**Fig. 13.31** (same case) As stated above, bladder washing showed uncertain cytology. UroVysion FISH test on a prefixed and Pap-prestained conventional smear showed chromosomal aberrations (chromosome 3 red, 7 green, 17 blue) and anomalies of the 9p21 area (arrows) with up to 6 signals in 29 of 30 nuclei.
*Cytology and FISH study:* Morphologic atypia along with molecular genetic results (polysomia and gene amplification) indicate dysplastic lesions somewhere in the mucosa of the urinary system.
*Tissue diagnosis* (multiple endoscopic biopsies): Mild urothelial dysplasia.

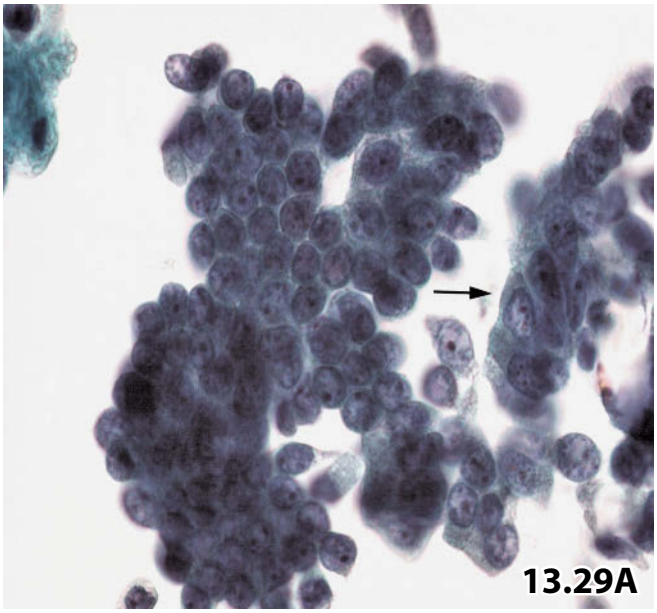
13.29A

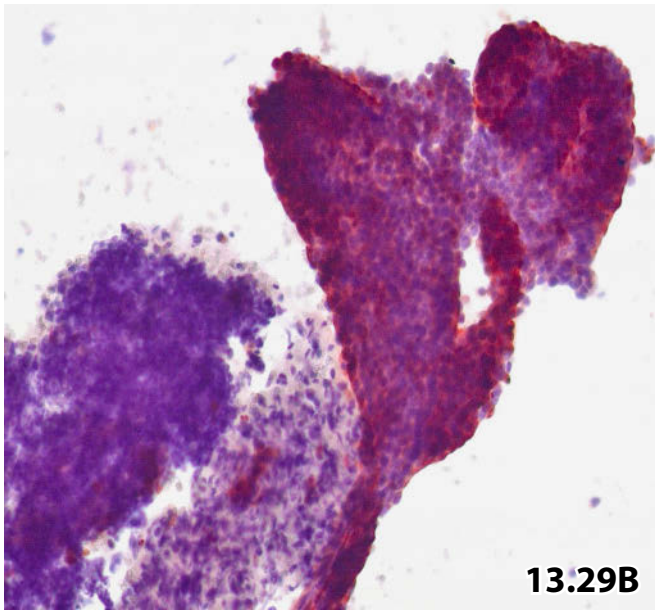
13.29B

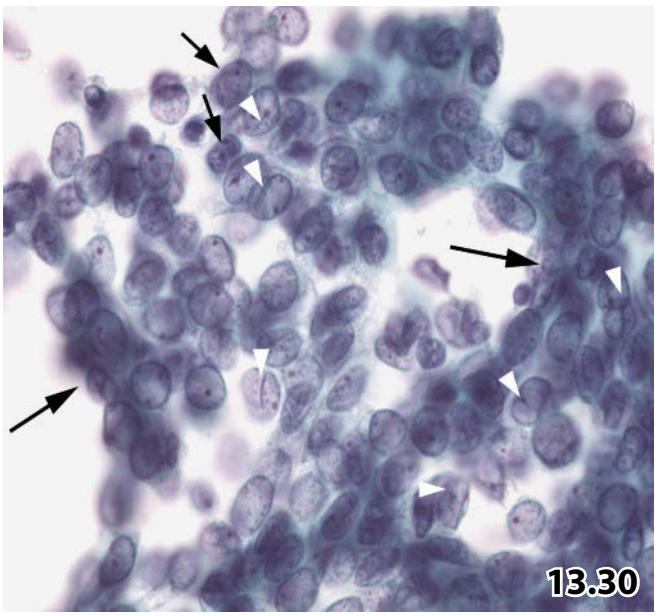
13.30

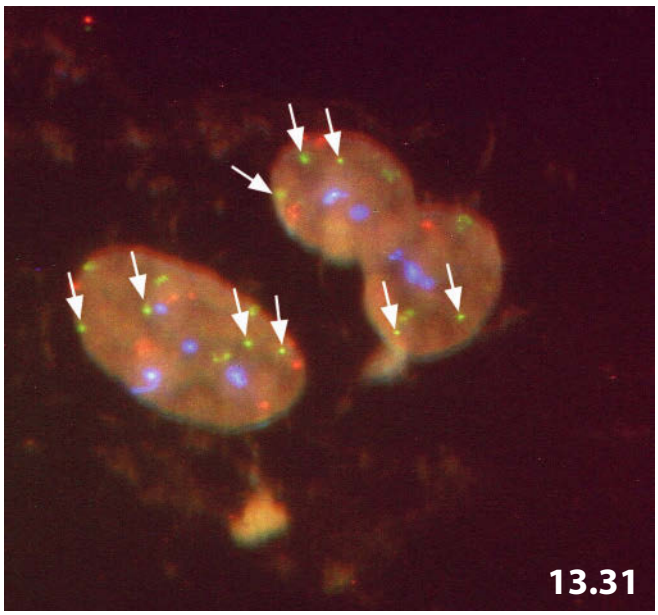
13.31

**Fig. 13.32 Moderate urothelial dysplasia.**
Direct sediment smears of a bladder washing from an elderly man show cytomorphologic characteristics of moderate urothelial dysplasia. Note in particular the monotonous cell appearance, cellular crowding, loss of polarity, high N/C ratio, and usually loose granular chromatin texture. Digital image cytometry (not shown) revealed aneuploid DNA distribution pattern indicating high-grade urothelial lesion. There is no follow-up available (Pap stain, high magnification).

**Fig. 13.33 Severe urothelial dysplasia and impact of ancillary tests.**
A 65-year-old woman underwent multiple cystoscopic controls over a period of 2 years because of well-established interstitial cystitis. Histologic biopsies always rendered a benign result, unlike bladder washings, which yielded without exception atypical cytologic results. Digital image cytometry was also performed on the atypical cell population, disclosing an abnormal (tetraploid) DNA distribution pattern (not shown). A recent bladder washing showed highly atypical transitional cells compatible with high-grade dysplasia. Additional UroVysion FISH test was mandated due to previous atypical cytologic findings: unequivocal chromosomal aberrations were found (not shown) (direct sediment smear, Pap stain, high magnification).
*Cytologic diagnosis supported by FISH study:* Severe urothelial dysplasia. Carcinoma in situ or invasive transitional cell neoplasm cannot be ruled out.
*Histologic diagnosis, not earlier than 21 months after positive cytology* (cystoscopic biopsies from the bladder mucosa): High-grade urothelial dysplasia.

**Figs. 13.34–13.37 Urothelial carcinoma in situ.**
Three different examples of carcinoma in situ (CIS) are discussed together with the diagnostic impact of static DNA cytometry.

**Fig. 13.34** (case #1) Classical CIS in a Cytospin specimen. Loose aggregation of malignant cells is characteristic of the liquid-based preparation mode. Note in particular the vacuolated cytoplasm and clean background of the specimen (bladder washing, Pap stain, high magnification).
*Cytologic follow-up* by cystoscopic bladder washings resulted in persistent CIS. Biopsies were not performed.

**Fig. 13.35** (case #2) CIS, clear cell variant. Both pale clear nuclei and partial low N/C ratio may give rise to diagnostic difficulties between benign and malignant transitional cells. Still, cell size, extreme variation in N/C ratio, irregular nuclear membrane, radiating filiform chromatin (arrow), and pronounced polymorphic nucleoli suggest malignancy. Compare tumor cells with unequivocally benign urothelial cells (arrowheads) (bladder washing, direct sediment smear, Pap stain, high magnification).

**Fig. 13.36** (same case) DNA quantitation by digital image cytometry was very helpful in order to render a conclusive cytologic diagnosis: Polyploidizing hypotetraploid stemline and numerous aneuploid single cells indicating severe dysplasia or malignancy.
*Tissue diagnosis* (multiple biopsies from the bladder mucosa): Urothelial carcinoma in situ.

**Fig. 13.37** (case #3) Concomitant CIS and low-grade papillary carcinoma was found in a 76-year-old man presenting with microhematuria. A voluminous papillary tumor was detected during cystoscopic exploration. Bladder washing and excisional biopsies were simultaneously performed.
Bladder washing: Lower magnification shows numerous isolated fusiform and slightly atypical urothelial cells indicating low-grade papillary transitional cell carcinoma, but highly abnormal urothelial cells are present as well (arrow); distinct cellular enlargement, nuclear polymorphism, hyperchromasia, and pronounced nucleoli are readily identified when compared to the basic cell population (direct sediment smear, Pap stain).
ICM-DNA (not shown): The low-grade neoplastic cell population revealed a diploid DNA pattern unlike the isolated highly atypical cells; the latter disclosed a definite aneuploid DNA histogram.
*Cytologic diagnoses supported by DNA analysis:*
(1) Low-grade papillary transitional cell neoplasia.
(2) Most probably concomitant second high-grade neoplastic lesion (severe dysplasia, CIS or invasive carcinoma).
*Histologic diagnoses:*
(1) Papillary transitional cell carcinoma pTa, grade 2.
(2) Severe urothelial dysplasia was detected in a single biopsy from the bladder mucosa not earlier than 50 months after the positive cytologic findings.

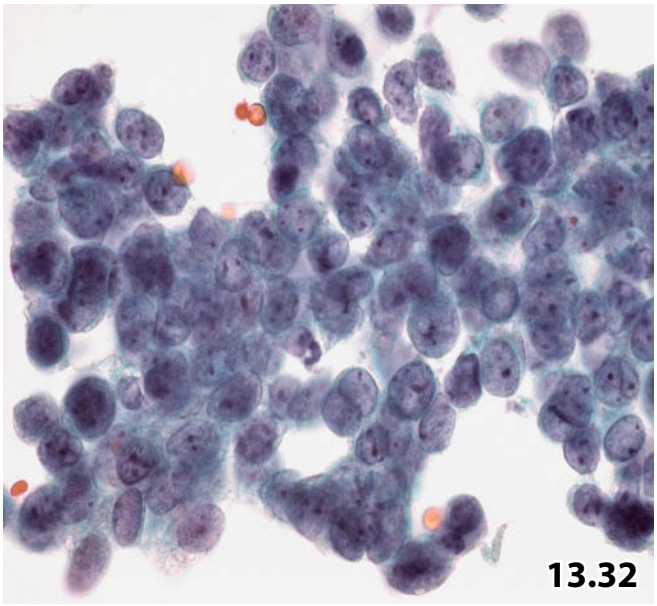
13.32

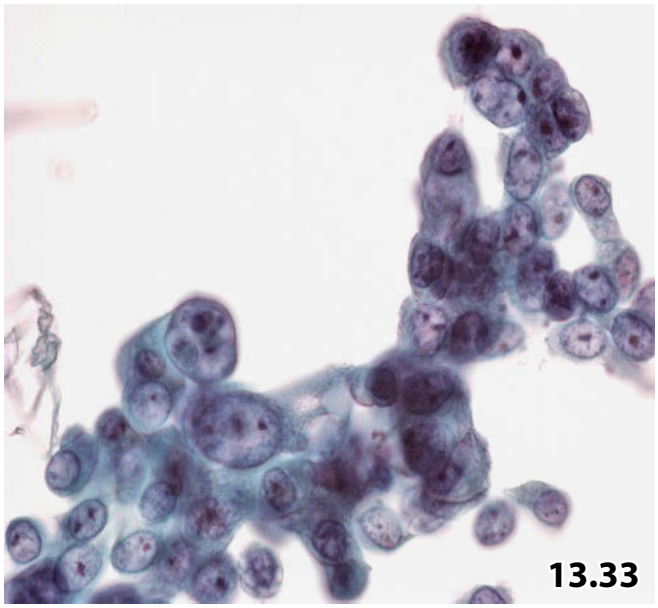
13.33

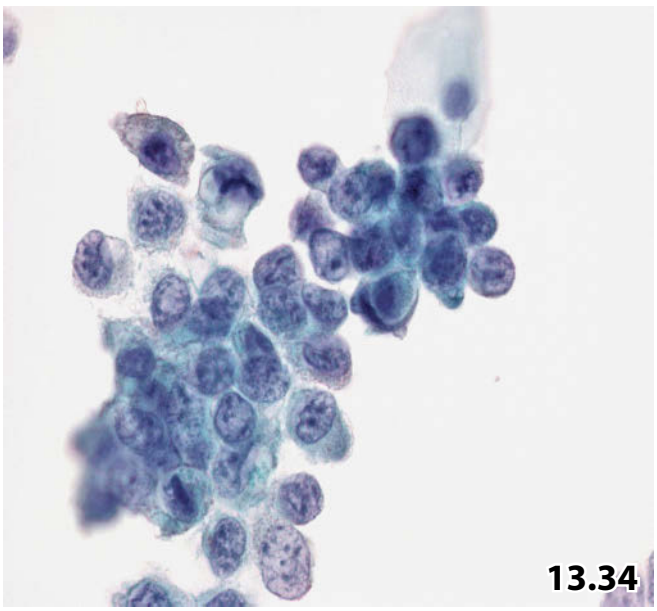
13.34

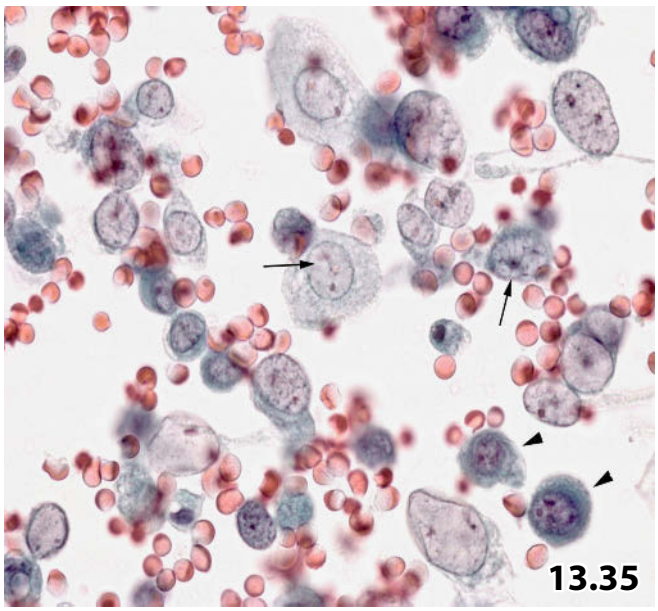
13.35

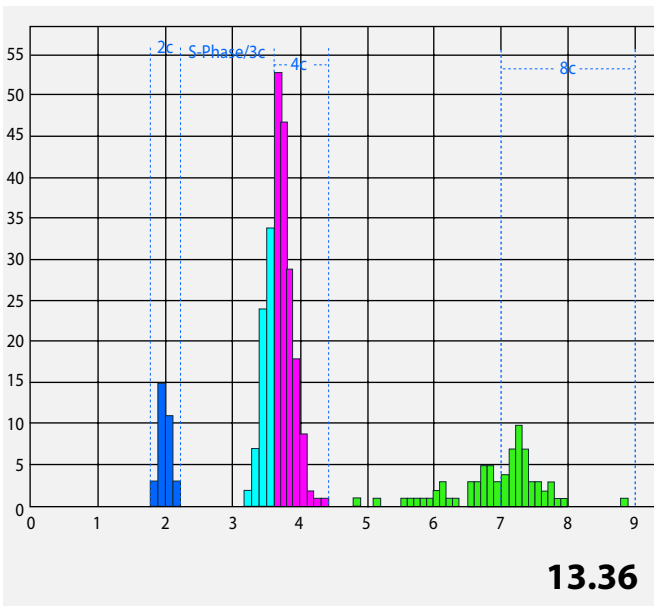

13.36

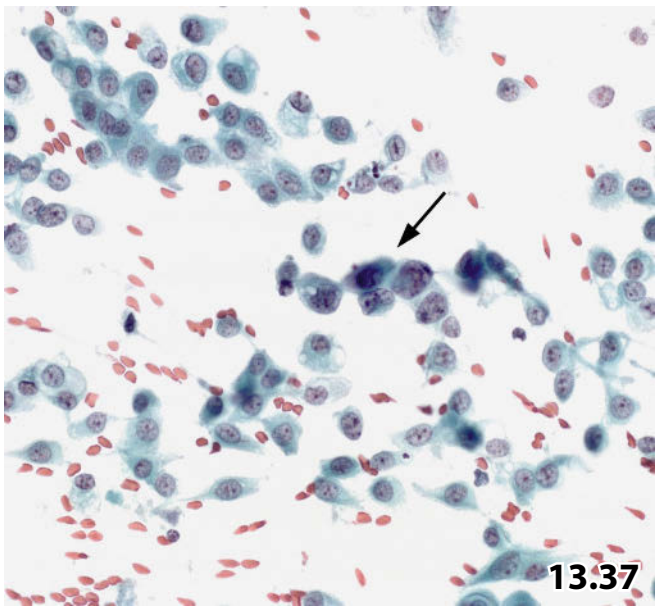
13.37

**Figs. 13.38 and 13.39 Papillary transitional cell carcinoma, grade 1.**
Two papillary low-grade neoplasms from different patients are highlighted focusing on key cytologic features.

**Fig. 13.38** (case #1) Higher magnification reveals papillary fronds. Fibrovascular cores are coated with uniform neoplastic cells exhibiting mild nuclear atypias. Note the characteristic nuclear opacity. ICM-DNA showed a diploid histogram (not shown) (bladder washing, direct sediment smear, Pap stain).
*Cytologic diagnosis:* Papillary transitional cell carcinoma, grade 1 (confirmed by histology: pTa,G1).

**Fig. 13.39A–C** (case #2) Cytologic hallmarks are demonstrated using different microscopic magnifications.
*Cytologic diagnosis:* Papillary transitional cell carcinoma, grade 1. ICM-DNA showed a diploid histogram(not shown).
*Tissue diagnosis:* Papillary transitional cell carcinoma pTa,G2.
**A** Two typical cytologic features of low-grade papillary tumor are demonstrated at low magnification (ureteral washing, direct sediment smear, Pap stain): (1) A small papillary frond exhibiting distinct palisading of the superficial cell layer (right). (2) Numerous isolated uniform neoplastic cells. They are spindle-shaped or exhibit eccentric cytoplasm. Focal evidence of cellular palisading (arrows) and vague streaming cell formation (arrowheads). **B** A large palm-frond-like cell aggregation is shown at higher magnification comprising cell stream pattern (arrow) and rosette-like formations (arrowheads).**C** High magnification focuses on nuclear hallmarks of low-grade papillary tumors: wrinkled cleaved and grooved nuclear membranes (arrows), loose granular or opaque chromatin, indistinct nucleoli, and absence of nuclear hyperchromasia.

**Fig. 13.40 Papillary transitional cell carcinoma, grade 2.**
Increased cell size, coarse clumping chromatin, mild hyperchromasia, occasional pronounced nucleoli separate G2-papillary neoplasms from G1-tumors (Fig. 13.39C). ICM-DNA revealed an aneuploid histogram(not shown) (washing of renal pelvis, direct sediment smear, Pap stain, high magnification).

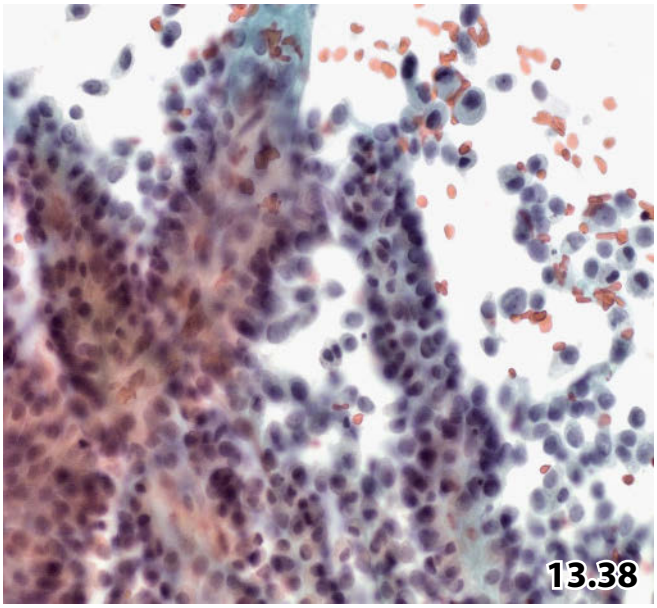
13.38

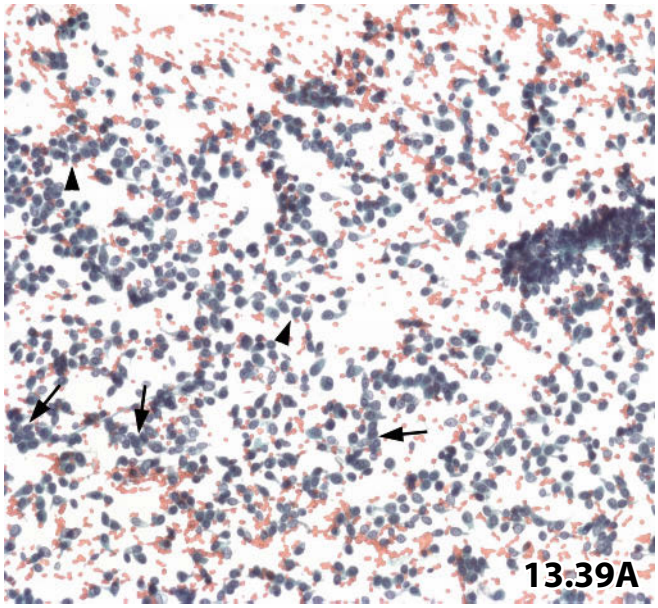
13.39A

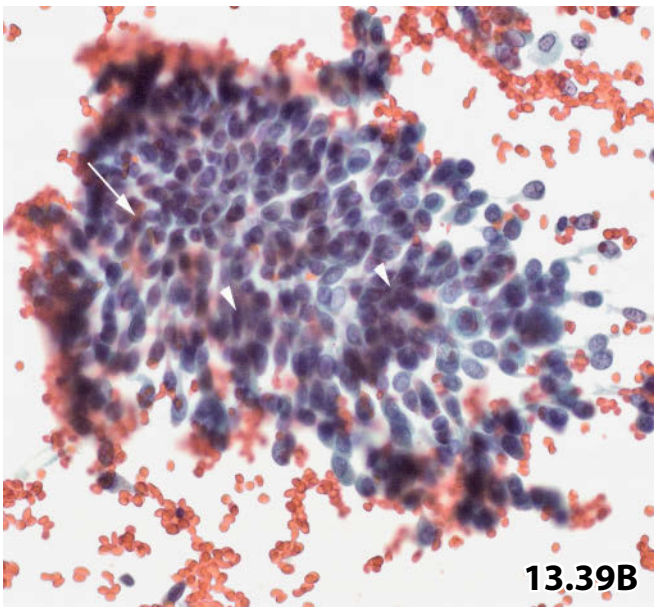
13.39B

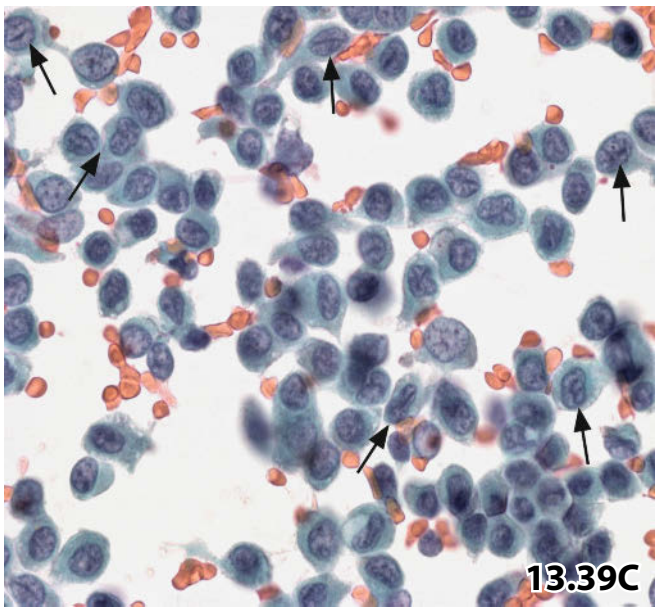
13.39C

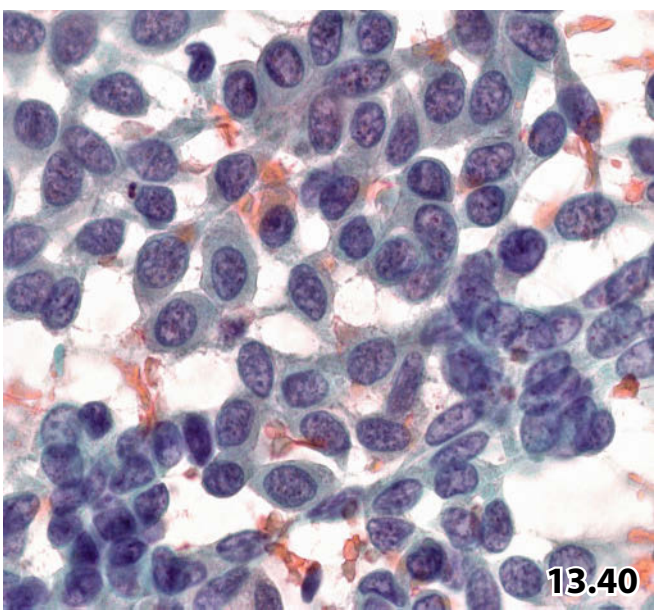
13.40

**Fig. 13.41A, B Papillary transitional cell carcinoma, grade 3.**
Example of a G3-papillary neoplasia in a bladder washing (direct sediment smear, Pap stain).
*Cytologic diagnosis:* Papillary transitional cell carcinoma, grade 3.
*Tissue diagnosis:* Invasive papillary transitional cell carcinoma, grade 3.
**A** Crowded malignant cells showing a remarkably high N/C ratio, pleomorphic nuclei, and coarse clumping chromatin. The papilliform structure of the cell cluster is faintly discernible (arrow). Invasive growth cannot be diagnosed by cytology (high magnification). **B** Lower magnification exhibits a large papillary formation and papillary fronds that are partially covered by neoplastic urothelium. Note subepithelial capillary vessels containing red blood cells, a phenomenon that is best identified upon uncoated fronds (arrows).

**Fig. 13.42 Invasive nonpapillary transitional cell carcinoma, common type.**
Key features of invasive transitional cell carcinoma: overt malignant cells occurring alone or grouped in compact three-dimensional clusters, necrotic debris is nearly always present (top and lower left) (bladder washing, direct sediment smear, Pap stain, higher magnification).

**Fig. 13.43 Invasive transitional cell carcinoma with focal mucus production.**
Higher magnification reveals a urothelial carcinoma composed of medium-sized and large cells. Interspersed signet ring-like cells indicate focal mucin production. Note the glassy appearance and pink staining of the cytoplasmic inclusions, which show a positive staining reaction for Alcian blue/PAS (not shown) (bladder washing, direct sediment smear, Pap stain).
*Cytologic diagnosis:* Transitional cell carcinoma focally associated with mucoid differentiation. Diagnosis was confirmed by histology.

**Fig13.44 Well-differentiated / verrucous squamous cell carcinoma.**
An 86-year-old man who presented with a bladder condition indicating cystitis or bladder neoplasia underwent cystoscopy. Bladder washing was performed, direct sediment smears (after centrifugation) were Pap-stained. Hypercellular smears revealed polymorphic, strongly keratinized, nucleated and anucleated squamous cells. Nuclei showed mere mild atypia. Careful evaluation of the cytologic specimen detected occasional pearl formations (top) (high magnification).
*Tentative cytologic diagnosis:* Keratinizing squamous cell carcinoma versus widespread atypical squamous metaplasia.
*Tissue diagnosis* (endoscopic biopsy): Verrucous squamous cell carcinoma.

**Fig. 13.45 Adenocarcinoma: particular diagnostic challenge following electro-cauterization.**
A 75-year-old woman with a diagnosis of ureteral papillary adenocarcinoma underwent follow-up cystoscopy and bladder washing 2 weeks after the initial histologic diagnosis. Cellular artifacts caused by electrocauterization (elongation of the cytoplasm of a large proportion of the cell population, and opaque nucleoplasm) hampered correct cytologic diagnosis (direct sediment smear, Pap stain, high magnification).
*(False) cytologic diagnosis:* Altered dysplastic urothelial cells following cauterization.
*Discussion:* However, these cells represent adenocarcinoma when compared to the neoplastic cells in histologic sections. Note: Indistinct nuclear membrane irregularities, partially well-preserved granular chromatin (arrows) and a single prominent nucleolus (arrowheads) may be helpful to avoid underinterpretation or misinterpretation.
*Final diagnosis:* Multifocal primary adenocarcinoma in the urinary tract.

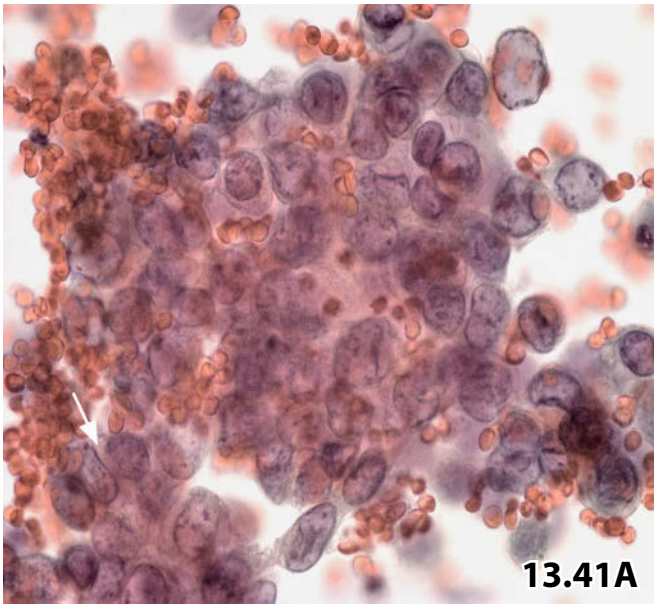
13.41A

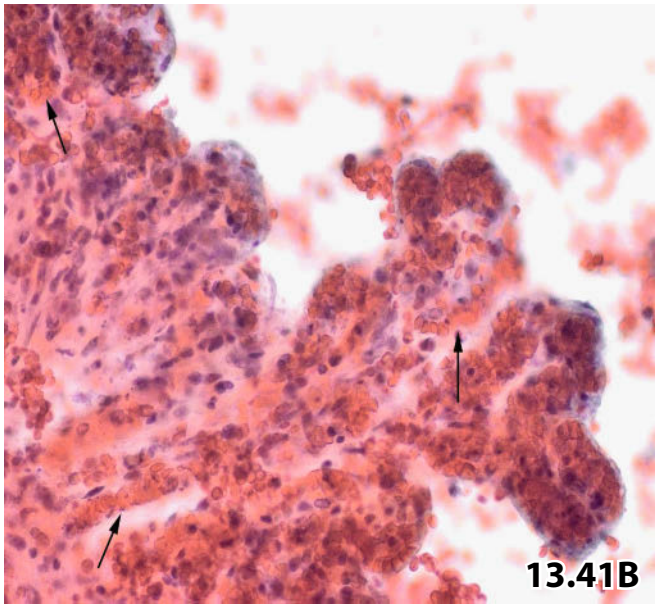
13.41B

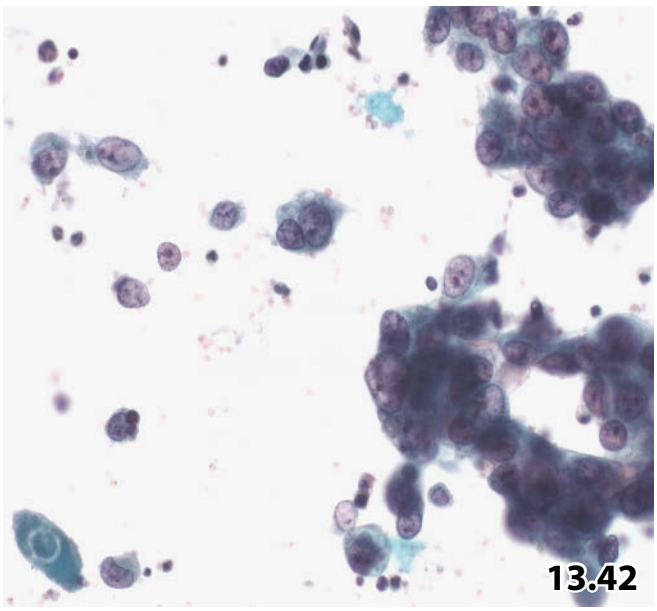
13.42

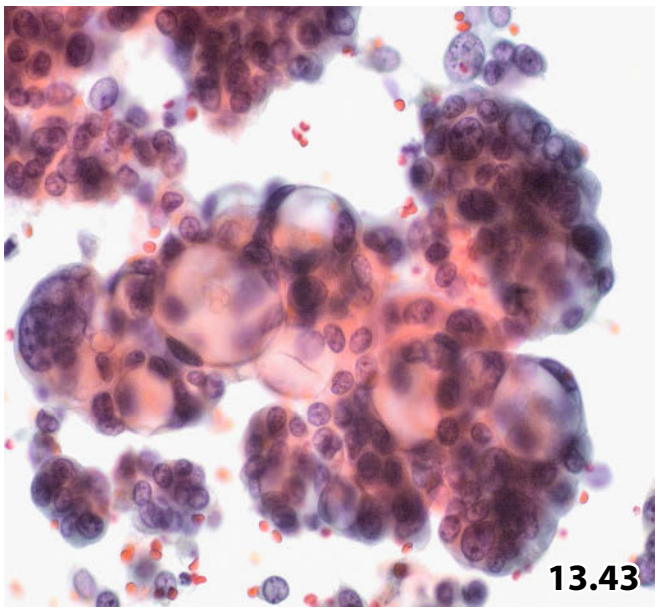
13.43

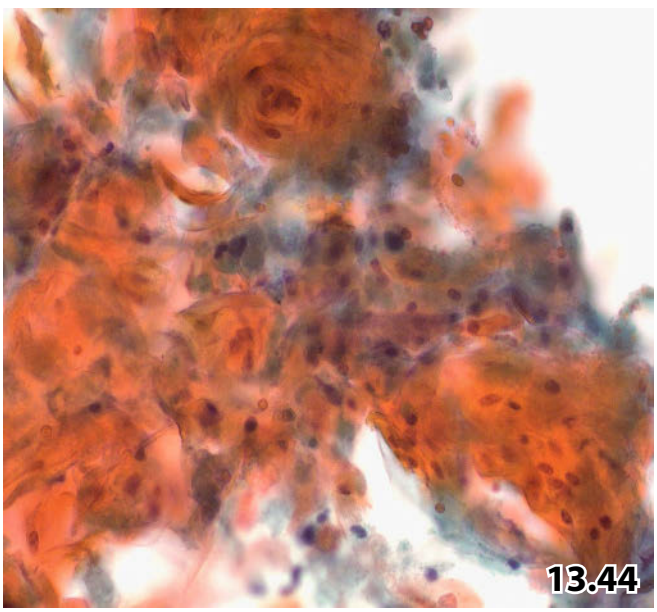
13.44

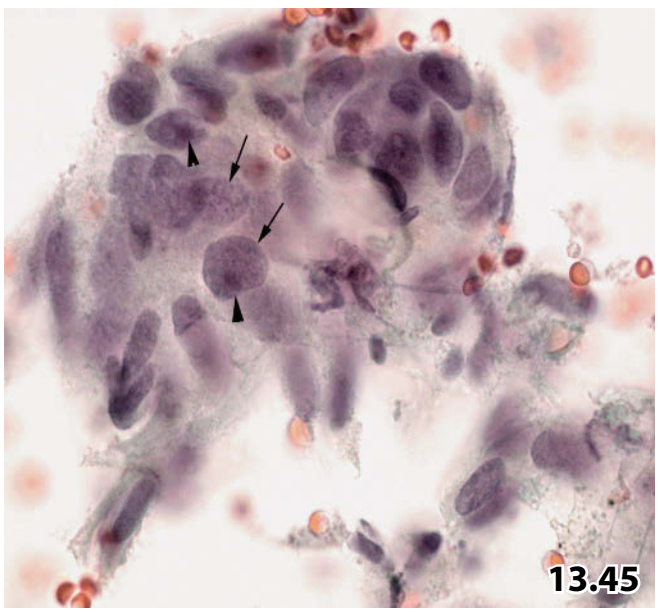
13.45

**Fig. 13.46A, B Prostatic adenocarcinoma.**
An 84-year-old man with a positive history of poorly differentiated prostatic adenocarcinoma presented cystoscopically with inflammatory changes of the bladder mucosa. Direct smears were performed from the sediment after conventional centrifugation of the bladder irrigation fluid. **A** Cytoarchitecture (arrangement of the fairly uniform tumor cells in a sheet-like formation) and cell features (round to oval nuclei exhibiting evenly distributed granular chromatin, distinct nucleoli, and abundant foamy cytoplasm) favor carcinoma of prostatic origin. A conclusive cytologic diagnosis requires adequate immunostainings (Pap stain, higher magnification). **B** Strong positive immunocytochemical reaction of the tumor cells for prostatic acid phosphatase verified cytomorphologic diagnosis (Pap-prestained direct smear).
*Cytologic diagnosis* was confirmed by postmortem examination of body tissues.

**Fig. 13.47 Colonic adenocarcinoma.**
Cystoscopy detected a papillary tumor formation in an 87-year-old man's urinary bladder. High magnification exhibits characteristic cytologic features of colonic adenocarcinoma invading the urinary collecting system: palisade cell arrangement and glandular formations (lower left), polymorphic nuclei, clearly defined nuclear borders, pronounced nucleoli, abundant cuboid and columnar cytoplasm occasionally containing mucin (lower left) (bladder washing, direct sediment smear, Pap stain).
*Tissue diagnosis:* Invading mucinous carcinoma of the colon sigmoids was histologically assessed in retrospect.

**Figs. 13.48 and 13.49 Renal cell adenocarcinoma.**
Two examples of renal cell carcinoma of the clear cell type with their peculiarities in fluids obtained from the urinary collecting system. Cytomorphology and diagnostic dilemmas are discussed.

**Fig. 13.48** (case #1) Washing of the renal pelvis in a 70-year-old man. Imaging studies suggested transitional cell carcinoma of the renal pelvis. Direct sediment smears (after conventional centrifugation) were Pap-stained(higher magnification).
*Cytology* rendered a vague diagnosis: Urothelial dysplasia versus low-grade transitional cell neoplasia, among others.
*Comments:* Atypical/malignant epithelial cells exhibiting histiocytoid nuclei and abundant foamy cytoplasm may simulate activated histiocytes (arrows). However, notable compact sheets are indicative of carcinoma of the clear cell type.
*Tissue diagnosis* (tumor excision): Renal cell adenocarcinoma of the clear cell type, grade 2.

**Fig. 13.49** (case #2) An elderly woman presenting with the clinical diagnosis of a tumoral renal lesion underwent cystoscopy, which provided negative findings. Bladder washing was performed for cytologic investigations. The fluid was processed using the Cytospin method (Pap stain). Picture detail presents five epithelial cells. The two cells on the left and at the bottom show substantial degeneration. However, morphologic abnormalities are readily made out by comparing with the remaining apparently benign urothelial cells (upper right). Cell alterations closely match those of degenerating malignant cells, degenerating histiocytes, and cells affected by a virus.
*Tentative cytologic diagnosis:* A few degenerating atypical epithelial cells most likely exfoliated from a carcinoma of the large-cell type.
*Tissue diagnosis:* Renal cell adenocarcinoma of the clear cell type, grade 3.

**Fig. 13.50 Extranodal marginal zone lymphoma of the MALT type.**
A 61-year-old woman cystoscopically presented with nodular lesions in the mucosa of her urinary bladder. Direct smears made from the sediment of a bladder washing (conventional centrifugation) were extremely rich in slightly atypical lymphocytes: Note pronounced nuclear irregularities and polymorphic nucleoli. Attention should be paid to the coarse chromatin texture in accordance with that of benign lymphocytes. Urothelial cells are also present. (Pap stain, high magnification).
*Tentative cytologic diagnosis:* Reactive lymphocytosis or low-grade non-Hodgkin lymphoma. Neither immunophenotyping of the lymphoid population nor molecular clonality analysis were performed using the cytologic material.
*Tissue diagnosis* (excisional biopsy of nodules located in the bladder mucosa): Non-Hodgkin lymphoma of the B-cell phenotype, low-grade, MALT type.

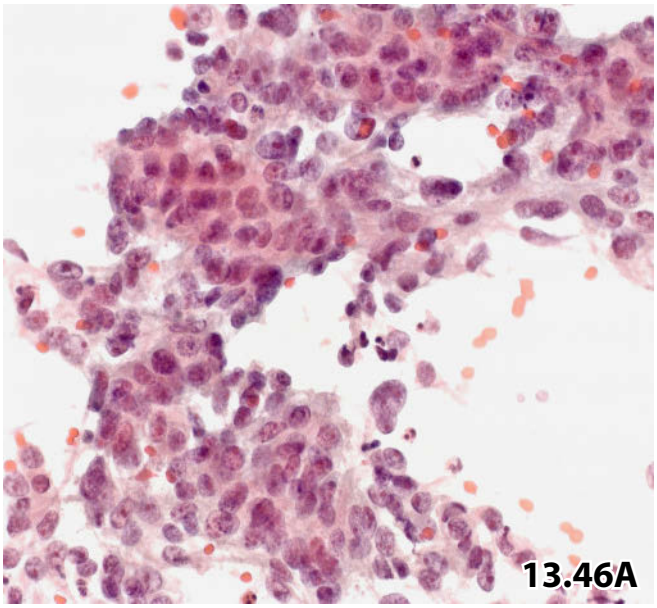
13.46A

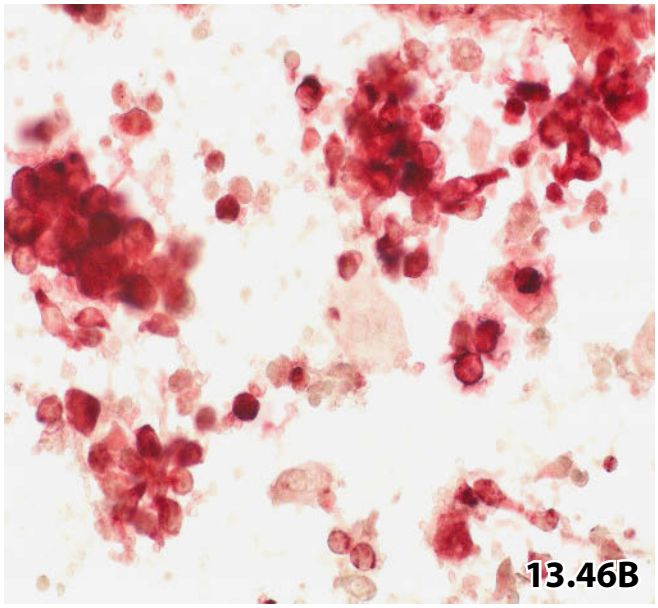
13.46B

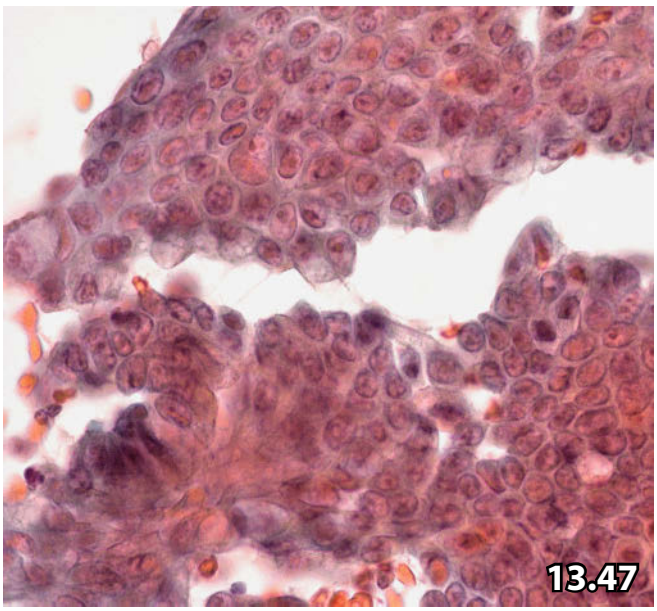
13.47

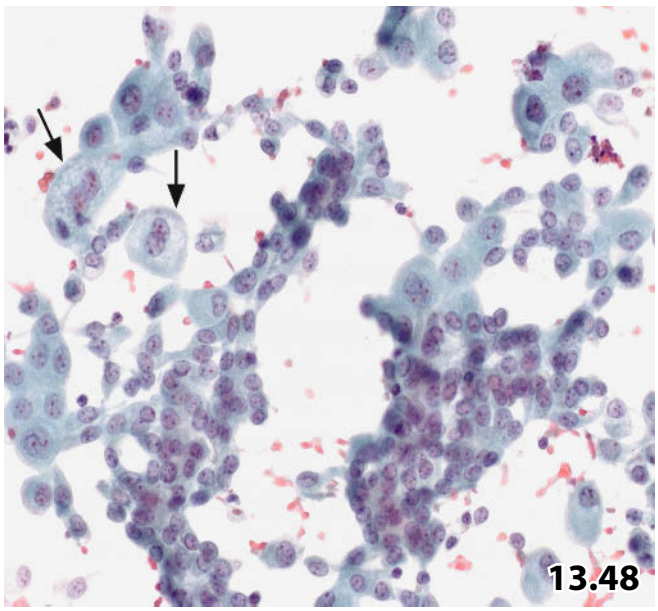
13.48

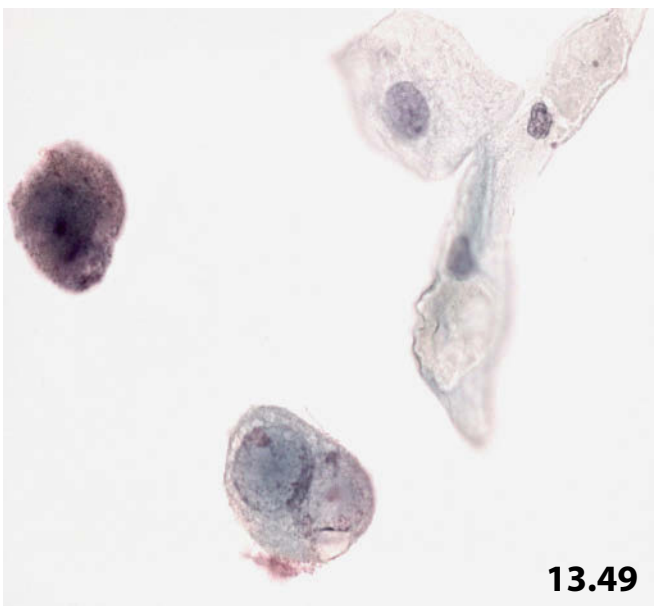
13.49

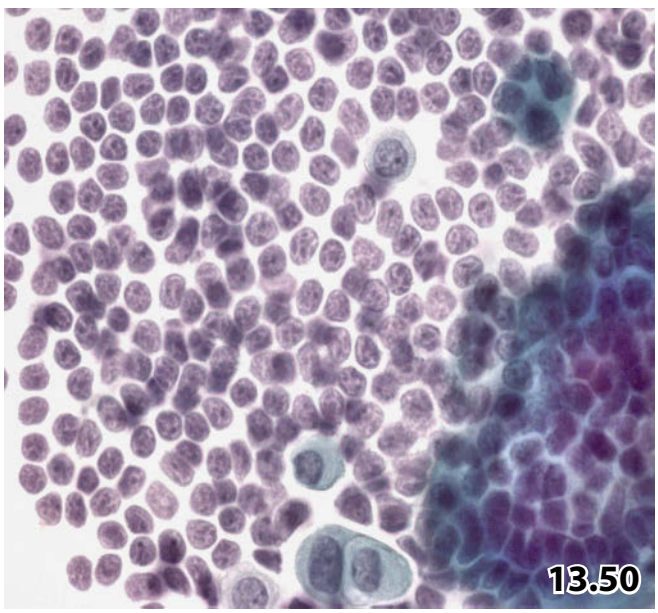
13.50

# Male Genital Organs 14



## Synopsis and Algorithms




Spieler/Rössle, *Nongynecologic Cytopathology. A Practical Guide. Essentials of Diagnostic Pathology*,
DOI 10.1007/978-3-642-24719-4_14,

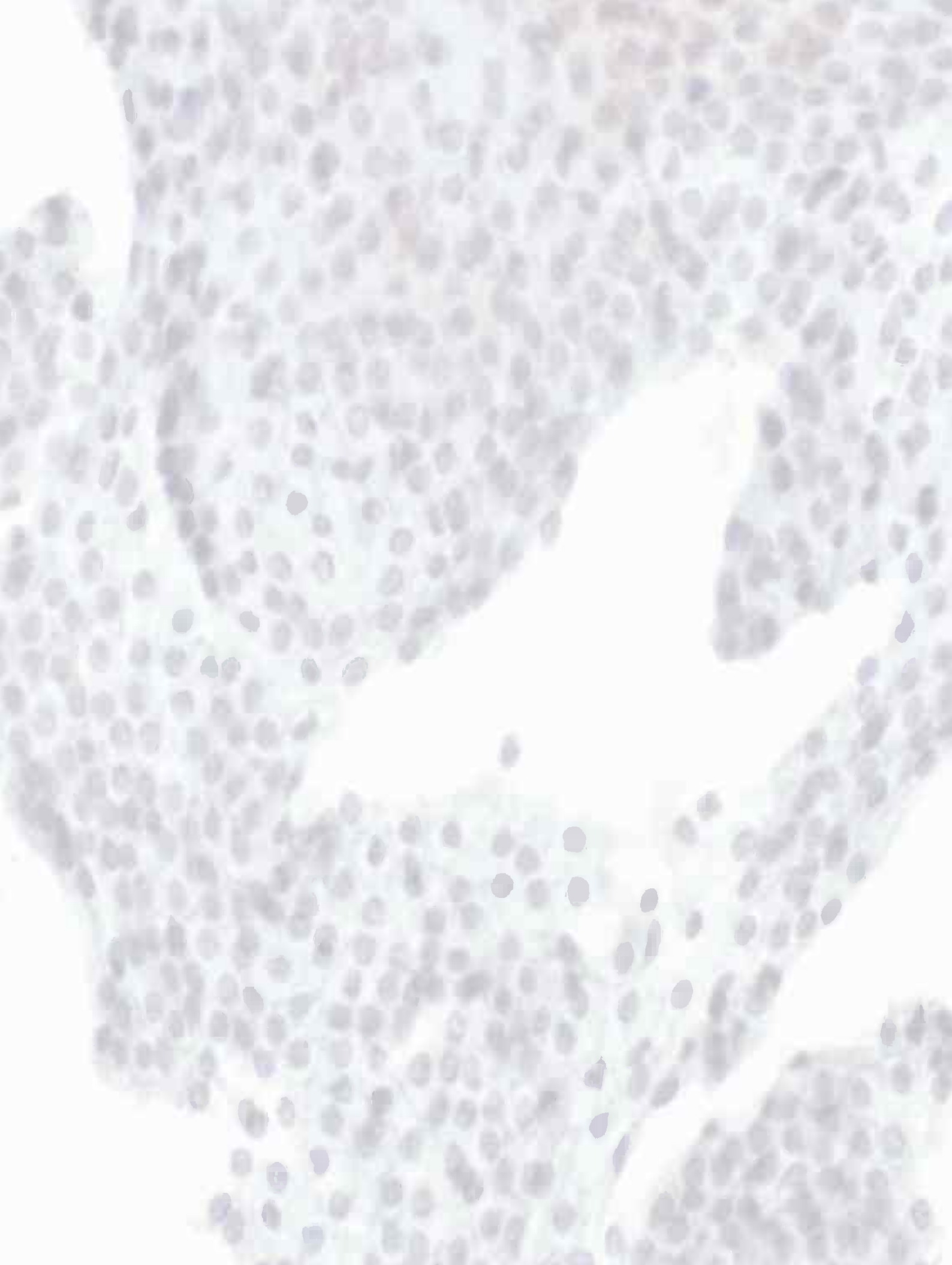

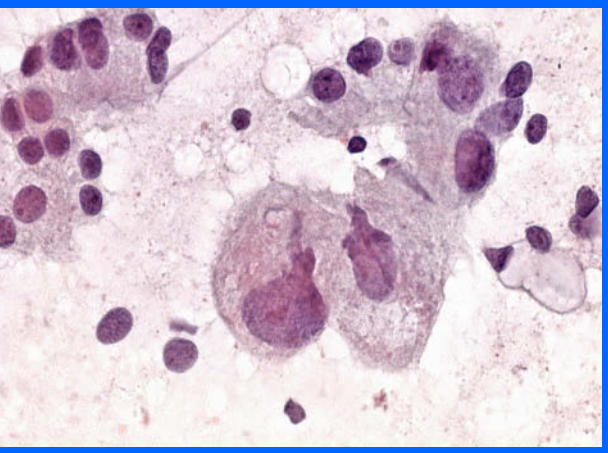

# Section 14.1
# Prostate

**Note to the reader concerning fine-needle aspiration biopsy (FNAB) of the testes**

- FNAB of enlarged testes and of sonographically presenting testicular lesions is rarely performed and requires a stringent indication. We refer to selected series in the literature.
- FNAB of the testes as the first-line procedure for evaluation of male infertility is not discussed in this book. We refer the reader to pertinent publications [24A, 30, and others], distinguished textbooks, and internet data bases.

## 14.1.1 Introduction

**General Comments**

- Nowadays, FNAB of the prostate has almost completely disappeared worldwide in routine clinical practice. Refinement of core-needle biopsy, scarcity of urologists well trained in the FNAB method, and few pathologists experienced in cytodiagnosis of the prostate are the main reasons for this situation.
- Prostate cancer is the second leading cause of cancer-related death among men.
- 75% of all prostate cancers occur in men over 65 years of age. That is why we are convinced this method should urgently be reactivated because more and more elderly males will be presenting with prostatic lesions.
- For men aged older than 75 years, FNAB should be considered the most efficient diagnostic procedure because it is economic, safe, quickly performed, sensitive, and reliable. In younger males, FNAB is a highly efficient and quickly performed diagnostic procedure to confirm lesions that are clinically judged to be benign [33].
- Transrectal FNAB of the prostate under digital or ultrasound control is an inexpensive and rapid method for diagnostic evaluation of palpable and nonpalpable prostatic lesions, yielding high sensitivity (95%), high specificity, and a low complication rate (< 1%). Reported rates of a large series published by Esposti showed false-negative diagnoses ranging from 2.7% to 13.6%, and false-positive results in five cases (2.4%) when compared to subsequent histologic examinations [15]. A breakdown of 19 papers with a total of 5007 FNABs of the prostate gland by Böcking provides a mean sensitivity of 86% and a specificity of 96% [9].
- The most commonly used instrument and technique for digitally-guided transrectal aspiration of the prostate is that developed by Sixten Franzén in the 1950s. In 1960, Franzén and colleagues reported for the first time on cytologic diagnosis of prostate carcinoma [20]. Urologists with high-level skills in rectal palpation and FNAB technique provide aspirates with high cellularity and high quality. The most common cause for a missed diagnosis of malignancy is inadequate cellularity.
- In our experience, diagnosis of prostatic lesions is one of the least challenging fields in FNAB cytology. The most common neoplastic lesion is prostatic adenocarcinoma of the acinar type (>90%), a carcinoma type that is characterized by distinct and easily reproducible cytologic features.
- Overviews of the FNAB technique of the prostate are provided in individual articles [29, 9].

- The description of pitfalls and infrequent findings in FNABs of the prostate are presented by Pérez-Guillermo and coauthors [34].
- Prostatic FNAB containing solely unaltered epithelial sheets virtually never occur. The morphology of normal prostatic epithelium is shortly described in Chapter 18, Sect. 14.1, "Synopsis and Algorithms, " p. 1224.

## 14.1.2 Epithelial Hyperplasia and Metaplasia

### 14.1.2.1 Adenomatous Hyperplasia

(Figs. 14.1–14.5)

#### Microscopic Features

- Hallmarks: Honeycomb pattern of the cell sheets comprising palisade arrangement of the outermost cells. Cell buds and acinar structures are common.
  Nuclear membranes are distinct and sharply outlined (in contrast to malignant prostatic cell nuclei where the dense packed chromatin breaks off abruptly). This major morphologic difference is best seen at a lower magnification (Fig. 14.1B).
- The N/C ratio occasionally is high, and the cytoplasm is constantly clear and foamy.
- Foamy histiocytes are frequently encountered in the background of the smears intermingled with a few inflammatory cells.

**Caution**

- Focally severe cell changes may be found in very active hyperplastic sheets and cell clusters.
- Individual nuclei and cells, which are clustered in small groups, may even reveal the typical characteristics of malignancy (Fig. 14.3). Nevertheless, these findings should not be overdiagnosed as either atypical or malignant.
- A diagnosis of prostate carcinoma is only permitted if cell sheets display distinct nucleoli and the typical chromatin texture in each nucleus; further comments are given in Sect. 14.1.7.2, p. 859 (Figs. 14.29, 14.30, 14.32B).

#### Additional Comments

- "Adenomatous hyperplasia" or "glandular hyperplasia" are the most suitable terms in the cytodiagnostic procedure because a hyperplastic fibromuscular proportion is usually not present in FNABs of the prostate (Fig. 14.4).
- Cytoplasmic lipofuscin deposits do not have any additional diagnostic value (Fig. 14.5).
- It is not possible to distinguish between acinar and ductal cell proliferation by cytology.
- Hyperplastic prostate sheets are sometimes difficult to distinguish from rectal mucosal epithelium, but a correct cell typing is not important as long as the cells can be classified as benign.

### 14.1.2.2 Squamous Metaplasia (Figs 14.6 and 14.7)

#### Etiology

Benign transformation of the glandular prostate epithelial cells into immature squamous cells mainly occurs [41]:

- In the prostatic ducts at the periphery of an infarct.
- Following surgical interventions on the prostate gland.
- Following infection.
- Following hormonal therapy with estrogens.

#### Microscopic Features

- Hallmarks:
  Small to medium-sized polygonal cells in cobblestone arrangement.
  Dense cyanophilic cytoplasm.
  Evenly distributed granular or homogeneous chromatin.
  Smooth nuclear outline.
- FNA smears usually contain only a few small sheets of metaplastic cells sporadically associated with mesenchymal cells and fibrotic tissue fragments.
- Mature squamous cells exhibiting keratinization and glycogen storage may occasionally occur (Fig. 14.7).

**Caution**

- Enlarged and activated squamous metaplastic cells may mimic seminal vesicle epithelium or may even lead to a false diagnosis of carcinoma. Yet, seminal vesicle cells exhibit gross variations in nuclear size along with intra- and extranuclear lipofuscin inclusions (see Sect. 14.1.6.2, p. 857), whereas prostatic carcinoma cells are associated with the typical morphologic characteristics of malignancy (see Sect. 14.1.7.2, p. 859).
- Prominent squamous metaplasia comprising activated nuclei should not be confused with squamous cell carcinoma.

#### Additional Comments

- Squamous metaplastic lesions of the prostate share morphologic features with squamous metaplastic sheets in bronchial exfoliative cytology and in smears from the transformation zone of the uterine cervix.
- On digital rectal palpation, areas of infarction may be suggestive of prostatic carcinoma.

## 14.1.3 Prostatitis (Figs. 14.8–14.14)

#### Etiology

The frequency of prostatitis in larger series of FNABs averages 4%. The route of infection remains uncertain in most cases.

Chronic prostatitis as a result of autoimmune response against prostate antigens is discussed, though the current knowledge of this disease remains scant [32].

### Microscopic Features

The type of inflammation is defined by the dominating cell pattern.

Prostate epithelial cells in the context of an inflammatory process may exhibit completely bland morphology or different degrees of reactive/regenerative atypia.

- *Acute and chronic prostatitis* (Figs. 14.8 and 14.9) exhibit large numbers of neutrophils or lymphocytes.
- *Xanthogranulomatous prostatitis* (Fig. 14.10) is characterized by large amounts of xanthoma cells (cholesterol-laden histiocytes).
- *Granulomatous prostatitis* (Figs. 14.11 and 14.12) is easily recognized if a dominant epithelioid cell pattern is present. Histiocytic giant cells of the Langhans type are diagnostically helpful but not indispensable. Accompanying neutrophils, lymphocytes, plasma cells, and histiocytes may give an impression of the stage of the inflammatory process.
- *Tuberculosis* (Figs. 14.13 and 14.14) also shows an epithelioid-granulomatous pattern, but epithelioid cells accompanying tuberculosis are usually degenerated and associated with caseous necrotic material in the background of the smear.
- *Malakoplakia* rarely occurs in prostate glands. The disorder is thought to be a particular reaction to a chronic infection. Accumulation of histiocytes and a mixed inflammatory cell component comprising lymphocytes, plasma cells, neutrophils, and eosinophils are characteristic. A granulomatous component is absent. A definite diagnosis depends on the detection of Michaelis-Gutmann bodies as well as intracellular and extracellular particles displaying a target-like or ring-like structure [46] (see also Sect. 12.1.5.4, p. 735).

**Caution**

- In the setting of severe inflammation, most diagnostic difficulties arise in the differentiation between reactive epithelial atypia and carcinoma (Figs. 14.15 and 14.16).
- Please note that granulomatous prostatitis is frequently accompanied by marked alteration of the epithelial cells.
- Recommended procedure:
  - If well-differentiated cancer is taken into consideration one should refrain from rendering a definite diagnosis (see Sect. 14.1.4.1, p. 856): repeated FNAB or histologic investigation are appropriate procedures in these cases.
  - Poorly differentiated prostate carcinoma should be easily recognized in most of the cases.
- Chronic prostatitis comprising huge amounts of lymphocytes is infrequently encountered. The presence of a uniform lymphoid cell pattern requires further immunocytochemical and molecular genetic investigations in order to distinguish between an inflammatory process and malignant lymphoma (see Sect. 14.1.10.2, p. 864).
- Do not confuse small stripped nuclei of benign prostate epithelium with lymphocytes: the epithelial nuclear chromatin is reticular, whereas lymphocytic chromatin is coarsely granular.
- Mycobacterial infection associated with a caseous necrotic background should not be misinterpreted as tumor necrosis. Tumor necrosis goes along with undifferentiated epithelial and stromal prostate cancer, urothelial carcinoma, high-grade lymphoma, or metastatic tumors.
- Prostatitis developing nodular or diffuse fibrosis may clinically simulate carcinoma on rectal palpation. This clinical misinformation should not misdirect our diagnostic decision-making!

### Additional Comments

- FNABs of hyperplastic prostate glands with dilated ducts may yield secretory masses containing inflammatory cells; this finding should not be overdiagnosed as an inflammatory process.
- Admixture of eosinophilic leukocytes is encountered in most types of prostatic inflammatory processes. Large amounts of eosinophils should be reported; an obvious presence of parasites should be excluded, particularly in immunosuppressed individuals.
- Granulomatous prostatitis of long duration with marked fibrosis usually yields specimens of low cellularity, and it may be impossible to render a proper diagnosis.
- Small numbers of epithelioid cells and fibroblasts, occasionally accompanied by small sclerotic tissue fragments, should not be overinterpreted as a granulomatous prostatitis. In this setting, a reparative granulomatosis after a surgical procedure or infarction should be taken into consideration.
- If tuberculosis is suspected, a search for acid-fast bacilli using Ziehl-Neelsen stain on smear preparations can contribute to a conclusive diagnosis. Nontuberculous mycobacterial infection (MOTT) rarely occurs in prostatic glands. Culture or molecular genetic analyses using PCR are essential for an exact *Mycobacterium* typing.

## 14.1.4 Atypical Prostatic Epithelium and Prostatic Intraepithelial Neoplasia

### 14.1.4.1 Atypical Prostatic Epithelium

**Definition**

Cellular changes differing from unequivocal benign cells are not always clear enough to indicate malignancy. The diagnostic challenge is illustrated by means of several pictures (Figs. 14.3, 14.15–14.18).

**Microscopic Features**

- *Mild atypia*
  - The cells are enlarged in comparison to benign prostatic epithelial cells, but the N/C ratio is within the normal range.
  - Variable nuclear size, indistinct indentations of the nuclear membranes, and usually reticular chromatin.
  - Rounded centrally located nucleoli of varying size.
- *Moderate to severe atypia*
  - The cells are greatly enlarged.
  - Decreased nuclear spacing clearly appears as compared to completely benign and slightly atypical cell clusters.
  - Irregular nuclear shape and granularity of the chromatin are striking.
  - Single and multiple nucleoli display marked polymorphism.

**Diagnostic Procedure**

- *Reactive cellular atypia* is rather likely (see also Sect. 14.1.4.2):
  - In cases where individual or grouped atypical cells (independent of grade of atypia) appear together with clearly benign cell clusters.
  - In context with a general cell pattern of inflammation with or without prostatic calculi.
  - In combination with a hyperplastic cell pattern.
- *Severe atypia favoring carcinoma* should be rendered as a tentative diagnosis if each cell in several clusters demonstrates atypical changes of varied degrees, including nuclei presenting with one or multiple distinct nucleoli. Scattered cells should display comparable cellular changes. Repeated FNAB or punch biopsies are mandatory [8].

**Caution**

- Definite adenocarcinoma diagnosis in cytologic smears depends on the amount of unequivocal and well-preserved malignant cells.
- Myoepithelial cells are an unreliable parameter distinguishing between benign and premalignant/malignant cell changes.

**Additional Analyses**

Immunocytochemistry

Evaluation of prostatic cell markers (PSA and PAP) and myoepithelial cell markers (p63, alpha-SMA, SM-myosin, S100 protein, HMW CK) has no value in assessing or ruling out malignancy in equivocal cytologic settings.

DNA ploidy (ICM DNA)

Digital cytometry could be an option in order to assess the malignant potential of highly atypical cells [8]. However, DNA measurement cannot always differentiate between benign and malignant prostatic lesions. While aneuploidy is in good agreement with precancerous and malignant lesions, euploid-diploid DNA profiles do not discriminate between a benign reactive cell population and a well-differentiated prostatic adenocarcinoma (see Sect. 14.1.7.1., p. 858).

### 14.1.4.2 Prostatic Intraepithelial Neoplasia

- Neoplastic transformation of the lining epithelium of prostatic ducts is referred to as prostatic intraepithelial neoplasia (PIN).
- Distinguishing between PIN and focal glandular atypia or atypical small acinar proliferation is hardly ever possible by cytology. Obviously, prostatic intraepithelial neoplasia is an architectural pattern; therefore, PIN and atypical acinar proliferation can only be identified histologically.
- In FNAB specimens, low-grade intraepithelial neoplasia usually mimics reactive cellular atypia; on the other hand, high-grade intraepithelial neoplasia matches severe epithelial atypia and carcinoma. Consequently high-grade PIN may lead to a false-positive diagnosis of carcinoma.
- Unequivocally benign prostatic epithelial sheets interspersed with a few malignant cell sheets may indicate a high-grade intraepithelial lesion.

**Caution**

- A cytologic prostate cancer diagnosis should solely be rendered in the presence of a representative number of malignant cell clusters, each expressing unequivocal criteria of malignancy.
- Still, high-grade PIN is reported to be commonly associated with prostate cancer [31]

## 14.1.5 Benign Soft Tissue Lesions and Rare Benign Tumors

- FNABs of benign pseudotumorous and benign neoplastic stromal lesions will exceptionally provide representative samples presenting adequate cellularity.
- Benign stromal cell tumors may provide single large atypical cells lacking all typical signs of malignancy; the cell changes may reflect degenerative phenomenons.

Atypical stromal cells exhibiting minor mitotic activity and large nucleoli may originate from a benign pseudosarcomatous tumor.

- The morphology of other rare benign prostatic lesions, such as blue nevus, paraganglioma, neurofibroma, schwannoma, and ganglioneuroma is described in the literature [47] and discussed in various chapters of this book.

**Caution**

Spindle cells showing increased mitotic activity and necrosis, together with cellular pleomorphism, strongly indicate a malignant stromal cell neoplasia.

## 14.1.6 Contaminants Originating from Adjacent Organs and Tissues

### 14.1.6.1 Rectal Mucosa (Figs. 14.19–14.21)

**Microscopic Features**

In general, single cells and epithelial tissue fragments are easy to classify as originating from the rectal mucosa. They are characterized by the following hallmarks:

- The cylindric intestinal epithelial cells are frequently palisading and usually larger than prostatic epithelial cells.
- True glands are enclosed in large epithelial fragments; the glands are lined with mucin-producing cells.
- The nuclei are clear; they often show indistinct chromatin structure and deeply cleaved prominent membranes.

**Caution**

Cell clusters originating from markedly hyperplastic rectal mucosa may exhibit pleomorphic overlapping nuclei and large nucleoli (Fig. 14.21).

Regenerative hyperplastic clusters from the intestinal epithelium may easily be mistaken for:

- Poorly differentiated prostatic carcinoma.
- Mucinous prostatic carcinoma.
- Invasive or metastatic adenocarcinoma of the rectum or of a remote primary neoplasm.

**Immunocytochemistry**

All types of prostate carcinoma should yield positive immunostaining with antibodies against PSA and/or PAP. Additional immunostainings (e.g., for CK7 and CK20) can be used for differential diagnostic purposes if a sufficient number of cytologic smears is available.

### 14.1.6.2 Seminal Vesicle Epithelium (Figs. 14.22–14.27)

**Microscopic Features**

- Hallmarks (Fig. 14.22):
  - Extreme variation in cell size.
  - The nuclei have a dark and homogeneous appearance or show a loose granular chromatin texture.
  - Nuclear cytoplasmic inclusions may appear empty or may show lipofuscin deposits.
  - The nucleoli may be prominent.
  - The cytoplasm is cyanophilic and densely structured and/or vacuolated.
  - Cytoplasmic lipofuscin inclusions are common.
- Admixture of mature sperms is a strong indicator as to the seminal vesicle origin of the aspirated material (Figs. 14.23B, 14.25, 14.26).

**Caution**

- Seminal vesicle epithelial cell clusters composed of uniform cells exhibiting distinct nucleoli and absence of lipofuscin can easily lead to a false-positive diagnosis of prostatic carcinoma (Figs. 14.24, 14.26, 14.27A).
- Seminal vesicle epithelium may contain huge and polymorphic cells (Fig. 14.27B). Such cells should not be interpreted as atypical or malignant unless single cell morphology and cytoarchitectural criteria are consistent with malignancy; nuclei of prostatic cancer cells exhibit closely packed granular chromatin in contrast to the nuclei of seminal vesicle cells.
- Seminal vesicle carcinoma is extremely rare.

**Additional Comments**

- Enlargement and strong hyperchromasia of seminal vesicle nuclei are due to euploid polyploidization of the nuclear DNA: ICM-DNA studies would provide a diploid stemline with repeated doubling of the euploid DNA content.
- By rectal palpation, enlargement of the seminal vesicles may occasionally be misinterpreted as a tumor of prostatic origin. Erroneous clinical information should not influence the cytologic decision making.

**Immunocytochemistry**

Prostatic epithelial cells normally show a positive immunostaining with antibodies against PSA and/or PAP, while cells originating from seminal vesicles yield a negative result.

### 14.1.6.3 Ganglion Cells (Fig. 14.28)

**Microscopic Features**

Hallmarks:

- Mature ganglion cells occur as huge cells with a low N/C ratio.
- The centrally positioned nucleus is even and pale, and the chromatin appears finely granular. One large round nucleolus is usually prominent.
- The large cytoplasm exhibits multiple processes that taper off into neuronal fibers. Paranuclear granulation may be distinct.

**Caution**

One should be aware of the chance that the needle hits a large pelvic ganglion; crowded ganglion cells in an aspirate from the prostate gland should not mislead to a tumor diagnosis of the large-cell type.

**Immunocytochemistry**

Prostatic epithelial cells normally show a positive immunostaining with antibodies against PSA and/or PAP, while ganglion cells express neuroendocrine markers such as chromogranin A, synaptophysin, and neuron-specific enolase (NSE).

### 14.1.6.4 Further Potential Contamination

- Squamous cells from the anal mucosa.
- Urothelial cells from the urethra and bladder. These cells can properly be classified by an immunocytochemical analysis using antibodies against CK7, CK20, and CK13.
- Smooth muscle fibers from the wall of the rectum and urinary bladder.
- Striated muscle fibers from the pelvic floor musculature.
- Intrapelvic fatty tissue.

## 14.1.7 Common Adenocarcinoma of the Prostate (Acinar Origin)

### 14.1.7.1 Introduction, Tumor Grading, Quantitative DNA Cytometry

- Prostate cancer is the second leading cause of cancer related death in men: 75% of all prostate cancers occurs in men over 65 years of age.
- Prostatic adenocarcinoma histogenetically originates from the acinar or ductal epithelium. However, an overwhelming proportion of all prostatic carcinomas arise in the acinar epithelium: they are referred to as carcinoma of the acinar type (>90%) or simply called common prostatic carcinoma.
- In general, the histogenetic distinction is not considered by cytology, unless a distinct tumor type is present in the cytologic smear such as prostatic ductal adenocarcinoma or mucinous adenocarcinoma (Fig. 14.46).
- Acinar-type carcinoma is characterized by distinct cytologic features permitting an accurate diagnosis in the majority of cases.
- Varied subtypes of prostatic carcinoma have been described by Pérez-Guillermo and coauthors [34]

**Tumor Grading**

- The tissue grading system according to the Gleason score is based on the histologic architecture and cannot be applied to cytology. However, correlation of cytological grading with the Gleason score system has been discussed in several publications [11, 25, 28, 44].
- At our institution, cytologic grading is routinely performed based on the German score system: recommendation of the Pathologisch-Urologischer Arbeitskreis – Prostatakarzinom [24] (Table 14.1.1, below).
- Malignant cells and cell sheets in cytologic smears should be graded according to the least differentiated tumor fraction.

**DNA Ploidy: Methodology and Impact on Tumor Biology**

- Cytologic prostatic cancer grading may be completed by quantitative DNA measurement using flow cytometry (FCM) or static image cytometry (ICM-DNA) [2, 6, 18, 27, 36, 37, 39]:
  - For final tumor grade at radical prostatectomy.
  - For pretreatment decisions.
  - For prediction of prognosis.
  - For posttreatment tumor follow-up, especially in patients with localized cancer .
- The nuclear DNA content of prostate cancer cells is strongly related to the tumor grade and stage [1]. Prostate carcinoma can be divided into different ploidy types and grades by means of image cytometry:
  - Peridiploid, grade 1.
  - Peritetraploid, grade 2.

**Table 14.1.1** Cytologic grading of prostate carcinomas according to *Pathologisch-Urologischer Arbeitskreis – Prostatakarzinom* [24]

| Cellular criteria | Score: low (1) to high (3) |
|---|---|
| 1. Medium nuclear size | (1) (2) (3) |
| 2. Variability in nuclear size | (1) (2) (3) |
| 3. Medium nucleolar size | (1) (2) (3) |
| 4. Nucleolar variability (size, shape, number) | (1) (2) (3) |
| 5. Cellular and nuclear dissociation | (1) (2) (3) |
| 6. Nuclear arrangement | (1) (2) (3) |

Score 6–10 corresponds to malignancy grade 1

Score 11–14 corresponds to malignancy grade 2

Score 15–18 corresponds to malignancy grade 3

– Aneuploid and X-ploid, grade 3.
– Multiploid, grade 4.

Biologically, however, prostatic carcinomas mainly fall into two classes, namely:
Low grade (peridiploid and peritetraploid tumors) , and high grade (unequivocal aneuploid/multiploid tumors) [18, 19].

- The DNA histogram has been found to be a stable and reproducible tumor characteristic. At our institution, the following algorithms have proved to be consistent for ploidy-interpretation using Feulgen-restained routine Pap smears:

**DNA-peridiploid:**
1.8c ≤ DNA index of the stemline (SL) ≤2.2c, and a few nuclei exhibiting DNA values in the 3c and 4c area
**DNA-peritetraploid:**
3.6c ≤ SL ≤ 4.4c (modal DNA peak), a varied amount of diploid nuclei, and/or a few nuclei exhibiting DNA values in the 8c area and in noneuploid areas
**DNA-aneuploid:**
1. aneuploid SL: SL < 0.9c, **or** 1.1c < SL < 1.8c, **or** 2.2c < SL < 3.6c, **or** SL > 4.4c
2. diploid **or** tetraploid SL and >15% nuclei exhibiting varying aneuploid DNA values

**DNA-multiploid:**
occurrence of multiple aneuploid SLs (Manhattan skyline)

– A stemline contains more than 20% of all cells measured.
– Single-cell and stemline interpretation follow the standards of the 2001 consensus report of the European Society for Analytical Cellular Pathology for ICM-DNA [23].

- Diagnostic DNA cytometry is able to identify cancer patients:
  – At low risk for tumor progression.
  – With a better chance of survival even without therapy (peridiploid and peritetraploid DNA distribution pattern).
  – With tumors responding poorly to either irradiation or endocrine therapy [9, 39].
- Basic information on cytogenetics and clinical relevance of quantitative DNA cytometry using FNAB specimens from the prostate are pointed out in a report by Böcking [9].
- The advantages, disadvantages, and methodological differences between flow cytometric (FCM) and static (ICM-DNA) DNA measurement have been studied by several groups [4, 16, 35].
- Methodologic sources of errors using image and flow DNA cytometry as to assessing the malignant potential of prostate carcinomas are discussed in detail in a paper by Falkmer [17].

**Caution**

Prostate carcinoma may exhibit strong tumor heterogeneity. Therefore, one has to adopt two rules applying DNA quantification to standard cytologic specimens:
1. DNA measurement should be applied to cells of the least differentiated tumor fraction.
2. ICM-DNA grading by means of nuclei from FNA smears requires a sample presenting adequate cellularity. The sample should be regarded as representative if cellular material is obtained from the whole tumor volume by extensive fan-like aspiration [22].

### 14.1.7.2 Cytomorphology of Common Prostatic Adenocarcinomas (Acinar Origin)

#### 14.1.7.2.1 Common Microscopic Features

(Figs. 14.29–14.31)
The following hallmarks concern acinar-type adenocarcinoma of any malignancy grade:

- Malignant nuclei are invariably larger as compared with benign prostatic epithelial cells in the same smear.
- Irregularities of the malignant nuclear outline are distinct; nuclear protrusions occasionally occur (Fig. 14.31).
- The typical granular densely packed chromatin pattern erases the otherwise prominent nuclear membrane of benign prostatic epithelial nuclei.
- An eccentric condensation of the chromatin in a certain number of malignant nuclei strongly indicates malignant degeneration.
- A reliably diagnostic characteristic of malignancy in prostatic cell sheets is a single distinct eosinophilic nucleolus appearing in each nucleus.

**Note**

In general, it is possible to identify all these features already at low power magnification (Figs. 14.29 and 14.32A)

#### 14.1.7.2.2 Well-Differentiated Adenocarcinoma

(Fig. 14.32 and 14.33)
**Microscopic Features**

- Well-differentiated prostatic carcinomas are characterized by uniformly enlarged cells and nuclei.
- The clear and foamy cytoplasm usually shows sharply defined borders.
- The chromatin is densely granular.
- A single large nucleolus is centrally located.
- Slightly increased N/C ratio compared to benign prostatic epithelial cells; monolayer sheets exhibit decreased nuclear spacing as compared to hyperplastic prostatic cell sheets; a few individual tumor cells occasionally occur.

**Caution**

- Malignant cell sheets strongly mimic benign hyperplastic epithelium exhibiting reactive nuclear changes. This is why a sufficient number of tumor cell sheets have to fulfill all diagnostic requirements of malignancy to make a conclusive cytologic diagnosis possible.
- Small-cell type prostate carcinoma should not give rise to a false-negative diagnosis.
- It is highly important to check atypical cells against unequivocal benign single cells and cell sheets in each cytological slide available (of the same aspirate). Neoplastic cells are always larger than benign epithelial cells.

#### 14.1.7.2.3 Moderately Differentiated Adenocarcinoma (Figs. 14.34–14.36)

The distinct atypical clustering of neoplastic cells in combination with unequivocal nuclear features of malignancy should rule out major diagnostic problems.

**Microscopic Features**

- Hallmarks: Malignant cells occur in cohesive three-dimensional clusters with sharp borders. The cells are tightly packed and cell dissociation is almost absent.
- Increased N/C ratio. The cell borders are partially ill defined.
- The tumor cells are enlarged and irregular in shape.
- The nuclei show densely packed chromatin.
- The pronounced nucleoli may occur singly or multiply.

#### 14.1.7.2.4 Poorly Differentiated Adenocarcinoma (Figs. 14.37–14.40)

**Microscopic Features**

- Poorly differentiated adenocarcinomas exhibit unequivocal malignant morphologic features.
- Hallmarks: Irregular malignant sheets and clusters. Cell dissociation and many single tumor cells.
- The tumor cells and nuclei are enlarged and polymorphous.
- Variable N/C ratio. Ill-defined pleomorphic cytoplasm.
- The chromatin is densely granular and coarse.
- Multiple pleomorphic nucleoli.
- Cellular debris may exceptionally occur.

#### 14.1.7.2.5 Additional Analyses and Additional Comments

- Immunocytochemistry (Fig. 14.41):
  p53 may have a predictive role in advanced prostate cancer and could be helpful in therapeutic decision-making [7].
  Prostatic cancer cells normally show positive immunostaining for PSA and/or PAP. Secondary cancer in the prostate gland should be reliably differentiated with ABs against cytokeratins, CA epitopes, and other tumor antigens.
- Quantitative DNA analysis: see Sect. 14.1.7.1, "DNA Ploidy: Methodology and Impact on Tumor Biology," p. 858.
- In a limited number of common prostatic adenocarcinomas, the nucleoli may appear indistinct or nearly invisible, although all other criteria of malignancy are overt (Figs. 14.33, 14.39, 14.40). Careful examination of all available smears make an accurate diagnosis possible also in cases of well-differentiated carcinomas. In equivocal cases one should render a vague diagnosis of atypia suggestive of cancer.
- Nuclear protrusions cannot be found on benign prostate nuclei, which may be helpful in assessing a diagnosis of malignancy (Fig. 14.31).
- Necrosis is an extremely rare feature of prostatic adenocarcinomas. If present, another type of malignancy (primary or metastatic) has to be taken into consideration and the use of an adequate immunopanel is mandatory (Figs. 14.51 and 14.52).
- Cytoplasmic lipofuscin deposits may occasionally be observed in carcinoma cells, independent of tumor grade.
- Myoepithelial cells have no decisive relevance distinguishing between benign and malignant prostatic lesions.
- Descriptions of rare primary carcinomas in FNABs of the prostate are provided in Sect. 14.1.9, p. 862, of this book and by Pérez-Guillermo and colleagues [34].

## 14.1.8 Common Prostatic Adenocarcinoma After Therapy, Hormonal and/or Radiation

[24, 26, 38, 41, 48]

### 14.1.8.1 General Comments

- The typical cellular changes may be observed both after radiotherapy and hormone therapy.
- The interval between the beginning of the therapy and the appearance of therapy-induced changes on tumor cells depends on the type of therapy chosen and the grade of the primary tumor. With estrogen-treated tumors, this interval may take up to 6 months, whereas the cellular effects of radiation can reliably be determined at the earliest 12–18 months after completion of treatment.
- Since patients usually tolerate transrectal FNAB well, it can be repeatedly used during long-term follow-up in order to obtain a complete therapy monitoring.

### 14.1.8.2 Cytomorphology of Regressive Changes
(Figs. 14.42–14.45)

Regressive changes subsequent to hormone therapy and irradiation are related to the cytoplasm, the nuclei, and cell clusters. Stromal degeneration may occasionally be encountered as well.

- *The cytoplasm* may exhibit a varied quality depending on the degree of cell regression:
  1. Multiple large bubble-like empty vacuoles; the nucleus is marginally positioned. Vacuoles of neighboring cells frequently coalesce, resulting in dense crowding of adjacent nuclei (Fig. 14.42).
  2. Shrinking and tightening of the cytoplasm together with apoptosis of the nucleus (Fig. 14.43).
  3. The cytoplasm withers as a result of progressive degeneration of the cell.
- *Single cells and cell clusters* develop increasing regressive changes during the degeneration process:
  1. Apoptotic changes of the nuclei together with shrinking and tightening of the cytoplasm; the nucleoli exhibiting a reduced volume (Fig. 14.43).
  2. The nuclei are hyperchromatic and tightly packed together with coarsely condensed chromatin. Simultaneous vanishing of the nucleoli can be observed. The cytoplasm can be arranged as a dense mass around clusters of nuclei (Fig. 14.44A).
  3. Coalesced homogeneous and deep-colored nuclei are clustered together. The nucleoli and cytoplasm have almost completely disappeared (Fig. 14.44B).
  4. Greatly enlarged nuclei, possibly lobulated and vacuolated. Criteria of nuclear malignancy are still clearly discernible (unlike in condensed and pyknotic nuclei as stated in the three points above) (Fig. 14.45).
- *Stromal changes* vary from myxoid degeneration to strong sclerosis; the latter may hamper FNAB.

**Caution**

- A well-performed FNAB presenting with fragments of sclerotic soft tissue and complete absence of epithelial elements may argue for an excellent response to the previous therapy, provided that the clinical results are in accordance.
- Squamous cell metaplasia should not be taken into consideration as a parameter for the therapeutic effect. Squamous cell metaplasia is a particular epithelial transformation that can be observed under different nontumoral conditions concerning benign prostatic epithelium; it can be found in carcinomas with good response to therapy as well as in nonresponders (see also Sect. 14.1.2.2, "Squamous Metaplasia," p. 854).

**Table 14.1.2** Grading of the therapeutic response, applied by the Cytology Division, Kantonsspital St. Gallen

| Therapy-induced changes on primary tumor cells and tissue | Therapeutic effect | | |
|---|---|---|---|
| | Good | Moderate | Poor |
| Cytoplasm vacuoles | +++ | ++ | + |
| Nuclear changes: apoptosis, karyorrhexis, karyolysis, giant nuclei, loss of nucleoli | ++ | + | none |
| Unaltered carcinoma cells and tumor tissue | None or few | ++ | +++ |

### 14.1.8.3 Grading of the Therapeutic Response

Some authors have proposed more than three categories to classify therapeutic effects on carcinoma cells [3, 26]. Our in-house classification of the therapeutic effects based upon qualitative and quantitative changes of tumor cells is presented in Table 14.1.2 [41].

### 14.1.8.4 Regression Grade and Prognosis

Several authors have studied the correlation between morphologic regression grade of the primary tumor and the prognosis of the patient [5, 14, 26, 48].

It is a well-known fact that primary and metastatic prostate carcinoma may exhibit strong tumor heterogeneity. Thus, varied cell clones of the same tumor may respond in a different way to a given treatment modality, which should be taken into account in patients with a discrepancy between the morphologic response to treatment and the clinical course of the tumor.

**Caution**

- Radiation-treated cancers are less suitable for FNAB than hormone-treated tumors due to rapid and strong sclerosis of the connective tissue.
- Cytologically, squamous metaplasia should not be taken into consideration when judging the therapeutic effects on prostate carcinomas.
- Different cell clones in a tumor may respond differently to a given treatment modality; therefore, cytomorphologically recorded tumor regression is not always in line with the clinical course of the tumor.

## 14.1.9 Rare Primary Carcinomas other than Conventional Prostatic Adenocarcinoma

### 14.1.9.1 Prostatic Adenocarcinoma: Mucinous and Signet Ring Cell Type (Fig. 14.46)

- These terms are reserved for tumors meeting the widely accepted criteria that have frequently been published [32A]. Adenocarcinoma exhibiting prostate-like cell features and marked intracytoplasmic mucin inclusions or lakes of extracellular mucin should give rise to differential diagnostic reflection on the rare type of mucin-producing prostate carcinoma versus metastatic carcinoma, e.g., extending from the adjacent colorectal compartment into the prostate gland.
- Immunocytochemically, colorectal carcinoma shows a negative staining for PSA/PAP and positivity for cytokeratin 20 and CDX2.
  Coexpression of CK7 can be observed in cases with primary gastric cancers.

### 14.1.9.2 Prostatic Adenocarcinoma: Ductal Type [10, 12, 13, 42, 43, 45] (Fig. 13.29)

#### General Comments

- Usually, these rare tumors initially present with polypoid masses in the prostatic urethra. Based on their clinical symptoms, they are frequently discovered in transurethral resection or – depending on the spreading pattern – in samples from urine or bladder washings. See also Sect. 13.3.1.2, p. 831.
- It is important to recognize this rare tumor type because it is an aggressive variant among prostate cancers.

#### Microscopic Features

- Hallmark is the striking papillary and tubulopapillary growth pattern.
- Tubules and papillae are lined with a single cell layer or a complex layer of tall columnar cells exhibiting elongated and often stratified nuclei and large nucleoli.
- Most ductal carcinomas show high-grade atypias and enhanced mitotic activity as compared to common prostatic adenocarcinoma [21, 34, 45].

#### Immunocytochemistry

The ductal-type prostate carcinoma shows immunoreactivity for PSA and PAP and negative staining results for CK7, CK20, and CK13.

#### Differential Diagnosis

- The ductal carcinoma type may mimic high-grade papillary transitional carcinoma, but the latter usually lacks tubular differentiation and positive immunoreactivity for prostate specific epitopes.
- By reading the overall cell pattern carefully, a minor component of conventional prostate carcinoma is detected in up to 50% of ductal-type neoplasms.

### 14.1.9.3 Urothelial Carcinoma (Figs. 14.47–14.49)

Primary transitional cell carcinoma may arise from transitional epithelium of the periurethral glands and perhaps on the background of transitional cell metaplasia of the prostatic epithelium

#### Microscopic Features

Hallmarks:

- Cytologic specimens usually contain numerous individual polymorphic tumor cells.
- The N/C ratio is increased.
- The highly irregular nuclei display indentations, coarse chromatin, and multiple polymorphous nucleoli.
- The cytoplasm is cyanophilic, dense, or vacuolated.
- Pronounced cell detritus and tumor necrosis are highly indicative of transitional cell carcinoma.

#### Differential Diagnosis and Immunocytochemistry

- Urothelial cells yield a positive immunostaining with antibodies against CK7, CK20, and CK13 (Fig. 14.49B), the latter of which is rather specific. No positive immunostaining can be achieved using antibodies for the common prostatic markers.
- Proper typing of poorly differentiated transitional cell carcinoma may be difficult as typical cell markers may have disappeared in the course of dedifferentiation, or immunopositivity is weakly expressed and encountered only in a small proportion of the tumor cell population. In this setting, the differential diagnosis should consider primary prostatic or metastatic undifferentiated large-cell carcinoma, nonpigmented malignant melanoma, large-cell lymphoma, and sarcoma. Melanoma cells exhibit typical immunomarkers such as S100 protein, Melan, and HMB-45. Malignant lymphomas are recognized by their specific immunocytochemical staining patterns (see Sect. 15.3, “Lymph Nodes: Malignant Lesions,” p. 950).

### 14.1.9.4 Extremely Rare Prostatic Carcinoma

The neoplasms are similar to those observed in other organs of the human body; the specific cytomorphology is described in the respective chapters of this book.

#### 14.1.9.4.1 Adenosquamous, Squamous, and Basaloid Neoplasia (Fig. 14.50)

It is difficult to rule out secondary spread from the bladder, urethra, or anal/cloacal area; an appropriate clinical work-up is essential.

Distinguishing between squamous cell carcinoma and squamous cell metaplasia is considered in Sect. 14.1.2.2, "Squamous Metaplasia," p. 854.

#### 14.1.9.4.2 Adenoid Cystic Carcinoma

The basic features of this neoplasia are described in Sect. 5.1.5.2, p. 415.

#### 14.1.9.4.3 Primary Small-Cell Carcinoma

- Primary small-cell carcinomas of the prostate are rare and highly aggressive tumors. According to reports in the literature, microscopic features are akin to those of small-cell carcinoma of the lung and small-cell carcinoma originating from other organs; however, primary small-cell cancer of the prostate is frequently associated with fractions of acinar-type carcinoma.
- Remember nonepithelial tumors composed of small cells including malignant lymphoma, and small round cell tumors of different histogenesis. Immunocytochemical studies are necessary for a correct diagnosis [34, 40A, 47A].

#### 14.1.9.4.4 Undifferentiated Large-Cell Carcinoma

(Figs. 14.51 and 14.52)

Cytology as well as immunocytochemical investigations may not provide successful distinction between rare primary undifferentiated prostatic cancer and other undifferentiated neoplasms.

#### 14.1.9.4.5 Sarcomatoid Carcinoma

This tumor entity may be considered an undifferentiated variant of prostatic adenocarcinoma [40].

## 14.1.10 Nonepithelial and Biphasic Malignancies of the Prostate

### 14.1.10.1 Sarcoma [47]

#### General Comments

- Sarcoma of the prostate constitutes less than 0.1% of all prostatic malignant tumors.
- Most of the soft tissue tumors clinically mimic nodular or diffuse prostatic hyperplasia. Except in children, prostatic hyperplasia or adenocarcinoma will be the initial clinical diagnosis, so the pathologist will be the first physician to establish the diagnosis of a stromal tumor by histologic or cytologic studies.
- Even if mesenchymal neoplasms are unlikely to ever be seen cytologically, cytopathologists should always be aware of running across an odd tumor entity.

#### Microscopic Features

The main morphologic characteristics of sarcomas are cellular/nuclear pleomorphism, mitotic activity, necrosis, and invasion. However, necrosis may be absent and invasion cannot be evaluated by cytology.

- *Leiomyosarcoma* (Fig. 14.53) is the most frequent sarcoma of the prostate in adults. The tumor displays large atypical and pleomorphic spindle cells, increased mitotic activity, and necrosis.
- *Rhabdomyosarcoma* is most frequently found in the prostate of children. The tumor reveals the typical signs of malignancy. The atypical cells are rounded with an epithelioid arrangement; they exceptionally show a cross-striated cytoplasm.
- *Stromal sarcoma* is characterized by a distinct immunoprofile (see the next paragraph below).

#### Immunocytochemistry

The majority of soft tissue tumors will stain like sarcomas in other organs and anatomic regions of the body. For definite typing, a complete immunohistochemical work-up should be performed on histologic-bioptic material [47].

A few typical immunopatterns are worth mentioning:

- Desmin is a relatively specific immunomarker for leiomyosarcoma and is also very sensitive for rhabdomyosarcoma.
- Myogenin positivity is proof of rhabdomyoblastic differentiation.
- Stromal sarcomas stain positive for CD34 with additional but variable expression of muscle-related markers (smooth muscle actin, HHF-35, and desmin).
- Hormone receptors (estrogen receptor and progesterone receptor) may be expressed as well.

#### Differential Diagnosis

Poorly differentiated urothelial carcinoma, undifferentiated prostate carcinoma, and metastatic undifferentiated large-cell cancers should be taken into consideration.

**Caution**

- Benign stromal tumors may also exhibit large atypical cells. In comparison to sarcomatous lesions, they show minor if any mitotic activity and usually inconspicuous nucleoli; necrosis is absent.
- The morphology of many malignant soft tissue tumors may overlap to some degree. Hence appropriate cytochemical, immunocytochemical, and molecular genetic analyses are essential in to reaching a conclusive diagnosis.
- Caseous tuberculosis exhibiting pronounced granular necrosis and poorly preserved shadowy fusiform cellular elements may give rise to diagnostic dilemmas!

### 14.1.10.2 Malignant Lymphoma and Myeloid Neoplasia [12A, 30A]

#### General Comments

- Primary lymphoma in the prostatic gland occurs less frequently than secondary lymphomatous and leukemic involvement. The entire spectrum of hematolymphoid malignancies may involve the prostate such as Hodgkin and non-Hodgkin lymphomas, lymphoid and myeloid leukemias, as well as plasmacytoma.
- Approximately 10–20% of leukemias involve the prostate, leukemic lymphocytic lymphoma (chronic lymphocytic leukemia, CLL) is the most commonly encountered tumor type.
- A tumoral manifestation of myeloid lesions is called myelogenic sarcoma, granulocytic sarcoma, or chloroma.
- More information is provided in Sect. 15.3, "Lymph Nodes: Malignant Lesions," p. 950.

#### Microscopic Features

- *Lymphocytic NHL, CLL.* Monomorphic cell pattern composed of mature-appearing small lymphocytes. Nonetheless, the nuclei are slightly enlarged (as compared to benign lymphocytes) exhibiting dense granular chromatin and distinct medium-sized to large nucleoli.
- *Follicular NHL.* Mixed lymphoid cell pattern. Distinct nuclear atypia are largely dependent on the grade of the follicular lymphoid tumor, especially in medium-sized and large lymphoid cells. The nuclei exhibit molding and cleaving, dense granular chromatin, and pronounced single and multiple nucleoli.
  Large numbers of starry sky macrophages may be present.
- *Large-cell anaplastic NHL.* Large undifferentiated blastoid cells, isolated and occasionally arranged in diffuse sheets. The latter are interspersed with small and medium-sized lymphocytes.
- *Myeloid neoplasia.* Atypical cells that are preferably medium-sized. The nuclei demonstrate cleaving and molding of their membranes. Rather indistinct wide and pale cytoplasm. Immunocytochemical investigations are essential in order to distinguish myeloid lesions from malignant lymphoid lesions.

Classifying and subtyping of primary lymphomas has to follow the established criteria. More information on this issue is provided in Sect. 15.3, "Lymph Nodes: Malignant Lesions," p. 950.

#### Differential Diagnosis

- NHLs that show a mixed lymphoid cell pattern must be distinguished from benign hyperplastic/follicular lymphoid lesions.
- Monomorphic NHLs that are composed of small tumor cells exhibiting dense clustering may mimic small-cell carcinoma.
- Large-cell blastic NHL can give rise to diagnostic dilemmas with undifferentiated large cell carcinoma.
- Distinguishing between myeloid neoplasia and clear cell carcinoma may be a challenge.

#### Additional Analyses

Immunocytochemistry

Application of an appropriate panel of antibodies is helpful to solve diagnostic problems:

- Cytokeratins and CD45 distinguish between epithelial (CK**+**) and lymphoid cells (CD45**–**).
- Neuroendocrine markers such as CD56, chromogranin A, synaptophysin, and TTF-1 demonstrate cytoplasmic positivity in small-cell carcinoma of the lung, with exceptions.
- Myeloperoxidase is helpful in establishing the diagnosis of a myeloid neoplasia.
- Enumeration of B lymphocytes (CD20) and T lymphocytes (CD3) may frequently help in distinguishing between benign lymphoproliferative lesions and neoplastic lymphoid disorders.

Molecular Genetics

If B-/T-cell enumeration is not diagnostic, polymerase chain reaction (PCR) using nuclear DNA of cells from a cytologic sample can establish clonality of the lymphoid population (see also Sect. 15.1.4.3, p. 911).

**Caution**

- CLL typically shows strong expression for CD23, whereas the reaction for Pan-B cell markers appears dimly.
- It may be difficult to distinguish myeloid neoplasia from malignant lymphoma. In cases with equivocal cytologic and clinical results, further investigations (immunocytochemistry, molecular genetics) are indispensable to avoid a misdiagnosis of malignant lymphoma.
- Starry-sky macrophages are not at all a reliable indicator of benign follicular hyperplasia. They occur as a pathognomonic admixture, particularly in follicular lymphoma and Burkitt lymphoma. In addition, they appear as reactive elements in lymphoma with high mitotic activity and a high apoptotic index.

### 14.1.10.3 Rare Miscellaneous Tumors

There have been a few cases reported in the histopathologic literature, such as germ cell tumors, paraganglioma, Wilms tumor, biphasic neoplasms, and unusual soft tissue tumors. Most of these tumors will be diagnosed by histology in combination with immunohistochemical and/or cytogenetic investigations; an initial cytologic diagnosis is exceptional. The neoplasms usually show a similar morphologic appearance in comparison to their counterparts in other organs and areas of the body.

The specific cytomorphology is described in the respective chapters of this book, in pertinent publications, and in distinguished textbooks.

#### 14.1.10.3.1 Biphasic Neoplasms

- *Phylloides tumor:* a biphasic growth pattern of epithelial and stromal components with variable degree of cellular atypia argues for phylloides tumor mimicking its counterpart in the breast.
- *Sarcomatoid carcinoma*, occasionally comprising heterologous components (areas of osseous or chondroid differentiation), is mainly encountered in patients with a previous history of prostatic adenocarcinoma treated with radiation or hormones. The spindle cell component may be considered as metaplastic change of the prostatic epithelium following the therapeutic intervention. Both epithelial and sarcomatoid components of sarcomatoid carcinoma may show focal immunoreactivity for PSA, PAP, and cytokeratins.

## 14.1.11 Metastases

- Secondary tumors to the prostate gland account for 0.5–3% of all malignant prostatic tumors: they are usually detected at autopsy. Clinical work-up and a selective panel of immunocytochemical stains are important in cases where secondary prostatic neoplasia is suspected.
- Hematogenous tumor spread to the prostate is extremely rare; infiltrates of disseminated hematolymphoid neoplasms occur a lot more commonly, as do tumors extending from adjacent organs and soft tissue into the prostate gland.

### 14.1.11.1 Selected Tumor Entities

- *Transitional cell carcinoma* from the bladder and proximal urethra.
  Cytologically, it is not possible to resolve whether an urothelial carcinoma is of prostatic origin or invasive. Regardless of the primary site of the tumor, urothelial cells yield positive immunostainings for CK7, CK20, and CK13; the latter being rather specific for urothelial cells. See also Sect. 14.1.9.3, p. 862.
- *Mucinous adenocarcinoma* from the colon and rectum.
  Clinical history and immunocytochemical staining with antibodies against prostatic epitopes (negative) and CK20 and/or CDX2 (positive) provide diagnostic clarification. See also Sect. 14.1.9.1, p. 862.
- *Squamous cell carcinoma, basaloid cell carcinoma,* and *undifferentiated small-cell carcinoma* from the anal/cloacal region.
  Cytomorphology and immunocytochemical investigations are valuable tools for proper typing but not for determining the primary site of the neoplasm; a broad clinical work-up is mandatory. The immunocytochemical reaction for CK5/6 is positive on cells of squamous and basaloid cell carcinomas.
  Metastatic small-cell carcinoma of the lung stain positive for TTF-1, CD56, chromogranin, and synaptophysin, whereas small cell carcinoma of the anal canal usually shows a negative result.

**Caution**

- The lung seems to be the most frequent primary site for tumors that hematogenously metastasize into the prostate gland [33]
- Malignant melanoma should always be taken into consideration in cases presenting with large and mainly single tumor cells,
- Metastasis of clear cell renal carcinoma may strongly mimic prostatic adenocarcinoma. Positive immunoreactivity for RCCMa is helpful to recognize a renal cell carcinoma; however, RCCMa is not very sensitive.
- Small-cell tumors need a proper immunocytochemical work-up: carcinoma versus malignant lymphoma versus tumors of mesenchymal/neural origin.

## 14.1.12 Further Reading


1. Adolfsson J. Prognostic value of desoxyribonucleic acid content in prostate cancer: a review of current results. Int J Cancer 1994;58:211-216.
2. Ahlgren G, Lindholm K, Falkmer U, Abrahamsson PA. A DNA cytometric proliferation index improves the value of the DNA ploidy pattern as a prognosticating tool in patients with carcinoma of the prostate. Urology 1997;50:379-384.
3. Alken CE, Dhom G, Straube W, et al. Therapie des Prostatakarzinoms und Verlaufskontrolle. Urologe(A) 1975;14:112.
4. Badalament RA, O'Toole RV, Young DC, Drago JR. DNA ploidy and prostate specific antigen as prognostic factors in clinically resectable prostate cancer. Cancer 1991;67:3014-3023.
5. Bandhauer K, Spieler P. The value of cytology for the follow-up of prostatic cancer after hormone and irradiation therapy. Eur Urol 1985;11:224-227.
6. Bantis A, Gonidi M, Athanassiades P, Tsolos Ch, Liossi A, et al. Prognostic value of DNA analysis of prostate adenocarcinoma: correlation to clinicopathologic predictors. J Exp Clin Cancer Res 2005;24:273-278.
7. Berner A, Harvei S, Tretlie S, et al. Prostatic carcinoma. A multivariate analysis of prognostic factors. Br J Cancer 1994;69:924-930.
8. Berner A, Skjorten FJ, Fossa SD. Follow-up of prostatic intraepithelial neoplasia. Eur Urol 1996;30:256-260.
9. Böcking A. Cytopathology of the prostate. Der Pathologe 1998;19:53-58.
10. Brinker DA, Potter SR, Epstein JI. Ductal adenocarcinoma of the prostate diagnosed on needle biopsy: correlation with clinical and radical prostatectomy findings and progression. Am J Surg Pathol 1999;23:1471-1479.
11. Chodak GW, Bibbo M, Straus FH, Wied GL. Transrectal aspiration biopsy versus transperineal core biopsy for the diagnosis of carcinoma of the prostate. J Urol 1984;132:480-482.
12. Christensen WN, Steinberg G, Walsh PC, Epstein JI. Prostatic duct adenocarcinoma. Findings at radical prostatectomy. Cancer 1991;67:2118-2124.

12A. Chu PG, Huang Q, Weiss LM. Incidental and concurrent malignant lymphomas discovered at the time of prostatectomy and prostate biopsy: a study of 29 cases. Am J Surg Pathol 2005;29: 693-699.

13. Eble JN, Sauter G, Epstein JI, Sesterhenn IA. (Eds.): World Health Organization Classification of tumors. Pathology and Genetics of tumors of the urinary system and male genital organs. IARC Press: Lyon 2004.
14. Egle N, Spieler P. Zytologische und Histologische Verlaufskontrollen beim hochvoltbestrahlten Prostatakarzinom Helv Chir Acta 1976;43:337.
15. Esposti PL. Aspiration biopsy cytology in the diagnosis and management of prostatic carcinoma. Stal & Accidenstryck, Stockholm 1974.
16. Falkmer UG. Methodological aspects on flow and image cytometric nuclear DNA assessment in prostatic adenocarcinoma. Acta Oncol 1991;30:201-203.
17. Falkmer UG. Methodologic sources of errors in image and flow cytometric DNA assessments of the malignancy potential of prostatic carcinoma. Hum Pathol 1992;23:360-367.
18. Forsslund G, Esposti PL, Nilsson B, Zetterberg A. The prognostic significance of nuclear DNA content in prostatic carcinoma. Cancer 1992;69:1432-1439.
19. Forsslund G, Nilsson B, Zetterberg A. Near tetraploid prostate carcinoma. Methodologic and prognostic aspects. Cancer 1996;78:1748-1755.
20. Franzen S,Gierth G,Zajicek J. Cytological diagnosis of prostatic tumors by transrectal aspiration biopsy: a preliminary report. Brit J Urol 1960;32:193-196
21. Gong Y, Caraway N, Stewart J, Staerkel G. Metastatic ductal adenocarcinoma of the prostate: cytologic features and clinical findings. Am J Clin Pathol 2006;126:302-309.
22. Häggarth L, Auer G, Busch C, Norberg M, et al. The significance of tumor heterogeneity for prediction of DNA ploidy of prostate cancer. Scand J Urol Nephrol 2005;39:387-392.
23. Haroske G, Baak JP, Danielsen H, et al. Fourth updated ESACP consensus report on diagnostic DNA image cytometry. Anal Cell Pathol 2001;23:89-95.
24. Helpap B, Boecking A,Dhom G et al. Klassifikation, histologisches und zytologisches Grading sowie Regressionsgrading des Prostatakarzinoms. Der Pathologe 1985;6:3-7.

24A. Jha R, Sayami G. Testicular fine needle aspiration in evaluation of male infertility. JNMA J Nepal Med Assoc 2009;48:78-84.

25. Layfield LJ, Mukamel E, Hilborne LH et al. Cytological grading of prostatic aspiration biopsy: a comparison with the Gleason grading system. J Urol 1987;138:798-800.
26. Leistenschneider W, Nagel R. Praxis der Prostatazytologie. Springer Verlag Berlin Heidelberg 1984.
27. Lieber MM. DNA content/ploidy as prognostic factors in prostate cancer. The Prostate 1992;4:119-124.
28. Maksem JA, Johenning PW. Is cytology capable of adequately grading prostate carcinoma? Urology 1988;31:437-444.
29. Maksem JA, Berner A, Bedrossian C- Fine needle aspiration biopsy of the prostate gland. Diagn Cytopathol 2007;35:778-785.
30. Mehrotra R, Chaurasia D. Fine needle aspiration cytology of the testis as the first-line diagnostic modality in azoospermia: a comparative study of cytology and histology. Cytopathology 2008;19: 363-368.

30A. Mermershtain W, Benharroch D, Lavrenkov K, et al. Primary malignant lymphoma of the prostate-a report of three cases. Leuk Lymphoma 2001;42:809-811.

31. Mostofi FK, Sesterhenn IA, Davis Jr CJ. Prostatic intraepithelial neoplasia (pin): morphological clinical significance. The Prostate Supplement 1992;4:71-77.
32. Motrich RD, Maccioni M, Riera CM, et al. Autoimmune prostatitis: state of the art.
Scand J Immunol 2007;66:217-27.

32A. Nagakura K, Hayakawa M, Mukai K, et al. Mucinous adenocarcinoma of prostate: a case report and review of the literature. J Urol 1986;135:1025-1028.

33. Pérez-Guillermo M, Acosta-Ortega J, Garcia-Solano J. The continuing role of fine-needle aspiration of the prostate gland into the 21st century. Diagn Cytopathol 2005;32:315-320.
34. Pérez-Guillermo M, Acosta-Ortega J, Garcia-Solano J. Pitfalls and infrequent findings in fine-needle aspiration of the prostate gland. Diagn Cytopathol 2005;33:126-137.
35. Pindur A, Chakraborty S, Welch DG, Wheeler TM. DNA ploidy measurements in prostate cancer: differences between image analysis and flow cytometry and clinical implications. The Prostate 1994;25:189-198.
36. PretoriusME, Waehre H, Abeler VM, et. al. Large scale genomic instability as an additive prognostic marker in early prostate cancer. Cell Oncol 2009;31:251-259.
37. Ross JS, Sheehan CE, Ambros RA, et al. Needle biopsy DNA ploidy status predicts grade shifting in prostate cancer. Am J Surg Pathol 1999;23:296-301.
38. Schmeller NT, Jocham D, Staehler G, et al. Cytologic Regression Grading of Hormone-treated Prostatic Cancer The Prostate 1986;9:1-7.
39. Schroeder F, Tribukait B, Boecking A, et al. Clinical utility of cellular DNA measurements in prostate carcinoma. Consensus conference on Diagnosis and Prognostic Parameters in Localized Prostate Cancer. Scand J Urol Nephrol Suppl 1994;162:51-63
40. Shannon RL, Ro JY, Grignon DJ, et al. Sarcomatoid carcinoma of the prostate. A clinicopathologic study of 12 patients. Cancer 1992;69:2676-2682.

40A. Simon RA, di Sant'Agnese PA, Huang LS, et. al. CD44 expression is a feature of prostatic small cell carcinoma and distinguishes it from its mimickers. Hum Pathol 2009;40:252-258.
41. Spieler P, Gloor F, Egle N, Bandhauer K. Cytological findings in transrectal aspiration biopsy on hormone- and radio-treated carcinoma of the prostate. Virchows Arch A Path Anat and Histol 1976;372:149-159.
42. Stamatiou K, Alevizos A, Mariolis A, et al. Adenocarcinomas of the prostatic duct in necropsy material. Can J Urol 2007;14:3502-3506.
43. Takazawa R, Kawakami S, Yamamoto K, et al. A case of prostatic duct adenocarcinoma: its clinical significance in comparison with typical acinar adenocarcinoma. Hinyokika Kiyo 2008;54:243-247.
44. Tannenbaum M, Bostwick DG,Maksem J, Shevchu K. The prostate gland. In: Silverberg, editor. Principles and Practice of Surgical Pathology and Cytopathology. 3rd ed, New York: Churchill-Livingston, Inc. 1997;pp 2321-2333.
45. Vandersteen DP, Wiemerslage SJ, Cohen MB. Prostatic duct adenocarcinoma: a cytologic and histologic case report with review of the literature. Diagn Cytopathol 1997;17:480-483.
46. Wagner D, Joseph J, Huang J, Xu H. Malakoplakia of the prostate on core needle biopsy: a case report review of the literature. Int J Surg Pathol 2007;15:86-89.
47. Wagner GW, Jorge LY, Anthony di Sant'Agnese et al. Soft tissue tumors of the prostate. A review. Anal Quant Cytol Histol 2007;29:341-350.
47A. Wang W, Epstein JI. Small cell carcinoma of the prostate. A morphologic and immunohistochemical study of 95 cases. Am J Surg Pathol 2008;32:65-71.
48. Zajicek J, Prostatic gland and seminal vesicles, in: Aspiration Biopsy Cytology Part 2:Cytology of Infradiaphragmatic Organs. ed, Wied GL Chicago, S.Karger Basel. 1979;pp 129-166.

**Figs. 14.1–14.5 Adenomatous hyperplasia.**
All transrectal FNABs were performed under digital control using Franzèn's device. Aspirated material was directly smeared onto several glass slides, immediately fixed with a fixative spray, and Pap-stained. Morphologic key features are demonstrated with the focus on potential diagnostic problems.

**Fig. 14.1A, B** (case #1) **A** Very low magnification shows the distinct features of prostatic hyperplasia. Note in particular the large ramified sheets frequently exhibiting sharp borders, acinar formations (small arrows), cellular palisading (large arrows), and epithelial buds (arrowheads). **B** Higher magnification is most suitable to identify honeycomb cell arrangement, the fine and loose chromatin dispersed in a pale nucleoplasm, and the distinct smooth nuclear borders.

**Fig. 14.2** (case #2) High magnification shows many of the features described in Fig. 14.1 (epithelial buds, honeycomb structure, and the typical nuclear morphology). Small nucleoli in epithelial cell nuclei occasionally occur, and dark elongated nuclei belonging to myoepithelial cells are also present.

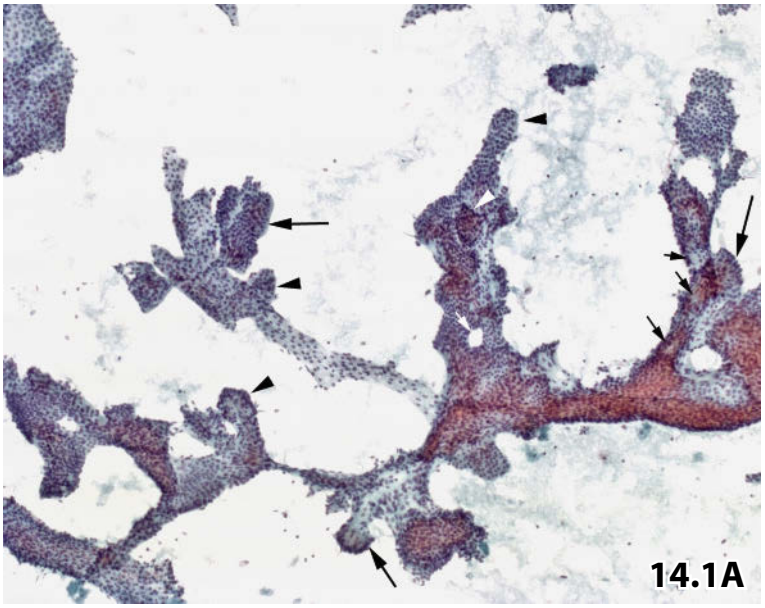

14.1A

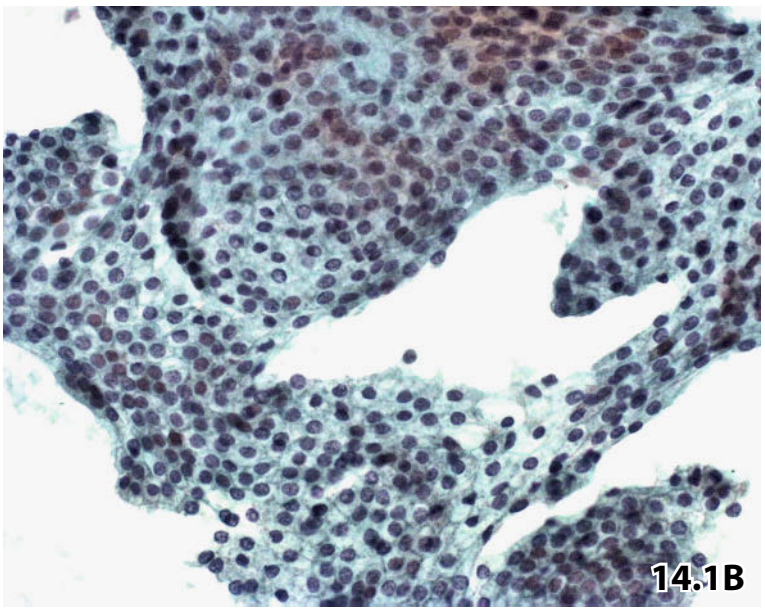

14.1B

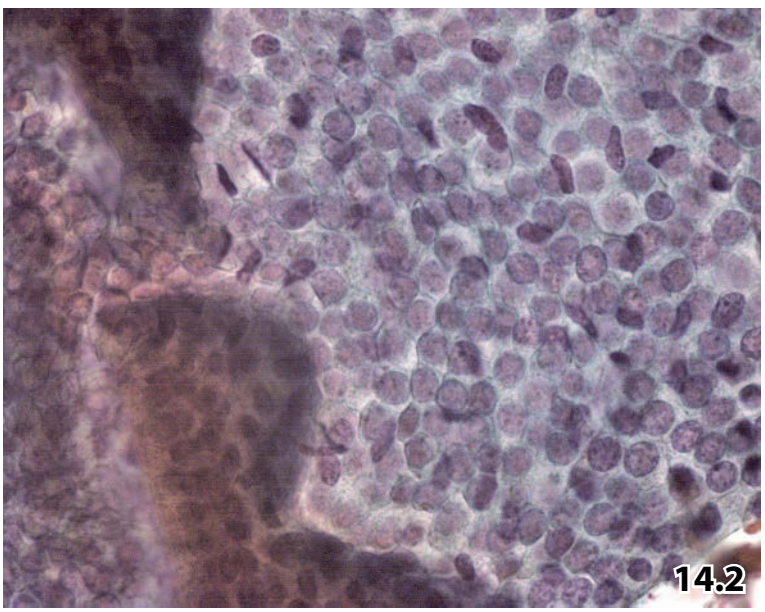

14.2

**Fig. 14.3A, B** (case #3) Regenerative cell changes can give rise to diagnostic dilemmas. **A** An epithelial area depicted at high magnification shows adenomatous hyperplasia exhibiting regenerative atypias that mimic well-differentiated prostatic adenocarcinoma (compare with Figs. 14.30 and 14.31). **B** The diagnostic dilemma can readily be solved switching to low power magnification: the area mimicking carcinoma is presented on the left (arrow), whereas the other areas of this large sheet exhibit all features of benign epithelial hyperplasia (monomorphic nuclei, absence of nucleoli, budding, among other benign features).

**Fig. 14.4** (case #4) An FNAB exceptionally providing a multitude of hyperplastic fibromuscular fragments associated with adherent epithelial cell clusters (arrows) (lower magnification).

**Fig. 14.5** (case #5) Intracytoplasmic lipofuscin deposits are demonstrated at high magnification. Staining quality of lipofuscin may range from blue-gray to golden-brown using the Papanicolaou method.

**Figs. 14.6 and 14.7 Squamous metaplasia.**
Two cases demonstrating varied degrees of maturation of metaplastic squamous cells.

**Fig. 14.6** (case #1) Immature squamous metaplasia.
High magnification shows an epithelial sheet composed of hyperplastic prostatic epithelial cells in a honeycomb arrangement (left) and immature metaplastic squamous cells growing in a cobblestone arrangement (right). Metaplastic squames exhibit sharply outlined dense and cyanophilic cytoplasm, and they are larger than prostatic epithelial cells. The nuclei of both cell types exhibit bland reticular chromatin texture but signs of activation (mild nuclear irregularity and more or less distinct nucleoli).

**Fig. 14.7** (case #2) Maturing squamous metaplasia.
Prostatic epithelium (upper left) and squamous metaplasia at different stages of maturation are demonstrated at lower magnification: immature metaplastic squamous cells (arrows), maturing squames (small arrowheads), and mature squamous cells storing glycogen and/or keratin in their cytoplasm (large arrowheads).

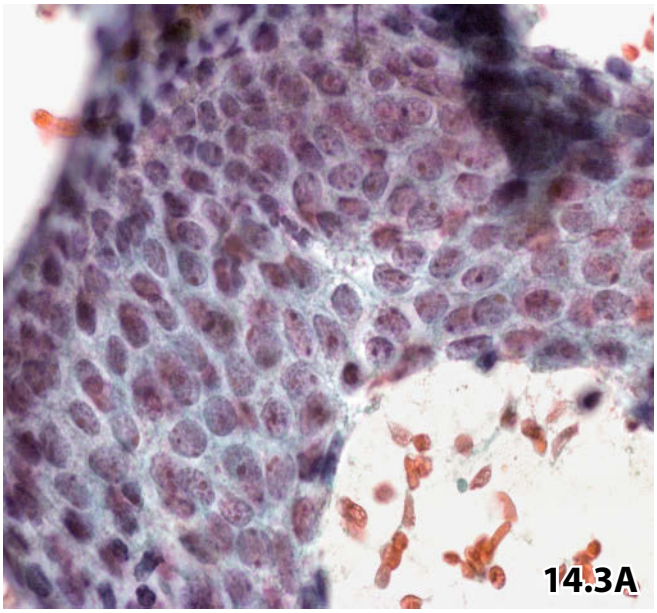
14.3A

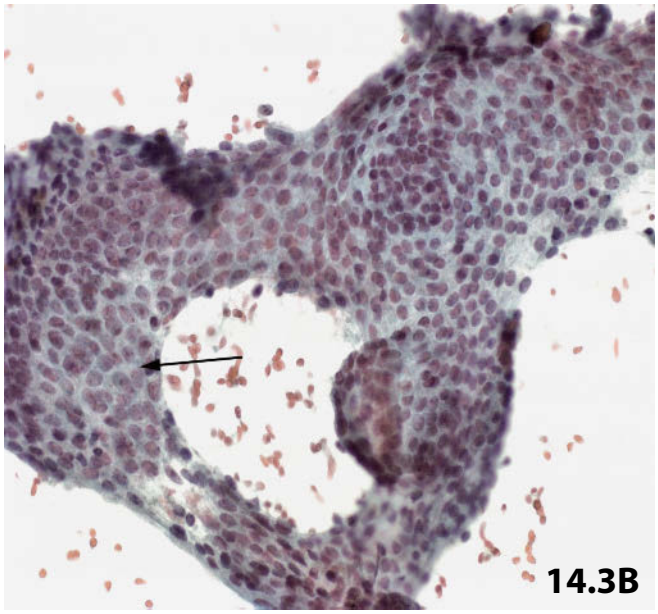
14.3B

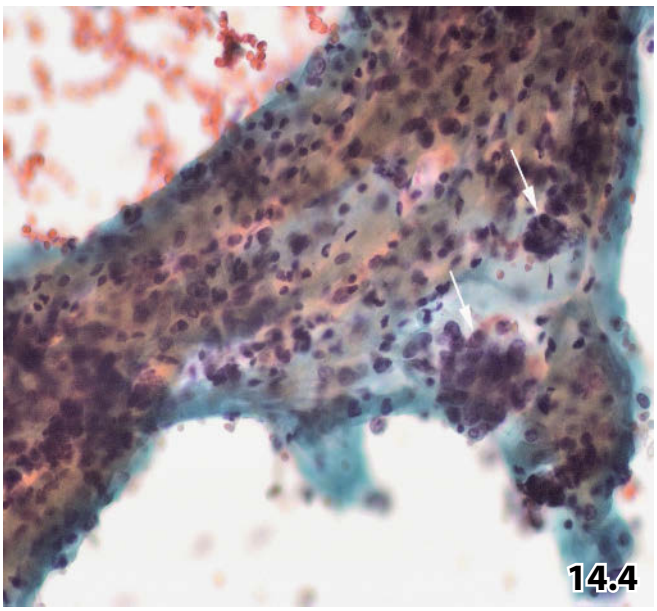
14.4

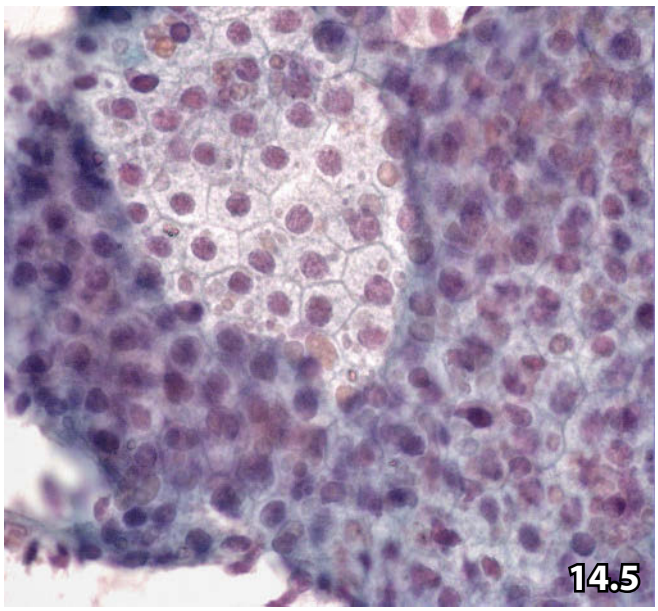
14.5

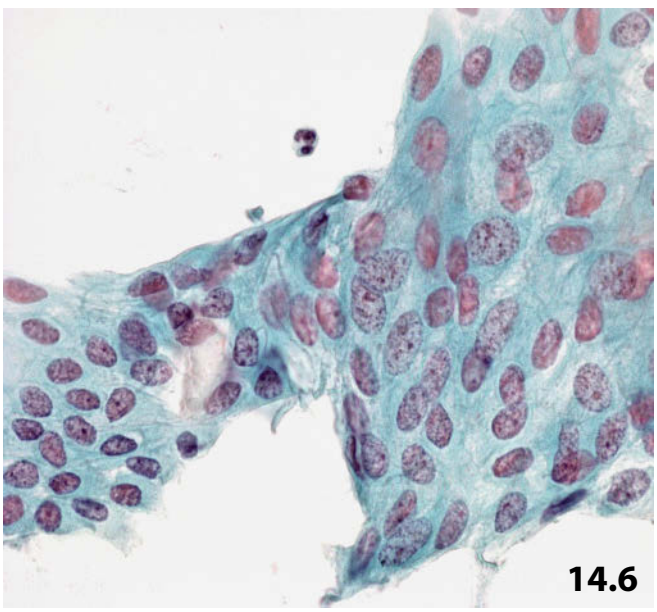
14.6

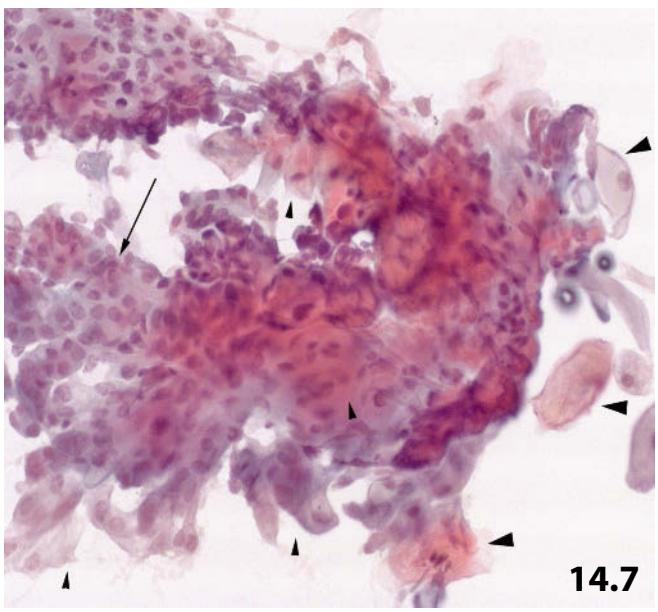
14.7

**Fig. 14.8 Acute prostatitis.**
A sheet composed of slightly polymorphic prostatic epithelial cells occurs in a background of neutrophil granulocytes. Note that the epithelial sheet itself is interspersed with neutrophils (FNAB, direct smear, Pap stain, lower magnification).

**Fig. 14.9 Chronic prostatitis.**
Higher magnification shows similar alterations of the prostatic epithelial cells as mentioned in Fig. 14.8. Contrary to Fig. 14.8, lymphocytes are infiltrating the epithelial sheets and are scattered in the background of the smear (FNAB, direct smear, Pap stain).

**Fig. 14.10 Xanthogranulomatous prostatitis.**
Lower magnification shows that cholesterol-laden histiocytes – also referred as to xanthoma cells (arrows) – may mimic reactive prostatic epithelial cells in combination with foamy cytoplasm (arrowhead). Compared to prostatic epithelial cells, xanthoma cells usually exhibit increased variability in size, coarser cytoplasmic vacuoles, increased polymorphism of the nuclei, and flimsy chromatin (FNAB, direct smear, Pap stain).

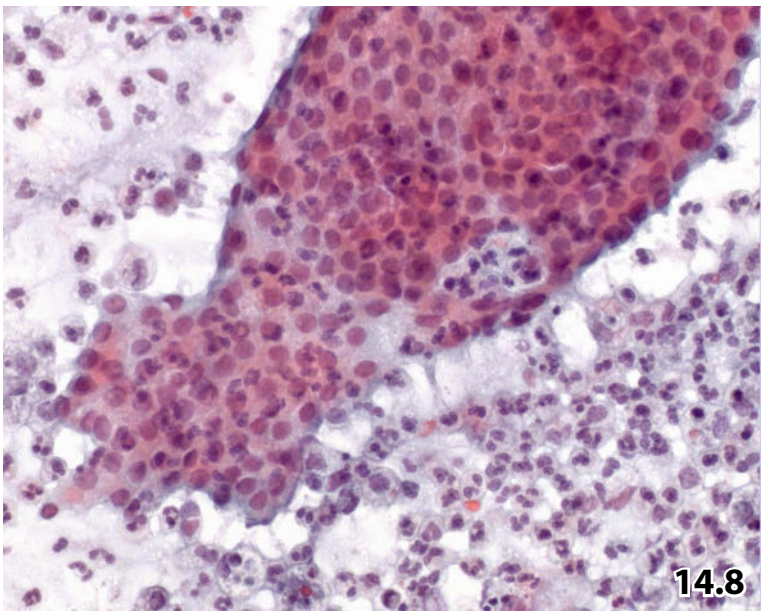
14.8

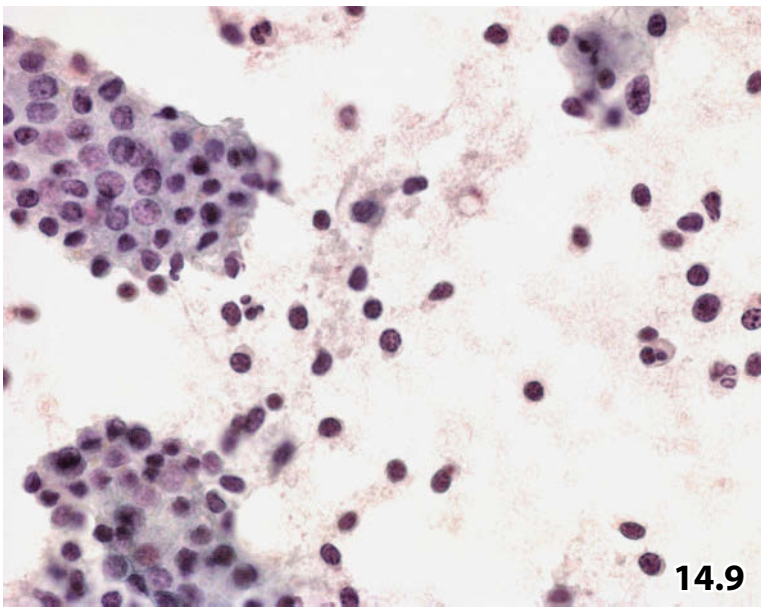
14.9

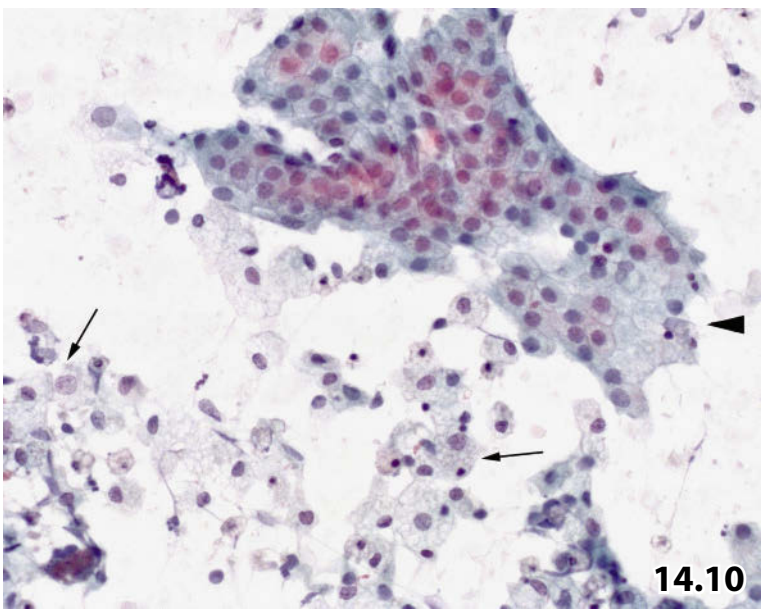
14.10

**Figs. 14.11 and 14.12 Granulomatous prostatitis.**
FNABs from two patients exhibit characteristic cytologic features of granulomatous prostatitis (direct smears, Pap stain).

**Fig. 14.11** (case #1) A sheet of epithelial prostate cells is depicted (right), mild cellular reactivity is overt (mild nuclear irregularities, sporadic small nucleoli, focally irregular nuclear spacing). A histiocytic giant cell of the Langhans type (center) is surrounded by activated epithelioid histiocytes; a few lymphocytes and granulocytes are scattered in and between the histiocytes (arrows). The background of the smear is completely clean (higher magnification).

**Fig. 14.12** (case #2) High magnification shows the characteristic mixture of nonepithelial cellular elements: epithelioid histiocytes (upper left), foamy histiocytes and macrophages (bottom left), numerous maturing and mature plasma cells (top and lower right), and neutrophils.

**Figs. 14.13 and 14.14 Prostatic tuberculosis.**
Figure 14.13 shows morphologic features that are pathognomonic for tuberculosis. Figure 14.14 emphasizes activated epithelioid histiocytes giving rise to diagnostic confusion (FNABs, direct smears, Pap stain).

**Fig. 14.13** (case #1) A 51-year-old man. No clinical information available. Polymorphous, activated, and degenerating epithelioid histiocytes are embedded in a background of granular/caseous detritus (high magnification).
*Cytologic diagnosis and metachronous histology:* Necrotic epithelioid granulomatosis, consistent with tuberculosis.

**Fig. 14.14** (case #2) A 55-year-old man with positive history of urinary tract tuberculosis presented with a firm uneven prostate gland by digital exploration. Clinical findings suggested carcinoma. A hypercellular smear mainly exhibits loose aggregates of large atypical cells (especially upper left) associated with wide ill-defined foamy cytoplasm (high magnification).
*Tentative cytologic diagnosis:* Highly suggestive of poorly differentiated prostatic adenocarcinoma.
*Discussion:* However, too little attention was paid to the few scattered unambiguous epithelioid histiocytes (arrows) and sparse granular debris (arrowheads), indicating tuberculosis. A majority of the activated epithelioid cells are rounded and grouped in loose clusters mimicking poorly differentiated carcinoma cells.
*Microbiologic and histologic studies:* Prostatic tuberculosis.

Aggregates of activated epithelioid histiocytes– comprising rounded nuclei, granular chromatin, nucleoli and foamy cytoplasm – may mislead to a false cytologic diagnosis of poorly differentiated prostatic adenocarcinoma.

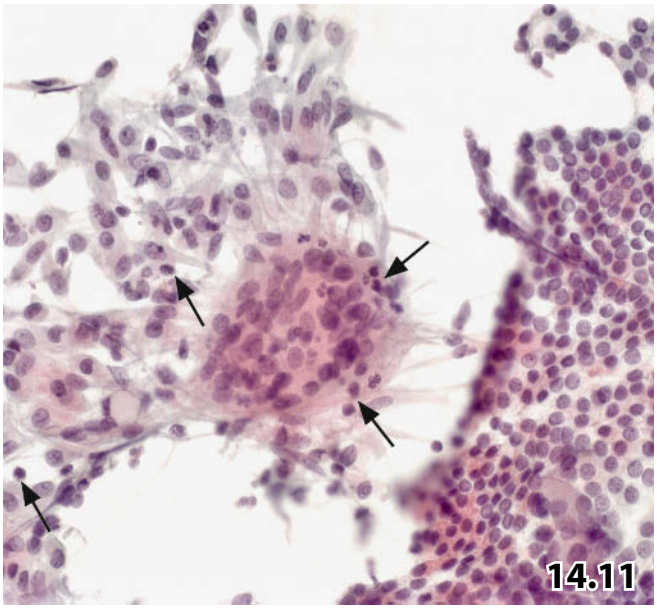
14.11

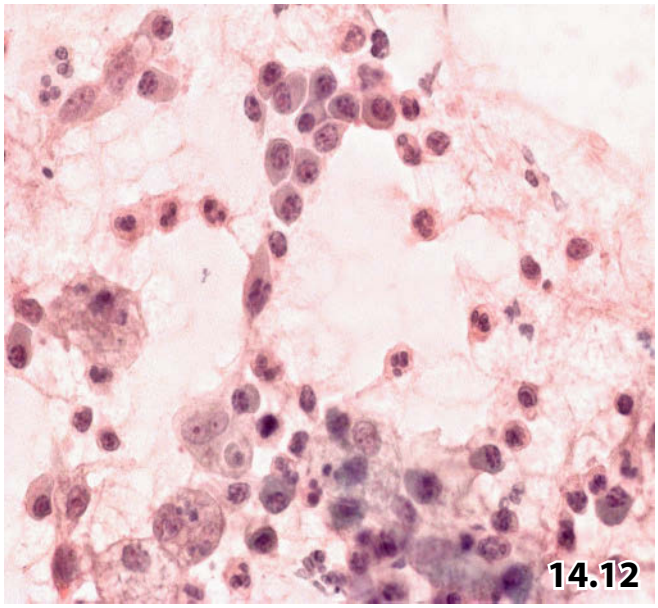
14.12

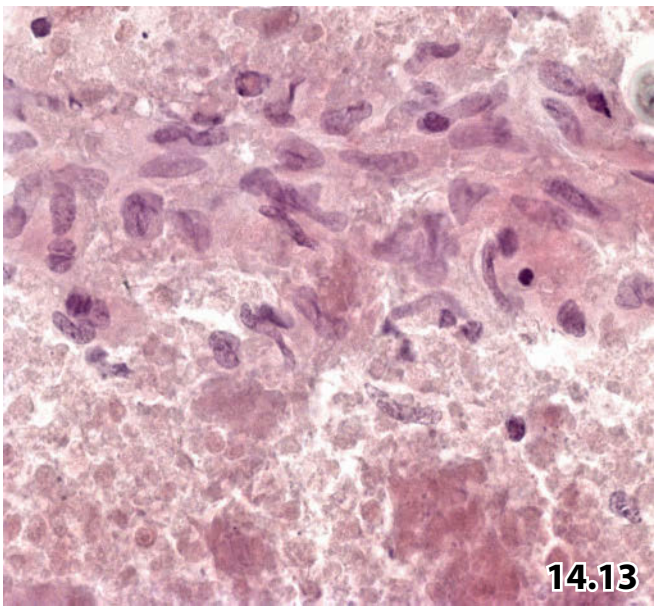
14.13

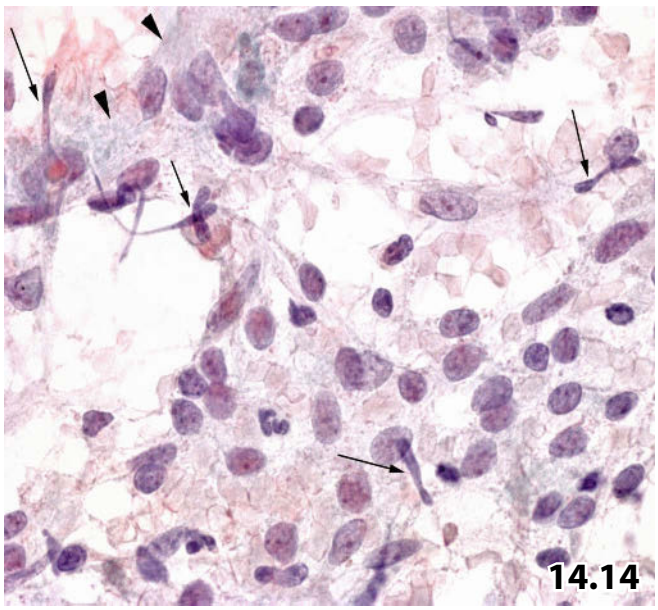
14.14

**Figs. 14.15–14.18 Atypical prostatic epithelium: a differential diagnostic challenge.** Atypias of prostatic epithelial cells are mainly encountered in combination with an inflammatory process in the prostate gland. Severe reactive cell changes may closely resemble prostatic adenocarcinoma. In terms of the potential diagnostic problems, it is highly important to consider overall cytologic appearance in all available smears. Four prostatic FNABs from different patients are presented highlighting particular diagnostic difficulties. Direct smears of the aspirated cell material were Pap-stained.

**Fig. 14.15** (case #1) Granulomatous prostatitis is frequently associated with marked epithelial atypias, as demonstrated herein (high magnification).
*Features suggesting malignancy:* The epithelial sheet is composed of monomorphic atypical cells exhibiting regular nuclear spacing, distinct nucleoli in each nucleus, and dense granular chromatin; morphologic features that may suggest well-differentiated prostatic adenocarcinoma.
*Features arguing for reactive cell changes:* Clinging mesenchymal fragments containing epithelioid nuclei (bottom) would be extremely unusual in the context of carcinoma, and inflammatory cells in the background of the specimen require caution as to diagnostic decision-making.
*Final diagnosis:* Granulomatous prostatitis.

**Fig. 14.16** (case #2) Strongly atypical epithelial cell clusters of a prostatic gland that is affected by an acute inflammatory process (high magnification).
*Features suggesting malignancy:* The compact sheet exhibits closely arranged epithelial cells including nuclear overlapping. The cells show pronounced eccentrically located nucleoli and dense granular chromatin. Cytology may suggest moderately differentiated prostatic adenocarcinoma.
*Features arguing for reactive cell changes:* Unevenly distributed and clumped chromatin is rarely encountered in the nuclei of prostatic carcinoma cells. Neutrophils, both in the background and infiltrating the cell sheets (arrows), additionally favor regenerative disorder.
*Final diagnosis:* Acute prostatitis associated with a severe regenerative epithelial process.



**Fig. 14.17** (case #3) Another case displays epithelial atypia associated with acute prostatitis. In spite of the concomitant acute inflammation, cell alterations strongly favor carcinoma. High magnification shows a cluster composed of epithelial cells exhibiting severe atypias: irregular cell arrangement, nuclear overlap, varied size of nuclei and nucleoli, distinct nuclear irregularities, and dense granular chromatin. Dispersed atypical cells with and without cytoplasm are also present (arrows).
*Tentative cytologic diagnosis:* Acute prostatitis and strong suspicion of prostate carcinoma.
*Histologic diagnosis:* Poorly differentiated prostatic adenocarcinoma and acute prostatitis.

**Fig. 14.18** (case #4) Epithelial atypia associated with prostatic lithiasis. Lower magnification exhibits calcific deposits, debris, and inflammatory cells (left). A three-dimensional epithelial cluster (right) shows irregular cell arrangement and nuclear irregularities, but bland chromatin and indistinct nucleoli suggest reactive cell changes.
*Final diagnosis* (histology was not performed): Prostatic lithiasis and prostatitis.

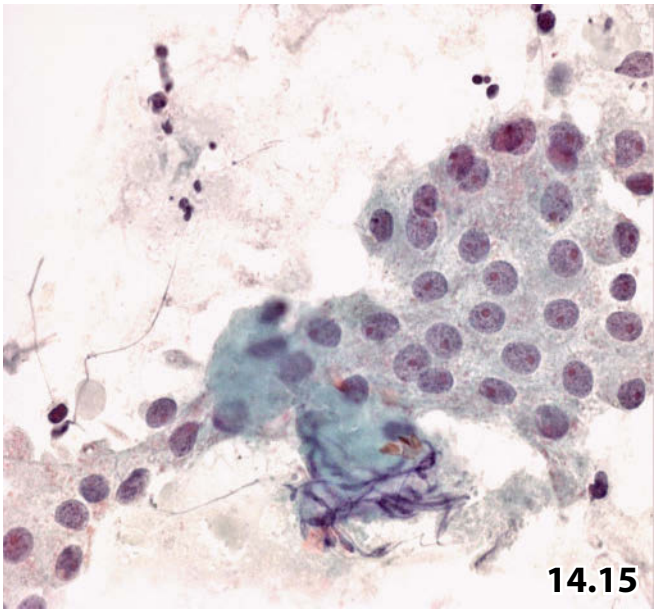
14.15

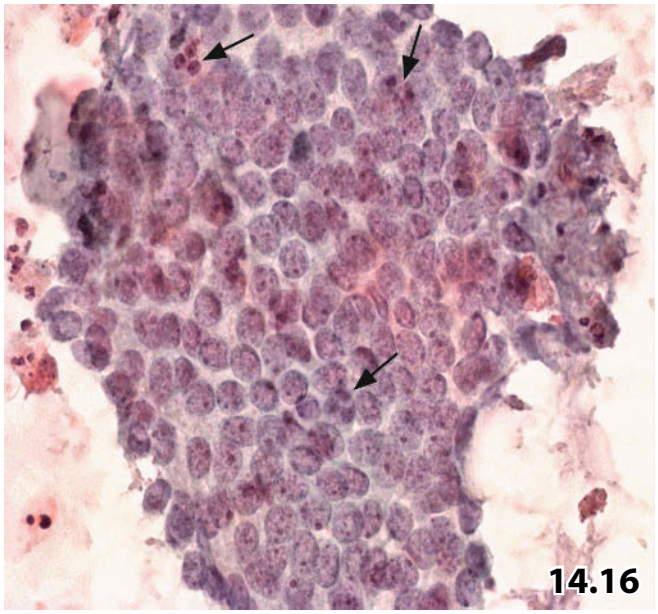
14.16

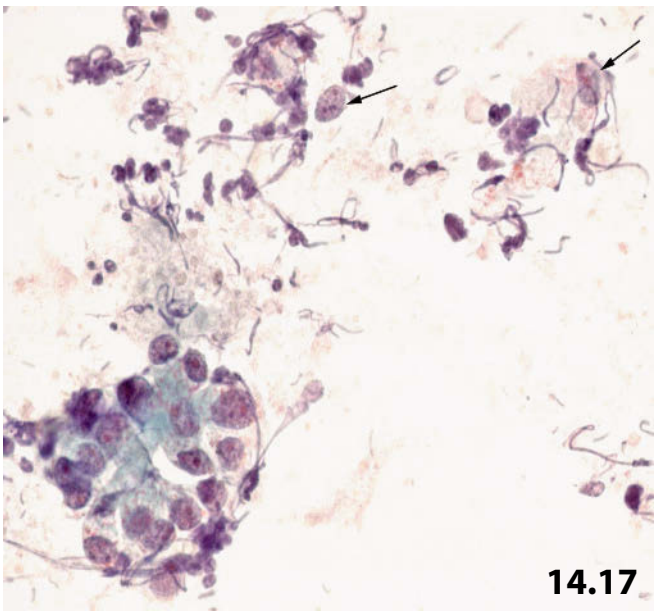
14.17

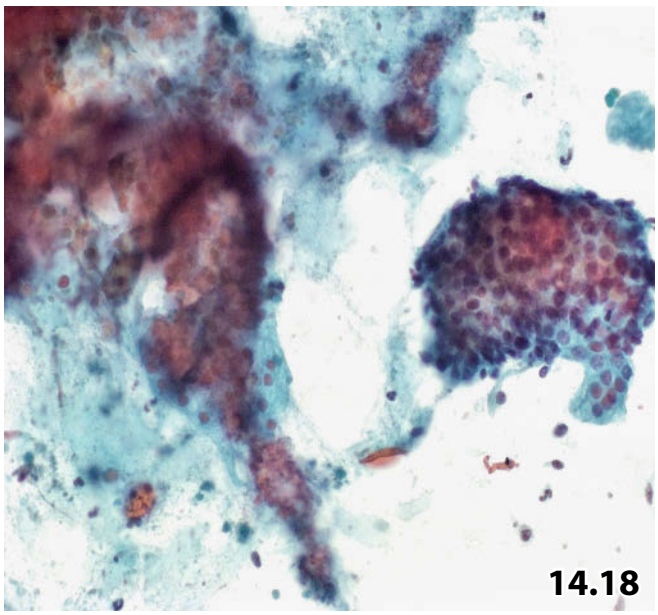
14.18

**Figs. 14.19–14.21 Rectal mucosa.**
Fragments of rectal mucosa frequently occur as contaminants in transrectal FNAB of the prostate. Cytomorphology of rectal mucosa is illustrated and diagnostic dilemmas are discussed. All direct smears were Pap-stained.

**Fig. 14.19A** (case #1) Two epithelial fragments originating from rectal mucosa are depicted at higher magnification. The classic cytologic features indicative of colonic epithelium comprise regular cell arrangement, cells exhibiting cuboidal to columnar shape, cellular arrangement in palisades and true glands, intracytoplasmic mucus and free mucus, pale nucleoplasm and indistinct chromatin, nuclear irregularities comprising pronounced nuclear molding and cleaving. **B** (case #2) Distinguishing between rectal mucosa and prostatic adenomatous hyperplasia may be a diagnostic challenge. High magnification presents a cell sheet that is difficult to assign to a specific type of epithelium. Solely distinct columnar shape of a few cells (arrows) and mucoid mass in the background (arrowheads) favor intestinal origin of the epithelial cells.

**Fig. 14.20** (case #3) Rectal mucosa versus prostatic epithelium.
The picture contrasts a fragment of rectal mucosa (right) with a fragment of prostatic epithelium (left) at lower magnification. Note the significant nuclear and cytoplasmic differences between the two cell types.

**Fig. 14.21** (case #4) Regenerative rectal mucosa versus carcinoma (high magnification).
A sheet of rectal mucosa exhibits irregular cell arrangement, mild nuclear irregularities, dense granular chromatin, and small nucleoli, features that may give rise to a misdiagnosis of well-differentiated colonic adenocarcinoma. Note that unambiguous nuclear criteria of malignancy are absent.

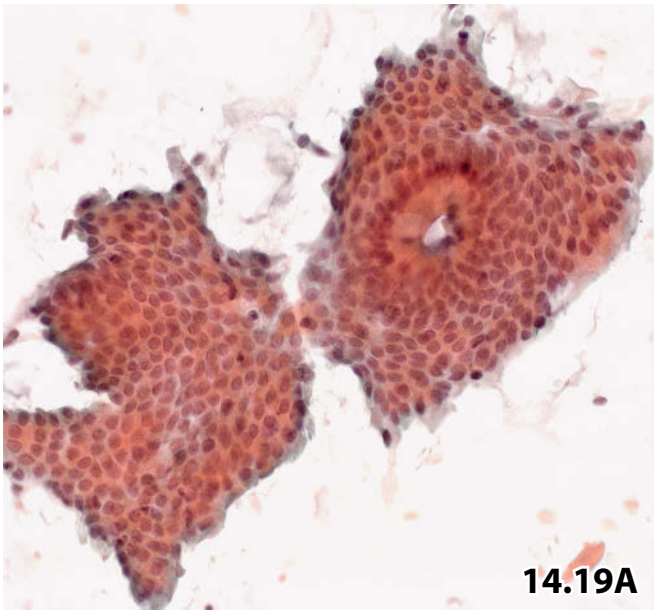

14.19A

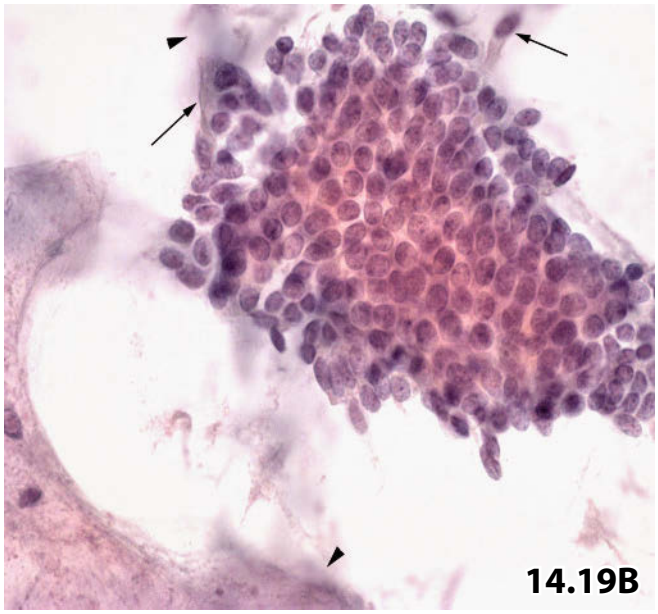

14.19B

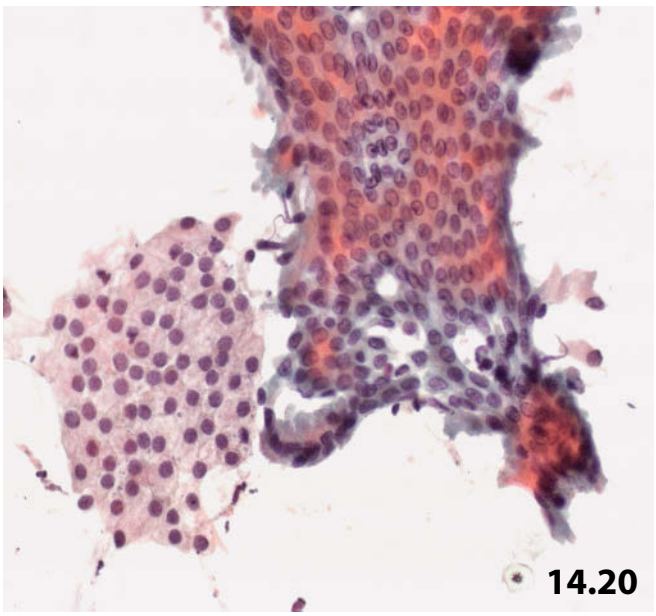

14.20

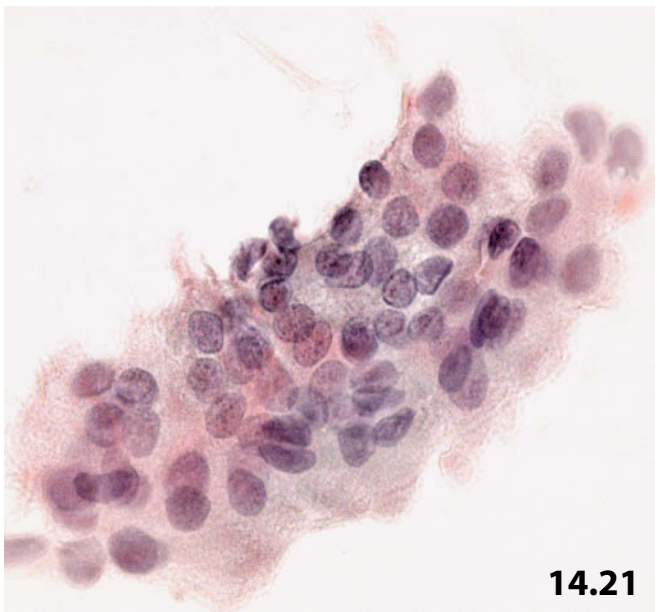

14.21

**Figs. 14.22–14.27 Seminal vesicle epithelium.**
Cells from the seminal vesicles are frequently sampled in the course of transrectal FNAB of the prostate. Varied cytologic phenotypes of single cells and epithelial fragments originating from seminal vesicle are illustrated and possible diagnostic confusions are disclosed. Direct smears were Pap-stained.

**Fig. 14.22A, B** (case #1) Classic features of seminal vesicle cells are demonstrated. **A** Flat sheets are composed of epithelial cells showing extreme variation in cell size and dark staining nuclei (low magnification). **B** A picture detail presenting the morphologic clues of seminal vesicle cells comprising lipofuscin pigment.

**Fig. 14.23A, B** (case #2) Cell clusters of seminal vesicle can mimic prostatic hyperplasia and well-differentiated prostate carcinoma. **A** At low magnification, large epithelial clusters from a seminal vesicle may show similarity to prostatic adenomatous hyperplasia and well-differentiated prostatic carcinoma. **B** Microscopic examination using high magnification solves the diagnostic problems. Benign cells of the seminal vesicle exhibit strong variability in size, dark staining nuclei, and absence of nucleoli. Lipofuscin pigment is rather sparse and of minor diagnostic value in this setting. Single mature sperms (arrow) are encountered in the current field.

**Fig. 14.24** (case #3) The problem of nonpigmented seminal vesicle epithelium.
A cluster originating from seminal vesicle epithelium is composed of comparatively monomorphic nonpigmented cells (higher magnification). In this setting, proper histogenetic classification is only possible by comparing the target cell cluster with prostatic and intestinal-mucosal cell sheets of the same smear (or by using adequate immunostainings).

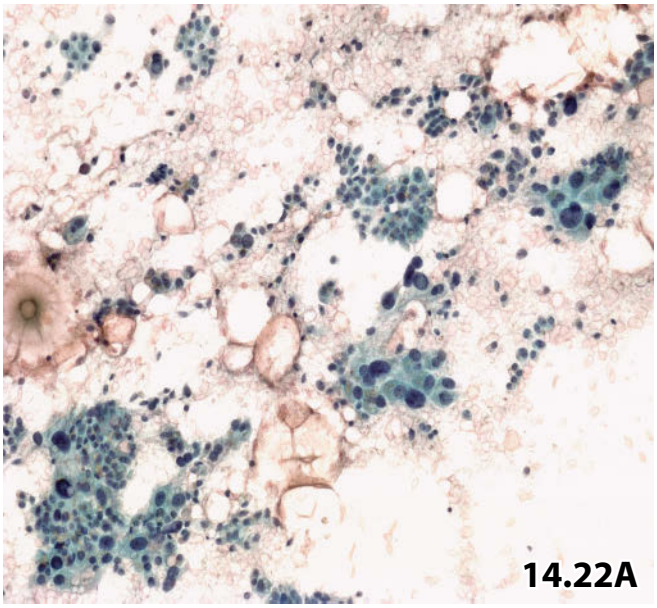
14.22A

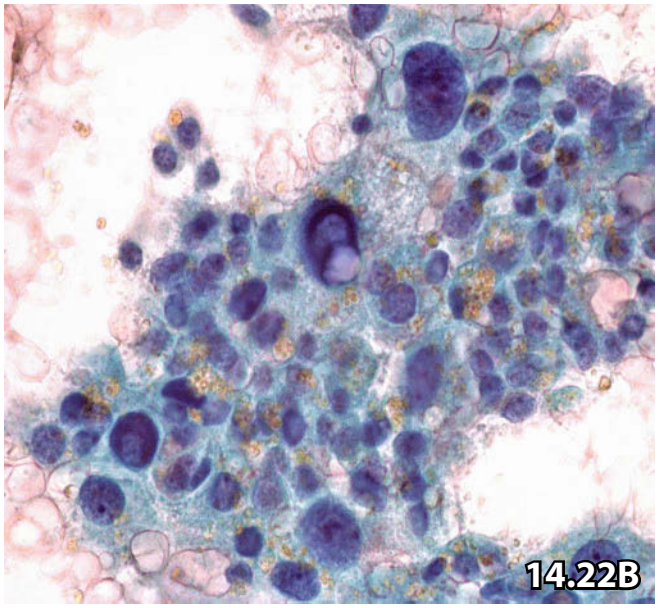
14.22B

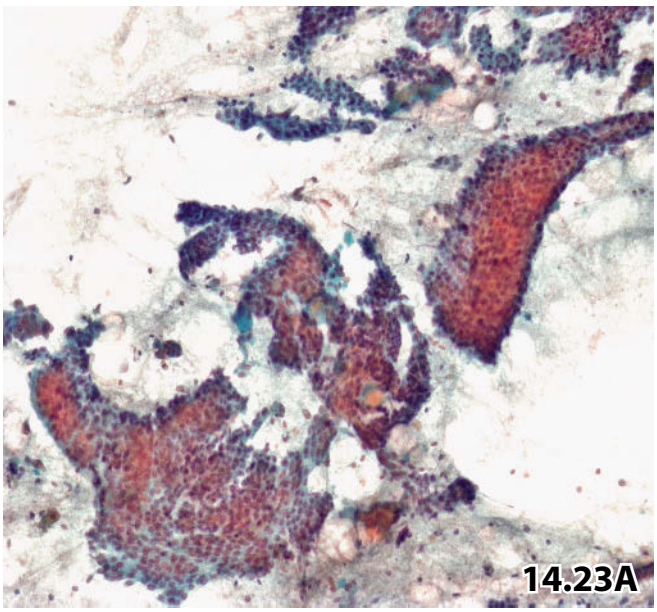
14.23A

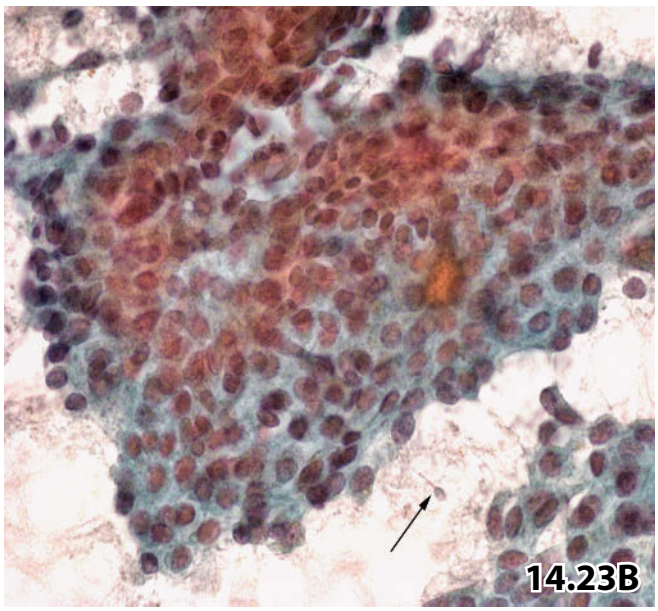
14.23B

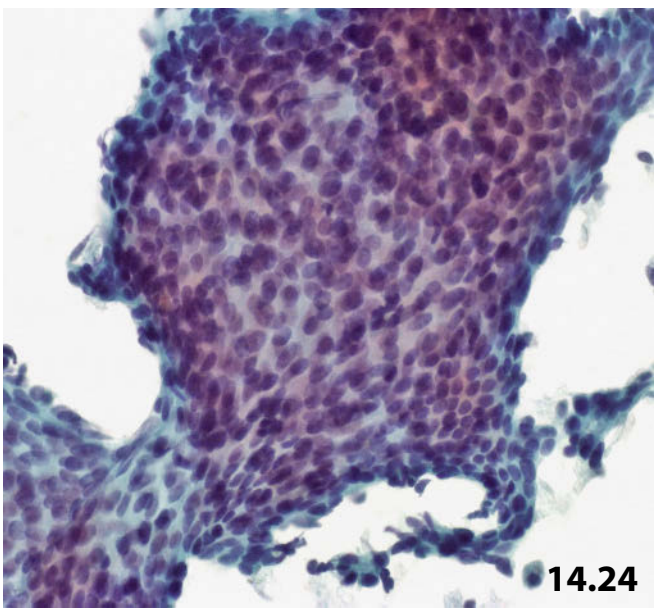
14.24

**Fig. 14.25** (case #4) Mature sperms can serve as a powerful diagnostic marker for seminal vesicle cells. High magnification shows a regular flat sheet originating from seminal vesicle epithelium but mimicking adenomatous prostatic hyperplasia. Surrounding mature sperms and spermiophages are helpful in classifying the cell sheet.

**Fig. 14.26** (case #5) Seminal vesicle epithelium showing extremely distinct nucleoli (arrows) and absence of lipofuscin pigment should not mislead to a false-positive diagnosis of poorly differentiated prostatic adenocarcinoma. Nuclear polymorphism, varying cell size, deep-staining nuclei, and mature sperms are key features for an accurate classification. Nucleoli as presented here may represent activated/regenerative seminal vesicle epithelium (high magnification).

**Fig. 14.27A, B** (case #6) Another case emphasizing diagnostic problems between seminal vesicle epithelium and carcinomatous lesion. Comparison of the different cell types and the background features in the same smear is extremely helpful in reaching an accurate diagnosis by cytology. **A** The depicted cell sheet, originating from regenerative seminal vesicle epithelium, is extremely difficult to distinguish from well-differentiated prostatic adenocarcinoma (high magnification). **B** Another field of the same smear indicates a seminal vesicle aspirate comprising a characteristic cell pattern and specimen background (mature sperms embedded in proteinaceous fluid, though barely reognizable) (low magnification). The dispersed huge polymorphous and dark staining stripped nuclei of seminal vesicle origin should not be misinterpreted as undifferentiated malignant neoplastic cells (arrows).

**Fig. 14.28 Ganglion cells.**
High magnification shows a typical ganglion cell (transrectal FNAB of prostate, direct smear, Pap stain). Note the characteristic chromatin, eccentric nucleus, huge nucleolus, and the delicate cytoplasmic processes that are not completely in focus (arrows).

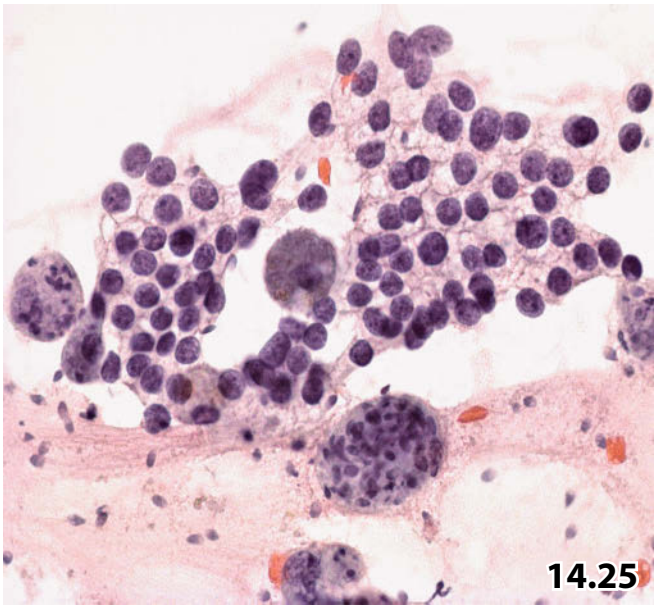
14.25

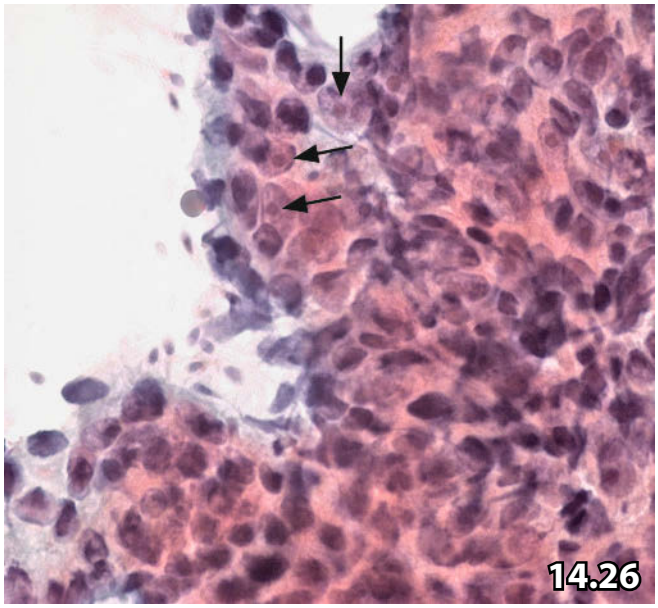
14.26

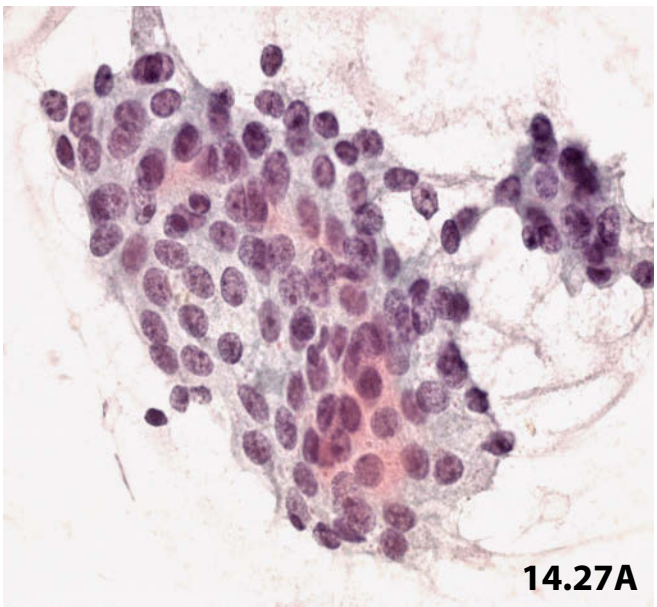
14.27A

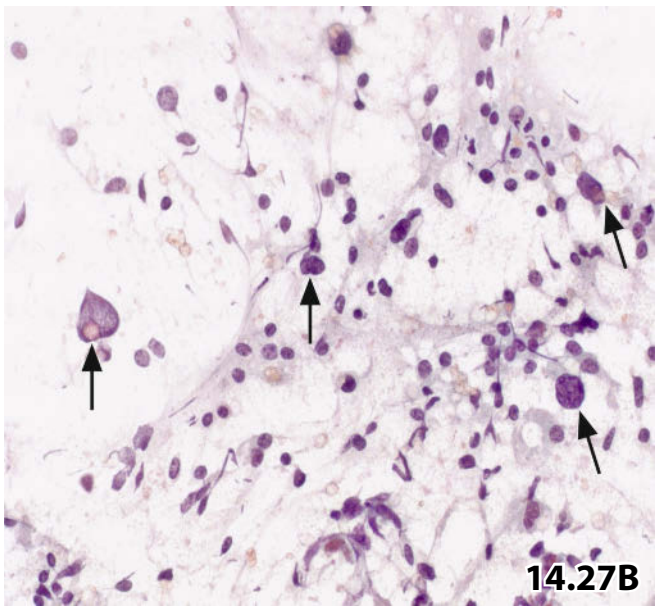
14.27B

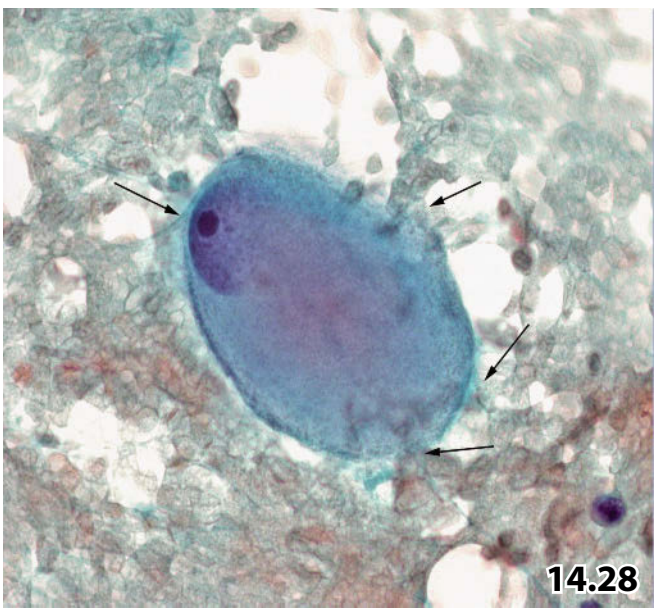
14.28

**Figs. 14.29–14.31 Cytologic key features of common prostatic adenocarcinomas irrespective of malignancy grade.**
Transrectal FNAB from three patients. Direct smears were Pap-stained.

**Fig. 14.29** (case #1) Distinctive structural and cytomorphologic features of benign (arrow) and malignant prostatic cell sheets are presented at lower magnification. Note in particular that benign and malignant cells are associated with abundant vacuolated cytoplasm, but malignant cells and their nuclei have increased size, and the nuclei of the malignant cells harbor distinct nucleoli (arrowheads).

**Fig. 14.30** (case #2) We emphasize the nuclear details of malignant prostatic epithelial cells. Note in particular the nuclear monomorphism, faint nuclear membrane, dense granular chromatin, a conspicuous nucleolus in each nucleus.

**Fig. 14.31** (case #3) We present a case giving rise to diagnostic confusion between well-differentiated prostate carcinoma and prostatic adenomatous hyperplasia. The malignant cell sheet exhibits regular cell arrangement, and absence of distinct nucleoli; but numerous nuclear protrusions and buds (arrows) are a strong argument in favor of malignancy, together with the dense granular chromatin erasing the nuclear membranes (high magnification).

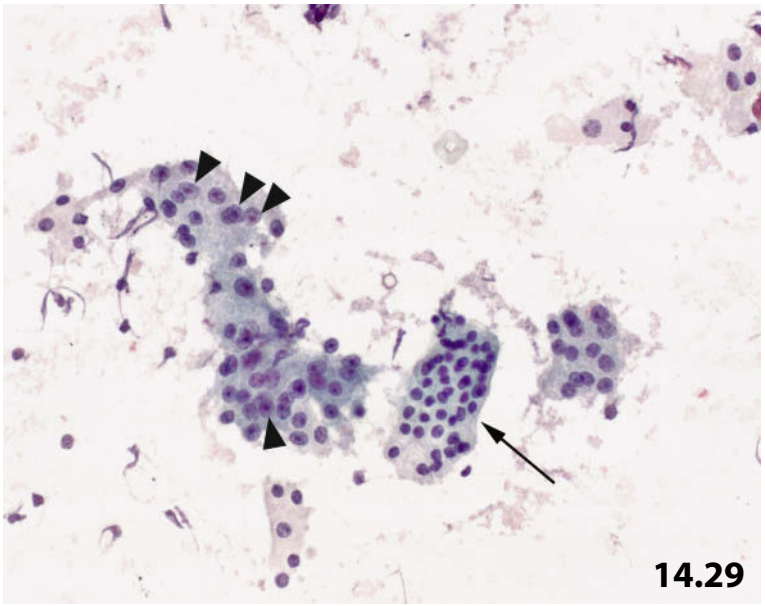

14.29

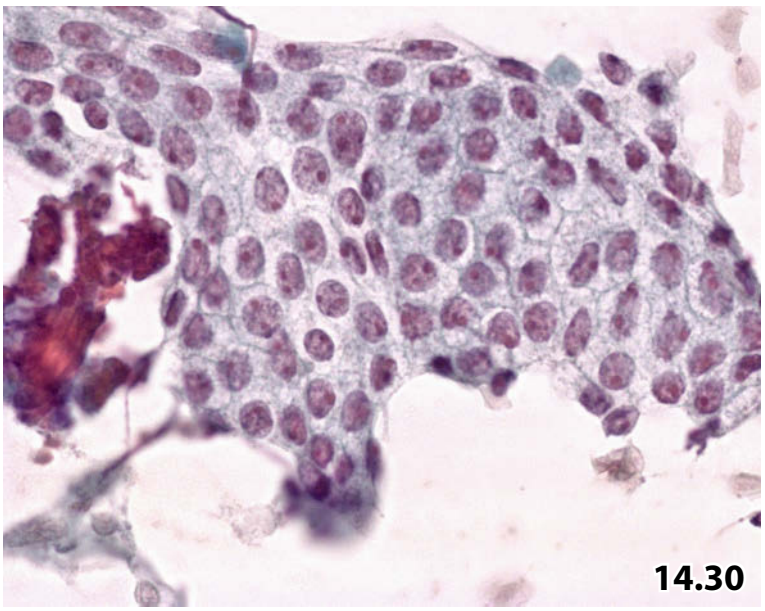

14.30

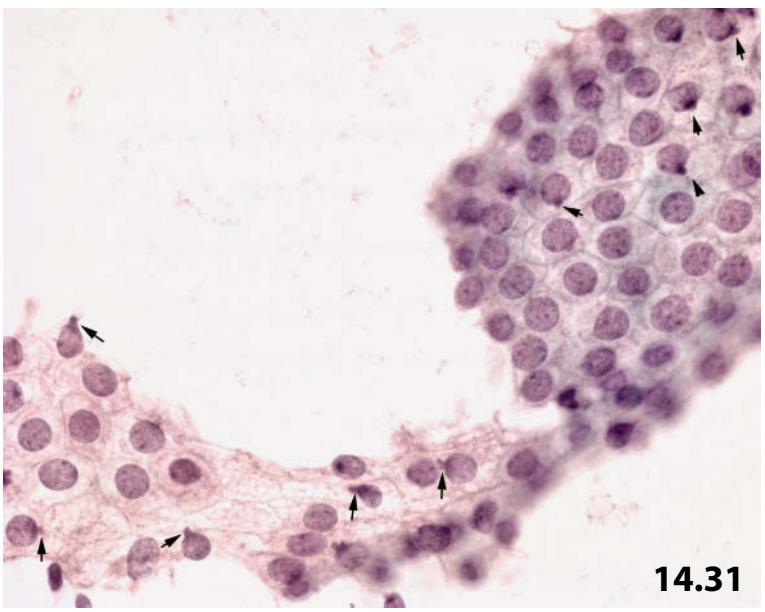

14.31

**Figs. 14.32 and 14.33 Well-differentiated adenocarcinoma of the prostate.**
Transrectal FNAB from two patients. Direct smears were Pap-stained.

**Fig. 14.32A, B** (case #1) Morphologic key features of well-differentiated prostate carcinoma are demonstrated in comparison to benign prostatic epithelium.
*Cytologic diagnosis:* Well-differentiated adenocarcinoma of the prostate, grade 1, score 10.
*Tissue diagnosis:* Prostatic adenocarcinoma, grade 1 (15×15×5 mm in size).
**A** A large branching sheet of a well-differentiated adenocarcinoma is shown at low magnification. Note the slender benign cell sheet (arrows) partly superimposed on the carcinomatous epithelial fragment. Check for the main discriminatory diagnostic features in this setting: nuclear spacing, nuclear size, and nuclear shade of color! **B** Same case: morphologic details of the benign (top) and the malignant cell sheet are highlighted at high magnification. Please note the difference in nucleolar appearance.

**Fig. 14.33** (case #2) A second case emphasizes the potential diagnostic difficulties between well-differentiated carcinoma and benign adenomatous hyperplasia. High magnification shows a well-differentiated, extremely uniform prostatic adenocarcinoma. Nuclear size, mainly small and indistinct nucleoli, and regular nuclear spacing may suggest benign adenomatous hyperplasia.
*Cytologic diagnosis:* Well-differentiated prostatic adenocarcinoma, grade 1, score 7.
*Discussion:* Finely dispersed dense chromatin erasing the nuclear membrane and a certain dyschromasia (note the grey-pinkish shade) indicate malignancy. Considering the overall cell pattern allows a definite cytologic diagnosis of well-differentiated prostatic carcinoma.
*Tissue diagnosis* (transurethral resection of the prostate): Prostatic adenocarcinoma, grade 1.

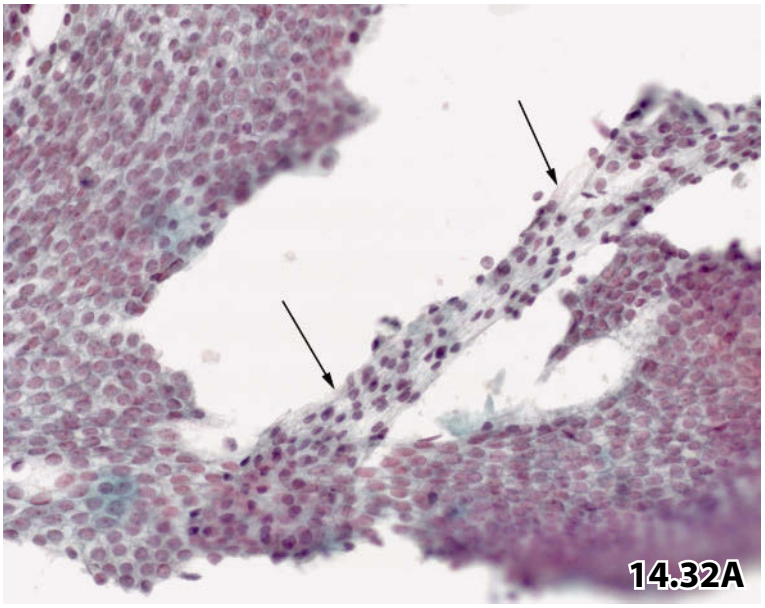
14.32A

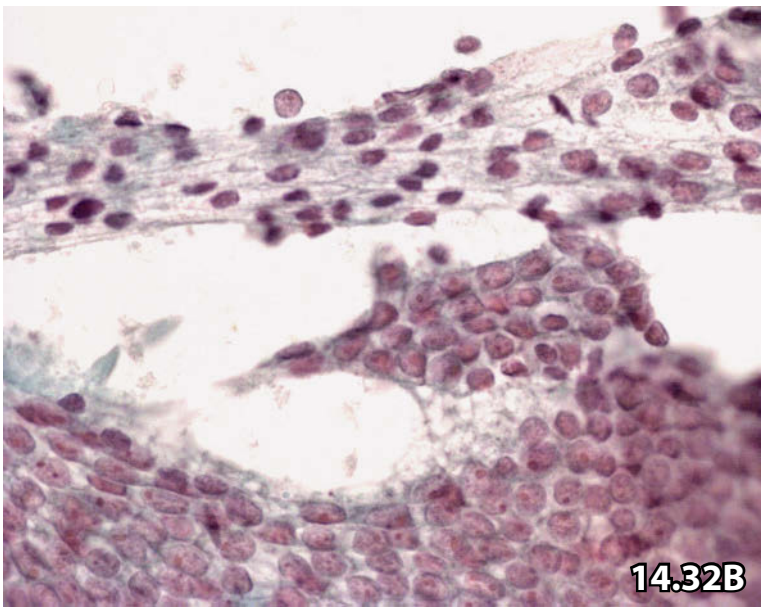
14.32B

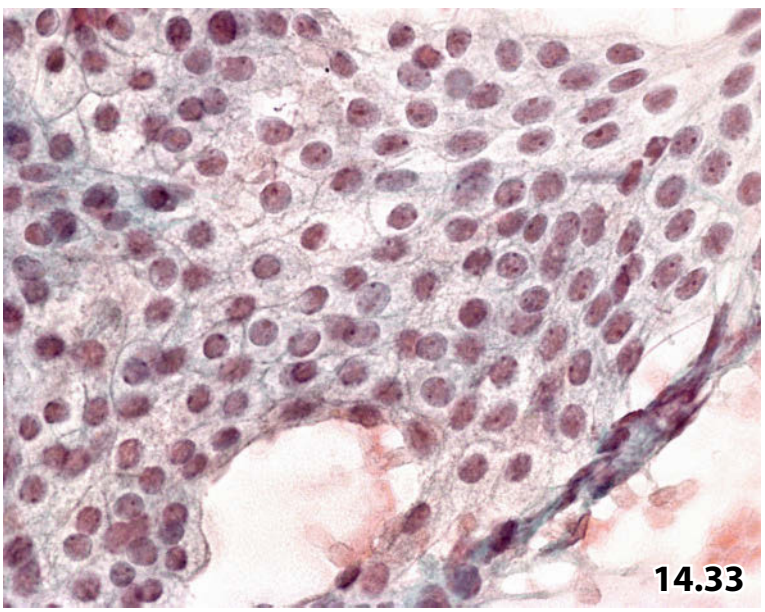
14.33

**Figs. 14.34–14.36 Moderately differentiated adenocarcinoma of the prostate.**
Cytomorphologic hallmarks are presented in transrectal FNABs from three different patients. Direct smears were Pap-stained.

**Fig. 14.34** (case #1) Key features of a moderately differentiated carcinoma at low magnification: compact and sharply outlined three-dimensional cell clusters along with few individual tumor cells.

**Fig. 14.35** (case #2) Cellular details indicating malignancy are evident: three dimensional cluster, irregular nuclear arrangement, very dense and fine granular chromatin fusing with nuclear membrane, and pronounced nucleoli.
*Cytologic diagnosis:* Moderately differentiated prostatic adenocarcinoma, grade 2, score 12. (no histologic work-up).

**Fig. 14.36** (case #3) A benign hyperplastic prostatic cell sheet (upper right) in comparison with a carcinomatous cell cluster (bottom). One should note the neutrophils (arrows), indicating an additional acute inflammation (lower magnification).
*Cytologic diagnosis:* Moderately differentiated prostatic adenocarcinoma, grade 2, score 13.
*Histology and final diagnosis:* Microscopic examination of transurethrally resected prostatic tissue yielded a false-negative result, but the positive cytology, clinical findings, and serologic results altogether ascertained malignancy.

> Prostatic tissue sampled by transurethral resection of small carcinomas located at the periphery of the prostate gland usually reveal a tumor-negative histologic result.

**Fig. 14.37 Poorly differentiated adenocarcinoma of the prostate: cytologic characteristic.**
A 59-year-old man with a positive history of a prostate carcinoma presented with locally relapsing disease. A transrectal FNAB was performed and direct smears were Pap-stained. Higher magnification shows the characteristic appearance of a poorly differentiated adenocarcinoma: loose and irregular grouping of large malignant cells, numerous dispersed stripped pleomorphic nuclei, and abundant ill-defined cytoplasm. Chromatin texture and nucleoli match those of well-differentiated and moderately differentiated prostatic adenocarcinomas.
*Cytologic diagnosis:* Relapsing poorly differentiated prostatic adenocarcinoma, grade 3, score 16. No histologic work-up.

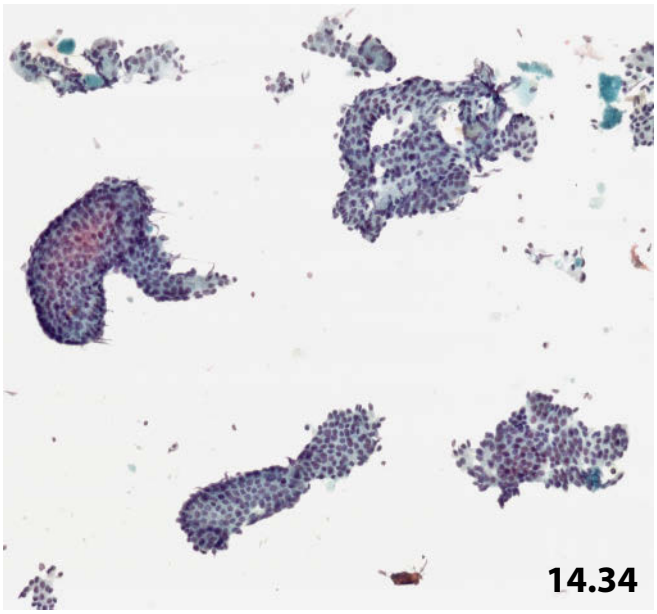

14.34

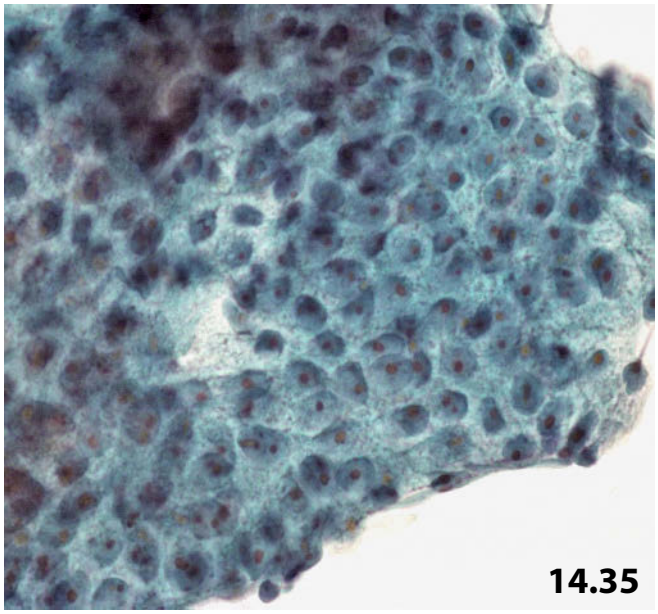

14.35

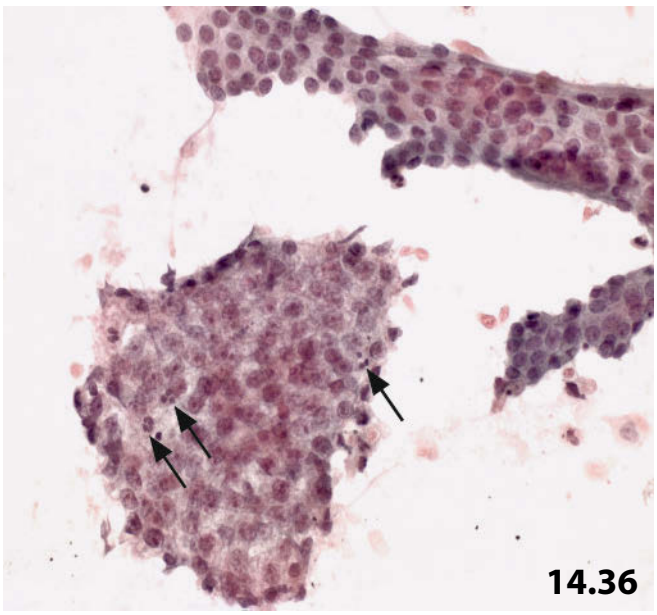

14.36

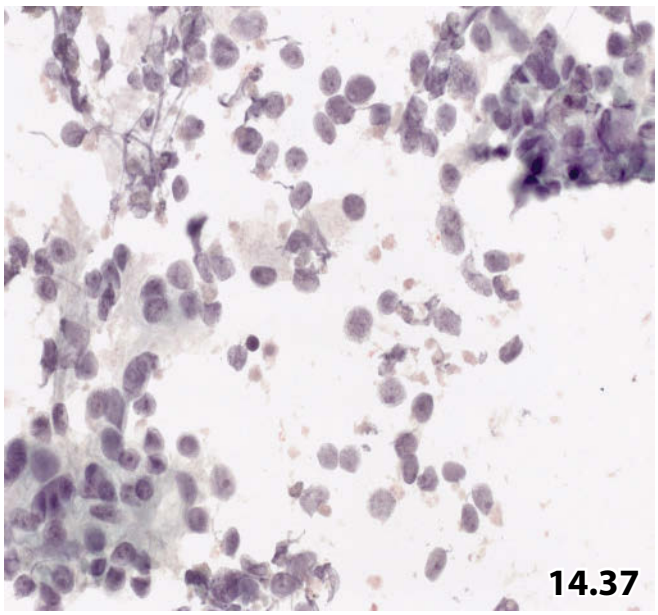

14.37

**Fig. 14.38 Poorly differentiated adenocarcinoma of the prostate versus seminal vesicle.**
It should be remembered that epithelial sheets of the seminal vesicle (lower right) can closely mimic poorly differentiated carcinoma (upper left) (high magnification). Seminal vesicle epithelial cells mainly differ from carcinoma cells in their varying nuclear size, a sharply defined and dense cytoplasm, and a high proportion of intracytoplasmic lipofuscin deposits. Note also Fig. 14.26.

**Fig. 14.39 Poorly differentiated and well-differentiated prostatic adenocarcinoma occurring simultaneously**
Higher magnification shows two epithelial sheets originating from both poorly differentiated (right) and well-differentiated (left) prostatic adenocarcinoma. Note the practically complete absence of nucleoli in the well-differentiated tumor cells causing a diagnostic dilemma with adenomatous hyperplasia. Yet the densely packed finely granular chromatin indicates malignancy.

**Fig. 14.40 Poorly differentiated prostatic adenocarcinoma: unusual absence of nucleoli.**
High magnification shows poorly differentiated carcinoma cells with rare occurrence of nucleoli, but one should be aware of all other textural and cellular criteria that are compatible with prostatic adenocarcinoma.

**Fig. 14.41A, B Immunocytochemical properties of prostatic adenocarcinoma.**
The two figures demonstrate positive immunocytochemical reactivity for the two prostate-typic immunomarkers. Immunostaining was performed using Pap-prestained direct smears from fine-needle aspirates. **A** Strong diffuse positivity for prostate-specific antigen (PSA). **B** Strong granular and dot-like positivity for prostate acid phosphatase (PAP).

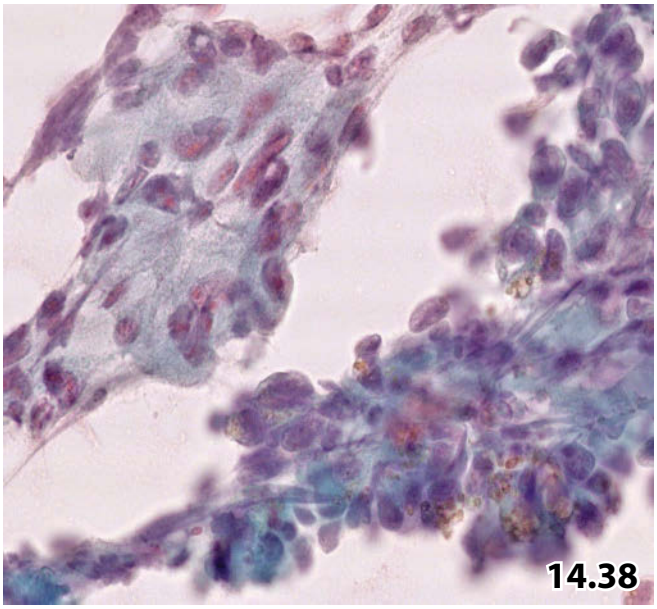
14.38

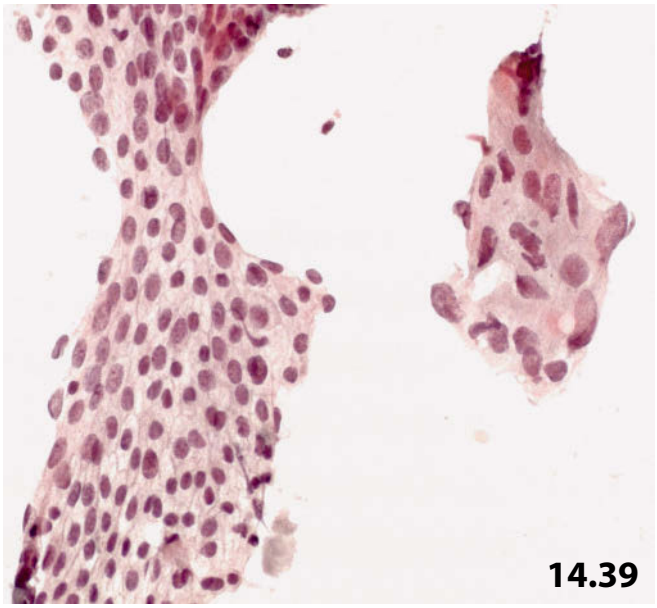
14.39

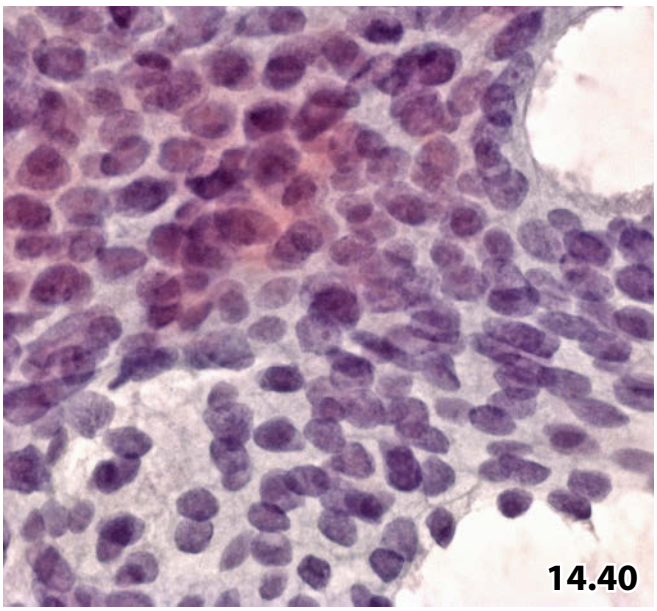
14.40

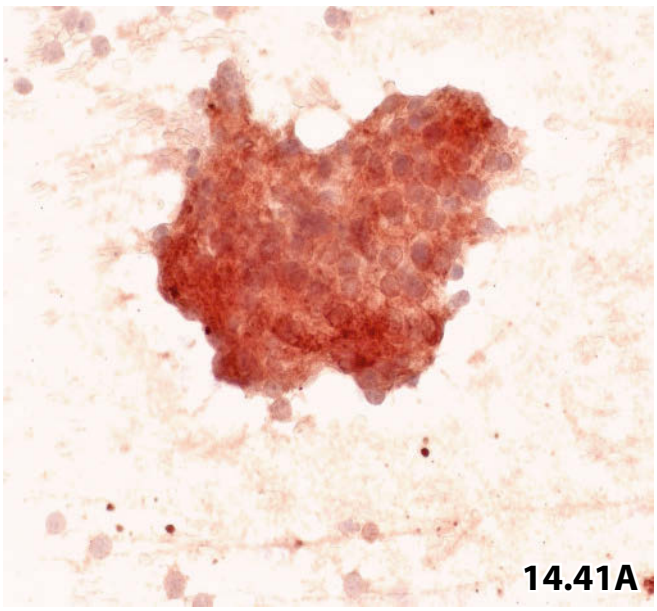
14.41A

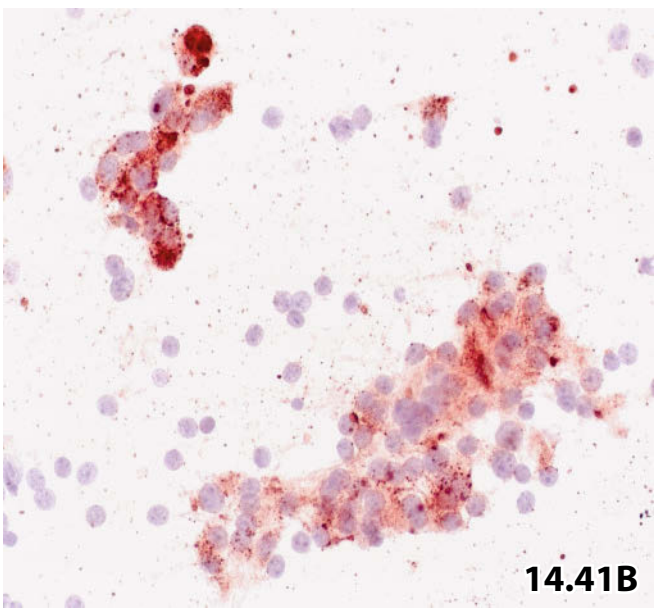
14.41B

**Figs. 14.42–14.45 Therapeutic effects on cells of the prostatic adenocarcinoma of common type.**

Five patients were treated by many diverse clinical protocols for prostatic carcinoma. Subsequently, periodical transrectal FNABs were performed monitoring tumor response to treatment and tumor follow-up. Direct smears were Pap-stained. Varied therapy-induced effects on the tumor cells are demonstrated and classified.

**Fig. 14.42** (case #1) An 81-year-old man presented with a history of poorly differentiated prostatic carcinoma. Estrogen treatment was given for the past 2 years. A majority of the tumor cells exhibit intracytoplasmic large empty vacuoles (arrows). Vacuoles of neighboring cells focally fuse, resulting in nuclear crowding (arrowheads) (lower magnification).
*Cytologic therapeutic effect:* Poor.

**Fig. 14.43** (case #2) A 78-year-old man presented with a history of irradiated prostatic carcinoma of moderate differentiation. Cytoplasmic shrinking and tightening (arrows), and nuclear pyknosis (arrowheads) clearly emerge at high magnification, as does obvious absence of nucleoli.
*Cytology of therapeutic effect:* Moderate.

**Fig. 14.44A** (case #3) A 62-year-old man has a positive history of prostatic adenocarcinoma and estrogen therapy extending over several years. Tumor cells show both good preservation of the cellular morphology (lower right) and varying degrees of therapeutic response. The latter comprise vacuolization and tightening of the cytoplasm, apoptotic nuclei, tightly packed degenerating nuclei associated with small dense cytoplasm (arrows), and disappearance of nucleoli (high magnification).
*Cytology of therapeutic effect:* Moderate.
**B** (case #4) An elderly man with a positive history of prostate carcinoma and estrogen therapy over the past few years. High magnification shows a few relatively well-preserved carcinoma cells (upper right). However, the vast majority of the tumor cells exhibit strong regressive changes. Note coalesced, deeply stained pyknotic nuclei clustered together (center); the cytoplasmic bodies and the nucleoli have practically disappeared.
*Cytology of therapeutic effect:* Good.

**Fig. 14.45** (case #5) A 72-year-old man presented with a history of estrogen-treated poorly differentiated prostatic carcinoma over a long period. Nuclear features of malignancy are consistently present. Distinct enlargement of nuclei associated with increased pleomorphism, large empty cytoplasmic vacuoles, and sporadic apoptotic nuclei are observed as well (lower right) (high magnification).
*Cytology of therapeutic effect:* Moderate to poor.

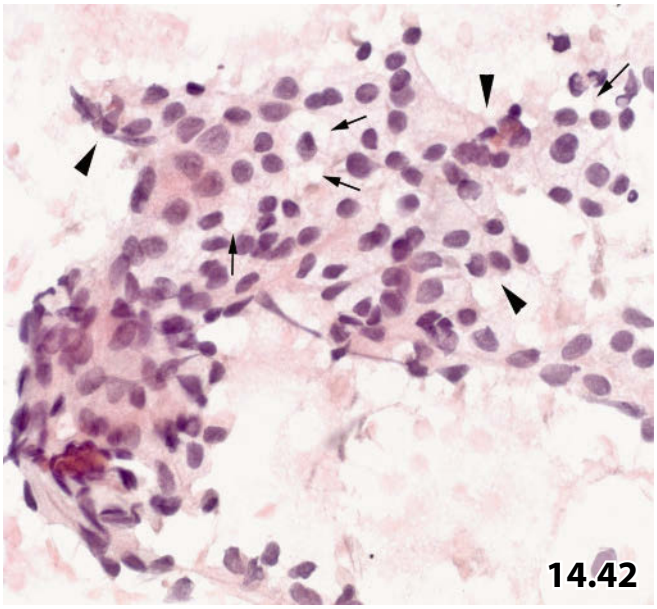
14.42

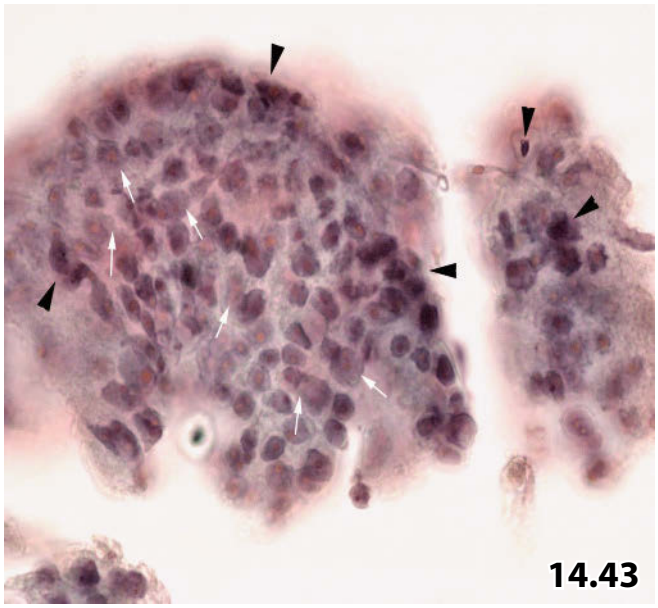
14.43

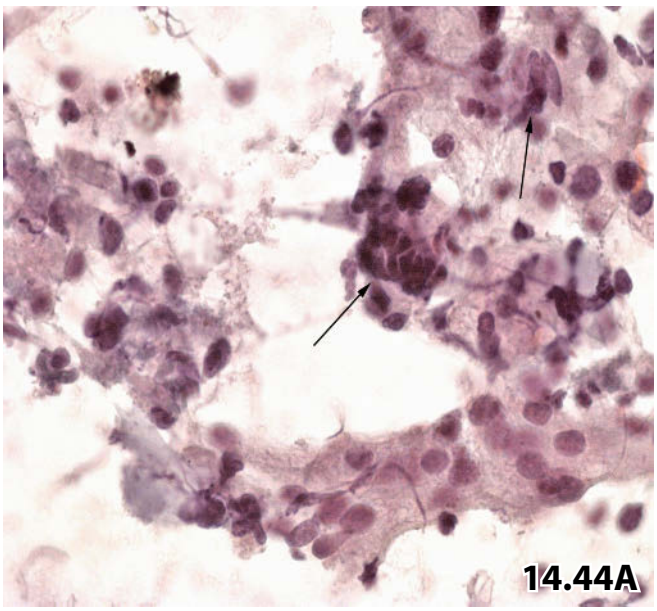
14.44A

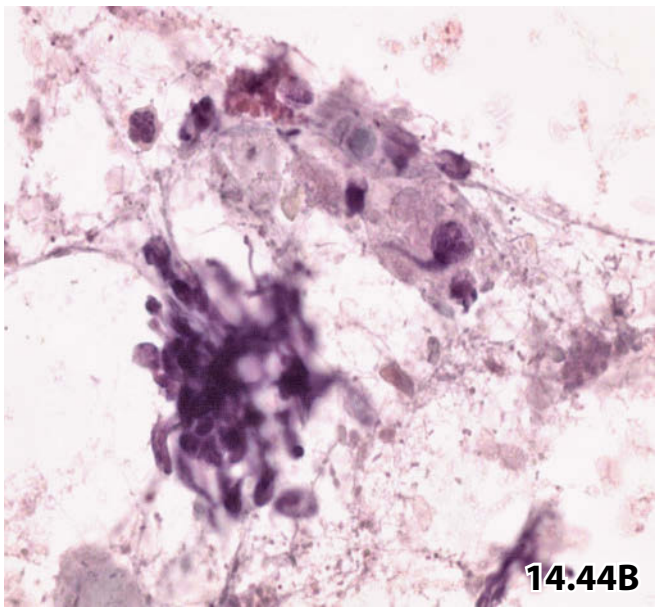
14.44B


14.45

**Fig. 14.46A, B Mucinous prostatic adenocarcinoma.**
Transrectal FNAB of an 85-year-old man's prostate, the patient having no particular clinical history. Pap-stained direct smears. **A** Sheets and clusters composed of carcinoma cells exhibiting the typical features of prostatic origin. Cellular material is embedded in thick mucoid masses (high magnification). Cytoplasmic storage of mucus may be presumed in conventional staining. **B** Strong immunopositive reaction of the tumor cells for prostate acid phosphatase (Pap-prestained smear, nuclear counterstain was not performed) rules out a primary tumor site other than the prostate gland.
*Cytologic diagnosis:* Mucinous prostatic adenocarcinoma (surgical exploration and histologic examination were refused by the patient).

**Figs. 14.47–14.49 Urothelial carcinoma in the prostate gland.**
Three elderly male patients with a history of transitional cell carcinoma of the urinary bladder underwent FNAB of their enlarged prostate gland. Direct smears were Pap-stained.

**Fig. 14.47** (case #1) Distinguishing between urothelial carcinoma and prostatic adenocarcinoma may be difficult. Tumor cells showing morphologic characteristics of prostatic origin are depicted using high magnification: dense granular chromatin, faint nuclear membranes, pronounced nucleoli, ill-defined vacuolated cytoplasm, acinic-like formations (arrows). The negative immunocytochemical staining result for prostate acid phosphatase is not shown.
*Tentative cytologic diagnosis:* Poorly differentiated carcinoma, the result of immunolabeling favors urothelial cancer.
*Tissue diagnosis* (transurethral resection of the prostate): Poorly differentiated transitional cell carcinoma invading the wall of the urinary bladder and prostate.

**Fig. 14.48** (case #2) The classical morphologic features of urothelial carcinomas are shown: nuclear polymorphism, granular and coarse chromatin, vacuolated and dense cyanophilic cytoplasm, cell-in-cell formation (arrows), high mitotic rate, and background necrosis (high magnification).



**Fig. 14.49A, B** (case #3) An elderly man presenting with a history of urothelial carcinoma. **A** Extreme nuclear pleomorphism, coarse clumping chromatin, dense cytoplasm, and an extremely high mitotic rate are features of this undifferentiated neoplasm (high magnification). **B** Strong immunopositivity of the tumor cells for CK7. The epithelial sheets composed of benign prostatic cells show a negative staining result (lower left).
*Cytologic diagnosis:* The cytokeratin pattern indicates relapsing undifferentiated urothelial carcinoma apparently invading the prostate gland (no histologic follow-up).

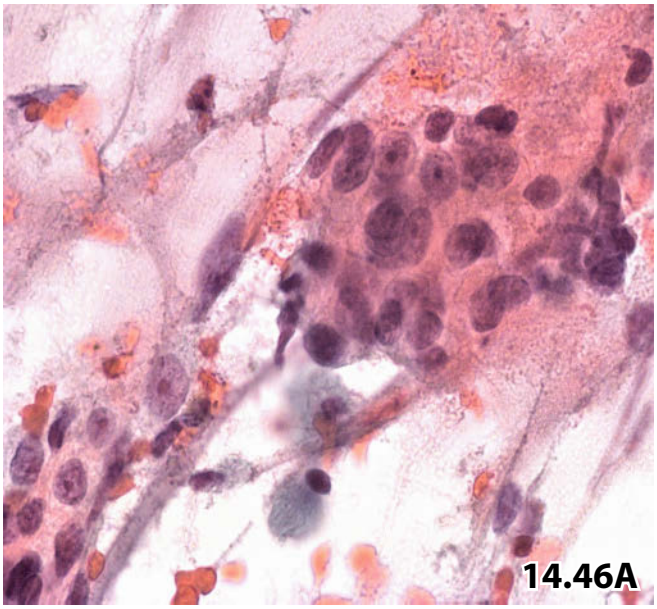
14.46A

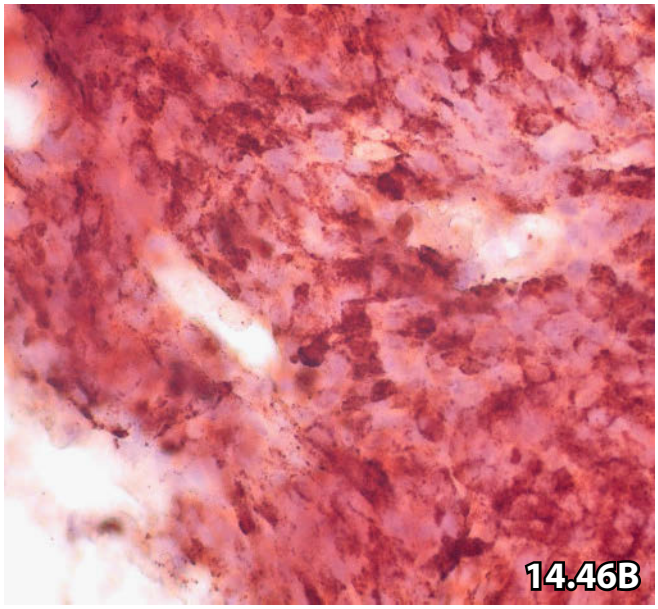
14.46B

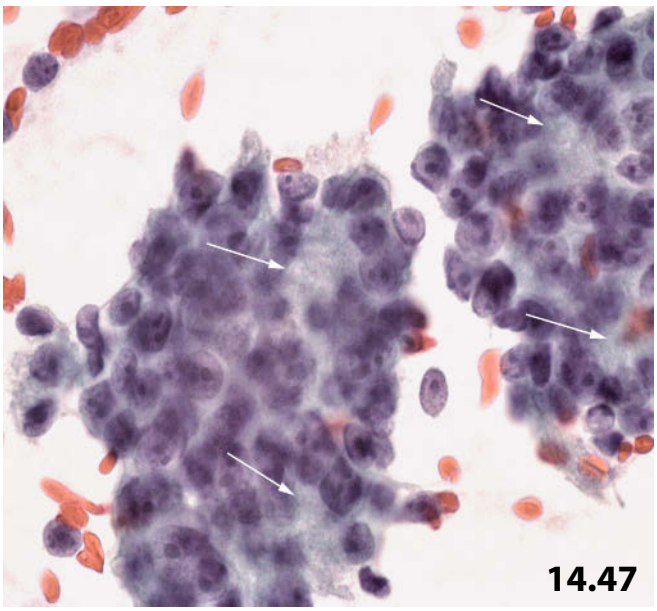
14.47

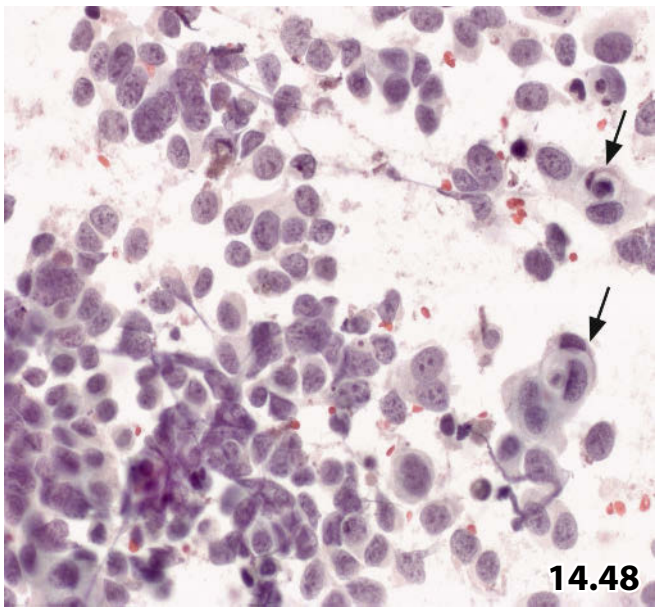
14.48

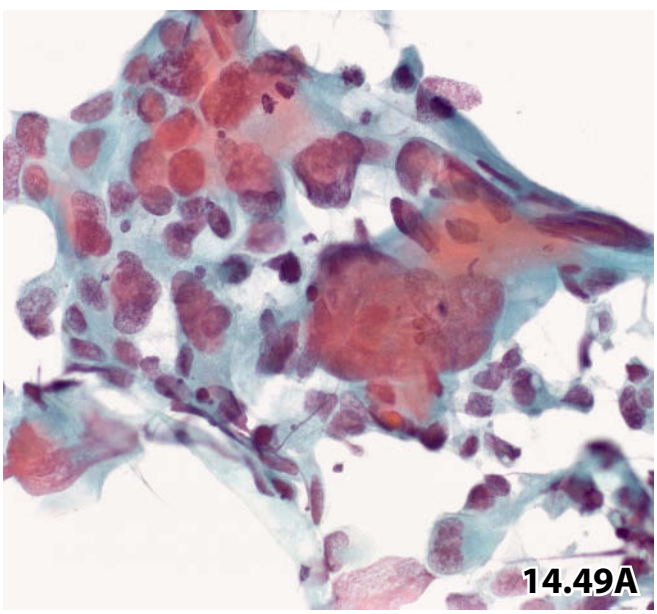
14.49A

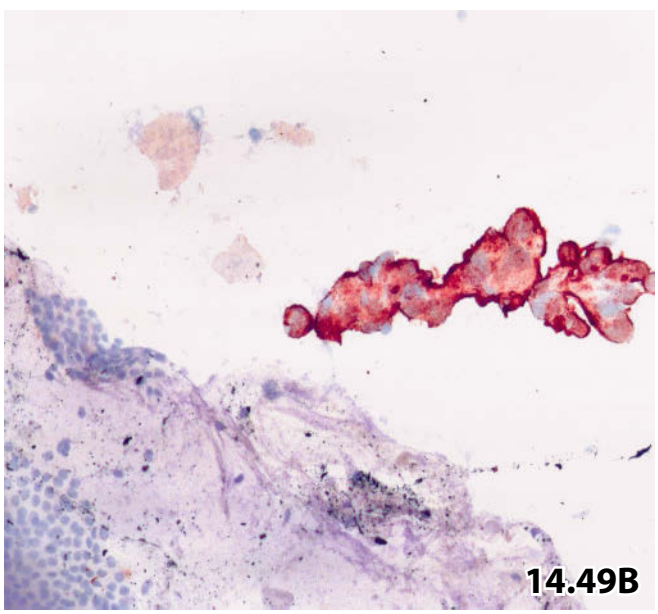
14.49B

**Fig. 14.50 Adenosquamous carcinoma of the prostate.**
A 74-year-old man presenting with a history of repeatedly relapsing poorly differentiated prostatic adenocarcinoma. Surprisingly, the tumor shows a biphasic cell pattern in the latest follow-up-FNAB (direct smears, Pap stain). Adenomatoid cell sheets are consistent with moderately to poorly differentiated prostatic adenocarcinoma. In addition, the background of the smear reveals numerous polymorphic and hyperkeratotic squamous cells occasionally comprising atypical nuclei (arrow) (lower magnification).
*Cytologic diagnosis:* Adenosquamous carcinoma (no histologic follow-up).

**Figs. 14.51 and 14.52 Undifferentiated prostatic carcinoma.**
Two examples of undifferentiated carcinoma of the prostate.

**Fig. 14.51A, B** (case #1) Laboratory testing revealed an increased PSA level in a 64-year-old man. FNAB of the prostate was initially undertaken. The direct smears were Pap-stained. **A** Nuclei show attributes of prostatic adenocarcinoma; irregular cell aggregates, cellular pleomorphism, and necrotic background argue for an undifferentiated prostatic neoplasm (high magnification). **B** Immunocytochemical staining for prostate acid phosphatase are positive in both cytoplasm of intact tumor cells (arrows) and in cytoplasmic debris (arrowheads) (Pap-prestained smears).
*Cytologic diagnosis:* Necrotic undifferentiated prostatic carcinoma (confirmed by histology).

**Fig. 14.52** (case #2) Uncommon cytologic appearance of a prostatic carcinoma in a 76-year-old man (higher magnification):
(1) Generally, the tumor cells are dissociated.
(2) Compact cell clusters (right) appear ball-like and are associated with whorled configuration and vague palisading of the tumor cells.
*Tentative cytologic diagnosis:* Large-cell carcinoma of the pleomorphic subtype, most likely of prostatic origin (immunocytochemistry was not performed for technical reasons).
*Comment:* Differential diagnostic consideration should include poorly differentiated intestinal adenocarcinoma and squamous cell carcinoma.
*Postmortem histologic diagnosis:* Solid undifferentiated prostatic carcinoma.



**Fig. 14.53A, B Leiomyosarcoma of the prostate gland.**
A 45-year-old man presented with an enormous tumor mass filling the prostatic area. Sarcoma was clinically suggested. FNAB was performed and direct smears were Pap-stained with the Papanicolaou method. **A** Low magnification shows several microfragments of hyalinized and sclerotic mesenchymal tissue. Encased spindle-shaped nuclei occur singly or in tightly packed strands. **B** High magnification from another spot of the slide displays epithelioid arrangement of fusiform malignant cells (Pap-restained smear after negative immunocytochemical staining). Initial negative immunocytochemical reaction for pancytokeratin (Lu-5) and immunopositivity for vimentin are not shown. Further immunostains were not performed for lack of cytologic material.
*Tentative cytologic diagnosis:* Stromal spindle cell neoplasia.
*Tissue diagnosis:* Moderately differentiated leiomyosarcoma of undetermined origin (prostate versus seminal vesicle).

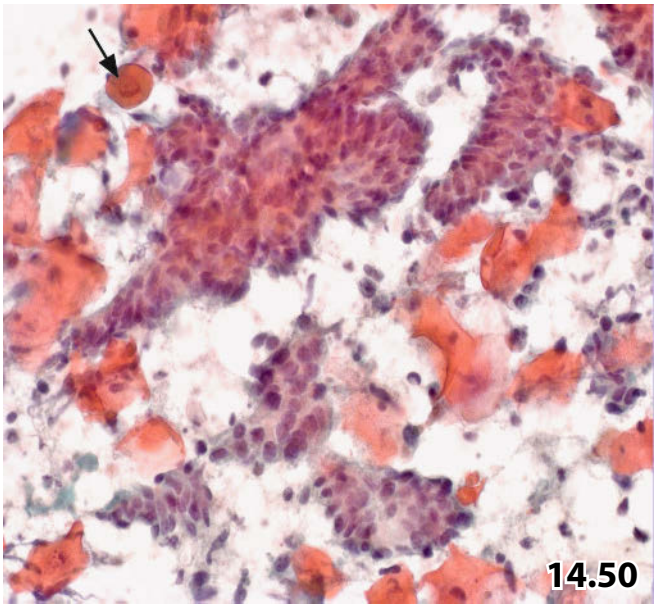
14.50

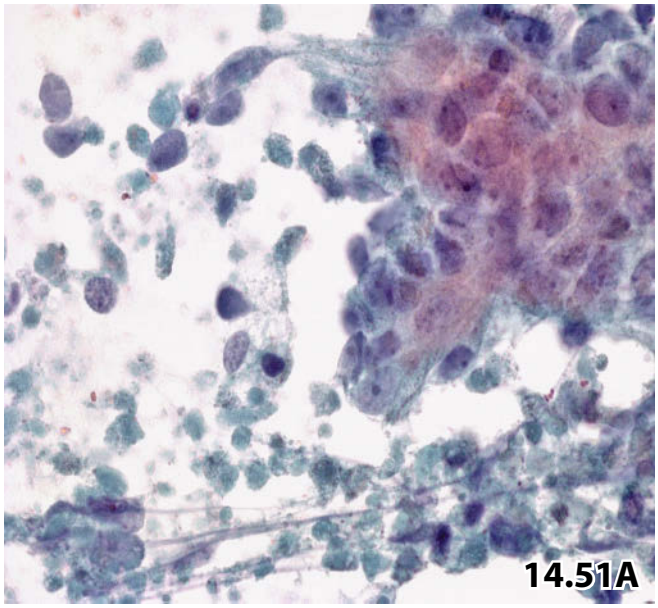
14.51A

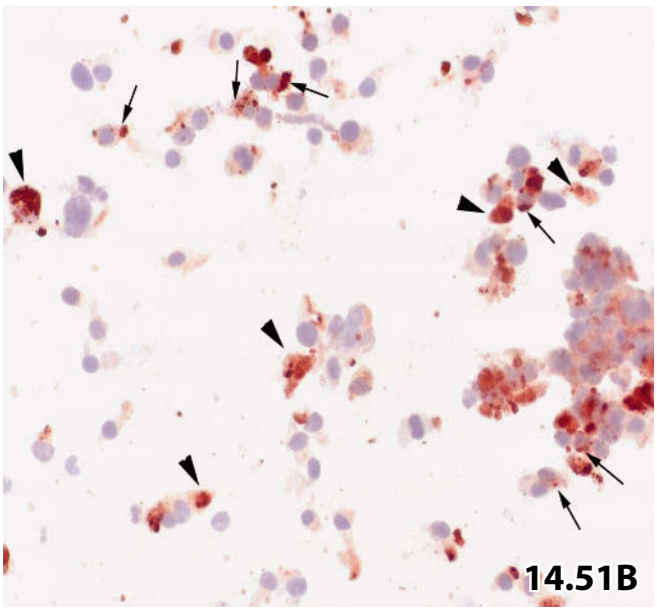
14.51B

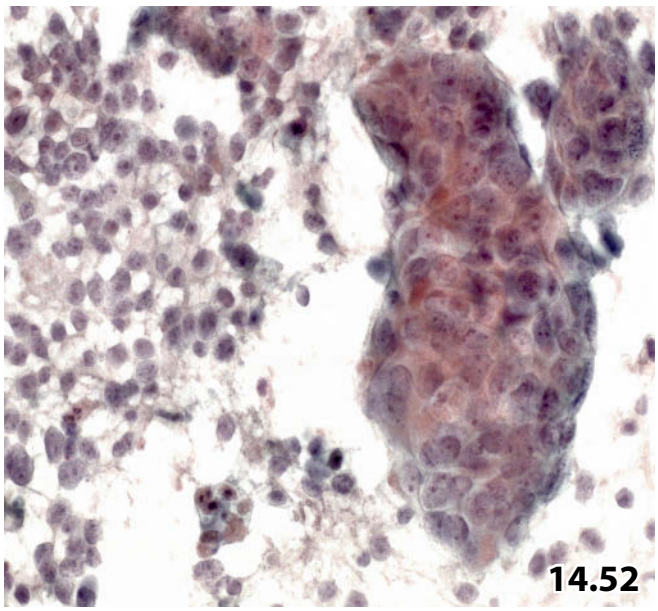
14.52

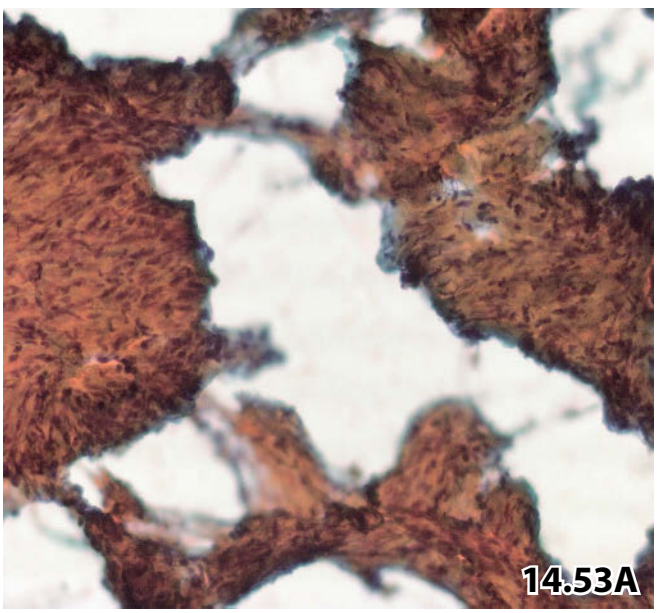
14.53A

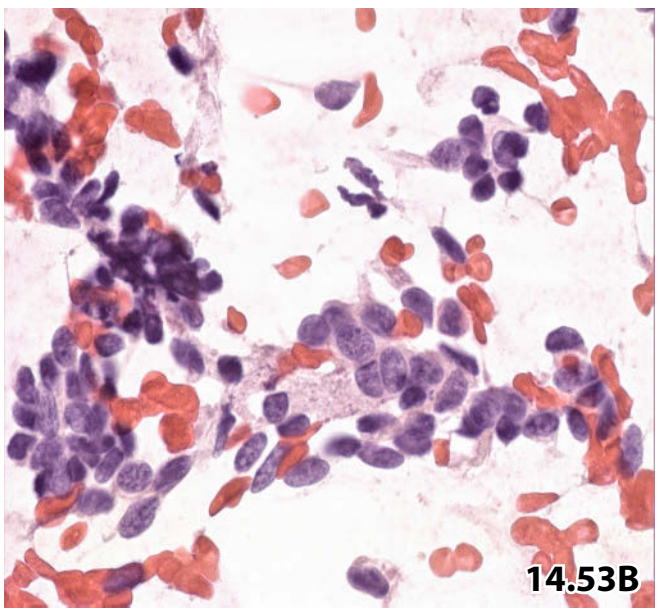
14.53B

# Section 14.2
# Penis

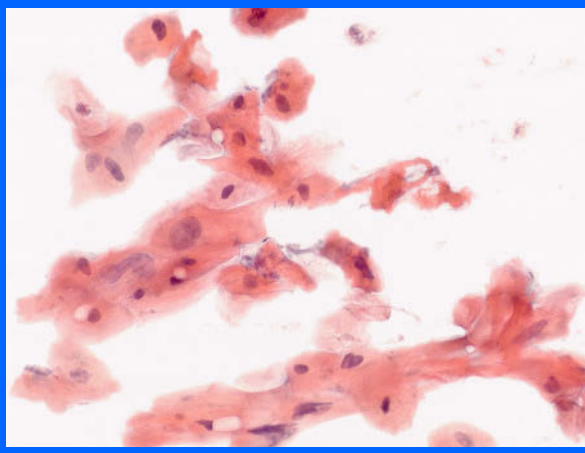

## 14.2.1 Introduction

**General Comments** [1, 3, 18, 19, 20]
Squamous cell carcinoma (SCC) is by far the most common penile carcinoma subtype. Squamous cell carcinoma usually originates in the epithelium of the glans, coronal sulcus, and foreskin.

**Etiology**
Etiologic factors and predisposing conditions are phimosis, poor genital hygiene, chronic inflammation, lack of circumcision, human papilloma virus infection, lichen sclerosus, and smoking. There is a strong evidence that human papilloma viruses (in particular types 16 and 18) are associated with penile carcinoma in about 50% of all cases.

### 14.2.1.1 Groin Lymph Node Metastases

- In general, superficial inguinal lymph nodes are the first metastatic site of penile carcinomas. Clinically occult, superficially spreading squamous cell carcinoma concealed due to phimosis may primarily appear as swelling of an inguinal lymph node.
- Depending on the preference of the attending physician, FNAB of palpable inguinal lymph nodes may be performed instead of an initial surgical excision. US-guided FNAB can be helpful as an initial investigation tool in the evaluation of patients with positive imaging results of the groin but a clinically occult situation [10, 19].

## 14.2.2 Cytology of Penile Lesions

Cytology as a diagnostic technique is not extensively used in the evaluation of penile lesions. At our institution, exfoliative cytology is selectively applied by urologists, particularly in tumor follow-up.

The scraping technique is mainly applied on flat and ulcerative disorders in order to obtain initial information with minimal waste of time and cost. Surgical biopsy followed by histologic investigation is indispensable in doubtful, precancerous, and malignant lesions.

**Sampling Methods and Sample Processing**
- *Scraping*. The simplest method is the scraping of a lesion over its whole area. Most suitable are Cytobrush or a sharp-edged device (edge of a glass slide, dermatological curette, etc.) with intent to prepare conventional smears or liquid-based preparations.
- *The curette technique* allows collecting both cells and small tissue fragments; the latter may be utilized as microbiopsies.
- *Touch imprints* commonly provide inadequate and scanty cellular material originating from the superficial cell layers only.
- *FNAB* may be used with lesions presenting in a nodular fashion such as the marginal area of an ulcer.
- *Liquid-based cytology* is superior to conventional direct smears in terms of optimal cell preservation, cell recognition, adequacy of the sample, and ability to provide material for further investigations such as immunocytochemistry and DNA ploidy studies.

## 14.2.3 DNA Ploidy

Flow Cytometry

Several studies investigated quantitative DNA distribution patterns of penile cancer by means of flow cytometric analysis. A correlation could be shown between the histologic type of invasive cancer and a high DNA index indicating an increased risk for tumor progression [6, 8, 13].

DNA Image Cytometry

- Our initial experience with image cytometry (ICM DNA) on a series of cases with atypical squamous cells suggests that DNA ploidy testing can identify individuals at increased risk of malignancy.
- ICM-DNA standards as used in our study are in accordance with the consensus statements of the European Society of Analytical Cellular Pathology (ESACP) [7].
- Histogram algorithms have been applied according to ploidy evaluation of squamous lesions in other organs such as the uterine cervix, oral mucosa, esophagus, and respiratory tract [5, 9, 12, 15, 16]:

DNA algorithms for squamous lesions are presented in Chapter 8 "Oral Cavity and Oropharynx", Sect. 8.4, p. 565.

- We conclude that DNA image cytometry is a reliable adjuvant tool for early identification of neoplastic squamous cells in cytologic samples of penile lesions. DNA aneuploidy is a reliable marker for malignancy and its precursors. Further studies will be needed to confirm our observations and to evaluate the clinical impact of cytometric analyses.

**Caution**

Nuclear DNA content can be abnormal in cells with incorporated DNA of human papilloma virus, DNA histograms may display a distinct polyploid DNA pattern including scattered nuclei with aneuploid DNA content. However, nuclei with ninefold or more chromosome sets (9c exceeding events) should be absent.

## 14.2.4 Inflammation and Infection

[17, 18] (Fig. 14.54)

- The penis mucosa can be affected by infections and inflammatory dermatosis. Bacteria, fungi, and protozoa can be detected in cytologic specimens by means of selective staining methods such as Gram, PAS, Grocott, and Ziehl-Neelsen. Koilocytic atypia (HPV changes) is a definite sign of human papilloma virus infection (Fig. 14.54).
- Epithelial atypias in the setting of inflammation are usually a challenge for cytopathologists. The cell changes should not be overestimated as dysplastic, although a premalignant and malignant squamous lesion can virtually not be ruled out on light microscopy alone (Fig. 14.55). ICM-DNA is believed to be an effective method distinguishing between regenerative and dysplastic cellular atypia (see Sect. 14.2.3).

## 14.2.5 Atypical Squamous Cells in Cytologic Samples

In this setting, several issues should be considered and be kept in mind:

**Caution**

- Squamous cells collected by superficial scraping may exhibit variously pronounced changes due to regenerative activity.
- Benign reactive cell changes are rarely accompanied by cell detritus.
- It is not possible to differentiate between squames with severe reactive atypia and high grade dysplasia or invasive cancer by cytology alone. DNA image cytometry may be used as an objective adjuvant tool for the early identification of primary malignancy and precursor lesion (see Sect. 14.2.3).
- Both the precancerous (dysplastic) squamous lesion and differentiated squamous cell carcinoma may be covered by a hyperkeratotic/acanthotic squamous cell layer preventing the exfoliation of diagnostic target cells.
- Squamous cell atypias in the setting of inflammation should not be overestimated as dysplastic or malignant changes.

## 14.2.6 Squamous Cell Carcinoma and Its Variants

### 14.2.6.1 Common Squamous Cell Carcinoma

Common SCC is easily diagnosed based on pleomorphic malignant squamous cells, keratinized or less differentiated, together with necrotic debris. The overall cytologic features of SCC are identical to their counterparts occurring in other body sites (e.g., respiratory tract, esophagus, oral cavity, cervix uteri) and include:

- Pleomorphic cyanophilic, amphophilic, or orangeophilic cytoplasm.
- An increased N/C ratio.
- Enlarged deeply stained, hyperchromatic, and irregularly shaped nuclei.
- Granular and coarse chromatin.
- Occasional prominent nucleoli.

More information is provided in Sect. 2.2.2.2, "Invasive SCC," p. 139).

### 14.2.6.2 Well-Differentiated and Verrucous Squamous Cell Carcinoma (Figs. 14.55–14.57)

Strongly keratinized and verruciform squamous neoplasms usually give rise to diagnostic difficulties. Unambiguous malignant cells are frequently absent in exfoliative cytologic samples due to a marked acanthotic and hyperkeratotic superficial coating.

*A verrucous neoplasm* may be suspected if the following cell alterations are present:

- Large numbers of polymorphic anucleated keratinized squamous cells accompanied by cellular debris.
- The cytoplasm appearing eosinophilic to orangeophilic and densely structured.
- Scattered squamous cells may exhibit indistinct atypical or apoptotic changes.

**Caution**

Pleomorphic acanthosis and hyperkeratosis may also be observed in benign conditions. Multiple punch biopsies or wide surgical excision are mandatory in this setting.

### 14.2.6.3 Condylomatous Carcinoma

Condylomatous carcinoma (synonym: warty carcinoma) is characterized by an arborizing growth of epithelial cells overlying a connective tissue core. The cytologic features of the lining epithelium are similar to verrucous SCC, but this tumor subtype is virus-related and koilocytic changes should be present.

### 14.2.6.4 Basaloid Squamous Cell Carcinoma

**Microscopic features and Differential Diagnosis**

- The tumor cells are small, showing scanty cytoplasm.
- The nuclei are irregular and hyperchromatic, exhibiting densely packed granular chromatin and inconspicuous nucleoli.
- Tumor cells palisading at the periphery of the cell clusters together with keratinized squamous elements are key features of this tumor entity.

Papillary basaloid carcinoma and small-cell carcinoma of the neuroendocrine type are composed of cells sharing many features with cells of basaloid SCC.

Neuroendocrine small-cell carcinomas exhibit immunoreactivity for neuroendocrine markers such as chromogranin A and synaptophysin, contrary to SCC cells.

### 14.2.6.5 Sarcomatoid Carcinoma [11]

Sarcomatoid carcinoma (synonym: spindle cell carcinoma) is a subtype of SCC composed of pleomorphic spindle cells displaying pronounced nuclear atypia. Occasional epithelial-like aggregates of undifferentiated tumor cells and keratinized carcinoma cells can be observed.

Differentiating from true sarcoma requires immunocytochemical tests; a correct diagnosis is based mainly on immunopositivity for cytokeratins (MNF-116) and other epithelial markers.

### 14.2.6.6 Adenosquamous and Mucoepidermoid Carcinoma [1, 4]

These two entities are very uncommon biphasic neoplasms. They are characterized by both fractions of squamous cell carcinoma and mucin-producing adenocarcinoma.

## 14.2.7 Other Rare Primary Tumors

### 14.2.7.1 Penile Intraepithelial Malignant Lesions

Penile intraepithelial malignant lesions include pagetoid spreading squamous cell carcinoma, classic Paget disease, and urothelial carcinoma.

**Caution**

Superficial scraping usually misses atypical and malignant cells that are embedded in the lower layers of the penile epidermis.

### 14.2.7.2 Malignant Melanoma [2]

The rare primary penile melanoma is located in the glans penis in a high percentage of cases. The diagnosis can be established by means of scrape specimens from exophytic lesions.

Cytomorphologic hallmarks:

- Large cells frequently occurring singly. They show abundant granular cytoplasm that may contain melanin pigment.
- The nuclei are large, pale, grooved, and folded; and frequently multiple.
- Large pleomorphic nucleoli are obvious.

Positive immunoreaction for melanoma-typical markers (Melan A, HMB45, S100 protein) is diagnostic for this tumor type.

A comprehensive overview of this tumor entity and related pictures are provided in Sect. 16.2.9, p. 1030.

### 14.2.7.3 Extremely Unusual Primary Malignant Neoplasms

Benign and malignant primary penile soft tissue tumors are rare. The most frequently encountered entities are Kaposi sarcoma and leiomyosarcoma [3,14]. Other rare primary malignant neoplasms of the penis are not discussed further.

## 14.2.8 Secondary Tumors

Tumors metastasizing to the penis are rare. Prostate and bladder are reported to be the most frequent primary tumor sites followed by kidney and colon. Clinical history, clinical findings (most often multinodular superficial growth pattern), along with immunocytochemical results are important diagnostic tools.

## 14.2.9 Further Reading


1. Cubilla AL. Carcinoma of the penis. Modern Pathology 1995;8:116-118.
2. Donate Moreno MJ, Ruiz Mondejar R, Giménez Bachs JM, et al. Malignant melanoma of the penis. Report of one case. Arch Esp Urol 2005;58:672-674.
3. Eble JN, Sauter G, Epstein JI, Sesterhenn IA (Eds.):World Health Organization Classification of tumours. Pathology and genetics of tumours of the urinary system and male genital organs. IARC Press: Lyon 2004.
4. Froehner M, Schöbl R, Wirth MP. Mucoepidermoid penile carcinoma: clinical, histologic, and immunohistochemical characterization of an uncommon neoplasm. Urology 2000;56:154.
5. Gockel I, Kammerer P, Brieger J, et al. Image cytometric analysis of mucosal biopsies in patients with primary achalasia. World J Gastroenterol 2006;12:3020-3025.
6. Hall MC, Sanders JS, Vuitch F, et al. Deoxyribonucleic acid flow cytometry and traditional pathologic variables in invasive penile carcinoma: assessment of prognostic significance. Urology 1998;52:111-116.
7. Haroske G, Baak JP, Danielsen H, et al. Fourth updated ESACP consensus report on diagnostic DNA image cytometry. Anal Cell Pathol 2001;23:89-95.
8. Hoofnagle RF Jr, Kandzari S, Lamm DL. Deoxyribonucleic acid flow cytometry of squamous cell carcinoma of the penis. W V Med J 1996;92:271-273.
9. Itakura Y. Sasano H, Mori S, Nagura H. DNA ploidy in human esophageal squamous dysplasias and squamous cell carcinomas as determined by image analysis. Mod Pathol 1994;7:867-873.
10. Kroon BK, Horenblas S, Duerloo EE. Ultrasonography-guided fine-needle aspiration cytology before sentinel node biopsy in patients with penile carcinoma. BJU Int 2005;95:517-521.
11. Lont AP, Gallee MP, Snijders P, Horenblas S. Sarcomatoid squamous cell carcinoma of the penis: a clinical and pathological study of 5 cases. J Urol 2004;172:932-935.
12. Nguyen VQ, Grote HJ, Pomjanski N, Knops K, Böcking A. Interobserver reproducibility of DNA image-cytometry in ASCUS or higher cervical cytology. Cell Oncol 2004;26:143-150.
13. Ornellas AA, Mendes Campos M, Ornellas MH, et al. Penile cancer: flow cytometry study of ploidies in 90 patients. Prog Urol 2000;10:72-77.
14. Piana M, Martinez Mansur R, Codone J, et al. Penile leiomyosarcoma: case report and bibliographic review. Arch Esp Urol 2006;59:728-731.
15. Remmerbach TW, Mathes SN, Weidenbach H, et al. Noninvasive brush biopsy as an innovative tool for early detection of oral carcinomas. Mund Kiefer Gesichts Chir 2004;8:229-236.
16. Remmerbach TW, Weidenbach H, Pomjanski N et al. Cytologic and DNA-cytometry early diagnosis of oral cancer. Anal Cell Pathol 2001;22:211-221.
17. Rossi R, Urbano F, Tortoli E, et al. Primary tuberculosis of the penis. J Eur Acad Dermatol Venereol 1999;12:174-176.
18. Schneede P, Frimberger D, Hungerhuber E, Hofstetter A. Papules, fungi, protozoa – or cancer? Many skin conditions of the penis can be confirmed with biopsy. MMW Fortschr Med 2003;145:52-54.
19. Solsona E, Algaba F, Horenblas S, et al. EAU Guidelines on penile cancer European Urology 2004;46:1-8.
20. Soria IC, Theodore C, Gerbaulet A. Epidermoid carcinoma of the penis. Bull Cancer 1998;85:773-784.

**Figs. 14.54 and 14.55A Inflammation/infection: reactive squamous cell changes versus squamous cell carcinoma.**

**Fig. 14.54** ( case #1) Scrape specimen from a superficial lesion of the glans penis in a 26-year-old man. Direct smears were Pap-stained. Higher magnification shows atypical superficial squamous cells including mild HPV cytopathic effects: nuclear enlargement, irregularity of the nuclear contour, bi- and multinucleation (arrow), occasional hyperchromasia.
*Tentative cytologic diagnosis:* Assumed HPV-associated cell changes and patient's age favors a benign HPV-induced lesion.
*Comment:* However, the nuclear atypias associated with a polymorphic shape of the keratinized cytoplasms may suggest well-differentiated squamous cell carcinoma, first and foremost condylomatous carcinoma.
*Histologic diagnosis* (excisional biopsy of the lesion): Condylomata acuminata.

**Fig. 14.55A** (case #2) Superficial squamous cells showing nuclear atypia (enlargement, irregular outline, hyperchromasia) are positioned adjacent to a stromal fragment. Note neutrophils that are both embedded in the stromal tissue and scattered in the background of the smear (scraping specimen from the preputial cavity, direct smear, Pap stain, high magnification).
*Cytology:* In this setting, cytology cannot differentiate between reactive/regenerative cell change and well-differentiated squamous cell carcinoma (see also Fig. 14.55B, same case but different field).

**Figs. 14.55B and 14.56 Well-differentiated squamous cell carcinoma of the prepuce/glans of the penis.**
Two examples are presented. Direct scrape smears were Pap-stained.

**Fig. 14.55B** (case #1) Scraping of a nodular lesion at the glans penis was performed in a 46-year-old man presenting with a positive history of squamous cell carcinoma at the same location. High magnification showing numerous strongly keratinized atypical squamous cells. Nuclear irregularities and hyperchromasia are obvious. Absence of an inflammatory background strongly suggests relapsing well-differentiated squamous cell carcinoma (see also Fig. 14.55A, same case but different field).
*Tentative cytologic diagnosis:* Most likely keratinized squamous cell carcinoma.
*Histologic diagnosis* (excisional biopsy of the lesion): Keratinized well-differentiated squamous cell carcinoma.

**Fig. 14.56** (case #2) A 61-year-old man presented with an ulcerous lesion at the inner prepuce. Scraping yields hypercellular direct smears mainly composed of anucleated markedly keratinized squames and cellular detritus (low magnification). Note polymorphism of the cytoplasm and occasional severe nuclear atypias (arrows).
*Cytologic diagnosis:* Well-differentiated keratinizing squamous cell carcinoma (histologically confirmed by an excisional biopsy).

**Fig. 14.57 Verrucous squamous cell carcinoma of the penile prepuce.**
Hypercellular cytologic smears were obtained by scraping a middle-aged man's ulcerous lesions in the preputial cavity. Dispersed and aggregate squamous cells are markedly keratinized. The cytoplasmic bodies are stained red, orangeophilic, and yellowish showing distinct polymorphism. Vague pearl formations (arrow) and cell detritus are also present. Note minor nuclear irregularities (higher magnification, Pap stain).
*Tentative cytologic diagnosis* (supported by clinical findings): Well-differentiated keratinizing squamous cell carcinoma.
*Histologic diagnosis* (excisional biopsy of the whole lesion): Verrucous squamous cell carcinoma.

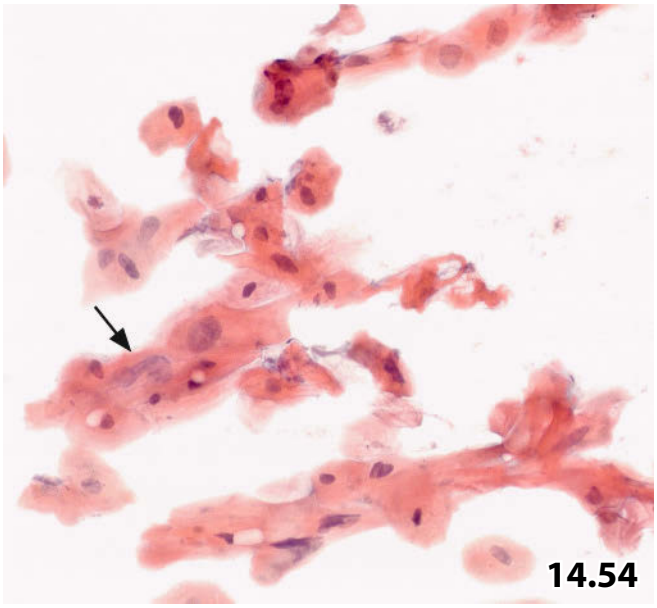
14.54

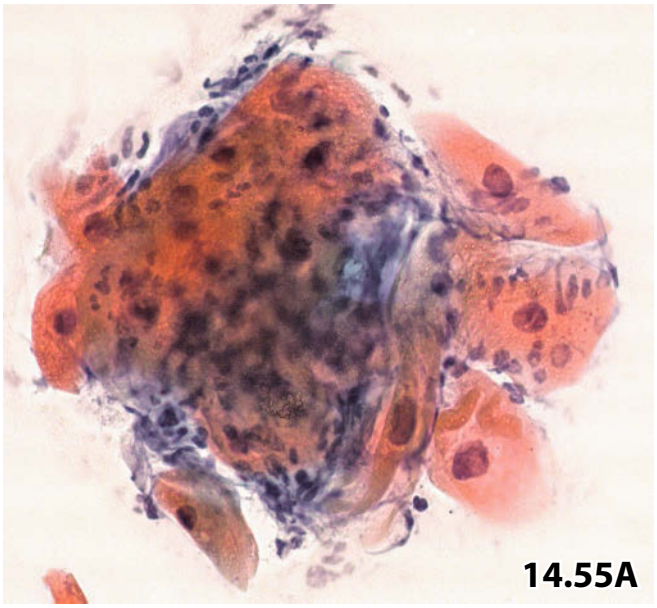
14.55A

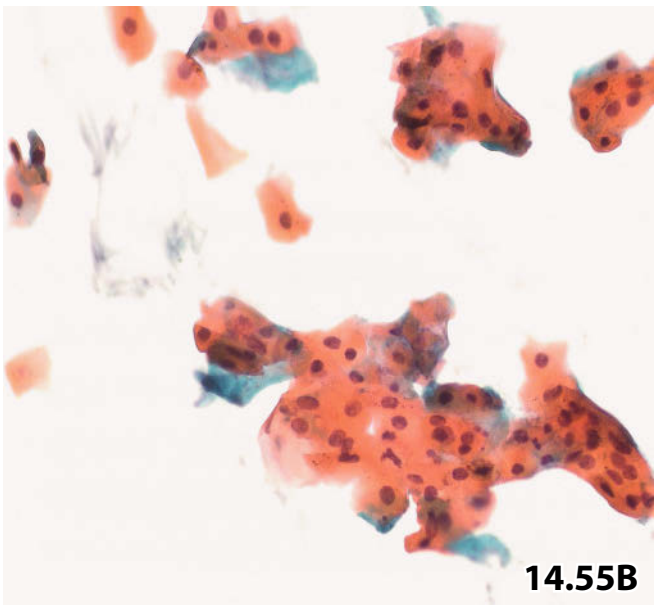
14.55B

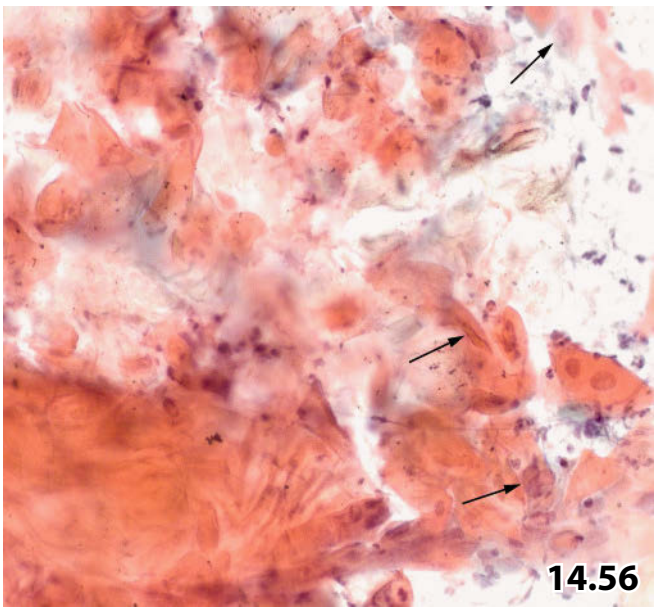
14.56

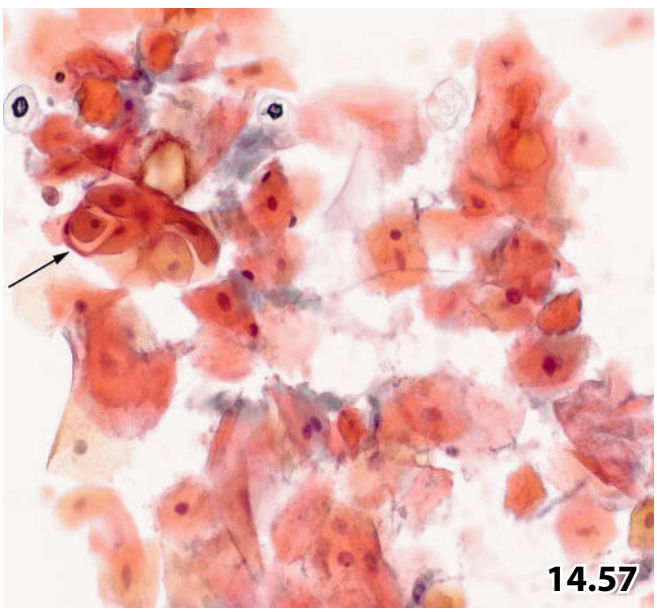
14.57

# 15 Lymph Nodes




Spieler/Rössle, *Nongynecologic Cytopathology. A Practical Guide. Essentials of Diagnostic Pathology*,
DOI 10.1007/978-3-642-24719-4_15, © Springer-Verlag Berlin Heidelberg 2012

## Synopsis and Algorithms

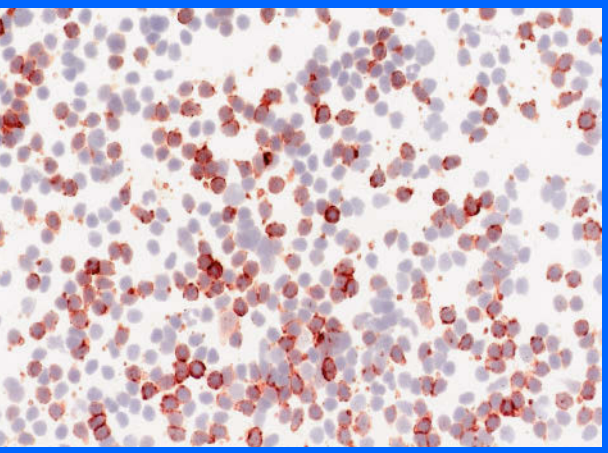

# Section 15.1
# Lymph Nodes



## 15.1.1 Introduction


**Acknowledgement**

The authors of this book wish to express their gratitude to PD Sergio B. Cogliatti, MD, for his support in producing the lymph node chapter. As an expert in lymphoma pathology, he worked on the entire manuscript and made valuable suggestions and improvements as to diagnostics and adjuvant analyses on the cytology level. In spite of his tremendous work load in a large, service-oriented institute, he always found time for discussions and technical explanatory notes.


**General Comments**

- Enlarged lymph nodes are a common finding in clinical practice as lymph nodes are an important part of the immune system and a frequent destination of spreading malignant cells. Thus lymph nodes become enlarged in a wide spectrum of diseases and fine-needle aspiration biopsy (FNAB) is often used as an initial investigation in diagnosing and triaging patients; not only for superficial (palpable) nodes but more and more for abnormal deep-seated nodular lesions located in complex body compartments. Deep-seated lesions can be detected by different imaging techniques and may be investigated by laborious and expensive invasive interventional procedures [25]; this is why a definite diagnosis by aspiration biopsy is of prime importance in many instances, particularly in patients whose condition is too poor for anesthesia and open surgical biopsy.
- FNAB of lymph nodes is one of the most challenging fields in routine cytodiagnostic practice [8]. In particular, separating reactive proliferative lymphatic lesions from low-grade malignant lymphoma can be extremely delicate. The challenge for cytopathologists, therefore, is to apply modern practices on both diagnostic and laboratory levels in order to achieve the most specific diagnosis; and there is no question that close interdisciplinary cooperation is absolutely necessary. Several recent studies and reviews have attested high overall accuracy to cytomorphologic diagnosis of lymphomas. The success rate of FNA cytology ranges from 80% to over 90% in diagnosis of NHL, yielding lower values in lymphoma subclassification [3, 8, 18]. The combination of cytomorphology and ancillary methods (cellular immunophenotyping, molecular biology techniques) on aspirated cell samples can reliably distinguish between benign and malignant lymphatic conditions [33] achieving high sensitivity and specificity for the diagnosis and classification of lymphomas [35].
- The future role of surgical lymphoma diagnostics in comparison with minimally invasive procedures has recently been discussed by Morris-Stiff and coauthors [24].
- A false-negative FNA diagnosis involves a potentially significant diagnostic delay from FNAB to bioptic diagnosis. This occurs particularly in patients with indistinct clinical symptoms from their malignant lymphoid tumor [28].
- Over a period of two decades (1987–2007) more than 10,000 superficially located lymph nodes were cytologically evaluated at the Cytologic Department of the Kantonsspital St. Gallen. The majority of them were sampled by our cytopathologists using free-hand FNAB and ultra-

sound-guided fine-needle aspiration biopsy (US-FNAB). In recent years, hundreds of image-guided lymph node aspirations from the abdominal, retroperitoneal, and mediastinal compartment have been added to by means of ultrasound, computed tomography, endoscopy, and endoscopic ultrasound.

## 15.1.2 Fine-Needle Aspiration Biopsy

### 15.1.2.1 Indications for FNAB of Lymph Nodes [8]

FNAB can give important information as a first-line investigation for abnormal nodular lesions that are or are suspected of being lymph nodes, and during the follow-up of previously diagnosed malignant lymphomas and nonlymphoid neoplasms.

Relevant indications for fine-needle aspiration cytology include:

- Detection of lesions that mimic a lymph node such as nodular hyperplastic or ectopic organ tissue, cysts, sharply demarcated benign and malignant tumors whithin or at the outer margin of parenchymatous organs, extranodal circumscribed tumors of soft-tissue origin, and others.
- Triaging enlarged lymph nodes: nonspecific reactive lymphadenopathy versus specific lymphadenitis versus malignant lymphoma versus metastatic neoplasm.
- Staging of proven lymphoma and lymphadenopathies at multiple sites in the patients' bodies.
- Investigation of suspected extranodal tissue involvement by a malignant tumor.
- Lymphoma patients suffering from residual disease or recurrences during long-term follow-up.
- Lymphoma patients who develop additional lymphadenopathy in disagreement with the clinical and laboratory results.
- Patients at high surgical risk.
- Enlarged lymph nodes that are not accessible by means of a simple surgical excision (mediastinal, intraabdominal, retroperitoneal).
- Assessment of tumor progression from a low-grade to a high-grade lymphoma, taking into account the morphologic and biologic (S-phase fraction, proliferation index, mitotic rate) indices established by previous cytologic and/or histologic investigations.
- Identification of a second type of lymphoid malignancy, for instance Hodgkin lymphoma following non-Hodgkin lymphoma.

### 15.1.2.2 FNAB: Sampling Techniques

1. Palpable lymph nodes are frequently sampled by freehand aspiration. However, our experience has shown that US-FNAB can minimize sampling error, particularly on large palpable lesions (see Sect. 15.1.2.6, "FNAB and Sonography," p. 909).
2. At our institution, cytologic specimens from superficial nonpalpable lymph nodes are routinely obtained by US-FNAB and occasionally by FNAB supported by PET-CT imaging. PET-CT imaging is a combined investigation using computed tomography (CT) together with positron emission tomography (PET). Lesions showing enhanced metabolic activity in PET are precisely localized in comparison with the concomitant CT image; subsequently they are easily detected by ultrasound imaging.
3. Deep-seated lymph nodes are sampled by standard techniques such as US-FNAB, aspiration under direct endoscopic vision, endoscopic ultrasound-guided fine-needle aspiration (EUS-FNAB) [26] and CT-guided access. At our hospital, such FNABs are performed by radiologists, chest physicians, and gastroenterologists.

### 15.1.2.3 FNAB: Technical Details

- Aspiration is performed with standard needles (22- to 25-gauge). Using needles with a larger caliber in many cases yields blood-rich aspirates that contain only a few target cells; such samples are generally not sufficient for diagnosis.
- With regard to superficial nodules, the target lesion must be immobilized with one hand. Thus, it is highly recommended to hold the syringe with the needle attached in a pistol-type holder, unless a vacuum system is connected to the needle.
- It is important to perform an excessive aspiration with multiple needle passes and suctions in a fan-like manner in order to collect an adequate sample.
- The needling technique without suctioning may occasionally yield enough cellular material from lymphatic tissues.
- Further specifications on FNAB technique can be found in several chapters of this book and in the literature.

### 15.1.2.4 FNAB Performed by Cytopathologists

- FNAB of abnormal superficial lymph nodes (palpable or nonpalpable) at various sites of the body has proved to be a simple, rapid, and cost effective technique with limited complications if performed by well-trained physicians; it can replace a large number of surgical biopsies.
- However, the best results are obtained when all steps are performed by a cytopathologist skilled in the fields as listed:
  - Ultrasound imaging giving information on structural properties of the lesion, size and shape of the nodule, and anatomic relationship to surrounding tissues.
  - Decision on the interventional procedure: FNAB with or without sonographic guidance.

- Decision on specimen processing: conventional smear versus Cytospin preparation versus ThinPrep method versus cell-block technique.
- Adequate cell collection for auxiliary laboratory investigations.
- Microscopic evaluation and cytologic decision-making taking into account the ancillary test results.

#### 15.1.2.5 FNAB Performed by Attending Physicians and Practitioners

- Inexperienced operators and physicians who do not follow established aspiration and preparation techniques reduce the diagnostic sensitivity; FNABs often yield inadequate, diagnostically inconclusive, poorly preserved, and potentially misleading material. Therefore, during the interventional procedure the operator should be assisted by a cytotechnologist, who is responsible for optimal smear preparation and adequate collection of cell material for additional tests.
- On the other hand, liquid-based thin-layer technology (Cytospin, ThinPrep) has proved to be a perfect tool for clinic-based FNAB if a cytopathologist or cytotechnologist is not available on site:
  - The total amount of aspirate, including needle rinse and syringe rinse material, is available and the cell preservation is excellent.
  - An optimal preparation of the lymphoid cells can be achieved for morphologic evaluation as well as for additional laboratory tests. Thin-layer preparations are particularly well-suited for immunocytochemistry and fluorescence in situ hybridization.

#### 15.1.2.6 FNAB and Sonography

- Sonographic findings can be extremely helpful to pre-estimate the nature of a lymph node enlargement. It further enables the operator to place the needle in the sonographically most suspicious area, thus acquiring a representative sample and providing enough smears containing adequate cellularity and adequately preserved material for additional analyses.
- Normal lymph nodes usually appear sonographically as flattened hypoechogenic structures showing an echogenic hilus. Fatty replacement of lymphoid tissue is easily recognized as reflective defects inside the hypoechogenic lymphoid tissue.
- On the other hand, ultrasonographic investigation supports the clinical suspicion of a malignant lymphoma: large nodules appear singly or tightly packed together, showing neat margins and homogeneous hypodensity, restricted to one location or disseminated.

#### 15.1.2.7 FNAB and Histology

- A combination of FNAB and core-needle biopsy can reduce the number of interventions that provide inadequate material and may increase the diagnostic yield at least for certain lymphoma subgroups [15].
- At the oncologic unit of the Kantonsspital St. Gallen, core-needle biopsy is performed solely on patients whose general condition is too poor for surgical exploration and frequently subsequent to a prior indeterminate FNAB diagnosis.
- Excisional biopsy of the entire pathological lymph node should be sought whenever the situation allows a surgical intervention [28].

### 15.1.3 Laboratory Procedures, Technical Aspects

#### 15.1.3.1 Conventional Smears

For lymphoid disorders, it is highly recommended to prepare both wet-fixed and air-dried smears.

##### 15.1.3.1.1 Wet-Fixed Preparation

At least one or two specimens should be prepared. Aspirate material (or part of it) is expelled one or two drops at a time directly on the glass slides. The material is spread with a second slide in flat position, and wet fixed within 2–3 s in Delauney solution (or another alcohol fixative), or using a spray fixative. The essential goal of the procedure is to obtain a cellular thin layer with well-preserved morphologic details, but without any squash artifacts.

##### 15.1.3.1.2 Air-Dried Smears

They should be prepared like thin cell films that allow rapid drying of the cell material. Drying should be supported by waving the slide in the air or using a fan.

##### 15.1.3.1.3 Staining Procedures

- Wet-fixed specimens are routinely Pap-stained and air-dried smears are stained using May-Grünwald-Giemsa (MGG) or Diff-Quik. Pap-stained cells usually qualify for better evaluation of the nuclear details, whereas cytoplasmic features are better recognized using the MGG staining procedure.
- We prefer wet-fixed and Pap-stained smears for other reasons: they are the most suitable for (1) comparative studies of the cell morphology in cytologic specimens and histologic sections of the same lesion and (2) the majority of immunocytochemical tests.

### 15.1.3.2 Liquid-Based Cytology

- As already mentioned above, a transport medium is best used by clinicians performing FNABs who are not familiar with the proper preparation and fixation technique and if cytology staff attendance is not available.
- Furthermore, a liquid-based method is often superior to conventional smears with regard to clear background, thin-layer preparation, cell preservation (Figs. 15.18, 15.35, 15.48), and a large number of cytologic specimens, which is a prerequisite for the application of complete antibody panels. Optimal and standardized preparation is mandatory for additional studies, in particular immunocytochemistry, molecular techniques (e.g., FISH), or static DNA cytometry [13] (Figs. 15.65, 15.68, 15.69).
- Therefore, the residual material in the needle and syringe should routinely be washed out and suspended in a vial containing a cell medium. The cell suspension can be processed by cytocentrifugation (Cytospin) or by means of processors such as ThinPrep, SurePath, etc. The type of transport medium depends on the kind of processor and thin-layer preparations can be performed as instructed by the manufacturers.

**Caution**

We know from our experience and from the literature that the morphologic features may be altered using liquid-based methods; as a result cell interpretation requires modification. The most challenging morphologic changes of lymphoid cells in liquid-based specimens compared to conventional smears are nuclear shrinking, disruption of the cytoplasm, and more pronounced nucleoli.

15

### 15.1.3.3 Processing of Sanguineous Aspirates

Regardless of the operator, CytoLyt (Hologic, Marlborough, MA, USA) among other hemolyzing fixatives, has been shown to be indispensable as an initial transport medium for FNABs providing bloody aspirates. CytoLyt is best used in combination with the ThinPrep modality. CytoLyt lyses erythrocytes and provides well-preserved lymphoid cells and a clear smear background.

### 15.1.3.4 Cell-Block Technique

The use of the cell-block technique depends on the amount of the aspirated cell material and is a matter of individual preference. The great advantage of this method, particularly in lymph node cytology, is the possibility of producing extra slides for ancillary tests, such as a large battery of immunocytochemical stains.

## 15.1.4 Ancillary Techniques [9]

- The main objectives of auxiliary techniques such as immunocytochemistry, PCR, and FISH to aspirates of lymph nodes are the detection of phenotypic and genotypic profiles including clonality, translocation of specific gene loci, and more complex genetic aberrations. At our institution, cytomorphologic evaluation combined with the auxiliary techniques mentioned above are standard diagnostic procedures in lymphohematologic disorders.
- Clonality assessment is largely used to differentiate between malignant non-Hodgkin lymphoma and reactive lymphoproliferative disorders. Numerous non-Hodgkin lymphomas providing inconclusive cytologic results can be elucidated by adequate immunophenotyping and molecular characterization, a benefit particularly for those patients in whom surgical biopsy is contraindicated [35].

### 15.1.4.1 Immunocytochemistry [7, 31, 32, 33, 35]

- Immunocytochemistry (IC) is a reliable method, particularly when performed on Cytospin samples or even better on liquid-based thin layer specimens (ThinPrep) devoid of background debris.
- Immunocytochemical staining results are difficult to interpret in conventional smears comprising dense proteinaceous background and/or debris; the diffuse positive immunostaining of the background material may obscure individual cells.
- Poor sample cellularity may prevent the application of an adequate immunocytochemical panel or actually any immunocytochemical testing.
- Immunocytochemistry is a suitable way to:
  - Recognize B-cell and T-cell lineage (Figs. 15.65 and 15.81).
  - Identify polyclonality of a benign reactive lymphoid lesion (Figs. 15.1 and 15.2) and monoclonality of a malignant lymphoid proliferation.
  - Diagnose and classify B-cell non-Hodgkin lymphomas (κ and λ light chain restriction, and specific CD marker profiles, and others) (Fig. 15.3).
  - Diagnose malignant lymphomas of the T-cell phenotype (always in accordance with cytomorphology!) (Figs. 15.81 and 15.89).
  - Diagnose Hodgkin lymphomas (CD15- and CD30- and PAX-positive tumor cells) (Figs. 15.96 and 15.97).
  - Define the proliferative activity of lymphoid tumor cell populations (MIB-1 index based on the immunopositive nuclear rate).
  - Distinguish between anaplastic/large-cell NHLs and non-lymphoid malignant neoplasms (lymphoid cell markers versus nonlymphoid markers).
- For diagnostic purposes and subtyping, fresh wet-fixed smears, Pap-stained smears, and Pap-stained archival

cytologic specimens qualify for the vast majority of immunocytochemical stains. The target antigens include B- and T-cell markers, plasma cell-associated markers, myeloid cell-associated markers, surface and cytoplasmic immunoglobulins, CD markers, and specific gene products.

- As already mentioned, liquid-based thin layer preparations (e.g., ThinPrep) are superior to conventional smears for the immunocytochemical work-up of lymphomatous lesions.

**Caution**

- It is of utmost importance that cytology laboratories properly utilize immunolabeling methods.
- Each institution should develop internal protocols for processing the cell aspirate from standardized sampling to staining procedures, and for rules ensuring the validity and reproducibility of the results.
- Those immunotests that have provided untrustworthy results have to be evaluated with special attention. Whenever possible, they should be substituted with other markers and by another biological or technical approach.

- Differentiation of Leukocytes: CD Markers (Cluster of Differentiation) See Table 15.1.1. p. 912.

### 15.1.4.2 Flow Cytometry [3, 4, 10, 11, 30 ]

- Together with immunocytochemistry, flow cytometry (FCM) is the most commonly used auxiliary method to distinguish between a benign and malignant B-cell lymphoid proliferation in lymph node aspirates. For B-cell NHLs, several study groups have reported a correlation between cytology combined with flow cytometric immunophenotyping and histologic results ranging around 85% [22].
- FCM has the same diagnostic targets as indicated for immunocytochemistry, but has the following advantages:
  - Rapid immunophenotyping using fluorescence-activated cell sorting (e.g., FACS®: Becton Dickinson, San Jose, CA, USA).
  - A large number of specific monoclonal antibodies can be used simultaneously.
  - Multiparametric analysis and possibility to recognize coexpression of CD markers in order to define cell profile and monoclonality.
  - Automation and objective interpretation.

  A disadvantage of the FCM method is the loss of direct visualization of the antigen-antibody product and the complete loss of the evaluated cell material.
- Limitations of flow cytometric evaluation may be given by:
  - Loss of the target cells after processing.
  - Partial lymph node involvement leading to discrepant samples for morphologic and cytometric evaluation.
  - T-cell-rich or lymphohistiocytic-rich lymphoma variants comprising only a small tumor cell population of monoclonal B cells.
  - Poor tumor preservation.
  - Low viability.
  - T-cell NHLs lacking aberrant immunophenotype.
  - Others [16, 23, 33].

The limitations as listed may partly hold true for other adjunct analyses, in particular for IC.

### 15.1.4.3 Molecular Genetics [18]

The molecular techniques generally used in routine practice are PCR gene amplification and FISH. Other methods such as comparative genomic hybridization (CGH), Southern blot analysis, or microarray technologies are restricted to fresh or liquid frozen tissue and may currently play a pivotal role in research work.

A complete molecular diagnostic palette may not only help refine the diagnosis, but is also valuable for prognosis assessment and planning treatment protocols.

Molecular diagnostic assays in lymph node aspirates are suitable for

- Clonality analysis.
- Sequencing.
- The detection of mutational status.
- The detection of chromosomal translocations.
- The detection of more complex genetic abnormalities.

#### 15.1.4.3.1 Polymerase Chain Reaction

[29, 35] (Figs. 15.4 and 15.5)

- PCR using DNA extracted from nuclei in cytologic samples allows the amplification of nucleic acid sequences. Either followed by gel electrophoresis or fragment analysis, it is a reliable assay to assess both clonal variable diversity joining (VDJ) rearrangement of heavy and variable joining (VJ) rearrangement of light immunoglobulin chain genes in lymphoid B-cell proliferations, or of T-cell receptor genes in T-cell populations. Amplification of oncogene breakpoints may still have a certain value in the setting of long distant PCR in detecting Bcl-2 rearrangements.
- PCR is more sensitive in detecting clonality than immunocytochemical and flow cytometric tests, and the same is true when applied to tissue samples [1].
- At our institution, routinely prestained cytologic smears have been available for PCR investigations. The cells are scraped from the stained slides and prepared using standard procedures [18]. Several studies could show that prestained smears, coverslipped archival glass slides, and unstained fresh cytologic material are suitable for PCR studies [2, 12, 19]. Furthermore, Torlakovic and coworkers found various cytologic laboratory procedures valuable for PCR detecting IgH gene rearrangement [34].

**Table 15.1.1** Synopsis of clusters of differentiation (markers of cytologic relevance only) regarding lymphoid and nonlymphoid cells, and lymphoid tumors

| CD # | Predominant cellular specificity | CD positivity as an indicator of selected tumor entities |
|---|---|---|
| 1a | Cortical thymocytes<br>Langerhans cells, interdigitating reticulum cells | Langerhans cell histiocytosis |
| 2 | Thymocytes, peripheral T-cells (sheep-erythrocyte receptors) | Most T-cell lymphomas |
| 3 | All T lymphocytes | Most T-cell lymphomas |
| 4 | Helper/inducer T-cells | CD4-restricted T-cell lymphomas |
| 5 | T lymphocytes | Small lymphocytic lymphoma/CLL<br>T-cell lymphomas<br>Mantle cell lymphoma |
| 7 | T lymphocytes (immature and mature) | Most T-ALLs<br>Peripheral T-cell lymphoma |
| 8 | Cytotoxic/suppressor T cells | CD8-restricted T-cell lymphomas |
| 10 | precursor B-cells, germinal center cells | B-ALL<br>common type follicular lymphoma<br>DLBCL, GCB-type |
| 11c | Monocytes, macrophages, granulocytes<br>Some T and B cells | Hairy cell leukemia<br>Marginal zone B-cell lymphoma |
| 15 | Granulocytes, myeloic cells, histiocytes | Hodgkin lymphoma (HRS cells)<br>Myelogenic sarcoma |
| 19 | Precursor B cells, peripheral B cells | B-cell lymphomas |
| 20 | All peripheral B lymphocytes | Most B-cell NHLs<br>10–20% positivity in tumor cells of Hodgkin lymphomas |
| 21 | Follicular dendritic cells, marginal zone cells | Dendritic reticulum cell neoplasm |
| 22 | All B lymphocytes, marginal zone cells | B-cell lymphomas |
| 23 | Mature B lymphocytes, follicular dendritic cells | CLL<br>Marginal zone B-cell lymphoma |
| 25 | | Hairy cell leukemia |
| 30 | | B- and T-cell lymphomas<br>Hodgkin lymphoma (HRS cells)<br>Anaplastic large-cell lymphoma |
| 34 | Myeloid and lymphoid precursor cells | Precursor cell neoplasms |
| 38 | Plasma cells, wide spectrum of activated lymphocytes | Plasma cell tumors |
| 43 | T lymphocytes<br>Myeloid cells and various B cells | T-cell lymphomas<br>some B-cell lymphomas<br>myelogenic sarcoma |
| 45 | Leukocyte common antigen | B- and T-cell lymphomas |
| 56 | NK/T cells, plasma cells | NK-/T-cell lymphomas<br>Plasma cell neoplasms<br>Blastic plasmacytoid dendritic cell neoplasm |
| 68 | Multiple types of histiocytic cells | Histiocytic sarcoma |
| 79a | B lymphocytes, wide spectrum of maturation stages | Most B-cell NHLs<br>B-ALL |
| 117 | Myeloid cells<br>Mast cells | Myelogenic sarcoma<br>Mastocytoma |
| 123 | Blastic plasmacytoid dendritic cells | Blastic plasmacytoid dendritic cell neoplasm |
| 138 | Plasma cells | Multiple myeloma<br>Lymphoplasmacytic lymphoma |

ALL, acute lymphoblastic leukemia; CLL, chronic lymphocytic leukemia; NHL, non-Hodgkin lymphoma; HRS cells, Hodgkin and Reed-Sternberg cells; MZ, marginal zone; DLBCL, diffuse large B-cell lymphoma; GCB, germinal center B-cell-type

**Caution**

- Immunocytochemical staining prohibits subsequent PCR-based DNA analysis [34].
- Both Pap staining and MGG staining can inhibit PCR. Removal of the inhibition seems to be possible using a simple destaining method [6, 34].

#### 15.1.4.3.2 Southern Blot

Southern blot analysis has been shown to be a reliable tool to detect a monoclonal B-cell and T-cell gene rearrangement. However, the method is not easy to practice and requires unfixed material in large amounts.

#### 15.1.4.3.3 Fluorescence In Situ Hybridization (FISH)

[5, 14, 17, 29]

- FISH can be applied on intact nuclei and on isolated DNA molecules. FISH using interphase nuclei is highly suitable for cytologic specimens with the objective of detecting structural and numerical chromosomal changes.
- Detecting specific gene translocations is an excellent tool for lymphoma subtyping. The method has been routinely applied to establish t(14;18)(q32;q21) translocation in lymphoma of follicle center cell origin and t(11;14)(q13;q32) translocation in mantle cell lymphoma, and others (Fig. 6.1).
- FISH can also detect chromosomal aberrations in patients with small-cell lymphocytic lymphoma, which may in the future provide a basis for prognostic and therapeutic considerations [5].
- Unstained wet-fixed, unstained air-dried smears, and smears stained according to the Papanicolaou or MGG method, as well as archival cytologic specimens [27] comparably qualify for FISH assays. Monolayer cell spreading on conventional smears is accurate for FISH analyses, but optimal results have been achieved using liquid-based cytology (e.g., ThinPrep) in respect of standardized preparation, technical handling, and interpretation.

### 15.1.5 The Lymph Node and Its Architecture (Fig. 15.6)

- Lymph nodes are bean-shaped organs located throughout the lymphatic system filtering the lymphatic fluid. The nodes store white blood cells, which are precursors of active immunocompetent cells. Furthermore, lymph nodes are places where special cells can trap cancer cells or bacteria as well as foreign particles that are traveling in the lymphatic fluid through the human body.
- The lymph nodes are coated by a fibrous capsule from which trabeculae of loose connective tissue extend into the parenchyma and concentrate at the hilus. The trabeculae embedding blood vessels, histiocytic cells, and lymphoid sinuses.
- The lymph circulates to the lymph nodes via afferent lymphatic vessels that cleave the capsule and drain into the sinus just beneath the capsule. The subcapsular sinus drains into trabecular sinuses and finally into medullary sinuses. The lymph then leaves the lymph node via the efferent lymphatic vessels at the hilus.
- The peripheral area of the lymph node is called cortex and the inner area medulla. The parenchymatous area between the cortex and medulla is referred to as the paracortex.

#### 15.1.5.1 Cortex

The cortex contains nodules that are predominantly composed of densely packed B lymphocytes:

– *The primary follicles* contain small inactive/resting lymphocytes.
– *The secondary follicles* exhibit germinal centers resulting from an antigenic stimulus. Secondary follicles consist of an outer rim of small lymphocytes and a central area called the germinal center comprising small and large lymphatic cells at various stages of transition; mitotic activity is obvious. These lymphoid cells are intermingled with nonphagocytic antigene presenting dendritic reticulum cells/histiocytes and phagocytic macrophages. The latter are known as tingible-body or starry-sky macrophages. Large rounded cells moved from the germinal center into the interfollicular space are the B immunoblasts, which have the potential to differentiate into plasma cells.

#### 15.1.5.2 Medulla

The medulla is made up of cell cords that are composed of B and T lymphocytes, plasma cells, histiocytes, and occasional mast cells.

#### 15.1.5.3 Paracortex

The paracortical area is the T-cell compartment of the pulp, where resting T lymphocytes develop into immunocompetent cells in a similar manner as the B cells.

## 15.1.6 Cytology of Benign Lymph Nodes

The cytology pattern of benign lymph nodes as described below refers to aspirates from reactive hyperplastic lymph nodes. Inactive lymph nodes usually are very small, not palpable and consequently an extremely rare target for FNAB.

The morphologic features of the cells listed next were first described by Lukes, Collins, and Lennert [20, 21].

- *Resting lymphocytes* (Fig. 15.7)
  - These cells are small, ranging from 4 to 10 $\mu$m (depending on fixation and staining modalities). A small rim of cytoplasm, usually not surrounding the whole nucleus, exhibits a pale blue to cyanophilic staining quality. The nuclei are round, generally exhibiting smooth outlines; wrinkling is rarely seen. The chromatin appears as loosely distributed or clumped coarse granules. Nucleoli are absent or inconspicuous in air-dried MGG-stained smears, but often seen as centrally placed small dots in Pap-stained specimens.
- *Germinal center cells* (Figs. 15.8 and 15.9)
  These cells represent a variegated population composed of small and large cleaved and noncleaved cells.
  - *Centroblasts:* Large follicle center cells are referred to as centroblasts, two to three times larger than small lymphocytes. Their cytoplasm is scant and slightly basophil. The nuclei are rounded, exhibiting indistinct irregularities. The chromatin is fine and evenly distributed. Multiple nucleoli are peripherally located.
  - *Centrocytes:* Small cleaved cells, called centrocytes develop from centroblasts. They are only slightly larger than small lymphocytes and show characteristic irregularities of the nuclear shape, nuclear indentations, and occasional deep cleaves. The chromatin is fine and evenly distributed, and tiny nucleoli are usually seen. The cytoplasm is small, pale, and hardly recognizable.
- *Immunoblasts, plasmablasts, plasmacytoid cells, and plasma cells* (Figs. 15.10–15.12)
  - *The immunoblast* is similar in size to centroblasts. However, in contrast to the latter the nuclei are usually completely round, comprising an accentuated membrane, mostly one pronounced centrally located rounded nucleolus, and evenly distributed loose and fine granular chromatin. The cytoplasm forms a broad rim with neat margins and deep basophilic staining; small sharply outlined vacuoles are frequent.
  - *The plasmablast* is a transitional stage between immature blasts and mature plasma cells and can usually be detected. Plasmablasts have approximately the size and appearance of immunoblasts, but the nucleus is eccentrically positioned and the basophilic cytoplasm is occasionally triangular in shape, showing a distinct paranuclear halo. Binucleation may occur.
  - *The plasmacytoid cell* is an intermediate stage of differentiation between immunologically determined inactive lymphocytes and plasma cells showing both morphologic features of lymphocytes and plasma cells.
  - *Mature plasma cells* exhibit pathognomonic morphologic features: an eccentrically placed nucleus, the whole cytoplasmic body measures twice the size of the included nucleus exhibiting a deep basophilic staining quality including paranuclear clearing. The chromatin is coarse and densely packed with several aggregates that are typically arranged in a spokelike pattern.
- *Monocytoid B lymphocytes* are lymphocytes related to the marginal zone surrounding the lymph follicles.
  - The cells show centrocyte-like nuclear features and a moderate to abundant pale cytoplasm that may lead to a monocytoid appearance of the cells.
- *Macrophages and other histiocytic cells* (Figs. 15.9, 15.13–15.16)
  The term "histiocyte" has been used for multiple purposes, but the cell is generally considered a relatively inactive constituent of the mononuclear phagocytic system found in normal connective tissue.
  - *Histiocytic cells* (Fig. 15.13) in common use comprise a vesicular kidney-shaped nucleus and a large clear cytoplasm that may become pale and eosinophilic. The cytoplasmic structure and its inclusions depend on the phagocytic activity of the individual cell. The nuclear contour is smooth and the chromatin loose and reticular. The number of nucleoli and their shapes are regulated by cellular activity.
  - *Tingible-body cells,* also referred to as starry-sky macrophages (Figs. 15.9 and 15.14), appear in general as huge cells with abundant clear and ill-defined cytoplasm containing phagocytosed cellular fragments and debris. The nuclei are of the histiocytic type but frequently barely visible. The chromatin is fine and loosely distributed, one to multiple small but distinct nucleoli occur.
  - *Reticulum cell* is, in the current sense of the term, a cell of the reticuloendothelial system. But in lymph nodes, the term is frequently used for histiocytes and histiocytoid stromal cells.
  - *Interdigitating reticulum cells* (Fig. 15.15) are histiocytes with the potential to present antigen; they are found in T-cell areas of lymph nodes. The cells are mainly characterized by interdigitating cytoplasmic surface projections and longitudinal nuclear grooves.
  - *Epithelioid histiocytes* (Fig. 15.16) show a characteristic nuclear shape that has a striking resemblance to a footprint.

### 15.1.6.1 Immunoprofiles of Histiocytic Cells

**Table 15.1.2** Histiocytic subsets and their immunoprofile

| Cell type | CD68/ CD163 | CD21/CD23 | CD35 | S100 | CD1a | CD45 |
|---|---|---|---|---|---|---|
| – Common histiocytes in reactive sinus histiocytosis<br>– Macrophages<br>– Epithelioid cells | ++ | | – | – | – | + |
| SHML cells in Rosai-Dorfman disease | ++ | | – | ++ | – | |
| Follicular dendritic histiocytes | | + | ++ | | | |
| Interdigitating reticulum cells of T-cell area | – | | – | + | + Variable | |
| Langerhans cells | (+) Variable | | | ++ | ++ | (+) Variable |

SHML, sinus histiocytosis with massive lymphadenopathy

– completely negative (+) negative or weak + moderate ++ distinct

## 15.1.7 Further Reading


1. Aiello ADD, Giardini R, Alasio L, et al. PCR analysis of IgH and BCL2 gene rearrangement in the diagnosis of follicular lymphoma in lymph node fine-needle aspiration. A critical appraisal. Diagn Mol Pathol 1997;6:154-160.
2. Alcan SLC, Sarago C, Sidawy MK, et al. Polymerase chain reaction detection of immunoglobulin gene rearrangement and bcl-2 translocation in archival glass slides of cytologic material. Diagn Mol Pathol 1995;4:25-31.
3. Bangerter M, Brudler O, Heinrich B, Griesshammer M. Fine needle aspiration cytology and flow cytometry in the diagnosis and subclassification of non-Hodgkin's lymphoma based on the World Health Organization Classification. Acta Cytol2007;51:390-398.
4. Barroca H, Marques C, Candeias J.Fine needle aspiration cytology diagnosis, flow cytometry immunophenotyping and histology in clinically suspected lymphoproliferative disorder. A comparative study. Acta Cytol 2008;52:124-132.
5. Caraway NP, Thomas E, Khanna A, et al. Chromosomal abnormalities detected by multicolor fluorescence in situ hybridization in fine-needle aspirates from patients with small lymphocytic lymphoma are useful for predicting survival. Cancer(Cancer Cytopathol) 2008;114:315-322.
6. Chen J-T, Lane MA, Clark DP. Inhibitors of the polymerase chain reaction in Papanicolaou stain. Removal with a simple destaining procedure. Acta Cytol 1996;40:873-877.
7. Chhieng DC, Cohen JM, Cangiarella JF. Cytology and immunophenotyping of low- and intermediate-grade B-cell non Hodgkin's lymphomas with a predominant small-cell component: a study of 56 cases. Diagn Cytopathol 2001;24:90-97.
8. Das DK. Value and limitations of fine-needle aspiration cytology in diagnosis and classification of lymphomas: a review. Diagn Cytopathol 1999;21:240-249.
9. Dey P. Role of ancillary techniques in diagnosing and subclassifying non-Hodgkin's lymphomas on fine needle aspiration cytology. Cytopathology 2006;17:275-287.
10. Dey P, Amir T, Al Jassar A, et al. Combined applications of fine needle aspiration cytology and flow cytometric immunophenotyping for diagnosis and classification of non-Hodgkin lymphoma. Cytojournal2006;3:24.
11. Dong HY, Harris NL, Preffer FI, et al. Fine-needle aspiration biopsy in the diagnosis and classification of primary and recurrent lymphoma: a retrospective analysis of the utility of cytomorphology and flow cytometry. Mod Pathol 2001;14:472-481.
12. Gall K, Pavicic D, Pavelic J, et al. PCR amplification of DNA from stained cytological smears. J Clin Pathol 1993;46:378-379.
13. Garbar C, Remmelink M, Mascaux C. Fine needle aspiration cytology of lymph node: experience of 2 university hospitals with conventional smears and liquid-based cytology.Acta Cytol 2008;52:418-423.
14. Gong Y, Caraway N, Gu J, et al. Evaluation of interphase fluorescence in situ hybridization for the t(14;18)(q32;q21) translocation in the diagnosis of follicular lymphoma on fine-needle aspirates: a comparison with flow cytometry immunophenotyping.Cancer 2003;99:385-393.
15. Gong JZ, Snyder MJ, Lagoo AS, et al. Diagnostic impact of core-needle biopsy on fine-needle aspiration of non-Hodgkin lymphoma.Diagn Cytopathol 2004;31:23-30.
16. Hanley KZ, Holden JT, Mosunjac MB. Fine-needle aspiration cytology of high-grade non-Hodgkin lymphomas - when flow cytometry does not support the diagnosis. (abstract)Cancer(Cancer Cytopathol) Suppl. 2008;114:418-419.
17. Jiang F, Katz RL. Use of interphase fluorescence in situ hybridization as a powerful diagnostic tool in cytology.Diagn Mol Pathol 2002;11:47-57.
18. Kocjan G. Best Practice No 185: Cytological and molecular diagnosis of lymphoma. J Clin Pathol 2005;58:561-567.
19. Kube MJ, McDonald DA, Quin JW, Greenberg ML. Use of archival and fresh cytologic material for the polymerase chain reaction. Analyt Quant Cytol Histol 1994;16:174-182.
20. Lennert K. Histopathologie der Non-Hodgkin-Lymphome (nach der Kiel Klassifikation). Springer Verlag Berlin-Heidelberg 1981.
21. Lukes RJ, Collins RD. A functional approach to the classification of malignant lymphoma. Recent Results in Cancer Res1974;46:18-30.
22. Mathiot C, Decaudin D, Klijanienko J, et al. Fine-needle aspiration cytology combined with flow cytometry immunophenotyping is a rapid and accurate approach for the evaluation of suspicious superficial lymphoid lesions. Diagn Cytopathol 2006;34:472-478.
23. Meda BA, Buss DH, Woodruff RD, et al. Diagnosis and subclassification of primary and recurrent lymphoma: the usefulness and limitations of combined fine-needle aspiration cytomorphology and flow cytometry.Am J Clin Pathol2000;113:688-699.
24. Morris-Stiff G, Cheang P, Key S, et al. Does the surgeon still have a role to play in the diagnosis and management of lymphomas?World J Surg Oncol 2008;6:13.
25. Pugh JL, Jhala NC, Eloubeidi MA, et al. Diagnosis of deep-seated lymphoma and leukemia by endoscopic ultrasound-guided fine-needle aspiration biopsy. Am J Clin Pathol2006;125:703-709.
26. Ribeiro A, Vazquez-Sequeiros E, Wiersema LM, et al. EUS-guided fine-needle aspiration combined with flow cytometry and immunocytochemistry in the diagnosis of lymphoma. Gastrointest Endosc 2001;53:485-491.
27. Richmond J, Bryant R, Trotman W, et al. FISH detection of t(14;18) in follicular lymphoma on Papanicolaou-stained archival cytology slides.Cancer 2006;108:198-204.
28. Roh JL, Lee YW, Kim JM. Clinical utility of fine-needle aspiration for diagnosis of head and neck lymphoma.Eur J Surg Oncol 2008;34:817-821.
29. Safley AM, Buckley PJ, Creager AJ, et al. The value of fluorescence in situ hybridization and polymerase chain reaction in the diagnosis of B-cell non-Hodgkin lymphoma by fine-needle aspiration. Arch Pathol Lab Med 2004;128:1395-1403.

30. Sigstad E, Dong HP, Davidson B, et al. The role of flow cytometric immunophenotyping in improving the diagnostic accuracy in referred fine-needle aspiration specimens. Diagn Cytopathol 2004;31:159-163.
31. Simsir A, Fetsch P, Stetler-Stevenson M, Abati A. Immunophenotypic analysis of non-Hodgkin's lymphomas in cytologic specimens: a correlative study of immunocytochemical and flow cytometric techniques. Diagn Cytopathol 1999;20:278-284.
32. Sneige N, Dekmezian RH, Katz RL, et al. Morphologic and immunocytochemical evaluation of 220 fine needle aspirates of malignant lymphoma and lymphoid hyperplasia.Acta Cytol 1990;34: 311-322.
33. Stewart CJR, Duncan JA, Farquharson M, Richmond J. Fine needle aspiration cytology diagnosis of malignant lymphoma and reactive lymphoid hyperplasia.J Clin Pathol 1998;51:197-203.
34. Torlakovic E, Berner A, Risberg B. Detection of immunoglobulin heavy chain gene rearrangements by polymerase chain reaction analysis on lymph node imprints and fine-needle aspirate smears: a comparison of five different imprint preparations. Diagn Cytopathol 1999;20:333-338.
35. Venkatraman L, Catherwood MA, Patterson A, et al. Role of polymerase chain reaction and immunocytochemistry in the cytological assessment of lymphoid proliferations. J Clin Pathol 2006;59:1160-1165.

**Figs. 15.1 and 15.2 Defining clonality using CD markers.**
A 50-year-old woman presenting with a single enlarged cervical lymph node. FNAB specimens showed a heterogeneous cell pattern including polymorphic lymphoid blasts. Cytology could not reliably distinguish between a benign and malignant lymphoid lesion (conventional stain is not shown).
*Immunocytochemistry* was applied on Pap-prestained conventional smears in order to define the clonality of the lymphoid population. Immunostains using antibodies against CD3 and CD20 can distinguish between a benign and a malignant lymphoproliferative disorder: a balanced CD3/CD20 ratio (50:50) was found, which reliably excludes B non-Hodgkin lymphoma. The proliferation index was calculated as the percentage of MIB-1-stained nuclei (9%, not shown).
*Tissue diagnosis* (excisional biopsy of the lymph node): Reactive lymphadenopathy with evidence of progressive transformation of the germinal centers.

**Fig.15.1** CD3 immunostaining: please note that only monomorphic small lymphocytes are decorated and that the background of the smear is clean.

**Fig. 15.2** CD20 immunostaining: please note the positive staining of small lymphocytes, plasmacytoid cells, and blasts. Plasmacytoid cells are characterized by their triangular cytoplasm (arrows). Unlike the CD3-stained specimen, the background of the CD20-stained specimen exhibits immunopositive material.

**Fig. 15.3 Defining clonality using immunostains for immunoglobulin light chains.**
Small lymphocytic non-Hodgkin lymphoma in an aspirate of a cervical lymph node. All neoplastic cells immunocytochemically express cytoplasmic Ig kappa light chains (Cytospin preparation, nuclear counterstaining was not performed). Note the faintly positive granular background staining pattern, which is usually observed in Cytospin specimens. Positive immunostaining for the B-cell marker CD22 and negative staining for Ig lambda light chains are not shown.
*Cytologic/ immunocytochemical diagnosis:* Small lymphocytic B non-Hodgkin lymphoma, monoclonal kappa.
*Tissue diagnosis* (excisional biopsy of a lymph node): Small lymphocytic non-Hodgkin lymphoma of the B phenotype, monoclonal expression of Ig kappa and IgM.



**Figs 15.4 and 15.5 Fine-needle aspiration and polymerase chain reaction.**
Two cases in which PCR was followed by gel electrophoresis and fragment analysis, respectively. Cell sampling by FNAB.

**Fig. 15.4** (case #1) A patient with a positive history of peripheral T-NHL presented with clinical findings suggestive of relapsing disease.
*PCR amplification* (followed by gel electrophoresis) of DNA extracted from cell nuclei sampled by FNAB of the spleen: clonal rearrangement of T-cell receptor gamma genes.
(MWM, molecular weight marker; – C, negative control; + C, positive control; TCR, T-cell receptor).

**Fig. 15.5** (case #2) A patient suffering from high-grade B-NHL. FNAB of a large abdominal lymph node yielded an ambiguous cytologic diagnosis: the cytologic smears showed a large number of small lymphocytes intermingled with atypical blastic B-cells; MIB-1 immunostaining demonstrated a high percentage of positive blasts (high proliferation index of the blast cell population).
*PCR amplification* (followed by fragment analysis) of DNA extracted from cell nuclei of a Pap-prestained conventional smear: Clonal rearrangement of immunoglobulin heavy chain genes (blue-stained peak, framework 2).

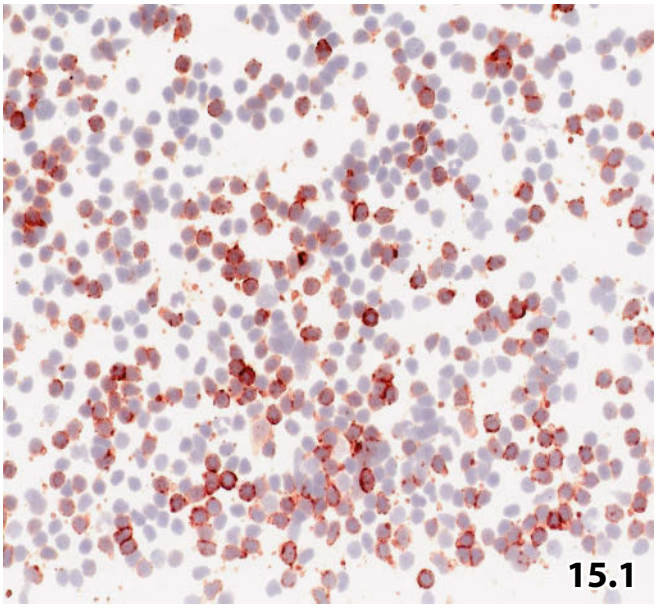
15.1

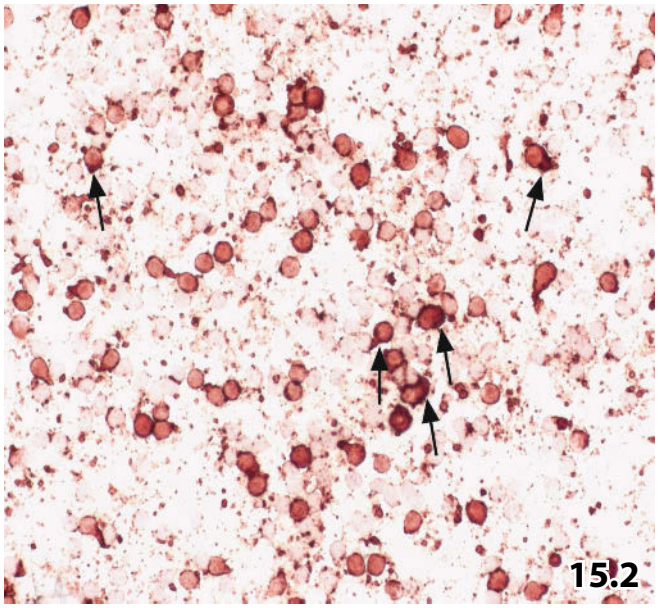
15.2

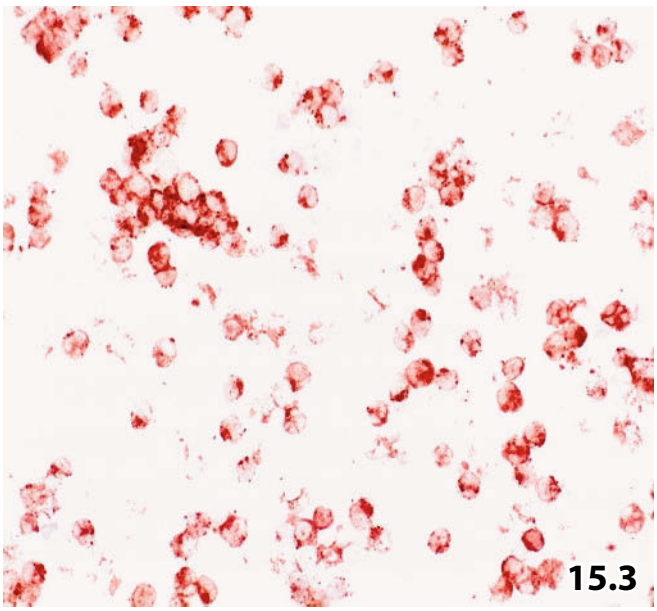
15.3

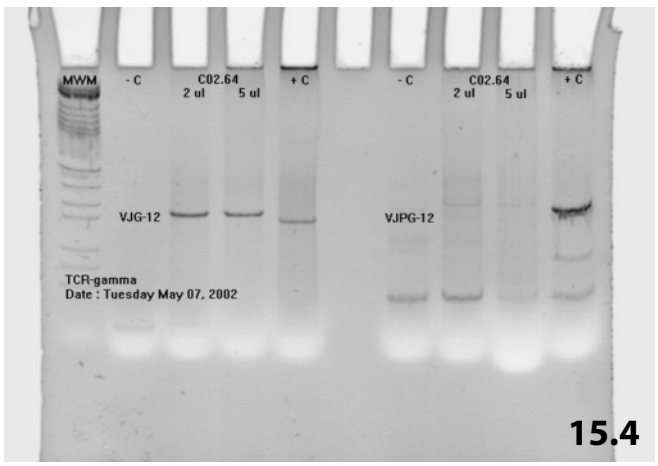

15.4

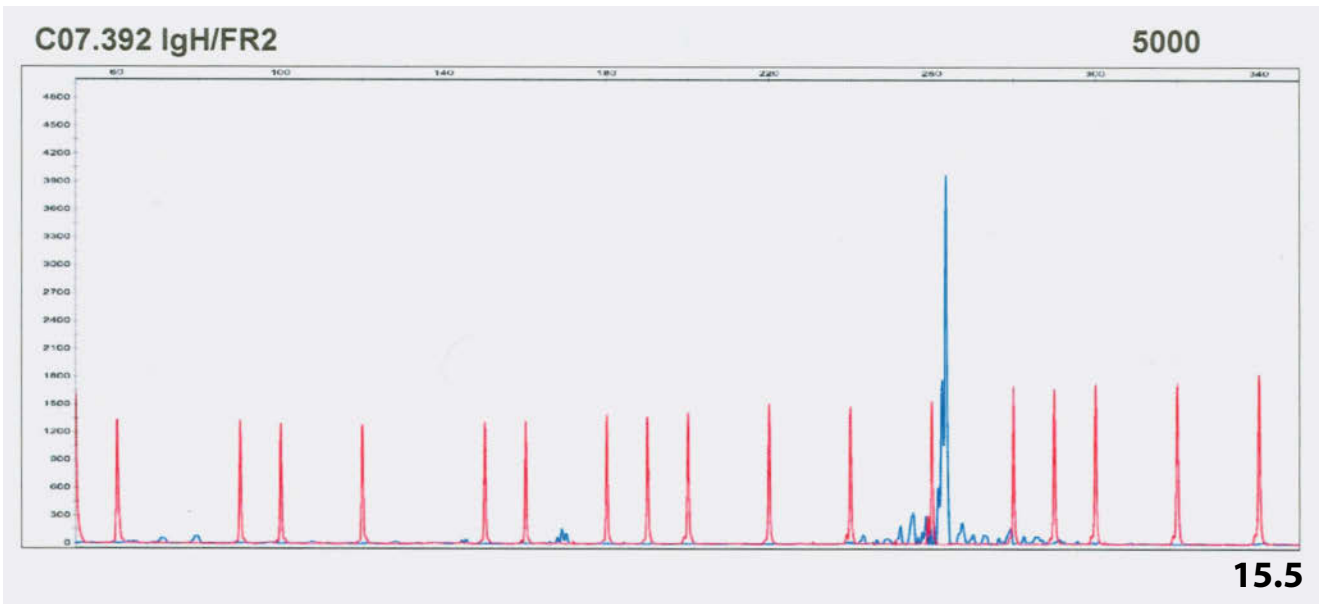

15.5

**Fig. 15.6 Histology of a benign reactive lymph node.**
Very low magnification of an enlarged benign lymph node showing reactive changes (histologic section, HE stain). Short description of the architectural features, elucidated by arrows from right to left:

- Fibrous capsula.
- Subcapsular sinus.
- Cortex and secondary follicles; note starry-sky pattern of the germinal centers.
- Paracortex.
- Medulla; note the distinct cell cords.
- The hilus is composed of loose connective tissue, capillaries and thick-walled vessels (containing red blood cells), and lymphatic vessels (their lumen is devoid of cellular elements).

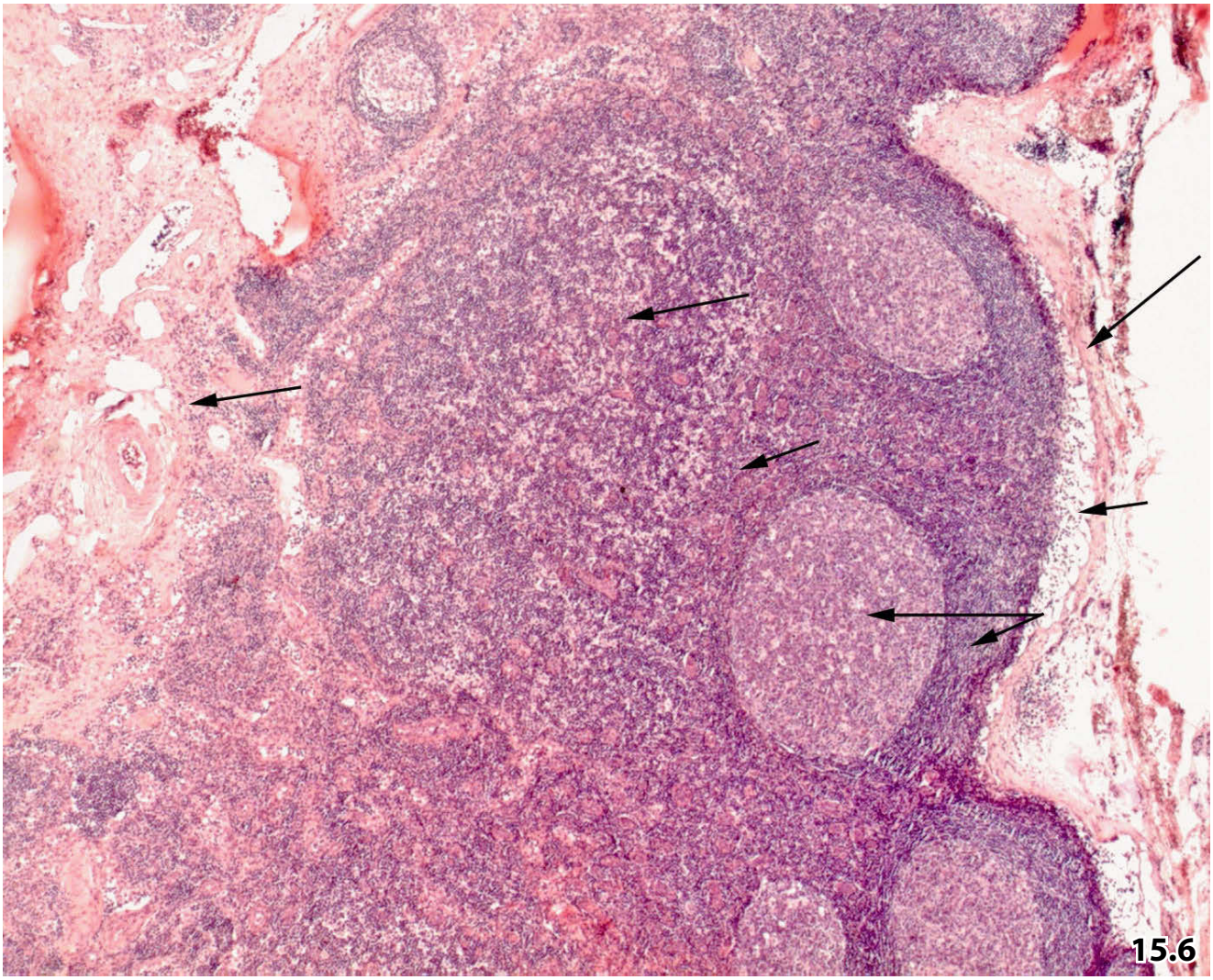
15.6

**Figs. 15.7–15.16 Benign lymphoid cells and variants of histiocytes in FNABs of lymph nodes.**
Cells in aspirates of benign reactive lymph nodes. Direct smears were MGG- and/or Pap-stained.

**Fig. 15.7** *Resting lymphocytes* stained with MGG are presented at high magnification. The distinct nuclear cleaving indicates T lymphocytes (arrows).

**Fig. 15.8** *Germinal center cells* stained with MGG (direct smear, high magnification):
1. A few resting lymphocytes
2. A centroblast exhibits characteristic cytoplasm and nucleoli (particularly easy to recognize when Pap stain is used; see Fig. 15.9); the nucleoli are shifted to the nuclear periphery (arrow)
3. Centrocytes showing pronounced irregular nuclear outline (small arrowheads)
4. A histiocyte is also present (large arrowhead)

**Fig. 15.9** *Germinal center cells,* Pap-stained, are presented at lower magnification: centroblasts (arrows), centrocytes (arrowheads), and a single tingible-body macrophage (center) are clearly discernible. Note the chromatin texture of benign lymphoid cells: loosely arranged granules and small clumps.

**Fig. 15.10** *Immunoblasts and plasmablasts* (arrows) vary in their cytoplasmic shape: deep-basophilic rim vs eccentric basophilic cytoplasmic body exhibiting flimsy paranuclear halo (high magnification, MGG stain).

**Fig. 15.11** *Mature plasma cell* (arrow) *and plasmacytoid cells* (arrowheads) show discriminative morphologic features. Unlike plasmacytoid cells, mature plasma cells comprise coarsely clumped chromatin, absence of nucleoli, and abundant eccentric cytoplasm, but both cell types exhibit a paranuclear clear area (MGG stain, lower magnification).

The eccentric cytoplasmic area of mature plasma cells exhibits an identical diameter to the associated nucleus.



**Fig. 15.12** Two *typical immunoblasts* are depicted from a Pap-stained smear. One of the two nuclei displays a centrally placed nucleolus (arrow lower right), the other nucleus exhibits four large nucleoli (arrow paracentral left). Numerous centroblasts comprising multiple nucleoli, and small cleaved and noncleaved lymphocytes are also present (lower magnification).

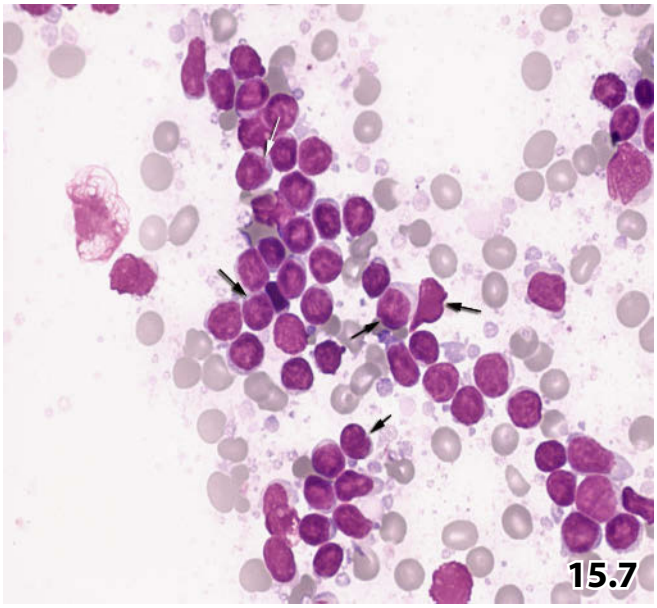
15.7

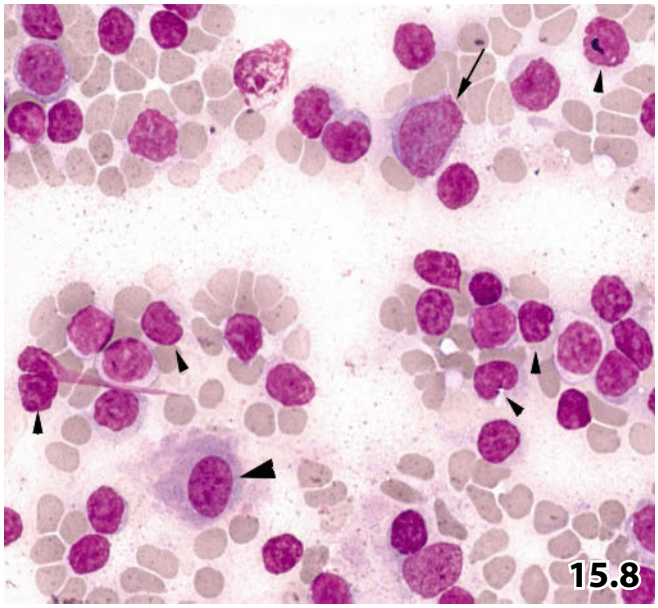
15.8

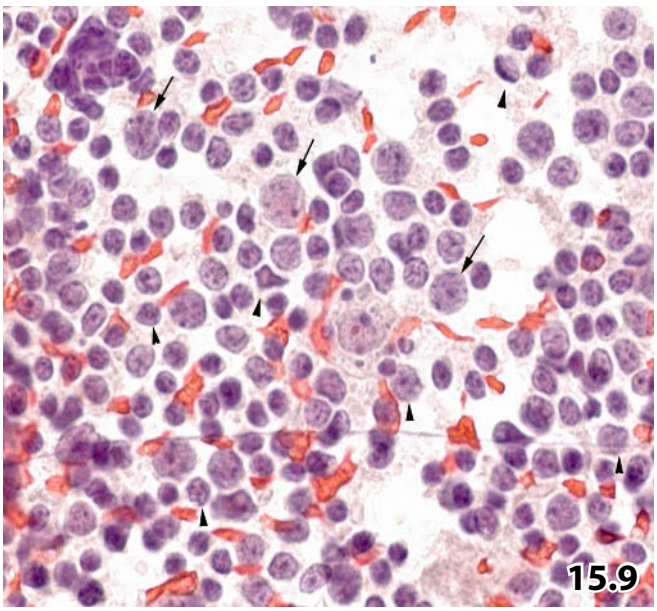
15.9

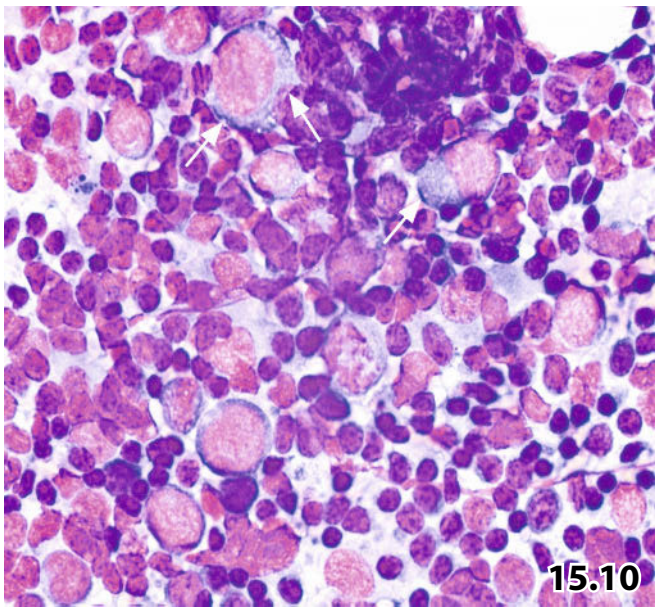
15.10

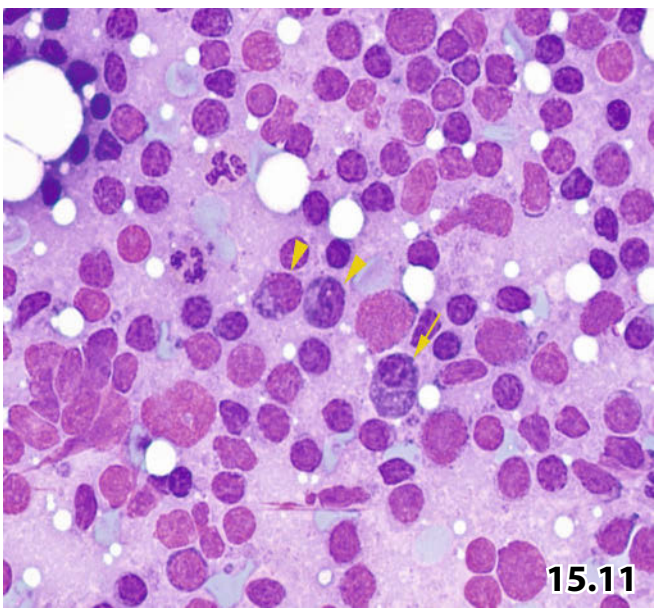
15.11

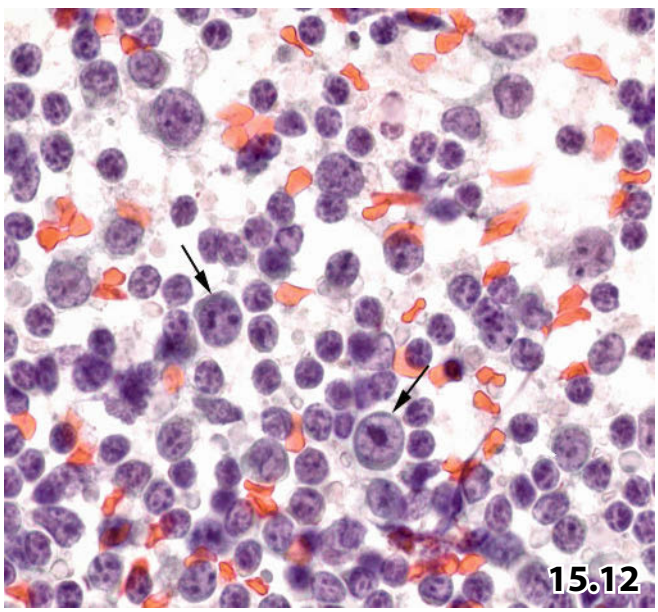
15.12

**Fig. 15.13** *Activated histiocytes* are scattered between lymphoid cells. Round or ovoid smooth nuclei associated with a distinct nucleolus indicate cell activation (arrows). Note the abundant ill-defined foamy cytoplasm (Pap stain, lower magnification).

**Fig. 15.14** Two *classic tingible-body macrophages* are shown in detail (MGG stain). Please note that the nucleus can be strongly covered by phagocytosed cellular fragments (macrophage, lower left).

**Fig. 15.15** *Interdigitating reticulum cells* are characterized by interdigitating cytoplasmic projections and longitudinal nuclear grooves (Pap stain, high magnification).

**Fig. 15.16** *Epithelioid histiocytes* occurring in a loose cluster show the characteristic nuclear shape. Cell activation gives rise to rounded nuclei and pronounced nucleoli (arrows) (Pap stain, high magnification).

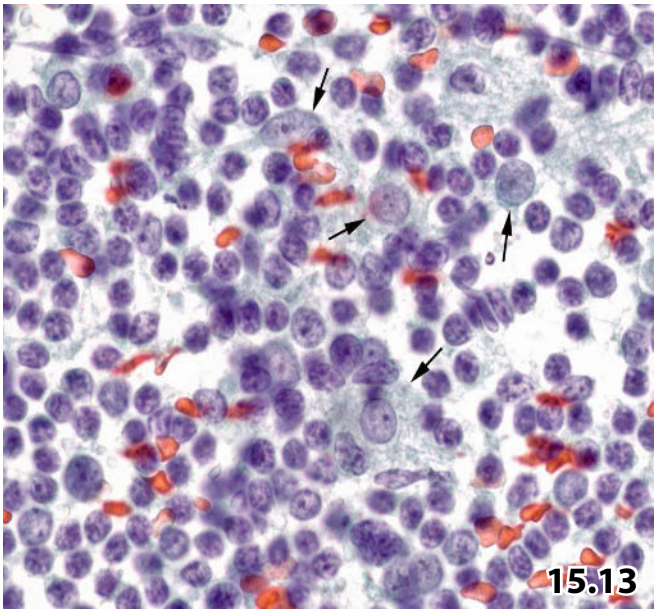
15.13

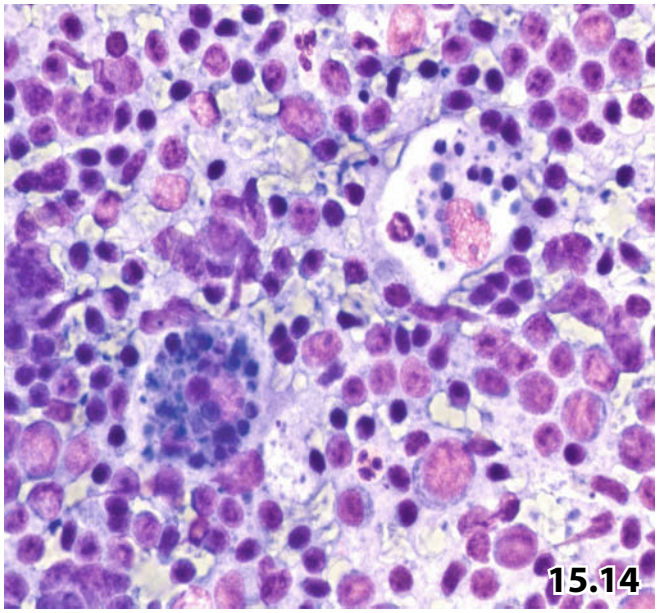
15.14

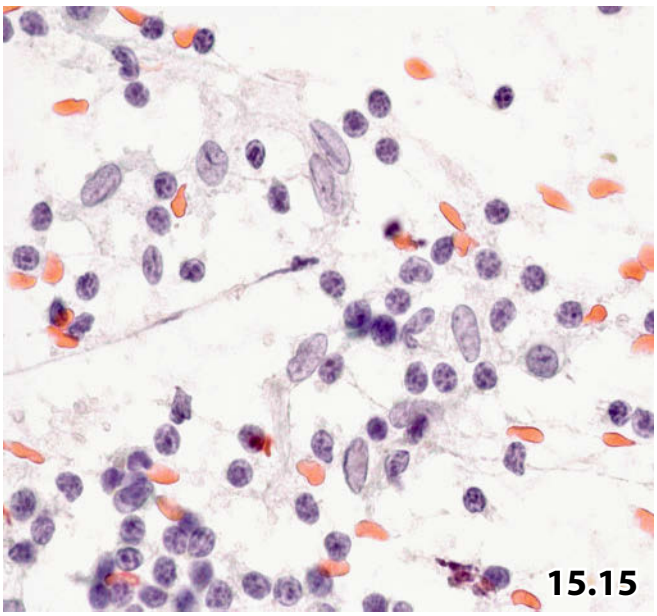
15.15

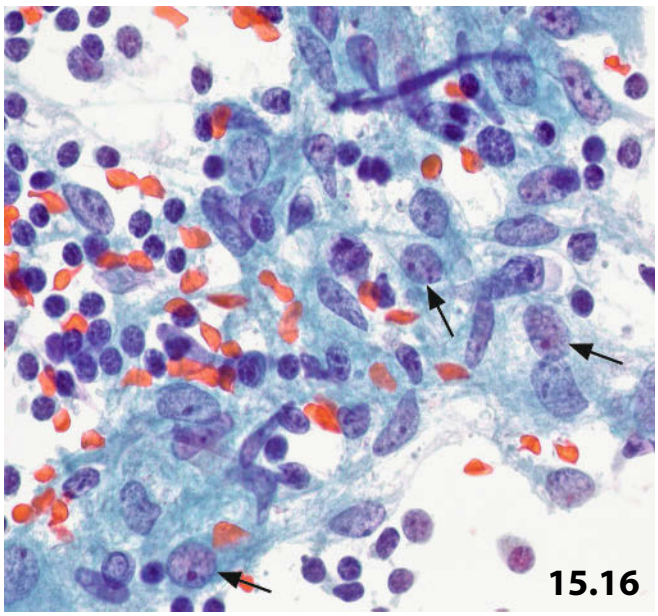
15.16

# Section 15.2
# Lymph Nodes

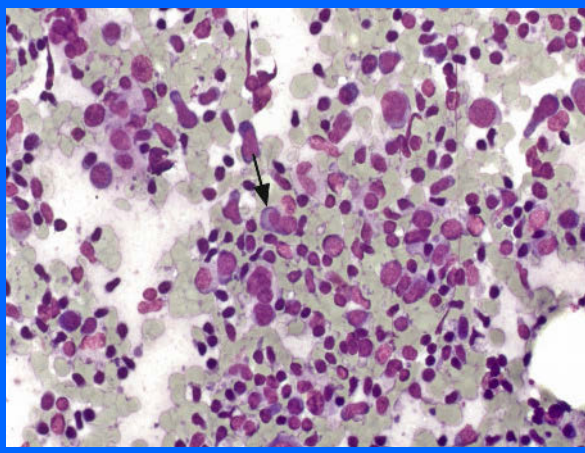

## Common Lymphadenopathy
## Infections
## Particular Benign Lesions

### 15.2.1 Introduction

- Lymph nodes become enlarged in a broad spectrum of diseases:
  - Common reactive lymphadenopathy.
  - Infectious diseases.
  - Malignant lymphatic disorders.
  - Malignant metastatic disease.
- Among these classes, cytologic patterns of reactive-proliferative lymphatic lesions are particularly delicate to distinguish from malignant lymphoma.
- Dorfman and Warnke presented a comprehensive summary of lymphadenopathies simulating malignant lymphomas in tissue samples [9].

**Caution**

The cellularity of the cytologic specimen, the appearance of the entire cell population (pleomorphic versus monomorphic), and unusual cell types (concerning size, shape, nuclear color, cell crowding) are in a first step best evaluated at low microscopic magnification.

- Causes of benign lymphadenopathy and related morphologic patterns can be categorized as listed in Table 15.2.1, p. 927.

### 15.2.2 Common Reactive Lymphadenopathy (Figs. 15.17 and 15.18)

**Synonyms and Definition**

Synonyms: Reactive lymphoid hyperplasia, reactive hyperplasia, and follicular hyperplasia.

Common reactive lymphadenopathy (LDP) is defined as a proliferation of cells in all compartments of the lymph node including germinal centers. As a result, cytologic specimens are composed of a variegated cell population providing patterns that can lead to a false-positive diagnosis of malignant lymphoma (see caution, p. 927).

**Microscopic Features** [47]

- The cytomorphologic characteristics of the diverse cell types are described and shown in detail in Sect. 15.1.6, "Cytology of Benign Lymph Nodes," p. 914.
- The smears are hypercellular showing an overall polymorphic cytologic pattern due to different stages of cellular transformation. In cytologic preparations, the structure of the secondary follicles is not really preserved but may occasionally be suggested.
- Small B and T lymphocytes are in general the predominant component accompanied by a varying number of germinal center cells (centrocytes, centroblasts, preimmunoblasts) and cells from the interfollicular area (immunoblasts, plasmablasts, plasmacytoid cells, and plasma cells).
- Small B cells of the centrocytic type and small T lymphocytes share many morphologic features such as small nuclear indentations and cleaves, occasional

**Table 15.2.1** Causes and morphologic patterns of benign lymphadenopathy/lymphadenitis

| Cause of the disorder | Common morphologic pattern and key features |
|---|---|
| Nonspecific | – Reactive hyperplasia including secondary follicles |
| Infectious: bacterial / protozoal / fungal | – Suppurative lymphadenitis<br>– Granulomatosis<br>– Reactive hyperplasia |
| Infectious: viral | – Pulpa hyperplasia<br>– Follicular hyperplasia |
| Immunologic disorders<br>Postvaccinial lymphadenitis | – Reactive hyperplasia including secondary follicles and variable plasmacytoid hyperplasia |
| Miscellaneous disorders | |
| – Dermatopathic lymphadenopathy | – Reactive hyperplasia, interdigitating reticulum cells, melanin |
| – Rosai-Dorfman disease | – Large histiocytes with lymphophagocytosis, small lymphocytes and plasma cells |
| – Castleman disease | – Reactive hyperplasia, histiocytes with crumpled nuclei |
| – Kikuchi lymphadenitis | – Apoptosis, karyorrhexis, granular debris. Phagocytic histiocytes with crescent nuclei. Reactive hyperplasia. No granulocytes |
| – Sarcoidosis | – Epithelioid granulomatosis, Langhans type giant cells |
| – Langerhans cell histiocytosis | – Langerhans cells, eosinophils, EM: Birbeck granules |

**Caution**

Sinus histiocytosis can be extremely pronounced and is particularly present in inflammatory lesions of various etiologies, in connection with malignancies, and in lymph nodes draining limbs (inguinal lymph nodes!). Ordinary reactive sinus histiocytes stain immunocytochemically positive for CD68 and usually for common leukocyte antigen (CD45), but they are indispensably negative for S100 protein and CD35.

small nucleoli (more frequently encountered in nuclei of centrocytes), and a faint cytoplasmic rim. Actually, the two cell populations can only be reliably distinguished by immunophenotyping.

- A great number of tingible-body macrophages is a key indicator of secondary follicles.
- Histiocytes of varying types occur either scattered throughout the smear or as cohesive sheets and clusters. Diagnostically representative histiocytic patterns and the underlying disorders are discussed in Sects. 15.2.3, p. 928, and 15.2.5, p. 931.
- Neutrophils, eosinophils, and mast cells (best visualized by MGG staining) may occasionally be seen.

**Caution**

- Basically, a polymorphic (variegated) cell pattern is indicative of benign follicular hyperplasia, whereas a monomorphic appearance of the cell population is suggestive of malignant lymphoma.
- Cytological misdiagnoses may occur in the following situations [49, 50]:
  - *False-positive diagnosis* in cases with pronounced reactive changes including active germinal centers, and/or atypical plasmacytoid hyperplasia, and increased mitotic activity. In such cases, blasts and transitional lymphoid cells are falsely classified as malignant (e.g., Fig. 15.28).
  - *Potential false-negative diagnosis* can occur in lymphomas:
    1. That present with an unusual pleomorphic cell pattern (lymphomas of the mixed cell type in particular follicular lymphoma, angioimmunoblastic T-cell lymphoma, and others) [35] (e.g., Figs. 15.70 and 15.85A).
    2. Admixed with a large amount of reactive lymphoid tissue.
    3. With a significant population of reactive T lymphocytes.
    4. With a predominance of histiocytes.
    5. Partially involving the target lymph node. Inadequate lymph node sampling may lead to an erroneous negative diagnosis [46].

    In all these cases, the overall cell pattern is misleading because tumor cells are sparse, or completely absent, or masked by the dominant benign infiltrate.
- It is important for cytopathologists to be aware of a so called false-positive FNAB result, due to surgical excision of a benign lymph node other than that previously aspirated (having provided a malignant cytologic result).

**Additional Comments**

- In the majority of FNABs, clinicians expect a reliable cytodiagnostic result. Vague diagnostic phrases such as "suggestive of," "suspicious of," "cannot rule out," "consistent with," and others are not useful for further considerations and therapeutic decisions, especially in patients who are not disposed or willing to accept more invasive tissue sampling.
- Thus, the requirement of cytologists is to apply expert cytopathologic practice in combination with ancillary methods (immunotyping, molecular biology techniques) in order to reliably distinguish between benign and malignant lymphatic conditions in as many cases as possible [37].

**Additional Analyses**

Immunophenotyping of the lymphoid population by immunocytochemistry (IC) or flow cytometry (FCM), assessment of polyclonality (by IC, FCM, or PCR), and low Bcl-2 expression of reactive B and T cells (detected by IC, FCM, or molecular assays) are suitable tools to differentiate between reactive lymphoid hyperplasia and NHL [26] (see also Sect. 15.1.4, "Ancillary Techniques," p. 910).

## 15.2.3 Bacterial, Parasitic, and Mycotic Infections

### 15.2.3.1 Bacterial Infections

Bacterial infections (e.g., by *Staphylococcus aureus*) result in a suppurative lymphadenitis. Bacteria are best demonstrated with the Gram staining procedure.

**Microscopic Features**

- Acute purulent reaction in the initial inflammatory phase is recorded by numerous neutrophils, free macrophages, and a varying number of lymphocytes.
- In the florid stage, frank purulent material is aspirated containing well-preserved and heavily degenerate neutrophils, macrophages, and cellular debris.
- Infections fading away, spontaneously or under antibiotic therapy, may show lymphocytes, plasma cells, histiocytes, and a decrease in the number of neutrophilic granulocytes.

### 15.2.3.2 Mycobacteriosis (Figs. 15.19–15.21)

Mycobacteriosis of lymph nodes is caused by different type species of Gram-positive acid-fast bacilli. Infections due to *Mycobacterium tuberculosis* have completely different epidemiologic implications as compared to mycobacteria other than tuberculosis (MOTT), also referred to as atypical mycobacteriosis. Atypical mycobacteriosis in children is typically accompanied by cervical lymphadenitis; the common cause for atypical mycobacteriosis is *Mycobacterium avium*.

**Microscopic Features**

- Common hallmarks:
  - Epithelioid cells in mycobacterial infections, unlike epithelioid cells in sarcoidosis, are more elongated and more slender, disclosing thinly elongated nuclei that are frequently pyknotic.
  - Langhans-type histiocytic giant cells typically show up with the nuclei clustered together at the periphery of the cytoplasm, frequently in a horseshoe-like arrangement.
  - Fragments of granulomatous tubercles may be encountered in FNAB samples showing characteristic palisading of the epithelioid cells.
- Tuberculosis [11]: the occurrence of Langhans-type giant cells and epithelioid cells, together with caseous detritus and neutrophils, is highly suggestive of tuberculosis. Caseous necrosis consists of fine granular material randomly distributed in an opaque background (Figs. 15.20 and 15.21).

The search for acid-fast bacilli in cytologic material using Ziehl-Neelsen stain should be a routine procedure, but the reaction has rather low sensitivity [3]: Mycobacteria present as Gram-positive, acid-fast, slender, straight, or slightly curved rods (Fig. 2.18B). Appropriate tests in a specialized laboratory are recommended for an accurate diagnosis including mycobacterial typing.

**Caution**

- Atypical mycobacteriosis may come along with cytologic features identical to tuberculosis, i.e., caseous detritus is not a definite proof of tuberculosis.
- Caseous detritus may exceptionally be found in sarcoidosis as well.

**Differential Diagnosis**

- Distinguishing between mycobacterioses and other granulomatous lesions is often difficult, especially in cases where acid-fast bacilli cannot be established. Epithelioid granulomatosis is encountered in other types of nonspecific and specific chronic inflammatory processes and is likewise seen in lymph nodes located in the lymph-drain sector of malignant disorders (Fig. 15.22).
- In contrast to mycobacterial infections, sarcoid granuloma is usually composed of large activated epithelioid histiocytes that are packed together in dense aggregates interspersed with small lymphocytes (Fig. 15.39). The cytoplasm of Langhans-type giant cells occasionally contains asteroid bodies [36] (Fig. 2.89B).
- Caseous necrosis should not be misinterpreted as tumor necrosis.

- Elongated and somewhat pleomorphic epithelioid cells comprising dense cytoplasm and darkly stained pyknotic nuclei may mimic malignant squamous cells; additional coarse background debris may lead to an erroneous diagnosis of squamous cell carcinoma.

**Caution**

Both malignant lymphoma (in particular Hodgkin lymphoma) and lymph node metastases of carcinomas associated with a pronounced granulomatous component can mimic epithelioid-granulomatous lymphadenitis [20, 61].

### 15.2.3.3 Cat-Scratch Disease [27] (Fig. 15.23)

Cat-scratch disease is a bacterial infection typically causing swelling of the lymph nodes, particularly in the axilla and in the head and neck region. It usually results from the scratch, lick, or bite of a cat.

Lymphadenopathy can appear days to months after the original injury. More than 90% of affected people have had some kind of contact with cats. *Bartonella henselae* is the bacterium that causes cat-scratch disease; it is found in all parts of the world.

**Microscopic Features** [8, 44]

Cat-scratch disease usually reveals a heterogeneous appearance in cytologic smears paralleling tissue pathology; the cellular composite in smears frequently do not meet distinct cytodiagnostic criteria.

In histology, plasmacytoid monocytes and monocytoid B cells are seen in close association with epithelioid cell granulomas. The varying number of the different cell types and granuloma formation depend on the stage of the infection [21].

- Monocytoid B cells are medium-sized cells with round or indented nuclei and abundant pale clear cytoplasm.
- Plasmacytoid monocytes show eccentrically positioned round nuclei, coarsely clumped chromatin, and dense cytoplasm. Immunocytochemically, they express a high level of CD4, CD68, and CD123.

Both cell types are in functional relationship with the formation of the pathognomonic granulomatous response in cat-scratch disease.

- The cytologic hallmark is the suppurative granulomas exhibiting peripherally palisading epithelioid histiocytes and centrally located neutrophilic granulocytes.

**Cytochemistry**

A modified silver stain may identify the pleomorphic bacteria (*Bartonella henselae*) appearing as coccoid rods; the bacteria are Gram-negative [8].

**Differential diagnosis** [44]

- Cytologic diagnoses encompass a wide spectrum ranging from acute bacterial lymphadenitis to nonspecific granulomatosis, to common lymphoproliferative lesions; such disorders may include lymphadenopathies with suppurative granulomas (lymphogranuloma venereum, *Yersinia* lymphadenitis, listeriosis, fungal infection, and others), and any lesion accompanied by epithelioid granulomatosis (sarcoidosis, mycobacteriosis, toxoplasmosis, malignant lymphomas, etc.).
- Modified silver stain and clinical information are valuable tools to reach a conclusive diagnosis.

### 15.2.3.4 Toxoplasmic (Piringer-Kuchinka) Lymphadenitis

[14, 34, 42, 56] (Figs. 15.24 and 15.25)

Toxoplasmosis is a parasitic disease caused by the protozoan *Toxoplasma gondii*. Cats have been shown to be a major reservoir of this agent, but the protozoan is also transmitted from mother to fetus.

Up to one-third of the world's population is estimated to be carriers of Toxoplasma infection.

**Microscopic Features**

- Cytological hallmarks:
  Predominance of a polymorphous cell population including cell components from the germinal centers and histiocytes.
  Epithelioid histiocytes discretely arrayed or grouped in small clusters (microgranulomas) are a characteristic finding. These cells have abundant clear cytoplasm and eccentric nuclei.
- Parasites can occasionally be identified by careful evaluation of the cytological smears, parasites occur both free in the background and ingested in the cytoplasm of monocytes. Papanicolaou staining shows Toxoplasma cysts with bradyzoites, whereas May-Grünwald-Giemsa preparations can better visualize tachyzoites [34, 59].

**Additional Analyses**

Immunocytochemical staining demonstrates positivity for *Toxoplasma gondii* antigen.

Tachyzoites emit autofluorescence by fluorescence microscopy, improving identification of the parasite [34, 59].

**Differential Diagnosis**

- Other lymph node lesions with small epithelioid cell groups must be considered in the differential diagnosis. In contrast, sarcoidosis and tuberculosis usually exhibit large granulomatous clustering of epithelioid cells.
- Caseous necrosis, giant cells, and suppurative changes argue against toxoplasmic lymphadenitis.

- Lymphadenopathies, caused both by sinus histiocytosis and grouped proliferation of epithelioid cells may present diagnostic dilemmas for toxoplasmic lymphadenitis because they do not demonstrate prominent lymphoid hyperplasia, and germinal centers are absent to a large extent.

**Caution**

Lymph nodes showing lymphoid hyperplastic features and small groups of epithelioid cells may be an indicator of a malignant process in the environments of the aspirated node. In this setting, groups of epithelioid cells are referred to as sarcoid-like lesions.

**Additional Comment**

FNAB is a valuable tool for the diagnosis of Toxoplasma lymphadenitis in combination with serologic testing (presence of IgM-specific antibodies to *Toxoplasma gondii*). The latter confirms the diagnosis on a high level, avoiding surgical biopsies [34, 56].

### 15.2.3.5 Leishmania Lymphadenitis [6, 24, 39]

Leishmaniasis is a parasitic disease that is found in parts of the tropics, subtropics, and in Southern Europe. The most common route of infection is through the bite of infected sand flies. The most common forms are cutaneous and visceral leishmaniasis.

**Caution**

Leishmaniasis is an uncommon cause of lymphadenitis, but the possibility of this disease should be included in the differential diagnosis in patients living in or coming from endemic areas.

**Microscopic Features**

Leishmania lymphadenitis may be divided into different groups according to the prevalent cellular composition [24]:

- Cytology: The cytologic smears have a polymorphic appearance and are composed of various types of lymphocytes, plasma cells, mono- and multinucleated histiocytes, and starry-sky cells. Histiocytic and epithelioid granulomas, mast cells, and lymphoglandular bodies (cytoplasmic fragments of lymphocytes) may also be encountered in cytologic preparations.
- Parasites: It is emphasized that parasites appear as so-called Leishman-Donovan bodies (LDB); these bodies can be identified in practically all cases, but their number differs from case to case. LDBs are small round or oval spherical bodies and may occur both extracellularly and in the cytoplasm of histiocytes, epithelioid cells, and giant cells [24, 39].

**Additional Comments**

- The term "Leishman-Donovan bodies" is generally used for the intracellular stages of the nonflagellated form of *Leishmania donovani* (visceral leishmaniasis) and similar forms of *Leishmania tropica* (in lesions of cutaneous leishmaniasis).
- FNAB diagnosis is very helpful and spares more invasive diagnostic procedures on this self-limited disorder, which needs no further treatment.

### 15.2.3.6 Fungal Infections and Worms

Histoplasmosis [55], cryptococcosis [13], and coccidioidomycosis [38] are the most common fungal infections affecting lymph nodes. Microfilariae are rarely detected in cytologic aspirates, but they may incidentally be found in the peripheral blood [45]. We refer the reader to the specialized sources in the cytologic literature (as advised).

## 15.2.4 Virus-Induced Lymphadenitis

Several virus types may cause reactive lymphadenopathy such as EBV, HIV, varicella-herpes zoster, and vaccinia. The most common disorders are presented in the following sections, comprising the morphologic findings in aspirates of affected lymph nodes and the diagnostic challenge.

### 15.2.4.1 EBV-Specific Lymphadenopathy (Infectious Mononucleosis)

[19, 48] (Figs. 15.26–15.29)

Infectious mononucleosis is caused by the *Epstein-Barr virus (EBV)*, which is related to a group of herpes viruses. The virus affects B cells providing lymphocytes with characteristic atypical and plasmacytoid changes useful for diagnostic purposes.

EBV infection is nearly ubiquitous; anyone at any age can develop mononucleosis. It occurs most often in young adults between the ages of 15 and 35. People with weakened immune systems such as AIDS patients, or those with an organ transplant, are particularly vulnerable; this patient group may occasionally produce serious complications.

**Microscopic Features**

- Hallmarks
  - Lymph node aspirates reveal an extremely polymorphous pattern exhibiting a characteristic cell mix comprising the whole spectrum from small lymphocytes to large polymorphic immunoblasts.
  - A high proportion of the cells exhibit a pronounced dense cytoplasm staining, deep cyanophilic with Pa-

panicolaou and deep blue with May-Grünwald-Giemsa, DiffQuik, and Pappenheim.
  - Prominent plasmacytoid differentiation and mature plasma cells are key features for infectious mononucleosis.
  - Many of the medium-sized and large cells show multinucleation and prominent nucleoli. The nucleoli can appear strongly enlarged, pleomorphic, and multiple. The nucleoplasm is clear and the finely stippled chromatin texture is that of benign lymphoid cells.
- A considerably increased mitotic rate is present.

**Immunocytochemistry**

Unlike malignant lymphoma, the immunocytochemical pattern of mononucleosis exhibits a mixture of B and T cells, numerous T cells having a cytotoxic/suppressor phenotype [19].

**Differential Diagnosis**

- A variegated appearance of the cytologic smear in combination with polymorphic blasts may initially give the impression of a malignant disorder. Large-cell lymphoma of the blastic subtype, plasmacytoma with pronounced plasmacytoid features (immature and anaplastic tumor form), a myelogenic sarcoma, and even large-cell carcinoma are easily misdiagnosed (Fig. 15.28).
- Binucleated immunoblasts and plasmablasts can mimic Reed-Sternberg cells (as found in Hodgkin lymphoma) (Fig. 15.29); The polymorphic reactive background in FNAB samples may enhance a possible misinterpretation by careless interpreters.

**Caution**

- In most cases, a polymorphic cell pattern with a pronounced lymphoplasmacytoid appearance allows a correct diagnosis of a benign proliferative lesion.
- In rare cases, fulminant infectious mononucleosis may lead to severe cellular alterations that are cytologically difficult to differentiate from large-cell lymphoma; smears containing large pleomorphic blastic cells intermingled with lymphoid cells showing plasmacytoid differentiation should always raise the alarm of an EBV-induced lymphoproliferative lesion.
- Benign polymorphic lymphoid blasts generally have a high potential for a false-positive diagnosis.
- In cases with ambiguous diagnostic findings, it is highly recommended to exclude an EBV infection by serologic tests for virus antibodies and/or await a tissue diagnosis before rendering a tentative or false diagnosis of malignancy to the attending physician.
- Binucleated immunoblasts and plasmablasts should not mislead to the diagnosis of Hodgkin lymphoma; however, the risk of Hodgkin lymphoma (EBV-positive) after a mononucleosis infectiosa-related infection appears to be increased [15].

#### 15.2.4.2 AIDS-Related Lymphadenopathy (Fig. 15.30)

- Diffuse lymphadenopathy, with the cervical nodes most frequently affected, is one of the earliest and most common findings in patients with AIDS.
- FNAB is a minimally invasive and helpful tool in HIV-positive patients, not only for an efficient diagnosis of reactive lymphoid hyperplasia, but also for early detection of a malignant neoplasm (in particular malignant lymphoma), and in the assessment of opportunistic infections such as mycobacteriosis (Fig. 15.31), toxoplasmosis, mycoses, and others [17, 29, 40, 41].
- Aspiration cytology has also turned out to be a reliable procedure for monitoring pathologic lymph nodes in AIDS patients over a long period [2].

**Microscopic Features**

- The morphologic features of AIDS-related reactive lymphoid hyperplasia are not specific.
- B-cell predominance was found by immunocytochemistry in most of the evaluated aspirates, but light chain clonal rearrangement was not detected in any of the cases [30].
- Mycobacteriosis of retroperitoneal lymp nodes may occur in the course of HIV infection (Fig. 15.31).

### 15.2.5 Miscellaneous Disorders and Diseases of Unknown Etiology

#### 15.2.5.1 Reactive Lymphadenopathy in Immunologic Diseases (Fig. 15.32)

Inflammations induced by autoimmune disorders can affect various organs, including the lymph nodes. Lymphadenopathy is predominantly encountered in the setting of systemic lupus erythematosus and rheumatoid arthritis. In this group of patients, aspiration cytology is helpful to distinguish rapidly between an immune-related condition and infectious and malignant diseases [33].

**Microscopic Features**

- Aspirates are composed of follicle center cells and cells from the parafollicular areas comprising immunoblasts and plasma cells.

#### 15.2.5.2 Dermatopathic Lymphadenopathy [16, 51] (Figs. 15.33–15.36)

Dermatopathic lymphadenopathy (DL), also referred to as dermatopathic lymphadenitis, is a disorder secondary to various forms of dermatitis and mycosis fungoides. Enlargement of the lymph nodes is caused by a lymphoid hy-

perplastic process and by proliferation of histiocytes and macrophages usually containing fat and melanin.

**Microscopic Features**

- Hallmarks: The cellular smears exhibit a loose network of large histiocytes, so-called interdigitating reticulum cells interspersed with lymphocytes.
  Interdigitating reticulum cells are T-zone-specific histiocytes characterized by:
  - Elongated, clear vesicular nuclei showing longitudinal grooves, folds, and convolutions along with
  - Wide pale and ill-defined cytoplasmic bodies with multiple connecting processes and containing variable amounts of granular melanin pigment
- The dual cell pattern is completed by lymphoid elements related to a reactive lymphadenopathy; germinal center cells are occasionally present.
- Histiocytic aggregates containing centrally located small blood vessels may occasionally be seen.

**Immunocytochemistry** [16, 51]

Interdigitating reticulum cells express positive immunoreactivity for S100 protein, variable positivity for CD1a, and negativity for CD68. Sinus histiocytes provide the opposite immunoprofile.

**Differential Diagnosis**

- Interdigitating reticulum cells resemble Langerhans cells both morphologically and by immunocytochemistry. Confusion with Langerhans cell histiocytosis may occur, particularly in lymph node aspirates from children (Fig. 15.40A). Both types of histiocytes share fairly equivalent immunoreactivity.
- Large activated melanin-laden histiocytic cells should not lead to diagnostic confusion with malignant melanoma (Fig. 15.36). A misdiagnosis of melanoma is more likely in samples exhibiting additional small clusters of melanocytic nevoid cells [60].

**Caution**

- Dermatopathic lymphadenopathy and cell aggregates of a (lymph) nodal nevus should not be confused with malignant melanoma.
- Melanin-laden macrophages may be encountered in DL, as well as in reactive lymphadenopathy of patients without a clinically manifest cutaneous disorder.

### 15.2.5.3 Rosai-Dorfman Disease

[1, 7, 23, 31] (Fig. 15.37)

This disorder is also referred to as sinus histiocytosis with massive lymphadenopathy (SHML). The cause of the lesion is still unknown, although a viral etiology is suspected. Rosai-Dorfman disease commonly occurs in young people as massive, painless, bilateral lymph node enlargement in the neck area; with a predilection in black people.

Rare extranodal sites can be involved, including the skin, central nervous system, eyes, upper respiratory tract, and others [12].

**Microscopic Features and Immunocytochemistry**

- Hallmark: Numerous large histiocytes exhibiting phagocytized well-preserved lymphocytes in their cytoplasm, a condition that is referred to as lymphophagocytosis or emperipolesis. A halo is seen around each incorporated cell. The remaining cytoplasmic body of the histiocyte shows fine vacuolization.
- The typical histiocytes are scattered in a background of mature lymphocytes and plasma cells.
- SMHL histiocytes show invariable S100 positivity by immunocytochemistry.

**Caution**

Halos surrounding ingested lymphocytes in SMHL histiocytes are evidence of true emperipolesis ruling out an accidental overlay of lymphocytes.

**Differential Diagnosis**

- SMHL in FNAB samples may mimic common reactive sinus histiocytosis, in contrast to tissue sections where Rosai-Dorfman disease is unequivocally recognized. Emperipolesis is absent or extremely rarely seen in reactive histiocytosis, and S100 is never expressed in histiocytes of reactive sinus histiocytosis.
- Langerhans cells show distinct morphologic (grooved nuclei), ultrastructural (Birbeck granules) and immunocytochemical (positive CD1a expression) characteristics differing from SMHL cells (emperipolesis and CD1a immunonegativity). Immunostaining for S100 protein is positive in specific histiocytes of both disorders.
- Reed-Sternberg-like giant cells rarely occurring in Rosai-Dorfman disease may raise diagnostic confusion with Hodgkin lymphoma; binucleated histiocytes of SMHL comprising large pleomorphic nucleoli and absence of lymphophagocytosis differ from true Reed-Sternberg cells in Hodgkin lymphoma for the positive immunoreactivity for S100 protein [7].
- Shiran and coworkers recently called attention to multifocal combined nodal and extranodal SMHL that can cause diagnostic confusion with histiocytic sarcoma [43].

### 15.2.5.4 Castleman Disease [28] (Fig. 15.38)

Castleman disease is also called angiofollicular hyperplasia. It is a very rare disorder characterized by a hyperproliferation of benign B lymphocytes, plasma cells, vessels, and endothelial cells [4].

– Unicentric Castleman disease involves lymphoid organs at a single site of the body, frequently in the mediastinal space. Removal of the lymphoid mass is curative.
– Multicentric Castleman disease compromises patients with widespread hyperplastic disorders. In the majority of cases, the lesion is associated with gamma herpes virus (KSHV), which may also be found in Kaposi sarcoma and in primary effusion lymphoma.

References are provided in Sect. 2.4.3.7.1, p. 214.

**Microscopic Features and Differential Diagnosis**

- In general, a variegated lymphoid cell population is encountered: predominantly small mature lymphocytes (B and T phenotype), eosinophils, follicle center cells, including immunoblasts, and plasma cells.
- Furthermore, large atypical histiocytoid cells (follicular dendritic cells) are present, showing ill-defined cytoplasm and enlarged nuclei with distinctly irregular outline or crumpled appearance.
  The chromatin appears granular to coarse.
  The nucleoli are distinct.
- The *plasma cell type of angiofollicular hyperplasia* exhibits sheets of plasma cells and many follicle center cells originating from large germinal centers. In this setting, plasmacytoma has to be ruled out. KSHV-related disorders are closely associated with the plasmacytic type of Castleman disease.
- *Castleman disease of the hyaline vascular variant* shares the overall cytologic pattern with other reactive lymphoid disorders. Large histiocytes with crumpled appearance of the nuclei are a distinct indicator of angiofollicular hyperplasia, but the histiocytes may mimic follicular dendritic cells, immunocytochemically exhibiting CD35.

### 15.2.5.5 Kikuchi Lymphadenitis [32, 53, 54, 57]

Kikuchi disease (Kikuchi-Fujimoto disease), also referred to as histiocytic necrotizing lymphadenitis, is an uncommon idiopathic, generally self-limiting lymphadenopathy in young adults. The most common clinical manifestation of Kikuchi disease (KD) is cervical lymphadenopathy with or without systemic signs and symptoms. Concomitant cutaneous involvement is occasionally observed.

**Microscopic Features**

- Hallmarks: An increase of apoptotic cells, and karyorrhectic or eosinophilic granular debris are typical features in aspirates of Kikuchi lymphadenitis.
  Unlike apoptotic cells, karyorrhectic and granular debris occur in the abundant cytoplasmic bodies of histiocytes. The latter have twisted (crescentic) nuclei that are eccentrically positioned.
  A reactive lymphoid cell population practically devoid of classic starry-sky cells and neutrophilic granulocytes is another key feature.
- Two other types of histiocytes are seen:
  Common nonphagocytic histiocytes with characteristic kidney-shaped nuclei, and medium-sized histiocytic elements (plasmacytoid monocytes) comprising eccentric round nuclei, coarsely clumped chromatin, and dense cytoplasm.
- A granulomatous component is absent.

**Differential Diagnosis** [32, 53, 54, 57]

There is a substantial morphologic overlap between KD and other forms of lymphadenopathy and lymphadenitis:

- Nonspecific lymphadenopathy may be diagnosed by mistake in cases of KD associated with a pronounced reactive lymphoid background.
- Morphologic overlap between KD and tuberculosis is obvious on the strength of polymorphous debris; but the combination of apoptosis, intra- and extracellular karyorrhexis and/or granular debris, and typical crescentic nuclei in macrophages will usually permit a correct diagnosis.
- Malignant lymphoma may rarely raise diagnostic confusion with KD.

### 15.2.5.6 Sarcoidosis [52, 58] (Fig. 15.39)

- Sarcoidosis is a multisystem disorder characterized by noncaseating granulomas; young adults are most commonly affected. The cause of the disease is still unknown. Virtually any organ can be affected, but sarcoid granulomas most often appear in the lung or in lymph nodes with a preponderance of the mediastinum and neck.
- The exclusive presentation of sarcoidosis in lymph nodes without other organ manifestations rarely occurs and may pose diagnostic problems [5].

**Microscopic Features**

- Hallmarks
  – Cohesive, noncaseating epithelioid cell granuloma associated with Langhans-type giant cells. The granulomatous fragments are loosely interspersed with mature lymphocytes.
  – The epithelioid cells are large elongated mononucleated histiocytic elements. However, strongly activated epithelioid cells may show a more spherical configuration.
  – Langhans-type giant cells are multinucleated histiocytes; the nuclei are clustered together at the periphery or in a horseshoe-like arrangement along the inner cytoplasmic margin.
  – The nuclei of both cell types mentioned above show characteristic elongation with one end broader than

the other bearing striking resemblance to a footprint. The chromatin texture is bland, and the size and number of nucleoli depend on the cellular activity.
  - Asteroid bodies in the background of the preparation or included in the cytoplasm of Langhans giant cells may support the diagnosis of sarcoidosis [36] (Fig. 2.89B).
- The background of the smear appears as reactive lymphadenopathy associated with follicular hyperplasia.

**Differential Diagnosis**

Differentiation from other granulomatous lesions, in particular from mycobacteriosis (see Sect. 15.2.3.2, p. 928) may be difficult. Yet, in the majority of the cases FNAB is a reliable tool for the diagnosis of sarcoidosis in conjunction with clinical, radiographic, and laboratory results.

**Caution**

- Caseous detritus may exceptionally be found in sarcoidosis.
- Extra- and intracellular asteroid bodies may support the diagnosis of sarcoidosis, but these elements rarely occur.

### 15.2.5.7 Granulomatous Lymphadenitis

A broad spectrum of infectious and malignant disorders is responsible for the occurrence of more or less typical epithelioid granulomas in lymphatic tissues. Granulomatous reactions may be caused by bacteria, fungi, sarcoidosis, malignant non-Hodgkin lymphoma, Hodgkin lymphoma, and solid malignant tumors located in the lymph draining region. Granulomas may be encountered in many other pathologic conditions.

Koo and coauthors showed that FNAB in combination with ancillary investigations can achieve a definitive diagnosis in over 80% of granulomatous lymphadenitis cases [22].

### 15.2.5.8 Lymph Node Involvement by Langerhans Cell Histiocytosis [18, 25] (Fig. 15.40)

Langerhans cell histiocytosis (LCH) may be confined to lymph nodes without other organ involvement. Although exclusive manifestation of LCH in lymph nodes is rarely encountered, this lesion should always be remembered in daily cytologic practice.

More information on LCH is provided in Sect. 2.3.7.1, p. 189.

**Microscopic Features**

- Hallmarks
  - In comparison to macrophages, Langerhans cells may appear larger and they are multinucleated. The nuclei are oval to kidney-shaped, showing deep grooves and indentations, and the chromatin is vesicular. The cytoplasm is wide with neat margins and an eosinophilic staining quality. Distinct nucleoli are sometimes present.
  - Birbeck granules are intracytoplasmic organelles unique for Langerhans cells. They are detected by electron microscopy showing the characteristic shape of tennis rackets or rods.
- Varying numbers of eosinophils and neutrophils are present. Plasma cells are rarely seen.
- Charcot-Leyden crystals may be encountered together with degenerating eosinophilic granulocytes [25].
- The background pattern is that of a reactive lymphadenopathy, it is more or less distinct.

**Immunocytochemistry** (Fig. 15.40B)

Langerhans cells show strong positivity for S100 protein and CD1a, a pattern that is characteristic of this cell type.

**Differential Diagnosis** [10, 18]

- Other disorders to be considered are those comprising a cell fraction with vesicular nuclei showing grooves, folds, and convolutions. Such lesions include:
  - Dermatopathic lymphadenopathy.
  - Castleman disease.
  - Kikuchi lymphadenitis.
  - Sinus histiocytosis.
  - Malignant histiocytosis.
  - Hodgkin lymphoma.
- Focal involvement of a lymph node by LCH may remain unrecognized because of the low incidence of Langerhans cells. This setting is challenging regarding both cytologic smears and tissue sections. The prevalent misdiagnosis in such cases is common lymphadenopathy.

## 15.2.6 Further Reading


1. Alvarez Alegret R, Martinez Tello A, Ramirez T, et al. Sinus histiocytosis with massive lymphadenopathy (Rosai-Dorfman disease): diagnosis with fine-needle aspiration in a case with nodal and nasal involvement. Diagn Cytopathol 1995;13:333-335.
2. Bart PA, Meuwly JY, Corpataux JM, et al. Sampling lymphoid tissue cells by ultrasound-guided fine needle aspiration of lymph nodes in HIV-infected patients. Swiss HIV Cohort Study. AIDS 1999;13:1503-1509.
3. Bezabih M, Mariam DW, Selassie SG. Fine needle aspiration cytology of suspected tuberculous lymphadenitis. Cytopathology 2002;13:284-290.
4. Castleman B, Iverson L, Menendez VP. Localized mediastinal lymph node hyperplasia resembling thymoma. Cancer 1956;9: 822–30.
5. Chen HC, Kang BH, Lai CT, Lin YS. Sarcoidal granuloma in cervical lymph nodes. J Chin Med Assoc 2005;68:339-342.
6. Daneshbod Y, Daneshbod K, Khademi B, et al. New cytologic clues in localized Leishmania lymphadenitis. Acta Cytol 2007;51:699-710.
7. Deshpande V, Verma K. Fine needle aspiration (FNA) cytology of Rosai Dorfman disease. Cytopathology 1998;9:329-335.
8. Donnelly A, Hendricks G, Martens S, et al. Cytologic diagnosis of cat scratch disease (CSD) by fine-needle aspiration. Diagn Cytopathol 1995;13:103-106.
9. Dorfman RF, Warnke R. Lymphadenopathy simulating the malignant lymphomas. Human Pathol 1974;5:519-550.
10. Edelweiss M, Medeiros LJ, Suster S, Moran CA. Lymph node involvement by Langerhans cell histiocytosis: a clinicopathologic and immunohistochemical study of 20 cases. Hum Pathol 2007;38:1463-1469.
11. Ersöz C, Polat A, Serin MS, et al. Fine needle aspiration (FNA) cytology in tuberculous lymphadenitis. Cytopathology 1998;9:201-207.
12. Gaitonde S. Multifocal, extranodal sinus histiocytosis with massive lymphadenopathy: an overview. Arch Pathol Lab Med 2007;131:1117-1121.
13. Garbyal RS, Basu D, Roy S, Kumar P. Cryptococcal lymphadenitis: report of a case with fine needle aspiration cytology. Acta Cytol 2005;49:58-60.
14. Gupta RK. Fine needle aspiration cytodiagnosis of toxoplasmic lymphadenitis. Acta Cytol 1997;41:1031-1034.
15. Hjalgrim H, Askling J, Rostgaard K, et al. Characteristics of Hodgkin's lymphoma after infectious mononucleosis. N Engl J Med 2003;349:1324-1332.
16. Iyer VK, Kapila K, Verma K. Fine needle aspiration cytology of dermatopathic lymphadenitis. Acta Cytol 1998;42:1347-1351.
17. Jayaram G, Chew MT. Fine needle aspiration cytology of lymph nodes in HIV-infected individuals. Acta Cytol 2000;44:960-966.
18. Kakkar S, Kapila K, Verma K. Langerhans cell histiocytosis in lymph nodes. Cytomorphologic diagnosis and pitfalls. Acta Cytol 2001;45:327-332.
19. Kardos TF, Kornstein MJ, Frable WJ. Cytology and immunocytology of infectious mononucleosis in fine needle aspiration of lymph nodes. Acta Cytol 1988;32:722-726.
20. Khurana KK, Stanley MW, Powers CN, Pitman MB. Aspiration cytology of malignant neoplasms associated with granulomas and granuloma-like features: diagnostic dilemmas. Cancer 1998;84:84-91.
21. Kojima M, Morita Y, Shimizu K, et al. Plasmacytoid monocytes in cat scratch disease with special reference to the histological diversity of suppurative lesions. Pathol Res Pract 2006;202:17-22.
22. Koo V, Lioe TF, Spence RA. Fine needle aspiration cytology (FNAC) in the diagnosis of granulomatous lymphadenitis. Ulster Med J 2006;75:59-64.
23. Kumar B, Karki S, Paudyal P. Diagnosis of sinus histiocytosis with massive lymphadenopathy (Rosai-Dorfman disease) by fine needle aspiration cytology. Diagn Cytopathol 2008;36:691-695.
24. Kumar PV, Moosavi A, Karimi M, et al. Subclassification of localized Leishmania lymphadenitis in fine needle aspiration smears. Acta Cytol 2001;45:547-554.
25. Kumar PV, Mousavi A, Karimi M, Bedayat GR. Fine needle aspiration of Langerhans cell histiocytosis of the lymph nodes. A report of six cases. Acta Cytol 2002;46:753-756.
26. Laane E, Tani E, Björklund E, et al. Flow cytometric immunophenotyping including Bcl-2 detection on fine needle aspirates in the diagnosis of reactive lymphadenopathy and non-Hodgkin's lymphoma. Cytometry B Clin Cytom 2005;64:34-42.
27. Lamps LW, Scott MA. Cat-scratch disease: historic, clinical, and pathologic perspectives. Am J Clin Pathol 2004;121 Suppl:S71-80.
28. Mallik MK, Kapila K, Das DK, et al. Cytomorphology of hyaline-vascular Castleman's disease: a diagnostic challenge. Cytopathology 2007;18:168-174.
29. Martin-Bates E, Tanner A, Suvarna SK, et al. Use of fine needle aspiration cytology for investigating lymphadenopathy in HIV-positive patients. J Clin Pathol 1993;46:564-566.
30. Oertel J, Oertel B, Lobeck H, Huhn D. Immunocytochemical analysis of lymph node aspirates in patients with human immunodeficiency virus infection. J Clin Pathol 1990;43:844-846.
31. Ohsaki H, Nakamura M, Kagawa A, et al. Fine needle aspiration cytology of an enlarged inguinal lymph node. Cytopathology 2008;19:389-393.
32. Osborn M, Aqel N, Levine TS. The fine needle aspiration appearances of Kikuchi's lymphadenitis. Cytopathology 2009;20:36-43.
33. Pai MR, Adhikari P, Coimbatore RV, Ahmed S. Fine needle aspiration cytology in systemic lupus erythematosus lymphadenopathy. A case report. Acta Cytol 2000;44:67-69.
34. Pathan SK, Francis IM, Das DK, et al. Fine needle aspiration cytologic diagnosis of toxoplasma lymphadenitis. A case report with detection of a Toxoplasma bradycyst in a Papanicolaou-stained smear. Acta Cytol 2003;47:299-303.
35. Pilotti S, Di Palma S, Alasio L, et al. Diagnostic assessment of enlarged superficial lymph nodes by fine needle aspiration. Acta Cytol 1993;37:853-866.
36. Rajasekharan P, Narurkar S, Patel K, Rajpal A. Asteroid bodies in a lymph node aspirate. A case report. Acta Cytol 2007;51:66-67.
37. Renshaw AA. Reporting risk of malignancy/dysplasia in cytology. A potential way to improve communication, if not reputation. Cancer (Cancer Cytopathol) 2007;111:465-466.
38. Robertson S, Kovitz KL, Moroz K. Disseminated coccidioidomycosis. The role of cytology in multidisciplinary clinical approach and diagnosis. J La State Med Soc 1999;151:409-413.
39. Sah SP, Prasad R, Raj GA. Fine needle aspiration of lymphadenopathy in visceral leishmaniasis. Acta Cytol 2005;49:286-290.
40. Saikia UN, Dey P, Jindal B, Saikia B. Fine needle aspiration cytology in lymphadenopathy of HIV-positive cases. Acta Cytol 2001;45:589-592.
41. Shapiro AL, Pincus RL. Fine-needle aspiration of diffuse cervical lymphadenopathy in patients with acquired immunodeficiency syndrome. Otolaryngol Head Neck Surg 1991;105:419-421.
42. Shimizu K, Ito I, Sasaki H, et al. Fine needle aspiration of toxoplasmic lymphadenitis in an intramammary lymph node. A case report. Acta Cytol 2001;45:259-262.
43. Shiran MS, Tan GC, Kenali MS, et al. Multifocal nodal and extranodal Rosai-Dorfman disease initially diagnosed as histiocytic lymphoma. Malays J Pathol 2008;30:63-65.
44. Silverman JF. Fine needle aspiration cytology of cat scratch disease. Acta Cytol 1985;29:542-547.
45. Sivakumar S. Role of fine needle aspiration cytology in detection of microfilariae: report of 2 cases. Acta Cytol 2007;51:803-806.
46. Sneige N, Dekmezian RH, Katz RL, et al. Morphologic and immunocytochemical evaluation of 220 fine needle aspirates of ma-

lignant lymphoma and lymphoid hyperplasia. Acta Cytol 1990;34:311-322.
47. Stani J. Cytologic diagnosis of reactive lymphadenopathy in fine needle aspiration biopsy specimens. Acta Cytol 1987;31:8-13.
48. Stanley MW, Steeper TA, Horwitz CA, et al. Fine-needle aspiration of lymph nodes in patients with acute infectious mononucleosis. Diagn Cytopathol 1990;6:323-329.
49. Steel BL, Schwartz MR, Ramzy I. Fine needle aspiration biopsy in the diagnosis of lymphadenopathy in 1103 patients. Role, limitations and analysis of diagnostic pitfalls. Acta Cytol 1995;39:76-81.
50. Stewart CJR, Duncan JA, Farquharson M, Richmond J. Fine needle aspiration cytology diagnosis of malignant lymphoma and reactive lymphoid hyperplasia. J Clin Pathol 1998;51:197-203.
51. Sudilovsky D, Cha I. Fine needle aspiration cytology of dermatopathic lymphadenitis. Acta Cytol 1998;42:1341-1346.
52. Tambouret R, Geisinger KR, Powers CN, et al. The clinical application and cost analysis of fine-needle aspiration biopsy in the diagnosis of mass lesions in sarcoidosis. Chest 2000;117:1004-1011.
53. Tong TR, Chan OW, Lee KC. Diagnosing Kikuchi disease on fine needle aspiration biopsy: a retrospective study of 44 cases diagnosed by cytology and 8 by histopathology. Acta Cytol 2001;45:953-957.
54. Tsang WY, Chan JK. Fine-needle aspiration cytologic diagnosis of Kikuchi's lymphadenitis. A report of 27 cases. Am J Clin Pathol 1994;102:454-458.
55. Tuon FF, Gomes V, Pagliari C, et al. Isolated lymphadenitis due to Histoplasma capsulatum diagnosed by fine-needle aspiration biopsy and immunohistochemistry. Rev Iberoam Micol 2008;25:50-51.
56. Viguer JM, Jimenez-Heffernan JA, Lopez-Ferrer P, et al. Fine needle aspiration of toxoplasmic (Piringer-Kuchinka) lymphadenitis: a cytopathologic correlation study. Acta Cytol 2005;49:139-143.
57. Viguer JM, Jimenez-Heffernan JA, Perez P, et al. Fine-needle aspiration cytology of Kikuchi's lymphadenitis: a report of ten cases. Diagn Cytopathol 2001;25:220-224.
58. Wakely PE Jr, Silverman JF, Holbrook CT, et al. Fine needle aspiration biopsy cytology as an adjunct in the diagnosis of childhood sarcoidosis. Pediatr Pulmonol 1992;13:117-120.
59. Zaharopoulos P. Demonstration of parasites in toxoplasma lymphadenitis by fine-needle aspiration cytology: report of two cases. Diagn Cytopathol 2000;22:11-15.
60. Zaharopoulos P, Hudnall SD. Nevus-cell aggregates in lymph nodes: fine-needle aspiration cytologic findings and resulting diagnostic difficulties. Diagn Cytopathol 2004;31:180-184.
61. Zardawi IM, Barker BJ, Simons DP. Hodgkin's disease masquerading as granulomatous lymphadenitis on fine needle aspiration cytology. Acta Cytol 2005;49:224-226.

**Figs. 15.17 and 15.18 Cytology of common reactive lymphadenopathy.**
The appearance of common reactive lymphadenopathy (LDP) in FNAB specimens is demonstrated using varied magnifications, staining methods, and preparation techniques.

**Fig. 15.17A, B** (case #1) Conventional smears stained according to the MGG and Papanicolaou procedure. **A** High magnification shows a heterogeneous pattern due to different stages of transformation of the lymphoid cells. An eosinophilic leukocyte (arrow) and a mast cell (arrowhead, upper right) are also present. The different cell types are easily interpretable using MGG staining. **B** Same aspirate but the current smear is Pap-stained. The characteristic heterogeneous cell population and a tingible-body macrophage are shown at lower magnification. Coarse-granular chromatin in the nuclei of small lymphocytes and loose chromatin in the nuclei of blastic cells indicate a benign lymphoid population.

**Fig. 15.18** (case #2) Thin layer preparation (Cytospin) may be the most suitable for accentuating the overall appearance of LDP at low magnification: small and large cleaved and noncleaved lymphoid cells interspersed with starry-sky cells (arrow) (Pap stain).

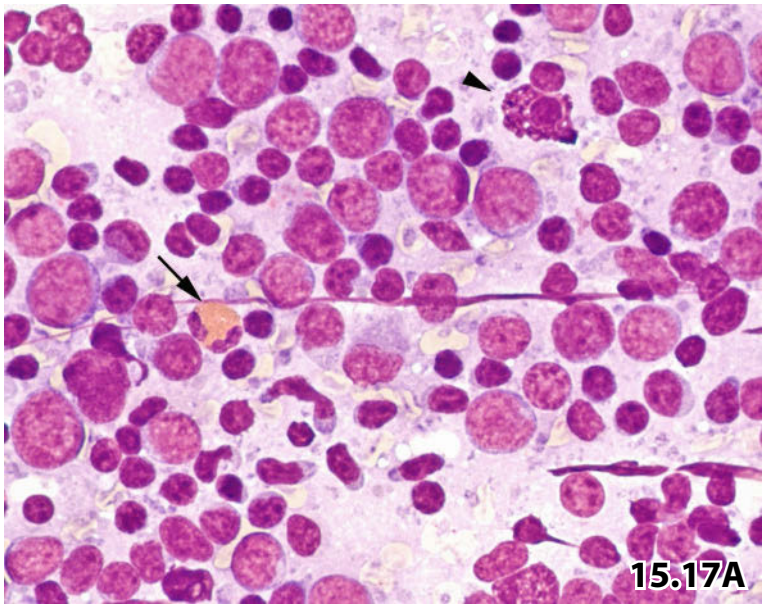
15.17A

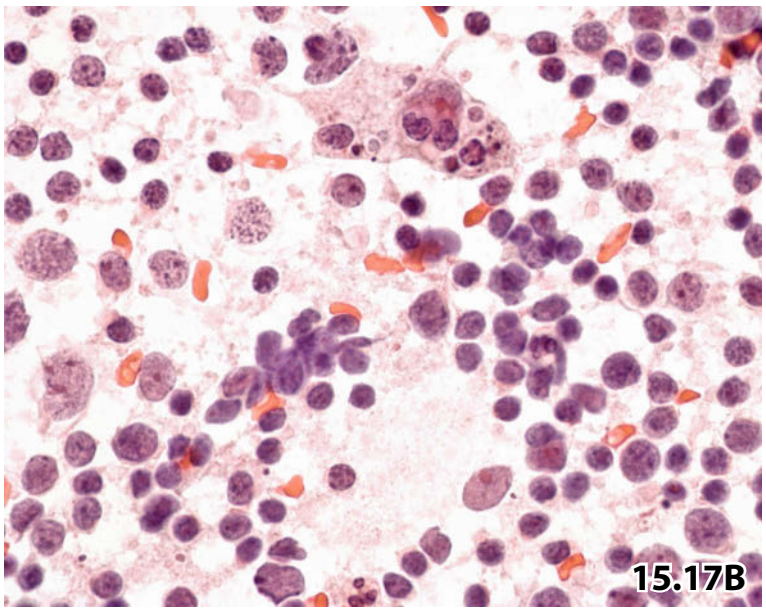
15.17B

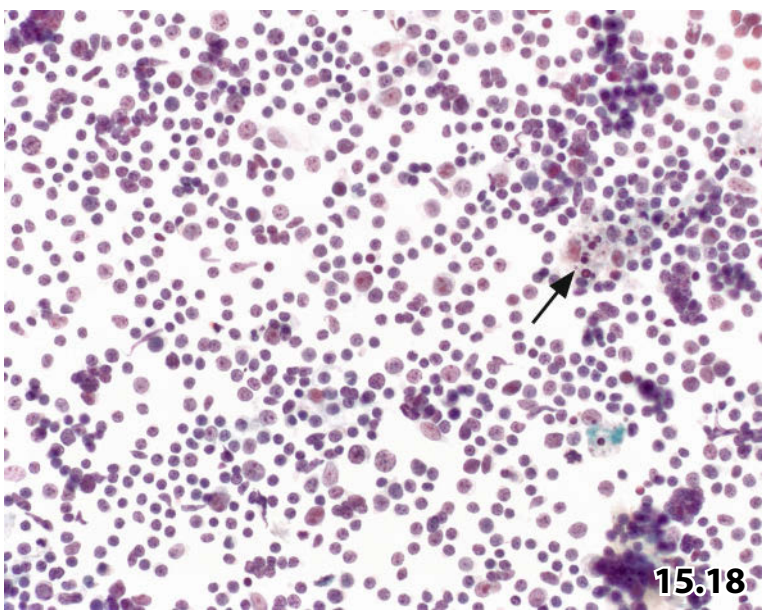
15.18

**Fig. 15.19 Atypical mycobacteriosis: MOTT.**
FNAB of a preauricular lymph node in a 1-year-old boy. Large irregular aggregates of activated epithelioid histiocytes in combination with minor cellular detritus in the background favor a cytologic diagnosis of MOTT (mycobacteriosis other than tuberculosis) (direct smear, Pap stain, lower magnification).
*Microbial culture* from the aspirated material determined the mycobacterial subtype: *Mycobacterium avium-intracellulare*.

**Figs. 15.20 and 15.21 Tuberculosis.**
Two young men presented with enlarged cervical lymph nodes. FNABs were performed from both sides of the neck in each patient. Aspirates were conventionally processed.
*Microbiological tests* from aspirates of both patients found *Mycobacterium tuberculosis*.

**Fig. 15.20** (case #1) Low magnification shows mainly degenerating epithelioid histiocytes entrapped in caseous detritus. Neutrophils are scattered in the background (Pap stain). Ziehl-Neelsen staining using a Pap-prestained smear provided a positive reaction for acid-fast bacilli (not shown).

**Fig. 15.21** (case #2) MGG staining shows epithelioid histiocytes and a Langhans-type giant cell (upper left) at high magnification.

**Fig. 15.22 Epithelioid cell granulomatosis in lymph nodes neighboring malignant neoplasia.**
An elderly woman presented with an enlarged supraclavicular lymph node.
Loose clusters of activated epithelioid histiocytes associated with cells originating from reactive lymphoid tissue (upper left) are shown at lower magnification (FNAB, direct smear, Pap stain).
*Tentative cytologic diagnosis:* Reactive LDP including numerous epithelioid histiocytes. A conclusive diagnosis is not possible (mycobacteriosis, toxoplasmosis, other disorder?)
*Histologic examination* of an excised lymph node, adjacent to the aspirated one, revealed diffuse large B-cell lymphoma, centroblastic variant.

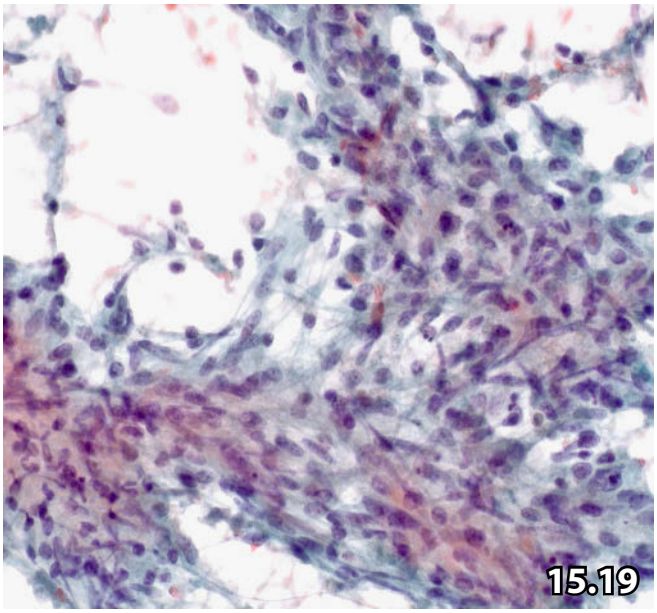
15.19

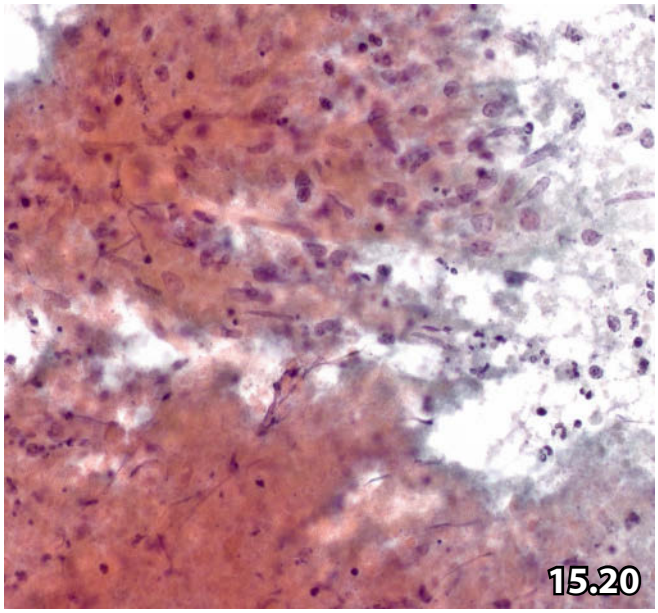
15.20

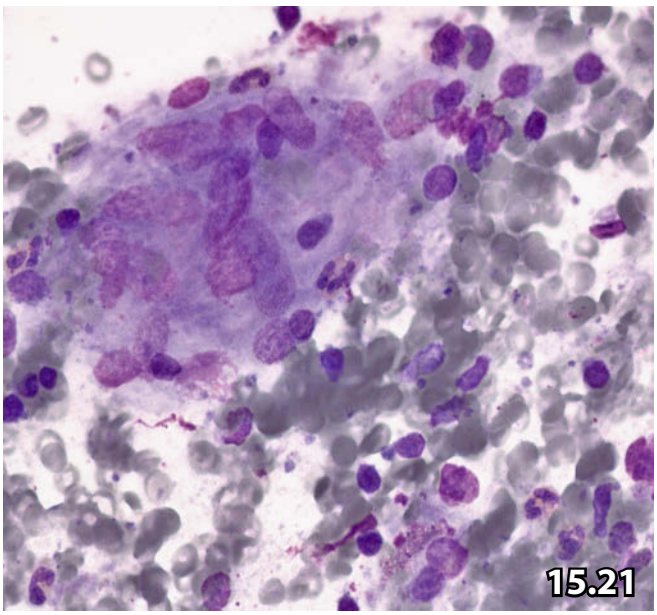
15.21

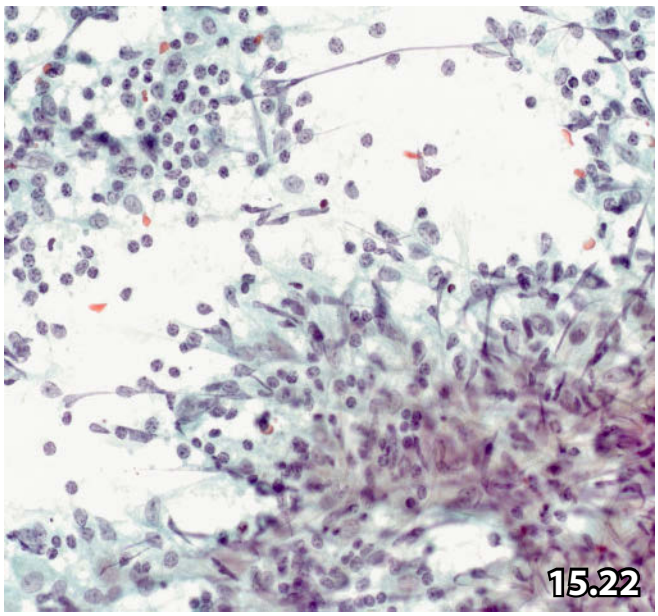
15.22

**Fig. 15.23 Cat-scratch disease.**
Fine needle aspirate of a 24-year-old man's axillary lymph node. Direct smears and MGG staining were performed. Low magnification shows suppurative lymphadenitis associated with peripheral palisading of epithelioid histiocytes (arrows).

**Figs. 15.24 and 15.25 Toxoplasmic lymphadenitis: morphology and parasites.**
Enlarged submandibular lymph nodes in two boys, 8 and 11 years old. FNAB was performed and direct smears were MGG- and Pap-stained.
*Cytologic diagnoses:* LDP comprising distinct follicular hyperplasia and aggregates of epithelioid cells; findings suggest toxoplasmic lymphadenitis.
*Subsequent serotest* results revealed positive toxoplasma antibody titer in both patients.

**Fig. 15.24** (case #1) Higher magnification of an MGG-stained smear exhibits a loose aggregate of activated epithelioid cells surrounded by a variegated lymphoid cell population.

**Fig. 15.25** (case #2) High magnification of a Pap-stained smear is focused on parasites enclosed in the cytoplasm of histiocytes and macrophages (arrows). Note coexistence of parasites and cellular detritus in the cytoplasm of a macrophage (paracentral, left).

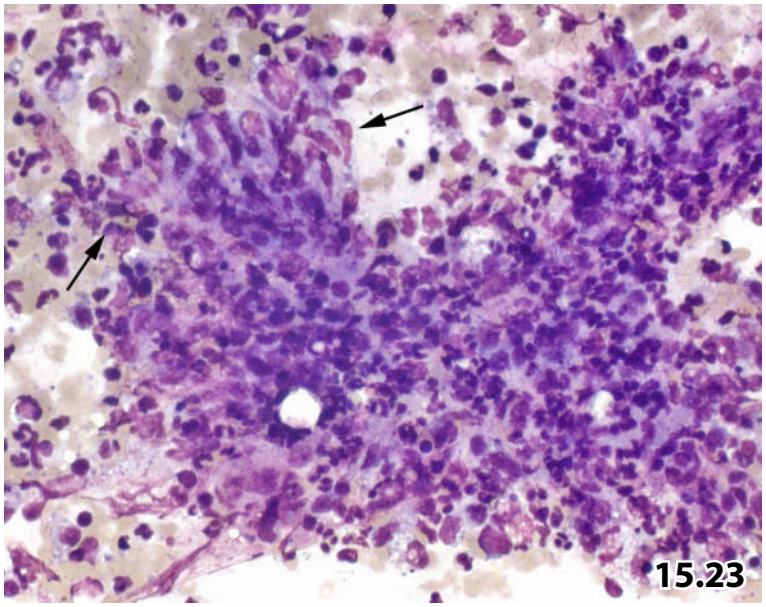
15.23

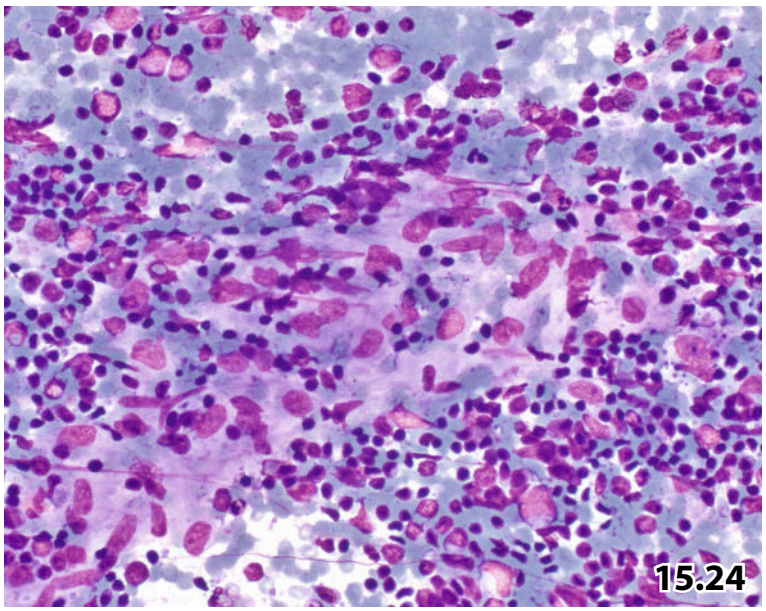
15.24

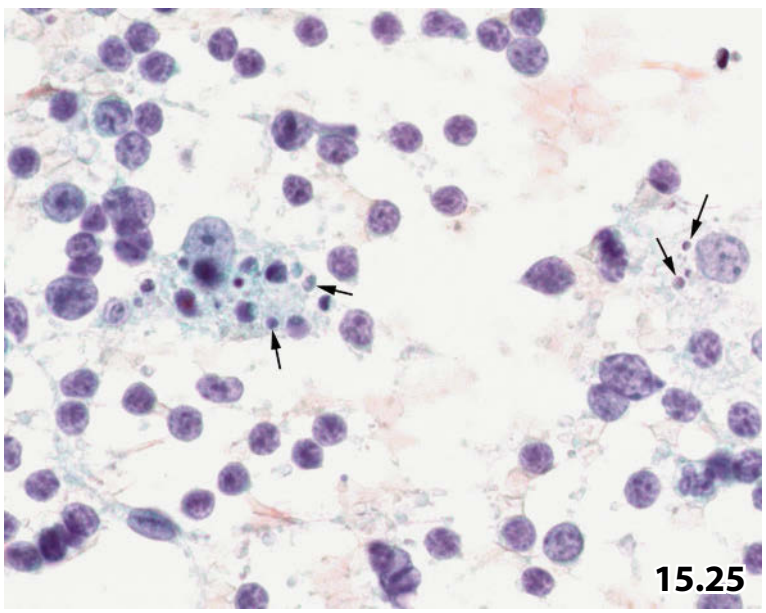
15.25

**Figs. 15.26 and 15.27 EBV-specific lymphadenopathy: infectious mononucleosis.**
Two young female patients presented with enlarged cervical lymph nodes. FNAB was performed followed by direct smearing of the aspirated material.
*Cytologic diagnoses:* Pronounced LDP associated with plasmacytoid hyperplasia highly suggesting mononucleosis.
*Subsequent serologic results* confirmed mononucleosis infectiosa.

**Fig. 15.26** (case #1) The lymph node aspirate shows a high proportion of cells with plasmacytoid features: immunoblasts, plasmablasts, and mature plasma cells (arrow) (MGG stain, lower magnification).

**Fig. 15.27** (case #2) High magnification shows mainly immunoblasts and plasmablasts accompanied by small lymphocytes and macrophages/starry-sky cells (upper left). Lucid and pale chromatin argue against malignancy (Pap stain).

**Figs. 15.28 and 15.29 Cytologic features suggestive of EBV-associated lymphadenopathy: possible diagnostic pitfall.**
Two young patients were found to have enlarged lymph nodes in the submandibular area.
*FNAB cytology* suggested EBV infectious disease.
*Follow-up:* Both patients had no further examinations. Results of serologic tests, if any, were not disclosed.

**Fig. 15.28** (case #1) Image detail shows an extremely heterogenous cell pattern, the cell size ranging from small lymphocytes to immunoblasts (direct smear, Pap stain). The overall cell pattern, coarse-granular nuclear chromatin of small and medium-sized lymphocytes, and loose reticular chromatin of the nuclei of the blast cells particularly indicate benign lymphoproliferative disease.

**Fig. 15.29** (case #2) A Reed-Sternberg-like cell (upper left) within a variegated lymphoid background comprising numerous benign blasts and cells with plasmacytoid features (arrows) (lower right). This setting may be misinterpreted as Hodgkin lymphoma (direct smear, Pap stain, high magnification).



**Figs. 15.30 and 15.31 AIDS-related lymphadenopathy and retroperitoneal mycobacteriosis.**
Two male patients with a positive history of AIDS presented with supraclavicular and retroperitoneal lymphadenopathy, respectively. FNABs were performed and direct smears were prepared.

**Fig. 15.30** (case #1) Aspirates from three supraclavicular lymph nodes provide a heterogeneous cell pattern comprising the whole spectrum ranging from small lymphocytes to blasts. A high proportion of the cells exhibit plasmacytoid features. The mitotic activity is high (arrow) (MGG stain, high magnification).

**Fig. 15.31** (case #2) Image-guided FNAB of a retroperitoneal lymph node in the other patient reveals histiocytes filled with acid-fast bacilli (direct smear, Ziehl-Neelsen stain, high magnification). Mycobacteriosis of retroperitoneal lymph nodes is another version of opportunistic infection in patients with AIDS.

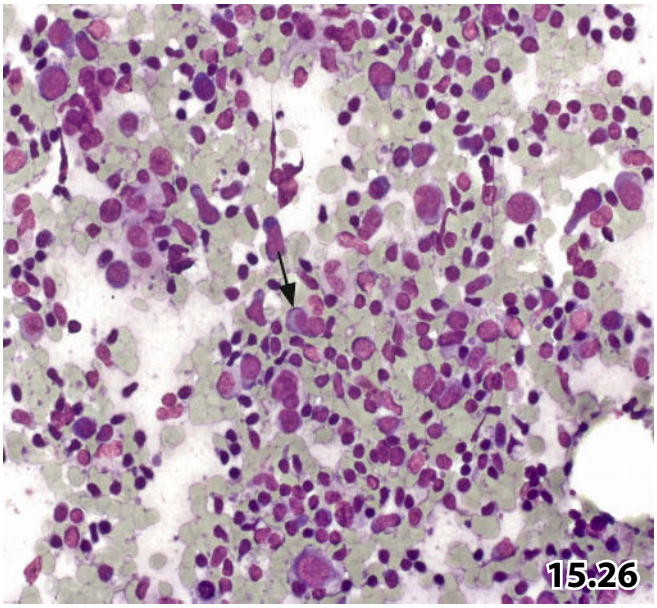
15.26

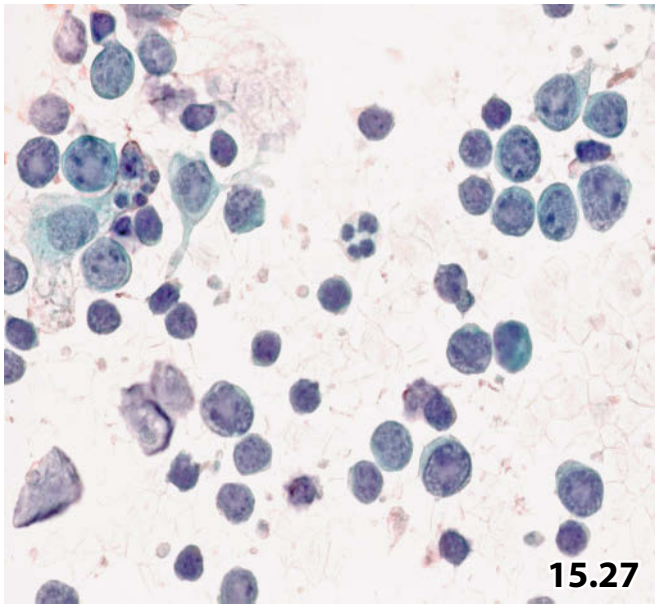
15.27

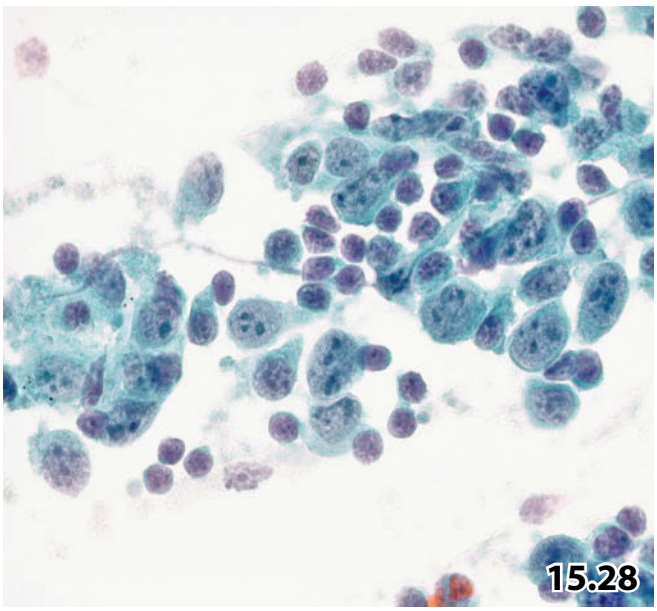
15.28

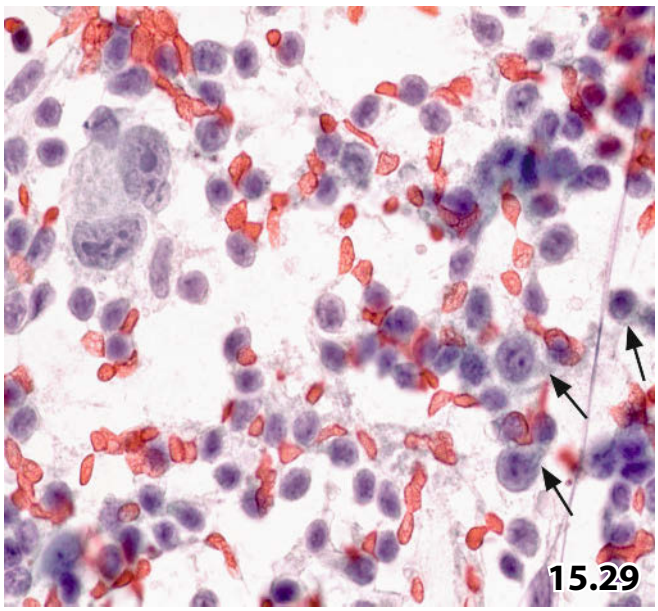
15.29

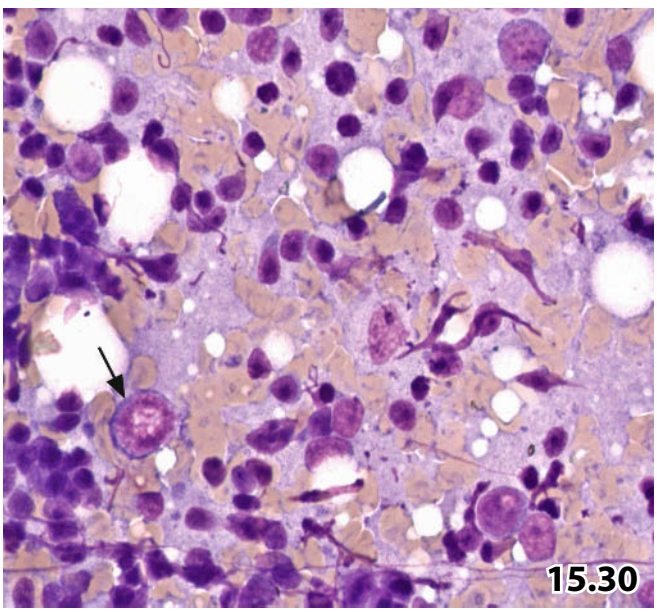
15.30

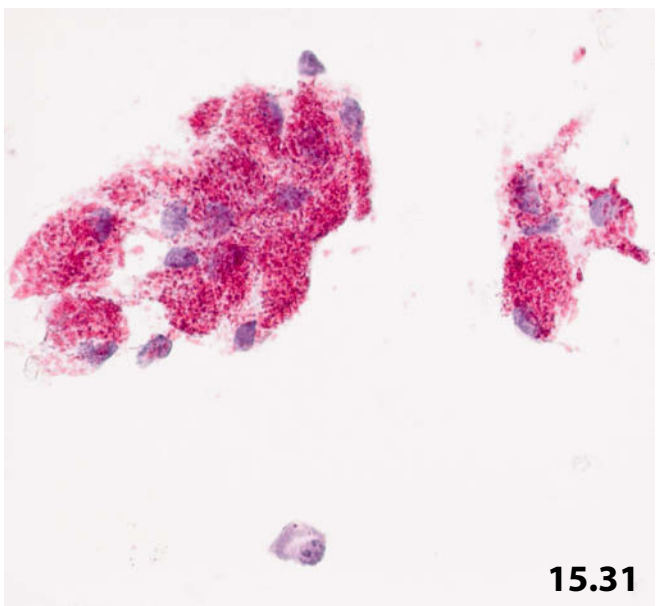
15.31

**Fig. 15.32 Reactive lymphadenopathy in immunologic disease.**
A 54-year-old woman with a positive history of chronic polyarthritis presented with markedly enlarged inguinal lymph nodes.
Aspirates exhibit small lymphocytes, numerous plasmablasts (arrows), maturing and mature plasma cells. Regrettably, MGG staining was not done (direct smear, Pap stain, higher magnification).

**Figs. 15.33–15.36 Dermatopathic lymphadenopathy.**
Cytologic characteristics of dermatopathic LDP are presented on the basis of four cases (FNAB of lymph nodes) using different staining methods and preparation techniques.

**Fig. 15.33** (case #1) Low magnification reveals a loose network of interdigitating reticulum cells (arrows) spreading out between reactive lymphoid cells (direct smear, MGG stain).

**Fig. 15.34** (case #2) High magnification of a Pap-stained direct smear shows a dense network of interdigitating reticulum cells. Cytoplasmic and nuclear properties of the specific histiocytes are readily recognized.

**Fig. 15.35** (case #3) In comparison to the conventional smears, cytoplasmic and nuclear features of interdigitating reticulum cells are well preserved in liquid-based preparation, but the cytoarchitecture is poorly maintained (ThinPrep method, Pap stain, higher magnification).

**Fig. 15.36** (case #4) Crowded interdigitating reticulum cells exhibiting intracytoplasmic melanin pigment. This particular setting should not be misinterpreted as malignant melanoma of the spindle cell variant (direct smear, Pap stain, high magnification).

Please note that melanin-laden interdigitating reticulum cells usually occur sporadically, contrary to the pattern presented herein.

**Fig. 15.37 Rosai-Dorfman disease.**
A 4-year-old girl presented with an enlarged cervical lymph node. FNAB was performed, and direct smears were MGG- and Pap-stained. High magnification is focused on incorporated lymphocytes in large histiocytes (so-called emperipolesis). Note halos around the ingested cells (arrows) and the vacuolated cytoplasm (Pap stain).

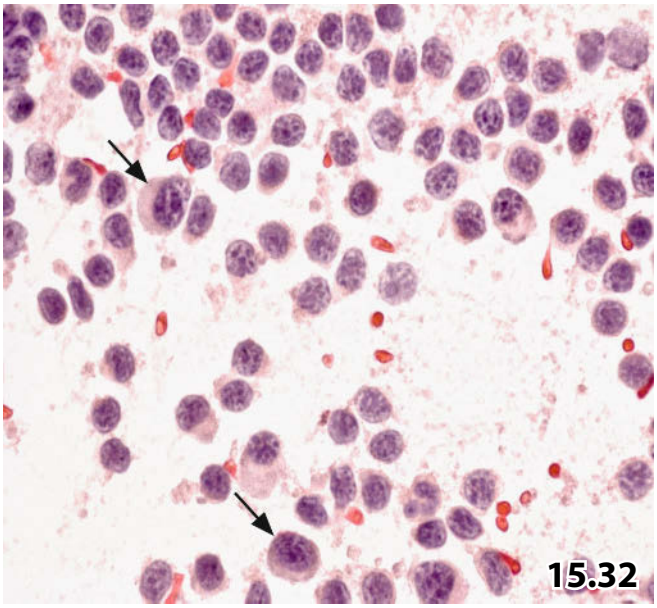
15.32

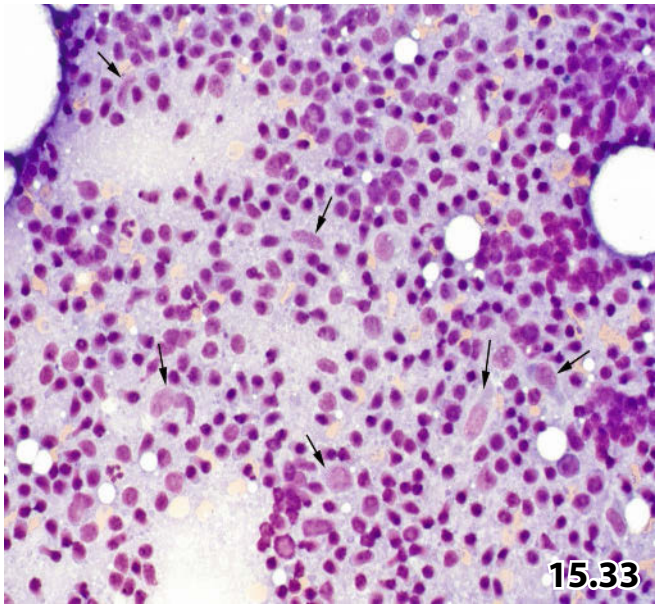
15.33

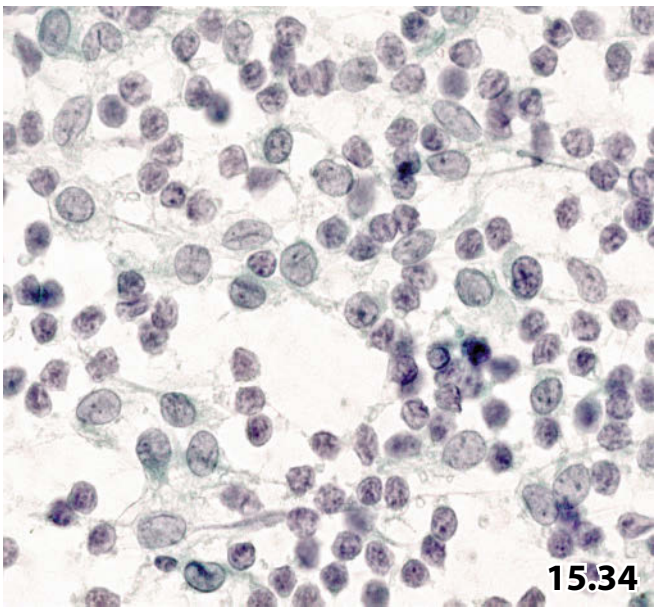
15.34

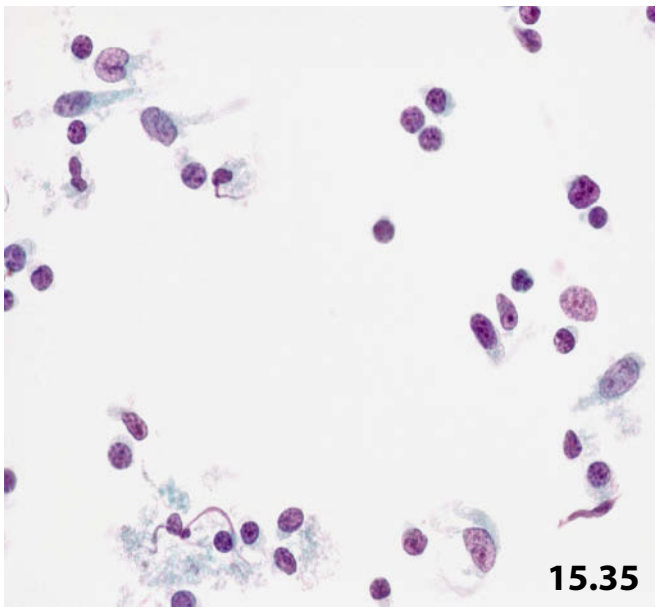
15.35

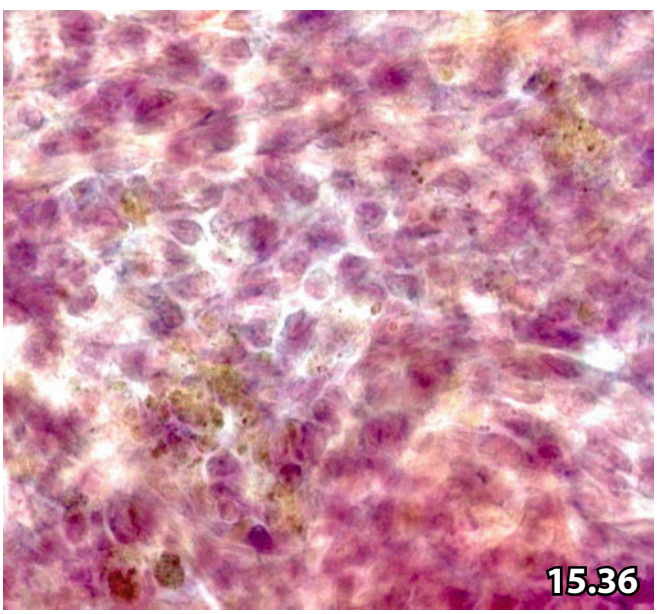
15.36

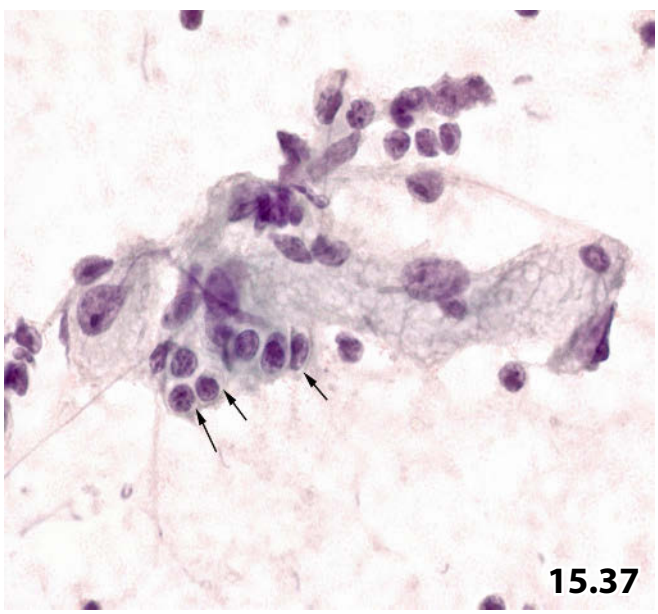
15.37

**Fig. 15.38A, B Castleman disease.**
A 16-year-old male presented with a greatly enlarged lymph node at the right side of his neck. Direct smears were prepared from the aspirate. Only Pap-stained specimens are available.
*A nonspecific cytologic diagnosis was made:* Reactive LDP, Castleman's disease, Hodgkin lymphoma, others?
*Histologic diagnosis* of the same lymph node: Castleman tumor of the hyaline vascular variant.
**A** A predominantly small-cell lymphoid pattern and scattered large histiocytes (arrows) may suggest Castleman disease (lower magnification). **B** Key feature of Castleman disease: numerous small and large histiocytes, their nuclei show crumpled appearance and are readily detected at high magnification (arrows).

**Fig. 15.39 Sarcoidosis.**
FNAB of an enlarged cervical lymph node in a young female patient. High magnification shows a fragment of granulomatous tissue that is composed of large activated epithelioid histiocytes comprising a Langhans-type giant cell (lower right). The granulomatous tissue is penetrated by small lymphocytes (bottom). Ziehl-Neelsen stain provided a negative result (not shown) (Pap stain).
*Tentative cytologic diagnosis:* Epithelioid cell granulomatosis.
*Clinical follow-up and final diagnosis:* Sarcoidosis (no histologic investigation).

**Fig. 15.40A, B Langerhans cell histiocytosis.**
A 49-year-old woman was afflicted with persistent lymphadenopathy. FNAB was performed on an enlarged lymph node at the right side of the neck. Direct smears were Pap-stained.
*Cytologic/immunocytochemical diagnosis:* Langerhans cell histiocytosis.
*Comment:* Differential diagnosis should consider dermatopathic lymphadenopathy, but large histiocytes, multinucleation, and pronounced nucleoli do not match interdigitating reticulum cells.
*Tissue diagnosis:* Cytologic diagnosis was confirmed by histologic examination of a lymph node.
**A** Characteristic Langerhans cells scattered in a reactive lymphoid background are presented at high magnification. **B** Immunostaining is helpful in distinguishing between Langerhans cell histiocytosis and dermatopathic lymphadenopathy: Langerhans cells stain positive for S100 antigen (Pap-prestained conventional smear).

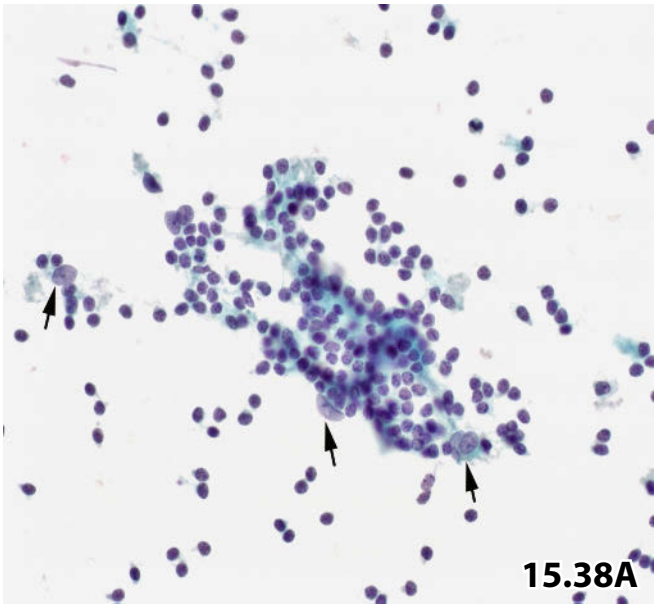
15.38A

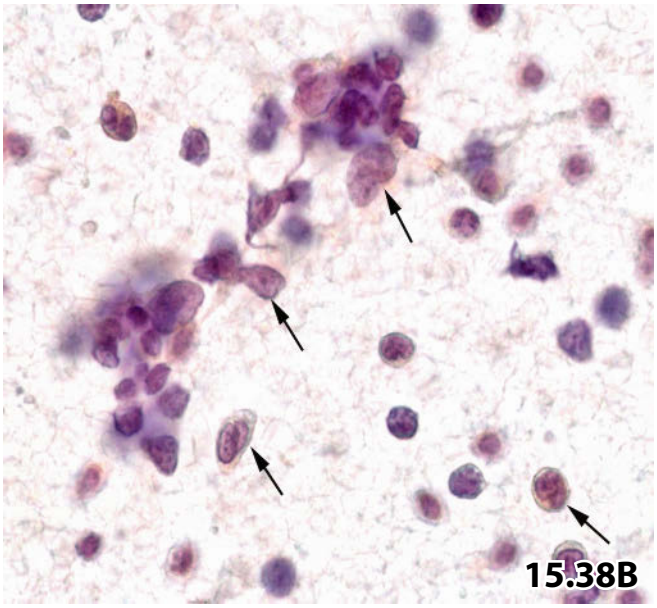
15.38B

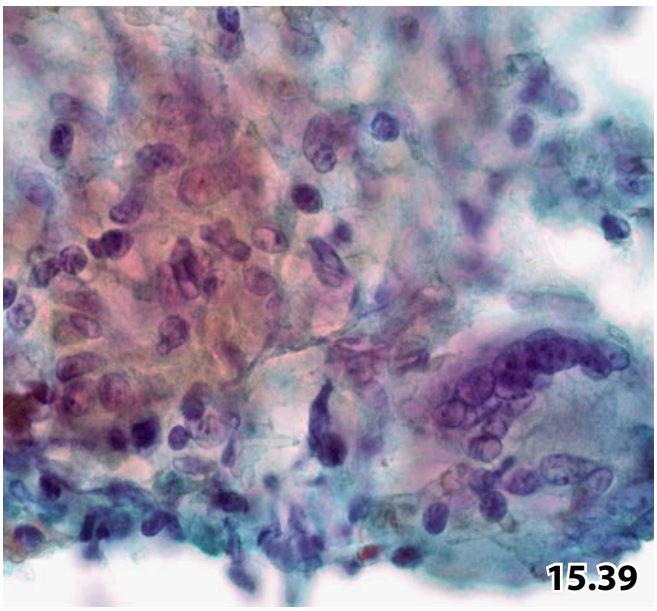
15.39

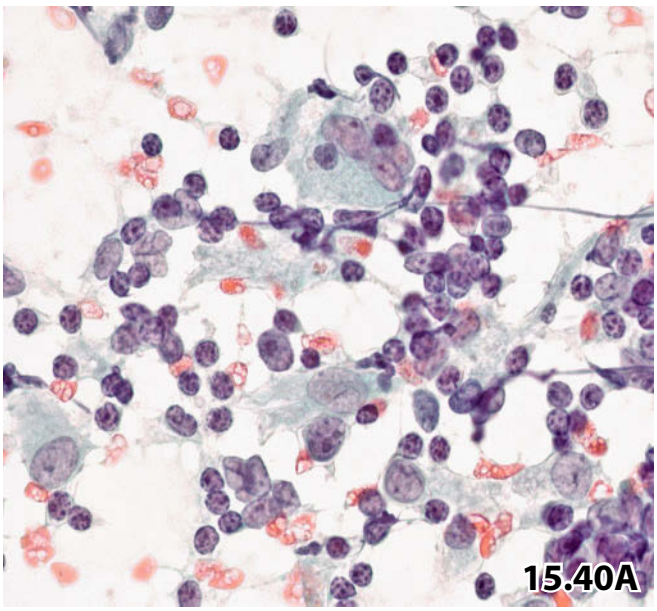
15.40A

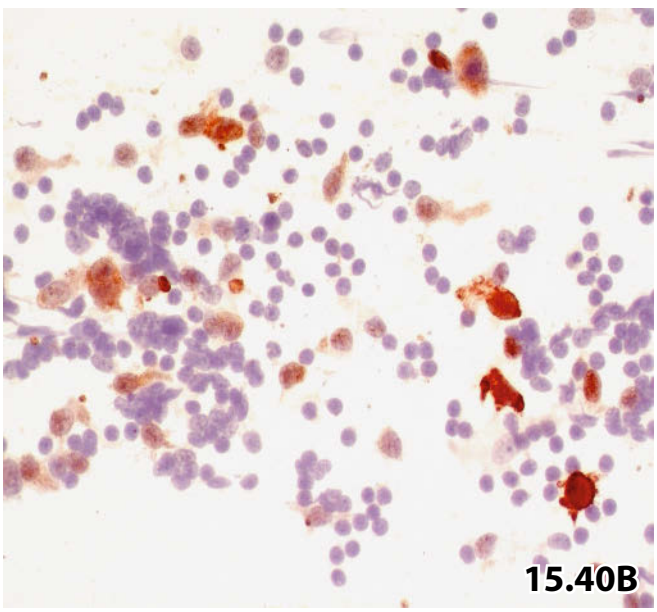
15.40B

# Section 15.3
# Lymph Nodes

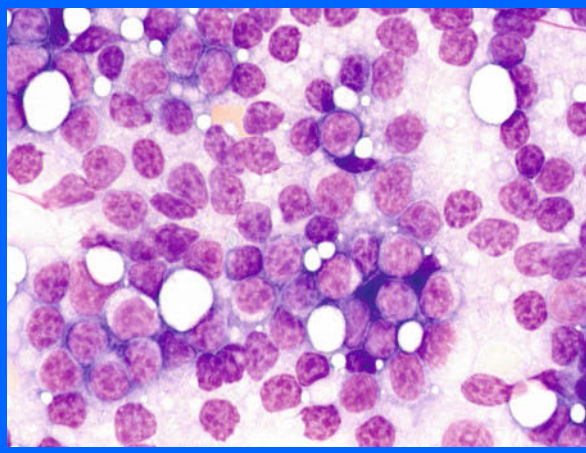

## B- and T-Cell Non-Hodgkin Lymphomas
## Hodgkin Lymphomas
## Histiocytic Sarcoma
## Myeloproliferative Disorders
## Metastatic Neoplasms

### 15.3.1 Introductory Comments on Non-Hodgkin Lymphomas and Hodgkin Lymphomas [17]

#### 15.3.1.1 General Comments

- According to a large number of studies, the incidence of malignant lymphoma is steadily increasing, both in industrial and in developing countries [17]. In addition, an increasing number of abnormal deep-seated lesions that are located in complex body compartments are visualized by different imaging techniques and investigated by means of laborious and expensive interventional procedures [74]. This is why economical, minimally invasive diagnostic techniques such as image-guided fine-needle aspiration biopsy (FNAB) will gradually be more and more requested in the future.
- Conclusive tumor diagnoses including accurate subclassification of lymphomas by aspiration cytology are desired.
- Vague differential diagnostic issues are of little value to attending physicians for further planning and therapeutic decision-making [79]. This is particularly true for:
  - Patients who are not disposed or willing to undergo more invasive tissue sampling.
  - Patients whose condition is too poor for anesthesia and open surgical biopsy.
  - Patients in a restricted medical setting such as in developing countries.
- Thus, cytologic laboratories must apply expert cytodiagnostic practices in combination with ancillary methods (immunotyping, molecular biologic techniques) that can reliably distinguish between benign and malignant lymphoproliferative disorders [86] and that are suitable to classify a high percentage of malignant lymphomas [22]. In general, ancillary techniques are applicable to cytology specimens without difficulty [51]. Several studies have shown the effectiveness of these methods; even so the diagnosis and subtyping of malignant lymphoma by aspiration cytology alone remains controversial [4, 17, 36, 40, 43, 81, 83].
- The new 2008 WHO classification of lymphomas is based on morphologic, genetic, and molecular criteria, and also on clinical features [88].

#### 15.3.1.2 Basic Diagnostic Rules

- Large lymph nodes tightly packed together, restricted to one location or disseminated, are suggestive of malignant lymphoma. Ultrasonographic investigation would reveal large rounded nodules with neat margins and homogeneous hypodensity.
- The process of diagnosing malignant lymphomas by cytology is mandatory requiring close interdisciplinary cooperation among the clinical disciplines involved.

- The best reproducible diagnoses in FNAB specimens are high grade B-cell non-Hodgkin lymphomas (NHL) and classical Hodgkin lymphoma.
- Major difficulties diagnosing and subtyping of malignant lymphoma, and distinguishing between malignant lymphoma and reactive lymphadenopathy arise from:
  - NHL predominantly composed of small cells [12].
  - Low-grade NHL of follicular center-cell origin exhibiting a pronounced variegated cell pattern.
  - Lymphocyte-predominant Hodgkin lymphoma.
  - Hodgkin lymphoma with a dominating reactive background masking single tumor cells (Hodgkin-Reed-Sternberg [HRS] cells).

### 15.3.1.2.1 Basic Remarks on Lymphoma Diagnostics by Cytology

#### Microscopic Features

- In general, a polymorphic cell pattern in cytologic preparations favors benign follicular lymphoid hyperplasia, whereas monomorphic appearance instead suggests malignant lymphoma.
- Nuclei of lymphoma cells are invariably enlarged as compared to nuclei of small benign lymphocytes.
- The chromatin of the nuclei of small-cell malignant lymphomas and of many malignant large blastic cells is finely granular and densely packed, thus the nuclei become deeply stained and appear in a three-dimensional fashion (ballooned). Conspicuous nucleoli are frequent but arbitrary.
- Dense focal crowding of the tumor cells is a typical feature for malignant lymphoma of any grade (Figs. 15.44 and 15.61). Loose or dense aggregation of both small lymphoma cells and large blast cells may easily be misinterpreted as carcinomatous clusters (small-cell carcinoma and undifferentiated large-cell carcinoma, respectively) (Fig. 15.78A).

#### Additional Analyses

- The diagnostic impact of phenotypic and/or genotypic profiling must be re-emphasized. Thus, it is recommended to save a certain proportion of the cells from each sample for auxiliary analyses such as immunocytochemistry, flow cytometry (FCM), polymerase chain reaction (PCR), and fluorescence in situ hybridization (FISH).
- CD markers and their diagnostic properties are listed in Sect. 15.1.4.1, Table 15.1.1, p. 912.
- However, not only cytomorphology but also adjuvant analyses are affected with limited diagnostic specificity. Immunophenotyping, flow cytometric procedure, and molecular tests may fail to identify aberrant T-cell sets or monoclonal B-cell populations for various reasons such as:
  - Incomplete tumor involvement of the targeted lymph node resulting in sampling error.
  - T-cell-rich or histiocyte-rich variants of B-cell lymphoma containing too few malignant (monoclonal) B blasts.
  - Marked tumor sclerosis providing paucicellular aspirates.
  - Poor cell preservation.
  - T-cell NHLs devoid of specific immunophenotype.

#### Major Cytodiagnostic Challenges

**Caution**

- Distinguishing between benign and malignant lymphoid disorders may give rise to difficulties, as stated below [85, 86]:

  *False positive diagnosis of lymphoma* may occur in cases with:

  1. Pronounced reactive changes in lymph nodes, including active germinal centers, and/or atypical plasmacytoid hyperplasia, together with increased mitotic activity. Blasts and plasmacytoid transitional cells may be overestimated as being malignant (Fig. 15.28, 15.29, 15.41).
  2. Uniform appearance of the overall cell population due to an excessive benign hyperplasia of T-zone lymphocytes. Diagnostic considerations include NHLs composed of a monotonous lymphocytic pattern such as small lymphocytic lymphoma, lymphoblastic lymphoma, and mantle cell lymphoma (Fig. 15.42).

  *False negative diagnosis may occur in:*

  1. Lymphomas presenting with a distinct heterogeneous cell pattern (lymphomas of the mixed cell type) [70], in particular:
     - Follicular lymphoma (Fig. 15.60).
     - Marginal zone lymphoma (Fig. 15.70).
     - DLBCL-centroblastic variant (Fig. 15.76).
     - Certain T-cell lymphomas, in particular angioimmunoblastic T-cell lymphoma (Fig. 15.85A).
     - Hodgkin lymphoma (Fig. 15.93).
  2. Lymphomas admixed with a large proportion of reactive lymphoid tissue.
  3. Lymphomas of the B-cell phenotype with a significant admixture of reactive T-lymphocytes (Fig. 15.75).
  4. Lymphomas admixed with a predominant proportion of benign proliferative histiocytes.

  The overall cell pattern is misleading in the particular settings recorded as (2), (3), and (4) due to the dominant benign lymphocytic/histiocytic infiltration; the tumor cells are too sparse or masked by the benign cell population.
- FNAB sampling from a lymph node with partial tumor involvement may lead to an erroneous negative diagnosis [82].

- Extranodal and extramedullary (bone) infiltrates of malignant lymphomas are infrequently encountered in fine-needle aspirates [65, 100] but can give rise to diagnostic pitfalls. The diagnostic consideration includes extramedullary hematopoiesis, granulocytic sarcoma, and nonlymphohematopoietic malignancies, in particular undifferentiated carcinoma. The most common lymphoma subtypes forming extranodal tumor masses are large-cell lymphoma and plasma cell myeloma. The preferred extranodal sites of lymphoid neoplasms are the skin and soft tissues, but also many parenchymatous organs can be affected, in particular the kidney, liver, salivary glands, and breast.
- It is important that cytopathologists be aware of a pretended false-positive FNAB result due to excision of a benign lymph node (LDP) other than the previously aspirated node (yielding a malignant cytologic result).
- Diagnostic limitations of adjuvant analyses, see Sect. 15.3.1.2.1, p. 951.

### 15.3.1.2.2 Non-Hodgkin Lymphomas in general

#### General Comments

- Non-Hodgkin lymphomas (NHL) are by definition clonal proliferations of lymphatic immature precursor cells, or peripheral functionally determinated lymphoid cells that are morphologically and immunologically similar to, or even indistinguishable from their benign counterparts.
- The neoplastic cells are characterized by cytomorphologic and pheno- and/or genotypic features according to former and recent classification schemes, i.e., Rappaport's classification (in the 1960s), the International Working Formulation (in the early 1980s), the Kiel update (in 1992), the Revised European-American Lymphoma Classification (REAL 1994), and the World Health Organization classifications (WHO 2001 and 2008). Completing the established morphologic properties, recent characteristic marker profiles and genetic/karyotypic peculiarities of the various malignant lymphoma entities are compiled in the 2008 WHO classification scheme [88]. The 2008 WHO classification generally defines entities irrespective of their presentation as solid tumors (lymphomas) or leukemic disorders (lymphatic leukemias).
- Some lymphomas may show specific cytologic characteristics so that an accurate diagnosis and subtyping can be rendered on the basis of cytomorphology alone.
- To discuss the multitude of different variants of B-cell NHLs and particular T-/NK-cell NHLs is beyond the scope of this work. We limit our explanations to selected entities presumed to be of major interest and importance in aspiration cytology of lymph nodes, parenchymatous organs, and soft tissue masses.

#### Grading

- Grading of malignant non-Hodgkin lymphomas is one of the greatest challenges in cytological diagnosis. Cytologic grading systems are largely based upon well-established diversity in cell size ("cyte" versus "blast") and the flow cytometric or morphometric approach. Low- and high-grade lymphomas vary in their biological behavior, the former are usually composed of small cells (cytes) and the latter of pleomorphic large cells (blasts).
- An elementary cytologic grading into the two subtypes, low-grade and high-grade, may sometimes provide reasonable information to the attending physicians:
  - A minimally invasive procedure together with basic grading will be suitable for therapeutic decision-making in patients presenting in a poor general condition.
  - Assessment of a progression from low-grade to high-grade lymphoma in the tumor follow-up.
  - However, aspirations that show meager cellularity prevent reliable subtyping and grading.
- Intermediate tumor variants composed of a mixed tumor cell population or a conspicuous admixture of blastic cells usually cause severe grading problems by cytology.
- The proliferation index of a cell population defined by the percentage of tumor cell nuclei that stained positive with antibodies against Ki-67/MIB-1 [1] or determination of the flow cytometric S-phase fraction [72] may serve as complementary biological parameters for tumor aggressiveness. These tools are particularly valuable in correlation with corresponding data collected from previous histologic or cytologic investigations. Proliferation indices should be completed by cut off points for different grades of malignancy as proposed by several authors.
- For more details and references, we refer to Sect. 15.3.6, "Follicular Lymphoma: Cytologic Grading," p. 959.

**Caution**

- Cytologic specimens of NHLs exhibiting a mixed cell lymphoid population comprising "cytes" and "blasts" give rise to serious problems regarding tumor classification.
- The cytologic classification of certain high-grade malignant NHLs that are composed of small- to medium-sized cells can be difficult (e.g., mantle cell lymphoma). A conclusive diagnosis including tumor subtyping and grade requires ancillary analyses.
- Keep in mind that both benign and malignant lymphoid cells in liquid-based cytologic specimens tend to appear more pleomorphic compared to their counterparts in conventional smears including nuclear irregularities, distinct nucleoli, and loose chromatin texture; a reliable tumor grading is often more difficult than in conventional aspirate smears (incidentally, the same effect on lymphoid cells is observed in sediment smears of body fluids).

#### 15.3.1.2.3 Non-Hodgkin Lymphomas of the B-Cell Phenotype

**General Comments**

The antibody panel used for immunocytochemical characterization and subtyping of B-NHL is largely dependent on the antecedent cytomorphological interpretation. A substantial predominance of CD20-positive and/or other B-cell marker-positive atypical lymphoid cells usually allows the cytologic diagnosis of non-Hodgkin lymphoma of the B-cell phenotype (B-NHL) [106].

- The following results can establish, or at least suggest, a diagnosis of B-NHL:
  - Accurate cytomorphologic features that are in accordance with the established rules for the various tumor variants listed below.
  - A substantial predominance of B-cell marker-positive atypical lymphoid cells detected by immunophenotyping (CD20 and others) (Fig. 15.65).
  - Phenotypic or genotypic kappa or lambda light chain restriction. The kappa:lambda ratio that favors malignant lymphoma must be high or low, according to the properties of the cell clone (Fig. 15.3). It is most helpful to establish reliable internal immunoglobulin (Ig) light chain ratios using immunocytochemical or flow cytometric tests for defining monoclonality in cytologic specimens [4, 82].
- A proper subtyping of B-cell NHLs usually needs a broad spectrum of additive analyses.

#### 15.3.1.2.4 Non-Hodgkin Lymphomas of the T-Cell Phenotype

**General Comments**

- T-cell lymphomas are rare neoplasms accounting worldwide for about 10% of all non-Hodgkin lymphomas. Accordingly, these tumors are rarely encountered in fine-needle aspirates and the cytodiagnostic experience is poor. The varying cytologic appearance and a variegated cell pattern in many T-cell lymphomas are one of the greatest diagnostic challenges for cytopathologists [2].
- Park and Kim studied the usefulness of FNAB on malignant lymphomas in an area with a high incidence of T-cell lymphoma (Korea). They found significant limits for FNAB used as a first-line diagnostic procedure in T-cell lymphomas [68].
- The following features can establish, or at least suggest, a diagnosis of a non-Hodgkin lymphoma of T-cell phenotype (T-NHL):
  - A characteristic but nonspecific morphologic indicator for tumor cells of the T-cell lineage are the polylobated cerebriform nuclei comprising loose chromatin structure and rather indistinct nucleoli.
  - Positive immunostaining for T-cell markers of a high percentage of the tumor cells established by immunocytochemical or flow cytometric tests (Fig. 15.81).
  - Clonal rearrangement of T-cell receptor (TCR) genes (Fig. 15.4) by molecular genetic testing.
- Appropriate subtyping of T-NHL usually needs the whole battery of additive analyses.
- T-cell lymphomas can be classified into two main groups: (1) precursor T-cell neoplasms and (2) mature T-/NK- (natural killer) cell neoplasms.

Some variants of T-cell and NK-cell lymphomas have been selected and are presented hereinafter, considering the morphological and biological characteristics. The selected entities are thought to be most likely encountered in daily FNA practice for enlarged lymph nodes, for tumoral masses in particular organs (e.g., spleen, liver, gastrointestinal tract), and for infiltrates in soft tissues, particularly in the subcutis:

- T lymphoblastic leukemia/lymphoma.
- T-cell prolymphocytic leukemia.
- Adult T-cell leukemia/lymphoma.
- Mycosis fungoides/Sézary syndrome.
- Peripheral T-cell lymphoma NOS.
- Angioimmunoblastic T-cell lymphoma.
- T anaplastic large-cell lymphoma.

**Caution**

The broad spectrum of cytologic appearance of the mature T-cell lymphomas is a major reason for pitfalls in standard cytology of T-cell neoplasms.

### 15.3.1.2.5 Hodgkin Lymphomas

#### Introduction and Classification

- Hodgkin lymphoma (HL) is a malignant disorder of the lymphoid cell system characterized by a mixed lymphocytic and histiocytic background interspersed with large mononucleated and multinucleated tumor cells that derive from mature germinal center B-cells. The disease usually affects lymph nodes preferably in the neck area followed by mediastinal nodes. Young adults are the preferred age group for HL with a second peak in the older age group, dependent on the HL subtype. Hodgkin lymphomas account for about 30% of all malignant lymphomas.
- Human herpesvirus (HHV-6) and Epstein-Barr virus are reported to be frequently present in lymph nodes of patients affected by Hodgkin lymphoma [48]; in approximately 50% of the classical HL types, Reed-Sternberg cells are infected by the Epstein-Barr virus.
- The cytodiagnostic accuracy of Hodgkin lymphoma is reported to be high in practically all studies documented in the literature, ranging from 85% to 95%. In contrast, initial cytologic subtyping of HL reaches a much lower percentage of accuracy, ranging from 60% to 70% [18, 37].
- Hodgkin lymphoma is currently divided into two groups:
  1. *Classical Hodgkin lymphoma*
     Classical HL is further divided into four histologic subtypes that may differ in many morphological and clinical respects but not in immunophenotypic or genetic pecularities. The four HL subtypes comprise:
     - Mixed cellularity.
     - Nodular sclerosis.
     - Lymphocyte-rich variant.
     - Lymphocyte-depleted variant.
  2. *Nodular lymphocyte predominant Hodgkin lymphoma*
     This entity differs from classical HL in its clinical behaviour, in the cellular composition, and particularly in immunophenotypic pecularities.
- The classic HL subtypes share similar morphologic characteristics:
  - Varying number of pathognomonic large tumor cells typically mononucleated or bi-/multinucleated, referred to as Hodgkin cells and Reed-Sternberg cells (HRS cells).
  - Heterogeneous inflammatory component preferentially composed of small and enlarged (reactive) lymphocytes supplemented by varying proportions of eosinophilic and neutrophilic granulocytes.
  - Enlarged lymphocytes are benign although they may display distinct nuclear irregularities.
  - The inflammatory infiltrate is usually intermingled with histiocytes and/or epithelioid histiocytes and/or dendritic cells. Occasionally, histiocytic cells may represent a large proportion of the background cell population.
  - Epithelioid granulomas are not uncommon [33].

#### Major Cytodiagnostic Challenges

**Caution**

- *False negative diagnosis #1* [13] may occur when tumor cells (HRS cells) are sparse, completely absent, or obscured by a dense background infiltrate. This situation may be caused by:
  - Partial tumor involvement of the examined lymph node.
  - A pronounced inflammatory background.
  - Pronounced fibrosis.
  - A pronounced (epithelioid) granulomatous reaction [105].
  - The lymphocyte-rich and nodular lymphocyte-predominante subtype of HL.
- *False-negative diagnosis #2* may be caused by:
  - A polymorphous background population in HL simulating reactive lymphadenopathy: HRS cells are misinterpreted as benign blasts (Fig. 15.93).
  - Suppurative and necrotizing changes mimicking lymphadenitis [98].
- *False-positive diagnosis* of HL is easily possible:
  - In cases of virus-induced lymphadenopathy, in particular Epstein-Barr virus, comprising lymphoplasmacytoid cells and multinucleated blasts mimicking HRS cells (Fig. 15.29).
- *Misinterpretation of HRS cells* [32, 45]. Sporadic HRS cells devoid of an adequate lymphocytic background, or in combination with a particular background pattern may lead to a false diagnosis of:
  - B- or T-NHL with HRS cell-imitating large lymphoid blasts.
  - Metastatic carcinoma of the large-cell type (Fig. 15.98B).
  - Metastatic lymphoepithelial carcinoma.
  - Metastatic malignant melanoma.
  - Undifferentiated nonepithelial/nonlymphoid neoplasms.
- Differentiation between classical HL-lymphocyte rich variant and nodular lymphocyte predominant HL, Table 15.3.2, p. 974.
- Combined HL and NHL. Several reports in the literature document the occasional occurence of composite (both tumor types in the same lymph node), simultaneous (both tumor types in separate lymph nodes), and sequential lymphatic tumors (Hodgkin lymphoma may follow NHL and vice-versa). The most common NHL subtype associated with HL is follicular lymphoma [35].
- HL and liquid-based preparation. HRS cells usually exhibit a smaller size in liquid-based preparations as compared with conventional smears (Fig. 15.90).

The following sections focus on the cytological features and the relevant immunologic and molecular properties of select-

ed types of malignant lymphomas that are of major interest for cytopathologists. Diagnostic considerations and pitfalls are discussed as well. The information is based on our experience in this field and data from the current literature [83]. The various entities are classified and presented according to the specifications indicated in the recent 2008 WHO nomenclature [88]. For further information, particularly with respect to the variability in immunophenotyping and of genetic abnormalities, we refer the reader to the 2008 WHO classification book and to specialized sources in the literature.

## 15.3.2 B Lymphoblastic Leukemia/ Lymphoma [34, 39] (Fig. 15.43)

### General Comments

- Synonyms: the neoplasm is also referred to as acute lymphoblastic leukemia (B-ALL) and precursor B lymphoblastic leukemia /lymphoma.
- B lymphoblastic leukemia/lymphoma is an aggressive neoplasm of B lymphoblasts, i.e., progenitor cells. The tumor may present as a sole tumor mass (lymphoblastic lymphoma, B-LBL), a lesion with extensive involvement of bone marrow, and leukemic disorder (lymphoblastic leukemia). Extramedullary involvement occurs frequently with predilection of the liver, spleen, central nervous system, and with involvement of the testes.
- B-ALL is a disease of childhood: 75% of cases occur in children under 6 years of age. In childhood, B-LBL occurs less frequently than lymphoblastic lymphoma of T-cell lineage. See also Sect. 15.3.12, p. 966.

### Microscopic Features

- Size of the immature blasts varies from small to intermediate:
  - *Small blasts* exhibit fuzzy nucleoli, and a scant cytoplasmic rim.
  - *Medium-sized blasts* show one or multiple variably prominent nucleoli; the distinct cytoplasm is of light-blue to grey staining quality. Cytoplasmic vacuoles and/or coarse granules are occasionally present.
- The nuclei consistently exhibit hyperchromasia, a finely granular condensed and evenly distributed chromatin, and frequently irregular contours and/or convolutions.
- Mitotic activity is pronounced.
- A focal starry-sky pattern may occasionally be observed.

**Caution**

Morphologic features of B lymphoblastic neoplasms are indistinguishable from those of T lymphoblastic lymphomas (see Sect. 15.3.12, p. 966).

### Additional Analyses

Immunophenotyping

Variable immunophenotype correlates with the degree of lymphoblast differentiation.

- Immunostaining for CD45 yields variable positivity.
- *Key markers for B-LBL*: terminal deoxynucleotidyl transferase (TdT) shows strong nuclear immunoreactivity, and CD10 decorates tumor cells of common B-ALL. CD34 shows variable immunolabeling.
- B-cell markers: CD19+, CD79a+, CD22+, PAX5+ (nuclear). CD20 shows variable labeling.
- Surface Ig is absent.

Molecular Genetics

- Rearrangements: IgH gene in practically all cases and T-cell receptor gene in the majority of cases.
- Chromosomal abnormalities: several quantitative (gain and loss) and structural (translocations) changes (see specialized literature).

### Differential Diagnosis

- T-ALL/LBL show variable positivity for many T-cell associated antigens, in particular CD3 (lineage specific). Further CD99+, TdT+, and CD1a+.
- Burkitt lymphoma is a diagnostic challenge in cases of LBL with extensive components of medium sized blasts and starry-sky pattern. However, Burkitt lyphoma exhibits particular immunophenotypic and genetic characteristics.
- Acute myeloid leukemia is a diagnostic challenge in cases of LBL presenting with medium-sized blasts. However, myeloid leukemic cells exhibit positive myeloperoxidase reaction and rare positivity for PAX5.

### Additional Comments

- It could be shown that fine needle aspiration is a valuable tool in order to detect recurrent ALL/LBL in general [101], and testicular recurrence in particular [20].
- Chromosomal abnormalities are in many cases related to particular prognostic features.

## 15.3.3 Small Lymphocytic Lymphoma/ Chronic Lymphocytic Leukemia

(Figs. 15.44–15.49)

### General Comments

- Small lymphocytic lymphoma (SLL) is a low-grade tumor due to abnormal neoplastic proliferation of B cells in the peripheral blood, bone marrow, and lymph nodes. Initially, the tumor cells accumulate in the peripheral blood and bone marrow; but the two compartments may occasionally become involved only at a later stage of the disease.
- SLL is a disease of adults and most patients are over 50 years old. CLL is the most common type of leukemia of adults in Western countries.

- The leukemic variant of the disorder is referred to as chronic lymphocytic leukemia (CLL) usually infiltrating lymph nodes, spleen, and liver.

### Microscopic Features

- Hallmarks: Predominantly small lymphocytes that are slightly larger than normal lymphocytes.
  - The clumped chromatin texture matches that of normal lymphocytes.
  - A pronounced centrally located nucleolus occurs in about 90% of all nuclei.
  - The nuclei are round, but focal irregularities and small indentations are commonly detected by careful microscopic evaluation.
  - A scant slightly basophilic (MGG) or cyanophilic (Pap) cytoplasmic rim is obvious.
  - The small tumor cells usually show focal dense crowding.
- The mitotic rate is very low.
- If present, tumor proliferation centers provide scattered medium-sized and large cells:
  - Prolymphocytes morphologically mimic SLL cells, but the former are obviously larger.
  - Paraimmunoblasts are blastic cells showing irregular nuclei, finely dispersed chromatin, large central nucleoli, and a distinct basophilic cytoplasm.
- Occasionally, small lymphocytic lymphoma exhibits features of lymphoplasmacytoid differentiation, a tumor variant characterized by considerably more Ig expression (Fig. 15.46).

**Caution**

- Cytologic aspirates of lymph nodes affected by SLL/CLL, accompanied by tumor proliferation centers, yield a mixed cellular pattern that is difficult to differentiate from other low-grade NHLs of the mixed type, progressive transformation, or reactive lymphadenopathy (Fig. 15.47).
- In liquid-based thin-layer preparations, nucleoli and irregularities of the nuclear outline of benign lymphocytes occur more frequently and more prominently than in conventional smears. Therefore, one should not overvalue these features and provide an erroneous diagnosis of small-cell lymphocytic lymphoma.

### Additional Analyses

Immunophenotyping

- *Key markers for SLL:* typically strong coexpression for CD5 and CD23.
- CD10– and cyclin D-1–.
- B-cell markers: CD20+ (slightly positive), CD22+, CD79a+.
- Surface Ig is weakly expressed.

Molecular Genetics

- Cytogenetic abnormalities (chromosomal gains and losses) are detected in the majority of cases.
- Trisomy 12 is characteristic.

### Differential Diagnosis

- SLL including cells of tumor proliferation centers should be differentiated against:
  - Other low-grade B-NHL showing CD5-, CD23-, and surface immunoglobulines strongly positive.
  - Transformation of CLL into diffuse large-cell lymphoma (Richter's syndrome) exhibiting increased proliferative activity (Ki-67) and chromosomal aberrations [10].
  - Benign proliferative lymphadenopathy (it is composed of a polyclonal lymphoid population).
- Metastases of small-cell carcinoma show a typical morphology expressing cytokeratins +, TTF-1+ (primary lung cancer), endocrine markers +, and are negative for lymphoid markers.
- Certain types of small round-cell tumors exhibit particular cytologic and cytoarchitectural, cytochemical, and immunocytochemical features (see Sect. 12.1.10.2.2, "Wilms tumor," p. 743).

### Additional Comments

Certain characteristic chromosomal abnormalities may have a great impact on the clinical behavior and the therapy modulation in patients afflicted with small-cell lymphocytic NHL (10).

## 15.3.4 Lymphoplasmacytic Lymphoma

### General Comments

- Lymphoplasmacytic lymphoma (LPL) is a rare small-cell lymphoid tumor with a considerable proportion of cells showing plasmacytoid and plasmacytic differentiation. The tumor usually involves bone marrow, less frequently lymph nodes and spleen. LPL occurs in middle-aged adults.
- Waldenström macroglobulinemia concerns a patient cohort afflicted with lymphoplasmacytic lymphoma including tumor involvement of the bone marrow and IgM monoclonal gammopathy [66].

### Microscopic Features

- Hallmark is a pure triple population comprising small lymphocytes, plasmacytoid lymphocytes and mature plasma cells showing PAS-positive nuclear inclusions (Dutcher bodies).
  Mast cells and hemosiderin are usually present.
- Cells from residual germinal centers may give rise to a more variegated cell pattern.
- An increased number of clear monocytoid B-cells may occasionally be observed.

**Additional Analyses**

Immunophenotyping

- CD5–, CD10–, CD23–.
- B-cell markers: CD79a+ (strongly positive), CD19+, CD20+, and CD22 shows variable positivity.
- Plasma cell-typical markers: CD138+ and CD38+ are exclusively expressed in plasma cells.
- Surface Ig: monotypic, strongly expressed.
- Cytoplasmic Ig: monotypic in plasmacytic cells (mainly IgM).

**Differential Diagnosis**

- Reactive lymphadenopathy is a diagnostic challenge if LPL is associated with cells from prominent germinal centers of residual benign lymphatic tissue.
- Marginal zone lymphoma.
- Small lymphocytic lymphoma/CLL (cytoplasmic Ig is absent and CD5 immunostaining is positive in SLL).
  Small lymphocytic lymphoma is a diagnostic challenge if cytoplasmic Ig is absent in LPL.
- Any small-cell lymphoma with plasmacytic differentiation.

## 15.3.5 Plasma Cell Neoplasms

**General Comments**

- Plasma cell neoplasms are composed of mature end-stage B cells that produce a single uniform, so-called monoclonal Ig (paraprotein or M-protein).
- Plasma cell neoplasms, which are of cytologic interest, encompass plasma cell myeloma, solitary plasmacytoma of the bone, and extraosseous plasmacytoma.

### 15.3.5.1 Plasma Cell Myeloma

Synonyms: multiple myeloma, myelomatosis, Kahler disease.

Myeloma is a bone marrow-based plasma cell neoplasm associated with paraprotein in the serum and/or urine. Generalized bone marrow involvement is a characteristic finding, whereas focal tumor cell masses occur at an early stage of the disease. The disease is observed in middle-aged or elderly people (average age at diagnosis, 70 years). Children are never affected and young adults only rarely.

### 15.3.5.2 Solitary Plasmacytoma of the Bone

This is a plasma cell neoplasm that occurs as a localized medullary bone tumor; there is no evidence of disseminated bone marrow involvement. Most commonly involved bones are those having an active hematopoiesis such as vertebrae, ribs, and skull. The tumor occurs in middle-aged people, particularly in males.

### 15.3.5.3 Extraosseous Plasmacytoma [6]

- This is a localized plasma cell neoplasm involving tissues other than bone marrow. In most cases, it may occur as a single extramedullary manifestation, or as a metastasis originating from multiple myeloma.
- Approximately 80% of extramedullary plasmacytomas occur in the upper respiratory tract (pharynx, sinuses, and larynx), but they may also be found in other sites of the body (lymph nodes, soft tissue, breast, thyroid, gastrointestinal tract, bladder, central nervous system, and others). The average age at diagnosis is 50 years, with a predilection for males.
- The anaplastic subtype of extraosseous plasmacytoma has a distinctive affinity for the oral cavity and frequently occurs as an HIV-associated tumor [24].

**Microscopic Features**

The cytologic preparations of all afore-mentioned variants of plasma cell neoplasms generally demonstrate high cellularity and broadly similar morphologic features depending on the grade of differentiation.

- *Mature tumor form* (Figs. 15.50): The tumor cells are practically indistinguishable from mature plasma cells, see Sect. 15.1.6, "Cytology of Benign Lymph Nodes," p. 914. Immature plasma cells are occasionally scattered between mature plasma cells.
- *Immature tumor form* (Figs. 15.51–15.53): Immature plasma cells display a higher N/C ratio, a more dispersed granular chromatin, and usually a more or less prominent nucleolus as compared to mature neoplastic plasma cells. The eccentric position of the nucleus and cytoplasmic plasmacytoid features are quite preserved.
- *Anaplastic tumor form* [49, 78] (Fig. 15.54): Aspirates show the typical morphological appearance of a high-grade blastic non-Hodgkin lymphoma, but some cells exhibit plasmablastic/cytic features, including paranuclear cytoplasmic clearing.
  The predominant population of blasts consists of large monomorphic cells with a high N/C ratio. The nuclei are round to oval and often marginally located, they exhibit coarse unevenly dispersed chromatin and one prominent central nucleolus or multiple large nucleoli. The cytoplasm is pale blue (MGG) or eosinophilic/amphophilic (Pap).
  Pronounced mitotic activity and tingible body macrophages are generally seen.
  Necrotic debris in the background is observed in virtually all cases.
  Tumor cells may aggregate in sheets and clusters.

Cytoplasmic Ig inclusions: The cytoplasm of myeloma cells may contain crystallized or condensed Ig. The most common phenotypes of Ig inclusions are mentioned below:

– Accumulation of multiple grape-like arranged inclusions, they are sharply outlined, homogeneously structured, and stain pale blue.
– Red-staining single refractile round bodies (Russell bodies) that may entirely occupy the cytoplasm.
– Crystalline rods (Fig. 15.55). Most of these elements may also be seen in the cytoplasm of benign and reactive plasma cells.

**Additional Analyses** (Fig.15.56)

Immunophenotyping

Similar immunocytochemical patterns exhibit plasma cell myeloma, solitary plasmacytoma of the bone, and extraosseous plasmacytoma.
– CD45 in most cases is negative.
– CD5–, CD10 shows variable positivity, CD56+.
– B-cell markers: CD19–, CD20 shows variable positivity, CD79a+.
– Plasma cell-associated markers: CD38+, CD138+, MUM-1+. Cyclin D-1 shows variable positivity.
– Surface Ig: nearly absent.
– Cytoplasmic Ig: monotypic, strongly expressed (IgG > A > D >> M).

Molecular Genetics

Similar molecular patterns exhibit plasma cell myeloma, solitary plasmacytoma of the bone, and extraosseous plasmacytoma.
– Antigen receptor genes: heavy and light chain restriction (Ig heavy chain and κ/λ light chain gene rearrangement).
– Chromosomal abnormalities: numerical and structural in the majority of the cases, in particular: t(4;14) (p16.3;q32). t(11;14) (q13;q32) represents translocation of cyclin D1 oncogen.

**Differential Diagnosis** [78]
- A plasma cell neoplasia composed of a thoroughly mature tumor cell population must be distinguished from benign plasma cell hyperplasia. Hence, the diagnostic consideration strongly depends on the clinical, laboratory, and radiologic results.
- Plasma cell neoplasias showing a mixed population including tumor cells with plasmacytoid features and/or numerous blasts could mimic the following lesions:
  – Reactive lymph node with germinal centers and proliferation of the plasma cell-line, such as infectious mononucleosis. But reactive lymphadenopathy shows the whole lymphocyte maturation sequence, strong CD45 and CD20 positivity, and polyclonal Ig expression.
  – Marginal zone lymphoma with pronounced plasmacytic differentiation. It is particularly important in this setting to distinguish between extranodal marginal zone B-cell lymphoma of the MALT type and extraosseous plasmacytoma.
  – Burkitt lymphoma. However, the cells of this tumor entity lack plasmacytoid cell features and they are immunocytochemically positive for CD20 and PAX-5, and negative for CD138.
  – Plasmablastic subtype of diffuse large B-cell lymphoma: A tumor entity that expresses IgM/A and is associated with distinct clinical features (affinity to the oral cavity, HIV-association, etc.).
  – Immunoblastic lymphoma. Immunocytochemistry should reliably distinguish between plasma cell neoplasm and immunoblastic lymphoma. Cells of the latter are CD20-positive and CD138-negative.
  – Large-cell carcinoma. The tumor cells of plasmablastic and pleomorphic plasma cell neoplasms often aggregate in sheets and clusters, strongly mimicking undifferentiated carcinoma. Immunocytochemical work-up readily solves the diagnostic problems: carcinoma cells express cytokeratins and at best lineage-specific antigens, but they do not show positivity for B-cell markers, plasma cell-specific immunomarkers, and Ig.

**Caution**

Plasmacytoma of the plasmablastic and pleomorphic subtype may raise diagnostic confusion with carcinoma if the tumor cells are arranged in pseudoepithelial clusters and sheets. This misinterpretation most likely occurs if the plasma cell tumor is extramedullary localized. An appropriate panel of immunocytochemical stains should be applied for diagnostic purposes covering epithelial, lymphoid, and plasma cell markers.

## 15.3.6 Follicular Lymphoma (Figs. 15.57–15.64)

**General Comments and Definitions**
- Follicular lymphoma (FL) is a lymphatic tumor composed of follicular (germinal center) B cells expressing a homogeneous immunophenotype.
- FL accounts for about 20% of all lymphomas, the highest incidence occurs in the United States and in Western Europe. The disease rarely affects individuals in the first and second decades of their lives and has the highest incidence in adults whose average age is 60.
- FL typically involves lymph nodes, spleen, and bone marrow. Primary involvement of extranodal sites may occasionally occur, mainly affecting the skin, gastrointestinal tract, breast, and testes.
- Variants of FL:
  1. Lymphoma with follicular architecture: Tumoral follicle center cells (centrocytes and centroblasts) forming distinct or partial follicles that are readily recognized in paraffin sections.
  2. Diffuse large B-cell lymphoma: Follicular tumors that reveal histologically diffuse areas of centroblasts, and

tumors that display a diffuse growth pattern composed of neoplastic centroblasts and centrocytes.

- A follicular pattern is an exclusive histologic criterion [17]. In spite of this handicap, FLs can cytologically be recognized or at least suggested with a high degree of accuracy by their characteristic biphasic cell component.
- The majority of follicular lymphomas are grade 1–2 (80–90% in different series). Grades 1, 2, and 3a follicular lymphomas are regarded as being low-grade tumors with indolent clinical behavior (incurable disease). Thus, low-grade FLs are usually treated with a more conservative therapeutic schedule. However, transformation into secondary high-grade lymphoma of the centroblastic type is frequent.
- High-grade FLs (grade 3b) have a more aggressive course and are treated with aggressive chemotherapeutic schemes (potentially curable disease).

**Caution**

Follicular structures are not really recognizable in cytologic smears of FL.

**Cytologic Grading** [1, 27, 50, 52] (Figs. 15.57 vs 15.62)

The grading system as applied for follicle center cell lymphomas in histology is not fully adaptable to cytologic preparations since cytology does not provide architectural information. It has been proposed and widely accepted that cytological grading is based on microscopic evaluation of the tumor cell type (cytes vs blasts). Depending on the method applied, the threshold values range between 10% and 20% blast cells for low-grade NHL, and between 20% and 40% blast cells for high-grade lymphoma in relation to the whole tumor cell population [27, 104]. The highest accuracy for cytologic grading has been reached for low-grade NHLs, in comparison with the histologic grading results in the corresponding tumors.

**Microscopic Features**

Smears of follicular lymphomas are typically composed of a dual cell pattern comprising centroblasts and centrocytes in which the centrocytes usually predominate, but centroblasts are present as well. The number of mitoses depends on the proportion of the blastic transformed lymphoid cells.

*Centrocytes*

- The small cell component of FL consists of lymphoid cells exhibiting a variable nuclear shape such as angulated, cleaved, intended, twisted, or elongated.
- The nuclear chromatin may occasionally be coarse, but in the majority of the nuclei it is fine, granular, and densely packed, giving the nuclei a hyperchromatic appearance.
- Nucleoli are frequently seen but they are inconspicuous.
- The cytoplasm is scant, dense, and pale.

*Centroblasts*

- Centroblasts are large cells, two to five times the size of normal lymphocytes. Their nuclei are vesicular with either cleaved or noncleaved contours showing dispersed chromatin.
  - The noncleaved cell type has two or three distinct nucleoli typically located close to the nuclear membrane.
  - The cleaved cell type shows irregularly cleaved and lobated nuclei and rather indistinct nucleoli.
- The cytoplasm is scant and basophilic but not as intensely stained as in immunoblasts.

*Starry-sky macrophages and epithelioid cells* may be present (Figs. 15.60 and 15.63). The latter usually appear in a nodular arrangement.

**Additional Analyses** [28] (Fig.15.65)

Immunophenotyping

- CD45+.
- CD5–, CD10+, CD38 (weak expression), CD43–.
- B-cell markers: CD19+, CD20+, CD22+, CD79a+.
- Specific gene products: Bcl-2+, Bcl 6+.
- Surface Ig: monotypic.

Molecular Genetics

- Antigen receptor genes: heavy and light chain restriction.
- Chromosomal abnormalities: translocation t(14;18) (q32;q21) represents *Bcl-2* gene rearrangement that is characteristic for FL.

**Additional Comments**

- Bcl-2 protein is expressed in the vast majority of the grade 1 and grade 2 follicular lymphomas, but only in about half of the grade 3 follicular lymphomas. The reported results concerning FLs exhibiting the highest Bcl-2 expression are variable [47, 80].
- Translocation t(14;18) can be detected in up to 90% of the low-grade (Grade 1-2) follicular lymphomas.
- Identical immunocytochemical and molecular genetic features can also be found in diffuse large B-cell lymphomas of germinal center origin (GCB-type of diffuse large B-cell lymphoma), however at a much lower frequency.
- It must be assumed that FISH is the most efficient method for detecting chromosomal translocations.

**Caution**

- It can be difficult to distinguish between small blastic cells and enlarged cytes exhibiting pronounced nucleoli.
- Smears of follicular lymphomas displaying a considerable proportion of centroblasts (> 20%) are difficult to classify and to grade precisely by cytology alone.

- In FNAB specimens, the identification of follicle-derived large B-cell lymphomas is only possible by identifying the immunocytochemical characteristics, and the chromosomal translocation t(14;18) by FISH [28]

**Differential Diagnosis**

- Reactive lymphadenopathy (LPD) may strongly mimic low-grade follicular lymphoma (Figs. 15.59 and 15.60). However, the overall cytologic pattern in LPD is more heterogeneous with various stages of transformation of the follicle center cells and plasma cells as well as tingible-body macrophages. Nuclear cleaving and nucleoli are less pronounced in transformed cells of reactive lymphoid lesions as compared with tumor cell nuclei of FL. In contrast to FL, LPD is further characterized by polyclonality of the lymphoid population and by the absence of chromosomal abnormalities [41]. Negative Bcl-2 expression of reactive B and T cells (detected by IC, FC, or molecular assays) is also suitable for primary differentiation between reactive hyperplasia and NHL.
- Mantle cell lymphoma is often difficult to differentiate cytologically from follicular lymphoma, due to the striking morphologic similarity between mantle cells and centrocytes (matching nuclear size and angulated and twisted tumor cell nuclei) (Fig. 15.61).
  An accurate diagnostic result requires immunophenotyping and cytogenetic studies: mantle cell lymphoma shows a distinct immunophenotype (CD5**+**, CD10**–,** cyclin D1**+**), Bcl-6 negativity, and cyclin D1 positivity, the latter due to the specific chromosomal translocation t(11;14) [77]
  Further information is provided in Sect. 15.3.7, below.



## 15.3.7 Mantle Cell Lymphoma

(Figs. 15.66–15.69)

**General Comments**

- Mantle cell lymphoma (MCL) is a B-cell neoplasm, composed of monomorphic small to medium-sized lymphoid cells with characteristic nuclear shapes. Distinguishing between MCL and other types of small cell non-Hodgkin lymphomas can be difficult by cytology. MCL takes a more aggressive course in comparison with other small-cell NHLs; the median survival time is 3–5 years.
- MCL comprises up to 10% of all non-Hodgkin lymphomas. It is encountered in middle-aged to older individuals and has a male predilection.
- Lymph nodes, spleen, bone marrow, and peripheral blood are the most common sites of involvement.

**Microscopic Features**

- Hallmarks of classic MCL:
  - Aspirates are composed of a monomorphous lymphatic population.
  - The tumor cells are small to medium-sized, exhibiting moderate and pronounced irregularities of the nuclear outline.
  - The nuclei are angulated, cleaved, and twisted in a similar fashion as compared to centrocytes of follicular lymphoma (Fig. 15.61).
  - The nuclear chromatin is finely dispersed and the nucleoli are inconspicuous.
  - Transformed neoplastic cells such as centroblasts and paraimmunoblasts are absent.
- Apoptotic tumor cells generally occur in large numbers.
- Scattered histiocytes and epithelioid histiocytes may be seen.

**Additional Analyses** [8, 9] (Figs. 6.1., 15.68, 15.69)

Immunophenotyping

- CD45+.
- CD5+, CD10–, CD23–, CD43+.
- B-cell markers: CD20+, CD22+.
- Specific gene products: cyclin D-1+ (nuclear), SOX-11+.
- Surface Ig: monotypic ($\lambda > \kappa$).

Molecular Genetics

- Antigen receptor genes: light chain restriction.
- Chromosomal abnormalities (Fig. 6.1): translocation t(11;14) (q13;q32) represents cyclin D-1 gene rearrangement that is characteristic of MCL.

**Additional Comments**

Generally, mantle cell lymphoma is not graded, but proliferative activity (mitotic rate) is the most important prognostic factor and has an impact on therapy modulation. Immunocytochemistry is best used to assess the proliferation fraction in cytologic specimens; proliferative activity is defined by a proliferating cell nuclear antigen labeling index (MIB-1).

**Differential Diagnoses**

Both classical MCL and MCL subtypes may give rise to diagnostic challenges.

- Tumor cells of classical MCL obviously share morphological features with the centrocytes of FL, but the dual cell pattern of FL comprising centrocytes and centroblasts is absent in MCL.
- The small-cell variant of MCL mimics small lymphocytic lymphoma (see Sect. 15.3.3, p. 955).
- MCLs exhibiting foci composed of large monocytoid B-cell-like elements (abundant pale cytoplasm) may mimic marginal zone B-cell lymphoma or small lymphocytic lymphoma/CLL associated with proliferation centers.
- The blastoid variant of MCL resembles lymphoblastic NHL (Sect. 15.3.2, p. 955), both revealing pronounced mitotic activity. Apoptosis is less pronounced in lymphoblastic NHL as compared to MCL.

- The pleomorphic subtypes of MCL consist of pleomorphic, large tumor cells with irregular nuclei, large nucleoli, and broad cytoplasm. Diagnostic considerations include diffuse large-cell lymphomas of the centroblastic variant and undifferentiated nonlymphoid neoplasms.

## 15.3.8 Marginal Zone Lymphoma

(Figs. 15.70 and 15.71)

**General Comments** [90]

- Marginal zone B-cell lymphomas (MZL) are tumors of the marginal zone B cells of secondary lymph follicles and Peyer patches. MZLs are related to predetermined cells at different sites of the body and are suspected of being associated with chronic antigenic stimulation by microbial pathogens and/or autoantigens. The relevant cells of origin are mainly localized in lymphoid organs such as spleen and lymph nodes, and in nonlymphoid organs where they give rise to mucosa-associated lymphoid tissue (MALT).
- Marginal zone lymphomas are relatively uncommon neoplasms accounting for approximately 2–4% of all B-cell lymphomas in adults.
- Most of the MZLs occur in adults, with a median age of 60 years.

### 15.3.8.1 Categories of Marginal Zone Lymphomas

- MZLs are categorized into three groups depending on the site of involvement [88]:
  1. *Extranodal MZL of the MALT type*.
     MALT lymphoma is the most frequent subtype of MZL, accounting for 50–70% of all MZLs.
     - Several autoimmune disorders, such as Hashimoto thyroiditis, myoepithelial sialadenitis (MESA) with or without systemic Sjögren's syndrome, and lymphoid interstitial pneumonitis have been related to an increased risk of MALT lymphoma.
     - *Helicobacter pylori* is the best-characterized microbial organism associated with MALT lymphoma, namely lymphoma affecting gastric mucosa. Other chronic infections are susptected of playing a possible pathogenetic role in the acquisition of lymphatic tissue in various organs and subsequent malignant transformation [90].
  2. *Splenic MZL*.
     Splenic MZL accounts for 20% of all MZLs.
  3. *Primary nodal MZL (with or without monocytoid B cells)*.
     Nodal MZL is the least frequent lesion in this tumor group and accounts for about 10% of all MZLs.
- Splenic and nodal MZL accounts for less than 1% of all non-Hodgkin lymphomas.
- Patients affected with extranodal (MALT) and splenic MZL usually present with an indolent course of their disease, unlike patients with nodal MZL, which can show more aggressive progress.
- MZLs display a broad morphological spectrum concerning both histologic growth pattern and heterogeneous cellular composition. This variability is independent of the anatomical site of MZL.
- All three categories of MZLs share immunophenotypic, genetic, and chromosomal similarities, even though nodal and extranodal lesions are more akin to each other than to splenic tumors.
- Difficulties distinguishing between MZL and other low-grade lymphomas and benign reactive lymphoproliferation, together with the rarity of this tumor entity, hamper the use of FNAB as an initial diagnostic test. Consequently, cytologic findings are sparsely discussed in the cytologic literature [16, 53].

**Caution**

Nodal dissemination of a MALT lymphoma should be ruled out before assessing a diagnosis of primary nodal MZL.

**Microscopic Features** [16, 53]

- Hallmarks favoring MZL include first and foremost a heterogeneous cellular pattern with predominance of a small and medium-sized lymphoid cell population.
  The classic marginal zone B cells express lymphocytoid and monocytoid features:
  - Centrocytoid features are expressed by irregularly shaped nuclei (akin to centrocytes); the cells show dispersed chromatin, indistinct nucleoli, and a more or less abundant cytoplasm.
  - Monocytoid appearance of the tumor cells is caused by a wide pale cytoplasm.
  - Plasmacytoid differentiation comprises a greater amount of eccentric, densely structured, and basophilic cytoplasm.
  - Nuclear indentations, cleaves, and grooves of all cell variants mentioned above may be obscured by a dense distribution of the chromatin.
- Transformed cells in various stages.
- Variable proportions of plasma cells, histiocytic aggregates, and tingible body macrophages may be encountered.
- MZL in the parotid gland: Epithelioid granulomatous reaction may occur in FNABs of salivary gland MALT-type MZL [96].
- MZL in lymph nodes (Fig. 15.71): Plasmacytoid or plasmacytic differentiation, and large transformed cells with a high mitotic rate are common findings in nodal MZL. Cellular heterogeneity seems to be more pronounced in nodal MZLs as compared to extranodal tumor manifestations [93].

**Additional Analyses**

Immunophenotyping [46]

- CD5–, CD10–, DBA44 exhibits variable immunopositivity.
- CD11c shows variable positivity and is particularly expressed in splenic MZL.
- CD19+, CD43 shows variable positivity, cyclin D-1–.
- B-cell markers: CD20+, CD79a+.
- Marginal zone cell-associated antigens: CD21+, CD23+, CD25+, CD35+.
- Surface Ig: monotypic (typically IgM).

Molecular Genetics

- Antigen receptor genes: heavy and light chain restriction.
- Chromosomal abnormalities:
  - t(11;18) (q21;q21) API2-MALT 1 fusion gene; it is a characteristic translocation for MZL but variable in relation to the primary tumor site.
  - t(1;14) (p22;q32) BCL10-IgH.
  - Trisomy of various chromosomes is not uncommon but nonspecific.

**Additional Comments**

- All three categories of marginal zone B-cell lymphomas share immunophenotypic, genetic, and chromosomal pecularities, with exceptions.
- The frequency at which the chromosomal translocations and trisomies occur varies broadly depending on the primary site of the tumor [88]. Recent cytogenetic studies have shown that translocation t(11;18) is a recurring abnormality in extranodal MALT-type marginal zone B-cell lymphoma; the translocation has so far not been reported in nodal or splenic MZL.
- Currently, a specific marker for MALT lymphoma does not exist.

**Caution**

A monoclonal B-cell population is detected by molecular genetic methods in more than 50% of all salivary glands affected by lymphoepithelial sialadenitis without clinical and histologic evidence of malignant degeneration [3, 11, 91].
Accordingly, establishing the clonality of a lymphoid population by immunocytochemistry, flow cytometry, or molecular genetic methods may produce a false-positive tumor diagnosis in cytology samples of salivary glands.

**Differential Diagnosis**

- A polymorphous cell pattern with the typical individual cell features may be highly suggestive of MALT lymphoma in FNABs from extranodal lymphoid disorders. But the same pattern will pose many more difficulties differentiating between MZL and reactive lymphadenopathy when found in FNABs of lymph nodes (Fig. 15.70). Phenotypic and/or genotypic clonality analyses are crucial to reach an accurate diagnosis.
- CD5 and CD10 are important immunocytochemical markers distinguishing between MZL and other B-cell NHLs of the small-cell type. In contrast to MZL, small lymphocytic lymphoma exhibits CD5 positivity while CD10 positivity favors FL.
- MZL with marked plasma cell differentiation may mimic plasmacytoma [44].
- Mantle cell lymphoma may share strong cytologic overlap with MZL, but the latter lacks expression of CD5 and cyclin D1 [60].

## 15.3.9 Hairy Cell Leukemia (Fig. 15.72)

**General Comments**

- Hairy cell leukemia (HCL) was originally referred to as histiocytic leukemia, malignant reticulosis, and leukemic reticuloendotheliosis.
- HCL is a low-grade neoplasm of small B lymphoid cells. The tumor involves peripheral blood, bone marrow, and spleen [58, 71], but tumorous infiltrates may also occur in other organs, particularly in the liver and lymph nodes [56]; the latter are usually affected in advanced disease.
- The patients affected with HCL are middle-aged, with few exceptions. The disease is almost absent in children.

**Microscopic Features** [58, 71]

- Hallmarks:
  - The lymph node aspiration smears show a monotonous population of small atypical lymphoid cells.
  - The cytoplasm is abundant and pale. A proportion of the tumor cells exhibit thin, hair-like cytoplasmic protrusions and projections (villi) in a circumferential mode.
- The nuclei are oval or bean-shaped.
- The chromatin is more or less homogeneous, unlike the coarse clumping in normal lymphocytes.
- Nucleoli are indistinct or absent.

**Additional Analyses** (Fig. 15.72B)

Cytochemistry

Tartrate-resistant acid phosphatase(TRAP) is a characteristic biochemical marker for HCL but it shows variable positivity.

Immunophenotyping

- *Typical CD markers:* CD11c+, CD19+, CD25+.
- CD5–, CD10–, CD43–, cyclin D-1 shows variable positivity.
- *Key markers for HCL:*
  - Annexin A1+, TRAP+, CD103+, DBA44+.
  - MIB-1 near zero is a very typical feature for this tumor entitity.
- B-cell markers: CD20+, CD22+.
- Surface Ig: monotypic, strongly positive.

Molecular Genetics

Antigen receptor genes: VH genes are present in the majority of cases.

### Additional Comments

- Typically, all cases of HCL will comprise at least a few cells with evidence of strong granular tartrate-resistant acid phosphatase (TRAP) positivity. Cytochemical TRAP-positivity is established using air-dried unfixed slide specimens.
- TRAP immunoreactivity has a high specificity and sensitivity in the diagnosis of HCL. Please note that weak staining has no diagnostic value.
- Annexin A1 (ANXA1) is an extremely useful marker for diagnostic purposes in this setting as it is not expressed in any B-cell lymphoma other than HCL. But ANXA1 can also be expressed by myeloid cells and T lymphocytes.
- CD123 has been found to be a useful marker for cells of classical hairy cell leukemia [21].

### Differential Diagnosis

- Splenic marginal zone lymphoma with villous lymphocytes and some uncommon clonal small B-cell lymphoid disorders of the spleen share a villous cytology. The cells of splenic small B-cell lymphomas with villous lymphocytes lack cytochemical expression of TRAP and the immunostain pattern is different as compared to hairy cell leukemia [21, 88].
- Distinguishing between HCL and other small-cell neoplastic lymphoproliferative disorders such as chronic lymphocytic leukemia, T-cell prolymphocytic leukemia, follicular lymphomas, and mantle cell lymphoma (in leukemic phase) is possible using clinical, immunocytologic, molecular genetic, and definitely morphologic criteria.
- Rare variants (prolymphocytic, blastic, and others) of HCL may be difficult to distinguish from other non-Hodgkin lymphomas (lymphoblastic lymphoma, Burkitt lymphoma, diffuse large-cell NHL, etc.).

## 15.3.10 Diffuse Large B-cell Lymphoma, Not Otherwise Specified

### General Comments

- Diffuse large B-cell lymphoma is a largely heterogeneous tumor group comprising variants that are defined by morphological, immunophenotypical, and molecular features, or by distinct clinical characteristics. These tumor subtypes are listed in the 2008 WHO lymphoma classification, p.234 [88].
- In the current chapter, we address only the main variants of the large group of diffuse large B-cell lymphomas, hereafter referred to as DLBCL.
- DLBCL is a malignant lymphoma composed of large B lymphoid cells; a particular cytoarchitectural pattern is absent. Cellular and nuclear size is equal to or exceeds normal histiocytes/macrophages.
- This tumor group encompasses up to 30% of all adult non-Hodgkin lymphomas in Western countries and still has a higher percentage in developing countries. The disorder commonly affects elderly people with higher rates among men. DLBCL may present as a nodal disorder or extranodal mass. The most frequently affected extranodal sites include gastrointestinal tract, bones, salivary glands, thyroid, and kidney.
- DLBCL usually arises as a primary tumor, but it may also appear as a progressive disorder of primarily low-grade lymphomas such as small lymphocytic lymphoma, follicular lymphoma, and Hodgkin lymphoma, among others.
- The etiology of this tumor type is not clear, but immunodeficiency is an established significant risk factor.

### Microscopic Features

The cytomorphology of DLBCL exhibits broad variability. The most common variants distinguished in the 2008 WHO classification include:

*DLBCL, centroblastic variant* (Figs. 15.73–15.76)

- The tumor is composed of medium-sized and large lymphoid blastic cells, the overall pattern is monotonous (>90% centroblasts); however, a polymorphic appearence may occur due to the admixture of immunoblasts.
- The nuclei are round and vesicular, but cleaving and multilobation can occasionally predominate.
- The chromatin is fine, densely packed, and evenly dispersed.
- At least two conspicuous nucleoli are placed at the inner surface of the nuclear membrane.
- The cytoplasm is scanty, either vacuolated or basophilic.

*DLBCL, immunoblastic variant* (Fig. 15.77)

- Immunoblasts dominate the cellular composite (>90%).
- The nuclei are round, showing indistinct irregularities.
- The distribution of chromatin is similar to that seen in centroblasts.
- A single large and round nucleolus is centrally located.
- The cytoplasm is readily recognized as a broad, deep-basophilic rim (cyanophilic in Pap-stain).
- Plasmacytoid differentiated blasts are present in a higher percentage of all cases.

*DLBCL, anaplastic variant* (Fig. 15.78)

- Large and oversized round to polyhedral cells are typical for the anaplastic tumor variant.
- The tumor cells may occur in crowded aggregates, cohesive sheets, or compact clusters, and occasionally even in papillary formations.

- The nuclei are large, pleomorphic, and bizarre.
- The chromatin may be finely dispersed or accumulated in coarse clusters.
- The cytoplasm is usually abundant, vacuolated, or more densely structured, and fading away at the periphery.

### Additional Analyses

Immunophenotyping

- B-cell markers: CD19+, CD20+, CD22+, CD79a+.
- Immunostaining is variable for CD10, CD30, Bcl-6, MUM-1, and FOXP1 according to different subtypes (germinal center B-cell-like (GCB) DLBCL vs activated B-cell-like (ABC) DLBCL).
- Proliferation index: >40% to nearly 100% using Ki67/MIB-1 (nuclear positivity).
- Surface and/or cytoplasmic Ig: monotypic positive in up to 80% of the cases.

Molecular Genetics

- Antigen receptor genes: Ig heavy and light chain restriction.
- Chromosomal translocations: Bcl-2, Bcl-6, and c-MYC.

### Additional Comments

The impact of gene expression profiling, other molecular genetic abnormalities, and cellular immunophenotypes for subtyping and prognostication of DLBCLs are discussed in specialized sources [88], as is the role of FNAB in this setting.

### Differential Diagnosis

- DLBCLs that are characterized by a medium-sized cell population may be confused with other non-large cell blastic lymphoid malignancies such as Burkitt lymphoma, mantle cell lymphoma with blastoid features, medium-sized lymphoblastic lymphoma, and myelo-monocytic leukemic infiltrates. DLBCL express neither cyclin D1 nor myelogenic cell markers.
- Admixture of numerous benign T lymphocytes or histiocytes is a well-known phenomenon in a certain percentage of DLBCLs (Fig. 15.75). In this setting, diagnostic considerations include:
  - Histiocyte-rich large B-cell lymphoma or true T-cell lymphoma (in general, the former is a highly aggressive lymphoma) [92].
  - Peripheral T-cell non-Hodgkin lymphoma.
  - Hodgkin lymphoma (foremost the lymphocyte-predominant subtype).
  - A hyperplastic T-cell population interspersed with single nonlymphoid neoplastic cells such as carcinoma, melanoma, and others.
  - Primary or metastatic lymphoepithelial carcinoma in FNABs from extranodal soft tissue masses and lymph nodes, respectively.
  - Reactive lymphoid disorder comprising abundant T-cell hyperplasia.
- The DLBCL-centroblastic variant with a considerable proportion of immunoblasts, plasmacytoid cells, and small lymphocytes may mimic reactive lymphoid hyperplasia with a pronounced plasmacellular component such as infectious mononucleosis (Fig. 15.76).
- The immunoblastic variant of DLBCL is difficult to differentiate from plasmablastic DLBCL and immature plasma cell myeloma by cytologic features alone.
- The anaplastic variant displays morphologic overlap with anaplastic large-cell lymphoma (a disorder of cytotoxic T cells) and anaplastic kinase protein (ALK) positive large B-cell lymphoma. Both tumors have different biological and clinical properties compared to DLBCL.
- Furthermore, the anaplastic subtype of DLBCL can strongly mimic undifferentiated large-cell carcinoma, malignant melanoma, and lymphocyte-depleted Hodgkin lymphoma, in cytologic specimens exhibiting crowding and clustering of the lymphoid blasts. A basic immunocytochemical work-up (e.g., CD45, CD20, CD3 vs MNF116 and melanoma-associated antigens) should be performed on any cytological specimen that contains large pleomorphic blastoid cells (Fig. 15.78).

**Caution**

- DLBCL with a pronounced admixture of T lymphocytes and/or histiocytes may be misinterpreted as benign lymphoproliferative lesion; or the scattered tumor cells are obscured, hampering correct identification and conclusive tumor diagnosis.
- The polymorphic variant of centroblastic DLBCL comprising high proportions of lymphocytes, immunoblasts, and plasmacytoid cells can easily lead to a misdiagnosis of EBV-induced reactive lymphadenopathy (mononucleosis infectiosa), and vice versa.
- The anaplastic variant of DLBCL can strongly mimic undifferentiated carcinoma and other undifferentiated malignancies, including malignant melanoma. Differentiation is easily achieved by an appropriate immunocytochemical evaluation.

## 15.3.11 Burkitt Lymphoma

(Figs. 15.79 and 15.80)

### General Comments

- Burkitt lymphoma (BL) is a highly aggressive peripheral B-cell lymphoma that is predominantly composed of medium-sized blastic cells of germinal center cell origin. The tumor may arise in lymph nodes and in extranodal sites; it rarely presents with leukemia.
- BL shows broad variation in morphologic, biologic, and clinical features; there exists no diagnostically specific parameter.
- Three variants of BL differ for clinical purposes:

1. *Endemic BL* occurs most of all in Africa and is the most common malignant tumor in the pediatric population of the equatorial area. The incidence peak is reached in the first decade of life. Jaws and other facial bones are affected by this tumor in about 50% of cases; another predilection site is the abdomen (with or without involvement of the jaw). Epstein-Barr virus (EBV) DNA/RNA is detected in tumor cells of endemic Burkitt lymphomas in up to 90% of cases.
2. *Sporadic BL* is encountered throughout the world, mainly affecting children and young adults. Tumor incidence in Western Europe and in the United States is low, accounting for 1–2% of all lymphomas, but BL accounts for about 50% of all childhood lymphomas. The majority of sporadic BLs manifests as an abdominal mass with the most frequent primary site in the ileocecal region. Primary tumor manifestation in the facial bones is rare. EBV positivity is detected in roughly 30% of sporadic Burkitt lymphomas.
3. *Immunodeficiency-associated BL* is primarily seen in HIV-positive patients, mainly affecting lymph nodes, and BL may occur as the initial manifestation of acquired immunodeficiency syndrome (AIDS). A few cases of Burkitt lymphoma arising in organ transplant recipients are documented in the literature [26].

**Caution**

- The vast majority of nonendemic Burkitt lymphomas present with an abdominal tumor mass, affecting children and young adults.
- BL associated with HIV infection can occur as the initial manifestation of AIDS.
- In addition to the manifold clinical manifestions, Burkitt lymphomas reveal a considerable variability in their morphologic spectrum. Therefore, FNAB diagnosis of BL requires the whole battery of cytomorphologic, immunocytochemical, and molecular genetic tests.

**Microscopic Features** [94]

*The classical BL* cytologic features can be observed in all three above-mentioned variants of BL:

- The cells are medium-sized, giving rise to a diffuse monotonous pattern in cytologic smears. Cell aggregates rarely occur, but the tumor cells show a tendency to cohesiveness throughout the smear.
- The nuclei are round, showing occasional indentations with dispersed granular and clumped chromatin.
- The nucleoli occur multiply, centrally, or paracentrally situated, basophilic, and usually inconspicuous.
- The cytoplasm is medium-sized, deeply basophilic (dense and cyanophilic in Pap stain), and frequently shows small and sharply outlined vacuoles containing lipids.
- A striking starry-sky pattern (numerous tingible body macrophages) is usually present but not diagnosis-specific.
- Exceptionally large numbers of mitotic figures are encountered in most cases together with a high fraction of apoptotic cells.
- A granulomatous reaction occurs frequently and can occasionally be very pronounced.

*Variants of BL* with their cytologic manifestations:

- Tumors composed of cells with eccentric nuclei, basophilic cytoplasmic bodies, and one distinct centrally placed nucleolus are referred to as BL with plasmacytoid differentiation.
- Tumors exhibiting more cellular pleomorphism and large nucleoli have been termed atypical BL.

**Additional Analyses** [94]

Immunophenotyping

- *Key markers for BL:* CD10+, Bcl-6+, Bcl-2 shows variable positivity.
- CD5–, TdT–.
- B-cell markers: CD20+, CD19+, CD22+.
- Proliferation index: nearly 100% using Ki67/MIB-1 (nuclear positivity).
- Oncogen LMP1-EBV+ (latent membrane protein 1 oncogene of Epstein-Barr virus) is characteristic for the endemic BL.
- Surface Ig: rarely monotypic expression (typically IgM).

Molecular Genetics

- Antigen receptor genes: light chain restriction
- Characteristic translocation: c-MYC translocations
- Evidence of Epstein-Barr-encoded RNA (EBER)
- Specific gene-expression signature for core Burkitt

**Additional Comments**

- Monotonous proliferation of cohesively growing medium-sized peripheral blastic cells, extremely high growth fraction, and c-MYC translocation are prototypic and phenotypic of the most valuable diagnostic parameters for the diagnosis of Burkitt lymphoma [14].
- BL with plasmacytoid differentiation is predominantly seen in children and immunocompromized patients.
- The latent membrane protein 1 (LMP-1) oncogene of the Epstein-Barr virus is believed to contribute to the development of many EBV-associated tumors; and EBV small RNAs (EBER) are detectable in tumour cells of many BLs by in situ hybridization.
- Gene expression profiling has recently been studied by two separate groups, which have identified a solid gene expression signature for core Burkitt lymphoma [19, 31].
- The combination of morphologic, immunocytochemical, and molecular genetic parameters is in many cases adequate for an initial FNA diagnosis of BL [61].

**Caution**

- Translocation c-MYC is highly characteristic but not specific for Burkitt lymphoma.
- About 10% of core BLs lack MYC translocation using the FISH technique.
- Highly proliferating diffuse large-cell B-cell lymphomas may likewise show c-MYC translocation.

**Differential Diagnosis**

- Diffuse medium-sized and large cell B-cell lymphomas that exhibit a very high proliferation rate (with or without a starry-sky pattern) and those with c-MYC translocation (detected in approximately 15% of diffuse large-cell B-cell lymphomas) must be differentiated from BL.
- BL with plasmacytoid differentiation may show cytomorphologic overlap with the immature type of plasma cell neoplasms.
- Blastoid mantle cell lymphoma and B-ALL are two entities that may share cytologic features with BL.

## 15.3.12 T Lymphoblastic Leukemia/Lymphoma (Figs. 15.43 and 15.81)

**General Comments** (see also Sect. 15.3.2, "B Lymphoblastic Leukemia/Lymphoma," p. 955)

- T lymphoblastic leukemia/lymphoma is a high-grade neoplasm of immature precursor cells of the T lineage. The bone marrow is always affected and mediastinum/thymus frequently involved in contrast to B lymphoblastic lymphoma/leukemia.
- T lymphoblastic lymphoma encompasses up to 90% of all lymphoblastic lymphomas; it is seen in all age groups but most frequently in adolescent males.
  - The leukemic tumor form (T-ALL) occurs more commonly in older children and in males.
  - In adults, acute lymphoblastic leukemia of the T phenotype accounts for about 25% of all patients affected with a lymphoblastic leukemic disorder.

**Microscopic Features**

- The morphologic features of T lymphoblastic neoplasms are indistinguishable from those of B lymphoblastic tumoral disorders [34, 39]. Still, the rate of mitotic figures was found to be higher in T lymphoblastic lymphoma as compared with B-LBL (see Sect. 15.3.2, "B Lymphoblastic Leukemia/Lymphoma," p. 955).

**Additional analyses**

Cytochemistry

There is dot-like positive acid phosphatase activity, but this reaction is not specific for T-LBL.

Immunophenotyping

- CD45 shows variable positivity.
- CD99+, CD34 and TdT (nuclear positivity) show variable positivity.
- B-cell markers: CD79a shows variable positivity.
- T-cell markers: CD3+ (lineage-specific marker!), CD1a+, CD7+, CD2 shows variable positivity.
- Myeloid-associated antigens: CD13 and CD33 show variable positivity, myeloperoxydase-negative.

Molecular Genetics

Chromosomal rearrangements: T-cell receptor gene rearrangement is present in almost all T-ALL/LBLs, accompanied by IgH gene rearrangements in a few cases.

**Differential Diagnosis**

- B-ALL/B-LBL show positivity for many B-cell associated antigens. Common B-ALL (CALLA) shows positivity for CD10.
- Acute myeloid leukemia can be confused with T lymphoblasic lymphoma that presents with medium-sized blasts (myeloid lesions express immunocytochemically myeloperoxydase, PAX5 is rarely positive).

## 15.3.13 T-Cell Prolymphocytic Leukemia

**General Comments**

T-cell prolymphocytic leukemia is a rare aggressive leukemia of peripheral T cells. The lesion frequently presents with generalized lymphadenopathy; other organs including the skin may be involved. The median age of the affected patients is 65 years.

**Microscopic Features**

- Aspirates are composed of small to medium-sized lymphoid cells.
- The nuclei are round, showing marked nuclear irregularities, including cleaves, indentations, and deep grooves. The nuclear outline may exhibit a cerebriform appearance.
- The nucleoli are usually distinct.
- The cytoplasm is dense, basophilic, and devoid of granula. Cytoplasmic protrusions are seen in cytologic preparations from body fluids rather than in specimens from fine needle aspirates.

**Additional Analyses**

Cytochemistry

- Strong cellular positivity for alpha-naphthyl acetat esterase.
- Dot-like cytoplasmic positivity for acid phosphatase.

Immunophenotyping

- TdT–, CD1a-, TCL1+ (overexpression).
- T-cell markers:
  - CD2+, CD3+, CD7+, CD52+.
  - CD4+/CD8– staining pattern in 60% of cases.
  - CD4+/CD8+ coexpression in 25% of cases.

Molecular Genetics
- Antigen receptor genes: T-cell receptor (TCR) clonally rearranged.
- Most frequent chromosomal abnormalities are found in chromosome 14 and chromosome 8.

**Differential Diagnosis**
Other mature T-cell neoplasms such as adult T-cell leukemia/lymphoma.

## 15.3.14 Adult T-Cell Leukemia/Lymphoma

**General Comments**
- Adult T-cell leukemia/lymphoma (ATLL) is a mature T-cell neoplasm caused by a retrovirus known as human T-cell lymphotropic virus type 1 (HTLV-1). ATLL is endemic in many regions of the world; the distribution is closely linked to the prevalence of HTLV-1 in the particular population. ATLL occurs exclusively in adults between the third and eighth decades.
- About one-third of patients present with a lymphomatous form of the disease, but involvement of the peripheral blood commonly occurs. The clinical course of the disease is aggressive, resulting in diffuse infiltration of many organs including the skin.

**Microscopic Features**
The variability of the cytologic appearance of ATLL is striking, ranging from the pleomorphic small-cell type to the anaplastic large-cell type.
- The lymphoid tumor cells are usually medium-sized to large, but tumors may occur that are predominantly composed of small pleomorphic cells.
- The nuclei show pronounced pleomorphism with highly irregular contour caused by deep indentations and polylobation. The nucleoli may be prominent.
- The chromatin is coarse and irregularly distributed.
- Blast-like cells (finely dispersed chromatin, pronounced nucleoli, distinct dense cytoplasm) and giant tumor cells exhibiting cerebriform nuclei may be present in varied proportions. Hodgkin-like and Reed Sternberg-like (HRS) cells scattered in a background of mild abnormal lymphoid cells may also be encountered.

**Additional Analyses**
Immunophenotyping
- CD 25+.
- T-cell markers:
  - CD2+, CD3+, CD5+, CD7–.
  - CD4+/CD8– constellation occurs in most cases.
  - CD4+/CD8+ coexpression rarely occurs.
  - Activation-related antigen CD30: variable immunoreactivity on large blastic cells.
  - ALK–.

Molecular Genetics
- Antigen receptor genes: T-cell receptor (TCR) is clonally rearranged.
- Viral genome: monoclonal integration of human T-cell lymphotropic virus type 1 (HTLV-1).
- Chromosomal abnormalities: nonspecific structural and numerical occurrences.

**Differential Diagnosis** [54]
- The differential diagnosis of ATLL includes other types of T-cell neoplasms such as T-cell prolymphocytic leukemia, Sézary syndrome, and peripheral T-cell lymphomas.
- A particular heterogeneous appearance of the cell population may suggest angioimmunoblastic T-cell lymphoma.
- Small-cell variants exhibiting mild atypical lymphoid cells interspersed with HRS-like cells can give rise to a misinterpretation of Hodgkin lymphoma.

## 15.3.15 Mycosis Fungoides/ Sézary Syndrome

**General Comments**
Mycosis fungoides (MF) and Sézary syndrome (SS) are the most common cutaneous T-cell lymphomas; their etiology is unknown. The diseases typically affect middle-aged and older people. Sézary syndrome is the leukemic conversion of mycosis fungoides frequently in combination with extensive organ involvement (lymph nodes, liver, spleen, and lung). Histologic, cytologic, immunocytochemical, and molecular features of MF may be very similar to those of SS. Characteristics that separate the two disorders are listed in Table 15.3.1, p. 968.

**Microscopic Features** [7, 67]
- Unlike nodal infiltration in mycosis fungoides, the nodal tumor cell infiltrates associated with Sézary syndrome are mostly uniform. All atypical lymphoid cells exhibit morphologic features referred to as Sézary cells.
- Two variants of the Sézary cell may be seen, primarily defined by their size:
  - *Small Sézary cells* are slightly larger than normal lymphocytes (<12 $\mu$m in diameter).
  - *Large Sézary cells* are larger than 12 $\mu$m and may be more than four times as large as small lymphocytes in the same smear.
  - Intermediate-sized cells are common.
- Nuclear hallmarks: The nuclei of small cells usually show relatively mild indentations in comparison to the nuclei of enlarged cells with marked indentations resulting in a grooved or cerebriform appearance.

**Table 15.3.1** Mycosis fungoides vs Sézary syndrome

| Features | Mycosis fungoides | Sézary syndrome |
|---|---|---|
| **Clinical** | – Cutaneous manifestations ranging from patches to tumorous infiltrates<br>– Indolent course | Syndrome defined by the triad:<br>– Erythroderma<br>– Lymphadenopathy<br>– Sézary cells in skin, lymph nodes, and peripheral blood |
| **Lymph node status** | Lymphadenopathy in advanced stages of the disease | Generalized lymphadenopathy from the beginning |
| **Morphology of enlarged lymph nodes** | – Initially often dermatopathic lymphadenopathy (see Sect. 15.2.5.2, p. 931)<br>– Partial or complete tumor involvement in later stages of the disease | Monotonous infiltrate of tumor cells (Sézary cells) |

- The nuclear chromatin is condensed and irregularly distributed.
- The nucleoli can be prominent.
- The cytoplasm appears as a narrow rim around the nucleus.
- The presence of eosinophils, histiocytes, and tingible body macrophages is variable.

**Additional Analyses** [67]

Immunocytochemical and molecular features are virtually identical in MF and SS.

Immunophenotyping

– *Key marker for MF/SS:* cutaneous lymphocytic antigen+
– T-cell markers:
  – CD2+, CD3+, CD4+, CD5+, TCRβ+.
  – CD7-, CD8-, CD25-.

Molecular Genetics

– Antigen receptor genes: T-cell receptor (TCR) clonally rearranged.
– Common chromosomal abnormalities: structural and numerical occurences.

**Differential Diagnosis**

The cytodiagnostic accuracy of lymph node aspiration samples is strongly determined by the extent of the tumor cell infiltrates:

- Mycosis fungoides with scattered atypical lymphoid cells in the background of dermatopathic lymphadenopathy may suggest a reactive disorder rather than a tumorous infiltrate [25].
- A heterogeneous cytologic appearance due to lymph node involvement by small and large atypical lymphoid cells (mainly in SS) may simulate peripheral T-NHL or Hodgkin lymphoma.

**Caution**

Mycosis fungoides and Sézary syndrome have an increased risk of developing a secondary malignancy, in particular Hodgkin lymphoma [30].

## 15.3.16 Peripheral T-Cell Lymphoma, Not Otherwise Specified (Figs. 15.82–15.84)

**General Comments**

- Peripheral T-cell lymphoma, NOS (PTCL) is a lumping category of tumors covering all mature T-cell lymphomas that are not otherwise specified [102]. This group encompasses about 30% of all T-cell lymphomas in Western countries. PTCLs mainly occur in adults.
- PTCL is a heterogeneous tumor group exhibiting a broad cytologic spectrum.
- Lymph node involvement is a common feature of this tumor entity, but many other anatomical sites of the body can be affected, predominantly the skin and gastrointestinal tract.

**Microscopic Features** [2]

The cytomorphologic appearance is extremely heterogeneous, varying from monomorphic to highly pleomorphic cell patterns.

- In the majority of cases, the cytologic specimens are composed of medium-sized and large tumor cells.
- The nuclei are irregular and often pleomorphic due to molding and grooves.
- The vesicular or coarse chromatin is irregularly distributed. Hyperchromasia is common.
- The nucleoli are large and prominent.
- Mitotic activity is high.
- Reed-Sternberg-like cells may be intermingled.
- Inflammatory infiltrates frequently dominate the background of the smears; they are composed of small and transformed lymphocytes, plasma cells, eosinophils, and epithelioid histiocytes (Figs. 15.82B and 15.83).

- Cases with a large number of epithelioid histiocytes are referred to as lymphoepithelioid cell variant (Lennert's lymphoma) of PTCL [97].

**Additional Analyses** [2]

Immunophenotyping

- An aberrant T-cell phenotype is characteristic:
  - CD2+, CD3+, CD5 and CD7(variable positivity) is a frequent constellation.
  - CD4+/CD8– is the usual constellation.
  - TCRβ+ is the usual constellation.
  - CD30+, CD56 (variable positivity) is a possible constellation.
- The proliferation index is usually high using Ki67/MIB-1 (nuclear positivity).

Molecular Genetics

Antigen receptor genes: T-cell receptor (TCR) is clonally rearranged.

**Differential Diagnoses**

- A variegated PTCL cell pattern caused by a considerable admixture of reactive lymphoid elements, histiocytes, and starry-sky macrophages may mimic malignant lymphoma of the B-cell phenotype, angioimmunoblastic T-cell lymphoma, or severe reactive lymphoproliferation (Fig. 15.82A).
- A mixed pattern composed of typical PTCL cells may be misinterpreted as mycosis fungoides, adult T-cell leukemia/lymphoma, or Hodgkin lymphoma.
- Clustering of large tumor cells gives rise to diagnostic dilemmas between PTCL and pleomorphic carcinoma, melanoma, and other undifferentiated nonlymphoid neoplasms.
- Rare PTCLs composed of small monocytoid lymphocytes (Fig. 15.83) with abundant clear cytoplasm may mimic marginal zone B-cell lymphoma [95].
- The lymphoepithelioid cell variant of PTCL may share many morphologic features with epithelioid cell-rich NHLs and Hodgkin lymphoma (Fig. 15.82B).

**Caution**

Appropriate cytologic typing of peripheral T-cell lymphoma is challenging both by light microscopy and the use of additional biological tests, the latter often turn out to be of limited value.

## 15.3.17 Angioimmunoblastic T-Cell Lymphoma (Figs. 15.85 and 15.86)

**General Comments**

Angioimmunoblastic T-cell lymphoma (AILD-T) is a mature T-cell lymphoma presenting with constitutional symptoms and with generalized lymphadenopathy in practically all patients. The tumor is known as one of the more frequent variants of peripheral T-cell lymphomas. It accounts for 1–2% of all non-Hodgkin lymphomas and affects middle-aged and older people.

**Microscopic Features** [23, 62]

- Hallmarks: A distinct heterogeneous cell population, the clustering of reticulum cells and small tissue fragments that contain small hyalinized capillary-sized vessels are key features for the identification of AILD-T by cytology.
- The tumor cells present as small to medium-sized lymphocytes with minor atypias, i.e., mild nuclear irregularities and clear cytoplasm.
- The inflammatory component consists of small and enlarged reactive lymphocytes, immunoblasts, plasma cells, eosinophils, and histiocytes.
- Follicular dendritic cell networks are widely spread and interspersed with lymphocytes.
- Reed-Sternberg-like cells may be observed.
- Tingible body macrophages and increased mitotic activity are rarely seen.

**Additional Analyses**

Immunophenotyping

- CD10 shows variable positivity.
- CXCL13+, PD-1+.
- T-cell markers: CD2+, CD3+, CD5+, CD4+ >CD8+.

Molecular Genetics

- Antigen receptor genes: T-cell receptor (TCR) is clonally rearranged (biallelic) in 75–90% of cases.
- Immunoglobulin genes: clonal rearrangement in approximately 30% of cases.
- Most common chromosomal abnormalities: trisomy 3, trisomy 5, and additional X chromosome.

**Additional Comments**

- Follicular dendritic cells show positive immunoreactivity for CD21, CD23, and CD35.
- The B-cell population, including immunoblasts and plasma cells, is polytypic.
- It should be remembered that secondary malignant lymphomas of the B-cell lineage such as diffuse large B-cell lymphoma, plasmacytoma, and even Hodgkin lymphoma can occur.

**Differential Diagnosis**

- AILD-T presenting a variegated cell population may strongly mimic reactive proliferation (Fig. 15.85A). The close resemblance of the two differing entities may additionally be enhanced by:
  - The abundance of germinal center cells from hyperplastic secondary follicles in an early tumor stage.
  - A minor population of neoplastic T-cells.

- A peripheral T-cell lymphoma containing numerous epithelioid cells may share morphologic characteristics with AILD-T.
- Cases exhibiting Reed-Sternberg-like cells may simulate Hodgkin lymphoma.

## 15.3.18 Anaplastic Large-Cell Lymphoma: ALK-Positive [55, 63, 76, 88] (Figs. 15.87–15.89)

### General Comments

- *Anaplastic large-cell lymphoma, anaplastic lymphoma kinase protein (ALK)* protein-*positive* (ALCL-ALK+) is a T-cell lymphoma consisting of large pleomorphic lymphoid cells. ALCL-ALK+ is a rare tumor frequently occuring in the first three decades of life. It accounts for 3% of all adult NHLs, but for 10–20% of the non-Hodgkin lymphomas in children. Both lymph nodes and extranodal sites are involved by this tumor type. The most commonly affected extranodal sites include skin, soft tissues, liver, and lung. The mediastinum is less frequently involved by ALCL-ALK+ than Hodgkin lymphoma.
- *ALK-negative anaplastic large-cell lymphoma* lacks anaplastic lymphoma kinase protein but is indistinguishable from the ALK-positive tumor entity by its morphology and the genetic phenotype (except ALK negativity).
- At the least, tumors with and without ALK expression must be considered as separate entities because ALK expression is associated with a significant prognostic benefit. Further information is provided in the literature, for instance in the 2008 WHO lymphoma classification [88].

15

### Microscopic Features

Similar to other T-cell NHLs, ALCLs appear with a heterogeneous morphologic pattern; but most cases contain a variable proportion of characteristic tumor cells.

- Hallmarks
  - Medium-sized to large anaplastic cells with abundant vacuolated amphophilic cytoplasm.
  - Multinucleated giant cells are outnumbered; their nuclei are arranged in a wreath-like pattern resembling Reed-Sternberg cells (Fig. 15.88).
  - The nuclei are eccentrically placed and are kidney-shaped or have an embryo-like shape.
  - Cells containing nuclei with cytoplasmic invaginations are termed doughnut cells.
  - The chromatin is dispersed or finely granular.
  - The nucleoli are most often multiple and prominent, rod-shaped, or pleomorphic, staining eosinophilic or basophilic.
- An inflammatory background is frequently present composed of small lymphocytes, granulocytes, histiocytes, and macrophages.
- *Small-cell variant:* There is a predominant population of small to medium-sized tumor cells exhibiting irregular nuclei, a single distinct nucleolus, and plasmacytoid features (eccentrically placed nuclei and usually pale cytoplasm). A proportion of hallmark cells is always present; in addition, small tumor cells will usually exhibit the nuclear characteristics of hallmark cells.
- *Lymphohistiocytic variant:* Neoplastic cells are admixed with a large number of histiocytic cells. In this setting, the tumor cells may be masked.

### Additional Analyses (Fig. 15.89B)

Immunophenotyping

- *Key markers for ALCL-ALK+:*
  - CD30 shows invariable positivity (membranous and paranuclear).
  - ALK+ (cytoplasmic and nuclear).
  - Epithelial membrane antigen (EMA)+.
  - CD15–.
- CD43 and CD45 both show variable immunoreactivity.
- T-cell markers: CD4+, CD5+, CD3 shows variable positivity.
- Histiocytic marker: CD68+ (reactivity is antibody-dependent).

Molecular Genetics

- Antigen receptor genes: T-cell receptor (TCR) is clonally rearranged in up to 90% of cases.
- Chromosomal abnormalities: the most common chromosomal translocation is t(2;5) (p23;q35); various translocations in addition.

### Additional Comments

- Small-cell tumor variant: CD30 expression is rather weak or negative in small neoplastic cells, and ALK positivity is often confined to the nucleus.
  Other staining disparities are influenced by genetic alterations of the tumor cells [88].
- EMA immunopositivity correlates with ALK expression in ALCL-ALK+.
- Some of the ALCLs can only be recognized as T-cell tumors on the basis of molecular clonality analysis, due to the absent expression of T-cell markers by immunocytochemistry.

### Differential Diagnosis [76, 88]

- Other B- or T-cell lymphomas with anaplastic features and/or CD30 expression. Anaplastic diffuse large B-cell lymphomas may be ALK-positive but do not stain positive for T-cell markers by means of immunocytochemistry.
- Diffuse large B-cell lymphoma with plasmacytoid features may immunocytochemically express ALK protein correspondent with EMA positivity; but CD30 antigen is not detectable.
- The small-cell variant of ALCL can be misinterpreted as peripheral T-cell lymphoma (Fig. 15.89A).

- Sporadic tumor cells may be missed in a polymorphous background of benign reactive lymphocytes, but ALCL tumor cells can be visualized by CD30 immunostaining.
- ALCL combined with a heterogeneous cellular infiltrate of lymphocytes, tingible body macrophages, and atypical lymphoid cells that mimic immunoblasts may mislead to a diagnosis of severe reactive lymphadenopathy, probably virus-induced such as mononucleosis infectiosa.
- Hodgkin lymphoma, sarcomatous neoplasm, carcinoma, melanoma, and germ cell tumors may be positive for ALK and/or CD30 and may show a confusing cell pattern. On the other hand, most of these tumors exhibit distinct immunocytochemical features and/or molecular profiles unlike those of ALCL. In this respect, we refer to the literature and to various chapters of this book such as Sects. 15.3.19, "Hodgkin Lymphoma," p. 971, 17.2, "Malignant Lesions of Soft Tissue and Bone," p. 1092, and 15.3.24, Table 15.3.3, p. 978 [76].

**Caution**

Many malignant tumors with anaplastic cell morphology may express CD30 antigen and/or ALK protein. Such tumors include diffuse large B-cell lymphoma, embryonal carcinoma, and others.

## 15.3.19 Classic Hodgkin Lymphoma

(Figs. 15.90–15.95)

### General Comments

- Classical Hodgkin lymphoma (CHL) accounts for more than 90% of all Hodgkin lymphomas. Previous Epstein-Barr virus infection is associated with a higher incidence of CHL. Therefore, it is presumed that EBV plays a certain role in the pathogenesis of this tumor entity.
- The anatomic sites of CHL vary by tumor subtype. Localized disease is common. Cervical and mediastinal lymph nodes are most frequently involved. Nodular sclerosis is frequently seen as mediastinal disorder. Primary extranodal involvement (e.g., lung) is rarely encountered, whereas splenic involvement is relatively common.
- Introductory comments and major cytodiagnostic challenges are condensed in Sect. 15.3.1.2.5, p. 954

### Microscopic Features

- Hallmarks of classic CHL:
  - *Reed-Sternberg (RS) cells* are large atypical cells. They either have a bilobated nucleus or the nucleus consists of multiple segments resembling multinucleation.
    The two nuclear lobes frequently occur in a pathognomonic mirror-inverted arrangement and multiple segments may be arranged in a wreath-like pattern.
    The nuclear membranes are wrinkled or molded and folded; smooth nuclear borders occur exceptionally.
    The chromatin is finely granular, dense, and regularly dispersed, giving the nucleus a certain pale and dyschromatic appearance as compared to benign nuclei in the same smear.
    The number of nucleoli varies; they are very prominent, usually eosinophilic, and round, bar-like, comma-shaped, or bent.
    The cytoplasm is abundant and stains slightly basophilic (MGG-staining) or cyanophilic (Pap-staining method) showing a distinct border. Small and large vacuoles occur sporadically.
  - *Hodgkin cells* are the mononuclear counterpart of RS cells with identical morphologic characteristics. The size clearly exceeds that of normal lymphocytes and small histiocytes but may be equal to large activated histiocytes.
- HRS tumor cells commonly represent a small fraction of all cells in a cytologic specimen.
- The composition of the reactive cellular background is variable, depending on the histological subtype of CHL. The benign fraction of CHL usually consists of small benign lymphocytes, neutrophils, eosinophils, plasma cells, histiocytes, epithelioid histiocytes, and enlarged atypical lymphocytes.
- *Atypical lymphocytes* are benign reactive cells; they are larger than their small benign counterparts, comprising irregular nuclei with indentations and cleaves, dense granular chromatin, and usually pronounced nucleoli. Occasionally, they can account for a relatively high proportion of the inflammatory cell population. Reactive atypical lymphoid cells are sometimes indistinguishable from non-Hodgkin lymphoma cells and from small mononuclear Hodgkin cells (Fig. 15.94).

**Caution**

- Hodgkin cells can vary in size and morphology (such as atypical chromatin texture and prominent but small nucleoli instead of the typical large and polymorphic ones) and may mimic large activated histiocytes or activated lymphocytes. Thus, an initial diagnosis of Hodgkin lymphoma should never be rendered in cases suggestive of HL based on the presence of Hodgkin cell-like cells alone (and complete absence of Reed-Sternberg cells).
- Cytologic smears being rich in atypical reactive lymphocytes but devoid of unambiguous HRS cells can easily lead to a false diagnosis of non-Hodgkin lymphoma.
- Scattered epithelioid histiocytes and small fragments of granulomatous tissue are not uncommon in cytologic samples of Hodgkin lymphoma (Fig. 15.95).
- The presence of eosinophilic granulocytes in FNAB specimens is not mandatory for a cytological diagnosis of HL.

**Additional Analyses** (Figs. 15.96 and 15.97)

Immunophenotyping

*HRS cells:*

– CD30 +, CD15 +, MUM-1+ are reliably diagnostic for HRS cells.
– On the contrary, HRS cells are negative for CD45 and macrophage-specific markers.
– B-cell markers: PAX5 shows an intense positive reaction; CD20 and CD79a exhibit variable positivity.
– T cell-markers: variable positivity in a minority of the tumor cells.

Molecular Genetics

Rearrangements in HRS cells:

– Clonal Ig gene occurs in practically all cases (single cell PCR).
– T-cell receptor gene is present in rare cases.

**Caution**

- CD30 is invariably expressed in HRS cells.
- Immunopositivity for CD15 occurs in the majority of CHL , but it may be expressed in only a minority of all tumor cells . The staining pattern is membrane-accentuated and/or intracytoplasmic globular .
- HRS cells are CD45-negative by immunolabeling .
- Immunoreactivity for PAX5 is typically weaker in HRS cells as compared to reactive B-cells.

### 15.3.19.1 Mixed Cellularity Classical HL

**General Comments and Microscopic Features**

- The mixed cellularity classical HL (MCCHL) variant of CHL predominantly involves peripheral lymph nodes and less frequently the spleen; mediastinal involvement is uncommon.
- MCCHL should be correctly identified by cytology in up to 100% of all cases. Individual exceptions are mentioned (see "Differential Diagnosis" immediately below).
  - Histologic and cytologic key features
    Typical HRS cells, highly variable variegated cellular background; very little extra sclerosis.

**Differential Diagnosiss**

- Cytologic specimens of MCCHL that are rich in HRS cells may mislead to a diagnosis of lymphocyte-depleted classical HL, anaplastic large T-cell lymphoma (immunocytochemical distinction, see Sects. 15.3.18, p. 970, and 15.3.19.4, p. 973) or the anaplastic variant of diffuse large B-cell lymphoma (particularly in cases with CD30 expression); see Sect. 15.3.10, p. 963.
- A marked polymorphic cytologic appearance of MCCHL can give rise to diagnostic difficulties: small and large HRS cells may overlap with pleomorphic tumor cells of non-Hodgkin lymphomas; such tumors include angioimmunoblastic T-cell lymphoma, Mycosis fungoides, peripheral T-NHL, and adult T-cell lymphoma.
- MCCHL exhibiting excessive amounts of epithelioid histiocytes and granulomatous tissue fragments may be easily confused with granulomatous (infectious) diseases such as mycobacteriosis, sarcoidosis, and others.

### 15.3.19.2 Nodular Sclerosis Classical HL

**General Comments and Microscopic Features**

- Nodular sclerosis classical HL (NSCHL) involves the mediastinum in 80% of all CHL patients.
- FNAB sampling error in nodular sclerosing Hodgkin lymphomas most likely occurs in cases with pronounced collagenous fibrosis.
- The syncytial variant of NSCHL is characterized by clustering of HRS cells (Fig. 15.98B). Cytologic features of the syncytial variant of NS have been described by Stanley and Powers [84].
  - Histologic key features
    Hodgkin and Reed-Sternberg cells usually present as lacunar cells that are characterized by an artificial retraction of the cytoplasm, leaving an empty space around the tumor cell. A nodular growth pattern with compact collagenous bundles surrounding one or several nodules is pathognomonic.
  - Cytology [38, 84]
    The diagnosis of Hodgkin lymphoma can be assessed in the majority of cases of NSCHL, but proper subtyping is often impossible because collagenous material will be absent to a large extent in cytologic samples.
    – *Lacunar-type HRS cells* are not as distinctive in cytologic smears as in histologic sections; HRS cell nuclei showing enhanced and deep lobation, less prominent nucleoli, and more abundant cytoplasm may suggest lacunar cells (Fig. 15.98A).

**Caution**

- Paucity of cells or absence of typical HRS cells in fine-needle aspirates of NSCHL due to distinct fibrosis and sclerosis hampers a correct diagnosis; the diagnosis may even be inconclusive with regard to the malignancy status of the aspirated lesion.
- The syncytial variant of NSCHL is distinguished by sheets and clusters of HRS cells, which can be misinterpreted in cytologic specimens as metastatic carcinoma or other large-cell neoplasms [84] (Fig. 15.98B)

### 15.3.19.3 Lymphocyte-Rich Classical Hodgkin Lymphoma

**General Comments and Microscopic Features**

In lymphocyte-rich classical Hodgkin lymphoma (LRCHL), the vast majority of cases involve peripheral lymph nodes.

This is a rare tumor variant that comprises roughly 5% of all classical Hodgkin lymphomas.

- Histologic key features
  LRCHL most commonly exhibits a nodular growth pattern. The nodules are composed of small lymphocytes and may harbor small germinal centers. Eosinophils are mostly absent and neutrophils are usually absent.
- Cytology
  Smears of aspirates are dominated by small benign lymphocytes. A false-negative cytologic diagnosis seems to be likely when HRS cells are extremely scarce, completely absent, or masked by the lymphocyte-rich background (Fig. 15.99).

**Differential Diagnosis**

- LRCHL may easily be confused with nodular lymphocyte predominant Hodgkin lymphoma. A correct subtyping demands immunophenotyping that reveals the profile of HRS cells in LRCHL in comparison to the tumor cells of nodular lymphocyte predominant HL (see Table 15.3.2, p. 974).
- Cellular smears of LRCHL, which are dominated by a large number of small lymphocytes interspersed with follicle center cells and inconspicuous HRS cells, reflect reactive lymphadenopathy.

### 15.3.19.4 Lymphocyte-Depleted Classical HL

**General Comments and Microscopic Features**

- Lymphocyte-depleted classical HL (LDCHL) is the rarest subtype of CHL comprising less than 1% of all HL cases in Western countries. This variant is closely associated with HIV infection. The tumor mainly involves lymph nodes in the retroperitoneum and abdominal organs.
  - Histologic and cytologic key features:
    Unlike other forms of classical Hodgkin lymphoma, HRS cells are numerically dominating in LDCHL. Some cases appear with a marked pleomorphism of the HRS cells.

**Differential Diagnosis**

- Large HRS cells of LDCHL forming aggregates and clumps in aspirate specimens can mimic large-cell epithelial tumors and occasionally malignant melanoma. An appropriate panel of immunocytochemical stains (e.g., CD15, CD30, LMP, PAX5, MUM-1 vs cytokeratins and melanocytic markers) will help render a definite diagnosis.
- Cases that are composed of marked pleomorphic HRS cells are difficult to distinguish from sarcomatous neoplasm and anaplastic large-cell lymphoma. Unlike HRS cells, ALCL-ALK+ tumor cells are immunocytochemically negative for PAX5 and positive for ALK protein and EMA. Furthermore, HRS cells can be reliably differentiated from ALK-negative ALCLs by expression of PAX5.

## 15.3.20 Nodular Lymphocyte-Predominant Hodgkin Lymphoma (Fig. 15.100)

**General Comments**

- Nodular lymphocyte-predominant Hodgkin lymphoma (NLPHL) is a monoclonal B-cell neoplasm characterized by large neoplastic cells popularly known as popcorn cells or lymphocyte-predominant (LP) cells (formerly called L&H cells) scattered in a background of B-phenotypic lymphocytes. Popcorn cells represent variants of HRS cells exhibiting particular cytologic and phenotypic features (see Table 15.3.2, below).
- NLPHL predominantly occurs in the middle of life and affects men. Most patients present with peripheral lymphadenopathy in the cervical, axillary, and inguinal regions.
- Distinguishing between NLPHL and lymphocyte-rich classical HL is difficult by cytology alone. Still, NLPHL can be differentiated by an adequate immunopanel if ample aspiration smears are available containing enough relevant tumor cells [107].

**Microscopic Features**

- Histologic key features
  The lymph node architecture is completely replaced by a nodular or nodular and diffuse infiltrate that is composed of a large proportion of small lymphocytes and histiocytes and epithelioid cells. Popcorn cells are usually embedded in a meshwork of follicular dendritic cells. Sclerosis and residual germinal centers are rarely seen.
- Cytology
  Table 15.3.2 (p. 974) highlights the morphological and biological disparity between nodular lymphocyte-predominant Hodgkin lymphoma and lymphocyte-rich classical Hodgkin lymphoma.

**Differential Diagnosis**

- As stated above, diagnostic problems in FNAB material arise in particular between NLPHL and lymphocyte-rich classical Hodgkin lymphoma.
- It may also be difficult to differentiate between NLPHL and T-cell lymphomas and/or histiocyte-rich large B-cell lymphomas. Several studies suggest a close relationship between these two entities [108].

## 15.3.21 Histiocytic Lymphoma and Histiocytic Sarcoma [15, 57, 88, 99] (Fig. 15.101)

**General Comments**

- Histiocytic lymphoma: The term "histiocytic lymphoma" is a misnomer even though it is now and then still in use. Many tumors that were once referred to as histiocytic lymphoma are now established as variants of B- or T-cell lymphomas.

**Table 15.3.2** Comparison of the relevant morphological and immunocytochemical features between nodular lymphocyte-predominant Hodgkin lymphoma and lymphocyte-rich classical Hodgkin lymphoma

| Features | Nodular lymphocyte-predominant HL | Lymphocyte-rich classical HL |
|---|---|---|
| **Morphology** | | |
| – Tumor cells | **Popcorn- or LP cells:** large, usually mononucleated cells. | **HRS: Classical Hodgkin and Reed-Sternberg cells**. Large Reed-Sternberg cells: bi- or multinucleated. |
| – Nucleus | **Distinct folding and multilobation** (popcorn-like). | **Less polymorphic** aspect. |
| – Nucleoli | Usually multiple, smaller than in HRS cells, **usually basophilic.** | Single and multiple, **markedly prominent, usually eosinophilic.** |
| – Background population | Follicular dendritic cells, predominantly B lymphocytes and numerous T cells. **Neutrophils and eosinophils nearly absent**. | Predominantly mantle cells together with germinal center cells. **Varied proportions of neutrophils and eosinophils** (particularly in MCCHLs). |
| **Immunophenotyping of the tumor cells** | | |
| – B-cell markers | | |
| – CD20 and CD79a | Positive (Fig . 15.100B). | – Not in all cases and in a minority of tumor cells positive. |
| – PAX5 | Positive. | – Weak nuclear positivity (with few exceptions) **.** |
| – J chain | **Positive in the majority of cases.** | **Negative.** |
| – CD45 | **Positive.** | **Negative.** |
| – CD30 | **Positive** (with a few exceptions: weak staining). | **Positive (invariably and strongly).** |
| – CD15 | **Negative**. | **Positive** in the majority of cases, but not in all tumor cells. |
| – BcL-6 | **Positive.** | **Negative.** |
| – MUM-1 | **Negative.** | **Positive.** |
| – EMA | Positive in the majority of cases (>50%). | Positive in 20–30% of all cases. |

Bold text: differential diagnostically important features and immunoprofiles

15

- *Histiocytic sarcoma* is a very rare tumor of high-grade malignancy composed of neoplastic cells showing morphologic and immunophenotypic features of mature histiocytes.
- Detailed information on the clinical features, cytomorphology, immunophenotyping, and genetics is available in the specialized literature, as indicated above.

### Microscopic Features and Immunocytochemistry

True histiocytic sarcoma is characterized as follows:

- The large pleomorphic tumor cells are usually round to oval but occasionally spindle-shaped. Multinucleation is common.
- The cytoplasm is abundant, dense, or vacuolated.
- The nuclei are pleomorphic and eccentrically placed, displaying a reniform shape and frequent irregular folds.
- In general, the chromatin is vesicular.
- The nucleoli vary in size.
- Erythrophagocytic (emperipolesis) tumor cells are occasionally encountered.
- The inflammatory background is sparse, consisting of neutrophils, eosinophils, lymphocytes, plasma cells, and benign histiocytes; but occasionally the inflammatory infiltrate may be pronounced and compact to such an extent that it obscures the tumor cell fraction.

One or more histiocyte-associated markers are positive: CD68, CD163, and lysozyme. CD45 and CD4 show a positive immunoreaction in a high percentage of the cells.

### Differential Diagnosis [57]

- The cytomorphologic features of histiocytic sarcoma are not specific and provoke a large differential diagnosis including Rosai-Dorfman disease, diffuse large B-cell lymphoma, anaplastic large-cell lymphoma, myeloid tumors, histicytosis X, pleomorphic carcinoma, malignant melanoma, and rare pleomorphic sarcomas.

- A definitive diagnosis of histiocytic sarcoma demands a panel of immunocytochemical stains that should include histiocyte-associated markers, alternately combined with T- and B-lymphocytic markers, myeloid markers, CD1a, CD30, cytokeratins, and melanoma-typical antigens. Composing the full immunocytochemical set of tests depends on the morphologic analysis and the clinical history.

## 15.3.22 Extramedullary Hematopoiesis

[73, 75] (Fig. 15.102)

### General Comments

In general, extramedullary hematopoiesis (EMH / myeloid metaplasia) develops subsequently to a myeloproliferative or myelosuppressing disorder. EMH may present as tumorous mass lesion in lymph nodes, soft tissues, or various organs (liver, spleen, kidney, breast, lung, and others) [42, 75]; it may clinically and radiologically mimic a real neoplasm. Thus, FNAB is in many cases applied as an initial investigation and misdiagnosis of malignancy seems likely in cases with unsuspected EMH due to a bland clinical history.

### Microscopic Features

- Hallmarks:
  Hematopoietic cells of all three hematologic cell lines are present in various proportions and different stages of maturation. The cell population comprises normoblasts, myeloid precursors (myelocytes, metamyelocytes, promyelocytes), and large megakaryocytes. The latter present as large cells with multilobated/multisegmented dark nuclei and abundant cytoplasm. Nucleoli are practically absent.
- Varying amounts of normal and activated lymphocytes in cases with involvement of lymphatic tissues.
- Usually cell-rich smears.

### Differential Diagnosis and Immunocytochemistry

Pathognomonic cytologic findings and the clinical/hematologic context are sufficient for a conclusive diagnosis in most cases; however, diagnostic dilemmas may sometimes occur:

- The heterogeneous appearance of the cytologic smears including normal lymphocytes, scattered plasma cells and histiocytes, normoblasts and myeloid precursors at various stages of maturation, together with megakaryocytes that are potentially mistaken for activated multinucleated histiocytes, may mislead to a diagnosis of an inflammatory (granulomatous) process.
- In particular, the mature variant of myeloid sarcoma must be distinguished from myeloid metaplastic tumor-forming infiltrates.
  Granulocytic sarcoma typically comprises immature myeloid elements and a decrease in erythroid (normoblasts) and megakaryocytic cells. Immature myeloid cells express the precursor markers CD34 and CD117.
- Polymorphous, multilobated megakaryocytes may appear as bizarre giant cells simulating Reed-Sternberg cells or pleomorphic carcinoma cells.
- The background cell pattern and immunophenotypical pecularities of the atypical cells are helpful to establish a conclusive diagnosis:
  - Megakaryocytes: factor VIII +
  - Myeloid precursor cells: myeloperoxydase-positive, CD34+, CD117+
  - HRS cells: CD15+, CD30+, PAX5+, MUM-1 (IRF4)+
  - Carcinoma cells: cytokeratin-positive/immunoreactivity for lineage-typical or specific cell markers

**Caution**

Accidental bone marrow sampling during FNAB of the breast, thoracic wall, posterior medastinum, and paraverebral retroperitoneal area may provoke a misdiagnosis of benign or neoplastic extramedullary myeloproliferation.

## 15.3.23 Granulocytic Sarcoma [69]

### General Comments

- Synonyms: myelogenic sarcoma, chloroma.
- Granulocytic sarcoma (GS) is an extramedullary-located neoplasm composed of myeloid cells including precursor cells. It is usually associated with a myeloproliferative disorder and may develop during the course of acute myeloid leukemia, chronic myeloid leukemia, or myelodysplastic disorders. But GS can also occur as an antecedent acting as the first sign of a primary or relapsing myeloproliferative lesion; or GS may follow a leukemic manifestation. The cytologic diagnosis is particularly challenging in the case of GS developing prior to leukemic manifestations or bone marrow involvement [5].
- Extramedullary tumorous leukemic lesions may be seen in any age and can occur anywhere in the body. They are most commonly found in lymph nodes, soft tissue, skin, and bone [69, 87]. More than one body site can be involved [89]. Simultaneous malignant lymphoma and GS in lymph nodes have occasionally been reported in the literature.
- FNAB is an effective and quick tool to distinguish between nodular GS and other malignant neoplasms. FNAB material is highly suitable for cytomorphologic evaluation as well as for cytochemical, immunocytochemical, and flow cytometric studies [29, 65, 89, 100]. However, an accurate subtyping of hematologic neoplasms requires sophisticated clinical-hematologic investigations on the morphologic, cytochemical, immunologic, and genetic levels.

**Caution**

- Benign and malignant extramedullary myeloproliferative disorders involving lymph nodes, soft tissue, skin, or parenchymatous organs can easily be misinterpreted by cytology; particularly in patients whose clinical information is incomplete or in patients who have developed an extramedullary myeloproliferative lesion before leukemia and bone marrow involvement become evident.
- Special attention must be paid to GS involving parenchymatous organs, a setting in which a fatal misinterpretation can very likely occur. A well-known target organ for this tumor entity is the breast [64].

### Microscopic Features

GS may occur as a mature, immature, or blastic variant:

- *The mature variant* is characterized by a trilineage hematopoietic cell proliferation consisting of precursor cells, immature cells, and mature cells of erythropoiesis, granulopoiesis, and megakaryopoiesis. Promyelocytes and other precursor cells, as well as eosinophilic granulocytes are common components in the mature tumor variant.
  Maturing myeloid cells are associated with lobulation of the nuclei, indistinct nucleoli, prominent eosinophilic granules, and cytoplasmic Auer rods.
- *The immature variant* (Fig. 15.103) exhibits a great proportion of promyelocytes and myeloblasts. Eosinophilic myelocytes usually occur.
- *Blastic variant* (Fig. 15.104): Erythroid and megakaryocytic elements are decreased or completely absent. Myeloid blasts occur in large numbers. The blastic cells are large, showing clear and rounded nuclei with indentations; they frequently have a histiocytoid appearance. The chromatin is finely dispersed and the nucleoli are prominent but rarely pleomorphic. The N/C ratio is medium to high. The cytoplasm is basophilic and usually agranular.
- *Acute monocytic leukemias:* The smears contain myeloblasts, monoblasts, and promonocytes. The predominant cell type is the promonocyte showing typical nuclear folds, nuclear lobulation, and granular cytoplasm (Fig. 15.105).
- A varying number of benign lymphoid cells are additionally seen in aspirates obtained from GS-involved lymph nodes.

### Additional Analyses

#### Cytochemistry

Naphtol AS-D chloroacetate-esterase positivity is a characteristic biochemical marker for myeloid blastic cells.

#### Immunophenotyping

- Immunostains for CD30 and CD45 yield a negative and a variably positive result, respectively.
- *Key markers for myeloid cells:* myeloperoxidase (MPO) positive, lysozyme positive, CD15+.
- Precursor cell markers (immature myeloid cells): CD34 and CD117 exhibit variable positivity.
- Megakaryocyte lineage: Factor VIII shows strong immunopositivity.
- B-cell markers: CD20 negative, CD79a shows variable labeling.
- T cell-markers: CD3–, CD43+ (not line-specific).
- Histiocyte-associated marker: CD68+.

#### Molecular Genetics

- Molecular genetic markers are applied according to different kinds of AML subtypes.
- FISH: *bcr/abl* gene fusion t(9;22).

### Additional Comments

- Cytochemical studies may be helpful in determining the lineage of myeloid blasts. However, cytochemistry is currently replaced by immunophenotyping using immunocytochemistry or flow cytometry.
- The proportion of immunostained cells varies with the tumor grade. Poorly differentiated and blastic tumor cells tend to be completely negative or may show only focal staining.
- Anti-myeloperoxydase is the most sensitive and specific antibody to identify a myeloid cell population [69].
- CD68 determines the monocytic differentiation of a myeloid leukemia.
- The bcr/abl fusion signal using the FISH technique rapidly and reliably detects the myeloid origin of blasts in chronic myeloic leukemia. The test excludes malignant large-cell elements originating from non-Hodgkin lymphomas and Hodgkin lymphomas [103].
- Cytogenetic and molecular genetic assays are required for the initial diagnosis and genetic characterization of leukemic neoplasms and for the assessment of potential tumor behavior. Post-therapy follow-up studies can detect evolving genetic properties of myeloid cells.

### Differential Diagnosis [64]

- Misdiagnosis most likely occurs in GS showing a low degree of cellular differentiation. It can be extremely difficult to distinguish GS from other neoplasias in patients presenting without hematologic pathology and an appropriate clinical history.
- The most common misdiagnosis in GS is non-Hodgkin lymphoma [69].
- The following diagnostic considerations should be taken into account depending on the location of the granulocytic sarcomatous infiltration, the degree of myeloid cell differentiation, and the amount of a monocytoid tumor component:

- Large-cell non-Hodgkin lymphoma, especially in cases of immature/blastic GS located in lymph nodes.
- Hodgkin lymphoma in cases of GS with a prominent immature blastic and megakaryocytic component, comprising tumor cells exhibiting large nucleoli and associated with inflammatory infiltrates.
- Metastatic discohesive undifferentiated carcinoma, in cases of GS with poorly differentiated myeloblastic cells (Fig. 15.104B).
- Particular primary carcinoma variants, in cases of GS affecting glandular organs, such as breast, salivary glands, and prostate. Greater detail is provided in Sects. 1.3.15.3, p. 67, 5.1.5.7, p. 419, and 14.1.10.2, p. 864.
- Metastatic malignant melanoma and histiocytic sarcoma, in cases of GS that are composed of large blasts, numerous monocytoid elements, and abnormal megakaryocytes.
- GS showing a variegated cellular appearance attended by numerous lymphocytes should not be mistaken for an inflammatory process (Fig. 15.103).
- Extramedullary hematopoiesis may be misdiagnosed if FNAB provides cells of the mature GS variant comprising myeloid precursors at an advanced stage of maturation and megakaryocytic elements.

Appropriate panels of antibodies, together with clonality analyses (using FISH or PCR) are helpful in achieving a correct diagnosis.

**Caution**

GS cells showing immunoreactivity for CD45 and CD43, or for other T-cell markers, may mislead to a diagnosis of T-cell non-Hodgkin lymphoma; hence, CD3 should be used as a first-line T-cell marker.
Similar differential diagnostic problems occur if myeloid tumor cells exhibit immunoreactivity for CD45 and CD79a [59]; an erroneous diagnosis of B-cell non-Hodgkin lymphoma is rather likely.

## 15.3.24 Metastatic Neoplasms and Their Immunocytochemical Characteristics

### General Comments

- Fine-needle aspiration is a widely used diagnostic tool for lymph nodes that are suggestive of metastatic tumor involvement. The method is highly accurate and reliable and is widely accepted by clinicians.
  It is useful:
  - To confirm a metastatic lesion in patients with known primary tumors.
  - To detect tumorous lymph node involvement in patients having an occult primary neoplasm.
  - To detect recurrences during tumor follow-up.
  - To diagnose a second lymphoid or nonlymphoid neoplasm.
  - To discern or exclude infectious diseases in tumor patients undergoing treatment with immunocompromising therapeutic regimes.
  - For staging newly detected cancer.
  - To establish potential changes in the biological nature of a cancer that has previously been diagnosed.
- The large majority of such lesions are correctly identified in cytologic aspirates due to their morphologic characteristics, selective immunostaining properties, and genetic features.
- Squamous cell carcinoma, adenocarcinoma, and poorly differentiated large-cell carcinoma are most commonly encountered in daily routine practice.
- Morphologic features, immunocytochemical properties, and diagnostic dilemmas of organ-typical carcinomas are presented in the chapters of this book devoted to the specific organs.

**Caution**

- Cytology alone can provide a false-negative diagnosis or an incorrect tumor typing. Selected lesions giving rise to diagnostic difficulties are presented in photographs and discussed in the corresponding legends:
  - Breast carcinoma, clear cell type (Fig. 15.106).
  - Breast carcinoma, monomorphic cell type (Fig. 15.107).
  - Cystic papillary thyroid carcinoma (Fig. 15.108).
  - Keratinizing squamous cell carcinoma (Fig. 15.109).
  - Lymphoepithelial carcinoma (Fig. 15.110).
  - Amelanotic malignant melanoma (Fig. 15.111).
  - Example of concomitant neoplasms (Fig. 15.112).
- Determinate cytologic reports should never be rendered based on poorly preserved cytologic smears (Fig. 15.113).

### Immunocytochemistry

- A synopsis of the most common tumor cell markers that are detectable by routine immunocytochemical testing is given in Table 15.3.3, p. 978. The list includes a majority of markers and antigens that play a crucial role in the diagnostic spectrum of epithelial neoplasms and selected nonepithelial and nonlymphoid tumors.
- CD markers of leukocytes and lymphoid tumors are listed in Table 15.1.1, Sect. 15.1.4.1, p. 912.

**Table 15.3.3** Common nonlymphoid tumor cell markers detectable in cytologic specimens using immunocytochemical methods

| Marker groups | Individual markers | Immunopositivity relevant for diagnosis[a] |
|---|---|---|
| **Cytokeratins** | Pancytokeratins (MNF116, Lu-5) | Carcinomas |
| | CK 5/6, 34betaE12 | Squamous cell carcinoma |
| | CK7 and CK20 | Transitional cell carcinoma, Pancreas and bile duct carcinoma |
| | CK7 | Adenocarcinoma of the lung and breast |
| | CK13 | Transitional cell carcinoma |
| | CK20 | Colonic adenocarcinoma |
| **CA (carcinoma antigen) markers** | CA 19-9 | Pancreatic and bile duct carcinoma |
| | CA 125 | Ovarian carcinoma |
| **CD (cluster of differentiation) marker** | CD1 | Langerhans cell histiocytosis |
| **Tumor-typical markers** | CEA | Carcinomas |
| | TTF-1 | Thyroid neoplasms, Adenocarcinoma of the lung, Small cell carcinoma in particular of the lung, Neuroendocrine tumors |
| | Mammaglobin | Breast carcinoma |
| | E-cadherin | Ductal breast carcinoma |
| | Vimentin (frequently coexpressed with cytokeratins in cytologic smears!) | Soft tissue tumors |
| **Tumor markers – more or less specific** | Thyroglobulin | Thyroid follicular neoplasm |
| | Calcitonin | Thyroid medullary carcinoma |
| | PHRP | Tumors of the parathyroid gland |
| | PSA, PAP | Carcinoma of the prostate |
| | AFP, Hep Par 1 | Hepatocellular carcinoma |
| | CDX-2 | Intestinal, particularly colorectal carcinoma |
| | CgA, synaptophysin, NSE | Neuroendocrine tumors, parathyroidal tumors |
| | Hormone receptors | Breast carcinoma, Endometrial carcinoma, Ovarian carcinoma |
| | PLAP, hCG, AFP | Germ cell tumors |
| | RCCMA | Renal cell carcinoma |
| | Calretinin | Mesothelioma |
| | PMC, HMB-45, Melan A, Tyrosinase | Malignant melanoma |
| | S100 (in general has low specificity!) | Melanoma, granulosa cell tumor, Langerhans cell histiocytosis |
| | GFAP | Peripheral nerve sheath tumors |
| | Alpha SMA | Smooth muscle tumors, myoepithelial tumors |

[a] See details in the specific chapters of this book.

AFP, alpha-feto protein; CgA, chromogranin A; GFAP, glial fibrillary acidic protein; hCG, human chorionic gonadotrophin; Hep Par 1, hepatocyte antigen; LMW CK, low-molecular-weight cytokeratins; NSE, neuron-specific enolase; PAP, prostate acid phosphatase; PHRP, parathyroid hormone-related protein; PLAP, placental alcaline phosphatase; PMC, pan melanoma cocktail; PSA, prostate-specific antigen; RCCMA, renal cell carcinoma-associated cell marker; SMA, smooth muscle actin; TTF-1, thyroid transcription factor-1

**Caution**

- Each institution should develop individual protocols for the processing of cell aspirates from standardized sampling to staining-procedures and establish reliable rules to ensure the validity and reproducibility of the immunocytochemical results.
- Immunotests that have been found to provide untrustworthy results must be evaluated with special attention. Whenever possible, they should be substituted with another immunopanel, another technical approach, or if need be a different biological assay.

## 15.3.25 Further Reading


1. Ali EA, Boerner SL, Geddie WR, et al. Grading B-cell Non-Hodgkin lymphoma using MIB-1 proliferative index in fine needle aspirates. 2008; 114 Suppl:445.
2. Al Shanqeety O, Mourad WA. Diagnosis of peripheral T-cell lymphoma by fine-needle aspiration biopsy: a cytomorphologic and immunophenotypic approach. Diagn Cytopathol 2000;23:375-379.
3. Bahler DW, Swerdlow SH. Clonal salivary gland infiltrates associated with myoepithelial sialadenitis (Sjögren's syndrome) begin as nonmalignant antigen-selected expansions. Blood 1998;91:1864-1872.
4. Bangerter M, Brudler O, Heinrich B, Griesshammer M. Fine needle aspiration cytology and flow cytometry in the diagnosis and subclassification of non-Hodgkin's lymphoma based on the World Health Organization Classification. Acta Cytol 2007;51:390-398.
5. Bangerter M, Hildebrand A, Waidmann O, Griesshammer M. Diagnosis of granulocytic sarcoma by fine-needle aspiration cytology. Acta Haematol 2000;103:102-108.
6. Bangerter M, Hildebrand A, Waidmann O, Griesshammer M. Fine needle aspiration cytology in extramedullary plasmacytoma. Acta Cytol 2000;44:287-291.
7. Basu D, Kumar S, Shome DK, Chauhan S. Cutaneous T-cell lymphoma diagnosed by fine-needle aspiration: a case report with clinical, cytological, and immunophenotypic features. Diagn Cytopathol 1994;11:174-177.
8. Bentz JS, Rowe LR, Anderson SR, et al. Rapid detection of the t(11;14) translocation in mantle cell lymphoma by interphase fluorescence in situ hybridisation on archival cytopatholgic material. Cancer 2004;102:124-131.
9. Caraway NP, Gu J, Lin P, et al. The utility of interphase fluorescence in situ hybridisation for the detection of the translocation t(11;14)(q13;q32) in the diagnosis of mantle cell lymphoma on fine-needle aspiration specimens. Cancer 2005;105:110-118.
10. Caraway NP, Thomas E, Khanna A, et al. Chromosomal abnormalities detected by multicolor fluorescence in situ hybridization in fine-needle aspirates from patients with small lymphocytic lymphoma are useful for predicting survival. Cancer(Cancer Cytopathol) 2008;114:315-322.
11. Carbone A, Gloghini A, Ferlito A. Pathological features of lymphoid proliferations of the salivary glands: lymphoepithelial sialadenitis versus low-grade B-cell lymphoma of the MALT type. Ann Otol Rhinol Laryngol 2000;109:1170-1175.
12. Chhieng DC, Cohen J-M, Cangiarella JF. Cytology and immunophenotyping of low- and intermediate-grade B-cell non-Hodgkin's lymphomas with a predominant small-cell component: A stuy of 56 cases. Diagn Cytopathol 2001;24:90-97.
13. Chhieng DC, Cangiarella JF, Symmans WF, Cohen JM. Fine-needle aspiration cytology of Hodgkin disease: a study of 89 cases with emphasis on false-negative cases. Cancer 2001;93:52-59.
14. Cogliatti SB, Novak U, Henz S, et al. Diagnosis of Burkitt lymphoma in due time: a practical approach. Brit J Haematol 2006;134:294-301.
15. Copie-Bergman C, Wotherspoon AC, Norton AJ, et al. True histiocytic lymphoma: a morpholgic, immunohistochemical, and molecular genetic study of 13 cases. Am J Surg Pathol 1998;22:1386-1392
16. Crapanzano JP, Lin O. Cytologic findings of marginal zone lymphoma. Cancer 2003;99:301-309.
17. Das DK. Value and limitations of fine-needle aspiration cytology in diagnosis and classification of lymphomas: a review. Diagn Cytopathol 1999;21:240-249.
18. Das DK, Gupta SK, Datta BN, Sharma SC. Fine needle aspiration cytodiagnosis of Hodgkin's disease and its subtypes. I. Scope and limitations. Acta Cytol 1990;34:329-336.
19. Dave SS, Fu K, Wright GW, et al. Molecular diagnosis of Burkitt's lymphoma. N Engl J Med 2006;354:2431-2442.
20. de Almeida MM, Chagas M, de Sousa JV, Mendonca ME. Fine-needle aspiration cytology as a tool for the early detection of testicular relapse of acute lymphoblastic leukemia in children. Diagn Cytopathol 1994;10:44-46.
21. Del Giudice I, Matutes E, Morilla R, et al. The diagnostic value of CD123 in B-cell disorders with hairy or villous lymphocytes. Haematologica 2004;89:303-308.
22. Dey P. Role of ancillary techniques in diagnosing and subclassifying non-Hodgkin's lymphomas on fine needle aspiration cytology. Cytopathology 2006;17:275-287.
23. Dey P, Radhika S, Das A. Fine-needle aspiration biopsy of angioimmunoblastic lymphadenopathy. Diagn Cytopathol 1996;15:412-414.
24. Folk GS, Abbondanzo SL, Childers EL, Foss RD. Plasmablastic lymphoma: a clinicopathologic correlation. Ann Diagn Pathol 2006;10:8-12.
25. Galindo LM, Garcia FU, Hanau CA, et al. Fine-needle aspiration biopsy in the evaluation of lymphadenopathy associated with cutaneous T-cell lymphoma (mycosis fungoides/Sézary syndrome). Am J Clin Pathol 2000;113:865-871.
26. Gong JZ, Stenzel TT, Bennett ER, et al. Burkitt lymphoma arising in organ transplant recipients: a clinicopathologic study of five cases. Am J Surg Pathol 2003;27:818-827.
27. Gong JZ, Williams DC Jr, Liu K, Jones C. Fine-needle aspiration in non-Hodgkin lymphoma: evaluation of cell size by cytomorphology and flow cytometry. Am J Clin Pathol 2002;117:880-888.
28. Gong Y, Caraway N, Gu J, et al. Evaluation of interphase fluorescence in situ hybridization for the t(14;18)(q32;q21) translocation in the diagnosis of follicular lymphoma on fine-needle aspirates: a comparison with flow cytometry immunophenotyping. Cancer 2003;99:385-393.
29. Gujral S, Kumar R, Jain P, et al. Fine needle aspiration of extramedullary myeloid cell tumor in myelodysplastic syndrome. A report of three cases. Acta Cytol 1999;43:647-651.
30. Huang KP, Weinstock MA, Clarke CA, et al. Second lymphomas and other malignant neoplasms in patients with mycosis fungoides and Sézary syndrome: evidence from population-based and clinical cohorts. Arch Dermatol 2007;143:45-50.
31. Hummel M, Bentink S, Berger H, et al. A biologic definition of Burkitt's lymphoma from transcriptional and genomic profiling. N Engl J Med 2006;354:2419-2430.
32. Iacobuzio-Donahue CA, Clark DP, Ali SZ. Reed-Sternberg-like cells in lymph node aspirates in the absence of Hodgkin's disease: pathologic significance and differential diagnosis. Diagn Cytopathol 2002;27:335-339.
33. Iyengar KR, Mutha S. Discrete epithelioid cells: useful clue to Hodgkin's disease cytodiagnosis. Diagn Cytopathol 2002;26:142-144.

34. Jacobs JC, Katz RL, Shabb N, et al. Fine needle aspiration of lymphoblastic lymphoma. A multiparameter diagnostic approach. Acta Cytol 1992;36:887-894.
35. Jaffe ES, Zarate-Osorno A, Kingma DW, et al. The interrelationship between Hodgkin's disease and non-Hodgkin's lymphomas. Ann Oncol 1994;5 Suppl 1:7-11.
36. Jeffers MD, Milton J, Herriot R, McKean M. Fine needle aspiration cytology in the investigation of non-Hodgkin's lymphoma. J Clin Pathol 1998;51:189-196.
37. Jimenez-Heffernan JA, Vicandi B, Lopez-Ferrer P, et al. Value of fine needle aspiration cytology in the initial diagnosis of Hodgkin's disease. Analysis of 188 cases with emphasis on diagnostic pitfalls. Acta Cytol 2001;45:300-306.
38. Jogai S, Dey P, Al Jassar A, et al. Role of fine needle aspiration cytology in nodular sclerosis variant of Hodgkin's lymphoma. Acta Cytol 2006;50:507-512.
39. Kardos TF, Sprague RI, Wakely PE Jr, Frable WJ. Fine-needle aspiration biopsy of lymphoblastic lymphoma and leukemia. A clinical, cytologic, and immunologic study. Cancer 1987;60:2448-2453.
40. Katz RL, Gritsman A, Cabanillas F, et al. Fine-needle aspiration cytology of peripheral T-cell lymphoma. Am J Clin Pathol 1989;91:120-131.
41. Kishimoto K, Kitamura T, Fujita K, et al. Cytologic differential diagnosis of follicular lymphoma grades 1 and 2 from reactive follicular hyperplasia: cytologic features of fine-needle aspiration smears with Pap stain and fluorescence in situ hybridization analysis to detect t(14;18)(q32;q21) chromosomal translocation. Diagn Cytopathol 2006;34:11-17.
42. Koch CA, Li CY, Mesa RA, Tefferi A. Nonhepatosplenic extramedullary hematopoiesis: associated diseases, pathology, clinical course, and treatment. Mayo Clin Proc 2003;78:1223-1233.
43. Kocjan G. Best Practice No 185: Cytological and molecular diagnosis of lymphoma. J Clin Pathol 2005;58:561-567.
44. Kojima M, Nakamura S, Motoori T, et al. Primary marginal zone B-cell lymphoma of the lymphnode resembling plasmacytoma arising from a plasma cell variant of Castleman's disease. A clinicopathological and immunohistochemical study of seven patients. APMIS 2002;110:875-880.
45. Kollur SM, El Hag IA. Fine-needle aspiration cytology of metastatic nasopharyngeal carcinoma in cervical lymph nodes: comparison with metastatic squamous-cell carcinoma, and Hodgkin's and non-Hodgkin's lymphoma. Diagn Cytopathol 2003;28:18-22.
46. Kost CB, Holden JT, Mann KP. Marginal zone B-cell lymphoma: a retrospective immunophenotypic analysis. Cytometry B Clin Cytom 2008;74:282-286.
47. Laane E, Tani E, Björklund E, et al. Flow cytometric immunophenotyping including Bcl-2 detection on fine needle aspirates in the diagnosis of reactive lymphadenopathy and non-Hodgkin's lymphoma. Cytometry B Clin Cytom 2005;64:34-42.
48. Lacroix A, Jaccard A, Rouzioux C, et al. HHV-6 and EBV DNA quantitation in lymph nodes of 86 patients with Hodgkin's lymphoma. J Med Virol 2007;79:1349-1356.
49. Lin O, Gerhard R, Zerbini MC, Teruya-Feldstein J. Cytologic features of plasmablastic lymphoma. Cancer 2005;105:139-144.
50. Mann R, Berard C. Criteria for the cytologic subclassification of follicular lymphomas: a proposed alternative method. Hematol Oncol 1982;1:187-192.
51. Mathiot C, Decaudin D, Klijanienko J, et al. Fine-needle aspiration cytology combined with flow cytometry immunophenotyping is a rapid and accurate approach for the evaluation of suspicious superficial lymphoid lesions. Diagn Cytopathol 2006;34:472-478.
52. Mathur S, Dawar R, Verma K. Diagnosis and grading of non-Hodgkin's lymphomas on fine needle aspiration cytology. Indian J Pathol Microbiol 2007;50:46-50.
53. Matsushima AY, Hamele-Bena D, Osborne BM. Fine-needle aspiration biopsy findings in marginal zone B cell lymphoma. Diagn Cytopathol 1999;20:190-198.
54. Matutes E. Adult T-cell leukaemia/lymphoma. J Clin Pathol 2007;60:1373-1377.
55. McCluggage WG, Anderson N, Herron B, Caughley L. Fine needle aspiration cytology, histology and immunohistochemistry of anaplastic large cell Ki-1-positive lymphoma. A report of three cases. Acta Cytol 1996;40:779-785.
56. Meara RS, Reddy V, Arnoletti JP, et al. Hairy cell leukemia: a diagnosis by endoscopic ultrasound guided fine needle aspiration. Cytojournal 2006;3:1.
57. Miliauskas JR. Fine-needle aspiration cytology: true histiocytic lymphoma/histiocytic sarcoma. Diagn Cytopathol 2003;29:233-235.
58. Moriarty AT, Schwenk GR Jr, Chua G. Splenic fine needle aspiration biopsy in the diagnosis of lymphoreticular diseases. A report of four cases. Acta Cytol 1993;37:191-196.
59. Mourad WA, Sneige N, Huh YO, et al. Fine needle aspiration cytology of extramedullary chronic myelogenous leukemia. Acta Cytol 1995;39:706-712.
60. Murphy BA, Meda BA, Buss DH, Geisinger KR. Marginal zone and mantle cell lymphomas: assessment of cytomorphology in subtyping small B-cell lymphomas. Diagn Cytopathol 2003;28:126-130.
61. Nakamura N, Nakamine H, Tamaru J, et al. The distinction between Burkitt lymphoma and diffuse large B-cell lymphoma with c-myc rearrangement. Mod Pathol 2002;15:771-776.
62. Ng WK, Ip P, Choy C, Collins RJ. Cytologic findings of angioimmunoblastic T-cell lymphoma: analysis of 16 fine-needle aspirates over 9-year period. Cancer 2002;96:166-173.
63. Ng WK, Ip P, Choy C, Collins RJ. Cytologic and immunocytochemical findings of anaplastic large cell lymphoma: analysis of ten fine-needle aspiration specimens over a 9-year period. Cancer 2003;99:33-43.
64. Ngu IW, Sinclair EC, Greenaway S, Greenberg ML. Unusual presentation of granulocytic sarcoma in the breast: a case report and review of the literature. Diagn Cytopathol 2001;24:53-57.
65. Orucevic A, Reddy VB, Selvaggi SM, et al. Fine-needle aspiration of extranodal and extramedullary hematopoietic malignancies. Diagn Cytopathol 2000;23:318-321.
66. Owen RG, Treon SP, Al Katib A, et al. Clinicopathological definition of Waldenstrom's macroglobulinemia: consensus panel recommendations from the Second International Workshop on Waldenstrom's macroglobulinemia. Semin Oncol 2003;30:110-115.
67. Pai RK, Mullins FM, Kim YH, Kong CS. Cytologic evaluation of lymphadenopathy associated with mycosis fungoides and Sézary syndrome. Role of immunophenotypic and molecular ancillary studies. Cancer(Cancer Cytopathol) 2008;114:323-332.
68. Park IA, Kim CW. FNAC of malignant lymphoma in an area with a high incidence of T-cell lymphoma. Correlation of accuracy of cytologic diagnosis with histologic subtype and immunophenotype. Acta Cytol 1999;43:1059-1069.
69. Paydas S, Zorludemir S, Ergin M. Granulocytic sarcoma: 32 cases and review of the literature. Leuk Lymphoma 2006;47:2527-2541.
70. Pilotti S, Di Palma S, Alasio L, et al. Diagnostic assessment of enlarged superficial lymph nodes by fine needle aspiration. Acta Cytol 1993;37:853-866.
71. Pinto RG, Rocha PD, Vernekar JA. Fine needle aspiration of the spleen in hairy cell leukemia. A case report. Acta Cytol 1995;39:777-780.
72. Pinto AE, Cabecadas J, Nobrega SD Mendonca E. Flow-cytometric S-phase fraction as a complementary biological parameter for the cytological grading of non-Hodgkin's lymphoma. Diagn Cytopathol 2003;29:194-199.
73. Policarpio-Nicolas ML, Bregman SG, Ihsan M, Atkins KA. Mass-forming extramedullary hematopoiesis diagnosed by fine-needle aspiration cytology. Diagn Cytopathol 2006;34:807-811.
74. Pugh JL, Jhala NC, Eloubeidi MA, et al. Diagnosis of deep-seated lymphoma and leukemia by endoscopic ultrasound-guided fine-needle aspiration biopsy. Am J Clin Pathol 2006;125:703-709. 75.

75. Raab SS, Silverman JF, McLeod DL, Geisinger KR. Fine-needle aspiration cytology of extramedullary hematopoiesis (myeloid metaplasia). Diagn Cytopathol 1993;9:522-526.
76. Rapkiewicz A, Wen H, Sen F, Das K. Cytomorphologic examination of anaplastic large cell lymphoma by fine-needle aspiration cytology. Cancer(Cancer Cytopathol) 2007;111:499-507.
77. Rassidakis GZ, Tani E, Svedmyr E, et al. Diagnosis and subclassification of follicular center and mantle cell lymphomas on fine-needle aspirates: a cytologic and immunocytochemical approach based on the Revised European-American Lymphoma (REAL) classification. Cancer 1999;87:216-223.
78. Reid-Nicholson M, Kavuri S, Ustun C, et al. Plasmablastic lymphoma: cytologic findings in 5 cases with unusual presentation. Cancer(Cancer Cytopathol) 2008;114:333-341.
79. Renshaw AA. Reporting risk of malignancy/ dysplasia in cytology. A potential way to improve communication, if not reputation. Cancer (Cancer Cytopathol) 2007;111:465-466.
80. Saikia UN, Dey P, Saikia B, Das A. Fine-needle aspiration biopsy in diagnosis of follicular lymphoma: cytomorphologic and immunohistochemical analysis. Diagn Cytopathol 2002;26:251-256.
81. Skoog L, Tani E. The role of fine-needle aspiration cytology in the diagnosis of non-Hodgkin's lymphoma. Diagn Oncol 1991;1:12-18.
82. Sneige N, Dekmezian RH, Katz RL, et al. Morphologic and immunocytochemical evaluation of 220 fine needle aspirates of malignant lymphoma and lymphoid hyperplasia. Acta Cytol 1990;34:311-322.
83. Spieler P, Schmid U. How exact are the diagnosis and classification of malignant lymphomas from aspiration biopsy smears? A comparison between histologic and cytologic diagnoses of 20 Hodgkin's and 54 non-Hodgkin's lymphomas according to Rappaport (1966) and Kiel (1974) nomenclatures. Path Res Pract 1978;163:232-250.
84. Stanley MW, Powers CN. Syncytial variant of nodular sclerosing Hodgkin's disease: fine-needle aspiration findings in two cases. Diagn Cytopathol 1997;17:477-479.
85. Steel BL, Schwartz MR, Ramzy I. Fine needle aspiration biopsy in the diagnosis of lymphadenopathy in 1103 patients. Role, limitations and analysis of diagnostic pitfalls. Acta Cytol 1995;39:76-81.
86. Stewart CJR, Duncan JA, Farquharson M, Richmond J. Fine needle aspiration cytology diagnosis of malignant lymphoma and reactive lymphoid hyperplasia. J Clin Pathol 1998;51:197-203.
87. Suh YK, Shin HJ. Fine-needle aspiration biopsy of granulocytic sarcoma: a clinicopathologic study of 27 cases. Cancer 2000;90:364-372.
88. Swerdlow SH, Campo E, Harris NL, et al. (Eds.). WHO Cassification of Tumours of Haematopoietic and Lymphoid Tissues. IARC: Lyon 2008.
89. Tao J, Wu M, Fuchs A, Wasserman P. Fine-needle aspiration of granulocytic sarcomas: a morphologic and immunophenotypic study of seven cases. Ann Diagn Pathol 2000;4:17-22.
90. Thieblemont C. Clinical presentation and management of marginal zone lymphomas. Hematology Am Soc Hematol Educ Program 2005;307-313.
91. Tiemann M, Asbeck R, Wacker HH. Clonal B-cell reaction in Sjögren disease and Hashimoto autoimmune thyroiditis. Pathologe 1996;17:289-295.
92. Tong TR, Lee KC, Chow TC, et al. T-cell/histiocyte-rich diffuse large B-cell lymphoma. Report of a case diagnosed by fine needle aspiration biopsy with immunohistochemical and molecular pathologic correlation. Acta Cytol 2002;46:893-898.
93. Traverse-Glehen A, Felman P, Callet-Bauchu E, et al. A clinicopathological study of nodal marginal zone B-cell lymphoma. A report on 21 cases. Histopathology 2006;48:162-173.
94. Troxell ML, Bangs CD, Cherry AM, et al. Cytologic diagnosis of Burkitt lymphoma. Cancer 2005;105:310-318.
95. Uherova P, Ross CW, Finn WG, et al. Peripheral T-cell lymphoma mimicking marginal zone B-cell lymphoma. Mod Pathol 2002;15:420-425.
96. Vaillo A, Gutierrez-Martin A, Ballestin C, Ruiz-Liso JM. Marginal zone B-cell lymphoma of the parotid gland associated with epithelioid granulomas. Report of a case with fine needle aspiration. Acta Cytol 2004;48:420-424.
97. Vaillo Vinagre A, Gutierrez MA, Perez Barrios A, et al. Lymphoepithelioid cell lymphoma (Lennert's lymphoma). Report of a case with fine needle aspiration cytology. Acta Cytol 2004;48:234-238.
98. Vicandi B, Jimenez-Heffernan JA, Lopez-Ferrer P, et al. Hodgkin's disease mimicking suppurative lymphadenitis: a fine-needle aspiration report of five cases. Diagn Cytopathol 1999;20:302-306.
99. Vos JA, Abbondanzo SL, Barekman CL, et al. Histiocytic sarcoma: a study of five cases including the histiocyte marker CD163. Mod Pathol 2005;18:693-704.
100. Wakely P Jr, Frable WJ, Kneisl JS. Soft tissue aspiration cytopathology of malignant lymphoma and leukemia. Cancer 2001;93:35-39.
101. Wakely PE Jr, Kornstein MJ. Aspiration cytopathology of lymphoblastic lymphoma and leukemia: the MCV experience. Pediatr Pathol Lab Med 1996;16:243-252.
102. Yao JL, Cangiarella JF, Cohen JM, Chhieng DC. Fine-needle aspiration biopsy of peripheral T-cell lymphomas. A cytologic and immunophenotypic study of 33 cases. Cancer 2001;93:151-159.
103. Yashima-Abo A, Satoh T, Abo T, et al. Distinguishing between proliferating nodal lymphoid blasts in chronic myelogenous leukemia and non-Hodgkin lymphoma: report of three cases and detection of a bcr/abl fusion signal by single-cell analysis. Pathol Int 2005;55:273-279.
104. Young NA, Al-Saleem TI, Al-Saleem Z, et al. The value of transformed lymphocyte count in subclassification of non-Hodgkin's lymphoma by fine-needle aspiration. Am J Clin Pathol 1997;108:143-151.
105. Zardawi IM, Barker BJ, Simons DP. Hodgkin's disease masquerading as granulomatous lymphadenitis on fine needle aspiration cytology. Acta Cytol 2005;49:224-226.
106. Zardawi IM, Jain S, Bennet G. Flow-cytometric algorithm on fine-needle aspirates for the clinical workup of patients with lymphadenopathy. Diagn Cytopathol 1998;19:274-278.
107. Zhang JR, Raza AS, Greaves TS, Cobb CJ. Fine-needle aspiration diagnosis of Hodgkin lymphoma using current WHO classification – re-evaluation of cases from 1999-2004 with new proposals. Diagn Cytopathol 2006;34:397-402.
108. Zhao FX. Nodular lymphocyte-predominant Hodgkin lymphoma or T-cell/histiocyte rich large B-cell lymphoma: the problem in "grey zone" lymphomas. Int J Clin Exp Pathol 2008;1:300-305.

**Fig. 15.41 Mononucleosis infectiosa mimicking malignant lymphoma.**
FNAB of a young woman's enlarged neck lymph node. Higher magnification shows a high proportion of atypical lymphocytes: cellular enlargement, irregular nuclear shape, and distinct nucleoli (direct smear, Pap stain, no MGG stained specimen available).
*Tentative cytologic diagnosis:* Overall cell pattern suggests malignant lymphoma on Pap staining.
*Comments:*EBV-typical immunoblasts, plasmablasts, and mature plasma cells rarely occur or are very difficult to distinguish.
Note the loose but coarse granular chromatin texture indicating benign (reactive) lymphoid cells.
In this particular case, MGG stain would be extremely helpful in order to accentuate plasmacytoid features of the atypical cells.
*Final diagnosis:* Subsequent positive serologic results confirmed mononucleosis infectiosa.

**Fig. 15.42 Hyperplasia of the lymphonodular T-zone mimicking low-grade non-Hodgkin lymphoma.**
A 67-year-old woman presented with enlarged peripheral lymph nodes and a retroperitoneal mass.
Lower magnification shows a high proportion of small to medium-sized lymphocytes in combination with blasts (arrows), intermediate cells, and histiocytes (arrowheads) (FNAB, direct smear, MGG stain).
*(False-positive) cytologic diagnosis:* Low-grade NHL associated with scattered centroblasts (likely follicular lymphoma, grade 1–2).
*Comment:* Pronounced nuclear irregularities in size and shape of the proliferating T cells suggested malignancy.
*Histology of the same lymph node:* Reactive lymphadenopathy associated with enlarged T-zones.

**Fig. 15.43A–C Lymphoblastic lymphoma.**

Morphological features of B lymphoblastic neoplasms are indistinguishable from those of malignant T lymphoblastic proliferations.



A 53-year-old man having a positive history of relapsing NHL presented with an enlarged inguinal lymph node. The patient was referred to FNAB with the clinical issue: relapse of lymphoma vs viral infection. Direct smears were MGG- and Pap-stained.
*Cytologic and subsequent histologic diagnosis* (the latter by lymph node excision): Lymphoblastic lymphoma.
**A** Lower magnification shows a heterogeneous cell population composed of small and intermediate cells (MGG staining method). It is rather difficult to recognize blast cell features but the N/C ratio is consistently high. **B** Detail from a Pap-stained smear clearly exhibits lymphoblastic features: irregularly shaped nuclei, evenly distributed fine and coarse granular chromatin, and occasionally indistinct multiple nucleoli. Usually extremely small cytoplasmic rims; the larger cytoplasmic bodies harbor distinct vacuoles (arrows). **C** Only 20–30% of the malignant blasts express leukocyte common antigen (CD45) (immunostaining of a Pap-prestained specimen).

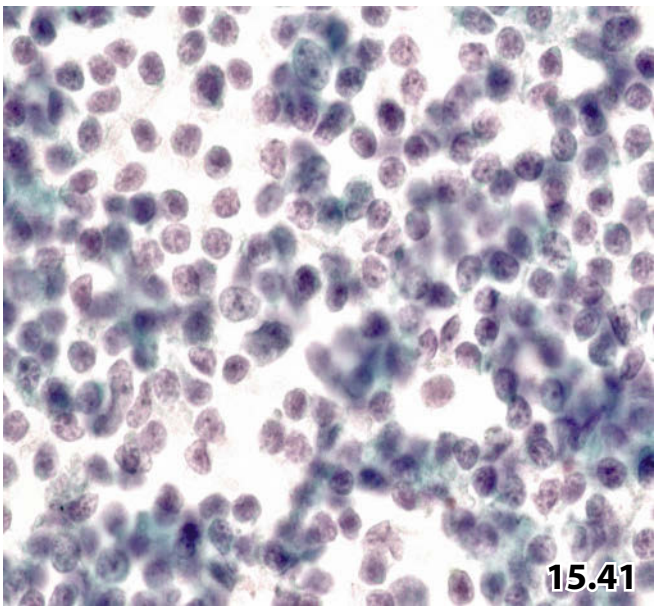
15.41

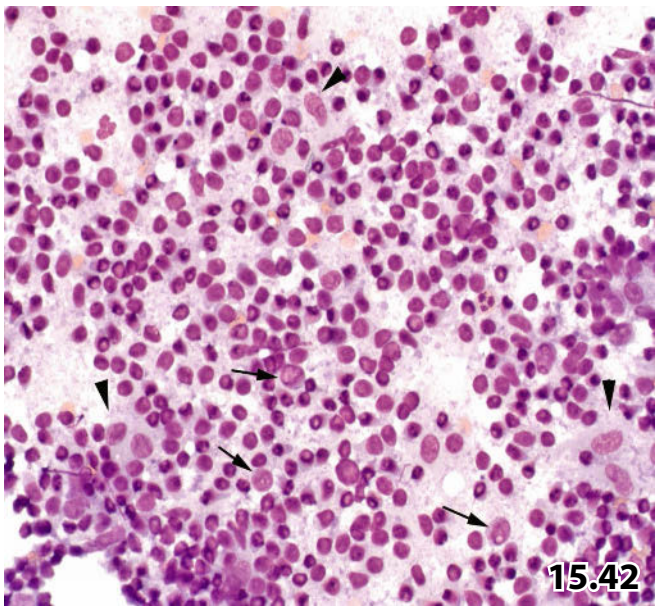
15.42

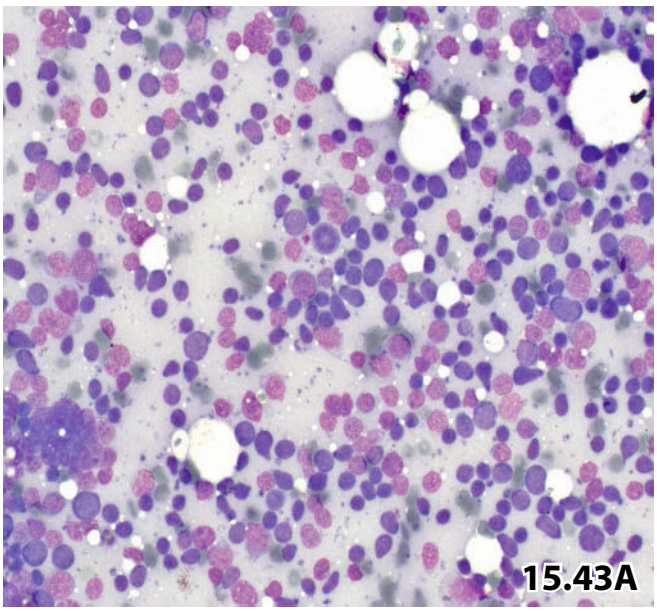
15.43A

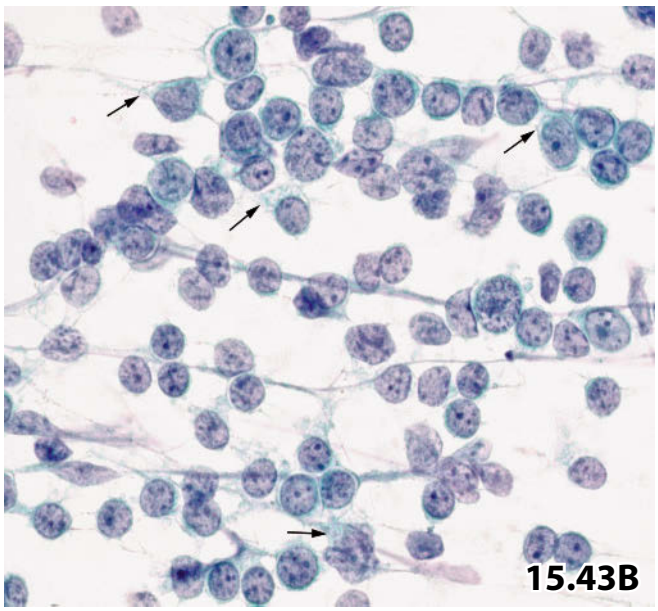
15.43B

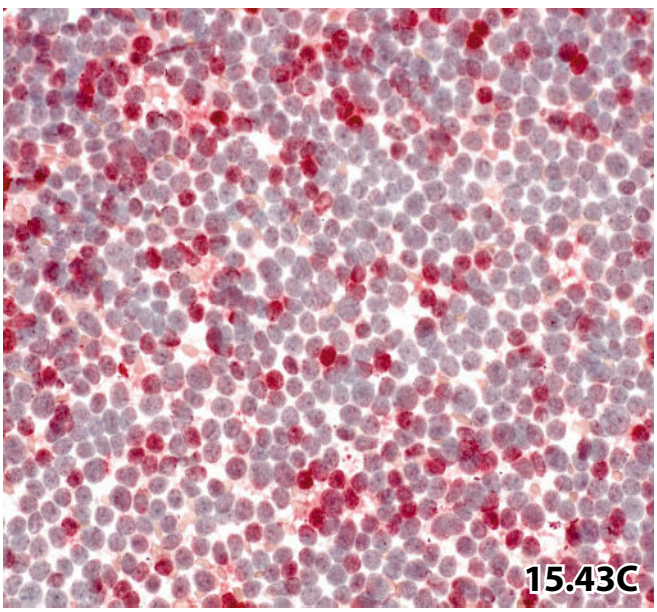
15.43C

**Figs. 15.44–15.49 Small lymphocytic lymphoma.**
The morphology of classic small lymphocytic lymphoma (SLL) and the established tumor variants is explained using fine-needle aspirates from different patients. Varied preparation techniques, staining methods, and immunocytochemical properties are demonstrated.

**Fig. 15.44** (case #1) Classic tumor variant.
Low magnification (direct smear, Pap stain) reveals the uniform appearance of the classic type of small lymphocytic lymphoma. Note in particular:
(1) Slightly enlarged lymphoid tumor cells in comparison to benign small lymphocytes.
(2) Pronounced nucleoli.
(3) Numerous small compact aggregations of the tumor cells.

**Fig. 15.45** (case #2) Classic tumor variant.
High magnification (direct smear, MGG stain) is focused on slightly enlarged and irregular nuclei, pronounced nucleoli and the clumped chromatin. The chromatin texture is comparable to that in nuclei of benign lymphocytes.

**Fig. 15.46** (case #3) Plasmacytoid variant.
This tumor type corresponds to lymphoplasmacytoid immunocytoma under the terms of the Kiel classification scheme. Note the plasmacytoid features (arrows) in the majority of small and intermediate tumor cells, and the coarse chromatin texture in the majority of the tumor cell-nuclei (direct smear, MGG stain, high magnification).

**Fig. 15.47** (case #4) SLL associated with tumor proliferation centers in a direct smear.
Small lymphocytic lymphoma comprising prolymphocytes (arrows) and paraimmunoblasts (arrowheads) that originate from tumor proliferation centers (direct smear, MGG stain).

**Fig. 15.48** (case #5) SLL associated with tumor proliferation centers in a ThinPrep® specimen.
High magnification exhibits numerous prolymphocytes (arrows). A paraimmunoblast is also present (upper left). Compare with Fig. 15.47.

**Fig. 15.49** (case #6) Small lymphocytic lymphoma and immunocytochemistry.
Typical strong expression of the B-cell marker CD23 (Pap-prestained direct smear).

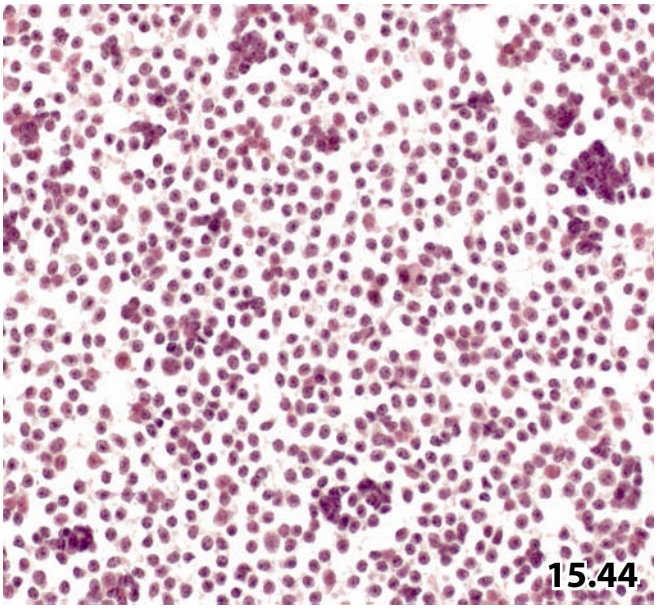
15.44

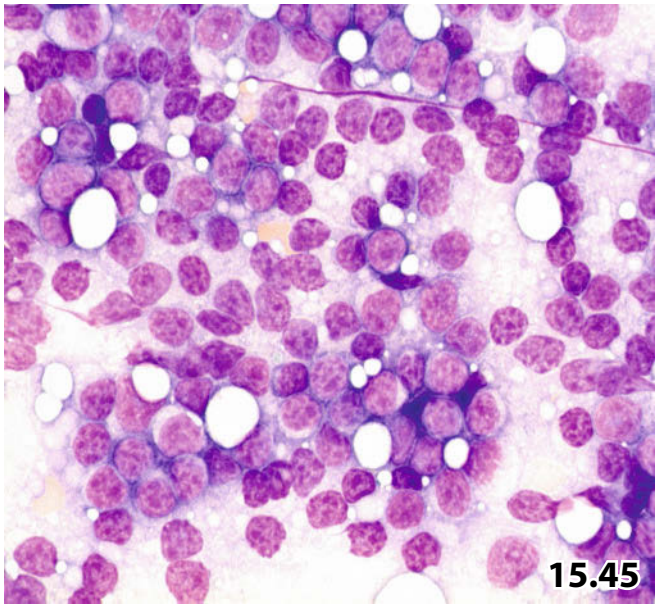
15.45

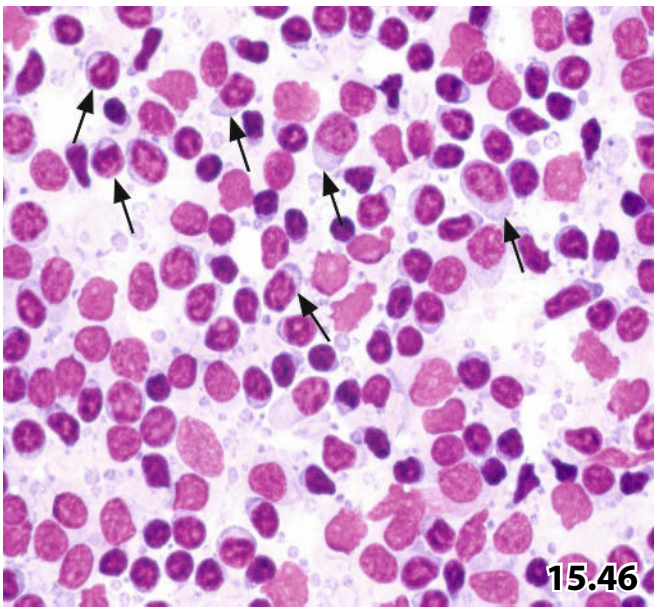
15.46

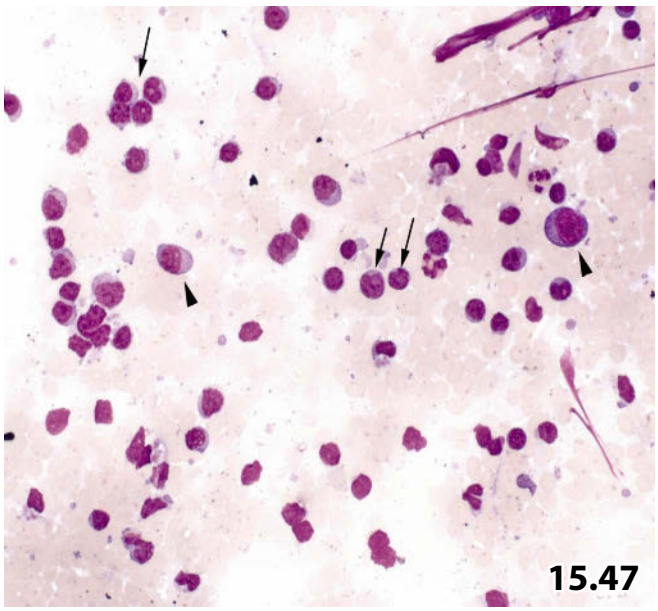
15.47

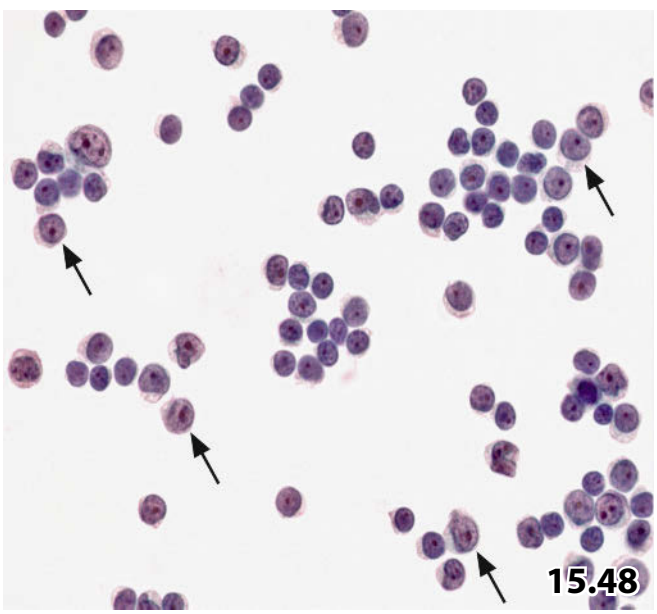
15.48

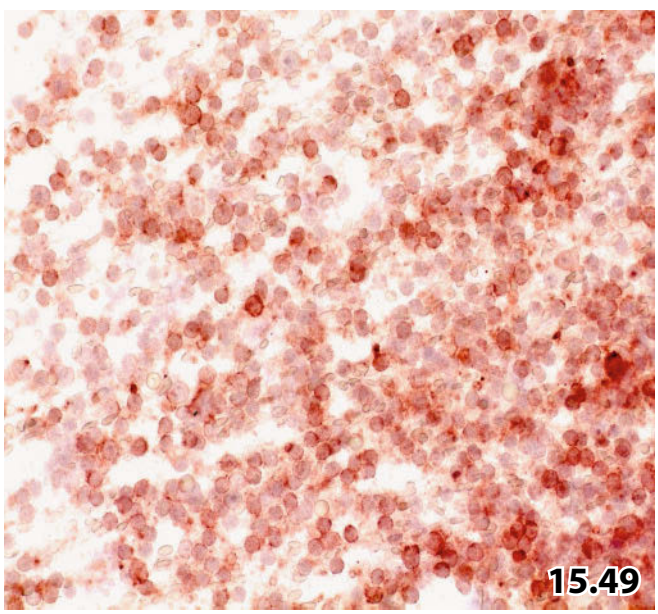
15.49

**Figs. 15.50–15.56 Variants of plasma cell neoplasm.**
Both plasmacytoma of the bone and extraosseous plasmacytoma are presented in FNAB samples from different patients. Tumor variants, varied preparation techniques, varied staining methods, and immunocytochemistry are highlighted. Diagnostic difficulties are reviewed. Each cytologic diagnosis was verified by histology.

**Fig. 15.50** (case #1) Plasmacytoma: mature tumor form.
FNAB of an osteolytic lesion located in the os sacrum. The aspirate reveals a high percentage of mature tumor cells exhibiting plasmacytic features and a few less mature tumor cells (arrow). The cells are scattered in a background composed of blood and small lymphocytes (direct smear, MGG stain, lower magnification).

**Fig. 15.51** (case #2) Plasmacytoma: immature tumor form in a liquid-based specimen.
FNAB of a plasmacytoma located in soft tissues of the shoulder area. A ThinPrep specimen shows less mature tumor cells exhibiting a higher N/C ratio, both coarsely clumped and loose chromatin, more prominent nucleoli, vacuolated less basophilic cytoplasm, and less voluminous eccentric cytoplasm as compared to mature plasmacytic tumor cells (Pap stain, high magnification).

One should always remember that:
1. Cells of plasmacytoma appear smaller both in conventional Pap-stained smears and liquid-based preparations compared to MGG-stained specimens (after air drying).
2. In Pap-stained specimens, the cytoplasm of immature plasma cells usually appears finely granular and vacuolated compared to dense and cyanophilic cytoplasm of mature plasma cells.
3. The cytoplasmic paranuclear clearing frequently appears indistinct in Pap-stained smears (see also Fig. 15.53).

**Fig. 15.52** (case #3) Plasmacytoma: immature tumor form (MGG stain).
An aspirate of a cervical lymph node. High magnification exhibits the same appearance of the tumor cell population as shown in Fig. 15.51, but plasmacytoid features (basophilia and paranuclear clearing of the cytoplasm) perform better in air-dried MGG-stained specimens. Note the mitotic figure at the bottom of the field indicating proliferative activity.

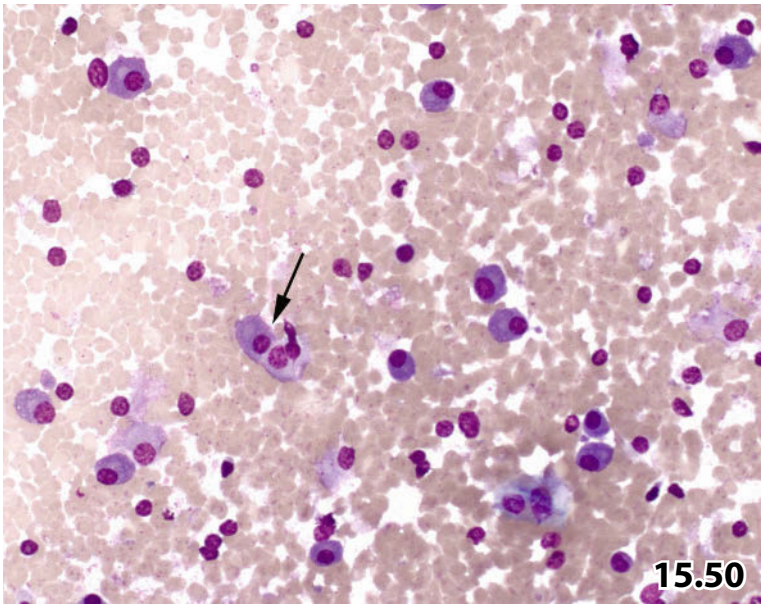
15.50

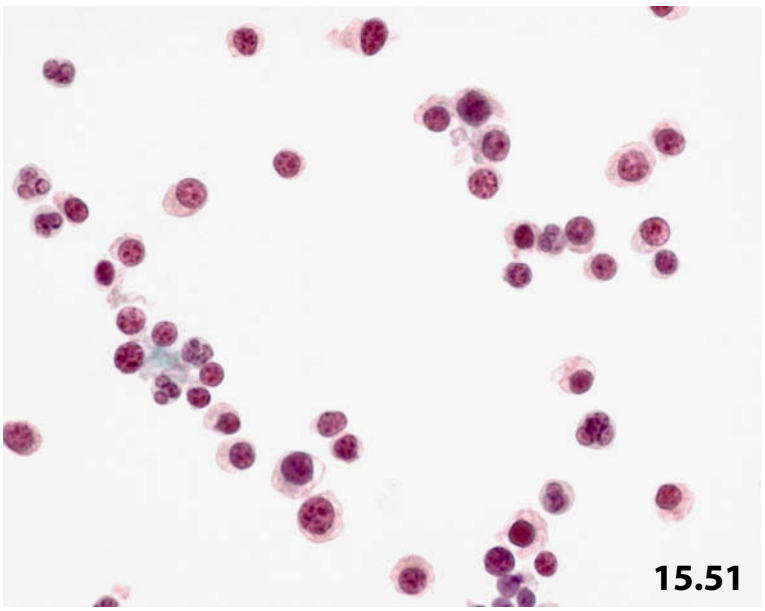
15.51

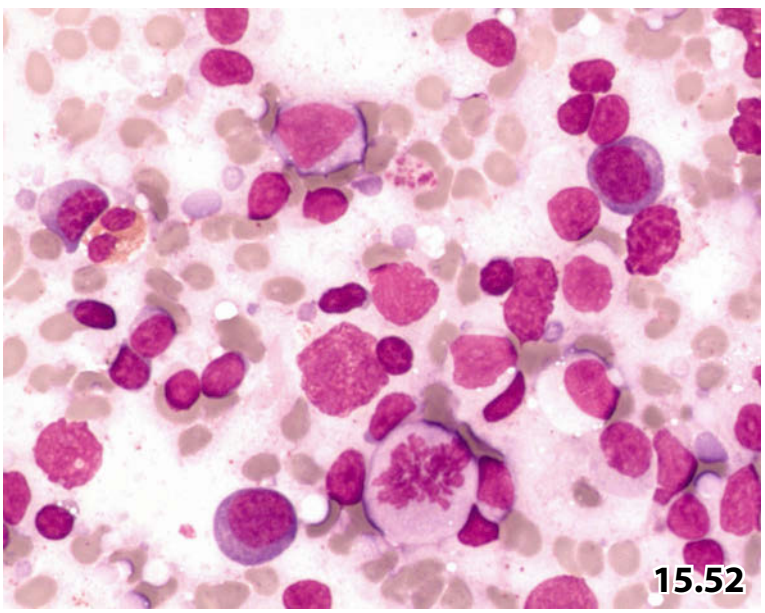
15.52

**Fig. 15.53** (case #4) Plasmacytoma: immature tumor form (Pap stain).
An aspirate of a pleural nodular mass that was associated with disintegration of a nearby rib. Plasmacytoid features are vaguely discernible, and nucleoli are extremely prominent (direct smear, high magnification).

**Fig. 15.54** (case #5) Plasmacytoma: anaplastic tumor form.
An FNAB of the sternum from a patient presenting with a positive history of anaplastic plasmacytoma. Pleomorphic tumor cells with loss of the plasmacytoid features, high mitotic activity, and scarce cell detritus (arrows) (direct smear, Pap stain, high magnification).
*Comment:* The positive history of an anaplastic plasmacytoma made it possible to render a conclusive diagnosis by standard cytology; unlike patients with an uneventful history and/or inadequate clinical information, making cytologic diagnosis challenging.

**Fig. 15.55** (case #6) Plasmacytoma with immunoglobulin inclusion.
High magnification shows a crystalline rod (arrow) incorporated into the cytoplasm of an immature tumor cell (direct smear, MGG stain).

**Fig. 15.56** (case #7) Immature plasmacytoma and immunocytochemistry.
Strong expression of the plasma cell-associated marker CD38 (Pap-prestained direct smear). Note the background immunopositivity frequently occurring in conventional cytologic smears.

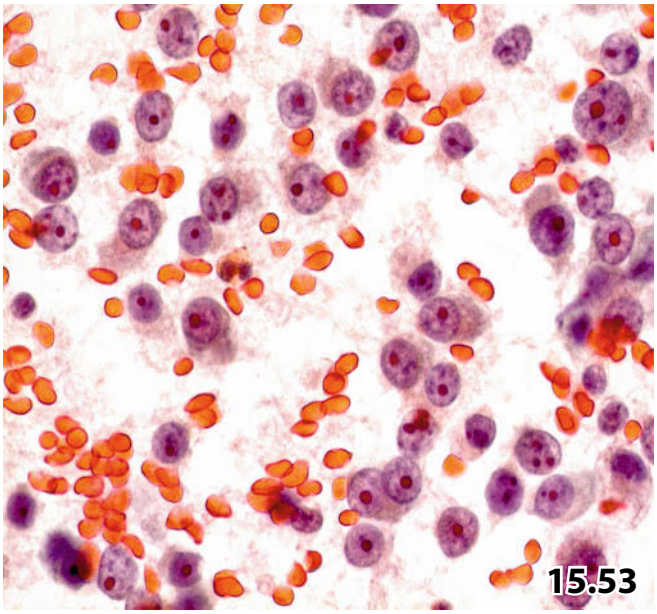
15.53

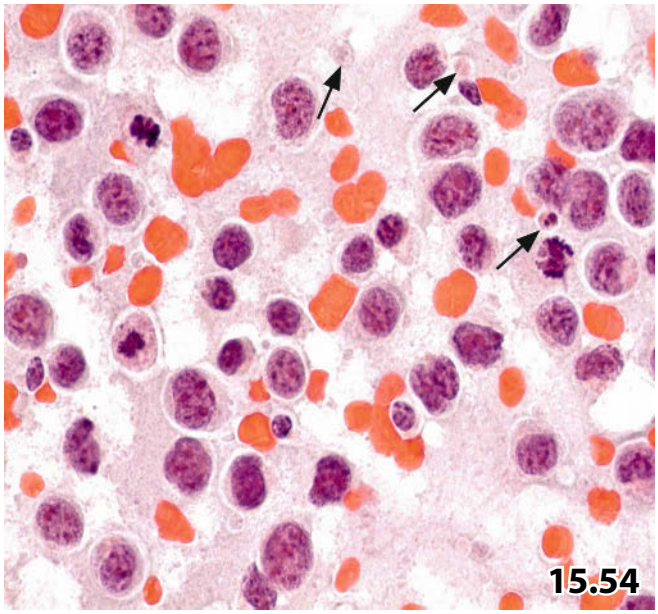
15.54

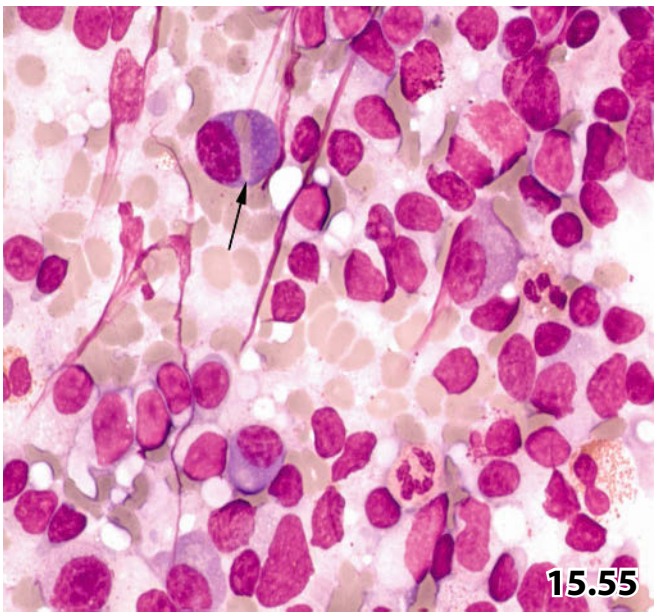
15.55

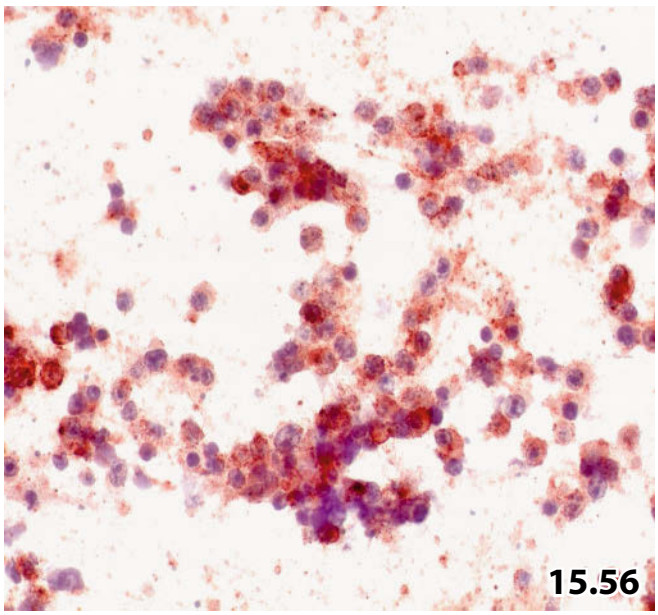
15.56

**Figs. 15.57–15.65 Follicular lymphoma, low-grade and high-grade variant, and diagnostic dilemmas.**
Several patients were selected who revealed a follicular lymphoma (FL) in FNABs of enlarged lymph nodes. In each patient, the diagnosis of FL and its subtype were established previous to the cytologic investigation or were confirmed metachronously by histologic examination of a lymph node. Varied preparation techniques, varied staining methods, immunocytochemical attributes, and diagnostic challenge are presented and discussed.

**Fig. 15.57** (case #1) Low-grade FL (histologically grade 1).
An elderly man presented with polylymphadenopathy. Lower magnification shows a uniform small cell pattern where atypical centrocytes (characterized by irregular nuclei) and small lymphocytes (characterized by dark staining nuclei) predominate (direct smear, MGG stain).

**Fig. 15.58** (case #2) Low-grade FL (histologically grade 2).
It is often difficult to ascertain the cytologic grade of FL in liquid-based preparations (the current specimen has been prepared using the ThinPrep technique), particularly for two reasons:
(1) Enhancement of the nucleoli, with each nucleus exhibiting a single nucleolus or multiple pronounced nucleoli.
(2) Distinguishing between centrocytes and small centroblasts is extremely difficult due to the decreased variability of the cell sizes. (Liquid-based preparation Pap stain, high magnification).

**Fig. 15.59** (case #3) Low-grade FL (histologically grade 2) vs reactive lymphadenopathy.
Physical examination showed an enlarged inguinal lymph node in an elderly female patient. FNAB-direct smears prepared for Pap staining show a heterogenous appearance. The cell population is composed of small, intermediate, and large cleaved and noncleaved cells. It is difficult to distinguish between a reactive lymphoid lesion and low-grade follicular lymphoma. However, the overall cell pattern suggests a lymphoid neoplasm because of the absence of small benign lymphocytes and large cells other than centroblasts (arrows), meaning that all cells may originate from the same cell clone (direct smear, high magnification).

**Fig. 15.60** (case #4) Low-grade FL (histologically grade 2) vs reactive lymphadenopathy.
Relapsing FL in an elderly female patient. Direct smears (FNAB of a cervical lymph node) were air dried and MGG-stained. Cellular appearance is similar to that demonstrated in Fig. 15.59, but faint plasmacytoid cell features and tingible-body macrophages (arrow) definitely mimic reactive lymphadenopathy (high magnification).

**Fig. 15.61** (case #5) Low-grade FL (histologically grade 2) vs mantle cell lymphoma.
History of relapsing FL in a 53-year-old woman. A monomorphic population of centrocytes showing variation in nuclear shape is highly characteristic of low-grade FL. Note compact clustering of tumor cells (upper left and upper right) indicating malignancy (high magnification, direct smear, Pap stain).
*Comments:* In cases with a predominance of centrocytes, mantle cell lymphoma has to be considered in the differential diagnosis. A definite diagnosis requires immunophenotyping and cytogenetic studies.

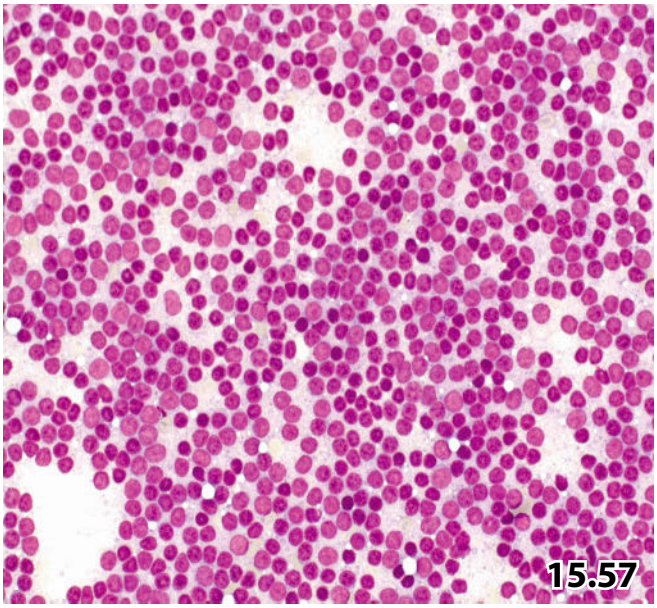
15.57

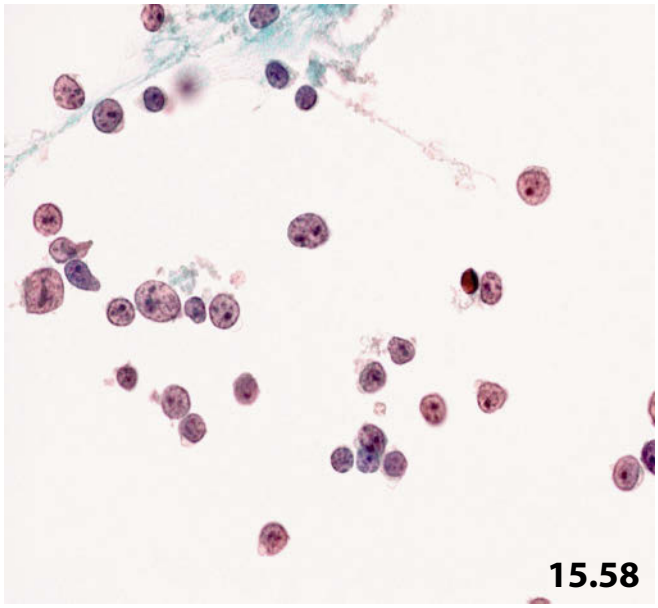
15.58

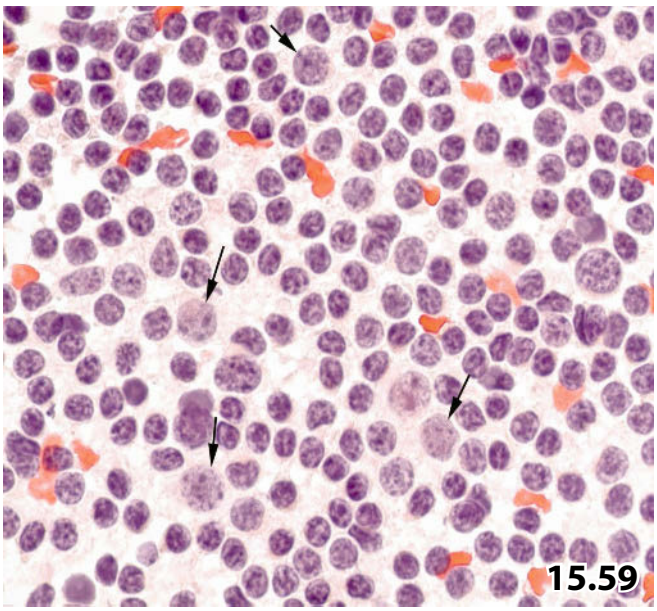
15.59

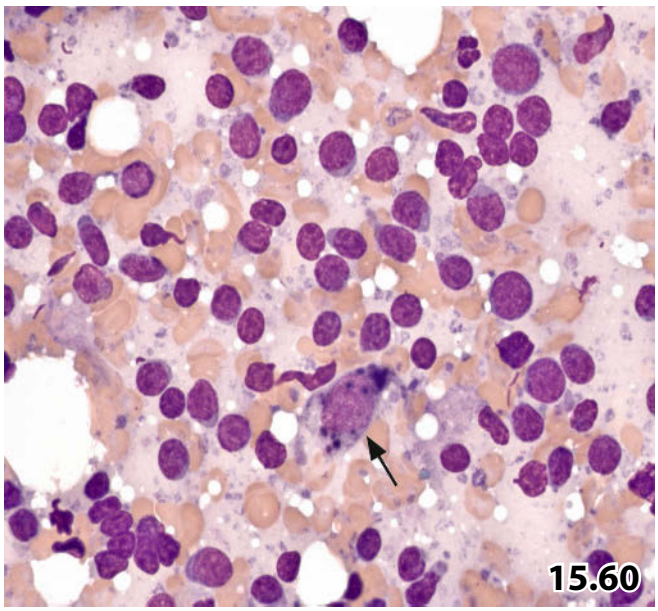
15.60

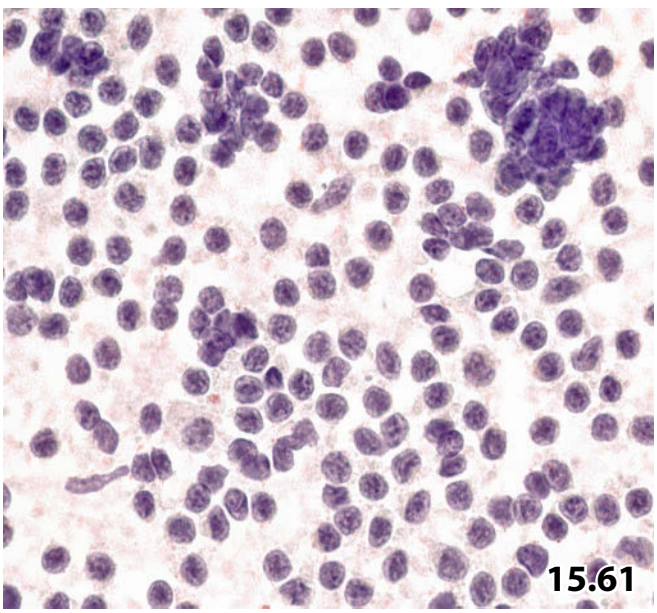
15.61

**Fig. 15.62** (case #6) Intermediate- to high-grade FL (histologically grade 3a).
A patient suffering from relapsing malignant lymphoma. Lower magnification reveals a mixed cell pattern (direct smear, MGG stain). Centroblastic tumor cells (arrows)account for more than 30% of the whole cell population. As a result, cytology suggests high-grade FL.

**Fig. 15.63** (case #7) Low- to intermediate-grade FL (histologically grade 3a) associated with epithelioid histiocytes.
An elderly woman presented with multiple enlarged lymph nodes suggestive of malignant lymphoma. High magnification reveals predominantly atypical centrocytes showing pronounced nuclear cleaving and grooves. A loose aggregate of activated histiocytes occasionally showing epithelioid nuclei (arrows) is also present in this field.

Activated epithelioid cells associated with rounded nuclei and distinct nucleoli can potentially be misinterpreted as blast cells.

**Fig. 15.64** (case #8) High-grade FL (histologically grade 3b) atypical centrocytes vs small blasts.
A middle-aged woman with a history of malignant lymphoma of the tongue presented with enlarged cervical lymph nodes. The cleaved atypical nuclei indicate a malignant lymphoma originating from germinal center cells. According to our experience, it is often difficult to distinguish between medium-sized centrocytes and small centroblasts by standard cytology (direct smear, MGG stain, high magnification).

**Fig. 15.65A, B** (case #9) Low-grade FL, diagnostic impact of lymphocyte immunophenotyping.
A 61-year-old woman with low-grade follicular lymphoma in remission for many years, presented with a nodule located in the left parotid area. Diagnostic consideration includes a tumor of the parotid gland, a reactive lymph node, and relapsing lymphoma. An FNAB was performed, direct smears and ThinPrep specimens were prepared, the latter with the intention of performing immunocytochemical studies (conventional MGG- and Pap-stained cytology is not shown).
*Cytology and immunocytochemistry:* The result of the immunocytochemical work-up classifies the atypical lymphoid population as malignant lymphoma of the B-cell phenotype.
**A** An antibody for the B-cell marker CD20 decorates all medium-sized and large atypical cells (ThinPrep specimen, high magnification). **B** Opposite immunoprofile: the T-cell marker CD3 demonstrates positivity in small benign T-lymphocytes (ThinPrep specimen, high magnification).

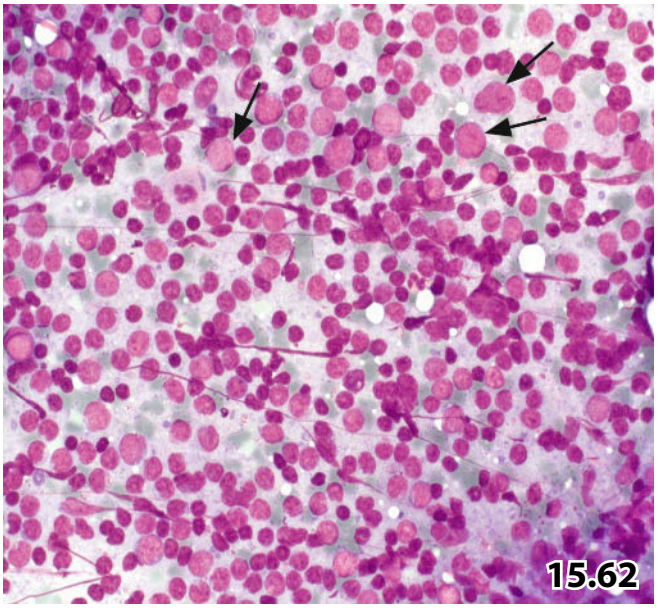
15.62

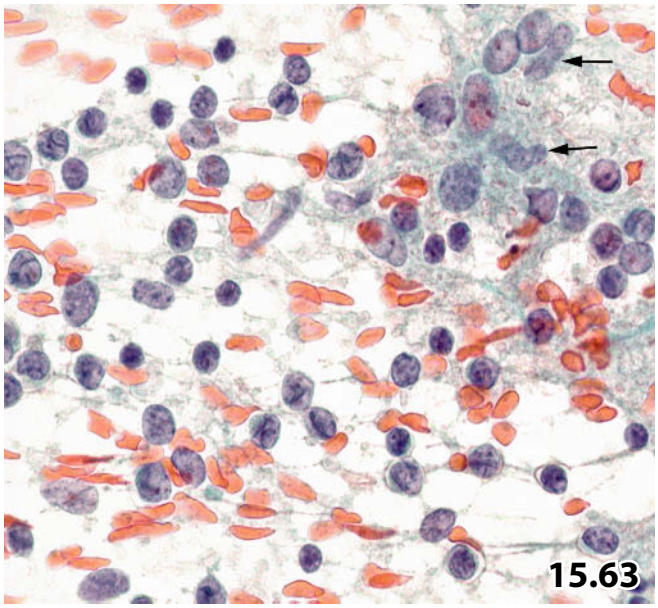
15.63

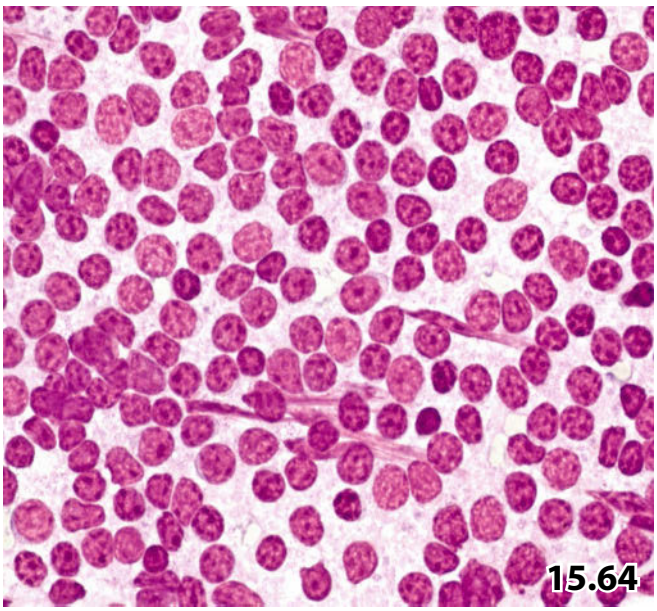
15.64

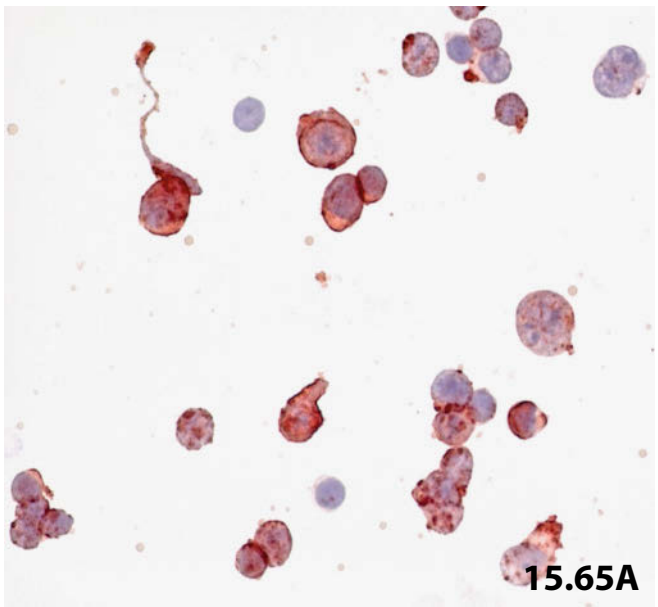
15.65A

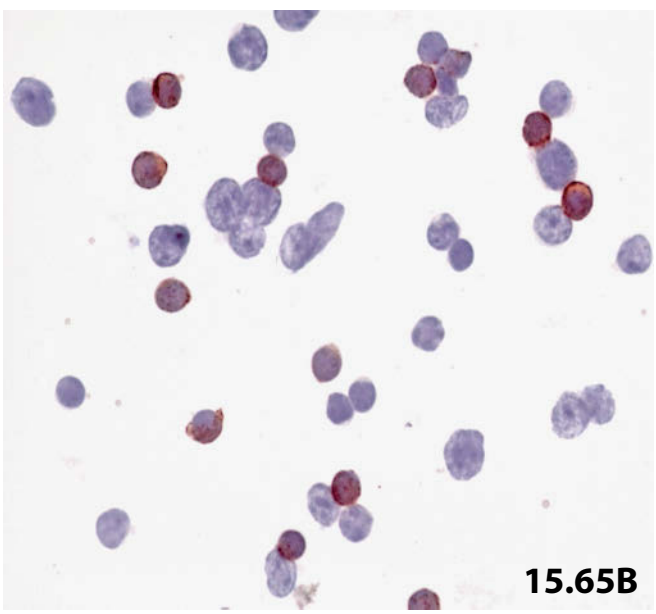
15.65B

**Fig. 15.66 and 15.67 Mantle cell lymphoma: classic cytologic features.**
FNAB on two patients presenting with enlarged lymph nodes. The direct smears show the classic cell features of mantle cell lymphoma.

**Fig. 15.66** (case #1) Lower magnification of an MGG-stained direct smear exhibits uniform appearance. Note nuclear irregularity, inconspicuous nucleoli, and a few apoptotic cells (arrows).

**Fig. 15.67** (case #2) High magnification focuses on (1) variability in cell size, (2) pronounced irregularities of nuclear outline, (3) chromatin texture, and (4) usually indistinct nucleoli (Pap staining). Compare tumor cell morphology with that of a histiocyte (upper right).

**Figs. 15.68 and 15.69 Mantle cell lymphoma and immunocytochemistry.**
A patient with a positive history of mantle cell lymphoma presented with a mass in the soft tissue of his upper arm. FNAB was performed and liquid-based method was applied with the intention of immunocytochemical investigations. Conventional cytology is not shown, but selected immunostains are demonstrated:

**Fig. 15.68A** Tumor cells strongly express CD43 by immunolabeling (lower magnification, ThinPrep specimen). **B** Immunopositivity for Cyclin D1 is distinct (ThinPrep specimen, lower magnification, ).

**Fig. 15.69** A minor proportion of the tumor cell nuclei stain positive for MIB-1. Proliferation index: 12% (ThinPrep specimen, high magnification).

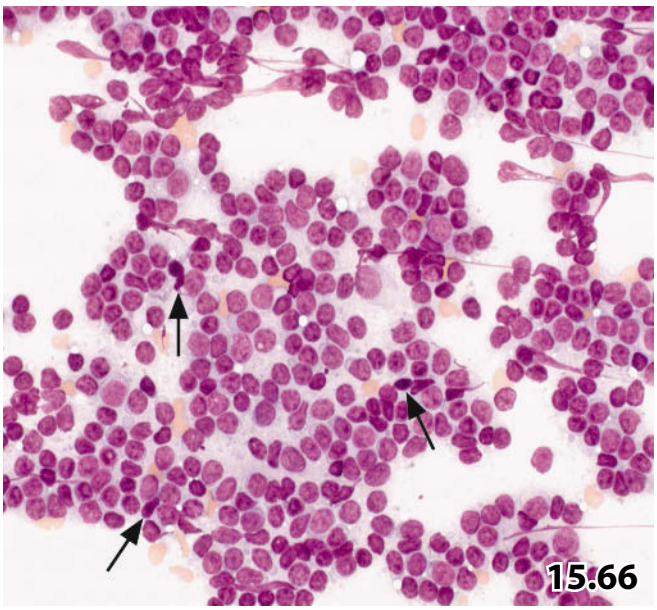
15.66

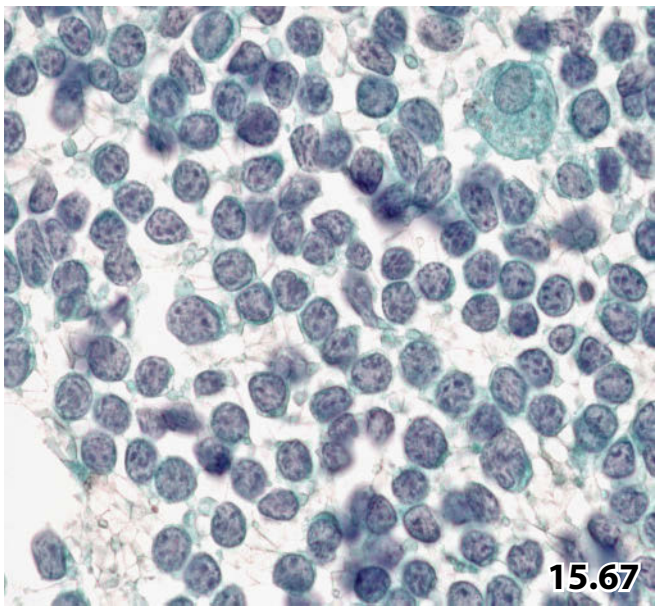
15.67

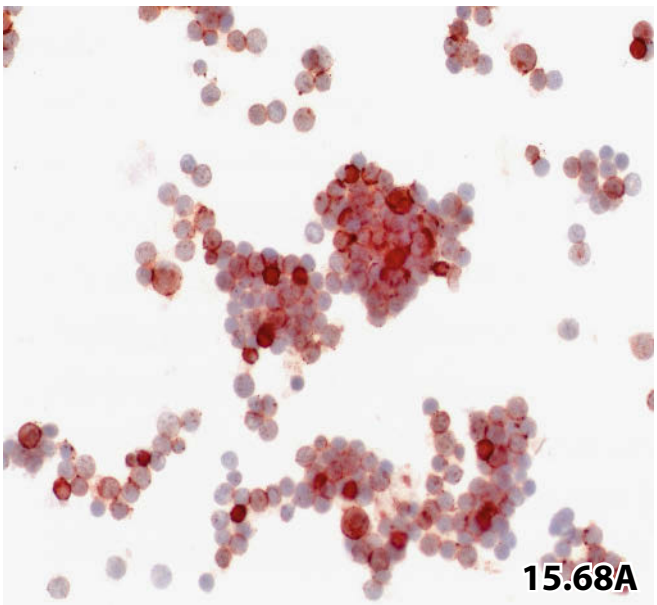
15.68A

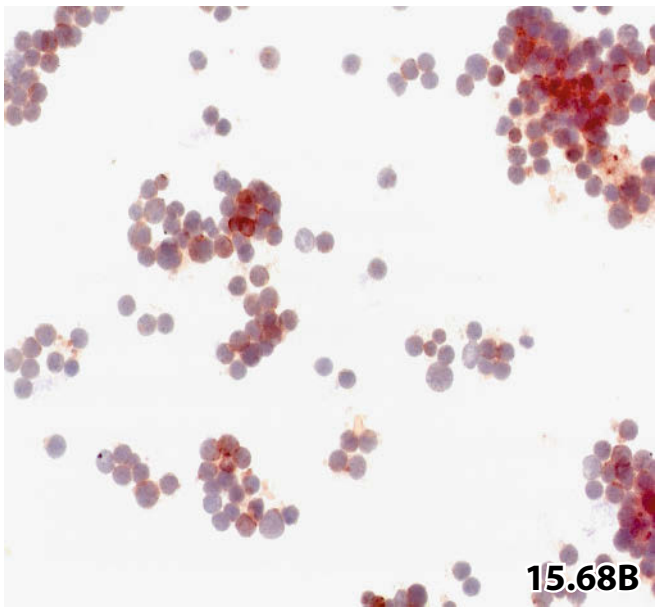
15.68B

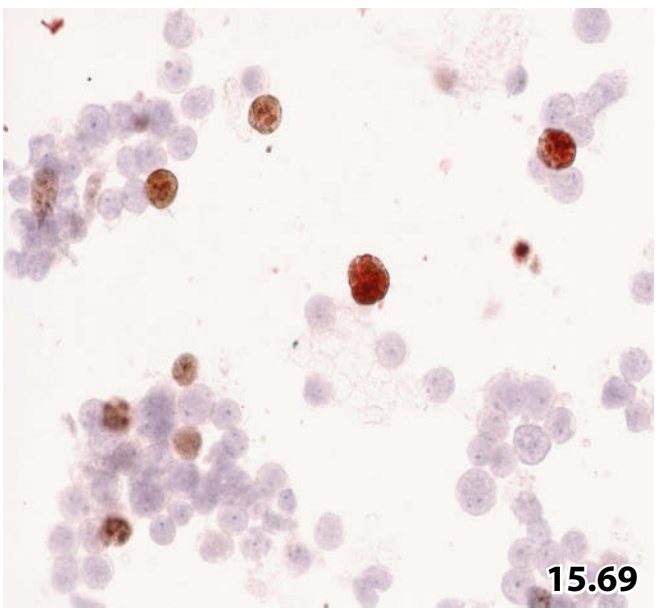
15.69

**Figs. 15.70 and 15.71 Nodal marginal zone lymphoma.**
These two cases of marginal zone lymphoma in lymph node aspirates emphasize the difficulties in both assessing malignancy and proper subtyping by standard cytology.

**Fig. 15.70** (case #1) A 62-year-old woman presented with a solitary lymph node at her neck (a specific clinical history was not available). Direct FNAB smears were prepared for both Pap-staining and May-Grünwald-Giemsa-staining (the latter is not shown). Low magnification shows a mixed cell population comprising small and medium-sized lymphoid cells, occasional large transformed cells, histiocytes, monocytoid cells, and a tingible-body macrophage. Distinct cellular atypias are not identifiable, at neither low nor high magnification (Pap stain).
*Cytologic misdiagnosis:* Reactive lymphadenopathy.
*Tissue diagnosis* (lymph node excision biopsy): Low-grade non-Hodgkin lymphoma of the B-cell phenotype, most likely marginal zone lymphoma.

**Fig. 15.71** (case #2) A healthy 70-year-old woman detected a solitary lymph node at the right side of her neck. FNAB was performed, both direct smears and liquid-based specimens were prepared. A more pronounced cellular polymorphism is obvious compared with the preceding case: blasts account for a high fraction of the whole cell population, and medium-sized lymphoid cells exhibit distinct atypias (irregular nuclei, dense granular chromatin, polymorphic nucleoli) (arrows), but numerous tingible-body macrophages are also present (lower left and lower right) (direct smear, Pap stain, high magnification). A high percentage of the cells expressed B-cell markers, and immunostaining for MIB-1 revealed an extremely low proliferation index (immunostains are not shown).
*Cytologic diagnosis:* Low-grade malignant non-Hodgkin lymphoma of the B phenotype. A further subtyping is not possible.
*Tissue diagnosis* (lymph node excision biopsy): Nodal marginal zone lymphoma, low grade.

**Fig. 15.72A, B Hairy cell leukemia.**
Image-guided FNAB of retroperitoneal lymph nodes in a man with a long history of hairy cell leukemia. Direct smears were Pap-stained. **A** Higher magnification shows small lymphoid cells with mild nuclear irregularities, homogeneous chromatin, and occasional distinct nucleoli. Please note particularly the pale cytoplasm (arrows) and hair-like cytoplasmic protrusions (arrowheads). **B** Positive immunostaining for DBA44 makes the particular cytoplasmic tails of the tumor cells clearly visible (Pap-prestained direct smear).

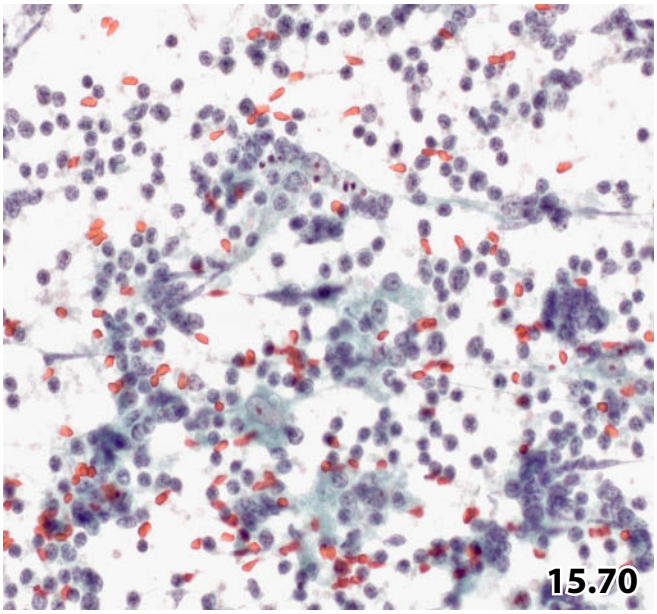

15.70

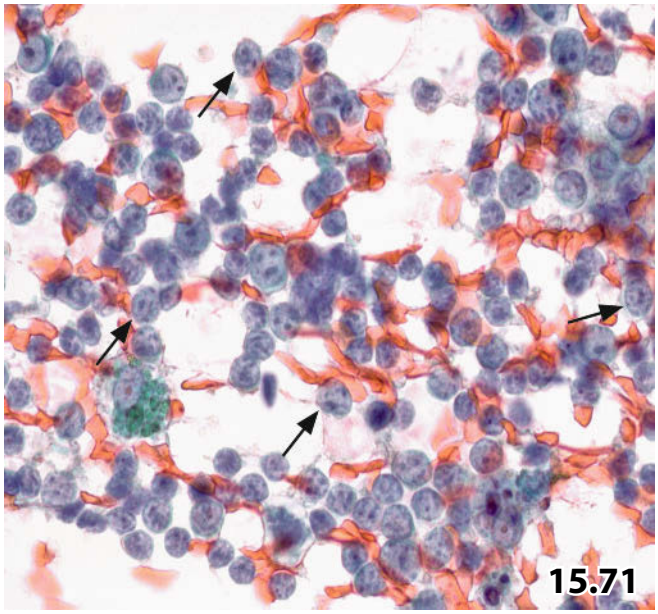

15.71

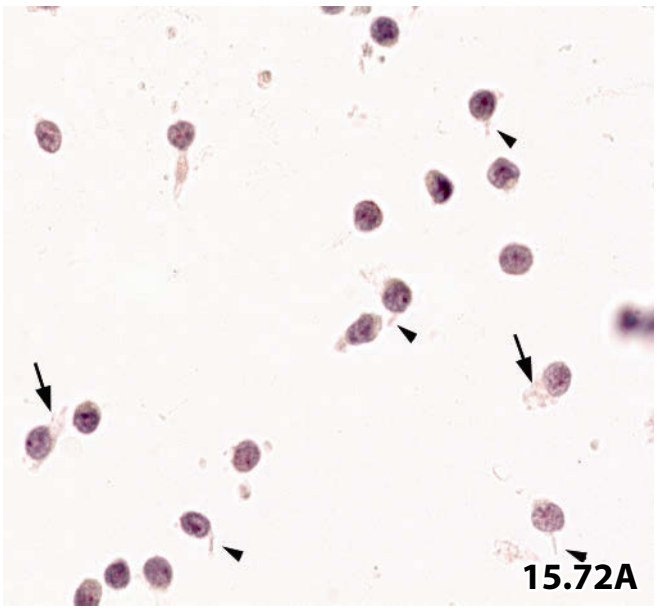

15.72A

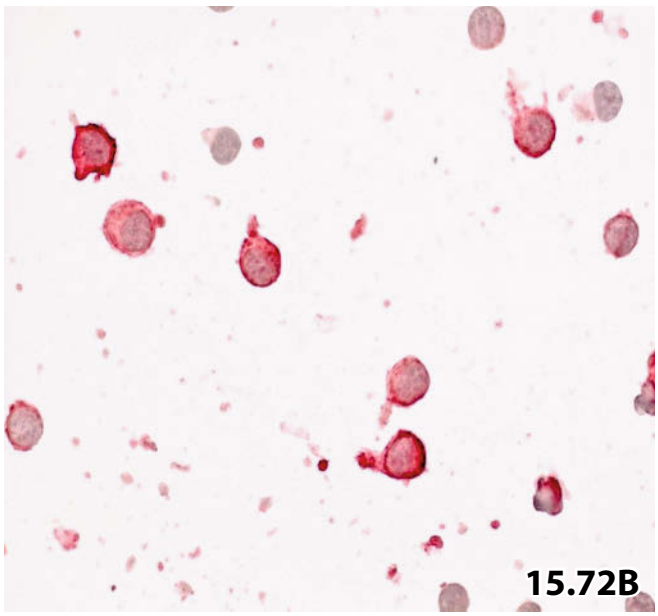

15.72B

**Figs. 15.73–15.76 Diffuse large B-cell lymphoma: centroblastic variant.**
Four cases illustrate the varied phenotypes of centroblastic diffuse large B-cell lymphoma (DLBCL) in terms of the diagnostic challenges. Direct smears were prepared for MGG and Pap stain.

**Fig. 15.73** (case #1) A 46-year-old man with a recent diagnosis of high-grade NHL; complete tumor staging was performed with multiple FNABs. High magnification shows a fairly monotonous appearance of the cell population composed of large neoplastic cells exhibiting irregular nuclear outline, occasional lobated nuclei, and an extremely high N/C ratio (MGG stain).
*Cytologic diagnosis:* Blastic large-cell NHL.
*Histology* provided definite subtyping (DLBCL, centroblastic variant).

**Fig. 15.74** (case #2) A 74-year-old woman presented with clinical symptoms suggesting malignant lymphoma. Initial FNAB of an enlarged lymph node was performed. The same cellular features as demonstrated above are readily identified in a Pap-stained smear (lower magnification). Note evenly dispersed fine chromatin, distinct nucleoli usually shifted to the inner surface of the nuclear membrane, amorphous background debris, and several starry-sky macrophages (lower right). In this setting, macrophages indicate substantial tumor necrosis.
*Cytologic diagnosis:* High-grade large-cell B-cell lymphoma, most probably DLBCL of the centroblastic variant.
*Tissue diagnosis* (lymph node excision biopsy): Diffuse large B-cell lymphoma, centroblastic variant.

**Fig. 15.75** (case #3) DLBCL comprising a major proportion of hyperplastic T lymphocytes. A 40-year-old man presented with enlarged cervical lymph nodes. FNAB was performed and direct smears were prepared for Pap stain. The admixture of a high proportion of benign (but activated) lymphocytes can give rise to diagnostic dilemmas: activated T lymphocytes are enlarged, exhibiting small but distinct nucleoli (arrows); in addition, the field contains histiocytes and a single large malignant cell (upper right). Epithelioid histiocytes were also present but are not shown (lower magnification).
*Tentative cytologic diagnosis:* Overall cell pattern suggests lymphocyte-rich Hodgkin lymphoma or non-Hodgkin lymphoma of the mixed cell type. Histologic examination is required for a definite diagnosis and tumor typing.
*Tissue diagnosis* (lymph node excision biopsy): T-cell-rich DLBCL, centroblastic variant.

**Fig. 15.76** (case #4) DLBCL exhibiting a variegated appearance.
A 68-year-old male patient with a history of gastric DLBCL presented with enlarged cervical lymph nodes. The patient was referred to FNAB, direct smears were MGG-stained. The extremely heterogeneous microscopic appearance mimics reactive lymphoid hyperplasia. The cell population consists of small lymphocytes, medium-sized atypical lymphoid cells (arrows), lymphoblasts (arrowheads), and tingible body macrophages (a single cell, lower left).
*Cytology:* Together with the clinical history, the correct diagnosis of DLBCL could easily be established by standard cytology.

> *Comment:* One should be aware that the cell pattern presented here can give rise to diagnostic confusion in cases with an uneventful patient history and/or inadequate clinical information. The cellular pattern most likely suggests mononucleosis infectiosa.

*Tissue diagnosis* (lymph node excision biopsy): DLBCL, centroblastic variant.

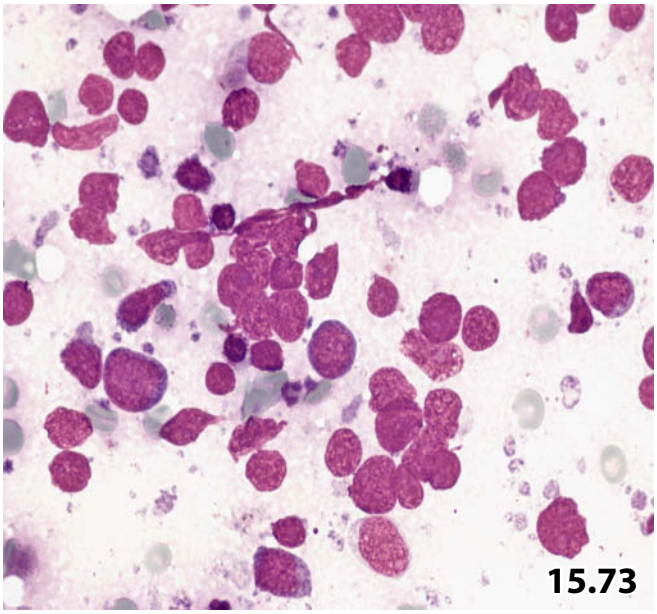
15.73

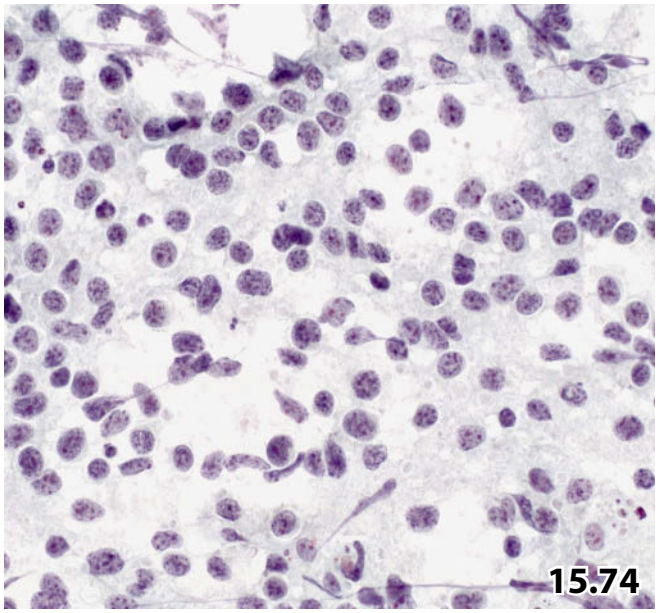
15.74

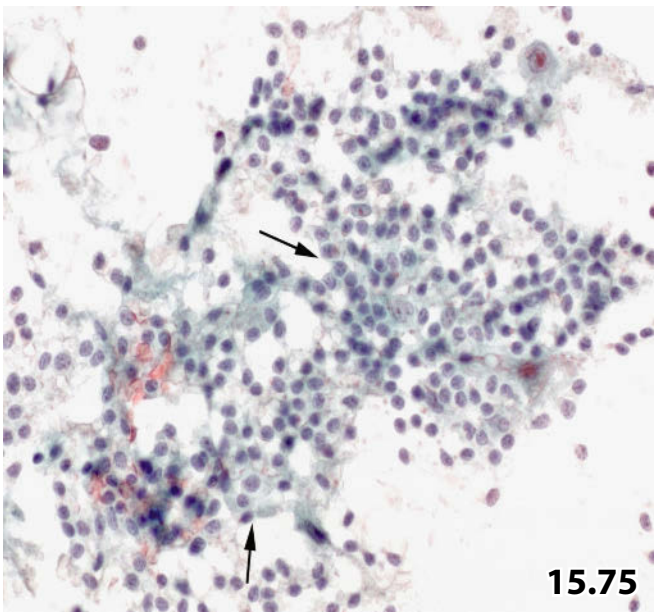
15.75

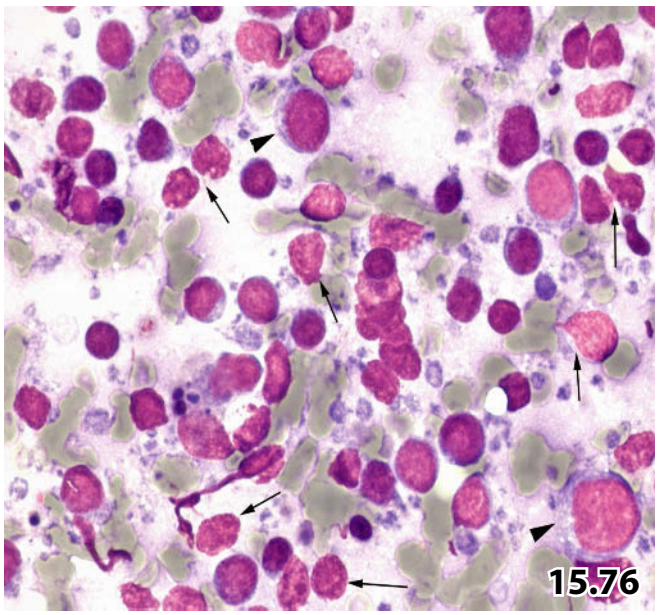
15.76

**Fig. 15.77 Diffuse large B-cell lymphoma: immunoblastic variant.**
Image-guided FNAB of a retroperitoneal mass in an 71-year-old man. Direct smears were Pap-stained. Immunoblast-like neoplastic cells dominate the smear pattern. Mitotic activity (lower right) and background detritus are obvious (high magnification).
*Cytology:* An accurate cytologic diagnosis was not possible due to unavailable immunocytochemical studies. Blastic NHL and large-cell carcinoma were assumed. Repeated FNAB or surgical biopsy had been recommended.
*Comment:* The cells exhibiting huge, frequently centrally positioned nucleoli are compatible with immunoblasts.
*Histologic diagnosis* (surgical biopsy of the retroperitoneal tumor): DLBCL, immunoblastic variant.

**Fig. 15.78A, B Diffuse large B-cell lymphoma: anaplastic variant.**
A 69-year old man with a history of testicular large-cell non-Hodgkin lymphoma, NOS, presented with a recently detected enlarged cervical lymph node. FNAB of the lymph node was performed; direct smears and liquid-based preparations were prepared for Pap stain.
*Cytologic/ immunocytochemical diagnosis:* Large B-cell NHL, anaplastic subtype.
*Tissue diagnosis:* DLBCL, centroblastic and anaplastic variant.
**A** High magnification shows pleomorphic malignant cells (conventional smear, Pap stain). Abundant vacuolated cytoplasm and loose cell aggregation give rise to difficulties distinguishing between blastic lymphoma and anaplastic carcinoma. **B** Immunostaining for the B-cell marker CD20 clearly decorates all neoplastic cells, both isolated and grouped. Thus, carcinoma can be excluded by cytology (Pap-prestained ThinPrep specimen, lower magnification).

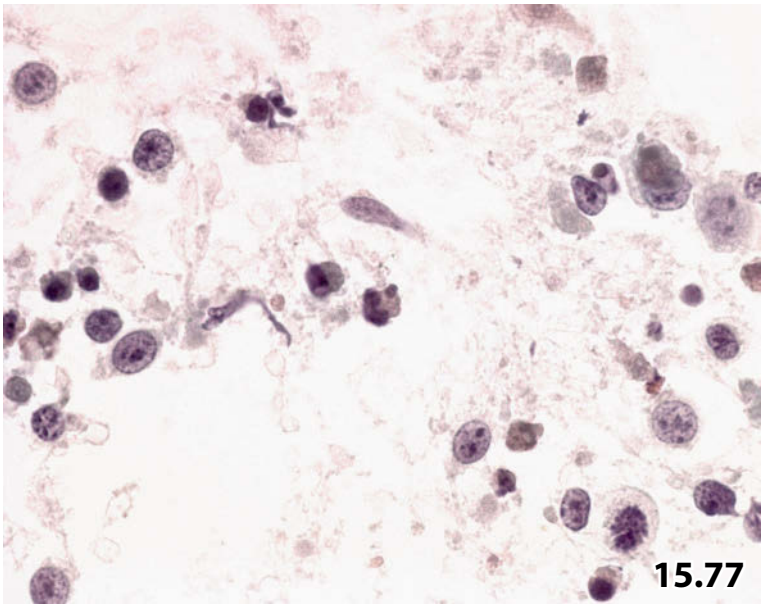

15.77

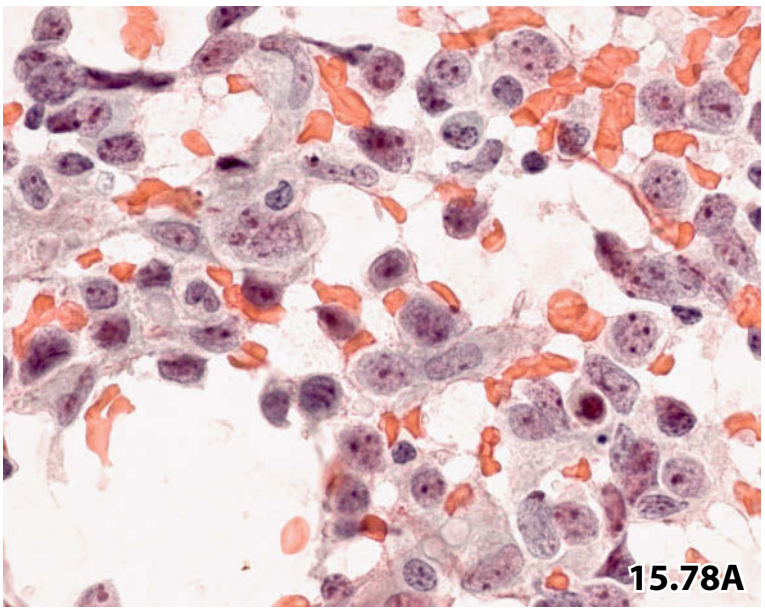

15.78A

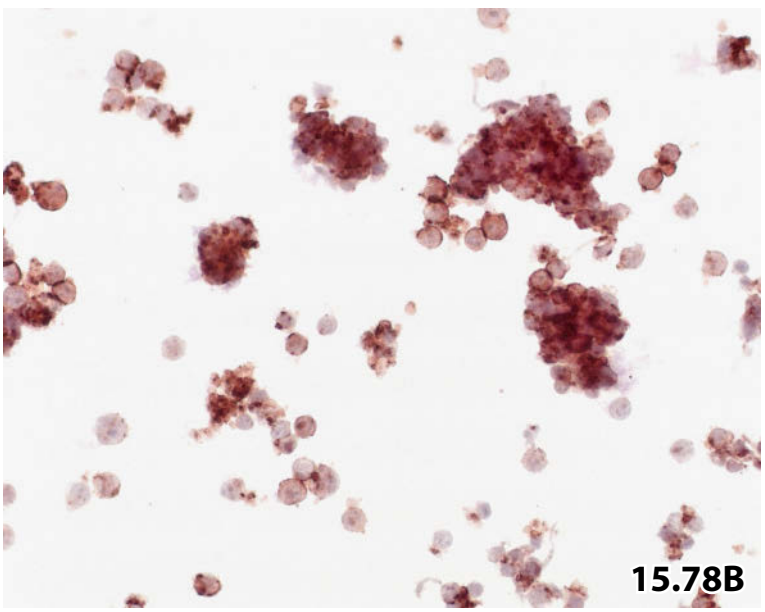

15.78B

**Figs. 15.79 and 15.80 Cytologic features of classical Burkitt lymphoma.**
FNAB of inguinal lymph nodes in two middle-aged patients. Both patients had no specific personal history.
*Cytologic diagnosis:* Burkitt lymphoma (confirmed by histologic examination in both patients).

**Fig. 15.79** (case #1) Lower magnification demonstrates a monotonous cell pattern and loose aggregations of the blastic tumor cells. Note the sharply outlined vacuoles embedded in a deeply basophilic cytoplasm (direct smear, MGG stain). Generally, cytoplasmic key features are much better displayed in MGG-stained specimens than Pap-stained smears.

**Fig. 15.80** (case #2) Irregularities of the nuclear membrane, characteristic chromatin texture, and nucleoli are perfectly expressed using the Papanicolaou staining procedure. Numerous tingible body macrophages are also present (lower right) (direct smear, high magnification).

**Fig. 15.81 T lymphoblastic lymphoma.**
An elderly man with a positive history of relapsing lymphoblastic NHL presented with an enlarged lymph node at his neck. Immunocytochemically, nearly 100% of the tumor cells express the T-cell marker CD3 determining T-cell lineage of the lymphoma (FNAB, Pap-prestained direct smear). Cytomorphologic features of lymphoblastic lymphoma are demonstrated in Fig. 15.43A and 15.43B by means of MGG and Pap staining.

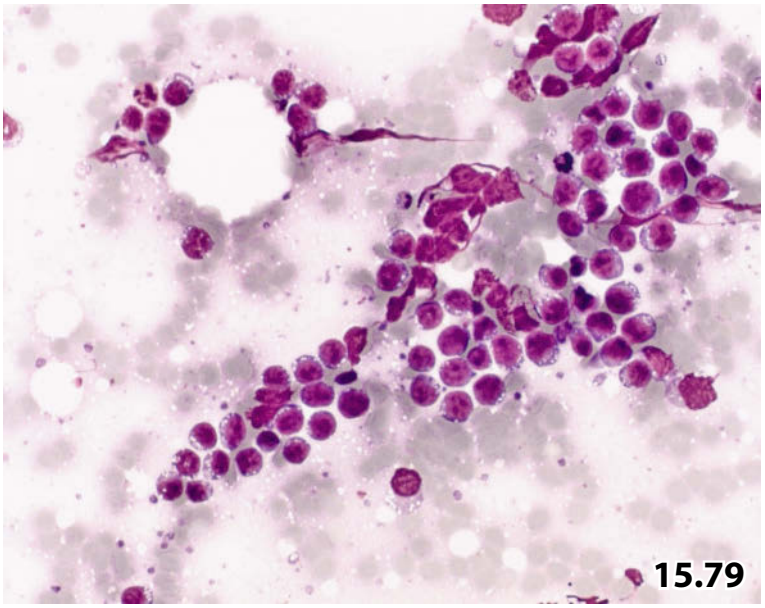
15.79

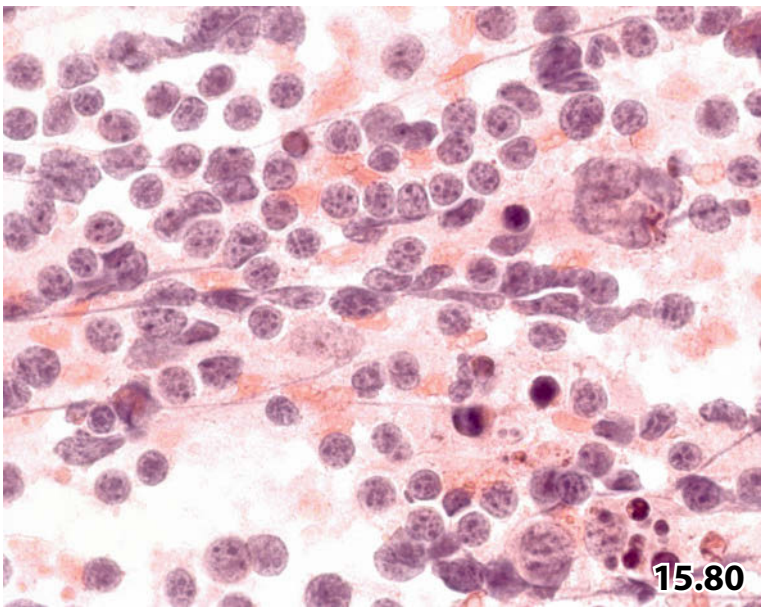
15.80

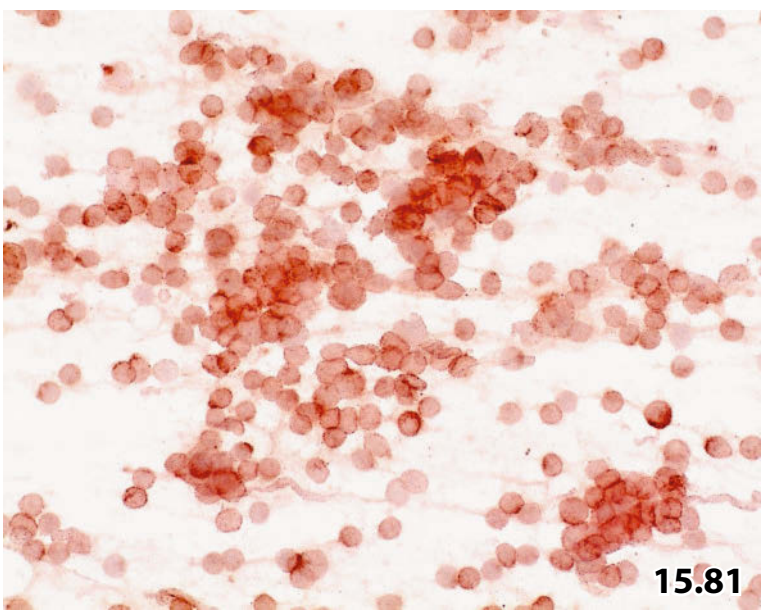
15.81

**Figs. 15.82–15.84 Peripheral T-cell lymphoma.**
FNABs of peripheral lymph nodes from three different patients afflicted with peripheral T-cell lymphoma. Initial aspiration of the lymph nodes was followed by excisional biopsy and histologic examination. Direct smears were prepared from material of the aspirates for MGG and Pap stains. Tumor variants, typical cytologic features, and diagnostic considerations are discussed.

**Fig. 15.82A, B** (case #1) A 75-year-old man presented with enlarged axillary lymph nodes. Initial FNAB was performed.
*Tentative cytologic diagnosis:* Most likely malignant NHL. Epithelioid cell-rich Hodgkin lymphoma, among other lesions, should be considered in this setting.
*Discussion:* The heterogeneous appearance of the cell population may mimic a benign lymphoid hyperplastic lesion, but pronounced nuclear polymorphism, dense and granular chromatin, hyperchromasia, and compact cell clustering favor malignancy. Histologic examination is essential in order to exclude reactive lymphadenopathy.
*Tissue diagnosis:* Peripheral T-cell lymphoma.
**A** A heterogeneous cell pattern is disclosed at lower magnification. The cell population is composed of small lymphoid cells, medium-sized atypical cells (small arrows), cells showing plasmacytoid features (large arrows), and histiocytes (arrowheads). Tingible body macrophages are also present (left) (MGG stain). **B** High magnification again exhibits cellular heterogeneity (MGG stain) including active epithelioid histiocytes (top).

**Fig. 15.83** (case #2) T-cell NHL, small-cell variant.
A 38-year-old woman presented with enlarged lymph nodes and pleural effusion. Initial FNAB of an inguinal nodule. A peripheral T-cell lymphoma of the monomorphic small-cell variant (compare nuclear size of tumor cells with red blood cells and neutrophils) is pictured at high magnification. Note the characteristic chromatin and nuclear irregularities (direct smear, MGG stain).
*Cytologic/ cytochemical diagnosis:* T-cell NHL, small-cell variant. A cytochemical test verified the T-phenotype of the lymphoma cells providing dot-like acid phosphatase activity (not shown). Subsequent histologic studies are not available.



**Fig. 15.84** (case #3) T-cell lymphoma, large-cell pleomorphic variant.
A middle-aged male patient with a history of long-standing T-CLL presented with an enlarged submandibular lymph node. Initial aspiration of the lymph node was performed in order to confirm tumor relapse. High magnification is focused on nuclear abnormalities (molding, indentations, grooves) that are pathognomonic for the vast majority of malignant T lymphocytes. The lymphoid cells exhibit the T-cell marker CD3 by immunolabeling (not shown) (direct smear, Pap stain).
*Cytologic/ immunocytochemical diagnosis:* T-cell lymphoma, large tumor cell variant.
*Tissue diagnosis:* Pleomorphic NHL of the T-cell phenotype.

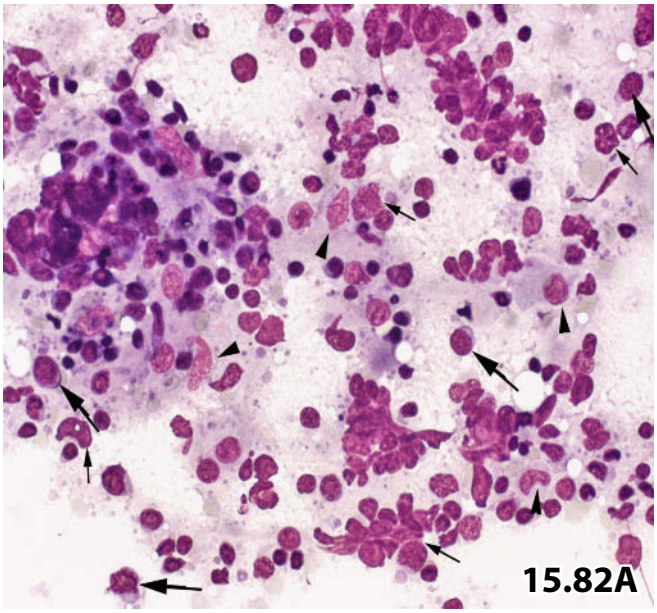
15.82A

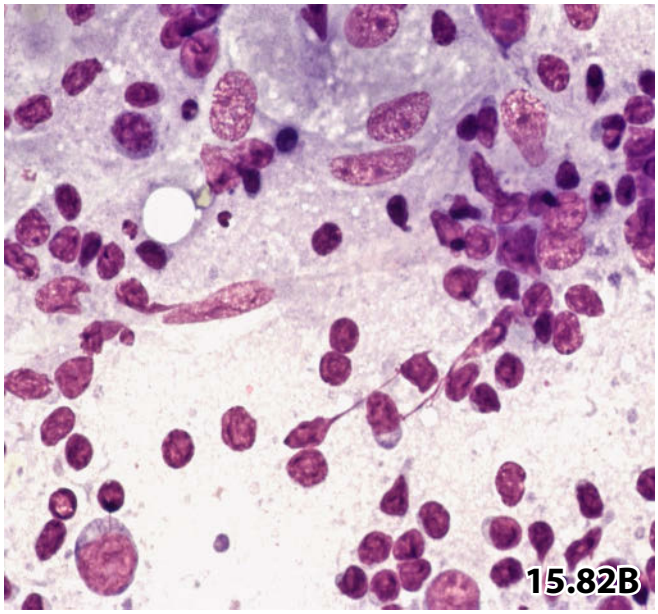
15.82B

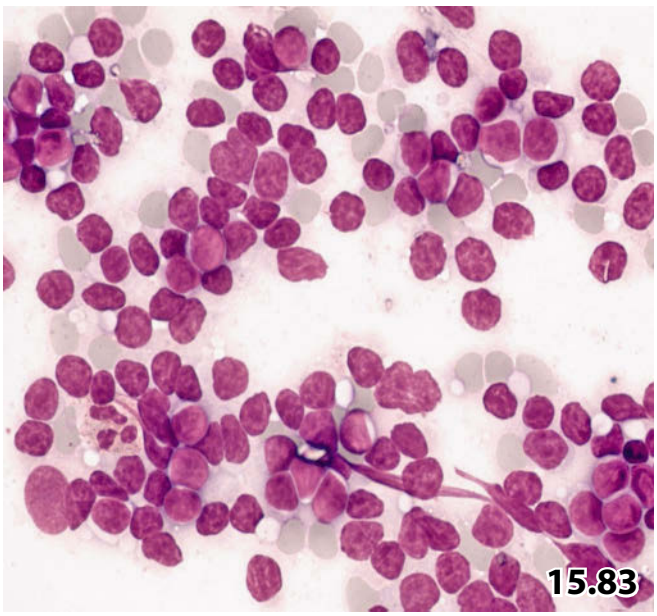
15.83

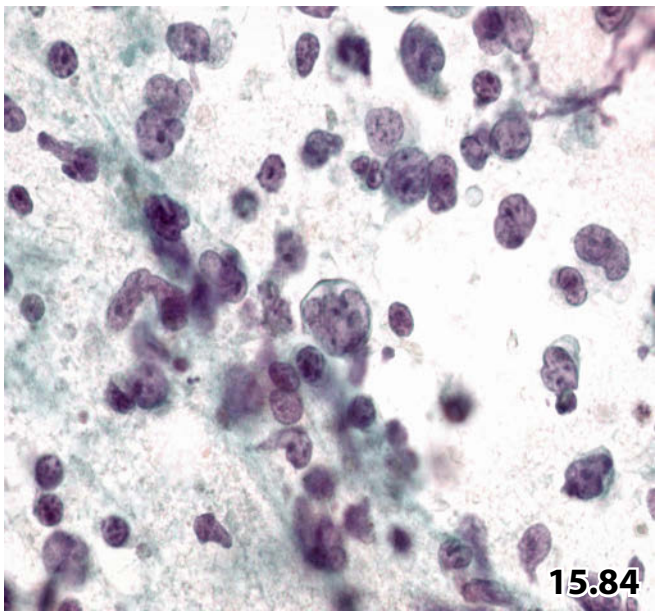
15.84

**Figs. 15.85 and 15.86 Angioimmunoblastic T-cell lymphoma.**
We present two examples of angioimmunoblastic T-cell lymphoma (AILD-T) from two different patients. FNAB of enlarged lymph nodes was performed; the overall cell appearance primarily suggested reactive lymphadenopathy in both patients.

**Fig. 15.85A–C** (case #1) A 72-year-old man presented with enlarged axillary lymph nodes, with no specific clinical history. Primary FNAB was performed. Direct smears were prepared for MGG and Papanicolaou stains.
*Tentative cytologic diagnosis:* Diagnostic considerations comprised reactive lymphoid lesion, angioimmunoblastic lymphoma, and other variants of NHL.
*Comment:* We would like to emphasize that careful evaluation of the cytologic specimens will usually reveal scattered tumor cells with distinct features indicating AILD-T.
*Postmortem histologic diagnosis:* Disseminated AILD-T.
**A** A distinct heterogeneous cell population is shown at lower magnification (MGG stain). The typical tumor cells (arrows) clearly differ from inflammatory cells (an immunoblast, a plasma cell, an eosinophilic granulocyte, and a histiocyte are marked by arrowheads). **B** The details of angioimmunoblastic T-lymphoma cells are shown at high magnification (arrows) (MGG staining). **C** Low magnification displays a soft tissue fragment comprising hyalinized capillary-sized vessels (arrows) (Pap stain).

**Fig. 15.86** (case #2) Another key feature of AILD-T is shown at lower magnification: a loose aggregate of reticulum cells interspersed by atypical lymphoid elements (arrow). In addition, numerous tumor cells occur isolated or crowded together(right) (direct smear, Pap stain).

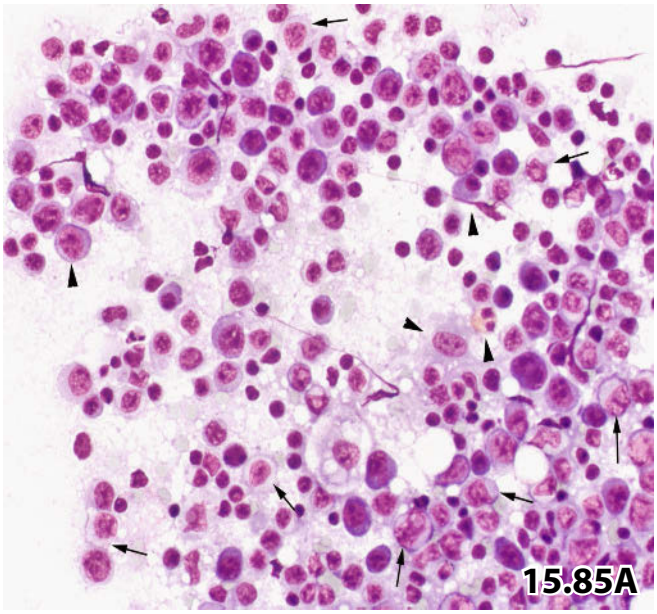
15.85A

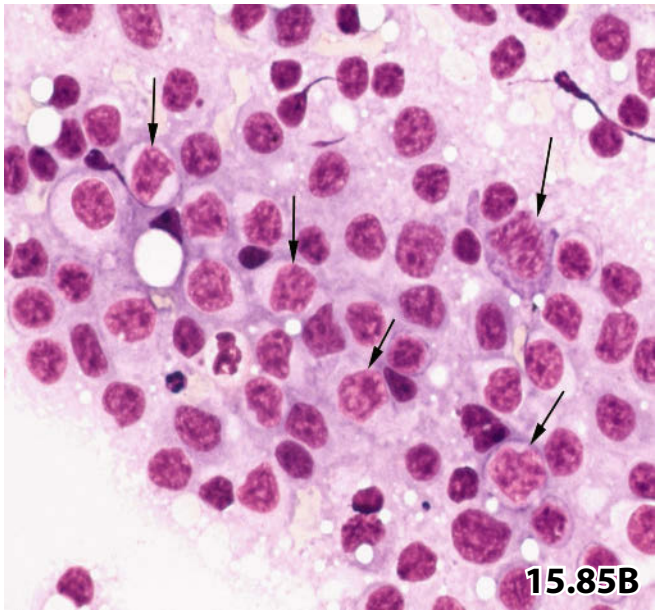
15.85B

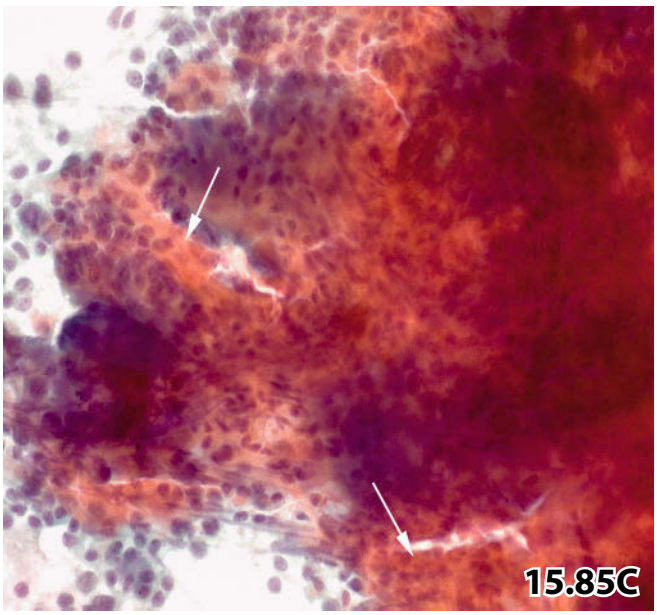
15.85C

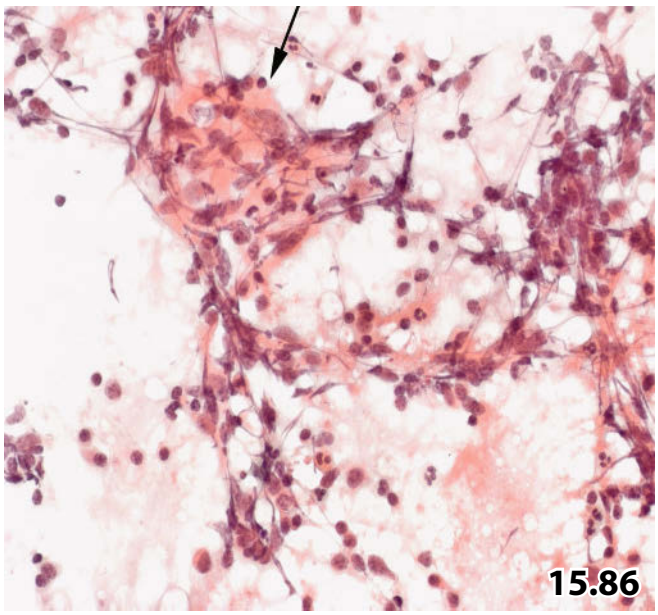
15.86

**Figs. 15.87–15.89 Anaplastic large-cell lymphoma.**
Three different patients: FNAB of primary and relapsing anaplastic large-cell lymphomas.

**Fig. 15.87** (case #1) A middle-aged man without a specific clinical history presented with an axillary tumor mass. The characteristic cytomorphology of anaplastic large-cell lymphoma is shown in detail. Key features include multinucleation, kidney-shaped nuclei, abundant basophilic cytoplasm associated with sharply defined vacuoles, and an inflammatory background (direct smear, MGG stain).
*Tentative cytologic diagnosis:* Pleomorphic malignant neoplasia. Immunocytochemistry was not performed for technical reasons.
*Tissue and immunohistochemical diagnosis* (surgical excision of the axillary mass): Large-cell anaplastic T-cell non-Hodgkin lymphoma.

**Fig. 15.88** (case #2) FNAB of a submammary lymph node in a patient with a history of anaplastic large-cell lymphoma. The detail (Pap-stained direct smear) exhibits a tumor giant cell with a wreath-like arrangement of the nuclei (left). Such cells may closely resemble Reed-Sternberg cells in Hodgkin lymphoma.
*Cytology:* The diagnosis of anaplastic large-cell lymphoma was easily made based on the patient's well-established history.

**Fig. 15.89A, B** (case #3) Example of large-cell anaplastic T-cell NHL, small to medium-size cell variant.
Relapse of an anaplastic large-cell lymphoma in a 60-year-old woman. FNAB of a lump at the back (direct smears for conventional microscopy, Pap stain). **A** Cytomorphology of the tumor cells is comparable to that shown in case #1 (Fig. 15.87) (high magnification). **B** The tumor cells exhibit strong immunopositivity for CD30 (ThinPrep specimen).

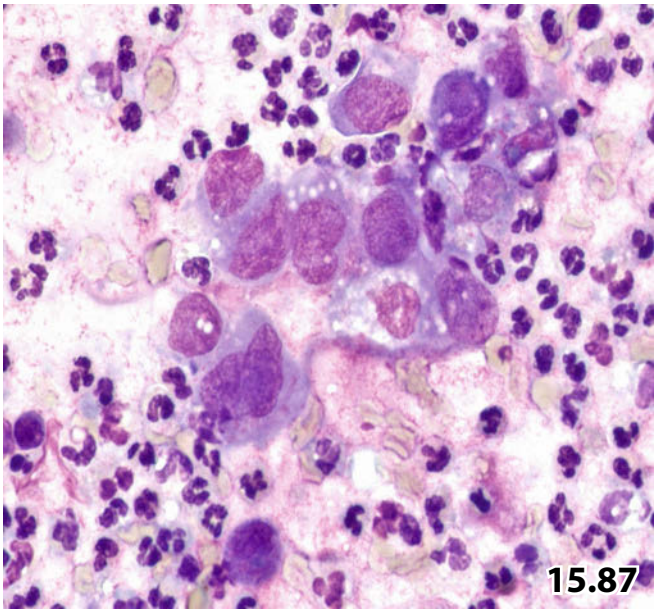
15.87

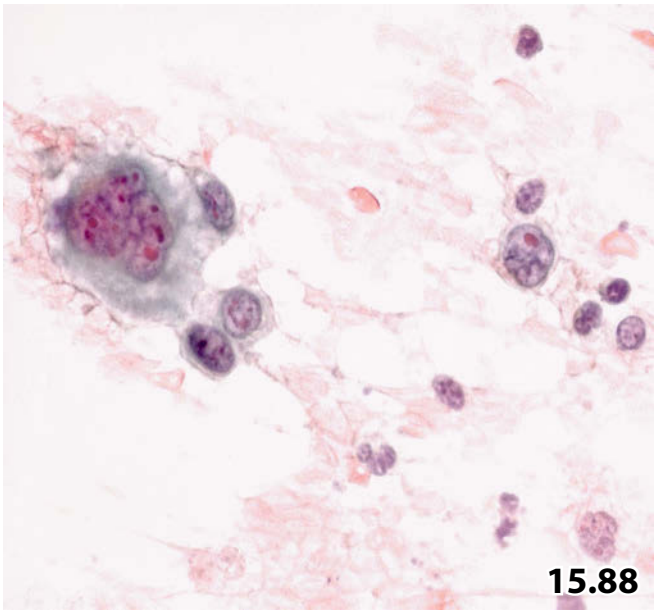
15.88

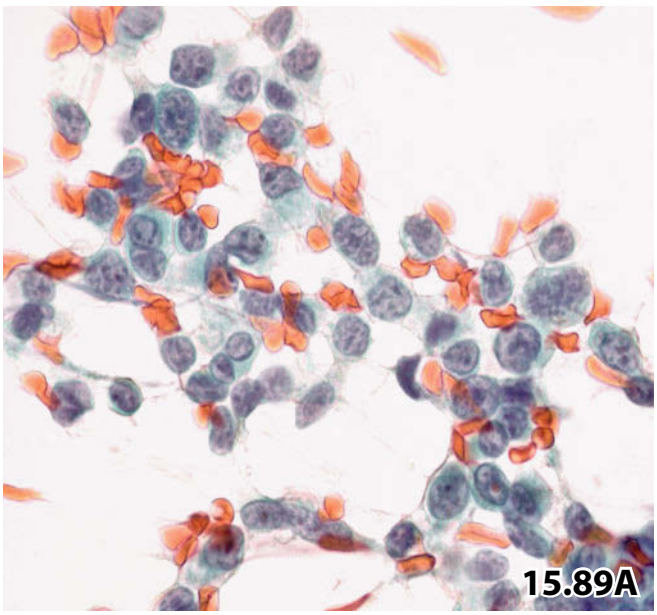
15.89A

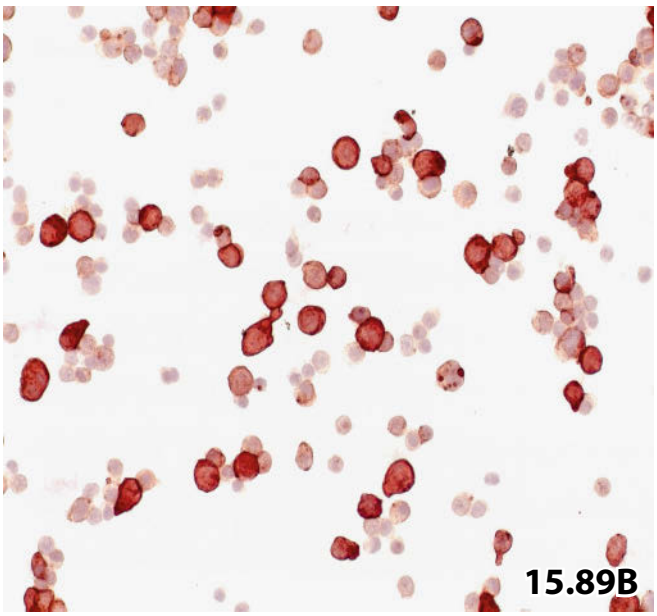
15.89B

**Fig. 15.90 Hodgkin cells in liquid-based preparation.**
High magnification reveals a Hodgkin cell (arrow), two histiocytes (arrowheads), and dispersed small to medium-sized atypical elements representing either atypical lymphocytes or small Hodgkin cells (upper left) (FNAB, ThinPrep specimen, Pap stain).

**Figs. 15.91–15.95 Classical Hodgkin lymphoma corresponding to the mixed cellular variant.**
Cytologic characteristics of classical Hodgkin lymphoma (CHL) are shown through fine-needle aspirates from different patients.

**Fig. 15.91** (case #1) Reed-Sternberg cells showing exemplary chromatin, nucleolus, and cytoplasm (arrows). Take note of mirror-inverted arrangement of the two nuclear lobes (center) (direct smear, Pap stain, high magnification).

**Fig. 15.92** (case #2) A classic Reed-Sternberg cell showing multiple nuclear segments arranged in a wreath-like pattern. Note the characteristic abundant pale-staining cytoplasm (direct smear, Pap stain, high magnification).

**Fig. 15.93** (case #3) Classic heterogeneous appearance of CHL.
An MGG-stained cytologic specimen (air-dried direct smear) reveals the classic heterogeneous appearance of CHL at low magnification. The background population is composed of small and transformed lymphocytes, plasma cells (small arrow), neutrophils and eosinophils (large arrows), and HRS cells (a Hodgkin cell is marked by an arrowhead).

**Fig. 15.94** (case #4) Characteristic fraction of atypical lymphocytes.
Higher magnification is focused on benign but enlarged atypical lymphocytes illustrating a characteristic component of the reactive background of classical Hodgkin lymphomas mixed cellular variant. A single Hodgkin cell is clearly discernible (arrow), medium-sized atypical cells containing large nucleoli may represent either atypical lymphocytes or small Hodgkin cells (arrowheads); distinguishing small Hodgkin cells may be difficult (direct smear, Pap stain).

15

Please note that the atypical lymphocytes encountered in HL closely share morphologic features with the tumor cells of non-Hodgkin lymphomas such as follicular lymphoma, mantle cell lymphoma, and others.

**Fig. 15.95** (case #5) Activated epithelioid histiocytes.
A Pap-stained cytologic specimen shows a large proportion of atypical lymphocytes associated with aggregates of activated epithelioid histiocytes (upper left and lower right). Hodgkin cells (arrows) clearly differ from epithelioid cells (direct smear, low magnification).

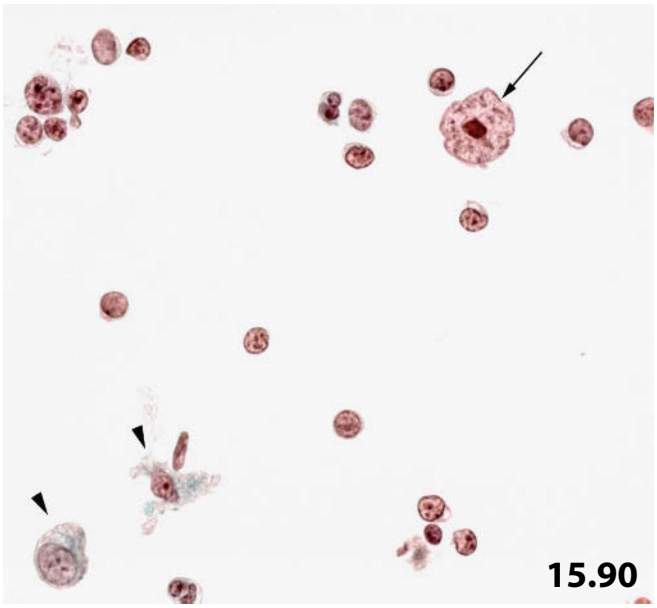
15.90

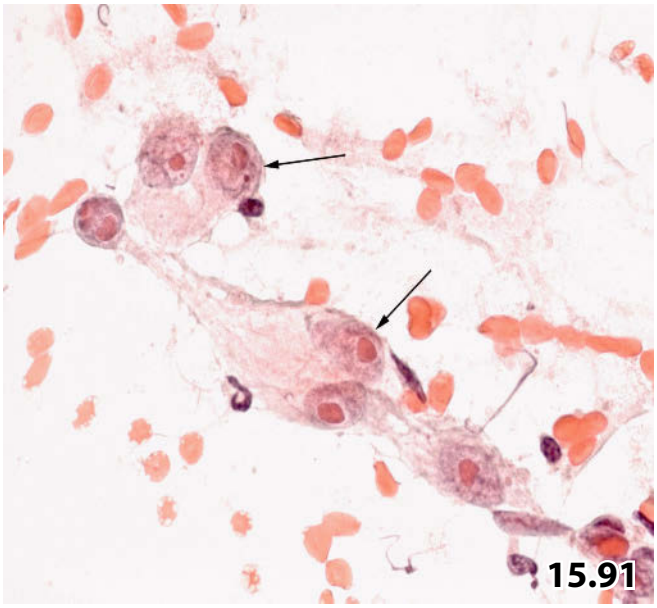
15.91

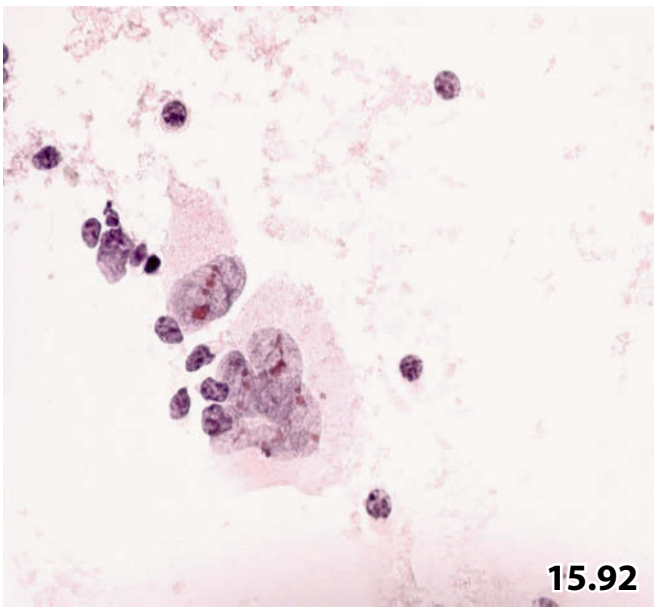
15.92

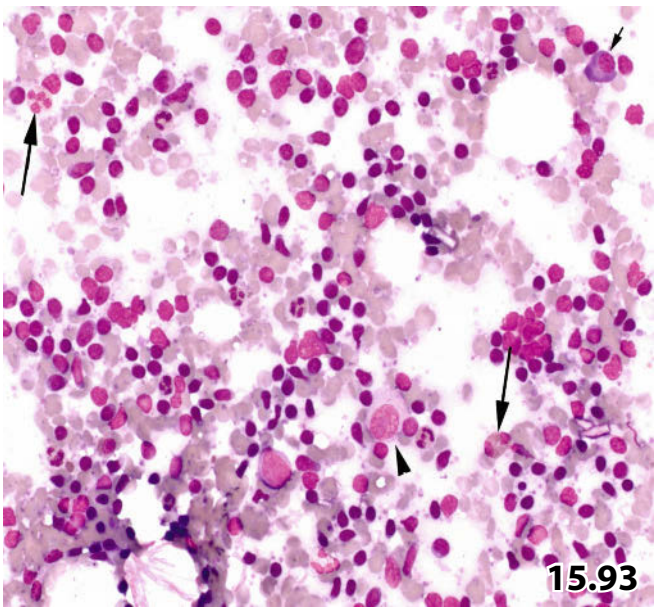
15.93

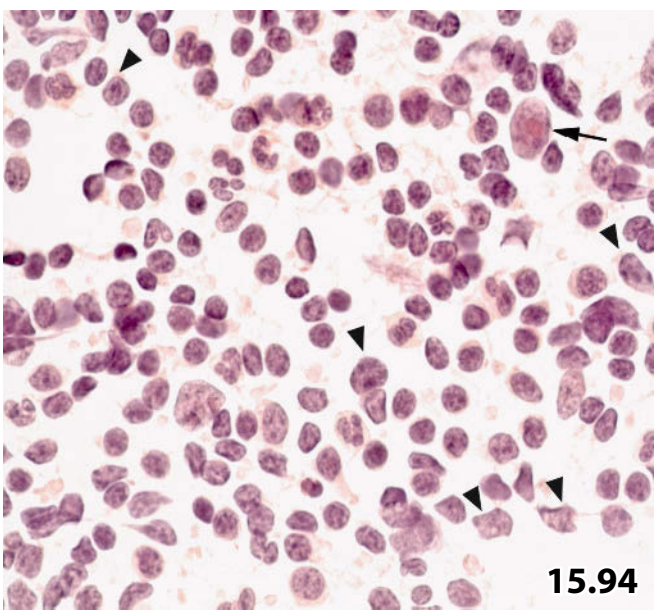
15.94

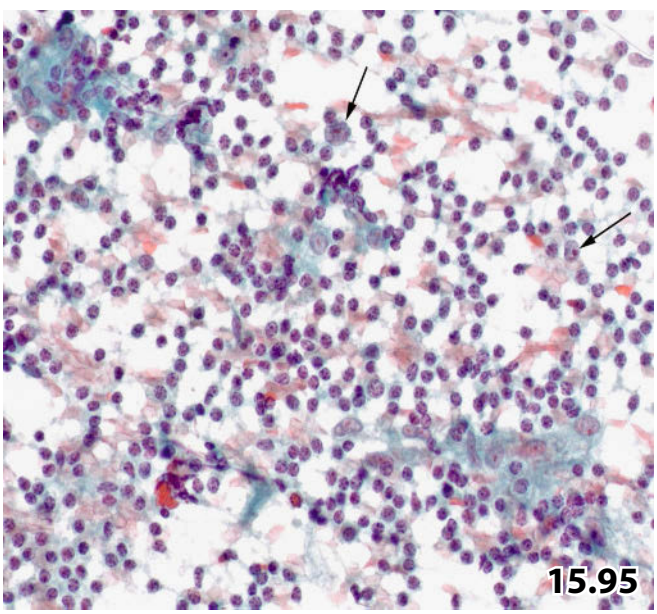
15.95

**Figs. 15.96 and 15.97 Immunocytochemical properties of HRS cells.**
Staining properties are shown using conventional smears and a liquid-based specimen originating from different aspirates.

**Fig. 15.96A** An antibody for CD30 decorates large and medium-sized Hodgkin cells in a dot-like fashion (Pap-prestained ThinPrep specimen). **B** The B-cell marker PAX5 shows a positive immunoreaction in the cytoplasm of HRS cells (Pap-prestained conventional smear).

**Fig. 15.97** An antibody for CD15 decorates HRS cells (Pap-prestained conventional smear). The diffuse staining pattern suggests membrane-accentuated staining mode.

**Fig. 15.98A, B Classical HL nodular sclerosis, classical and syncytial variant.**
Two variants of HL nodular sclerosis are shown; the FNAB specimens originate from two patients. **A** (case #1) FNAB of a lymph node in a 32-year-old man presenting with densely packed, enlarged cervical lymph nodes. Tumor cells exhibit features of classic HRS cells except for less prominent nucleoli compared to HRS cells in a CHL-mixed cellular variant. The cells exhibit abundant delicate cytoplasm and accentuated grooves (not in focus). Findings are consistent with HRS cells of the lacunar type, indicating CHL nodular sclerosis (direct smear, Pap stain, high magnification).
*Tentative cytologic diagnosis* was HL nodular sclerosis (confirmed by histologic examination of a lymph node from the neck).
**B** (case #2) This case shows an example of HL nodular sclerosis, syncytial variant: dense aggregation of HRS cells raise difficulties distinguishing between HL and anaplastic carcinoma (direct aspirate smear, Pap stain, high magnification).

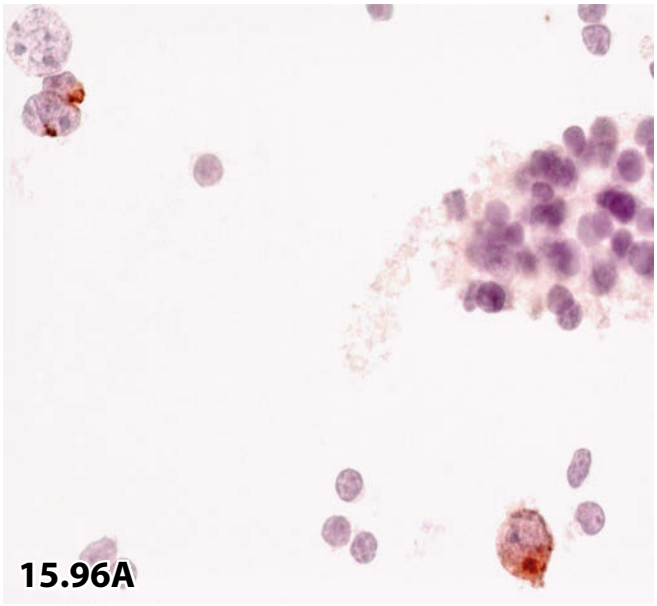
15.96A

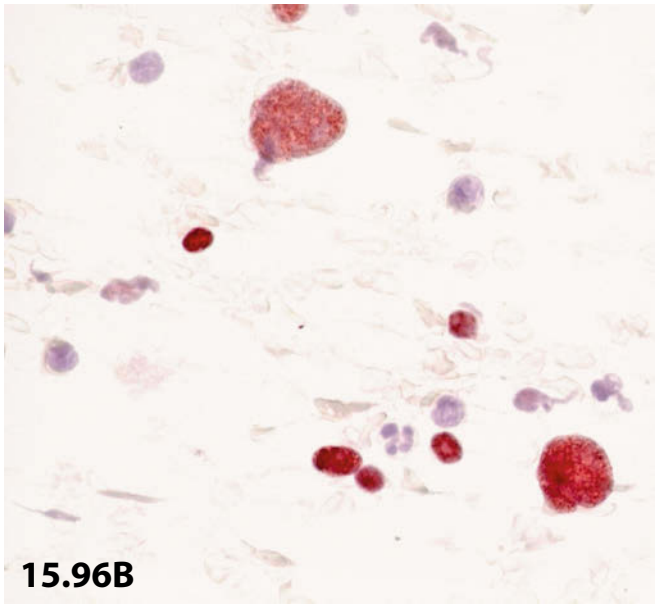
15.96B

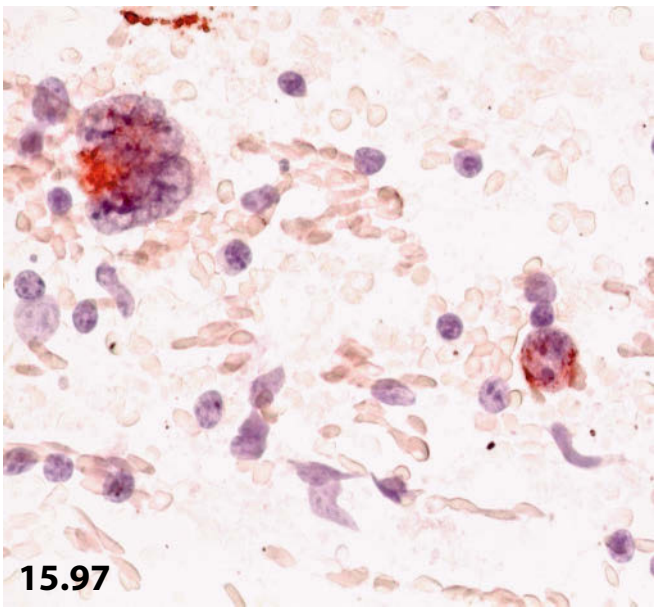
15.97

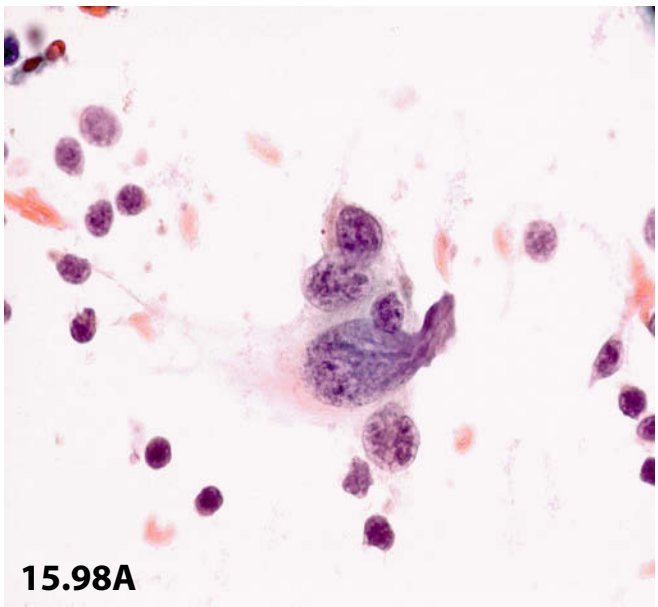
15.98A

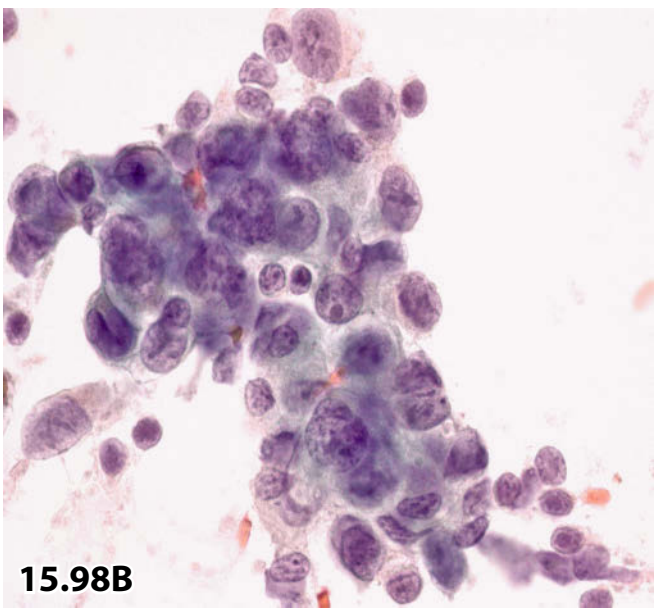
15.98B

**Fig. 15.99 Lymphocyte-rich classical Hodgkin lymphoma.**
During the course of a physical examination, a 59-year-old woman was found to have two enlarged supraclavicular lymph nodes. The attending physician referred the patient to FNAB. Low magnification shows a heterogeneous cell pattern apparently caused by various stages of lymphocytic transformation. However, numerous enlarged lymphocytes are present showing nucleoli (arrows) (direct smear, MGG stain).
*Tentative cytologic diagnosis:* Probably reactive lymphoid lesion, but low-grade non-Hodgkin lymphoma cannot be excluded.
*Discussion* Unambiguous HRS cells could not be detected in the course of the first examination or by rescreening the smears. In the end, the question remained open as to whether the aspirated cell population originated from benign proliferative zones of the lymph node or from neoplastic areas.
*Histology* from the excised lymph node: Lymphocyte-rich HL, subtotal infiltration of the lymph node!!

**Fig. 15.100A, B Nodular lymphocyte predominant Hodgkin lymphoma.**
A 12-year-old presented with an enlarged lymph node (3 cm in diameter) at her neck. FNAB was performed. Direct smears and liquid-based preparations were prepared.
*Cytologic diagnosis:* Nodular lymphocyte predominant Hodgkin lymphoma (negative immunoreactions for CD30 and CD15 are not shown). Subsequent histology confirmed the cytologic diagnosis.
**A** High magnification reveals atypical lymphocytes and L&H cells. The popcorn-like cells in the center is characterized by pronounced folding and lobation of the nucleus and multiple basophilic nucleoli (direct smear, Diff-Quik stain). **B** B-cell marker CD20 immunocytochemically decorates both atypical lymphocytes and the L&H cell presented in this field (Pap-pre-stained direct smear).

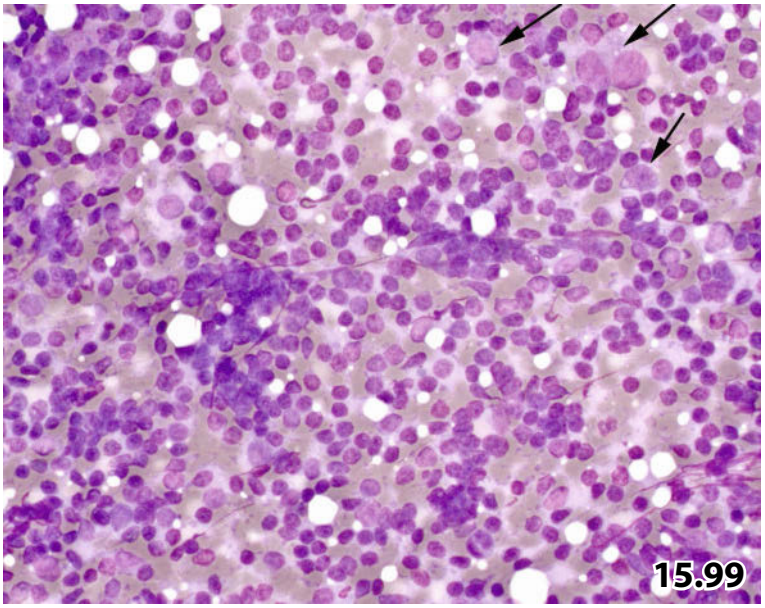
15.99

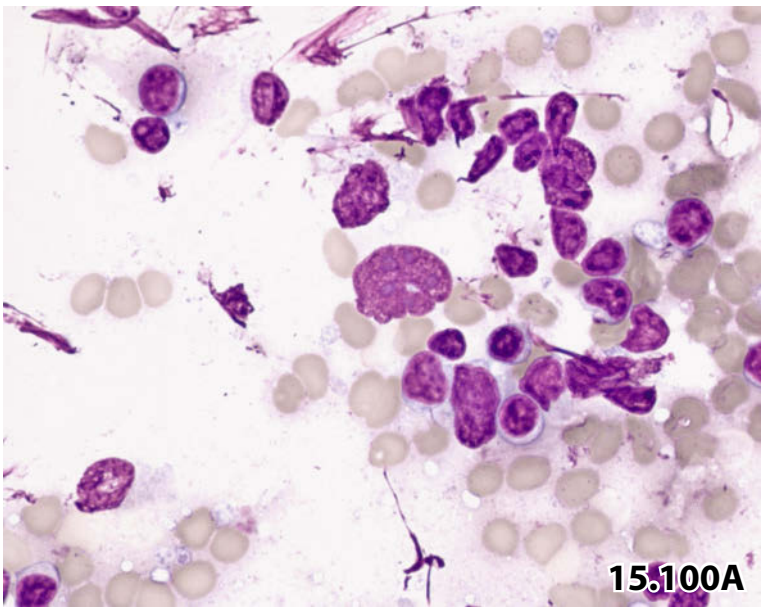
15.100A

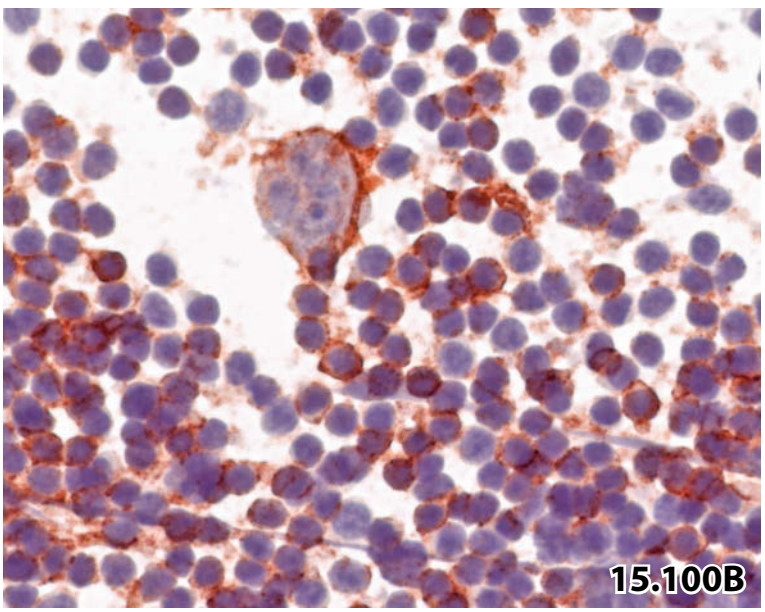
15.100B

**Fig. 15.101 Histiocytic sarcoma.**
A 58-year-old man presenting with a cervical tumor mass was referred to FNAB. Direct smears were Pap-stained. High magnification mainly exhibits fusiform pleomorphic neoplastic cells. Vesicular chromatin and abundant clear cytoplasm fading away at the periphery are striking features. Tumor cells showed negative staining results for pancytokeratin-Lu5 and common leukocyte antigen-CD45 (immunostains are not shown).
*Tentative cytologic diagnosis:* Undifferentiated malignant neoplasia, most likely sarcoma. Amelanotic spindle cell melanoma cannot be ruled out.
*Tissue diagnosis* (based on a large panel of antibodies and according to repeated evaluations by consultant pathologists): Sarcoma originating from dendritic reticulum cells.

**Fig. 15.102 Extramedullary hematopoiesis in a lymph node.**
Extramedullary hematopoiesis in a patient suffering from polycythemia vera. MGG-stained specimen shows hematopoietic cells of all three hematologic cell lines (trilineage cell component) comprising varied degrees of cellular maturation. A megakaryocyte is located in the center of the field (FNAB of a lymph node, direct smear, high magnification).

**Figs. 15.103 and 15.104 Granulocytic sarcoma.**
Extramedullary located myeloid tumor mass in two different patients; aspiration cytology revealed immature and blastic variant of granulocytic sarcoma.

**Fig. 15.103** (case #1) Granulocytic sarcoma, immature variant.
A 36-year-old man with a positive history of acute myeloid leukemia. The patient presented with an enlarged cervical lymph node. High magnification shows a heterogeneous cellular appearance caused by immature myeloid cells (myeloblasts, promyelocytes) and an admixture of lymphocytes. An eosinophilic myelocyte is depicted as well (arrow) (direct smear, MGG stain).

Myelogenic sarcoma located in lymph nodes may easily be misinterpreted as severe reactive lymphoid disorder (e.g., EBV-induced lymphadenopathy) caused by a mixture of benign lymphocytes and myeloid cells, the latter mimicking immature and blastic lymphoid cells.



**Fig. 15.104A, B** (case #2) Granulocytic sarcoma, blastic variant.
A middle-aged man with a positive history of acute myeloid leukemia presented with a lymph node in the subcutis; the patient was referred to FNAB. **A** The vast majority of the cells are immature blood cells often with a histiocytoid appearance (arrows). Cells with granular cytoplasm are also present (top) (direct smear, MGG stain, high magnification). **B** Same case: a direct smear was Pap-stained (lower magnification). Again, morphologic similarity between immature myeloid elements and histiocytes is striking. A single-file row (upper right) may simulate epithelial neoplasia, e.g., small-cell carcinoma, breast carcinoma, and others.

**Fig. 15.105 Acute monocytic leukemia.**
A 60-year-old man with a positive history of AML,M5a,b presented with infraclavicular subcutaneous infiltrates. The patient was referred to FNAB. Note the characteristic cytology of promonocytes, in particular the nuclear lobation, and the distinct cytoplasm containing dispersed granules (arrows). Regrettably, MGG staining was not performed (direct smear, Pap stain, high magnification).

Morphologic features of myeloid blasts call for differential diagnostic considerations including in particular non-Hodgkin lymphoma of the T-cell phenotype and thyroid carcinoma or breast carcinoma of the clear cell type, in cases with pseudo-epithelial aggregation of the myelogenic tumor cells.

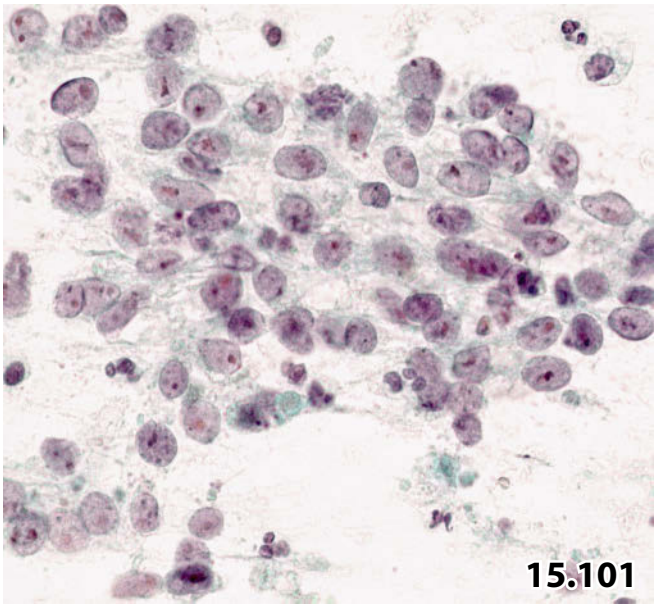
15.101

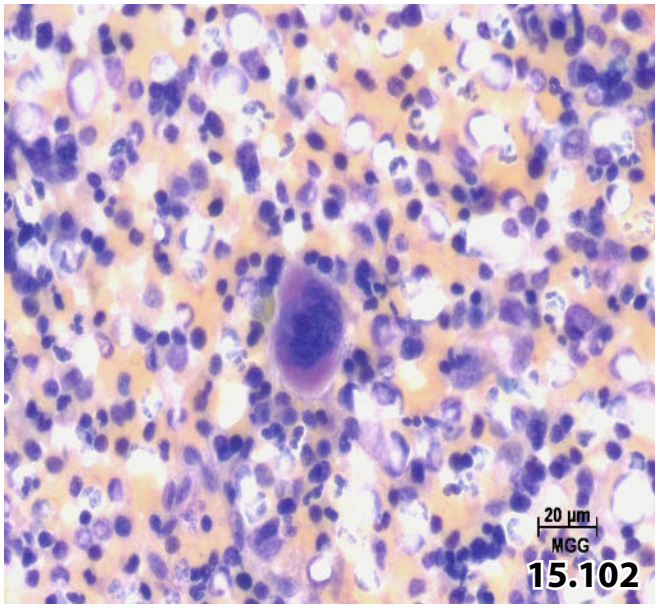

15.102

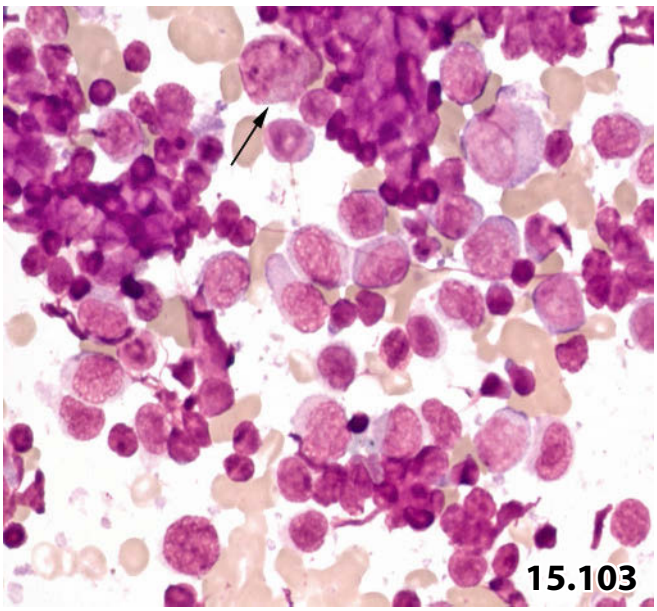
15.103

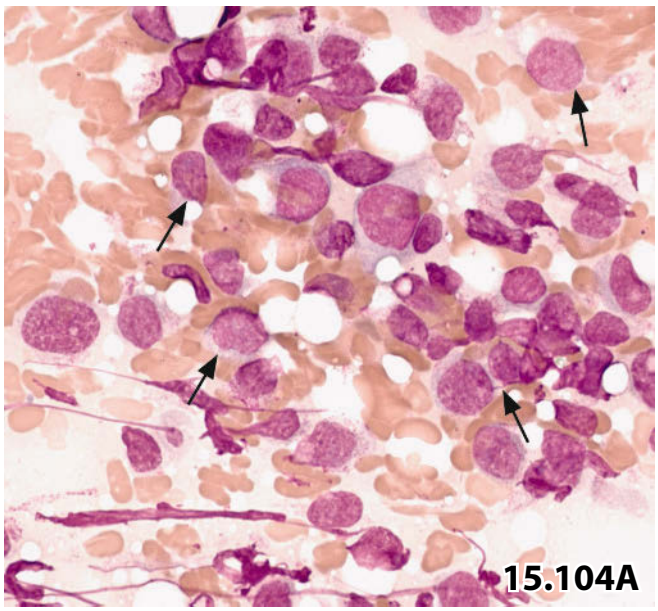
15.104A

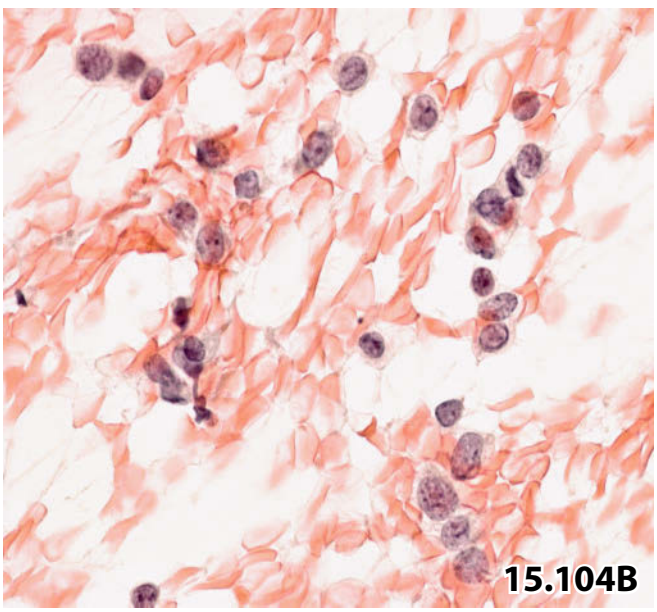
15.104B

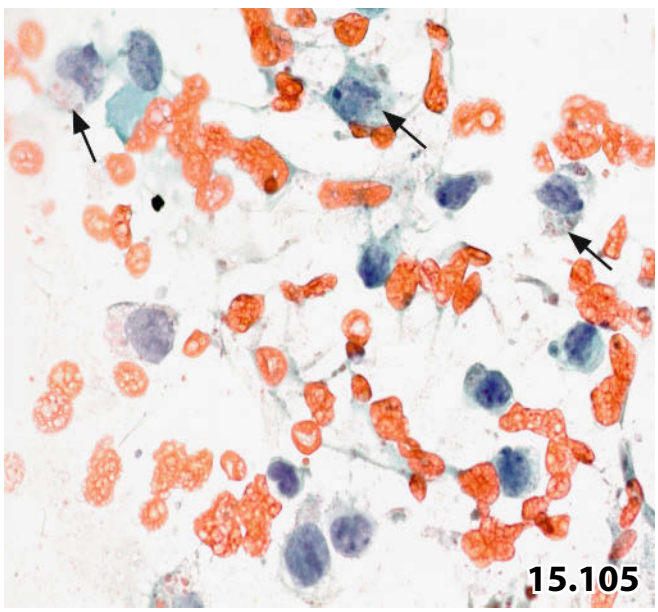
15.105

**Figs. 15.106–15.112 Metastatic neoplasms.**
The selected lesions as presented below most likely give rise to diagnostic difficulties in standard aspiration cytology. Additional analyses, in particular immunocytochemistry, are indispensable for an accurate cytologic diagnosis. In each case, aspirated cell material was directly smeared and Pap-stained (except for case #5, Fig. 15.110A exhibiting a cell population stained with MGG).

**Fig. 15.106** (case #1) Breast carcinoma: clear cell type, well differentiated.
High magnification reveals small benign lymphocytes and dispersed medium-sized cells exhibiting abundant clear cytoplasm, loose chromatin, and nuclear indentations (lower right) (FNAB of a cervical lymph node).
*Cytologic differential diagnosis:*
– Well-differentiated clear cell carcinoma of unclear primary origin (thyroid, kidney, among others).
– Activated histiocytes.
– Atypical lymphoid cells.
– Immature myeloid cells.
– Other clear cell lesions.
*Tissue diagnosis:* Ductal breast carcinoma, tubular variant.

**Fig. 15.107** (case #2) Breast carcinoma: monomorphic, well differentiated.
This variant of breast carcinoma may exhibit papilliform clusters composed of uniform cells, as demonstrated here at high magnification (FNAB of a cervical lymph node).

Regarding breast carcinoma, bear in mind that mucinous cytoplasmic inclusions are common and psammoma bodies may occasionally occur.

*Cytologic differential diagnosis:* Cytoarchitecture, the nuclear features (indentations, grooves, fine granular chromatin, and nucleolar variability), and cellular palisading (arrows) may mimic:
– Papillary thyroid carcinoma.
– Bronchioloalveolar carcinoma.
– Renal cell carcinoma.



**Fig. 15.108** (case #3) Papillary thyroid carcinoma: cystic variant.
This tumor entity is most difficult to recognize in fine-needle aspirates of lymph nodes. Compare the small tumor cell cluster (upper right) with the scattered histiocytes. Note in particular the nuclear grooves (arrow), clear nuclear areas, compact cytoplasm, and high N/C ratio exhibited by the carcinoma cells (FNAB of a cervical lymph node, higher magnification).
*Cytologic differential diagnosis:*
– Breast carcinoma.
– Bronchioloalveolar carcinoma.
– Renal cell carcinoma.

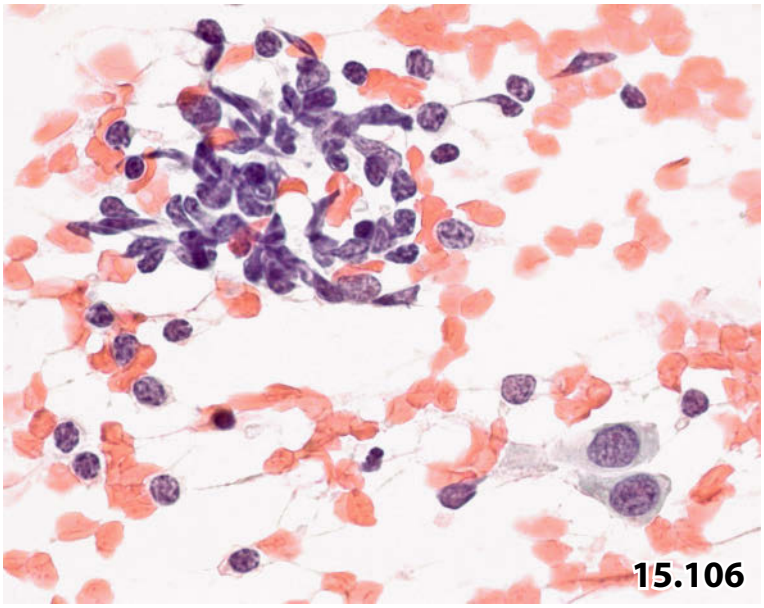
15.106

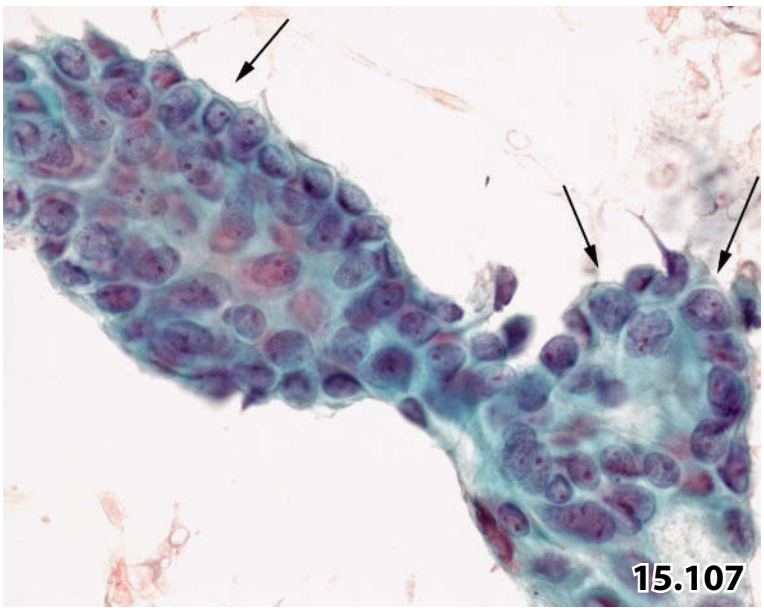
15.107

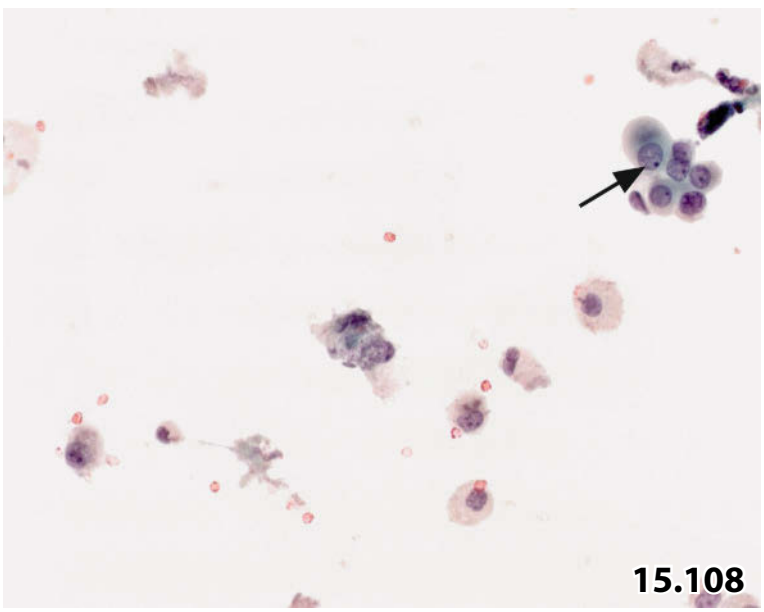
15.108

**Fig. 15.109** (case #4) Well-differentiated keratinizing squamous cell carcinoma.
Pronounced cytoplasmic polymorphism and varied staining quality (red, orange, yellowish) favor well-differentiated SCC. In this setting, an extensive search for atypical/malignant squamous cells is of great diagnostic relevance (such as the cell in the center, arrow) (FNAB of a cervical node, high magnification).
*Cytologic differential diagnosis:* Branchial cleft cyst and other cervical cysts lined with atypical squamous epithelium.

**Fig. 15.110A, B** (case #5) Lymphoepithelial carcinoma.
A 25-year-old man presented with an enlarged lymph node at the right side of his neck. FNAB was performed as an initial investigation. The cytologic challenge and impact of immunocytochemistry of this particular carcinomatous lesion are highlighted.
*Cytologic differential diagnosis:*
– Reactive lymphadenopathy.
– Hodgkin lymphoma.
– Reactive lymphoid lesion associated with isolated malignant lymphoid blasts.
– Reactive lymphoid lesion associated with isolated undifferentiated carcinoma cells.

**A** A heterogeneous lymphoid cell pattern together with scattered histiocytes and large atypical cells (arrows) are presented at lower magnification. Few dispersed carcinoma cells are frequently encountered in aspirates of lymph nodes affected by lymphoepithelial carcinoma; distinguishing between carcinoma cells and benign blast cells and activated histiocytes is usually impossible by light microscopic investigation alone. Immunocytochemical work-up is mandatory in this setting (FNAB of a cervical lymph node, MGG stain, lower magnification). **B** A few small clusters composed of carcinoma cells are identified (right) using immunostaining for pancytokeratin-MNF116. Note the reactive lymphoid background and loosely arranged epithelioid histiocytes (upper left) (Pap-prestained direct smear).

**Fig. 15.111** (case #6) Amelanotic malignant melanoma.
A 53-year-old woman presented with a firm cervical lymph node. There was no specific clinical history available. FNAB yielded cellular aspirates. The smears exhibit numerous medium-sized to large cells dispersed and grouped in loose aggregates. Note the abundant homogeneous eosinophilic cytoplasm (higher magnification).
*Tentative cytologic diagnosis and differential diagnosis:* Large-cell carcinoma comprising oxyphilic cell features: the primary tumor may be located in the thyroid gland, kidney, or liver. Nonpigmented malignant melanoma, epithelioid sarcoma, and blastic lymphoma should also be considered, the latter being rather unlikely. Immunocytochemical tests could not be performed.
*Tissue diagnosis* (excised cervical lymph node): Lymph node metastasis of an amelanotic melanoma.

**Fig. 15.112** (case #7) Concomitant malignant neoplasms.
A 69-year-old man with a clinical history of both lymphocytic non-Hodgkin lymphoma and squamous cell carcinoma of the floor of mouth presented with enlarged cervical lymph nodes. High magnification of a direct aspirate smear reveals a population of atypical lymphocytes (in line with lymphocytic NHL) interspersed with large undifferentiated neoplastic cells consistent with poorly differentiated SCC.
*Note the great significance of the clinical feed back:* Initially, history of SCC was not included in the clinical information accompanying the cytologic sample sent to our laboratory. Hence, diagnostic dilemma resulted between Hodgkin lymphoma, metastatic undifferentiated malignant neoplasia, metastatic malignant melanoma, and other large cell malignancies.

**Fig. 15.113 Poorly preserved cytologic specimen.**
FNAB of an enlarged cervical lymph node: The aspirated material was inadequately spread, and the delay in fixation resulted in air-drying artifacts. It was impossible to render a useful cytologic diagnosis (Pap stain, lower magnification).

Never make a conclusive diagnosis on cytologic smears that have been poorly prepared!!

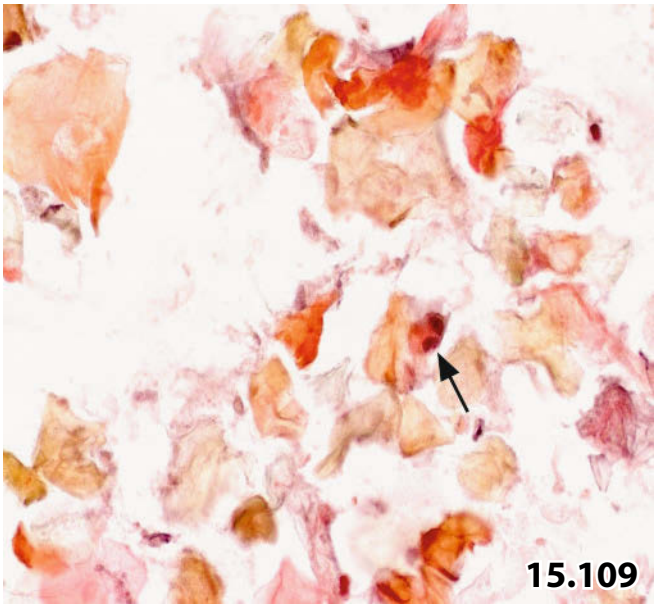
15.109

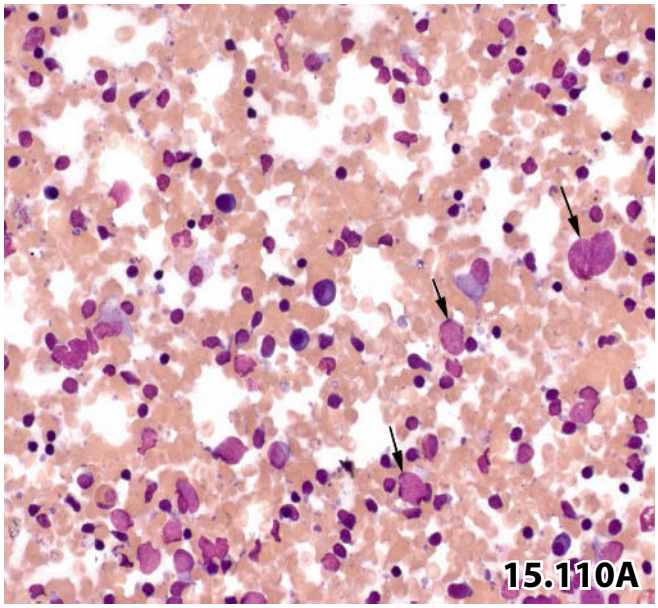
15.110A

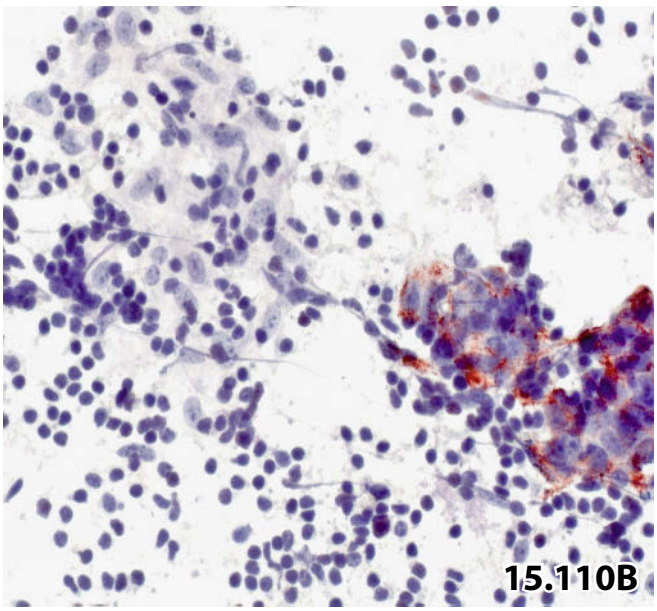
15.110B

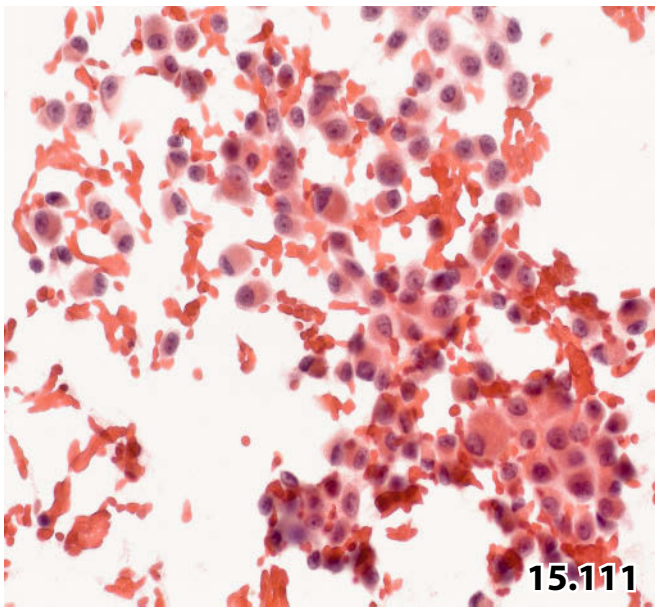
15.111

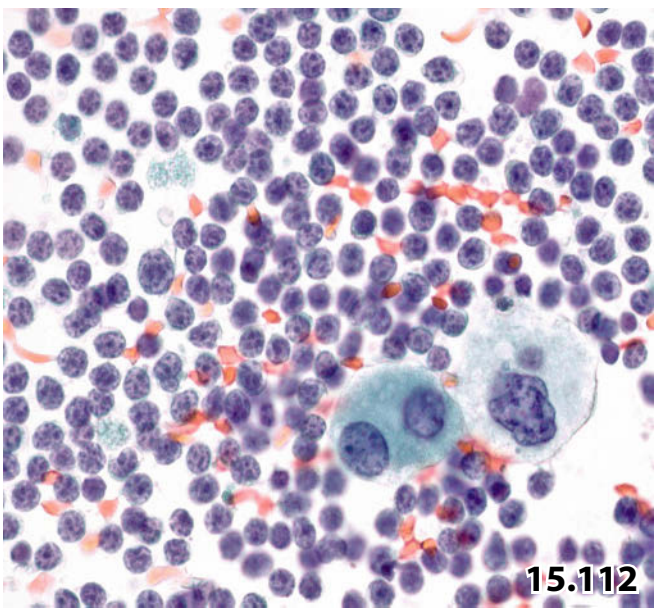
15.112

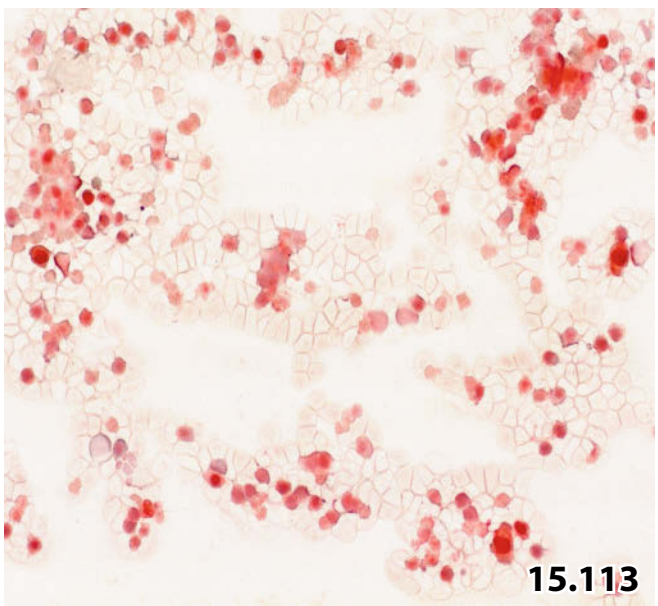
15.113

# 16 Skin Lesions and Unusual Subcutaneous Lesions




Spieler/Rössle, *Nongynecologic Cytopathology. A Practical Guide. Essentials of Diagnostic Pathology*,
DOI 10.1007/978-3-642-24719-4_16, © Springer-Verlag Berlin Heidelberg 2012

## Synopsis and Algorithms

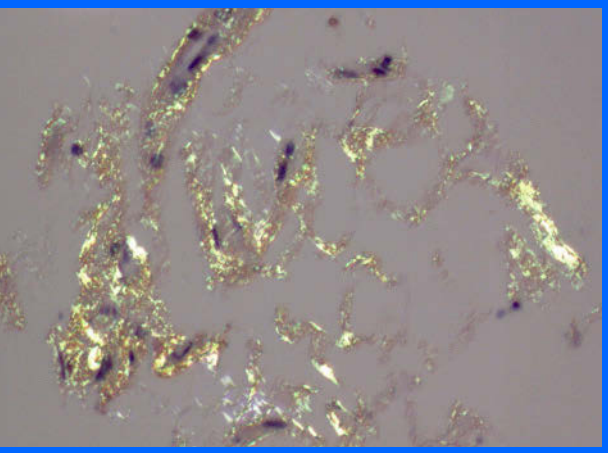

# Skin Lesions and Unusual Subcutaneous Lesions

## 16.1 Introduction

**General Comments**

Dermatologic cytology is not widely used, even though cutaneous lesions are clearly visible and generally well-defined. The reasons for this neglect are comprehensible:

- It is easy to obtain a tissue probe by biopsy.
- In many cases, cytology cannot provide a determinant diagnosis because skin disorders are frequently associated with inflammatory background and reactive cell changes.
- Many cutaneous lesions are covered by an intact epidermis and the number of valid scraping samples is limited.
- Many of the cutaneous nodules are undersized for FNAB.
- The histologic architecture of many tumors of the skin and their relationship to the adjacent cutaneous/subcutaneous structures is decisive for a final diagnosis.

In recent years, however, several studies have indicated the utility of FNAB in the diagnosis and differential diagnosis of primary tumors of the skin and skin adnexa [20, 21, 56, 81].

### 16.1.1 Sampling, Processing, and Staining

- *Surface scraping*. Lesions on the skin surface may be accessible for surface scraping. Adequate cellular material is likely obtained from ulcerative lesions and from lesions with damaged epidermal cover. The sample can be taken by scalpel blades, with the edge of common glass slides, or by curettes. If the latter provide small fragments of tissue, the scrape material should not be transferred onto glass slides but processed using the cell-block method.
- *FNAB* may be applied to nodular or to diffuse gross lesions. Nodules have to be immobilized with one hand. Thus, it is highly recommended to hold the syringe with the needle attached in a pistol-type holder unless a vacuum system is connected to the needle. FNAB utilizes 21- to 27-gauge needles. A 26-gauge needle is most appropriate for small-sized tumors ranging from less than 1 mm up to 5 mm.
- If available, *sonography* may be helpful to distinguish the type of lesion (solid versus cystic), and its outline.
- *Direct smearing* of the aspirate onto a glass slide for immediate fixation in an alcohol solution or by means of a spray fixative should be the standard method in dermatologic cytology. The wet-fixed specimens are stained using the Papanicolaou or Hematoxylin-Eosin staining method. Additional air-dried smears are particularly recommended in cases where a lymphoid lesion is presumed; the smears are stained using the May-Grünwald-Giemsa or similar staining techniques.
- *Liquid-based methods* such as cytospin, ThinPrep, and others are best used by operators who are not familiar with proper preparation and fixation technique, and for samples with an obvious paucity of cells. The advantages and disadvantages of thin-layer preparation are discussed in Sects. 1.1.4.2, p. 4, 2.4.1.2, p. 205, 10.1.2.2, p. 634, and 15.1.3.2, p. 910.
- The *cell-block technique* should be applied to tissue fragments and clots obtained by curetting or aspiration.

### 16.1.2 Histology and Cytology of Normal Skin

Epidermis and dermis are the two basic layers of the skin.

1. The outermost layer of the *epidermis* is the stratum corneum, it is composed of flatly laminated keratinized anucleated cells. Bottommost is the germinal layer with its small cuboid to columnar cells attached to the basement membrane. The small nuclei are dense and darkly stained and obviously patternless. Melanocytes that produce melanin pigment are located between the cells of the germinal layer.
   - ○ Scrape specimens from the normal skin contain anucleated squamous cells and a few nucleated superficial and intermediate squames.
2. The *dermis* consists of connective tissue that is mainly composed of a network of various types of fibers comprising hair follicles, sebaceous glands, sweat glands, vessels, nerve cells, and lymphoid tissue.

### 16.1.3 Cutaneous Appendages and Their Cells

(Fig. 16.1)

- The base of the hair follicle is called *hair bulb* placed in the dermis and the subdermal tissue. The pluripotential hair matrix cells in the hair bulb give rise to the hair and the inner root sheath.
  - ○ The matrix cells show large vesicular nuclei and a basophilic cytoplasm. Melanocytes are interspersed between the matrix cells.
- *Sebaceous glands* are embedded in dermal tissue. The large lipid-containing cells are carried in the secretory duct toward the surface; the cells eventually disintegrate and release the sebaceous content into the hair follicle.
  - ○ Sebaceous cells are large with abundant rounded cytoplasm due to fatty storage. Lipid droplets give rise to a characteristic cytoplasmic texture comprising a mix of multiple small and large well-defined vacuoles. The nuclei are often pyknotic, well-preserved nuclei are small, showing bland chromatin (Fig. 16.1A and 16.1B).
- *Sweat glands* are embedded within the dermal and subdermal soft tissue, the epithelial layer is composed of cuboidal cells. The secretory cells consist of two types: serous and mucinous. The nuclei exhibit a regular shape and bland chromatin.
  - ○ The serous cells are clear, containing small inconspicuous cytoplasmic granules and glycogen (Fig. 16.1C).
  - ○ The mucin-secreting cells (dark cells) embody numerous basophilic granules and PAS-positive mucopolysaccharides.

## 16.2 Common and Rare Skin Lesions, Benign and Malignant (Selected Entities)

### 16.2.1 Skin Lesions Presenting Diagnostic Dilemmas

A number of skin lesions with different biological behaviors and variable macroscopic and histologic appearance may exhibit distinctive superficial hyperkeratosis and acanthosis. Superficial scraping will be diagnostically less conclusive; the specimens usually contain abundant anucleated and/or keratinized superficial squames together with a variable inflammatory background. However, deep scraping, or scraping the rim or bottom of an ulcer, may produce accurate cell material. A small selected series of such lesions is specified.

- *Seborrheic keratosis* is a very common lesion in older people.
- *Keratoacanthoma*. Excision is required to rule out well-differentiated squamous cell carcinoma in cases with doubtful clinical features.
- *Senile keratosis* may undergo malignant transformation. Exclusion of carcinoma requires wide local excision.
- *Bowen disease* is an intraepidermal squamous cell carcinoma that occurs in unexposed parts of the body. Depending on the cellular differentiation of the uppermost epidermal layer, the exfoliated cells range from slightly atypical superficial squamous cells to undifferentiated malignant cells of the basaloid type; the latter match the cells sampled from carcinoma in situ of the uterine cervix.
- *Paget disease of the nipple* is a secondary cutaneous lesion due to an underlying ductal breast carcinoma. The carcinoma cells are located in the deeper layers of the epidermis and therefore unlikely reached by simple scraping of the surface nipple area. This issue is detailed in Sect. 1.3.14.2, p. 65.

### 16.2.2 Noninfectious Granulomas and Epidermoid Cyst

#### 16.2.2.1 Fat Necrosis (Fig. 1.20)

Fat necrosis may follow trauma, surgery, and irradiation.

**Microscopic Features**

- ○ A mixture of well-preserved and degenerating fat cells, lipophages, and amorphous debris.
- ○ A mixed inflammatory cell pattern is interspersed with multinucleated macrophages and few activated fibroblasts.

**Caution**

A reliable diagnosis is not possible in cases of hypocellular aspirates.

#### 16.2.2.2 Suture Granuloma (Fig. 16.2)

Suture granuloma is located in or adjacent to a scar. A subcutaneous nodule caused by foreign body type granulomatous reaction to surgical material may mimic a tumor, or a local recurrence of malignancy respectively.

**Microscopic Features**

- Excessive foreign body reaction, cell pattern comprising numerous multinucleated macrophages.
- Suture material is ingested in multinucleated macrophages appearing as tightly packed bars with strong birefringence under polarized light, but it is also readily recognized in light microscopy by its refractile behavior.

#### 16.2.2.3 Epidermoid Cyst (Fig. 16.3)

- Epidermoid cysts are the most common cutaneous cysts, occurring most commonly on the face, scalp, neck, and trunk, resulting from proliferation of epidermal cells within a localized area of the dermis. Epidermoid cysts are benign lesions, may occur at any age, and are approximately twice as common in men as in women.
- Epidermoid cysts are asymptomatic but may occasionally become inflamed or secondarily infected resulting in swelling and tenderness.
- Spontaneous discharge or aspiration of foul-smelling cheese-like material is diagnostic.

**Microscopic Features**

- Hallmark: Anucleated superficial squamous cells, although small dark nuclei may occasionally be seen (Fig. 16.3A).
- A chronic inflammatory process may lead to destruction of the cyst wall followed by a granulomatous reaction of the foreign body type. Granulomatous tissue and histiocytic giant cells may be arranged in close contact to squamous cells (Fig. 16.3B).

**Caution**

Strongly activated polymorphous histiocytes (and fibroblasts) originating from granulomatous tissue may mimic undifferentiated carcinoma cells.
Immunocytochemical stains are helpful in doubtful cases: pancytokeratins reliably demonstrate positivity on carcinoma cells, and activated histiocytes are positive for CD68.

### 16.2.3 Amyloid Protein Deposits in Subcutaneous Tissue of the Abdominal Wall [12, 24, 98] (Fig. 16.4)

- Fine-needle aspiration of subcutaneous abdominal fat is a simple, fast, and reliable method to detect systemic amyloidosis. Several studies have reported sensitivity ranging from 78% to 93% [24, 66, 98].
- The four-quadrant aspiration procedure around the umbilicus is the preferred method at our institution.
- It is advantageous to process the aspirated material by means of the cell-block technique:
  - The amyloid strands are accurately visible, superior to their performance in smear specimens.
  - Amyloid deposits in the wall of blood vessels become more apparent as compared to those in cytologic smears.

**Microscopic Features**

- Cytologic findings include homogeneous and cylindric material intimately associated with the fat tissue. The strands are refractile, staining brightly eosinophilic using the Papanicolaou or Hematoxylin-Eosin staining methods.
- Amyloid protein is positive for Congo red staining (Fig. 16.4A) and shows birefringence in a bottle-green manner (Fig. 16.4B). Bottle-green birefringence is a diagnostic hallmark for amyloid protein but collagen may react in a similar way; although collagen appears as long and slender strands without intimate contact with the adipose tissue.

### 16.2.4 Pemphigus Vulgaris [10, 51, 96, 97]

Pemphigus vulgaris is a group of mucocutaneous diseases of unclear – possibly autoimmune – etiology, characterized by formation of bullae within the epidermis. Loss of the intercellular connections in the stratum spinosum results in loss of cohesion between keratinocytes (acantholysis) as a major characteristic of pemphigus vulgaris. Fluid samples present abundant regenerating parabasal and basal cells exhibiting increased mitotic activity. The activated cell population may suggest malignancy.

**Microscopic Features**

- Hallmarks: High cellularity of the cytologic samples.
  - Uniform cell pattern composed of small cells exhibiting increased N/C ratio and nuclei with pronounced single or multiple irregular nucleoli.
  - Increased mitotic rate.
  - The nuclei are well preserved but the cytoplasm shows degenerative changes.

- The chromatin texture is generally loose and fairly even, but irregular distribution may occur.
- Hyperchromasia is exceptional.
- Occasional cell-in-cell arrangements may be seen.

## 16.2.5 Viral Infections [11]

### 16.2.5.1 Herpes Simplex Virus

Hallmark: Cellular changes produced by this virus type are distinctive (Fig. 11.3):

- Immature squamous cells are enlarged, showing mono- or multinucleation, and a distinct, small cytoplasmic rim.
- The nuclei exhibit a characteristic ground-glass texture and/or eosinophilic inclusions combined with granular condensation of the chromatin against the nuclear periphery.
- Nuclear molding frequently occurs.

The multinucleated cells may give rise to suspicion of pemphigus vulgaris; but in pemphigus the cells are usually smaller, the chromatin pattern is well preserved, and the cytoplasm is degenerating.

### 16.2.5.2 Herpes Zoster and Varicella

Both viral infections present similar cell changes as described above (check specialized sources in the literature).

### 16.2.5.3 Molluscum Contagiosum

This is a common skin disease caused by a virus that affects the top layers of the skin.

- The fluid obtained from vesicles contains numerous superficial squamous cells, their cytoplasm is loaded with masses of virus particles compressing the nuclei against the cytoplasmic membrane. This is a cell phenotype referred to as a molluscum body.

## 16.2.6 Pilomatrixoma

[25, 76, 87, 100, 102] (Figs. 16.5–16.7)

**General Comments**

Pilomatrixoma, also known as calcifying epithelioma of Malherbe, is a benign tumor of the hair follicle composed of cells with differentiation toward hair cells. Cytologically, the lesion is almost exclusively diagnosed by FNAB. The tumor is frequently seen in the head and neck area and at the upper extremity of younger people, but pilomatrixoma can also occur in unusual locations of the human body [1, 100].

**Microscopic Features**

- Hallmarks:
  - Shadow cells: Anucleated squamous cells staining faintly yellow by the Papanicolaou method; the lost nuclei are substituted by a centrally placed unstained clear area.
  - Basaloid cells from the germinal layer: Small cells comprising darkly stained nuclei and sparse cytoplasm. Nucleoli and nuclear molding may be prominent. Degenerating cells disclose pyknotic nuclei. Most of the cells are tightly clustered but regularly arranged.
  - Calcium deposits
- Squamous cells at various stages of maturation. The nuclei are vesicular, slightly irregular, and frequently stripped.
- Cellular discohesion may be pronounced.
- Proliferation of melanocytes may be present [84].
- A granulomatous component including foreign-body giant cells is frequently present.
- Amorphous debris may be encountered.

**Differential Diagnosis** [33, 87]

Several reports in the literature emphasize pilomatrixoma for its high potential to masquerade as a malignant tumor, especially in patients with an abnormal clinical presentation of this particular tumor such as in the skin of the breast.

- Dense clustering of basaloid cells closely resembles tumor cell aggregates as seen in basal cell carcinoma.
- Crowded aggregates of degenerating basaloid cells in combination with detritus may mimic metastatic small-cell carcinoma [29].
- Metastatic neuroendocrine carcinoma and primary cutaneous Merkel cell tumor should always be taken into consideration.
- Squamous cell carcinoma or odontogenic tumor should be considered in cases consisting of squamous cells from different layers, numerous isolated cells, and debris [9, 90].
- Pilomatrixoma presenting as a lump of the breast or as locoregional subcutaneous nodule may readily be overdiagnosed as breast carcinoma of the monomorphic small-cell type (Fig. 16.7A and 16.7B) [1] (see also Sect. 1.3.1.2, p. 57).
- The presence of numerous deep-stained naked nuclei containing nucleoli may lead to a false diagnosis of malignant lymphoma.

### 16.2.6.1 Pilomatrix Carcinoma

On rare occasions, pilomatrixomas show invasiveness and sporadic metastases to distant sites [27]. We have found a single case documented in the cytologic literature [22].

**Caution**

Cutaneous FNAB rich in basaloid cells (and inconspicuous admixture of squamous cells and shadow cells) should always raise the suspicion of pilomatrixoma, particularly in young and middle-aged patients [33].

## 16.2.7 Basal Cell Carcinoma

[30, 34, 63, 105] (Figs. 16.8–16.10)

### General Comments

- Synonyms of basal cell carcinoma (BCC) are basal cell epithelioma, or rodent ulcer.
- Cytologic investigation is useful to differentiate BCC from many skin lesions imitating BCC by macroscopic inspection. The majority of the basal cell carcinomas are ulcerated or show at least a cellular or crusty surface that can easily be removed, thus obtaining an adequate sample by scraping will be no problem in a high percentage of the cases [23]. FNAB is a perfect tool for larger tumors [30, 34, 63].
- BCCs are tumors of the hair-bearing skin most particularly involving the face of adults. A high percentage of patients who suffer from basal cell carcinoma may develop one or more metachronous tumors within 10 years.
- As a general rule, basal cell carcinoma does not metastasize. In case of metastatic BCCs, most of the metastases are limited to regional lymph nodes. Metastasizing tumors cannot be distinguished from nonmetastasizing BCCs using cytologic parameters.
- A few studies have been conducted regarding immunocytochemical results in fine needle aspirates of BCC [34].

### Microscopic Features

- Hallmarks:
  - Cohesive clusters of uniform small cells varying in size and shape occasionally exhibiting distinct borders. Cells at the periphery of the clusters are focally arranged in palisade formation (Fig. 16.8A and 16.8B).
  - Solitary cells may occur casually showing scanty and poorly defined cytoplasm.
  - Intercellular bridges are absent and mitoses are rare.
  - The nuclei are monomorphic round to oval and occasionally elongated. The chromatin pattern is loose or finely granular. Nucleoli may be encountered in activated tumor cells.
- Basal cell carcinomas are usually populated by a few melanocytes and Langerhans cells [34].

### 16.2.7.1 Variants of Basal Cell Carcinoma

Many histologic variants of basal cell carcinoma are established; some of them may be recognized in cytologic preparations eventually causing diagnostic problems.

The tumor variants of major cytologic interest include the following entities:

- *Keratotic BCC* is a variant showing differentiation toward hair structures (Fig. 16.10). The tumors express parakeratotic-like squamous cells that occur in strands or concentric whorls surrounding horn cysts. The cells and their nuclei are elongated, the cytoplasm is dense, eosinophilic, or cyanophilic. The horn cysts are composed of fully keratinized cells.
- *Cystic BCC* shows differentiation toward sebaceous glands. Solid BCC tissue fragments may be interspersed with typical sebaceous cells.
- *Adenoid BCC* shows a differentiation toward apocrine and eccrine glands. The tumor contains tubular and gland-like structures; their lumen may be filled with secretion.
- *Pigmented basal cell carcinoma* may contain variable amounts of melanin. The granular pigment is stored in the cytoplasm of melanocytes, melanophages (located in the adjacent stroma), and exceptionally in tumor cells.
- *Granular cell BCC* shows a differentiation to granular cells occurring within some portion of the tumor or involving the entire tumor [7, 82].

### Differential Diagnosis

- Solid adenoid cystic carcinoma devoid of mucoid inclusions, pilomatrixoma lacking ghost cells and keratinization, and metastatic small-cell carcinoma may mimic basal cell carcinoma.
- Eccrine spiradenoma predominantly composed of small cells comprising dark nuclei and scant amounts of cytoplasm can mimic basal cell carcinoma in cytologic samples.
- Neuroendocrine carcinoma of the skin (Merkel cell carcinoma) belongs to a group of small-cell neoplasms with striking cytomorphologic resemblance to basal cell carcinoma. A distinct immunocytochemical pattern can easily distinguish between Merkel cell carcinoma and BCC (see Sect. 16.2.10, “Differential Diagnosis,” p. 1032).
- Trichoepithelioma is characterized by horn cysts and a surrounding tumor component which are similar in appearance to that of basal cell carcinoma; distinction from keratotic BCC may be practically impossible. Immunomarkers, tested by the use of histologic sections, seem to be of uncertain value distinguishing between BCC and trichoepithelioma [80].
- Basal cell carcinoma associated with chromatin coarsening, conspicuous nucleoli, and mitotic activity may simulate poorly differentiated squamous cell carcinoma (SCC). BCC may be distinguished from nonkeratinizing SCC by cohesive closely packed cells and the absence of intercellular bridges.
- The keratotic variant of BCC causes most differential diagnostic problems, though keratotic horn cysts in basal cell carcinoma appear differently from keratin pearls in SCC.

- Granular cell tumor may strongly resemble granular cell basal cell carcinoma in cases with granular differentiation of the majority of the basaloid tumor cells.

## 16.2.8 Squamous Cell Carcinoma

Among other causes, invasive squamous cell carcinoma (SCC) frequently occurs in association with actinic keratosis, with or without preceding or concomitant in situ carcinoma.

### 16.2.8.1 SCC of the Common Type (Fig. 16.11)

SCCs of the common type demonstrate an unequivocal malignant cell pattern with the characteristic features as seen in various organs such as bronchus, uterine cervix, oral cavity, and esophagus.

**Microscopic Features**

- Single tumor cells and three-dimensional irregular clusters.
- Tumor cells showing pronounced variation in size and shape.
- Nuclear key features:
  - Marked nuclear pleomorphism included molding and cleaving
  - Nuclear hyperchromasia
  - Unevenly distributed clumped chromatin or a homogeneous deep-staining chromatin texture
- Large pleomorphic nucleoli often occur multiply. Giant cells and mitotic activity may be common.
- The cytoplasm is polyhedral from round to polygonal to spindle shaped. The N/C ratio varies, but on the whole it is low.
  The sharply outlined cytoplasm of poorly differentiated cells is partly dense and cyanophilic, partly vacuolated, and often shows concentric lamination. In contrast, the cytoplasm of the keratinized cells is densely structured and pleomorphic or fusiform, exhibiting a bright red, orange, or yellow coloration.
- Keratin pearls commonly occur.
- Intercellular bridges are commonly observed.

### 16.2.8.2 Variants of Squamous Cell Carcinomas and Their Differential Diagnosis

See also Sect. 5.2.7.2, p. 468

#### 16.2.8.2.1 Well-Differentiated and Verrucous SCC

(Figs. 14.55B, 14.56, 14.57)
Accurate cell material can be obtained from the base and rims of malignant ulcers.

**Microscopic Features and Differential Diagnosis**

- These SCC variants are characterized by minimal cellular atypia.
- A certain degree of dyskaryosis and nuclear pleomorphism may be observed in abundantly keratinized cells. Numerous anucleated cells are present as well.
- The cytoplasm generally exhibits bright red and orange color.
- Pearl formation may occur.

By cytology, it is difficult to differentiate between well-differentiated SCCs and strongly hyperkeratotic/acanthotic benign or premalignant skin lesions, such as seborrheic keratosis, keratoacanthoma, senile keratosis, epidermal inclusion cyst, and others.

#### 16.2.8.2.2 Poorly Differentiated Squamous Cell Carcinoma

- *Large-cell SCC* (nonkeratinizing) may mimic numerous undifferentiated large-cell cancers such as poorly differentiated adenocarcinoma, nonpigmented malignant melanoma, malignant lymphoma of the blastic type, undifferentiated nonepithelial neoplasms, and others.
- *Small-cell SCC* comprising focal keratinization and horn pearls may mimic keratotic basal cell carcinoma. However, poorly differentiated SCCs show more pronounced cellular and nuclear pleomorphism, a higher N/C ratio, considerable loss of nuclear polarity, and no trend for palisading when compared to BCC. As already mentioned in Sect. 16.2.7.1, p. 1029, basal cell carcinoma shows horn cysts and not horn pearls, and intercellular bridges are absent.

#### 16.2.8.2.3 Spindle Cell Squamous Cell Carcinoma

(Fig. 5.77)
May mimic various epithelial and mesenchymal spindle cell lesions, including unpigmented spindle cell melanoma.

## 16.2.9 Malignant Melanoma [19, 40, 67, 77, 104]

**General Comments**

- Surgical biopsy is a well-established first-line diagnostic procedure in malignant melanomas of the skin. Garcia Rojo and coauthors studied the value of FNAB for the diagnosis of various melanocytic proliferations of the skin regarding feasibility of proper subtyping and differential diagnostic dilemmas [32].
- On the other hand, both FNAB and exfoliative cytology may be an accurate and helpful tool for the detection of:
  - Primary noncutaneous melanomas (e.g., vaginal, cervical, intraocular, among other sites) [19, 67].
  - Recurrent malignant melanoma [41, 89].
  - Metastatic melanoma [26, 77, 85].
- Tumor cells originating from malignant melanomas can exhibit a wide morphologic spectrum mimicking other

neoplasms; this is particularly true for nonpigmented malignant melanomas. However, the phenotype of epithelioid melanoma cells will allow a conclusive diagnosis in a majority of the cases.

- A few studies compared the cytologic features of malignant melanoma in conventional smears with those in liquid-based preparations. Good preservation and comparability of the cytological feature are yielded with both techniques [6, 72].

### 16.2.9.1 Epithelial-Type Malignant Melanoma

(Figs. 16.12–16.15)

**Microscopic Features** (Figs. 16.12–16.14)

- Hallmarks: Loss of cellular cohesion, bi- and multinucleation, intranuclear cytoplasmic invaginations, macronucleoli, and melanin pigment are distinct cellular characteristics of epithelioid malignant melanoma in comparison with other tumors.
- Binucleation is found in up to 20% of all tumor cells [93]. Anisocytosis and anisokaryosis vary from case to case.
- The nuclei are eccentrically positioned. The nucleoplasm may be lucid or dark. The nuclear membranes appear as a thin but distinct rim with pronounced irregularities comprising wrinkling and indentations. Intranuclear vacuoles are sharply outlined.
- The chromatin is finely to moderately granular and evenly distributed.
- The pronounced round or pleomorphic nucleoli usually stain red with the Papanicolaou staining method; bizarre nucleolar shapes may be encountered.
- In general, the cytoplasm is clear, showing ill-defined margins, large vacuoles may be present.
- The N/C ratio tends to be rather low.
- Melanin pigment occurs both in melanoma cells and macrophages; the latter are referred to as melanophages or melanophores. Melanophages may outnumber pigmented melanoma cells.

  The pigment in melanoma cells appears as clumps, as densely packed dirty greenish-brown granules, or fine light brownish cytoplasmic dust (Fig. 16.14); in contrast, the pigment in melanophages usually is coarse granular and densely packed.

  An abundance of melanin pigment may overshadow the cellular morphology, the cells are consequently difficult to classify as macrophages and tumor cells.

**Immunocytochemistry and Differential Diagnosis**

- The immunochemistry characterization of epithelioid melanoma cells is almost always successful using the melanoma-typical markers HMB-45, Melan A, pan melanoma cocktail (PMC), and tyrosinase (Fig. 16.15A and 16.15B); every marker is highly specific but variably sensitive.
- S100 protein immunolabeling usually provides a strong positive reaction in each cell of any melanocytic tumor type [92].
- Cytokeratins (CK) are well known for distinguishing between melanoma cells and carcinoma cells, but positive cytokeratin expression has been described in a low percentage of malignant melanomas as well. Additionally, CK immunopositivity has been found to occur more commonly in metastases of melanoma compared with primary tumors [5, 53].
- Smooth muscle actin may rarely provide a positive reaction in spindle cell melanomas [83].

Occasionally, melanoma cells may resemble undifferentiated malignant lymphoma of the large-blast type. In particular, lymphoma of the T-cell phenotype associated with pronounced nuclear polymorphism and grooving may be difficult to distinguish from melanoma. Immunocytochemical work-up using a panel of melanoma-typical and lymphocytic antibodies is extremely helpful to establish a definite diagnosis.

### 16.2.9.2 Variants of Malignant Melanoma

The most important variants of malignant melanoma and their differential diagnoses are discussed.

#### 16.2.9.2.1 Spindle Cell Melanoma [19, 77, 79, 104]

(Fig. 7.15)

**Microscopic features**

- This tumor type shows a predominant spindle cell pattern, occasionally interspersed with epithelioid tumor cells. Spindle cells occur dispersed or arranged in cohesive fascicles and whorls.
- Their nuclei are centrally placed, exhibiting an oval or elongated shape.
- Malignant melanoma spindle cells may exhibit a wide range of atypias from small virtually bland cells with regular nuclei and inconspicuous nucleoli to highly pleomorphic cells.

**Differential Diagnoses**

- Bland spindle cells may mimic granulomatosis, benign/low-grade soft tissue tumors of various types, and neuroendocrine tumors with fusiform cells [5, 49].
- Pleomorphic spindle melanoma cells may be indistinguishable from high-grade sarcomatous neoplasms and pleomorphic carcinoma [89].
- Melanotic spindle cell tumors comprise cutaneous spindle cell melanoma, melanotic schwannoma, and melanotic malignant peripheral nerve sheath tumor [52, 65].
- The antibody against S100 protein labels not only spindle melanoma cells but also a variety of mesenchymal neoplasms and occasionally carcinomas. Peripheral nerve

sheath tumors show strong immunocytochemical expression of S100 protein.
- Smooth muscle actin may aberrantly be detected in spindle cell melanoma [83].

**Caution**
- Primary melanoma and metastatic tumor of the same patient frequently exhibit discrepancies in their morphology: metastases may predominantly be composed of spindle cells, whereas the primary counterpart is composed of epithelioid cells.
- Spindle melanoma cells may lose the diagnostically important expression of melanoma-associated immunomarkers (except for S100 protein), even though scattered epithelial-type tumor cells may retain positive immunoreactivity, which is helpful in establishing a conclusive diagnosis.

#### 16.2.9.2.2 Balloon Cell Melanoma [4, 73]

This entity is entirely composed of large cells exhibiting an abundant vacuolated cytoplasm. The latter do not contain glycogen or fat. Generally, the tumor cells meet the pathognomonic cytologic features of epithelial type melanoma, showing positive immunoreactivity for melanoma-typical antibodies, but melanin pigment is completely absent. One must pay attention to the fact that the primary tumor may have a common morphology, contrary to the balloon-type metastases in the same patient [73].

Balloon cell melanoma should always be considered in the differential diagnosis of primary and secondary clear cell tumors, such as breast carcinoma of the secretory, lipid-rich or glycogen-rich type, clear cell renal cell carcinoma, hepatocellular carcinoma of the clear cell type, and others.

#### 16.2.9.2.3 Melanoma of the Monomorphic Small-Cell Type

The diagnosis may become uncertain in melanocytic tumors, which are composed of small cells lacking both melanin pigment and the typical nuclear morphology of melanoma cells. Consequently, these cells mimic cells from breast carcinomas and other carcinomas composed of a uniform cell population.

Furthermore, a population of relatively small individual monomorphic melanoma cells associated with eccentric nuclei and dense cyanophilic cytoplasm of the plasmacytoid type could lead to a false diagnosis of neuroendocrine tumor or plasmacytoid/plasmacytic malignant lymphoma. A correct diagnosis should be possible using an appropriate panel of antibodies.

#### 16.2.9.2.4 Other Rare Tumor Variants

Tumor variants such as melanoma with rhabdoid features [92] or signet-ring cell-like melanoma [95] have been discussed in a limited number of studies including differential diagnostic considerations.

### 16.2.10 Merkel Cell Carcinoma

[46, 69, 78, 88] (Fig. 16.16)

**General Comments**
- Merkel cell carcinoma (MCC) is a malignant cutaneous neoplasm showing neuroendocrine and epithelial differentiation. Therefore, it has been suggested that the tumor is not derived from neuroectodermal Merkel cells but from the epithelium [43]. The recently detected Merkel cell polyomavirus (MCV) seems to play an important role in the etiology and pathogenesis of Merkel cell carcinoma [30A].
- MCC usually occurs in the dermis but occasionally as well in the subcutaneous tissue. Privileged localizations of the tumor are in the skin of the head and neck and the skin of extremities in the elderly population. The tumor has a striking tendency for local recurrence and for spreading into the regional lymph nodes, but distant metastases may occur as well [103].

**Microscopic Features**

The cytomorphological findings are those of a small round blue cell malignant tumor.
- Hallmarks:
  - The aspirates are highly cellular.
  - Tumor cells occur in small clusters forming rosettes and single-file rows. The cells are often molding against each other. Single cells and stripped nuclei are present in addition to the aggregated cells. The small tumor cells are uniform and round to oval in shape.
  - The eccentrically placed and irregularly outlined nuclei contain a fine granular chromatin and an inconspicuous nucleolus. The nuclear membrane is well defined.
  - There is pronounced nuclear hyperchromasia.
  - The cytoplasm is scanty and sometimes faintly granular.
  - Mitotic figures are frequently encountered.

**Immunocytochemistry** (Fig. 16.16D)
- The tumor cells exhibit intense staining for Pan-cytokeratins, CK20, and neuron-specific enolase (NSE). CK20 positivity is characterized by prominent paranuclear dot-like globules; however, it is an inconstant phenomenon [45, 91].
- The neuroendocrine markers synaptophysin and chromogranin demonstrate immunopositivity in a high percentage of MCC cells [88].
- CK7 reactivity may be seen in a subset of MCCs [45].
- Negative immunoreactivity is achieved for TTF-1 and leukocyte common antigen (LCA and CD45). Positive immunostaining for CK20 and simultaneously for TTF-1 is a powerful aid in distinguishing between secondary small-cell carcinoma to the skin (TTF-1 **+**, CK20 **–**) and MCC (opposite immunoprofile) [15, 16, 58].

- In doubtful cases, an immunostaining (or PCR) for the Merkel cell virus can be performed [87A].

**Differential Diagnosis** [78]

- TTF-1 and CK20 can reliably distinguish between metastatic small-cell carcinoma of various sites and Merkel cell carcinoma. However, a small percentage of extrapulmonary small-cell carcinomas provide immunopositivity for CK20. Furthermore, the two markers do not reliably distinguish between cutaneous metastases of pulmonary small-cell carcinoma and extrapulmonary small-cell carcinoma due to overlap in the immunophenotypic signatures [16].
- Poorly differentiated neoplasms of the small round blue cell malignant tumor group lacking the characteristic cytoarchitectural features and a possible specific smear background may be indistinguishable from MCC. Immunophenotyping can be helpful, at least to suggest a diagnosis. In such cases, the individual clinical history is of utmost importance in preventing a misdiagnosis.
- Basal cell carcinoma. An appropriate immunocytochemical work-up should permit a correct diagnosis excluding MCC. Basal cell carcinoma is negative for neuroendocrine markers.
- Nonpigmented small-cell malignant melanoma devoid of the typical nuclear morphology may mimic MCC, but the different immunoprofiles should help make a conclusive diagnosis.
- Lymphoblastic lymphoma/malignant lymphoma of the small-cell type and granulocytic sarcoma. Immunopositivity for CK20 and endocrine markers in MCC is completely different from the immunoreactivity of cells from NHL and hematopoietic disorders.
- Cells of salivary gland small-cell carcinoma frequently exhibit CK20 immunopositivity, which hampers distinguishing these salivary gland tumors from MCC [15].

## 16.2.11 Kaposi Sarcoma [31, 42] (Fig. 16.17)

Kaposi sarcoma is a malignant vascular tumor usually associated with immunosuppression and human herpes virus 8 (HHV-8) infection. Kaposi sarcoma is usually investigated by a surgical biopsy, but secondary tumor manifestations may sporadically be detected using fine-needle aspiration obtained from enlarged lymph nodes [71].

The immunocytochemical detection of HHV-8 components is diagnostic for Kaposi sarcoma.

**Microscopic Features and Differential Diagnosis**

- The most typical cytological features are tissue fragments composed of spindle cells exhibiting distorted nuclei and an ill-defined cytoplasmic outline. Loosely or radially arranged spindle-shaped cells and discrete spindle cells are likewise observed.
- Nuclear crush artifacts are reported to be a diagnostic key feature [31].

Other mesenchymal neoplasms and granulomatous lesions may show similar morphologic features as compared with Kaposi sarcoma. However, granulomatous lesions are usually associated with histiocytic cells, such as foamy cells or epithelioid histiocytes [18].

## 16.2.12 Malignant Lymphoma of the Skin [61, 64]

- Malignant lymphomas of the skin are only sporadically investigated by cytology; it most likely occurs when FNAB or skin scraping is used as the initial investigation in ulcerating cutaneous lesions.
- Cutaneous lymphoma may occur as a primary or secondary manifestation of the disease. NHL presenting as skin lesion can be assigned to the B-cell or T-cell phenotype. The predominance of one or the other phenotype varies, depending on country and continent.
- Skin involvement of Hodgkin disease is occasionally seen in an advanced tumor stage [44].
- Malignant hematopoietic disorders rarely cause cutaneous manifestations. Immunocytochemical peculiarities differentiate between granulocytic sarcoma and malignant lymphoma [54, 60, 61].
- Immunocytochemical panels are extremely helpful in distinguishing between lymphoid, epithelial, and mesenchymal disorders. Differentiating malignant lymphoma from cutaneous lymphoid hyperplasia is practically impossible based on cytologic findings alone.
- Various ancillary techniques should be applied to cytologic samples of lymphoid skin lesions in order to separate NHL from reactive lymphoid hyperplasia and to subclassify malignant lymphomas. These methods include immunocytochemical or multicolor flow cytometric immunophenotyping; and assessment of the clonality by immunocytochemical kappa/lambda staining or by molecular genetic analyses [68, 99]. Fluorescence in situ hybridization may be applied to detect specific translocations of gene loci occurring in particular lymphoma variants. The methods are detailed in several chapters of this book and summarized in Sect. 15.1.4, “Ancillary Techniques,” p. 910.
- Primary cutaneous malignant lymphomas are discussed in Sect. 15.3, p. 950, and especially in Sect. 15.3.15, “Mycosis fungoides/Sézary syndrome,”, p. 967.

## 16.3 Primary Cutaneous Tumors Mimicking Metastatic Deposits and Vice-Versa

Gupta and Naran have documented a large series of metastatic epithelial tumors to the skin and subcutis detected by FNAB [39].

### 16.3.1 Cutaneous Cylindroma

Cutaneous cylindroma is a predominantly benign tumor probably originating from cutaneous glands. The lesion is typically localized to the scalp but it may also occur on the face and in other skin areas.

**Microscopic Features and Differential Diagnosis**

- The cells are tightly packed and vary considerably in size.
- Epithelial cell aggregations encase globules of basement-membrane-like material.
- Solid and/or tubular tumor cell clusters may be surrounded by hyaline stroma (Fig. 16.18).

Primary adenoid-cystic carcinoma of the salivary glands or the breast should be considered in cases in which the tumor is located on the face or on the breast skin [13].

### 16.3.2 Mucinous Adenocarcinoma of the Skin

Mucinous adenocarcinoma is a rare tumor originating from skin adnexa. The neoplasm occurs most often on the head and neck of elderly patients. It is a slow-growing tumor occasionally metastasizing to regional lymph nodes; the prognosis is good.

**Microscopic Features and Differential Diagnosis**

- The cytologic smears are composed of loosely dispersed mucin-forming cells scattered in a background of mucoid material [50]

- Primary cutaneous mucinous adenocarcinoma closely mimics metastatic mucinous adenocarcinoma.
- Primary mucinous skin carcinoma at an axillary site is extremely rare but will likely mislead to a diagnosis of metastatic mucinous mammary carcinoma [94].

**Caution**

Axillary presentation of cutaneous mucin-producing carcinoma should raise the possibility of metastatic mucinous breast carcinoma and vice-versa.

### 16.3.3 Breast Cancer Versus Pilomatrixoma [1], Basal Cell Carcinoma, and Melanoma of the Monomorphic Small-Cell Type

**Caution**

- Pilomatrixoma, basal cell carcinoma, and small-cell variants of malignant melanoma as described earlier in this chapter may particularly mimic breast carcinoma.
- One has to keep in mind that breast cancer provides the majority of secondary tumors in the skin and in scars on the breast after successful surgical treatment of the primary tumor (At our institution, follow-up monitoring patients with suspicion of cutaneous breast cancer recurrence/metastasis is usually performed by fine-needle aspiration).
- In general, the common type of breast carcinoma is easily recognized in cytologic specimens, but metastases of mammary carcinoma of the monomorphic subtype can be challenging.

## 16.4 Unusual Nonneoplastic Masses in Skin and Subcutaneous Regions

### 16.4.1 Pseudosarcomatous Reactive Soft Tissue Lesions

Nodular fasciitis and other disorders represent benign proliferation of fibroblasts and myofibroblasts in subcutaneous tissues. The cause of this reactive lesion is unknown.

The lesions commonly occur in the upper extremities of adults and in the head and neck region of infants and children. Nodular fasciitis is most commonly seen in young adults between 30 and 40 years of age. Spontaneous regression generally occurs within a few months.

Cytomorphologic characteristics and additional informations are provided in Sect. 17.1.3, “Fibroblastic and Myofibroblastic Lesions,” p. 1059.

### 16.4.2 Kimura Disease and Angiolymphoid Hyperplasia with Eosinophilia

Both disorders, although widely accepted as separate disease entities, present clinically as inflammatory nodules mainly in the head and neck region. Their cytomorphologic features are closely related to each other.

Detailed information on the two entities are presented in Sects. 5.2.4.1.2, p. 465, and 5.2.4.2.3, p. 466.

### 16.4.3 Endometriosis [14, 36, 38, 75] (Fig. 16.19)

#### General Comments

- Endometriosis consisting of ectopic endometrial tissue is most frequently implanted in the pelvic serosa and on the surface of the pelvic organs, but it may also involve adjacent connective tissue.
- Rare implantations occur in the skin and in subcutaneous soft tissue of which the predilection sites are:
  - Scars of the lower abdominal area in women with a prior history of abdominal and pelvic surgery, in particular those with a history of previous cesarean section [70, 75].
  - The umbilical region [28].
  - The inguinal region [14].
  - The perineum and rectovaginal septum [59].
- Cutaneous/subcutaneous endometriosis is an extremely rare disorder in females without a history of abdominal surgery or preexisting endometriosis [28].
- Endometriosis can present as a palpable mass, hence a minimally invasive method such as FNAB is most likely chosen for initial investigation in patients with an unremarkable clinical history. However, the lesion can present a multitude of clinical signs and symptoms and may be painful in a cyclical modality.
- (Clear-cell-) adenocarcinoma may occur in a background of peripheral endometriosis [86].

**Caution**

- Endometriosis can cause diagnostic problems in fine-needle aspirates if the cytopathologist is unaware of the related clinical symptoms and/or a history of earlier abdominal surgery.
- Malignant transformation starting from extraabdominal endometriosis has been described.

#### Microscopic Features

- Hallmarks:
  - The smears are usually highly cellular.
  - The background is composed blood, detritus, and hemosiderin-laden macrophages.
  - A varying number of syncytial clusters, tubular formations, and epithelial sheets forming a honeycomb pattern are present together with aggregates of fusiform stromal cells. The stromal cell nuclei may show crowding and overlapping.
- Endometrial glandular cells are small to medium-sized. The nuclear membranes are distinct and wrinkled. The nucleoli are usually inconspicuous and the chromatin is granular and evenly distributed.
- The cytoplasm is scant and cyanophilic.
- Transition from glandular epithelium to squamous metaplasia may be observed: immature squamous cells exhibit large dense polygonal cytoplasm and cobblestone arrangement.
- Mild to moderate epithelial atypia may be observed depending on hormonal cell activation.
- Endometrial decidualization rarely occurs; it is characterized by enlarged active stromal cells that are embedded in a distinctive myxoid background [8].
- The morphologic variability of cutaneous endometriosis as seen in histologic biopsies has recently been studied by Kazakov and contributors [48].

#### Differential Diagnosis and Immunocytochemistry

- Glandular endometrial cell groups composed of enlarged reactive cells comprising nuclear hyperchromasia, irregular nuclear outline, and nuclear overlapping could lead to a false-positive diagnosis of metastatic adenocarcinoma [3].
- Soft tissue fragments combined with the absence of glandular cells in aspirates from endometriosis of the abdominal wall may lead to a false diagnosis of nodular and proliferative fasciitis, myxoma, or low-grade sarcoma [8].
- Immunocytochemistry is an important tool in determining a definite cytologic diagnosis, but it cannot rule out malignancy; epithelial endometrial cells reliably show positivity for hormone receptors (Fig. 16.19C).

### 16.4.4 Tumor Mass in the Groin Due to Particle Disease and Osteoarthritic Hydrarthrosis

(Figs. 3.82, 3.83, 3.88, 16.20)

#### General Comments

- Particle disease is a lesion following arthroplasty. It refers to the host's adverse biologic response to wear debris generated from the prosthesis. Particulate wear debris causes periprosthetic bone destruction (aseptic osteolysis) that results in an inflammatory response comprising macrophage activation and phagocytosis [2]. Varying types of debris such as polymethylmethacrylate (cement disease), polyethylene, and metal components (metallosis) can generate an inflammatory process. [35, 47]. Particle disease may lead to implant failure.
- Particle disease rarely induces a huge granulomatous mass with cystic degeneration, presenting as either an intrapelvic tumor [62], a thigh mass [55], or an inguinal tumor [57].

  A groin mass can particularly result from:
  - The extent of iliopsoas bursitis to the groin caused by hip prosthetic complications including wear particle disease. Direct communication between bursa and joint is possible but not always traceable [17, 37].
  - The extent of pronounced hydrarthrosis to the subcutaneous tissue due to osteoarthritis (Fig. 16.20).

- At our institution, we have observed a few patients presenting with an inguinal tumor mass caused by disorders as described above. All patients have had clinical suspicion of malignant neoplasia.

**Caution**

Elderly patients with dementia are likely to forget about previous hip replacement, which will often make it impossible to complete their clinical history.

**Microscopic Features** [55, 57, 74]

1. The microscopic hallmarks of wear particle disease (Fig. 3.88) are the following:
   - Most of the aspirates are turbid and viscous.
   - The smears are hypercellular consisting of proliferating fibroblasts and histiocytes. The fusiform mesenchymal cells are scattered or densely packed. Macrophages may also be present, comprising activated irregular nuclei and vacuolated or foamy cytoplasm; phagocytic activity may be pronounced.
   - Inflammatory cells and multinucleated histiocytic giant cells are frequently present.
   - Particulate wear debris from the prosthesis (from joint surfaces and interfaces) is closely associated with macrophages and foreign-body-type giant cells. The debris is refractile, and certain components such as polyethylene are birefringent upon polarization.
2. Detailed microscopic features of osteoarthritic joint fluid (Figs. 3.82, 3.83, 16.20) are provided in Sect. 3.4.1.2, "Osteoarthritis and Trauma," p. 314.

**Differential Diagnosis** (Fig. 16.20A)

- Polymorphous detritus should not be misread as tumor necrosis; attention should be paid to refractile behavior of certain components of the background material.
- Activated histiocytes can mimic undifferentiated carcinoma, sarcoma, and large-cell anaplastic lymphoma.
- A selective panel of immunocytochemical stains is helpful in reaching an accurate cytologic diagnosis.

### 16.4.5 Inguinal Tumor Mass Due to Hydatid Cyst of the Hip Joint and Pelvic Bone

- Bone and joint involvement with hydatid disease is rare; however, it is occasionally observed in countries where echinococcosis is quite common. The second most common skeletal location is the pelvis and hip joint [65A].
- The pseudotumorous swelling may extend from the hip joint or pelvic bones to the groin area presenting as subcutaneous palpable mass. The clinical diagnosis is in many cases that of a malignant tumor [101].
- For information on the morphologic features and diagnostic cautions regarding hydatid disease, see Sect. 9.1.7.3, p. 590.

## 16.5 Further Reading


1. Ali MZ, Ali FZ. Pilomatrixoma breast mimicking carcinoma. Coll Physicians Surg Pak 2005;15:248-249.
2. Amstutz HC, Campbell P, Kossovsky N, Clarke IC. Mechanism and clinical significance of wear debris-induced osteolysis. Clin Orthop Relat Res 1992;276:7-18.
3. Ashfaq R, Molberg KH, Vuitch F. Cutaneous endometriosis as a diagnostic pitfall of fine needle aspiration biopsy. A report of three cases. Acta Cytol 1994;38:577-581.
4. Baehner FL, Ng B, Sudilovsky D. Metastatic balloon cell melanoma: a case report. Acta Cytol 2005;49:543-548.
5. Banerjee SS, Harris M. Morphological and immunophenotypic variations in malignant melanoma. Histopathology 2000;36:387-402.
6. Barkan GA, Rubin MA, Michael CW. Diagnosis of melanoma aspirates on ThinPrep: The University of Michigan experience. Diagn Cytopathol 2002;26:334-339.
7. Barr RJ, Graham JH. Granular cell basal cell carcinoma. Arch Dermatol 1979;115:1064-1067.
8. Berardo MD, Valente PT, Powers CN. Cytodiagnosis and comparison of nondecidualized and decidualized endometriosis of the abdominal wall. A report of two cases. Acta Cytol 1992;36:957-962.
9. Bhadani PP, Sen R, Bhadani UK, et al. Is fine needle aspiration cytology (FNAC) useful in skin adnexal masses? A study on 5 cases of pilomatrixoma. Indian J Pathol Microbiol 2007;50:411-414.
10. Blank H, Burgoon CF. Abnormal cytology of epithelial cells in pemphigus vulgaris: a diagnostic aid. J Invest Dermatol 1952; 18:213-223.
11. Blank H, Burgoon CF, Baldridge G, Urbach F. Cytologic smears in diagnosis of herpes simplex, herpes zoster and varicella. JAMA 1951;146:1410-1412.
12. Blumenfeld W, Hildebrandt RH. Fine needle aspiration of abdominal fat for the diagnosis of amyloidosis. Acta Cytol 1993;37:170-174.
13. Bondeson L, Lindholm K, Thorstenson S. Benign dermal eccrine cylindroma. A pitfall in the cytologic diagnosis of adenoid cystic carcinoma. Acta Cytol. 1983;27:326-328.
14. Catalina-Fernandez I, Lopez-Presa D, Saenz-Santamaria J. Fine needle aspiration cytology in cutaneous and subcutaneous endometriosis. Acta Cytol 2007;51:380-384.
15. Chan JK, Suster S, Wenig BM, et al. Cytokeratin 20 immunoreactivity distinguishes Merkel cell (primary cutaneous neuroendocrine) carcinomas and salivary gland small cell carcinomas from small cell carcinomas of various sites. Am J Surg Pathol 1997; 21:226-234.
16. Cheuk W, Kwan MY, Suster S, Chan JK. Immunostaining for thyroid transcription factor 1 and cytokeratin 20 aids the distinction of small cell carcinoma from Merkel cell carcinoma, but not pulmonary from extrapulmonary small cell carcinomas. Arch Pathol Lab Med 2001;125:228-231.
17. Cheung YM, Gupte CM, Beverly MJ. Iliopsoas bursitis following total hip replacement. Arch Orthop Trauma Surg 2004;124:720-723.
18. Corkill M, Stephens J, Bitter M. Fine needle aspiration cytology of mycobacterial spindle cell pseudotumor. A case report. Acta Cytol 1995;39:125-128.
19. Czerniak B, Woyke S, Domagala W, Krzysztolik Z. Fine needle aspiration cytology of intraocular malignant melanoma. Acta Cytol 1983;27:157-165.
20. Daskalopoulou D, Galanopoulou A, Statiropoulou P, et al. Cytologically interesting cases of primary skin tumors and tumor-like conditions identified by fine-needle aspiration biopsy. Diagn Cytopathol 1998;19:17-28.
21. Daskalopoulou D, Maounis N, Kokalis G, et al. The role of fine needle aspiration cytology in the diagnosis of primary skin tumors. Arch Anat Cytol Pathol 1993;41:75-81.
22. Deolakar MV, Brown DC, Desai SA. Malignant pilomatrixoma: a case report with fine needle aspiration (FNA) cytology. Cytopathology 1999;10:270-275.
23. Derrick EK, Smith R, Melcher DH, et al. The use of cytology in the diagnosis of basal cell carcinoma. Br J Dermatol 1994;130:561-563.
24. Dhingra S, Krishnani N, Kumari N, Pandey R. Evaluation of abdominal fat pad aspiration cytology and grading for detection in systemic amyloidosis. Acta Cytol 2007;51:860-864.
25. Domanski HA, Domanski AM. Cytology of pilomatrixoma (calcifying epithelioma of Malherbe) in fine needle aspirates. Acta Cytol 1997;41:771-777.
26. Doubrovsky A, Scolyer RA, Murali R, et al. Diagnostic accuracy of fine needle biopsy for metastatic melanoma and its implications for patient management. Ann Surg Oncol 2008;15:323-332.
27. Dutta R, Boadle R, Ng T. Pilomatrix carcinoma: case report and review of literature. Pathology 2001;33:248-251.
28. Elm MK, Twede JV, Turiansky GW. Primary cutaneous endometriosis of the umbilicus: a case report. Cutis 2008;81:124-126.
29. el Hag IA, Kollur SM. Fine needle aspiration cytology of pilomatrixoma of the neck region: differentiation from metastatic undifferentiated nasopharyngeal carcinoma. Acta Cytol 2003;47:526-528.
30. Fang X, Ma B. Fine needle aspiration cytology of basal cell carcinoma of the skin: a clinical and cytopathological appraisal. J Dermatol 1999;26:640-646.

30A. Feng H, Shuda M, Chang Y, Moore PS. Clonal integration of a polyomavirus in human merkel cell carcinoma. Science 2008;319(5866):1096-1100.31.

31. Gamborino E, Carrilho C, Ferro J, et al. Fine needle aspiration diagnosis of Kaposi's sarcoma in a developing country. Diagn Cytopathol 2000;23:322-325.
32. Garcia Rojo B, Garcia Solano J, Sanchez Sanchez C, et al. On the limited value of fine-needle aspiration for the diagnosis of benign melanocytic proliferations of the skin. Diagn Cytopathol 1998; 19:441-445.
33. Garcia Solano J, Acosta-Ortega J, Perez-Guillermo M. Pilomatrixoma: never lower your guard. Diagn Cytopathol 2007;35:457-458.
34. Garcia-Solano J, Garcia-Rojo B, Sanchez-Sanchez C, et al. Basal-cell carcinoma: cytologic and immunocytochemical findings in fine-needle aspirates. Diagn Cytopathol 1998;18:403-408.
35. Goodman S. Wear particulate and osteolysis. Orthop Clin North Am 2005;36:41-48, vi.
36. Griffin JB, Betsill WL Jr. Subcutaneous endometriosis diagnosed by fine needle aspiration cytology. Acta Cytol 1985;29:584-588.
37. Grosclaude S, Adam P, Besse JL, Fessy MH. Iliopsoas bursal distension revealing complication of total hip arthroplasty: five cases. Rev Chir Orthop Reparatrice Appar Mot 2006;92:351-357.
38. Gupta RK. Fine-needle aspiration cytodiagnosis of endometriosis in cesarean section scar and rectus sheath mass lesions – a study of seven cases. Diagn Cytopathol 2008;36:224-226.
39. Gupta RK, Naran S. Fine needle aspiration cytology of cutaneous and subcutaneous metastatic deposits from epithelial malignancies. An analysis of 146 cases. Acta Cytol 1999;43:126-130.
40. Gupta SK, Rajwanshi AK, Das DK. Fine needle aspiration cytology smear patterns of malignant melanoma. Acta Cytol 1985;29:983-988.
41. Hafström L, Hugander A, Jönsson PE, Lindberg LG. Fine-needle-aspiration cytodiagnosis of recurrent malignant melanoma. J Surg Oncol 1980;15:229-234.
42. Hales M, Bottles K, Miller T, et al. Diagnosis of Kaposi's sarcoma by fine-needle aspiration biopsy. Am J Clin Pathol 1987;88:20-25.
43. Heenan PJ, Elder DE, Sobin LH. Histological typing of skin tumours, 2nd ed. World Health Organization. Springer 1996
44. Jain S, Nigam S, Kumar N, Reddy BS. Cutaneous relapse in Hodgkin's disease: a case report. Acta Cytol 2005;49:191-194.

45. Jensen K, Kohler S, Rouse RV. Cytokeratin staining in Merkel cell carcinoma: an immunohistochemical study of cytokeratins 5/6,7,17, and 20. Appl Immunohistochem Mol Morphol 2000;8:310-315.
46. Kabukcuoglu F, Sungun A, Polat N, et al. Fine needle aspiration cytology of Merkel cell carcinoma. Acta Cytol 2003;47:311-313.
47. Kadoya Y, Kobayashi A, Ohashi H. Wear and osteolysis in total joint replacements. Acta Orthop Scand Suppl 1998;278:1-16.
48. Kazakov DV, Ondic O, Zamecnik M, et al. Morphological variations of scar-related and spontaneous endometriosis of the skin and superficial soft tissue: a study of 71 cases with emphasis on atypical features and types of müllerian differentiations. J Am Acad Dermatol 2007;57:134-146.
49. King R, Busam K, Rosai J. Metastatic malignant melanoma resembling malignant peripheral nerve sheath tumor: report of 16 cases. Am J Surg Pathol 1999;23:1499-1505.
50. Kotru M, Manucha V, Singh UR. Cytologic and histologic features of primary mucinous adenocarcinoma of skin in the axilla: a case report. Acta Cytol 2007;51:571-574.
51. Kraskina NA, Strod AK. Diagnostic value of cytological picture of the focus of the disease in pemphigus. Vestn Venerol Dermatol 1955;No 5:10-14.
52. Krausz T, Azzopardi JG, Pearse E. Malignant melanoma of the sympathetic chain: with a consideration of pigmented nerve sheath tumours. Histopathology 1984;8:881-894.
53. Kucher C, Zhang PJ, Acs G, et al. Can Melan-A replace S-100 and HMB-45 in the evaluation of sentinel lymph nodes from patients with malignant melanoma? Appl Immunohistochem Mol Morphol 2006;14:324-327.
54. Kumar PV. Leukemia cutis. Fine needle aspiration findings. Acta Cytol 1997;41:666-671.
55. Lachiewicz PF. Case report: a thigh mass resulting from polyethylene wear of a revision total hip arthroplasty. Clin Orthop Relat Res 2007;455:274-276.
56. Layfield LJ, Glasgow BJ. Aspiration biopsy cytology of primary cutaneous tumors. Acta Cytol 1993;37:679-688.
57. Lecuit M, Chatelain D, Courpied JP, et al. Tissue reactions to wear debris of joint prostheses. Apropos 2 cases. Rev Chir Orthop Reparatrice Appar Mot 1999;85:636-639.
58. Leech SN, Kolar AJ, Barrett PD, et al. Merkel cell carcinoma can be distinguished from metastatic small cell carcinoma using antibodies to cytokeratin 20 and thyroid transcription factor 1. J Clin Pathol 2001;54:727-729.
59. Leiman G, Markowitz S, Veiga-Ferreira MM, Margolius KA. Endometriosis of the rectovaginal septum. Diagnosis by fine needle aspiration cytology. Acta Cytol 1986;30:313-316.
60. Long JC, Mihm MC. Multiple granulocytic tumors of the skin: report of six cases of myelogenous leukemia with initial manifestations in the skin. Cancer 1977;39:2004-2016.
61. Long JC, Mihm MC, Qazi R. Malignant lymphoma of the skin: a clinicopathological study of lymphoma other than mycosis fungoides. Cancer 1976;38:1282-1296.
62. Mak KH, Wong TK, Poddar NC. Wear debris from total hip arthroplasty presenting as an intrapelvic mass. J Arthroplasty 2001;16:674-676.
63. Malberger E, Tillinger R, Lichtig C. Diagnosis of basal-cell carcinoma with aspiration cytology. Acta Cytol 1984;28:301-304.
64. Mandal S, Varma K, Jain S. Cutaneous manifestations in non-Hodgkin's lymphoma. Acta Cytol 2007;51:853-859.
65. Marco V, Sirvent J, Alvarez Moro J, et al. Malignant melanotic schwannoma fine-needle aspiration biopsy findings. Diagn Cytopathol 1998;18:284-286.
65A. Martinez AA, Herrera A, Cuenca J, Herrero L. Hydatidosis of the pelvis and hip. Int Orthop 2001;25:302.304.
66. Masouye I. Diagnostic screening of systemic amyloidosis by abdominal fat aspiration: an analysis of 100 cases. Am J Dermatopathol 1997;19:41-45.
67. Masubuchi S Jr, Nagai I, Hirata M, et al. Cytologic studies of malignant melanoma of the vagina. Acta Cytol 1975;19:527-532.
68. Mathiot C, Decaudin D, Klijanienko J, et al. Fine-needle aspiration cytology combined with flow cytometry immunophenotyping is a rapid and accurate approach for the evaluation of suspicious superficial lymphoid lesions. Diagn Cytopathol 2006;34:472-478.
69. Mellblom L, Akerman M, Carlen B. Aspiration cytology of neuroendocrine (Merkel-Cell) carcinoma of the skin. Report of a case. Acta Cytol 1984;28:297-300.
70. Minaglia S, Mishell DR Jr, Ballard CA. Incisional endometriomas after Cesarean section: a case series. J Reprod Med 2007;52:630-634.
71. Morelli L, Pusiol T, Piscioli I, et al. Fine needle aspiration cytology determinants of the diagnosis of primary nodal Kaposi's sarcoma as the first sign of unknown HIV infection: a case report. Acta Cytol 2007;51:602-604.
72. Morrison C, Young DC, Wakely PE Jr. Cytopathology of malignant melanoma in conventional and liquid based smears. Am J Clin Pathol 2002;118:435-441.
73. Mowat A, Reid R, Mackie R. Balloon cell metastatic melanoma: an important differential in the diagnosis of clear cell tumours. Histopathology 1994;24:469-472.
74. Parwani AV, Yang B, Clark DP, Ali SZ. Particle disease: cytopathologic findings of an unusual case. Diagn Cytopathol 2004;31:259-262.
75. Pathan SK, Kapila K, Haji BE, et al. Cytomorphological spectrum in scar endometriosis: a study of eight cases. Cytopathology 2005;16:94-99.
76. Perez-Guillermo M, Garcia Solano J, Acosta Ortega J. FNA of pilomatrixoma: smear vs. cell block. Diagn Cytopathol 2006;34:384-385.
77. Perry MD, Gore M, Seigler HF, Johnston WW. Fine needle aspiration biopsy of metastatic melanoma. A morphologic analysis of 174 cases. Acta Cytol 1986;30:385-396.
78. Pettinato G, De Chiara A, Insabato L, Iaffaioli V. Neuroendocrine (Merkel-cell) carcinoma of the skin. Fine needle aspiration cytology and clinicopathologic study of a case. Acta Cytol 1984;28:283-289.
79. Piao Y, Guo M, Gong Y. Diagnostic challenges of metastatic spindle cell melanoma on fine-needle aspiration specimens. Cancer (Cancer Cytopathol) 2008;114:94-101.
80. Poniecka AW, Alexis JB. An immunohistochemical study of basal cell carcinoma and trichoepithelioma. Am J Dermatopathol 1999;21:332-336.
81. Rege J, Shet T. Aspiration cytology in the diagnosis of primary tumors of skin adnexa. Acta Cytol 2001;45:715-722.
82. Reichel M. Granular cell basal cell carcinoma. Cutis 1997;59:88-90.
83. Riccioni L, Di Tommaso L, Collina G. Actin-rich desmoplastic malignant melanoma: report of 3 cases. Am J Dermatopathol 1999;21:537-541.
84. Rizzardi C, Brollo A, Colonna A, et al. A tumor with composite pilo-folliculosebaceous differentiation harboring a recently described new entity – melanocytic matricoma. Am J Dermatopathol 2002;24:493-497.
85. Rodrigues LK, Leong SP, Ljung BM, et al. Fine needle aspiration in the diagnosis of metastatic melanoma. J Am Acad Dermatol 2000;42:735-740.
86. Rust MM, Susa J, Naylor R, Cavuoti D. Clear cell carcinoma in a background of endometriosis. Case report of a finding in a midline abdominal scar 5 years after a total abdominal hysterectomy. Acta Cytol 2008;52:475-480.
87. Sanchez Sanchez C, Gimenez Bascunana A, Pastor Quirante FA, et al. Mimics of pilomatrixomas in fine-needle aspirates. Diagn Cytopathol 1996;14:75-83.
87A. Satoshi K. Recent advances in the biology of Merkel cell carcinoma. Human Pathology 2011;42(8):1063-1077.

88. Sharma A, Rana DN, Desai M. Cytomorphological evaluation of a small round blue cell tumour of the head and neck. Cytopathology 2007;18:197-199.
89. Siddaraju N, Yaranal PJ, Mishra MM, et al. Fine needle aspiration cytology in recurrent amelanotic melanoma: a case report. Acta Cytol 2007;51:829-832.
90. Sivakumar S. Pilomatrixoma as a diagnostic pitfall in fine needle aspiration cytology: a case report. Acta cytol 2007;51:583-585.
91. Skoog L, Schmitt FC, Tani E. Neuroendocrine (Merkel-cell) carcinoma of the skin: immunocytochemical and cytomorphologic analysis on fine-needle aspirates. Diagn Cytopathol 1990;6:53-57.
92. Slagel DD, Raab SS, Silverman JF. Fine needle aspiration biopsy of metastatic malignant melanoma with "rhabdoid" features. Frequency, cytologic features, pitfalls and ancillary studies. Acta Cytol 1997;41:1426-1430.
93. Spieler P, Gloor F. Identification of types and primary sites of malignant tumors by examination of exfoliated tumor cells in serous fluids. Comparison with the diagnostic accuracy on small histologic biopsies. Acta Cytol 1985;29:753-767.
94. Terada T, Sato Y, Furukawa K, Sugiura M. Primary cutaneous mucinous carcinoma initially diagnosed as metastatic adenocarcinoma. Tohoku J Exp Med 2004;203:345-348.
95. Tsang WY, Chan JK, Chow LT. Signet-ring cell melanoma mimicking adenocarcinoma. A case report. Acta Cytol 1993;37:559-562.
96. Tzanck A, Melki GR, Aron-Brunetiere R. Cytodiagnosis of pemphigus. Acta Unio Int Contra Cancrum 1951;7:727-729.
97. Vadasz E. Cytological differential diagnosis of pemphigus vulgaris and other bullous dermatoses and their cytological changes as demonstrated by Tzanck's test during treatment with steroids. Z Haut Geschlechtskr 1958;25:287-290.
98. van Gameren II, Hazenberg BP, Bijzet J, et al. Diagnostic accuracy of subcutaneous abdominal fat tissue aspiration for detecting systemic amyloidosis and its utility in clinical practice. Arthritis Rheum 2006;54:2015-2021.
99. Venkatraman L, Catherwood MA, Patterson A, et al. Role of polymerase chain reaction and immunocytochemistry in the cytological assessment of lymphoid proliferations. J Clin Pathol 2006;59:1160-1165.
100. Viero RM, Tani E, Skoog L. Fine needle aspiration (FNA) cytology of pilomatrixoma: report of 14 cases and review of the literature. Cytopathology 1999;10:263-269.
101. Wahane RN, Pangarkar MA, Bobhate SK. Fine needle aspiration cytology of a hydatid cyst of the pelvis and hip joint. Acta Cytol 2008;52:381-384.
102. Wang J, Cobb CJ, Martin SE, et al. Pilomatrixoma: clinicopathologic study of 51 cases with emphasis on cytologic features. Diagn Cytopathol 2002;27:167-172.
103. Wick MR, Goellner JR, Scheithauer BW, et al. Primary neuroendocrine carcinomas of the skin (Merkel cell tumors): a clinical, histologic, and ultrastructural study of thirteen cases. Am J Clin Pathol 1983;79:6-13.
104. Woyke S, Domagala W, Czerniak B, Strokowska M. Fine needle aspiration cytology of malignant melanoma of the skin. Acta Cytol 1980;24:529-538.
105. Youngberg GA, Laucirica R, Leicht SS. Frequency of occurrence of diagnostic cytologic parameters in basal cell carcinoma. A retrospective review of 25 cases. Am J Clin Pathol 1989;91:24-30.

**Fig. 16.1A–C Normal cells of cutaneous appendage.**
Cells and tissue fragments are depicted from Pap-stained direct smears at high magnification (FNAB material).
**A** *Sebaceous gland:* Acinar microfragment representing secretory gland tissue.
**B** *Sebaceous gland:* A single cell cluster originating from duct epithelium. The mild nuclear irregularity is caused by the acute inflammation.
**C** *Serous sweet gland:* Flat discohesive sheet of glandular epithelial cells.

**Fig. 16.2 Suture granuloma.**
A 34-year-old man after the extirpation of his left testis for seminoma presented with a nodular formation located on his scrotal sack. FNAB was performed to rule out metastatic disease. Lower magnification shows an inflammatory infiltrate composed of histiocytes, macrophages, foreign body giant cells, and leukocytes. Histiocytic giant cells adhesive to a birefringent bar-like element (upper right) substantiate suture granuloma (direct smear, Pap stain).

**Fig. 16.3A, B Epidermoid cyst.**
Two illustrations demonstrate key features of epidermoid cysts (FNAB, direct smears, Pap stain, higher magnification). **A** Anucleated superficial squamous cells exhibiting abundant translucent eosinophilic and cyanophilic cytoplasm. Small dark nuclei are rarely encountered (upper left). **B** Inflammatory epidermoid cysts are characterized by close contact between histiocytic giant cells and squamous cells. Only sporadic leukocytes in this field.

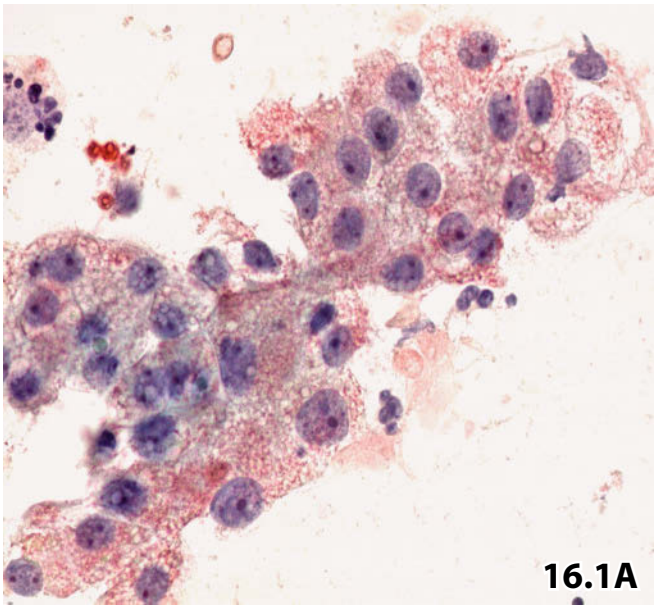
16.1A

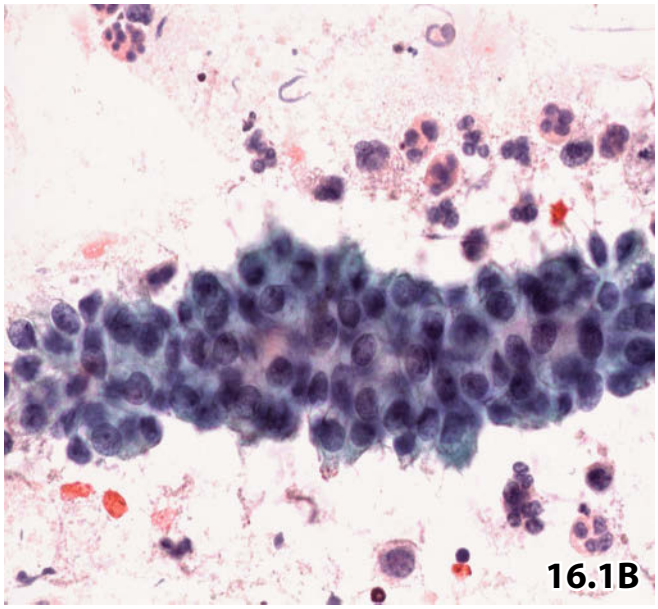
16.1B

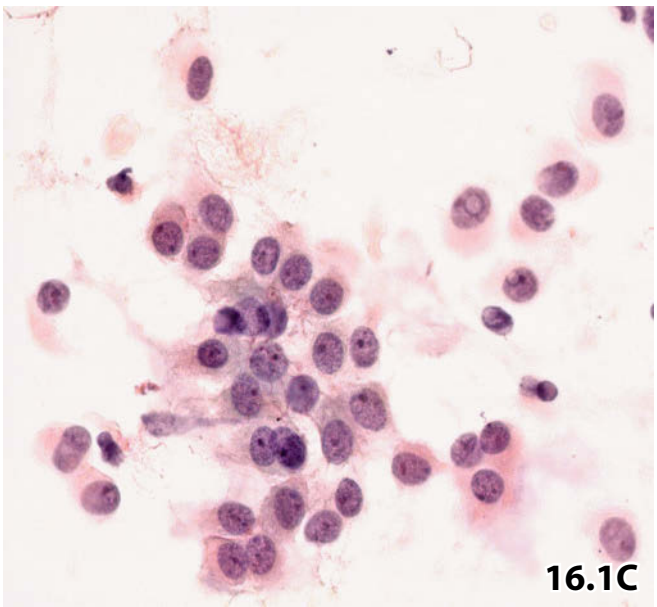
16.1C

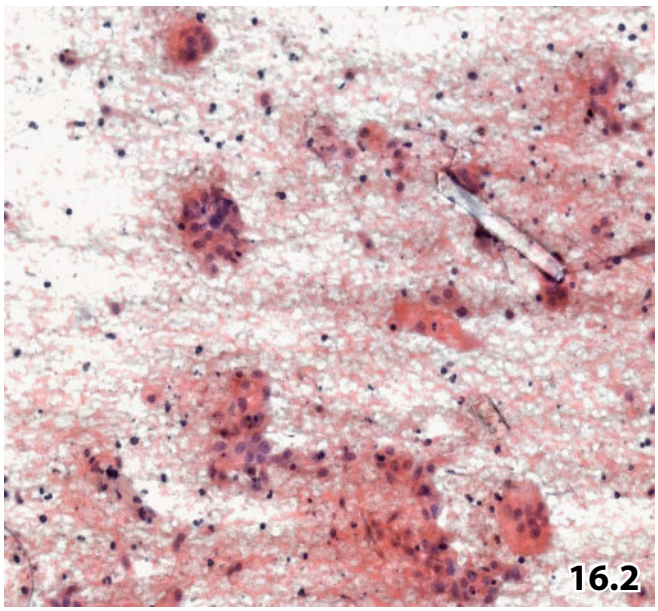
16.2

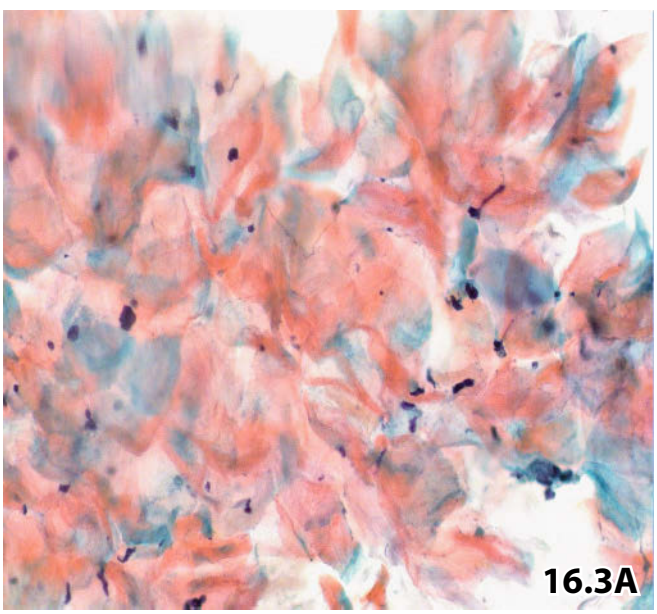
16.3A

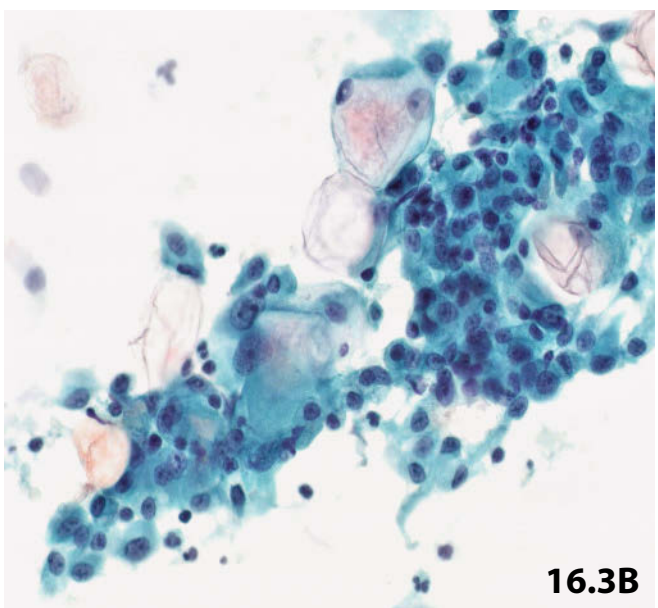
16.3B

**Fig. 16.4A, B Amyloidosis.**
Systemic amyloidosis was suspected in a 60-year-old man. A four-quadrant aspiration of the subcutaneous tissue around the umbilicus was performed. Aspirated small tissue fragments were processed by means of the cell-block technique. **A** Amyloid protein is visualized using Congo red stain. Amyloid deposits occur both in fat tissue and in the wall of small blood vessels (arrows) (lower magnification). **B** Bottle-green birefringence upon polarization is a feature of amyloid protein (after Congo red stain).

**Figs. 16.5–16.7 Pilomatrixoma.**
Cytologic hallmarks of pilomatrixoma are demonstrated by means of fine-needle aspirates from three patients. Direct smears were Pap-stained. Case #3 exemplarily demonstrates that a particular location of pilomatrixomas may give rise to diagnostic dilemmas.

**Fig. 16.5** (case #1) The characteristic heterogeneous cytologic appearance of a pilomatrixoma is presented at low magnification:
1. Large compact clusters composed of small basaloid cells (left).
2. Groups of shadow cells and scattered shadow cells embedded between basaloid cells (center, small arrows).
3. Mature squamous cells (large arrow).
4. Foreign-body histiocytic giant cells (arrowheads).

**Fig. 16.6** case #2) High magnification shows ghost cells (shadow cells) in close contact to basaloid cells (upper left) and to histiocytic giant cells (bottom). Shadow cells display an unstained pale area in place of the vanished nucleus (arrows).

**Fig. 16.7A, B** (case #3) An 80-year-old woman with a history of carcinoma of her left breast (successfully treated about 40 years before) presented with a skin nodule in the immediate vicinity of her left breast. FNAB was performed, direct smears were Pap-stained.
*(False) cytologic diagnosis:* Moderately differentiated carcinoma, cytology suggests recurrence/metastasis of the previous breast carcinoma (comments see legend Fig. 16.7B).
*Tissue diagnosis* (excisional biopsy): Pilomatrixoma.
**A** Lower magnification shows a pilomatrixoma that is mainly composed of hyperplastic basaloid cells. Shadow cells (arrow) and maturing squames (not shown) are rarely encountered.
**B** Similarities between activated basaloid cells and neoplastic epithelial breast cells are striking (relatively monomorphic cell pattern, eccentric nuclei, minor nuclear irregularities, occasional nuclear grooves (arrows), fine granular/reticular chromatin, dense cytoplasm). Cellular detritus in the background of the smear (upper right) may additionally act as an indicator of a neoplastic disorder (high magnification).

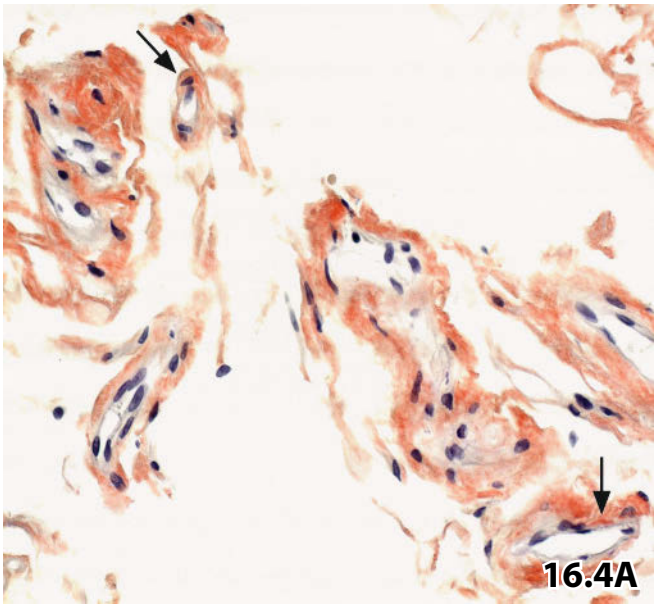
16.4A

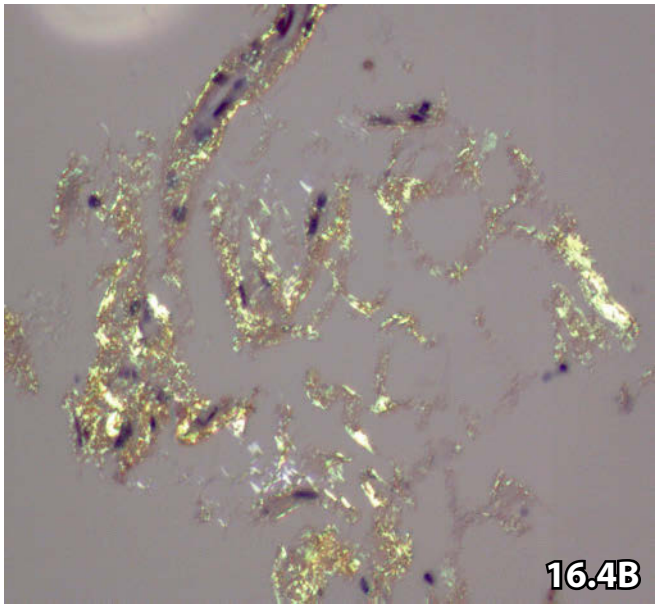
16.4B

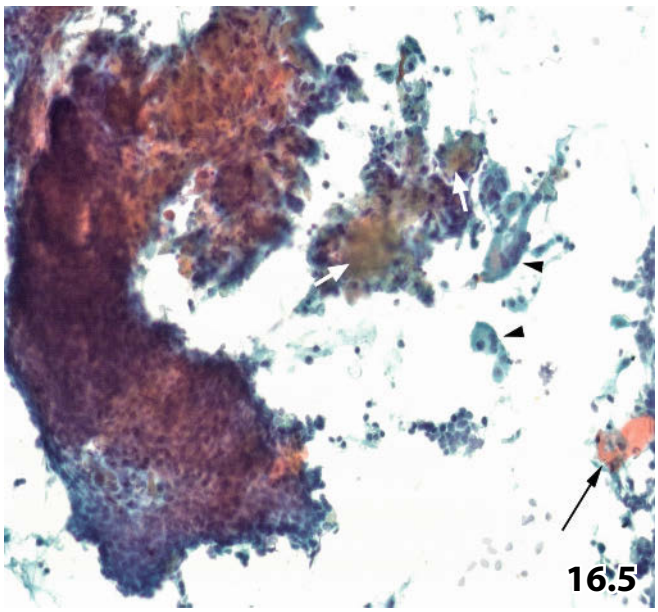
16.5

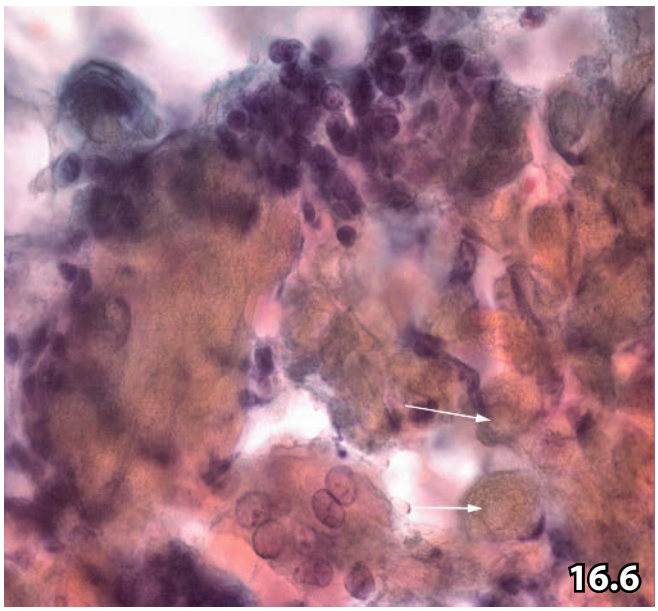
16.6

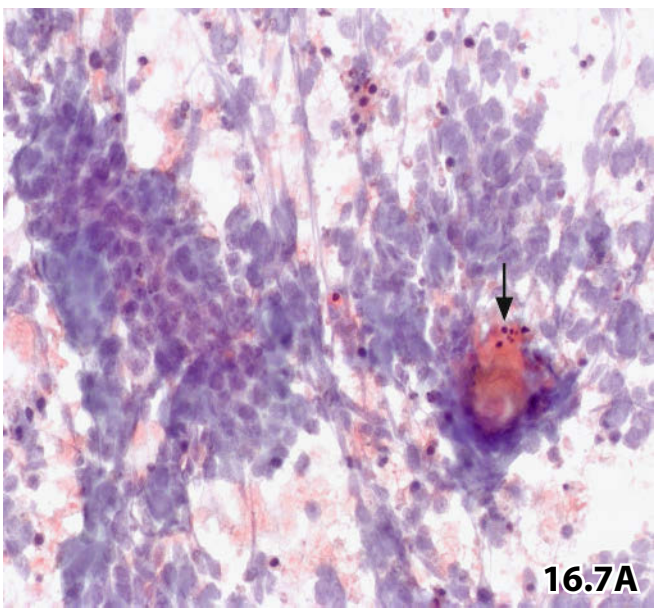
16.7A

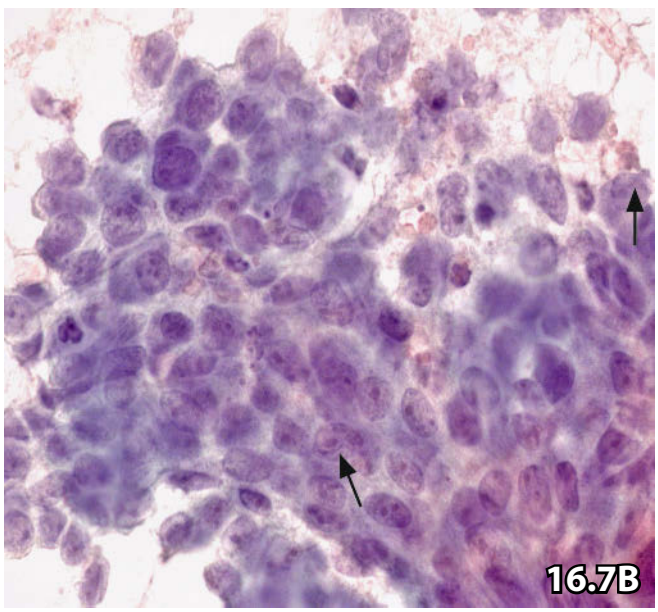
16.7B

**Figs. 16.8–16.10 Basal cell carcinoma.**
Classic type and variants of basal cell carcinoma are shown in fine-needle aspirates from three patients. Direct smears were Pap-stained. The firm cytologic diagnoses have been verified by metachronous histiologic examination (excisional biopsies).

**Figs. 16.8A, B** (case #1) Classic cytologic appearance of basal cell carcinoma. FNAB of a small nodule in the cheek of an 89-year-old woman. **A** Compact, three-dimensional and usually sharply demarcated tumor cell clusters are demonstrated at low magnification. Note the uniform appearance of the cell pattern and the regular cell clustering. Focal palisade arrangement of the peripheral cell layer is clearly visible (arrows). **B** Morphologic details of the tumor cells are focused at high magnification. Please note in particular the cuboidal and fusiform cell shapes and the cellular palisading at the lower right periphery of the cluster.

**Fig. 16.9** (case #2): Lower magnification reveals a basal cell carcinoma which is predominantly composed of spindle shaped tumor cells.

**Fig. 16.10** (case #3) Detail of the keratotic variant of basal cell carcinoma is presented comprising activated nonkeratinizing fusiform squamous cells forming strands (arrows) and a whorl composed of keratinized cells (upper left). The latter is also referred to as horn cyst.

**Fig.16.11 Squamous cell carcinoma: common type.**
Scraping from an ulcerous skin lesion of a 65-year-old man. Lower magnification reveals keratinizing atypical and frankly malignant squamous epithelial cells intermingled with an inflammatory component. Cell detritus is also present.

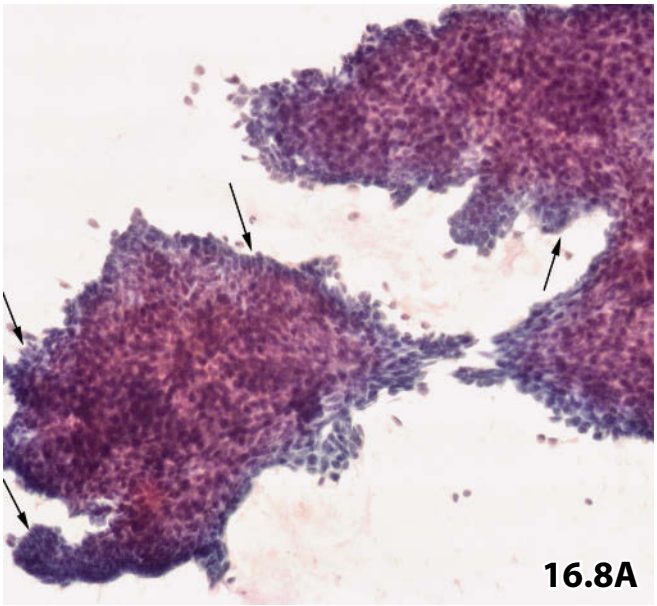
16.8A

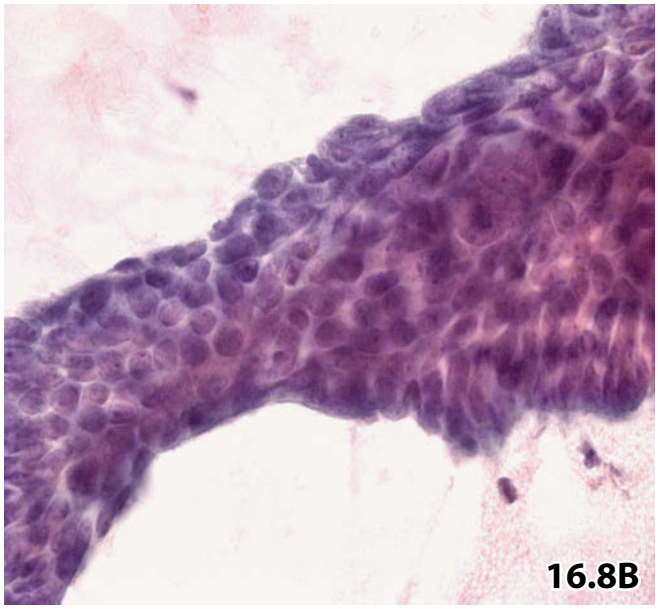
16.8B

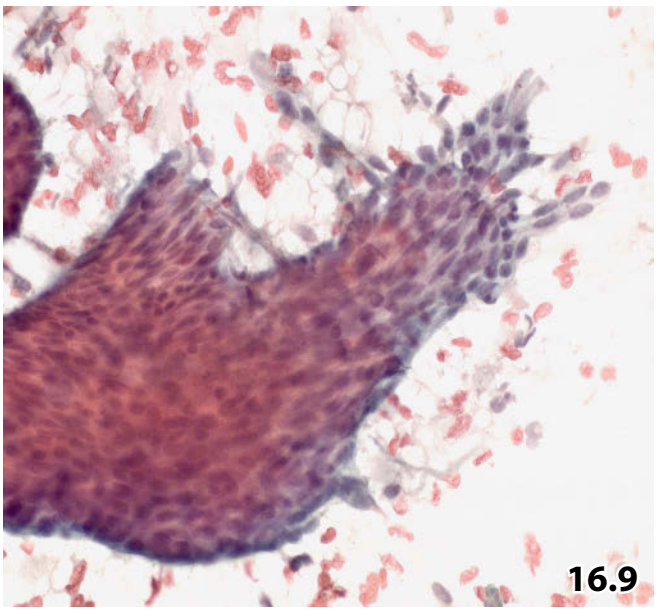
16.9

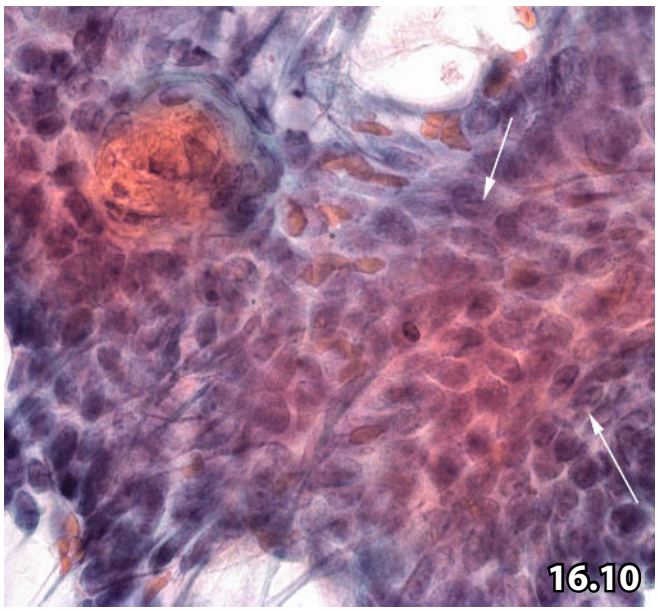
16.10

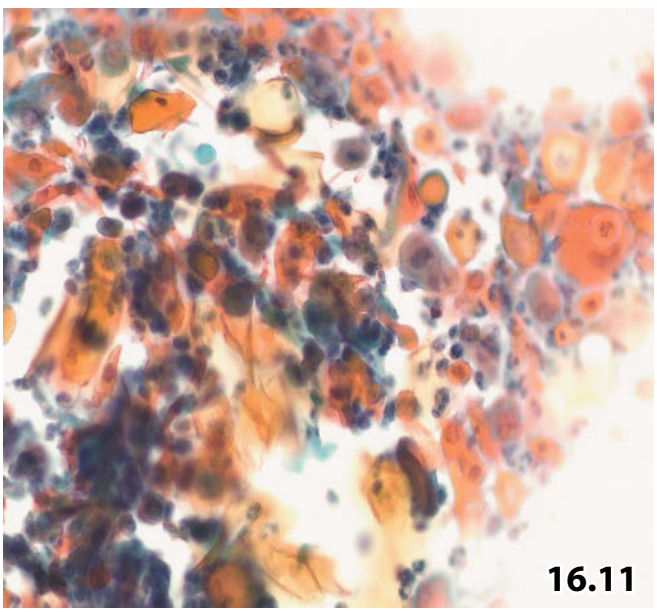
16.11

**Figs. 16.12–16.15 Malignant melanoma.**
Cytologic key features of malignant melanoma and its immunocytochemical properties are demonstrated. Aspirated cell material was directly smeared onto glass slides and Pap-stained.

**Fig. 16.12** (case #1) Cytomorphologic appearance of the classic melanoma variant is exhibited at lower magnification.
Note in particular:
– Discohesive cell pattern.
– Abundant cytoplasm, usually elongated.
– Bi- and multinucleation.
– Eccentrically positioned nuclei.
– Distinct nucleoli.

**Fig.16.13** (case #2) High magnification focuses on the morphology of single tumor cells.
Note in particular:
– Evenly distributed chromatin: fine granules and few clumps.
– Granular cytoplasm.
– Nuclear vacuoles (arrows).
– A macrophage loaded with melanin pigment (arrowhead) referred to as a melanophore/melanophage.

**Fig. 16.14** (case #3) Classic manifestation of melanin pigment ingested in the cytoplasm of melanoma cells (higher magnification):
– Clumps (small arrows).
– Coarse granules (large arrows).
– Powdery (arrowheads), largely not in focus.

**Fig. 16.15A, B** (case #4) Positive immunostaining for melanoma-typical antigens. Staining pattern may vary from case to case. **A** A vast majority of melanoma cells are immunopositive for Pan-melanoma cocktail-PMC (Pap-prestained direct smear). **B** A minority of tumor cells are immunocytochemically decorated with antibodies for HMB-45 (Pap-prestained direct smear).

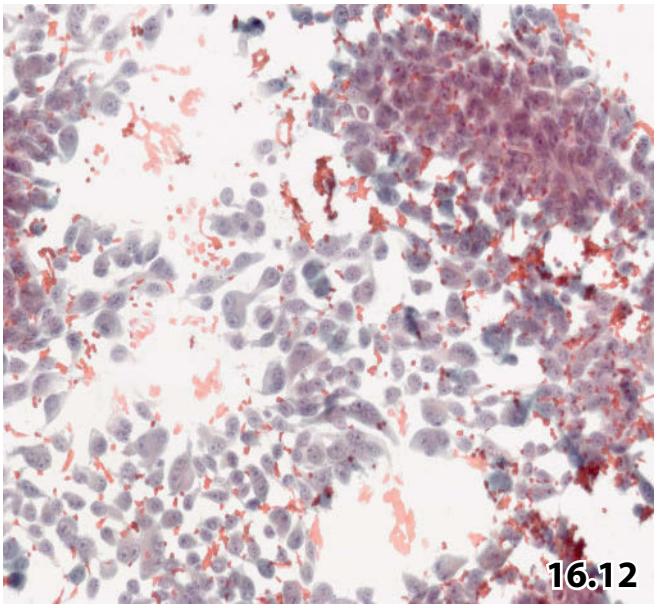
16.12

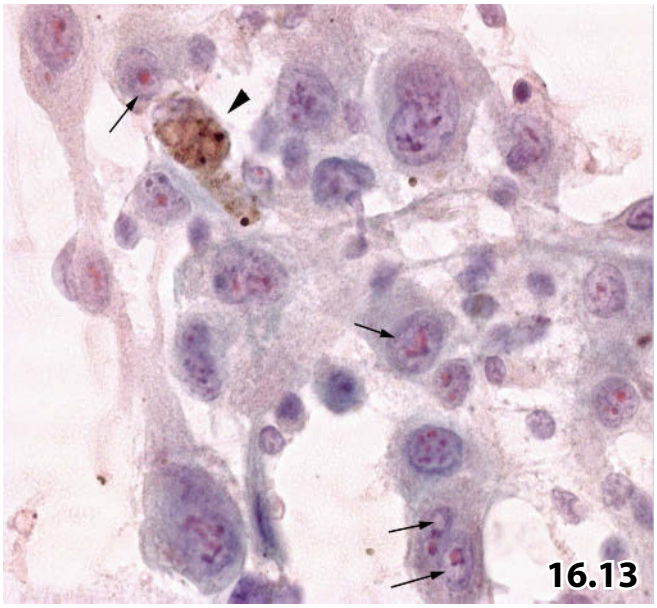
16.13

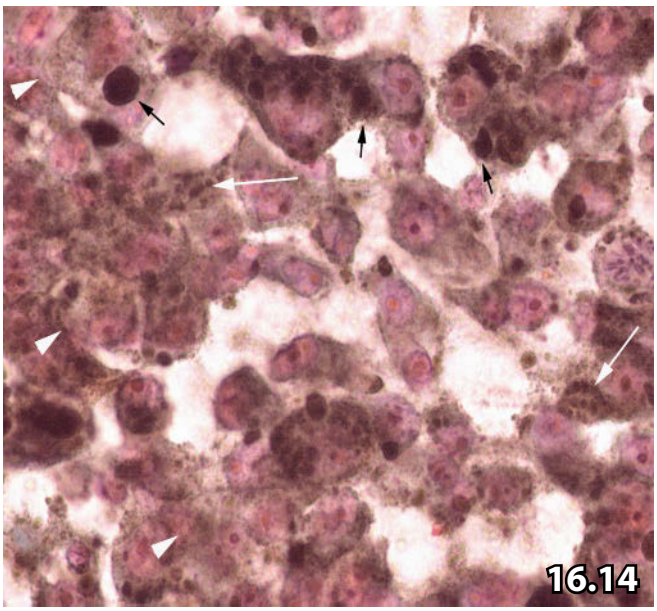
16.14

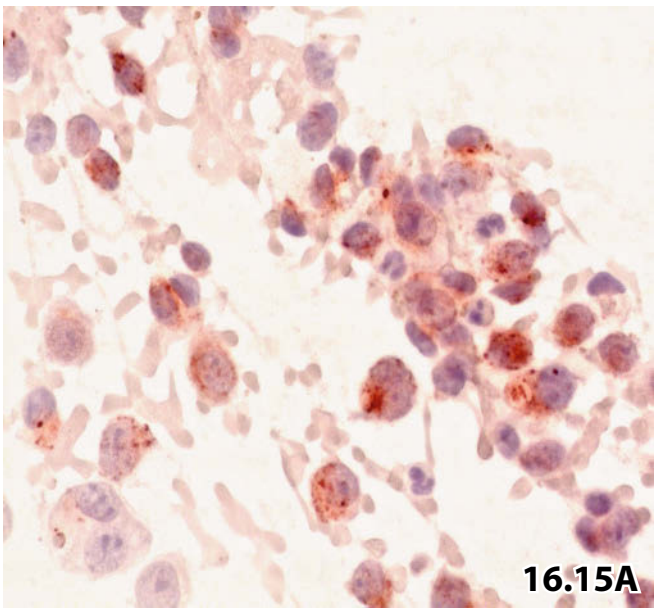
16.15A

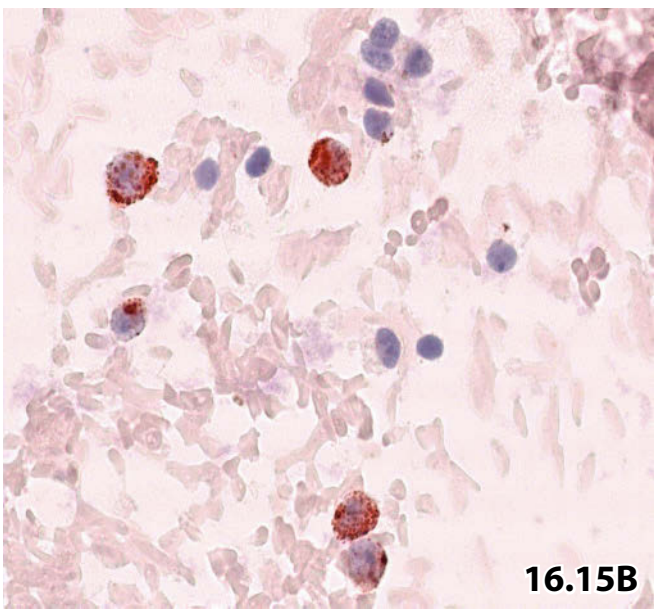
16.15B

**Fig. 16.16A–D Merkel cell carcinoma.**
A 68-year-old man with a history of non-small-cell lung cancer presented with a subcutaneous nodule at his elbow. FNAB was performed in order rule out or confirm metastatic disease. Cytologic material was processed using varied laboratory methods. The specimens were Pap-stained.
*Cytologic/ immunocytochemical diagnosis:* Merkel cell carcinoma.
**A** Note the heterogeneous cytoarchitecture at higher magnification: single cells, rows, and clusters (direct smear). **B** Cellular details are depicted. Note suggested rosette formation (upper right) (direct smear). **C** Cellular appearance of Merkel cell carcinoma in liquid-based preparation (ThinPrep). Compare with the cellular morphology in Fig. 16.16B (same magnification). Liquid-based preparation frequently gives rise to certain alterations of the cells: more coarse and dense chromatin, cellular crowding, and shrinking of cytoplasm and nuclei as compared to the conventional smears. **D** Immunostaining for CK20 provides large paranuclear dot-like globules (arrows) (Pap-prestained direct smear). Further immunoreactions are not shown: MNF-116 (dot-like positivity) and TTF1-negative staining result.

**Fig. 16.17 Kaposi sarcoma.**
A 58-year-old man with an uneventful clinical history presented with multiple nodules in his lung and subcutis. FNAB of a subcutaneous nodule (direct smears, Pap stain). Lower magnification reveals a heterogeneous cell pattern: small and large polyhedral and spindle-shaped atypical cells. The nuclei are distorted and the cytoplasm is ill defined. Note the high mitotic activity (arrows).
*Tentative cytologic diagnosis:* Malignant mesenchymal neoplasia. Diagnostic consideration includes malignant fibrous histiocytoma and pleomorphic liposarcoma.
*Tissue diagnosis* (surgical excision of a nodule): Angiosarcoma of the Kaposi variant.

**Fig. 16.18 Cutaneous cylindroma.**
FNAB of a subcutaneous parasternal nodule in a 68-year-old woman with a positive history of malignant non-Hodgkin lymphoma. Direct smears were Pap-stained. At lower magnification, features of a cylindromatous neoplasia become readily apparent:
– Compact clusters are composed of uniform small to medium-sized cells.
– Homogeneous basement membrane material coating some of the cell clusters.
– A few translucent homogeneous globules are surrounded by tumor cells (center). It is impossible to distinguish between a primary cutaneous cylindroma and a metastasis of a cylindromatous tumor in a remote organ.



*Cytologic diagnosis:* Cylindroma, not otherwise specified.
*Histologic diagnosis* (surgical excision of the nodule): Cylindromatous tumor, most likely primary skin tumor.

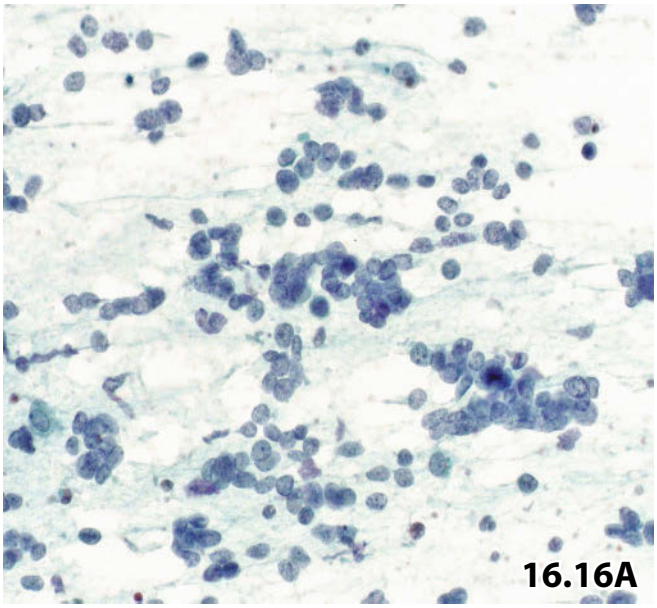
16.16A

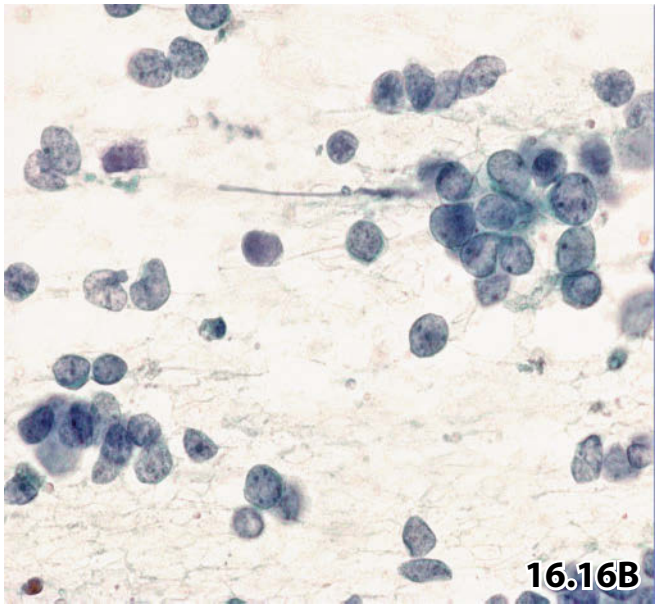
16.16B

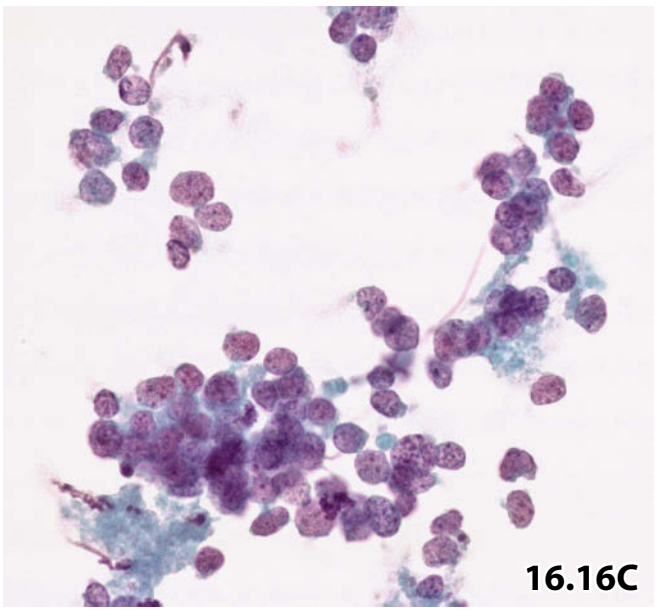
16.16C

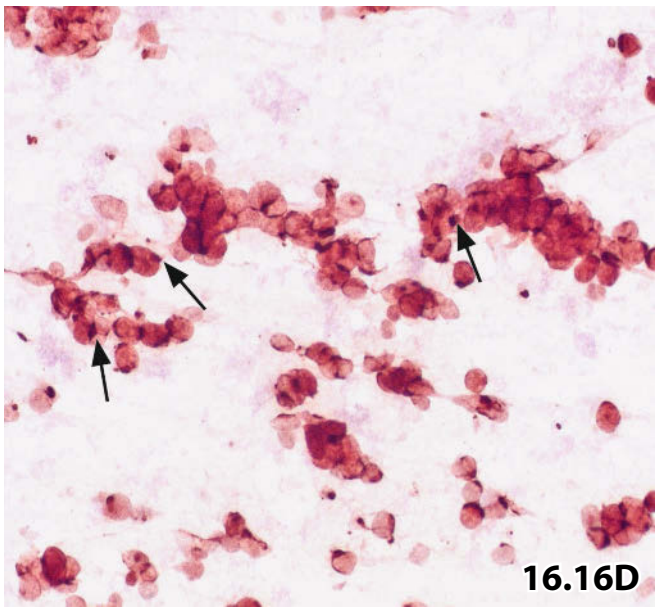
16.16D

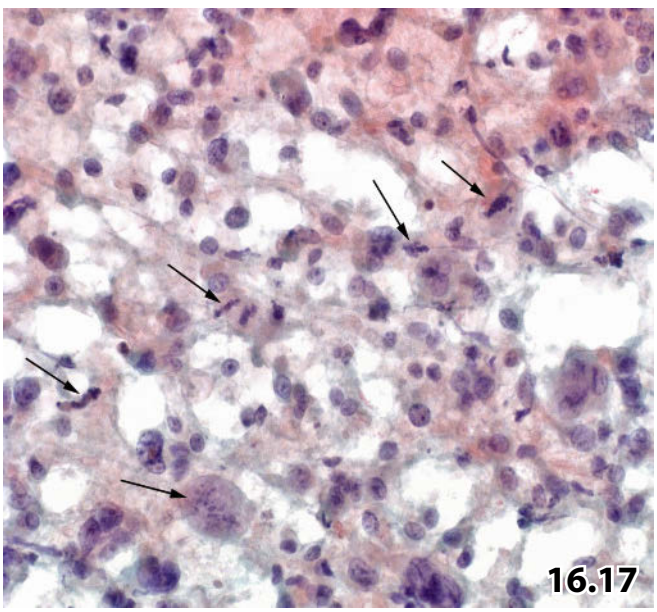
16.17

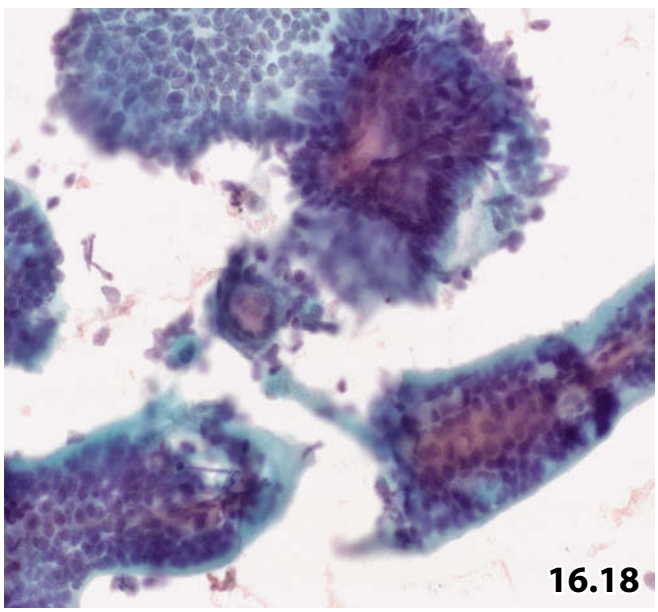
16.18

**Fig. 16.19A–C Endometriosis.**
Sonographic routine investigation revealed a hypoechoic formation in the inguinal region of a 46-year-old woman. Re-FNAB was requested after an inconclusive diagnosis of a first aspirate. Vigorous ultrasound-guided aspiration eventually yielded adequate material (direct smears, Pap stain).
*Cytologic/immunocytochemical diagnosis:* Endometriosis.
*Histologic diagnosis* (excisional biopsy): Multiple foci of endometrial tissue.
**A** High magnification exhibits a benign compact cluster composed of small cuboidal to columnar epithelial cells in a background containing hemosiderophages (left), positive iron stain is not shown. Immunocytochemical staining for calretinin was performed in order to exclude a mesothelial fragment (the negative staining result is not shown). **B** Lower magnification shows a small tissue fragment composed of epithelial cells and cellular stroma (arrows) indicating endometrial tissue. Detritus was absent in the available cytologic specimens. **C** Cytologic diagnosis was confirmed by positive nuclear immunoreaction using specific antibodies against estrogen receptors.

**Fig. 16.20A, B Hydrarthrosis involving the inguinal region.**
An 87-year-old woman presented with a firm tumor located slightly above the left groin. The patient's personal medical history was vague. Clinical and image findings led to suspicion of a malignant lymphoma. The patient was referred to FNAB in order to avoid more invasive procedures. A viscous aspirate was directly smeared onto slides, which were Pap-stained. **A** High magnification revealing activated histiocytes scattered in a detritic background may mislead to a false-positive diagnosis of malignancy such as undifferentiated necrotizing carcinoma, malignant blastic lymphoma, among other lesions. **B** Lower magnification additionally shows a fragment of chondroid tissue (upper right) and calcific deposits (the latter is obscured by masses of detritus), indicating a degenerative disorder.
*Cytologic diagnosis:* Distinctive hydrarthrosis presenting as inguinal tumor mass. The results are compatible with long-standing osteoarthrosis. No further examinations were performed.

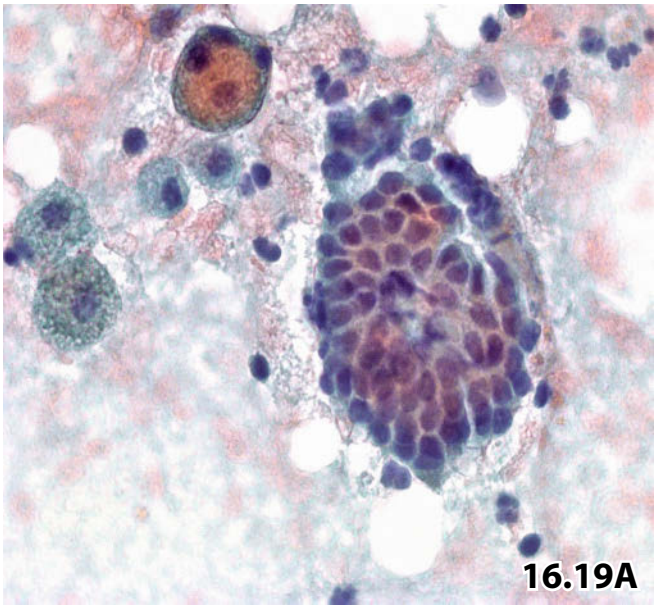
16.19A

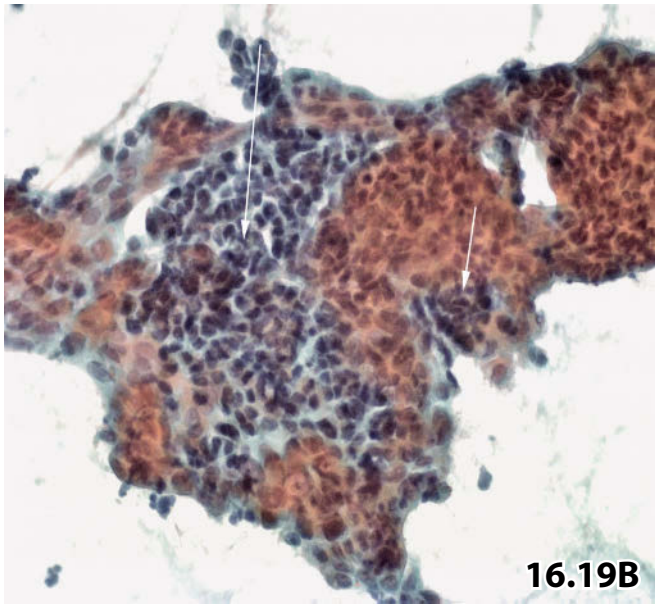
16.19B

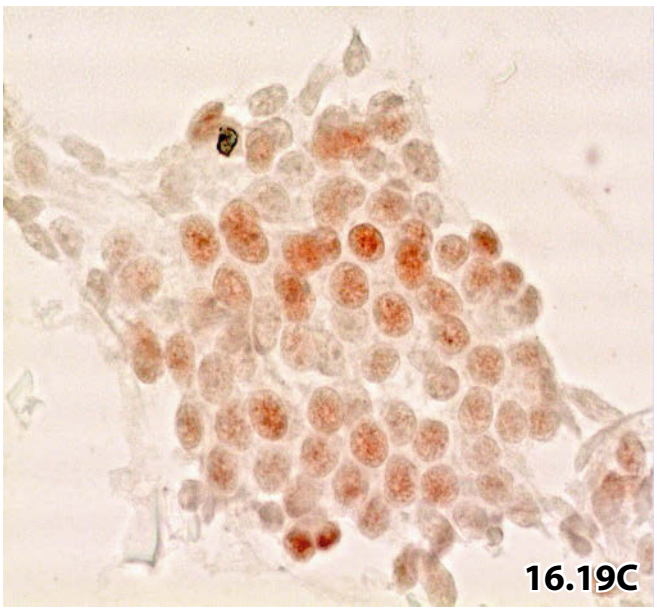
16.19C

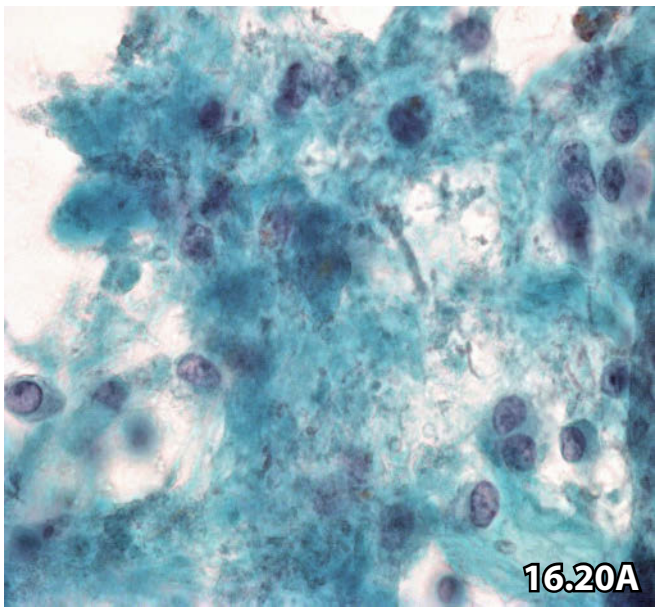
16.20A

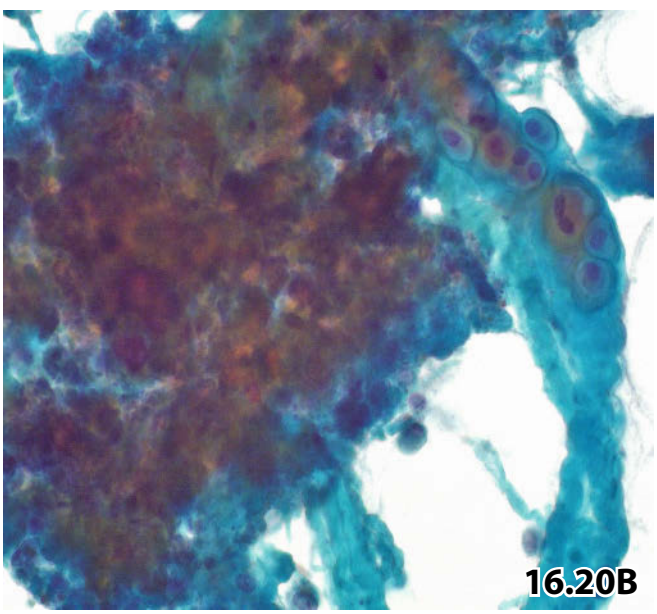
16.20B

# Soft Tissue and Bone 17



Spieler/Rössle, *Nongynecologic Cytopathology. A Practical Guide*. *Essentials of Diagnostic Pathology*,
DOI 10.1007/978-3-642-24719-4_17, 

## Synopsis and Algorithms

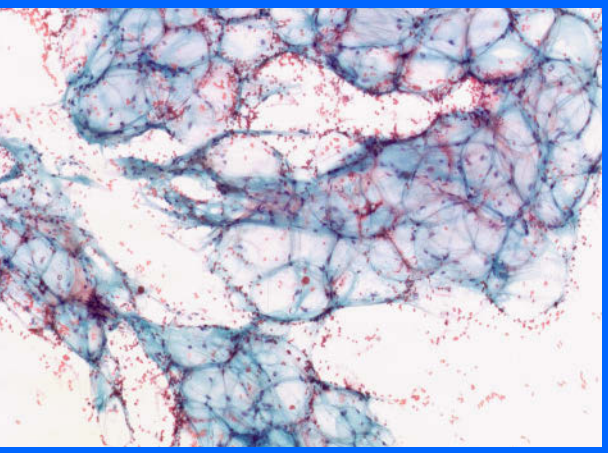

# Section 17.1
# Soft Tissue and Bone

## Benign and Intermediate Tumoral Lesions

### 17.1.1 Introduction

**General Comments**

- FNAB can serve as the initial minimally invasive approach to diagnosing primary soft tissue tumors and bone lesions, including sarcomas. Actually FNAB is widely used at orthopedic tumor centers where cytopathologists with extensive experience in the interpretation of benign and malignant soft tissue lesions are available, and the interdisciplinary orthopedic tumor team is familiar with the FNAB procedure. Even so, FNAB is accepted and very popular for the diagnosis of tumor recurrence and metastasis in previously established soft tissue malignancies.
- Every cytopathologist should be familiar with benign and intermediate soft tissue lesions since such disorders are often unexpectedly encountered in FNAB of superficial nodules, giving rise to diagnostic problems and limitations in standard cytology. Generally speaking, most cytopathologists are on a permanent learning curve rather than fully equipped with expert diagnostic knowledge in this field.
- In the last two decades, the cytopathologists at our institution have acquired extensive experience in the diagnosis of benign mesenchymal disorders with FNAB. However, only occasionally do we have the opportunity to perform FNABs on previously undiagnosed or suspected sarcomas.
- FNAB will be less rewarding or completely fail to collect cells from hard and sclerotic intraosseous lesions and circumscribed sclerotic nodules of soft tissues. On the other hand, the thinning or complete destruction of the cortical bone permits the use of fine needles; bony lesions and sclerotic mesenchymal tumors extending into the surrounding soft tissue may be successfully diagnosed by aspirating the diffuse marginal areas of the disorder with ultrasound guidance.
- We refer the reader to many excellent comprehensive books and specialized sources in the literature relating to those aspects of FNA cytology that will increase our knowledge and understanding of the performance, diagnostic accuracy, histogenetic subtyping, advantages, and diagnostic challenges [14, 24, 28, 45, 63, 68, 70]. Comprehensive histologic classification and completive information on each tumor entity is provided by Fletcher and associates in the 2002 WHO tumor nomenclature [22].

#### 17.1.1.1 Overview Section 17.1

- This section covers benign and intermediate soft tissue and bone tumors that:
  - Are most likely to be encountered in FNAB samples.
  - Exhibit a distinct cytologic pattern.
  - Give rise to difficulties in diagnosis.

  Many lesions will not be considered due to their rare incidence or peculiar locations unsuitable as FNAB targets.
- Benign and intermediate lesions of soft tissues are broadly discussed. The presentation of benign and intermediate bone lesions is limited to the most common entities (Sects. 17.1.11–17.1.13, p. 1066); fibrohistiocytic, fibrogenic, myogenic, lipogenic, vascular, and neural non-malignant

bone lesions are counterparts to the respective soft tissue lesions described in Sects. 17.1.2.-17.1.10, below.

- The various tumoral entities are presented in a dual mode (the range of the disorders follows the same order in the text and tables).
  1. Selective comments, a more extensive description of the cytomorphologic features, differential diagnostic considerations, and diagnostically important ancillary tests are provided in the subsequent Sects. 17.1.2–17.1.13.
     The individual tumors have been grouped histogenetically according to the 2002 WHO classification of soft tissue tumors [22].
  2. The cytomorphologic features and cytoarchitectural properties of the tumors are neatly arranged in Table 17.1.1, "Synopsis and Algorithms: Benign Lesions," p. 1250.
     Table 17.1.2, "Synopsis and Algorithms: Benign Lesions", p. 1252 summarizes the age groups, gender-based preference, common location, and the differential diagnostic spectrum of each entity.

#### 17.1.1.2 FNAB: Technical Aspects

- Free-hand and image-guided aspiration techniques (for both palpable and deep-seated lesions), and laboratory procedures are similar to those presented in several chapters of this book. The techniques used at our institution are virtually identical to the technique recommended by Ward and associates [68].
- On-site attendance of a cytopathologist allows immediate examination of the aspirated material assessing the adequacy of the specimen, rapid diagnosis, and a decision on additional needle passes. Additional sampling is highly recommended for cell-block analysis; and it is frequently helpful to achieve enough cells for ancillary tests, including special stains, immunocytochemistry, static and/or flow cytometry, molecular genetics, and electron microscopy.
- FNAB may completely fail to obtain cell material from intraosseous lesions that are capped by intact cortical bone and/or composed of abundant bony tumor matrix. Yet, thinning or destruction of the cortical bone permits the successful use of the fine-needle technique; and bony tumors extending into surrounding soft tissue may be diagnosed by vigorous aspiration of the diffuse marginal tumor areas (with the assistance of ultrasound guidance).

#### 17.1.1.3 Definition of Intermediate Soft Tissue Lesions

Soft tissue tumors of the intermediate category are associated with infiltrative and locally destructive behavior. In addition, some of them may have a low risk for distant metastases.

### 17.1.2 Adipocytic Tumors [1, 37]

#### 17.1.2.1 Lipoma (Fig. 17.1)

- Lipomas are the most common form of soft tissue tumors. They are commonly found in adults with a preponderance in obese individuals, and frequently occur multiply. Lipomatosis is a hereditary condition where the patients present with multiple lipomas.
- Lipomas may be small but can enlarge to sizes up to 10 cm and sometimes more. The nodules are soft to the touch and generally clearly moveable.
- Lipomas arise in subcutaneous tissue (superficial lipoma) or within deep soft tissues including skeletal muscles (deep-seated lipoma). Malignant transformation of lipomas into liposarcomas occurs very rarely, and subcutaneous lipomatous tumors are unlikely to be malignant [10, 69].

**Microscopic Features**

- Three-dimensional cohesive lobular arrangement of mature lipocytes; loose fibrous connective tissue and capillary vessels may surround the lobuli, vessels are rarely branching.
- The adipocytes are usually enlarged in comparison to cells of normal adipose tissue; they are round, uniform, and vacuolated with an eccentrically placed nucleus.
- Scattered lipoblasts (spheric cells exhibiting fine granular and multivacuolated cytoplasm, and occasional nuclear irregularities) and inflammatory cells may be encountered.

#### 17.1.2.2 Lipoblastoma [32, 47]

Synonyms: Fetal lipoma, embryonic lipoma, infantile lipoma. Lipoblastoma is a rare benign tumor of embryonal fat that occurs almost exclusively in infants and children.

**Microscopic Features**

- The smears usually show moderate cellularity composed of lipocytes in various stages of maturation, including undifferentiated mesenchymal cells.
- Lipoblast-looking cells have a multivacuolated cytoplasm and a centrally placed small bland nucleus.
- Individual tumor cells and cell clusters are embedded in a stromal matrix, occasionally of myxoid nature, containing a delicate plexiform vascular network.
- Large cells with granular cytoplasm resembling hibernoma cells may be found.

**Differential Diagnosis**

Lipoma (versus lipoma-like lipoblastoma), myxoid liposarcoma (versus lipoblastoma exhibiting abundant myxoid matrix), and well-differentiated liposarcoma may cause diagnostic confusion. However, liposarcoma is rare under the age of

10 years, and features of malignant adipose tumors such as nuclear atypia, nuclear hyperchromasia, and mitotic figures are absent in lipoblastomas.

**Additional Analyses** [51]
Molecular genetic analysis, using the FISH technique, may be helpful in differentiating between lipoblastoma and other lipogenic tumors, particularly lipoblastoma rich in myxoid matrix versus myxoid liposarcoma. Lipoblastomas are characterized by the deletion of 8q11-13, mostly associated with a rearrangement of the *PLAG1* gene (8q12), with the *HAS2* gene (8q24), or *COL1A2* gene (7q22). In other cases, a polysomy of chromosome 8 may be observed. In contrast, myxoid liposarcoma exhibits a characteristic t(12;16) translocation.

### 17.1.2.3 Angiolipoma [7, 66] (Fig. 1.62)

Angiolipomas appear most often as multiple small subcutaneous nodules during the late teens and in young adults.

**Microscopic Features**
- The tumor is composed of fat cells and vessels. Mature adipocytes are intermingled with branched thick-walled vessels of the capillary type.
- The characteristic intravascular fibrin thrombi may also be detectable in cytologic smears.

**Differential Diagnosis**
A neoplasm almost completely composed of vascular channels is referred to as cellular angiolipoma. This angiolipoma variant is difficult to differentiate from angiosarcoma and Kaposi sarcoma, particularly in cytologic specimens.

### 17.1.2.4 Myolipoma

Myolipoma is an extremely rare lesion in adults. The benign tumor, consisting of mature adipose tissue and mature smooth muscles, is in the majority of cases deeply located and large: the average size of the tumors reaching 15 cm in diameter.

**Microscopic Features**
- The aspirates contain mature smooth muscle cells and mature fat tissue, whereas the smooth muscle component usually outweighs fat tissue.
- The smooth muscle tissue fragments are compact and composed of elongated cells arranged in a parallel fashion.
- The nuclei are centrally placed, showing fine chromatin and a small inconspicuous nucleolus.
- The cytoplasm is dense, acidophilic, and fibrillary.
- The biphasic cell component shows neither cellular atypia nor mitotic activity.

**Additional Analyses**
Immunostaining demonstrates strong positivity for smooth muscle actin (SMA) and desmin related to smooth muscle cells.

### 17.1.2.5 Angiomyolipoma

Angiomyolipoma is a tumor that usually affects the kidney and pararenal soft tissue of adults. Other primary sites have only rarely been reported.

**Microscopic Features and Differential Diagnosis**
- Angiomyolipoma is a well-characterized tumor composed of cells and tissue fragments as seen in myolipoma, including thick-walled, tortuous capillary blood vessels.

Cytomorphologic criteria and further details concerning renal angiomyolipoma are covered in Sect. 12.1.7.1, p. 737.

Angiomyolipoma may mimic angiolipoma.

### 17.1.2.6 Chondroid Lipoma [39, 50]

Chondroid lipoma is a benign tumor with evidence of embryonal fat (lipoblasts), mature adipose tissue, and embryonal chondroid matrix. The tumor primarily affects adults, with a female predilection.

**Microscopic Features**
- The cell pattern includes abundant uni- and multivacuolated lipoblasts and a variable proportion of mature adipose tissue. The nuclei of the lipoblast are small, exhibiting smooth borders or indentations, finely dispersed chromatin, and inconspicuous nucleoli. Cells having eosinophilic granular cytoplasm resemble hibernoma cells and chondroid cells.
- Cells and tissue fragments are embedded in a myxoid-chondroid matrix with hyalinized areas.
- Capillary-type vessels may be encountered.

**Differential Diagnosis**
Chondroid lipoma may easily masquerade as myxoid liposarcoma or extraskeletal myxoid chondrosarcoma.

According to the preponderant cell type, chondroid lipoma can also simulate chondroma, lipoblastoma, hibernoma, and other benign and malignant neoplasms.

**Immunocytochemistry** [39]
Immunocytochemically, the tumor cells uniformly demonstrate positivity for S100 protein and for vimentin, and sporadically for cytokeratins. Epithelial membrane antigen (EMA) is always negative.

### 17.1.2.7 Myelolipoma

Myelolipoma is a lesion showing a unique combination of adipose tissue and hematopoietic cells. The vast majority of these tumors are found in the adrenal glands, but any type of lipoma may contain areas of hematopoietic tissue.

Further details on myelolipoma are provided in Sect. 12.2.3.1.2, "Adrenal Myelolipoma," p. 767.

### 17.1.2.8 Spindle Cell and Pleomorphic Lipoma (Fig. 17.2)

Spindle cell and pleomorphic lipomas are benign neoplasms of the adipose tissue representing the two ends of a common cytohistologic spectrum.
The subcutis of the neck and back area is typically affected. There is a male predilection over the age of 50.

#### Microscopic Features

- *Spindle cell lipoma* [17, 26] is composed of spindle cells arranged in parallel streaks, their cytoplasm is elongated, and the nuclei are bland.
  Small fragments of collagen tissue and collagen fibers meet the characteristic collagen bundles in histologic sections.
  Mature adipose cells are part of this tumor entity (Fig. 17.2A).
  Myxoid stromal changes and large numbers of mast cells are typical features but not always present.
- *Pleomorphic lipoma* [57, 76] is characterized by a mixture of spindle cells, pleomorphic rounded cells, and pleomorphic multinucleated giant cells.
  The nuclei of the giant cells are hyperchromatic and show a characteristic radial arrangement (floret cells) (Fig. 17.2B).
  Mature fat tissue, lymphocytes, and plasma cells are usually observed in the background of the smears.

**Caution**

Intermediate cell patterns between classic spindle cell lipoma and pleomorphic lipoma occur frequently.

#### Differential Diagnosis

- Spindle cell lipoma may mimic other spindle cell tumors and myxoid lesions including low-grade liposarcoma and atypical lipomatous tumor.
- Numerous mesenchymal lesions containing pleomorphic histiocytoid cells and multinucleated giant cells must be considered, including fat necrosis, lipogranuloma, myositis ossificans, pleomorphous histiocytoma, and liposarcoma.

#### Additional Analyses

- All spindle cells both in spindle cell lipomas and pleomorphic lipomas express CD34 using immunocytochemical staining. In spindle cell lipoma, there exists a coexpression with bcl-2 [26].
- Monosomy or partial loss of chromosome 16, and aberrations of chromosome 13 are typical of spindle cell/pleomorphic lipoma, distinguishing them from well-differentiated liposarcoma [22].

### 17.1.2.9 Hibernoma [23, 30, 46] (Fig. 17.3)

- Hibernoma is a particular variant of benign lipoma occurring in young adults. The tumor mainly occurs in the subcutaneous tissue of the thigh, back, upper extremity, head, and neck; but hibernomas can develop at almost any site of the human body. The etiology of hibernoma is unknown, but it is assumed to arise from the remnants of fetal brown adipose tissue. The latter is a specialized form of fat normally found in hibernating and nonhibernating animals.
- In addition to typical hibernoma, three variants of this tumor entity have been described [23]:
  - Lipoma-like.
  - Myxoid.
  - Spindle cell.

#### Microscopic Features

- *Classic hibernoma* includes numerous polygonal multivacuolated adipocytes comprising lipochrome pigment-rich, coarsely granulated cytoplasm.
  The tumor cells exhibit unequal staining quality varying from eosinophilic to pale or mixed; they are frequently arranged in tight aggregates surrounded by branching capillaries or thick-walled vessels.
  The nuclei are small, centrally or eccentrically located, and exhibit a dense chromatin structure.
- The *hibernoma lipoma-like variant* consists of normal white fat and scattered hibernoma cells.
- The *hibernoma myxoid variant* goes along with a basophilic matrix.
- *Spindle cell hibernoma* is a biphasic lesion composed of spindle cell lipoma and hibernoma.

#### Differential Diagnosis [30]

It may be difficult to differentiate between hibernoma and proliferative myositis, lipoblastoma, histiocytoma, granular cell tumor, oncocytoma, and other lesions.

#### Additional Analyses

- Immunocytochemistry provides variable positivity for S100 protein.
- The exclusive CD34-positivity in spindle cells of the spindle cell hibernoma variant is shared with that in spindle cells of spindle cell lipomas [23].

### 17.1.2.10 Atypical Lipomatous Tumor

[22] (Fig. 17.4)

Synonyms: Well-differentiated liposarcoma, atypical lipoma, lipoma-like liposarcoma, spindle cell liposarcoma, inflammatory liposarcoma, among others.

Atypical lipomatous tumor (ALT) is a locally aggressive malignant neoplasm which is – in whole or in part – composed of a population of proliferating mature adipocytes. It has virtually no metastatic potential but can undergo dedifferentiation.

The tumor occurs in middle-aged adults with a peak incidence in the 6th decade.

**Caution**

- Atypical lipomatous tumors usually develop in deep soft tissues; the limbs (thigh), retroperitoneum, and mediastinum are the primarily affected sites.
- Paratesticular areas with the spermatic cord is another typical location for this tumor entity.
- The presence of lipoblasts is neither a conclusive argument nor a prerequisite for the diagnosis of liposarcoma.
- Generally speaking, atypical lipomatous tumors are difficult to distinguish by FNA cytology.

#### Microscopic Features

- *Lipoma-like atypical lipomatous tumors*
  Aspirates from lipoma-like atypical lipomatous tumors [12, 73] are composed of clusters of mature adipocytes and dispersed adipocytes, sharing many features with common lipomas. But the adipocytes show variation in cytoplasmic and nuclear size, and nuclear atypia may be recognized in both adipocytes and stromal cells.
  In addition, scattered atypical multinucleated stromal cells and multinucleated lipoblasts are present, the latter exhibiting single or multiple cytoplasmic vacuoles and granulation, and enlarged hyperchromatic nuclei with an irregular outline.
- Other histologic variants of atypical lipomatous tumors include [41]:
  - *Sclerosing type:* Multinucleated floret cells (Fig. 17.2B) and collagen occur in addition to the cell pattern as described for the common adipocytic variant of atypical lipomatous tumors [61]
  - *Inflammatory type:* This tumor variant is commonest in the retroperitoneal space. A chronic inflammatory infiltrate can predominate to such an extent that the nature of the underlying neoplastic tissue is barely discernible.
  - *Spindle cell type:* This variant is associated with a fibrous and myxoid matrix, and a distinct proportion of proliferative spindle cells showing minor cellular irregularities.
- A rare finding in ALT is the heterologous differentiation of mesenchymal cells into bone, smooth muscle fibers, and striated muscle components.

#### Differential Diagnosis

- Lipoma-like atypical lipomatous tumor (ALT) has to be distinguished from spindle cell and pleomorphic lipoma. The two entities differ in their biological behaviour, morphology, and cytogenetic features.
- Sclerosing-type ALT raise differential diagnostic problems with varied types of liposarcoma, as well as pleomorphic lipoma and spindle cell lipoma.
- Inflammatory ALT most of all suggests a benign inflammatory lesions (e.g., inflammatory pseudotumor), reactive lymphoid lesion (e.g., Castleman disease), or malignant lymphoma.
- Spindle cell ALT may mimic spindle cell lipoma, myxoma, myxoid liposarcoma, myxoid leiomyosarcoma, myxoid chondrosarcoma, chordoma, and other lesions.

#### Cytogenetics

Molecular genetic analysis using FISH can detect amplification of the MDM2 gene locus in chromosome 12 (12q14-15). This feature may help distinguish between ALT and benign adipocytic tumors [22] ( see also Sect. 17.2.3, “Cytogenetics and Immunocytochemistry”, p. 1094.

## 17.1.3 Fibroblastic and Myofibroblastic Lesions

### 17.1.3.1 Nodular Fasciitis

[9, 56] (Figs. 17.5–17.7)

Synonym: Pseudosarcomatous fasciitis.

Nodular fasciitis is a rapidly growing nonneoplastic lesion of proliferating fibroblastic or myofibroblastic cells that are loosely and haphazardly arranged. The lesion may be well delineated or locally spreading. It usually occurs in subcutaneous tissues of the upper extremities, trunk, head, and neck.

All age groups are involved but the disorder is common in young adults. Experts suggest that trauma is an important factor in the etiology of the disorder.

#### Microscopic Features

- Cytologic smears are usually cellular, composed of slender and plump fusiform fibroblasts or myofibroblasts bearing bland nuclei. The cells are grouped in loose aggregates or occur in isolation. Osteoclast-like giant cells may be present.
- Occasionally, the overall cell pattern appears pleomorphic due to articulate variations in cellular size and shape of the proliferating stromal cells.
- Varying proportions of chronic inflammatory cells are present.

- Numerous small vessels can usually be found as well as hyaline and myxoid masses. Hyalinized mesenchymal fragments and osseous metaplasia are occasionally encountered.

**Differential Diagnosis** [13, 28]

- Cell-rich cytologic specimens including dense clusters of spindle cells frequently pose a diagnostic challenge. Schwannoma or other spindle cell lesions, such as fibrous histiocytoma, solitary fibrous tumor, fibromatosis, desmoid tumor, smooth muscle tumors, fibrosarcoma, and adipose tissue tumors of the myxoid and spindle cell variants must be taken into consideration.
- In contrast to nodular fasciitis, schwannomas lack single cells and inflammation, and their stroma appears both myxoid and finely fibrillar. Furthermore, the immunocytochemical profile of nodular fasciitis differs from that of the benign peripheral nerve sheath tumor (Schwannoma: S100 **+**, SMA **–**) [44].

**Additional Analyses**

Immunocytochemistry

Vimentin, smooth muscle actin (SMA), and muscle specific actin (MSA) decorate myofibroblasts by immunocytochemical staining procedures.

Antibody against CD68 identifies histiocytic elements.

ICM-DNA

Ploidy analysis yields a diploid DNA distribution pattern not only in nodular fasciitis but also in other (myo)fibroblastic pseudotumors such as proliferative fasciitis and proliferative myositis [19, 52].

### 17.1.3.2 Proliferative Fasciitis and Proliferative Myositis [13, 72] (Fig. 17.8)

These two proliferative disorders are rapidly growing and poorly delineated, but they are less common than nodular fasciitis. They occur in middle-aged and older adults.

#### 17.1.3.2.1 Proliferative Fasciitis

Proliferative fasciitis is most commonly found in the upper extremity (forearm), followed by the lower extremity and trunk.

The lesion comprises a subcutaneous proliferation of mesenchymal cells mimicking nodular fasciitis, but in addition, proliferative fasciitis exhibits pathognomonic ganglion-like cells.

#### 17.1.3.2.2 Proliferative Myositis

Proliferative myositis develops particularly in the trunk, shoulder girdle, and upper arm, exhibiting the same cellular composite as described for proliferative fasciitis; it is the intramuscular counterpart of proliferative fasciitis.

**Microscopic Features**

The basic cell pattern of these two entities is very similar to that of nodular fasciitis, but an additional cell type is encountered:

- Scattered large, plump cells with a rounded eccentrically positioned nucleus, a prominent nucleolus, and abundant amphophilic cytoplasm exhibiting long slender and interdigitating processes. The cells display morphologic similarities to ganglion cells and have been described as ganglion-cell-like cells.

**Differential Diagnosis and Additional Analyses**

Differential diagnostic considerations are the same as stated above, and secondary analyses as mentioned for nodular fasciitis provide virtually identical results. However, ganglion-cell-like cells immunocytochemically exhibit MSA less frequently.

### 17.1.3.3 Myositis Ossificans [20, 65] (Fig. 17.9)

Synonyms: Pseudomalignant osseous tumor of soft tissue, myositis ossificans traumatica, fibrodysplasia ossificans progressiva, and others.

- Myositis ossificans can develop anywhere in the body with a predilection for body sites that are more likely exposed to traumas. Myositis ossificans has a broad age distribution, but it occurs most frequently in young adults bearing a significant relation to physical activity.
- It is a reparative nonneoplastic extra- and intramuscular lesion associated with heterotopic osteogenesis. The lesion is composed of cellular fibrous tissue and bone, including cellular atypia and strong mitotic activity.

**Microscopic Features**

The cellular components may vary considerably in cytologic preparations, giving rise to diagnostic dilemmas.

- The cytologic specimens usually contain numerous isolated cells:
  - Round to oval cells(immature mesenchymal cells), sometimes with elongated cytoplasm.
  - Spindle-shaped cells (fibroblasts) embedded in amorphous metachromatic stroma occasionally exhibiting loose clustering.
  - The cytoplasm varies in size and contains fine granules. Perinuclear clearing has frequently been observed.
- Imitation of osteoblasts has been described, comprising eccentrically placed rounded to oval nuclei, one or two nucleoli, and bland chromatin.
- Mature skeletal muscle, multinucleated (osteoclast-like) giant cells and mitoses may occasionally be found. Inflammatory infiltrates are inconspicuous.

**Differential Diagnosis** [28, 65]

- Diagnostic considerations should particularly include bone-forming lesions such as extraskeletal osteosarcoma, osteoblastoma, osteoid osteoma, and callus.
- Furthermore, other lesions of the pseudosarcomatous tumor group and epithelioid sarcoma must be distinguished from myositis ossificans.

**Immunocytochemistry**

All cells irrespective of their differentiation stain immunocytochemically positive for vimentin and usually for S100 protein. Myofibroblasts coexpress actin, SMA, and desmin. Osteoblasts and osteocytes coexpress osteocalcin.

### 17.1.3.4 Fibroma [28] (Fig. 17.10)

Synonyms and related terms: Dermatofibroma, fibroma of tendon sheath, desmoplastic fibroblastoma, calcifying fibrous tumor, and many others.

Fibromas are ubiquitous benign neoplasms that can be found in different types of mesenchymal tissues, including nerve sheaths, muscles, and bones; the most common sites of fibromas are the soft tissues of the extremities, especially the fingers.

Young males are most frequently affected.

**Microscopic Features**

The lesion is composed of fibroblasts at various stages of differentiation and a pronounced stromal component with metaplastic areas. Unlike in histology, distinguishing morphologic features of fibromas from different body sites do not exist for cytology.

- Cytologic specimens contain slender and plump fibroblasts and fibrocytes, bundles of collagen matrix, myxoid matrix, and thick-walled vessels.
- The nuclei are bland, showing fine chromatin structure and sporadic small nucleoli.
- Both calcified deposits and fragments of metaplastic osseous, and/or chondroid tissue may be present.

**Differential Diagnosis**

A variety of tumors of the fibroblastic/myofibroblastic category share morphologic features with fibromas; furthermore peripheral nerve tumors, gastrointestinal tumor (GIST), callus, spindle cell sarcomas, osteosarcoma, and others.

### 17.1.3.5 Desmoid-Type Fibromatosis

[11, 54] (Fig. 17.11)

Synonyms: Aggressive fibromatosis, desmoid, extraabdominal desmoid, abdominal (mesenteric) fibromatosis, and others.

- Desmoid-type fibromatosis is a low-grade lesion of the deep soft tissues, showing a strong tendency for local invasion and recurrence but inability to metastasize.
- It is usually found in extraabdominal sites in children (head and neck, thoracic area, thigh), in the abdominal wall in younger adults (musculoaponeurotic structures), and in a variety of anatomic locations in later adulthood.
- Intraabdominal fibromatosis is located in the pelvis and mesentery.

A few recent reports that address findings of FNAB samples are available in the literature [11, 54].

**Microscopic Features**

- Desmoid-type fibromatosis is composed of proliferating fibroblasts. The lesion shares cytologic features with fibroma.
- Variable mitotic activity.
- Extensive collagen and stromal hyalinization is characteristic for this tumor entity, often preventing successful aspiration of adequate cellular material.
- Extensive myxoid changes may occur, particularly in intra-abdominal desmoid-type fibromatosis.

**Differential Diagnosis** [54]

Lesions raising diagnostic problems are listed in Sect. 17.1.3.4, "Differential diagnosis", above.

Under- and overdiagnosis of malignancy may occur in FNAB specimens; diagnostic problems are frequently caused by inadequate cell sampling.

**Additional Analyses**

Immunocytochemistry

All cells strongly express vimentin. Cells of myofibroblastic origin stain positive for muscle-specific markers. Desmin, CD34, c-kit, and S100 protein are rarely expressed.

Molecular Genetics

We refer the reader to standard soft tissue textbooks [22] and to relevant reports in the literature.

### 17.1.3.6 Fibromatosis Colli

Congenital muscular torticollis is discussed in Sect. 5.2.2.1.2, p. 461.

### 17.1.3.7 Myofibroblastic Tumor of the Subcutis

This lesion is also known under the term "inflammatory pseudotumor" and is usually located in visceral organs, particularly in the lung (see Sect. 2.2.1.9.3, p. 137). The subcutaneous location is not very well documented.

The pleomorphic cytologic appearance in fine-needle aspirates may easily lead to confusion with malignant soft tissue tumors [48, 62].

## 17.1.4 Fibrohistiocytic Tumors

### 17.1.4.1 Giant Cell Tumor of Soft Tissue [3, 34, 38]

Synonyms: Osteoclastoma of soft tissue, giant cell tumor of low malignant potential.

This rare neoplasm of superficial soft tissues is the histological analog of giant cell tumor of bone. It particularly affects middle-aged patients (5th decade) but is also seen in children and elderly patients. The superficial soft tissue of the upper and lower extremities is most frequently involved, followed by the trunk, and the head and neck. Metastases are extremely uncommon.

#### Microscopic Features

- Aspirates are composed of numerous round to oval, strictly mononuclear tumor cells and osteoclast-like giant cells.
- The nuclei of the mononuclear tumor cells share the morphologic properties of the nuclei in osteoclast-like giant cells: loose and finely granular chromatin, smooth borders, and a conspicuous centrally placed nucleolus. A few mitoses may be observed.
- The background material usually consists of loose fragments of fibrous tissue interspersed with hemosiderin-laden macrophages and branching vessels. Foamy macrophages, metaplastic bone, and a great deal of blood (aspirated from blood-filled spaces that are clearly visible in histologic sections) may be present.

#### Immunocytochemistry

Immunocytochemical staining for CD68 strongly decorates the giant cells, unlike mononuclear tumor cells, which simply show focal positivity.

A few cells may show positive immunoreaction for SMA, keratins, and S100 protein.



### 17.1.4.2 Giant Cell Tumor of the Tendon Sheath and Diffuse Type [2, 22] (Fig. 3.84)

This term encompasses many tumors generally arising from the synovium of joints, bursae, and tendon sheaths. The tumor subtypes (discussed below) are characterized by their site of origin, involvement of the adjacent joints, and their growth pattern. Thus biological behavior and clinical presentation can vary greatly.

- *The localized form of giant cell tumor* is frequent and is referred to as giant cell tumor of the tendon sheath; synonyms are tenosynovial giant cell tumor and nodular tenosynovitis. A circumscribed proliferation is characteristic of this tumor type.

The tumor usually occurs in middle-aged people (between 30 and 50 years of age), with a slight female preponderance.

Giant cell tumors of tendon sheath are one of the most common tumors in the hand. Tumor locations adjacent to other small and large joints are uncommon.

- *Diffuse giant cell tumors* appear as a destructive intra- or extraarticular proliferative disorder; extraarticular tumors show intramuscular or subcutaneous spreading. Synonyms are pigmented villonodular (teno-) synovitis (Fig. 3.84).

This tumor type usually affects younger patients, most frequently before 40 years of age. Intraarticular lesions involve the knee and less frequently the hip, ankle, and elbow, whereas extraarticular tumors are found adjacent to the knee, thigh, and foot. Exceptional sites may be encountered for both tumor types. The risk of recurrence is relatively high but malignancy is very uncommon.

#### Microscopic Features

- The cellular aspirates are composed of osteoclast-like giant cells and synovial-like mononuclear cells.
- *Mononuclear cells:*
  - The small spindle-shaped cells of the stromal type disclose nuclei with longitudinal grooves, finely granular chromatin, and small but distinct nucleoli.
  - The large epithelioid cells are composed of rounded nuclei and abundant clear cytoplasm; the nuclei are typically lobulated, exhibiting pronounced nucleoli and thin dispersed chromatin.
- *Osteoclastic giant cells:* In the diffuse tumor variant, osteoclastic giant cells occur less commonly or are completely absent as compared to the localized form of giant cell tumors.
- Foam cells, hemosiderophages together with extracellular hemosiderin deposits, chronic inflammatory infiltrates, and fragments of fibrotic tissue are usually present.
- Mitoses are common.

#### Differential Diagnosis and Immunocytochemistry

- Large mononuclear epithelioid cells may be misinterpreted as malignant cells.
- Cells of both the localized and diffuse type of giant cell tumors exhibit identical immunocytochemical staining properties. Mononuclear cells are strongly positive for histiocytic markers such as CD68. A certain fraction of the spindle cells may stain positive for desmin; positivity for specific muscle actin is rare.

Giant cells express both CD68 and CD45.

## 17.1.5 Smooth Muscle Tumors and Perivascular Tumors

### 17.1.5.1 Leiomyoma of Deep Soft Tissues

Leiomyoma occurs in the deep somatic soft tissue of the extremities, retroperitoneum, and abdominal cavity [22, 24]: it is one of the most common benign soft tissue tumors in the human body.

The cytologic features of leiomyomas are fairly characteristic.

**Microscopic Features**

The tumor cells of leiomyomas closely resemble normal smooth muscle cells. The cells generally appear tightly cohesive, usually in parallel arrangement.

- The nucleus is centrally placed, elongated, and typically blunt-ended or cigar-shaped. The chromatin is fine and regularly dispersed.
- The nucleoli are inconspicuous or completely absent.
- The cytoplasm is dense, acidophilic, and fibrillar.
- Interstitial matrix is absent.
- Large leiomyomas frequently exhibit regressive cell changes.

**Differential Diagnosis and Immunocytochemistry**

- Distinguishing between leiomyoma and well-differentiated leiomyosarcoma can be difficult by cytology alone.
- Cells of leiomyomatous tumors are always positive for smooth muscle actin (SMA) and less frequently for desmin. The cells may contain abundant intracytoplasmic glycogen (PAS-positive and diastase-sensitive).

### 17.1.5.2 Perivascular Myoid Tumors (Fig. 17.12)

The following tumor types form a morphologic continuum: angioleiomyoma, myopericytoma (hemangiopericytoma), myofibroma, and infantile hemangiopericytoma.

**Microscopic Features and Immunocytochemistry**

- The tumors are composed of bundles of smooth muscle cells or at least spindle-shaped myoid-appearing cells. (In histologic sections, the cells show a striking affinity to the perivascular space.)

The spindle-shaped myoid cells exhibit a positive immunocytochemical staining for SMA, unlike endothelial cells that show positivity for CD31 and factor VIII. The staining profile can vary strongly depending on the tumor subtype, itself dependent on its cellular composition [22].

### 17.1.5.3 Glomus Tumor [29, 31]

Glomus tumors usually occur as small, painful subungual nodules but may also be encountered at any anatomic site of the human body. The glomus tumor is a disorder of young adults but it may be seen at any age.

The glomus tumor is a neuromyoarterial benign hamartoma, with most cells resembling a special type of smooth muscle cells of the normal glomus body. Malignant transformation occurs extremely rarely.

**Microscopic Features and Immunocytochemistry**

- The aspirates reveal uniform round to oval, polygonal cells that are generally tightly clustered together. Glomus cells, smooth muscle cells, and vascular elements may occur in a variable proportion to each other depending on the tumor subtype.
- Stripped nuclei and/or spindle cells are present, although they vary in number.
- The nuclei are smoothly outlined, the chromatin is finely granular.
- Nucleoli and mitotic figures are absent.
- The background matrix shows hyalinization or myxoid features; mast cells are usually present.

Immunocytochemical stains demonstrate tumor cell positivity for alpha-SMA and vimentin. Other cell markers such as desmin, CD34, S100 protein, and cytokeratin are usually not expressed.

**Differential Diagnosis** [29, 31]

Aggregation of the epithelioid tumor cells can mislead to a diagnosis of a benign or malignant monomorphic epithelial tumor (metastasis of breast carcinoma, neuroendocrine tumor, neoplasms of the glandular adnexa of the skin, and others).

## 17.1.6 Skeletal Muscle Tumors: Rhabdomyoma

Rhabdomyoma is a rare benign neoplasm of striated muscles. The tumors are classified into cardiac and extracardiac subtypes; the extremely rare genital rhabdomyoma found in the vagina of middle-aged women is not further discussed.

Extracardiac rhabdomyomas are subdivided into two classes defined by a particular morphologic appearance:

- Adult-type rhabdomyoma.
- Fetal-type rhabdomyoma.

#### 17.1.6.1 Adult-Type Rhabdomyoma

[15, 49] (Fig. 17.13)

Adult-type rhabdomyoma has a predilection site in the mouth, throat, and the soft tissues of head and neck. An elderly male population is mainly affected.

**Microscopic Features**

- The tumor exhibits mature skeletal muscle differentiation: the aspirates contain scattered and closely packed cells with abundant polyhedral eosinophilic cytoplasm with evidence of granulation, vacuolization, rod-shaped crystalline inclusions (Pap stain: orange, MGG stain: pink), and occasional cross-striation.
- The nuclei are small, round to oval, and eccentrically located, revealing a prominent nucleolus.
- Multinucleated cells are frequently seen. Cytoplasmic glycogen can easily be demonstrated (PAS-positive and diastase-sensitive).

**Differential Diagnosis**

An appropriate immunocytochemical panel (as stated in "Immunocytochemistry" below) differentiates most adult rhabdomyomas from morphologically related tumors, such as granular cell tumor (strong S100 positivity), hibernoma, oncocytic tumors (cytokeratin positivity), and specific sarcomas.

#### 17.1.6.2 Fetal-Type Rhabdomyoma [67]

Most of the tumors are located in the head and neck area (soft tissue and mucosa-affiliated). Fetal rhabdomyoma is a neoplasm of young children.

**Microscopic Features and Differential Diagnosis**

- Fetal type rhabdomyoma is composed of immature skeletal muscle cells. Cytologic specimens are composed of loosely arranged intermediate striated muscle cells and undifferentiated spindle-shaped mesenchymal cells embedded in a myxoid matrix.
- The complete absence of cellular atypia distinguishes between fetal-type rhabdomyoma and rhabdomyosarcoma.

**Immunocytochemistry**

A skeletal muscle immunophenotype is expressed by the cells of both tumor variants: strong positivity for muscle-specific actin (MSA), myoglobin, and desmin.

Negative or weak focal immunoreactivity may be obtained using antibodies against vimentin, SMA, and S100 protein.

### 17.1.7 Vascular Tumors: Angiomas

- Benign vascular tumors are ubiquitous but occur most commonly in the skin.
- In a given case, it is often difficult to decide whether the disorder is a malformation, a reactive process, or a true neoplasm.
- Cytology is frequently unable to render a firm diagnosis of angioma due to lack of pathognomonic endothelial cells; to distinguish between distinct tumor variants is practically impossible.

**Microscopic Features and Immunocytochemistry**

- Repeated aspiration of masses of erythrocytes in correlation with clinical data may suggest hemangioma.
- Aspirates from lymphangiomas usually provide a typical turbid, milky fluid containing normal lymphocytes.
- Spindle-shaped flattened endothelial cells may now and then be present, positive immunoreactivity will clearly identify the nature of these cells.

Morphologically, endothelial cells from blood vessels cannot be differentiated from those of lymphatic vessels. Positive immunoreactivity for factor VIII and/or lymphoendothelial markers (D2-40, podoplanin) will clarify the nature of the cells.

### 17.1.8 Benign Peripheral Nerve Tumors: Schwannoma, Neurofibroma

[16, 24, 42] (Figs. 17.14–17.18)

**General Comments**

- Benign peripheral nerve sheath tumors encompass many synonyms and related terms conditioned by a highly differing microscopic composition of the individual tumors corresponding to size, location, and duration of the tumor.
- Schwannoma (neurilemoma) and neurofibroma are the two most common types of benign tumors arising from peripheral nerves. They are common tumors and may occur singly or multiply. They may affect any part of the body and appear at any age, but preferentially in young adults.
- The pigmented benign peripheral nerve tumor is a rare tumor variant.
- Schwannomas and neurofibromas originate from the Schwann cells, which are a variety of glial cells, and produce the insulating myelin sheath covering peripheral nerves.
- Neurofibromatosis Type 1 is a genetically inherited disease (von Recklinghausen disease) presenting with multiple tumor nodules throughout the body in association with cutaneous café-au-lait spots.

**Microscopic Features**

- Hallmarks:
  - The pathognomonic element of all peripheral nerve tumors is a slender spindle cell with a long hair-like cytoplasmic process.
  - The nucleus is small, oval, or elongated with tapered ends and varying angulation.
  - The cytoplasmic processes of neighboring cells may be arranged in twisting bundles.
  - The nuclei frequently form parallel rows or palisades, a type of tissue called Antoni type A.
- Antoni type A areas may merge with Antoni type B areas. The latter are composed of small epithelioid cells with granular cytoplasm embedded in a myxoid background.
- Dense aggregations of fat-laden macrophages may be present.
- Cellularity of schwannomas can vary quantitatively and qualitatively. The matrix may decrease to a minimum with increasing cellularity, and mono- and multinucleated giant cells showing pleomorphic nuclei may appear in association with mitotic activity.

**Differential Diagnosis**

Most schwannomas exhibit cytologic features allowing a conclusive diagnosis, but microscopic overlap with other benign and malignant tumors can lead to awkward misinterpretations. Differential diagnostic considerations should include the following tumor entities:

- Nodular fasciitis, fibrohistiocytic tumors, and pleomorphic adenoma. Intact individual cells and inflammation are absent in schwannomas by contrast with nodular fasciitis. The stroma of schwannomas may be myxoid but it appears more fibrillar as compared to the matrix of (myo) fibroblastic lesions or of pleomorphic adenomas.
- Melanotic schwannoma can mimic desmoplastic spindle cell melanoma.
- Malignant peripheral nerve sheath tumor and other sarcomas have to be differentiated from benign peripheral nerve sheath tumors.
- A variety of cytokeratin-positive malignomas must be considered, including sarcomatoid carcinoma, synovial sarcoma, and mesothelioma.

**Immunocytochemistry** (Fig. 17.17B)

- Immunocytochemical staining is strong positivity for S100 protein, especially in Antoni type A tumor areas.
- Furthermore, glial fibrillary acidic protein (GFAP) and CD57 give rise to a positive immunoreaction in the majority of the cases.
- The immunoreactivity for various types of cytokeratins, particularly in cells of retroperitoneal schwannomas, may be due to cross-reactivity with GFAP intermediate filament proteins [21].

## 17.1.9 Chondro-osseous Tumors of Soft Tissue

Some bone-forming lesions are subsumed as variants of (myo-)fibroblastic lesions (see Sect. 17.1.3, p. 1059).

**Soft Tissue Chondroma** (Fig. 17.19)

Synonyms: Extraskeletal fibrochondroma, myxochondroma, osteochondroma.

This tumor occurs in extraosseous and extrasynovial areas, predominantly in the vicinity of the finger joints and tendons; other locations are uncommon.

A middle-aged patient group is predominantly affected.

**Microscopic Features**

- Soft tissue chondroma is typically composed of adult-type hyaline cartilage and foci of osseous, fibrous, and/or myxoid stroma.
- Aspirates primarily contain hyaline chondroid fragments. The chondrocytes are poorly outlined cells with indistinct cellular borders, abundant pale or vacuolated cytoplasm, and small pyknotic nuclei. Binucleation and mitotic activity are rare. However, mild atypias comprising nuclear variation in size and shape, and hyperchromasia may focally be present (chondroblasts).
- Chondrocyte-surrounding matrix may be myxoid or sclerotic. Prominent ossification may also occur, but it is barely encountered in FNAB material.
- A number of cases exhibit strong calcification.
- Soft tissue chondroma may give rise to extensive granuloma-like reactions in the adjacent soft tissue areas, including epithelioid cells and multinucleated giant cells.

**Differential Diagnosis**

- Soft tissue chondroma occurring as a neck mass may be misinterpreted as pleomorphic adenoma with extensive chondroid metaplasia.
- Numerous tumorous disorders comprising chondroid components pose diagnostic challenges, including callus, chondroid metaplasia, osteochondroma, pulmonary hamartoma, chondrosarcoma, osteosarcoma, among others.

**Immunocytochemistry**

As normal chondrocytes, neoplastic chondroid cells also exhibit positive immunostaining for S100 protein.

## 17.1.10 Soft Tissue Tumors of Uncertain Differentiation

**Intramuscular Myxoma** (Figs. 17.20 and 17.21)
Intramuscular myxoma is a benign tumor; the most frequent sites are the large muscles of the thigh, shoulder, buttocks, and upper arm.

The tumor has a predilection for middle-aged and older females.

### Microscopic Features

- Smears contain abundant myxoid stroma with a few capillary vessels. Cystic changes within the myxoid masses may occur.
- The matrix is interspersed with bland spindle- and stellate-shaped cells, the nuclei are small, and the cytoplasm is eosinophilic.
- Focal areas might be associated with an increase in cell number and an increase in collagen fibers in the matrix.

### Differential Diagnosis and Immunocytochemistry

- Immunocytochemically, the tumor cells stain positive for vimentin and variably for CD34, desmin, and actin. S100 protein is not exhibited.
- Other intramuscular disorders with myxoid stromal changes must be taken into consideration.

## 17.1.11 Cartilage Tumors

### 17.1.11.1 Osteochondroma [28] (Fig. 17.22)

### General Comments

- Osteochondroma is actually the most common benign bone tumor. Osteochondromas occur in children and young adults, and most tumors are diagnosed during the second decade of life.
- The lesion is most often found at the metaphysis of long bones; the distal end of femurs and the proximal end of the tibia and humerus are the most common anatomic sites of involvement.
- The vast majority of osteochondromas present as solitary lesions. Approximately 15% of osteochondromas occur as multiple lesions (hereditary multiple osteochondromas), a disorder that is inherited in an autosomal dominant manner [40].
- Malignant transformation is rare and has been reported in older patients.

### Microscopic Features and Differential Diagnosis

The tumor presents morphologically as cartilage-capped outgrowth on the surface of the bone, the outer surface of the tumor consists of a fibrous membrane (perichondrium) that is continuous with the adjacent periosteum.

- The chondroid tumor fraction is composed of well-differentiated chondrocytes occurring in cohesive nests or in distinct rows embedded in a hyalinized matrix.
- Calcification may be present.

Diagnostic considerations include all tumors containing cartilage such as callus, chondroid metaplasia, osteochondroma, chondroid lipoma, (myo-)fibroblastic lesions, chondrosarcoma, and osteosarcoma.

### 17.1.11.2 Chondroblastoma [6, 25, 36] (Fig. 17.23)

Synonyms: Calcified giant cell tumor, epiphyseal giant cell tumor, and others.

Chondroblastoma is a rare benign cartilage-producing neoplasm of the bones commonly diagnosed during the second and third decades of life, with a male predilection.

The characteristic anatomic sites are the epiphysis of long bones such as distal and proximal femur, proximal tibia, and proximal humerus; a rare classical primary origin in other bones is well known. The location in temporomandibular bones may lead to diagnostic problems by cytology with regard to tumors of the parotid region [6].

### Microscopic Features

The overall morphologic appearance of chondroblastoma allows a conclusive cytologic diagnosis in most cases.

- The cytologic specimens are usually cell-rich.
- Mature and immature chondroid cells occur in isolation or in groups.
- Less differentiated chondroid cells are small to medium-sized round or polygonal in shape, containing a round to oval nucleus. Mitoses are occasionally encountered.
- The nuclei may show indentations and grooves.
- The cytoplasm is finely vacuolated and sharply defined. It frequently contains granular calcifications and hemosiderin pigment.
- Numerous multinucleated osteoclast-like giant cells are a characteristic feature of this tumor entity.
- Matrix substance of a chondromyxoid appearance surrounds the chondroid cells; granular calcified inclusions are common.
- Focal cystic and hemorrhagic degeneration is common.

### Differential Diagnosis

- Differential diagnosis includes both lesions with chondroid matrix and lesions with giant cells.
- Chondroblastomas consisting of cystic and hemorrhagic areas may mimic aneurysmal bone cyst, giant cell tumor of bone, fibrous histiocytoma, and other pathologic conditions, whereas extensive chondroid matrix may raise suspicions of chondrosarcoma and osteosarcoma.

- Undifferentiated chondroblasts accompanied by a sparse stromal component can mislead to a diagnosis of undifferentiated sarcoma, lymphoma, or carcinoma.
- Chondroblastomas that are located in the temporomandibular area associated with a well-developed chondroid matrix may mimic mixed tumor of the salivary gland type [6].

**Additional Analyses**

Immunocytochemistry

As usual, chondroid cells immunocytochemically express S100 protein and vimentin. However, immunopositivity for cytokeratin has also been reported [18, 60].

DNA Ploidy

DNA aneuploidy has been found by flow cytometry in a case of malignant chondroblastoma. Whether DNA aneuploidy correlates with the development of metastatic disease is not yet clear [53].

## 17.1.12 Osteogenic Tumors

### 17.1.12.1 Osteoblastoma [28]

Synonyms: Ossifying giant cell tumor and giant osteoid osteoma.

Osteoblastoma is a rare benign neoplasm producing osteoid. It affects young males during the second and third decades of life. Preferential primary site of this tumor is the spine. Long bones are uncommonly involved and other locations are rare. Osteoblastoma typically grows intraosseously but tumors at the surface of the bone have also been observed.

**Microscopic Features**

- Aspirates contain osteoblasts characterized by abundant granular cytoplasm and round nuclei.
- The cell pattern tends to be monomorphic, but occasional enlarged osteoblasts exhibit distinct nuclei, nucleoli, and mitoses. Bony trabeculae-lining and osteoid mass-lining tumor cells are frequently observed.
- The intertrabecular matrix includes spindle cells, osteoclast-like giant cells, and a vascular-myxoid background.
- The osteoid matrix is focally calcified. Hyaline cartilage is rarely present.

**Differential Diagnosis**

- It is acknowledged that the diagnosis of osteoblastoma by FNA cytology can be difficult. The tumor can closely resemble osteoid osteoma, aneurysmal bone cyst, giant cell tumor, and osteosarcoma.
- Differential diagnoses concerning benign and tumor-like lesions of the spine have recently been discussed by Knoeller and coauthors [43]

### 17.1.12.2 Giant Cell Tumors of Bone

[35, 22, 58, 59, 64] (Fig. 17.24)

Synonyms: osteoclastoma and giant cell myeloma.

Giant cell tumors are uncommon primary bone tumors affecting the ends of long bones, in particular the subchondral epiphyseal area of the distal femur and the proximal tibia. Flat bones of the pelvis and the vertebrae of the sacral area are also typically involved; other tumor locations are very rare [35, 59]. Giant cell tumors account for 20% of the benign primary bone tumors.

The tumor is locally aggressive, and distant metastases are rarely encountered.

The peak incidence occurs in the 20- to 50-year-old age group.

**Microscopic Features**

- Hallmarks:
  Aspirates contain a dual cell population consisting of mononucleated tumor cells and osteoclasts. The mononuclear cells are of mesenchymal origin, representing the true tumorous component; they are assumed to induce the proliferation of osteoclastic giant cells.
  - *Mononucleated tumor cells* are usually tightly clustered, and a few cells may occur as single elements. They show a round to polygonal to elongate shape. The cytoplasm is abundant and ill defined.
  - *Osteoclastic giant cells* are in close contact with clustered tumor cells or occur interspersed between dissociated mononuclear cells. The cells may reach an enormous size, comprising a few dozen nuclei.
- Both the nuclei of tumorous stromal cells and osteoclasts exhibit strikingly similar morphology, comprising pale chromatin and one or two distinct nucleoli. Mitoses are rarely seen.
- Hematopoietic cells may be admixed with the osteoclasts.
- Modifications of the basic tumor pattern include a distinct spindle shape of the mononuclear tumor cells, fragments of fibrotic tissue, bone formation, necrotic debris (particularly in large tumors), and focal nuclear atypia.

**Differential Diagnosis [64]**

A variety of tumors comprising giant cells should not be classified as true benign giant cell tumors of bone. The following lesions should be taken into consideration:

- Aneurysmal bone cyst.
- Simple bone cyst.
- Variants of giant cell tumors of soft tissue [27].
- Brown tumor of hyperparathyroidism.
- Chondroblastoma.
- Osteoid osteoma.
- Osteoblastoma.
- Osteosarcoma.
- Undifferentiated pleomorphic sarcoma (MFH).
- And other tumors.

**Caution**

Brown tumor of hyperparathyroidism is a localized non-neoplastic bone lesion resulting from abnormal bone metabolism in hyperparathyroidism. It rarely occurs as the prime manifestation of hyperparathyroidism. Only a limited number of reports are available regarding aspiration cytology [55].

## 17.1.13 Tumors of Undefined Neoplastic Nature

### 17.1.13.1 Aneurysmal Bone Cyst

[8, 74, 75] (Fig. 17.25)

Current synonyms: Multilocular hematic bone cyst, giant cell reparative granuloma.

- Aneurysmal bone cyst is a benign osteolytic bone lesion. Histologically, it is composed of blood-filled spaces that are separated by a fibrovascular stroma containing fibroblasts, osteoclast-type giant cells, and trabeculae of bone rimmed with osteoblasts.
- Aneurysmal bone cyst may occur as a primary lesion or secondarily in the context of benign and malignant bone tumors [22].
- Common locations are the metaphyseal ends of the long bones (femur, tibia, humerus) and vertebral bodies.
- The disorder affects all age groups with a predilection for children and young adults.

**Microscopic Features**

Aneurysmal bone cysts share many cytomorphologic features with giant cell tumors of bone (see Sect. 17.1.12.2, p. 1067).

- Aspirates are most often rich in blood, displaying isolated and clustered mononuclear cells. The cells may occur in close contact with the hyaline extracellular matrix.
- Multinucleated osteoclast-like giant cells are numerous.
- Mesenchymal spindle cells, fibrovascular stromal fragments, and mitoses are usually present.

**Differential Diagnosis**

- Rendering a conclusive diagnosis of aneurysmal bone cyst is difficult by cytology. In particular, true tumors complicated by aneurysmal bone cysts can pose severe diagnostic problems that lead to misdiagnoses.
- There exist numerous differential diagnostic considerations (see Sect. 17.1.12.2, "Giant Cell Tumors of Bone, Differential Diagnosis" page number cited above) primarily including giant cell tumor of bone and brown tumor of hyperparathyroidism.

### 17.1.13.2 Langerhans Cell Histiocytosis

[22, 77] (Figs. 17.26 and 17.27)

Synonyms: Langerhans cell granulomatosis, histiocytosis X, eosinophilic granuloma.

The terms "Hand-Schüller-Christian disease" and "Letterer-Siwe disease" are used for clinical purposes.

- Langerhans cells are epidermal dendritic cells derived from bone-marrow cells. They play a role in triggering the immune response through antigen uptake and presentation to the T lymphocytes [4].
- Langerhans cell histiocytosis (LCH) is a rare and poorly understood disease. Its key feature is the proliferation of a cell population exhibiting Langerhans cell characteristics. The etiology of the disease remains uncertain. A possible role of viral infection, immune dysfunction, and reactive conditions are discussed. Still, molecular genetic studies have shown that LCH is a clonal disease rather than a polyclonal reactive disorder [4, 71].
- The disorder presents with different clinical patterns. Currently, it is best classified according to the number and type of involved organ systems (single-system disease versus multisystem disease) and the degree of organ dysfunction [33].
- A wide age distribution has been reported for LCH involving bones, with a predilection for children and young adults.
- The most common sites for osseous LCH are the skull, proximal femur, mandible, and bones of the pelvis. Ribs are frequently affected in adults.

**Microscopic Features**

- Hallmarks:
  - The cytologic specimens show many histiocytoid cells of intermediate size occurring in isolation or in loose aggregates.
  - The cytoplasm is clear or faintly eosinophilic, exhibiting delicate borders.

- The nuclei show an irregular outline and contortion as a consequence of indentations and characteristic grooves.
- The chromatin is thinly dispersed.
- The nucleoli are small but often distinct.
- Inflammatory cells are usually scattered between tumor cells. The inflammatory infiltrates consist of a high percentage of eosinophilic granulocytes along with lymphocytes, plasma cells, and neutrophilic granulocytes.

○ Degenerating eosinophils can give raise to Charcot-Leyden crystals.
○ Osteoclast-like giant cells and foamy histiocytes are occasionally present.
○ Necrosis and mitotic activity are commonly encountered.

### Additional Analyses

Immunocytochemistry

Langerhans cells exhibit pathognomonic positivity for CD1a and S100 protein (Fig. 17.27D); both nuclei and cytoplasms show pronounced reactivity. CD101 is an additional marker for the diagnosis of LCH [5].

Immunoreactivity for common leukocyte antigen (CD45) is definitely absent in cells of LCH.

Electron Microscopy

Tennis racket-shaped condensates, so-called Birbeck granules, are found as intracytoplasmic inclusion. They are unique to LCH.

### Differential diagnosis

The cytologic features are considered fairly unique of this particular tumor entity. Malignant lymphoma and fibrous histiocytoma may mimic LCH and may give rise to a diagnostic dilemma. An appropriate panel of immunocytochemical stains can solve the diagnostic problems.

## 17.1.14 Further Reading


1. Akerman M, Rydholm A. Aspiration cytology of lipomatous tumors: a 10-year experience at an orthopedic oncology center. Diagn Cytopathol 1987;3:295-302.
2. Batra VV, Jain S, Singh DK, Kumar N. Cytomorphologic spectrum of giant cell tumor of tendon sheath. Acta Cytol 2008;52:152-158.
3. Beal M, Mayerson J, Wakely PE Jr. Fine-needle aspiration cytology of giant cell tumor of soft tissue (soft tissue giant cell tumor of low malignant potential). Ann Diagn Pathol 2003;7:365-369.
4. Bechan GI, Egeler RM, Arceci RJ. Biology of Langerhans cells and Langerhans cell histiocytosis. Int Rev Cytol 2006;254:1-43.
5. Bouloc A, Boulland ML, Geissmann F, et al. CD101 expression by Langerhans cell histiocytosis cells. Histopathology 2000;36:229-232.
6. Cabrera RA, Almeida M, Mendoca ME, Frable WJ. Diagnostic pitfalls in fine-needle aspiration cytology of temporomandibular chondroblastoma: report of two cases. Diagn Cytopathol 2006;34:424-429.
7. Chhieng DC, Cangiarella JF, Waisman J, et al. Fine-needle aspiration cytology of spindle cell lesions of the breast. Cancer 1999;87:359-371.
8. Creager AJ, Madden CR, Bergman S, Geisinger KR. Aneurysmal bone cyst: fine-needle aspiration findings in 23 patients with clinical and radiologic correlation. Am J Clin Pathol 2007;128:740-745.
9. Dahl I, Akerman M. Nodular fasciitis a correlative cytologic and histologic study of 13 cases. Acta cytol 1981;25:215-223.
10. Dalal KM, Antonescu CR, Singer S. Diagnosis and management of lipomatous tumors. J Surg Oncol 2008;97:298-313.
11. Dalen BP, Mels-Kindblom JM, Sumathi VP, et al. Fine-needle aspiration cytology and core needle biopsy in the preoperative diagnosis of desmoid tumors. Acta Orthop 2006;77:926-931.
12. Dey P. Fine needle aspiration cytology of well-differentiated liposarcoma. A report of two cases. Acta Cytol 2000;44:459-462.
13. Dodd LG, Martinez S. Fine-needle aspiration cytology of pseudosarcomatous lesions of soft tissue. Diagn Cytopathol 2001;24:28-35.
14. Domanski HA. Fine-needle aspiration cytology of soft tissue lesions: diagnostic challenges. Diagn Cytopathol 2007;35:768-773.
15. Domanski HA, Dawikiba S. Adult rhabdomyoma in fine needle aspirates. A report of two cases. Acta Cytol 2000;44:223-226.
16. Domanski HA, Akerman M, Engellau J, et al. Fine-needle aspiration of neurilemoma (schwannoma). A clinicopathologic study of 116 patients. Diagn Cytopathol 2006;34:403-412.
17. Domanski HA, Carlen B, Jonsson K, et al. Distinct cytologic features of spindle cell lipoma. A cytologic-histologic study with clinical, radiologic, electron microscopic, and cytogenetic correlations. Cancer 2001;25:93:381-389.
18. Edel G, Ueda Y, Nakanishi J, et al. Chondroblastoma of bone. A clinical, radiological, light and immunohistochemical study. Virchows Arch A Pathol Anat Histopathol 1992;421:355-366.
19. el-Jabbour JN, Wilson GD, Bennett MH, et al. Flow cytometric study of nodular fasciitis, proliferative fasciitis, and proliferative myositis. Hum Pathol 1991;22:1146-1149.
20. Estrada-Villasenor E, Cedillo ED, Martinez GR. Scrape cytology of myositis ossificans: Report of a case and analysis of the cytologic findings described previously. Diagn Cytopathol 2008;36:50-53.
21. Fanburg-Smith JC, Majidi M, Miettinen M. Keratin expression in schwannoma; a study of 115 retroperitoneal and 22 peripheral schwannomas. Mod Pathol 2006;19:115-121.
22. Fletcher CDM, Unni KK, Mertens F (Eds.). World Health Organization Classification of Tumours. Pathology and Genetics of Tumours of Soft Tissue and Bone. IARC Press: Lyon 2002.
23. Furlong MA, Fanburg-Smith JC, Miettinen M. The morphologic spectrum of hibernoma: a clinicopathologic study of 170 cases. Am J Surg Pathol 2001;25:809-814.

24. Gonzalez-Campora R. Cytoarchitectural findings in the diagnosis of primary soft tissue tumors. Acta Cytol 2001;45:115-146.
25. Granados R, Martin-Hita A, Rodriguez-Barbero JM, Murillo N. Fine-needle aspiration cytology of chondroblastoma of soft parts: case report and differential diagnosis with other soft tissue tumors. Diagn Cytopathol 2003;28:76-81.
26. Guo Z, Voytovich M, Kurtycz DF, Hoerl HD. Fine-needle aspiration diagnosis of spindle-cell lipoma: a case report and review of the literature. Diagn Cytopathol 2000;23:362-365.
27. Gupta K, Dey P, Goldsmith R, Vasishta RK. Comparison of cytologic features of giant-cell tumor and giant-cell tumor of tendon sheath. Diagn Cytopathol 2004;30:14-18.
28. Hajdu SI, Hajdu EO. Cytopathology of Soft Tissue and Bone Tumors. Basel, S Karger 1989.
29. Handa U, Palta A, Mohan H, Punia RP. Aspiration cytology of glomus tumor: a case report. Acta Cytol 2001;45:1073-1076.
30. Hashimoto CH, Cobb CJ. Cytodiagnosis of hibernoma: a case rport. Diagn Cytopathol 1987;3:326-329.
31. Holck S, Bredesen JL. Solid glomus tumor presenting as an axillary mass: report of a case with morphologic study, including cytologic characteristics. Acta Cytol 1996;40:555-562.
32. Hong R, Choi DY, Do NY, Lim SC. Fine-needle aspiration cytology of a lipoblastoma: a case report. Diagn Cytopathol 2008;36:508-511.
33. Howarth DM, Gilchrist GS, Mullan BP, et al. Langerhans cell histiocytosis: diagnosis, natural history, management, and outcome. Cancer 1999;85:2278-2290.
34. Icihikawa K, Tanino R. Soft tissue giant cell tumor of low malignant potential. Tokai J Exp Clin med 2004;29:91-95.
35. Jain M, Aiyer HM, Singh M, Narula M. Fine-needle aspiration diagnosis of giant cell tumor of bone presenting at unusual sites. Diagn Cytopathol 2002;27:375-378.
36. Jain M, Kaur M, Kapoor S, Arora DS. Cytological features of chondroblastoma: a case report with review of the literature. Diagn Cytopathol 2000;23:348-350.
37. Kapila K, Ghosal N, Gill SS, Verma K. Cytomorphology of lipomatous tumors of soft tissue. Acta Cytol 2003;47:555-562.
38. Kim NR, Han J. Primary giant cell tumor of soft tissue. Report of a case with fine needle aspiration cytologic and histologic findings. Acta Cytol 2003;47:1103-1106.
39. Kindblom LG, Meis-Kindblom JM. Chondroid lipoma: an ultrastructural and immunohistochemical analysis with further observations regarding its differentiation. Hum Pathol 1995;26:706-715.
40. Kitsoulis P, Galani V, Stefanaki K, et al. Osteochondromas: review of the clinical, radiological and pathological features. InVivo 2008;22:633-646.
41. Klijanienko J, Caillaud JM, Lagacé R. Fine-needle aspiration in liposarcoma: cytohistologic correlative study including well-differentiated, myxoid, and pleomorphic variants. Diagn Cytopathol 2004;30:307-312.
42. Klijanienko J, Caillaud JM, Lagacé R. Cytohistologic correlations in schwannomas (neurilemomas), including „ancient", cellular, and epithelioid variants. Diagn Cytopathol 2006;34:517-522.
43. Knoeller SM, Uhl M, Adler CP, Herget GW. Differential diagnosis of benign tumors and tumor-like lesions in the spine. Own cases and review of the literature. Neoplasma 2004;51:117-126.
44. Kong CS, Cha I. Nodular fasciitis: diagnosis by fine needle aspiration biopsy. Acta Cytol 2004;48:473-477.
45. Kumar S, Chowdhury N. Accuracy, limitations and pitfalls in the diagnosis of soft tissue tumors by fine needle aspiration cytology. Indian J Pathol Microbiol 2007;50:42-45.
46. Lemos MM, Kindblom LG, Meis-Kindblom JM, et al. Fine-needle aspiration characteristics of hibernoma. Cancer 2001;93:206-210.
47. Lopez-Ferrer P, Jimenez-Heffernan JA, Yebenes L, et al. Fine-needle aspiration cytology of lipoblastoma: a report of two cases. Diagn Cytopathol 2005;32:32-34.
48. MacSweeney F, Desai SA. Inflammatory pseudotumour of the subcutis: a report on the fine needle aspiration findings in a case misdiagnosed cytologically as malignant. Cytopathology 2000;11:57-60.
49. McGregor DK, Krishnan B, Green L. Fine-needle aspiration of adult rhabdomyoma: a case report with review of the literature. Diagn Cytopathol 2003;28:92-95.
50. Mentzel T, Remmler K, Katenkamp D. Chondroid lipoma. Clinicopathological, immunohistochemical, and ultrastructural analysis of six cases of a distinct entity in the spectrum of lipomas. Pathologe 1999;20:330-334.
51. Morerio C, Nozza P, Tassano E, et al. Differential diagnosis of lipoma-like lipoblastoma. Pediatr Blood Cancer 2009;52:132-134.
52. Ooe M, Ishiguro N, Kawashima M. Nuclear DNA content and distribution of Ki-67 positive cells in nodular fasciitis. J Dermatol 1993;20:214-218.
53. Ostrowski ML, Johnson ME, Truong LD, et al. Malignant chondroblastoma presenting as a recurrent pelvic tumor with DNA aneuploidy and p53 mutation as supportive evidence of malignancy Skeletal Radiol 1999;28:644-650.
54. Owens CL, Sharma R, Ali SZ. Deep fibromatosis (desmoid tumor): cytopathologic characteristics, clinicoradiologic features, and immunohistochemical findings on fine-needle aspiration. Cancer 2007;111:166-172.
55. Pavlovic S, Valyi-Nagy T, Profirovic J, David O. Fine-needle aspiration of brown tumor of bone: cytologic features with radiologic and histologic correlation. Diagn Cytopathol 2009;37:136-139.
56. Raab SS, Silverman JF, McLeod DL, et al. Fine needle aspiration biopsy of fibromatoses. Acta Cytol 1993;37:323-328.
57. Rigby HS, Wilson YG, Cawthorn SJ, Ibrahim NB. Fine needle aspiration of pleomorphic lipoma: a potential pitfall of cytodiagnosis. Cytopathology 1993;4:55-58.
58. Roux S. Giant cell tumors of bone. Rev Rhum Engl Ed 1998;65:139-147.
59. Saikia B, Goel A, Gupta SK. Fine-needle aspiration cytologic diagnosis of giant-cell tumor of the sacrum presenting as a rectal mass: a case report. Diagn Cytopathol 2001;24:39-41.
60. Semmelink HJ, Pruszczynski M, Wiersma-van Tilburg A, et al. Cytokeratin expression in chondroblastomas. Histopathology 1990;16:257-263.
61. Shattuck MC, Victor TA. Cytologic features of well-differentiated sclerosing liposarcoma in aspirated samples. Acta Cytol 1988;32:896-901.
62. Shukla S, Sharma S, Langer S, Sinha M. FNAC of inflammatory myofibroblastic tumour of the subcutis: a diagnostic dilemma. Indian J Pathol Microbiol 2007;50:875-877.
63. Singh HK, Kilpatrick SE, Silverman JF. Fine needle aspiration biopsy of soft tissue sarcomas: utility and diagnostic challenges. Adv Anat Pathol 2004;11:24-37.
64. Vetrani A, Fulciniti F, Boschi R, et al. Fine needle aspiration biopsy diagnosis of giant-cell tumor of bone. An experience with nine cases. Acta Cytol 1990;34:863-867.
65. Wakely PE, Almeida M, Frable WJ. Fine-needle aspiration biopsy cytology of myositis ossificans. Mod Pathol 1994;7:23-25.
66. Walaas L, Kindblom LG. Lipomatous tumors: a correlative cytologic and histologic study of 27 tumors examined by fine needle aspiration cytology. Hum Pathol 1985;16:6-18.
67. Walsh SN, Hurt MA. Cutaneous fetal rhabdomyoma: a case report and historical review of the literature. Am J Surg Pathol 2008;32:485-491.
68. Ward WG, Savage P, Boles CA, Kilpatrick SE. Fine-needle aspiration biopsy of sarcomas and related tumors. Cancer Control 2001;8:232-238.
69. Weiss SW. Lipomatous tumors. Monogr Pathol 1996;38:207-239.
70. Weiss SW, Goldblum JR (eds) (2007), Enzinger and Weiss's Soft Tissue Tumors, 5th rev. ed, Mosby

71. Willman CL, McClain KL. An update on clonality, cytokines, and viral etiology in Langerhans cell histiocytosis. Hematol Oncol Clin North Am 1998;12:407-416.
72. Wong NL. Fine needle aspiration cytology of pseudosarcomatous reactive proliferative lesions of soft tissue. Acta Cytol 2002;46: 1049-1055.
73. Woyke S, Kapila K, Goswami KC. Atypical lipoma as a potential pitfall in the cytodiagnosis of subcutaneous tumors. A report of two cases. Acta Cytol 1997;41:897-902.
74. Yadavrao KA, Rajaram DS, Vijaykumar WJ, Langade YB. Fine needle aspiration cytology diagnosis of aneurysmal bone cyst: a case report. Indian J Pathol Microbiol 2007;50:425-426.
75. Yamamoto T, Nagira K, Akisue T, et al. Fine-needle aspiration biopsy of solid aneurysmal bone cyst in the humerus. Diagn Cytopathol 2003;28:159-162.
76. Yong M, Raza AS, Greaves TS, Cobb CJ. Fine-needle aspiration of a pleomorphic lipoma of the head and neck: a case report. Diagn Cytopathol 2005;32:110-113.
77. Zhu H, Hu DX. Langerhans cell histiocytosis of the thyroid diagnosed by fine needle aspiration cytology. A case report. Acta Cytol 2004;48:278-280.

**Fig. 17.1A, B Classic lipoma.**
FNAB of a tender lobate subcutaneous tumor. Direct smears were stained according to the Papanicolaou method. **A** Classic lipoma is characterized by lobular arrangement of mature fat cells (low magnification). **B** Higher magnification displays large round mature lipocytes with eccentrically placed small nuclei. Scanty loose connective tissue and capillaries sporadically intersect the fat cells (upper left).

**Fig. 17.2A Spindle cell lipoma.**
A lipoma predominantly composed of spindle-shaped lipocytes comprising bland nuclei is shown at higher magnification. Collagen fiber bundles are also present (FNAB, direct smear, Pap stain).
**B Pleomorphic lipoma.**
Round and fusiform adipocytes reveal nuclear polymorphism: varying size, irregular nuclear outline, as well as cleaved and grooved nuclei. A multinucleated floret cell exhibiting radial nuclear arrangement is also depicted (arrow). The nuclear chromatin is thinly dispersed or patternless (FNAB, direct smear, Pap stain, higher magnification).

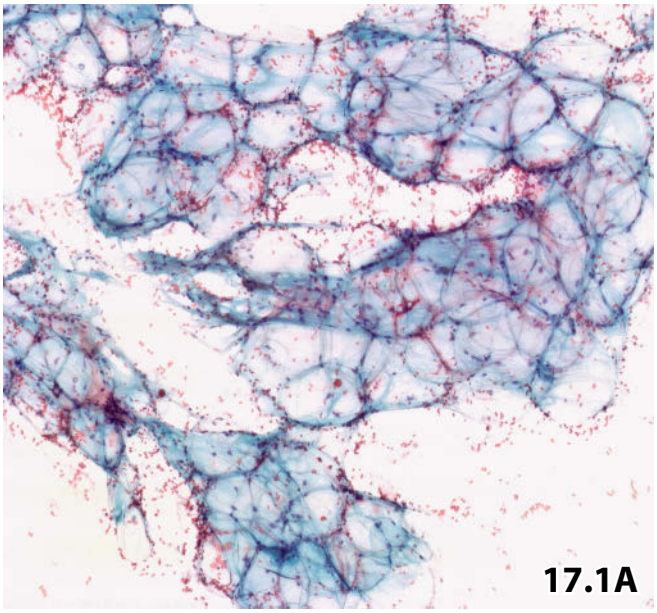
17.1A

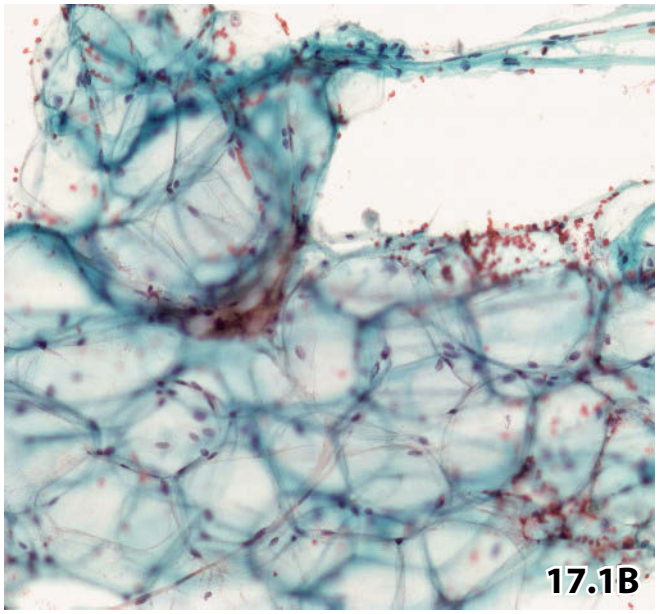
17.1B

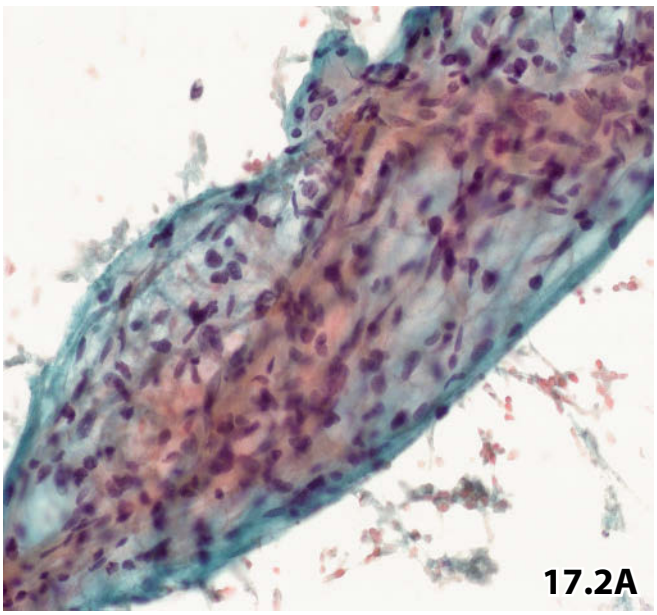
17.2A

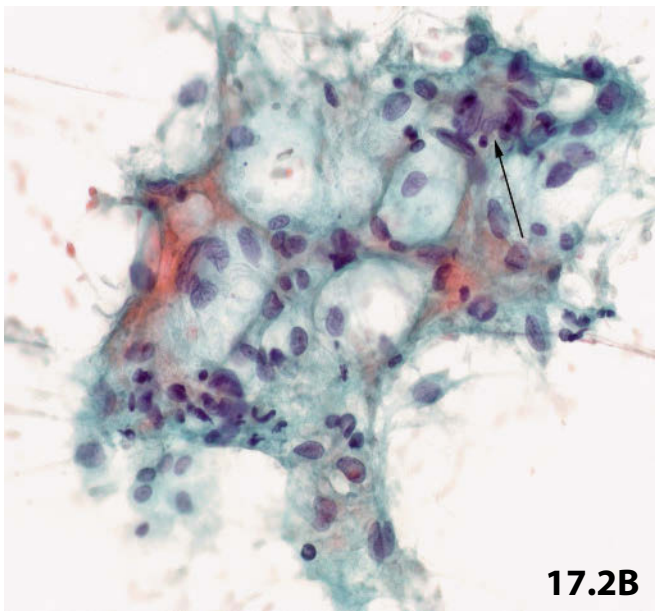
17.2B

**Fig. 17.3A, B Hibernoma.**
FNAB of a palpable supraclavicular nodule in a younger female patient. Direct smears were Pap-stained. **A** Low magnification contrasts a cluster of common benign fat cells (left) with a lipocyte-cluster of the hibernoma variant (right). **B** The cellular details of hibernoma cells are highlighted. Note the tightly packed cells, particular cytoplasmic features (vacuolated, dense, and granular; redish-brown color), mild nuclear irregularities, and occasional dense granular chromatin.

**Fig. 17.4A, B Well-differentiated lipoma-like liposarcoma versus atypical lipoma.**
A 42-year-old woman presented with a voluminous mass (10×20 cm) situated in the muscles of her left thigh. Ultrasound-guided FNAB was performed and wet-fixed direct smears were prepared from the aspirated material for Pap staining.
*Tentative cytologic diagnosis:* Lipoma-like atypical intramuscular lipoma and well-differentiated liposarcoma must be considered. Distinguishing between a benign and malignant lipomatous disorder is not possible in this setting.
*Tissue diagnosis* (complete excision of the lesion): Well-differentiated lipoma-like liposarcoma.
**A** Lower magnification readily reveals a lipomatous lesion; note that nuclear irregularities in both adipocytes and spindle-shaped stromal cells are clearly visible. **B** High magnification sets focus on irregular cell arrangement, distinct nuclear irregularities, and bland chromatin.

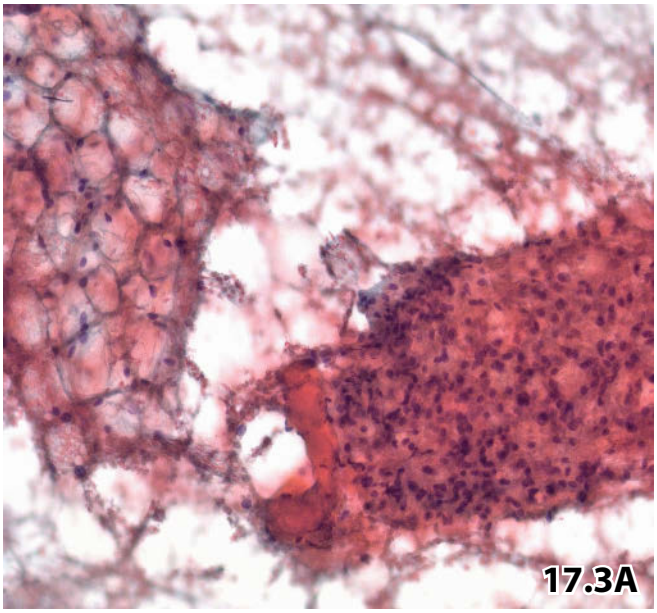
17.3A

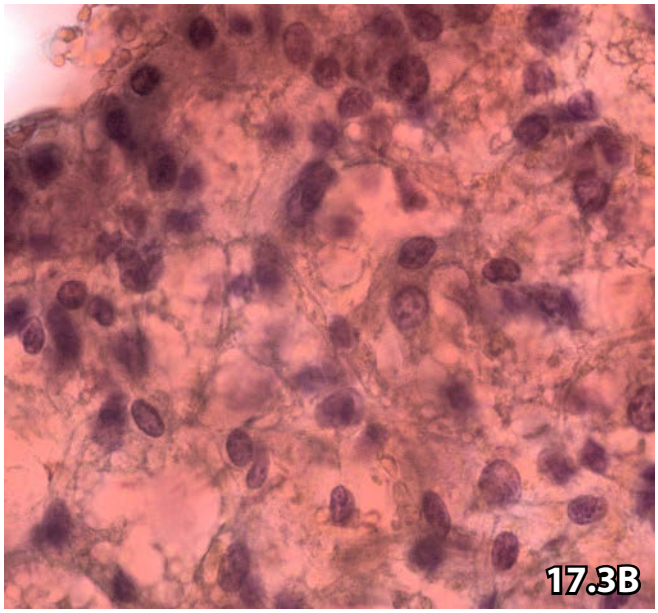
17.3B

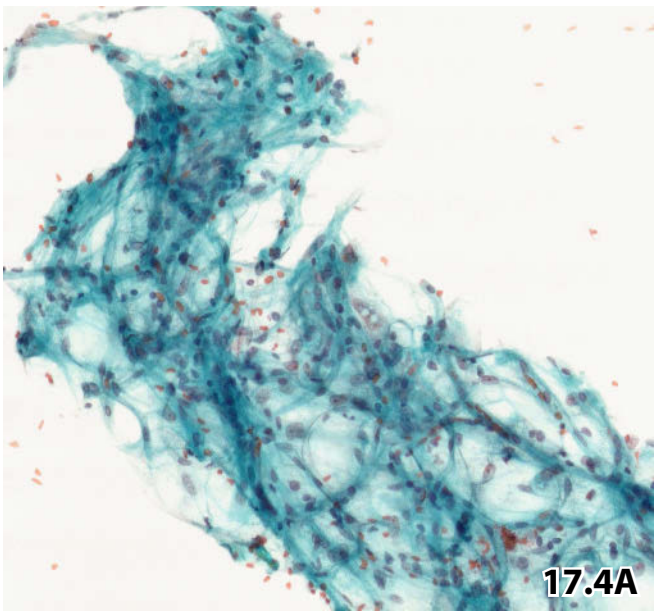
17.4A

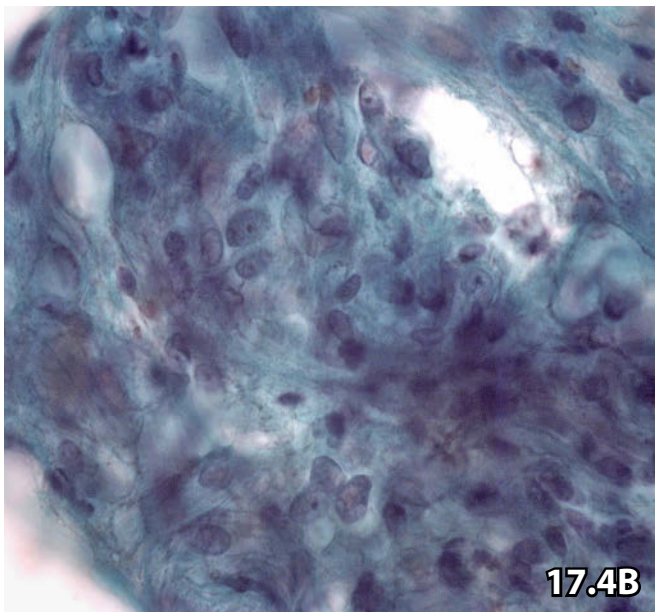
17.4B

**Figs. 17.5–17.7 Nodular fasciitis.**
Cytologic features of nodular fasciitis are demonstrated in FNAB material from three patients. Aspirates were processed by direct smears and the Papanicolaou staining technique.

**Fig. 17.5** (case #1) A small, firm nodular lesion was detected at the right forearm of a 52-year-old woman. Lower magnification reveals activated fibro- and myofibroblasts occuring in isolation or in aggregates. Multinucleated giant cells showing osteoclastic features (crowded nuclei with pronounced centrally placed nucleoli).

**Fig. 17.6** (case #2) A 41-year-old woman presented with a subcutaneous nodule at her right thigh. High magnification calls attention to the combination of nuclear/nucleolar polymorphism and bland chromatin.

The large empty bubbles in the background of the smear may be misinterpreted as cytoplasmic bodies of adipocytes.

**Fig. 17.7** (case #3) Another peculiarity of nodular fasciitis is shown by means of the aspirate from a 34-year-old man's pretibial swelling located in the right lower leg. Lower magnification displays activated myofibroblastic cells (arrows) embedded in fibromyxoid tissue loosely interspersed with inflammatory cells (bottom).

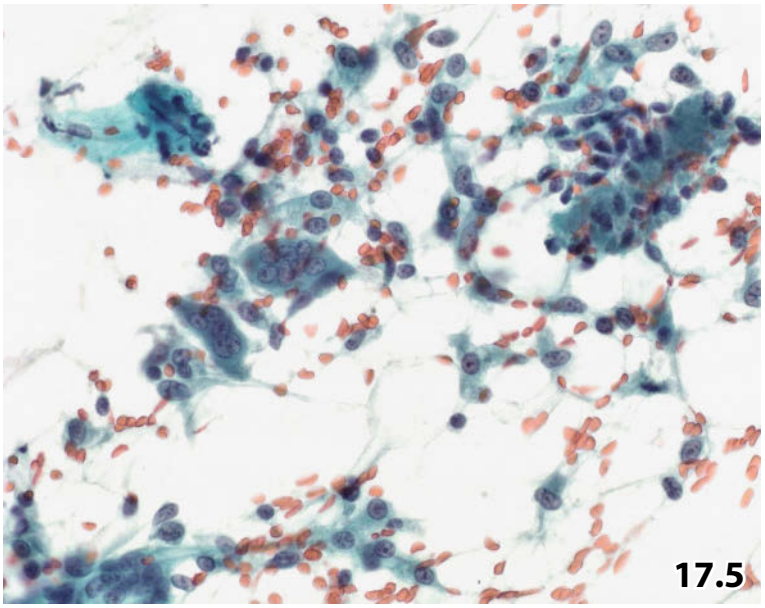
17.5

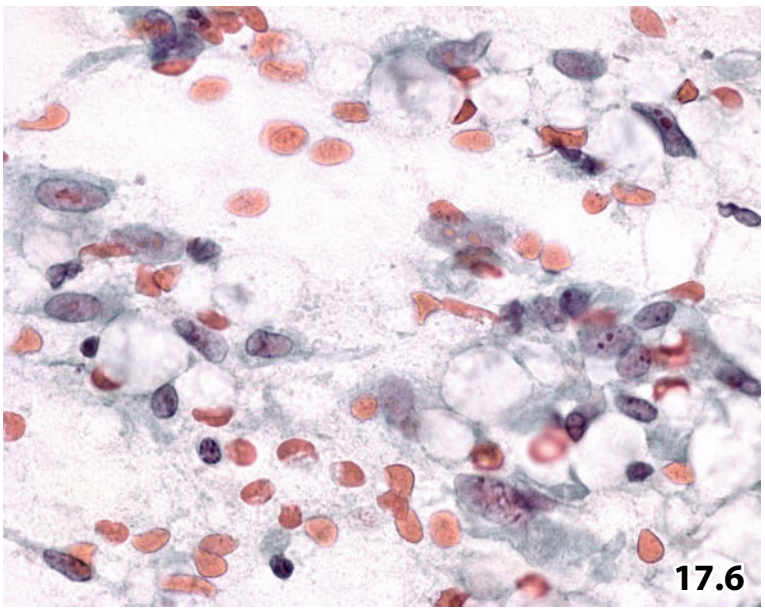
17.6

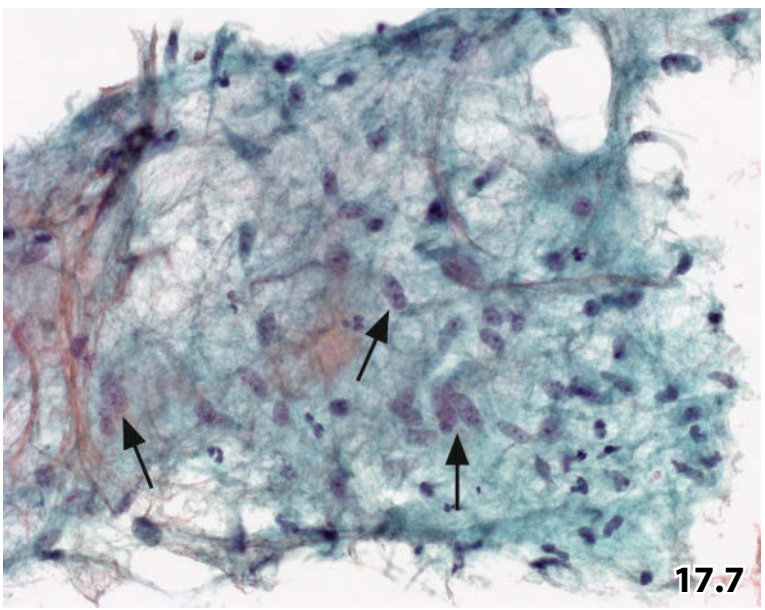
17.7

**Fig. 17.8A, B Proliferative fasciitis/proliferative myositis.**
A 54-year-old woman presented with an aching swelling in the skeletal muscles of the right thigh. Ultrasound-guided FNAB was performed providing cellular direct smears (Pap stain). **A** Microfragments of tissue and single cells exhibiting the cytologic appearance of proliferative myositis:
– Myofibroblastic cells embedded in fibromyxoid tissue matching the appearance of nodular fasciitis.
– Bundles of skeletal muscles (upper left).
– Ganglion-cell-like cells exhibiting distinct nucleoli (arrows).
**B** A typical ganglion-cell-like cell is presented at high magnification. Note the eccentrically placed nucleus and the implied slender cytoplasmic process extending to the right. Ganglion-cell-like cells are an integral part for the diagnosis of both proliferative fasciitis and proliferative myositis.

**Fig. 17.9A, B Myositis ossificans.**
Ultrasound-guided FNAB of a diffuse infraclavicular swelling in a 38-year-old woman. Direct smears were prepared followed by Pap staining. **A** Numerous dispersed immature mesenchymal cells with polyhedral cytoplasm are embedded in an amorphous background; a microfragment of skeletal muscle tissue is also present in the chosen field (higher magnification). **B** High magnification exhibits amorphous background material and perinuclear clearing (upper left); both are considered as typical features of myositis ossificans.

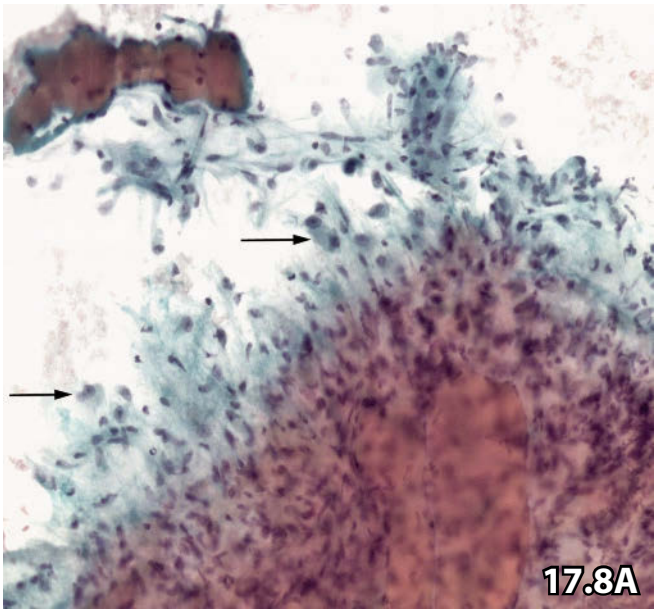
17.8A

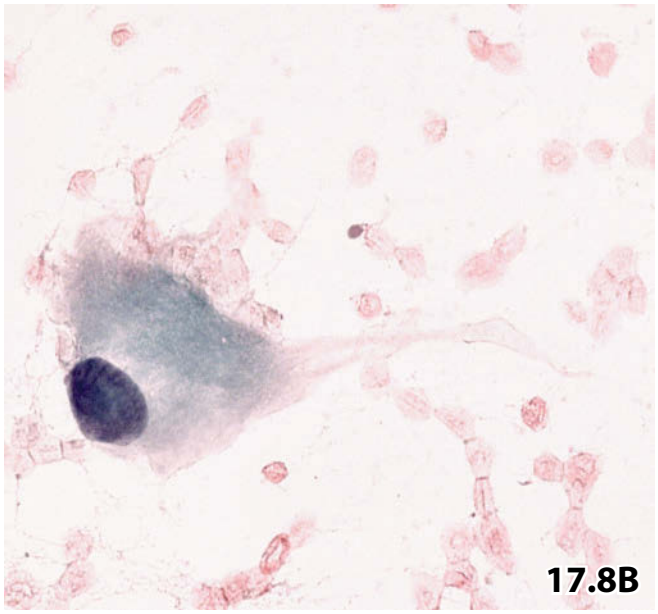
17.8B


17.9A

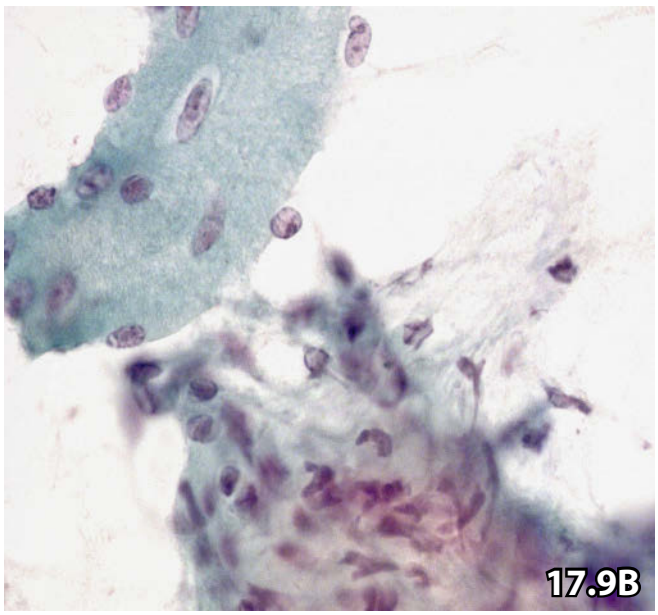
17.9B

**Fig. 17.10A, B Fibroma.**
A 20-year-old woman presented with a nodular lesion in her left axilla. FNAB was performed (direct smears, Pap stain). **A** Tightly packed gross and mainly fusiform fibroblasts occur in a background of collagen matrix (lower magnification). **B** Cellular details and structural features of the collagen matrix are highlighted. Note bland chromatin and often indistinct nucleoli.

**Fig. 17.11 Desmoid-type fibromatosis.**
Imprint and scraping cytology of the cut surface of a paravertebral mass removed by surgical excision. Lower magnification showss conspicuously activated fibroblasts and a fragment of hyalinized collagenous tissue (upper left) (Pap stain).
*Histologic diagnosis:* Extra-abdominal fibromatosis (desmoid).

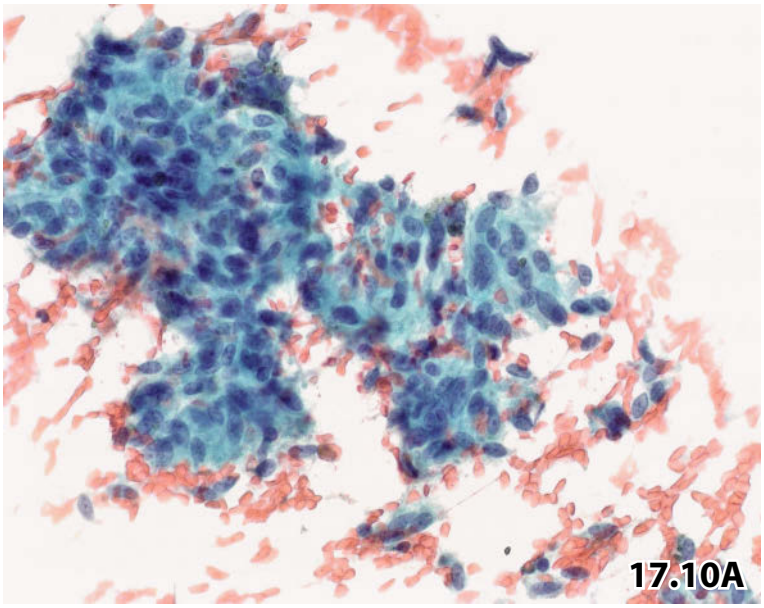
17.10A

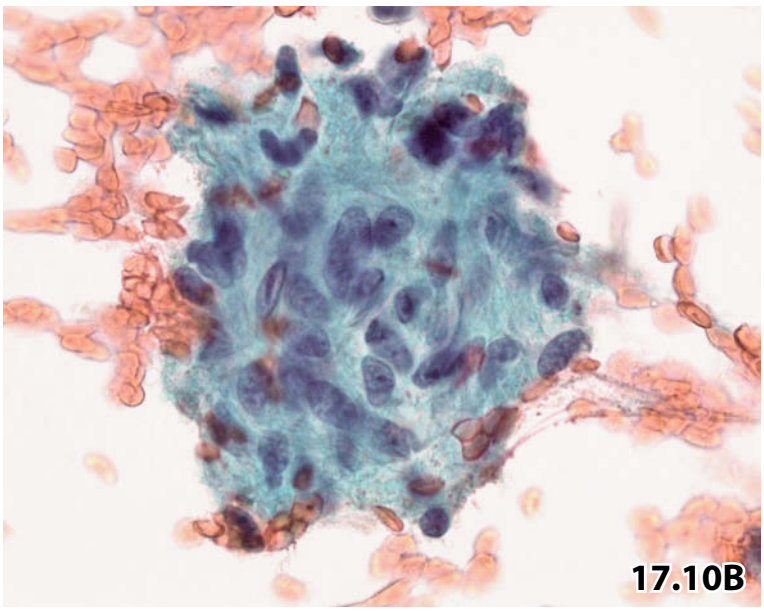
17.10B

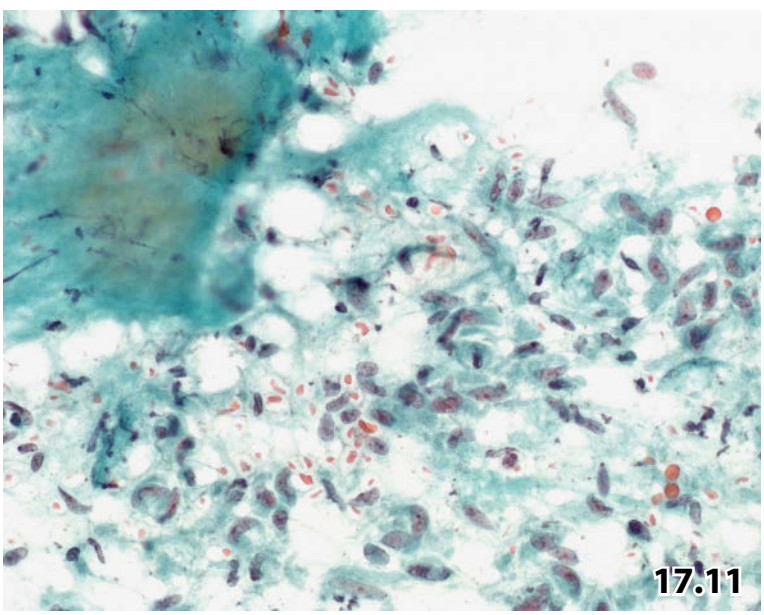
17.11

**Fig. 17.12 Hemangiopericytoma.**
A 51-year-old man presented with a tumor mass in his left parotid area. Tentative clinical diagnosis was cystic Warthin tumor. FNAB was performed yielding hypercellular direct smears, which were Pap-stained.
*Tentative cytologic/immunocytochemical diagnosis:* Spindle cell neoplasia. Immunostaining indicates myoid cell origin, tumor cells express strong positivity for alpha smooth muscle actin (not shown).
*Differential diagnoses:* Spindle cell myoepithelioma and parotid pleomorphic adenoma of myoepithelial variant were considered initially.
*Tissue diagnosis* (excisional biopsy): Encapsulated hemangiopericytoma.
**A** Lower magnification discloses bundles of myoid-type spindle-shaped cells. **B** High magnification shows blunt-ended nuclei usually occuring in parallel arrangement. Nucleoli are absent.

**Fig. 17.13A, B Adult type rhabdomyoma.**
FNAB of a submandibular tumor in a 58-year-old man. Direct smears were Pap-stained.
*Cytologic/immunocytochemical diagnosis:* Rhabdomyoma, adult type. The cytoplasm of the tumor cells showed positive immunoreaction for desmin (not shown). The diagnosis was confirmed by histology.
**A** A single tumor cell is depicted at extremely high magnification (Oil immersion by slightly closing the substage diaphragm of the microscope, ×100). Note two eccentrically placed nuclei, the granular cytoplasm, and rod-shaped crystalline cytoplasmic inclusions (arrows).
**B** Detail from another field displays a cluster of crowded tumor cells intermingled with fusiform cells. The tumor cells have abundant compact and homogeneous cytoplasm harboring eccentrically placed nuclei (arrows).

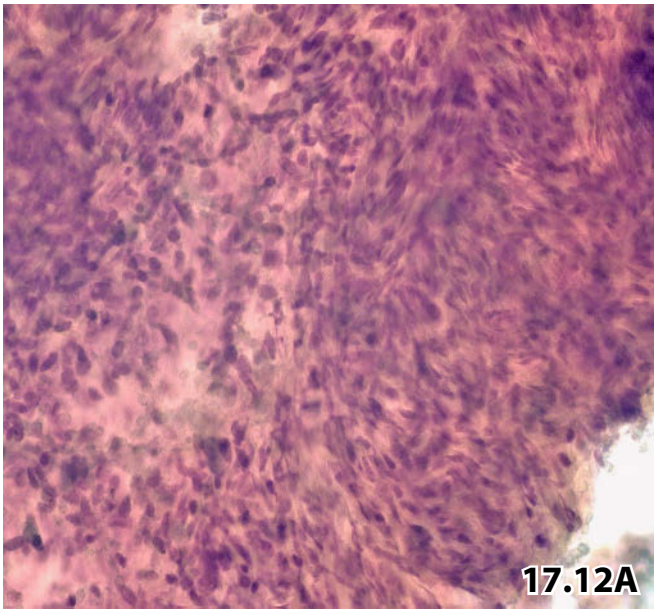
17.12A

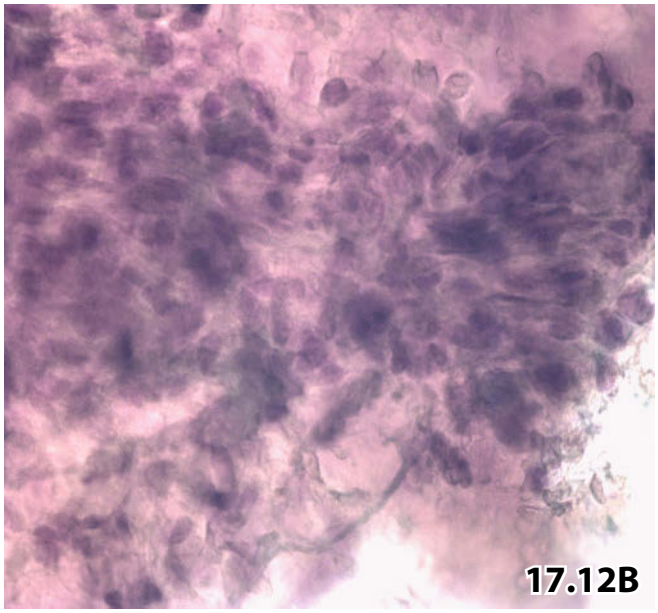
17.12B

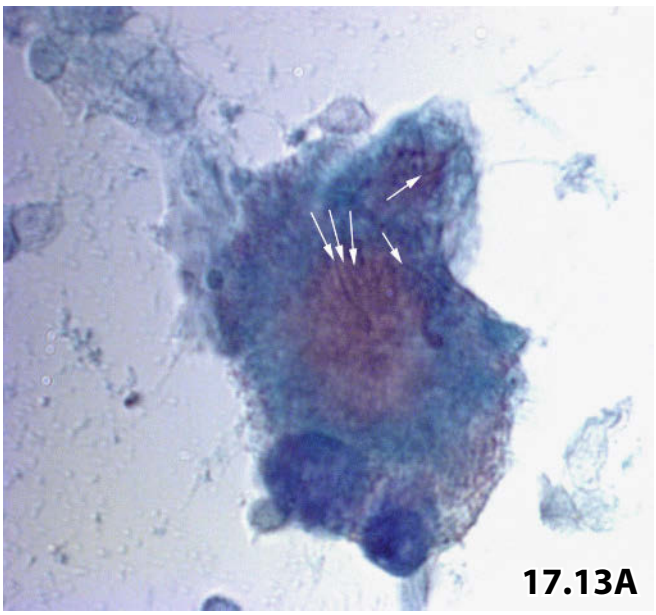
17.13A

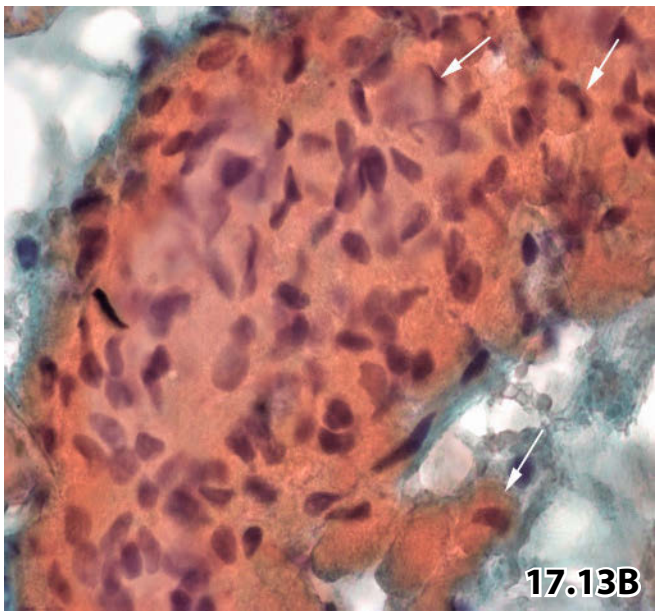
17.13B

**Figs. 17.14–17.18 Schwannoma and neurofibroma.**
Cytologic key features are presented by means of fine-needle aspirations and imprint cytology (case #5) of five patients with schwannoma/neurofibroma. Aspirated material was directly smeared onto glass slides with the exception of case #2 (thin layer preparation). Each specimen was Pap-stained.

**Fig. 17.14** (case #1) A classic microfragment originating from a peripheral nerve sheath tumor: spindle cells are mostly arranged in bundles and embedded in loose fibrillar matrix (arrows) (lower magnification).

**Fig. 17.15** (case #2) High magnification reveals the classic cytoarchitecture of a microfragment of schwannoma tissue including an Antoni type A nuclear arrangement (asterisk). Note slender spindle cells containing nuclei with tapered ends and discrete nuclear angulation (arrows). Loose fibrillar background matrix is seen at the bottom of the picture. Material depicted in this figure was processed using a liquid-based method (ThinPrep).

**Fig. 17.16** (case #3) Another example highlighting nuclear features and the long hair-like cytoplasmic processes of the peripheral tumorous glial cells (high magnification). Note the variability of nucleus size.

**Fig. 17.17A, B** (case #4) Example of a cellular schwannoma located in the pelvis minor of a 80-year-old woman with a history of malignant melanoma that had been successfully treated, without evidence of metastasis. Image-guided FNAB of the pelvic mass (direct smears, Pap stain)
*Tentative cytologic diagnosis:* Malignant spindle cell neoplasm, most likely malignant fibrous histiocytoma or malignant schwannoma (S100 positivity).
*Discussion:* A spindle cell melanoma could not completely be ruled out in spite of the unsuitable background matrix. The accentuated cellular polymorphism resulted in an erroneous interpretation of malignancy.
*Tissue diagnosis* (surgical biopsy): Degenerating benign cellular schwannoma.
**A** Higher magnification exhibits irregular cell arrangement, multinucleation, and nuclear pleomorphism of the spindle cells. Please note the loose fibrillar background. **B** Tumor cells show immunocytochemical expression of the S100 protein.

**Fig. 17.18** (case #5) A younger woman with a long-standing history of neurofibromatosis underwent another excisional biopsy of a cutaneous nodule. Imprint cytology specimens from the cut surface of this tumor were prepared and Pap-stained. Higher magnification shows hyaline matrix encasing stromal cells, which are often considerably elongated and contain slender and variegated nuclei.
*Tissue diagnosis:* Focally atypical neurofibroma.

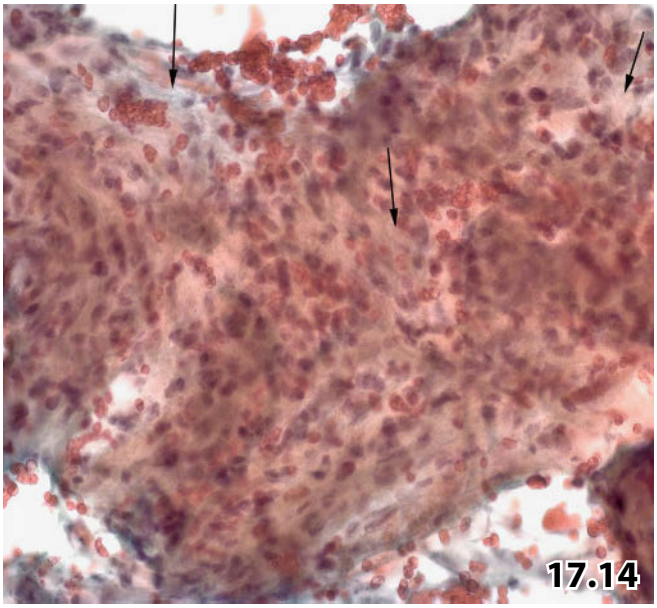
17.14

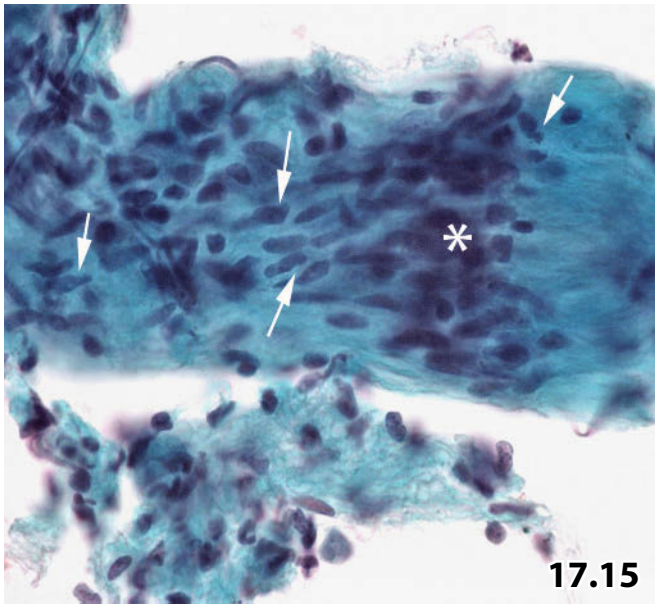
17.15

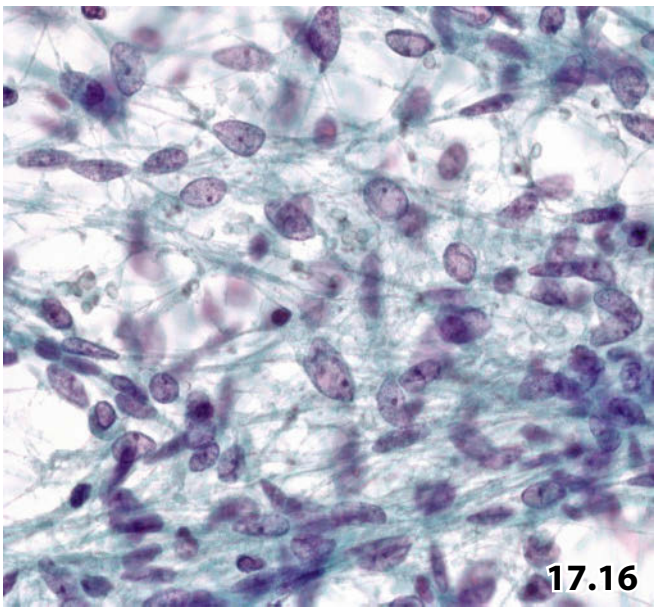
17.16

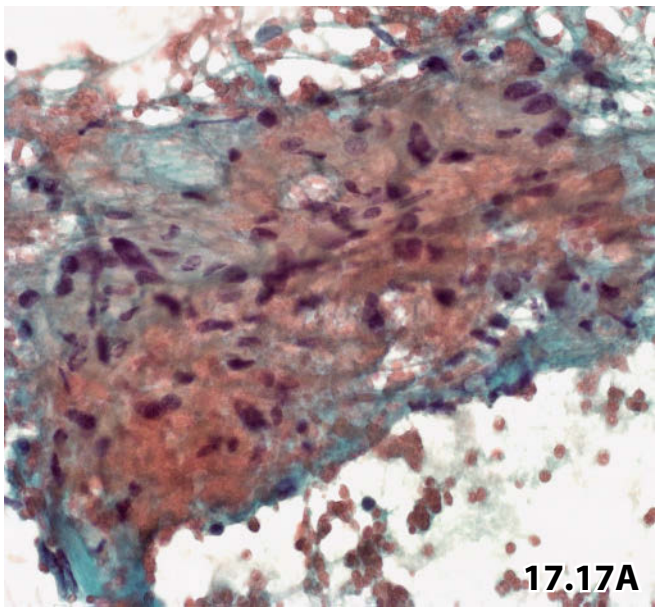
17.17A

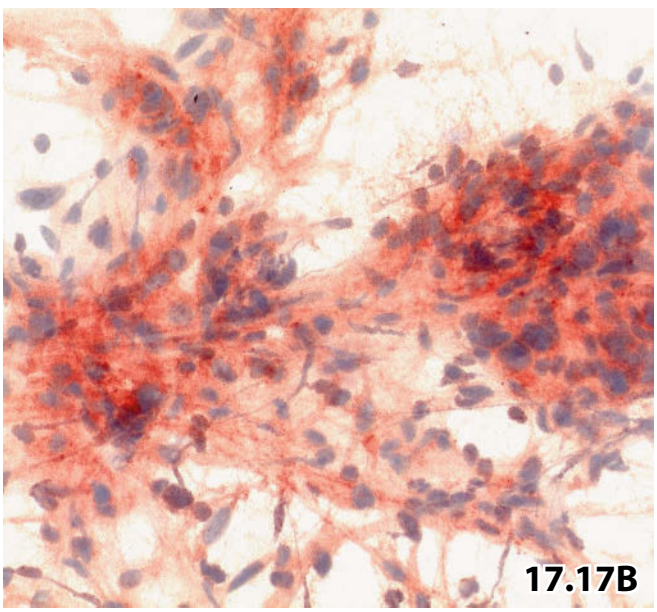
17.17B

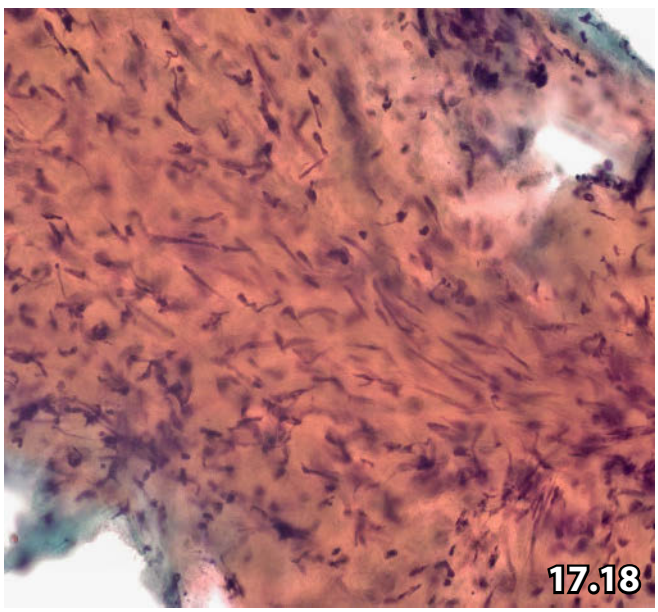
17.18

**Fig. 17.19 Soft tissue chondroma.**
A 55-year-old man presented with a firm nodule at his neck. FNAB was performed, and the direct smears were Pap-stained. High magnification shows a fragment of chondroid tissue exhibiting chondroid matrix and slightly atypical chondrocytes (variation of nuclear size and distinct nucleoli).
*Cytologic diagnosis:* Chondroid tumor.
*Tissue diagnosis* (excisional biopsy): Chondroid tumor, potential low-grade malignancy.
No tumor relapse was observed during a 5-year follow-up period,.

**Figs. 17.20 and 17.21 Intramuscular myxoma.**
Two middle-aged man presenting with an intramuscular mass in their buttock and thigh, respectively. Ultrasound-guided FNABs were performed, the direct smears were Pap-stained.
*Cytologic diagnosis* (both cases): Mesenchymal myxoid lesion without signs of malignancy.
*Tissue diagnosis* (both cases): Intramuscular myxoma.

**Fig.17.20** (case #1) Low magnification reveals a paucicellular myxoma: thin myxoid-mucoid matrix enclosing scattered stellate and spindle-shaped cells.

**Fig. 17.21** (case #2) Cytologic detail of the second tumor shows a hypercellular tissue microfragment: a mesh of collagen fibers pervades the myxoid matrix. The cells exhibit a certain nuclear polymorphism; the cytoplasmic bodies are polyhedral, stellate or spindle-shaped.

**Fig. 17.22 Osteochondroma.**
A 69-year-old woman presented with a tumor on her right forefinger. Clinical findings suggested ecchondroma. The direct smear of the aspirated material was Pap-stained. Cohesive aggregations of mature chondrocytes are embedded in hyaline chondroid matrix. Calcium deposits are also present at the upper margin of the picture (lower magnification).
*Cytologic and subsequent tissue diagnosis:* Osteochondroma.

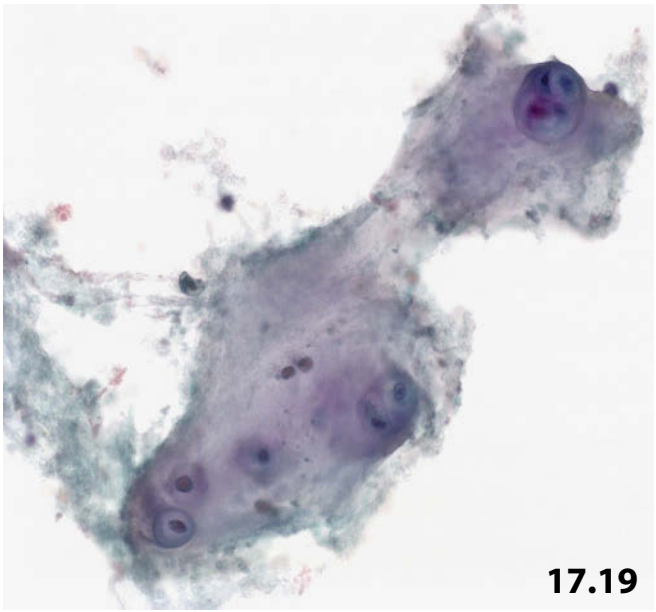

17.19

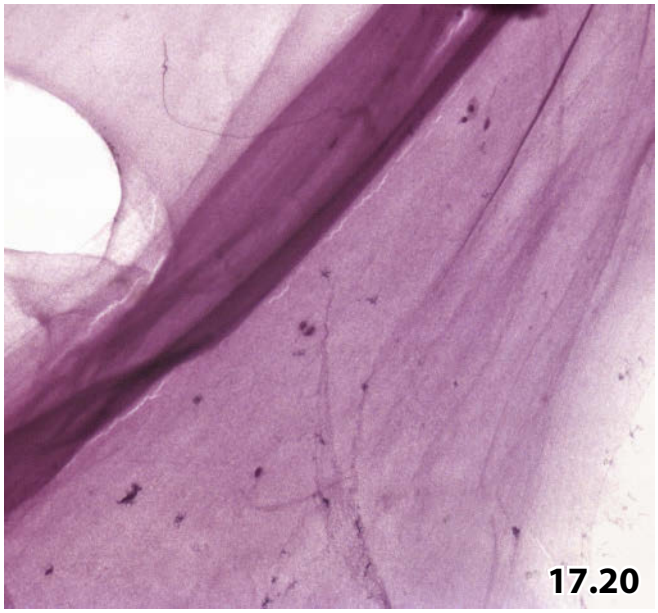

17.20

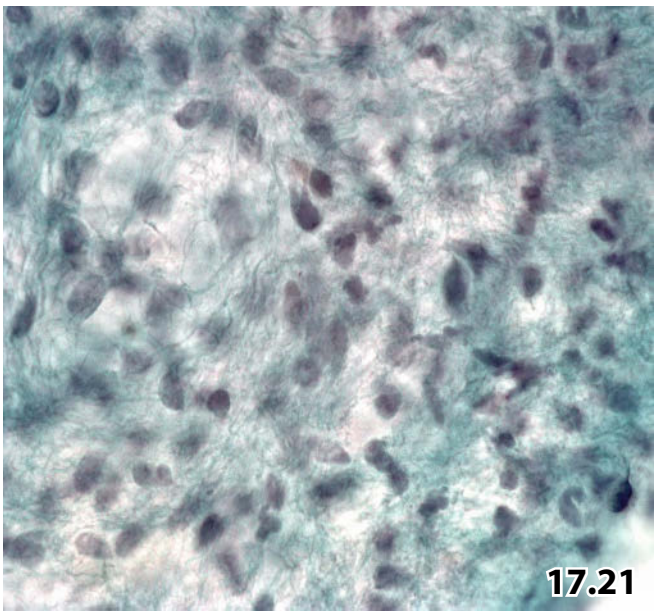

17.21

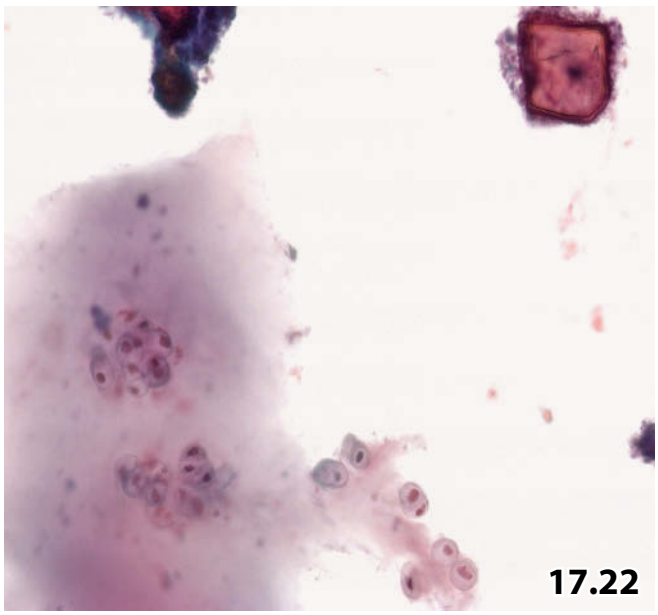

17.22

**Fig. 17.23A–C Chondroblastoma.**
Imprint cytology specimens from the cut surface of a tumor that was removed by surgical excision. The tumor was located adjacent to the humerus of an 18-year-old man. The cytologic specimens were Pap-stained. Cytologic appearance of the tumor is presented using various microscopic magnifications.
*Histologic diagnosis* of chondroblastoma was verified by several pathologists.
**A** Immature chondrocytes occurring dispersed or in loose aggregates. Note the intracellular calcium deposit (arrow) (lower magnification). **B** High magnification exhibits morphologic details of immature chondroid cells: nuclear polymorphism and sharply outlined cytoplasm. **C** This figure shows another microscopic field comprising a multinucleated osteoclast-like giant cell (upper right) (high magnification).

**Fig. 17.24A, B Giant cell tumor of bone.**
Surgical biopsy from a tumor located at the medial condyle of the right femur in a 50-year-old woman. Imprint cytology specimens were prepared from the cut surface of the surgically removed neoplastic tissue (Pap stain). **A** Low magnification demonstrating the characteristic dual cell population of a giant cell tumor of bone. Please note in particular the dense crowding of the mononucleated tumor cells, and the enormous size of single osteoclastic giant cells (upper right). **B** High magnification is focused on the striking morphologic similarity of mononucleated tumor cells and osteoclasts concerning both nuclear and cytoplasmic features.

**Fig. 17.25 Aneurysmal bone cyst.**
Image-guided FNAB of a 12-year-old's bone-destructive tumor of the sacrum. Direct smears were Pap-stained.
Characteristic cytologic appearance of aneurysmal bone cyst is shown at lower magnification: Bloody background of the smear, usually clustered degenerating mononucleated cells (arrow), osteoclast-like giant cells, scattered mesenchymal spindle cells (right). Overall cell pattern may mimic giant cell tumor of bone; still, cells in aspirates of aneurysmal bone cysts tend to undergo degenerative changes.
*Cytology:* An accurate diagnosis could not be rendered by cytology due to sparse cellularity of the aspirate.
*Tissue diagnosis:* Aneurysmal bone cyst, solid variant.

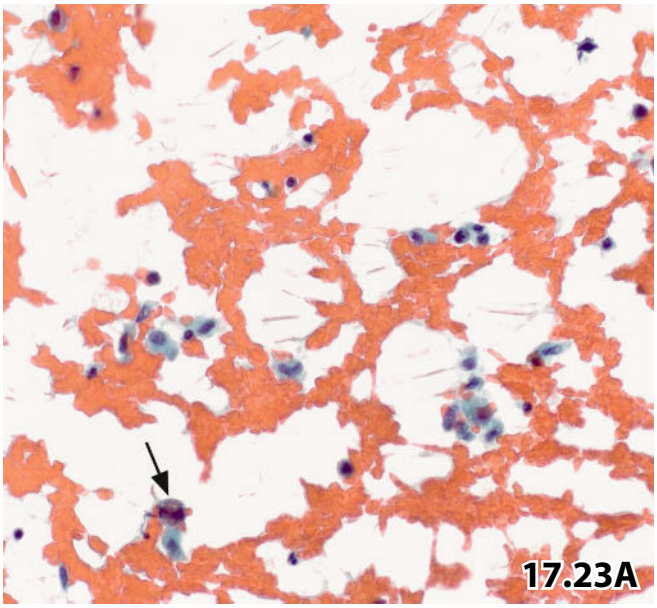
17.23A

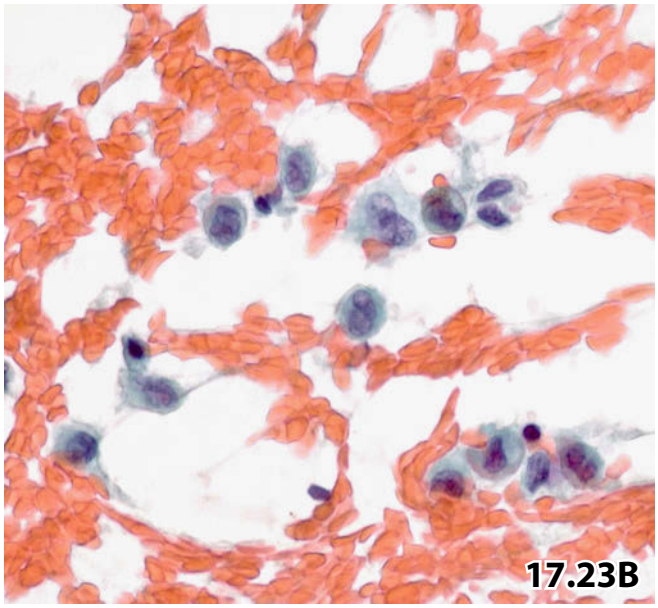
17.23B

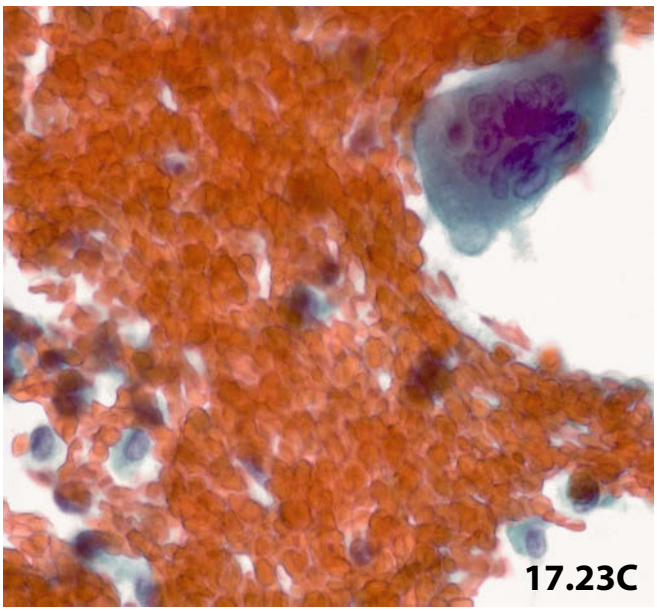
17.23C

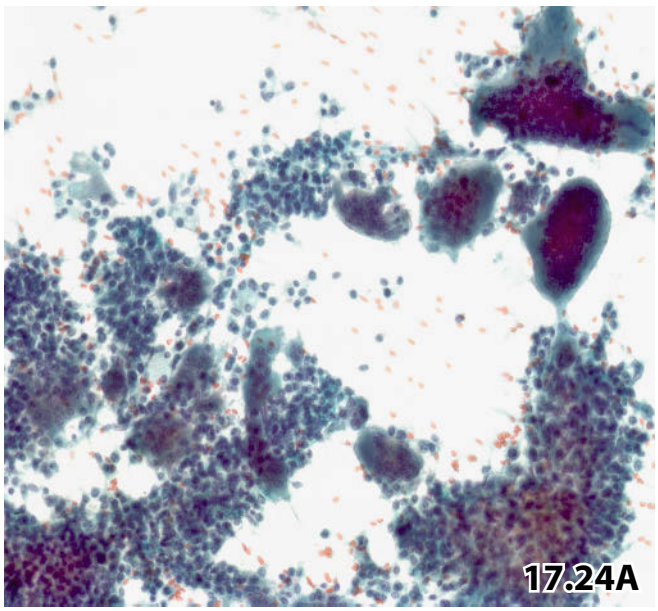
17.24A

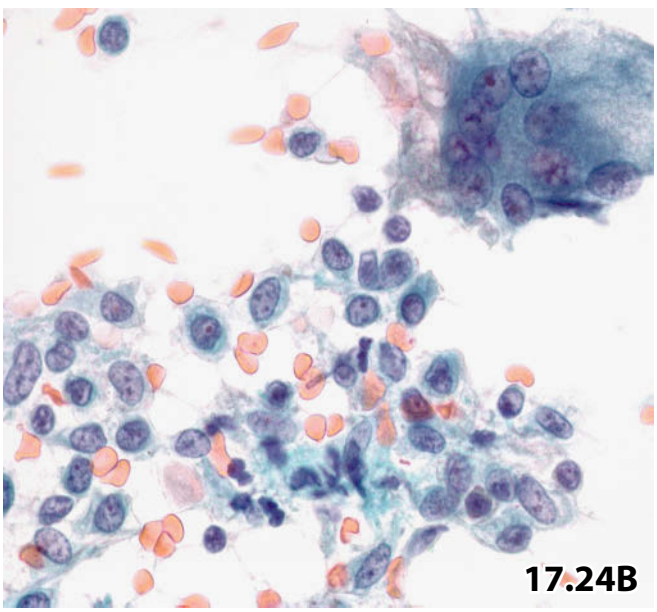
17.24B

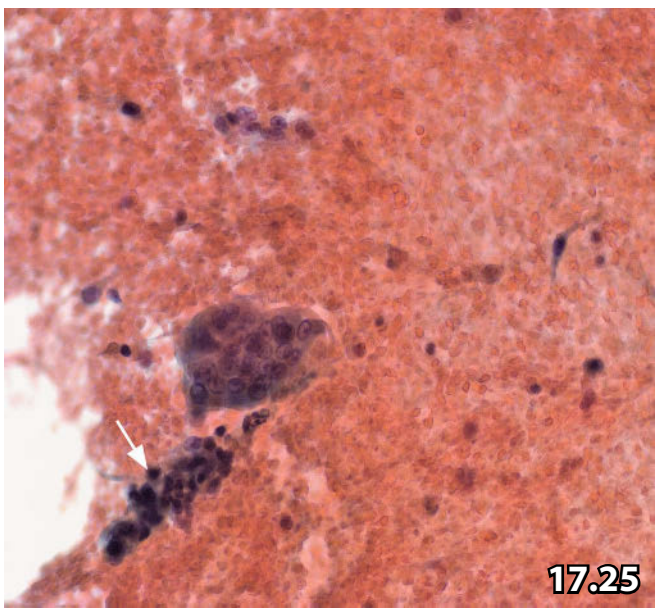
17.25

**Figs. 17.26 and 17.27 Langerhans cell histiocytosis.**
Two cases of Langerhans cell histiocytosis are presented with respect to morphology and immunocytochemistry. Image-guided FNABs were performed in both patients, direct smears were MGG- and/or Pap-stained.

**Fig. 17.26** (case #1) A 13-year-old male patient presented with a swelling in the right temporal area. Imaging revealed a subjacent bone defect. High magnification shows loosely clustered atypical histiocytoid elements. The nuclei are variably sized and irregularly outlined, whereas the cytoplasm is mainly dense and occasionally biphasic (compact central area versus ill-defined vacuolated outer edge). Note that scattered eosinophilic granulocytes are barely distinguishable in the Pap-stained smear (arrows).
*Cytologic and histologic diagnosis:* Langerhans cell histiocytosis.

**Fig. 17.27A–D** (case #2) A 23-year-old man presented with a tumor in the right temporal orbita boundary region. The pictures demonstrate morphologic and immunocytochemical key features using varied staining procedures.
*Cytologic and subsequent histologic diagnosis:* Langerhans cell histiocytosis.
**A** The characteristic appearance of this lesion comprises histiocytoid cells showing atypical nuclei (arrows), inflammatory background (neutrophils and eosinophils), multinucleated osteoclast-like giant cells, and background debris (MGG stain, lower magnification). **B** Same cell pattern, but the picture is taken from a smear that was Pap-stained. **C** High magnification highlights the morphology of Langerhans cells: note in particular nuclear identations and grooves, both vacuolated and dense cytoplasm, and degenerative cell changes. Eosinophilic and neutrophilic granulocytes are scattered among the tumor cells (Pap stain). **D** Langerhans cells reveal strong positive immunocytochemical reaction for S100 protein (Pap-prestained smear).

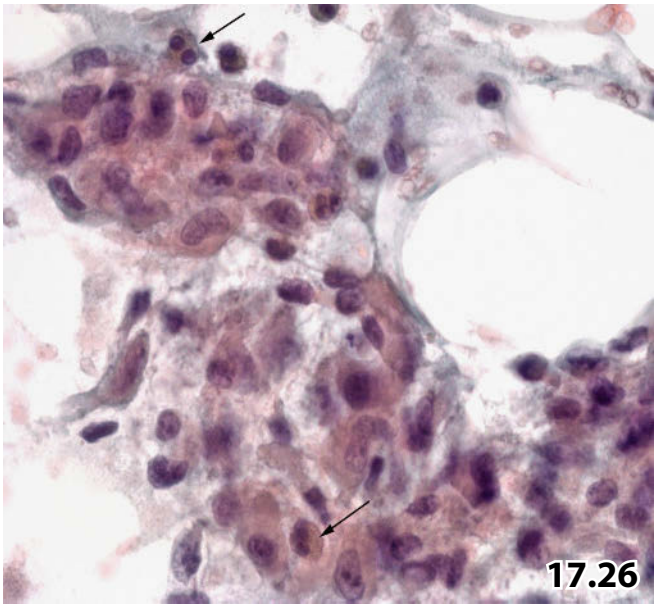
17.26

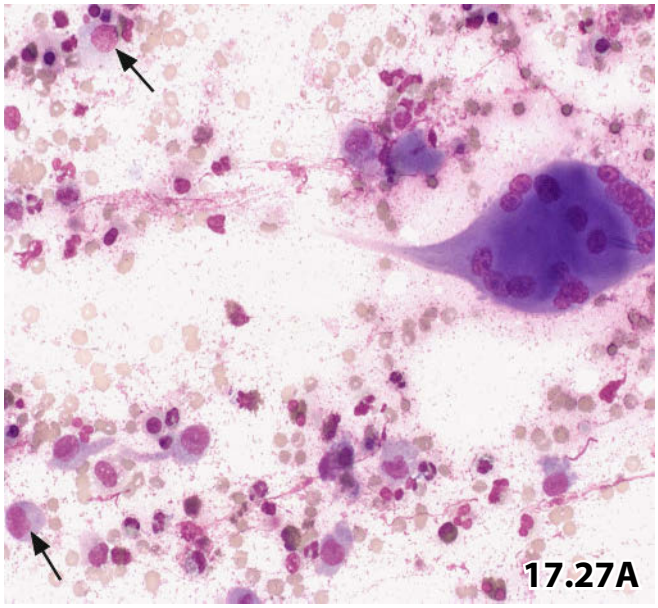
17.27A

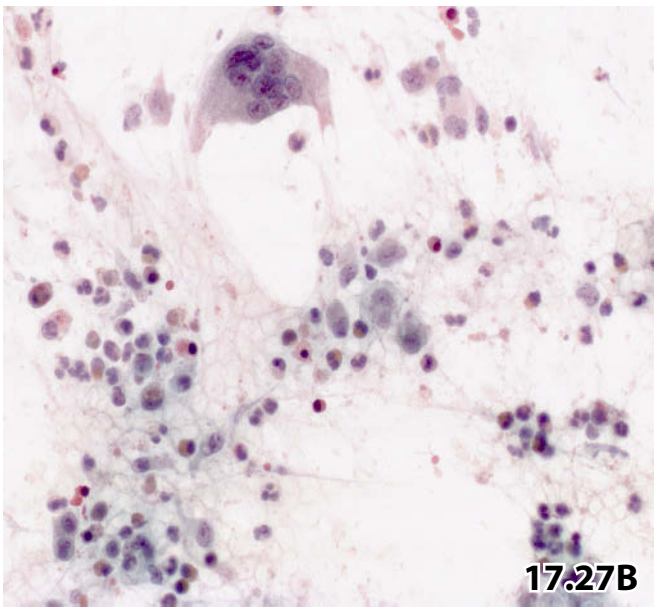
17.27B

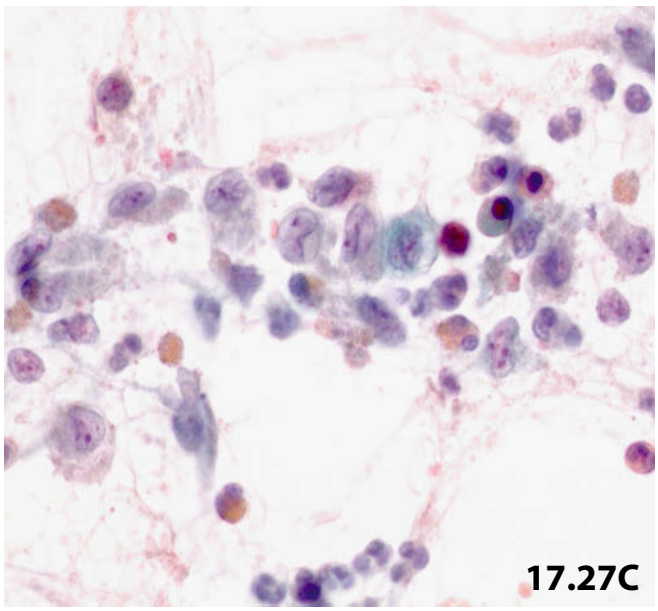
17.27C

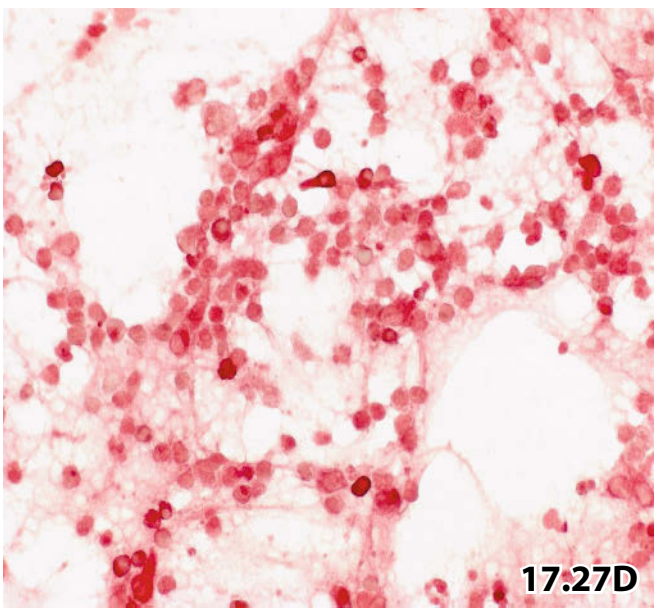
17.27D

# Section 17.2
# Soft Tissue and Bone

## Malignant Tumoral Lesions

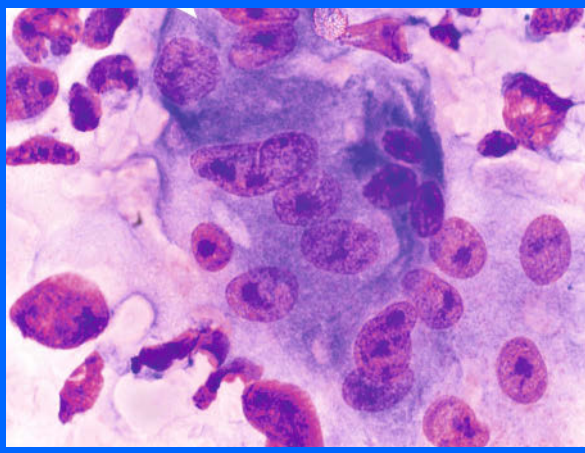

## 17.2.1 Introduction

### 17.2.1.1 Background and Acknowledgment

- During the past 10–15 years, we have gained wide experience in aspiration cytology of benign soft tissue lesions.
- However, the expert knowledge in the cytologic diagnosis of primary malignant soft tissue and bone tumors has only slightly increased over the years because orthopedic oncologists rarely referred patients and samples to our cytologic department for primary diagnosis of malignant soft tissue and bone lesions.
  On the other hand, FNAB was frequently required to complete tumor staging or to prove tumor relapse and metastases once a primary diagnosis has been established.
- Therefore, the authors of this book express their gratitude to Walter Hoebling, MD, PMPH, director of Institute of Pathology at the Klinikum Wels-Grieskirchen (Austria), who has contributed to this chapter and provided us with a selection of relevant illustrations.

### 17.2.1.2 Fine-Needle Aspiration Biopsy: General Comments

- Actually FNAB is widely used as the initial diagnostic approach to suspected malignant orthopedic tumors; particularly at orthopedic tumor centers where both cytopathologists with extensive experience in the interpretation of malignant soft tissue lesions are available and the interdisciplinary orthopedic-oncologic team is familiar with the cytologic procedure.
- However, many practicing cytopathologists are still inexperienced in the diversity of malignant soft tissue neoplasms and their broad morphologic heterogeneity. Hence, diagnostic limitations to accurate cytologic diagnoses and the risk of misdiagnoses clearly exist.
- On the other hand, FNAB is on the rise to serve as the initial minimally invasive diagnostic approach toward lesions located in soft tissues and bones, in particular deep-seated lesions. Therefore, all cytopathologists should be on the alert to meet unexpected primary sarcomas in daily practice.
- Moreover, FNAB is accepted and widely popular for the diagnosis of tumor recurrence and metastasis of previously established soft tissue malignancies.
- Operators should be aware that FNAB will be less rewarding or will even completely fail to obtain cells from both intraosseous lesions and hard/sclerotic soft tissue nodules.
  - Yet, thinning or complete destruction of the cortical bone permits the use of the fine needle technique.
  - Osseous or sclerotic mesenchymal tumors extending into the soft tissue may be successfully diagnosed by vigorous aspiration of the diffuse marginal areas; ultrasound-guided needle insertion is a must in such cases.
- As mentioned above, we have only sporadically performed FNABs on previously undiagnosed sarcomatous lesions. We refer the reader to many excellent comprehensive books and specialized sources in the literature dealing with the different aspects of aspiration cytology of malignant soft

tissue disorders and bone lesions such as FNAB in relation to utility, limitations, performance, diagnostic accuracy, histogenetic subtyping, and complementary analyses; we restrict ourselves to selected references that have been published in recent years [1, 4, 5, 8–13, 17–22].

- Benign and intermediate soft tissue tumors are presented in Sect. 17.1, p. 1055.
  Soft tissue tumors of the intermediate category are associated with infiltrative and locally destructive behavior. In addition, some of the intermediate tumors have a low risk for distant metastases.

#### 17.2.1.3 Fine-Needle Aspiration Biopsy: Technical Aspects

- Aspiration techniques (for palpable and deep-seated lesions) and laboratory procedures are similar to those that have been discussed in several chapters of this book. The techniques used at our institution are virtually identical to the technique recommended by Ward and associates [20].
- On-site attendance of a cytopathologist allows immediate examination of the aspirated material for assessment of the adequacy of the specimen, a rapid diagnosis, and a decision as to whether there is a need for additional needle passes. Additional sampling is highly recommended for cell-block analysis and is helpful in achieving enough cells for ancillary tests, including special stains, immunocytochemistry, static and/or flow cytometry, molecular genetics, and electron microscopy.

#### 17.2.1.4 Molecular Genetics and Other Ancillary Methods

Cytogenetic and molecular genetic information have a significant impact on the classification, subtyping, and categorization of the biological behavior of soft tissue tumors. Comprehensive histologic classification and completive information as to molecular genetisc and other adjuvant analyses are provided by Fletcher and associates in the 2002 WHO tumor nomenclature and in the 2006 update [6, 7]. Progress in genomics of sarcoma is described in a recent report by Conley and coauthors [3].

Application of immunocytochemistry, electron microscopy, and cytogenetics to cytologic specimens will have a substantial effect on increasing the cytodiagnostic accuracy [1, 4, 8, 17].

#### 17.2.1.5 Histologic and Cytologic Grading

- Histologic grading is considered one of the most important prognostic parameters for malignant soft tissue tumors; several grading systems are in use throughout the world. Yet, diagnostic imaging, molecular genetic results, and other advanced tests are undisputable for current and future grading systems, in addition to morphologic criteria, [2, 15].
- A majority of primary soft tissue sarcomas can be graded using cell material obtained by fine-needle aspiration [14, 16], but limitations of the cytologic grading should be respected:
  - FNAB material may not be representative of the whole lesion.
  - The aspirated cell population may be not sufficient to establish correct subtyping, not to mention proper grading.
  - Tumor typing should be clearly established prior to any attempt at tumor grading.
  - Cytohistopathological correlation studies have shown the best diagnostic agreement for the category of high-grade sarcomatous lesions.
  - Major grading problems occur with myxoid tumors and spindle cell sarcomas.
  - Grading should not be used on intermediate soft tissue lesions and on potential pseudosarcomatous disorders.
  - Grading may have no prognostic value in certain tumor entities [7].

### 17.2.2 Cytologic Diagnosis of Primary Soft Tissue Sarcomas

**General Comments**

- The most common malignant soft tissue tumors are presented herein considering basic cytomorphologic features, differential diagnostic aspects, and diagnostically important ancillary tests. Detailed information is available in individual series, review articles, distinguished textbooks, and internet databases; and a selection of references is provided in Sect. 17.2.1.2, p. 1092.
- Histogenetically, the individual tumors have been grouped according to the 2002 WHO classification of soft tissue tumors [7].
- Diagnostic algorithms of the selected entities are compiled in a synoptical table referring to cytoachitectural patterns and cellular details (17.2, "Synopsis and Algorithms," Table 17.2.1, p. 1254).

#### 17.2.2.1 Basic Diagnostic Approach

The overwhelming variety and complexity of the clinicopathologic tumor entities require a sophisticated diagnostic approach; six major aspects have to be taken into account in order to achieve reliable diagnostic conclusions:

1. Cytomorphology.
2. Cytologic criteria of malignancy.
3. Adjuvant analyses: immunocytochemistry, molecular biology, and electron microscopy.

4. Clinical characteristics of the lesion: the patient's history, tumor location, characteristics of tumor growth, and type of pain.
5. Radiologic data.
6. Close multidisciplinary teamwork.

#### 17.2.2.1.1 Cytomorphology

*Cytoarchitectural patterns* have to be considered in the context of cytologic details (below):
- Cellularity of the cytologic specimen.
- Degree of cellular dyshesion.
- Myxoid matrix.
- Chondroid/osteoid matrix.
- Fibrillar matrix.
- Inflammatory background.
- Presence of necrotic debris.

*Cytologic details*. The majority of soft tissue tumors can be classified into five groups:
- Pleomorphic pattern.
- Spindle cell pattern.
- Round cell pattern.
- Epithelioid cell pattern.
- Predominant giant cells.

#### 17.2.2.1.2 Cytologic Criteria of Malignancy

Six criteria indicate malignancy:
- Necrosis.
- Cellular and nuclear pleomorphism.
- Mitotic activity.
- Atypical chromatin texture.
- Particular cytoplasmic features.
- Size and shape of the nucleoli.

**Caution**

- Distinct morphologic criteria of malignancy may be absent in lesions of low-grade malignancy.
- On the contrary, pseudosarcomatous lesions may exhibit unequivocal cytologic features of malignancy.
- In dubious pathomorphologic settings, a correlation with clinical and radiologic findings is crucial.

#### 17.2.2.1.3 Adjuvant Analyses

We refer the reader to many excellent comprehensive books and specialized sources in the literature. References are given in Sects. 17.2.1.2, p. 1092, and 17.2.1.4, p. 1093.

Immunocytochemical and molecular characteristics of selected neoplasms are described in Sects. 17.2.3–17.2.12.

### 17.2.3 Malignant Adipocytic Tumors: Liposarcomas (Figs. 17.28–17.30)

#### 17.2.3.1 Well-Differentiated Liposarcoma / Atypical Lipomatous Tumor (Fig. 17.28)

**Microscopic Features**
- The aspirates are generally composed of mature adipose tissue fragments including a few scattered atypical adipocytes and lipoblasts exhibiting features that have been described in Sect. 17.1.2, "Adipocytic Tumors" p. 1056.
- Mitotic figures are also present.

**Cytogenetics and Immunocytochemistry**

Detection of giant marker and ring chromosomes, consisting of amplicons of chromosome 12q13-15, are useful in distinguishing between benign lipoma variants and well-differentiated liposarcoma/atypical lipomatous tumor. The chromosomal aberration is associated with an amplification of the *MDM2* gene, which can be shown by means of FISH and immunocytochemical (nuclear) positivity for the MDM2 protein.

**Differential Diagnosis**
- A majority of lipoma-like well-differentiated liposarcomas may be indistinguishable from common benign lipomas. The above-mentioned MDM2 tests are helpful in achieving a definite diagnosis.
- The cytologic pattern of well-differentiated liposarcomas usually wholly overlaps with that of atypical lipoma.

#### 17.2.3.2 Myxoid Liposarcoma

Myxoid liposarcoma belongs to the large group of malignant soft tissue tumors associated with a myxoid matrix.
- The tumor is characterized by lipoblasts and scattered bland rounded to fusiform cells embedded in a highly vascularized myxoid matrix (Fig. 17.29).

#### 17.2.3.3 Round Cell Myxoid Liposarcoma

This is a variant of myxoid liposarcoma that is characterized by a substantial admixture of primitive round cells indicating high-grade malignancy.
- The round tumor cells are lipoblasts exhibiting cytoplasmic lipid vacuoles and pleomorphic nuclei with prominent nucleoli.

**Cytogenetics**

The traditional variants of myxoid liposarcoma are characterized by the chromosomal translocation t(12;16)(q13;p11), which is detectable by FISH.

#### 17.2.3.4 Dedifferentiated Liposarcoma (Fig. 17.30)

- A liposarcoma is composed of obvious malignant, pleomorphic rounded and fusiform tumor cells.
- The histogenesis is determined by a variable number of distinguishable lipoblasts.

**Caution**

Dedifferentiated liposarcoma may morphologically resemble the so-called pleomorphic liposarcoma (see Sect. 17.2.3.5 below), but it is clearly distinguishable from the latter by ring chromosomes and amplification of the *MDM2* gene.

#### 17.2.3.5 Pleomorphic Liposarcoma

**Microscopic Features**

- Pleomorphic liposarcoma consists of pleomorphic multivacuolated lipoblasts, neoplastic spindle cells, and multinucleated giant cells. Distinguishing between pleomorphic liposarcoma and dedifferentiated liposarcoma can be difficult by morphology alone.

**Differential Diagnosis and Cytogenetics**

Pleomorphic liposarcoma may resemble dedifferentiated liposarcoma. The latter tumor entity usually shows both multivacuolated lipoblasts and multinucleated giant cells to a lesser extent, but larger numbers of isolated pleomorphic mononucleated tumor cells. In doubtful cases, the presence of *MDM2* amplification argues for a dedifferentiated liposarcoma.

### 17.2.4 Malignant Fibroblastic/Myofibroblastic Tumors: Myxofibrosarcoma/Fibrosarcoma (Fig. 17.31)

Myxofibrosarcoma was formerly referred to as myxoid malignant fibrous histiocytoma.

**Microscopic Features**

- Myxofibrosarcoma and fibrosarcoma are malignant tumors composed of fusiform, polygonal or stellate fibroblast-like cells that are largely arranged in sheets and fascicles; dissociated cells are often present.
- Tumors are designated as myxofibrosarcomas containing a more or less prominent myxoid matrix crossed by capillary networks.
- The term "fibrosarcoma" should be used only in rare cases of fibroblastic tumors completely devoid of myxoid matrix.
- In the vast majority of cases, the tumor cells exhibit mild atypia, but a varying degree of nuclear pleomorphism may occur.

**Differential Diagnosis**

- Regarding the virtually absent cellular atypias, myxofibrosarcoma is cytologically often misdiagnosed as a benign condition such as myxoma. In general, this misdiagnosis is of limited clinical relevance since all myxoid tumors should be removed surgically and referred to subsequent histologic analyses.
- Lipoblasts are absolutely necessary in oder to differentiate between myxoid liposarcoma and myxofibrosarcoma.
- Fibrosarcoma shares many common morphologic features with other spindle cell sarcomas including leiomyosarcoma, variants of monophasic synovial sarcoma, malignant peripheral nerve sheath tumor, dermatofibrosarcoma protuberans, and spindle cell GIST. Consequently, the diagnosis of fibrosarcoma is only valid for those tumors lacking any indicator of a specific cytogenetic differentiation; typical tumor attributes can be identified by means of appropriate additive analyses such as immunocytochemistry, molecular genetic tests, electron microscopy, among others.

### 17.2.5 So-called Fibrohistiocytic Tumors: Undifferentiated Pleomorphic Sarcoma

#### 17.2.5.1 Undifferentiated High-Grade Pleomorphic Sarcoma (Figs. 17.32 and 17.34)

(Formerly Pleomorphic and Storiform Malignant Fibrous Histiocytoma)

This tumor entity is (by definition of the 2002 WHO classification) reserved for a small group of pleomorphic sarcomas showing no definable line of differentiation using current technologies.

**Microscopic Features**

- The tumors are composed of either numerous plump spindle cells arranged in a storiform pattern or of pleomorphic cells that tend to be randomly scattered.
- The myxoid variant exhibits large amounts of vascularized myxoid stroma, more than 50% of the entire tumor mass (Fig. 17.34).

**Differential Diagnosis**

In most cases, additional analyses (immunocytochemistry, FISH, etc.) will reveal a definitive lineage allocation distinguishing undifferentiated high-grade pleomorphic sarcoma from pleomorphic liposarcoma, rhabdo- or leiomyosarcoma, anaplastic carcinoma, sarcomatous melanoma, anaplastic large-cell lymphoma, and other tumors.

If a definitive allocation is not possible on cytological material, undifferentiated high-grade pleomorphic sarcoma should be used as a preliminary working diagnosis; the conclusive diagnosis should be left to histologic evaluation of surgically removed tumor tissue.

#### 17.2.5.2 Undifferentiated Pleomorphic Sarcoma with Giant Cells (Fig.17.33)

(Formerly the Giant Cell Variant of Malignant Fibrous Histiocytoma)

This is a small group of undifferentiated sarcomas that contain a high proportion of osteoclast-like giant cells showing no lineage differentiation using current technologies.

In most cases of cytologically undifferentiated pleomorphic sarcoma, additional analyses (immunocytochemistry, FISH, etc.) and/or extensive sampling (for histology) of the surgically removed tumor tissue will provide a definitive lineage allocation that may include extraskeletal osteosarcoma, leiomyosarcoma, soft tissue giant cell tumor, among other tumors.

#### 17.2.5.3 Undifferentiated Pleomorphic Sarcoma with Prominent Inflammation

(Formerly the Inflammatory Variant of Malignant Fibrous Histiocytoma)

This tumor type microscopically displays a high proportion of benign and malignant xanthomatous cells, usually in combination with an acute, chronic, or mixed inflammatory background.

Additional analyses may enable precise tumor type assessment such as dedifferentiated liposarcoma, leiomyosarcoma, inflammatory myofibroblastic tumor, carcinoma, and lymphoma.

### 17.2.6 Malignant Smooth Muscle Tumor: Leiomyosarcoma (Fig. 17.35)

Leiomyosarcoma is a classic representative of the spindle cell tumor group.

**Microscopic Features**

- Diagnostic key features comprise intersecting fascicles composed of atypical elongated eosinophilic cells containing myofibrils. The nuclei exhibit segmentation and blunt-end or cigar-shaped outline.
- Scattered atypical stripped tumor cell nuclei are occasionally observed outside the fascicles.

**Differential Diagnosis and Immunocytochemistry**

- Immunopositivity for alpha smooth muscle actin, desmin, myogenin, or calponin is diagnostic for leiomyosarcomas.
- Spindle cell squamous cell carcinoma and spindle cell malignant melanoma can be excluded on the basis of tumor-typical immunocytochemical features.
- Leiomyosarcoma shares many common features with other spindle cell sarcomas (see Sect. 17.2.4, p. 1095).

### 17.2.7 Malignant Skeletal Muscle Tumor: Rhabdomyosarcoma

Rhabdomyosarcomas are composed of cells exhibiting varied degrees of skeletal muscle differentiation. Morphology of the tumor cells ranges from:

(A) Undifferentiated small round elements showing a small rim of cytoplasm, to
(B) Spindle cells having eosinophilic cytoplasm with cross-striations (so-called tadpole cells), to
(C) Large polyhedral rhabdomyoblasts characterized by abundant eosinophilic cytoplasm and prominent nucleoli.

Three clinicopathologic tumor entities are well defined and briefly mentioned in Sects. 17.2.7.1–17.2.7.3, below.

**Additional Analyses**

Immunocytochemistry

Rhabdomyoblastic differentiation of immature cells may be identified by positive staining for muscle-specific proteins (desmin, myoglobin, among others).

Electron Microscopy

Electron microscopy detects rhabdomyoblastic differentiation by evidence of cytoplasmic filaments.

#### 17.2.7.1 Embryonal Rhabdomyosarcoma

This tumor occurs mostly in children and adolescents.

**Microscopic Features and Molecular Genetics**

- The common variant of embryonal rhabdomyosarcoma is composed of immature rounded cells embedded in predominantly myxoid stroma.
- Rhabdomyoblasts are present in variable proportions, showing various degrees of differentiation

There may be loss of heterozygosity (LOH) at chromosome 11.

#### 17.2.7.2 Alveolar Rhabdomyosarcoma (Fig. 17.36)

Alveolar rhabdomyosarcoma is a tumor of adolescents and young adults.

**Microscopic Features and Molecular Genetics**

- This tumor variant features alveolar spaces lined with primitive round cells showing varied degrees of cytoplasmic differentiation.
- Eosinophilic giant cells are occasionally encountered.

Chromosomal translocation t(2;13)(q36;q14).

**Differential Diagnosis**

The solid form of alveolar rhabdomyosarcoma may closely mimic small round cell tumors of childhood, small-cell carcinoma, small-cell melanoma, and lymphoblastic lymphoma. Immunocytochemical studies are of great value in differentiating these neoplasms.

### 17.2.7.3 Pleomorphic Rhabdomyosarcoma

(Fig. 17.37)

This is a rare tumor variant mainly occurring in older adults.

**Microscopic Features and Differential Diagnosis**

- The tumor is almost exclusively composed of large atypical and polyhedral rhabdomyoblasts or rhabdomyoblast-like cells.

Pleomorphic rhabdomyosarcomas share morphologic attributes with sarcomas exhibiting distinct epithelioid cell features (see also Sect. 17.2.8, "Differential Diagnosis," below).

## 17.2.8 Vascular Tumors: Epithelioid Hemangioendothelioma and Epithelioid Angiosarcoma (Fig. 17.38)

Peculiarities of malignancy (degree of cellular pleomorphism, mitotic rate, etc.) defines the tumor type (angiosarcoma vs hemangioendothelioma), the rate of local recurrence, the potential of distant spreading, and eventually the tumor outcome.

**Microscopic Features**

The epithelioid tumor's appearance is based on cells forming compact epithelium-like aggregations, with the cells exhibiting the following features:

- Round, polygonal and fusiform cells exhibiting abundant dense cytoplasm with sharply defined outline.
- Nuclei displaying mild to moderate and occasionally severe atypia.
- Nuclear inclusions are rather common (Fig. 17.38).
- One or multiple nucleoli are usually prominent.
- A spindle cell component may be seen exhibiting malignant cell features.
- Focally, tumor cells may show a tendency toward dehiscence.

**Differential Diagnosis and Immunocytochemistry**

The tumor cells express cytokeratins, CD31, CD34, and factor VIII antigen.

- The cytomorphological overlap between epithelioid hemangioendothelioma and epithelioid sarcoma, clear cell sarcoma, alveolar soft part sarcoma, malignant rhabdoid tumor, or epithelioid cell GIST may be distinct.
- Hemangioendotheliomas mainly composed of polygonal cells may closely resemble undifferentiated carcinoma and melanoma.
- Nuclear cytoplasmic inclusions are relatively common in histogenetically different tumors such as clear cell sarcoma, myxofibrosarcoma, melanoma, paraganglioma, and several carcinoma types (e.g., of thyroid, breast, and renal origin).

**Caution**

Angiosarcomas often arise in parenchymatous organs such as the thyroid gland, breast, or liver where both primary and metastatic carcinomas are the most common tumor types; diagnostic confusion can easily occur.

## 17.2.9 Neural Tumor: Malignant Peripheral Nerve Sheath Tumor (Fig. 17.39)

**Microscopic Features**

Malignant peripheral nerve sheath tumors (MPNST) are composed of spindle cells arranged in fascicles exhibiting varied degrees of neural differentiation:

- Tissue fragments consisting of palisades of tightly packed elongated nuclei in parallel formations (Verocay bodies) and areas of fibrillary matrix.
- Numerous scattered polyhedral and pleomorphic tumor cells are usually present as well.
- Nuclei with tapered ends are a nearly constant finding; furthermore, the nuclei may exhibit varying types of angulation.

**Differential Diagnosis and Immunocytochemistry**

MPNST may resemble fibrosarcoma, undifferentiated pleomorphic sarcoma, and other spindle cell tumors.

S100 protein and other neural markers are expressed.

**Caution**

- Unlike in benign schwannoma, positive immunoreactivity for S100 is only sporadically found in MPNST.
- Distinguishing between benign schwannoma and MPNST is difficult by cytology alone since malignant cell features (such as large bizarre nuclei, hyperchromasia, mitotic activity, and others) may also be found in benign peripheral nerve sheath tumors. On the other hand, the absence of malignant cell features in a hypocellular cytologic smear does not rule out MPNST: the aspirate may originate from areas of benign neural tissue within a sarcoma.

## 17.2.10 Malignant Chondro-osseous Tumors

Primary chondrosarcoma and osteosarcoma can occur both in soft tissues and in bones.

### 17.2.10.1 Chondrosarcoma

The neoplastic cells of chondrosarcoma usually appear at different stages of maturation producing chondroid matrix. Four major tumor variants are distinguishable:

- *Well-differentiated chondrosarcoma* is characterized by chondrocytes and abundant hyaline-chondroid masses. This tumor variant shows striking resemblance to chondroma. Still, an admixture of a few chondroblasts enclosed in a myxoid matrix indicates chondrosarcoma.
- *Myxoid chondrosarcoma* is characterized by trabecular formations consisting of chondroblasts embedded in a myxoid matrix. Hyaline cartilage is usually absent.
- *Mesenchymal chondrosarcoma* mainly consists of poorly differentiated rounded chondroblastic cells arranged within sparsely fibrillary and myxoid matrix. Nests of hyaline cartilage may be encountered.
- *Dedifferentiated chondrosarcoma* is dominated by pleomorphic fibrohistiocyte-like cells and fibroblast-like spindle cells. Small areas of immature or maturing hyaline cartilage are also present. Diagnostic considerations include fibrosarcoma and undifferentiated pleomorphic sarcoma.

### 17.2.10.2 Osteosarcoma

Osteosarcoma is a high-grade neoplasia. The appearance of the tumor cells varies from undifferentiated small round cells to large pleomorphic cells associated with osteoid matrix with or without cartilage. Multiple microscopic tumor variants are distinguished depending on the predominant cell type.

## 17.2.11 Malignant Soft Tissue Tumors of Uncertain Differentiation

### 17.2.11.1 Clear Cell Sarcoma of Soft Tissue

(Fig. 17.40)

**Microscopic Features**

- Clear cell sarcoma is composed of relatively uniform clear epithelioid cells comprising round clear nuclei with prominent nucleoli. Multinucleation and nuclear cytoplasmic inclusions are frequent.
- Cytoplasmic melanin deposits frequently occur.
- The tumor cells are usually arranged in fascicles and clusters.

**Differential Diagnosis and Molecular Genetics**

- Clear cell sarcoma may share morphologic characteristics with other neoplasms presenting with clear cell features such as leiomyosarcoma, peripheral nerve tumors, angiosarcoma, renal cell carcinoma, etc.
- Nuclear cytoplasmic inclusions, a hallmark of clear cell sarcoma, occur relatively often in histogenetically different malignant tumors such as myxofibrosarcoma, melanoma, paraganglioma, and several types of carcinoma (thyroid carcinoma, breast carcinoma, and renal cell carcinoma).
- Misdiagnosis of metastatic malignant melanoma can easily occur considering the melanotic tumor variant of clear cell sarcoma.

Chromosomal translocation t(12;22)(q13;q12) is a characteristic feature of this tumor entity.

### 17.2.11.2 Epithelioid Sarcoma

**Microscopic Features**

- A morphologic hallmark of epithelioid sarcoma are centrally necrotic epithelioid nodules.
- The cell population at the edge of necrotic areas is composed of slender and plump epithelioid spindle cells with granular and clear cytoplasm
- Lymphoid aggregates are occasionally present.

**Differential Diagnosis and Immunocytochemistry**

- Epithelioid sarcoma may be confused with other nonepithelial tumors of the epithelioid category.
- Metastases of malignant melanoma and epidermoid carcinoma as well as other secondary neoplasms may mimic epithelioid sarcoma.
- Furthermore, nonneoplastic granulomatous disorders (e.g., rheumatoid nodule, foreign body granuloma), and nonneoplastic tumorous lesions (e.g., fasciitis) must be considered for diagnosis.

The epithelioid cells immunocytochemically exhibit coexpression for cytokeratins and vimentin.

### 17.2.11.3 Synovial Sarcoma

Classic synovial sarcoma of the mixed variant is a typical example of the category of malignant biphasic soft tissue tumors.

**Microscopic Features**

- The tumor is composed of:
  - *Epithelioid cells* arranged in sheets, clusters, and pseudoglandular (alveolar) formations.
  - *Slender fusiform cells* in a spreading pattern.
- The epithelioid cells show uniform round to oval nuclei.

### Additional Analyses

Immunocytochemistry

There is a positive reaction for cytokeratins, epithelial membrane antigen, and vimentin. Immunopositivity is most distinct on cells lining pseudoglandular structures.

Molecular Genetics

Chromosomal translocation t(X;18)(p11;q11).

### Differential Diagnosis

- Malignant epithelioid mesothelioma, neuroendocrine carcinoma, undifferentiated pleomorphic sarcoma among others may share morphologic features with synovial sarcoma.
- Monophasic spindle cell synovial sarcomas are extremely difficult to distinguish from other spindle cell neoplasms.
- The undifferentiated variant of synovial sarcoma may mimic small round cell tumors.

## 17.2.12 Miscellaneous Malignant Soft Tissue Tumors

Several chapters of this book address individual tumor entities and special groups of malignant nonepithelial tumors. Readers are in particular referred to the following sections covering selected tumors, including corresponding illustrations:


– Sect. 2.3.7.1, “Langerhans Cell Histiocytosis,” p. 189 and 17.1.13.2, p. 1068.
– Sect. 3.2.1, “Mesothelial Tumors,” p. 260.
– Sect. 5.2.6.2, “Paraganglioma,” p. 467.
– Sects. 5.2.3.5, “Chordoma,” p. 464, and 11.3.3.6.2, “Chordoma,” p. 710.
– Sect. 12.1.10.2.2, “Wilms Tumor/Small Round Cell Tumors,” p. 743.
– Sect. 12.2.3.3.2.: “Neuroblastoma, Ganglioneuroblastoma, Ganglioneuroma,” p. 769.
– Sect. 15.3. “Lymph Nodes: Malignant Lymphomas,” p. 950, “Histiocytic Sarcoma,” p. 973, and “Myeloproliferative Disorders,” p. 975–977.
– Sect. 16.2.11, “Kaposi Sarcoma,” p. 1033.


## 17.2.13 Further Reading


1. Akerman M, Domanski HA. The cytology of soft tissue tumours. Monogr Clin Cytol 2003;16:IX-X,1-112.
2. Coindre JM. Grading of soft tissue sarcomas: review and update. Arch Pathol Lab Med 2006;130:1448-1453.
3. Conley AP, Trent J, Zhang W. Recent progress in the genomics of soft tissue sarcomas. Curr Opin Oncol 2008;20:395-399.
4. Domanski HA. Fine-needle aspiration cytology of soft tissue lesions: diagnostic challenges. Diagn Cytopathol 2007;35:768-773.
5. Fleshman R, Mayerson J, Wakely PE Jr. Fine-needle aspiration biopsy of high-grade sarcoma. A report of 107 cases. Cancer (Cancer Cytopathol) 2007;111:491-498.
6. Fletcher CD. The evolving classification of soft tissue tumours: an update based on the new WHO classification. Histopathology 2006;48:3-12.
7. Fletcher CDM, Unni KK, Mertens F (Eds.). World Health Organization Classification of Tumours. Pathology and Genetics of Tumours of Soft tissue and Bone. IARC Press: Lyon 2002.
8. Gonzalez-Campora R. Cytoarchitectural findings in the diagnosis of primary soft tissue tumors. Acta Cytol 2001;45:115-146.
9. Hajdu SI, Hajdu EO. Cytopathology of Soft Tissue and Bone Tumors. Basel, S Karger 1989.
10. Kilpatrick SE, Geisinger KR. The usefulness and limitations of fine-needle aspiration biopsy. Am J Clin Pathol 1998;110:50-68.
11. Kilpatrick SE, Cappellari JO, Bos GD, et al. Is fine-needle aspiration biopsy a practical alternative to open biopsy for the primary diagnosis of sarcoma? Experience with140 patients. Am J Clin Pathol 2001;115:59-68.
12. Kumar S, Chowdhury N. Accuracy, limitations and pitfalls in the diagnosis of soft tissue tumors by fine needle aspiration cytology. Indian J Pathol Microbiol 2007;50:42-45.
13. Layfield LJ. Cytologic diagnosis of osseous lesions: a review with emphasis on the diagnosis of primary neoplasms of bone. Diagn Cytopathol 2009;37:299-310.
14. Mallik MK, Dey P, Gupta SK, Vasishta RK. Grading of soft tissue sarcomas on fine-needle aspiration cytology smear. Diagn Cytopathol 2009 Aug 17; Epub.
15. Oliveira AM, Nascimento AG. Grading of soft tissue tumors: principles and problems. Skeletal Radiol 2001;30:543-559.
16. Palmer HE, Mukunyadzy P, Culbreth W, Thomas JR. Subgrouping and grading of soft-tissue sarcomas by fine-needle aspiration cytology: a histopathologic correlation study. Diagn Cytopathol 2001; 24:307-316.
17. Singh HK, Kilpatrick SE, Silverman JF. Fine needle aspiration biopsy of soft tissue sarcomas: utility and diagnostic challenges. Adv Anat Pathol 2004;11:24-37.
18. Wahane RN, Leie VR, Bobhate SK. Fine needle aspiration cytology of bone tumors. Acta Cytol 2007;51:711-720.
19. Ward WG Sr, Kilpatrick S. Fine needle aspiration biopsy of primary bone tumors. Clin Orthop Relat Res 2000;373:80-87.
20. Ward WG, Savage P, Boles CA, Kilpatrick SE. Fine-needle aspiration biopsy of sarcomas and related tumors. Cancer Control 2001;8:232-238.
21. Weiss SW, Goldblum JR (eds) (2007), Enzinger and Weiss’s Soft Tissue Tumors, 5th rev. ed, Mosby
22. Yang YJ, Damron TA. Comparison of needle core biopsy and fine-needle aspiration for diagnostic accuracy in musculosceletal lesions. Arch Pathol Lab Med 2004;128:759-764.

**Figs. 17.28–17.30 Liposarcoma.**
The three pictures represent distinct variants of the malignant adipocytic tumor group. Fine-needle aspiration biopsy specimens come from three tumors of different patients. Air-dried direct smears were MGG-stained.

**Fig. 17.28** (case #1) Well-differentiated liposarcoma.
An elderly woman presented with a pelvic and retroperitoneal tumor mass (postmortem examination verified the cytologic diagnosis). Note lipoblasts (arrows) and adipocytes showing moderately atypical nuclei (arrowheads) (higher magnification).

**Fig. 17.29** (case #2) Myxoid liposarcoma.
An 86-year-old woman was referred to FNAB of a tumor located in the forearm, aspiration (rendering a correct cytologic diagnosis) was followed by excision of the tumor. Lower magnification exhibits myxoid background vascularized by thick-walled upper right and slender capillary vessels. Note the heterogeneous cell population ranging from (atypical) lipocytes to pleomorphic lipoblasts (arrows).

**Fig. 17.30** (case #3) Dedifferentiated and pleomorphic liposarcoma.
Cytologic diagnosis(FNAB) of a tumorous process in the pelvic space of a 65-year-old man. High magnification reveals dispersed pleomorph polyhedral tumor cells and a dirty background. A highly atypical lipoblast showing characteristic cytoplasmic multivacuolation (arrow) indicates lipoid origin of this otherwise undifferentiated neoplasm.

**Fig. 17.31 Myxofibrosarcoma/fibrosarcoma.**
A 73-year-old man presenting with a lump in the soft tissue of his upper left arm (FNAB, air-dried direct smears, MGG staining procedure). High magnification illustrates the fusiform character of the tumor cells and their arrangement in fascicles (left) and sheets (right). Cell dissociation and varied nuclear pleomorphism are overt.

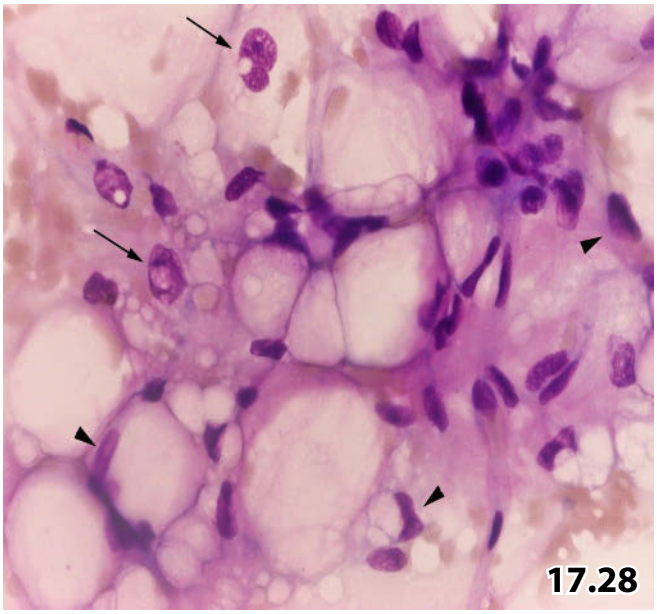
17.28

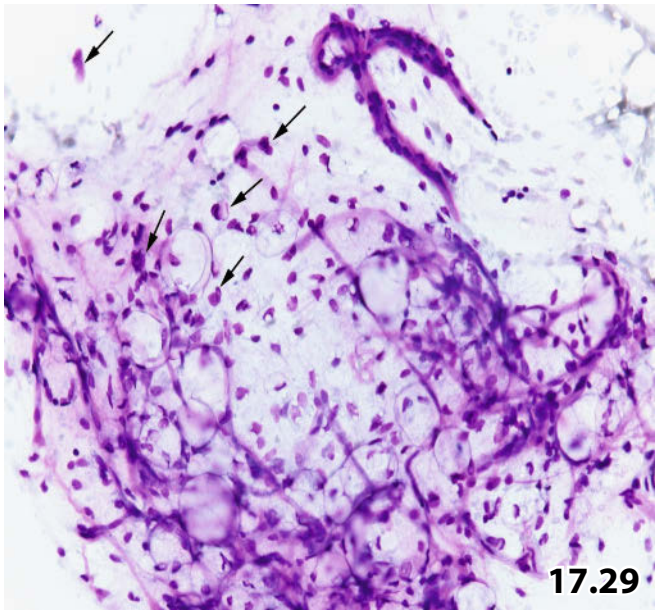
17.29

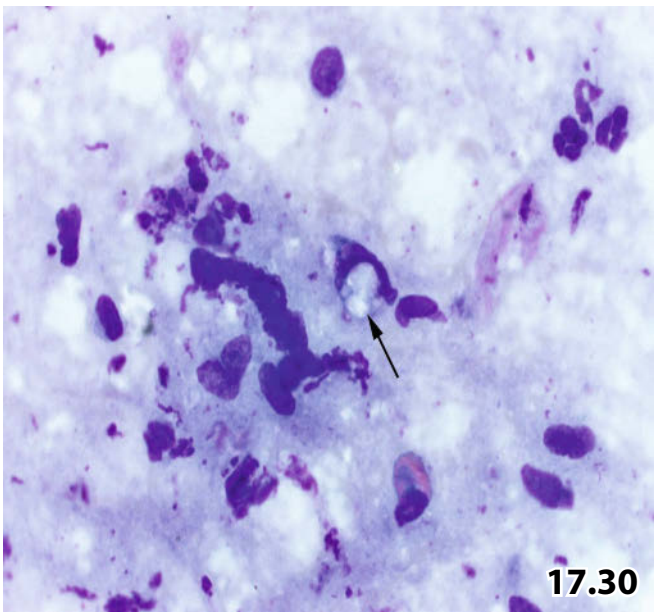
17.30

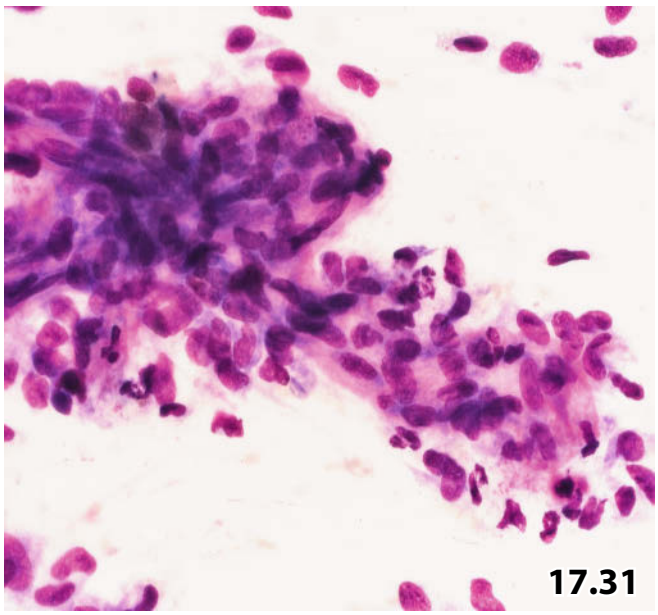
17.31

**Figs. 17.32–17.34 Undifferentiated pleomorphic sarcoma (former MFH).**
Three representative examples of undifferentiated pleomorphic sarcomas are demonstrated by means of aspirate specimens from two patients. The FNA diagnoses were confirmed by subsequent histologic analysis. Direct smears were stained according to two different staining procedures.

**Fig. 17.32** (case #1) Undifferentiated high-grade pleomorphic sarcoma.
Tumor relapse 2 years after the initial diagnosis (the primary tumor of this patient is presented in Fig. 17.33, case #2). The high-grade pleomorphic tumor variant is characterized by storiform-like arrangement of spindled tumor cells (arrows) and by the presence of isolated fusiform and large pleomorphic tumor cells (arrowheads) (air-dried smear, MGG stain, low magnification).

**Fig. 17.33** (case #2) Undifferentiated pleomorphic sarcoma with giant cells.
The tumor was located on the left side of the back in the left thoracic area of a 77-year-old man. High magnification highlights an osteoclast-like giant cell (multiple monomorphic nuclei showing pronounced nucleoli) (arrow) along with pleomorphic tumor cells (nuclear pleomorphism, coarse chromatin, hyperchromasia, and small cytoplasmic rim). Air-dried smear, MGG stain. The particular cytology of the relapsing tumor is depicted in Fig. 17.32, case #1.

**Fig. 17.34** (case #3) Myxoid variant of undifferentiated high grade pleomorphic sarcoma.
A 61-year-old man presented with a tumor in his upper left arm. Wet-fixed slides were Pap-stained. Cytologic appearance of this tumor variant is shown at lower magnification: Pleomorphic tumor cells (arrows), apoptotic cells, and necrotic debris are embedded in a myxoid/mucoid matrix.

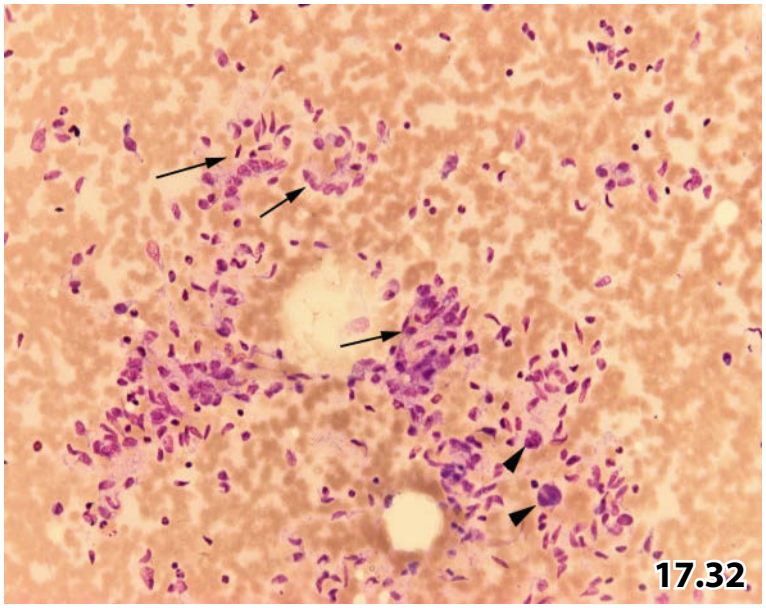
17.32

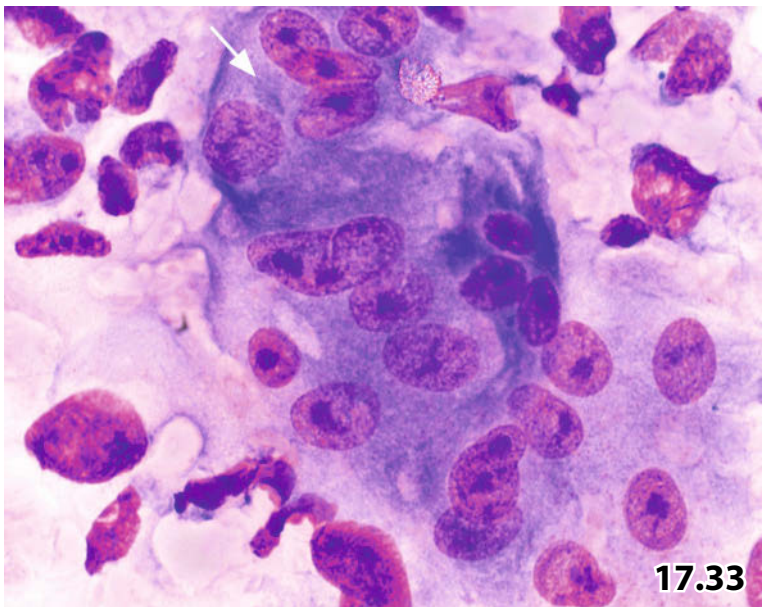
17.33

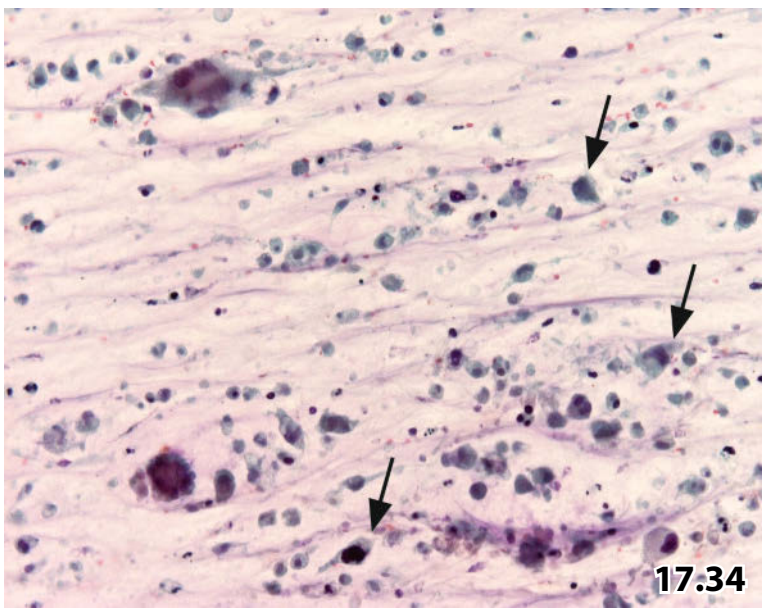
17.34

**Fig. 17.35 Pleomorphic leiomyosarcoma, G3.**
A man aged 55 years presenting with a history of pleomorphic cardiac leiomyosarcoma. The patient was referred to cytologic investigation to confirm tumor metastasis in the duodenal area. Fine-needle aspiration provided multiple microfragments of tissue, thus the aspirated material was processed using the cell-block technique (HE stain). The intersecting fascicles composed of elongated atypical cells are readily identifiable at lower magnification. Note typical nuclear shape appearing blunt-ended/cigar-shaped.

**Figs. 17.36 and 17.37 Rhabdomyosarcoma.**
Cytologic examples of two variants of rhabdomyosarcoma. FNA material was directly smeared onto glass slides followed by air-drying or wet fixation.

**Fig. 17.36** (case #1) Alveolar rhabdomyosarcoma.
Metastatic alveolar rhabdomyosarcoma in a 28-year-old man. FNAB was performed on a single nodule located in the right parietal pleura. High magnification shows a loosely clustered group of primitive mononucleated rounded cells forming alveolar nests (arrows). A few large rhabdomyoblast-like cells are also present (left) (air-dried smear, MGG stain).

**Fig. 17.37** (case #2) Pleomorphic rhabdomyosarcoma.
Pleomorphic rhabdomyosarcoma is characterized by rhabdomyoblasts. The shape of the rhabdomyoblasts ranges from round to fusiform to polygonal with abundant cytoplasm; however, distinct cross-striation is not detectable. In this detail, the epithelioid arrangement of the cells is striking (wet-fixed smear, Pap stain, high magnification).

**Fig. 17.38 Epithelioid angiosarcoma.**
A 67-year-old woman presented with an enlarged cervical lymph node. FNAB of the lymph node was performed providing air-dried direct smears for MGG staining. Cytology clearly exhibits epithelioid aggregation of the tumor cells, showing abundant dense cytoplasm that is almost invariably sharply outlined. Note nuclear cytoplasmic inclusions (arrows) and prominent nucleoli (arrowheads).
*Tentative cytologic diagnosis:* Malignant large cell tumor, most likely metastatic undifferentiated carcinoma.
*Clinical and surgical work-up and multiple biopsies:* Epithelioid angiosarcoma of the thyroid with a metastasis in a single neck lymph node.

**Fig. 17.39 Malignant peripheral nerve sheath tumor.**
FNAB of a metastasis located in the thoracic wall of a 18-year-old woman, 1 year after removal of the primary tumor in the left thigh. Detail of a direct smear (wet-fixed smear, Pap stain) showing signs of neural differentiation: tapered ends and angulation of the nuclei, faint palisading of elongated nuclei (arrows). Scattered large tumor cells are occasionally encountered (arrowheads).
*Cytologic diagnosis:* Metastasis of a well- to moderately differentiated MPNST (a biopsy was not performed).

**Fig. 17.40 Clear cell sarcoma of soft tissue.**
A tumoral swelling located in the forefoot of a 28-year-old woman. FNAB was followed by an excisional biopsy. Abundant clear round or elongated cytoplasm is a key feature of this tumor entity together with rounded nuclei exhibiting lucid nucleoplasm, coarse clumping chromatin, and prominent nucleoli. Occasional nuclear cytoplasmic inclusions are also present (arrows) (wet-fixed direct smear, Pap stain, high magnification).

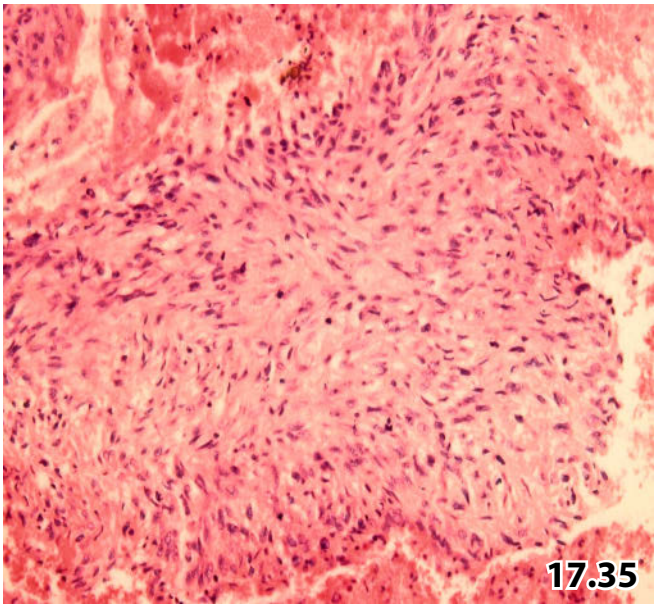
17.35

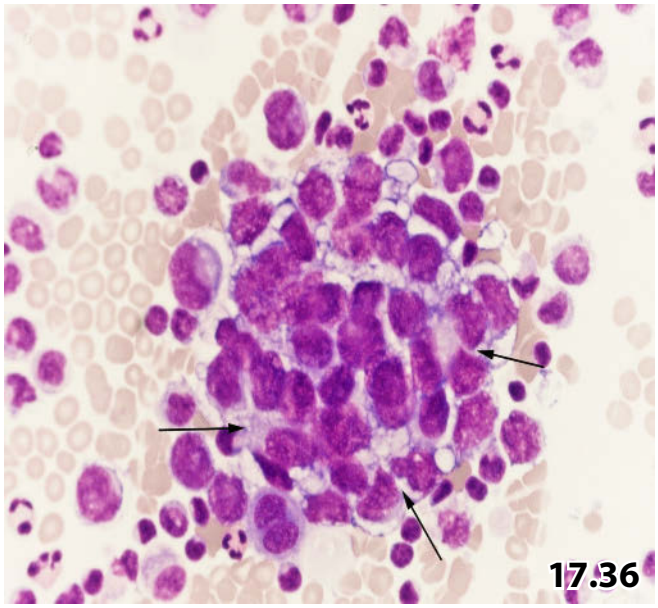
17.36

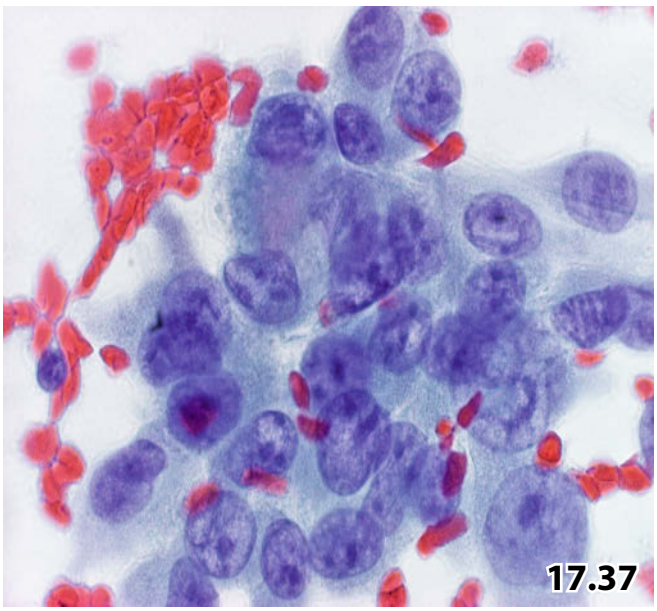
17.37

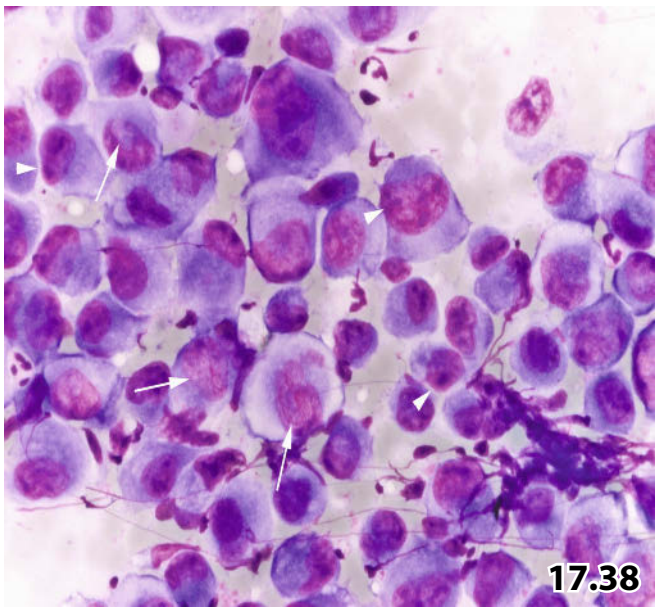
17.38

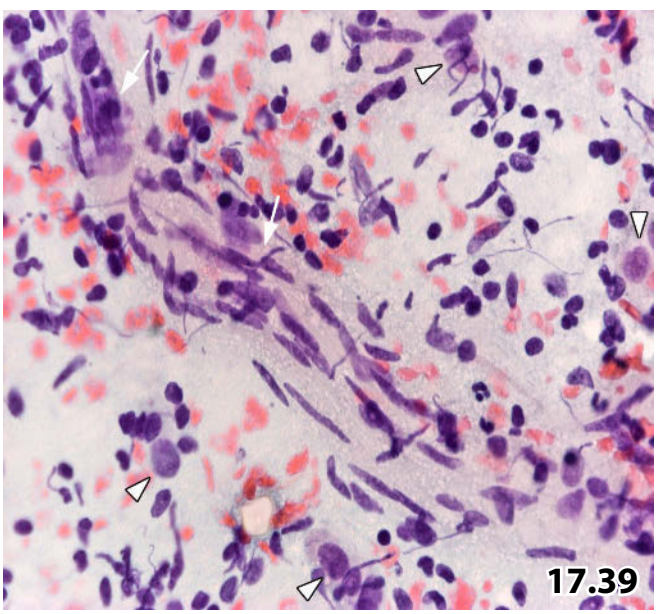
17.39

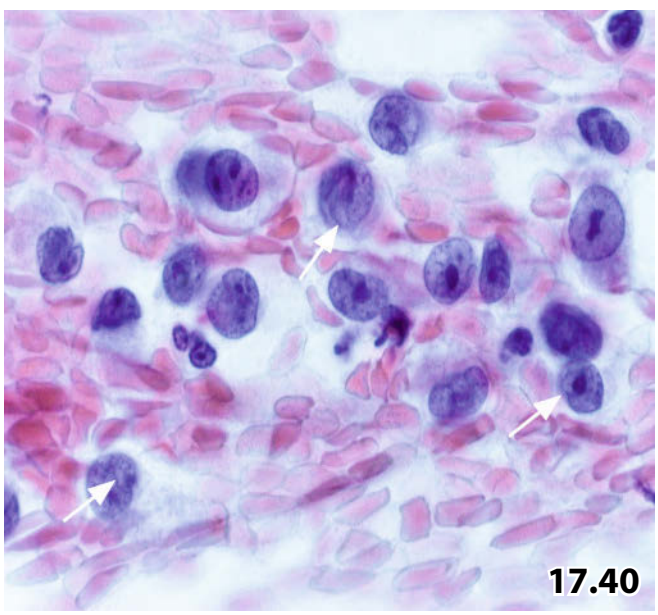
17.40

# Synopsis and Algorithms 18



Spieler/Rössle, *Nongynecologic Cytopathology. A Practical Guide*. *Essentials of Diagnostic Pathology*,
DOI 10.1007/978-3-642-24719-4_18, 

# Chapter 1 Breast

## Section 1.2
## Breast: Fine-Needle Aspiration Biopsy

- Benign Disorders
- Benign Tumors
- Proliferative Breast Disease with Atypia

## Cytology of Normal Breast Tissue Section 1.2.1, p. 16

### Normal Lining of the Duct System

| Basic cell pattern | Particular and/or additional features | Differential diagnosis or possible diagnostic pitfall |
|---|---|---|
| – Regular honeycomb sheets<br>– Uniform cuboid and columnar epithelial cells, focally overlapping<br>– Nuclei with smooth margins, loose and evenly distributed chromatin<br>– Sporadic small distinct nucleoli, centrally located<br>– Small dark bipolar nuclei attached to the periphery of the cell clusters and a few myoepithelial cells in the background | | |

### Fragment of the Normal Lobular Unit

| Basic cell pattern | Particular and/or additional features | Differential diagnosis or possible diagnostic pitfall |
|---|---|---|
| – Typical acini embedded in loosely structured stroma, frequently appended tubular terminal duct fragments<br>– Thin or gross, but distinct basal lamina<br>– Cells showing cuboidal to cylindric shape, smooth nuclear margins, and bland chromatin<br>– Surrounding myoepithelial cells are flat or rounded showing clear delicate cytoplasm | | |

## Cystic Lesion and Duct Ectasia Section 1.2.2, p. 17

### Duct Ectasia / Benign Cyst

| Basic cell pattern | Particular and/or additional features | Differential diagnosis or possible diagnostic pitfall |
|---|---|---|
| – Foamy histiocytes, often degenerated<br>– Varying amounts of apocrine epithelial cells<br>– Neutrophils – variable<br>– Cellular debris and serous fluid in the background – variable | – Macroscopically: bloody fluid<br>– Microscopically: old blood | **Do not miss intracystic neoplasia! Search carefully for atypical/malignant cells!** |

### Simple Cyst with Modified Epithelium in Regeneration and Repair

| Basic cell pattern | Particular and/or additional features | Differential diagnosis or possible diagnostic pitfall |
|---|---|---|
| – Typical cyst sediment as stated above<br>– Large polymorphous epithelial cells – single and grouped:<br>  – Abundant clear cytoplasm often elongated with delicate margins<br>  – Nuclei intended and cleaved<br>  – Pale and usually darkly stained nucleoplasm<br>  – Indistinct chromatin structure<br>  – Large nucleoli | | – Malignant neoplasia |

1

## Infection and Inflammation Secs. 1.2.3–1.2.7, p. 17

### Acute Mastitis

| Basic cell pattern | Particular and/or additional features | Differential diagnosis or possible diagnostic pitfall |
|---|---|---|
| – Neutrophils and macrophages<br>– Histiocytes and epithelial cells with cytophagocytosis<br>– Loose epithelial clusters focally interspersed with neutrophils:<br>  – Cell enlargement<br>  – Normal N/C ratio<br>  – Bland chromatin pattern<br>  – Centrally located prominent and round nucleoli | – Numerous degenerating neutrophils and abundant background debris | – Atypical epithelial hyperplasia<br>– Carcinoma, low-grade type<br>– Breast abscess |

### Subareolar Abscess

| Basic cell pattern | Particular and/or additional features | Differential diagnosis or possible diagnostic pitfall |
|---|---|---|
| – Squamous cells partly anucleated<br>– Cellular elements indicating chronic inflammation – variable<br>– Foreign body reaction and granulation tissue – variable | | – Squamous cell carcinoma<br>– Metaplastic carcinoma |

### Fat Necrosis

| Basic cell pattern | Particular and/or additional features | Differential diagnosis or possible diagnostic pitfall |
|---|---|---|
| – Mixed inflammatory cell pattern<br>– Multinucleate macrophages<br>– Lipophages with abundant vacuolated cytoplasm<br>– Small clusters of anucleated fat cells and bland fat tissue<br>– Amorphous debris | – Activated fibroblasts – variable | – Single carcinoma cells |

### Suture Granuloma

| Basic cell pattern | Particular and/or additional features | Differential diagnosis or possible diagnostic pitfall |
|---|---|---|
| – Pronounced foreign body reaction<br>– Huge multinucleate macrophages<br>– Tightly packed intracytoplasmic birefringent bars | | |

### Granulomatous Mastitis NOS / Sarcoidosis / Tuberculosis

| Basic cell pattern | Particular and/or additional features | Differential diagnosis or possible diagnostic pitfall |
|---|---|---|
| – Mixed inflammatory cell pattern, lymphocyte predominant<br>– Small and large fragments of cell-rich granulomatous tissue<br>– Epithelial cell groups with inflammatory atypias – variable<br>– Sporadic epithelioid cells and Langhans giant histiocytes | – Activated fibroblasts embedded in fibrous matrix<br>– Numerous epithelioid cells<br>– Langhans giant histiocytes<br>– Caseous/granular debris | – Single carcinoma cells<br>– Epithelioid granulomatosis (sarcoidosis)<br>– Epithelioid granulomatosis (tuberculosis) |

## Infection and Inflammation Secs. 1.2.3–1.2.7, p. 17 (continued)

### Pseudolymphoma

| Basic cell pattern | Particular and/or additional features | Differential diagnosis or possible diagnostic pitfall |
|---|---|---|
| – High cellularity<br>– Small lymphocytes, plasmacytoid elements, histiocytes | – Immature lymphocytic population<br>– Large numbers of immature blastic cells | – Malignant lymphoma<br>– Large-cell carcinoma (along with lymphatic hyperplasia) |

### Plasma Cell Mastitis

| Basic cell pattern | Particular and/or additional features | Differential diagnosis or possible diagnostic pitfall |
|---|---|---|
| – Numerous lymphocytes and plasma cells | – The lymphocytes may be outnumbered by mature plasma cells | – Plasmacytoma |

## Noncellular Elements Sect. 1.2.8, p. 19

### Liesegang Rings

| Basic cell pattern | Particular and/or additional features | Differential diagnosis or possible diagnostic pitfall |
|---|---|---|
| – Concentrically laminated ring-shaped elements, more or less shadowy | | |

### Collagenous Spherulosis

| Basic cell pattern | Particular and/or additional features | Differential diagnosis or possible diagnostic pitfall |
|---|---|---|
| – Cellular sample<br>– Bland and proliferative epithelial cell groups<br>– Closely packed cohesive cells surrounding translucent acellular spherules<br>– Benign nuclear features: smooth borders and fine chromatin<br>– Background with dispersed naked bipolar nuclei | | – Atypical ductal hyperplasia<br>– Adenoid cystic carcinoma<br>– Cribriform ductal carcinoma (in situ or invasive) |

### Mucocele-Like Lesion

| Basic cell pattern | Particular and/or additional features | Differential diagnosis or possible diagnostic pitfall |
|---|---|---|
| – Mucus: globular and diffuse<br>– Scant cellularity<br>– Compact monolayer epithelial sheets, minor or missing nuclear atypia | – Florid epithelial proliferation with nuclear atypia | – Mucinous adenocarcinoma |

### Silicone Granuloma

| Basic cell pattern | Particular and/or additional features | Differential diagnosis or possible diagnostic pitfall |
|---|---|---|
| – Numerous vacuolated histiocytes<br>– Multinucleated giant cells<br>– Minimal inflammatory component | | |

### Amyloid

| Basic cell pattern | Particular and/or additional features | Differential diagnosis or possible diagnostic pitfall |
|---|---|---|
| – Refractile material (eosinophilic with Pap stain)<br>– Pathognomonic properties stained with Congo red, subsequently showing bottle-green birefringence | | |

1

## Pregnancy and Lactation Sect. 1.2.9, p. 20

### Hormonal Cell Stimulation

| Basic cell pattern | Particular and/or additional features | Differential diagnosis or possible diagnostic pitfall |
|---|---|---|
| – Grossly enlarged epithelial cells occurring mostly dispersed<br>– Round and frequently naked nuclei with smooth borders<br>– Regular fine granular chromatin<br>– Prominent nucleoli<br>– Low N/C ratio<br>– Foamy and coarse-vacuolated cytoplasm | | – Secretory carcinoma |

### Lactating Adenoma

| Basic cell pattern | Particular and/or additional features | Differential diagnosis or possible diagnostic pitfall |
|---|---|---|
| – High cellularity<br>– Cellular morphology as described above<br>– Many benign acinic formations<br>– Dirty background due to secretory material | | |

## Fibrocystic Breast Changes Sect. 1.2.10, p. 20

### Fibrocystic Breast Disease

| Basic cell pattern | Particular and/or additional features | Differential diagnosis or possible diagnostic pitfall |
|---|---|---|
| – Low cellularity<br>– Few fragments of adipose and fibrotic tissue<br>– Benign flat sheets and small acinic clusters with myoepithelial cells<br>– Round and oval nuclei with smooth borders<br>– Finely dispersed chromatin<br>– Small round nucleoli – variable<br>– Small sheets of apocrine cells – variable<br>– Foam cells | | |

## Proliferative Breast Disease with and Without Atypia Sects. 1.2.11–1.2.13, p. 21

### Ductal Hyperplasia Without Atypia

| Basic cell pattern | Particular and/or additional features | Differential diagnosis or possible diagnostic pitfall |
|---|---|---|
| – High cellularity<br>– Regular sheets and papilliform clusters including myoepithelial cells<br>– Groups of elongated epithelial cells exhibiting streaming and swirling pattern<br>– Focally enlarged epithelial cells: bland nuclear pattern with indistinct indentations and coloration, sporadic large regular nucleoli<br>– Small sheets of apocrine cells – variable<br>– Foam cells | | – Nipple duct adenoma<br>– Fibroadenoma<br>– Papilloma<br>– Juvenile papillomatosis |
| | – Cellular and nuclear pleomorphism<br>– Detritus | – Florid ductal hyperplasia<br>– Nipple duct adenoma<br>– Proliferative disease with atypia<br>– Carcinoma |

### Ductal Hyperplasia with Atypia

| Basic cell pattern | Particular and/or additional features | Differential diagnosis or possible diagnostic pitfall |
|---|---|---|
| – Same basic cell pattern as described above, but :<br>– Dense and loose cell clusters, more irregular nuclear spacing<br>– Loss of nuclear polarity<br>– Cell dissociation<br>– Anisonucleosis and nuclear irregularities<br>– Coarse granular and clumping chromatin, hyperchromasia<br>– Macronucleoli | | – Florid ductal hyperplasia<br>– Cellular fibroadenoma<br>– Papilloma<br>– Ductal carcinoma in situ, low-grade<br>– Papillary carcinoma, low-grade |

## Proliferative Breast Disease with and Without Atypia (continued) Sects. 1.2.11–1.2.13, p. 21

### Tubular Adenoma / Adenosis

| Basic cell pattern | Particular and/or additional features | Differential diagnosis or possible diagnostic pitfall |
|---|---|---|
| – Cellular specimen<br>– Elements of benign ductal hyperplasia and tubular formations of different size with bland nuclei<br>– Large number of myoepithelial cells<br>– Foam cells<br>– Secretory masses and debris<br>– Scarce stromal component | | |

### Sclerosing Adenosis / Radial Scar / Complex Sclerosis

| Basic cell pattern | Particular and/or additional features | Differential diagnosis or possible diagnostic pitfall |
|---|---|---|
| – Low cellularity<br>– Cells are arranged singly, in small groups, and single-file rows<br>– Occasionally pleomorphic excentrically positioned nuclei<br>– Few fragments of sclerotic stroma | | – Invasive breast carcinoma – common type |

### Gynecomastia

| Basic cell pattern | Particular and/or additional features | Differential diagnosis or possible diagnostic pitfall |
|---|---|---|
| – Few large and dense three-dimensional, branching cell clusters<br>– Variable nuclear size, round to oval nuclei with smooth borders<br>– Regularly distributed fine granular chromatin<br>– Distinct nucleoli<br>– Myoepithelial cells<br>– Cellular stroma often edematous or myxoid | **Extremely polymorphous cell pattern:**<br>– Strong variation in cell and nuclear size<br>– Nuclei may show indentations and prominent nucleoli<br>– Occasional mitotic figures | – Florid phase of gynecomastia<br>– Carcinoma |

### Hamartoma

| Basic cell pattern | Particular and/or additional features | Differential diagnosis or possible diagnostic pitfall |
|---|---|---|
| – High cellularity<br>– Two tissue components, epithelial and mesenchymal:<br>(1) Lobular acinic and ductal glandular structures, intact lobular units embedded in fibrous stroma, bland and proliferative ductal epithelial cells, focal apocrine change<br>(2) Fibrous and adipose tissue, components of histogenetically different stromal tissue may occur<br>– Myoepithelial cells and bipolar nuclei<br>– Foam cells | | – Fibroadenoma<br>– Adenosis |

1

## Papillary Tumor Sect. 1.2.14, p. 23

### Papilloma

| Basic cell pattern | Particular and/or additional features | Differential diagnosis or possible diagnostic pitfall |
|---|---|---|
| – High cellularity<br>– Papillary arborizing cell clusters with fibrovascular cores<br>– Bland epithelial cell morphology<br>– Heterogeneous cell population (epithelial and myoepithelial features) | | – Fibroadenoma |
| | -Cystic background and hemosiderophages | – Intracystic papilloma |

### Suggestive of Papilloma

| Basic cell pattern | Particular and/or additional features | Differential diagnosis or possible diagnostic pitfall |
|---|---|---|
| – True papillary formations comprising fibrovascular cores are absent<br>– Small papilliform and stellate clusters with palisading cylindrical cells<br>– Bland columnar cells in compact rows<br>– Single cells with elongated and cylindric cytoplasm<br>– Bipolar nuclei at the periphery of clusters or in the background<br>– Apocrine metaplasia – variable<br>– Sporadic squamous metaplasia | | – Marked ductal hyperplasia |
| | – Lack of myoepithelial cells<br>– Irregular epithelial cells with focal stratification<br>– Mild hyperchromasia<br>– Enlarged nucleoli | – Highly proliferative papilloma<br>– Ductal hyperplasia with atypia<br>– Low-grade papillary carcinoma |

## Fibroadenoma and Phylloides Tumor Sect. 1.2.15, p. 24

### Fibroadenoma

| Basic cell pattern | Particular and/or additional features | Differential diagnosis or possible diagnostic pitfall |
|---|---|---|
| – Marked cellularity<br>– Large cohesive sheets and antler-horn-like cell clusters<br>– Apocrine metaplasia is common<br>– Nuclei with smooth borders, regular chromatin, centrally placed nucleoli<br>– Large numbers of stripped epithelial-cell nuclei and bipolar nuclei<br>– Multinucleated giant histiocytes are common<br>– Myxoid degeneration of small and large stromal fragments | | – Phylloides tumor<br>– Papilloma<br>– Hamartoma<br>– Pleomorphic breast adenoma |
| | – Nuclear polymorphism<br>– Large nucleoli<br>– Numerous isolated epithelial cells<br>– Discohesive cell clusters<br>– Loss of nuclear polarity in cell clusters | – Juvenile fibroadenoma<br>– Carcinoma |

### Phylloides Tumor

| Basic cell pattern | Particular and/or additional features | Differential diagnosis or possible diagnostic pitfall |
|---|---|---|
| – Epithelial component as stated for fibroadenoma, in addition:<br>  – Hypercellular stromal component with spindle-shaped fibroblastic cells polymorphous or sarcomatoid in appearance, but bland nuclei | | – Fibroadenoma |
| | – Marked sarcomatoid cell features | – Phylloides tumor with sarcoma-like stromal component<br>– Malignant phylloides tumor |

## Selected Benign Epithelial and Mesenchymal Breast Lesions Sects. 1.2.16–1.2.18, p. 25

### Adenomyoepithelioma

| Basic cell pattern | Particular and/or additional features | Differential diagnosis or possible diagnostic pitfall |
|---|---|---|
| – Biphasic cell pattern:<br>(1) Large epithelial cell clusters, ductal and acinar<br>(2) Large number of myoepithelial cells:<br>cohesive groups of spindle-shaped cells appearing in a streaming pattern enclosed in epithelial sheets,<br>or as single elongated cells,<br>or as naked bipolar nuclei<br>– Marked hypercellularity<br>– Bland nuclei with fine chromatin texture<br>– Normal N/C ratio<br>– Proliferative activity with nuclear atypias – variable | | – Pseudoangiomatous stromal hyperplasia<br>– Hamartoma<br>– Fibroadenoma<br>– Phylloides tumor<br>**Further differential diagnoses should be considered dependent on the dominant cell pattern and the degree of atypia** |

### Lipoma / Angiolipoma / Hibernoma

| Basic cell pattern | Particular and/or additional features | Differential diagnosis or possible diagnostic pitfall |
|---|---|---|
| – Ballooned-appearing uniform lipocytes in groups of different sizes<br>– Rare individual lipocytes | – Branching vascular network spreading among lipocytes<br>– Myxoid matrix<br>– Numerous small, densely packed fat droplets in the cytoplasm of lipocytes giving a reddish-brown staining to the cells, mimicking cytoplasmic granulation | – **Angiolipoma**<br>– Lipoma-like liposarcoma<br>– **Hibernoma**<br>– Granular cell tumor<br>– Apocrine lesion |

### Granular Cell Tumor

| Basic cell pattern | Particular and/or additional features | Differential diagnosis or possible diagnostic pitfall |
|---|---|---|
| – Highly cellular cytologic samples<br>– Single cells and loose cell clusters, uniform large cells<br>– Abundant but ill-defined fine granular cytoplasm<br>– Small, excentrically positioned nuclei<br>– Bland chromatin<br>– Inconspicuous nucleoli<br>– Occasional nuclear polymorphism and distinct nucleoli<br>– Background with granular material | | – Foam cells (cystic fluid)<br>– Hibernoma<br>– Apocrine carcinoma<br>– Clear cell carcinoma<br>– Malignant melanoma |

## Rare Benign Breast Lesions

Rare epithelial, cystic, and mesenchymal lesions that are occasionally observed in daily cytology practice and/or cited in the literature are listed in Sect. 1.2.19, p. 27. They may give rise to diagnostic confusion, leading to an incorrect benign diagnosis or a diagnosis of malignancy, respectively.

1

# Section 1.3
# Breast: Fine-Needle Aspiration Biopsy – Malignant Lesions

## Infiltrating Ductal Carcinoma Sect. 1.3.1, p. 56

### Invasive Ductal Carcinoma: Common Type

| Basic cell pattern | Particular and/or additional features | Differential diagnosis or possible diagnostic pitfall |
|---|---|---|
| – Cohesive cell groups, nuclear overlapping and loss of polarity<br>– Three-dimensional dense clusters mainly well defined<br>– Shoe-/boot-shaped and V-shaped clusters and single-file rows<br>– Individual cells – variable<br>– Eccentric nuclei and triangular dense cytoplasm are common<br>– Medium-sized round to oval nuclei:<br>  – Wrinkled saw-blade-like membrane<br>  – Molding and cleaving<br>  – Hyperchromasia or dyschromasia<br>  – Distinct nuclear clearing, grooves and inclusions – variable<br>– Chromatin: characteristically dense and finely granular, or patternless, occasionally glassy or dusty<br>– Indistinct nucleoli<br>– Cytoplasm densely structured and triangular, target-like inclusions<br>– Myoepithelial cells are absent<br>– Tumor cell necrosis is infrequent | | – Sclerosing adenosis<br>– Florid benign epithelial proliferation<br>– Actinic cell changes |
| | – Pronounced nuclear clearing, grooves, and inclusions<br>– Patternless, glassy, or dusty chromatin | – **Keep in mind metastatic papillary thyroid carcinoma!** |
| | – Smears containing only a few single carcinoma cells | – Malignant lymphoma |

### Infiltrating Ductal Carcinoma: Monomorphic, Small-Cell Type

| Basic cell pattern | Particular and/or additional features | Differential diagnosis or possible diagnostic pitfall |
|---|---|---|
| – Small carcinoma cells (size of two to three erythrocytes)<br>– Architectural and cellular criteria as listed above but usually less distinct<br>– Overall monomorphic cell pattern<br>– Sporadic small nucleoli | | – Benign hyperplastic breast lesions<br>– **Pilomatrixoma**<br>– Low-grade DCIS<br>– Small-cell carcinoma of varied origin |

### Infiltrating Ductal Carcinoma, Large-Cell Type

| Basic cell pattern | Particular and/or additional features | Differential diagnosis or possible diagnostic pitfall |
|---|---|---|
| – Highly cellular specimen<br>– Loose aggregates of large polymorphic highly atypical cells<br>– Numerous isolated cells, mitotic activity<br>– Nuclear indentations and foldings<br>– Coarse chromatin, hyperchromasia<br>– Large nucleoli, often multiple<br>– Increased N/C ratio<br>– Bizarrely shaped cytoplasm<br>– Usually necrotic background | | – High-grade DCIS<br>– Florid benign epithelial proliferation<br>– Nipple duct adenoma with necrosis<br>– Lactational cell changes<br>– Actinic cell changes |

## Infiltrating Lobular Carcinoma Sect. 1.3.2, p. 58

### Classic Lobular Carcinoma

| Basic cell pattern | Particular and/or additional features | Differential diagnosis or possible diagnostic pitfall |
|---|---|---|
| – Low cellularity<br>– Predominantly dissociated small to medium-sized tumor cells<br>– Pronounced single-file cell arrangement, lack of large tumor cell clusters<br>– Eccentric vesicular nuclei with molding and cleaving<br>– Tiny nucleoli<br>– Finely dispersed chromatin and/or pronounced nuclear clearing<br>– Frequent targetoid cytoplasmic inclusions<br>– Sporadic signet ring cells | | – Lobular carcinoma in situ<br>– Invasive ductal carcinoma |

### Pleomorphic Lobular Carcinoma

| Basic cell pattern | Particular and/or additional features | Differential diagnosis or possible diagnostic pitfall |
|---|---|---|
| – Cellular morphology as described above, but:<br>  – Increased cellularity<br>  – Enlarged cells<br>  – Pleomorphic nuclei and distinct nucleoli | | – as stated above |

## Ductal Intraepithelial Neoplasia / Carcinoma In Situ (DIN/DCIS) Sect. 1.3.3, p. 59

### Ductal Carcinoma In Situ, Low-Grade Type

| Basic cell pattern | Particular and/or additional features | Differential diagnosis or possible diagnostic pitfall |
|---|---|---|
| – Monotonous population of monomorphic small- to medium-sized cells<br>-– Numerous cohesive three-dimensional cell clusters, loss of nuclear polarization<br>– Few single cells<br>– Nuclei round to oval, wrinkled saw-blade-like membranes, nuclear molding and cleaving<br>– Indistinct nucleoli<br>– No myoepithelial cells | | – Invasive ductal carcinoma (common or small-cell type) |

### Ductal Carcinoma In Situ, High-Grade Type

| Basic cell pattern | Particular and/or additional features | Differential diagnosis or possible diagnostic pitfall |
|---|---|---|
| – Cellular aspirate<br>– Polymorphic malignant cells<br>– Dirty background with necrosis – common<br>– Apoptotic and degenerating tumor cells | | – Invasive ductal carcinoma (large-cell type)<br><br>**Distinction of high-grade DCIS from invasive ductal high-grade carcinoma is practically impossible by cytology** |

1

## Common and Rare Variants of Breast Carcinoma Sects. 1.3.4–1.3.14, p. 60

### Tubular Carcinoma

| Basic cell pattern | Particular and/or additional features | Differential diagnosis or possible diagnostic pitfall |
|---|---|---|
| – Cohesive flat sheets with lack of myoepithelial cells<br>– Focal nuclear overlapping<br>– Three-dimensional tubular structures<br>– Nuclear changes are similar as compared to lobular carcinoma: slight variation in size, irregularities of the nuclear membrane, finely dispersed chromatin, weak nuclear staining, absence of hyperchromasia<br>– Generally small nucleoli<br>– Occasionally solitary cytoplasmic vacuoles<br>– Cell dissociation is uncommon | – Numerous three-dimensional tubular structures | – Benign hyperplastic breast lesions<br>– Microglandular-like breast lesions / microglandular adenosis<br>– Invasive ductal and papillary carcinoma<br>– Adenoid cystic carcinoma |

### Papillary Carcinoma (Less Well Differentiated)

| Basic cell pattern | Particular and/or additional features | Differential diagnosis or possible diagnostic pitfall |
|---|---|---|
| – Highly cellular smears<br>– True complex papillary fragments with fibrovascular cores<br>– Three-dimensional papilliform clusters<br>– Cells are larger than those in low-grade papillary tumors<br>– Increased N/C ratio, nuclear indentations, coarse chromatin, hyperchromasia<br>– Conspicuous nucleoli<br>– Necrotic background and hemosiderophages may be present | | |

### Suggestive of Papillary Carcinoma

| Basic cell pattern | Particular and/or additional features | Differential diagnosis or possible diagnostic pitfall |
|---|---|---|
| – Absence of true papillae and distinct papilliform clusters<br>– Atypical columnar cells isolated or in palisade arrangement, occurrence of small and large cell chains | | |

Distinguishing between **low-grade papillary carcinoma** and **benign papilloma**; see Chap. 1.2, Sect. 1.2.14, p. 23.

### Mucinous Carcinoma

| Basic cell pattern | Particular and/or additional features | Differential diagnosis or possible diagnostic pitfall |
|---|---|---|
| – Three-dimensional cell balls, flat sheets and single cells floating in thick mucinous material<br>– Mucus is often concentrically condensed<br>– Occasional signet ring cells<br>– Nuclei with mild degree of atypia: vesicular, occasional nuclear grooves, no hyperchromasia<br>– Rare nucleoli<br>– Cells of common ductal carcinoma type – variable | | – Mucocele-like lesions<br>– Fibroadenoma **with excessive myxoid stroma!**<br>– Mucinous eccrine carcinoma such as axillary cutaneous tumor |

### Medullary Carcinoma

| Basic cell pattern | Particular and/or additional features | Differential diagnosis or possible diagnostic pitfall |
|---|---|---|
| – Highly cellular smears with unequivocal malignant epithelial cells<br>– Numerous lymphocytes and plasma cells, occasionally neutrophilic granulocytes<br>– Epithelial Tumor cells:<br>  – Syncytial epithelial sheets and occasional clusters<br>  – Large numbers of scattered tumor cells and stripped nuclei<br>  – Nuclei variable in size and shape, coarse chromatin<br>  – Prominent polymorphic nucleoli<br>  – Cytoplasm of varying size, usually vacuolated | | – High-grade ductal carcinoma<br>– Malignant lymphoma<br>– Lymph node in the breast affected by metastatic disease<br>– Intramammary reactive lymph node |

## Common and Rare Variants of Breast Carcinoma Sects. 1.3.4–1.3.14, p. 60 (continued)

### Apocrine Carcinoma

| Basic cell pattern | Particular and/or additional features | Differential diagnosis or possible diagnostic pitfall |
|---|---|---|
| – Tumor cells showing abundant cytoplasm with sharply defined margins<br>– Variable eosinophilic granulation, usually coarse<br>– Excentrically located large, round, and vesicular nuclei<br>– Prominent nucleoli<br>– Foam cells from cystic areas – possible | | – Lipid-rich carcinoma<br>– Carcinoma with squamous differentiation<br>– Granular cell tumor<br>– **In the axilla: axillary primary apocrine carcinoma** |

### Secretory (Juvenile) Carcinoma

| Basic cell pattern | Particular and/or additional features | Differential diagnosis or possible diagnostic pitfall |
|---|---|---|
| – Cellular smears<br>– Grape-like clusters composed of mucinous globular structures and single globuli<br>– Sparse extracellular mucus in an otherwise clean background<br>– Lack of significant cellular atypia<br>– Occasional signet ring cells | | |

### Lipid-Rich Carcinoma

| Basic cell pattern | Particular and/or additional features | Differential diagnosis or possible diagnostic pitfall |
|---|---|---|
| – Large cells with abundant rounded cytoplasm (abundant fat storage)<br>– Mix of multiple, variably sized, well-defined cytoplasmic vacuoles **unique: cytoplasmic droplets of variable size**<br>– Numerous single cells, occasional cell clustering<br>– Eccentrically located nuclei, clumped or finely granular chromatin<br>– Prominent nucleoli (single or multiple) | | – Apocrine carcinoma |

### Clear Cell (Glycogen-Rich) Carcinoma

| Basic cell pattern | Particular and/or additional features | Differential diagnosis or possible diagnostic pitfall |
|---|---|---|
| – Mixed cell pattern: clusters, loose groups, and single cells<br>– Large cells with abundant clear cytoplasm<br>– Focally fine granular eosinophilic cytoplasm<br>– Abundant intracytoplasmic glycogen (positive PAS reaction)<br>– Nuclei are pleomorphic, hyperchromatic, and excentrically located, as in common breast cancer | | – Lipid-rich carcinoma<br>– Ductal breast carcinoma, large-cell type/ secretory<br>– Apocrine tumors<br>– Metastatic renal cell carcinoma<br>– Other rare clear cell tumors |

### Adenoid Cystic Carcinoma

| Basic cell pattern | Particular and/or additional features | Differential diagnosis or possible diagnostic pitfall |
|---|---|---|
| – Cell-rich sample **presenting two cell types and spherical acellular material:** Small basaloid and few larger eosinophilic cells occur in tightly cohesive three-dimensional cell nests. The cells are arranged around cores of homogeneous acellular material, background with acellular spheres and cylinders<br>– The cells are basically small and uniform with scant cytoplasm<br>– Minor nuclear atypia: angular membranes<br>– Numerous naked bipolar nuclei in the background | | – Collagenous spherulosis<br>– Myospherulosis<br>– Ductal carcinoma with secretory material<br>– Cribriform carcinoma |

1

## Common and Rare Variants of Breast Carcinoma Sects. 1.3.4–1.3.14, p. 60 (continued)

### Metaplastic Carcinoma

| Basic cell pattern | Particular and/or additional features | Differential diagnosis or possible diagnostic pitfall |
|---|---|---|
| – Mixture **of frank carcinoma cells and mesenchyma-like cells**:<br>  – Carcinoma cells of common ductal type or large-cell type<br>  – Bland or pleomorphic spindle tumor cells with sarcomatoid features and phagocytic activity<br>– Atypical histiocyte-like multinucleated cells with intracytoplasmic vacuoles and debris<br>– Chondroid, osseous, or squamous metaplasia exhibiting varied cellular atypia – variable | | – Fibromatosis<br>– Pseudosarcomatous fasciitis<br>– Phylloides tumor with epithelial atypia<br>– Pleomorphic breast carcinoma<br>– Secondary Ca – poorly differentiated<br>– Primary and metastatic sarcoma |

### Squamous Cell Carcinoma of the Breast

| Basic cell pattern | Particular and/or additional features | Differential diagnosis or possible diagnostic pitfall |
|---|---|---|
| – Densely keratinized cytoplasm<br>– Hyperchromatic dense nuclei and highly irregular nuclear membranes<br>– Coarse or patternless chromatin<br>– Large pleomorphic nucleoli<br>– Necrosis in the background | | – Metastatic squamous cell carcinoma<br>**Distinction of primary from metastatic squamous cell carcinoma is not possible by morphologic features alone** |

### Carcinoma with Osteoclastic Giant Cells

| Basic cell pattern | Particular and/or additional features | Differential diagnosis or possible diagnostic pitfall |
|---|---|---|
| – **Biphasic component** of atypical epithelial cells and giant cells:<br>  – Epithelial component: irregular cell clusters and cell dissociation, mild to moderate nuclear pleomorphism<br>  – Giant cells with osteoclastic features: huge cells with abundant cytoplasm, nuclei crowded on one side, one conspicuous nucleolus in each nucleus | | |

### Primary Breast Carcinoma with Neuroendocrine Differentiation

| Basic cell pattern | Particular and/or additional features | Differential diagnosis or possible diagnostic pitfall |
|---|---|---|
| – Monomorphic small to intermediate cells, frequently isolated<br>– Clustered cells: rosette-like and alveolar arrangement<br>– Few enlarged cells with homogeneous dark-staining nuclei<br>– Regular nuclei with mildly wrinkled contour and finely dispersed chromatin<br>– Indistinct rounded or plasmacytoid cytoplasm, frequently fine eosinophilic granularity<br>– Common mammary carcinoma cells – variable | | – Metastatic endocrine cancer |
| | – Predominant uniform spindle cell pattern | – Mesenchymal lesion |
| | – Dominant small-cell pattern (oat cell type) | – Metastatic small-cell carcinoma (mainly lung)<br>– Metastatic Merkel cell carcinoma |

### Inflammatory Carcinoma

| Basic cell pattern | Particular and/or additional features | Differential diagnosis or possible diagnostic pitfall |
|---|---|---|
| – Paucicellular FNA specimen<br>– Cytologic findings of invasive ductal carcinoma: usually large pleomorphic tumor cells | | **A conclusive cytologic diagnosis is only possible considering the characteristic clinical features** |

## Common and Rare Variants of Breast Carcinoma Sects. 1.3.4–1.3.14, p. 60 (continued)

### Paget Disease (Microscopic Description Applies to Scrape Specimens)

| Basic cell pattern | Particular and/or additional features | Differential diagnosis or possible diagnostic pitfall |
|---|---|---|
| – Sparsely isolated large pleomorphic cells<br>– Nuclei with pronounced irregularities<br>– Coarse chromatin, hyperchromasia<br>– Irregular prominent nucleoli<br>– Distinctly outlined cytoplasm, clear or densely structured<br>– Possibly detritus material | | – Malignant melanoma |
| | – Smears with abundance in tumor cells | – Bowen disease |

Other sporadic carcinomas are listed in Sect. 1.3.14.3, p. 65.

## Malignant Lymphoma and Myeloid Lesions Sect. 1.3.15, p. 65

### Non-Hodgkin Lymphoma, high-grade

| Basic cell pattern | Particular and/or additional features | Differential diagnosis or possible diagnostic pitfall |
|---|---|---|
| – Large number of pleomorphic single tumor cells as well as loose cell groups and dense clusters<br>– Irregular nuclei: indentations, coarse chromatin, hyperchromasia<br>– Pleomorphic nucleoli<br>– Variable cytoplasm as to size and density<br>– Variable admixture of small to medium-sized bland and atypical lymphoid cells | | – Breast carcinoma, large-cell type<br>– Malignant melanoma<br>– Sarcoma |
| | – Basophilic/cyanophilic tumor cell cytoplasm with small vacuoles<br>– large numbers of starry-sky cells | – Suggesting Burkitt lymphoma |
| | – Large clear cytoplasm and<br>– Multilobated nuclei | – Suggestive of multilobated B-NHL<br>– Suggestive of T-cell NHL<br>– Suggestive of HRS cells indicating Hodgkin lymphoma |

### Non-Hodgkin Lymphoma, Mixed Cell Type

| Basic cell pattern | Particular and/or additional features | Differential diagnosis or possible diagnostic pitfall |
|---|---|---|
| – High cellularity<br>– Atypical lymphocytic population<br>– Small lymphocytes, plasmacytoid elements, and large numbers of immature, blastoid cells<br>– Histiocytes | | – Pseudolymphoma of the breast<br>– Hyperplasia of intraglandular lymphatic tissue |
| | – Hodgkin and Reed-Sternberg cells (HRS) | – Hodgkin lymphoma |

### Myelogenic Sarcoma, Immature and Blastic Variant

| Basic cell pattern | Particular and/or additional features | Differential diagnosis or possible diagnostic pitfall |
|---|---|---|
| – Numerous large atypical cells<br>– Mostly lobated or histiocytoid clear nuclei<br>– Cytoplasm vacuolated or granular<br>– Myeloid precursor cells<br>– Immature granulocytes | | – NHL , large-cell type<br>– Undifferentiated carcinoma<br>– Malignant melanoma |
| | – Trilineage hematopoietic cell proliferation consisting of precursor cells, immature cells, and mature cells of erythropoiesis, granulopoiesis and megakaryopoiesis | – Mature variant of myelogenic sarcoma<br>– Extramedullary hemopoiesis |

1

## Malignant Mesenchymal Lesions

A list composed of selected tumor entities with their morphologic and immunocytochemical properties together with differential diagnostic options is given in Sect. 1.3.16, p. 67.

## Metastatic Cancers

Differential diagnostic considerations are offered in each section of the current Chap. 1.3. The most important immunoreactions and immunopanels to distinguish metastatic lesions from primary breast cancer are listed in Sect. 1.3.17, p. 68.

# Section 1.4
# Breast: Nipple Discharge

| Microscopic Features in correlation with the Etiology of the Lesion | | Sect. 1.4.3, p. 97 |
|---|---|---|
| **Bland Smear, Occurring Together with Both Benign and Malignant Breast Disorders** | | |
| **Basic cell pattern** | **Particular and/or additional features** | **Differential diagnosis or possible diagnostic pitfall** |
| – Proteinaceous background<br>– Acellular smear<br>  – Or a few foam cells<br>  – And/or a few bland ductal cells, dispersed or tightly clustered | | |
| **Duct Ectasia** | | |
| **Basic cell pattern** | **Particular and/or additional features** | **Differential diagnosis or possible diagnostic pitfall** |
| – A large amount of proteinaceous material<br>– Background with cellular debris – variable<br>– Large numbers of activated foam cells, occasionally multinucleated<br>– Few bland duct cells | | – True cystic lesion |
| **Galactorrhea** | | |
| **Basic cell pattern** | **Particular and/or additional features** | **Differential diagnosis or possible diagnostic pitfall** |
| – Background material: abundant lipoproteinaceous material, and masses with clear droplets of varying size<br>– Numerous foam cells<br>– Epithelial cells are sparse or absent | | |
| **Infection / Inflammation** | | |
| **Basic cell pattern** | **Particular and/or additional features** | **Differential diagnosis or possible diagnostic pitfall** |
| – Varying number of neutrophilic granulocytes<br>– Foam cells and macrophages may be present | – Purulent discharge with detritic neutrophils | – Abscess |

## Microscopic Features in correlation with the Etiology of the Lesion (continued) Sect. 1.4.3, p. 97

### Benign and Low-Grade Proliferative Lesions Presenting with an Almost Identical Cytologic Pattern: Benign Florid Ductal Epithelial Hyperplasia / Proliferative Breast Disease With Atypia / Intraductal Papilloma / Low-Grade Papillary Carcinoma / Low-Grade DCIS

| Basic cell pattern | Particular and/or additional features | Differential diagnosis or possible diagnostic pitfall |
|---|---|---|
| – Hemorrhagic and inflammatory background – variable<br>– Varied cellularity<br>– Tight papilliform clusters and single cells<br>– Mild cellular atypia<br>– Cleaved and wrinkled nuclei<br>– Small nucleoli are common<br>– Apocrine cells may be present | | – invasive breast carcinoma monomorphic subtype (ductal or lobular variant) |

### Malignant High-Grade Lesions Presenting with an Almost Identical Cytologic Pattern: Poorly Differentiated Ductal Intraepithelial Neoplasia / High-Grade, Comedo-Type Invasive Ductal Carcinoma

| Basic cell pattern | Particular and/or additional features | Differential diagnosis or possible diagnostic pitfall |
|---|---|---|
| – Variable background, usually hemorrhagic and necrotic<br>– Enlarged pleomorphic cells, individual or in discohesive groups<br>– Generally strong cellular degeneration<br>– Pleomorphic nuclei grooved and folded, hyperchromatic<br>– Coarse chromatin<br>– Prominent irregular nucleoli<br>– Calcifications may be present | | |

### Discharge from Lactiferous Ducts

| Basic cell pattern | Particular and/or additional features | Differential diagnosis or possible diagnostic pitfall |
|---|---|---|
| – Squamous cells<br>– Squamoid detritus<br>– Histiocytic giant cells<br>– Variable number of neutrophils | – Squamous cells with regressive and regenerative changes: irregular amphophilic or keratinized cytoplasm, small pleomorphic and dark nuclei | – Squamous cell carcinoma |

**Paget Disease** see Chap. 1.3, Sect. 1.3.14.2, p. 65.

# Chapter 2 Respiratory Tract and Mediastinum



## Section 2.1 Respiratory Tract: FNAB and Exfoliative Cytology

- Normal and Abnormal Cells
- Granulomatous and Infectious Diseases

### Normal Cytology and Benign Cellular Components (Selected Entities) Sect. 2.1.3, p. 110

#### Superficial Squamous Cells

| Basic cell pattern | Particular and/or additional features | Differential diagnosis or possible diagnostic pitfall |
|---|---|---|
| – Small pyknotic nuclei<br>– Broad orangeophilic cytoplasm | | |

#### Intermediate Squamous Cells

| Basic cell pattern | Particular and/or additional features | Differential diagnosis or possible diagnostic pitfall |
|---|---|---|
| – Round to oval monomorphic nuclei with smooth membrane and fine loose chromatin<br>– Low N/C ratio<br>– Thin cyanophilic cytoplasm | | |

#### Columnar Bronchial Epithelial Cells

| Basic cell pattern | Particular and/or additional features | Differential diagnosis or possible diagnostic pitfall |
|---|---|---|
| – Column-shaped cells ending in a tail; the other pole of the cytoplasm ends in a terminal plate with their anchored cilia<br>– The nuclei are displaced toward the cytoplasmic tail; they are round to oval with a smooth outline<br>– Loose chromatin texture<br>– Small nucleoli | | |

#### Bronchial Goblet Cells

| Basic cell pattern | Particular and/or additional features | Differential diagnosis or possible diagnostic pitfall |
|---|---|---|
| – Molded or flattened nuclei, displaced to the cell periphery<br>– The mucoid inclusions stain light-pink and are lucent (Pap stain) | | |

#### Basal/Parabasal Cells and Reserve Cell Hyperplasia

| Basic cell pattern | Particular and/or additional features | Differential diagnosis or possible diagnostic pitfall |
|---|---|---|
| – Extremely small cells, smaller than small lymphocytes, round to polygonal shape<br>– Small and densely structured rim of cytoplasm, often polygon-shaped similar to bronchial metaplastic squamous cells<br>– Tiny homogeneous nuclei, deep-dark staining<br>– Cells are usually grouped in cohesive sheets of variable size | | – Small-cell carcinoma |

## Normal Cytology and Benign Cellular Components (Selected Entities) (continued) Sect. 2.1.3, p. 110

### Alveolar Macrophage

| Basic cell pattern | Particular and/or additional features | Differential diagnosis or possible diagnostic pitfall |
|---|---|---|
| – Large polyhedral cells, frequent bi- and multinucleated<br>– Nuclei excentric and typically bean-shaped<br>– Loose thinly dispersed chromatin<br>– One or multiple small but distinct nucleoli<br>– Abundant and foamy cytoplasm<br>– Various types of phagocytized material | – Numerous sharply outlined small and large cytoplasmic vacuoles | – Lipid pneumonia<br>– Adenocarcinoma<br>– Liposarcoma |

### Epithelioid Histiocytes

| Basic cell pattern | Particular and/or additional features | Differential diagnosis or possible diagnostic pitfall |
|---|---|---|
| – Mononucleated elongated histiocytoid elements<br>– Typically elongated nucleus with one end broader than the other<br>– Nuclei with bland chromatin and characteristic configuration | – Variable cell, nucleus, and nucleolus size dependent on the cell activity<br>– Heavily activated epithelioid cells<br>– Heavily activated rounded epithelioid cells, densely aggregated | – Langerhans cells<br>– Clear cell carcinoma |

### Langhans-Type Giant Cells

| Basic cell pattern | Particular and/or additional features | Differential diagnosis or possible diagnostic pitfall |
|---|---|---|
| – Histiocytic giant cells with multiple elongated epithelioid nuclei, frequently horseshoe-like crowded together at the periphery of the cytoplasm | – Rare cytoplasmic asteroid bodies | |

## Abnormal and Atypical Epithelial Cells Sect. 2.1.4, p. 112

### Squamous Metaplasia

| Basic cell pattern | Particular and/or additional features | Differential diagnosis or possible diagnostic pitfall |
|---|---|---|
| – Monomorphic polygon-shaped immature squamous cells in monolayered cobblestone arrangement<br>– Dense cyanophilic cytoplasm, sharply outlined<br>– Perinuclear halo<br>– Nuclear structure usually dense and patternless, smooth membranes, frequent karyopyknosis, light-blue or gray coloring (in Pap-stain), | – Larger metaplastic squamous cells may show mild keratinization | |

### Atypical Squamous Metaplasia

| Basic cell pattern | Particular and/or additional features | Differential diagnosis or possible diagnostic pitfall |
|---|---|---|
| – Basic cell pattern as stated above, but<br>  – Increased N/C ratio<br>  – Nuclei are irregularly outlined showing granular chromatin, hyperchromasia and nucleoli | | |

## Abnormal and Atypical Epithelial Cells Sect. 2.1.4, p. 112 (continued)

### Mild Reactive Hyperplasia: Respiratory Cells (Bronchial, Terminal Bronchiolar) and Alveolar Lining Cells

| Basic cell pattern | Particular and/or additional features | Differential diagnosis or possible diagnostic pitfall |
|---|---|---|
| **Variants of cell aggregation:**<br>– Cohesive cell clusters with regularly arranged cells<br>– Small clusters with monolayered cells<br>– Large papilliform clusters with tightly packed cells (so-called Creola bodies)<br>– Typical: cytoplasmic and nuclear molding of adjoining cells<br>– Pale and reticular nuclei, inconspicuous irregularities<br>– Nucleoli enlarged but uniform and rounded<br>– Often highly vacuolated and mucus producing cytoplasm<br>– Focal preservation of ciliated respiratory cells | | – Bronchioloalveolar carcinoma<br>– Adenocarcinoma (primary and metastatic) |

### Severe Reactive Hyperplasia: Respiratory Cells (Bronchial, Terminal Bronchiolar) and Alveolar Lining Cells

| Basic cell pattern | Particular and/or additional features | Differential diagnosis or possible diagnostic pitfall |
|---|---|---|
| – The cells are considerably enlarged as compared to their normal counterparts<br>– N/C ratio normal or slightly increased<br>– Loose or tight cell clusters with irregular cell arrangement, loss of nuclear polarization, overlapping of cells and nuclei<br>– Three-dimensional papilliform or acinar cell groups – variable, cells show centroacinar nuclear clustering and clear and vacuolated cytoplasm protruding to the periphery. The contour of the clusters is sharply delineated or knobby<br>– Nuclear outlines are smooth or molded and cleaved – variable<br>– Loose or fine stippled chromatin, coarse clusters may occur<br>– Nucleoplasm may be clear or deep blue in color<br>– Significantly enlarged nucleoli, often pleomorphic, multiplicity is frequent<br>– Terminal plates and cilia are hardly ever observed<br>– Atypical squamous metaplasia – variable | | – Bronchioloalveolar carcinoma<br>– Adenocarcinoma (primary and metastatic) |
| | – N/C ratio and nuclear staining quality covering a wide range, combined with numerous scattered hyperplastic cells | – Malignant lymphoma<br>– Melanoma |

### Cellular Response to Irradiation and Chemotherapy: Respiratory Cells (Bronchial, Terminal Bronchiolar) and Alveolar Lining Cells

| Basic cell pattern | Particular and/or additional features | Differential diagnosis or possible diagnostic pitfall |
|---|---|---|
| – Strongly enlarged atypical cells<br>– Frequent multinucleation<br>– N/C ratio more or less in normal range<br>– Pleomorphic nuclei showing frequent indentations and grooves<br>– Chromatin texture: fine and coarse granules and thin strands separating empty nuclear areas from each other<br>– Sharply demarcated nuclear vacuoles<br>– Macronucleoli<br>– Cytoplasmic vacuoles – numerous and prominent | | – Malignant neoplasia |

## Endogenous and Exogenous Noncellular Components, and Nonhuman Cellular Components

Their morphology, differential diagnosis, and implications are discussed in Sect. 2.1.5, p. 115.

## Granulomatous and Infectious Diseases Sect. 2.1.6, p. 116

### Sarcoidosis

| Basic cell pattern | Particular and/or additional features | Differential diagnosis or possible diagnostic pitfall |
|---|---|---|
| – Epithelioid cells crowded together and interspersed with small lymphocytes<br>– Cell detritus is exceptional | | – Tuberculosis<br>– Epithelioid granulomatosis |

### Tuberculosis / Atypical Mycobacteriosis

| Basic cell pattern | Particular and/or additional features | Differential diagnosis or possible diagnostic pitfall |
|---|---|---|
| – Elongated notedly slender epithelioid cells<br>– Thinly elongated nuclei, frequently pyknotic<br>– Caseous necrosis – fine and coarse granules in an opaque background | | – Nonspecific granulomatous process<br>– Chronic inflammation<br>– Peritumoral reaction<br>– Necrotic malignant tumor |

### Nonspecific Viral Cell Alterations

| Basic cell pattern | Particular and/or additional features | Differential diagnosis or possible diagnostic pitfall |
|---|---|---|
| – Enlarged cells and enlarged hyperchromatic nuclei<br>– Bland chromatin texture<br>– Prominent nucleoli<br>– Normal N/C ratio<br>– Occasional multinucleation and nuclear inclusions<br>– Nuclear irregularities – variable | – Ciliocytophthoria | – Adenocarcinoma<br>– Tumor necrosis |

### Herpes Simplex Virus Infection

| Basic cell pattern | Particular and/or additional features | Differential diagnosis or possible diagnostic pitfall |
|---|---|---|
| – Bronchial epithelial cells enlarged and rounded, mono- or multinucleation, distinct small cytoplasmic rim<br>– Nuclei with characteristic ground-glass texture and/or eosinophilic inclusions<br>– Frequent nuclear molding<br>– Granular chromatin condensation at the nuclear periphery | | – Cancer cells |

### Cytomegalovirus Infection

| Basic cell pattern | Particular and/or additional features | Differential diagnosis or possible diagnostic pitfall |
|---|---|---|
| – Striking enlargement of cells containing a huge nucleus<br>– Nuclei with a single deep basophilic inclusion exhibiting inhomogeneous areas; the inclusions are surrounded by a clear halo (owl eye appearance),<br>– Condensed chromatin compressed against the nuclear membrane showing a pearl necklace-like configuration<br>– Intracytoplasmic, orangeophilic inclusions – variable | – Exceptional multinucleated giant cells with virus-induced changes | – Cancer cells |

### Respiratory Syncytial Virus Infection

| Basic cell pattern | Particular and/or additional features | Differential diagnosis or possible diagnostic pitfall |
|---|---|---|
| – Syncytial cell aggregates of enormous size<br>– Intracytoplasmic deeply stained inclusions with clear halos | | |

### Measles

| Basic cell pattern | Particular and/or additional features | Differential diagnosis or possible diagnostic pitfall |
|---|---|---|
| – Large multinucleated giant cells<br>– Tiny cytoplasmic and nuclear inclusion bodies | | |

## Granulomatous and Infectious Diseases Sect. 2.1.6, p. 116 (continued)

### *Candida Albicans* Infection

| Basic cell pattern | Particular and/or additional features | Differential diagnosis or possible diagnostic pitfall |
|---|---|---|
| – Round to oval yeast cells: single, in dyads, and forming long chains (referred to as pseudohyphae)<br>– Accompanying purulent infiltrate | | |

### Aspergillosis / Aspergilloma

| Basic cell pattern | Particular and/or additional features | Differential diagnosis or possible diagnostic pitfall |
|---|---|---|
| – Uniformly wide, and septate hyphae with rectangular branching<br>– Accompanying purulent infiltrate – variable | – Eosinophilic granulocytes (in exfoliative cytologic samples) | – **Allergic bronchopulmonary aspergillosis** |

### Mucormycosis

| Basic cell pattern | Particular and/or additional features | Differential diagnosis or possible diagnostic pitfall |
|---|---|---|
| – Hyphae with similar morphology as compared to Aspergillus<br>– Branching of the hyphae at 90°, **but mind the difference:** hyphae are nonseptate varying greatly in width<br>– Presence of conidiophores<br>– Usually pronounced neutrophilic infiltrate and detritus | | |

### *Pneumocystis jirovecii (carinii)*

| Basic cell pattern | Particular and/or additional features | Differential diagnosis or possible diagnostic pitfall |
|---|---|---|
| – Tiny spherical organisms (4–5 µm in diameter): the capsule is smooth and darkly stained, focal thickenings of the capsule<br>– Disintegrated cysts are deeply grooved, crescent shaped, or crinkled | – Cysts presenting as a dense, foamy mass are easily recognized<br>– **Scattered organisms and small numbers of organisms can be detected only with special stains !** | – Degenerating or washed out erythrocytes<br>– Yeast-form fungi (Candida, Histoplasma)<br>– Other organisms |

References concerning cytodiagnosis of pulmonary parasitic infections are indicated in Sect. 2.1.6.4, p. 118.

# Section 2.2
# Respiratory Tract: FNAB and Exfoliative Cytology

- Tumor-Like Lesions
- Benign Tumors
- Malignant Tumors

## Benign Tumors and Pseudotumorous Lesions of the Lung (Selected Entities)
Sect. 2.2.1, p. 134

### Squamous Cell Papilloma

| Basic cell pattern | Particular and/or additional features | Differential diagnosis or possible diagnostic pitfall |
|---|---|---|
| – Regular squamous cells of superficial and intermediate type<br>– Small basal cells may be present<br>– Nonkeratinizing squamous cells arranged in regular groups<br>– Minor cytoplasmic and nuclear irregularities – variable | – Koilocytosis may be present | |
| | – Distinct cytoplasmic and nuclear irregularities | – Squamous cell carcinoma |

### Mucinous Glandular Adenoma / Papilloma / Cystic Lesions

| Basic cell pattern | Particular and/or additional features | Differential diagnosis or possible diagnostic pitfall |
|---|---|---|
| Dissociated and/or clustered cells:<br>– Benign mucus-producing cells<br>– Goblet cells<br>– Squamous cell component – variable | | – Low-grade mucoepidermoid carcinoma |
| | – Chondromyxoid background | – Pulmonary hamartoma |

### Pulmonary Hamartoma

| Basic cell pattern | Particular and/or additional features | Differential diagnosis or possible diagnostic pitfall |
|---|---|---|
| Mesenchymal components:<br>– Fibrous tissue<br>– Fibromyxoid stroma<br>– Chondroid masses<br>– Smooth muscle cells and lipomatous tissue – sporadic<br>Epithelial components:<br>– Columnar cells ciliated and non-ciliated<br>– Mucin producing cells – variable<br>– Cellular atypia and detritus possible | – Predominant chondroid tissue | – Costochondral or bronchial cartilage<br>– Chondroma<br>– Other tumors with a distinct cartilage component |
| | – Predominant epithelial cells | – Low-grade epithelial tumor<br>– Mucinous cystadenoma<br>– Adenocarcinoma |
| | – Stellate cells scattered in a fibromyxoid background | – Peritumoral fibrosis<br>– Pseudotumor<br>– Low-grade spindle cell tumor |

## Benign Tumors and Pseudotumorous Lesions of the Lung (Selected Entities) Sect. 2.2.1, p. 134 (continued)

### Granular Cell Tumor

| Basic cell pattern | Particular and/or additional features | Differential diagnosis or possible diagnostic pitfall |
|---|---|---|
| – Usually abundant tumor cells (both in exfoliative and FNAB samples)<br>– Uniform large cells showing ill-defined borders and abundant, finely granular cytoplasm<br>– The fragile cells occur singly or grouped<br>– The nuclei are small and may be eccentrically positioned<br>– Bland granular chromatin<br>– Inconspicuous nucleoli<br>– Granular background material | | – Foamy alveolar macrophages<br>– Low-grade oxyphilic lesions primary or metastatic<br>– Malignant melanoma |

### Primary Lung Teratoma

| Basic cell pattern | Particular and/or additional features | Differential diagnosis or possible diagnostic pitfall |
|---|---|---|
| – Pattern of common cystic lesions comprising mature squamous cells | – Atypical squamous cells | – **Metastasis of an extrapulmonary germ cell tumor**, e.g., after successful therapy of the remote primary tumor<br>– Squamous cell carcinoma |

### Clear Cell Sugar Tumor

| Basic cell pattern | Particular and/or additional features | Differential diagnosis or possible diagnostic pitfall |
|---|---|---|
| – Polygonal and spindle-shaped cells: either solitary or arranged in irregular cohesive clusters<br>– Low N/C ratio,<br>– Oval to elongated nuclei with bland features comprising finely dispersed chromatin and smooth contours<br>– Stripped nuclei are frequent<br>– Abundant cytoplasm, vacuolated and granular (glycogen!)<br>– Delicate small vessels transgressing cell clusters | | – Clear cell carcinoma, both lung primary and metastases from many remote organs<br>– Mesenchymal tumor |

### Pulmonary Oncocytoma

| Basic cell pattern | Particular and/or additional features | Differential diagnosis or possible diagnostic pitfall |
|---|---|---|
| – Round to ovoid cells<br>– Granular and eosinophilic cytoplasm or condensed deeply eosinophilic stained cytoplasmic body<br>– Small bland nuclei | | – Oncocytic carcinoid<br>– Metastatic renal cell carcinoma, granular cell type and chromophobe type |

### Amyloid Tumor

| Basic cell pattern | Particular and/or additional features | Differential diagnosis or possible diagnostic pitfall |
|---|---|---|
| – Amorphous pale protein masses<br>– Congo-red stain positivity and apple-green birefringence<br>– Lymphoid infiltrate and foreign body giant cells – variable | | |

### Endometriosis

| Basic cell pattern | Particular and/or additional features | Differential diagnosis or possible diagnostic pitfall |
|---|---|---|
| – Usually highly cellular smears<br>– Glandular cells occur in sheets, syncytial clusters, and tubular formations<br>– Small to medium-sized cells<br>– Distinct nuclear wrinkled membranes<br>– Granular and evenly distributed chromatin<br>– Usually inconspicuous nucleoli<br>– Scant cyanophilic cytoplasm | | – Low-grade adenocarcinoma (primary or metastatic) |

## Benign Tumors and Pseudotumorous Lesions of the Lung (Selected Entities) Sect. 2.2.1, p. 134 (continued)

| Basic cell pattern | Particular and/or additional features | Differential diagnosis or possible diagnostic pitfall |
|---|---|---|
| | – Hemorrhagic background<br>– Hemosiderin-laden macrophages<br>– Detritus | – Hemorrhagic infarct of the lung<br>– Granulomatosis |
| | – Aggregates of fusiform stromal cells<br>– Nuclei of stromal cells exhibiting crowding and overlapping | – Granulomatosis<br>– Stromal neoplasia |
| | – Activated epithelial cells and/ or decidualized stromal cells | – Epithelial neoplasia |

### Inflammatory Pseudotumor

| Basic cell pattern | Particular and/or additional features | Differential diagnosis or possible diagnostic pitfall |
|---|---|---|
| – Proliferation of spindle cells and histiocytes<br>– Small and large stromal fragments – variable<br>– Reactive cell changes and atypias – variable<br>– Varying numbers of lymphoid cells and plasma cells | | – Various spindle cell lesions, benign and malignant |

## Malignant Tumors of the Lung Sect. 2.2.2, p. 138

### In-Situ Squamous Cell Carcinoma (SCC)

| Basic cell pattern | Particular and/or additional features | Differential diagnosis or possible diagnostic pitfall |
|---|---|---|
| – Single small cells of round to oval shape<br>– The nuclei exhibit obvious malignant features:<br>  – Dense granular chromatin structure<br>  – Hyperchromasia<br>  – Irregularity of the membrane<br>– Nucleoli – variable<br>– Most of the cells show densely keratinized cytoplasm<br>– Notably increased N/C ratio<br>– Rare necrosis and inflammatory infiltrates | | – Invasive SCC<br>– **Primary SCC of the oropharyngeal region** |

### Invasive Keratinizing SCC

| Basic cell pattern | Particular and/or additional features | Differential diagnosis or possible diagnostic pitfall |
|---|---|---|
| – Cells are obviously malignant including:<br>Extreme cellular polymorphism, varied cytoplasmic shape, typical tadpole cells<br>– N/C ratios from extremely high to extremely low<br>– Marked nuclear hyperchromasia<br>– Homogenized or clumped chromatin, often nucleoplasmic clearing<br>– Rarely visible nucleoli<br>– Cytoplasm:<br>Intense eosinophilia and orangeophilia or deep cyanophilic staining, hyaline appearance and concentric lamination, occasional keratin pearls and intercellular bridges<br>– Neoplastic cells occur singly and in loose groups, tissue fragments are commonly encountered in FNABs and brushings<br>– Usually tumor necrosis and a sanguineous smear background | | – Severely degenerated atypical metaplastic squames<br>– Squamous metaplasia with atypias/ dysplasia<br>– **Malignant squamous cells may occasionally mimic plant cells** |

## Malignant Tumors of the Lung Sect. 2.2.2, p. 138 (continued)

| Basic cell pattern | Particular and/or additional features | Differential diagnosis or possible diagnostic pitfall |
|---|---|---|
| | – Predominance of small, round SCC cells | – In-situ SCC |
| | – Highly elongated slender malignant squamous cells<br>– Small, deep-stained nuclei with smooth contour<br>– Eosinophilic cytoplasm | – Benign mesenchymal cells<br>– Smooth muscle fibers |
| | – Predominance of degenerating malignant squames | – Benign or malignant squamous cells with severe actinic change |

### SCC with Clear Nuclei

| Basic cell pattern | Particular and/or additional features | Differential diagnosis or possible diagnostic pitfall |
|---|---|---|
| – Large squamous cells exhibiting:<br>  – Broad lucid cytoplasm with hyaline appearance eosinophilic or cyanophilic staining<br>  – Pale vesicular nuclei showing inconspicuous chromatin texture, variably sized nucleoli, and indistinct membrane irregularities<br>– Necrosis is usually not pronounced | | – Benign regenerative squamous cells<br>– **Primary SCC in the oropharyngeal area** |

### Poorly Differentiated SCC

| Basic cell pattern | Particular and/or additional features | Differential diagnosis or possible diagnostic pitfall |
|---|---|---|
| – Keratinized tumor cells are sparse or completely absent<br>– Cyanophilic cytoplasm is sharply outlined, dense, and concentrically structured, varying irregular cytoplasmic vacuolization<br>– Pleomorphic nuclei with pronounced irregular outlines, indentations and cleaving<br>– Irregularly distributed and coarsely clumped chromatin<br>– Conspicuous polymorphous nucleoli<br>– Marked necrotic debris | | – Proliferative bronchial/alveolar epithelial cells<br>– Proliferative cells of histiocytic origin<br>– Poorly differentiated adenocarcinoma<br>– Large-cell undifferentiated carcinoma<br>– Mesothelioma (undifferentiated epithelial or sarcomatoid type)<br>– Secondary neoplasms: transitional cell Ca, amelanotic melanoma, large cell lymphoma |

### SCC, Small-Cell Variant

| Basic cell pattern | Particular and/or additional features | Differential diagnosis or possible diagnostic pitfall |
|---|---|---|
| – Small tumor cells with properties of malignant squamous cells<br>– Nuclei with coarse chromatin and prominent nucleoli<br>– Conspicuous cytoplasm, elongated and sharply outlined<br>– Occasional intercellular bridges, **only visible in loose tumor cell sheets and clusters** | | – Tumor composed of small-cell carcinoma and SCC |
| | – Obvious squamous differentiation is absent | – True small-cell pulmonary or metastatic carcinoma |

## Malignant Tumors of the Lung Sect. 2.2.2, p. 138 (continued)

### Adenocarcinoma, Conventional Type

| Basic cell pattern | Particular and/or additional features | Differential diagnosis or possible diagnostic pitfall |
|---|---|---|
| – Both single cells and clusters<br>– Syncytial cell groups, compact balls, true acini, or papillary fragments, possibly groups with radiating flower petal pattern<br>– Eccentrically placed nuclei, vesicular, variably lobulated, the nuclear membranes exhibit varied irregularities<br>– Chromatin finely granular or powdery, regularly dispersed<br>– One centrally placed macronucleolus<br>– Cytoplasm extremely variable in structure and size: Homogeneous, or foamy or vacuolated, huge vacuoles may lead to an eccentric position of the nucleus<br>– Cytoplasmic mucus inclusion – variable | **Well-differentiated pulmonary adenocarcinoma**:<br>– Monomorphic tumor cell pattern<br>– Minor nuclear atypia | – Reactive-regenerative bronchial/alveolar epithelium<br>– Bronchioloalveolar carcinoma |
| | **Poorly differentiated pulmonary adenocarcinoma:**<br>– Pleomorphic tumor cells<br>– Marked cell dissociation<br>– Tumor necrosis | – Large-cell cancer, primary and metastatic such as nonkeratinizing SCC, undifferentiated carcinoma, amelanotic melanoma, large-cell lymphoma |
| | **Mucinous pulmonary adenocarcinoma**<br>– Pronounced mucinous features | – Carcinomas of salivary gland type (bronchial gland origin)<br>– Metastatic mucinous cancer |

### Papillary Adenocarcinoma

| Basic cell pattern | Particular and/or additional features | Differential diagnosis or possible diagnostic pitfall |
|---|---|---|
| – Papillary fragments, fibrovascular cores<br>– Epithelial layer composed of low-columnar cells, or tall polygonal to columnar cells. Varied cellular atypia.<br>– Mucin production – variable | | – Bronchioloalveolar carcinoma |

### Bronchioloalveolar Carcinoma (BAC)

| Basic cell pattern | Particular and/or additional features | Differential diagnosis or possible diagnostic pitfall |
|---|---|---|
| – Cell groups and sparse single cells<br>– Small to medium-sized uniform cells<br>– Tightly packed spherical or papilliform clusters, flat sheets, and radiating flower-petal pattern<br>– Distinct depth of focus for the cells arranged in three-dimensional clusters, lack of nuclear overlapping<br>– Round to oval nuclei, extremely uniform in size: nuclear grooves are common, occasional cytoplasmic invaginations<br>– Powdery/fine granular, evenly distributed chromatin<br>– Indistinct nucleoli (with exceptions)<br>– Cytoplasm varies in volume from modest to abundant: homogeneous, granular, foamy, or coarsely vacuolated<br>– Clean background in cytologic preparations | – Occasional psammoma bodies | – **Pronounced regenerative bronchiolar/ alveolar epithelium**<br>– Low-grade mucoepidermoid carcinoma<br>– Papillary carcinomas – primary and metastatic<br>– Metastatic adenocarcinoma |
| | – Clear nuclei<br>– Marked nuclear grooves and vacuoles<br>– Distinct fine granular, powdery, evenly distributed chromatin | – **Particular metastatic carcinomas** such as breast cancer, clear cell renal cell carcinoma, well-differentiated papillary transitional and papillary thyroid carcinoma |
| | – Only few scattered BAC cells | – **Activated histiocytes/ macrophages** |

## Malignant Tumors of the Lung Sect. 2.2.2, p. 138 (continued)

| Basic cell pattern | Particular and/or additional features | Differential diagnosis or possible diagnostic pitfall |
|---|---|---|
| | **BAC of mucinous type:**<br>– Numerous mucus producing cells<br><br>**Poorly differentiated BAC:**<br>– Polymorphic tumor cells | – Mucinous cell hyperplasia<br><br>– Primary poorly differentiated adenocarcinoma of common type<br>– Metastatic adenocarcinomas |

### Large-Cell Undifferentiated Carcinoma

| Basic cell pattern | Particular and/or additional features | Differential diagnosis or possible diagnostic pitfall |
|---|---|---|
| – Preponderance of very large single cells, occasionally tumor cells in a syncytial arrangement<br>– Giant cells<br>– High N/C ratio<br>– Highly abnormal nuclear contour, cleaved and lobulated<br>– Irregularly dispersed chromatin as strands and clusters<br>– Hyperchromatic or pale parachromatin<br>– Large and pleomorphic nucleoli varying from cell to cell<br>– Cytoplasm is frequently ill defined and variably stained<br>– Tumor necrosis | | – Cell changes due to chemotherapy/irradiation<br><br>– Metastatic undifferentiated carcinoma<br><br>– Mesothelioma (undifferentiated epithelial or sarcomatoid type)<br><br>– Amelanotic melanoma<br>– Sarcoma<br>– Large-cell lymphoma |

### Adenosquamous Carcinoma

| Basic cell pattern | Particular and/or additional features | Differential diagnosis or possible diagnostic pitfall |
|---|---|---|
| Tumor composed of two different cell types:<br>– Malignant squamous cells with keratinization<br>– Adenocarcinoma cells with mucin secretion | | |

### Small-Cell Carcinoma, Oat Cell Type

| Basic cell pattern | Particular and/or additional features | Differential diagnosis or possible diagnostic pitfall |
|---|---|---|
| – Tumor cells 1.5 to 2 times the size of a lymphocyte<br>– Tumor cells individually distributed or arranged in small tight clusters, or in linear single-file pattern<br>– Round nuclei with wrinkled membrane or nuclei with extremely irregular shape and outline<br>– Very dense and evenly distributed salt and pepper chromatin<br>– Hyperchromasia or dyschromasia<br>– Nucleoli are usually absent or inconspicuous<br>– Cytoplasm as thin cyanophilic rim<br>– Intercellular molding of cells and nuclei and nuclear compression<br>– Apoptosis and tumor necrosis are frequent | | – Basal cell hyperplasia<br><br>– Carcinoid tumor<br>– Merkel cell carcinoma |

### Small-Cell Carcinoma, Intermediate Cell Type

| Basic cell pattern | Particular and/or additional features | Differential diagnosis or possible diagnostic pitfall |
|---|---|---|
| – Same basic cytologic features as stated for oat cell tumor type as to nuclear shape, nuclear outline, chromatin texture, and staining properties but:<br>  – Slightly enlarged cells<br>  – Conspicuous nucleoli<br>  – Distinct cytoplasmic body, often elongated | | – Poorly differentiated nonkeratinizing SCC of small-cell variant<br>– Malignant lymphoma<br>– Carcinoid tumors |
| | – Distinct fusiform cell pattern | – Varied spindle cell tumors such as spindle cell SCC, benign or malignant stromal tumor, non pigmented spindle cell melanoma, spindle cell carcinoid |

## Malignant Tumors of the Lung Sect. 2.2.2, p. 138 (continued)

### Carcinomas of the Salivary Gland Type

| Basic cell pattern | Particular and/or additional features | Differential diagnosis or possible diagnostic pitfall |
|---|---|---|
| **The basic cytologic features of these tumors are briefly discussed in Sect. 2.2.2.7, p. 146, and described in detail in Sect. 5.1.5, p. 414.** | | |
| – **Adenoid cystic carcinoma** | | – Well-differentiated adenocarcinomas of the lung<br>– Carcinoid (endocrine tumors composed of a pure epithelial small-cell component)<br>– Mucin-producing adenocarcinomas with cribriform pattern |
| – **Mucoepidermoid carcinoma, low grade** | | – Mucus gland adenoma<br>– Bronchioloalveolar carcinoma<br>– Mucinous adenocarcinomas – primary and metastatic |
| – **Mucoepidermoid carcinoma, high grade** | | – Adenosquamous carcinoma, SCC |

### Lung Metastasis: Breast Carcinoma

| Basic cell pattern | Particular and/or additional features | Differential diagnosis or possible diagnostic pitfall |
|---|---|---|
| – Small to medium-sized fairly monomorphic tumor cells<br>– Nuclei with irregular shape and deep grooves<br>– Fine granular and pale chromatin<br>– Inconspicuous nucleoli<br>– Single-file tumor cell arrangement | | – Bronchioloalveolar carcinoma<br>– **Other secondary carcinomas with akin nuclear features** such as papillary carcinoma of the thyroid, renal cell carcinoma, and others |

### Lung Metastasis: Colon Carcinoma

| Basic cell pattern | Particular and/or additional features | Differential diagnosis or possible diagnostic pitfall |
|---|---|---|
| – Malignant cells with distinct columnar shape arranged in small and large tightly palisaded clusters<br>– Hyperchromatic and coarsely structured nuclei<br>– Frequent pleomorphic tumor cell detritus | | – Papillary adenocarcinoma of the lung |

### Lung Metastasis: Poorly Differentiated Transitional Cell Carcinoma

| Basic cell pattern | Particular and/or additional features | Differential diagnosis or possible diagnostic pitfall |
|---|---|---|
| – Large cells with pleomorphic nuclei<br>– Large nucleoli<br>– Dense cyanophilic cytoplasm, vague concentric lamellation may occur<br>– Pronounced necrotic debris | | – Poorly differentiated, nonkeratinizing SCC (primary and metastatic)<br>– Secondary high-grade cancer |

### Lung Metastasis: Adenocarcinoma of the Prostate

| Basic cell pattern | Particular and/or additional features | Differential diagnosis or possible diagnostic pitfall |
|---|---|---|
| – Monomorphous, medium-sized to large tumor cells<br>– Distinctive round nuclei<br>– Single pronounced nucleolus<br>– Evenly distributed granular chromatin<br>– Regular tumor cell arrangement | | – Atypical carcinoid |

## Malignant Tumors of the Lung Sect. 2.2.2, p. 138 (continued)

### Lung Metastasis: Amelanotic Malignant Melanoma

| Basic cell pattern | Particular and/or additional features | Differential diagnosis or possible diagnostic pitfall |
|---|---|---|
| – Large undifferentiated tumor cells, rare cell clustering<br>– Pleomorphic nuclei, nuclear inclusions, clumped chromatin<br>– Huge nucleoli<br>– Cytoplasm: variable in size | | – Poorly differentiated SCC<br>– Poorly differentiated adenocarcinoma<br>– Undifferentiated lung carcinoma<br>– Nonepithelial cancer / mesothelioma<br>– Large-cell lymphoma |

### Lung Metastasis: Pigmented Malignant Melanoma

| Basic cell pattern | Particular and/or additional features | Differential diagnosis or possible diagnostic pitfall |
|---|---|---|
| – Same basic cytologic features as stated above<br>– Intracytoplasmic melanin pigment | | – Atypical carcinoid tumor – with melanin production |

### Lung Metastasis: Sarcoma

| Basic cell pattern | Particular and/or additional features | Differential diagnosis or possible diagnostic pitfall |
|---|---|---|
| – Large undifferentiated tumor cells<br>– Pleomorphic nuclei and nucleoli<br>– Varied chromatin patterns<br>– Cytoplasm : variable, often elongated and spindle-shaped | – Tight tumor cell clustering | – Primary pulmonary sarcoma<br>– Spindle cell carcinoma of lung<br>– Sarcomatoid type mesothelioma<br>– Undifferentiated carcinoma (primary or secondary) ! |

Other rare primary tumors of the lung and malignant lymphoid/myelogenic tumors are discussed in Sects. 2.2.2.8, p. 146, and 2.2.2.9, respectively, p. 147.

## Neuroendocrine Lung Tumors Sect. 2.2.3, p. 149

### Typical Carcinoid and Tumorlet

| Basic cell pattern | Particular and/or additional features | Differential diagnosis or possible diagnostic pitfall |
|---|---|---|
| – Uniformity of neoplastic cells throughout the smear<br>– Tumor cells appear singly, in loose sheets or in three-dimensional cohesive clusters<br>– Numerous cell clusters with acinar and rosette cell formation- Occasionally nests of small spindle cells<br>– Round to ovoid shaped small to medium-sized cells and nuclei<br>– Variable N/C ratio<br>– Occasional greatly enlarged tumor cells<br>– Nuclei are usually eccentrically located giving the cell a plasma cell-like appearance<br>– Fine granular chromatin pattern, inconspicuous nucleoli<br>– Medium-sized rim of fine granular basophilic or eosinophilic cytoplasm<br>– Very few mitoses, necrosis is absent | – Numerous isolated monomorphous tumor cells<br>– Single-file cell arrangement of the tumor cells exhibiting small cytoplasmic rims | – Adenoid cystic carcinoma lacking hyaline globules<br>– Metastatic monomorphic small cell adenocarcinomas (e.g., from the breast)<br>– Low-grade non-Hodgkin lymphoma<br>– Small-cell lung carcinoma |

Cells of tumorlets: very uncommon in cytologic samples

## Neuroendocrine Lung Tumors Sect. 2.2.3, p. 149 (continued)

### Atypical Carcinoid

| Basic cell pattern | Particular and/or additional features | Differential diagnosis or possible diagnostic pitfall |
|---|---|---|
| – Same cytological features as listed above, but:<br>– Pronounced cellular polymorphism<br>– Cells more frequently spindle-shaped<br>– Nuclei more irregular in shape, occasionally molded<br>– Coarse chromatin<br>– Hyperchromasia<br>– Distinct nucleoli<br>– Common mitotic figures and necrosis | | – Squamous cell carcinoma, small-cell variant<br>– Adenocarcinoma<br>– Mucoepidermoid carcinoma lacking mucus production<br>– Prostatic carcinoma, small-cell type<br>– Mesenchymal neoplasms<br>– Amelanotic melanoma of small spindle cell type<br>– Plasmacytoid malignant non-Hodgkin lymphoma<br>– Paraganglioma, small-cell, epitheloid type |
| | – Cytoplasmic melanin inclusions (uncommon) | – Pigmented melanoma of small spindle cell type |
| | – Single-file cell arrangement of the tumor cells and tight clustering | – Small-cell lung carcinoma, intermediate cell type |

### Large-Cell Neuroendocrine Carcinoma

| Basic cell pattern | Particular and/or additional features | Differential diagnosis or possible diagnostic pitfall |
|---|---|---|
| – Hypercellular smears<br>– Tumor cells of medium to large size, numerous single tumor cells and stripped nuclei<br>– Three-dimensional tumor cell clusters, focally peripheral palisading, and occasionally rosette-like formations<br>– Giant cells – variable<br>– Pleomorphic nuclei with irregular contours, frequent molding<br>– Fine or coarse granular chromatin<br>– Usually single and prominent nucleoli<br>– Cytoplasmic bodies varying in size, occasional granulation<br>– Apoptosis, necrosis, and mitotic figures are common | | – Poorly differentiated SCC<br>– Poorly differentiated adenocarcinoma, primary and metastatic<br>– Prostatic adenocarcinoma, large-cell type |

# Section 2.4
# Mediastinum

2

## Cytology of Nontumorous Mediastinal Disorders (Selected Entities) Sect. 2.4.2, p. 206

### Acute Mediastinitis

| Basic cell pattern | Particular and/or additional features | Differential diagnosis or possible diagnostic pitfall |
|---|---|---|
| – Abundant frequently degenerating neutrophilic granulocytes<br>– Debris<br><br>**An adequate proportion of the cytologic sample should be used for microbiological testing!** | | |

### Florid Inflammatory/Infectious Granulomatosis

| Basic cell pattern | Particular and/or additional features | Differential diagnosis or possible diagnostic pitfall |
|---|---|---|
| – Cells and tissue fragments of granulomatous tissue | | – Granulomatosis associated with cancer such as germ cell tumors, Hodgkin- and non-Hodgkin lymphoma |

### Sarcoidosis

| Basic cell pattern | Particular and/or additional features | Differential diagnosis or possible diagnostic pitfall |
|---|---|---|
| – Epithelioid cells, often activated<br>– Giant cells of Langhans type<br>– Occasionally caseating necrosis<br>– Lymphocytes | – Marked caseating detritus | – Atypical mycobacteriosis<br><br>– Tuberculosis/atypical mycobacteriosis |

### Fibrotic and Sclerotic Inflammatory Process

| Basic cell pattern | Particular and/or additional features | Differential diagnosis or possible diagnostic pitfall |
|---|---|---|
| – Hypocellular aspirate<br>– Few stromal cells<br>– Small fragments of fibrotic tissue | | – Neoplasms with a sclerotic component such as<br>  – Sarcomas<br>  – Hodgkin lymphoma of nodular sclerosing type<br>  – Sclerosing non-Hodgkin lymphoma |

### Bronchogenic Cyst

| Basic cell pattern | Particular and/or additional features | Differential diagnosis or possible diagnostic pitfall |
|---|---|---|
| – Ciliated columnar cells and cuboidal cells<br>– Squamous metaplastic cells<br>– Small bronchial glands<br>– Occasional calcification<br>– Smooth muscle cells and cartilage<br>– Birefringent, needle-shaped crystals – variable | – Inflammatory background, debris, cholesterol crystals | – Esophageal cyst<br><br>– Thymic cyst |

### Esophageal Cyst

| Basic cell pattern | Particular and/or additional features | Differential diagnosis or possible diagnostic pitfall |
|---|---|---|
| – Same elements as in bronchogenic cyst fluid, except cartilage | | – Bronchogenic cyst<br>– Thymic cyst |

## Cytology of Nontumorous Mediastinal Disorders (Selected Entities) (continued) Sect. 2.4.2, p. 206

### Gastroenteric Cyst

| Basic cell pattern | Particular and/or additional features | Differential diagnosis or possible diagnostic pitfall |
|---|---|---|
| – Gastric-type and intestinal-type epithelium<br>– Mucin-secreting cells<br>– Ciliated columnar cells | | |

### Pericardial/Mesothelial Cyst

| Basic cell pattern | Particular and/or additional features | Differential diagnosis or possible diagnostic pitfall |
|---|---|---|
| – Watery and clear fluid, usually acellular<br>– Regular flattened sheets of large polygonal cells with bland nuclei | | |

### Cystic Fluid Comprising Pancreatic Tissue

| Basic cell pattern | Particular and/or additional features | Differential diagnosis or possible diagnostic pitfall |
|---|---|---|
| – Cystic background<br>– Typical pancreatic tissue fragments: ducts, acini and islet cells | | – Teratoma with pancreatic tissue<br>– Pancreatic pseudocyst distending into the mediastinal space |

Mediastinal deposits and other congenital cysts, acquired cystic disorders, and thymic cysts: see sections concerned.

## Thymus Gland and Its Diseases (Selected Entities) Sect. 2.4.3, p. 208

### Thymoma

| Basic cell pattern | Particular and/or additional features | Differential diagnosis or possible diagnostic pitfall |
|---|---|---|
| **Epithelial cells (epithelioid type)**<br>– Round to oval, variable in size<br>– Bland nuclei with smooth outline and pale chromatin<br>– Crowded nuclei and cytoplasmic invaginations – variable<br>– Distinct but small nucleoli<br>– Cytoplasm varies from scant to medium-sized showing indistinct borders; clear and delicate, or densely structured and squamoid<br>**Epithelial cells (spindle type), common, but in minority**<br>– Elongated cytoplasm and nuclei<br>– Nuclei are regular with evenly distributed chromatin<br>**Lymphoid cells**<br>– Predominantly small lymphocytes of mature T phenotype<br>– Occasionally activated lymphocytes<br>-– Plasma cells – extremely uncommon<br>**Other elements**<br>– Clear cells with abundant pale cytoplasm – variable<br>– Hassall corpuscles – occasionally present<br>– Foam cells<br>– Fibrotic tissue fragments<br>– Calcification<br>– No mitotic activity | – Predominant epithelioid component<br>– Predominant small-cell component<br>– Predominant spindle cell component<br>– Predominant lymphocytic component | – Thyroid papillary carcinoma<br>– Germinomas, embryonal carcinoma<br>– Thymic carcinoid<br>– Metastatic carcinomas/melanoma<br>– Non-Hodgkin lymphomas<br>– Small-cell carcinoma<br>– Neuroblastoma/paraganglioma<br>– Granuloma and cell-rich fibrotic lesion<br>– Sarcomas, nerve sheath tumors<br>– Spindle cell squamous carcinoma<br>– Spindle cell melanoma, nonpigmented<br>– Spindle cell carcinoid<br>– Non-Hodgkin lymphoma |

## Thymus Gland and Its Diseases (Selected Entities) Sect. 2.4.3, p. 208 (continued)

### Invasive Thymoma

| Basic cell pattern | Particular and/or additional features | Differential diagnosis or possible diagnostic pitfall |
|---|---|---|
| – Clearly predominant epithelioid cell pattern (as stated above)<br>– Nuclear enlargement and pronounced nucleoli<br>– Mitotic activity | | |

Thymic Carcinoma, see Sect. 2.4.3.4.3, p. 211.

### Thymic Carcinoid

| Basic cell pattern | Particular and/or additional features | Differential diagnosis or possible diagnostic pitfall |
|---|---|---|
| – Cellular smears<br>– Single cells and cell clusters<br>– Round to oval nuclei, fine granular chromatin<br>– Scant granular cytoplasm<br>– Sporadic fusiform tumor cells | – Usually scattered very large tumor cells exhibiting abundant granular cytoplasm and macronucleoli<br><br>– Marked apoptosis and pyknosis | – Thymoma<br>– Adenocarcinoma<br>– Large-cell carcinoma<br><br>– **Do not misinterpret as lymphoid cells of a thymoma!** |

### Thymic Spindle Cell Carcinoid

| Basic cell pattern | Particular and/or additional features | Differential diagnosis or possible diagnostic pitfall |
|---|---|---|
| – Abundant spindle-shaped tumor cells (same nuclear and cytoplasmic texture as stated above) | | – A variety of spindle cell lesions (benign and malignant) |

### Benign Teratoma

| Basic cell pattern | Particular and/or additional features | Differential diagnosis or possible diagnostic pitfall |
|---|---|---|
| – Mature squamous cells<br>– Squamous cell detritus<br>– Sebaceous cells<br>– Cells of mesodermal/entodermal origin – possible<br>– Granulomatous tissue, foreign body giant cells and calcification – variable | | – Other cystic lesions of the mediastinum |

### Seminoma (Germinoma)

| Basic cell pattern | Particular and/or additional features | Differential diagnosis or possible diagnostic pitfall |
|---|---|---|
| – Highly cellular smears<br>**Dual cell population:** large monomorphic frankly malignant tumor cells mainly discohesive, and reactive lymphocytes/mature plasma cell<br>– Tumor cells having large vesicular nuclei, membrane irregularities and hyperchromasia<br>– One or multiple prominent nucleoli<br>– The cytoplasm is usually scanty: well-defined margins with intermittent double-contour and thickening<br>– Naked nuclei<br>– Necrosis and tigroid background – variable<br>– Granulomatous tissue reaction – possible | – Sporadic histiocytic multinucleated giant cells | – Thymoma<br>– Undifferentiated large-cell carcinoma<br>– Non-Hodgkin lymphoma, large-cell type<br>– May mimic syncytiotrophoblasts ! |

Characteristics of Embryonal Carcinoma, Yolk Sac Tumor, Choriocarcinoma are provided in Sects. 12.3.7.2 and 12.3.7.3, p. 784.

## Benign and Malignant Lymphoid Disorders in Thymus and Mediastinal Lymph Nodes, Sect. 2.4.3.7, p. 214

### Castleman Disease: Angiofollicular Hyperplasia, Hyaline Vascular Variant

| Basic cell pattern | Particular and/or additional features | Differential diagnosis or possible diagnostic pitfall |
|---|---|---|
| – Small mature lymphocytes (B and T phenotype)<br>– Follicle center cells including immunoblasts<br>– Plasma cells and eosinophilic granulocytes<br>– Large atypical histiocytoid cells, irregular nuclear outline, distinct nucleoli, granular or coarse chromatin | | – Thymoma<br>– Hodgkin lymphoma |

### Castleman Disease: Angiofollicular Hyperplasia, Plasma Cell Type

| Basic cell pattern | Particular and/or additional features | Differential diagnosis or possible diagnostic pitfall |
|---|---|---|
| – Sheets of plasma cells and many follicle center cells originating from large germinal centers | | – Plasmacytoma |

### Lymphoblastic Non-Hodgkin Lymphoma

| Basic cell pattern | Particular and/or additional features | Differential diagnosis or possible diagnostic pitfall |
|---|---|---|
| – Cellular smears<br>– Monotonous-appearing lymphoblasts:<br>  – Tumor cells about twice the size of small lymphocytes<br>  – Nuclei with characteristic indentations and grooves<br>  – Granular and powdery chromatin<br>  – Inconspicuous nucleoli<br>– High mitotic rate<br>– Very small cytoplasmic rim<br>– Numerous tingible body macrophages<br>– Pronounced background necrosis | | |
| | – A considerable proportion of normal epithelial thymic tissue | – Lymphocyte-rich thymoma |

### Large-Cell Non-Hodgkin Lymphoma of the Mediastinum

| Basic cell pattern | Particular and/or additional features | Differential diagnosis or possible diagnostic pitfall |
|---|---|---|
| – Usually highly cellular aspirates<br>– Predominantly large atypical lymphocytes<br>– Small atypical lymphocytes in varying numbers<br>– Nuclei often cleaved and lobulated, frequent hyperlobulation<br>– Vesicular chromatin<br>– Prominent single or multiple nucleoli, sometimes huge<br>– Small cytoplasmic rims are often basophilic (MGG stain)<br>– N/C ratio strongly varying within the same tumor | | – Hodgkin lymphoma<br>– Thymic carcinoma<br>– Metastatic carcinoma<br>– Germinoma |
| | – A considerable proportion of normal epithelial thymic tissue | – Thymoma |
| | – Fragments of sclerotic tissue and mesenchymal spindle cells (dependent on the intensity of tumor sclerosis) | – **False-negative results or misdiagnoses**, see Sect. 2.4.3.7.3, p. 215. |

## Benign and Malignant Lymphoid Disorders in Thymus and Mediastinal Lymph Nodes, Sect. 2.4.3.7, p. 214 (continued)

### Hodgkin Lymphoma

| Basic cell pattern | Particular and/or additional features | Differential diagnosis or possible diagnostic pitfall |
|---|---|---|
| – **Often sparse cellular aspirates due to tumor sclerosis**<br>– Polymorphous lymphoid cell population: Small lymphocytes intermingled with atypical lymphoid elements, enlarged irregular nuclei, hyperchromatic, pronounced nucleoli, indistinct cytoplasm<br>– Plasma cells, eosinophils, and histiocytes are common<br>**Specific tumor cells (HRS cells):**<br>– Mononuclear Hodgkin cells and<br>– Reed-Sternberg cells: huge cells with at least two large, mirror-image nuclei, mild hyperchromasia, red-colored comma-shaped nucleoli, densely packed and evenly distributed fine granular chromatin | | |
| | – Predominant benign and atypical lymphocytes<br>– Sporadic HRS cells | – Benign reactive lymphocytic population<br>– Non-Hodgkin lymphoma |
| | – Numerous HRS cells | – Castleman disease<br>– Large-cell non-Hodgkin lymphoma of the mediastinum<br>– Germ cell tumors<br>– Pleomorphic carcinoma, metastatic |
| | – Occasionally marked epithelioid cell granulomatosis | – Granulomatous inflammation |
| | – Pronounced cystic changes of the Hodgkin lymphoma and a few lymphoid cells and ambiguous HRS cells | – Any mediastinal cystic lesion |

# Chapter 3 Effusions

## Section 3.1
## Pleural – Pericardial – Peritoneal – Tunica Vaginalis Testis

– Benign and Equivocal Lesions

### Benign Mesothelial Cells and Histiocytes / Common Effusion Sect. 3.1.2 and 3.1.3, p. 242

#### Mesothelial Cells

| Basic cell pattern | Particular and/or additional features | Differential diagnosis or possible diagnostic pitfall |
|---|---|---|
| – Dense cytoplasm with a fading, finely vacuolated periphery<br>– Nucleus is often positioned eccentrically, distinct smooth membranes, typical kidney shape<br>– Loose and evenly distributed chromatin<br>– Distinct rounded nucleoli variable in size<br>– Often cell pairs and short chains with empty windows between the cells<br>– Smoothly contoured three-dimensional cell clusters – variable<br>– Sporadic cores of homogeneous collagen | | |
| | – Strong cytoplasmic vacuolization | – Carcinoma cells containing mucus/ signet ring cells |
| | – Irregular dense cytoplasm, dark-red staining (Pap stain), and deep-dark staining pyknotic nuclei, and irregular nuclear outline | – **Degenerate mesothelial cells**<br>– Squamous cell carcinoma |

#### Activated Mesothelial Cells/Mesothelial Proliferation

| Basic cell pattern | Particular and/or additional features | Differential diagnosis or possible diagnostic pitfall |
|---|---|---|
| – Same cell pattern as stated above, but:<br>Cells showing enlargement, rounded nuclei, multinucleation, and very prominent nucleoli<br>– Papillary clusters and three-dimensional spheres with irregular outlines, blackberry-like! | | – Markedly activated histiocytes showing tight clustering<br>– Monomorphic mesothelioma<br>– Carcinoma |
| | – Cells strongly enlarged, vacuolized and bizarrely shaped, high N/C ratio, cleaved and folded nuclei, pleomorphic nucleoli | – Large-cell carcinoma<br>– Large-cell anaplastic lymphoma<br>– Sarcoma |

#### Histiocytes

| Basic cell pattern | Particular and/or additional features | Differential diagnosis or possible diagnostic pitfall |
|---|---|---|
| – Irregular foamy or dense cytoplasm<br>– Nuclear polymorphism with distinct indentations<br>– Bright nucleoplasm, fine chromatin<br>– Small round nucleoli | | – Mesothelial cells |

#### Benign effusion, Common Appearance

| Basic cell pattern | Particular and/or additional features | Differential diagnosis or possible diagnostic pitfall |
|---|---|---|
| **Mixed cell pattern:**<br>– Typical mesothelial cells<br>– Histiocytes<br>– Neutrophils, lymphocytes<br>– A few eosinophils | | |

## Particular Leukocytic and Histiocytic Patterns Sects. 3.1.4–3.1.7, p. 243

### Acute Inflammation and Empyema

| Basic cell pattern | Particular and/or additional features | Differential diagnosis or possible diagnostic pitfall |
|---|---|---|
| – Preponderance of neutrophilic granulocytes | – Markedly degenerated neutrophils | – Empyema |

### Eosinophilic Effusion

| Basic cell pattern | Particular and/or additional features | Differential diagnosis or possible diagnostic pitfall |
|---|---|---|
| – Cell pattern of benign effusions, but: **> 10% eosinophilic granulocytes** | | |

### Benign Reactive Lymphocytosis, NOS

| Basic cell pattern | Particular and/or additional features | Differential diagnosis or possible diagnostic pitfall |
|---|---|---|
| – Cell pattern of benign effusions, but: **≥ 50% lymphocytes**<br>– Reactive changes of the lymphocytes – variable<br>– Benign lymphoid blasts – variable | | – Malignant NHL with minor blastic cell component<br>– Hodgkin lymphoma, absence of HRS cells in effusion |

### Benign Reactive Lymphocytosis with Marked Lymphocytic Transformation

| Basic cell pattern | Particular and/or additional features | Differential diagnosis or possible diagnostic pitfall |
|---|---|---|
| – Pure reactive lymphoid cell population with benign but atypical lymphoid blasts | | – B-cell NHL with a proportion of blastic tumor cells<br>– Blast-type NHL with pronounced hyperplasia of benign T cells<br>– Marked T-cell hyperplasia intermingled with large carcinoma cells |

### Florid Pleural Tuberculosis

| Basic cell pattern | Particular and/or additional features | Differential diagnosis or possible diagnostic pitfall |
|---|---|---|
| – Monotonous pure lymphoid cell population consisting of exclusively small benign lymphocytes:<br>  – Slightly enlarged<br>  – Small centrally placed nucleoli in about 50% of all nuclei | **Epithelioid histiocytes, Langhans giant cells, and caseous debris are virtually always absent** | – Small lymphocytic lymphoma / chronic lymphatic leukemia |

### Liver Cirrhosis

| Basic cell pattern | Particular and/or additional features | Differential diagnosis or possible diagnostic pitfall |
|---|---|---|
| – Mainly small histiocytes with polymorphic but otherwise bland nuclei and hyaline cyanophilic cytoplasmic inclusions<br>– Enhanced phagocytic activity<br>– Mesothelial cells and leukocytes – variable<br>– Mesothelial cells usually exhibit hyperplastic changes | | |

### Cyst Content

| Basic cell pattern | Particular and/or additional features | Differential diagnosis or possible diagnostic pitfall |
|---|---|---|
| – Numerous large histiocytoid foam cells<br>– Absence of typical effusion-background (mesothelial cells and leukocytes)<br>– Cholesterol deposits – variable | | – Histiocytosis X |

## Particular Leukocytic and Histiocytic Patterns Sects. 3.1.4–3.1.7, p. 243 (continued)

### Rheumatoid Serositis

| Basic cell pattern | Particular and/or additional features | Differential diagnosis or possible diagnostic pitfall |
|---|---|---|
| – **Spindle cells often exhibiting multiple deep-staining nuclei**<br>– Histiocytes<br>– Langhans giant cells<br>– Cellular degeneration and debris | | – (Spindle cell) neoplasia |

### Effusion After Surgery

| Basic cell pattern | Particular and/or additional features | Differential diagnosis or possible diagnostic pitfall |
|---|---|---|
| – Granuloma fragments and lymphocytes | | – Sarcoidosis |

## Crystalline Deposits Sect. 3.1.8, p. 247

### Immunoglobulins

| Basic cell pattern | Particular and/or additional features | Differential diagnosis or possible diagnostic pitfall |
|---|---|---|
| – Refractile bright green-yellow bar-like and needle-like elements, mainly intracytoplasmic in histiocytes and mesothelial cells | | |

### Cholesterol

| Basic cell pattern | Particular and/or additional features | Differential diagnosis or possible diagnostic pitfall |
|---|---|---|
| – Extracellular birefringent crescents and plates | – Fluid from the abdominal cavity containing cholesterol deposits | – **most likely cystic lesion;** check the cellular background! |

## Background Material Sects. 3.1.9 and 3.1.10, p. 247

### Detritic Background

| Basic cell pattern | Particular and/or additional features | Differential diagnosis or possible diagnostic pitfall |
|---|---|---|
| – Cell degeneration<br>– Necrosis | | – Rheumatoid pleuritis: look for the typical cells!<br>– Tumor necrosis: undifferentiated malignant neoplasm most likely of epithelial or lymphatic origin |

### Mucoid Masses

| Basic cell pattern | Particular and/or additional features | Differential diagnosis or possible diagnostic pitfall |
|---|---|---|
| – Mucus as background in smears without tumor cells | | – Content of a simple mucinous cyst<br>– Common in pseudomyxoma peritonei<br>– Extremely rare in mucinous adenocarcinomas |
| | – Mucinous cells showing bland morphology or mild atypias | – Pseudomyxoma peritonei<br>– Metastatic well-differentiated mucinous adenocarcinoma |
| | – Clearly atypical or malignant mucinous cells | – Mucinous adenocarcinoma |

## Rare Events Including Unexpected Cell Sampling from Neighboring Organs

See Sect. 3.1.11, p. 247.

# Section 3.2
# Pleural – Pericardial – Peritoneal – Tunica Vaginalis Testis

## – Malignant Lesions



## Primary Neoplasms of the Serosal Membranes Sects. 3.2.1 and 3.2.2, p. 260

### Epithelial Mesothelioma

| Basic cell pattern | Particular and/or additional features | Differential diagnosis or possible diagnostic pitfall |
|---|---|---|
| – Tumor cells basically exhibit the same morphologic features as benign mesothelial cells, but:<br>– Cellular enlargement compared with benign mesothelial cells<br>– Irregular nuclear outline<br>– Dense granular and coarse chromatin<br>– Hyperchromasia<br>– Often prominent nucleolus<br>– Abundant cytoplasm with peripheral vacuolization and fading<br>– Cell clusters: ball- or morula-like, faint hobnail contour, central homogeneous hyaline cores | – Sporadic psammoma bodies | – Different types of adenocarcinoma (see metastases, Sect. 3.2.3, p. 263)<br>– Rare tumor types, such as endocrine tumors |

### Well-Differentiated Peritoneal Papillary Mesothelioma

| Basic cell pattern | Particular and/or additional features | Differential diagnosis or possible diagnostic pitfall |
|---|---|---|
| – Same cell pattern as stated above<br>– Papillary fragments | **In females:**<br>– Psammoma bodies accompanying papillary tumors in abdominal fluids | – Metastatic papillary carcinoma<br>– Ovarian and peritoneal serous papillary carcinoma |

### Small-Cell Variant of Mesothelioma

| Basic cell pattern | Particular and/or additional features | Differential diagnosis or possible diagnostic pitfall |
|---|---|---|
| – Tumor cells of undifferentiated small-cell type | | – Small-cell cancer particularly of pulmonary origin<br>– Small round cell tumors<br>– Malignant lymphoma |

### Mesothelioma with Single Cell Degeneration and Mesothelioma with Squamous Differentiation

| Basic cell pattern | Particular and/or additional features | Differential diagnosis or possible diagnostic pitfall |
|---|---|---|
| – Cells of malignant mesothelioma as described above<br>– Cells with polymorphous red-stained cytoplasm and deep-staining polymorphic nuclei (Pap-stain) – variable | | – Metastatic squamous cell carcinoma |

### Sarcomatous mesothelioma

| Basic cell pattern | Particular and/or additional features | Differential diagnosis or possible diagnostic pitfall |
|---|---|---|
| – Oval to spindle-shaped neoplastic cells, large and pleomorphic<br>– Irregular hyperchromatic nuclei<br>– Occasionally prominent giant cells<br>– Rare metaplastic osteoid or cartilage components | | – Miscellaneous malignant soft tissue tumors |

### Biphasic Malignant Mesothelioma

| Basic cell pattern | Particular and/or additional features | Differential diagnosis or possible diagnostic pitfall |
|---|---|---|
| **Biphasic cell pattern:** mesothelial tumor cells of epithelial and sarcomatous subtype | | – Biphasic sarcoma<br>– Spindle cell carcinoma<br>– Carcinosarcoma<br>– Carcinoma with atypical stromal reaction |

## Primary Neoplasms of the Serosal Membranes Secs. 3.2.1 and 3.2.2, p. 260 (continued)

### Primary Nonmesothelial Neoplasm: Primary Effusion Lymphoma (PEL)

| Basic cell pattern | Particular and/or additional features | Differential diagnosis or possible diagnostic pitfall |
|---|---|---|
| – Numerous large and polymorphic lymphoid blast cells, high N/C ratio<br>– Irregular nuclear outline<br>– Coarse chromatin<br>– Hyperchromasia<br>– Multiple pleomorphic nucleoli<br>– Small rim of cytoplasm – vacuolated or densely structured | **The diagnosis of PEL depends on distinct immunocytochemical and molecular genetic test results** | – Benign lymphoproliferative disorder, **in particular EBV-associated**!!<br>– Infiltrating blastic lymphoma |

## Tumors Spreading to Serosal Membranes (Direct Invasion / Metastases) Sect. 3.2.3, p. 263

### Selected Entities of the Most Frequent Metastatic Neoplasms Based on Their Cytoarchitectural and Cellular Characteristics

#### A. Adenocarcinomas Characterized by Three-dimensional Spheres and Papillary Clusters

| Basic cell pattern | Particular and/or additional features | Differential diagnosis or possible diagnostic pitfall |
|---|---|---|
| – Three-dimensional morulae and papillary clusters<br>– Clusters with **hobnail contour, rarely sharply delineated**<br>– Variable number of clusters with cores of homogeneous hyaline material<br>– Single tumor cells – variable<br>– Unambiguous malignant cells with variable N/C ratio<br>– Dense and finely granular or clumped chromatin<br>– Hyperchromasia<br>– Distinct nucleoli<br>– Cytoplasm irregularly outlined<br>– Possible mucoid component (cytoplasmic and/or background) | | Primary adenocarcinomas of<br>– Colon<br>– Stomach<br>– Gallbladder<br>– Endometrium<br>– Hyperplastic mesothelium<br>– Malignant mesothelioma |
| | – Striking **multinucleation** of the tumor cells | – Adenocarcinoma of lung |

#### B. Adenocarcinomas characterized by slender papillary clusters

| Basic cell pattern | Particular and/or additional features | Differential diagnosis or possible diagnostic pitfall |
|---|---|---|
| – Small- and large-sized slender papillary clusters<br>– Small glandular cells with distinct focal palisading<br>– Clear nuclei with bizarre shape: cleaved and folded<br>– Chromatin: finely dispersed sometimes patternless | | Primary adenocarcinomas of<br>– Ovary (low-grade papillary adenocarcinoma and borderline serous tumors)<br>– Lung (bronchioloalveolar carcinoma) |
| | – Single large rounded malignant cells<br>– Most cells with intracytoplasmic mucus<br>– Mucinous background is common | Primary adenocarcinoma of pancreas and bile ducts |

#### C. Carcinomas Characterized by Sharply Delineated Compact Cell Balls

| Basic cell pattern | Particular and/or additional features | Differential diagnosis or possible diagnostic pitfall |
|---|---|---|
| **(1) Compact cell balls with smooth contours**<br>– Papillary clusters – variable<br>– Single tumor cells – variable<br>– Monomorphic tumor cells with distinct, sharply outlined cytoplasm<br>– Dense granular chromatin,<br>– Discrete or absent hyperchromasia<br>– Medium-sized nuclei with sporadically wrinkled membrane and/or deep identations<br>– Small nucleoli | | Primary carcinomas of<br>– Breast (common breast carcinoma)<br>– Lung (bronchioloalveolar carcinoma)<br>– Uterus (endometrial carcinoma, well differentiated)<br>– Varied sites: endocrine carcinoma, well differentiated<br>– Benign hyperplastic mesothelium<br>– Benign mesothelial spheres with collagen core<br>– Epithelial malignant mesothelioma |

## Tumors Spreading to Serosal Membranes (Direct Invasion / Metastases) Sect. 3.2.3, p. 263 (continued)

### Selected Entities of the Most Frequent Metastatic Neoplasms Based on Their Cytoarchitectural and Cellular Characteristics

| Basic cell pattern | Particular and/or additional features | Differential diagnosis or possible diagnostic pitfall |
|---|---|---|
| **(2) Compact cell balls with concentric lamination of the outermost cells**<br>– Single tumor cells – variable<br>– Medium-sized and large pleomorphic cells<br>– Nuclei with indentations and hyperchromasia | | Primary SCC of lung, esophagus, uterine cervix, among others:<br>– Nonkeratinizing squamous cell carcinoma |
| **D. Diffuse Sheets and Papillary Groups of Polymorphic Cells** | | |
| **Basic cell pattern** | **Particular and/or additional features** | **Differential diagnosis or possible diagnostic pitfall** |
| – Large cells with huge, markedly vacuolated cytoplasm<br>– Pleomorphic nuclei, coarsely clumping chromatin<br>– Multiple large nucleoli<br>– Intracytoplasmic mucinous material<br>– Background mucus – possible | | Primary adenocarcinomas of<br>– Ovary (poorly differentiated ovarian carcinoma)<br>– Lung, colon, breast, pancreas, bile duct (poorly-differentiated adenocarcinoma)<br>– Rare neoplasms, such as epithelioid sarcoma |
| **E Small-Cell Pattern: Tumor Cells in Single-File Arrangement and Tight Balls** | | |
| **Basic cell pattern** | **Particular and/or additional features** | **Differential diagnosis or possible diagnostic pitfall** |
| – Small tumor cells **but larger than lymphocytes!**<br>– Small densely packed cell balls and characteristic single-file cell arrangement<br>– Cytoplasm absent or scant cytoplasmic rim<br>– Nuclei are round, oval, or elongated with wrinkled membrane<br>– Striking hyperchromasia or nucleoplasm with dirty blue-grey or pinkish color<br>– Finely granular chromatin, larger nuclei with salt-and-pepper pattern<br>– Nucleoli: small inconspicuous, or absent<br>– Apoptotic bodies<br>– Necrosis possible | | Primary cancers of varied origin:<br>– Small-cell carcinoma<br>– Small round blue cell tumors<br>– Merkel cell carcinoma<br><br>– Reactive lymphocytosis<br>– Malignant non-Hodgkin lymphoma |
| **F. Tumors Characterized Mainly by Single Histiocytoid Cells** | | |
| **Basic cell pattern** | **Particular and/or additional features** | **Differential diagnosis or possible diagnostic pitfall** |
| – Discohesive histiocytoid cells of varying size<br>– Usually wide and foamy cytoplasm<br>– Nuclei frequently kidney-shaped<br>– Chromatin either coarse and clumping, or pale and fine dispersed | | – Malignant histiocytosis (primary tumor usually in the lung)<br>– Liver cirrhosis<br>– Cyst content<br>– Reactive histiocytosis |
| | **Mucus**<br>– Abundant cytoplasmic mucus may give rise to signet ring cells<br>– Mucinous background – variable | Primary tumor: gastric carcinoma |
| **G. Tumors Characterized Mainly by Single Polymorphous Large Cells and Keratinizing Cytoplasm** | | |
| **Basic cell pattern** | **Particular and/or additional features** | **Differential diagnosis or possible diagnostic pitfall** |
| – Pleomorphic large cells, also fusiform<br>– Abundant dense, eosinophilic, or cyanophilic cytoplasm<br>– Hyperchromatic nuclei with indentations<br>– Coarse chromatin, or dense and patternless nucleus<br>– Usually necrotic debris | | Primary SCC of lung, esophagus, uterine cervix, among others:<br>– Squamous cell carcinoma, keratinizing |
| | – Cytoplasm dense or vacuolated<br>– Sporadic keratinization | Transitional cell carcinoma of the urothelial tract |

## Tumors Spreading to Serosal Membranes (Direct Invasion / Metastases) Sect. 3.2.3, p. 263 (continued)

### Selected Entities of the Most Frequent Metastatic Neoplasms Based on Their Cytoarchitectural and Cellular Characteristics

#### H. Tumors Characterized Mainly by Large Single Cells with Nuclear Inclusions and Granular Cytoplasm

| Basic cell pattern | Particular and/or additional features | Differential diagnosis or possible diagnostic pitfall |
|---|---|---|
| – Large single cells, frequently multinucleated<br>– Distinct abundant cytoplasm, usually granular<br>– Nuclei with smooth margins, indentations and folding, sharply outlined nuclear inclusions<br>– Fine and evenly dispersed chromatin<br>– Huge pleomorphic nucleoli | | Primary cancers of varied origin:<br>– Nonpigmented malignant melanoma<br>– Hepatocellular carcinoma<br>– Oncocytic tumors<br>– Benign activated liver parenchyma cells |
| | – Melanophages<br>– Cytoplasmic melanin pigment – variable amount | Pigmented malignant melanoma |

#### I Tumors Characterized by Particular Presentation of Mucin

| Basic cell pattern | Particular and/or additional features | Differential diagnosis or possible diagnostic pitfall |
|---|---|---|
| – Cytoplasmic vacuoles presenting central **droplets of mucus**, target like | | Breast carcinoma |
| – Nuclei displaced by mucin-filled vacuoles, so-called **signet-ring cells** | | Adenocarcinoma of the stomach |
| – Masses of **mucinous material in peritoneal cavity fluids**<br>– Tumor cells sparse or absent<br>– Tumor cells appear benign or of low-grade malignancy and usually occur embedded in masses of mucin | | Pseudomyxoma peritonei<br>Low-grade mucinous adenocarcinomas of varied origin |

#### K. Benign and neoplastic lesions associated with Psammoma Bodies

| Basic cell pattern | Particular and/or additional features | Differential diagnosis or possible diagnostic pitfall |
|---|---|---|
| – Psammoma bodies incorporated in epithelial clusters and/or background psammoma bodies | | Primary adenocarcinoma of<br>– Thyroid<br>– Lung<br>– Breast<br>– Pancreas<br>– Endometrium<br>– Stomach |
| | – Psammoma bodies encased in the fibrovascular cores of true papillae | Papillary ovarian adenocarcinoma |
| | – Psammoma bodies as a background element, or encased in clusters of mesothelia cells exhibiting mild atypia (usually encountered in abdominal fluid samples) | Metastatic well-differentiated adenocarcinoma<br>Endosalpingiosis and other benign mesothelial lesions |

## Malignant Lymphoma and Myeloid Lesions Involving Serosal Membranes Sect. 3.2.3.2, p. 267

### Selected Entities Based on Their Cytoarchitectural and Cellular Characteristics

#### Pure Lymphocytic Pattern, Uniform

| Basic cell pattern | Particular and/or additional features | Differential diagnosis or possible diagnostic pitfall |
|---|---|---|
| – Pure lymphocytic smear, uniform cell pattern<br>– Minor nuclear enlargement<br>– Nuclei with fine granular chromatin<br>– Distinct, centrally placed nucleolus – variable<br>– Scant cytoplasm | | Potential malignant lymphoid disorders:<br>– Lymphocytic lymphoma<br>– Chronic lymphatic leukemia (CLL)<br><br>benign T-cell hyperplasia<br>florid pleural tuberculosis |

#### Mixed Lymphoid Cell Pattern

| Basic cell pattern | Particular and/or additional features | Differential diagnosis or possible diagnostic pitfall |
|---|---|---|
| – Mixed cell pattern: **≥ 50% lymphoid cells**<br>– Atypical lymphoid cells of varied size:<br>Irregular nuclei with flattening and molding, fine granular chromatin<br>– Nucleoli variable in size<br>– Large blastoid cells – variable | | Potential malignant lymphoid disorders:<br>– Malignant B-NHL with blast component<br>– Large-cell lymphoma along with marked reactive T cell hyperplasia<br>– putative Hodgkin lymphoma<br><br>Myeloid neoplasia<br><br>Florid reactive lymphocytosis: benign |
| | – Scattered large atypical blastoid cells | Pronounced reactive lymphocytosis interspersed with carcinoma cells |
| | – Obvious **Hodgkin** and **Reed-Sternberg** cells | Hodgkin lymphoma |

#### Large Number of Malignant Lymphoid Blastic Cells

| Basic cell pattern | Particular and/or additional features | Differential diagnosis or possible diagnostic pitfall |
|---|---|---|
| – Numerous large pleomorphic blastic cells<br>– Unequivocal malignant features<br>– Frequent cell degeneration<br>– Necrosis<br>– Only a few benign lymphocytes | | – Large-cell lymphoma – different types<br><br>– Large-cell anaplastic carcinoma<br><br>– Other undifferentiated malignoma<br><br>– Large amounts of immature lymphocytes in viral infections |

## Rare Secondary Neoplasms Spreading to Serosal Membranes Sect. 3.2.3.3, p. 269

### Check Also Differential Diagnosis Considerations Specified Above

It concerns a large group of neoplasms that are rarely encountered in effusions, in particular:

- **Carcinoma and nonepithelial malignancies** infrequently metastasizing to body cavities
- **Spindle cell tumors** and pleomorphic **spindle sarcoma** of different histogenesis. Sarcomatous mesothelioma should always be kept in mind.
- The large group of **small blue cell tumors**
- **Germ cell neoplasms**

Descriptions of single cases and reviews are reported in the literature. A comprehensive description of rare neoplasms in effusions is published in the book by Hajdu and Hajdu [29].

# Section 3.3
# Effusions, Aspiration and Washing
# Peritoneal Cavity – Cul-de-Sac – Douglas Pouch

## Mesothelial Layer and Fallopian Tube Sects. 3.3.2 and 3.3.3, p. 301

### Benign Sheets from the Mesothelial Layer

| Basic cell pattern | Particular and/or additional features | Differential diagnosis or possible diagnostic pitfall |
|---|---|---|
| – Cell components as in benign effusions<br>– Small and large flat cohesive sheets<br>– Centrally placed pale nuclei cleaved and folded<br>– Low N/C ratio<br>– Indistinct chromatin pattern<br>– Distinct nucleolus<br>– Polygonal cytoplasm with distinct borders<br>– Common cell degeneration | – Intermediate and superficial squamous cells | – Highly suggestive of transvaginal aspiration |
| | – Hyaline globules surrounded by activated histiocytes and mesothelial cells | – Low-grade adenocarcinoma<br>– Adenoid cystic carcinoma |

### Degenerating Mesothelial Cells

| Basic cell pattern | Particular and/or additional features | Differential diagnosis or possible diagnostic pitfall |
|---|---|---|
| – Same cell pattern as stated above<br>– Cells showing large eosinophilic cytoplasm and abnormal deeply stained nuclei | | – Atypical / malignant squamous cells |

### Cells Derived from the Fallopian Tube and Fimbriae

| Basic cell pattern | Particular and/or additional features | Differential diagnosis or possible diagnostic pitfall |
|---|---|---|
| – Ciliated columnar cells, single or in small clusters<br>– Detached ciliary tufts | | – Well-differentiated adenocarcinoma focally exhibiting ciliated tumor cells (an extremely rare occurrence!) |

## Spillage of Cyst Content into Body Cavities Sect. 3.3.4, p. 301

### Cystic Fluid from Lesions of Different Sources

| Basic cell pattern | Particular and/or additional features | Differential diagnosis or possible diagnostic pitfall |
|---|---|---|
| – The typical effusion cell pattern is absent<br>– Large foamy histiocytes with phagocytosis<br>– Cellular debris | | – Cystic fluid NOS |
| | – Follicle epithelium | – Follicle cyst |
| | – Detached ciliary tufts | – Simple serosal cyst |
| | – Epithelial clusters of cuboidal cells | – Serous cystadenoma |
| | – Epithelial clusters of mucinous cells | – Mucinous cystadenoma |
| | – Squamous cells | – Dermoid cyst |
| | – Endometrial-type cells, or merely hemosiderophages and debris | – Endometriotic cyst |
| | – Mesothelial cells | – Mesothelial cyst<br>– Effusion with degenerate mesothelial cells |
| | – Hooklets and/or scolices and/or chitin masses | – Abdominal hydatid cyst<br>– Ruptured hydatid cyst in an abdominal organ (e.g. in the liver) |

## Endosalpingiosis Sect. 3.3.5, p. 302

### Endosalpingiosis and Mesothelial Cell Hyperplasia

| Basic cell pattern | Particular and/or additional features | Differential diagnosis or possible diagnostic pitfall |
|---|---|---|
| – **Psammoma bodies surrounded by mesothelial cells**<br>– The mesothelial cells are bland occurring in small compact clusters, spheres, or papillary groups<br>– Mesothelial-like single cells<br>– Stimulated round or elongated mesothelial cells with increased N/C ratio – variable. Round nuclei with fine chromatin and enlarged nucleoli | | – Borderline serous tumor of the ovary<br>– Low-grade serous papillary carcinoma of the ovary<br>– Low-grade serous papillary carcinoma of the peritoneum |

## Endometriosis Sect. 3.3.6, p. 302

| Basic cell pattern | Particular and/or additional features | Differential diagnosis or possible diagnostic pitfall |
|---|---|---|
| – Hemosiderin-loaded macrophages<br>– Pronounced background debris | **In rare cases in addition:**<br>– Tight clusters of small and medium-sized cells<br>– Wrinkled nuclei and tiny nucleoli<br>– Tendency to squamous metaplasia – variable<br>– Small fragments of stromal tissue adherent to the clusters | – Highly suggestive of endometriosis<br>– Well-differentiated endometrial adenocarcinoma<br>– Varied low-grade epithelial tumors of the ovary and peritoneum |

## Low-Grade Neoplastic Tumors of the Ovary and Peritoneum Sect. 3.3.7, p. 303

### Well-Differentiated Nonpapillary Neoplasms

| Basic cell pattern | Particular and/or additional features | Differential diagnosis or possible diagnostic pitfall |
|---|---|---|
| – Numerous cell clusters: rounded or papilliform<br>– Usually columnar cell shape, distinct cell borders<br>– Cellular palisading – variable<br>– Nuclear molding and finely granular chromatin<br>– Indistinct hyperchromasia and variable nucleoli<br>– Psammoma bodies – variable | | – Serous borderline tumor of ovary or peritoneum<br>– Well-differentiated serous ovarian cystadenocarcinoma<br>– Well-differentiated endometrial carcinoma<br>– Endosalpingiosis |
| | – Innumerable psammoma bodies | – Psammoma carcinoma of the ovary |
| | – Mucin-containing tumor cells | – Well-differentiated mucinous ovarian cystadenocarcinoma |

### Well-Differentiated Neoplasms, Unequivocal Papillary Variant

| Basic cell pattern | Particular and/or additional features | Differential diagnosis or possible diagnostic pitfall |
|---|---|---|
| – Same basic cell pattern as stated above<br>– Branching papillary cell clusters with fibrovascular core<br>– Micropapillary structures with fibrovascular core | | – Low-grade papillary serous adenocarcinoma of ovary or peritoneum<br>– Well-differentiated peritoneal papillary mesothelioma |
| | – Psammoma bodies and mucin-containing tumor cells | – Papillary variants of ovarian carcinomas as stated above |

Few selected rare gynecologic tumors are presented in Sect. 3.3.8, p. 303

Cytomorphologic descriptions relative to the most frequent secondary tumors encountered in abdominal fluids are given in Sect. 3.2.3 "Metastases to Serous Membranes", p. 263.
Cytology of gastrointestinal malignant lesions in peritoneal washings is discussed in a report by Martin and Goellner [13].

# Chapter 4 Thyroid

## Section 4.2
## Thyroid and Parathyroid Glands

### Thyroiditis Sect. 4.2.1, p. 336

#### Suppurative Thyroiditis

| Basic cell pattern | Particular and/or additional features | Differential diagnosis or possible diagnostic pitfall |
|---|---|---|
| – Masses of degenerating neutrophilic granulocytes<br>– Debris | – Search for pathogenic organisms! | |

#### Thyroiditis de Quervain

| Basic cell pattern | Particular and/or additional features | Differential diagnosis or possible diagnostic pitfall |
|---|---|---|
| – Aggregation of:<br>Epithelioid cells and mulitinucleated giant cells of Langhans type<br>– Large and pale epithelioid cell nuclei, fine and loose chromatin<br>– Small and large conspicuous nucleoli<br>– Lymphocytes, neutrophils, eosinophils, plasma cells<br>– Debris and abundant colloid<br>– Small sheets of follicular cells, nuclei are bland or degenerated | – **Variable cytologic patterns related to disease stage**<br>– Cytoplasm of giant cells may contain condensed colloid | |

#### Subacute Lymphocytic Thyroiditis Occurring Sporadically or Postpartum

| Basic cell pattern | Particular and/or additional features | Differential diagnosis or possible diagnostic pitfall |
|---|---|---|
| – Numerous mature lymphocytes<br>– Sheets of follicular cells, bland or slightly activated | – Sporadic psammoma bodies<br>– Only sporadic lymphocytes | – Hyperplastic thyroid lesion/adenoma |

#### Hashimoto Autoimmune Thyroiditis

| Basic cell pattern | Particular and/or additional features | Differential diagnosis or possible diagnostic pitfall |
|---|---|---|
| – Aspirates with abundant cellularity<br>– Large numbers of mature lymphocytes, plasma cells, and follicle center lymphoid cells including starry sky cells<br>– Small and large regular sheets of oncocytic cells:<br>Polygonal cells with well-defined borders, dense eosinophilic cytoplasmic granularity<br>– Round nuclei, evenly and darkly stained, finely granular chromatin, central nucleolus<br>– Activated mesenchymal cells – variable<br>– Scant colloid | – Giant cells and psammoma bodies – variable<br>– Samples devoid of epithelial cells<br>– Samples with sparse lymphoid cells<br>– Numerous activated stromal cells | – Malignant lymphoma<br>– Oncocytic neoplasm<br>– Granulomatous thyroiditis |

Rare forms of **chronic lymphocytic thyroiditis, fibrotic and granulomatous thyroiditis**, see Sects. 4.2.1.2.4 and 4.2.1.2.5, p. 337.

## Thyroid Cysts (Selected Subtypes) Sect. 4.2.2, p.338

### Colloid Cyst

| Basic cell pattern | Particular and/or additional features | Differential diagnosis or possible diagnostic pitfall |
|---|---|---|
| – Viscous aspirate<br>– Abundant dense colloid, often cracked in a mosaic pattern<br>– Few small monolayer sheets of follicular cells<br>– Pyknotic nuclei<br>– Sparse foam cells, if any | | – Colloid-filled giant follicle |

### Cystic Change in Goiters

| Basic cell pattern | Particular and/or additional features | Differential diagnosis or possible diagnostic pitfall |
|---|---|---|
| – Aspirated fluid is clear, translucent brown, or bloody<br>– Variable numbers of histiocytes<br>– Cytoplasmic hemosiderin inclusions – variable<br>– Red blood cells: sparse or abundant | – Foreign-body giant cells, diverse inflammatory cells – variable | – Parathyroid cyst |
| | – Strongly activated histiocytes, and<br>– Regenerative follicular cells:<br>  – Gross cell enlargement<br>  – Pleomorphic cytoplasm and nuclei<br>  – Prominent nucleoli<br>  – Coarse clumping chromatin | – Malignant neoplasm |

### Long-Standing Cyst

| Basic cell pattern | Particular and/or additional features | Differential diagnosis or possible diagnostic pitfall |
|---|---|---|
| – Cholesterol crystals<br>– Calcium particles<br>– Small connective tissue fragments and fibroblasts | – Psammoma bodies | – Cystic thyroid papillary carcinoma |

### Thyroglossal Duct Cyst

| Basic cell pattern | Particular and/or additional features | Differential diagnosis or possible diagnostic pitfall |
|---|---|---|
| – Columnar cells<br>– Squamous cells, occasionally keratinized<br>– Squamous cell debris<br>– Inflammatory background, histiocytes | | – Branchial cleft cyst |

**Cystic degeneration in malignant neoplastic lesions**, see Sect. 4.2.2, "Cystic Degeneration of Neoplastic Disorders," p. 338.

## Hyperplastic Thyroid Lesions Sect. 4.2.3, p. 339

### Goiter: Diffuse and Nodular

| Basic cell pattern | Particular and/or additional features | Differential diagnosis or possible diagnostic pitfall |
|---|---|---|
| – Cellular smears comprising colloid, epithelial single cells, sheets, and tissue fragments<br>– **Follicular cells:** Isolated or grouped in small sheets and in large regular tissue fragments with or without micro- and mediofollicular pattern, oncocytic metaplasia is frequent<br>– Small nuclei: neat margins and regular spacing,<br>– Varied numbers of stripped small, pyknotic, dark-staining nuclei,<br>– Fine granular and evenly distributed chromatin,<br>– Distinct, clear or pale and well-defined cytoplasm<br>– **Follicles** retain their three-dimensional form, bordered by uniform cuboid cells with luminal colloid<br>– **Background-colloid:** thin and lucid, crumpled or mosaic-like cracked film | **Variable:**<br>– Stromal cells and areas of granulomatous or fibrous tissue<br>– Degenerated follicular cells: polymorph nuclei, conspicuous nucleoli<br>– Recent and old hemorrhage, histiocytes, hemosiderophages,<br>– Foreign body-type giant cells<br>– Calcification, sporadic psammoma bodies | – Parathyroid benign lesions |
| | – Hyperplastic follicular cells: enlarged, bland nuclei with pronounced nucleoli | – Follicular carcinoma<br>– Adenomatous nodules |
| | – Papilliform and even papillary tissue fragments | – Papillary thyroid carcinoma<br>– Renal clear cell adenocarcinoma |
| | – Pronounced inflammatory cell component (lymphocytes!)<br>– combined with abundant oncocytic metaplasia | – Lymphocytic thyroiditis<br>– Hashimoto thyroiditis |

### Hyperthyroidism

| Basic cell pattern | Particular and/or additional features | Differential diagnosis or possible diagnostic pitfall |
|---|---|---|
| – Rather paucicellular aspirate<br>– Follicular cells occur dispersed or in loose syncytial sheets<br>– Follicular formations are vague<br>– Flare cells: large cytoplasm, pale and finely granular with marginal vacuoles (fire-flare appearance), in MGG staining<br>– Scant colloid as thin, pale slightly eosinophilic film<br>– Frequent multinucleation, epithelioid granulomatous component, and focal lymphocytic infiltration | – Oncocytic cells as an inconstant finding | |
| | **Activated cells:** eccentrically located nuclei varying in shape and size, small but distinct nucleoli | |
| | – **Mainly grossly activated follicular cells** | – Carcinoma, primary or secondary |
| | – **Mainly activated spindle cell component** | – Anaplastic carcinoma<br>– Medullary carcinoma |

## Follicular Neoplasia: Benign and Malignant Sect. 4.2.4, p. 340

### Simple (Follicular) Adenoma and Colloid Adenoma

| Basic cell pattern | Particular and/or additional features | Differential diagnosis or possible diagnostic pitfall |
|---|---|---|
| – Identical to nodular goiter and macrofollicular goiter, respectively (see Sect. 4.2.3, p. 339) | | – Nodular goiter or macrofollicular goiter, respectively |

### Microfollicular Adenoma / Adenomatous Nodule / Well-Differentiated Follicular Carcinoma

| Basic cell pattern | Particular and/or additional features | Differential diagnosis or possible diagnostic pitfall |
|---|---|---|
| – Abundance of monomorphic follicle cells, single, in loose sheets or in three-dimensional arrangement<br>– Microfollicles, a few of them containing pale staining colloid<br>– Round to oval nuclei, smooth, slightly increased in size<br>– Granular chromatin evenly distributed<br>– Small nucleoli – variable<br>– Pale cytoplasm of variable size<br>– Background colloid is absent | | – Parathyroid lesions<br>– **Distinguishing between follicular adenoma and well-differentiated follicular carcinoma is rarely possible by cytology** |

### Hyalinizing Trabecular Adenoma

| Basic cell pattern | Particular and/or additional features | Differential diagnosis or possible diagnostic pitfall |
|---|---|---|
| – Cells occurring isolated or in loose aggregates and syncytial clusters<br>– Frequently radially oriented cells surrounding a central hyaline core<br>– Cells are oval to spindle-shaped<br>– Thin dispersed chromatin and small inconspicuous nucleoli<br>– Huge and elongated cytoplasm with rounded pale inclusion bodies<br>– Frequent hyaline background material | – Oval to spindle-shaped and mildly pleomorphic nuclei<br>– Nuclear longitudinal grooves and cytoplasmic nuclear inclusions | – Medullary thyroid carcinoma<br>– Papillary thyroid carcinoma |

### Atypical Adenoma and Follicular Carcinoma

| Basic cell pattern | Particular and/or additional features | Differential diagnosis or possible diagnostic pitfall |
|---|---|---|
| – Aspirates with marked cellularity<br>– Syncytial cellular aggregates, loose or crowded<br>– Focally marked cellular overlapping<br>– Many empty microfollicles<br>– Polymorphic nuclei showing bizarre indentations and folds<br>– Large nucleoli<br>– Irregular chromatin distribution and hyperchromasia | | – Parathyroid lesions |

### Poorly Differentiated Follicular Carcinoma

| Basic cell pattern | Particular and/or additional features | Differential diagnosis or possible diagnostic pitfall |
|---|---|---|
| – Cell-rich aspirates<br>– Syncytial epithelial tissue fragments: loose or tight<br>– **Follicles:** irregularly formed, intraluminal colloid is rare<br>– Focally pronounced nuclear crowding and overlapping<br>– Clearly enlarged nuclei, variable in size, rounded and smooth, or pleomorphic with irregular outline<br>– Irregularly distributed, coarsely granular chromatin<br>– Distinct hyperchromasia<br>– Nucleoli of varying size are always present<br>– Background colloid is sparse, but necrosis is common | | |

**Insular carcinoma**, see Sect. 4.2.4.4.3, p. 342.

## Benign Oncocytes and Oncocytic Tumors Sect. 4.2.5, p. 342

### Benign Oncocytes

| Basic cell pattern | Particular and/or additional features | Differential diagnosis or possible diagnostic pitfall |
|---|---|---|
| – Large polygonal cells<br>– Abundant cytoplasm with well-defined margins appearing either as close-grained or extremely dense-structured, staining either eosinophilic, cyanophilic or amphophilic (with Pap stain)<br>– Nuclei are large and round in central or eccentric position<br>– Nucleoli are prominent and red-colored | | |

### Oncocytic Adenom

| Basic cell pattern | Particular and/or additional features | Differential diagnosis or possible diagnostic pitfall |
|---|---|---|
| – Distinct monomorphic cell pattern<br>– Single cells and loose cohesive cell groups<br>– Occasional follicles<br>– Typical oncocytes with a low N/C ratio:<br>  – Nuclei are round, uniform in size with a single round nucleolus<br>  – Finely granular chromatin pattern | – Presence of colloid and lymphocytes favor a benign lesion | – goiter with oncocytic metaplasia<br>– Hashimoto thyroiditis |

### Oncocytic Carcinoma

| Basic cell pattern | Particular and/or additional features | Differential diagnosis or possible diagnostic pitfall |
|---|---|---|
| – Many isolated cells and syncytial-type tissue fragments<br>– Cells are smaller (compared to benign oncocytes) exhibiting an increased N/C ratio<br>– Variations in nuclear size and shape<br>– Focal irregular nuclear crowding<br>– Macronucleoli, frequently multiple and irregular<br>– Occasional psammoma bodies and cellular debris<br>– Colloid is absent | – Papillary growth pattern – variable | – Graves disease<br>– Goiter with oncocytic metaplasia<br>– Medullary carcinoma<br>– Parathyroid lesions, oncocytic variants<br>– Oncocytic papillary carcinoma |

## Papillary Thyroid Carcinoma and Its Variants Sect. 4.2.6, p. 343

### Papillary Carcinoma, Common Type

| Basic cell pattern | Particular and/or additional features | Differential diagnosis or possible diagnostic pitfall |
|---|---|---|
| **Key features:**<br>– Papillary formations<br>– Monolayered cohesive sheets<br>– Nuclear grooves and longitudinal folds<br>– Intranuclear cytoplasmic invaginations<br>– Finely granular and dusty chromatin<br>**Other features:**<br>– High cellularity<br>– Scant colloid, viscous and bubble-gum smearing effect<br>– Psammoma bodies – variable<br>– Histiocytes, histiocytic giant cells, lymphocytes – variable | | – Parathyroid lesions<br><br>**Caution:**<br>– **Nuclear grooves and longitudinal folds also in nonpapillary thyroid carcinoma – variable**<br><br>– **Intranuclear cytoplasmic invaginations also in:**<br>  – **Adenoma and follicular neoplasms**<br>  – **Oncocytic, medullary and anaplastic carcinoma**<br>  – **Metastases of renal cell carcinoma**<br><br>– **Psammoma bodies also in:**<br>  – **Benign thyroid hyperplastic lesions**<br>  – **Lymphocytic / Hashimoto thyroiditis** |

## Papillary Thyroid Carcinoma and Its Variants Sect. 4.2.6, p. 343 (continued)

### Follicular Variant Papillary Carcinoma

| Basic cell pattern | Particular and/or additional features | Differential diagnosis or possible diagnostic pitfall |
|---|---|---|
| – Nuclear key features of common papillary carcinoma, and pronounced follicular architecture<br>– Papillary pattern is absent<br>– Colloid may be thick and abundant<br>– Generally a large number of histiocytes | | – Benign follicular neoplasm<br>– Goiter with macrofollicles and abundant colloid |

### Tall Cell Variant Papillary Carcinoma

| Basic cell pattern | Particular and/or additional features | Differential diagnosis or possible diagnostic pitfall |
|---|---|---|
| – Nuclear key features of common papillary carcinoma, but cells are large with polygonal to columnar shape<br>– Dense cytoplasm staining either cyanophilic or eosinophilic with sharply defined margins | – Papillary fronds and lymphoid infiltrates – variable | – Oxyphilic cell variant of papillary carcinoma<br>– Metastasis of breast carcinoma<br>– Hashimoto thyroiditis |

### Columnar Cell Variant Papillary Carcinoma

| Basic cell pattern | Particular and/or additional features | Differential diagnosis or possible diagnostic pitfall |
|---|---|---|
| – Papillae and syncytial tissue fragments are frequent<br>– Monomorphic cells with palisade arrangement<br>– Pale and clear cytoplasm, columnar-shaped<br>– Elongated nuclei, overlapped and pseudostratified<br>– Finely granular or dusty chromatin<br>– Nucleoli are small or inconspicuous | **Absence of nuclear grooves and intranuclear inclusions!!** | – all cell variant of thyroid papillary carcinoma<br>– Metastatic adenocarcinoma |

### Oncocytic Variant Papillary Carcinoma

| Basic cell pattern | Particular and/or additional features | Differential diagnosis or possible diagnostic pitfall |
|---|---|---|
| – Frequent papillary fronds<br>– Pure oncocytic population<br>– Variably sized large cells grouped in loose clusters and syncytial fragments<br>– Nuclear grooves and nuclear cytoplasmic inclusions – variable<br>– Dense granular chromatin<br>– Prominent central nucleolus<br>– Abundant granular cytoplasm<br>– Rare psammoma bodies | – Pronounced lymphoplasmacytic background<br>– Oncocytes showing sparse nuclear grooves and inclusions | – Nonpapillary oncocytic tumors<br>– Tall cell variant of papillary carcinoma<br>– Hashimoto thyroiditis |

### Papillary Carcinoma with Clear-Cell Change

| Basic cell pattern | Particular and/or additional features | Differential diagnosis or possible diagnostic pitfall |
|---|---|---|
| – Nuclear key features of common papillary carcinoma and frequently stripped nuclei and barely visible enlarged clear cytoplasm with poorly defined outline | | – Medullary thyroid carcinoma<br>– Mesenchymal lesions<br>– Metastatic tumors |

Comments on **cystic papillary carcinoma** are given in Sect. 4.2.6.1.6, p. 346.

## Medullary Thyroid Carcinoma (MTC) Sect. 4.2.7, p. 347

| Basic cell pattern | Particular and/or additional features | Differential diagnosis or possible diagnostic pitfall |
|---|---|---|
| – Abundant isolated cells, marked variation in size and shape<br>– Occasionally loosely arranged cell groups but rarely dense clusters<br>– Nuclei are round to oval or spindle-shaped, always eccentrically located, frequently bi- and multinucleated<br>– Coarse chromatin scattered throughout the nucleus<br>– Intranuclear cytoplasmic inclusions are frequent<br>– Nucleoli of variable shape and size<br>– Amyloid protein in the background – variable | | – Parathyroid lesions |
| | – **MTC monomorphic cell type** versus | – Other thyroid adenoma or carcinoma |
| | – **MTC spindle cell type** | – Papillary thyroid carcinoma |
| | – **MTC pleomorphic cell type** | – Anaplastic carcinoma |
| | – Heterogeneous pattern consisting of polygonal cells and fusiform cells | – Proliferative granulation tissue |
| | – Dense cytoplasm: often granular, showing typical plasmacytoid appearance and cytoplasmic processes (single or multiple) | – Oncocytic carcinoma |
| | – Dense acellular and cloudy background material (amyloid), and paucity of cells | – Thyroid gland amyloidosis |

## Anaplastic Thyroid Carcinoma Sect. 4.2.8, p. 348

| Basic cell pattern | Particular and/or additional features | Differential diagnosis or possible diagnostic pitfall |
|---|---|---|
| – Cellular aspirates comprising two cell types*<br>  – Each cell type showing significant pleomorphism in size and shape<br>  – Cells are dispersed or loosely grouped, rarely occurring in dense clusters<br>  – Frequent tumor giant cells<br>– Nuclei with highly irregular contour, lobulation and cytoplasmic inclusions – variable<br>– Irregularly distributed bizarre chromatin clumps<br>– Multiple irregular nucleoli<br>– Mitoses<br>– Abundant and dense cytoplasm, occasionally vacuolated<br>– Necrotic and sanguineous background exhibiting variable inflammatory component | – Multinucleated cells of osteoclastic type – variable | |
| | – * **Predominant spindle cell pattern** | – Proliferating mesenchymal cells<br>– Spindle cell medullary carcinoma<br>– Fibrosarcoma, angiosarcoma<br>– Hemangiopericytoma |
| | – * **Predominant polygonal and rounded cells, small or large** | – Atypical follicular cells, after radioiodine therapy / irradiation<br>– Malignant lymphoma – blastic type<br>– Poorly differentiated carcinoma |
| | – * **Mixed cell pattern** | – Nonkeratinizing squamous cell carcinoma<br>– Malignant fibrohistiocytoma<br>– Angiosarcoma, malignant<br>– Hemangioendothelioma |

## Uncommon Rare Thyroid Neoplasms Sect. 4.2.9, p. 348

## Malignant Lymphoma Sect. 4.2.10, p. 349

### Low-Grade Malignant Lymphoma and Malignant Lymphoma of the MALT Type

| Basic cell pattern | Particular and/or additional features | Differential diagnosis or possible diagnostic pitfall |
|---|---|---|
| – Immature / atypical small-cell and mixed lymphoid population | | – Reactive / atypical lymphoid hyperplasia<br>– Varied small-cell carcinomas |
| | – A considerable number of oncocytic follicle cells | – Hashimoto thyroiditis<br>**MALT-lymphoma usually coexists with Hashimoto thyroiditis** |

### Malignant Lymphoma, Small Blast Type

| Basic cell pattern | Particular and/or additional features | Differential diagnosis or possible diagnostic pitfall |
|---|---|---|
| – Dissociated small to medium-sized pleomorphic cells<br>– Irregularly outlined hyperchromatic nuclei<br>– Granular and coarse chromatin<br>– Variable cytoplasm in size, shape, and structure | | – Thyroid small-cell anaplastic carcinoma<br>– Metastatic small-cell carcinoma |

### Malignant Lymphoma, Large Blast Type

| Basic cell pattern | Particular and/or additional features | Differential diagnosis or possible diagnostic pitfall |
|---|---|---|
| – Large pleomorphic cells bearing resemblance to those in anaplastic carcinoma | | – Anaplastic thyroid carcinoma<br>– Metastatic undifferentiated large-cell carcinoma |

Further comments on thyroid malignant lymphomas, see Sect. 4.2.10, p. 349.
A comprehensive synopsis of the cytology of malignant lymphoma is given in Sect. 15.3 "Lymph Nodes: Malignant Lymphomas," p. 950.

## Selected Metastatic Cancers Masquerading as Primary Thyroid Tumor Sect. 4.2.11, p. 350

### Metastatic Renal Cell Carcinoma

| Renal tumor variants | Particular cell features | Differential diagnosis or possible diagnostic pitfall |
|---|---|---|
| – **Clear cell renal cell carcinoma** | – Intranuclear inclusions | – Follicular thyroid carcinoma |
| – **Papillary renal cell carcinoma** | – Nuclear indentations, grooves, and inclusions | – Papillary thyroid cancer |
| – **Chromophobe renal cell carcinoma** | – Oncocytic features | – Oncocytic thyroid carcinoma |

### Metastatic Breast Carcinoma

| Breast carcinoma variants | Particular cell features | Differential diagnosis or possible diagnostic pitfall |
|---|---|---|
| – **Poorly differentiated or metaplastic breast carcinoma** | – Pleomorphic cell pattern | – Medullary thyroid carcinoma<br>– Anaplastic carcinoma of the thyroid |
| – **Breast carcinoma, lobular and common ductal type** | – Papilliform cytoarchitecture<br>– Clear chromatin<br>– Nuclear grooves and inclusions<br>– Eccentric nuclei and dense eosinophilic cytoplasm | – Tall cell variant of papillary thyroid carcinoma |

## Selected Metastatic Cancers Masquerading as Primary Thyroid Tumor (continued) Sect. 4.2.11, p. 350

### Metastatic Adenocarcinoma

| Adenocarcinoma variants | Particular cell features | Differential diagnosis or possible diagnostic pitfall |
|---|---|---|
| – **Common colonic adenocarcinoma**<br>– **Endometrial adenocarcinoma** | – Distinct columnar cell pattern | – Columnar cell papillary carcinoma |
| – **Mucinous adenocarcinoma** | – Marked mucinous features | – Mucinous thyroid cancer |
| – **Mucoepidermoid carcinoma** | – (Mucinous features and) squamous cells | – Thyroid cancer with (mucinous and) squamous features |

## Parathyroid Glands Sect. 4.2.12, p. 351

### Parathyroid Cyst

| Basic cell pattern | Particular and/or additional features | Differential diagnosis or possible diagnostic pitfall |
|---|---|---|
| – Watery clear fluid<br>– Cells are usually absent<br>– No debris | | – cysts of variable thyroidal and neck origin |

### Parathyroid Hyperplasia and Parathyroid Adenoma

| Basic cell pattern | Particular and/or additional features | Differential diagnosis or possible diagnostic pitfall |
|---|---|---|
| – Cell-rich aspirate,<br>– Usually monomorphic overall cell pattern<br>– Proteinaceous background<br>– Colloid is completely absent<br>– Slightly smaller cells as compared to thyroid follicle cells<br>– Cells are dissociated and occur in loose syncytial groups, or in large cohesive clusters<br>– Vague microfollicular structures<br>– Nuclei are smooth, stripped nuclei are frequent<br>– Micronucleoli – variable<br>– Coarse granular chromatin, evenly distributed<br>– Pale cytoplasm with both ill-defined and sharply outlined borders | | – Hyperplastic goiter<br>– Follicular thyroid adenoma<br>– Follicular thyroid carcinoma<br>– Papillary thyroid carcinoma |
| | – Cytoplasm with pronounced eosinophilic granularity | – Hashimoto thyroiditis<br>– Oncocytic neoplasms<br>– Medullary thyroid carcinoma |
| | – Heterogeneous cell pattern: significant change in epithelial cell size and cell shape | – Carotid body tumor |

# Chapter 5 Salivary Glands

## Section 5.1 Salivary Glands

- Crystalloids
- Nonneoplastic Cells and Disorders
- Benign and Malignant Neoplasms



## Crystalloids Sect. 5.1.2, p. 403

### Amylase Crystalloids

| Basic cell pattern | Particular and/or additional features | Differential diagnosis or possible diagnostic pitfall |
|---|---|---|
| – Numerous nonbirefringent polyhedral crystalloids<br>  – Varying sizes and shapes<br>  – Predominantly needle-shaped with pointed ends<br>  – Smaller crystalloids are tabular-shaped<br>MGG staining: deep-blue, Pap staining: bright orange | – Inflammatory infiltrate – variable | |

### Tyrosine Crystalloids

| Basic cell pattern | Particular and/or additional features | Differential diagnosis or possible diagnostic pitfall |
|---|---|---|
| – Irregular crystals in floral or rosette arrangement<br>Pap staining: usually pink | | |

### Collagen-Rich Crystalloids

| Basic cell pattern | Particular and/or additional features | Differential diagnosis or possible diagnostic pitfall |
|---|---|---|
| – Sunburst-like structures: collagen fibers are radially arranged around a clear central area | | |

## Cytology of Normal Salivary Glands and Nonneoplastic Disorders Sect. 5.1.3, p. 404

### Normal Salivary Glands

| Basic cell pattern | Particular and/or additional features | Differential diagnosis or possible diagnostic pitfall |
|---|---|---|
| – A few small parenchymatous tissue fragments with loosely clustered acini, scattered cells, and stripped nuclei<br>– Acinar cells are grouped in spherical formations:<br>  – Small round nucleus, peripherally located<br>  – Loose chromatin, indistinct nucleoli<br>  – Pronounced nuclear membrane<br>– Secretory ducts appear as regular tubular structures composed of cuboid and columnar cells interspersed with myoepithelial cells<br>– Benign lymphoid cells are usually present | – Cells of serous glands showing abundant granular and foamy cytoplasm<br>– Cells of mucus glands showing abundant clear cytoplasm | – Well-differentiated acinic cell carcinoma |

### Retention Cyst

| Basic cell pattern | Particular and/or additional features | Differential diagnosis or possible diagnostic pitfall |
|---|---|---|
| – Watery fluid and foam cells or viscous mucoid fluid<br>– Squamous metaplastic cells are common<br>– Cuboid and columnar-shaped epithelial cells are sparse<br>– Varying degrees of inflammation<br>– Occasional stone fragments | – Atypical metaplastic squamous cells | – Low-grade mucoepidermoid carcinoma<br>– Cystic squamous cell carcinoma |

## Cytology of Normal Salivary Glands and Nonneoplastic Disorders (continued) — Sect. 5.1.3, p. 404

### Mucus Retention Cyst

| Basic cell pattern | Particular and/or additional features | Differential diagnosis or possible diagnostic pitfall |
|---|---|---|
| – Mucinous background, few epithelial cells<br>– No inflammation | | |

### Polycystic Disease

| Basic cell pattern | Particular and/or additional features | Differential diagnosis or possible diagnostic pitfall |
|---|---|---|
| – Secretion with inclusion of eosinophilic laminated spheroliths<br>– Clean background with histiocytes and clusters of ductal epithelial cells<br>– No inflammatory changes, no lymphocytes | | – Various benign cystic lesions<br>– Cystic neoplasms |

### Lymphoepithelial Cyst

| Basic cell pattern | Particular and/or additional features | Differential diagnosis or possible diagnostic pitfall |
|---|---|---|
| – Proteinaceous background<br>– Metaplastic squamous epithelial cells and numerous anucleated squames<br>– Mixed population of small lymphocytes, plasma cells, histiocytes, and follicle center cells (centroblasts, immunoblasts)<br>– Rarely amylase crystalloids | | – Salivary duct cysts<br>– Chronic inflammation<br>– Pleomorphic adenoma<br>– Warthin tumor<br>– Malignant lymphoma |

### Sialadenosis

| Basic cell pattern | Particular and/or additional features | Differential diagnosis or possible diagnostic pitfall |
|---|---|---|
| – Cellular specimens comprising salivary gland tissue fragments: Both acini and acinar cells are enlarged<br>– Edematous background<br>– No inflammation | | |

### Oncocytic Hyperplasia

| Basic cell pattern | Particular and/or additional features | Differential diagnosis or possible diagnostic pitfall |
|---|---|---|
| – Numerous typical oncocytes, singly or arranged in clusters<br>– Moderate nuclear polymorphism – variable | | – Benign and malignant oncocytic neoplasia |

### Acute Sialadenitis

| Basic cell pattern | Particular and/or additional features | Differential diagnosis or possible diagnostic pitfall |
|---|---|---|
| – Cellular aspirates<br>– Masses of degenerating neutrophilic granulocytes<br>– Lymphocytes and histiocytes – variable<br>– Cellular debris and fibrin<br>– Fragments of calculi – possible | | |

### Chronic Sialadenitis: Nonobstructive inflammatory Disorder

| Basic cell pattern | Particular and/or additional features | Differential diagnosis or possible diagnostic pitfall |
|---|---|---|
| – Specimens with low cellularity<br>– Small duct fragments and few atrophic acinic cells<br>– Scattered fibroblasts<br>– Mixed population of inflammatory cells | | |

### Chronic Sialadenitis with Ductal Obstruction

| Basic cell pattern | Particular and/or additional features | Differential diagnosis or possible diagnostic pitfall |
|---|---|---|
| – Masses of mucoid background originating from dilatated ducts<br>– Metaplastic ductal epithelial cells (squamous and mucoid)<br>– Histiocytes, macrophages, lymphocytes, granulocytes | – Miscellaneous crystalloids – variable | – Low-grade mucoepidermoid Ca |

## Cytology of Normal Salivary Glands and Nonneoplastic Disorders (continued) — Sect. 5.1.3, p. 404

### Chronic Sclerosing Sialadenitis (Küttner Tumor)

| Basic cell pattern | Particular and/or additional features | Differential diagnosis or possible diagnostic pitfall |
|---|---|---|
| – Dense lymphocytic infiltrate: Conglomerate of small lymphocytes and lymphoid cells from secondary lymph follicles<br>– Clusters of ductal cells surrounded by collagen and infiltrated by lymphocytes<br>– Paucity or absence of acinic cells<br>– Fibroblasts and fragments of sclerotic tissue – variable | Low cellularity of FNA smears despite extensive needling indicates progressed fibrosis | – Nonspecific chronic inflammation<br>– Malignant lymphoma |

### Extravasation Mucocele / Mucus Granuloma

| Basic cell pattern | Particular and/or additional features | Differential diagnosis or possible diagnostic pitfall |
|---|---|---|
| – Mucoid masses<br>– Foam cells<br>– Foreign-body giant cells and macrophages | | – Other granulomatous disorders |

### Necrotizing Sialometaplasia / Salivary Gland Infarct

| Basic cell pattern | Particular and/or additional features | Differential diagnosis or possible diagnostic pitfall |
|---|---|---|
| – Necrotic acini<br>– Gland ducts with goblet cells and pronounced squamous cell metaplasia | | – Low-grade mucoepidermoid carcinoma |

Cytology of **sarcoidosis**, **tuberculosis**, and **other infectious diseases**, see Sects. 5.1.3.5.2 and 5.1.3.5.3, p. 407.

### Benign Nonspecific Lymphoproliferative Lesions

| Basic cell pattern | Particular and/or additional features | Differential diagnosis or possible diagnostic pitfall |
|---|---|---|
| – Abundant lymphoid infiltrate: Small lymphocytes and follicle center cells | | – Intraparotid lymph node<br>– Lymphoid hyperplasia associated with benign and malignant lesions<br>– Malignant lymphoma |

### Lymphoepithelial Sialadenitis: MESA

| Basic cell pattern | Particular and/or additional features | Differential diagnosis or possible diagnostic pitfall |
|---|---|---|
| – Abundant lymphoid infiltrate: Small lymphocytes and follicle center cells<br>– Myoepithelial islands | | – Malignant non-Hodgkin lymphoma (MALT lymphoma) |

– Diagnostic considerations in **various lymphoproliferative disorders** are specified in Sect. 5.1.3.6, p. 409.
– Regarding **Castleman disease**, see Section 2.4.3.7.1, p. 214.

## Benign Neoplasms of the Salivary Glands Sect. 5.1.4, p. 409

### Pleomorphic Adenoma

| Basic cell pattern | Particular and/or additional features | Differential diagnosis or possible diagnostic pitfall |
|---|---|---|
| – **Gelatinous mass:** myxoid, mucoid, chondroid and hyaline material<br>MGG stain: red to dark-purple<br>Pap stain: gray-greenish to pale pink with fibrillar structure<br>– **Epithelial cells** are numerous:<br>– Monomorphous, medium-sized<br>– Rounded or plasmacytoid in appearance<br>– Bland nuclei with finely reticular chromatin<br>– Inconspicuous nucleoli<br>– Sharply demarcated dense and cyanophilic cytoplasm<br>– **Myoepithelial cells** are spindle-shaped, focally streaming into the stroma | – Epithelial component may exhibit **variable architectural patterns** and **different cell types:**<br>– Cystic change<br>– Squamous metaplasia<br>– Mucus-producing cells<br>– Occasional cellular/ nuclear atypia<br>– Variable detritic mass deposits | – A variety of benign and malignant salivary gland lesions and metastases |

### Warthin Tumor

| Basic cell pattern | Particular and/or additional features | Differential diagnosis or possible diagnostic pitfall |
|---|---|---|
| – Smears with protein-rich background, appearing dirty and granular, occasional cholesterol deposits<br>– Mixed population of lymphocytes<br>– Typical oncocytes arranged in regular flat sheets strongly varying in size and multitude<br>– Squamous metaplasia is common, occasionally atypical | | – Miscellaneous oncocyte-predominant benign salivary gland lesions<br>– Sebaceous (lymph-) adenoma |
| | – Warthin tumor with sparse lymphocytic fraction | – Oncocytoma |
| | **Cyst content with degenerated epithelial component:**<br>– Scattered mature lymphocytes in a typical background<br>– Merely degenerating oncocytes showing typical features:<br>– Polygonal, columnar or pyramidal cell shape, variable in size<br>– Salmon-colored, thick and homogeneous cytoplasm<br>– Pyknotic nuclei<br>– Sharply outlined cytoplasmic remnants of oncocytes with features as stated above | – Nonspecific cyst content<br>– Tumor necrosis |
| | – **Pronounced metaplasia:** Squamous or mucinous and cellular atypia and necrosis | – Squamous cell carcinoma<br>– Mucoepidermoid carcinoma, low-grade<br>– Sialometaplasia (in minor salivary glands) |

## Benign Neoplasms of the Salivary Glands Sect. 5.1.4, p. 409 (continued)

### Oncocytoma

| Basic cell pattern | Particular and/or additional features | Differential diagnosis or possible diagnostic pitfall |
|---|---|---|
| – Cell-rich aspirates<br>– Numerous oncocytes: isolated, in clusters, and in papillary fragments<br>– Few lymphocytes<br>– Scanty proteinaceous material | | – Oncocyte-predominant salivary gland lesions<br>– Warthin tumor |
| | – Preponderance of clear cells | – Myoepithelioma<br>– Low-grade clear cell carcinoma<br>– Metastases of clear cell cancers<br>– Low-grade mucoepidermoid carcinoma<br>– Acinic cell carcinoma |
| | Infrequent:<br>– Squamous or mucinous metaplasia<br>– Cellular atypia<br>– Necrosis | – Squamous cell carcinoma<br>– Mucoepidermoid carcinoma, low-grade<br>– Sialometaplasia (in minor salivary glands) |

### Basal Cell Adenoma

| Basic cell pattern | Particular and/or additional features | Differential diagnosis or possible diagnostic pitfall |
|---|---|---|
| – Cellular smears<br>– Numerous cohesive cell clusters and branching cords<br>– Monomorphic individual cells:<br>  – Round to ovoid nuclei<br>  – Granular chromatin, occasionally one distinct nucleolus<br>– Cytoplasm occurring as small pale rim<br>– Rare single cells, usually as naked nuclei<br>– Sparse hyaline and homogeneous material:<br>Occasionally attached to the border of the cell clusters<br>MGG stain: bright red<br>Pap stain: almost translucent<br>– Completely absent: myxoid stroma of pleomorphic adenoma<br>– Occasionally cystic changes:<br>Smears with watery proteinaceous background and bland epithelial cells either scattered, or in dense clusters, or in papillary fragments | | – Basal cell adenocarcinoma<br>– Pleomorphic adenoma, cellular variant<br>– Adenoid-cystic carcinoma, solid form<br>– Basaloid squamous cell carcinoma<br>– Small-cell carcinoma<br>– Other primary and metastatic tumors with predominant basaloid features |

Cytology and differential diagnoses of other **rare benign tumors of the salivary gland such as cystadenoma, clear cell adenoma, canalicular adenoma, sebaceous adenoma, myoepithelioma, mesenchymal tumors**, see Sect. 5.1.4.5, p. 413.

## Malignant Tumors of the Salivary Glands Sect. 5.1.5, p. 414

### Low-Grade Mucoepidermoid Carcinoma

| Basic cell pattern | Particular and/or additional features | Differential diagnosis or possible diagnostic pitfall |
|---|---|---|
| **Mucin-producing cells**<br>– Large polyhedral cytoplasm well defined and finely vacuolated<br>– Small nuclei bland in shape and structure<br>– Cell clusters and individual cells<br>**Intermediate epidermoid cells**<br>– Multilayered tightly packed clusters<br>– Single cells may occur<br>– Bland nuclei: small, round to oval, dark staining, small nucleoli<br>– Moderate N/C ratio<br>– Homogeneous sharply outlined cytoplasm, rare keratinization<br>– Cytoplasmic vacuoles – variable<br>**Squamous cells** (in the majority of cases sparsely present)<br>– Keratinized cytoplasm and minimal nuclear atypia | – Mucin-rich background and possibly cystic background<br><br>Infrequent:<br>– Pronounced lymphocytosis | – Retention cyst<br>– Sialadenitis<br>– Pleomorphic adenoma: cystic and with various metaplastic cell changes<br><br>**Caution:**<br>**Isolated mucoid cells and intermediate cells may mimic histiocytes**<br><br>– Various mucinous cysts<br><br>– Warthin tumor |

### High-Grade Mucoepidermoid Carcinoma

| Basic cell pattern | Particular and/or additional features | Differential diagnosis or possible diagnostic pitfall |
|---|---|---|
| – Rarely cystic background<br>– Mucoid material, cellular debris, inflammation – variable<br>– Low number of mucus-producing cells<br>– Numerous keratinized squamous cells, pleomorphic, intercellular bridges – variable<br>– Increased mitotic activity | | – Primary and secondary epithelial cancers, such as:<br>  – Salivary duct carcinoma<br>  – Squamous cell carcinoma<br>  – Adenosquamous carcinoma |

### Adenoid Cystic Carcinoma

| Basic cell pattern | Particular and/or additional features | Differential diagnosis or possible diagnostic pitfall |
|---|---|---|
| – Small polyhedral cells, minor variation in cell size<br>– Nuclei are round to oval and hyperchromatic coarse chromatin, irregular nucleoli<br>– Cytoplasmic bodies appear as small rim<br>– Tumor cells are generally tightly clustered<br>– Characteristic extracellular globular material: homogeneous spherical bodies surrounded by carcinoma cells. Pap stain: translucent; MGG stain: pink | | – Basal cell adenoma<br>– Pleomorphic adenoma<br>– Polymorphous low-grade adenocarcinoma (in intraoral minor salivary glands)<br>– Benign and malignant epithelial-myoepithelial tumors |

### Well-Differentiated Acinic Cell Carcinoma

| Basic cell pattern | Particular and/or additional features | Differential diagnosis or possible diagnostic pitfall |
|---|---|---|
| – Hypercellular smears with abundant tumor cells: Marked monotonous cell pattern Numerous stripped nuclei<br>– Absence of ductal elements and mesenchymal cells<br>– Rare calcium deposits, possibly psammoma body-like | – Abundance of stripped nuclei<br><br>– Cohesive tumor cell clusters showing more or less well-formed acinic structures<br>– Monomorphic nuclei, round or oval, centrally located nucleolus<br>– Granular chromatin<br>– Mild atypias may be present<br>– Cytoplasm appears foamy and often granular | **Caution:**<br>**Do not mistake stripped nuclei for lymphocytes! (possible misdiagnosis: Warthin tumor)**<br><br>**Caution:**<br>**Cytoarchitecture strongly resembles benign acini (possible misdiagnosis: normal salivary gland tissue)** |

## Malignant Tumors of the Salivary Glands Sect. 5.1.5, p. 414 (continued)

| Basic cell pattern | Particular and/or additional features | Differential diagnosis or possible diagnostic pitfall |
|---|---|---|
| | – Cells with dense cytoplasm (MGG stain: grey) resembling oncocytes | – Oncocytic tumor |
| | **Variable:**<br>– Cells with abundant clear vacuolated cytoplasm | – Clear cell carcinoma<br>– Mucoepidermoid carcinoma<br>– Myoepithelial carcinoma |
| | **Infrequent:**<br>– Papillary clusters and cystic features | – Various cystic lesions<br>– Primary salivary gland tumor with cystic and papillary features<br>– Metastatic papillary neoplasia (e.g., thyroid papillary carcinoma) |
| | **Variable:**<br>– Lymphocytic component | – Warthin tumor |

### Poorly Differentiated Acinic Cell Carcinoma

| Basic cell pattern | Particular and/or additional features | Differential diagnosis or possible diagnostic pitfall |
|---|---|---|
| – Clearly malignant cell population:<br>– Polymorphic cells and nuclei, irregular chromatin,<br>– Enlarged polymorphic nucleoli | | – Primary and metastatic undifferentiated pleomorphic carcinomas |

### Polymorphous Low-Grade Adenocarcinoma

| Basic cell pattern | Particular and/or additional features | Differential diagnosis or possible diagnostic pitfall |
|---|---|---|
| – Cell-rich smears comprising monomorphous cells forming a variety of papillae, sheets, and clusters<br>– Small to medium-sized cells with bland chromatin texture<br>– Occasional nucleoli<br>– Dense and eosinophilic stained cytoplasm | | – Monomorphic adenoma |
| | – Tubular structures containing hyaline globules | – Adenoid cystic carcinoma |
| | – Myxoid matrix | – Pleomorphic adenoma |

Morphological features and further information on **rare malignant neoplasms** of the salivary glands, see Sects. 5.1.5.5 and 5.1.5.6, p. 417. Entities include **epithelial**, **epithelial-myoepithelial**, **lymphoepithelial**, and **mesenchymal tumors**.

### Common Low-Grade Non-Hodgkin Lymphomas

| Basic cell pattern | Particular and/or additional features | Differential diagnosis or possible diagnostic pitfall |
|---|---|---|
| – Monotonous lymphoid cell population<br>– Small and enlarged lymphoid cells, variably atypical<br>– Deeply stained nuclei:<br>– Irregular outline and indentations<br>– Nucleoli – variable<br>– Starry-sky cells – variable<br>– Small mature lymphocytes are rare<br>– Absence of epimyoepithelial cell groups | | – Benign lymphoproliferative lesions (for various reasons)<br>– Various types of small-cell malignant tumors |

## Malignant Tumors of the Salivary Glands Sect. 5.1.5, p. 414 (continued)

### Marginal Zone Lymphoma (MALT-Type Lymphoma)

| Basic cell pattern | Particular and/or additional features | Differential diagnosis or possible diagnostic pitfall |
|---|---|---|
| – Heterogeneous population of lymphocytes, predominance of enlarged lymphoid cells<br>– Tingible body macrophages<br>– Absence of typical follicle center cells | | – Benign lymphoproliferative lesions (for various reasons)<br>– Myoepithelial sialadenitis<br>– The lymphoid background may be strongly suggestive of Hodgkin lymphoma |

### Myeloid Sarcoma

| Basic cell pattern | Particular and/or additional features | Differential diagnosis or possible diagnostic pitfall |
|---|---|---|
| – Medium to large atypical cells, isolated and loosely clustered<br>– Usually clear and lobated nucleus with histiocytoid shape<br>– Large vacuolated or granular cytoplasm | | – NHL – large-cell type<br>– Undifferentiated carcinoma<br>– Malignant melanoma |

## Selected Metastatic Cancers Masquerading as Primary Salivary Gland Tumor Sect. 5.1.5.8, p. 420

### Metastatic Lymphoepithelioma-like Carcinoma / Poorly Differentiated Pleomorphic Carcinoma

| Basic cell pattern | Particular and/or additional features | Differential diagnosis or possible diagnostic pitfall |
|---|---|---|
| – Cohesive and isolated clearly malignant cells intermingled with mature lymphocytes | | – Malignant lymphoepithelial lesions<br>– Large-cell malignant lymphoma (associated with T-lymphocytic hyperplasia) |

### Metastatic Papillary Thyroid Carcinoma / Pulmonary Adenocarcinoma

| Basic cell pattern | Particular and/or additional features | Differential diagnosis or possible diagnostic pitfall |
|---|---|---|
| – Cytologic smears with cystic background and papillary tufts | | – Cystic salivary gland tumors with papillary projections |

### Metastatic Breast Carcinoma / Thyroid carcinoma / Renal Cell Carcinoma / Melanoma

| Basic cell pattern | Particular and/or additional features | Differential diagnosis or possible diagnostic pitfall |
|---|---|---|
| – Clear cells with lobated nuclei and possibly nuclear cytoplasmic inclusions | | – Various neoplasms with clear cell predominance |

# Section 5.2
# Head and Neck Lesions



## Congenital Neck Lesions Sect. 5.2.2, p. 460

### Branchial Cleft Cyst (Lesion in the Lateral Neck Area)

| Basic cell pattern | Particular and/or additional features | Differential diagnosis or possible diagnostic pitfall |
|---|---|---|
| – Benign squamous cells:<br>  – Mild nuclear irregularities<br>  – Distinct but small nucleoli – variable<br>– Respiratory epithelium – uncommon<br>– Lymphocytes (from cyst-surrounding lymphoid tissue)<br>– Mixed inflammatory infiltrate – variable<br>– Occasionally cholesterol crystals | | – Cervical cysts, congenital or acquired<br>– Odontogenic neoplasm<br>– Salivary gland lesions with squamous metaplasia<br>– Parotid lymphoepithelial cyst/ lymphangioma |
| | – Atypical squamous cells | – Metastatic squamous cell carcinoma (SCC)<br>– SCC ex-branchial cyst, in situ or invasive |
| | – Smears devoid of cellular elements, or merely abundant inflammatory infiltrate | – Inflammatory disorder of varied origin: salivary glands, odontogenic, cystic granuloma |

### Congenital Muscular Torticollis (Lesion in the Lateral Neck Area)

| Basic cell pattern | Particular and/or additional features | Differential diagnosis or possible diagnostic pitfall |
|---|---|---|
| – Benign slender, spindle-shaped fibroblast cells singly or arranged in clusters<br>– Ovoid nuclei with bland morphologic features<br>– Atrophic skeletal muscle and multinucleated cells with abundant cytoplasm (degenerating muscle fibers)<br>– Invariably fragments of collagen<br>– Inflammatory infiltrate – variable amount<br>– Clean or pink granular background | | – Infantile fibromatosis colli<br>– Calcifying aponeurotic fibrosis |

### Thyroglossal Duct Cyst (Lesion in the Midline Neck Area)

| Basic cell pattern | Particular and/or additional features | Differential diagnosis or possible diagnostic pitfall |
|---|---|---|
| – Aspirates with low cellularity<br>– Colloid in the background<br>– Epithelial cells of:<br>Columnar type<br>Or metaplastic squamous type<br>Or normal-looking superficial squamous type<br>– Variable inflammatory cell patterns, neutrophils are frequently predominant | | – Common cystic thyroid nodule<br>– Teratomatous lesions: teratoma, dermoid cyst<br>– Epidermal inclusion cyst |
| | – Numerous columnar epithelial cells, usually ciliated | – Bronchogenic cyst |

Other lesions arising in the midline neck area such as **ectopic thyroid tissue**, **dermoid cyst**, **teratoma**, **plunging ranula** are described in Sect. 5.2.2.2, p. 461.

### Cervical Thymoma (Lesion Occurring in any Neck Area)

| Basic cell pattern | Particular and/or additional features | Differential diagnosis or possible diagnostic pitfall |
|---|---|---|
| – Cellular smears with small mature lymphocytes, less frequently large activated lymphocytes, monocytes, and only a few epithelial cells (thymocytes) | | – Ectopic thymic tissue<br>– Malignant lymphoma<br>– Lymphocytic thyroiditis |
| | – Predominant epithelial cells, few lymphocytes | – Thyroid carcinoma |

## Congenital Neck Lesions Sect. 5.2.2, p. 460 (continued)

### Thymic Cyst (Lesion Occurring in any Neck Area)

| Basic cell pattern | Particular and/or additional features | Differential diagnosis or possible diagnostic pitfall |
|---|---|---|
| – Cystic fluid, serous or sanguineous<br>– Background of the smears with inflammatory cells, erythrocytes, debris, calcium deposits, and frequently cholesterol crystals<br>– Cuboid, columnar, ciliated columnar, or squamous epithelial cells | | – Various types of neck cysts<br>– Cystic neoplasms |

### Bronchogenic Cyst (Lesion Occurring in any Neck Area)

| Basic cell pattern | Particular and/or additional features | Differential diagnosis or possible diagnostic pitfall |
|---|---|---|
| – Ciliated columnar cells and ciliary tufts<br>– Sheets of squamous metaplastic cells<br>– Cartilage, smooth muscles and bronchial glands | | – Thyroglossal duct cyst<br>– Branchial cleft cyst<br>– Tracheal diverticula |

**Malformation of lymphatic vessels** and **very rare congenital neck disorder**s see Sects. 5.2.2.3.2. and 5.2.2.4, p. 463.

## Pseudotumors and Neoplasms from Adjacent Structures (Selected Entities) Sect. 5.2.3, p. 464

### Mycotic Aneurysm

| Basic cell pattern | Particular and/or additional features | Differential diagnosis or possible diagnostic pitfall |
|---|---|---|
| – Neutrophils<br>– Cellular debris | | – Necrotic neoplasm |

### Chordoma

| Basic cell pattern | Particular and/or additional features | Differential diagnosis or possible diagnostic pitfall |
|---|---|---|
| – Conspicuous background composed of myxoid matrix<br>– **Biphasic cell pattern:**<br>  – Physaliferous cells in variable numbers: Medium-sized to large cells with a bubbly cytoplasm<br>  – Small epithelial-like cells and spindle cells may dominate<br>– Relatively uniform nuclei with considerable pleomorphism, bland chromatin texture<br>– Cytoplasm may be eosinophilic, mimicking oncocytes<br>– Anaplastic cellular components – variable | – Cartilaginous areas – variable | – Myxoid liposarcoma<br>– Metastatic carcinomas, various types<br>– Hyaline-type chondrosarcoma |

## Benign Noncongenital, Nonneoplastic Lesions of the Head and Neck Sect. 5.2.4, p. 465

### Nodular Fasciitis / Proliferative Fasciitis / Desmoid-Type Fibromatosis

| Basic cell pattern | Particular and/or additional features | Differential diagnosis or possible diagnostic pitfall |
|---|---|---|
| – Usually cell-rich smears comprising proliferative cells of varied types:<br>  – Spindle-shaped cells<br>  – Round cells with eccentric nuclei resembling plasma cells<br>  – Large plump cells with eccentric nuclei resembling Ganglion cells<br>– Conspicuous nucleoli and abundant cytoplasm<br>– Chromatin is finely granular and evenly distributed<br>– Varying proportions of inflammatory cells<br>– Small fragments of hyaline and myxoid masses – variable | – Conspicuous preponderance of fusiform cells | – Schwannoma<br>– Other spindle cell tumors |

### Proliferative Myositis

| Basic cell pattern | Particular and/or additional features | Differential diagnosis or possible diagnostic pitfall |
|---|---|---|
| – Same basic cell pattern as stated above | – Atrophic muscle fibers | – As listed for pseudosarcomatous proliferative lesions |

### Angiolymphoid Hyperplasia / Kimura Disease

| Basic cell pattern | Particular and/or additional features | Differential diagnosis or possible diagnostic pitfall |
|---|---|---|
| – Hypercellular smears<br>– **Inflammatory cells:**<br>  – Mixed lymphoid population<br>  – Numerous scattered eosinophils<br>– **Proliferative endothelial cells:**<br>  – Spindle-shaped and polygonal cells<br>  – Nuclei are vesicular, cytoplasm is deeply eosinophilic<br>– Fragments of collagenous tissue – variable | – Polymorphic proliferative endothelial cells<br><br>– Mixed lymphoid population<br>– Scattered eosinophils<br>– Proliferative endothelial cells mimicking HRS cells | – Angiomatous tumors<br><br>– Undifferentiated carcinoma with associated inflammation<br><br>– Hodgkin lymphoma |

**Common lymphadenopathy** and **miscellaneous infectious lymph node disorders** are presented in Sect. 15.2 "Lymph Nodes: Benign Lesions," p. 926.

## Benign and Malignant Neoplasms Sect. 5.2.6, p. 467

### Pilomatrixoma

| Basic cell pattern | Particular and/or additional features | Differential diagnosis or possible diagnostic pitfall |
|---|---|---|
| – **Shadow cells:** faintly yellow-staining cells (Pap method) the area of lost nuclei remains unstained<br>– **Basaloid cells**<br>  – Cells are tightly but regularly clustered<br>  – Small cells comprising darkly stained nuclei<br>  – Little cytoplasm<br>  – Nucleoli may be prominent<br>  – Degenerating cells with pyknotic nuclei<br>  – Numerous naked nuclei with nucleoli<br>– **Calcium deposits**<br>– Squamous cells in various stages of maturation<br>– Granulomatous component and foreign-body giant cells – variable<br>– Amorphous debris – variable | | |

## Benign and Malignant Neoplasms Sect. 5.2.6, p. 467 (continued)

| Basic cell pattern | Particular and/or additional features | Differential diagnosis or possible diagnostic pitfall |
|---|---|---|
| | – (Almost) exclusively basaloid cells | – Basal cell carcinoma<br>– Undifferentiated carcinoma<br>– Small-cell carcinoma<br>– Endocrine – Merkel cell tumor<br>– Monomorphic cell breast carcinoma **(in cases of pilomatrixoma presenting as breast lump! )** |
| | – Considerable number of naked basaloid-cell nuclei with nucleoli | – Malignant lymphoma |
| | – Squamous cells in various stages of maturation. Vesicular nuclei, slightly irregular and frequently stripped<br>– Marked cellular discohesion | – Squamous cell carcinoma<br>– Odontogenic tumor |

### Carotid Body Paraganglioma

| Basic cell pattern | Particular and/or additional features | Differential diagnosis or possible diagnostic pitfall |
|---|---|---|
| – Hypercellular sanguineous smears<br>– Single cells and loose cellular grouping:<br>  – Pseudorosettes including acinar structures,<br>  – Cells vary in shape from round to fusiform,<br>  – Moderate anisokaryosis<br>– Considerable anisonucleosis and enlarged nuclei, nuclei are round, ovoid, or crescent-shaped<br>– Abundant pale cytoplasm poorly outlined<br>– Eosinophilic granules – variable<br>– A few small spindle-shaped cells | | – Fibrous/neural neoplasms<br>– Melanotic melanoma<br>– Thyroid carcinoma, follicular and medullary<br>– Undifferentiated carcinoma, metastases |
| | – Marked cytoplasmic eosinophilic granulation | – Neuroendocrine tumors |

### Merkel Cell Carcinoma

| Basic cell pattern | Particular and/or additional features | Differential diagnosis or possible diagnostic pitfall |
|---|---|---|
| – Highly cellular aspirates<br>– Tumor cells in small clusters, rosettes, single file, and rows: cells are often molded against one another<br>– Single cells and stripped nuclei<br>– Tumor cells are small, uniform, and round to oval in shape<br>– Nuclei are eccentrically placed and irregularly outlined:<br>  – Well-defined nuclear membrane<br>  – Finely granular chromatin structure<br>  – Pronounced hyperchromasia<br>  – Inconspicuous nucleolus<br>– Scanty cytoplasm, occasionally exhibiting faint granularity<br>– Frequent mitotic figures | | – Metastatic small-cell carcinoma<br>– Small round blue cell tumors<br>– Basal cell carcinoma<br>– Small-cell nonpigmented malignant melanoma,<br>– Malignant lymphomas of small-cell type<br>– Small-cell carcinoma of the salivary gland<br>– Pilomatrixoma |

## Selected Metastatic Tumors in the Head and Neck Area

Cytomorphology, differential diagnoses, immunocytochemical properties, and commentaries, see Sect. 5.2.7, p. 468.

# Chapter 6 Central Nervous System

## Section 6.1
## Central Nervous System: Cerebrospinal Fluid

### Cytology of Normal Cerebrospinal Fluid and Contaminants Sect. 6.1.2, p. 492



#### Normal Cerebrospinal Fluid (CSF)

| Basic cell pattern | Particular and/or additional features | Differential diagnosis or possible diagnostic pitfall |
|---|---|---|
| – Colorless watery fluid<br>– Paucity of cells: a few lymphocytes and monocytes | | |

#### Choroid Plexus Cells / Ependymal Cells (Mainly in Lumbar CSF)

| Basic cell pattern | Particular and/or additional features | Differential diagnosis or possible diagnostic pitfall |
|---|---|---|
| – Cuboidal cells: isolated or in papillary fragments | | – Choroid plexus papilloma<br>– Secondary low-grade papillary tumor |

#### Choroid Plexus Fragments (Mainly in Ventricular CSF)

| Basic cell pattern | Particular and/or additional features | Differential diagnosis or possible diagnostic pitfall |
|---|---|---|
| – Numerous cuboidal cells in large papillary fragments, and isolated cells in variable numbers | | – Choroid plexus papilloma<br>– Secondary low-grade papillary neoplasia (e.g., of thyroidal origin) |

#### Leptomeningeal Cells or Astrocytes (Mainly in Lumbar CSF)

| Basic cell pattern | Particular and/or additional features | Differential diagnosis or possible diagnostic pitfall |
|---|---|---|
| – Benign spindle cells, usually sparse | | |

#### Melanin Pigment

| Basic cell pattern | Particular and/or additional features | Differential diagnosis or possible diagnostic pitfall |
|---|---|---|
| – Pigment occurring, intra- and extracytoplasmic in various benign and malignant primary CNS lesions<br>(see Sect. 6.1.2.5 "CSF and melanin pigment," p. 493) | | – Metastatic melanoma<br>– Other secondary melanotic lesions |

#### Bone Marrow from a Vertebral Body (Contaminants in Lumbar CSF)

| Basic cell pattern | Particular and/or additional features | Differential diagnosis or possible diagnostic pitfall |
|---|---|---|
| – Mature and immature hematopoietic cells<br>– Megakaryocytes – variable | | – Lymphoma<br>– Leukemia |

#### Chondrocytes from an Intervertebral Disk (Contaminants in Lumbar CSF)

| Basic cell pattern | Particular and/or additional features | Differential diagnosis or possible diagnostic pitfall |
|---|---|---|
| – Large cells, single or in small sheets<br>– Small, round, deeply stained pyknotic nuclei, occasionally multiple<br>– Pale and vacuolated cytoplasm surrounded by a capsule-like dense substance | | – Neoplastic cells |

#### Brain Tissue Fragments (Contaminants in Ventricular CSF)

| Basic cell pattern | Particular and/or additional features | Differential diagnosis or possible diagnostic pitfall |
|---|---|---|
| – Small tissue fragments composed of a dense network of fibrillary elements interspersed with small dark nuclei<br>– Capillaries containing red blood cells | | |

## Reactive and Atypical Cell Changes Sect. 6.1.3, p. 493

### Activated Monocytes / Histiocytes

| Basic cell pattern | Particular and/or additional features | Differential diagnosis or possible diagnostic pitfall |
|---|---|---|
| – Large cells: generally isolated, but occasionally clustered<br>– Horseshoe-shaped nuclei with bizarre indentations, or multilobated, smooth membranes<br>– Thinly dispersed chromatin<br>– Prominent nucleolus – variable<br>– Cytoplasm wide and polyhedral, focally vacuolated | | – Malignant neoplasia of the clear cell type |

### Activated Leptomeningeal Cells / Astrocytes

| Basic cell pattern | Particular and/or additional features | Differential diagnosis or possible diagnostic pitfall |
|---|---|---|
| – Large spindle cells<br>– Elongated nuclei with indentations<br>– Granular chromatin<br>– Signs of incipient degeneration – variable | | – Spindle cell neoplasia |

### Monomorphic Reactive Lymphoid Hyperplasia

| Basic cell pattern | Particular and/or additional features | Differential diagnosis or possible diagnostic pitfall |
|---|---|---|
| – Monomorphic population of small activated lymphocytes:<br>  – Coarse chromatin texture<br>  – Prominent nucleoli – variable<br>  – Mild nuclear membrane irregularities | | – Chronic lymphocytic leukemia / small lymphocytic lymphoma |

### Variegated Reactive Lymphoid Infiltrate

| Basic cell pattern | Particular and/or additional features | Differential diagnosis or possible diagnostic pitfall |
|---|---|---|
| – Mixed lymphoid population – mature and immature cells<br>– Lymphoid and plasmacytoid cells with:<br>  – Coarse chromatin texture<br>  – Prominent nucleoli<br>  – Nuclear membrane irregularities | | – Malignant lymphoma |

### Encephalomalacia

| Basic cell pattern | Particular and/or additional features | Differential diagnosis or possible diagnostic pitfall |
|---|---|---|
| – Cell debris and degenerated glial cells<br>– Possibly enlarged reactive glial cells and lipophages | | – Tumor necrosis |

## CSF in Nontumoral Conditions (Selected Disorders) Sect. 6.1.4, p. 494

### Lyme Disease

| Basic cell pattern | Particular and/or additional features | Differential diagnosis or possible diagnostic pitfall |
|---|---|---|
| – Cell-rich sediment<br>– Numerous lymphoid cells, mainly immunoblasts and plasma cells<br>– Numerous foamy macrophages | | – Variant types of viral infections<br>– Multiple sclerosis<br>– Malignant lymphoma |

### Cryptococcosis

| Basic cell pattern | Particular and/or additional features | Differential diagnosis or possible diagnostic pitfall |
|---|---|---|
| – Round-shaped elements (5–15 µm in diameter) surrounded by a mucopolysaccharide capsule, additional thin-necked buds<br>– Usually marginal inflammatory reaction | **Caution:**<br>**In AIDS patients, malignant lymphoma and strong cellular response to another infectious agent can occur simultaneously with cryptococcosis, thus *cryptococci* may be difficult to recognize** | Nonfungal elements:<br>– Degenerating erythrocytes<br>– Water drops<br>– Air bubbles<br>– Others |

**Bacterial**, **mycobacterial**, **viral** (including AIDS) **infections**, **eosinophilia**, and **demyelinating diseases**, see Sect. 6.1.4, p. 494.

## CSF and Neoplastic Lesions in the Central Nervous System (Selected Entities) Sect. 6.1.5, p. 496

### Metastatic Melanoma

| Basic cell pattern | Particular and/or additional features | Differential diagnosis or possible diagnostic pitfall |
|---|---|---|
| -Typical malignant melanoma cells (cytomorphology see elsewhere) | | – Primary meningeal melanoma: extremely rare! |
| | – Melanotic | – Activated melanophages<br>– Non-melanoma neoplastic cells |
| | – Nonpigmented | – Undifferentiated large-cell neoplasms:<br>– Large-cell carcinoma<br>– Large-cell lymphoma and others |

### Metastatic Breast Carcinoma

| Basic cell pattern | Particular and/or additional features | Differential diagnosis or possible diagnostic pitfall |
|---|---|---|
| – Breast carcinoma cells (cytomorphology, see elsewhere) | | |
| | – Toothed wheel-like cytoplasmic protrusions and blebs | – **This is a signature of breast cancer cells in CSF, but not absolutely specific!** |

### Metastatic Squamous Cell Carcinoma

| Basic cell pattern | Particular and/or additional features | Differential diagnosis or possible diagnostic pitfall |
|---|---|---|
| – Distinct malignant squamous cells or atypical squamous cells | | – Craniopharyngioma<br>– Contaminants |

## CSF and Neoplastic Lesions in the Central Nervous System (Selected Entities) Sect. 6.1.5, p. 496 (continued)

### Large-Cell-Type Leukemic Lymphoma

| Basic cell pattern | Particular and/or additional features | Differential diagnosis or possible diagnostic pitfall |
|---|---|---|
| – Monomorphic single-cell pattern<br>– Large malignant elements, high N/C ratio<br>– Nuclei with finely granular chromatin and irregular membrane<br>– Pronounced nucleoli | – Paucicellular fluid<br>– Nuclear convolutions and grooves (typical of T-NHL)<br>– Cytoplasmic granularity | – Poorly differentiated malignant neoplasia<br>– Metastatic large-cell tumors showing nuclear convolutions, such as:<br>– Pulmonary adenocarcinoma<br>– Breast carcinoma<br>– Renal cell carcinoma<br>– Malignant melanoma<br>– Myelogenous leukemias |

### Anaplastic Glial Tumors

| Basic cell pattern | Particular and/or additional features | Differential diagnosis or possible diagnostic pitfall |
|---|---|---|
| – Highly pleomorphic cells – scattered or loosely grouped<br>– Pronounced variability in cell size<br>– Nuclei with coarse chromatin and large nucleoli, irregular nuclear membranes | | – Undifferentiated metastatic neoplasms |

### Low-Grade Glioma

| Basic cell pattern | Particular and/or additional features | Differential diagnosis or possible diagnostic pitfall |
|---|---|---|
| – Benign looking monocytoid cells<br>– Bland nuclei<br>– Loose chromatin structure | | – Macrophages<br>– Monocytes |

### Choroid Plexus Papilloma

| Basic cell pattern | Particular and/or additional features | Differential diagnosis or possible diagnostic pitfall |
|---|---|---|
| – Papillary projections<br>– Monomorphic cells with bland nuclei regularly arranged | | – Normal choroid plexus<br>– Secondary low-grade papillary tumor |

### Choroid Plexus Carcinoma

| Basic cell pattern | Particular and/or additional features | Differential diagnosis or possible diagnostic pitfall |
|---|---|---|
| – Papillary projections<br>– Frankly malignant cells with irregular arrangement | | -Secondary papillary adenocarcinoma |

### Medulloblastoma

| Basic cell pattern | Particular and/or additional features | Differential diagnosis or possible diagnostic pitfall |
|---|---|---|
| – Highly cellular specimens<br>– Anaplastic small cells with the size of large lymphocytes<br>– High N/C ratio<br>– Hyperchromatic pleomorphic nuclei<br>– Cells isolated or densely clustered, rosette formation and necrosis – variable | | – Small round cell tumors<br>– Small-cell carcinoma of the lung<br>– Retinoblastoma<br>– Neuroblastoma |

Commentaries on **various other neoplastic disorders** are provided in Sects. 6.1.5.2–6.1.5.4 p. 496.

# Chapter 8 Oral Cavity and Oropharynx

- Benign Oral Lesions
- Leukoplakia
- Benign and Malignant Tumors



## Cytology of Benign Oral Lesions Sect. 8.5, p. 566

### Normal Epithelial Cells

| Cell types and their origin | Particular and/or additional features | Differential diagnosis or possible diagnostic pitfall |
|---|---|---|
| – **Squamous cells:** almost identical to squamous cells in samples from saliva, sputa, cervix/vagina)<br>– **Columnar cells:** point of origin are the nasopharyngeal area and/or salivary gland ducts<br>– **Acinar formations:** originating from salivary glands<br>– **Lymphocytes:** originating from tonsillae or hyperplastic lymph nodes | | |

### Abnormal Squamous Cells: Sporadically or Caused by Varied Mucosal Irritations (NOS)

| Basic cell pattern | Particular and/or additional features | Differential diagnosis or possible diagnostic pitfall |
|---|---|---|
| – Cell enlargement<br>– Bland cytoarchitecture comprising normal N/C ratio | **Variable:**<br>– Binucleation<br>– Nuclear pleomorphism<br>– Nuclear inclusions<br>– Giant nucleoli<br>– Cytoplasmic vacuolization | – Anemias<br>– Tropical sprue<br>– Drugs<br>– Chemotherapeutics<br>– Postirradiation |

### Reactive/Reparative Squamous Cell Changes Due to Inflammation, Ulceration, Infection (Bacterial, Mycotic)

| Basic cell pattern | Particular and/or additional features | Differential diagnosis or possible diagnostic pitfall |
|---|---|---|
| – Abnormal acidophilic irregular cytoplasm<br>– Hyper-/parakeratotic cells<br>– Enlarged nuclei with smooth borders<br>– Loose chromatin pattern,<br>– Frequently increased N/C ratio<br>– Infrequent prominent and multiple nucleoli<br>– Neutrophils, lymphocytes, histiocytes – variable | Abnormal chromatin texture – variable | – Dysplasia<br>– Well-differentiated squamous cell carcinoma |

### Pemphigus Vulgaris

| Basic cell pattern | Particular and/or additional features | Differential diagnosis or possible diagnostic pitfall |
|---|---|---|
| – Highly cellular cytologic sample and uniform cell pattern<br>– Small squamous cells with increased N/C ratio<br>– Single or multiple irregular nucleoli<br>– Generally loose and even chromatin texture<br>– Hyperchromasia is exceptional<br>– Occasional cell-in-cell arrangement | | – Squamous cell carcinoma |

## Cytology Performed on Clinically Leukoplakic Lesions Sect. 8.6, p. 567

### Most Likely Benign Leukoplakic Lesion

| Basic cell pattern | Particular and/or additional features | Differential diagnosis or possible diagnostic pitfall |
|---|---|---|
| – Uniform, keratinized, red, orange, or yellow stained anucleated squamous cells<br>– Occasional bland and regularly shaped nuclei | | |

### Indeterminate Verrucous Plaque

| Basic cell pattern | Particular and/or additional features | Differential diagnosis or possible diagnostic pitfall |
|---|---|---|
| – Marked keratinized anucleated squamous cells comprising certain pleomorphism<br>– Sporadic pearl formation<br>– Few squamous cells containing nuclei with minor irregularities<br>– Bland chromatin texture and bland nucleoplasmic coloring | | – Dysplastic epithelium with hyperkeratosis<br>– Well-differentiated SCC / verrucous SCC<br>– Keratinizing squamous cell papilloma<br>– Verruca vulgaris |

### Dysplastic/Premalignant Squamous Lesion or Squamous Cell Carcinoma In Situ

| Basic cell pattern | Particular and/or additional features | Differential diagnosis or possible diagnostic pitfall |
|---|---|---|
| – Distinct cytoplasmic and nuclear pleomorphism<br>– Nuclei show indentations and cleaving<br>– Increased N/C ratio<br>– Dense chromatin pattern, finely granular or coarse<br>– Hyperchromasia<br>– Nucleoli are variable in size and shape | – Cytoplasmic keratinization – variable | – Invasive squamous cell carcinoma |

## Squamous Cell Carcinoma and Its Variants Sect. 8.7, p. 568

### Keratinized SCC: Well-Differentiated SCC and Verrucous SCC

| Basic cell pattern | Particular and/or additional features | Differential diagnosis or possible diagnostic pitfall |
|---|---|---|
| – Abundantly keratinized anucleated cells<br>– Brightly red- and orange-stained cytoplasm<br>– Few squamous cells containing nuclei with minor irregularities,<br>– Most nuclei exhibiting bland outline, texture, and coloring | – Mild cellular pleomorphism and pearl formation – variable | – Strongly keratinized leukoplakic lesions, benign or dysplastic |

### SCC, Moderately to Poorly Differentiated

| Basic cell pattern | Particular and/or additional features | Differential diagnosis or possible diagnostic pitfall |
|---|---|---|
| – In general less prominent keratinization, extreme variations in tumor cell maturation<br>– Sporadic anucleated, heavily keratinized cells<br>– Enlarged nuclei with marked pleomorphism:<br>  – Irregular borders usually prominent,<br>  – Distinct hyperchromasia,<br>  – Irregular chromatin texture,<br>  – Single or multiple prominent nucleoli<br>– Increased N/C ratio<br>– Usually necrotic debris, red blood cells, leukocytes | | – Metastatic SCC |

### Lymphoepithelial carcinoma

| Basic cell pattern | Particular and/or additional features | Differential diagnosis or possible diagnostic pitfall |
|---|---|---|
| – Syncytial sheets of large undifferentiated cells<br>– Vesicular and pale nuclei with marked irregular borders<br>– Indistinct chromatin structure<br>– Nucleoli variable in size and shape<br>– Cytoplasm tends to be wide, clear, and delicate<br>– Background infiltrate of benign lymphoplasmoid cells | | – Non-Hodgkin lymphoma of blastic type associated with benign lymphoplasmacytoid hyperplasia<br>– Benign follicle-center blasts originating from hyperplastic follicles<br>**Caution: in cases with single scattered cancer cells, tumor cells are often misinterpreted as activated histiocytes** |

## Rare Primary Tumors and Metastases Sect. 8.8, p. 568

### Granular Cell Tumor

| Basic cell pattern | Particular and/or additional features | Differential diagnosis or possible diagnostic pitfall |
|---|---|---|
| – Highly cellular cytologic specimens<br>– Uniform large fragile cells, single or grouped<br>– Small nuclei often excentrically positioned<br>– Bland granular chromatin<br>– Inconspicuous nucleoli<br>– Ill-defined and abundant finely granular cytoplasm<br>– Background comprising abundant granular material | – Well defined cytoplasm (rare finding) | – Foamy cells from a cystic fluid<br>– Malignant melanoma<br>– Metastasis of renal cell carcinoma, and other clear cell neoplasms<br>– Onocytic tumor |

**Other rare primary and secondary tumors** are discussed in Sect. 8.8, p. 568.

# Chapter 9 Liver

## Section 9.1 Liver

- Normal Cytology
- Benign Lesions, Inflammation/Infections
- Benign Tumors
- Equivocal Lesions
- Premalignant Lesions

## Liver Parenchyma Sects. 9.1.2–9.1.4, p. 588

### Benign Hepatocytes

| Basic cell pattern | Particular and/or additional features | Differential diagnosis or possible diagnostic pitfall |
|---|---|---|
| – Many small to medium-sized monolayer sheets or dense clusters, regular nuclear spacing<br>– Round nuclei of variable size with neat margins<br>– Fine and smooth chromatin structure<br>– Numerous clear nuclear inclusions, sharply outlined<br>– Usually one small nucleolus, centrally located<br>– Large distinct cytoplasm, eosinophilic cytoplasmic granulation | – Intracytoplasmic lipofuscin – variable | |

### Fragments of Bile Ductules

| Basic cell pattern | Particular and/or additional features | Differential diagnosis or possible diagnostic pitfall |
|---|---|---|
| – Tightly packed elongated or tubular clusters consisting of small cells<br>– The cells are cuboid and of small columnar shape<br>– Occasional cellular palisading | | |

### Fatty Liver / Steatosis

| Basic cell pattern | Particular and/or additional features | Differential diagnosis or possible diagnostic pitfall |
|---|---|---|
| – Enlarged hepatocytes<br>– Medium-sized and large cytoplasmic vacuoles<br>– Marginalized nuclei<br>– Normally structured cell sheets | | |

### Pigment in Benign Hepatocytes

| Basic cell pattern | Particular and/or additional features | Differential diagnosis or possible diagnostic pitfall |
|---|---|---|
| **Lipofuscin**<br>– Pale golden brown finely granular pigment<br><br>**Bile**<br>– Intracytoplasmic granules, usually yellow or green in color, considerable variation in size and density<br><br>**Hemosiderin**<br>– Large and coarse granular elements with inhomogeneous particle size and shape<br>MGG stain: brown staining,<br>Pap stain: greenish-brown in color | | |

## Myeloid Metaplasia Sect. 9.1.5, p. 588

### Extramedullary Hematopoiesis

| Basic cell pattern | Particular and/or additional features | Differential diagnosis or possible diagnostic pitfall |
|---|---|---|
| – Trilineage hematopoietic cells:<br>  – Normoblasts<br>  – Premature and maturing myeloid cells<br>  – Megakaryocytes | | – Myelogenic sarcoma<br>– Large-cell carcinoma<br>– Malignant lymphoma |

## Inflammation / Infection Sect. 9.1.6, p. 589

### Acute Inflammation NOS

| Basic cell pattern | Particular and/or additional features | Differential diagnosis or possible diagnostic pitfall |
|---|---|---|
| – Mainly neutrophils, well preserved<br>– Phagocytic macrophages | | |

### Pyogenic Abscess

| Basic cell pattern | Particular and/or additional features | Differential diagnosis or possible diagnostic pitfall |
|---|---|---|
| – Mainly neutrophils, markedly degenerated<br>– Phagocytic macrophages | | – Amebic abscess |

### Chronic and Viral Hepatitis

| Basic cell pattern | Particular and/or additional features | Differential diagnosis or possible diagnostic pitfall |
|---|---|---|
| – Lymphoid cells – varying degrees of differentiation<br>– Plasma cells | | – Malignant lymphoma |

### Infectious Granulomatosis, Sarcoidosis, Mycobacteriosis

| Basic cell pattern | Particular and/or additional features | Differential diagnosis or possible diagnostic pitfall |
|---|---|---|
| – Epithelioid cells<br>– Common histiocytes, partly multinucleated<br>– Giant cells of the Langhans type<br>– Small epithelioid granuloma fragments<br>– Lymphocytes | | – Noninfectious granulomatosis, sarcoidosis |
| | – Caseous necrosis | – Caseating tuberculosis |
| | – Eosinophils<br>– Foreign-body giant cells<br>– Macrophages<br>– Birefringent crystals | – Granulomas following drug use |

### Talc Granulomatosis

| Basic cell pattern | Particular and/or additional features | Differential diagnosis or possible diagnostic pitfall |
|---|---|---|
| – Birefringent crystals<br>– Foreign-body giant cells<br>– Macrophages | | – Other foreign-body granulomas |

## Cystic Lesions Sect. 9.1.7, p. 589

### Primary Congenital or Simple Cysts

| Basic cell pattern | Particular and/or additional features | Differential diagnosis or possible diagnostic pitfall |
|---|---|---|
| – Smear with proteinaceous background<br>– Foam cells | | |
| | – Glandular cells<br>– Occasional mucus | – Cysts of the intrahepatic bile ducts<br>– Cysts in cholangiocellular tumors |
| | – Ciliated epithelial cells | – Foregut cyst |
| | – Mesothelial cell sheets | – Mesothelial cyst |

### Secondary Cyst: Necrotic Malignancy

| Basic cell pattern | Particular and/or additional features | Differential diagnosis or possible diagnostic pitfall |
|---|---|---|
| – Detritus and necrosis<br>– Apoptosis<br>– Macrophages<br>– Inflammatory component (optional) | | – Caseating tuberculosis |

### Hydatid Cyst (Echinococcosis)

| Basic cell pattern | Particular and/or additional features | Differential diagnosis or possible diagnostic pitfall |
|---|---|---|
| – Debris partly homogeneous and opaque<br>– **Unusually nucleated cells**<br>– Single hooklets – variable<br>– Scolices – variable | – Cystic fluid devoid of specific tapeworm elements | – Simple cyst |

## Nonneoplastic Epithelial Lesions, Mass Presenting Sect. 9.1.8, p. 591

### Cirrhosis Comprising Regenerative Parenchymatous Nodules

| Basic cell pattern | Particular and/or additional features | Differential diagnosis or possible diagnostic pitfall |
|---|---|---|
| – Hepatocytes often binucleated, marked variation in size and shape<br>– Dense chromatin structure<br>– Distinct large and irregular nucleoli | | – Well-differentiated HCC |
| | – **Optional**:<br>– Proliferating bile ducts<br>– Inflammatory infiltrate<br>– Fragments of fibrous tissue<br>– Active fibroblasts | – Focal nodular hyperplasia |

### Focal Nodular Hyperplasia

| Basic cell pattern | Particular and/or additional features | Differential diagnosis or possible diagnostic pitfall |
|---|---|---|
| – Normal hepatocytes<br>– Fragments of fibrous tissue associated with individual epithelial and mesenchymal elements<br>– Activated fibroblasts<br>– Proliferating bile ducts | | – Liver cirrhosis |

## Benign Epithelial Tumors Sect. 9.1.9, p. 591

### Liver Cell Adenoma

| Basic cell pattern | Particular and/or additional features | Differential diagnosis or possible diagnostic pitfall |
|---|---|---|
| – Benign hepatocytes large, usually pale<br>– Uniform regular nuclei with smooth borders and inclusions; the nucleoplasm may be patternless and pale<br>– Distinct amphophilic nucleoli<br>– Gland-like formations with bile plugs<br>– No bile ducts<br>– No mitoses | | – Well-differentiated HCC |

### Noncystic Cholangiocellular Tumors: Bile Duct Adenoma, Biliary Microhamartoma, Biliary Adenofibroma

| Basic cell pattern | Particular and/or additional features | Differential diagnosis or possible diagnostic pitfall |
|---|---|---|
| – Benign cuboidal to columnar cells<br>– Basally situated monomorphic nuclei<br>– No mitoses<br>– Varying amount of stromal tissue | – Possibly focal mucin production | |

9

## Cholangiocellular Tumors of Equivocal Malignant Potential Sect. 9.1.10, p. 592

### Hepatobiliary Mucinous Cystadenoma

| Basic cell pattern | Particular and/or additional features | Differential diagnosis or possible diagnostic pitfall |
|---|---|---|
| – The same basic pattern as described for benign cholangiocellular tumors<br>– Overt mucin production<br>– Polypoid clusters and papillary fronds – variable | – **Foci of dysplastic cells as an indicator of increased malignant potential** | |

### Biliary Papillomatosis

| Basic cell pattern | Particular and/or additional features | Differential diagnosis or possible diagnostic pitfall |
|---|---|---|
| – The same basic pattern as described for benign cholangiocellular tumors<br>– Papillary fragments with fibrovascular stalks<br>– Palisade arrangement of columnar cells<br>– Cells from acute or chronic inflammation<br>– Regressive cell changes | – **Foci of dysplastic cells as an indicator of increased malignant potential** | |

## Liver Cell Dysplasia Sect. 9.1.11, p. 593

### Liver Cell Dysplasia, Large-Cell Type

| Basic cell pattern | Particular and/or additional features | Differential diagnosis or possible diagnostic pitfall |
|---|---|---|
| – Sheets and clusters of mildly atypical hepatocytes<br>– Scattered nuclear pleomorphism<br>– High N/C ratio<br>– Densely granular irregular chromatin<br>– Pleomorphic nucleoli | | – Regenerative nodule/liver cell adenoma<br>– Well-differentiated HCC |

### Liver Cell Dysplasia, Small-Cell Type

| Basic cell pattern | Particular and/or additional features | Differential diagnosis or possible diagnostic pitfall |
|---|---|---|
| – Atypical small hepatocytes in microtrabecular and acinar arrangement<br>– Round to oval nuclei<br>– Irregular granular chromatin<br>– Inconspicuous nucleoli | | – Small-cell malignant tumor |

## Rare Benign Primary Liver Tumors Sect. 9.1.12, p. 593

A few lesions of this large tumor group are worth mentioning where aspiration cytology may be helpful as an initial diagnostic tool: **cavernous hemangioma**, **angiomyolipoma**, **myelolipoma**, **dermoid cyst**.

# Section 9.2
# Liver – Malignant Lesions

## Hepatocellular Carcinoma (HCC) and Its Variants Sects. 9.2.1 and 9.2.2, p. 604

### HCC, Well-Differentiated

| Basic cell pattern | Particular and/or additional features | Differential diagnosis or possible diagnostic pitfall |
|---|---|---|
| – Mostly large cohesive and regular sheets<br>– Endothelial cells coating tumor cell trabeculae<br>– Minimal atypical cells of the hepatoid type, not enlarged as compared to normal hepatocytes<br>– Well-defined granular cytoplasm<br>– Round nucleus with finely granular chromatin<br>– A single conspicuous nucleolus, centrally located<br>– No bile duct cells | | – Reactive / hyperplastic hepatocytes<br>– Regenerative liver nodule<br>– Liver cell adenoma<br>– Liver cell dysplasia (large-cell type)<br>– Well-differentiated neuroendocrine tumor |

### HCC, Well- to Moderately Differentiated

| Basic cell pattern | Particular and/or additional features | Differential diagnosis or possible diagnostic pitfall |
|---|---|---|
| – Atypical cells of the hepatoid type<br>– Large cytoplasm with coarse granulation<br>– Increased N/C ratio<br>– Irregular nuclei with densely packed coarse chromatin<br>– Enlarged nucleoli, centrally located or multiple<br>– Monolayer sheets arborizing fingerlike, focally nuclear overlapping and crowding<br>– Stripped atypical nuclei with cauliflower shape<br>– Characteristic endothelial cell pattern | | |

### HCC, Poorly Differentiated

| Basic cell pattern | Particular and/or additional features | Differential diagnosis or possible diagnostic pitfall |
|---|---|---|
| **Cell features indicative of hepatocytic tumor origin:**<br>– Pleomorphic cells, nuclei, and nucleoli<br>– Intranuclear cytoplasmic inclusions<br>– Varying N/C ratio<br>– Irregular sheets and dense clusters<br>– Frequently isolated tumor cells<br>– Stripped atypical nuclei with cauliflower shape<br>– Cytoplasmic bile pigment | | – Poorly differentiated large-cell endocrine carcinoma<br>– Poorly differentiated adenocarcinoma<br>– Undifferentiated large-cell carcinoma<br>– Malignant melanoma |

### Fibrolamellar variant of HCC

| Basic cell pattern | Particular and/or additional features | Differential diagnosis or possible diagnostic pitfall |
|---|---|---|
| – Extremely large hepatoid cells, single or in small sheets<br>– Normal N/C ratio<br>– Dense granular chromatin<br>– Huge centrally located nucleolus<br>– Abundant polygonal oncocytic cytoplasm<br>– Fibrous and sclerotic tissue | | – Pronounced reactive liver disorders associated with fibrosis<br>– Secondary large-cell neoplasms with oncocytic features |

### Clear cell Variant of HCC

| Basic cell pattern | Particular and/or additional features | Differential diagnosis or possible diagnostic pitfall |
|---|---|---|
| – Sheets or clusters of obvious malignant cells exhibiting abundant clear cytoplasm<br>– Atypical polymorphous hyperchromatic nuclei<br>– Coarse chromatin | | – Metastasis of renal cell carcinoma<br>– Rare secondary clear cell tumors |

## Hepatocellular Carcinoma (HCC) and Its Variants (continued) Sects. 9.2.1 and 9.2.2, p. 604

### Small-Cell Variant of HCC

| Basic cell pattern | Particular and/or additional features | Differential diagnosis or possible diagnostic pitfall |
|---|---|---|
| – Cellular smears showing clusters of small uniform neoplastic cells<br>– Round to oval nuclei with irregular outline<br>– Dense granular chromatin<br>– Inconspicuous or even absent nucleolus<br>– Usually indistinct cytoplasm | | – Various types of small-cell tumors<br>– Neuroendocrine tumor, common type or small-cell variant<br>– Liver cell dysplasia of the small-cell type |

## Neuroendocrine Tumor Sect. 9.2.3, p. 607

### Common Neuroendocrine Tumor (NET)

| Basic cell pattern | Particular and/or additional features | Differential diagnosis or possible diagnostic pitfall |
|---|---|---|
| – Abundant cellular material<br>– Small to medium-sized tumor cells with plasmacytoid features, single and in loose clusters<br>– Eccentrically placed nuclei<br>– Distinct cytoplasm with reddish granulation<br>– Rosette-like and acinar formations | – Huge stripped polymorphous nuclei – variable | – Well-differentiated HCC<br>– Breast cancer metastasis |

### NET of the Large-Cell Type

| Basic cell pattern | Particular and/or additional features | Differential diagnosis or possible diagnostic pitfall |
|---|---|---|
| – Large atypical hepatoid cells, polygonal in shape, often arranged in branching sheets<br>– Dense granular nuclear chromatin<br>– Prominent nucleolus<br>– Eosinophilic cytoplasmic granulation – variable | | – Hepatocellular carcinoma<br>– Metastatic carcinoma of the large-cell type<br>– Metastasis of medullary thyroid carcinoma |

### Small-Cell Neuroendocrine Carcinoma, Poorly Differentiated

| Basic cell pattern | Particular and/or additional features | Differential diagnosis or possible diagnostic pitfall |
|---|---|---|
| – Cell-rich sample<br>– Small malignant cells, occasionally fusiform<br>– Cells occur singly and focally clumping<br>– Very small or absent cytoplasmic rim<br>– Dense granular chromatin and salt-and-pepper pattern | | – Other small-cell cancers in particular metastases<br>– Malignant tumors of the small round cell tumor group |
| | – Predominant fusiform tumor cells | – Varied spindle cell neoplasms<br>– Small-cell, spindle cell amelanotic melanoma |

## Cholangiocarcinoma Sect. 9.2.4, p. 609

### Classic Cholangiocarcinoma

| Basic cell pattern | Particular and/or additional features | Differential diagnosis or possible diagnostic pitfall |
|---|---|---|
| – Classical cytologic features of adenocarcinomas<br>– Palisading malignant columnar cells<br>– Intracytoplasmic and background mucus – variable | | – Secondary adenocarcinomas |

## Uncommon Primary Liver Neoplasia Sect. 9.2.5, p. 609

### Combined Hepatocellular-Cholangiocarcinoma

| Basic cell pattern | Particular and/or additional features | Differential diagnosis or possible diagnostic pitfall |
|---|---|---|
| – Typical neoplastic cells of HCC-type<br>**combined with**<br>– Unequivocal adenocarcinoma | | – **Collision tumors:**<br>(1) HCC and cholangiocarcinoma<br>(2) HCC and metastatic adenocarcinoma |
| **Further uncommon neoplasms**, see Sect. 9.2.5, p. 609 | | |

## Metastatic Tumors

A synopsis of the most frequent secondary cancers and their immunocytochemical features is given in Sects. 9.2.6. and 9.2.7, p. 610, respectively.

# Chapter 10 Pancreas

## Section 10.1 and 10.2
## Pancreas, Extrahepatic Bile Ducts, Ampullary Region

### Cytology of the Pancreas and Bile Ducts Sects. 10.1.4., p. 636 and 10.2.4, p. 682

#### Pancreatic Acinar Cells and Tissue

| Basic cell pattern | Particular and/or additional features | Differential diagnosis or possible diagnostic pitfall |
|---|---|---|
| – Small acinar formations and fragments of acinar tissue in lobular arrangement<br>– Small round to ovoid uniform nuclei, mild variation in size, and smooth distinct membranes<br>– Usually eccentrically and basally placed nuclei<br>– Fine granular and evenly distributed chromatin<br>– Conspicuous small and round nucleoli<br>– Abundant and fine granular cytoplasm, granularity may appear fuzzily in Papanicolaou stain | | |

#### Cells of Small Pancreatic Ducts

| Basic cell pattern | Particular and/or additional features | Differential diagnosis or possible diagnostic pitfall |
|---|---|---|
| – Regular flat sheets of cuboidal to columnar cells<br>– Small round nuclei, occasionally with a tiny nucleolus<br>– Regularly distributed granular chromatin<br>– Relatively scant and poorly defined cytoplasm | | |

#### Cells of Large Pancreatic Ducts (Typical Finding in Brushings or direct Juice Aspiration, But Rarely Found in Fine-Needle Aspirates)

| Basic cell pattern | Particular and/or additional features | Differential diagnosis or possible diagnostic pitfall |
|---|---|---|
| – Small to medium-sized cells of cuboidal and columnar shape, isolated, in palisade arrangement, or in regular flat honeycomb sheets<br>– Round nuclei, distinctly outlined<br>– Evenly dispersed and granular chromatin<br>– Distinct nucleoli – variable<br>– Well-defined, densely structured or vacuolated cytoplasm<br>– Cell degeneration – variable | – Markedly elongated cytoplasm<br>– Pronounced cellular degeneration | – Bile-duct lining epithelial cells<br>– Tumor necrosis |

#### Islet Cells of the Endocrine Fraction of the Pancreas

| Basic cell pattern | Particular and/or additional features | Differential diagnosis or possible diagnostic pitfall |
|---|---|---|
| – Cells singly or in loose aggregates<br>– Nuclei sharing morphologic features of common pancreatic acinar cells<br>– Usually blurred cytoplasm | | – Acinar cells of benign pancreatic parenchyma |

#### Cells of Large Bile Ducts (Typical Finding in Brushings and Duodenal Secretions, But Rarely Found in Fine-Needle Aspirates)

| Basic cell pattern | Particular and/or additional features | Differential diagnosis or possible diagnostic pitfall |
|---|---|---|
| – Slender, elongated columnar cells, so-called **matchstick cells**<br>– Basally located small round nuclei with regular outline<br>– Bland chromatin<br>– Small round nucleolus – variable<br>– Smoothly outlined pale cytoplasm, dense or vacuolated | – A variety of metaplastic lesions – variable: pyloric gland, intestinal, and squamous metaplasia<br>– Numerous cuboidal epithelial cells | – Pancreas-duct lining epithelial cells |

## Cytology of the Pancreas and Bile Ducts (continued) Sects. 10.1.4., p. 636 and 10.2.4, p. 682

### Cells of Duodenal Lining Epithelium (Typical Finding in Brushings, Juice Collected from the Orifice of the Ampulla of Vater, and Duodenal Secretions)

| Basic cell pattern | Particular and/or additional features | Differential diagnosis or possible diagnostic pitfall |
|---|---|---|
| – Cuboid to cylindric cells with a prominent brush border arranged in regular flat sheets<br>– Sheets with honeycomb appearance interspersed with goblet cells | – Numerous isolated superficial duodenal cells, lacking brush borders | – Cells of biliary and/or pancreatic duct origin |

### Cell Damage Due to Thermal Cautery (Typical Finding in Brushings Combined with Endoscopic Retrograde Cholangiography)

| Basic cell pattern | Particular and/or additional features | Differential diagnosis or possible diagnostic pitfall |
|---|---|---|
| – Degenerated mucosal epithelial cells appear isolated and clustered<br>– Pronounced elongation of the cytoplasm and nuclei<br>– Deeply stained, homogeneous nuclei | | – Spindle cell neoplasia, benign or malignant |

## Contaminants in FNABs and Brushings Sects. 10.1.4, p. 636 and 10.2.4, p. 682

### Mesothelial Cells (Typical Finding in Transcutaneous FNA Samples)

| Basic cell pattern | Particular and/or additional features | Differential diagnosis or possible diagnostic pitfall |
|---|---|---|
| – Large sheets of flattened cells, some sheets may be folded<br>– Centrally placed and widely spaced nuclei<br>– Indented nuclei, clear nucleoplasm and blurred chromatin texture<br>– Conspicuous nucleoli – variable | – Activated, regenerative mesothelial cells with distinct nucleoli | – Carcinoma |

### Gastrointestinal Epithelium (Presenting Diagnostic Dilemmas in Endoscopic-Guided Aspirations)

| Basic cell pattern | Particular and/or additional features | Differential diagnosis or possible diagnostic pitfall |
|---|---|---|
| – Sheets and single cells of the gastric and intestinal epithelial layers<br>– Nuclear irregularities and overlapping – variable<br>– Intracytoplasmic and background mucus – variable | **Variable morphologic appearance dependent on the origin of the cells (stomach, duodenum, small bowel, large bowel)**<br>– Endoscopic-guided FNAB of the pancreas comprising numerous mucinous cells, single cells, and sheets (as a contaminant) | – Mucinous cystic pancreatic tumor |

### Intramural Ampullary and Duodenal Glands (Generally Resulting from Vigorous Brushing the Ampullary Area)

| Basic cell pattern | Particular and/or additional features | Differential diagnosis or possible diagnostic pitfall |
|---|---|---|
| – Polygonal and more voluminous cells (as compared to duct-lining cells)<br>– Nuclei varying in size and shape<br>– Distinct nucleoli of variable size<br>– Usually abundant clear cytoplasm, coarsely vacuolated<br>– Irregular cell clustering and nuclear crowding – variable | | – Adenocarcinoma of the clear cell type |

## Inflammation, Infection, and Infectious Cysts: Findings in Pancreatic Aspirates
Sect. 10.1.5, p. 637

### Early Form of Acute Pancreatitis

| Basic cell pattern | Particular and/or additional features | Differential diagnosis or possible diagnostic pitfall |
|---|---|---|
| – Degenerated fat cells (fat necrosis)<br>– Foam cells: lipid-laden vacuolated macrophages<br>– Numerous neutrophils<br>– Granular debris<br>– Degenerating and necrotic acinar and ductal cells showing small pyknotic dark-staining nuclei – variable | | |

### Healing Form of Acute Pancreatitis

| Basic cell pattern | Particular and/or additional features | Differential diagnosis or possible diagnostic pitfall |
|---|---|---|
| – Same basic cell pattern as stated above, and<br>– Granulation tissue with reactive immature fibroblasts<br>– Activated histiocytes and proliferating capillaries<br>– Frequent granular calcium deposits<br>– Numerous leukocytes of various types | – Pronounced activation of fibroblasts, histiocytes, and endothelial cells | – Large-cell carcinoma and fibrosclerosis |

10

### Chronic Pancreatitis

| Basic cell pattern | Particular and/or additional features | Differential diagnosis or possible diagnostic pitfall |
|---|---|---|
| – Minor acinar cell component<br>– Ductal cells are the dominant cell type, arranged in small cohesive slightly irregular sheets<br>– Loose and regular chromatin distribution<br>– Usually vacuolated cytoplasm<br>– Background with lymphocytes, plasma cells, and fragments of fibrosclerotic tissue | – Duct cell squamous metaplasia: densely structured and sharply outlined cytoplasm, small bland nuclei | |
| | – Ductal cells may display atypical features:<br>– Sheets with focal nuclear overlapping<br>– Slightly enlarged nuclei (compared to normal cells) varying in size and shape<br>– N/C ratio normal or slightly increased<br>– Nuclear wrinkling and indentations – variable<br>– Conspicuous nucleoli, variable in size | – Adenocarcinoma of the pancreas, well to moderately differentiated |
| | – Dense lymphoplasmacytic infiltrates | – Autoimmune pancreatitis |

### Tuberculosis

| Basic cell pattern | Particular and/or additional features | Differential diagnosis or possible diagnostic pitfall |
|---|---|---|
| – Caseous necrosis<br>– Epithelioid histiocytes<br>– Langhans giant cells<br>– Neutrophils and/or lymphoplasmacytic infiltrate | | – Nonspecific granulomatous disease<br>– Mycotic infection<br>– Cancer necrosis |

### Hydatid Cyst (Echinococcosis)

| Basic cell pattern | Particular and/or additional features | Differential diagnosis or possible diagnostic pitfall |
|---|---|---|
| – Typical homogeneous and opaque debris<br>– Hooklets – variable, often extremely scanty!<br>– Scolices – often missing<br>– Sporadic nucleated cells | | |

**Cystic lesions** caused by other **protozoal and helminth infections** are describe in distinguished textbooks.

## Inflammation and Infection: Selected Entities in Bile Duct Cytology and Duodenal Aspirates Sect. 10.2.5, p. 683

### Nonspecific Inflammations and Infections

| Basic cell pattern | Particular and/or additional features | Differential diagnosis or possible diagnostic pitfall |
|---|---|---|
| – Cell-rich samples<br>– Mixture of inflammatory cells and epithelial cells<br>– Poor preservation of epithelial cells: degenerated cells show cytoplasmic vacuolization or shrinkage together with chromatin clumping and karyorrhexis.<br>– Numerous stripped nuclei<br>– Bile pigment is usually present | | |

### *Giardia lamblia*

| Basic cell pattern | Particular and/or additional features | Differential diagnosis or possible diagnostic pitfall |
|---|---|---|
| – The stained parasite has a characteristic appearance, looking like a smiley face<br>– Trophozoites have large karyosomes and lack of peripheral chromatin, giving the two nuclei a halo appearance | | |

Further comments on inflammation and infections are provided in Sect. 10.2.5, p. 683.

## Nontumorous Cystic Lesions: Findings in Aspirates Sect. 10.1.6, p. 639

### Pseudocyst

| Basic cell pattern | Particular and/or additional features | Differential diagnosis or possible diagnostic pitfall |
|---|---|---|
| – Practically lacking cyst-lining epithelial cells<br>– Mixed inflammatory component – variable<br>– Usually hemosiderin-laden macrophages<br>– Background with debris, blood, and hemosiderin<br>– Bile pigment may be observed | | – Retention cyst |

### Retention Cyst

| Basic cell pattern | Particular and/or additional features | Differential diagnosis or possible diagnostic pitfall |
|---|---|---|
| – Cytologic features similar to those of pseudocysts, but cyst-lining epithelial cells often occur | – Mucinous epithelial cells<br>– Islet cells from neighboring pancreatic tissue | – Pseudocyst<br>– Mucinous cystic neoplasia<br>– Cystic islet cell tumor |

### Congenital Cyst

| Basic cell pattern | Particular and/or additional features | Differential diagnosis or possible diagnostic pitfall |
|---|---|---|
| – Scant cellularity<br>– Single cuboid epithelial cells with bland nuclei<br>– Usually basophilic cytoplasm, sharply outlined | – Bland squamous epithelial cells – variable | – Other squamous cell-lined cysts (e.g., dermoid cyst) |

## Nontumorous Cystic Lesions: Findings in Aspirates Sect. 10.1.6, p. 639 (continued)

### Lymphoepithelial Cyst

| Basic cell pattern | Particular and/or additional features | Differential diagnosis or possible diagnostic pitfall |
|---|---|---|
| – Cell-rich cytologic samples<br>– Benign superficial squamous cells and anucleated squames<br>– Histiocytes and lymphocytes<br>– Cholesterol crystals | **Extremely scarce or absent lymphocytes prevent a conclusive diagnosis** | – Dermoid cyst<br>– Congenital cyst<br>– Parapancreatic squamous cysts |
| | – Mucin-secreting cells may rarely be encountered | – Retention cyst<br>– Mucinous cystic neoplasia |

**Rare cystic lesions** are discussed in Sect. 10.1.6.5, p. 640.

## Neoplastic Cysts: Findings in Aspirates Sect. 10.1.7, p. 640

### Serous Cystadenoma

| Basic cell pattern | Particular and/or additional features | Differential diagnosis or possible diagnostic pitfall |
|---|---|---|
| – Proteinaceous background<br>– Scarce epithelial cells with cuboidal or small-columnar shape arranged in small regular sheets<br>– Round smooth nucleus with bland chromatin texture,<br>– Usually indistinct nucleoli,<br>– Clear vacuolated and sharply outlined cytoplasm, Intracytoplasmic glycogen<br>– Foamy macrophages – variable<br>– Fragments of fibrous stroma – variable | **Extremely scarce or absent epithelial cells usually prevent a conclusive diagnosis** | – Other benign cystic lesions |
| | – Gastrointestinal epithelium contaminants (EUS-FNAB !) | – Mucinous cystic tumor |

### Mucinous Cystic Neoplasm

| Basic cell pattern | Particular and/or additional features | Differential diagnosis or possible diagnostic pitfall |
|---|---|---|
| – Background mucin<br>– Columnar shaped cells containing mucin, arranged in honeycomb-patterned flat sheets and palisading rows<br>– Isolated cells mucin producing or appearing as goblet cells<br>– Bland nuclei, indistinct nucleoli | | – Intraductal papillary-mucinous tumor<br>– **Simple cyst or serous cystadenoma attended by gastrointestinal epithelium contaminants (EUS-FNAB !)** |
| | – Numerous activated foamy histiocytes and mucin-containing macrophages | – Poorly differentiated adenocarcinoma |

### Mucinous Cystic Adenoma

| Basic cell pattern | Particular and/or additional features | Differential diagnosis or possible diagnostic pitfall |
|---|---|---|
| – Background mucin<br>– Aspirates of low to moderate cellularity<br>– Round nuclei, bland chromatin, and small nucleoli<br>– Cytoplasmic mucin | | – Mucin-producing retention cyst |

### Mucinous Cystic Borderline Tumor

| Basic cell pattern | Particular and/or additional features | Differential diagnosis or possible diagnostic pitfall |
|---|---|---|
| – Enlarged cells as compared with benign cyst-lining epithelium<br>– Size-variable nuclei with membrane irregularities<br>– Increased N/C ratio<br>– Distinct nucleoli<br>– Granular and coarse chromatin<br>– More pronounced cellular palisading as compared to benign cystic neoplasms and varying complexity of clustering | | – Intraductal papillary-mucinous tumor |

## Neoplastic Cysts: Findings in Aspirates Sect. 10.1.7, p. 640 (continued)

### Mucinous Cystadenocarcinoma, Noninvasive or Invasive

| Basic cell pattern | Particular and/or additional features | Differential diagnosis or possible diagnostic pitfall |
|---|---|---|
| – Highly cellular aspirates<br>– Three-dimensional cell clusters showing acinar or small papilliform formation<br>– Marked cellular dyshesion<br>– Cells with unambiguous features of malignancy:<br>  – High N/C ratio<br>  – Wrinkled and folded nuclei, dark nucleoplasm<br>  – Irregularly distributed granular and coarse chromatin<br>– Frequently multiple prominent nucleoli | | – Cystic degenerative adenocarcinoma (primary or secondary pancreatic cancer)<br>– Intraductal papillary-mucinous tumor |
| | – Substantial mitotic activity and necrosis | – Usually: invasive cystadenocarcinoma |

### Intraductal Papillary-Mucinous Neoplasm (IPMN)

| Basic cell pattern | Particular and/or additional features | Differential diagnosis or possible diagnostic pitfall |
|---|---|---|
| – Abundant extracellular viscous mucin<br>– Entrapped in background mucin or aside:<br>  – Cohesive sheets of mucinous epithelial cells,<br>  – Goblet-cells commonly occurring,<br>  – Papillary clusters – variable<br>– Histiocytes and mucin-laden macrophages<br>– Inflammatory infiltrates – rarely encountered | – Varied degrees of cellular atypia | – Mucinous cystic neoplasms<br>– Common ductal carcinoma with varying degrees of differentiation |
| | – Clusters with irregular cell arrangement<br>– Numerous nonmucinous epithelial cells and large number of single cells<br>– Severe nuclear atypia with nuclear clearing<br>– Necrosis | – Suggestive of malignant IPMN |

### Solid Pseudopapillary Tumor

| Basic cell pattern | Particular and/or additional features | Differential diagnosis or possible diagnostic pitfall |
|---|---|---|
| – Highly cellular smears<br>– Numerous branching papillary fragments with:<br>  – Delicate fibrovascular cores surrounded by myxoid stroma<br>  – Superficial neoplastic cells: mono- or multilayered<br>– Myxoid and mucoid tissue fragments with or without cell cover<br>– Monomorphic neoplastic cells:<br>  – Usually oval vesicular nuclei with distinct grooves and inclusions<br>  – Fine granular chromatin<br>  – Small but conspicuous nucleoli<br>  – Amphophilic ill-defined cytoplasm, occasionally granulated<br>– Background: macrophages and necrosis | | |

**Rare cystic tumors** and **tumors with variable cystic components** are summarized in Sect. 10.1.7.5, p. 642.

**Benign epithelial and mesenchymal tumors of the extrahepatic biliary tract and ampullary region are briefly discussed in Sect. 10.2.6, p. 684**

## Invasive Carcinomas of the Duct Cell Type (Pancreas, Biliary Tree, Ampullary Area) Sects. 10.1.8, p. 643 and 10.2.7, p. 684

### Well-Differentiated Ductal Adenocarcinoma

| Basic cell pattern | Particular and/or additional features | Differential diagnosis or possible diagnostic pitfall |
|---|---|---|
| – Usually cellular smears<br>– Small and large cohesive sheets with sharply defined margins, peripheral dissociation of cells is absent<br>– Flat sheets with honeycomb appearance, or tightly packed cells with nuclear crowding and overlapping<br>**Typical nuclear morphology:**<br>– Considerable variations in size<br>– Nuclear membrane irregularities detectable on each nucleus comprising tiny wrinkles, folds, or subtle lobation<br>– Chromatin clearing or fine granular irregular chromatin texture<br>– Conspicuous small nucleoli – variable<br>– Clear and sharply outlined cytoplasm, vacuolated or mucinous<br>– Mitoses – variable in number<br>– Rare necrosis | | – Secondary adenocarcinoma |

### Moderately Differentiated Ductal Adenocarcinoma

| Basic cell pattern | Particular and/or additional features | Differential diagnosis or possible diagnostic pitfall |
|---|---|---|
| – Same basic cytological features as stated above, but<br>– Increased irregular cell arrangement and three-dimensional cell clusters<br>– Nuclear pleomorphism: indentations, cleaving and lobulation<br>– Coarse chromatin and hyperchromasia<br>– Micronucleoli and occasional macronucleoli<br>– Mitoses and necrosis | | – Secondary adenocarcinoma |

### Poorly Differentiated Ductal Adenocarcinoma

| Basic cell pattern | Particular and/or additional features | Differential diagnosis or possible diagnostic pitfall |
|---|---|---|
| – Irregular three-dimensional cell clusters<br>– Marked dissociation, numerous single cells<br>– Marked cellular and nuclear pleomorphism, high N/C ratio<br>– Coarse chromatin and pronounced hyperchromasia<br>– Numerous mitoses<br>– Extensive necrosis | – In cases exhibiting only sporadic tumor cells | – Secondary undifferentiated carcinoma<br>– Non-Hodgkin lymphoma, blastic type<br>– Markedly activated histiocytes/ macrophages |

### Adenosquamous Carcinoma

| Basic cell pattern | Particular and/or additional features | Differential diagnosis or possible diagnostic pitfall |
|---|---|---|
| – Biphasic tumor growth pattern: Mucinous and squamoid (keratinized) malignant cells<br>– Varying degrees of cellular differentiation<br>– **Squamous component should account for > 30%** of the whole tumor cell population | – Exceptionally high proportion of malignant squamous cells | – Secondary adenosquamous carcinoma<br>– Squamous cell carcinoma (primary or metastatic) |

## Invasive Carcinomas of the Duct Cell Type (Pancreas, Biliary Tree, Ampullary Area) Sects. 10.1.8, p. 643 and 10.2.7, p. 684 (continued)

### Clear Cell Pancreatic Carcinoma

| Basic cell pattern | Particular and/or additional features | Differential diagnosis or possible diagnostic pitfall |
|---|---|---|
| – Malignant epithelial cells with abundant clear cytoplasm<br>– **Clear cell component accounts for >90%** | | – Clear cell pancreatic endocrine tumor<br>– Any metastatic clear cell carcinoma:<br>Renal clear cell carcinoma<br>Adrenocortical carcinoma<br>Tumors of the female genital tract<br>Lung cancer<br>Clear cell neoplasms of other body sites |
| | – Many isolated, degenerating tumor cells | – Strongly activated histiocytes/ macrophages |

### Oncocytic Neoplasm: Ductal Type

| Basic cell pattern | Particular and/or additional features | Differential diagnosis or possible diagnostic pitfall |
|---|---|---|
| Typical oncocytoid cells:<br>– Large cytoplasm with distinct eosinophilic granulation<br>– Rounded nuclei with smooth border<br>– Large nucleolus<br>– Cellular atypias according to the tumor grade | | – Endocrine tumor of the pancreas<br>– Acinar cell carcinoma<br>– Metastases of oncocytic-type carcinoma |

**Other rare variants of ductal carcinoma of the pancreas** and **precursor lesions**, see Sects. 10.1.8.2. and 10.1.8.3, p. 644.

**Carcinomas of the bile ducts and the ampulla of Vater** usually exhibit related morphologic features; for details see Sect. 10.2.7, p. 684.

## Other Malignant Neoplasms of the Exocrine Pancreas Sect. 10.1.9, p. 645

### Pancreatic Undifferentiated Small-Cell Carcinoma

| Basic cell pattern | Particular and/or additional features | Differential diagnosis or possible diagnostic pitfall |
|---|---|---|
| – Undifferentiated small carcinoma cells share morphologic features with those of small-cell carcinomas from other sites of the human body, in particular of the lung | | – Metastatic small-cell carcinomas |

### Acinar Cell Carcinoma

| Basic cell pattern | Particular and/or additional features | Differential diagnosis or possible diagnostic pitfall |
|---|---|---|
| – Highly cellular smears<br>– Monomorphic tumor cells, slightly enlarged compared to benign acinar cells<br>– Large and small loosely cohesive clusters comprising prominent acinar and acini-like formations<br>– Numerous isolated cells often stripped<br>– Bland chromatin texture<br>– Granular cytoplasm, scant to moderate in size<br>– One or two prominent nucleoli | | – Benign pancreatic parenchymatous tissue<br>– Endocrine pancreatic tumor |
| | – Nuclear grooves and inclusions | – Solid pseudopapillary tumor of the pancreas |

## Other Malignant Neoplasms of the Exocrine Pancreas Sect. 10.1.9, p. 645 (continued)

### Osteoclastic Giant Cell Tumor

| Basic cell pattern | Particular and/or additional features | Differential diagnosis or possible diagnostic pitfall |
|---|---|---|
| Two different cell types:<br>– Multinucleated giant cells of osteoclast type with bland appearing nuclei<br>– Mononuclear cells showing variable nuclear pleomorphism<br>– Pleomorphic spindle cells – variable | | – Pleomorphic giant cell carcinoma |

### Pancreatoblastoma

| Basic cell pattern | Particular and/or additional features | Differential diagnosis or possible diagnostic pitfall |
|---|---|---|
| Cell-rich cytologic preparations with a biphasic cell pattern:<br>– Mesenchymal tissue fragments composed of primitive spindle cells<br>– Epithelial cells: Cohesive sheets and loose aggregates with acinar differentiation and occasional squamoid corpuscles | – Heterologous elements such as cartilage – variable | – Acinar cell carcinoma<br>– Endocrine tumor<br>– Other pancreatic tumors |

## Endocrine Tumors of the Pancreas, Bile Ducts, and Ampullary Region Sect. 10.1.10, p. 646



### Endocrine Tumor of the Common Type

| Basic cell pattern | Particular and/or additional features | Differential diagnosis or possible diagnostic pitfall |
|---|---|---|
| – Highly cellular smears<br>– Homogeneous cell population<br>– Predominantly isolated cells but also loose cell aggregates and rosette-like structures<br>– Monomorphic round to oval nuclei, smooth membranes<br>– Finely granular and evenly distributed chromatin<br>– Large cytoplasm vacuolated and ill defined, or dense and sharply outlined with eccentrically placed nuclei (plasmacytoid appearance)<br>– Fibrovascular stromal fragments are usually present<br>– Multiple nuclei, hyperchromasia, small nucleoli – variable<br>– Mitoses – variable | | – Dissociation of pancreatic acini<br>– Islet cell hyperplasia<br>– Solid pseudopapillary tumor of the pancreas<br>– Pancreatic acinar cell carcinoma<br>– Malignant melanoma<br>– Malignant lymphoma |
| | – Only individual tumor cells with plasmacytoid appearance | – Plasmacytoma |

### Poorly Differentiated Endocrine Carcinoma

| Basic cell pattern | Particular and/or additional features | Differential diagnosis or possible diagnostic pitfall |
|---|---|---|
| – Large pleomorphic tumor cells<br>– Nuclei, variable in size and shape<br>– Large nucleoli<br>– Dense coarsely granular chromatin<br>– Eosinophilic cytoplasmic granularity – variable<br>– Mitoses<br>– Necrotic debris is common | | – Poorly differentiated pancreatic adenocarcinoma<br>– Metastatic poorly differentiated carcinoma |

### Clear Cell Endocrine Tumor

| Basic cell pattern | Particular and/or additional features | Differential diagnosis or possible diagnostic pitfall |
|---|---|---|
| – Tumor cells with abundant clear and vacuolated cytoplasm<br>– Cellular and nuclear polymorphism – variable | | – Clear cell ductal pancreatic carcinoma<br>– Any metastatic clear cell carcinoma |

## Endocrine Tumors of the Pancreas, Bile Ducts, and Ampullary Region (continued) Sect. 10.1.10, p. 646

### Oncocytic Endocrine Tumor

| Basic cell pattern | Particular and/or additional features | Differential diagnosis or possible diagnostic pitfall |
|---|---|---|
| – Characteristic oxyphilic cells:<br>  – Large polygonal or round cytoplasm, densely packed with granules<br>  – Round and dark-stained nuclei,<br>  – Centrally placed large nucleoli<br>– Cellular polymorphism – variable | | – Oncocytic pancreatic neoplasm – ductal type<br>– Acinar cell pancreatic carcinoma<br>– Metastases of oncocytic-type carcinomas |

### Mucinous Variant of Pancreatic Endocrine Tumor

| Basic cell pattern | Particular and/or additional features | Differential diagnosis or possible diagnostic pitfall |
|---|---|---|
| – Mucinous tumor cells<br>– Goblet cells – variable<br>– Cellular and nuclear polymorphism – variable | | – Mucinous adenocarcinomas – primary or metastatic |

Comments on various rare tumors of the pancreas and bile ducts including metastases are provided in Sects:

**Sect. 10.1.11, "Other Pancreatic Tumors and Metastases to the Pancreas," p. 647**

**Sect. 10.2.10, "Metastases to the Biliary Tract," p. 686**

# Chapter 11 Gastrointestinal Tract

## Esophagus – Barrett Esophagus – Stomach – Bowel – Anal canal – Perirectal area

### Normal Cytology and Benign Nontumoral Lesions of the Esophagus
Sect. 11.2.2, p. 702, and 11.2.3, p. 703

#### Normal cytology

| Basic cell pattern | Particular and/or additional features | Differential diagnosis or possible diagnostic pitfall |
|---|---|---|
| – Superficial and intermediate squamous cells<br>– Nuclear pyknosis – variable<br>– Rare keratinization<br>– Rarely parabasal and basal squamous cells<br>– Round to oval nuclei with smooth contour and vesicular chromatin pattern | – Glandular cells with or without mucus secretion | – Esophageal mucosal glands<br>– Intestinal metaplasia (Barrett esophagus)<br>– Gastric mucosa |

#### Granulomatous Diseases (Various Types)

| Basic cell pattern | Particular and/or additional features | Differential diagnosis or possible diagnostic pitfall |
|---|---|---|
| – Neutrophilic granulocytes and lymphocytes<br>– Epithelioid histiocytes, histiocytic giant cells<br>– Granuloma fragments / microgranulomas<br>– Reactive changes of squamous cells | | |

#### Reflux Esophagitis

| Basic cell pattern | Particular and/or additional features | Differential diagnosis or possible diagnostic pitfall |
|---|---|---|
| – Mixed inflammatory cell pattern<br>– Superficial and intermediate squames<br>– Parabasal and basal squamous cells | – Reactive cell changes – variable<br>– Numerous parabasal/ basal squames | – Undifferentiated small cell carcinoma |

#### Eosinophilic Esophagitis (Suggestive of)

| Basic cell pattern | Particular and/or additional features | Differential diagnosis or possible diagnostic pitfall |
|---|---|---|
| – Superficial and intermediate squames<br>– Numerous eosinophilic granulocytes | | |

#### Acute Esophagitis

| Basic cell pattern | Particular and/or additional features | Differential diagnosis or possible diagnostic pitfall |
|---|---|---|
| – Purulent exudate: numerous degenerating neutrophilic granulocytes<br>– Cellular debris<br>– Squamous cells – variable | **Acute esophagitis is frequently caused by fungi!**<br><br>**Additional staining methods are inevitable for detection of microbial pathogens** | |

## Normal Cytology and Benign Nontumoral Lesions of the Esophagus Sect. 11.2.2, p. 702, and 11.2.3, p. 703 (continued)

### Herpes simplex virus infection

| Basic cell pattern | Particular and/or additional features | Differential diagnosis or possible diagnostic pitfall |
|---|---|---|
| – Considerably enlarged immature squamous cells<br>– Peculiar narrow rim of cytoplasm<br>– Nuclei present in a three-dimensional fashion (ballooned) with smooth margins, either pale ground glass nucleoplasm or a single eosinophilic inclusion surrounded by a halo<br>– Granular chromatin located at the inner surface of the nuclear membrane<br>– The affected cells are often multinucleated | | **Virus-altered cells should not be mistaken for carcinoma !** |

### Reactive/Reparative Squamous Cell Changes

| Basic cell pattern | Particular and/or additional features | Differential diagnosis or possible diagnostic pitfall |
|---|---|---|
| – Cytoplasm of the squamous cells with abnormal acidophilia and irregularities in shape<br>– Enlarged nuclei, but their borders tend to be smooth<br>– Loose chromatin pattern – possibly abnormalities<br>– Prominent and multiple nucleoli – variable<br>– Increased N/C ratio – variable | | – Mild to moderate dysplastic epithelial cell changes |

**Benign Tumors of the Esophagus see Sect. 11.2.4, p. 703.**

## Esophageal Premalignant Lesions and Squamous Cell Carcinoma Sects. 11.2.5 – 11.2.7, p. 704

### Low-Grade Squamous Cell Dysplasia

| Basic cell pattern | Particular and/or additional features | Differential diagnosis or possible diagnostic pitfall |
|---|---|---|
| – Keratinized superficial squamous cells, either anucleated or containing pyknotic nuclei<br>– Parakeratotic squamous cells<br>– Orangeophilic and eosinophilic cytoplasm<br>– Mild cytoplasmic and nuclear polymorphism (similar to regenerative cell changes) | | – Benign hyperkeratosis/parakeratosis<br>– Reactive/regenerative cell changes<br><br>**Bear in mind: underlying severe dysplasia or carcinoma!** |

### High-Grade Squamous Cell Dysplasia And Carcinoma In Situ

| Basic cell pattern | Particular and/or additional features | Differential diagnosis or possible diagnostic pitfall |
|---|---|---|
| – Marked cytoplasmic and nuclear pleomorphism<br>– Coarse chromatin texture<br>– Increased N/C ratio<br>– Mitotic activity<br>– Detritus rarely occurs | | – Invasive squamous cell carcinoma |

### Keratinized Squamous Cell Carcinoma: Well-Differentiated

| Basic cell pattern | Particular and/or additional features | Differential diagnosis or possible diagnostic pitfall |
|---|---|---|
| – Abundant keratinized anucleated cells<br>– Dense red and orangeophilic cytoplasm<br>– Scant cytoplasmic pleomorphism, and pearl formation – variable<br>– A few squamous cells contain nuclei with minor irregularities: irregular outline, abnormal texture and abnormal color | | – Reactive/reparative cell changes<br><br>– Intensely keratinized leukoplakic lesions, benign or dysplastic |

## Esophageal Premalignant Lesions and Squamous Cell Carcinoma
## Sects. 11.2.5 – 11.2.7, p. 704 (continued)

### Squamous Cell Carcinoma: Moderate to Poor Differentiation

| Basic cell pattern | Particular and/or additional features | Differential diagnosis or possible diagnostic pitfall |
|---|---|---|
| **Extreme variation in tumor cell maturation:** keratinization is much less prominent and variable, but anucleated intensely keratinized cells may occur<br>– Enlarged nuclei with marked pleomorphism<br>  – Usually prominent and irregular nuclear borders<br>  – Distinct hyperchromasia<br>  – Irregular chromatin texture<br>  – One or multiple prominent nucleoli<br>  – Increased N/C ratio<br>  – Usually leukocytes, red blood cells, and necrotic debris | | – High-grade intraepithelial neoplasia (dysplasia)<br>– Poorly differentiated adenocarcinoma and large-cell undifferentiated carcinoma (in cases with absent keratinized tumor cells)<br>– Metastatic squamous cell carcinoma |

## Barrett Esophagus (Intestinal Metaplasia) Sect. 11.2.8, p. 705

### Benign Barrett Epithelium

| Basic cell pattern | Particular and/or additional features | Differential diagnosis or possible diagnostic pitfall |
|---|---|---|
| – Columnar cells and few goblet cells appearing isolated, or in palisade alignment closely attached to each other, or in tightly cohesive regular sheets<br>– Uniform nuclear spacing, nuclear overlapping is absent<br>– Small round to oval nuclei, situated at the base of the cytoplasm<br>– Loose chromatin and pale nucleoplasm<br>– Indistinct nucleoli<br>– Low N/C ratio | | – Esophageal mucosal glands<br>– Gastric mucosa |
| | – Slightly enlarged nuclei with inconspicuous irregularities of the membrane<br>– Distinct round, centrally placed nucleoli<br>– Low mucus production | – Reactive/regenerative Barrett mucosa<br>– Barrett mucosa with low-grade dysplasia |

### Barrett Mucosa with Low-Grade Dysplasia

| Basic cell pattern | Particular and/or additional features | Differential diagnosis or possible diagnostic pitfall |
|---|---|---|
| – Columnar cells and a few goblet cells<br>– Enlarged nuclei:<br>  – Moderate membrane irregularities<br>  – Faint hyperchromasia<br>  – Fine granular or reticular chromatin<br>– Distinct single or multiple nucleoli<br>– Cuboid to cylindric cytoplasm, occasionally rounded<br>– Irregular basal position of the nuclei<br>– Irregular sheets and irregular cellular palisading | | – Reactive/regenerative Barrett mucosa |

### Barrett Mucosa with High-Grade Dysplasia

| Basic cell pattern | Particular and/or additional features | Differential diagnosis or possible diagnostic pitfall |
|---|---|---|
| – Distinct cytoplasmic and nuclear pleomorphism<br>– Three-dimensional cell clustering<br>– Irregular nuclear membranes<br>– Finely granular or coarse chromatin texture<br>– Hyperchromasia – variable<br>– Conspicuous nucleoli<br>– Increased N/C ratio<br>– Mitotic activity | | – Adenocarcinoma |
| | – Marked mucus production<br>– Signet ring cells<br>– Necrosis | – Invasive esophageal adenocarcinoma<br>– Metastatic adenocarcinoma |

## Stomach, Bowel, Anal Canal, Perirectal Area (Selected Entities) Sect. 11.3, p. 707

### Extraneous Cells and Material

| Basic cell pattern | Particular and/or additional features | Differential diagnosis or possible diagnostic pitfall |
|---|---|---|
| – Bronchial columnar cells, ciliated columnar cells, mucus producing cells<br>– Pulmonary macrophages, intracytoplasmic anthracotic and blood pigment | | – Swallowed material from the respiratory tract |
| – Intestinal epithelial cells<br>– Feces<br>– Mature superficial and intermediate squamous cells | | – Rectovaginal fistula |
| – Intestinal epithelial cells<br>– Feces<br>– Urothelial cells | | – Rectovesical fistula |
| – Vegetable cells<br>– Meat fibers | | – Food particles<br>**Caution: can mimic tumor cells or vermicular eggs!** |
| – Other ingested foreign material | | |

### Gastrointestinal Stromal Tumor

| Basic cell pattern | Particular and/or additional features | Differential diagnosis or possible diagnostic pitfall |
|---|---|---|
| Cytologic specimens with abundant cellularity and biphasic cellular pattern:<br>– **Spindle cell fraction**<br>– Uniform spindle cells arranged in fascicles or whorls<br>– Focal nuclear palisading<br>– Bland nuclei<br>– Ill-defined cytoplasmic borders<br>– Myxoid stroma<br>– **Epithelioid cell fraction**<br>– Epithelioid cells<br>– Tumor cells arranged singly or in small clusters<br>– Often irregularly outlined round nuclei<br>– Frequently multinucleated cells<br>– Small nucleoli<br>– Rim of eosinophilic or clear cytoplasm, well-defined cytoplasmic borders, occasionally with plasmacytoid features<br>– Collagenous stromal fragments | | |
| | – Cellular pleomorphism<br>– Mitoses and necrosis | – Poorly differentiated carcinoma (e.g., squamous cell carcinoma) |
| | – Pure spindle cell pattern | – Benign tissue fragments from the gastrointestinal wall<br>– Intra-abdominal fibrosis<br>– Fibrous tumors<br>– Leiomyomatous tumors<br>– Kaposi sarcoma<br>– Nerve-sheath tumor |
| | – Pure epithelioid cell pattern | – Adenocarcinoma |

## Stomach, Bowel, Anal Canal, Perirectal Area (Selected Entities) (continued) Sect. 11.3, p. 707

### Chordoma

| Basic cell pattern | Particular and/or additional features | Differential diagnosis or possible diagnostic pitfall |
|---|---|---|
| – Physaliferous cells with vacuolated and bubbly cytoplasm<br>– The spectrum of cellular types including:<br>  – Mono- or binucleated large cells<br>  – Uniform small cells<br>  – Rounded epithelium-like cells<br>  – Spindle-shaped cells<br>  – Giant cells<br>– In the majority of cells the cytoplasm is clear and vacuolated<br>– Cells occur dissociated and in small groups<br>– Distinct chondroid extracellular matrix | | – Chondrogenic tumors<br>– Myxoid liposarcoma<br>– Ependymoma<br><br>– Metastatic clear cell carcinoma<br>– Mucin-producing adenocarcinoma |

### Squamous Cell Carcinoma with Basaloid Features

| Basic cell pattern | Particular and/or additional features | Differential diagnosis or possible diagnostic pitfall |
|---|---|---|
| – Small malignant cells (imitating small-cell carcinoma of the lung)<br>– The tumor cells may focally occur in palisade arrangement | | – Basal cell carcinoma<br><br>– Metastases of small-cell carcinomas<br><br>– Endocrine tumor |

**Additional lesions** of the gastrointestinal tract are discussed in Sect. 11.3, p. 707.

# Chapter 12 Kidney, Adrenal Glands, Retroperitoneum

## Section 12.1 Kidney

- Benign and Malignant Lesions
- Pediatric Renal Tumors

### Cytology of Normal Renal Parenchyma Sect. 12.1.4, p. 734

#### Glomerulus

| Basic cell pattern | Particular and/or additional features | Differential diagnosis or possible diagnostic pitfall |
|---|---|---|
| – Large, sharply circumscribed three-dimensional structures with lobule-like appearance composed of small epithelial and endothelial cells<br>– Small capillary vessels, focal intraluminal erythrocytes | | |

#### Proximal Convoluted Tubule

| Basic cell pattern | Particular and/or additional features | Differential diagnosis or possible diagnostic pitfall |
|---|---|---|
| – Medium-sized cells, individual or grouped in flat sheets<br>– Inconspicuous nucleoli<br>– Abundant granular cytoplasm, usually eosinophilic<br>– Microvilli / brush borders barely recognizable | | |

#### Henle Loop and Distal Convoluted Tubule

| Basic cell pattern | Particular and/or additional features | Differential diagnosis or possible diagnostic pitfall |
|---|---|---|
| – Small cells with central nuclei<br>– Cells occurring singly or arranged in flat sheets, sporadic multilayered tubules<br>– Less granular cytoplasm when compared with proximal tubular cells | | |

#### Collecting Ducts

| Basic cell pattern | Particular and/or additional features | Differential diagnosis or possible diagnostic pitfall |
|---|---|---|
| – Cells varying in size<br>– Cell shape is cuboidal and the cytoplasm sharply outlined (apart from that, similar cellular morphology as described for Henle loop and distal convoluted tubules) | | |

## Inflammatory Disorders and Infections Sect. 12.1.5, p. 735

### Abscess of the Kidney

| Basic cell pattern | Particular and/or additional features | Differential diagnosis or possible diagnostic pitfall |
|---|---|---|
| – Abundant degenerating neutrophils and histiocytes<br>– Large amounts of debris<br>– Organisms can be identified using special staining | | |

### Xanthogranulomatous Pyelonephritis

| Basic cell pattern | Particular and/or additional features | Differential diagnosis or possible diagnostic pitfall |
|---|---|---|
| – Abundant necrosis and neutrophilic granulocytes<br>– Xanthomatous cells in the form of foamy macrophages<br>– Multinucleated giant histiocytes<br>– Fibroblasts and fibrocytes – variable | | – Malakoplakia |
| | – Predominantly xanthomatous cells | – Clear cell renal cell carcinoma |
| | – Large numbers of multinucleated giant histiocytes, sporadically of the Langhans cell type | – Tuberculosis |
| | – Considerably activated fibroblasts | – Malignant spindle cell tumors |

### Tuberculosis

| Basic cell pattern | Particular and/or additional features | Differential diagnosis or possible diagnostic pitfall |
|---|---|---|
| – Epithelioid histiocytes<br>– Histiocytic giant cells of the Langhans type<br>– Caseous necrosis and leukocytes | | – Xanthogranulomatous pyelonephritis |

### Malakoplakia

| Basic cell pattern | Particular and/or additional features | Differential diagnosis or possible diagnostic pitfall |
|---|---|---|
| – **Michaelis-Gutmann bodies:** concentrically laminated cytoplasmic inclusions in epithelioid/histiocytic cells<br>– Accumulation of proliferative epithelioid histiocytes<br>– Foamy histiocytes, histiocytic giant cells<br>– Pleomorphic histiocytes<br>– Lymphocytes, plasma cells and granulocytes<br>– A distinct granulomatous pattern is absent | | – Miscellaneous infections<br>– Xanthogranulomatous pyelonephritis<br>– Iatrogenic inflammatory process<br>– Previous surgery |
| | – Dense grouping of pleomorphic histiocytes | – Clear cell renal cell carcinoma |

### Renal Infarct

| Basic cell pattern | Particular and/or additional features | Differential diagnosis or possible diagnostic pitfall |
|---|---|---|
| – Necrotic debris<br>– Degenerating and atypical epithelial cells | | – Tumor necrosis |

## Cystic Lesions of the Kidney Sect. 12.1.6, p. 736

### Congenital and Acquired Cysts

| Basic cell pattern | Particular and/or additional features | Differential diagnosis or possible diagnostic pitfall |
|---|---|---|
| – Numerous foam cells<br>– Occasional neutrophilic granulocytes<br>– A few benign epithelial cells, variably degenerated<br>– Rarely blood, hemosiderophages, and calcified concretions<br>– Liesegang rings occur extremely rarely | – Blood<br>– Necrosis<br>– Atypical epithelial cells | – Malignant tumor, cystic and necrotic |

Comments concerning **complex cysts**, see Sect. 12.1.6.2, p. 736.

## Benign Renal Tumors Sect. 12.1.7, p. 737

### Angiomyolipoma

| Basic cell pattern | Particular and/or additional features | Differential diagnosis or possible diagnostic pitfall |
|---|---|---|
| – Mature adipose tissue fragments, usually abundant<br>– Smooth muscle cells: isolated, in groups, or in dense clusters<br>  – Pleomorphism may be distinct<br>  – Variable cell size and shape<br>  – Variable chromatin pattern, fine to coarse granular<br>– Thick-walled blood vessels lined by endothelial cells | – Pronounced clustering of rounded stromal cells | – Sarcomatoid renal cell carcinoma<br>– Sarcoma<br>– Renal cell carcinoma |

### Renal Cortical Adenoma

| Basic cell pattern | Particular and/or additional features | Differential diagnosis or possible diagnostic pitfall |
|---|---|---|
| – High cellularity<br>– Cells with abundant clear cytoplasm<br>– Centrally positioned small nuclei showing indistinct irregularities<br>– No mitoses | – Papillary and tubular formations – variable | – Renal cell carcinoma of low-grade malignancy |

### Renal Oncocytoma

| Basic cell pattern | Particular and/or additional features | Differential diagnosis or possible diagnostic pitfall |
|---|---|---|
| – Highly cellular aspirates<br>– Monotonous population of polygonal cells, isolated or in regular clusters<br>– Abundant eosinophilic cytoplasm, homogeneous or granular with distinct cell borders<br>– Single or multiple deeply stained nuclei, minor membrane irregularities<br>– Occasionally apoptotic or enlarged hyperchromatic nuclei<br>– Evenly distributed chromatin<br>– The nucleoli may be prominent | | – Well-differentiated renal cell carcinoma mainly composed of granular cells<br>– Chromophobe renal cell carcinoma |

## Renal Cell Carcinomas Sect. 12.1.8, p. 738

### Clear Cell Renal Cell Carcinoma

| Basic cell pattern | Particular and/or additional features | Differential diagnosis or possible diagnostic pitfall |
|---|---|---|
| – Clear cells:<br>  – Abundant clear cytoplasm (lipids and glycogen), fine and coarse granules, and vacuoles<br>  – Eosinophilic cytoplasmic globules – variable<br>  – Well-defined or indistinct cell borders<br>  – Low N/C ratio<br>  – Usually small nuclei showing accentuated membranes and finely dispersed chromatin<br>  – Small nucleoli (large nucleoli in less differentiated tumors)<br>– Occasional stripped nuclei<br>– Tumor cells may occur singly or in loose sheets, papilliform clusters; few papillary fronds may be observed<br>– Branching capillaries are usually evident<br>– Hemorrhage and necrosis (particularly in less differentiated tumors) | – Other cell types – variable:<br>  – Granular cells: eosinophilic dense and granular cytoplasm<br>  – Oncocytic cells: extremely dense eosinophilic, and sharply demarcated cytoplasm<br>– Nuclear grooves and pseudoinclusions – variable | – Xanthogranulomatous pyelonephritis<br>– Benign tubular epithelial clusters<br>– Angiomyolipoma<br><br>– Adrenocortical carcinoma<br>– Wilms tumor (in pediatric patients)<br>– Transitional cell carcinoma |
| | **Varying cell types – predominant:**<br>– Tumor cells with a mix of granular and dense cytoplasm | – Chromophobe renal cell carcinoma |
| | – Oncocytic cells: extremely dense eosinophilic cytoplasm or marked granularity, the cytoplasm is sharply demarcated | – Oncocytoma |
| | **Varying cytoarchitecture combined with particular nuclear features comprising distinct grooves and pseudoinclusions**<br>– Single tumor cells or<br>– Tumor cells in loose sheets showing alveolar pattern or<br>– Tumor cells in papilliform clusters or<br>– A few papillary fronds | – Papillary transitional cell carcinoma<br>– Papillary renal cell carcinoma<br>– Follicular / papillary thyroid carcinoma (metastasis) |

### Papillary Renal Cell Carcinoma

| Basic cell pattern | Particular and/or additional features | Differential diagnosis or possible diagnostic pitfall |
|---|---|---|
| – Cellular aspirates exhibit three-dimensional papillary fragments with fibrovascular cores<br>– Occasionally papilliform clusters without cores<br>– Cell shape is cuboidal or columnar<br>– A few single cells<br>– N/C ratio is moderate to high<br>– Nuclear outline may be smooth or irregular, nuclear grooves are frequently observed<br>– Generally dense and finely granular chromatin<br>– Nucleoli are single and small, except in high-grade tumors<br>– Striking intracytoplasmic hemosiderin storage<br>– Large numbers of lipid-laden macrophages<br>– Common hemorrhage, necrosis, and cystic change | – Nuclear pseudoinclusions – variable<br><br>– Variable amounts of psammomatous bodies | – Clear cell renal cell carcinoma<br><br>– Papillary transitional cell carcinoma<br><br>– Renal cell carcinoma of Bellini collecting ducts<br><br>– Metastases:<br>Gastrointestinal stromal tumor<br>Colonic adenocarcinoma<br>Thyroid papillary carcinoma |

### Renal Cell Carcinoma, Chromophobe Variant

| Basic cell pattern | Particular and/or additional features | Differential diagnosis or possible diagnostic pitfall |
|---|---|---|
| – Cellular aspirate comprising single cells and cell groups<br>– Large polygonal cells with abundant pale cytoplasm<br>– Neither necrosis nor calcification | Granular and/or dense eosinophilic cytoplasm – variable | – Vegetable cells<br>– Koilocytes |
| | – Cell membrane sharply outlined<br>– Conspicuous perinuclear halos<br>– Pronounced granular and/or dense eosinophilic cytoplasm | – Granular cell variant of clear cell renal cell carcinoma<br>– Oncocytoma |

## Renal Cell Carcinomas Sect. 12.1.8, p. 738 (continued)

### Renal Cell Carcinoma, Sarcomatoid Differentiated

| Basic cell pattern | Particular and/or additional features | Differential diagnosis or possible diagnostic pitfall |
|---|---|---|
| – Epithelial cells with clear or granular cytoplasm (as seen in common RCC)<br>– Pleomorphic sarcomatoid cell component, cytology matching sarcomatous lesions | | – High-grade renal cell carcinoma<br>– Sarcoma (primary or metastatic) |

**Rare primary** and **secondary tumors of the kidney**, see Sect. 12.1.8.2, p. 741.

## Tumors of the Renal Pelvis Sect. 12.1.9, p. 742

### Papillary Transitional Cell Carcinoma, Low-Grade

| Basic cell pattern | Particular and/or additional features | Differential diagnosis or possible diagnostic pitfall |
|---|---|---|
| – Monotonous cell pattern<br>– Minimally atypical cells, singly or in loose aggregates<br>– Usually papilliform cell clusters, papillary clusters with fibrovascular core may occur<br>– Eccentrically located nuclei, mild irregular outline<br>– **Nuclear grooves** frequently occur<br>– Fine granular chromatin, evenly dispersed<br>– Small nucleoli are common<br>– Homogeneous and slightly cyanophilic cytoplasm | | – Clear cell renal cell carcinoma<br>– Well-differentiated papillary renal cell carcinoma<br>– Thyroid papillary carcinoma |

### Transitional Cell Carcinoma, High-Grade

| Basic cell pattern | Particular and/or additional features | Differential diagnosis or possible diagnostic pitfall |
|---|---|---|
| – Large columnar, spindle, or polygonal cells occurring in isolation or irregularly grouped<br>– Hyperchromatic nuclei, coarse and clumped chromatin<br>– Irregular nucleoli<br>– High N/C ratio<br>– Dense or vacuolated cytoplasm, sharply defined<br>– Bizarre cells and necrosis are common | – Squamous or adenomatous metaplastic differentiation – variable<br>– Occasionally papilliform or even papillary clusters<br>– Marked squamous or adenomatous differentiation | – High-grade renal cell carcinoma<br>– Sarcomatoid differentiated renal cell carcinoma<br>– Non-Hodgkin lymphoma of the blast type<br>– Metastatic squamous cell carcinoma or<br>– Metastatic adenocarcinoma or<br>– Mucoepidermoid carcinoma |

## Pediatric (and Young Adult) Renal Tumors Sect. 12.1.10, p. 743

### Metanephric Adenoma / Adenofibroma

| Basic cell pattern | Particular and/or additional features | Differential diagnosis or possible diagnostic pitfall |
|---|---|---|
| – Cellular cytologic samples<br>– Small deeply stained cells with scant cytoplasm<br>– The nuclei with loose chromatin and usually small nucleoli<br>**Caution: the cells may mimic lymphocytes**<br>– Tight acinar, tubular, glomeruloid, and occasionally papillary structures | – Psammoma bodies may be encountered<br>– Fibroblastic component in metanephric adenofibroma | – Mesoblastic nephroma<br>– Renal clear cell sarcoma<br>– Wilms tumor |

### Pediatric Renal Cell Carcinoma

| Basic cell pattern | Particular and/or additional features | Differential diagnosis or possible diagnostic pitfall |
|---|---|---|
| – Cytologic features of renal cell carcinomas in the pediatric age group are virtually identical when compared with those in adults (microscopy and differential diagnoses as stated above) | | |

### Wilms Tumor

| Basic cell pattern | Particular and/or additional features | Differential diagnosis or possible diagnostic pitfall |
|---|---|---|
| – **Blastemal cells:**<br>  – Extremely scant cytoplasm<br>  – Strongly basophilic, small, round, or mildly irregular nuclei<br>  – Granular and coarse chromatin, evenly distributed<br>  – Nucleoli are inconspicuous or absent<br>  – Cells are haphazardly grouped<br>  – Frequent smearing artifacts<br>– **Epithelial cells:**<br>  – Mildly enlarged nuclei compared to blastemal cells<br>  – The cytoplasmic rims are increased as well<br>  – Rosettes, tubules, and abortive glomerulus-like structures<br>  – Epithelial cell clusters may be surrounded by a basal lamina<br>– **Stromal cells:**<br>  – Spindle-shaped and loosely arranged<br>– Myxoid background material<br>– Hemorrhage, necrosis, and cyst formation are not pronounced | – Smooth or skeletal muscle, fat, or cartilage may be seen | Small round cell tumors:<br>– Embryonal rhabdomyosarcoma,<br>– Neuroblastoma,<br>– Non-Hodgkin lymphoma,<br>– Ewing sarcoma/PNET |

Cytology of **other rare pediatric tumor entities** is described in Sect. 12.1.10.2.3, p. 745.

# Section 12.2 Adrenal Glands

## Normal Adrenal Gland Sect. 12.2.2, p. 767

### Adrenal Cortex

| Basic cell pattern | Particular and/or additional features | Differential diagnosis or possible diagnostic pitfall |
|---|---|---|
| Basic nuclear features:<br>– Small round nuclei, occasionally eccentrically located<br>– Regularly distributed loose chromatin<br>– Inconspicuous single nucleoli<br>– Distinct intranuclear sharply demarcated cytoplasmic inclusions | | |

### Adrenal Cortex: Zona Glomerulosa

| Basic cell pattern | Particular and/or additional features | Differential diagnosis or possible diagnostic pitfall |
|---|---|---|
| – Basic nuclear features as stated above<br>– Small aggregates and cords of cuboidal cells, the cells exhibiting variable staining quality | | |

### Adrenal Cortex: Zona Fasciculata

| Basic cell pattern | Particular and/or additional features | Differential diagnosis or possible diagnostic pitfall |
|---|---|---|
| – Basic nuclear features as stated above<br>– Abundant cytoplasm, single or multiple clear vacuoles | | |

### Adrenal Cortex: Zona Reticularis

| Basic cell pattern | Particular and/or additional features | Differential diagnosis or possible diagnostic pitfall |
|---|---|---|
| – Basic nuclear features as stated above<br>– Dense and compact cyanophilic cytoplasm<br>– Cytoplasmic fine granular golden-brown lipofuscin pigment | | |

### Adrenal Medulla

| Basic cell pattern | Particular and/or additional features | Differential diagnosis or possible diagnostic pitfall |
|---|---|---|
| – Irregularly shaped large cells that may be adhering to blood vessels | | |

## Benign and Malignant Primary Lesions of the Adrenals Sect. 12.2.3, p. 767

### Adrenal Cyst

| Basic cell pattern | Particular and/or additional features | Differential diagnosis or possible diagnostic pitfall |
|---|---|---|
| – Cystic fluid: clear, turbid, brown or bloody<br>– Foam cells and few epithelial cells<br><br>**Caution: Always search for hydatid features!** | – Leukocytes<br>– Hemosiderophages<br>– Necrosis | – Inflammation<br>– Previous hemorrhage<br>– Degenerating malignant tumor (primary or metastatic) |

### Adrenal Myelolipoma

| Basic cell pattern | Particular and/or additional features | Differential diagnosis or possible diagnostic pitfall |
|---|---|---|
| – Mature adipose tissue<br>– Trilineage hematopoiesis:<br>  – Immature and mature cells of myeloid and erythroid origin and megakaryocytes<br>– Lymphocytes | | – Renal angiomyolipoma<br>– Lipoma / well-differentiated liposarcoma |

## Benign and Malignant Primary Lesions of the Adrenals Sect. 12.2.3, p. 767 (continued)

### Adrenal Hyperplasia and Adrenal Adenoma

| Basic cell pattern | Particular and/or additional features | Differential diagnosis or possible diagnostic pitfall |
|---|---|---|
| – Usually hypercellular smears<br>– Numerous small round stripped nuclei<br>– Intact lipid-laden vacuolated cytoplasm – variable<br>– Stromal spindle cells and endothelial cells – variable<br>– Granular or bubbly background | | – Benign hepatocytes **in FNABs of the right adrenal gland**<br>– Adrenocortical carcinoma<br>– Small round cell tumors, in particular metastasis of small-cell carcinoma |

### Adrenocortical Carcinoma

| Basic cell pattern | Particular and/or additional features | Differential diagnosis or possible diagnostic pitfall |
|---|---|---|
| – Hypercellular smears<br>– Tumor cells are isolated or aggregated in dense groups<br>– **Irrespective of the tumor grade:**<br>  – Nuclear enlargement and prominent nucleoli (as compared to benign adrenocortical cells)<br>  – Mitosis and necrosis<br>  – Cytoplasm varies from spindle-shaped to polyhedral<br>  – Rarely: oncocytic and adenosquamous cell features<br>  – Rare myxoid background | – **Well-differentiated tumors:** wide clear lipid-laden cytoplasm<br>– **Less well-differentiated tumors:** enhanced granular cytoplasm, pleomorphic nuclei<br>– **Poorly differentiated tumors:** extreme cellular pleomorphism and multinucleation | – Benign cortical lesions<br>– Low-grade endocrine tumor<br>– Renal cell carcinoma<br>– Poorly differentiated carcinoma<br>– Pheochromocytoma<br>– Melanoma<br>– High-grade sarcoma |

### Pheochromocytoma

| Basic cell pattern | Particular and/or additional features | Differential diagnosis or possible diagnostic pitfall |
|---|---|---|
| – Hypercellular smears<br>– Single cells, loose cellular clusters, and pseudorosettes<br>– Three different cell types, varying distribution pattern:<br>  – Neuroendocrine cell type<br>  – Spindle cells<br>  – Large cells | | – Small round cell neoplasms |
| | – Predominant neuroendocrine cell type:<br>  – Medium-sized polygonal cells<br>  – Finely granular cytoplasm<br>  – Nuclei: eccentric, round to oval, regular<br>  – Granular chromatin and indistinct nucleoli | – Adrenocortical tumors |
| | – Predominant spindle cells with abundant cytoplasm, elongated nuclei, and coarse chromatin | – Spindle cell adrenal cortical carcinoma<br>– Desmoplastic malignant melanoma<br>– Mesenchymal spindle cell tumor |

### Neuroblastoma

| Basic cell pattern | Particular and/or additional features | Differential diagnosis or possible diagnostic pitfall |
|---|---|---|
| – Small uniform cells<br>– Hyperchromatic dense nuclei and coarse chromatin<br>– Small cytoplasmic rims<br>– Fibrillary matrix<br>– Necrosis | – Cell clustering and rosette formation – variable<br>– Differentiating neuroblasts – variable | Adults:<br>– Small-cell carcinoma<br>– Malignant lymphoma<br><br>Pediatric group:<br>– Malignant lymphoma<br>– Small blue cell tumors |

## Benign and Malignant Primary Lesions of the Adrenals Sect. 12.2.3, p. 767 (continued)

### Ganglioneuroblastoma

| Basic cell pattern | Particular and/or additional features | Differential diagnosis or possible diagnostic pitfall |
|---|---|---|
| – Neuroblastoma component (as stated above)<br>– Differentiating neuroblasts<br>– Differentiated ganglion cells – variable<br>– Nerve fibers | | |

### Ganglioneuroma

| Basic cell pattern | Particular and/or additional features | Differential diagnosis or possible diagnostic pitfall |
|---|---|---|
| – Differentiated ganglion cells<br>– Nerve fibers | | |

**Metastases see Comments in Sect. 12.2.4, p. 770.**

# Section 12.3 Retroperitoneum

- Benign and Malignant Lesions
- Germ Cell Tumors

## Nonneoplastic Lesions of the Retroperitoneum Sect. 12.3.2, p. 779

- Cysts
- Abscess
- Mycobacterial infection
- Hydatid cyst
- Malakoplakia
- Lymphangiomyomatosis
- Extramedullary hemopoiesis
- Endometriosis
- Idiopathic retroperitoneal fibrosis

**Cytologic characteristics** and **differential diagnoses** of these entities, see Sect. 12.3.2, p. 779, with links to other chapters of this book.

## Benign Tumors Sect. 12.3.4, p. 781

### Lipoma

| Basic cell pattern | Particular and/or additional features | Differential diagnosis or possible diagnostic pitfall |
|---|---|---|
| – Mature fatty tissue<br>– Rarely mild nuclear atypia | – A varying number of lipoblasts<br>– Stromal spindle cell component | – Well-differentiated liposarcoma |

### Hibernoma

| Basic cell pattern | Particular and/or additional features | Differential diagnosis or possible diagnostic pitfall |
|---|---|---|
| – Tightly clustered adipocytes<br>– Centrally placed dark nuclei<br>– Pigment-rich, granular cytoplasm | | – Proliferative myositis<br>– Oncocytoma<br>– Granular cell tumor<br>– Histiocytoma<br>– Alveolar soft part sarcoma |

## Benign Tumors Sect. 12.3.4, p. 781 (continued)

### Leiomyoma

| Basic cell pattern | Particular and/or additional features | Differential diagnosis or possible diagnostic pitfall |
|---|---|---|
| – Individual and clustered spindle cells<br>– Abundant eosinophilic cytoplasm, indistinct cell borders<br>– The nuclei are predominantly cigar-shaped/blunt ended<br>– Fine granular chromatin<br>– Inconspicuous nucleolus<br>– Mild cellular atypia – variable | | – Various low-grade spindle cell lesions |

### Schwannoma (Neurilemoma)

| Basic cell pattern | Particular and/or additional features | Differential diagnosis or possible diagnostic pitfall |
|---|---|---|
| – Numerous single spindle-shaped cells<br>– Pale and wavy cytoplasm<br>– Nuclei are elongated with pointed ends (blunted ends may occur as well) | – **Hallmark but infrequently observed:** Organoid cell arrangement, so-called Verocay bodies | – Various low-grade spindle cell lesions |

## Sarcomas (Commonest Entities) Sect. 12.3.5, p. 782

### Well-Differentiated Liposarcoma

| Basic cell pattern | Particular and/or additional features | Differential diagnosis or possible diagnostic pitfall |
|---|---|---|
| – **Two dominating cell types:**<br>– Lipoid cells round, spindle, or stellate in shape, small bland nuclei<br>– Lipoblasts with eccentrically located hyperchromatic and folded nuclei. The nuclei are surrounded by cytoplasmic fat vacuoles | | – Fatty tissue necrosis<br>– Lipoma |

### Myxoid Low-Grade Liposarcoma

| Basic cell pattern | Particular and/or additional features | Differential diagnosis or possible diagnostic pitfall |
|---|---|---|
| – Two dominating cell types as stated above<br>– Gelatinous background material (myxoid matrix)<br>– Delicate branching capillaries | | – Myxoma<br>– Schwannoma<br>– Myxoid fibrosarcoma<br>– Chordoma<br>– Other tumors with myxoid component |

### Leiomyosarcoma

| Basic cell pattern | Particular and/or additional features | Differential diagnosis or possible diagnostic pitfall |
|---|---|---|
| – Spindle cells, individual or in clusters<br>– Abundant syncytial cytoplasm<br>– Predominantly cigar-shaped and blunt-ended nuclei<br>– Degree of nuclear atypia depends on tumor grade | | – Low-grade leiomyosarcoma: various spindle cell lesions<br>– High-grade leiomyosarcoma: malignant fibrous histiocytoma |

### Malignant Schwannoma

| Basic cell pattern | Particular and/or additional features | Differential diagnosis or possible diagnostic pitfall |
|---|---|---|
| – Loose cell clusters and fascicular cell arrangement<br>– Spindle cells with blunt ends<br>– Nuclear atypia and nucleolar size depend on tumor grade<br>– Mitotic activity | – Fibrillary background – variable<br>– Verocay bodies are rarely present | – Varied spindle cell lesions |

## Sarcomas (Commonest Entities) Sect. 12.3.5, p. 782 (continued)

### Undifferentiated Pleomorphic Sarcoma (Malignant Fibrous Histiocytoma)

| Basic cell pattern | Particular and/or additional features | Differential diagnosis or possible diagnostic pitfall |
|---|---|---|
| – **Two main cell types:**<br>  – Mononucleated, polymorphic histiocyte-/fibroblast-like cells<br>  – Bizarre multinucleated giant cells<br>– Pleomorphic nuclei<br>– Irregular chromatin<br>– Distinct nucleoli<br>– Phagocytosis, debris, leukocytes, red blood cells | | – Pleomorphic liposarcoma<br>– Leiomyosarcoma<br>– Rhabdomyosarcoma<br>– Other tumors |
| | – Myxoid background | – Myxoid liposarcoma<br>– Myxoid leiomyosarcoma |

### Pleomorphic Liposarcoma

| Basic cell pattern | Particular and/or additional features | Differential diagnosis or possible diagnostic pitfall |
|---|---|---|
| – Lipoblasts with sharply defined cytoplasmic fat-vacuoles<br>– Eccentrically located scalloped nuclei<br>– Gelatinous, myxoid background – variable | | – Malignant fibrous histiocytoma<br>– Myxoid fibrosarcoma<br>– Extraskeletal myxoid chondrosarcoma<br>– Chordoma |

**Round cell sarcomas** mainly include round cell liposarcoma in adults, and both embryonal rhabdomyosarcoma and extraskeletal Ewing sarcoma in infancy and childhood; comments see Sect. 12.3.5.3, p. 783.

## Malignant Lymphomas Sect. 12.3.6, p. 784

Detailed cytomorphologic description of the various lymphoma subtypes, ancillary methods applicable on cytologic material, and differential diagnostic considerations are provided in Sect. 15.3, "Lymph Nodes: Malignant Lesions," p. 950.

## Germ Cell Tumors Sect. 12.3.7, p. 784

### Seminoma / Dysgerminoma

| Basic cell pattern | Particular and/or additional features | Differential diagnosis or possible diagnostic pitfall |
|---|---|---|
| – Large single cells interspersed with mature lymphocytes<br>– The tumor cells are rounded<br>– High N/C ratio<br>– Large single nucleus, irregularly wrinkled membrane<br>– One prominent central nucleolus<br>– Clear cytoplasm, well-defined borders with characteristic intermittent double-contours and thickenings<br>– Necrosis is common | | – Large-cell lymphoma, blastic type |

### Embryonal Carcinoma

| Basic cell pattern | Particular and/or additional features | Differential diagnosis or possible diagnostic pitfall |
|---|---|---|
| – Tumor cells are arranged in syncytial groups<br>– Usually large and anaplastic cells<br>– Variable nuclear size and shape<br>– Multiple prominent nucleoli<br>– Coarse and clumped chromatin<br>– Multinucleated giant cells – variable<br>– Large cytoplasm with indistinct membrane | | – Undifferentiated carcinoma<br>– Undifferentiated sarcoma |

## Germ Cell Tumors Sect. 12.3.7, p. 784 (continued)

### Endodermal Sinus Tumor

| Basic cell pattern | Particular and/or additional features | Differential diagnosis or possible diagnostic pitfall |
|---|---|---|
| – Similar cell pattern as described above, but:<br>– Less pronounced cellular pleomorphism<br>– Papillary and acinar formations<br>– Cytoplasmic vacuolization<br>– Intra- and extracytoplasmic eosinophilic bodies | | |

### Choriocarcinoma

| Basic cell pattern | Particular and/or additional features | Differential diagnosis or possible diagnostic pitfall |
|---|---|---|
| – Two different cell types:<br>– **Syncytiotrophoblasts:** pleomorphic multinucleated giant cells with bizarrely shaped nuclei and deeply stained large nucleoli<br>– **Cytotrophoblasts:** large to medium-sized rounded cells with irregular and coarsely structured nuclei, high N/C ratio, sharply outlined cytoplasm | | |

**Teratomas**, see Sect. 12.3.7.4, p. 785.

## Retroperitoneal Metastases Sect. 12.3.8, p. 785

### Selected Differential Diagnostic Problems

| Tumor type | Particular and/or additional features | Differential diagnosis or possible diagnostic pitfall |
|---|---|---|
| – Nonkeratinizing squamous cell carcinoma | – Solely dissociated tumor cells | – Undifferentiated large-cell carcinoma<br>– Poorly differentiated adenocarcinoma<br>– Spindle-/round cell tumors of the kidney<br>– Spindle-/round cell sarcoma<br>– Spindle-/round cell melanoma<br>– Large-cell lymphoma, blastic type |
| – Poorly differentiated large-cell tumors | | – Dedifferentiated adeno- and squamous cell carcinoma<br>– Transitional cell carcinoma<br>– Large-cell tumors of the kidney and adrenals<br>– Germ cell tumors<br>– Poorly differentiated round cell sarcoma<br>– Large-cell malignant lymphoma<br>– Melanoma<br>– Chordoma |
| – Tumors with myxoid / mucinous background | | – Metastatic mucinous adenocarcinoma<br>– Chordoma of the sacral region<br>– Myxoid ependymoma<br>– Extraskeletal myxoid chondrosarcoma<br>– Other tumors with myxoid / mucoid features |

# Chapter 13 Urinary Tract

## Section 13.2 Urinary Tract

- Normal and Metaplastic Findings
- Cell Degeneration and Reactive Atypia
- Nonneoplastic Lesions and Benign Tumors

## Normal Cytology and Metaplastic Lesions Sect. 13.2.1, p. 808

### Superficial Urothelial Cells

| Basic cell pattern | Particular and/or additional features | Differential diagnosis or possible diagnostic pitfall |
|---|---|---|
| – Cells of variable size: isolated, loosely grouped, or tightly clustered<br>– Frequent bi-/multinucleation<br>– Nuclei with irregular outline<br>– Loosely arranged granular chromatin, chromocenters<br>– Large cytoplasm, wide and pale, variable structure, sharply outlined<br>– Characteristic cytoplasmic molding in cell clusters | | |

### Intermediate, Basal, and Atrophic Urothelial Cells

| Basic cell pattern | Particular and/or additional features | Differential diagnosis or possible diagnostic pitfall |
|---|---|---|
| – Cells are smaller as compared to superficial cells, elongated or round in shape<br>– Cell clusters: regular, compact, three-dimensional, narrow spacing of the nuclei<br>– Densely structured nuclei, smooth margins, deep-blue staining<br>– Small and dense cytoplasm, sharply outlined | | |

### Elongated / Columnar Urothelial Cells

| Basic cell pattern | Particular and/or additional features | Differential diagnosis or possible diagnostic pitfall |
|---|---|---|
| – Cell shape: elongated or distinctly columnar<br>– Nuclei with smooth and/or irregular outline<br>– Thinly dispersed granular chromatin<br>– Clear cytoplasm<br>– N/C ratio in a normal range<br>– The nucleoli may be prominent<br>– Frequently shrunk and dark nuclei | | – Papillary transitional cell carcinoma grade 1<br>– Benign glandular cells<br>  – Intestinal metaplasia<br>  – Periurethral gland cells<br>  – Prostatic epithelial cells |

### Metaplastic Squamous Cells of the Urothelial Lining

| Basic cell pattern | Particular and/or additional features | Differential diagnosis or possible diagnostic pitfall |
|---|---|---|
| – Superficial and intermediate squamous cells<br>– Bland nuclei | – Marked keratinization – variable | – Squames of urethral origin<br>– Squames of vaginal (vulvar) origin<br>– Vesicovaginal fistula (**in the presence of Döderlein bacilli!**) |

### Glandular / Intestinal Metaplasia of the Urothelial Lining

| Basic cell pattern | Particular and/or additional features | Differential diagnosis or possible diagnostic pitfall |
|---|---|---|
| – Elongated or distinctly columnar<br>– Mucin secreting cylindric cells | | – Periurethral gland epithelium<br>– Prostatic epithelial cells<br>– Low-grade urothelial papillary neoplasia |

## Normal Cytology and Metaplastic Lesions Sect. 13.2.1, p. 808 (continued)

### Cells from Ileal Bladder Mucosa

| Basic cell pattern | Particular and/or additional features | Differential diagnosis or possible diagnostic pitfall |
|---|---|---|
| – High cellularity<br>– Cells of intestinal type frequently with strong signs of degeneration, columnar configuration partly well preserved<br>– Signs of degeneration: nuclear pyknosis and karyorrhexis, cytoplasmic vacuolization and inclusions (eosinophil and cyanophil)<br>– Well-preserved intestinal cell nuclei are small and regular in shape with thinly dispersed chromatin<br>– Background with debris and mucus<br>– Granulocytes and bacteria may be present | | |

### Cells of Renal Origin

| Basic cell pattern | Particular and/or additional features | Differential diagnosis or possible diagnostic pitfall |
|---|---|---|
| – Medium-sized cells<br>– Round nuclei with inconspicuous chromatin texture<br>– Distinct cytoplasm, granular or vacuolated<br>– Possibly renal casts | | **Caution: individual renal cells are barely identifiable** |

## Transitional Cell Degeneration and Reactive/Reparative Atypia Sect. 13.2.2, p. 810

### Reversible Urothelial Atypia Caused by Varied Irritating Agents (NOS)

| Basic cell pattern | Particular and/or additional features | Differential diagnosis or possible diagnostic pitfall |
|---|---|---|
| – Urothelial cells frequently enlarged, normal N/C ratio<br>– Large cytoplasm: Clear or coarsely vacuolated, sharply demarcated<br>– Irregular nuclei: Molded and cleaved membranes, nucleoplasm with clear areas and scattered chromatin condensates<br>– Prominent nucleoli – variable | – Numerous distinct multiple nucleoli, occasionally polymorphic | – Highly activated urothelial cells<br>– Low-grade dysplasia<br>– Low-grade papillary transitional cell tumor |
| | – Disintegration of the cytoplasm<br>– Nuclear pyknosis and karyolysis<br>– Indistinct nucleoli<br>– Cell detritus | – Urothelial cell degeneration<br>– Necrotic neoplasia |
| | – Prominent nucleoli and cytoplasmic leukophagocytosis | – Concomitant inflammation |

### Lithiasis

| Basic cell pattern | Particular and/or additional features | Differential diagnosis or possible diagnostic pitfall |
|---|---|---|
| – Striking cellular variability in shape and size<br>– Binucleation or multinucleation, and nuclear hyperchromasia<br>– Cytoplasm often occurring as small rim<br>– Three-dimensional cell balls and papillary clusters – variable<br>– Refractile crystalline deposits in the cytoplasm and birefringent crystals in the background<br>– Neutrophils from secondary inflammation/infection – variable | | Transitional cell carcinoma |

## Transitional Cell Degeneration and Reactive/Reparative Atypia (continued) Sect. 13.2.2, p. 810

### Postirradiation

| Basic cell pattern | Particular and/or additional features | Differential diagnosis or possible diagnostic pitfall |
|---|---|---|
| – Strongly enlarged urothelial cells mostly bi- or multinucleated<br>– Nuclei are present in a three-dimensional fashion (ballooned): bright or hyperchromatic and lucid, occasionally pyknotic and karyorrhectic<br>– Normal N/C ratio<br>– Huge nucleoli<br>– Intranuclear and cytoplasmic vacuoles | | – Actinic changes of dysplastic or malignant cells<br>– Transitional carcinoma |

### Postchemotherapy

| Basic cell pattern | Particular and/or additional features | Differential diagnosis or possible diagnostic pitfall |
|---|---|---|
| – Pronounced nuclear irregularities<br>– Strong nuclear hyperchromasia<br>– Coarse chromatin or homogeneous nuclear texture | | – High-grade dysplasia/carcinoma in situ<br>– Transitional cell carcinoma |

**Transitional cell artifacts** caused by other diagnostic and therapeutic interventions, see Sect. 13.2.2.1.6, p. 811.

## Benign Urothelial and Nonurothelial Lesions, and Benign Tumors (Selected Entities) Sect. 13.2.3, p. 812

### Von Brunn Nests

| Basic cell pattern | Particular and/or additional features | Differential diagnosis or possible diagnostic pitfall |
|---|---|---|
| – Small urothelial tissue fragments with bland cells, embedded in loose connective tissue<br>– Nests of urothelial cells are surrounded by basal-membrane material<br>– Gland-like spaces lined with columnar urothelial cells | | |

### Endosalpingiosis

| Basic cell pattern | Particular and/or additional features | Differential diagnosis or possible diagnostic pitfall |
|---|---|---|
| – Mesothelial cells or tubal-type epithelial cells<br>– Ciliated cells – variable<br>– Small cohesive cell aggregations or papilliform cell clusters | | |

### Endometriosis

| Basic cell pattern | Particular and/or additional features | Differential diagnosis or possible diagnostic pitfall |
|---|---|---|
| – Uniform small epithelial cells, high N/C ratio<br>– Rounded nuclei, smooth margins, variable indentations<br>– Fine and evenly distributed chromatin<br>– Indistinct nucleoli<br>– Small darkly stained stromal spindle cells – variable | – Large nucleoli in activated epithelial cells | – Urothelial carcinoma, small-cell type<br>– Adenocarcinoma, low-grade, small cell type |

### Vesicointestinal Fistula

| Basic cell pattern | Particular and/or additional features | Differential diagnosis or possible diagnostic pitfall |
|---|---|---|
| – Masses of feces<br>– Vegetable cells<br>– Inflammatory background – variable<br>– Epithelial cells of transitional and intestinal type – variable | – Markedly activated intestinal epithelial cells | – Bladder-invasive intestinal adenocarcinoma |

## Benign Urothelial and Nonurothelial Lesions, and Benign Tumors (Selected Entities) Sect. 13.2.3, p. 812 (continued)

### Vesicovaginal Fistula

| Basic cell pattern | Particular and/or additional features | Differential diagnosis or possible diagnostic pitfall |
|---|---|---|
| – Superficial and intermediate squamous cells<br>– Döderlein bacilli | | |

### Transitional Cell Papilloma

| Basic cell pattern | Particular and/or additional features | Differential diagnosis or possible diagnostic pitfall |
|---|---|---|
| – Papillary fragments with fibrovascular cores<br>– Bland urothelial cells<br>– Bland thickness of the epithelial layer | | – Papillary neoplasm of low malignant potential |

Selected **nonurothelial tumors** (granular cell tumor and pheochromocytoma), see Sect. 13.2.3.2.3, p. 813.

## Inflammation, Infections, Granulomatosis Sect. 13.2.4, p. 813

### Inflammation and Infection (Particularly Bacterial and Mycotic)

| Basic cell pattern | Particular and/or additional features | Differential diagnosis or possible diagnostic pitfall |
|---|---|---|
| – Neutrophil granulocytes<br>– Necrotic debris<br>– Histiocytes<br>– Variable numbers of regenerative urothelial cells | – Pathogens may be visible by conventional stainings | |
| | – Urothelial cells showing marked regenerative atypia | – Carcinoma with concomitant inflammation! |

### Tuberculosis and Bacillus Calmette-Guerin Therapy

| Basic cell pattern | Particular and/or additional features | Differential diagnosis or possible diagnostic pitfall |
|---|---|---|
| – Epithelioid cells<br>– Giant cells of the Langhans type<br>– Caseous-necrotic background material<br>– Large numbers of neutrophils<br>– Occasionally granuloma fragments of epithelioid cell type | | |

### Granuloma-Like Epithelioid/Histiocytic Inflammatory Pattern

| Basic cell pattern | Particular and/or additional features | Differential diagnosis or possible diagnostic pitfall |
|---|---|---|
| – Accumulation of proliferative epithelioid histiocytes<br>– Foam cells and foamy giant cells<br>– Lymphocytes, plasma cells, and granulocytes<br>– No distinct granulomatous pattern | | – Iatrogenic<br>– Miscellaneous infections<br>– Preceding surgery<br>– Xanthogranulomatous cystitis<br>– Malakoplakia |

## Inflammation, Infections, Granulomatosis Sect. 13.2.4, p. 813 (continued)

### Malakoplakia

| Basic cell pattern | Particular and/or additional features | Differential diagnosis or possible diagnostic pitfall |
|---|---|---|
| – Accumulation of proliferative epithelioid histiocytes<br>– Foam cells and foamy giant cells<br>– Lymphocytes, plasma cells, and granulocytes<br>– No distinct granulomatous pattern | – Michaelis-Gutmann bodies: concentrically laminated cytoplasmic inclusions in epithelioid cells and histiocytes<br><br>**Caution: Michaelis-Gutmann bodies are rarely encountered in cytologic specimens** | – Differential diagnostic considerations as stated in granuloma-like inflammatory pattern |

### Cytomegalovirus-Affected Cell

| Basic cell pattern | Particular and/or additional features | Differential diagnosis or possible diagnostic pitfall |
|---|---|---|
| – Strikingly enlarged, rounded, mononucleated cells<br>– Deeply basophilic nuclear inclusion:<br>  – Homogeneous or inhomogeneous structured<br>  – Sharply demarcated<br>  – Surrounded by a clear halo<br>– Chromatin condensed to the nuclear membrane (dark small dots) | | – Polyomavirus-affected cell (decoy cell type 2) |

### Polyomavirus-Affected Cell

| Basic cell pattern | Particular and/or additional features | Differential diagnosis or possible diagnostic pitfall |
|---|---|---|
| – **Enlarged and rounded epithelial cells with a nuclear inclusion, so-called decoy cells:**<br>  – **Type 1:** dense, basophilic, homogeneous inclusion completely filling the nucleus, thickened nuclear membrane<br>  – **Type 2:** centrally positioned granular inclusion surrounded by an incomplete halo<br>  – **Type 3:** diffusely distributed coarse chromatin, no particular halo, variable multinucleation<br>  – **Type 4:** vesicular nucleus with aggregations of coarse chromatin, single nucleolus<br><br>– Cytoplasm occurring as a small rim or attached as tag, variably preserved<br>– Usually cellular debris and neutrophilic granulocytes | | – **Type 2:** cytomegalovirus affected cell<br><br>– **Type 4:** carcinoma |

**Koilocytic lesion** (HPV infection) and **parasitic disease**, see Sects. 13.2.4.5.2 and 13.2.4.6, p. 815.

# Section 13.3 Urinary Tract

– Precancerous Urothelial Lesions
– Malignant Lesions

## Urethra Sect. 13.3.1, p. 830

### Clear Cell Adenocarcinoma

| Basic cell pattern | Particular and/or additional features | Differential diagnosis or possible diagnostic pitfall |
|---|---|---|
| – Frequent papillary cytoarchitecture<br>– Cells with abundant clear cytoplasm<br>– Moderate to marked nuclear pleomorphism<br>– Granular to vesicular chromatin<br>– Prominent, occasionally multiple nucleoli<br>– Distinct mitotic activity | | – Nephrogenic adenoma<br>– Metastatic clear cell carcinoma |

### Prostatic Ductal Adenocarcinoma

| Basic cell pattern | Particular and/or additional features | Differential diagnosis or possible diagnostic pitfall |
|---|---|---|
| – Papillary and tubulopapillary clusters lined by tall columnar cells in a single layer or in a pseudostratified fashion<br>– Elongated nuclei and large nucleoli<br>– High-grade cellular pleomorphism<br>– Nuclear grooves may be distinct<br>– Mitotic activity | – This tumor entity is frequently combined with common acinar tumor fractions | – High-grade papillary transitional carcinoma<br>– Common acinar prostatic adenocarcinoma |

**Caution: Primary squamous cell carcinoma, common adenocarcinoma, and malignant melanoma of the urethra may present identical or similar cytomorphology compared to their counterparts at other body sites; each of these tumor types may mimic urothelial carcinoma.**

## Bladder, Ureter, and Renal Pelvis: Precancerous Urothelial Lesion Sect. 13.3.3, p. 832



### Mild Dysplasia

| Basic cell pattern | Particular and/or additional features | Differential diagnosis or possible diagnostic pitfall |
|---|---|---|
| – Benign urothelium, but:<br>the cells are slightly enlarged, sometimes crowded and elongated<br>– Monomorphic bland nuclei, but:<br>sporadically irregular outlines and longitudinal grooves<br>– Opaque nucleoplasm or dense granular chromatin<br>– Small nucleoli – variable | | – Nonspecific cellular atypias<br>– Papillary urothelial neoplasm – low-grade<br>– Papillary urothelial neoplasm of low malignant potential |

### Moderate Dysplasia

| Basic cell pattern | Particular and/or additional features | Differential diagnosis or possible diagnostic pitfall |
|---|---|---|
| – High cellularity<br>– Overall monotonous pattern of enlarged cells, crowded and elongated with loss of polarity<br>– Hyperchromatic nuclei with distinct irregular outline<br>– Longitudinal nuclear grooves and granular chromatin<br>– Distinct small to medium-sized nucleoli<br>– N/C ratio normal or slightly increased<br>– The cytoplasm is sharply defined and dense | | – Severe reactive/regenerative urothelial atypia<br>– Transitional cell papillary carcinoma grade 2 |

### Severe Dysplasia

| Basic cell pattern | Particular and/or additional features | Differential diagnosis or possible diagnostic pitfall |
|---|---|---|
| – High cellularity<br>– Highly abnormal enlarged urothelial cells, rounded or elongated occasionally crowded with marked loss of polarity<br>– The nuclei are hyperchromatic and polymorphous with granular and coarse chromatin<br>– Increased N/C ratio<br>– Medium-sized to large nucleoli<br>– Increased mitotic activity | | – Severe reactive/regenerative urothelial atypia<br>– Transitional cell papillary carcinoma grade 3<br>– Transitional cell carcinoma in situ<br>– Invasive transitional cell cancer |

## Bladder, Ureter, and Renal Pelvis: Precancerous Urothelial Lesion (continued) Sect. 13.3.3, p. 832

### In Situ Transitional Cell Carcinoma

| Basic cell pattern | Particular and/or additional features | Differential diagnosis or possible diagnostic pitfall |
|---|---|---|
| – High cellularity – monotonous cell pattern<br>– Clean background, no detritus and no signs of inflammation<br>– Numerous individual, highly abnormal cells, round or polygonal in shape<br>– Cell clusters rarely occur<br>– Hyperchromatic nuclei, wrinkled and folded<br>– Coarse granular and clumped chromatin<br>– High N/C ratio<br>– Large pleomorphic nucleoli<br>– Small cytoplasmic rims, variably structured | | – Invasive transitional cell carcinoma |
| | – **Exceptionally**: all tumor cells showing clear pale nuclei | – False-negative diagnosis (normal urothelial cells) |

## Bladder, Ureter, and Renal Pelvis: Papillary Transitional Cell Carcinoma Sect. 13.3.4, p. 833

### Papillary Transitional Cell Carcinoma (PTC) Grade 1

| Basic cell pattern | Particular and/or additional features | Differential diagnosis or possible diagnostic pitfall |
|---|---|---|
| – Cells slightly enlarged (as compared to intermediate urothelial cells)<br>– Eccentric nuclei showing mild irregularities<br>– Nuclei show flexed, longitudinal nuclear grooves<br>– Evenly dispersed, dense and granular chromatin or opaque nucleoplasm<br>– Usually small nucleoli<br>– Homogeneous cytoplasm, slightly cyanophilic, elongated, fusiform, or columnar<br><br>**Obvious features for PTC-G1 diagnosis:**<br>– **Cells in papillary and papilliform aggregates:**<br>  – Syncytial sheets with nuclear overlapping<br>  – Focally vague loss of cellular polarity<br>– **Single tumor cells:**<br>  – Loosely scattered and/or<br>  – Close-packed forming streaming pattern and occasionally rosette-like formations | | – Benign columnar/spindle urothelial cells<br>– Proliferating intermediate urothelial cells<br>– Reactive/reparative cell changes<br><br>– Flat mild transitional cell dysplasia<br>– Papillary urothelial neoplasm of low malignant potential |

### PTC Grade 2

| Basic cell pattern | Particular and/or additional features | Differential diagnosis or possible diagnostic pitfall |
|---|---|---|
| – High cellularity, overall monotonous cell pattern<br>– Clearly enlarged cells, crowded and frequently elongated<br>– Focally distinct loss of polarity<br>– Hyperchromatic nuclei with distinct irregular outline<br>– Nuclei show flexed, longitudinal nuclear grooves<br>– Dense granular and focally coarse chromatin<br>– N/C ratio slightly increased<br>– Distinct small to medium-sized nucleoli in numerous nuclei<br><br>**Obvious features for PTC-G2 diagnosis:** Diagnostic cytoarchitecture, as described above for PTC grade 1 | | – Severe reactive/regenerative atypia<br><br>– Flat moderate transitional cell dysplasia |

### PTC Grade 3

| Basic cell pattern | Particular and/or additional features | Differential diagnosis or possible diagnostic pitfall |
|---|---|---|
| – Cytomorphologic pattern as described for invasive nonpapillary transitional cell carcinoma (see, p. 1222)<br><br>**Single diagnostic indicator for PTC-G3 diagnosis:** True papillary fragments | | Nonpapillary transitional cell carcinoma |

## Bladder, Ureter, and Renal Pelvis: Invasive Nonpapillary Transitional Cell Carcinoma Sect. 13.3.5, p. 835

### Invasive Transitional Cell Carcinoma

| Basic cell pattern | Particular and/or additional features | Differential diagnosis or possible diagnostic pitfall |
|---|---|---|
| – Highly cellular bladder irrigation specimen and urine sample<br>– Numerous individual tumor cells<br>– Three-dimensional irregular clusters infrequently occur<br>– Cells are large and pleomorphic, increased N/C ratio<br>– Irregular pleomorphic nuclei, marked hyperchromasia, coarsely granular and clumped chromatin<br>– Usually multiple and pleomorphic prominent nucleoli<br>– Dense homogeneous or vacuolated cytoplasm<br>– Sporadic atypical squamous cells<br>– Necrotic debris and blood | | – Transitional cell carcinoma in situ **(Take into account the pathognomic cell morphology and pattern of in situ carcinomas!)**<br>– Primary and secondary malignant tumors – epithelial, mesenchymal, lymphatic |
| | – Numerous atypical and malignant squamous cells | – Urothelial carcinoma with squamous component<br>– Squamous cell carcinoma – primary or metastatic |

## Bladder, Ureter, and Renal Pelvis: Selected Other Primary Cancers Sect. 13.3.6, p. 835

### Squamous Cell Carcinoma

| Basic cell pattern | Particular and/or additional features | Differential diagnosis or possible diagnostic pitfall |
|---|---|---|
| – Malignant squamous cells:<br>Pleomorphic, keratinized, and nonkeratinized cytoplasm<br>Nuclear pleomorphism<br>Hyperchromasia and coarse chromatin<br>– Necrosis | | – Urothelial carcinoma with squamous cell component<br>– Invading or metastatic squamous cell carcinoma |
| | – Predominant nonkeratinizing malignant squamous cells | – Transitional cell carcinoma<br>– Metastatic undifferentiated large cell carcinoma |

### Verrucous Squamous Cell Carcinoma

| Basic cell pattern | Particular and/or additional features | Differential diagnosis or possible diagnostic pitfall |
|---|---|---|
| – Polymorphous, keratinized anuclear squamous cells, dense eosinophilic and orange-colored cytoplasm<br>– A few squamous cells with minimal nuclear atypia<br>– Apoptotic nuclei | | – Acanthotic / atypical squamous metaplasia |

### Primary Adenocarcinoma of the Urinary Bladder

| Basic cell pattern | Particular and/or additional features | Differential diagnosis or possible diagnostic pitfall |
|---|---|---|
| – Three-dimensional clusters with scalloped contour, single cells variably occur<br>– Cuboidal or columnar cells with vacuolated/foamy cytoplasm<br>– Large irregular nuclei:<br>– Hyperchromatic, vesicular, and glassy, or dense granular, or chromatin strands<br>– Large round or pleomorphic nucleoli<br>– Intracytoplasmic mucus and signet ring cells – variable | | – Invading or metastatic adenocarcinoma |
| | – Masses of background mucus | – Adenocarcinoma of colloid type – primary or secondary |

## Bladder, Ureter, and Renal Pelvis: Selected Other Primary Cancers (continued) Sect. 13.3.6, p. 835

### Primary Undifferentiated Small-Cell Carcinoma

| Basic cell pattern | Particular and/or additional features | Differential diagnosis or possible diagnostic pitfall |
|---|---|---|
| – Small to medium-sized atypical and malignant cells<br>– Wrinkled and folded hyperchromatic nuclei<br>– Densely packed irregular chromatin<br>– Small cytoplasmic rims | | – Metastatic small-cell carcinoma<br>– Malignant lymphoma |

## Carcinoma from Adjacent Organs Invading the Urinary Collecting System Sect. 13.3.7, p. 836

### Prostatic Adenocarcinoma

| Basic cell pattern | Particular and/or additional features | Differential diagnosis or possible diagnostic pitfall |
|---|---|---|
| – Small and large sheets of monomorphic cuboidal cells<br>– Broad foamy or vacuolated cytoplasm<br>– Rounded nuclei presenting in three-dimensional fashion, exhibiting mild irregularities<br>– Dense and evenly distributed granular chromatin<br>– One prominent centrally located nucleolus<br>– Usually no detritus | | – Monomorphic urothelial carcinoma |

### Common Colonic Adenocarcinoma

| Basic cell pattern | Particular and/or additional features | Differential diagnosis or possible diagnostic pitfall |
|---|---|---|
| – Large columnar cells with palisade arrangement<br>– Pleomorphic hyperchromatic nuclei<br>– Coarsely granular chromatin texture<br>– Multiple nucleoli are common<br>– Large vacuolated cytoplasm showing variable mucin content<br>– Generally background necrosis | | – Other metastatic adenocarcinomas<br>– Primary bladder adenocarcinoma |

### Well-Differentiated Renal Cell Carcinoma

| Basic cell pattern | Particular and/or additional features | Differential diagnosis or possible diagnostic pitfall |
|---|---|---|
| – Medium-sized to large atypical clear cells<br>– Clear nuclei with scattered chromatin<br>– Varied nuclear pleomorphism<br>– Huge foamy or vacuolated cytoplasm<br>– Cell clustering is usually absent<br>– Frequent cellular degeneration | | – Clear cell adenocarcinoma of extrarenal origin<br>– Activated and degenerating histiocytes **Caution: individual renal carcinoma cells with signs of degeneration are virtually indistinguishable from activated or degenerating histiocytes**<br>– Degenerating urothelial cells<br>– Nephrogenic adenoma |

## Rare Nonurothelial Primaries and Metastatic Malignant Tumors

Selected entities having potential relevance for cytology are described in Sect. 13.3.8, p. 837.

# Chapter 14 Male Genital Organs

## Section 14.1 Prostate

### Normal Prostate, Epithelial Hyperplasia, Metaplasia Sect. 14.1.2, p. 854

#### Normal Prostatic Parenchyma

| Basic cell pattern | Particular and/or additional features | Differential diagnosis or possible diagnostic pitfall |
|---|---|---|
| – Uniform cuboidal cells<br>– Small nuclei with distinct smooth borders<br>– Nucleoli are completely absent<br>– Monolayer sheets showing regular nuclear spacing | | |

#### Adenomatous Hyperplasia

| Basic cell pattern | Particular and/or additional features | Differential diagnosis or possible diagnostic pitfall |
|---|---|---|
| – Cuboid and particularly cylindrical cells, focally palisading<br>– Variable nuclear size<br>– Occasional nucleoli<br>– Monolayer sheets with irregular nuclear spacing<br>– Sheets exhibit honeycomb pattern and buds | | |

#### Squamous Metaplasia of Prostatic Duct Epithelium

| Basic cell pattern | Particular and/or additional features | Differential diagnosis or possible diagnostic pitfall |
|---|---|---|
| – Polygonal cells exhibiting varying size<br>– Prominent dense cyanophilic cytoplasm, sharply defined<br>– Sheets: monolayered, cobblestone-like cell arrangement | | |



### Prostatitis and Atypical Prostatic Epithelium Sects. 14.1.3, p. 854 and 14.1.4, p. 856

#### Acute, Purulent Prostatitis

| Basic cell pattern | Particular and/or additional features | Differential diagnosis or possible diagnostic pitfall |
|---|---|---|
| – Varying quantities of neutrophil granulocytes<br>– Debris – variable | | |

#### Recurrent Prostatitis

| Basic cell pattern | Particular and/or additional features | Differential diagnosis or possible diagnostic pitfall |
|---|---|---|
| – Neutrophil granulocytes<br>– Lymphocytes<br>– Histiocytes | | |

#### Granulomatous Prostatitis

| Basic cell pattern | Particular and/or additional features | Differential diagnosis or possible diagnostic pitfall |
|---|---|---|
| – Aggregates of :<br>  – Histiocytes<br>  – Epithelioid cells and Langhans giant cells<br>– Occasional multinucleated hi stiocytes<br>– Neutrophils, lymphocytes, plasma cells – variable | Caseous detritus (rare occurrence) | Mycobacterial prostatitis |

## Prostatitis and Atypical Prostatic Epithelium (continued) Sects. 14.1.3, p. 854 and 14.1.4, p. 856

### Chronic Prostatitis

| Basic cell pattern | Particular and/or additional features | Differential diagnosis or possible diagnostic pitfall |
|---|---|---|
| – Few common histiocytes and epithelioid histiocytes<br>– Small sclerotic tissue fragments<br>– Possibly a few leukocytes | | – post-surgery or post-infarction |

### Mycobacterial (Tuberculous) Prostatitis

| Basic cell pattern | Particular and/or additional features | Differential diagnosis or possible diagnostic pitfall |
|---|---|---|
| – Caseation necrosis<br>– Degenerating epithelioid histiocytes<br>– Occasional Langhans giant cells<br>– Mixed inflammatory background | – Mild to marked reactive atypias of the epithelial cells may occur<br>– Pronounced caseating detritus<br>– **Activated rounded epithelioid cells may mimic carcinoma cells** | – Tumor necrosis<br>– Poorly differentiated prostate carcinoma |

### Mild epithelial atypia, NOS

| Basic cell pattern | Particular and/or additional features | Differential diagnosis or possible diagnostic pitfall |
|---|---|---|
| – Cellular and nuclear enlargement<br>– N/C ration within normal range<br>– Focal nuclear crowding<br>– Indistinct nuclear irregularities<br>– Reticular chromatin<br>– Distinct rounded nucleoli of varying size, centrally positioned | | – Mild reactive cell changes<br>– Low-grade PIN |

### Moderate to Severe Atypia, NOS

| Basic cell pattern | Particular and/or additional features | Differential diagnosis or possible diagnostic pitfall |
|---|---|---|
| – Strong cellular and nuclear enlargement<br>– Irregular nuclear shape<br>– Pronounced granular chromatin<br>– One or multiple nucleoli, marked polymorphism – variable<br>– Irregular cell sheets showing decreased nuclear spacing | | – Severe reactive cell changes<br>– High-grade PIN<br>– Prostatic adenocarcinoma |

**General rules regardless of the grade of epithelial atypia:**
- **Focally atypical cells** interspersed throughout hyperplastic epithelial sheets or in combination with inflammation favor reactive/regenerative epithelial cell changes
- **Atypical cells of varying degree throughout the cytologic specimen (lacking a particular background pattern)** cannot differentiate between severe reactive atypia and (pre)neoplasia

## Benign Soft Tissue Lesions and Rare Benign Tumors see Sect. 14.1.5, p. 856.

## Contaminants Originating from Adjacent Organs and Tissues Sect. 14.1.6, p. 857

### Rectal Mucosa

| Basic cell pattern | Particular and/or additional features | Differential diagnosis or possible diagnostic pitfall |
|---|---|---|
| – Sheets and clusters of tall cylindrical cells (larger than prostatic epithelial cells) focally palisading and frequently forming true glands that are often lined by goblet cells<br>– Nuclei showing clear indistinct chromatin and deep indentations | – Enlarged glandular cells with polymorphous overlapping nuclei, and large nucleoli | – Severe regenerative cell change (hyperplastic rectal mucosa)<br>– Mucinous adenocarcinoma (primary or secondary) |

### Seminal Vesicle Epithelium

| Basic cell pattern | Particular and/or additional features | Differential diagnosis or possible diagnostic pitfall |
|---|---|---|
| – Polymorphous polygonal cells, extremely variable in size<br>– Monolayer sheets and numerous isolated cells<br>– Extreme variation of nuclear shape and size<br>– Dark hyperchromatic nuclei, most often homogeneous<br>– Occasional nucleoli<br>– Prominent dense cyanophilic cytoplasm<br>– Lipofuscin inclusions – cytoplasmic and/or nuclear<br>– Mature sperms – variable | – A pronounced pleomorphic nucleolus in virtually every nucleus<br>– Absence of lipofuscin pigment | **Caution:**<br>**Cellular polymorphism and dark-staining nuclei may mimic malignant neoplasia, particularly in cases lacking lipofuscin pigment and/or showing distinct nucleoli** |

### Ganglion Cells

| Basic cell pattern | Particular and/or additional features | Differential diagnosis or possible diagnostic pitfall |
|---|---|---|
| – Huge isolated cells<br>– Large cytoplasm with star-like arrangement of neuronal processes<br>– The nucleus is pale or shows fine granular chromatin<br>– Usually one large round nucleolus | – As a rare event: conglomeration of ganglion cells | – Discrete tumor cells<br>– Undifferentiated large-cell carcinoma |

**Further potential contamination** from periprostatic organs and tissues, see Sect. 14.1.6.4, p. 858.

## Common Adenocarcinomas of the Prostate (Acinar Origin) Sect. 14.1.7, p. 858

**Nuclear hallmarks of prostatic adenocarcinoma independent of the malignancy grade:**
- Enlarged monomorphic nuclei with protrusions, nuclear irregularities are tumor grade-dependent
- The granular, densely packed chromatin pattern erases the otherwise prominent nuclear membrane
- Eccentric condensation of the chromatin in a limited number of malignant nuclei

### Well-Differentiated Adenocarcinoma

| Basic cell pattern | Particular and/or additional features | Differential diagnosis or possible diagnostic pitfall |
|---|---|---|
| – Uniformly enlarged cells and nuclei<br>– Slightly increased N/C ratio. Cytoplasm usually sharply outlined<br>– Dense granular chromatin<br>– One large single nucleolus in each nucleus<br>– Monolayer sheets:<br>  – Decreased nuclear spacing<br>  – Focally mild nuclear crowding<br>-Only a few isolated carcinoma cells | | – Reactive cellular transformation |

## Common Adenocarcinomas of the Prostate (Acinar Origin) (continued) Sect. 14.1.7, p. 858

### Moderately Differentiated Adenocarcinoma

| Basic cell pattern | Particular and/or additional features | Differential diagnosis or possible diagnostic pitfall |
|---|---|---|
| – Enlarged irregular cells<br>– Increased N/C ratio. Cytoplasm partially ill-defined<br>– Nuclei display irregular shape and dense granular chromatin<br>– Single or multiple large nucleoli in each nucleus<br>– Three-dimensional tight cell clusters, sharply outlined<br>– Only a few isolated tumor cells | | |

### Poorly Differentiated Adenocarcinoma

| Basic cell pattern | Particular and/or additional features | Differential diagnosis or possible diagnostic pitfall |
|---|---|---|
| – Enlarged pleomorphic cells and nuclei<br>– Ill-defined pleomorphic cytoplasm<br>– Dense granular and coarse chromatin<br>– Multiple pleomorphic nucleoli<br>– Irregular clusters showing marked cell dissociation | – Exceptionally: tumor necrosis | – Metastatic adenocarcinoma |

## Common Prostatic Adenocarcinoma After Therapy

Microscopic features and grading of the therapeutic response, see Sect. 14.1.8, p. 860, and Table 14.1.2.

## Rare Primary Carcinomas Other than Conventional Prostatic Adenocarcinoma Sect. 14.1.9, p. 862

### Mucinous Prostatic Adenocarcinoma / Signet Ring Cell Prostatic Carcinoma

| Basic cell pattern | Particular and/or additional features | Differential diagnosis or possible diagnostic pitfall |
|---|---|---|
| – Malignant columnar cells<br>– Cytoplasmic and background mucus | – Signet ring cells | – invading / metastatic mucinous adenocarcinoma |

### Prostatic Adenocarcinoma, Ductal Type (Usually Discovered in Samples from Urine or Bladder Washings)

| Basic cell pattern | Particular and/or additional features | Differential diagnosis or possible diagnostic pitfall |
|---|---|---|
| – Tubulopapillary clusters<br>– Stratified tall columnar cells, focally palisading<br>– Highly atypical / malignant nuclei of the prostatic type, large nucleoli<br>– Mitotic activity (more pronounced compared to common prostatic adenocarcinoma) | | – Papillary transitional cell carcinoma, high-grade |

### Urothelial Carcinoma, Primary or Secondary

| Basic cell pattern | Particular and/or additional features | Differential diagnosis or possible diagnostic pitfall |
|---|---|---|
| – Pleomorphic cells – usually isolated<br>– Irregular nuclei with indentations<br>– Increased N/C ratio<br>– Coarse chromatin<br>– Multiple pleomorphic nucleoli<br>– Dense and vacuolated cyanophilic cytoplasm<br>– Pronounced detritus / necrosis | | – Undifferentiated prostatic adenocarcinoma<br>– Amelanotic melanoma<br>– Large-cell anaplastic lymphoma<br>– Sarcoma |

**Further rare types of primary prostatic carcinoma: adenosquamous, squamous, basaloid, adenoid-cystic, small-cell undifferentiated (NOS), sarcomatoid,** see Sect. 14.1.9.4, p. 862.

## Nonepithelial and Biphasic Malignancies of the Prostate Sect. 14.1.10, p. 863

### Primary Spindle Cell Sarcoma of Varying Histogenesis

| Basic cell pattern | Particular and/or additional features | Differential diagnosis or possible diagnostic pitfall |
|---|---|---|
| – Atypical spindle cells<br>– Cellular and nuclear pleomorphism<br>– Marked mitotic activity<br>– Necrosis | | – Caseous necrotic tuberculosis<br>– Sarcomatoid prostate carcinoma<br>– Urothelial carcinoma<br>– Spindle cell melanoma |

### Primary Rhabdomyosarcoma

| Basic cell pattern | Particular and/or additional features | Differential diagnosis or possible diagnostic pitfall |
|---|---|---|
| – Basic pattern as stated above | – Atypical rounded cells with epithelioid arrangement<br>– Usually eccentric nuclei<br>– Large cytoplasm possibly with cross-striation | – Undifferentiated prostate carcinoma<br>– Urothelial carcinoma<br>– Undifferentiated large-cell carcinoma<br>– Amelanotic melanoma<br>– Large-cell anaplastic lymphoma |

### Biphasic Prostatic Neoplasms of Varying Types (Such as Phylloides Tumor, Sarcomatoid Carcinoma)

| Basic cell pattern | Particular and/or additional features | Differential diagnosis or possible diagnostic pitfall |
|---|---|---|
| – Epithelial and stromal cells and tissue fragments exhibiting variable atypia<br>– Marked mitotic activity<br>– Necrosis | | |

### Non-Hodgkin Lymphoma: Small-Cell, Lymphocytic Variant

| Basic cell pattern | Particular and/or additional features | Differential diagnosis or possible diagnostic pitfall |
|---|---|---|
| – Numerous small lymphoid cells<br>– Monomorphic cell pattern<br>– **Mild nuclear atypia:**<br>  – Minor nuclear enlargement<br>  – Dense granular chromatin<br>  – Centrally located distinct nucleoli | | – Chronic prostatitis |

### Non-Hodgkin Lymphoma: Follicular Variant

| Basic cell pattern | Particular and/or additional features | Differential diagnosis or possible diagnostic pitfall |
|---|---|---|
| – Variegated lymphoid cell pattern<br>– **Nuclear atypia:**<br>  – Medium-sized nuclei with molding and cleaving<br>  – Dense granular chromatin<br>  – Distinct nucleoli possibly multiple | | – Chronic prostatitis comprising secondary lymph follicles<br>– Intraprostatic or paraprostatic hyperplastic lymph node |

### Large-Cell Blastic and Anaplastic non-Hodgkin Lymphoma

| Basic cell pattern | Particular and/or additional features | Differential diagnosis or possible diagnostic pitfall |
|---|---|---|
| – Large undifferentiated blastoid cells, possibly arranged in diffuse pseudo-sheets<br>– Interspersed small and medium-sized benign and atypical lymphocytes<br>– Cellular detritus | | – Undifferentiated prostatic carcinoma<br>– Transitional cell carcinoma<br>– Sarcoma<br>– Malignant melanoma |

## Nonepithelial and Biphasic Malignancies of the Prostate (continued) Sect. 14.1.10, p. 863

### Myeloid Neoplasia

| Basic cell pattern | Particular and/or additional features | Differential diagnosis or possible diagnostic pitfall |
|---|---|---|
| – Mainly medium-sized atypical cells<br>– The nuclei are clear with cleaving and molding<br>– Rather indistinct but wide and pale cytoplasm | – Loose aggregation of the tumor cells | – Non-Hodgkin lymphoma<br>– Clear cell carcinoma |

More information about **malignant lymphomas** and **myeloid lesions** is provided in Sect. 15.3, "Lymph Node: Malignant Lesions," p. 950.

Rare miscellaneous tumors such as **germ cell tumors**, **paraganglioma**, **Wilms tumor**, **unusual soft tissue tumor**, see Section 14.1.10.3, p. 865.

## Metastases

The most important secondary neoplasms to the prostatic gland are mentioned above as considerations in differential diagnosis. Additional informations, see Sect. 14.1.11, p. 865.

# Chapter 15 Lymph Nodes

## Section 15.2 Lymph Nodes

- Lymphadenopathies
- Infections
- Miscellaneous Benign Lesions

### Reactive Lymphadenopathy Sect. 15.2.2, p. 926

**Common Reactive Lymphoid Hyperplasia, AIDS-Related Lymphadenopathy, Reactive Lymphoid Hyperplasia in Immunologic Diseases, Background Pattern Along with Benign and Malignant Disorders with Similar Appearance**

| Basic cell pattern | Particular and/or additional features | Differential diagnosis or possible diagnostic pitfall |
|---|---|---|
| – Hypercellular polymorphic pattern exhibiting various stages of cellular transformation, but small lymphocytes, B and T cells predominate<br>– **Germinal center cells:**<br>  – Centrocytes, centroblasts, pre-immunoblasts<br>  – Tingible-body macrophages<br>– **Cells from the interfollicular area:**<br>  – Immunoblasts, plasmablasts, plasmacytoid cells, plasma cells<br>– Histiocytes – individual or in cohesive aggregates<br>– Neutrophils, eosinophils and mast cells – variable | | – Non-Hodgkin lymphoma of follicle center cell origin<br>– Hodgkin lymphoma (in cases of reactive lymphadenopathy with multinucleated blastic cell component) |

### Bacterial, Parasitic, Mycotic Infections Sect. 15.2.3, p. 928

**Common Bacterial Infection: Initial Phase**

| Basic cell pattern | Particular and/or additional features | Differential diagnosis or possible diagnostic pitfall |
|---|---|---|
| – Reactive lymphadenopathy<br>– Numerous neutrophilic granulocytes | | – Cat-scratch disease |

**Common Bacterial Infection: Florid Stage**

| Basic cell pattern | Particular and/or additional features | Differential diagnosis or possible diagnostic pitfall |
|---|---|---|
| – Frank purulent material<br>– Abundant degenerating neutrophils | | |

**Mycobacteriosis: Tuberculosis, Atypical Mycobacteriosis**

| Basic cell pattern | Particular and/or additional features | Differential diagnosis or possible diagnostic pitfall |
|---|---|---|
| – Epithelioid cells, elongated showing pyknotic nuclei<br>– Langhans-type histiocytic giant cells<br>– Caseous detritus<br>– Neutrophilic granulocytes | – Markedly elongated epithelioid cells<br>  – Nuclei frequently pyknotic<br>  – Dense eosinophilic cytoplasm<br>– Extremely polymorphic detritus | – Sarcoidosis<br>– Malignant squamous cells<br>– Tumor necrosis |

**Cat-Scratch Disease**

| Basic cell pattern | Particular and/or additional features | Differential diagnosis or possible diagnostic pitfall |
|---|---|---|
| – Suppurative granulomas:<br>  – Peripherally palisading epithelioid histiocytes<br>  – Centrally located neutrophils<br>– Polymorphic lymphohistiocytic population | – Dispersed epithelioid histiocytes – variable | – Acute bacterial lymphadenitis<br>– Common reactive lymphadenitis<br>– Nonspecific granulomatosis |

## Bacterial, Parasitic, Mycotic Infections Sect. 15.2.3, p. 928 (continued)

### Toxoplasmic Lymphadenitis

| Basic cell pattern | Particular and/or additional features | Differential diagnosis or possible diagnostic pitfall |
|---|---|---|
| – Polymorphous reactive lymphoid cell population<br>– Histiocytes<br>– Small groups of epithelioid histiocytes, microgranulomas<br>– Absence of caseous necrosis, giant cells, neutrophils | – **Occasional parasites! extracellular and intracytoplasmic** | **All disorders with small epithelioid cell groups:**<br>– Mycobacteriosis<br>– Sarcoidosis<br>– Sinus histiocytosis<br>– Lymph node adjacent to a malignant tumor |

### Leishmania Lymphadenitis

| Basic cell pattern | Particular and/or additional features | Differential diagnosis or possible diagnostic pitfall |
|---|---|---|
| – Polymorphous cell pattern<br>– Various types of lymphocytes and atypical plasma cells<br>– Mono-/multinucleated histiocytes and starry-sky cells<br>– Lymphoglandular bodies (hyaline bodies)<br>– Histiocytic/epithelioid granulomas, mast cells | – **Frequently identifiable parasites! So-called Leishman-Donovan bodies, occurring extracellular and within histiocytes, epithelioid cells, and giant cells** | |

**For fungal infections and worms** we refer the reader to specialized sources in the literature.

## Virus-Induced Lymphadenitis Sect. 15.2.4, p. 930

### Infectious Mononucleosis

| Basic cell pattern | Particular and/or additional features | Differential diagnosis or possible diagnostic pitfall |
|---|---|---|
| – Extremely polymorphous but mixed cell pattern with the whole range from lymphocytes to polymorphic immunoblasts<br>– Many cells with pronounced dense cytoplasmic staining: deep cyanophilic (Pap) and deep blue (MGG, DiffQuik)<br>– Prominent plasmacytoid differentiation and mature plasma cells<br>– Prominent nucleoli and multinucleation<br>– Nucleoli may be markedly enlarged, pleomorphic and multiple<br>– Nucleoplasm is clear and the chromatin rather finely stippled<br>– Obvious mitotic activity | | – NHLs with pronounced plasmacytoid features<br>– Myeloid leukemia |
| | – Atypical immunoblasts | – Large-cell NHL, blastic type |
| | – Multinucleated immunoblasts and plasmablasts | – Reed-Sternberg-like cells indicating Hodgkin lymphoma |

## Miscellaneous Disorders and Diseases of Unknown Etiology Sect. 15.2.5, p. 931

### Dermatopathic Lymphadenopathy

| Basic cell pattern | Particular and/or additional features | Differential diagnosis or possible diagnostic pitfall |
|---|---|---|
| – Common reactive lymphoid hyperplasia<br>– Loose network of large histiocytes:<br>  – Clear vesicular nuclei showing longitudinal grooves, folds and convolutions<br>  – The cytoplasm has multiple connecting processes, often ill defined | – Clustered histiocytes with blood vessels in the center – variable | – Langerhans cell histiocytosis |
| | – Specific histiocytes containing melanin pigment<br>– Melanin-laden macrophages – variable | – Metastatic malignant melanoma<br>– Melanocytic aggregates in a lymph node<br>– Intranodal nevus |

## Miscellaneous Disorders and Diseases of Unknown Etiology (continued) Sect. 15.2.5, p. 931

### Rosai-Dorfman Disease

| Basic cell pattern | Particular and/or additional features | Differential diagnosis or possible diagnostic pitfall |
|---|---|---|
| – Numerous large histiocytes showing **lymphophagocytosis/ emperipolesis:** Cytoplasmic inclusions of well-preserved lymphocytes with a halo around each incorporated cell<br>– Histiocytes scattered in the background<br>– Mature lymphocytes and plasma cells | | – Reactive sinus histiocytosis<br>– Langerhans cell histiocytosis<br>– Reed-Sternberg-like cells indicating Hodgkin lymphoma<br>– Histiocytic sarcoma |

### Castleman Disease (CD)

| Basic cell pattern | Particular and/or additional features | Differential diagnosis or possible diagnostic pitfall |
|---|---|---|
| – Variegated lymphoid cell population: Predominantly small mature lymphocytes, eosinophils, follicle center cells (including immunoblasts) plasma cells<br>– Large atypical histiocytoid cells (follicular dendritic cells):<br>– Ill-defined cytoplasm and enlarged crumpled nuclei<br>– Granular to coarse chromatin, and nucleoli | – **Plasmacytic variant of CD**: sheets of plasma cells and many follicle center cells | – Another type of reactive lymphoid disorders<br>– Plasmacytoma |

### Kikuchi Lymphadenitis

| Basic cell pattern | Particular and/or additional features | Differential diagnosis or possible diagnostic pitfall |
|---|---|---|
| – Increase of apoptotic cells<br>– Three different types of histiocytes:<br>(1) Phagocytic histiocytes with marginalized twisted nuclei, the cytoplasm containing karyorrhectic and granular debris<br>(2) Common non-phagocytic histiocytes with kidney-shaped nuclei<br>(3) Medium-sized histiocytic elements (plasmacytoid monocytes) with eccentric round nuclei, coarse chromatin and dense cytoplasm<br>– Reactive lymphoid background lacking classic starry-sky cells<br>– Neutrophils are practically absent<br>– No granulomatous component | – Karyorrhectic and/or eosinophilic granular debris | – Nonspecific lymphadenopathy<br>– Malignant lymphoma<br>– Tuberculosis<br>– Tumor necrosis |

### Sarcoidosis

| Basic cell pattern | Particular and/or additional features | Differential diagnosis or possible diagnostic pitfall |
|---|---|---|
| – Cohesive, noncaseating epithelioid cell granuloma interspersed with mature lymphocytes<br>– Langhans-type giant cells<br>– Activated epithelioid cells with spherical configuration, the chromatin texture is bland, size and number of nucleoli depends on the cell activity | – Asteroid bodies – rarely seen<br>– Caseous detritus – unusual | – Various other granulomatous lesions<br>– Tuberculosis |

### Langerhans Cell Histiocytosis

| Basic cell pattern | Particular and/or additional features | Differential diagnosis or possible diagnostic pitfall |
|---|---|---|
| – Histiocytes usually enlarged and often multinucleated: nuclei are oval to kidney-shaped and frequently show deep grooves and indentations, vesicular chromatin<br>– Wide cytoplasm with neat margins<br>– Distinct eosinophilic nucleoli – variable<br>– Varying numbers of eosinophils and neutrophils, rare plasma cells<br>– Rare Charcot-Leyden crystals, always together with degenerating eosinophilic granulocytes<br>– Background pattern of reactive lymphadenopathy – variable | **Electron microscopy:**<br>**Specific intracytoplasmic organelles (Birbeck granules) showing characteristic tennis-racket shape and rod shape** | – Reactive sinus histiocytosis<br>– Dermatopathic lymphadenopathy<br>– Castleman disease<br>– Kikuchi lymphadenitis<br>– Malignant histiocytosis<br>– Hodgkin lymphoma |

# Section 15.3 Lymph Nodes

- Malignant Non-Hodgkin Lymphomas
- Hodgkin Lymphomas
- Histiocytic Sarcoma
- Myeloproliferative Disorders

## A Small and Medium-Sized B-Cell Non-Hodgkin Lymphomas
### Low Grade and High grade

### Small Lymphocytic Lymphoma (SLL)/Chronic Lymphocytic Leukemia Sect. 15.3.3, p. 955

| Basic cell pattern | Particular and/or additional features | Differential diagnosis or possible diagnostic pitfall |
|---|---|---|
| – Small lymphocytes<br>  – Slightly larger compared with normal lymphocytes<br>  – Focal cell crowding into dense aggregates<br>– Round nuclei, but focal membrane irregularities and small indentations<br>– Clumped chromatin similar to that of normal lymphocytes<br>– Pronounced centrally positioned nucleolus<br>– Scanty slightly basophilic (MGG) or cyanophilic (Pap) cytoplasm<br>– Very low mitotic rate | | – Benign T(B)-cell hyperplasia<br>**Caution: liquid-based preparations providing more prominent nucleoli and nuclear irregularities!**<br>– Other B-NHLs<br>– Small-cell carcinoma |

### SLL: Variant with Tumor Proliferation Centers Sect. 15.3.3, p. 955

| Basic cell pattern | Particular and/or additional features | Differential diagnosis or possible diagnostic pitfall |
|---|---|---|
| – Cell features as described above, but additional scattered medium-sized and large cells:<br>  – **Prolymphocytes** are similar to small lymphoma cells but slightly larger in size<br>  – **Paraimmunoblasts** are large cells with irregular nuclei, finely dispersed chromatin, large centrally placed nucleoli, and dense cytoplasm | – Distinct basophilic cytoplasm | – Transition of SLL into high-grade NHL<br>– Reactive lymphadenopathy<br>– Small round blue cell tumors |

### SLL: Lymphoplasmacytoid Variant Sect. 15.3.3, p. 955

| Basic cell pattern | Particular and/or additional features | Differential diagnosis or possible diagnostic pitfall |
|---|---|---|
| – Cell features as described for common SLL, but<br>  – Interspersed plasmacytoid cells<br>  – Varying numbers of plasmablastic cells | | – Reactive lymphadenopathy<br>– Plasma cell neoplasm<br>– Marginal zone lymphoma |

### Lymphoplasmacytic Lymphoma Sect. 15.3.4, p. 956

| Basic cell pattern | Particular and/or additional features | Differential diagnosis or possible diagnostic pitfall |
|---|---|---|
| – Smears comprising **three cell lines**:<br>  – Small lymphocytes,<br>  – Plasmacytoid lymphocytes,<br>  – Plasma cells<br>– PAS-positive nuclear inclusions<br>– Mast cells and hemosiderin are usually present | – Distinct mixed cell pattern due to residual germinal centers<br>– Varying numbers of clear monocytoid (B-) cells | – Another type of small lymphocytic lymphoma / CLL<br>– Another type of small-cell NHL with plasmacytic differentiation<br>– Reactive lymphadenopathy<br>– Marginal zone lymphoma |

## A Small and Medium-Sized B-Cell Non-Hodgkin Lymphomas (continued)
### Low Grade and High Grade

**Follicular Lymphoma: Classical Type** Sect. 15.3.6, p. 958

| Basic cell pattern | Particular and/or additional features | Differential diagnosis or possible diagnostic pitfall |
|---|---|---|
| – Smears comprising a dual cell pattern: predominating centrocytes, and centroblasts to a lesser extent<br>– **Centrocytes**:<br>– Small to medium-sized lymphocytes<br>– Variable nuclear shapes: angulated, cleaved, indented, twisted, or elongated<br>– Finely granular, occasionally coarse chromatin<br>– Nuclear hyperchromasia<br>– Frequent but inconspicuous nucleoli<br>– Scant cytoplasm, dense and pale<br>– **Centroblasts:**<br>– Large cells, 2 to 5 times the size of normal lymphocytes<br>– Vesicular nuclei or dispersed dense chromatin<br>– Cleaved or noncleaved nuclear contour<br>– Two or three nucleoli – variable, **located close to the nuclear membrane**<br>– Scant and basophilic cytoplasm<br>– Mitotic figures – variable | – **Starry sky cells and epithelioid cells – variable**<br><br>**>20% Centroblasts** | – Reactive lymphadenopathy<br>– Mantle cell lymphoma<br><br>– Suggesting follicle-derived large B-cell lymphoma, intermediate- or high-grade |

**Mantle Cell Lymphoma, Classical Type** Sect. 15.3.7, p. 960

| Basic cell pattern | Particular and/or additional features | Differential diagnosis or possible diagnostic pitfall |
|---|---|---|
| – Aspirates with a monomorphic lymphocytic population<br>– Tumor cells are small to medium-sized<br>– Nuclear outline with moderate or pronounced irregularities: angulated, cleaved and twisted, very similar to centrocytes!<br>– Finely dispersed chromatin<br>– Inconspicuous nucleoli<br>– No transformed cells (such as centroblasts or paraimmunoblasts)<br>– Scattered histiocytes and epithelioid histiocytes – variable<br>– Mitotic figures – variable | | – Follicle center cell lymphoma having a preponderance of centrocytes |

**Variants of mantle cell lymphomas** and related differential diagnoses, see Sect. 15.3.7, p. 960.

**Marginal Zone Lymphoma (MZL)** Sect. 15.3.8, p. 961

| Basic cell pattern | Particular and/or additional features | Differential diagnosis or possible diagnostic pitfall |
|---|---|---|
| – Polymorphic cellular pattern<br>– Predominance of small and medium-sized lymphoid tumor cells, typically expressing monocytoid features with increased pale cytoplasm<br>– Transformed benign lymphoid cells in various stages<br>– Plasma cells, monocytoid cells, histiocytic aggregates, and tingible body macrophages – in variable numbers | | – Reactive lymphadenopathy |
| | – Numerous tumor cells exhibiting **centrocyte-like features:**<br>– Irregularly shaped nuclei, dispersed chromatin, and small nucleoli | – Mantle cell lymphoma |
| | – Numerous tumor cells with **plasmacytoid appearance:**<br>– Wide eccentric and densely structured basophil cytoplasm | – B-cell NHLs of small-cell type such as follicular lymphomas, small lymphocytic lymphoma, immature plasma cell neoplasia |
| | – Marked plasma cell component | – Plasma cell tumor |

The presence of distinct **cellular heterogeneity** is more often observed among **nodal MZLs.**

## A Small and Medium-Sized B-Cell Non-Hodgkin Lymphomas (continued)
### Low Grade and High Grade

**Hairy Cell Leukemia** Sect. 15.3.9, p. 962

| Basic cell pattern | Particular and/or additional features | Differential diagnosis or possible diagnostic pitfall |
|---|---|---|
| – Monotonous population of small atypical lymphoid cells<br>– Abundant and pale cytoplasm:<br>  – Circumferential thin, hair-like cytoplasmic protrusions and projections (villi) – not detectable on each cell<br>– Oval or bean-shaped nuclei<br>– More or less homogeneous chromatin<br>– Nucleoli are absent or indistinct | | – Other small-cell lymphoid neoplasms, such as<br>  – Chronic lymphocytic leukemia<br>  – Prolymphocytic leukemia<br>  – Follicular NHL<br>  – Mantle-cell lymphoma<br><br>**In FNABs of the spleen:**<br>– Splenic MZL,<br>– Rare small B-cell tumors of the spleen comprising villous cytoplasmic features |

## B Plasma Cell Neoplasms (PCN) Sect. 15.3.5, p. 957

**Cytoplasmic inclusions occur variably, comprising crystallized or condensed immunoglobulins (selected phenotypes):**
– Multiple grape-like arranged inclusions: sharply outlined, homogeneously structured, and pale-blue staining
– Red-staining single refractile round bodies (Russell bodies)
– Crystalline rods

**PCN: Mature Tumor Form**

| Basic cell pattern | Particular and/or additional features | Differential diagnosis or possible diagnostic pitfall |
|---|---|---|
| – Cell-rich smears<br>– Tumor cells simulating mature plasma cells<br>– Scattered immature plasma cells – variable | | – Benign plasma cell hyperplasia |

**PCN: Immature Tumor Form**

| Basic cell pattern | Particular and/or additional features | Differential diagnosis or possible diagnostic pitfall |
|---|---|---|
| – Smears are rich in immature plasma cells:<br>  – Eccentric position of the nucleus<br>  – Dispersed granular chromatin<br>  – Usually one variably prominent nucleolus<br>– High N/C ratio<br>– Cytoplasmic plasmacytoid features are well preserved | | – Benign lymphadenopathy with plasmacytoid hyperplasia<br><br>– Burkitt lymphoma with plasmacytoid differentiation<br>– Marginal zone lymphoma with plasmacytoid features |

**PCN: Anaplastic Tumor Form**

| Basic cell pattern | Particular and/or additional features | Differential diagnosis or possible diagnostic pitfall |
|---|---|---|
| – Cellular aspirates<br>– Morphological appearance is basically that of a high-grade blastic NHL, but: a number of cells having plasmacytoid appearance comprising (vague) paranuclear cytoplasmic clearing<br>– Large monomorphic blast cells: high N/C ratio, nuclei are round to oval, usually marginally displaced coarse unevenly dispersed chromatin, one prominent central nucleolus or multiple large nucleoli, pale blue (MGG) or eosinophilic/amphophilic (Pap) cytoplasm<br>– Generally pronounced mitotic activity and tingible body macrophages<br>– Necrotic background debris in virtually all cases | | – Immunoblastic lymphoma<br>– Diffuse large B-cell lymphoma, plasmablastic subtype |
| | – Tumor cell aggregates forming sheets and clusters – variable | – **Large-cell carcinoma!!** |
| | – Pronounced cellular pleomorphism including prominent multinucleation and polylobulation | – Anaplastic large-cell lymphoma<br>– Anaplastic carcinoma |

## C Blastic B-Cell Non-Hodgkin Lymphomas
### Small Cell / Medium-Sized Cell / Large Cell

**B-Lymphoblastic Leukemia/Lymphoma** Sect. 15.3.2, p. 955

| Basic cell pattern | Particular and/or additional features | Differential diagnosis or possible diagnostic pitfall |
|---|---|---|
| Small to medium-sized blast cells:<br>– Small blasts: fuzzy nucleoli, scant cytoplasmic rim<br>– Medium-sized blasts: variably prominent single or multiple nucleoli, distinct cytoplasm of light blue to grey staining quality, occasionally cytoplasmic vacuoles and/or coarse granules<br>– Hyperchromatic nuclei, frequently irregular contour and/or convolutions<br>– Finely granular, condensed and evenly distributed chromatin<br>– Pronounced mitotic activity | – Focally starry-sky pattern – variable | – Acute myeloid leukemia<br>– Burkitt lymphoma |

**T-lymphoblastic leukemia/lymphoma exhibiting identical cytomorphologic features!!** Sect. 15.3.12, p. 966

**Burkitt Lymphoma (BL): Classical Type** Sect. 15.3.11, p. 964

| Basic cell pattern | Particular and/or additional features | Differential diagnosis or possible diagnostic pitfall |
|---|---|---|
| – Diffuse monotonous pattern of medium-sized tumor cells<br>– Tendency to cellular cohesiveness but hardly any compact aggregates<br>– Round nuclei with occasional indentations<br>– Dispersed granular and clumped chromatin<br>– Multiple basophilic nucleoli, centrally or paracentrally situated<br>– Medium-sized, deeply basophilic (cyanophilic) cytoplasm often small, sharply outlined lipid vacuoles<br>– A starry-sky pattern is usually present and striking<br>– Exceptionally high number of mitotic figures but a high proportion of apoptotic cells<br>– Granulomatous reaction is frequent, occasionally pronounced | | – Lymphoblastic lymphoma , medium-sized<br>– Blastoid mantle cell lymphoma<br>– Diffuse large B-cell lymphoma |

**BL with Plasmacytoid Differentiation** Sect. 15.3.11, p. 964

| Basic cell pattern | Particular and/or additional features | Differential diagnosis or possible diagnostic pitfall |
|---|---|---|
| – Same cell pattern as stated above<br>– Many cells with eccentric situated nuclei and one centrally placed nucleolus, basophilic cytoplasm | | – Plasma cell neoplasm, immature type |

**BL: Borderline Type** Sect. 15.3.11, p. 964

| Basic cell pattern | Particular and/or additional features | Differential diagnosis or possible diagnostic pitfall |
|---|---|---|
| – Cell features as described for classic BL<br>– Overall more pronounced cellular pleomorphism and large nucleoli | | – Diffuse large B-cell lymphoma |

**Diffuse Large B-Cell Lymphoma, DLBCL, Centroblastic Variant** Sect. 15.3.10, p. 963

| Basic cell pattern | Particular and/or additional features | Differential diagnosis or possible diagnostic pitfall |
|---|---|---|
| – Pronounced cellular pleomorphism comprising large nucleoli<br>– Overall monotonous cell pattern, >90% centroblasts<br>– Medium-sized and large lymphoid blastic cells<br>– Round and vesicular nuclei<br>– Fine, densely packed and evenly dispersed chromatin<br>– At least two conspicuous nucleoli, marginally placed<br>– Scanty cytoplasm, either vacuolated or basophilic | – Occasionally dominant nuclear cleaving and multilobation<br>– A high proportion of immunoblasts and plasmacytoid cells producing a polymorphic cell pattern | – Other medium-/large-cell blastic lymphomas<br>– Burkitt lymphoma<br>– Myelomonocytic leukemic infiltrate<br>– **Mononucleosis infectiosa!!** |

## C Blastic B-Cell Non-Hodgkin Lymphomas (continued)
### Small Cell / Medium-Sized Cell / Large Cell

**DLBCL, T-cell rich** Sect. 15.3.10, p. 963

| Basic cell pattern | Particular and/or additional features | Differential diagnosis or possible diagnostic pitfall |
|---|---|---|
| – Same cell pattern as stated above<br>– A high proportion of benign T lymphocytes | | – Reactive lymphadenopathy with T-cell hyperplasia<br>– Peripheral T-cell non-Hodgkin lymphoma<br>– Hodgkin lymphoma, , lymphocyte-predominant<br>– Single carcinoma cells (lymph node metastasis)<br>– Single melanoma cells (lymph node metastasis)<br>– Lymphoepithelial carcinoma (lymph node metastasis) |

**DLBCL, Histiocyte-Rich** Sect. 15.3.10, p. 963

| Basic cell pattern | Particular and/or additional features | Differential diagnosis or possible diagnostic pitfall |
|---|---|---|
| – Cell features as described for DLBCL, centroblastic type<br>– A high proportion of histiocytes | | – T-cell lymphoma |

**DLBCL, Immunoblastic Variant** Sect. 15.3.10, p. 963

| Basic cell pattern | Particular and/or additional features | Differential diagnosis or possible diagnostic pitfall |
|---|---|---|
| – Dominating immunoblastic component >90% atypical immunoblasts<br>– Round nuclei with indistinct irregularities<br>– Chromatin is similar to that in centroblasts<br>– A single large and round nucleolus, centrally located<br>– Broad rim of deeply basophilic cytoplasm<br>– Plasmacytoid differentiated blasts – variable | | – Plasmablastic DLBCL<br>– Immature plasma cell myeloma<br>– ALK-positive large B-cell lymphoma |

**DLBC, Anaplastic Variant** Sect. 15.3.10, p. 963

| Basic cell pattern | Particular and/or additional features | Differential diagnosis or possible diagnostic pitfall |
|---|---|---|
| – Large, oversized round to polyhedral cells<br>– Tumor cells may occur in crowded aggregates, cohesive sheets or compact clusters, occasionally papillary formations<br>– Large, pleomorphic, and bizarre nuclei<br>– Finely dispersed or coarse chromatin<br>– Abundant cytoplasm, vacuolated or densely structured, fading away at the periphery | | – Anaplastic large cell lymphoma<br>– Hodgkin lymphoma<br>– Undifferentiated large cell carcinoma (lymph node metastasis)<br>– Malignant melanoma (lymph node metastasis) |

## D T-Cell Neoplasms Sects. 15.3.12–15.3.18, p. 966

### T-Cell Prolymphocytic Leukemia Sect. 15.3.13, p. 966

| Basic cell pattern | Particular and/or additional features | Differential diagnosis or possible diagnostic pitfall |
|---|---|---|
| – Small to medium-sized lymphoid cells<br>– Round nuclei showing marked nuclear irregularities:<br>  – Cleaves, indentations, and deep grooves<br>  – Nuclei may exhibit cerebriform appearance<br>– Usually distinct nucleolus<br>– Dense and basophilic cytoplasm, devoid of granules<br>– Cytoplasmic protrusions – variable | | – Other variants of mature T-cell neoplasms e.g., adult T-cell leukemia/lymphoma<br>– Prolymphocyte leukemia – B-type |

### Adult T-Cell Lymphoma / Leukemia Sect. 15.3.14, p. 967

| Basic cell pattern | Particular and/or additional features | Differential diagnosis or possible diagnostic pitfall |
|---|---|---|
| – Usually medium-sized to large lymphoid tumor cells<br>– Nuclei show pronounced pleomorphism: highly irregular contour caused by deep indentations and multilobulation, cerebriform shape<br>– Prominent nucleoli – variable<br>– Coarse and irregularly distributed chromatin<br>– Blast-like cells with distinct nucleoli – variable<br>– Giant tumor cells – variable | | – Other variants of mature T-cell neoplasms |
| | – Heterogeneous cell population<br>– Predominance of small pleomorphic cells | – Angioimmunoblastic T-cell lymphoma |
| | – Small lymphoid cells with mild atypias<br>– Large tumor cells showing HRS cell-like features | – Hodgkin lymphoma |

### Mycosis Fungoides (Appearance in FNABs of Affected Lymph Nodes) Sect. 15.3.15, p. 967

| Basic cell pattern | Particular and/or additional features | Differential diagnosis or possible diagnostic pitfall |
|---|---|---|
| – Polymorphic smear pattern<br>– **Small Sézary cells slightly larger compared to normal lymphocytes:** relatively indistinct nuclear indentations<br>– Large Sézary cells – variable<br>– Condensed and irregularly distributed chromatin<br>– Prominent nucleoli – variable<br>– Narrow cytoplasmic rim around the nucleus<br>– Presence of inflammatory infiltrates – variable eosinophils, histiocytes, and tingible body macrophages | | |
| | – Heterogenous cell pattern: numerous large Sézary cells | – Peripheral T-cell NHL<br>– Hodgkin lymphoma |
| | – Dermatopathic lymphadenopathy comprising scattered tumor cells, **generally associated with mycosis fungoides in the early stage of disease** | – Reactive (dermatopathic) lymphadenopathy |

## D T-Cell Neoplasms Secs. 15.3.12–15.3.18, p. 966 (continued)

### Sézary Syndrome (Appearance in FNABs of Affected Lymph Nodes) Sect. 15.3.15, p. 967

| Basic cell pattern | Particular and/or additional features | Differential diagnosis or possible diagnostic pitfall |
|---|---|---|
| – Rather monotonous smear pattern<br>– Large Sézary cells, their size is more than four times that of small lymphocytes: distinct nuclear indentations, grooved/cerebriform aspect<br>– Small Sézary cells – variable<br>– Condensed and irregularly distributed chromatin<br>– Prominent nucleoli – variable<br>– Narrow cytoplasmic rim around the nucleus<br>– Presence of inflammatory infiltrates – variable<br>  – Eosinophils, histiocytes, and tingible body macrophages | | – Peripheral T-cell NHL<br>– Hodgkin lymphoma |
| | – Heterogeneous appearance: mixture of small and large Sézary cells | – Reactive lymphadenopathy |

### Peripheral T-Cell Lymphoma (PTCL), NOS Sect. 15.3.16, p. 968

| Basic cell pattern | Particular and/or additional features | Differential diagnosis or possible diagnostic pitfall |
|---|---|---|
| – Cytomorphology is of very diverse appearance, usually medium-sized and large tumor cells<br>– Irregular pleomorphic nuclei, molding, and grooves<br>– Vesicular or coarse, and irregular chromatin<br>– Hyperchromasia is common<br>– Large and prominent nucleoli<br>– High mitotic activity<br>– Reed-Sternberg-like cells – variable | | – Mycosis fungoides<br>– Adult T-cell lymphoma<br>– DLBCL – centroblastic variant<br>– Hodgkin lymphoma<br><br>– Carcinoma<br>– Melanoma<br>– Other undifferentiated neoplasms |
| | – Intense inflammatory infiltrates | – B-cell non-Hodgkin lymphomas<br>– Angioimmunoblastic T-cell non-Hodgkin lymphomas<br>– Reactive lymphadenopathy |

### PTCL: Lymphoepithelioid Variant (Lennert Lymphoma) Sect. 15.3.16, p. 968

| Basic cell pattern | Particular and/or additional features | Differential diagnosis or possible diagnostic pitfall |
|---|---|---|
| – Same cell pattern as stated above<br>– Numerous epithelioid histiocytes | | – Epithelioid cell-rich non-Hodgkin lymphomas<br>– Hodgkin lymphoma |

### Angioimmunoblastic T-Cell Lymphoma Sect. 15.3.17, p. 969

| Basic cell pattern | Particular and/or additional features | Differential diagnosis or possible diagnostic pitfall |
|---|---|---|
| – Pronounced heterogeneous cell population comprising clustering of reticulum cells and tissue fragments that contain hyalinized small vessels<br>– Small to medium-sized lymphoid tumor cells, minor atypias, clear cytoplasm<br>– Inflammatory component: small and reactive lymphocytes, immunoblasts, plasma cells, eosinophils, histiocytes, rare tingible body macrophages<br>– Follicular dendritic cells forming a dense cellular meshwork interspersed with lymphocytes | | – Reactive lymphadenopathy<br><br>– Peripheral T-cell lymphoma |
| | – Reed-Sternberg-like cells – variable | – Hodgkin lymphoma |

## D T-Cell Neoplasms Secs. 15.3.12–15.3.18, p. 966 (continued)

### T Anaplastic Large-Cell Lymphoma Sect. 15.3.18, p. 970

| Basic cell pattern | Particular and/or additional features | Differential diagnosis or possible diagnostic pitfall |
|---|---|---|
| – Medium-sized to large pleomorphic cells<br>– Eccentrically placed nuclei, kidney- or embryo-shaped; a few nuclei with cytoplasmic invaginations (doughnut cells)<br>– Dispersed or fine granular chromatin<br>– Usually multiple and prominent nucleoli: rod-shaped or pleomorphic, eosinophilic, or basophilic<br>– Abundant vacuolated amphophilic cytoplasm<br>– Inflammatory background: lymphocytes, granulocytes, histiocytes | | – B-cell lymphoma with anaplastic features<br>– Diffuse large B-cell lymphoma<br>– Hodgkin lymphoma<br>– Sarcomatous neoplasms<br><br>– Carcinoma<br>– Melanoma<br>– Germ cell tumors |
| | – Occasional multinucleated giant cells with their nuclei arranged in a wreath-like pattern | – Reed-Sternberg-like cells, indicating Hodgkin lymphoma |
| | – **Small-cell pattern:** dominating small to medium-sized tumor cells, irregular nuclei, one distinct nucleolus, plasmacytoid features<br>– A certain proportion of large tumor cells is always present | – Peripheral T-cell non-Hodgkin lymphoma |
| | – Variegated tumor cell pattern comprising plasmacytoid features, combined with a distinct inflammatory infiltrate | – Reactive lymphadenopathy – **Mononucleosis infectiosa!!** |
| | Lymphohistiocytic pattern:<br>– Neoplastic cells associated with numerous histiocytic cells | – **Do not miss scattered neoplastic cells!** |

## E Hodgkin Lymphomas Secs. 15.3.19 and 15.3.20, p. 971

RS = Reed-Sternberg cells / HRS cells = Hodgkin cells and Reed-Sternberg cells

15

### Basic Cytologic Features of Classical Hodgkin Lymphoma/Mixed Cellularity Classical HL Secs. 15.3.19, p. 971, and 15.3.19.1, p. 972

| Basic cell pattern | Particular and/or additional features | Differential diagnosis or possible diagnostic pitfall |
|---|---|---|
| **Reed-Sternberg cells**<br>– Large atypical cells<br>– The nuclei are either bilobulated and typically mirror-inverted, or showing multiple nuclear segments simulating multinucleation<br>– Nuclear membranes are mostly wrinkled, molded and folded<br>– Finely granular chromatin, dense and regularly dispersed, often pale and dyschromatic<br>– Single or multiple and very prominent nucleoli, eosinophilic and round, bar-like, comma-shaped or bent<br>– Abundant cytoplasm with a distinct border slightly basophilic (MGG) or cyanophilic (Pap), small and large vacuoles – variable<br><br>**Hodgkin cells**<br>– They are the mononuclear variant of RS cells showing basically identical morphologic characteristics<br>– Cell size exceeds that of lymphocytes and small histiocytes | – The structure of the reactive infiltrate is variable, dependent on the Hodgkin lymphoma subtype | – Reactive lymphadenopathy, in particular virus-induced (**EBV!**)<br><br>– T non-Hodgkin lymphomas with mixed tumor cell pattern and HRS cell features |

## E Hodgkin Lymphomas Sects. 15.3.19 and 15.3.20, p. 971 (continued)

**RS = Reed-Sternberg cells / HRS cells = Hodgkin cells and Reed-Sternberg cells**

### Basic Cytologic Features of Classical Hodgkin Lymphoma/Mixed Cellularity Classical HL (continued) Sects. 15.3.19, p. 971, and 15.3.19.1, p. 972

| Basic cell pattern | Particular and/or additional features | Differential diagnosis or possible diagnostic pitfall |
|---|---|---|
| **Cellular background**<br>– Contains small benign lymphocytes, atypical lymphocytes, neutrophils, eosinophils, plasma cells, and (epithelioid) histiocytes<br>– **Specification of the atypical lymphocytes: enlarged, irregular nuclei with indentations and cleaves, dense granular chromatin and pronounced nucleoli. These cells are benign but may masquerade of non-Hodgkin lymphoma cells.** | – A few scattered HRS cells | – **Single cells of carcinoma, melanoma, or other large-cell tumors!!** |
| | – Overall paucity of cells | – Benign lymphatic tissue / reactive lymphadenopathy |
| | – Numerous epithelioid histiocytes and granuloma fragments<br>– Inflammatory background<br>– Sporadic HRS cells | – Varying granulomatous diseases, mycobacteriosis, sarcoidosis |

**Nodular Sclerosis Classical HL** Comments see Sect. 15.3.19.2, p. 972.

### Lymphocyte-Rich Classical Hodgkin Lymphoma Sect. 15.3.19.3, p. 972

| Basic cell pattern | Particular and/or additional features | Differential diagnosis or possible diagnostic pitfall |
|---|---|---|
| – Lymphocyte-rich background<br>– A few HRS cells | | – Nodular lymphocyte predominant Hodgkin lymphoma<br>– Reactive lymphadenopathy |

**Differential diagnostic aspects** of lymphocyte-rich classical Hodgkin lymphoma and nodular lymphocyte predominant Hodgkin lymphoma are listed in Table 15.3.2, p. 974.

### Lymphocyte-Depleted Classical Hodgkin Lymphoma Sect. 15.3.19.4, p. 973

| Basic cell pattern | Particular and/or additional features | Differential diagnosis or possible diagnostic pitfall |
|---|---|---|
| – HRS cells in great numbers<br>– Minor typical HL-background | | – Carcinoma<br>– Melanoma |
| | – Pronounced cellular and nuclear pleomorphism | – Anaplastic large cell lymphomas<br>– DLBCL – anaplastic variant<br>– Pleomorphic carcinoma and sarcomas |

### Nodular Lymphocyte Predominant Hodgkin Lymphoma Sect. 15.3.20, p. 973

| Basic cell pattern | Particular and/or additional features | Differential diagnosis or possible diagnostic pitfall |
|---|---|---|
| **Popcorn or LP cells:**<br>– Large tumor cells usually mononucleated<br>– Pronounced nuclear folding and multilobulation<br>– Nucleoli usually multiple and basophilic, smaller than in nuclei of common HRS cells<br>– Granulocytes are virtually absent | | – Lymphocyte-rich classical Hodgkin lymphoma |
| | – Abundance of small lymphocytes, histiocytes, and epithelioid histiocytes | – Benign lymphatic tissue / reactive lymphadenopathy<br>– T-cell NHL<br>– Histiocyte-rich large B-cell lymphoma |

**Differential diagnostic aspects** of nodular lymphocyte predominant HL and lymphocyte-rich classical Hodgkin lymphoma are listed in Table 15.3.2, p. 974.

## F Histiocytic Sarcoma Sect. 15.3.21, p. 973

### Histiocytic Sarcoma (Histiocytic Lymphoma)

| Basic cell pattern | Particular and/or additional features | Differential diagnosis or possible diagnostic pitfall |
|---|---|---|
| – Large pleomorphic tumor cells, usually round to oval but sometimes spindle-shaped, multinucleation is common<br>– Abundant, dense or vacuolated cytoplasm<br>– Pleomorphic, eccentrically placed nuclei with reniform shapes but usually with irregular folds<br>– Vesicular chromatin<br>– Tumor cell erythrophagocytosis – variable<br>– Inflammatory background (granulocytes, lymphocytes, plasma cells, histiocytes) – variable. Occasionally abundant! | | – Rosai-Dorfman disease<br>– Histiocytosis X<br>– Diffuse large B-cell lymphoma<br>– Anaplastic large-cell lymphoma<br>– Extramedullary myeloid tumors<br>– Pleomorphic carcinoma and sarcoma<br>– Malignant melanoma |

## G Myeloproliferative Disorders

### Extramedullary Hematopoiesis Sect. 15.3.22, p. 975

| Basic cell pattern | Particular and/or additional features | Differential diagnosis or possible diagnostic pitfall |
|---|---|---|
| – Smears comprising **three cell lines:**<br>– Precursors and mature cells of erythropoiesis<br>– Granulopoiesis and<br>– Megakaryopoiesis<br>– Scattered lymphocytes, plasma cells, and histiocytes – variable | – Pleomorphic megakaryocytes | – **Inadvertent sampling of bone marrow!!**<br>– Inflammatory process<br>– Granulocytic sarcoma – mature variant<br>– Reed-Sternberg-like cells indicating Hodgkin lymphoma<br>– Undifferentiated carcinoma |

### Granulocytic Sarcoma: Mature Variant Sect. 15.3.23, p. 975

| Basic cell pattern | Particular and/or additional features | Differential diagnosis or possible diagnostic pitfall |
|---|---|---|
| -Trilineage cell component as in extramedullary hematopoiesis<br>-A few myeloid blasts | | – Extramedullary hematopoiesis<br>– Inflammatory process |

### Granulocytic Sarcoma: Immature/and Blastic Variant Sect. 15.3.23, p. 975

| Basic cell pattern | Particular and/or additional features | Differential diagnosis or possible diagnostic pitfall |
|---|---|---|
| – Trilineage cell component as in extramedullary hematopoiesis, but: preponderance of myeloid blasts, up to 100% | – Distinct atypical megakaryocytic component | – Large-cell non-Hodgkin lymphoma<br>– Malignant melanoma<br>– Histiocytic sarcoma<br>– Metastatic undifferentiated carcinoma<br>– Hodgkin lymphoma |

### Acute Monocytic Leukemias Sect. 15.3.23, p. 975

| Basic cell pattern | Particular and/or additional features | Differential diagnosis or possible diagnostic pitfall |
|---|---|---|
| – Predominate cell type is the promonocyte:<br>– Nuclear folds, nuclear lobulation, granular cytoplasm<br>– Further myeloblasts and monoblasts | | – Malignant melanoma<br>– Histiocytic sarcoma |

## H Metastatic Neoplasms

**Comments on metastatic carcinomas and their most important immunocytochemical attributes for cytodiagnostic purpose** are provided in Sect. 15.3.24, p. 977 and Table 15.3.3, p. 978.

# Chapter 16 Skin Lesions and Unusual Subcutaneous Lesions

The current synopsis **comprises merely a selection of benign and malignant cutaneous and subcutaneous nonneoplastic lesions and tumors**. Further lesions are described in Sects. 16.2.1, p. 1026, 16.2.2, p. 1026, 16.2.12, p. 1033 and 16.3, p. 1034.

## Common and Rare Skin Lesions, Benign and Malignant: Selected Entities from Sect. 16.2, p. 1026

### Pemphigus Vulgaris

| Basic cell pattern | Particular and/or additional features | Differential diagnosis or possible diagnostic pitfall |
|---|---|---|
| – High cellularity of the cytologic specimen<br>– Small dissociated squamous cells, uniform cell pattern<br>– Increased N/C ratio<br>– The nuclei are well preserved, containing pronounced singular or multiple irregular nucleoli<br>– Loose and fairly even chromatin texture, irregularities are possible<br>– Hyperchromasia is exceptional<br>– Degenerating cytoplasm<br>– Occasional cell-in-cell phenomenon | | – Squamous cell carcinoma |

### Herpes Simplex Virus Infection

| Basic cell pattern | Particular and/or additional features | Differential diagnosis or possible diagnostic pitfall |
|---|---|---|
| – Enlarged rounded immature squamous cells, mono- or multinucleated<br>– Frequent nuclear molding<br>– Distinct small cytoplasmic rim<br>– Nuclei exhibit ground-glass texture or eosinophilic inclusions<br>– Granular condensation of the chromatin to the nuclear periphery | | – (Squamous) carcinoma cells |

### Molluscum Contagiosum

| Basic cell pattern | Particular and/or additional features | Differential diagnosis or possible diagnostic pitfall |
|---|---|---|
| **Molluscum bodies:**<br>– Numerous superficial squamous cells<br>– Cytoplasm loaded with masses of virus particles compressing the nucleus against the cytoplasmic membrane | | |

### Pilomatrixoma

| Basic cell pattern | Particular and/or additional features | Differential diagnosis or possible diagnostic pitfall |
|---|---|---|
| **Shadow cells:**<br>– Faintly yellow stained cells (Pap method)<br>– The lost nuclei are substituted by an unstained clear area<br>**Basaloid cells from the germinal layer:**<br>– Small cells are tightly but regularly clustered and are made up of deep-staining nuclei<br>– Scanty cytoplasm<br>– Nucleoli may be prominent<br>– Degenerating cells with pyknotic nuclei<br>**Calcium deposits**<br>**Squamous cells:**<br>– In various stages of maturation<br>– Nuclei are vesicular, slightly irregular and frequently stripped<br>– Pronounced cellular discohesion | Variable:<br>– Granulomatous component and foreign body giant cells<br>– Amorphous debris<br><br>– Predominance of basaloid cells, absence of ghost cells<br><br>– Numerous naked basaloid cell nuclei with distinct nucleoli<br><br>– Predominance of maturing and mature squamous cells | – Basal cell carcinoma<br>– Undifferentiated carcinoma<br>– Small-cell carcinoma<br>– Endocrine tumor/Merkel cell tumor<br>– Monomorphic breast carcinoma **if pilomatrixoma presents as a breast lump**<br><br>– Malignant lymphoma<br><br>– Squamous cell carcinoma<br>– Odontogenic tumor |

## Common and Rare Skin Lesions, Benign and Malignant: Selected Entities from Sect. 16.2, p. 1026 (continued)

### Basal Cell Carcinoma (BCC)

| Basic cell pattern | Particular and/or additional features | Differential diagnosis or possible diagnostic pitfall |
|---|---|---|
| – Cohesive clusters of small cells<br>  – Clusters varying in size and shape<br>  – No intercellular bridges<br>– Cells at the periphery of the clusters show palisade arrangement<br>– Monomorphic, round to oval nuclei, sometimes elongated<br>– Chromatin pattern loose or finely granular<br>– Occasional nucleoli in activated tumor cells<br>– Very few mitoses<br>– Individual cells with scanty and poorly defined cytoplasm | – Melanocytes and Langerhans cells – variable | – Breast carcinoma, monomorphous subtype<br>– Solid adenoid cystic carcinoma<br>– Pilomatrixoma<br>– Metastatic small-cell carcinoma<br>– Eccrine spiradenoma<br>– Neuroendocrine tumor (**in particular Merkel cell carcinoma**) |

### Keratotic BCC

| Basic cell pattern | Particular and/or additional features | Differential diagnosis or possible diagnostic pitfall |
|---|---|---|
| – The same cell pattern as stated above<br>– Strands or concentric whorls of parakeratotic-like spindle cells surrounding horn cysts filled with fully keratinized cells | | – Trichoepithelioma<br>– Poorly differentiated SCC |

### Granular cell BCC

| Basic cell pattern | Particular and/or additional features | Differential diagnosis or possible diagnostic pitfall |
|---|---|---|
| – The same cell pattern as stated above<br>– Basaloid cell differentiation to granular tumor cells | – Preponderance of granular basaloid tumor cells | – Granular cell tumor |

### Pigmented BCC

| Basic cell pattern | Particular and/or additional features | Differential diagnosis or possible diagnostic pitfall |
|---|---|---|
| – The same cell pattern as stated above<br>– Variable amounts of melanin in melanocytes, melanophages, and rarely in tumor cells | | – Malignant melanoma |

### Squamous Cell Carcinoma (SCC) Common Type

| Basic cell pattern | Particular and/or additional features | Differential diagnosis or possible diagnostic pitfall |
|---|---|---|
| – Single cells and three-dimensional irregular clusters<br>– Tumor cells with pronounced variation in size and shape<br>– **Nuclei:**<br>  – Marked pleomorphism, molding and cleaving,<br>  – Hyperchromasia<br>  – Unevenly distributed and clumped chromatin,<br>  – Large nucleoli, often multiple and polymorph<br>– Nuclei of in keratinized tumor cells: Darkly stained and homogeneous<br>– Giant cell forms and mitoses<br>– N/C ratio variable, but rather low<br>– **Cytoplasm of poorly differentiated cells:**<br>  – Polyhedral cytoplasm , round, polygonal or spindle shaped<br>  – Partly dense and cyanophilic, partly vacuolated<br>  – Generally sharply outlined<br>  – Occasionally concentric rings<br>– **Cytoplasm of keratinized cells:**<br>  – Pleomorphic, polygonal, or spindle shaped,<br>  – Bright red, orange, and yellow stained,<br>  – Densely structured<br>– Intercellular bridges and keratin pearls | | |

## Common and Rare Skin Lesions, Benign and Malignant: Selected Entities from Sect. 16.2, p. 1026 (continued)

### Well-Differentiated Keratinized SCC and Verrucous SCC

| Basic cell pattern | Particular and/or additional features | Differential diagnosis or possible diagnostic pitfall |
|---|---|---|
| – Mildly pleomorphic anucleated squamous cells showing abundant keratinization and pearl formation<br>– Few squamous cells containing nuclei with minor irregularities:<br>  – Rare irregularities of nuclear outline, texture, and color | | – Epidermal inclusion cyst<br>– Hyperkeratotic/acanthotic skin lesions, benign and premalignant |

### Poorly Differentiated SCC, Small-Cell Type

| Basic cell pattern | Particular and/or additional features | Differential diagnosis or possible diagnostic pitfall |
|---|---|---|
| – Small undifferentiated carcinoma cells<br>– Focal keratinization and horn pearls | | – Keratotic basal cell carcinoma |

### Spindle Cell SCC

| Basic cell pattern | Particular and/or additional features | Differential diagnosis or possible diagnostic pitfall |
|---|---|---|
| – Fusiform squamous carcinoma cells, nonkeratinized | | – Other spindle cell lesions consisting of polymorphic spindle cells<br>– In particular **nonpigmented spindle cell melanoma** |

### Malignant Melanoma, Epithelial Cell Type

| Basic cell pattern | Particular and/or additional features | Differential diagnosis or possible diagnostic pitfall |
|---|---|---|
| – Loss of cellular cohesion<br>– **Bi- and multinucleated tumor cells:**<br>  – Low N/C ratio<br>  – Anisocytosis and anisokaryosis – variable<br>  – Eccentrically positioned nuclei<br>  – Macronucleoli and sharply edged intranuclear vacuoles<br>  – Clear or dark nuclei<br>– Granular chromatin pattern evenly distributed, varied coarseness<br>– Irregular nuclear membrane, microscopically small but distinct nuclear wrinkling and indentations<br>– Melanin pigment in tumor cells and macrophages – variable<br>– Clear and indistinct cytoplasm, variable coarse vacuolization | – Complete absence of melanin pigment | – Undifferentiated carcinoma, large cell type<br>– Malignant lymphoma:<br>  – Large blast type, NOS<br>  – Lymphomas of T-cell phenotype! |

### Malignant Melanoma, Spindle Cell Type

| Basic cell pattern | Particular and/or additional features | Differential diagnosis or possible diagnostic pitfall |
|---|---|---|
| – Predominantly atypical spindle cells (similar nuclear morphology as stated above), dispersed or in cohesive fascicles and whorls<br>– Oval or elongated centrally placed nuclei | – Virtually always interspersed epithelial-type melanoma cells | |
| | – Tumor spindle cells with **fairly bland morphology** | – Granulomatosis<br>– Varied soft tissue tumors, benign or low grade<br>– Endocrine tumor consisting of spindle-shaped tumor cells |
| | – Tumor spindle cells – **highly pleomorphic** | – High-grade sarcoma<br>– Pleomorphic carcinoma |
| | – Tumor spindle cells – **melanotic** | – Melanotic schwannoma<br>– Melanotic peripheral nerve sheath tumor |

## Common and Rare Skin Lesions, Benign and Malignant: Selected Entities from Sect. 16.2, p. 1026 (continued)

### Balloon Cell Melanoma

| Basic cell pattern | Particular and/or additional features | Differential diagnosis or possible diagnostic pitfall |
|---|---|---|
| – Typical large malignant melanoma cells (nuclear morphology, see above) exhibiting abundant vacuolated cytoplasm | | – Primary and secondary clear cell tumors such as subtypes of:<br>– Breast carcinoma<br>– Clear cell renal cell carcinoma,<br>– Others |

### Malignant Melanoma, Monomorphic, Small-Cell Type

| Basic cell pattern | Particular and/or additional features | Differential diagnosis or possible diagnostic pitfall |
|---|---|---|
| – Monomorphic small tumor cells usually lacking typical nuclear features of melanoma cells<br>– Melanin pigment is absent | | – Monomorphic carcinomas such as small-cell-type breast cancer, and others |
| | – Small tumor cells with plasmacytoid cytoplasm | – Neuroendocrine tumor<br>– Malignant lymphoma, particularly plasmocytoma |

### Merkel Cell Carcinoma

| Basic cell pattern | Particular and/or additional features | Differential diagnosis or possible diagnostic pitfall |
|---|---|---|
| – Highly cellular aspirates<br>– Tumor cells in small clusters, rosettes, single-file rows; cells are often molded against one another<br>– Single cells and stripped nuclei<br>– Tumor cells are small, uniform, and round to oval in shape<br>– The nucleus is eccentrically placed and irregularly outlined:<br>– Fine granular chromatin<br>– Pronounced hyperchromasia<br>– Inconspicuous nucleoli<br>– Well-defined nuclear membrane<br>– Scanty cytoplasm, sometimes exhibiting faint granularity<br>– Frequent mitotic figures | | – Metastatic small-cell carcinoma<br>– Basal cell carcinoma<br>– Small-cell carcinoma of the salivary gland type<br>– Small-cell malignant melanoma, nonpigmented<br>– Malignant lymphomas of the small-cell type<br>– Small round blue cell tumors |

### Kaposi Sarcoma

| Basic cell pattern | Particular and/or additional features | Differential diagnosis or possible diagnostic pitfall |
|---|---|---|
| – Tissue fragments composed of spindle cells<br>– Tumor cells are loosely and radially arranged<br>– Discrete spindle cells – variable<br>– Distorted nuclei<br>– Ill-defined cytoplasm<br>– Nuclear crush artifacts | | – Various mesenchymal neoplasms<br>– Granulomatous lesions |

**Malignant lymphoma of the skin:** differential diagnoses have been considered above and are discussed in Sect. 16.2.12, p. 1033.

## Primary Cutaneous Tumors Mimicking Metastatic Deposits (and Vice-Versa) Sect. 16.3, p. 1034

### Cutaneous Cylindroma

| Basic cell pattern | Particular and/or additional features | Differential diagnosis or possible diagnostic pitfall |
|---|---|---|
| – Cell-rich cytologic specimens<br>– Cell sizes vary considerably<br>– Three-dimensional tightly cohesive cell clusters encasing globules of basement-membrane-like material | **Further morphologic details on adenoid cystic carcinomas are presented in Sects. 1.3.9, p. 63 and 5.1.5.2, p. 415** | – Adenoid cystic carcinoma of salivary glands<br>– Adenoid cystic carcinoma of the breast |

### Primary Cutaneous Mucinous Adenocarcinoma

| Basic cell pattern | Particular and/or additional features | Differential diagnosis or possible diagnostic pitfall |
|---|---|---|
| – Loosely dispersed mucinous cells in a mucinous background | | – Metastatic mucinous adenocarcinoma<br>**Beware of the axillary presentation of mucinous breast carcinomas!** |

Primary cutaneous tumors mimicking **monomorphic small-cell breast carcinoma metastasizing** to the skin are considered above.

## Unusual Nonneoplastic Masses in Skin and Subcutaneous Regions Sect. 16.4, p. 1034

### Nodular Fasciitis / Proliferative Fasciitis

| Basic cell pattern | Particular and/or additional features | Differential diagnosis or possible diagnostic pitfall |
|---|---|---|
| – Usually cellular smears mainly composed of proliferative mesenchymal cells:<br>(1) Spindle-shaped cells – variable<br>(2) Round cells with eccentric nuclei resembling plasma cells<br>(3) Large plump cells with eccentric nuclei resembling ganglion cells (typical of proliferative fasciitis)<br>– Conspicuous nucleoli<br>– Abundant cytoplasm<br>– Finely granular and evenly distributed chromatin<br>– Varying proportions of inflammatory cells | – Small fragments of hyalin and myxoid masses – variable | |
| | – Predominance of spindle-shaped cells | – Schwannoma<br>– Other spindle cell tumors |

### Proliferative Myositis

| Basic cell pattern | Particular and/or additional features | Differential diagnosis or possible diagnostic pitfall |
|---|---|---|
| – Generally the same cell pattern as stated above<br>– Typical ganglion cell-like cells | – Atrophic muscle fibers | |

### Angiolymphoid Hyperplasia / Kimura Disease

| Basic cell pattern | Particular and/or additional features | Differential diagnosis or possible diagnostic pitfall |
|---|---|---|
| – Hypercellular smears<br>– Mixed lymphoid population<br>– Numerous scattered eosinophilic granulocytes<br>– Proliferative endothelial cells: spindle-shaped and polygonal cells with vesicular nuclei and deep eosinophilic cytoplasm | – Fragments of collagenous tissue – variable | – Angiomatous tumors<br>– Undifferentiated carcinoma<br>– Hodgkin lymphoma |

## Unusual Nonneoplastic Masses in Skin and Subcutaneous Regions (continued) — Sect. 16.4, p. 1034

### Endometriosis

| Basic cell pattern | Particular and/or additional features | Differential diagnosis or possible diagnostic pitfall |
|---|---|---|
| – Usually highly cellular smears<br>– **Background**:<br>  – Hemorrhagic<br>  – Detritic<br>  – Hemosiderin-laden macrophages<br>– **Epithelial cells** in sheets, syncytial clusters, tubular formations<br>  – Small to medium-sized glandular cells<br>  – Scant and cyanophilic cytoplasm<br>  – Distinct nuclear membranes, wrinkled<br>  – Granular and evenly distributed chromatin<br>  – Usually inconspicuous nucleoli<br>– Aggregates of fusiform stromal cells, the nuclei are crowded and focally overlapping | Squamous metaplasia – possible | – Metastasis of a well-differentiated endometrial carcinoma<br>– Other metastatic carcinomas – monomorphic variants |
| | – Complete absence of glandular cells | – Nodular/proliferative fasciitis |
| | – Activated or decidualized stromal cells | – Low-grade sarcoma |
| | – Myxoid background | – Myxoma |

### Endometriosis: Hormonal Cell Activation

| Basic cell pattern | Particular and/or additional features | Differential diagnosis or possible diagnostic pitfall |
|---|---|---|
| – Enlarged atypical epithelial cells<br>– Hyperchromatic nuclei with irregular outline<br>– Dense cell clustering and throughout nuclear overlapping | | – Carcinoma emerging from endometriosis<br>– Metastatic (adeno)carcinoma |
| | – Pronounced squamous metaplasia | – Metastatic squamous cell carcinoma |

## Tumor Mass in the Groin Due to Particle Disease and Osteoarthritic Hydrarthrosis
Sect. 16.4.4, p. 1035

### Particle Disease Following Arthroplasty

| Basic cell pattern | Particular and/or additional features | Differential diagnosis or possible diagnostic pitfall |
|---|---|---|
| – Often turbid and viscous aspirates<br>– Hypercellular smears, cohesive aggregates of spindle cells<br>– Proliferating fibroblasts and histiocytes exhibiting pronounced phagocytosis<br>– Macrophages with activated, irregular nuclei, vacuolated or foamy cytoplasm<br>– Frequent inflammatory cells and multinucleated giant cells<br>– Debris – variable | – Refractile elements, and birefringent components upon polarization<br><br>– A lot of debris associated with macrophages and foreign-body giant cells | – Undifferentiated carcinoma<br>– Undifferentiated sarcoma<br>– Large-cell malignant lymphoma<br>– Tumor necrosis |

### Osteoarthritic Hydrarthrosis and Traumatic Arthritis

| Basic cell pattern | Particular and/or additional features | Differential diagnosis or possible diagnostic pitfall |
|---|---|---|
| – Chondrocytes embedded in cartilaginous matrix<br>– Inflammatory infiltrate – variable | – Debris and proteinaceous background<br>– Hemosiderophages – variable | – **Suggestive of traumatic arthritis** |

# Chapter 17 Soft Tissue and Bone

## Section 17.1 Soft Tissue and Bone – Benign and Intermediate Tumoral Lesions

**Table 17.1.1** Synopsis of selected entities of benign/intermediate soft tissue and bone lesions considering cell types, particular cytologic features, and characteristics of the extracellular matrix

| Cell types<br>Particular cytologic features<br>Background features | Entities | | | | | | | | | | | | | |
|---|---|---|---|---|---|---|---|---|---|---|---|---|---|---|
| | Lipoma | Lipoblastoma | Angiolipoma | Myolipoma | Angiomyolipoma | Chondroid Lipoma | [1]Spindle cell lipoma[a] Pleomorphic lipoma | Hibernoma | Atypical lipomatous tumor | Nodular fasciitis | Proliferative fasciitis/myositis | Myositis ossificans | Fibroma | Desmoid-type fibromatosis |
| **Spindle cells** | | (+) | | ++ | ++ | | +++ | (+) | (+) | ++ | ++ | (+) | ++ | ++ |
| Slender | | | | | | | + | | | ++ | ++ | | ++ | ++ |
| Plump | | | | + | + | | | | | ++ | ++ | | ++ | ++ |
| Nuclei blunt-ended | | | | + | + | | | | | | | | | |
| Nuclei with tapered ends | | | | | | | | | | | | | | |
| **Round cells** | | | | | | | ++ | | ++ | | | ++ | | |
| **Epithelioid cell type** | | | | | | | | | | | | | | |
| **Histiocytic elements** | | | | | | | | | | | | | | |
| Histiocytes | | | | | | | | | + | + | + | | | |
| Macrophages | | | | | | | | | | | | | | |
| Hemosiderophages | | | | | | | | | | | | | | |
| **Multinucleated giant cells** | | | | | | | ++ | | + | | | | | |
| **Osteoclast (-like) giant cells** | | | | | | | | | | + | | (+) | | |
| **Adipocytes** | | | | | | | | | | | | | | |
| Mature adipocytes | +++ | ++ | ++ | + | + | ++ | + | (+) | ++ | | | | | |
| Immature adipocytes/lipoblasts | | ++ | | | | +++ | | | ++ | | | | | |
| Hibernoma (-like) cells | | (+) | | | | + | | +++ | + | | | | | |
| **Skeletal muscle cells** | | | | | | | | | | | | + | | |
| **Chondroid/osteoid cells** | | | | | | | | | | | | | | |
| **Ganglion cells** | | | | | | | | | | | | | | |
| **Ganglion cell-like cells** | | | | | | | | | | | ++ | | | |
| **Particular cytologic features** | | | | | | | | | | | | | | |
| Hypercellular smears | +++ | | | | | | | +++ | (+) | ++ | ++ | | | |
| Tissue fragments | +++ | | | ++ | ++ | (+) | ++ | | + | | | | ++ | ++ |
| Cell aggregates | | | | | | ++ | | ++ | + | ++ | ++ | (+) | | |
| Numerous single cells | | | | | | | | | ++ | ++ | ++ | ++ | | |
| Numerous bare nuclei | | | | | | | | | | | | | | |
| Mitoses | 0 | 0 | | 0 | | + | 0 | 0 | | ++ | ++ | + | | + |
| Pleomorphic cells/nuclei | 0 | 0 | | 0 | | | ++ | 0 | ++ | 0 | 0 | 0 | 0 | 0 |
| Melanin pigment | | | | | | | | | | | | | | |
| Hemosiderin intra- or extracellular | | | | | | | | | | | | | | |
| **Background** | | | | | | | | | | | | | | |
| Mucoid/myxoid | (+) | (+) | | | | +++ | (+) | (+) | (+) | + | + | | ++ | (+) |
| Fibrillary collagen | (+) | | | | | | ++ | | (+) | | | | ++ | +++ |
| Fine fibrillar/glial | | | | | | | | | | | | | | |
| Chondroid/osteoid | (+) | | | | | +++ | | | + | + | + | (+) | (+) | |
| Inflammatory | + | | | (+) | | | + | | (+) | + | + | | | |
| Granulomatous | | | | | | | | | | | | | | |
| Mast cells | | | | | | | ++ | | | | | | | |
| Vessels/capillary network | + | ++ | ++ | | +++ | + | | + | | ++ | | | + | ++ |
| Calcium deposits | | | | | | | | | | | | | + | |

**Table 17.1.1** (continued)

+++ abundant
++ numerous
+ few or not always present
(+, ++, +++) variable (according to subtype)
0 completely absent or extremely rare
[1a] Intermediate cell patterns between the two classic end points are common
[2b] Basic cell pattern of various tumor forms

| Cell types<br>Particular cytologic features<br>Background features | Entities | | | | | | | | | | | | | |
|---|---|---|---|---|---|---|---|---|---|---|---|---|---|---|
| | Soft tissue giant cell tumor | [2]Tendon sheath giant cell tumor[b] | Leiomyom | Glomus tumor | Rhabdomyoma, adult/ fetal type | Peripheral nerve tumor | Soft tissue chondroma | Intramuscular myxoma | Osteo chondroma | Chondroblastoma | Osteoblastoma | Bone giant cell tumor | Aneurysmal bone cyst | Langerhans cell histiocytosis |
| **Spindle cells** | | ++ | +++ | (+) | (++) | +++ | | ++ | | | + | (+) | ++ | |
| Slender | | | + | | | | | | | | | | | |
| Plump | | | | | | | | | | | | | | |
| Nuclei blunt-ended | | | + | | | | | | | | | | | |
| Nuclei with tapered ends | | | | | | + | | | | | | | | |
| **Round cells** | ++ | | | ++ | | | | | | +++ | +++ | +++ | +++ | |
| **Epithelioid cell type** | | ++ | | | | (++) | | | | | | | | |
| **Histiocytic elements** | | + | | | | | | | | | | | | +++ |
| Histiocytes | | | | | | | + | | | | | | | + |
| Macrophages | | | | | | (+) | | | | | | | | + |
| Hemosiderophages | ++ | + | | | | | | | | | | | | |
| **Multinucleated giant cells** | | | + | | | (+) | | | | | | | | |
| **Osteoclast (-like) giant cells** | ++ | (++) | | | | | | | | ++ | ++ | +++ | +++ | + |
| **Adipocytes** | | | | | | | | | | | | | | |
| Mature adipocytes | | | | | | | | | | | | | | |
| Immature adipocytes/lipoblasts | | | | | | | | | | | | | | |
| Hibernoma (-like) cells | | | | | | | | | | | | | | |
| **Skeletal muscle cells** | | | | | ++ | | | | | | | | | |
| **Chondroid/osteoid cells** | | | | | | | + | | ++ | +++ | +++ | (+) | | |
| **Ganglion cells** | | | | | | | | | | | | | | |
| **Ganglion cell-like cells** | | | | | | | | | | | | | | |
| **Particular cytologic features** | | | | | | | | | | | | | | |
| Hypercellular smears | | + | | ++ | | | | | | ++ | | | | ++ |
| Tissue fragments | | | ++ | | | +++ | | | | | | | | |
| Cell aggregates | | | | + | | ++ | | | ++ | ++ | | ++ | ++ | ++ |
| Numerous single cells | | | | + | | | | | | | | ++ | ++ | ++ |
| Numerous bare nuclei | | | | (+) | | | | | | | | | | |
| Mitoses | + | ++ | | 0 | 0 | (+) | | | | + | | + | + | + |
| Pleomorphic cells/nuclei | 0 | | 0 | 0 | 0 | (+) | + | | | | + | (+) | | +++ |
| Melanin pigment | | | | | | (+) | | | | | | | | |
| Hemosiderin intra- or extracellular | | ++ | | | | | | | | ++ | | | | |
| **Background** | | | | | | | | | | | | | | |
| Mucoid/myxoid | | | | + | (+) | ++ | (+) | +++ | | ++ | + | | | |
| Fibrillary collagen | | + | | | | | (+) | (+) | | | | (+) | + | |
| Fine fibrillar/glial | | | | | | ++ | | | | | | | | |
| Chondroid/osteoid | + | | | | | | ++ | | ++ | ++ | ++ | | ++ | |
| Inflammatory | | + | | | | | | | | | | | | ++ |
| Granulomatous | | | | | | | + | | | | | | | |
| Mast cells | | | | + | | | | | | | | | | |
| Vessels/capillary network | + | | | (+) | | | | + | | | | | + | |
| Calcium deposits | | | | | | | + | | + | ++ | ++ | | | |

**Table 17.1.2** Synopsis of the age groups, common locations, and the differential diagnostic spectrum of the lesions listed in Table 17.1.1

| Entities | Common age groups<br>Years of age<br>Gender preference | Most common sites of origin | Differential diagnoses |
|---|---|---|---|
| **Lipoma** | 40–60 years of age<br>Rare in children unless as part of inherited disease | Superficial and deep-seated lipoma in:<br>Neck, shoulder, chest, back, abdomen, thigh | Other benign lipomatous tumors<br>Well-differentiated liposarcoma |
| **Lipoblastoma** | Infants and young children up to 5 y. | Subcutaneous tissues of:<br>Upper and lower extremities | Lipoma, well-differentiated liposarcoma, myxoid liposarcoma |
| **Angiolipoma** | 15–30 years of age | Subcutaneous tissue of: Upper arm, forearm, trunk | Angiosarcoma<br>Kaposi sarcoma |
| **Myolipoma** | Exclusively in adults | Subcutaneous tissue (with deep growth) of groin, trunk, extremities.<br>Abdominal cavity, retroperitoneum | Angiomyolipoma |
| **Angiomyolipoma** | Adults | Kidney and perirenal soft tissue | |
| **Chondroid lipoma** | Adults with few exceptions | Subcutaneous or deep-seated:<br>Proximal upper and lower extremities | Myxoid liposarcoma, extraskeletal myxoid chondrosarcoma, and others |
| **Spindle cell lipoma/<br>Pleomorphic lipoma** | Elderly people | Dermal or subcutaneous tissue of:<br>Neck (predominantly posterior), shoulder girdle, back | A variety of lesions with predominant spindle cells or pleomorphic mono- and multinucleated giant cells |
| **Hibernoma** | Young adults | Subcutaneous tissue of:<br>Thigh, back, upper extremity, head /neck | Primarily lesions with granular cells:<br>Lipoblastoma, histiocytoma, granular cell tumor, oncocytoma |
| **Atypical lipomatous tumor** | Middle-aged adults | Deep soft tissues:<br>Thigh, retroperitoneum, mediastinum, and note (!) spermatic cord | According to tumor variants:<br>Pleomorphic lipoma, liposarcomas, benign and malignant myxoid tumors, inflammation, lymphoid hyperplasia, malignant lymphoma |
| **Nodular fasciitis** | All age groups, but mainly in young adults | Subcutaneous tissue of:<br>Upper extremities, trunk, head and neck | Schwannoma and other spindle cell lesions (histiocytic, fibrous, lipomatous) |
| **Proliferative fasciitis (PF)<br>Proliferative myositis (PM)** | Middle-aged and older adults | PF: forearm, lower extremity, trunk<br>PM: trunk, shoulder girdle, upper arm | Comparable to those in nodular fasciitis |
| **Myositis ossificans** | Broad age distribution with a predilection for young adults | Intramuscular: anywhere in the body<br>In favor: sites exposed to trauma | Benign and malignant bone-forming lesions, other pseudosarcomatous lesions and sarcomas |
| **Fibroma** | Mainly in younger male adults | Ubiquitous<br>Extremities, particularly fingers | Many entities of the fibroblastic tumor category and callus, schwannoma, GIST, spindle cell sarcomas, osteosarcoma, etc. |
| **Desmoid-type fibromatosis** | Broad age distribution | Deep soft tissues (also intraabdominal):<br>– Extraabdominal (pediatric population)<br>– Abdominal wall (younger adults)<br>– Various sites (older age group) | See: fibroma |
| **Giant cell tumor of soft tissue** | Predominantly in middle-aged patients | In superficial soft tissues of upper and lower extremities (in about 70% of tumors) | |
| **Giant cell tumors of:**<br>**– tendon sheath**<br>**– diffuse type** | Middle-aged patients<br>Younger patients ( < 40 years) | Hands, predominantly in the fingers<br>Elbows, hip, ankle, knee, thigh, foot | Malignant neoplasms |
| **Leiomyoma** | | – Very common<br>– Rare in deep somatic soft tissue | Well-differentiated leiomyosarcoma |
| **Glomus tumor** | Typically in young adults | Skin and superficial soft tissue mainly subungual. Deep soft tissue and viscera are rarely affected | Monomorphic epithelial neoplasms: benign and malignant, primary and metastatic |
| **Rhabdomyoma**<br>**– Adult type**<br>**– Fetal type** | Elderly male population<br>Young children | Head and neck soft tissue, mouth, throat | Granular cell tumor, hibernoma, oncocytic tumors, sarcoma<br>Rhabdomyosarcoma |

**Table 17.1.2** (continued)

| Entities | Common age groups<br>Years of age<br>Gender preference | Most common sites of origin | Differential diagnoses |
|---|---|---|---|
| **Benign peripheral nerve tumor** | At any age<br>Schwannoma and neurofibroma: young adults | Any part of the body | Fibrohistiocytic tumors, pleomorphic adenoma, malignant peripheral nerve tumor, spindle cell melanoma, certain cytokeratin positive malignancies |
| **Soft tissue chondroma** | Middle-aged patients | Fingers | Neck tumor: pleomorphic adenoma<br>Many lesions with chondroid features |
| **Intramuscular myxoma** | Middle-aged and older females | Large muscles of thigh, shoulder, upper arm, buttock | Intramuscular lesions with myxoid features |
| **Osteochondroma** | Children and young adults | Metaphysis of long bones | Tumors containing cartilage |
| **Chondroblastoma** | Mostly in the second and third decade | Epiphysis of long bones | Various lesions with chondroid matrix and/or giant cells.<br>Parotid area: biphasic tumors of salivary gland |
| **Osteoblastoma** | Teenager and third decade (especially males) | Spine | Osteoid-osteoma, aneurysmal bone cyst, giant cell tumor, osteosarcoma |
| **Giant cell tumor of bone** | Between 20 and 50 years | Ends of long bones (distal femur, proximal tibia).<br>Sacrum | All tumors and reactive lesions associated with osteoclast-like giant cells |
| **Aneurysmal bone cyst** | Children and young adults | Ends of long bones, vertebral bodies | Giant cell tumor of bone and related lesions.<br>Brown tumor of hyperparathyroidism |
| **Langerhans cell histiocytosis** | Children and young adults | Bone sites only: Skull, femur, mandible, bones of pelvis, ribs (in adults) | Malignant lymphoma,<br>Fibrous histiocytoma |

# Section 17.2 Soft Tissue and Bone – MalignantTumors

**Table 17.2.1** Synopsis of selected malignant soft tissue/bone lesions considering cytoarchitectural patterns and cellular details

| Cytoarchitectural pattern | Entities | | | | | | | | | | | | |
|---|---|---|---|---|---|---|---|---|---|---|---|---|---|
| | Adipocytic tumors | | | | | Undifferentiated pleomorphic sarcoma (former MFH) | | | | Myogenic sarcomas | | | |
| | Well-differentiated liposarcoma | Myxoid liposarcoma | Round cell myxoid liposarcoma | Dedifferentiated and pleomorphic liposarcoma | **Fibrosarcoma** | High grade | With giant cells | With inflammation | | Leiomyosarcoma | Embryonal rhabdomyosarcoma | Alveolar rhabdomyosarcoma | Pleomorphic rhabdomyosarcoma |
| **Cell dyshesion** | | | | | ++ | (++) | (++) | (++) | | + | | | ++ |
| **Myxoid matrix** | | +++ | +++ | + | (++) | (++) | | | | | ++ | | |
| **Chondroid/osteoid matrix** | | | | | | | + | | | | | | |
| **Fibrillar matrix** | | | | | | | | | | | | | |
| **Inflammatory infiltrate** | | | | | | | | ++ | | | | | |
| **Background necrosis** | | | | | | + | + | + | | | | | |
| **Cytologic details** | | | | | | | | | | | | | |
| **Pleomorphic** | 0 | | ++ | (++) | ++ | +++ | +++ | +++ | | | (++) | (+) | +++ |
| **Spindle cell** | | + | + | ++ | +++ | (+++) | (+++) | (++) | | +++ | (+) | | |
| **Round cell** | | + | ++ | ++ | | (++) | (++) | (++) | | | ++ | +++ | |
| **Epithelioid** | | | | | | (++) | (++) | (++) | | | | | ++ |
| **Giant cells** | | | | | | | ++ | | | | | + | |
| **Mature-like tumor cell component** | +++ | | | | | | | | | | | | |

**Table 17.2.1** (continued)

| | | | |
|---|---|---|---|
| +++ | abundant | (+, ++, +++) | variable (according to subtype) |
| ++ | numerous | 0 | completely absent or extremely rare |
| + | few or not always present | | |

| Cytoarchitectural pattern | Epithelioid hemangioendothelioma and angiosarcoma | Malignant peripheral nerve sheath tumor | Chondro-osseous tumors | | | | | Clear cell sarcoma | Epithelioid sarcoma | Synovial sarcoma |
|---|---|---|---|---|---|---|---|---|---|---|
| | | | Well-differentiated chondrosarcoma | Myxoid chondrosarcoma | Mesenchymal chondrosarcoma | Dedifferentiated chondrosarcoma | Osteosarcoma | | | |
| **Cell dyshesion** | ++ | ++ | | | | | | | | |
| **Myxoid matrix** | + | | | +++ | + | | | | + | |
| **Chondroid/osteoid matrix** | | | +++ | 0 | 0 | + | ++ | | | |
| **Fibrillar matrix** | | + | | | | | | | | |
| **Inflammatory infiltrate** | | | | | | | | | + | |
| **Background necrosis** | | | | | | | | | ++ | 0 |
| **Cytologic details** | | | | | | | | | | |
| **Pleomorphic** | (++) | (++) | + | ++ | | ++ | (++) | | | |
| **Spindle cell** | (++) | +++ | | | | ++ | (++) | | ++ | ++ |
| **Round cell** | (++) | | | | +++ | | (++) | | | |
| **Epithelioid** | +++ | | | | | | | +++ | ++ | ++ |
| **Giant cells** | | | | | | | | (++) | | 0 |
| **Mature-like tumor cell component** | | (+) | ++ | 0 | 0 | | | | | |

# Glossar

| | |
|---|---|
| **AB** | Antibody |
| **AFP** | Alpha-feto protein |
| **AG** | Antigen |
| **AIDS** | Aquired immune deficiency syndrome |
| **ALK** | Anaplastic lymphoma kinase protein |
| **Ca** | Carcinoma |
| **CA** | Cancer antigen (cancer associated carbohydrates) |
| **CB** | Core biopsy |
| **CC** | Cholangiocarcinoma |
| **CD** | Cluster of differentiation (cellular surface antigen) |
| **CEA** | Carcinoembryonic antigen |
| **CgA** | Chromogranin A |
| **CK** | Cytokeratin |
| **CLL** | Chronic lymphocytic leukemia |
| **CMV** | Cytomegalovirus |
| **CNB** | Core needle biopsy |
| **COPD** | Chronic obstructive pulmonary disease |
| **CT** | Computed tomography |
| **DLBCL** | Diffuse large B-cell lymphoma |
| **DNA** | Desoxyribonucleic acid |
| **DQ** | Diff Quick stain |
| **EBV** | Ebstein-Barr virus |
| **EMA** | Epithelial membrane antigen |
| **ER** | Estrogen receptor |
| **EUS** | Endosonography |
| **EUS-FNP** | Endosonography-guided fine-needle aspiration biopsy |
| **FA** | Fragment analysis by gene analizer |
| **FACS** | Fluorescence activated cell sorting (the acronym FACS is trademarked and owned by Becton Dickinson, Franklin Lakes, NJ, USA) |
| **FCM** | Flow cytometry |
| **FISH** | Fluorescence in situ hybridization |
| **FNAB** | Fine-needle aspiration biopsy |
| **FNH** | Focal nodular hyperplasia |
| **GFAP** | Glial fibrillary acidic protein |
| **HCA** | Hepatocellular adenoma |
| **HCC** | Hepatocellular carcinoma |
| **HCG** | Human chorionic gonadotrophin |
| **Hep Par 1** | Hepatocyte antigene |
| **HHF-35** | Monoclonal antibody recognizing the muscle-specific isoforms of actin |
| **HHV** | Human Herpesvirus |
| **HIV** | Human immunodeficiency virus |
| **HMW CK** | High molecular weight cytokeratins |
| **HPV** | Human papillomavirus |
| **HR** | Hormone receptors |
| **HRS CELL** | Hodgkin- and Reed-Sternberg cell |
| **HTLV-1** | Human T-cell lymphotropic virus type 1 |
| **IC** | Immunocytochemistry |
| **ICM** | Image cytometry (systems:Ahrens Cytometrie-System, Bargteheide,DE; AutoCyte, TriPath, Burlington NC, USA; Zeiss-Kontron/Cires 3.1,DE) |
| **ICM DNA** | Quantitative DNA analysis by image cytometry |
| **IPMN** | Intraductal papillary mucinous neoplasm |
| **LCA** | Leukocyte common antigen (CD45) |

| | |
|---|---|
| **L&H cell** | Lymphocytic / histiocytic cell ('popcorn' cell) |
| **LAVysion™** | Probe set for Fluorescence in situ hybridization (Abbott Molecular Inc., Des Plaines, IL, USA) |
| **LOH** | Loss of heterozygosity |
| **MALT-lymphoma** | Marginal-zone B-cell lymphoma of mucosa-associated lymphoid tissue |
| **MFH** | Malignant fibrous histiocytoma |
| **MGG** | May-Gruenwald-Giemsa stain |
| **MOTT** | mycobacteria other than tuberculosis |
| **MRI** | Magnetic resonance imaging |
| **MSA** | Muscle specific actin |
| **N/C ratio** | Nuclear/cytoplasmic ratio |
| **NET** | Neuroendocrine tumor |
| **NOS** | Not otherwise specified |
| **NSCLC** | Non small cell lung cancer |
| **NSE** | Neuron-specific enolase |
| **PanIN** | Pancreatic intraepithelial neoplasia |
| **PAP** | Prostate acid phophatase |
| **Pap** | Papanicolaou-stain |
| **PAS** | Periodic-acid-Schiff stain |
| **PCEA** | Polyclonal carcinoembryonic antigen |
| **PCR** | Polymerase chain reaction |
| **PET** | Positron Emission Tomography |
| **PET-CT** | Positron Emission Tomography combined with computed tomography |
| **PIN** | Prostatic intraepithelial neoplasia |
| **PLAP** | Placental alcaline phosphatase |
| **PR** | Progesterone receptor |
| **PMC** | Pan melanoma cocktail |
| **PSA** | Prostate specific antigen |
| **RCCMa** | Renal cell carcinoma associated cellmarker |
| **RS CELL** | Reed-Sternberg cell |
| **SCLC** | Small cell lung cancer |
| **SM** | Smooth muscle |
| **SMA** | Smooth muscle actin |
| **SL** | Stemline (DNA index) |
| **TdT** | Terminal deoxynucleotidyl transferase |
| **TP** | ThinPrep® Pap Test (Cytyc/Hologic Corp, Marlborough,MA, USA) |
| **TTF-1** | Thyroid transcription factor-1 |
| **UroVysion™** | Probe set for Fluorescence in situ hybridization (Abbott Molecular Inc., Des Plaines, IL, USA) |
| **US-FNAB** | Ultrasound-guided fine-needle aspiration biopsy |

# Subject Index

## D

## F



## G



## H

## M

## N

## O



## P

## Q



## R



## S